AIEE Transactions Index for Part I, Volume 70, 1951

1. Technical Subject Index

Accelerators, Dielectric Loading for Waveguide Linear. Flesher, Cohn.........887-93
Acoustic Models of Transformer Installations. Gettys, Conover.........333-6; disc. 336
Admittance Functions, Loci of Complex Impedance and. Michaels.........299-303
Admittance Remains Constant as Load Varies, Networks for Which Magnitude or Phase Angle of Input Impedance or Transfer. Berkowitz..286-91
Aging of Class-B Insulating Material in Nitrogen. Stewart, Whitman.........436-7; disc. 437
Air Blast Circuit Breaker, A New 69-Kv. Shores, Beatty.........202-07; disc. 207
Air Circuit Breakers, A Spring Mechanism for Hand Closing of Magnetic Power. Dickinson, Findley.........189-92; disc. 192
Aircraft D-C Systems, Fault Transients in. Scorgie.........713-20; disc. 720
Alignment Techniques for Phase-Rotation Single Side-Band Transmitters, Output Analysis and. Whitby, Scheuch.........209-12
Alloy Sheaths for Underground Power Cable, Lead-. Halperin, Betzer.........423-9; disc. 429
Alternating and Direct Voltage Endurance Studies on Mica Insulation for Electric Machinery. Moses.........763-8; disc. 768
A-C Arc Adjacent to Refractory Surfaces, A Study of Conduction Phenomena Near Current Zero for an. Browne, Strom.........398-407; disc. 407
A-C Arc Welders with Saturable Reactor Control. Oestreicher.........787-90
A-C Generators, Relay Protection of. (Committee Report).........275-81; disc. 281
A-C Impedances of Machine Conductors, Circuit Analysis Method for Determination of. Babb, Williams.........661-5; disc. 665
A-C Instruments, Frequency Compensation of. Miller.........217-20; disc. 220
A-C Multiple-Car Control for the Pennsylvania Railroad, New. Newhouse.........645-7; disc. 647
A-C Multiple-Unit Car Control Equipment. O'Kelly.........652-6
A-C Multiple-Unit Car Motor. Kreitler.........648-50; disc. 650
A-C Servomechanisms, Effects of Carrier Shifts on Derivative Networks for. Attura.........612-18
A-C Servomechanisms, Network Synthesis by Graphical Methods for. Bjornson.........619-25
Alternators, Static Magnetic Exciter for Synchronous. Storm.........1014-17
American Gas and Electric Company, Corona Investigation on Extra-High-Voltage Lines—500-Kv Test Project of the. Gross, Wagner, Naef, Tremaine.........75-91; disc. 91
American Gas and Electric Company, Line Insulator Loss Under Normal Conditions—500-Kv Test Project of the. Naef, Tremaine, Jones.........1073-8
American Gas and Electric Company, Radio Influence Tests in Field and Laboratory—500-Kv Test Project of the. Lippert, Pakala, Bartlett, Fahrnkopf.........251-65; disc. 265
American Gas and Electric Company, Techniques of Corona Loss Measurement and Analysis—500-Kv Test Project of the. Naef, Tremaine, Jones.........496-505; disc. 505
American Gas and Electric Company, The 300-315 Kv Extra High-Voltage Transmission System of the. Sporn, Peterson, Gross, St. Clair...64-72; disc. 72
Amplifier Subcommittee, Progress Report of the AIEE Magnetic. (Committee Report)..445-9; disc. 449
Amplifiers Based on Linear Approximations of the Magnetization Curve, Steady-State Analysis of Self-Saturating Magnetic. Esselman.........451-9
Amplifiers—Cases of Negligible Commutation, The Transient Response of Magnetic. Finzi, Chandler, Beaumariage.........934-42; disc. 942
Analogue Computers, A Diode Bridge Limiter for Use with Electronic. Medkeff, Parent.........913-16
Analogue Computing Techniques Applied to Economics. Strotz, Calvert, Morehouse.........557-62; disc. 562
Analysis and Alignment Techniques for Phase-Rotation Single Side-Band Transmitters, Output. Whitby, Scheuch.........209-12
Analysis Method for Determination of A-C Impedances of Machine Conductors, Circuit. Babb, Williams.........661-5; disc. 665
Analysis of a 3-Phase Inverter with Resistive Load. Turkington.........1055-61
Analysis of Grounding Banks to Balance Distribution Feeder Voltages, An. Long.........823-7
Analysis of Rotating Machines and Stationary Networks by Means of Rotating Reference Frames. Ku.........943-54; disc. 954
Analysis of Self-Saturating Magnetic Amplifiers Based on Linear Approximations of the Magnetization Curve, Steady-State. Esselman.........451-9
Analyzer Study of Harmonic Power Generation with Nonlinear Impedance Element, Differential. Russell, Peterson.........917-20
Angle-Shaped Conductors, Geometric Mean Distances of. Magnusson.........121-3
Angular Velocity, A Tachometer for Measurement of Instantaneous Variations in. Bartles....1102-05
Annulus by the Method of Subareas, Calculation of the Capacitance of a Circular. Higgins, Reitan.........926-31; disc. 931
Apparatus Protection, Some Effects of Lightning Arrester Protective Characteristics and Location upon Station. Kalb.........379-83; disc. 383
Application, Economics of Power Transformer. Barkle, Witzke.........440-4; disc. 444
Application of a Series Capacitor to a Synchronous Condenser for Reducing Voltage Flicker, The. Black, Lischer.........144-50
Application of Microwave Channels. Cheek..813-17
Application of Resonant Grounding in Power Systems in the United States. Gross, Atherton.........389-93; disc. 393
Application of Shunt Capacitors at Transmission and Distribution Stations. Porter, Zimmerman.........112-18; disc. 118
Applications, 940-960 Megacycle Communications Equipment for Industrial. Gunter......807-12
Approach to Control Room Lighting, An Engineering. Dzwonczyk.........852-7; disc. 857
Approach to the Compensation of Saturating Servomechanisms, A Phase-Plane. Hopkin......631-9
Approximations of the Magnetization Curve, Steady-State Analysis of Self-Saturating Magnetic Amplifiers Based on Linear. Esselman.........451-9
Arc Adjacent to Refractory Surfaces, A Study of Conduction Phenomena Near Current Zero for an A-C. Browne, Strom.........398-407; disc. 407
Arc Chokes Power Flow in New Lightning Arresters, Spiral. Ackermann, DeVal.........995-8
Arc Rectifier on the Central Railway of Brazil, Regeneration With a Mercury. Schmidt.........1092-6
Arc Welders with Saturable Reactor Control, A-C. Oestreicher.........787-90
Arcs and Their Relation to the Welding Arc, The Physical Mechanism of Low and High-Current. Finkelnburg.........800-03
Arcs, New Electrodes for Stabilizing Inert-Gas Welding. Cobine, Gallagher.........804-06
Armatures, Winding Insulation Tester for D-C. Catlin, Rohats.........465-8
Arrester Protective Characteristics and Location upon Station Apparatus Protection, Some Effects of Lightning. Kalb.........379-83; disc. 383
Arresters, Spiral Arc Chokes Power Flow in New Lightning. Ackermann, DeVal.........995-8
Arresters, The Power Interruption Testing of Lightning. Ackermann.........1-5; disc. 5
Audio Noise in Substation Type Transformers, An Investigation of. Vivian, Peck...328-31; disc. 331
Automatic Controls, Some Design Criteria for. Nims.........606-11
Automatic Devices, Switching of Distribution Capacitors by Manual and. Hopkins, Schultz...138-43
Automatic Private-Line Teletypewriter Switching System, A Full. Bacon, Locke.........473-80
Automatic Trunk Selection in Reperforator Switching. Blanton.........481-9

B

Balancing of Large Turbine-Generator Rotors, Modern Practice in the. Laffoon, Hagg, Janthey, Heller.........593-8; disc. 598
Ballasts, Noise Evaluation of Fluorescent Lamp. Hayes, Gould.........573-9
Banks, A New Carrier-Current Frequency-Shift System for Use with Differential Protection of Transformer. Beckwith.........832-5; disc. 835
Banks, Switching High-Voltage Shunt Capacitor. Funkhouser, VanSickle, Shankle.........129-33; disc. 134
Banks to Balance Distribution Feeder Voltages, An Analysis of Grounding. Long.........823-7
Bar Induction Motor, A Contribution to the Theory of the Deep-. Douglas.........862-6
Basic Heat-Transfer Data in Electron Tube Operation. Buckland.........1079-85
(Basic Sciences) A New Method for Treating Electron Tubes When Used as Oscillators in the Free as Well as in the Synchronized States. Mostafa, Bey.........999-1004
(Basic Sciences) Calculation of Flux Distributions with Saturation. Poritsky.........309-19; disc. 319
(Basic Sciences) Calculation of the Capacitance of a Circular Annulus by the Method of Subareas. Higgins, Reitan.........926-31; disc. 931
(Basic Sciences) Contact Transients in Simple Electric Circuits. Martin, Stauss.........304-07; disc. 307
(Basic Sciences) Dependence of Direct Sparkover Voltage of Gaps on Humidity and Time. Jacob, Sommerman.........921-4; disc. 924
(Basic Sciences) Loci of Complex Impedance and Admittance Functions. Michaels.........299-303
(Basic Sciences) Networks for Which Magnitude or Phase Angle of Input Impedance or Transfer Admittance Remains Constant as Load Varies. Berkowitz.........286-91
(Basic Sciences) Tables of Green's Functions, Fourier Series, and Impulse Functions for Rectangular Coordinate Systems. Smith.........22-30
(Basic Sciences) The Generalized Transmission Matrix Stability Criterion. Honnell....292-6; disc. 296
Bibliography of Relay Literature—1947-1949. (Committee Report).........247-50
Blast Circuit Breaker, A New 69-Kv Air. Shores, Beatty.........202-07; disc. 207
Brazil, Regeneration with a Mercury Arc Rectifier on the Central Railway of. Schmidt.........1092-6
Breakdown Voltage, A Gas Tube Inverter with the Supply Voltage Below the. Cage, Schuder.........908-12
Breaker, A New 69-Kv Air Blast Circuit. Shores, Beatty.........202-07; disc. 207
Breakers, A Spring Mechanism for Hand Closing of Magnetic Power Air Circuit. Dickinson, Findley.........189-92; disc. 192
Bridge Limiter for Use with Electronic Analogue Computers, A Diode. Medkeff, Parent.........913-16
Buried Cables, Thermal Transients on. Buller.........45-52; disc. 52, 1106

C

Cab Signaling and Train Control System for Railroads, A Modern. Allison.........232-8; disc. 238
Cable, Lead-Alloy Sheaths for Underground Power. Halperin, Betzer.........423-9; disc. 429
Cable, Washington, D. C., 69-Kv Medium-Pressure Gas-Filled. Clark.........418-21; disc. 421
Cable with Submerged Repeaters, A Submarine Telephone. Gilbert.........564-72
Cables, Thermal Expansion Effects in Power. Schifreen.........160-8; disc. 168
Cables, Thermal Transients on Buried. Buller.........45-52; disc. 52, 1106
Calculation of Flux Distributions with Saturation. Poritsky.........309-19; disc. 319
Calculation of the Capacitance of a Circular Annulus by the Method of Subareas. Higgins, Reitan.........926-31; disc. 931
Calculations—Effect of Conductor Configuration in Overhead Lines, Welding. Tietze.........784-6
Calculator, A New Train Performance. Smith..657-60
Capacitance of a Circular Annulus by the Method of Subareas, Calculation of the. Higgins, Reitan.........926-31; disc. 931
Capacitor Banks, Switching High-Voltage Shunt. Funkhouser, VanSickle, Shankle..129-33; disc. 134
Capacitor in Series with a Synchronous Condenser, Technical Problems Associated with the Application of a. Witzke, Michelson.........519-25
Capacitor Switching Phenomena. Van Sickle, Zaborszky.........151-8; disc. 158

Capacitor to a Synchronous Condenser for Reducing Voltage Flicker, The Application of a Series. Black, Lischer 144–50
Capacitors at Transmission and Distribution Stations, Application of Shunt. Porter, Zimmerman . . . . . . 112–18; disc. 118
Capacitors by Manual and Automatic Devices, Switching of Distribution. Hopkins, Schultz 138–43
Capacitors in High-Voltage Transmission Lines, Fundamental Effects of Series. Johnson, Barkle, Povejsil . . . . 526–35; disc. 535
Capacity by the Probability Method Effect of Interconnections, Determination of Reserve. Calabrese 1018–20
Car Control Equipment, A-C Multiple-Unit. O'Kelly 652–6
Car Control for the Pennsylvania Railroad, New A-C Multiple-. Newhouse . . . . 645–7; disc. 647
Car Equipments?, Why 4-Motor Multiple-Unit. Williamson 240–2
Car Motor, A-C Multiple-Unit. Kreitler . . . . 648–50; disc. 650
Car Motor for the Pennsylvania Railroad, A New Multiple-Unit. Jungk . . . . 243–5; disc. 245
Carrier Communication Channel, Vibracode System of Supervisory Control on a. Allen, Daniel . . . . 818–22; disc. 822
(Carrier Current) Application of Microwave Channels. Cheek 813–17
Carrier Current Communications Circuits, Signal and Supervision Systems Used on. Mayer 990–4
Carrier-Current Frequency-Shift System for Use with Differential Protection of Transformer Banks, A New. Beckwith . . . . 832–5; disc. 835
(Carrier Current) 940–960 Megacycle Communications Equipment for Industrial Applications. Gunter 807–12
Carrier Current Supervisory System for Distribution Circuits. Podolsky, Lubin 1096–1101
Carrier Relaying System, Measurements and Tests on a Power Line. Miller, Worthington 1005–07
Carrier Shifts on Derivative Networks for A-C Servomechanisms, Effects of. Attura 612–18
Cars, Electric Equipment and Performance of Lightweight Rapid Transit. Ellis, Sloman . . . . 227–30; disc. 230
Cars, Selection of Equipment for Multiple-Unit. Hutchison . . . . 640–3; disc. 643
Changer Welders, Ignitrons for Frequency-. Rottier 900–07
Channel Time-Division-Multiplex Telegraph System for Long-Distance Radio Circuits, Four- or Two-. Peterman, Minc 362–72
Channel, Vibracode System of Supervisory Control on a Carrier Communication. Allen, Daniel . . . . 818–22; disc. 822
Channels, Application of Microwave. Cheek . . 813–17
Channels for a Power System, Choice of Telemetering Systems and. Duff 1086–91
Characteristics and Location upon Station Apparatus Protection, Some Effects of Lightning Arrester Protective. Kalb . . . . 379–83; disc. 383
Charge in Electrostatic Mineral Separation, Distribution of. Fraas, Ralston 1028–30
Choice of Telemetering Systems and Channels for a Power System. Duff 1086–91
Chokes Power Flow in New Lightning Arresters, Spiral Arc. Ackermann, DeVal 995–8
Circuit Analysis Method for Determination of A-C Impedances of Machine Conductors. Babb, Williams . . . . 661–5; disc. 665
Circuit Breaker, A New 69-Kv Air Blast. Shores, Beatty . . . . 202–07; disc. 207
Circuit Breakers, A Spring Mechanism for Hand Closing of Magnetic Power Air. Dickinson, Findley . . . . 189–92; disc. 192
Circuits and Their Application in Designing Shaded Pole Motors, Equivalent. Chang . . 690–8; disc. 698
Circuits, Carrier Current Supervisory System for Distribution. Podolsky, Lubin 1096–1101
Circuits, Contact Transients in Simple Electric. Martin, Stauss . . . . 304–07; disc. 307
Circuits, Four- or Two-Channel Time-Division-Multiplex Telegraph System for Long-Distance Radio. Peterman, Minc 362–72
Circuits, Signal and Supervision Systems Used on Carrier Current Communications. Mayer 990–4
Circular Annulus by the Method of Subareas, Calculation of the Capacitance of a. Higgins, Reitan . . . . 926–31; disc. 931
Class-B Insulating Material in Nitrogen, Aging of. Stewart, Whitman . . . . 436–7; disc. 437
Closing of Magnetic Power Air Circuit Breakers, A Spring Mechanism for Hand. Dickinson, Findley . . . . 189–92; disc. 192
Coach Power Supply, Economics of Trolley. McDonald, Price 687–9
(Committee Report) Bibliography of Relay Literature—1947–1949. (51–38) 247–50
(Committee Report) Inductive Co-ordination Aspects of D-C Systems Supplied by Rectifiers. (51–206) 1034–54
(Committee Report) Marking of Varmeters. (51–3) . . . . 12–14; disc. 14
(Committee Report) Power System Fault Control. (51–66) 410–17
(Committee Report) Progress Report of the AIEE Magnetic Amplifier Subcommittee. (51–71) . . . . 445–9; disc. 449
(Committee Report) Relay Protection of A-C Generators. (51–42) . . . . 275–81; disc. 281
(Committee Report) Results of a Questionnaire Covering Current Practices in Electrical Tests on Dielectrics in the Field. (51–186) 986–9
(Communication) A Full Automatic Private-Line Teletypewriter Switching System. Bacon, Locke 473–80
(Communication) A Submarine Telephone Cable with Submerged Repeaters. Gilbert 564–72
(Communication) Automatic Trunk Selection in Reperforator Switching. Blanton 481–9
Communication Channel, Vibracode System of Supervisory Control on a Carrier. Allen, Daniel . . . . 818–22; disc. 822
(Communication) Operational Study of a Highway Mobile Telephone System. Dorff 31–7
(Communication) Pulse-Time Modulation Telemetering Systems for Rocket Application. Mengel 599–605
(Communication) Shielded Dielectric-Rod Waveguides. Beam, Wachowski 874–80
(Communication) Single-Frequency Signaling System for Supervision and Dialing over Long-Distance Telephone Trunks. Newell, Weaver 489–95
Communications Circuits, Signal and Supervision Systems Used on Carrier Current. Mayer 990–4
Communications Equipment for Industrial Applications, 940–960-Megacycle. Gunter 807–12
Commutating Reactor Control for Mechanical Rectifiers. Diebold 1062–5
Commutation in Universal-Type Motors. Packer . . . . 170–6; disc. 176
Commutation, The Transient Response of Magnetic Amplifiers—Cases of Negligible. Finzi, Chandler, Beaumariage . . . . 934–42; disc. 942
Compensation of A-C Instruments, Frequency. Miller . . . . 217–20; disc. 220
Compensation of Saturating Servomechanisms, A Phase-Plane Approach to the. Hopkin 631–9
Compensators for Watt-hour and Var-hour Meters Improvements in Transformer-Loss. Schleicher 973–7
Complex Impedance and Admittance Functions, Loci of. Michaels 299–303
Computers, A Diode Bridge Limiter for Use with Electronic Analogue. Medkeff, Parent 913–16
Computers, A Method of Gating for Parallel. Ratz, Smith 510–16
Computers, Systematization of Tube Surveillance in Large-Scale. Spence 516–19
(Computing Devices) The Input-Output System of the EDVAC. Snyder 507–09
Computing Techniques Applied to Economics, Analogue. Strotz, Calvert, Morehouse . . . . 557–62; disc. 562
Condenser for Reducing Voltage Flicker, The Application of a Series Capacitor to a Synchronous. Black, Lischer 144–50
Condenser, Technical Problems Associated with the Application of a Capacitor in Series with a Synchronous. Witzke, Michelson 519–25
Conditionally Stable Feedback Systems, A Note on the Design of. Travers 626–30
Conduction Phenomena Near Current Zero for an A-C Adjacent to Refractory Surfaces, A Study of. Browne, Strom . . . . 398–407; disc. 407
Conductor Configuration in Overhead Lines, Welding Calculations—Effect of. Tietze 784–6
Conductors, Circuit Analysis Method for Determination of A-C Impedances of Machine. Babb, Williams . . . . 661–5; disc. 665
Conductors, Geometric Mean Distances of Angle-Shaped. Magnusson 121–3
Conductors—Service Experience and Further Experimental Work, The Torsional Damper for. Burgess, Hogg 1031–3
Configuration in Overhead Lines, Welding Calculations—Effect of Conductor. Tietze 784–6
Constant as Load Varies, Networks for Which Magnitude or Phase Angle of Input Impedance or Transfer Admittance Remains. Berkowitz 286–91
Constants, A Per-Unit Interpretation of Transmission Line. Povejsil, Johnson . . . . 194–200; disc. 200
Contact Resistance—The Contribution of Non-uniform Current Flow. Kouwenhoven, Sackett 791–5
Contact Testing, An Electronic Power Source for Large D-C. Pettit 320–2
Contact Transients in Simple Electric Circuits. Martin, Stauss . . . . 304–07; disc. 307
Contribution of Nonuniform Current Flow, Contact Resistance—The. Kouwenhoven, Sackett . . 791–5
Contribution to the Theory of the Deep-Bar Induction Motor, A. Douglas 862–6
Control, A-C Arc Welders with Saturable Reactor. Oestreicher 787–90
Control Equipment, A New Lightweight Rapid Transit. Lichtenfels, Moore 224–6
Control Equipment, A-C Multiple-Unit Car. O'Kelly 652–6
Control for Mechanical Rectifiers, Commutating Reactor. Diebold 1062–5
Control for the Pennsylvania Railroad, New A-C Multipe-Car. Newhouse . . . . 645–7; disc. 647
Control on a Carrier Communication Channel, Vibracode System of Supervisory. Allen, Daniel . . . . 818–22; disc. 822
Control, Power System Fault. (Committee Report) 410–17
Control Room Lighting, An Engineering Approach to. Dzwonczyk . . . . 852–7; disc. 857
Control System for Railroads, A Modern Cab Signaling and Train. Allison . . . . 232–8; disc. 238
Controllers, The Effects of Loads and Disturbances upon Feedback. Jones 460–4
Controls, Some Design Criteria for Automatic. Nims 606–11
Co-ordination Aspects of D-C Systems Supplied by Rectifiers, Inductive. (Committee Report) 1034–54
Core, A 2,000,000-Kva Transformer. Sealey 8–11
Core Form Transformer Winding, Improved. Grimmer, Teague . . . . 962–5; disc. 965
Corona Investigation on Extra-High-Voltage Lines—500-Kv Test Project of the American Gas and Electric Company. Gross, Wagner, Naef, Tremaine . . . . 75–91; disc. 91
Corona Loss Measurement and Analysis—500-Kv Test Project of the American Gas and Electric Company, Techniques of. Naef, Tremaine, Jones . . . . 496–505; disc. 505
Criteria for Automatic Controls, Some Design. Nims. 606–11
Criterion, The Generalized Transmission Matrix Stability. Honnell . . . . 292–6; disc. 296
Crystals as Sensing Elements of Pressure, Temperature, and Humidity, Piezoelectric. Roberts, Goldsmith 968–72
Current Flow, Contact Resistance—The Contribution of Nonuniform. Kouwenhoven, Sackett . . . 791–5
Current Supervisory System for Distribution Circuits, Carrier. Podolsky, Lubin 1096–1101
Current, Transformer Magnetizing Inrush. Specht . . . . 323–7; disc. 327
Current Zero for an A-C Arc Adjacent to Refractory Surfaces, A Study of Conduction Phenomena Near. Browne, Strom . . . . 398–407; disc. 407
Curve, Steady-State Analysis of Self-Saturating Magnetic Amplifiers Based on Linear Approximations of the Magnetization. Esselman 451–9
Cyclic Light Flicker, Effect of the Duration of Voltage Dip on. Brieger . . . . 894–8; disc. 899

D

Damper for Conductors—Service Experience and Further Experimental Work, The Torsional. Burgess, Hogg 1031–3
Damping and Synchronizing Torques, Synchronous Machine. Concordia 731–7
Data in Electron Tube Operation, Basic Heat-Transfer. Buckland 1079–85
Deep-Bar Induction Motor, A Contribution to the Theory of the. Douglas 862–6
Delta System, Neutral Inversion of a Single Potential Transformer Connected Line-to-Ground on an Isolated. Gleason . . . . 103–10; disc. 110
Dependence of Direct Sparkover Voltage of Gaps on Humidity and Time. Jacob, Sommerman . . . . 921–4; disc. 924
Derivative Networks for A-C Servomechanisms, Effects of Carrier Shifts on. Attura 612–18
Design Criteria for Automatic Controls, Some. Nims 606–11
Design, Ice Testing and Its Influence Upon Switch. Heberlein, Field . . . . 37–42; disc. 42
Design Method for Polyphase Reluctance Synchronous Motors, A. Crouse 957–62
Design of Conditionally Stable Feedback Systems, A Note on the. Travers 626–30
Designing Frog-Leg Windings of D-C Machines, Rules for. Dwight, Haltmaier . . . . 707–11; disc. 711
Detection of Turn-to-Turn Faults in Large High-Voltage Turbine Generators. Sexton, Alke . . . . 270–3; disc. 273
Deterioration of Transformer Oil and Paper Insulation by Temperatures. Vogel, Petersen, Matsch . . . . 18–20; disc. 21
Determination of A-C Impedances of Machine Conductors, Circuit Analysis Method for. Babb, Williams . . . . 661–5; disc. 665
Determination of Generator Stand-by Reserve Requirements. Strandrud . . . . 179–87; disc. 18

Determination of Reserve Capacity by the Probability Method Effect of Interconnections. Calabrese..........1018–20
Development of a Pumpless Ignitron. Herskind, Remscheid..........1066–9
Development of Large Turbine Generators, Progress in the. Huntley, Taylor..........580–9; disc. 589
Devices, Switching of Distribution Capacitors by Manual and Automatic. Hopkins, Schultz..........138–43
Dialing over Long-Distance Telephone Trunks, Single-Frequency Signaling System for Supervision and. Newell, Weaver..........489–95
Dielectric Loading for Waveguide Linear Accelerators. Flesher, Cohn..........887–93
Dielectric-Rod Waveguides, Shielded. Beam, Wachowski..........874–80
Dielectrics in the Field, Results of a Questionnaire Covering Current Practices in Electrical Tests on. (Committee Report)..........986–9
Differential Analyzer Study of Harmonic Power Generation with Nonlinear Impedance Element. Russell, Peterson..........917–20
Differential Protection of Transformer Banks, A New Carrier-Current Frequency-Shift System for Use with. Beckwith..........832–5; disc. 835
Diode Bridge Limiter for Use with Electronic Analogue Computers, A. Medkeff, Parent..........913–16
Dip on Cyclic Light Flicker, Effect of the Duration of Voltage. Brieger..........894–8; disc. 899
D-C Armatures, Winding Insulation Tester for. Catlin, Rohats..........465–8
D-C Contact Testing, An Electronic Power Source for Large. Pettit..........320–2
D-C Machine Parameters, Measurement of. Saunders..........700–05; disc. 705
D-C Machines, Rules for Designing Frog-Leg Windings of. Dwight, Haltmaier..........707–11; disc. 711
D-C Power Supplies and Isolation of Faults on Electric Transit Systems. Watkins, Reagan.
  Part I. D-C Power Supply..........537–42; disc. 542
  Part II. Isolation of D-C Faults..543–50; disc. 550
D-C Power Systems, Factors Affecting Minimum Surface Leakage Distances in. Hart, Rosenberry, McClinton..........738–42
D-C Systems, Fault Transients in Aircraft. Scorgie..........713–20; disc. 720
D-C Systems Supplied by Rectifiers, Inductive Coordination Aspects of. (Committee Report)..........1034–54
Direct Sparkover Voltage of Gaps on Humidity and Time, Dependence of. Jacob, Sommerman..........921–4; disc. 924
Direct Voltage Endurance Studies on Mica Insulation for Electric Machinery, Alternating and. Moses..........763–8; disc. 768
Distances in D-C Power Systems, Factors Affecting Minimum Surface Leakage. Hart, Rosenberry, McClinton..........738–42
Distances of Angle-Shaped Conductors, Geometric Mean. Magnusson..........121–3
Distribution Capacitors by Manual and Automatic Devices, Switching of. Hopkins, Schultz..138–43
Distribution Circuits, Carrier Current Supervisory System for. Podolsky, Lubin..........1096–1101
Distribution Feeder Voltages, An Analysis of Grounding Banks to Balance. Long..........823–7
Distribution of Charge in Electrostatic Mineral Separation. Fraas, Ralston..........1028–30
Distribution Stations, Application of Shunt Capacitors at Transmission and. Porter, Zimmerman..........112–18; disc. 118
Distributions with Saturation, Calculation of Flux. Poritsky..........309–19; disc. 319
Disturbances upon Feedback Controllers, The Effects of Loads and. Jones..........460–4
Division Multiplex Telegraph Set, An Electronic Time. Hansen, Slayton..........354–61; disc. 361
Division Multiplex Telegraph System for Long-Distance Radio Circuits, Four-or-Two-Channel Time-. Peterman, Minc..........362–72
Duration of Voltage Dip on Cyclic Light Flicker, Effect of the. Brieger..........894–8; disc. 899

E

Economics, Analogue Computing Techniques Applied to. Strotz, Calvert, Morehouse..557–62; disc. 562
Economics of Extra-High-Voltage Transmission, System. St. Clair, Peterson..........841–8; disc. 848
Economics of Power Transformer Application. Barkle, Witzke..........440–4; disc. 444
Economics of Trolley Coach Power Supply. McDonald Price..........687–9
EDVAC, The Input-Output System of the. Snyder..........507–09
Effect of the Duration of Voltage Dip on Cyclic Light Flicker. Brieger..........894–8; disc. 899
Effects of Carrier Shifts on Derivative Networks for A-C Servomechanisms. Attura..........612–18
Effects of Lightning Arrester Protective Characteristics and Location upon Station Apparatus Protection, Some. Kalb..........379–83; disc. 383
Effects of Loads and Disturbances upon Feedback Controllers, The. Jones..........460–4
Effects of Series Capacitors in High-Voltage Transmission Lines, Fundamental. Johnson, Barkle, Povejsil..........526–35; disc. 535
Efficiency, Transmission Line Load Impedance for Maximum. Lutz..........283–5
Electric Circuits, Contact Transients in Simple. Martin, Stauss..........304–07; disc. 307
Electric Equipment and Performance of Lightweight Rapid Transit Cars. Ellis, Sloman..........227–30; disc. 230
Electric Home Heating. Parks..........828–31
(Electric Welding) Effect of the Duration of Voltage Dip on Cyclic Light Flicker. Brieger..........894–8; disc. 899
(Electric Welding) Probabilities of Interference Between Resistance Welders. Boice..........775–83
Electrodes for Stabilizing Inert-Gas Welding Arcs, New. Cobine, Gallagher..........804–06
Electromagnetic Induction Method of Measuring Oscillating Fluid Flow, An. Morris, Chadwick..346–50
Electromechanical Transducer, An. Engelberger, Kretsch..........213–16
Electron Tube Operation, Basic Heat-Transfer Data in. Buckland..........1079–85
Electron Tubes When Used as Oscillators in the Free as Well as in the Synchronized States, A New Method for Treating. Mostafa, Bey..........999–1004
Electronic Analogue Computers, A Diode Bridge Limiter for Use with. Medkeff, Parent..........913–16
Electronic Power Source for Large D-C Contact Testing, An. Pettit..........320–2
Electronic Time Division Multiplex Telegraph Set, An. Hansen, Slayton..........354–61; disc. 361
(Electronics) A Gas Tube Inverter with the Supply Voltage Below the Breakdown Voltage. Cage, Schuder..........908–12
(Electronics) Analysis of a 3-Phase Inverter with Resistive Load. Turkington..........1055–61
(Electronics) Development of a Pumpless Ignitron. Herskind, Remscheid..........1066–9
(Electronics) Distribution of Charge in Electrostatic Mineral Separation. Fraas, Ralston..........1028–30
(Electronics) Electrostatic Sources of Ionizing Energy. Trump..........1021–7
(Electronics) Progress Report of the AIEE Magnetic Amplifier Subcommittee. (Committee Report)..........445–9; disc. 449
(Electronics) Steady-State Analysis of Self-Saturating Magnetic Amplifiers Based on Linear Approximations of the Magnetization Curve. Esselman..........451–9
Electrostatic Mineral Separation, Distribution of Charge in. Fraas, Ralston..........1028–30
Electrostatic Sources of Ionizing Energy. Trump..........1021–7
Element, Differential Analyzer Study of Harmonic Power Generation with Nonlinear Impedance. Russell, Peterson..........917–20
Elements of Pressure, Temperature, and Humidity, Piezoelectric Crystals as Sensing. Roberts, Goldsmith..........968–72
Eleven Year Operating Record—Rural Line Sectionalizing by Repeater Fuses. Schahfer, Strout..680–6
Endurance Studies on Mica Insulation for Electric Machinery, Alternating and Direct Voltage. Moses..........763–8; disc. 768
Energy, Electrostatic Sources of Ionizing. Trump..........1021–7
Engineering Approach to Control Room Lighting, An. Dzwonczyk..........852–7; disc. 857
Equipment, A New Lightweight Rapid Transit Control. Lichtenfels, Moore..........224–6
Equipment, A-C Multiple-Unit Car Control. O'Kelly..........652–6
Equipment and Performance of Lightweight Rapid Transit Cars, Electric. Ellis, Sloman..........227–30; disc. 230
Equipment for Industrial Applications, 940–960 Megacycle Communications. Gunter..........807–12
Equipment for Multiple-Unit Cars, Selection of. Hutchison..........640–3; disc. 643
Equipments?, Why 4-Motor Multiple-Unit Car. Williamson..........240–2
Equivalent Circuits and Their Application in Designing Shaded Pole Motors. Chang..........690–8; disc. 698
Evaluation of Fluorescent Lamp Ballasts, Noise. Hayes, Gould..........573–9
Exciter for Synchronous Alternators, Static Magnetic. Storm..........1014–17
Expansion Effects in Power Cables, Thermal. Schifreen..........160–8; disc. 168
Experimental Study of Induction Machine End-Turn Leakage Reactance, An. Barnes..671–7; disc. 677
Experimental Work, The Torsional Damper for Conductors—Service Experience and Further. Burgess, Hogg..........1031–3

F

Factor in Synchronous Machines, Telephone Influence. Oscarson, Benson..........743–8
Factor Meter, A Hook-On Power. Corson, Nylander..........468–72
Factors Affecting Minimum Surface Leakage Distances in D-C Power Systems. Hart, Rosenberry, McClinton..........738–42
Fault Control, Power System. (Committee Report)..........410–17
Fault Locator, The Linascope Transmission Line. Kidd..........1008–13
Fault Transients in Aircraft D-C Systems. Scorgie..........713–20; disc. 720
Faults in Large High-Voltage Turbine Generators, Detection of Turn-to-Turn. Sexton, Alke..........270–3; disc. 273
Faults on Electric Transit Systems, D-C Power Supplies and Isolation of. Watkins, Reagan.
  Part I. D-C Power Supply..........537–42; disc. 542
  Part II. Isolation of D-C Faults...543–50; disc. 550
Feedback Controllers, The Effects of Loads and Disturbances upon. Jones..........460–4
Feedback Systems, A Note on the Design of Conditionally Stable. Travers..........626–30
Feeder Voltages, An Analysis of Grounding Banks to Balance Distribution. Long..........823–7
Feeders, Group Regulation of Urban 4-Kv. Grim, Peck..........551–6
Field and Laboratory—500-Kv Test Project of the American Gas and Electric Company, Radio Influence Tests in. Lippert, Pakala, Bartlett, Fahrnkopf..........251–65; disc. 265
500-Kv Test Project of the American Gas and Electric Company, Corona Investigation on Extra-High-Voltage Lines—. Gross, Wagner, Naef, Tremaine..........75–91; disc. 91
500-Kv Test Project of the American Gas and Electric Company, Line Insulator Loss Under Normal Conditions—. Naef, Tremaine, Jones..........1073–8
500-Kv Test Project of the American Gas and Electric Company, Radio Influence Tests in Field and Laboratory—. Lippert, Pakala, Bartlett, Fahrnkopf..........251–65; disc. 265
500-Kv Test Project of the American Gas and Electric Company, Techniques of Corona Loss Measurement and Analysis—. Naef, Tremaine, Jones..........496–505; disc. 505
Flicker, Effect of the Duration of Voltage Dip on Cyclic Light. Brieger..........894–8; disc. 899
Flicker, The Application of a Series Capacitor to a Synchronous Condenser for Reducing Voltage. Black, Lischer..........144–50
Flow, An Electromagnetic Induction Method of Measuring Oscillating Fluid. Morris, Chadwick..........346–50
Flow, Contact Resistance—The Contribution of Nonuniform Current. Kouwenhoven, Sackett..791–5
Flow in New Lightning Arresters, Spiral Arc Chokes Power. Ackermann, DeVal..........995–8
Fluid Flow, An Electromagnetic Induction Method of Measuring Oscillating. Morris, Chadwick..346–50
Fluorescent Lamp Ballasts, Noise Evaluation of. Hayes, Gould..........573–9
Flux Distributions with Saturation, Calculation of. Poritsky..........309–19; disc. 319
Form Transformer Winding, Improved Core. Grimmer, Teague..........962–5; disc. 965
Four-Motor Multiple-Unit Car Equipments?, Why. Williamson..........240–2
Four- or Two-Channel Time-Division-Multiplex Telegraph System for Long-Distance Radio Circuits. Peterman, Minc..........362–72
Fourier Series, and Impulse Functions for Rectangular Co-ordinate Systems, Tables of Green's Functions. Smith..........22–30
Frames, Transient Analysis of Rotating Machines and Stationary Networks by Means of Rotating Reference. Ku..........943–54; disc. 954
Frequency-Changer Welders, Ignitrons for. Rottier..........900–07
Frequency Compensation of A-C Instruments. Miller..........217–20; disc. 220
Frequency-Modulation Telegraph Network, A Nationwide. Bramhall, Smith..........373–8; disc. 378
Frequency-Shift System for Use with Differential Protection of Transformer Banks, A New Carrier-Current. Beckwith..........832–5; disc. 835
Frequency Signaling System for Supervision and Dialing over Long-Distance Telephone Trunks, Single-. Newell, Weaver..........489–95
Frog-Leg Windings of D-C Machines. Rules for Designing. Dwight, Haltmaier..........707–11; disc. 711
Functions, Fourier Series, and Impulse Functions for Rectangular Co-ordinate Systems, Tables of Green's. Smith..........22–30
Functions, Loci of Complex Impedance and Admittance. Michaels..........299–308
Fundamental Effects of Series Capacitors in High-Voltage Transmission Lines. Johnson, Barkle, Povejsil..........526–35; disc. 535

Fuses, 11-Year Operating Record Rural Line Sectionalizing by Repeater. Schahfer, Strout..680-6
Fuses for Resistance Welding Machines, Selection of. Stadum........796-9

G

Gaps on Humidity and Time, Dependence of Direct Sparkover Voltage of. Jacob, Sommerman........921-4; disc. 924
Gas-Filled Cable, Washington, D. C., 69-Kv Medium-Pressure. Clark........418-21; disc. 421
Gas Tube Inverter with the Supply Voltage Below the Breakdown Voltage, A. Cage, Schuder....908-12
Gas Welding Arcs, New Electrodes for Stabilizing Inert-. Cobine, Gallagher........804-06
Gating for Parallel Computers, A Method of. Ratz, Smith........510-16
Generalized Transmission Matrix Stability Criterion, The. Honnell........292-6; disc. 296
Generation with Nonlinear Impedance Element, Differential Analyzer Study of Harmonic Power. Russell, Peterson........917-20
Generator Rotors, Modern Practice in the Balancing of Large Turbine-. Laffoon, Hagg, Janthey, Heller........593-8; disc. 598
Generator Standby Reserve Requirements, Determination of. Strandrud........179-87; disc. 187
Generator Stator Windings, A New High-Voltage Insulation for Turbine-. Laffoon, Hill, Moses, Berberich........721-6; disc. 726
Generator Stators, The Use of Preferred Orientation Strip Steel in Turbine-. Apperson, Fontaine........836-9; disc. 839
Generators, Detection of Turn-to-Turn Faults in Large High-Voltage Turbine. Sexton, Alke........270-3; disc. 273
Generators, Progress in the Development of Large Turbine. Huntley, Taylor........580-9; disc. 589
Generators, Relay Protection of A-C. (Committee Report)........275-81; disc. 281
Geometric Mean Distances of Angle-Shaped Conductors. Magnusson........121-3
Graphical Methods for A-C Servomechanisms, Network Synthesis by. Bjornson........619-25
Green's Functions, Fourier Series, and Impulse Functions for Rectangular Co-ordinate Systems, Tables of. Smith........22-30
Ground on an Isolated Delta System, Neutral Inversion of a Single Potential Transformer Connected Line-to-. Gleason........103-10; disc. 110
Grounding Banks to Balance Distribution Feeder Voltages, An Analysis of. Long........823-7
Grounding in Power Systems in the United States, Application of Resonant. Gross, Atherton........389-93; disc. 393
Group Regulation of Urban 4-Kv Feeders. Grim, Peck........551-6

H

Hand Closing of Magnetic Power Air Circuit Breakers, A Spring Mechanism for. Dickinson, Findley........189-92; disc. 192
Harmonic Power Generation with Nonlinear Impedance Element, Differential Analyzer Study of. Russell, Peterson........917-20
Heat-Transfer Data in Electron Tube Operation, Basic. Buckland........1079-85
Heating, Electric Home. Parks........828-31
Hemispherical Radiometers, Total. Gier, Dunkel........339-43; disc. 343
Heterodyne Oscillators, A Servo System for. Slonczewski........1070-2
High-Voltage Insulation for Turbine-Generator Stator Windings, A New. Laffoon, Hill, Moses, Berberich........721-6; disc. 726
High-Voltage Lines—500-Kv Test Project of the American Gas and Electric Company, Corona Investigation on Extra-. Gross, Wagner, Naef, Tremaine........75-91; disc. 91
High-Voltage Shunt Capacitor Banks, Switching. Funkhouser, VanSickle, Shankle..129-33; disc. 134
High-Voltage Transmission Lines, Fundamental Effects of Series Capacitors in. Johnson, Barkle, Povejsil........526-35; disc. 535
High-Voltage Transmission, System Economics of Extra-. St. Clair, Peterson........841-8; disc. 848
High-Voltage Transmission System of the American Gas and Electric Company, The 300-316 Kv Extra-. Sporn, Peterson, Gross, St. Clair........64-72; disc. 72
High-Voltage Turbine Generators, Detection of Turn-to-Turn Faults in Large. Sexton, Alke........270-3; disc. 273
Highway Mobile Telephone System, Operational Study of a. Dorff........31-7
Home Heating, Electric. Parks........828-31
Hook-On Power Factor Meter, A. Corson, Nylander........468-72
Humidity and Time, Dependence of Direct Sparkover Voltage of Gaps on. Jacob, Sommerman........921-4; disc. 924
Humidity, Piezoelectric Crystals as Sensing Elements of Pressure, Temperature, and. Roberts, Goldsmith........968-72

I

Ice Testing and Its Influence Upon Switch Design. Heberlein, Field........37-42; disc. 42
Ignitron, Development of a Pumpless. Herskind, Remscheid........1066-9
Ignitron Rectifiers for Urban Transit Power Supply, Sealed. Borst........770-4
Ignitrons for Frequency-Changer Welders. Rottier........900-07
Impedance and Admittance Functions, Loci of Complex. Michaels........299-303
Impedance Element, Differential Analyzer Study of Harmonic Power Generation with Nonlinear. Russell, Peterson........917-20
Impedance for Maximum Efficency, Transmission Line Load. Lutz........283-5
Impedance or Transfer Admittance Remains Constant as Load Varies, Networks for Which Magnitude or Phase Angle of Input. Berkowitz........286-91
Impedances of Machine Conductors, Circuit Analysis Method for Determination of A-C. Babb, Williams........661-5; disc. 665
Impregnated Paper Insulation, Radial and Tangential Stresses in. Whitehead........56-9; disc. 59
Improved Core Form Transformer Winding. Grimmer, Teague........962-5; disc. 965
Improvements in Transformer-Loss Compensators for Watthour and Var-hour Meters. Schleicher........973-7
Impulse Functions for Rectangular Co-ordinate Systems, Tables of Green's Functions, Fourier Series, and. Smith........22-30
Induction Machine End-Turn Leakage Reactance, An Experimental Study of. Barnes...671-7; disc. 677
Induction Method of Measuring Oscillating Fluid Flow, An Electromagnetic. Morris, Chadwick..346-50
Induction Motor, A Contribution to the Theory of the Deep-Bar. Douglas........862-6
Induction Motor Performance, A Simplified Method for Predicting. Webking........667-70; disc. 671
Induction Motors, Transient Response of Small 2-Phase. Hopkin........881-6
Inductive Co-ordination Aspects of D-C Systems Supplied by Rectifiers. (Committee Report)..1034-54
Industrial Applications, 940-960 Megacycle Communications Equipment for. Gunter........807-12
(Industrial Control) An Electronic Power Source for Large D-C Contact Testing. Pettit........320-2
Inert-Gas Welding Arcs, New Electrodes for Stabilizing. Cobine, Gallagher........804-06
Influence Factor in Synchronous Machines, Telephone. Oscarson, Benson........743-8
Influence Tests in Field and Laboratory—500-Kv Test Project of the American Gas and Electric Company, Radio. Lippert, Pakala, Bartlett, Fahrnkopf........251-65; disc. 265
Input Impedance or Transfer Admittance Remains Constant as Load Varies, Networks for Which Magnitude or Phase Angle of. Berkowitz........286-91
Input-Output System of the EDVAC, The. Snyder........507-09
Inrush Current, Transformer Magnetizing. Specht........323-7; disc. 327
Inspection Program for Large Rotating Machines, A Maintenance. Johnson........749-54; disc. 755
Installations, Acoustic Models of Transformer. Gettys, Conover........333-6; disc. 336
Instantaneous Variations in Angular Velocity, A Tachometer for Measurement of. Bartles..1105-02
(Instruments) A Servo System for Heterodyne Oscillators. Slonczewski........1070-2
(Instruments) An Electromechanical Transducer. Engelberger, Kretsch........213-16
Instruments, Frequency Compensation of A-C. Miller........217-20; disc. 220
(Instruments) Marking of Varmeters. (Committee Report)........12-14; disc. 14
(Instruments) Results of a Questionnaire Covering Current Practices in Electrical Tests on Dielectrics in the Field. (Committee Report)........986-9
(Insulated Conductors) Lead-Alloy Sheaths for Underground Power Cable. Halperin, Betzer........423-9; disc. 429
(Insulated Conductors) 69-Kv Medium-Pressure Gas-Filled Cable, Washington, D. C. Clark........418-21; disc. 421
(Insulated Conductors) Thermal Expansion Effects in Power Cables. Schifreen........160-8; disc. 168
(Insulated Conductors) Thermal Transients on Buried Cables. Buller........45-52; disc. 52, 1107
Insulating Material in Nitrogen, Aging of Class-B. Stewart, Whitman........436-7; disc. 437
Insulation by Temperatures, Deterioration of Transformer Oil and Paper. Vogel, Petersen, Matsch........18-20; disc. 21
Insulation for Electric Machinery, Alternating and Direct Voltage Endurance Studies on Mica. Moses........763-8; disc. 768
Insulation for Turbine-Generator Stator Windings, A New High-Voltage. Laffoon, Hill, Moses, Berberich........721-6; disc. 726
Insulation, Radial and Tangential Stresses in Impregnated Paper. Whitehead........56-9; disc. 59
Insulation Tester for D-C Armatures, Winding. Catlin, Rohats........465-8
Insulation Testing of Synchronous Machines, Routine. Hunt, Vivian........756-62
Insulator Loss Under Normal Conditions—500-Kv Test Project of the American Gas and Electric Company, Line. Naef, Tremaine, Jones..1073-8
Interconnections, Determination of Reserve Capacity by the Probability Method Effect of. Calabrese........1018-20
Interference Between Resistance Welders, Probabilities of. Boice........775-83
Interruption Testing of Lightning Arresters, The Power. Ackermann........1-5; disc. 5
Inversion of a Single Potential Transformer Connected Line-to-Ground on an Isolated Delta System, Neutral. Gleason........103-10; disc. 110
Inverter with Resistive Load, Analysis of a 3-Phase. Turkington........1055-61
Inverter with the Supply Voltage Below the Breakdown Voltage, A Gas Tube. Cage, Schuder.....908-12
Investigation of Audio Noise in Substation Type Transformers, An. Vivian, Peck......328-31; disc. 331
Investigation on Extra-High-Voltage Lines—500-Kv Test Project of the American Gas and Electric Company, Corona. Gross, Wagner, Naef, Tremaine........75-91; disc. 91
Ionizing Energy, Electrostatic Sources of. Trump........1021-7
Isolation of Faults on Electric Transit Systems, D-C Power Supplies and. Watkins, Reagan:
  Part I. D-C Power Supply.....537-42; disc. 542
  Part II. Isolation of D-C Faults..543-50; disc. 550

L

Laboratory—500-Kv Test Project of the American Gas and Electric Company, Radio Influence Tests in Field and. Lippert, Pakala, Bartlett, Fahrnkopf........251-65; disc. 265
Lamp Ballasts, Noise Evaluation of Fluorescent. Hayes, Gould........573-9
(Land Transportation) A Modern Cab Signaling and Train Control System for Railroads. Allison........232-8; disc. 238
(Land Transportation) A New Lightweight Rapid Transit Control Equipment. Lichtenfels, Moore........224-6
(Land Transportation) A New Lightweight Rapid Transit Motor. Pettersen........222-3
(Land Transportation) A New Multiple-Unit Car Motor for the Pennsylvania Railroad. Jungk........243-5; disc. 245
(Land Transportation) A New Train Performance Calculator. Smith........657-60
(Land Transportation) A-C Multiple-Unit Car Control Equipment. O'Kelly........652-6
(Land Transportation) A-C Multiple-Unit Car Motor. Kreitler........648-50; disc. 650
(Land Transportation) Economics of Trolley Coach Power Supply. McDonald, Price........687-9
(Land Transportation) Electric Equipment and Performance of Lightweight Rapid Transit Cars. Ellis, Sloman........227-30; disc. 230
(Land Transportation) New A-C Multiple-Car Control for the Pennsylvania Railroad. Newhouse........645-7; disc. 647
(Land Transportation) Regeneration With a Mercury Arc Rectifier on the Central Railway of Brazil. Schmidt........1092-6
(Land Transportation) Why 4-Motor Multiple-Unit Car Equipments? Williamson........240-2
Lead-Alloy Sheaths for Underground Power Cable. Halperin, Betzer........423-9; disc. 429
Leakage Distances in D-C Power Systems, Factors Affecting Minimum Surface. Hart, Rosenberry, McClinton........738-42
Leakage Reactance, An Experimental Study of Induction Machine End-Turn. Barnes........671-7; disc. 677
Light Flicker, Effect of the Duration of Voltage Dip on Cyclic. Brieger........894-8; disc. 899
Lighting, An Engineering Approach to Control Room. Dzwonczyk........852-7; disc. 857
Lightning Arrester Protective Characteristics and Location upon Station Apparatus Protection, Some Effects of. Kalb........379-83; disc. 383
Lightning Arresters, Spiral Arc Chokes Power Flow in New. Ackermann, DeVal........995-8
Lightning Arresters, The Power Interruption Testing of. Ackermann........1-5; disc. 5

Lightning Incidence Is High, Protection of Transmission Lines Over Mountainous Region Where. Housley, Harper........124-6; disc. 126
Lightweight Rapid Transit Cars, Electric Equipment and Performance of. Ellis, Sloman........227-30; disc. 230
Lightweight Rapid Transit Control Equipment, A New. Lichtenfels, Moore........224-6
Lightweight Rapid Transit Motor, A New. Pettersen........222-3
Limiter for Use with Electronic Analogue Computers, A Diode Bridge. Medkeff, Parent........913-16
Linascope Transmission Line Fault Locator, The. Kidd........1008-13
Line Carrier Relaying System, Measurements and Tests on a Power. Miller, Worthington........1005-07
Line Constants, A Per-Unit Interpretation of Transmission. Povejsil, Johnson........194-200; disc. 200
Line Fault Locator, The Linascope Transmission. Kidd........1008-13
Line Insulator Loss Under Normal Conditions—500-Kv Test Project of the American Gas and Electric Company. Naef, Tremaine, Jones........1073-8
Line Load Impedance for Maximum Efficiency, Transmission. Lutz........283-5
Line Sectionalizing by Repeater Fuses, 11-Year Operating Record—Rural. Schahfer, Strout........680-6
Linear Accelerators, Dielectric Loading for Waveguide. Flesher, Cohn........887-93
Linear Approximations of the Magnetization Curve, Steady-State Analysis of Self-Saturating Magnetic Amplifiers Based on. Esselman........451-9
Lines—500-Kv Test Project of the American Gas and Electric Company, Corona Investigation on Extra-High-Voltage. Gross, Wagner, Naef, Tremaine........75-91; disc. 91
Lines, Fundamental Effects of Series Capacitors in High-Voltage Transmission. Johnson, Barkle, Povejsil........526-35; disc. 535
Lines Over Mountainous Region Where Lightning Incidence Is High, Protection of Transmission. Housley, Harper........124-6; disc. 126
Lines, Welding Calculations—Effect of Conductor Configuration in Overhead. Tietze........784-6
Load, Analysis of a 3-Phase Inverter with Resistive. Turkington........1055-61
Load Impedance for Maximum Efficiency, Transmission Line. Lutz........283-5
Load, Transient Response of Saturable Reactors with Resistive. Storm........95-102
Load Varies, Networks for Which Magnitude or Phase Angle of Input Impedance or Transfer Admittance Remains Constant as. Berkowitz........286-91
Loading for Waveguide Linear Accelerators, Dielectric. Flesher, Cohn........887-93
Loads and Disturbances upon Feedback Controllers, The Effects of. Jones........460-4
Locator, The Linascope Transmission Line Fault. Kidd........1008-13
Loci of Complex Impedance and Admittance Functions. Michaels........299-303
Long-Distance Radio Circuits, Four- or Two-Channel Time-Division-Multiplex Telegraph System for. Peterman, Minc........362-72
Long-Distance Telephone Trunks, Single-Frequency Signaling System for Supervision and Dialing over. Newell, Weaver........489-95
Loss Compensators for Watt-hour and Var-hour Meters, Improvements in Transformer-. Schleicher........973-7
Loss Measurement and Analysis—500-Kv Test Project of the American Gas and Electric Company, Techniques of Corona. Naef, Tremaine, Jones........496-505; disc. 505
Loss Under Normal Conditions—500-Kv Test Project of the American Gas and Electric Company, Line Insulator. Naef, Tremaine, Jones........1073-8

M

Machine Conductors, Circuit Analysis Method for Determination of A-C Impedances of. Babb, Williams........661-5; disc. 665
Machine Damping and Synchronizing Torques, Synchronous. Concordia........731-7
Machine End-Turn Leakage Reactance, An Experimental Study of Induction. Barnes........671-7; disc. 677
Machine Parameters, Measurement of D-C. Saunders........700-05; disc. 705
Machinery, Alternating and Direct Voltage Endurance Studies on Mica Insulation for Electric. Moses........763-8; disc. 768
Machines, A Maintenance Inspection Program for Large Rotating. Johnson........749-54; disc. 755
Machines and Stationary Networks by Means of Rotating Reference Frames, Transient Analysis of Rotating. Ku........943-54; disc. 954
Machines, Routine Insulation Testing of Synchronous Hunt, Vivian........756-62
Machines, Rules for Designing Frog-Leg Windings of D-C. Dwight, Haltmaier........707-11; disc. 711
Machines, Selection of Fuses for Resistance Welding. Stadum........796-9
Machines, Telephone Influence Factor in Synchronous. Oscarson, Benson........743-8
Magnetic Amplifier Subcommittee, Progress Report of the AIEE. (Committee Report)........445-9; disc. 449
Magnetic Amplifiers Based on Linear Approximations of the Magnetization Curve, Steady-State Analysis of Self-Saturating. Esselman........451-9
Magnetic Amplifiers—Cases of Negligible Commutation, The Transient Response of. Finzi, Chandler, Beaumariage........934-42; disc. 942
Magnetic Exciter for Synchronous Alternators, Static. Storm........1014-17
Magnetic Power Air Circuit Breakers, A Spring Mechanism for Hand Closing of. Dickinson, Findley........189-92; disc. 192
Magnetizing Inrush Current, Transformer. Specht........323-7; disc. 327
Magnitude or Phase Angle of Input Impedance or Transfer Admittance Remains Constant as Load Varies, Networks for Which. Berkowitz........286-91
Maintenance Inspection Program for Large Rotating Machines, A. Johnson........749-54; disc. 755
Manual and Automatic Devices, Switching of Distribution Capacitors by. Hopkins, Schultz........138-43
Marking of Varmeters. (Committee Report)........12-14; disc. 14
Material in Nitrogen, Aging of Class-B Insulating Stewart, Whitman........436-7; disc. 437
Matrix Stability Criterion, The Generalized Transmission. Honnell........292-6; disc. 296
Maximum Efficiency, Transmission Line Load Impedance for. Lutz........283-5
Mean Distances of Angle-Shaped Conductors, Geometric. Magnusson........121-3
Measurement and Analysis—500-Kv Test Project of the American Gas and Electric Company, Techniques of Corona Loss. Naef, Tremaine, Jones........496-505; disc. 505
Measurement of D-C Machine Parameters. Saunders........700-05; disc. 705
Measurement of Instantaneous Variations in Angular Velocity, A Tachometer for. Bartles........1102-05
(Measurements) A Hook-On Power Factor Meter. Corson, Nylander........468-72
Measurements and Tests on a Power Line Carrier Relaying System. Miller, Worthington........1005-07
Measurements of Resistance, Three-Phase. Matsch, Basu, Horcher........350-2; disc. 352
(Measurements) Total Hemispherical Radiometers. Gier, Dunkle........339-43; disc. 343
Measuring Oscillating Fluid Flow, An Electromagnetic Induction Method of. Morris, Chadwick........346-50
Mechanical Rectifiers, Commutating Reactor Control for. Diebold........1062-5
Mechanism for Hand Closing of Magnetic Power Air Circuit Breakers, A Spring. Dickinson, Findley........189-92; disc. 192
Mechanism of Low and High Current Arcs and Their Relation to the Welding Arc, The Physical. Finkelnburg........800-03
Megacycle Communications Equipment for Industrial Applications, 940-960. Gunter........807-12
Mercury Arc Rectifier on the Central Railway of Brazil, Regeneration with a. Schmidt........1092-6
Meter, A Hook-On Power Factor. Corson, Nylander........468-72
Meters, Improvements in Transformer-Loss Compensators for Watt-hour and Var-hour. Schleicher........973-7
Method Effect of Interconnections, Determination of Reserve Capacity by the Probability. Calabrese........1018-20
Method for Determination of A-C Impedances of Machine Conductors, Circuit Analysis. Babb, Williams........661-5; disc. 665
Method for Polyphase Reluctance Synchronous Motors, A Design. Crouse........957-62
Method for Predicting Induction Motor Performance, A Simplified. Webking........667-70; disc. 671
Method for Treating Electron Tubes When Used as Oscillators in the Free as Well as in the Synchronized States, A New. Mostafa, Bey........999-1004
Method of Gating for Parallel Computers, A. Ratz, Smith........510-16
Method of Measuring Oscillating Fluid Flow, An Electromagnetic Induction. Morris, Chadwick........346-50
Methods for A-C Servomechanisms, Network Synthesis by Graphical. Bjornson........619-25
Mica Insulation for Electric Machinery, Alternating and Direct Voltage Endurance Studies on. Moses........763-8; disc. 768
Microwave Channels, Application of. Cheek........813-17
Mineral Separation, Distribution of Charge in Electrostatic. Fraas, Ralston........1028-30
Mobile Telephone System, Operational Study of a Highway. Dorff........31-7
Models of Transformer Installations, Acoustic. Gettys, Conover........333-6; disc. 336
Modern Cab Signaling and Train Control System for Railroads. Allison........232-8; disc. 238
Modern Practice in the Balancing of Large Turbine-Generator Rotors. Lafloon, Hagg, Janthey, Heller........593-8; disc. 598
Modulation Telegraph Network, A Nationwide Frequency. Bramhall, Smith........373-8; disc. 378
Modulation Telemetering Systems for Rocket Application, Pulse-Time. Mengel........599-605
Motor, A Contribution to the Theory of the Deep-Bar Induction. Douglas........862-6
Motor, A New Lightweight Rapid Transit. Pettersen........222-3
Motor, A-C Multiple-Unit Car. Kreitler........648-50; disc. 650
Motor for the Pennsylvania Railroad, A New Multiple-Unit Car. Jungk........243-5; disc. 245
Motor Multiple-Unit Car Equipments?, Why Four-. Williamson........240-2
Motor Performance, A Simplified Method for Predicting Induction. Webking........667-70; disc. 671
Motors, A Design Method for Polyphase Reluctance Synchronous. Crouse........957-62
Motors, Commutation in Universal-Type. Packer........170-6; disc. 176
Motors, Equivalent Circuits and Their Application in Designing Shaded Pole. Chang........690-8; disc. 698
Motors, Split-Winding Starting of 3-Phase. Alger, Ward, Wright........867-72; disc. 872
Motors, Transient Response of Small 2-Phase Induction. Hopkin........881-6
Mountainous Region Where Lightning Incidence Is High, Protection of Transmission Lines Over. Housley, Harper........124-6; disc. 126
Multiple-Car Control for the Pennsylvania Railroad, New A-C. Newhouse........645-7; disc. 647
Multiple-Unit Car Control Equipment, A-C. O'Kelly........652-6
Multiple-Unit Car Equipments?, Why 4-Motor. Williamson........240-2
Multiple-Unit Car Motor, A-C. Kreitler........648-50; disc. 650
Multiple-Unit Car Motor for the Pennsylvania Railroad, A New. Jungk........243-5; disc. 245
Multiple-Unit Cars, Selection of Equipment for. Hutchison........640-3; disc. 643
Multiplex Telegraph Set, An Electronic Time Division. Hansen, Slayton........354-61; disc. 361
Multiplex Telegraph System for Long-Distance Radio Circuits, Four- or Two-Channel Time-Division. Peterman, Minc........362-72

N

Nationwide Frequency-Modulation Telegraph Network, A. Bramhall, Smith........373-8; disc. 378
Network, A Nationwide Frequency-Modulation Telegraph. Bramhall, Smith........373-8; disc. 378
Network Synthesis by Graphical Methods for A-C Servomechanisms. Bjornson........619-25
Networks by Means of Rotating Reference Frames, Transient Analysis of Rotating Machines and Stationary. Ku........943-54; disc. 954
Networks for A-C Servomechanisms, Effects of Carrier Shifts on Derivative. Attura........612-18
Networks for Which Magnitude or Phase Angle of Input Impedance or Transfer Admittance Remains Constant as Load Varies. Berkowitz........286-91
Neutral Inversion of a Single Potential Transformer Connected Line-to-Ground on an Isolated Delta System. Gleason........103-10; disc. 110
New Lightweight Rapid Transit Control Equipment, A. Lichtenfels, Moore........224-6
New Lightweight Rapid Transit Motor, A. Pettersen........222-3
New 69-Kv Air Blast Circuit Breaker, A. Shores, Beatty........202-07; disc. 207
Nitrogen, Aging of Class-B Insulating Material in. Stewart, Whitman........436-7; disc. 437
Noise Evaluation of Fluorescent Lamp Ballasts. Hayes, Gould........573-9
Noise in Substation Type Transformers, An Investigation of Audio. Vivian, Peck........328-31; disc. 331
Nonlinear Impedance Element, Differential Analyzer Study of Harmonic Power Generation with. Russell, Peterson........917-20
Nonuniform Current Flow, Contact Resistance—The Contribution of. Kouwenhoven, Sackett........791-5
Note on the Design of Conditionally Stable Feedback Systems, A. Travers........626-30
(Nucleonics) Dielectric Loading for Waveguide Linear Accelerators. Flesher, Cohn........887-93

O

Oil and Paper Insulation by Temperatures, Deterioration of Transformer. Vogel, Petersen, Matsch........18-20; disc. 21
Operating Record—Rural Line Sectionalizing by Repeater Fuses, 11-Year. Schahfer, Strout........680-6
Operation, Basic Heat-Transfer Data in Electron Tube. Buckland........1079-85

Operational Study of a Highway Mobile Telephone System. Dorff.....31-7
Orientation Strip Steel in Turbine-Generator Stators, The Use of Preferred. Apperson, Fontaine.....836-9; disc. 839
Oscillating Fluid Flow, An Electromagnetic Induction Method of Measuring. Morris, Chadwick..346-50
Oscillators, A Servo System for Heterodyne. Slonczewski.....1070-2
Oscillators in the Free as Well as in the Synchronized States, A New Method for Treating Electron Tubes When Used as. Mostafa, Bey.....999-1004
Output Analysis and Alignment Techniques for Phase-Rotation Single Side-Band Transmitters. Whitby, Scheuch.....209-12
Output System of the EDVAC, The Input-. Snyder.....507-09
Overhead Lines, Welding Calculations—Effect of Conductor Configuration in. Tietze.....784-6

P

Paper Insulation by Temperatures, Deterioration of Transformer Oil and. Vogel, Petersen, Matsch.....18-20; disc. 21
Paper Insulation, Radial and Tangential Stresses in Impregnated. Whitehead.....56-9; disc. 59
Parallel Computers, A Method of Gating for. Ratz, Smith.....510-16
Parameters, Measurement of D-C Machine. Saunders.....700-07; disc. 705
Pennsylvania Railroad, A New Multiple-Unit Car Motor for the. Jungk.....243-5; disc. 245
Pennsylvania Railroad, New A-C Multiple-Car Control for the. Newhouse.....645-7; disc. 647
Per-Unit Interpretation of Transmission Line Constants, A. Povejsil, Johnson.....194-200; disc. 200
Performance, A Simplified Method for Predicting Induction Motor. Webking.....667-70; disc. 671
Performance Calculator, A New Train. Smith..657-60
Performance of Lightweight Rapid Transit Cars, Electric Equipment and. Ellis, Sloman.....227-30; disc. 230
Phase Angle of Input Impedance or Transfer Admittance Remains Constant as Load Varies, Networks for Which Magnitude or. Berkowitz.....286-91
Phase-Plane Approach to the Compensation of Saturating Servomechanisms, A. Hopkin.....631-9
Phase-Rotation Single Side-Band Transmitters, Output Analysis and Alignment Techniques for. Whitby, Scheuch.....209-12
Phenomena, Capacitor Switching. VanSickle, Zaborszky.....151-8; disc. 158
Phenomena Near Current Zero for an A-C Arc Adjacent to Refractory Surfaces, A Study of Conduction. Browne, Strom.....398-407; disc. 407
Physical Mechanism of Low and High-Current Arcs, and Their Relation to the Welding Arc, The. Finkelnburg.....800-03
Piezoelectric Crystals as Sensing Elements of Pressure, Temperature, and Humidity. Roberts, Goldsmith.....968-72
Plane Approach to the Compensation of Saturating Servomechanisms, A Phase-. Hopkin.....631-9
Pole Motors, Equivalent Circuits and Their Application in Designing Shaded. Chang....690-8; disc. 698
Polyphase Reluctance Synchronous Motors, A Design Method for. Crouse.....957-62
Potential Transformer Connected Line-to-Ground on an Isolated Delta System, Neutral Inversion of a Single. Gleason.....103-10; disc. 110
Power Air Circuit Breakers, A Spring Mechanism for Hand Closing of Magnetic. Dickinson, Findley.....189-92; disc. 192
Power Cable, Lead-Alloy Sheaths for Underground. Halperin, Betzer.....423-9; disc. 429
Power Cables, Thermal Expansion Effects in. Schifreen.....160-8; disc. 168
Power Factor Meter, A Hook-On. Corson, Nylander.....468-72
Power Flow in New Lightning Arresters, Spiral Arc Chokes. Ackermann, DeVal.....995-8
(Power Generation) An Engineering Approach to Control Room Lighting. Dzwonczyk..852-7; disc. 857
(Power Generation) Progress in the Development of Large Turbine Generators. Huntley, Taylor.....580-9; disc. 589
Power Generation with Nonlinear Impedance Element, Differential Analyzer Study of Harmonic. Russell, Peterson.....917-20
Power Interruption Testing of Lightning Arresters, The. Ackermann.....1-5; disc. 5
Power Line Carrier Relaying System, Measurements and Tests on a. Miller, Worthington.....1005-07
Power Source for Large D-C Contact Testing. An Electronic. Pettit.....320-2
Power Supplies and Isolation of Faults on Electric Transit Systems, D-C. Watkins, Reagan:
  Part I. D-C Power Supply.....537-42; disc. 542
  Part II. Isolation of D-C Faults..543-50; disc. 550
Power Supply, Economics of Trolley Coach. McDonald, Price.....687-9
Power Supply, Sealed Ignitron Rectifiers for Urban Transit. Borst.....770-4
Power Supply Study and New Rectifier Installation for the United Electric Railways of Providence. Whitman, Schaller.....978-85; disc. 985
Power System, Choice of Telemetering Systems and Channels for a. Duff.....1086-91
Power System Fault Control. (Committee Report).....410-17
Power Systems, Factors Affecting Minimum Surface Leakage Distances in D-C. Hart, Rosenberry, McClinton.....738-42
Power Systems in the United States, Application of Resonant Grounding in. Gross, Atherton.....389-93; disc. 393
Power Transformer Application, Economics of. Barkle, Witzke.....440-4; disc. 444
Practice in the Balancing of Large Turbine-Generator Rotors, Modern. Laffoon, Hagg, Janthey, Heller.....593-8; disc. 598
Preferred Orientation Strip Steel in Turbine-Generator Stators, The Use of. Apperson, Fontaine.....836-9; disc. 839
Pressure Gas-Filled Cable, Washington, D. C., 69-Kv Medium-. Clark.....418-21; disc. 421
Pressure, Temperature, and Humidity, Piezoelectric Crystals as Sensing Elements of. Roberts, Goldsmith.....968-72
Private-Line Teletypewriter Switching System, A Full Automatic. Bacon, Locke.....473-80
Probabilities of Interference Between Resistance Welders. Boice.....775-83
Probability Method Effect of Interconnections, Determination of Reserve Capacity by the. Calabrese.....1018-20
Problems Associated with the Application of a Capacitor in Series with a Synchronous Condenser, Technical. Witzke, Michelson.....519-25
Program for Large Rotating Machines, A Maintenance. Johnson.....749-54; disc. 755
Progress in the Development of Large Turbine Generators. Huntley, Taylor.....580-9; disc. 589
Progress Report of the AIEE Magnetic Amplifier Subcommittee. (Committee Reportt).....445-9; disc. 449
Project of the American Gas and Electric Company, Techniques of Corona Loss Measurement and Analysis—500-Kv Test. Naef, Tremaine, Jones.....496-505; disc. 505
Protection of A-C Generators, Relay. (Committee Report).....275-81; disc. 281
Protection of Transformer Banks, A New Carrier-Current Frequency-Shift System for Use with Differential. Beckwith.....832-5; disc. 835
Protection of Transmission Lines Over Mountainous Region Where Lightning Incidence is High. Housley, Harper.....124-6; disc. 126
Protection, Some Effects of Lightning Arrester Protective Characteristics and Location upon Station Apparatus. Kalb.....379-83; disc. 383
Protective Characteristics and Location upon Station Apparatus Protection, Some Effects of Lightning Arrester. Kalb.....379-83; disc. 383
(Protective Devices) Application of Resonant Grounding in Power Systems in the United States. Gross, Atherton.....389-93; disc. 393
(Protective Devices) 11-Year Operating Record—Rural Line Sectionalizing by Repeater Fuses. Schahfer, Strout.....680-6
(Protective Devices) Power System Fault Control. (Committee Report).....410-17
(Protective Devices) Spiral Arc Chokes Power Flow in New Lightning Arresters. Ackermann, DeVal.....995-8
Providence, Power Supply Study and New Rectifier Installation for the United Electric Railways of. Whitman, Schaller.....978-85; disc. 985
Pulse-Time Modulation Telemetering Systems for Rocket Application. Mengel.....599-605
Pumpless Ignitron, Development of a. Herskind, Remscheid.....1066-9

Q

Questionnaire Covering Current Practices in Electrical Tests on Dielectrics in the Field, Results of a. (Committee Report).....986-9

R

Radial and Tangential Stresses in Impregnated Paper Insulation. Whitehead.....56-9; disc. 59
Radio Circuits, Four- or Two-Channel Time-Division-Multiplex Telegraph System for Long-Distance. Peterman, Minc.....362-72
Radio Influence Tests in Field and Laboratory—500-Kv Test Project of the American Gas and Electric Company. Lippert, Pakala, Bartlett, Fahrnkopf.....251-65; disc. 265
(Radio) Operational Study of a Highway Mobile Telephone System. Dorff.....31-7
Radiometers, Total Hemispherical. Gier, Dunkle.....339-43; disc. 343
Railroad, New A-C Multiple-Car Control for the Pennsylvania. Newhouse.....645-7; disc. 647
Railroads, A Modern Cab Signaling and Train Control System for. Allison.....232-8; disc. 238
Railway of Brazil, Regeneration with a Mercury Arc Rectifier on the Central. Schmidt.....1092-6
Railways of Providence, Power Supply Study and New Rectifier Installation for the United Electric. Whitman, Schaller.....978-85; disc. 985
Rapid Transit Cars, Electric Equipment and Performance of Lightweight. Ellis, Sloman.....227-30; disc. 230
Rapid Transit Control Equipment, A New Lightweight. Lichtenfels, Moore.....224-6
Rapid Transit Motor, A New Lightweight. Pettersen.....222-3
Reactance, An Experimental Study of Induction Machine End-Turn Leakage. Barnes.....671-7; disc. 677
Reactor Control, A-C Arc Welders with Saturable. Oestreicher.....787-90
Reactor Control for Mechanical Rectifiers, Commutating. Diebold.....1062-5
Reactors with Resistive Load, Transient Response of Saturable. Storm.....95-102
Record—Rural Line Sectionalizing by Repeater Fuses, 11-Year Operating. Schahfer, Strout.....680-6
Rectangular Co-ordinate Systems, Tables of Green's Functions, Fourier Series, and Impulse Functions for. Smith.....22-30
Rectifier Installation for the United Electric Railways of Providence, Power Supply Study and New. Whitman, Schaller.....978-85; disc. 985
Rectifier on the Central Railway of Brazil, Regeneration with a Mercury Arc. Schmidt.....1092-6
Rectifiers, Commutating Reactor Control for Mechanical. Diebold.....1062-5
Rectifiers for Urban Transit Power Supply, Sealed Ignitron. Borst.....770-4
Rectifiers, Inductive Co-ordination Aspects of D-C Systems Supplied by. (Committee Report).....1034-54
Reference Frames, Transient Analysis of Rotating Machines and Stationary Networks by Means of Rotating. Ku.....943-54; disc. 954
Refractory Surfaces, A Study of Conduction Phenomena Near Current Zero for an A-C Arc Adjacent to. Browne, Strom.....398-407; disc. 407
Regeneration with a Mercury Arc Rectifier on the Central Railway of Brazil. Schmidt.....1092-6
Regulation of Urban 4-Kv Feeders, Group. Grim, Peck.....551-6
Relay Literature-1947-1949, Bibliography of. (Committee Report).....247-50
Relay Protection of A-C Generators. (Committee Report).....275-81; disc. 281
Relaying System, Measurements and Tests on a Power Line Carrier. Miller, Worthington.....1005-07
Reluctance Synchronous Motors, A Design Method for Polyphase. Crouse.....957-62
Repeater Fuses, 11-Year Operating Record—Rural Line Sectionalizing by. Schahfer, Strout.....680-6
Repeaters, A Submarine Telephone Cable with Submerged. Gilbert.....564-72
Reperforator Switching, Automatic Trunk Selection in, Blanton.....481-9
Report of the AIEE Magnetic Amplifier Subcommittee, Progress. (Committee Report)...445-9; disc. 449
Requirements, Determination of Generator Stand-by Reserve. Strandrud.....179-87; disc. 187
Reserve Capacity by the Probability Method Effect of Interconnections, Determination of. Calabrese.....1018-20
Reserve Requirements, Determination of Generator Stand-by. Strandrud.....179-87; disc. 187
Resistance—The Contribution of Nonuniform Current Flow, Contact. Kouwenhoven, Sackett...791-5
Resistance, Three-Phase Measurements of. Matsch, Basu, Horcher.....350-2; disc. 352
Resistance Welders, Probabilities of Interference Between. Boice.....775-83
Resistance Welding Machines, Selection of Fuses for. Stadum.....796-9
Resistive Load, Analysis of a 3-Phase Inverter with. Turkington.....1055-61
Resistive Load, Transient Response of Saturable Reactors with. Storm.....95-102
Resonant Grounding in Power Systems in the United States, Application of. Gross, Atherton.....389-93; disc. 393
Response of Magnetic Amplifiers—Cases of Negligible Commutation, The Transient. Finzi, Chandler, Beaumariage.....934-42; disc. 942
Response of Saturable Reactors with Resistive Load, Transient. Storm.....95-102
Response of Small 2-Phase Induction Motors, Transient. Hopkin.....881-6
Results of a Questionnaire Covering Current Practices in Electrical Tests on Dielectrics in the Field. (Committee Report).....986-9

Rocket Application, Pulse-Time Modulation Telemetering Systems for. Mengel....599–605
Rod Waveguides, Shielded Dielectric-. Beam, Wachowski....874–80
Room Lighting, An Engineering Approach to Control. Dzwonczyk....852–7; disc. 857
(Rotating Machinery) A New High-Voltage Insulation for Turbine-Generator Stator Windings. Laffoon, Hill, Moses, Berberich....721–6; disc. 726
(Rotating Machinery) Aging of Class-B Insulating Material in Nitrogen. Stewart, Whitman....436–7; disc. 437
Rotating Machines, A Maintenance Inspection Program for Large. Johnson....749–54; disc. 755
Rotating Machines and Stationary Networks by Means of Rotating Reference Frames, Transient Analysis of. Ku....943–54; disc. 954
Rotation Single Side-Band Transmitters, Output Analysis and Alignment Techniques for Phase-. Whitby, Scheuch....209–12
Rotors, Modern Practice in the Balancing of Large Turbine-Generator. Laffoon, Hagg, Janthey, Heller....593–8; disc. 598
Routine Insulation Testing of Synchronous Machines. Hunt, Vivian....756–62
Rules for Designing Frog-Leg Windings of D-C Machines. Dwight, Haltmaier....707–11; disc. 711
Rural Line Sectionalizing by Repeater Fuses, 11-Year Operating Record—. Schahfer, Strout....680–6

S

Saturable Reactor Control, A-C Arc Welders with. Oestreicher....787–90
Saturable Reactors with Resistive Load, Transient Response of. Storm....95–102
Saturating Magnetic Amplifiers Based on Linear Approximations of the Magnetization Curve, Steady-State Analysis of Self-. Esselman....451–9
Saturating Servomechanisms, A Phase-Plane Approach to the Compensation of. Hopkin....631–9
Saturation, Calculation of Flux Distributions with. Poritsky....309–19; disc. 319
Scale Computers, Systematization of Tube Surveillance in Large-. Spence....516–19
Sealed Ignitron Rectifiers for Urban Transit Power Supply. Borst....770–4
Sectionalizing by Repeater Fuses, 11-Year Operating Record—Rural Line. Schahfer, Strout....680–6
Selection in Reperforator Switching, Automatic Trunk. Blanton....481–9
Selection of Equipment for Multiple-Unit Cars. Hutchison....640–3; disc. 643
Selection of Fuses for Resistance Welding Machines. Stadum....796–9
Self-Saturating Magnetic Amplifiers Based on Linear Approximations of the Magnetization Curve, Steady-State Analysis of. Esselman....451–9
Sensing Elements of Pressure, Temperature, and Humidity, Piezoelectric Crystals as. Roberts, Goldsmith....968–72
Separation, Distribution of Charge in Electrostatic Mineral. Fraas, Ralston....1028–30
Series, and Impulse Functions for Rectangular Coordinate Systems, Tables of Green's Functions, Fourier. Smith....22–30
Series Capacitor to a Synchronous Condenser for Reducing Voltage Flicker, The Application of a. Black, Lischer....144–50
Series Capacitors in High-Voltage Transmission Lines, Fundamental Effects of. Johnson, Barkle, Povejsil....526–35; disc. 535
Series with a Synchronous Condenser, Technical Problems Associated with the Application of a Capacitor in. Witzke, Michelson....519–25
Service Experience and Further Experimental Work, The Torsional Damper for Conductors—. Burgess, Hogg....1031–3
Servo System for Heterodyne Oscillators, A. Slonczewski....1070–2
Servomechanisms, A Phase-Plane Approach to the Compensation of Saturating. Hopkin....631–9
Servomechanisms, Effects of Carrier Shifts on Derivative Networks for A-C. Attura....612–18
Servomechanisms, Network Synthesis by Graphical Methods for A-C. Bjornson....619–25
Shaded Pole Motors, Equivalent Circuits and Their Application in Designing. Chang..690–8; disc. 698
Sheaths for Underground Power Cable, Lead-Alloy. Halperin, Betzer....423–9; disc. 429
Shielded Dielectric-Rod Waveguides. Beam, Wachowski....874–80
Shift System for Use with Differential Protection of Transformer Banks, A New Carrier-Current Frequency. Beckwith....832–5; disc. 835
Shifts on Derivative Networks for A-C Servomechanisms, Effects of Carrier. Attura....612–18
Shunt Capacitor Banks, Switching High-Voltage. Funkhouser, VanSickle, Shankle..129–33; disc. 134
Shunt Capacitors at Transmission and Distribution Stations, Application of. Porter, Zimmerman....112–18; disc. 118
Side-Band Transmitters, Output Analysis and Alignment Techniques for Phase-Rotation Single. Whitby, Scheuch....209–12
Signal and Supervision Systems Used on Carrier Current Communications Circuits. Mayer....990–4
Signaling and Train Control System for Railroads, A Modern Cab. Allison....232–8; disc. 238
Signaling System for Supervision and Dialing over Long-Distance Telephone Trunks, Single-Frequency. Newell, Weaver....489–95
Simplified Method for Predicting Induction Motor Performance, A. Webking....667–70; disc. 671
Single-Frequency Signaling System for Supervision and Dialing over Long-Distance Telephone Trunks. Newell, Weaver....489–95
69-Kv Air Blast Circuit Breaker, A New. Shores, Beatty....202–07; disc. 207
69-Kv Medium-Pressure Gas-Filled Cable, Washington, D. C. Clark....418–21; disc. 421
Some Design Criteria for Automatic Controls. Nims....606–11
Some Effects of Lightning Arrester Protective Characteristics and Location upon Station Apparatus Protection. Kalb....379–83; disc. 383
Source for Large D-C Contact Testing, An Electronic Power. Pettit....320–2
Sources of Ionizing Energy, Electrostatic. Trump....1021–7
Sparkover Voltage of Gaps on Humidity and Time, Dependence of Direct. Jacob, Sommerman....921–4; disc. 924
Spiral Arc Chokes Power Flow in New Lightning Arresters. Ackermann, DeVal....995–8
Split-Winding Starting of 3-Phase Motors. Alger, Ward, Wright....867–72; disc. 872
Spring Mechanism for Hand Closing of Magnetic Power Air Circuit Breakers. Dickinson, Findley....189–92; disc. 192
Stability Criterion, The Generalized Transmission Matrix. Honnell....292–6; disc. 296
Stabilizing Inert-Gas Welding Arcs, New Electrodes for. Cobine, Gallagher....804–06
Stable Feedback Systems, A Note on the Design of Conditionally. Travers....626–30
Stand-by Reserve Requirements, Determination of Generator. Strandrud....179–87; disc. 187
Starting of 3-Phase Motors, Split-Winding. Alger, Ward, Wright....867–72; disc. 872
State Analysis of Self-Saturating Magnetic Amplifiers Based on Linear Approximations of the Magnetization Curve, Steady-. Esselman....451–9
States, A New Method for Treating Electron Tubes When Used as Oscillators in the Free as Well as in the Synchronized. Mostafa, Bey....999–1004
Static Magnetic Exciter for Synchronous Alternators. Storm....1014–17
Station Apparatus Protection, Some Effects of Lightning Arrester Protective Characteristics and Location upon. Kalb....379–83; disc. 383
Stationary Networks by Means of Rotating Reference Frames, Transient Analysis of Rotating Machines and. Ku....943–54; disc. 954
Stations, Application of Shunt Capacitors at Transmission and Distribution. Porter, Zimmerman....112–18; disc. 118
Stator Windings, A New High-Voltage Insulation for Turbine-Generator. Laffoon, Hill, Moses, Berberich....721–6; disc. 726
Stators, The Use of Preferred Orientation Strip Steel in Turbine-Generator. Apperson, Fontaine....836–9; disc. 839
Steady-State Analysis of Self-Saturating Magnetic Amplifiers Based on Linear Approximations of the Magnetization Curve. Esselman....451–9
Steel in Turbine-Generator Stators, The Use of Preferred Orientation Strip. Apperson, Fontaine....836–9; disc. 839
Stresses in Impregnated Paper Insulation, Radial and Tangential. Whitehead....56–9; disc. 59
Strip Steel in Turbine-Generator Stators, The Use of Preferred Orientation. Apperson, Fontaine....836–9; disc. 839
Studies on Mica Insulation for Electric Machinery, Alternating and Direct Voltage Endurance. Moses....763–8; disc. 768
Study of a Highway Mobile Telephone System, Operational. Dorff....31–7
Study of Conduction Phenomena Near Current Zero for an A-C Arc Adjacent to Refractory Surfaces, A. Browne, Strom....398–407; disc. 407
Study of Harmonic Power Generation with Nonlinear Impedance Element, Differential Analyzer. Russell, Peterson....917–20
Study of Induction Machine End-Turn Leakage Reactance, An Experimental. Barnes....671–7; disc. 677
Subareas, Calculation of the Capacitance of a Circular Annulus by the Method of. Higgins, Reitan....926–31; disc. 931
Subcommittee, Progress Report of the AIEE Magnetic Amplifier. (Committee Report)..445–9; disc. 449
Submarine Telephone Cable with Submerged Repeaters, A. Gilbert....564–72
Substation Type Transformers, An Investigation of Audio Noise in. Vivian, Peck...328–31; disc. 331
(Substations) Group Regulation of Urban 4-Kv Feeders. Grim, Peck....551–6
Supervision Systems Used on Carrier Current Communications Circuits, Signal and. Mayer..990–4
Supervisory Control on a Carrier Communication Channel, Vibracode System of. Allen, Daniel....818–22; disc. 822
Supervisory System for Distribution Circuits, Carrier Current. Podolsky, Lubin....1096–1101
Supply, Economics of Trolley Coach Power. McDonald, Price....687–9
Supply Study and New Rectifier Installation for the United Electric Railways of Providence, Power. Whitman, Schaller....978–85; disc. 985
Supply Voltage Below the Breakdown Voltage, A Gas Tube Inverter with the. Cage, Schuder...908–12
Surface Leakage Distances in D-C Power Systems, Factors Affecting Minimum. Hart, Rosenberry, McClinton....738–42
Surfaces, A Study of Conduction Phenomena Near Current Zero for an A-C Arc Adjacent to Refractory. Browne, Strom....398–407; disc. 407
Surveillance in Large-Scale Computers, Systematization of Tube. Spence....516–19
Switch Design, Ice Testing and Its Influence Upon. Heberlein, Field....37–42; disc. 42
(Switchgear) A New 69-Kv Air Blast Circuit Breaker. Shores, Beatty....202–07; disc. 207
Switching, Automatic Trunk Selection in Reperforator. Blanton....481–9
Switching High-Voltage Shunt Capacitor Banks. Funkhouser, VanSickle, Shankle....129–33; disc. 134
Switching of Distribution Capacitors by Manual and Automatic Devices. Hopkins, Schultz....138–43
Switching Phenomena, Capacitor. VanSickle, Zaborszky....151–8; disc. 158
Switching System, A Full Automatic Private-Line Teletypewriter. Bacon, Locke....473–80
Synchronous Alternators, Static Magnetic Exciter for. Storm....1014–17
Synchronous Condenser for Reducing Voltage Flicker, The Application of a Series Capacitor to a. Black, Lischer....144–50
Synchronous Condenser, Technical Problems Associated with the Application of a Capacitor in Series with a. Witzke, Michelson....519–25
Synchronous Machine Damping and Synchronizing Torques. Concordia....731–7
Synchronous Machines, Routine Insulation Testing of. Hunt, Vivian....756–62
Synchronous Machines, Telephone Influence Factor in. Oscarson, Benson....743–8
Synchronous Motors, A Design Method for Polyphase Reluctance. Crouse....957–62
Synthesis by Graphical Methods for A-C Servomechanisms. Bjornson....619–25
System, A Full Automatic Private-Line Teletypewriter Switching. Bacon, Locke....473–80
System Economics of Extra-High-Voltage Transmission. St. Clair, Peterson....841–8; disc. 848
System Fault Control, Power. (Committee Report)....410–17
System for Heterodyne Oscillators, A Servo. Slonczewski....1070–2
System for Supervision and Dialing over Long-Distance Telephone Trunks, Single-Frequency Signaling. Newell, Weaver....489–95
System, Measurements and Tests on a Power Line Carrier Relaying. Miller, Worthington..1005–07
System, Neutral Inversion of a Single Potential Transformer Connected Line-to-Ground on an Isolated Delta. Gleason....103–10; disc. 110
System of Supervisory Control on a Carrier Communication Channel, Vibracode. Allen, Daniel....818–22; disc. 822
System of the American Gas and Electric Company, The 300–315 Kv Extra-High-Voltage Transmission. Sporn, Peterson, Gross, St.Clair....64–72; disc. 72
System of the EDVAC, The Input-Output. Snyder....507–09
System, Operational Study of a Highway Mobile Telephone. Dorff....31–7
Systematization of Tube Surveillance in Large-Scale Computers. Spence....516–19
Systems, A Note on the Design of Conditionally Stable Feedback. Travers....626–30
Systems, Factors Affecting Minimum Surface Leakage Distances in D-C Power. Hart, Rosenberry, McClinton....738–42
Systems, Fault Transients in Aircraft D-C. Scorgie....713–20; disc. 720
Systems in the United States, Application of Resonant Grounding in Power. Gross, Atherton....389–93; disc. 393
Systems Supplied by Rectifiers, Inductive Co-ordination Aspects of D-C. (Committee Report)....1034–54
Systems Used on Carrier Current Communications Circuits, Signal and Supervision. Mayer....990–4

T

Tables of Green's Functions, Fourier Series, and Impulse Functions for Rectangular Co-ordinate Systems. Smith.........22-30
Tachometer for Measurement of Instantaneous Variations in Angular Velocity, A. Bartles.....1102-05
Tangential Stresses in Impregnated Paper Insulation, Radial and. Whitehead...........56-9; disc. 59
Technical Problems Associated with the Application of a Capacitor in Series with a Synchronous Condenser. Witzke, Michelson.........519-25
Techniques Applied to Economics, Analogue Computing. Strotz, Calvert, Morehouse..557-62; disc. 562
Techniques of Corona Loss Measurement and Analysis—500-Kv Test Project of the American Gas and Electric Company. Naef, Tremaine, Jones..........496-505; disc. 505
Telegraph Network, A Nationwide Frequency-Modulation. Bramhall, Smith..........373-8; disc. 378
Telegraph Set, An Electronic Time Division Multiplex. Hansen, Slayton...............354-61; disc. 361
Telegraph System for Long-Distance Radio Circuits, Four- or Two-Channel Time-Division-Multiplex. Peterman, Minc.........362-72
Telemetering Systems and Channels for a Power System, Choice of. Duff.........1086-91
Telemetering Systems for Rocket Application, Pulse-Time Modulation. Mengel.............599-605
Telephone Cable with Submerged Repeaters, A Submarine. Gilbert.........564-72
Telephone Influence Factor in Synchronous Machines. Oscarson, Benson.........743-8
Telephone System, Operational Study of a Highway Mobile. Dorff.........31-7
Telephone Trunks, Single-Frequency Signaling System for Supervision and Dialing over Long-Distance. Newell, Weaver.........489-95
Teletypewriter Switching System, A Full Automatic Private-Line. Bacon, Locke.............473-80
Temperature, and Humidity, Piezoelectric Crystals as Sensing Elements of Pressure. Roberts, Goldsmith.........968-72
Temperatures, Deterioration of Transformer Oil and Paper Insulation by. Vogel, Petersen, Matsch.........18-20; disc. 21
Test Project of the American Gas and Electric Company, Corona Investigation on Extra-High-Voltage Lines—500-Kv. Gross, Wagner, Naef, Tremaine.........75-91; disc. 91
Test Project of the American Gas and Electric Company, Line Insulator Loss Under Normal Conditions—500-Kv. Naef, Tremaine, Jones..........1073-8
Test Project of the American Gas and Electric Company, Techniques of Corona Loss Measurement and Analysis—500-Kv. Naef, Tremaine, Jones.........496-505; disc. 505
Tester for D-C Armatures, Winding Insulation. Catlin, Rohats.........465-8
Testing, An Electronic Power Source for Large D-C Contact. Pettit.........320-2
Testing and Its Influence Upon Switch Design, Ice. Heberlein, Field...............37-42; disc. 42
Testing of Lightning Arresters, The Power Interruption. Ackermann.........1-5; disc. 5
Testing of Synchronous Machines, Routine Insulation. Hunt, Vivian.........756-62
Tests in Field and Laboratory—500-Kv Test Project of the American Gas and Electric Company, Radio Influence. Lippert, Pakala, Bartlett, Fahrnkopf.........251-65; disc. 265
Tests on a Power Line Carrier Relaying System, Measurements and. Miller, Worthington......1005-07
Tests on Dielectrics in the Field, Results of a Questionnaire Covering Current Practices in Electrical. (Committee Report).........986-9
Theory of the Deep-Bar Induction Motor, A Contribution to the. Douglas.........862-6
Thermal Expansion Effects in Power Cables. Schifreen.........160-8; disc. 168
Thermal Transients on Buried Cables. Buller.........45-52; disc. 52, 1106
300-315 Kv Extra-High-Voltage Transmission System of the American Gas and Electric Company, The. Sporn, Peterson, Gross, St.Clair....64-72; disc. 72
Three-Phase Inverter with Resistive Load, Analysis of a. Turkington.........1055-61
Three-Phase Measurements of Resistance. Matsch, Basu, Horcher.........350-2; disc. 352
Three-Phase Motors, Split-Winding Starting of. Alger, Ward, Wright.........867-72; disc. 872
Time, Dependence of Direct Sparkover Voltage of Gaps on Humidity and. Jacob, Sommerman.........921-4; disc. 924
Time Division Multiplex Telegraph Set, An Electronic. Hansen, Slayton.........354-61; disc. 361
Time-Division-Multiplex Telegraph System for Long-Distance Radio Circuits, Four- or Two-Channel. Peterman, Minc.........362-72
Time Modulation Telemetering Systems for Rocket Application, Pulse-. Mengel.............599-605
Torques, Synchronous Machine Damping and Synchronizing. Concordia.........731-7
Torsional Damper for Conductors—Service Experience and Further Experimental Work, The. Burgess, Hogg.........1031-3
Total Hemispherical Radiometers. Gier, Dunkle.........539-43; disc. 343
Train Control System for Railroads, A Modern Cab Signaling and. Allison..........232-8; disc. 238
Train Performance Calculator, A New. Smith..657-60
Transducer, An Electromechanical. Engelberger, Kretsch.........213-16
Transfer Admittance Remains Constant as Load Varies, Networks for Which Magnitude or Phase Angle of Input Impedance or. Berkowitz..........286-91
Transfer Data in Electron Tube Operation, Basic Heat-. Buckland.........1079-85
Transformer Application, Economics of Power. Barkle, Witzke.........440-4; disc. 444
Transformer Banks, A New Carrier-Current Frequency-Shift System for Use with Differential Protection of. Beckwith.........832-5; disc. 835
Transformer Connected Line-to-Ground on an Isolated Delta System, Neutral Inversion of a Single Potential. Gleason.........103-10; disc. 110
Transformer Core, A 2,000,000-Kva. Sealey....8-11
Transformer Installations, Acoustic Models of. Gettys, Conover.........333-6; disc. 336
Transformer-Loss Compensators for Watt-hour and Var-hour Meters, Improvements in. Schleicher.........973-7
Transformer Magnetizing Inrush Current. Specht.........323-7; disc. 327
Transformer Oil and Paper Insulation by Temperatures, Deterioration of. Vogel, Petersen, Matsch.........18-20; disc. 21
Transformer Winding, Improved Core Form. Grimmer, Teague.........962-5; disc. 965
(Transformers) An Analysis of Grounding Banks to Balance Distribution Feeder Voltages. Long.........823-7
Transformers, An Investigation of Audio Noise in Substation-Type. Vivian, Peck.....328-31; disc. 331
Transient Analysis of Rotating Machines and Stationary Networks by Means of Rotating Reference Frames. Ku.........943-54; disc. 954
Transient Response of Magnetic Amplifiers—Cases of Negligible Commutation, The. Finzi, Chandler, Beaumariage.........934-42; disc. 942
Transient Response of Saturable Reactors with Resistive Load. Storm.........95-102
Transient Response of Small 2-Phase Induction Motors. Hopkin.........881-6
Transients in Aircraft D-C Systems, Fault. Scorgie.........713-20; disc. 720
Transients in Simple Electric Circuits, Contact. Martin, Stauss.........304-07; disc. 307
Transients on Buried Cables, Thermal. Buller.........45-52; disc. 52, 1106
Transit Cars, Electric Equipment and Performance of Lightweight Rapid. Ellis, Sloman.........227-30; disc. 230
Transit Control Equipment, A New Lightweight Rapid. Lichtenfels, Moore.........224-6
Transit Motor, A New Lightweight Rapid. Pettersen.........222-3
Transit Power Supply, Sealed Ignitron Rectifiers for Urban. Borst.........770-4
Transit Systems, D-C Power Supplies and Isolation of Faults on Electric. Watkins, Reagan.
  Part I. D-C Power Supply.....537-42; disc. 542
  Part II. Isolation of D-C Faults..543-50; disc. 550
Transmission and Distribution Stations, Application of Shunt Capacitors at. Porter, Zimmerman.........112-18; disc. 118
(Transmission) Corona Investigation on Extra-High-Voltage Lines—500-Kv Test Project of the American Gas and Electric Company. Gross, Wagner, Naef, Tremaine.........75-91; disc. 91
Transmission Line Constants, A Per-Unit Interpretation of. Povejsil, Johnson.......194-200; disc. 200
Transmission Line Fault Locator, The Linascope. Kidd.........1008-13
(Transmission) Line Insulator Loss Under Normal Conditions—500-Kv Test Project of the American Gas and Electric Company. Naef, Tremaine, Jones.........1073-8
Transmission Line Load Impedance for Maximum Efficiency. Lutz.........283-5
Transmission Lines, Fundamental Effects of Series Capacitors in High-Voltage. Johnson, Barkle, Witzke.........526-35; disc. 535
Transmission Lines Over Mountainous Region Where Lightning Incidence is High, Protection of. Housley, Harper.........124-6; disc. 126
Transmission Matrix Stability Criterion, The Generalized. Honnell.........292-6; disc. 296
(Transmission) Radio Influence Tests in Field and Laboratory—500-Kv Test Project of the American Gas and Electric Company. Lippert, Pakala, Bartlett, Fahrnkopf.........251-65; disc. 265
Transmission, System Economics of Extra-High-Voltage. St.Clair, Peterson.........841-8; disc. 848
Transmission System of the American Gas and Electric Company, The 300-315 Kv Extra-High-Voltage. Sporn, Peterson, Gross, St.Clair....64-72; disc. 72
(Transmission) Techniques of Corona Loss Measurement and Analysis—500-Kv Test Project of the American Gas and Electric Company. Naef, Tremaine, Jones.........496-505; disc. 505
Transmitters, Output Analysis and Alignment Techniques for Phase-Rotation Single Side-Band. Whitby, Scheuch.........209-12
(Transportation, Air) Fault Transients in Aircraft D-C Systems. Scorgie.........713-20; disc. 720
(Transportation, Land) A Modern Cab Signaling and Train Control System for Railroads. Allison.........232-8; disc. 238
(Transportation, Land) A New Lightweight Rapid Transit Control Equipment. Lichtenfels, Moore.........224-6
(Transportation, Land) A New Lightweight Rapid Transit Motor. Pettersen.........222-3
(Transportation, Land) A New Multiple-Unit Car Motor for the Pennsylvania Railroad. Jungk.........243-5; disc. 245
(Transportation, Land) A New Train Performance Calculator. Smith.........657-60
(Transportation, Land) A-C Multiple-Unit Car Control Equipment. O'Kelly.........652-6
(Transportation, Land) A-C Multiple-Unit Car Motor. Kreitler.........648-50; disc. 650
(Transportation, Land) Economics of Trolley Coach Power Supply. McDonald, Price.........687-9
(Transportation, Land) Electric Equipment and Performance of Lightweight Rapid Transit Cars. Ellis, Sloman.........227-30; disc. 230
(Transportation, Land) New A-C Multiple-Car Control for the Pennsylvania Railroad. Newhouse.........645-7; disc. 647
(Transportation, Land) Regeneration with a Mercury Arc Rectifier on the Central Railway of Brazil. Schmidt.........1092-6
(Transportation, Land) Why 4-Motor Multiple-Unit Car Equipments? Williamson.........240-2
Trolley Coach Power Supply, Economics of. McDonald, Price.........687-9
Trunk Selection in Reperforator Switching, Automatic. Blanton.........481-9
Trunks, Single-Frequency Signaling System for Supervision and Dialing over Long-Distance Telephone. Newell, Weaver.........489-95
Tube Inverter with the Supply Voltage Below the Breakdown Voltage, A Gas. Cage, Schuder.........908-12
Tube Operation, Basic Heat-Transfer Data in Electron. Buckland.........1079-85
Tube Surveillance in Large-Scale Computers, Systematization of. Spence.........516-19
Tubes When Used as Oscillators in the Free As Well as in the Synchronized States, A New Method for Treating Electron. Mostafa, Bey.......999-1004
Turbine-Generator Rotors, Modern Practice in the Balancing of Large. Laffoon, Hagg, Janthey, Heller.........593-8; disc. 598
Turbine-Generator Stator Windings, A New High-Voltage Insulation for. Laffoon, Hill, Moses, Berberich.........721-6; disc. 726
Turbine-Generator Stators, The Use of Preferred Orientation Strip Steel in. Apperson, Fontaine.........836-9; disc. 839
Turbine Generators, Detection of Turn-to-Turn Faults in Large High-Voltage. Sexton, Alke.........270-3; disc. 273
Turbine Generators, Progress in the Development of Large. Huntley, Taylor........580-9; disc. 589
Turn-to-Turn Faults in Large High-Voltage Turbine Generators, Detection of. Sexton, Alke.........270-3; disc. 273
Two-Channel Time-Division-Multiplex Telegraph System for Long-Distance Radio Circuits, Four or. Peterman, Minc.........362-72
2,000,000-Kva Transformer Core, A. Sealey.....8-11
Two-Phase Induction Motors, Transient Response of Small. Hopkin.........881-6

U

Underground Power Cable, Lead-Alloy Sheaths for. Halperin, Betzer.........423-9; disc. 429
Unit Car Control Equipment, A-C Multiple-. O'Kelly.........652-6
Unit Car Equipments?, Why 4-Motor Multiple-. Williamson.........240-2
Unit Car Motor, A-C Multiple-. Kreitler.........648-50; disc. 650
Unit Car Motor for the Pennsylvania Railroad, A New Multiple-. Jungk.........243-5; disc. 245
Unit Cars, Selection of Equipment for Multiple-. Hutchison.........640-3; disc. 643
Unit Interpretation of Transmission Line Constants, A Per-. Povejsil, Johnson........194-200; disc. 200
United Electric Railways of Providence, Power Supply Study and New Rectifier Installation for the. Whitman, Schaller.........978-85; disc. 985

United States, Application of Resonant Grounding in Power Systems in the. Gross, Atherton..........389–93; disc. 393

Universal-Type Motors, Commutation in. Packer..........170–6; disc. 176

Urban 4-Kv Feeders, Group Regulation of. Grim, Peck..........551–5

Urban Transit Power Supply, Sealed Ignitron Rectifiers for. Borst..........770–4

Use of Preferred Orientation Strip Steel in Turbine-Generator Stators, The. Apperson, Fontaine..........836–9; disc. 839

V

Variations in Angular Velocity, A Tachometer for Measurement of Instantaneous. Bartles..1102–05

Var-hour Meters, Improvements in Transformer Loss Compensators for Watt-hour and. Schleicher..........973–7

Varmeters, Marking of. (Committee Report)..........12–14; disc. 14

Velocity, A Tachometer for Measurement of Instantaneous Variations in Angular. Bartles..1102–05

Vibracode System of Supervisory Control on a Carrier Communication Channel. Allen, Daniel..........818–22; disc. 822

Voltage Below the Breakdown Voltage, A Gas Tube Inverter with the Supply. Cage, Schuder..908–12

Voltage Dip on Cyclic Light Flicker, Effect of the Duration of. Brieger..........894–8; disc. 899

Voltage Endurance Studies on Mica Insulation for Electric Machinery, Alternating and Direct. Moses..........763–8; disc. 768

Voltage Flicker, The Application of a Series Capacitor to a Synchronous Condenser for Reducing. Black, Lischer..........144–50

Voltage of Gaps on Humidity and Time, Dependence of Direct Sparkover. Jacob, Sommerman..........921–4; disc. 924

Voltage Transmission, System Economics of Extra-High-. St.Clair, Peterson.......841–8; disc. 848

Voltages, An Analysis of Grounding Banks to Balance Distribution Feeder. Long..........823–7

W

Washington, D. C., 69-Kv Medium-Pressure Gas-Filled Cable. Clark..........418–21; disc. 421

Watt-hour and Var-hour Meters, Improvements in Transformer-Loss Compensators for. Schleicher..........973–7

Waveguide Linear Accelerators, Dielectric Loading for. Flesher, Cohn..........887–93

Waveguides, Shielded Dielectric-Rod. Beam, Wachowski..........874–80

Welders, Ignitrons for Frequency-Changer. Rottier..........900–07

Welders, Probabilities of Interference Between Resistance. Boice..........775–83

Welders with Saturable Reactor Control, A-C Arc. Oestreicher..........787–90

Welding Arc, The Physical Mechanism of Low and High Current Arcs and Their Relation to the. Finkelnburg..........800–03

Welding Arcs, New Electrodes for Stabilizing Inert-Gas. Cobine, Gallagher..........804–06

Welding Calculations—Effect of Conductor Configuration in Overhead Lines. Tietze..........784–6

Welding Machines, Selection of Fuses for Resistance. Stadum..........796–9

Winding, Improved Core Form Transformer. Grimmer, Teague..........962–5; disc. 965

Winding Insulation Tester for D-C Armatures. Catlin, Rohats..........465–8

Winding Starting of 3-Phase Motors, Split-. Alger, Ward, Wright..........867–72; disc. 872

Windings, A New High-Voltage Insulation for Turbine-Generator Stator. Lafloon, Hill, Moses, Berberich..........721–6; disc. 726

Windings of D-C Machines, Rules for Designing Frog-Leg. Dwight, Haltmaier.......707–11; disc. 711

Z

Zero for an A-C Arc Adjacent to Refractory Surfaces, A Study of Conduction Phenomena Near Current. Browne, Strom..........398–407; disc. 407

2. Author Index

Ackermann, Otto. The Power Interruption Testing of Lightning Arresters. (51–1).......1–5; disc. 7

Ackermann, Otto; E. J. DeVal. Spiral Arc Chokes Power Flow in New Lightning Arresters. (51–189)..........995–8

Aicher, L. C., Jr. Disc..........924

Alger, P. L., Disc..........665, 678

Alger, P. L.; H. C. Ward, Jr.; F. H. Wright. Split-Winding Starting of 3-Phase Motors. (51–160)..........867–72; disc. 872

Alke, Roger J.; R. M. Sexton. Detection of Turn-to-Turn Faults in Large High-Voltage Turbine Generators. (51–41)..........270–3; disc. 274

Allen, T. J. Disc..........126

Allen, T. J.; J. Daniel. Vibracode System of Supervisory Control on a Carrier Communication Channel. (51–146)..........818–22; disc. 822

Allison, L. R. A Modern Cab Signaling and Train Control System for Railroads. (51–34)..........232–8; disc. 239

Amchin, Howard K. Disc..........394

Anderson, E. R.; L. J. Anderson. Disc..........344

Anderson, L. J.; E. R. Anderson. Disc..........344

Apperson, J. W.; C. B. Fontaine. The Use of Preferred Orientation Strip Steel in Turbine-Generator Stators. (51–154)..........836–9; disc. 840

Arnold, G. W. Disc..........711

Atherton, Edward W.; E. T. B. Gross. Application of Resonant Grounding in Power Systems in the United States. (51–64)..........389–93; disc. 396

Atkinson, R. W. Disc..........60, 168, 353, 429

Attura, George M. Effects of Carrier Shifts on Derivative Networks for A-C Servomechanisms. (51–100)..........612–18

B

Babb, D. S.; J. E. Williams. Circuit Analysis Method for Determination of A-C Impedances of Machine Conductors. (51–109)..........661–5; disc. 665

Bacon, W. M.; G. A. Locke. A Full Automatic Private-Line Teletypewriter Switching System. (51–76)..........473–80

Balentine, C. J.; E. B. Rietz. Disc.....118, 135, 159

Bany, H. Disc..........14

Barkle, J. E.; A. A. Johnson, D. J. Povejsil. Fundamental Effects of Series Capacitors in High-Voltage Transmission Lines. (51–89)....526–35; disc. 535

Barkle, J. E.; R. L. Witzke. Economics of Power Transformer Application. (51–70)..........440–4

Barnes, E. C. An Experimental Study of Induction Machine End-Turn Leakage Reactance. (51–111)..........671–7; disc. 678

Barnes, H. C.; J. H. Kinghorn. Disc..........282

Bartles, S. P. A Tachometer for Measurement of Instantaneous Variations in Angular Velocity. (51–238)..........1102–05

Bartlett, S. C.; G. D. Lippert, W. E. Pakala, C. D. Fahrnkopf. Radio Influence Tests in Field and Laboratory—500-Kv Test Project of the American Gas and Electric Company. (51–40)..........251–65; disc. 269

Basu, N. C.; L. W. Matsch, G. R. Horcher. Three-Phase Measurements of Resistance. (51–59)..........350–2; disc. 352

Beam, Robert E.; H. M. Wachowski. Shielded Dielectric-Rod Waveguides. (51–162)..........874–80

Beatty, J. W.; R. B. Shores. A New 69-Kv Air Blast Circuit Breaker. (51–27).......202–07; disc. 208

Beaumariage, D. C.; L. A. Finzi, D. P. Chandler. The Transient Response of Magnetic Amplifiers—Cases of Negligible Commutation. (51–175)..........934–42; disc. 942

Beck, Edward. Disc..........134

Beckwith, R. W. A New Carrier-Current Frequency-Shift System for Use with Differential Protection of Transformer Banks. (51–153)....832–5; disc. 835

Beckwith, Sterling. Disc..........591

Beeman, D. L. Disc..........444

Bellaschi, P. L. Disc..........21, 72

Benson, Ikel C.; G. L. Oscarson. Telephone Influence Factor in Synchronous Machines. (51–124)..........743–8

Berberich, L. J.; C. M. Laffoon, C. F. Hill, G. L. Moses. A New High-Voltage Insulation for Turbine-Generator Stator Windings. (51–121)..........721–6; disc. 730

Berkowitz, Raymond S. Networks for Which Magnitude or Phase Angle of Input Impedance or Transfer Admittance Remains Constant as Load Varies. (51–45)..........286–91

Betzer, C. E.; H. Halperin. Lead-Alloy Sheaths for Underground Power Cable. (51–68)..........423–9; disc. 434

Bewley, L. V. Disc..........386

Bey, M.El-Shishini; Abd El-Samie Mostafa. A New Method for Treating Electron Tubes When Used as Oscillators in the Free as Well as in the Synchronized States. (51–191)..........999–1004

Bjornson, George A. Network Synthesis by Graphical Methods for A-C Servomechanisms. (51–101)..........619–25

Black, P. M.; L. F. Lischer. The Application of a Series Capacitor to a Synchronous Condenser for Reducing Voltage Flicker. (51–20)..........144–50

Blanton, W. B. Automatic Trunk Selection in Reperforator Switching. (51–78)..........481–9

Bliss, T. J.; R. L. Witzke. Disc..........386

Boice, W. K. Probabilities of Interference Between Resistance Welders. (51–137)..........775–83

Borst, David W. Sealed Ignitron Rectifiers for Urban Transit Power Supply. (51–131)..........770–4

Boyajian, A. Disc..........966

Brainerd, Arthur A. Disc..........858

Bramhall, F. B.; L. A. Smith. A Nationwide Frequency-Modulation Telegraph Network. (51–62)..........373–8; disc. 378

Brancato, E. L. Disc..........438

Brazier, L. G. Disc..........421

Brieger, L. Effect of the Duration of Voltage Dip on Cyclic Light Flicker. (51–165)...894–8; disc. 899

Brown, H. F. Disc..........542, 550, 643

Browne, T. E., Jr.; A. P. Strom. A Study of Conduction Phenomena Near Current Zero for an A-C Arc Adjacent to Refractory Surfaces. (51–65)..........398–407; disc. 409

Buchanan, L. W. Disc..........678

Buckland, Mrs. B. O. Basic Heat-Transfer Data in Electron Tube Operation. (51–227)....1079–85

Buller, F. H. Thermal Transients on Buried Cables. (51–9)..........45–52; disc. 54, 1107

Buller, R. M. Disc..........200

Burgess, T. J.; A. D. Hogg. The Torsional Damper for Conductors—Service Experience and Further Experimental Work. (51–205)..........1031–3

Burrell, R. W. Disc..........430

Butler, R. M. Disc..........535

C

Cage, John M.; J. C. Schuder. A Gas Tube Inverter with the Supply Voltage Below the Breakdown Voltage. (51–168)..........908–12

Cain, B. M. Disc..........840

Calabrese, G. Determination of Reserve Capacity by the Probability Method Effect of Interconnections. (51–198)..........1018–20

Calvert, J. F.; R. H. Strotz, N. F. Morehouse. Analogue Computing Techniques Applied to Economics. (51–93)..........557–62; disc. 562

Camilli, G. Disc..........327

Carfrae, W. J. Disc..........589

Carpenter, T. J. Disc..........6

Carroll, Joseph S. Disc..........93, 506

Catlin, F. H.; N. Rohats. Winding Insulation Tester for D-C Armatures. (51–74)..........465–8

Chadwick, Joseph H.; A. J. Morris. An Electromagnetic Induction Method of Measuring Oscillating Fluid Flow. (51–58)..........346–50

Chandler, D. P.; L. A. Finzi, D. C. Beaumariage. The Transient Response of Magnetic Amplifiers—Cases of Negligible Commutation. (51–175)..........934–42; disc. 942

Chang, S. S. L. Equivalent Circuits and Their Application in Designing Shaded Pole Motors. (51–116)..........690–8; disc. 699

Cheek, R. C. Application of Microwave Channels. (51–145)..........813–17

Clark, H. W. 69-Kv Medium-Pressure Gas-Filled Cable, Washington, D. C. (51–67)..........418–21; disc. 422

Cobine, J. D.; C. J. Gallagher. New Electrodes for Stabilizing Inert-Gas Welding Arcs. (51–143)..........804–06

Coggeshall, I. S. Disc..........378

Cohn, George I.; G. T. Flesher. Dielectric Loading for Waveguide Linear Accelerators. (51–164)..........887–93

Cole, H. L. Disc..........966

Concordia, Charles. Synchronous Machine Damping and Synchronizing Torques. (51–122).....731–7

Conover, William B.; B. Gettys. Acoustic Models of Transformer Installations. (51–56)..........333–6; disc. 337

Cook, S. S. Disc..........394

Corson, A. J.; A. L. Nylander. A Hook-On Power Factor Meter. (51–75)..........468–72

Cowles, Laurence G. Disc..........297

Craig, A. B. Disc..........17, 118

Crary, S. B. Disc..........73, 850

Crouse, C. H. A Design Method for Polyphase Reluctance Synchronous Motors. (51–177)..957–62

Crowdes, G. J. Disc..........168

Cybulski, John; J. O'Connor. Disc..........705

D

D'Andrade, H. E. Disc..........859

Dana, George. Disc..........395

Daniel, Joel; T. J. Allen. Vibracode System of Supervisory Control on a Carrier Communication Channel. (51–146)..........818–22; disc. 822

Darrow, K. G. Disc..........193

de Bellis, A. M. Disc..........207

Del Mar, William A. Disc..........52, 61, 168, 421

Derr, W. A. Disc..........822

DeVal, E. J.; O. Ackermann. Spiral Arc Chokes Power Flow in New Lightning Arresters. (51–189) 995–8
DeWeese, Fred C. Disc........127
Dickinson, R. C.; J. D. Findley. A Spring Mechanism for Hand Closing of Magnetic Power Air Circuit Breakers. (51–25)........189–92; disc. 192
Diebold, Edward J. Commutating Reactor Control for Mechanical Rectifiers. (51–211)......1062–5
Dillow, N. E. Disc........135
Doggett, L. A. Disc........698
Dorff, Louis A. Operational Study of a Highway Mobile Telephone System. (51–7)........31–7
Dorfman, L. O. Disc........768
Douglas, John F. H. A Contribution to the Theory of the Deep-Bar Induction Motor. (51–159)..862–6
Douglas, John F. H. Disc........665, 873
Dovjikov, Alexander. Disc........135
Duff, C. K. Choice of Telemetering Systems and Channels for a Power System. (51–229)......1086–91
Dunkle, R. V.; J. T. Gier. Total Hemispherical Radiometers. (51–57)........339–43; disc. 345
Dwight, H. B. Disc........931
Dwight, H. B.; R. G. Haltmaier. Rules for Designing Frog-Leg Windings of D-C Machines. (51–119)........707–11; disc. 712
Dzwonczyk, V. L. An Engineering Approach to Control Room Lighting. (51–157)...852–7; disc. 860

E

Ebel, L. C.; L. F. Roehmann. Disc........59
Eckel, John F. Disc........431
Ellis, W. R.; M. L. Sloman. Electric Equipment and Performance of Lightweight Rapid Transit Cars. (51–33)........227–30; disc. 231
El Samie Mostafa, Abd; M. El-Shishini Bey. A New Method for Treating Electron Tubes When Used as Oscillators in the Free as Well as in the Synchronized States. (51–191)........999–1004
El-Shishini Bey, M.; Abd El-Samie Mostafa. A New Method for Treating Electron Tubes When Used as Oscillators in the Free as Well as in the Synchronized States. (51–191)........999–1004
Engelberger, J. F.; H. W. Kretsch. An Electromechanical Transducer. (51–29)........213–16
Espenschied, Lloyd. Disc........361
Esselman, Walter H. Steady-State Analysis of Self-Saturating Magnetic Amplifiers Based on Linear Approximations of the Magnetization Curve. (51–72)........451–9
Estoppey, R. F. Disc........221
Evans, Byron. Disc........393

F

Fahrnkopf, C. D.; G. D. Lippert, W. E. Pakala, S. C. Bartlett. Radio Influence Tests in Field and Laboratory—500-Kv Test Project of the American Gas and Electric Company. (51–40)..251–65; disc. 269
Ferri, Louis F. Disc........110
Field, E. J.; G. E. Heberlein. Ice Testing and Its Influence Upon Switch Design. (51–8)........37–42; disc. 43
Findley, J. D.; R. C. Dickinson. A Spring Mechanism for Hand Closing of Magnetic Power Air Circuit Breakers. (51–25)........189–92; disc. 192
Fink, L. H. Disc........169
Finkelnburg, Wolfgang. The Physical Mechanism of Low- and High-Current Arcs, and Their Relation to the Welding Arc. (51–142)........800–03
Finzi, L. A.; D. P. Chandler, D. C. Beaumariage. The Transient Response of Magnetic Amplifiers—Cases of Negligible Commutation. (51–175)........934–42; disc. 942
Flesher, Gail T.; G. I. Cohn. Dielectric Loading for Waveguide Linear Accelerators. (51–164)........887–93
Fontaine, C. B.; J. W. Apperson. The Use of Preferred Orientation Strip Steel in Turbine-Generator Stators. (51–154)........836–9; disc. 840
Fowler, C. J.; R. M. Showers. Disc........267
Fraas, Foster; O. C. Ralston. Distribution of Charge in Electrostatic Mineral Separation. (51–202)........1028–30
Frick, C. W. Disc........265
Funkhouser, A. W.; R. C. Van Sickle, D. F. Shankle. Switching High-Voltage Shunt Capacitor Banks. (51–18)........129–33; disc. 137

G

Gallagher, C. J.; J. D. Cobine. New Electrodes for Stabilizing Inert-Gas Welding Arcs. (51–143)........804–06
Gault, J. S. Disc........671, 677
Gerdel, R. W. Disc........344
Gettys, Briggs; W. B. Conover. Acoustic Models of Transformer Installations. (51–56)........333–6; disc. 337
Gier, J. T.; R. V. Dunkle. Total Hemispherical Radiometers. (51–57)........339–43; disc. 345
Gilbert, J. J. A Submarine Telephone Cable with Submerged Repeaters. (51–94)........564–72
Gleason, Lyle L. Neutral Inversion of a Single Potential Transformer Connected Line-to-Ground on an Isolated Delta System. (51–14)..103–10; disc. 110
Goldsmith, P.; E. A. Roberts. Piezoelectric Crystals as Sensing Elements of Pressure, Temperature, and Humidity. (51–180)........968–72
Goodrich, R. D., Jr. Disc........200
Gordy, T. D. Disc........319, 331, 337
Gould, H. R.; C. P. Hayes. Noise Evaluation of Fluorescent Lamp Ballasts. (51–95)........573–9
Grim, C. L.; H. B. Peck. Group Regulation of Urban 4-kv Feeders. (51–92)........551–6
Grimmer, E. J.; W. L. Teague. Improved Core Form Transformer Winding. (51–178)..962–5; disc. 967
Griscom, S. B. Disc........850
Grobel, L. P. Disc........598
Gross, Eric T. B.; E. W. Atherton. Application of Resonant Grounding in Power Systems in the United States. (51–64)........389–93; disc. 396
Gross, I. W. Disc........384
Gross, I. W.; P. Sporn, E. L. Peterson, H. P. St. Clair. The 300–315 Kv Extra-High-Voltage Transmission System of the American Gas and Electric Company. (51–11)........64–72; disc. 73
Gross, I. W.; C. F. Wagner, O. Naef, R. L. Tremaine. Corona Investigation on Extra-High-Voltage Lines—500-Kv Test Project of the American Gas and Electric Company. (51–12)........75–91; disc. 94
Grover, F. W. Disc........931
Gunter, Frank B. 940–960 Megacycle Communications Equipment for Industrial Applications. (51–144)........807–12

H

Hagg, A. C.; C. M. Laffoon, C. H. Janthey, P. R. Heller. Modern Practice in the Balancing of Large Turbine-Generator Rotors. (51–97)........593–8; disc. 598
Halperin, Herman; C. E. Betzer. Lead-Alloy Sheaths for Underground Power Cable. (51–68)........423–9; disc. 434
Halperin, Herman. Disc........729
Haltmaier, R. G.; H. B. Dwight. Rules for Designing Frog-Leg Windings of D-C Machines. (51–119)........707–11; disc. 712
Hamilton, W. S. H. Disc........650
Hansen, T. A.; R. D. Slayton. An Electronic Time Division Multiplex Telegraph Set. (51–60)........354–61
Harder, E. L. Disc........450
Harper, John D.; J. E. Housley. Protection of Transmission Lines Over Mountainous Region Where Lightning Incidence is High. (51–17)........124–6; disc. 126
Harrison, H. R.; A. H. Powell. Disc........43
Hart, J. E.; W. W. Rosenberry, A. T. McClinton. Factors Affecting Minimum Surface Leakage Distances on D-C Power Systems. (51–123)...738–42
Hayes, C. P.; H. R. Gould. Noise Evaluation of Fluorescent Lamp Ballasts. (51–95)........573–9
Heberlein, G. E.; E. J. Field. Ice Testing and Its Influence Upon Switch Design. (51–8)........37–42; disc. 43
Heil, V. E.; F. Spayth. Disc........307
Heller, P. R.; C. M. Laffoon, A. C. Hagg, C. H. Janthey. Modern Practice in the Balancing of Large Turbine-Generator Rotors. (51–97)........593–8; disc. 598
Herskind, C. C.; E. J. Remscheid. Development of a Pumpless Ignitron. (51–212)........1066–9
Herzog, E. Disc........396
Hickernell, L. F.; C. J. Snyder. Disc........433
Higgins, Thomas James; D. K. Reitan. Calculation of the Capacitance of a Circular Annulus by the Method of Subareas. (51–174)..926–31; disc. 932
Hill, C. F.; C. M. Laffoon, G. L. Moses, L. J. Berberich. A New High-Voltage Insulation for Turbine-Generator Stator Windings. (51–121)..721–6; disc. 730
Hoffmann, Banesh. Disc........296
Hogg, A. D.; T. J. Burgess. The Torsional Damper for Conductors—Service Experience and Further Experimental Work. (51–205)........1031–3
Honnell, Pierre M. The Generalized Transmission Matrix Stability Criterion. (51–46)........292–6; disc. 298
Hopkin, Arthur M. A Phase-Plane Approach to the Compensation of Saturating Servomechanisms. (51–103)........631–9
Hopkin, A. M. Transient Response of Small 2-Phase Induction Motors. (51–163)........881–6
Hopkins, R. J.; N. R. Schultz. Switching of Distribution Capacitors by Manual and Automatic Devices. (51–19)........138–43
Horcher, G. R.; L. W. Matsch, N. C. Basu. Three-Phase Measurements of Resistance. (51–59)........350–2; disc. 352
Housley, J. Elmer; J. D. Harper. Protection of Transmission Lines Over Mountainous Region Where Lightning Incidence is High. (51–17)........124–6; disc. 126
Howard, S. B. Disc........385
Hunt, L. F.; J. H. Vivian. Routine Insulation Testing of Synchronous Machines (51–126)......756–62
Huntley, E. D.; H. D. Taylor. Progress in the Development of Large Turbine Generators. (51–96)........580–9; disc. 591
Hutchison, W. M. Selection of Equipment for Multiple-Unit Cars. (51–104)........640–3; disc. 643

I

Ingersoll, L. R. Disc........53

J

Jacob, P. B., Jr.; G. M. L. Sommerman. Dependence of Direct Sparkover Voltage of Gaps on Humidity and Time. (51–173)........921–4; disc. 925
Janthey, C. H.; C. M. Laffoon, A. C. Hagg, P. R. Heller. Modern Practice in the Balancing of Large Turbine-Generator Rotors. (51–97)........593–8; disc. 598
Johnson, A. A.; J. E. Barkle, D. J. Povejsil. Fundamental Effects of Series Capacitors in High-Voltage Transmission Lines. (51–89)....526–35; disc. 535
Johnson, A. A.; D. J. Povejsil. A Per-Unit Interpretation of Transmission Line Constants. (51–26)........194–200; disc. 201
Johnson, I. B.; L. E. Saline. Disc........127, 384
Johnson, I. B.; J. R. Stevenson. Disc........136
Johnson, John S. A Maintenance Inspection Program for Large Rotating Machines. (51–125)...749–54
Jones, A. R. Disc........92
Jones, A. R.; O. Naef, R. L. Tremaine. Line Insulator Loss Under Normal Conditions—500-Kv Test Project of the American Gas and Electric Company. (51–224)........1073–8
Jones, A. R.; O. Naef, R. L. Tremaine. Techniques of Corona Loss Measurement and Analysis—500-Kv Test Project of the American Gas and Electric Company. (51–80)........496–505; disc. 506
Jones, R. W. The Effects of Loads and Disturbances upon Feedback Controllers. (51–73)........460–4
Jungk, H. G. A New Multiple-Unit Car Motor for the Pennsylvania Railroad. (51–36)..243–5; disc. 245

K

Kalb, J. W. Some Effects of Lightning Arrester Protective Characteristics and Location upon Station Apparatus Protection. (51–63)..379–83; disc. 387
Karr, J. H. Disc........177
Kelham, W. O. Disc........408
Kelly, C. F. Disc........344
Kidd, K. H. The Linascope Transmission Line Fault Locator. (51–194)........1008–13
Kilbourne, C. E. Disc........726
Killian, S. C. Disc........43
Kinghorn, J. H.; H. C. Barnes. Disc........282
Knight, M. H. Disc........72
Knowlton, A. E. Disc........16
Knudsen, H. Lottrup. Disc........1106
Komives, L. I. Disc........61, 421, 433
Kouwenhoven, W. B.; W. T. Sackett, Jr. Contact Resistance—The Contribution of Nonuniform Current Flow. (51–140)........791–5
Krabbe, Ulrik. Disc........449, 942
Kreitler, F. C., Jr. A-C Multiple-Unit Car Motor. (51–106)........648–50; disc. 651
Kretsch, H. W.; J. F. Engelberger. An Electromechanical Transducer. (51–29)........213–16
Ku, Y. H. Transient Analysis of Rotating Machines and Stationary Networks by Means of Rotating Reference Frames. (51–176)....943–54; disc. 955

L

Laffoon, C. M.; A. C. Hagg, C. H. Janthey, P. R. Heller. Modern Practice in the Balancing of Large Turbine-Generator Rotors. (51–97)........593–8; disc. 598
Laffoon, C. M.; C. F. Hill, G. L. Moses, L. J. Berberich. A New High-Voltage Insulation for Turbine-Generator Stator Windings. (51–121)..721–6; disc. 730
Lamborn, R. Disc........245
Lane, Frederic A. Disc........589
Langstaff, H. A. P. Disc........134, 273, 860
Lenehan, B. E. Disc........220
Leonard, M. G. Disc........5
LeVesconte, Lester B. Disc........444
Lichtenfels, I. W.; H. G. Moore. A New Lightweight Rapid Transit Control Equipment. (51–32)........224–6

Lippert, G. D.; W. E. Pakala, S. C. Bartlett, C. D. Fahrnkopf. Radio Influence Tests in Field and Laboratory—500-Kv Test Project of the American Gas and Electric Company. (51-40)......251-65; disc. 269
Lischer, L. F. Disc......281
Lischer, L. F.; P. M. Black. The Application of a Series Capacitor to a Synchronous Condenser for Reducing Voltage Flicker. (51-20)......144-50
Locke, G. A.; W. M. Bacon. A Full Automatic Private-Line Teletypewriter Switching System. (51-76)......473-80
Long, Leonard W. An Analysis of Grounding Banks to Balance Distribution Feeder Voltages. (51-148)......823-7
Lubin, S.; L. Podolsky. Carrier Current Supervisory System for Distribution Circuits. (51-236)......1096-1101
Lunge, G. S. Disc......835
Lutz, S. G. Transmission Line Load Impedance for Maximum Efficiency. (51-44)......283-5

M

MacLeod, D. R. Disc......643
Magnusson, P. C. Geometric Mean Distances of Angle-Shaped Conductors. (51-16)......121-3
Manning, M. L. Disc......438
Martin, E. R. Disc......711
Martin, Frank E.; H. E. Stauss. Contact Transients in Simple Electric Circuits. (51-48)......304-07; disc. 308
Matsch, L. W.; N. C. Basu, G. R. Horcher. Three-Phase Measurements of Resistance. (51-59)......350-2; disc. 352
Matsch, L. W.; F. J. Vogel, C. C. Petersen. Deterioration of Transformer Oil and Paper Insulation by Temperatures. (51-4)......18-20; disc. 21
Maust, Charles I. Disc......119
Mayer, Robert Lyon. Signal and Supervision Systems Used on Carrier Current Communications Circuits. (51-188)......990-4
McClinton, A. T.; J. E. Hart, W. W. Rosenberry. Factors Affecting Minimum Surface Leakage Distances on D-C Power Systems. (51-123)...738-42
McCoy, R. L. Disc......266
McDonald, G. R.; J. C. Price. Economics of Trolley Coach Power Supply. (51-115)......687-9
Meador, J. R. Disc......965
Medkeff, Russell J.; R. J. Parent. A Diode Bridge Limiter for Use with Electronic Analogue Computers. (51-170)......913-16
Mengel, John T. Pulse-Time Modulation Telemetering Systems for Rocket Application. (51-98)......599-605
Merrell, Edwin J. Disc......61, 433
Meyerhoff, L. Disc......60
Michaels, Edward L. Loci of Complex Impedance and Admittance Functions. (51-47)......299-303
Michelson, E. L.; R. L. Witzke. Technical Problems Associated with the Application of a Capacitor in Series with a Synchronous Condenser. (51-88)......519-25
Miller, C. J., Jr. Disc......267
Miller, John H. Frequency Compensation of A-C Instruments. (51-30)......217-20
Miller, R. H.; A. R. Worthington. Measurements and Tests on a Power Line Carrier Relaying System. (51-192)......1005-07
Minc, A.; W. C. Peterman. Four- or Two-Channel Time-Division-Multiplex Telegraph System for Long-Distance Radio Circuits. (51-61)...362-72
Moore, H. G. Disc......230
Moore, H. G.; I. W. Lichtenfels. A New Lightweight Rapid Transit Control Equipment. (51-32).224-6
Morehouse, N. F.; R. H. Strotz, J. F. Calvert. Analogue Computing Techniques Applied to Economics. (51-93)......557-62; disc. 562
Morgan, W. A. Disc......535, 848
Morris, Albert J.; J. H. Chadwick. An Electromagnetic Induction Method of Measuring Oscillating Fluid Flow. (51-58)......346-50
Morton, W. B. Disc......42, 857
Moses, Graham Lee. Alternating and Direct Voltage Endurance Studies on Mica Insulation for Electric Machinery. (51-127)......763-8; disc. 769
Moses, Graham Lee; C. M. Laffoon, C. F. Hill, L. J. Berberich. A New High-Voltage Insulation for Turbine-Generator Stator Windings. (51-121)......721-6; disc. 730
Mostafa, Abd El-Samie; M. El-Shishini Bey. A New Method for Treating Electron Tubes When Used as Oscillators in the Free as Well as in the Synchronized States. (51-191)......999-1004
Murray, C. S. Disc......337

N

Naef, O.; I. W. Gross, C. F. Wagner, R. L. Tremaine. Corona Investigation on Extra-High-Voltage Lines—500-Kv Test Project of the American Gas and Electric Company. (51-12)......75-91; disc. 94
Naef, O.; R. L. Tremaine, A. R. Jones. Line Insulator Loss Under Normal Conditions—500-Kv Test Project of the American Gas and Electric Company. (51-224)......1073-8
Naef, O.; R. L. Tremaine, A. R. Jones. Techniques of Corona Loss Measurement and Analysis—500-Kv Test Project of the American Gas and Electric Company. (51-80)......496-505; disc. 506
Nau, Robert H. Disc......407
Neher, J. H. Disc......52
Nevins, B. R. Disc......14
Newell, N. A.; A. Weaver. Single-Frequency Signaling System for Supervision and Dialing over Long-Distance Telephone Trunks. (51-79)......489-95
Newhouse, S. E. New A-C Multiple-Car Control for the Pennsylvania Railroad. (51-105)......645-7; disc. 647
Nims, Paul T. Some Design Criteria for Automatic Controls. (51-99)......606-11
Noest, John G. Disc......590
Nylander, A. L.; A. J. Corson. A Hook-On Power Factor Meter. (51-75)......468-72

O

O'Connor, John; J. Cybulski. Disc......705
Oestreicher, S. A-C Arc Welders with Saturable Reactor Control. (51-139)......787-90
Ogden, H. S. Disc......647
O'Kelly, W. S. A-C Multiple-Unit Car Control Equipment. (51-107)......652-6
O'Neill, D. J. Disc......859
Opsahl, A. M. Disc......383
Ordas, A. F. Disc......872
Oscarson, G. L.; I. C. Benson. Telephone Influence Factor in Synchronous Machines. (51-124).743-8
Owens, J. B. Disc......42

P

Packer, L. C. Commutation in Universal-Type Motors. (51-24)......170-6; disc. 178
Packer, L. C. Disc......698
Pakala, W. E.; G. D. Lippert, S. C. Bartlett, C. D. Fahrnkopf. Radio Influence Tests in Field and Laboratory—500-Kv Test Project of the American Gas and Electric Company. (51-40)......251-65; disc. 269
Parent, Robert J.; R. J. Medkeff. A Diode Bridge Limiter for Use with Electronic Analogue Computers. (51-170)......913-16
Parks, Earl E. Electric Home Heating. (51-150)......828-31
Parmelee, Georve V. Disc......343
Peck, H. B.; C. L. Grim. Group Regulation of Urban 4-Kv Feeders. (51-92)......551-6
Peck, R. R.; J. H. Vivian. An Investigation of Audio Noise in Substation Type Transformers. (51-55)......328-31; disc. 332
Peterman, W. C.; A. Minc. Four- or Two-Channel Time-Division-Multiplex Telegraph System for Long-Distance Radio Circuits. (51-61)...362-72
Petersen, C. C.; F. J. Vogel, L. W. Matsch. Deterioration of Transformer Oil and Paper Insulation by Temperatures. (51-4)......18-20; disc. 21
Peterson, E. L.; H. P. St. Clair. System Economics of Extra-High-Voltage Transmission. (51-156)......841-8; disc. 850
Peterson, E. L.; P. Sporn, I. W. Gross, H. P. St. Clair. The 300-315 Kv-Extra-High-Voltage Transmission System of the American Gas and Electric Company. (51-11)......64-72; disc. 73
Peterson, H. A.; P. E. Russell. Differential Analyzer Study of Harmonic Power Generation with Nonlinear Impedance Element. (51-172)......917-20
Peterson, Thomas F. Disc......93
Pettersen, R. A. A New Lightweight Rapid Transit Motor. (51-31)......222-3
Pettit, D. L. An Electronic Power Source for Large D-C Contact Testing. (51-51)......320-2
Podolsky, L.; S. Lubin. Carrier Current Supervisory System for Distribution Circuits. (51-236)......1096-1101
Poritsky, H. Calculation of Flux Distributions with Saturation. (51-50)......309-19; disc. 319
Porter, F. M.; C. P. Zimmerman. Application of Shunt Capacitors at Transmission and Distribution Stations. (51-15)......112-18; disc. 119
Porter, F. M.; C. P. Zimmerman. Disc......134, 159
Povejsil, D. J.; A. A. Johnson. A Per-Unit Interpretation of Transmission Line Constants. (51-26)......194-200; disc. 201
Povejsil, D. J.; A. A. Johnson, J. E. Barkle. Fundamental Effects of Series Capacitors in High-Voltage Transmission Lines. (51-89)....526-35; disc. 535
Powell, A. H.; H. R. Harrison. Disc......43
Price, J. C.; G. R. McDonald. Economics of Trolley Coach Power Supply. (51-115)......687-9
Puchstein, A. F. Disc......176

R

Ralston, Oliver C.; F. Fraas. Distribution of Charge in Electrostatic Mineral Separation. (51-202)......1028-30
Ratz, A. G.; V. G. Smith. A Method of Gating for Parallel Computers. (51-83)......510-16
Reagan, M. E.; S. S. Watkins. D-C Power Supplies and Isolation of Faults on Electric Transit Systems
  Part I—D-C Power Supply. (51-90)......537-42; disc. 542
  Part II—Isolation of D-C Faults. (51-91)......543-50; disc. 550
Reitan, Daniel Kinseth; T. J. Higgins. Calculation of the Capacitance of a Circular Annulus by the Method of Subareas. (51-174)..926-31; disc. 932
Remscheid, E. J.; C. C. Herskind. Development of a Pumpless Ignitron. (51-212)......1066-9
Richards, N. W. Disc......924
Rietz, E. B.; C. J. Balentine. Disc......118, 135, 159
Robert, J. R. Disc......91, 119, 267, 505
Roberts, E. A.; P. Goldsmith. Piezoelectric Crystals as Sensing Elements of Pressure, Temperature, and Humidity. (51-180)......968-72
Robertson, Lawrence M. Disc......394
Roehmann, L. F.; L. C. Ebel. Disc......59
Rohats, N.; F. H. Catlin. Winding Insulation Tester for D-C Armatures. (51-74)......465-8
Rorden, H. L. Disc......268, 387
Rosenberg, L. T. Disc......591
Rosenberry, W. W.; J. E. Hart, A. T. McClinton. Factors Affecting Minimum Surface Leakage Distances on D-C Power Systems. (51-123)..738-42
Ross, M. D. Disc......590
Rottier, Richard R. Ignitrons for Frequency-Changer Welders. (51-166)......900-07
Rowell, Ralph M. Disc......14, 221
Runciman, A. S. Disc......127
Russ, J. C. Disc......395
Russell, Paul E.; H. A. Peterson. Differential Analyzer Study of Harmonic Power Generation with Nonlinear Impedance Element. (51-172)......917-20

S

Sackett, W. T., Jr.; W. B. Kouwenhoven. Contact Resistance—The Contribution of Nonuniform Current Flow. (51-140)......791-5
St. Clair, H. P.; E. L. Peterson. System Economics of Extra-High-Voltage Transmission. (51-156)......841-8; disc. 850
St. Clair, H. P.; P. Sporn, E. L. Peterson, I. W. Gross. The 300-315 Kv Extra-High-Voltage Transmission System of the American Gas and Electric Company. (51-11)......64-72; disc. 73
Saline, L. E.; I. B. Johnson. Disc......127, 384
Salmonson, W. G. Disc......238
Salter, E. H. Disc......352
Satterlee, W. W. Disc......21, 438
Saunders, Robert M. Measurement of D-C Machine Parameters. (51-118)......700-05; disc. 705
Saunders, R. M.; Otto J. M. Smith. Disc......562
Schahfer, R. M.; F. H. Strout. 11-Year Operating Record—Rural Line Sectionalizing by Repeater Fuses. (51-112)......680-6
Schaller, F. F.; W. C. Whitman. Power Supply Study and New Rectifier Installation for the United Electric Railways of Providence. (51-185)......978-85; disc. 985
Scheuch, Donald R.; O. Whitby. Output Analysis and Alignment Techniques for Phase-Rotation Single Side-Band Transmitters. (51-28)......209-12
Schifreen, C. S. Thermal Expansion Effects in Power Cables. (51-22)......160-8; disc. 169
Schleicher, George B. Improvements in Transformer-Loss Compensators for Watt-hour and Var-hour Meters. (51-182)......973-7
Schmidt, A., Jr. Regeneration with a Mercury Arc Rectifier on the Central Railway of Brazil. (51-232)......1092-6
Schroeder, T. W. Disc......394
Schuder, John C.; J. M. Cage. A Gas Tube Inverter with the Supply Voltage Below the Breakdown Voltage. (51-168)......908-12
Schultz, N. R. Disc......158
Schultz, N. R.; R. J. Hopkins. Switching of Distribution Capacitors by Manual and Automatic Devices. (51-19)......138-43
Scorgie, Donald G. Fault Transients in Aircraft D-C Systems......713-20; disc. 720
Sealey, W. C. A 2,000,000-Kva Transformer Core. (51-2)......8-11
Sexton, Robert M.; R. J. Alke. Detection of Turn-to-Turn Faults in Large High-Voltage Turbine Generators. (51-41)......270-3; disc. 274
Shanck, R. B. Disc......378
Shankle, D. F.; A. W. Funkhouser, R. C. VanSickle. Switching High-Voltage Shunt Capacitor Banks. (51-18)......129-33; disc. 137
Shildneck, L. P. Disc......839

Shores, R. B.; J. W. Beatty. A New 69 Kv Air Blast Circuit Breaker. (51–27)........202–07; disc. 208
Short, H. D. Disc..................................429
Showers, R. M.; C. J. Fowler. Disc..............267
Slayton, R. D.; T. A. Hansen. An Electronic Time Division Multiplex Telegraph Set. (51–60)..354–61
Sloman, M. L.; W. R. Ellis. Electric Equipment and Performance of Lightweight Rapid Transit Cars. (51–33)..........................227–30; disc. 231
Slonczewski, T. A Servo System for Heterodyne Oscillators. (51–218)......................1070–2
Smith, Arthur Bessey. Disc.........................268
Smith, H. B. Disc.....................................15
Smith, J. J. Tables of Green's Functions, Fourier Series and Impulse Functions for Rectangular Coordinate Systems. (51–6)..................22–30
Smith, L. A.; F. B. Bramhall. A Nationwide Frequency-Modulation Telegraph Network. (51–62)..............................373–8; disc. 378
Smith, Otto J. M.; R. M. Saunders. Disc..........562
Smith, S. V. A New Train Performance Calculator. (51–108).......................................657–60
Smith, V. G.; A. G. Ratz. A Method of Gating for Parallel Computers. (51–83)..............510–16
Smythe, W. R. Disc..................................932
Snyder, R. L., Jr. The Input-Output System of the EDVAC. (51–82).......................507–09
Sommerman, G. M. L.; P. B. Jacob, Jr. Dependence of Direct Sparkover Voltage of Gaps on Humidity and Time. (51–173)............921–4; disc. 925
Spayth, Frank; V. E. Heil. Disc.....................307
Specht, T. Transformer Magnetizing Inrush Current. (51–53)...........................323–7; disc. 327
Specht, T. R. Disc...............................331, 336
Spence, Homer W. Systematization of Tube Surveillance in Large-Scale Computers. (51–84)..516–19
Sporn, Phillip; E. L. Peterson, I. W. Gross, H. P. St. Clair. The 300–315 Kv Extra-High-Voltage Transmission System of the American Gas and Electric Company. (51–11).......64–72; disc. 73
Stadum, C. B. Selection of Fuses for Resistance Welding Machines. (51–141)....................796–9
Stauss, Henry E.; F. E. Martin. Contact Transients in Simple Electric Circuits. (51–48)...........................304–07; disc. 308
Stevenson, J. R.; I. B. Johnson. Disc.............136
Stewart, H. C.; L. C. Whitman. Aging of Class-B Insulating Material in Nitrogen. (51–69)...........................436–7; disc. 438
Storm, H. F. Static Magnetic Exciter for Synchronous Alternators. (51–196)......................1014–17
Storm, H. F. Transient Response of Saturable Reactors with Resistive Load. (51–13)........95–102
Strandrud, H. T. Determination of Generator Standby Reserve Requirements. (51–23).......179–87
Strom, A. P.; T. E. Browne, Jr. A Study of Conduction Phenomena Near Current Zero for an A-C Arc Adjacent to Refractory Surfaces. (51–65)..............................398–407; disc. 409
Strotz, R. H.; J. F. Calvert, N. F. Morehouse. Analogue Computing Techniques Applied to Economics. (51–93)....................557–62; disc. 562
Strout, F. H.; R. M. Schahfer. 11-Year Operating Record—Rural Line Sectionalizing by Repeater Fuses. (51–112).............................680–

T

Taylor, G. J. Disc....................................858
Taylor, H. D.; E. D. Huntley. Progress in the Development of Large Turbine Generators. (51–96)..............................580–9; disc. 591
Taylor, P. L. Disc.....................................208
Teague, W. L.; E. J. Grimmer. Improved Core Form Transformer Winding. (51–178)..962–5; disc. 967
Tietze, H. Watson. Welding Calculations—Effect of Conductor Configuration in Overhead Lines. (51–138)..784–6
Tovee, E. H. Disc......................................768
Travers, Paul. A Note on the Design of Conditionally Stable Feedback Systems. (51–102).......626–30
Tremaine, R. L.; I. W. Gross, C. F. Wagner, O. Naef. Corona Investigation on Extra-High-Voltage Lines —500-Kv Test Project of the American Gas and Electric Company. (51–12).......75–91; disc. 94
Tremaine, R. L.; O. Naef, A. R. Jones. Line Insulator Loss Under Normal Conditions—500-Kv Test Project of the American Gas and Electric Company. (51–224)......................................1073–8
Tremaine, R. L.; O. Naef, A. R. Jones. Techniques of Corona Loss Measurement and Analysis—500-Kv Test Project of the American Gas and Electric Company. (51–80)............496–505; disc. 506
Trump, J. G. Electrostatic Sources of Ionizing Energy. (51–199)......................................1021–7
Turkington, Robert E. Analysis of a 3-Phase Inverter with Resistive Load. (51–210)...........1055–61

V

Van Sickle, R. C. Disc...............................407
Van Sickle, R. C.; A. W. Funkhouser, D. F. Shankle. Switching High-Voltage Shunt Capacitor Banks. (51–18)..........................129–33; disc. 137
Van Sickle, R. C.; J. Zaborszky. Capacitor Switching Phenomena. (51–21)............151–8; disc. 158
Vikoren, O. B. Disc...................................193
Vivian, J. H.; L. F. Hunt. Routine Insulation Testing of Synchronous Machines. (51–126).....756–62
Vivian, J. H.; R. R. Peck. An Investigation of Audio Noise in Substation Type Transformers. (51–55)..............................328–31; disc. 332
Vogel, F. J.; C. C. Petersen, L. W. Matsch. Deterioration of Transformer Oil and Paper Insulation by Temperatures. (51–4)...........18–20; disc. 21

W

Wachowski, Hillard M.; R. E. Beam. Shielded Dielectric-Rod Waveguides. (51–162).......874–80
Wagner, C. F.; I. W. Gross, O. Naef, R. L. Tremaine. Corona Investigation on Extra-High-Voltage Lines—500-Kv Test Project of the American Gas and Electric Company. (51–12)...75–91; disc. 94
Walters, T. R. Disc....................................437
Ward, H. C., Jr.; P. L. Alger, F. H. Wright. Split-Winding Starting of 3-Phase Motors. (51–160)..............................867–72; disc. 872
Watchorn, C. W. Disc.........................187, 849
Watkins, S. S.; M. E. Reagen. D-C Power Supplies and Isolation of Faults on Electric Transit Systems.
  Part I—D-C Power Supply. (51–90)..............................537–42; disc. 542
  Part II—Isolation of D-C Faults. (51–91)..............................543–50; disc. 550
Weaver, A.; N. A. Newell. Single-Frequency Signaling System for Supervision and Dialing over Long-Distance Telephone Trunks. (51–79).....489–95
Webb, R. L. Disc......................................192
Weber, Ernst. Disc....................................931
Webking, Henry E. A Simplified Method for Predicting Induction Motor Performance. (51–110)..667–70
Wentz, E. C. Disc.....................................111
Whitby, Oliver; D. R. Scheuch. Output Analysis and Alignment Techniques for Phase-Rotation Single Side-Band Transmitters. (51–28).........209–12
Whitehead, J. B. Radial and Tangential Stresses in Impregnated Paper Insulation. (51–10)..............................56–9; disc. 62
Whitman, L. C.; H. C. Stewart. Aging of Class-B Insulating Material in Nitrogen. (51–69)..............................436–7; disc. 438
Whitman, W. C.; F. F. Schaller. Power Supply Study and New Rectifier Installation for the United Electric Railways of Providence. (51–185)..............................978–85; disc. 985
Wieseman, R. W. Disc................................769
Wildes, Karl L. Disc..................................954
Williams, J. E.; D. S. Babb. Circuit Analysis Method for Determination of A-C Impedance of Machine Conductors. (51–109)...........661–5; disc. 665
Williamson, R. A. Why 4-Motor Multiple-Unit Car Equipments? (51–35).......................240–2
Wiseman, Robert J. Disc.............................431
Witzke, R. L.; J. E. Barkle. Economics of Power Transformer Application. (51–70)..............440–4
Witzke, R. L.; T. J. Bliss. Disc.....................386
Witzke, R. L.; E. L. Michelson. Technical Problems Associated with the Application of a Capacitor in Series with a Synchronous Condenser. (51–88)..519–25
Woods, G. M. Disc....................................985
Worthington, A. R.; R. H. Miller. Measurements and Tests on a Power Line Carrier Relaying System. (51–192)......................................1005–07
Wright, F. H.; P. L. Alger, H. C. Ward, Jr. Split-Winding Starting of 3-Phase Motors. (51–160)..............................867–72; disc. 872

Y

Yarbrough, C. T. Disc................................755
Young, R. E. Disc.....................................898

Z

Zaborszky, J.; R. C. Van Sickle. Capacitor Switching Phenomena. (51–21)...........151–8; disc. 158
Zimmerman, C. P.; F. M. Porter. Application of Shunt Capacitors at Transmission and Distribution Stations. (51–15).........112–18; disc. 119
Zimmerman, C. P.; F. M. Porter. Disc.....134,159

The Induction Galvanometer, a Sensitive Instrument Converter

R. W. GILBERT
ASSOCIATE AIEE

IT IS broadly conceded that the most effective method of sensitive d-c amplification for measurement purposes is preliminary conversion to alternating current and amplification as alternating current. The resolution sensitivity of an a-c amplifier is, in good practice, limited only by fundamental noise levels, and conductive decoupling allows greater circuit flexibility for feedback. As a class, systems comprising a network loop of error conversion, amplification, phased rectification and degenerative feedback to cancel the error are extensively used in many effective devices for d-c amplification as a measurement process.

Performance of such systems is largely contingent upon the detailed characteristics of the sensitive converter, and considerable developmental effort has been expended to produce the several methods and devices in contemporary use; for example, the contact modulator and the thermally modulated resistance. In some cases characteristic gain is obtained as in the saturable reactor amplifier, certain nonlinear resistance element circuits, and impedance modulators such as the capacitance modulator.

The method of choice is naturally determined by the details of requirement, but in general the following are the functional objectives.

1. Conversion should be efficient at levels sufficiently low to maintain an adequate feedback ratio.

2. The converting device should not introduce spurious components additive to the input level.

3. The converting device should not be subject to excessive drift in terms of input level.

4. The frequency of conversion should be sufficiently high for a high resolution sensitivity in terms of differential time.

Contemporary devices are probably most deficient in the last objective, being limited generally to audio frequencies. In closed-feedback systems the feedback period must be made long with respect to the periodicity of modulation, usually by peaking the amplifier, to avoid oscillation around the circuit loop or a step-function response. The overall system will then have a phase velocity insufficient for many requirements, or will be objectionable in applications where complicating corrective measures are admissible. Also, practical amplifier problems are considerably alleviated by increasing the operating frequency above the range of power-frequency hum, power rectifier harmonics and microphonic impulses.

The induction galvanometer here described is a sensitive d-c to a-c converter having an advantage of high operating frequency; into the megacycle region if desired. With suitable amplification reasonably peaked to the operating frequency, feedback periods in the millisecond region are readily obtainable. It has an inherently high conversion gain, of 10^8 order on an energy basis, and delivers a high amplifier input level. In practice the attendant circuit and component economy may be a considerable advantage.

Galvanometer Structure

The induction galvanometer is essentially a conventional permanent magnet movable coil instrument structure, but including means for injecting an a-c component of magnetic flux into the permanent field flux path. The functional construction is shown in Figure 1 wherein the a-c field component is injected by an a-c magnetic shunt. When the movable coil is in the normal center-zero position the flux linkage is zero. But deflection causes the coil to link proportionally the a-c component of field flux, and an a-c component of potential having a magnitude and phase-direction proportional to the degree and direction of deflection is induced in the coil. Thus deflection of the coil in response to a d-c current will produce an a-c potential which can be extracted by the external circuit for amplification.

Of necessity the connected external circuit presents an effective a-c impedance across the coil, and an a-c component of current will circulate through the coil causing a force reaction with the a-c component of field flux. The induced potential is in quadrature with the field flux, and if the coil circuit is entirely resistive the alternating current will likewise be in quadrature and the reaction force will be entirely alternating. However, reactance in the coil circuit impedance will develop an in-phase component of coil current, and the coil will be subjected to a steady-state component of parasitic torque, which must be minimized. The torque appears as mechanical stiffness, similar to that imposed by a mechanical spring, but may be of either sign, positive or negative when the coil circuit is inductive or capacitive respectively. It is, therefore, essential that the phase angle of the coil and the connected circuit be considered.

Actually the reaction torque effect is useful because the coil circuit can include a resonated transformer which can be trimmed to cancel the torque of the filaments required for conductive connection to the coil. Transformer tuning thus serves as an adjustment to the point of infinite sensitivity by virtue of an infinite net mechanical compliance, or as close an

---

Paper 51-183, recommended by the AIEE Instruments and Measurements Committee and approved by the AIEE Technical Program Committee for presentation at the AIEE Summer General Meeting, Toronto, Ont., Canada, June 25–29, 1951. Manuscript submitted November 9, 1950; made available for printing April 23, 1951.

R. W. Gilbert is with the Weston Electrical Instrument Corporation, Newark, N. J.

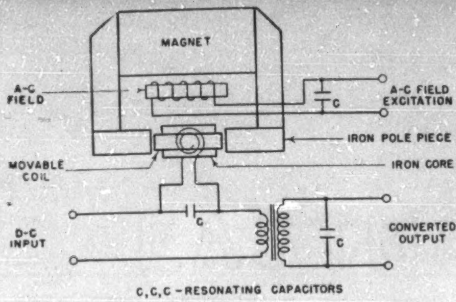

Figure 1. Galvanometer structure

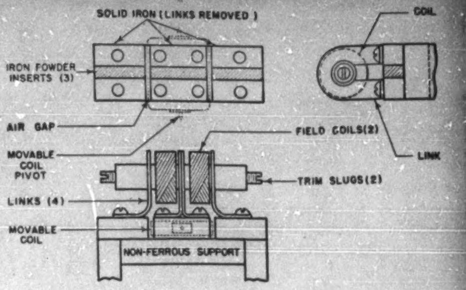

Figure 2. Iron powder inserts with link excitation

approach as practical permanency of adjustment will permit.

The developed a-c coil potential is directly proportional to frequency, whereas the reaction force is a current-flux product. Thus for a constant conversion sensitivity the a-c flux level may be reduced by raising the operating frequency, and the torque effect reduced in proportion. In fact, the operational quality of the system is proportional to increasing frequency until limited by some secondary consideration such as losses in the field structure or the movable coil.

The solid iron flux paths normally used in d-c instrument structures are not efficient for the high-frequency component of flux, and conversely magnetic materials good at high frequencies have permeabilities insufficient for the relatively high level of steady flux from the permanent magnet. It is thus necessary to have a composite magnetic structure including materials individually efficient for both components of the field flux. Figure 2 illustrates a composite pole structure wherein inserts of high-frequency material, iron powder-resin binder compacts, are included in each pole piece and the core.

In this arrangement the inserts are excited by links connected to the pole and core faces, forming single-turn loops around the inserts by conduction through the poles and the core. The outside ends of the links are coupled to a field coil connected to the high-frequency excitation source and resonated to the operating frequency. The flux is air-returned as is permissible at higher frequencies, and will not return in any appreciable amount through the solid iron and magnet structure. A compact design for tightness of coupling between the field coil and the inserts is desirable to minimize leakage reactance which would cause phase shift. Particularly the line impedance of the links should be a minimum consistent with practical design.

In the operating circuit both the movable coil and field coils are individually resonated to the operating frequency, and for small coil deflections the quadrature phase-shift characteristic to loosely coupled resonated circuits obtains. Thus the useful movable coil output appears in quadrature to the excitation, which permits the frequency-shift operating circuit described later.

Figure 3 shows the production design of the induction galvanometer in which the link and insert structure of Figure 2 is discernible. It is intended only as an error detector in feedback systems, and so is designed to have a minimum of mechanical restoring force; the conducting filament connections to the movable coil are as light as adequate mechanical strength will permit. Also, the angle of necessary coil motion is small, and a simple rectangular air gap design is used instead of the usual radial design.

A zero corrector is included in the cover, but it serves only to adjust the filaments to the position of zero force when the coil is at the point of zero coupling.

Galvanometer Performance

The structure allows some design and performance optimums not usual to d-c instrument mechanisms. For example:

1. The small deflection angle allows concentration of the permanent magnetic field to a high density.
2. The movable coil carries no load such as a pointer or mirror, allowing an unusually light coil design having a low moment of inertia.
3. The alternating component of torque reduces friction to an undetectable order, allowing pivot and jewel bearings at sensitivities normally requiring a suspension design.
4. Electrical cancellation of the filament torque provides resolution sensitivity as a function of adjustment rather than as a design limit.

The design of Figure 3 has an operating frequency of 200 kc, largely dictated by amplifier considerations. At a nominal excitation level of 0.5 watt a 100 turn movable coil of approximately 50 ohms resistance will develop an output potential of about 1.6 rms volts per degree de-

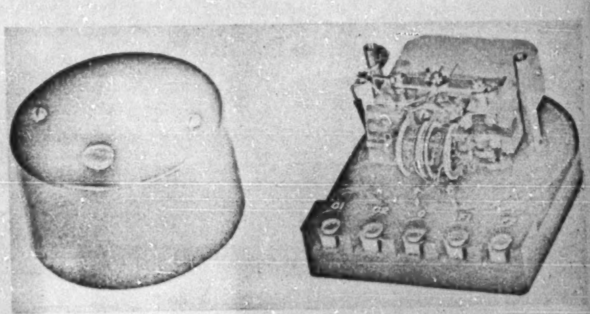

Figure 3. Induction galvanometer design for 200-kc conversion

flection. The permanent field flux density at the coil is about 8,000 gausses, and the d-c sensitivity against the restraint of the conducting filaments is about 6×10^{-8} ampere per degree deflection. Neglecting electrical torque the conversion gain, defined as the ratio of energy developed in the movable coil impedance (about 300 ohms) to the d-c energy producing it, calculates on this basis to about 4×10^{10}.

Actually the figure of conversion gain is illustrative only because in operation the circuit may be adjusted for cancellation of the restoring force of the filaments, in which case the gain is adjustable through infinity to a negative sign.

In practise the conversion gain is more than adequate to present other limitations even when used with an amplifier of comparatively low gain. In low range operation at high response speed, thermal agitation of the movable coil is apparent, and imposes a noise level limit. Also, drift influences become apparent, mainly thermo-electric potentials between the filament alloy and the copper in the coil and circuit connections; a special filament alloy is used to minimize this effect. But other than in these respects performance appears to be a matter of critical adjustment, with a reasonable expectancy in terms of energy of about 10^8 minimum gain.

Circuit Application

The major result of the high conversion gain is the large feedback ratio obtainable using an amplifier of nominal gain. This in combination with the high phase velocity permitted by the high operating frequency provides an unusually short feedback period for a system including mechanical motion in its operating cycle. For example, an amplifier input resolution of 1 millivolt alternating current will require a galvanometer movable coil operating excursion of only a few seconds of angle. This, together with a relatively low mechanical moment of the coil, is capable of exhibiting feedback periods in the order of a few milliseconds on input ranges compatible with drift influences. Feedback ratios as high as 10^6 are entirely practical.

The induction galvanometer as a converter could be used with the customary peaked amplifier, phased rectifier, and d-c degenerating feedback network, to form a d-c amplifying system. But the quadrature phase relationship between the field excitation and the converted output to the amplifier led to the development of a frequency-shift system of operation that proved simpler and more effective than the usual magnitude system. In particular it avoids a separate field excitation source. Also it is capable of adjustment to a condition of infinite effective gain with a nominal order of actual magnitude gain.

Frequency-Shift System

In explanation Figure 4(A) shows an idealized amplifier having a transconductance (G_a) of positive sign, coupled back upon itself by a pi-network comprising an output admittance Y_2, an input admittance Y_1 and a feedback conductance G_3. Such a system will oscillate when the amplifier transconductance is larger than the real component of the feedback admittance. The general admittance of the loop may be stated as:

$$G_a - \frac{Y_1 Y_2 + Y_1 G_3 + Y_2 G_3}{G_3} = 0 \qquad (1)$$

which must have a real solution for oscillation. In practical amplifiers the transconductance is amplitude-limited by the energy output of the amplifier, so a solution can develop by an amplitude reduction of G_a provided the phase solution is real, which requires some frequency where the feedback network is entirely conductive. Thus the system, if capable will oscillate at a frequency (f_0) where the coupling network has a zero phase angle and at an amplitude of oscillation where G_a is reduced to equality with the transfer conductance of the coupling network.

When the input and output admittances are large with respect to the feedback conductance, as is permitted when G_a is of a usual order, equation 1 may be approximated as:

$$G_a - \frac{Y_1 Y_2}{G_3} = 0 \qquad (2)$$

Now consider the addition of a susceptive feedback element B_3 in parallel with the original feedback conductance G_3. The simplified impedance, equation 2 now becomes:

$$G_a - \frac{Y_1 Y_2}{G_3 + B_3} = 0 \qquad (3)$$

The frequency of oscillation will now shift to a frequency where the input and

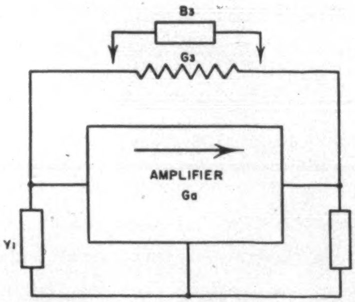

(A) EXPLANATORY FREQUENCY— SHIFT OSCILLATOR

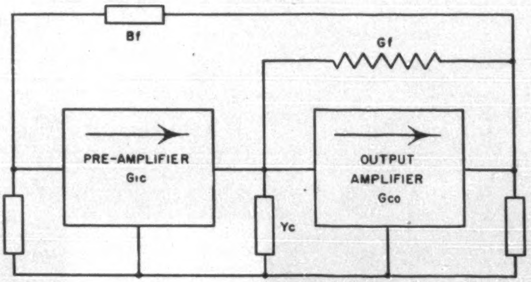

(B) ADDITION OF PRE-AMPLIFIER SECTION

Figure 4. Equivalent networks for frequency-shift oscillation system

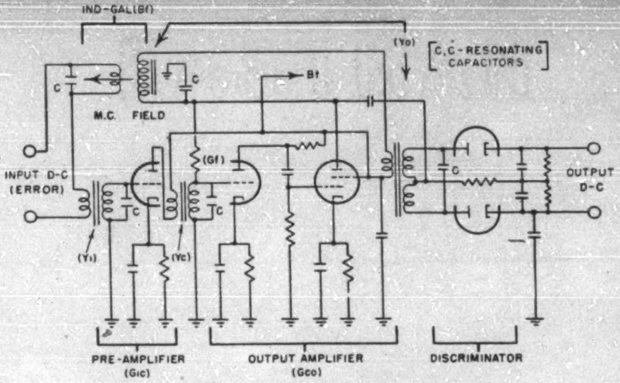

Figure 5. Circuit diagram, frequency-shift amplifier

output admittances will have a composite phase angle opposing that introduced by B_3, and a real solution demands that:

$$\angle(Y_1Y_2) = \angle(G_3+B_3) \qquad (4)$$

to keep the coupling network phaseless to match the phaseless amplifier transconductance G_a.

Y_1 and Y_2 are parallel inductance-capacitance circuits phase-resonant at f_0, and the frequency shifts in response to an appearance of B_3 in a direction and to a degree proportional to the sign and magnitude of B_3 respectively.

The induction galvanometer is applied to the circuit to effect a frequency shift in the manner of B_3. The galvanometer field circuit is included as part of the output admittance Y_2, and the movable coil as part of the input admittance Y_1. With both parallel-resonant, and loosely coupled by a small movable coil deflection, the feedback component due to deflection will be shifted in quadrature phase, and will appear as the susceptive feedback B_3. The equivalent B_3 component is zero with the movable coil at center position, and appears in sign and amount proportional to the coil deflection.

The conductive feedback element G_3 is still necessary to maintain oscillation, but only in sufficient amount to insure stable operation.

Figure 4(B) differs essentially from the explanatory circuit of Figure 4(A) in the addition of the preamplifier section G_{ic} effective upon feedback through the galvanometer coupling parameter, here B_f. This increases the sensitivity of the system to B_f without requiring an impractical low value of conductive feedback, here G_f, for maintenance of oscillation. When B_f is zero the preamplifier section is quiescent, but the second amplifier section is in stable oscillation. Y_i, Y_c and Y_0 are the input, interstage coupling, and output admittances respectively.

The general simplified impedance of the loop now is:

$$G_{co} - \frac{Y_iY_cY_0}{G_{ic}B_f+G_fY_i} = 0 \qquad (5)$$

which is similar to that for the illustrative circuit, equation 3. The output section transconductance G_{co} is amplitude limited as before, but the input section transconductance G_{ic} is normally constant because of the low input level. Note that when B_f is zero the expression neglects G_{ic}, but is much more sensitive to appearance of B_f because of the gain of the input section G_{ic}.

To complete the amplifying system the output admittance Y_0 includes a frequency discriminating rectifier to supply the output direct current in response to the frequency shift.

D-C Degeneration

The amplifier system as described wherein a large useful d-c output obtains upon injection of a very small d-c input is generally combined with degeneration by including a d-c feedback path in degenerative sense. The amplifier then serves as an error-resolver and may function for example as an automatic potentiometer. The error amplifier then need only have a high gain but not necessarily stability, gain producing the necessary stability by the feedback mechanism.

D-c degeneration may be applied in many forms familiar to practise, the simplest being a single resistance mutual to the input and output circuits. It may include functions of time integration or differentiation for purposes of damping or for control of response time. It may include motor driven components such as a slide wire combined with reactive elements for damping. But in general the freedom with which various forms and amounts of degeneration may be successfully applied is contingent upon a high phase-velocity in the error resolving function; otherwise phase reversals may develop in the operating loop, leading to instability or limiting the designed response speed.

In any event, while the methods of degeneration are too numerous to discuss, a common requirement for high resolution sensitivity and phase velocity dictates the best obtainable performance in these respects for the broadest usage. To this end a practical design applicable to many degenerative systems is described without reference to any specific method of degeneration or application.

Amplifier Circuit

The circuit of the frequency-shift amplifier, including the output frequency discriminator, is shown in Figure 5 in which the components corresponding to the equivalent network elements are identified. The output-input d-c degenerative network with which the amplifier is normally used is not shown. The preamplifier is one half of the dual triode, and the amplifier section is the other half of the dual triode and a power pentode in cascade. Two stages are required in the output section to phase the conductive feedback G_f in regenerative sense.

The input, interstage coupling and output (discriminator) transformers are of conventional cup-core construction, resonated to a center frequency of 200 kc with slug trimmers. The bulk of the output impedance is in the galvanometer field and its associated resonating capacitor, with the discriminator transformer coupled by insertion of its primary winding in series with the galvanometer field inductance, which phases the discriminator properly. The discriminator primary has relatively few turns, the number determining the coefficient of coupling between the separately resonated galvanometer field circuit and the secondary, which is connected to the dual diode rectifier.

The frequency discriminator is a conventional balanced type as commonly used in radio practise, and is phased by the capacitive connection to the output stage plate. The output direct current is thus balanced at center frequency and polarized with respect to frequency-shift as the galvanometer deflects. As a power output element it is reasonably efficient, particularly when designed for supplying high-impedance load circuits. However, it is a peak rectifier and develops current pips having frequency components orders higher than the operating frequency, and so requires decoupling and by-passing not shown in the circuit. Otherwise interference with the sensitive input end of the amplifier may occur.

An amplifier strip comprising the Figure 5 circuit is illustrated in Figure 6. A complete production design instrument amplifier, including the amplifier strip, power supply components and a plug-in degenerating network, is shown in Figure 7.

The output is a current having a range of one milliampere into an external burden not exceeding 5,000 ohms. The degenerating network unit, or "range standard," can be of either the potential-input or current-input type, and both types maintain balance in the input source circuit; in this sense the amplifier is an automatic potentiometer.

Coupling Conditions

Note that the galvanometer field and the discriminator transformer secondary are separately tuned to the same center frequency and coupled. The coupling coefficient may then be selected to slightly overcouple the two resonant circuits, to develop a double-peaked impedance and phase characteristic identified with the overcoupled condition. In the operating loop this compound impedance appears in shunt to the single-peak impedance of the interstage transformer, and by proper adjustment of the Q factors of the circuits in relation to the coupling coefficient an overall flat-topped impedance and phase characteristic may be developed.

A flat-topped phase characteristic of the overall total shunt impedance requires a relatively large excursion of frequency to produce a minor order of phase angle for balance against the feedback through B_f, and a correspondingly small appearance of B_f causes a large frequency shift. Theoretically a truly flat top would make the system infinitely sensitive to B_f.

Overcoupling in proper amount thereby provides a method of simple adjustment to any desired incremental sensitivity about the center-frequency point, and a relatively high sensitivity over reasonable excursions from center. Apparently the system is considerably superior to a conventional amplitude amplifier of similar component complement, unless regenerated for extra gain which is ordinarily not as tractable of adjustment as simple resonant impedances.

It would appear that excess overcoupling resulting in double-peaking of the total impedance could cause instability by making the frequency of oscillation jump discontinuously from peak to peak, as commonly occurs in coupled oscillators. However, in use the system includes a d-c degenerative feedback loop which exerts a corrective action. When the system is highly degenerated excess overcoupling may in fact be perfectly stable, and is evidenced by reversal of the balancing action of the galvanometer; in this case the galvanometer exerts restraint upon the frequency shift rather than initiating the shift. Sensitivity in terms of galvanometer deflection is then past infinity and negative. But actually the ideal adjustment condition is still the point of disappearing galvanometer deflection, with ability of the system to accommodate excess overcoupling considered as an adjustment tolerance.

Performance

It is difficult to present a concrete analysis of the performance of a system where results are dependent almost entirely upon adjustment. Some adjustment tolerance must be determined as a permanent condition from the standpoint of engineering design, as a basis for evaluation. Upon this basis the following details of performance are offered:

1. Galvanometer excursion for full output excursion is in the order of 5 seconds of angle. This has not been measurable by direct observation, but determined from the developed coil potential and/or the time-constant of feedback in a degenerated system against the mechanical moment of the coil.

2. Galvanometer resolution in terms of deflection and spring compliance is by far sufficient to make other limiting conditions, thermal drift for example, the effective limit upon the input sensitivity.

3. The small mechanical moment of the coil, the short excursion angle and the high phase velocity of the amplifier operating at a high frequency combine to result in a short feedback period. For example degeneration to an input range of 1 millivolt will result in a feedback period of about 0.1 second under a condition of considerable misadjustment.

4. When the amplifier is closely adjusted and critically examined, limiting noise due to thermal motion impacts upon the movable coil is observable. This is the generally

Figure 6 (below). Amplifier strip assembly using frequency-shift system

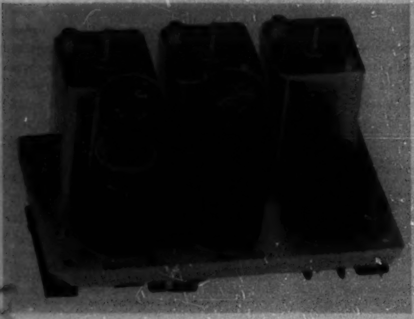

Figure 7 (right). Complete amplifier including plug-in degenerating network and power supply

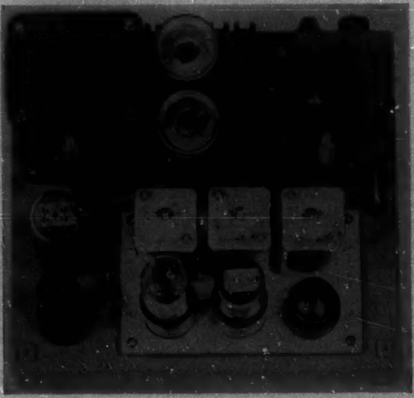

recognized limit to the sensitivity of galvanometers beyond which amplification involves bandwidth considerations.

The short feedback period is perhaps most useful in providing stability when the feedback circuit is designed for differentiation or integration functions. For example current may be time-integrated by feedback through a capacitor, and potential may be time-integrated by feedback through a mutual inductor. In such cases even short phase delays in the amplifier will lead to over-all feedback oscillation around the operating loop.

In feedback systems such as those to which this circuit is applicable it has apparently only been recently appreciated that the sensitivity of error detection may be raised through infinity to function with stability on the negative side. The normal action of initiating control then has become restraint upon a system that spontaneously desires to initiate the change. Stability, whether operation is by initiation or restraint, is a function of the time parameters of the system, and transition through the point of infinite error resolution need include no discontinuous function leading to instability.

In the production design of Figure 7 a warm-up thermal drift having a stated 5-microvolt maximum essentially determines the resolution sensitivity of the system. This corresponds to about 0.1 microampere in the 50-ohm galvanometer movable coil. Zero adjustment of the galvanometer after warm-up will resolve most of this error. The working error is this resolution sensitivity figure added to the adjustment figure of the range standard resistors, which may be made 0.1 per cent of the range. Therefore, on ranges below about 5 millivolts or 100 microamperes resolution sensitivity is limiting, and on higher ranges the standardized resistor adjustment is limiting. On still higher ranges the resolution sensitivity warrants a resistor adjustment accuracy beyond that normally feasible; for example on a 1-volt range the possible precision is 5 parts per million.

Discussion

John H. Miller (Weston Electrical Instrument Corporation, Newark, N. J.): It is quite possible that Mr. Gilbert has not sufficiently stressed the extremely high accuracy capable with his amplifier. It will be noted that the conversion accuracy is strictly associated with the feedback resistor within the bounds of the magnitude of the error signal required for rebalancing. Because of the very high frequency used in the converting system, even a moderate phase velocity gives very rapid rebalancing to the end that extremely tight feedback coupling can be used.

Obviously there is no restriction to the form of the feedback network and where extremely high accuracy is wanted a resistor of the National Bureau of Standards standard type can be used, and since a 4-terminal connection is applicable this resistance may be external to the amplifier and oil immersed and temperature controlled if that refinement is deemed desirable.

Thus it is quite possible to apply this amplifier to the measurement of low values of current and voltage to the best accuracy possible with modern deflectional instruments, 1/10 of 1 per cent. Those instruments usually take power of the order of several milliwatts, an amount of power frequently not available from low energy sources.

As a specific example, let us assume a potential of up to 20 millivolts from a noble metal thermocouple of moderately high resistance which is to be measured with a deflectional instrument to a good degree of accuracy. The potential can be connected to the amplifier which will have a coupling resistor of 20 ohms and of high accuracy. The output can then be placed on a 1/10 of 1 per cent standard deflectional instrument from which full accuracy can be obtained; at the same time the measurement is made with effectively infinite resistance in the input circuit since the only current taken is a very minute amount. A resolution of one part in 5,000 will actually be obtained in the amplifier. Such an arrangement can be found very useful in laboratory measurement of temperatures and, of course, the millivolt value may be obtained from any other transducing element.

We feel that this dependence of the accuracy of the amplifier only on the coupling or feedback resistor is a very important part of the system as a whole and may well be most useful in the accurate measurement of currents and voltages in brackets which heretofore could not be placed on deflectional-type instruments.

A Study of Carrier-Frequency Noise on Power Lines

Part I. Theoretical Considerations and Measuring Techniques

R. C. CHEEK
MEMBER AIEE

J. D. MOYNIHAN
ASSOCIATE AIEE

ONE of the basic criteria of the performance of any communication or signaling circuit is its signal-to-noise ratio. In a power-line carrier communication channel, poor signal-to-noise ratio may result in unsatisfactory service of a degree varying from barely perceptible background noise* to complete masking and total loss of intelligibility of the speech signal. In telegraphic types of channels, poor signal-to-noise ratio can cause misoperation ranging from an occasional spike on a telemetered chart record to incorrect tripping of a circuit breaker through a carrier remote tripping system.

Although the application of power-line carrier equipment is still in some respects as much an art as it is a science, methods of estimating the attenuation of a proposed channel are available.[1,2] These methods are largely empirical, but they give fairly good results for well-trapped channels. It is possible, therefore, to estimate the signal that will be delivered to a receiving point by a carrier transmitter of a given power and frequency, provided sufficient information on the intervening system layout is available. This is only half the story, however, because the noise level must be known or estimated in order for the signal-to-noise ratio to be predicted.

A search of the literature has failed to reveal any quantitative information on carrier-frequency conducted noise levels on power transmission lines. This is remarkable in view of the present-day importance of a knowledge of noise levels at proposed carrier receiving points, but is probably explained by the fact that only during the last decade, which has seen a trend toward longer carrier channels, lower transmitter power, and increased receiver sensitivity, has the problem of noise on carrier channels become an acute one.

In an effort to establish benchmarks for estimating noise levels on transmission lines of various voltage classes and various types of construction, the authors have undertaken a program of carrier-frequency noise measurement which, it is hoped, will eventually permit signal-to-noise ratios to be predicted with reasonable accuracy. A necessary preliminary step in this program was a search of the literature on radio noise and its measurement, with a view toward establishing from theoretical considerations the properties of noise most likely to affect carrier channel performance, and adapting noise-measuring techniques already developed in the radio field to the measurement of these properties of carrier-frequency noise on power lines.

Concurrently with the actual measurement of noise in the field, a study is being made of the effect of different noise levels and the resulting signal-to-noise ratios upon the performance of actual carrier equipment in various applications.

The study thus resolves itself into three major divisions, that is:

1. Study of the theoretical aspects of noise leading to development of measuring techniques and procedures.
2. Measurement in the field of noise characteristics on actual lines of various voltage classes and types of construction.
3. Correlation of measured noise characteristics and required signal-to-noise ratios for given grades of service with typical carrier receiving equipment in various applications.

This paper describes the studies made under division 1 above, including a review of some of the theoretical aspects of noise and a discussion of measuring instruments and recommended measuring techniques. A companion paper[3] gives the results of a series of field measurements of carrier-frequency noise on representative transmission lines. A later paper will report on the effects of transmission-line noise of known characteristics on typical carrier receiving equipment in various applications.

Characteristics of Noise

Noise due to all causes can be divided into two broad classifications: random noise and impulse noise. The properties of these two types of noise are markedly different, and their relative effects vary in a different manner from each other when receiving equipment characteristics vary. Hence, the two will be discussed separately. Both types are present simultaneously on power lines, but the tests reported in the companion paper[3] indicate that impulse noise always predominates to a greater or lesser extent.

---

* The general term "noise" is used in this paper to designate all electrical disturbances that may give rise to unwanted frequency components within the acceptance band of a receiver, exclusive of intentionally generated continuous-wave signals. The term "noise" thus applies regardless of whether reception is aural or mechanical.

Paper 51-187, recommended by the AIEE Carrier Current Committee and approved by the Technical Program Committee for presentation at the AIEE Summer General Meeting, Toronto, Ont., Canada, June 25–29, 1951. Manuscript submitted March 27, 1951; made available for printing April 23, 1951.

R. C. CHEEK and J. D. MOYNIHAN are with Westinghouse Electric Corporation, East Pittsburgh, Pa.

The authors acknowledge the invaluable suggestions and assistance of W. E. Pakala and C. D. Fahrnkopf.

RANDOM NOISE

Random noise is noise with a continuous frequency spectrum resulting from the random occurrence of an infinite number of elementary discharges or fluctuations that are not in themselves separately distinguishable. The audio output of a communication receiver to which true random noise is applied is a soft hissing or rushing sound.

Noise approaching true random noise in its characteristics may appear on power-line carrier channels as a result of thermal agitation in the power-line conductors, pick-up of distant atmospheric discharges or static by the power-line conductors acting as antennas, and tube or resistor noise in carrier receivers. The aggregate of the almost infinite number of small random discharges that occur constantly on an extensive power system also probably approaches random noise in its characteristics if these random discharges are considered separately from the large, separately distinguishable, and more or less regular pulses which predominate.

IMPULSE NOISE

Because impulse noise is the predominant type of noise on power lines, it will be discussed in somewhat greater detail below.

Impulse noise consists of sharp, discrete, well-separated impulses, each identifiable with a specific electrical discharge. The repetition rate of the impulses may be random or regular. If the repetition rate is irregular, the noise contains all frequencies in the spectrum and the amplitudes of the individual frequency components vary only gradually over a given band of frequencies. If the pulses are uniform and have a regular repetition rate, their frequency spectrum contains discrete frequency components separated by a frequency equal to the repetition rate, that is, it consists of the fundamental and harmonics of the repetition frequency.

It is reasonable to expect impulse noise on power lines to have a more or less uniform repetition rate because of the cyclic nature of the power voltage that gives rise to the electrical discharges. However, random pulses also can be expected as a result of switch operations, faults, and lightning discharges on or near the power line. In a carrier communication channel, typical power-line noise produces a harsh, raspy buzz upon which are superimposed strong clicks or pops of random occurrence, indicating that regular as well as random pulses are present in the channel.

A convenient type of pulse to use in a mathematical analysis of the effect of impulse noise in reception is a unit pulse occurring at $t=0$. Such a pulse has infinitesimal duration and infinite amplitude, such that its time integral is unity. The frequency spectrum of the unit pulse can be deduced from its Fourier integral representation,

$$i(t)=\frac{1}{2\pi}\int_{-\infty}^{\infty}e^{j\omega t}d\omega \tag{1}$$

which shows that all frequencies are present in such a pulse and further that all frequency components have the same amplitude.

In reference 4 it is shown that if an impulse is of such short duration that the system to which it is applied does not respond appreciably before the impulse is completed, its operational form is simply Ap, where A is the force-time area of the pulse. This is an important result, not only because of the usefulness of such a representation in an analysis of the effect of impulse noise upon receiving equipment, but also because it demonstrates the fact that the response of a receiver to a sharp pulse, or to a continuous train of well-separated sharp pulses, is independent of the actual amplitude or shape of the individual pulses at the input to the receiver and is dependent only upon their areas.

IMPORTANCE OF RECEIVER CHARACTERISTICS IN EVALUATING EFFECTS OF NOISE

The ultimate harmful effects of noise of any kind occur in the end device connected to the output circuit of a receiver, for example, a telephone receiver or a telemetering instrument. Because the noise is radically modified in passing through the tuned circuits and the detector of a receiver, it is necessary to consider the effect of receiver characteristics upon noise in any evaluation of the relative importance of the various parameters that may be used to describe the noise.

The tuned circuits of the receiver have a major modifying effect upon noise in its passage through the receiver, because only those frequency components of the noise that are accepted by the tuned circuits are detected and passed on to the end device. It is evident, therefore, that the selectivity of the receiver is an important factor in evaluating the ultimate effect of noise of a given type.

The most commonly used measure of selectivity is the width of the experimentally determined receiver selectivity curve between the two points at which the gain is 3 decibels down from the midband value G_0. A more specific measure is the power bandwidth, which is defined as

$$B_0=\frac{\int_0^{\infty}G^2(f)df}{G_0^2} \tag{2}$$

where $G(f)$ is the response of the receiver as a function of frequency. The power bandwith B_0 is the width of an ideal (rectangular) response curve which would result in the same noise power output if substituted for the actual response curve $G(f)$ with random noise applied to the receiver. In Appendix I it is shown that the power bandwidth of a cascade amplifier with "n" single-tuned circuits is, for ordinary values of Q,

$$B_0=\frac{\pi f_0(2n-2)!}{Q2^{2n-1}(n-1)!^2} \tag{3}$$

where f_0 is midband frequency and n is the number of tuned circuits. The Q of all the tuned circuits is assumed to be the same. By application of Stirling's formula,[5] this expression reduces to (approximately)

$$B_0=\frac{f_0}{2Q}\sqrt{\frac{\pi}{n-1}} \tag{4}$$

For $n\geqq 5$, the power bandwidth approaches to within a few per cent the bandwidth specified on the basis of 3-decibels drop in gain.[6]

RESPONSE OF A RECEIVER TO RANDOM NOISE

If the individual components of random noise have the same amplitude e at all frequencies, the mean square output of a receiver to which it is applied is

$$E^2=\int_0^{\infty}G^2(f)e^2df \tag{5}$$

which from equation 2 can be expressed as

$$E^2=e^2G_0^2B_0 \tag{6}$$

so that

$$E_{rms}=eG_0\sqrt{B_0} \tag{7}$$

Actually e will not have the same value at all frequencies, but due to the random nature of the amplitude distribution, the result is the same when the analysis is made on a statistical basis with e equal to the mean value of the component voltages.[6] Thus, the rms noise output of a selective amplifier to which random noise is applied is proportional to the square root of the bandwidth of the amplifier.

The peak and the average values of the envelope of random noise are both statistically related to the rms value, and these relations are independent of the frequency interval. Hence, the peak and the average values of random noise also

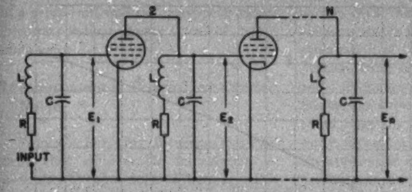

Figure 1. Selective amplifier with *n* tuned circuits used in analysis of response of a receiver to impulse noise

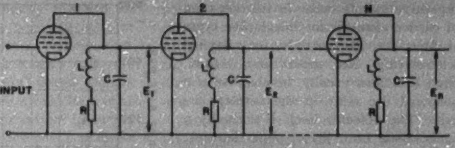

Figure 2. N-stage tuned amplifier with signal injected directly at first-stage grid. The ratio of pulse response to midband gain for this amplifier is the same as that for the amplifier of Figure 1

are proportional to the square root of the bandwidth. Jansky[7] has reported a measured value of four for the ratio of peak to rms voltage, and a value of 0.85 for the ratio of average to rms voltage for random noise over a wide range of bandwidths. Landon[8] also has confirmed experimentally the variation of rms and peak values of random noise with the square root of the bandwidth and has reported a ratio of 3.4 of the peak to the rms value. Strictly speaking the peak value is indeterminate and can be defined only in terms of a voltage which is equalled or exceeded a certain number of times during a given period. It is probably the arbitrary nature of this kind of definition that leads to the divergence of the results of the several investigators.

RESPONSE OF A RECEIVER TO IMPULSE NOISE

The term "shock excitation" is often used to describe the phenomena associated with the application of a sharp impulse to a selective circuit. It is well known that the result is an oscillation at the natural frequency of the circuit involved.

In the case of a sharp impulse applied to a receiver, which usually contains a number of tuned circuits, all of the tuned circuits oscillate but the envelope of the oscillation is different for each. Consider the case of a receiver having *n* single-tuned circuits preceding the detector, as shown in Figure 1. For a sharp pulse applied at $t=0$ in series with the inductance of the input circuit (for example, from an untuned coupling coil) the envelope of the oscillatory voltage applied to the detector by the *n*th tuned circuit is approximately (for Q large, as in the usual receiver tuned circuits)

$$E(t)=2A_0aG_0\frac{e^{-at}(at)^{n-1}}{(n-1)!} \qquad (8)$$

in which A_0 is the integrated volt-time area of the original pulse, $a=R/2L=\pi f_0/Q$, and G_0 is the over-all gain of the stages considered for a continuous-wave signal at the midband frequency f_0, to which all the circuits are assumed to be tuned. Equations equivalent in form to equation 8 have been given by Landon[8] and Thomas and Burgess[9] but neither of these authors gives a derivation. An independent derivation is given in Appendix II.

Equation 8 also holds for the case of a pulse applied to the first-stage grid of an amplifier of the type shown in Figure 2. Note, however, that the value of G_0 is different for the two cases.

If equation 8 is divided by the midfrequency gain G_0, and the resulting expression is plotted as a function of time for several different values of n, the effect of the tuned circuits upon the oscillation envelope can be examined. This is done in Figure 3, in which the output for $n=1$ to four tuned circuits is plotted.

It is evident from Figure 3 that the effect of the tuned circuits is to lengthen the pulse and to reduce its peak value. Also, the peak value occurs at a longer and longer time after application of the pulse as n is increased beyond a single stage. This peak occurs at

$$t=\frac{n-1}{a} \qquad (9)$$

at which time the amplitude of the envelope is

$$E_{\max}=2A_0aG_0\frac{e^{(1-n)}(n-1)^{n-1}}{(n-1)!} \qquad (10)$$

and from equations 4 and 10, again by application of Stirling's Formula,[5]

$$E_{\max}=2\sqrt{2}A_0G_0B_e \qquad (11)$$

Hence, the peak value of the envelope is directly proportional to the bandwidth, the gain of the receiver, and the area of the original impulse.

The peak value of the response of a receiver to impulses is an important factor in the operation of carrier communication channels. In an automatic simplex carrier assembly a transfer unit performs the switching operations between the transmit and the receive conditions and vice versa. The transfer unit responds to noise peaks when they exceed a certain preset level, normally well below the minimum received carrier signal level, and under these conditions the carrier transmitter may be intermittently or permanently blocked. In other types of communication channels, impulse noise produces a masking or distracting effect which is roughly a function of the peak value of the noise at the output of the receiver (and also of the repetition rate, as will be discussed later).

The average value of the envelope of the receiver detector output is the most important factor in evaluating the effect of

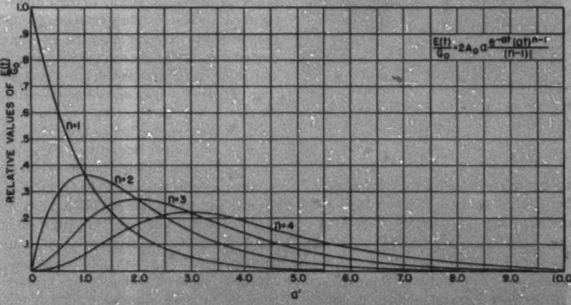

Figure 3. Effect of number of tuned circuits *n* in Figures 1 and 2 upon pulse response. Increasing *n* lengthens the pulse response and reduces its peak value

repetitive impulse noise in the operation of carrier channels for telegraphic types of functions, for example, for relaying, telemetering, and supervisory control. Such functions usually involve use of a polarized d-c relay in the detector circuit. The detector itself is normally a linear diode or a linear plate detector. The average value of the response of such a system to sharp impulses can be found by first integrating equation 8 with respect to time as follows:

$$\int_0^\infty E(t)dt = 2A_0 aG_0 \times$$

$$\int_0^\infty \frac{e^{-at}(at)^{n-1}dt}{(n-1)!} = 2A_0 G_0 \qquad (12)$$

Then, if the pulses have a repetition rate of m per second, and provided that the repetition rate is such that the wave trains in the tuned circuits do not overlap appreciably, the average response is

$$E_{av} = 2mA_0 G_0 \qquad (13)$$

which is independent of the bandwidth.

Since the spectrum of a unit impulse contains all frequencies with equal amplitudes, it follows that the noise energy in a given interval is proportional to the interval. Hence, the rms value of receiver response with impulse noise is proportional to the square root of the bandwidth, as with random noise. The rms value of the response is of less importance than peak and average values in evaluating the harmful effects of noise in power-line carrier applications, as previously indicated.

Response of Receiver to Combination of Random and Impulse Noise

In the preceding discussions, the assumption of purely random noise or purely impulse noise has been made throughout. Also, the impulses were assumed to be sharp and well separated in the case of impulse noise. If the noise is a composite type, made up of random noise and impulse noise with neither markedly predominant, the peak value of the noise at the receiver output can be expressed as

$$E_{max} = k_1 B_0^\beta \qquad (14)$$

where β has a value between 0.5 and 1.0. The average value of the output can be expressed as

$$E_{av} = k_2 B_0^\gamma \qquad (15)$$

where γ has a value between 0 and 0.5.

If the noise consists of sharp impulses, the separation of the impulses determines for a given bandwidth whether equations 11 and 13, which were derived on the assumption of a single sharp impulse, are applicable. If the repetition rate is sufficiently high to cause appreciable overlapping of the resulting wave trains in the receiver, the conditions for composite random and impulse noise, equations 14 and 15, apply. An idea of the bandwidths and pulse rates at which this begins to occur is given by Figure 4, which shows for a 100-kc amplifier the pulse repetition rates at which the response to each individual pulse (equation 8) is down to 1 per cent of its maximum value before the next pulse occurs.

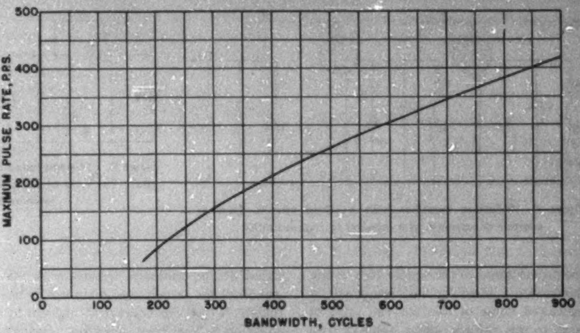

Figure 4. Maximum pulse repetition rates for which the response of a 100-kc selective amplifier to a particular pulse is down to 1 per cent of peak value before the next pulse occurs

Lippert et al[9] report that the noise field in the vicinity of 3-phase transmission lines has an average pulse repetition rate on the order of 20 pulses per second, the pulses resulting primarily from corona discharges on the negative half-cycles of the 60-cycle voltage. Although at least 60 pulses per second might reasonably be expected, the erratic nature of the corona bursts produces an effective pulse rate below this figure, according to these investigators. These conclusions agree fairly well with the findings reported for conducted line noise in the companion paper,[8] and it is therefore possible to conclude from Figure 4 that in carrier receivers of the usual bandwidths, the reponse to noise consisting predominantly of impulses is as given by equations 11 and 13. Thus, increasing carrier communication receiver selectivity should reduce proportionally the peak value of the response to impulses of the type found in power lines, up to the maximum selectivity that can be used in such receivers. In telegraphic channels, however, where the average response to noise is most important, increased selectivity cannot be expected to reduce materially the effects of impulse noise until the extremely sharp selectivity is reached at which the wave trains resulting from the pulses begin to overlap. Further increases in selectivity should provide reductions in average response approaching proportionality to the square root of the resulting bandwidths.

Quasi-Peak Value of Impulse Noise

The American Standards Association[10] has published proposed standards for radio noise meters including provision for measurement of a "quasi-peak" value of noise. The quasi-peak value is based on the use of a detector output circuit which has a fast charging time (1 millisecond) and a relatively slow discharging time (600 milliseconds). These time constants result in a reading which is near the peak value of the response of the detector to pulses occurring at a rate of approximately 15 or more per second. Experience in the radio noise measurement field has shown that quasi-peak readings are approximately proportional to the masking or distracting effects of noise in aural reception of modulated signals. Hence, it is logical to expect quasi-peak readings of conducted carrier-frequency noise to be indicative of the probable effects of such noise on carrier communication channels of the duplex or manual simplex types. In the automatic simplex type, as has already been pointed out, the actual peak value is of more importance because it is the factor that determines whether the transfer unit operates.

With irregular pulses, or pulses of high amplitude that occur infrequently, the quasi-peak reading is somewhat less than the absolute peak value reached. When transfer unit operation is not involved, however, the masking effect of such peaks is not as great as if they were repetitive at a rapid rate, and the quasi-peak value is correspondingly lower than the maximum value.

Measurement of Power Line Carrier Noise

From the foregoing discussion it is evident that considerable information is necessary to define noise of the type existing on transmission lines if measurements of such noise are to be generally useful. Noise essentially random in its characteristics can be specified simply on the basis of its rms or its average voltage in a given bandwidth, but impulse noise requires several parameters for its definition. Because the noise response at the output of a receiver to which impulse noise is applied is of more practical interest than the detailed characteristics of the original noise pulses themselves, it does not appear necessary to include such parameters as the original pulse amplitude or duration. What is required is a measurement of the peak, quasi-peak, and average values of the response of a receiver (that is, a noise meter) of known bandwidth, the bandwidth being sufficiently large to avoid overlapping of the pulse response. These values can then be referred to different bandwidths, using the relations previously derived, provided that the pulse repetition rate is not so great that overlapping of the pulse response occurs at the new bandwidth considered. Thus a knowledge of the pulse rate also is desirable.

The noise levels measured at a given point on a power system can be expected to vary with the frequency at which the measurement is made, partly because the attenuation of the system to noise components from distant sources will vary with frequency as for actual signals. Hence, the noise levels should be investigated over the entire carrier frequency range, unless the measurement is made for the application of a specific channel at a predetermined frequency.

It is well known that noise on carrier channels varies radically with weather conditions, and isolated readings of noise have little value unless correlated with weather. The most desirable method of taking this factor into account is to record the noise level (for example, the quasi-peak level) continuously at some convenient frequency over a period long enough to include a representative variety of weather conditions at the test location. The relative variation of peak, quasi-peak, and average readings under different weather conditions should also be investigated.

DISCUSSION OF NOISE METERS

An ideal meter for measuring power-line carrier noise would include a means of determining the relative amounts of conducted random and impulse noise present in a given bandwidth in the carrier spectrum. In addition it would be able to indicate the pulse repetition rate for the impulse noise present, and to indicate and record the peak, quasi-peak, and the average values of the noise.

Although several available types of noise meters approach this ideal, practical limitations prevent their reaching it completely. There is no meter available that can separate random and impulse noise and measure the characteristics of the two independently. However, a comparison of the quasi-peak reading with the average reading of a given composite noise provides an indication as to whether one type or the other is predominant. The manufacturer of the Stoddart type *NM-10A* noise meter, for example, recommends that the noise be considered predominantly impulsive in nature if the ratio of quasi-peak to average reading exceeds 1.8. This appears reasonable on the basis that random noise peaks do not exceed 1.8 times the average value often enough to provide a quasi-peak meter reading approaching this figure.

For impulse noise consisting of short, sharp pulses the ratio of peak to average readings in a given bandwidth is roughly

Figure 5. Noise meters suitable for measuring conducted noise on power lines. (Below) Stoddart type *NM-10A* (right) Ferris model *64-AB*

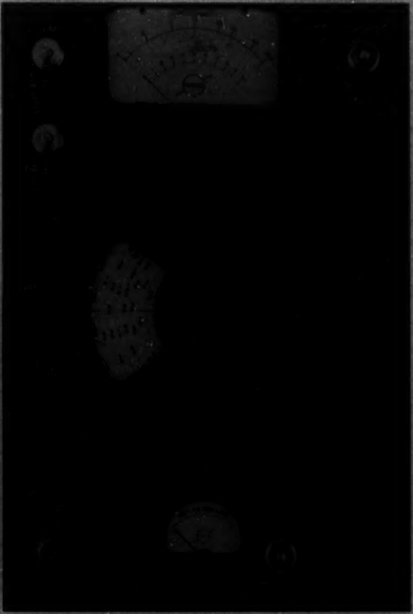

proportional to the pulse repetition rate. However, since both random and impulse noise may be present on a power line, it appears preferable to examine the output of the meter on an oscilloscope with a calibrated sweep oscillator for a more accurate determination of the pulse rate.

A limitation of practical noise meters is their inability to record peak values continuously. At present, peak values are obtained by a slide-back method which does not lend itself to continuous recording.

In spite of these limitations, much valuable and useful information can be obtained with modern noise meters meeting the proposed American Standard Association standard.[10] At least two makes of such instruments covering the power-line carrier spectrum are available. Two typical noise meters suitable for measuring carrier-frequency conducted noise are shown in Figure 5.

It should be noted that an attempt to measure noise with a conventional carrier receiver calibrated on continuous-wave signals, using a milliammeter to measure the rectified (diode detector) current, will yield information only on the average value of the noise envelope. This information, although it may be useful in connection with the application of telegraphic channels, is not of much value in the application of voice communication channels. The same limitations apply to noise measurements made with tunable carrier-frequency voltmeters not provided with quasi-peak weighting circuits. In both cases the average readings obtained are too low to be indicative of the masking effect of the noise in communication applications. If such measurements are made in connection with other applications, the relative bandwidths of the measuring device and the apparatus to be applied must be taken into account.

Conclusions

From the foregoing theoretical analyses and the subsequent discussions, the following conclusions have been reached:

1. More information is needed on the conducted noise levels existing on power lines at power-line carrier frequencies.
2. The average, peak, and rms values of the response of a carrier receiver to random noise are proportional to the square root of the bandwidth of the receiver.
3. The peak value of the response of a carrier receiver to impulse noise consisting of sharp, well-separated pulses is proportional to the bandwidth of the receiver and to the volt-time area of the original pulses, but it is independent of the actual peak amplitude of the latter.
4. The average value of the response of carrier receivers of the usual bandwidths to sharp, well-separated impulse is independent of the bandwidths of the receivers but is proportional to the volt-time area and the repetition rate of the original pulses. The rms value of the response is proportional to the square root of the bandwidth, as with random noise, in addition to these factors.
5. Knowledge of the peak values of the response of a receiver to impulse noise is important in the application of automatic simplex carrier communication channels. Quasi-peak values are more indicative of the probable interfering properties of noise in other types of communication channels. Average values are more important in the application of telegraphic types of channels.
6. Radio noise meters designed in accordance with modern proposed standards can provide information on the conducted carrier-frequency noise levels on power lines which will be useful in the application of both voice and telegraphic types of carrier channels. Calibrated receivers, or other instruments not provided with quasi-peak weighting circuits, in general provide information only on the average value of noise response, which is not indicative of the actual masking effect of impulse noise in voice communication circuits.
7. Measurements of carrier-frequency noise at a given point in a power line should include determination of whether random or impulse noise predominates, measurements of peak, quasi-peak, and average noise over the carrier spectrum with a noise meter of known bandwidth, a record of the approximate pulse repetition rate if impulse noise is predominant, and a continuous record of a representative noise response (for example, quasi-peak) over a period of time sufficient to include a variety of weather and switching conditions.

Appendix I. Bandwidth of Cascade Amplifier with "N" Single Tuned Circuits

In a cascade amplifier, for example, Figure 1, comprising n single-tuned circuits all tuned to the same resonant frequency f_0 and having the same high Q, and with each circuit isolated from the others by tube stages, the power bandwidth is the same whether the input voltage for each stage is injected in series with the inductance from a low-impedance source, or across the parallel circuit from a high-impedance source. The assumption is made in the case of series injection that the output voltage to the grid of the following stage is proportional only to the current in the circuit, that is, that the reactance of the capacitor C is constant, which is permissible with negligible error for the small bandwidths being considered. Also, it is assumed that the reactance around each circuit is $2X_0(f-f_0)/f_0$, where X_0 is the reactance of either branch at f_0, and that R is constant.

Consider as an example the case where the input voltage is applied from a high-impedance source across the parallel circuit. The response as a function of frequency for this case is proportional to the parallel impedance, which under the assumptions stated is for each stage

$$Z(f)=\frac{L/C}{\sqrt{R^2+[2X_0(f-f_0)/f_0]^2}} \tag{16}$$

The response of each stage at f_0 is proportional to

$$Z_0=Q\omega_0L=L/RC \tag{17}$$

and the power bandwidth, by equation 2, for n stage is

$$B_0=\frac{\int_0^\infty Z^{2n}(f)df}{Z_0^{2n}} =\int_0^\infty \frac{df}{[1+4Q^2(f-f_0)^2/f_0^2]^n} \tag{18}$$

or

$$B_0=\int_0^\infty \frac{f_0^{2n}df}{[f_0^2+4Q^2f_0^2-8Q^2f_0f+4Q^2f^2]^n} \tag{19}$$

which by use of Forms 67 and 71 of Peirce's Tables and after some manipulation is, for the usual values of Q,

$$B_0=\frac{\pi f_0(2n-2)!}{Q2^{2n-1}(n-1)!^2} \tag{20}$$

A similar derivation for the case of series injection of the input signal to each stage leads to an expression identical to equation 18, and therefore equation 20 also applies.

Appendix II. Impulse Response of Cascade Amplifier with "N" Tuned Circuits

In reference 4 it is shown that (with certain mathematical restrictions that are met in practical physical cases) the operational form of short impulse is Ap, where A is the area of the impulse. This form can be used to represent any impulse of such short duration that the impulsed system does not respond appreciably before the impulse is completed.

Assuming that a sharp impulse of area A_0 is applied in series with the first tuned circuit of the amplifier of Figure 1, the voltage E_1 applied to the grid of the first tube is (in operational form)

$$E_1=\frac{A_0}{LC}\frac{p}{p^2+Rp/L+1/LC} \tag{21}$$

The current applied to the second tuned circuit is, for a pentode amplifier, approximately

$$I_2=g_mE_1 \tag{22}$$

and E_2, the output voltage, is

$$E_2=\frac{g_mA_0p}{LC^2(p^2+Rp/L+1/LC)}\times \frac{p+R/L}{(p^2+Rp/L+1/LC)} \tag{23}$$

and similarly the output of E_n of the nth tuned circuit is

$$E_n=\frac{g_m^{n-1}A_0p(p+2a)^{n-1}}{LC^n[(p+a)^2+b^2]^n} \tag{24}$$

where $a=R/2L$ and

$$b=\sqrt{(1/LC)-(R^2/4L^2)}$$

To find E_n as a function of t, we substitute equation 24 in the Bromwich-Wagner complex integral, changing p to the complex parameter s, which gives

$$E_n(t)=\frac{g_m^{\,n-1}A_0}{LC^n}\frac{1}{2\pi i}\times\int_{Br_1}\frac{e^{ts}(s+2a)^{n-1}ds}{(s+a+ib)^n(s+a-ib)^n} \qquad (25)$$

The integrand in equation 25 has two poles of order n, one at $s=-a-ib$ and one at $s=-a+ib$. To determine the residue at $s=-a+ib$ we expand $(s+2a)^{n-1}$ and $(s+a+ib)^{-n}$ in powers of $(s+a-ib)$, multiply the resulting series term by term, and then multiply the expansion of e^{ts} in powers of $(s+a-ib)$ by the result. Following this procedure we get

$$(s+2a)^{n-1}=(a+ib)^{n-1}+(n-1)(a+ib)^{n-2}(s+a-ib)+\frac{(n-1)(n-2)(a+ib)^{n-3}}{2!}\times(s+a-ib)^2+\ldots\ldots \qquad (26)$$

$$(s+a+ib)^{-n}=(2ib)^{-n}+(-n)(2ib)^{-n-1}(s+a-ib)+\frac{(-n)(-n-1)(2ib)^{-n-2}}{2!}\times(s+a-ib)^2+\ldots\ldots \qquad (27)$$

The product of equations 26 and 27 is

$$(s+2a)^{n-1}(s+a+ib)^{-n}=\frac{(a+ib)^{n-1}}{(2ib)^n}+\left[\frac{(n-1)(a+ib)^{n-2}}{(2ib)^n}-\frac{n(a+ib)^{n-1}}{(2ib)^{n+1}}\right]\times(s+a-ib)+\ldots\ldots \qquad (28)$$

If a is small compared to b (that is, if Q is large) only the first term of equation 28 is significant, and equation 28 can be expressed approximately as

$$(s+2a)^{n-1}(s+a+ib)^{-n}=1/2^n ib \qquad (29)$$

Then since

$$\frac{e^{ts}}{(s+a-ib)^n}=\frac{e^{(-a+ib)t}}{(s+a-ib)^n}+\frac{te^{(-a+ib)t}}{(s+a-ib)^{n-1}}+\frac{t^2e^{(-a+ib)t}}{2!(s+a-ib)^{n-2}}+\ldots\ldots \qquad (30)$$

the coefficient of $(s+a-ib)^{-1}$ in the product of equations 29 and 30 is, for n stages

$$C_1=\frac{t^{n-1}e^{(-a+ib)t}}{2^n ib(n-1)!} \qquad (31)$$

and the coefficient of the corresponding term in the similar expansion about $s=-a-ib$ is

$$C_2=-\frac{t^{n-1}e^{(-a-ib)t}}{2^n ib(n-1)!} \qquad (32)$$

The value of the integrand in equation 25 is $2\pi i$ times the sum of the residues C_1 and C_2, and we have

$$E_n(t)=\frac{A_0 g_m^{\,n-1}e^{-at}t^{n-1}}{LC^n 2^{n-1}b(n-1)!}\,\frac{e^{ibt}-e^{-ibt}}{2i} \qquad (33)$$

The gain of the amplifier for a continuous signal at the resonant frequency is approximately

$$G_0=(1/R^n)(g_mL/C)^{n-1}\sqrt{L/C} \qquad (34)$$

so that (assuming $b=1/\sqrt{LC}$)

$$E_n(t)=2A_0aG_0\frac{e^{-at}(at)^{n-1}}{(n-1)!}\sin\sqrt{1/LC}\,t \qquad (35)$$

The envelope of $E_n(t)$ is the coefficient of $\sin\sqrt{1/LC}\,t$ or

$$E(t)=2A_0aG_0\frac{e^{-at}(at)^{n-1}}{(n-1)!} \qquad (36)$$

References

1. Power-Line Carrier Application, R. C. Cheek. *Electrical Transmission and Distribution Reference Book*, fourth edition, Westinghouse Electric Corporation, East Pittsburgh, Pa., chapter 12, 1950.

2. Application of Carrier to Power Lines, F. M. Rives. *AIEE Transactions*, volume 62, 1943, pages 835–844.

3. A Study of Carrier Frequency Noise on Power Lines, Part II, Results of Field Measurements, R. C. Cheek, J. D. Moynihan. *AIEE Transactions*, volume 70, 1951 (*Proceedings T1-245*).

4. Complex Variable and Operational Calculus (book), N. W. McLachlan. The Macmillan Company, New York, N. Y., 1942.

5. Higher Mathematics for Engineers and Physicists (book), I. S. and E. S. Sokolnikoff. McGraw-Hill Book Company, New York, N. Y., 1941.

6. Survey of Existing Information and Data on Radio Noise over the Frequency Range 1–30 Mc/S, H. A. Thomas, R. E. Burgess. *Special Report Number 15*, National Physical Laboratory (London, England), 1947.

7. An Experimental Investigation of the Characteristics of Certain Types of Noise, K. G. Jansky. *Proceedings*, Institute of Radio Engineers (New York, N. Y.), volume 27, 1939, pages 763–68.

8. A Study of the Characteristics of Noise, V. D. Landon. *Proceedings*, Institute of Radio Engineers (New York, N. Y.), volume 24, 1936, pages 1514–21.

9. Radio Influence Tests in Field and Laboratory—500 Kv Test Project of the American Gas and Electric Company, G. D. Lippert, W. E. Pakala, S. C. Bartlett, C. D. Fahrnkopf. *AIEE Transactions*, volume 70, 1951, pages 251–69.

10. Proposed American Standard Specification for a Radio Noise Meter 0.015 to 25 Megacycles/Second. *C63.2*, American Standards Association (New York, N. Y.), 1949.

Discussion

J. C. G. Carter (Westinghouse Electric Corporation, Baltimore, Md.): In their paragraph entitled Discussion of Noise Meters the authors state that measurements made with conventional carrier receivers calibrated on actual signals are of little value. Actually some use can be and has been made of such readings as follows:

1. For adjustment of an automatic simplex system, the control of the transfer unit in a transmitter-receiver can be set so that the line noise in the absence of a signal will just trigger it. The receiver can then be disconnected from the line and a signal generator substituted. The generator can be tuned to the carrier frequency to be received, and its voltage adjusted until it too will just trigger the transfer unit. As the transfer unit operates on peak voltages, the peak value of the signal from the generator is a measure of the peak value of the line noise. For operation of the equipment, the control of the transfer unit can then be set at a safe margin above this. The peak noise value thus deduced can be used as an indication of the peak line noise level to be expected at about that carrier frequency at that particular point. This may be useful if other equipment is contemplated to operate at that point either as an addition or as a result of a rearrangement of equipment.

2. To determine the suitability of the line for keyed carrier applications such as protective relaying or carrier on-off telemetering which work on rectified radio frequency, a conventional receiver can be connected to the line, and the sensitivity adjusted so that the line noise gives a convenient diode reading. A signal generator can then be substituted as suggested above to give an equivalent signal. This will be a measure of the average line noise. Corrections will, of course, have to be made for the relative bandwidths of the measuring receiver and the proposed operating receiver.

3. To determine the masking effect of the noise for voice systems other than automatic simplex, a communication-type receiver similar to the one contemplated for installation might be connected to the line at the same time as an applied modulated signal. This could be an actual signal from a distant station or more conveniently a local signal generator capable of being modulated by speech. The level of the speech modulated input signal could then be adjusted so that the speech was barely intelligible against the background of the noise. While it is difficult to substitute another masking signal for the noise and so determine the actual quasi-peak noise level, one could deduce from the above test that a received signal would have to have a certain minimum level.

R. C. Cheek and J. D. Moynihan: The authors appreciate the discussion offered by Mr. Carter, especially because it rounds out the paper by describing practical methods of taking noise voltages into account in the setting up of specific carrier channels. These methods are quite useful when the carrier receiving equipment used in making the tests is the same as that which will be used later in the actual operation of the channels. However, quantitative data taken in this manner with a variety of types of carrier receivers and line tuning and coupling arrangements cannot be correlated because of the large number of variables involved. It was for these reasons that the authors preferred to use standardized noise meters in making the studies described.

It is hoped that the results of these

studies will stimulate others to make similar measurements so that the over-all fund of knowledge of carrier-frequency noise phenomena can be increased. The only possible way to assure consistency of results among different investigators is for all to use standard procedures and equipment.

The procedures described by Mr. Carter give results predicated upon the existence of a noise level no greater than that prevailing at the time such tests were made. Therefore, care should be taken to select for such measurements a time at which the noise level is known to be unusually high, for example during a thunderstorm.

The Duty on Lightning Arresters for A-C Systems

EDWARD BECK
MEMBER AIEE

THE duty of lightning arresters is to protect the electric equipment against damage and the service against outage from transient overvoltages. The duty on lightning arresters is the continuous normal system voltage to which they are subjected; the frequency with which they discharge; the character, that is, crest value and wave shape of the surge currents and the power follow current which they are called upon to handle.

This paper concerns itself not with the protective characteristics of lightning arresters but with the duty on them and suggests tests which will demonstrate their ability to perform their operating duty cycle under conditions which are expected in service. The test procedures suggested pertain to valve-type lightning arresters. Significant duty cycle tests on expulsion-type lightning arresters are under study. A paper[1] by O. Ackermann discusses that subject.

Normal System Voltage

Lightning arresters are subjected to 60-cycle voltage continuously, for all practical purposes. Unless discharged by a surge, they are expected to be insulators, or very high resistances, depending on their construction. Their insulating qualities are expected to remain as constant as those of other insulation in wet as well as dry weather and under reasonable degrees of contamination of the outer surfaces. However, there are unusual conditions of installation which may require special consideration. Present standards cover this phase.[2]

General Discussion of Lightning Arrester Discharge Currents

The characteristics of lightning arrester discharge currents are not definite, fixed quantities, but have a statistical distribution. The selection of a current for laboratory or routine tests must bear this in mind. The conclusions reached in this paper are based on field research, theory, and experience. As in many matters involving probability, there may be differences of opinion regarding the conclusions, but it is believed that those drawn in this paper are logical in the present state of knowledge.

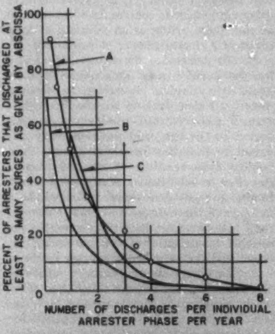

Figure 1. Distribution of discharges through individual lightning arresters[4]

A. 34 single-phase lightning arrester years[4]
B. 1,020 lightning arrester years[9]
C. 73 lightning arrester years[11]

Estimates of lightning arrester discharge current magnitudes have been made on a theoretical basis[3] and data have been accumulated in the field by recording currents discharged through lightning arresters in actual service. It is of interest to note the rather good agreement between the conclusions of the early paper by A. M. Opsahl[3] and the field data. Considerable information has been accumulated on the expected frequency of discharge and on the crest magnitudes of lightning arrester discharge currents. A limited amount of data is available on wave shapes of the discharge currents. For descriptions of the recording devices used in the field researches the reader is referred to the list of references given at the end of this paper.

Frequency of Lightning Arrester Discharge

Data in statistical curve form from two sources are shown in Figures 1 and 2.[4,5] Additional data on distribution lightning arresters on distribution systems are published in references 6 and 7. The data in Figures 1 and 2, gathered principally on distribution and highly insulated unshielded medium voltage lines, are representative of the available information.

The majority of the records have been obtained by means of devices with a lower limit of recording ability of 50 or several hundred amperes. It has been found by the use of more sensitive instruments in limited number that under some conditions lightning arresters apparently discharge surges of quite low magnitude and short duration more frequently.[8] Some records in addition to those published have given evidence of a large number of short duration discharges of less than 50-amperes crest in a particular station during certain periods. These, it was concluded, were not caused by lightning, but by surges produced by some system disturbances. These small discharges through lightning arresters are sometimes

---

Paper 51-190, recommended by the AIEE Protective Devices Committee and approved by the Technical Program Committee for presentation at the AIEE Summer General Meeting, Toronto, Ont., Canada, June 25–29, 1951; Manuscript submitted January 31, 1951; made available for printing April 23, 1951.

EDWARD BECK is with the Westinghouse Electric Corporation, East Pittsburgh, Pa.

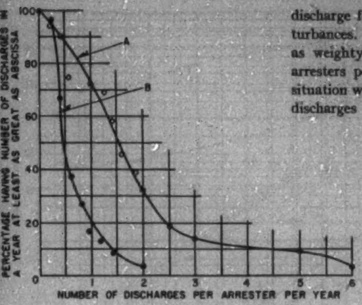

Figure 2. Average number of single-pole lightning arrester discharges per year[5]

A. Lightning arresters in stations, 133.5 lightning arrester years

B. Distribution lightning arresters, 160 lightning arrester years

accompanied by power follow current and sometimes not. It requires a surge of some minimum magnitude and duration timed in the proper relation to the phase of the system voltage to start power follow. The records of small magnitude were obtained on valve lightning arresters on a subtransmission system. On these the ratio of lightning arrester sparkover to system voltage is relatively low. On distribution systems the ratio of lightning arrester sparkover to system voltage is relatively high in most cases, and it is believed that most distribution lightning arresters would not be discharged by such small surges, even if present. The low current, short discharges are not considered significant as far as duty on lightning arresters or effect on apparatus is concerned. Hereafter they are neglected.

It is concluded from the available data that in isokeraunic levels of 30 to 40, lightning arresters on rural distribution systems may be expected to discharge, on the average, about once per year. On urban distribution systems the expected frequency of operation is less because of the more effective shielding from buildings. In stations connected to wood pole lines without shield wires, the number of discharges per lightning arrester pole is estimated at about 1.5 per year. The figure may be affected by the number of lines entering a station and the number of lightning arresters in the station.[8] Lightning arresters in stations such as those mentioned discharge more frequently than lightning arresters on distribution systems. This may be explained by the fact that, in general, there is a lower density of such stations per mile of line than distribution transformers with lightning arresters. Distribution lightning arresters are lower in voltage ratings and sparkover than lightning arresters on subtransmission systems, and might be expected to discharge for a higher percentage of disturbances. Apparently this factor is not as weighty as the density of lightning arresters per mile of circuit. A similar situation was found in an investigation of discharges through expulsion lightning arresters of the transmission line type.[10] Such lightning arresters at isolated locations discharged about once per year, whereas lightning arresters of the same type distributed along the lines at every second pole discharged on the average of 0.35 times per year.

In high-voltage stations connected to lines shielded adequately against direct strokes for at least a half to one mile out from the station, the frequency of operation is less than in the more exposed stations. This is indicated by field investigations[8,11] and by calculation.[12]

Crest Magnitudes of Lightning Arrester Discharge Currents

There exists a large volume of data on the crest magnitudes of lightning arrester discharge currents, recorded principally by the surge crest ammeter.[13] Although this device has certain limitations, they are not serious. The lower limit of sensitivity is usually 50 or more amperes. In the case of several surges of the same polarity, the maximum is recorded. If several surges occur between inspections, they cannot be distinguished. However, the probabilities of this happening are not great. It is considered unlikely that this possibility has a significant effect on the data.

Figure 3 shows the statistical distribution of measurements of crest currents reported by a number of investigators. The data comprise records of generally

Figure 3. Statistical distribution of records of crest currents obtained on various investigations

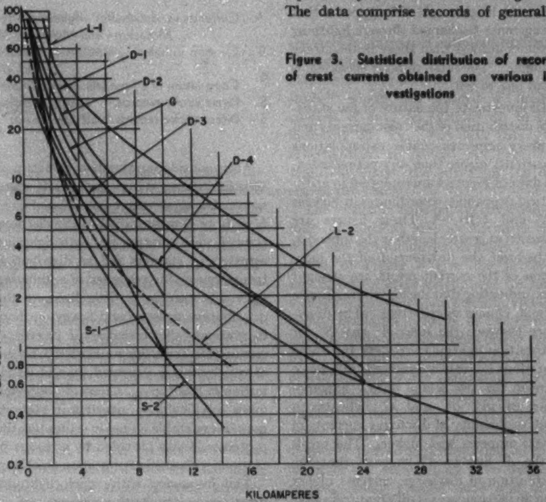

D-1. Wilbur and McMorris. Lightning arresters on 4,800 volt delta distribution system,[25] 500 records

D-2. McEachron and McMorris, distribution lightning arresters,[4] 1,608 records

D-3. McCann and Beck. Distribution lightning arresters,[5] 114 records

D-4. McCarthy, Stann, Edge and McKinley. Distribution lightning arresters,[7] 1,685 records

G. Grunewald. Lightning arresters in Germany

L-1. Andrews and McCann. Expulsion lightning arresters on 33-kv wood pole lines,[10] 73 records

L-2. Collins. Lightning arresters on 24-kv wood pole lines.[26] 499 records

S-1. McCann and Beck. Lightning arresters in stations,[5] 266 records

S-2. Gross and McMorris. Lightning arresters in stations,[9] 459 records not less than 50 to several hundred amperes. The surges of small magnitude mentioned under Frequency of Discharge are not included. Possibly differences in the limits of measurement affect the curves in some degree so that they may not all actually be on the same basis. It is believed that the probable effect of this on the over-all picture is small.

In Figure 4 the data of Figure 3 are compiled. The curves of Figure 3 indicate that there may be a difference between the data for distribution lightning arresters and those in stations. Therefore three curves are shown in Figure 4 as explained in its caption. The maximum current indicated in Figure 4 is 35,000 amperes. Examination of the spark gap electrodes of lightning arresters that had been in service on rural distribution lines has given some evidence of occasional higher currents.[14,15] The dashed curves are the crest currents recorded in an investigation of direct strokes to masts and rods.[16] These have been plotted for comparison. The crest currents of strokes to lines are probably of the same magnitudes as those to masts and rods of moderate heights. It thus appears that the currents discharged through lightning arresters are less than those in the stroke terminal. The ratio, roughly speaking, is about one to ten.

To investigate the nature of the statistical distribution of the crest currents and to make some reasonable extrapolations to currents higher than any yet recorded, the data of Figure 4 are replotted to arithmetical probability coordinates in Figures 5(A) and 5(B).[17,18] These figures are discussed at greater length in the appendix. To be brief, the distribution of the logarithms of the current crests are straight lines, indicating that the logarithms have a normal, chance distribution. The divergence between the lines *A′* and *B′* for distribution lightning arresters and those in stations indicate a significant difference between the two sets of data. Extrapolation of *A′*, *B′*, and *C′* indicates a small probability of discharge currents of 65,000 amperes and higher. The break in the *A′* line to *A″* suggests that the distribution of discharge currents higher than 20,000 amperes is different from that below this value, and that the probability of very high currents is less than one might expect. Unfortunately data at the high currents are scarce. For the present it must be admitted that we do not know the facts. If the data for direct strokes, all components, from Figure 13 of reference 16 are plotted in the same manner, they do not show this aberration.

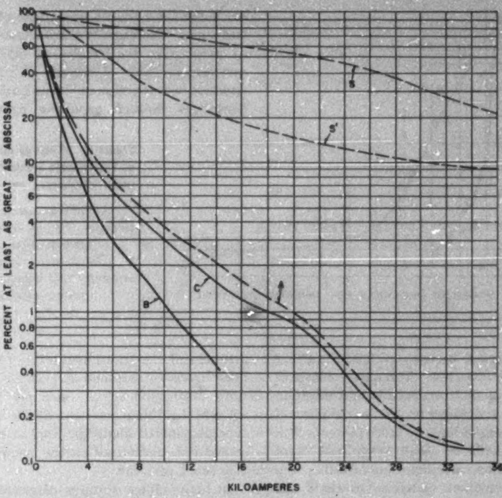

Figure 4. Statistical distribution of discharge records compiled from data of Figure 3

A. Currents in distribution lightning arresters, 3,907 records. Wilbur and McMorris, McEachron and McMorris, McCann and Beck, McCarthy et al

B. Currents in lightning arresters in stations, 1,184 records. Collins, Gross and McCann, McCann and Beck

C. Compilation of all records except Grunewald, 5,164 records

S. Direct stroke records.[16] Maximum component in strokes

S′. Direct stroke records,[16] all components

After considering the data and its possible limitations at high currents, it seems reasonable to assume curve *C′* of Figure 5(B) to be representative of the distribution of crest currents for both lightning arresters in stations and at distribution transformers, for purposes of estimating duty. It may be a little light on the distribution arresters and heavy on those in stations. Nevertheless, if it errs, it errs on the severe side for station arresters of which more is expected than of distribution or line types. Curve *B′*, applying more specifically to arresters in stations may be preferable for use in estimating the protective levels provided by arresters in stations without line or station shielding.

The frequency with which lightning arresters on distribution systems and in stations connected to unshielded lines may be expected to discharge currents with crests at least as great as any probable magnitude is shown by the solid curves in Figure 6. They are derived from curve *C′* of Figure 5(B) assuming average frequencies of discharge of 1/2, 1, and $1^1/_2$ times per year per lightning arrester. The station data alone are plotted dashed, for information. On the basis of one discharge per year, any lightning arrester may be expected to discharge currents at least as high as stated in the first column of Table I as often as stated in the second column.

The rare occurrence of very high discharge currents is apparent, and is corroborated by the fact that none has been recorded. It is the author's opinion that the 65,000- and 100,000-ampere tests now in use as criteria of the ability of a lightning arrester to stand up in service have not been well chosen although the magnitudes may be impressive. At least, they do not seem significant for valve lightning arresters. A high surge current has merit for expulsion lightning arresters, because

Table I

Amperes	Frequency			
100,000	Once	in	14,300	year
65,000	"	"	4,000	"
20,000	"	"	200	"
10,000	"	"	45	"
5,000	"	"	13	"
1,500	"	"	$3^1/_2$	"
830	"	"	2	"
100	"	"	1	"

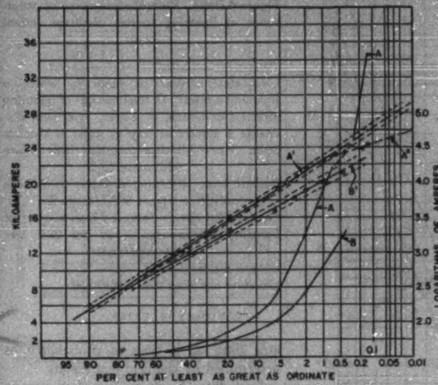

Figure 5(A). Probable distribution of crest currents

A. Arithmetic distribution of crest currents in distribution lightning arresters. Use ordinates on left

B. Arithmetic distribution of crest currents in lightning arresters in stations. Use ordinates on left

A'. Distribution of logarithms of crest currents in distribution lightning arresters. Use ordinates on right

A''. Possible distribution of logarithms of crest currents above 20,000 amperes in distribution lightning arresters. Use ordinates on right

B'. Distribution of logarithms of crest currents in lightning arresters in stations. Use ordinates on right

The dashed lines embracing A' and B' are the boundaries of their confidence envelopes for a probability of 0.95

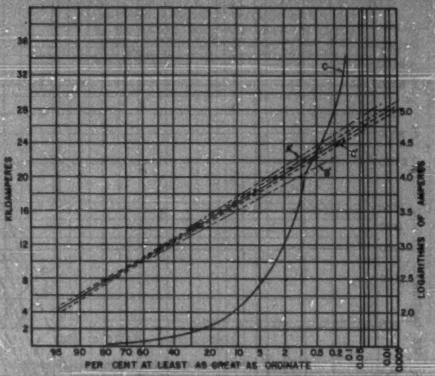

Figure 5(B). Probable distribution of all crest currents. Includes both distribution and lightning arresters in stations, 5,164 records

C. Arithmetic distribution of all currents. Use ordinates on left

C'. Distribution of logarithms of all currents. Use ordinates on right. The dashed lines embracing C' are the boundaries of the confidence envelope for a probability of 0.95. A' and B' correspond to A' and B' of Figure 5(A), for reference

it subjects the arcing chambers of these lightning arresters to great mechanical forces as a result of the high and sudden gas pressures produced by high surge currents. Experience indicates it to be a good criterion for expulsion lightning arresters.

It has already been said that the data of Figure 6 are based on records obtained, for the most part, on highly insulated and unshielded lines of medium voltage. Although the volume of data on high-voltage lines, both unshielded and shielded, is not large enough to warrant conclusions based on records, it would seem that the curves of Figure 6 should be valid for unshielded high-voltage lines also. They may be pessimistic to some degree. On the other hand, high-voltage conductors are located farther above the ground and should be subjected to more disturbances of significant magnitude. Lightning arresters in stations that have adequate direct stroke shielding, connected to lines that are also well shielded for at least a half mile or a mile from the station, will experience high surge currents less frequently. The high currents result from strokes to the circuits near the arrester.[3] In well shielded systems the probability of this is remote. It would result from a backflash from the shield wires to the system conductors or from a stroke that side flashes to the conductors despite the shielding. This is a possibility, but in well shielded systems it is a rare occurrence, as is evident from the excellent flashover records of well shielded lines. The probable distribution of discharge currents in high voltage, shielded stations is affected by numerous factors such as the arrangement and extent of the shielding and the ground resistances. Field measurements in significant number are lacking. It can be said with some confidence that in a well shielded high-voltage station, the lightning arrester discharge currents seldom will exceed 5,000 amperes, except in the case of a side flash to a conductor which is unlikely. A theoretical study of the probable occurrence of certain lightning arrester discharge currents based on definite assumptions will be found in reference 12.

The effect of line insulation and shielding on the frequency and the crests of discharge currents through lightning arresters in stations is indicated in Figure 7, reproduced from reference 9. Similar indications have been obtained in another study[11] which has yielded a limited amount of data on systems up to and including 230 kv. The data from this investigation, if plotted on Figure 6, would lie above the curve for 0.5 discharge per year.

The available data on the crest magnitudes of lightning arrester discharge currents may be summarized as follows. The curves of Figure 6 give the probable expectancy of crest magnitudes for rural distribution systems and medium voltage, highly insulated systems in isokeraunic levels of 30 to 40 in altitudes below 5,000 feet. The curves may be corrected in proportion for other isokeraunic levels, by increasing or decreasing the average number of discharges per lightning arrester per year. It is possible but not definitely proved generally, that at high altitudes the curves may have different shapes, having greater slope and ordinates even for a higher frequency of discharge.[10] It is believed that the curves are valid also for high-voltage unshielded systems. For high-voltage systems well shielded against direct strokes, it is probable that the frequency of discharge is less and that the discharge currents seldom exceed 5,000 amperes. The curves lie too low for urban distribution systems, on which both the frequency and magnitude of the discharge currents are lower.[8]

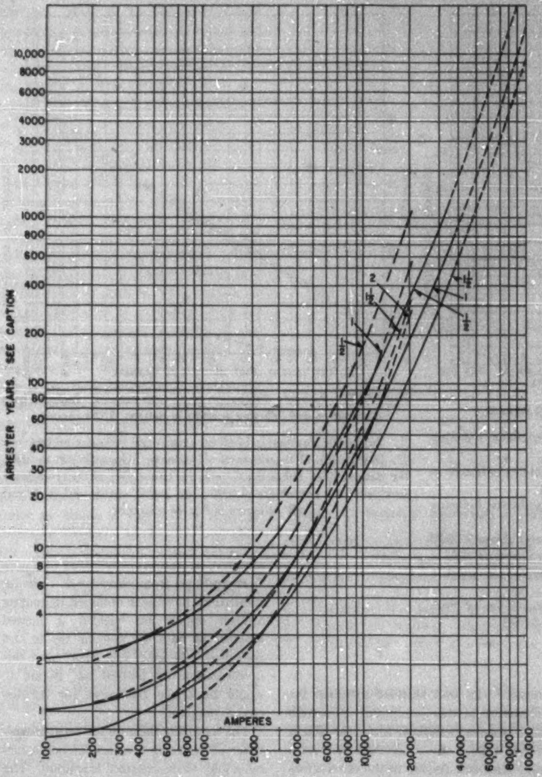

Figure 6 (left). Probable frequency of occurrence of lightning arrester discharge current crests

Abscissae—amperes

Ordinates—number of years in which a lightning arrester, or total number of lightning arresters of which, in a year, one will discharge a current at least as great as abscissa

Solid lines—All data compiled from Figure 5(B) curve C′

Dashed lines—lightning arresters in stations only, from Figure 5(A), curve B′

Numbers on curves—assumed total number of lightning arrester discharges per year per lightning arrester

Isokeraunic level—30

Elevation not more than 5,000 feet

Wave Fronts or Rates of Rise of Lightning Arrester Discharge Currents

Wave fronts of currents discharged by lightning arresters in service have been measured by magnetic surge front recorders.[20] A few have been obtained with cathode-ray oscillographs.[21] Conclusions drawn from the available data are plotted in Figure 8. They are derived from the background data of Figure 9[8] and additional data accumulated later. Both figures indicate that the shortest fronts accompany low currents, such as curve *E* of Figure 9 for currents of less than 1,000-ampere crest, and the point on Figure 8 marked 28. This point signifies that out of 100 lightning arresters, 28 might discharge per year, currents whose crests are not more than 500 amperes with fronts of not more than 1 microsecond. Because of the low crest currents these records are not of practical interest in a consideration of the effect on lightning arresters or apparatus protected by lightning arresters. The rapid rise of current in the case of a large number of the low crest magnitude discharges results from the abrupt change in the surge circuit produced by the sudden sparking of the lightning arrester series gap.[8,9,21] The rate of rise of current in the system before lightning arrester sparkover can be considerably slower. It is thus not reasonable to lump all of the recorded wave fronts together in a statistical distribution curve and to apply this wave front curve to crest currents of all magnitudes. Some discretion must be used in estimating the probable wave fronts or rates of rise that are significant. Figure 8, compiled by A. M. Opsahl, presents the available data on a basis of probability as determined by the field test results.

Excluding the short front, low current discharges, the shortest fronts appear to be $1^1/_2$ microseconds. The highest lightning arrester current measured with this front is 7,900 amperes,[8] indicating an average rate of rise of about 5,000 amperes per microsecond. That is the highest rate of rise recorded so far. It is reported that rates of rise of 43,000 amperes per microsecond have occurred in strokes. The most significant curve of the statistical distribution of wave fronts is curve *C* of Figure 9, for above 5,000 amperes. From Figure 8 it appears that the probability of occurrence of 5,000 amperes per microsecond is two out of 100 lightning arresters per year in isokeraunic levels of 30 to 40, on the kinds of systems studied; subtransmission on wood poles with no shielding. The recording equipment was placed in locations where past experience had indicated that lightning disturbances were likely to be more severe than elsewhere. With a probability of two discharges per 100 lightning arresters per year on wood pole, unshielded lines the probability on shielded systems will be much less.

Calculations of the probability of 5,000 amperes per microsecond on high voltage, shielded systems[12] indicate that it may be from zero to five per 100 lightning arresters per year, depending on the shielding, the ground resistance, the insulation levels of the lines, and the lightning arrester ratings. The probability of zero applies to highly insulated (1,500 kv, $1^1/_2$×40) shielded lines with tower footing resistances of 10 to 20 ohms or less. The higher probabilities apply to lower insulated (500 kv, 1.5×40) shielded lines with tower footing resistances of 50 ohms. It is apparent that tower footing resistance plays an important part in this matter, and that it should be low, at

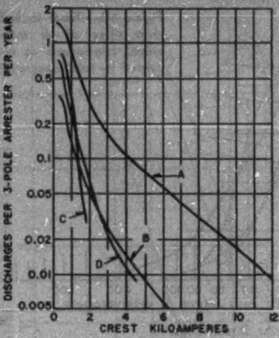

Figure 7 (above). Effect of shielding on number and crest magnitude of lightning arrester currents[3]

Curves show number of discharges per three pole lightning arrester year with crest current at least as great as abscissa

A. Wood pole lines without ground wires
B. Wood pole lines with ground wires
C. Steel tower lines without ground wires
D. Steel tower lines with ground wires

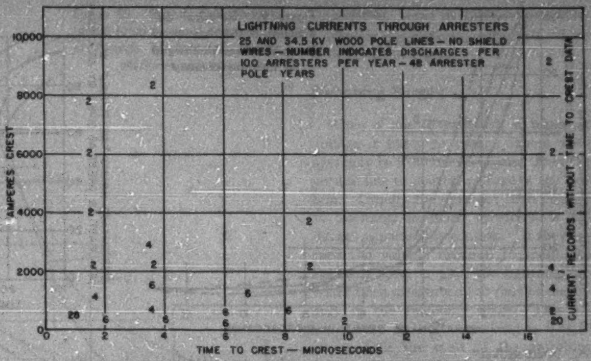

Figure 8. Probability of times to crest of lightning arrester discharge currents of various magnitudes

least for the first several towers out from the station.

There are several considerations that make the rate of rise of arrester discharge current of interest. They involve the discharge characteristics of valve lightning arresters and inductive drops in leads. The voltage across a valve element generally reaches its crest in a shorter time than the current. The actual voltage and its rate of rise for any practical discharge current can be determined in the laboratory from cathode-ray oscillograms. With the relation between lightning arrester discharge current and voltage known from test, the rates of rise of the currents, if they are of appreciable crest magnitude, give an indication of the front of the surge voltage produced at the lightning arrester by lightning. This may be important from the standpoint of the oscillations that may be set up at the terminals of protected apparatus. Furthermore, the crest value of the voltage across the valve element is a function of the rate of rise rather than the crest of the discharge current.[23] It should be noted, however, that the crest of the lightning arrester discharge voltage for steep rates of rise of current has only a short duration.

As far as it has been determined, the rate of rise of the discharge current does not affect the ability of valve lightning arresters to withstand severe discharges and interrupt power follow current.

Times to Half Crest Value of Lightning Arrester Discharge Currents

Two instruments have been used to record the general wave shape of lightning arrester discharge current; the fulchronograph,[29] later followed by the photo-recorder.[30] The limitations of the fulchronograph are that the individual links are spaced about 40 microseconds apart, so that fast fronts are not readily recorded. Also, the lower limit of sensitivity of the device is about 50 amperes. Its particular usefulness resides in its ability to record wave tails and multiple discharges of significant magnitude.

The photo-recorder is a current recording device of greater current sensitivity. It can record currents from 0.2 ampere to very high magnitudes. It cannot, however, distinguish very short time intervals. In this it is less sensitive than the fulchronograph. The usefulness of the photo-recorder is in its ability to record currents of long duration and low magnitude. It does not lend itself readily to the recording of wave fronts or times to half crest value.

Data from field records on the time from the beginning of discharge current to the point where the current has passed through its crest and decayed to half its crest value are given in Figure 10. On this figure is shown also the time to half value for currents in direct strokes. It appears that the median value for lightning arresters in stations is about 26 microseconds and that 80 per cent of the discharge currents had times to half value of not more than 40 microseconds. In the case of the 83 records obtained on distribution lightning arrester discharges, the times to half value were greater, the median value being about 40 microseconds and 80 per cent being not more than 75 microseconds. The times to half value of currents in direct strokes are in general longer than of currents in lightning arresters, although the curves for direct strokes and distribution lightning arresters are similar. There seems to be no conspicuous reason for the difference in times to half value between distribution and station lightning arresters shown in Figure 10, unless it be the fact that almost all of the records on distribution lightning arresters were obtained on delta systems, whereas most of the records on lightning arresters in stations were obtained on systems where the neutrals of the source transformers were grounded solidly or through resistance.

Total Durations of Lightning Arrester Discharge Currents

The total duration of the discharge currents as recorded by fulchronographs and photo-recorders are shown in Figure 11. In the case of the total durations recorded by fulchronographs, the duration is that time to the point where the current decays to 50 amperes or less, since the fulchronograph does not record currents lower than this. In the records obtained with the photo-recorder, it is the time to practically zero current. The photo-recorder data includes the power follow current, if present. Power follow current of valve arresters is not likely to appear on the fulchronograph. Of interest in Figure 11 are the greater durations recorded with the photo-recorder than with the fulchronograph, indicating

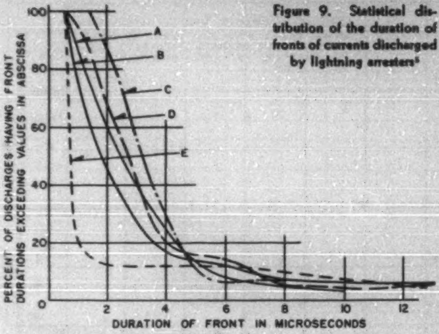

Figure 9. Statistical distribution of the duration of fronts of currents discharged by lightning arresters[5]

A. Direct strokes[16]
B. All lightning arrester records[5]
Discharges with crests:—
C. Above 5,000 amperes, 17 records
D. Between 1,000 and 5,000 amperes, 29 records
E. Between 0 and 1,000 amperes, 25 records

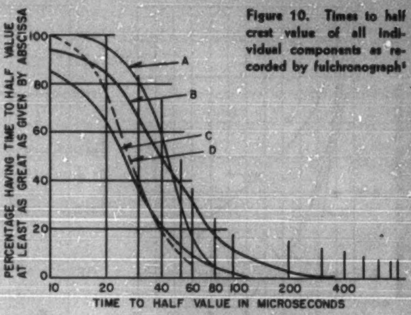

Figure 10. Times to half crest value of all individual components as recorded by fulchronograph[5]

A. Direct strokes[16]
B. Distribution lightning arresters, 83 records
C. Lightning arresters in stations, all records, 223
D. Lightning arresters in stations. Records with crests above 1,000 amperes only, 83

that there are likely to be tails below 50 amperes of some duration. The photorecorder data were obtained on two systems, both wood pole, unshielded; one with isolated neutral and the other grounded through resistance. Longer durations of lightning arrester discharge currents may be expected on such systems than on those effectively grounded.[15] The fulchronograph data were obtained on various systems, solidly grounded, isolated and resistance grounded.

The curves for currents in lightning arresters and direct strokes are similar, except that there are more currents in strokes of durations of several tens of thousands of microseconds, than there are in lightning arresters. The longest durations in lightning arresters were found on a distribution system of the Wisconsin Public Service Corporation, a delta system in a region of high soil resistivity. From the background data of the Wisconsin Public Service Corporation curve,[23] it appears that the maximum crest current recorded was 6,000 amperes, and that it was the discharges of relative low crest magnitude, 2,000 amperes or less that had the long durations.

Considering the fulchronograph data, it appears that 50 per cent of the discharges through lightning arresters in stations are above 50 amperes for not more than 80 microseconds, and about 5 per cent for more than 400 microseconds. In the case of distribution lightning arresters, excluding the Wisconsin data, 50 per cent have durations above 50 amperes for not more than 200 microseconds and 5 per cent may exceed 4,000 microseconds. The maximum durations recorded with the fulchronograph in Wisconsin were no longer than recorded through distribution lightning arresters elsewhere, but 50 per cent of the Wisconsin records exceeded 4,000 microseconds and 5 per cent exceeded 7,000 microseconds.

Coulombs Discharged by Lightning Arresters

The coulombs discharged by lightning arresters in service can be determined by integration of the discharge current waves. In some cases they have been recorded by means of the magnetic integrator.[20]

The available data indicate that the charge in most cases varied between a small fraction of a coulomb and about one coulomb. One record was obtained which indicated 3.7 coulombs in a lightning arrester in a station on an isolated neutral system. It is, however, not certain that this record was one discharge or consisted of more than one superimposed on the fulchronograph. On the Wisconsin distribution system eight records were obtained indicating charge greater than 1 coulomb, three of which barely reached 1.5 coulombs. Two of these last three were associated with crest currents of less than 1,500 amperes and the third with a crest current of slightly over 6,000 amperes. In the Wisconsin investigation it was indicated that charges of more than one coulomb associated with crest currents of less than about 2,000 amperes damaged the distribution valve type lightning arresters on which the measurements were carried out, whereas similar charges associated with crest currents of 4,000 amperes or more did not,[23] suggesting that lightning arresters of this type are more vulnerable to low currents of long duration than high currents of short duration, with the same charge. This has been indicated by laboratory tests. On the other hand, it was later found that on the Wisconsin system crosses occurred between the ungrounded distribution system and a 69-kv circuit on the same poles. It was concluded that at least some of the lightning arrester damage was caused by this. Furthermore, it is possible that the coulombs registered may have been influenced by such crosses. The Wisconsin data therefore cannot be regarded as conclusive, in respect to coulombs and damage to distribution lightning arresters. No records other than those obtained in Wisconsin were associated with damage to modern lightning arresters.

The charges involved in direct strokes are considerably higher.[16] About 50 per cent of the strokes have at least 9 coulombs, and a total charge of more than 160 coulombs has been reported. Except for discharges of few components and short duration, resulting in small amounts of charge, the great preponderance of the total charge occurs during the flow of the continuing stroke current of low magnitude. The high current peak portion of a stroke current may be 100,000 amperes or more, but its duration is too short to involve more than a few coulombs.[16] This fact may account to a large measure for the lower coulombs found in lightning arresters, since it is likely that the low current tails are drained away through paths other than a lightning arrester, or that the lightning arrester ceases to discharge before the surge on the system is exhausted.[24]

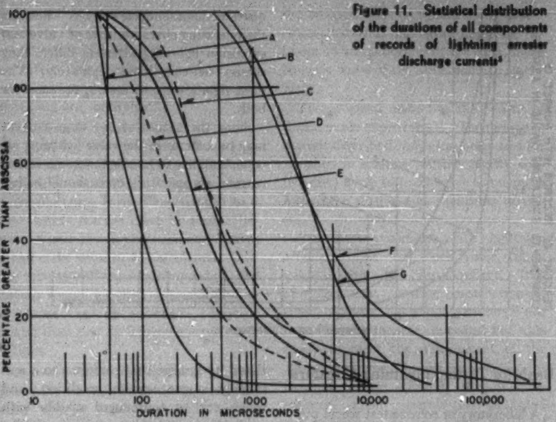

Figure 11. Statistical distribution of the durations of all components of records of lightning arrester discharge currents[4]

I. As measured by fulchronograph, sensitivity 50 amperes:

A. Direct strokes,[18] 123 records

B. Lightning arresters in stations. All records, 268

C. Wisconsin Public Service Corporation, distribution lightning arresters, 56 records

D. Other distribution records, 41

E. All distribution records, 97

II. As measured with photo recorder, sensitivity 0.2 ampere:

F. Direct strokes,[18] 30 records

G. Lightning arresters in stations, 137 records

Multiple Discharges

Multiple or repetitive discharges are those that have more than one impulse or well defined crest occurring in the same disturbance. The several crests are called components. Between these components the current may actually cease, or there may be a continuing current of low magnitude. The available data on the statistical distribution of the numbers of components in lightning arrester discharges are given in Figure 12. It is possible that some of the components considered to occur in the same discharge actually occurred in separate discharges. However, after considering the probability of this it is believed that the curves of Figure 12 are reasonably representative. The data plotted in Figure 12 were obtained on lightning arresters in stations. The data secured on distribution lightning arresters are not included. Since it was not practical to service the distribution lightning arrester installations as frequently as those in stations, the distribution records were not considered sufficiently significant to use. The installations in stations were serviced on the average of once a week and usually after every storm.

Comparison between the sets of data obtained with the fulchronograph and the photo-recorder show more components for the photo-recorder. This may indicate components of less than 50-amperes crest, not detected by the fulchronograph, or some of the apparent components may be the result of system disturbances such as those mentioned in the section under Frequency of Lightning Arrester Discharges. As far as duty on the lightning arresters is concerned, the fulchronograph curve is considered the significant one. On this basis, about half the discharges may have more than one component and 5 per cent may have more than seven.

General Comparison of the Characteristics of Currents in Strokes and in Lightning Arresters

Crest magnitude. Considerably less in lightning arresters. In general terms, ratio is about one to ten.

Duration of front. About the same in lightning arresters as in strokes.

Rate of rise of current. Less in lightning arresters. Ratio is about one to ten.

Times to half crest value. Less in lightning arresters in stations than in strokes. Roughly the same in distribution lightning arresters as in strokes.

Total duration. Fulchronograph records less in lightning arresters in stations than in strokes. Slightly less in distribution lightning arrester than in strokes.

Coulombs. Less in lightning arresters.

Number of significant components. Less in lightning arresters.

Switching Surges

When a line is switched, a transient voltage is likely to occur. These voltages may be from one to several times the normal line to neutral voltage of the system. Usually they are not high enough to discharge lightning arresters, or endanger apparatus insulation. If they exceed the voltage required to spark the lightning arrester gap, the lightning arrester must dissipate all or part of the energy in the switching surge. This energy, very generally speaking is $0.5CE^2$ where E is the crest of the switching surge voltage. If a lightning arrester discharges on a switching surge, the discharge current is of low crest magnitude with a long tail. It may be said to be similar to a low, long duration, lightning discharge.

Power Follow Current

A distinction must be made between the duty imposed by power follow current on valve and expulsion lightning arresters. In the case of the valve lightning arresters, the magnitude of the power follow current is independent of the short circuit capacity of practical systems. It is determined by the 60-cycle voltage across the lightning arrester terminals and on the relations of the instantaneous values of the surge and 60-cycle voltage across the lighting arrester during discharge. The latter factor will influence also the duration of the power follow current. Usually the duration of power follow in a valve lightning arrester, if the 60-cycle voltage applied to it does not exceed the lightning arrester voltage rating, is less than a half cycle. It may vary between zero and almost a half cycle depending on the already mentioned relation of surge and system voltage waves. Lightning arresters usually do not have 60-cycle voltage equal to their rating impressed on them, except in laboratory tests or during abnormal system voltage conditions. Records obtained with the photo-recorder indicate that occasionally the power follow current may persist for more than a half cycle without damage to the lightning arrester. The background data obtained with the photo-recorder, used to derive the curves of Figure 11, show that only 25 per cent of the component discharges had power follow durations approaching a half cycle or more of 60-cycles; 75 per cent were less. On one system, with isolated neutral, three records indicated power follow

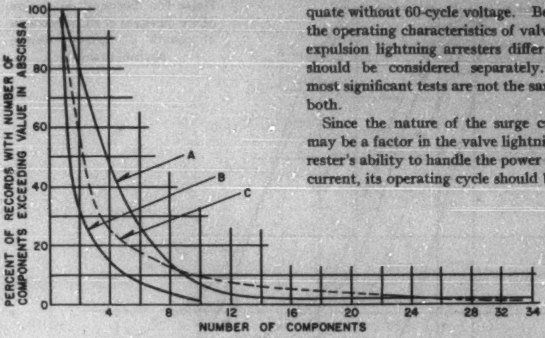

Figure 12. Statistical distribution of numbers of components in records of lightning arrester discharge currents[5]

A. Measured with photo recorder, sensitivity 0.2 ampere, 31 records

B. Measured with fulchronograph, sensitivity 50 amperes, 228 records

C. Direct strokes[18]

current of three half cycles and six of two half cycles. On a similar system grounded through resistance and located in a different part of the country, two records of amost three half cycles and two of two half cycles were obtained.[5] This may result from a long continuing discharge, or a multiple discharge, or restriking in the lightning arrester. Restriking in the lightning arrester may be caused by 60-cycle voltage across the lightning arrester in excess of its rating, not unlikely on isolated or resistance grounded systems.

Generalized Wave Shape of Lightning Arrester Discharge Currents

It is evident from the recorded data that the characteristics of the surge currents discharged through lightning arresters in service vary widely. There is no fixed duty for these devices. Figure 13 is an attempt to present a generalized wave shape with values that are thought to be significant. It is quite possible that when more data accumulate changes in the values may be in order. For the time being Figure 13 seems a representative aggregate of the expected discharges.

Basis for Testing Lightning Arresters

A laboratory or routine test whose purpose is to verify the ability of a lightning arrester to withstand severe service should involve discharging the lightning arrester by a surge of some severity while the lightning arrester is connected to a source of 60-cycle voltage so that power follow current will flow. This is the so-called operating duty cycle test referred to in AIEE and NEMA standards for lightning arresters. Tests with surge current alone, with the lightning arrester not connected to a 60-cycle source, do not have sufficient significance. Tests made to verify the impulse protective characteristics of lightning arresters, that is, the voltages that appear across their terminals when discharged by surges, are adequate without 60-cycle voltage. Because the operating characteristics of valve and expulsion lightning arresters differ, they should be considered separately. The most significant tests are not the same for both.

Since the nature of the surge current may be a factor in the valve lightning arrester's ability to handle the power follow current, its operating cycle should be initiated by a surge that conforms to a reasonably severe service condition, and which can be reproduced readily with available surge testing equipment. The 60-cycle voltage applied to its terminals should be equal to the lightning arrester voltage rating. The short circuit capacity of the 60-cycle source should be sufficient to maintain at least 90 per cent of the open circuit voltage during the flow of power follow current. This conforms with existing standards. In view of the severe duty imposed on valve lightning arresters by long surges, the discharge current used should have a long duration.

The most substantial lightning arresters are those identified as station type lightning arresters. The duty cycle tests on these should be more rigorous than on line or distribution types. AIEE and NEMA standards presently prescribe a duty cycle test for station lightning arresters of 30 discharges with 60-cycle voltage connected, using a surge current of 10,000 amperes crest and 10 by 20 microsecond wave shape. This test is not representative of the conditions with which lightning arresters of this type may have to contend because the duration of the surge current is not long enough. The present test is no longer a criterion that distinguishes between lightning arresters of the station and other types, nor is it indicative of what modern station type lightning arresters will do. The standards also require a surge discharge of 100,000 amperes crest of 5 by 10 wave shape with no 60-cycle voltage connected. This is impressive but not as significant as a lower current of relatively long duration with 60-cycle voltage. It is suggested that this requirement for valve lightning arresters be discarded.

This paper proposes that a different discharge current be used for the purpose of verifying the ability of station type light-

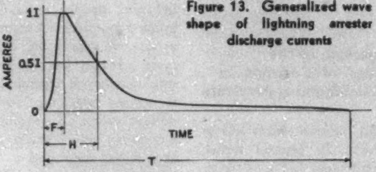

Figure 13. Generalized wave shape of lightning arrester discharge currents

I. Crest currents from less than 100 amperes up

	Distribution and Station	Station Only
Median Value	830 a	710 a
1,500 a or more	32%	27%
5,000 a	8	5
10,000 a	2.5	1.15
20,000 a	0.6	0.2

F. Fronts, 1.5–25 microseconds (μs). Durations of fronts increase with currents; maximum recorded rate of rise, about 5,000 amperes per μs

H. Times to half value from less than 10 to 75 μs. Median value for arresters in stations, 26 μs; for distribution lightning arresters, 40 μs

T. Total significant durations 40–10,000 μs. Median for lightning arresters in stations, 80 μs; for distribution lightning arresters, 200 μs ning arresters to stand up under the demands of service, and to classify the several types of lightning arresters more accurately than is now the case, so that purchasers may have a clear picture of what they are specifying.

Consideration must be given to laboratory facilities and problems. It is suggested that the crest magnitude of 10,000 amperes be retained, but that the shape of the discharge current be changed to a wave which reaches crest in a time between 5 and 15 microseconds and decays to half crest value in 45–60 microseconds. The time to half value corresponds to the median found for distribution lightning arresters, which is about 50 per cent greater than that for lightning arresters in stations.

In power follow testing the total duration of the wave through the lightning arrester will be determined both by the surge circuit constants and by the 60-cycle power source in parallel with the lightning arrester. An energized transformer shunting the arrester is a circuit with inductance and resistance and will discharge some of the long tail of a surge.[15] In defining the total duration of the surge discharge through the lightning arrester this must be taken into account. Therefore it is recommended that the source of power follow be a two winding transformer. The technique of determining the total duration is to connect the secondary of the transformer to the test specimen's terminals, to disconnect the primary from the source of power, to short circuit the primary to simulate a source of low impedance, and then to discharge the surge generator into this circuit. The duration of the discharge through the lightning arrester can be measured with a cathode-ray oscillograph either by recording current or voltage. It is recommended that measured in this manner, the total duration of the surge current actually discharged through the lightning arrester be not less than 600 microseconds. Testing with such surges has indicated that with the transformer disconnected from the lightning arrester, the total duration of the discharge is well over 2,000 microseconds.

During the actual duty cycle test, the short circuit is removed from the transformer primary and it is connected to a 60-cycle source. The present standards specify 30 operations. From Figure 6 this number may appear excessive. However, probabilities are involved to a high degree, multiple discharges and switching surges occur, and modern arresters are quite able to handle the situation. Therefore it is recommended that the 30 operations be retained. It is recommended that the firing angle be between 15 and 0 degrees of the crest of the 60-cycle wave of the same polarity as the surge.

The proposal made has the benefit of considerable experience.[15] The discharge current described above has been used for 15 years in making routine quality control duty cycle tests on valve elements of Autovalve station type lightning arresters.

The field experience with lightning arresters built with such surge tested valve elements has been excellent. It is of interest that on earlier constructions of these station lightning arresters, not tested in the manner described but able easily to meet the requirement of the 100,000 ampere 5 by 10 wave, sufficient cases of damage occurred to cause some concern. Field research then indicated the importance of long tailed surges of lower magnitude and led to the adoption of a rigorous routine duty cycle testing procedure.

To summarize the proposed test criterion for station type lightning arresters, it is suggested that it be a duty cycle test, with the test specimen connected to a source of 60-cycle voltage equivalent to its rating. The number of operations suggested is 30, with the firing angle 15–0 degrees ahead of the crest of the 60-cycle voltage of the same polarity as the surge. The proposed discharge current is one with a crest of 10,000 amperes, a front of 5–15 microseconds, a time to half value of 45–60 microseconds, and a total duration determined as discussed earlier of not less than 600 microseconds.

The test is suggested as a design verification test. It is not recommended that test specimens subjected to it be put in service, because of the severity of the test. The life of a lightning arrester subjected to such duty cycles will not be unlimited.

For line and distribution lightning arresters it is suggested that a similar, modified, surge be adopted. It might be a lower current, a shorter time to half value and duration, or fewer discharges. Although the field data indicate that the probability of severe duty may be greater in the case of distribution lightning arresters, it is not practical to expect distribution or line lightning arresters to withstand tests as severe as those which station lightning arresters will handle. The station lightning arresters are expected to be the most durable and most effective arresters that can be made economically. The others are smaller and less expensive.

The foregoing tests are not intended to check the protective characteristics of valve lightning arresters. For this purpose it is believed that the 10 by 20 microsecond waves now prescribed in standards are adequate.

In the case of expulsion lightning arresters, the power follow current is of major importance. It is influenced by numerous factors such as the short circuit capacity and recovery voltage of the system, the location of the lightning arrester, its characteristics, the power factor of the follow current circuit including the lightning arrester, and the electrical angle of the 60-cycle voltage at which it is fired. These conditions vary in service. The subject is discussed in reference 1. The present paper does not attempt to make any recommendations except that the duty cycle tests for expulsion lightning arresters be different from those for valve lightning arresters.

Appendix I. The Probability Curves, Figures 5(A) and 5(B)

The method of plotting the curves of Figures 5(A) and 5(B) with their confidence envelopes, the meaning of the confidence envelopes and the conclusions that can be drawn from such curves are discussed in references 17 and 18. Normal chance distribution is indicated if the data fall on a straight line when plotted on probability graph paper. The distributions of the amperes of crest current, curves *A*, *B*, and *C* of Figures 4 and 5(A) and 5(B) are not straight lines. However, the distributions of the logarithms of the currents, A', B', and C' are straight lines and therefore indicate a normal distribution. In Figure 5(A), the high currents appear to deviate from the line A'.

The confidence envelopes for a probability level of 0.95, shown by the dashed lines above and below the curves of the logarithms, are derived from the data[18] and, as the term indicates, denote the degree of confidence with which the data may be regarded. They signify that in 100 investigations of the kind made, the data from at least 95 would fall within the confidence zone, or that for one additional set of data, the chances would be 19 to 1 that it would fall within the zone.

The confidence envelopes for A' and B' do not overlap at currents higher than about 100 amperes. Therefore it may be assumed that there is a significant difference between these two sets of data. A', B', and C' being straight lines, extrapolation to higher currents than any recorded by extending the lines appears justified. However, a question is posed by the observation that the highest points of A' lie outside of its confidence zone. It appears that the logarithms for currents higher than 20,000 amperes may have a different distribution, lying on another straight line A'', and that their probability of occurrence may be less than one would expect from the considerable volume of data at lower currents. There is, on the other hand, the possibility that the high currents recorded reached the limit of sensitivity of the recording devices, and that the actual currents may have been higher than indicated. This would tend to put the measurements into the confidence envelope.

All of the data are gathered together into one curve, *C'*, in Figure 5(B). The same tendency is discernible at the high currents, although now the points lie within the confidence zone for *C'*. Apparently, in the region above 20,000 amperes some speculation will be involved until there is available a larger volume of data at those currents. However, some conjectures seem warranted. After considering Figures 5(A) and 5(B), the possibility of a lower probability of currents above 20,000 amperes than indicated by *A'* or *C'*, and the limitations of our present knowledge, it is concluded that *C'* is reasonably representative of the distribution of the lightning arrester discharge current crests for all lightning arresters. Curve *C'* passes through the logarithm 5, corresponding to 100,000 amperes, at the probability of about 0.007. This is seven in 100,000 or one in 14,300 discharges. Since the confidence envelope boundaries pass through the probabilities of 0.012 and 0.005 at this same logarithm, the probability might be, in 95 cases out of 100, 12 or five in 100,000. Considering the trend indicated by the line *A"* of Figure 5(A), even the probability of five discharges of 100,000 amperes or more in 100,000 may be too high. Nevertheless, it is probably safer to err on the high than on the low side, consequently *C'* is assumed to be the distribution.

References

1. THE POWER INTERRUPTION TESTING OF LIGHTNING ARRESTERS, **Otto Ackermann.** *AIEE Transactions*, volume 70, part 1, 1951, pages 1–7.

2. REPORT ON STANDARD FOR VALVE AND EXPULSION TYPE LIGHTNING ARRESTERS, AIEE Standard number 28A, February 1950.

3. SURGE CURRENTS IN PROTECTIVE DEVICES, **A. M. Opsahl.** *Electrical Engineering* (*AIEE Transactions*), volume 54, February 1935, pages 200–04.

4. FIELD INVESTIGATION OF THE CHARACTERISTICS OF LIGHTNING CURRENTS DISCHARGED BY ARRESTERS, **I. W. Gross, G. D. McCann, E. Beck.** *AIEE Transactions*, volume 61, 1942, pages 266–71.

5. FIELD RESEARCH ON LIGHTNING ARRESTER DISCHARGES, **G. D. McCann, E. Beck.** *AIEE Transactions*, volume 66, 1947, pages 625–29.

6. DISCHARGE CURRENTS IN DISTRIBUTION ARRESTERS, **K. B. McEachron, W. A. McMorris.** *Electrical Engineering* (*AIEE Transactions*), volume 57, June 1938, pages 307–14.

7. LIGHTNING INVESTIGATION ON A RURAL DISTRIBUTION SYSTEM, **D. A. MacCarthy, D. A. Stann, D. R. Edge, W. C. McKinley.** *AIEE Transactions*, volume 68, 1949, pages 428–37.

8. LIGHTNING INVESTIGATION ON THE 25 KV SYSTEM OF THE WEST PENN POWER COMPANY, **William C. Bowen, Edward Beck.** *AIEE Transactions*, volume 66, 1947, pages 831–6.

9. LIGHTNING CURRENTS IN ARRESTERS IN STATIONS, **I. W. Gross, W. A. McMorris.** *AIEE Transactions*, volume 59, 1940, pages 417–22.

10. LIGHTNING INVESTIGATION ON 33 KV WOOD POLE LINES, **F. E. Andrews, G. D. McCann.** *AIEE Transactions*, volume 64, 1945, pages 768–77.

11. AN EIGHT YEAR INVESTIGATION OF LIGHTNING CURRENTS AND PREVENTIVE LIGHTNING PROTECTION ON A TRANSMISSION SYSTEM, **E. Hansson, S. K. Waldorf.** *AIEE Transactions*, volume 63, 1944, pages 251–8.

12. *Discussion* by **C. F. Wagner** of BASIC IMPULSE INSULATION LEVELS FOR HIGH VOLTAGE SYSTEMS, **J. E. Clem, J. R. Meador, W. J. Rudge, A. H. Powell.** *AIEE Transactions*, volume 69, part II, 1950, pages 953–60.

13. THE SURGE CREST AMMETER, **C. M. Foust, H. P. Kuehni.** *General Electric Review* (Schenectady, N. Y.), volume 35, 1932, page 644.

14. LIGHTNING CURRENTS IN FIELD AND LABORATORY, **P. L. Bellaschi.** *Electrical Engineering* (*AIEE Transactions*), volume 54, August 1935, pages 837–43.

15. LIGHTNING AND LIGHTNING PROTECTION ON, DISTRIBUTION SYSTEMS, **R. C. Bergvall, E. Beck.** *AIEE Transactions*, volume 59, 1940, pages 442–9.

16. THE MEASUREMENT OF LIGHTNING CURRENTS IN DIRECT STROKES, **G. D. McCann.** *AIEE Transactions*, volume 63, 1944, pages 1157–64.

17. GRAPHICAL STATISTICS—AN ENGINEERING APPROACH, **L. R. Hill, P. L. Schmidt.** *Westinghouse Engineer* (East Pittsburgh, Pa.), March 1950, page 121.

18. GRAPHICAL STATISTICS—AN ENGINEERING APPROACH, **L. R. Hill, P. L. Schmidt.** *Westinghouse Engineer* (East Pittsburgh, Pa.), May 1950, page 157.

19. LIGHTNING INVESTIGATION AT HIGH ALTITUDES IN COLORADO, **L. M. Robertson, W. W. Lewis, C. M. Foust.** *AIEE Transactions*, volume 61, 1942, pages 201–08.

20. NEW INSTRUMENTS FOR RECORDING LIGHTNING CURRENTS, **C. F. Wagner, G. D. McCann.** *AIEE Transactions*, volume 50, 1940, pages 1061–8.

21. FIELD INVESTIGATION OF LIGHTNING SURGES AT SUBSTATIONS, **I. W. Gross, G. D. McCann.** *AIEE Transactions*, volume 66, 1947, pages 569–76.

22. *Discussion* by **A. M. Opsahl** of BASIC IMPULSE INSULATION LEVELS FOR HIGH VOLTAGE SYSTEMS, **J. E. Clem, J. R. Meador, W. J. Rudge, A. H. Powell.** *AIEE Transactions*, volume 69, part II, 1950, pages 953–60.

23. FIELD INVESTIGATION OF LIGHTNING, **C. F. Wagner, G. D. McCann, E. Beck.** *AIEE Transactions*, volume 60, 1941, pages 1222–9.

24. *Discussion* by **E. Beck** of THE MEASUREMENT OF LIGHTNING CURRENTS IN DIRECT STROKES, **G. D. McCann.** *AIEE Transactions*, volume 63, 1944, pages 1157–64.

25. MEASURED LIGHTNING CURRENTS THROUGH DISTRIBUTION ARRESTERS ON 4800 VOLT RURAL CIRCUITS, **H. R. Wilbur, W. A. McMorris.** *General Electric Review* (Schenectady, N. Y.), volume 44, March 1941, page 159.

26. LIGHTNING CURRENTS MEASURED, **H. W. Collins.** *Electrical World* (New York, N. Y.), May 12, 1934.

Discussion

W. A. Sumner (Westinghouse Electric Corporation, Sharon, Pa.): We are glad to note that Mr. Beck recognizes the merit of the high surge current test for expulsion lightning arresters and finds that it is a good criterion for this type of lightning arrester. From a close field follow of expulsion lightning arresters mounted in distribution transformers, representing some 2,500,000 lightning arrester years and representing a nation-wide distribution, much of which experience was associated with rural lines having severe lightning exposure, we agree, in general, with the trend as shown for the "Probable Frequency of Occurrence for Lightning Arrester Discharge Current Crests," as set forth in Figure 6. However, our data would indicate that the frequency of occurrence of the heavier currents in the range of 65,000 to 100,000 amperes might be appreciably greater than shown in the curve. It is true that one stroke per year at 65,000 amperes for each 4,000 lightning arresters, or 0.025 per cent per lightning arrester year, is a relatively small figure. However, when one considers the volume with which these expulsion lightning arresters are manufactured for distribution transformer application, it is realized that a high state of perfection is required. We, therefore, consider it essential to maintain at least the present 65,000 surge ampere requirements for these distribution-type expulsion lightning arresters.

O. Ackermann (Westinghouse Electric Corporation, East Pittsburgh, Pa.): Only a rather short section of Mr. Beck's paper is allotted to power follow, mainly because valve-type lightning arresters limit this current to a very small amount compared to their surge discharge capacity. That the matter is quite different with expulsion-type lightning arresters is indicated but briefly by the author. The subject is, however, all important as far as the service life of expulsion lightning arresters is concerned; therefore I wish to enlarge on this point at least in a discussion to the paper on lightning arrester duty.

Expulsion lightning arresters do not limit power follow current nearly as much as the valve type; in fact, many of them limit it hardly at all. The latter in particular must therefore be designed to handle full system fault current for about one cycle at a time. For a 1,000-ampere rms fault, the flow of charge per cycle amounts to 15 coulombs. If one compares this with the figures reported to be critical to valve-type lightning arresters in Mr. Beck's paper, one comes to realize that expulsion lightning arresters, built to handle power flow are not sensitive to surge discharges. On the other hand, current flow in the expulsion type is accompanied by the consumption of gas producing material. Therefore, the weight of the question of service duty is shifted from the characteristics of lightning surges to the frequency and character of power follow operations.

Regarding lightning arresters for distribution service, the sparkover of expulsion and of valve types is nearly enough the same to warrant the conclusion that expulsion lightning arresters operate as frequently as valve arresters which, according to Mr. Beck is, on the average, about once per year. Another source of information, reporting expulsion lightning arrester operations only, is the lightning investigation paper by McCarthy and others.[1] Based on experience covering 4,054 expulsion lightning arrester years, that paper states that, on the average, an expulsion lightning arrester carries power follow 0.65 times a year, and that this power follow is restricted to one half cycle or less in all but 1 per cent of the cases. It is gratifying to note that the results of these two separate investigations are, as I am to show, surprisingly much alike.

It is well known that expulsion lightning arresters discharge surge currents without power follow if the surge occurs at times of low instantaneous power voltage. With many types of expulsion lightning arresters this region roughly covers the time within 30 electrical degrees of voltage zero, which is one-third of the total voltage cycle. As random surge discharges are distributed uniformly over the range of the voltage cycle, and as most of them last only a short part of such a cycle, one must conclude that only about two-thirds of them cause power follow. Hence, the 0.65 figure for yearly power follow operations per lightning arrester indicates that the total surge discharges per unit are about one per year; this checks Mr. Beck's estimate.

The American standards consider an expulsion lightning arrester to give satisfactory service if it is in acceptable operating condition after five test operations of the most severe kind. This most severe test condition is approached only if the lightning arrester discharge starts at an early moment in the voltage cycle. For any other moment, the follow current is lower in amplitude and shorter in duration. Therefore, lightning arrester life in terms of power follow operations is considerably longer with random firing than with firing timed for maximum severity discharge, even if the lightning arrester is installed at a location of maximum permissible fault current. If one appraises this effect by the factor of 2.5, the multiplication of all factors involved indicates that an expulsion arrester, installed at the most critical location permitted by its rating, has an average life of 19 years (1/0.65 × 5 × 2.5). Now, remembering that expulsion lighting arrester life increases about as the ratio of the maximum current rating to the available fault current, it is evident that, on the average, an expulsion lightning arrester has a service life well over 20 years just like any other piece of properly designed and applied distribution equipment.

It would, of course, be assuring if this contention could be proved by some sort of life test. I feel that this can be done and, therefore, I wish to conclude this discussion by calling attention to what I consider a significant life test for high current rating expulsion lightning arresters, applying to ratings of 6,000 amperes or more. It is testing at 90 per cent of rated lightning arrester voltage, and advancing the moment of firing by 80 electrical degrees for successive discharges. Tests of this nature are reported and discussed in the paper on the spiral groove lightning arrester[2] which also is being presented in this session.

REFERENCES

1. See reference 5 of the paper.
2. SPIRAL ARC CHOKES POWER FLOW IN NEW LIGHTNING ARRESTERS, Otto Ackermann, E. J. DeVal. *AIEE Transactions*, volume 70, 1951, pages 905–98.

H. A. Cornelius (Public Service Company of Northern Illinois, Chicago, Ill.): The author is congratulated for presenting a clear, comprehensive paper which discusses several topics of value to the industry.

The use of probability theory in regard to lightning arrester discharge currents, as has been done in this paper, should be quite helpful in providing forecasting data for users of lightning arresters.

The mention of 5,000-ampere discharge currents and rates of rise, the frequency with which they may be expected on shielded and unshielded lines, is of considerable interest. Figure 5(B) curve C, for example, shows the distribution of crest currents in valve-type lightning arresters in stations and at distribution transformers. This figure shows that 90 per cent of the surge currents discharged through lightning arresters are 5,000 amperes or less. Another measure of this 5,000-ampere co-ordination criterion is its frequency of occurrence. This is given in the paper as once in 13 years.

The analysis regarding the probabilities of having a rate of rise of 5,000 amperes occur is of considerable interest. However, the probabilities of having from 0 to 5 such rates of rise on shielded lines and 2 such rates of rise on unshielded lines per 100 lightning arresters per year, do not appear to be consistent. Perhaps more discussion of this point would clarify it.

Having a current discharge through a lightning arrester in a station of 65,000 amperes once in 4,000 years has been calculated and is shown in Figure 6 of the paper. An analysis of the field data made for another purpose corroborates this. That is, the records over many years show that only 0.5 of 1 per cent of the currents discharged are 30,000 amperes or more. On this basis, the use of duty cycle tests on valve-type lightning arresters of 65,000 or 100,000 amperes is much higher than necessary.

The statement is made that "both Figures 8 and 9 indicate that the shortest fronts accompany low currents." This is apparently based on 25 records shown in curve E of Figure 9 and on the 28 points with less than 2-microsecond fronts and magnitudes below 2,000 amperes. This does not appear to be sufficient data to use for such a conclusion.

The crest value of the voltage across a valve element is a function of the rate of rise of current rather than of the current crest value. Because of this characteristic behavior, what is the magnitude of the discharge voltage across a 37-kv station-type lightning arrester, for example, when it is subjected to a 5,000-ampere per microsecond, 5,000-ampere crest current, compared to what it would be on the standard 5,000-ampere, 10-microsecond front-test wave?

The proposed current, wave shape, and duration duty cycle test is a 10,000-ampere wave which reaches its crest in 5 to 15 microseconds and decays to half tail value in 45 to 60 microseconds, which is applied for 600 microseconds, with a 60-cycle power follow source connected to the lightning arrester. It is suggested that a 5-microsecond front, a 45-microsecond half tail and a duration of 600 microseconds would be more satisfactory to use from a users point of view.

Another related problem, which is not discussed, is the need for a low current, long duration test for valve-type lightning arresters. The author's comments on the use of a 300-ampere crest with a 4- or 5-microsecond front and half tail value at 1,000 microseconds would be appreciated.

J. W. Kalb (Ohio Brass Company, Barberton, Ohio): Mr. Beck's proposal should go far toward better defining lightning arrester performance with respect to actual service conditions. The field data cited and statistical analysis thereof offer convincing evidence for the generalized wave shape proposed in Figure 13 of the paper. It is in the application of this test wave that some question may arise.

The proposed timing of this impulse with respect to the 60-cycle voltage does not differ essentially from the present standard duty cycle test, that is, with the impulse and 60-cycle voltage of the same polarity. This may have been chosen originally because it was thought to be the most severe condition, but it is known now that this is not necessarily true.[1] Furthermore, natural lightning is apt to strike at any point on either polarity of 60-cycle voltage. Would it not be more representative to space the timing angle of each successive operation some value such as 15 degrees.

As in the existing standard duty cycle test, Mr. Beck is concerned with the ability of the valve element to withstand service conditions. The requirement of a high fault current 60-cycle supply circuit imposes the most severe duty on the valve element, but not necessarily the gap element. In such a circuit the follow current flow is limited almost entirely by the lightning arrester valve resistor, and the circuit recovery voltage appearing across the gap element at follow current zero is very low. In a lower fault current circuit the higher circuit reactance causes a greater disparity in time between follow current zero and 60-cycle voltage zero. The circuit recovery voltage, though still very low, is larger than in the high current test circuit. The multiple gaps' ability to withstand these very small recovery voltages determines the lightning arrester's ability to interrupt 60-cycle follow current.

A considerable proportion of lightning arrester failures in stations have been ascribed to excessive system voltage. This implies gap failure, admittedly under conditions of abnormally high follow current through the valve resistor element. Since severe system voltage conditions as well as abnormal lightning conditions impose severe duty upon the lightning arrester, should we not consider a test which explores lightning arrester performance under more severe recovery voltage conditions. Such a test could be an additional combined impulse and power voltage test using not a high fault current circuit, but one whose short circuit impedance was at least 3 ohms per kilovolt of arrester rating, predominantly reactive. Crest magnitude of the impulse current would be unimportant, but total duration should be in the order of 100 microseconds to start follow current easily. Polarity would be chosen as that at which follow current could be started at the earliest point on the voltage wave, or if preferred the timing could be spaced 15 degrees between operations as suggested above.

Mr. Beck has suggested an apparently logical change in the impulse wave shape used on the standard lightning arrester duty cycle test. The long tail portion is moderate enough to represent possible severe operating conditions even though a transformer winding will by-pass considerable long duration current from the lightning arrester. The preceding comments are merely for consideration in further increasing the usefulness of the duty cycle test.

REFERENCE

1. ESTIMATION OF LIGHTNING ARRESTER CHARACTERISTICS AND ASSOCIATED MEASUREMENT PROB-

LEMS, Bror Svensson. *Report 337*, International Conference on Large High-Voltage Electric Systems (Paris, France), 1946.

Arthur R. Koerber (General Electric Company, Pittsfield, Mass.): Mr. Beck has carefully reviewed field data from many independent sources and has suggested a composite impulse test wave shape to be used in combination with power. A test, similar to this, that combines a long-duration impulse wave such as encountered in service with a duty cycle test would be highly desirable.

Any test to be used as a basis for standardization should be easily duplicated in different laboratories and should not require complex specifications to insure identical test conditions.

Mr. Beck specifies that the duration of the impulse discharge be determined with the primary of the power transformer short circuited to simulate a source of low impedance. In making the actual test, however, the reactance of the power source is, of course, inserted in the circuit. This additional reactance increases the duration of the impulse discharge. Since the reactance of the power source will not be the same for different laboratories, the duration of the impulse used in the actual test will vary from laboratory to laboratory, making the severity of the test nonuniform.

The principal difference between the proposed test and the present standard duty cycle test is the long-duration tail of the impulse wave. The amplitude of the tail of the impulse current wave should be more exactly defined than to simply state that the total duration of the surge current actually discharged through the lightning arrester be not less than 600 microseconds with the primary of the test transformer short circuited.

Past attempts to combine long-duration impulse and power have led to considerable difficulty due to the interaction between the impulse and power circuits. Svennson reported in 1946 that this interaction directly affects the severity of the duty on the arrester.[1] Our tests have confirmed his results. Furthermore, this interaction is dependent upon the test circuit constants which can be varied without departing from Mr. Beck's specifications.

Although Mr. Beck may have used this test for some time, it would appear that more study is necessary to arrive at a set of specifications which will insure that different laboratories, using impulse generators and power circuits with different constants, can obtain equivalent results.

To demonstrate the adequacy of lightning arresters to handle long-duration discharges, we have proposed,[2] in addition to the present standard test, a long-duration surge-withstand test for station-type lightning arresters. This test consists of 20 successive applications of a surge having an essentially constant magnitude of 150 amperes (less than 10 per cent decrement), to be maintained for at least 2,000 microseconds. This test wave is believed to be a fair representation of the long-time low-current discharge resulting from lightning or switching surges. The present standard discharge current withstand test together with the proposed long-duration test should demonstrate the adequacy of the discharge capacity of the lightning arrester at both extremes expected in the field, the high-current short-duration component and the low-current long-duration discharge.

If specifications can be drawn up for the combined long-duration power test which will permit all laboratories to obtain uniform results without these specifications becoming overly complex, then such a combined test should be reconsidered by the industry.

REFERENCE

1. See reference 1 of preceding discussion.

2. LONG DURATION SURGE TESTING OF LIGHTNING ARRESTERS, S. B. Howard, T. J. Carpenter, H. Schwartz. *AIEE Transactions*, volume 70, 1951, pages 1487–92.

R. H. Mertz (The Detroit Edison Company, Detroit, Mich.): My discussion resolves itself in the form of a question which the operator is confronted with after the lightning arresters have seen some service.

Let us assume that the lightning arresters have been built to meet the conditions suggested by Mr. Beck. They have had, let us say, ten years of service, they are then removed for some reason such as a rebuilding operation. What tests are necessary to determine if they are satisfactory for reuse?

For present types of 6-kv distribution lightning arresters that have been removed from service, we are thinking in terms of an impulse of around 100 kv, 2,000 amperes and a power follow current of 400 amperes. No wave-shape control. Is this sufficient current to determine if the lightning arrester is satisfactory for reuse?

H. L. Rorden (Bonneville Power Administration, Portland, Oreg.): In recent trends for reduction of insulation levels for the transmission of power at high voltages, lightning arresters have been recognized as the protective device upon which the insulation levels are based. Major economies can be achieved by establishing as close a margin as is feasible between basic insulation levels and the levels to which lightning surges may be limited by protective devices. This becomes of increasing importance with the higher voltages.

If lightning arresters are to become a major part of our scheme of protection, the system designer must know the limitations as well as the protective characteristics of lightning arresters that are to be used on his system. Mr. Beck's paper contains a vast amount of information useful to the system designer which has not been previously available to the industry, and which can only come from one who has devoted a major effort to understanding the performance characteristics of lightning arresters. We are particularly impressed with his suggestions and recommendations for duty cycle tests and his discussion of power-follow currents. Data of this nature are necessary in the application of lightning arresters if the system designer is to provide adequate protection without excessive and too conservative margins, which in turn dictate high and expensive insulation levels.

We believe that Mr. Beck's suggestions, particularly those recommending a long-wave duty-cycle test and elimination of the high-current short-time tests, should be considered for inclusion in national standards. The power-follow current that a lightning arrester can be expected to withstand has always been an interesting question. Mr. Beck has included data that should be helpful in determining the degree of risk that a user may anticipate for dynamic overvoltages.

It has been the experience of the Bonneville Power Administration that lightning arrester failures rarely occur from lightning, and that the greatest hazard is the dynamic transients that exceed the lightning arrester rating. We find that lightning arresters are most susceptible to failure from (1) dynamic overvoltages of short duration but of high enough magnitude to flashover the lightning arrester series gaps, or (2) dynamic overvoltages of relatively long duration which do not flash over the series gaps but result in excessive heating of the lightning arrester blocks. Voltages in the first category may occur from unusual switching surges or from faults on delta-connected systems. Voltages of the latter type may occur from overspeed accompanying load rejection.

Good economy dictates that some degree of risk must be assumed in balancing cost versus the degree of protection. We would appreciate Mr. Beck's comments relative to these hazards and the probability of lightning arrester failure from them.

E. Beck: The discussions by Sumner and Ackermann are useful contributions to the information needed to develop satisfactory tests for expulsion-type distribution lightning arresters. We have no comments to make except to suggest that more detailed discussion of a proposal for practical test criteria for these lightning arresters would be of value to the standardizing committees.

The discussion by Cornelius raises several questions. One pertains to the probabilities of rates of rise of lightning arrester discharge current of 5,000 amperes or more per microsecond on unshielded and shielded systems. It is well that this question is raised because the wording of the paper is not exactly clear on this point. The paper states that on shielded lines the probabilities of such steep currents are less than on unshielded systems. This was intended to apply to very well shielded systems where the probability of back flashes from the shield wires to the conductors is negligible. In another paragraph of the paper the statement is made that on high-voltage shielded systems the probability of lightning arrester discharge currents of 5,000 or more amperes per microsecond may be from zero to 5 per 100 arresters per year. These figures might indicate off hand that on shielded systems there can be a greater probability of steep currents than on unshielded systems, which, as Cornelius points out, is not consistent. The shielded systems with a higher probability of steep lightning arrester currents are not well shielded. The analysis made by C. F. Wagner, reference 12 of the paper, from which the data were taken, brings this out. Wagner calculated the probabilities of steep arrester currents on the basis of the probability of back flashes. If a back flash occurs, the voltage and current on the line conductors rise abruptly, more or less regardless of the rate of rise of current that the lightning has produced in the shield wires before the back flash occurs. Thus there

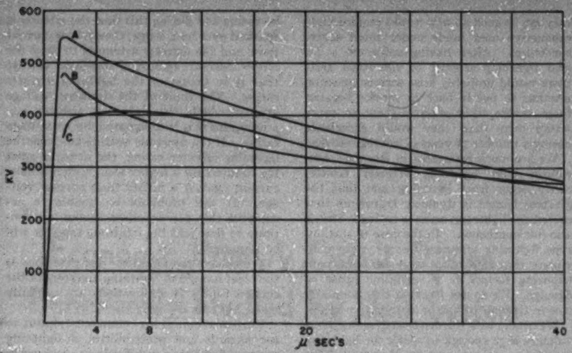

Figure 1. 121-kv station type autovalve lightning arrester. Discharge voltages for discharge currents of two different wave shapes, compared to basic impulse insulation level of 115-kv class

Curve A. 1.5×40 microsecond voltage, basic impulse insulation level of 115-kv class
B. Lightning arrester discharge voltage, discharge current of 4,800 amperes, 3×23 microseconds
C. Lightning arrester discharge voltage, discharge current of 4,800 amperes, 10×28 microseconds

may be a greater probability of steep arrester discharge currents in a poorly shielded system than in an unshielded one. As indicated by Wagner, the higher probabilities of steep currents are associated with systems that have overhead ground wires but lower insulation and higher ground resistances, on which back flashes are more probable. That low tower footing resistances in the vicinity of a station are highly desirable for this reason, is pointed out by Wagner and in the paper.

Cornelius questions the validity of the conclusions that the shortest fronts of lightning arrester discharge currents accompany low magnitudes of current. The data available indicate this to be so. It is recognized that the volume of data is not great. More data would be useful and we hope that more may be accumulated. The operators of transmission and distribution systems could contribute to such an accumulation of data. The conclusion is based on all the data that are available to the industry at present. There are certain considerations that also point toward the same conclusion, such as the one mentioned in the paper that when an arrester gap sparks, a sudden rise in current in the lightning arrester is to be expected, up to a magnitude depending on the characteristics of the lightning arrester and the voltage across the lightning arrester at the instant sparkover occurs. This is something like the case of a back flash from a struck shield wire to a line conductor. In a paper[1] by I. W. Gross and G. D. Lippert results are given of measurements on rates of rise of surge voltage. Figure 4 of that paper is of a special interest and indicates again the considerably greater prevalence of moderate rates of rise over steep ones.

Cornelius asks for the magnitude of the discharge voltage of a 37-kv station-type lightning arrester while discharging a current with a rate of rise of 5,000 amperes per microsecond, with a crest of 5,000 amperes. Before replying to this question we wish to make the following remarks. The meaning of rate of rise of discharge current should be defined accurately. A discharge current as described is difficult to obtain in the laboratory. From certain available data we do not think that the current crest has much, if any, effect on the crest of the discharge voltage provided the initial rate of rise of current is held constant. We urge caution in using crest magnitude of discharge voltage without consideration of the wave shape in relating lightning arrester performance to insulation withstand strength because insulation withstand strength, basic impulse insulation level, is itself defined on the basis of both crest and wave shape. We estimate that an initial rate of rise of 5,000 amperes per microsecond will produce, in a 37-kv Autovalve station-type lightning arrester, a discharge voltage crest of the order of 147 kv. This is about the same as the voltage crest produced by a 10 by 20 discharge current of 20,000 amperes crest, although the discharge voltage wave shapes will be different.

It is not recommended that the crest voltage just estimated be used as a basis for comparison with insulation. For this purpose the discharge voltages obtained with the 10 by 20 current wave now standard are more suitable. The change in both crest and wave shape of the voltage produced by change in the time to crest of the discharge current is shown by A. M. Opsahl in reference 22 of the paper. In Figure 1 of this discussion, Opsahl's data are used to plot the discharge voltages of a 121-kv Autovalve station-type lightning arrester with two discharge currents, both of 4,800 amperes crest but with different wave shapes as indicated in the figure's caption. The 1.5 by 40 wave of voltage that designates the basic impulse insulation level of 115-kv class insulation is shown for reference. Comparing curves *B* and *C* with *A* and considering the areas under them it appears likely that there is actually less margin between *C* and *A* than between *B* and *A*. From this standpoint alone the 10 by 20 wave of discharge current should be preferable because it produces discharge voltages which in magnitude and wave shape seem to approximate the severity of the 1.5 by 40 voltage wave that determines the insulation level of equipment.

Cornelius suggests that instead of the discharge current wave shape proposed in the paper for the duty cycle test, a wave shape of 5 by 45 microseconds with a total duration of 600 microseconds would be more satisfactory from the users' point of view. We have no particular comment on this although we would question why this wave should be more satisfactory. We would like to point out that in arriving at these tests, there are some limitations as to what can be done in laboratories and routine test floors. The wave shape proposed in the paper has been used for a number of years and it seems to satisfy the criterion that is really the most important; that is, that lightning arresters which meet these tests give good service in the field.

We are not entirely convinced that tests in addition to those proposed in the paper are necessary to control the performance of lightning arresters and to differentiate between the different types. We would however, go so far as to say that a low current long duration test of perhaps the general order proposed by Cornelius at the end of his discussion has more significance than the 65,000- and 100,000-ampere test now specified for valve lightning arresters in standards. We are of the opinion that the 65,000-ampere tests should be retained for distribution-type expulsion lightning arresters but we think these high current tests might well be discarded in the case of the valve lightning arresters.

Kalb raises several points of interest in reference to the tests. The firing angle suggested in the paper was proposed because its use in such tests over a number of years[2] has resulted in good service experience indicating the test procedure to be a good criterion. Also, it is a convenient firing point. In selecting a test procedure it is not practical to cover all possible conditions covered by their statistical distribution. One selects a criterion that is representative, is severe enough to assure satisfactory service and can be obtained by practical means in the laboratory or shop. We do not believe varying the firing angle is necessary in case of valve lightning arresters.

Kalb's suggestion of a reactive circuit has merit for lightning arresters whose follow current depends significantly on the impedances of the power system. This is the case with expulsion lightning arresters. In the case of practical systems and valve lightning arresters the power follow circuit is highly resistive because of the characteristic of the valve element. The effect that phase displacement between voltage and current may have on the ability of gaps to recover and interrupt is well known but we do not believe it is a problem in arresters of the valve types as they are made today.

In reply to Koerber's discussion, we agree that there are interactions between impulse and power circuits that affect the duty on the lightning arrester. This was considered when the duty cycle test proposed in the paper was established as a routine quality control test for station-type Autovalve lightning arresters some years ago.[2] This is a factor to a degree also in testing with 10 by 20 waves of discharge current. The tail of that discharge current is less well defined than the wave proposed in the paper. We recognize that probably debate and discussion is to be expected before a new standard is evolved. The industry has had similar problems that have been reconciled.

A long duration test of the general character mentioned by Koerber has merit, in our opinion, as a surge current withstand test and we are in general agreement with a proposal of this nature. As in the case of the other proposal, some further discussion of it is desirable. We do not believe it takes the place of a duty cycle test such as that proposed in the paper.

The question raised by Mertz opens a subject on which much discussion might take place. If there is no limitation as to test facilities and the expense warranted, a series of tests might be desirable. One test we would consider to be significant is a 60-cycle sparkover or withstand test in accordance with AIEE standards. To check the protective characteristics of valve lightning arresters, we believe that a volt time oscillogram using a 10 by 20 discharge current would be desirable. For such a test a current crest of 1,500 amperes would be adequate although other current magnitudes might be used. In the case of the expulsion lightning arresters, inspection of the series gap and the interrupter should be sufficient. To check the follow current interrupting ability of a valve lightning arrester that has been in service for 10 years, a test such as Mertz describes, that is 2,000 amperes surge current and a 60-cycle circuit of 400 amperes should, in our opinion, be satisfactory. We assume the 400 amperes mentioned by Mertz applies to the short circuit current capacity of the 60-cycle power circuit. On the expulsion lightning arresters this would be a rather mild circuit and on these we recommend inspection rather than the duty cycle test. Such tests will not tell whether these 10-year lightning arresters are as good as new in all respects but they will indicate that more service can be expected from them. To make tests to determine whether they are as good as new would require more exhaustive ones made under more severe conditions. After having subjected a 10-year lightning arrester to the latter tests there would probably arise serious question whether to put it back in service because these severe tests subject them to more severe duty than they would experience during a number of years of average service.

We are much interested in Rorden's conclusion that lightning arrester failures rarely occur from lightning and that the greatest hazard is dynamic transients that exceed the lightning arrester rating. This is also our conclusion. In the case of station-type lightning arresters we are quite convinced that lightning alone without contributing factors is a negligible cause of damage. We do not feel that this is equally true in the case of line or distribution types.

We concur with Rorden that dynamic overvoltages high enough to spark the lightning arrester series gap produce damage. This would require considerable voltage in the case of station-type lightning arresters since their 60-cycle sparkover, dry or wet, is at least $1^{1}/_{2}$ times and usually more than $1^{1}/_{2}$ times the lightning arrester rating. In the case of high-voltage lightning arresters, other than the station type, contamination and moisture on the outside surfaces can cause trouble of this nature. Such a condition will reduce the 60-cycle sparkover below normal. This is the major reason why the use of line-type lightning arresters with ratings higher than 73 kv is not recommended.

Mr. Rorden mentions, also as a cause of lightning arrester damage, dynamic overvoltages of long duration which do not sparkover the series gaps but result in excessive heating of the lightning arrester blocks. This question must be examined in some detail. It seems to us that a dynamic voltage in excess of the lightning arrester rating but below the sparkover voltage of the lightning arrester, not accompanied by any other transient system disturbance, would not be harmful because if the gaps do not spark, the current through the arrester is limited to that which is passed by the shunting resistance elements that parallel the series gap elements. This current is small and to the best of our knowledge would not damage the lightning arrester valve elements. If, however, there is a dynamic voltage on the lightning arrester in excess of its rating and during this time the arrester is sparked over by a surge, then follow current flows and the arrester attempts to clear the follow current against a dynamic voltage that is in excess of the lightning arrester rating. The limit of the dynamic voltage against which the lightning arrester can accomplish this is designated by its voltage rating. If the dynamic voltage is above the lightning arrester rating, the arrester must try to interrupt a higher than normal follow current against a higher than normal voltage. It will probably be unable to accomplish this, power follow current will continue to flow and the lightning arrester will be damaged.

We believe the situation just described is the chief hazard to lightning arresters of the station type. If applications are carefully made, the risk is negligible.

Rorden's request for comments relative to the hazards and probabilities of lightning arrester damage is a difficult one to answer quantitatively. The risk of damage increases as the dynamic voltage applied across the lightning arrester increases beyond the lightning arrester rating. With the voltage no higher than the arrester rating, the probability of damage is negligible, and this seems to have been borne out very well by service experience. If the dynamic voltage applied across the arrester terminals increases above the arrester rating the risk mounts. As the dynamic voltage applied to the lightning arrester terminal increases, the risk increases and finally if the dynamic voltage becomes equal to gap sparkover, damage is practically certain.

In closing, I wish to express appreciation to the discussors of the paper because the discussions have raised points of interest and provided an opportunity for expanding on the subject beyond the original scope of the paper.

References

1. Lightning Investigation on 132-Kv System of the American Gas and Electric Company, I. W. Gross, G. D. Lippert. *AIEE Transactions*, volume 64, 1945, pages 74–84.

2. Control of Lightning Arrester Quality, T. L. Dyer, E. Beck. *Westinghouse Engineer* (East Pittsburgh, Pa.), May 1951, pages 100–01.

3. Surging Lightning Arresters Connected to Power Voltage, A. D. Forbes. *Electric Journal* (East Pittsburgh, Pa.), May 1935, pages 162–65.

Economic Primary Circuit Design Beneficially Studied by Unit System

D. K. BLAKE
MEMBER AIEE

IT IS convenient, in the study of distribution system economics, to make two distinctions or divisions. They are the secondary system and the primary system. The secondary system is thought of as being composed of distribution transformers and their secondary (120/240 volt) mains. The primary system is conveniently thought of as being composed of primary or feeder circuit, and distribution substations to supply the feeders or circuits.

In practice it is easier to design for field conditions by thinking of and treating the primary system and the secondary system separately. It is believed this separation of treatment results in no substantial error involving an economic choice but it is recognized that one system does have an economic reaction to the other system. This paper will confine its discussion to the principal economic considerations of the primary system focusing most attention on that portion of the primary circuit that covers the load area. Overhead construction supplying domestic areas is predominantly in mind, but small power loads and commercial areas cannot be ignored in practical applications.

Studies of Ideal Uniform Conditions, a Valuable Aid to the Judgment

Field conditions confronting the distribution planning engineers are very complex. Uniform distribution of the load over substantial areas is not the rule. The exact determination of the most economical design is not practical and an approximate determination is laborious and consequently has deterred many from giving primary circuit economic design the study it deserves. It is believed much benefit can be obtained from theoretical studies of ideal uniform conditions. Before one can design for complex conditions he must understand well the principal factors determining an economic choice for ideal uniform conditions. After this it is in order to see how ideal studies can be modified to represent conditions known to commonly occur in the field. After these effects are understood it then becomes in order to analyze field conditions to see how they can be modified in a study to approximate ideal conditions. The large individual loads in the area, for example, can be set aside and the remaining load assumed as distributed in an approximate manner. This will enable determination of design for distributed load conditions. Then the concentrated loads present, or anticipated, can be added and their effect on the circuit design observed. This procedure educates the judgment, and judgment must always be relied upon in making final decisions of distribution circuit design in practice. This paper offers no substitute for the engineer's judgment. It is hoped the ideas presented will be an aid to his judgment.

Voltage Drop Principal Design Requirement

In the process of the design of any part of a distribution system there are two requirements to be met that are uppermost in the mind of the engineer. One is good voltage and the other is continuity of supply. This paper is concerned exclusively with the good voltage aspect it being assumed that the resulting circuit is satisfactory or can easily be made so, from the continuity viewpoint. It is believed to be a more informative procedure to first design for voltage requirements and then modify for continuity requirements.

Voltage requirements are usually expressed by some upper limit and some lower limit. This spread in voltage is thought of as being at the consumer's service entrance. The amount of this spread in volts is a matter of opinion. Whatever the value chosen, the voltage drops through successive parts of the system are so allocated that a certain value of voltage drop is allotted to the primary circuit between the first transformer nearest the feed point and the last transformer, or transformer receiving the lowest voltage on its primary. It is this voltage drop between the first transformer and the last transformer that determines or controls the economic circuit design. The lowest primary system (not circuit alone) cost is obtained when the circuit can be so designed that the maximum load can be picked up at one point. The reason is that the more load that can be picked up from one point and still meet the prescribed voltage drop, the fewer the number of feeders or substations required to feed the area and the better is the total primary copper in the area utilized though this latter may not always be so.

Pattern Studies First in Importance

If a feed point in a given area is selected and lines are drawn on paper to feed the individual distribution transformers a particular circuit pattern will result. The lines may be run in a different manner and another pattern will be seen. The location of the feed point may be changed resulting in another pattern. Patterns therefore may be influenced by street spacings, routings, obstacles and

---

Paper 51-193, recommended by the AIEE Transmission and Distribution Committee and approved by the AIEE Technical Program Committee for presentation at the AIEE Summer General Meeting, Toronto, Ont., Canada, June 25–29, 1951. Manuscript submitted October 13, 1950; made available for printing May 14, 1951.

D. K. Blake is with the General Electric Company, Schenectady, N. Y.

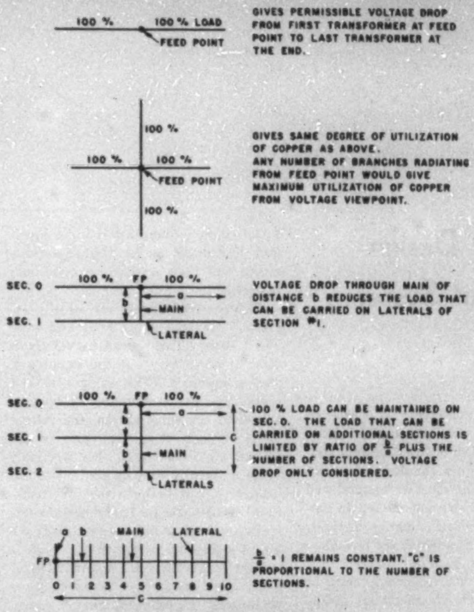
100 %
100 % LOAD
FEED POINT
GIVES PERMISSIBLE VOLTAGE DROP FROM FIRST TRANSFORMER AT FEED POINT TO LAST TRANSFORMER AT THE END.
100 %
100 %
100 %
FEED POINT
100 %
GIVES SAME DEGREE OF UTILIZATION OF COPPER AS ABOVE.
ANY NUMBER OF BRANCHES RADIATING FROM FEED POINT WOULD GIVE MAXIMUM UTILIZATION OF COPPER FROM VOLTAGE VIEWPOINT.
SEC. 0
100 %
FP
100 %
a
b
MAIN
SEC. 1
LATERAL
VOLTAGE DROP THROUGH MAIN OF DISTANCE b REDUCES THE LOAD THAT CAN BE CARRIED ON LATERALS OF SECTION #1.
SEC. 0
100 %
FP
100 %
a
SEC. 1
b
c
b
MAIN
SEC. 2
LATERALS
100 % LOAD CAN BE MAINTAINED ON SEC. 0. THE LOAD THAT CAN BE CARRIED ON ADDITIONAL SECTIONS IS LIMITED BY RATIO OF b/a PLUS THE NUMBER OF SECTIONS. VOLTAGE DROP ONLY CONSIDERED.
a
b
MAIN
LATERAL
FP
0 1 2 3 4 5 6 7 8 9 10
c
b/a = 1 REMAINS CONSTANT. "c" IS PROPORTIONAL TO THE NUMBER OF SECTIONS.

Figure 1. Beginning with a straight line fed at the middle as the base of a unit system one can study a variety of patterns

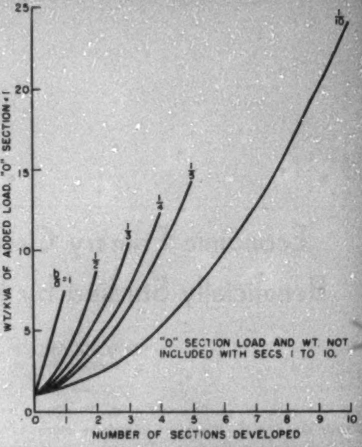

Figure 3. The group of curves is related to those of Figure 2 and indicates the degree of copper utilization

the points available for the selection of feed points. It is important to study what influence the choice of pattern or extension of a pattern will have on the amount of load that can be picked up at one point and the resulting utilization of copper.

It is important that the method used to study these factors of circuit design be made as simple and as convenient as possible, not only because of better understanding but to reduce the labor involved. In the initial stages it is not necessary to be specific about voltage, voltage drop, kilovolt-amperes, power-factor, or wire size. To study patterns one begins by choosing the simplest pattern which is a straight line fed from the middle, Figure 1. The load is assumed to be 100 per cent distributed, the weight of wire 100 per cent, the wire size unity, the length unity, the prescribed voltage drop from the feed point is unity, and the weight/kva is unity. All values are referred from the feed point to the end of each branch or lateral.

It is obvious that we could superimpose a duplicate straight line at right angles to the first one and feed the four points of the compass from the same feed point and maintain the same full utilization of copper. Any number of duplicate

Figure 4 (below). The voltage drop in the mains is seen to offer the most benefits of voltage drop reduction by the use of larger copper

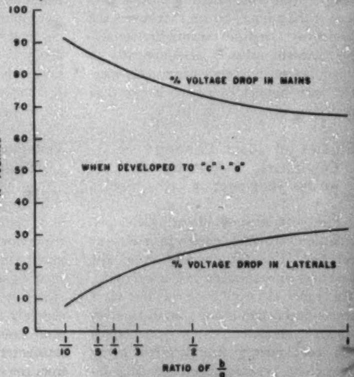

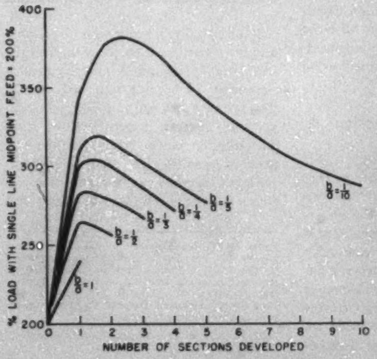

Figure 2 (left). Pattern development is related to the length ratio of mains to laterals and the number of sections developed until the total length of mains equals the length of the unit lateral. This group of curves indicates the amount of load that can be picked up from one feed point and give unit voltage drop

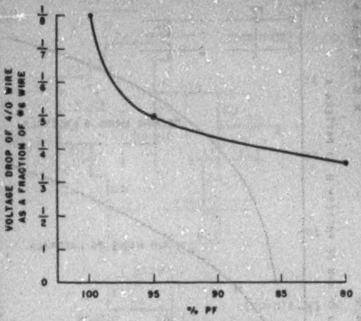

Figure 5 (left). Copper sizes are best thought of in terms of the resulting voltage reduction. The amount of voltage reduction quickly levels off as the power factor decreases

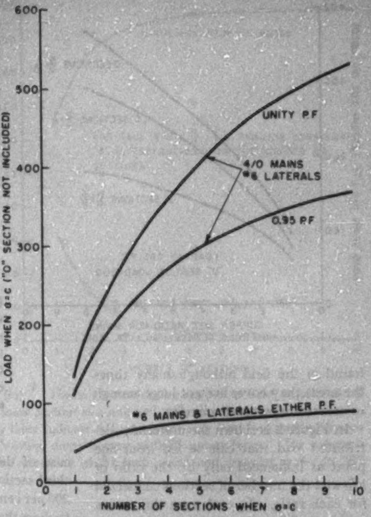

Figure 7 (right). Larger copper in the mains gives substantially greater load carrying ability to keep within the prescribed unit voltage drop

branches could radiate from the feed point like spokes in a wheel and also give a maximum utilization of copper. Such a pattern with more than four spokes however departs too far from practical conditions.

If we consider a duplicate straight line separated a distance "*b*" but parallel to the original line, we introduce an important factor that prevents getting full copper utilization on the second straight line, although it does not change the full utilization on the original line unless we change the original feed point. It is convenient to assume the original feed point as fixed and to run a conductor called a "main" from the feed point to the middle of the second line. For simplicity, no load is considered to be connected to the main "*b*."

The voltage drop through the main must be included in the total allowable drop and therefore reduces the load that can be carried on the two halves of the duplicate line now labeled as "laterals." Thus we have added more copper and carry less load.

A third straight line parallel to the other two can be added and supplied by extending the main "*b*" making it longer and increasing its importance as a consumer of valuable voltage drop and further reducing the amount of load that can be carried per lateral.

A convenient way of analyzing symmetrical patterns is to use various ratios of b/a and adding individual straight lines or sections until the total length of the "*b*" mains called "*c*" is equal to the length of a lateral. This process covers the field conditions where the length of the mains is of the same order as the laterals or shorter.

A convenient way of studying patterns where the length of main is much greater than the length of the laterals is to assume a fixed ratio like $b/a=1$ and simply add sections successively until the total length becomes a limiting factor.

These symmetrical patterns do, to some extent, approximate conditions frequently

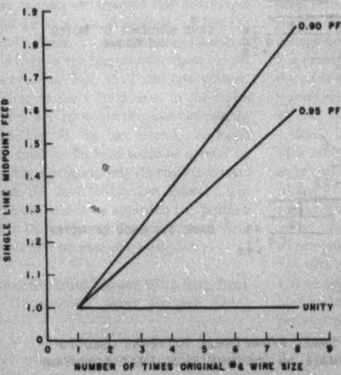

Figure 6 (left). The weight/kva increases linearly with larger copper if kilovars accompany the kilowatts

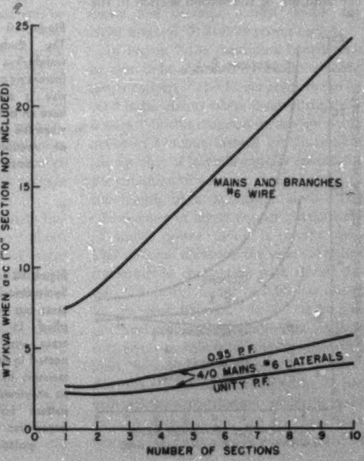

Figure 8 (right). The large load in Figure 7 is carried at a corresponding reduction in weight/kva because the laterals are better loaded

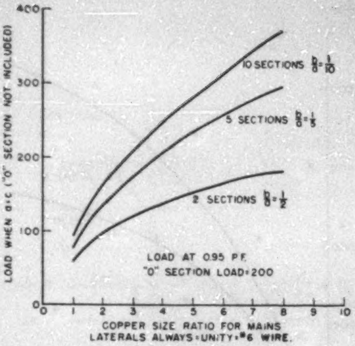

Figure 9 (left). This is a study in load carrying ability as influenced by increasing the wire size expressed in terms of ratio of area or weight to the unit conductor

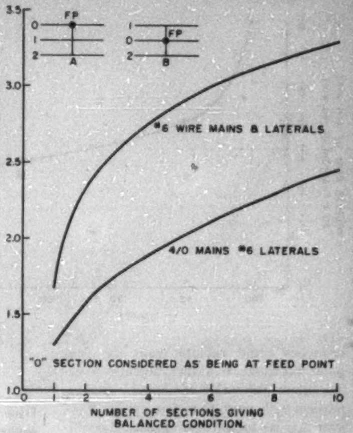

Figure 11 (right). Pattern variations can be made easily by relocating the feed point. Copper size benefits can be combined to observe combination benefits

found in the field although many times the areas they cover are not large enough to constitute complete circuits.

In Figure 2 is shown the uniformly distributed load that can be fed from one point as influenced only by the ratio of *b/a* and the number of sections connected for each ratio. In each case the curves terminate when the total length of mains "*c*" equals the length of laterals "*a*." No consideration at this point is given to wire size or power factor. Any wire size would give the same result as long as all wires, "mains and laterals" are the same size. Likewise, the power factor does not matter as long as it is the same for all cases.

It is seen that the smaller the ratio of *b/a* becomes, the greater the load that can be picked up from one feed point and that the amount of load diminishes after the addition of the second section in the case of the higher ratios and after the third section for the lowest ratio. Using 200 per cent as a reference base load helps to show that the adding of sections 1 to 10 fails to give a loading equal to the original "O" section.

It is seen from Figure 3 that the lowest weight/kva is obtained with the lowest ratio when it is restricted to the same number of sections as the others which, of course, is due entirely to its shorter total length of main "*c*." When all ratios are

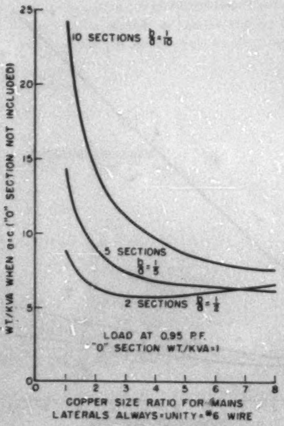

Figure 10 (left). The study of weight/kva with increasing copper size is seen to have an optimum when the number of sections is small

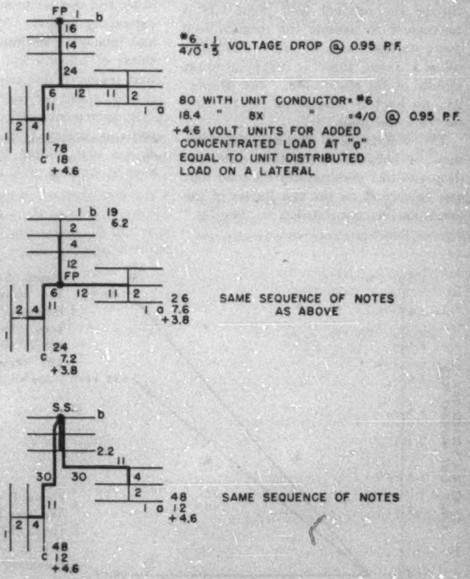
FP
1
b
16
14
24
6
12
11
2
1
0
11
2
4
1
1
78
C
18
+4.6
#6/4/0 = 1/5 VOLTAGE DROP @ 0.95 P.F.
80 WITH UNIT CONDUCTOR=#6
18.4 " 8X " =4/0 @ 0.95 P.F.
+4.6 VOLT UNITS FOR ADDED
CONCENTRATED LOAD AT "0"
EQUAL TO UNIT DISTRIBUTED
LOAD ON A LATERAL
1
b
19
6.2
2
4
12
FP
6
12
11
2
1
0
2.6
7.6
+3.8
2
4
11
1
24
C
7.2
+3.8
SAME SEQUENCE OF NOTES
AS ABOVE
S.S.
b
2.2
11
30
30
4
2
1
0
48
12
+4.6
11
2
4
1
48
C
12
+4.6
SAME SEQUENCE OF NOTES

THREE SMALL SYMMETRICAL PATTERNS USED TO APPROXIMATE AN UNSYMMETRICAL FIELD CONDITION

Figure 12 (right). Symmetrical patterns can be applied to small areas and connected in various manners to form an unsymmetrical pattern from a larger area viewpoint

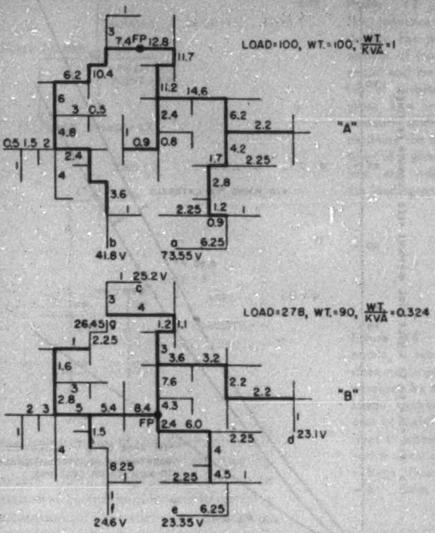
LOAD=100, WT.=100, $\frac{WT.}{KVA}$=1
"A"
FP
b
41.8V
a
73.55V
LOAD=278, WT.=90, $\frac{WT.}{KVA}$=0.324
"B"
25.2V
c
FP
d
23.1V
f
24.6V
e
23.35V

TWO PATTERNS APPLIED TO ASSUMED FIELD CONDITIONS

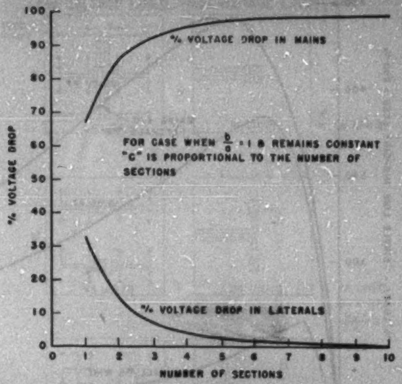

Figure 13 (left). The unit system can be applied to field conditions by choosing some portion as a unit and analyzing that area in those terms. The heavy lines indicate 4/0 conductor and light line number 6 conductor. Voltage drops figured at 0.95 power factor. The pattern is changed by relocation of the feed point and benefits shown in "B"

Figure 14 (above). The voltage drop in laterals rapidly becomes insignificant when the total length of mains is large compared to the length of lateral. Compare with Figure 4

developed to the same distance of "a" = "c" then the weight/kva increases substantially with the lower ratio. This is due to the fact that voltage drop in the mains is greater, and therefore the permissible voltage drop in the laterals to keep with the same limit is less for the lower ratios as shown by Figure 4. The more voltage drop permissible in the laterals, the better the copper utilization. Observe that there are more laterals with lighter loads per lateral as these ratios become smaller. The voltage drop in the last laterals determines the distributed load for all the other laterals. While the total voltage drop in the other laterals is less than in the last laterals, these cannot carry more load than the last without adding to the voltage drop in the mains which in turn would decrease the permissible load in the last lateral. However the total circuit load could be greater by having a progressively decreasing density from the first to the last lateral. The purpose here is to approach the problem from the uniformly distributed load viewpoint first because of its simplicity.

Benefits from Larger Wire Size Best Understood After Pattern Study

At this point it is pertinent to introduce wire size and power factor to see what influence they will have on loads that can be fed from one point and copper utilization expressed in weight/kva.

The place of course to use more copper is in the mains for that is where most of the voltage drop occurs. Assume that the original size for mains and laterals is the smallest wire commonly used for distribution primaries, number 6 wire. The maximum voltage reduction that can be made is of course the largest wire size commonly used in dictribution primaries, 4/0. Instead of thinking in terms of ohms resistance and reactance or B and S gauge, think in terms of the ratios of voltage drops and cross section or weights. For example, a 4/0 copper is eight times the cross section and weight of a number 6 conductor and gives 1/8 the voltage drop at unity power factor.

Going back to the original single line with midpoint feed, it can carry about eight times the load at unity power factor with a 4/0 instead of number 6 and the weight/kva will be the same as before or unity. If, however, the power factor is 95 per cent then the voltage drop is about 1/5 with distribution spacings instead of 1/8 so we can carry only five times the load and the weight/kva has gone up 60 per cent to 1.6. Figure 5 shows the voltage drop of a 4/0 as a fraction of number 6. This means that the voltage correction possibilities by changing wire sizes are greatly restricted by power factors below unity. Instead of being an 8:1 spread in voltage drop it is 5:1 for 0.95 power factor and less than 4:1 at 0.8 power factor. Figure 6 shows how the weight/kva remains constant for unity power factor and increases uniformly as the cross sections increase for other power factor and becomes almost double for eight times (4/0) at 0.90 power factor.

In Figure 7 the maximum benefit can be seen to be obtained by means of using larger copper. This larger copper is to be used in the mains where most of the drop occurs. In this diagram we are not using ratios of b/a but instead are increasing the number of laterals equally spaced for the condition of a length of main equal to the length of a lateral or $a=c$. The effectiveness of larger copper particularly at unity power factor is clearly seen. This also can illustrate the value of shunt capacitors in connection with circuit design. A power factor of 0.95 has about 31 per cent kilovars. It would be impractical to distribute individual capacitors equal to this total amount to every load, or every lateral for that matter. Fortunately the drop produced by 31 per cent kilovars distributed with the load can be compensated for by half that amount or 16 per cent kilovars located at

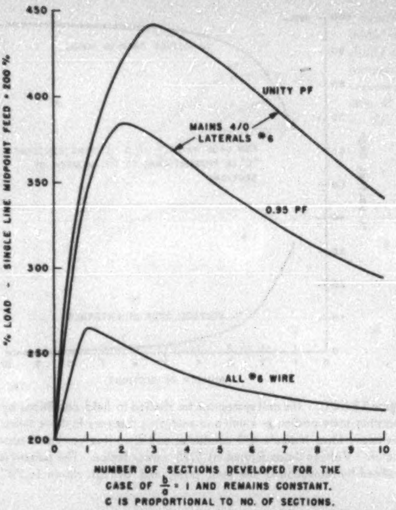

Figure 15. The voltage drops in the mains seriously limit the maximum load that can be picked up after the first few sections. Patterns of this kind are greatly benefited by the addition of supplementary regulators located at one or more points in the circuit

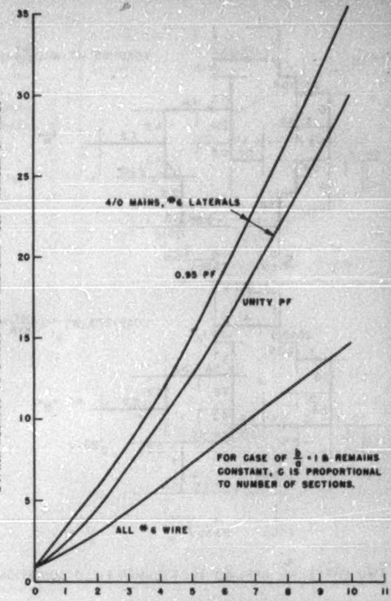

Figure 16 (right). The weight/kva of course goes up rapidly because the greater amount of copper caused by length carries less load per foot

the end of the mains. The load of the "O" section is not included in the figures because it may be any amount up to 200 per cent without exceeding the prescribed voltage drop for the circuit. It also may be looked at as a concentrated load comparable to all the load on all the other laterals. In the field such a situation would at once indicate the location of the feed point.

The weight/kva for the load indicated in Figure 7 is shown in Figure 8. The benefits of larger copper in the mains is clearly evident. Increasing the number of sections increases the weight/kva because the load carried per lateral goes down as the number of laterals goes up. The additional weight/kva is easy to justify in view of the greater load permitted and consequent reduction in the number of feeders or substations as the case may be. Figure 9 shows how the load that can be picked up, increases with increasing copper size. The larger number of laterals gets a more pronounced benefit because every portion of a voltage drop taken out of the mains enables all the laterals to carry a corresponding increase in load. When the number of laterals is less than five, the weight/kva increases as the copper size approaches the maximum. Figure 10 shows this to occur at about five times the cross section when the pattern has two sections. This up turn of course is due to the great weight put into the mains not benefiting a large enough number of sections or laterals.

Pattern Benefits Are to Be Compared with Larger Copper Benefits

In Figure 11 is illustrated a combination study of pattern and copper size.

The pattern is simply modified by a change in location of the feed point. The benefit from a purely pattern viewpoint is very pronounced but when combined with copper benefits the benefit of pattern change is substantially reduced. In this kind of study it is essential to take into account the source that supplies the feed point. If the source is a feeder from a distant substation then the length of that feeder is increased with the accompanying cost and added voltage drop. This voltage drop in the express feeder portion substantially exceeds the voltage reduction in the pattern itself. For the three section pattern illustrated in Figure 11 this amounts to a 50 per cent increase. This of course would be unacceptable if it were not for the ability to compensate for all voltage drop occurring in the feeder portion. Even then it may not be acceptable due to the added feeder cost and the complication of an added circuit on the pole structures for some or all portions of distance within the circuit area.

Feed Points Can Be Considered as a Bus Regulated Substation

This is a good place to emphasize that these feed points could very well be the location of bus regulated substations in lieu of feeders from a distant substation. Figure 11 in that case shows how the size of load that can be bus-regulated is increased by locating them at the load center. In such cases the added voltage drop of the higher voltage subtransmission is divided by the square of the ratio of voltages and will usually not be significant. Field conditions may prevent full realization of theoretical benefits.

From the foregoing considerations it seems that the proper procedure in load area studies is to first determine the number and location of feed points. The remainder of the primary system study then becomes the determination of the number,

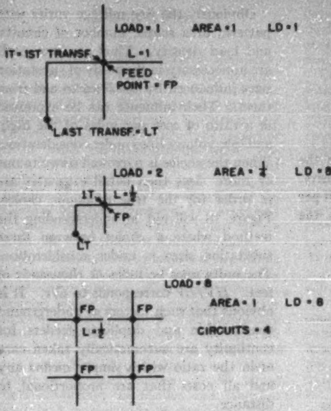

Figure 17 (left). The influence load density has on the amount of load per circuit and the number of circuits in a given area is conveniently studied by changing the dimensions of a given pattern and adjusting the load accordingly

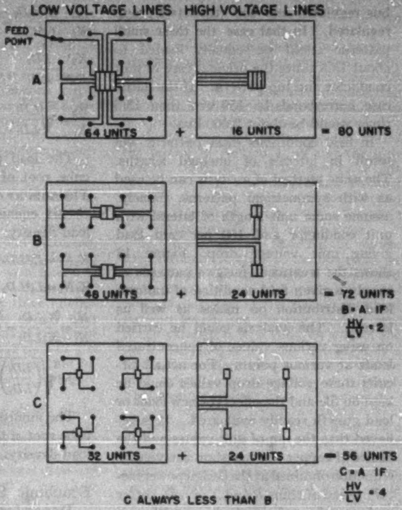

Figure 18. Economic substation sizes are largely determined by the relation between the cost of high-voltage lines to supply them and the cost of low-voltage lines from them

size, and location of the distribution substations. Obviously there are two extremes. Each circuit feed point can be connected by means of feeders to one large substation for the entire area. The other extreme is to locate a substation at each feed point. The economic choice may be a number of smaller substations each with a few shorter feeders.

Small Symmetrical Patterns Can Be Grouped to Approximate Nonuniform Field Conditions

Field conditions, of course, are not uniform and a study of uniform patterns alone is of limited value in designing for nonuniform field conditions. However, the benefits to be derived from a study of symmetrical patterns can be extended by grouping a number of small symmetrical patterns to form a larger nonsymmetrical pattern. Such a combination is shown in Figure 12. A feed point is first assumed as indicated in the upper pattern. Load is uniformly distributed giving unit voltage drop for the unit length of lateral. Starting at the end of the smaller symmetrical patterns and working backwards to the feed point, the voltage drops in the individual portion of mains are calculated mentally keeping in mind that the unit length of mains has twice the voltage drop of unit length of lateral because the lateral load is assumed to be distributed. These voltage drops are then totaled and that value then is used as a reference to determine what modifications will accomplish in load carrying ability. With unit conductor the total drop to the end of the small pattern "*a*" is 80 and for "*b*" is 78. The extreme benefit from increase in copper size would occur by going from a number 6 to 4/0. This would give a voltage drop 1/5 at 0.95 power factor. If applied as shown by the heavy lines it would reduce the total voltage drop to 18.4 for "*a*" and 18 for "*b*." For the same voltage requirement the load carrying ability by increasing copper size as indicated becomes $80 \div 18.4 = 4.35$ times. Any concentrated loads in the area could then be added and their resulting voltage drop added to the 18.4. If, for example, we superimpose a concentrated load, equal to the distributed load along the lateral, at the end of the last lateral for pattern "*a*" 4.6 should be added to 18.4 giving 23 volts. This would decrease the total load to $80 \div 23 = 3.5$ times. The pattern's load is thus reduced to 80 per cent by the addition of this concentrated load. Observe that 2 volts of this 4.6 occurs in the lateral itself and could be reduced by larger copper of intermediate size.

If now the feed point is located as shown in the middle figure of Figure 12, then on the face of it the pattern change alone gives $80 \div 26 = 3.08$ times. Adding the benefits of large copper we have $18.4 \div 7.6 = 2.42$ showing that the copper benefits reduce the pattern change benefits. But a closer examination will show that each small pattern can now be considered separately. Pattern "*b*" can be loaded $7.6 \div 6.2 = 1.23$ times "*a*" and pattern "*c*" $7.6 \div 7.2 = 1.05$ times "*a*."

Suppose now we consider the bottom figure of Figure 12, and that the first feed point becomes a substation which cannot be located at such a convenient spot as in the middle figure. The smaller patterns "*a*," "*b*," and "*c*" are considered as radial feeders. With bus regulation the load on "*b*" could be built up to $6.2 \div 2.2 = 2.8$ times what it would be if substation was located as in the middle figure assuming 4/0 copper for the mains. "*a*" and "*c*" however would be diminished to 63 and 60 per cent, respectively, on account of the long feeder drop. On the other hand individual feeder regulators in the feeders to "*a*" and "*c*" would compensate for the 30/6 volts and permit loadings $7.6 \div 6 = 1.27$ times for "*a*" and $7.2 \div 6 = 1.2$ times for "*c*." All values are referred to the middle figure. To summarize: The copper benefits give 4.35 times the load carrying ability in the top pattern. The shift in feed point combined with the copper benefits raises this to 10.5. If advantage could be taken of more load on the shorter branches this 10.5 could be raised to 11.5. Locating substation at feed point of bottom figure permits 16.3 times for the total area but requires a much heavier load near the substation to be realized, a very unlikely situation. Feeder voltage regulators increase the loading potentialities to nearly 21 times but still require the doubtful benefit of having such a heavy load on the feeder next to the substation. Another way the lower figure of Figure 12 could be evaluated would be to have one feeder bus regulated and the other two group regulated. In that case the three small patterns could be equally loaded to about 13.5 times the original case of unit conductor and top pattern. If the initial case corresponds to 150 kva then 13.5 times would be about 2,000 kva.

In field conditions most patterns will result in laterals of unequal lengths. The same method of analysis can be used as with symmetrical patterns, namely, assume some unit length of lateral with unit conductor and 100 per cent load giving unit voltage drop. Figure 13 shows the treatment for two patterns to supply a given field condition of uniform load distribution on mains as well as laterals. The analysis could be carried on using various values of concentrated loads at various points. For actual circuits these voltage drop values could be kept on file and the effects of new loads or load growth readily evaluated. It is believed that the use of unit values and the choice of copper size based on the voltage reduction obtained at the design power factor instead of ohms R and X gives a better understanding of circuit design although the labor involved is still substantial. It is obvious from the examples shown that the load carrying possibilities cover a wide range and therefore such study is essential if circuits in practice are to carry the maximum load per foot of distribution circuit.

Figures 14, 15, and 16 show the voltage, load and weight/kva for a fixed pattern extended in length. The amount of load that can be picked up is seen to increase rapidly to a maximum and then taper more slowly with increasing length, an effect due to voltage drop in the mains which can be improved by larger copper. This kind of a situation is ideal for subdivision of the circuit by the use of supplementary regulation and of capacitance to produce a voltage rise and is common in farm lines.

Economic Loading Increases with Load Density

In Figure 17 is illustrated the ease with which the effect of load density can be studied by changing the scale of dimensions of a given pattern. Let L=length, K=kilovolt-ampere of load per circuit, N=number of circuits, and LD=load density. The subscripts indicate the first and second cases.

$K_1L_1=K_2L_2$ for same voltage drop, or $\frac{L_2}{L_1}=\frac{K_1}{K_2}$

L_1^2=area of original circuit

$$LD_1=\frac{K_1}{L_1^2} \qquad LD_2=\frac{K_2}{L_2^2}$$

$$\frac{K_2}{K_1}=\frac{L_2^2LD_2}{L_1^2LD_1}=\frac{K_1^2LD_2}{K_2^2LD_1}$$

$$\frac{K_2^3}{K_1^3}=\frac{LD_2}{LD_1}$$

$$\frac{K_2}{K_1}=\sqrt[3]{\frac{LD_2}{LD_1}}$$

The load per circuit increases as the cube root of the ratio of load density. The number of circuits times the load per circuit equals the total area times the load density.

$$K_2N_2=L_1^2LD_2$$

$$K_1N_1=L_1^2LD_1$$

$$\frac{N_2}{N_1}=\frac{K_1LD_2}{K_2LD_1}=\sqrt[3]{\frac{LD_1}{LD_2}\frac{LD_2}{LD_1}}$$

$$=\sqrt[3]{\left(\frac{LD_2}{LD_1}\right)^2}$$

The number of circuits increases as the cube root of the square of the ratio of the load density.

Economic Substation Size Dependent on Economic Circuit Size

It is not the scope of this paper to go into the determination of economic substation size. The problem is composed essentially of the three variables (1) high-voltage lines to the substation, (2) the substations themselves, and (3) the low-voltage lines from the substation to the feed points in the circuit areas. The influence of each variable can best be understood by omitting the substation cost variable and observing how the miles of high-voltage lines increase and the miles of low-voltage lines decrease as the substation size decreases. For any particular pattern or shape of load area, the sum of the costs of the high-voltage plus low-voltage lines for one size of substation can be equated to that of another size, and the result expressed as a ratio of high-voltage line cost per mile to low-voltage line cost per mile that would give equal total line cost for either substation size. This ratio is then compared with the actual ratio of cost per mile to see how much margin there is left to make up for the omitted substation cost. If C=cost of high-voltage lines per mile, c=low voltage, M=high-voltage line total miles, m=low voltage and subscripts 1 and 2= substation size then

$$CM_1+cm_1=CM_2+cm_2$$

$$C(M_1-M_2)=c(m_2-m_1)$$

$$\frac{C}{c}=\frac{m_2-m_1}{M_1-M_2}$$

Obviously the line mileage varies with pattern, area shape, number of circuits, and load density. Thus accurate costs are unnecessary in the study of substation sizes influenced by the lines to and from them. Their influence can be expressed in a ratio of cost per miles of the high- and low-voltage lines under consideration. When the choice is narrowed down to one or more sizes then detail estimates are in order for the true economic choice. Figure 18 will aid in understanding the method where a choice between three substation sizes is under consideration. The units may be miles or thousands of feet. HV/LV corresponds to C/c. It is obvious that such factors as underground construction and duplicate feeders for continuity are automatically taken care of in the ratio which simply means any and all costs that are proportional to distance.

This paper could be made much more comprehensive by more examples but it would also be much longer. It is believed enough has been included to show that the best understanding of distribution system economic design is obtained by the approach that considers the secondary system first which establishes the transformer locations. The primary circuit to cover the area is then determined using the distribution transformers as units to determine the load that can be picked up from the economic location of the feed point limited by the voltage drop from the first transformer to the last transformer. The feed points are then utilized as load units to determine the size and the location of distribution substations. It also has been shown that the unit system can go a long way in an analyses made for the benefit of the understanding and thus avoid the clouding effect produced when one tries to understand by using kilovolt-amperes values, conductor sizes in ohms or B & S gauge, miles, power factors, and so forth. Such a simplified method can never replace detailed studies for actual costs but they could easily reduce the volume of such estimates made for purposes of comparison. Furthermore the unit system is useful in conveying a better understanding to others who work in a different area but are nevertheless affected by a distribution system choice. Obviously much depends on the ingenuity and judgment of the one using such simplified methods.

Reference

1. *Electrical World* (New York, N. Y.), March 12, 1949, pages 107–08.

Discussion

D. R. Samson (General Electric Company, Schenectady, N. Y.): The "unit system" of feeder analysis described in this paper was suggested by Mr. Blake to a small group of engineers several years ago. Since that time the individual ingenuity which he speaks of in his paper has expanded this idea. The unit system has been proposed to several utility companies and accepted. An application engineer in the Denver Office of the General Electric Company has developed a unique portable calculating board for use with this unit system of circuit analysis.

By this simplified approach it is possible to analyze a distribution area without the confusing parameters of wire size, equivalent spacing, power factor, or exact transformer location. Having completed an elementary study it is possible to obtain more exacting data by convenient conversion factors. In his paper Mr. Blake makes no mention of single or 3-phase branches. Under actual field conditions, the feeders and branches may be a combination of single and three phase. The area may be analyzed as though it were all three phase, and then convert the 3-phase unit voltage drops into single-phase values. If the load density is the same over the entire area, the unit drop for a single-phase branch can be obtained by doubling the 3-phase drop for a delta system or by multiplying by the factor $2\sqrt{3}$ for line to neutral drops on a Y-connected system. These factors are based upon 3-phase line-to-line voltage drops. It should also be noted that if the system is a multigrounded wye, the neutral impedance may be considerably lower than the phase wire impedance. This means that the correction factor $2\sqrt{3}$ can be reduced as determined by local grounding conditions.

In the use of this system, it has been found convenient to separate the larger concentrated load, and then assume the remaining load of a feeder or an area to be relatively uniformly distributed. In particular areas where no feeder loading exists, the calculations are simplified because the distributed loading effect in these sections may be omitted. Thus it is possible to very conveniently simulate actual loading conditions.

As pointed out by the author, the unit system of feeder analysis is not intended to supplant a detailed study. However, it has been found that this method of analysis enables one to quickly analyze the effects of relocating a feed point or a substation, to observe the behavior of concentrated and distributed loads, to evaluate the efficiency of present and future copper installations, to calculate voltage benefits from capacitors to primary systems, and to insure good consumer voltage.

In the analysis of the load carrying ability of the circuit configurations shown in Figure 1, the author has assumed full loading of the "O" section and uniform load density for the rest of the area considered. It may be pointed out that if the loadings of each lateral become progressively less as one moves away from the feed point, the load carrying ability of the main and the combined laterals can be increased when the voltage drop at the end of each lateral is equal to that at the end of the "O" section. Progressively decreasing loads on the lateral is not a practical field condition for heavy residential areas, but in the urban fringes this condition can quite often exist.

Consider a circuit as shown in Figure 1 which has three additional sections and a length ratio of main to lateral of $1/3(b/a = 1/3)$. From Figure 2 of the paper it can be seen that the total load carried by the original section "O" and the three additional laterals is 266 per cent, or section "O" carries 100 per cent load for each half and the three additional laterals carry a total of only 66 per cent load. If the load carried on each lateral had not all been equal, the total load carried by these laterals could be increased. Thus with loading conditions such that the voltage drop at the end of each lateral is equal to the drop at the end of the "O" section, the total load of the three laterals could be increased from the 66 per cent value to 100 per cent. The combination of laterals and section "O" would then be 300 per cent as compared with 266 per cent for uniform load conditions as shown in Figure 2.

Similarly the load carrying ability of the main and laterals could be increased if the length of each lateral becomes shorter as one progresses away from the substation. The load to be picked up by these laterals would be at a uniform rate per unit of length or the load density would be considered uniform. The load area would have a geometric shape of an isosceles triangle with the feed point located at the midpoint of the base side of the triangle. Thus it would be possible to feed a large uniformly distributed load area by dividing the load area into a number of triangular sections.

B. M. Jones (Duquesne Light Company, Pittsburgh, Pa.): I think the author has made a very good paper, but believe that it is somewhat too theoretical for a lot of the people who have to do with primary circuit design, particularly the designers, the young engineers coming along, and others.

I suggest that the writer work up some typical examples using certain definite lengths, certain sizes of copper, and certain assumed loads.

D. K. Blake: For a numerical example dealing in amperes and volts, let us begin with the straight line in Figure 1. First we assume number 6 conductor as our unit conductor size and 3 per cent voltage drop as the unit design value. Next assumptions are 2,400/4,160 Y circuit and a load power factor of 95 per cent.

With balance load we need consider the impedance of only one wire in which we can allow $2{,}400 \times 0.03 = 24$ volts impedance drop.

$$R \cos \theta + X \sin \theta = 0.432 \text{ for 1,000 foot length}$$

$$24 \text{ volts} \div 0.432 = 55.5 \text{ amperes}$$

which turn out to be

$$\frac{55.5 \times 2{,}400 \times 3}{1{,}000} = 400 \text{ kva 3-phase balanced load}$$

For distributed load we can double either the load or the length. This turns out to be our 100 per cent load whichever we decide to do.

Next we add a parallel line of the same length to study the effect of pattern. Our first line is called "O" Section and our second is called Section 1. The main b connecting the midpoints is for illustration assumed to be equal to c which is also equal to a. In calculating the voltage drop to the end of the lateral of Section 1 we use the unit system. Each lateral is assumed to be unit conductor of the same length and assumed to carry the same 100 per cent load carried by the laterals of Section "O." Therefore the voltage drop in each lateral is one.

To this voltage must be added the voltage drop through the main b. At this point we must decide whether load is distributed along this main or not. Let us assume it is not. Main b then carries 200 per cent load for unit length and the voltage drop produced through it is 2 volts for double the load. This in turn must be multiplied by a factor of two, since we assumed our load on unit lateral a is uniformly distributed. This gives us a 4-volt drop in the main b.

Next, we add the 1-volt drop in the lateral of Section 1 to the 4 volts to get a total of 5 volts drop from the feed point to the end of the laterals in Section 1. Since, 100 per cent load gives five times the voltage drop, we must limit the load we can supply along the laterals of Section 1 to 1/5 to meet our design requirements of unit voltage drop.

If we had chosen for our reference 800 kva of distributed load for 1,000 feet then we could have carried only 160 kva on each lateral or a total of 320 kva for the two laterals of Section 1. If instead we had taken the benefit of distributed load in distance, the kilovolt-ampere values would be cut in one-half while the length of both b and the laterals would be doubled.

The weight/kva of Section 1 load is easily obtained by dividing 3/2 times the length (Section $1+b$) by 1/5 the load which gives a factor of 7.5 times the value of Section "O." There is no need of converting this into pounds/kva because one is only interested in comparative weights as a measure of copper utilization.

Now suppose b is 1/2 instead of unity then the 4 volts become 2 volts to make a total of 3. The load then increases in the ratio of 5/3 (533 kva), and the weight/kva is the reciprocal —5/3 for the same unit or 3 per cent voltage drop.

Suppose again we use larger copper in b where most of the voltage drop occurs.

$$R \cos \theta + X \sin \theta = 0.0865 \text{ for 4/0 copper}$$

Dividing this into 0.432 for number 6 gives 5 which means 1/5 the voltage drop. Therefore, $4/5 = 0.8$ volt drop in the main plus 1 volt for lateral $= 1.8$. Dividing the 5 volts for the original case by $1.8 = 2.78$ $320 \times 2.78 = 890$ kva we can now carry from the feed point to the ends of the two laterals of Section 1.

Nor do we need to assume uniform conditions. One branch of Section 1 could be twice the length of the other and for the same load would give 2 volts drop in the larger lateral. In the same density this would be twice the load and twice the distance making 4 volts. This load also would pass through b and would add another 2 volts for number 6 wire or 0.4 volt for 4/0. We would then have $0.8+0.4+4 = 5.2$ volts drop when 300 per cent load was flowing through *b*, 100 per cent on the short lateral and 200 per cent on the long lateral. To keep within the allowable voltage drop the load on the short and long lateral would need to be limited in the ratio of 1/5.2 or 154 kva on the short and 308 kva on the long branch, the total being 462 kva.

Instances of unbalanced loads also may be analyzed with the unit system. Sticking to our simple pattern of Section "O" and Section 1 we can assume one lateral of Section 1 is three phase and the other single-phase line to neutral. Calculate first the 3-phase drop. Half the load through Section *b* gives 2 volts drop for 3-phase load through number 6 wire. Single-phase load line to neutral requires the current to flow through the neutral doubling the impedance, and since we still assume 100 per cent load over one phase instead of over three phases we have three times the current. So twice the impedance and three times the current gives six times the voltage drop. This means 6 volts in the lateral instead of 1 volt and 12 volts in the main *b*. This 12 volts in main *b* must be added to the 3-phase drop of 2 volts giving 14 volts in the main. The end of the 3-phase lateral is 15 volts, and the single phase is 20 volts. This is four times the voltage drop for balanced 3-phase load and means the load must be limited to 1/4 or 80 kva instead of 320 kva. Obviously no one would design such an unbalanced circuit for it manifestly fails to utilize the other two phases.

The examples should make clear the procedure. Time and labor is saved and I think a better understanding of the benefits of larger copper and attention to pattern design. Obviously a lot of work is still required.

Current Carrying Capacity of ACSR Conductors

J. H. WAGHORNE
NONMEMBER AIEE

V. E. OGORODNIKOV
NONMEMBER AIEE

CURRENT-carrying capacities of ACSR conductors are presented in nomogram form. One nomogram covers several sizes of conductors for ranges of wind velocities and ambient temperatures. A simpler nomogram applicable to one or more particular transmission lines is recommended for operating use.

On most transmission lines the thermal rating of the conductors is not the factor which limits current under normal operation even under conditions of no wind and maximum ambient temperatures. Line losses, voltage regulation, and stability dictate currents below the thermal limit. Hence any chart or table giving maximum permissible currents for a range of conductor sizes is primarily for use under abnormal conditions where a line is required to carry extra current because of either scheduled or unscheduled interruptions on other circuits. To be readily useful to an operating staff, such tables and charts must be simple and the values of current presented must be safe for use at any time. For these reasons they are usually based on the minimum wind speed and maximum ambient temperature experienced in the district concerned, even though ambient conditions at any particular time may differ sufficiently to make the safe value of current 50 per cent larger than that shown by the table.

Figure 1 indicates values suggested by various investigators for use in their countries. Conditions differ of course, but the conservatism of those responsible for the suggestions probably differs even more. The problem of making satisfactory joints in the earlier transmission lines may also have influenced these suggested values. Modern joints, however, when well made, are reliable and need not be treated more conservatively than the rest of the line.

Most of the published work on this subject has concentrated on a more precise establishment of the limiting conditions of wind and temperature. The mathematical equations used[1,2] are far more precise than the knowledge of the variables warrants. In this paper some of this unwarranted precision is sacrificed in favour of a simplified presentation to enable advantage to be taken of the wind and ambient temperature prevailing at the time extra capacity is required.

Consider briefly the variables involved:

Ambient Temperature T

Ambient temperature is probably known more accurately than any other variable. Some care must be taken to ensure that the highest ambient anywhere along the transmission line is used. If one value is to be chosen which will be safe at all times it must be at least 40 degrees centigrade in this area.

Conductor Temperature T_c

Permissible conductor temperature is really a function of time, as pointed out for copper conductors by Olmsted.[1] For aluminum conductors operating up to 80 degrees centigrade, annealing time is long enough to be considered infinite and above 120 degrees centigrade is short enough to be considered zero. Between these limits annealing times have not yet been completely determined. A value of 80 degrees centigrade may be chosen as safe for present purposes.

Time

In addition to the influence of time already mentioned, a conductor requires some time to reach equilibrium temperature after a given current increase. This factor would allow larger currents to be used for short periods but will be neglected in the following presentation.

Emissivity E

Various values of emissivity from 0.22 to 1.0 are quoted for the range from new to blackened conductors.[2] Used conductors measured in the Hydro-Electric Power Commission's Laboratory had emissivities ranging from 0.5 to 0.8. A value of 0.6 is considered to be reasonable and will be used. New conductors should reach this value after about a year's exposure.

Solar Absorption Coefficient α

The coefficient of solar absorption is not necessarily the same as emissivity except for black conductors and may vary from 0.6 to 1.0. A value of 0.8 will be

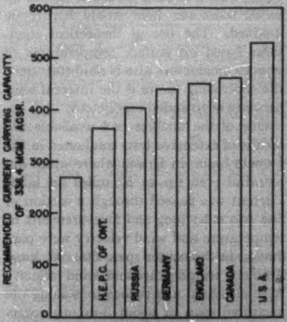

Figure 1. Values of current-carrying capacity of 336,400 circular mil ACSR recommended for general use by various investigators in the countries named. For the value to the left see text

---

Paper 51-195, recommended by the AIEE Transmission and Distribution Committee and approved by the AIEE Technical Program Committee for presentation at the AIEE Summer General Meeting, Toronto, Ont., Canada, June 25–29, 1951. Manuscript submitted March 27, 1951; made available for printing May 11, 1951.

J. H. WAGHORNE and V. E. OGORODNIKOV are with The Hydro-Electric Power Commission of Ontario, Toronto, Ont., Canada.

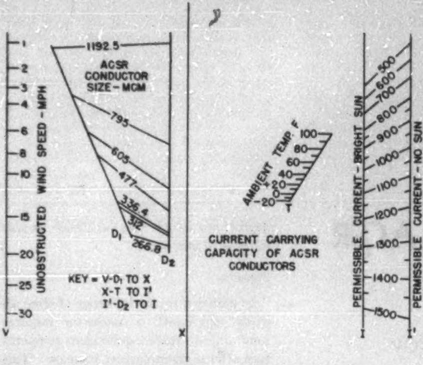
1
2
3
4
6
8
10
15
20
25
30
V
UNOBSTRUCTED WIND SPEED - MPH
1192.5
ACSR CONDUCTOR SIZE - MCM
795
605
477
336.4
312
266.8
D_1
D_2
KEY = V-D_1 TO X
X-T TO I'
I'-D_2 TO I
X
AMBIENT TEMP. F
100
80
60
40
+20
0
-20
T
CURRENT CARRYING CAPACITY OF ACSR CONDUCTORS
PERMISSIBLE CURRENT - BRIGHT SUN
PERMISSIBLE CURRENT - NO SUN
500
600
700
800
900
1000
1100
1200
1300
1400
1500
I
I'

Figure 2. Nomogram of current-carrying capacity of several sizes of ACSR conductors. Wind speed values shown are observed values and include a safety factor of 2.5. No reduction has been made for ferrous-type hardware

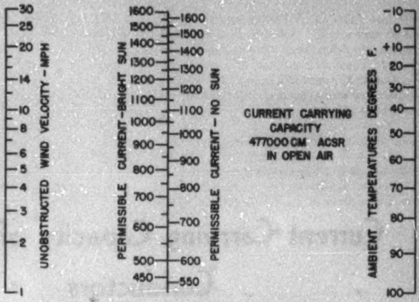
30
25
20
14
10
8
6
5
4
3
2
1
UNOBSTRUCTED WIND VELOCITY - MPH
PERMISSIBLE CURRENT - BRIGHT SUN
1600
1500
1400
1300
1200
1100
1000
900
800
700
600
500
450
PERMISSIBLE CURRENT - NO SUN
1600
1500
1400
1300
1200
1100
1000
900
800
700
600
550
CURRENT CARRYING CAPACITY 477000 CM ACSR IN OPEN AIR
AMBIENT TEMPERATURES DEGREES F.
-10
0
+10
20
30
40
50
60
70
80
90
100

Figure 3. Nomogram of current-carrying capacity of 477,000 circular mil ACSR with no reduction for ferrous-type hardware

used because if for a particular conductor it should be larger than this, then the emissivity would be larger than the assumed value of 0.6.

Wind Speed V

The effect of wind on the current-carrying capacity of the conductor is large and in practice it is the least accurately known of all the variables. Even with the use of a wind tunnel in the Laboratory, the accurate determination of the effect of this variable is extremely difficult, particularly at the higher wind speeds. Hutchings and Parr[2] have made many measurements at wind velocities from one-half to two miles per hour, but extrapolation of their values to speeds up to 30 miles per hour would hardly be justified. The use of theoretical equations based on surface temperatures of smooth conductors also is doubtful, since the controlling factor is the internal temperature of stranded conductors.

One of the authors had available the results of extensive tests conducted in the Donetz basin in Russia where winds are plentiful even up to 50 miles an hour. Current was passed through a section of line two miles long and measurements of temperature and wind velocity were conducted in the center span, 600 feet long. Ambient temperature and wind velocity were measured at five locations along the measured span at about 3-minute intervals during tests. Temperature measurements were made with thermocouples embedded under the outer layer of aluminum, a special measurement platform being used near the center of the span. Five different sizes of ACSR conductors were tested over a period of two years. Considerable reliance has been placed on these results since no other comparable tests are known.

Tests are conducted with, and equations assume that winds are at right angles to the conductors; in practice, however, this may not be so. Shielding of trees and valleys also may reduce the effective wind somewhat from measured or observed values. For these reasons, values of 40 per cent of the observed values, as suggested by Olmsted,[1] are used in the equations used for plotting the nomograms. Since wind speeds are not generally measured or recognized as readily as temperatures the effect of different speeds is given here as taken from the Beaufort scale.

If a value of wind speed which would be always safe were based on data taken at Hanlan's Point on Lake Ontario, two miles per hour should be chosen. However, data over a 23-year period from Agincourt, ten miles inland, show that for 12 per cent of the hours during July, less than one mile of wind passes an anemometer 40 feet above ground. Since this wind may be parallel to the line, an effective speed of not more than one-half mile per hour would have to be chosen to be always safe.

Conductor Hardware

If such line hardware as suspension clamps and vibration dampers are of low-loss types, the conductors inside the clamps will operate cooler than in open air as a result of the additional radiating surface. However, as shown by Crabb and Sheadel[3] as well as others, all-ferrous clamps may have sufficient magnetic losses to raise the temperature of the conductor within the clamp considerably above that in open air. This means that on 60-cycle lines such hardware imposes very serious limitations to the current-carrying capacity. This fact will not be considered in the initial presentation but will be included later.

A value of current which would be safe at all times in this area, with all factors considered would therefore have to be based on values: $V=1/2$, $T=40$, $T_c=80$, $E=0.22$, $\alpha=0.6$. For 336,400 circular mils this current would be only 270 amperes assuming low-loss hardware (shown at left on Figure 1).

Reduction of Equation

Starting with the equation of Hutchings and Parr:[2]

Table I

Range of Wind Speed, Miles per Hour	For Use on Land, Based on Observations Made at Land Stations
Less than 1	Calm, smoke rises vertically
1 to 3	Direction of wind shown by smoke drift, but not by wind vanes
4 to 7	Wind felt on face, leaves rustle; ordinary wind vane moved by wind
8 to 12	Leaves and small twigs in constant motion; wind extends light flag
13 to 18	Raises dust and loose paper; small branches are moved
19 to 24	Small trees in leaf begin to sway; crested wavelets form on inland waters
25 to 31	Large branches in motion, whistling heard in telegraph wires; umbrellas used with difficulty
32 to 38	Whole trees in motion; inconvenience felt when walking against wind

$$I^2R+\alpha S'D=13.8\times10^{-4}(VD)^{0.448}\theta+\pi DES[(\theta+T+273)^4-(T+273)^4]$$

where

I = current in amperes
R = resistance of one centimeter of conductor in ohms
α = solar absorption coefficient
S' = intensity of solar radiation, watts per square centimeter
D = conductor diameter in centimeters
V = wind velocity in centimeters per second
θ = temperature rise of conductor, degrees centigrade
E = emissivity of conductor surface
S = Stefan's constant, 5.7×10^{-12} watts per square centimeter
T = ambient temperature, degrees centigrade

a practical simplification can be effected. If a limiting conductor temperature of 80 degrees centigrade be chosen $T+\theta=80$ and the last term of the equation becomes

$$\pi DES[353^4-(353-\theta)^4]$$

Since this term is always the smaller some error can be tolerated in it; hence it may be written

$$\pi DES(3\times353^3)\theta$$

For a range of θ from 40 to 100 this assumption produces an error in this term ranging from -11 to $+15$ per cent but the error produced in the value of I is always less than 2 per cent.

When the powers of V and D in the first term on the right-hand side are checked from the Russian data it is found that 0.5 is a better choice than 0.448.

Assuming $\alpha=0.8$; $S'=90$ milliwatts per square centimeter; $E=0.6$; and changing V to miles per hour and D to inches

$$I^2R=(aV^{0.5}D^{0.5}+0.0036)\theta-0.183D$$

where a is a constant to be determined from experimental data. For ACSR conductors

$$R=\frac{1.09\times10^{-6}}{D^2}$$

with only very small error on a few sizes.

$$\therefore I^2=3{,}300\left(\frac{a}{0.0036}V^{0.5}D^{2.5}+D^2\right)\theta-0.166\times10^6D^3$$

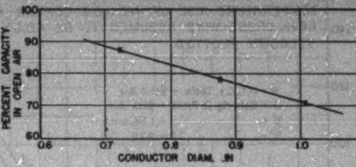

Figure 4. Per cent current-carrying capacity of ACSR conductors inside all-ferrous suspension clamps compared to that in open air

From the Russian, English, and American data $a/0.0036$ is chosen as 3.0

$$\therefore I^2=3{,}300(3.0V^{0.5}D^{2.5}+D^2)\theta-0.166\times10^6D^3$$

This is in a form that can be plotted on a Nomogram[4] and this is done in Figure 2. Instead of D the nominal conductor sizes are shown, the θ scale is marked in ambient degrees F, and the V scale is multiplied by 2.5 as previously decided.

For a particular conductor, say 477,000 circular mils with $D=0.858$ this equation simplifies to

$$I^2=2{,}080(3.24V^{0.5}+1)\theta-0.105\times10^6$$

and can be shown on the very simple nomogram of Figure 3.

Influence of Conductor Hardware

Since very little information was available regarding the limitation imposed on current-carrying capacity by conductor hardware, some tests were conducted by the Commission's Research Division. As a high degree of accuracy was not considered essential, these tests used natural wind on the roof of the Laboratory and also a "rough and ready" wind tunnel. Three sizes of ACSR conductors were used, 795,000, 477,000, and 336,400 circular mils with a galvanized malleable-iron type of suspension clamp having no armour over the conductor. The 477,000 circular mil clamp was eight inches long and had a seat diameter of one inch.

Over a range of wind velocities from zero to ten miles per hour and temperature rises up to 100 degrees centigrade it was found that for any particular conductor tested a single percentage reduction in current-carrying capacity was applicable. This information is presented in Figure 4 with conductor diameter as abscissa. However, this curve should not be considered as generally applicable; the only safe method is to conduct experiments covering the particular hardware in question.

It is obvious that for a particular transmission line this factor can be applied to any nomogram similar to Figure 3 by adjusting the current scale by the appropriate amount.

Conclusion

It has been shown that the current-carrying capacities of a wide range of conductors can be included in one nomogram, Figure 2. However, since the nomogram generally will be used hurriedly under the pressure of abnormal operating conditions, it should be as simple as possible. Hence the simpler nomogram, Figure 3, applicable to only one combination of conductor and line hardware is recommended for operating use.

References

1. SAFE RATINGS FOR OVERHEAD LINE CONDUCTORS, Leonard M. Olmsted. *AIEE Transactions*, volume 62, 1943, pages 844–53.

2. CURRENT CARRYING CAPACITY OF BARE STRANDED CONDUCTORS, Second Report, E. E. Hutchings, R. G. Parr. The British Electrical and Allied Industries Research Association, Ref. O/T5.

3. MAGNETIC HEATING OF TRANSMISSION LINE CLAMPS, V. L. Crabb, J. M. Sheadel. *AIEE Transactions*, volume 68, part II, 1949, pages 1032–35.

4. EMPIRICAL EQUATIONS AND NOMOGRAPHY (book), Dale S. Davis. McGraw-Hill Book Company, New York, N. Y., 1943.

Discussion

Leonard M. Olmsted (Duquesne Light Company, Pittsburgh, Pa.): This paper constitutes another valuable addition to the growing store of information about the rating of overhead lines. Those who undertook the subject, seeking to procure additional capacity to speed up war production some eight to ten years ago, were faced with a great scarcity of data relating to the effect of moderate temperatures upon the mechanical strength of conductors. In our early work, we utilized available data as fully as possible, then allowed a 20 per cent margin of safety to compensate for the suspected inaccuracies in available data and to allow for other limitations which had not then been evaluated. Every important subsequent addition to the literature has been reviewed carefully and incorporated into the basic data from which we determine operating ratings. It appears that the 20 per cent margin originally allowed was a good choice, as most of the additions to basic data otherwise would have required a reduction in operating ratings.

Our efforts have been applied mostly to hard-drawn copper conductors, as we have no lines which are entirely aluminum cable steel-reinforced (ACSR) and it appears that the copper portions are somewhat more limited in rating than the ACSR of equiva-

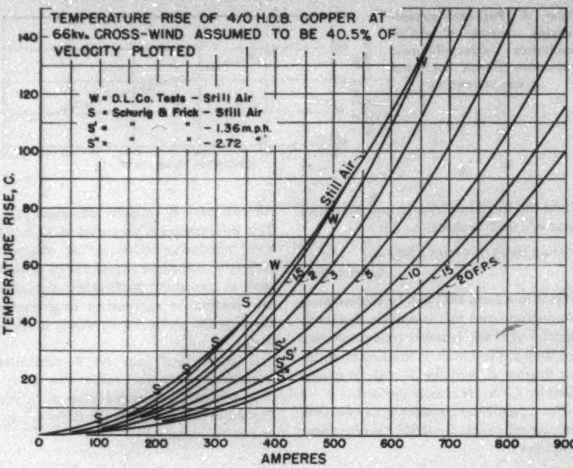

Figure 1

lent conductivity. During this period, the problem of splices and connectors suitable for heavy-current operation has been investigated and satisfactorily solved. Nonmagnetic suspension clamps have been utilized to eliminate the heating formerly caused by magnetic losses. New standards have been developed to provide the ground clearances required for conductors at higher operating temperatures. Last, but not least, our knowledge of the problem has developed to the point where we can confidently give higher ratings for emergency operation, and modify these ratings for seasonal variations in load and atmospheric conditions, with reasonable assurance of retaining adequate margins of safety throughout the economic life of the conductors.

As long as we are considering normal operation of lines, it appears that proper use of annual or seasonal equivalents of ambient temperature, conductor temperature, wind velocity and sun heating are adequate to determine ratings. When we set aside a certain portion of the useful life to provide for emergency operation at a higher rating for a limited number of hours, however, then we are permitting a considerable increase in heating which could cause deterioration of joints or dangerous ground clearances if the emergency should occur during a period of relatively high ambient temperature and little or no wind.

From our experience with the application of equations for current capability in moving air to an essentially still air condition, we are inclined to believe that the only safe procedure is to calculate low velocity conditions both as moving air and as still air. We have found it desirable to revert to the original test data of Dr. I. Langmuir[1] and Dr. C. W. Rice[2,3] to determine the current capability of a given conductor under annual equivalent temperature, wind, and sun-heating conditions, then to determine the conductor temperature for other atmospheric combinations by use of the approximation $I=CD^{1.25}(T_c-T_0)^{0.5}V^{0.2}$

where D = outside diameter of conductor, inches

T_c = conductor temperature, C

T_0 = air temperature, corrected for sun heating, C

V = wind velocity, feet per second

C = constant derived from comparison with I from more exact determination for annual equivalent conditions

With this method, approximately correct results are obtained from "still air" if it is assumed to have a velocity of $0.0880D^{0.5}(T_C-T_0)^{0.5}$ feet per second normal to the line conductor. For a given conductor, it is convenient to work from a curve such as Figure 1, which shows how the "still air" limit may indicate a lower extreme conductor temperature than any formula developed for moving air. Various test points are noted; keeping in mind that 1.36 miles per hour normal to the conductor corresponds to 4.93 feet per second of random direction, it appears that the data are within reasonable agreement.

It should be emphasized that the law of diminishing returns definitely applies to the up-rating of overhead conductors. Preparing a circuit for higher capability not only may involve a sizable expenditure for joints, non-ferrous hardware and improved ground clearances, but also paves the way for increased energy losses. To a certain point, these expenditures are justified, but there certainly must be a point where the construction of new facilities will be the better solution for normal use. In case of emergency, however, it is essential that the fullest possible use be made of line capability to reduce customer interruptions and to reduce investment for emergency use only.

For our system, it is believed that an emergency rating 50 per cent above the normal is desirable, and obtainable without excessive expenditure. A typical example is a 4/0 hard-drawn copper circuit which has been rehabilitated for winter operation at 430-amperes normal, 650-amperes one hour emergency followed by 23 hours at 610 amperes, with an expected life of 75 years. If no margin had been required for the high emergency loading, the same circuit could have been rated 470 amperes, although such loading entails a 20 per cent increase in line losses which tend to reduce the economic gain. The operating advantage of the high emergency rating more than justifies the small reduction in normal rating.

REFERENCES

1. CONVECTION AND RADIATION OF HEAT, I. Langmuir. *Transactions*, American Electro Chemical Society, (New York, N.Y.) volume 23, 1913, pages 299–332.

2. FREE AND FORCED CONVECTION OF HEAT IN GASES AND LIQUIDS, C. W. Rice. *AIEE Transactions*, volume 42, 1923, pages 653–706.

3. FREE CONVECTION OF HEAT IN GASES AND LIQUIDS—II, C. W. Rice. *AIEE Transactions*, volume 43, 1924, pages 131–44.

Elements of System Capacity Requirements

C. W. WATCHORN
MEMBER AIEE

THE assigned subject embraces all the factors that must be considered in the determination and planning of the capacity to be provided for an electric system, so that the load as a whole will be supplied most economically with reasonable assurance of continuity of service. Such planning requires a determination of the level of service reliability, or the risk of failure to carry the load, as a measure of the assurance of continuity of service. This in turn is a basis for decision, not only as to the amount of the capacity to be provided, but also the manner in which it is to be provided.

The level of service reliability, insofar as generating capacity is involved, depends on the amount of installed capacity, the probable load conditions, the capacities and pressures of individual steam boilers and turbines, the probable forced outage rates of the steam turbines and boilers, the extent to which they may be interconnected steamwise, the maintenance schedules, both as to frequency and duration, and also whether on a 1-, 2-, or 3-shift basis, routine maintenance requirements, and the seasonal and miscellaneous capacity reductions. In the event hydro capacity is installed or is being considered for installation on the system, the capacities, probable forced outage rates and scheduled maintenance requirements of the hydro units, the stream flow characteristics, the chronological relationship of the seasonal load variations to the stream flow characteristics, the reservoir capacity and scheme of operation are additional factors upon which the level of service reliability is dependent.

Wide differences in the installed capacity required for the same assurance of service, or the same level of service reliability, result from different pressures and arrangements of boilers and turbines, different sizes of boilers and turbines, different maintenance schedules and different characteristics of seasonal load variations, and so forth, all for very nearly the same annual peak load conditions. Such results demonstrate that the use of some fixed percentage reserve requirement, applicable to all conditions is unreasonable. Probability methods applied to generating capacity problems, provide much valuable data that are not obtainable in any other way. Such methods supply a rational basis for the design of the general features of the generating facilities so as to provide the desired level of over-all system reliability at the minimum total over-all system cost.

Probability methods provide a tool by means of which it is possible to calculate the risk being taken to carry some given load with some given installed capacity; they do not and cannot provide a guarantee against forced outages of generating facilities nor against failures to carry the load. The chance of failure to carry a particular load with some given installed capacity is the same whether or not probability methods have been applied. The application of probability methods does not prevent the installation of any amount of additional capacity that it may be desired to provide, but it does measure the increase in system reliability obtained thereby, thus furnishing a basis upon which can be decided whether such added capacity is worth its many millions of dollars of cost.

Table I. Method of Computing Probabilities of Availability of Various Numbers of a Group of Boilers or Turbines

The probability all or n units will be available (the first term)
$= q^n$
The probability $n-1$ units will be available (the second term)
$= (n)(\text{the first term})(p/q)$
The probability $n-2$ units will be available (the third term)
$= [(n-1)/2](\text{the second term})(p/q)$
The probability $n-3$ units will be available (the fourth term)
$= [(n-2)/3](\text{the third term})(p/q)$, and
The probability $n-4$ units will be available (the fifth term)
$= [(n-3)/4](\text{the fourth term})(p/q)$, etc.

The application of probability methods to capacity problems do not involve complicated mathematics, but rather only two very simple principles, that are inherent in many games of chance: (1) the probability that two or more independent events will happen simultaneously is the product of the probabilities that each will happen independently, and (2) the probability that some one of two or more similar independent events will happen is the sum of the probabilities that each of such similar events will happen independently. Calculations made according to these principles are much more simple than many others that engineers are frequently called upon to make. A very large number of arithmetical computations may be involved in the applications of these principles to generating capacity problems, particularly when many different conditions are being studied. Still, the computations are basically simple, involving only

Table II. Numerical Computation of the Probabilities of Availability of Various Numbers of Boilers or Turbines of a Group of Four Units

The first term $= (0.99)^4 = 0.9605960$
The second term $= 4(0.9605960)(0.01/0.99) = 0.0388120$
The third term $= (3/2)(0.0388120)(0.01/0.99) = 0.0005880$
The fourth term $= (2/3)(0.0005880)(0.01/0.99) = 0.0000040$
The fifth term $= (1/4)(0.0000040)(0.01/0.99) = 0.0000000$
1.0000000

Paper 51-197, recommended by the AIEE Power Generation Committee and approved by the Technical Program Committee for presentation at the AIEE Summer General Meeting, Toronto, Ont., Canada, June 25–29, 1951. Manuscript submitted February 8, 1951; made available for printing April 30, 1951.

C. W. WATCHORN is with the Pennsylvania Water & Power Company, Baltimore, Md.

Table III. Probability of Availability of the Indicated Number of Boilers or Turbines for Forced Outage of Individual Boilers or Turbines Equal to 0.01, 0.02, and 0.03

Number of Boilers or Turbines in Group

Units Available	p=0.01	p=0.02	p=0.03	Units Available	p=0.01	p=0.02	p=0.03	Units Available	p=0.01	p=0.02	p=0.03	Units Available	p=0.01	p=0.02	p=0.03
		1				2				3				4	
1	0.9900000	0.9800000	0.9700000	2	0.9801000	0.9604000	0.9409000	3	0.9702990	0.9411920	0.9126730	4	0.9605960	0.9223682	0.8852928
0	100000	200000	300000	1	198000	392000	582000	2	294030	576240	846810	3	388120	752954	1095208
				0	1000	4000	9000	1	2970	11760	26190	2	5880	23050	50809
								0	10	80	270	1	40	314	1047
												0			8
	1.0000000	1.0000000	1.0000000		1.0000000	1.0000000	1.0000000		1.0000000	1.0000000	1.0000000		1.0000000	1.0000000	1.0000000
		5				6				7				8	
5	0.9509900	0.9039208	0.8587340	6	0.9414801	0.8858424	0.8329720	7	0.9320653	0.8681256	0.8079828	8	0.9227447	0.8507631	0.7837434
4	480298	922368	1327939	5	570594	1084705	1545721	6	659036	1240179	1749241	7	745652	1389001	1939159
3	9703	37648	82141	4	14409	55342	119515	5	19971	75929	162301	6	26361	99214	209909
2	98	768	2541	3	194	1506	4929	4	336	2583	8366	5	533	4049	12984
1	1	8	39	2	2	23	114	3	4	53	259	4	7	103	502
				1			1	2			5	3		2	12
	1.0000000	1.0000000	1.0000000		1.0000000	1.0000000	1.0000000		1.0000000	1.0000000	1.0000000		1.0000000	1.0000000	1.0000000
		9				10				11				12	
9	0.9135172	0.8337478	0.7602311	10	0.9043820	0.8170729	0.7374241	11	0.8953382	0.8007314	0.7153014	12	0.8863848	0.7847167	0.6938424
8	830470	1531373	2116107	9	913517	1667495	2280693	10	994820	1797560	2433500	11	1074406	1921755	2575085
7	33555	125010	261786	8	41524	153137	317416	9	50244	183425	376314	10	59689	215708	438030
6	791	5953	18892	7	1119	8334	26179	8	1523	11230	34916	9	2010	14674	45158
5	12	182	876	6	20	298	1417	7	31	458	2160	8	46	674	3142
4		4	27	5		7	53	6		13	93	7	1	22	155
3			1	4			1	5			3	6			6
	1.0000000	1.0000000	1.0000000		1.0000000	1.0000000	1.0000000		1.0000000	1.0000000	1.0000000		1.0000000	1.0000000	1.0000000
		13				14				15				16	
13	0.8775209	0.7690225	0.6730271	14	0.8687458	0.7536420	0.6528363	15	0.8600583	0.7385692	0.6332512	16	0.8514577	0.7237978	0.6142536
12	1152300	2040264	2705985	13	1228529	2153263	2826714	14	1303119	2260926	2937763	15	1376093	2363421	3039606
11	69837	249828	502142	12	80661	285637	568257	13	92140	322990	636010	14	104250	361748	705063
10	2587	18694	56944	11	3259	23317	70300	12	4033	28564	85238	13	4914	34452	101762
9	66	954	4403	10	91	1309	5979	11	122	1749	7909	12	168	2285	10229
8	1	35	245	9	2	54	370	10	3	79	538	11	4	112	759
7			10	8			17	9			29	10		4	43
								8			1	9			2
	1.0000000	1.0000000	1.0000000		1.0000000	1.0000000	1.0000000		1.0000000	1.0000000	1.0000000		1.0000000	1.0000000	1.0000000

NOTE: p=0.01 for boilers or turbines operating at pressures of 1,000 pounds per square inch and below. (based on EEI data)
p=0.02 " " " " " " " " about 1,300 pounds per square inch. (based on EEI data)
p=0.03 " " " " " " " " " 1,500 " " " " (assumed for illustration only)

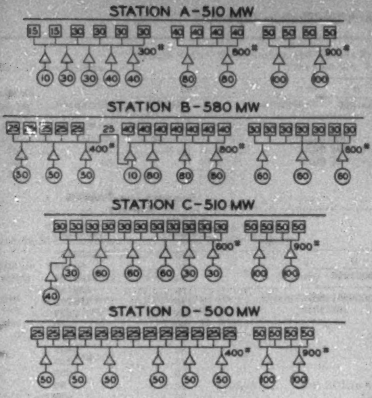

Figure 1 (left). Boiler and turbine arrangements, capacities and pressures for present generating stations—in operation, under construction and planned — total capacity 2,100 mw

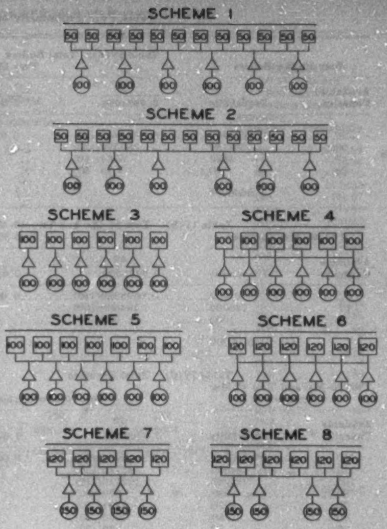

Figure 2 (right). Various schemes for boiler and turbine arrangements and capacities under consideration for a proposed future generating station, Station E—total capacity 600 mw with 900, 1,300, and 1,500 pounds per square inch pressures

multiplication and addition, and are readily kept in an intelligible order by recording the results in a systematic manner. Such data relating to any one station or group of stations, when once determined, are always thereafter available for subsequent studies, thus greatly reducing the amount of calculation required at such time.

These probability calculations provide the means for making one or both of two different general types of determinations, (1) the level of service reliability of a generating system for use as a basis for decision regarding provision of additional capacity, and (2) the levels of service reliability resulting from the installation of various alternative facilities as a basis for a very accurate determination of the relative merits, capacity-wise of such alternative schemes. Short-cut methods may be useful in the first of these determinations; however, the latter determination cannot be made satisfactorily by means of any of the generally known short-cut methods, consequently the longer detailed arithmetical method must be used. In view of the very large value of the information thus obtained, particularly as a factor in the determination of the design of the overall most economical system, the time and cost of making such detailed calculations are justified many times over.

There are many mathematical niceties or refinements that are not incorporated in the calculations shown herein, since if they were included, the number of computations that would be required to be made would be increased several thousandfold and the differences obtained by including them as compared with omitting them are relatively small and are of no practical significance.

General

There are three principal phases in the application of probability methods to generating capacity problems, viz., (1) the determination of the availability of capacity, (2) the determination of the loads to be carried, and (3) the combining of these two groups of data to determine the probability of failure to carry the load.

One element of the first of these phases is made available by forced outage data on steam turbines and boilers and hydroelectric units collected by various committees of the Edison Electric Institute that have been published by the AIEE, under the sponsorship of the AIEE Joint Subcommittee on the Application of Probability Methods to Power System Problems.[1] These data show that the average forced outage rates, or probabilities of unavailability, for steam turbines and also for steam boilers operating at pressures below 1,000 pounds per square inch, are 1.0 per cent for all practical purposes; and for both steam turbines and boilers operating at higher pressures, about 2.0 per cent. Since these outage rate data were collected at a time prior to the present general availability of equipment operating at the nominal 1,500 pounds per square inch pressure, the forced outage rate data for turbines and boilers operating at pressures higher than 1,000 pounds per square inch is here assumed to apply to turbines and boilers operating at the nominal 1,300 pounds per square inch pressure. For the purpose of further illustrating the effect of forced outage rates on capacity requirements, the probabilities of unavailabilities of both turbines and boilers operating at the nominal 1,500 pounds per square inch pressure have here been assumed to be 3.0 per cent. These rates are not based on actual experience and it should be clearly understood that they are not intended as predictions of the performance of such high pressure units. If higher forced outage rates than these are applicable to the reheat cycle for these various pressure ranges this is then a further factor to be considered in the determination of capacity requirements; but this particular situation has not been used in the subsequent illustrations.

Since the probability of unavailability of a turbine or boiler operating at pressures below 1,000 pounds per square inch is 0.01, and since it is a certainty that the unit (either turbine or boiler) will either be available or unavailable, the probability of availability for a turbine or boiler operating in this pressure range is 0.99.

The two basic principles previously stated can now be applied to two turbines or two boilers. For example, the probability that the two turbines will be available at the same time is equal to 0.99 multiplied by 0.99 or 0.9801; the proba-

Table IV. Probability of Availability of Station A Low-Pressure Capacity

Table IV(A). Total Boilers

Four 30-Mw Boilers		Two 15-Mw Boilers		
Available Capacity	Probability	30 0.9801000	15 0.0198000	0 0.0001000
120	0.9605960	0.9414801(150)	0.0190199(135)	960(120)
90	388120	380396(120)	7685(105)	39(90)
60	5880	5764(90)	115(75)	1(60)
30	40	39(60)	1(45)	
	1.0000000			

Table IV(B). Two 30-Mw and Two 40-Mw Turbines

Two 40-Mw Turbines		Two 30-Mw Turbines		
Available Capacity	Probability	60 0.9801000	30 0.0198000	0 0.0001000
80	0.9801000	0.9605960(140)	0.0194060(110)	0.0000980(80)
40	198000	194060(100)	3920(70)	20(40)
0	1000	980(60)	20(30)	
	1.0000000			

Table IV(C). Total Turbines

Two 30-Mw and Two 40-Mw Turbines		One 10-Mw Turbine	
Available Capacity	Probability	10 0.9900000	0 0.0100000
140	0.9605960	0.9509901(150)	0.0096059(140)
110	194060	192119(120)	1941(110)
100	194060	192119(110)	1941(100)
80	980	970(90)	10(80)
70	3920	3881(80)	39(70)
60	980	970(70)	10(60)
40	20	20(50)	
30	20	20(40)	
	1.0000000		

Summary Low-Pressure Capacity

Available Capacity	Probability
150	0.8953382
140	90438
135	182704
120	558186
110	193795
105	7679
100	1940
90	6770
80	3891
75	115
70	1009
60	50
50	20
45	1
40	20
	1.0000000

Table IV(D). Total Low-Pressure Capacity

Total Turbines		Total Boilers							
Available Capacity	Probability	150 0.9414801	135 0.0190199	120 0.0381356	105 0.0007685	90 0.0005803	75 0.0000115	60 0.0000040	45 0.0000001
150	0.9509901	0.8953382(150)	0.0180878(135)	0.0362666(120)	0.0007308(105)	0.0005518(90)	0.0000110(75)	0.0000038(60)	0.0000001(45)
140	96059	90438(140)	1826(135)	3663(120)	74(105)	56(90)	1(75)		
120	192119	180876(120)	3655(120)	7326(120)	148(105)	111(90)	2(75)	1(60)	
110	194060	182704(110)	3691(110)	7400(110)	149(105)	113(90)	2(75)	1(60)	
100	1941	1828(100)	37(100)	74(100)	1(100)	1(90)			
90	970	913(90)	18(90)	37(90)	1(90)	1(90)			
80	3891	3663(80)	74(80)	149(80)	3(80)	2(80)			
70	1009	950(70)	19(70)	38(70)	1(70)	1(70)			
60	10	9(60)		1(60)					
50	20	19(50)		1(50)					
40	20	19(40)		1(40)					
	1.0000000								

bility that one of the two turbines will be available at the same time the other is unavailable is equal to twice (since there are two ways in which this event can happen) 0.99 multiplied by 0.01 or 0.0198, and the probability that both turbines will be unavailable at the same time is equal to 0.01 multiplied by 0.01 or 0.0001. The sum of these three amounts is equal to unity, since it is a certainty (as indicated by a probability of 1.0) that the units will both be available, one will be available with the other unavailable or both will be unavailable. Such probabilities can be numerically determined, for any number of units or for any probability of outage, from successive terms in the binominal expression $(q + p)^n$, where "n" is the number of turbines or boilers, "p" the probability of unavailability and "q" the probability of availability. These various terms are readily computed from the expressions shown in Table I, from which, for four turbines or boilers operating at pressures below 1,000 pounds per square inch, we have the numerical results shown in Table II.

This is all there is to the fundamental or basic principles of probability methods applicable to generating capacity problems. They certainly are neither complicated nor difficult either to understand or to apply. Care must be taken as to the details of making the calculations to arrange the results in a systematic and orderly manner for purposes of control, otherwise they would soon become hopelessly confused.

Table III, computed in the manner shown in Tables I and II, shows the probabilities of availability for various numbers, from one to 16, of boilers or turbines for forced outage rates or probabilities of unavailability of single units of 0.01, 0.02, and 0.03. These data provide all the basic probability information required for most systems. If these data are insufficient, or if other outage rates are required, the expansions, as shown in Tables I and II, are easily made.

Application

THE PROBLEM

The method of applying the foregoing developed fundamental principles to generating capacity problems can be best

Table V. Probability of Availability of Station B 400 Pounds and 800 Pounds Pressure Capacity

Table V(A). Total Station 400 Pounds Pressure

Five 25-Mw Boilers		Three 50-Mw Turbines			
Available Capacity	Probability	150	100	50	0
		0.9702990	0.0294030	0.0002970	0.0000010
125	0.9509900	0.9227447(125 25T)	0.0279620(100)	0.0002824(50)	0.0000010(0)
100	480298	466032(100 25T)	14122(100)	143(50)	
75	9703	9415(75 25T)	285(75 25T)	3(50)	
50	98	95(50 25T)	3(50 25T)		
25	1	1(25 25T)			
	1.0000000				

Table V(B). 800 Pounds Pressure Turbines

Three 80-Mw Turbines		One 10-Mw Turbine	
Available Capacity	Probability	10	0
		0.9900000	0.0100000
240	0.9702990	0.9605960(250 B)	0.0097030(240)
160	29430	291090(170 B)	2940(160)
80	2970	2940(90 B)	30(80)
0	10	10(10 B)	
	1.0000000		

Table V(C). Total Station 800 Pounds Pressure

Turbines		Seven 40-Mw Boilers				
Available Capacity	Probability	280	240	200	160	120
		0.9320653	0.0659036	0.0019971	0.0000336	0.0000004
250 B	0.9605960	0.8953382(250 25B)	0.0633067(240)	0.0019184(200)	0.0000323(160)	0.0000004(120)
240	97030	90438(240)	6395(240)	194(200)	3(160)	
170 B	291090	271316(170 25B)	19183(170 25B)	581(170 25B)	10(160)	
160	2940	2740(160)	194(160)	6(160)		
90 B	2940	2740(90 25B)	194(90 25B)	6(90 25B)		
80	30	28(80)	2(80)			
10 B	10	9(10 25B)	1(10 25B)			

Table V(D). Total 400 Pounds and 800 Pounds Pressure Capacity

Total High Pressure		Total Low Pressure							
Available Capacity	Probability	125 25T	100 25T	100	75 25T	50 25T	50	25 25T	0
		0.9227447	0.0466032	0.0293742	0.0009700	0.0000098	0.0002970	0.0000001	0.0000010
250 25B	0.8953382	0.8261686(400)	0.0417256(375)	0.0262998(350)	0.0008685(350)	0.0000088(325)	0.0002659(300)	0.0000001(300)	0.0000009(250)
240	729900	673510(365)	34016(340)	21441(340)	708(315)	7(290)	217(290)		1(240)
200	19378	17881(325)	903(300)	569(300)	19(275)		6(250)		
170 25B	291080	268593(320)	13565(295)	8551(270)	282(270)	3(245)	86(220)		
160	3276	3023(285)	153(260)	96(260)	3(235)		1(210)		
120	4	4(245)							
90 25B	2940	2713(240)	137(215)	86(190)	3(190)		1(140)		
80	30	28(205)	1(180)	1(180)					
10 25B	10	9(160)	1(135)						
	1.0000000								

Summary 400 Pounds and 800 Pounds Pressure Capacity

Available Capacity	Probability
400	0.8261686
375	417256
365	673510
350	271683
340	55457
325	17969
320	268503
315	708
300	4132
295	13565
290	224
285	3023
275	19
270	8833
260	249
250	15
245	7
240	2714
235	3
220	86
215	137
210	1
205	28
190	89
180	2
160	9
140	1
135	1
	1.0000000

illustrated by their application to an actual problem. Although the system considered herein for illustrative purposes is an all-steam system, the illustration could also have been made with respect to a combined hydro and steam system. The illustrated all-steam system is made up of four generating stations, Stations A, B, C, and D, with a total capacity of 2,100,000 kw, shown schematically on Figure 1. These four stations will be fully developed within the next several years, after which a new site will be required for additional capacity. The site available for the next plant (Station E) can be developed for an ultimate capacity of 600,000 kw.

The problem is two-fold, (1) to determine the risk or chance of failure to carry the load for some future year for various designs of the new station when it is complete, and (2) to determine the general design layout of this plant for maximum over-all system economy which overall most economic determination is beyond the scope of this paper. Although the most economical design of Station E, without regard to the system as a whole, would possibly be one with large high pressure boilers and turbines installed as a unit system, possibly with reheat, such a plant may not result in the most economical design for the system as a whole. If the design results in low availability of capacity, additional capacity will be required to be otherwise provided, at least from time to time, to maintain the requisite level of service reliability. The cost associated with such additional capacity is obviously a charge against the plant design; and in some cases, this cost may more than offset the greater economies of the particular plant when considered by itself and without regard to the effect on the system as a whole. The capacity effect of the several elements that enter into this phase of the problem can be evaluated only by means of probability methods, as illustrated for eight possible design layouts for the future Station E, shown on Figure 2. To show further the effect of different forced outage rates as influenced by station design, the capacity requirements are determined for each of these layouts with Station E built for 900, 1,300, and 1,500 pounds per square inch pressures. The number of answers is still further increased by consideration of single and double shift maintenance schedules and three characteristics of seasonal load variations.

Availability of Capacity

A first step in the solution of most generating capacity problems is the determination of the effect of forced outages on

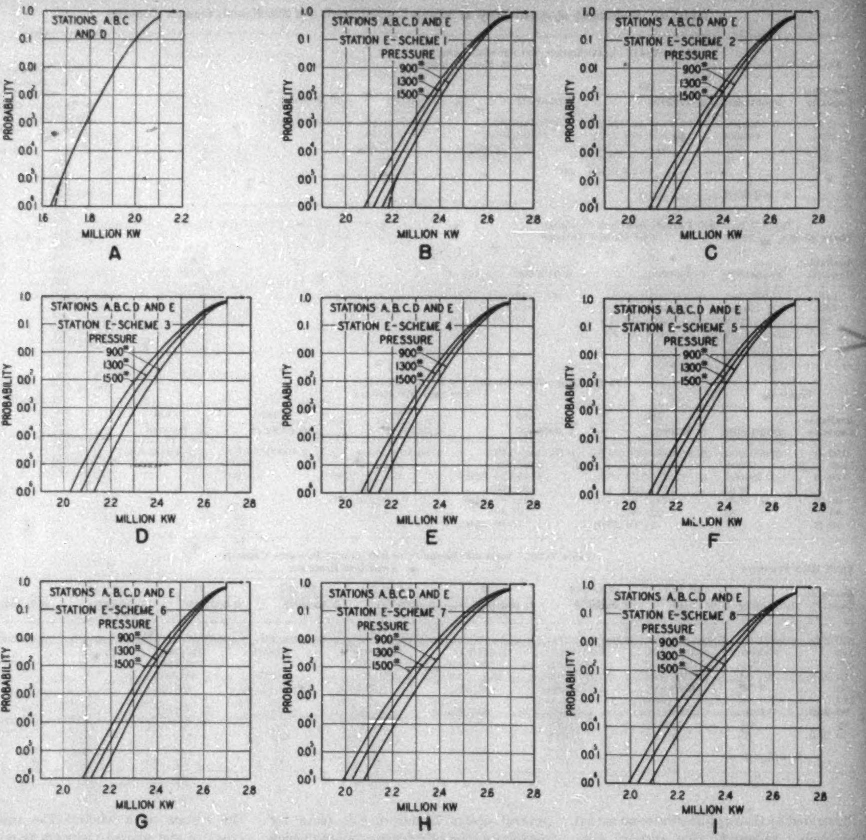

Figure 3. Probability of availability of total system capacity equal to and smaller than the amount shown—schemes 1 to 8 for Station E at 900, 1,300, and 1,500 pounds per square inch pressures

the probable availability of generating capacity. Table IV, which treats of the low-pressure capacity of Station A, was prepared to show the general manner in which such calculations may be made. Table IV(A) of this table shows the method of computing the probabilities of availability of various amounts of the boiler capacity. These calculations are shown in a form that has been found to be most adaptable for accounting for all the various combinations under consideration. The basic probabilities are taken from Table III and are shown to the right of the capacities for one, two, three, and four of the four 30-megawatt (mw) boilers available and below the capacities for zero, one and two of the two 15-mw boilers available. The probabilities that various numbers of the 30-mw boilers will be available at the same time that various numbers of the 15-mw boilers also will be available are the products of the separate probabilities that each will be available (application of the first basic principle previously discussed). Each must be multiplied by each value of the probabilities shown in the column to the left, and these products are entered in the computation form, as shown, directly below and opposite the respective component probabilities. The next step identifies each of these probabilities with the available boiler capacity with which they are associated, as shown in parentheses directly to the right of the various probabilities previously computed. Such capacities are the sum of the two boiler capacities that enter into each of the combinations.

The computations of the probable availability of the low-pressure turbine capacity of Station A are similarly made as shown in Tables IV(B) and IV(C), the results of IV(B) being used in the left hand column of Table IV(C).

Table IV(D) shows the method of combining the probable availabilities of the

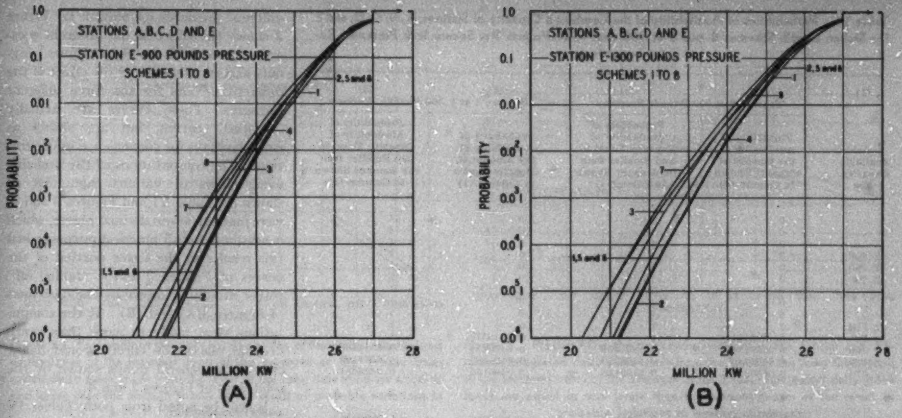

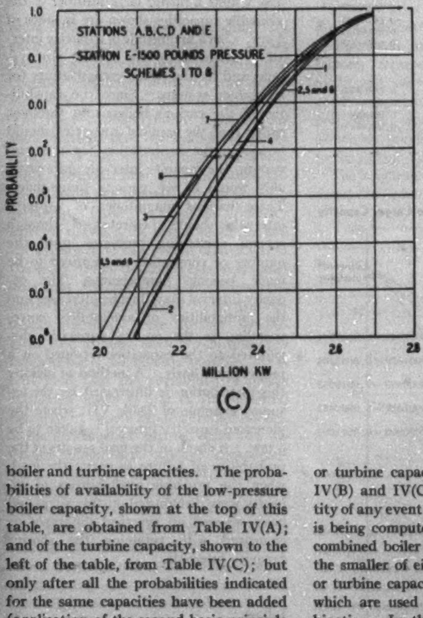

Figure 4. Probability of availability of total system capacity equal to and smaller than the amount shown—900, 1,300, and 1,500 pounds per square inch pressures for Station E with schemes 1 to 8

boiler and turbine capacities. The probabilities of availability of the low-pressure boiler capacity, shown at the top of this table, are obtained from Table IV(A); and of the turbine capacity, shown to the left of the table, from Table IV(C); but only after all the probabilities indicated for the same capacities have been added (application of the second basic principle previously discussed). Again, the computations of the various probabilities of availability of turbine and boiler combinations in Table IV(D) are obtained as the products of the component probabilities at the top and to the left of the table. In this case, the boiler and turbine capacities are being combined rather than boiler capacities alone as in Table IV(A), or turbine capacities alone as in Tables IV(B) and IV(C). Therefore, the identity of any event for which the probability is being computed, that is, the available combined boiler and turbine capacity, is the smaller of either the available boiler or turbine capacities, the probabilities of which are used in that particular combination. In this case there are fairly numerous combinations that result in the same available combined boiler and turbine capacity. Again the application of the second basic probability principle calls for the summation of the probabilities for the same available capacity, producing the results shown in the summary at the right of the table.

Because each of these calculations requires the multiplication of two series of fractions, of which the sum should always be equal to unity, it is important as well as convenient to check the sum of the products, and if necessary to make adjustments to bring the sum to unity.

Table V is shown to illustrate the treatment of the 10-mw superposed capacity of Station B. These calculations should be clear from the above discussion of Table IV and reference to the schematic diagram of Station B shown on Figure 1. It will be noted from Figure 1 that the exhaust from this superposed unit is capable of producing 25-mw generation at 400 pounds per square inch pressure. Accordingly, Tables V(A) and V(D) indicate by the designation "25T," in the event identification in parentheses, when there is 25 mw more 400 pounds turbine capacity than boiler capacity available to utilize such exhaust steam. The "B" in the parentheses in Tables V(B) and V(C) indicates that the superposed unit is available, while the designation, "25B" in Tables V(C) and V(D) indicates that exhaust steam capable of producing 25 mw at 400 pounds pressure is available from the superposed unit.

The computations of the probabilities of availability of various amounts of capacity for the other stations of the system and combinations of stations, present

Table VI. Probabilities of Availability of the Combined Capacity of Stations A, B, C, D, and E for Station E with Schemes 2 and 3 at 900 and 1500 Pounds Per Square Inch Pressures, Respectively

(1)	(2)	(3)	(4)	(5)
	Scheme 2 at 900 Pounds Pressure		Scheme 3 at 1,500 Pounds Pressure	
Available Capacity, Mw	Probability of Availability of the Amount of Capacity Shown in Column (1)	Probability of Availability of Capacity Equal to and Smaller than the Amount Shown in Column (1)	Probability of Availability of the Amount of Capacity Shown in Column (1)	Probability of Availability of Capacity Equal to and Smaller than the Amount Shown in Column (1)
...	0	1	0	1
...	0	1	0	1
...	0	1	0	1
2,800	0	1	0	1
2,790	0	1	0	1
2,780	0	1	0	1
...	0	1	0	1
...	0	1	0	1
...	0	1	0	1
2,710	0	1	0	1
2,700	0.4102601	1	0.3645570	1
2,690	0.0539144	0.5897399	0.0400234	0.6954430
2,680	0.0169145	0.5358255	0.0125565	0.6554196
2,670	0.0660284	0.5189110	0.0490163	0.6428631
...	...	...	...	...
...	...	...	...	...
...	...	...	...	...
2,220	0.0000005	0.0000010	0.0000260	0.0000939
2,210	0.0000002	0.0000005	0.0000137	0.0000679
2,200	0.0000002	0.0000003	0.0000191	0.0000542
2,190	0.0000001	0.0000001	0.0000093	0.0000351
2,180	0.0000000	0.0000000	0.0000050	0.0000258
...	0.0000000	0.0000000		
...	0.0000000	0.0000000		
...	0.0000000	0.0000000		
2,070	0.0000000	0.0000000	0.0000003	0.0000005
2,060	0.0000000	0.0000000	0.0000001	0.0000002
2,050	0.0000000	0.0000000	0.0000001	0.0000001
2,040	0.0000000	0.0000000	0.0000000	0.0000000
	1.0000000		1.0000000	

Table VII. Method of Adjusting Probabilities of Availability of Capacity to Larger Capacity Intervals

Available Capacity	Original Probability			Adjusted Probability
700		+	+	=
696	0.0013261			
695	0.0036216	+0.8×0.0013261	+0.4×0.0002341	=0.0047761
692	0.0002341			
690	0.0043216	+0.6×0.0002341	+0.6×0.0001072	=0.0045264
688	0.0001072			
685	0.0017854	+0.4×0.0001072	+0.8×0.0000963	=0.0019053
684	0.0000963			
680	0.0021420	+0.2×0.0000963	+0.8×0.0001321	=0.0022669
679	0.0001321			
675	0.0010421	+0.2×0.0001321	+0.6×0.0000902	=0.0011226
673	0.0000902			
670		+	+	=
	1.0000000			1.0000000

and future, are made in the same general manner as those shown on Tables IV and V, using the proper forced outage rates for the various pressures of the different stations involved. These calculations become very long, involving numerous multiplications and additions; nevertheless, the effects of different station designs on capacity requirements cannot be determined by any other method. The use of automatic digital computers, that are particularly adaptable to making these calculations, greatly reduces the time required.

Columns (2) and (4) of Table VI show the probabilities of availability of various specific amounts of capacity computed for the system made up of Stations A, B, C, and D of Figure 1 and Station E of Figure 2 at 900 pounds per square inch pressure for Scheme 2, and at 1,500 pounds pressure for Scheme 3, respectively. Columns (3) and (5) show the probabilities of availability of capacity equal to and smaller than that shown in Column (1).

The curves of Figures 3 and 4 show plots of similar data as Columns (3) and (5) of Table VI for the system as computed for each of the eight layouts and the three different pressures for Station E; Figure 3 shows the effect of the different pressures for each of the eight different layouts and Figure 4 shows the effect of the different layouts for the three different pressures. These curves are actually "stepped" curves, but are shown as smooth curves for convenience in illustration. The computations of the probable availabilities of various capacities, as shown on Table VI and Figures 3 and 4, were made to seven decimal places, which is adequate for all practical purposes, but this results in the lower portion of the curves of Figures 3 and 4 "falling off" rather rapidly as shown by the dash lines of Figures 3(A) and (B). If the computations were made to more than seven decimal places the curves would follow closely the general trends shown by the solid lines of Figures 3 and 4.

It will be noted from both Tables IV and V that a rather large number of the available capacities shown are in steps of 5 mw. Such magnitude of capacity interval is desirable for the smaller size systems and for the initial computations for the larger systems. Since the capabilities of the various boilers and turbines, rather than the nominal capacities, should be used in the computations for an actual system, the capacity intervals quite probably would be of various magnitudes. These various magnitudes of capacity intervals should be retained through several combining processes until the number of computations required to be made become cumbersome. The capacity interval may then be increased and the probabilities of availability corresponding to the omitted capacities distributed to the capacities retained on a proportional basis. A method of making this distribution is illustrated by the assumed example of Table VII, where the increased capacity interval is taken to be 5 mw. A check of the final results of the probability of failure to carry the load, when the probable availabilities of capacity were distributed on this suggested basis, showed no practical difference as compared with retaining the shorter capacity intervals.

Loads

In studies of future capacity requirements the loads can never be known with certainty. The usual practice in such studies has been to estimate the annual peak loads for the future period and then, largely ignoring the effect on the estimates of possible seasonal and business variations, to determine capacity requirements on the basis of an arbitrary reserve for-

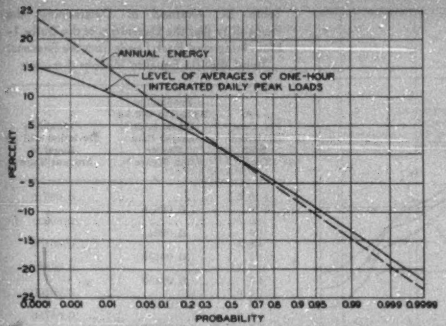

Figure 5. Probabilities the per cent deviations of the annual energy and of the level of the seasonal trend of the averages of the 1-hour integrated daily peak loads from the level of the long time trend are equal to and larger than the amount shown as the result of probable variations in business conditions

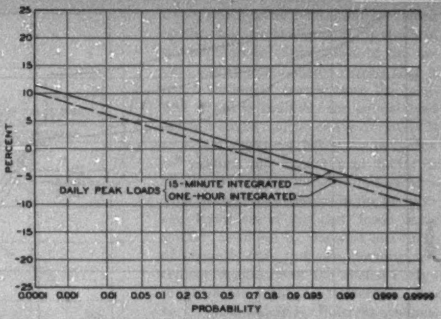

Figure 7. Probabilities the per cent deviations of the 1-hour and 15-minute integrated daily peak loads from the level of the long time trend of the seasonal trend of the averages of the 1-hour integrated daily peak loads are equal to and larger than the amount shown as the result of probable variations in weather conditions

mula. Practice is slowly changing; for example, change in seasonal load shapes on many systems has made it necessary to consider estimated loads for the entire year rather than the annual peak alone. The reserve requirement formulas for some systems give recognition to maintenance, or may even be based on probability computations; but still the estimated loads are treated more or less as a certainty. However, since the necessary interval between the initial planning and the operation of new steam capacity is in the order of two to three years, it is desirable that the variability of future estimated loads be recognized. Also as probability methods were further investigated and applied, such recognition on a rational basis has become possible. It is here held that the variability of future estimated loads is one of the essential elements in system capacity requirements.

An estimate of future loads can be broken down into several component parts: the long time trend, variations from this trend caused by business cycles, the seasonal load trend, and variations from the normal seasonal load caused by weather or other conditions of relatively short duration. Two of these components for any system as of some particular time might be considered as fixed characteristics. The long time trend and seasonal load trend usually change rather slowly. For any particular estimate of future loads (not too far in the future) they can be projected, if properly based on past experience, as relatively certain conditions that must be provided for. The other two components can be based on past experience also; but these represent the uncertainties of the future—the possible deviations from the long time and seasonal load trends. Such variable factors, representing the chance that loads will vary from relatively certain conditions, can be readily handled in a probability study by the two simple principles previously stated and applied to the forced outage data.

The long time trend of load growth may determine when various increments of capacity are to be added. It may also influence the economics of the size of such additions. But the trend of growth has no influence on the amount of system capacity required for an estimated load for some particular period, and consequently it is not an element to be considered further in this discussion.

It is then relatively simple to determine the experienced frequency of occurrence

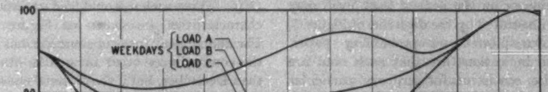

Figure 6. Seasonal trend of the averages of the 1-hour integrated daily peak loads

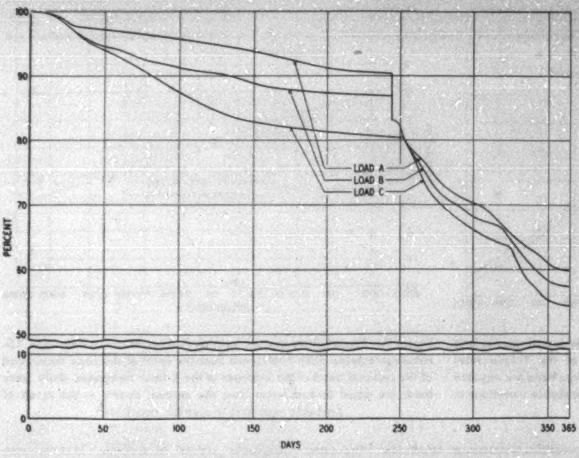

Figure 8. Duration of the seasonal trend of the averages of the 1-hour integrated daily peak loads for the seasonal load trend at the level of the long time trend

of deviations of various percentage magnitudes from the long time load trend once this trend is determined. Such experienced data, which in general are measures of the effects of the relative business activities on the annual energy requirements or on the general load level, may be illustrated by the dash line of Figure 5, shown plotted on probability paper. The indications are that such data are quite consistent for any one particular geographical area but that they may vary quite widely for different areas.

The seasonal load characteristics are determined on the basis of the averages of the weekday peak loads, over a period of recent years, adjusted for the long time load trend indicated for the load year for which it is desired to study the capacity requirements. A smooth curve is then drawn through the points thus determined. The same general analysis may also be made for Saturdays and minor holidays and for Sundays and major holidays; however, generally these latter data are not necessary for capacity studies, as shown by the relatively small magnitude of the amounts shown in the lower portion of the last four columns of Table XIII, particularly columns (9) and (10). Three such seasonal load variation characteristics are shown on Figure 6. The annual peak loads of some sections of the country may occur in months other than December, but if the seasonal curves are shifted to adjust for this fact, they might still show the general characteristics of Figure 6. The effect of these differences in characteristics of the seasonal load variations on the installed system capacity requirements is very marked. Load A requires more installed capacity to maintain some given level of service reliability than either Load B or Load C, all other conditions being equal. Similarly Load B requires more installed capacity than Load C in order to meet the same requirements as to service reliability.

Table VIII. Adjustment of the Duration Curve of the Seasonal Trend of Average 1-Hour Integrated Peak Loads for Load A for Variations in Weather Conditions

Mw Load	Days in Load Band		Per Cent Deviation		
			+'0.5	+9.5	+8.5
		Probability	0.00010	0.00031	0.00104
2,160	12		0.0012(2,386)	0.0037(2,366)	0.0125(2,344)
2,150	7		0.0007(2,375)	0.0020(2,355)	0.0073(2,333)
2,140	3		0.0003(2,364)	0.0009(2,344)	0.0031(2,322)
2,130	0		0 (2,354)	0 (2,333)	0 (2,311)
2,120	5		0.0005(2,342)	0.0016(2,322)	0.0052(2,300)
2,110	20		0.0020(2,331)	0.0062(2,311)	0.0208(2,289)
2,100	9		0.0009(2,320)	0.0028(2,300)	0.0094(2,278)

Note: The quantities shown in parentheses are the loads adjusted for the per-cent deviation.

Table IX. Method of Determining the Probability that the Deviations of the Daily 1-Hour Integrated Peak Loads from the Seasonal Trend Will Be Equal to Various Amounts

Per Cent Deviation from Trend	Probability Deviation will be Equal to or Larger than Shown From Figure 7	Probability Deviation will be Equal to Amount Shown
+10.5		0.00010
+10	0.00010	
+9.5		0.00031
+9	0.00041	
+8.5		0.00104
+8	0.00145	
+7.5		0.00275
+7	0.00420	
+6.5		0.00800
+6	0.01220	
+5.5		0.01780
+5	0.03000	
		1.00000

The daily peak loads will necessarily vary above or below those shown on Figure 6, since the values shown thereon are obtained as averages. Such variations would be the result of deviations in weather conditions from those usually experienced for the various seasons of the year, and also of the differences in the day to day habits and activities of the people in the geographical area under study. These load variations will be referred to hereinafter as being the result of variations in weather conditions. The frequency of such variations, on a one-hour integrated basis, in percentage of the seasonal trend values, may be illustrated by the dash line curve shown on Figure 7, also shown plotted on probability paper. These characteristics may also vary quite widely for different areas or for different seasons in the same area.

Figure 8 shows the duration curves for Loads A, B, and C, based on the normal seasonal trend of the averages of the daily peak loads as shown on Figure 6. These duration data for Load A, adjusted for the variations from the average caused by variations in weather conditions, as illustrated by Figure 7, are shown by the solid line curve on Figure 9. This latter curve has the familiar general characteristics expected for an annual duration curve of daily peak loads.

The manner of making these calculations, by application of our two general probability principles, is indicated on Table VIII. The data to the left of Table VIII are on the basis of Load A, as shown on Figure 8, for 2,167 mw annual peak of the seasonal trend of the averages of the weekday 1-hour integrated peak loads, assumed for the year 1958. The data at the top of this table are obtained from the dash line of Figure 7 as indicated

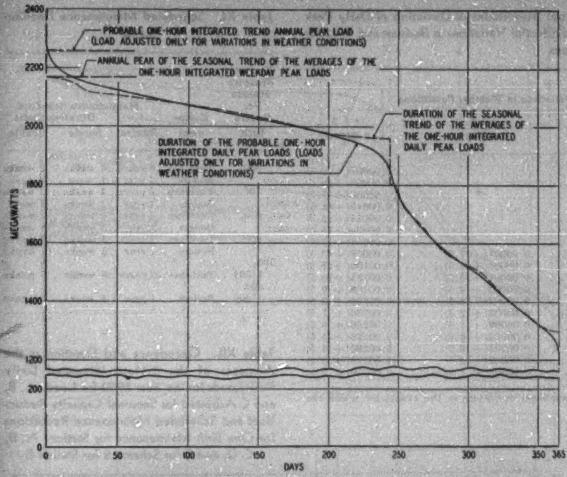

Figure 9. Comparison between the durations of the probable 1-hour integrated daily peak loads and the seasonal trend of the averages of the 1-hour integrated daily peak loads—for Load A—for the seasonal load trend at the level of the long time trend—for the year 1958

in Table IX. Since the total of the probabilities of the various per cent deviations shown in the calculations indicated on Table VIII is equal to unity, as shown in Table IX, and the total number of days in a year is equal to 365, the total of the number of days resulting from the calculations also will be equal to 365. The days shown computed in Table VIII are tallied with respect to the loads shown in parentheses and a new load duration curve determined which reflects the adjustment for variations in weather conditions, assuming that the load level coincides with the long time trend. This is the curve shown by the solid line on Figure 9, for Load A for the year 1958. The dash line is the same as that for Load A of Figure 8, converted to megawatts, also for the year 1958.

The effect of the variations of business conditions on the daily peak loads can be derived from the deviations of the annual energy requirements from the long-time trend, which latter relationship is shown by the dash line of Figure 5. A study of the relationship of the peaks to the annual energy requirements reveals that if the deviation of energy from the long-time trend is positive, the annual load factor is larger than when the deviation is zero, and vice versa, when the deviation is negative the annual load factor is smaller than when the deviation is zero. This characteristic results in the percentage deviations of the peak loads being smaller, as shown by the solid line curve of Figure 5, than the corresponding percentage deviations of the annual energy requirements. This characteristic also varies quite widely for different systems.

The variations in the daily peak loads that result from the combined effect of variations in both business and weather conditions are determined next. This is accomplished by combining the probability data for the effect of business conditions, shown by the solid line curve of Figure 5, with the corresponding data for the effect of weather conditions, shown by the dash line curve of Figure 7. This combining process, again by the application of the two basic probability principles previously described, is indicated on Table X. The accumulated values of the probabilities computed in the manner shown in Table X, or the probability that the percentage deviations of the one-hour integrated daily peak loads will be equal to or larger than the amount shown, are shown by the dash line curve of Figure 10.

These data of Figure 10 are of particular interest and importance in the determination of the system capacity require-

Figure 10. Probabilities the per cent deviations of the 1-hour and 15-minute integrated daily peak loads from the level of the long time trend of the seasonal trend of the averages of the 1-hour integrated daily peak loads are equal to and larger than the amount shown as the result of probable variations in both business and weather conditions

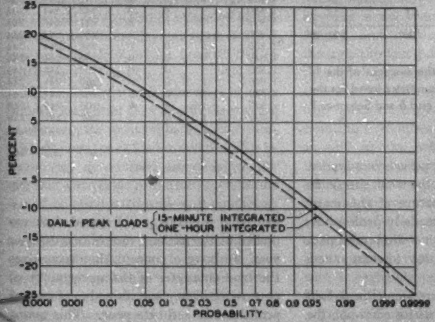

Figure 11. Probable average frequency of occurrence of 1-hour integrated peak loads equal to and larger than the amount shown—for the year 1958

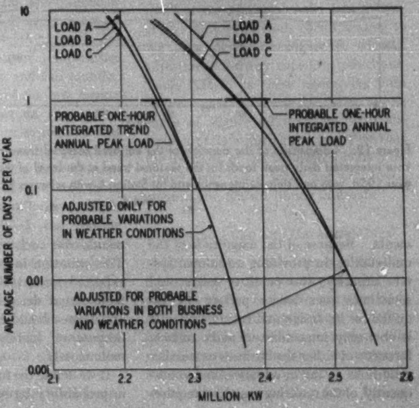

Table X. Determination of Probabilities of Various Magnitudes of Deviation of Daily Peak Loads from the Trend Resulting from the Combined Effect of Variations in Business and Weather Conditions

Variations in Business Conditions		Variations in Weather Conditions		
Per Cent Deviation	Probability	+10.5 0.00010	+9.5 0.00031	+4.5 0.03500
+15	0.00021			0.00001(+19.5)
+14	0.00058			0.00002(+18.5)
+13	0.00141			0.00005(+17.5)
+12	0.00340			0.00012(+16.5)
+11	0.00590			0.00021(+15.5)
+10	0.00950			0.00034(+14.5)
+9	0.01600			0.00054(+13.5)
+8	0.02200		0.00001(+17.5)	0.00078(+12.5)
+7	0.03000		0.00001(+16.5)	0.00105(+11.5)
+6	0.03800		0.00001(+15.5)	0.00135(+10.5)
+5	0.04800	0.00001(+15.5)	0.00002(+14.5)	0.00168(+ 9.5)
+4	0.05900	0.00001(+14.5)	0.00002(+13.5)	0.00206(+ 8.5)
+3	0.06700	0.00001(+13.5)	0.00002(+12.5)	0.00236(+ 7.5)
+2	0.07500	0.00001(+12.5)	0.00002(+11.5)	0.00260(+ 6.5)
+1	0.07900	0.00001(+11.5)	0.00003(+10.5)	0.00276(+ 5.5)
0	0.08000	0.00001(+10.5)	0.00003(+ 9.5)	0.00280(+ 4.5)
−1	0.07800	0.00001(+ 9.5)	0.00002(+ 8.5)	0.00273(+ 3.5)
−2	0.07100	0.00001(+ 8.5)	0.00002(+ 7.5)	0.00250(+ 2.5)

Note: The quantities shown in parentheses are the combined deviations or the events for which the amounts immediately to the left are the probabilities.

Table XI. Scheduled Maintenance Requirements

Nominal Pressure Pounds Per Square Inch	Equipment	Maintenance Schedule Interval	Duration Shifts Single	Double
300	Turbines	6 years	4 weeks	2 weeks
	Boilers	1 year	1 week	4 days
400	Turbines	5 years	4 weeks	2 weeks
	Boilers	1 year	2 weeks	1 week
600	Turbines	4 years	4 weeks	2 weeks
	Boilers	1 year	3 weeks	11 days
800	Turbines	3 years	5 weeks	18 days
	Boilers	1 year	3 weeks	11 days
900, 1,300	Turbines	3 years	6 weeks	3 weeks
and 1,500	Boilers	1 year	4 weeks	2 weeks

Table XII. Occurrence and Duration of the Averages of the 1-Hour Integrated Daily Peak Loads for the Year 1958 for Loads A, B, and C Adjusted for Seasonal Capacity Reductions and Scheduled Maintenance Reductions for One Shift Maintenance for Stations A, B, C, D, and E for Scheme 2 for Station E

(1)	(2)	(3)	(4)	(5)	(6)	(7)
	Number of Days the Adjusted Load is in the Load Bands up to 10 Mw Greater than the Load Shown in Column (1)			Number of Days the Adjusted Load is Equal to and Larger than the Load Shown in Column (1)		
	Load					
Load, Mw	A	B	C	A	B	C
2,200	8			8		
2,190	30			38		
2,180	36			74		
2,170	66			140		
2,160	57	17	17	197	17	17
2,150	24	5	5	221	22	22
2,140	19	10	5	240	32	27
2,130	4	10	5	244	42	32
2,120	0	23	0	244	65	32
2,110	0	40	5	244	105	37
2,100	0	43	0	244	148	37
2,090	0	48	5	244	196	42
2,080	0	25	0	244	221	42
2,070	0	13	5	244	234	47
2,060	0	5	5	244	239	52
2,050	0	5	1	244	244	53
2,040	0	0	10	244	244	63
...	0	0	...	244	244	...
...	0	0	...	244	244	...
...	0	0	...	244	244	...
1,890	0	0	0	244	244	244
1,880	1	0	0	245	244	244
1,870	2	0	0	247	244	244
1,860	4	0	0	251	244	244
1,850	2	0	0	253	244	244
1,840	2	0	0	255	244	244
1,830	4	0	0	259	244	244
1,820	1	0	0	260	244	244
1,810	5	0	0	265	244	244
1,800	1	4	4	266	248	248
1,790	1	3	1	267	251	249
...	..	..	..	...	...	...
...	..	..	..	...	...	...
...	..	..	..	365	365	365
	365	365	365			

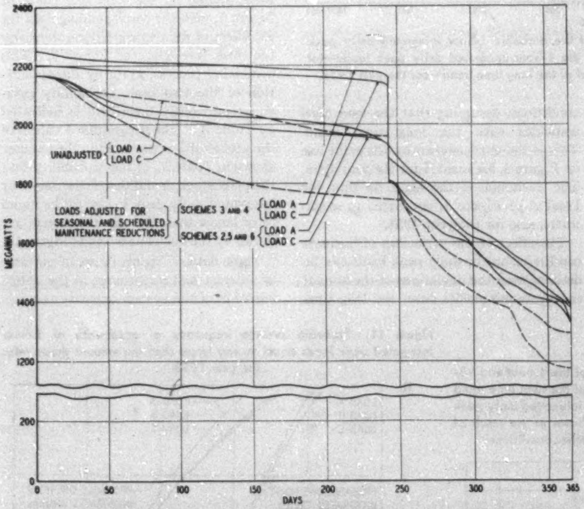

Figure 12. Comparison of the duration of the adjusted seasonal trend of the averages of the 1-hour integrated daily peak loads for the seasonal trend at the level of the long time trend for the year 1958, with one shift maintenance and for Station E with schemes 2, 5, and 6 and Schemes 3 and 4

ments. Because of the magnitude of the undertaking in providing additional system capacity, two or three years, and sometimes even longer periods are required for its design and installation. It is obviously impossible to make reliable forecasts of either the business or weather conditions so far in advance, and consequently, of the resulting peak load requirements, over such long periods in advance. This situation is exactly what should be expected from the nature of the many factors that determine daily peak loads; and there should be no disappointment because of inability to forecast them more closely.

If we define the future annual peak load in probability terms, as for example, the load that is likely to be equaled or exceeded at the average rate of one day per year, we have a concept that recognizes the true character of the uncertainty of occurrence of any specific value of annual peak load in a future year. This quan-

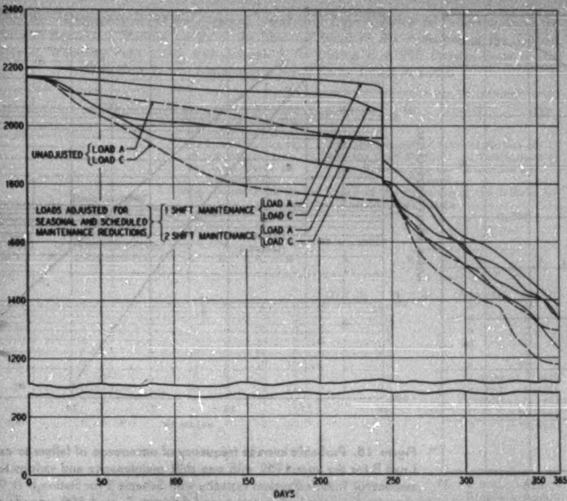

Figure 13. Comparison of the duration of the adjusted seasonal trend of the averages of the 1-hour integrated daily peak loads for the seasonal trend at the level of the long time trend for the year 1958, with one and two shift maintenance and for Station E with Schemes 2, 5, and 6

tity is calculated in the same manner as that indicated on Table VIII by substituting for the data shown thereon, obtained from the dash line curve of Figure 7, which shows the effect of variations of weather conditions only, the data from the dash line curve of Figure 10, as computed in Table X, for the combined effect of variations in both business and weather conditions. Such computations, when plotted, result in the right-hand group of curves of Figure 11, which are based on the annual peak of the seasonal trend of the averages of the weekday peak loads for the year 1958 of 2,167 mw. These computations resulted in probable 1-hour integrated annual peak loads, defined as above, as the 1-hour integrated peak load that would be equaled or exceeded at the average rate of one day per year, of 2,383 mw for Load A, 2,367 for Load B, and of 2,363 mw for Load C.

If it is desired to risk a forecast of some definite load level as of two to three years in advance, the most probable 1-hour integrated annual peak load would be different from that determined above, since the effect of variations in business conditions would be eliminated and such conditions would be treated as a certainty. If we assume such future load level to be that corresponding to the long time load trend, the probable 1-hour integrated trend annual peak load, defined as suggested above, would be as obtained directly from the computations indicated on Table VIII and as shown by the left-hand group of curves of Figure 11. These computations result in values of the probable 1-hour integrated trend annual peak loads of 2,257 mw for Load A, and of 2,251 mw for both Loads B and C for these conditions for the year 1958.

Seasonal and Miscellaneous Capacity Reductions and Scheduled and Routine Maintenance Requirements

It is assumed that the older units of Stations A, B, C, and D are subject to seasonal capacity reductions with increased circulating water temperature during spring, summer, and fall months, reaching a maximum of 60 mw during August and continuing at this value through the first part of September and then gradually reducing to zero prior to the end of the fall season in early December. Such capacity reductions and those resulting from other miscellaneous causes as well as the scheduled and routine maintenance requirements, should be added to the load chronologically. All the capacity can then be considered to be available for operation and operated except for forced outages, thus reducing the required computations many-fold with a negligible practical effect on the final results.

Table XI shows the scheduled maintenance requirements assumed for all conditions other than for weekend maintenance, which latter was ignored since it has been found to have no practical effect on the system capacity requirements. This maintenance time was applied to the boiler and turbine capacity of Stations A, B, C, and D and to the various schemes for Station E to determine the capacity reductions resulting therefrom. It should be noted that no capacity reductions result from the maintenance of one boiler for the 600 pounds and 400 pounds pressure facilities of Stations B and D, respectively, and for Schemes 2, 5, 6, and 8 for Station E, and that a smaller reduction than the boiler capacity is experienced for the 400 pounds and 800 pounds pressure facilities of Station B and the 600 pounds pressure facilities of Station C. The maintenance reductions were then applied chronologically to the three seasonal load trends in such a manner as to raise the resulting maximum effective load level the minimum possible amount consistent with the maintenance periods required and other considerations of a practical nature.

The solid line curves of Figure 12 show the duration curves of the seasonal trends of the averages of the 1-hour integrated daily peak loads for Loads A and C for the year 1958, after adjustment for seasonal capacity reduction and capacity reductions resulting from scheduled maintenance with Schemes 2, 5, and 6 and with Schemes 3 and 4 for Station E and with one shift maintenance at all plants. The solid line curves of Figure 13 show the corresponding data for Schemes 2, 5, and 6 for Station E with both one and two shift maintenance at all plants. The dash line curves of these figures show the corresponding duration curves of the trend of the averages of the 1-hour integrated daily peak loads corresponding to the data shown on Figure 8, without adjustment for any capacity reductions. Table XII gives these underlying data for Scheme 2, as shown by the solid line curve of Figure 12, together with the number of days during the year 1958 that the averages of the adjusted 1-hour integrated daily peak loads are of various magnitudes, within 10-mw intervals.

Combining Load and Capacity Data

The event in which we are ultimately interested is the probability of failure to carry the load. Failure to carry the load, as used herein, contemplates any situation in which it is impossible to perform the maintenance as scheduled, no capacity available for spinning reserve, or a still worse condition resulting from further

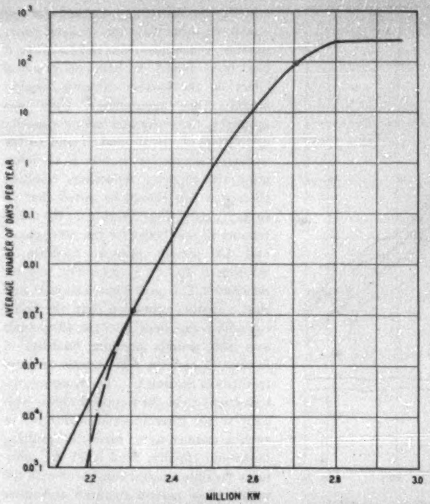

Figure 14. Probable average frequency of occurrence of failure to carry the load for various levels of the annual peak of the averages of the 1-hour integrated weekday peak loads for Load B with a total installed system capacity of 2,700 mw, one shift maintenance and Scheme 2 for Station E at 900 pounds per square inch pressure

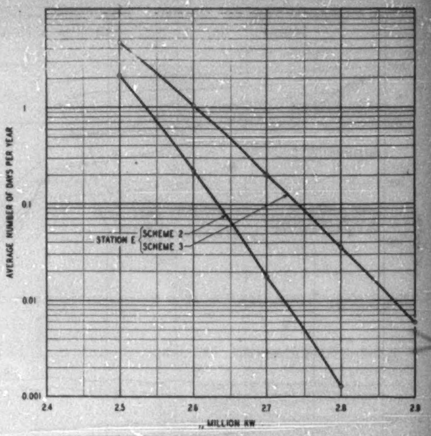

Figure 15. Probable average frequency of occurrence of failure to carry Load B for the year 1958 with one shift maintenance and various total amounts of installed system capacity with Scheme 2 for Station E at 900 pounds per square inch pressure and Scheme 3 at 1,500 pounds per square inch pressure

unavailability of capacity that requires a reduction in system frequency, voltage reductions, actual dropping of various amounts of load, or a combination of any such emergency measures. Such conditions occur when the actual available capacity, without such emergency measures, would be equal to or smaller than the load unadjusted for capacity reductions.

The probability of failure to carry the load is the sum of the probabilities of the occurrence of each of such conditions; it may be expressed either as a pure probability (which would require that the duration data of Table XII and Figures 12 and 13 be expressed as ratios rather than days in the period) or expressed in terms of the average number of days of failure per year. This latter quantity appears to be the more significant to most people. This computation can be made in either one of two ways. One way is to multiply the probabilities of availability of specific amounts of capacity, as shown by columns (2) and (4) of Table VI, by the number of days the corresponding adjusted load, as shown by columns (5), (6), and (7) of Table XII, is equal to and greater than such available capacity. The other way is to multiply the probabilities of availability of capacity equal to and smaller than various amounts, as shown by columns (3) and (5) of Table VI, by the number of days that the corresponding adjusted load, as shown by columns (2), (3), and (4) of Table XII, is within the 10-mw load band above the load shown. These two methods will result in exactly the same answer. The latter is the more convenient because of the smaller magnitude of the number of days in columns (2), (3), and (4) of Table XII as compared with those in columns (5), (6), and (7) thereof. Typical computations are indicated in Table XIII, for Scheme 2 at 900 pounds pressure for Station E and Loads A and B with one shift maintenance at all plants.

It is necessary to make these computations for a number of different magnitudes of load (unadjusted for variations in business and weather conditions) to provide a basis for subsequent calculations that allow for the effect on the capacity requirements of the load variations that result from changing business and weather conditions. The calculations indicated in Table XIII are for annual peaks of the trend of the averages of the 1-hour integrated week-day peak loads of 2,307 mw and 2,707 mw. Other similar calculations were made at 100-mw intervals; smaller systems would require smaller steps and larger systems might permit the use of larger steps. These calculations were made for the different magnitudes of the annual peaks of the trend of the averages of the 1-hour integrated weekday peak loads without any modifications of the adjusted seasonal trend of the averages of the daily peak load data, such as might actually be the case for loads that might deviate from the long time load trend. The data in Table XIII, corresponding to columns (2) and (3) of Table XII, were shifted in Table XIII, as shown by columns (3) and (5), and (4) and (6), respectively, thereof, relative to the probable availabilities of capacity data corresponding to column (3) of Table VI as shown in column (2) of Table XIII; vertically downward to allow for assumed smaller loads and upward to allow for larger loads.

The probable average number of days of failure per year, computed for Load B in columns (8) and (10) of Table XIII are plotted on Figure 14. The curve of Figure 14 was drawn through these points and others similarly computed. The dash line of the lower portion of the curve was that actually computed while the solid line portion of the curve in this lower range of probability is a projection or extrapolation of the upper part of the curve. This lower solid line portion of the curve is more nearly correct than the

Table XIII. Determination of the Average Number of Days Per Year of Failure to Carry the Load with Respect to Various Levels of the Seasonal Trend of the Averages of the 1-Hour Integrated Weekday Peak Loads with Scheme 2 for Station E at 900 Pounds Pressure and One Shift System Maintenance Schedule for Loads A and B

(1)	(2)	(3)	(4)	(5)	(6)	(7)	(8)	(9)	(10)
Available Capacity and Load, Mw	Probability of Availability of Capacity Equal to and Smaller than the Amount Shown in Column (1)	Number of Days the Adjusted Load is in the Load Band up to 10 mw Greater than the Load Shown in Column (1)				Average Number of Days of Failure to Carry the Load Within Load Bands up to 10 mw Greater than the Load Shown in Column (1)			
		Mw Annual Peak of the Trend of the Averages of the 1-Hour Integrated Weekday Peak Loads							
		2,307		2,707		2,307		2,707	
		Load							
		A	B	A	B	A	B	A	B
						(2)×(3)	(2)×(4)	(2)×(5)	(2)×(6)
2,750	1	0	0	0	0	0	0	0	0
2,740	1	0	0	8	0	0	0	8	0
2,730	1	0	0	30	0	0	0	30	0
2,720	1	0	0	36	0	0	0	36	0
2,710	1	0	0	66	0	0	0	66	0
2,700	1	0	0	57	17	0	0	57	17
2,690	0.5897399	0	0	24	5	0	0	14.1538	2.9487
2,680	0.5358255	0	0	19	10	0	0	10.1807	5.3583
2,670	0.5189110	0	0	4	10	0	0	2.0756	5.1891
2,660	0.4528826	0	0	0	23	0	0	0	10.4163
2,650	0.4010898	0	0	0	40	0	0	0	16.0436
....	....	0	0	....	....	0	0		
....	....	0	0	....	....	0	0		
....	....	0	0	....	....	0	0		
2,350	0.0001394	0	0	5	0	0	0	0.0007	0
2,340	0.0000975	8	0	1	4	0.0007800	0	0.0001	0.0004
2,330	0.0000677	30	0	1	3	0.0020310	0	0.0001	0.0002
2,320	0.0000514	36	0	0	3	0.0018504	0	0	0.0002
2,310	0.0000348	66	0	3	2	0.0022968	0	0.0001	0.0001
2,300	0.0000252	57	17	2	6	0.0014364	0.0004284	0.0001	0.0001
2,290	0.0000168	24	5	4	8	0.0004032	0.0000840	0.0001	0.0001
2,280	0.0000115	19	10	2	4	0.0002185	0.0001150	0.0000	0.0000
2,270	0.0000084	4	10	2	1	0.0000336	0.0000840	0.0000	0.0000
2,260	0.0000056	0	23	2	2	0	0.0001288	0.0000	0.0000
2,250	0.0000037	0	40	0	1	0	0.0001480	0	0.0000
2,240	0.0000024	0	43	1	1	0	0.0001032	0.0000	0.0000
2,230	0.0000015	0	48	1	4	0	0.0000720	0.0000	0.0000
2,220	0.0000010	0	25	2	0	0	0.0000250	0.0000	0
2,210	0.0000005	0	13	1	4	0	0.0000065	0.0000	0.0000
2,200	0.0000003	0	5	3	3	0	0.0000015	0.0000	0.0000
2,190	0.0000001	0	5	0	1	0	0.0000005	0	0.0000
2,180	0.0000000	0	0	2	2	0	0	0.0000	0.0000
....	0.0000000					0.0000000	0.0000000	0.0000	0.0000
....	0.0000000					0.0000000	0.0000000	0.0000	0.0000
....	0.0000000					0.0000000	0.0000000	0.0000	0.0000
		365	365	365	365	0.009050	0.001197	223.42	92.078

dash line portion, which is the result of computations of probabilities limited to seven decimal places. This characteristic was previously discussed with respect to Figures 3(A) and (B). It is of no practical consequence, as will be seen later from the computations of Table XIV. The actual curve of Figure 14 is a series of small scalloped segments concaved downward. However, a smooth curve drawn through a sufficiently large number of computed points is satisfactory for all practical purposes.

Adjustment for Probable Load Variations

The next and last step in the calculations is to incorporate the effect of the load variations that result from changes in both business and weather conditions. The method of incorporating the effects of these factors in the calculations is shown in Table XIV. These calculations are carried through for the data of Figure 14 by combining them with the load probability data previously derived in Table X, and as shown by the dash line curve of Figure 10. Since these load data are on a 1-hour integrated basis and it is desired to make the computations on a 15-minute integrated basis, 1.5 per cent was added to the per cent deviations computed in Table X, resulting in the solid line curve of Figure 10. Table XIV, like Table XIII and several of the earlier computations, is calculated by applying the same two basic probability principles applicable to generating capacity problems. The event in this latter calculation is the probability of failure to carry the load when adjusted for variation in both business and weather conditions, for the year 1958 for which the annual peak of the seasonal trend of the averages of the one-hour integrated weekday peak loads, taken as 100 per cent load or zero deviation in the calculations, is 2,167 mw as shown in Table XIV. The result thus obtained for these conditions for Load B and a total installed capacity of 2,700 mw, with one shift maintenance at all plants and with Scheme 2 for Station E at 900 pounds per square inch pressure, is a chance of failure to carry the load at the average rate of 0.01794 day per year, or a failure to carry the load at the average rate of one day in 55.7 (1/0.01794) years.

The results, similarly computed for all the other conditions studied with a total installed capacity of 2,700 mw for the same magnitude as above of the long time load trend for Loads A, B, and C, with one and two shift maintenance, Schemes 1 to 8, inclusive, for Station E at 900 pounds, 1,300 pounds, and 1,500 pounds per square inch pressures, are tabulated in Table XV in order of preference of various schemes for Load B with one shift maintenance. It will be noted from this table that even though there is the same total amount of installed capacity and even though the annual peaks of the trends of the averages of the 1-hour integrated weekday peak loads are the same for all cases, the risk or chance of failure to carry the load varies from an average rate of more than one day per year to a rate smaller than one day in 130 years. This variation is the composite effect of the differences in the characteristics of Loads A, B, and C, one or two shift maintenance, arrangement of the boilers and turbines of Station E, whether or not there is extra boiler capacity therein, and the pressure thereof.

Equivalent Capacity of Various Schemes for Station E

It is believed that a reasonable and adequate degree of reliability is provided with an objective risk of failure to carry the load at the average rate of one day in 10 years, or 0.1 day per year, provided the effect of all the factors affecting capacity requirements are evaluated as shown herein. The conditions for which the risk of failure to carry the load is smaller than this rate are shown to the right and above the stepped line on Table XV while those for which the risk is larger are shown to the left and below this line. This means that less capacity than 2,700 mw is required for reliable service on this assumed system for the conditions to the right and above this line, and more capacity for those conditions to the left and below.

The determination of the differences in the equivalent capacities provided by various schemes for Station E is made by assuming one and two less and more units installed in Station E and repeating the calculations through Table XIV for the various conditions. The results of such

Table XIV. Determination of the Average Number of Days per Year of Failure to Carry the Load, Including the Effect of Variations in Business and Weather Conditions, with Scheme 2 for Station E at 900 Pounds Pressure and One Shift System Maintenance Schedule for Load B

(1)	(2)	(3)	(4)	(5)
Annual Peak of the Trend of the Averages of the 15-Minute Integrated Weekday Peak Loads for Various Load Levels of the Seasonal Load Trend		Probability of Deviation, as Shown in Column (1), of Daily Peak Loads from the Trend, that are the Result of the Combined Effect of Variations in Business and Weather Conditions	Average Number of Days per Year of Failure to Carry the Load With Respect to Annual Peaks, as Shown in Column (2), of the Trend of the Averages of the 15-Minute Integrated Weekday Peak Loads	Average Number of Days per Year of Failure to Carry the Load, Including the Effect of Variations in Business and Weather Conditions
Per Cent Deviation from Long Time Load Trend	Mw	Table X	(2) and Fig. 14	(3) × (4)
+21	2,622	0.00005	18.0	0.00090
+20	2,600	0.00012	11.0	0.00132
+19	2,579	0.00028	6.5	0.00182
+18	2,557	0.00054	3.8	0.00205
+17	2,535	0.00106	2.1	0.00223
+16	2,514	0.00193	1.15	0.00222
+15	2,492	0.00329	0.60	0.00197
...	...	...	...	...
...	...	...	...	...
...	...	...	...	...
+5	2,275	0.05839	0.00039	0.00002
+4	2,254	0.06402	0.00018	0.00001
+3	2,232	0.06784	0.000077	0.00001
+2	2,210	0.06954	0.000032	0.00000
+1	2,189	0.06887	0.000014	0.00000
0	2,167	0.06600	0.0000061	0.00000
−1	2,145	0.06121	0.0000027	0.00000
−2	2,124	0.05511	0.0000012	0.00000
...	...	...	...	0.00000
...	...	...	...	0.00000
...	...	...	...	0.00000
		1.00000		0.01794

Table XV. Number of Years for Which Failures to Carry the Load Will Occur at the Average Rate of One Day for the Long Time Load Trend Load for the Year 1958 for Loads A, B, and C, Including the Effect of Variations in Business and Weather Conditions, for Various Schemes and Pressures for Station E with One and Two Shift System Maintenance Schedules and a Total Installed System Capacity of 2,700 Mw

	Station E		Load					
		Nominal Pressure in Pounds per Square	A		B		C	
			Number of Scheduled Maintenance Shifts					
Line	Scheme	Inch	1	2	1	2	1	2
1	5	900	11.74	33.7	57.3	105.1	125.3	131.1
2	6	900	11.76	32.6	55.9	104.0	121.1	127.3
3	2	900	11.35	32.2	55.7	102.0	123.5	133.3
4	2	1,300	7.02	18.4	28.7	54.6	67.5	74.0
5	6	1,300	6.79	18.0	28.6	55.1	67.1	71.9
6	8	900	6.08	18.2	28.4	58.9	72.1	76.8
7	1	900	4.55	22.5	28.3	85.2	98.9	113.6
8	5	1,300	7.01	18.2	28.2	54.2	66.7	72.1
9	4	900	4.19	17.93	23.4	63.7	74.4	85.4
10	3	900	3.39	15.26	21.4	53.9	64.4	75.1
11	2	1,500	4.61	10.85	17.9	33.6	41.2	44.6
12	5	1,500	4.55	10.61	17.6	32.3	39.1	42.8
13	6	1,500	4.49	10.74	17.3	31.1	40.1	42.6
14	1	1,300	2.74	11.94	15.34	45.1	53.2	59.5
15	8	1,300	3.30	9.09	13.17	25.6	32.8	35.9
16	7	900	2.17	10.15	11.74	35.3	40.2	53.0
17	4	1,300	2.16	8.61	11.74	30.2	36.6	42.5
18	1	1,500	1.85	7.46	9.40	25.3	30.7	36.0
19	3	1,300	1.82	6.55	8.96	21.8	25.8	31.6
20	8	1,500	2.06	5.11	7.29	14.3	18.4	20.2
21	4	1,500	1.46	5.35	7.07	18.2	21.9	26.3
22	7	1,300	1.19	4.67	5.42	15.8	17.4	23.7
23	3	1,500	1.07	3.57	4.99	10.97	13.58	16.4
24	7	1,500	0.776	2.74	3.24	8.76	10.11	13.72

computations are shown plotted on Figure 15 for Scheme 2 for Station E at 900 pounds per square inch pressure and Scheme 3 at 1,500 pounds, both for Load B and one shift maintenance. These curves show that for the above stated objective level of service reliability (that is, one day of failure in 10 years) 2,632 mw total installed capacity is required with Scheme 2 for Station E and 2,742 mw for Scheme 3. Thus an increase of 110 mw in the equivalent capacity for Station E with Scheme 2 as compared with Scheme 3 results solely from the different designs assumed for those two schemes, including the difference in pressures. Such a difference is quite impressive and important, and points up one of the often overlooked effects of recent trends in the design of modern steam power plants. (In this connection it should be recalled that the forced outage rates for 1,500 pound pressure units are assumed rather than experienced.)

Table XVI shows results of similar computations for all the other conditions studied, also in order of preference of various schemes with Load B and one shift maintenance as for Table XV. The differences in the equivalent capacities of the various schemes for Station E, as compared with the most reliable scheme for each of the load characteristics and maintenance schedules, are shown to be very substantial for many conditions. The differences shown in the right-hand portion of Table XVI show only the differences resulting from changes in Station E (i.e., are limited to the capacity differences in a single column). Even greater differences exist when comparison is made among the results in the several columns. A maximum difference of 280 mw is indicated between the total required installed capacity shown in line 24 for Station E at 1,500 pounds per square inch pressure with Scheme 7 for Load A and one shift maintenance and that shown in line 1 for Station E at 900 pounds per square inch pressure with Scheme 5 for Load C and two shift maintenance. Such differences as these in the installed capacity requirements for different conditions, whether large or small, could not be revealed other than by a proper application of probability methods.

The differences in the equivalent capacities of the various schemes for Station E, as shown to the right of Table XVI, would be reduced for a level of service reliability lower than a chance of failure to carry the load at the average rate of one day in 10 years, and would be increased for higher objective levels of

Table XVI. Total Installed Capacity Required to Maintain a Level of Service Reliability of a Risk or Chance of Failure to Carry the Load at the Average Rate of One Day in 10 Years and the Resulting Difference in the Equivalent Capacity of Station E Both for the Long Time Load Trend Load for the Year 1958 for Loads A, B, and C, Including the Effect of Variations in Business and Weather Conditions, for Various Schemes and Pressures for Station E and One and Two Shift System Maintenance Schedules

			Total Required Installed Capacity						Difference in Equivalent Capacity of Station E for Various Schemes and Pressures					
			Load											
		Station E Nominal Pressure in Pounds Per Square Inch	A		B		C		A		B		C	
			Number of Scheduled Maintenance Shifts											
Line	Scheme		1	2	1	2	1	2	1	2	1	2	1	2
1	5	900	2,693	2,651	2,631	2,604	2,595	2,590	0	0	0	0	0	0
2	6	900	2,693	2,652	2,632	2,604	2,596	2,591	0	1	1	0	1	1
3	2	900	2,695	2,652	2,632	2,605	2,600	2,596	2	1	1	1	5	6
4	8	900	2,728	2,669	2,647	2,610	2,596	2,591	35	18	16	6	1	1
5	6	1,300	2,717	2,672	2,653	2,622	2,613	2,608	24	21	22	18	18	18
6	5	1,300	2,717	2,673	2,653	2,622	2,613	2,608	24	22	22	18	18	18
7	2	1,300	2,716	2,673	2,653	2,623	2,616	2,612	23	22	22	19	21	22
8	1	900	2,734	2,668	2,660	2,612	2,609	2,602	41	17	29	8	14	12
9	4	900	2,740	2,676	2,664	2,620	2,615	2,607	47	25	33	16	20	17
10	3	900	2,753	2,681	2,666	2,622	2,616	2,608	60	30	35	18	21	18
11	2	1,500	2,738	2,696	2,672	2,642	2,633	2,627	45	45	41	38	38	37
12	5	1,500	2,739	2,697	2,673	2,641	2,630	2,624	46	46	42	37	35	34
13	6	1,500	2,741	2,697	2,673	2,644	2,629	2,625	48	46	42	40	34	35
14	1	1,300	2,760	2,693	2,681	2,635	2,627	2,619	67	42	50	31	32	29
15	8	1,300	2,767	2,706	2,684	2,643	2,626	2,621	74	55	53	39	31	31
16	7	900	2,781	2,700	2,692	2,637	2,630	2,614	88	49	61	33	35	24
17	4	1,300	2,773	2,707	2,692	2,650	2,640	2,632	80	56	61	46	45	42
18	1	1,500	2,785	2,714	2,703	2,656	2,647	2,638	92	63	72	52	52	48
19	3	1,300	2,794	2,723	2,706	2,658	2,650	2,639	101	72	75	54	55	49
20	4	1,500	2,800	2,730	2,716	2,670	2,661	2,651	107	79	85	66	66	61
21	8	1,500	2,804	2,741	2,720	2,676	2,661	2,652	111	90	89	72	66	62
22	7	1,300	2,828	2,743	2,736	2,674	2,669	2,650	135	92	105	70	74	60
23	3	1,500	2,832	2,760	2,742	2,695	2,683	2,672	139	109	111	91	88	82
24	7	1,500	2,870	2,779	2,769	2,709	2,699	2,681	177	128	138	105	104	91

reliability. This characteristic is shown by the two curves of Figure 15, which converge for decreasing levels of service reliability and diverge for increasing levels. Such differences vary both as to megawatt and percentage amount for the various schemes and conditions. These differences would be increased slightly if the adjustment for variations in business conditions were omitted from the calculations and also for smaller loads than those assumed herein.

Figure 15 shows that the installed capacity requirements decrease with a reduction in the objective level of service reliability and increase for higher levels, so that for the conditions assumed herein, the installed capacity requirements would be reduced varying amounts, depending primarily on the layout and pressure assumed for Station E. The decrease would be about 25 mw to 45 mw for a reduction in the objective level of service reliability by half to a chance of failure to carry the load at the average rate of one day in five years; and the increase would be about 65 mw to 105 mw for a five-fold increase in the objective level of service reliability to a chance of failure to carry the load at the average rate of one day in 50 years.

The inclusion of the adjustment for the effect of variations in business conditions increased the installed capacity requirements for the conditions illustrated herein by about 5 per cent. Other system conditions would show an increase in the capacity requirements of a different amount. For example, if we consider a generating system made up of only Stations A and E, and an annual peak of averages of the 1-hour integrated weekday peak loads of 825 mw, adjustment for the effect of variations in business conditions of the same percentage amounts as shown in Figure 5, increased the installed capacity requirements only 3 per cent.

Installed Reserve

A generally standard practice that has developed over many years is to consider or measure the adequacy of both the planned and available installed capacity in terms of a percentage "reserve." The reserve requirement is usually stated as the percentage the excess of the effective rating or capability of the installed capacity (without reduction for scheduled and routine maintenance or miscellaneous and seasonal capacity reductions) over the "expected" or forecast one-hour integrated annual peak load, is of such load.

Because load forecasts made two to three years in advance are subject to considerable uncertainty, one factor in the consideration of an adequate allowance for installed reserve requirements is the load forecasting error. Then, if some percentage of reserve requirement is set for design purposes, and a large positive load forecasting error occurs, the actual available reserve will be considerably reduced as compared with the objective requirement. Such a situation might be interpreted as an indication that inadequate capacity was provided, even though a portion of the capacity was provided for just such a contingency; such an interpretation is illogical, and often confusing and difficult both to explain satisfactorily and to understand.

One very important objection to the use of a percentage reserve requirement is the resultant tendency to compare the relative adequacy of the reserve provided for different systems on the basis of the loads experienced during the one maximum peak load hour of the year, without regard to the capacity situation during other periods of the year when it may be equally "tight" or even more "tight" than for the annual peak load hour and also different for different systems. The widely different degrees of over-all system reliability for the same total installed capacity and the same general level of peak loads, shown by the results of Table XV for the different conditions considered thereon, demonstrate the inapplicability of percentage comparisons as a measure of the relative adequacy of the reserve. These widely different degrees of system reliability for various conditions were obtained with very nearly the same percentage reserve capacity (as defined above) being 13.3 per cent for Load A, 14.1 per cent for Load B, and 14.3 per cent for Load C.

Table XVI provides the basis for determining the wide range in the reserve requirements for these various conditions in order to maintain the level of service reliability constant at the average rate of failure to carry the load of one day in 10 years. This reserve requirement (as defined above) varies from about 9.5 per cent with Schemes 2, 5, and 6 for Station E at 900 pounds per square inch pressure with Load C and two shift maintenance to about 20.5 per cent for Scheme 7, and 19 per cent with Scheme 3 for Station E, both at 1,500 pounds per square inch pressure with Load A and one shift maintenance.

This characteristic of a widely varying percentage reserve requirement is still further emphasized if we consider a generating system made up of only Stations A and E, as previously considered, again with an annual peak of the averages of the 1-hour integrated weekday peak load of 825 mw, for which the probable 1-hour integrated annual peak load for Load A is 908 mw and for Load C is 900 mw.

With Scheme 2 for Station E at 900 pounds per square inch pressure, with Load C and two shift maintenance, about 15.5 per cent "reserve" is required to maintain the desired level of service reliability of a chance of failure to carry the load at the average rate of one day in 10 years. About 44.5 per cent is required with Scheme 3 for Station E at 1,500 pounds per square inch pressure with Load A and one shift maintenance. Based on these results there is a serious question as to the significance of a so-called system reserve expressed either in percentage or absolute amount, as a measure of either the absolute or relative adequacy of the capacity provided.

Conclusion

The foregoing discussion and results demonstrate that the complex composite effect of all the factors that affect system capacity requirements can be evaluated by the use of two simple basic probability principles applied arithmetically. The results also show wide differences in the capacity requirements for various conditions; it is believed that these differences can be evaluated in no other way than by the application of probability methods. Such results are important in the determination of the over-all most economical design of generating capacity arrangement and pressure and the most economical co-ordination of capacity planning with operating practices and policies.

In general, the most reliable system conditions or the smallest amount of capacity required to be installed in order to maintain some given level of service reliability is with the lower pressures, the smaller size boilers and turbines, extra boiler capacity and cross-overs or a common header.

The results definitely demonstrate the questionableness of the use of a so-called reserve as a measurement of either the absolute or relative adequacy of the capacity provided. A much more significant basis for stating the capacity situation is in terms of the probable average number of years for a failure to carry the load, as defined herein, for one day.

The specific results obtained for one particular system and a given set of conditions are of little use in any other system; consequently the problems relating to each system should be treated with respect to the conditions peculiar to each.

Reference

1. Outage Rates of Steam Turbines and Boilers and of Hydro Units, **AIEE Committee Report**. *AIEE Transactions*, **volume 68, part I, 1949, pages 450–57.**

Discussion

F. J. Maginniss (General Electric Company, Schenectady, N.Y.): Mr. Watchorn's stimulating paper is a very real advance in the application of statistical methods to system and generation outage problems. We feel sure that this approach will be more appreciated by system engineers as its application becomes better understood, and that it will be extended to cover not only problems of a single system but also to determine the reliability and economic justification of various system interconnections as well as the optimum economic operating conditions under any given load distribution.

It is almost self-evident that the probability method of determining system reliability becomes itself more reliable as the size of the system (or number of units involved) becomes larger and larger. In this connection it has seemed worthwhile to us to make some quite idealized calculations to determine the increased reliability of several of the schemes for station *E*, as described in the paper, extended to larger systems than the one in the paper. In addition we have tried to apply some relative cost figures to the various schemes in order to arrive at a "cost of reliability" comparison.

The four schemes to be discussed are schemes 1, 3, 5, and 7, of the paper. A system is assumed to consist of a number of 600,000-kw stations, each of identical arrangement. Thus there is one system made up of 600,000-kw stations with twelve 50,000-kw boilers and six 100,000-kw turbines on a common header as in scheme 1; another system of 600,000-kw stations, each of which contains six 100,000-kw boiler and turbine units as in scheme 3; et cetera. A further idealization is made in that for purposes of comparison a 1 per cent forced outage rate is assumed for each boiler and for each turbine. No recognition is made of any of the many other variables involved, such as load variations, steam pressure, system interconnection, or others.

The results of the calculation are shown in Figure 1 of this discussion. The ordinate of this figure gives the per cent of total system capacity which can be assumed to be available on all except one day in 10 years. Scheme 5, which incorporates an extra 100,000-kw boiler, is seen to be most reliable, whereas scheme 7, consisting of five 120,000-kw boilers and four 150,000-kw turbines on a common header, is least reliable. The gain resulting from the use of small units is evident from the position of the curve for scheme 1.

In order to give some indication of the economic justification of each of these schemes, approximate station cost figures have been applied to each of the schemes studied. On the basis of some December 1948 cost figures, if scheme 3, the unit scheme, is considered as the base station with unit cost, the cost of a station with the arrangement of scheme 1 is about 1.17; for scheme 5 about 1.13; and for scheme 7 about 0.97.

If the ordinates of the curves of Figure 1 are divided by these relative cost figures, the result will be the per cent of the total capacity of a system made up of scheme 3 stations which can be relied on for the same total cost as was required to construct the scheme 3 system. For example, a dollar will buy less system capacity using scheme 1 than scheme 3; consequently other things being equal, less kilowatts can be depended on. Figure 2 of this discussion shows the result of applying the cost figures in the curves previously shown. Scheme 7 employing the largest units, is now seen to give the greatest reliability per dollar, while scheme 1 with the smaller and consequently more expensive boilers and scheme 5 with the reserve boiler capacity in each station are shown to be considerably less reliable per dollar spent. The effect of system size is more readily apparent in Figure 2, since here each of the curves except the scheme 3 curve is approaching a value different from 100 per cent as system size increases.

The most obvious conclusion which I feel can be drawn is that a large amount of ef-

Figure 1 (left)

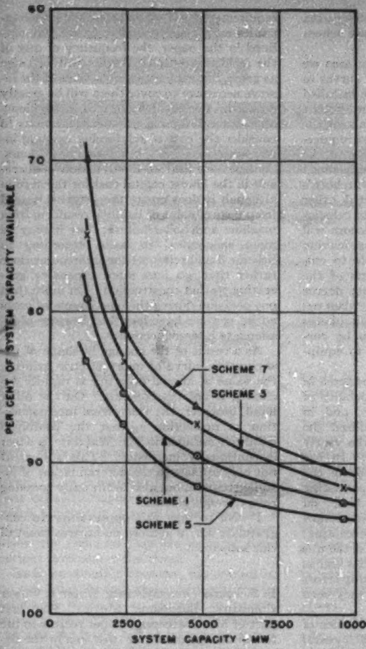

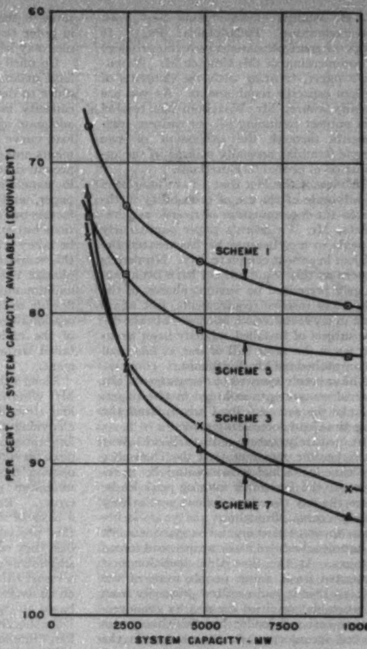

Figure 2 (right)

fort can be profitably expended in extending the work so adequately presented by Mr. Watchorn and others. I believe it also is obvious that the cost factor must be seriously considered in any evaluation of reliability data obtained by statistical methods.

Wayne C. Astley (Philadelphia Electric Company, Philadelphia, Pa.): Mr. Watchorn is to be congratulated on his thoroughness and the tremendous amount of work he has undertaken in the development of this paper. Although the use of probability methods to determine reserve requirements has been the subject of considerable discussion recently, Mr. Watchorn has emphasized a new element. It is that the variability of future estimated loads is one of the essential elements in system capacity requirements and should be treated with probability methods.

Heretofore, it has been the practice to project the present load duration curve into the future, based on an estimate of the annual peak load. The loads were then considered as certain events and were compared with the probable amounts of capacity available. Mr. Watchorn's scheme to treat the annual peak load as the load that is likely to be equaled or exceeded at the average rate of one day per year seems very logical.

A comparison which might be of interest would be a determination of the reserve requirements for the various schemes at Station E based on "short cut" methods. I agree that these methods would not give the proper answer, but an indication of the magnitude of the error would emphasize the point.

The paper properly points out that the reliability of service to be obtained can not be determined when only the per cent of installed reserve is known. The interconnected system with which the discusser is associated has come to realize this. For a number of years the installed reserve obligation of the interconnection has been 10 per cent of the annual peak. The spinning reserve of 6 per cent was adequate to protect against the largest error in estimating load that might be expected to occur once in four years as determined by probability methods. It also was sufficient to cover the loss of the largest unit. The cold reserve of 4 per cent served as a back up which could be placed on the line in 24 hours or less.

The post-war load with its higher summer peaks has made it impossible to conduct a proper maintenance schedule with only 10 per cent reserve, and an additional 2 per cent has been added to provide room for maintenance. In the meantime a probability study has been initiated to determine the true reserve requirement to maintain the desired level of service reliability.

Mr. Watchorn has indicated that the capacity requirements may be lessened by conducting the maintenance on a 2-shift basis. This results in increased maintenance cost only when it is necessary to pay overtime premiums, and the increased cost is the amount of the premium. In most cases the increased cost of maintenance due to premium overtime payments will be more than offset by the operating savings resulting from the reduction in outage time. I should like to cite a typical example from the records of the system previously mentioned.

A 182,000-kw machine was overhauled on a 3-shift schedule using a centralized maintenance group. It was necessary to pay a back shift differential to the afternoon and night shifts. Furthermore, time and one-half was paid on the first day of rest and double time for the second day of rest. The total amount of these premiums amounted to approximately $1,700 per week. While the unit was out, the additional cost of generating the replacement energy on other units was $7,000 per day.

If maintenance had been performed on a 2-shift basis five days a week, it is estimated that the work would have been completed in nine working days or 11 elapsed days including one Saturday and one Sunday. The premium overtime payments would have been only $100. In other words, generating costs would have been increased $28,000 and maintenance costs reduced only $1,600. In the face of these facts all maintenance on the economical machines is performed around the clock. Even on the minor machines single shift maintenance has not been considered.

Mr. Watchorn has produced a timely paper which should arouse much interest.

W. H. Phillips (Pennsylvania–New York Interconnection, Philadelphia, Pa.): It gives me great pleasure to have the privilege of commenting at this time on Mr. Watchorn's paper, treating with the elements of system capacity requirements. As you are already aware, Mr. Watchorn has treated this subject including all its various components through the utilization of two simple formulas normally utilized in the application of probability methods.

In view of the fact that I have long been an advocate of the use of probability methods in the determination of reserve requirements, Mr. Watchorn's paper particularly appeals to me, because he has treated the subject in a most complete way. Numerous papers on this same subject have been previously presented on various phases of the subject of reserve requirements, but at no time in my recollection, however, has the entire subject of installed capacity been wrapped up in the same ball of wax as has been accomplished by Mr. Watchorn.

I have been requested to discuss two of the several components included in the paper, namely the seasonal load trend; and the long-time load forecasting errors.

Immediately subsequent to World War II, it became apparent that the December day-time loads had grown materially in relation to the December evening peak loads. Since the day-time load follows a relatively steady course throughout the year, it became apparent that much less space was left to handle scheduled maintenance and forced outages. At the time this condition first presented itself many people were of the opinion that it had resulted primarily from an unstable condition created by reconversion to post-war loads; but this theory was proved incorrect when the change in the shape of the December load curve continued to exist throughout the years 1947 and 1948.

In the eastern Pennsylvania–New Jersey area during the pre-war years, 1934–35, immediately following the depression, monthly peak loads from November through to the following October averaged 84.2 per cent of the maximum monthly peak load experienced in that period. I have selected the period November 1 to October 31 in analyzing this problem because it covers the period for which new capacity is installed, and in the area which I have studied and from which I come, this period is known as a service year, since capacity is normally installed about the first of November to cover increasing loads above those of the previous December and the new capacity installed at that time is expected to carry the load until the end of the following October.

When the average monthly peak load during the service year was 84.2 per cent of the maximum peak load, there was adequate room for conducting scheduled maintenance and handling forced outage.

Over this same series of months during the service years 1946–47 and 1947–48, the average monthly peak load amounted to 97.92 per cent of the maximum load during the same period leaving only about 2 per cent in which to conduct scheduled maintenance as well as handle forced outages. I believe it is obvious to all of you that a normal maintenance schedule cannot be accomplished with such a relatively small drop in load during the year. As a result it has been necessary to increase the installed reserve in the Pennsylvania–New Jersey area in order that adequate maintenance schedules may be performed.

Up until the present time, in our area we have utilized only the seasonality curves in order to determine how much the installed capacity must be increased, in order that adequate space will be available above the load curve for the various outage requirements and capacity reductions. But at the present time we are engaged in a study which in some degree parallels Mr. Watchorn's paper, and when this is completed other factors not normally included in our calculations but emphasized by Mr. Watchorn will be taken into consideration. Before leaving this subject, I believe it desirable to emphasize the fact that certain parts of the maintenance schedule are in some degree flexible so that during those years when exceptional conditions occur, certain phases of the maintenance schedule can be curtailed without appreciable harm to equipment.

Along with the other factors considered in Mr. Watchorn's paper is the probability of long-time load forecasting errors, and in analyzing this subject he has utilized the long-time trend and determined the yearly peak deviations from this trend. In my opinion this procedure would indicate the minimum probability of load forecasting errors. Relatively few companies, on a basis of my knowledge of the fact, follow this procedure in their load forecasting; but, they rather attempt to forecast the ups and downs created by business cycles and as a result the ultimate load forecasting errors on an average are worse than had they been based on the long-time trend.

In the area which I represent, studies of long-time load forecasting errors ($2^1/_2$ years) were made covering a period of 10 years and the company in this area which exhibited the poorest load forecasting showed a probability of load 25 per cent above the estimate once every 10 years. The other two groups were not as bad, but the diversified estimates of all of the three groups indicated a load 13 per cent above the estimate once every 10 years.

I believe this statement is emphasized by the fact that in June 1944, we were requested by the Office of War Utilities to estimate loads for 1945, 1946, 1947 with the Japanese war continuing and with the Japanese war over. Our combined load estimate for 1947 made $2^1/_2$ years in advance indicated a load in December 1947 (with the Japanese war over) of 3,300,000 kw, while actually in December 1947, we experienced a load of 3,935,000 kw or 19 per cent more than that estimated $2^1/_2$ years in advance. I am sure that the error in forecasting during this period was not limited to our own group since there was a general countrywide pessimistic view of what might happen to the loads after the war was over, but I am bringing up this case to emphasize the fact that extremely large errors in load forecasting errors can be made as little as $2^1/_2$ years in advance. As a result of this forecasting error, maintenance was severely curtailed and occasionally it was necessary for us to drop voltage or frequency in order to prevent the interruption of service to customers.

Before closing I would like to emphasize one point which has not been covered in Mr. Watchorn's paper, namely the effect of interconnection on reducing installed reserve requirements. If we assume that two companies exist exactly similar to the one outlined in the paper, the frequency of any of the incidents outlined therein will be twice as great, but each company's share of the reserve necessary to cover them will be greatly reduced. For this reason, it is highly desirable when designing generating stations to consider the cost of reinforcing existing interconnections or building new ones. Scheme 3 for Station E will undoubtedly result in the lowest capital cost for the station although it does create the greatest hazard from a standpoint of liability resulting from machine and boiler failure; but it may be more economical to build according to Scheme 3 and reinforce the interconnections rather than go into more expensive generating station construction. On more than one occasion during the past couple of years entire systems have been lost because of inadequate interconnection.

As a result of the change in shape of the seasonality curve of many electric utilities, the value of annual diversity is rapidly declining, if not disappearing. On the other hand, however, the value from interconnection as protection against the combined liabilities outlined in Mr. Watchorn's paper is continually increasing. This statement not only applies to the determination of installed reserve, but also to the daily spinning reserve requirements.

I wish to take this opportunity to congratulate Mr. Watchorn on his treatment of this subject.

E. S. Loane (Pennsylvania Water & Power Company, Baltimore, Md.): The first part of Mr. Watchorn's paper relates to the forced outage data and their use in the determination of the probable availability of capacity. In several previously published papers, other investigators have proposed the use of various short cut methods for at least part of the problem here involved. Mr. Watchorn, however, prefers to make all his computations by a rather simple but lengthy arithmetical process. Possible use of automatic computation, plus the simplicity and reliability of the process probably justify this choice.

In the second part of the paper, relating to load estimates and particularly in the consideration of the long term effects of business conditions and the resultant variations in loads estimated 2 to 4 years in advance, the author has proposed a departure from previous general practice.

There is little reason to question the general statements that a load record extending over a sufficient period of years can be used to establish a trend or growth curve, and that a summary of all the annual percentage variations from this trend will form a more or less normal distribution curve as has been plotted in Figure 5 of the paper. In the application of such a curve, however, there may be a question as to whether or not we are actually picking a year entirely at random when we center our attention on a specific period 2 to 4 years in the future as the basis for some capacity study. Suppose, for example, we were at a time and place where analysis of past loads and present conditions indicated that loads were running 5 to 10 per cent below the long time trend. In this situation it has been assumed, rather than demonstrated in the

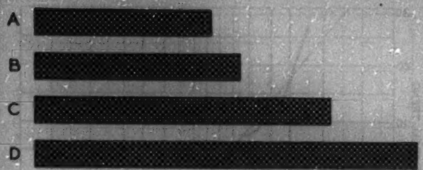

Figure 3. Effect of considering variations in annual peak load from trend on calculated reserve requirements

A. Reserve for outages only
B. Reserve for load variations
C. Joint reserve
D. Sum of A and B

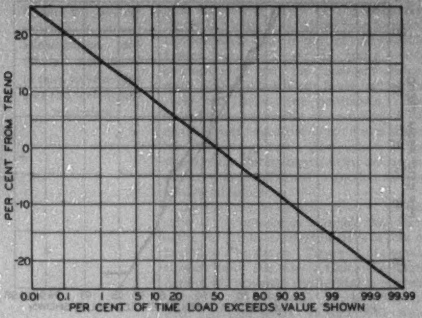

Figure 5 (right). Assumed variation in annual peak from trend on probability scale

paper, that 3 years hence we are just as likely to have loads 5 to 10 per cent above the trend as we are to have loads 5 to 10 per cent below.

On the other hand, suppose the situation were reversed and loads were currently running 5 to 10 per cent above the long time trend. Then it may be unduly hazardous to base capacity requirements on an estimate which apparently says that the loads in 3 years are just as likely to be 5 to 10 per cent below the trend as they are to be at their current level above the trend.

Such questioning, however, can detract in no way from the importance of variations in estimated loads as an element in system capacity requirements. Even if we choose to estimate the loads, taking into account current conditions, rather than to project a long time trend, we must know for a certainty that the loads will not be just what we estimate; they may be more or less than our best possible guess. With loads below the trend or below our estimate and with a reasonable installed capacity there is a very small chance of failure, in fact the available reserve at times may appear excessive. But such excess reserve is no better than just enough reserve, and the added safety at light loads is no compensation for added risk when the loads are heavy. It is not surprising then that consideration of the variability of future estimated loads, as contrasted with a definite estimate of load growth along the trend, increased the installed capacity requirements 3 and 5 per cent in the two cases investigated by the author.

The variability of future loads was found to be a more important element in the installed capacity requirements of the larger system because the other risks, particularly failure of units, become generally less important percentage wise, as the system grows.

Once an investigator has established the effect of variability in estimated loads on the capacity requirements of his system, the indicated effect could perhaps be incorporated in successive capacity studies on some approximate basis. Considering the several elements of judgment that necessarily enter into the determination of capacity requirements, particularly the desired level of reliability and the probable future loads, it is questionable whether there is advantage to be had from detailed investigation of loads in connection with each capacity study. Generally it should be sufficient that the over-all judgment be well informed by periodic checks or investigations that establish what the author has sometimes referred to as "bench marks" for a particular system's capacity requirements.

In the last section of Mr. Watchorn's paper, comparison is made among various layouts for Station B for various system load shapes and various maintenance schedules. The type of problem presented in such comparison is particularly suitable for solution by probability methods based on experienced outage data. Earlier papers have pointed out, as the author does again, that there are two different types of capacity problems (1) the need for installed generating capacity, which still involves judgment, no matter what theories may be applied as aids thereto, and (2) the comparison of alternative schemes, which to a large extent, but not quite entirely, is unaffected by the desired level of service reliability, or by any other elements of judgment, so long as it is within a reasonable range. It also might be noted that the first class of problems is susceptible to solution by short cut methods, while the second class will generally require the detailed computation, here used by the author.

It is unfortunate that limitations of space deterred the author from further discussion of the summarized results in Table XVI. Although it is necessary to keep in mind his admonition that specific results obtained for one particular system and given set of

Figure 4. Effect of including reserve for variations in annual peak load from trend when evaluating capacity additions

Incremental reserve in per cent of added load
A. Plan A, unit system station
B. Plan B, common header and reserve boiler capacity
(A-B). Differential Plans A and B

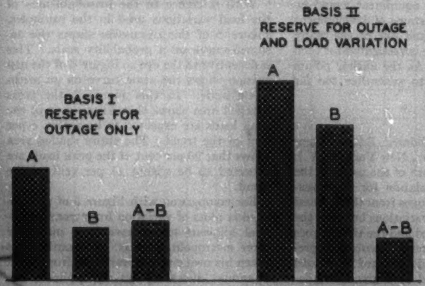

Figure 6. Assumed variation in annual peak from trend on arithmetic scale

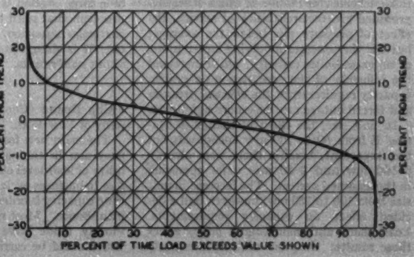

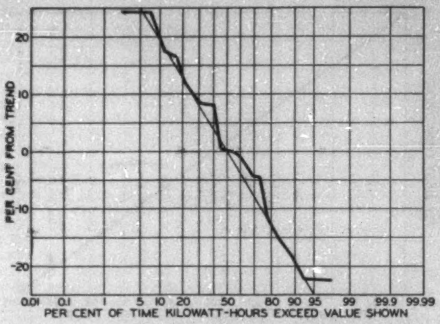

Figure 7. Actual variation in annual kilowatt-hour sales from trend in first metropolitan area and straight line equivalent

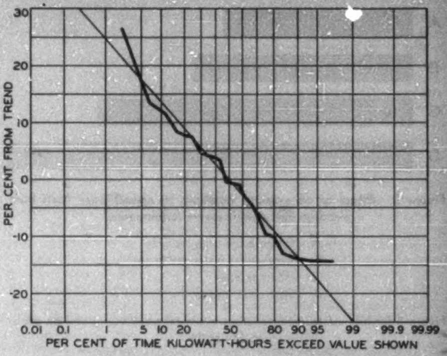

Figure 8. Actual variation in annual kilowatt-hour sales from trend in second metropolitan area and straight line equivalent

conditions are of little use in any other system, certain general results may be useful as indication of those things that may require more detailed examination in other situations.

Let us look first at the loads and maintenance practice. Load B with one shift maintenance requires about 50 megawatt (mw), or 2 per cent more installed capacity than Load C; and Load A which has the least valley for maintenance, requires about 75 mw more capacity than Load B. But because A has an expected annual peak about 20 mw higher than B, the effect of shape alone is again approximately 50 mw. This effect of load shape is reduced somewhat by the possibility of two shift maintenance. As might be expected, this maintenance policy has greatest effect for Load A, where the maintenance situation is "tight." Two-shift maintenance there saves 60 mw in required capacity installation, while for Load B the saving is about 40 mw, and for Load C only about 10 mw. The saving from 2-shift maintenance is naturally smaller in all those cases in which there is extra boiler capacity in the proposed new Station E.

Each step in the assumed forced outage rate, that is, the 1, 2, and 3 per cent, identified respectively with nominal pressures of 900, 1,300, and 1,500 pounds per square inch, apparently requires an increased installed capacity of about 30 mw or 5 per cent of the proposed Station E capacity. Load shapes and maintenance schedules had relatively little influence on these results. For those schemes for Station E which otherwise provided greatest reliability of service, the effect of pressure was below the average; but for the schemes involving larger units, or no extra boiler capacity, which increased the influence of the new station on system capacity requirements, the effect of pressure and forced outage rate was more significant.

In unit size, the effect of change in Station E from 50 to 100 mw boilers was not too important, because there were already 6–100 mw and 3–80 mw units operating in the assumed system. The increase in unit size from 100 to 150 mw, however, had a decided effect on capacity requirements. Load shape and maintenance policy affect these results; the more difficult it is to do the required maintenance the less desirable it is to have the larger units. For the higher assumed outage rates, corresponding to the higher pressures, the larger units also are less desirable from the points of view of capacity requirements, amounting in one case to a disadvantage of 70 mw.

The extra boiler capacity provided in three layouts had a capacity value of about 30 mw on the average, or 5 per cent of Station E capacity. This added value ranged from 5 to 65 mw, being low where maintenance was no problem and the unit sizes and pressures were low. The larger benefits from the extra boiler are associated with a tight maintenance situation and the less reliable layouts of the station.

The value of steam interconnection, without any extra boiler capacity is indicated by comparison of two 6-unit plants. The common steam header provided in scheme 4 provides capacity savings from 0 to about 30 mw. Just as for the extra boiler, the saving is high where higher forced outage rates create the greater risks of unit outages. The effect of an extra boiler and of a steam header have been evaluated here for a large plant, and in some situations they were found more valuable than in others. It should be recognized, however, that the cost of such equipment could be credited with relatively little capacity savings when only 2, 3, or perhaps even 4 units are installed in a plant. Whether such equipment would be justified during initial stages of development of a large station is just one of the many problems that must be investigated for each particular situation. As the author points out, it is dangerous to generalize too far about such results.

Philip Doane (Consolidated Edison Company of New York, Inc., New York, N. Y.):

The main new feature of the paper is the provision in the calculation for the possibility of load level changes from the forecast due to business cycle variations between the time capacity is ordered and the time it goes into service. Most reserve calculations previously made have determined the load which could be carried by a given installation with any specified chance of loss of load. The necessary allowance for forecast uncertainties was a separate problem.

Figure 3 of the discussion shows the effect of the indicated provision to be sizable in a representative case, as compared with reserve against outages only.

Figure 4 of the discussion shows an example of the effect of including load level variations when comparing alternative system arrangements, different design features, or differing interconnections. The figure shows rates of increase per megawatt of allowable added load for two alternative capacity additions. The indicated differential in required reserve capacity between plans A and B is less on Basis II, which allows for load level variations. This decreased difference in capacity requirements would be only partly offset by the reduction in the credit for economy generation from the differential reserve capacity. Thus the lesser differential on Basis II favors higher outage risks, usually associated with unit system or higher pressure installations. Credit for differences in generating efficiency between Plans A and B applies to all the new capacity except that part considered in evaluating the capacity differential. Consequently the larger capacity requirement indicated on Basis B, which allows for load level variations, favors high efficiency installations.

With reference to the reasonableness of the load variations used in the examples, Figure 5 of this discussion shows the assumed curve on a probability scale. This is deceptive to the eye so Figure 6 of the discussion shows the same curve on an arithmetic scale. In this Figure 6 the cross hatched area shows that 50 per cent of the peak loads are expected to be within 5 per cent of the trend. The entire shaded area shows that 90 per cent of the peak loads are expected to be within 11 per cent of the trend.

For comparison with Figure 5 of the discussion plots of variation from trend of annual kilowatt hours have been made for three metropolitan areas. The author has taken his own curve of variation from trend of annual kilowatt hours and applied a cor-

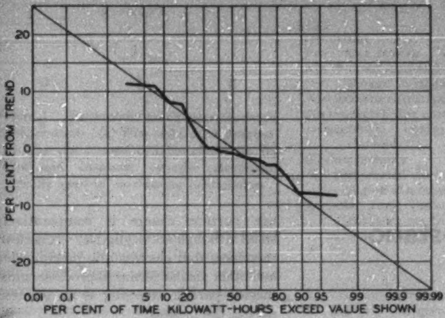

Figure 9. Actual variation in annual kilowatt-hours distributed from trend in third metropolitan area and straight line equivalent

rection factor for changes in load factor with business conditions to obtain variations in load from trend. This discussion neglects that refinement and presents Figures 7, 8, and 9 only to suggest that the slope of the assumed curve in Figure 5 of the discussion is not too steep.

The curve of Figure 5 of the discussion may not be steep enough for a reason now to be considered. The author's method is understood as projecting trend-up-to-date to a future time and applying as possible variations at that time the actual variations from actual past trend. This belittles the possibility that the trend projected today may differ appreciably from the trend which will be fixed by actual data covering the next ten years as well as past years. It is one thing in 1951 to determine a trend curve for the period 1905–1950 and thus locate the trend position for 1931. It was a very different thing in 1929 to take the data for the period 1905–1928 and estimate the trend position for 1931. What we want to know is the expectancy of variation from the forecast trends as they are estimated year by year; not the variations from the final historical trend which will not be known until ten or more years after the event. Such a set of variations might be established by actually determining in each of a series of years, by some method excluding knowledge of later years, the trend fixed by the data up to that year, projecting each such trend to the third annual peak following (that is, data up to and including 1940 peak projected to 1943 peak) and tabulating differences between actual loads and the corresponding projected trend values. An alternative procedure might be to record the differences between each peak and the estimate therefor made 30 months prior to the peak date. Figure 10 of the discussion shows such a set of variations from forecast. Unfortunately the record of comparable figures does not cover an entire major business cycle and the judgment assignment of the values to the lower half of the cycle may be a little pessimistic. The straight line equivalent of variation of annual kilowatt hours from trend is also shown for the same system. Comparison of the slopes of the curves suggests that uncertainties in trend location and projection may be a material factor.

Coming now to interpretation of the results of the calculation it is felt that some detail on the distribution of days of loss of load should be shown. Figure 11 of the discussion shows the way in which the larger part of the expected loss of load is concentrated in the relatively infrequent years with high load levels. If we exclude from consideration the years with annual peaks equaled or exceeded once in 50 years or for 2 per cent of the time we then exclude three fourths of the expected days of loss of load. To elaborate, if we take the same standard of reliability as before for 49 out of 50 years and disregard what happens one year in 50 then the increase in joint reserve requirements over reserve for outage only shown in Figure 3 of the discussion is reduced by 28 per cent. Whether the investment for full protection is justifiable becomes a question. From another viewpoint we may put a limit on the maximum assumed variation in load from trend. If this ceiling is set at 15 per cent in our example then the incremental reserve requirement over that for outage only is cut by 12 per cent, with all years being considered.

The authors' work thus poses two questions for each user of his method. The first is that of forecast accuracy. The author shows how to put a price on forecast uncertainties. The second question is that of interpreting and applying the reliability figures produced by the calculation. For this, consideration of the distribution is necessary, much as information on expected dispersion of material strength values is needed in considering strength tests. These two questions are of minor importance in the second of the two specific applications shown by the author, since in comparing alternative development plans, considerable variations in selected reliability level have little effect. The two questions are of major importance when fixing the required reserve, as for the first of the two applications.

Figure 10. Comparison of errors in peak forecasts made 30 months in advance with variations in annual kilowatt-hours distributed from trend for same system

A. Actual forecast errors—assumed to belong to lower half of complete business cycle
B. Straight line approximation of A, above
C. Straight line equivalent of actual variation in kilowatt-hours distributed from trend

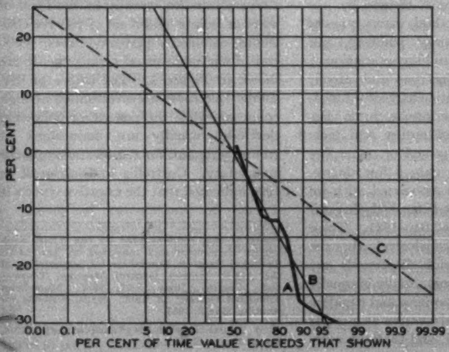

Figure 11. A. Per cent of time annual peak exceeds given value
B. Accumulated total of average weekdays per year of loss of load for all years with annual peaks equal to or less than given value

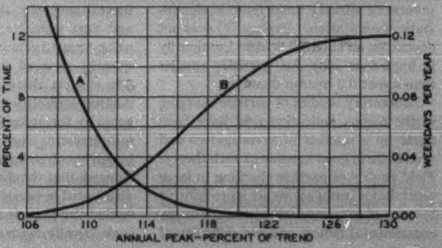

Particle Charging in Electrostatic Precipitation

H. J. WHITE
MEMBER AIEE

ELECTRIC charging of aerosols is basic to electrostatic precipitation and related technical processes, and also has inherent scientific interest. Experience indicates that the unipolar corona discharge provides by far the best practical means of highly charging suspended particles in gases. Early workers in electrostatic precipitation did not investigate particle charging itself, but rather regarded it as an integral part of the overall precipitation process. Studies carried out during the past 25 years, however, have provided a satisfactory theoretical and experimental foundation for the particle-charging process. The object of the paper is to give a connected account of these studies, including some heretofore unpublished results, and to portray the present state of development of the particle-charging art.

Theoretical studies indicate that two particle-charging mechanisms are present in the unipolar corona discharge: (1) bombardment of the particles by ions moving in the d-c field, and (2) attachment of ions to the particles by ion diffusion. It is shown that process (1) leads to a particle charge which is proportional both to the d-c field strength and to the surface area of the particle, and is the process of primary importance in electrostatic precipitation. Process (2) does not depend on an external field and ordinarily is important only for particles smaller than about 0.2 micron diameter.

Laboratory studies of particle charging in the corona ionization field have been made by a number of investigators and results are in good agreement with theory. Field studies of particle charging in large precipitator installations are more difficult because of inherent lack of control of the experimental factors and the difficulty of obtaining small samples which are representative of the large gas flows and weights of dispersoids treated, but results thus far obtained appear to be in general agreement with the theory. Several disturbing effects which may adversely affect particle charging under practical electrostatic precipitation conditions are discussed briefly.

Electrostatic precipitation derives fundamentally from the mechanical or Coulomb force which is exerted on an electrically charged particle in an electric field. Although other forces of electric origin may act on particles, these are generally insignificant compared with the Coulomb force and are of minor importance in electrostatic precipitation. The widespread applications of the Coulomb force in modern science and technology are perhaps the best indication of its importance. For example, in addition to electrical precipitation these applications include atomic particle accelerators such as the cyclotron, determination of the fundamental electronic charge by the Millikan oil-drop method, many types of electronic tubes, spray painting, pile fabric manufacture, and ore separation.

In contrast to electrons and atomic nuclei for which electric charge is a fundamental property, the smoke, fume, fog, and dust particles of nature and technology may be uncharged or, more frequently, charged to only a low degree. The electric charges associated with industrial aerosols were extensively investigated by the writer in 1940–1941. These measurements show conclusively that the majority of industrial dispersoids are charged, that the charge usually is equally distributed between positive and negative so that the particle suspension as a whole is electrically neutral, and that the average particle charge is comparatively small although not negligible. It is clear, therefore, that electrostatic precipitation and other similar technical processes must include particle charging as an inherent part of the process.

Electrical activity is associated with so many physical and chemical phenomena that it becomes a matter of choosing the best method of charging particles rather than searching for a single available method. Methods which have been suggested include X rays or γ-rays, friction, flames, photo-electricity and various types of electric discharges. The historic and by far the best method, however, appears to be the use of the unipolar corona or brush discharge. The earliest experiments of Hohlfeld,[1] the pioneer work of Lodge,[2] and the successful commercial development of the electrostatic precipitation process by Cottrell[3] were all based on the unidirectional corona discharge. The subsequent broad application of the process in industry, and more recently in air cleaning, has been dependent on the corona particle-charging method. Several other important but more recent technical processes, including, for example, spray painting and the electric method of printing and image reproduction, also utilize this method of particle charging.

In an electrical precipitator the corona discharge is established between a set of active electrodes, usually in the form of wires or points, and a set of passive electrodes, commonly plates or tubes. Several of the more usual arrangements are shown in Figure 1. The active or discharge electrodes are maintained at high potential, while the passive or collecting electrodes usually are maintained at ground potential for reasons of simplicity and safety. Cottrell's earliest work in 1906 indicated that the negative corona is

---

Paper 51-200, recommended by the AIEE Electronics Committee and approved by the AIEE Technical Program Committee for presentation at the AIEE Summer General Meeting, Toronto, Ont., Canada, June 25–29, 1951. Manuscript submitted October 23, 1950; made available for printing May 3, 1951.

H. J. WHITE is with the Research Corporation, Bound Brook, N. J.

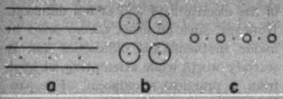

Figure 1. Electrostatic precipitator electrode configurations: (a) Wire and plate electrodes, (b) Wire and co-axial cylinder electrodes, (c) Wire and co-planar cylinder electrodes, chiefly used in air-cleaning precipitators

Nomenclature

i = current
j = current density
$A(n)$ = cross-sectional area of ion current stream to suspended particle
N_0 = ion concentration
$\psi(n)$ = electric flux entering particle
e = electronic charge = 4.80×10^{-10} statcoulomb
K = ion mobility
E_0 = undistorted electric field strength in the region of a suspended particle
θ_0 = polar angle through which flux enters particle; see Figure 2(B)
a = particle radius
n = particle charge at time t
n_s = limiting or saturation particle charge
t = time
t_0 = time constant of particle charging
D = dielectric constant of particle
q = particle charge
m = particle mass
ρ = particle density
C = kinetic theory root-mean-square velocity of ions
k = Boltzmann constant
T = absolute temperature
V = potential energy of ions in the electric field of a charged particle

much superior to the positive for electrical precipitation because of its greater stability and higher permissible operating currents and voltages. All experience since then has confirmed this result. However, positive corona has been used in air-cleaning precipitators because of its possibly lower ozone production.

Corona discharges have been studied for many years, but it is only recently that the detailed physical mechanisms involved have been reasonably well clarified, largely by Loeb[4] and his group. The essential features of the discharge for electrostatic precipitation purposes are the existence of a highly active but restricted region close to the discharge electrode which contains both positive and negative ions, and a passive region throughout the remainder of the discharge space which contains a dense concentration of unipolar ions. These latter ions are generated predominantly by electron bombardment of gas molecules in the active region of the discharge, and then are selectively carried by the d-c field through the passive region to the collecting electrodes. In atmospheric air the unipolar ion concentrations under electrostatic precipitation conditions commonly range from 10^8 to 10^9 ions per cubic centimeter, with corresponding electric field strengths of from 1 to 10 kv per centimeter. Corona current-voltage characteristics are a strong function of gas composition and in practice vary widely depending on the nature of the gas. The electric field in the passive region in all cases is primarily due to the space charge of the unipolar ions rather than to direct surface charges on the electrodes.

Theoretical Particle Charging Equations

Theoretical calculations of particle charging necessarily are based on a number of simplifying but not invalidating assumptions:

1. The particles are assumed to be spherical.
2. Particle spacing is assumed large compared to particle diameter.
3. Ion concentration and electric field in the region of any given particle are assumed uniform.

Assumption (1) is true for many types of particles and is a reasonable approximation for many others. Assumptions (2) and (3) are closely true for nearly all industrial and natural aerosols. Two distinct particle charging mechanisms are active in the corona discharge. The most important one is the bombardment of the particles by the ions moving under the force of the electric field. A secondary mechanism is the diffusion of ions to the particles. Under precipitator conditions this is usually of practical importance only for relatively small particles of less than about 0.2 micron diameter.

The charging of particles in the unipolar ion field by the ordered or Coulomb motions of ions along the lines of force was first studied theoretically by Rohmann[5] and later in somewhat more detail by Pauthenier and Moreau-Hanot.[6] The problem is essentially one in electrostatics. Figure 2(A) represents the electric field in the neighborhood of an uncharged conducting sphere placed in a uniform electric field. It may be shown that the electric flux passing through the sphere is increased by a factor of three as compared to the undistorted field and that the maximum field at the surface of the sphere, which occurs along the axis parallel to the field direction, is also increased by a factor of three. The dashed lines represent the limit of the field which passes through the sphere. Gas ions travelling within these limits at the initial instant after the sphere is placed in the field will strike the sphere and impart charge by attachment. This charge in turn produces a repulsive force which alters the field configuration and thereby reduces the rate of charging.

Figure 2(B) shows the field configuration when the sphere has received half of its theoretical maximum or saturation charge. Both the electric flux entering the sphere and the maximum field on the side of the sphere facing the oncoming ions have been reduced through the repulsive effect of the ion charge on the sphere. Ultimately sufficient charge is received to completely counteract the external field; the electric flux entering the sphere is reduced to zero, and charging ceases.

The theoretical particle charging equation under these conditions is derived as follows. The gas ion current i to the particle is

$$i=jA(n) \tag{1}$$

The ion current density j in the undistorted region outside the immediate influence of the particle is given by

$$j=N_0eKE_0 \tag{2}$$

The cross-sectional area $A(n)$ of the ion current stream which enters the particle

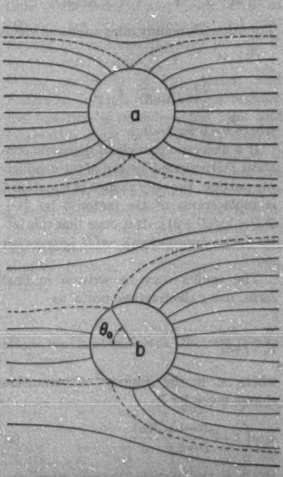

Figure 2. Electric field near charged and uncharged conducting spheres placed in a uniform field. (a) Uncharged sphere. (b) Charged sphere (one-half of saturation charge)

Table I. Typical Values of Saturation Charge n_s and Charging Constant t_0 for the Field-Dependent Ion-Bombardment Charging Process

E_0, Kv/Cm	a, Microns	n_s	K, Cm/Sec/Volt/Cm	N_0, Ions/Cm³	t_0, Second
1	0.1	2	1	10^7	0.2
10	0.1	20	1	10^8	0.02
1	1	2×10^2	1	10^9	0.002
10	1	2×10^3	10	10^7	0.02
1	10	2×10^4	10	10^8	0.002
10	10	2×10^5	10	10^9	0.0002
1	100	2×10^6			
10	100	2×10^7			

when its charge is n is determined by the electric flux $\psi(n)$ as follows:

$$A(n)=\frac{\psi(n)}{E_0} \tag{3}$$

Determination of the flux $\psi(n)$ is a problem in electrostatics. Omitting details not essential to the present argument, the result for a conducting particle is given by the integral

$$\psi(n)=\int_0^{\theta_0}\left(3E_0\cos\theta-\frac{ne}{a^2}\right)2\pi a^2\sin\theta d\theta$$

$$=3\pi a^2E_0\left(1-\frac{ne}{3E_0a^2}\right)^2 \tag{4}$$

substituting equations 2, 3, and 4 in equation 1, there results

$$i=\frac{d(ne)}{dt}=3\pi a^2N_0eKE_0\left(1-\frac{ne}{3E_0a^2}\right)^2 \tag{5}$$

Equation 5 is readily integrated and yields

$$n=\frac{3E_0a^2}{e}\cdot\frac{t}{t+\dfrac{1}{\pi N_0eK}} \tag{6}$$

where $n=0$ for $t=0$.

If a dielectric particle of dielectric constant D is assumed instead of the conducting particle, the only change in equation 6 is replacement of the factor 3 by $[1+2(D-1)/(D+2)]$. It is clear that this latter factor approaches 3 as D approaches ∞.

The results may be written in final form, using electrostatic units, as

$$\frac{n}{n_s}=\frac{t}{t+t_0} \tag{7}$$

where n_s is the limiting or saturation charge given by

$$n_s=\left(1+2\frac{D-1}{D+2}\right)\cdot\frac{E_0a^2}{e} \tag{8}$$

and t_0 is the particle-charging time constant given by

$$t_0=\frac{1}{\pi N_0eK} \tag{9}$$

Several important conclusions may be drawn from these formulas. The particle charge n given by equation 7 is an asymptotic function of time, approaching the saturation value n_s for large values of t. It is seen, for example, that half the final charge is reached at $t=t_0$ and 91 per cent at $t=10t_0$. The saturation or limiting charge n_s is directly proportional both to the electric field E_0 and to the surface area of the particle represented by a^2. The charging time constant t_0 is inversely proportional both to ion concentration N_0 and to ion mobility K; that is, the larger the ion concentration and the higher the ion mobility the faster the particle becomes charged.

Table I gives orienting values of these quantities for a range of typical corona discharge conditions in air. The saturation charge is seen to be roughly of the order of magnitude of 10 electronic charges for a 0.2-micron particle, increasing to 10^3 electronic charges for a 2-micron particle and to 10^7 charges for a 200-micron particle. The time constant of charging ranges from about 10^{-1} to 10^{-4} seconds, but charging ordinarily may be considered reasonably complete in about 10^{-2} seconds. This latter value shows that particle charging in a precipitator at gas velocities of 5 to 10 feet per second is completed in the first few inches of gas flow path in the corona field.

The ratio of particle charge to particle mass q/m is of physical interest and may be easily calculated. For this purpose consider a conducting particle of diameter 2a and of density ρ. Formula 8 gives the charge

$$q=n_se=3E_0a^2 \tag{10}$$

while the mass is given by

$$m=\frac{4}{3}\pi a^3\rho \tag{11}$$

so that

$$q/m=\frac{9E_0}{4\pi a\rho} \tag{12}$$

As an example, assume $E_0=6$ kv per centimeter $=20$ electrostatic units, $a=0.5\times10^{-4}$ centimeters, and $\rho=1$. Then $q/m=2.9\times10^5$ statcoulombs per gram.

Charging by Ion Diffusion

The charging of particles by ion motion in the electric field, considered in the preceding section, becomes less effective as particle size decreases, and it is necessary to determine the importance of ion diffusion in the charging of small particles. An exact theory of particle charging would take into account the simultaneous effects of the electric field and of ion diffusion. However, such an exact theory leads to undue mathematical difficulties and is scarcely worth while attempting, at least from a practical standpoint. For particles larger than about 0.5-micron diameter the exact solution would not be appreciably different from the result already obtained. Likewise, by considering ion diffusion alone, a sufficiently valid result is obtained for the case of very fine particles of less than about 0.1-micron diameter.

Gas ions present in a gas share the heat motions of the gas molecules and in general obey the laws of kinetic theory. The thermal motions of the ions cause them to diffuse through the gas, and in particular to collide with any liquid or solid particles which may be present. Such ions will in general adhere to the particles because of the attractive electrical image forces which come into play as soon as the ions approach the particles very closely. The diffusion of the ions, therefore, provides a particle-charging mechanism which does not depend on an externally applied electric field. Such a field will aid in charging the particle but is not necessary for the diffusion charging process.

The accumulation of electric charge on a particle gives rise to a repelling field which tends to prevent additional ions from reaching the particle. The rate of charging, therefore, decreases as charge accumulates on a particle, and ultimately will proceed at a negligible rate or stop entirely. The particle charge will depend on the thermal energies of the ions, on the particle size, and on the time of exposure.

The first significant study of particle charging by diffusion of unipolar ions seems to have been made by Arendt and Kallmann[7] who give the following equation for the rate of particle charging, valid for the case where the particle has already taken on appreciable charge

$$\frac{dn}{dt}\left(1+\frac{a^2C}{4nKe}\right)=\pi a^2CN_0e^{-\frac{ne^2}{akT}} \tag{13}$$

The derivation of the Arendt and Kallmann equation is rather elaborate. Essentially the same result is obtained by the simpler method given here. In kinetic theory[8] it is shown that the density of a gas in a potential field is not uniform but varies according to the equation

$$N=N_0e^{\frac{V}{kT}} \tag{14}$$

In the case of gas ions in the neighborhood of a suspended particle having a charge ne, the potential energy V of an

Table II. Representative Values of Particle Charge n for the Ion-Diffusion Charging Process

a, Centimeters	t, Seconds 10^{-3}	10^{-2}	10^{-1}	1	10
10^{-5}	3	7	11	15	19
10^{-4}	70	110	150	190	230
10^{-3}	1,100	1,510	1,930	2,340	2,750
10^{-2}	15,100	19,300	23,400	27,500	31,700

ion of the same polarity at a distance r from the center of the particle is

$$V = -\frac{ne^2}{r} \tag{15}$$

The ion density near the particle surface is given by

$$N = N_0 e^{-\frac{ne^2}{akT}} \tag{16}$$

From kinetic theory the number of ions which strike the surface of the particle per second is $\pi a^2 NC$. Assuming that all ions which reach the particle are attached by image forces, the ion current to the particle is

$$\frac{dn}{dt} = \pi a^2 C N_0 e^{-\frac{ne^2}{akT}} \tag{17}$$

An elementary integration gives, for an initially uncharged particle, the charging equation

$$n = \frac{akT}{e^2} \ln\left(1 + \frac{\pi a C N_0 e^2}{kT} t\right) \tag{18}$$

Representative values of n calculated from equation 18 are given in Table II for $T = 300°K$ and $N_0 = 5 \times 10^8$ ions per cubic centimeter.

In general it may be said that in electrostatic precipitation the external-field particle-charging mechanism predominates for particles larger than about 0.5-micron diameter, and that the ion diffusion process becomes predominant only for particles smaller than about 0.2-micron diameter. For most electrostatic precipitation applications, the external-field charging process may be used in calculating particle charges, and only in exceptional cases need ion diffusion be considered.

Experimental Work on Particle Charging

Laboratory experimental measurements on particle charging in the corona ion field have been made by a number of investigators. These researches have established the essential validity of the theoretical particle-charging formulas discussed in the preceding sections. Some of the more important of the work will now be reviewed, and it will be seen that reasonable agreement exists between theory and experiment.

The first measurements of particle charging in the corona field appear to have been made by Rohmann[5] in connection with a particle-size analysis method utilizing preliminary corona charging followed by an air-blast particle-mobility apparatus. Particle charge was an essential though secondary objective of the work. A typical result of these experiments, which were made using Fe_3O_4 particles under conditions where the ion-bombardment process predominated, gave for a 2-micron particle a value of 480 electronic charges, compared with a theoretical value of 400 electronic charges.

Ladenburg[9] studied experimentally the limiting charge attained by suspended particles of from 10^{-5} to 10^{-4} centimeter radius in the corona discharge between a negative wire and a grounded plane. He found close agreement with theoretical formulas 6 and 8 for all except the very small particles of less than 1-micron radius charged in a field of very low ion density. For these the charge was larger than predicted by formulas 6 and 8, and varied linearly with the radius a rather than with a^2 as in formulas 6 and 8. This linear relation may be derived from the Arendt and Kallmann theory[7] as restricted by the conditions of Ladenburg's experiments.

More comprehensive measurements were made by Pauthenier and Moreau-Hanot.[6] Their experiments were of two types. In one type both metallic and insulating spheres ranging in size from about 10 to about 200 microns diameter were released in a negative corona field maintained between a fine wire and a coaxial cylinder, and the trajectories of the individual particles as they moved to the cylinder wall were photographed. Analysis of these trajectories together with the known values of the corona parameters made it possible to calculate the individual particle charges. Within the experimental error of a few per cent it was found that the limiting or saturation charge obeyed formulas 6 and 8, while the time rate of charging agreed with formula 7. The agreement was more exact for the larger particles.

Table III. Comparison of Theoretical and Experimental Particle Charge Values for the Ion-Diffusion Charging Process

a, Microns	N_0, Ions/Cm³	t, Seconds	n, Experimental	n, Theoretical
0.5	515	1,500	20	32
0.5	515	3,000	32	38
0.5	515	6,000	40	44
2.25	67,000	1,500	170	493
2.25	67,000	3,000	260	520
2.25	67,000	6,000	280	548

In the second type of experiment, much larger spheres of a few millimeters up to 1-centimeter diameter were individually dropped through the same cylindrical corona field and caught, after emerging from the field, in the Faraday cage of a low-capacity electrometer. The charges in this case were sufficiently large to permit individual measurements by the electrometer, thus allowing direct experimental tests of the particle-charging formulae, using single spheres. The formulas were verified in detail by studying each parameter separately.

Arendt and Kallmann[7] were able to obtain reasonable experimental checks of their theoretical ion-diffusion charging equation 13 by repeated observations of the charges adsorbed by individual particles placed in very low ion concentrations of the order of magnitude of 10^3 to 10^4 ions per cubic centimeter, and continuing observations for long periods of up to several hours.

The usefulness of the Arendt and Kallmann formula 13 is limited because the equation is in differential form and integration must be carried out numerically for each case, and also because it applies only to the case where the particle has already accumulated appreciable charge. It is therefore of interest to compare a few of their measurements with the theoretical values predicted by the simpler formula 18 developed in this paper.

Table IV. Experimental Results on Particle Charging in the Unipolar Corona Discharge for the Ion-Bombardment Process

a, Microns	t, Seconds	E_0, Volts/cm	N_0	t/t_0	n	n_s	$\frac{n}{n_s}$ (Exp.)	$\frac{n}{n_s}$ (Th.)
1	0.0165	560	1.98×10^7	0.292	14	64	0.218	0.226
2	0.0165	560	1.98×10^7	0.292	54	258	0.209	0.226
3	0.0165	560	1.98×10^7	0.292	125	578	0.216	0.226
1	0.0172	730	2.70×10^7	0.420	23	84	0.273	0.296
2	0.0172	730	2.70×10^7	0.420	93	336	0.277	0.296
2.5	0.0172	730	2.70×10^7	0.420	144	525	0.274	0.296
1	0.015	940	3.4×10^7	0.459	32	109	0.294	0.314
2	0.015	940	3.4×10^7	0.459	140	436	0.321	0.314

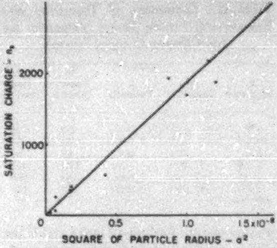

Figure 3. Experimental results showing linear relation between particle charge and square of particle radius

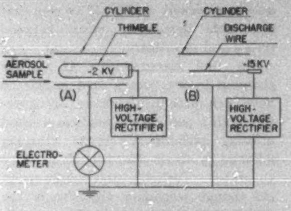

Figure 4. Schematic diagram of cylindrical-condenser-type particle-charge analyzer. Part A collects negative particles on cylinder and positive particles on thimble. Part B collects residual uncharged particles on cylinder by normal precipitation action

Table III lists the comparative values of particle charge n for two particle sizes and ion densities and for several values of time. The agreement is seen to be correct in order of magnitude, but not very close numerically. This is not surprising in view of the approximate nature of the theory and the inherent inaccuracies in experiments of this kind. The results do indicate, however, the range of validity of the theory, and that one is justified in concluding that the ion-diffusion process is of very limited importance in electrostatic precipitation.

Fuchs and Petranoff[10] charged oil mist droplets in an experimental precipitator by shooting a small jet of the oil mist through a short trajectory near the collecting pipe surface and parallel to the coaxial discharge wire. The theoretical particle charge was calculated from measurements of the corona current density and the time of exposure of the droplets to the charging field. The actual charges were determined experimentally by photographing their motions in a known oscillatory field between condenser plates. Representative results of this work are given in Table IV. The measurements were made for rather low values of field strength E_0 and ion density N_0, and the agreement between experiment and theory is good for this difficult type of work.

Some experiments on the charging of individual particles in a small test precipitator made by the writer in 1940 are of interest. Oil mist was charged by passing it through a small tube-type precipitator. Charge and diameter of individual particles of the charged mist were determined by the Millikan oil-drop method. The results for a charging time of 0.5 second and an average field of 5.6 kv per centimeter are shown in Figure 3 in which particle charge is plotted as a function of the square of particle radius. The theoretical straight line relationship between these quantities predicted by equation 8 is seen to be approximately true. The slope of the experimental line corresponds to a value of the field E_0 equal to about 1.5 times the space-average field in the tube, a not unreasonable value when it is considered that the oil mist was fed through a nozzle directed at the discharge wire where the charging field is maximum.

Particle Charge Measurements on Precipitator Dispersoids

The experimental results on particle charging up to this point have been given in terms of the charges on individual particles. Although the determination of individual particle charge is valuable in checking the theory, it is obviously a tedious and somewhat impractical method for measuring the over-all charge properties of dispersoids. For the latter purpose it is necessary to determine the charge properties of the dispersoid as a whole.

In practice, a particle charge analyzer, Figure 4, has been used to measure the charge and the charge distribution of dispersoids. A sample of the gas containing the dispersed suspended particles is drawn through a nozzle (not shown). The gas then passes through a d-c field maintained between the concentric cylinder and thimble electrodes. This field removes the charged particles from the gas, negative particles going to one electrode and positive particles to the opposing electrode. The electric charge received by either electrode is measured by means of a suitably connected sensitive electrometer. The mass of the particles collected on the corresponding electrode is measured by weighing on a sensitive balance. Any uncharged particles present are unaffected by the condenser field, and will be collected in the precipitation field which follows. Measurements made on both laboratory and field precipitators using this apparatus are given in Table V. The measurements were made on the residual or uncollected fraction of charged material leaving the precipitators, but nevertheless are representative of the degree of charging attained. These results do not of course show the charge of the material collected in the precipitator itself, but elementary considerations show that this material also must be negatively charged and to a substantial degree.

The net conclusion is that dispersoids in precipitators under normal operating conditions become charged to the degree of 10^5 to 10^6 statcoulombs per gram. Inasmuch as average particle size usually lies between 0.5 and 10 microns, a simple calculation shows that the average individual particle charges range between 10^2 and 10^5 electronic charges.

Abnormal Particle Charging Conditions

Disturbing conditions are sometimes present in precipitators which cause particle charge to be abnormally low. This in turn lowers the precipitation rate and interferes with normal operation. A brief discussion of these conditions is of considerable interest in any study of particle charging in the corona field.

SPACE-CHARGE SUPPRESSION OF CORONA CURRENT

This may occur with medium concentrations of fine fumes or smokes, or with very heavy concentrations of larger particles.

The particles which are suspended in the corona field, being charged to the same polarity as the unipolar corona ions, tend to reduce the electric field at the discharge electrode and, with high particle concentrations, may even reduce the field to its incipient corona-starting value. The corona current may then be reduced by a factor of 100 or more, and normal particle charging becomes impossible until the

Table V. Electrostatic Precipitator Particle Charge Measurements

Precipitator	Aerosol	q/m
Laboratory	Cement-mill raw-mix dust	10^5
	Fine particle fraction of fly ash	2×10^5
	Oil fume	9×10^5
Field	Lead oxide fume	2×10^6
	Fly ash	2×10^6

particle concentration is sufficiently decreased.

Back Corona

Back corona[12] is the localized discharge which occurs at the collecting electrode surface when that surface becomes coated with a layer of poorly conducting particles. Theory, experiment and long-accumulated field experience have all shown that back corona phenomena occur in a precipitator when the bulk electrical resistivity of the collected particle layer exceeds approximately 2×10^{10} ohm-centimeter, and become severe for resistivities greater than about 10^{11} ohm-centimeter. Incipient back corona lowers the sparking voltage, while severe back corona produces a positive ion discharge at the collecting electrode (assuming negative corona from the wires) which tends to neutralize the negative ions from the discharge electrode. Under this latter condition particle charge is greatly reduced, and positive and neutral particles may be present in numbers approaching or even exceeding the negative particles.

Particle Erosion from Collecting Electrode

This may occur in dry collection when gas velocity is high or gas-flow distribution is poor or exceptionally turbulent. Particles at the surface of the collected layer are caught up and resuspended by the wind force, somewhat as in a dust or sand storm.

Such eroded particles usually tend to be positively charged due to pith-ball effect (again assuming negative corona). Usually the corona discharge will rapidly recharge and recollect these particles, but if erosion is severe particle charge may be substantially reduced and numbers of both positive and neutral particles begin to appear.

References

1. The Precipitation of Smoke by Electrical Means, **Hohlfeld.** *Kastner Archiv Naturlehre*, volume ii, 1824, pages 205–06.

2. The Electrical Collection of Dust and Smoke, with Special Reference to the Collection of Metallic Fume, and to a Possible Purification of the Atmosphere, **O. J. Lodge.** *Journal*, Society of Chemical Industry (London, England), volume V, number 11, 1886, pages 572–76.

3. Art of Separating Suspended Particles from Gaseous Bodies, **F. G. Cottrell.** United States Patent 895,729.

4. Fundamental Processes of Discharges in Gases, **L. B. Loeb.** John Wiley and Sons, Inc., New York, N. Y., 1939.

5. Method of Size Measurement for Suspended Particles, **H. Rohmann.** *Zeitschrift fur Physik* (Berlin, Germany), volume 17, 1923, pages 253–65.

6. Charging of Spherical Particles in an Ionizing Field, **M. M. Pauthenier, M. Moreau-Hanot.** *Journal de Physique et Le Radium* (Paris, France), series 7, volume 3, 1932, pages 590–613.

7. The Mechanism of Charging of Mist Particles, **P. Arendt, H. Kallmann.** *Zeitschrift fur Physik* (Berlin, Germany), volume 35, 1925, pages 421–41.

8. Kinetic Theory of Gases, **L. B. Loeb.** McGraw-Hill Book Company, New York, N. Y., 1934.

9. Research on the Physical Basis of Electrical Gas Purification, **R. Ladenburg.** *Annalen der Physik* (Leipzig, Germany), volume 4, 1930, pages 863–97.

10. Rate of Charging a Droplet by an Ionic Current, **N. Fuchs, Petranoff.** *Transactions*, Faraday Society, 1936, pages 1131–38.

11. The Physical Basis of Electrical Gas Purification, **Mierdel and Seeliger.** *Transactions*, Faraday Society (London, England), 1936, page 1284.

12. Characteristics and Fundamentals of the "Back Corona" Discharge, **H. J. White.** Gas Discharge Conference, Brookhaven National Laboratory, Brookhaven, N. Y., October 1948.

Discussion

F. Fraas (Bureau of Mines, College Park Md.): Dr. White has presented an interesting paper. I would like to inquire as to what studies he has made with respect to superimposing a radio frequency ripple on the constant potential supplied to the ionizing wires. In a specific example of our studies a positive corona wire spaced parallel to a grounded metal cylinder emitted a 0.09-milliampere corona current at a maximum constant or d-c potential of 31 kv. Above this maximum potential for the wire there is a spark discharge to the grounded cylinder. However, by inserting a radio frequency potential in series with the constant potential the d-c corona emission increased tenfold to 1.1 milliampere with the constant potential at the same 31 kv.

Power to the radio frequency oscillator was supplied through a 1:1 isolating transformer with the secondary at 31 kv above ground potential. Estimated power output of the Tesla coil of the oscillator was approximately 10 watts with a frequency of approximately 50 megacycles.

H. J. White: The discussion by Mr. Fraas raises an important point. Various types of a-c and transient voltages superposed on direct current have been tried in electrical precipitation. Certain of these arrangements do give somewhat higher corona currents. However, it must be noted that in Cottrell electrostatic precipitators negative polarity is used almost universally in preference to positive because of the higher corona currents possible. The example given by Mr. Fraas is for positive corona and therefore cannot be compared directly to the electrostatic precipitation case. Another significant difference which must be taken into account is the fact that large precipitators have appreciable capacitance which in turn makes it very difficult or impossible to obtain large voltage swings with high radio frequencies, for example, the 50 megacycles quoted by Mr. Fraas.

Electrostatic Precipitation of High-Resistivity Dust

G. W. PENNEY
FELLOW AIEE

IN electrostatic precipitation of high-resistivity dust, the voltage drop across the layer of collected dust on the large electrodes of the ionizer may be sufficiently high to cause electrical breakdown through this layer of dust. The high local voltage gradient, at these points of breakdown, results in a glow at the surface of the dust. This glow is a source of ions of a sign opposite to that of the ions liberated at the wire. The resulting partial neutralization of the charge acquired by the suspended dust particles causes a loss in cleaning efficiency. Other troubles are wire vibration and increased ozone generation. This trouble can usually be eliminated by operating at a higher relative humidity, or by the liberal use of adhesives.

In electrostatic precipitation it is obvious that a dust of high electrical conductivity may give trouble due to excessive electrical leakage through a layer of conducting dust on insulators. It may not be as obvious that high resistivity dust can cause very serious trouble and is in fact much more likely to cause trouble under typical operating conditions.

The resistivity of most dusts will in general be high only when the relative humidity is low. At times of low humidity a trouble frequently occurs called "reverse-ionization" or "back-ionization." This results in low efficiency, severe vibration of ionizing wires, and excessive ozone generation.

The trouble occurs in all types of precipitators but this paper is restricted to the condition in low-voltage 2-stage precipitators having a positive ionizing wire and used for air conditioning.

Characteristics of Reverse-Ionization

In the normal operation of an ionizer the ions are generated in a small region immediately surrounding the ionizing wire. If the wire is positive, as in electrostatic precipitators designed for air-conditioning applications, the electrons or negative ions are immediately collected by the wire, while the positive ions travel away from the wire, to the large negative electrode. In passing through the air some of these positive ions are collected by suspended dust particles. The amount of charge which a particle can obtain depends on the voltage gradient, the density of ions, and the time of charging.[1,2] A typical 1-micron particle may acquire a few hundred elementary charges, and a 10-micron particle a few tens of thousands of elementary charges.

During operation a layer of dust accumulates on the large electrode of the ionizer. The ions formed at the wire and which pass through the air to the large electrode constitute a current which must be conducted through the dust layer. If the resistivity of the dust is increased, the resulting voltage drop across the dust increases and the ionizing current decreases until the dust layer breaks down electrically. This breakdown tends to occur at points leaving local regions of high-voltage gradient at the surface of the dust. This causes a glow discharge or corona which if viewed in a darkened room appears as minute glowing spots. A glow at the large or negative electrode provides a source of negative ions which move toward the wire partially neutralizing the effect of the positive ions from the wire. This condition is called "reverse-ionization." With increasing resistivity of the dust the number of glowing spots on the negative electrode increases until at times the entire area appears to glow. The negative ions tend to neutralize the normal positive charge on the dust particles leaving the ionizer. This tends to increase the ionizer current, decreases the efficiency, and causes other troubles.

The conditions under which this trouble called reverse-ionization occurs can be predicted if the electrical characteristics of the dust are known. The resistivity of the dust as measured in bulk, multiplied by the current density (ionizer current per-unit area) gives the voltage gradient. If this voltage gradient is greater than that needed to produce breakdown, reverse-ionization is to be expected. As an example a dust having a resistivity of 3×10^{10} ohm–centimeters will be considered. A typical current density is 0.5×10^{-6} amperes per square centimeter. This current density multiplied by the resistivity gives a voltage gradient of 1.5×10^{4} volts per centimeter. Many samples of dust when subjected to a voltage test will break down below this voltage gradient.

In estimating the condition at which reverse-ionization will occur the resistivity of the dust and the electrical breakdown voltage are primary factors. The uniformity of the dust deposit is also important. The resistivity of collected dusts may vary from a fraction of an ohm–centimeter to 10^{13} ohm–centimeter or even higher. The breakdown voltage varies through a much smaller range. General experience seems to indicate that reverse-ionization is probable if the resistivity of the dust is greater than 10^{11} ohm–centimeter and is improbable if the resistivity of the dust is less than 5×10^{9} ohm–centimeter.

Tests of High Resistivity Dust

In order to study the effect of high resistivity dust and the nature of reverse-

---

Paper 51-201, recommended by the AIEE Electronics Committee and approved by the AIEE Technical Program Committee for presentation at the AIEE Summer General Meeting, Toronto, Ont., Canada, June 25–29, 1951. Manuscript submitted March 20, 1951; made available for printing May 7, 1951.

G. W. Penney is with Carnegie Institute of Technology, Pittsburgh, Pa.

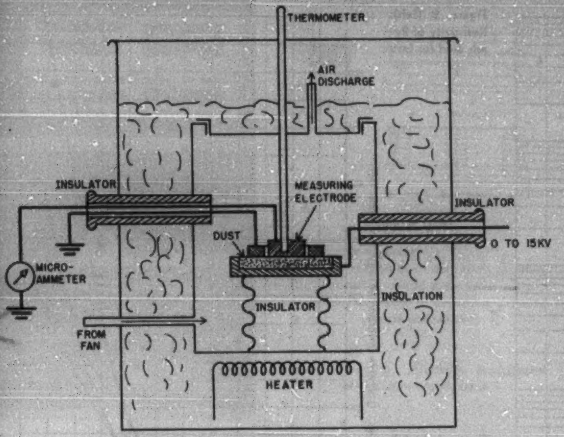

Figure 1. Cross section of apparatus for measuring resistivity

ionization a series of tests were made using electrically precipitated fly ash. The sample used was taken from a power plant burning a type of coal under conditions which were known to give trouble in electrostatic precipitation. This was a convenient way to get a large homogeneous sample of a dust. It is of course a material which frequently is discharged into the atmosphere and must be removed by air cleaning devices. The sample used was chosen because it had an unusually high resistivity at moderately low humidities. It was therefore a good sample to demonstrate trouble, but it should not be regarded as a typical dust.

In an agglomeration of particles such as a layer of collected dust, the resistivity as measured on a large sample depends largely on the surface resistivity of the separate particles and so it is to be expected that the resistivity as measured will depend on the humidity. Tests were made in which a sample of dust was placed in a test cup with a measuring electrode surrounded by a guard electrode resting on the dust. The temperature and dew point of the air surrounding the sample could be controlled. Potentials from 0 to 15,000 volts could be applied across the sample and the current measured. Figure 1 is an illustration of the apparatus. A fan was used to slowly circulate air through the test oven. The relative humidity was varied by controlling the temperature of the sample. In order to get a high dew point, a few tests were made in which the ingoing air was bubbled through water. The temperature of the air surrounding the sample was held constant for approximately two hours before taking readings. This seemed to give equilibrium conditions. The measuring electrode was 2 inches in diameter and the sample of dust 9/32 inches thick. For resistivities less than 5×10^{10} ohm–centimeters the current could be read with a microammeter. For higher resistivities a galvanometer was used to measure the current. The pressure on the sample was approximately 4.75 grams per square centimeter. Under these conditions the resistivity measured is a function of dew point, temperature, packing, and applied voltage. Tests were made in which the dew point varied from 35 to 80 degrees Fahrenheit. In Figure 2 the resistivities measured are plotted as a function of relative humidity. The curve shown is for 3,000 volts across the sample giving a voltage gradient of 4,200 volts per centimeter. At 2,800 volts per centimeter the resistivity is approximately 18 per cent higher, and for 5,600 volts per centimeter about 10 per cent lower.

To study the effect of a layer of dust on the ionizing current, the large electrodes of the precipitator cell shown in Figure 4(A) were coated by slowly blowing dust into a cell with the ionizer energized until the dust layer reached a thickness of about 1/32 inch. The cell was then mounted on insulators in a box in which the temperature could be controlled. The dew point in the box remained constant at 65 degrees Fahrenheit. The box was heated to 176 degrees Fahrenheit over a period of 4 hours and then cooled slowly. During the cooling period curves of current versus voltage were taken. These curves are shown in Figure 3 together with a curve for a clean cell. Curve A for the clean cell was essentially the same as a curve for the electrodes coated with dust and tested at 60 per cent relative humidity. It has been found that the rate of cooling used to obtain curves B and C, of Figure 3 was too rapid to give an equilibrium condition. For this reason the dust at 32 per cent humidity when curve C was measured would not have exactly the resistance that would be obtained from Figure 2. Nevertheless the curves of Figure 3 do show qualitatively the manner in which current changes with humidity. High resistivities give severe reverse-ionization and currents large as compared to that for a clean cell. Moderate resistivities particularly at lower voltage give a reduction in current. A thick dust layer would give a greater reduction in current than the thin dust layer used in these tests.

In another series of tests the efficiency of a precipitator was measured when the large electrodes of the ionizer were coated with a thin layer of this fly ash. The precipitator was tested when cleaning normal city air and the efficiency measured using the filter paper discoloration method.[3] A duct added for test purposes reduced the air flow slightly below rated velocity. Under these test conditions the efficiency measured at 54 per cent relative humidity was 95.5 per cent. This is approximately the efficiency of the precipitator with clean electrodes. At a humidity of 15 per cent the efficiency dropped to 71 per cent and at 7 per cent relative humidity the efficiency was 54 per cent. Three tests were made at 12 per cent relative humidity but regulating the ionizer voltage by means of a separate power supply so as to maintain the current at approximately the normal value for a clean cell. In tests 4, 5, and 6 the current was 500, 550, and 600 microamperes respectively and resulted in efficiencies of 80 to 83 per cent. These tests indicate that if the resistivity is high, satisfactory performance is not secured by adjusting the voltage to give a normal ionizing current.

The dust layer was then saturated with "Celluflex" which is a tricresyl phosphate base adhesive with a wetting agent added so that the resistivity of the adhesive is relatively low. The unit was then tested at humidities duplicating tests 1, 2, and 3. With the dust saturated with low resistivity adhesive the efficiency remained at 95.5 to 96 per cent regardless of humidity.

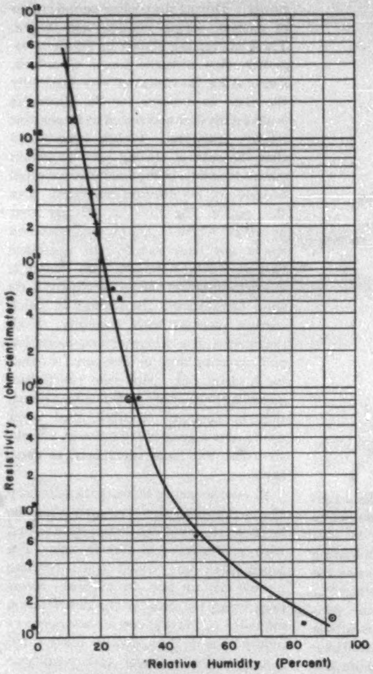

Figure 2 (left). Resistivity of fly-ash used for tests

+ Dew point between 35 °F and 40 °F
× Dew point between 40 °F and 45 °F
· Dew point between 45 °F and 50 °F
⊙ Dew point 80 °F

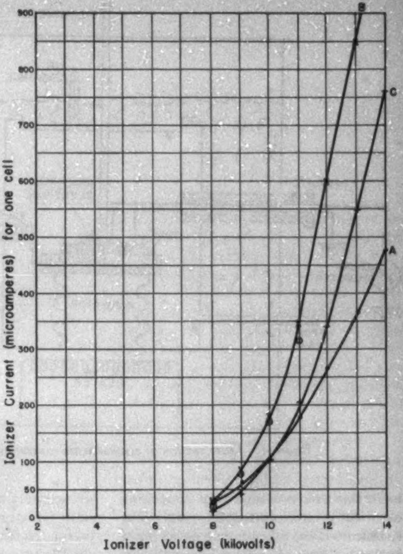

Figure 3 (right). Ionizer current of one cell. The large electrodes of the ionizer were coated with fly ash

A. 80 °F —60% relative humidity
B. 149 °F— 9% relative humidity
C. 106 °F—32% relative humidity

Photographs were taken to show the appearance of the ionizer discharge under typical conditions. Figure 4(A) shows the appearance of the ionizer with the thin deposit of dust, Figure 4(B) was taken in a darkened room with the ionizer energized under conditions giving no reverse-ionization. This was a 15-minute exposure at f4.5 and shows the glow along the ionizer wire as it appears when viewed in a darkened room. Figure 4(C) is similar to 4(B) except taken under conditions giving reverse-ionization. The glow at the large electrodes as well as along the wires is clearly visible. Most of the center large electrode is behind the member which supports the ionizer so that only a little of the glow on this electrode is visible.

Discussion of Test Results

The tests that have been described were intended to study the nature of reverse-ionization and to investigate means for eliminating it. The nature of the trouble seems clearly indicated, however, the resistivity at which the trouble starts is more difficult to determine. The resistivity tests were intended to approximate the condition of the dust on electrodes but there are several uncertainties. For example, the packing of the dust as deposited is probably different from the packing in the test cup. Electrically deposited dust tends to be spongy or porous so that probably the dust in the test cup may be more dense. Then dust seems to exhibit a type of hysteresis so that the resistivity measured at a given humidity depends partly on previous history. A dust reaches equilibrium very slowly. The tests shown in Figure 2 are reasonably reproducible but the resistivity as given by the curve of Figure 2 would only approximate the resistivity at the same humidity under the conditions of the tests shown in Figure 3. Further tests are also needed to verify the correlation between resistivity and relative humidity. These uncertainties do not influence the qualitative analysis of the nature of reverse-ionization but do prevent an exact

Table I. Effect of Humidity on Efficiency Electrodes Coated with Fly Ash

Test Number	Surface Condition of Large Electrode	Air Temp., Degrees Fahrenheit	Air Relative Humidity, Per Cent	Current	Efficiency, Per Cent
1	Coated with fly-ash dry	63	54	550	95.5
2		79	15	800	71
3		102	7	1,150	54
4		118	12	500*	83
5		118	12	550*	82
6		118	12	600*	80
7	Coated with fly-ash saturated with celluflex	63	50	600	95.8
8		83	14	not measured	95.6
9		109	6	600	96

* Ionizer voltage was varied to maintain specific current.

Figure 4 (left).

A. Structure of ionizer
B. Photograph taken in dark-room showing normal discharge at the wires
C. Photograph taken in dark-room showing reverse-ionization

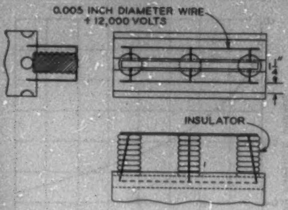

Figure 5 (above). Electrode arrangement of unit shown in Figure 4

determination of the resistivity at which the trouble begins. Such a determination on this particular dust would however be of rather limited value because of the wide variation in types of dust that must be precipitated.

Further tests to study the point at which the efficiency is impaired seem very desirable. Tests 4, 5, and 6 of Table I exhibit a serious loss in efficiency even though the current was normal. These tests were made with a thin dust layer. A thicker deposit of dust would exhibit a larger decrease in current just below the resistivity at which reverse-ionization starts.

The increased generation of ozone which accompanies reverse-ionization is very noticeable to the sense of smell but was not measured in these tests. This increase is probably due to several factors. The increase in current would of course give a corresponding increase in ozone. Then the generation of ozone due to negative corona is normally higher than for positive corona. The most important factor is probably the change in the type of discharge when both positive and negative corona occur simultaneously.

Another difficulty that accompanies reverse-ionization is the increased tendency of the wire to vibrate. Wire vibration is troublesome because it shortens the life of the wire and because of the humming noise created. In cases of severe vibration the amplitude may be sufficiently great to cause spark-over between the wire and the large electrode. Even slight reverse-ionization increases the tendency of the wires to vibrate.

Elimination of Reverse-Ionization

Since reverse-ionization is caused by electrical breakdown of the layer of collected dust, it has been suggested that the trouble can be eliminated by frequent cleaning of the electrodes. This is not always successful because an extremely thin layer of high resistivity dust can cause trouble. In these tests the electrodes were wiped off with a dry rag and yet a considerable increase in current occurred at low humidities indicating reverse-ionization.

Reducing the ionizer voltage reduces the ionizer current and the resulting voltage gradient in the dust. While the voltage can be lowered until reverse-ionization ceases, this is not generally practical. The resistivity of dust may be 20 times the resistivity required to cause reverse-ionization at normal voltage, so that the ionizing current would need to be reduced to 5 per cent of normal to eliminate reverse-ionization.

Since a small change in humidity results in a large change in resistivity, the control of humidity is usually an effective and feasible means of eliminating reverse-ionization. Humidities considered desirable from a comfort standpoint usually result in a sufficiently low resistivity of the collected dust. Usually in precipitators cleaning normal ventilating air, little reverse-ionization is experienced when the humidity of the air entering the precipitator is controlled.

Adhesives have been found desirable as a means of retaining the precipitated dust. Most adhesives incorporate wetting agents to improve washability. This also results in a relatively low resistivity liquid. Saturating the dust with these adhesives is a very effective means for reducing the resistivity of the dust. A liberal amount of adhesive may be required because the surface layer of dust must be wetted.

Conclusion

High resistivity dusts may result in excessive voltage gradients across the layer of collected dust on the large electrodes of the ionizer. This results in electrical breakdown through this dust layer and a negative corona at the surface of the large electrode. This supplies negative ions to partially neutralize the normal positive charge imparted to dust particles. Reverse-ionization reduces the efficiency of precipitation and causes excessive ozone generation and wire vibration. Reverse-ionization is probable if the resistivity of the dust is greater than 10^{11} ohm–centimeters and is improbable below 5×10^9 ohm–centimeters.

Control of humidity can keep the resistivity of the collected dust below objectionable limits and is usually an effective and feasible means of eliminating reverse-ionization. The use of liberal amounts of adhesive also is an effective means of eliminating trouble.

References

1. A New Electrostatic Precipitator, G. W. Penney. *Electrical Engineering* (*AIEE Transactions*), volume 56, January 1937, pages 159–63.

2. Untersuchungen uber die Physikalischen Vorgange bei der Sogenannten Elektrischen Gasreinigung, Rudolf Ladenburg. *Annalen der Physik* (Leipzig, Germany), volume 4, fifth Series, 1930, pages 863–97.

3. A Test Method for Air Filters, Richard S. Dill. *Transactions*, American Society of Heating and Ventilating Engineers (New York, N. Y.), volume 44, 1938, page 379.

4. Collection of Fly Ash, H. J. White, L. M. Roberts, C. W. Hedberg. *Mechanical Engineering* (New York, N. Y.), November 1950, pages 873–80.

Discussion

John R. Coolidge (Borg-Warner Central Research Laboratory, Bellwood, Ill.): Dr. Walker and I presented[1] some initial results of our program of study of electrostatic precipitation at Pennsylvania State College. In particular, in addition to a general survey of electrostatic precipitation, we discussed the effects of relative humidity and voltage on the precipitation efficiency of gypsum—a high resistivity dust. Figures C and D from the paper illustrate our results. In discussing these tests we said: "If the material comes in contact with the collector plate, it is then necessary that the particle give up its charge and assume the charge of the collector plate. If the resistivity of the deposited layer is extremely high this charge transfer becomes difficult, back voltages are built up, sparking and uneven current flow result and precipitation is difficult. Some studies have correlated the resistivity of the precipitated material with the efficiency of precipitation of the material. These studies indicate that if the resistance is less than 8×10^8 ohm–centimeter precipitation is easy, but if it reaches 10^{13} ohm–centimeter precipitation is almost impossible.

"Many investigators have mentioned the desirability of humidifying the gas in order to improve precipitation under certain conditions. In accordance with this practice laboratory investigations show that relative humidity plays a prominent role in the precipitation of gypsum compound. . . . Figure C represents the dependence of precipitator current on the relative humidity before, during, and after a precipitator run with gypsum. The theory behind these changes is not understood but they illustrate the pronounced effect of humidity and dust on the electric discharge. . . . Typical results are shown in Figure D. The experimental precipitator used in these investigations is shown in Figure B and employs 13 16-gauge, 4 inch by 12 inch plates; spaced 1 inch apart with 4 wires, 20 mils in diameter, spaced equal distance between each pair of plates. The data suggest a relation for efficiency.

$$\text{"}E=1-\epsilon^{-Kh(V-V_c)} \tag{1}$$

where

V=applied voltage
V_c=critical corona voltage
h=fractional humidity
K=constant for the system

"This relation is applicable to the gypsum compound only. It appears however to agree with the aforementioned resistivity studies . . . the effect of the moisture probably giving a reduction in resistivity."

It is indeed comforting to read that Dr. Penney's experiments corroborate our results and confirm our speculations on the action of high resistivity dust at the collector plates.

The correlation of the resistivity of the dust with its precipitability is interesting. However, I must agree with Dr. Penney that the results of his resistivity measurements bear somewhat a tenuous relationship to the resistivity of the material as it exists in a precipitator.

REFERENCE

1. A Survey of Electrostatic Precipitation, E. A. Walker, J. E. Coolidge. *Heating, Piping, and Air Conditioning* (Chicago, Ill.), March 1951.

G. W. Hewitt (Westinghouse Electric Corp., East Pittsburgh, Pa.): This paper shows the serious effects of reverse-ionization on cleaning efficiency. Dr. White's paper[1] also describes this abnormal condition. It is indicated that the cause of the lower efficiency is the decrease in particle charge resulting from the presence of ions of the opposite sign.

A theoretical calculation of the effect of opposite-sign ions on the charging of particles by the electric field can be made very easily. This is done by modifying the theoretical field charging analysis[1,2] developed for a unipolar ion stream, so as to include both positive and negative ions incident upon the particle. Figure 1 of this discussion shows the effects of rather small relative current densities of opposite-sign ions, for two values of charging time.

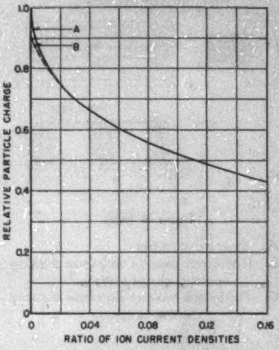

Figure 1. Effects of opposite-sign ions on particle charging by electric field

Curve A. Saturation charge, $mNt=\infty$
Curve B. Practical charging time which produces 90 per cent of saturation charge when no opposite-sign ions are present, $mNt=6\times10^8$

Let

m=mobility of the charging ions, centimeter per second per statvolt per centimeter
N=concentration of the charging ions, number per cubic centimeter
t=charging time, seconds

For curve A, $mNt=\infty$ and the particle has its "saturation" charge. For curve B, mNt has the practical value of 6×10^8 for which the particles acquire 90 per cent of the saturation charge in a unipolar ion stream. Curve B indicates a 42 per cent reduction in particle charge for an opposite-sign ion current density of one-tenth the charging ion current density. A 9 per cent loss in charge results when the ratio of ion current densities is only 0.01.

Calculations of opposite-sign ion effects in the case of diffusion charging do not yield results as simple as those for field charging. However, they indicate that in the particle size range where diffusion charging is important, the effect is fully as pronounced as that for field charging.

No accurate check of this theoretical curve with the experimental results can be made without additional information on the ratio of negative to positive ion currents in Test 2, Table I of the paper and on the efficiency-particle charge characteristic of the test precipitator. However, a very rough comparison, which can be obtained by making the following assumptions, may be of some interest:

1. Assume the increase in current caused by reverse-ionization to be divided between positive and negative ions in the ratio of their mobilities, about 480:660, after taking into account the voltage drop across the dust layer.

2. Assume the effect on efficiency of the decrease in particle charge in Test 2 to be the same as that of an equal increase in air velocity in tests on precipitators of similar type. In Tests 1 and 2, Table I, reverse-ionization caused a change in cleaning efficiency from 95.5 per cent to 71 per cent. The efficiency-velocity characteristic of a similar precipitator, as given in one of Professor Penney's earlier papers,[3] shows this same decrease in efficiency for an air velocity increase of 2.3:1. From this it is estimated that the particle charge in Test 1 was approximately 2.3 times the particle charge in Test 2. Then from curve B, the corresponding ratio of ion-current densities in Test 2 is about 0.19. For the 800 microamperes total current, this would indicate a negative ion current of 130 and an increase in positive ion current of 90, making a total current increase caused by reverse-ionization of 220. The observed increase in Test 2 over Test 1 was 250, but correction for the voltage drop across the dust layer would increase this considerably, perhaps to 300 or 400. While no definite conclusions can be drawn from this comparison, no great discrepancy is indicated. The theoretical effects of opposite-sign ions on particle charging by the electric field, appear reasonable.

REFERENCES

1. Particle Charging in Electrostatic Precipitation, H. J. White. *AIEE Transactions*, volume 70, 1951, pages 1186–91.

2. Charging of Spherical Particles in an Ionizing Field, M. M. Pauthenier, M. Moreau-Hanot. *Journal De Physique et La Radium* (Paris, France), Series 7, volume 3, 1932, pages 590–613.

3. A New Electrostatic Precipitator, G. W. Penney. *Electrical Engineering (AIEE Transactions)*, volume 56, January 1937, pages 159–63.

G. W. Penney: I would interpret Mr. Coolidge's data in a somewhat different manner from that implied in his discussion. He emphasizes the current resulting from the deposition of charged dust. In general this current is very small compared to the current carried by the air ions in the corona discharge. So the primary difficulty seems to be the conduction of the ion or corona current through the layer of collected dust on the large electrodes opposite the high potential wire.

Mr. Coolidge suggests an equation expressing efficiency as a function of the product of humidity and voltage. While this would appear to be a reasonable approximation for the curve drawn through the few points shown, other curves could be drawn through these same points which would not be represented by the equation suggested. Furthermore there are many reasons to believe that this simple exponential equation cannot represent efficiency in general. For example with many dusts between 40 and 90 per cent relative humidity the efficiency is substantially independent of humidity. So until further information is available it seems that this should be regarded as merely a suggested equation.

Mr. Hewitt has made a valuable contribution by suggesting a method of calculating the reduction in the charge on a dust particle and the resultant decrease in efficiency caused by reverse ionization.

Analysis of Total and Incremental Losses in Transmission Systems

L. K. KIRCHMAYER
ASSOCIATE AIEE

G. W. STAGG
NONMEMBER AIEE

AS INTEGRATED power systems are developed, larger steam and hydrogenerating plants become concentrated in the most favorable economic locations; and the problem of including transmission losses in the economic scheduling of generation becomes increasingly important. The first steps toward the solution of this problem have been made by George[1] in expressing the total transmission losses in terms of generator powers. The application of the network analyzer to determine a similar loss formula was developed later by Ward, Eaton, and Hale.[2] A method of co-ordinating fuel costs and transmission losses has been described by George, Page, and Ward[3] which requires the use of a transmission loss formula.

This paper describes an improved method of obtaining a transmission loss formula which involves considerably less network analyzer data and a fraction of the arithmetic calculations of the methods previously described in the literature.[1,2] The proposed method essentially requires impedance measurements on the open-circuited transmission network and a normal load flow study. The derivation of the proposed method involves a number of fundamental concepts of tensor analysis[4] as presented in the companion paper by G. Kron.[5] The various assumptions made in obtaining the loss formula have been evaluated in a study of the American Gas and Electric System.

Assumptions

The assumptions made in obtaining the loss formula are the following:

1. The equivalent load current at any bus remains a constant complex fraction of the total equivalent load current. The equivalent load current at a bus is defined to be the sum of the line-charging, synchronous condenser, and load current at that bus.
2. The generator bus voltage magnitudes are assumed to remain constant.
3. The ratio of reactive power to real power of any source is assumed to remain a fixed value.
4. The generator bus angles are assumed to remain constant.

These assumptions are similar to those of reference 2. Because of the generality of the tensor approach, other assumptions, if necessary, may be made about system operation. However, this paper is restricted to the assumptions listed above. A summary of the tensor method is given in Appendix I.

Description of American Gas and Electric System[6]

The American Gas and Electric Company is composed of the Indiana, Ohio, and Appalachian operating divisions and maintains transmission facilities in portions of seven states. The outside perimeter encloses approximately 80,000 square miles. Principal interconnections

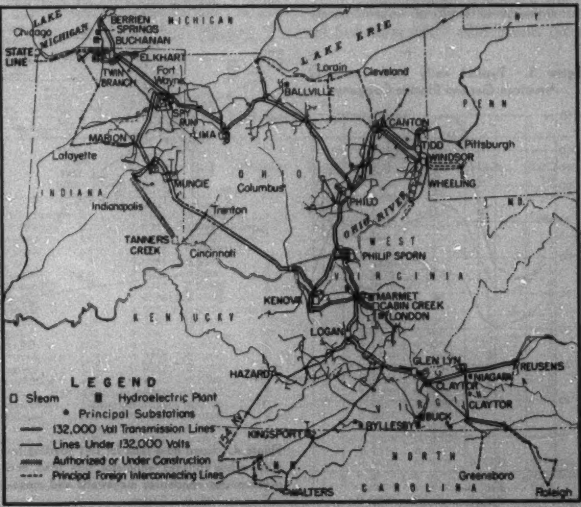
LAKE MICHIGAN
Chicago
STATE LINE
BERRIEN SPRINGS
BUCHANAN
MICHIGAN
ELKHART
TWIN BRANCH
Fort Wayne
SPY RUN
LIMA
LAKE ERIE
Lorain
Cleveland
BALLVILLE
N. Y.
PENN
CANTON
TIDD
Pittsburgh
WINDSOR
WHEELING
MD.
MARION
Lafayette
INDIANA
MUNCIE
Indianapolis
OHIO
Columbus
Trenton
PHILO
OHIO RIVER
TANNERS CREEK
Cincinnati
WEST VIRGINIA
PHILIP SPORN
KENOVA
MARMET
CABIN CREEK
LONDON
KENTUCKY
LOGAN
GLEN LYN
REUSENS
NIAGARA
CLAYTOR
HAZARD
VIRGINIA
BUCK
BYLLESBY
KINGSPORT
TENN.
NORTH CAROLINA
Greensboro
Raleigh
WALTERS
LEGEND
Steam
Hydroelectric Plant
Principal Substations
132,000 Volt Transmission Lines
Lines Under 132,000 Volts
Authorized or Under Construction
Principal Foreign Interconnecting Lines

Figure 1. Map of 1950 American Gas and Electric Company System

---

Paper 51-204, recommended by the AIEE Transmission and Distribution Committee and approved by the AIEE Technical Program Committee for presentation at the AIEE Summer General Meeting, Toronto, Ont., Canada, June 25–29, 1951. Manuscript submitted March 28, 1951; made available for printing May 11, 1951.

L. K. Kirchmayer is with the General Electric Company, Schenectady, N. Y., and G. W. Stagg is with the American Gas and Electric Service Corporation, New York, N. Y.

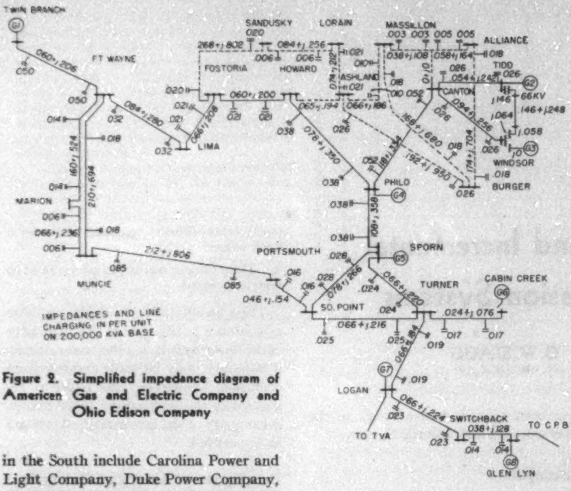
TWIN BRANCH
G1
FT WAYNE
SANDUSKY
LORAIN
MASSILLON
ALLIANCE
FOSTORIA
HOWARD
ASHLAND
TIDO
CANTON
66KV
G2
WINDSOR
G3
BURGER
LIMA
PHILO
G4
MARION
SPORN
G5
PORTSMOUTH
MUNCIE
TURNER
CABIN CREEK
G6
SO. POINT
G7
LOGAN
SWITCHBACK
TO C P B L
TO T VA
G8
GLEN LYN
IMPEDANCES AND LINE CHARGING IN PER UNIT ON 200,000 KVA BASE

Figure 2. Simplified impedance diagram of American Gas and Electric Company and Ohio Edison Company

in the South include Carolina Power and Light Company, Duke Power Company, Virginia Electric and Power Company, and the Tennessee Valley Authority; on the northern fringe, Ohio Edison Company; toward the East, West Penn Power Company; and in the western portion, the Northern Indiana Public Service Company, Public Service Co. of Indiana, and Cincinnati Gas and Electric Company. The American Gas and Electric Company is predominantly a steam system and had in operation during 1950 nine major steam plants interconnected with a 132-kv transmission network of approximately 3,800 circuit miles. The peak load for 1950 was 2,386,000 kw. A map of the American Gas and Electric 132-kv transmission system showing major generating plants and principal foreign interconnections is shown in Figure 1.

For the purposes of developing techniques and to determine the accuracy of the assumptions made in obtaining a transmission loss formula, a simplified representation of the American Gas and Electric System was used maintaining, however, the wide variation of operating conditions experienced in actual practice.

Physical simplifications included the following:

1. Radial lines were omitted.
2. Stations within the same vicinity were bussed together.
3. Multicircuit lines were paralleled.
4. Small tap stations were omitted.
5. Principal interconnections were shown at the nearest generating station to minimize the number of terms involved in the loss formula.

The transfer of power between the Ohio and Indiana Divisions of the American Gas and Electric Company may cause additional losses in the Ohio Edison transmission system. Consequently a simplified representation of the Ohio Edison System also is considered, and a loss formula was obtained to include the total losses in both simplified systems. The simplified American Gas and Electric System and Ohio Edison System impedance diagram is shown in Figure 2. The dotted lines designate the Ohio Edison Company.

Hourly summer peaks for a typical weekday, Saturday, and Sunday were grouped and averaged to produce step load curves typifying five periods of operation common on the American Gas and Electric System. These five periods are designated as A, B, C, D, and E in Figure 3. For each of these periods, individual station loads were determined maintaining the variations in load en-

Figure 3. Typical daily load cycles of American Gas and Electric Company

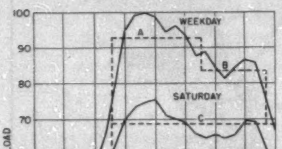

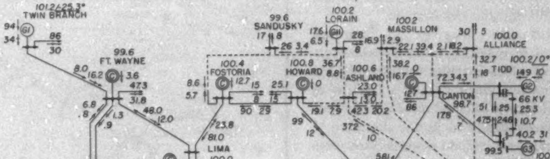
TWIN BRANCH
FT. WAYNE
SANDUSKY
LORAIN
MASSILLON
ALLIANCE
FOSTORIA
HOWARD
ASHLAND
TIDO
CANTON
66 KV
WINDSOR
LIMA
MARION
PHILO
BURGER
PORTSMOUTH
SPORN
MUNCIE
TURNER
CABIN CREEK
SO. POINT
O.P.
A.E.P.
LOGAN
TO TVA
SWITCHBACK
TO C.P.B.L.
GLEN LYN
10 MW
10 MVAR
LINE FLOWS UNCORRECTED FOR LINE CHARGING

Figure 4. Load flow data for D-1 loading including bus voltages, generator, line, load, and synchronous condenser megawatts and megavars

countered between the three operating divisions. Stub loads were added at the major substations and tap loads were proportioned between these stations. The Kenova generating plant and all small steam and hydrogeneration were assumed to vary as the loads and were netted at the major substations. The Burger and Lorain steam plants of the Ohio Edison Company were considered as negative loads that varied in the same manner as the loads of the Ohio Edison Company.

Operating conditions on the American Gas and Electric System afford a strenuous test of the assumptions involved in obtaining a loss formula and include the following:

1. Large industrial loads subject to long strikes affecting the load pattern.

2. Divisions with independent load variations.

3. Transmission of large blocks of power over considerable distances which in turn cause large variations in:
   a. Generator angular bus position.
   b. Power factor of generating stations to maintain voltage.

4. Regulation of 132-kv system with reactive capacity principally in the form of synchronous condensers which operate lead to lag from peak to off-peak, causing reactive load to remain at proportionally higher value during light load periods. (The variation in voltage on the 132 kv is approximately 3 to 4 per cent drooping for light load periods.)

Network Analyzer Measurements Required

In the following analysis the word generator is understood to be either a steam generator, hydrogenerator, or an interconnection that is to be included in the loss formula. For a given base case it is necessary to record the following quantities most of which would be recorded in a normal load flow study.

Load Flow Study

1. Record generator voltage magnitudes, megawatts, megavars, and angles.

2. Record scalar values of all line currents.

3. With the network analyzer reference chosen such that the summation of the currents of the generators included in the loss formula equal a real number, record all generator vector currents and the real part of all equivalent load currents.

4. For a check on the system operation, it is desirable to record load voltages, load and line megawatts and megavars, and synchronous condenser megavars.

The preceding data are shown in Figures 4 and 5 for a typical D loading.

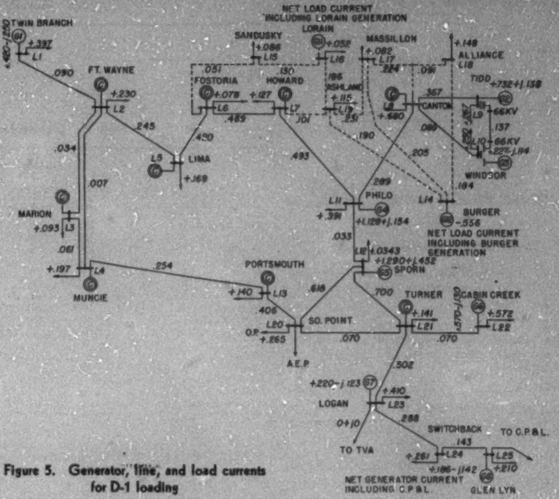
TWIN BRANCH
G1
+.420-j.250
+.397
L1
.090
FT. WAYNE
+.230
L2
.245
.034
.007
L5
LIMA
+.169
MARION
+.093
L3
.061
+.197
L4
MUNCIE
.254
SANDUSKY
+.086
L15
NET LOAD CURRENT INCLUDING LORAIN GENERATION
LORAIN
G11
+.052
L16
MASSILLON
+.082
L17
.224
.091
+.148
ALLIANCE
L18
.051
FOSTORIA
+.078
+.127
L6
.483
.130
HOWARD
L7
.101
.186
ASHLAND
+.115
L19
.231
.430
.493
.190
L8
+.680
.367
CANTON
.088
.205
TIDD
+.732+j.138
G2
L9
66KV
.137
L10
66KV
+.227-j.114
G3
WINDSOR
.184
.289
PHILO
L11
+.391
G4
+1.128+j.154
L14
BURGER
-.556
NET LOAD CURRENT INCLUDING BURGER GENERATION
.033
L12
+.0343
+1.290+j.452
G5
SPORN
PORTSMOUTH
+.140
L13
.406
.616
.700
TURNER
+.141
L21
+.570-j.130
CABIN CREEK
G6
+.572
L22
L20
SO. POINT
O.P.
+.265
.070
.070
A.E.P.
.502
+.220-j.123
G7
LOGAN
+.410
L23
0+j0
.288
TO TVA
SWITCHBACK
TO C.P.&L.
.143
+.261
L24
L25
+.186-j.142
+.210
G8
NET GENERATOR CURRENT INCLUDING C.P.&L.
GLEN LYN

Figure 5. Generator, line, and load currents for D-1 loading

Table I. Measured R_{Gn-Gm} Resistances

		Twin Branch G1	Tidd G2	Windsor G3	Philo G4	Sporn G5	Cabin Creek G6	Logan G7	Glen Lyn G8
Twin Branch	G1	0.2493	0.0235	0.0235	0	0.0419	0.0507	0.0507	0.0507
Tidd	G2	0.0235	0.1275	0.0976	0	0.0050	0.0063	0.0063	0.0063
Windsor	G3	0.0235	0.0976	0.1473	0	0.0050	0.0063	0.0063	0.0063
Philo	G4	0	0	0	0	0	0	0	0
Sporn	G5	0.0419	0.0050	0.0050	0	0.1005	0.0987	0.0987	0.0987
Cabin Creek	G6	0.0507	0.0063	0.0063	0	0.0987	0.1662	0.1422	0.1422
Logan	G7	0.0507	0.0063	0.0063	0	0.0987	0.1422	0.2082	0.2082
Glen Lyn	G8	0.0507	0.0063	0.0063	0	0.0987	0.1422	0.2082	0.3122

Table II. Measured R_{Lj-Gm} Resistances

		Twin Branch G1	Tidd G2	Windsor G3	Philo G4	Sporn G5	Cabin Creek G6	Logan G7	Glen Lyn G8
Twin Branch	L1	0.2493	0.0237	Same as Tidd	0.000	0.0420	0.0507	....	
Ft. Wayne	L2	0.1803	0.0237		....	0.0420	0.0507	....	
Marion	L3	0.1640	0.0203		....	0.0530	0.0650	....	
Muncie	L4	0.1533	0.0190		....	0.0580	0.0710	....	
Lima	L5	0.1333	0.0276		....	0.2880	0.0348	....	
Fostoria	L6	0.0830	0.0303		....	0.0178	0.0220	Same as Cabin Creek	Same as Cabin Creek
Howard	L7	0.0460	0.0300		....	0.0100	0.0125	....	
Canton	L8	0.0235	0.0805		....	0.0050	0.0063	....	
Tidd	L9	0.0235	0.1275	0.0977	....	0.0050	0.0063	....	
Windsor	L10	0.0235	0.0988	0.1443	....	0.0050	0.0063	....	
Philo	L11	0.000	0.000	0.000	....	0.000	0.000	....	
Sporn	L12	0.0417	0.0050	Same as Tidd	....	0.1005	0.0983	....	
Portsmouth	L13	0.0757	0.0000		....	0.0890	0.1088	....	
Burger	L14	0.0325	0.0670		....	0.0065	0.0080	....	
Sandusky	L15	0.0567	0.0430		....	0.0125	0.0145	....	
Lorain	L16	0.0480	0.0475		....	0.0100	0.0125	....	
Massillon	L17	0.0310	0.0690		....	0.0067	0.0075	....	
Alliance	L18	0.0300	0.0790		....	0.0055	0.0068	....	
Ashland	L19	0.0400	0.0505		....	0.0063	0.0100	....	
South Point	L20	0.0593	0.0075		....	0.0950	0.1163	....	
Turner	L21	0.0507	0.0063		....	0.0990	0.1422	....	
Cabin Creek	L22	0.0507	0.0063		....	0.0990	0.1622	0.1422	0.14222
Logan	L23	0.0507	0.0063		....	0.0990	0.1422	0.2088	0.20823
Switchback	L24	0.0507	0.0063		....	0.0990	0.1422	0.2082	0.24
Glen Lyn	L25	0.0507	0.0063		....	0.0990	0.1422	0.2082	0.12 37

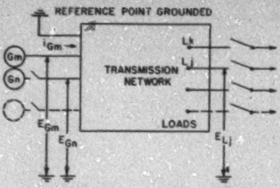
REFERENCE POINT GROUNDED
i_{Gm}
Gm
Gn
TRANSMISSION NETWORK
L_k
L_j
LOADS
E_{Gm}
E_{Gn}
E_{Lj}

Figure 6. Measurement of R_{Gn-Gm} and R_{LjG-m}

IMPEDANCE MEASUREMENTS

1. Remove from ground all line-charging capacitors, synchronous condenser, loads, and generators.

2. Ground the reference point. It is best to choose one of the major plants as the reference point which, in this case, was Philo.

3. Impress a known current at a given generator m and read the real part of the voltages at all busses with impressed current as reference.

This test is indicated schematically in Figure 6 and specifically in Figure 7 with Twin Branch energized. In Figure 6

$$R_{Gn-Gm}=R_{Gm-Gn}=\text{real part of } \frac{E_{Gn}}{i_{Gm}} \qquad (1)$$

$$R_{Lj-Gm}=R_{Gm-Lj}=\text{real part of } \frac{E_{Lj}}{i_{Gm}} \qquad (2)$$

Table III. Calculation of d_1

In general

$$d_m=\frac{1}{\sum\limits_n i_{Gn}} \sum_j i_{Lj} R_{Lj-Gm}$$

$$d_1=\frac{1}{\sum\limits_n i_{Gn}} \sum_j i_{Lj} R_{Lj-G1}$$

Load Number	i_{Lj}	R_{Lj-G1}	$(i_{Lj}\times R_{Lj-G1})$
L1	+0.397	0.2493	0.09897
L2	+0.230	0.1893	0.04354
L3	+0.093	0.1640	0.01525
L4	+0.197	0.1533	0.03020
L5	+0.169	0.1333	0.02253
L6	+0.078	0.0830	0.00647
L7	+0.127	0.0460	0.00584
L8	+0.680	0.0235	0.01598
L9	+0.267	0.0235	0.00627
L10	+0.250	0.0235	0.00563
L11	+0.391	0.0000	0.00000
L12	+0.0343	0.0419	0.00143
L13	+0.140	0.0757	0.01060
L14	−0.556	0.0325	−0.01807
L15	+0.086	0.0567	0.00488
L16	+0.052	0.0480	0.00250
L17	+0.082	0.0310	0.00254
L18	+0.148	0.0300	0.00444
L19	+0.115	0.0400	0.00460
L20	+0.265	0.0593	0.01571
L21	+0.141	0.0507	0.00715
L22	+0.572	0.0507	0.02900
L23	+0.410	0.0507	0.02079
L24	+0.261	0.0507	0.01323
L25	+0.210	0.0507	0.01065

$$\sum_j i_{Lj} R_{G1-Lj}=0.3604$$

$$d_1=\frac{1}{4.78}(0.3604)=0.0754$$

where $\sum\limits_n i_{Gn}=4.78$

Table IV. d_m Matrix

	1	2	3	4	5	6	7	8
$d_m=$	0.0754	0.0316	0.0323	0.00	0.0534	0.0750	0.0843	0.0925

Table V. Generation Schedules for Base Cases

		D-1 Loading				B-1 Loading			
		P Mw	Q Mvar	V Per Cent	θ Degrees	P Mw	Q Mvar	V Per Cent	θ Degrees
Twin Branch	1	94	34	101.2	−25.3	240	62	105.5	−32.6
Tidd	2	149	10	100.2	0.0	217	33	101.4	6.8
Windsor	3	40.2	31	100.1	−2.5	149	31	101.5	6.4
Philo	4	238	23	104	0.0	410	15	108.4	0.0
Sporn	5	285	−29	105	0.0	295	57	105.5	−10.8
Cabin Creek	6	116	36	103.6	− 9.0	196	50	103.9	−22.8
Logan	7	45.8	24.3	102.8	−14.7	62	41	105.5	−30.9
Glen Lyn	8	81	16.4	104	−18.9	108	33	105.5	−37.4
Net Glen Lyn		41	26.4	104	−18.9	68	43	105.5	−37.4
TVA		0	0			0	0		
CPL		40	−10			40	−10		
Burger		111	43			132	43		
Lorain		17.6	6.5			25	12.4		
Ohio to Indiana		99.4				123.1			
Ohio to Appalachian		185.2				163.8			

Applying the preceding definitions to Figure 7

$$R_{G1-G1}=\frac{0.748}{3.0}=0.2493$$

$$R_{G2-G1}=R_{G1-G2}=\frac{0.0705}{3.0}=0.0235$$

$$R_{L2-G1}=R_{G1-L2}=\frac{0.568}{3.0}=0.1893$$

This same test is repeated with generators 2, 3, 5, 6, 7, and 8. The R_{Gn-Gm} matrix is given in Table I; the R_{Lj-Gm} matrix, in Table II.

Calculations

In general, the total transmission losses are given by

$$\begin{aligned} P_{\text{losses}} &= \text{total transmission losses} \\ &= \sum_m\sum_n P_m B_{nm} P_n \end{aligned} \qquad (3)$$

where

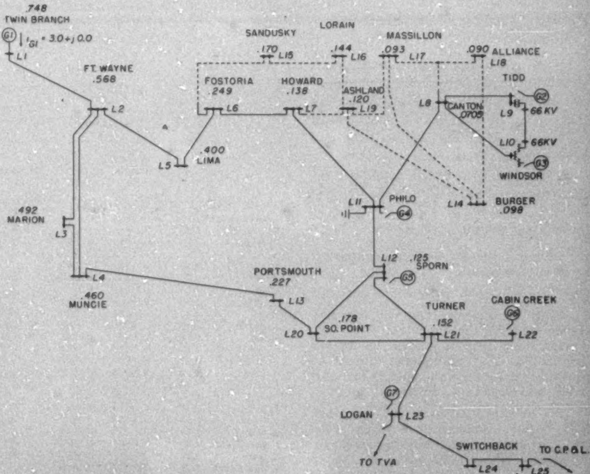
.748
TWIN BRANCH
G1
$i_{G1}=3.0+j0.0$
L1
FT. WAYNE
.568
L2
.400
LIMA
L5
492
MARION
L3
L4
.460
MUNCIE
SANDUSKY
.170
L15
LORAIN
.144
L16
MASSILLON
.093
L17
.090
ALLIANCE
L18
FOSTORIA
.249
L6
HOWARD
.138
L7
ASHLAND
.120
L19
L8
CANTON
.0705
TIDD
G2
L9
66 KV
L10
66KV
G3
WINDSOR
L11
PHILO
G4
L14
BURGER
.098
L12
.125
SPORN
G5
PORTSMOUTH
.227
L13
L20
.178
SO. POINT
TURNER
.152
L21
CABIN CREEK
G6
L22
G7
LOGAN
L23
TO TVA
SWITCHBACK
L24
L25
TO C.P.&L.
G8
GLEN LYN

Figure 7. Resistance measurements on open-circuited transmission network

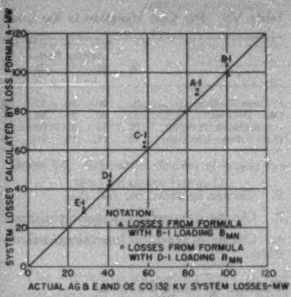

Figure 8. Comparison of actual losses and results from loss formula

Table VI. Comparison of R_{n-m} and B_{nm} for D-1 and B-1 Loading

m	n	R_{n-m} D-1	R_{n-m} B-1	B_{nm} D-1	B_{nm} B-1	m	n	R_{n-m} D-1	R_{n-m} B-1	B_{nm} D-1	B_{nm} B-1
1	1	0.1570	0.1495	0.1734	0.1411	2	8	−0.0593	−0.0584	−0.0455	−0.0246
2	2	0.1228	0.1216	0.1229	0.1210	3	4	+0.0262	+0.0243	+0.0263	+0.0234
3	3	0.1412	0.1400	0.2847	0.1418	3	5	−0.0222	−0.0281	−0.0210	−0.0255
4	4	0.0585	0.0559	0.0546	0.0513	3	6	−0.0425	−0.0425	−0.0526	−0.0356
5	5	0.0522	0.0506	0.0478	0.0447	3	7	−0.0518	−0.0517	−0.0719	−0.0300
6	6	0.0747	0.0759	0.0703	0.0726	3	8	−0.0600	−0.0591	−0.0848	−0.0288
7	7	0.0981	0.0995	0.1190	0.1324	4	5	+0.0051	+0.0030	+0.0046	+0.0025
8	8	0.1857	0.1887	0.2429	0.2373	4	6	−0.0165	−0.0172	−0.0151	−0.0133
						4	7	−0.0258	−0.0264	−0.0218	−0.0131
1	2	−0.0250	−0.0294	−0.0197	−0.0202	4	8	−0.0340	−0.0338	−0.0258	−0.0138
1	3	−0.0257	−0.0301	−0.0339	−0.0221	5	6	+0.0288	+0.0286	+0.0236	+0.0253
1	4	−0.0169	−0.0220	−0.0132	−0.0146	5	7	+0.0195	+0.0194	+0.0136	+0.0152
1	5	−0.0284	−0.0330	−0.0180	−0.0274	5	8	+0.0113	+0.0120	+0.0067	+0.0085
1	6	−0.0411	−0.0443	−0.0413	−0.0418	6	7	+0.0414	+0.0427	+0.0442	+0.0425
1	7	−0.0504	−0.0535	−0.0583	−0.0574	6	8	+0.0332	+0.0353	+0.0347	+0.0326
1	8	−0.0586	−0.0609	−0.0700	−0.0617	7	8	+0.0899	+0.0921	+0.1119	+0.1188
2	3	+0.0922	+0.0910	+0.0938	+0.0912						
2	4	+0.0269	+0.0250	+0.0260	+0.0239						
2	5	−0.0215	−0.0274	−0.0205	−0.0242						
2	6	−0.0418	−0.0418	−0.0391	−0.0333						
2	7	−0.0511	−0.0510	−0.0439	−0.0262						

B_{nm} = constants which are calculated from network analyzer data
P_m = real power output of generator m

Also the incremental transmission loss at generator n is given by

$$\frac{\partial P_{\text{losses}}}{\partial P_n}=\sum_m 2B_{nm}P_m \qquad (4)$$

Several steps are taken to calculate B_{nm}.

(1) *Calculate*

$$d_m=\frac{1}{\sum_n i_{Gn}}\sum_j i_{Lj}R_{Lj-Gm} \qquad (5)$$

where

i_{Lj} = real part of equivalent load current j from base case
R_{Lj-Gm} = measured resistance between generator m and load j (Table II)
$\sum_n i_{Gn}$ = summation of base case generator and interconnection currents included in loss formula (See Figure 5)

A sample of calculation of d_1 is given in Table III. The d_m matrix obtained is given in Table IV.

(2) *Calculate*

$$R_{n-m}-w'=R_{Gn-Gm}-d_n-d_m \qquad (6)$$

where

R_{Gn-Gm} = measured resistance between generator n and generator m (Table I)
R_{n-m} = symmetrical through resistance in equivalent circuit between generators and hypothetical load

Thus

$$R_{1-2}-w'=R_{G1-G2}-d_1-d_2$$

$$R_{1-2}-w'=0.0235-0.0754-0.0316 = -0.0835 \qquad (7)$$

(3) *Determine w' From Relationship*

$$w'=\frac{\sum_k i_k^2R_k-\sum_m\sum_n(i_{dm}i_{dn}+i_{qm}i_{qn})\times(R_{Gn-Gm}-d_m-d_n)}{\sum_m\sum_n(i_{dm}i_{dn}+i_{qm}i_{qn})} \qquad (8)$$

where

R_k = resistance of line k (Figure 2)
i_k = scalar current in line k for base case (Figure 5)
$\sum_k i_k^2R_k$ = total transmission losses of base case
i_{dm} = real component of generator m current for base case (Figure 5)
i_{qm} = imaginary component of generator m current for base case (Figure 5)

For the D-1 base case $w'=0.0585$. A derivation of this method of calculating w' is given in Appendix I.

(4) *Calculate*

$$R_{n-m}=R_{Gn-Gm}-d_n-d_m+w'$$

Thus $R_{1-2}=R_{G1-G2}-d_1-d_2+w'=-0.0835+0.0585=-0.0250$. This quantity R_{n-m} is a term similar to K_{nm} obtained in reference 2.

(5) *Calculate*

$$B_{nm}=\frac{1}{V_mV_n}\left\{(1+s_ms_n)\cos\theta_{mn}+(s_m-s_n)\sin\theta_{mn}\right\}R_{n-m} \qquad (9)$$

V_m = bus voltage of generator m (Figure 4)
θ_m = angular position of terminal voltage of generator m (Figure 4)

Figure 9. Variation in total system losses for B loading for shift in generation between Twin Branch and Philo

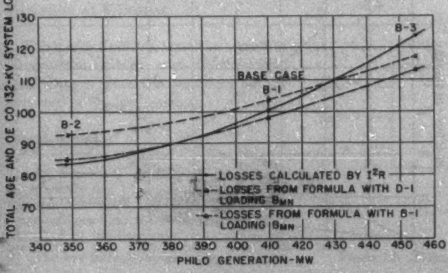

Figure 10. Variation in total system losses for D loading for shift in generation between Twin Branch and Philo

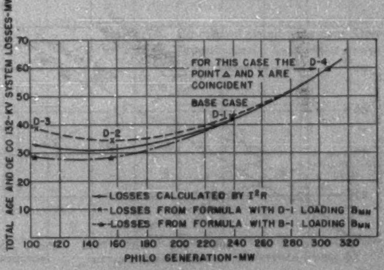

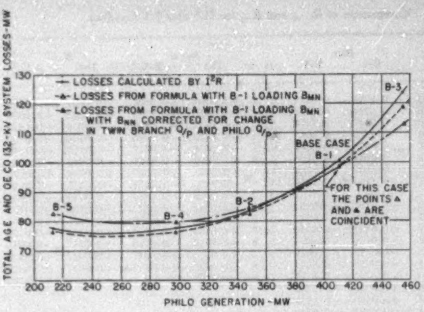

Figure 11 (left). Variation in total system losses for B loading for shifts in generation between Twin Branch and Philo with corrected B_{nn}

Table VII. Per Cent Variation in Kw Load

	Loading Period				
	A	B	C	D	E
Indiana Division	21	20	20	17	17
Ohio Division	35	36	39	38	40
Appalachian Division	32	33	31	35	34
Ohio Edison Company	12	11	10	10	9

Q_m = reactive power output of generator m

$s_m=\frac{Q_m}{P_m}$ of generator m for base case

Thus

$$B_{11}=\frac{1}{V_1^2}(1+s_1^2)R_{1-1}=\frac{1}{(1.012)^2}\times [1+(0.362)^2](0.1570)=0.1734$$

$$B_{12}=\frac{1}{V_1V_2}\left\{(1+s_1s_2)\cos\theta_{12}+ (s_1-s_2)\sin\theta_{12}\right\}R_{1-2}$$

$$=\frac{1}{(1.012)(1.002)}[(1+0.362\times 0.067)\times \cos(-25.3)+(0.362-0.067)\times \sin(-25.3)](-0.0250)=-0.0197$$

Results

For the American Gas and Electric System, the two most important periods relative to economical loading are the B and D. Consequently, these loadings were chosen as base conditions to study the effects of the variations in load pattern and in generator bus voltages, angles, and power factors upon the results obtained by the loss formula. The generation schedules for the B-1 and D-1 base cases are tabulated in Table V. A comparison of R_{n-m} and B_{nm} for the two base cases is given in Table VI.

A comparison of the actual losses and the results from the loss formula for the probable economic generation schedules for A, B, C, D, and E loading conditions are given in Figure 8. As indicated by the points in the Figure, constants calculated from both the B-1 and D-1 cases were used in the loss formula. If a B_{nm} corresponding to the average of the B_{nm} from both of these cases is used, the results will lie midway between those shown in Figure 8. Inspection of Figure 8 indicates that a single loss formula using the average B_{nm} of the B and D loadings may be used to cover the entire daily load cycle.

The discrepancies involved in the application of a given loss formula result chiefly from the following:

1. Change in equivalent load current pattern.
2. Change in generator Q_m/P_m.
3. Change in generator angular position.
4. Change in generator bus voltage magnitudes.

Change in Load Pattern

The formula is derived assuming all equivalent load currents remain a constant complex proportion of each other. In actual hourly operation, the individual kilowatt loads of the Ohio Edison Company and the three operating divisions of the American Gas and Electric Company do not remain a fixed per cent of the total combined kilowatt load. The variation in the loads represented in the simplified system are tabulated in Table VII.

It will be noted that the R_{n-m} for the two cases in Table VI agree very closely, the discrepancy resulting largely from small changes in the relative complex magnitudes of the load currents between the D and B periods. Thus the effect of the variation in kilowatt load during the daily load cycle can be closely approximated by assuming the equivalent load currents vary proportionally.

However, in the case of strikes the load pattern may be changed considerably. Analysis indicates the most severe change in the load pattern to occur for a coal strike during the A loading condition and a steel strike during the D loading condition. The results obtained are tabulated in Table VIII.

Figure 12. Variation of Twin Branch reactive megavolt amperes with megawatts

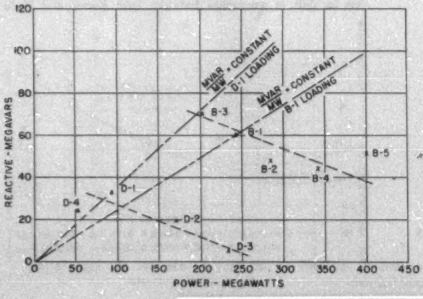

Figure 13. Variation of Philo reactive megavolt amperes with megawatts

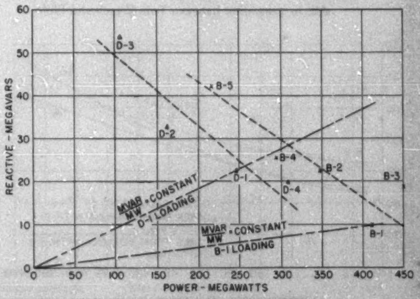

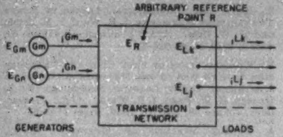

Figure 14. Schematic diagram of power system (Reference Frame 1)

Effect of Swinging Blocks of Generation

The discrepancies encountered in the application of the loss formula when swinging large blocks of generation are largely the result of changes in the Q/P ratios and angles of the generators. To illustrate these discrepancies, large blocks of power were swung between the relatively high cost generation at Twin Branch and the relatively low cost generation at Philo. The results are shown in Figures 9 and 10 for the B and D loading period respectively. To check the assumption that the Q/P ratios of the generators remain constant the variation of the generator reactive as a function of generator megawatts was plotted for each plant for the various system operating conditions. Typical results for the Twin Branch and Philo plants are plotted in Figures 12 and 13. Operation for the constant Q/P assumption is indicated by a broken diagonal line extending from the origin.

If the diagonal B_{nn} terms are corrected for the changes in Q/P ratios of the individual generators the results obtained from the loss formula agree more closely with the actual losses as indicated in Figure 11. For the cases of Figure 11, it was only necessary to correct the B_{nn} terms corresponding to Twin Branch and Philo since the Q/P ratios of the other sources remained essentially constant. Inspection of Figure 11 indicates the effect of the changes in generator angles to be of minor importance.

Variation of Voltages

The results indicate that the variation of generator voltages over the daily load cycle have a second order effect on the accuracy of the loss formula.

Conclusions

1. An improved method of obtaining a loss formula has been presented which involves considerably less measurements and computations than the methods previously described in the literature.

2. The loss formula obtained by averaging the B and D loading B_{nm} is applicable for:

   a. A normal variation in load pattern as during the daily load cycle, and

   b. Normal variations in generator bus voltage and angle and moderate variations in generator Q/P ratios.

3. For extreme swings in generation, it may be necessary to correct the diagonal B_{nn} terms for large variations in generator Q/P ratio for more accurate results.

4. For large variations in load pattern such as strikes, it may be necessary to determine a separate loss formula.

Appendix I. Summary of Derivation

In the following analysis, the lower case indices $n, m, j,$ and k are tensor indices, and the capitals G and L are identification indices. Whenever a repeated tensor index appears in a product (one upper and the other a lower index) a summation on that index is indicated. (This is the Einstein summation convention.) For example

$$a_n = Z_{Gn-Lk} l^k$$

is equivalent to

$$a_n = \sum_k Z_{Gn-Lk} l^k$$

Measurement Reference Frame (Reference Frame 1)

In general, the operation of a power system may be given by the following set of linear equations:

$$\mathbf{E}_1 = \mathbf{Z}_{11}\mathbf{I}^1$$

or

$$\boxed{\begin{array}{c} E_{Gn}-E_R \\ \hline E_{Lj}-E_R \end{array}} = \begin{array}{|c|c|} \hline i^{Gm} & i^{Lk} \\ \hline Z_{Gn-Gm} & Z_{Gn-Lk} \\ \hline Z_{Lj-Gm} & Z_{Lj-Lk} \\ \hline \end{array} \qquad (10)$$

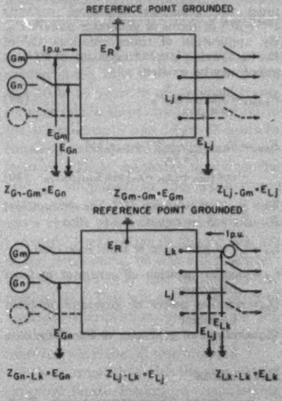

Figure 15. Definition of impedances

Table VIII

Case	Losses By $I_k^2R_k$	Losses From Loss Formula: Average B_{nm}	D-1 Loading B_{nm}	B-1 Loading B_{nm}	Comments
A-2	80.0	67.9	66.6	69.2	Coal strike—approximately 185 mw less load in Appalachian Division
D-9	41.2	31.3	31.4	31.2	Steel strike—100 mw less load in Canton

where the variables are defined in Figure 14. The reference point R is usually chosen to be one of the major generators. The $\mathbf{Z}_{11}$ impedances are defined as shown in Figure 15.

Reference Frame 2

It is known in general that if a set of currents I^j is related to a set of currents I^k by a tensor C_k^j such that

$$I^j = C_k^j I^k \qquad (11)$$

and if the power remains invariant, then

$$E_k = \mathbf{C}_k^{j*} E_j \qquad (12)$$

and

$$Z_{kk} = \mathbf{C}_k^{j*} Z_{jj} C_k^j \qquad (13)$$

Define

$$\sum_k i^{Lk} = i^L \qquad (14)$$

Assume that

$$\frac{i^{Lk}}{i^L} = l^K \qquad (15)$$

Then

$$\boxed{\begin{array}{c} i^{Gm} \\ \hline i^{Lk} \end{array}} = \begin{array}{|c|c|} \hline i^{Gm} & i^L \\ \hline 1 & \\ \hline & l^k \\ \hline \end{array} \qquad (16)$$

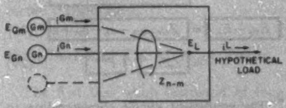

Figure 16. Equivalent circuit from generators to single hypothetical load (Reference Frame 3)

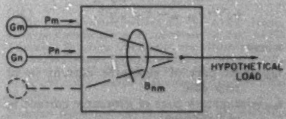

Figure 17. Equivalent circuit with impressed generator powers (Reference Frame 6)

$$\mathbf{I}^1 = \mathbf{C}_2^1 \mathbf{I}^2 \qquad (17)$$

$$\mathbf{C}_2^1 = \begin{array}{|c|c|}\hline 1 & \\ \hline & t^k \\ \hline\end{array} \qquad (18)$$

Applying the transformations indicated by equations 11, 12, and 13

$$\begin{array}{c|c|c} & i^{Gm} & i^{L} \\ \hline E_{Gn}-E_R & Z_{Gn-Gm} & a_n \\ \hline E_L-E_R & b_m & w \end{array} \qquad (19)$$

where

$$a_n = Z_{Gn-Lk} t^k \qquad (20)$$

$$b_m = t^{j*} Z_{Lj-Gm} \qquad (21)$$

$$w = t^{j*} Z_{Lj-Lk} t^k \qquad (22)$$

$$E_L = t^{j*} E_{Lj} \qquad (23)$$

Reference Frame 3

Since

$$i^L = -\sum_n i^{Gn}$$

the load current may be eliminated by the transformation

$$\mathbf{I}^2 = \mathbf{C}_3^2 \mathbf{I}^3 \qquad (24)$$

where

$$\mathbf{I}^3 = \begin{array}{|c|}\hline i^{Gm} \\ \hline\end{array}, \qquad \mathbf{I}^2 = \begin{array}{|c|}\hline i^{Gm} \\ \hline i^{L} \\ \hline\end{array} \qquad (25)$$

and

$$\begin{array}{c|c} & i^{Gm} \\ \hline i^{Gm} & 1 \\ \hline i^{L} & t_m \end{array} \qquad (26)$$

where $t_m = -1$ for all m. Thus,

$$\mathbf{C}_3^2 = \begin{array}{|c|}\hline 1 \\ \hline t_m \\ \hline\end{array} \qquad (27)$$

Applying transformations indicated by equations 11, 12, and 13

$$\begin{array}{c|c} & i^{Gm} \\ \hline E_{Gn}-E_L & Z_{Gn-Gm}-a_n-b_m+w \end{array} \qquad (28)$$

$$= \begin{array}{|c|}\hline Z_{n-m} \\ \hline\end{array} \; \begin{array}{|c|}\hline i^{Gm} \\ \hline\end{array} \qquad (29)$$

The equivalent circuit corresponding to the preceding equation is given in Figure 16. The power losses in this equivalent circuit are

$$\begin{aligned} P_{\text{losses}} &= \text{real part of } i^{Gm*} Z_{n-m} i^{Gn} \\ &= i^{dm} R_{m-n} i^{dn} + i^{qm} R_{n-m}{}^{qn} \\ &\quad + i^{dm}(X_{n-m} - X_{m-n}) i^{qn} \end{aligned} \qquad (30)$$

where

i_{dm} = real part of generator current m of base case

i_{qm} = imaginary part of generator current m of base case

In general, $X_{n-m} - X_{n-m}$ is negligibly small. Thus

$$P_{\text{losses}} = i^{dm} R_{n-m} i^{dn} + i^{qm} R_{n-m} i^{qn} \qquad (31)$$

The asymmetrical R_{n-m} in equation 31 may be replaced by the symmetrical R_{n-m}. Then from equations 20, 21, and 28

$$\begin{aligned} \text{Symmetrical } R_{n-m} & \\ &= \text{real part of } \frac{Z_{n-m} + Z_{m-n}}{2} \qquad (32) \\ &= R_{Gn-Gm} - d_n - d_m + w' \qquad (33) \end{aligned}$$

where

$$d_m = \text{real part of } \frac{i^{Lk}}{i^{L}} R_{Lk-Gm} \qquad (34)$$

$$w' = \text{real part of } w \qquad (35)$$

The losses in the transmission network may be obtained by summing the I^2R losses in each line.
Thus

$$P_{\text{losses}} = \sum_k i_k^2 R_k \qquad (36)$$

R_k = Resistance of line k
i_k = Scalar current in line k

Equating equations 31 and 36 and using equation 33

$$\begin{aligned} \sum_k i_k^2 R_k = {} & i^{dm}(R_{Gn-Gm} - d_n - d_m + w') i^{dn} + \\ & i^{qm}(R_{Gn-Gm} - d_n - d_m + w') i^{qn} \end{aligned} \qquad (37)$$

Solving for w'

$$w' = \frac{\sum_k i_k^2 R_k - i^{dm}(R_{Gn-Gm} - d_n - d_m) i^{dn} - i^{qm}(R_{Gn-Gm} - d_n - d_m) i^{qn}}{i^{dm} \delta_{mn} i^{dn} + i^{qm} \delta_{mn} i^{qn}} \qquad (38)$$

where δ_{mn} = square matrix all of whose elements are unity.

Transformation from Frame 3 to Reference Frame 6

It is next necessary to obtain the equivalent circuit with impressed powers instead of impressed currents as indicated in Figure 17. That is, it is necessary to express the generator impressed currents $i^{dm} + ji^{qm}$ in terms of generator powers P_m. By application of transformations $\mathbf{C}_t^3$ of the companion paper,[5] equation 31 of this paper may be written

$$P_{\text{losses}} = \sum_m \sum_n P_m B_{mn} P_n \qquad (39)$$

$$\begin{aligned} B_{nm} = B_{mn} = \frac{1}{V_n V_m} & [(1 + s_m s_n) \times \\ & \cos\theta_{mn} + (s_m - s_n) \sin\theta_{mn}] R_{n-m} \end{aligned} \qquad (40)$$

The R_{n-m} of equation 40 is the symmetrical R_{n-m} given by equation 33. Also

$s_m = \dfrac{Q_m}{P_m}$ of generator m from base case

θ_m = angular position of generator m from base case

Q_m = reactive power of generator m from base case

V_m = voltage of generator m from base case

References

1. INTRASYSTEM TRANSMISSION LOSSES, E. E. George. *Electrical Engineering (AIEE Transactions)*, volume 62, March 1943, pages 153–58.

2. TOTAL AND INCREMENTAL LOSSES IN POWER TRANSMISSION NETWORKS, J. B. Ward, J. R. Eaton, and H. W. Hale. *AIEE Transactions*, volume 69, part I, 1950, pages 626–32.

3. CO-ORDINATION OF FUEL COST AND TRANSMISSION LOSS BY USE OF THE NETWORK ANALYZER TO DETERMINE PLANT LOADING SCHEDULES, E. E. George, H. W. Page, J. B. Ward. *AIEE Transactions*, volume 68, part II, 1949, pages 1152–63.

4. TENSOR ANALYSIS OF NETWORKS (book), G. Kron. John Wiley and Sons, Inc., New York, N. Y., 1939.

5. TENSORIAL ANALYSIS OF INTEGRATED TRANSMISSION SYSTEMS—PART I. THE SIX BASIC REFERENCE FRAMES, G. Kron. *AIEE Transactions*, volume 70, 1951, pages 1239–48.

6. THE INTEGRATED POWER SYSTEM (book), Philip Sporn. McGraw-Hill Book Company, Inc., New York, N. Y., 1950.

Discussion

E. E. George (Ebasco Services Inc., New York, N. Y.): This paper contributes several new improvements on previous methods of loss determination:

1. It uses a normal load flow condition instead of an equal-angle condition to determine basic losses, thus preserving normal voltage levels.
2. It selects typical load levels to represent the daily load curve.
3. It analyzes the effects of each simplifying assumption.
4. It permits more general assumptions about system operation than are possible with previous methods.

The authors refer to open-circuit impedance measurements of the transmission system as a new method. Both J. B. Ward and the discusser have used this method in place of the old superposition method since early in 1950. Although nothing has been published in AIEE literature, this impedance measurement method has been used on the network analyzers at Lafayette, Pittsburgh, Schenectady, Atlanta, and College Station during 1950.

The method of computation used by the authors is apparently very similar to that used by Ward, and it is simpler than the equivalent star network with mutual impedances used by the discusser.

In spite of efforts to popularize tensor algebra, it is still an unknown shorthand to most power engineers, young and old. Fortunately, the authors have confined it to the Appendix. Additional explanation of tensor index notation would be helpful.

L. K. Kirchmayer and **G. W. Stagg**: We wish to thank Mr. George for his comments on our paper. Regarding the second and third paragraphs of Mr. George's discussion, we have the following comments:

The use of open circuit impedance measurements of a given network to determine self and mutual impedances, from several points of entry to a given point, is well known in circuit analysis. The authors do not refer to the use of open circuit impedance measurements as a new method; however, the use of the particular open circuit measurements described in the paper in conjunction with normal load flow data to obtain a loss formula is, to our knowledge, a new method.

Since the methods of Ward and George have not been published, we are not in a position to make a detailed comparison of their method with ours; however, according to conversations we have had with Ward and Hale early this year (1951), the impedance measurements we suggest are different from those used by Ward. Ward's method does not use measurements of the mutual impedances between generators and loads as in Table II of our paper. In addition, it is our understanding that the method proposed by Ward assumes that all lines have the same R/X ratio, and involves the determination of an equal angle loading condition by means of a superposition method. To the best of our knowledge the calculations suggested by Ward and Hale differ in several other important respects from those proposed in our paper.

Transmission loss formulas have proved to be very valuable tools in the economic analysis and operation of power systems. In particular, transmission loss formulas have been used to advantage in the following manner:

1. To co-ordinate incremental fuel costs and incremental transmission losses for optimum economic system operation.
2. To determine the change in transmission losses under different interconnection transactions for purposes of billing. These changes in losses can be evaluated by means of a total system loss formula in which the various external interconnections are included as specified variables.

Inhibited Oils for Transformers

HERMAN HALPERIN
FELLOW AIEE

H. A. ADLER
MEMBER AIEE

INSULATING oil plays an important role in the operation of the equipment of an electric utility, but its cost constitutes only a minor portion of the total investment in equipment. In the Commonwealth Edison Company, there is on the average 0.6 of a gallon of oil in oil-filled transformers and associated regulators and circuit breakers for each kilovolt-ampere of transformer capacity. For each kilowatt of generating capacity, there are about 4 kva of connected transformer capacity on the basis of nameplate ratings. Therefore, for each kilowatt of generating capacity the system uses 2.4 gallons of insulating oil, exclusive of oil in cable systems. The cost of the oil in the transformers, circuit breakers, and regulators represents only about 2 per cent of the total installed cost of this equipment.

In view of the importance of oil in the operating performance of expensive equipment and of its relatively low cost, the continued efforts over the years to obtain improved oil have been well justified. Recognition of the need for better oils was the reason for initiating a research project on Insulating Oils and Cable Saturants in 1935 at the Massachusetts Institute of Technology. This work was conducted with support from electric-utility companies, equipment manufacturers, and oil refiners, and under various sponsorships, including the AIEE. The project was discontinued in 1943 on account of war requirements.

The interest in obtaining transformer oil with improved resistance to oxidation received new impetus at the end of World War II when system loads began to increase rapidly and higher unit costs for equipment accentuated the need for greater loading of equipment. For the Commonwealth Edison Company, the ratio of maximum loading to nameplate ratings has been increasing during the past 15 years. For example, the average of the annual peak loads of the 4-kv distribution transformers was 30 per cent higher in 1949 than in 1939. The ratio of this average to the nameplate ratings was 95 per cent in 1949. For 12/4-kv substation transformers, the load has increased on the average about 15 per cent in the last five years, and now the ratio of peak loads to nameplate ratings is over 80 per cent on the average. In this case, as well as for distribution transformers, emergency loading is not considered.

It is estimated that in the past 15 years, the top oil temperatures have risen on the average by 5 to 18 degrees centigrade, depending on the type of transformer and the nature of service. Assuming that the rate of deterioration doubles for about each 8 degrees centigrade, such increases in temperature would mean a reduction in oil life of 30 to 75 per cent. Additional life is consumed in connection with loading at still higher temperatures during emergencies caused by failures of parallel-connected equipment.

It is estimated that with loading as it existed in the 1930's, the average oil life was 10 to 15 years in unprotected transformers (air in direct contact with oil in the transformers), and 15 to 25 years in conservator-type and semisealed transformers. These estimates apply to the original oil placed in the transformers when new. It has been observed that when change of oil was necessary due to excessive deterioration in service, the life of the replacement oil was much shorter; in some cases only half as long as the original oil. This was due to the effect of residual deterioration products in the insulation which could not be completely removed when the oil was replaced.

It is apparent that with the present and expected future loading, a considerable increase in the frequency of changes of conventional oil must be expected. This would cause a large increase in problems of oil handling and transformer maintenance, and a consequent large increase in maintenance costs. In connection with the latter point, the cost of the oil itself is only a portion of the cost of oil replacement, which involves in addition cost of labor, testing, and transportation. Since much of the replacing of oil has to be done during periods of low load, a decrease in the needed frequency of replacements is desirable. Another factor worth consideration is the possibility of service failures occurring in old deteriorated transformers as a consequence of the handling necessary for cleaning and changing oil. Therefore, an oil with improved aging characteristics may readily be attractive from both economic and operating standpoints, even if it is somewhat more expensive than ordinary oil.

In view of these considerations, an immediate interest developed in inhibited oil when it became commercially available in 1946. A program of tests was initiated at that time to determine the extent of the superiority of inhibited oil over conventional oil. The first and most direct interest in inhibited oil was for use as replacement oil in transformers in service where excessive deterioration made replacement of oil necessary. For this reason, the first set of heat-aging tests was made on transformers representing unprotected transformers.

First Series of Transformer Tests

The first test setup consisted of four 2,170-120/240-volt distribution transformers. Two were new 15-kva transformers, the other two were old 10-kva transformers which had been in service

---

Paper 51-208, recommended by the AIEE Transformers Committee and approved by the AIEE Technical Program Committee for presentation at the AIEE Summer General Meeting, Toronto, Ont., Canada, June 25–29, 1951. Manuscript submitted March 27, 1951; made available for printing May 10, 1951.

HERMAN HALPERIN and H. A. ADLER are with the Commonwealth Edison Company, Chicago, Ill.

The authors acknowledge the helpful contributions in these studies by L. B. Schofield, who supervised the testing done in Chicago.

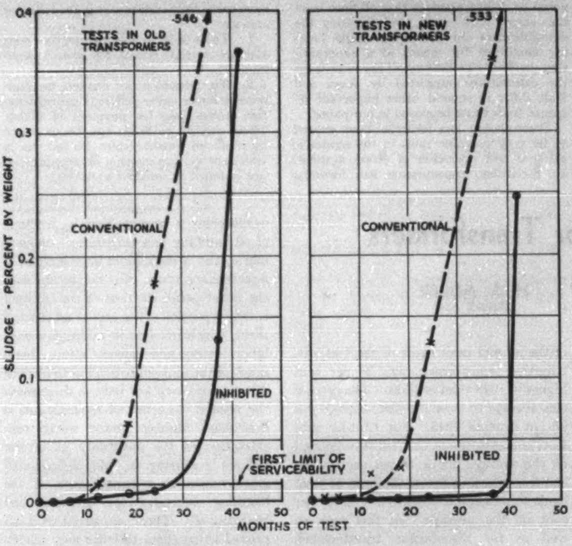

Figure 1. Sludge content of oil in first series of transformer tests

Sludge was determined in accordance with ASTM method D670-42T[3] after sample removed from transformer was permitted to stand in dark overnight

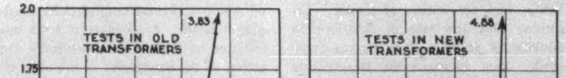

Figure 2. Neutralization number of oil in first series of transformer tests

Determinations in accordance with ASTM D663-46T[4]

for about 22 years. For one of the new transformers, the free conventional oil was merely drained and replaced by inhibited oil *A*.

The old transformers were reconditioned in accordance with usual procedures. The reconditioning process consisted of removal of the core and coils from the case, cleaning and flushing of the core and coils with clean oil. A considerable amount of sludge was, however, still in evidence on the core and coils. Then one transformer was filled with conventional oil and the other one with inhibited oil *A*.

The pair of old transformers was intended to give information on the performance of replacement oil in transformers on the system. The pair of new transformers was expected to give comparable information on oil in new transformers which may not be effectively protected from air throughout their lives. In order to represent conditions in unprotected transformers, access of air to the oil was permitted by leaving the covers resting on the top of the transformer cases without being bolted down. This permitted some breathing, and not an unrestricted access of air which would have existed if the covers had been propped up or completely removed.

In these aging tests, the transformers were operated with a top oil temperature of 90 degrees centigrade. From August 1946 to November 1946 a continuous top oil temperature of 90 degrees centigrade was maintained. From November 1946 to October 1947 a cooling period of 64 hours each week was introduced in order to provide for breathing action. Starting in October 1947, the weekly cooling period was cut down to 16 hours in order to accelerate the aging. The tests were terminated in February 1950, after 42 months.

The four transformers were installed in a closed celotex box 8 feet long, 28 inches wide, and 38 inches deep. In order to obtain closely similar operation, the primaries of each pair were operated in series with the secondaries short circuited. Balance was obtained by a lamp in parallel with the high-voltage winding of the transformer of each pair tending to show the higher temperature, the size of lamp being varied until correct balance was obtained. By this method it was possible to maintain the same top oil temperature on all four transformers throughout the tests in spite of differences in amount of sludging. Temperatures were measured by thermocouples placed about one inch below the surface of the oil in each transformer and in the air between the two transformers at each end of the box. During the normal work-week, transformer currents were adjusted manually as required to maintain proper temperatures. This setup proved adequate to maintain top oil temperatures at 90 degrees centigrade within one degree with occasional slight adjustments of current to compensate for the seasonal changes in average room temperature. The celotex box was open during the cooling periods.

Samples of oil were taken after 3, 6, 12, 18, 24, 37, and 42 months. The sampling procedure was essentially in accordance with the methods recommended in a standard by the American Society for Testing Materials (ASTM) D923-49.[1] Following the removal of the 24-month samples, two gallons of oil were added to each of the 15-kva transformers and $1^1/_2$ gallons to each of the 10-kva transformers to make up for the loss due to the various samplings. Following the removal of the 37-month samples, two quarts of oil were added to each of four transformers.

In the Commonwealth Edison Company, the serviceability of transformer oil on the system is judged mainly on the basis of sludge content and acidity of the oil as determined by tests of oil samples periodically removed from the transformers. Oil is considered to have reached the end of serviceability if the sludge content reaches 0.015 per cent by weight, or if the neutralization number reaches a value of 0.6 milligram KOH per gram of oil. Many years of experience have led to the conclusion that on the basis of these criteria it is possible to remove oil from service before the transformers reach a serious degree of deterioration. However, no claim is made that after these limits have been passed there is a direct correlation between acidity and sludge content of removed oil samples and the condition of the transformer.

The change of these two properties during the aging tests is shown graphically in Figures 1 and 2. The limits of serviceability are indicated by horizontal lines on the graphs. The conventional oil reached the end of serviceability on the basis of sludge content before the limit for neutralization number was reached. The inhibited oil reached the limits for sludge and for neutralization number at about the same time. The conventional oil reached the end of its useful life after one year in the old transformer and after about 14 months in the new transformer. The inhibited oil reached the end of its life after about 27 months in the old transformer and after about 40 months in the new transformer.

Table I. Comparison of New Inhibited Oil A with New Conventional Oil in Short-Time Laboratory Tests*

Test Method	Inhibited Oil A	Conventional Oil	Ratio of Life of Inhibited Oil to Life of Conventional Oil
Proposed ASTM Transformer Oil Oxidation Test at 95 C (TOOT)**			
Life to reach interfacial tension of 15 dynes/cm, days	107	6	18
Life to reach NN of 0.5 milligram KOH/g, days	101	7	14
Modified Continental Oil Co. Test at 135 C			
Time for oxygen pressure to drop 60 millimeters, hours	67.5	6.8	10
Modified Dornte Test at 120 C			
Time to absorb 650 milliliters of oxygen per 100 grams of oil, hours	136	9.9	14
ASTM Bomb Test			
Sludge by weight, per cent	0	0.02	
ASTM Sludge-Accumulation Test			
Sludge by weight, per cent			
3-day test	0	0.01	
7-day test	trace	0.05	
14-day test	trace	0.19	

*Oils were furnished in 1946. NN = Neutralization Number.

**Proposed method under study by ASTM Committee D-9 Subcommittee IV.

On this basis, the life of inhibited oil *A* can be expected to be twice the life of conventional oil when used as replacement oil in old transformers of the unprotected type. In new transformers of the unprotected type, the ratio is about three to one. Since, as stated before, the make-up oil was added after the 24-month sampling, the ratio of two to one for oil in old transformers is not affected by the addition of new oil. The ratio of three to one for the oil in new transformers may be somewhat affected, however, by the addition of make-up oil.

In accordance with service experience, Figure 1 shows a shorter life of conventional oil when used as replacement oil in old transformers than when used in new transformers. Inhibited oil *A* shows a similar behavior.

It is impossible to determine a definite relation between the life of oil in these aging tests and life in service on account of the variety of loading conditions and types of service. It is estimated that one year of life in these tests represents approximately five to 20 years of life in service. On this basis, the life of inhibited oil A would be about ten to 40 years, depending on operating conditions, when used as replacement oil in old unprotected transformers.

These transformer tests were designed to give information on the performance of the oils under conditions of accelerated aging in unprotected transformers, but at

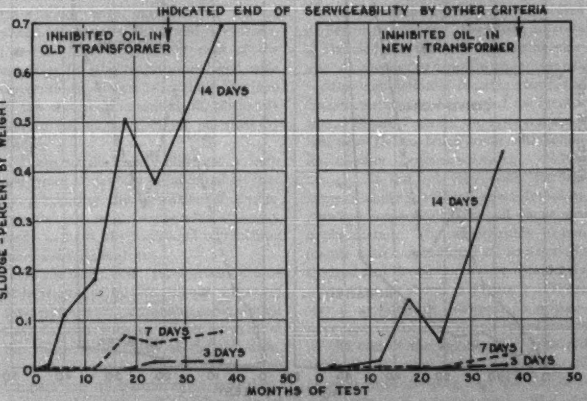

Figure 3. ASTM sludge accumulation test for inhibited oil in first series of transformer tests

Determinations in accordance with ASTM D670-42T[3]

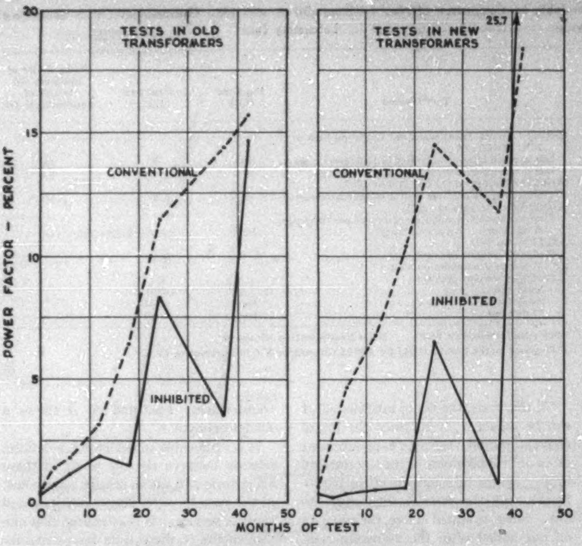

Figure 4. Power factor at 100 degrees centigrade of oil in first series of transformer tests

Determinations in accordance with ASTM D924-49[5]

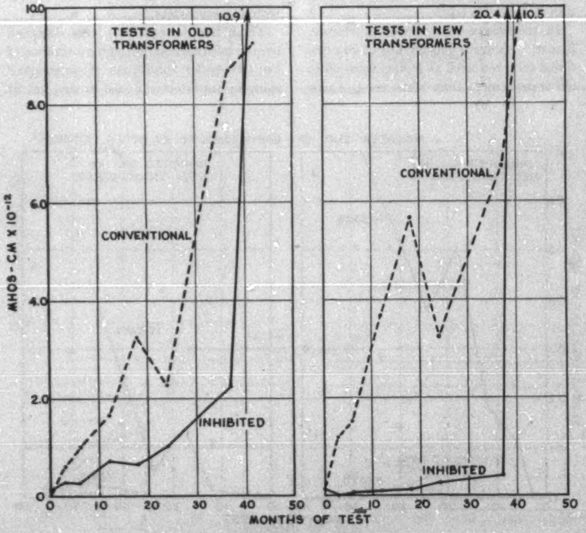

Figure 5. D-c conductivity at 100 degrees centigrade of oil in first series of transformer tests

Calculated from resistivity determined according to ASTM D257-49T[6]

the same time not too much different from service conditions. The superiority of inhibited over conventional oil in these accelerated transformer tests, while substantial, is not so great as indicated by some of the highly accelerated short-time laboratory tests. Table I gives a comparison of inhibited oil *A* with conventional oil on the basis of such short-time tests, and shows for inhibited oil *A*, a life 10 to as much as 18 times the life for conventional oil. It is believed that the accelerated-aging tests in transformers give a more realistic idea of the superiority of inhibited oil than the short-time laboratory tests.

The opinion has been expressed that the deterioration of some inhibited oils will take a sharp upturn when the inhibitor has been expended. This is confirmed by the data in Figures 1 and 2. There appears to be, however, no reason for concern, since oil would not be allowed to remain in transformers to this stage of deterioration. As with conventional oil, it is planned to continue periodic tests of samples of oil in service and to remove the oil from the transformer when it approaches a critical value. The ASTM sludge-accumulation test and the ASTM bomb test, while not originally designed for this purpose, appear to be useful criteria to predict the approaching end of the inhibition period.

Figure 3 shows the results of the ASTM sludge-accumulation test during the various stages of the transformer oxidation tests. Samples of inhibited oil removed from old transformers began showing appreciable sludge in the 3-day test after two years of aging, indicating that the inhibitor had been completely or almost completely used up at that time. The 7-day test gave a warning after 18 months. For the new transformer, the inhibited oil began showing sludge in the 3-day test after 37 months of aging. The amount was small, but it was appreciable in the 7-day test. It may be assumed, therefore, that the inhibitor was nearly used up after three years of accelerated aging.

The results of the ASTM bomb test present similar conclusions with regard to the end of the inhibition period. The sludge values in this test were very low for the inhibited oil until a sharp upturn occurred after two years of aging in the old transformer and after three years of aging in the new transformer. In the old transformer, the bomb sludge value was 0.023 per cent after 18 months and 5.7 per cent after two years. Similarly, in the new transformer the bomb sludge value was 0.006 per cent after two years and 5.1 per cent after three years.

In general, it should be expected that any accelerated laboratory test should be a quite sensitive indicator of the point where the inhibitor has been used up. For example, in agreement with the results of the ASTM bomb test and the ASTM sludge-accumulation test, the Modified Continental Oil Company test showed that the inhibitor had been nearly expended after three years of aging in the new transformer. The 3-year sample had a test life of only one hour in the Modified Continental Oil Company test, compared with 67.5 hours for the new oil as shown in Table I. All available data indicate that such tests will predict the approaching end of the inhibition period long before actually serious deterioration of the oil occurs and, therefore, will allow ample time for removal of the oil.

Other tests made periodically during these transformer-aging tests confirm the superiority of inhibited oil over conventional oil, such as measurements of power factor, d-c conductivity, and interfacial tension, as shown in Figures 4, 5, and 6. The latter test has been under investigation for some time by the Commonwealth Edison Company as an additional criterion of oil in service. Some investigators have suggested that oil be considered to be in a critical condition when the interfacial tension falls below 15 dynes per centimeter. The conventional oil reached this limit after six months of tests of the old and new transformers, while the inhibited oil fell below this limit after two years or more of aging. After completion of 42 months of the aging tests, the inhibited oil in the new transformer was yellow, while that in the old transformer was reddish-brown, and the conventional oil in both transformers was nearly black.

These additional data in the tables and figures support the conclusion given earlier that the life of inhibited oil was twice the life of conventional oil in the old transformers and three times that in the new transformers.

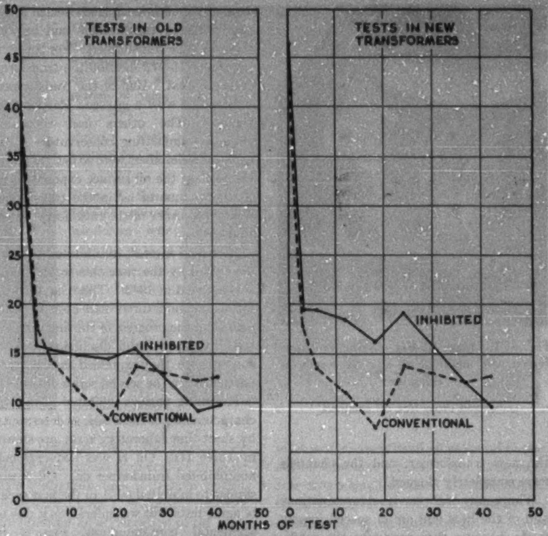

Figure 6. Interfacial tension of oil in first series of transformer tests

Determinations in accordance with ASTM D971-50[7]

Table II. Heat Run on 15-Kva Unprotected Transformers* After Completion of 42 Months of Aging Tests

	Temperature Rise†, °C. Inhibited Oil A	Temperature Rise†, °C. Conventional Oil
High voltage winding (avg)**	50	113
Low voltage winding (avg)**	47	90
Top oil	39	46

*Transformers were new at start of aging tests. These measurements were obtained in accordance with standard temperature test by opposition method, ASA C57.22.[3]

†Ambient in tests was 22 or 23 degrees centigrade; allowable maximum ambient according to AIEE Standards is 40 degrees centigrade.

**Maximum rise permitted by AIEE Standards is 55 degrees centigrade for new transformers.

At the end of these aging tests, the two 15-kva transformers were subjected to a heat run at rated current in order to determine temperature rises. The results are shown in Table II. The rises for the transformer with inhibited oil are as would be expected for brand new transformers. The temperature rises of the windings for the transformer aged with conventional oil were twice those obtained in the test with inhibited oil, obviously due to the clogging of oil passages by sludge.

These results clearly illustrate a very important advantage of inhibited oil that by preventing the formation of sludge, transformers may be operated at heavy loads without the likelihood of reaching excessive temperatures.

On the other hand, for a given permissible length of oil life, higher operating temperatures are permissible for inhibited than for conventional oil on account of the difference in rate of deterioration. Of course, in any increase of the operating temperature of transformers, consideration must be given to the performance of other constituents, especially of the solid insulation, in connection with their own heat-aging characteristics as well as the effects of oil-deterioration products on them.

While Table II shows different top oil temperatures for the transformers at the same load, it should be noted that in the aging tests the top oil temperatures were kept at 90 degrees centigrade within one degree for each transformer as stated earlier in the paper. Therefore, in spite of the sludging the test was not accelerated on account of temperature increases.

After completion of the aging tests, the transformers were dismantled for inspection. Figure 7 shows the appearance of the new 15-kva transformer with inhibited oil after 42 months of aging. While the details are not very clear, the absence of sludge is evident, as was found by personal inspection. The oil ducts are unobstructed. The comparable transformer with conventional oil was heavily sludged and the oil ducts were completely obstructed, as shown in Figure 8. There was a considerable difference in appearance also in the old 10-kva transformers at the end of the aging tests. The old transformer aged with inhibited oil showed some sludging, but the oil channels were still unobstructed. The old transformer with conventional oil was very heavily sludged, more heavily than

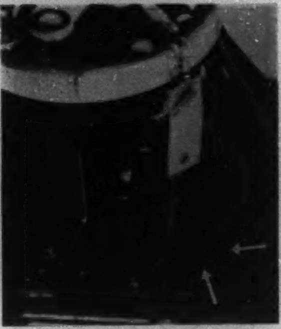

Figure 7. New 15-kva distribution transformer with inhibited oil after 42 months of aging tests

Arrows show free oil channels

the new transformer, and the channels were completely clogged.

The results of these visual examinations and of the heat run are of special importance, because they represent the condition of the transformers after the inhibitor was used up and after a period of operation beyond the permissible service limits. In spite of such operation in excess of the limits which would be permitted in service, the condition of the transformers with inhibited oil was satisfactory, especially for the 15-kva transformer.

On the basis of the results of this first series of tests, the Commonwealth Edison Company adopted, early in 1950, the general practice of using only inhibited oil as replacement oil for all transformers where the condition of the oil required its removal from service. This was put into effect in July 1950. In order to have only one oil in stock, inhibited oil is being used as replacement oil for circuit breakers and other equipment using transformer oil.

Second Transformer Test Setup

While the first investigation demonstrated the advantages and need for inhibited oil for use as replacement oil for existing transformers, the question still remained unsettled as to whether the use of inhibited oil would be justified for new modern transformers. Most of the existing transformers are of the unprotected or conservator type, while in modern transformers the oil is completely or partly protected from contact with air. For this reason, a second transformer setup was built to simulate the performance of the oil in completely-sealed nitrogen-blanketed transformers and in conservator-type transformers. For this purpose, new 15-kva distribution transformers were used. Half of the transformers were sealed with a nitrogen blanket over the oil. The others had expansion chambers simulating conservators. The expansion chambers were so designed that the ratio of the oil surface exposed to air to the volume of oil in the transformer was of the order of the ratio found in actual service.

Increased interest in inhibited oils had developed by the time this second setup was planned in 1948. Three large transformer manufacturers had been kept informed of the progress of the first series of tests by reports and discussions. As a consequence, they expressed an interest to participate in the second series of tests by contributing various inhibited oils. The characteristics of these oils, as determined by short-time laboratory tests, are shown in Table III. Oil *H* was conventional, noninhibited transformer oil. Oil *F* was similar to inhibited oil *A* in the first series of aging tests, but was inferior to it due to accidental contamination. Figures in parentheses show test results of a more representative oil of this type. It may be seen that some of the other inhibited oils showed little superiority to conventional oil in these short-time tests.

The transformer setup, as finally constructed, contained ten transformers with four inhibited oils selected from the six submitted and one conventional oil.

The second series of transformer-aging tests was run at a top oil temperature of 95 degrees centigrade. This increase of 5 degrees centigrade over the previous test temperature was adopted to accelerate the aging, because it was anticipated that the duration of the tests would be lengthened considerably by the protection given the oil in this setup. The current was interrupted each week for 16 hours in order to create a breathing action. The tests were started in August 1948 and terminated in May 1950, after 21 months of operation, because leaks had developed in the bushings of most of the transformers.

This investigation did not last long enough to furnish definite conclusions. The results showed a number of inconsistencies which were probably due at least partly to the disturbing effects of the leaks. All conservator-type transformers lost oil through leaks with the result that 6 to 21 quarts of new oil had to be added to make up for the lost oil.

One interesting result of these tests was the indication given for the effectiveness of conservators and nitrogen blankets in retarding deterioration of oil. In spite of the fact that the tests with conservator-type and sealed transformers were run at higher temperatures, the conventional oil showed less deterioration than in the unprotected transformer in the first series of aging tests.

Third Transformer Setup

When the aging tests of various oils in the second transformer setup were discontinued, it was decided to build a similar setup on account of the important interest in the value of inhibited oil in modern transformers. In order to avoid leaks, it was decided to replace the gasket seals by solder seals and the gasketed compound-filled bushings by special solder-sealed glass bushings. Figure 9 shows this new test setup without the celotex housing.

In October 1950, several manufacturers of transformers announced in a meeting of

Table III. Short-Time Laboratory Tests of Oils Submitted in 1948 for Second Series of Transformer Tests

Test	Oil B	C	D	E	F	G	H*
Proposed ASTM Transformer Oil Oxidation Test, TOOT							
Time to reach interfacial tension of 15, days	13	....	69.5	13	66(107)**	8.5	6
Time to reach NN of 0.5, days	13.5	....	72.5	9	69(101)	8	7
Time to reach sludge of 100 mg, days		45.5					
Modified Dornte Test at 120 C							
Time to absorb 650 milliliters of oxygen per 100 grams of oil, hours	9.4	132	144	10.9	57(136)	9.5	9.9
Modified Continental Oil Co. Test at 135 C							
Time for oxygen pressure to drop 60 millimeters, hours	11.6	....	61.4	....	49.3	10.6	6.8
ASTM Bomb Test							
Sludge by weight, per cent	0.025	....	0.04	....	0.005	0.01	0.04
ASTM Sludge-Accumulation Test							
Sludge by weight after 14 days, per cent	0.077	....	0.006	....	0.004	0.241	0.309

*All except oil H are inhibited oils.

**Figures in parentheses represent values obtained on a more representative 1948 sample than the one actually used in the transformer tests.

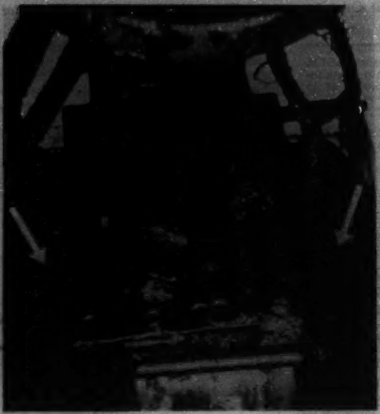

Figure 8. New 15-kva distribution transformer with conventional oil after 42 months of aging tests

Arrows show clogged oil channels

Figure 9. Setup for third series of transformer tests

Six transformers have conservator-type expansion chambers and four transformers are sealed with nitrogen above oil. Enclosure for setup was removed for picture

the Edison Electric Institute that they had decided to use inhibited oil. All stated that they would use DBPC (ditert-butyl-para-cresol) as the inhibitor in commercial production. This inhibitor is chemically identical with the inhibitor which was used in the inhibited oil in the first series of transformer tests and in one or two oils of the second series. However, the various inhibited oils are not necessarily identical, because the base of the oils and the degree of refining might be different. It is of interest to note that this inhibitor was one of those studied in the research project at the Massachusetts Institute of Technology mentioned earlier in this paper.

With this new policy of the transformer manufacturers, most of the oils used for the second transformer setup became obsolete. It was decided to use, in the third setup, the oils embodying the latest ideas for inhibited oils. Table IV shows the results of short-time tests for these oils which are, on the whole, better than found for the 1948 samples. (In February 1951, some of the manufacturers suspended, partly or completely, the furnishing of inhibited oil in new transformers, mainly because of a shortage which developed in the supply of DBPC incidental to defense needs.)

The aging tests of the third transformer set up were begun in February 1951 and are expected to continue for several years. Provisions have been made to obtain periodic oil samples in small quantities with a minimum of disturbance. Since the size of the samples will be much smaller than for the previous setups, it is expected that little or no make-up oil will need to be added to the transformers. As in the second series of tests, the transformers operate at a top oil temperature of 95 degrees centigrade with a 16-hour cooling period once a week. While this temperature provides an acceleration of the aging it is considered not so high that it would produce in the oil or in the solid insulation processes of deterioration different in type from those expected in service. Paper tapes were suspended in the oil in the transformers, in order to compare their mechanical strength after completion of the aging tests with initial results.

This project is of a co-operative nature, and the suppliers of the oil samples will be given progress reports.

Mixing of Oils

Problems of mixing inhibited oil with other oils must be considered when adopting the use of inhibited oil. Such problems may arise in connection with work on transformers requiring the addition of make-up oil or in connection with limitations in storage facilities which, in some cases, may make it inconvenient to keep inhibited oil completely separated from conventional oil. Table V shows the stability of various mixtures of inhibited oil *A* with conventional oil as found in one set of laboratory tests. The data indicate that a small addition of conventional oil to inhibited oil will not seriously reduce the life of the inhibited oil. A 50-50 mixture had a life of less than a quarter of the life of the inhibited oil. The results of similar tests made by two other investigators have been shown to the authors, and these data were about the same as those obtained in Chicago.

These findings lead to the conclusion that relatively small additions of conventional oil to inhibited oil are not objectionable, but that from an economic standpoint, large additions of conventional oil should be avoided. From a technical standpoint, there appears to be no harm in any such mixture because its life will be still in excess of the life of the conventional oil, but greater watchfulness will be desirable to detect the end of the inhibition period.

There is no apparent objection to mixing the various inhibited oils used in this latest investigation, since the same pure chemical is presumably utilized as the inhibitor in each instance. Therefore, the problem of compatibility should not arise for at least these oils.

Table IV. Short-Time Laboratory Tests of Oils Submitted in 1950 for Third Series of Transformer-Aging Tests

	Oil					
Test	I	J	K	L	M	N*
Proposed ASTM Transformer Oil Oxidation Test at 95 C, TOOT Days to reach interfacial tension of 15	19	98	88	63	130+	6
Modified Continental Oil Co. Test at 120 C Hours	32	228	142.5	197	219	24.5
Modified Dornte Test at 120 C Hours to absorb 825 milliliters of O_2 per 100 grams of oil	39	191	140	48	250+	

*All except oil N are inhibited oils.

Additions of Inhibitor to Oil by User

Consideration has been given to the feasibility of adding inhibitor to new or reclaimed-used oil by the user. In neither case was such a procedure found to be financially attractive.

The premium paid for inhibited oil is not large enough to warrant the purchase of conventional oil and the inhibitor separately. The cost for the latter method, including fixed charges on mixing equipment and cost of labor, is about the same as the cost of inhibited oil as now commercially available. In addition, the mixing involves some inconvenience for the user, loss of time, and divided responsibility.

Studies have been made from time to time for Chicago conditions on the costs and problems involved in connection with reclaiming deteriorated oil removed from transformers. The latest study indicates that the total cost for reclaiming and inhibiting deteriorated transformer oil is practically identical with the cost of new inhibited oil. This means that nothing would be gained in cost per year of service, even if the reclaimed and inhibited oil had the same life in service as the new inhibited oil. This economic analysis of reclaiming and inhibiting old oil took into account the following factors:

1. The charges for the necessary equipment and space.
2. The costs of operating, testing, and labor.
3. The costs of materials.
4. The salvage value of the old oil for use as fuel oil.

Use of Inhibited Oil in Circuit Breakers

As stated before, inhibited oil has been adopted as replacement oil in circuit breakers in Chicago. This decision was reached as a matter of economy and expediency, in order to avoid the need of storing and handling of two oils.

Consideration was given to the suitability of inhibited oil for this use. From theoretical considerations, there should be neither much advantage nor disadvantage in using inhibited oil in circuit breakers. Discussion of this problem has centered around the settling rate of carbon. Some claims were made that the settling rate would be faster than for conventional oil because the inhibitor would retard the formation of oxidation products and such products would have the effect of keeping colloidal particles such as carbon in suspension. Others claimed inhibited oil could have a slower carbon-settling rate. This problem is not of very great importance for the Commonwealth Edison Company, because the circuit breakers are generally not subjected to reclosing duty except for 4-kv distribution feeders. For the latter circuit breakers, there may be one or two reclosures after circuit breaker openings due to the occasional failures on the outside plant. In addition, all types of circuit breakers are frequently inspected after opening faults.

Table V. Oxidation Stability of Oil Mixtures

Inhibited Oil A, Per Cent	Conventional Oil, Per Cent	Days in Proposed ASTM TOOT Test to Reach Interfacial Tension of 15 Dynes/Cm
100	0	107
98	2	104
50	50	24
0	100	6

Test data made available to the authors for up to 100 interruptions of about 400 amperes in a recloser showed higher dielectric strength and faster carbon-settling rate for an inhibited oil than for conventional oil. One equipment manufacturer expressed the opinion that inhibited oil with DBPC is satisfactory from a technical angle for use in oil circuit breakers.

Two years ago one industrial firm adopted the use of inhibited oil of type *A* for 12-kv circuit breakers. These circuit breakers operated frequently under overloads and subjected the oil to severe operating conditions and heavy carbon formation. The user has concluded from this and other operating experiences that inhibited oil is satisfactory for such service. Several electric utilities have been using inhibited oil as replacement oil in some or all of their circuit breakers for a couple of years; and no adverse reports on operating performance have been received.

Summary and Conclusions

1. Incerased loading of transformers has accentuated the need for improved insulating oil, especially for replacement purposes for unprotected or partly protected transformers in service.

2. Information on the performance of inhibited oils has been, and is being, obtained in accelerated heat-aging tests of transformers under reasonably severe conditions in regard to both temperature and duration of loading.

3. Based on these tests of transformers, the service life of one inhibited oil in unprotected transformers has been indicated to be twice the life of conventional oil when used as replacement in old transformers.

4. This ratio becomes three to one for new transformers of the unprotected type.

5. Laboratory tests on samples of oil, running from a few hours to several months, indicate 10 to 18 times as much life for one inhibited oil as for conventional oil. However, the results of tests of oil in transformers extending over a period of years are considered to be more reliable and realistic.

6. Additional samples of inhibited oil representing present ideas of various transformer manufacturers are under investigation. Short-time tests have been completed and long-time tests in transformers are under way.

7. From an economic standpoint, the use of inhibited oil is very attractive when replacement of oil is necessary for transformers in service.

8. Studies made for Chicago conditions show no financial advantage to the user for him to adopt the general practice of adding an inhibitor to new or reclaimed old oil.

9. Sludging may lead to poor heat dissipation and excessive temperatures. The use of inhibited oil by preventing sludge formation permits heavy loading without the danger of excessive temperatures developing.

10. Due to the slower rate of deterioration of inhibited oil, higher operating temperatures are permissible for the same oil life, provided other components of the transformer do not limit the maximum temperature.

11. Available information indicates that inhibited oil is satisfactory for use in circuit breakers.

12. The life of both inhibited oil and of conventional oil in modern protected transformers is expected to be longer than in unprotected transformers. Tests are under way to compare the performance of inhibited oils in sealed nitrogen-blanketed and in conservator-type transformers with the performance of conventional oil.

References

1. Method for Sampling Electrical Insulating Oils. *D923-49*, American Society for Testing Materials (Philadelphia, Pa.), 1949.

2. Distribution, Power, and Regulating Transformers. *C57.22-1948*, American Standards Association (New York, N. Y.), 1948, section 100, page 18.

3. Methods of Test for Sludge Formation in Mineral Transformer Oil. *D670-42T*, American Society for Testing Materials (Philadelphia, Pa.), 1949, part 6, pages 214–21.

4. Method of Test for Acid and Base Numbers of Petroleum Oils by Color Indicator Titration. *D663-46T*, American Society for Testing Materials (Philadelphia, Pa.), 1946, part III-A, pages 819–23.

5. Method of Test for Power Factor and Dielectric Constant of Electrical Insulating Oils of Petroleum Origin. *D924-49*, American Society for Testing Materials (Philadelphia, Pa.), 1949, part 5, pages 1074–76.

6. Methods of Test for Electrical Resistance of Insulating Materials. *D257-49T*, American Society for Testing Materials (Philadelphia, Pa.), 1950, part 6, pages 396–410.

7. Method of Test for Interfacial Tension of Oil Against Water by the Ring Method. *D971-50*, American Society for Testing Materials (Philadelphia, Pa.), 1950, pages 412–14.

Discussion

Frank C. Doble (Doble Engineering Company, Belmont, Mass.): The authors are to be congratulated for their excellent report on the results of their study which represents a great deal of work over a long period of time.

While they state that DBPC is chemically identical with the inhibitor which was used in the inhibited oil in the first series of transformer tests (those in 1946) and in one or two oils of the second series (those in 1948), as well as being one of those studied in the research project at the Massachusetts Institute of Technology from 1935 to 1943, it should be noted that considerable improvements have been made in the manufacture and degree of purity of DBPC during this period, resulting in extensive improvements in its performance as an oxidation inhibitor for insulating oils. One effect of this improvement has been a decrease in the degree of refinement required to obtain a desirable receptivity of the oil to the inhibitor. With the older type of DBPC it was necessary to refine the oil to the point where a sharp break occurred in the life characteristics of the oil following exhaustion of the inhibitor. This sharp break is quite evident in the curves shown in the paper which are based on the first series of transformer tests. Oil inhibited with the DBPC now available exhibits a break equal to or better than uninhibited oil, thus increasing the period, spoken of by the authors, "for tests to predict the approaching end of the inhibition period long before actually serious deterioration of the oil occurs and, therefore, will allow ample time for removal of the oil."

Was consideration given to renewal of the inhibitor at this stage before it is exhausted and oxidation deterioration of the oil begins in arriving at the authors' conclusion number 8, that "studies made for Chicago conditions show no financial advantage to the user for him to adopt the general practice of adding an inhibitor to new or reclaimed old oil?"

This conclusion may be misleading when taken without reference to the balance of the paper which states that "the latest study indicates that the total cost for reclaiming and inhibiting deteriorated transformer oil is practically identical with the cost of new inhibited oil." As the cost of adding inhibitor is relatively a fixed amount, presumably the cost for Chicago conditions refers mainly to the costs for reclamation as being the deciding factor. If so, conclusion number 8 would not hold for those utilities who do find an economic advantage in reclaiming oil now that it is possible to renew its resistance to oxidation by the addition of DBPC. Most experience to date on the reclamation of oil shows diminishing returns from a life expectancy standpoint unless an oxidation inhibitor is used to restore the oil at least to its original life expectancy. Consequently, whenever it is found economically desirable to reclaim deteriorated oil, there is certainly a very definite financial advantage to be derived by adding DBPC to the reclaimed oil to restore its resistance to oxidation.

It might be noted that the test conditions during the first series of transformer tests, on which the curves of Figures 1 to 6 are based, are somewhat favorable to the uninhibited oils in that the "vicious spiral of sludging and heating" is discounted by the maintenance of the same top oil temperature in all four transformers, a condition which would not occur in normal operation, once sludging began, as demonstrated by the heat run.

The authors state that the results of the heat run "illustrate a very important advantage of inhibited oil, that by preventing the formation of sludge, transformers may be operated at heavy loads without the likelihood of reaching excessive temperatures." Do the authors consider this practice to be extreme in view of the statement in another paper at this session that "one extreme view is that no sludge should be permitted?"

Reference

1. Relative Performance of Normal Oils With and Without DBPC Inhibitor in Semisealed Transformers, E. D. Treanor, E. L. Roab. *AIEE Transactions*, volume 70, 1951, pages 1414–21.

T. K. Sloat (Westinghouse Electric Corporation, Sharon, Pa.): The paper emphasizes that inhibited oil in pole-type distribution transformers will be of distinct advantage since these are the most difficult to keep sealed and nitrogen protection equipment is not practical. The test data shows that we can expect to obtain three times the life from the new distribution transformers with inhibited oil and twice the life in used transformers as compared to the conventional oils.

The problem of recovery of used oils is entirely one of economics. Since used transformer oil has a marketable value as fuel oil, and if you consider the cost of the oil recovery, new inhibitor cost, and make-up oil cost, which is about 10 to 15 per cent, you approach closely the cost of new inhibited oil. There still remains the question of whether or not this inhibited-recovered oil is the equivalent of new oil. Further studies will be necessary to satisfy this question.

The authors did not emphasize the interfacial tension tests. There are those who feel that this is the single test required for evaluating oils in service and advocate limits of 15–20 dynes as the criterion for replacing or reconditioning oil. The interfacial tension data, in this work, does not show much difference between the inhibited or the uninhibited oil nor does it predict the formation of sludge.

It will be interesting to see the results of the additional tests in progress.

George H. von Fuchs (Consultant, Niagara Falls, N. Y.): The paper deals with a timely subject in a very interesting and highly informative manner. For someone who has been closely associated with the development of inhibited turbine and transformer oils, field test reports of this type are "the proof of the pudding."

Turbine and transformer oils are both essential to the electric power industry. Thus experience gained with inhibited turbine oils, the practical application of which preceded inhibited transformer oil by a decade, should be of interest to you. The inhibited turbine oil and the turbine oil stability test (the present ASTM-D 943)[1] were developed simultaneously. With this test a 10- to 20-fold increase in oil life was predicted for inhibited oils. It was also found, however, that deterioration products from a previous oil fill would appreciably reduce the life expectancy of oils and that dirty oil system had to be cleaned in order to reap the maximum benefits predicted for inhibited oils by the laboratory test. More recently a joint ASTM-ASME committee has drafted recommended practices for cleaning new and used turbine systems.

It has been shown in the paper that sludge in a transformer accelerates oil breakdown. But what is even more important, sludge also interferes with the cooling action of the oil; the resulting heat rise hinders full utilization of the transformer even at its normal rating and definitely prevents its operation at heavier loads.

Sludged transformers represent a reclaiming problem of considerable magnitude and of great economic importance. With the aid of inhibited oil, some utilities are able to reclaim sludged power transformers by the use of attached clay filters without loss in operating time. DBPC is not removed by the clay filters while the transformers are gradually restored to their rated capacity. For distribution transformers other reclaiming methods must be developed and I predict that AIEE will soon find the subject of sufficient general interest to organize a working committee for this purpose.

Reference

1. Oxidation Characteristics of Inhibited Steam Turbine Oils, *D-943*, American Society for Testing Materials (Philadelphia, Pa.).

Herman Halperin and **H. A. Adler:** The interest in inhibited transformer oil will probably continue to increase, as loads on transformers continue to increase and their effect upon the aging of the oil becomes more pronounced. This is particularly true for presently installed transformers which have varying degrees of exposure of the oil to air. As we see it, the value of the use of inhibited oil is not so much the increase of the life of the oil as obtained under previous loading conditions, but rather the possibility of operating existing transformers at higher loads and, therefore, at a more economic utilization without excessive oil trouble.

With regard to Mr. Doble's remarks that the quality of the inhibitors has been greatly improved in recent years, we made the observation that the stability in short-time laboratory tests of recent shipments of inhibited oil was much superior to earlier shipments.

Short-time laboratory tests available so far indicate that the inhibition period of conventional oils with inhibitor added is shorter than for oils specially refined for best inhibitor susceptibility.

The statements in the paper with regard to reclaiming and inhibiting old oil apply to Chicago conditions, including consideration of the fact that old transformer oil is used in Chicago as fuel oil. The considerations for Chicago conditions were quite similar to those mentioned in Mr. Sloat's discussion.

The fact that a test with controlled maximum temperature would be favorable to sludging oils was recognized when designing these tests, but this method was preferred to a constant-current test. It was felt the constant temperature test would give a more conservative comparison of the oils while the constant-current test might lead to exaggerated conclusions.

While it would be desirable to avoid any sludging in service, it is recognized that this goal is neither practical nor economical, but efforts are made to keep sludging to a minimum and the criterion of serviceability is set accordingly.

As Mr. Sloat points out, the interfacial tension test does not give a clear-cut distinction between inhibited and noninhibited oil, mainly due to the rapid drop of the interfacial tension test values during the first few months of aging. The interfacial tension test is very sensitive to contamination of the oil by varnishes and other materials in the transformer and this may be the reason for the initial rapid change of interfacial tension test in the aging tests. However, after this initial effect there was a distinct difference in interfacial tension test between inhibited and noninhibited oils.

As Dr. von Fuchs points out, the problem of cleaning sludged transformers is of great importance and it is being studied. It is difficult to remove sludge which has precipitated out, especially in oil ducts between windings.

On the Mechanics of Magnetic Amplifier Operation

ROBERT A. RAMEY
MEMBER AIEE

THERE have been many analyses of magnetic amplifiers presented in the literature, many showing remarkably close check with experimental results. But there still seems to be room for a discussion of the mechanics of amplifier operation as nearly devoid of mathematical elegance as possible. This paper is essentially an effort to "talk through" an analysis of magnetic amplifier operation. More exacting mathematical analyses based upon the concepts presented herein are being prepared by the Naval Research Laboratory and will be published as they are concluded.

In order to provide understanding rather than a method of general mathematical solution a semidescriptive or quasi-mathematical technique is utilized. Since this problem is quite complex, "exact" mathematical prediction seldom leads to a clear picture. This paper is designed to give such a picture of the physics of magnetic amplifier operation and to give examples of the usefulness of the fundamental concepts. It will seem light reading for many of our mathematically-minded scientists—that truly is the author's aim. It is hoped that this presentation will answer many of the questions raised by the engineers in this field who seldom have the time available to analyze the general solutions published in the literature. A further object of this paper is the introduction of examples of certain new magnetic amplifier circuits the author has developed as a direct result of this study.

Summary

In this paper certain magnetic amplifier circuits will be illustrated and their circuit equations presented subject to certain assumptions. The equations will be interpreted in as clear a manner as the author thinks possible and some conclusions will be drawn. Since the mathematics of analysis of magnetic amplifiers is quite complex as viewed from continuous theory a clearer period by period interpretation will be pursued during which periods the equations may be considered as a continuous, elementary and reasonably accurate representation of the phenomena. The two periods which will be used are those during which the amplifier output current is large (conducting period); and during which the amplifier output current is of the order of the magnetizing current (nonconducting period). Equivalent circuits for each period will be set up. The final conditions of one period will represent the initial conditions of the following period.

The two assumptions utilized in this analysis are "ideal" magnetization curves for the core materials, Figure 1, and "ideal" rectifiers. The best core materials and rectifiers manufactured today rather closely approximate these assumed conditions. A resistive load impedance will be used for simplification of the mathematics.

The conclusions drawn from these elementary considerations will form a basis for predicting the performance of examples of certain novel circuits which shall have properties of an unusual nature. Practical discussion of these circuits is beyond the scope of this paper and will be presented elsewhere.

A relation will be derived in an elementary manner between the response time of magnetic amplifiers and the factors which influence this phenomenon. A rectified sinusoidal signal will be used to avoid the consideration of certain transcendental equations which would arise in the consideration of a d-c signal. The resulting expression will be a sequence whose terms will approach a final value in the nth term. The number n will directly measure the response time. The final value of the sequence will be the steady-state firing angle for the output current.

There will be presented a discussion of the function of the control voltage in magnetic amplifier operation. It will be shown that the control source need never supply the power for the amplifier control. The energy storage in the amplifier cores in steady-state operation can be supplied entirely from the a-c power source. The result is a very efficient amplifier with response time of approximately one-half cycle. Remarks regarding power gain will be difficult to interpret since the control source will never be required to supply any power to the amplifier circuit.

This approach to the magnetic amplifier problem has resulted from a recognition of the fact that the magnetic amplifier is a voltage-sensitive device and not, as generally believed, a current-sensitive device. The only truly independent variable is the control voltage. Of course control means which are "current sources" provide exceptions to these remarks.

Concerning the "Simple" Series Magnetic Amplifier

Two Transformers and One Transformer

The simple series amplifier shown schematically in Figure 2 consists of a pair of single phase transformers I and II connected in series in the primary or "output" circuit and energized from an a-c source E_{ac} in series with a load circuit impedance R_L. The secondary or "con-

---

Paper 51-217, recommended by the AIEE Magnetic Amplifiers Committee and approved by the AIEE Technical Program Committee for presentation at the AIEE Summer General Meeting, Toronto, Ont., Canada, June 25–29, 1951. Manuscript submitted February 5, 1951; made available for printing May 1, 1951.

Robert A. Ramey is with the Naval Research Laboratory, Washington, D. C.

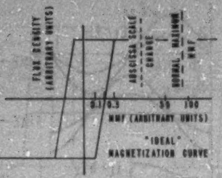

Figure 1. "Ideal" magnetization curve

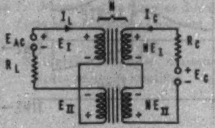

Figure 2. Series magnetic amplifier

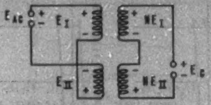

Figure 3. Equivalent circuit for nonconducting period (Core I proceeding to saturation)

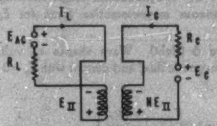

Figure 4. Equivalent circuit for conducting period (core I saturated)

trol" circuit has the two transformer secondaries connected in series opposition (for a-c voltages of fundamental frequency) in series with a control circuit resistance R_c and a control voltage source E_c. The equations for this circuit configuration are:

$$E_{ac} = E_{\mathrm{I}} + E_{\mathrm{II}} + I_L R_L \text{ (primary circuit)} \quad (1)$$

$$NE_{\mathrm{I}} = NE_{\mathrm{II}} + E_c - I_c R_c \text{ (secondary circuit)} \quad (2)$$

where E_{I} and E_{II} are the instantaneous primary voltages on transformers I and II respectively, I_L and I_c are the instantaneous primary and secondary currents respectively and N is the ratio: secondary turns/primary turns.

However during the periods of time during which transformer cores *I* and *II* are unsaturated simultaneously, currents I_L and I_c are assumed quite negligibly small, Figure 1. During these periods the circuit equations become from 1 and 2:

$$E_{ac} = E_{\mathrm{I}} + E_{\mathrm{II}} \text{ (primary circuit)} \quad (3)$$

$$NE_{\mathrm{I}} = NE_{\mathrm{II}} + E_c \text{ (secondary circuit)} \quad (4)$$

This will be called the nonconduction period. The equivalent circuit for this period is shown in Figure 3.

Whenever either transformer core is saturated the primary and secondary voltages of that transformer ideally cease to exist and currents I_L and I_c can no longer be neglected. If core I is saturated the circuit equations become from 1 and 2:

$$E_{ac} = E_{\mathrm{II}} + I_L R_L \text{ (primary circuit)} \quad (5)$$

$$0 = NE_{\mathrm{II}} + E_c - I_c R_c \text{ (secondary circuit)} \quad (6)$$

The output current I_L must equal the reflected control current NI_c for core II remains unsaturated and can have no net ampere turns beyond that needed for magnetization. This period of time will be called the conducting period. The equivalent circuit for this period is shown in Figure 4. If core II is saturated (negative half-cycle of a-c voltage) the circuit equations become from equations 1 and 2:

$$E_{ac} = E_{\mathrm{I}} + I_L R_L \text{ (primary circuit)} \quad (7)$$

$$0 = -NE_{\mathrm{I}} + E_c - I_c R_c \text{ (secondary circuit)} \quad (8)$$

where I_L equals $(-)NI_c$. Another equivalent circuit like that of Figure 4 would redundantly represent this.

A MATTER OF TIMING

To say that the foregoing equations are the only ones to be observed would hardly tell the whole story. One must determine when each is to be used. In setting up the equations it was stated that one set of equations was for the periods during which both cores were unsaturated simultaneously (nonconducting period) and the other set was for the periods during which either one of the cores was saturated (conducting period). It is clear from the above considerations that the flux level in both cores must be known at all times if the equations are to be useful.

There exists only one fundamental relation between magnetic flux and the electrical quantities one can conveniently measure. This relation between rate of change of flux and applied voltage was first published by Faraday and has been subsequently called Faraday's Law of Electromagnetic Induction. It is this relation which will be used herein.

Since the equations being used in this paper concern only voltages and currents it is deemed advisable for clarity to keep this magnetic flux measurement in the same units. This will avoid the confusion associated with the introduction of a magnetic quantity. The integral of the voltages E_{I} and E_{II} will measure flux changes in their respective cores. The transformer core will be saturated when the integral of its terminal voltage attains a value in volt-seconds equivalent to that which may be stored by the transformer. A convenient measure of this value is obtained from the a-c source voltage E_{ac} which time integral over a half-cycle is equivalent to the volt-second storage of both cores. That is to say,

$$1/2 \int_0^{1/2f} E_{ac} dt$$

will be the volt-second capacity of one transformer core on a traverse of flux from its negative maximum value to its positive maximum value. The term $1/2f$ is the time of one half-cycle of a-c supply voltage where f is the line frequency in cycles per second. These amplifiers are regarded as being supplied from an a-c source which voltage is the maximum that can be applied and still keep the cores from saturating at any time due to alternating current alone.

Elimination of E_{II} from equations 5 and 6 gives:

$$\left(E_{ac} + \frac{E_c}{N}\right) = \left(\frac{R_c}{N^2} + R_L\right) I_L \quad (9)$$

From this relation it is apparent that the output current will lag the a-c voltage by an angle dependent upon the voltages E_{ac} and E_c when E_c is a constant d-c voltage. This lag can be eliminated by utilization of a rectified a-c voltage for E_c which frequency and phase is the same as that of the a-c source. This type of control voltage is in quite wide use and is almost indistinguishable from d-c control with the same average voltage. This step results in quite a simplification when one recognizes that the initial instant of each period of operation now is clearly defined. The conducting period begins when one of the cores saturates; the nonconducting period begins when the a-c voltage reaches zero.

In all problems involving definite integrals some set of initial conditions must be specified—a starting point. The author has chosen the no-load condition ($E_c = 0$) sufficiently long after application of the a-c voltage E_{ac} so that all transients due to the application of alternating current have ceased to exist. At this time the amplifier is operating according to equations 3 and 4 with $E_{\mathrm{I}} = E_{\mathrm{II}}$, $E_c = 0$ and both E_{I} and E_{II} simultaneously equal to $1/2\ E_{ac}$. Since the cores are identical and the two transformers are in series the magnetizing currents are identical and flow in the primary circuit.

The flux in the cores is swinging from knee to knee on the magnetization curves 90 degrees behind the a-c voltage wave (that is, maximum flux deviation at zero applied voltage) and the magnetization current is exactly that indicated by the magnetization loops. These relations are shown in Figures 5 and 6. When E_{ac} is zero and going positive the line current is zero and the fluxes in the cores are at points A. Subsequently, the a-c voltage becomes positive, the current I_L assumes the values at B and continues to increase according to the magnetization loop (proportional to Φ) until E_{ac} approaches zero at C and becomes zero at D. During the succeeding negative half-cycle the line current assumes the values of E, F, and when E_{ac} becomes zero, A. Since the magnetization loops are identical, I_L+NI_c and I_L-NI_c are equal. Consequently, $I_c=0$ with $E_c=0$ no matter how "fat" the magnetization loop. A current I_c can only flow when there is a difference in magnetization level between the two cores. The magnetization currents are carried by the primary circuit as the quiescent current. This is a reasonably accurate picture of the relations existing with $E_c=0$.

The exact instant of application of E_c will be designated as point A, when E_{ac} is zero and dE_{ac}/dt is positive—the beginning of a nonconducting period. Time will be called zero at this instant and will attain a value $1/2f$ second at the end of the half-cycle; at the beginning of each half-cycle time measurement will be zero.

The Magnetizing Voltages

Equations 3, 4, 5, 6, 7, and 8 show the voltage and current relations existing in the simple series magnetic amplifier in non-conducting and conducting states. From these equations expressions for the magnetizing voltages E_I and E_{II} may be derived.

During periods of nonconduction equations 3 and 4 are applicable. Solution of these equations gives:

$$E_I=1/2\left(E_{ac}+\frac{E_c}{N}\right);\quad E_{II}=1/2\left(E_{ac}-\frac{E_c}{N}\right)$$

Since all subsequent calculations will involve only a half-cycle at a time it will be convenient to work with magnitudes without regard to direction. The equations for the nonconducting period become:

$$|E_I|=1/2\left[|E_{ac}|+\frac{|E_c|}{N}\right]$$

(core I proceeding to saturation)

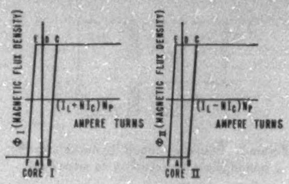

Figure 5. Magnetization loops showing instantaneous magnetomotive force for $E_c=0$

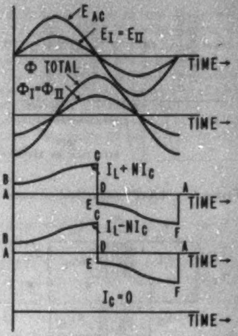

Figure 6 (right). Wave shapes of voltage, magnetic flux, and current with $E_c=0$

$$|E_{II}|=1/2\left[|E_{ac}|-\frac{|E_c|}{N}\right]$$

(core II deviating from saturation)

during the positive half-cycles. During the negative half cycles:

$$|E_I|=1/2\left[|E_{ac}|-\frac{|E_c|}{N}\right]$$

(core I deviating from saturation)

$$|E_{II}|=1/2\left[|E_{ac}|+\frac{|E_c|}{N}\right]$$

(core II proceeding to saturation)

During periods of conduction with core I saturated (positive half-cycle of a-c voltage) equations 5 and 6 yield:

$$|E_{II}|=\frac{|E_{ac}|-\dfrac{NR_L}{R_c}|E_c|}{1+\dfrac{N^2R_L}{R_c}}$$

In summary:

(1) Either core proceeding to saturation will have:

$$|E_I|=|E_{II}|=1/2\left[|E_{ac}|+\frac{|E_c|}{N}\right]\text{ volts}\qquad(10)$$

across its primary terminals in such a direction as to produce the desired saturation.

(2) Either core deviating from saturation during nonconducting period will have:

$$|E_I|=|E_{II}|=1/2\left[|E_{ac}|-\frac{|E_c|}{N}\right]\text{ volts}\qquad(11)$$

(3) Either core deviating from saturation during a conducting period will have:

$$|E_I|=|E_{II}|=\frac{|E_{ac}|-\dfrac{NR_L|E_c|}{R_c}}{1+\dfrac{N^2R_L}{R_c}}\text{ volts}\qquad(12)$$

across its primary terminals in the appropriate direction.

Since the subsequent calculations will begin and end within a half-cycle the use of magnitudes will not prove cumbersome. The symmetry between expressions for E_I and E_{II} during conducting and nonconducting periods will, however, prove extremely convenient.

Concerning Transients

In the preceding discussion a review of the circuit equations of the series magnetic amplifier indicated two modes of operation could be expected, and for each of these modes a simple equivalent circuit could be used. It has further been determined that the times of validity of these equivalent circuits could be definitely and conveniently established. Convenient initial conditions have been designated and described.

The problem has been set up in this manner to illustrate the fundamental physics involved. Since the magnetic amplifier is transient by nature any discussion disregarding this fact would fail to present a clear picture of its operation. To understand what goes on in "steady-state" operation one must also clearly understand the transient operation.

The following discussion will picture period by period the operation of the magnetic amplifier in transient until the general term is recognized.

During the first half-cycle of a-c voltage immediately following the application of E_c equations 3 and 4 are applicable and will remain effective until core I reaches saturation. This will occur at a time t_1 defined by the relation:

$$\int_0^{t_1}E_Idt=1/2\int_0^{1/2f}E_{ac}dt=\Delta_0\text{ volt-seconds}$$

The value E_I is determined from equation 10.

There follows in the interval (t_1 to $1/2f$) a period of conduction during which the

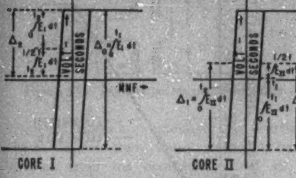

Figure 7. Magnetization changes during first cycle after initiation of transient

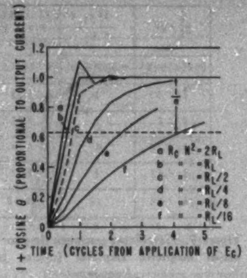

Figure 8 (right). Response characteristics series magnetic amplifier

voltage across transformer $I(E_I)$ is zero and the currents I_L and I_c are determined by equations 5 and 6. Core II in the first half-cycle has E_{II} across its terminals causing it to deviate from its saturated value by an amount:

$$\Delta_1=\int_0^{t_1}E_{II}dt+\int_{t_1}^{1/2f}E_{II}dt \text{ volt-seconds}$$

The value of E_{II} for the nonconducting period (0 to t_1) is defined by equation 11 and for the conducting period (t_1 to $1/2f$) by equation 12. The resultant changes in the core fluxes are shown in Figure 7. This pictures the mechanism of the first (positive) half-cycle of a-c supply voltage.

During the second (negative) half-cycle of a-c supply voltage core II will saturate at a time t_2 defined by:

$$\int_0^{t_2}E_{II}dt=\Delta_1 \text{ volt-seconds}$$

That is, in order to saturate, core II must return to its saturated value and the only mechanics available is by releasing the volt-seconds absorbed during the previous half-cycle. After saturation E_{II} becomes zero and a conducting period ensues until the a-c voltage reaches zero.

Core I meanwhile has E_I across its terminals causing it to deviate from its saturated value by an amount:

$$\int_0^{t_2}E_Idt+\int_{t_2}^{1/2f}E_Idt=\Delta_2 \text{ volt-seconds}$$

where E_I is defined according to equation 11 in the nonconducting interval (0 to t_2) and by equation 12 in the conducting interval (t_2 to $1/2f$). The resultant changes in the core fluxes are shown in Figure 7. This pictures the mechanics of the second (negative) half-cycle of a-c supply voltage.

During the third (positive) half-cycle of a-c voltage the steps of the first half-cycle are repeated with the same equations effective. The only change is in the initial conditions, that is, instead of being

$$\frac{1}{2}\int_0^{1/2f}E_{ac}dt \text{ volt-seconds from saturation}$$

Core I is Δ_2 volt-seconds from saturation. The saturation will occur at a time t_3 defined by:

$$\int_0^{t_3}E_Idt=\Delta_2 \text{ volt-seconds}$$

Or, more generally, saturation in any odd $(n-1)^{st}$ half-cycle will occur at a time t_{n-1} defined by:

$$\int_0^{t_{n-1}}E_Idt=\Delta_{n-2} \text{ volt-seconds}$$

Core II meanwhile has E_{II} across its terminals and will deviate from its saturated value in any odd $(n-1)^{st}$ half-cycle by an amount:

$$\int_0^{t_{n-1}}E_{II}dt+\int_{t_{n-1}}^{1/2f}E_{II}dt=\Delta_{n-1} \text{ volt-seconds}$$

During the succeeding even (nth) half-cycle saturation will occur at time t_n defined by:

$$\int_0^{t_n}E_{II}dt=\Delta_{n-1} \text{ volt-seconds}$$

or:

$$\int_0^{t_n}E_{II}dt=\int_0^{t_{n-1}}E_{II}dt+\int_{t_{n-1}}^{1/2f}E_{II}dt$$

However, E_I and E_{II} have the same magnitudes during each respective part of a half-cycle (equations 10, 11, and 12). A general expression defining t_n for any nth half-cycle can be found by substituting those values for E_I and E_{II} in the equation above. This fundamental relation for transient operation is:

$$1/2\left[|E_{ac}|+\frac{|E_c|}{N}\right]\int_0^{t_n}\sin\omega tdt$$
$$=1/2\left[|E_{ac}|\frac{|E_c|}{N}\right]\int_0^{t_{n-1}}\sin\omega tdt$$
$$+\frac{|E_{ac}|-\frac{NR_L}{R_c}|E_c|}{1+N^2R_L/R_c}\int_{t_{n-1}}^{1/2f}\sin\omega tdt$$

Since E_{ac} is a known constant the bracketed coefficients may be replaced by the following functions of E_c:

$$f_1(E_c)=1/2\left[|E_{ac}|+\frac{|E_c|}{N}\right],$$

$$f_2(E_c)=1/2\left[|E_{ac}|-\frac{|E_c|}{N}\right],$$

$$f_3(E_c)=\frac{|E_{ac}|-\frac{NR_L}{R_c}|E_c|}{1+N^2R_{L/R_c}}.$$

This gives:

$$f_1(E_c)\int_0^{t_n}\sin\ \omega tdt=f_2(E_c)\int_0^{t_{n-1}}\times$$
$$\sin\omega tdt+f_3(E_c)\int_{t_{n-1}}^{1/2f}\sin\omega tdt \quad (13A)$$

When the definite integrals are evaluated one finds:

$$\cos\omega t_n=\frac{-f_2(E_c)-f_3(E_c)+f_1(E_c)}{f_1(E_c)}+$$
$$\frac{f_2(E_c)-f_3(E_c)}{f_1(E_c)}\cos\omega t_{n-1}$$

or in terms of the saturation angle θ_n:

$$\cos\theta_n=1-f_5(E_c)+f_4(E_c)\cos\theta_{n-1}\ (n>1) \quad (13)$$

where:

$$f_5(E_c)=\frac{f_2(E_c)+f_3(E_c)}{f_1(E_c)},\ f_4(E_c)$$
$$=\frac{f_2(E_c)-f_3(E_c)}{f_1(E_c)}$$

The saturation angle for the first half-cycle may be calculated from equation 13A:

$$\cos\theta_1=-f_2(E_c)/f_1(E_c)$$

These preceding equations show that the saturation time or "firing angle" is directly determined by the previous saturation time and the magnitude of the signal voltage. From the general expressions above one can construct the transient output current as a function of time after application of a signal voltage. Current "firing" will occur in any nth half-cycle at the time t_n and the current will have instantaneous values determined by equation 9 for the remaining part of the half-cycle. The angle at which saturation occurs will change according to equation 13 until such time as θ_n equals θ_{n-1}; this will be the steady-state condition. The "response time" could be defined as that number of cycles needed for the firing angle to reach some predetermined part of its final value.

OF CURRENTS AND TIME

Since firing occurs at angle θ determined by equation 13 and the magnitude of current is determined by equation 9, calculation of current for transient and steady-state conditions is a relatively easy problem. The average current for any nth half-cycle is:

$$I_L(\text{avg}) = \frac{1}{\pi}\int_{\theta_n}^{\pi} I_L d\theta = \frac{1}{\pi}\int_{\theta_n}^{\pi} \frac{E_{ac}+\frac{E_c}{N}}{\frac{R_c}{N^2}+R_L}\times$$

$$d\theta = \frac{1}{\pi}\frac{E_{ac}+\frac{E_c}{N}}{\frac{R_c}{N^2}+R_L}[1+\cos\ \theta_n] = f_6(E_c)\times$$

$$[1+\cos\theta_n]\ \text{(transient and steady-state average current)} \qquad (14)$$

That is, for any given amplifier, the output current is directly proportional to $(1+\cos\theta_n)$ and to a function of E_c. For any given set of initial conditions $f_6(E_c)$ would become a constant and $(1+\cos\theta_n)$ would be directly proportional to the averaged output current. The value $\cos\theta_n$ can be obtained from equation 13 for transient conditions so it is possible to plot the average output current as a function of time from known initial conditions. Steady-state firing angle θ_{ss} can be determined from equation 13 by setting $\theta_n = \theta_{n-1} = \theta_{ss}$. This will give:

$$\cos\theta_{ss} = \frac{1-f_5(E_c)}{1-f_4(E_c)} \qquad (15)$$

relating the steady-state firing angle θ_{ss} and the circuit parameters. By substitution of this expression in place of θ_n in equation 14:

$$I_L(\text{avg}) = f_6(E_c)\left[1+\frac{1-f_5(E_c)}{1-f_4(E_c)}\right]\times$$

(steady-state average current)

Substitution of the appropriate expressions for the function of E_c gives:

$$I_L(\text{avg}) = \frac{2}{\pi}N\frac{E_c}{R_c} = N\frac{E_c(\text{avg})}{R_c} \qquad (16)$$

that is, the average load ampere turns equal the average control ampere turns in steady-state operation.

Using equation 14, an example magnetic amplifier is analyzed in transient. The values: $E_{ac} = 100$ volts, $N = 1/2$ and $R_L = 50$ ohms are chosen as circuit parameters. For purposes of comparison several values of R_c were chosen and the control voltage E_c was adjusted to always give a final value of θ_n of 90 degrees; $(1+\cos\theta_n)$ equal to unity. Steady-state current firing at 90 degrees is accomplished by setting $\cos\theta_n$ equal to $\cos\theta_{n-1}$, and both equal to zero in equation 13. This gives:

$$1-f_5(E_c) = 0$$

the relation between E_c and R_c for 90-degree firing. Initial conditions are made the same as described in the section on A Matter of Timing. The plot of these transients of $(1+\cos\theta_n)$ is shown in Figure 8. The time of response is measured by the time required for $(1+\cos\theta_n)$ to reach 63 per cent of its final value (shown as the dashed line in Figure 8).

Direct calculation of response time of the series magnetic amplifier appears to be a step-by-step process when the general solutions are involved. However, considerable simplification of the mathematics may be attained by specifying convenient test conditions. A steady-state firing angle of 90 degrees will prove convenient since the expression $(1\text{-}f_5(E_c))$ of equation 13 becomes zero. Since the time response of the simple series magnetic amplifier is considered to be independent of the applied signal voltage this simplification seems to be completely justified.

So equation 13 becomes:

$$\cos\theta_n = f_4(E_c)\cos\theta_{n-1}\ (n>1) \qquad (17)$$

with the condition: $1-f_5(E_c)=0$, wherein E_c and R_c are always adjusted so that the steady-state firing angle is 90 degrees.

Substitutions of the firing angle θ_n for each succeeding nth half-cycle in equation 14 gives:

$$I_{L_1}(\text{avg}) = f_6(E_c)\left[1-\frac{f_2(E_c)}{f_1(E_c)}\right]$$

(first half-cycle)

$$I_{L_2}(\text{avg}) = f_6(E_c)\left[1+f_4(E_c)\left(-\frac{f_2(E_c)}{f_1(E_c)}\right)\right]$$

(second half-cycle)

$$I_{L_3}(\text{avg}) = f_6(E_c)\left[1+f_4^2(E_c)\left(-\frac{f_2(E_c)}{f_1(E_c)}\right)\right]$$

(third half-cycle)

R_c/N^2	$\frac{N^2R_L}{4R_c}$	RESPONSE TIME BY EQUATION 18
OHMS/TURN^2	CYCLES	CYCLES
$R_L/4$	1	1.28
$R_L/8$	2	2.26
$R_L/16$	4	4.24
$R_L/32$	8	8.21
$R_L/64$	16	16.18

Figure 9. Calculated response time for simple series magnetic amplifier (cycles of line frequency)

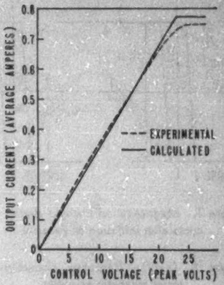

Figure 10. Transfer characteristic series magnetic amplifier

or generally:

$$I_{L_n}(\text{avg}) = f_6(E_c)\left[1+f_4^{n-1}(E_c)\left(-\frac{f_2(E_c)}{f_1(E_c)}\right)\right]$$

(nth half-cycle)

The final steady-state current will be from equation 17:

$$I_{L_{ss}}(\text{avg}) = f_6(E_c)[1+f_4(E_c)\ \cos 90°] = f_6(E_c)$$

The time of response is that time at which the output current reaches $(1-1/e)$ of its final value so the expression determining the nth half-cycle at which the output current reaches this quantity is

$$\frac{I_{L_n}}{I_{L_{ss}}} = \left(1-\frac{1}{e}\right) = 1+f_4^{n-1}(E_c)\left(-\frac{f_2(E_c)}{f_1(E_c)}\right)$$

Substituting the expressions for the functions of E_c and utilizing the conditional equations above in this expression gives:

$$\left[\frac{\frac{N^2R_L}{R_c}-1}{\frac{N^2R_L}{R_c}+1}\right]^{n-1} = \frac{\frac{N^2R_L}{R_c}+1}{\frac{N^2R_L}{R_c}e}$$

or the response time:

$$T_R = \frac{n}{2} = \frac{1}{2}\left[1+\frac{\ln\frac{k+1}{ke}}{\ln\frac{k-1}{k+1}}\right]\text{cycles} \qquad (18)$$

where:

$$k = \frac{N^2R_L}{R_c}$$

As H. F. Storm[1] demonstrates, the response time is a function of the resistance ratios and is quite independent of the transformer inductances

$$\left(T_R = \frac{N^2R_L}{4R_c}\right)_1$$

Substitution of typical values as shown in the table of Figure 9 yields resulting

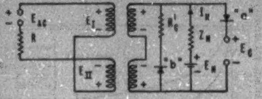

Figure 11. New series magnetic amplifier

response times approximately one fourth cycle higher than those predicted by Storm from his consideration of the "apparent inductance" of the control circuit.

Average output current as a function of control voltage calculated from equation 16 for a laboratory amplifier is compared to the experimental data in Figure 10. The check is not good at values of output current approaching amplifier maximum output since the experimental amplifier has inductive impedance when saturated whereas the theoretical amplifier does not.

REMARKS

The preceding analysis has been performed with the application of only one basic assumption. This assumption is that the transformer cores saturate completely at a very low value of magnetizing current. The use of a rectified sinusoidal control voltage is hardly an assumption but rather a recognition of existing practice. The ensuing simplification of the mathematical process is so great as to allow a direct viewing of the operation of these amplifiers in all normal modes of operation.

Direct calculation of transients gives response times in good agreement with those published heretofore and the output and control currents are subject to the same "current transformer principle" observed by all investigators in this field.

During the nonconducting period the control ampere turns have a minute value dependent upon the magnetization loops. During the conducting period the control ampere turns have a value equal to the output ampere turns, except for the ampere turns designated by the magnetization loops.

The remarkable fact that the time of response of the series magnetic amplifier does not depend upon the inductance of the transformers as reactors seems to be adequately shown by this analysis.

A New Series Amplifier

A CHANGE OF FUNCTION

In the previous analysis the control current during nonconduction was considered to be such a small quantity that its existence did not effect the voltage relations. During the conducting period the ampere turns in the output circuit (determined by equation 9) differed from the control ampere turns in magnitude only by the negligibly small magnetizing ampere turns. It is readily apparent from these considerations that the major need for power from the control source occurs during the conducting period.

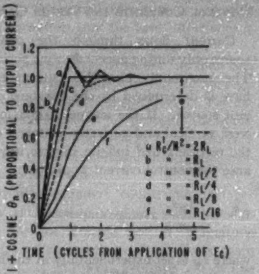

Figure 12. Response characteristics new series magnetic amplifier

During the nonconducting period the flux level in the two cores is altered. One core goes through its complete flux change, equation 10, to saturation while the other core deviates from its saturated value according to equation 11. During the conducting period the flux in the unsaturated core deviates further from saturation according to equation 12.

This section of the paper will be a study of a new type of series magnetic amplifier circuit which shall be governed by the same equations as the simple magnetic amplifier during the nonconducting period but which shall not include the control voltage in the equations governing the conducting period. In order to divorce the control voltage from the circuit during periods of conduction it is necessary to block the control voltage circuit during these periods. This is accomplished in the example to be analyzed by placing a rectifier "a" in series opposition to the control voltage, Figure 11. This means no forward current may be carried by the control source. However, since some current is needed during nonconduction to assure operation of the constraint imposed by the control voltage, this minute current is supplied from a "constant current" source. This source, shown parallel to the control voltage circuit, consists of a high impedance Z_M and a voltage E_M of sufficient value to assure a value of current I_M as large as any current needed for the control circuit's operation. A path for control-circuit currents during the conduction periods is provided through rectifier "b" and resistance R_c' also shown parallel to the control voltage circuit.

Examination of the nonconducting period shows:

$$E_{ac} = E_{I} + E_{II} \text{ (primary circuit)} \tag{3}$$

$$NE_{I} = NE_{II} + E_c \text{ (secondary circuit)} \tag{4}$$

These are the same relations as those which governed the simple series amplifier during nonconduction.

For the conducting period (core I saturated):

$$E_{ac} = E_{II} + I_L R_L \text{ (primary circuit)} \tag{5}$$

$$0 = NE_{II} - I_c R_c' \text{ (secondary circuit)} \tag{19}$$

These are the same relations as those which governed the simple series amplifier during conduction with the exception that E_c no longer appears.

Elimination of E_{II} from equations 5 and 19 gives:

$$E_{ac} = \left[\frac{R_c'}{N^2} + R_L\right] I_L \tag{20}$$

The instantaneous magnitude of output current is no longer a function of the control voltage as in equation 9. The control voltage may effect only the angle of firing.

Examination of the transient operation follows as in the section on Concerning Transients of this paper. One finds the general expression defining the time of firing to be:

$$f_1(E_c)\int_0^{t_n} \sin\ \omega t dt = f_2(E_c)\int_0^{t_{n-1}} \times$$

$$\sin \omega t dt + K\int_{t_{n-1}}^{1/2f} \sin \omega t dt$$

where:

$$K = \frac{|E_{ac}|}{1 + \dfrac{N^2 R_L}{R_c'}}$$

When the definite integrals are evaluated one finds:

$$\cos\theta_n = 1 - f_7(E_c) + f_8(E_c)\cos\theta_{n-1}\ (n > 1) \tag{21}$$

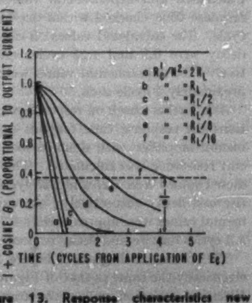

Figure 13. Response characteristics new series magnetic amplifier

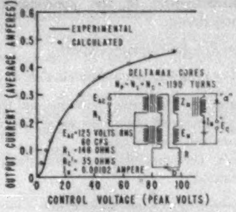

Figure 14. Transfer characteristic new series magnetic amplifier

where:

$$f_7(\boldsymbol{E}_c) = \frac{f_2(\boldsymbol{E}_c)+K}{f({}_1\boldsymbol{E}_c)}, \text{ and } f_8(\boldsymbol{E}_c) = \frac{f_3(\boldsymbol{E}_c)-K}{f_1(\boldsymbol{E}_c)}$$

From any set of initial conditions current firing will occur in the *n*th half-cycle according to equation 21 and will have instantaneous value determined by equation 20.

Using the same initial conditions and final conditions as used in the section on Concerning Transients, the transient response of a magnetic amplifier calculated for rise of output current is shown in Figure 12. The calculated response for decay of output current is shown in Figure 13.

To check the results of calculations with the equations developed above, a magnetic amplifier was set up in the Naval Research Laboratory and its transfer characteristics and response times predicted. Figure 14 shows a plot of the transfer characteristics obtained. The extreme closeness of the check is not significant because a mean value was chosen for the rectifier "b" resistance. This value was not sufficiently high at low output currents causing the noted deviation. At high current the effect of the amplifier's saturated impedance has apparently compensated for the drop in rectifier resistance below the chosen mean value. Calculated and experimental values for response time checked within one-fourth cycle. The calculated values on rise and decay were 0.9 and 1.25 cycles respectively; the experimental values were approximately 1 cycle each.

As a further check on response calculations the response time for this experimental amplifier with doubled load circuit resistance was calculated. The predicted values were 1.25 and 2.25 cycles on rise and decay respectively; the experimental values were approximately 1.3 and 2.3 cycles for rise and decay respectively.

The schematic diagram of Figure 14 is electrically the same as that of Figure 11. Electrical isolation makes the constant current source more easily obtained.

CONTROL CURRENTS AND POWER GAIN

Current flows through the control source only during nonconducting periods. The maximum value this current may have is determined by the constant current source. If the magnetization loops were vertical and perfectly matched and the rectifiers had infinite inverse impedance the control current would be:

$$I_c = (-)\,\frac{I_M\theta_n}{\pi} \text{ average amperes} \qquad (22)$$

where I_M is set experimentally at the lowest value which will assure full amplifier output.

Using the expression above, the theoretical control current for the amplifier of Figure 14 (with I_M equal to 1.02 milliamperes) was calculated and is shown in Figure 15 along with the experimental results. The character of the two curves is essentially the same. However, the experimental curve has smaller magnitude indicating the practical amplifier does not quite possess the ideal characteristics noted in the theoretical calculation. The relative importance of the factors causing this deviation is the subject of further investigations.

The power amplification of this type of magnetic amplifier is a most unusual function. Discussion of this factor is complicated by the facts: (1) no power is required from the control source (power must be absorbed instead) and (2) the control current magnitude is an inverse function of the control voltage and can be made to become zero at maximum output power by proper choice of I_M.

If power absorbed in the control source be considered the input power and that absorbed by the load impedance the output power the "gain" of the amplifier may be examined. One finds this "gain" is a function of the control voltage with a range of "gain" values (for the practical amplifier heretofore discussed) from only a few hundred at low control voltage to infinity at maximum power output with a response time of approximately one cycle. "Gain" at one-half maximum output power was approximately 5,000.

The theoretical amplifier would always have a gain of infinity since I_M could be made zero.

REMARKS

One of the most interesting aspects of the preceding analysis has been the role of the control voltage. The control source is not actively engaged in the magnetization of the transformer cores—it has rather assumed the function of a passive circuit which is used for a standard or measurement reference. The power needed for the operation of the amplifier has all been drawn from the major power sources—even that power needed for the measurement of E_c. The control circuit's maximum current I_M is determined by the requirements of the cores and rectifiers and seems quite independent of the other parameters of the circuit. With appropriate materials and circuits it is readily conceivable that tremendous power gains may be obtained with a response time of one cycle.

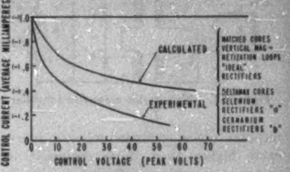

Figure 15. Control current characteristic new series magnetic amplifier

There are two very serious disadvantages inherent in the type of magnetic amplifier discussed here. Reference to Figure 14 will show the output currents do not bear a linear relation to the control voltage. Further, since the a-c source must supply the losses associated with R_c', full use of the capabilities of the transformer cannot be attained.

The net result is that, though this type of circuit configuration exhibits fast response with high gain, it is nonlinear and has relatively low power output, for a given transformer size.

A New Parallel-Connected Magnetic Amplifier

AN OBVIOUS IMPROVEMENT

Examination of the series magnetic amplifier has shown it to have serious limitations. One of the most notable arrives from the fact that a change in the magnetic flux level of each core occurs during times when full output current flows in the transformer windings. Any voltage across the transformer during these periods of conduction subtracts directly from that voltage which is available for application to the load impedance. The gain is high and the response time short but the transformers are quite large for any given output and the output characteristic is far from linear.

The following section of this paper will deal with an example of a type of magnetic amplifier with self-magnetizing features similar to those previously discussed but which shall not require a

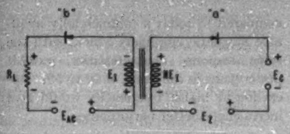

(A) SINGLE CORE MAGNETIC AMPLIFIER

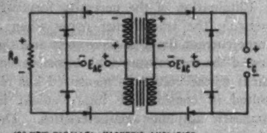

(B) NEW PARALLEL MAGNETIC AMPLIFIER

Figure 16. (A) Single core magnetic amplifier, (B) New parallel magnetic amplifier

change of magnetization in a conducting transformer.

An obvious method for eliminating the need for changing the flux level in a core whose windings are carrying output current is to allow that transformer to conduct only during alternate half-cycles and to set the magnetization level during the other half-cycles. To accomplish this, the a-c supply voltage is applied to a transformer primary winding only during positive half-cycles (see Figure 16A); during negative half-cycles a rectifier "b" blocks the a-c voltage from the transformer winding. In the transformer secondary or control circuit the now familiar rectifier "a" is placed in series opposition to the control voltage which is in series with a magnetizing voltage E_z. A single winding (autotransformer) connection would serve for illustration but would hardly seem as versatile.

The properties the magnetizing voltage E_z needs to possess are readily recognizable. During positive half cycles E_z must prevent flow of current in the control circuit due to voltage transformed from the primary circuit (NE_{ac}) and during negative half-cycles E_z must accomplish the appropriate magnetization of the transformer core. From these considerations it is seen E_z can be NE_{ac}.

The output current of the single-transformer magnetic amplifier is of half-wave rectified form. Full-wave rectified output is obtained by appropriate paralleling of two single-transformer amplifiers. It is this parallel amplifier with full-wave rectified output which will be the subject of the following discussion.

One example of this type of circuit is shown in Figure 16. The primary or output circuit is the same as the well-known self-saturating bridge-type parallel magnetic amplifier. The transformer secondary terminals are connected in the same way to the same bridge-type circuit with the exception that the load impedance is replaced by the control voltage E_c.

In the primary circuit the full load current flows in alternate half-cycles through core I and core II respectively. The existence of rectifier "b" prevents the application of the line voltage E_{ac} to the core which is not to conduct during any particular half-cycle.

In the secondary circuit the voltages E_{ac}' is chosen to be of the same phase as the a-c line voltage and of magnitude NE_{ac}. The control voltage E_c is again chosen as full wave rectified a-c of line frequency and with variable amplitude.

The equations which govern the circuit during the non-conducting period (positive half-cycle) are:

$$E_{ac} = E_{I}$$
$$NE_{ac} - E_c = NE_{II}$$

and during negative half-cycles:

$$E_{ac} = E_{II}$$
$$NE_{ac} - E_c = NE_{I}$$

During periods of conduction:

$$E_{ac} = I_L R_L$$
$$NE_{ac} - E_c = NE_{II} \text{ (positive half-cycles)}$$
$$-NE_{ac} - E_c = NE_{II} \text{ (negative half-cycles)}$$

This may be summarized using magnitudes as before:

(1) Either core proceeding to saturation will have

$$|E_{I}| = |E_{II}| = |E_{ac}| \tag{23}$$

across its primary terminals in the appropriate direction.

(2) Either core deviating from the saturated state will have in both the conducting and nonconducting periods:

$$|E_{I}| = |E_{II}| = |E_{ac}| - \frac{|E_c|}{N} \tag{24}$$

across its primary terminals in the appropriate direction.

(3) Either core which is saturated will be considered to have zero volts across its primary terminals.

(4) During conducting periods the output current will be:

$$I_L = \frac{E_{ac}}{R_L} \tag{25}$$

Solution of the equations above for the angle at which firing occurs (using the same technique and with the same assumption as in the preceding analyses) gives:

$$\cos\theta_n = \frac{2|E_c|}{|NE_{ac}|} - 1 \quad (n > 1) \tag{26}$$

This means the firing angle for any nth half-cycle is dependent entirely upon the control voltage of the previous half-cycle.

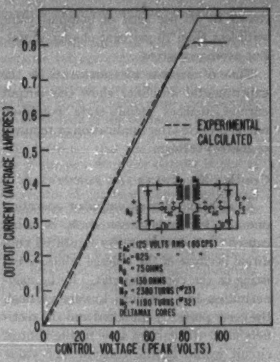

Figure 17. Transfer characteristic new parallel magnetic amplifier

In other words the time for full response is a half-cycle of a-c voltage no matter what be the other parameters of the circuit.

The average output current would be:

$$I_L(\text{avg}) = \frac{1}{\pi}\frac{|E_{ac}|}{R_L}(1+\cos\theta_n) = \frac{2|E_c|}{\pi N R_L} \tag{27}$$
$$= \frac{E_c(\text{avg})}{NR_L}$$

From this it is seen that the average output current is directly proportional to the average control voltage. Further, this output magnitude is independent of the a-c supply voltage. Changes in the line voltage will not affect these relationships so long as the output current is below the saturation value for the amplifier setup.

EXPERIMENTAL VERIFICATION

An experimental amplifier using the circuit herein discussed was assembled and tested. The resulting transfer characteristic is shown in Figure 17 along with the calculated "ideal" characteristic. The results nicely confirm the relationships predicted both in character and magnitude.

The component of R_L, due to the rectifier impedance, is a variable which average value was determined experimentally from voltage measurements at one-half of maximum output current. The minor deviations of the experimental curve for that predicted can, to a great extent, be explained by this choice of constant rectifier impedance.

The output current's independency of line voltage was checked experimentally also. With the control voltage set a constant value to give one-fourth maximum output current the line voltage was reduced to 50 per cent of nominal value with less than 10 per cent change in output average current.

Time of response measurements for the experimental amplifier show the output current reaches steady-state condition one-half cycle after application or removal of control voltage.

Control Currents and Power Gain

At all times during amplifier operation one of the transformer cores is being caused to deviate from its saturated condition because of the voltage relations existing in the control circuit. If the magnetization loops, Figure 1, were vertical, the cores perfectly matched and the rectifiers ideal the current flow in the control circuit would be the constant d-c value corresponding to one-half the width of the magnetization loop. This constant d-c control current would flow through the control source in the direction opposite to the control voltage, that is, the "control power" must be absorbed by the control source. If, however, a constant current of the same constant magnitude were drawn from the control source the net current could be made ideally zero and consequently the "input power" would be zero allowing amplifier "gain" to be infinite. The control current for the experimental amplifier herein used is shown in Figure 18 along with the "ideal" characteristic. Rectifier leakage in the output circuit and "nonideal" cores are easily seen to be principal causes for the decrease in control current as control voltage increases. It has been experimentally determined that the major difficulty arises from the rectifiers.

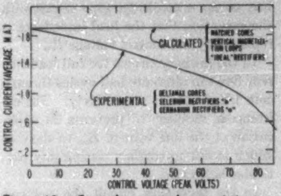

Figure 18. Control current characteristic new parallel magnetic amplifier

It has been experimentally determined that "gains" of more than a thousand can be obtained at 60 cycles per second (with 100 per cent response within a cycle) using materials now abundantly available commercially and without compensating for control current. With care in selections of core materials and rectifiers, "gains" of the order of 10,000 at 60 cycles per second are possible with appropriate circuitry. The response time will remain less than one cycle. This performance is compared to today's commercially available magnetic amplifiers which, with the same response characteristics, exhibit power gains in the range of 20 to 50. Operation at higher frequencies would give increasingly better performance.

Remarks

Elimination of the necessity for magnetizing the transformer cores when a large current flows in their coils and the use of the control source as a passive element whose voltage is measured has resulted in considerable improvement in magnetic amplifier characteristics. The obvious improvement is simultaneous availability of: short response time, high gain, good linearity, wide output range, virtual independence of supply voltage and good output power/weight ratios.

This approach to the magnetic amplifier problem has resulted from a recognition of the fact that the magnetic amplifier is a voltage-sensitive device and not, as generally believed, a current-sensitive device. The only truly independent variable is the control voltage.

Reference

1. Series Connected Saturable Reactor with Control Source of Comparatively Low Impedance, H. F. Storm. *AIEE Transactions*, volume 69, part II, 1950, pages 756–65.

Discussion

Ulrik Krabbe (Thomas B. Thrige, Odense, Denmark): The new coupling for a magnetic amplifier, developed by R. A. Ramey is very promising in some respects, even if it is not as promising as the paper indicates. I am sorry that it is introduced with theoretical considerations on a much lower level.

A reader of this paper not familiar with literature on magnetic amplifiers could easily get the impression that Mr. Ramey's approach to the magnetic amplifier is quite new, and further that engineers working with magnetic amplifier have not understood how it really works. ("The magnetic amplifier is a voltage-sensitive device and not, as generally believed, a current-sensitive device.")

Since Mr. Ramey did not make any acknowledgments to earlier authors, I should like to call his attention to Uno Lamm's work on the transductor.[1] Mr. Ramey's assumptions are nearly the same as Lamm's: idealizing the iron core with a saturation core consisting of two straight lines, the parting of the interval in conducting and nonconducting time interval. Other authors have used the same method, and it seems to me with more consequence than Mr. Ramey.

Does the author mean that the transductor is current-sensitive or voltage-sensitive? Ohms law applies to the control circuit and therefore the one expression may be as good as the other. However there may be a little difference in the expression. It is natural to say that an electronic tube is voltage-sensitive because it is an electrostatic field in the zone around the grid which determines the action. In the same way it is natural to say that the self-saturated magnetic amplifier is current-sensitive since it is a magnetomotive force which determines the flux variation. Mr. Ramey's coupling has a control-circuit with a current partly determined as a difference between a control voltage and an a-c voltage and therefore it may be natural to say that Mr. Ramey's coupling is voltage-sensitive, but that does not change the fact that the correct expression for other couplings is that they are current-sensitive.

The experiments show that the magnetic amplifier is made with Deltamax core and germanium rectifiers, that means the best material available. The control current changes from 1.9 to 0.75 milliamperes when the control voltage changes 80 volts. The output is changed 46 watts. This gives an input of 0.09 watt (the fact that control current changes in opposite direction to the voltage makes no principal difference) therefore the power amplification is 500 and the response time, half a cycle.

This amplification is compared with amplification of "commercially available magnetic amplifiers" with power gain of 20 to 50. This comparison is not just. It would have been considerably more interesting to get a comparison between the new coupling and the conventional type using exactly the same components (rectifiers and iron cores).

Since the power gain 500 is obtained with best possible materials used it is hard to see how it should be possible to get amplification of 10,000 as the author mentions.

When I, in spite of the criticism find the coupling promising, it is because the figure showing the output to control voltage shows very good linearity. A comparison with conventional circuits and the same component should be very interesting.

Reference

1. Some Fundamentals of a Theory of the Transductor or Magnetic Amplifier, A. Uno Lamm. *AIEE Transactions*, volume 66, 1947, pages 1078–85.

F. S. Malick (Westinghouse Electric Corporation, Pittsburgh, Pa.). Mr. Ramey is to be commended for his new approach to magnetic amplifier analysis as well as for his new circuit. I feel that this new circuit will find extensive application as the output stage of multistage amplifiers for the following reasons.

The control voltage which must be used must be of a rather large value in order to overcome the threshold voltage of the rectifiers in the control circuit. Practical linear operation can be attained with saturation occurring at control voltages as low as three volts. Probably the majority of error detecting devices are operated with maximum error voltages considerably less than this. This means that a preamplifier of the simple reactor or self-saturating type must be used to increase the voltage level to a value sufficiently large to control this new circuit.

This new circuit presents an economical means of reducing the time delay in the high power stages. Inexpensive frequency multiplication equipment can be built for the preamplifier stage to reduce the reactor size and consequently the time delay but this method becomes expensive for large powers.

This new circuit does not appear to be suitable for adding signals or operating with bias to shift the characteristic. This means that signal mixing would have to be accomplished in low level stages of the simple reactor or self-saturating type.

Robert A. Ramey: The author wishes to acknowledge the discussions by Mr. Krabbe and Mr. Malick. It is apparent there exists need for clarification of several points made in the paper.

The author regrets that space limitations have not allowed inclusion of reference to the many score of excellent publications which have contributed directly to this study. It was felt that the inclusion of one required inclusion of all.

Superficial examination of the use of a multivalued loop instead of a single-valued function for the magnetization characteristic lends credulence to Mr. Krabbe's remarks regarding their equivalence. In the analysis or the series amplifier the error introduced is indeed quite small. However, when changes (such as additional nonlinear elements, different voltages and frequencies) are made in the control circuit this equivalence disappears. The use of a single-valued magnetization curve cannot anticipate the control circuit currents. These currents are determined by the properties of the materials utilized and consequently realistic assumptions regarding them are required. In all analyses it is the assumptions which dictate the attainable results not the mathematical tools thereafter used. The assumption of a single-valued relation between flux density and magnetomotive force provides a convenient simplification for analyzing these circuits. However this assumption is not realistic except in amplifiers using materials whose a-c magnetization characteristic approximate such relations. These materials are seldom used in high-gain amplifiers.

Recognition of conducting and nonconducting time intervals does not constitute assumption but rather the obvious result of the usual assumption of core saturation.

The author's remarks regarding the voltage-sensitivity nature of magnetic amplifiers are based upon the fact that magnetomotive force does not determine flux variation as the assumption of a single-valued magnetization characteristic would lead one to believe. One has only to look at a family of "hysteresis" loops of any ferromagnetic material and note their variation with voltage, frequency, et cetera to realize the impossibility of determining flux variation from knowledge of magnetomotive force. To assume or infer that this quantity is the independent or controlling variable seems to the author to be a grave tactical error in the attack on the magnetic amplifier problem. However, knowledge of the reactive voltages involved allows one to determine flux variation uniquely. From the practical point of view this means if one has the problem of producing amplifiers which have characteristics which are linear, independent of line voltage and frequency, he must not allow this highly variable control circuit current to affect the circuit operation. In the series magnetic amplifier (wherein the control circuit resistance is relatively low) this problem does not often arise, hence the linear character and independence of a-c line. However in the currently-popular self-saturating circuits (wherein the control circuit resistances are relatively high and magnetizing currents and rectifier leakage constitute a considerable part of the total control circuit current) this problem is quite formidable. Recognition of the fundamental voltage sensitivity of the magnetic amplifier provides solution to this problem through circuits of the type illustrated. Often it is through the results that one sees the value of a point of view. In the magnetic amplifier control circuit, as in the vacuum tube grid circuit, currents exist. The trick in each case is to prevent these currents from affecting the device's operation.

Comparison between the new control circuits and the conventional type using the exactly same components (rectifiers and iron cores) has been made. Experience in the laboratory has shown an improvement of one to two orders of magnitude can be attained in the gain-response time ratio of magnetic amplifiers obtained commercially, when circuits of the new type are simply substituted in place of the conventional resistance-voltage control circuit combination. This is even more remarkable when one realizes that core and winding design was based upon other circuitry and does not take advantage of the properties of the new type of control.

The inference that the superior performance of the new amplifier circuits is due to the use of better materials is unfounded. The results of the researches of industrial laboratories have shown the gain-response time ratio of conventional magnetic amplifiers using Deltamax cores does not essentially differ from that being attained with other materials. The principal advantage to the use of this material lies in its higher saturating flux density. The principal disadvantage lies in its wider magnetization loop (some ten times that of other materials such as Supermalloy). The selenium output circuit rectifiers are stock items of the same quality as those used in commercial amplifiers. The position in which the germanium rectifiers are used has no counterpart in conventional circuitry and therefore cannot be compared.

One of the ways of improving the gain of the new circuits is to utilize materials with narrower magnetization loops. However, until improvement can be made in the output circuit rectifiers, cancellation of control circuit currents offers the most immediate method of realizing higher gain. Since the control circuit relations depend only upon the existence of a control circuit current and not upon its magnitude, functional and average negation of this current may be accomplished by appropriate auxiliary circuitry. The circuit illustration in the paper does not represent the maximum gain attainable with the given materials.

The results Mr. Malick has achieved very nicely confirm those obtained in this laboratory with a single rectifier as the nonlinear control circuit element. It will be interesting to note the results he accomplishes when he examines the use of other types of nonlinear elements in the control circuit.

The author anticipates no considerable difficulty in adding signals or shifting the characteristic. Signals can be added in series and characteristic shift can be accomplished by series constant voltage.

Economic Factors Which Influence Dieselization and Electrification

CHARLES KERR, JR.
MEMBER AIEE

THE DIESEL-electric locomotive has been adopted extensively for new motive power purchases in North America. In many other regions throughout the world (South America, Australia, Europe, Africa, India), electrification has been selected for operation of major railway systems. These differing trends have led to speculation concerning the economic status of these two types of motive power. This paper briefly explains the reasons which have led to these diverse decisions, and attempts to show that they are the logical result of conditions which currently prevail in various parts of the world.

Major railroad systems were created around the steam locomotive with its reciprocating drive. Until the advent of the electric drive, there was no available alternative to the steam reciprocating locomotive for universal railroad application. The remarkable developments which have taken place in the electric drive have shown its superiority to the reciprocating steam locomotive to be so great that the trend today is almost exclusively towards some form of locomotive incorporating the electric drive.

Locomotives utilizing the electric drive may be powered by diesel engines, steam turbines, gas turbines or by overhead trolley systems fed from large central stations. For purposes of this discussion, the diesel-electric and electrification only are considered because the turbine locomotives, either steam or gas, have not received wide commercial application.

Since the diesel-electric and the straight electric locomotive both employ electric transmission of power to the driving wheels of a locomotive, they have, or can be made to have, many identical characteristics for haulage purposes which are superior to the characteristics of the reciprocating steam locomotive. The main difference in these two types lies in the primary source of power for the electric drive. When these primary power sources for the diesel and the electric locomotive are analyzed, it is found that three major differences exist between the two types of locomotives:

1. The diesel-electric locomotive, which must carry its own prime mover, is definitely limited in horsepower output by the capacity of this prime mover, and by the limitations placed on this capacity from weight and clearance restrictions which will differ widely on rail systems throughout the world. The electric locomotive, which receives power from large stationary power sources, is not subject to these same restrictions. Consequently, higher horsepower electric locomotives can always be produced, providing a higher standard of rail operations within the same weight and clearance restrictions.

2. Diesel operation must carry the maintenance expense which accompanies a multiplicity of small mobile prime movers, while electric operation, when electric energy is purchased, avoids this expense. The maintenance of these prime movers comprises 40–50 per cent of the total diesel locomotive repair cost. The maintenance expense of the electric locomotive, including a pro rata share of the distribution system, should be lower when the mobile prime movers are eliminated.

3. Electrification provides a broader range of possible fuels. Electric energy may be produced from residual oils, natural gas, or coal in large steam stations, and in many localities from water power. On the contrary, diesel operation is restricted to diesel fuel which is often in scarce supply and high in price. When available sources of fuel are restricted in volume or in kind, electrification will provide an insurance against fuel shortages or adverse prices to a greater degree than any other type of railroad motive power.

Beside these basic differences in the two types of motive power, there are many others, of a nature peculiar to specific localities or countries, which may have a very controlling influence on the adoption of either diesel or electric motive power. A thorough knowledge of these specific conditions usually will explain why the proper answer to the railroad operating problems of one country does not necessarily apply to all countries.

Dieselization in North America

The widespread adoption of the diesel-electric locomotive by the railroads of North America has created the impression, in some quarters, that railroad electrification is an obsolete form of motive power. An analysis of the conditions which brought about this dieselization does not necessarily substantiate this conclusion.

Most major railroads in North America are privately owned corporations which must have profitable operation for their existence. At the close of the second World War, these railroads were faced with rapidly rising operating expenses which were not accompanied by a proportionate increase in operating revenues, a combination that produced a very unfavorable operating ratio. Motive power on the railroads consisted predominantly of reciprocating steam locomotives whose operation was handicapped by rising fuel costs, and even worse, by labor troubles in the coal industry which caused, on several occasions, serious curtailment of railroad operations and threatened continuation of railroad service. These conditions forced the adoption of a new type of motive power capable of being installed in a short period of time; and a type which would provide immediate operating economies and immediate relief from

---

Paper 51-220, recommended by the AIEE Land Transportation Committee and approved by the AIEE Technical Program Committee for presentation at the AIEE Summer General Meeting, Toronto, Ont., Canada, June 25–29, 1951. Manuscript submitted March 16, 1951; made available for printing May 3, 1951.

CHARLES KERR, JR. is with Westinghouse Electric Corporation, East Pittsburgh, Pa.

troubles incident to the use of coal as the major railroad fuel. The diesel-electric locomotive was the logical answer to the problems which beset these railroads.

The diesel, by its use of the electric transmission, provides a locomotive capable of delivering constant horsepower at the rail over the normal working range. This speed-tractive effort characteristic permits larger trains to be hauled on faster schedules, eliminates double-heading of locomotives, and reduces helper service. These provide operating economies of considerable magnitude. They are the operating benefits of any locomotive which incorporates the electric drive.

The diesel-electric locomotive is a type which lends itself to a high degree of standardization, allowing production of a few models. American industry was prepared to produce this type of locomotive in large quantities. The diesel, therefore, met the demand for a better locomotive which could be produced in a short period of time and which could be operated without demanding extensive changes to the road way and other railroad fixed property. Under prevailing circumstances, it was an immediate answer to a pressing railroad situation which confronted the North American railroad industry.

The tremendous distances spanned by the main line railroads of North America have been an obstacle to extensive electrification and have worked to the adoption of the diesel. To secure the greatest benefits from any type of motive power on these far-flung systems, it is necessary to operate locomotives on long runs. In the case of electrification, this would require installations extending over several hundred or thousands of miles of line. Such installations naturally involve expenditures of great magnitude, especially if detour routes are provided for emergency conditions.

Where railroad systems are privately owned corporations, funds for improvements must be secured from private banks, insurance companies, or by the sale of securities to the public. The credit of many railroads was not sufficiently sound to secure the large funds required for major electrifications at favorable interest rates due to the nature of the credit situation which exists under private ownership.

Locomotives themselves can be purchased on equipment trust loans where the only security offered to the lender is a mortgage on the locomotives purchased. These loans have enjoyed such prestige that money can be readily secured in this manner. More recently, insurance companies have purchased locomotives for rental to the railroads, the latter being under no obligations other than periodical rental payments. With these methods of financing, locomotives are readily securable by any privately owned railroad, more or less regardless of its financial condition because locomotives can be reclaimed and resold should a railroad default on its payments.

The wayside facilities, trolley transmission lines, substations, which are a part of all electrifications, cannot be financed in North America in the easy manner available for locomotive purchases. Money for this type of apparatus requires the sale of bonds, secured by a mortgage on the railroad. This increased fixed indebtedness is not welcomed by any railroad financed by private capital.

Of all factors influencing motive power developments in North America, the fuel situation is probably paramount. This region is fortunately blessed with an abundant amount of diesel fuel which can be secured in practically all sections at a reasonable price. On the contrary, electric power, in the regions through which the densest rail traffic moves, is produced predominantly from coal, a fuel which has risen rapidly in price and has been subject to serious shortages.

One of the past economies of electrification in North America has been a substantial saving in fuel expense, especially comparing electric operation to steam operation. Today, diesel oil can be secured for 8 to 11 cents a gallon almost universally throughout the country, while electric power produced from coal costs 0.8 to 1.0 cents per kilowatt-hour if exceptionally good load factors are secured, and may be even higher if purchased under adverse conditions. With these prevailing prices of diesel oil and electric power, electrification cannot show economy in fuel expense. This particular relationship between these two major sources of energy does not exist in other parts of the world except in limited cases.

There is no evidence that North America will be faced in the immediate future with a shortage of diesel fuel for railroad operations or with a marked increase in its price. In contrast to this ample supply of diesel fuel, the nation has faced a shortage of electric power continuously since the conclusion of the second World War. This shortage has been so serious that the electric power industry has not been in a particularly favorable position to assume major loads such as extensive railroad electrifications. In spite of the greatest expansion of the power industry in history during the past five years, a shortage of power has existed.

In the past decade the railroads of North America have been forced to find an economical type of motive power to replace the reciprocating steam locomotives. The type of motive power selected had to be one of proven economy, one which could be produced rapidly, one which could be readily financed without impairing railroad credit, and one which operated on an abundant, inexpensive and readily available fuel. The diesel-electric locomotive met these conditions for the privately owned railroads.

The diesel-electric locomotive has revolutionized railroad operations in North America. Its use will be extended more and more not only here, but elsewhere throughout the world. But this extended use should not imply that the electric locomotive is an obsolete type of motive power, nor that its use should not be extended wherever conditions exist which make its operation economical.

Motive Power Situation Outside of North America

The conditions which have made the diesel imperative for the railroads of North America do not exist to a similar extent in many other countries.

In spite of its operating advantages, the diesel-electric locomotive would never have reached universal acceptance in North America if that region had not had an abundant supply of oil, with an assured source of supply under all world conditions and with a favorable price level.

A comparison between current fuel prices in the United States and those in a foreign country having an extensive electrified service, is representative of the different conditions which may exist throughout the world, as shown in tabulation below:

	United States	Foreign
Coal per ton (2,000 lb.)	$5.34	$16.80
Diesel oil per gallon	9.09¢	16.1¢
Electricity per kw-hr	1.061¢	0.667¢

With these fuel prices, the relative cost of producing 1,000 horsepower hours of useful work at the locomotive driving wheels is as follows:

	United States	Foreign
With coal	$1.06	$3.38
With diesel oil	$0.80	$1.43
With electric power	$1.06	$0.67

In the United States the average cost of electric power is 133 per cent that of diesel oil, while in the selected foreign country it is only 47 per cent that of diesel oil. In other words, the fuel situation in the foreign country is roughly $2^{3}/_{4}$ times more favorable to electric operation. Conditions similar to these might be cited for other countries which have limited coal and oil resources.

The fuel situation, price, availability, and assurance of supply must be a paramount consideration in any selection of motive power. In any area without an assured supply of oil, electrification offers the widest protection against all uncertainties in sources of fuel for railroad operations. Again, in most countries where a questionable supply of oil exists or where its price is relatively high, electrification will produce a marked operating economy in the operation of heavy traffic rail lines.

Besides economies in fuel, electrification will show other savings, generally speaking, compared to the diesel. Locomotive maintenance should be lower on the straight electric locomotive because the mobile prime movers are eliminated. On most railroads outside of North America smaller trains are operated. The number of locomotives owned per mile of railroad is, therefore, greater, producing a proportionately increased economy in locomotive maintenance by the avoidance of locomotive prime movers.

Most railroads of the world, exclusive of North America, are built for maximum loads per axle of 35,000–40,000 pounds against 60,000–65,000 in North America. It is a more difficult problem to build high capacity diesel-electric locomotives for these roads with weight, clearance and gauge restrictions. On the contrary, high capacity electric locomotives, which do not carry their own prime movers, can be constructed satisfactorily for operation under these prevailing restrictions. Wherever the desire exists to produce a very high standard of service under restricted loadings and clearances, the advantages of electric power become more pronounced. Electric locomotives have been constructed to produce 4,000 rail horsepower per 100 tons on drivers while no American diesel has yet exceeded 1,650 rail horsepower per 100 tons on drivers. This advantage of the electric locomotive under limited weight and clearance restrictions is not appreciated.

Generally speaking, rail systems outside of North America do not extend over comparable distances. Because of this fact, it is often possible to reap the benefits of electrification through rather modest investments for installations of relatively small mileage. The nature of the traffic, supplemented by a higher percentage of locomotives per mile of track makes electrification a more lucrative investment. As most foreign rail systems are government owned, the peculiar financial problems incident to North America do not exist.

The diesel locomotive was made practical by standardization. There has always been a reluctance to standardize electrification systems and their component parts. The economy of electrification could be greatly improved if the railroads would permit a greater degree of standardization, not only as it pertains to trolley voltage, but also motive power. The manufacturers of electric motive power and machinery would welcome standardization. The railroads should reach agreement on a few basic standards and cease preparing difficult specifications to suit some fictitious requirement. This practice has ceased with the diesel, otherwise present prices could never have been attained. The principal need in railroad electrification is to find means to reduce first cost, and if this can be made possible, the field for its economical use will be expanded.

General Summary

Wherever it can be economically justified by traffic density or favorable fuel sources and prices, electrification remains, as it has in the past, the finest method yet devised for operation of the world's major rail systems. By its use a higher standard of service can be produced, the maintenance expense lowered, and in many parts of the world, a decided economy affected in the cost of fuel or energy. Unfortunately, conditions in North America have made it impossible to expand electric operation. The trend in this area, nevertheless, should not prejudice the views of railroad management elsewhere who must operate under radically different economic conditions.

At the moment, two types of power are available with assured background of experience, the straight electric and the diesel-electric. Each type can be built to give a most creditable performance. The important factor is to see that each is applied where conditions are suited for best over-all economy.

In closing this discussion of dieselization and electrification, mention should be made of the gas turbine. In the not too distant future, this type of electric locomotive may be available for general application in road passenger or freight service. It offers certain promising features, especially an ability to burn residual fuels and possibly coal. Its major characteristics as a motive power unit will closely follow those of the diesel, and its widest applications appear to be in services now handled by the larger diesel road locomotives. Where electrification now is justified in comparison with the diesel, it likely will be justified in comparison with the gas turbine.

Discussion

P. A. McGee (Great Neck, N. Y.): Mr. C. Kerr's presentation of the position of diesel motive power on our railroads, I believe, is altogether too apologetic.

Electric transmission of power to the wheels of a locomotive is, of course, ideal, and could just as well be applied to a locomotive with steam power as to a diesel locomotive.

However, the steam electric locomotive, despite the ideal transmission gear and the large amount of money spent on its development has not proved economically practical. There are other reasons for the employment of diesel power besides the electric transmission gear.

In suburban, subway and rapid-transit services where train weight and power demand for frequent rapid accelerations are the controlling factors, direct electric power is the logical and, as of this date, the economic source of power.

The advantages of direct electric power in these services follows from the short time rating of electric transmission which can be fully exploited in this type of service, and the extraordinary light weight of the electric propulsion equipment when applied direct to the car trucks and underframe. A subway train may, for a matter of seconds during acceleration, take over 15,000 horsepower, and the weight of the electric propulsion equipment is less than 30 pounds per horsepower.

Where locomotives are employed as in mainline service the conditions are radically different. With motor car operation, the passenger and his supporting structure supplies the weight necessary to permit the motors to develop the required adhesion for rapid acceleration. Locomotives must have the necessary axle weights to develop their power and to accelerate the trains. With the present development of the art, diesel power plants normally employed in locomotive services in this country weigh around 20 pounds per horsepower. The electric transmission may weigh around 25 pound per horsepower in passenger service. In freight service, the electric transmission

Table I

	Switching per Hour	Freight Per 1,000 Gross-Ton-Miles Inc. L. and T.	Passenger per Car Mile
Coal steam, pounds	887.00	122.00	20.50
Oil steam, gallons	62.88	8.54	1.07
Oil diesel, gallons	6.34	1.60	.28
Kw-hr Electric (1948)	124.00	29.29	3.60

Table II

	United States			Foreign		
	Switching Service per Hour	Freight per 1,000 Gross-Ton-Miles	Passenger per Car Mile	Switching Service per Hour	Freight per 1,000 Gross-Ton-Miles	Passenger per Car Mile
Steam coal	$2.36	$0.33	$0.055	$7.46	$1.03	$0.173
Diesel	$0.58	$0.15	$0.025	$1.03	$0.26	$0.045
Electric	$1.32	$0.31	$0.038+0.004	$0.69	$0.19	$0.024+0.008
*Electric			$0.042			$0.032

* Diesel fuel costs for heating of 0.05 gallon per car mile added to electric passenger costs.

may be considerably heavier. The supporting structure trucks and auxiliary gear may weigh around 100 pounds per horsepower. This gives a total diesel locomotive weight of approximately 150 pounds per horsepower.

Experience in highspeed passenger service indicates that very little advantage would be gained by reduction in locomotive total weight from the 150 pounds per horsepower value, except on practically level track. In freight service today, the tendency is to add ballast to any locomotive unit weighing less than 150 pounds per horsepower. The switching service weights of 250 to 300 pounds per horsepower are found to be the most practical.

Diesel engines in transportation services operating at 1,200 rpm to 2,500 rpm weigh as low as 5 pounds per horsepower. Such power could be applied to locomotives but there would be little sense in reducing the weight of the diesel power plant with a corresponding reduction in reliability, and then add dead ballast to a locomotive to obtain adhesion.

The value of relative lightness of electric locomotives is largely a paper advantage. Our experience with diesel locomotives as stated indicates this fact.

The development of the possible short time rating of an electric locomotive may, in many cases, be very costly. It may seriously increase the maximum power demand and penalize the cost of electric power with negligible operating advantages. The original Chicago, Milwaukee & St. Paul electrification included an elaborate arrangement to control maximum power demands.

In main line service, the self-contained diesel locomotive capable of operating on any rail line without the addition of vulnerable transmission and distribution systems on the right-of-way has a great inherent advantage over any other type of power developed to date, provided it meets the economic requirements of the operation.

The explanation for the wholesale adoption of diesel power on our American railroads is the large economic advantage of this type of power: it is cheaper to buy. A diesel locomotive costs less per horsepower than a thermal plant requires with electrification. It is more flexible in operation, permitting large assignment and crew savings.

Diesel power saves in maintenance and servicing expenses. It is thermodynamically the most efficient unit available.

It gives a large fuel economy when diesel fuel is available.

In this country, the out-of-pocket expenses with diesel locomotive operation are less than half those of steam operation in practically all regions.

It is a matter of passenger-car-mile and freight-ton-mile performance required to determine the period over which the diesels will pay for themselves.

The diesel situation in foreign countries today is just about in the position in which it was in this country 10 or 12 years ago. It is changing rapidly, and I believe since Mr. Kerr's paper was written, at least one of the continents mentioned in the opening paragraph of his paper, as being committed to electrification, has now decided on extensive diesel application.

It is true that axle loads permissible on foreign railroads are limited. However, this requirement is in part compensated for by the fact that they require less horsepower per locomotive and haul much lighter trains with less buff and pulls than normally required in the United States. As a result, designs have been completed and units actually built which, I believe, meet the majority of foreign requirements on standard or larger gauge.

Mr. Kerr mentions that the railroads in this country are privately owned and must obtain their financial support for development and improvement through private sources.

Mr. Kerr also states that due to rapidly rising operating costs with what might be implied to be obsolete steam power, that the railroads were forced to radically change their motive power, and to change it quickly as possible.

The diesel locomotive, as developments show, supplied the answer, and note, without any support from our government.

In referring to railroads outside of North America, Mr. Kerr points out that they are mostly government owned, and as such can more easily finance the heavy expenditures required with electric railroad distribution and transmission systems.

There is no doubt that diesel fuel is scarce in certain countries as is also gasoline. However, it is extremely doubtful that the economy of Africa, Australia, India, or South America could dispense with the automobile, bus, and truck. When you come right down to actual requirements, I believe that you will find that the amount of fuel oil required in these continents to operate their limited rail operations would be negligible in comparison with their gasoline requirements. The fuel situation with regard to diesel power is generally overstressed.

In this connection, I would like to refer to Mr. Kerr's comparison of fuel prices and fuel operating costs.

The fuel unit costs assumed, appear to be quite representative, with the possible exception of foreign electric power. The situation, I feel, is rather unique where electric power at a possible load factor of 40 per cent, with a possible seasonal factor cost of 6.67 mils where coal costs $16.80 per ton and diesel fuel costs 16 cents per gallon.

In measuring the amount of work performed in a given railroad operation, I fear that Mr. Kerr has oversimplified the problem in taking the 1,000-horsepower-hours as a direct operation with the three types of power. To start with, a 1,000-horsepower unit would take between two or three hours to develop 1,000-horsepower-hours of work in main line service, and a switcher locomotive would take at least 10 or 12 hours to produce this work.

To those seriously interested in the relative fuel consumption and cost values with different types of power on American railroads, reference may be made to the excellent records of the Interstate Commerce Commission or Association of American Railroads. If we take the Association of American Railroads record for the latest year published (1949), the unit values of fuel consumption are shown in Table I of this discussion for the three major operations on Class I railroads, on the accounting basis per locomotive hour in switching service, per 1,000 gross-ton-miles in freight service, and per car mile in passenger service.

With domestic fuel costs of: $5.34 per ton coal; 9.09 cents per gallon, diesel; and 10.6 mils per kilowatt-hour, electric; and comparative fuel costs of $16.80 per ton; 16.1 cent per gallon, diesel; and 6.67 mils per kilowatt-hour for electric, respectively, as assumed in Mr. Kerr's paper. See Table II of this discussion which shows the approximate costs that result in the United States and foreign countries with the three types of services considered.

Comparing Mr. Kerr's values with those given in this discussion, it will be noted that with domestic operation, the savings with diesel power over steam or electric is 76 per cent in switching, and over 50 per cent in road services, instead of the 20 per cent shown in Mr. Kerr's table.

In foreign operation, the diesel costs are 50 per cent greater in switching and between 37 per cent and 40 per cent greater in road service, rather than the over 100 per cent shown in Mr. Kerr's table.

In domestic operation, the large fuel savings are well known and understood to be of the order of 50 per cent over coal and electric. In foreign services, I feel that a more thorough investigation is necessary to develop the exact fuel costs before rushing to the foreign and United States treasuries for funds to exploit some hastily conceived projects.

There are many railroad problems which can be most economically answered today with straight electrification.

An abundance of cheap electric power is a most favorable factor, and short-haul mountain or tunnel operation on heavy grades can very well be handled economically with electric power.

With the progress of the automotive industry, and our world-wide economic dependence on liquid fuel, coupled with the very promising developments of liquid fuel from solid fuel, the diesel locomotive deserves a more thorough understanding by foreign railroads, and those interested in their development.

Charles Kerr, Jr.: P. A. McGee's discussion of this paper principally raises only one issue, namely, the relative fuel costs of diesel and electric locomotives. In all other respects he seems to be in virtual agreement with the author.

In his presentation of relative fuel costs, Mr. McGee has taken the comparative figures published by the Interstate Commerce Commission. The author is well acquainted with these reports, but refrained from using them as a basis of comparison in the paper because they are not strictly comparable.

Most electrifications in the United States operate in territory where operating conditions are more severe than average railroad service requirements. Naturally, the power consumed to haul trains in electrified territory is higher than the national average, the latter however being representative of diesel operations.

Consequently, in presenting figures on fuel comparisons, the author felt that strictly comparable costs could best be secured by assuming that all types of locomotives should perform the same amount of work, and from this basis, derives fuel costs from realistic estimates of overall system efficiencies. This presents a more truly representative comparison than that given by Mr. McGee.

Economic Evaluation of Fuel and Energy Sources for Railway Motive Power

T. M. C. MARTIN
ASSOCIATE AIEE

Synopsis: The trend towards widespread utilization of diesel-electric motive power in main-line operations continues unabated with some authorities predicting complete dieselization in the relatively near future. There can be no denying the physical superiority of diesel-electric locomotives over the fast disappearing steam locomotives that have dominated the American motive power scene for over 100 years. There are, however, economic questions of some importance raised by the phenomenal speed with which the change-over is being accomplished and the consequent demand imposed on the nation's middle distillate capacity and the petroleum resources upon which this capacity depends. Locomotives with electric traction motors are probably here for the long pull, but there may be reason to believe that the electrical energy to supply their traction motors can be produced at lower cost in ways other than with diesel-electric prime movers. Under certain circumstances of petroleum product demand and supply the gas-turbine electric locomotive may be found to have an economic justification. Similarly, the trolley-electric locomotive can undoubtedly be justified in situations where hydroelectric, and perhaps other low cost electric generating facilities create a competitive price differential sufficient to overcome the initial cost handicap occasioned in providing the fixed facilities required to bring energy to the pantographs of trolley-electric locomotives. In the Pacific Northwest, for example, it can be demonstrated that on the basis of present prices of electric energy and diesel fuel the extra investment required for operation of trolley-electric locomotives can be recovered from operating savings in about ten years.

Economic Changes Since 1948

IN 1948 the author presented a paper[1] which discussed the comparative costs of coal, residual oil, diesel oil, and electric energy for motive power operation in the Pacific Northwest. Some of the questions raised in that paper have been resolved or at least the solutions have been fairly well determined in the interim. However, at least one new factor, that is, the gas-turbine locomotive has entered the picture, and the basic question of comparative fuel economy remains largely unsolved. It is believed appropriate, therefore, to re-examine the analyses then offered in the light of technologic changes in motive power utilization in the meantime, and with particular regard for the present and prospective national defense program and its probable impact on the availability and price of various fuels.

In the 1948 paper[1] attention was invited to the impressive growth in the numbers of diesel-electric locomotives in use on American railroads, and the prediction was made that before long 50 per cent of all railway motive power work units would be performed by diesel-electric locomotives. That point is virtually here now. By the time this paper is delivered, the Interstate Commerce Commission statistics will reveal that the total work units performed on Class I carriers in the United States are at least 50 per cent attributable to diesel-electric motive power. Some of our railroads have become nearly 100 per cent diesel operated and others, among which are a few of our largest transcontinental carriers, are approaching the 75 per cent point.

At the time the previous paper was written the author was not inclined to make the prediction that the reciprocating steam locomotive would pass entirely from the rosters of American railroads, and he is not now inclined to suggest that this is likely to happen very soon. However, it now is apparent that the reciprocating steam locomotive has suffered a blow that may eventually prove fatal. The latter is no figure of speech, for in the past few years a number of thousands of steam locomotives have been melted down in an endeavor to cash in on present high scrap prices and clear the way for a widespread swing to diesel-electric motive power. It is also in point to record the fact that locomotive builders in this country have virtually ceased the manufacture of reciprocating steam locomotives, and have retooled their facilities for the production of diesel and gas-turbine-electric units. In the previous paper it did not seem worth-while to mention the gas-turbine-electric locomotive, although two were in experimental development at the time. It still does not seem appropriate to deal with the coal-fired gas-turbine locomotive for it has not yet at least been convincingly demonstrated that it is a practical contender in the motive power field. It is possible, however, to set forth some tentative observations on the probable economics of the oil-fired gas turbine, since one of these types now has a reasonable amount of actual road operating experience in back of it, and its builders have, as a result thereof, a sizable order for additional units for early delivery.

Era of the Electric Traction Motor

There can be little remaining doubt that the railroads have embarked on a course from which there is no easy reversal. Except in the event of an extreme national emergency requiring a drastic cut in petroleum use and a return to coal as an energy source, it seems unlikely that railroads will ever again rely strongly on the reciprocating steam locomotive. The electric traction motor has revolutionized railroading to the point that barring phenomenal developments in the field of hydraulic torque converters it is a reasonable expectation that what-

---

Paper 51-221, recommended by the AIEE Land Transportation Committee and approved by the AIEE Technical Program Committee for presentation at the AIEE Summer General Meeting, Toronto, Ont., Canada, June 25–29, 1951. Manuscript submitted March 26, 1951; made available for printing May 2, 1951.

T. M. C. MARTIN is with Bonneville Power Administration, Portland, Oreg.

Table I. Illustrating Method of Computing Average Tractive Resistance of Selected Sections of Railroad

(1) Compensated Gradient Per Cent	(2) Miles Per Hundred Miles, Per Cent	Tractive Resistance: (3) Grade, Pounds	Tractive Resistance: (4) Traction, Pounds	Tractive Resistance: (5) Total, Pounds	(6) Column (2) × Column (5) (Plus Values)	(6) Column (2) × Column (5) (Minus Values)
Typical Light Profile						
0.0	35	0	6	6	210	
0.2	55	4	6	10	550	
0.3	5	6	6	12	60	
0.8	5	16	6	22	110	
Total	100				930	
R_m = 9.3 pounds per ton						
Typical Medium-Heavy Profile						
0.2	10	4	6	10	100	
0.4	10	8	6	14	140	
0.8	15	16	6	22	330	
1.6	20	32	6	38	760	
−1.4	20	−28	6	−22		−440
−0.6	15	−12	6	− 6		− 90
−0.3	10	− 6	6			
Total	100				1,330	−530

R_m = 13.3 pounds per ton.
R_r = 5.3 pounds per ton.

ever the primary energy source employed the means of creating actual tractive effort at the rail will be the electric traction motor. The question of whether main-line railway motive power will be electric or not is largely decided—it will be. What has not been fully determined as yet is whether the electricity which drives the traction motors of the locomotives will be generated in a central station and conveyed to the locomotive through a transmission-trolley-pantograph system, or whether it will be generated on the locomotive with a relatively small internal-combustion engine or turbine as prime mover. As was stated in the previous paper, generation of power on the locomotive has certain undeniable advantages. The locomotive is rendered independent of all trolley limitations. This is not an unmixed blessing, however, either technologically or economically speaking. Relatively small locomotive-borne prime movers have a number of limitations largely associated with space and weight considerations that influence their design within railway clearance diagrams. The most serious limitations of the self-contained prime mover types of locomotives arise, however, from economic factors. With the failure of the coal-fired, internal-combustion turbine thus far to qualify, it becomes apparent that the self-contained units are now, and promise for some time to come to be dependent upon petroleum in some form as fuel. The diesel utilizes a middle-distillate product and the gas turbine at present utilizes a special product, apparently a form of residual but somewhat higher in cost than the ordinary run of bunker fuel.

Table II. Fuel and Energy Requirements for Operation over the Typical Profile Illustrated in Table I

	Light Profile	Medium-heavy Profile
Ruling grade (per cent)	0.8	1.6
Total tractive resistance on ruling grade (pounds per ton)	22	38
Average tractive resistance		
Motoring (R_m) pounds per ton	9.3	13.3
Regenerating (R_r) pounds per ton		5.3
Total weight of locomotive, tons	230	460
Continuous tractive effort at 16 per cent adhesion, pounds	73,600	147,200
Ratings		
Gross tons	3,340	3,870
Gross tons trailing	3,110	3,410
Fuel and energy requirements per *KGTM*		
Gallons of diesel fuel	1.58	2.26
Gallons of gas-turbine fuel	2.32	3.32
Kilowatt-hours	27.9	33.0
Fuel and energy requirements per locomotive mile (including locomotives)		
Gallons of diesel fuel	5.28	8.75
Gallons of gas-turbine fuel	7.75	12.85
Kilowatt-hours	93.2	127.7

Derivation of Working Equations

It is the purpose of this paper to compare the competitive costs of operating diesel-electric, gas-turbine-electric, and trolley-electric locomotives under varying conditions of profile. The basic physical relationships and working equations that are useful in analyzing the comparative costs are:

$$\text{work} = \text{energy} = \text{distance} \times \text{force} \qquad (1)$$

$$\text{energy} = \text{power} \times \text{time} \qquad (2)$$

The basic units of the above equations are feet, pounds, foot pounds, et cetera, and are seldom used in practical applications. The more familiar practical units and equivalents between the electrical, mechanical, and thermal units involved will be derived. These latter relationships are not exact, but are entirely adequate for the purpose.

Energy Units

One horsepower hour = 1,980,000 foot pounds

One kilowatt-hour = 2,640,000 foot pounds

Power Units

One horsepower = 33,000 foot pounds per minute

One horsepower = 1,980,000 foot pounds per hour

One kilowatt = 44,000 foot pounds per minute

One kilowatt = 2,640,000 foot pounds per hour

Thermal Units

One British thermal unit = 780 foot pounds

Let

KGTM = thousands of gross ton miles
R = average total tractive resistance in pounds per ton
W = work done against *R* per *KGTM*

Taking

$$\text{work} = \text{distance} \times \text{force} \qquad (1)$$

and converting to practical units

$$W = 1{,}000 \times 5{,}280R$$

Expressing *W* in heat units

$$W = \frac{1{,}000 \times 5{,}280}{780} R$$

$$W = 6{,}800R \text{ (in Btu)} \qquad (3)$$

It is necessary to assume heat values for the fuels to be considered, and to fix some practical values for the over-all utilization efficiencies that can reasonably be expected when recognition is given the everyday working load factors that locomotives will be likely to be operated at in main-line service. The efficiencies assumed below are the result of test data assembled over a period of years on two Western railroads.

Let

D = gallons of diesel fuel per *KGTM* as burned in Diesel-electric road locomotives
G = gallons of gas-turbine fuel per *KGTM* as burned in gas-turbine road locomotives

Table III. Comparative First and Operating Costs of Diesel-Electric and Trolley-Electric Locomotives Operating over 400-Mile Division

Typical Medium-heavy Profile—Price Levels of Mid-1951

	Diesel-Electric		Trolley-Electric	
Primary energy source		diesel fuel		hydroelectric energy
Total annual locomotive miles		3,000,000		3,000,000
Annual miles per locomotive		150,000		150,000
Gross tons trailing per locomotive		3,410		3,410
First cost of items that vary with type of motive power				
20 locomotives at $600,000 each		$12,000,000		$12,000,000
Electrification fixed facilities				
400 miles of trolley and transmission line and structures at $22,500 per mile				9,000,000
50,000 kva frequency changers at $75.00 per kva				3,750,000
100,000 kva trackside substations at $12.50 per kva				1,250,000
Communication and signal changes				2,000,000
Total first costs where differentials exist		$12,000,000		$28,000,000
Operating Costs	Per Locomotive Mile	Per Year	Per Locomotive Mile	Per Year
Fuel and energy				
8.75 gallons diesel fuel per locomotive mile at 11.0 cents per gallon	$0.96	$2,880,000		
127.7 kilowatt-hours electric energy per locomotive mile at 4.0 mils per kilowatt-hour			$0.51	$1,530,000
Lubrication	0.04	120,000	0.01	30,000
Locomotive repairs	0.64	1,920,000	0.32	960,000
Locomotive depreciation at 5.0 per cent	0.20	600,000	0.20	600,000
Electrification fixed property costs				
Depreciation at 3.0 per cent			0.16	480,000
Operation and maintenance			0.10	300,000
Total annual costs where differentials occur	$1.84	$5,520,000	$1.30	$3,900,000

Assumed heat contents of fuels as received are:

Diesel fuel = 140,000 Btu per gallon
Gas-turbine fuel = 150,000 Btu per gallon

and over-all utilization efficiencies are assumed to be:

Diesel fuel = 40,000 Btu per gallon or 28.6 per cent efficiency
Gas-turbine fuel = 27,000 Btu per gallon or 18.0 per cent efficiency

Substituting in

$$W = 6{,}800R \qquad (3)$$

$$D = \frac{6{,}800}{40{,}000}R = 0.17R \qquad (4)$$

$$G = \frac{6{,}800}{27{,}000}R = 0.25R \qquad (5)$$

Equations 4 and 5 are basic equations which will permit determination of the approximate quantities of diesel oil and gas-turbine fuel required per thousand gross ton miles against varying values of average tractive resistance.

Additional notation is required for derivation of expressions for electric energy requirements as follows:

Let

$SKWH_m$ = kilowatt-hours per $KGTM$ (as measured at the 3-phase 60-cycle supply sides of substations feeding railway loads, motoring)

$SKWH_r$ = kilowatt-hours per $KGTM$ (as measured at the 3-phase 60-cycle supply sides of substations feeding railway loads, regenerating)

e = average over-all electric efficiency between the rail and the 3-phase 60-cycle supply sides of substations feeding railway loads

A number of different values of e will be appropriate depending on the particular type of transmission system, voltage, current, trackside substations, locomotives, et cetera, which are employed. Experience with the 12-kv 25-cycle system of the Great Northern Railway has demonstrated the accuracy of using e equal to two-thirds, and for the purposes of this paper that value of efficiency will be assumed.

Therefore

$$\text{Work} = \text{distance} \times \text{force} \qquad (1)$$

$$SKWH_m = \frac{5{,}280 \times 1{,}000 \times 3}{2{,}640{,}000 \times 2}R_m = 3.0R_m \qquad (6)$$

and

$$SKWH_r = \frac{5{,}280 \times 1{,}000 \times 2}{2{,}640{,}000 \times 3}R_r = 1.3R_r \qquad (7)$$

and net input energy will be

$$SKWH_m - SKWH_r \qquad (8)$$

Note the subscripts on the average tractive resistances used in equations 6 and 7.

R_m = the average total tractive resistance opposing movement

R_r = the average net tractive resistance assisting movement in all cases where the component resulting from downgrade movement exceeds numerically the components attributable to all other types of resistance

Equations 6 and 7 must be computed separately and then offset as in equation 8 to obtain final net energy requirements in all cases where regeneration is a factor to be considered.

Profile Analysis

Table I illustrates a suggested short-cut method of computing the average tractive resistance that has been found very useful. It yields adequate approximations where the principal purpose is a comparison of the same profile operated with different kinds of motive power. Where absolute accuracy is requisite a more rigorous and detailed treatment will be appropriate. The light profile is typical of many miles of railroads located in the East and Midwest, whereas the medium-heavy profile is typical of a good deal of mileage of the Western group of carriers.

It is important to recognize that fuel and energy must be expended moving locomotives as well as trailing loads, and some method of quickly compensating for fuel and energy required by locomotives is desirable, and fortunately rather easily devised. The method which will be described rests upon the assumption that most modern locomotives which utilize electric traction motors as the means of creating tractive effort motorize all axles which means that total weight and weight on drivers are equal. Further, it has been fairly well established that good everyday conservative rating of these same locomotives limits normal continuous tractive effort to 16 per cent of locomotive weight. Engineers cheerfully argue this continuous adhesion question at great length and with little practical result, but the fact remains that a considerable body of empirical evidence points to 16 per cent as being something railroad men can live with. In any event where the same adhesion is used for all motive power types being compared, the absolute value of adhesion chosen cancels out, and the argument becomes academic.

Equivalent Fuel Requirements

It now is possible to demonstrate the use of equations 4, 5, 6, and 7 utilizing the tractive resistance values shown in Table I.

The proper resistance values are:

For light profiles:

$R_m = 9.3$ pounds per ton

For medium-heavy profiles:

$R_m = 13.3$ pounds per ton
$R_r = 5.3$ pounds per ton

Taking the light profile:

$$\begin{aligned} D &= 0.17R_m \\ &= 0.17\times 9.3 \\ &= 1.58 \text{ gallons of diesel fuel per } KGTM \end{aligned} \tag{4}$$

$$\begin{aligned} G &= 0.25R_m \\ &= 0.25\times 9.3 \\ &= 2.32 \text{ gallons of gas-turbine fuel per } KGTM \end{aligned} \tag{5}$$

$$\begin{aligned} SKWH_m &= 3.0R_m \\ &= 3.0\times 9.3 \\ &= 27.9 \text{ kilowatt-hours per } KGTM \end{aligned} \tag{6}$$

The medium-heavy profile yields:

$$\begin{aligned} D &= 0.17R_m \\ &= 0.17\times 13.3 \\ &= 2.26 \text{ gallons of diesel fuel per } KGTM \end{aligned} \tag{4}$$

$$\begin{aligned} G &= 0.25R_m \\ &= 0.25\times 13.3 \\ &= 3.32 \text{ gallons of gas-turbine fuel per } KGTM \end{aligned} \tag{5}$$

$$\begin{aligned} SKWH_m &= 3.0R_m \\ &= 3.0\times 13.3 \\ &= 39.9 \text{ kilowatt-hours per } KGTM \end{aligned} \tag{6}$$

$$\begin{aligned} SKWH_r &= 1.3R_r \\ &= 1.3\times 5.3 \\ &= 6.9 \text{ kilowatt-hours per } KGTM \end{aligned} \tag{7}$$

$$\begin{aligned} SKWH_m - SKWH_r &= 39.9-6.9 \\ &= 33.0 \text{ kilowatt-hours per } KGTM \end{aligned} \tag{8}$$

By assuming reasonable weights of locomotives operating over the profiles shown in Table I it will be feasible to calculate the comparative quantities of fuel required per locomotive mile. An appropriate locomotive for the light profile might consist of two average diesel-electric cabs which may be assumed to be 115 tons each giving a locomotive weight of 230 tons. For the medium-heavy profile a locomotive corresponding to four diesel-electric cabs having a total weight of 460 tons seems to be indicated. Gas-turbine-electric and trolley-electric locomotives of weights equal to the diesel locomotives are assumed in each case. These latter two types might, however, consist of less cabs than their diesel counterparts. Table II sets forth the resulting calculations of fuel and energy quantities for the two types of profiles.

Example—Electrification versus Dieselization

It is likewise possible to take a selected example and compare the probable costs to operate a given section of railroad by different methods. Let the comparison, for example, be related to electrification or dieselization for a 400-mile section of medium-heavy profile such as shown in Table I with a ruling grade of 1.6 per cent, and as a further assumption employ the locomotive weights used in Table II. The section of railroad chosen may be assumed to be in the Pacific Northwest, and the prices used may be taken as those actually prevailing as of Mid-1951. Principal factors and related comments follow:

1. Diesel fuel cost delivered on locomotive. (average over the area) = 11 cents per gallon

2. Electric energy cost delivered to 3-phase 60-cycle sides of railway substations = 4.0 mils per kilowatt-hour.

3. First cost of locomotives are assumed to be equal at $60,000 each, and annual depreciation at 5.0 per cent is likewise assumed to apply to both the diesel-electric and trolley-electric types.

4. The cost of locomotive running repairs is taken at two-thirds of direct fuel cost for the diesel-electric type and the same item for trolley-electric locomotives is taken at one-half the diesel-electric cost. The first assumption is well borne out by data collected from a number of roads and published by one of the diesel manufacturers. The latter assumption arises from analyses of actual repair costs of both types on a Western carrier.

5. The first cost of electrification (fixed property) is based on Mid-1951 estimated prices for structures, trolley, transmission, frequency conversion, trackside substations, and includes an allowance of 14 per cent for engineering, tools, contingencies, supervision, taxes, and clerical exclusive of communication and signal changes which are provided for in a separate item.

6. Depreciation rate for electrification fixed properties is taken at 3.0 per cent.

7. Traffic for this section has, for convenience, been assumed to be consolidated on a freight basis only. All locomotives are assumed to run with trailing loads equal to their rated capacity on the 1.6 per cent ruling grade, and the entire rosters of 20 locomotives of both types are assumed to average 150,000 miles each per year. The total annual locomotive mileage is thus taken at 3,000,000, and therefore, the total annual consolidated traffic is 10,230,000 thousands of gross ton miles trailing. This is equivalent to an average of approximately 35,000 tons each way per day over the 400-mile section.

The above factors, combined to illustrate the effect of motive power choice upon initial capital costs as well as annual operating expenses, are shown in Table III.

Only such items of cost and expense as vary with the type of locomotive are shown in this analysis.

Under the assumed circumstances it is evident that although it would cost $16,000,000 more in the first instance to install the necessary transmission, catenary, and other trackside equipment to permit the use of trolley-electric locomotives on such a hypothetical 400-mile section, it would cost $1,620,000 per year less to operate such a system than to operate the same section with diesel-electric locomotives. Annual savings of such magnitude would permit the amortization of the additional first cost in approximately 10 years. In view of the fact that the prices used for diesel fuel and electric energy are those currently in effect it is clear that the possibility of paying out in less than 10 years cannot be entirely ruled out. Most authorities are of the opinion that further upward adjustment of prices is far more likely in the petroleum field than in hydroelectric power.

Reference

1. THE PRESENT COMPETITIVE POSITION OF COAL, RESIDUAL OIL, DIESEL OIL, AND ELECTRICITY AS ENERGY SOURCES FOR MOTIVE POWER OPERATION IN THE PACIFIC NORTHWEST, T. M. C. Martin. *AIEE Transactions*, volume 67, part II, 1948, pages 1664–69.

Discussion

W. A. Brecht (Westinghouse Electric Corp., East Pittsburgh, Pa.): Mr. Martin's estimates of the savings that can be made with electrification as compared with dieselization in the Pacific Northwest are based on 4 mils per kilowatt hour for electric energy. This is a very favorable rate, probably only half the rate that can be obtained for steam generated power in the East.

Based on a similar economic study made at Westinghouse, Figure 1 has been prepared which shows the per cent return on the additional investment for electrification

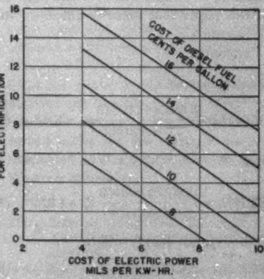

Figure1

with varying costs of diesel fuel and electric power. Mr. Martin's figures of 4 mils for electric power and 11 cents per gallon for diesel fuel show a return of 9.5% on this chart, which agrees very closely with his estimate of a 10 per cent return. Figure 1 of the discussion shows that, at prevailing costs for diesel fuel, electrification can be justified only with very cheap power.

Future trends in liquid fuel and power costs will determine the future of railroad electrification. The probabilities are that liquid fuels will rise more rapidly over the next decade than electric power.

Mr. Martin's first-cost estimates for frequency changers and substations are lower than present day prices for this type of equipment.

Static Capacitors for High-Voltage Use in Japan

K. KITAGAWA
ASSOCIATE AIEE

T. OMORI
NONMEMBER AIEE

Synopsis: Over 4,000,000 kilovars of static capacitors designed for power-factor improvement and voltage regulations have been manufactured in Japan. About half have been used for voltage regulation at primary substations in place of synchronous condensers and are directly connected to lines operating from 11 to 77 kv. The largest installation has a capacity of 80,000 kilovars. More than 60 per cent of the electric power in Japan comes from hydroelectric sources that are remote from their load centers and synchronous condensers are generally installed at the end of the long transmission lines for voltage regulation. This offers an excellent field for static capacitors. The development of a paper dielectric several times thicker than standard capacitor papers has permitted the construction of single capacitors rated as high as 500 kilovars. The cost of a comparable new unit is less than a third of that of a conventional unit of 30 kilovars, the largest generally made. This has made the static capacitor a strong competitor of the synchronous condenser. A number of technical difficulties have been encountered. Waveform distortion, in particular, has caused abnormal current flow resulting in false operation of relays and excessive vibration and noise in transformers. This distortion was found to be due to magnetic saturation of the transformer cores and could be avoided by inserting a suitable reactor in series with the capacitor. Another technical problem concerned the development of a switch for frequent operation in the range from 11 to 77 kv. Operation of these capacitors and switches over a period of 10 years has proved their effectiveness. The first 66-kv series capacitor in the world was placed in service in March 1945.

Use of Static Capacitors in Japan

AT THE end of 1932, not more than 10,000 kilovars of static power capacitors were installed in Japan.[1,2] At this time, low-cost oil-filled capacitors were put on the market by Sumitomo Electric Industries, Limited, of Osaka. The demand increased gradually and there are now more than 4,000,000 kilovars of capacitors installed for both power-factor correction and for voltage regulation of transmission lines, some of which are in Korea, Manchuria, and Formosa.

An outstanding feature of these installations is that more than half are used for voltage regulation in place of synchronous condensers. Table I lists the principal installations, the highest working voltage being 77 kv and the largest capacity being 80,000 kilovars. The largest single bank that is switched on and off by a single switch is rated at 10,000 kilovars. Single capacitor units are designed for operation up to 30 kv and have capacities as great as 500 kilovars. Units of 200 to 300 kilovars are common. For large installation at voltages exceeding 33 kv, these units are connected in series-parallel as shown in Figures 1 and 2.

More than 60 per cent of the electric power generated in Japan is obtained from hydroelectric installations that are located at substantial distances from the load centers that they serve. Large synchronous condensers supply capacitive kilovars at the end of the long transmission lines to provide voltage regulation. Static capacitors could be used in place of the synchronous condensers if the relative costs justify their use.

With conventional dielectric paper having a thickness of 0.01 millimeter, it is difficult mechanically to build large capacitors and they are generally restricted to sizes of about 30 kilovars. Their costs have been higher than for comparable synchronous condensers on a kilovar basis.

A paper of suitable quality that is several times thicker than the conventional paper has been developed by the writers and their collaborators. This paper permits the construction of units of about 500 kilovars at a cost that is less than a third of the former cost. These static power capacitors are now economically and technically competitive with the synchronous condenser and are sometimes used in parallel with it. The capacitors may be mounted in the open and as a 200-to-300-kilovar unit weighs about a ton, they may be conveniently handled without special equipment.

If only static capacitors are used for voltage regulation, the rotating equipment and the third winding on the associated transformer may be avoided. The initial installation of these new capacitors was made in 1937 and comprised a bank rated at 22,000 kilovars. Operation was at 22 kv and through the transformer provided voltage control of a 154-kv transmission line at the Suishako power plant near Seoul, Korea. Many additional installations have been made since then in Japan and as may be seen in Table I permit great flexibility as some operate independently, others are associated with on-load tap changers, and some are paralleled with static reactors or with existing synchronous condensers. In the latter installations, Table I shows only the rating of the static capacitors and does not include that of the associated synchronous condenser.

Various technical difficulties were encountered in the early installations. One of the chief troubles was due to waveform distortion. It caused abnormally high current to flow at the higher harmonics and resulted in faulty operation of relays as well as excessive vibration and noise from the transformers or induction motors connected to the line. A satisfactory remedy was to insert a suitable reactor in series with the capacitor.[3]

Paper 51-223, recommended by the AIEE Transmission and Distribution Committee approved by the AIEE Technical Program Committee for presentation at the AIEE Summer General Meeting, Toronto, Ont., Canada, June 25–29, 1951. Manuscript submitted October 25, 1950; made available for printing May 15, 1951.

K. KITAGAWA is with the Sumitomo Electric Industries, Ltd., Osaka, Japan, and T. OMORI is with the Nisshin Electric Company, Ltd., Kyoto, Japan.

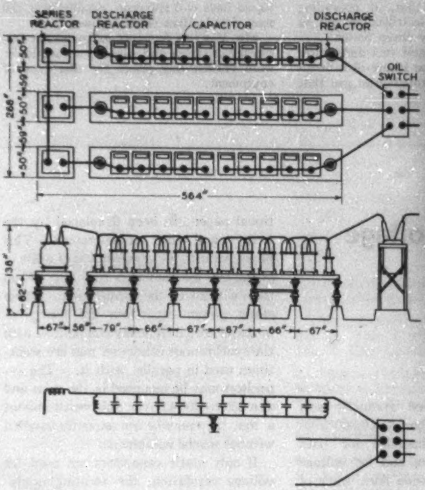

Figure 1 (left). Connection diagram of 66-kv 3-phase 50-cycle 10,000-kilovar capacitor consisting of 24 units of 334 kilovars each

Figure 2 (above). Installation of 66-kv 10,000×3-kilovar capacitor for voltage regulation of a 154-kv transmission line

This improved the waveform so that it was better than it had been before the insertion of the capacitor. The effectiveness of the capacitor in improving power factor and voltage regulation was retained.

The size of the series reactor is related to the order of the harmonics that are emphasized. The reactor aids also in minimizing switching transients and in suppressing restriking in switching.

Another difficulty was the design of switches for these capacitors. It is necessary to vary the amount of kilovars as the load changes and particular difficulties were encountered in switching large-capacitance banks in the range from 11 to 77 kv. Ordinary switches with some modifications served for circuits up to 33 kv, and several types of oil switches were developed for use above 22 kv. Figure 3 is a representative oil switch for use at 66 or 77 kv. It uses a "slit" type of contact system in which there are eight contacts in series. Operation is satisfactory and capacitors may be disconnected without restriking.[4] It is desirable, however, that simpler and more economical designs be developed.

Table II lists a group of installations using series capacitors. These installations in general result in overcompensation of line reactance. The first 66-kv series capacitor in the world[5,6] was put in service in March 1945.

Table I. List of Installation of High-Voltage Capacitors for Voltage Control of the Transmission Lines up to 1950 (Japanese Made)

Voltage, Kv	Total Capacity of Static Capacitor, Kva	Bank Capacity, Kva	Year Set up	Location
77	60,000	10,000	1948	Osaka with R.C.
	30,000	10,000	1947	Kobe with R.C.
	30,000	10,000	1947	Itami with R.C.
	30,000	10,000	1947	Osaka with R.C.
66	7,200	3,600	1938	Sendai S.C. only
	30,000	10,000	1942	Korea with R.C.
	36,000	6,000	1942	Korea S.C. only
	24,000	6,000	1943	Manchuria S.C. only
	27,000	4,000	1947	Kyushu S.C. only
		5,000	1942	Kyushu S.C. only
	15,000	5,000	1949	Kyushu S.C. only
	30,000	10,000	1950	Tokyo with R.C.
There are 13 other 66 kv installations				
44	40,000	10,000	1941	Manchuria S.C. only
	20,000	5,000	1948	Ube with T.C.
33	1,500	1,500	1935	Kyoto S.C. only
	40,000	10,000	1944	Formosa with R.C.
	15,000	5,000	1948	Tokyo S.C. only
7 other installations are set besides the above				
22	32,000	2,000	1937, 1941	Korea with T.C.
	20,000	5,000	1943	Manchuria with T.C.
	20,000	5,000	1949	Hokkaido S.C. only
9 other installations are set besides				
11	80,000	5,000	1938, 1942	Kobe with R.C.
		7,125	1943	
	42,000	6,000	1942	Manchuria with T.C.
	60,000	5,000	1943	Korea S.C. only
There are 6 other installations of more than 30,000 kva capacity				

R.C. = Static capacitor with rotary condenser.
T.C. = Static capacitor with on-load tap changer.
S.C. only = Static condenser only.

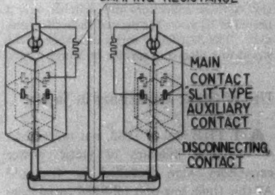

Figure 3. Construction of slit-type 8-contact capacitor switch for 77-kv use

Figure 4 (left). 22.3-kv single-phase 60-cycle 334-kilovar unit for 3-phase 77-kv use

Figure 6 (right). The extinguishing chamber and mounting of balancing resistors

Capacitors

Capacitors for use at voltages between 2,200 and 77,000 are manufactured according to the same principles and methods as are used for oil-filled cables. Several capacitor elements using kraft paper from 0.05 to 0.125 millimeter in thickness and between 500 and 850 millimeters in width, together with 0.015-millimeter aluminum foils are hermetically sealed in a sheet-metal box. Metallic pipe connections to the box permit thorough vacuum drying and impregnation with a refined insulating oil so that no voids are left within the dielectric.

The volume of the elements and impregnant will vary with temperature as a result of ambient changes and operation. This is automatically compensated for by using a reservoir having flexible metallic walls. The internal pressure is maintained slightly above atmospheric to prevent any air invasion from outside.

Figure 4 shows a group of capacitors rated at 334 kvar for operation at 22,300 volts and 60 cycles. The flexible-walled reservoir may be seen at the top. Externally, capacitors for 3-phase operation differ from these only in size and in the number of insulated terminals. Capacitors shown in Figure 4 are 58 inches high; $29^{5}/_{8}$ inches wide; and $42^{7}/_{8}$ inches deep.

While the use of thick paper may appear to be a backward step in capacitor design, the electrical characteristics of the capacitors made with cable paper are more stable than are obtained with the use of tissue paper. The high voltages and kilovar ratings also are evidence of the adequacy of the design and the materials.

A capacitor is a complex structure of insulating paper and impregnant. A third important consideration is the moisture content and voids that may exist in the dielectric path. It has been found that the elimination of moisture and voids can be attained more readily with cable paper than with tissue paper. Moreover, the tissue paper is weakened mechanically by heating and evacuation to remove moisture and voids and is more liable to be damaged in the process of manufacture than is cable paper. Also, it is more expensive to handle tissue paper than cable paper in the capacitor-manufacturing processes.

Cable paper in widths up to 800 millimeters can be readily handled in manufacture and permits the size of the capacitor element to be greater than if tissue paper were employed. This is one reason why units as large as 500 kilovars may be assembled from as many as ten individual capacitor windings.

The cost per kilogram of cable paper is only a third that of tissue paper. These factors are significantly instrumental in making cable-paper capacitors low enough in cost to compete effectively with synchronous condensers. Figure 5 shows relative cost plotted against kilovar rating for capacitors in the range from 3.3 to 11 kv and operation at 60 cycles.

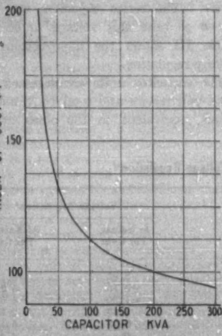

Figure 5. Index of cost of capacitors for 3.3-kv to 11-kv 60-cycle use

Waveform Distortion

The increase in the intensity of harmonics that accompany the use of capacitive loading of lines may become so serious as to challenge the use of the capacitors. The source of these higher harmonics is attributed chiefly to magnetic saturation of the iron cores of transformers, induction regulators, and similar equipment. The waveform distortion[8] due to the higher harmonics is

Table II. Series Capacitors in Japan, Korea, and Manchuria

			Line Constant			Rating of Capacitor		
Case No.	Place Installed	Year Installed	Voltage and Cycles	Distance, Km.	R & JX Ohm	Normal Current, Amperes	Normal Voltage	X Ohm
1	Kyushu	1938	3,300 50	27.8	85 +j2.6	20	1,600	80
2	Manchuria	1939	22,000 50	93.0	51.4 +j23.1	65	4,500	69.4
3	Okayama	1941	3,300 60	20.0	13.7 +j8.76	47	520	11
4	Tohoku	1942	3,300 50	9.4	4.9 +j7.2	60	194	3.23
5	Osaka	1944	3,300 60	10.8	10.17 +j5.22	72	215	3.01
6	Korea	1944	22,000 60		37.1 +j24	140	2,520	18
7	Korea	1945	66,000 60	136.0	22.8 +j25	275	9,100 (11,000)	32 (40)

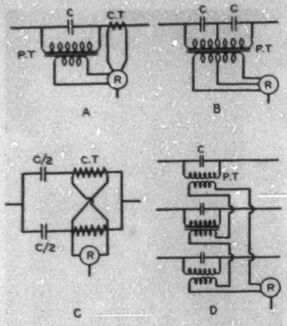

Figure 7 (left). Protection devices for dielectric faults in series capacitors

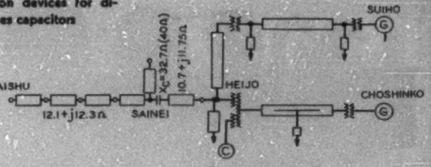

Figure 8. Outline of transmission system to which a 66-kv series capacitor was added

likely to be greatest in the case of light loading of the line. It is considered good practice in some countries to disconnect the capacitor under these conditions through the use of a relay sensitive to currents or voltages at the significant higher harmonics. Another method is to distribute the capacitors over the system at the nearest possible position to the load. In Japan, this problem has been met by the use of a series reactor of such value as to make the load inductive at the higher harmonics.

The use of delta-connected transformers in 3-phase distribution systems makes the third harmonic unimportant so that only the fifth or higher harmonics need be considered. A series reactor will be effective if its inductive reactance at the fifth harmonic is greater than the capacitive reactance of the capacitor at this frequency. As the operating conditions of a circuit are not generally known, a practical arrangement is to use a series reactor having a reactance slightly more than 4 per cent greater than the capacitive reactance of the capacitor so as to resonate or give a total inductive reactance at the fifth harmonic. By this means, the waveform of any circuit can be corrected. The reactor will also serve to restrict the transient phenomena set up by switching operations.

Consideration is being given to the use of a reactor to resonate the third harmonic to earth as a method of eliminating the tertiary windings of transformers.

Switches

When several capacitor groups in the voltage range of 3,300 to 11,000 volts are installed, disconnect switches[4] are usually provided for each group and a main circuit breaker for over-all bank protection. Switches for capacitors must meet some special requirements: they must be nonrestriking; suppress excessive inrush current; and permit frequent operation. The usual type of circuit breaker has been designed for switching large inductive loads and does not always meet the requirements for capacitive loads.

For voltages up to 11,000, restriking may be avoided by increasing the opening speed with plain break contacts. Although this type may be used on circuits as high as 33 kv, a multicontact arrangement has been developed for the range from 22 to 77 kv. Oil or gas-pressure types also have been tried. Figure 6 illustrates the construction of the extinguishing chamber of the capacitor switch known as the "Saigeki" or slit type, in which eight contacts are arranged in series. In each slit contact, the arc is confined to the narrow space between special fiber plates. This multicontact principle permits the opening speed to be held to 2.5 meters per second on circuits between 22 and 77 kv. To reduce the inrush current to reasonable values when the capacitors are connected to the circuit, damping resistors are inserted during part of the opening and closing operation. The resistance is about 10 or 20 per cent of the reactance of the capacitors being switched.

The effectiveness of the multicontact arrangement is fully realized only if all contacts have the same resistance and recent practice has been to provide so-called balancing resistances to bridge each contact.

Series Capacitors

The first series capacitors[5,6] in Japan were installed in 1938 on a 3,300-volt line. Several sets ranging up to 66 kv have since been put in service and are listed in Table II. Their general characteristics are as follows:

1. Overcompensation for the inductive reactance of the line is the normal condition as the main purpose of the installation is to increase the load capacity of the system.
2. Ordinary induction-type relays without high-speed devices are used to protect the capacitors from overvoltage on the 3,300-volt lines. For 22,000 volts and over, simple sphere gaps (Cases 6 and 7) or a modified device of the Westinghouse type (Case 2) are used.
3. Abnormal behaviour such as may occur in switching transformers under light load is suppressed by connecting in parallel to the capacitor a reactor having an inductive reactance about 10 per cent of the capacitive reactance.
4. In case of fault, the capacitor is short circuited by one of the methods shown in Figure 7; scheme "A" being used for Case 2, scheme "B" for Case 7, scheme "C" for Case 3, and scheme "D" for Case 6.

66-Kv Series Capacitor

The first 66-kv series capacitor ever to be put in service was installed in Korea in March 1945. It was designed to increase the load capacity as well as to improve voltage regulation.

In the transmission line shown in Figure 8, the voltage at Kaishu was expected to drop to 56 and to 52 kv for loads of 10,000 and 15,000 kw, respectively. The series capacitor was designed to raise this voltage to 66 kv. Table III shows the improvement in voltage regulation.

The capacitor units are designed for 6,600-volt service and total 14.73 microfarads, equivalent to 180 ohms at 60

Table III. Improvement of Voltage Regulation

Power Factor of Load, Per Cent	X	Voltage Regulation* At Sainei, Per Cent	Voltage Regulation* At Kaishu, Per Cent
80	Without capacitor	3.95	10.1
	With capacitor of 30 ohm	−0.30	5.2
	With capacitor of 40 ohm	−1.00	4.0
90	Without capacitor	2.25	8.7
	With capacitor of 30 ohm	0.62	5.1
	With capacitor of 40 ohm	0	4.4

* Percentage of voltage difference between 6,000 and 15,000-kw loads, based on the voltage at 6,000-kw load.

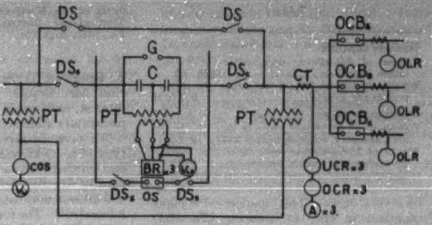

Figure 9. General connections and protective devices for 66-kv series capacitor

BR:	Voltage balance relay	OCB:	Oil circuit breaker
UCR:	Under current relay	OS:	Oil switch
OCR:	Over current relay	DS:	Disconnecting switch
OLR:	Over load relay	CT:	Current transformer
V:	Volt-meter	PT:	Potential transformer
A:	Ammeter	G:	Spark gap
COS:	Change over switch	C:	Series capacitor

cycles per second. A total of 66 capacitors are required for the 3-phase system. There are 11 capacitors in parallel and two such groups in series for each phase, providing a reactance of 32.7 ohms. Sixty and 54 capacitors will provide 36 and 40 ohms, respectively. The normal maximum load current is 275 amperes and the terminal voltage at the series capacitors is 9,000 to 11,000 volts corresponding to kilovar ratings of 7,400 and 9,150 and impedances of 32.7 and 40 ohms. The rated voltage of the unit capacitor is 6,600 and the apparent total capacity of the 66 units amounts to 16,000 kilovars.

The capacitor bank is protected against overvoltage by being short circuited by a spark gap and by an oil switch operated by an overcurrent relay of the induction type. The overvoltage is computed to vary between 28,000 and 140,000 volts. Excessive excitation current may flow in the transformer associated with the capacitor when switching under no load or light load. To avoid this, the series capacitor is automatically short circuited under these conditions and is inserted in the circuit only when the load current exceeds some predetermined value. This arrangement does not limit the usefulness of the series capacitor because it is required only when the load current is large.

If any single capacitor unit fails, the entire bank will be short circuited by a relay responsive to the voltage unbalance across the two series capacitor groups. Figure 9 shows the general connections and protective devices.

Although several synchronous machines are used both before and behind this series capacitor, no instability problems were encountered and the anticipated improvements in increasing the output voltage were attained. It is regretted that no further operational data can be presented as the war ended shortly after installation was placed in service.

References

1. Power Condensers in Japan, S. Bekku. Conference on Large High-Voltage Electric Systems (Paris, France), June 1939.

2. Power Condensers, K. Kitagawa. Ohm Company, Japan, 1942.

3. Improvement of Voltage Waveform by Static Condensers for Power-Factor Improvement, K. Kitagawa, T. Tanaka. *Electrotechnical Journal* (Tokyo, Japan), April 27, 1939.

4. On the New Oil Switch for Condenser Use, K. Kitagawa, R. Arai. *Journal*, Japanese Institute of Electrical Engineers, April 1942.

5. On the Protective Device of Series Condenser, K. Kitagawa, R. Arai. *Journal*, Japanese Institute of Electrical Engineers, April 1941.

6. Installation of Series Condenser on Extra High Voltage Long Transmission Line, T. Omori. *Journal*, Japanese Electrical Manufacturers' Association, September-December 1945, page 17.

Discussion

Hamilton Brooks (Westinghouse Electric Corp., East Pittsburgh, Pa.). The authors have given an interesting survey of Japanese capacitor applications and designs. Certain statements, however, may lead to false conclusions unless amplified. For example, the authors state: "The cost of a comparable new unit (that is 300 to 500 kilovars) is less than a third the cost of a conventional unit of 30 kilovars, the largest generally made. This has made the static capacitor a strong competitor of the synchronous condenser." This is not challenged in so far as it may apply to Japanese practice, but it is not generally true, and does not apply to American designs. American capacitor units of 15- and 25-kilovar unit ratings are produced at a lower cost per kilovar than can be realized with 500-kilovar units, and equipments using these units are lower in cost than synchronous condensers.

Large unit or tank type capacitors are by no means new, having been supplied by various European concerns for some 25 years, and are still manufactured by some companies. The small unit or cell type capacitor was chosen for American development, and the few attempts to introduce tank type designs in this country have been abandoned because they were not competitive.

The design factors of the two types of construction have little in common. With the cell construction, the thermal and mechanical aspects are minimized and the maximum use can be made of the dielectric qualities of the insulation. Accordingly, American development has emphasized improvements in dielectrics and this has resulted in greatly increased kilovar ratings without increasing the volume of material. Thus the American cell type of unit has progressed from the 2-kilovar unit of 1922, through stages of 5, 10, 15, and 25 kilovars with little if any change in unit volume. The early 2-kilovar units used thick, cable-type paper and transformer oil, as is evidently now used in Japan. These 2-kilovar units gave good service, even when made with available conventional materials and superficial processing, simply because of the mass of insulation employed. The modern 25-kilovar unit, no larger than the original 2-kilovar design, has been made possible only because of the development of extremely pure and uniform thin papers, synthetic dielectric liquids of high stability, refinements in processing, and advances in manufacturing control. The cell type of construction permits the designer to make full use of these dielectric improvements.

With the tank type of construction thermal and mechanical problems are paramount. The volume and thickness of insulation necessary to satisfy these requirements is such as to make it uneconomical to perfect the dielectric properties beyond the level of general insulation quality. For tank construction, therefore, it is fitting to use cable-type papers and oil impregnation. With the thick insulation, satisfactory levels of insulation strength may be attained with the degree of processing that is possible with the large unit.

Because the design factors appropriate to the cell construction are not applicable to tank construction, a 500-kilovar unit using the practices employed in a modern 25-kilovar unit would be unworkable. Similarly, a 25 or 30-kilovar unit using the design factors of a Japanese 500-kilovar unit would be highly uneconomical as is shown by the authors curve, Figure 5. Sufficient information is not contained in the paper to allow a close comparison of American cell type capacitors with the Japanese tank type. However, the dimensions of a 334-kilovar unit are given, and a statement made to the effect that a 200 to 300 kilovar installation weighs about a ton. Table I is obtained from these data.

A cost comparison between capacitors and synchronous condensers may be made

Table I

Japanese Capacitor	
Volume of 334-kilovar unit, cubic inches per kvar	220. 0
Weight of 200 to 300-kilovar unit, pounds per kvar	6.7 to 10
American Capacitor	
Volume of 12–25-kilovar units in an open assembly, cubic inches per kvar	77.0
Weight of 12–25-kilovar units in an open assembly, pounds per kvar	3.8

on several bases. The Japanese cable paper capacitor is said to compete effectively with synchronous condensers. A recently published American comparison[1] is reproduced in Figure 1 of the discussion. The curve shows the approximate relative cost of shunt capacitors and synchronous condensers. The capacitors are Y-connected and switched in five steps. Costs do not include main circuit breakers, land space, foundations or spare parts but do include freight, automatic control, erection, capacitor fuses, and coolers on the synchronous condenser. In curves *A* and *B* the losses are evaluated at 150 and 250 dollars per kilowatt respectively. The American capacitor using 25-kilovar units is lower in cost than the synchronous condenser up to very large ratings, and is much lower in all cases when losses are evaluated.

The adaptability of the cell type of capacitor to mass production contributes in no small degree to its economic manufacture. The requirements for distribution circuits as well as transmission line applications can be met in the majority of cases by one of five standard voltage ratings of 25-kilovar unit. In addition to low cost, small size, and light weight; the American cell type capacitor has many other advantages. Among these are simplification of stock and spare parts, flexibility of application, interchangeability, and extreme over-all reliability in large installations when properly applied with individual unit fuses.

REFERENCE

1. ELECTRICAL TRANSMISSION AND DISTRIBUTION REFERENCE BOOK (book), Central Station Engineers of the Westinghouse Electric Corporation. Westinghouse Electric Corp., East Pittsburgh, Pa., 1950, page 255.

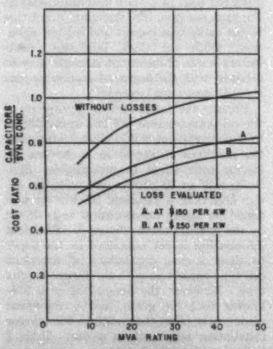

Figure 1. Approximate relative cost of shunt capacitors and synchronous condensers

K. Kitagawa, T. Omori: The authors have read Mr. Brooks' discussion with much interest, and would like to add some complementary statements.

We have compared the costs between cell type 15 to 25-kilovar units using thin paper and synthetic oil as dielectrics, as generally used in America, and our tank type 200 to 500-kilovar unit using cable type paper and mineral oil. The former, as far as we know, cost $5.00 to $7.00 (1,800 to 2,500 yen), and the latter, $1.95 to $2.20 per kilovar (700 to 800 yen), in 1950 when our report was prepared. Now, however, as of April of 1951, the cost of ours has risen to between $3.00 and $3.30 (1,100 to 1,200 yen), per kilovar.

Small capacity cell type units (30 kilovar or lower) are manufactured in Japan too, and the cost of them is about $4.50 per kilovar.

In comparison with synchronous condensers, the capacitor is more advantageous in Japan than in America. Figure 2 of the discussion shows an example of cost ratio in April 1951, of an 11-kv, 5 × 9,000-kilovar capacitor installation (including installation frame, series reactors, discharge reactors, oil switches, control panel, and so forth), to an 11-kv 45,000-kva hydrogen-cooled outdoor synchronous condenser. Other conditions are the same as those indicated by Mr. Brooks and are only for the case without loss considerations. The capacitor costs only one half or one third as much as the synchronous condenser. This might be a peculiar case, but capacitors generally cost less than synchronous condensers in Japan.

As Mr. Brooks says, thermal and mechanical problems which are not important in the cell type capacitor, become paramount in tank type (large capacity unit) capacitors. Many of these problems have been successfully overcome in our type of capacitor.

Table II

60 cycle 30-kilovar unit..................cell type
volume 104.6 cubic inches per kilovar
weight 6.6 pounds per kilovar
60 cycle 300-kilovar unit..................tank type
volume 89.3 cubic inches per kilovar
(excluding feeding tank portion)
weight 6.7 pounds per kilovar
(including feeding tank portion)

Temperature restraint is one of the fundamental factors, and in our case the allowable temperature at the hottest point can be taken as 80 degrees centigrade or higher because of the high stability or high durability of dielectrics. This is a result of using high refining methods, cable type paper, and low viscosity mineral oil.

On the other hand, the most desirable case is when the heat generation is equal to heat dissipation at allowable highest temperature. That is, the volume of the capacitor cannot be less than that which provides the necessary dissipation area. Lowering of volume of the capacitor to less than this limitation has no meaning. And so, if the large capacity unit is designed well economically and technically—from the over-all aspect both of manufacturing and application—it is needless to decrease the volume of the capacitor by using expensive dielectrics of high dielectric-constant unless there is a great decrease of dielectric loss factor.

Synthetic oil was once tried for cell type capacitors in Japan also, but was soon abandoned mainly for economical reasons.

Electrical properties of our capacitor are excellent and its reliability, long durability and nondeterioration, are highly recognized in all fields. For example, the insulation thickness is not taken in as much as the discusser supposes. The 334-kilovar unit in

Figure 2 (right). Cost ratio of capacitors to synchronous condensers in America and Japan

(A). 45,000-kva synchronous condenser is taken as 67,500 kva (150 per cent nominal rating for the consideration of lagging kilovar operation

(B). Without consideration for lagging kilovar operation

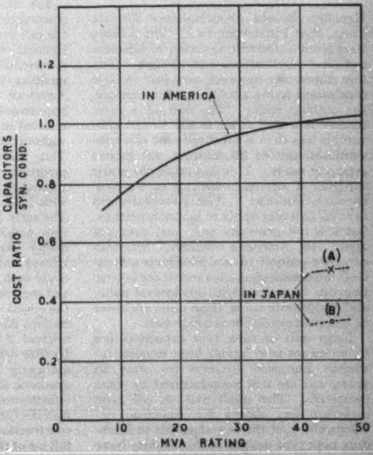

Figure 4 of the paper whose volume Mr. Brooks estimated is for 77-kv line use, and is designed with a somewhat lower voltage gradient, such as 10,000 volts per millimeter, than the ordinary case which takes the greater safety factor for probable abnormal voltage in extra-high-tension lines into account. For 3,300 volt use, for example, the volume and weight of capacitor are as shown in Table II.

From these figures, compared with those in America as shown by Mr Brooks, it is seen that the difference of volume or weight comes mainly from difference of dielectric constant.

Volume per kilovar estimated by Mr. Brooks from Figure 4 may be corrected by excluding the feeding tank portion: volume of 334-kilovar unit for 77-kv use is 125 cubic inches per kilovar.

Furthermore the thin capacitor paper costs about three times the thick paper, and with thick paper we can easily construct a 25-kilovar element against a 5-kilovar element with thin paper. These are the main reasons for the lower price of Japanese capacitors compared with American ones.

It must be added that large unit capacitors are more advantageous for large group capacity installations. For example, in making up 10,000 kilovar, 20 units of 500 kilovars are easier to assemble than 400 units of 25 kilovars.

The tank type is more stable physically and mechanically for open air use.

Tensorial Analysis of Integrated Transmission Systems

Part I. The Six Basic Reference Frames

GABRIEL KRON
MEMBER AIEE

Synopsis: A method of analysis is outlined to solve steady-state problems arising in the operation of large interconnected transmission systems exchanging power between their own operating divisions and outside companies. Special attention is paid to the calculation of total and incremental losses for economic loading studies and to the allocation of incremental losses between the various subsidiary and outside companies. This first part restricts itself to lay the necessary foundations for the numerical study made in a companion paper[1] on the system of the American Gas and Electric Company.

Introduction

The Pioneering Works of George and Ward

As power transmission systems grow in size and the ties between them multiply, many new problems arise in their steady-state operation that cannot be solved entirely on an a-c network analyzer. Such problems are for instance the determination of the most economic loading of various plants, the allocation of transmission losses among the various divisions of the integrated system or among outside companies that merely transfer power across portions of the system. The demand for a systematic and scientific solution of such problems to replace the present-day approximations is increasing rapidly.

After the publications of Steinberg and Smith[2] on fuel rates, the pioneering work in placing the study of economic loading of transmission systems on a more rational basis is due to E. E. George.[3] The use of the a-c analyzer in connection with such studies has been pioneered by Ward, Eaton and Hale[4] who also extended the concepts of George and placed them on an analytical foundation. Their work primarily concerned the evaluation of the effect of transmission-line losses upon the economic loading of power plants of a system.

This present paper restricts attention to the formulas of reference 4 for finding the total and incremental I^2R losses of a transmission system. At this point it also is necessary to state some of the assumptions concerning the operation of a system under which the loss formula (equation 5) of reference 4 is valid. Most of these assumptions are not stated explicitly in reference 4 but are emphasized here to help the step-by-step development of the reasoning to follow:

1. All load currents, charging currents, and synchronous-condenser currents of the system vary in the same manner.

2. Whatever values the load currents have at normal load, the ratio of these values remains unchanged, as the loads vary.

3. Whatever values the generator currents have at normal load, these currents remain fixed in phase angle relative to each other but stretch in magnitude individually, as the generator powers vary.

4. As the generator currents stretch, the absolute potentials of the generator and load points of entry automatically assume values to satisfy the voltage drop in the lines. (That is neither the generator voltages nor the load voltages are adjustable.)

5. The generator currents are projected at all loads upon the terminal voltages existing at normal load and these current projections are considered as representing the generator powers.

The Inadequacy of Conventional Analytical Tools

These contributions bring into sharper focus the inadequacy of present-day methods of thinking to cope with the large-scale analytical needs of the power system engineer. Although the above assumptions about the operating behavior of a single system are about the simplest possible, nevertheless the amount of measurements involved and the amount of numerical calculations needed grow to prohibitive proportions with the size of many present-day systems.

A far more serious objection to the use of conventional methods is their inflexibility. For instance both the total loss formula of reference 4 and the method of measurements are valid only for the above-mentioned limited assumptions. If the engineer attempts to add one more assumption (for instance two hypothetical loads in place of one, or swinging terminal voltages with constant absolute values) the whole loss formula collapses and so does the suggested method of measurement. For every added assumption the engineer is forced to start from scratch to develop an entirely new loss formula and to devise an entirely new procedure of measurements.

There seems to be no question that the solution of the problems of modern interconnected transmission systems require an analytical tool possessing the speed, versatility, and range of an airplane rather than those of an old-fashioned horse and buggy.

The Tensorial Method of Attack

The purpose of the present paper is to introduce a new method of thinking to

---

Paper 51-225, recommended by the AIEE Transmission and Distribution Committee and approved by the AIEE Technical Program Committee for presentation at the AIEE Summer General Meeting, Toronto, Ont., Canada, June 25-29, 1951. Manuscript submitted March 28, 1951; made available for printing May 11, 1951.

Gabriel Kron is Consulting Engineer with the General Electric Company, Schenectady, N. Y.

The writer is indebted to S. B. Crary for initiating the long-range study, to L. Kirchmayer and Charles Imburgia for helpful suggestions.

attack vigorously the problems arising in the every day operation of integrated power systems having several divisions that exchange powers among each other and with outside operating companies. The main characteristics of the new analytical approach are as follows:

1. A set of constants (self and mutual impedances) are established for the transmission system, that are independent of any future assumptions to be made concerning the problems in which the constants are to be used. These constants are to be changed only if the transmission system itself changes. (Either an a-c network analyzer or analytical methods may be used to find these constants).

2. The formulation of the problem, the various assumptions and the steps leading to the final solution are performed in terms of a minimum number of symbols (so-called "tensors") each symbol representing a large group of generators, or loads, or metering points, or relations between them.

3. At each stage of the development the engineer may arbitrarily extend or restrict his assumptions at will to suit his immediate needs, without jeopardizing the validity of any other portion of his analysis.

4. The necessary numerical computations come out automatically in such a systematic form (in terms of matrices) that they may be performed by digital computing devices.

In short, the analytical tool is similar to a high-grade living organism, that can adapt itself equally to the needs of the simplest of system problems, or to those of the most highly elaborate ones that the system engineer may dare or care to undertake.

Problems Solved to Date by The New Method

The following extensions and generalizations already performed may be mentioned as illustrations for the power and possibilities of the new method of thinking:

1. The concepts of "hypothetical" loads, generators, metering points, etc., are introduced, that replace the large number of actual loads, generators, or metering points by a small number, or by one only.

2. Instead of assuming that the ratio of the load currents remains constant as the generator powers vary, it has been assumed that the ratio of the real components of the load currents remain constant and also the ratio of their reactive components.

3. Instead of assuming that the generator and load terminal voltages vary merely to satisfy the voltage drop requirements of the current changes, it has been assumed that as the loads vary, all generators and loads swing in angle, so that the absolute value of their terminal voltage remains constant, or assumes preassigned values.

These last two assumptions enable the engineer to think and talk freely about generator and load powers (real and reactive) instead of merely generator and load currents. A correct accounting for the swing of the reactive powers is thereby assured.

The system to be analyzed may consist of several operating divisions with different types of loads, each division supplying power to the others and to outside companies. The following problems arising in their operation have already been solved, in addition to those mentioned:

1. Calculation of the effects on losses and economic loadings of the interchange powers transferred between the operating divisions themselves, between outside companies across the system, or between the system and outside companies.

2. Determination of the I^2R and I^2X losses incurred in the territory of each division due to a transfer of power across its lines between any other two divisions or outside companies.

3. Determination of the I^2R and I^2X losses incurred due to the utilization of only a limited group of generators to transfer power to outside companies.

4. Determination of the I^2R and I^2X losses due to the existence of "circulating" powers flowing between two neighboring divisions and of "sneak" powers flowing between several companies connected in closed meshes.

Problems relating to interchange power and those relating to the charging for losses incurred in transmitting power through the lines of other companies are often independent of economic loading considerations and need be solved separately.

In attacking any of the above problems it has been necessary to introduce some or all of the following additional complications:

1. Autotransformers exist in the system whose turn-ratio currents also must be considered.

2. Large charging currents exist, that cannot be lumped together with the loads but must be considered as independent variables.

3. The synchronous condensers are treated not as loads but as generators of purely reactive power.

The Algebra of Tensors

The types of system problems under consideration involve steady-state operation and as such they are comparatively very simple mathematically. Their solution involves merely the addition and multiplication of a large number of complex numbers. However in reducing a large number of numerical information to a smaller number, many pitfalls and many unnecessary operations must be avoided along the road. It is true that for such short-range travel a jet-propelled airplane might be uneconomical, nevertheless a helicopter would prove quite helpful in getting to places.

Tensor algebra is a tool par excellence for such a purpose. Since the main goal of transmission line studies is to transform information in terms of complex voltages, currents, and impedances into information in terms of real powers and real losses, such transformations may be accomplished simply, smoothly, and with the least amount of labor by a series of mental operations called "transformations of reference frames." The study of single and integrated transmission systems will involve chiefly the establishment of a series of reference frames (each step characterized by a matrix of transformation). Quite a large variety of reference frames will have to be introduced gradually, such as:

1. Physically existing reference frames and hypothetical reference frames.

2. Reference frames in space and reference frames in time.

3. Stationary reference frames and moving reference frames.

4. Reference frames within the reference frames.

Similarly symbols of tensors will occur, each component of which also is a tensor, whose components again might be still tensors. Moreover the transmission networks themselves will be looked upon partly as mesh-networks, partly as junction networks, and partly as orthogonal networks, when demanded by the immediate problem at hand. In spite of the large number of lines, generators, loads, metering points, and other system components, the manipulation of the multiply compound tensors and of the entire networks will nevertheless be almost as simple as the manipulation of ordinary scalar quantities and single lines or generators.

Constant reference will be made to the author's "Tensor Analysis of Networks",[1] as for instance (TAN page 29). As the development of new physical concepts unfolds, and the complexity of the assumptions increases, eventually the whole apparatus of tensor algebra published in the above book will be put to practical use. Any new concept not covered in that text will be treated here or in future publications in greater detail.

(The solution of many problems relating to the stability of integrated transmission systems will require however a jet-propelled airplane—instead of a helicopter—to arrive at some of the desired goals. The more advanced concepts of tensor analysis will supply such transportation.)

A New, Basic Set of Linear Equations for Power System Studies

The basic set of linear equations available for the analysis of power systems is ohm's law, $\mathbf{E}=\mathbf{ZI}$ where $\mathbf{E}$ and $\mathbf{I}$ represent the real and reactive components of the terminal voltages and currents of all generators and all loads. Unfortunately none of these latter quantities are known, neither are system operators interested in these quantities. What the system operators usually know are the following:

1. The real powers $\mathbf{P}$ supplied by each generator.
2. The real powers exchanged between operating divisions.

What the system operators are interested to find out (from the point of view of this paper) are the following:

1. The total and incremental transmission line losses (both I^2R and I^2X) occurring in each division.
2. The transmission line losses occurring in the territory of each operating division due to the transmission of various types of exchange powers across its lines by other companies.

The purpose of the present paper is to express the performance of integrated power systems as a set of linear equations between the real powers P supplied by the generators and the incremental losses L in the transmission system. In the new set of equations $\mathbf{L}=\mathbf{MP}$ the matrix $\mathbf{M}$ represents a set of real constants that is independent of $\mathbf{P}$ and $\mathbf{L}$, (but does depend upon the state of the system at an arbitrary average load).

The studies mentioned, relating to loss and exchange power calculations and to economic loadings, should be considered merely as opening chapters on a much wider variety of steady-state power-system problems to which the above power equation, and others to be developed, could be applied. The equations to be shown will include both reactive and active generator powers, also terminal voltages with variable absolute values and many other known or unknown system parameters.

The Current-Flow Reference Frames

The Assumptions

In the companion paper[1] an extensive numerical study is made on a simplified representation of the system of the American Gas and Electric Company in order to determine the adequacy or limitations of various assumptions which may be made in economic loading studies. The analytical formulation of that numerical work will serve as the skeleton around which the more general assumptions will eventually be developed.

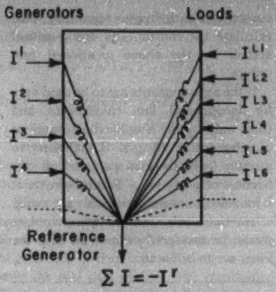

Figure 1. "Measurement" reference frame number 1

George and Ward in their published works restrict their method of measurements and their formulas to obtain merely the I^2R losses of a system. In consequence they do not measure, nor do they calculate any system impedance, $z=r+jx$ not even a resistance r. They measure and calculate "loss coefficients" only. On the other hand the measurements and formulas to be developed here do give the general impedances of the system, so that the results are valid for many other studies besides that of I^2R losses. The real and symmetrical part of all impedance matrices (complex and asymmetrical) here given are identical with the coefficients of equation 5, reference 4. Only in one respect is the present study less general. In the numerical study of the companion paper it was assumed that no autotransformers exist. That assumption is retained temporarily here in analytical study also, in order to strip the latter from all extra encumbrances and reduce it to its barest outline for greater clarity and simplicity. The study will consist of three main steps:

1. The basic measurements, basic constants, and basic impedance matrices of a transmission system are outlined in the conventional "current-flow" reference frames.
2. The currents are replaced by real power and the voltages by incremental I^2R losses.
3. The study of the "power-flow" reference frame begins.

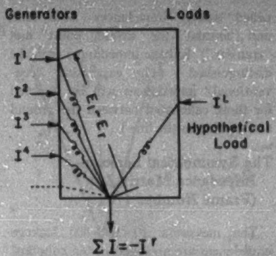

Figure 2. "Leakage" reference frame number 2

To establish the minimum framework, the following simplifying assumptions are made:

1. The whole system is considered as one unit with no subdivisions.
2. Any outside company is represented by one generator at each point of interconnection.
3. No autotransformers exist.
4. Synchronous condenser currents and charging currents are considered as load currents.
5. All loads are replaced by one hypothetical load.

In the second part of the study the previously mentioned approximate assumptions concerning the variation of generator power are considered. The introduction of more general assumptions (such as the variation of generator voltages and reactive powers) is left for future consideration.

The Measurements

Assume normal load conditions and measure all currents and voltages of the generators and loads (Figure 1). The currents in the lines need not be measured, but it is preferable to do so, in order to serve as checks on the calculations, say of the I^2R losses.

For convenience let it be assumed that there are eleven generators and 50 loads. The system constants are measured as follows:

1. Remove all generators, loads, line-charging capacitors, and synchronous condensers.
2. Select any one point as a reference point, say the most heavily loaded generator point of entry.
3. Impress unit current between each remaining *generator* point of entry and the reference point.
4. Measure the differences of potentials (complex numbers) appearing between the reference point and all the generator and load points of entry. (Sixty voltages with each impressed unit current.)

These differences of potentials will be

called "leakage" impedances. Both "self" and "mutual" (or "driving point" and "transfer") leakage-impedances will be distinguished. (The expression "conventional" impedances will be reserved for those calculated between the ground and a point on the line.)

The Symmetrical Leakage-Impedance Matrix $\mathbf{Z}_{11}$ (Frame Number 1)

The measured 10×60=600 leakage impedances are arranged in ten columns, representing one part of the symmetrical "leakage-impedance" matrix.

$$\mathbf{Z}_{11}=\begin{array}{r|cccc|cccc|} & 1 & 2 & \cdots & 10 & L1 & L2 & \cdots & L50\\ \hline 1 & Z_{1,1} & Z_{1,2} & \cdots & Z_{1,10} & & & & \\ 2 & Z_{2,1} & Z_{2,2} & \cdots & Z_{2,10} & & & & \\ & \cdots & \cdots & \cdots & \cdots & & & & \\ 10 & Z_{10,1} & Z_{10,2} & \cdots & Z_{10,10} & & & & \\ \hline L1 & Z_{11,1} & Z_{11,2} & \cdots & Z_{11,10} & & & & \\ L2 & Z_{12,1} & Z_{12,2} & \cdots & Z_{12,10} & & & & \\ & \cdots & \cdots & \cdots & \cdots & & & & \\ L50 & Z_{60,1} & Z_{60,2} & \cdots & Z_{60,10} & & & & \\ \hline \end{array}$$

$$=\begin{array}{c|c|c|} & g & L\\ \hline g & \mathbf{Z}_{gg} & \mathbf{Z}_{gL}\\ \hline L & \mathbf{Z}_{Lg} & \mathbf{Z}_{LL}\\ \hline \end{array} \qquad (1)$$

Because of the symmetry of $\mathbf{Z}_{11}$ the 500 $\mathbf{Z}_{gL}$ components are also known, since $\mathbf{Z}_{gL}=(\mathbf{Z}_{Lg})_t$. However the 50×50=2,500 components of $\mathbf{Z}_{LL}$ are not measured and are left unknown.

The impressed voltage vector is denoted (not calculated) as

$$\mathbf{E}_1=\begin{array}{|cccc|cccc|} 1 & 2 & \cdots & 10 & L1 & L2 & \cdots & L50\\ \hline E_1-E_r & E_2-E_r & \cdots & E_{10}-E_r & E_{L1}-E_r & E_{L2}-E_r & \cdots & E_{L50}-E_r\\ \hline \end{array}=\begin{array}{|c|c|} g & L\\ \hline \mathbf{E}_g-\mathbf{E}_r & \mathbf{E}_L-\mathbf{E}_r\\ \hline \end{array}$$

The current vector is

$$\mathbf{I}^1=\begin{array}{|cccc|cccc|} 1 & 2 & .. & 10 & L1 & L2 & \cdots & L50\\ \hline I^1 & I^2 & .. & I^{10} & I^{L1} & I^{L2} & \cdots & I^{L50}\\ \hline \end{array}=\begin{array}{|c|c|} g & L\\ \hline \mathbf{I}^g & \mathbf{I}^L\\ \hline \end{array}$$

Remarks on the Measurements

On many a-c boards the measurements of currents may be more accurate than those of voltages. In such cases the currents flowing in each line are measured and—knowing the line impedances—the desired difference of potentials are calculated from them by $\mathbf{C}_t{}^*\mathbf{e}$ or by inspection.

When no a-c board is available, the above constants may nevertheless be calculated by subdividing the given network into several sub-networks with a small number of meshes, calculating their leakage impedances, then reestablishing the original network. Procedures are given in TAN pages 133–140.

When the system is large, or is composed of several operating divisions, it is often more convenient to measure the constants of each division separately, then calculate the constants of the resultant system by the above mentioned procedure.

If the measurements are to be used only for incremental loss calculations and those only by the simplified assumptions of reference 4, then it is sufficient to measure only the real parts of all differences of potentials. When however it is intended to consider correctly the swing of reactive powers, the complex voltages should be measured even when only the losses are to be found.

The Introduction of One Hypothetical Load (Frame Number 1-2)

Let the 50 load currents $\mathbf{I}^L$ (complex numbers) measured during normal load be summed up into one resultant current, the "hypothetical" load current

$$I^L=I^{L1}+I^{L2}+\ldots I^{Ln} \qquad (2)$$

Let it be assumed that at any other load the ratio of the load currents remains the same as it is at normal load. That is let, at normal load, the following 50 complex ratios be established:

$$l_n=\frac{I^{Ln}}{I^L}(n=1,\ \ldots\ 50) \qquad (3)$$

The summation of all l_n is unity

$$l_1+l_2+\ldots l_{50}=\frac{I^{L1}+I^{L2}+\ldots I^{Ln}}{I^L}=1$$

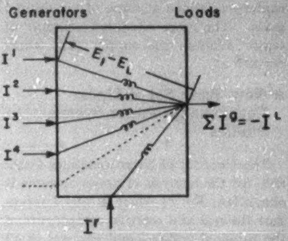

Figure 3. "Through" reference frame number 3

The preceding assumptions are equivalent to establishing a matrix of transformation $\mathbf{C}_L$ between the actual and hypothetical load currents as (TAN pages 141–173).

$$\begin{aligned} I^{L1}&=l_1I^L\\ I^{L2}&=l_2I^L\\ I^{L50}&=l_{50}I^L \end{aligned}\qquad \mathbf{C}_L=\begin{array}{r|c|} & L\\ \hline 1 & l_1\\ \hline 2 & l_2\\ \hline & \\ \hline 50 & l_{50}\\ \hline \end{array}\qquad \mathbf{I}^L=\mathbf{C}_L\mathbf{I}^{L'}$$

(There exists no exactly analogous transformation in TAN.) The currents of the reduced system are

$$\mathbf{I}^2=\begin{array}{|cccc|c|} 1 & 2 & .. & 10 & L\\ \hline I^1 & I^2 & .. & I^{10} & I^L\\ \hline \end{array}=\begin{array}{|c|c|} g & L\\ \hline \mathbf{I}^g & \mathbf{I}^L\\ \hline \end{array}$$

Since the generator currents remain unchanged, the system currents are transformed by (TAN page 216).

$$\mathbf{I}^1=\mathbf{C}_2{}^1\mathbf{I}^2 \quad \Big| \quad \mathbf{C}_2{}^1=\begin{array}{c|c|c|} & g & L\\ \hline g & 1 & \\ \hline L & & \mathbf{C}_L\\ \hline \end{array} \qquad (4)$$

where 1 is the unit matrix.

The Voltage Vector $\mathbf{E}_2$

Next let it be assumed that the power of the single hypothetical load is the same as the sum of the powers of the 50 individual loads (TAN pages 101 and 326). With that assumption the single hypothetical load voltage at normal load could be calculated (if needed) as the weighted average of 50 load voltages.

$$\mathbf{E}_L{}'=(\mathbf{C}_L)_t{}^*\mathbf{E}_L$$

$$E_L=l_1{}^*E_{L1}+l_2{}^*E_{L2}+\ldots l_{50}{}^*E_{L50} \qquad (5)$$

The impressed voltage is by $(\mathbf{C}_2{}^1)_t{}^*\mathbf{E}_1$

$$\mathbf{E}_2=\begin{array}{|cccc|c|} 1 & 2 & \cdots & 10 & L\\ \hline E_1-E_r & E_2-E_r & \cdots & E_{10}-E_r & E_L-E_r\\ \hline \end{array}=\begin{array}{|c|c|} g & L\\ \hline \mathbf{E}_g-\mathbf{E}_r & E_L-E_r\\ \hline \end{array}$$

where each E represents the difference of potential between the ground and a point on the network, Figure 2.

The Asymmetrical Leakage-Impedance Matrix $\mathbf{Z}_{22}$ (Frame Number 2)

Since the system power remains invariant when the fifty load currents are replaced by one hypothetical load current, the measured $\mathbf{Z}_{11}$ is transformed by (TAN pages 109, 327, and 222).

$$\mathbf{Z}_{22}=(\mathbf{C}_2^1)_t{}^*\mathbf{Z}_{11}\mathbf{C}_2^1$$

$$\mathbf{Z}_{22}=\begin{array}{c|c|c} & g & L \\ \hline g & \mathbf{Z}_{gg} & Z_{gL}\mathbf{C}_L \\ \hline L & \mathbf{C}_{Lt}{}^*\mathbf{Z}_{Lg} & \mathbf{C}_{Lt}{}^*\mathbf{Z}_{LL}\mathbf{C}_L \end{array}$$

$$\mathbf{Z}_{22}=\begin{array}{c|cccc|c} & 1 & 2 & & 10 & L \\ \hline 1 & Z_{1,1} & Z_{1,2} & \dots & Z_{1,10} & a_1 \\ 2 & Z_{2,1} & Z_{2,2} & \dots & Z_{2,10} & a_2 \\ .. & \dots & \dots & \dots & \dots & \dots \\ 10 & Z_{10,1} & Z_{10,2} & \dots & Z_{10,10} & a_{10} \\ \hline L & b_1 & b_2 & \dots & b_{10} & w \end{array}=\begin{array}{c|c|c} & g & L \\ \hline g & \mathbf{Z}_{gg} & \mathbf{a} \\ \hline L & \mathbf{b} & \mathbf{w} \end{array} \qquad (6)$$

The resultant impedance matrix is no longer symmetrical. The four groups of components are found as follows:

1. The generator impedances $\mathbf{Z}_{gg}$ remain unchanged. They still form a symmetrical square.
2. The vertical set of mutual impedances **a** between the generators and the hypothetical load are found by $\mathbf{Z}_{gL}\,\mathbf{C}_L$, that is by multiplying each column of the measured impedances by $\mathbf{C}_L$, each 50 multiplications giving one complex impedance "a".
3. The horizontal set of mutual impedances **b** are similarly found by $\mathbf{C}_{Lt}{}^*\,\mathbf{Z}_{Lg}$. Both **a** and **b** are functions of the normal-load currents.
4. The self-impedance w of the hypothetical load cannot be found by $\mathbf{C}_{Lt}{}^*\,\mathbf{Z}_{LL}\,\mathbf{C}_L$, since the 2,500 components of $\mathbf{Z}_{LL}$ have not been measured. There are several simple ways to calculate w however:

   a. One method is to substitute into the last equation of the set (6) the normal-load values of the currents and E_L-E_r. Then the unknown w may be solved.

   b. Another method is shown in the companion paper.[1]

   c. A general method, valid also for several hypothetical loads, will be shown in connection with equation 9.

These self and mutual impedances will serve as the starting points of any future analysis. The following two properties should be noted:

1. The load impedances **a** and **b** are asymmetrical.
2. The load impedances are functions of the load currents existing at normal load.

REMARKS

The same products are used in finding the b impedances that are used for the a impedances, except that the products are added up differently.

$$a=(l'+jl'')(z'+jz'')=l'z'-l''z''+j\times(l'z''+l''z')$$

$$b=(l'-jl'')(z'+jz'')=l'z'+l''z''+j\times(l'z''-l''z')$$

Division by I^L may be performed in equation 6 in place of equation 3. The number of divisions is thereby decreased.

When the measurements are to be used only for incremental loss calculations and those only by the simplified assumptions of reference 4, then it is sufficient to use only the real part of $\mathbf{C}_L$. The resultant $\mathbf{Z}_{22}$ matrix contains again only *real* components, it is symmetrical and the a and b coefficients become equal, each being $(a+b)/2=d$. However if it is intended to consider the reactive power flow correctly even for the loss calculations, or if other types of transmission system studies are to be made, the asymmetrical, complex $\mathbf{Z}_{22}$ must be established.

Physical Interpretation of $\mathbf{E}_2=\mathbf{Z}_{22}\mathbf{I}^2$

The equation $\mathbf{E}_2=\mathbf{Z}_{22}\mathbf{I}^2$ is the basic equation that defines the whole system. It serves as the starting point of all analysis.

The equation refers to a junction network and not to a mesh network (TAN pages 354–378). That is $\mathbf{I}^2$ represents a set of currents, each leaving the network at the reference point of entry (Figure 2) and entering it either at a generator or at the hypothetical load. Similarly each component of $\mathbf{E}_2$ represents the difference of potential between the reference point (a generator) and the points of entry of the various currents. The equation $\mathbf{E}_2=\mathbf{Z}_{22}\mathbf{I}^2$ is merely the inverse of the more customary equation of a junction network $\mathbf{I}^2=\mathbf{Y}^{22}\mathbf{E}_2$.

The active and reactive losses in any network are found by the quadratic form (TAN page 455).

$$P_L=P_L'+jP_L''=\mathbf{I}^{2*}\mathbf{Z}_{22}\mathbf{I}^2=\mathbf{I}^{2*}\mathbf{E}_2 \qquad (7)$$

Nevertheless this reference frame cannot be used for the loss calculations, since the losses come out as differences of large numbers, namely

Losses = generator powers − load powers

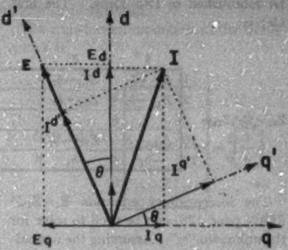

Figure 4. "Time" reference frame number 4

Transformation to the "Through" Reference Frame (Frame Numbers 2-3)

It is necessary to introduce next a reference frame in which the hypothetical load current I^L does not occur as a variable. Its place is going to be taken by the current in the reference generator $I^r=I^{11}$.

To perform the transformation, the following constraint is noted to exist among the system currents (TAN page 157).

$$I^1+I^2+\dots I^{10}+I^{11}+I^L=0$$

From this I^L may be expressed in terms of I^{11} as

$$I^L=-I^1-I^2-\dots-I^{10}-I^{11}$$

Hence the transformation matrix is

$$\mathbf{C}_3^2=\begin{array}{c|ccccc} & 1 & 2 & & 10 & 11 \\ \hline 1 & 1 & & & & \\ 2 & & 1 & & & \\ & & & & & \\ 10 & & & & 1 & \\ \hline L & -1 & -1 & & -1 & -1 \end{array} \qquad \mathbf{I}^2=\mathbf{C}_3^2\mathbf{I}^3 \qquad (8)$$

Note that the two indices of **C** denote the two reference frames between which the transformation is being made.

The new current vector contains only the generator currents.

$$\mathbf{I}^3=\begin{array}{|c|c|c|c|c|} 1 & 2 & .. & 10 & 11 \\ \hline I^1 & I^2 & .. & I^{10} & I^{11} \\ \hline \end{array}$$

The new voltage vector is by $(\mathbf{C}_3^2)_t{}^*\mathbf{E}_2$, Figure 3.

$$\mathbf{E}_3=\begin{array}{|c|c|c|c|c|} 1 & 2 & \dots & 10 & 11 \\ \hline E_1-E_L & E_2-E_L & .. & E_{10}-E_L & E_{11}-E_L \\ \hline \end{array}$$

The Intermediary Equation $\mathbf{E}_3=\mathbf{Z}_{33}\mathbf{I}^3$

The new "through" impedance matrix is found by $(\mathbf{C}_3^2)_t{}^*\mathbf{Z}_{22}\mathbf{C}_3^2$. This product will be established in two steps. The first step is:

$$\mathbf{Z}_{32}=\mathbf{C}_{3}{}^{2}{}_{t}\mathbf{Z}_{22}=\begin{array}{c|c|c|c|c|c|}
 & 1 & 2 & \cdots\cdot & 10 & L \\
\hline
1 & Z_{1,1}-b_1 & Z_{1,2}-b_2 & \cdots & Z_{1,10}-b_{10} & a_1-w \\
2 & Z_{2,1}-b_1 & Z_{2,2}-b_2 & \cdots\cdot & Z_{2,10}-b_{10} & a_2-w \\
\cdots & \cdots\cdot & \cdots\cdot & \cdots\cdot & \cdots\cdot & \cdots\cdot \\
10 & Z_{10,1}-b_1 & Z_{10,2}-b_2 & \cdots\cdot & Z_{10,10}-b_{10} & a_{10}-w \\
11 & -b_1 & -b_2 & \cdots\cdot & -b_{10} & -w \\
\hline
\end{array} \tag{9}$$

The intermediary equation $\mathbf{E}_3=\mathbf{Z}_{32}\mathbf{I}^2$ (TAN page 178) can be used to solve for the unknown "w". Assuming the normal-load generator currents and voltages as known, the first two equations may be solved for the unknown w and E_L. (Hence it is not necessary to measure 50 normal-load voltages to find the hypothetical load voltage E_L by equation 5. But the measurements may serve as a check).

The Asymmetrical "Through" Impedance Matrix $\mathbf{Z}_{33}$ (Frame Number 3)

Performing the second multiplication $\mathbf{Z}_{32}\mathbf{C}_3{}^2$ the resultant is the asymmetrical "through" impedance matrix.

$$\mathbf{Z}_{33}=\begin{array}{c|c|c|c|c|}
 & 1 & 2 & \cdots\cdot & 11 \\
\hline
1 & Z_{1,1}+w-a_1-b_1 & Z_{1,2}+w-a_1-b_2 & \cdots\cdot & w-a_1 \\
2 & Z_{2,1}+w-a_2-b_1 & Z_{2,2}+w-a_2-b_2 & \cdots\cdot & w-a_2 \\
\cdots & \cdots\cdots\cdot & \cdots\cdots\cdot & \cdots\cdot & \cdots\cdot \\
11 & w-b_1 & w-b_2 & \cdots\cdot & w \\
\hline
\end{array} \tag{10}$$

$$\mathbf{Z}_{33}=\begin{array}{c|c|c|c|c|}
 & 1 & 2 & \cdots\cdot & 11 \\
\hline
1 & Z_{1-1} & Z_{1-2} & \cdots\cdot & Z_{1-11} \\
2 & Z_{2-1} & Z_{2-2} & \cdots\cdot & Z_{2-11} \\
\cdots & \cdots\cdot & & \cdots\cdot & \cdots\cdot \\
11 & Z_{11-1} & Z_{11-2} & \cdots\cdot & Z_{11-11} \\
\hline
\end{array}$$

The matrix $\mathbf{Z}_{33}$ is asymmetrical and complex. It may be subdivided into a real part and an imaginary part, each being an asymmetrical matrix

$$\mathbf{Z}_{33}=\mathbf{R}_{33}+j\mathbf{X}_{33}$$

The Calculation of Powers

When the voltage equation $\mathbf{E}=\mathbf{ZI}$ of any network (not necessarily stationary) is given, where $\mathbf{Z}$ is a complex, asymmetrical matrix, then the I^2R losses and the I^2X powers are found by the following steps (proofs will be given in another publication):

1. Divide $\mathbf{Z}$ into a real and imaginary component as $\mathbf{Z}=\mathbf{R}+j\mathbf{X}$.

2. Divide $\mathbf{R}$ and $\mathbf{X}$ each into a symmetrical and a skew-symmetrical part (TAN page 42).

$$\begin{array}{l|l}
\mathbf{R}=\mathbf{R}_s+\mathbf{R}_k & \mathbf{X}=\mathbf{X}_s+\mathbf{X}_k \\
\mathbf{R}_s=(\mathbf{R}+\mathbf{R}_t)/2 & \mathbf{X}_s=(\mathbf{X}+\mathbf{X}_t)/2 \\
\mathbf{R}_k=(\mathbf{R}-\mathbf{R}_t)/2 & \mathbf{X}_k=(\mathbf{X}-\mathbf{X}_t)/2
\end{array} \tag{11}$$

3. The real part of the stored power (the I^2R losses) is found by

$$P'=\mathbf{I}^*(\mathbf{R}_s+j\mathbf{X}_k)\mathbf{I} \tag{12}$$

In most transmission systems the second term is negligible, hence for loss calculations it is sufficient to use only the real, symmetrical part of $\mathbf{Z}$, namely $\mathbf{R}_s$.

4. The reactive part of the stored power I^2X is found by

$$jP''=\mathbf{I}^*(\mathbf{R}_k+j\mathbf{X}_s)\mathbf{I} \tag{13}$$

It is of interest to point out that in equation 6 of reference 4 the coefficients K_{mn} represent the symmetrical part of $\mathbf{R}_{33}$ namely $\mathbf{R}_s$ and the coefficients H_{mn} represent the skew-symmetric part of $\mathbf{X}_{33}$ namely $\mathbf{X}_k$. The former would have been found by transforming only the real, symmetrical part of $\mathbf{Z}_{33}$ with the aid of $\mathbf{C}_3{}^2$.

Physical Interpretation of $\mathbf{E}_3=\mathbf{Z}_{33}\mathbf{I}^3$

The components of $\mathbf{E}_3$ represent the differences of potential appearing between all the generators point of entry and the hypothetical load point, Figure 3. Similarly the currents $\mathbf{I}^3$ represent a set of generator currents, each entering at a generator and leaving the network at the hypothetical load point. The load voltages and currents have disappeared from the picture.

The currents in this reference frame represent the correct load-flow in the system. Hence the powers $\mathbf{I}^{3*}\mathbf{E}_3$ represent the I^2R and I^2X losses in the transmission system in terms of generator currents only, without introducing differences of large numbers.

Transformations from Current Flow to Power Flow

The Four Steps

The second part of the analytical study consists of replacing the generator currents $\mathbf{I}^3$ by the real generator powers $\mathbf{P}$ as variables. For that purpose four successive changes have to be made on the load-flow equations $\mathbf{E}_3=\mathbf{Z}_{33}\mathbf{I}^3$.

1. A new time reference frame is introduced by $\mathbf{C}_4{}^3$ expressing the generator currents in terms of their real and reactive power components existing at normal load.

2. All complex numbers in $\mathbf{E}_4=\mathbf{Z}_{44}\mathbf{I}^4$ are replaced by real numbers. (This change is not considered here as a "transformation of reference frame".)

3. The reactive-power components of the generator currents are expressed in terms of their real-power components by $\mathbf{C}_5{}^4$. Only an approximate method will be shown here for this step, equivalent to the assumptions of reference 4. A more correct method will be given in a subsequent publication.

4. The real-power components of generator currents are replaced by the real powers $\mathbf{P}$ of generators by the transformation $\mathbf{C}_6{}^5$.

The Introduction of New Time Reference Frame Number 4 (Frame Number 3-4)

All complex E and I have the same origin in time, (usually the total load current I^L existing at normal load is taken as the real axis $\mathbf{d}$). Let at normal load the angle of lag of a generator voltage be θ, Figure 4. Also let $I=I^d+jI^q$ and $E=E_d+jE_q$. Then $\tan\theta=E_q/E_d$.

Let now a new time reference frame $\mathbf{d}'$ and $\mathbf{q}'$ be introduced for each generator along its terminal voltage and at right angles to it. Then the components of I', namely $I^{d'}$ and $I^{q'}$ represent the real and reactive power components of I.

The problem is to find $\mathbf{C}_T$ that changes each complex I to I' when the time reference frame is rotated by an angle θ. It is well known that a rotation of a reference frame—while the vector remains stationary—is equivalent to the rotation of the vector in the opposite direction, assuming the reference frame stationary. Hence from Figure 4 for one current

$$I=\epsilon^{-j\theta}I' \qquad \mathbf{C}_T=\boxed{\epsilon^{-j\theta}}$$

where $\epsilon^{-j\theta} = \cos\theta - j\sin\theta$. For all 11 generator currents

$$\mathbf{C}_4^3 = \begin{array}{c|cccc} & 1 & 2 & \dots & 11 \\ \hline 1 & \epsilon^{-j\theta_1} & & & \\ 2 & & \epsilon^{-j\theta_2} & & \\ \dots & & & \dots & \\ 11 & & & & \epsilon^{-j\theta_{11}} \end{array} \qquad (14)$$

The new through matrix $\mathbf{Z}_{44}$ is found by $(\mathbf{C}_4^3)_t^*\mathbf{Z}_{33}\mathbf{C}_4^3$.

Transformations with Diagonal C

Since $\mathbf{C}_4^3$ is a diagonal matrix, $\mathbf{Z}_{44}$ may be found by the following simplified steps, without calculating $\epsilon^{-j\theta_1}$.

1. Form a matrix containing all possible combination of $\epsilon^{j\theta_n}\epsilon^{-j\theta_k} = \epsilon^{j(\theta_n-\theta_k)}$ containing only differences of angles.

$$\mathbf{A} = \begin{array}{c|cccc} & 1 & 2 & & 11 \\ \hline 1 & \epsilon^{j(\theta_1-\theta_1)} & \epsilon^{j(\theta_1-\theta_2)} & & \epsilon^{j(\theta_1-\theta_{11})} \\ 2 & \epsilon^{j(\theta_2-\theta_1)} & \epsilon^{j(\theta_2-\theta_2)} & & \epsilon^{j(\theta_2-\theta_{11})} \\ & & & & \\ 11 & \epsilon^{j(\theta_{11}-\theta_1)} & \epsilon^{j(\theta_{11}-\theta_2)} & & \epsilon^{j(\theta_{11}-\theta_{11})} \end{array} \qquad (15)$$

The angles form a skew-symmetric matrix with unity along main diagonal.

2. Multiply each component of $\mathbf{Z}_{33}$ of equation 10 by the corresponding component of the above matrix and by no other number. The product gives the corresponding component of $\mathbf{Z}_{44}$.

$$\mathbf{Z}_{44} = \begin{array}{c|cccc} & 1 & 2 & \dots & 11 \\ \hline 1 & Z_{1-1} & Z_{1-2}\epsilon^{j(\theta_1-\theta_2)} & \dots & Z_{1-11}\epsilon^{j(\theta_1-\theta_{11})} \\ 2 & Z_{2-1}\epsilon^{j(\theta_2-\theta_1)} & Z_{2-2} & \dots & Z_{2-11}\epsilon^{j(\theta_2-\theta_{11})} \\ \dots & \dots & \dots & \dots & \dots \\ 11 & Z_{11-1}\epsilon^{j(\theta_{11}-\theta_1)} & Z_{11-2}\epsilon^{j(\theta_{11}-\theta_2)} & & Z_{11-11} \end{array} \qquad (16)$$

$$\mathbf{Z}_{44} = \begin{array}{c|cccc} & 1 & 2 & \dots & 11 \\ \hline 1 & Z_{1-1}' & Z_{1-2}' & \dots & Z_{1-11}' \\ 2 & Z_{2-1}' & Z_{2-2}' & \dots & Z_{2-11}' \\ \dots & \dots & \dots & \dots & \dots \\ 11 & Z_{11-1}' & Z_{11-2}' & \dots & Z_{11-11}' \end{array}$$

The voltage vector (still representing the voltage drop between the generators and the hypothetical load) becomes

$$\mathbf{E}_4 = \begin{array}{cccc} 1 & 2 & \dots & 11 \\ \hline |E_1| - E_L\epsilon^{j\theta_1} & |E_2| - E_L\epsilon^{j\theta_2} & \dots & |E_{11}| - E_L\epsilon^{j\theta_{11}} \end{array} \qquad (17)$$

For total and incremental loss studies $\mathbf{E}_4$ need not be calculated.

Changing Complex Equations into Real Equations

The next step is to express the complex equations $\mathbf{E}_4 = \mathbf{Z}_{44}\mathbf{I}^4$ in terms of real quantities. That may be accomplished by introducing twice as many equations and twice as many variables. If

$\mathbf{I} = \mathbf{I}_d + j\mathbf{I}_q$, $\mathbf{E} = \mathbf{E}_d + j\mathbf{E}_q$, $\mathbf{Z} = \mathbf{R} + j\mathbf{X}$

then the new $\mathbf{I}_4$, $\mathbf{E}_4$, and $\mathbf{Z}_{44}$ matrices assume the following form (reference 5, page 147).

$$\mathbf{I}^4 = \begin{array}{cc} d & q \\ \hline \mathbf{I}_d & \mathbf{I}_q \end{array}$$

$$\mathbf{Z}_{44} = \begin{array}{c|cc} & d & q \\ \hline d & \mathbf{R} & -\mathbf{X} \\ q & \mathbf{X} & \mathbf{R} \end{array} \qquad (18)$$

$$\mathbf{E}_4 = \begin{array}{cc} d & q \\ \hline \mathbf{E}_d & \mathbf{E}_q \end{array}$$

The real axes are denoted by **d**, the imaginary by **q**.

The I^2R losses are found by $\mathbf{I}_t^4\mathbf{Z}_{44}\mathbf{I}_t^4$. Calculations of the reactive losses I^2X is left for future consideration.

The Assumption of Constant Generator Q/P (Frame Number 5)

In order to express I^q as a function of I^d, as a first approximation let it be assumed next that as the loads vary, the generator currents stretch in magnitude, while the terminal voltages follow merely the voltage drop requirement of the static network. In that case each generator current I may be replaced by its projection upon the terminal voltage existing at normal load, namely by I^d. That is

$$I^q = sI^d \qquad \mathbf{C}_p = \begin{array}{c|c} & d' \\ \hline d & 1 \\ q & s \end{array} \qquad (19)$$

where s is a real constant, found from normal load measurements as

$$s = \frac{I^{q0'}}{I^{d0'}} = \frac{Q_0}{P_0} \qquad (20)$$

The constant s also represents the ratio of the reactive to active power of each generator at normal load.

The transformation matrix of the whole system is

$$\mathbf{I}^4 = \mathbf{C}_5^4\mathbf{I}^5 \quad \mathbf{C}_5^4 = \begin{array}{c|ccc} & d_1' & d_2' & .. \\ \hline d_1 & 1 & & \\ d_2 & & 1 & \\ .. & & & .. \\ \hline q_1 & s_1 & & \\ q_2 & & s_2 & \\ & & & .. \end{array} = \begin{array}{c|c} & d' \\ \hline d & 1 \\ q & \mathbf{s} \end{array} \qquad (21)$$

The resultant $\mathbf{Z}_{55}$, containing only real numbers, is

$$\mathbf{Z}_{55} = \begin{array}{c|c} & d' \\ \hline d & (\mathbf{R} + \mathbf{sRs}) + (\mathbf{sX} - \mathbf{Xs}) \end{array} = \boxed{\mathbf{R}_{55} + \mathbf{X}_{55}} \qquad (22)$$

Since $\mathbf{s}$ is a diagonal matrix, $\mathbf{Z}_{55}$ is the sum of two matrices.

$$\mathbf{R}_{55} = \begin{array}{c|cccc} & 1 & 2 & \dots & 11 \\ \hline 1 & R_{1-1}'(1+s_1^2) & R_{1-2}'(1+s_1s_2) & \dots & R_{1-11}'(1+s_1s_{11}) \\ 2 & R_{2-1}'(1+s_2s_1) & R_{2-2}'(1+s_2^2) & \dots & R_{2-11}'(1+s_2s_{11}) \\ \dots & \dots & \dots & \dots & \dots \\ 11 & R_{11-1}'(1+s_{11}s_1) & R_{11-2}'(1+s_{11}s_2) & \dots & R_{11-11}'(1+s_{11}^2) \end{array} \qquad (23)$$

$$\mathbf{X}_{55} = \begin{array}{c|cccc} & 1 & 2 & \dots & 11 \\ \hline 1 & 0 & (X_{1-2}')(s_1-s_2) & \dots & (X_{1-11}')(s_2-s_{11}) \\ 2 & (X_{2-1}')(s_2-s_1) & 0 & \dots & (X_{2-11}')(s_1-s_{11}) \\ \dots & \dots & \dots & \dots & \dots \\ 11 & (X_{11-1}')(s_{11}-s_1) & (X_{11-2}')(s_{11}-s_2) & \dots & 0 \end{array}$$

Their sum is (containing only real numbers)

$$\mathbf{Z}_{55} = \begin{array}{c|cccc} & 1 & 2 & & 11 \\ \hline 1 & Z_{1-1}'' & Z_{1-2}'' & & Z_{1-11}'' \\ 2 & Z_{2-1}'' & Z_{2-2}'' & & Z_{2-11}'' \\ & & & & \\ 11 & Z_{11-1}'' & Z_{11-2}'' & & Z_{11-11}'' \end{array} \qquad (24)$$

The impressed voltage is by $(\mathbf{C}_5^4)_t^*\mathbf{E}_4$

$$\mathbf{E}_5 = \begin{array}{c} d \\ \hline \mathbf{E}_d + \mathbf{sE}_q \end{array} \qquad (25)$$

Each component of $\mathbf{E}_5$ represents that portion of $|E_q|$ that is consumed as a voltage drop, while I flows from the generator to the hypothetical load.

The equation $\mathbf{E}_5 = \mathbf{Z}_{55}\mathbf{I}^5$ contains as many scalar equations as there are generators.

This transformation matrix $\mathbf{C}_5^4$ is the key to the flow of the reactive power of the system during a load variation. A more correct form, in which the ratio Q/P is variable, will be presented in another publication.

The exact $\mathbf{C}_5^4$ will include components of the complex asymmetrical $\mathbf{Z}_{33}$ also.

Transformation of Real Currents into Real Powers
(Frame Number 5-6)

Let it be assumed furthermore that the deviation of the generator terminal voltages from their normal-load values is small. That is let the real power of each generator be

$$P = I^{d'}|E|_o \tag{26}$$

where the subscript *o* represents normal-load values.

From this

$$I^{d'} = (1/|E|_o)P \qquad \mathbf{C}_g = d' \overset{d}{\boxed{1/|E|_o}} \tag{27}$$

The resultant matrix of transformation for the whole system is the diagonal matrix

$$\mathbf{C}_6^5 = \begin{array}{c|c|c|c|c|} & 1 & 2 & & 11 \\ \hline 1 & 1/|E_1|_o & & & \\ \hline 2 & & 1/|E_2|_o & & \\ \hline & & & \ldots\ldots & \\ \hline 11 & & & & 1/|E_{11}|_o \\ \hline \end{array} \tag{28}$$

The Power-Flow Reference Frame
(Frame Number 6)

The "Loss" Matrix

The final "loss" matrix $\mathbf{Z}_{66}$ is found in a simplified manner by dividing each component of $\mathbf{Z}_{55}$ by the corresponding component of another matrix $\mathbf{E}_{nk}$. The general component of the latter matrix is the product $E_{nk} = |E_n|_0|E_k|_0$

$$\mathbf{Z}_{66} = \begin{array}{c|c|c|c|c|} & 1 & 2 & \ldots\ldots & 11 \\ \hline 1 & Z_{1-1}''/E_{11} & Z_{1-2}''/E_{12} & \ldots\ldots & Z_{1-11}''/E_{1,11} \\ \hline 2 & Z_{2-1}/E_{21} & Z_{2-2}''/E_{22} & \ldots\ldots & Z_{2-11}''/E_{2,11} \\ \hline \ldots & \ldots\ldots & \ldots\ldots & \ldots\ldots & \ldots\ldots \\ \hline 11 & Z_{11-1}''/E_{11,1} & Z_{11-2}''/E_{11,2} & \ldots\ldots & Z_{11-11}''/E_{11,11} \\ \hline \end{array} \tag{29}$$

where $E_{2,11}$ represents the product $|E_2|_0 |E_{11}|_0$.

$$\mathbf{Z}_{66} = \begin{array}{c|c|c|c|c|} & 1 & 2 & & 11 \\ \hline 1 & Z_{1/1} & Z_{1/2} & \ldots & Z_{1/11} \\ \hline 2 & Z_{2/1} & Z_{2/2} & & Z_{2/11} \\ \hline & \ldots & \ldots & \ldots & \ldots \\ \hline 11 & Z_{11/1} & Z_{11/2} & & Z_{11/11} \\ \hline \end{array}$$

It should be noted that, because of the diagonal matrices $\mathbf{C}_4^3, \mathbf{C}_5^4$, and $\mathbf{C}_6^5$, each component of $\mathbf{Z}_{66}$ (a real number) may be found from the corresponding component of $\mathbf{Z}_{33}$, equation 10 without utilizing the other components of $\mathbf{Z}_{33}$.

That is if the general term of the "through" matrix $\mathbf{Z}_{33}$ is $Z_{n-k} = R_{n-k} + jX_{n-k}$, then the general term of the final "loss" matrix is

$$Z_{n/k} = \{[R_{n-k}\cos(\theta_n-\theta_k) - X_{n-k}\times \sin(\theta_n-\theta_k)](1+s_ns_k) + [R_{n-k}\sin(\theta_n-\theta_k) + X_{n-k}\cos(\theta_n-\theta_k)](s_n-s_k)\} / |E_n|_0|E_k|_0$$

If only the symmetrical part of R_{n-k} and the skew-symmetrical part of X_{n-k} is used, the resultant $Z_{n/k}$ would be identical with B_{nk} of reference 4, equation 10.

The Final Loss Equation $\mathbf{E}_6 = \mathbf{Z}_{66}\mathbf{I}_6$

The components of $\mathbf{I}_6$ represent the real power P supplied by each generator. The components of $\mathbf{E}_6 = (\mathbf{C}_6^5)_t\mathbf{E}_5 = \mathbf{L}$ are fractions (less then unity). They represent the "incremental" losses ∂(loss)/∂(power)$=\mathbf{L}$ that is the percentage I^2R losses that a power P_g suffers while it flows from a generator to the hypothetical load. The components of $\mathbf{L}$ may be called "directional" incremental losses. The product L_1P_1 represents the total I^2R loss λ_1 suffered by P_1 while it flows to the hypothetical load.

The dimension of $\mathbf{I}^6 = \mathbf{P}$ is that of power, $\mathbf{E}_6 = \mathbf{L}$ is a numeric and the dimension of $\mathbf{Z}_{66} = \mathbf{M}$ is the inverse of power, $Z/E^2 = 1/P$.

Knowing $\mathbf{P}$ and $\mathbf{L}$, the reactive powers $\mathbf{Q}$ supplied by the generators, also the I^2X losses and other pertinent information may be calculated.

Total Losses

If the real power of each generator is given, then the total I^2R losses are found by

---

$$\lambda = \mathbf{PMP} = \mathbf{PL} = \mathbf{I}^6\mathbf{Z}_{66}\mathbf{I}^6 = \mathbf{I}^6\mathbf{E}_6 \tag{30}$$

The same answer is found if:

1. Only the symmetrical part of $\mathbf{Z}_{66}$ is used, to be denoted by $\mathbf{R}_{66} = \mathbf{B}$.
2. Only the symmetrical part of $\mathbf{R}_{n-k}$ and the skew-symmetric part of $\mathbf{X}_{n-k}$ is used with the transformations $\mathbf{C}_4^3$, $\mathbf{C}_5^4$, and $\mathbf{C}_6^5$.

Each component of $\mathbf{I}^6\mathbf{E}_6$ represents the I^2R loss due to one generator current, while their sum gives the total losses in the whole system.

Economic Loading Studies

Differentiating λ with respect to $\mathbf{P}$ (TAN page 32) the "incremental losses", to be used in economic loading studies, are

$$\frac{\partial\lambda}{\partial \mathbf{P}} = 2\mathbf{R}_{66}\mathbf{P} \tag{31}$$

represented by a one-matrix (vector). It should be noted that $\mathbf{R}_{66}$ is only the symmetrical part of $\mathbf{Z}_{66} = \mathbf{M}$ and $\partial\lambda/\partial P$ differs from $\mathbf{L}$. The latter two concepts represent different types of incremental losses.

The sum of the fuel cost $\mathbf{F}$ (a diagonal matrix) and 2 $\mathbf{R}_{66}$ (a square matrix) are used in reference 3 for the co-ordination equation to determine the most economic loadings of the system.

References

1. ANALYSIS OF TOTAL AND INCREMENTAL LOSSES IN TRANSMISSION SYSTEMS, L. K. Kirchmayer, G. W. Stagg. *AIEE Transactions*, volume 70, 1951, pages 1197-1205.

2. ECONOMY LOADING OF POWER PLANTS AND ELECTRIC SYSTEMS (book), Steinberg, Smith. John Wiley and Sons, New York, N. Y., 1943.

3. INTRASYSTEM TRANSMISSION LOSSES, E. E. George. *Electrical Engineering* (*AIEE Transactions*), volume 62, March 1943, pages 153-58.

4. TOTAL AND INCREMENTAL LOSSES IN TRANSMISSION NETWORKS, J. B. Ward, J. R. Eaton, H. W. Hale. *AIEE Transactions*, volume 69, 1950, pages 626-31.

5. TENSOR ANALYSIS OF NETWORKS (book), G. Kron. John Wiley and Sons, New York, N. Y., 1939.

6. THE APPLICATION OF TENSORS TO THE ANALYSIS OF ROTATING ELECTRICAL MACHINERY (book), G. Kron. *General Electric Review* (Schenectady, N. Y.), 1942.

7. CO-ORDINATION OF FUEL COST AND TRANSMISSION LOSS BY USE OF THE NETWORK ANALYZER TO DETERMINE PLANT LOADING SCHEDULES, E. E. George, H. W. Page, J. B. Ward. *AIEE Transactions*, volume 68, 1949, pages 1152-60.

8. MATRIX ANALYSIS OF ELECTRIC NETWORKS (book), Le Corbeiller. John Wiley and Sons, New York, N. Y., 1950.

Discussion

E. E. George (Ebasco Services Inc., New York, N. Y.): The author has used tensor analysis to develop improvements in procedure in making loss formulas, and apparently has developed a general approach to other power problems.

The mathematical procedure in this paper is largely a mystery to the average engineer. Any comment on this must be left to the few mathematicians who understand tensor notation and tensor algebra.

The author has contributed several important items:

1. The use of constant power to replace previous constant current *or* constant voltage concepts.
2. The concept of a separate impedance matrix, susceptible of modification.
3. The concept of a separate load matrix, susceptible of modification.

Perhaps the author should state, as he has in previous papers, that tensor analysis is a shorthand notation, useful in developing formulas, but that the application of these formulas to physical problems requires just as many arithmetical operations as if the formulas had been developed by other methods.

Gabriel Kron: Let Mr. George not confuse short-hand "notation" with short-hand "thinking!"

George had observed that the load variations in a transmission system are more or less uniform. So he assumed in his analysis that all load-currents vary together in the same ratio that they happen to have at normal load. Both his and Ward's method of measurements are based upon this observation. No amount of knowledge of tensors would have ever led them to this simplification; it needed a close acquaintance with the practical operation of actual power systems and good engineering judgment.

Once I became convinced that here is a key assumption, my quarter-century background of tensorial analysis immediately put into high gear—(entirely in an automatic manner) a chain-reaction of reasoning. The chain of thought may be described as follows.

Here is an assumption that compels 50 load-currents to go up and down together in unison instead of allowing them to vary independently. In order to fit an isolated girder into some bigger structure I am going to consider this constraint not as a "constraint," as is always done conventionally, but as a "transformation" of something into something else. Evidently in this constraint "50 load currents" are transformed into "one load-current." So the first link in the chain of thoughts brought to life the concept of a single "hypothetical" load current I^L.

Next, if there is a transformation, there must also exist a "matrix of transformation" $\mathbf{C}_L$ that establishes a relation between the 50 "old" currents and the one "new" current as $\mathbf{i} = \mathbf{C}_L\mathbf{i}'$. Moreover, if there is a transformation usually there exists something in the physical set-up that is not transformed but remains "invariant." Obviously the new hypothetical load carries the same real and reactive powers that the 50 old loads do. This "invariance of power" automatically makes available the "laws of transformation" of many physical entities connected with the transmission system.

Now that I have a "matrix of transformation" $\mathbf{C}_L$ and "laws of transformation," I must get hold of some physical entity to transform it with $\mathbf{C}_L$. The entity that first comes into mind in stationary network studies is the "impedance" tensor $\mathbf{Z}$. It is true, $\mathbf{C}_L$ has nothing whatever to do with the 100 self- and mutual-impedances that exist between the ten generators, since no constraint was placed upon the generator currents. However, the 500 mutual impedances that the 50 load currents form with the ten generators, can be transformed into *ten* new impedances. Since $\mathbf{C}_L$ contains complex numbers I also knew that I would need 20 mutual impedances instead of ten, as they (the **a** and **b** coefficients) would be nonreciprocal.

Having on my hands both generator and load currents (and impedances) each set behaving in quite different manners, I had to draw upon my experience with "compound" tensors (tensors within tensors) to realize that the **a** mutual impedances can be found by the simple multiplications $\mathbf{C}_L\mathbf{Z}$ and the **b** mutual impedances by a conjugate formula $(\mathbf{C}_L)_t{}^*\ \mathbf{Z}$ that gives a set of different numbers with hardly any additional work. I could also visualize that to obtain 20 important hypothetical impedances, it would be worth-while to measure 500 conventional impedances or voltages on the actual system. Thus was born the concept of "load-impedance" measurement—without using the loads themselves—for this particular problem, in place of the "loss-coefficient" measurements of George and Ward.

Of course similar load-impedance measurements must have been performed previously for other types of problems ever since transmission lines existed. I merely realized that the measured load impedances may be transformed even under the handicap of placing restrictions upon the load variations.

It should also be emphasized that in the writings of George and Ward no traces whatever can be found of the concept of one single hypothetical load current. They always talk of a large number of loads constrained to vary in the same manner. Hence, the concept of an asymmetrical mutual impedance between the hypothetical load and a generator remains a total stranger to anyone who maintains the physical picture of "constraint" instead of "transformation."

To obtain the single self-impedance "*w*" of the hypothetical load by $\mathbf{C}_t{}^*\ \mathbf{Z}\ \mathbf{C}$, a very important key number by the way, at first I was appalled by the necessity of measuring 2,500 impedances merely to calculate one single number. Sheer instinct of survival dictated that there ought to be some other way of calculating one wee-bit of a number without doubly multiplying 2,500 numbers together with 50 other numbers. Eventually I found several short-cuts and Kirchmayer found many more still simpler ways of calculating *w*.

I will terminate now the enumeration of the links in this ever-expanding chain of thought and will ask Mr. George the $64 question: Would you call the above chain of reasoning a short-hand "notation"?

It definitely is a short-hand "reasoning," fully automatic, requiring no understanding of the fourth dimension, only a well-defined "pattern of thinking." It requires the same type of automatic thinking that any power engineer employs as soon as he is confronted with a 3-phase problem. "Let's introduce symmetrical components" (which by the way, is also a "transformation"). Nevertheless if the engineer is not acquainted with the tensorial chain of thought it is most unlikely that he would ever stumble upon the above-indicated method of calculating the 20 nonreciprocal mutual impedances existing between the 50 uniformly varying loads and the ten independent generators. Of course there are no reasons why anyone should not eventually discover some still simpler method.

It is true, a short-hand "thinking" automatically introduces as one of its by-products a short-hand "notation." But bringing that up in any discussion over the merits of tensors is like emphasizing that an airplane is a useful noise-making gadget, as its racket scares the enemy on the battlefront. Einstein did not discover his $E = mc^2$ formula by leaving out the summation signs in his notes! He discovered that formula by confronting the "matrix of transformation" $\mathbf{C}$ of the Lorentz "transformation" $x = \mathbf{C}\ x'$ with the question: What physical entities will remain "invariant" under this $\mathbf{C}$? He found that, among others, the sum of the mass and energy of a particle will also remain invariant.

George claims that a formula requires the same amount of numerical computations whether the formula was derived by tensorial reasoning or by some other conventional reasoning. If he has in mind the formulas employed in the steps establishing the required loss-coefficients (the purpose of all these papers under discussion) he picked a poor occasion to assert such a claim. The George-Ward formulas are definitely nontensorial, while my formulas definitely are tensorial. The amount of measurements and calculations involved in arriving at the same final goal, the loss-coefficients (using the same initial assumptions) happen to involve with the tensorial reasoning only 5 to 10 per cent of the work involved by the use of their nontensorial method. When the calculations for one transmission system take several weeks, a reduction of working time to one tenth of its previous value certainly shows up the tensorial method of attack in a rather favorable light.

Nevertheless no serious students of tensors ever claimed, I never claimed, and I still do not claim now, that the tensorial reasoning saves, or ever intended to save, *arithmetical* calculations. Every engineering problem inherently involves a certain amount of numerical computation that no method under the sun can circumvent. Also, with every particular problem there are associated short-cuts, whose discovery depends entirely on the alertness and background of the analyst himself. When a method requires an unreasonably large amount of computation, that is not the merit of other methods; it is rather the failing of the employed method or of the computer himself.

As a matter of fact, if I had stuck blindly to the steps offered by the tensorial method, I would have been forced to calculate the self-impedance *w* of the hypothetical load by 2,500 measurements and by several times as many multiplications. Nevertheless the tensorial procedure supplies a steel framework that enables the engineer to fill in the empty spaces by any imaginable method that may strike his fancy. The strong but slim steel girders of tensor analysis allow plenty of elbow-room to draw upon the resources of every other mathematical or physical science, or upon just ordinary horsesense.

The tensorial reasoning is intended primarily to save mental labor, to attack in an organized systematic manner complicated problems that look hopelessly involved, such as are most of the problems that arise in integrated transmission system operation: the kind of problems that power engineers are apt to consider unsolvable. Yes, their solution does look hopeless with the conventional analytical tools employed by power engineers. But the systematic method of tensors, plus modern calculating devices, do promise definite answers.

There are no reasons why the solutions of many presently-ignored steady-state problems of integrated transmission systems should not be part of a mere everyday office routine, performed by trained calculators, by punch-card machines or by special electronic calculating devices. The analytical tool is already available and many of the methods have already been worked out in detail. It is only a question of how fast the power companies themselves will utilize the facilities already available along these lines.

Perhaps the greatest handicap to overcome, before power engineers can even start solving their integrated system problems by analytical methods, is their awe, their fear of the "mysteries" of tensors.

Determination of Instantaneous Currents and Voltages by Means of Alpha, Beta, and Zero Components

W. C. DUESTERHOEFT
ASSOCIATE AIEE

MAX W. SCHULZ, JR.
NONMEMBER AIEE

EDITH CLARKE
FELLOW AIEE

APPLICATIONS of the method of alpha, beta, and zero components (conveniently written $\alpha,\beta,0$ components) to the determination of phase currents and voltages of fundamental frequency in unbalanced 3-phase power systems have been given.[1-3] The advantages of $\alpha,\beta,0$ components over symmetrical components, in the determination of fundamental-frequency phase quantities, is largely restricted to unsymmetrical 3-phase systems in which the positive- and negative-sequence impedances of the rotating machines of the system can be assumed equal. This restriction is not present in the determination of instantaneous phase quantities by the method of $\alpha,\beta,0$ components.

The purpose of this paper is to present a method of analysis rather than to develop new equations. For this reason, well-known equations previously derived by outstanding engineers have been selected for redevelopment here in order to show the simplifications made possible by the application of $\alpha,\beta,0$ components. Sincere admiration is hereby expressed for the ability of these engineers to carry through the original development without the benefit of $\alpha,\beta,0$ components.

The paper is divided into three parts. In Part I, relations are established between instantaneous phase quantities and their $\alpha,\beta,0$ components, and between α and β components and direct- and quadrature-axis components. Park's equations for an ideal synchronous machine,[4,5] in terms of direct-axis, quadrature-axis, and zero-sequence components, are expressed in terms of $\alpha,\beta,0$ components for use in Part II and Part III.

In Part II, equations for instantaneous phase currents and voltages at the terminals of an unloaded ideal synchronous machine during all types of short circuits are derived by means of $\alpha,\beta,0$ components. It is thought the method of developing the complete harmonic series for instantaneous currents and voltages, given in the Appendix I, has not been presented previously.

In Part III, equations for circuit-breaker recovery voltages derived by Park and Skeats[6] are redeveloped using $\alpha,\beta,0$ components. The simplification in development made possible by the application of $\alpha,\beta,0$ components can be seen readily by comparison with the original development.

Part I. Equations for Use in Parts II and III

NOTATION

Let i, ψ, and e with appropriate subscripts represent instantaneous armature current, flux linkage, and voltage, respectively; let subscripts a, b, c refer to phase a, b, c, respectively; let subscripts α, β, 0 refer to α, β, and 0 components, respectively; let subscripts d and q refer to the direct- and quadrature-axis components, respectively.

Relations Between Phase Quantities and Their $\alpha,\beta,0$ Components

By definition, instantaneous phase currents i_a, i_b, i_c of normal phase order abc at any point in a 3-phase system, in terms of their instantaneous $\alpha,\beta,0$ components of current, are

$$i_a = i_\alpha + i_0 \tag{1}$$

$$i_b = -\frac{1}{2}i_\alpha + i_0 + (\sqrt{3}/2)i_\beta \tag{2}$$

$$i_c = -\frac{1}{2}i_\alpha + i_0 - (\sqrt{3}/2)i_\beta \tag{3}$$

Simultaneous solution of the preceding equations gives

$$i_\alpha = \left(\frac{2}{3}\right)\left[i_a - \frac{(i_b + i_c)}{2}\right] \tag{4}$$

$$i_\beta = \frac{(i_b - i_c)}{\sqrt{3}} \tag{5}$$

$$i_0 = \frac{(i_a + i_b + i_c)}{3} \tag{6}$$

If i in equations 1–6 is replaced ψ or e, equations relating instantaneous flux linkages (ψ) or voltages (e), respectively, in the phases and in the α, β, and 0 circuits will be obtained. Equations 1–6 are general equations which apply under all conditions. No simplifying assumptions need be made; the quantities involved may be expressed in per unit of stated base quantities, or in any consistent system of units.

Ideal Synchronous Machine

In developing equations involving synchronous machines[4,5] the work is greatly simplified if per unit quantities are used, and an ideal synchronous machine is assumed with saturation, hysteresis and eddy currents in the iron neglected, these latter effects to be taken into account later if of importance.

Unit or Base Armature Quantities

Unit armature current and voltage are crest values of rated phase current and rated phase voltage, respectively; unit

---

Paper 51-226, recommended by the AIEE Transmission and Distribution Committee and approved by the AIEE Technical Program Committee for presentation at the AIEE Summer General Meeting, Toronto, Ont., Canada, June 25–29, 1951. Manuscript submitted February 26, 1951; made available for printing May 3, 1951.

W. C. Duesterhoeft and Edith Clarke are both with the University of Texas, Austin, Tex., and Max W. Schulz, Jr., is with the General Electric Company, Pittsfield, Mass.

The authors wish to express their appreciation for the assistance given by Mr. Chwan-Chang Lee in the preparation of this paper.

impedance is the ratio of rated phase voltage to rated phase current; unit speed of the rotor is synchronous speed; unit time is one electrical radian; unit armature linkage will generate unit armature voltage at rated speed; unit armature magnetomotive force is the magnetomotive force produced by rated positive-sequence armature currents; unit permeance when multiplied by unit magnetomotive force produces unit armature linkages.

RELATIONS BETWEEN DIRECT- AND QUADRATURE-AXIS COMPONENTS AND α AND β COMPONENTS

As zero-sequence components (written 0 components in the α, β, 0 system) are the same in both systems, it is unnecessary to consider them in establishing relations between the two systems of components. If equations 1, 2, and 3 are substituted for i_a, i_b, and i_c, respectively, in the equations for i_d and i_q in reference 5, and the resultant equations solved for i_α and i_β, the following equations are obtained:

$$i_d=i_\alpha \cos \theta+i_\beta \sin \theta \tag{7}$$

$$i_q=-i_\alpha \sin \theta+i_\beta \cos \theta \tag{8}$$

$$i_\alpha=i_d \cos \theta-i_q \sin \theta \tag{9}$$

$$i_\beta=i_d \sin \theta+i_q \cos \theta \tag{10}$$

If i in the preceding equations is replaced by ψ or e, equations relating direct- and quadrature-axis components and α and β components of flux linkage ψ or voltage e, respectively, result.

PARK'S EQUATIONS FOR AN IDEAL SYNCHRONOUS MACHINE IN TERMS OF $\alpha,\beta,0$ COMPONENTS

The development of these equations (which are expressed in terms of direct- and quadrature-axis components) by using $\alpha,\beta,0$ components instead of phase quantities, and the expression of them in terms of $\alpha,\beta,0$ components have been given.[7] For the initial conditions following a short circuit at the terminals of an unloaded machine, operating at rated speed, these equations in terms of $\alpha,\beta,0$ components are

$$e_\alpha=-I_f \sin \theta-p(x+y \cos 2\theta)i_\alpha-py\times \sin 2\theta i_\beta-ri_\alpha \tag{11}$$

$$e_\beta=I_f \cos \theta-py \sin 2\theta i_\alpha-p\times (x-y \cos 2\theta)i_\beta-ri_\beta \tag{12}$$

$$e_0=-px_0i_0-ri_0 \tag{13}$$

$$x=\frac{(x_d''+x_q'')}{2};\quad y=\frac{(x_d''-x_q'')}{2} \tag{14}$$

where $p=d/dt$; r is per-unit armature resistance, assume the same in all component networks; θ is the angular displacement in electrical radians of the direct-axis of the rotor from the axis of phase a, measured in the normal direction of the rotor. x_d'' and x_q'' are per-unit direct- and quadrature-axis reactances, respectively; e is per unit armature voltage rise to machine terminals; i is per unit current flowing from machine terminals; and I_f=d-c field current in per unit of that base field current which will produce unit armature linkage at no load and rated speed, with saturation neglected, and generate unit armature voltage.

During the first instant after a disturbance, the speed of the rotor can be assumed constant at rated speed because of rotor inertia. At rated speed, the speed of the rotor in per unit of synchronous speed is unity; and the angle θ, at any time t in electrical radians, may be written

$$\theta=\theta_0+t \tag{15}$$

where $\theta_0=\theta$ at time $t=0$, from which time in electrical radians is measured. In the work which follows in Parts I and II, constant rotor speed will be assumed, and armature resistance (r) in equations 11, 12, and 13 will be neglected to permit ready solution without a differential analyzer. As armature resistance is small relative to reactance, neglecting it will not appreciably affect initial currents and voltages; for subsequent values, appropriate decrement factors can be applied, as will be explained later.

Part II. Short-Circuit Currents and Voltages at the Terminals of an Unloaded Ideal Synchronous Machine, Operated at Rated Speed

Equations 11–14, with resistance neglected and constant rotor speed assumed, will be used to determine phase currents and voltages at the machine terminals in terms of their harmonic components during the first instant after various types of short circuits. Subsequent values of current and voltage may be obtained by application of appropriate decrement factors. Even harmonics (including d-c components) and natural-frequency terms are attenuated by armature time constants; odd harmonics (including fundamental-frequency terms) are attenuated by rotor time constants. As capacitance of the generator is neglected, there will be no natural frequency terms. In determining maximum currents and voltages, action of voltage regulators can be neglected as any change in the voltage of the field exciter will have negligible effect during the first cycle or less required for currents and voltages to reach their maximum values.

LINE-TO-LINE SHORT CIRCUIT

Let the fault be between phases b and c. The conditions imposed by the fault are: $i_a=0$; $i_b=-i_c$; $e_b=e_c$. These equations substituted in equations 4 and 6, and in 5 with i replaced by e, give $i_\alpha=0$; $i_0=0$; $e_\beta=0$. The above equations allow the reduction of equation 12, with $r=0$, to

$$I_f \cos \theta=p(x-y \cos 2\theta)i_\beta \tag{16}$$

If each side of equation 16 is integrated, there results

$$I_f (\sin \theta-\sin \theta_0)=(x-y \cos 2\theta)i_\beta$$

The current i_β, being zero immediately before the fault at $t=0$, must be zero immediately after the fault; hence, $I_f \sin \theta_0$ appears in the preceding equation as the integration constant. Solution for i_β gives

$$i_\beta=\frac{I_f(\sin \theta-\sin \theta_0)}{(x-y \cos 2\theta)} \tag{17}$$

Substitution of equation 17 and $i_\alpha=0$ in equation 11 gives

$$e_\alpha=-I_f \sin \theta-\frac{py \sin 2\theta I_f (\sin \theta-\sin \theta_0)}{(x-y \cos 2\theta)} \tag{18}$$

HARMONIC SERIES FOR CURRENTS

Currents i_β in equation 17 can be expanded in a harmonic series in terms of x and y by application of equations 99 and 96 with Z given by equation 94, if a and b in these equations are replaced by x and y, respectively. When x and y are then replaced by their values in terms of x_d'' and x_q'' from equation 14 and i_β multiplied by $\sqrt{3}/2$ to give $i_b=-i_c$ (since $i_\alpha=i_0=0$), the harmonic series at the first instant is obtained

$$i_b=-i_c=[\sqrt{3}\, I_f/(x_d''+\sqrt{x_d''x_q''})]\times \sum_{n=1}^{\infty} Z^{n-1} \sin (2n-1)\theta-(\sqrt{3/2})\times [I_f \sin \theta_0/\sqrt{x_d''x_q''}]\times \left[1+2\sum_{n=1}^{\infty} Z^n \cos 2n\theta\right] \tag{19}$$

where

$$Z=\frac{(\sqrt{x_d''}-\sqrt{x_q''})}{(\sqrt{x_d''}+\sqrt{x_q''})} \tag{20}$$

Equation 19 checks the work of Doherty and Nickle.[8] As pointed out by these authors, it is interesting to note that the coefficients in the harmonic series are the constant Z, which is less than unity, taken to increasingly higher powers for the higher harmonics. The first series in 19 gives the fundamental and odd-harmonic terms; the second series gives the d-c and even-harmonic terms.

HARMONIC SERIES FOR VOLTAGES

Voltage e_a, in equation 18, can be simplified by integration of the first term and indicated differentiation, as in the following equation

$$e_a = pI_f\left[\cos\theta - \frac{y\sin 2\theta(\sin\theta - \sin\theta_0)}{(x-y\cos 2\theta)}\right]$$

$$= pI_f\left[\frac{(x-y)\cos\theta + y\sin\theta_0\sin 2\theta}{(x-y\cos 2\theta)}\right] \qquad (21)$$

Equation 21 can be expanded in harmonic series in terms of x and y by application of equations 100 and 97 with Z given by equation 94, if a and b in these equations are replaced by x and y, respectively.

$$e_a = pI_f\frac{2(x-y)\sum_{n=1}^{\infty}Z^{n-1}\cos(2n-1)\theta}{x-y+\sqrt{x^2-y^2}} + 2pI_f\sin\theta_0\sum_{n=1}^{\infty}Z^n\sin 2n\theta \qquad (22)$$

When x and y in the fraction in equation 22 are replaced by their values in terms of x_d'' and x_q'' from equation 14 and numerator and denominator multiplied by $\sqrt{x_d''/x_q''}$, and the indicated differentiation performed, $e_a = e_\alpha$ is

$$e_a = e_\alpha = \frac{-2I_f\sqrt{x_d''x_q''}\sum_{n=1}^{\infty}(2n-1)Z^{n-1}\sin(2n-1)\theta}{(x_d''+\sqrt{x_d''x_q''})} + 4I_f\sin\theta_0\sum_{n=1}^{\infty}nZ^n\cos 2n\theta$$

$$e_b = e_c = -\frac{1}{2}e_a \qquad (23)$$

where Z is given by equation 20.

LINE-TO-GROUND SHORT CIRCUIT

Let the fault be between phase a and ground. The conditions imposed by the fault are: $e_a=0$; $i_b=i_c=0$. These equations substituted in equations 4, 5, and 6 and in equation 1, with i replaced by e, give

$$i_\beta=0;\quad i_\alpha=2i_0;\quad e_\alpha=-e_0 \qquad (24)$$

Equations 24 substituted in equations 11 and 13 reduce these equations to expressions which can be solved for i_α

$$e_\alpha = -e_0 = px_0i_0 = p\tfrac{1}{2}x_0i_\alpha$$
$$= -I_f\sin\theta - p(x+y\cos 2\theta)i_\alpha \qquad (25)$$

$$p(x+\tfrac{1}{2}x_0+y\cos 2\theta)i_\alpha = -I_f\sin\theta \qquad (26)$$

If each side of equation 26 is integrated and the condition is satisfied that i_α must be zero at $t=0$

$$i_\alpha = \frac{I_f(\cos\theta - \cos\theta_0)}{(x+\frac{1}{2}x_0+y\cos 2\theta)} \qquad (27)$$

When i_α from equation 27 and $i_\beta=0$ are substituted in equation 12

$$e_\beta = I_f\left[\cos\theta - \frac{py\sin 2\theta(\cos\theta-\cos\theta_0)}{(x+\frac{1}{2}x_0+y\cos 2\theta)}\right] \qquad (28)$$

HARMONIC SERIES FOR CURRENTS

The series for i_α, equation 27, in terms of x, y, and x_0 can be obtained by using Equations 100 and 96, with Z given by equation 94 if a and b in these equations are replaced $(x+\frac{1}{2}x_0)$ and $-y$, respectively. When x and y are replaced by values in terms of x_d'' and x_q'' from equation 14 i_α and Z are determined. Since $i_a=i_\alpha+i_0$, and $i_0=\frac{1}{2}i_\alpha$

$$i_a = \left(\frac{3}{2}\right)i_\alpha$$

$$= \frac{3I_f\sum_{n=1}^{\infty}Z^{n-1}\cos(2n-1)\theta}{[x_d''+\frac{1}{2}x_0+\sqrt{(x_d''+\frac{1}{2}x_0)(x_q''+\frac{1}{2}x_0)}]} - \frac{3I_f\cos\theta_0\left[1+2\sum_{n=1}^{\infty}Z^n\cos 2n\theta\right]}{2\sqrt{(x_d''+\frac{1}{2}x_0)(x_q''+\frac{1}{2}x_0)}} \qquad (29)$$

where

$$Z = \frac{\sqrt{x_q''+\frac{1}{2}x_0}-\sqrt{x_d''+\frac{1}{2}x_0}}{(\sqrt{x_q''+\frac{1}{2}x_0}+\sqrt{x_d''+\frac{1}{2}x_0})} \qquad (30)$$

HARMONIC SERIES FOR VOLTAGES

The α-component of voltage can be found from equation 25 if i_α in this equation is replaced by $(2/3)i_a$ given by equation 29, and the indicated differentiation performed.

$$e_\alpha = p\tfrac{1}{2}x_0i_\alpha$$

$$= \frac{-x_0I_f}{x_d''+\frac{1}{2}x_0+\sqrt{(x_d''+\frac{1}{2}x_0)(x_q''+\frac{1}{2}x_0)}} \times \sum_{n=1}^{\infty}(2n-1)Z^{n-1}\sin(2n-1)\theta + \frac{2x_0I_f\cos\theta_0}{\sqrt{(x_d''+\frac{1}{2}x_0)(x_q''+\frac{1}{2}x_0)}} \times \sum_{n=1}^{\infty}nZ^n\sin 2n\theta \qquad (31)$$

where Z is given by equation 30.

Integration and indicated differentiation of the first term of e_β in equation 28, and simplification, give

$$e_\beta = \frac{pI_f[(x-y+\frac{1}{2}x_0)\sin\theta - y\cos\theta_0\sin 2\theta]}{(x+\frac{1}{2}x_0+y\cos 2\theta)} \qquad (32)$$

Equation 32 can be expanded in a series in terms of x, y, and x_0 by application of equations 99 and 97, where Z is given by equation 94. When expressed in terms of x_d'', x_q'', and x_0 by a procedure similar to that used to obtain i_a in equation 29, and the indicated differentiation performed

$$e_\beta = \frac{2I_f\sqrt{(x_d''+\frac{1}{2}x_0)(x_q''+\frac{1}{2}x_0)}}{x_d''+\frac{1}{2}x_0+\sqrt{(x_d''+\frac{1}{2}x_0)(x_q''+\frac{1}{2}x_0)}} \times \sum_{n=1}^{\infty}(2n-1)Z^{n-1}\cos(2n-1)\theta - 4I_f\cos\theta_0\sum_{n=1}^{\infty}nZ^n\cos 2n\theta \qquad (33)$$

where Z is given by equation 30.

PHASE VOLTAGES

From equations 1, 2, and 3 with i replaced by e,

$$e_a = e_\alpha + e_0 = 0 \qquad (34)$$

$$e_b = -\frac{3e_\alpha}{2} + \frac{\sqrt{3}e_\beta}{2} \qquad (35)$$

$$e_c = -\frac{3e_\alpha}{2} - \frac{\sqrt{3}e_\beta}{2} \qquad (36)$$

After e_α from equation 31 and e_β from equation 33 have been substituted in equations 35 and 36, the resultant equations can be simplified by application of the equation:

$$A\sin\delta + B\cos\delta = \sqrt{A^2+B^2}\sin(\delta-\gamma)$$

where

$$\gamma = \tan^{-1}(B/A)$$

Thus

$$e_b = \frac{\sqrt{3}I_f\sqrt{x_d''x_q''+(\frac{1}{2}x_0)(x_d''+x_q'')+x_0^2}}{x_d''+\frac{1}{2}x_0+\sqrt{(x_d''+\frac{1}{2}x_0)(x_q''+\frac{1}{2}x_0)}} \times \sum_{n=1}^{\infty}(2n-1)Z^{n-1}\sin[(2n-1)\theta+\gamma] - \frac{2\sqrt{3}I_f\cos\theta_0\sqrt{x_d''x_q''+(\frac{1}{2}x_0)(x_d''+x_q'')+x_0^2}}{\sqrt{(x_d''+\frac{1}{2}x_0)(x_q''+\frac{1}{2}x_0)}} \sum_{n=1}^{\infty}nZ^n\sin(2n\theta+\gamma) \qquad (37)$$

where

$$\gamma = \tan^{-1}\frac{2\sqrt{(x_d''+x_0/2)(x_q''+x_0/2)}}{\sqrt{3}x_0}$$

and Z is given by equation 30. The equation for e_c differs from that for e_b only in that sign before γ is negative instead of positive.

DOUBLE LINE-TO-GROUND FAULT

Let the fault be between phases b and c and ground. The conditions imposed by the fault are: $i_a=0$, and $e_b=e_c=0$. These equations substituted in equation 1, and in equations 4, 5, and 6 with i replaced by e, give

$$i_\alpha=-i_0 \quad e_\beta=0 \quad e_\alpha=2e_0 \tag{38}$$

Equations 38 with equations 11, 12, and 13 give

$$p(x+2x_0+y\cos 2\theta)i_\alpha+py\times \sin 2\theta i_\beta=-If(\sin\theta)$$

$$py\sin 2\theta i_\alpha+p(x-y\cos 2\theta)i_\beta=I_f(\cos\theta)$$

If both sides of the preceding equations are integrated and the integration constants evaluated, there results

$$(x+2x_0+y\cos 2\theta)i_\alpha+y\times \sin 2\theta i_\beta=I_f(\cos\theta-\cos\theta_0) \tag{39}$$

$$y\sin 2\theta i_\alpha+(x-y\cos 2\theta)i_\beta=I_f(\sin\theta-\sin\theta_0) \tag{40}$$

Simultaneous solution of equations 39 and 40 for i_α and i_β gives

$$i_\alpha=\frac{I_f[(x-y)\cos\theta-x\cos\theta_0+y\cos 2\theta\cos\theta_0+y\sin\theta_0\sin 2\theta]}{x^2-y^2+2x_0x-2x_0y\cos 2\theta} \tag{41}$$

$$i_\beta=\frac{I_f[(2x_0+x-y)\sin\theta-(2x_0+x)\sin\theta_0-y\sin\theta_0\cos 2\theta+y\cos\theta_0\sin 2\theta]}{x^2-y^2+2x_0x-2x_0y\cos 2\theta} \tag{42}$$

HARMONIC SERIES FOR CURRENTS

To apply the equations of Appendix I to equations 41 and 42, a and b must have the following values in equations 100, 97, 96, and 98, and in Z given by equation 94

$$a=x^2-y^2+2x_0x=x_d''x_q''+x_0(x_d''+x_q'')$$

$$b=2x_0y=x_0(x_d''-x_q'')$$

The procedure for determining the complete harmonic series for i_α and i_β, and then substituting them in the equations for i_b and i_c, and combining terms, is similar to that used to obtain e_b in equation 37. It will not be given here; instead, the odd-harmonic terms of i_b will be expressed in a form suitable for use in Part III.

From equation 38, $i_0=-i_\alpha$; therefore from equation 2

$$i_b=-3i_\alpha/2+\sqrt{3}i_\beta/2 \tag{43}$$

When the terms in the numerators of equations 41 and 42 involving θ_0 (even harmonics) are omitted, and these equations are substituted in equation 43

$$i_b=I_f\frac{-3(x-y)\cos\theta+\sqrt{3}(x-y+2x_0)\sin\theta}{2[x^2-y^2+2x_0(x-y\cos 2\theta)]} \tag{44}$$

HARMONIC SERIES FOR VOLTAGES

From equations 38 and 13

$$e_\alpha=2e_0=-2px_0i_0=2px_0i_\alpha \tag{45}$$

If equation 41 for i_α is expressed in its harmonic series, then substituted in equation 45, and the differentiation performed, e_α is obtained. The voltage $e_a=e_\alpha+e_0=(3/2)e_\alpha$ is

$$e_a=\frac{-6x_0x_q''I_f}{x_q''(x_d''+2x_0)+\sqrt{x_d''x_q''(x_d''+2x_0)(x_q''+2x_0)}}\times\sum_{n=1}^{\infty}(2n-1)Z^{n-1}\sin(2n-1)\theta-\frac{6x_d''x_q''I_f\cos\theta_0}{\sqrt{x_d''x_q''(x_d''+2x_0)(x_q''+2x_0)}}\times\sum_{n=1}^{\infty}nZ^n\sin 2n\theta+6I_f\times\sin\theta_0\sum_{n=1}^{\infty}nZ^n\cos 2n\theta \tag{46}$$

where

$$Z=\frac{\sqrt{x_d''(x_q''+2x_0)}-\sqrt{x_q''(x_d''+2x_0)}}{\sqrt{x_d''(x_q''+2x_0)}+\sqrt{x_q''(x_d''+2x_0)}} \tag{47}$$

THREE-PHASE FAULT

The conditions imposed by the fault, in a grounded or unground system are: $i_a+i_b+i_c=0$, and $e_a=e_b=e_c$. These equations substituted in equation 3, and in equations 4, 5, and 6 with i replaced by e, give $i_0=0$, $e_\alpha=0$, and $e_\beta=0$. When $e_\alpha=0$ and $e_\beta=0$ are substituted in equations 11 and 12, these equations will be the same as those for a double line-to-ground fault with the terms containing x_0 omitted. There $i_a=i_\alpha+i_0=i_\alpha$ can be written from equation 41 by omitting the terms in the denominator containing x_0.

$$i_a=I_f\frac{(x-y)\cos\theta-x\cos\theta_0+y\cos(2\theta-\theta_0)}{(x^2-y^2)} \tag{48}$$

$$=I_f\left[\frac{\cos\theta}{x_d''}-\frac{(x_d''+x_q'')\cos\theta_0-(x_d''-x_q'')\cos(2\theta-\theta_0)}{(2x_d''x_q'')}\right] \tag{49}$$

Part III. Circuit Breaker Recovery Voltage

Circuit breaker recovery voltage may be defined as the voltage appearing across the poles of a circuit breaker after it has interrupted a current. The first analytical treatment of the subject is given in a paper by Park and Skeats.[6] They divide the effects of recovery voltage into high- and low-frequency effects and treat these two effects separately. High-frequency effects depend upon the capacitance in the system. Two types of systems are considered for low-frequency effects: (1) those in which the impedances of stationary equipment are much greater than the impedances of rotating machines, so that the effects of unequal reactances in the direct and quadrature axes of rotating machines are relatively unimportant; (2) those in which the impedances of rotating machines predominate. It is the latter type which will be considered here, the purpose being to check the final equations in Appendices B, C, and D of the reference paper[6] by using $\alpha,\beta,0$ components.

The equations for fault current, developed in Part II, will be used to determine the voltage across the poles of the circuit breaker for the first phase to clear of a fault at the terminals of an unloaded ideal synchronous machine operating at rated speed. In the case of multiple pole breakers, the resistance of an arc formed by an uninterrupted phase current is assumed to be zero. Natural frequency effects caused by capacitance will be neglected.

External reactances can be added to the machine reactances but, as the length of externally connected circuits increases, the capacitance assumes greater importance. Resistance will be treated as in the reference paper;[6] its effect on the initial magnitudes of currents and voltages is small and will be neglected, but the attenuation of currents and voltages is included in the decrement factors. Use will be made of the method of superposition, whereby a current is interrupted (made zero) by superposing an equal and opposite current without changing the system. The voltage drop across the switch terminals caused by the application of a current equal and opposite to the fault current will be the same as the voltage across the switch caused by opening the switch. When faults involving ground in a grounded system are treated, the voltage across the circuit breaker is equal to the phase voltage to ground of the opened phase. In ungrounded faults or ungrounded systems, the circuit breaker voltage will be the difference between two phase voltages.

FLUX LINKAGES AND VOLTAGES

The following equations relate sudden changes in Ψ_α, Ψ_β, and Ψ_0 with sudden changes in i_α, i_β, and i_0.

$$\Psi_\alpha' = -i_\alpha'(x+y\cos 2\theta) - i_\beta' y \sin 2\theta \tag{50}$$

$$\Psi_\beta' = -i_\alpha' y \sin 2\theta - i_\beta'(x-y\cos 2\theta) \tag{51}$$

$$\Psi_0' = -i_0 x_0 \tag{52}$$

$$x = \frac{(x_d''+x_q'')}{2}; \quad y = \frac{(x_d''-x_q'')}{2} \tag{53}$$

where primes indicate sudden changes from previous values; and the negative, signs with currents follow the convention for signs of the reference papers:[4,6] flux linkages due to the main field are positive, those due to current in the positive direction are negative. Voltage rise to the machine terminals in any circuit, a, is written

$$e_a = p\Psi_a \tag{54}$$

where Ψ_a included all linkages with circuit a.

DECREMENT FACTORS

The equations for short-circuit currents given in Part II are for initial currents. By the time a circuit breaker operates to interrupt a fault current, the magnitude of the current will have changed. Let

k_r = decrement factor for odd harmonics which may combine effects of rotor transient and subtransient time constants with exciter response

k_a = decrement factor for even harmonics which depends upon the armature time constant

OPENING A DOUBLE LINE-TO-GROUND FAULT

Let the fault involve phases b and c in a grounded system, and assume that phase b opens before phase c, after armature transients have died away. The fault current i_b, at the instant phase b clears, is k_r times that given by equation 44 with I_f replaced by unity for rated voltage before the fault. Let i_b' indicate the current to be superposed on existing conditions. Then,

$$i_b' = \frac{-k_r[-3(x-y)\cos\theta + \sqrt{3}(x-y+2x_0)\sin\theta]}{2[x^2-y^2+2x_0(x-y\cos 2\theta)]} \tag{55}$$

Before phase b opens, which is before i_b' is applied, $e_b=e_c=0$ and $i_a=0$. With resistance neglected and $e_b=e_c=0$, $\Psi_b=\Psi_c=0$; from equation 5, with i replaced Ψ, $\Psi_\beta=0$. After i_b' is applied, as phase a remains open and phase c remains grounded, $i_a'=0$ and $\Psi_c'=0$; e_b, Ψ_b, and Ψ_β, which were zero before i_b' was applied, will take on new values. In the development given below, as all quantities are increments due to the application of i_b', the primes will be omitted. With $i_a=0$, in equation 1, $i=-i_0$. Therefore from equations 2 and 3

$$i_b' = -3\frac{i_\alpha}{2} + \sqrt{3}\frac{i_\beta}{2} \tag{56}$$

$$\Psi_0 = -i_0 x_0 = i_\alpha x_0 \tag{57}$$

If i in equations 2 and 3 is replaced by Ψ and $\Psi_c=0$ subtracted from Ψ_b, there results

$$\Psi_b = \sqrt{3}\Psi_\beta \tag{58}$$

Ψ_β is given by equation 51 in terms of i_α and i_β. The procedure to determine i_α and i_β is to substitute equations 50, 51, and 57 in the equation $\Psi_c=0$; then from simultaneous solution of the resultant equation and equation 56, i_α and i_β in terms of i_b' are obtained. When i_α and i_β are substituted in equation 51, Ψ_β in terms of i_b' is determined. From equation 58, Ψ_b is obtained in terms i_b'; i_b' is then replaced by the negative of the fault current at the instant phase b clears, given by equation 55. With Ψ_b known, $e_b=p\Psi_b$ = circuit breaker recovery voltage.

When equations 50, 51, and 57 are substituted in $\Psi_c=0$, equation 3 with i replaced by Ψ, the resultant equation is

$$i_\alpha(x+y\cos 2\theta+\sqrt{3}y\sin 2\theta+2x_0) + i_\beta[y\sin 2\theta+\sqrt{3}(x-y\cos 2\theta)] = 0 \tag{59}$$

Simultaneous solution of equations 59 and 56 gives equations for i_α and i_β in terms of i_b'. When these equations are substituted in equation 51 and the resultant equation multiplied by $\sqrt{3}$, Ψ_b is obtained.

$$\Psi_b = \frac{-i_b'[x^2-y^2+2x_0(x-y\cos 2\theta)]}{(2x+x_0-y\cos 2\theta+\sqrt{3}y\sin 2\theta)} \tag{60}$$

When i_b', given by equation 55, replaces i_b' in equation 60, Ψ_b becomes

$$\Psi_b = \frac{k_r[-3(x-y)\cos\theta+\sqrt{3}(x-y+2x_0)\sin\theta]}{2[2x+x_0-y\cos 2\theta+\sqrt{3}y\sin 2\theta]} \tag{61}$$

As the assumption is made[6] that phase b clears at current zero, the value of voltage $e_b=p\Psi_b$ at that instant will be determined. At current zero, the numerator of the fraction in equation 44 for fault current i_b must be zero. To satisfy this condition, the following equations are required

$$-3(x-y)\cos\theta+\sqrt{3}(x-y+2x_0)\sin\theta = 0 \tag{62}$$

$$\tan\theta = \frac{\sqrt{3}(x-y)}{(x-y+2x_0)} \tag{63}$$

Let Ψ_b in equation 61 be written $\Psi_b = N/D$. Then $e_b = p\Psi_b = (DpN-NpD)/D^2$. To satisfy the condition of equation 62 at the instant phase b clears, $N=0$; but pN is not zero. Therefore, $e_b = pN/D$ at the instant phase b clears.

$$e_b = p\Psi_b = \left(\frac{k_r}{2}\right)\times \frac{[3(x-y)\sin\theta+\sqrt{3}(x-y+2x_0)\cos\theta]}{[2x+x_0-y\cos 2\theta+\sqrt{3}y\sin 2\theta]} \tag{64}$$

where for current zero, $\sin\theta$, $\cos\theta$, $\cos 2\theta$, and $\sin 2\theta$ must have the following values determined by equation 63.

$$\sin\theta = \frac{\sqrt{3}(x-y)}{\sqrt{3(x-y)^2+(x-y+2x_0)^2}}$$

$$\sin 2\theta = \frac{2\sqrt{3}(x-y)(x-y+2x_0)}{3(x-y)^2+(x-y+2x_0)^2}$$

$$\cos\theta = \frac{x-y+2x_0}{\sqrt{3(x-y)^2+(x-y+2x_0)^2}}$$

$$\cos 2\theta = \frac{(x-y+2x_0)^2-3(x-y)^2}{3(x-y)^2+(x-y+2x_0)^2} \tag{65}$$

When these trigonometric functions are substituted in equation 64, the resultant equation simplified, and x and y replaced by their values in terms of x_d'' and x_q'' from equation 53, e_b is given by the following equation

$$e_b = \frac{2\sqrt{3}(x_q''^2+x_q''x_0+x_0^2)^{3/2}k_r}{x_d''(2x_q''+x_0)^2+x_0(2x_q''+x_0)(x_q''+2x_0)} \tag{66}$$

Equation 66, which gives the voltage across the switch terminals at the instant phase b clears, checks equation D-28 of the reference paper.[6]

OPENING A 3-PHASE FAULT TO GROUND IN A GROUNDED SYSTEM

It will be assumed that phase a is the first to clear after d-c and second harmonic components of current have disappeared. The fault current i_a at the instant phase a clears is k_r times the first terms of equation 48, with I_f replaced by E, the line-to-neutral voltage before the fault occurs. The current i_a' to be superposed on existing conditions, therefore, is

$$i_a' = \frac{-k_r E(x-y)\cos\theta}{x^2-y^2} \tag{67}$$

As phases b and c remain grounded after i_a' is applied, $\Psi_b'=\Psi_c'=0$. If equations 2 and 3 with i replaced by Ψ', are added and then subtracted the following equations are obtained

$$\Psi_\alpha' = 2\Psi_0' \qquad (68)$$

$$\Psi_\beta' = 0 \qquad (69)$$

From equation 1 with i replaced by Ψ'

$$\Psi_a' = \Psi_\alpha' + \Psi_0' = 3\Psi_0' \qquad (70)$$

As Ψ_a was zero before i_a' was applied, Ψ_a' in equation 70 is the actual flux linkage Ψ_a after phase a clears. For convenience, the primes will be omitted in the development which follows, but it is understood that all values of Ψ and i are increments due to the application of i_a'.

From equations 50–52 and 68–70, the following equations are obtained

$$-i_\alpha(x+y\cos 2\theta) - i_\beta y \sin 2\theta = 2\Psi_0 = -2i_0x_0$$

$$-i_\alpha y \sin 2\theta - i_\beta(x-y\cos 2\theta) = 0$$

Simultaneous solution of the preceding equations gives i_α in terms of i_0; i_β is not required.

$$i_\alpha = \frac{2i_0x_0(x-y\cos 2\theta)}{(x^2-y^2)} \qquad (71)$$

$$i_a' = i_\alpha + i_0$$

$$= \frac{2i_0x_0(x-y\cos 2\theta + i_0(x^2-y^2)}{(x^2-y^2)} \qquad (72)$$

From equation 72, i_0 in terms of i_a' is

$$i_0 = \frac{i_a'(x^2-y^2)}{[2x_0(x-y\cos 2\theta)+x^2-y^2]} \qquad (73)$$

From equations 70, 52, and 73,

$$\Psi_a = 3\Psi_0 = -3i_0x_0$$

$$= \frac{-i_a'3x_0(x^2-y^2)}{[2x_0(x-y\cos 2\theta)+x^2-y^2]} \qquad (74)$$

When i_a' in equation 74 is replaced by its value from equation 67

$$\Psi_a = \frac{3k_rEx_0(x-y)\cos\theta}{[2x_0(x-y\cos 2\theta)+x^2-y^2]} \qquad (75)$$

The assumption is made[6] that phase a clears at current zero. From equations 48 and 67, this requires that $\cos\theta = 0$; therefore, $\theta = \pi/2$ or $3\pi/2$. After equation 75 is differentiated, and then θ replaced by $3\pi/2$, e_a is given by the following equation at the instant phase a clears

$$e_a = p\Psi a = \frac{3x_0k_rE(x-y)}{2x_0(x+y)+x^2-y^2}$$

When x and y are replaced by their values from equation 53, the magnitude of e_a, the recovery voltage is

$$e_a = \frac{k_rE_a(3x_0x_q'')}{x_d''(x_q''+2x_0)} \qquad (76)$$

Equation 76 checks equation C-15 of reference 6. If $\theta = \pi/2$ instead of $3\pi/2$, the sign of e_a in equation 76 would be negative.

OPENING A 3-PHASE FAULT (NOT TO GROUND) IN AN UNGROUNDED SYSTEM

It will be assumed that phase a clears first. Two cases will be considered: (1) d-c and second harmonic components of currents have disappeared when phase a clears, and (2) they have not disappeared. The current to be superposed on existing condition in either case will be indicated by i_a'; and Ψ_a in terms of i_a' will be determined before substitution is made for i_a'. All values of Ψ and i used below are understood to be changes in Ψ and i due to the application of i_a'.

Without a neutral conductor or ground return path, $i_0 = 0$ and $\Psi_0 = 0$. Therefore, $i_a' = i_\alpha$ and $\psi_a = \Psi_\alpha$. As phases b and c are connected, $e_c = e_b$; and with resistance neglected, $\Psi_b = \Psi_c$. From equation 5, with i replaced by Ψ, $\Psi_\beta = 0$. Simultation solution of equations 50 and 51 for i_α, with $\Psi_\beta = 0$ and $\Psi_\alpha = \Psi_a$, gives

$$i_\alpha = i_a' = \frac{-\Psi_a(x-y\cos\theta)}{(x^2-y^2)} \qquad (77)$$

$$\Psi_a = \frac{-i_a'(x^2-y^2)}{(x-y\cos 2\theta)} \qquad (78)$$

With $\Psi_\beta = \Psi_0 = 0$, $\Psi_b = -\Psi_\alpha/2 = -\Psi_a/2$. Then

$$\Psi_{ba} = \Psi_a - \Psi_b = \frac{3\Psi_a}{2} = \frac{-\left(\frac{3}{2}\right)i_a'(x^2-y^2)}{(x-y\cos 2\theta)} \qquad (79)$$

Case 1

The value of i_a' to be substituted in equation 79 is the same as that given in equation 67; and if phase a clears at current zero, $\cos\theta = 0$ and $\theta = \pi/2$ or $3\pi/2$. If equation 67 is substituted for i_a' in equation 79, the differentiation performed, and θ replaced by $3\pi/2$

$$e_{ba} = p\Psi_{ba} = \left(\frac{3}{2}\right)k_rE\frac{(x-y)}{(x+y)} = \left(\frac{3}{2}\right)k_rE\frac{x_q''}{x_d''} \qquad (80)$$

The equation for this case and that given in reference 6 agree.

Case 2

The value of i_a' to be substituted in equation 79 is the negative of i_a given by equation 48 with appropriate decrement factors, and I_r replaced by unity.

$$i_a' = -\frac{[k_r(x-y)\cos\theta - k_ax\cos\theta_0 + k_ay \times \cos(2\theta-\theta_0)]}{(x^2-y^2)} \qquad (81)$$

Equation 81 checks equation B-4 of reference 6, when the same notation is used. When equation 81 is substituted in equation 79, with the last term in the numerator expanded, Ψ_{ba} becomes

$$\Psi_{ba} = \frac{3[k_r(x-y)\cos\theta - k_ax\cos\theta_0 + k_ay \times \cos 2\theta\cos\theta_0 + k_ay\sin 2\theta\sin\theta_0]}{2(x-y\cos 2\theta)}$$

$$= \frac{3}{2}\frac{[k_r(x-y)\cos\theta + k_ay\sin 2\theta\sin\theta_0]}{x-y\cos 2\theta} - \frac{3}{2}k_a\cos\theta_0$$

The equation for Ψ_{ba} can be expanded in series by equations 100 and 97 where Z is given by 94, if x and y replace a and b, respectively, in these equations. When x and y are then replaced by their value in terms of x_d'' and x_q'' from equation 53, and Ψ_{ba} differentiated, an expression for e_{ba}, the circuit breaker recovery voltage will be obtained.

$$e_{ba} = \left[-3k_rx_q''/(x_q''+\sqrt{x_d''x_q''}\right] \times \left[\sum_{n=1}^{n=\infty}(2n-1)Z^{n-1}\sin(2n-1)\theta\right] + 6k_a\sin\theta_0\sum_{n=1}^{n=\infty}nZ^n\cos 2n\theta \qquad (82)$$

where

$$Z = \frac{(\sqrt{x_d''} - \sqrt{x_q''})}{\sqrt{x_d''} + \sqrt{x_q''}}$$

As in the reference paper, the recovery voltage at current zero depends upon θ_0, θ and x_q''/x_d''. Equation 82 should check equation B-59 of the reference paper.[6] However, as there are only two series in equation 82 and four in equation B-59 in addition to five other terms, the agreement between the two has not been established at the present writing. When the development of equation 82 is compared with that of equation B-59, the advantages of $\alpha,\beta,0$ components and also of the harmonic series of Appendix I are apparent.

Appendix I. Special Trigonometric Series

The following trigonometric functions will be expanded in harmonic series.

$$f_1(\theta) = \frac{1}{(a-b\cos 2\theta)} \qquad (83)$$

$$f_2(\theta) = \frac{b\sin 2\theta}{(a-b\cos 2\theta)} \qquad (84)$$

$$f_3(\theta) = \frac{b\cos 2\theta}{(a-b\cos 2\theta)} \qquad (85)$$

$$f_4(\theta) = \frac{\sin\theta}{(a-b\cos 2\theta)} \qquad (86)$$

$$f_5(\theta) = \frac{\cos\theta}{(a-b\cos 2\theta)} \qquad (87)$$

where a and b are scalars, and $b<a$.

Consider the following expression, expanded by long division,

$$1/(1-Z)=1+Z+Z^2+\ldots Z^n+\ldots$$
$$=1+\sum_{n=1}^{\infty} Z^n$$

Let

$$Z=Z/\underline{\phi}=Z\epsilon^{j\phi}=Z(\cos\phi+j\sin\phi)$$

Then

$$\frac{1}{1-Z(\cos\phi+j\sin\phi)}=1+\sum_{n=1}^{\infty}(Z/\underline{\phi})^n$$
$$=1+\sum_{n=1}^{\infty}Z^n(\cos n\phi+j\sin n\phi)$$

Rationalization of the left-hand side, and equating real and imaginary terms, gives

$$\frac{Z\sin\phi}{1-2Z\cos\phi+Z^2}=\sum_{n=1}^{\infty}Z^n\sin n\phi \qquad (88)$$

$$\frac{1-Z\cos\phi}{1-2Z\cos\phi+Z^2}=1+\sum_{n=1}^{\infty}Z^n\cos n\phi \qquad (89)$$

If unity is subtracted from each side of equation 89

$$\frac{Z\cos\phi-Z^2}{1-2Z\cos\phi+Z^2}=\sum_{n=1}^{\infty}Z^n\cos n\phi \qquad (90)$$

From the addition of equations 89 and 90, there results

$$\frac{1-Z^2}{1-2Z\cos\phi+Z^2}=1+2\sum_{n=1}^{\infty}Z^n\cos n\phi \qquad (91)$$

Equations 88–91 are given by Bromwich;[10] the work which follows is an extension. If equation 89 is multiplied by Z^2 and added to equation 90, and both sides of the resultant equation divided by $(1-Z^2)$, there results

$$\frac{Z\cos\phi}{1-2Z\cos\phi+Z^2}=\frac{Z^2}{1-Z^2}+\frac{1+Z^2}{1-Z^2}\times\sum_{n=1}^{\infty}Z^n\cos n\phi \qquad (92)$$

If each side of equation 91 is multiplied by $(1+Z^2)/(1-Z^2)$, the resultant equation is

$$\frac{1}{1-\frac{2Z}{1+Z^2}\cos\phi}=\frac{1+Z^2}{1-Z^2}\times\left[1+2\sum_{n=1}^{\infty}Z^n\cos n\phi\right] \qquad (93)$$

Let $2Z/(1+Z^2)=b/a$. Then, $Z=(a-\sqrt{a^2-b^2})/b$, where the negative sign before the radical satisfies the condition that the series in equation 93 will approach unity as b approaches zero, which means that Z must be zero when b is zero. Thus,

$$\lim_{b\to 0} Z=\lim_{b\to 0}\frac{a-\sqrt{a^2-b^2}}{b}$$
$$=\lim_{b\to 0}\frac{a^2-(a^2-b^2)}{b(a+\sqrt{a^2-b^2})}=\lim_{b\to 0}\frac{b}{2a}=0$$

If both numerator and denominator of the expression for Z are multiplied by 2, $+b$ and $-b$ added to the numerator, and $+a$ and $-a$ added to the denominator, the equation for Z becomes

$$Z=\frac{a-\sqrt{a^2-b^2}}{b}$$
$$=\frac{(a+b)-2\sqrt{a^2-b^2}+(a-b)}{(a+b)-(a-b)}$$
$$=\frac{\sqrt{a+b}-\sqrt{a-b}}{\sqrt{a+b}+\sqrt{a-b}} \qquad (94)$$

The following equations involving Z will be found useful

$$\frac{2Z}{1+Z^2}=\frac{b}{a};\quad 1+Z^2=\frac{2aZ}{b};$$
$$1-Z^2=\frac{2(b-aZ)}{b};\quad \frac{1+Z^2}{1-Z^2}=\frac{aZ}{b-aZ};$$
$$\frac{Z}{b-aZ}=\frac{1}{\sqrt{a^2-b^2}} \qquad (95)$$

If ϕ in equation 93 is replaced by 2θ, and both sides of the equation divided by a, the resultant equations when simplified by substitutions from equation 95 becomes

$$\frac{1}{a-b\cos 2\theta}=\frac{1}{\sqrt{a^2-b^2}}\times\left[1+2\sum_{n=1}^{\infty}Z^n\cos 2n\theta\right] \qquad (96)$$

Equation 96 expresses equation 83 as a series, where Z is given by equation 94.

If ϕ in equation 88 is replaced by 2θ, $(1+Z^2)$ in the denominator of the fraction replaced by its value from equation 95, numerator and denominator then divided by Z, and both sides of the resultant equation multiplied by 2, there results

$$\frac{b\sin 2\theta}{a-b\cos 2\theta}=2\sum_{n=1}^{\infty}Z^n\sin 2n\theta \qquad (97)$$

Equation 97 expresses equation 84 as a series, where Z is given by equation 94.

When ϕ in equation 92 is replaced by 2θ, and substitutions are made from equations 94 and 95, the equation becomes

$$\frac{b\cos 2\theta}{a-b\cos 2\theta}=\frac{a-\sqrt{a^2-b^2}}{\sqrt{a^2-b^2}}+\frac{2a}{\sqrt{a^2-b^2}}\times\sum_{n=1}^{\infty}Z^n\cos 2n\theta \qquad (98)$$

Equation 98 expresses equation 85 as a series where Z is given by equation 94.

The series for equation 86 can be obtained by multiplying both sides of equation 96 by $\sin\theta$ and simplifying the resultant equation.

$$\frac{\sin\theta}{a-b\cos 2\theta}=\frac{1}{\sqrt{a^2-b^2}}\times\left[\sin\theta+2\sum_{n=1}^{\infty}Z^n\cos 2n\theta\sin\theta\right]$$
$$=\frac{1}{\sqrt{a^2-b^2}}\left[\sin\theta+\sum_{n=1}^{\infty}Z^n\times\sin(2n+1)\theta-\sum_{n=1}^{\infty}Z^n\sin(2n-1)\theta\right]$$
$$=\frac{1}{\sqrt{a^2-b^2}}\times\left[\sin\theta-Z\sin\theta+\sum_{n=1}^{\infty}Z^n\times\sin(2n+1)\theta-\sum_{n=2}^{\infty}Z^n\sin(2n-1)\theta\right]$$
$$=\frac{1}{\sqrt{a^2-b^2}}\left[\sin\theta-Z\sin\theta+\sum_{n=2}^{\infty}Z^{n-1}\sin(2n-1)\theta-\sum_{n=2}^{\infty}Z^n\sin(2n-1)\theta\right]$$
$$=\frac{1-Z}{\sqrt{a^2-b^2}}\sum_{n=1}^{\infty}Z^{n-1}\sin(2n-1)\theta$$
$$=\frac{2}{a+b+\sqrt{a^2-b^2}}\sum_{n=1}^{\infty}Z^{n-1}\times\sin(2n-1)\theta \qquad (99)$$

The series for equation 87 can be obtained by multiplying both sides of equation 96 by $\cos\theta$.

The development is analogous to that given in equation 99.

$$\frac{\cos\theta}{a-b\cos 2\theta}=\frac{2}{a-b+\sqrt{a^2-b^2}}\times\sum_{n=1}^{\infty}Z^{n-1}\cos(2n-1)\theta \qquad (100)$$

Equations 99 and 100 express equations 86 and 87, respectively, as series where Z is given by equation 94.

References

1. PROBLEMS SOLVED BY MODIFIED SYMMETRICAL COMPONENTS, Edith Clarke. *General Electric Review* (Schenectady, N. Y.), November and

December, 1938, volume 41, numbers 11 and 12, pages 488–94 and 545–49.

2. Two-Phase Co-ordinates of a Three-Phase Circuit, **Edward W. Kimbark.** *AIEE Transactions*, volume 58, 1939, pages 894–910.

3. Circuit Analysis of A-C Power Systems, **Edith Clarke.** John Wiley and Sons, New York, N. Y., volume 1, chapter X, 1943.

4. Definition of an Ideal Synchronous Machine and Formula for the Armature Flux Linkages, **R. H. Park.** *General Electric Review* (Schenectady, N. Y.), volume 31, June 1928, pages 332–34.

5. Two Reaction Theory of Synchronous Machines—Generalized Method of Analysis—Part I, **R. H. Park.** *AIEE Transactions*, volume 48, July 1929, pages 716–30.

6. Circuit Breaker Recovery Voltages, **R. H. Park, W. F. Skeats.** *AIEE Transactions*, volume 50, March 1931, pages 204–39.

7. Circuit Analysis of A-C Power Systems, **Edith Clarke.** John Wiley and Sons, New York, N. Y., volume II, 1950.

8. American Standard Definitions of Electrical Terms, AIEE, 1942.

9. Synchronous Machines IV—Single Phase Circuits, **R. E. Doherty, C. A. Nickle.** *AIEE Transactions*, volume 47, April 1928, pages 457–92.

10. Theory of Infinite Series, **T. J. I'a. Bromwich.** Macmillan and Company, Limited, London, England, 1942.

Discussion

Eric T. B. Gross (Illinois Institute of Technology, Chicago, Ill.): It has not been recognized until a few years ago that Clarke components are very useful in many unbalanced 3-phase problems, and this paper indicates clearly some of the distinct advantages of Clarke components. The complex operator a, so significant in symmetrical components sometimes introduces complications. Since the unbalances of great practical importance are the short circuit of "one phase" alone or "between two phases," which are "single axis" unbalances, they may be studied by replacing the 3-phase machine by a 2-phase machine. Dreyfus (1911, 1912, 1916), Biermanns (1915), Rudenberg (1925) made valuable investigations along these lines in Europe some time ago and a close relation to the treatment with Clarke components should not be surprising. See also reference 1.

In some cases, especially in connection with the application of the network analyzer, symmetrical components can not be used whereas Clarke components provide a basis for the solution. One such example concerns the study of transients in power systems[2] by means of the transient analyzer when single-phase circuits are used to reproduce 3-phase phenomena.[3]

References

1. Damping and Resonance in Polyphase Generators, **R. Willheim.** *Archiv fuer Elektrotechnik*, (Berlin, Germany), 1929, pages 593–611.

2. Transient Analysis of Three-Phase Power Systems, Part I, **Eric T. B. Gross, Leonard Rabins.** *Journal*, Franklin Institute (Philadelphia, Pa.), volume 251, 1951, pages 333–41.

3. Transient Analysis of Three-Phase Power Systems, Part II, **Leonard Rabins, Eric T. B. Gross.** *Journal*, Franklin Institute (Philadelphia, Pa.), volume 251, 1951, pages 521–37.

A High-Speed Telemetering System With Automatic Calibration

W. E. PHILLIPS
MEMBER AIEE

Synopsis: This paper describes a high-speed telemetering system which uses frequency as a translating means. Equipment for two different frequency bands of 20 to 25 cycles and 80 to 100 cycles has been developed. The system is electronic and the lag between a change in the primary quantity to a change in the receiver is less than 0.4 second. The system is independent of the wave shape and amplitude of the signal over extremely wide limits. Means are provided for automatic calibration at frequent intervals which compensate for changes in vacuum tubes and other circuit elements.

THE USE of a variable frequency as a translating means for a telemetering system was proposed as early as 1917.[1] This early system, which was installed on the Chicago, Milwaukee and St. Paul Railway, used motor generator sets to generate the variable frequency for telemetering. The advent of the vacuum tube makes such a system cumbersome when judged by present-day standards, however, at the time of its installation it was a real achievement.

Since the date of the above installation numerous commercial telemetering systems using frequency as a means of translation have been developed. The application of these systems has not been general because the need for high-speed carrier current telemetering was not so acute as at present and also the characteristics of the telemetering systems were not well suited to carrier current. The recent requirement of higher telemetering speeds has resulted in new developments in this field and this paper describes a high-speed telemetering system developed to fulfill the present day requirements of electrical power systems.

Idealized Telemetering System

Before discussing the telemetering system which is the subject of this paper, it would be well to outline some of the characteristics of a more or less idealized frequency telemetering system. The characteristics of such a system would be:

1. The frequency band should be as narrow as possible in order that it takes the minimum possible space in the carrier frequency spectrum, also certain types of power line carrier equipment require that the frequency change be very small. The same requirement must be met on the submultiplexing of microwave transmission.
2. The frequency used should be low. It should be noted that the use of a very low frequency will be disadvantageous from the standpoint of telemetering speed and modulation on certain carrier channels.
3. The telemetering receiver should be independent of harmonics and extraneous frequencies which may be present in the received signal.
4. The telemetering receiver should be independent of the amplitude of the received signal over extremely wide limits.
5. There should be no error due to temperature variations.
6. There should be no error due to aging of components.
7. The system should be instantaneous in response.
8. The accuracy should be within the generally accepted limits for telemetering systems applicable to carrier current transmission and should be sustained over periods of many months.
9. The system should be independent of power supply variations.

Basic Concepts

The primary objective in this development was to provide a high-speed telemetering system in which the initial movement of the receiving recorder occurs within 0.5 second or less after the change in primary load. It should be noted that it is not the purpose of this paper to prove the need for a high-speed telemetering system. It will suffice merely to state at this point that it has been found, that for those applications which require fast changes in generation for the automatic control of load and frequency, this high-speed telemetering will make possible improved control with a reduction in the maneuvering of generator loads.

Frequency was selected as a translating means for a high-speed telemetering system for the following reasons:

1. Frequency can be transmitted long distances without losing any of its intelligence due to high attenuation.
2. Frequency may be transmitted continuously and thus it constitutes a medium for a continuous telemetering system.
3. Frequency lends itself ideally to being varied instantly to a value proportional to a varying measured quantity.

In the development of this telemetering system particular attention was given to insure that it was suitable for application to carrier frequency and microwave channels.

Telemetering Transmitter

The equipment at the transmitting end consists of a primary element, thermal converter,[2,3] a Speedomax recorder,[4] and a phase shift type of oscillator.

The thermal converter is connected to the current and potential transformers and produces a d-c potential, proportional to a-c power, which is recorded potentiometrically by the Speedomax recorder. The recorder, which is cali-

---

Paper 51-228, recommended by the AIEE Joint Subcommittee on Telemetering and approved by the AIEE Technical Program Committee for presentation at the AIEE Summer General Meeting, Toronto, Ont., Canada, June 25–29, 1951. Manuscript submitted March 26, 1951; made available for printing May 11, 1951.

W. E. Phillips is with Leeds and Northrup Company, Philadelphia, Pa.

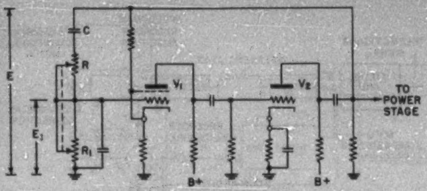

Figure 1. Schematic diagram of oscillator frequency determining network

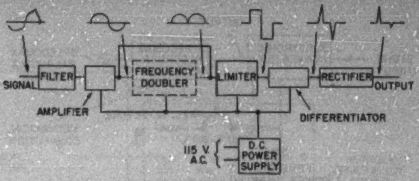

Figure 2. Block diagram of frequency converter showing wave shapes at several stages

brated in primary power, has a retransmitting slidewire, the resistance of which is varied in accordance with the recorder reading. This slidewire is connected in a phase-shift oscillator circuit in such a manner that a variation in slidewire resistance causes a change in the oscillator frequency.

All of these things have been amply described previously, however, since we are particularly interested in the variable frequency oscillator circuit and the method of varying it, a review of this circuit will be helpful. This oscillator and its control circuit are shown schematically in Figure 1.

The frequency determining network consists of R, R_1, C, and C_1. This network has the property that the voltage E_1 (Figure 1) will be in phase with the voltage E at only one frequency. This frequency is determined from the following relation

$$W^2 = \frac{1}{RR_1CC_1} \tag{1}$$

where

$W = 2\pi f$.

As shown in Figure 1, there are two stages of amplification, V_1 and V_2, between the grid of V_1 and its feedback circuit from the output of V_2. Thus there is 360 degree phase shift, 180 degrees in each tube, in the feedback circuit exclusive of any phase shift in the frequency determining network. Since to maintain oscillation, the feedback must be in phase with the original signal this means there must be zero phase shift in the network consisting of R, R_1, C, and C_1. For oscillation, the frequency will be automatically maintained at a value which keeps this phase shift at zero. If R and R_1 are changed, the frequency instantly varies to a new value which will satisfy the relation in equation 1.

The capacitors and resistors in the frequency determining network are extremely stable and have low temperature coefficients so that the over-all temperature coefficient of the oscillator frequency output is 0.003 per cent per degree Fahrenheit. The frequency of the oscillator is not dependent on normal changes in tube characteristics since if the tube is operating the phase shift between the grid and plate circuit voltages is 180 degrees.

Tests conducted over a period of several months show the oscillator drift to be 0.05 per cent.

In the case of the telemetering system, resistors R and R_1, Figure 1, are mounted on the shaft of the recorder and their value changes with the recorder reading as noted previously. For each recorder position there is a definite value of frequency. Thus for each value of primary load there is established a definite frequency. Oscillators having ranges of 20 to 25 cycles or 80 to 100 cycles are used. As will be explained later both of these frequencies may be used simultaneously as two tones on a multitone carrier channel.

Telemetering Receiver

The receiving end of the telemetering system consists of an electronic converter which produces a d-c voltage proportional to frequency, and a Speedomax potentiometer recorder which is connected to the output of the electronic converter.

The electronic converter, shown schematically in Figure 2, consists of a filter, an amplifier section, a frequency doubler section—this is used only for the 20-25 cycle range, a limiter section, a differentiating section, a rectifier section, and a d-c power supply.

Filter

The filter for the 20–25 cycle converter is of the low-loss type and consists of 2 Constant K low pass sections and one shunt M derived section. The loss at operating frequencies is less than 6 decibels and the attenuation at frequencies of 60 cycles or above is 60 decibels or greater.

The filter for the 80–100 cycle converter consists of $2^1/_2$ Constant K band pass sections. The loss at operating frequencies is less than 6 decibels and the attenuation at 60 cycles and below and at 150 cycles and above is greater than 60 decibels.

The wave forms shown in Figure 2 indicate graphically the elimination of harmonics by the filter.

Frequency Doubler Section

As indicated previously, the frequency doubler section is used only on the 20-to-25 cycle range. The reason for this doubling is that with frequencies of low values, a high-speed recorder needs additional filtering in order that it does not tend to follow the cyclic variations in the final output current. Any additional filtering added because of the use of a low frequency will increase the time lag of the telemetering system.

The frequency doubler section consists of a phase inverter stage the output of which is fed in push-pull to the grids of a twin triode. The twin triode is connected as a cathode follower so that the resultant cathode current is of double frequency.

Limiter Section

The limiter section consists of three pentode stages; the first two stages serve to give identical limiting to both the positive and negative half waves of the signal voltage. Sharp cutoff tubes are used which give a square wave when the grids go negative, however, there is some rounding of the wave shape when the grids draw grid current on the positive half wave. After passing through the first two limiters, the wave shape is reshaped to a form roughly resembling a sine wave and this modified wave form is applied to the grid of the third limiter stage. The reshaping circuit in combination with the third limiter stage produce essentially a square wave shown in Figure 2, which is constant in amplitude and wave shape for a wide range of input signals.

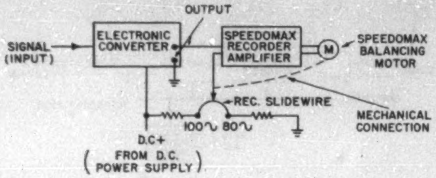
OUTPUT
SIGNAL (INPUT)
ELECTRONIC CONVERTER
SPEEDOMAX RECORDER AMPLIFIER
M
SPEEDOMAX BALANCING MOTOR
REC. SLIDEWIRE
MECHANICAL CONNECTION
100∿ 80∿
D.C+ (FROM D.C. POWER SUPPLY)

Figure 3. Schematic diagram of recorder measuring circuit

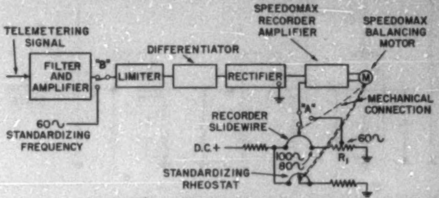
TELEMETERING SIGNAL
FILTER AND AMPLIFIER
"B"
LIMITER
DIFFERENTIATOR
RECTIFIER
SPEEDOMAX RECORDER AMPLIFIER
SPEEDOMAX BALANCING MOTOR
M
MECHANICAL CONNECTION
"A"
RECORDER SLIDEWIRE
60∿ STANDARDIZING FREQUENCY
D.C+
100∿
80∿
60∿
R₁
STANDARDIZING RHEOSTAT

Figure 4. Schematic diagram of method employed to standardize receiving recorder

Differentiator Section

This section, as the name indicates, differentiates the square waves derived from the limiter section. The differentiator circuit is conventional in design and consists of a capacitor of small capacitance in series with a comparatively low resistance. Thus the impedance is determined primarily by the capacitor.

Due to the low time constant of the circuit and the fact that the reactance of the capacitor is small for the very high rates of change experienced with square waves, current will flow, through the capacitor only at a time when the square wave is changing sharply.

A true derivative of the square waves, which are shown in Figure 2 at the input to this section, would have a vertical amplitude but zero width. This would not be satisfactory for the end use which, as will be described later, is to integrate the positive pulses. After the derivative is obtained, the wave is amplified and reshaped so as to have some width as shown in Figure 2.

Rectifier Section

The rectifier section consists of a twin diode (*6H6*) so connected that the positive current pulses are permitted to flow through a parallel combination of resistance and capacity. The voltage across this resistance–capacitance network is proportional to the average number of impulses and it is this voltage which is recorded by the potentiometer recorder. The negative pulses are short circuited by the other half of the *6H6* so that they do not appear in the output.

D-C Power Supply

The d-c power supply is electronically regulated using a *VR-150* tube as a reference. The d-c voltage is held within 1/4 per cent for a change of 95 to 130 volts in the a-c input.

Recorder and Calibrating Circuit

The recorder measuring circuit is shown schematically in Figure 3.

The output of the electronic converter is opposed to the electromotive force set-up by the recorder slidewire circuit so that any unbalance will cause the balancing motor, by means of its amplifier, to move the slidewire until the two potentials are equal. This is the conventional potentiometer method of measuring a potential. The slidewire circuit voltage is obtained from the d-c power supply which supplies the electronic converter. If the d-c voltage changes it affects both the output of the converter and the slidewire voltage in the same direction. By the use of proper constants in these circuits the effects of changing d-c voltage are minimized.

As described previously, the electronic converter contains vacuum tubes; variations in some of these tubes will have an effect on the output. This variation in tube characteristics is a relatively slow process and if some automatic means can be provided for checking and compensating for these variations at intervals of once a week we will have no significant changes in the telemetering calibration. As a practical matter it is convenient to perform this automatic calibration at 45 minute intervals.

Figure 4 is a schematic diagram of the method used to automatically calibrate or standardize the telemetering converter. Switches *A* and *B* are normally closed as shown and the recorder balancing motor is mechanically connected only to the recorder slidewire. Thus the circuit functions exactly as described previously when measuring the telemetering frequency.

As noted in Figure 4 the potential at the one end of the recorder slidewire corresponds to the converter output at 80

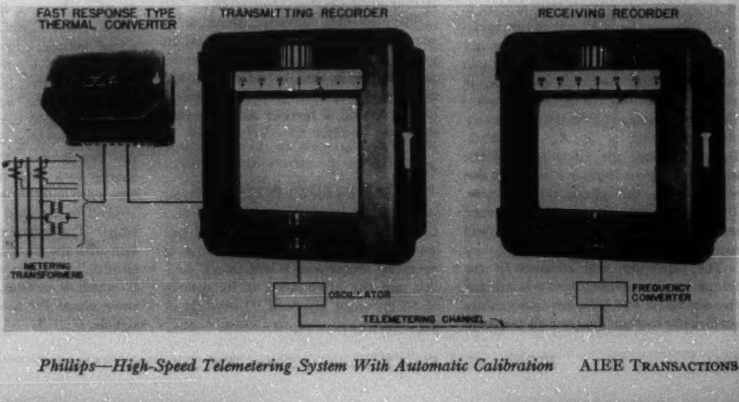
FAST RESPONSE TYPE THERMAL CONVERTER
TRANSMITTING RECORDER
RECEIVING RECORDER
METERING TRANSFORMERS
OSCILLATOR
FREQUENCY CONVERTER
TELEMETERING CHANNEL

Figure 5. Pictorial diagram of telemetering channel equipment

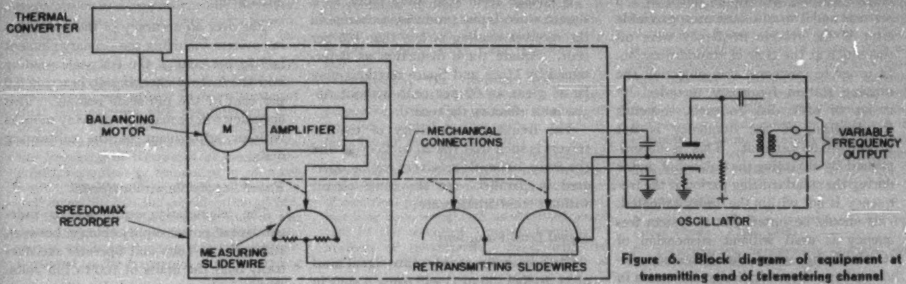
THERMAL CONVERTER
BALANCING MOTOR
M
AMPLIFIER
MECHANICAL CONNECTIONS
SPEEDOMAX RECORDER
MEASURING SLIDEWIRE
RETRANSMITTING SLIDEWIRES
VARIABLE FREQUENCY OUTPUT
OSCILLATOR

Figure 6. Block diagram of equipment at transmitting end of telemetering channel

cycles and the other end of the slidewire to the output at 100 cycles. If 60 cycles were the converter input, its output would be a potential which is designated as 60 cycles at resistor R_1.

For purposes of explanation, it is assumed that with an 80-cycle input the recorder will balance at the 80-cycle point on the slidewire and with a 60 cycle input the converter output will equal the potential at the 60 cycle point on R_1. This relation, once potentiometrically established, is fixed since the slidewire and the coils shown are made of high grade, low temperature coefficient resistance wire.

After a period of operation the converter output may change due to some change in tube characteristics or other elements in the converter. If for example the output decreases, then it will be low by the same percentage at either the 80- or 60-cycle frequency. By connecting the converter to a known 60-cycle frequency we can check the converter calibration in the following manner. Referring to Figure 4, switches *A* and *B* are connected to the calibrating or standardizing position which is the position opposite to that shown in figure. Switch *B* connects a known 60-cycle frequency to the converter input just after the filter and switch *A* connects one side of the Speedomax recorder amplifier to the 60-cycle point on R_1. The same recorder mechanism which controls switches *A* and *B* also controls the mechanical connection between the recorder balancing motor and the standardizing rheostat. This is shown as a double dashed line on Figure 4. When switches *A* and *B* are thrown to the standardizing position, this mechanical connection is made. This mechanism has been used on potentiometer recorders for a great many years.

If, as assumed, the output of the converter is low when connected to 60 cycles, then to achieve a balance with the 60-cycle point on R_1, it will be necessary to reduce the potential of the 60-cycle point. The unbalance in the recorder amplifier will, through the medium of the balancing motor, cause the standardizing rheostat to decrease its resistance. This decrease in resistance shunts more of the current out of the slidewire circuit which lowers the potential of the 60-cycle point and also the recorder slidewire potential. When the recorder is returned to its normal measuring state, the recorder slidewire will again be correctly calibrated for 80 to 100 cycles for the conditions existing in the converter at this time.

It should be noted that any change in the d-c potential to the slidewire circuit as well as changes in the converter will be compensated.

The use of a 60-cycle standardizing frequency has just been discussed. This may be either system frequency or a standard 60-cycle frequency which is now quite commonly available in generating stations and dispatching centers. When a standard frequency is available, there is no question of inaccuracy from this source. When system frequency is used,

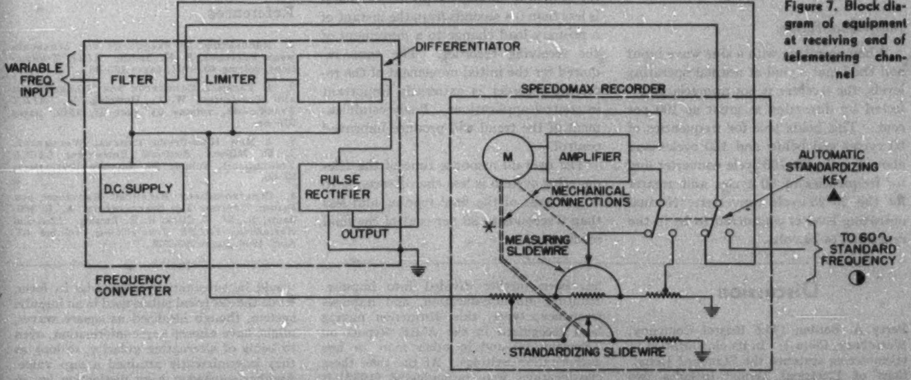
VARIABLE FREQ. INPUT
FILTER
LIMITER
DIFFERENTIATOR
SPEEDOMAX RECORDER
M
AMPLIFIER
D.C. SUPPLY
PULSE RECTIFIER
OUTPUT
MECHANICAL CONNECTIONS
*
MEASURING SLIDEWIRE
AUTOMATIC STANDARDIZING KEY ▲
TO 60∿ STANDARD FREQUENCY ◐
FREQUENCY CONVERTER
STANDARDIZING SLIDEWIRE

Figure 7. Block diagram of equipment at receiving end of telemetering channel

* THIS CONNECTION MADE ONLY WHEN STANDARDIZING.

▲ CONTACTS CLOSED TO OPPOSITE SIDE WHEN STANDARDIZING.

◐ SYSTEM FREQUENCY CAN BE USED IN CONJUNCTION WITH CONTACTS IN EXISTING SYSTEM FREQUENCY RECORDER.

it may possibly deviate as much as 1/3 per cent and it would cause an appreciable error if the system frequency were off this much at the time of standardization. In order to overcome this objection the existing station frequency recorder, by means of back disk contacts, suspends standardizing if the frequency is not within ±0.05 per cent. This is accomplished by disabling the balancing motor during the standardizing period if the frequency is not within the limits indicated.

It should be noted that if system frequency is used without suspension of standardizing when the frequency deviates beyond certain limits, the errors in calibration will not be cumulative but will result only in temporary errors proportional to the frequency deviation.

The over-all telemetering system is shown in pictorial form on Figure 5. Figure 6 shows the transmitting end equipment in schematic form and Figure 7 shows the receiving end equipment also in schematic form. It will be interesting to compare the performance and characteristics of this telemetering system with those of the idealized telemetering system which were outlined earlier.

Telemetering Frequencies

The method used for generating and measuring the telemetering frequencies is extremely flexible and any desired frequency can be used for the translation of readings. The telemetering systems which are now installed have made use of two different frequencies. Some of the present installations use a frequency of 80 to 100 cycles and the remainder of the installations employ a frequency of 20 to 25 cycles. Other frequencies can be used if there is a justifiable need for them.

Interference Factors

When operating with a sine wave input and the input signal at normal operating levels, the receiver is not appreciably affected by distortion as great as 100 per cent. This holds true for frequencies of 60 cycles and below and 150 cycles and above for the 80–100 cycle converter and for frequencies of 60 cycles and greater for the 20–25 cycle converter. Normal operating level is considered to be in the range of 1 to 10 volts.

A change from sine wave input to a square wave input produces a change in the receiver reading of less than 0.5 per cent. Square wave distortion as determined by Mark and Space relations may be as great as 60 per cent without appreciable effect on the record.

The frequency selectivity of the receivers is such that the 20 to 25 cycle and the 80 to 100 cycle receivers can be operated in parallel over the same circuit without cross interference.

Signal Level Variations

Changes in the steady state signal level of 34 decibel (50 to 1) will cause a shift in the receiver record of approximately 0.2 per cent. Instantaneous changes in signal level of 50 per cent cause a momentary deviation of 0.5 per cent in the receiver reading.

Temperature Effects

The temperature coefficient of the oscillator (transmitter) output frequency is 0.003 per cent per degree Fahrenheit. The temperature coefficient of the telemetering receiver is 0.016 per cent per degree Fahrenheit before the receiver is standardized at the new temperature. After standardization this error is reduced to 0.004 per cent per degree Fahrenheit.

Effects of Tube Variations

The receiver is independent of wide changes in vacuum tube characteristics. This is due to the fact that the telemetering receiver is periodically standardized.

Response Time

The over-all response of the telemetering system including the primary element is less than 0.4 seconds from the instant of a primary load change to a movement of the receiving recorder. The time required for the initial movement of the receiving recorder is extremely important in control applications. Early establishment of the trend will produce improved control.

The over-all response time of the telemetering system is less than 2 seconds to 90 per cent of the final reading and less than 3 seconds to 99 per cent of the final reading.

Accuracies

The over-all accuracy of the telemetering system including the primary element is 1.75 per cent of the full scale reading and the factory checking accuracy is 0.9 per cent of the full scale reading. This accuracy will be maintained many months without adjustment of the calibrating dials.

Power Supply Variation Effects

The telemetering equipment is independent of power supply changes between 105 and 125 volts and operates satisfactorily over the limits of 100 to 135 volts. Either instantaneous or slow changes in this voltage supply, within these limits, will have little effect on the receiver.

Conclusion

A comparison of the performance data of this telemetering system with the characteristics outlined for an idealized system shows that the latter has been closely approached. The ability of the telemetering system to operate with sustained accuracy over a wide variety of carrier channels has been demonstrated by installations over a period of more than two years. One installation on the Tennessee Valley Authority system transmits the telemetered load for a distance of 500 miles and employs three different types of carrier current circuits in traversing this distance.

This installation has also permitted practical demonstration of the fact that the over-all response of the telemetering system is comparable to that of an indicating wattmeter.

References

1. Regulation of Frequency for Measurement Purposes, B. H. Smith. *AIEE Transactions*, volume 40, 1921, pages 425–38.

2. A Thermal Converter for Telemetering and Totalizing, W. C. Downing, Jr. *AIEE Transactions*, volume 68, part II, 1949, pages 879–84.

3. A New High-Speed Thermal Wattmeter, J. H. Miller. *Electrical Engineering* (*AIEE Transactions*), volume 60, January 1941, pages 37–40.

4. Electronically Balanced Recorder for Flight Testing and Spectroscopy, A. J. Williams, Jr., W. R. Clark, R. E. Tarpley. *Electrical Engineering* (*AIEE Transactions*), volume 65, April 1946, pages 205–208.

Discussion

Perry A. Borden (The Bristol Company, Waterbury, Conn.): In its classification of telemetering systems, the Standard Definitions of Electrical Terms[1] includes two categories, "Frequency" telemeters and "Impulse" telemeters. The latter group has been further divided into impulse-counting, impulse-duration, and impulse-frequency, types, this distinction having been recognized in the AIEE Report on Telemetering[2] and in other more or less authoritative writings. At the time these classifications were promulgated (1932) it was tacitly assumed that the currents or voltages utilized in a frequency system would be substantially sinusoidal in form, while the electrical pulses used in an impulse system, though idealized as square waves, might have almost any conformation, even to being of alternating polarity, so long as they intermittently attained a zero value. Another somewhat hazy distinction lay in the former system having a frequency sufficiently high (say, over 16 cycles) to be predominantly governed by the laws of transmission in a-c circuits, while the latter, whose frequency might range down to zero, could be considered as a succession of discrete electrical impulses.

Less inhibited by tradition, the radio group and the exponents of mobile telemetering do not appear to have burdened their terminologies with the foregoing distinction; and their term "pulse-rate" seems generic to all measurements based on the frequency of recurrence of electric impulses, regardless of symmetry or of wave form. The soundness of this reasoning is well exemplified in the consideration of Mr. Phillips' paper. The receiving end of the system which he describes includes a converter which produces a d-c voltage proportional to the frequency of the incoming signal, this voltage being measured in a conventional manner. The conversion of the a-c signal to a measurable voltage involves several steps, in which the identity of the incoming wave form is completely lost.

Eventually, the rectifier section of the receiving network delivers a voltage proportional to the average number of impulses; and it is this voltage which is recorded by the potentiometer.

The idea of producing a measurable potential proportional to the number-in-a-selected-time, or frequency, of a succession of electrical pulses is of course not new, and has long been recognized as standard practice in the so-called "impulse-frequency" systems of telemetering. Now, with its definite application in a refined form to a telemetering system in which the transmitted signals approximate a sine wave, it may be said that there no longer exists any distinction between the two classes. Thus, it appears that such line of demarcation as may have existed between frequency systems and any of the subclasses of impulse systems is becoming most indefinite, and that the joint efforts of the several committees now collaborating on definitions in telemetering should seriously consider such grouping as will eliminate the present nebulosity in classification.

References

1. American Standard Definition of Electrical Terms. AIEE, 1942.

2. Telemetering, Supervisory Control, and Associated Circuits. AIEE, 1948.

Rapid Transit Developments In Toronto

J. G. INGLIS
MEMBER AIEE

Synopsis: The construction of Canada's first subway is scheduled for completion in the City of Toronto by the end of 1953. Since there were no standards to be continued, full advantage was taken of new methods and materials. A brief description is given of much of the equipment, particularly the cars which will be 130 in number and of the lightweight Presidents' Conference Committee(PCC) type.

A Century of Progress

WHEN public transportation commenced in Toronto in 1851 with four horse-drawn omnibuses, who could have foretold that the next century would see the little city of 24,000 become a bustling metropolitan area of a million; or that public transportation facilities would have increased to over 1,000 street cars, 600 busses, 85 trolley coaches, 6 ferry boats, and 1,000 miles of interurban motor coach system; or that these facilities would still be inadequate, and that exactly 100 years after public transportation began here, the construction of Canada's first subway would be started in Toronto, thereby permitting it to join the ranks of approximately 15 world cities which have this type of mass transportation.

Preliminary Planning

Actual construction of the subway commenced in September 1949, with the completion scheduled for the latter part of 1953 although construction was preceded by several years of study and planning.

An unusual opportunity was presented in the construction of the subway. Since it was entirely new, it was unnecessary to conform to any existing standards, and free choice was possible in the selection of methods and materials. Full advantage was taken of this opportunity and much detail study was made of practices existing on this Continent and abroad.

Description of Route and Service

Many details concerning the project have been given in an earlier paper.[1] The 1-way length of the line is 4.56 miles and it extends from the Union Station on the south, thence along Front Street to Yonge Street, then north on Yonge to Eglinton Avenue. The southerly portion, approximately 7,000 feet long, will be under city streets, and will be built by the cut-and-cover method. North of this point the lower cost of property made it possible for the line to follow an off-street route closely parallel to Yonge Street. The off-street route reduced the cost, permitted easier grades, and permitted better transfer arrangement with intersecting car and bus lines. The off-street portion of the route is partially in subway and partially in a depressed open cut. The closed portion will be approximately two-thirds of the total length, and the open portion the remainder.

The system will be a 2-track line, with 12 stations to be spaced about 0.4 miles apart. Local service on the Yonge Street surface route will be provided by busses, making connections at each subway station. Also, at all stations but two, connecting rail or bus lines will intersect the subway, and transfers between the surface and the underground systems may be made. At the northerly terminal at Eglinton Avenue and Yonge Streets, a radiating network of bus and trolley coach lines operating from ten loading platforms will serve the surrounding section of the City and the two adjoining suburbs. Wherever possible, passenger transfer between surface and subway vehicles will be made entirely on Commission property to avoid the inconvenience and delay of paper transfers.

The maximum capacity of the system will be 40,000 passengers per hour in each direction. This is between two and three times the expected initial loads, and should provide liberally for expected expansion. The base schedule speed will be approximately 18 miles-per-hour with a 1-way running time of 15 minutes. In the rush hours this will be increased to 16 or 17 minutes.

Train length and headway will vary with the traffic. In the rush hour periods, the headways will decrease to two minutes and the train length increase to 6, 8, or even 10 cars. All details such as the power supply, signalling, station platforms, and car equipment are being designed for an ultimate operation of 10-car trains on 2-minute headways.

Power Supply

The propulsion power will be supplied at 600 volts direct current from mercury arc rectifiers located in automatic stations. Current collection will be by means of an overrunning 150 pound third rail. Additional feed cable will not be used as it is considered more economical to add intermediate stations at a later date if or when the system approaches its ultimate carrying capacity.

A supervisory control system will be provided to give remote control of all traction power circuit breakers. It also will control the ventilating system, and will indicate failure of any pump or auxiliary power supply. A series of emergency alarm boxes will be located in the subway and the operation of these will automatically cut off the power supply in that area and send in an alarm to the load dispatcher. A telephone will be located beside each box.

Paper 51-230, recommended by the AIEE Land Transportation Committee and approved by the AIEE Technical Program Committee for presentation at the AIEE Summer General Meeting, Toronto, Ont., Canada, June 25–29, 1951. Manuscript submitted March 26, 1951; made available for printing May 3, 1951.

J. G. Inglis is with the Toronto Transportation Commission, Toronto, Canada.

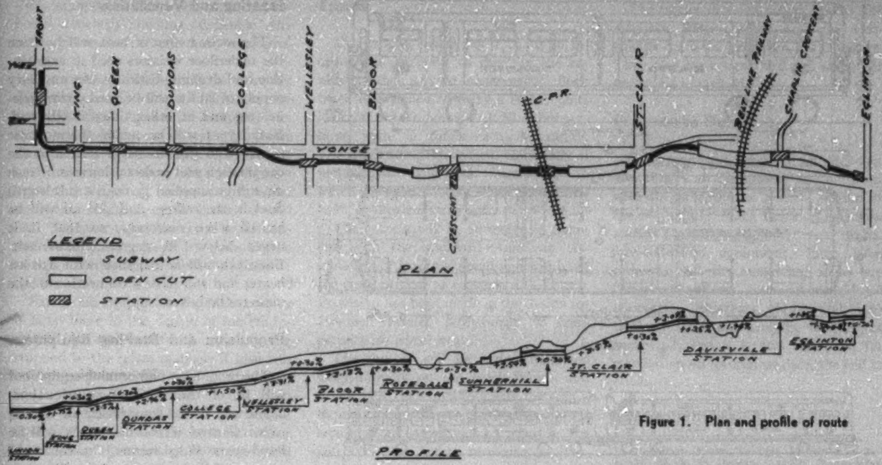

Figure 1. Plan and profile of route

Fluorescent subway lighting will be used and 60-cycle energy will be available. Lighting intensities will be higher than those generally used in subways. The proposed intensities are:

	Foot-Candles
Mezzanine or control areas	7.5 to 12.0
Stairways and escalators	10.0 to 12.0
Loading platforms	7.5 to 12.0
Train tubes	1.0

A standby battery supply will provide instantaneous and automatic emergency lighting in case of a power failure.

Operation of the trains will be regulated by a 3-aspect wayside signal system, complete with track trip throughout and with speed control on the steepest down grades. The interlocking plants at the terminals will function automatically, but will have overriding manual control. Yard approach signals will be semiautomatic, with track occupancy indicated automatically but switch movements controlled manually. The automatic interlocking features associated with each switch and signal will prohibit conflicting train movements.

The Car Equipment

The car design provides for speed, safety, comfort, quietness, appearance, and economy. It has been prepared in conjunction with the Transit Research Corporation together with interested manufacturers and operators, in order to take full advantage of the economies incident to standardization between properties and to the use of PCC car equipment wherever possible.

A full-size model of a car body was made in the Commission's shops to permit final decisions on certain matters affecting appearance or comfort and which could not be settled readily from blueprints or calculations, see Figures 3 and 4.

Following the two steps just described, the final specification was sent out for bids in February 1951, but not before a preliminary one had been sent to all the known major suppliers for their comments.

There will be 130 cars, arranged in 65 2-car units semipermanently connected. The two cars in a unit will not be disconnected except in emergency or on overhaul. There will be only one cab in each car, and two cars will be connected back-to-back so that, for operating purposes, each unit is the equivalent of a 96-foot car with a cab at each end. The arrangement just described was chosen for economy in cost and space. In each car the cost of erecting and fitting one cab is saved, while there is a reduction in coupler expense, and an increase in the car body seating space.

Table I

Length of 2-car unit over drawbar faces	96′7″
Length of car over anticlimbers	48′1/2″
Length over bulkheads	45′
Width over doors	10′4″
Width over side sheets	10′
Weight, light—not more than	45,000 lbs
Door openings per car side	3
Door height	6′6″
Door width	45′
Door spacing	15′2″
Seating capacity	50
Floor height above rail (maximum)	3′9″
Roof height above rail (maximum)	11′11″
Floor to ceiling	7′5″
Wheel diameter	28″
Track gauge	4′10¹/₂″

The general dimensions of the car are given in Table I.

Two main objectives in the general arrangement of the car body were maximum comfortable seating capacity and minimum station stop time. The combination of transverse and longitudinal seats provides seating for 50, and allows maximum freedom of passenger movement. The seats themselves were designed specially to combine maximum comfort in minimum space. They will be upholstered in colorful washable fabric and will have rubber cushions and backs.

The doors are of ample width (45 inches) for two streams of passengers closely spaced. They are on 15-foot centers and no passenger is more than four adult steps from a seat to a door. The expected heavy transfer movement at the majority of the stations renders it necessary to ensure minimum stop time in order to achieve the full benefits of rapid transit.

The door mounting is on the outside of the car. This is rather uncommon but has the advantages of weight reduction, elimination of troublesome door pockets

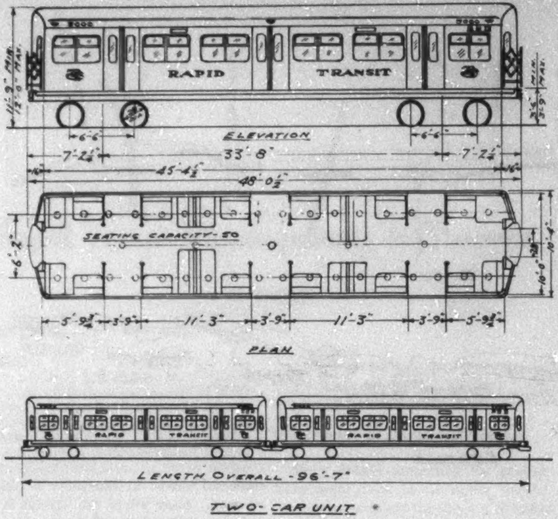

Figure 2. Plan and elevation of car

and double glazing. The doors will be controlled from an operating position in an unused motorman's cab. An interior step in each cab, together with a full-drop sash on the side will permit the guard to view the station platform above passengers' heads. The usual door signal lights will be mounted externally on each car, as well as one in each cab.

The lighting will be provided by incandescent fixtures, with one over every seat. An intensity of approximately 20 foot-candles will be provided on the reading plane, together with an adequate intensity on the ceiling, advertising cards, aisles and doors to provide high general illumination. In case of a power failure, the emergency car body lights will at once come on automatically.

The windows will be of the picture type, with the top half movable and on the outside. By this arrangement, car windows can be closed quickly from the outside, preparatory to movement through the automatic washer. Fixed sash will be set in rubber. All glass openings in the car body proper, together with those in the doors and cab, are shaped and located to enhance the appearance and sales appeal of the car.

Heating and Ventilation

The main source of heat will be from the underfloor resistors used in acceleration and dynamic braking. An auxiliary supply of 20 kw will be used during preheating and at other times if required. Both types will be under thermostatic control and will discharge heat into the car through seat pedestal louvres. Fresh air will be supplied through a full length duct in the ceiling, and this air will be heated when necessary, so that it is never below 50 degrees Fahrenheit. Each cab will be supplied with a 3-kw heater and will have a connection to the main car body heat supply.

Propulsion and Braking Equipment

The propulsion and braking equipment will be of the PCC all-electric type. There will be no compressed air on the cars. Control of car movement will be hand-operated by means of a combined motor and braking controller. The controller handle will have the usual dead man feature with a foot pedal which will nullify this feature during braking only.

Acceleration and braking will both be automatic. An innovation in lightweight rapid transit equipment will be the use of a load weighing device by which the rates of acceleration and braking will be uniform, regardless of load. On level track, the maximum rate of acceleration will be 2.3 miles per hour per second. The corresponding maximum rate of service braking will be 2.8 miles per hour per second. By adopting this device, the motors can be worked closer to their maximum capacity without danger of overloading. In Toronto, the combination of grade, load, car weight, and length of run, impose greater duty on the motors than in any other city where

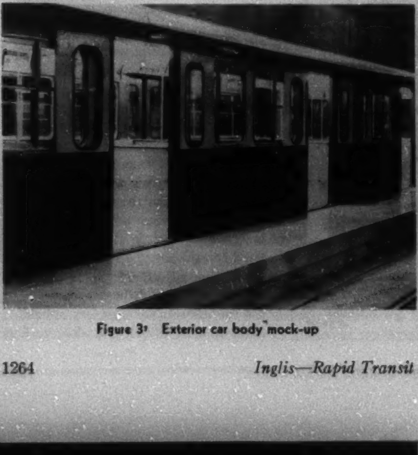

Figure 3. Exterior car body mock-up

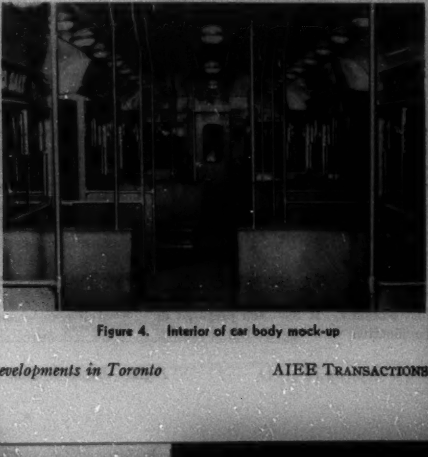

Figure 4. Interior of car body mock-up

PCC equipment has been used or proposed, thereby making desirable the extra protection which has been provided.

The normal braking will be done by dynamic means, with a supplementary propeller shaft brake to complete the cycle and hold the car at rest. Magnetic track brakes will be supplied, with their use limited to times when emergency braking is required, or for an automatic substitute if the dynamic brakes should fail. At other times the track brake cannot be applied except by operating a separate controller, in order to minimize rail wear.

Safety has been given the high priority it must have in the design of the equipment. In addition to the train being stopped in the usual manner, it also will be stopped automatically if the controller handle is released, if the train passes the raised track trip at a red signal light, if the train should break in two, or if the "stop" button should be depressed from any cab in a train.

Trucks

The trucks will be of PCC type increased in capacity to care for the car weight and service concerned. Each truck is designed to carry a center plate load of 25,000 pounds at 50 miles-per-hour, with an ample factor of safety. The truck structure consists essentially of rectangular structural framework to which the axles, motors, truck bolster and track brakes are attached.

The wheels will be 28 inches in diameter with the standard American Association of Railroad tread and will be of the resilient type as on surface PCC cars. Provision has been made in the design for $1^1/_2$-inch bolster adjustment to compensate for wheel wear.

The motors will be spring-supported longitudinally on the truck frame, and drive their corresponding axle through a hypoid drive. Motor bearings and truck bearings are designed to operate for 750,000 miles before requiring replacement.

The trucks have two sets of brakes, the magnetic track brakes and the electrically-operated propeller shaft brakes. They also have two third rail shoes per truck and a track trip.

Progress to Date

Contracts have been let for the construction of all the subway and open cut with the exception of a small section at the north end. Many items such as substation equipment, signals, track, cables, fare-collection equipment, have been ordered, and the remaining items are being ordered as soon as considered necessary. Shortages of material, particularly steel, are delaying the project somewhat, but it is still scheduled for completion on its original date, the end of 1953.

Reference

1. Proposed Rapid Transit System for Toronto, W. E. P. Duncan. *AIEE Transactions*, volume 66, 1947, pages 939–46.

Discussion

G. M. Woods (Westinghouse Electric Corporation, East Pittsburgh, Pa.): The appreciation which the Toronto Transportation Commission has of the needs of the city and its efforts to meet those needs is shown by the public's extensive use of the facilities provided. As is common in many American cities, street traffic on Yonge Street had become very congested and seriously interfered with the movement of street cars which formed the principal means of transportation.

The number of people to be moved in the foreseeable future warranted the investment in a rapid transit system. This step is surely more logical than the step taken in many other cities, that is, the provision of a boulevard or parkway for the private automobiles which have only a small fraction of the subway's passenger capacity.

As Mr. Inglis states the engineers had a free hand in the construction of the subway because it was entirely new. From the standpoint of equipment, a car which conformed in general to Transit Research Corporation standards was adopted. The electric equipment specified is an adaptation of the PCC surface car equipment with such modifications as called for by the heavier loads, longer runs and higher speeds of rapid transit service. The use of a load-weighing device in both acceleration and braking assists in getting the most out of the equipment without excessive overloading.

The use of off-street and open cut sections on the northern portion of the line is especially noteworthy. It reduces the extremely high cost of subway construction. In the United States the East Boston Tunnel is being extended on a surface private right-of-way and Cleveland has well advanced plans for a 13-mile rapid transit line, largely on railroad private right-of-way. This type of rapid transit affords a means of reducing traffic congestion most effectively and at minimum cost.

Electrical Characteristics of a 3-Phase Delta Submarine Power Cable Circuit Using Earth As One Conductor

F. O. WOLLASTON
MEMBER AIEE

THE RECENT installation by British Columbia Electric Company of a 3-phase delta-connected submarine power cable circuit in which two of the conductors are single-core cables and the third conductor is the ground path, appears to be an innovation in submarine cable practise. The circuit is laid in the Pacific Ocean from the British Columbia mainland to an island about three miles off shore. The depth of the sea water in the channel is about 800 feet. For this combination of geographic conditions the circuit selected has decided economic advantages. It requires only two single-conductor cables and yet has a load carrying capacity equal to that of a 3-conductor cable circuit. It requires no joints in the submarine cable, a feature of much practical value. If one cable should fail, the other cable would not be damaged and could be used to supply single-phase service to the load. These advantages are readily apparent. However, it is not easy to determine whether the electrical features of the circuit would be acceptable. A complete analysis has been made from which it has been found that the electrical characteristics are decidedly superior to that of either an equivalent 3-conductor submarine cable or an open-wire line. The magnitude of the currents flowing in the sea water and earth are negligible. The total copper losses plus sheath losses of the circuit are less than would obtain for an equivalent 3-conductor submarine cable or for a 3-phase open-wire line. The average impedance of the circuit is lower than that of an equivalent open-wire line. The impedances of the individual phases are considerably unbalanced but this is not considered to be objectionable.

These economic and electrical features do not appear to have been brought out previously in American technical literature. They are discussed here to draw attention to the possibilities of this type of cable circuit. The electrical analysis can be useful as a guide in considering the operating features of such circuits.

Limitations of 3-Conductor Cable

Three-conductor cables have been universally used for submarine power cable circuits. This type of cable is most readily adaptable to shorter distances. When the length does not exceed about one mile, the cable can be manufactured in one piece and shipped on a single reel. This provides the most convenient set-up for installation, as the reel can be mounted on a barge and the cable installed by paying it off the reel as the barge is towed along. The braking is easily done by using a hand-brake acting on the rim of the cable reel. When the cable length exceeds about a mile, several inconvenient limitations are introduced. If the cable is to be manufactured in one piece it may be necessary to lay it out for shipment on two or more flat cars. On arrival at its destination, it must be transferred to a barge or a cable ship, laying it out in a special way to avoid kinking and twisting during installation. The extra handling at the shipping and destination points requires a large amount of manual labor and adds greatly to the installation cost as compared to the cost of installing a single reel-length. If the length necessitates manufacturing the cable in two or more pieces, there will be one or more joints in the submarine portion of the cable. Most operators would prefer to avoid this if possible. The presence of joints is not only undesirable electrically, but may introduce several real difficulties in the installation procedure. Only one of the difficulties will be mentioned here. This concerns the braking. It is of great importance, particularly in deep-water installations, to brake the cable accurately so that it does not fall slackly to the bottom in loops which can kink, yet at the same time the tension must not exceed the tensile strength of the cable assembly. There is no type of braking device that will permit the smooth passage of a joint while maintaining proper tension on the cable. The laying of a joint in deep water is therefore a tricky procedure which should be avoided if possible.

Advantages of Single-Conductor Cable

Single-conductor cable, because of its smaller physical size and weight, can be handled in much longer reel lengths than 3-conductor cable. Lengths of at least three miles can be handled on a single reel with no unusual difficulty. This compares with a limitation of about one mile for 3-conductor cable. Thus for installations exceeding one mile in length, single-conductor cable becomes quite attractive.

One possibility is the use of single-conductor cable with grounded sheath return, where the load to be served is single phase. Special attention is directed to the fact that load currents flowing in the cable sheath would not raise the cable temperature appreciably. Thus they would have no effect on the carrying capacity. Where 3-phase service is required, two single-conductor cables could

---

Paper 51-233, recommended by the AIEE Insulated Conductors Committee and approved by the AIEE Technical Program Committee for presentation at the AIEE Summer General Meeting, Toronto, Ont., Canada, June 25–29, 1951. Manuscript submitted February 27, 1951; made available for printing May 3, 1951.

F. O. Wollaston is with the British Columbia Electric Railway Company, Ltd., Vancouver, B. C., Canada.

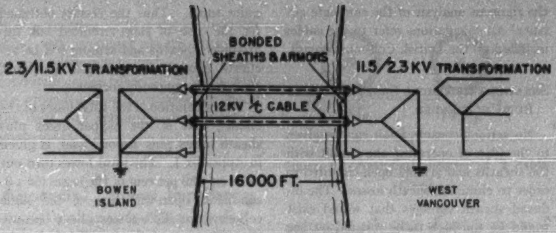

Figure 1. Schematic of grounded delta submarine cable circuit

be installed and the grounded sheaths used for the third conductor. These possibilities have both been seriously considered in Norway,[1] although no actual installations have been made. In that country, a comparatively great part of the population lives along the coast. The coast is characterized by countless deeply indented fiords and numerous offshore islands. The depth of the water is usually around 600 to 1,000 feet, although many fiords are from 2,000 to 4,000 feet deep. The electrification of the coastal communities necessitates the use of submarine cables to the islands. Likewise for crossing the fiords, submarine cable is indicated as land lines would have to follow extremely circuitous routes through difficult terrain. The conditions along the British Columbia coast are rather similar. Thus numerous practical cases exist where the special advantages of single-conductor submarine cable merit careful consideration.

As the cost of the single-core cable is less than 50 per cent of the 3-core cable it is quite possible that projects which would otherwise be too expensive, could be economically accomplished by the use of single conductor cable. The transformer installations at the sending and receiving ends would not add to the cost, as such transformations would be required anyway in most cases. For 3-phase circuits, the installed cost of two single-conductor cables would always be less than that of a 3-conductor cable, if the route length is such that no joints are required in the single-conductor cable. The terminal transformations required for the 3-phase 2-cable installation would present no economic disadvantage where a step-up and step-down bank at either end would have been required in any case. However, under some circumstances the 3-phase 2-cable circuit might not be advantageous. For example, if it were to be used as a link connecting two 15-kv systems with multigrounded neutrals, a 1-to-1 transformation would be required at both ends. Such transformations would not be required for a 3-conductor cable installation.

There are some points favoring an installation of three single-core cables, rather than one 3-conductor cable. The reliability of the single-core cable circuit would be much greater, since a failure of one cable would not put the circuit out of commission. Three-phase service could be restored with the two remaining cables, using the water as the third conductor. The single core cable circuit fits in well with system growth. At first, when the load is small it can be served single phase with one single core cable using sheath return. When the load has grown to the point where three phase service is desirable, it can be taken care of by installing a second single core cable. If the load develops to the point where reliability becomes a prime consideration, a third single-core cable can be installed. At a later stage, the circuit capacity can be doubled by adding a fourth single-core cable.

The British Columbia Installation

Two single-core 12-kv cables were laid between West Vancouver and Bowen Island.[3] Each cable was 16,300 feet long and was made in one length. The cable is paper-insulated, lead covered, with wire armoring. Conductor size is number 0. The armor is composed of *57S* aluminum alloy. The total weight of each length of cable on its special reel was 26 tons. This presented no particular difficulty in shipping or handling during the installation. The depth of the water in which the cable was laid is about 800 feet. The sea bottom is sandy and comparatively flat.

The usual steel-wire armor was not considered desirable for these cables, due to the increased sheath losses which it would produce. Convincing evidence of the excellent resistance of *57S* aluminum alloy to salt-water corrosion was presented. A Canadian coast patrol boat fitted with hull plates of this alloy, has had 20 years continuous service in both temperate and tropical waters without corrosion damage to the hull. The alloy armor, being nonmagnetic, does not add to the losses and its high conductivity is particularly advantageous for carrying the current of the grounded phase.

The circuit is connected to a 4-wire star-connected 4-kv line through a star-delta 2,300/11,500-volt transformation at the supply end. At the load end the circuit is connected to one large customer's 3-phase load through a 11,500/2,300-volt delta-delta transformation. The remainder of the customers are domestic, some connected directly to the grounded-delta circuit through single-phase, 11,500/115/230-volt transformers and others to single-phase 6,900-volt multigrounded neutral circuits derived from the grounded-delta submarine circuit by 11,500/6,900-volt transformations. The sheaths and armors of both cables are interconnected and solidly grounded. They are metallically connected to one phase lead of the transformer bank at each end. The circuit diagram is shown in Figure 1.

Electrical Characteristics of the Circuit

The best appreciation of the electrical characteristics of the 2-cable grounded-delta circuit is gained by comparing its features one at a time with the equivalent characteristic of an ordinary 3-conductor circuit. The total circuit losses will be compared to the losses of a 3-conductor overhead line and also to the losses of a submarine circuit consisting of three single-conductor cables. The circuit impedance will be compared in the same manner. The magnitude of the currents flowing in the ground will be calculated. The small magnitude of these currents seems to be surprising to many engineers with whom the subject has been discussed. There seems to be a general misapprehension that because salt water is a comparatively good conductor, the ground currents will be large. It will be shown that this is not the case.

In the discussion that follows, the term "ground path" means the combined path through salt water and earth is parallel, through which the ground currents can flow. The analysis of ground currents will be approximate but sufficiently accurate for a practical understanding of the performance of the circuit. The approximate analysis is easier to follow than the rigorous analysis of the complete circuit. All calculations refer to the cables installed on the British Columbia circuit.

Sheaths and Armors Short-Circuited But Ungrounded

No serious consideration can be given to the idea of operating the circuit with the sheaths and armors open-circuited in order to eliminate sheath losses. The induced sheath voltages that would exist would be too high to be resisted by the jute bedding between the sheath and armor and the layer of jute over the armor. It is not worth while to calculate these induced voltages for the grounded delta circuit, due to the complication introduced by the presence of currents flowing in the ground. A sufficiently good idea of their magnitude can be more easily obtained by evaluating them for a circuit of three single-conductor cables operating with ordinary electrical connections, that is, with no grounded phase. The values can be readily obtained by a published method.[3] With a circuit length of 16,000 feet and full load current of 300 amperes, the induced longitudinal voltage in the sheath is 481 volts. The induced voltage in the armor is 429 volts. The voltage difference between the sheath and armor is 52 volts. The values for a 2-cable grounded-delta circuit would be of the same order of magnitude. Even if the jute were replaced by a layer of special insulating material, the risk of defects developing over a long period of service is appreciable. These voltages could cause severe damage to the sheath or armor by burning, if a puncture should develop.

It is concluded that the sheaths and armors should be short circuited by thorough grounding at both ends of the circuit. In the British Columbia installation, this was done by bonding all sheaths and armors together at each end and connecting them to two large metallic plates buried in the seashore at the lowest low-tide mark. The bonded sheaths and armors were also metallically connected to the grounded phase of the transformer bank, which had additional grounding through driven ground rods. Thus the sheaths and armors formed a metallic conductor for the grounded phase.

It is much easier to calculate the circuit losses and impedances for the case where ground currents are not permitted to flow. Accordingly, the first calculation will be made for short-circuited sheaths and armors which are used as the conductor of the third phase but are not grounded. It will be shown later that if the sheaths and armors are grounded, the currents which flow in the ground are quite small. Thus the results obtained for the case of short-circuited but ungrounded sheaths and armors will be accurate enough for practical purposes, though not rigorously correct.

The calculation of the total losses of the circuit, that is, the copper losses plus sheath losses plus armor losses, is given in Appendix I. The total losses turn out to be only 89 per cent of the losses for a 3-conductor open-wire line of the same copper size. This comes about because the resistance of the paralleled sheaths and armors, which form one phase of the circuit, is less than half that of the copper conductor. Thus the I^2R losses in this phase are much less than they would be if the copper conductor were used.

The magnitude of the total losses is very much less than for an ordinary circuit of three single-conductor cables with short-circuited sheaths and armors. The losses for the 3-cable circuit are 132 per cent of the losses for a 3-conductor open-wire line of the same copper size. The calculation is given in Appendix I.

The impedance of the 2-cable circuit with sheaths and armors short circuited but ungrounded is calculated in Appendix I. The impedances of the two phases having the copper conductors are about equal and their average is 0.85 ohm per mile. The impedance of the phase consisting of the cable sheaths is much lower, only 0.14 ohm per mile. The average for the three phases is 0.61 ohm per mile. This compares with 0.88 ohm per mile for the average impedance of a 3-conductor open-wire line of the same copper size and spacing. The regulation of the 2-cable circuit is, therefore, somewhat lower than for an equivalent open-wire circuit. The inequality of the phase impedances would indicate that if voltage regulators are required on the circuit, the regulators should be single-phase units.

The magnitude of the currents in the sheaths of the two cables is of some interest. Part of the load current flows in one sheath and the remainder in the other sheath. Besides this, there is a circulating current which flows out on one of the sheaths and back on the other. Calling I the load current, the current in each sheath expressed as a percentage of the load current, is:

Cable Number 1 sheath current $=(0.87-j0.63)I=108$ per cent I

Cable Number 2 sheath current $=(0.13+j0.63)I=64$ per cent I

The sum of the two currents is equal to the load current, since the sheath circuit is isolated and therefore the vectorial sum of the circulating currents in it must be zero.

Sheaths and Armors Short Circuited and Grounded at Both Ends

Connecting the sheath circuit to ground at both ends will permit the load current I_B flowing on the sheaths to divide between the sheath path and the ground path. The proportion of the current which will flow in the ground can be approximated with sufficient accuracy by utilizing the analysis given by Wagner and Evans[5] for the single-phase impedance of a cable circuit with grounded-sheath return. The 2-cable grounded delta circuit can be treated as a single-phase circuit. Since $(I_A+I_C)=-I_B$, the load current can be thought of as a single-phase current flowing out in the two copper conductors in parallel and returning in the sheaths and ground. Thus the analysis becomes the same as for the single-phase circuit. The calculation is given in Appendix II. It turns out that the current in the ground will be only 16 per cent of the phase current.

This result may seem surprising but is entirely consistent with published information. Wagner and Evans[5] have demonstrated theoretically that when single-phase current flows out on the conductors of a cable and returns through the lead sheath and ground in parallel, practically all of it will return on the sheath, if the latter has the low resistance which is characteristic of lead sheaths of usual dimensions. They also give sufficient information to show that if the same cable were laid in salt water, the majority of the current would still return on the sheath, although the amount returning in the ground path would be somewhat larger than before. The author has received from Norway the results of an actual test on a submarine cable which fully substantiates this conclusion. The use of aluminum armor intensifies the tendency of the return current to confine itself to the sheath path, since the aluminum armor adds considerably to the conductivity of the sheath path.

The calculated value of 16 per cent for the current flowing in the ground is higher than could actually occur in practise. This is because the resistance of the grounding plates was ignored in the calculation. An idea of the effect of resistance in the grounds at each end of the circuit is obtained easily. The impedance of the ground path is 0.84 ohm per mile (see Appendix II) and since the circuit is about three miles long, the total impedance of the ground path is 2.52 ohms. If it is assumed that the ground

Table I

Conductor radius, inches	r_c	0.187
Insulation thickness, inches		0.205
Inner diameter of sheath, inches		0.800
Outer diameter of sheath, inches		1.000
Thickness of jute over sheath, inches		0.157
Inner diameter of armor, inches		1.314
Outer diameter of armor, inches		1.570
Spacing between cables, inches	S	24
Mean sheath radius, inches	r_s	0.450
Mean armor radius, inches	r_a	0.721
Resistance of lead sheath at 20°C., ohm/foot		31.7×10^{-6}
Resistance of wire armor at 20°C., ohm/foot		6.27×10^{-6}
Paralleled resistance of sheath and armor, ohm/foot	Rs	5.23×10^{-6}
Conductor resistance at 78°C., ohm/feet	Rc	12.3×10^{-6}
Mean radius of equivalent sheath, inches	r	0.592
$5.3 \log S/r$, ohm/foot	X	8.50×10^{-6}
$5.3 \log S/r_s$, ohm/foot	X_s	9.14×10^{-6}
$5.3 \log S/r_a$, ohm/foot	X_a	8.06×10^{-6}
$5.3 \log r/r_c$, ohm/foot	X_c	3.22×10^{-6}
$5.3 \log 2$, ohm/foot		1.59×10^{-6}
$Rs/(X+5.3 \log 2)$	M	0.52
$Rs/(X-1.77 \log 2)$	N	0.66
Full load current per phase, amperes	I	300
Length of circuit, feet		16,000
Circuit configuration is flat and untransposed.		

plates have a resistance of 0.5 ohm at each end of the circuit, the impedance of the ground path becomes 2.81 ohms. This will reduce the ground current to only 14 per cent instead of 16 per cent.

It is to be observed that in some single-conductor cable circuits with solid-bonded sheaths, a residual induced longitudinal voltage can exist between the two ends of the circuit. This occurs when the circuit arrangement is not completely symmetrical, as for example in a circuit of three single-conductor cables in flat configuration. The residual voltage referred to is an internal generated voltage resulting from electromagnetic induction. If the sheaths are grounded at both ends of the circuit, the residual induced voltage will cause a circulating current to flow out on the sheaths and back through the ground. In the case of the 2-cable grounded-delta circuit, this voltage is zero. This can be clearly seen from equation 6, Appendix I, which states that the voltage between the end bonds of the sheath circuit consists of only the voltage drop of the load current flowing through the resistance of the paralleled sheaths. Accordingly there can be no ground current from this source and it does not appear in the calculations.

Conclusions

The use of single-conductor cables in submarine circuits is economically attractive in some circumstances and is not objectionable from the standpoint of electrical operation, particularly when the cable armoring is composed of a non-magnetic metal having high conductivity. It is permissible to use a single-conductor cable with grounded sheath return for serving single-phase loads. Two single-conductor cables connected in delta, with the grounded sheaths forming one leg of the delta, are permissible for serving 3-phase loads.

Appendix I. Losses, Impedances, and Voltages for Ungrounded Circuits

It is desired to obtain the induced sheath voltages for a circuit of three single-conductor cables with open-circuited sheaths; and the copper and sheath losses for the same circuit when the sheaths are short circuited. These data are for comparison with similar data for a circuit of two single-conductor cables operated as a 3-phase delta-connected circuit, the third phase consisting of the paralleled sheaths and armors of the two cables. The desired results can be readily obtained by a published method[3] with very little calculation. The cable has a Number 0, standard-stranded single-copper conductor, with 0.205-inch insulation, 0.1-inch lead sheath and a single layer of aluminum-alloy armor wire having 35 per cent conductivity. There is a layer of jute between the lead sheath and the armor. To save unnecessary complication in the calculations dealing with short-circuited sheaths, the sheath and armor will be replaced by an equivalent sheath having the inner diameter of the lead sheath, the outer diameter of the wire armor and a resistance equal to the paralleled resistances of the lead sheath and the wire armor. As this equivalent sheath has substantial thickness, its geometric mean radius is not equal to its mean radius. In this Appendix the mean sheath radius is sufficiently accurate for the problems considered and is used throughout. In Appendix II, the geometric mean radius (g.m.r.) is more convenient and is used throughout. The data required in the calculations are given in Table I.

Three-Cable Circuit: Induced Voltages in Open-Circuited Sheath and Armor

From Table III, reference 3, Cable Arrangement Number IV, equation 1 or 3, the induced voltage in the lead sheath of each outer cable for full load of 300 amperes on the 16,000 foot circuit is

$$E = 300 \times 16{,}000 \times j0.5[(-X_s + 5.3 \log 2) + j\sqrt{3}(X_s + 5.3 \log 2)] = 481 \text{ volts}$$

Similarly for the armor, using X_a instead of X_s, the induced voltage is $E_a = 429$ volts. The voltage difference between sheath and armor is $(E_s - E_a) = 52$ volts.

Three-Cable Circuit: Impedance to Neutral When Sheaths and Armors Are Open Circuited

The impedance to neutral when the sheaths and armors are open circuited is the same as for an open-wire line. Although the circuit is untransposed, the average impedance of the three phases is the most convenient value to use in comparisons with other impedances which will be calculated later. This is the same as the impedance of a transposed line and thus can be obtained from published tables. Using the tables given in reference 4, the average impedance to neutral per phase is

$Z = 0.88$ ohm per mile

Three-Cable Circuit: Total Losses when Sheaths Are Short Circuited

The sheath and armor are replaced by the equivalent sheath described earlier. Reference 3, Table III, equation 9, gives the total sheath losses in the form of a ratio, W_s/I^2R_s. To get the total sheath losses as a percentage of the total copper losses, this is multiplied by $I^2R_s/3I^2R_c$. We then have

$$W_s/3I^2R_c = W_s/I^2R_s \, . \, I^2R_s/3I^2R_c$$
$$= \frac{I^2R_s}{3I^2R_c} \cdot \frac{3(M^2+N^2+2)}{2(M^2+1)(N^2+1)} = 0.32$$

Thus the sheath losses are 32 per cent of the copper losses and the total circuit losses are 132 per cent of the copper losses alone.

Two-Cable Circuit: Sheaths Short-Circuited but Not Grounded

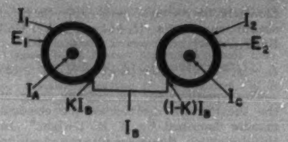

Figure 2. Analytical diagram of 2 cable circuit

Figure 2 represents diagramatically the 2-cable circuit. The sheath and armor are combined into the equivalent sheath described earlier. The left-hand cable has A-phase current I_A flowing in the conductor. The sheath has an induced current I_1 flowing in it and a voltage drop E_1 along it. Similarly the right-hand cable has a conductor current I_C, an induced sheath current I_2 and a voltage drop E_2. The B-phase current flows in the two sheaths in parallel, and is divided between them in the ratio KI_B in the left-hand sheath and $(1-K)I_B$ in the right-hand sheath. Let the B-phase current be chosen as the reference vector and let "a" be the usual operator indicating a phase shift of 120 degrees.

Then

$$I_A = aI_B; \quad I_C = a^2I_B; \quad I_A + I_B + I_C = 0 \qquad (1)$$

Since the sheaths are bonded at both ends but not grounded, the vector sum of all circulating sheath currents is zero. Also, the voltage drop in one sheath is equal to the voltage drop in the other. This drop is not zero and will be called the residual voltage E_R. Expressing the foregoing in the form of equations

$$I_1 + I_2 = 0; \quad E_1 = E_2 = E_R \qquad (2)$$

The total current in the sheath of the left-hand cable is $(I_1 + KI_B)$. Call this $I_{s\cdot1}$.

Similarly, for the right-hand cable, the total sheath current is $[I_2+(1-K)I_B]$. Call this I_{s2}.

$$I_{s1}=[I_1+KI_B];\quad I_{s2}=[I_2+(1-K)I_B] \qquad (3)$$

The equations for the voltage drops in the sheaths are derived in the classical manner described by H. B. Dwight.[6] In this derivation, fluxes are integrated out to some very large distance "p". The distance "p" need not be defined, since it cancels out when the vector sum of all the currents in the system is zero, as is the case in the present problem. The term "ln" means natural logarithm.

The equations for sheath voltage drops are:

$$E_1=E_R=I_1R_S+KI_BR_S+2j\omega\left(I_A\ln\frac{p}{r}+I_1\ln\frac{p}{r}+KI_B\ln\frac{p}{r}+I_c\ln\frac{p}{s}+I_2\times\ln\frac{p}{s}+(1-K)I_B\ln\frac{p}{s}\right) \qquad (4)$$

$$E_2=E_R=I_2R_S+(1-K)I_BR_S+2j\omega\left(I_A\ln\frac{p}{s}+I_1\ln\frac{p}{s}+KI_B\ln\frac{p}{s}+I_c\times\ln\frac{p}{r}+I_2\ln\frac{p}{r}+(1-K)\,I_B\ln\frac{p}{r}\right) \qquad (5)$$

After putting all phase currents in terms of I_B as given in equation 1, simplifying, and adding equations 4 and 5, there is

$$2E_R=I_BR_S$$

or

$$E_1=E_2=E_R=I_BR_S/2 \qquad (6)$$

Substituting this value into equation 4 and solving for the total sheath current, there is

$$I_{s1}/I_B=(R_s/2-a.2j\omega\ln s/r)/\times(R_s+2j\omega\ln s/r) \qquad (7)$$

Similarly for the sheath current of the other cable:

$$I_{s2}/I_B=1-(R_s/2-a.2j\omega\ln s/r)/\times(R_s+2j\omega\ln s/r) \qquad (8)$$

The term $2j\omega\ln s/r$ is the same as the term "x" listed in Table I, when converted from absolute units into practical units. Accordingly equations 7 and 8 now can be evaluated numerically. They are:

$$I_{s1}=(0.87-j0.63)I_B=108\%\ I_B \qquad (7)$$

$$I_{s2}=(0.13+j0.63)I_B=64\%\ I_B \qquad (8)$$

The vector sum of I_{s1} and I_{s2} is equal to I_B.

The total losses in the circuit when expressed as a percentage of the losses in the conductors of a 3-wire circuit of the same conductor size, are:

$$W_T/3I^2R_c=(I_{s1}^2R_s+I_{s2}^2R_s+2I^2R_c)/\times 3I^2R_c=\overline{1.08}^2R_s/3R_c+\overline{0.64}^2R_s/3R_c+2/3=89\% \qquad (9)$$

The impedance of a conductor is the voltage drop in it divided by the current flowing in it. The voltage drop in the cable conductor is derived in the same manner as for the sheath. It is convenient to express the self-reactance in two parts, one representing the flux linkages external to the mean sheath radius, and the other representing the flux linkages internal to the mean sheath radius. The latter will be called X_c and is $X_c=2j\omega I\ln r/r_c+$conductor internal reactance, where r_c is the conductor radius. The voltage drop in the A-phase cable conductor now may be written

$$E_A=I_A(R_c+jX_c)+2j\omega\left(I_{s1}\ln\frac{p}{r}+I_c\times\ln\frac{p}{s}+I_{s2}\ln\frac{p}{s}+I_A\ln\frac{p}{r}\right) \qquad (10)$$

Similarly for the C-phase conductor

$$E_c=I_c(R_c+jX_c)+2j\omega\left(I_{s1}\ln\frac{p}{s}+I_c\times\ln\frac{p}{r}+I_{s2}\ln\frac{p}{r}+I_A\ln\frac{p}{s}\right) \qquad (11)$$

After simplifying, dividing equation 10 through by I_A and dividing equation 11 through by I_c, there is

$$Z_A=E_A/I_A=R_c+jX_c+2j\omega\ln\frac{s}{r}(I_{s1}/I_A+1) \qquad (12)$$

$$Z_c=E_c/I_c=R_c+jX_c+2j\omega\ln\frac{s}{r}(I_{s2}/I_c+1) \qquad (13)$$

The voltage drops and the currents in the sheath circuit have already been derived (see equations 6 and 7) and so the impedances of the two sheaths may be written down at once. They are

$$Z_{s1}=E_1/I_{s1}=(R_s/2)(R_s+2j\omega\ln s/r)/\times(R_s/2-a\times2j\omega\ln s/r) \qquad (14)$$

$$Z_{s2}=E_2/I_{s2}=(R_s/2)(R_s+2j\omega\ln s/r)/\times[R_s/2+(1+a)\times2j\omega\ln s/r] \qquad (15)$$

The impedance of the two sheaths in parallel is determined in the usual way, that is,

$$Z_s=\frac{Z_{s1}Z_{s2}}{Z_{s1}+Z_{s2}}$$

When this operation is performed it is found that

$$Z_s=Z_B=R_s/2 \qquad (16)$$

and this is the B-phase impedance.

All the numerical quantities necessary for evaluating equations 12, 13, and 16 are included in Table I. The impedances when evaluated are

$$Z_A=(0.855+j0.174)=0.872 \text{ ohm per mile} \qquad (12)$$

$$Z_c=(0.750+j0.350)=0.824 \text{ ohm per mile} \qquad (13)$$

$$Z_B=(0.138)=0.138 \text{ ohm per mile} \qquad (16)$$

The average impedance $=(Z_A+Z_B+Z_C)/3=0.613$ ohm per mile.

Appendix II. Ground Currents in 2-Cable Grounded-Delta Circuit

Let the load current on the grounded phase be I_B and let I_B be the reference vector in the calculations. Since $(I_A+I_C)=-I_B$, the circuit can be thought of as a single-phase circuit, in which the load current flows out in the two copper conductors in parallel and returns in the sheath and ground in parallel. Wagner and Evans[5] have given the analysis for such a circuit. Following Wagner and Evans, the impedance of the sheath branch of the ground-return circuit is

$$Z_s=R_s/2=0.138 \text{ ohm per mile}$$

The impedance of the ground branch is

$$Z_g=0.095+j0.279\log D_e/\text{g.m.r. sheaths}=0.095+j0.833=0.84 \text{ ohm per mile}$$

In the above, D_e is taken as 280 feet (3,360 inches) as given by Wagner and Evans[5] for submarine cable in deep salt water. The g.m.r. of one sheath is 0.508 inch. The g.m.r. of the two sheaths in parallel at 24-inch spacing is 3.52 inches. In the analysis of the complete circuit given by Wagner and Evans, the impedance of the conductor branch of the circuit also is evaluated. This does not concern us in the present problem, as we are interested only in determining the relative magnitudes of the currents flowing in the sheath and ground respectively.

The current in the grounded phase will divide between the sheath path and the ground path in inverse proportion to the impedances of the two paths.

$$I_g/I_s=Z_s/Z_g=0.138/(0.095+j0.833)=(0.019-j0.164)=0.164$$

The total current I_B in the grounded phase is the sum of the currents in the sheath path and the ground path.

$$I_B=I_s+I_g=I_s+(0.019-j0.164)I_s=(1.019-j0.164)I_s=1.03I_s$$

The proportion of I_B which will flow in the ground is

$$I_g/I_B=0.164I_s/1.03I_s=0.16$$

The proportion of I_B which will flow in the sheaths is

$$I_s/I_B=1/1.03=0.97$$

Thus the current in the sheaths remains practically the same, whether the sheaths are grounded or not. The only significant change due to grounding the sheaths is that a current will flow in the ground which will be about 90 degrees out of phase with the current in the sheaths and which will have a magnitude of about 16 per cent of the total current of the grounded phase.

It was stated in the text of the paper that the analysis for the circuit with ungrounded sheaths could be used without serious error for the circuit with grounded sheaths. It will now be evident that this is the case. The grounding of the sheaths makes practically no change in the currents flowing in the copper conductors and in the sheaths. The only new factor introduced is the current in the ground. This is of quite small magnitude compared to the phase currents and is separated by a very large effective distance (280 feet) from the cables. Consequently it could make only negligible alteration in the numerical results obtained in Appendix 1.

References

1. Submarine Cables in Norway, C. W. Hirsch. *Electrical Communication* (New York, N. Y.), volume 25, number 1, March 1948.

2. Grounded Cable Sheath and Armor are Third Conductor of Submarine Circuit, F. O. Wollaston. *Electrical World* (New York, N. Y.), February 13, 1950.

3. Reduction of Sheath Losses in Single Conductor Cables, Herman Halperin, K. W. Miller. *AIEE Transactions*, volume 48, April 1929, pages 399–415.

4. Transmission and Distribution Reference Book. Westinghouse Electric and Manufacturing Company, East Pittsburgh, Pa., second edition, 1943.

5. Symmetrical Components (book), C. F. Wagner, R. D. Evans. McGraw-Hill Book Company, New York, N. Y., first edition, 1933.

6. Induced Voltages in Conductors, H. B. Dwight. *The Electric Journal* (East Pittsburgh, Pa.) volume 26, April 1928.

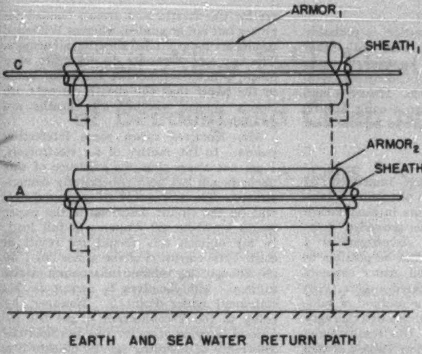

Figure 1 (above)

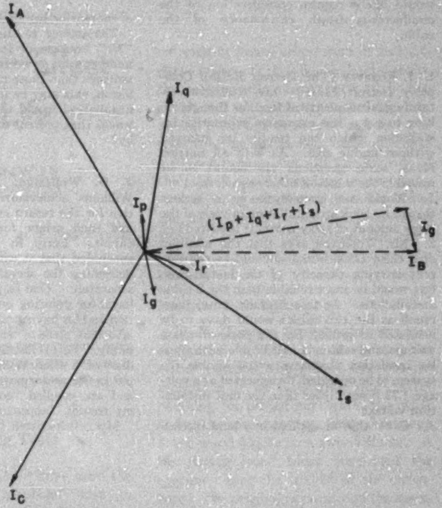

Figure 3 (right)

Discussion

J. S. Williams (Westinghouse Electric Corporation, East Pittsburgh, Pa.): An interesting extension of the author's calculation was to determine return currents in each sheath and in each armor. This involved consideration of self- and mutual-impedances, as indicated in Figure 1 of this discussion. The equations relating these are taken from Figure 2 and are listed below:

$$E_A=I_AZ_a+I_CZ_{ac}+I_pZ_{ap}+I_qZ_{aq}+I_rZ_{ar}+I_sZ_{as}$$

$$E_C=I_AZ_{ac}+I_CZ_c+I_pZ_{cp}+I_qZ_{cq}+I_rZ_{cr}+I_sZ_{cs}$$

$$0=I_AZ_{ap}+I_CZ_{cp}+I_pZ_p+I_qZ_{pq}+I_rZ_{pr}+I_sZ_{ps}$$

$$0=I_AZ_{aq}+I_CZ_{cq}+I_pZ_{pq}+I_qZ_q+I_rZ_{qr}+I_sZ_{qs}$$

$$0=I_AZ_{ar}+I_CZ_{cr}+I_pZ_{pr}+I_qZ_{qr}+I_rZ_r+I_sZ_{rs}$$

$$0=I_AZ_{as}+I_CZ_{cs}+I_pZ_{ps}+I_qZ_{qs}+I_rZ_{rs}+I_sZ_s$$

Figure 2

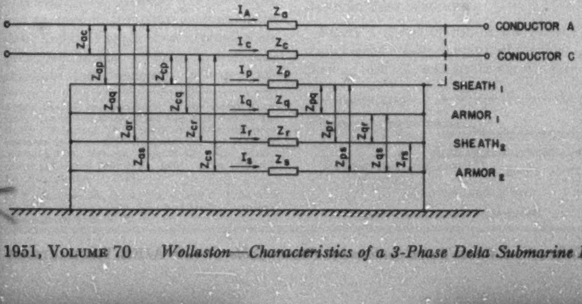

Each self- and mutual-impedance was evaluated with regard for the return path in earth and sea-water, based on a supposition that the equivalent return path was 280 feet distant from the cable:

$$Z_a=Z_c=r_a+\frac{r_e}{3}+j\left(X_a+\frac{X_e}{3}\right)=2.26+j3.69\text{ ohms}$$

$$Z_p=Z_r=r_p+\frac{r_e}{3}+j\left(X_p+\frac{X_e}{3}\right)=5.36+j3.26\text{ ohms}$$

$$Z_q=Z_s=r_q+\frac{r_e}{3}+j\left(X_q+\frac{X_e}{3}\right)=1.29+j3.09\text{ ohms}$$

$$Z_{ac}=Z_{ar}=Z_{as}=Z_{cp}=Z_{cq}=Z_{pr}=Z_{ps}=Z_{qr}=Z_{qs}=\frac{r_e}{3}+j\left(\frac{X_e}{3}-X_{ab}\right)=0.289+j1.82\text{ ohms}$$

$$Z_{ap}=Z_{cr}=\frac{r_e}{3}+j\left(\frac{X_e}{3}-X_{ap}\right)=0.289+j3.28\text{ ohms}$$

$$Z_{aq}=Z_{cs}=Z_{pq}=Z_{rs}=\frac{r_e}{3}+j\left(\frac{X_e}{3}-X_{aq}\right)=0.289+j3.11\text{ ohms}$$

The calculated currents are tabulated below and also sketched in vector form in Figure 3:

Phase "A" conductor... $I_A=1.0\underline{/120^\circ}$
Phase "C" conductor... $I_C=1.0\underline{/240^\circ}$
Sheath on conductor "A"................ $I_r=0.178\underline{/-24.5^\circ}$
Armor on conductor "A"................ $I_s=0.869\underline{/-34.7^\circ}$
Sheath on conductor "C"................ $I_p=0.131\underline{/93.1^\circ}$
Armor on conductor "C"................ $I_q=0.504\underline{/81.9^\circ}$
Ground return......... $I_g=0.155\underline{/-73.5^\circ}$

These results appear to match the author's conclusions quite closely.

Because the determination of earth return currents is dependent to some extent upon generalized earth impedance constants, it is perhaps realistic to ask whether the constants chosen as appropriate for this situation could be confirmed by any sort of test measurements. Possibly during some scheduled test period a single-phase 60-cycle test voltage could be applied between one conductor and ground at one terminal, with the same conductor connected solidly to ground at the remote end. Accurate evaluation of the results of such a test would likely require consideration of the conductor-to-sheath capacitance of the cable.

L. I. Komives (The Detroit Edison Company, Detroit, Mich.): Mr. Wollaston certainly gave us plenty of food for thought on how to get a less expensive submarine installation which can readily be enlarged without undue cost. As with all untried ideas, some questions are bound to be raised in the minds of other engineers.

1. Would a-c electrolysis be a serious thread for such an installation in view of the large amount of stray currents involved?
2. Mr. Wollaston says that the addition of a third cable would not add to the current-carrying capacity of the installation, but would be more reliable than the 2-cable installations. Is this literally true, inasmuch as the two cables would have to be insulated to ground for the phase-to-phase voltage, and adding a third cable with similar insulation thickness would enable the system to be operated Y-connected at a voltage 1.73 times higher than the first installation voltage.
3. Could this be applied in a land instead of submarine installation?

Table I

	Complete Solution	Approximate Solution
1. Ground current	$(0.03 - j0.15)\ I_B$	$(0.04 - j0.15)\ I_B$
2. Total current in grounded sheaths and armors of both cables together	$(0.97 + j0.17)\ I_B$	$(0.96 + j0.16)\ I_B$
3. Sum of sheath and armor currents in one cable: A phase cable	$(0.89 - j0.56)\ I_B$	$(0.87 - j0.63)\ I_B$
C phase cable	$(0.08 + j0.73)\ I_B$	$(0.13 + j0.63)\ I_B$

The answer to this question is probably "No" because of interference with other underground structures; however, at lower voltages than those mentioned by Mr. Wollaston, this may be feasible. If such a land installation would undergo a cable failure, would that present dangers to persons near by?

F. O. Wollaston: I am impressed by Williams' achievement in obtaining a solution for the return currents in each sheath and each armor for the grounded delta circuit. Early in my investigations I concluded that it would not be possible to determine the sheath and armor currents separately. One is indebted to Mr. Williams for pointing out the method of solution and for having carried through this very laborious piece of work. Our results agree nicely. This is illustrated in Table I of this discussion where Williams' results have been put in the vector notation used in the paper and are labelled "complete solution" and my results, "approximate solution."

My results listed in Item 3 of the table are for the sheaths and armors bonded together but not grounded, whereas Williams' results are for grounded sheaths and armors. The two sets of results do not differ very much, which confirms the statement made in the paper that the sheath currents are closely similar whether the sheaths are grounded or not.

Mr. Komives raises some interesting points. In the matter of a-c electrolysis, I am not aware that the existence of this phenomenon has been conclusively demonstrated. The amount of stray ground current on the circuit described in the paper would be about 50 amperes at full load. In my opinion this should not result in electrolytic corrosion of the armor but I do not know of any reliable information on the subject. Mr. Komives is correct in his statement under Point 2. However, by going to the Y-connection to get the increased carrying capacity, one sacrifices the possibility of restoring service quickly if a failure occurs on one of the cables. The possibility of using the grounded delta circuit for land lines seems to me to be ruled out because of probable interference with communication lines.

F-3 Lead Alloy Cable Sheath—Effect of Bending and Creep on Life

L. F. HICKERNELL
FELLOW AIEE

A. A. JONES
MEMBER AIEE

C. J. SNYDER
NONMEMBER AIEE

SINCE its commercial introduction in 1945,[1] *F-3* alloy has been tested on a continuing basis in order to evaluate it, comparatively, as a power cable sheathing material. The principal causes of power cable sheath failures in service are fatigue-cracking due to slow bending of the cable in manholes or at duct mouths caused by expansion and contraction incident to daily load cycles; and gradual expansion (creep) of the sheath due to static internal pressure caused by differences in elevation along the cable run and/or the "ratcheting" effect due to thermal expansion, particularly when oil-filled joints or terminals are used. Therefore, to be of value, accelerated laboratory tests should be designed to measure the resistance of the sheathing material, in actual cable sheath form, to these two principal causes of failure. This has been accomplished by:

1. A cable slow-bending test, using a test specimen comprising an 87-inch length of commercially produced paper-lead cable.
2. A cable-sheath creep test, using a test specimen comprising a 15-inch length of commercially produced cable sheath.

In addition, as a relatively quick test of ductility, stress fracture (high-internal-pressure burst) tests also were made.

A description of these test procedures and equipment, test data, analyses of the data, and their application to practice are presented herein. These further substantiate the previously indicated advantages of *F-3* alloy as a power-cable sheathing material.[1,2,3]

Cable Constructions

Table I shows the cable core constructions. Various sheaths were applied over these cores to obtain samples for test. Table II shows the sheath constructions tested.

Cable Slow-Bending Tests

Other investigators[3,4,5,6] have used the so-called "dummy manhole" test to evaluate slow-bending characteristics of cable sheaths. However, this test requires a relatively long test specimen with a complete cable joint installed at the midpoint. The cable slow-bending test as used by the authors, while not directly comparable to the "dummy manhole" test, evaluates cable sheaths in the same comparative manner. In addition, it is a simpler test to set up and operate, requires a relatively short test specimen (87 versus 240- to 300-inches; hence, more tests can be made with the same total length of cable), and does not introduce the additional variables due to installation of cable joints and arc-proofing.

Bending Test Specimen

Figure 1 shows in outline the 87-inch straightened specimen prepared for cable-bending test. Cracks in the sheath were detected by loss of air pressure in the lead-sleeve reservoir. For double-lead sheaths, the outer sheath was cut back at the reservoir and both sheaths sealed together at that point and at the pulling eye. The specimens were then bent uniformly over a 42-inch radius form with the flat side of the pulling eye in the plane of curvature.

In bending a 2.40-inch diameter cable, the lead sheath permanently stretched 2.75 per cent on the outside, and compressed 2.75 per cent on the inside of the bend.

Bending Test Equipment

Figure 2 shows the cable-bending test equipment. With the cross-head at center position, the pulling eye was attached to it by a bearing pin. After checking for proper curvature, the other end of the specimen was clamped between fitted wood blocks in a swivel frame. A free-sliding wood block supported the specimen near the middle of the curvature. The original curvature of the specimen was increased and decreased alternately by the reciprocating motion of the cross-head along the chord of the arc. A pressure relay soldered to the reservoir energized the driving-motor circuit at 5 pounds and de-energized it at 2 pounds pressure. A specimen was considered to have failed when it would not hold pressure overnight (15 hours).

Bending Strain

Figure 3 shows the dial gauge with an 8-inch span used for strain measurement. Strain readings were taken along the outer curvature of the specimen during the initial stages of test. The gauge measured the maximum and minimum deviation from straightness during one bending

Figure 1. Specimen for cable-bending test

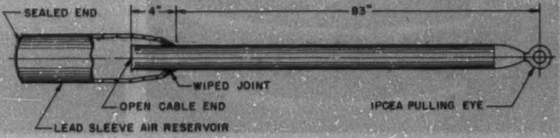

Paper 51-234, recommended by the AIEE Insulated Conductors Committee and approved by the AIEE Technical Program Committee for presentation at the AIEE Summer General Meeting, Toronto, Ont., Canada, June 25–29, 1951. Manuscript submitted March 21, 1951; made available for printing May 7, 1951.

L. F. Hickernell, A. A. Jones, and C. J. Snyder are with the Anaconda Wire and Cable Company, Hastings-on-Hudson, N. Y.

Table I. Cable Core Constructions

Cable Core Designation	No. Condrs.	Conductor Size Awg Mcm	Conductor Shape	Paper Thickness, Mils	Type	Binder	Core Diameter, Inches
A	3	350	SS	203	CB-Sh	Metal	2.00
B	3	350	SS	345	CB-Sh	Metal	2.69
C	3	350	SS	345	CB-Sh	CB Paper	2.69
D	3	500	SS	150	CB-Sh	CB Paper	2.12
E	3	500	SS	365	CB-Sh	CB Paper	3.03
F	3	350	CS	215	CB-Sh	CB Paper	2.11
G	3	500	CS	250	CB-Sh	CB Paper	2.47
H	1	500	R	240	CB-Sh		1.27
I	3	350	CS	150 x 150	Belted		2.11
J	3	500	SS	190	CB-Sh	CB Paper	2.29
K	1	750	R	240	CB-Sh		1.42
L	3	500	CS	240	CB-Sh-GF	Metal	2.41
M	3	750	SS	175*	CB-Sh	CB Paper	2.60
N	3	500	CS	240	CB-Sh-GF	CB Paper	2.41
O	3	400	CS	78 x 55	Belted		1.62
P	3	800	CS	215	CB-Sh	Metal	2.67
Q	3	500	SS	150	CB-Sh	Metal	2.18
R	1	2,500	C Sg	240	CB-Sh		2.35
S	3	500	SS	148	CB-Sh	CB Paper	2.05
U	3	#4/0	SS	218 x 218	Belted		2.30
V	3	500	CS	150	Sh	Al-Paper	2.07
W	3	500	CS	175	CB-Sh	CB Paper	2.18

Legend:
SS = standard sector
CS = compact sector
C Sg = compact segmental
R = round (concentric)
CB = carbon black
Sh = shielded
GF = gas-filled
Al = aluminum foil
* = dry paper

Table II. Sheath Constructions

Sample Number	Cable Core Designation	Sheath Thickness, Mils	Cable Diameter, Inches	Sheath Tensile Strength, Psi
F-3 Alloy				
6903	C	146	3.02	2,692
6974	B	140	3.01	2,702
7162	E	157	3.35	2,702
7390	E	105	3.24	—
7392	E	99-103*	3.50	—
7394	G	84	2.64	2,901
7396	G	75–82*	2.89	2,900
7397	G	266	2.99	2,774
7398	F	78	2.27	3,016
7400	F	75–57*	2.46	3,000
7402	D	127	2.42	2,864
7404	D	85	2.30	3,018
7405	D	85	2.31	2,957
7441	I	125	2.38	2,809
7776	W	130	2.43	2,971
8140	H	103**	1.63	—
8142	K	113**	1.80	—
8427	M	141	2.89	3,102
8526	D	125	2.42	3,040
8652	U	125	2.57	2,615
8653	U	87	2.49	2,819
8680	Q	90	2.37	—
8681	Q	87–88*	2.66	—
8682	P	96	2.88	3,077
8700	V	122	2.32	2,718
9186	W	125	2.39	2,607
9275	L	133	2.65	3,058
Copper-Lead				
7389	E	144	3.33	—
7391	E	99	3.24	2,239
7393	E	95–97*	3.50	2,200
7395	G	80	2.64	2,205
7399	F	75	2.26	2,207
7403	D	122	2.39	2,200
7440	I	125	2.85	2,109
8474	N	133	2.69	—
8651	U	125	2.56	2,077

* Double sheath; reinforced with two 5-mil copper tapes, each intercalated with an 8-mil paper tape.

** Fluted sheath; dimension shown is to bottom of flute. Flutes, 75-mil deep x 100-mil wide; teeth, 125-mil wide.

cycle from which the corresponding bending radii were calculated:

$$R=\frac{8}{H}+\frac{H}{2}-r$$

where

R = radius of curvature of cable axis
r = radius of cable
= $^1/_2$ diameter of cable
H = reading of gauge

The strain produced by one test cycle was computed from:

$$\epsilon=\frac{r}{R_{max}}-\frac{r}{R_{min}}$$

where

ϵ = strain
R_{max} = maximum radius of curvature
R_{min} = minimum radius of curvature

Figure 4 shows the measured strain versus movement obtained on various cable constructions. For any one cycle, the largest strain along the curvature of the specimen was plotted. For comparison, the theoretical strain was calculated from the above formula having determined R_{min} and R_{max} from geometry. The largest measured strains usually were a little greater than theoretical because the cables seldom bent uniformly.

Life versus Cable Diameter and Movement

Figure 5 shows that for a given movement and material, the larger the cable diameter, the shorter is the sheath life. In general, the life of *F-3* alloy sheath is three or more times that of copper-lead.

Life versus Strain

Figure 6 is the data in Figure 5 replotted to show the effect of strain on sheath life. Depending upon the value of strain, *F-3* alloy sheath has two and one-half to five times the life of copper-lead. From these data, it is indicated that material and strain are the controlling factors in sheath life.

For a given cable, the data indicate that sheath life approaches infinity at some low strain (below 0.1 per cent), and

Figure 2 (below). Cable-bending test equipment

Figure 3 (right). Gauge used for determining strain

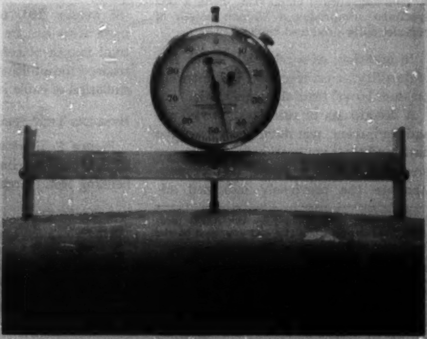

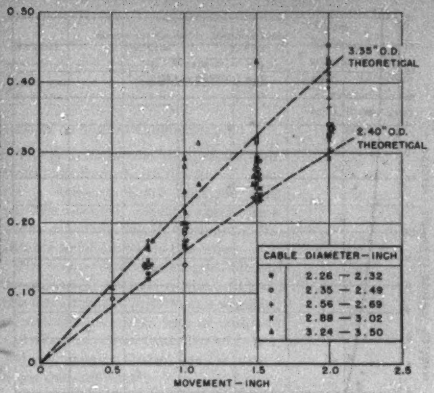

Figure 4 (above). Bending strain versus movement

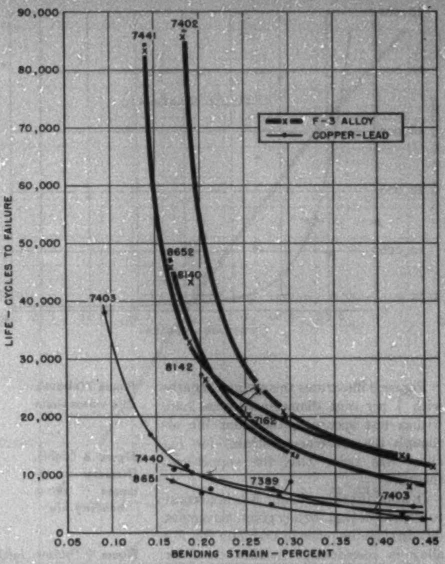

Figure 6 (right). Life versus strain

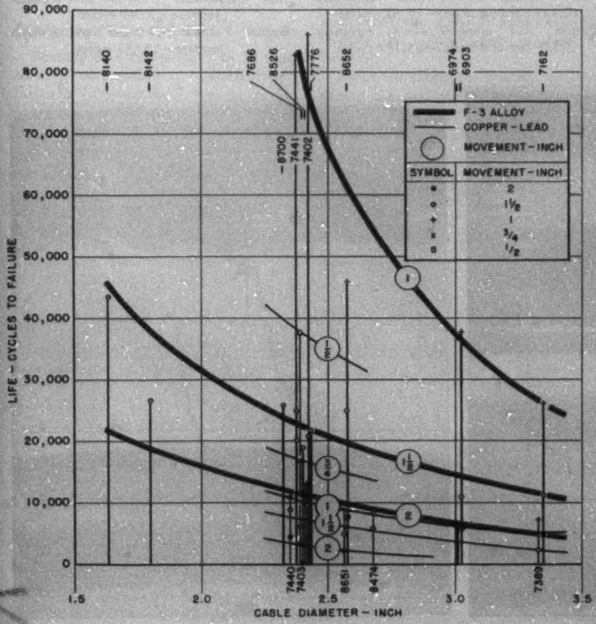

Figure 5 (below). Life versus cable diameter and movement

a low but nearly constant value at some high strain (above 1 per cent). This observation is confirmed by the data in the paper by Halperin-Betzer[8] as shown in Figure 7.

Figure 7 is replotted from Figure 1 of the Halperin-Betzer paper[8] using rectangular co-ordinates. This indicates a nearly constant life of 500 cycles between 1.25 and 2.0 per cent strain. Figure 6, analyzed by cable constructions, also indicates that at usual operating strains, 3-conductor shielded cable with carbon-black paper binder has somewhat longer sheath life than belted cable.

DIAMETER INCREASE VERSUS LIFE

At relatively high strains, the sheaths wrinkled and increased in diameter, and appeared to fail more from this cause than from bending fatigue. At very high strains, the increase in diameter was the controlling factor, and accounted probably for the life approaching the low constant value shown in Figure 7.

Figure 8 shows the relation between diameter increase at failure and sheath life. These data were obtained on many different cable constructions with standard sheath thickness of both copper-lead and *F-3* alloy. For any given increase in diameter, the life was independent of the sheath material tested.

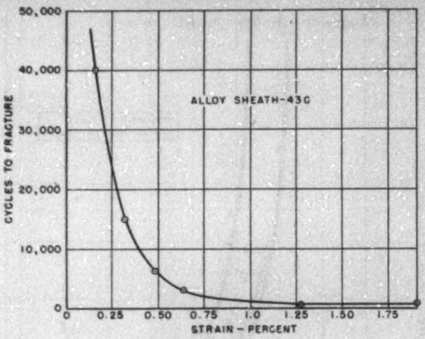

Figure 7 (above). Life versus strain

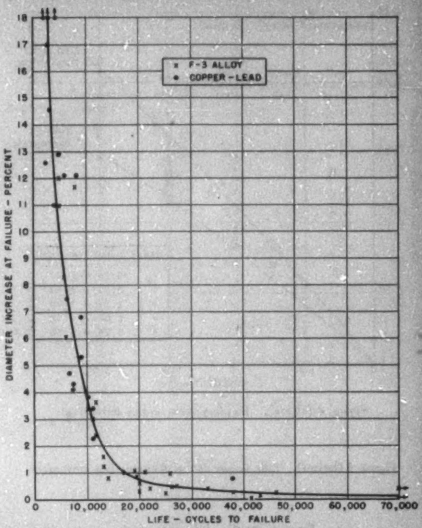

Figure 8 (right). Diameter increase versus bending life

Figure 9 illustrates this point. Sheaths with 1 per cent diameter increase had, within test accuracy, the same life although the movement (strain) for *F-3* alloy was twice that for copper-lead sheath.

In applying this relation, it is important to remember that for any given movement (strain), the increase in diameter for *F-3* alloy is considerably smaller than for copper-lead and therefore the life of *F-3* alloy sheath is significantly greater.

Figure 10 illustrates this observation. After bending with 2-inch movement, the results were:

Figure 9 (below, left). Sheaths after bending, 1 per cent diameter increase

Top: Copper-lead—3/4-inch movement (0.143 per cent strain)—17,000 cycles

Bottom: F-3 alloy—1 1/2-inch movement (0.289 per cent strain)—21,187 cycles

Figure 10 (below). Sheaths after bending, 2-inch movement (0.427 per cent strain)

Top: Copper-lead—14.6 per cent diameter increase—3,349 cycles

Bottom: F-3 alloy—1.2 per cent diameter increase—13,151 cycles

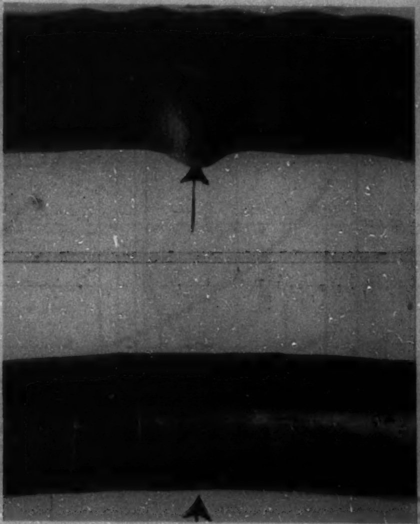

Material	Diameter Increase, Per Cent	Bending Life, Cycles
Copper-lead	14.6	3,349
F-3 Alloy	1.2	13,151

Effect of Sheath Construction

Figure 11 shows the life obtained with: twice standard sheath thickness; two-thirds standard sheath thickness; and reinforced-double sheaths, each two-thirds standard sheath thickness. Resistance to failure was in this order.

For reinforced-double sheaths, life was comparatively low and erratic. In part, this was attributed to noticeable wrinkling of both sheaths. In 11 tests on both lead and alloy, only two tests showed better, and the majority showed less life than a single thin-wall sheath.

For comparable constructions, *F-3* alloy maintained its ratio of superiority over copper-lead sheath.

Effect of Sheath Thickness

Figure 12 shows the life obtained with $1^1/_2$-inch movement on sheaths of varying thicknesses. For this strain (movement), reducing the thickness to two-thirds standard reduces the sheath life one-third for *F-3* alloy, and one-half for copper-lead.

Figure 12. Bending life versus sheath thickness, $1^1/_2$-inch movement (0.25 to 0.30 per cent strain)

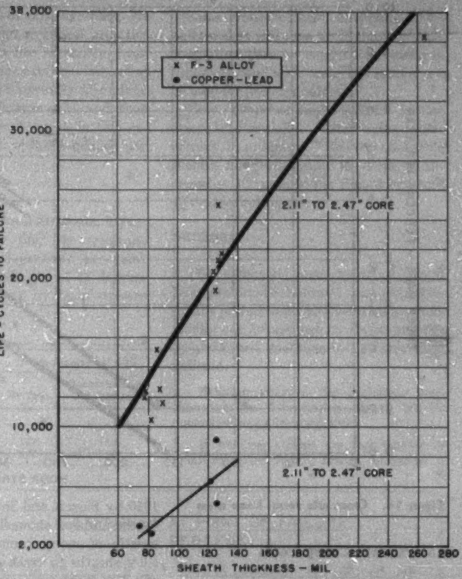

Life versus Testing Speed

Bending data in Figures 4 to 12 were obtained on a so-called "1-minute cycle" (actually 1.06 minutes). Since in service no more than a few cycles per day occur, tests were conducted at slower rates to determine the relative effect of speed of bending.

Figure 13 shows the relation between sheath life and speed of testing. For standard thickness, reducing the speed from 1 to 10 minutes per cycle reduces the life approximately 50 per cent. Further reduction in speed has little or no effect. Tentative indications are that, for the same material, the effect of speed is less at lower strains. More tests are in progress.

Figure 11 (left). Bending life versus sheath construction

Figure 13 (below). Bending life versus testing speed

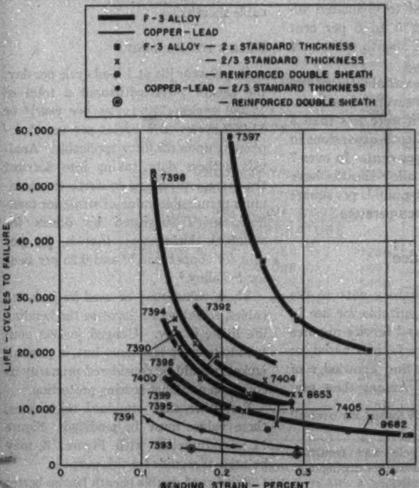

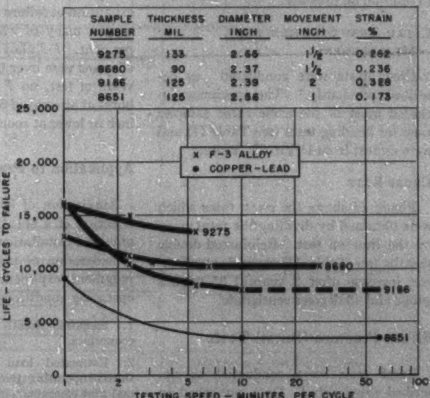

SAMPLE NUMBER	THICKNESS MIL	DIAMETER INCH	MOVEMENT INCH	STRAIN %
9275	133	2.66	$1^1/_2$	0.262
8680	90	2.37	$1^1/_2$	0.236
9186	125	2.39	2	0.328
8651	125	2.56	1	0.173

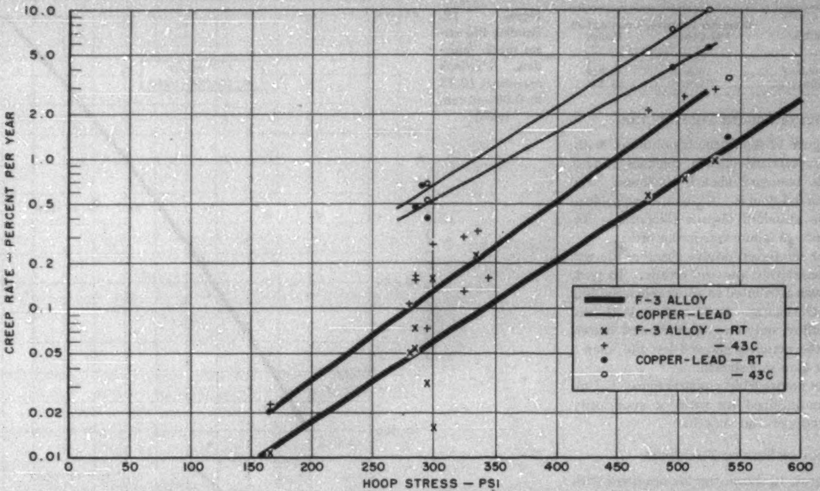

Figure 14. Creep rate versus hoop stress

Cable Sheath Creep Tests

Creep in cable sheaths is defined as the deformation (mostly increase in diameter) produced by subjecting the sheaths for long periods of time to stresses lower than the normal yield strength of the metal. In service, these stresses are created by internal pressures inside the sheath in oil-filled and gas-filled cables, and in solid-type cables by slopes and vertical risers or by oil-filled joints, if used. The test data were obtained by measuring increase in circumference of cable sheaths subjected to internal oil pressure.

CREEP TEST SPECIMEN AND MEASUREMENT

Creep tests were conducted as described previously.[1] The specimens included most of the same cable samples used for bending tests (see Table II) and were on test from $1^1/_2$ to $2^1/_2$ years.

CREEP RATE

Figure 14 shows the creep rates which were obtained by dividing the total creep by the time on test. Reinforced-double sheaths (see Table II) showed no diameter increase after 2 years at 35 pounds gauge and 43 degrees centigrade.

Stress-Fracture (Burst) Tests

Burst tests were conducted as described previously.[1] Data published in 1940 by Bassett and Snyder[7] and in 1946 by the authors[1] showed that it is characteristic of many commercial lead and alloy sheaths to crack or split with less and less diameter increase as the hoop stress is reduced from a value approximating its normal short-time tensile strength to 300 to 400 pounds per square inch. At 600 pounds per square inch and below, some sheath specimens stretch very little before splitting. Annual creep rates based on a few thousand hours of test cannot be applied to estimated 40-year service requiring 5 to 6 per cent total expansion, if the sheath splits at 1 to 4 per cent.

Figure 15 shows the variability in total expansion at failure of several sheath materials, many of which were less than 4 per cent. *F-3* alloy sheath expansions in all cases were over 6 per cent. In over 7 years of test, no *F-3* alloy sheaths have burst at stresses of 600 pounds per square inch or lower at room temperature.

Application to Practice

Application of laboratory data to the selection of a sheath suitable for use in practical installation and service requires consideration of many factors based on judgment, experience, and knowledge of operating conditions. Among these are:

1. Required sheath life based on over-all economics.
2. Estimated load cycle and resultant sheath operating temperatures during normal and emergency conditions.
3. Design of ducts and manholes in which cable is to be installed.
4. Possibility of wrinkling sheath during installation and training of cable in manhole, and expected loss in sheath thickness due to scoring and corrosion.
5. Relation between 1-minute (test) and 24-hour (operating) bending cycles.

Considering the difficulty of properly weighing these factors in advance, it would seem that conservative practice should be followed in the selection of cable sheaths.

DESIGN FOR BENDING

For 40-year life at 1 load cycle per day, the sheath must withstand a total of 12,480 cycles (312 cycles per year)[4] or 11,000 cycles (275 cycles per year)[8] depending upon the duty applicable. Analysis of these data, taking into account the several variables, confirms the maximum permissible value of strain for manhole design suggested by others for standard thicknesses; that is, 0.1 per cent for copper-lead,[8,9] and 0.25 per cent for *F-3* alloy.[8]

These values may be used for jacketed cables, since jackets increase the bending life little, if any. Unaged jackets contribute to creep resistance but, in general, jackets should be considered primarily as corrosion and duct-scoring protection.

For other than standard thicknesses, these values must be modified. Figure 11 in conjunction with Figure 13, may be used as a guide for this purpose.

Reinforced-double sheath has no better

bending resistance than a single sheath of the same thickness as the inner sheath; its primary value is to resist internal pressure. Accordingly, a permissible strain corresponding to the thickness of inner sheath should be selected.

If appreciably less than 40-year life is indicated by over-all economics, then diameter increase due to bending instead of maximum permissible value of strain becomes the determining factor in sheath selection.

Figure 15 shows that, before bursting, several sheaths will stretch 5$^1/_2$ per cent, which is adequate.[8] Thin-wall (two-thirds standard) sheaths may not always stretch 5 per cent without failing.

The authors have observed that on belted cables both *F-3* alloy and copper-lead sheaths increased in diameter more rapidly than on other cable constructions. Also, the *F-3* alloy sheaths with comparatively low original hardness increased in diameter more rapidly than sheaths that were harder. On the other hand, when the alloy sheath was very hard (so that it did not form wrinkles) and the strain was high, its life in bending was relatively poor. It appears that failure by increase in diameter is partially dependent on hardness (tensile strength), and that the optimum tensile strength in this respect is in the order of 3,000 pounds per square inch.

Design for Creep

If a 5$^1/_2$ per cent total expansion is permitted for 40-year life, the resultant creep rate is 0.1375 per cent per year. From Figure 14, this rate at 43 degrees centigrade is produced by hoop stresses as shown below:

	Hoop Stresses at 40C	
Sheath Material	By Test, Psi	Recommended for Design, Psi
Copper-Lead	167	150
F-3 Alloy	303	250

Some grades of lead, antimony alloy, and tin alloy will show appreciably greater creep rates than for copper-lead shown in Figure 14, and such materials should not be used for pressure cables.

New neoprene-hose jackets reduce creep substantially. After aging, their efficacy is unknown. Reinforced-double sheaths have practically no diameter increase at 300 pounds per square inch and 43 degrees centigrade.

Summary

The extensive tests reported herein have provided additional data on cable-sheath performance characteristics which readily can be applied to design practice by published methods.[5,9,10] These data indicate:

1. Bending strain is the important consideration in determining sheath life of expansion loops in manholes.

2. If bending strains are low (cables of small diameter, lightly loaded, or cables in

Figure 15. Expansion of tubes at failure

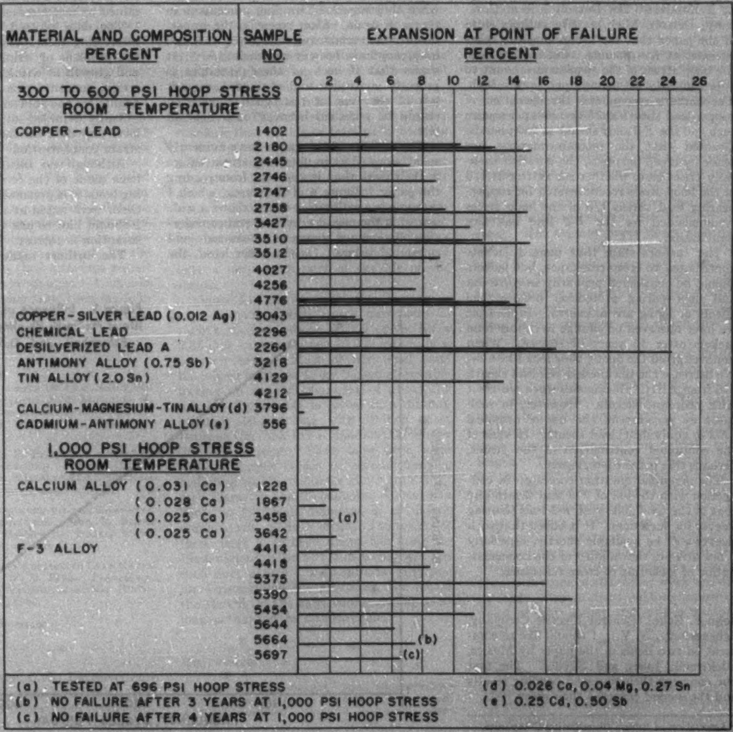

large manholes permitting large training radii), copper-lead or thin-wall alloy sheaths are satisfactory.

3. As cable diameter or loading increases, other factors being equal, strain increases.

4. Small expansion loops in restricted manholes increase the strain.

5. If bending strain exceeds a certain value, copper-lead will have a short life, and alloy sheaths should be used.

6. If the maximum permissible strain for standard alloy sheath is exceeded, additional strain resistance is best obtained by increased sheath thickness.

7. If bending strains are too high, the sheath increases in diameter, develops wrinkles and may fail from expansion rather than bending fatigue.

8. Thin-wall sheaths, in addition to lower resistance to bending and internal pressure, tend to wrinkle from handling. These wrinkles may cause stress concentrations and nonuniform bending resulting in short sheath life.

9. *F-3* alloy is further substantiated as a superior sheathing material by this extension of previously published data.[1,2,3]

In view of: increased cost of labor and materials; necessity to obtain the utmost from capital investment; possible future national emergencies and simultaneous critical shortage of materials; and unknown factors, it would seem that choice of a long-life sheath is well warranted.

References

1. F-3 Lead Alloy—An Improved Cable Sheathing, L. F. Hickernell, C. J. Snyder. *AIEE Transactions*, volume 65, 1946, pages 563–69.

2. Discussion by Herman Halperin of reference 1, page 1136.

3. Lead-Alloy Sheaths for Underground Power Cable, Herman Halperin, C. E. Betzer. *AIEE Transactions*, volume 70, part 1, 1951, pages 422-35.

4. Load Ratings of Cable, Herman Halperin. *Electrical Engineering* (*AIEE Transactions*), volume 58, October 1939, pages 535–53.

5. Load Ratings of Cable—II, Herman Halperin. *AIEE Transactions*, volume 61, 1942, pages 930–42.

6. Cyclic Movement of Cable—Its Causes and Effects on Cable-Sheath Life, Clement S. Schifreen. *AIEE Transactions*, volume 63, 1944, pages 1121–30.

7. The Testing of Lead Cable Coverings, W. H. Bassett, Jr., C. J. Snyder. *Proceedings*, American Society for Testing Materials (Philadelphia, Pa.), volume 40, 1940, pages 910–29.

8. Cable-Movement and Sheath-Life Data and Their Application in the Design of Cable Manholes, C. S. Schifreen. *Minutes*, 40th Meeting Transmission and Distribution Committee, Edison Electric Institute (New York, N. Y.), appendix A-77, 1946.

9. Oil-Filled Cable Forms Link in 66-Kv Philadelphia Loop, C. S. Schifreen. *Electric Light and Power* (Chicago, Ill.), volume 26, part I, July 1948, pages 44–49; part II, August 1948, pages 64–69.

10. Critical Inside Dimensions for Power Cable Manholes, Edward S. Halfmann. *AIEE Transactions*, volume 69, 1950, pages 1576–80.

Discussion

L. I. Komives (The Detroit Edison Company, Detroit, Mich.): The authors state in the paper that the motor pressure relay operates at five pounds. Calculating this, the hoop stress of the specimens amount to approximately 50 pounds per square inch. The authors recommend the operation of copper-lead sheath at 150 pounds per square inch and the *F-3* alloy sheath at 250 pounds. Granted that the recommendations are made for creep purposes, the question naturally arises as to whether such stress at 1/3 of the hoop stress recommended for copper-bearing lead versus 1/5 of the hoop stress recommended for the *F-3* lead has any significance.

The authors state that unaged jackets contributed to creep resistance, but jackets should be considered primarily as corrosion and duct-scoring protection because the effects of aging are unknown. In Detroit we have observed no change in rubber hose jackets after 15 years of service. When removed from the ducts, they look like new. We decrease the thickness of our lead sheath 1/6 from AEIC* thicknesses when we use it with neoprene jackets. However, in such cases we recommend the use of arsenical (*F-3* or equivalent) lead sheath. In view of the continued contribution of the jacket, perhaps this is too conservative.

The perennial question comes up in connection with the use of *F-3* lead sheath and that is the availability of *F-3* lead jointing sleeves for such lines. It is hoped that such sleeves will be available shortly, especially if one accepts the validity of the noncontribution of jacketing to creep resistance.

John F. Eckel (General Electric Company Schenectady, N. Y.): I should like to comment on two items in the paper by Messrs. Hickernell, Jones, and Snyder. The first one concerns their repeated bending results and the second concerns their creep tests.

It has been recognized for some time that Moore and Dollins[1] placed repeated bending tests of lead and its alloys on a sound basis when they expressed bending movement in terms of strain. More recently, the importance of the variables strain, temperature and frequency have been re-emphasized.[2,3,4] It seems that if each of these variables is properly controlled and evaluated, regardless of the type of test, good correlation should be obtained between each type of test.

The authors of this paper have evidently spent more effort in obtaining strain values in their work than is apparent from reading the paper. Figure 4 of the paper, which I presume is a calibration chart, shows a wide spread in the measured values and considerable divergence between measured and computed values. On the other hand, the curves of Figure 6 are of the general form expected. I should like to ask whether the strain values used in Figure 6 were determined by measurement or from Figure 4.

The data plotted in Figure 8 are very interesting and represent a new approach to the problem of wrinkling. The formation and growth of wrinkles introduce points of strain concentration which probably accounts for the shorter bending life observed in badly wrinkled samples. Do the authors have any data on the effect of wrinkles on strain concentration.

Although no mention appears to have been made of the temperature of the bending tests, it is presumed that at least most of them were made at ambient temperatures. I should like to ask the authors if this assumption is correct.

The authors made one statement with

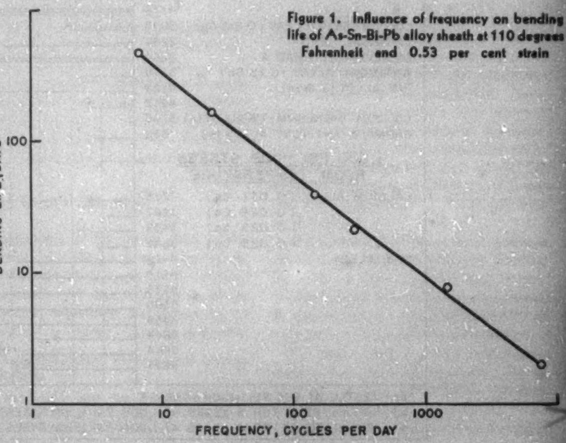

Figure 1. Influence of frequency on bending life of As-Sn-Bi-Pb alloy sheath at 110 degrees Fahrenheit and 0.53 per cent strain

---

* Association of Edison Illuminating Companies.

which I cannot agree. It is stated that frequency has little or no effect on bending life at cycle rates slower than the 10-minute cycle. In a recent paper[3] it was shown that a definite relationship exists between frequency and bending life at 110 degrees Fahrenheit in the strain range between 0.27 and 0.65 per cent. This may be expressed by the equation

$$\log l = \log b - m \log f \qquad (1)$$

where l is the bending life in days at frequency f, in cycles per day, b is the bending life when $f=1$ and m is the slope of the straight line. This equation was found to apply to acid lead from frequencies between 6.63 and 7,440 cycles per day. Recently, tests have been completed on chemical lead, common lead, and corroding lead and it was found that the bending life of each of these materials was affected by frequency in the same manner as that of acid lead.

We have had running for some time several repeated bending tests on samples of the As-Sn-Bi-Pb alloy cut from cable sheath. The tests at strains over 0.5 per cent are complete and again equation 1 expresses the relationship between bending life and frequency. Results at 0.53 per cent strain are shown in Figure 1 of this discussion. From these experiments it seems reasonable to believe that equation 1 expresses the relationship between bending life and frequencies for lead and its alloys, at least at strains above the endurance limit. Furthermore, the constants b and m seem to have values characteristic of each alloy.

In conclusion, I wish to make a brief comment on the author's creep tests. Although the *SR-4* type strain gauges are very useful I think we should recognize their limitations when used for strain measurements on lead. We have relied upon them for strain measurements in our bending tests but are aware of a definite restraining or stiffening effect. This effect was quantitatively demonstrated in a recent paper.[4] The creep tests made by the authors, according to their previous paper[5] employed *SR-4* strain gauges. I should like to ask if corrections have been made in the creep data of the authors to compensate for this restraining effect.

REFERENCES

1. FRACTURE AND DUCTILITY OF LEAD AND LEAD ALLOYS FOR CABLE SHEATHING, H. F. Moore, C. W. Dollins. *Bulletin*, University of Illinois Engineering Experiment Station (Urbana, Ill)., volume 41, number 1, 1943.

2. *Discussion* by John F. Eckel of LEAD-ALLOY SHEATHS FOR UNDERGROUND POWER CABLE, Herman Halperin, C. E. Betzer. *AIEE Transactions*, volume 70, 1951, part I, pages 430–32.

3. INFLUENCE OF FREQUENCY ON THE REPEATED BENDING LIFE OF ACID LEAD, John F. Eckel. *Proceedings*, American Society for Testing Materials (Philadelphia, Pa.), volume 51, 1951.

4. THE FATIGUE TEST AS APPLIED TO LEAD CABLE SHEATH, G. R. Gohn, W. C. Ellis. *Proceedings*, American Society for Testing Materials (Philadelphia, Pa.), volume 51, 1951.

5. See reference 1 of the paper.

Herman Halperin and **C. E. Betzer** (Commonwealth Edison Company, Chicago, Ill.): The authors of this paper have rendered a valuable service to the users of power cables through their development work on arsenical-lead cable sheathing. As was discussed in our recent paper[1] on such sheathing, such developments permit increased loading of the cables and longer life in service, and they came at an opportune time when increased loads and rising costs accentuated the need for better sheathing.

The test results that are presented are generally in agreement with our data. This discussion is mainly on a few points of differences.

The creep rates shown in the paper are lower than those which we obtained on the same and similar alloys. Based on those rates, the authors recommend a limiting hoop stress of 250 pounds per square inch at 43 degrees centigrade. Perhaps this limit would be all right for operation of the sheaths at 43 degrees centigrade. However, with the increased loadings of underground conduits, the ambient temperatures have increased considerably since the war. Duct temperatures above 45 degrees centigrade and sheath temperatures of 55 degrees or more have become rather common in Chicago. Furthermore, the cable in service is subjected to some vibration and movement which tends to increase the rate of creep above that measured in the laboratory. It appears to us that the present accepted limit of 175 pounds per square inch may be too conservative, and if the limit were increased, we would prefer to stop at 200 pounds per square inch for general application until more experience is obtained. Some trials at higher stresses on an experimental basis would be helpful.

Some of the data from our paper[1] are reproduced in Figure 7 from which the authors conclude that the life to fracture in bending is nearly constant at 500 cycles between 1.25 and 2.0 per cent strain. Actually, our data showed 40 per cent less life at 2.0 per cent strain than at 1.25 per cent. However, strains of the order of 2 per cent are encountered in service only very rarely in connection with emergency loading, and then for only a few cycles. Thus, they consume only a very small part of the life of the sheath.

Figure 5 of the paper shows a decrease in life in bending with 1-inch movement in their tests from about 80,000 cycles for a 2.35-inch cable to about 26,000 cycles for a 3.3-inch cable. Most of our bend tests have been made on 12-kv 3-conductor cable having an over-all diameter of about 2.4 inches. Such cable is tested in a dummy manhole 10-feet long with 19-inch offset between the cable in the duct and the center line of the joint. There have been some tests of larger cables of several designs, including single-conductor cable with 3.15-inch diameter and 3-conductor cables with 3.30- to 3.35-inch diameter in a 13-foot manhole with 25-inch offset. The results of these tests have been about the same for these various cables at 1/2 inch movement at each duct mouth. With suitable provision for expansion in the manholes, the life of the sheath on the large cables should be as long as that for the smaller cables.

REFERENCE

1. LEAD-ALLOY SHEATHS FOR UNDERGROUND POWER CABLE, Herman Halperin, C. E. Betzer. *AIEE Transactions*, volume 70, 1951, part I, pages 430–32.

W. J. Witte (Consolidated Gas, Electric Light and Power Company, Baltimore, Md.): The test data presented in this paper together with those data previously published by these authors and other investigators provide continuing indications that this arsenical lead alloy, designated *F-3*, is in many respects superior to copper lead as sheathing material for power cable.

The improved resistance to slow bending fatigue, resistance to creep, and resistance to burst from high internal pressures which are covered specifically in this paper appear to be adequately established for the relatively short periods of time covered by the laboratory tests and observations of those service installations upon which experience data have been collected since the commercial application of this alloy in 1945. However, over the period of the last 30 years other lead alloys have produced promising test results but after a period in service have proved unsatisfactory due to changes in the physical characteristics of the alloy. Therefore, the user of power cable is interested in establishing that this alloy will retain its physical properties for periods of time approximating the expected life of cables.

It appears additional experience and investigative data may be needed to establish whether these attractive fatigue and creep resistant properties are retained for periods of approximately 40 years, or will this alloy age-harden or self-anneal like so many of its predecessors, that is, the antimony, cadmium-antimony, cadmium-tin, and calcium alloys? It appears that additional time is necessary to provide sufficient conclusive data from which such an answer can be obtained.

L. Meyerhoff (General Cable Corporation, Bayonne, N. J.): Several papers have now appeared showing the superiority of arsenical lead alloy sheaths over copper bearing lead sheaths with respect to both bending and creep. The present paper deals with only one type of arsenical lead alloy, that designated as *F-3*. No less favorable results have however, been obtained with other arsenical lead alloys, notably with Gencalloy A, which has been produced commercially for several years by the company with which this discusser is associated.

In stressing the advantages of making cable bending tests with their 87-inch long samples as compared with the 240- to 300-inch samples used in much of the earlier work, the authors appear not to be familiar with the large amount of work that has been done with samples of comparable short length. Thus, Halperin and Betzer have for long used 96-inch samples on many of their tests and we adopted their sample and type of procedure some years ago. The shorter sample, either 87 or 96 inches, has been entirely adequate for studying the bending characteristics of the sheath itself, which is the authors' primary concern. However, much of the earlier work was done to study other matters, such as proper disposal of joint wipes and proper reinforcement of the sheath in the vicinity of wipes, for which conditions the use of the longer sample was required.

The paper does not make clear whether strain measurements were made throughout the tests or only at the start for the purpose of determining required movements to produce desired strains. Since the geometry of a given test specimen undergoes some change as the test progresses it may be quite important to measure strains throughout the test. We have found it very convenient for this purpose to use an instrument, known as an Arcmeter, by which we measure the radius of curvature and its change.

In the description of their test setup the authors state that a "free sliding wood block supported the specimen near the middle of the curvature." It may be wondered to what extent this block may affect free bending of the specimen. In the Halperin-Betzer sample no such support is used.

The authors state that "for a given cable, the data indicate that sheath life approaches . . . . . a low but nearly constant value at some high strain (above 1 per cent)." Since their data, as given in the paper, do not extend beyond 0.45 per cent strain, it is difficult to see how they can arrive at such a conclusion. The Halperin-Betzer data cited as confirmation of the quoted statement do not appear to this discusser to confirm it, particularly if all the pertinent data in Halperin-Betzer's Figure 1 are taken into account rather than only a selected part thereof.

We agree with the authors in their finding that where wrinkles are formed during the bending test, the life is short compared with what might have been expected from other tests in which wrinkling did not occur. Are we right in understanding that the authors attribute the damage that comes about as a result of wrinkling to be caused by the increase in diameter? We ourselves attribute the deleterious effects of the wrinkling primarily to increased concentration of stress, which occurs at the base rather than at the top of the wrinkle.

In the absence of wrinkles, we have found that the number of cycles to failure is closely proportional to sheath thickness, as is shown also by the authors' Figure 12 for the arsenical alloy. With wrinkles present, however, the life can be reasonably expected to go down more than in proportion as the thickness is reduced, since the severity of wrinkling varies inversely with the thickness. In this connection it may be stated that a tightly applied new jacket on a thin sheath will tend to reduce wrinkling and thereby improve the bending resistance, but how long such superiority can be maintained in service remains to be determined.

Figure 8 of the paper is worthy of some study. It may be observed that the data shown may very well be represented by two straight lines, one covering the range from zero to about 0.8 per cent increase in diameter and the other the range above 0.8 per cent. Evidently, two different causative factors are involved and it is probable that in one case it is bending fatigue and in the other it is wrinkling. About 80 per cent of the arsenical alloy samples are in the first group and about 90 per cent of the copper lead samples in the second.

It is shown that a double sheath, with the two component sheaths having the same thickness, does not have better bending resistance than a single sheath of the same thickness as one of the component sheaths. The authors relate the bending behavior of the double sheath to that of the inner sheath. Actually, the pertinent component sheath is the outer one, since when that fails, its primary function is no longer served. As an instance in point, we have made cable with double sheath, the inner sheath of which showed remarkable performance on bend test, but, since the outer sheath did not stand up any better than if the inner sheath had not been there we did not consider that we had made an effective gain. Incidentally, as we understand the authors' description of their preparation of bend samples with double sheath, it appears that both sheaths must fail before an indication of failure is obtained in their test. If this understanding is correct, the true bending behavior of the double sheath is even less favorable than indicated.

The creep data given are of interest and in general show about the same correlation between arsenical lead alloy and copper lead as has been reported by other observers. However, the creep rates shown are materially lower for both types of sheath than shown by other observers. It is noted that the specimens used for this test are pieces of sheath only 15 inches long. The question may well be raised as to whether the disposition of the ends of the specimens might not stiffen them and cause the readings to be too low.

R. W. Atkinson (General Cable Corporation, Bayonne, N. J.): I shall confine my comments largely to conclusions stated by the authors, particularly those stated under the Summary.

The authors should state the temperatures at which the fatigue tests were made. Were these made at room temperature? Life at temperatures found in operation is considerably lower than at room temperature, and relative values may be altered.

The rate of creep found is considerably lower for both types of lead than found in other laboratories, including tests reported by the University of Illinois. Do the authors have an explanation for this difference? Is it related to the shortness of their test specimen? What assurance have the authors that the strain gauges used have not furnished appreciable support, thus reducing creep rate? The scatter of the values for creep rate as shown is rather high; the values for copper lead and for *F-3* actually overlap. May this fact help toward an explanation of the lack of agreement with other observers?

The first four numbered items under the Summary are readily accepted without any new data. Indeed the paper gives little or nothing to add support to these statements.

If Item (5) is read in the light of Item (6) which shows that the alloy sheaths themselves have limitations, it is entirely correct.

Item (6) says, in part, "that . . . . . additional strain resistance is best obtained by increased sheath thickness." The best procedure—say from the standpoint of economics—might be, however, to use some means to keep down the strain.

In Item (7) it appears that the early failure of sheaths that accompanies wrinkling during bending is explained on the basis of the associated increased sheath diameter. In that case one would expect failure at the part of the sheath which reaches the largest diameter—at the top of the wrinkle or fold. Instead failure occurs normally at the smallest diameter. One wonders at the apparent different viewpoint in Item (7) and that indicated in Item (8) which gives an entirely different explanation of the failure of the wrinkled sheath and one with which I would generally agree.

I agree with Item (9) and would add that the favorable properties which are shown for *F-3* lead are also possessed by other arsenic-containing alloys.

L. F. Hickernell, A. A. Jones, and **C. J. Snyder:** None of the discussion questions the relative superiority of *F-3* alloy as compared to copper-lead as a cable sheathing material. It indicates general agreement with the data and results presented in the paper, and primarily is directed to details of the test methods, to speculation as to the mechanism of failure in bending, and to correlation of values of creep with other laboratories. This is to be expected since there are no universally accepted standard methods for evaluating the properties under investigation.

Specifically, in reply to the discussers, we offer the following:

(*Komives*) Our recommendation for the maximum hoop stress of 150 pounds per square inch for copper-lead and 250 pounds per square inch for *F-3* alloy sheath is based upon allowable creep. No attempt was made in the bending tests to include the effect of internal pressure. The 5-pounds gauge pressure used in the bending tests was selected as a means of detecting sheath failure solely on the basis of positively operating the pressure relays. Since the 5-pound indicating pressure results in such a low hoop stress (approximately 50 pounds per square inch), we doubt that this would affect the relative life of copper-lead and *F-3* alloy sheathed cables in bending.

The aging of neoprene-hose jackets should be correlated with the exposure conditions, especially temperature. Possibly the nondeterioration of jackets in Detroit is due to favorable operating conditions. Hose jackets, as long as they retain their initial physical properties, should contribute to creep resistance. However, there are no published data showing that they do contribute to bending resistance for the expected normal life of the cable. Until such data are available, we prefer to consider that the hose jackets are primarily for corrosion protection. However, since jackets do prevent duct scoring of the sheath, we believe that 10 to 20 per cent reduction in standard thicknesses may be warranted economically if *F-3* alloy is used.

Although *F-3* alloy joint sleeves have been furnished experimentally, present extrusion equipment is not adaptable for commercial production of heat-treated alloy sleeves in large sizes. It is hoped that eventually suitable equipment will be available for this purpose.

(*Eckel*) As indicated in the paper, Figure 4 of the paper shows the measured strain versus movement obtained on various cable constructions. This is not a calibration curve, but was included to show that cable movement and sheath strain are related, even though the correlation is affected by other variables such as core construction, and that strain is to be preferred to movement as an independent variable. The strain values used throughout the paper (including Figure 6) were measured values.

We have no measurements of the concentration of stress or strain in the wrinkles. The formation and growth of wrinkles probably are due to variations in strain at these points. The mechanism of failure in wrinkled sheaths probably is due to progressive increase in diameter at the wrinkles until the sheath fails. During testing at relatively high strains, the tension side of the sheath stretched permanently during each cycle. During the compression part of the bending cycle, little contraction in length occurred, therefore the extra length contributed to increasing the diameter of the sheath.

All bending tests were made at room temperature.

The statement on life versus testing speed (frequency) is substantiated by the data in Figure 13. Since submitting the paper, sample *9275* tested at 10 minutes per cycle gave a life to failure of 13,700 cycles. Figure 2 of this discussion is an amplification of Figure 13 of the paper to include this new value.

Figure 3 of this discussion shows an abstract of our data compared to that concurrently published by Gohn and Ellis[1] for antimony-lead alloy, and by Eckel[2] for acid-lead. For alloy material, the Gohn and Ellis data confirm our findings on the effect of testing speed even though the testing strain was higher (0.40 versus 0.24 per cent). For lead, the Eckel data do not appear to agree with ours, probably due to his testing strip specimens at high strains compared to our testing full-size cable constructions at strains approximately those normally encountered in service.

Possibly Eckel's equation for relating frequency and bending life is applicable at high strains (above the endurance limit), but at the lower, more practical, values of strain

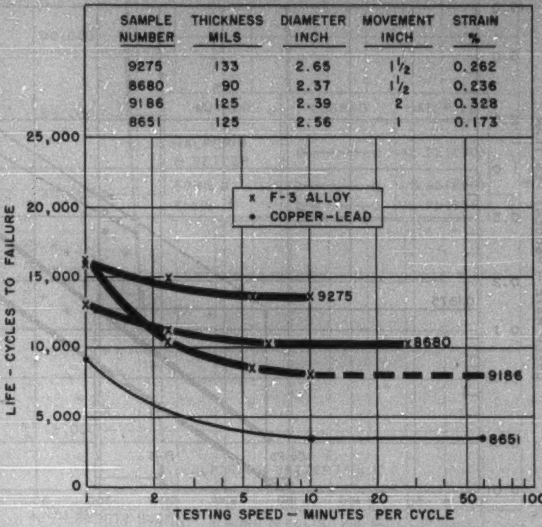

SAMPLE NUMBER	THICKNESS MILS	DIAMETER INCH	MOVEMENT INCH	STRAIN %
9275	133	2.65	1½	0.262
8680	90	2.37	1½	0.236
9186	125	2.39	2	0.328
8651	125	2.56	1	0.173

Figure 2 (above). Bending life versus testing speed

Figure 3 (below). Bending life versus testing speed

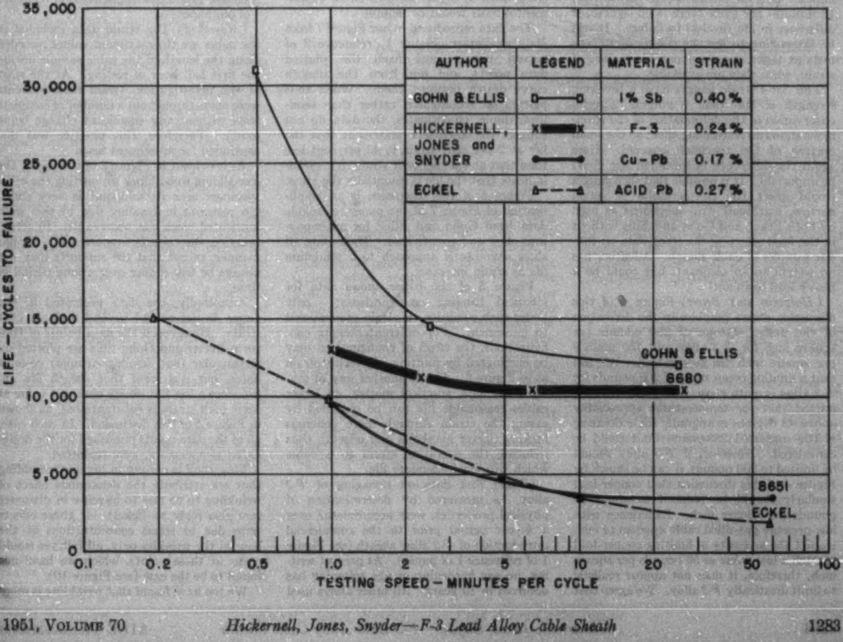

AUTHOR	LEGEND	MATERIAL	STRAIN
GOHN & ELLIS	□——□	1% Sb	0.40 %
HICKERNELL, JONES and SNYDER	x▬▬x	F-3	0.24 %
	●——●	Cu-Pb	0.17 %
ECKEL	Δ- - -Δ	ACID Pb	0.27 %

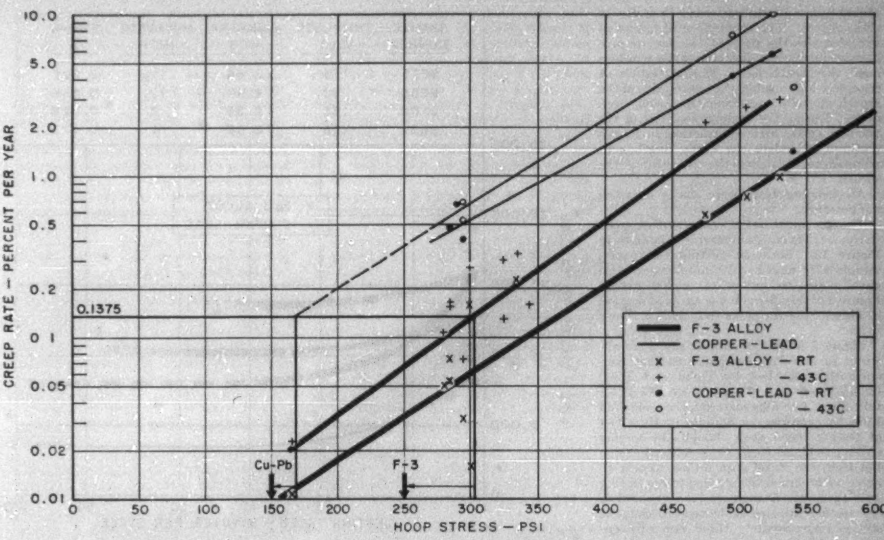

Figure 4. Creep rate versus hoop stress

(in the order of 0.15 per cent for lead, and 0.25 per cent for *F-3* alloy) our data do not support this relationship, but instead do indicate that for testing speeds slower than 10 minutes per cycle there is no significant difference in life (cycles) to failure. It will be interesting to see the results of Eckel's tests at lower, more comparable, values of strain, when they are available.

The *SR-4* strain gauges have a breaking strength of less than 1 pound. Careful observation of the deformation of the specimens shows no restraining effect on the small portion of the specimen covered. Here again the difference in specimen size could be important. It is possible that such gauges would affect the creep results of small, narrow, machined strip specimens as used by both Eckel, and Gohn and Ellis without in the least affecting the creep data on full-size samples of cable sheath. A feather has no weight to an elephant, but could be a heavy load to an ant!

(*Halperin* and *Betzer*) Figure 4 of this discussion shows graphically the derivation of the design stresses of 250 pounds per square inch for *F-3* alloy and 150 pounds per square inch for copper-lead. We feel that a limiting creep stress of 200 pounds for *F-3* alloy is quite conservative, but it is admitted that for temperatures appreciably above 43 degrees centigrade, some derating of the suggested 250-pound limit could be considered. However, if *F-3* alloy should be limited to 200 pounds, it can be shown by Figure 4 of this discussion that copper-lead similarly should be reduced to about 50 pounds per square inch. Experience with low-pressure gas-filled cable appears to contradict the necessity of limiting copper-lead to such a low value as 50 pounds per square inch, therefore, it does not appear realistic to limit drastically *F-3* alloy. We agree that some trials at higher stresses on an experimental basis would be helpful.

The data reproduced in our Figure 7 from Halperin-Betzer (Figure 1, reference 3 of paper) were copied from the plotted data points, and not from the smooth curve drawn between them. When thus plotted on rectangular, rather than semilogarithmic, co-ordinates, the data do not support the discussers' statement that the life at 2 per cent strain is 40 per cent less than that at 1.25 per cent strain, but rather indicate that the life is essentially the same.

Figure 5 of this discussion is an amplification of Figure 7 of the paper to include data from Gohn and Ellis[1] for antimony-lead alloy and copper lead. These data all show asymptotic approach to a minimum life as strain increases.

Figure 5 of the paper shows data for identical bending configurations; only under such conditions is strain proportional to movement. For different racking configurations, the effect of configuration may be eliminated by plotting life versus strain as in Figure 6. This is another way of saying that, as a practical matter, on larger cables reasonable life can be obtained by easing the strain through more generous racking (larger manholes and offsets), thus reducing the operating strain to a value which will yield adequate life.

(*Witte*) Test data on nonaging of *F-3* alloy, as measured by determination of physical properties, were accumulated over a 4-year period prior to the commercial introduction of *F-3* alloy sheath (see Figure 1 of reference 1 of paper). At present writing, no age hardening or age softening has occurred in 10 years. All other alloys used or proposed for power-cable sheathing have shown marked changes within the first few years. Furthermore, they have other undesirable properties as discussed in reference 1 of our paper.

(*Meyerhoff*) The strain data included in the paper are the maximum values recorded along the length of the cable sample during the first half hour of testing. At the start of the investigation, strain measurements were made throughout a number of complete tests without any significant change being found. Therefore, this practice was discontinued for subsequent tests.

As is evident in Figure 2 of the paper, the free-sliding wood block supporting the cable specimen near its midpoint is very short. No restraint in bending due to this well-lubricated block was observable. In actual practice, the cable is supported in a similar manner, except that the supports may not always be free-sliding over a long period of time.

Admittedly, the data presented in our paper do not extend beyond 0.45 per cent strain. However, if the data points of Halperin-Betzer and Gohn-Ellis are plotted on rectangular (not semilogarithmic) co-ordinates, our statement that sheath life approaches a low but nearly constant value at some high strain is substantiated, as shown in Figure 5 of this discussion. In each case, all of the data points published for the designated temperature, were replotted.

Meyerhoff is correct in his understanding that we attribute the deleterious effect of wrinkling to be due to increase in diameter (see also reply to Eckel). If these effects were due to stress concentrations at the base of the wrinkles only, all failures would occur at these points, which we have not found to be the case (see Figure 10).

We too have found that wrinkling is more pronounced in thin sheaths. The effectiveness of a tightly-applied new jacket depends on the degree to which the sheath is free of wrinkles prior to application of the jacket.

In reinforced double-sheath construction, it is our understanding that the primary purpose of the outer sheath is to provide protection to the bronze reinforcing tapes and the inner sheath. If the outer sheath fails first, it would take some time for the reinforcing tapes and/or inner sheath to fail, hence we have considered that the life of the inner sheath is dominant in bending. On this basis, the test specimens were prepared so that failure was not indicated until both sheaths had failed.

Most other investigators have determined creep on strips which to prepare require a certain amount of cold working of the metal; that is, flattening the original round sheath, cutting to size, and machining a reduced section. Our data were obtained on tubes prepared by removing the insulated core from the finished cable. We have conducted tests on strips and found the results were more erratic than with tubes, especially during the first 1,000 hours, or so. The more erratic results on strips are possibly caused by straightening of the strips when first placed under load together with a variable amount of strain hardening depending on the grain structure of the individual specimen. Possibly this accounts for some investigators' preference to measure creep between 1,000 and 2,000 hours; that is, discounting the creep during the first 1,000 hours. Accordingly, we prefer to evaluate creep rate on the total creep of a tube specimen because we believe the results are more indicative of the form in which the material is both manufactured and used in service. We believe that the difference between our results and those published by others is due more to the form of specimen and method of determining creep rate than to any problematical stiffening due to end fittings, gauges, et cetera.

(*Atkinson*) All bend tests were made at room temperature. We agree that at higher temperatures the life to failure will be lower, but we do not agree that the relative superiority of *F-3* alloy is not maintained. This was demonstrated in 1946 by Halperin's tests at 43 degrees centigrade (see reference 2 of paper).

In our replies to Eckel and Meyerhoff, we already have answered many of Atkinson's speculations regarding the factors affecting creep. In Figure 14, one set of values for copper-lead (at 540 pounds per square inch) is low, however, of the four curves in this figure, the largest "standard error of estimate" is 1.67. By any common statistical criterion, this scatter is not "rather high," but rather low.

Item 6 of the summary is directed to the problem of increasing the strain resistance of the cable sheath under a given set of conditions (cable diameter and manhole dimensions). Obviously, where practical and economical, the manhole should be designed to limit the strain to a permissible value for the sheath material.

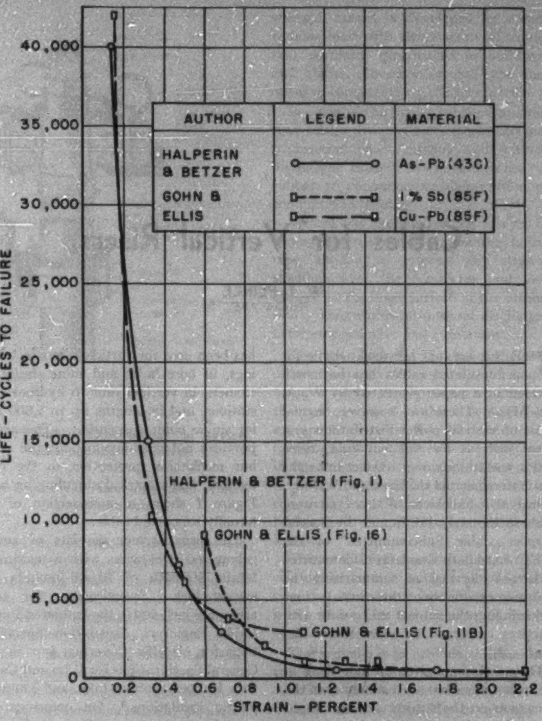

Figure 5. Life versus strain

In our opinion, Items 7 and 8 of the summary are not in conflict. Item 7 refers to cables which, although initially smooth, wrinkle and stretch during cyclic bending due to excessively high strain. This is the type of failure which is due to increase in diameter, as opposed to failure by bending fatigue which occurs at more reasonable strain. There is no consistency in this type of failure; it may occur at the top or bottom of the wrinkle, by tearing (expansion) or cracking, wherever the strain is greatest and the metal weakest. Item 8 refers to cables whose bending resistance has been lowered by formation of wrinkles due to handling prior to cyclic bending.

Naturally, we are gratified to note that the discussor agrees with point 9 of the Summary that *F-3* alloy is a superior sheathing material. Our data, of course, are confined to *F-3* alloy, which is produced by our company and its licensees under patents[3] covering composition and manufacturing processes, both of which contribute to obtaining the final desirable properties as a cable sheathing material. We will be very interested to see data published to substantiate the claim that other arsenical-lead alloys possess the same favorable properties.

References

1. The Fatigue Test as Applied to Lead Cable Sheath, G. R. Gohn, W. C. Ellis. *Proceedings*, American Society for Testing Materials (Philadelphia, Pa.), volume 51, 1951.

2. The Influence of Frequency on the Repeated Bending Life of Acid Lead, John F. Eckel. *Proceedings*, American Society for Testing Materials (Philadelphia, Pa.), volume 51, 1951.

3. United States Patents 2,300,788; 2,375,755; 2,504,600; Application Serial Number 686,461 (patent will issue in 1951).

Cables for Vertical Risers

W. T. PEIRCE
FELLOW AIEE

THE subject of terminal risers for paper insulated cables has been well covered in a paper presented by W. A. Del Mar.[1] There are, however, several types of vertical power distribution systems, such as for tall buildings, mine shafts, and tunnels over 100 feet in height which were beyond the scope of his study.

Several installations of this type were made in the early 1930's and the Special Purpose Cable Subcommittee* of the AIEE Insulated Conductor Committee undertook the task of summarizing the operating experience on these installations and bringing the subject up to date with practices employed on more recent designs.

The conclusions given are not those of the author alone but are a summary of the discussion on the subject and data submitted by other members of the AIEE Insulated Conductor Committee.

The distinctive feature of a vertical riser cable is the need for comprehending in the design some method of supporting the weight of cable and insulation. Consequently, our classification is based on method of support rather than type of insulation.

Type *A*. Top supported, by external round wire armor.

Type *B*. Top supported, by conductors alone.

Type *C*. Supported at regular intervals along the rise by clamps or grips external to cable.

Type *D*. Top supported, by internal supporting member separate from conductors.

Type *A*, external round wire armor type, has had the widest use, especially for suspensions of over 300 feet in height. It has been used for vertical risers in buildings, in bore holes and mine shafts, in tunnels, in vertical runs in hydroelectric stations, and in lengths up to 1,600 feet for single point suspension. The armor provides not only support for the cable but mechanical protection to the conductors, and electrical shielding as well. Figure 1 shows a cross-section of externally supported cable.

The usual armor consists of round galvanized steel wires with a maximum tensile strength of 70,000 pounds per square inch. Specifications for such armor are included in the Insulated Power Cable Engineers Association Specifications for Metallic Coverings,[2] or in the General Specifications for Wire and Cable with Rubber, Rubber-Like, and Thermoplastic Insulations.[3] On occasions for special purposes armor of copper, bronze, or copper-clad steel have been used.

Most mining regulations require the use of type *A* or armored cables in shafts or slopes where there is danger to personnel or equipment from contact with unshielded cables, or from cable burndown.

Type *B*, top supported by conductors, has been used extensively for bore holes, particularly in the single conductor or concentric multiple conductor types. Medium hard drawn copper conductors can support their own weight up to 1,000-foot lengths with a factor of safety of ten, and as this type is usually used in much shorter lengths, the additional factor of safety provides considerable assurance that the cable will not fall due to partial burnoff of conductors under fault conditions.

Type *C*, or continuously supported cable, is used more frequently in tunnel shafts where it is desired to use orthodox cable designs and where frequent support does not introduce any problem.

Type *D*, or top-supported cable with internal supporting strands, has been used for vertical risers in buildings and in bore holes of medium height with complete success. The general design is a 3-conductor cable with a steel supporting strand in each of the three interstices, and a rubber or neoprene jacket over-all. It is much lighter than the wire-armored type, and has the additional advantage that the outer jacket protects the steel supporting members from corrosion. On the other hand, as the steel supporting strands lie outside of the circle through the center of the conductors (except for special cases, such as elevator control cables), the tension on the supports tends to wedge them into the valleys between the insulated conductors. This causes more localized pressure on the insulation than with other methods of support and must be considered in the over-all design, particularly as to the weight to be supported. Figure 1 shows a cross-section of a typical cable construction with internal support.

Types of Insulation and Cable Design

The common insulations, such as rubber, varnished cambric, and saturated paper, have been used with all the types mentioned.

The most commonly used insulation for voltages up to 15 kv has been rubber, with varnished cambric as close second choice. For higher voltages, saturated paper has been the usual selection. In all cases where paper has been used for rises over 100 feet, either a special saturant,

---

* Other members of the Subcommittee are: G. W. Acock, J. F. Atkinson, A. Lee Barrett, E. D. Bent, E. W. Davis, R. A. Hopkins, J. F. Huguelet, R. H. Kolks, M. J. Lowenberg, R. B. McKinley, F. V. Smith, E. G. Sturdevant, C. F. Titus, R. K. Woodson, W. N. Zippler, and G. W. Zink.

Paper 51-235, recommended by the AIEE Insulated Conductors Committee and approved by the AIEE Technical Program Committee for presentation at the AIEE Summer General Meeting, Toronto, Ont., Canada, June 25–29, 1951. Manuscript submitted March 26, 1951; made available for printing May 4, 1951.

W. T. PEIRCE, Chairman of the Special Purpose Cable Subcommittee of the Insulated Conductors Committee is Chief Cable Engineer with the American Steel and Wire Company, Worcester, Mass.

The writer wishes to acknowledge the data submitted by C. T. Hatcher on operating experience with vertical riser cables in New York, and for information on system design submitted by C. F. Avilla, J. B. Johnson, and R. D. Woodson. Much of the data on supporting methods was made available by A. A. Jones and G. B. Shanklin.

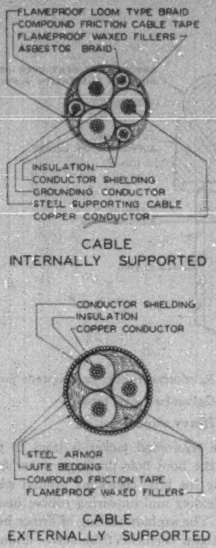
FLAMEPROOF LOOM TYPE BRAID
COMPOUND FRICTION CABLE TAPE
FLAMEPROOF WAXED FILLERS
ASBESTOS BRAID
INSULATION
CONDUCTOR SHIELDING
GROUNDING CONDUCTOR
STEEL SUPPORTING CABLE
COPPER CONDUCTOR
CABLE
INTERNALLY SUPPORTED
CONDUCTOR SHIELDING
INSULATION
COPPER CONDUCTOR
STEEL ARMOR
JUTE BEDDING
COMPOUND FRICTION TAPE
FLAMEPROOF WAXED FILLERS
CABLE
EXTERNALLY SUPPORTED

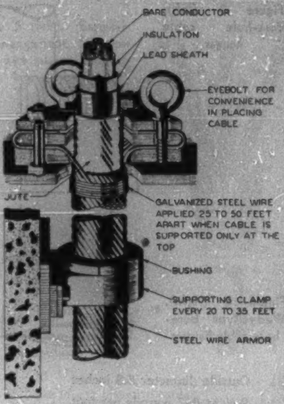
BARE CONDUCTOR
INSULATION
LEAD SHEATH
EYEBOLT FOR CONVENIENCE IN PLACING CABLE
JUTE
GALVANIZED STEEL WIRE APPLIED 25 TO 50 FEET APART WHEN CABLE IS SUPPORTED ONLY AT THE TOP
BUSHING
SUPPORTING CLAMP EVERY 20 TO 35 FEET
STEEL WIRE ARMOR

Figure 1 (left). Cross-sections of typical top-supported riser cables

Figure 2 (above). Three-ring clamp support for armored cables

which is a semisolid below its rated operating temperature, has been employed, or provision made for introducing oil at the top of the rise and periodically relieving static head pressure at the bottom. More recent installations have used special types of low gas pressure cables.[4]

The type of rubber used has been based on the individual manufacturers' recommendations. In the main, these have been for oil-base ozone-resisting rubber, although some manufacturers have preferred to use special high-voltage insulation and rubber with higher physical properties because of the mechanical strains involved. The service records available do not indicate any definite preference.

In the case of varnished cambric, the insulation has been applied with a butt wrap instead of with the usual overlap. The purpose of this is to provide a more compact insulation and to minimize slippage. Slipper compound between tapes has been omitted or else used sparingly to avoid oil migration troubles or leakage from lower terminals.

Where varnished cambric or paper has been used as insulation, both lead and nonmetallic (rubber or neoprene) sheaths have been employed. Lead sheaths introduce no problem where cables are supported at short intervals throughout their length. For top-supported cables, the use of lead limits the safe length to 500 feet unless special precautions are taken to transfer the weight of the lead to the supporting armor uniformly along the length. Otherwise, the lead will slip or sag under the armor and accumulate in accordion-like wrinkles at the bottom of the run. The use of lead makes it difficult to obtain high safety factors for the top support of long lengths. The minimum safety factors recommended by Insulated Power Cable Engineers Association[3] are four for leaded cable in buildings; five for bore holes; and seven for nonleaded vertical risers in buildings, while most mining laws require a factor of ten for working shafts. This safety factor is the rated breaking strength of the strength members in the cable divided by the total weight of cable in suspension.

Nonmetallic jackets, in the case of rubber-insulated cables, have been extruded and lead-vulcanized rubber such as used for portable cables. Since polychloroprene (neoprene) has been available, it has replaced rubber in most cases.

For varnished cambric and paper cables, nonmetallic jackets are composed of reinforced rubber or neoprene tapes with a varnished cloth or resin barrier tape between the core and the jacket. During vulcanization, the tapes bond into a homogeneous covering.

Conductor support is required with varnished cambric or paper insulation to prevent conductor slippage through the insulation. Soldered connectors have been found unreliable, as sufficient strength cannot be developed for a continuous load with the amount of vibration normally experienced in buildings and shafts. Pressure or gun-type mechanical connectors are the general rule.

In some of the earlier rubber-insulated riser cables, trouble was experienced due to internal ozone cutting and voltage discharges caused by nonadherence of rubber to conductor or deformation of conductor in bending.

Present-day designs include a layer of conducting rubber or conducting fabric tape applied as internal (or strand) shielding over the conductor and vulcanized to the inner surface of the insulation. This avoids all internal discharges between conductor and insulation.

The deformation or kinking of the conductor is due to the restriction of movement between the insulated conductors themselves when the cable is bent. When movement is restricted, the conductors cannot adjust themselves to the difference in the circumference of bend between the inner and outer surface of bend, and the conductor on the inside of the bend buckles as it occupies a position of shorter length.

The condition is aggravated when small conductors have a heavy wall of insulation and when the cable is bent sharply while under the compression of heavy mechanical loads.

The remedy is to provide slippage between conductor insulation surfaces and to reduce the adjustment required by using abnormally short lays in cabling.

To accomplish the first, the surface of the insulation may be lubricated or covered with separator tapes of paper or varnished cambric. There is a limit to the degree with which the conductors can be allowed to slide on each other without at the same time losing the support of the armor. It is desirable to use lays of eight or ten times the core diameter and to bend the cable as little as possible while it is under heavy strain. For this reason, hoisting the cable from the bottom imposes less severe strain on the cable structure than the usual method of lowering from the top.

It is sometimes required that the wire armor of type *A* cables be banded at intervals of from 25 to 50 feet, depending on the size of the cable. Such bands are usually about 4 inches long and consist of a serving of 12 Birmingham wire gauge galvanized steel wire. Their purpose is to prevent the armor from loosening and allowing the core to slip. The practice is not general, and no trouble has been reported on cables made to standard specifications which have not been so banded.

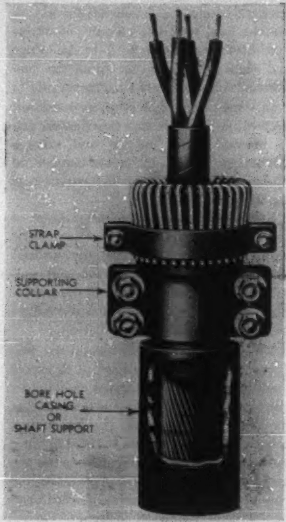

Figure 3 (left). Bore-hole cable hanger

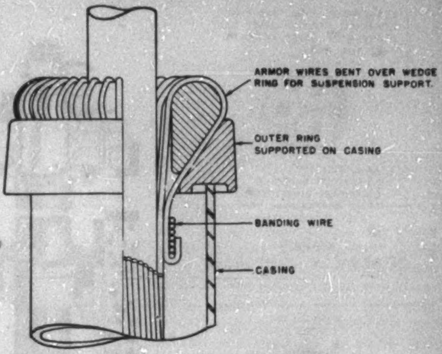
ARMOR WIRES BENT OVER WEDGE RING FOR SUSPENSION SUPPORT.
OUTER RING SUPPORTED ON CASING
BANDING WIRE
CASING

Figure 4 (right). Wedge-type bore-hole cable hanger

Specific Requirements for Various Types of Service

Building Risers

The electric power requirements of tall buildings are such that it is desirable to use a vertical a-c network for secondary distribution. Such a network requires high-voltage feed points for load centers at various levels, and vertical riser cables to service these load centers.

The riser cables are generally installed in conduit and consequently are of the top-supported types.

The majority of the installations have used wire armored cables. Common voltage rating is 15,000 volts and conductor sizes are 1/0 and smaller.

A typical cable construction should consist of:

(a). Number 1 19-wire strand

(b). Strand shielding

(c). 280 mils rubber (ozone resisting or manufacturer's recommendation) (or 250 mils rubber plus 3/64 varnished cambric tape)

(d). Copper shielding tape

(e). Three conductors cabled with jute fillers

(f). Fabric binder tape

(g). Double jute serving

(h). Number 6 American wire gauge galvanized steel armor

(i). Outside diameter 2.8 inches

(j). Weight 6–7 pounds per foot

For a varnished cambric cable, the insulation thickness would be 295 or 315 mils, and a reinforced rubber or neoprene jacket would be applied over the assembled conductors.

Bore-Hole Cables

Modern mining methods are highly mechanized and electrically-operated equipment predominates for underground workings. To avoid the use of cables in slopes and horizontal tunnels where they would occupy valuable space and be subject to injury from rock fall and mine equipment, it is desirable to feed the working faces from surface power lines through bore holes drilled vertically to the load centers. Since most mine equipment employs direct-current, rectifier stations at these load centers are commonly used.

These bore-hole cables must of necessity be of the top supported type. The usual a-c rating is 2,300 or 4,150 volts, although some of the larger mines are being forced to use higher voltages due to increasing power demands, and 600-volt d-c cables also are common to supply power to haulage locomotives.

Rubber insulation is used in the majority of cases, as bore holes are ordinarily wet. Conductor support also is very common, especially for the lower voltages and shorter runs. However, many mines use armored cable exclusively.

For armored types, the common construction is

(a). Stranded copper conductors

(b). Rubber insulation

(c). Metal shielding (above 6 kv)

(d). Three conductors cabled with jute fillers (ground wires are often included for system- ground or fault protection)

(e). Reinforced rubber or neoprene jacket

(f). Galvanized steel armor

(g). Heavy asphalt coating

The reinforced jacket is used to prevent the bore hole drainage water from rotting the jute, corroding ground wires, or shielding and impairing rubber insulation. The asphalt coating of armor helps to mitigate corrosion from active drainage water.

Conductor-supported types utilize medium hard-drawn conductors (sometimes reinforced with steel), rubber insulation, shielding above 3 kv, and a neoprene jacket. The use of several single conductors is perhaps more common than a 3-conductor cable. Shielding, with single conductor cables, is especially important, as the conductors are in loose contact with each other and the sides of the hole. They are subject to considerable movement due to repulsion from each other under load and are alternately wet and dry on the surface, so that continuity of ground contact is not always assured.

Copper tape shielding is usual except where the shield is used to operate sensitive ground fault relays in which case a concentric serving of copper wire is used having an area at least 50 per cent of the main conductor.

Mine Shafts

Cables for mine shafts and working slopes are of the armored type of the same general construction as the armored bore hole cables.

This is required by law in most cases and good practice in any case, since such cables are liable to mechanical injury from falling objects.

They may be top supported but generally they are clamped to the walls or shaft structure to keep them out of the way and to prevent swinging.

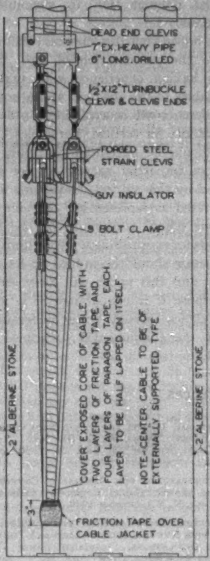
DEAD END CLEVIS
7" EX. HEAVY PIPE 6" LONG, DRILLED
1/2"X12" TURNBUCKLE CLEVIS & CLEVIS ENDS
FORGED STEEL STRAIN CLEVIS
GUY INSULATOR
3 BOLT CLAMP
COVER EXPOSED CORE OF CABLE WITH TWO LAYERS OF FRICTION TAPE AND FOUR LAYERS OF PARAGON TAPE. EACH LAYER TO BE HALF LAPPED ON ITSELF
NOTE-CENTER CABLE TO BE OF EXTERNALLY SUPPORTED TYPE
2' ALBERINE STONE
2' ALBERINE STONE
3'
FRICTION TAPE OVER CABLE JACKET

Figure 5 (left). Supporting arrangement for riser cable with internal supporting members

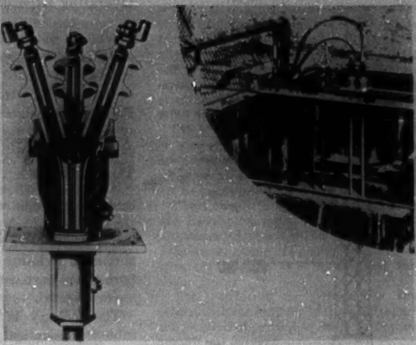

Figure 6 (right). Pothead for conductor-supported cables

TUNNEL ENTRANCES

In the transmission of power in cities it is often necessary to cross bodies of water in which submarine cables are vulnerable to dredging operations and ships' anchors. It is often more economical to drive tunnels, in which case there is a vertical entrance at both ends.

The cables in the vertical sections are but short sections in otherwise long horizontal runs, and it is usual to use cable that is compatible with the horizontal sections. The voltages used are 15,000 and higher.

Varnished cambric has been used for the 15,000-volt class, but the great majority of such cables have been insulated with saturated paper.

The general practice is to use lead-covered cables which are supported every 12 to 15 feet with split-type cable clamps or woven cable grips.

There is no one typical construction. Where saturated paper has been used, the problem of oil migration and static oil head has been overcome in one of the following ways:

1. Use of a saturant with a melting point above operating temperature.
2. Use of oil filling at the top and continuous drainage from the bottom.
3. Use of gas pressure cables.
4. Use of pressure-type pipe cables.

OTHER USE FOR RISER CABLES

In large hydroelectric developments, it often is necessary to conduct auxiliary power from the station to the top of the dam, or to connect the generator busses to transformers located at an upper level. Tunnels may be provided in the dam itself for such services.

The practice in such cases follows the ones described previously for similar installation conditions.

Methods of Support

A common method of support for wire-armored cables is to use a 3-plate bolted suspension clamp, as shown in Figure 2. This consists of three circular plates with holes in the center for the cable core. The armor wires are fanned between the first and second plates, bent over the outer edge of the second plate, and clamped again between the second and third plates.

Another method is to use a split cast iron throat that is bored to fit over the armored cable. The armor wires are bent back over the top edge of the throat and seized or clamped in place. Figure 3 shows a typical design and Figure 4 a modified type.

Cables with internal supporting members have these members clamped to strain insulators which are in turn supported, through turnbuckles, by a loose fitting section of pipe. The pipe, itself, is attached to the building frame or floor by dead-end devices or a collar. The general layout of such support is shown in Figure 5.

Several methods of support are used for cables supported by the conductors. The conductors may have a special drawn or mechanically-applied terminal fitting which can be attached to the top of the porcelain of a suspension-type pothead, providing both support and termination of the cable. This is illustrated in Figure 6.

For the lower voltages, a tripod arrangement can be mounted over the bore hole, and the bared conductors looped and clamped through strain insulators. If a 3-conductor cable is used, it is desirable to adjust the load on each conductor by means of individual turnbuckles.

Another common method is to loop the whole cable around a circular wooden disk with one or two turns, and to clamp the two protruding ends together.

There is a variety of split cable clamps available for supporting the sheath at 10- to 15-foot intervals. These are basically iron rings attached to the masonry of the shaft, with wooden or composition inserts carefully bored to 90 per cent of the actual cable diameter. It is important that the clamping action should be from the close fit of the inserts rather than from the strain put on the bolts.

Where the cable core is soft or easily deformed, split-type woven wire grips are available. The lower end of the grips is attached to the lead by a serving of friction tape, and the bridles of the grip either fastened to rings on a slope or to a forked bolt attached to the supporting structure. If vibration is anticipated, the bolts may be supported through compression-type springs. Figure 7 illustrates the general arrangement of such support.

If the supporting grips are to be used under corrosive conditions, it is desirable to interpose some insulation between bridles and support to avoid galvanic currents and to protect the lead sheath and grip from corrosion. This might

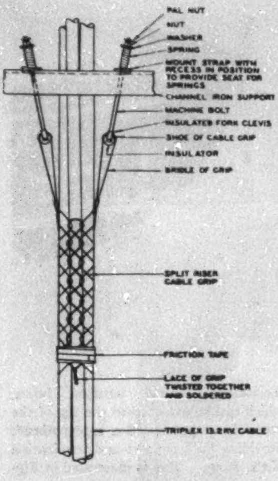

Figure 7. Basket grip for vertical support of lead-sheathed shaft cables

consist of tape between them or heavy asphalt paint over them.

In all cases of vertical support, the supporting means should be directly over the vertical section.

Methods of Installation

The easiest method of installing cables in the vertical position is to hoist the free end from the bottom. This cannot always be done as hoisting means may not be available; it may not be possible to set the cable up at the bottom of the lift, or the required horizontal slack at the top of the run cannot be provided for.

In such cases, the cables can be lowered from the top by using a pair of rope slings that alternately hold and lower. A long tapered wooden wedge is mounted above the vertical conduit, to be dropped into place in case the cable tends to slip.

For bore holes, the cable may be unreeled on the ground in a straightaway length. A pulling rope is attached to an eye formed in the lower end, and a corresponding hoist rope attached to the upper end as a brake.

In all cases, it is obvious that careful calculations of the loads involved must be made in order that equipment may be chosen properly.

The United States Bureau of Mines Circular *I.C. 6595*[5] provides a compilation of methods of installation used in shafts and bore holes.

Operating Experiences

While a wide variety of cable designs and methods of support has been used for vertically suspended cables, the operating experiences reported have been good. Barring early failures, due to faulty design or manufacture, the service record compares favorably with other types of service.

There has been some concern that a cable failure might result in burn-down of the cable. The relay system for vertical cables should be considered carefully and automatic reclosing avoided. No cable burn-downs have been reported and none are anticipated.

The industry is quite cognizant of cable expansion and contraction troubles for horizontal cables. A top-supported vertical cable is free to expand downward and, in addition, undergoes a slow stretch for the first few years of service. This stretch may be accompanied by a tendency to untwist. As much as $13^{19}/_{32}$ inches of permanent stretch have been experienced in a 732-foot length and up to 360 degrees of twist. Provision for such movements should be made at the bottom of each run.

It is desirable to provide an open chamber at the base of long vertical runs to permit the vertical movement to take place without constricting the movement of the cable. The tendency to untwist makes it advisable to clamp the cable before the joint to the vertical section or to provide free conductors between the joint and the vertical section, so that the twist is not imparted to the conductors within the joint itself.

Conclusions

It has been the intention of this paper to summarize the types of cable suitable for vertical power feeds, or for installations where a considerable vertical component is encountered. In general, each application has governing conditions which dictate the type which may be employed, and which determine the most practicable method of supporting the conductors so as to avoid slippage of the insulation.

The problem of vertical transmission can be solved by one of several fundamental cable constructions as described. Cables built for horizontal performance should not be used thus without consideration of modifications required for the vertical components if over 100 feet of rise are encountered.

Operating experience with vertical riser cable has been generally good, with the usual cause of trouble mechanical or physical damage due to surrounding conditions.

It is hoped that this summary will give rise to the presentation of data from others having experience with vertical riser cables to the end that an authoritative reference will be available of present-day practice for vertical riser cables.

It should be reiterated that this has been an impartial survey of the field covered by this subject, and is not to be interpreted as representing the views of any one school of thought on the best methods for engineering a given situation. Each usage should be judged on its own merits, and this paper will have served its purpose if it contributes to a more ready choice through better understanding of the fundamental principles involved.

References

1. TERMINAL RISERS FOR SOLID-TYPE IMPREGNATED PAPER CABLES, W. A. Del Mar. *AIEE Transactions*, volume 69, part II, 1950, pages 1592–99.

2. SPECIFICATIONS FOR METALLIC COVERINGS. Insulated Power Cable Engineers Association (New York, N. Y.), October 1946.

3. GENERAL SPECIFICATIONS FOR WIRE AND CABLE WITH RUBBER, RUBBER-LIKE AND THERMOPLASTIC INSULATIONS. Insulated Power Cable Engineers Association (New York, N. Y.) second edition, sections 6.4.2.2 and 6.4.2.5, 1951.

4. OPERATION OF LOW-PRESSURE GAS-FILLED CABLE, C. T. Hatcher. *AIEE Transactions*, volume 63, 1944, pages 788–92.

5. *Circular I.C. 6595*. United States Bureau of Mines (Washington, D. C.), April 1932.

Discussion

Wm. A. Del Mar (Phelps Dodge Copper Products Corporation, Yonkers, N. Y.): There are many problems connected with power cables which do not admit of a single solution to suit all circumstances and the Committee on Insulated Conductors is to be commended for sponsoring a series of papers which lay the groundwork for individual solutions of such problems. Mr. Peirce's committee has performed a valuable service of this kind in the present paper on Cables for Vertical Risers.

I would appreciate having further light thrown on the following questions:

The use of a saturant with a melting point above operating temperature implies that the saturant is solid at all operating temperatures. This means either some kind of wax saturant or a very low operating temperature. What does Mr. Peirce's committee have in mind?

Pipe cables of the compression type with oil compression medium, having equal heads of oil in and around the cable, present no question but where gas is the pipe medium the answer is not quite so clear. However vertical risers of considerable heights are used in European gas compression cable systems. For example a 75-foot vertical outdoor pipe connects an overhead line to a power station and considerably longer vertical pipes are used in mine shafts.

The following explanation is offered for the success of the installations: Whatever longitudinal channels may exist in a cable along which oil may migrate, no oil can reach the sheath to distend it except by passing *between* tapes and eventually between the outside tape and the tape under it, into the helical channel between turns of the outside tape. This is the only place where any oil from anywhere in the cable can come in contact with the sheath, as oil cannot be forced *through* impregnated paper. The channels take up only 1/25th of the length of the cable so that all internal head of oil that might exist, is exerted on 1/25th of the sheath area.

The sheath, usually of extruded polyethylene reinforced by bronze tapes, is a locally rigid structure having 200 pounds per square inch exerted on its outer surface. Hence in order for the internal pressure to lift the sheath, it must exert 25 times 200 or 5,000 pounds per square inch which is more than any riser can exert. Moreover, to more fully satisfy ourselves on this score, we installed an 80-foot gas compression cable riser and subjected it to daily load cycles under outdoor conditions for $2^{1}/_{2}$ years.

At the end of this period the saturation was complete from top to bottom, in insulation, butt spaces and strand spaces, and the polyethylene sheath was in perfect condition, having suffered no distortion or change in tensile strength.

Thus we have both a theoretical and an experimental verification of the practical results obtained in Europe.

L. I. Komives (The Detroit Edison Company, Detroit, Mich.): The author and his Subcommittee are to be congratulated for such a useful summary of data in the form of a committee report. It is felt that this subcommittee could continue the good work and supply design data for particular installations, especially those in tall buildings. Such data is very valuable to the designer of such systems.

Design data should include, if possible, recommendations on what to do with rather sharp bends (for instance, 90 degrees) near the top of a riser.

W. T. Peirce: Mr. Del Mar's comments are quite pertinent. The term "melting point" was not well chosen. "Flow or Pour Point" would be more technically correct.

As Mr. Del Mar points out, the major flow of oil in saturated paper is in the small oil channels between convolutions of tape and this tortuous path greatly impedes the movement of oil.

By using a compacted strand or a filling of semisolid material in the strand, together with an oil resisting barrier over the surface of the insulation on each conductor, migration of oil can be prevented in the strand or filler interstices. The paper insulation itself will retain the oil, especially if the pour point of the oil is above the operating temperature, and prevent migration or pressure build up in the cable.

The observations regarding the behavior of compression type cable in vertical runs are added confirmation that oil migration, when restricted to the insulation itself, is not a major problem for vertical risers.

The Committee will be glad to consider Mr. Komives' suggestion that the paper be supplemented with more detail design data. This was not done originally because it was apparent that no two installations were alike.

The architect is particularly concerned with the function of the building and the location of services is made to fit other considerations.

In the case of armored cables of the self-supporting type, the armor usually supplements a complete cable core. In this case the armor can be terminated at its support over the vertical rise and the core with armor removed installed in conduit for the required horizontal distance.

The original purpose of the Subcommittee was to survey operating experience with various designs of vertical cable. They are pleased to report that the general experience has been entirely satisfactory.

Application of Power Line Outage Monitor

JOHN F. ATKINSON
MEMBER AIEE

JAMES D. COOKE
NONMEMBER AIEE

THE PROBLEM of reporting outages on electric power distribution systems is as old as electric distribution itself. It has generally resolved itself by reliance upon the affected consumer reporting through the medium of the telephone. In urban or suburban areas little time is lost in receiving outage reports. However, in rural areas, such is not necessarily the case.

Telephone reporting of rural outages often involves long distance calls. Many affected consumers are reluctant to report outages by long distance telephone, preferring to let "someone else" do it. At the other extreme a single outage may cause a flood of long distance telephone calls.

In some rural areas outages occurring late at night or in the early morning hours may go unreported until daylight. In many rural areas telephone service is inadequate or nonexistent and it is not unusual for outages to be reported by postal card or letter.

The ideal solution to the outage reporting problem is a device which automatically and instantaneously reports to the dispatcher the existence of an outage and indicates its location. The development of such a device has been a challenge to the electric industry for many years.

In 1941 an automatic device[1,2] for reporting outages was installed experimentally on rural power distribution systems in Ohio, Minnesota, and Virginia. Work on these experimental installations was halted by World War II. After the war, further work was undertaken, utilizing more advanced techniques developed in the interim. As an outgrowth of this work, there has been developed a power line outage monitor described in detail in a companion paper.[3] The application of this power line outage monitor to rural electric power distribution systems is described herein.

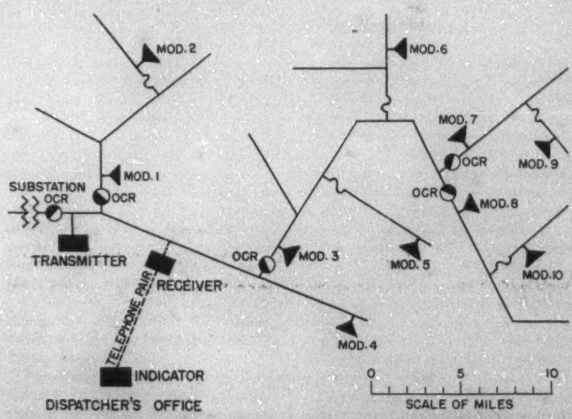

Figure 1. Arrangement of outage monitor components on a rural distribution system

The Outage Monitor

The outage monitor consists essentially of the following components arranged on a distribution system as shown in Figure 1: transmitter; receiver; indicator; and remote modulators.

The transmitter, shown in Figure 2, can be located near the substation. It supplies a continuous, unmodulated carrier signal which is propagated throughout the primary distribution system.

The receiver can be located at almost any point on the distribution system that is convenient to the dispatcher's office or service headquarters. Figure 3 shows a receiver installed adjacent to a transmitter.

The indicator, shown in Figure 4, can be located in the dispatcher's office or service headquarters. It is usually connected to the receiver by means of a 2-wire line such as a telephone pair.

The remote modulators are located on the distribution system at points that are to be monitored for outages. Each remote modulator sinusoidally alters the impedance of the distribution line at the point of attachment at a predetermined and selected audio frequency rate. This resulting dynamic impedance is reflected back to the transmitter as the transmitter

---

Paper 51-237, recommended by the AIEE Carrier Current Committee and approved by the AIEE Technical Program Committee for presentation at the AIEE Summer General Meeting, Toronto, Ont., Canada, June 25-29, 1951. Manuscript submitted March 21, 1951; made available for printing May 14, 1951.

JOHN F. ATKINSON is with the Rural Electrification Administration, United States Department of Agriculture, Washington, D. C., and JAMES D. COOKE is with the Central Virginia Electric Cooperative, Lovingston, Va.

The authors wish to express their gratitude to A. G. Loudon, Sr. and E. Altman of Clay Electric Cooperative, and to H. W. Kelley and J. M. McCutchen of Rural Electrification Administration for their work in conducting field tests of the outage monitor.

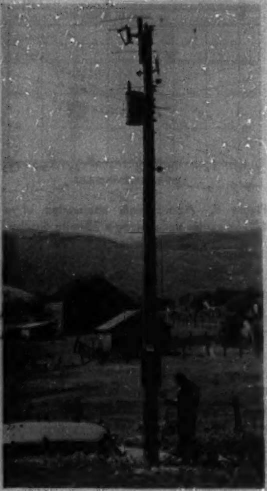

Figure 2. A transmitter installation

load impedance. Amplitude modulation of the carrier signal is thus produced. The modulating frequency is determined by the controlled audio-frequency source in each remote modulator. The per cent modulation varies along the line and is determined compositely by the impedance excursions of the remote modulator, the attenuation factor of the line connecting the transmitter to the remote modulator, the multiplicity of circuits comprising the radial feeders and the impedance of the transmitter tank circuit. Modulation is detected by the receiver and the resulting audio frequencies are passed on to the indicator unit which displays the energized or nonenergized condition of the monitored lines. A remote modulator installation is shown in Figure 5.

Figure 6 shows how the degree of modulation varies along a representative 35-mile line. The effect of taps and branch circuits are not shown in this illustration but will be discussed later. The modulator at point B may be adjusted to produce approximately 85 per cent modulation at that point. Per cent modulation decreases in the direction of the transmitter, but remains constant at 85 per cent out beyond the modulator. Figure 7 shows the approximate attenuation of the carrier signal on the same 35-mile line. From these two figures it can be seen that in the first 20-mile section of line in the illustration, the carrier level decreases with distance while percent modulation increases with distance. This condition may be used to advantage in that the receiver can be located effectively at almost any point on the line. If the receiver is located near the transmitter, the per cent modulation level received is low but the carrier level is high. On the other hand, if the receiver is located at, say, the 15-mile point, the carrier level is lower but the percent modulation level is higher. The net result in either case is a demodulated signal of relatively constant level. The receiver may be located out beyond the modulator to a maximum distance where the carrier signal level approaches line noise level. This is possible because of the higher modulation level available out beyond the modulator.

Test Installations

Experimental installations of the outage monitor have been made on the lines of Central Virginia Electric Cooperative, Lovingston, Va. and on the lines of Clay Electric Cooperative, Keystone Heights, Fla. Both of these systems are typical rural distribution systems, each encompassing over 1,000 miles of 7.2/12.5-kv distribution circuits and serving approximately three rural consumers per mile of line. Each of these experimental installations consists of a transmitter, a receiver, an indicator, and ten modulators.

The amount of experimental equipment available was limited and consequently the entire systems could not be monitored. The purpose of the tests was to determine operational and performance characteristics of the outage monitor when applied to a rural distribution system.

Distance Capability

One of the factors of prime interest in the operation of the outage monitor was the distance over which it would reliably operate. It has been found that it would operate satisfactorily, without special line treatment, over distances up to about 40 miles. On some lines where considerable carrier energy was lost in resonant taps, this distance was reduced to about 20 miles. If the distribution lines are treated so as to confine the carrier energy to the desired feeders, the range of operation can be increased considerably. Typical rural distribution systems are made up of radial feeders operating out of one or more substations. Such being the case, it has been found convenient to locate a transmitter at or near each substation with receivers located between transmitters and their associated remote modulators.

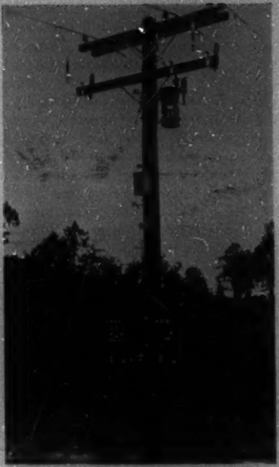

Figure 3. Outage monitor receiver installed adjacent to transmitter

Automatic sectionalizing devices on rural distribution systems are normally installed from zero all the way out to 25 miles from the substation. Under such conditions, with the transmitter at or near the substation, sufficient operating range can be obtained to monitor practically all sectionalizing points energized from the substation. Separate transmitters and receivers are usually required for each substation, although under certain conditions it is possible to couple the carrier energy to another substation through a suitable filter network.

Line Noise

High-voltage distribution circuits are characterized by a rather high ambient

Figure 4. Indicator unit installed in radio dispatcher's office

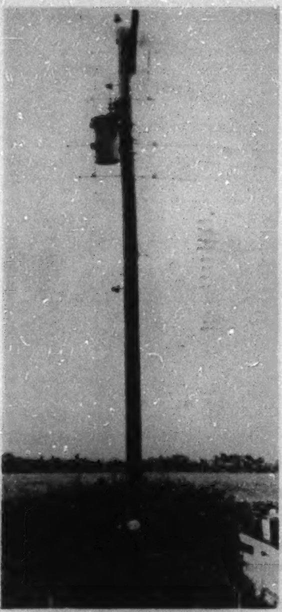

Figure 5. Remote modulator installation

noise level in the radio frequency spectrum, particularly in the 50 to 150 kc range. This radio frequency noise is caused by corona, defective equipment, static discharges on loose hardware, loose connections, poor ground bonding, induced atmospheric static, and defective or inherently noisy consumer appliances. High ambient noise level usually limits the distance over which carrier circuits can be made to operate. The outage monitor principle of operation permits locating the receiver near the transmitter where a strong carrier signal is always assured. Thus the carrier signal overrides almost all types of line noise except power arcs occurring near the receiver. Line noise has not proved to be an operating problem, even during violent thunderstorms.

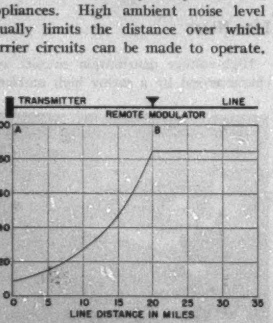

Figure 6. Per cent modulation along distribution line with remote modulator located at the 20-mile point

Taps and Branch Circuits

Distribution taps and branch circuits whose effective lengths are odd multiples of one quarter wavelength tend to act as low impedance bridging circuits. In some cases it has been found necessary to effectively shorten, lengthen or isolate such taps or branch circuits by the insertion of a choke coil or by installation of a termination unit. Such treatment is necessary only when the tap approximates the critical length. Shifting the carrier frequency of the transmitter by a few kilocycles may solve this problem without resorting to line treatment.

Another scheme that has been utilized is to make use of such critical taps by installing a remote modulator at the outer end of the tap. Since the remote modulator acts to alternately short circuit and open circuit the tap at a given audio frequency rate, such impedance alternations are reflected to the input end of the tap. This modulates the carrier signal appearing on the main feeder. Such installations of remote modulators have proved effective.

Standing Waves

Standing waves are generally present, since it is not feasible to terminate distribution lines in their r-f characteristic impedance nor to maintain impedance matches on all branch circuits or taps. Such standing waves, however, have not been found to be detrimental. The r-f power loss introduced is made up by increasing the transmitter power output as required. Standing wave patterns must be taken into account when locating the remote modulators on the line, the best results being obtained when the modulators are located at voltage antinodes.

Transformers, Oil Circuit Reclosers, Voltage Regulators, and Other Apparatus

It has been found that while such items as distribution transformers and lightning arresters introduce slight impedance discontinuities in the line, the attenuation of the carrier signal due to this bridging effect is not significant.

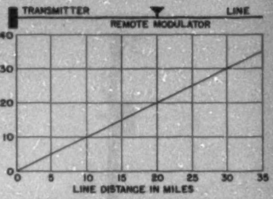

Figure 7. Approximate attenuation of a 100-kc carrier signal along a 35-mile distribution line

Oil circuit reclosers contain series connected solenoids which operate the reclosures when fault conditions occur. The inductance of these solenoids acts as an r-f choke which tends to attenuate the carrier signal. Fortunately, reclosers of higher ampere rating have less inductance and consequently produce less attenuation. Such reclosers are always located nearer the substation where minimum attenuation is more important. By-passing these solenoids with small capacitors has been resorted to in unusual circumstances, but as a general rule no special treatment of oil circuit reclosers is required.

Line type voltage regulators offer more serious attenuation and it has usually been found necessary to by-pass the series coils with capacitors of about 0.05 microfarad.

Shunt capacitors act as a direct short circuit to carrier frequencies. Small series r-f chokes must be inserted in the shunt capacitor leads to prevent short circuiting of the carrier signal. Here again, use can be made of the one quarter wavelength tap. By installing the capacitor bank on the outer end of such a tap, the input end of the tap becomes a high impedance point. Under such conditions, neither the tap nor the shunt capacitor is detrimental to the operation of this type of carrier equipment.

Weather Effects

Operation of the outage monitor was noted particularly during mild icing of

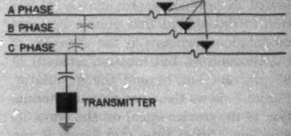

Figure 8. Phase-to-ground method of coupling transmitter to line

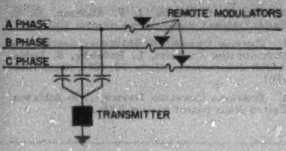

Figure 9. Alternate method of phase-to-ground coupling

distribution lines in the winter of 1950 on the Virginia installation. No appreciable degradation of signal was observed.

On the Florida installation, no change in operation has been observed during extremely wet weather or during thunderstorms.

Interference with and From Other Services

In early experimental models the remote modulators were found to emit harmonics which were objectionable in the broadcast band. A low-pass filter was incorporated in the modulator circuit which suppressed these harmonics to a level that was satisfactory for radio receivers located immediately adjacent to the modulator.

Tests were made to determine the effect of interference from other carrier sources.

The outage monitor was tuned to within 3 kc of a carrier channel used by a neighboring power utility for voice communication. Signal level from this carrier was sufficiently strong for reception of loud and clear speech on a carrier frequency receiver. This interfering carrier signal had no noticeable effect on the operation of the outage monitor. However, if a resulting carrier beat frequency were to coincide with one of the utilized modulating frequencies, false operation would probably occur during the outage period.

Although there is no reason why the outage monitor would not interfere with other nearby carrier equipment utilizing the same channel, to date no complaints of carrier interference have been received from neighboring utilities known to be using adjacent carrier channels.

Method of Coupling Transmitter and Receiver to Line

The most effective method of coupling the transmitter to the distribution system has been found to be phase-to-ground coupling such as is shown in Figure 8. Coupling between phases is accomplished by mutual inductive and capacitive coupling.

Coupling between all three phases and ground as shown in Figure 9 has also been tried. Although this gives more even carrier distribution, line attenuation is much greater than in the single-phase method. The receiver is normally coupled to the line between one phase and ground. When the transmitter and receiver are physically located at the same spot, the receiver is coupled directly into the transmitter thereby saving the installation of a separate coupling capacitor.

Locating the Remote Modulators

Optimum performance of remote modulators is obtained if special attention is given to their location on the distribution system. Since standing waves are usually present, it has been found best to locate the remote modulators at or near voltage antinodes. Such points represent high impedance points on the line and are most responsive to dynamic impedance variations produced by the modulators.

A portable survey instrument has been devised which performs the function of a remote modulator, and is used to determine suitable installation points. It consists of a vacuum tube voltmeter, a battery powered modulator and a special coupling capacitor[4] built into a "hot stick."

Figure 10. Portable survey instrument with "hot stick" coupler

This coupling device is used to quickly couple the survey instrument to the line at any desired point. Carrier voltage level can be read on the meter and the modulated signal produced can be detected and measured at the central receiving point. Figure 10 shows the portable survey instrument.

Location of the remote modulators is not limited to voltage antinode points, but insufficient modulation usually results if the modulators are coupled to the line at voltage nodes. Intermediate points usually produce satisfactory results.

Locating Transmitter and Receiver

Location of the transmitter and receiver is not critical and installation can usually be made almost anywhere on the system. However, for practical considerations, it has been found desirable to locate the transmitter near the substation supplying the distribution system. The reason for this is twofold. The transmitter can distribute its carrier power more evenly to all of the radial feeders of the system, and it is less susceptible to power outages when located near the substation.

A principal consideration in locating the receiver is its location with respect to the dispatcher's office so that the wire line to the indicator can be reasonably short. Another consideration is reliability of power source supplying the receiver.

Modulation Levels and Signal Levels

Modulation levels as measured at the receiver input have been found to range from a high of 5 per cent to a minimum usable level of 0.01 per cent. Using the portable survey instrument, it has been found that a 2-volt carrier level at the remote modulator location will produce usable modulation at the transmitter site. Carrier level in the vicinity of the transmitter may range up to 250 volts.

Power Line Harmonics

Power line harmonics interact with the carrier signal within the remote modulators to produce modulation. Modulation levels produced by these power line harmonics are sometimes of the same order of magnitude as the desired signals produced by the modulators. This factor must be taken into consideration in the selection of modulating frequencies, and the use of power line harmonic frequencies must be avoided.

Experience gained from the two experimental installations in Virginia and Florida has proved that the principle of operation of the outage monitor equipment is sound and practical. These installations are providing valuable application data under a variety of conditions. Improvements in the equipment and in techniques of application to rural power distribution systems are being made as a result of this experience.

References

1. Carrier Indicator Reports Rural Outages, D. E. Basler, J. F. Atkinson. *Electrical World* (New York, N. Y.), volume 115, number 8, February 22, 1941, pages 52–54.

2. Outage Indicator, J. F. Atkinson, D. E. Basler. United States patent number 2,337,441.

3. Carrier Current Supervisory System for Distribution Circuits, L. Podolsky, S. Lubin. *AIEE Transactions*, volume 70, 1951, pages 1096–1101.

4. Portable Coupling Device, J. F. Atkinson. United States patent number 2,341,819.

No Discussion

A Magnetic Tape Oscillograph for Power System Analysis

E. C. SCHURCH
MEMBER AIEE

F. R. SCHLEIF
ASSOCIATE AIEE

THE inconvenience, expense, and delay of obtaining automatic records of power system phenomena and of obtaining records during staged field tests with conventional oscillographs has prompted the investigation of magnetic recording techniques for this purpose. While there is an abundance of information in engineering literature on the recording of sound by magnetic tape or wire, little information is available on the characteristics of applicability of magnetic recording to the field of oscillography. A review of current techniques and apparatus discloses that applicability to this field is limited by lack of a suitable pickup device. The development of a unique magnetic pickup device described here adapts magnetic tape recording to the field in which conventional oscillographs of both the automatic and laboratory types are usually employed. The advantage of reusability of the recording medium inherent in magnetic recording permits convenient incorporation of the "anticipator" feature in an automatic oscillograph. Transcription of the magnetic records at reduced tape speed by pen and ink recorder considerably enhances both automatic and laboratory oscillograph applications by elimination of the usual photographic processing. Both are made possible by the novel pickup device which delivers an output voltage independent of the speed of the tape. Construction and test of a model oscillograph using the new pickup device furnish a basis for design of a practical automatic recorder.

Advantages Offered

The possible advantages of magnetic recording for oscillographic purposes have long attracted interest. One of the first advantages to attract interest is the fact that the magnetic recording medium can be erased and reused practically an unlimited number of times. This permits continuous recording of phenomena, including steady state conditions, even where only transients or abnormal conditions are of interest. Thus, the transcription or examination of a small portion of the recorded information is substituted for the fast starting feature of the present conventional automatic oscillograph. In this substitution two benefits may be gained: The mechanical difficulties attending any fast starting feature are eliminated and the steady state conditions before the transient are recorded, whereas in conventional equipment, the recording is started by the transient or abnormal condition itself.

The economy aspect of the magnetic recording technique has not been overlooked. However, while it has previously permitted the continuous type of recording just mentioned, subsequent transcription of the desired portions of the recorded information has required some of the conventional photographic recording material and the conventional oscillograph itself. Although complete elimination of photographic materials and the delay and inconvenience of photographic processing is a desirable goal, it has not generally been achieved.

Previous Limitations

A brief review of some of the principles employed in magnetic recording and reproduction or transcription may clarify its previous limitations. In the most usual applications, the electric current representing the phenomenon to be recorded is passed directly through the main coil of the recording head producing magnetic impressions on the recording medium. A high-frequency bias current simultaneously applied to a coil of the recording head makes magnetic impressions closely proportional to the recording current over a wide range of current.[1]

For applications in which an especially wide range of frequencies is to be recorded, such as sound recording, self-demagnetization of the recording medium becomes a limitation in the recording of the higher frequencies. Self-demagnetization is a function of the ratio of the length to thickness of the small magnets set up by the recording process in the magnetic medium.[2] It is thus also a function of the ratio of frequency to speed of the recording medium. It may be regarded as a magnetic short circuiting of the flux as the magnetic poles get closer together. However, for available recording media and reasonable speeds the frequency at which self-demagnetization becomes appreciable is well above the range required for power system oscillographic applications. Thus, the recording process is readily accomplished by well-known means with suitable accuracy for the purposes described in this paper.

The usual means of reproducing the information which has been recorded in the form of magnetic impressions on the tape suffer more limitations than the recording process. The most commonly used pickup device is similar to the recording head. In fact, a single unit often serves both purposes for audio applications. The magnetic flux from the recording medium threads along the magnetic circuit of the pickup and through the pickup coil. The only voltage produced in the pickup coil is that due to the changes of magnetic flux. The rate of change of the flux and hence, for a given recording cur-

---

Paper 51-239, recommended by the AIEE Instruments and Measurements Committee and approved by the AIEE Technical Program Committee for presentation at the AIEE Summer General Meeting, Toronto, Ont., Canada, June 25–29, 1951. Manuscript submitted February 14, 1951; made available for printing May 14, 1951.

E. C. Schurch and F. R. Schleif are with the United States Bureau of Reclamation, Denver, Colo.

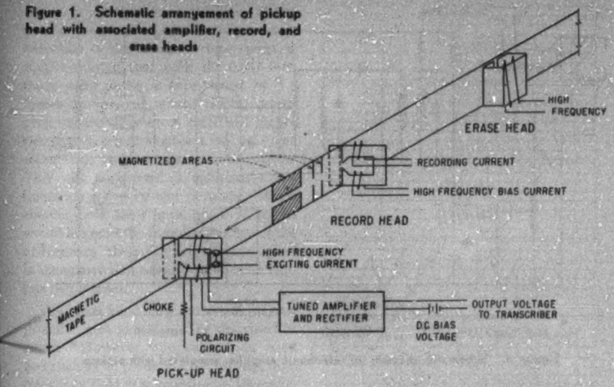

Figure 1. Schematic arrangement of pickup head with associated amplifier, record, and erase heads

rent, the voltage produced in reproduction is proportional to the frequency. If the frequency drops to zero, as for direct current, the output voltage becomes zero. For finite frequencies in the lower range where self-demagnetization is negligible, if the frequency doubles the output voltage doubles. Since output voltage is a function of frequency, and frequency during reproduction is a function of the speed of the magnetic medium past the pickup head, the output voltage is also directly a function of the speed of reproduction. Thus, aside from the inaccuracies introduced by drive speed variations, the range of applications to which this form of magnetic recording and reproducing has been adaptable has been limited by the ability of integrating and equalizing networks to compensate for the inherent characteristics. In the field of power system oscillography where transients and direct quantities or components are of importance, it is apparent why this form of recording and reproduction has not become popular.

A scheme of magnetic recording and reproducing which overcomes some of the foregoing difficulties is that of recording a carrier frequency which is frequency modulated as a function of the phenomenon to be recorded. Reproduction is then essentially a process of frequency discrimination. This technique has the obvious possibility of eliminating amplitude modulation and any inaccuracy due to nonuniformity of the magnetic medium. It is subject, however, to errors due to variations in drive speed in both the recording and reproducing processes and it is limited in range of response to a fraction of the range of frequencies[3] which can be resolved by the magnetic medium. The requirement for a separate oscillator to be frequency modulated by each quantity to be recorded imposes additional equipment.

A Pickup of Required Characteristics

From this review of the characteristics of magnetic recording and reproducing systems, it is evident that for full exploitation of the possibilities of magnetic recording for oscillographic purposes, a pickup head is needed which will produce an output voltage:

1. Proportional to the magnetomotive force exerted upon the pickup head by the portion of the tape being examined.
2. Polarity dependent upon the polarity of the magnetomotive force.
3. Independent of the speed of recording or reproduction.

The pickup head to be described in this paper is enabled to meet these requirements by the expedient of causing the reluctance of its magnetic circuit to vary in a cyclic manner at a frequency well above the highest frequency to be recorded. Of various possible means of varying the reluctance, such as by mechanical variation of air gaps in the magnetic circuit, mechanical strain of a portion of the magnetic circuit, or magnetic saturation of a portion of the magnetic circuit, the latter was chosen as offering the most practical solution. No moving parts are involved, permitting desirable simplification, and the frequency with which the reluctance can be varied is limited only by hysteresis and eddy current losses in the magnetic circuit.

The arrangement of the recording,

Figure 2. (A) Magnetizing forces and fluxes produced in pickup. (B) Production of double-frequency voltage in pickup coil by magnetizing forces and fluxes in (A)

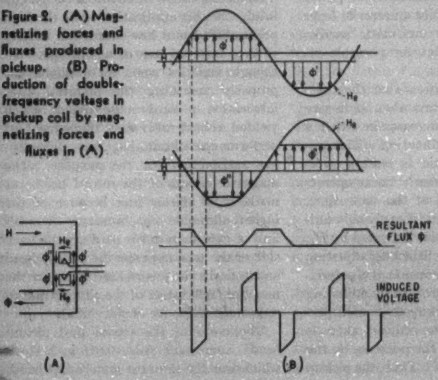

Figure 3. Variation of second harmonic component of output voltage with magnetizing force from tape

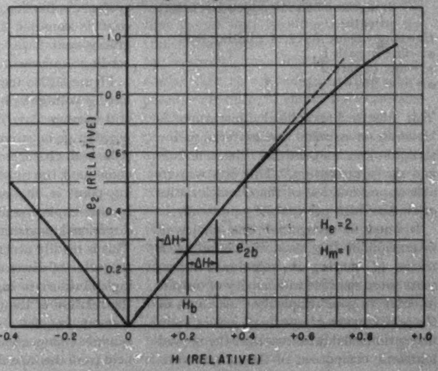

pickup, and erase heads is shown schematically in Figure 1. The magnetic circuits of the record and pickup heads are arranged to utilize a combination of transverse and perpendicular magnetization of the tape instead of the more common longitudinal magnetization. This is necessary to permit accurate reproduction of square waves or d-c pulses of unlimited duration. The pickup head has its magnetic circuit pierced by two small openings through which an auxiliary exciting coil is threaded to produce cyclic saturation of the part of the magnetic circuit indicated by the shaded areas of the pickup in Figure 1. As far as the pickup alone is concerned, greater sensitivity might be obtained by saturation of the entire magnetic circuit; however, the tape would then be demagnetized by the stray field set up. The balanced arrangement of the saturating part of the magnetic circuit serves to prevent appreciable stray field from the exciting frequency current from appearing at the pole faces which contact the magnetic tape. It also balances the exciting frequency component of voltage out of the main pickup coil. In this respect the pickup device differs from other magnetic pickups of which the authors have knowledge.

With this arrangement the effective reluctance of the magnetic circuit is increased once for each half cycle of the exciting current so that the predominant voltage produced in the main pickup coil is of twice the exciting current frequency and nearly proportional to the magnetomotive force exerted by the tape on the pole pieces of the pickup. Production of the double frequency output voltage by the balanced saturating core section of Figure 2(A) is illustrated by Figure 2(B). In this illustration

H = magnetizing force to be detected (magnetomotive force per-unit length of path)
H_e = magnetizing force of exciting field
ϕ' = flux in path 1
ϕ'' = flux in path 2
ϕ = total flux = $\phi' - \phi''$

This idealized graphical illustration is based on an assumed core material with a straight line magnetizing characteristic and sharp saturation. This is a reasonable approximation of the characteristics of modern high permeability materials.

It must be recognized that choice of saturation of the magnetic circuit as a means of varying its reluctance represents some sacrifice in linearity of output in order to gain simplicity. Analysis of the performance of saturated inductors in magnetic fields[4] indicates that the second harmonic component of the output voltage e_2 is expressed by

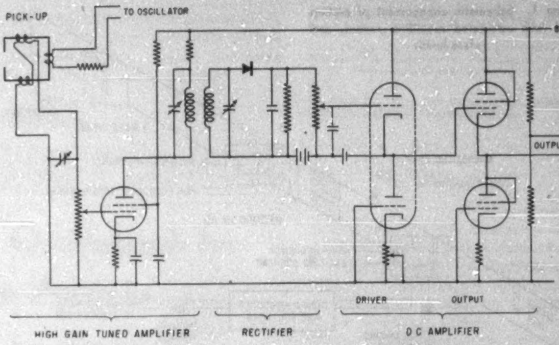

Figure 4. Schematic diagram of electronic amplifier associated with pickup

$$e_2 = \frac{4\rho NAH_e 10^{-8}}{3}\left(\left[1-\left(\frac{H_m+H}{H_e}\right)^2\right]^{3/2} - \left[1-\left(\frac{H_m-H}{H_e}\right)^2\right]^{3/2}\right)$$

in which

N = number of turns
$\rho = 2\pi$ times frequency of exciting field
A = area of the core
H_e = impressed (exciting) magnetizing force
H_m = magnetizing force required to saturate the core
H = magnetizing force to be detected

It is evident from the formula that e_2 is not a linear function of H; however, the relation between e_2 and H for $H_e = 2$ and $H_m = 1$, shown in Figure 3, indicates that an operating point can be chosen where the curvature is relatively slight. Although any curvature in this characteristic affects the over-all calibration curve of the instrument, a small amount of curvature can be tolerated for power system application, since an error of 5 per cent is common for automatic oscillographs and 2 per cent for portable recording equipment.

Figure 3 also illustrates that the alternating voltage e_2 is zero when H is zero and increases as H increases in either a positive or negative direction. This unpolarized characteristic is readily overcome, and the most nearly linear operating point is obtained at the same time, by the simple expedient of applying a unidirectional magnetic bias indicated by H_b. This is readily accomplished by adjusting the value of direct current in the polarizing coil shown in Figure 1 or by adjusting the relation of the pickup to a small permanent magnet. The output then is caused to vary about the point e_{2b} by the field from the tape ΔH. Thus, the pickup meets the requirements considered necessary to permit full exploitation of the possibilities of magnetic tape recording for oscillographic purposes on power systems.

Experimental Model

Oscillographic applications require an associated oscillator, amplifier, transcriber, and tape drive mechanism in addition to the magnetic tape, record, reproduce, and erase heads. These components have been assembled into an experimental model in order to verify the performance indicated by the foregoing theory. Pertinent features of the components of the model and experimental results will be described before considering possible features of more practical applications.

The physical arrangement of the pickup record, and erase heads is essentially as illustrated in Figure 1. Permalloy was used for the magnetic circuit of the pickup head. In this application both the high permeability and low saturation density of this material are of advantage. Although facilities were not available for properly annealing the material after fabrication, a compromise anneal, which yielded considerably less than the best performance obtainable, was nevertheless satisfactory for the purpose. The magnetic circuit of the record head was made from silicon iron because of the higher allowable flux density. A small link of core material is used on the back side of the tape opposite the pickup head and opposite the record head to reduce the magnetic reluctance of the circuits and to reduce the influence of stray fields.

The cores of the record and pickup heads were made from 0.015-inch stock which was the thinnest material at hand.

Although a reduction in thickness of the pole pieces would theoretically permit a reduction of the minimum tape speed, it was calculated that with the 0.015-inch thick pole pieces a tape speed of 1.8 inches per second would resolve a 60-cycle square wave and a speed of 5 inches per second would resolve a 60-cycle sine wave with only 1 per cent distortion. This was considered a sufficiently low minimum speed for test purposes. While thinner pole faces in a practical model would increase the frequency range of the instrument, the reduction of tape speed is of no particular advantage when an endless belt is used.

The erase head used embodied no new principle and so will not be described in detail. However, the orientation used was such as to produce a saturating, high frequency field in a longitudinal direction along the tape. Thus, even if minute magnetized areas are left in the tape by the erase system at the higher tape speeds, this remanent magnetism is perpendicular to the active recorded fields.

The electronic elements are assembled on one chassis in order to use one power supply. Such a combination also affords a desirable reduction of space required. The functions of the various electronic components are nevertheless sufficiently independent to permit separate explanation.

One oscillator serves three purposes: (1) supplying the high-frequency bias current for recording, (2) supplying the high-frequency exciting current for the pickup head, and (3) furnishing high-frequency power for the erase system. The power requirements of the erase system are the greatest of the three requirements and it is logical that a frequency should be chosen which will afford reasonable efficiency in this function. A frequency of 20 kc was selected for the experimental assembly on this basis. A push-pull oscillator circuit was used because of its inherent good wave form and high power output. As it is conventional in design, no diagram is included. A series resonant circuit is used with the erase head in order to simplify obtaining maximum power transfer. Delivery of the high-frequency bias current to the record head is effected through a control rheostat and through a winding on the record head separate from the main recording winding in order to keep the recording circuit isolated as much as possible. A resistance is used in series with the exciting coil of the pickup head to swamp out the effect of nonlinear impedance of this saturating circuit on the wave form of the exciting current. The value of the exciting current, although not critical, is adjusted for optimum performance by this series resistor.

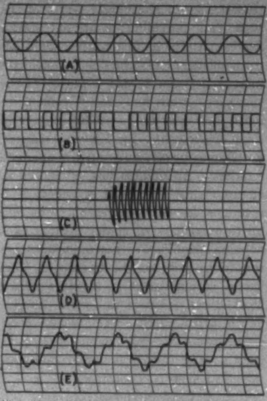

Figure 5. Oscillograms produced by magnetic tape oscillograph

(A) 60-cycle sine wave
(B) D-c pulses
(C) 60-cycle wave with initial offset
(D) Transformer magnetizing current
(E) Complex wave form

The amplifier contains a tuned section which operates at 40 kc, the second harmonic frequency of the exciting current to the pickup, a rectifier-detector, and a d-c amplifier to drive the pen and ink transcriber.

The tuned amplifier section is conventional but uses a sharp cut-off pentode amplifier tube to maintain a more linear relation between input and output at high signal levels. Here too, the high amplification possible in tuned amplifiers is used to advantage. The first part of the detector-rectifier circuit is conventional, but in order to handle the transcription of d-c phenomena from the tape the detector must be direct coupled to the d-c amplifier section. Here a d-c bias voltage is inserted to cancel the residual voltage produced by the unidirectional magnetic bias field applied to the pick-up head to obtain properly polarized performance and to shift operation to the best part of the magnetization characteristic illustrated by Figure 3. A schematic diagram of the electronic amplifier is shown in Figure 4.

The only unusual feature of the tape drive mechanism is that an adjustable speed drive having a range of from 2 to 15 inches per second is provided. A moderate tape speed is used for recording and a low tape speed is used for transcribing in order to bring the frequency of the quantity being transcribed within the range of accurate response of the transcribing pen. Actual tape speeds used in the tests will be described later.

The instrument used for transcribing the records has chart speeds of 5, 25, and 125 millimeters per second. The pen driving element is capable of reasonably flat frequency response up to 30 cycles per second. The instrument is of commercial design and needs no further description here.

Test Results

The minimum tape speed of 2 inches per second afforded by the tape drive mechanism produced satisfactory definition and amplitude in recordings of 60-cycle currents as determined by examination of the play-back with an oscilloscope. However, at this speed appreciable distortion occurs because the pole face width is an appreciable increment of the wave length. Recordings which were to be transcribed were made at higher tape speeds in order to reduce the frequency during transcription to within the flat frequency response range of the transcriber pen or to obtain sufficient time spread on the transcriber chart. For this reason tape speeds of from 5 to 15 inches per second were used in recording and tape speeds of from 2 to 5 inches per second were used in transcribing the records. Distortion due to pole face width was thereby limited to 1 per cent or less.

Samples of the results obtained are shown in Figure 5. These sample oscillograms are selected to illustrate the capability of this form of recording. Figure 5(A) shows a 60-cycle sine wave. Note that the time spread is greater than ordinarily obtainable with an automatic oscillograph. It is of interest to note that the time spread may be adjusted during the transcribing process to any value desired by controlling the relation between recorder tape speed and transcriber chart speed. Figure 5(B) shows the capability of the apparatus for resolving and reproducing d-c pulses. The pulses shown are of 3 seconds minimum duration and were transcribed at the same speed as recorded. The curvature of the chart ordinate due to the circular movement of the pen arm is evident. A recorder which transcribes onto a rectangular scale chart would be preferable.

The recording of an alternating current with an initial offset shown in Figure 5(C) is of interest in that it shows the capability of the system to record and reproduce both d-c and a-c components. This current was produced in a reactor and hence shows only a d-c decrement. The a-c decrement commonly visible in the short circuit current from synchronous machines is necessarily absent.

The trace shown in Figure 5(D) shows the distorted wave form of the exciting current of a transformer. The trace of Figure 5(E) was produced from a recording of a 60-cycle sine wave on a tape from which the previous higher frequency recording was not completely erased. It demonstrates the capability of the apparatus to transcribe a complex wave from the tape.

Possibilities of Practical Automatic Recorder

The principles and capabilities of the recording and transcribing scheme having been demonstrated, consideration of the possibilities of a design for employing the advantages of this magnetic recording technique for power system automatic oscillographic work will now be considered.

The burden imposed by a recording head upon the circuit to be monitored may be made very small. In the experimental model 0.04-volt-ampere was sufficient to utilize the full magnetic range of the tape. Unlike the Duddell type galvanometers of conventional oscillographs with their inherent low impedance, the recording heads for magnetic recording can be constructed with a wide range of impedances. If minimum burden is of importance with the circuits to be monitored the windings of the recording heads can be proportioned accordingly. Current shunts can be eliminated if necessary. High impedance windings on recording heads for potential circuits will reduce the current requirement to a small fraction of that required by conventional oscillographs.

Since the currents or voltages from power circuits may be recorded directly, without amplification, design may be expanded to provide additional recording channels by increasing the width of the tape and providing additional record heads. A 4-inch tape width should accommodate 12 channels with adequate margin between recorded paths. Continuous recording and erasing would eliminate fast starting mechanisms but a time delayed stop mechanism arranged for tripping by certain transients would be required. An endless belt 30 inches in circumference driven at a speed of 6 inches per second would permit preserving up to 5 seconds of power system phenomena including a section of steady state conditions prior to the transient. This would be equivalent to a 5-foot record from a conventional automatic oscillograph, although conventional automatic oscillograms average about 2 feet in length. The transients are usually contained within a 1-foot section.

If it is considered essential that the oscillograph be capable of producing a record of unlimited length, or several records in rapid succession, equipment could be arranged to automatically transfer the magnetic impressions from the endless belt to a stand-by supply of magnetic recording material by a rapid "contact printing" process in the presence of a high-frequency field.[5] The fault or transient detector would then operate to engage the transfer apparatus and the endless belt would never be stopped.

One oscillator and amplifier channel should be adequate for any reasonable number of recorded traces. Transcribing of the traces can be performed one at a time, requiring only one pen and ink transcriber and one pickup head. The time required for transcribing 12 traces would be in the order of 2 minutes–less time than required for photographic processing exclusive of washing and drying. Time marking of all traces simultaneously as they are recorded could be accomplished by linking all of the recording heads by a pulsed timing circuit operated by a cam on the tape drive synchronous motor or by an independent timing circuit. Matching of the independently transcribed traces could readily be effected by the timing marks. Automatic and continuous calibration of all traces could be effected by controlling the magnitude of the timing circuit pulses to a known value.

Conclusion

The advantages of flexibility in recording and transcribing speeds, the small amount of equipment required for recording a large number of quantities, the facility for recording a period of steady state conditions prior to a transient, the use of small quantities of low cost material for recording, the elimination of need for a dark room and wet photographic processing, and the time saved in obtaining usable records, appear to recommend this form of recording, especially for power system automatic oscillography. The large number of traces which can easily be recorded, the flexibility of speeds, and the elimination of the delay and inconvenience of photographic processing represent especially desirable features for field or laboratory oscillographic work. The unique fact that any number of graphical transcriptions may be made from any recording may be found an advantage in either application.

References

1. Supersonic Bias for Magnetic Recording, **Lynn C. Holmes, Donald L. Clark.** *Electronics* (New York, N. Y.), July 1945, pages 126–36.

2. Application of Experimental Test Procedures and Methods of Analysis of Results to Research Problems in Magnetic Recording, **C. S. Thompson.** *AIEE Transactions*, volume 68, part I, 1949, pages 407–17.

3. Frequency Modulation, **August Hund.** 1942, McGraw-Hill Book Company (New York, N. Y.), First edition, pages 29–31.

4. Air-Borne Magnetometers for Search and Survey, **E. P. Filch, W. J. Means, T. Slonczewski, L. A. Parratt, L. H. Rumbaugh, A. J. Tickner.** *AIEE Transactions*, volume 66, 1947, pages 641–51.

5. Duplicating Magnetic Tape by Contact Printing, **M. Camras, R. Herr.** *Electronics* (New York, N. Y.), volume 22, December 1949, pages 78–83.

Discussion

Lenard R. Engvall (Bureau of Reclamation, Coulee Dam, Wash.): The authors of this paper appear to have solved the fundamental problems in the use of magnetic tape for oscillography, and pointed the way in which development can proceed. For much routine field work, such as checking the timing and adjustment of circuit breakers, the accuracy and speed of response described is already ample. Such an instrument, compactly designed and readily portable should find many applications. The advantages pointed out in the conclusion are particularly applicable here.

A satisfactory automatic oscillograph based on magnetic tape recording would require extensive testing to prove its reliability. Its development, however, is highly desirable. High and uniform starting speed of the conventional automatic oscillograph during system trouble has always been a problem, and is becoming more important as the operating speed of relays and circuit breakers increases. The "anticipator" feature of the tape recorder, permitting reproduction of system conditions during the total fault time as well as a predetermined time prior to the fault, is therefore not merely an incidental feature but an important consideration.

As an indication of the possibilities of using an endless belt tape for such recording with immediate reproduction of records, during which time the tape would be unavailable, an examination was made of the system fault records at the switchyards of the Grand Coulee Power Plant, Columbia Basin Project, Coulee Dam, Wash. Over a period of 3 years, about 5 per cent of the records would have been missed by allowing a reproducing time of 2 minutes after each record, but this would be reduced to 1 per cent by decreasing the cycle to 1 minute.

E. C. Schurch and **F. R. Schleif:** Mr. Engvall's comments are appropriate and a valuable contribution to the subject. His experience data on the number of records that would have been lost by allowing reproducing times of 1 or 2 minutes during which the recording feature may be unavailable, to us indicate that in only the most important applications would it be necessary to employ the rapid "contact printing" transfer process mentioned in the paper and reference 5 of the paper. This transfer process could be started and stopped automatically to preserve desired records while the endless belt is in motion. In this case, recording on the endless belt would be continuous. However, in the majority of applications 100 per cent availability of the oscillographic equipment is not required, nor is it often actually realized with presently available equipment. An availability of 95 per cent would be a very satisfactory economic compromise.

Some Engineering Applications of the Electrolytic Field Analyzer

H. K. FARR
MEMBER AIEE

W. R. WILSON
MEMBER AIEE

MANY of the problems encountered by the electrical engineer require for their solution the determination of potential fields. He may wish to know the electrical stresses on the insulation in an apparatus, the a-c resistance of a group of conductors, or the hot-spot temperature on a transformer core. The mathematical solution to such problems is usually very arduous if not impossible. Direct measurements on conducting models, however, often provide answers quite rapidly and conveniently to even rather complex problems.

The electrolytic field analyzer or electrolytic tank is a device for measuring by analogy the physical quantities representing conditions in materials subjected to electric, magnetic, thermal, or other fields. Voltage and current are applied and measured around models consisting of conductors and insulators immersed in an electrolyte. The principle is an old one familiar to many engineers. Special circuits and model techniques have, however, permitted its extension to problems for which this instrument is not usually considered appropriate.

It has been found possible, for example, to represent the flow of heat in a material whose conductivity changes with direction, by distorting the shape of the model. A tank of special shape has been devised for the study of the magnetic field around circular coils. (The tank used for axially symmetric electric fields is of different shape.) Under certain conditions the distribution of high-frequency currents in conductors can be determined by setting up similar conductors in an electrolyte. A technique also has been worked out for the more difficult low-frequency condition, when it is necessary to connect capacitors in series with small electrodes to obtain the correct current distribution. A guarded bridge circuit has been used to determine the direct capacitance between any two conductors of a group by measurement of the resistance between electrodes of a model. These techniques have been applied by the authors during the past few years, in two industrial laboratories connected with the design of electric apparatus. The field plots and other data used to illustrate the discussion were obtained in the course of this work.

Table I summarizes the more important fields that may be studied by means of the electrolytic field analyzer. The present paper is concerned mainly with field types one through four. All of these fields are governed by similar laws; but field number three, the flow of an electric current in a conducting medium, is that of the electrolytic field analyzer itself. It is chosen to represent other fields because it is the simplest to control and measure.

Practical considerations may impose limitations on the types of problems that can be solved by this method. Some symmetry may be required for electrostatic fields in composite dielectrics or for magnetic fields due to electric currents. Though usually applied to static fields, the instrument may handle certain dynamic problems if lumped impedance elements are connected externally to the model.

Certain quantitative relations are needed to convert the data supplied by the field analyzer into quantities which characterize the "initial" field. (It is convenient to refer to the field of interest as the initial field and to its analogue in the field analyzer as the model.) These relations are derived in the Appendix, which discusses the model scale factors and which is intended to supply the necessary theoretical justification for the model techniques presented here.

Table I. Fields which may be Studied by Means of the Electrolytic Field Analyzer

Field Type	Fundamental Variables Potential	Flux	Examples
1. Electrostatic	Voltage	Electrostatic flux	Electrical stresses about a bushing or between windings of a transformer
2. Magnetic	Magnetic potential	Magnetic flux	Leakage inductance of transformer windings. Field in the air gap of a motor
3. Resistive flow of electric current	Voltage	Current	End ring of an induction motor. Current flow from point contact
4. Conductive heat flow	Temperature	Heat flow	Hot spot temperature of a transformer core
5. Fluid flow	Velocity potential	Fluid flow	Flow around streamlined objects
6. Gravitational	Gravitational potential	Force of gravity	Mapping of geological formations
7. Functions of a complex variable	Real part of the function	Imaginary part	Impedance function of an amplifier. Transient response of a network
8. Mechanical stress	Stress functions such as the sum of the principal stresses		Torsion of cylindrical shafts

---

Paper 51-240, recommended by the AIEE Instruments and Measurements Committee and approved by the AIEE Technical Program Committee for presentation at the AIEE Summer General Meeting, Toronto, Ont., Canada, June 25–29, 1951. Manuscript submitted March 26, 1951; made available for printing May 31, 1951.

H. K. FARR is with the General Electric Company Pittsfield, Mass., and W. R. WILSON is with the General Electric Company, Philadelphia, Pa.

The authors wish to acknowledge the interest and encouragement shown by T. R. Walters.

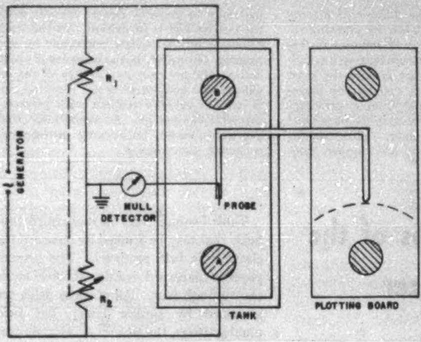

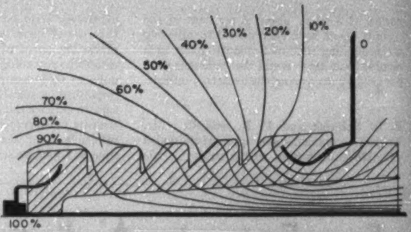

Figure 1 (left). Elements of the electrolytic field analyzer. The model consists of tank, electrolyte, and the electrodes *A* and *B*

Figure 3 (above). Potential field of a glass bushing obtained with the electrolytic field analyzer. The contours are equipotential lines with the voltage of each indicated as a percentage of the total applied voltage

General Construction and Operation of the Electrolytic Field Analyzer

Although the general principles have been discussed by others,[1,2,3] they will be outlined briefly. The basic equipment, sketched in Figure 1, comprises: the electrolytic tank and model; the external electric circuit; and a pantograph. The probe and bridge circuit measures the voltage at any point of the model with respect to some one fixed electrode. This voltage is conveniently expressed as a percentage of the total applied to the model. With the bridge arms set at any desired ratio the corresponding equipotential line may be traced with the pantograph, by moving the probe from point to point where a balance is shown on the null indicator. Although some workers[4,5,6] have constructed servo devices for automatic plotting, the labor of manual plotting with a pantograph may be much less than that of constructing a complicated model.

Figure 2. Equipment for field analysis

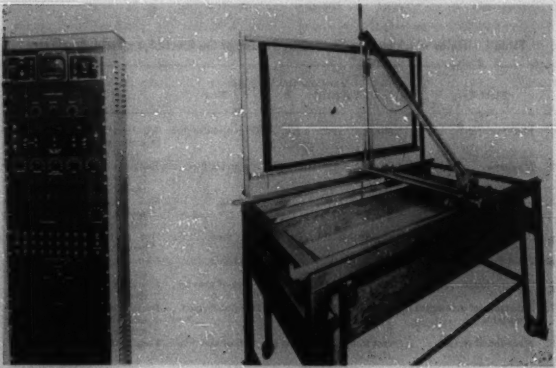

Figure 2 shows the field analyzer equipment arranged with a vertical plotting board. By substituting different tanks for different problems, one may use either a deep tank, or a shallow tank with a bottom that may be flat, sloping, or of hyperbolic contour.

An alternating voltage of about 1,000 cycles per second is supplied to the model. At lower frequencies errors may be caused by electrolytic films at the electrodes, whereas stray capacitances become troublesome at high frequencies. Because of its phase indication and rapid response a cathode-ray oscilloscope makes a good null indicator.

It is possible to use tap water (resistivity about 10,000-ohm centimeter) as the electrolyte. The electrodes, preferably copper, should be clean and the water renewed each day.

If it is desired to measure the resistance between two electrodes of the model, a third calibrated variable resistor may be connected in series with the electrodes so as to form a Wheatstone bridge. When the model requires a number of electrodes carrying specified currents, the electrodes may be connected to the generator circuit through individually variable series resistors. Also, one or more additional voltage dividers may be connected across the generator to maintain various electrodes at specified voltages.

Models for Plotting Equipotential Lines in Electrostatic Fields

The electrolytic field analyzer is especially well suited to the study of electric fields. In this connection it may be used to help in the design of insulation for high-voltage equipment,[7] to predict stresses on dielectric materials under test or to determine capacitances. For equipotential plots the model is constructed so that: electrodes have the same shape and position as those in the initial structure; and the electrolyte in the model has a conductivity which is everywhere proportional to the dielectric constant of the initial medium. Because of the practical difficulty of maintaining liquids with different conductivities, the application of the electrolytic field analyzer to problems involving several dielectrics is usually restricted to fields with sufficient symmetry to permit the use of a cross-sectional model in a shallow tank.

Symmetry Considerations

Geometries of two special types which lead to important simplifications in model construction are those of "translational" and "rotational" symmetry. Transla-

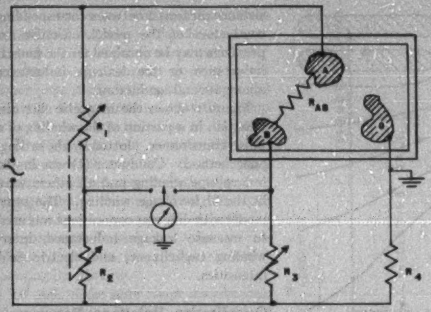

Figure 4. Guarded bridge circuit used with an electrolytic model for the determination of the partial capacitance between electrodes *A* and *B*

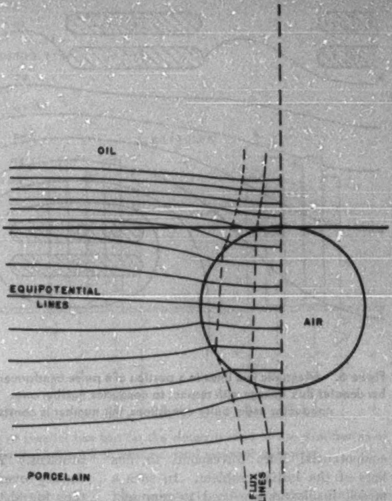

Figure 5 (right). The electrostatic field about a gas inclusion in porcelain near oil. Different models were used for the two types of lines

tional symmetry is represented by a group of long, straight, parallel conductors like a 3-phase cable or a system of bus bars. Rotational symmetry is that of a figure of revolution like a high-voltage bushing or a coaxial cable. For translational symmetry one uses a flat, shallow tank which represents a cross section of the initial structure. With rotational symmetry the model represents a wedge-shaped segment of the initial structure. This is set up in a tank with a sloping bottom. The axis of symmetry is the "shore line" where the top and bottom surfaces of the water meet.

If additional planes of symmetry are present, other portions of the model may be eliminated and the model enlarged to permit greater accuracy.

Composite Dielectrics

In the shallow tanks used for translational or rotational symmetry, it is possible to separate by special walls the liquids which represent various dielectrics. Fine, closely spaced, vertical, conducting, hair-pin paths carry the current over thin insulating barriers.[8]

The results of this technique are illustrated in Figure 3, an equipotential plot of the field around a glass bushing used on large capacitors. Askarel, glass and air were represented by electrolytes of different conductivities in a sloping tank.

With models of translational symmetry the conducting medium may be characterized by the "conductance per square." This is the specific conductivity of the electrolyte multiplied by the depth, and is similar to the surface conductivity of a material. It is the conductance measured between two plane vertical electrodes extending across a rectangular tank which has vertical insulating sides and a width equal to the separation of the electrodes. Practically, it may be determined by measuring the conductance between two vertical concentric cylinders placed in the tank and multiplying by an appropriate geometrical factor.

For translational symmetry, it is sufficient that the conductance per square be everywhere proportional to the dielectric constant. It is, therefore, possible to represent different dielectrics by variations in the depth of a single electrolyte with a constant specific conductivity. Even a dielectric whose permittivity changes gradually and continuously from point to point may be represented in this way. Where it changes abruptly, however, a line of vertical conducting pins should be placed along the edge of the step. Otherwise the step will distort the current pattern and cause a spurious voltage drop. When this technique is used in the sloping tank, the angle of slope is everywhere proportional to the dielectric constant; the change in depth at a boundary of the dielectric is the same as in a flat tank.

Capacitance Determination

The capacitance between two electrodes of the initial structure may be determined from a measurement of the resistance between corresponding electrodes of the model. For translational symmetry, the capacitance between two parallel conductors, per-unit length of one of the conductors, is $\epsilon/\sigma R$ where R is the resistance of the model, σ is the conductance per square of the electrolyte, and ϵ is the permittivity (inductive capacity) of the initial medium. This relation is developed in the Appendix. If R and σ are in ohms and mhos and ϵ is in rationalized meter-kilogram-second units, the resulting capacitance is expressed in farads per meter of conductor length.

If there are more than two conductors, the direct capacitance between any two (also called "partial" capacitance) may be determined from an electrolytic model using a guarded resistance bridge. This circuit is shown in Figure 4, connected so as to determine the capacitance between electrodes *A* and *B*. Electrode *G* in this diagram represents all the other conductors in the problem. The resistance R_{AB} is the partial resistance between electrodes *A* and *B*. With the null detector connected to *B* one adjusts R_3 so as to bring *B* and *G* to the same potential. The null detector is then switched over to the voltage divider (R_1 and R_2) which also is adjusted for a null reading. Then $R_{AB} = R_1R_3/R_2$ and the corresponding capacitance is $\epsilon/\sigma R_{AB}$.

Electrostatic Flux Plotting

By the methods already described, one plots equipotential lines of a model which correspond to equipotential lines of the initial electrostatic problem. For problems of translational symmetry, it is possible to construct a model whose

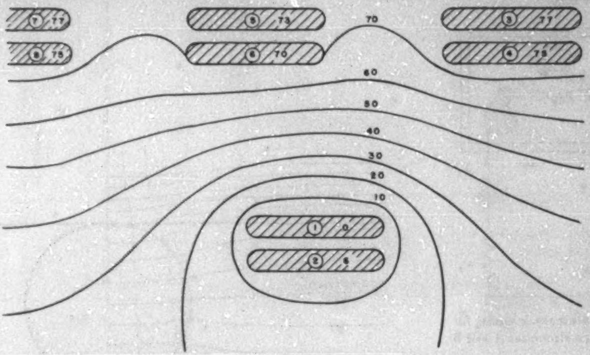

Figure 6. Magnetic flux lines in a portion of a pulse transformer winding. An uncircled number denotes flux linkage with respect to conductor number one. As very little flux penetrates a conductor under pulse conditions, this number is constant for each conductor

equipotential lines correspond to flux lines of the initial problem. In such a model, insulators are used to represent conductors of the initial problem, and the conductance per square of the electrolyte is made inversely proportional to the dielectric constant. Electrodes of the model are constructed to follow certain flux lines of the initial field. This is known as the conjugate or orthogonal method.

Figure 5 is a plot made from electrolytic models showing both equipotential lines and flux lines about a gas inclusion in porcelain near the porcelain surface. Because this problem was set up in the flat tank, the gas inclusion was represented as a cylinder. This approximates an actual inclusion which would be roughly spherical.

Magnetic Fields at High Frequencies

The most convenient method for plotting magnetic fields produced by electric currents is that which represents the initial magnetic flux lines as potential lines of the model: that is, the orthogonal representation.[9] The most tractable fields are those of translational symmetry at frequencies high enough so that currents flow only on the conductor surfaces (skin effect) but not so high that displacement currents are significant. For such fields, each conductor in the initial problem is accurately represented by a solid conductor of the same cross-sectional shape in the model. The current supplied by the external circuit to each conductor in the model is adjusted so as to be proportional to the total current flowing along the corresponding conductor of the initial problem. The distribution of current density over each conductor surface is then found to be the same in the model as in the initial structure. (The direction of this current is, of course, normal to the conductor surface in the model but along the surface in the initial problem.) Magnetic fields due to short pulse or transient currents may also be represented in this way. At any frequency it is correct to choose the conductance σ of the electrolyte so as to be everywhere inversely proportional to the magnetic permeability μ of the initial structure. Ferromagnetic materials of very high permeability may often be represented as insulators.

If two long, parallel conductors are connected together at one end, the self inductance of the loop per-unit length of one conductor is $\mu\sigma R$, where R is the resistance measured between corresponding conductors of the model. Similar expressions may be obtained for the mutual inductance or the leakage inductance among several conductors.

Figure 6 shows the magnetic flux distribution in a portion of the winding of a pulse transformer, plotted by the orthogonal method. Conductor (1) was in the low-voltage winding and all others were in the high-voltage winding. The same model with different connections was used to measure leakage inductance, interwinding capacitance, and electric field intensities.

Quantitative Relations Between Model and Prototype

Table II exhibits the correspondence between pairs of quantities which characterize electrostatic or magnetic fields of translational symmetry and their electrolytic models. Similar relations hold for fields of rotational symmetry and, in the case of electrostatics, for fields without symmetry. Their derivation is sketched in the Appendix. The expressions already given for capacitance and inductance follow from entries 3 and 8 of the table.

Flux Fields of Rotational Symmetry

It is possible to represent magnetic fields of rotational symmetry by the orthogonal method. In regions where the permeability is constant, the depth of the tank is made inversely proportional to the radius (measured from the axis of symmetry). This is in contrast to the direct representation for which one uses a sloping tank of depth proportional to the radius. This allows the convenient representation of circular windings. The

Table II. Analogous Quantities for Fields of Translational Symmetry

Electrostatic Field Direct Representation		Scale Factor		Electrolytic Model		Magnetic Field Orthogonal Representation
1. Length and co-ordinates of position	s_i ...	a	... s_m		... s_i	
2. Voltage	ϕ ...	b	... V	Voltage....................	ψ	Flux per-unit length
3. Permittivity	ϵ ...	k	... σ	Conductance per square....	$1/\mu$	Reciprocal of the permeability
4. Field intensity	E ...	b/a	... F	Field intensity.............	B	Flux density
5. Flux density	D ...	kb/a	... i	Current density per-unit length...	H	Field intensity
6. Charge (or flux) per-unit length	q ...	kb	... I	Total current..............	U	Total current
7. Charge density	m ...	kb/a^2	... p	Density of current sources per-unit area...	u	Current density per-unit area
8. Reciprocal of capacitance per-unit length	$1/c$...	$1/k$	... R	Resistance.................	l	Inductance per-unit length
9. Equipotential lines......................				Equipotential lines..............		Flux lines

Any magnetic or electrostatic quantity is equal to the scale factor times the corresponding quantity for the model when expressed in rationalized meter-kilogram-second units. F and i are in the same direction as E and D but at right angles to B and H. The scale factors a, b, and k are independent and may be chosen arbitrarily.

method has some practical limitations which do not apply to the sloping tank. The change in depth must be sufficiently gradual so that current flow is everywhere essentially horizontal. The model must be so proportioned that the region of interest is not too close to the deep part of the tank near the axis where the depth changes rapidly. A conducting surface is placed near the axis to replace the portion of the tank where the depth would otherwise become infinite and may be used as the return circuit for the currents supplied to the conductors representing the winding.

A tank of the same shape may be used for flux plotting in electrostatic fields of rotational symmetry.

Magnetic Fields at Low Frequencies

At frequencies below those at which skin effect predominates, the currents in the initial problem are distributed over the cross section of each conductor. It may then be necessary to use special methods to insure that the currents introduced into the model from the external circuit are correctly distributed and have the proper phase at each point.

At very low frequencies the currents are distributed over the cross section of an initial conductor uniformly and in phase. In the model the corresponding conductor, which would be solid in a high-frequency problem, now is broken up into an array of uniformly spaced vertical pins or small electrodes distributed over the area representing the cross section of the initial conductor. Equal current is supplied to each small electrode from an individual, variable, series resistor which is adjusted by trial and error. An alternative is the use of fixed series resistors of very high resistance. The number of electrodes which should be used to represent a given conductor (that is, the extent to which the subdivision should be carried) will depend on the size of the initial conductor and on the accuracy required. Karasev[10] uses a block of resistance material which makes contact with the surface of the electrolyte.

Table III. Current Distribution Determined by the Field Analyzer for the Bus System of Figure 7

Bar Number	Per Cent of Total I^2R Loss in Each Bar
1	9.6
2	10.2
3	32.2
4	48.0

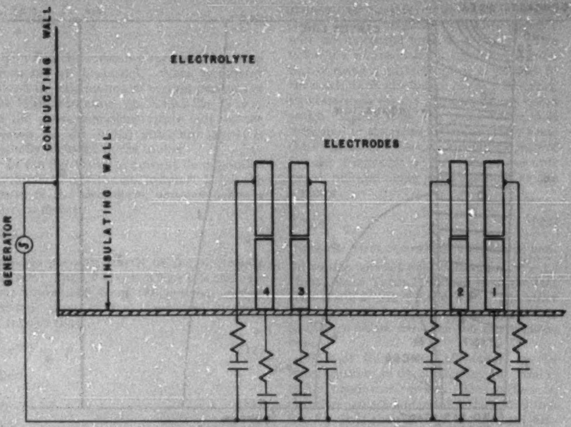

Figure 7. Model of a system of parallel bus bars for the determination of the distribution of current flowing under the influence of resistance and magnetic induction

At intermediate frequencies the conductor is subdivided in the same way. Instead of a resistor, however, one connects in series with each small electrode a capacitance equal to $f_i\mu\sigma/f_m\tau$, where τ is the d-c resistance per-unit length of the conductor or portion of a conductor in the initial problem corresponding to the area of the model apportioned to that particular electrode. The frequencies f_i and f_m are those of the initial problem and model respectively. The drop in the capacitor corresponds to the resistive drop in the initial problem and the drop in the electrolyte to the inductive voltage drop. In principle, the representation may be made exact provided a sufficiently large number of very small electrodes are used.

Figure 7 illustrates a model of this kind which was used in a problem of bus bar design. As the initial structure was symmetrical about two perpendicular planes, the model comprised only one quadrant of the cross section. One symmetry plane divided two groups of busses carrying opposing currents. In the model this plane was replaced by a conducting wall. The other symmetry plane, which bisected each bus bar, was replaced by an insulating wall. In this way, one half of the bus bars were eliminated completely and, of the remaining four bars, one half of each was included in the model. As two electrodes occupied an area corresponding to one half of the cross section of a bus bar, each electrode represented one quarter of a complete bus bar. An external resistor was also connected in series with each electrode to represent approximately the internal inductive effects for that portion of the conductor: that is, the drop that should occur in the electrolyte replaced by the conductor. Current from one generator terminal flows through the capacitors and resistors to the various electrodes, then through the electrolyte to the conducting wall of the tank, and back to the generator.

No equipotential plot is necessary for this test. A measurement of the voltage at each electrode allows a determination of the I^2R loss in the corresponding portion of the bus bar. The total power loss for each bar is shown in Table III, for a power frequency of $f_i = 60$ cycles per second. The current distribution is evidently very nonuniform.

Resistive Current Flow

For problems involving the flow of electric current through a medium obeying Ohm's law, the correspondence with the electrolytic model is not by an analogy but is direct. Regions in the initial problem which differ in conductivity are represented by electrolytes of proportional conductivity.

Figure 8, for example, shows the potential field throughout one of a pair of contacts in a circuit breaker. Each contact consists of an arc-resistant alloy plate brazed to a copper backing. This plot was made to show the effect of an incomplete braze. The alloy and the copper backing were represented in the model by electrolytes of different conductivities.

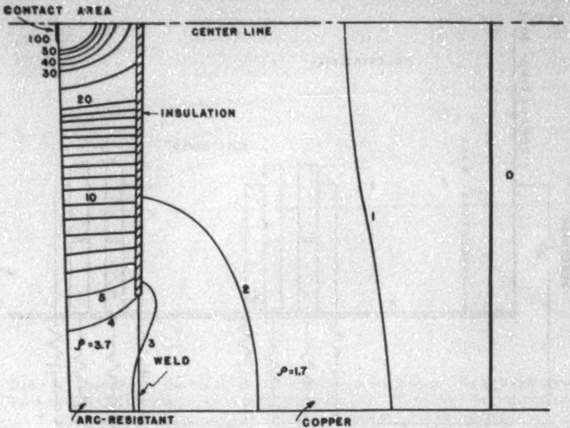

Figure 8. Voltage field produced by current flowing in a circuit-breaker contact assembly. The contours are equipotentials taken at intervals of 1 or 5 per cent of the total voltage applied to the model. The complete assembly includes two identical contacts of which only one is shown, and which make contact along the 100 per cent equipotential line. The insulating barrier in the model represents an incomplete braze. Values of ρ indicate resistivity. Electrodes in the model were along the 0 and 100 per cent equipotentials

Steady State Conductive Heat Flow in an Anisotropic Medium with Distributed Sources

The field analyzer also is well suited to the solution of problems in the conductive, steady-state flow of heat. Voltage in the model corresponds to temperature *T* and current density to heat flow *h* in watts per square inch.

Figure 9 is a temperature plot representing conditions in a transformer core. By taking advantage of the translational symmetry and of the two planes of mirror symmetry in the core, the model may be set up in a flat shallow tank covering an area corresponding to one quarter of the core cross section. The model presents several unusual problems. Corresponding to the fact that heat is generated uniformly throughout the core, current is introduced into the model through an array of vertical pins, uniformly spaced. One terminal of the generator is connected to these pins through series resistors which apportion equal currents to each pin. The heat conductivity (which corresponds to the electrical conductivity of the electrolyte) is higher along the laminations than across them. This situation is accurately represented by "stretching" the model in the direction perpendicular to the laminations by an amount equal to the square root of the ratio of the heat conductivities in the two directions. In the oil around the outside of the core, there is an abrupt temperature drop from the metal surface temperature to the constant temperature of the main body of oil. To represent this condition, small electrodes are placed along the two sides of the tank corresponding to the metal-oil boundary. Each of these electrodes is connected through a series resistor to the other terminal of the generator. The voltage at this terminal represents the temperature of the ambient oil, and the drop in the resistors, the temperature drop at the metal surface. These resistors are adjusted by trial and error in accordance with known laws of heat convection in oil. Thus, current flows from one generator terminal through resistors to pins distributed throughout the tank, through the electrolyte to the electrodes along the tank wall, then through other resistors to the other generator terminal.

Conclusions

The electrolytic field analyzer can supply answers to a surprising range of problems. It may be used not only to map fields, but to provide numerical values of such quantities as inductance, capacitance and a-c resistance. Although the accuracy may be poor for unfavorable geometries, it can be made quite satisfactory in many practical problems by observing certain precautions. A careful study of the theory of fields and models will often allow the application of the instrument to be extended to unusual problems by using special models or external circuits. Experience with the electrolytic field analyzer leads to an intuitive grasp of the analogies between fields of different types, which is very helpful in visualizing particular problems even when the instrument is not directly employed. The cost of assembling the basic equipment is low enough to be offset by the successful solution of even one or two important problems.

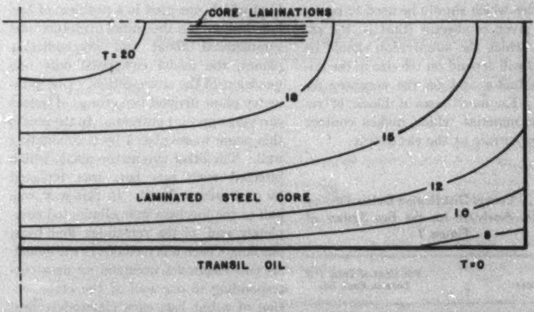

Figure 9. Temperatures in a cross section through one quarter of a transformer core. The contours are isothermal lines representing the temperature rise *T* in degree C with respect to the surrounding oil. No isothermal lines appear in the oil which is at a uniform temperature ($T=0$)

Appendix I. Mathematical Theory

The following analysis is made in terms of the rationalized meter-kilogram-second system of electromagnetic units.

Electrostatic Fields

The potential ϕ in an electrostatic field is determined by the equation

$$\nabla\cdot\epsilon\nabla\phi=-m \qquad (1)$$

where m is the charge density and ϵ is the permittivity. In a linear electrolyte, the voltage V satisfies the equation

$$\nabla\cdot\gamma\nabla V=-P \qquad (2)$$

where γ is the conductivity, and P is the density of the current which is introduced into the electrolyte from an external circuit, measured per-unit volume of the electrolyte. It is clear that V and ϕ will be everywhere the same if the source densities P and m and medium constants γ and ϵ are respectively equal at all points. Equation 2 involves four quantities P, V, γ and length, the last entering through the vector operator ∇. Three of these quantities can be scaled up or down at will; the remaining quantity will then bear a fixed ratio to its analogue in equation 1. Suppose scale factors a, b and k_0 are chosen for length, potential, and medium properties. Then

$$\nabla_m=a\nabla_i \qquad (3)$$

$$\phi=bV \qquad (4)$$

$$\epsilon=k_0\gamma \qquad (5)$$

The subscripts i and m refer respectively to the initial field and to the model. Combining equations 1 through 5 results in the relation

$$P=\frac{a^2}{bk_0}m \qquad (6)$$

for the source density scale factor.

Scale factors for other quantities are readily found from those already known. Thus for the field gradients $\boldsymbol{E}$ and $\boldsymbol{F}$ of the initial and model field,

$$\boldsymbol{E}=-\nabla_i\phi=-\frac{b}{a}\nabla_m V=\frac{b}{a}\boldsymbol{F} \qquad (7)$$

Also

$$\boldsymbol{D}=\epsilon\boldsymbol{E}=\frac{k_0b}{a}\gamma\boldsymbol{F}=\frac{k_0b}{a}\boldsymbol{J} \qquad (8)$$

where $\boldsymbol{D}$ is the initial electrostatic displacement and $\boldsymbol{J}$ is the current density per-unit area in the model. The total charge on a conductor of the initial problem is

$$Q=\int\int D\,dA_i=k_0ba\int\int J\,dA_m=k_0baI \qquad (9)$$

where I is the total current supplied from the external circuit to a conductor of the model. The integrals are taken over the conductor surface areas A_i and A_m which are in the ratio a^2. The capacitance between two electrodes is

$$C=\frac{Q}{\phi}=k_0a\frac{I}{V}=\frac{k_0a}{R} \qquad (10)$$

where R is the resistance measured between electrodes of the model. When symmetry allows the elimination of certain portions of the initial structure, quantities like Q or C in the above equations apply only to the portion of the initial structure which is actually included in the model.

In the flat tank the current flows parallel to the surface of the electrolyte. If h is the depth of the electrolyte, one can define a current density

$$\boldsymbol{i}=h\boldsymbol{J} \qquad (11)$$

amperes per-unit length of the electrolyte surface. Then $\nabla\cdot\boldsymbol{i}=p$, where p is the current introduced from the external circuit per-unit area of the electrolyte surface. It follows that

$$\nabla\cdot\sigma\nabla V=-p \qquad (12)$$

where

$$\sigma=h\gamma \qquad (13)$$

is the conductance per square of the electrolyte. If a new scale factor $k=k_0/h$ is used for translational symmetry, then

$$\epsilon=k\sigma \qquad (14)$$

The scale factors a and b remain the same. The relations in Table II for electrostatic quantities are derived by using equations 6 through 11 or by modifying their derivation and by the use of the relation $\boldsymbol{i}=\sigma\boldsymbol{F}$.

Magnetic Fields of Translational Symmetry

The magnetic fields considered here are those due to electric currents, not including displacement currents. It will be assumed that the materials are linear. The flux density $\boldsymbol{B}$ and the field intensity $\boldsymbol{H}$ are then related by $\boldsymbol{B}=\mu\boldsymbol{H}$ where μ depends on position but not on $\boldsymbol{H}$. If $\boldsymbol{B}$ is derived from a vector potential $\boldsymbol{A}$ then,

$$\nabla\times\frac{1}{\mu}\nabla\times\boldsymbol{A}=\boldsymbol{u} \qquad (15)$$

where $\boldsymbol{u}$ is the current density. For translational symmetry, derivatives with respect to z are zero, $\boldsymbol{u}$ is parallel to the z-axis and equation 15 reduces to $A_x=A_y=0$ and $A_z=\psi$ where

$$\nabla\cdot\frac{1}{\mu}\nabla\psi=-u \qquad (16)$$

Here ψ depends only on x and y and ∇ operates only in these co-ordinates. Comparison of equations 12 and 16 shows that this field may be represented in a flat tank if

$$\frac{1}{\mu}=k\sigma \qquad (17)$$

Then, since

$$\psi=bV \qquad (18)$$

$$u=\frac{kb}{a^2}p \qquad (19)$$

Since $\boldsymbol{B}=\nabla\times\boldsymbol{A}$, it follows that $B_x=\partial\psi/\partial y$ $B_y=-\partial\psi/\partial x$, and $B_z=0$. That is, $\nabla\psi$ and $\boldsymbol{B}$ are at right angles but are equal in magnitude. Hence, magnetic flux lines coincide with equipotential lines of ψ and V. The value of ψ at any point is equal to the total flux crossing a surface which is parallel to the z axis, is of unit length in the z direction, and intersects the x-y plane along any curve which extends from the point where ψ is measured to the reference point where ψ has the value zero. For an a-c magnetic field of angular frequency ω the voltage per-unit length induced along a path parallel to the z-axis is

$$\beta=j\omega\psi \qquad (20)$$

measured with respect to a reference conductor for which $\psi=0$. (Here, $j=\sqrt{-1}$.) Item four in Table II follows from the fact that $B=|\nabla\psi|$ and $\nabla\psi=(b/a)\boldsymbol{F}$. The other relations in that table are found by methods similar to those used for the electrostatic case.

At high frequencies, of course, in the space adjacent to the conductor, $\boldsymbol{B}$ is parallel to the conductor surface. This surface is, therefore, an equipotential surface for ψ and for V. It is then correct to represent conductors in the initial problem by conductors in the model. At low frequencies this is not necessarily true.

Electrostatic Flux Plotting

In simply-connected charge-free regions, $\boldsymbol{D}$ can be derived from a vector potential. Then for translational symmetry,

$$\nabla\cdot\frac{1}{\epsilon}\nabla\psi=0 \qquad (21)$$

where ψ now represents the electrostatic flux function. The above restriction requires that the model be constructed so that the electrolyte does not completely enclose any region representing a conductor of the initial structure.

Magnetic Fields of Rotational Symmetry

In magnetic fields of rotational symmetry equation 15 may be expanded in cylindrical co-ordinates. The current $\boldsymbol{u}$ has components in only the θ direction and θ derivatives of the $\boldsymbol{A}$ components are zero. This leads to $A_r=A_z=0$ and

$$\frac{\partial}{\partial z}\left[\frac{1}{\mu r}\frac{\partial(rA_\theta)}{\partial z}\right]+\frac{\partial}{\partial r}\left[\frac{1}{\mu r}\frac{\partial(rA_\theta)}{\partial r}\right]=-u \qquad (22)$$

where r is the distance from the axis. This time let

$$\psi=rA_\theta \qquad (23)$$

Then equation 22 reduces to

$$\nabla\cdot\frac{1}{\mu r}\nabla\psi=-u \qquad (24)$$

where ∇ operates in the variables r and z as though they were the rectangular co-ordinates x and y.

Comparison of equations 12 and 24 shows that the field is accurately represented in a shallow tank provided the current densities are represented in the same manner as for translational symmetry and the conductivity per square of the electrolyte varies as

$$\sigma=\frac{1}{k_1\mu r} \tag{25}$$

where k_1 is a constant. From equation 13 it is seen that the depth varies as

$$h=\frac{1}{k_1\gamma\mu r} \tag{26}$$

If a uniform electrolyte is used to represent a region of constant permeability μ, then h must be made proportional to $1/r$ and the tank cross section will be a hyperbola.

From the foregoing analysis, relations similar to those in Table II may be obtained for rotational symmetry.

Low-Frequency Magnetic Fields

At low frequencies one may not know the current density u. Equation 16 must then be replaced by one which relates the magnetic flux function ψ to the applied voltage rather than to the current. Only translational symmetry will be considered. The general equation for the electric gradient $\boldsymbol{E}$ in the initial magnetic field,

$$\nabla\times\boldsymbol{E}=-j\omega\nabla\times\boldsymbol{A} \tag{27}$$

is expanded in rectangular components. This leads to three differential equations that are satisfied by

$$E_z-\alpha+j\omega\psi=0 \tag{28}$$

Here α is a potential such that $\boldsymbol{e}=s\nabla\alpha$ where $\boldsymbol{e}$ comprises the x and y components of $\boldsymbol{E}$. All quantities in this equation are independent of z. Over the cross section of a conductor the potential α is equal to a constant value α_0 which represents the applied voltage per-unit length in the z direction. The induced voltage is, as was already pointed out, $\beta=j\omega\psi$. Finally, E_z inside a conductor is the resistive drop per-unit length. If ρ is the resistivity of the conductor, equation (16) leads to

$$E_z=\rho u=-\rho\nabla\cdot\frac{1}{\mu}\nabla\psi \tag{29}$$

The combination of equations 20, 28, and 29 results in

$$\beta+j\frac{\rho}{\omega_t}\nabla\cdot\frac{1}{\mu}\nabla\beta=\alpha_0 \tag{30}$$

inside a conductor. Outside a conductor this reduces to

$$\nabla\cdot\frac{1}{\mu}\nabla\beta=0 \tag{31}$$

In order to represent equations 30 and 31 by an electrolytic model β will be associated with the voltage V of the model. On account of equation 20 this is similar to the procedure adopted for high frequencies when ψ was associated with V. The region of the model which is to represent a conductor is broken up into a number of small areas into each of which current is introduced through a separate series capacitor c_n from a common source of voltage V_0. These capacitances are chosen so that $c_n=c_0A_n$, where A_n is the area apportioned to the corresponding electrode and c_0 is a constant. Then

$$V_0=V+\frac{p}{jc_0\omega_m} \tag{32}$$

which, when combined with equation 12, becomes

$$V+j\frac{1}{c_0\omega_m}\nabla\cdot\sigma\nabla V=V_0 \tag{33}$$

This is satisfied by V in the region of current sources. In the remainder of the model

$$\nabla\cdot\sigma\nabla V=0 \tag{34}$$

In order for equations 30 and 33 to be equivalent, the model conductivity must satisfy equation 17 and the capacities and frequencies must satisfy the relation,

$$\frac{a^2}{kc_0\omega_m}=\frac{\rho}{\omega_t} \tag{35}$$

The last equation is equivalent to

$$c_n=\frac{\omega_t\mu\sigma}{\omega_m r} \tag{36}$$

where r is the d-c resistance per-unit length of the conductor or section of a conductor in the initial device which corresponds to c_n in the model.

The relations given in Table II for magnetic quantities remain unchanged. In the case of item eight, however, R is to be interpreted as the equivalent series resistance of the model measured at the generator terminals so as to include the series capacitances with the model. The resultant l will then be the equivalent series inductance per unit length. If C is the effective series capacitance of the model, the a-c resistance of the corresponding conductor in the initial device is $\omega_t/(k\omega_mC)$ per meter.

Heat Flow in an Anisotropic Medium

If the co-ordinate axes are chosen to coincide with the principal axes of the material, the heat flow h in watts per square inch and the temperature T are related by the equations,

$$h_x=-g_x\frac{\partial T}{\partial x},\ h_y=-g_y\frac{\partial T}{\partial y},\ h_z=-g_z\frac{\partial T}{\partial z} \tag{37}$$

where g_x, g_y, and g_z are the heat conductivities along the x, y and z axes. If heat is being generated at a rate of w watts per cubic inch throughout the material, then $\nabla\cdot h=w$.

Hence, if the conductivity is the same at all points (medium homogeneous but anisotropic),

$$g_x\frac{\partial^2T}{\partial x_t^2}+g_y\frac{\partial^2T}{\partial y_t^2}+g_z\frac{\partial^2T}{\partial z_t^2}=-w \tag{38}$$

Suppose the model to be scaled so that

$$x_t=\sqrt{\frac{g_x}{g_0}}\,x_m,\ y_t=\sqrt{\frac{g_y}{g_0}}\,y_m,\ z_t=\sqrt{\frac{g_z}{g_0}}\,z_m \tag{39}$$

where g_0 is a constant. Then, in terms of the model co-ordinates, equation 38 becomes simply

$$g_0\nabla_m^2T=-w \tag{40}$$

For a uniform electrolyte (γ=constant) equation 2 has this same form. The voltage distribution in the model, therefore, represents the temperature distribution provided that currents P are introduced into the model proportional to the rate w of heat generation.

This principle may, of course, be applied to other fields such as electric or magnetic fields involving anisotropy in the permittivity or the permeability.

References

1. Electromagnetic Fields, Theory and Application, **Ernst Weber.** John Wiley and Sons, New York, N. Y., volume 1, 1950.

2. Methods of Plotting Electrostatic Fields, **P. E. Green, Jr.** *Bulletin Number 45*, North Carolina State College, Raleigh, N. C., June 1949, pages 35–42.

3. Electron Optics and the Electron Microscope, **V. K. Zworykin, G. A. Morton, E. G. Ramberg, J. Hillier, A. W. Vance.** John Wiley and Sons, New York, N. Y., 1945, pages 389, 477, 647.

4. Automatic Plotting of Electrostatic Fields, **Paul E. Green, Jr.** *Review of Scientific Instruments* (New York, N. Y.), 1948, pages 646–53.

5. Automatic Equipment and Techniques for Field Mapping, **J. K. Mickelsen.** *General Electric Review* (Schenectady, N. Y.), November 1949, pages 19–23.

6. Utilization of the Electric Tank in Different Problems Concerning High-Voltage Equipment, **G. Balachowski, Tirrolloy.** *Report Number 132*, International Conference of High-Voltage Electric Systems (Paris, France), 1950.

7. Cable Accessory Design Utilizing New Laboratory Techniques, **P. N. Bosworth, H. K. Farr.** *AIEE Transactions*, volume 69, part II, pages 1268–74 and *Electrical Engineering*, February 1950, pages 119–24.

8. **H. Schaefer, R. Stachowiak.** *Zeitschrift für Technische Physik* (Leipzig, Germany), volume 32, 1940, page 307.

9. Use of the Electrolytic Tank for Magnetic Problems, **R. E. Peierls.** *Nature* (London, England), 1946, pages 831–32.

10. **V. A. Karasev.** *Electrichestvo* (Moscow, Russia), May 1949.

Discussion

P. A. Abetti (General Electric Company, Pittsfield, Mass.): An electric machine may be considered as the site of several superimposed fields, namely: an electric field, a magnetic field, a current field, a field of mechanical forces, a field of conductive heat flow, a field of elastic forces in the material stressed by the mechanical forces, a field of fluid flow of the cooling medium. In some cases the transient response of the machine and its regulation characteristics are of interest. In order to meet the specifications the designer must be able to analyze and modify these fields, with the ultimate aims of safety, simplicity, efficiency and economy.

It is evident therefore that the accurate knowledge of these fields is essential for the electrical design engineer and useful for the power engineer, who writes the specifications and should make the best use of the machine's characteristics.

These fields satisfy in general Laplace's or Poisson's equation and the problems to be solved require the integration of these equations, that is, the determination values of the unknown function at any point of the region of interest, for assigned values on the boundary: (a) of this function (Dirichlet's problem), or (b) of its normal derivative (Neumann's problem), or (c) of a combination of both (a) and (b).

Aside from a purely mathematical "exact" solution, which is possible only for a limited number of cases, there are other "approximate" methods, which yield results of accuracy required for practical purposes. These methods may be divided in: numerical methods (iteration and relaxation processes) graphical methods (free-hand flux plotting with the Lehmann procedure) and experimental method (by field analogy). It is the last method which has been discussed by the authors, who have clearly shown its tremendous importance for the design of electric machinery. In fact, all the fields listed above are included in Table I of the paper, as well as the study of the transient performance of the apparatus.

In order to compare the three methods of approximate solution, it is necessary to know their relative accuracy. It would be therefore very interesting if the authors would indicate the accuracy which may be obtained with the electrolytic field analyzer in the measurement of the voltages and especially of the gradients. In fact, the latter are often more interesting than the former to the designer, particularly when they vary rapidly with the position of the point in consideration. Recently a method for obtaining directly the gradient has been described in the technical literature.[3] Are the authors planning to apply this method, or do they believe that it is better to measure directly and plot the voltages and then obtain the gradients from these voltages? It also would be very interesting to compare the three methods of approximate solution (numerical, graphical, and electrolytic tank) with respect to the labor involved, the accuracy of the results, and expense. In this comparison, allowance should be made for the time and expense necessary to build the model to be used in the tank.

Another type of field not mentioned by the authors may be studied[4] by means of the electrolytic field analyzer. This is the motion of filtering liquids, which follows Darcy's law, formally identical to Ohm's law. This application is of interest for the electrical industry, since the motion of water under a dam may be studied, in order to determine the uplift pressures which may reduce the stability of the dam. Another possible application is to diffusion processes, which also follow a law analogous to Ohm's law.

It is interesting to note that the principle of the method of the electrolytic tank goes back to Kirchoff[1] himself (1845) and that analogy between current flow and the functions of complex variables was first noted by Maxwell[2] (1881).

However, the first practical applications were made in the first years of this century and only in the recent years, as witnessed by the technical papers published on the subject, has there been a widespread interest in the electrolytic field analyzer. This fact is probably due to the ever-increasing requirements for faster, more accurate and rigorous solutions in the design of electric machinery which replace always more the empirical and semiempirical "rules of thumb" used in the past.

Finally it is worthwhile to mention that a complete bibliography of 64 items on the electrolytic field analyzer and on its applications is contained in a recent article by Dadda.[5]

References

1. Ueber den Durchgang eines elektrischen Stromes, G. Kirchoff. *Annalen der Physik* (Leipzig, Germany,) volume 64, 1845, pages 497–514.

2. A Treatise on Electricity and Magnetism, J. C. Maxwell, Oxford University Press, Oxford, England, 1881.

3. Direct Measurement in the Electrolytic Tank of the Gradient in an Electric Field, L. Dadda. *L'Energia Elettrica* (Milan, Italy), volume 26, 1949, pages 469–72.

4. Electrical Models for the Study of the Motion of Filtering Water, U. Puppini. *Comunicazioni all'Accademia delle Scienze* (Bologna, Italy), May 28, 1922.

5. The Electrolytic Tank of the Research Center on Electrical Models: Review of its Applications, L. Dadda. *L'Energia Elettrica* (Milan, Italy), volume 28, 1951, pages 23–39.

H. K. Farr and W. R. Wilson: The accuracy attainable and the labor involved in the use of the electrolytic field analyzer vary greatly depending on the type of problem, the quantity being measured and the extent of the precautions one is willing to take. It is possible, however, to make some rough comparisons with methods of hand plotting and numerical computation, respecting accuracy and labor costs.

For certain simple problems of translational symmetry, hand plotting may compete with the electrolytic field analyzer on the basis of time but not accuracy. It is doubtful whether the numerical method of relaxation can compete in any case on the basis of time, although, for certain problems, it might provide greater accuracy. The time required to build a model for the electrolytic field-analyzer varies from a few man hours to three or four man days. The cost of material is a few dollars. Setting up the model in the tank, mixing solutions, and making one or two plots will take about a 1-man day. Once a model is set up it is possible, in one day, to make several plots involving minor changes.

As regards accuracy, hand plotting is inferior to the electrolytic method. Since the hand-plotted curves must be drawn somewhat by eye, a certain amount of personal judgment is involved.

In problems to which the relaxation method may be applied, the error may be reduced to as small a value as desired by repeating the relaxation a sufficient number of times and by proceeding to finer nets. This method is appropriate to problems of translational symmetry involving a uniform medium, although the labor is usually considerable. For composite media or for rotational symmetry the computations become extremely tedious.

The accuracy obtained with the electrolytic field analyzer in specific applications has been reported by other workers. Boothroyd, Cherry and Makar,[1] for example, claim an accuracy of 1 per cent in the determination of certain impedance functions by means of a "double" electrolytic tank which eliminates errors due to the tank boundary. Loeb et al[2] report values within 1 to 5 per cent of computed quantities in the determination of the voltage around a hemispherically capped rod.

In determining the turn-to-turn capacitances of a winding, by means of the circuit shown in Figure 4, one of the present authors has obtained data which averaged within 2 or 3 per cent of theoretical values. Similar results have been obtained on other checks made using the flat tank. Where a sloping tank is used with problems of rotational symmetry, however, considerable error may be introduced by meniscus effects if the electrodes must be placed close to the axis where the electrolyte is very shallow. When the model must be kept small to avoid the perturbing effects of the tank boundaries, the error may reach 10 or 20 per cent. This error may usually be reduced considerably if the plot is made in two stages. The first model is made on a scale such as to minimize tank boundary effects. An enlarged model is then made of the region of interest by using the results of the first plot to lay out the new tank boundaries.

The accurate determination of field gradients by means of the electrolytic field analyzer is more difficult than the plotting of potentials. If, for example, one wishes to determine to an accuracy of 1 per cent, the average gradient over a distance in which the voltage drop is 1 per cent of the total applied voltage, this drop must be measured with an error of less than 1/10-thousanth of the applied voltage. The error in the measurement of distance must be reduced to a corresponding fraction of the total electrode spacing. The determination of gradients from an equipotential plot involves considerable error unless the model is built on a very large scale. Dadda's technique provides for the display of the direction as well as the magnitude of the field gradient, but apparently assures no greater accuracy than the usual double probe method. One technique, which the authors have found to give good results is the use of a special probe with a screw drive and a micrometer dial indicator whose readings are recorded when the probe position is adjusted for a balance at several settings of the voltage divider (R_1 and R_2 in Figure 1) differing by a small fixed interval, say 0.1 per cent. This technique has resulted in gradient values with an accuracy of 3 per cent or better for tests made in the flat tank.

References

1. An Electrolytic Tank for the Measurement of Steady-State Response, Transient Response, and Allied Properties of Networks, A. R. Boothroyd, E. C. Cherry, R. Makar. *Proceedings*, Institution of Electrical Engineers (London, England) volume 96, part 1, number 99, May 1949, pages 163–77.

2. The Choice of Suitable Gap Forms for the Study of Corona Breakdown and the Field Along the Axis of a Hemispherically Capped Cylindrical Point-to-Plane Gap, L. B. Loeb, J. H. Parker, E. E. Dodd, W. N. English. *The Review of Scientific Instruments* (New York, N. Y.), volume 21, January 1950, pages 42–47.

A Practical Application of Low-Frequency Magnetic Induction Theory

R. N. E. HAUGHTON
ASSOCIATE AIEE

THE inductive effects of power system ground currents on communication circuits due to faults such as grounds or other abnormal conditions are of great importance to communication engineers.[1,3,5,8,16] The effects may range from the noise created[7] by certain harmonic frequencies in the power circuit to the interruption and degradation of service and the exposure of personnel to hazardous voltages.

Low-frequency magnetic induction may be defined as the process by which power circuit currents induce voltages in the communication conductors at the fundamental power frequency. The induction may be due to the balanced or residual components of current in the power system under normal or abnormal conditions of operation.

Although induction arising from normal operation of the power system may result in the false operation of grounded ringing devices and other annoying effects, the magnitude of the induced voltages are much smaller than those due to power lines operating under abnormal conditions.

This paper deals entirely with abnormal low-frequency magnetic induction arising from power system fault currents. The severity of the effects depends upon the magnitude and duration of the fault current and the mutual impedance between the two circuits. The problem is to determine whether remedial measures are warranted and if so to what extent they should be undertaken. This requires consideration of the severity and probable frequency of the effects produced in communication lines by the induced voltages. Although such abnormal conditions existing in the power circuit are infrequent in occurrence and are usually of short duration, the resulting effects may be serious and consequently the selection and design of remedial measures is an important problem in the co-ordination of power and communication circuits.

Extensive research has been carried out in the past quarter century concerning the techniques necessary to evaluate low-frequency induction problems and to aid in deciding the need and type of remedial measures.

The purpose of this paper is to outline, in a simple and concise manner, the essential concepts of the theory of abnormal low-frequency magnetic induction and to describe their application to a practical field problem.

In order to facilitate a logical development of the subject the following important aspects will be discussed; the magnitude, frequency, and duration of the induced voltages in the communication circuits, their effects, and the types of remedial measures in current use.

Magnitude of Induced Voltages

When a fault occurs in a power system, a relatively large current many times greater than normal phase currents may be produced. If the power system is a star-connected grounded circuit or a delta line with suitable ground protection, the fault current is provided with a return path to the power source.

In the case of a delta line with no grounding facilities, the fault current will be insignificant since there is no ground return path, the only current being the "charging current" flowing through the distributed capacitance of the power wires to ground and possibly introducing noise in the communication system. If, however, a second ground develops, particularly on another phase then a path is completed and large fault currents may result.[5,6,16]

Fundamentally, the induced voltage in the communication conductors is a consequence of the electromagnetic field produced by the power circuit, which primarily depends upon the magnitude and frequency of the fault current and its distribution in the ground.

Referring to Figure 1, the fault current may be considered as flowing in an equivalent conductor at the geometric center of the power conductor configuration cross section, and due to the finite conductivity of the earth, returning to the power source through an image conductor below the surface of the earth.

The total induced voltage E in the communication conductor, Figure 1, may be considered as the resultant of two components, namely E_1 due to the fault current I_f in the equivalent power conductor at a distance r_1 from the communication conductor, and E_2 due to the fault current I_f in the image conductor at a distance r_2 from the communication conductor. The two voltages are 180 degrees apart with the neutralizing effect of E_2 depending on r_2 and therefore on the depth of the equivalent power conductor. The depth of the equivalent conductor increases with the earth resistivity.[3]

The existence of any grounded conductors either in the power system, the communication system, or in close proximity to either brings about a reduction in the induced voltage. This shielding[3] is due to the field created by the induced currents in the grounded shield conductors opposing the field established by the power system fault current. The amount of shielding depends upon the number of grounded conductors, their self and terminal ground impedances and their positions with respect to the power

---

Paper 51-242, recommended by the AIEE Wire Communications Systems Committee and approved by the AIEE Technical Program Committee for presentation at the AIEE Summer General Meeting, Toronto, Ont., Canada, June 25–29, 1951. Manuscript submitted March 15, 1951; made available for printing May 4, 1951.

R. N. E. HAUGHTON is with the Bell Telephone Company of Canada, Toronto, Ont., Canada.

Figure 1. Electromagnetic induction

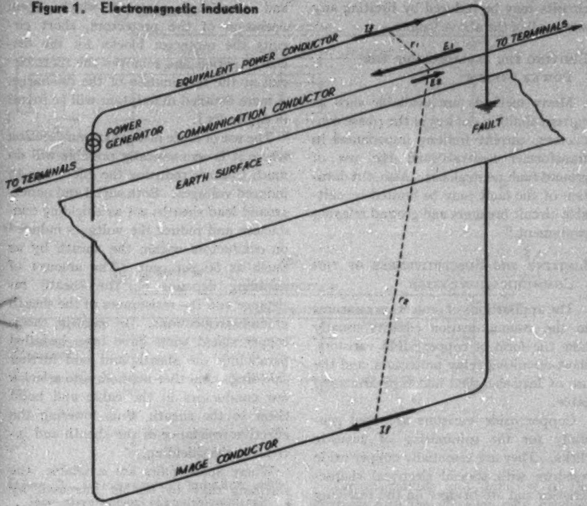

E - TOTAL INDUCED VOLTAGE IN COMMUNICATION CONDUCTOR = $E_1 + E_2$
E_1 - COMPONENT OF INDUCED VOLTAGE DUE TO I_f IN POWER CONDUCTORS
E_2 - COMPONENT OF INDUCED VOLTAGE DUE TO I_f IN THE IMAGE CONDUCTOR

and communication conductors. Such a conductor affords maximum shielding when closely coupled to either the power or communication system, when its admittance is high and the impedance of its ground connections are low.

Frequency of Occurrence of Induced Voltages

This factor, of course, depends on the frequency of occurrence of faults on the power line. Some factors which are responsible for power system faults are lightning surges, inadequate spacing and clearances of conductors and insufficient insulation.

One convenient method of expressing fault frequency is in terms of the "number of faults per hundred miles per year." If this can be obtained from the power company for any particular line, then the probable number of faults per year can be determined easily for any power exposure.

Duration of Induced Voltages

The duration of induced voltages depends on the duration of the power circuit fault, which in turn depends upon the type of protective relaying and circuit breakers employed. Obviously the length of time it takes the circuit breaker to operate, and the standard maintenance of the equipment are the most important factors.

Effects of Induced Voltages

Low-frequency induced voltages of up to 2,000 to 3,000 times the normal operating voltages of communication lines are not unusual. The effects they produce depend on their magnitude and duration and include service degradation or interruption, telegraph signal distortion, damage to plant, acoustic clicks, and electric shock.

Service Degradation and Interruption

The maintenance of high grade continuous service is part of the responsibility of a communication system to the public. Hence any situation in which the possibility of service degradation and interruption is high must be evaluated in terms of the importance of the service being rendered.

The main source of service interruption in low-frequency induction problems is the permanent operation of protectors thus grounding the communication conductors. In order to limit the maximum potential between each communication conductor and ground, an "open space cutout" protector, shown in Figure 2(A) is provided between each conductor and ground.

This device consists of two protector blocks. One of the blocks is of carbon and forms the ground electrode; the other is of porcelain with a small carbon insert. The carbon insert forms the line electrode and is depressed slightly below the bearing surface of the porcelain block so that when the two blocks are held together by a spring, a small gap exists between the carbon block and the carbon insert. The carbon insert is held in place in the porcelain block by means of glass cement. The protectors operate and clear twice every cycle for voltages in excess of about 350 volts peak value.[8]

The nature of the breakdown depends upon the magnitude and duration of the current through the blocks. For currents of short duration and small magnitude causing many protector operations over a period of time, the carbon dust collects on the electrodes after each operation, thus finally causing a permanent ground. For currents of long duration and high magnitude the glass cement will soften due to the heating effect of the current and allow the spring to push one block against the other and ground the conductor permanently.

Distortion of Telegraph Signals

The induced voltages, even though not sufficiently high enough to operate the protector blocks, may cause detrimental effects to telegraph signals ranging from distortion to momentary interruptions.

Damage to Offices and Associated Communication Equipment

The dielectric strength normally employed in the communication plant is adequate for the voltages used in normal operation with an appropriate factor of safety. Under high induced voltages dielectric failure may occur, notwithstanding any protective devices, thus damaging cables and wire, or apparatus in communication offices.

Acoustic Clicks

Acoustic clicks may occur during the operation of communication protector blocks. They are caused by protector blocks on a pair of wires not breaking down simultaneously.

Electric Shock

The possibility of communication personnel being in contact with conductors which have high induced voltages on them is always present and has an important bearing on the selection of the number and type of remedial measures employed. In many cases where the probability of permanent service interruption is low, additional remedial measures may be necessary to reduce the degree of hazard of electrical shock, especially if the frequency of power fault occurrence is high.

Remedial Measures

The effective and economical application of remedial measures[6,7] depends largely upon past experience in low-frequency induction problems and the application of certain principles to be discussed.

The interfering effects of a power system on communication circuits may be considered as having an intensity which is proportional to the product of three factors; influence, coupling, and susceptibility.[6,7]

"Influence Factors" refer to the characteristics of the power circuit which affect the communication system. In the case of low-frequency magnetic induction, the most important factors are the magnitude and duration of the ground fault current, the frequency of occurrence of the power system faults to ground and the presence of shielding conductors (such as ground wires) on the power line.

"Susceptiveness Factors" deal with certain characteristics of the communication circuits which determines its response to power system influence.

"Coupling Factors" are the mutual characteristics of the intervening medium that aids in determining the magnitude of the disturbance in the communication circuits.

Inductive effects on communication circuits may be reduced by limiting any one or all of the above factors.

Limiting the Influence of the Power System

Many methods are available such as current limiting devices in the phase conductors, current limiting impedances in transformer neutrals and the use of ground fault neutralizers. Also, the duration of the fault may be limited by suitable circuit breakers and ground relaying equipment.[17]

Limiting the Susceptiveness of the Communication System

The applications of protective measures to the communication circuits usually take the form of copper oxide varistors, short-circuiting relay protectors, and the use of lead-sheathed and tape-armoured cable.

Copper oxide varistors are used generally for the minimizing of acoustic clicks. They are essentially copper oxide resistors with special electrical characteristics and are bridged on the receiving branch of the operator's telephone set. When the varistor is under relatively low voltage due to speech, its impedance is high and therefore it takes negligible current from the receiver. On the other hand, when relatively high voltage is impressed on the operator's telephone circuit, the impedance of the varistor drops to a low value, thereby shunting the current from the receiver unit.

The short-circuiting relay protector, Figure 2(B) is a device designed to minimize permanent protector operation and service interruption. It consists of a relay and associated contacts which, upon operation of the protectors, short circuits the protector blocks for the discharge period and removes the short circuit at the termination of the discharge. A more detailed description will be found in Appendix I.

The use of cable in any exposure section where it is economically possible will do much towards reducing the effect due to induced voltages. Both aerial and underground lead sheaths act as shielding conductors and reduce the voltages induced on conductors within the sheath by as much as 50 per cent. The amount of shielding depends on the sheath resistance and the resistances of the sheath ground connections. In certain cases, copper shield wires have been installed paralleling the sheath and add further shielding. Another method is to select a few conductors in the cable and bond them to the sheath, thus lowering the effective resistance of the sheath and increasing the shielding.

Where spare pairs are available, the shielding may be further increased by bonding them to the sheath, thus lowering the effective sheath resistance.

Tape-armored cable consists of a wrapping of steel tape over a lead covering, thereby increasing the net conductivity of the sheath and providing a voltage reduction of up to 80 per cent.

Limiting the Mutual Coupling

If arranged in advance of construction, separations sufficient to limit the induced voltages to a reasonable value are possible.

This type of planning will do more to relieve inductive effects than any other precaution or type of remedial measure.

Figure 2. Communication protectors

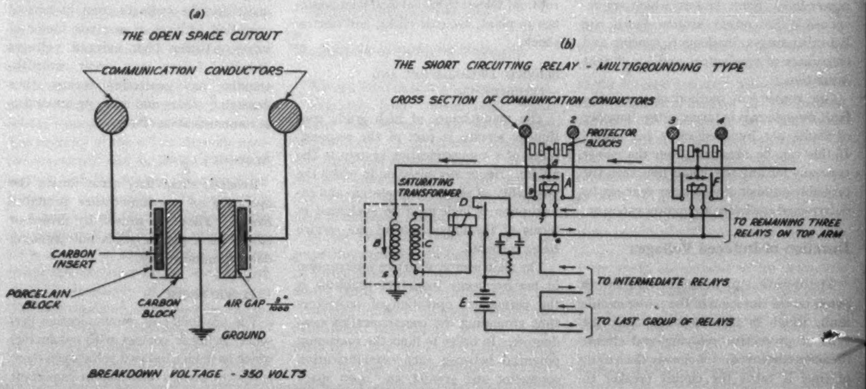
(a) THE OPEN SPACE CUTOUT

(b) THE SHORT CIRCUITING RELAY - MULTIGROUNDING TYPE

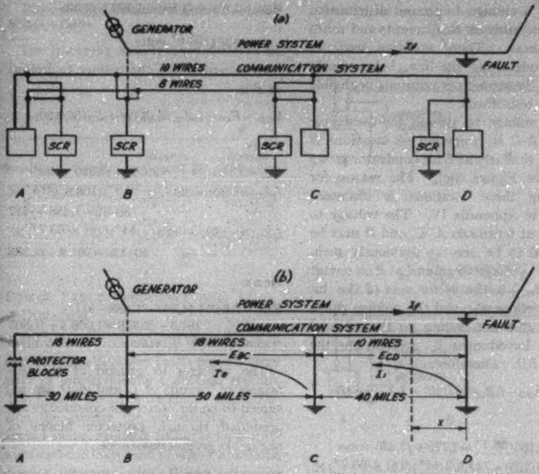

Figure 3. Low-frequency induction problem—development of equivalent circuit

Solution of a Low-Frequency Magnetic Induction Problem

The preliminary step in any low-frequency induction problem is to prepare a map showing the extent of the exposure and all separations between the two circuits. This should be followed with schematic drawings showing the number of conductors on the communication lines, the location of all terminals and protector blocks, a single line diagram for the power circuit and all pertinent data as shown on Figure 3.

In order to calculate induced voltages it is necessary to know the fault current and the mutual impedance between the power and communication conductors as explained in Appendix II. The fault current may be obtained by field tests, calculations,[10,11] or by the use of a network analyzer and is most useful in the form of a curve as shown in Figure 4. The "worst fault location" is next determined, and is the location that produces the maximum product of fault current and mutual impedance.

The induced open circuit voltages now are worked out for the worst fault location to permit an estimation to be made of protector operation. Assuming that the open circuit voltages are of such a value, say greater than 700 volts, that some or all of the protectors are operated, then the resulting currents may be readily determined.

The magnitude and duration of the currents and the voltages they produce between the conductors and between the conductors and ground are important factors in estimating the probability of permanent protector operation and the degree of electrical hazard to personnel.

The previous outline may be itemized in detail as follows:

1. Map prepared.
2. Fault current data obtained.
3. Determination of mutual impedance.
4. Calculation of induced voltage.
5. Determination of "worst fault location."
6. Determination of self and mutual impedance of communication conductors.
7. Calculation of induced currents.
8. Estimation of permanent protector operation.
9. Estimation of voltages to ground and voltage differences.
10. Estimation of the extent of electrical hazard to personnel.
11. Selection and application of remedial measures.

In order to illustrate the fundamental principles involved in low-frequency induction studies and to outline the general method of analysis the following typical problem will be studied:

Data

(a). Power system, star connected, multigrounded neutral, 60 cycles per second.

(b). Worst fault location—point *D*, Figure 3(C).

(c). I_f, power fault current, 650 amperes, Figure 4.

(d). Fault current duration—0.5 second.

(e). Fault frequency—10 faults per hundred miles per year.

(f). Communication system, open wire line, copper, 104-mil diameter.

(g). Exposure length, 90 miles, Figure 3(c).

(h). *d*, power and communication circuit separation, 3000 feet, Figure 3(c).

(i). ρ, average earth resistivity[8,9] for the exposure, 1,000 meter-ohms.

DETERMINATION OF MUTUAL IMPEDANCE

The following values of mutual resistance and reactance are derived from Figure 6, using a separation of 3,000 feet, and an earth resistivity of 1,000 meter-ohms.

Mutual resistance per kilofoot = 0.0155 ohm
Mutual reactance per kilofoot = 0.0255 ohm
Mutual impedance per kilofoot = $0.0155 + j0.0255 = 0.0298\underline{/58.7^\circ}$ ohms

Hence the mutual impedances for sections *BD*, *BC*, and *CD*, as shown in Figure 3, are therefore,

$$Z_{mBD} = 90 \times 5.28 \times 0.0298\underline{/58.7^\circ} = 14.1\underline{/58.7^\circ} \text{ ohms}$$

$$Z_{mBC} = 50 \times 5.28 \times 0.0298\underline{/58.7^\circ} = 7.86\underline{/58.7^\circ} \text{ ohms}$$

$$Z_{mCD} = 40 \times 5.28 \times 0.0298\underline{/58.7^\circ} = 6.29\underline{/58.7^\circ} \text{ ohms}$$

For a further discussion of mutual impedance see Appendix II.

CALCULATION OF OPEN CIRCUIT INDUCED VOLTAGES

As explained in Appendix II, the open circuit induced voltage in a conductor for any particular length of exposure is equal to the product of the power fault current and the mutual impedance for the section. The induced voltages in sections *BD*, *BC*, and *CD* are therefore

$$E_{BD} = I_f \quad Z_{mBD} = 650 \times 14.1\underline{/58.7^\circ} = 9{,}160\underline{/58.7^\circ} \text{ volts}$$

$$E_{BC} = I_f \quad Z_{mBC} = 650 \times 7.86\underline{/58.7^\circ} = 5{,}110\underline{/58.7^\circ} \text{ volts}$$

$$E_{CD} = I_f \quad Z_{mCD} = 650 \times 6.29\underline{/58.7^\circ} = 4{,}080\underline{/58.7^\circ} \text{ volts}$$

The communication protector blocks with an operating voltage of about 350 volts will obviously operate under the action of the above induced voltages at points *A*, *C*, and *D*, thus grounding all the communication conductors at these points.

CALCULATION OF CURRENTS

Assuming the communication conductors are grounded at *A*, *C*, and *D* through the operated protector blocks, see Figure 3(c), the resulting induced currents in circuit *A-D* will depend upon the induced voltages and the self and mutual impedances of the communication conductors in circuits *A-D* and *A-C* in accordance with the theory of coupled circuits.[12,13]

Let Z_{11} be the self impedance of circuit *A-D* in ohms, Z_{22} be the self impedance of circuit *A-C* in ohms, and Z_{12} be the mutual impedance between circuits *A-C* and *A-D*. Evaluating these impedances for our problem we have

$$Z_{11}=151.8\underline{/60.7^\circ}\text{ ohms}$$
$$Z_{22}=108.8\underline{/56.5^\circ}\text{ ohms}$$
$$Z_{12}=Z_{21}=75.2\underline{/84.6^\circ}\text{ ohms}$$

For details of the above results and a discussion of self and mutual impedances see Appendix III.

In Figure 3(c) let $\mathbf{E}_{BD}$, $\mathbf{E}_{BC}$ and I_1, I_2 be the induced voltages and resulting currents in circuits *A-D* and *A-C*. Applying Kirchoff's Law to circuit *A-C* and *A-D* we have the following system of linear equations

$$\mathbf{E}_{BD}=I_1Z_{11}+I_2Z_{12}$$
$$\mathbf{E}_{BC}=I_1Z_{21}+I_2Z_{22}$$

The solution of the above for I_1 and I_2 is obtained by expanding the associated determinants,[14,15]

$$I_1=\frac{\begin{vmatrix}\mathbf{E}_{BD} & Z_{12}\\ \mathbf{E}_{BC} & Z_{22}\end{vmatrix}}{\begin{vmatrix}Z_{11} & Z_{12}\\ Z_{21} & Z_{22}\end{vmatrix}}=\frac{\mathbf{E}_{BD}Z_{22}-\mathbf{E}_{BC}Z_{12}}{Z_{11}Z_{22}-Z_{21}Z_{12}}$$
$$=49.8\underline{/1.44^\circ}\text{ amperes}$$

and

$$I_2=\frac{\begin{vmatrix}Z_{11} & \mathbf{E}_{BD}\\ Z_{21} & \mathbf{E}_{BC}\end{vmatrix}}{\begin{vmatrix}Z_{11} & Z_{12}\\ Z_{21} & Z_{22}\end{vmatrix}}=\frac{\mathbf{E}_{BC}Z_{11}-\mathbf{E}_{BD}Z_{21}}{Z_{11}Z_{22}-Z_{21}Z_{12}}$$
$$=22.7\underline{/-40.8^\circ}\text{ amperes}$$

As mentioned previously, the possibility of permanent protector operation depends on the magnitude and duration of the current flowing through the operated protector. In this case, the magnitude of the current per conductor in circuit *A-D* is about 5 amperes and for circuit *A-C* about 2.3 amperes with a duration of 0.5 second. Assuming that for the type of protector blocks employed a current of 5 amperes for 0.5 second will cause permanent protector operation, then the likelihood of permanent grounding on circuit *A-D* is high.

VOLTAGE BETWEEN COMMUNICATION CONDUCTORS AND GROUND

After the protector blocks have operated, all the conductors in a group will assume a voltage to ground distribution which depends on the currents and series impedances. These voltages vary in magnitude along the line, being nearly zero at the protectors assuming negligible ground resistances.

The voltage to ground for conductor group *A-D* is computed at locations *B* and *C*; similarly at *B* for conductor group *A-C*, see Figure 3(c). The reason for selecting these locations is discussed briefly in Appendix IV. The voltage to ground at terminals *A*, *C*, and *D* may be assumed to be zero as previously mentioned. Voltage to ground at *B* on circuit *A-D* (V_{GB_1}) is the vector sum of the induced voltage $\mathbf{E}_{BD}$ and the voltage drops due to I_1 and I_2 acting on the self and mutual impedances Z_{11} and Z_{12} for the length *BD*. Therefore,

$$V_{GB_1}=\mathbf{E}_{BD}-I_1Z_{11}(90/120)-I_2Z_{12}(50/80)$$

where

$$\mathbf{E}_{BD}=9{,}160\underline{/58.7^\circ}=4{,}770+j7{,}830\text{ volts}$$
$$I_1Z_{11}(90/120)=(49.8\underline{/1.44^\circ})(151.8\underline{/60.7^\circ})\times 90/120=2{,}650+j5{,}010\text{ volts}$$
$$I_2Z_{12}(50/80)=(22.7\underline{/-40.86^\circ})(75.2\underline{/84.6^\circ})\times 50/80=770+j859\text{ volts}$$

Therefore

$$V_{GB_1}=4{,}770+j7{,}830-2{,}650-j5{,}010-770-j859=1{,}350+j1{,}961$$
$$=2{,}378\underline{/55.4^\circ}\text{ volts}$$

Similarly

$$V_{GC_1}=\mathbf{E}_{CD}-I_1Z_{11}(40/120)$$

where

$$\mathbf{E}_{CD}=4{,}080\underline{/58.7^\circ}=2{,}120+j3{,}500\text{ volts}$$
$$I_1Z_{11}(40/120)=(49.8\underline{/1.44^\circ})(151.8\underline{/60.7^\circ})\times 40/120=1{,}177+j2{,}222\text{ volts}$$

and

$$V_{GC_1}=2{,}120+j3{,}500-1{,}177-j2{,}222=943+j1{,}278$$
$$=1591\underline{/53.6^\circ}\text{ volts}$$

Also on circuit *A-C* the voltage to ground at *B* is

$$V_{GB_2}=\mathbf{E}_{BC}-I_2Z_{22}(50/80)-I_1Z_{11}(50/120)$$

where

$$\mathbf{E}_{BC}=5{,}110\underline{/58.7^\circ}=2{,}658+j4{,}360\text{ volts}$$
$$I_2Z_{22}(50/80)=(22.7\underline{/-40.8^\circ})(108.8\underline{/56.5^\circ})\times 50/80=1{,}488+j417$$
$$I_1Z_{11}(50/120)=(49.8\underline{/1.44^\circ})(151.8\underline{/60.7^\circ})\times 50/120=161.6+j2{,}338$$

Hence

$$V_{GB_2}=2{,}658+j4{,}360-1{,}488-417-161.6-j2{,}338=1{,}008.4+j1{,}605$$
$$=1{,}898\underline{/57.9^\circ}\text{ volts}$$

The voltages to ground at the terminals of circuits *A-C* and *A-D* are assumed to be zero since the conductors are grounded through protector blocks of negligible ground resistance.

VOLTAGE DIFFERENCES BETWEEN CIRCUIT *A-D* AND *A-C*

The voltage differences between conductor groups are important since personnel may come in contact with wires of group *A-C* and *A-D* Figure 3(c) simultaneously.

The voltage difference at any point between the two conductor groups such as *A-D* and *A-C*, Figure 3(c), is equal to the vector difference between the voltage to ground on each conductor group. For study purposes it will only be necessary to compute these differences at locations where they are likely to be greatest. This will be at *B* and *C* because at *B* both group *A-C* and *A-D* have a maximum voltage to ground due to coupling and shielding discontinuity while at *C* the voltage to ground on group *A-C* is assumed zero.

The voltage difference at point $B=V_{GB_1}-V_{GB_2}$.

$$V_{GB_1}-V_{GB_2}=2{,}378\underline{/55.4^\circ}-1{,}898\underline{/57.9^\circ}$$
$$=1{,}350+j1{,}961-1{,}008.4-j1{,}605-341.6+j356=494\underline{/46.2^\circ}\text{ volts}$$

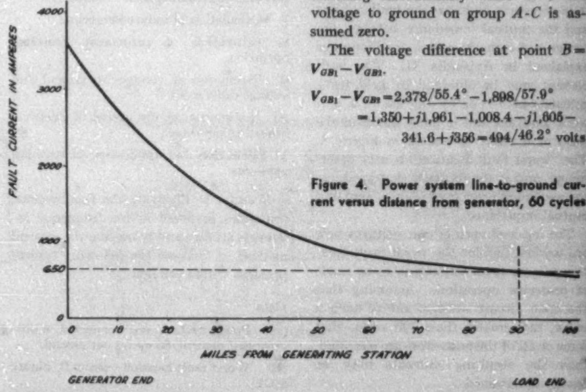

Figure 4. Power system line-to-ground current versus distance from generator, 60 cycles

The voltage difference at point $C = 1{,}591\underline{/53.6^\circ}$ volts.

The foregoing results are tabulated in Table I.

Table I

Location	Circuit	Voltage to Ground	Voltage Difference
B	A-D	$2378\underline{/55.4^\circ}$	$494\underline{/46.2^\circ}$
B	A-C	$1898\underline{/57.9^\circ}$	$494\underline{/46.2^\circ}$
C	A-D	$1591\underline{/53.6^\circ}$	$1591\underline{/53.6^\circ}$

POWER FAULT FREQUENCY AND DURATION

Information concerning the frequency and duration of power faults plays a large part in low-frequency induction studies. The higher the fault frequency and duration the greater the probability of personnel being exposed to hazardous voltages and the increased prospect of serious service interruptions. Power organizations usually keep records of fault frequencies occurring on their lines and also of fault durations.

In our example we have assumed a power line of appreciable fault frequency and duration namely 0.5 second and 10 faults per 100 miles per year.

ESTIMATION OF THE EXTENT OF ELECTRICAL HAZARD TO PERSONNEL

The probability of personnel being subjected to dangerous voltages is a difficult factor to estimate when we realize that contact must occur during the flow of abnormal ground current and that not all the fault locations are likely to produce hazardous conditions. Also, where the climbing of poles is necessary for maintenance or construction, personnel are exposed to possible voltage differences between conductor groups and even if the voltages are not high enough to cause bodily harm they may startle and cause a serious injury from falling.

Generally speaking, only the faults occurring within a particular length of power line, the length depending upon the specific problem, are effective in creating voltages likely to be excessive. A suggested criterion whose magnitude is proportional to the probability of personnel hazard may be taken as the product of the probable frequency of faults for the power exposure, the duration of the fault current and that fraction of the power line likely to produce hazardous conditions. This criterion will provide a means for comparing the relative probability of hazard between different remedial measures.

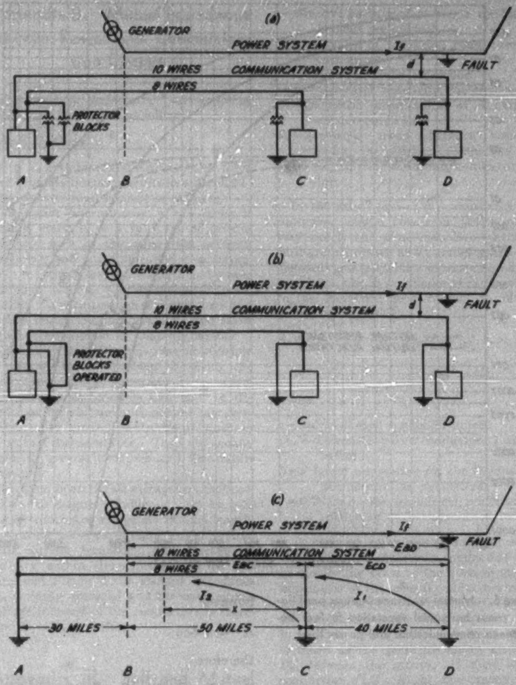

Figure 5. Low-frequency induction problem—application of short circuiting relays

In this problem, the likelihood of electrical hazard to personnel is assumed to be high, due to the excessive voltages to ground and voltage differences, the fault frequency, and the duration of the fault current.

Remedial Measures

One important remedial measure against permanent protector operation is to install short-circuiting relays of the multigrounding type at terminals *A* and *D*, Figure 5(a). This precaution, however, has no effect on the voltage to ground and voltage difference distribution in sections *A-C* and *A-D*.

To alleviate this hazard to personnel additional short-circuiting relays of the same type as at *A* should be considered for installation at *B* and *C* in order to provide a ground for all the conductors during protector operation and hence reduce the voltage to ground at these terminals to a value dependent on the resistance to ground of the short-circuiting relay installation. The voltage differences between conductor groups also will be eliminated since all conductors in a section, such as *B-C* Figure 5(b) have the same induced voltage.

The additional protection at *B* and *C* allows us to dispense with the need of short-circuiting relays at *A* insofar as permanent protector operation is concerned, since section *A-B* has no power exposure and hence no induced voltage. However, it is possible for the protector at *A* to operate before those at *B* and therefore the protectors at *A* will carry current and be exposed to possible protector operation. If this is deemed likely to happen then the short circuiting relays at *A* should remain.

The resulting currents with short circuiting relays operated at terminals *B*, *C*, and *D* are determined in a similar manner as before. In section *C-D*, Figure 5(b), the current is

$$I_1 = \frac{E_{CD}}{Z_{CD}} = \frac{4{,}080}{50.5}\,\frac{\underline{/58.7^\circ}}{\underline{/60.7^\circ}} = 81\underline{/-2.0^\circ} \text{ amperes}$$

and

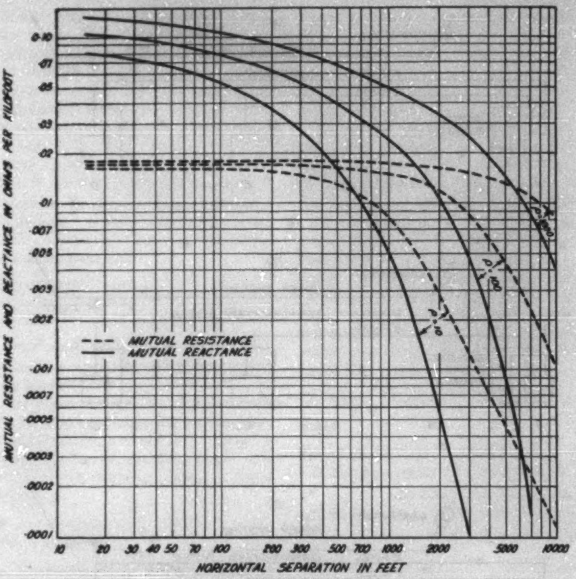

Figure 6. Mutual reactance in ohms per kilofoot versus horizontal separation in feet between communication and power lines

$$I_2 = \frac{E_{BC}}{Z_{BC}} = \frac{5,180}{55.4}\,\frac{/58.7°}{/69.8°} = 92.3\underline{/-11.1°}$$ amperes

where Z_{CD} and Z_{BC} are the self impedances of section *C-D* and *B-C* as determined in Appendix III.

The possibility of severely overloading the saturating transformers and relay contacts associated with the short circuiting relay protectors must not be overlooked. It is evident from the magnitude of I_1 and I_2 that the highest current to be handled by a saturating transformer is 92.3 amperes for 0.5 second at terminal *B*, while the highest current through a contact is 81/10 or 8.1 amperes at *C* and *D*. These values will be found to be within the operating range outlined in Appendix I.

The effect of placing short-circuiting relays of the multigrounding type at *B*, *C*, and *D* on the voltage to ground distribution is important and may be determined as follows: At a distance *X* miles from *D* in section *C-D* Figure 5(b) the voltage to ground is

$$V_{GX} = E_{CD}(X/40) - I_1 Z_{CD}(X/40)$$

however

$$I_1 = E_{CD}/Z_{CD}$$

therefore

$$V_{GX} = E_{CD}(X/40) - (E_{CD}/Z_{CD})Z_{CD}(X/40) = 0$$

Thus the voltage to ground at any point in section *C-D* and similarly in *B-C* is zero. This interesting fact is due to the voltage being uniformly induced in the communication conductors and thus consumed entirely by the resulting voltage drop in the impedance.

Table II. With Short Circuiting Relay Protection

Location	Circuit	Voltage to Ground	Voltage Difference Between Circuits
B	A-D	0	0
B	A-C	0	0
C	A-D	0	0

Table III. Without Short Circuiting Relay Protection

Location	Circuit	Voltage to Ground	Voltage Difference Between Circuits
B	A-D	$2,378\underline{/55.4°}$	$494\underline{/46.2°}$
B	A-C	$1,898\underline{/57.9°}$	$494\underline{/46.2°}$
C	A-D	$1,591\underline{/53.6°}$	$1,591\underline{/53.6°}$

With the proper selection and application of remedial measures permanent protector operation can be considerably reduced and the electrical hazard to personnel limited to tolerable values. Tables II and III show the benefits obtained with short-circuiting relay protection.

Figure 7. Geometric mean radius—A_g versus number of communication wires

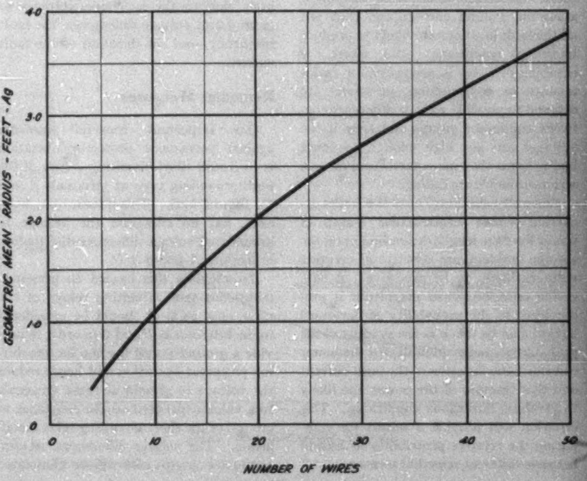

Conclusion

The methods presented here provide communication engineers with a practical means of predicting the effect of power system fault currents on communication lines. The induced voltages and resulting currents are shown to be easily calculated as illustrated by the field problem worked out in a step by step fashion. The results are analyzed and remedial measures selected and discussed.

Appendix I. Short-Circuiting Relay Protectors

Short-circuiting relay protectors[4] are employed on communication circuits where low-frequency induction is serious and the possibility of permanent protector operation is high.

There are in general two classes of short-circuiting relay protectors, namely the multigrounding type and the unit type.

The multigrounding-type relay protector is designed for group application whereby if one or more protector blocks operate then all the protector blocks on the remaining conductors in the assembly will be short circuited and brought to the same ground potential. This prevents possible potential differences from existing between various wires due to non-uniformity in protector block breakdown.

The unit-type relay, as its name implies, is designed for application to a single pair of wires, its operation placing a short circuit to ground on this pair only.

To understand the operation of the multigrounding short circuiting relay protector, shown in Figure 2(b) assume the voltage to ground on conductor 1 exceeds the breakdown voltage of the protector blocks (350 volts). This voltage will be impressed across points 1-8-5 as shown on the diagram. The resulting current flowing in coil *B* energizes coil *C* and operates relay *D*. This applies battery *E* to a closed circuit and current from *E* flows as indicated. Considering conductors 1 and 2, the potential difference between points 6 and 7 operates relay *A*. This action by-passes the induced current on the communication conductors through the path 1-9-8-5 to ground. Once coil *B* is energized all the relays such as *A* and *F* are operated, thereby placing a short circuit to ground on all protected pairs.

The contacts of the short circuiting relays Figure 2(b) are of special design to prevent their fusing together under heavy discharge currents. Tests have shown that 100 amperes may be carried safely for 2.5 seconds.

The master relay, *D*, Figure 2(b) will operate when approximately one ampere or more flows in the primary of the saturating transformer at 60 cycles. This can be adjusted to release when the current falls to below about 0.8 ampere.

The saturating transformer is designed to provide a safe range of voltages applied across the winding of the master relay for a wide range of current in the primary. The transformer will carry about 500 amperes for 10 seconds without overheating.

Appendix II. Mutual Impedance Between Power and Communication Circuits

The mutual impedance[5,6] or coupling factor may be defined as follows:

$$Z_m = E_c/I_f \text{ ohms}$$

where E_c is the induced electromotive force in the communication circuits in volts and I_f is the ground fault current in amperes.

The exact determination of this factor is difficult since it is a function of several variables such as the separation between the power and communication conductors, earth resistivity, exposure length and power system frequency. Curves such as Figure 6 relating Z_m with a range of separations and ground resistivities are available and allow rapid determination of coupling factors.

The earth resistivity[5,6] is a factor of prime importance in any problem involving the earth conduction of currents. It is usually expressed in meter-ohms and may be determined by voltage and current measurements using ground electrodes at spacings of up to a thousand feet. Tests are usually made at several locations and the results averaged.

Induced open circuit voltages on conductors due to magnetic induction may be estimated from a knowledge of exposure length, separation between circuits, power system fault current, frequency, and average resistivity within the exposure. With this data and Figure 6 the mutual impedance E_m is easily obtained and the open circuit voltage induced in the conductors is therefore $E_C = Z_m I_f$ volts.

Appendix III. Self and Mutual Impedance of Communication Conductors

For purposes of calculation, it is useful to represent the power and communications systems by equivalent single conductors.

In our low-frequency induction problem we are concerned with two groups of conductors namely the *A-D* group containing ten wires and the *A-C* group containing eight wires.

The self impedance of a circuit composed of n similar conductors in parallel is:

$$Z_{11} = r/n + (0.28)\times 10^{-3}\times f + j(0.882)\times 10^{-3}\times f\times \log_{10}\frac{2{,}280}{D_g\sqrt{\frac{f}{\rho}}} \text{ ohms per kilofoot} \quad (1)$$

The mutual impedance between two circuits composed of n conductors and m conductors respectively is:

$$Z_{12} = (0.28)\times 10^{-3}\times f + j(0.882)\times 10^{-3}\times f\times \log_{10}\frac{2{,}280}{D_g\sqrt{\frac{f}{\rho}}} \text{ ohms per kilofoot} \quad (2)$$

where

r = effective resistance of single conductor in ohms per kilofoot
m, n = number of paralleled conductors in each group
f = frequency in cycles per second
ρ = average earth resistivity, meter-ohms
A_g = geometric mean radius of n parallel conductors in feet
D_g = geometric mean distance between $n(1,2\ldots m)$ shielding conductors and $m(1,2\ldots m)$ disturbing conductors in feet

In the calculation of self impedance the equivalent single conductor which offers very nearly the same inductive reactance with ground return as a parallel group of n identical and not widely separated conductors $(1,2,3\ldots n)$ is a cylinder of radius equal to the geometric mean radius, A_g, of the group, see Figure 7.

$$A_g = [(pa)^n D_{12}^2 D_{13}^2 \ldots D_{1n}^2 D_{23}^2 D_{24}^2 \ldots \times D_{2n}^2 \ldots (D_{n-1,n})^2]^{\frac{1}{n^2}}$$

where

a = radius of each conductor in feet
D_{1n} = distance between conductors 1 and n in feet
p = a factor accounting for the internal inductance of the conductors
= 0.78 for a solid, cylindrical, nonmagnetic conductor

In order that the mutual impedance between the two equivalent conductors shall be closely the same as the average mutual impedance of the several conductors in the two groups which they represent, such as ten conductors in the one group and eight in another, see Figure 3(c), their separation is taken as the geometric mean distance, D_g, between the groups. If there are n conductors $(1,2\ldots n)$ in one group and $m(a,b\ldots m)$ in the other:

$$D_g = [D_{1a}D_{2a}\ldots D_{na}D_{1b}\ldots D_{nb}\ldots\ldots D_{nm}]^{\frac{1}{nm}}$$

where

$D_{nm} = \sqrt{(h_n - h_m)^2 - x^2}$ = radial separation of conductors n and m in feet

h_n, h_m = heights of conductors n and m in feet
x = horizontal separation of conductors n and m in feet

In our problem for circuit *A-D* and *A-C* we have

r = 1 ohm per kilofoot, resistance of 104-mil diameter copper
f = 60 cycles per second
ρ = 1,000 meter-ohms
A_g = 1.1 for $n = 10$, circuit *A-D*, and 0.82 for $n = 8$, circuit *A-C*
D_g = assumed to be 4 feet for circuit *A-D* and *A-C*

By substituting the above values in equations 1 and 2 we have,

Z_{11} per kilofoot = $0.239\underline{/60.7^\circ}$ ohms for circuit *A-D*
Z_{22} per kilofoot = $0.257\underline{/56.5^\circ}$ ohms for circuit *A-C*
Z_{12} per kilofoot = $0.1782\underline{/84.6^\circ}$ ohms for circuits *A-D* and *A-C*

Hence for circuit *A-D*, 120 miles long, the self impedance is

$$Z_{11}=120\times 5.28\times 0.239\underline{/60.7^\circ}=151.8\underline{/60.7^\circ}\ \text{ohms}$$

For circuit *A-C*, 80 miles long, the self impedance is

$$Z_{22}=80\times 5.28\times 0.257\underline{/56.6^\circ}=108.8\underline{/86.5^\circ}\ \text{ohms}$$

The mutual impedance for circuits *A-D* and *A-C* is

$$Z_{12}=80\times 5.28\times 0.1782\underline{/84.6^\circ}=75.2\underline{/84.6^\circ}\ \text{ohms}$$

For the condition of short circuiting relays at *B*, *C*, and *D*, Figure 5(b), we have

$r=1$ ohm per kilofoot; resistance of 104-mil diameter copper
$f=60$ cycles per second
$\rho=1000$ meter-ohms
$A_g=1.1$ for $n=10$, circuit *C-D*, and 1.8 for $n=18$, circuit *B-C*
$D_g=$ assumed to be 4 feet for both circuits

Again substituting in equations 1 and 2 we have

Z_{11} per kilofoot $=0.239\underline{/60.7^\circ}$ ohms for circuit *C-D*
Z_{22} per kilofoot $=0.210\underline{/69.8^\circ}$ ohms for circuit *B-C*

Hence for circuit *C-D*, 40 miles long, the self impedance is

$$Z_{11}=40\times 5.28\times 0.239\underline{/60.7^\circ}=50.5\underline{/60.7^\circ}\ \text{ohms}$$

And for circuit *B-C*, 50 miles long, the self impedance is

$$Z_{22}=50\times 5.28\times 0.210\underline{/69.8^\circ}=55.4\underline{/69.8^\circ}\ \text{ohms}$$

Appendix IV. The Effect of Coupling Discontinuities on the Voltage to Ground

Figure 3(c) illustrates a severe case of coupling discontinuity at point *B*. It will be shown that the voltage to ground in circuit *A-C* has a maximum at *B*.

Let *X* be any distance measured from *C* in section *B-C*. The voltage to ground at *X* is

$$V_{GX}=I_fZ_m\times X-I_2\times Z_{22}\times X-I_1Z_{12}X \qquad (3)$$

In section *A-B* the voltage to ground at *X*, $B\text{-}C<X<A\text{-}C$, is

$$V_{GX}=I_f\times Z_m\times BC-I_2\times Z_{22}\times X-I_1\times Z_{12}\times X \qquad (4)$$

Assuming that the above equations are linear in section *A-B* and *A-C* then their common point of intersection is the maximum voltage to ground for section *A-C*. At the point of intersection

$$I_fZ_mX-I_2X_{22}X-I_1Z_{12}X=I_fZ_mBC-I_2Z_{22}X-I_1Z_{12}X$$

from which $X=BC$. Therefore, at the point of coupling discontinuity *B* the voltage to ground is a maximum. This concept is a valuable aid in deciding at what locations the voltage to ground should be evaluated.

References

1. Inductive Interference Between Electric Power and Communication Circuits. Railroad Commission of the State of California, April 1919.

2. Coupling Factors for Ground Return Circuits, *Report Number 14*, Joint Subcommittee on Development and Research of the Edison Electric Institute and the Bell System (New York, N. Y.).

3. Shielding of Ground Return Circuits at Low Frequencies. *Report Number 26*, Joint Subcommittee on Development and Research of the Edison Electric Institute and the Bell System (New York, N. Y.).

4. Short Circuiting Relay Protectors, *Report Number 41*, Joint Subcommittee on Development and Research of the Edison Electric Institute and the Bell System (New York, N. Y.).

5. Earth Conduction Effects in Transmission Systems, **E. D. Sunde.** D. Van Nostrand Company Inc., New York, N. Y.

6. Earth Resistivity and Geological Structure, **R. H. Card.** *Bell System Technical Journal* (New York, N. Y.), 1936, volume XV, pages 167–71.

7. Status of Joint Development and Research on Noise Frequency Induction, **H. L. Willis, O. B. Blackwell.** *Bell System Technical Journal* (New York, N. Y.), April 1931, volume X, pages 184–205.

8. Status of Joint Development and Research on Low Frequency Induction, **R. N. Conwell, H. S. Warren.** *AIEE Transactions*, volume 50, 1931, pages 458–69.

9. Power Distribution and Telephone Circuits—Inductive and Physical Relations, **H. M. Trueblood, D. F. Cone.** *AIEE Transactions*, volume 44, 1925, pages 1052–64.

10. Circuit Analysis of A-C Power Systems. **Edith Clarke.** John Wiley and Sons, New York, N. Y., volumes 1 and 2.

11. Method of Symmetrical Components Applied to the Solution of Polyphase Networks, **C. L. Fortescue.** *AIEE Transactions*, 1918, volume 37, pages 1027–15.

12. Communication Networks, **Guillemin.** John Wiley and Sons, New York, N. Y.

13. Alternating Current Circuits, **Kerchner, Corcoran.** John Wiley and Sons, New York, N. Y.

14. Advanced Algebra, **Hawkes.** Ginn and Company, Boston, Mass.

15. Advanced Mathematics for Engineers and Physicists, **I. S. and E. S. Sokolnikoff,** McGraw-Hill Book Company, New York, N. Y.

16. Co-ordination of Power and Communication Circuits for Low Frequency Induction, **J. O'R. Coleman, H. M. Trueblood.** *AIEE Transactions*, volume 59, 1940, pages 403–11.

17. Power System Fault Control, **AIEE Committee Report.** *AIEE Transactions*, volume 70, part I, 1951, pages 410–17.

No Discussion

British Developments and Applications of Carrier Current Principles for Operating Requirements of Power Utilities

W. D. GOODMAN
NONMEMBER AIEE

Synopsis: Details are given of a wide-band coupling equipment for carrier current working with reasons for preferring inter-phase coupling followed by an investigation into the causes of noise on power line carrier circuits and the reasons for the adoption of single side-band equipment. Recent types of British communications and relaying equipment are then described.

THE EFFICIENT operation of modern interconnected high-voltage power networks with centralized control rooms demands that the power network shall be paralleled by a reliable and comprehensive communications network which provides facilities for telephony, supervisory control and indication, remote metering, and teleprinters. Where the distances involved are greater than about 20 miles, especially with lines of 66 kv and over, it is often found that these facilities together with feeder protection and intertripping can be most economically provided by means of carrier current equipment over the high-voltage lines. Such a communication network, with well-designed and constructed terminal equipment, is fundamentally as reliable as the power network it is used to control and with careful planning the loss of any line or circuit can be covered by the provision of alternative routes. Further, the whole of the equipment used is under the control of the power company and reliance does not have to be placed on circuits rented from other administrations.

The various components of such a network will now be dealt with in detail.

Lines and Coupling Equipment

The power lines are designed and constructed solely for the transmission of power at high voltages and low frequencies and their use for carrier current communication and protection is purely incidental. The design does, however, provide a circuit with a lower attenuation per unit length than that of most aerial telephone lines. The following important differences should, however, be noted. Where more than one telephone pair is run on the same route the wires are carefully transposed to avoid crosstalk between the circuits whereas with power lines the transpositions, inserted with no regard to communication requirements, are often more of an embarrassment than a help. They are inserted at intervals which are large compared with the wave length of the carrier frequencies used and cause reflections which produce small peaks in the attenuation-frequency characteristic. Another difference is that the considerably increased spacing of the conductors of the power line results in increased radiation. Whether phase-to-phase or phase-to-ground coupling is used there are phase wires which are unused for high-frequency transmission. These wires are closely coupled to the carrier circuit and from the crosstalk point of view tend to nullify the effect of any trap coils used. This will be referred to again later. A further point is that power lines normally terminate on bus bars and often transformers as well, which have an appreciable impedance, normally negative, to high frequencies. If these components are common to more than one line the common impedance is a source of coupling which will further modify the effect of the line traps. It should be noted also that this station capacity can cause the line traps to series resonate at some frequency below antiresonance.

In Britain phase-to-phase coupling to the power line has been adopted, in spite of the fact that it is more expensive than phase-to-ground coupling, for the following reasons.

1. The attenuation is less at any given frequency.
2. The variation of attenuation with changing weather conditions is less.
3. The radiation from the line is less.
4. There is less pickup of interference which results in an improved signal to noise ratio.
5. A phase-to-earth fault close to the transmitting end does not result in loss of signal at the receiving end.

The older types of coupling equipment were designed to pass either one or two bands of frequencies each about 6-kc wide. In coupling equipment of this type the line traps were regarded as a high impedance to prevent high-frequency energy being dissipated in the local switch gear and also to prevent changing switching conditions affecting the high-frequency circuit. They also were regarded as a means of minimizing crosstalk between circuits using the same frequency. Their efficiency from the crosstalk point of view is doubtful, due partly to the presence of the third phase wire. Using two sets of coupling equipment of this type tuned to the same frequency, crosstalk figures of 20 decibels have been measured between

---

Paper 51-244, recommended by the AIEE Carrier Current Committee and approved by the AIEE Technical Program Committee for presentation at the AIEE Summer General Meeting, Toronto, Ont., Canada, June 25–29, 1951. Manuscript submitted March 27, 1951; made available for printing May 14, 1951.

W. D. Goodman is with the General Electric Company Limited of England, Coventry, Warwickshire, England.

The author's thanks are due to the General Electric Co., Ltd. of England and to A. Reyrolle and Company Limited, and to his colleagues who have assisted in the preparation of this paper.

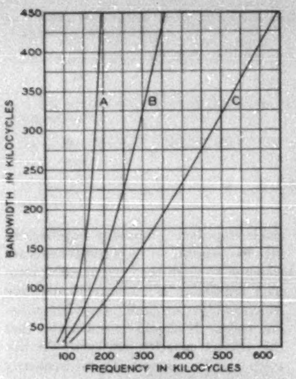

Figure 1. Curves showing variations of coupling filter bandwidth with frequency

Curves A and C are lower and upper limits of pass band. Curve B is tuning frequency

two feeders entering a substation from opposite directions and not connected to the same bus bars. This type of coupling equipment used the expensive line traps and coupling capacitors in a very inefficient manner and did not permit the use of multichannel carrier systems. As a result wide band coupling was developed in Britain which enables a frequency band, in some cases several hundred kilocycles wide, to be passed. The band width passed depends on the frequencies used. The curves in Figure 1 show how the band width obtained varies with frequency. This coupling equipment uses line traps with an inductance of 200 microhenrys and coupling capacitors of 0.002 microfarad. A further advantage of this coupling equipment is that no adjustment whatever is required on site as all the components are pretuned in the factory.

In this type of coupling equipment the line traps are regarded not primarily as traps but as elements of a band pass filter. Used thus, they guard against the variations of line attenuation with switching conditions but are less efficient with regard to crosstalk except at frequencies near the middle of the band. Crosstalk can however easily be guarded against by planning a network as a whole and not using the same frequency more than once in any one substation. Judging from the figures given in the preceding paragraph this is desirable even with the older type of coupling equipment. Figure 2 shows a typical attenuation frequency characteristic using the modern British type of coupling equipment with phase-to-phase working on a line 65 miles long under different switching conditions. The wide-band type of coupling equipment has a loss of approximately 1.5 decibels which is substantially constant over the band. This figure excludes the attenuation in the coaxial cable used to connect the coupling filter to the terminal equipment. Standard layouts of the coupling equipment in a switching station are preferred as by this means any stray capacities can be controlled, thus giving a more stable and constant performance. As with other types of line coupling equipment the coupling capacitors are capable of providing potential supplies for metering and relaying up to a burden of 150-volt amperes.

Power surges and lightning are both capable of providing impulses of very high voltages which the coupling equipment must be able to withstand. In some of the older types of equipment, fuses and gas discharge tubes were used to protect the equipment but the use of carrier relaying equipment means that the equipment must be fully operative immediately after such disturbances and the above devices are therefore unacceptable. The coupling equipment is therefore designed to withstand any impulse voltages that can reasonably be expected. Surge diverters incorporating spark gaps and nonlinear resistors are fitted in the line traps.

Although coupling equipment for any desired mid-band frequency can be made, in practice several standard bands have been selected to give adequate frequency coverage. Whenever possible all the coupling equipment on any power network is for the same band, this giving the advantage that a minimum of spare equipment need be stocked for use in case of breakdown, as all components throughout the network are interchangeable.

It is well known that variations in weather conditions cause variations in the attenuation of overhead lines. Measurements made in Great Britain tend to show that for the relatively short lines involved (up to 100 miles), and excluding the condition of the deposition of solid ice on the line, the variations to be expected only amount to a few decibels which would not seriously degrade a good quality telephone circuit. Turning now to the case of the deposition of solid ice on the conductors, which fortunately is rare in Great Britain, the attenuation rise is so considerable, possibly as much as eight times, that if it occurred over any appreciable length of line the signal to noise ratio would be reduced to such an extent as to make the circuit unusable. Because of this and the fact that experience over the last 20 years has provided no evidence of breakdown in Britain from this cause, automatic gain control does not appear to offer any appreciable advantages. Cases have been recorded when power line carrier circuits without automatic gain control have remained in operation when all other means of communication with power stations have broken down because of adverse weather conditions.

Communications Equipment

In the past most power line carrier communications equipment was of the amplitude-modulated (a-m) type which transmitted carrier and 2 side bands. These circuits, although they provided reasonable communication circuits, compared very unfavourably with modern long distance telephone circuits from the point of view of quality and signal-to-noise ratio, and further usually provided for the alternative, and not the simultaneous, transmission of speech and signaling (supervisory control, teleprinter working and so on) facilities required by power utilities.

In order to appreciate the reasons for the choice of single side-band carrier sup-

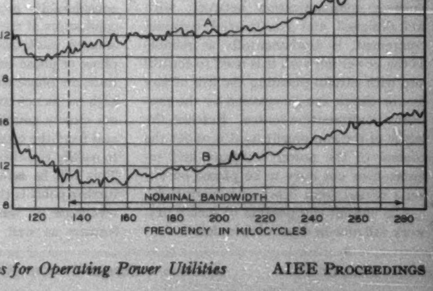

Figure 2. Insertion loss-frequency characteristic of 110 kv line 65 miles long using wide-band coupling equipment

Curve A with line earthed and curve B with line isolated pressed (s.s.b.) carrier equipment in Great Britain as the most suitable for power line carrier working, it is necessary to discuss briefly the causes of noise on power line carrier circuits. This noise may be divided into two types which will be called generated noise and induced noise. The first type is caused by the fact that on any energized power line, particularly in bad weather, innumerable leakage paths are continually forming over the insulators and being broken down by the high voltage on the line. These together with corona discharge act as rectifiers and modulate the carrier or any other high-frequency signal transmitted over the line. It will be clear that there will be no improvement in the signal to noise ratio due to generated noise if the high-frequency power transmitted to line is increased. On the other hand, if a suppressed carrier system is used, the absence of signals during silent periods avoids background noise due to modulation of the carrier. Hence it is an advantage to suppress the carrier. The second type of noise, induced noise, is wide-band noise caused by corona, insulator spitting, static and pickup from other energized lines and radio stations. This noise is directly proportional to the band width occupied by the signal. In this case, increasing the high-frequency power transmitted will improve the signal to noise ratio. Considering now a-m carrier systems it will be seen that these systems occupy twice as much frequency space as the original unmodulated audio-frequency band, and further they transmit a carrier frequency which is of no use in conveying intelligence. Both of these factors make the a-m system bad from the signal-to-noise ratio point of view.

Turning now to the possible alternatives to a-m, frequency modulation (f-m) at first sight appears to be an ideal solution. In this system the carrier is modulated with respect to frequency instead of amplitude, and any incidental amplitude modulation is eliminated by the use of limiters in the receiver. This type of modulation does however require a high deviation ratio to obtain a distortion-free circuit, and occupies a large amount of the available frequency spectrum. As the deviation ratio is decreased the signal to noise ratio also decreases and nonlinear distortion increases. It can be shown that to obtain an improvement in the signal-to-noise ratio of about 10 decibels over the equivalent a-m system a deviation ratio of about two is needed. Thus to obtain a 10-decibel improvement an audio band extending up to 4,000 cycles per second would require a bandwidth more than 16-kc wide for its transmission.

The second alternative to an a-m system is the s.s.b. system with carrier suppressed. This system is equivalent to translating the audio frequencies directly to the high frequency without the addition of carrier. It is a system on which considerable development work has been done over the last 20 years for use in long distance carrier telephone circuits. It can be calculated that compared with an a-m system the s.s.b. system gives an improvement of about 9 decibels in the signal-to-noise ratio for similar radiation from the line, and at the same time occupies only half the space in the frequency spectrum. The following figures show the order of improvement in signal-to-noise ratio to be expected in practice by using s.s.b. equipment instead of a-m equipment. The noise levels measured with a weighted psophometer at a zero level point on a typical a-m system working with interphase coupling on a 132-kv line 90 miles long were 2.5 millivolts with no carrier (induced noise) and 18.0 millivolts when carrier was being transmitted from the distant end (generated noise) with average weather conditions rising to 38.0 millivolts with rain and mist all along the line. The corresponding figures measured on the s.s.b. system to be described later were 0.75 millivolt under average weather conditions and 2.2 millivolts with rain and mist all along the line.

Considering now the relative merits of f-m and s.s.b. systems giving similar performance it is felt that the following factors weigh heavily in favour of the s.s.b. system:

1. The advantage of economy of frequency space.
2. Ease of maintenance.
3. It is easy to add superaudio signaling circuits, completely independent of the speech, but with an f-m system it is difficult to maintain a constant deviation ratio of 2-to-1 when transmitting a varying number of signals up to say eight independently.
4. Improved secrecy. Any signal radiated from the power line cannot be readily received on a normal domestic radio set because of the absence of carrier.
5. It is simpler to construct a flexible multicircuit s.s.b. system than it is to construct a flexible multicircuit f-m system. Such systems now are required to meet the needs of the control engineers of modern power systems.

On the older types of carrier equipment all frequency dependent equipment was made fully adjustable and the setting-up procedure often involved the selection of the most suitable operating frequency. This frequency adjustment was in the main made necessary by the lack of knowledge about coupling equipment. The present British wide-band coupling equipment makes it possible to decide the operating frequencies accurately in advance and provide s.s.b. terminal equipment without variable tuning. This equipment is built in conformity with modern carrier telephone technique instead of using radio technique as was previously done and is capable of providing power line carrier circuits which meet or closely approach the Comité Consultatif International des Communication Téléphoniques à Grande Distance requirements for long distance telephone circuits.

It will be appreciated that as, from the telephonic point of view, the power line is fundamentally a 2-wire circuit different frequencies must be used in the two directions of transmission in order to obtain full duplex operation. Two single side-band suppressed carrier systems with the development of which the author has been closely associated now will be described.

In both systems the basic audio-frequency band has been extended from the usual upper limit to 4,000 cycles per second. The subdivision of the band 300 to 4,000 cycles per second is as follows: 300 to 2,700 cycles is used for speech, a frequency of 3,060 cycles for telephone calling, the frequencies 3,300, 3,420, 3,540, 3,660, 3,780, and 3,900 cycles are used for independent signaling channels over which supervisory control and indication, remote metering, and teleprinter may be operated.

Any or all of these channels may be equipped either initially or at a later date. If it is desired to use an impulsing rate of greater than 40 impulses per second this can be done by using only 3 channels at 240 cycles spacing. The superaudio frequency of 3,060 cycles has been used for telephone calling to enable it to be kept on during speech for supervision of calls between automatic exchanges.

Another similarity between the two systems is that both have been designed to operate with 4-wire telephones. Owing to the complete absence of side tone, this type of telephone gives a considerable advantage when used in noisy situations. Both systems can, of course, be used with a normal 2-wire telephone by fitting a suitable 2-wire to 4-wire termination To cater for automatic operation with 4-wire telephones a 4-wire private automatic exchange also is available. A special feature of the 4-wire exchange is that it provides for the switching of the 3,060 cycle signaling tone in addition to

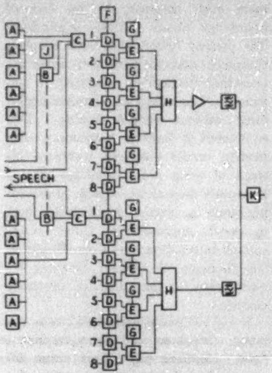

Figure 3. Block schematic of 8 circuit communications equipment

A—signaling equipment, B—ringing equipment, C—audio combining filter, D—first modem, E—second modem, F—12-kc oscillator, G—carrier oscillator, H—combining transformers, J—3,060-cycle oscillator, K—cable termination

the speech. The advantage of this facility is that on a call which is routed over several carrier circuits connected together by automatic exchanges the impulsing is carried out in each case by the original impulsed tone instead of by signals that have been regenerated at each exchange. The average impulse distortion using this method is usually less than with the repetition of impulses at each station. With impulse repetition the impulse distortion is variable depending on relay adjustment and can be increased greatly by the maladjustment of a single relay. With the other method however, although some distortion is introduced by each filter this is a fixed quantity that is not influenced by the quality of the maintenance carried out on the equipment. As an example of the impulse distortion to be expected using this method, a signal having an initial impulse ratio of 50-to-50 had a ratio of 45-to-55 after detection following the transmission over 8 carrier circuits in tandem.

The first system to be described is a multicircuit system which has been designed for maximum flexibility to allow any number of circuits to be equipped up to a maximum of eight for transmission over one feeder. Once the initial circuit or circuits have been installed further circuits easily can be added later up to the maximum of eight and within the system planning requirements mentioned earlier.

Figure 3 shows in simplified block schematic form an 8-circuit terminal. For clarity only channel 1 is terminated fully.

In order to provide maximum flexibility and simplicity of filter design double modulation is used. The eight 4,000 cycle audio bands are all used to modulate a 12 kc carrier, balanced metal rectifier modulators being employed. The appropriate side band 8 to 12 kc or 12 to 16 kc then is selected by a good coil and condenser filter. In the case of the odd numbered channels 1, 3, 5, and 7 the lower sideband 8 to 12 kc is selected, while the upper sideband 12 to 16 kc is selected for the even numbered channels 2, 4, 6, and 8. Then the selected sidebands of channels 1 and 2 are combined to form a subgroup containing 2 channels in the band 8 to 16 kc. Channels 3 and 4, 5 and 6, 7, and 8 also are combined in a similar manner, thus forming 4 subgroups each with a band 8 to 16 kc. In the second modulators each of these groups is used to modulate a carrier, whose frequency is chosen to translate the subgroup to the desired position in the frequency spectrum. The required sideband is selected by means of a simple coil and condenser filter. This filter can be kept fairly simple and at the same time minimize crosstalk by choosing the second carrier frequencies so that in each case the unwanted sidebands do not occupy the same frequencies as the wanted sidebands of other subgroups. After the second modulators the subgroups are brought together by the combining transformers to form a band 32 kc wide. This band is then amplified and after passing through the directional filters, which separate the transmit and receive frequency bands, is transmitted to line via the coaxial cable and wide-band coupling equipment. The receiving portion of the equipment is the reverse of the transmit portion except that there are no high-frequency amplifiers. Amplification and equalization are carried out at audio frequency before the audio band is split into its component parts. It should be noted that for flexibility first and second modulators and carrier oscillators need be equipped only for the circuits actually required. Extensions can, however, be carried out easily at a later date. Another feature is that a "through" circuit at any station need not be reduced to audio frequency but can be selected from the other circuits at intermediate frequency and after remodulation with a carrier frequency be retransmitted to line.

For reliability the oscillators and amplifiers which serve all circuits are provided in duplicate with automatic changeover. This applies to the 12 kc oscillator, the 3,060-cycle telephone signaling oscillator and the line amplifiers. If the user considers it desirable the carrier oscillators may also be duplicated but this is not usually considered necessary. Where several systems are installed in the same station it is uneconomic to fit each with spare line amplifiers, and up to 4 systems can be served by the same spare line amplifier with automatic selection and changeover facilities.

In order to obtain the required frequency stability accurate and stable oscillators are required. The 12 kc oscillator is a temperature stabilized coil and condenser oscillator while the carrier oscillator is of the crystal type. The maximum asynchronism of 2 terminals is 5 cycles per second over an ambient temperature range of 0 degree centigrade to 40 degrees centigrade.

The high-frequency power output when sending a 1 milliwatt 800-cycle tone at a zero level point on any one channel is a quarter of a watt. This has been found to be sufficiently high to provide zero equivalent audio circuits over lines with attenuations up to about 35 decibels. Further, by the adjustment of audio attenuator pads it is possible to obtain a zero equivalent circuit with audio extensions at each end each having attenuations of up to 10 decibels. The development of low-power carrier systems in Great Britain instead of the high-power systems used in the United States and Canada is mainly due to the severe radiation restrictions imposed by the British Post Office.

The second s.s.b. system to be described is a nonextensible single circuit system. It provides exactly the same facilities and quality as a single circuit of the multicircuit system described previously but will operate over lines having attenuations up to about 40 decibels. It is a single modulation system designed for carrier frequencies of between 80 kc and 200 kc. To economize in carrier oscillators, which are again of the crystal type, the same carrier frequency is used for both directions of transmission. Provision of full duplex operation is obtained by transmitting the lower sideband in one direction and the upper sideband in the other direction. Crystal filters are used to obtain the necessary suppression of the unwanted sideband. The high-frequency transmit and receive circuits are combined for connecting to the line coupling equipment by means of a high-frequency hybrid transformer.

On both these carrier systems monitoring facilities are provided. The alarm system is comprehensive, and wherever possible functional alarms instead of tube heater or anode alarms are used. Normally two types of alarm are given, an "urgent" alarm which indicates that the system has broken down and a "non-urgent" alarm which indicates that there is a fault but that the system is still operating on duplicate equipment. These two alarms can of course be combined into a single alarm if desired.

Feeder Protection

The most recent type of carrier relaying equipment installed in Britain is of the phase comparison type. This equipment requires a different carrier frequency for each direction of transmission. The output of a sequence network, fed from the feeder current transformers, is used to modulate the carrier with a square wave of power frequency. This is transmitted to the distant end for phase comparison with the output of the sequence network there to determine whether stabilization or tripping shall take place. The operating time of this equipment is about 3 cycles. The equipment gives a stabilizing angle of about 60 degrees to allow for the normal phase change along the line and ensure system stability.

Two stage starting is employed, the first stage starting the transmission of the modulated carrier and the second stage closing an isolating contact in the trip circuit.

This is to ensure that a signal is being transmitted from each end before the trip circuit is prepared. There are two types of starting equipment available. The first is for normal use which starts the equipment operating at a preset fault setting and the second for use on feeders connected to power stations where the amount of plant on load is frequently changing. Under these conditions situations will arise where the normal load current at some times is greater than the maximum fault current at others. To avoid either the frequent adjustment of fault setting or the transmission of carrier for long periods, a type of starting equipment is used which depends on the rate of change of current in the feeder. This starting equipment will bring the protection into operation for a few seconds each time there is a sudden change of feeder current due either to a fault or to a rapid change of load.

To ensure maximum reliability of the feeder protection in cases where the wide-band coupling equipment is used to transmit both carrier relaying and communications frequencies, the coaxial cable from the coupling equipment always is terminated in the relaying equipment. The connection to the communications equipment is made through a network which ensures that no fault in or maintenance work on the communications equipment can interfere with the efficiency of the feeder protection.

For intertripping a new type of carrier intertripping equipment now is in use with an operating time of about 70 milliseconds. It can be used for either one way or bothway intertripping and is fundamentally for use on twin feeders, but can be used equally well on single feeders.

This equipment operates on a phase comparison principle and inadvertent tripping of the feeder cannot take place as a result of interference picked up by the line. At the transmitting end the output of a 40-cycle oscillator is used to modulate both of two carrier frequencies. In each case the carrier frequency is suppressed and both sidebands are transmitted to line but in one case the phase of the 40-cycle input is changed by 45 degrees before modulation occurs. At the receiving end the pairs of sidebands are selected by filters and in each case one side band is demodulated against the other producing two 80 cycle signals which differ in phase by 90 degrees. The two 80 cycle signals are combined and rectified by a network that produces voltages which are equal in magnitude and polarity across the operating coils of two polarized relays connected in series. If it is desired to send a tripping signal for one feeder the phase of the 40-cycle input to the first modulator also is changed by 45 degrees, which results in the two 80-cycle signals at the receiving end being in phase causing a current to flow through the relay coils and operating one of them. To trip the other feeder the 40-cycle input to the other modulator is changed by a further 45 degrees which results in the two 80-cycle signals at the receiving end having a phase difference of 180 degrees. This causes a current to flow in the opposite direction through the relay coils, operate the other relay and cause tripping.

As with carrier relaying, the carrier intertripping equipment can be transmitted through the same coupling equipment as communication circuits without causing interference.

Power Supplies

All the carrier current equipment mentioned previously requires the same power supplies which are direct voltages of 250 volts and 50 volts and an a-c supply for tube heaters. These are obtained conveniently from the local low tension alternating current supply by using suitable rectifiers and transformers, a standby supply being obtained from an automatic starting rotary converter driven by the station switching battery or an alternator driven by a prime mover. Although this is usually satisfactory for communication equipment where an interval of several seconds can be tolerated while the standby machine is running up to speed, it cannot be tolerated for relaying equipment where the supply failure for a short time might easily result in the failure of the protection equipment to trip a faulty feeder. In this case special maintaining equipment is used to maintain the required outputs over the interval between the failure of the mains supply and the running to speed of the standby machine.

Discussion

A. D. Blachford (The Hydro Electric Power Commission of Ontario, Toronto, Ont., Canada): The author has presented a very enlightening paper on the developments and techniques of carrier current systems employed in the British Isles. It is evident that a considerable amount of engineering and planning has been done on the problems encountered and a new approach has been made to their solution.

The unique features of broad band coupling solve many problems when the need arises for multiple carrier channels, especially in these days when we are faced with a crowded frequency spectrum and facilities for the addition of extra channels. It might be interesting for the author to explain whether the capacity of the power line or station bus alters the tuning of the band-pass filter.

The choice of voice communication equipment has been made after a thorough study of the numerous systems on hand. His choice of single-side-band suppressed carrier is substantiated by the 20 years of development work which has been spent on this subject, and it has been found ideally suited to carrier current systems where additional frequencies are scarce.

The multichannel system employs 32 kc in both directions of transmission or a total of 64 kc and the separation between these channels is 32 kc, making a total bandwidth of 96. From Figure 1 of the paper this bandwidth would require an upper and lower frequency of 225 and 125 kc respectively. Assuming that the highest frequency allocated is 200 kc, would the author explain whether it would be economically possible to decrease this separation so that the upper frequency limit does not exceed 200 kc without impairing the over-all system?

The second single side-band system described is one of a less complex nature than the multichannel system and is ideally suited for use by a power utility where a nonextensible single circuit is required. One of the main features which is desirable in a communications circuit is reliability and continuity of service. The adoption of functional monitoring facilities has eliminated the loss of a channel by failure of some component part by making use of nonurgent alarms which will alert the operators to take the necessary steps to rectify the fault, while the system continues to operate on duplicate equipment.

The phase comparison relaying systems installed in England are similar in most respects to American methods. However it is noted that separate frequencies are employed for each direction of transmission. In conclusion would the author point out why they have adopted a 2-frequency system when the need for channel space is so urgent.

W. D. Goodman: The effect of the capacity of the power lines and station bus bars on the broad band coupling filter should be considered separately. In the case of the capacity of the lines this has no appreciable effect on the tuning of the filter but will affect the line attenuation. The impedance of the station bus bars and transformers is almost invariably negative at carrier frequencies and is equivalent to inserting a capacitor in series with the line traps which has the effect of series resonating a shunt arm of the filter at some frequency below the mid-band frequency. Unless steps are taken to avoid it, this will produce a sharp attenuation peak in the lower half of the pass band. The position of the peak will depend on the capacity of the station equipment. If this capacity is greater than about 0.002 microfarad, for interphase working with 200-microhenry line traps, no peak will occur as it will be outside the pass band of the filter. Two possible methods of eliminating this undesirable peak are to install a suitable capacitor behind the line traps to make sure that the peak falls outside the pass band of the filter or to fit a simple network to the line trap to eliminate the peak.

The frequency allocation for the multicircuit communications equipment referred to by Mr. Blatchford was originally decided on for operation in Britain. The equipment was centered on 200 kc which is the frequency of Droitwich high power radio transmitter and 16 kc was allowed on either side to keep well clear of the sidebands of this transmitter thus avoiding interference. If it was required to equip eight circuits below 200 kc it would not be difficult or expensive to change the carrier frequencies and redesign the directional filters to allow, say, 16 kc or 24 kc between the two directions of transmission. This would allow an 8-circuit system to be accommodated in the coupling filter bandwidth available.

Where phase comparison relaying is used over the same feeder as multicircuit communications equipment the economy of frequency space obtained by using the same relaying frequency for both directions of transmission is not so great as it appears at first sight if filter cost also is taken into account. The duplex multicircuit communications equipment transmit one group of frequencies in each direction and the use of a single relaying frequency for both directions would mean that a high level transmitted frequency would be near a low level received frequency. In order to avoid interference difficulties between the communications and relaying equipment, especially on long lines, it would be necessary either to increase the frequency separation between the two systems or to fit more complicated and expensive filters. If the same filters were used the greater frequency separation required would result in only a small economy of frequency space.

A Study of Carrier Frequency Noise on Power Lines

Part II. Results of Field Measurements

R. C. CHEEK
MEMBER AIEE

J. D. MOYNIHAN
ASSOCIATE AIEE

A CONTINUATION of the carrier-frequency noise studies described in the companion paper,[1] this paper gives the results of a series of measurements of conducted carrier-frequency noise levels on representative power transmission lines ranging in voltage class from 23 to 230 kv. Although the number of individual sets of measurements reported herein for each voltage class is too limited to permit many general conclusions to be drawn from the results, it is felt that in view of the dearth of published information of this type, the data obtained up to this time should be presented without delay. It is believed that this information, although inconclusive in some respects, will be of considerable value in the application of carrier to power lines. Additional measurements are planned, and more data will be presented in a later paper.

All noise voltage figures given refer to noise voltage to ground on the transmission line conductors. In estimating the total attenuation of a carrier channel, it is the usual practice to include in the estimate losses in coupling equipment at both ends of the channel.[2,3] In making an estimate of the signal-to-noise ratio however, the strength of the signal on the line itself at the receiving point should be estimated and compared with the measured or estimated noise voltage at that point. Additional attenuation in the channel due to losses in coupling equipment and coaxial cable to the receiver affects signal and noise alike and hence does not change the signal-to-noise ratio.

Equipment and Procedure Used In Making Measurements

The normal setup of the equipment used in making the measurements is shown in the block diagram of Figure 1. The equipment set up at one of the test locations, is shown in Figure 2.

In each series of tests a conventional coupling capacitor was used to connect the noise measuring equipment to the line. The impedance of a coupling capacitor is low at carrier frequencies compared to the impedance of the drain coil. At 100 kc, for example, the impedance of a typical drain coil is at least 75,000 ohms, and at the same frequency the impedance of a 0.001 microfarad capacitor is approximately 1,600 ohms. Consequently it is possible to obtain, with a noise meter of high input impedance, readings of noise voltage across a conventional drain coil essentially equal to the actual noise voltage on the line. However, it was deemed advisable because of possible resonant effects in the drain coils (some of which had unknown characteristics) to calibrate the drain coil used in each series of measurements with a capacitor of the same value as the coupling capacitor, in order to check the voltage-dividing properties of the network with respect to the frequency. Noise voltages measured at various frequencies were thus corrected to actual line noise values.

When measurements were made through a coaxial cable and a conventional tuner and coupling capacitor combination, the calibration procedure described previously was of course necessary in order to correct to the actual line value the widely different readings obtained as a result of coupling capacitor and tuner resonance, and the varying load presented by the coaxial cable and other connected equipment.

The general procedure used to obtain the data was as follows:

1. After calibration of the equipment with the drain coil and coupling capacitor to be used in a particular set of tests, the peak, quasi-peak, and average noise voltages during clear weather were measured at frequent intervals throughout the power line carrier spectrum. Measurements were made only at frequencies free of interfering signals, as determined by listening tests.
2. The wave form of the noise meter output was observed at several frequencies in the spectrum and photographed. The sweep frequency and the exposure was noted so that the approximate pulse repetition rate could be determined.
3. The noise meter was set to a convenient frequency clear of interfering signals and, after recalibration with a recording instrument, was left to record quasi-peak noise continuously. The recording period was sufficiently long to include a variety of weather conditions, of which a record was kept at most test locations, and switching operations, if any were regularly performed. Calibration was checked regularly during the recording period and at its conclusion.
4. In one test the peak, quasi-peak, and average noise voltages over the carrier spectrum were rechecked during stormy weather.

Description of Locations at Which Noise Was Measured

The measurements reported in this paper were made at a total of 10 locations on six different power systems. Figure 3 gives the details of typical line construc-

---

Paper 51-245, recommended by the AIEE Carrier Current Committee and approved by the AIEE Technical Program Committee for presentation at the AIEE Summer General Meeting, Toronto, Ont., Canada, June 25–29, 1951. Manuscript submitted March 28, 1951; made available for printing May 7, 1951.

R. C. CHEEK and J. D. MOYNIHAN are with the Westinghouse Electric Corporation, East Pittsburgh, Pa.

The authors acknowledge the co-operation of the Consolidated Gas, Electric Light and Power Company of Baltimore, the Ohio Power Company, the Pennsylvania Electric Company, the Pennsylvania Water and Power Company, the United States Steel Corporation, and the West Penn Power Company in the conduct of the tests reported in this paper.

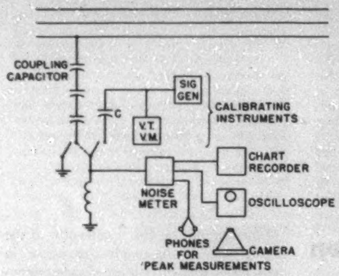

Figure 1. Block diagram of equipment used in making carrier-frequency noise studies

Capacitor C, equal in capacitance to the coupling capacitor, is used to calibrate the coupling capacitor and drain coil so that noise measured across the drain coil can be converted to actual line noise value

Figure 2 (right). Noise measuring equipment set up at a test location

The large box on the ground at the right of the noise meter is a weatherproof housing containing a second noise meter equipped with a chart recorder, used for obtaining a record of noise distribution with time. On the table beside the oscilloscope is the signal generator with built-in vacuum-tube voltmeter, used for calibration purposes

tion at each location. Locations A and B were at opposite ends of the same 31.5 mile double-circuit 132-kv line. Location A was the switchyard of a large steam generating station serving nine 132-kv lines. This location is known to be relatively noisy from the standpoint of carrier operation. Location B was the 132-kv bus of a large 132-kv switching and transformation station from which ten 132-kv lines emanate.

Location C was 18.3 miles from one end of a 67 mile 110-kv line which loops through but does not terminate in a 110/22-kv substation. Location D was the 22-kv bus of this same substation. A total of four 22-kv lines are connected to this 22-kv bus. Location E was another 22-kv bus, with four 22-kv lines, at a different substation on the same power system.

Locations F and G were on different power systems but at opposite ends of the same 50-mile 220-kv line. Location H was the 132-kv bus at a large steam generating station on a system interconnected with the system containing locations A and B. Location I was the 66-kv bus of a substation serving a large steel plant through a 4.3-mile double-circuit 66-kv line. The substation is served from a 66-kv ring surrounding a large metropolitan area. Location J was a 66-kv bus at the same generating station as location H.

General Nature of Conducted Carrier-Frequency Noise

A summary of the quasi-peak to average noise voltage ratios obtained at all locations is given in Table I for frequencies of 30, 100, and 200 kc. In all cases the ratio exceeds the figure of 1.8, which has been used as a criterion for the predominance of impulse noise.[1] In view of the narrow bandwidth of the noise meter (Stoddart *NM-10A*) used to obtain these figures, particularly at the lower end of the spectrum, these figures clearly indicate the general predominance of impulse noise over random noise on transmission lines. Higher ratios would have been obtained with a meter having a bandwidth more nearly equivalent to the usual carrier receiver bandwidths.

On most power systems, oscilloscope patterns of the voltages appearing directly across a drain coil cannot be expected to yield much significant information because of the presence of numerous carrier signals, one or more of which may exceed noise pulses in magnitude. At a few of the locations at which these tests were made, however, there were no nearby carrier channels in operation, and it was possible to obtain oscilloscope patterns of the voltage across the drain coils believed to be typical of noise alone. Voltages across the drain coils at locations D, E, and I, for example, are shown in Figure 4. The wave trains simulate the oscillations of a tuned circuit to which pulses are applied. It is possible that the drain coils themselves, responding to noise pulses with oscillations at their resonant frequencies, were primarily responsible for this effect. However, other resonances in the power systems involved may have played a part.

The 5-second exposure, Figure 4(d), indicates the more or less regular appearance of a pulse on each half-cycle of each phase voltage. In most of the observations of this type, however, it was noted that the wave train for a particular half-cycle of a single phase (presumably the phase to which the oscilloscope was coupled) predominated over the others. The predominance of this peak and the variable nature of its amplitude gave an effective pulse rate well below 60 pulses per second.

Typical of the several hundred photographs of the noise meter output obtained during these tests are those shown in Figure 5. These photographs show the a-c component of the rectified envelope appearing at the detector output in each case. The smoothing and delaying effect of the tuned circuits of the noise meter upon the pulse response is evident by comparison of Figures 4 and 5.

At some locations the noise pulses were relatively consistent and regular in amplitude and repetition rate. At others, especially in the lower voltage classifications, the pulses were so irregular both in occurrence and in amplitude that oscilloscope observation yielded little information. For example, Figures 5(a) and (b) taken at locations D and E respectively with 1/30 second exposure and sweep period, and the corresponding time exposures, Figures 5(c) and (d), indicate extreme irregularity of the pulses at these locations. Both of these were 22-kv busses. Figures 5(e) and (f) are 1/30 second exposures taken within a few seconds of each other at location I with the noise meter tuned to 200 kc. No prominent pulses occur in Figure 5(e), whereas several large peaks occur in Figure 5(f). (The extra traces in these and similar photographs in Figure 5 re-

Table I. Ratio of Quasi-Peak to Average Noise Voltage

Location	Kv	Frequency, Kc 30	100	200
A	132	2.0	4.0	4.0
B	132	2.0	2.25	2.04
C	110	4.12	5.0	5.0
D	22	2.36	2.8	2.34
E	22 (Fair Weather)	5.0	3.03	2.66
E	22 (Thunderstorm)	5.84	2.9	2.31
F	220	3.5	2.9	3.4
G	220	2.6	2.9	3.8
H	132	2.5	2.45	2.86
I	66	1.94	2.35	3.42
J	66	2.5	2.0	2.5

sulted from the persistence of the oscilloscope screen, which tended to retain previous traces to some extent.)

On the other hand, photographs of the noise meter output taken at all 110 to 220-kv locations indicate more nearly regular and consistent pulse repetition. Figure 5(g) and the corresponding time exposure, Figure 5(h) were taken at location C (110 kv) at 63 kc. These indicate the presence of a prominent pulse once each cycle of the 60-cycle frequency, such as might be caused by corona discharge at the peak of the negative half-cycle of the phase to which the instruments were coupled. Less prominent peaks are evident on the corresponding half-cycles of the other two phases. Similar photographs taken over the frequency range from 20 kc to 156 kc at this location are almost identical in appearance. All indicate that although the pulse amplitude is highly variable, the most prominent pulse occurs near the same point in the cycle. On many of the short exposures no prominent pulse is visible, indicating that on some cycles the pulse is missed completely. Similar results are indicated in Figures 5(i), (j), and (k), taken at location H (132 kv) at 100 kc. Figure 5(i) shows a prominent pulse at one point in the cycle which is practically absent in Figure 5(j) taken a few seconds later. Figure 5(k), a time exposure, shows predominance of a pulse at one particular point on each cycle and is similar to Figure 5(h) in this respect.

In Figure 5(l), the large pulse at the center of the trace appears to be predominant, but the time exposure, Figure 5(m), shows that the corresponding impulses on the other two phases were on the average almost equal in magnitude. These records were made at location A (132 kv) at 85 kc.

Records made at the two 220-kv locations (F and G) indicate regular occurrence of a pulse on one half cycle of each phase, voltage, with no particular phase strongly predominating. Figure 5(n) and (o), taken at 156 kc at location F, are representative of the records obtained at various frequencies over the carrier spectrum at both 220-kv locations.

Variation of Noise Voltage with Frequency

Curves of the peak, quasi-peak, and average noise voltages over the frequency range of 15 to 250 kc at all locations studied are shown in Figure 6. Data for these curves were taken with a Stoddart type *NM-10A* noise meter. The bandwidth of this instrument as a function of frequency is shown in Figure 7. In spite of the relatively narrower bandwidth of the meter at the lower end of the frequency range, all the curves show a general increase in noise level with decreasing frequency. This indicates that the rather general practice of reserving frequencies at the low end of the carrier spectrum for long-haul channels, to take advantage of the lower attenuation at these frequencies, may not result in as much gain with respect to signal-to-noise ratio as the attenuation figures alone would indicate, and in fact could conceivably result in a net loss.

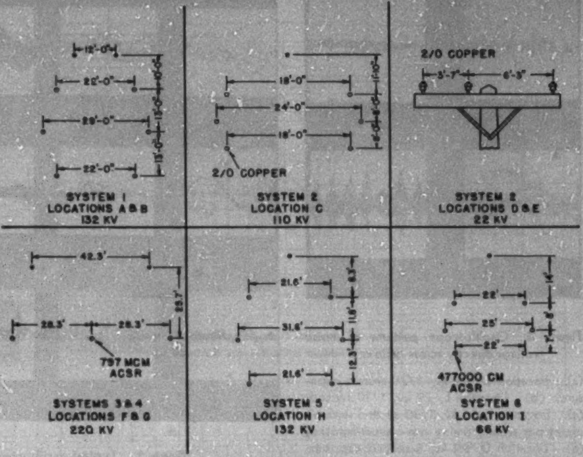

Figure 3. Details of typical line configurations at the test locations

A total of nine 66-kv lines of widely different construction emanate from location J, hence no particular configuration can be shown as typical for this location

The peaks and valleys that occur in the curves of Figure 6 are believed to be at least partly attributable to the presence of stub lines at or near the test locations, because in some cases they occur with a degree of regularity with respect to frequency. In Figure 6(b) for example, the peaks for all three types of noise are separated by intervals of almost exactly 40 kc, with the valleys halfway between. At location D, a 0.86 mile line is connected to the bus. Quarter-wave resonance of this line at 54 kc probably accounts for the extreme dip in Figure 6(d) at this frequency. If the assumption that stub lines are responsible for these effects is correct, it appears that noise is affected by such stub lines in much the same manner as signals, and that a large portion of the noise at a given location arrives from distant sources.

Figures 6(f) and (g), taken on successive days at opposite ends of a 50-mile 220-kv line, correspond closely in so far as the general noise level indicated is concerned. This suggests the possibility that noise measurements made at one point on a power system are closely indicative of the general noise level at neighboring points on the system. Although Figures 6(a) and (b) were taken from measurements made on the same 132-kv power system, the times at which the data were taken were widely separated, and hence the results are not necessarily indicative of what would have been obtained if the measurements had been made simultaneously. Figure 6(h) shows the results of measurements on an adjacent interconnected 132-kv system. These curves agree generally with Figure 6(b) but again the times of measurement were widely separated.

Variation of Noise Voltage with Time and with Weather Conditions

The dotted curves of Figure 6(e) show the results of a series of peak and average voltage measurements made during a heavy thunderstorm, as compared with the solid curves which show results of measurements made at the same location

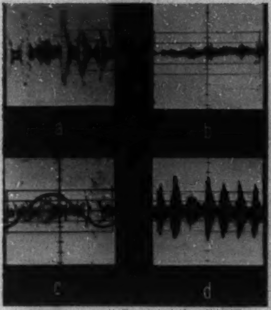

Figure 4. Oscilloscope patterns of noise voltage directly across drain coil

(a). Location D, 22 kv, 1/30-second exposure; (b). Location E, 22 kv, 1/30 second; (c). Location I, 66 kv, 1/30-second with 60 cycles per second timing wave superimposed; (d). Location D, 22 kv, 5-second exposure

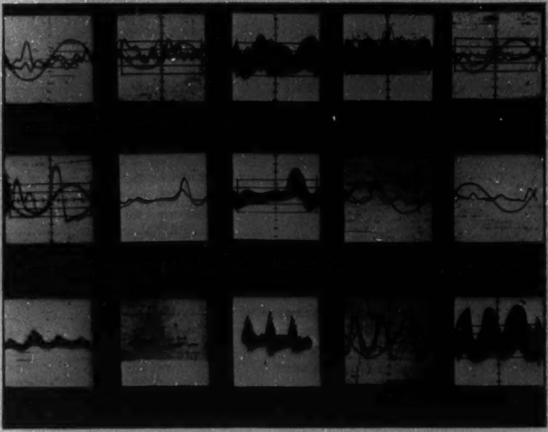

Figure 5. Typical oscilloscope patterns of noise meter output

All 1/30 second exposures were taken with 1/30-second oscilloscope sweep period and some have a 60-cycle timing wave superimposed. Extra traces result from previous sweeps. (a). location D, 22 kv, 1/30 second, 156 kc; (b). location E, 22 kv, 1/30 second, 156 kc; (c). location D, 22 kv, 5 seconds; (d). location E, 22 kv, 5 seconds; (e). location I, 66 kv 1/30 second, 200 kc; (f). location I, 66 kv, 1/30 second, 200 kc; (g). location C, 110 kv, 1/30 second, 63 kc; (h). location C, 110 kv, 5 seconds; (i). location H, 132 kv, 1/30 second (j). location H, 132 kv, 1/30 second; (k). location H, 132 kv, 3 seconds; (l). location A, 132 kv, 1/30 second; (m). location A, 132 kv, 5 seconds; (n). location F, 220 kv, 1/30 second; (o). location F, 220 kv, 3 seconds

during bright and clear weather. These measurements were made on successive days. In some portions of the spectrum the peak values during stormy weather were as much as ten times the fair-weather values. Quasi-peak readings taken during stormy weather were inconclusive because the behavior of the indicating instrument under these conditions was so extremely erratic that no definite values could be assigned to the indications. Readings of average voltage during stormy conditions followed very closely the curve taken for fair weather conditions. These results indicate that the major increase in the noise level during stormy weather resulted from the presence of extremely large impulses of entirely random occurrence. The repetition rate of these pulses was apparently too low to affect the average value of the noise response appreciably.

In an effort to determine the range of variation of noise levels over long periods of time and under a variety of weather conditions, continuous graphic recordings were made of quasi-peak noise voltage at all the locations studied. During most of these tests local records of weather conditions were kept and these were later transferred to the noise charts. A Ferris model *32A* noise meter was used in most of these tests, the majority of which were made at 156 kc. The bandwidth of this instrument at 156 kc is approximately 2,000 cycles, as compared with the 400-cycle bandwidth of the Stoddart type *NM-10A* noise meter used to obtain all the other data reported in this paper. The Ferris model *32A* instrument has a quasi-peak weighting circuit with 10-millisecond charge time as compared with the 1-millisecond charge time of the *NM-10A*, which meets the proposed new standards for noise meters.[4] A correction has therefore been applied to the data obtained with the model *32A* instrument to account for these differences.[5,6] The results can thus be compared without reference to differences between the two instruments actually used.

Typical segments of some of the chart records obtained are shown in Figure 8. Figure 8(a) is of interest because it shows a marked drop in noise level coincidental with a switch operation and restoration of the original noise level when the system returned to the previous setup. Fair weather prevailed throughout this sample record.

A marked increase in quasi-peak noise during thunderstorms is indicated by Figure 8(b), in which the chart pen continually ran off scale during thunderstorm conditions. Much lower values are indicated during subsequent light rain without thunder, however, indicating that the increase in noise level was more closely associated with lightning discharges than with rain itself.

A gradual increase in noise level with increasing cloudiness and subsequent light rain, followed by a return to lower values with clearing weather, is indicated by Figure 8(c) (location B).

In the tests at location B weather records from three additional widely separated points on the 132-kv system were examined in conjunction with the chart record of noise. It was found that rain or thunderstorm conditions reported at any one of these three points were accompanied by a marked increase in the noise recorded, even though fair weather prevailed at the recording point. This is further evidence that noise at a particular location on a power system contains

Figure 6. (On opposite and succeeding 3 pages). Peak, quasi-peak, and average noise voltage, phase-to-ground, as a function of frequency

All curves show fair-weather values except the dotted curves for location E, which show noise levels during a heavy thunderstorm

Figure 6(A)

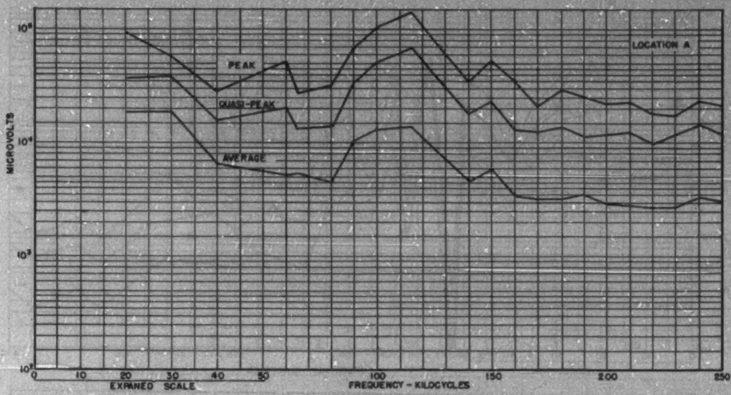

Figure 6(B)

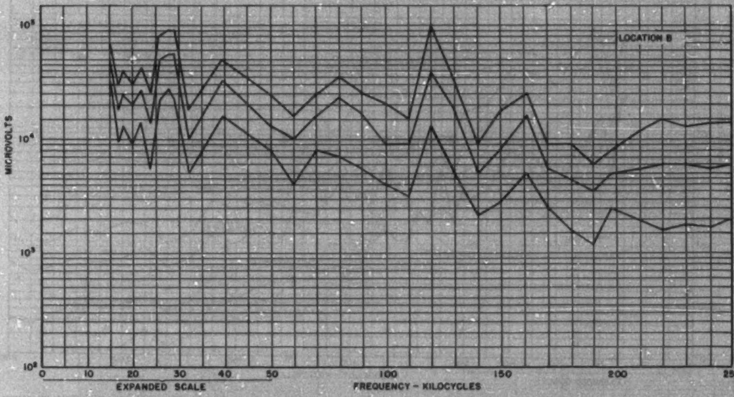

Figure 6(C)

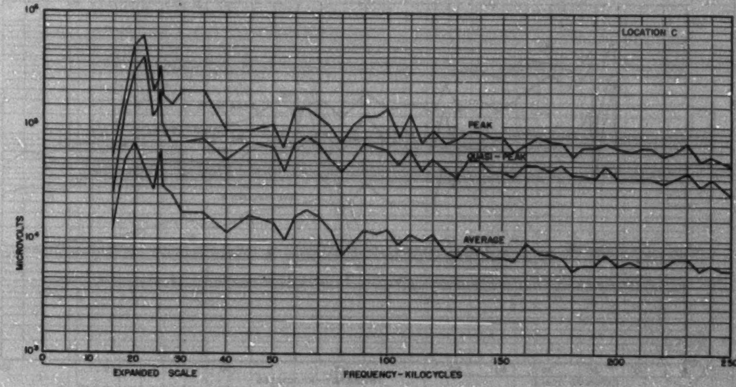

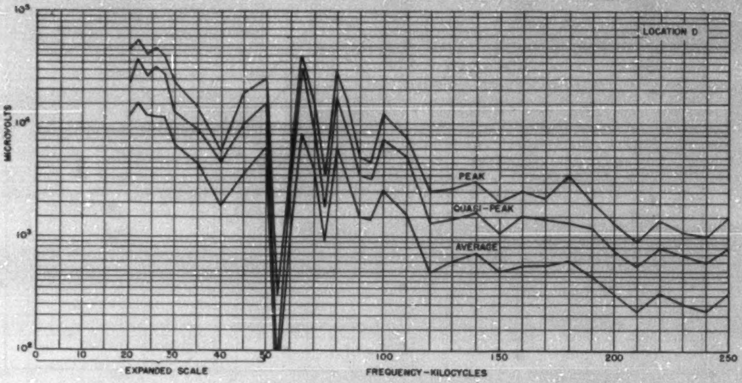

Figure 6(D)

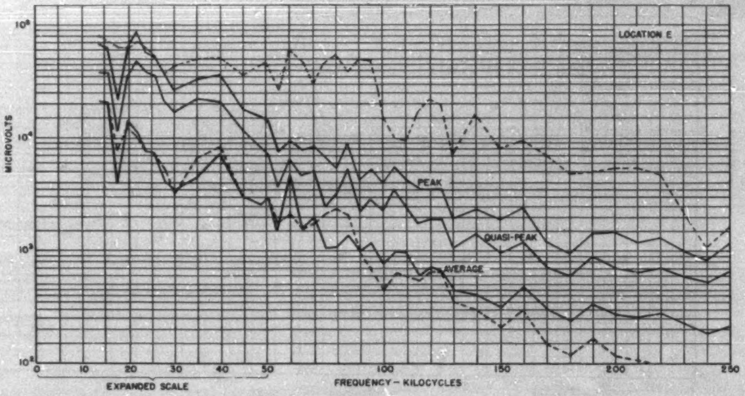

Figure 6(E)

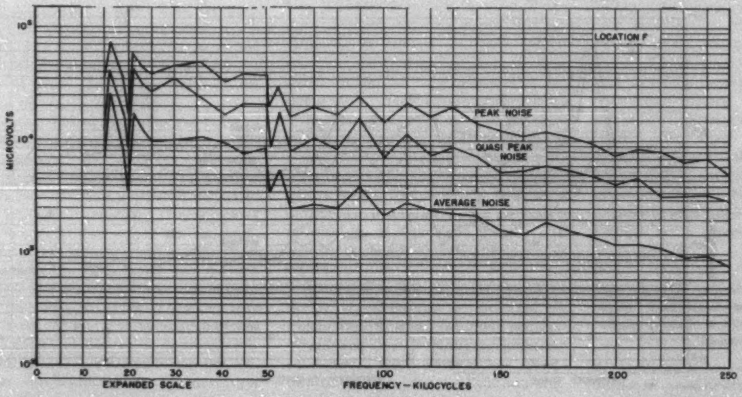

Figure 6(F)

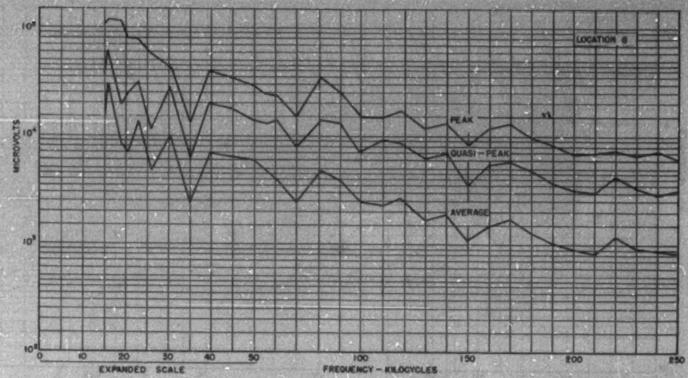

Figure 6(G)

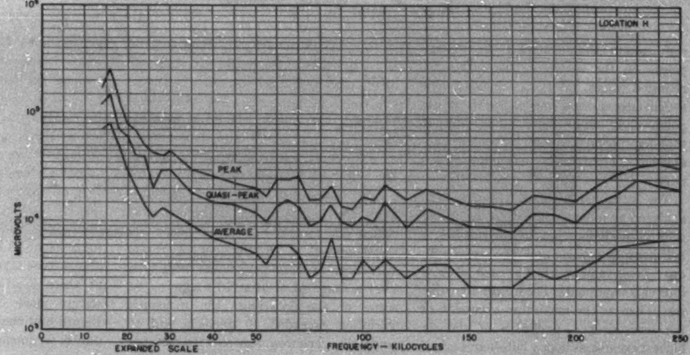

Figure 6(H)

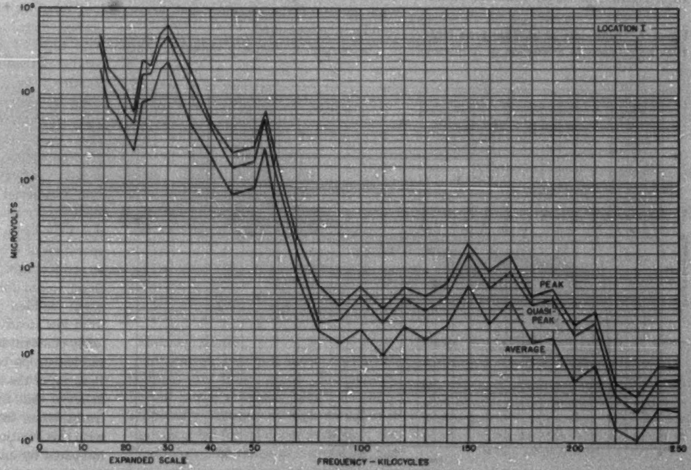

Figure 6(I)

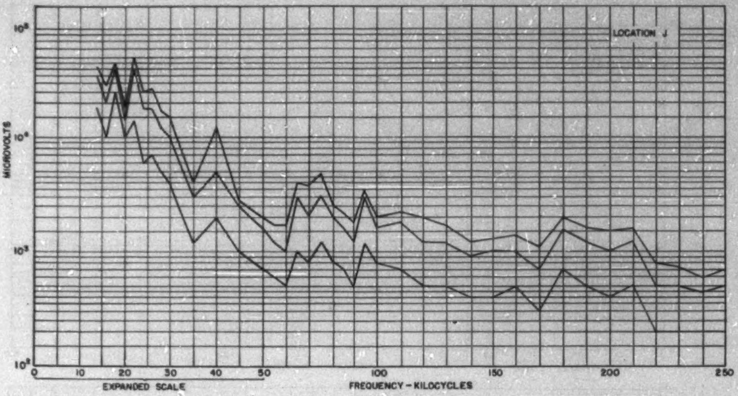

Figure 6(J)

components that originate at remote points on the system. The maximum recorded values, however, coincided with thunderstorm conditions at the recording point. Fog and light rain without thunder appeared to coincide with noticeable but not extreme increases in recorded noise.

The continuous chart records were analyzed as follows: The total recording time at each location was divided into half-hour intervals, and the maximum quasi-peak value reached in each of these intervals was noted. The maximum value was taken as the maximum excursion of the recorder pen, exclusive of the six highest excursions in any half-hour period. High isolated peaks of relatively infrequent occurrence were thus eliminated, on the basis that these would not seriously affect carrier channel operation in any of the usual applications. The number of time intervals during which the noise exceeded specific values was then plotted as a percentage of the total number of time intervals for each test.

Figure 7. Bandwidth of Stoddart type NM-10A noise meter as a function of frequency

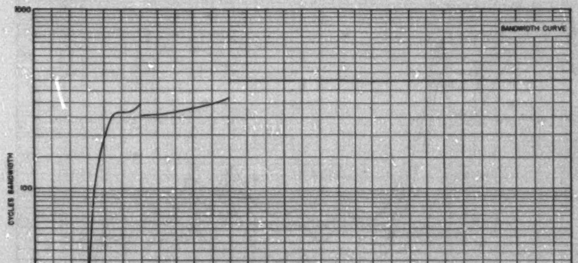

The results of the analysis of the quasi-peak records are shown in Figure 9, in which the curves for all the tests are superimposed. All the curves reveal variations in quasi-peak noise with time over a range of at least 20 decibels. At some of the locations, the measured variation exceeded 40 decibels and at some the variation was so extreme that the maximum values exceeded the full-scale range of the recorder and hence could not be measured.

The curves of Figure 9 show that the general noise level at a given location, is not a function of system voltage alone. Among the lowest over-all noise levels were those recorded at the 22-kv and 220-kv locations at 156 kc. These voltages are at the two extremes of the range of voltage classes studied.

Further evidence of the inverse variation of quasi-peak noise levels with frequency are the curves for noise at 63 kc at the two 22-kv locations. The curves for noise at 63 kc are roughly 25 decibels above those taken from the 156-kc records at these locations. These curves constitute more conclusive evidence than Figure 6 of the increase of noise with reduced frequency, because the data for these curves were taken over sufficiently long intervals to be representative of the normal distribution of the noise levels with time. For all except a small percentage of the total recording time at each location, the quasi-peak noise at the lower frequency is a fairly constant multiple of that at the higher frequency. The actual magnitude of the difference between the two sets of curves is not believed to be typical.

It is believed that the high noise level recorded for a portion of the time at location I (66 kv) was caused by intermittent operation of arc furnaces at the steel mill served from the bus at this location. The chart record for this location shows frequent sudden increases in noise level from low steady values to very high and fairly constant levels, followed by equally sudden drops back to the lower values. Because of the low minimum values, it is believed that the noise generated on the transmission lines themselves associated with this location was much lower than is indicated by analysis of the chart record

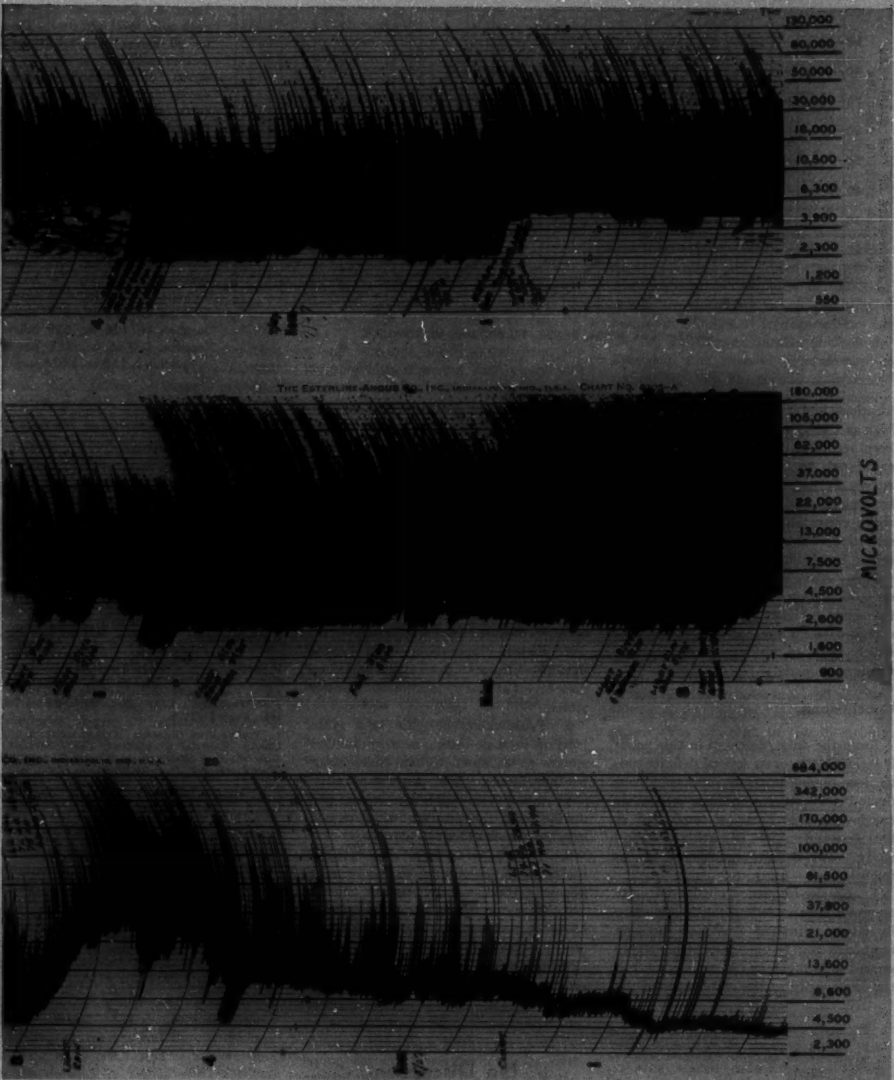

Figure 8. Typical chart records of quasi-peak noise

(a). Effect of switch operation; (b). Variation of noise during thunderstorms and subsequent rain without thunder; (c). Buildup of noise to thunderstorm value and return to fair-weather level

including this externally generated noise.

The curves of Figure 9 for locations F and G, two directly interconnected 220-kv stations, are almost identical. This is further evidence that a measurement of noise level at one point on a system is representative of the level at nearby interconnected points.

In general, Figure 9 shows that noise voltages at times reach considerably higher values than has been commonly supposed. Voltages as high as 0.5 volt were recorded for small percentages of the total recording times at several of the

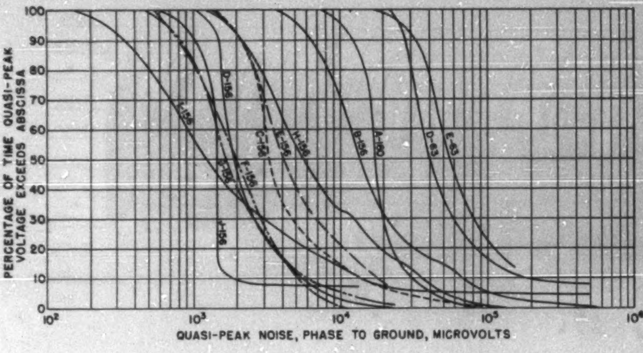

Figure 9. Distribution of quasi-peak noise level with time. Data for all curves were taken over periods sufficient to include a variety of weather conditions, except curve for location J. The curve for location I is not considered to be typical, for reasons discussed in text. Total recording time for each curve was as follows: Location A, 160 kc, 117 hours; location B, 156 kc, 1,076 hours; location C, 156 kc, 503 hours; location D, 156 kc, 323 hours, location D, 63 kc 110 hours; location E, 156 kc, 165 hours; location E, 63 kc, 74 hours; location F, 156 kc, 639 hours; location G, 156 kc, 619 hours; location H, 156 kc, 639 hours; location I, 156 kc, 317 hours; location J, 156 kc, 120 hours

locations, and it is believed that values as high as 1 volt or even greater would have been recorded if the recorder had been calibrated to measure them. These curves are based on noise in a 400-cycle bandwidth, and application of a bandwidth correction factor to obtain representative values for the usual carrier receiver bandwidths will result in higher values. Also, in view of the foregoing data on the variation of noise level with frequency, a higher general level could be expected below the 156-kc frequency at which most of the recorded measurements were made.

Conclusions

From the data presented in this paper it is possible to draw several definite conclusions regarding carrier-frequency conducted noise on power lines, and other conclusions that must be considered as tentative and subject to further tests and study. The definite conclusions are as follows:

1. Carrier-frequency conducted noise on power lines is predominantly impulsive in nature. Impulse repetition rates on most high-voltage lines varies from 60 per second to as much as 180 per second, but the irregularity of the amplitudes of the individual pulses results in an effective pulse rate considerably below these figures.
2. The general level of peak, quasi-peak, and average noise decreases with increasing frequency at a given location.
3. Carrier-frequency noise levels at times reach values considerably greater than has been commonly supposed to exist on power systems, with quasi-peak noise voltage in a 400 cycle bandwidth exceeding 0.5 volt for appreciable percentages of time on some systems.
4. Switch operations can cause marked changes in carrier-frequency noise levels at nearby locations on a power system.
5. Peak values of noise at a given location increase during nearby thunderstorms to as much as ten times clear-weather values. The increase in noise level under these conditions results primarily from the presence of extremely large pulses of random occurrence.
6. There is no direct relation between transmission line voltage class and carrier frequency conducted noise level.
7. Noise at a given location on a power system contains components that originate at distant points on the system.

The following conclusions must be regarded as tentative and subject to confirmation by further tests:

8. Noise levels measured at one point on a power system are closely indicative of the noise levels at neighboring interconnected points on the system.
9. Noise levels at a given location are affected by the presence of stub or tap lines in much the same manner as desired signals arriving from distant locations.

References

1. A Study of Carrier-Frequency Noise on Power Lines—Part I. Theoretical Considerations and Measuring Techniques, R. C. Cheek, J. D. Moynihan. *AIEE Transactions*, volume 70, 1951, pages 1127–34.

2. Power-Line Carrier Application, R. C. Cheek. *Electrical Transmission and Distribution Reference Book*, Westinghouse Electric Corporation (East Pittsburgh, Pa.), fourth edition, 1950.

3. Application of Carrier to Power Lines, F. M. Rives. *AIEE Transactions*, volume 62, 1943, pages 835–44.

4. Proposed American Standard Specification for a Radio Noise Meter .015 to 25 Megacycles/Second. *C63.2* American Standards Association (New York, N. Y.), 1949.

5. A Study of Wave Shapes for Radio Noise Meter Calibration, C. W. Frick. *AIEE Transactions*, volume 64, 1945, pages 890–901.

6. Radio Influence Tests in Field and Laboratory—500 KV Test Project of the American Gas and Electric Company, G. D. Lippert, W. E. Pakala, S. C. Bartlett, C. D. Fahrnkopf. *AIEE Transactions*, volume 70, part I, 1951, pages 251–69.

No Discussion

Transmission Considerations

G. E. BURRIDGE
ASSOCIATE AIEE

A. S. G. JONG
NONMEMBER AIEE

RECENT expansion in generating capacity of The Hydro-Electric Power Commission of Ontario together with the policy of centralized control has necessitated a power line carrier system of over 60 channels for the purpose of communication, telemetering, load-frequency control, and protective relaying. The carrier terminals, in general, are concentrated at specific station locations with one particular station utilizing over 20 operating carrier frequencies to provide the necessary services. The total carrier channel mileage is approximately 16,000 operating over 2,600 circuit miles of the power network.

The application of these carrier channels to an extensive power network is a difficult problem in that the system involves circuits of different physical characteristics, types of construction, and varying lengths of parallels in close proximity. These characteristics, which may not be of any importance at power frequencies, must be considered for carrier frequencies. In view of the complexities in operating conditions and requirements together with the limited frequency spectrum, 50–200 kc, a knowledge of the transmission characteristics of the power system at carrier frequencies is essential to the co-ordination of a power line carrier network for the reliable functioning of the channels with a minimum of interference.

The purpose of this paper is to present the method of measurement and quantitative results of the more important transmission factors and their consideration in the co-ordination of a power line carrier network.

Cross-Coupling

The plan or physical layout of a power system network has a direct bearing on the amount of carrier interference to be expected. Concentration of services at specific stations, physical parallels, and lengths of transmission lines, along with various possible switching conditions are of prime importance from a carrier interference viewpoint. Further, variable dimensions of transmission lines such as spacing, height and diameter of power conductors, and horizontal and vertical separation of disturbed and disturbing conductors are factors to be considered.

Theoretically, it is possible to determine by computations the effect of these factors, electrical as well as dimensional, for simple cases, but even with simplifying assumptions, the work is tedious and the results approximate. In complex cases when all factors are considered, quantitative results are best obtained by field measurements.

Variations in circuit conditions and types of service necessitate each carrier installation to be treated individually, with consideration given to multichannel operation and equipment characteristics. The allowable interference on any one channel will depend on the type of service in question. Should the service be an f-m voice communication channel, for example, considerable carrier interference could be tolerated; on the other hand, an a-m carrier employed for protective relaying could not tolerate carrier interference near or on the operating frequency where such a signal might cause incorrect circuit breaker operation.

The initial step in selecting operating frequencies would be to employ low frequencies (50-100 kc) for protective relaying carriers wherever possible, since present relay receivers are more selective at the lower frequencies. Further, these carriers operate intermittently and therefore their generated harmonics are not a continuous source of interference to other channels. Carriers used for voice communication, telemetering, and load control could be allocated within the band 100–200 kc, since they operate continually and harmonics are not a problem to carriers operating on lower frequencies. The problem is then one of selecting power levels and frequencies so that a minimum number of frequencies can be used on a maximum number of channels. Provided the channel interference is sufficiently low to permit satisfactory operation, the same carrier frequency may be repeated. The amount of interference can be determined by cross-coupling measurements. Cross-coupling loss is considered as a measure of the attenuation in carrier signal between coupled circuits. A method whereby these losses may be determined is included in Appendix I.

Curves for a typical set of cross-coupling measurements are included in Figures 1, 2, and 3 with the circuit separations and conductor configurations shown in Figures 4 and 5. In Figures 1, 2, and 3, the reference curve indicates the attenuation of carrier signal along the disturbing circuit. Figure 1 shows near-end and far-end cross-coupling loss measured on the phase wires adjacent to the disturbing conductor. The measured values indicate the similarity of near-end and far-end cross-coupling losses and the close approximation at some frequencies to the attenuation. The cross-coupling losses for the configuration shown in Figure 2 are generally higher than the losses for the circuit in Figure 1 primarily because of increased separation of the disturbed and disturbing conductors. A comparison is made in Figure 3 of phase-to-ground and phase-to-phase far-end cross-coupling loss, with a phase-to-phase disturbing signal transmitted on adjacent wires of a twin

---

Paper 51-246, recommended by the AIEE Carrier Current Committee and approved by the AIEE Technical Program Committee for presentation at the AIEE Summer General Meeting, Toronto, Ont., Canada, June 25–29, 1951. Manuscript submitted March 30, 1951; made available for printing May 16, 1951.

G. E. Burridge and A. S. G. Jong are with The Hydro-Electric Power Commission of Ontario, Toronto, Ont., Canada.

The authors wish to extend their appreciation to the Hydro-Electric Power Commission of Ontario for their permission to publish this paper and to Messrs. A. D. Blachford and S. C. Preston for their assistance in its preparation.

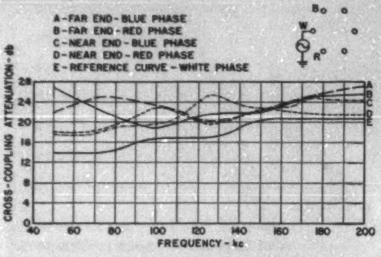

Figure 1 (left). Cross-coupling loss, phase-to-ground on adjacent conductors of a 96 mile twin circuit line

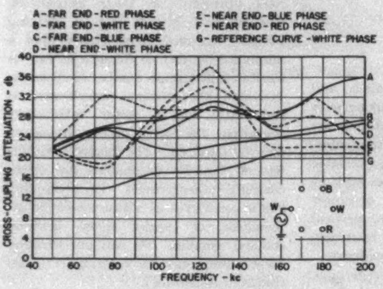

Figure 2 (left). Cross-coupling loss, phase-to-ground on conductors of adjacent circuit of a 96 mile twin circuit line

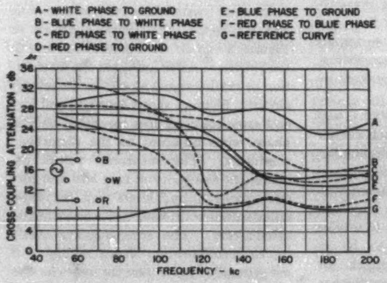

Figure 3 (left). Far end cross-coupling loss, phase-to-phase and phase-to-ground on conductors of adjacent circuit of a 96 mile twin circuit line

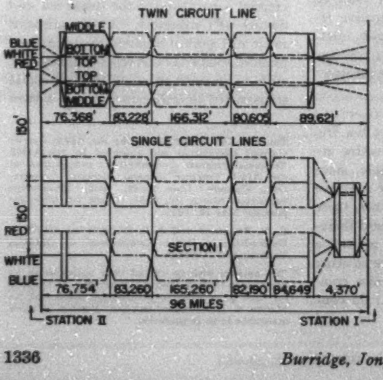
TWIN CIRCUIT LINE
BLUE
WHITE
RED
MIDDLE
BOTTOM
TOP
TOP
BOTTOM
MIDDLE
76,368'
83,228'
166,312'
80,605'
89,621'
150'
SINGLE CIRCUIT LINES
150'
RED
WHITE
BLUE
SECTION I
76,754'
83,260
165,260'
82,190'
84,649'
4,370'
96 MILES
STATION II
STATION I

Figure 4 (left). Plan view of twin circuit and single circuit 230 kv 60 cycles lines showing parallels and conductor phasing

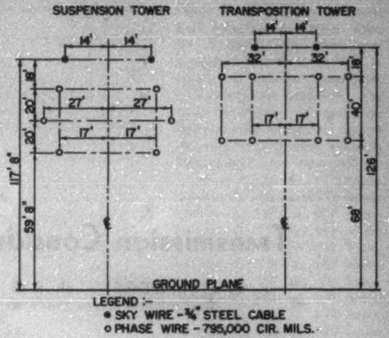
SUSPENSION TOWER
TRANSPOSITION TOWER
14'
14'
18'
20'
27'
27'
20'
17'
17'
117' 8"
59' 8"
32'
32'
18'
40'
126'
68'
GROUND PLANE
LEGEND:-
● SKY WIRE-¾" STEEL CABLE
○ PHASE WIRE-795,000 CIR. MILS.

Figure 5. Configuration, separation and height above ground conductors in twin circuit construction

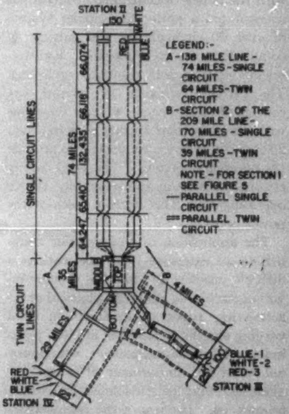
STATION II
130'
RED
WHITE
BLUE
SINGLE CIRCUIT LINES
74 MILES
66,074'
66,118'
132,435'
65,410'
64,247'
35 MILES
A
MIDDLE
TOP
BOTTOM
TWIN CIRCUIT LINES
29 MILES
B
4 MILES
RED
WHITE
BLUE
STATION IV
121'
BLUE-1
WHITE-2
RED-3
STATION III
LEGEND:-
A-138 MILE LINE-
74 MILES-SINGLE CIRCUIT
64 MILES-TWIN CIRCUIT
B-SECTION 2 OF THE 209 MILE LINE-
170 MILES-SINGLE CIRCUIT
39 MILES-TWIN CIRCUIT
NOTE-FOR SECTION I SEE FIGURE 5
—PARALLEL SINGLE CIRCUIT
═PARALLEL TWIN CIRCUIT

Figure 6. Plan view of composite 230 kv 60-cycle lines showing circuit separation and conductor phasing

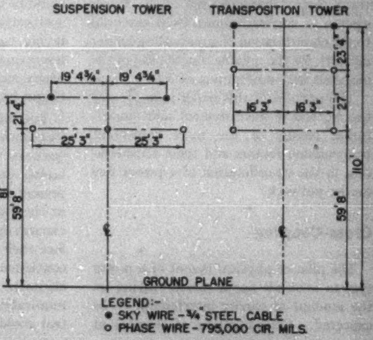
SUSPENSION TOWER
TRANSPOSITION TOWER
19' 4¾"
19' 4¾"
21' 4"
25' 3"
25' 3"
81'
59' 8"
23' 4"
27'
16' 3"
16' 3"
110'
59' 8"
GROUND PLANE
LEGEND:-
● SKY WIRE-¾" STEEL CABLE
○ PHASE WIRE-795,000 CIR. MILS.

Figure 7 (right). Configuration, separation and height above ground of power and ground conductors in single circuit construction

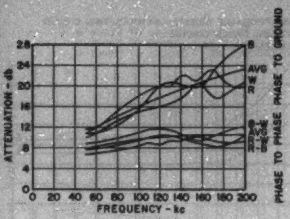

Figure 8 (left). Actual and average values of attenuation versus frequency for phase-to-phase and phase-to-ground transmission

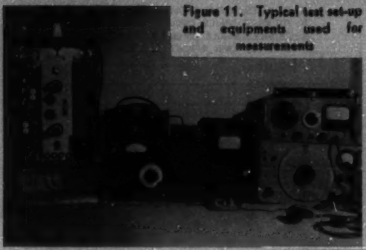

Figure 11. Typical test set-up and equipments used for measurements

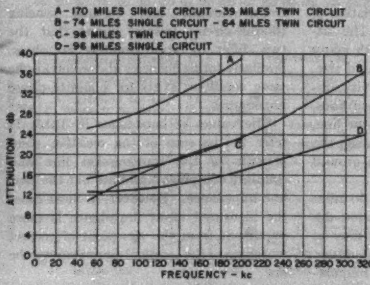

Figure 9 (left). Average attenuation versus frequency phase-to-ground transmission on single, twin and composite circuits

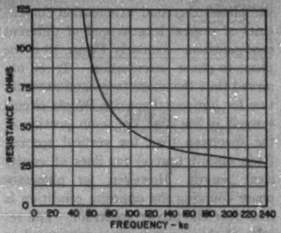

Figure 12. Magnitude of resistive component of coupling circuit at resonance versus frequency

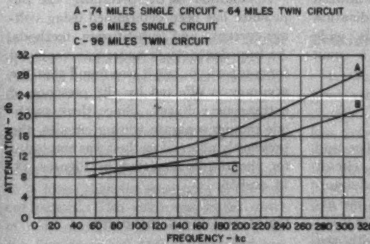

Figure 10 (left). Average attenuation versus frequency, phase-to-phase transmission on single, twin and composite circuits

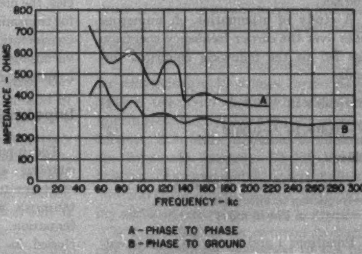

Figure 13 (right). Actual measured values of impedance phase-to-ground and phase-to-phase

circuit line. The losses decrease with increasing frequency and there is no defined difference in attenuation whether the terminating equipment is connected phase-to-ground or phase-to-phase.

One application of the results from these measurements may be made by referring to Figure 2. Consider two carriers operating while phase-to-ground on adjacent power circuits. The far-end and near-end cross-coupling loss at 115 kc is 29 decibels and the circuit attenuation 17 decibels. The interfering signal therefore will arrive 12 decibels below the level of the required signal.

The study of quantitative field measurements permits the optimum use of coupling loss in selecting the method of coupling and frequency. If measured values of coupling loss were not available, a margin of only 2 or 3 decibels could be safely assumed. It is practical to operate common frequencies on parallel power circuits by the judicious choice of frequencies where the coupling loss is high. The results were obtained under ideal conditions with the transmission line disconnected from associated power equipment. However, this same condition is approached when line traps are employed because the conductors are isolated at the operating frequencies by a high impedance.

Attenuation

Previous mention has been made of the selection of operating power levels. These levels must be sufficient to provide adequate signal-to-noise ratios at the receivers by exceeding the noise and the attenuation of line and coupling equipment, and must account for additional line losses due to weather conditions. The line losses may be determined by measuring input and output power levels. A satisfactory method is given in Appendix I with the testing equipment illustrated in Figure 11. The results of measurements made on several typical circuits are shown in Figures 8 to 10. The configurations are given in Figures 4 to 7.

The variation of attenuation with frequency for a 96 mile vertically spaced twin circuit line is given in Figure 8. Average curves have been shown in each of the graphs for phase-to-phase and phase-to-ground transmission. Figures 9 and 10 are also average values since in each case the over-all attenuation is essentially the same regardless of which phase conductor or conductors are employed. Figure 9 shows the variation of

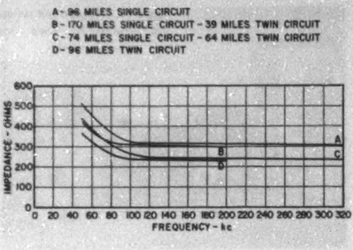

Figure 14 (left). Average phase-to-ground impedance of circuits of different construction and composition

Figure 15 (right). Average impedance phase-to-phase of circuits of different construction and composition

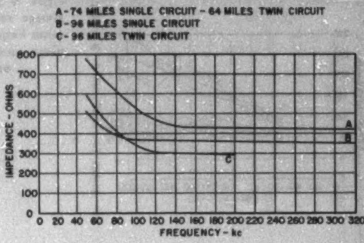

the phase-to-ground attenuation for circuits of several lengths and of different configuration. Similarly Figure 10 is the phase-to-phase attenuation. It is observed that the phase-to-ground attenuation for horizontal spacing (single circuit towers) is less over the main portion of the spectrum than for vertical spacing (twin circuit towers) for lines of equivalent length. However, for phase-to-phase coupling the opposite condition is true over the carrier spectrum. The results of these curves are summarized in Table I, where the attenuation is shown in decibels per mile of transmission line at 100 kc.

A study of attenuation on numerous lines over the carrier frequency spectrum has led to the following empirical formulas:

$$N=(0.5f\times10^{-3}+0.1)d \tag{1}$$

$$N=(0.4f\times10^{-3}+0.06)d \tag{2}$$

where

N = total attenuation in decibels
f = frequency in kilocycles
d = length of line in miles

Equations 1 and 2 may be used to calculate the phase-to-ground and phase-to-phase attenuation respectively. These equations are approximate in that they are derived from over-all average values. However results of sufficient accuracy can be obtained to predict the behaviour of a carrier wave on a line of given length.

The average curves (Figures 8–10) should not be interpreted as actual results to be expected on a line. Measured results will not show smooth variation of attenuation with frequency. The attenuation on a line will vary with many factors, for example, wire type and size, length of circuit, ground resistivity, insulator type, wire spacing, tapped lines, type and method of coupling to the line, changes in type of construction along the line length, and the presence of ground conductors.

In general for lines in excess of 50 miles in length, the value of attenuation derived from the empirical formulas may be used for engineering calculations. However in the selection of operating frequencies, the measured losses should be utilized for transmission quality and co-ordination considerations, due to possible wide variations in attenuation over a small frequency range.

Table I

Line Length, Miles	Line Configuration Miles Single Circuit	Miles Twin Circuit	Phase-to-Ground Attenuation, Db/Mile at 100 Kc	Phase-to-Phase Attenuation, Db/Mile at 100 Kc
96	96		0.14	0.10
96		96	0.17	0.10
138	74	64	0.18	0.09
209	170	39	0.14	

Impedance

The input impedance of the line and coupling equipment, with the circuit reactance tuned out, was measured simultaneously with the transmission line attenuation. A set of typical results is included in Figures 13 to 15, with the method of coupling to the line shown in Figures 18B and 18C.

The curve in Figure 12 denotes the magnitude of the resistive component of the coupling circuit at resonance, as a function of frequency. The measured values of input impedance include this component which contributes to the high impedance at the lower frequencies.

The phase-to-phase and phase-to-ground impedance is compared in Figure 13 from which average curves were derived. Similarly, Figures 14 and 15 display the average phase-to-phase and phase-to-ground impedance for circuits of different lengths and configuration. Table II is a summary of the impedance at 100 kc. In all cases, the phase-to-phase impedance is more than that for phase to ground.

A comparison of the phase-to-ground impedance for horizontal spacing (single-circuit towers) and vertical spacing (double-circuit towers) shows that the two differ by approximately 80 ohms. Similarly for frequencies above 100 kc the same condition exists for phase-to-phase impedance.

The values of impedance in Table II refer to the sum of the resistive components of the transmission line and coupling equipment, and are not the true line impedance. However, in most cases the measured input impedance is more important from the viewpoint of correct matching of the terminal equipment to the line.

In addition to the preceding, the impedance has been determined using voltage-current, and substitution methods. An Impedance-Angle meter was employed for comparison, but it was found that the accuracy is affected by the presence of extraneous voltages. Since these methods require separate testing circuits, the previously adopted method was employed for the results depicted in Figures 13, 14, and 15.

Noise and Field Intensity

The output power level of transmitting equipment is selected to provide an adequate signal-to-noise ratio at the carrier receiver terminals. The noise voltages present at a receiver input circuit will depend on the operating voltage of the power circuit and the type of transmission employed, that is, phase-to-phase or phase-to-ground. The value of noise measured with test instruments is difficult

Table II

Line Length, Miles	Line Configuration Miles Single Circuit	Miles Twin Circuit	Phase-to-Ground Impedance, Ohms	Phase-to-Phase Impedance, Ohms
96	96		330	370
96		96	240	340
138	74	64	270	530
209	170	39	310	

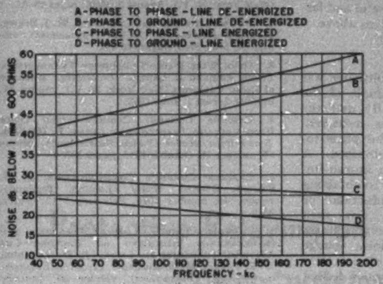

Figure 16 (left). Magnitude of noise with line energized and de-energized

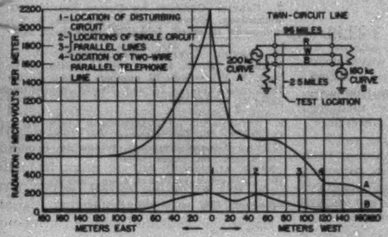

Figure 17 (left). Field intensity in the vicinity of transmission line produced by 3 watts at 200 kc and 2 watts at 160 kc

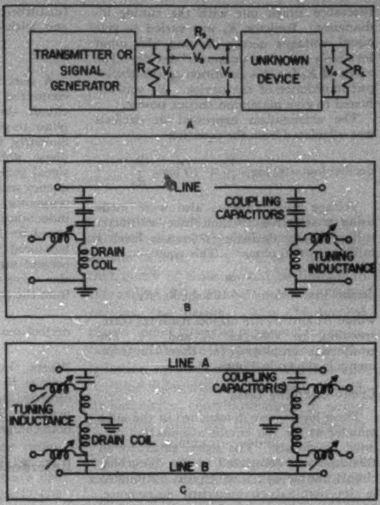

Figure 18 (right). Test set-up and methods of coupling used in field measurements

to relate to that obtained under actual operating conditions. However, the results will indicate the noise variation with frequency.

Noise in the carrier band of frequencies was measured on energized 230 and 115 kv lines. The measured value of the noise on the 115 kv lines tested was found to be lower than the sensitivity of the test equipment. This value was in the order of −70 decibels below 1 milliwatt with the line energized and de-energized but noise on 230 kv lines was considerably more. Figure 16 shows the magnitude of the noise obtained on one circuit. The method of measurement is outlined in Appendix I.

The phase-to-phase noise voltages are less than the phase-to-ground voltages. Further, for the de-energized line they decrease linearly with frequency and increase linearly with the line energized.

The magnitude of the field intensity in the vicinity of transmission lines produced by carrier waves is included, for general interest, in Figure 17. A standard radio noise and field intensity instrument was used to obtain these results. As only a limited number of radiation measurements were taken, insufficient data are available to arrive at any definite over-all conclusions; however the shielding effect of the parallel power transmission lines and telephone circuits is to be noted.

Conclusions

1. Far-end and near-end cross-coupling vary with frequency and method of coupling with the average cross-coupling loss generally increasing with frequency and separation of disturbed and disturbing circuits. Optimum use of coupling losses for carrier frequency co-ordination in a power network can be utilized only if measured values are available for consideration with noise and attenuation factors.

2. Attenuation on phase-to-phase transmission is less than that for phase-to-ground and in either case increases with frequency and varies with circuit configuration. It is possible to calculate the average attenuation with frequency from equations 1 and 2 for engineering purposes and on transposed circuits, the attenuation is essentially the same irrespective of which phase wire(s) is (are) employed.

3. The impedance of any circuit varies with line configuration and is higher for phase-to-phase than for phase-to-ground and at the higher frequencies tends to approach a constant value.

4. The amount of noise voltages present in the carrier frequency spectrum is directly proportional to the power circuit voltage and is more for phase-to-ground than for phase-to-phase. The noise will increase linearly with frequency for both types of coupling on an energized line and decrease linearly when the power circuit is de-energized.

5. In view of the transmission characteristics of high-voltage lines, carrier relay receiver selectivity characteristics and the intermittent but important nature of relay carriers, it appears advisable to allocate the frequency spectrum 50–100 kc for this type of service and the spectrum from 100–200 kc for communication, telemetering and load control purposes.

It is practical to use common frequencies for maximum utilization of the allocated carrier frequency spectrum where interference is low because of the geographic separation of equipment or where interference is relatively high as in the case of adjacent circuits by the optimum selection of transmission and equipment characteristics.

Appendix I. Attenuation, Cross-Coupling Loss and Noise Measurements

Attenuation

Attenuation measurements were made using the circuit in Figure 18(A). The transmission line circuit as shown in Figure 18(B) or (C) is inserted for the unknown device in Figure 18(A). The test procedure was as follows:

The output level of the signal generator, operating at frequency f, was set to produce voltage V_1 across resistor R and the circuit reactance tuned out with the tuning inductance. Resistor R_s was varied to give equal voltages across R_s and the input terminals of the unknown device. The value of R_s for this condition equals the input impedance of the device. R_L was adjusted to give maximum output power.

The attenuation expressed in decibels was calculated from the equation

$$\text{decibel loss} = 20 \log_{10} \frac{V_3}{V_4} + 10 \log_{10} \frac{R_L}{R_s}$$

Voltage measurements also were made using a selective vacuum tube voltmeter calibrated in decibels (reference level 1 milliwatt—600 ohms). This equation then becomes:

$$\text{decibel loss} = N_3 - N_4 + 10 \log_{10} R_L/R_s$$

where N_3 and N_4 are decibel readings corresponding to voltages V_3 and V_4. The equipment employed for these measurements is shown in Figure 11.

Cross-Coupling Loss

These losses were determined in the same manner as for the circuit attenuation outlined previously. The signal generator in this case was connected to the disturbing circuit, the far end of which was terminated in its nominal characteristic impedance. Measurements were made on adjacent lines (disturbed circuits) at the near-end and far-end, with each end terminated as above.

Noise

A selective vacuum tube voltmeter was connected to the input terminals of the circuit shown in Figure 18(B) and the phase-to-ground noise voltages measured. Similarly for Figure 18(C), the phase-to-phase noise voltages were obtained. A signal generator operating at a known frequency was employed as an aid to obtaining resonance with the tuning inductance or inductances. The voltmeter was then tuned to this frequency and noise voltages measured in decibels. The noise voltage present may be expressed as an equivalent sine wave voltage by calculation if desired from the equation

$$\text{decibel reading} = 20 \log_{10} \frac{V_N}{0.775}$$

Where V_N = equivalent sine wave noise voltage in volts. Figure 16 was plotted directly from measured values for convenience. This method may be used for both energized and de-energized power lines.

References

1. Measurement of Carrier Circuit Impedances, **W. H. Blankmeyer.** *Electrical World,* (New York, N. Y.), August 3, 1946, pages 49–51.

2. Power Line Carrier Channels, **M. J. Brown.** *Electrical Engineering* (*AIEE Transactions*), volume 64, May 1945, pages 246–50.

3. Open Wire Radio Frequency Transmission Lines, **Edmund A. Laport.** *Proceedings,* Institute of Radio Engineers (New York, N. Y.), volume 31, number 6, part 1, June 1943.

4. Carrier Current Communication Over High Voltage Transmission Lines, **E. Hanless.** *Brown Boveri Review* (Baden, Switzerland), volume 31, number 10, October 1945, pages 335–9.

5. Carrier Current Communication, **J. S. Forrest.** *Wireless World* (London, England), volume 48, number 1076, February 1942, pages, 26–9.

6. Carrier Current Losses Measured and Interference Minimized on Boulder—Los Angeles Transmission Lines, **J. D. Laughlin, W. E. Pakala, M. E. Reagan.** *Electrical Engineering* (*AIEE Transactions*), volume 59, January 1940, pages 4–9.

7. Carrier Current on Power Systems, **O. Richardson.** *Communications* (New York, N. Y.), volume 18, number 7, July 1938, pages 19–22, 24.

8. Carrier Current Transmission, **P. B. Wightman, H. H. Lyon.** *Communications* (New York, N. Y.), volume 23, numbers 8 and 9, August 1943, pages 13–15, 74 and 106–7; September, pages 32, 54, 56, 58.

9. Attenuation of Transmission Lines, **M. J. O. Strutt.** *Wireless Engineer and Experimental Wireless* (London, England), volume 10, number 114, March 1933, pages 139–40.

10. Operation of Power Line Carrier Channels, **H. W. Lensner.** *AIEE Transactions,* volume 66, 1947, pages 888–94.

Discussion

T. S. Dutton (Shawinigan Water and Power Company, Montreal, Canada): It is difficult to assess the practical value of the field tests on noise, the results of which are given in Figure 16.

The noise figures obtained with the apparatus and method of measurement as described in the Appendix would appear to be open to question.

In particular, no data is given regarding the bandwidth of the selective vacuum tube voltmeter over the frequency range covered, and it is not clear whether the noise decibel figures given relate to peak, quasi-peak, or some other degree of integration of the noise pulses.

No indication is given as to whether the vacuum tube voltmeter or other external means terminated the line with a load equal to the characteristic impedance of the line minus the resistive component of the series resonant coupling circuit. Likewise, no mention is made of the termination conditions of the distant end of the line, where mismatch would introduce a reflection factor.

With regard to the data given for the line energized condition, presumably wavetraps were not employed at each end of the line for each frequency in the range from 50 to 200 kcs at which measurements were taken. If this assumption is correct, then the figures given for the energized line condition may tend to show the impedance/-frequency relationship of the power equipment to which the line is connected rather than the noise/frequency relationship of the line itself. If traps were not used, then the figures given have little numerical significance, and even the finding that the noise increases with increasing frequency is suspect. Indeed this latter conclusion is contrary to the noise/frequency relationship that would be expected from a theoretical consideration of the probable relative amplitudes of the frequency components in a noise pulse.

In view of the considerable importance of accurate noise data as a means of co-ordinating and estimating transmitter power level requirements, and the scarcity of published field measurement data, an elucidation of the points raised would appear to serve a useful purpose.

G. E. Burridge: The authors wish to point out that conclusion 4 is too general to cover the experimental data included in the paper. A correct interpretation of the results is as follows:

"The amount of noise voltage present in the carrier frequency spectrum is greater for 230 kv than for 115-kv circuits, and is more for phase-to-ground than for phase-to-phase reception. The experimental results included for a particular circuit show; (a) the noise level increased linearly with frequency when the line was energized and (b) the noise level decreased linearly when the line was not energized."

Further measurements have indicated that the variation of noise with frequency did not follow any trend. Circuits of similar construction and voltage class have shown a decrease of noise with frequency in some cases and an increase in others with identical testing methods.

Several points have been raised by Mr. Dutton requesting further data dealing with the noise decibel readings given in Figure 16. This figure shows results obtained on one circuit of a 96-mile twin circuit transmission line. Details of this line and neighboring single circuit lines are given in Figure 4.

The noise readings were made with a selective vacuum-tube voltmeter having a bandwidth of 2 kc within the range 50–200 kc. This instrument indicates the average value of the noise envelope.

The field results were obtained without the use of terminations at each end of the line. This data approximates the noise voltages existing on the transmission circuit. Terminating the local end resulted in a decreased value of measured noise, but did not modify the shape or slope of the noise level-frequency curve. The effect of the distant end termination has not been determined experimentally. It is considered, however, that the reflection effects would be negligible due to the electrical length of the line at these frequencies and the appreciable circuit attenuation.

The noise results depicted in Figure 16 have been included to indicate the general noise levels present on a representative power circuit. The figure is not intended to represent the net result of an extensive study on the subject in question. The results were obtained without the use of line traps, since such a condition was not realizeable during measurements. It is possible that the slope of the curve may indicate the impedance-frequency characteristics of the terminating power circuit under certain conditions of relative bus-line impedance magnitudes and noise voltage ratios. The noise levels are representative of what would be expected under operating conditions where traps are not used or where trap circuit rejection is small.

Protective Relaying on Industrial Power Systems

CARL M. LATHROP
ASSOCIATE AIEE

CHARLES E. SCHLECKSER
NONMEMBER AIEE

THE trend of many industries such as the petroleum and chemical industries is toward the installation of continuous processing equipment wherein the individual units in the processing steps continuously receive and deliver raw materials, unfinished products, or finished products. As each individual unit is part of the processing chain, an emergency utility outage such as a power failure at any unit has an effect on the operation of all other processing units. Such an outage usually causes an upset in the operations which results in a large portion of the processing equipment having to be removed from service with the attendant dangers associated with such an operation.

Along with the above trend has come the trend toward complete electrification of the prime movers at the processing units. It is, therefore, becoming increasingly important that the electric power supply to a process unit be reliable and uninterrupted. Power supplies to process units in modern installations are, therefore, usually of the dual-feed type wherein two full capacity supplies are provided at the battery limits. However, duplicate equipment alone is not sufficient for a reliable power supply unless this equipment is properly co-ordinated by means of the power system relays.

Relaying on a modern industrial plant power system must be a compromise between:

1. Close protection of the electric equipment (motors, transformers or cable) wherein faulted circuits and equipment are disconnected from the power system in the shortest possible time and overload protection is paramount.

2. Power system co-ordination wherein short circuits cause minimum power system outage.

It has been the experience that this latter function of the relaying equipment is of greater importance than the first and that poor relay co-ordination may cause costlier results than problematical damage to electric equipment due to momentary overload. An example of poor relay co-ordination would be such that a short circuit on a motor feeder caused a main circuit breaker to trip instead of the motor feeder circuit breaker, with the resultant loss of the entire bus load. Loss of an entire bus at a major load for an extended time would cause the operation to be so upset as to require the unit to be removed from service. Many examples have been found where the relaying originally on the power system was co-ordinated, but that upon the addition of loads or generation to the system, the relaying was no longer co-ordinated. The system relaying cannot be held apart from the distribution system. It is determined by the distribution system and the loads.

It is possible by carefully analyzing the required power system co-ordination and protection requirements to select relaying equipment that will render the best possible results in satisfying the relaying problem. There are any number of different types of relays to be had. These range from the simple induction disk time overcurrent relay through differential, current balance, impedance distance, and all the others. It is believed, however, that many of these should be limited to the utility field in the interest of simplifying the design. Many industrial plants do not have the personnel for maintaining elaborate systems. Simple distribution systems with time-current and machine differential relaying will, through its simplicity, contribute more to power continuity than will the less adequately maintained elaborate system.

For any given arrangement of plant and load distribution it is possible to design several different systems. However, to demonstrate some principles, a system has been assumed that contains the usual machines. Some general recommendations and guides are given to aid in the selection of relaying equipment for both new and existing systems.

Desirable Protection For Electric Equipment and Machines

First let us look at what is desirable from the point of view of the equipment and machines. If possible, it is desirable that electric equipment be protected against system overloads and short circuits within certain limits, some of which are given here.

MOTORS

It is desirable that the overcurrent device on motor feeders open the motor circuit for line current values approaching 115 per cent of full load motor amperes for totally enclosed motors and 125 per cent of full load motor amperes for open-type motors.

Recent practice has been to obtain overload protection on large induction motors by means of thermal-type relays set to sound an alarm on occurrence of overloads. This is particularly attractive where operators are available to remove the overload cause. These are coupled with long time induction relays which are set to operate at approximately 250 per cent of full load motor rating. These latter units are used to trip the motor feeder circuit breaker. The induc-

---

Paper 51-248, recommended by the AIEE Industrial Power Systems Committee and approved by the AIEE Technical Program Committee for presentation at the AIEE Summer General Meeting, Toronto, Ont., Canada, June 25–29, 1951. Manuscript submitted March 5, 1951; made available for printing May 9, 1951.

CARL M. LATHROP and CHARLES E. SCHLECKSER are with the Standard Oil Development Company, Linden, N. J. Mr. Schleckser is now on leave with the United States Navy.

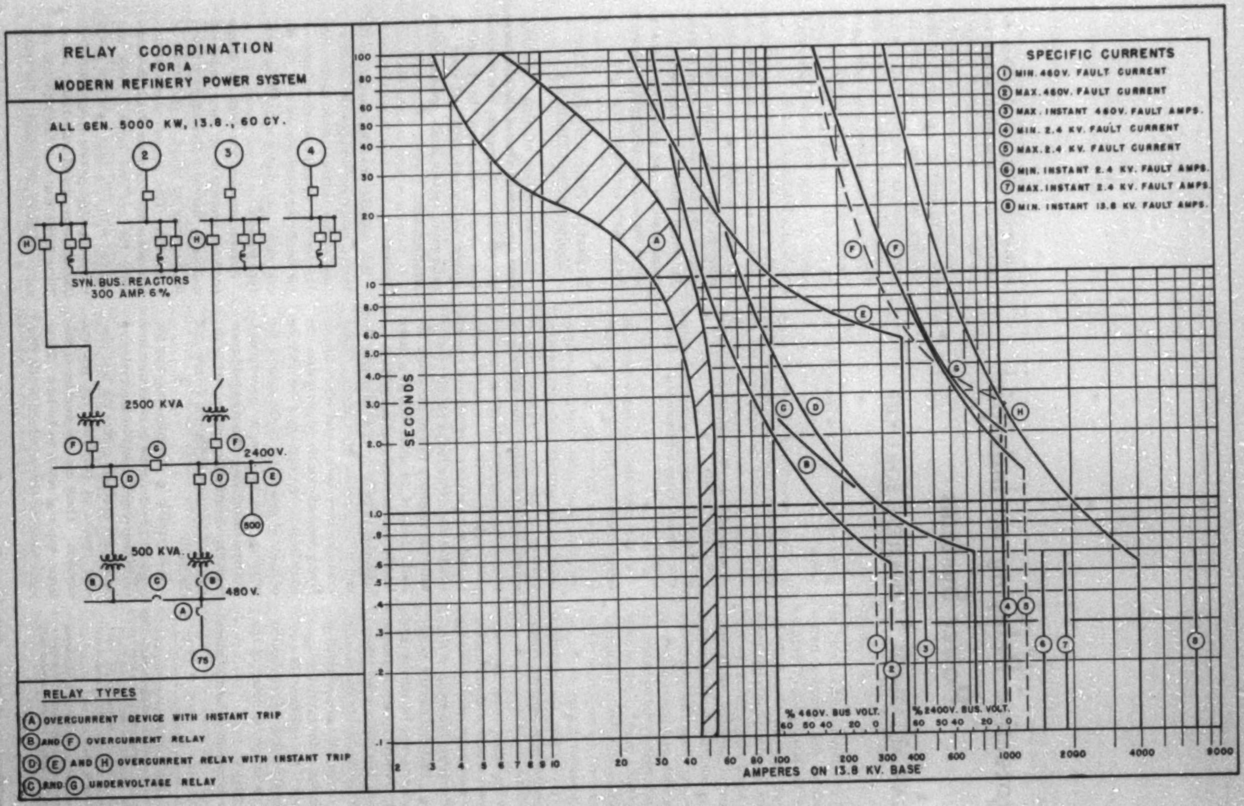

Figure 1. Relay co-ordination for a modern refinery power system

tion relay is usually timed so that at the starting current of the motor it will operate in approximately 125 per cent of the time required for the motor to fully accelerate. An instantaneous trip attachment on the induction relay is set to operate at approximately 10 to 15 times the full load motor amperes depending on inrush current value.

Large motors also are provided with time-delay undervoltage relays which are set to trip at a given percentage of rated voltage after an adjustable time delay.

CABLES

The National Electrical Code[1] permits a maximum overcurrent device setting of 150 per cent of the rated conductor current carrying capacity. From the cable life viewpoint it is desirable that a lower setting be used, but such as usually found impossible on an industrial power system where co-ordination is important.

TRANSFORMERS

The National Electrical Code permits a maximum overload protection setting on a transformer of 250 per cent; this protection being allowed either in the primary or secondary of the transformer. It is thought that this value is too high and it is usually found that a lower value may be used without effecting relay co-ordination or limiting motor starting.

GENERATORS AND POWERHOUSE BUSSES

Generators and powerhouse busses are generally protected against short circuits through the use of differential relaying equipment. Generator and bus overload protection is usually obtained indirectly by the settings on the feeder overcurrent devices and the surveillance of the operators.

It has been found difficult to obtain satisfactory overload protection for a generator by the use of overcurrent relays and even those with voltage restraint are questioned. When installed, these relays usually become merely "backup" protection for the differential relays.

Relay Co-ordination

By "co-ordination" it is meant that the settings applied to relays and trip devices that may be subjected to the same short circuit current are such as to cause the circuit clearing device nearest to the short circuit to open.

Figure 1 shows a portion of a modern industrial power system wherein a process unit or area is supplied through two 2,500-kva 13.2 to 2.4 kv transformers. This substation is assumed to be of the conventional secondary selective type. A 500-horsepower motor is shown connected to the 2.4-kv bus. Also two 500-kva 2,400 to 480 volt transformers are shown connected to the 2.4-kv busses arranged in the conventional secondary selective type system. The 2,500-kva transformers are connected each to a different powerhouse machine bus. The generation is assumed to consist of four 5,000-kw 13.8-kv generators connected through a synchronizing bus arrangement. The synchronizing bus reactors for this assumed system have been sized to maintain 80 per cent voltage on any given machine bus during a short circuit on an adjacent machine bus.

Equivalent arrangements can result when the power requirement is purchased from a utility company. Each machine bus then represents the bus on which an incoming utility feeder terminates. Smaller scale installations may be visualized by starting at the 5,000-kva substation level and letting the two 2,500-kva transformers represent the incoming power sources.

The 2.4-kv busses are shown connected through a normally open bus tie circuit breaker. Control wiring connections at this bus are such that for loss of voltage on a 2.4-kv bus section, the incoming circuit breaker to that bus section will open and the bus tie circuit breaker close. However, should the loss of voltage at a bus section be the result of a bus fault, lockout of the bus tie circuit breaker against closing is assumed to be by means of advance operation of the overcurrent relays on the incoming circuit breakers. The same arrangement is provided at the 460-volt bus sections.

It will be necessary to know system impedances and equipment ratings. The existence of such data is assumed and values used herein are typical. A relay setting study can best be visualized by plotting the time current characteristics of all of the protective elements of a section on the same curve sheet. All currents are converted to a common base by conventional means.

As a starting point vertical lines were placed on Figure 1 to represent the various maximum and minimum currents. See the numbered lines on the curve. The legend indicates the source.

Relay and trip device time-current characteristics are plotted in Figure 1 and indicate power system co-ordination that usually is adequate. The problem of co-ordinating a system of this type is begun at the load feeders connected to a 460-volt bus. For this particular demonstration it is assumed that the 75-horsepower motor is the largest load connected to the 460-volt bus and this governs.

Curve *A* on Figure 1 is a typical time-current curve of a device used for protection of a 75-horsepower motor feeder. It is the lower half of the curve usually associated with combined thermal-mechanical trip devices of the 600-volt class. The characteristics of this type device are effected by ambient temperature and hence is shown as a band. As it is desirable that only circuit breaker *A* is opened on short circuit or overload in this circuit, it is necessary that the time-current characteristic of overcurrent relay *B* lie "above" *A* for all possible currents up to short circuit currents. Automatic transfer (automatic closing of *C* upon power loss over *B*) at the 460-volt level is initiated by means of under-voltage relays. These undervoltage relays will close the bus tie circuit breaker *C* for any loss of voltage on either bus section. It is necessary, therefore, that the undervoltage relay equivalent time-current characteristic lie above that of the overcurrent relay at *B*. This is so the overcurrent relay at *B* will prevent the closing of the bus tie circuit breaker when the loss of voltage is the result of a bus fault.

In order to plot the undervoltage relay characteristic on the same curve sheet with the current actuated relays it is necessary to determine the "percentage of bus voltage" scale. This is done by determining the short circuit current that would flow for a 2-phase fault occurring during minimum generation (here assumed to be an outage of one generator). This current value is then the zero point on the voltage scale. The remainder of the scale is based on proration, that is, 90 per cent of the above current value is the 10 per cent bus voltage point, et cetera. For a 3-phase bus fault during maximum system generation, a higher fault current would flow and the voltage scale would move to the right so that the characteristic of the relay at *C* will always be co-ordinated with the current relay *B*.

At this point the first lumped impedance is encountered, the 2,400/480-volt transformer. Such impedances aid in reducing over-all tripping time by permitting the use of an instantaneous element.

The relay at *D* must co-ordinate with the relay at *B*. This is necessary to insure circuit breaker *B* operation for a 460-volt bus fault. The current relay at *D* is shown equipped with an instantaneous trip set to clear a minimum primary short circuit but not a maximum secondary short circuit. This is indicated by the vertical segment of the curve. All values on curve *D* lay above *B* and the curves do not intersect.

The relay *F* characteristic is shown to co-ordinate with relay *D* and relay *E* characteristics, that is, the curves do not intersect. This is necessary so that a load feeder fault will not trip the main incoming circuit breaker to a 2.4-kv bus. Relays at *G* have been set to co-ordinate with relays at *F* for the same reason that *C* was set to co-ordinate with *B*. Relay *H* is shown to co-ordinate with *F*.

It has been mentioned previously that the relays are "adjusted" to accomplish certain results. Let us say, for example, that curves *B* and *D* intersected. For low values of current the system would be co-ordinated but for values greater than those at the point of intersection the system would not be co-ordinated. Curve *D* can be moved unchanged to the right by changing current transformer ratios or more simply by changing the current taps on the relay. It may be moved vertically with some change in shape by adjusting the travel time of the induction disk which is done by varying the time lever or dial.

The generator and bus differential relay settings are independent of the foregoing system co-ordination. The usual practice is to set these relays as fast as possible without causing tripping on through faults, that is, faults beyond their area of protection.

Should it be desired to keep an induction motor connected during a transfer operation at the 460-volt or 2,400-volt bus, the characteristic of the motor undervoltage relay would be set "above" the transfer characteristic *C*. It is usually not possible to keep all motors on a substation connected during a transfer operation because the resulting inrush currents to the motors on the return of voltage would trip out the remaining incoming circuit breaker and result in a complete loss of power. It is, therefore, necessary to determine what motors are required to remain connected during a transfer and then determine what inrush current would result. Should the duration and magnitude of this current be such as to cause tripping of the remaining incoming circuit breaker, it would be necessary to reduce the number of motors to stay connected or increase the time setting on the incoming circuit breaker relay. In order to make an accurate calculation and decision on this type of problem, considerable information about motor and load characteristics is required.

Generally, low transfer times are desirable. On the type of system considered, the actual shape of the relay characteristic is important in reducing this transfer time. For example, relays at *B*, *D*, *F*, and *H* are shown having "very inverse" characteristics. Should relay *F* have an "inverse" characteristic, as shown dotted in Figure 1, a much longer transfer time would have resulted at the 2.4-kv bus.

It may be seen from Figure 1 that relay characteristics on feeders to large motors cause co-ordination difficulties. The 500-horsepower motor feeder relay *E* has an instantaneous trip setting of 15 times rated motor amperes. This setting has been necessary in many instances in order to start the motor, as the first cycle of current may reach this value, however, should the motor start satisfactorily with a lower setting the co-ordination and protection would be greatly improved. Should a motor have an inrush larger than the assumed 500-horsepower motor on the 2.4-kv bus, it would probably be necessary to use higher tap and time settings on relays at *F*, *G*, and *H* and thereby result in poorer protection for portions of the system these relays protect. There are several common causes of either poor relay co-ordination or poor equipment protection. The use of fuses for motor protection present a problem. The use of instantaneous trip devices on two successive relays or trip devices that do not have a lumped impedance intervening such as a transformer or reactor will not co-ordinate. For instance, relay *F* should not be equipped with an instantaneous trip attachment as there is no difference in the short circuit level from relay *F* to relays *D* and *E*. A short circuit on either relay *D* or *E* feeder would have caused relay *F* to trip which is, of course, undesirable. However, relay *H* and relay *F* are at locations having a definite difference in short circuit level as shown by currents (7) and (8). Cable impedance is usually not adequate to give the necessary change in level because it also is necessary to take into account system generation changes and the accuracy of the instantaneous trip device.

Trip devices on bus tie circuit breakers, if co-ordinated properly, generally result in poor system protection.

Often the reason for power systems being unco-ordinated is that upon addition of generating capacity or load to the system, the co-ordination had not been thoroughly checked and relay adjustments were not made to bring the system back into co-ordination. When contemplating system additions, the co-ordination problem should be thoroughly reviewed beforehand to determine the type of relaying equipment best suited for keeping the system in co-ordination.

As a matter of record, each system should have a set of relay curves such as is shown in Figure 1. As system changes and additions occur, it is an easy matter to evaluate the effect of the change.

REFERENCE

1. NATIONAL ELECTRICAL CODE. National Fire Protection Association (Boston, Mass.).

Discussion

H. P. Dupuis (Commonwealth Services Inc., Jackson, Mich.): The operation of station power for generating stations closely resembles industrial applications using continuous processing in that they both use a wide variety of motors, and uninterrupted service is of paramount importance.

A method of co-ordinating relay operation by use of selective curves as described by the authors, has been used very successfully by relay engineers of the Commonwealth Services Inc., on several industrial applications and on numerous installations of station power.

Since the relays to be co-ordinated usually involve two or more voltages it has been found that the interpretation of the curves can be simplified by using a kilovolt-ampere base rather than a current base referred to a particular voltage. It has also been found that where a number of applications is to be considered, the work of co-ordinating can be speeded up by plotting the characteristics of the commonly used relays to the same scale of log-log paper as used for the selectivity curves. By using semitransparent paper or a shadow box, the relay curves can then be traced directly on the selectivity sheet.

Satisfactory co-ordination between overcurrent relays and undervoltage relays is usually very difficult to obtain and where co-ordination is depended upon for proper transfer it would seem necessary to allow a large margin of safety. From an inspection of the typical curves of Figure 1, the operating time of relay *H* with some fault resistance may be in the order of 2 to 6 seconds for faults on the 2,400 side of the transformer. With this time delay the decrement in generator reactance may cause slower operation of the relay resulting in a delayed transfer that would cause a sufficient inrush of current to trip the power source to the good bus.

It would be of interest to know what objections the authors have to the commonly used scheme of having differential relays on the transformer banks supplying power to the various bus sections and using the differential relays to initiate transfer. Even on large industrial applications the distances are seldom too great to preclude the use of a simple differential scheme. This method results in a rather fast transfer and as shown in the paper by A. A. Johnson and H. A. Thompson,[1] it may result in higher inrush currents and greater stresses on the motor if the transfer is made when the motor residual voltage is out of phase with the new source voltage.

In the discussion of the Johnson and Thompson paper by J. A. Elzi and W. R. Brownlee it was pointed out that the high currents associated with the short-time transfer are confined to one-half cycle followed by normal current and that it is questionable whether this would produce undesirable stresses.

Mr. Johnson and Mr. Thompson further state in the discussion that the impedances of most industrial motor circuits are usually high enough to reduce the inrush current to a safe value. If the motor circuits and the characteristics of motors indicated the need for a greater time delay on transfer it could be easily obtained with undervoltage relays or by using one of the many devices available for that purpose.

REFERENCE

1. BUS TRANSFER TESTS ON 2,300-VOLT STATION AUXILIARY SYSTEM, A. A. Johnson, H. A. Thompson. *AIEE Transactions*, volume 69, part I, 1950, pages 386–94.

Carl M. Lathrop and Charles E. Schleckser: To a person as obviously experienced in the art of protective relaying as is H. P. Dupuis, this paper should appear to be elementary. It is. It was intended for the novice in the field of protective relaying. Many of the mechanisms used by those skilled in the art were purposely omitted for reasons of brevity. However, it is interesting to note the comments.

With regard to the use of the kilovolt-ampere base instead of the current scale referred to a particular voltage, the comment is that the kilovolt-ampere base has been used successfully.

In the final selection of tap and time dial setting, it is necessary to convert either kilovolt-ampere, or current referred to a particular voltage to the actual current, in which case it is of little consequence whether the original number is in kilovolt-amperes or in amperes.

The use of "overlays" showing commonly used relay characteristic curves plotted to the same log-log scale is a very useful time-saver mechanism. In addition, those getting into this detail may be interested in preparing templets from transparent material such as thick sheets of celluloid or transparent plastic. These templets can be moved around readily when it becomes necessary to fit a particular characteristic in between two existing characteristic curves.

On many occasions transformer differential relays or pilot wire relaying systems have been used to initiate automatic bus transfer. This is particularly desirable when two transformers are operating from the same source with very small values of impedance intervening. Basically this type of operation becomes necessary whenever a fault near one of two associated busses causes practically the same voltage condition on the other bus.

Industrial Plant Power Sources

RALPH T. WOODRUFF
MEMBER AIEE

WITH the limited amount of time and space available for this paper, no pretense will be made of treating the broad subject of industrial plant power sources in a comprehensive way. Rather, the intention is to take a quick look at all phases of the matter with the purpose of discovering, if possible, trends in one direction or another, examining the latest practices for technical advancement, and presenting pertinent economic data when available. Typical examples of the newest in industrial power plants in several widely different industries will be briefly described, and novel features pointed out. For more detailed discussions, reference must be made to the rather voluminous list of sources given at the end of this paper.

Power sources for industrial plants fall naturally into one of two general classes. They are: Public utilities and governmental agencies; and company-owned generating facilities.

Industry is progressively generating a smaller part of its own demand. According to one source, industry generated 40 per cent of its power requirements in 1939, only 33 per cent in 1948, and it was estimated that the figure will drop to 30 per cent by 1955.[1] A more recent figure quoted by another source and based on the census data of 1947 indicated that industrial plants were then generating only 17 per cent of their power requirements.[2] No matter which figures are more nearly correct, the trend toward purchased power seems evident.

Whenever power is needed for an industrial plant, the use of purchased power must be considered carefully. The factors that influence the choice of an industrial plant power source are so many and varied that it would be impossible to discuss all of them in this paper. However, it may be stated generally that wherever adequate amounts of purchased power are available at reasonable rates, purchased power will almost certainly be the most economical source unless there are special features of the industrial plant requirements. Some of these special features are listed below:

1. Heat needed in processes.
2. Heat available from processes.
3. Very large power demands.

The remainder of this paper will be devoted to a discussion of the features listed above and to some of the most recent means employed to provide economical power supplies in specific plants.

Plants Needing Heat in Processes

Many types of industrial plants belong in this category, including chemical plants, paper mills, oil refineries, and some manufacturing plants. It can be said almost axiomatically that where steam at relatively low temperature and pressure is needed in a process, as in many chemical plants, the power required can be generated at very low cost in topping units from steam produced at higher temperature and pressure than is needed for the process. Initial steam pressures utilized to date have gone as high as 1,250 pounds per square inch gauge, and initial temperatures as high as 900 degrees Fahrenheit. For small plants steam engines have been widely used as topping units, while for larger plants steam turbines of all types can be found, ranging from straight noncondensing to multiple-extraction, condensing units. Depending upon fuel and other costs, the actual out-of-pocket cost of the power thus generated may be as low as two mils per kilowatt-hour, or even less in the most favorable cases.

Perhaps the most outstanding example of a power plant of the type under consideration is the South Power House of the Dow Chemical Company at Midland, Mich. In size and design this power plant compares favorably with the latest public utility plants. Two 400,000 pounds per hour steam generators and one 30,000-kw turbogenerator form the initial unit which was placed in full operation on June 21, 1950. Figure 1 gives a view of the power plant and coal handling facilities. From the operating point of view, the plant is designed with nearly ideal lighting, ventilating facilities, and convenience. The building proper is designed so that the boilers and turbogenerator are contained within one room, and the boilers, boiler control panels, boiler feedwater pumps, and turbogenerator are arranged on the operating floor, so that a minimum of personnel is required on each shift. Additional space is provided in the building structure for two additional boilers and one additional turbogenerator unit.

Aside from the size of the boilers and turbogenerator and the high operating steam pressure of 1,250 pounds per square inch, there are several novel features involved in the South Power Plant which deserve mention. One of these features is the use of cyclone furnaces in which crushed coal carried in a high velocity stream of preheated air is introduced on a tangent through cylindrical primary burners at the furnace ends. Centrifugal forces in the spiralling mass throw out the coarser coal particles to a thin layer of molten slag coating the inside of the furnace, where they are rapidly burned by the scrubbing action of the high-velocity secondary air admitted tangentially along a part of the furnace length. Actual combustion of solid coal and combustible gases is said to be complete when the gases leave the cyclone furnace and enter the primary furnace in the boiler proper.

Another unusual feature is the use of completely pressurized furnaces. In-

---

Paper 51-250, recommended by the AIEE Industrial Power Systems Committee and approved by the AIEE Technical Program Committee for presentation at the AIEE Summer General Meeting, Toronto, Ont., Canada, June 25–29, 1951. Manuscript submitted March 8, 1951; made available for printing May 9, 1951.

RALPH T. WOODRUFF is with the Aluminum Ore Company, St. Louis, Mo.

Figure 1 (above). South Power Station, Dow Chemical Company, Midland, Mich.

Figure 2 (right). Firing aisle showing cyclone burners, South Power Station, Dow Chemical Company

duced draft fans are eliminated entirely and all air requirements are met by high-efficiency axial-flow variable-pitch blowers. Three such blowers are provided, each driven by an 800-horsepower d-c motor, with two in operation. Elaborate sealing arrangements are needed in the boiler to prevent gas leakage, including the installation of 60 pounds per square inch air jets which blow back the flames when small access doors are opened.

Figure 2 shows the firing aisle at the front of the boilers and gives a good view of the completely water cooled cyclone burners. It is worth noting that because of the very thorough heat recovery, the expected over-all efficiency of the steam generators is better than 90 per cent.[3]

Hydrogen cooling of the turbogenerator shown in Figure 3 is certainly not common industrial plants but becomes economically attractive in a machine of this size. As a matter of fact, this 30,000-kw turbogenerator is the largest double-extraction unit ever built. In the foreground two boiler feed pumps can be seen, one being motor-driven and the other turbine-driven. Figure 4 gives a good view of the console control board and boiler control panels. Above the boiler board at the left can be seen a uniscope television set which permits observation of hot slag drainage from the primary into the secondary furnace. The thought put into the design of the control boards is reflected in the compact arrangement and neat appearance.

Looking at the simplified steam flow diagram in Figure 5, it will be seen that steam is bled from the turbine at 425 and 165 pounds per square inch gauge pressure as required in the process, and exhausted at 25 pounds per square inch gauge pressure. Maximum flows at each pressure are indicated but, of course, these maximum flows cannot be taken simultaneously at all pressures. Exhausts from the turbine driven boiler feed pumps and forced draft blowers go to the 25 pounds per square inch pressure mains, the steam from which is used for boiler feed water and building heating, and for miscellaneous services.

From the foregoing brief description it is clear that one commonly used measure of power plant investment, namely; cost per installed kilowatt, is not applicable to plants of this type. In a base-loaded central station, the boiler capacity here installed could furnish steam to generate approximately 90,000 kw as compared to the 30,000-kw turbogenerator actually installed. Computing the cost per kilowatt on the basis of the installed generating capacity in a plant such as the South Power Station would result in a figure that would be inordinately large and hence misleading.

Means of providing heat for process other than by steam boilers and turbines are in use. One notable installation is that of a mercury boiler and turbine at the Pittsfield Works of the General Electric Company.[4] In this case, additional power and a considerable amount of steam at 640 pounds per square inch gauge pressure were required. The use of a 7,500-kw mercury-unit power plant enabled the generation of 7,500 kw of power and 113,000 pounds per hour of steam of the desired temperature and pressure, and the required ratio of electric power to steam production was obtained. No steam turbine topping unit could have met these requirements.

Figure 6 shows a heat-balance diagram at rated load for the Pittsfield installation. Note that the ratio of electric generation to steam produced is 66.5 kilowatt-hours per 1,000 pounds. Passing the steam flow from the mercury unit to existing extraction turbines results in a net over-all heat rate of 10,800 Btu per kilowatt-hours or a thermal efficiency of about 32

Figure 3 (left). 30,000-kw turbogenerator and auxiliaries, South Power Station, Dow Chemical Company

Figure 4 (below). Duplex control board, South Power Station, Dow Chemical Company

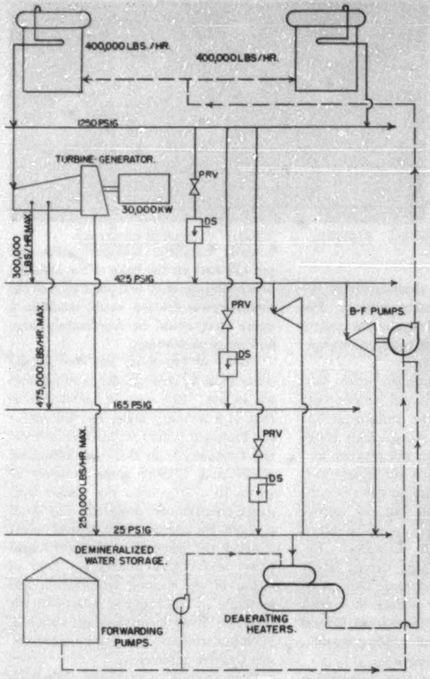
400,000 LBS./HR.
400,000 LBS./HR.
1250 PSIG
TURBINE-GENERATOR.
30,000 KW
PRV
DS
300,000 LBS/HR.MAX.
425 PSIG
PRV
DS
B-F PUMPS.
475,000 LBS/HR. MAX.
165 PSIG
PRV
DS
250,000 LBS/HR. MAX.
25 PSIG
DEMINERALIZED WATER STORAGE.
FORWARDING PUMPS.
DEAERATING HEATERS.

Figure 5 (left). Simplified flow diagram, South Power Station, Dow Chemical Company

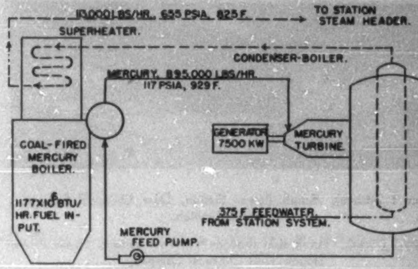
113,000 LBS/HR. 655 PSIA. 825 F.
TO STATION STEAM HEADER.
SUPERHEATER.
CONDENSER-BOILER.
MERCURY, 895,000 LBS/HR.
117 PSIA, 929 F.
COAL-FIRED MERCURY BOILER.
1177X10⁶ BTU/HR. FUEL INPUT.
GENERATOR 7500 KW
MERCURY TURBINE.
375 F FEEDWATER.
FROM STATION SYSTEM.
MERCURY FEED PUMP.

Figure 6 (above). Simplified heat balance at rated load, General Electric Company, Pittsfield, Mass.

per cent, which is remarkable for a plant of this capacity.

The gas turbine offers some interesting possibilities for generating power and furnishing heat requirements. Although no industrial applications appear to have been made to date, one central station installation might be mentioned as indicative of possible use in industry. At the Huey Station of the Oklahoma Gas and Electric Company, a simple cycle gas turbine in conjunction with a recuperator used for feed water heating from turbine exhaust gases, has been running very satisfactorily for more than a year.[5] Operating in conjunction with the steam station, the gas turbine reduces the overall heat rate, and increases the total capability. An increase of 7,400 kw in total capability for station at maximum load was obtained at an installed cost of less than $100 per kilowatt. The incremental heat rate for the gas turbine unit is 12,000 Btu's per kilowatt-hours.

At the present time it appears that gas turbines cannot compete with efficient steam or diesel generating plants because of the high first cost of units with efficient heat cycles, as well as because of fuel limitations. Where low cost gas or oil is available, a simple cycle low cost gas turbine may have a place particularly if heat can be recovered from exhaust gases.[6]

It is in order to mention here a proposal which has been made to apply gas turbine technique to steam power.[7] Briefly, the idea is to use superheated and compressed steam as the gaseous medium in a gas turbine instead of the usual gases of combustion. A portion of the exhaust steam from this turbine is then available to do work in a conventional condensing turbine and, after being condensed is added to the remainder of the exhaust from the gas turbine to desuperheat the steam. The desuperheated steam is then compressed, superheated and sent back to the gas turbine. Using this cycle with 1,200 degree Fahrenheit entrance steam temperature, and appropriate regenerators and air preheaters, the author computes a net plant efficiency of 40.85 per cent. With 1,600 degree Fahrenheit entrance temperature, the net plant efficiency is calculated at 48.2 per cent. Such efficiencies seem to be theoretically possible but there are practical difficulties involved in the operation of compressor, superheaters, and regenerators at the temperatures and pressure needed which, if not insoluble, would certainly make the cost of such installations enormous. Until some actual economic and operating data are available, this scheme cannot be of more than academic interest to industrial power plant engineers.

A case which frequently arises, especially in connection with chemical plants, is that in which an excess of power over and above the plant requirements can be generated economically by the steam needed for process. When such a condition occurs, an arrangement can often be worked out with the local public utility to sell the excess power to it at cost in return for a stand-by connection without the usual expensive charge. Both the industry and public utility can benefit by such an arrangement, not only from a cost standpoint, but also from the help that each may be able to give the other in emergencies.

Another condition is that in which the public utility undertakes to furnish steam for process use as well as power. A good example of such service is that of the Gulf Utilities Company sales to the industrial area of Baton Rouge, La.[8] In another instance, an industrial center in East Newark, N. J. supplies steam and power to 40 independent and diversified manufacturing firms within a small area.[9]

Plants Having Heat Available from Process

In order to simplify the classification, there have been included under the above heading all plants which may have heat available for power generation, whether in the form of waste heat directly from the process or in the form of by-product fuel. Many chemical plants, paper mills,

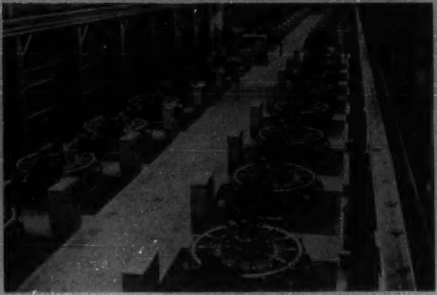

Figure 7 (left). Engine room, Aluminum Company of America, Point Comfort, Tex.

Figure 8 (right). 1,100-kw d-c generator, Aluminum Company of America, Point Comfort, Tex.

sugar cane refineries, saw mills, and the like may have heat available in some form or another. However, the steel industry tops them all in this respect and the discussion here will be confined to this industry.

A large and well-integrated steel plant will have waste heat and by-product fuel in the shape of blast furnace gas and coke oven breeze over and above the plant needs, and this fuel can be burned in boilers to produce a large amount of power. Coke oven gas and tar also may be available but it is usually more economical to burn this fuel elsewhere in the plant or sell it. Considerable low pressure steam is required for process and heating, and the demands for power are also very large. Designing a suitable power house for such a plant will necessitate a thorough knowledge of all steam and power demands, as well as of the by-product fuel availability.

Ordinarily, it will be found advisable to generate steam with the by-product fuel up to the maximum at all times. It will usually be desirable to generate this steam at some higher pressure than would be needed in the plant and supply the plant steam requirements through noncondensing turbogenerators, thus obtaining a portion of the plant power requirements at a very low heat rate. The balance of the high pressure steam can then be used to generate power in condensing turbogenerators. Generally the plant power requirements will be in excess of what can be supplied economically by the steam plant. In most cases, this excess power is best purchased from public utilities.[10,11]

A number of power plants have been built or are building for steel plants. Time will not permit detailed description of any one here but attention may be called to the trend to high temperature and pressures, as well as to the large size of some recent installations. For example, the Carnegie-Illinois Steel Corporation is just completing an installation in a plant near Chicago which consists of a 650,000 pounds per hour steam generator and a 60,000-kw turbogenerator.[11] The boiler burns blast furnace gas and the steam conditions are 1,025 pounds per square inch gauge pressure and 900 degrees Fahrenheit total temperature. Turbogenerator speed is 3,600 rpm and the turbine exhausts at 29 inches of vacuum with five bleed points for feed water heating. Hydrogen cooling is employed in the generator.

Very Large Power Requirements

Some industries are such large consumers of power that their demands are comparable to those of public utilities. These industries may elect to generate their own power requirements on the grounds that they can build the necessary power plants at as low costs and operate them as efficiently as the public utilities. If the needs of any industry dictate the location of its plants at points where large blocks of public utility power are not available except over long transmission lines, the proposition becomes increasingly attractive, particularly if extreme reliability of service is of prime importance in the operation of the plants.

The electrochemical industry is characterized by its disproportionately large use of power as compared to other types of industries. In this group, the aluminum industry is one of the best examples. Because of the large amounts of power needed to reduce the oxide of aluminum to metal, very low cost power is essential in order to produce the metal at reasonable cost. In the past, the demands were met by the construction of hydroelectric plants, at first by private enterprises, and more recently by government agencies. However, the unprecedented demands for aluminum since World War II have resulted in power demands beyond the capacity of existing hydroelectric systems to supply them.

In an effort to supplement its power generating facilities and thereby increase its aluminum-producing ability, Aluminum Company of America constructed and began operating last year a plant at Point Comfort, Tex., which embodies a number of novel features. Located on the Gulf of Mexico about 110 miles southwest of Houston, the Point Comfort plant has access to large quantities of natural gas at reasonable cost. To furnish the demands of the adjacent reduction works, 120 gas engine generators of new design have been installed in the engine rooms. These units furnish direct current at suitable voltage to the pot lines, doing away with the need for the conversion equipment normally required when alternating current power supply is employed.

The engine generators are housed in three engine rooms each containing forty units arranged in two rows of 20 each. Figure 7 gives a good view of one engine room showing clearly the horizontal radial-type engines, each with its own automatic control panel nearby. Rated 1,600 horsepower at 360 rpm, the engines are 2 cycle, 11 cylinder, and can be adapted with slight modification to gas, diesel fuel, or dual fuel operation. Thermal efficiencies are stated to be approximately 30 per cent.[13] Basically, the radial engine design is said to result in a simple, compact and sturdy arrangement, light weight, minimum foundations and small floor space. This engine with its welded base is a little over 12 feet wide, 9 feet 4 inches high, weighs about 85,000 pounds and can be shipped by rail as an assembled unit.[14]

Two noteworthy design features of this

radial gas engine will be mentioned. In most radial engines, master connecting rods are necessary to prevent rotation of the crank pin bearing. The same result is obtained in the new engine by an ingenious arrangement of gears so that all connecting rods are identical and are connected to a master gear which gyrates instead of rotating. A new ignition system was designed which is expected to operate for long periods of time without attention or maintenance, and also to insure a very low rate of spark plug electrode erosion. Ignition energy is supplied by a special impulse generator supplying accurately timed, unidirectional impulses. No cams, breaker points, brushes, collector rings, or rotor windings are involved in this generator.

The d-c generators in the Point Comfort installation are mounted beneath the engines and coupled directly to them. A net capacity of 1,150 kw is realized from each unit with engine auxiliaries motor driven from auxiliary a-c windings on the generators furnishing 425 volts at 24 cycles. An excellent view of a generator showing its accessibility for maintenance is given in Figure 8.

Space will not permit any more detailed description of this interesting power plant which is the largest of its kind in the world. Operating data on the new engines are not yet available, although it is known that they have been performing very satisfactorily to date. However, from the information which has been published, it is clear that in this plant its designers expected to utilize low-cost fuel efficiently without incurring transmission or conversion losses, and to secure lower first costs as well as greatly reduced maintenance costs through the compact, simplified design of the engine-generators. The power for the reduction plant might, of course, have been secured in other ways as from a steam generating plant or by purchase. As more information becomes public, it will be instructive to compare the costs for this gas engine-generator plant against the conventional power sources.

Other than the example given above, no outstanding applications of internal combustion engines for industrial power generation have been found. While the diesel engine inherently has a good thermal efficiency, the high first cost of the units, the relatively high cost of diesel fuel, and the operating labor and maintenance costs, together with the difficulty of obtaining any substantial heat recovery from the exhaust gases, seem to make the diesel engine unattractive to industries except, perhaps, as a standby source of power.

References

1. The Industrial Power System. *Electrical World* (New York, N. Y.), volume 131, May 12, 1949, number 21, page 13.

2. Census Data Reveal United States Power Pattern. *Power* (New York, N. Y.), volume 94, July 1950, page 120.

3. Pioneer Industrial Cyclone Furnaces for Dow Chemical's 1,250 PSIG Boiler. *Power* (New York, N. Y.), volume 93, March 1949, page 72.

4. Mercury Unit Tops Pittsfield Plant, Vorras A. Elliott. *Power* (New York, N. Y.), March 1950, volume 94, number 3, pages 77–84.

5. Hury Gas Turbine Ticks Off 3,400 Hours, J. W. Blake, R. W. Tumy. *Power* (New York, N. Y.), volume 94, February 1950, pages 96–101.

6. Economic Place of Today's Gas Turbines, A. G. Mellor. *Electrical World* (New York, N. Y.), volume 134, number 7, August 14, 1950, pages 88–92.

7. Application of Gas Turbine Technique to Steam Power, J. F. Field. *Combustion* (New York, N. Y.), volume 21, April 1950, number 10, pages 55–58.

8. The Industrial Power System. *Electrical World* (New York, N. Y.), volume 131, May 12, 1949, number 121, page 14.

9. How One Plant Serves 40 Industries, Comdr. Wm. J. Rotte, Jr. *Power* (New York, N. Y.), volume 94, November 1950, pages 120–22.

10. Power, Steam and Fuel Balances for a Modern Steel Plant, A. D. Mowry. *Proceedings*, Association of Iron and Steel Engineers (Pittsburgh, Pa.), 1947, pages 432–35.

11. Relation of the Power Load to Steam and Fuel Balances, Howard L. Halstead. *Proceedings*, Association of Iron and Steel Engineers (Pittsburgh, Pa.), 1947, pages 435–42.

12. Industry Seeks Fuel Flexibility. *Power* (New York, N. Y.), volume 94, December 1950, pages 90–100.

13. Aluminum Company of America, Point Comfort, Texas, Rex W. Wadman. *Diesel Progress* (New York, N. Y.), July 1950.

14. Design Features of the Nordberg Radial Engine, D. I. Bohn, Emil Grieshaber. *Paper number 50-OGP-1*, The American Society of Mechanical Engineers (New York, N. Y.), 1950.

No Discussion

Problems Confronting the Designer in Starting Large Motors

CARL M. LATHROP
ASSOCIATE AIEE

CHARLES E. SCHLECKSER
NONMEMBER AIEE

WITH the increase in use of electric power throughout industry and with large electric motors superseding the steam turbine in the large prime mover's field comes the accent on starting large motors. This problem is no respecter of system capacity. The petroleum industry, for example, finds itself in a period when product distribution and available crudes require the use of cracking processes. The fluid catalytic cracking process is popular in this field and among the major power consumers is the air blower and the gas compressor found in this type of unit. It is not unusual to find a 1,000-horsepower motor or larger on a system having a 4,000-kw demand.

It follows that the larger the motor and the smaller the system capacity, the more difficult the starting problem. Even with specially designed motors, that is, designed to have especially low inrush currents, the voltage drop may be appreciable. The effects of this sudden drop in voltage are not unknown. Among the effects that can be readily seen is the effect on lighting facilities supplied from the same system. Another effect is the increase in system current flowing to other motors on the system occasioned by the drop in voltage. Large voltage drops impair the ability of the motor being started to accelerate its load to full speed. There also are occasions where the power supply authority will allow only a certain maximum voltage fluctuation at the point of supply.

Quite apart from these factors are the more intangible factors, such as damage to the distribution system occasioned by the transient overvoltages that may be created by the sudden change in voltage. Other loads on the same system may require a relatively consistent voltage supply and will not tolerate excessive voltage variation.

When confronted with the problem of starting a motor, it is quite usual to determine first the allowable voltage drop under the particular circumstances. Many factors need to be evaluated including the number of starts expected in any period of time and the service. For example, the frequent starting of an air conditioning motor in an office building will require a voltage drop much less than that resulting from an equally large motor in the yard area of some industrial plant. Experience in many instances dictates this figure.

It will be first determined if the expected drop is within the system allowable limit. Then it will be determined if this drop is acceptable to the motor and load starting requirements. For purposes of this discussion, it is assumed that it has been determined that a 15 per cent voltage drop will be acceptable from the system or utility supply point of view if it is otherwise satisfactory.

For the complete investigation several items of information will be required. The Wr^2 of the combined motor and its load is required. These data are usually available from motor manufacturers and the manufacturers of equipment. In this instance a centrifugal pump is assumed. Also required is data on the variation of motor line current with speed. The power factor values at various speeds will be required if high accuracy is desired. The torque versus speed curve for the motor at rated voltage will be required, as well as the torque speed curve for the load for the conditions under which it will be accelerated.

To aid in visualizing the problem a typical example will be used. For the particular example, these data are as follows:

Wr^2 (pump) = 163 pound feet squared
Wr^2 (motor) = 3,400 pound feet squared
Wr^2 total = 3,563 pound feet squared
Motor—full load current = 211 amperes
Motor current and torque-speed (See Figure 2)
Pump torque-speed (See Figure 1)

The initial voltage drop can be determined from the equation

$$\%V_d = \frac{100X_s}{X_s + 0.577\dfrac{V_t}{I_m}}$$

in which X_s is the system phase to neutral impedance in ohms to the motor terminal, I_m is the inrush current for the assumed constant V_t. The system impedance can be obtained from several sources. If short-circuit current or the kilovolt-amperes of the system is known, the X_s can be calculated. If this information is not available, it can be approximated by assuming maintained voltage on the primary of the supply transformer and using only transformer impedance. If the motor is to be added to an existing system, it can be determined by starting one of the existing motors reading the drop in voltage and the current. These values are substituted in the foregoing equation and X_s determined.

For the present example X_s is taken at 0.236 ohms on a 3,300-volt base, V_t is 3,000 volts while I_m equals 1,310 amperes. When substituted above, the equation yields 15.2 per cent.

Having determined that the initial inrush current will create a voltage drop of 15.2 per cent and inasmuch as 15 per cent voltage drop had been assumed to be acceptable from the point of view of system requirements, the investigation can continue. However, had this voltage ex-

---

Paper 51-251, recommended by the AIEE Industrial Power Systems Committee and approved by the AIEE Technical Program Committee for presentation at the AIEE Summer General Meeting, Toronto, Ont., Canada, June 25–29, 1951. Manuscript submitted March 5, 1951; made available for printing May 7, 1951.

CARL M. LATHROP and CHARLES E. SCHLECKSER are with the Standard Oil Development Company, Linden, N. J. Mr. Schleckser now is on leave with the United States Navy.

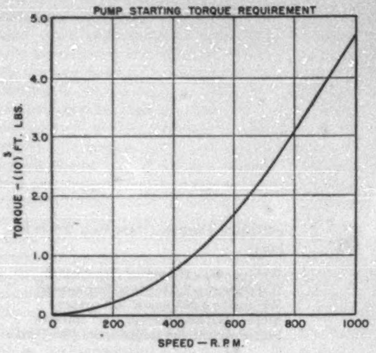

Figure 1 (left). Torque - speed characteristics of load used in the typical example

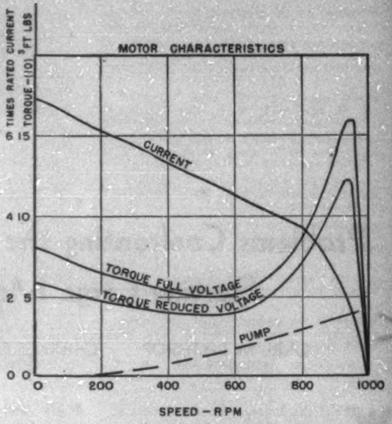

Figure 2 (right). Motor characteristics used in the typical example

ceeded the allowable limit, there are several things that could have been done to reduce the voltage drop. For example, an inspection of the foregoing calculations indicates that the system impedance has an effect on this voltage drop. Decreasing system impedance would assist materially in improving the voltage drop situation. The use of cable instead of open wire line construction may well be a factor in these determinations. It should be borne in mind that reducing system impedance will increase the interrupting duty.

After having reduced the system impedance to the practical minimum, the problem can next be solved by reducing the voltage at the motor terminals at the time of starting through the use of reduced voltage starters, or as is common in Europe, the reconnection of the motor from delta to star.

The use of a reduced voltage starter increases the cost over and above the minimum investment for an across-the-line starter. There is, therefore, the economic consideration of using larger system or substation transformers which have the effect of reducing system impedance with the attendant larger cost. This increment of cost should be contrasted with the incremental cost of reduced voltage starters. In making this economic comparison, one also must consider installation labor cost and not just material cost alone.

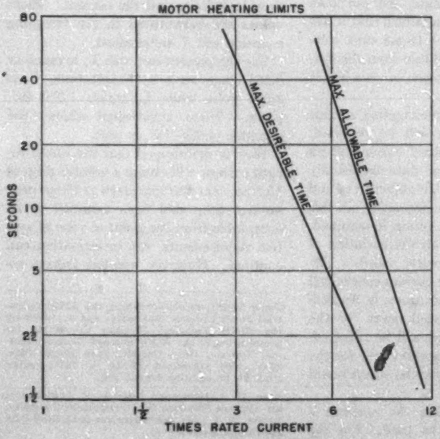

Figure 3. Maximum desirable and allowable motor heating limits

Motors specially designed to have a low inrush current may have an application. However, this also is an economic problem and should be so evaluated, keeping in mind that such motors have lower starting torque.

There is a further limitation placed on reduced voltage starting in that the torque the motor will develop decreases as the square of the applied voltage. A motor being started with 75 per cent normal voltage applied to its terminals will develop only 56 per cent as much torque as it would have had at full voltage and this torque may not be sufficient to accelerate the machine to full speed.

This later phase of the investigation will now be examined. Reference to Figure 2 will indicate the motor characteristics. It is to be noted that near half speed the motor torque is at one of its lowest values. For simplicity the load starting torque requirement has been added to this figure in the form of the dotted curve. The difference between the load torque requirement and the motor developed torque under the particular voltage condition is the torque available for acceleration. Should the motor torque curve intersect that of the load, the machine would fail to accelerate beyond the speed indicated by the point of intersection.

The fact that the motor torque curve always exceeds that of the load is not always a complete guarantee of satisfactory operation. Should, for example, the load requirement very nearly equal the value developed by the motor, the difference available for acceleration would be so small as to result in a long acceleration time. The high inrush current during starting can then be detrimental to the motor.

The determination of accelerating time is probably the most time-consuming part of the investigation. The method is probably best explained by actually following the procedure for the assumed example. The data in the first two columns of Table I is taken directly from the "motor characteristic curves" Figure 2. Convenient 100-rpm steps have been used. More accuracy would be had if the steps were more numerous and the increments less than 100 rpm; however, it is believed that in most cases the data could not support the presumed accuracy.

The motor impedance Z_m is first obtained by:

$$Z_m = 0.577\frac{V_t}{I_m}$$

where V_t is the nameplate voltage of the motor and I_m the full voltage current at the various speed steps. Actually, the motor current is somewhat less than tabulated due to the system voltage drop. This corrected current is obtained, and tabulated, by:

$$I_n = 0.577\frac{E}{Z_m + Z_e}$$

Z_e is the system impedance and E the system voltage on which it was determined. In the example, $V_t = 3{,}000$ and $E = 3{,}300$ volts. Z_m and Z_e should theoretically be added vectorially, however, over 80 per cent of the range of speed the motor power factor varies from 25 to 40 per cent. Normally system impedances are taken as entirely reactive, 0 per cent power factor, whereas actually resistance is present to the extent that system impedances and motor starting impedances are nearly in phase. For the present purposes they are added arithmetically.

The motor terminal voltage is then

$$V = I_n Z_m$$

which is translated to per cent, bearing in mind that V is a phase to neutral value.

The per cent of full voltage torque (% *FVT*) follows from the voltage thusly:

$$\% \, FVT = \left(\frac{V}{V_t}\right)^2 100$$

All of the values are a function of speed; therefore, the appropriate full voltage torque is read from Figure 2 and when multiplied by the corresponding % *FVT* results in the available reduced voltage torque.

For example, the zero speed motor voltage is 92.8 per cent, the % *FVT* is then 86.1 per cent. From the torque speed curve at zero speed is read 8,300 pound feet torque which when corrected by the 86.1 per cent factor becomes the tabulated 7,146 pound feet value.

The incremental acceleration time is obtained from

$$\Delta t = \frac{3.25(10)^{-3} Wr^2(N_2 - N_1)}{\Delta T}$$

which is derived as follows: conventionally

1. $f = ma$
2. $m = \frac{w}{g}$
3. $a = \frac{V_2 - V_1}{\Delta t}$
4. $f = \frac{w}{g}\,\frac{V_2 - V_1}{\Delta t}$

and $V = 2\pi rN$ generally which when substituted specifically in (3) becomes

$$a = \frac{2\pi r}{60}\,\frac{(N_2 - N_1)}{\Delta t}$$

With the force f being applied at the radius of gyration r, torque T being equal to fr; solving for Δt gives the required equation.

Incremental times are calculated for each increment of speed. The torque value in the equation is the average difference between the motor torque and the load requirement.

Applying this torque to the torque time equation results in a value of 0.170 second required to accelerate from 0 to 100 rpm. Similarly the other values are determined, entered in Table I and the total 2.65 seconds derived. The acceleration time of 2.65 seconds is not particularly long considering the size of the motor and the smallness of the system for the chosen example. However, it is known that rapid and successive starting of squirrel-cage induction motors, wherein large quantities of heat are suddenly liberated in the rotors, create undesirable situations. For example, the brazing material between the rotor bars and the ring construction is melted and thrown out of the machine by centrifugal force. This heat can in time be transmitted to stator windings with their more delicate insulating materials.

A set of limiting conditions is indicated by Figure 3. The data may vary between manufacturers and models of the same manufacturer, but, in general, the limits shown are probably not too unrealistic. Figure 3 shows a plot of allowable and desirable starting times in seconds as a function of current. In the chosen example, it is to be noted from the figure that the maximum desirable inrush current is about seven times normal. Had the conditions of the problem indicated that the motor was experiencing an inrush current of more than seven times normal, it then would have been in the region of the maximum allowable time. A calculated acceleration time and inrush current inconsistent with the maximum desirable and maximum allowable curves should seldom be tolerated.

Table I

Rpm	Motor Full Voltage Current*	Z_m	Z_m+Z_e	Motor Current In**	Motor Voltage †	Per Cent Motor Voltage	% FVT	RVT	Delta Torque	Seconds
0	1,310	1.32	1.56	1,220	1,610	92.8	86.1	7,146		
									6,820	0.170
100	1,250	1.39	1.63	1,170	1,626	94.0	88.4	6,545		
									6,070	0.190
200	1,200	1.44	1.68	1,130	1,627	94.0	88.4	5,845		
									5,260	0.220
300	1,140	1.52	1.76	1,080	1,642	94.6	89.5	5,306		
									4,537	0.255
400	1,080	1.60	1.84	1,035	1,656	95.7	91.6	4,942		
									3,820	0.308
500	1,025	1.69	1.93	987	1,668	96.4	92.9	4,650		
									3,275	0.354
600	965	1.79	2.03	940	1,682	97.0	94.1	4,800		
									2,280	0.501
700	900	1.92	2.16	885	1,700	98.0	96.0	5,760		
									4,273	0.278
800	835	2.07	2.31	825	1,708	98.5	97.0	8,135		
									7,012	0.168
900	750	2.31	2.55	747	1,725	99.5	99.0	12,840		
									5,533	0.209
990	200	3.66	3.90	215	1,862	107.0	114.0	6,876		
Total Seconds										2.65

*At 3,000 volts.

**At 3,300 volts.

†Phase to neutral values.

No Discussion

High-Voltage Motor Controllers Co-ordinated with Distribution Switchgear

T. B. MONTGOMERY
FELLOW AIEE

T. H. BLOODWORTH
MEMBER AIEE

IN DESIGN of distribution systems, protection from short circuits is provided by circuit breakers and relays. The prime requirement being the opening of the circuit with safety, the reclosing is of little concern, normally, beyond a few closed-open-closed cycles on automatic reclosing systems.

In applying motor controllers in a distribution system frequent closing and opening is normally required. In addition the controllers must either interrupt short circuit currents or withstand them thermally and mechanically until interruption takes place elsewhere.

The objective is to:

1. **Review the problems in applying circuit breakers and motor controllers to distribution systems.**
2. **Recite in chronological sequence typical steps that have been taken to meet short circuit protection in high-voltage a-c motor controllers.**
3. **Describe a controller arranged to perform the duty of control and co-ordinate its functioning with distribution switchgear by passing the interrupting duty on to the latter above the controller's interrupting rating.**

When the electrical engineer lays out a plant distribution system his concern principally is with:

1. Physical location—the arrangement of bus and cable runs to be nearest driven machines, and future ones, with least material and cost.
2. Voltage levels.
3. Voltage regulation.
4. Power factor.
5. Circuit protection.

Equipment for the protection and switching of his system is designed by switchgear engineers who deal with circuit breakers and relays which have evolved over many years for this specific purpose. Switchgear engineers are accustomed to thinking in terms of system short-circuit capacity but not in terms of motor characteristics and the control of the motor.

Equally well recognized is the fact that equipment to control motors, machines and processes is designed by control engineers and they are concerned with such items as: Initial starting current; starting; reversing; protection; speed control; stopping; braking.

The control engineer is not accustomed to thinking in terms of system short-circuit capacity. He has enough problems of his own and does not want to have to calculate short-circuit currents to properly apply his equipment. His standardization and cost would be affected if modifications were necessary to fit different system short-circuit values. Most of the manufacturers of control equipment do not make fault interrupting devices.

Yet high-voltage circuit breakers have been applied, for many years, in some types of motor controllers. Few, however, are being used today, the ones used being principally on very large motors, that start and stop infrequently.

Circuit breakers for controlling large motors are, for convenience, usually grouped in the same line with other plant switchgear units. Also, protection similar to that furnished generators is required, normally including differential protection, phase failure and reversal and over-temperature indication and alarm.

The Circuit Breaker—the Way It Is Rated

Table I shows the American Standard schedule of preferred ratings of power circuit breakers.

The function of a circuit breaker is to interrupt the flow of power in a circuit. This may be at light currents such as line charging or transformer magnetizing currents, rated load currents or at maximum short circuit currents. Normally, the circuit breaker remains closed at all times. In applying it as a power switch in motor control the repeated opening and closing it will stand, must be considered.

For application of distribution circuit breakers, such as (1) in Figure 1 in selecting from Table I the following factors are to be met:

1. Continuous current rating.
2. Rated voltage.
3. Short time current rating such as: momentary; and 4 second.
4. Tripping time.
5. Interrupting capacity.[1]

The values of continuous current rating given in Table I are for 60 cycles. Most manufacturers have established the same current values for 25 cycles and intermediate frequencies but circuit breakers are de-rated for frequencies higher than 60 cycles.

The distribution system short circuit current determination is based upon the direct axis rated voltage subtransient reactance of the connected synchronous generators and the direct axis rated voltage transient reactance for connected synchronous motors. The symmetrical rms short circuit current, is multiplied by

---

Paper 51-252, recommended by the AIEE Industrial Power Systems Committee and approved by the AIEE Technical Program Committee for presentation at the AIEE Summer General Meeting, Toronto, Ont., Canada, June 25–29, 1951. Manuscript submitted March 19, 1951, made available for printing May 14, 1951.

T. B. MONTGOMERY is with the Allis-Chalmers Manufacturing Company, Milwaukee, Wis., and T. H. BLOODWORTH is with the Allis-Chalmers Manufacturing Company, West Allis, Wis.

Table I. American Standard Schedules of Preferred Ratings of Power Circuit Breakers (ASA C37.6, 1949)

	Voltage Ratings			Insulation Level Withstand Test		Continuous Rating Amperes	Short Time			Interrupting Ratings		
	Rated Kv	Max. Design Kv	Min. Rated KV for Int. Mva	Low Freq. Rms Kv	Impulse Test Kv	Continuous 60 Cycles	Momentary	4 Second	3-Phase Rated Mva	Amperes at Rated Voltage	Max. Amperes	Time, Cycles
						Indoor Oil Power Circuit Breakers						
1	4.16	4.76	2.3	19	60	600	10,000	6,300	25	3,500	6,300	8
2	4.16	4.76	2.3	19	60	1,200	20,000	12,500	50	7,000	12,500	8
3	7.2	8.25	2.3	26	75	600	20,000	12,500	50	4,000	12,500	8
4	7.2	8.25	2.3	26	75	600	40,000	25,000	100	8,000	25,000	8
5	7.2	8.25	2.3	26	75	1,200	40,000	25,000	100	8,000	25,000	8
6	7.2	8.25	2.3	26	75	2,000	40,000	25,000	100	8,000	25,000	8
7	13.8	15.0	4.0	36	95	600	35,000	22,000	150	6,300	22,000	8
8	13.8	15.0	4.0	36	95	1,200	35,000	22,000	150	6,300	22,000	8
9	13.8	15.0	4.0	36	95	1,200	60,000	36,000	250	10,600	36,000	8
						Indoor Oilless Power Circuit Breakers						
1	4.16	4.76	2.3	19	60	600	20,000	12,500	50	7,000	12,500	8
2	4.16	4.76	2.3	19	60	1,200	20,000	12,500	50	7,000	12,500	8
3	4.16	4.76	3.5	19	60	600	40,000	25,000	150	21,000	25,000	8
4	4.16	4.76	3.5	19	60	1,200	40,000	25,000	150	21,000	25,000	8
5	4.16	4.76	3.5	19	60	2,000	40,000	25,000	150	21,000	25,000	8
6	4.16	4.76	3.85	19	60	1,200	60,000	37,500	250	35,000	37,500	8
7	4.16	4.76	3.85	19	60	2,000	60,000	37,500	250	35,000	37,500	8
8	7.2	8.25	4.6	36	95	1,200	51,000	32,000	250	20,000	32,000	8
9	7.2	8.25	4.6	36	95	2,000	51,000	32,000	250	20,000	32,000	8

a constant depending upon circuit breaker tripping time, to give the asymmetrical short circuit current to be interrupted.[1] The constant for a circuit breaker with an 8-cycle tripping time (standard for distribution circuit breakers) is unity, indicating that the d-c component of the short-circuit current will have decayed completely by the time the protective relays operate and the circuit breaker trips.

This method has served quite well in practice in making circuit breaker applications. It gives an approximation resulting from simplifying assumptions. Arc impedance and impedances of feeder lines, busses, and cables are neglected which tend to give conservative values. On the other hand, all induction generators and motors are neglected. As has been pointed out, in cases of large proportions of load in induction motors or generators, on phase-to-phase short circuits, a little less than one-half locked rotor current will be maintained on sustained short circuit. Also the growing use of static capacitors for power factor correction, particularly in metropolitan areas with resulting increase in excitation energy provides substantial contribution to 3-phase short circuits. These factors need to be taken into account.

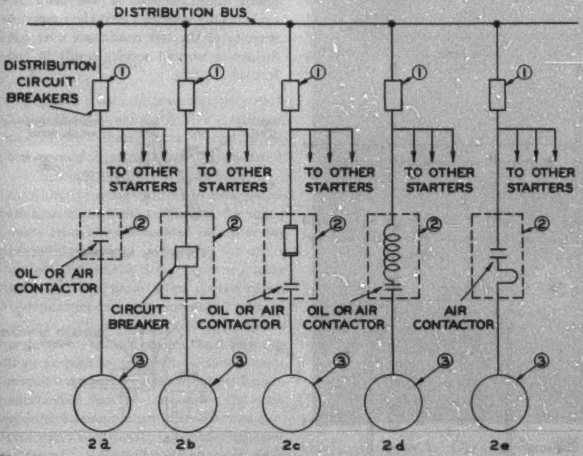

Figure 1. High-voltage controllers for a-c motors

The collection of statistical data which will show cost and risks involved in operating systems with short circuit currents above circuit breaker ratings, will be of great help to the engineer in industry.

The Motor Line Contactor—the Way It Is Rated

A definition which has been proposed for a controller is "apparatus for modulating the flow of power in a circuit."

In processes, for example, where controlling heating is involved the modulating may consist in connecting and disconnecting the power as is also the case in starting and stopping a motor where time is normally an element. This involves repeated opening and closing of the power handling contactor.

Unlike Table I for circuit breakers, in Table II the rated current for contactors is given on an 8-hour continuous basis. The reason for this difference in current rating is based on the difference in duty cycles in application and consequent difference in contact structures. The circuit breaker generally has a silver contact for current carrying and a separate copper or tungsten alloy contact for current interruption. This construction is illustrated in Figure 2. The contactor, using the same tip for current carrying and interrupting must utilize a material suitable for both functions. This construction is illustrated in Figure 3. Forged copper tips are satisfactory for an interruption (silver exhibits too great a tendency to welding) and excellent current carrying ability when contact surfaces are clean. Copper contacts held closed at full rated current for long periods may result in build-up of oxides on the current carrying

Table II. Standard High Voltage Air Break Contactors for Heavy-Duty Motor Starting 200 Amperes and 400 Amperes, 5,000 Volts, 25–60 Cycles

Number of Poles	Continuous Ampere Rating 8-Hr. Basis	KVA Interrupting Capacity at 2,500 Volts	KVA Interrupting Capacity at 5,000 Volts	Maximum Horsepower 2,000–2,500 Volts Synchronous 1.0 P.F.	2,000–2,500 Volts Synchronous 0.8 P.F.	2,000–2,500 Volts Induction	4,000–5,000 Volts Synchronous 1.0 P.F.	4,000–5,000 Volts Synchronous 0.8 P.F.	4,000–5,000 Volts Induction
3	200	25,000	25,000	900	700	700	1,500	1,250	1,250
3	400	25,000	35,000	1,750	1,500	1,500	3,000	2,500	2,500
3	400*	50,000	50,000	1,750	1,500	1,500	3,000	2,500	2,500

All ratings designed for following tests: 60-kv impulse; 19-kv dielectric; 35,000-rms ampere momentary through current with fuses.

* 50,000-kva contactor has a through current rating of 25,000 amperes for 30 cycles (0.5 second)—for use on motor

surfaces resulting in overheating. Operation every eight hours or less will break the oxide and insure a clean contact surface. In most cases operations are numbered per hour or minute.

The kilovolt ampere interrupting capacity is given only at rated voltage. Thus the 400-ampere contactor in Table II with an interrupting capacity of 50,000 kva will interrupt approximately 12,000 amperes at 2,500 volts and one-half this current value at 5,000 volts.

The method of calculating distribution system short-circuit kilovolt amperes in applying these contactors is unlike that used for circuit breakers in that it is based on symmetrical rms short-circuit current.[2,3] This is due to two conditions: the advent of the high-voltage power fuse, about which more will be said later; and the fact that most controllers are equipped with thermal overload relays. Thermal relays require more time to trip than circuit breakers through which power is fed.

This method is suitable for controllers using fuses that effectively limit the short-circuit current well below the peak of the first-quarter cycle. For controllers using fuses which pass a substantial part of the first-quarter cycle and for those passing the interrupting duty to circuit breakers elsewhere in the circuit, the d-c component of an unsymmetrical short-circuit current cannot be safely overlooked. Damage to contacts caused by through currents is greatest during the first-quarter cycle on through current faults.

The voltage rating is on the same basis as the motor, or similar apparatus which it controls. The contactor will withstand 10 per cent over its voltage rating and will remain closed down to 85 per cent normal voltage, being magnetically held closed and not latched in as is the case with the circuit breaker.

These contactors also have a maximum horsepower rating for synchronous and induction motors at rated voltage levels. This is based both on the 8-hour continuous current rating and the motor initial starting current which is the value of current when connected to the line with the rotor stationary. This value is determined, of course, solely by the impedance of the motor windings since no counter electromotive force is present without rotation. Other ratings include 60-kv impulse similar to the equivalent rated circuit breaker and 19-kv dielectric test.

While ratings have not been assigned, and probably none are necessary, Figure 4 shows closing time of 4.1 cycles with a 220-volt 60-cycle operating coil and Figure 5 an opening time of 4.1 cycles to the fully open position for the 200 and 400-ampere contactors. Contact separation occurs 1.4 cycles after the operating coil is deenergized.

These are important in many applications, particularly reversing dynamic braking and reversing plugging motor controllers. Since circuit breaker closing times are 15 to 30 cycles generally, and in such controllers motor stopping times are fixed at a minimum by law, operating times make the use of circuit breakers impractical.

In this connection, Figure 6 shows interrupting time at various values of current. It is interesting to note that, for example, in a reversing dynamic braking control with suitable mechanical interlocks to prevent two contactors being closed at once, from operating times in Figures 4 and 5, it is practical to have the dynamic braking contacts touch before the line contactor arc is extinguished, if only motor light running current (no load) is opened. This is of no concern since, with the momentary connection of the braking resistor to the line, current from the line is increased and from the curve of Figure 6 with such increase the interrupting time is lessened and the arc is quickly extinguished.

In connection with the curves of Figure 6, giving arcing time at light currents on the high-voltage contactors listed in Table II, there is an interesting comparison between operations in testing, in accordance with National Electrical Manufacturers' Association (NEMA) Standards, and actual conditions in service.

The curves show arcing time as measured in the short-circuit test laboratory with 15 per cent factor. Point *A* in Figure 6 shows time for interrupting the light running current of 12 amperes on a 150 horsepower, 2,300 volt, 3-phase, 60-cycle induction motor under service conditions. The time is less than 1/4 cycle. Points *B* and *C* show the opening of the circuit to a 300-horsepower 2,300-volt 3-phase 60-cycle synchronous motor with light running currents of 19.5 amperes and 27.4 amperes respectively. The arcing time likewise is less than 1/4 cycle. This indicates that the margin in severity of the test conditions over conditions in normal service result in conservative rating.

Figure 2 (below). Circuit breaker current carrying and interrupting contacts

Figure 3 (right). Contact tips of oil immersed contactor, showing arc interrupting and current carrying areas

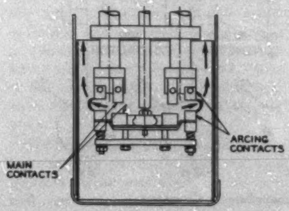

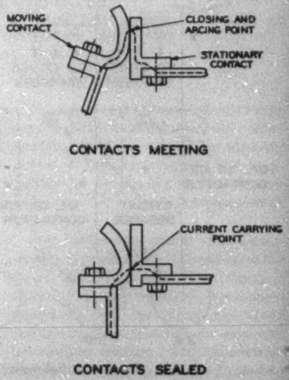

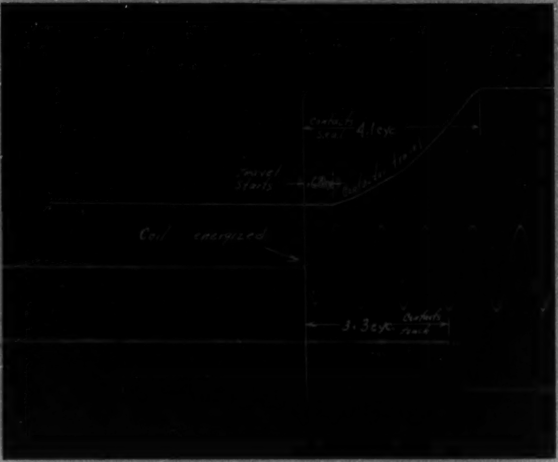

Figure 4. Closing time of 200-ampere 5,000-volt air break contactor

Still other ratings are 35,000 rms amperes momentary through current ratings for use with power fuses for all sizes in Table II, and 25,000 amperes through current rating for 30 cycles (0.5 second) for the 400 ampere size having 50,000-kva interrupting capacity. The description of, and reasons for, these ratings is the principal object of this paper. Steps in development which, over a period of years, have led to these ratings may be of interest and aid in evaluating them.

Control Evolution

Figure 1 shows diagrammatically various methods of across-the-line starting of motors on a distribution system giving the order of these steps in development.

Consider the motor (3) at 2a in Figure 1 for which a controller (2) is to be selected. On motors 550 volts and below, for many years contactors immersed in air as the insulating medium into which the arc is projected when the circuit is opened, have been used except in a few special cases. The practice has been successful because of three factors. At low voltages the impedances of the arc, cables, and busses is high enough in per cent to limit short-circuit currents to values which seldom do substantial damage. Secondly, the ratio of interrupting ability to continuous current carrying capacity in contactors is not constant. A contactor for example, with 8-hour current rating of 100 amperes will in general, interrupt considerably more than ten times this value on short circuit. This does not hold for a 3,000-ampere contactor. In the larger ratings, special blowout means and the like must be resorted to. The voltage level greatly affects the interrupting ability of a given design of apparatus. Often on d-c controllers where single break contacts are used on 250 volts, double break is used on 600 volts, employing the equivalent of two contactors.

Thirdly, the vast majority of controllers are 100 horsepower or less. The economics are such that the expense of replacing a single unit is not serious. However, the increase in short-circuit currents in distribution systems and the cost of outages in industrial processes is altering the importance of the problem. Until recently, on motors with voltages of 2,000–2,500 volts and 4,000–5,000 volts, representing the larger horsepower rating, oil contactors were used following the former trend in circuit breakers. The trend to increased use of the air contactor will be discussed later in the paper.

Let us leave for a time the interrupting duty on short circuits and consider only the requirements of starting and stopping the motor. The initial starting currents of induction and synchronous motors of 250 to 3,000 horsepower at speeds 300 to 3,600 rpm are shown in Table III.

As indicated, the maximum starting current when the motor is connected to the full line voltage at standstill is 625 per cent. The way controllers have been rated, and still are, for such motors is that line contactors shall handle ten times locked rotor current, thus allowing ample margin for any condition of operation. Such controllers are classified in NEMA Standards as class *A* controllers.[3]

Figure 7 shows such a controller, push-

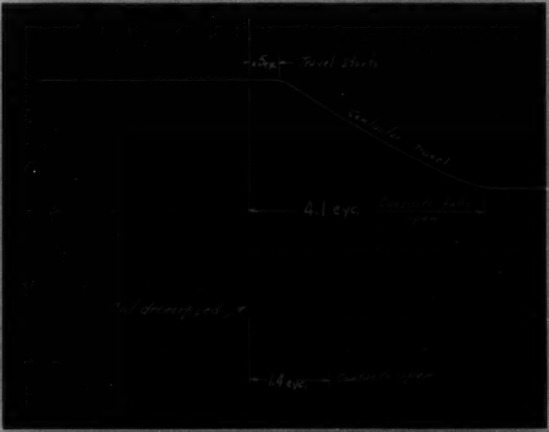

Figure 5. Opening time of 200-ampere 5,000-volt air break contactor

Forward contactor operation, 220 volts a-c, contact springs 14-117-500 mk 020

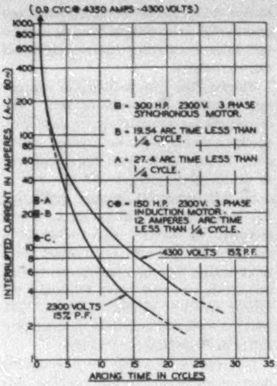

Figure 6 (left). Interrupting time of 200-ampere 5,000-volt air break contactor for small currents

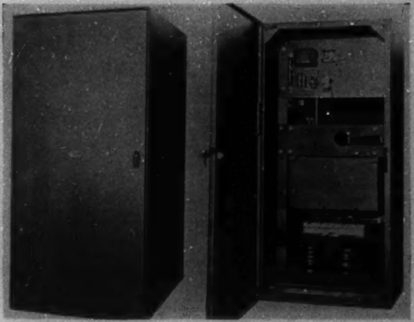

Figure 7 (right). Class A autotransformer reduced voltage controller having oil-immersed contactor. Left: Front view, door closed. Right: Rear view showing contactor and autotransformer

button operated, for auto transformer reduced voltage starting. A 3/5-pole oil immersed contactor is in the center and the auto transformer is at the bottom. This contactor is capable of handling any currents encountered in starting and stopping but is not intended to handle short circuits. The thermal overload has enough delay to cause another device such as circuit breaker 1 in 2a of Figure 1, to trip first in such cases. But since the controller is not tested for short circuit through currents there is no assurance it will withstand them thermally and mechanically while circuit breaker (1) is tripping. The connection for another and parallel type control for this same motor is shown at 2b in Figure 1.

Table III. Initial Starting (Locked Rotor) Currents, A-C Motors

Large Squirrel Cage Induction Motors; 250/3,000 Horsepower 440/2,300 Volts

Poles	Synch. Speed, Rpm	Initial Starting Current, Per Cent Full Load
2	3,600	575
4	1,800	590
6	1,200	590
8	900	590
10	720	575
12	600	575
14	514	550
16	450	540
18	400	525
20/24	360/300	500

Synchronous Motors

	Initial Starting Current			
	1.0 Power Factor		0.8 Per Cent	
Poles	Up to 500 Hp, Per Cent	Above, Per Cent	Up to 500 Hp, Per Cent	Above 500 Hp, Per Cent
4	675	625	600	575
6	600	550	550	500
8/14	575	500	500	450
16/28	300		275	
30 and above	275		250	

A circuit breaker is used for opening and closing the motor power circuit in place of the oil contactors of Figure 7. The controller may be backed up by the distribution circuit breaker (1) as before or it may be connected directly to the distribution bus depending on short-circuit current available at this point in the system. Here, however, the controller is rated in kilovolt ampere interrupting corresponding to the circuit breaker interrupting rating, and is classified in NEMA Standards[3] as a class *E1* controller if 25,000-kva or 50,000-kva circuit breakers are used.

Electrically operated circuit breaker mechanisms are not built for frequent starts and stops, whereas contactors operate thousands of times in rapid succession.

While this is a second type control, it is not necessarily a step in development since it has been used as long as the contactor type. It is rather a parallel type but is declining in use.

The connections for a third type controller are shown at 2c in Figure 1. This is a step in development in departure from previous control design for in addition to handling normal motor maximum currents it is given an interrupting rating. This controller is classified in NEMA Standards[3] as a class *E2* controller. The power fuses in the controller may or may not be of the current limiting type. As was mentioned earlier, the advent of power fuses made it necessary to know the available short-circuit kilovolt amperes in the system at the point at which the controller is connected. Fuses are available with current limiting characteristic up to 200 amperes. This corresponds to motor sizes up to 700 horsepower, 0.8 power factor, 2,300 volts and 1,250 horsepower, 0.8 power factor, 4,160 volts. Since interruption takes place in considerably less than the first 1/4 cycle (see Figure 8) the short-circuit current will never reach its peak either on a symmetrical or asymmetrical basis of available short circuit kilovolt amperage. Therefore, it is only necessary to insure that the available short-circuit kilovolt amperage at the point of application is within the short circuit kilovolt amperage rating of the fuse on a symmetrical basis.

NEMA Standards[3] define the available short current as "the average of the effective current in the 3 phases" and the effective current is the symmetrical rms value as determined from the last major loop preceding the instant of interruption (from oscillogram).

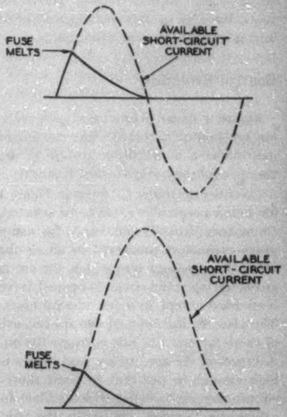
FUSE MELTS
AVAILABLE SHORT-CIRCUIT CURRENT
AVAILABLE SHORT-CIRCUIT CURRENT
FUSE MELTS

Figure 8. Typical curves illustrating current limiting action of one type of power fuse. Left: With symmetrical short circuit. Right: With assymetrical short circuit

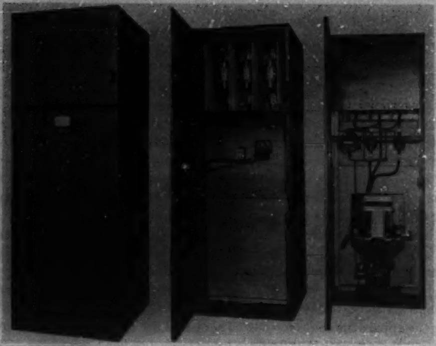

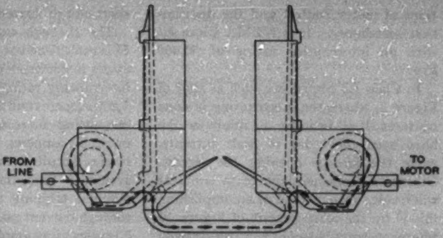

Figure 9 (left). Class E2 controller with power fuses and air break contactor. Left: Front view, with doors closed. Center: Front view, with doors open, showing power fuses. Right: Rear view with door open, showing air break contactor

Figure 10 (above). Current carrying members of air break contactor showing configuration minimizing blow off effect of high currents

Figure 9 shows a class *E2* controller. The front view in the center shows the power fuses at the top, where they are used both as fuse and disconnect. However, on larger motors, for contactors in the 400 ampere size, power fuses available are not current limiting to the same degree as those rated 200 amperes and below. For example, on one type fuse, that is available, which has a maximum continuous current rating of 234 amperes the actual peak current passed by the fuse in instantaneous amperes (including d-c component) is 38,000 for an available initial asymmetrical short-circuit current in rms amperes of 35,000.

The 35,000 amperes rms corresponds to the fuse rating of 150,000 kva at 2,500 volts. Therefore, the contactor and other components of the controller must be capable of withstanding this through current, both thermally and mechanically.

Extensive tests have shown that the contactors of NEMA class *A* standard controllers, handling 10 times motor current, will not satisfy this condition. When power fuses are used ahead of such contactors to substantiate the rating in accordance with NEMA Standards,[3] three close-open unit operations at rated interrupting kilovolt amperage are required.

On such tests with standard oil contactors welding of contacts result on closing or excessive gas is generated in the tank, because the contacts separate from the force of the heavy currents. With air contactors, the contacts weld on the closing stroke.

To meet values given in Table II, heavy duty construction is required and configuration of current carrying parts must minimize the blow open forces from heavy short circuit currents.

Oil Immersed and Air Break Types

The oil immersed contactor and the air break contactor each have design features which may make one more desirable than the other for special applications. For applications in corrosive or explosive atmospheres, since all contacts are located under oil, the oil contactor is applicable where the air break contactor is unsuitable.

Experience has shown that severe arcing on contacts under oil results in shorter life than for contacts operating in air under similar conditions. The oil contactor should not be applied where severe operating duty would result in excessive maintenance. One example is of crushers with line starters where the machine has to be lined up or spotted for lubrication at frequent intervals, say every six hours. The jogging with contacts handling locked rotor current results in severe duty on contact tips and oil. Any insulating oil will carbonize and sludge in time. For this reason parts must be cleaned and oil renewed at regular intervals. Also, the oil constitutes a fire hazard.

Following the trend in circuit breakers, industry is making use, more and more, of the air contactor illustrated in the controller of Figure 9. It is well suited for frequent starting and stopping of a motor, especially where it is expected that a considerable amount of jogging is needed. Fire hazard due to presence of oil is eliminated, maintenance is minimized, and contact life is increased. The arc products, liberated at each interruption, pass off in the air whereas in the oil type some oil carbonization, however minute, occurs. Blow out coils and arc chutes are required.

Reactors for limiting fault currents formerly had wide usage in distribution bus and feeder circuits. Figure 1 shows the connections at 2d to a controller of a fourth type with air core reactors for limiting fault currents to a value within the interrupting ability of the contactor. The use of this type of starter is limited to 600 horsepower and below as voltage loss, size of reactor, and reduction in accelerating torque becomes excessive with larger motors.[5]

The Co-ordinated Controller

Figure 1 at 2e shows the connections for a controller which co-ordinates the func-

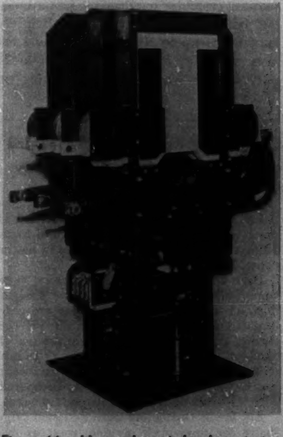

Figure 11. Heavy duty air break contactor, 400 amperes, 5,000 volts, 50,000 kva with through current rating of 25,000 amperes for 30 cycles

tions of motor control and the distribution switchgear. It is NEMA Class *E1* with an interrupting rating of 50,000 kva.

In Class *E2* controllers such as that of Figure 9, where the interrupting is done by fuses, it is desirable to minimize the blow open effect due to fault currents, while the fuse is opening the circuit. Otherwise excessive damage to contacts will result. One method of accomplishing this is by the arrangement of Figure 10 wherein current passes in nearly a straight line. Power fuses generally interrupt, even in largest sizes within approximately one-half cycle.

When, however, the controller is Class *E1*, and in fact any controller other than a Class *E2*, on faults above its own interrupting rating, it must safely withstand fault currents, thermally and mechanically until cleared elsewhere. The thermal capacity is dependent on maintenance of contact pressure. Normally operating magnets are energized from line voltage, which is reduced materially on fault.

The fact that two conductors in close proximity with current in opposite direction, repel each other may be used to maintain this contact pressure. This method is shown in Figure 11 with the motor or load lead disposed under the current carrying contacts in each phase. Short-circuit currents then produce forces on the moving contacts so as to act to force them closed.

The controller may have a thermal relay which operates in the conventional manner on motor overloads. Instantaneous relays cause the contactor to interrupt faults up to 50,000 kva. These relays preferably are equipped with lockout contacts which prevent opening at short-circuit currents above 50,000 kva.

The through current rating in Table II is established at 25,000 amperes for 30 cycles to correspond to the 25,000 ampere interrupting ratings of the 600 amperes, 1,200 amperes and 2,000 amperes continuous rating for circuit breakers to 150 megavolt-amperes listed in Table I for power circuit breakers for distribution systems.[1] Since these breakers all have a nominal tripping time of 8 cycles, the through current rating of the contactor of 30 cycles gives ample time margin for safe tripping.

While Class *E2* controllers, with power fuses, have greatly helped close the gap between control and distribution switchgear in fully protecting the apparatus controlled, users may question three points in their application:

1. Outage time while changing fuses.
2. Possible single phasing.
3. Gap in protection between functioning of thermal OL relay and minimum current at which fuse will blow.

These considerations have thus far caused no concern to users in the field. This is principally due to the fact that in normal service any short circuit results in the flow of full available short-circuit current. There are few little short circuits; but more completely integrated equipment has not been available

Conclusion

1. As late as 15 years ago there was no definite distinction between application of contactors and circuit breakers in motor controllers. Due principally to standardization work of NEMA, control of motors in horsepower ratings falling above 5,000 volts and 50,000-kva interrupting capacity are classified as switchgear. Ratings below these values are classified motor control. These classifications follow generally the dimensions of the duty cycles involved and requirements in the functioning of each class. In the switchgear sizes interrupting ratings are necessary. Also in these sizes highly repetitive operating cycles are not involved, as is the case in the lower kilovolt-ampere ratings.

2. High-voltage motor control has been evolved in recent years to meet the interrupting requirements needed in application and still provide control for rapidly repeated duty cycles.

3. The trend in both controller and circuit breaker design has been to the air-break type.

4. The requirements for a NEMA Class *E1* controller are outlined, namely highly repetitive duty cycle in starting and stopping motors and for protecting its connected load in service.

References

1. Standards for Power Circuit Breakers. *Publication number 46-116*, National Electrical Manufacturers Association (New York, N. Y.), part V, 1946, page 6.

2. High Voltage High Interrupting Capacity A.C. Motor Controllers, G. W. Heumann. *General Electric Review* (Schenectady, N. Y.), April 1950, page 15.

3. Standards for Industrial Control. *Publication number ICI-1949*, National Electrical Manufacturers Assocation (New York, N. Y.), 1949, pages 38–43.

4. System Short Circuit Currents, W. M. Hanna, H. A. Travers, C. F. Wagner, C. A. Woodrow, W. F. Skeats. *Electrical Engineering* (*AIEE Transactions*), volume 60, September 1941, pages 877–81.

5. The Use of Air-Core Reactors as Fault Limiting Means on High Interrupting Capacity Controllers, John D. Leitch. *AIEE Transactions*, volume 68, part I, 1949, pages 469–75.

Discussion

G. W. Heumann (General Electric Company, Schenectady, N. Y.): The author has described in his paper a new design of high-voltage air break contactor for use in motor controllers.

High-voltage air break contactors have been built for many years, some designs dating back 30 to 40 years. They are very important components available to the control engineer, especially since the use of 2,300-volt and 4,160-volt systems in industrial plants has grown considerably in recent years, because of economies as compared with 440-volt distribution in certain areas.

Air break contactors were designed originally for duty-cycle service, such as encountered on mine hoists, cableways, aerial tramways, and similar applications. Frequent starting and stopping of the motors made air break contactors a necessity; contact life is greater than with oil-immersed contactors, and any danger of a fire because of leaky oil tank is absent.

Old-style air break contactors were large and sprawley. When switching motor currents under heavy load conditions, sheets of flame and hot gases, and often parts of the arc, were emitted from the arc chutes. Thus, large spacings between phases and between the contactors and structural parts were required. While such spacings were tolerable on single-motor installations such as in the hoist house of a mine, they became a serious disadvantage when a number of high-voltage motor controllers had to be assembled into a line-up of enclosed control panels. For such applications oil-immersed contactors were normally used in spite of their above-mentioned shortcomings, in order to arrive at practicable control panel dimensions.

Perhaps the most significant feature of modern high-voltage air break contactors is the design of their arc chutes and associated parts. Current interruption takes place entirely within the arc chute, with little, if any, flame emitted. This makes it possible to reduce spacings between phases and between the contactor and adjacent parts. This evolution in design permits air break contactors to be used in enclosures having dimensions comparable to those required for oil-immersed contactors of equivalent rating. This makes it practicable to use air break contactors in enclosed panel line-ups. With the reduction in over-all space requirements, we may expect greatly increased usage of air break contactors for controlling general-purpose high-voltage motors, in addition to continuing their old use for heavy-duty material handling equipments.

J. W. Gibson (The General Electric Company Ltd. of England): The authors point out three difficulties that might arise in the application of power fuses to class $E2$ controllers. I consider that these difficulties are all avoided if there is correct co-ordination between the overload relays and the fuses, whereby the fuses are of sufficiently large current rating to operate only on electrical faults. For motors started on full voltage such co-ordination is usually obtained if the fuses are chosen to carry the locked rotor circuit, with the necessary margin for a time equal to the time of the start. The outage time while changing fuses becomes of no importance since the fuses only blow if there is an electrical fault which must in any case be rectified.

Single-phasing caused by overloading of the motor cannot occur, since under overload conditions the overload relays operate before the fuses.

Provided that an unnecessarily large fuse is not used, there is no gap in protection between the two devices, since the "take-over" value of current can be kept below the interrupting capacity of the contactor.

The Determination of Temperature Transients in Cable Systems by Means of an Analogue Computer

J. H. NEHER
MEMBER AIEE

THE calculation of the ultimate temperature rise of a cable system under a constant load is a relatively simple matter, and the only difficulty experienced is that of determining the proper thermal constants for the components of the thermal circuit. Once these have been determined, the procedure involves only simple arithmetic. If the temperature rise is desired at some time prior to reaching the ultimate, however, or if the load instead of being constant is varying in some prescribed manner, the calculation procedure immediately becomes extremely complicated involving many mathematical computations.

It is somewhat paradoxical that despite the fact that almost all practical cable rating calculations involve operating conditions which fall in the transient category, no satisfactory method of solving such problems on a transient basis is in general use. Although the majority of cable rating problems may be solved in a more or less satisfactory manner by the application of a simple modification of the steady state calculation technique, there is an increasingly greater demand for a satisfactory nonmathematical method of determining the transient temperature change which will occur under given operating conditions. This paper discusses such a method based on the use of electrical analogy and describes an electrical analogue computer designed specifically for the purpose.

General Considerations

In a paper recently presented before the Institute[1] F. H. Buller has presented a history of the attempts of various investigators to represent the constant load temperature transient of the conductor of a cable system mathematically and he has well demonstrated the complexity of the procedure. Even after this transient has been obtained, a considerable amount of laborious calculation remains to determine the transient response to a given varying load. This mathematical complexity results primarily from the fact that under transient conditions the thermal capacitance as well as the thermal resistance of the components of the thermal circuit must be taken into consideration, and also because discontinuities are present in the thermal circuit.[2]

If we consider that in the components where the thermal capacitance is actually distributed such as in the insulation and in the earth, the system may be treated as a series of lumped capacitances, then it will be evident that the entire thermal circuit may be represented by a network consisting of shunt capacitances and

---

Paper 51-253, recommended by the AIEE Computing Devices and Insulated Conductors Committee and approved by the AIEE Technical Program Committee for presentation at the AIEE Summer General Meeting, Toronto, Ont., Canada, June 25–29, 1951. Manuscript submitted March 6, 1951; made available for printing May 9, 1951.

J. H. Neher is with the Philadelphia Electric Company, Philadelphia, Pa.

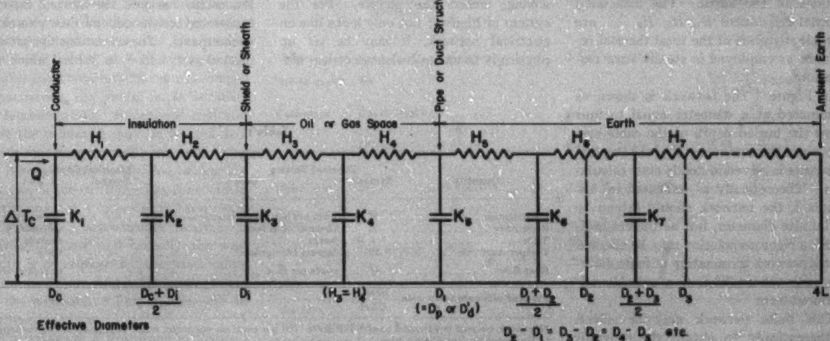

Figure 1. Equivalent thermal network for a buried cable system

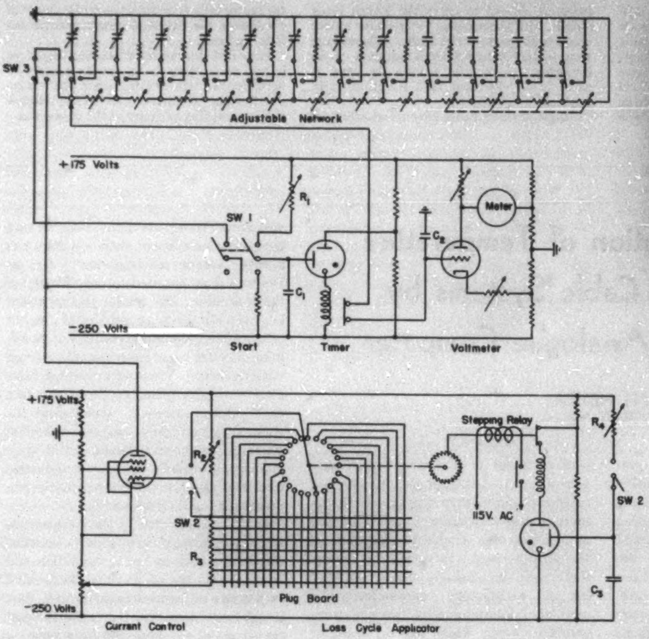

Figure 2 (left). Schematic diagram—analogue computer for cable systems

Figure 3 (above). Network and power supply unit of first model of computer

series resistances. Such a system is shown in Figure 1 applicable to either cables in duct or to a pipe type cable system. In the latter case K_1 represents the thermal capacitance of the conductor, K_2 the lumped thermal capacitance of the insulation, K_3 the capacitance of the skid wires and shielding tapes, K'_4 the lumped capacitance of the oil, K_5 the capacitance of the pipe, and K_6, K_7 . . . the lumped capacitances of successive cylindrical sections of the earth. The associated thermal resistances H_1, H_2, H_3 . . . are suitable divisions of the total thermal resistance as employed in steady state calculations.

In Figure 1 the network is shown as terminated at a diameter equal to four times the buried depth of the cable system, since this embraces all of the thermal resistance involved in steady state calculation. Theoretically as indicated in Appendix I, the network should extend to an infinite diameter, but as therein indicated, a rigorous solution may be effected with a network terminating at finite diameter with the addition of a suitable adjustment term.

This finite network may be solved mathematically to obtain the constant heat input—temperature transient with a degree of accuracy increasing with the number of sections which are employed to represent those components having distributed capacitances. But here again mathematical complexity increases rapidly with the number of sections employed and it would at first appear that nothing was gained by considering the system as such a network.

It is at this point that the electrical analogy enters the picture. For the system of Figure 1 not only looks like an electrical network, it may be set up physically as an equivalent electrical network and solved by the simple procedure of feeding an electric current into it and measuring the voltage developed as a function of time. The current may be either held constant or varied in accordance with any given loss cycle for the cable system under study and the voltage may be measured at any point in the network. The time relationships between the electrical transients and the thermal transients are simply a function of the relationships between the thermal capacitances and resistances and their electrical counterparts. These relationships are indicated as F_c and F_r in Table I which in-

Table I

Quantity	Thermal System Symbol	Thermal System Unit	Electrical Counterpart Symbol	Electrical Counterpart Unit
Capacitance	K	watt hrs per degree centigrade foot	$C = F_c K$	microfarads
Resistance	H	thermal ohm feet	$R = F_r H$	megohms
Time	t	hours	$S_t = F_c F_r t$	seconds
Temperature rise	ΔT	degrees centigrade	E	volts
Heat flow	Q	watts per foot	$I = \frac{E \text{ max*}}{\Sigma R}$	microamperes
Per cent ultimate temp. rise	$\frac{100\Delta T}{Q\Sigma H}$	%	ϕ	%

*Network current is adjusted to give full scale (100 per cent) on voltmeter when connected across the input to the network (capacitors open).

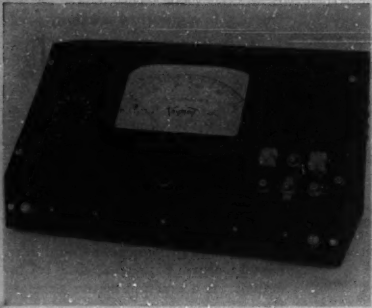

Figure 4 (left). Front view of control unit—first model of computer

Figure 5 (right). Rear view of control unit showing plug board for setting up a given loss cycle

dicates the general relationships between the quantities involved in the thermal system and their electrical counterparts.

The solution of transient heat flow problems in this manner is by no means new and a large and versatile analogue computer for this purpose has been built at Columbia University.[3] The computer described in this paper, however, being designed specifically for cable system analysis, constitutes a unit representing a fraction of the size, cost, and complexity of the Columbia installation.

Calculation of the Components of the Thermal Network

To obtain satisfactory results by this procedure presupposes that the basic thermal network has been set up properly and with the required accuracy, which involves mainly the manner of lumping the distributed capacitances in the insulation and earth portions. The general theory behind this procedure as outlined in Appendix II, consists in dividing these portions into a number of concentric zones of equal radial width in which case the lumped capacitance representation of each zone exceeds that of the preceding zone by a constant amount. The smaller the radial width of each zone or the smaller the incremental increase in lumped capacitances, the greater is the accuracy of representation. Experience indicates that the insulation may be treated as a single zone except possibly when studying oil flow problems in oil-filled cables. In the case of the earth portion, zone widths in the order of 4 inches have been found satisfactory. Considerable latitude is permissible here and actually the zone width is determined by the fixed values of the capacitors used in the earth portion of the computer. This matter will be discussed later on.

The values of K appearing in Figure 1 for each section or zone may be calculated by the equation

$$K = 155\kappa(D_2^2 - D_1^2)\frac{Q}{Q_1} \text{ watt hours per degree centigrade foot} \quad (1)$$

in which κ is the unit thermal capacitance of the medium in watt hours per degree centigrade cubic centimeters, D_1 and D_2 are the inner and outer diameters of the section in inches, Q_1 is the heat flow through the section, and Q is the reference heat flow on the basis of which the network is being set up (usually the losses per cable originating at the conductors).

The values of H appearing in Figure 1 are of course identical with those used in steady state calculations. In the cases of sections or zones having distributed capacitance, the distribution of thermal resistance on each side of the lumped capacitance as indicated in Appendix II is given by the equations

$$H_{1c} = 0.012\rho\frac{Q_1}{Q}\log_{10}\frac{D_1 + D_2}{2D_1} \text{ thermal ohm feet} \quad (2)$$

$$H_{c2} = 0.012\rho\frac{Q_1}{Q}\log_{10}\frac{2D_2}{D_1 + D_2} \text{ thermal ohm feet}$$

in which ρ is the thermal resistivity of the medium in thermal ohm centimeters. Table II gives values of κ and ρ applicable to the various sections and working formulas for K and H.

In a previous paper[6] the author presented a method of calculating the steady state temperature rise of cables in a duct bank in which the earth portion of the thermal circuit is considered to start with the geometric mean diameter of the working ducts D_d', neglecting any slight difference in thermal constants of the duct structure and of the surrounding earth. This procedure fully accounts for all of

Table II

Section	Medium	κ(watt hrs/Ccm)	ρ(Ccm/watt)	K(watt hrs/Cft)	H(thermal ohm feet)
Conductor	Copper	9.6×10^{-4}		$0.15nD_c^2$	
Insulation	Paper	5.7×10^{-4}	700	$0.088(D_i^2 - nD_c^2)$	$3.65G_1/n$** (center K_c)
	Oil filled & oilostatic	5.7×10^{-4}	550	$0.088(D_i^2 - D_c^2)$	$6.6\log_{10}\frac{D_i + D_c}{2D_c} +$ $6.6\log_{10}\frac{2D_i}{D_i + D_c}$
Sheath	Lead	3.9×10^{-4}		$0.060(D_s^2 - D_i^2)$	
Sheath-duct	Air				$\frac{Q_s}{Q}\left(\frac{2.59}{\sqrt{D_s}} + 0.33\right)$†
Cable-pipe	Gas (200 psi)				$0.69\frac{Q_s}{QD_s^{0.7}}$†
	Oil	5.0×10^{-4}		$0.077\frac{Q}{Q_s}(D_p^2 - 3D_s^2)$	$0.48\frac{Q_s}{Q\sqrt{D_s}}$† (center K_s)
Pipe	Steel	10.4×10^{-4}		$0.160\frac{Q}{Q_s}(D_p^2 - D_o^2)$	
Duct structure	Concrete	7.2×10^{-4}		$0.111\frac{Q}{Q_s}(D_d'^2 - N_dD_d^2)$*	
Earth	(per section)	$1/6.45\alpha\rho_e$	ρ_e	$\frac{24}{\alpha\rho_e}\frac{Q}{Q_s}(D_2^2 - D_1^2)$	$0.012\frac{Q_s}{Q}\rho_e\log_{10}\frac{D_1 + D_2}{2D_1} +$ $0.012\frac{Q_s}{Q}\rho_e\log_{10}\frac{2D_2}{D_1 + D_2}$

*See text.

**See reference 4.

†See reference 5.

Nomenclature

α = earth thermal diffusivity, square inches per hour
C = electrical capacitance, microfarads
D_1, D_2 = inner and outer diameters of a section, inches
D_c = conductor diameter, inches
D_i = insulation diameter, inches
D_s = sheath diameter, inches
D_o = inside diameter of pipe, inches
D_p = outside diameter of pipe, inches
D_x = effective diameter of network as set on the computer
D'_d = geometric mean diameter of working ducts in a duct bank, inches (see Reference 6)
E = electrical potential, volts
$Ei(-x)$ = exponential integral of $-x$. (See page 83 of Reference 7)
F_c = equivalence ratio, electrical/thermal capacitance
F_r = equivalence ratio, electrical/thermal resistance
G_1 = geometric factor for multiconductor cables (See Figure 2 of Reference 4)
H = thermal resistance, thermal ohm feet (degree centigrade foot per watt) in text, degree centigrade centimeter per watt in Appendix II
I = electric current, microamperes
$I_0()$, $J_0()$, $K_0()$ = Bessel functions
κ = unit thermal capacitance, watt hours per degree centigrade cubic centimeters
K = thermal capacitance, watt hours per degree centigrade foot in text and watt hours per degree centigrade centimeter in Appendix II
(LF) = loss factor
L = depth of burial of cable system or pipe, inches
n = number of conductors per cable
N_d = number of ducts per bank
ω = angular velocity, radians per hour
ϕ = per cent attainment
Q = heat flow emanating from a conductor, watts per foot
Q_1 = heat flow in a section, watts per foot
Q_a = heat flow in the air space for cables in duct, watts per foot
Q_e = heat flow in the earth, watts per foot in text and watts per centimeter in Appendix 1
Q_o = heat flow in the oil for oilostatic cables, watts per foot
ρ = thermal resistivity degree centigrade centimeter per watt
ρ_e = thermal resistivity of the earth, degree centigrade centimeter per watt
r = radius, centimeters
r_1, r_2 = inner and outer radii of a section, centimeters
R = electrical resistance, megohms
S_t = equivalent computer time setting, seconds
t = time in thermal system, hours
ΔT = temperature rise, degrees centigrade
ΔT_c = temperature rise at conductor, degrees centigrade
ΔT_{4L} = temperature rise at diameter $4L$, degrees centigrade
ΔT_x, T_x' = adjustment terms, degrees centigrade
ΔT_y = temperature rise at diameter D_y, degrees centigrade
ψ = angular displacement, radians

---

the resistance in the thermal circuit; but to include all of the thermal capacitance it is necessary to introduce a lumped capacitance at the start of the earth portion which is based on the area within D_d' less the void area of all of the ducts in the bank.

In setting up a thermal system such as shown in Figure 1 on an analogue computer, difficulty arises due to the extremely large amount of electrical capacitance required to represent the earth portion out to a diameter of $4L$ in respect to the amount required to represent the internal portion, the ratio being in the order of 400-to-1 for a typical pipe-type cable problem. As a practical matter, however, it is only necessary to extend the thermal circuit out to a diameter sufficient to effectively filter out the variations in input current when studying the effect of a cyclically varying load, since, as indicated in Appendix I, the temperature rise in the portion omitted is simply and accurately calculated by merely applying the loss factor of the cycle. This procedure reduces the required capacity to about 10 per cent of the value for representation out to a diameter of $4L$ with a corresponding reduction in the thermal resistance set on the computer to about 70 per cent of that of the total circuit in a typical case.

Similarly in reproducing the transients resulting from a constantly applied load, the computer network may be terminated at any convenient diameter at least five times the inner diameter of the earth portion with the addition of an adjustment term. This adjustment term developed in Appendix I, becomes effective after a period of time, which increases with the termination diameter. It should be noted that even with the network extended to a diameter of $4L$, there is still an adjustment term.

Analogue Computer Design

In the design of an analogue computer to be used specifically in the solution of transient heating problems in cable systems, portability and relative simplicity are of major importance since the device presumably will be set up and used in an engineering office. Portability is achieved by the use of electrical counterparts of relatively small electrical values and correspondingly small physical size. These in turn result in a relatively short duration of the electrical transient, and introduce problems as to the manner of its recording. The principal uses of the device may be summarized as follows:

1. Short time emergency ratings–determination of the per cent of ultimate temperature rise after a given time with constant load.
2. Effect of load factor–determination of the maximum temperature rise which will occur during a given cyclically applied loss cycle.
3. Oil flow problems–determination of the temperature rise at various points in the cable system as a function of time.

A consideration of these uses indicates that except in the somewhat special third case, a time plot of the transient is not required. As a practical matter therefore the additional expense and complication of a suitable curve drawing voltmeter involving a high speed chart and power amplifier is not justified provided that arrangements are made to take a voltage reading at the end of any desired time interval. With this system transient-time curves may be prepared by the point-to-point method if desired and the curves of Figures 7 to 9 were so obtained. Of course, a suitable graphical recorder may be added to the system if so desired.

Figure 2 shows schematically the principal elements of the computer, consisting of an adjustable resistor-capacitor network, a current control system, a vacuum tube voltmeter, an electronic timer, and a suitable power supply. The vacuum tube voltmeter may be connected to any point in the network and it serves to measure the voltage developed at that point without drawing any current from the network, and thus affecting the transient obtained. The electronic timer offers a means of disconnecting the voltmeter from the network at any desired time during the transient, and the voltage measured at the instant of disconnection is held on the relatively small capacitor C_2 associated with the voltmeter until the meter can be read. The desired time setting is made on the adjustable resistor R_1.

The network is connected in the plate circuit of a pentode vacuum tube which has the property that its plate current and therefore the network current is, under certain conditions, to a good approximation, a function of its grid potential and independent of its plate potential or the voltage developed across the network. Variation of this grid potential is accomplished by the tapped potentiometer R_3 and its series resistor R_2. With the grid connected to the 100 per cent tap, R_2 is adjusted until the network current is such that the voltmeter reads full scale (100 per cent) across the network. If the R_2R_3 circuit is properly proportioned, the

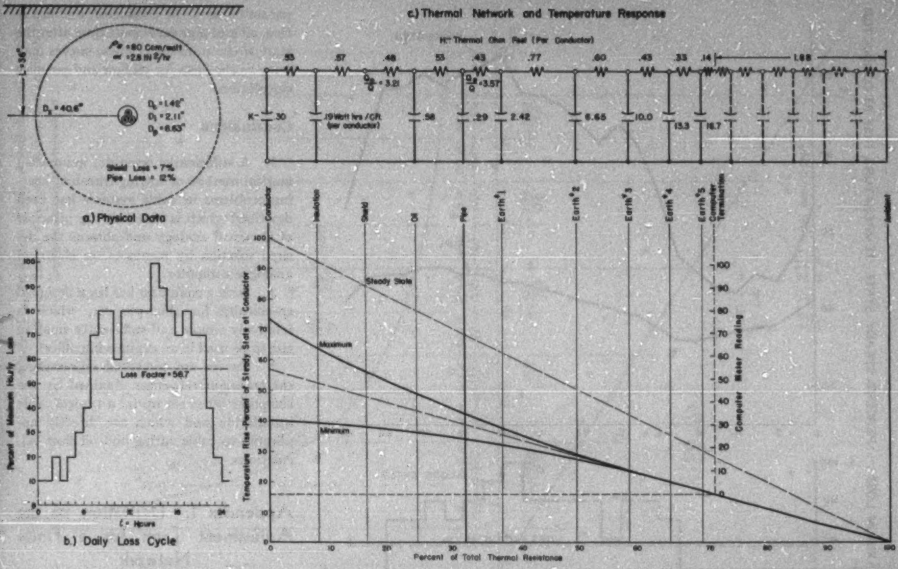

Figure 6. Pipe type temperature response to a cyclic load

relative values of the network current obtained on other taps on R_3 remain fixed irrespective of the total resistance in the network and consequent variation in R_3 for a full scale setting. The taps on R_4 are arranged to give 10 per cent steps in network current. The network current may be varied cyclically in accordance with a given loss cycle by a 24-point stepping relay which selects the proper tap on R_3 for each step through a plug board arrangement. The stepping rate is controlled by a relaxation oscillator and is adjusted by the adjustable resistor R_4. An auxiliary connection not shown in Figure 2 serves to permit a voltmeter reading at the end of any selected step of the cycle.

The network consists of 12 sections, of which the first seven are identical units having maximum values of 1.1 microfarads capacitance and 1.1 megohms resistance adjustable in 1 per cent steps. As many of these units as needed are used in setting up the internal portion of the thermal system. The eighth unit is similar except that the maximum capacitance is increased by 5 microfarads. The ninth unit is a composite affair embracing the last four sections which have nonadjustable capacitors of 10, 15, 20, and 25 microfarads respectively and suitably proportioned resistors gang adjusted in five steps to give a total resistance of the unit of 0, 1, 2, 3, or 4 megohms. The eighth and ninth units together with the resistor portion of the seventh unit are used in setting up the earth portion of the network for relatively small effective diameters of the cable system. For larger effective diameters such as a multicable in duct structure, the eighth capacitor is used to represent the lumped capacitance of the duct structure. A gang-operated switch is provided to disconnect and discharge each of the capacitors prior to making a transient run. This switch also sets up the circuit for adjusting the network current.

The network is set up by first determining values of F_c and F_r which will permit setting the earth portion exactly by the available settings on the eighth and ninth units. With these values established there is sufficient latitude in the range of the remaining units to set them accurately. For most problems it is possible to make the product F_cF_r equal to unity (one second electrical corresponds to one hour thermal) or some integer multiplier thereof, thus establishing an integer relationship between the time in hours in the simulated thermal system and time in seconds on the computer. In studying the very early portions of transients, it is desirable to expand the settings for the thermal network to the fullest extent by suitably combining the available units in the computer, thus increasing the F_cF_r product and effectively expanding the time scale of the computer for greater accuracy.

Figures 3, 4, and 5 show the first model of the computer which was assembled in two cabinets only to make use of a network and power supply assembly previously constructed for another purpose. The components are all standard radio parts with the exception of the plug board shown in Figure 5.

Application

A typical application of the computer is illustrated in Figure 6, which shows the equivalent thermal network for a typical 1,500,000 circular mil oilostatic cable installation. The portion of the network indicated was set up on the computer, and the loss cycle shown was then applied. The resultant maximum and minimum temperature rises at various points in the network are given by the curves shown directly below the network, which were taken after a large number of cycles had elapsed.

The fact that these curves converge with a line representative of the loss

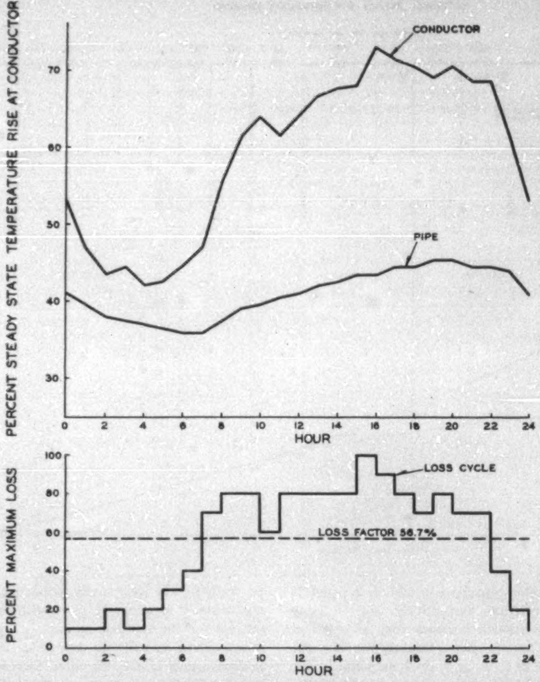

Figure 7. Pipe and conductor temperatures for a given loss cycle—1,500,000 circular mil oilostatic cable in a 6-inch pipe

factor of the cycle before the end of the portion of the network setup is reached indicated that a sufficient portion of the network has been included and that the temperature rise of the excluded portion may be simply calculated and added to the temperature rise obtained on the computer.

Figure 7 shows the cyclic variation of temperature rise both at the conductor, and at the pipe. The phase displacement between the maximums and minimums of these two curves is clearly indicated.

In similar manner the temperature-time transient curves for a constant load were obtained and are shown in Figure 8. When the time duration is sufficient for the adjustment term to become effective (in this case for times in excess of 30 hours) the adjustment indicated was calculated by equation 5 and added to the temperature rise measured by the computer.

Figure 9 shows the temperature rise per-unit loss at the conductor, midinsulation, oil and pipe for a short time after the start of the transient. These curves may serve as the basis for oil flow and pressure calculations.

Figure 8. Pipe and conductor temperatures for a constant load—1,500,000 circular mil oilostatic cable in 6-inch pipe

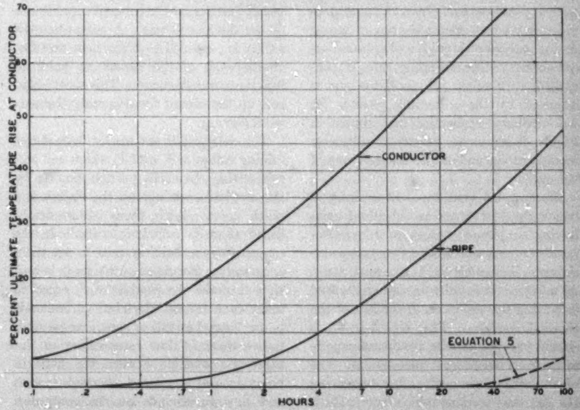

Conclusions

1. A sufficiently accurate, nonmathematical method of solving transient heating problems in cable systems has been described which is based on the principle of electrical analogy and obtains the desired solution by means of an electrical analogue computer.

2. Such a computer has been designed specifically for this purpose, which is relatively simple and sufficiently small in size to be used in an engineering office.

3. Curves are presented representing the transient responses obtained by the computer when set up for a typical cable installation and which are directly applicable to cable rating and oil flow calculations.

Appendix I. Derivation of the Adjustment Term for a Finite Network

Consider the network of Figure 1 as being infinite in extent. The value of ΔT_c obtained as a function of time would then represent the temperature rise at the conductor if the cable system were buried at an infinite depth. To determine the corresponding temperature rise if the system were buried at a finite depth L, we may apply the principle of images and subtract from ΔT_c

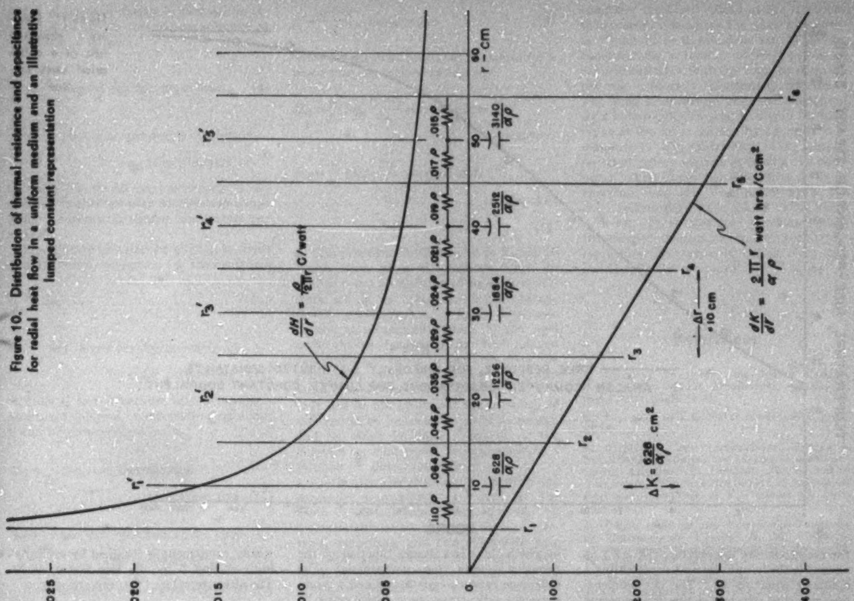

Figure 10. Distribution of thermal resistance and capacitance for radial heat flow in a uniform medium and an illustrative lumped constant representation

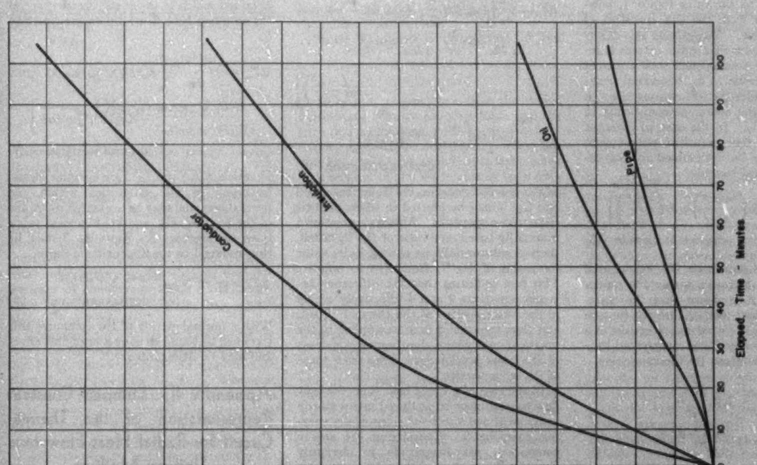

Figure 9. Short time conductor, insulation, oil and pipe temperature rise—1,500,000 circular mil oilostatic cable in 6-inch pipe

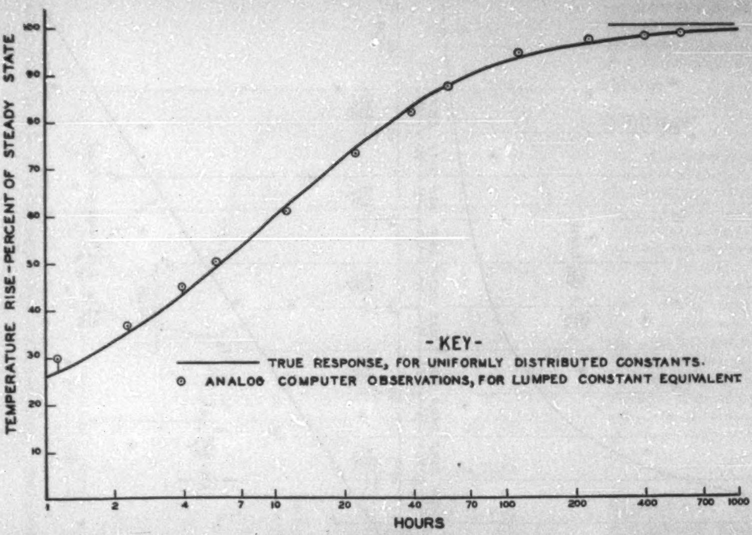

Figure 11. Heating characteristic of a cylindrical earth section

the corresponding temperature rise ΔT_{4L} at a point in the infinite network representing a diameter equal to $4L$. The net temperature rise thus obtained is the true transient temperature rise at the conductor of a cable system at depth L, since this procedure properly considers all of the basic factors involved.

The transient temperature rise ΔT_c obtained across the finite network terminated at $4L$ as shown in Figure 1, however, will differ from the true transient as determined above. To evaluate this difference let us assume that cable system is replaced by a line source, since such a system is readily amenable to mathematical treatment, and consider the temperature rise at a distance from the source corresponding to the diameter D_y. In the case of constant heat flow, the true transient temperature rise at D_y may be determined by the exponential integral formula[1]

$$\Delta T_y = \frac{Q_e\rho_e}{4\pi}\left[-Ei\left(\frac{-D_y^2}{16\alpha t}\right)+Ei\left(\frac{-L^2}{\alpha t}\right)\right] \quad \text{degrees centigrade} \quad (3)$$

in which $Ei(\ )$ represents the exponential integral of the quantity within the parenthesis.[7] It may be shown that the corresponding transient temperature rise for case where the earth is considered to consist of a cylinder of diameter D_x as represented by a finite network is given by the expression

$$\Delta T_y - \Delta T_x = \frac{Q_e\rho_e}{4\pi}\left[\log_e \frac{D_x^2}{D_y^2} - 2.56J_0\left(2.41\frac{D_y}{D_x}\right)\epsilon^{-23.2\frac{\alpha t}{D_x^2}} - 1.13J_0\left(5.52\frac{D_y}{D_x}\right)\epsilon^{-122\frac{\alpha t}{D_x^2}}\right] \quad \text{degrees centigrade} \quad (4)$$

in which $J_0(\ )$ is a Bessel function of the quantity within the parenthesis.[7] The difference between equations 3 and 4 represents the adjustment term which must be added to a temperature rise determined in a finite network terminated at a diameter D_x in order to obtain the true temperature rise which would be obtained with an infinite network. Thus

$$\Delta T_x = \frac{Q_e\rho_e}{4\pi}\left[\log_e 9.0\frac{\alpha t}{D_x^2} + 0.0006\frac{D_x^2}{\alpha t} + 2.53\epsilon^{-23.2\frac{\alpha t}{D_x^2}} + 1.05\epsilon^{-122\frac{\alpha t}{D_x^2}} + Ei\left(\frac{-L^2}{\alpha t}\right)\right]$$

$$= Q_e\rho_e\left[G_x\left(\frac{\alpha t}{D_x^2}\right) - G_L\left(\frac{\alpha t}{16L^2}\right)\right] \quad \text{degrees centigrade} \quad (5)$$

where for convenience the functions $G_x(\ )$ and $G_L(\ )$ may be plotted in terms of their respective arguments. Although equation 5 is actually based on a ratio of D_x/D_y of ten, there is substantially no change in its value for ratios of D_x/D_y from five to infinity. This fact indicates that the difference between equations 3 and 4 effectively occurs in the outer portion of the thermal circuit, and thus equation 5 may be applied to the practical case where the thermal constants of the inner portion may differ from those of the outer portion.

In the case of a cyclic heat flow, the heat flow pattern may be analyzed into a steady component and a series of sinusoidally varying components. Considering the steady component, its magnitude is obviously equal to the product of the maximum value of heat flow during the cycle by the loss factor of the load cycle producing the heat flow. Thus the adjustment term for the steady component is obtained by multiplying equation 5 by the loss factor, (LF). The ultimate value of this expression is

$$\Delta T_x = \frac{Q_e\rho_e}{2\pi}(LF)\log_e\frac{4L}{D_x} \quad \text{degrees centigrade} \quad (6)$$

Considering a sinusoidally varying component $q\epsilon^{j(\omega t+\psi)}$ the following expression is obtained which is the cyclic counterpart of the constant heat flow adjustment equation 5

$$\Delta T_x' = \frac{q\epsilon^{j(\omega t+\psi)}\rho_e}{2\pi}\left[K_0\left(D_x\sqrt{j\omega/4\alpha}\right)\times\frac{I_0\left(D_y\sqrt{j\omega/4\alpha}\right)}{I_0\left(D_x\sqrt{j\omega/4\alpha}\right)} - K_0\left(4L\sqrt{j\omega/4\alpha}\right)\right] \quad \text{degrees centigrade} \quad (7)$$

in which $K_0(\ )$ and $I_0(\ )$ are complex Bessel functions of the quantities within the parenthesis, and may be evaluated by means of the ber, bei, ker, and kei functions tabulated in reference 8. Equation 7 may be thus reduced to the approximate form

$$\Delta T_x' = q\epsilon^{j(\omega t+\psi)}\rho_e\epsilon^{-0.60D_x\sqrt{\omega/\alpha}(1+j1)} \quad \text{degrees centigrade} \quad (8)$$

With a normal setting of the computer this term will be found to have a negligible effect and may be disregarded.

Appendix II. Lumped Constant Representation of the Thermal Circuit for Radial Heat Flow in a Uniform Medium

The fundamental relationships for radial heat flow in a uniform medium may be stated in terms of change in thermal resistance and change in thermal capacitance as a function of radius r.

$$\frac{dH}{dr}=\frac{\rho}{2\pi r} \text{ degrees centigrade per watt} \qquad (9)$$

$$\frac{dK}{dr}=\frac{2\pi r}{\alpha\rho} \text{ watt hours per degree centigrade square centimeters} \qquad (10)$$

in which ρ is the thermal resistivity of the medium in thermal ohm centimeters and α is its diffusivity in square centimeters per hour.

Equation 10 also may be written in terms of unit thermal capacitance of the medium κ

$$\frac{dK}{dr}=2\pi\kappa r \qquad (10A)$$

$$\kappa=\frac{1}{\alpha\rho} \text{ watt hours per degree centigrade cubic centimeters} \qquad (11)$$

Thus H and K between any two radii r_1 and r_2 are obtained by integrating equations 9 and 10 between these limits.

$$H_{12}=\frac{\rho}{2\pi} \log_e r_2/r_1 \text{ thermal ohm centimeters} \qquad (12)$$

$$K_1=\frac{\pi}{\alpha\rho}(r_2 2-r_1 2) \text{ watt hours per degree centigrade centimeter} \qquad (13)$$

The equivalent network for the earth or a portion thereof may thus be formulated by dividing the earth into a number of concentric zones of radii r_1, r_2, r_3,...such that the difference between any two successive radii is a constant Δr. The lumped capacitance for each zone calculated by equation 13 is logically located at points on the thermal resistances for the respective zones corresponding to the median radii r_1', r_2', r_3',...where

$$r_1'=\frac{r_1+r_2}{2}\ldots\text{centimeters} \qquad (14)$$

Thus the thermal resistance branches for a given zone are divided as follows

$$H_{1c}=\frac{\rho}{2\pi} \log_e \frac{r_1+r_2}{2r_1} \text{ thermal ohm centimeters}$$

$$H_{c2}=\frac{\rho}{2\pi} \log_e \frac{2r_2}{r_1+r_2} \text{ thermal ohm centimeters} \qquad (15)$$

This procedure is illustrated in Figure 10 which shows plots of equations 9 and 10 against r and an illustrative equivalent network set up by taking $r_1=5$ centimeters, $r_2=15$ centimeters,.... Each resistance branch is numerically equal to the area under the resistance curve and each lumped capacitance is equal to the area over the capacitance curve (since this curve is drawn to an inverted ordinate).

It will be apparent that the accuracy of representation increases as Δr is decreased, and for infinitely small values of Δr the network solution would be equivalent to a solution by Bessel functions.

Practically the relationship between the successive capacitances involved in the earth network is fixed in the computer by commercially available unit sizes of electrical capacitors, and this effectively fixes the radius scale of Figure 10 for a particular problem under solution. Figure 10 as drawn is representative of the radius scale for small starting diameters, and the relatively large adjustment of r_1 required is accomplished by adjustment of the first capacitor in the network and its associated resistors.

For relatively large starting diameters the first section of the network is omitted and r_2 is suitably adjusted by changing the radius scale.

Figure 11 shows a comparison of the computer measured values of the transient temperature rise across the network shown in Figure 10 as it would be set up on the computer for a typical oil-filled pipe-type cable installation, with the true temperature rise for uniformly distributed constants. The time temperature rise was calculated for a hollow cylindrical section with the heat input at the inner surface by equation 6 of reference 1. The initial effect of the lumped constant representation in raising the computer values above the true curve is to be expected, but this disappears when the cable system network is joined to the earth network. It is therefore concluded that this lumped constant equivalent adequately represents the portion of the earth system included by the computer.

References

1. Thermal Transients on Buried Cables, F. H. Buller. *AIEE Transactions*, volume 70, part I, 1951, pages 44–55.

2. Discussion by J. H. Neher of reference 1, pages 52–53.

3. A Method for Determining Unsteady-State Heat Transfer by Means of an Electrical Analogy, V. Paschkis, H. D. Baker. *Transactions*, The American Society of Mechanical Engineers (New York, N Y.), volume 64, 1942, page 105.

4. Calculation of the Electrical Problems of Underground Cables, D. M. Simmons. *Electric Journal* (East Pittsburgh, Pa.), volume 29, 1932, equation 19, page 398.

5. The Thermal Resistance Between Cables and a Surrounding Pipe or Duct Wall, F. H. Buller, J. H. Neher. *AIEE Transactions*, volume 69, part 1, 1950, equations 1, 2, and 5 of author's closure, page 349.

6. The Temperature Rise of Cables in a Duct Bank, J. H. Neher. *AIEE Transactions*, volume 68, part I, 1949, pages 540–48.

7. Tables of Functions, Jahnke, Emde. Dover Publications, New York, N. Y., 1945.

8. Bessel Functions for A-C Problems, H. B. Dwight. *AIEE Transactions*, volume 48, July section 1929, pages 812–20.

Discussion

Wm. A. Del Mar: (Phelps Dodge Copper Products Corporation, Yonkers, N. Y.): The most ingenious feature of Mr. Neher's analogue computer is the use of an electronic timer whereby he is enabled to bridge the gap between slow thermal flow and fast electrical flow. Without this device it would be impossible to represent the thermal changes that take hours, by the charges and discharges of condensers which occur in seconds, a ratio of about 3,600 to 1, or a week in less than 3 minutes.

This computer is being used in committee work to mutually check calculations made by F. H. Buller[1] and by an approximate formula developed by Dr. R. J. Wiseman. It also is planned to use it in connection with a committee project for developing calculations on the hydraulics of pipe-type cables having oil as pressure medium.

It is exceedingly useful for computing the oil demand of oil-filled cables, a procedure that now requires laborious calculations with Bessel functions that may take longer for a manufacturer to carry out than the period between an inquiry for such cable and the time that a quotation must be furnished.

Long calculations are not only objectionable because of the time they consume but also because of the great chance they offer for mistakes. The computer overcomes this difficulty.

Reference

1. See reference 1 of the paper.

Dr. A. Gemant (The Detroit Edison Company, Detroit, Mich.): The author, in order to make his circuit much simpler than that of Paschkis', assumes radial symmetry to prevail. However, radial symmetry does not exist in the earth, and not at all in a duct bank; hence, the accuracy will suffer owing to this simplification. The general case is two-dimensional.

The results presented do not appear to contain a verification of the circuit by comparing its data with those obtained in a field installation.

If the method should prove, by experience, sufficiently accurate, it would provide a very elegant way of obtaining temperature transients in cables.

E. L. Harder (Westinghouse Electric Corporation, East Pittsburgh, Pa.): Several papers at the 1951 AIEE Summer General[1–8] Meeting outlining the solution of important engineering problems by the analogue computer show the general acceptance and value of this method, and a number of the other problems discussed could beneficially have used the analogue method. Where direct tests are impractical because of size or cost or inavailability of the equipment in the planning stage, and where calculations are quite involved, the computer or simulator provides an excellent possibility of obtaining the needed data most economically.

On the Anacom computer, which is our general purpose analogue computer, some 220 engineering problems falling into 52 different categories have been handled in a period of three years. Naturally we are enthusiastic.

The choice of general purpose versus

special purpose computer depends on the use and there is a definite field for each. Mr. Neher has mentioned the convenience of the special purpose unit. Where a particular problem must be solved many times for different conditions a special purpose computer is often justified. It can frequently be made more convenient for its particular problem than a general purpose machine used for that problem. The sizes, dial markings, and metering can all be ideal for that problem. Where many different problems are to be solved, the general purpose computer is usually more economical.

This particular computer has been most skillfully executed and the presentation shows the marks of thorough workmanship and care. The author is to be congratulated on presenting all of the information that is essential to understand and use the method with confidence, including the units and conversions and the mathematical background. The computer should prove a very worthwhile contribution to the users of cables.

There are a few detail questions that would clarify certain points in my mind and which might interest others in the audience.

1. How are the 7 per cent shield loss and 12 per cent pipe loss introduced in the analogue of Figure 6?
2. Why is the shield capacitance not used? Is it too small?
3. How are the maximum readings taken for Figure 6? Is this by plotting curves as in Figure 7 for each position or can they be read directly?
4. Why does 100 per cent computer meter reading in Figure 6 not correspond to the steady-state drop in that part of the thermal system represented on the computer?
5. I presume the study assumes equal heat in the other two conductors. (Figure 6)
6. In Appendix I where the rise for a depth D is taken equal to the rise above a cylinder of diameter $4D$. Does this not assume the earth surface to be the ambient, that is, an equithermal plane, above which temperature is measured? Is this justified practically? Might it not heat up?

REFERENCES

1. SOME ENGINEERING APPLICATIONS OF THE ELECTROLYTIC FIELD ANALYZER, **H. K. Farr, W. R. Wilson.** *AIEE Transactions*, volume 70, 1951, pages 1301–09.

2. THE HOT SPOT RISE SIMULATOR, **Clarence F. Book, V. V. Mason.** *AIEE Transactions*, volume 70, 1951, pages 1524–30.

3. A PORTABLE ELECTRONIC PILE KINETIC SIMULATOR, **Walter Pagels.** *AIEE Transactions*, volume 70, 1951, pages 1422–26.

V. Paschkis (Columbia University, New York, N.Y.): The increasing use of analogue computers for heat flow studies is always gratifying and the author is to be complimented on designing a small and compact unit.

The following questions came to this reader who has experience with the large computer mentioned in the paper as reference 3.

1. With the short times used (1 second electric = 1 hour heat), how well can readings be made, particularly shortly after load changes, when temperatures vary rapidly? With a high, but brief overload, say of 15 minutes duration, the "electric time" would be only 0.15 second. On a large computer ample time can be provided to read instruments.
2. In Figure 11 the time scale (abscissa) starts at 1 hour, and even at that time the recorded temperature is roughly 10 per cent too high. How large is the error at early times? Can the error, as shown, be attributed to inaccurate timing of the reading?
3. In equations 1 and 2 the addition of the ratios Q/Q_1 and Q_1/Q respectively needs explanation. The "rate of heat flow through the section" (Q_1) varies with time. What value is taken, and how is the use of the ratio justified?
4. In many instances a cable may be located in earth in the neighborhood of heat sources or sinks. (For example cables running parallel to other cables, to steam or water pipes). In this case, or if the surface of the earth undergoes temperature changes the network as shown is not sufficient.
5. Since a "portable calculator" in the office is of definite value, the reviewer wonders, if a "calibration" by means of a large computer might have any merits. A power company would then study for any of its cables which it considers critical, the total picture by means of a large computer. It might be possible to reduce the different influences mentioned in (4) in such a manner, that "quasi empirical" corrections could be found, to be applied to the portable network, which would be available for day to day solution of operating problems.
6. It would be interesting to see a discussion of the over-all accuracy covering errors caused by the circuit elements (leakage in condensers, nonlinearity in instrument amplifier, tolerance in resistors and condensers) and by the lumping. Such errors are of varying importance for different conditions; the speed of load changes being one example for such conditions. A check on over-all accuracy for various problems might be obtained by comparison with a more elaborate network.

These remarks are not made in a sense of criticism, but rather in the hope that they might enhance the usefulness of this tool.

J. H. Neher: I am very glad that Dr. Del Mar has mentioned the use being made of this analogue computer in connection with certain projects being undertaken by the Cable Characteristics Subcommittee, because these projects furnished the necessary urge to proceed with the development of this device at this time. Remarkably good agreement has been found by comparisons with calculations made on system setups under conditions relatively amenable to mathematical calculations and gives reassuring evidence that the device is theoretically sound. Furthermore, it has made possible the investigation of many more cases than could have been computed mathematically with the limited available personnel.

Dr. Gemant has suggested verification by comparing the data obtained on the computer with that measured in a field installation. It should be recognized that this computer does not present a direct solution of a particular cable heating problem in the same sense that Dr. Gemant obtains such a solution by the use of his reduced scale model.[1] Rather, the properly adjusted computer does only that which would otherwise require laborious mathematical solution of an elaborate thermal network. The formulation of this network, and the dependent settings for the computer require the same information as is needed for the rigorous mathematical calculation. Thus, an agreement between computer and field measured values would indicate primarily that the thermal constants and geometry were representative of the case under consideration. The computer also may be used readily if desired, to check results obtained by use of the Gemant reduced scale model.

The basis of this method is mathematical and it is unfortunate that it has been necessary to condense what could well fill an entire paper into a short appendix. Thus, in regard to the apparent radial symmetry which Dr. Gemant mentions, one might well assume from a casual reading of this paper, that the solution was based on radial heat flow in a system of diameter equal to four times the buried depth of the cable, part of this solution being obtained by setting up a radial system of a lesser diameter on the computer and the remainder of the solution by mathematical calculation for what was left over.

Actually a careful study of Appendix I will indicate that the basic solution involves assymmetry due to location of the cable near the earth's surface. This has been treated in a conventional manner, as previously discussed by the author before the Institute.[2] It so works out as shown in Appendix I that the solution is equivalent to the solution of a radial system as accomplished on the computer plus a calculated adjustment term which accounts for the assymmetry as well as the portion of the system not set up on the computer.

It is very gratifying to have discussions by Dr. Harder and Professor Paschkis, who have had a great deal of experience with analogue computers. Dr. Harder has raised an interesting point in respect to Figure 6 of the paper, and one which is not at first apparent in the figure. For the system shown the steady state temperature drop across the network setup is 72 per cent of the total drop in the system, and this 72 per cent corresponds to 100 per cent meter reading. The length of the meter reading scale shown should thus be 72 per cent of the ordinate of the figure. The base of this meter reading scale on the illustration, however, is placed on the calculated cyclic drop in the 28 per cent of the system omitted which is 18 per cent of the total steady state drop. Thus the 100 per cent meter reading point would fall at 90 per cent ordinate as shown in the figure.

In determining the curves of the figure it was merely necessary to watch the meter as it followed the transient and to note the highest value attained for each position of the voltmeter along the network. If there is any indication that the voltmeter needle cannot follow the transient and steady down during any hourly interval, the true position of the voltmeter at the end of that interval may be obtained by a selective cutout connection not shown in Figure 2.

Professor Paschkis is quite right in pointing out that with a time ratio of 1 second electric to 1 second thermal, a 15-minute transient in the thermal system could not be measured with sufficient accuracy. As indicated in the paper, however, this time ratio is not fixed in the computer, and desirably should be changed when studying short time transients. As an example the component values of the electrical network used in determining the curves of Figure 9 of the paper were so chosen that the time ratio was 10 seconds electric to 1 hour thermal. The 10 per cent disagreement between theoretical and measured values at the start of the curve of Figure 11 is due to the fact that in accordance with the method of formulation of the equivalent electrical network as given in Appendix II the first component of the network is a series resistance. Thus the instant current is applied to the network a voltage drop will appear across this resistance. The theoretical curve on the other hand, has zero temperature rise at the instant that heat flow starts. This disagreement disappears as the transient progresses, but it is still in evidence in this case after 1 hour thermal.

In an actual case the first component of the network is always a shunt capacitance (representing the conductor) and the above disagreement will not be noticeable.

In most cable systems heat is liberated due to losses at more than one point (conductor sheath and pipe where present) and in multiconductor systems, the heat flow in the earth is a multiple of the heat flow in the individual insulations. To simplify the solution for steady-state conditions it is customary to adjust the basic thermal constants involved to values which will give the proper thermal drop in the respective components on the assumption that there is a single source of heat flow originating at one conductor. The Q/Q_1 ratio mentioned by Professor Paschkis constitutes this adjustment. The extension of this procedure to transient solutions is rigorous as far as the multiple paths of heat flow are concerned but not in respect to the additional sheath and pipe losses which should properly be treated as additional current feeds to proper points in the electrical network. The complexity of such an arrangement is not considered to be justified, however, and the conventional adjustment represents a reasonable compromise.

In the case of interference by local heat source or sinks, this is simply handled by either calculating the interference temperature changes if steady state or determining it on the computer if transient and superimposing it upon the solution obtained neglecting the interference. The application of the principle of superposition in this respect has been discussed in a previous paper.[2]

The computer is simply calibrated or adjusted by setting up a simple resistance-capacitance circuit for which the response can be accurately calculated and then observing the response as obtained on the computer, and setting the timing circuits accordingly. The inherent accuracy of this computer is not too great but it is quite sufficient in view of the accuracy with which the components of the thermal network can be determined.

REFERENCES

1. DETERMINATION OF CABLE TEMPERATURES BY MEANS OF REDUCED-SCALE MODELS, Andrew Gemant, Joseph Sticher. *AIEE Transactions*, volume 65, 1946, pages 475–82.

2. THE TEMPERATURE RISE OF BURIED CABLES AND PIPES, J. H. Neher. *AIEE Transactions*, volume 68, part I, 1948, pages 9–17.

Voids and Wax In Solid High-Voltage Cables

FRANK J. POHNAN
MEMBER AIEE

Synopsis: A new method of inspection of impregnation of solid-type cable insulation was developed. This method is based on the property of oils and waxes to fluoresce when activated by ultraviolet light. This method reveals details of impregnation in new cables and wax formation in old cables that are not apparent with ordinary light.

WITH THE advent of higher and higher voltages on underground cables, many new difficulties and problems have arisen for both the cable manufacturers and cable users. It soon was learned that practically all insulation defects resulting either from manufacture, subsequent handling, or actual service of the cable, which remained unnoticed at the lower voltages, forcefully revealed themselves at the higher stresses. Closely controlled processes using the best known materials have greatly improved cables but have not solved all the problems for solid-type cables as indicated by the increased use of oil-filled, gas-filled, and compression cables.

In spite of all the precautions taken by the manufacturers, there still are unpredictable variations even in the best of the solid-type high-voltage cables, which sometimes result in differences in performance, for which there is no satisfactory explanation.

Observations of cable failures in service and failures and incipient failures on accelerated aging tests have led to the conclusion that two types of insulation breakdown are predominant. One is thermal while the other is caused by discharges in voids. When examination shows that a failure is caused by discharges in voids, evidence also indicates that a path (pinhole) is formed through the first, or first few tapes. Subsequently the impregnating compound between successive layers of tape carbonizes forming connected carbonized tracks or treeing, with the branches of the "tree" growing outward from the conductor. This treeing gives a definite, unmistakable and visible clue as to the origin of the breakdown. Except in belted three conductor cables, it almost always can be traced back to ionization in a void at the conductor, or, in a few, rather infrequent cases, to a void at the cable sheath.

To obtain some additional information about the cable insulation deterioration and the mechanism of its breakdown, we have made numerous laboratory tests, and over a period of years inspected and studied the condition of insulation of a great many solid-type impregnated-paper cables of various makes, types, and sizes, new and artificially aged, as well as those which for various reasons were removed from service.

During our investigation we have found, by studying the accompanying wax formations, that the cavitation or void formation in service started in each case in the dielectric wall at about one-third to one-half the distance from the conductor to the sheath. Although the cavitation slowly increases in size with time, in the cases examined, it remains isolated from the conductor until practically all or at least most of the impregnating oil is converted into wax and the cable becomes dry. It was, therefore, suspected that new cables are not void-free, and that there are voids near the conductor strands or sheath because the treeing started either at the conductor or sheath.

At the beginning of our wax studies we have used the magenta wax test developed by Hamilton and described by Robinson.[1] While the magenta wax test is an extremely helpful tool, it is quite laborious, and too slow where a detailed investigation of a large number of cables is involved.

Detailed investigations and studies of cable wax formations are quite difficult. In the absence of a standard method and nomenclature, it is an accepted practice to call the wax formations: a trace of wax, little wax, medium wax, heavy wax,

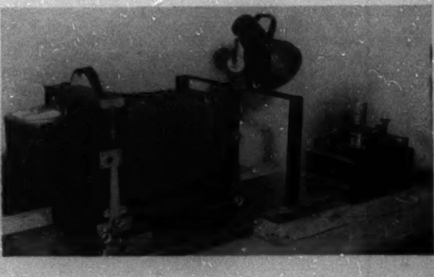

Figure 1. Arrangement of equipment for photographing cable insulation

---

Paper 51-254, recommended by the AIEE Insulated Conductors Committee and approved by the AIEE Technical Program Committee for presentation at the AIEE Summer General Meeting, Toronto, Ont., Canada, June 25–29, 1951. Manuscript submitted March 26, 1951; made available for printing May 9, 1951.

Frank J. Pohnan, now deceased, was with the Commonwealth Edison Company, Chicago, Ill.

The author expressed his appreciation and thanks to A. L. Brownlee for his encouragement and valuable suggestions, and to M. A. Vogt for his assistance in working out the procedure for taking photographs of the fluorescent samples.

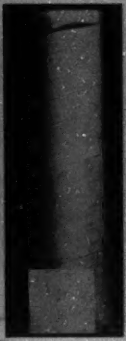

Figure 2 (left). A photograph of one conductor of a new 3-conductor cable, made by ordinary light showing how the insulation impregnation appears to the eye during a conventional inspection. The insulation impregnation seems to be thorough, with uniform oil distribution and without any voids

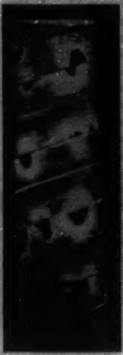

Figure 3 (right). A photograph taken with black light, of the sample shown in Figure 2, without any changes whatsoever being made on the sample between photographs. The distribution and the amount of oil in any spot are shown by the uniformity and degree of whiteness respectively. Poor oil distribution and numerous voids, of various sizes and shapes, not detectable by the conventional method of insulation inspection are clearly visible

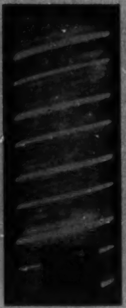

Figure 5 (left). A conductor of a new 3-conductor cable. The impregnation is thorough, distribution of oil is uniform, and the gaps between adjacent turns of tape are completely filled with oil. There are no voids except for two (small) bubbles in one of the gaps (the third white crossbar from the top). This shows that perfect insulation impregnation can be produced

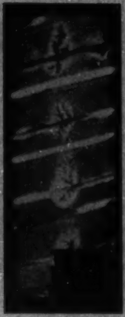

Figure 6 (right). A conductor of a new 3-conductor cable. The impregnation is poor, there is a genuine deficiency of oil, and dry gaps. Some of the voids have the tree-like shape

Figure 7 (left). A conductor of a new 3-conductor cable. Shows poor oil distribution, dry gaps and voids of different shapes and sizes

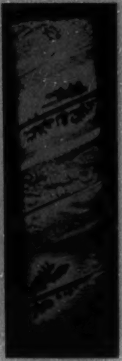

Figure 8 (right). A conductor of a new 3-conductor cable. Poor distribution of oil, dry gaps, and voids of strange patterns

and so forth. Furthermore, there is little consistency if more than one man does the dissecting because what one man calls light wax, the other may call medium wax, and what one calls medium wax, the next man may call heavy wax, and so on. The same is true for rating the degree and condition of the cable insulation impregnation. The need for a quicker, more accurate, reliable, and reproducible standard method of cable insulation inspection prompted a study of this problem. As a result of this study, a simple, rapid, and inexpensive cable insulation inspection technique was developed.

The new method is based on the fact that most oils and waxes will "fluoresce" when activated by ultraviolet radiant energy. They possess the property to absorb the energy of the impinging invisible ultraviolet rays and convert it immediately into light which falls within the visible spectrum. To use this property of the oils and waxes to the best advantage, they must be activated by a source of ultraviolet energy containing little or no visible (light) energy.

The most convenient sources of activating energy are the high-intensity mercury vapor lamps. However, to obtain the best effect, it is necessary to filter out the visible light. This can be accomplished with various kinds of glass filters. Such filters are available in several transmission ranges. Most of them contain nickel cobalt salts which make them appear black. Corning filter number *586*, for example, will transmit ultraviolet between *3880A* and *3280A* only.

For visual examination, an ultraviolet lamp with a filter or a black light is all the equipment required. Although a visual examination may be made in full daylight, a darkened room is very helpful in detecting and examining very small voids, or the distortion details of larger voids. Photographs must, of course, be taken in a dark room. It should be kept in mind that the intensity of the light given off by the fluorescence of the impregnating oil or of the cable wax is low, and that a time exposure will be necessary.

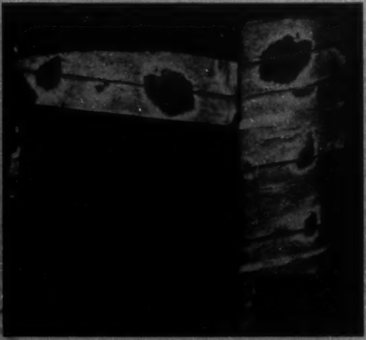

Figure 4. A conductor of a new 3-conductor cable. It shows poor distribution of oil, dry gaps, and the size of voids found in some new cables. To show that the voids were not created during unwinding of the tapes by lifting off of the oil from the tape underneath, the underside of the tape being unwound and the upperside of the tape still on the sample are shown, with the tape being unwound in place, the dark areas are directly overlaying. This shows a deficiency of oil in the dark area between the two tapes

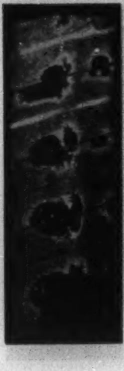

Figure 9 (left). A conductor of a new 3-conductor cable. General deficiency of oil, dry gaps, and numerous large voids

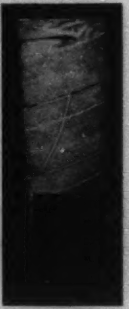

Figure 10 (right). A conductor of a used 3-conductor cable. Insulation is dry and uniformly waxed. Wax in gaps is clearly visible. A string of wax is hanging from the second gap

The exposure time depends on the speed of the film, opening of the lens, and the intensity of the fluorescence. Since only the fluorescence is to be photographed, all the ultraviolet rays reflected from the sample must be prevented from acting on the film. After considerable experimenting, we have found that a green filter mounted in the camera in back of the lens gives the best results. A film having a good response in the region of the wavelengths emitted by the fluorescence should be used. The cable photographs shown in Figures 2 to 11 were taken on Kodak XX Panchromatic film, using an F-8 lens opening and an exposure of 8 seconds.

While in visual examinations there is an appreciable difference between the hue of the oil and that of the wax, on photographs both appear white. There is, however, a difference between the two even on photographs. While areas covered with oil appear as soft, smooth white, wax shows up as a rougher, grainy white surface. The amount of oil or wax in any one spot is indicated by the degree of whiteness.

The new method of cable insulation inspection may very conveniently be used with the cable wrap overlay photography developed by Meyerhoff and Foster.[2]

Figure 1 shows the set-up used in our work. The equipment consists of a camera, a black light, a rotating film drum, and a sample holder. Almost any kind of a camera may be used for single photographs. For cable wrap overlay photography, a camera is required on which the ground glass or plate holder may be replaced by the rotating film drum after the camera is focused on the sample. The film drum in the photograph is an old oscillograph film holder with a dividing plate, having 120 divisions, fastened to its top. The number of divisions was determined by the length of the film on the drum and the width of the slit opening in the film holder. The activating source is a CH_4 or EH_4, 100 watt mercury vapor bulb with a Corning nickel-cobalt filter. The sample holder has a revolving chuck mounted on a sliding block, which permits rotation of the sample, and a stationary index against which the sample rests after the removal of each tape. Thus regardless of how many tapes have been unwound, the sample is always automatically in focus.

The brightness of the fluorescence is a function of the type and amount of the fluorescent material activated, and of the intensity of the activating source. The luminescent hue or color of the glow depends upon the chemical make-up of the excited material. Oils, paraffins, and waxes each have their own characteristic color of fluorescence which can be used not only in their detection, but may aid also in their identification. We have actually found that there is a considerable difference in color of the fluorescence exhibited by the impregnating oils used in the various makes of cables.

The new method permits a rapid inspection of the cable insulation, layer by layer, without extracting the impregnating oil. Each tape is examined before its removal from the cable, without disturbing in any way any of the evidence as it occurs in the cable. This method will not only detect even the slightest traces of cable wax in aged or used cable, but will, with equal sensitivity, detect a deficiency of impregnation in new cables. It should be helpful in post-mortem analyses and studies of arrested or incipient failures, particularly when wax formation studies of a large number of cables are to be made. Since it may be used either visually or photographically, it provides a reliable and reproducible technique, which may be standardized, of making permanent records of the exact condition of insulation of both new and used cables. If used photographically, the inconsistencies caused by the human factor, in grading the degree of impregnation as well as the degree or amount of waxing, are eliminated.

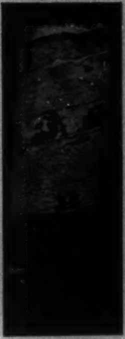

Figure 11. A conductor of a used 3-conductor cable. All the oil has been converted into wax, and the insulation is entirely dry. This shows that ionization of voids in the dielectric wall may produce only wax and no treeing or tracking. There was probably a deficiency of impregnation in the cable when new

Because of the suspicion that new cables are not void-free, and have voids near and at the conductor strands when received, samples of all available makes and types of new cables were subjected to a rigid inspection utilizing the newly developed method. It was found that most new cables are not void-free. Many have voids of irregular shapes and sizes, of random distribution throughout the entire insulation wall from the cable sheath to the conductor strands. In some cases the voids between an appreciable number of successive layers were found not only radially overlaying, but actually connected through dry channels between adjacent turns of tape in the affected layers. It also was found that in some 3-conductor shielded cables, the impregnation of the insulation of individual conductors in the same cable was, over the inspected length, widely different. In some cases one conductor was found to be quite bad while the other two conductors had relatively few voids. In other cases one conductor had fairly good impregnation while the other two conductors were bad. Still in other cases voids of various sizes were found in the insulation of all three conductors. The unequal degree of impregnation may perhaps throw some additional light on the strange behavior of some 3-conductor shielded cables during accelerated aging tests, where one conductor goes almost completely dry and develops hot spots while the other two conductors retain their compound and satisfactory dielectric properties. By examining samples taken from the cable so that an appreciable length of the cable was explored, longitudinal variations in the impregnation of a similar order were found.

It would be extremely difficult to describe adequately the condition of insulation in the new cables as we found it. With the new method it is quite easy and convenient to photograph the evidence.

Figures 2 to 11, inclusive, show the representative cases of impregnation and wax formation in the insulation wall of different cables.

With poor impregnation at the conductor strands, we have, in new cables, an essential prerequisite for ionization which may produce carbonization, treeing, and a subsequent failure. According to Atkinson[3] carbonization starts when the ionization becomes destructive.

Conclusions

The new method of inspection of impregnation of cable based on the properties of oils and waxes to fluoresce on exposure to ultraviolet radiation, is a valuable aid in the study of solid-type cable insulation. It can be used to determine the quality of impregnation of new cables and the nature and extent of deterioration in used cables.

References

1. Dielectric Phenomena in High Voltage Cables (book), D. M. Robinson. Chapman and Hall Ltd., London, England, 1936.

2. Cable Wrap Overlay Shown by Photography, Louis Meyerhoff, William P. Foster. *Electrical World* (New York, N. Y.), volume 123, number 7, February 17, 1945, pages 84–85.

3. High Voltage Cable Failure Mechanism, R. W. Atkinson. *Electrical Engineering*, volume 68, number 7, July 1949, pages 605–13.

Discussion

L. I. Komives (The Detroit Edison Company, Detroit, Mich.): Mr. Pohnan presented an original thought to help explain variations which occur in solid-type cables. His method looks like a very valuable new tool and it should be used by both the cable manufacturers and users in research on cables. Such a test, as suggested in this paper, may supply an answer to the age-old question as to what is the difference between conductors of a multiconductor cable which were made under quite similar conditions yet which show such great differences of life on accelerated aging tests, results which could not be explained by statistical scattering of values. The method will be recommended to be tried in the Research Laboratory of The Detroit Edison Company.

Wm. A. Del Mar (Phelps Dodge Copper Corporation, Yonkers, N. Y.): Dr. D. M. Robinson published[1] a theory of cable failure which, briefly described, is as follows:

Maximum stress, he says, occurs at the conductor surface giving rise to ionization and formation of carbonized corings or needles which extend into the insulation, carrying the potential of the conductor with them and thereby creating tangential stresses which give rise to lateral discharges in the oil or gas films between tapes. These discharges burn the oil into dendrites and failure is completed by discharges from the dendrites to the sheath.

Now Dr. Pohnan has provided a very elegant demonstration of something we already knew or suspected, namely that areas of subnormal impregnation exist in a solid-type paper insulated cable. Indeed it is the presence of such areas that distinguishes a solid type cable from an oil-filled cable.

While he shows that these areas, which he designates as cavitations, may exist in a new cable, he assumes that the dendrites that form therein, when failure is imminent, result, not from ionization native to the cavitations but from the Robinson effect.

My view is that Robinson may have put the cart before the horse and that failures may start, not at the conductor, but at the cavitations and may spread from there to the conductor and sheath. Robinson may be able to show corings without dendrites but dendrites without corings are much more common and Dr. Pohnan has given us a beautiful way of demonstrating the condition that gives rise to them.

The question may arise, how do Dr. Pohnan's cavitations become activated with destructive ionization deep in the insulation before the effects of ionization become visible near the conductor where the stress is supposedly greater?

The reason, I suggest, is that when ionization starts in a cable, it starts near the conductor due to the higher stress that exists there prior to ionization. This is in effect, a reduction of the resistivity of that part of the dielectric so that the potential distribution is no longer a function of the capacitance alone but becomes a function of the dielectric impedance.

Once that occurs, the region of maximum stress moves outward from the conductor into the insulation and it is at the new region of maximum stress that the cavitations develop dendritic burns.

I do not offer this explanation as a proved fact but as an alternative to the Robinson theory, to be checked by experimental research. Dr. Pohnan has given us a new tool to help such an investigation. It has always seemed queer to me that we do not believe the evidence of our eyes that slow failures start deep in the insulation and prefer to explain away this evidence because of blind faith in the immutability of the O'Gorman formula for maximum stress. Innumerable cables that I have examined which have been subjected to load cycle tests and taken off before failure occurred, have shown scattered dendrites deep in the insulation without any trace of burning near the conductor and cables which have failed on such tests usually show scattered dendrites not connected in any way with the failure. Which is the more probable, that one of these island dendrites developed into a failure or that some dendrites form as islands and others as the result of corings? It seems simpler to assume one origin than two. Dr. Pohnan's procedure may help us to get the final answer to this. However, one caution is necessary in using his procedure. While it reveals voids, these may not be the result of poor impregnation, but of loose taping.

The movement of the region of maximum stress is very clearly shown in a paper by E. Pugliese,[2] where it is shown as an extreme case, that with direct potential, the resistivity grading of the insulation by conductor heating may even put the maximum stress at the outside of the insulation. Migration of the region of maximum stress had also been pointed out by P. L. Hoover, in an AIEE paper[3] in which he used entirely different premises and mathematical procedure.

References

1. Breakdown Mechanism of Impregnated Papar Cables, D. M. Robinson. *Journal*, Institution of Electrical Engineers (London, England), volume 77, 1935, pages 90–108.

2. La Repartition Tranversale de la Tension Alternative et Continue Dans l' isolant des Cables À Haute Tension, E. Pugliese. *Bulletin*, Association Suisse des Electriciens (Zurich, Switzerland), 1950, volume 41, page 921.

3. The Mechanism of Breakdown in Dielectrics, P. L. Hoover. *AIEE Transactions*, volume 45, 1926, pages 983–97.

R. W. Atkinson (General Cable Corporation, Bayonne, N. J.): Pohnan's use of fluorescence for studying impregnation and wax formation is very intriguing and it should have some practical uses. Indeed, it may develop into another one of the useful tools for cable examination such as styrene wafers, radial power factor, and overlay photography. The extent of its usefulness probably depends upon certain characteristics not fully described in the text. This discussion is directed toward developing some of these.

It appears to this discusser that the method is not as sensitive as some other methods that have been used for measuring degree of impregnation. Pohnan speaks of completely impregnated solid-type cable. There is no such thing (at least not at, say, 20 degrees centigrade). Other methods are available which will show both qualitatively and quantitatively the degree of this lack of impregnation. In the process of manufacture a solid-type cable will usually be completely impregnated at some temperature considerably above 20 degrees centigrade. When subsequently cooled, the contraction of the compound will leave a space of 1 per cent of the oil volume for approximately each 14 degrees reduction in temperature. Moreover, after any subsequent heating (say to operating temperature, or even exposed to the sun in the storage yard on a hot day) the compound will expand and come out from the insulation and, in general, will not return. Therefore, if Pohnan's method has, in any case, appeared to indicate complete impregnation, it seems to lack the sensitivity which is obtainable by other means. It would be helpful to know the results of direct comparison with these methods.

From another standpoint, it appears that the method, inherently, might indicate differences in degree of impregnation when no such differences exist. It is understood that the density of the photographic negative produced by this method is a function of the amount of saturant adhering to the surface of the tape being photographed, and that the perfection of impregnation is judged by this density. But the thickness of the oil film is a function not only of the degree of impregnation but also of the radial distance between tapes. The latter may vary considerably in the same cable and even circumferentially in a single layer. Thus the density of the negative—or the whiteness of the print from it—is, by no means, a simple measure or indicator of perfection of impregnation. What is measured (approximately) is the total oil on the surface and not, as desired, how much that quantity differs from what would exist with complete impregnation. It will be helpful to know to what extent this comment affects the usefulness of Pohnan's method.

It is pertinent to indicate some of the other methods that have been used for indicating saturation. One widely used and probably the simplest is based on visual examination as the tapes are unwound layer by layer. Where air spaces exist under a tape, spots of lighter color appear. This method is a very quick and convenient way of showing roughly the completeness of saturation and, as contrasted to Pohnan's method, its indications are of the departure from complete impregnation, not of total oil present. However, the method has the various inaccuracies and difficulties in use that Pohnan has outlined for visual methods. Moreover, it is difficult to avoid false indications as a result of admitting air while the successive tapes are unwound. Another method is by unwinding the tapes under oil, which makes it possible to see any air bubbles that are freed and rise to the surface as the tapes are unwound. It is even possible to catch these bubbles and measure their volume. The unwinding under oil is tedious and messy and suitable only for special investigations. These, or some of the various other older methods could be used in comparison with Pohnan's method to evaluate it more definitely and to determine what use it may have as a practical tool.

Pohnan's method does not have some of the limitations of the older methods of measurement of impregnation and thus may have important uses for this purpose in spite of its own apparent limitations. Aside from this use, Pohnan's method seems to have particular adaptability to the measurement of "wax" formation.

C. E. Betzer (Commonwealth Edison Company, Chicago, Ill.): The illustrations presented in the paper reveal in striking manner the voids and deterioration due to ionization in high-voltage cable insulation. The technique of photographing under ultraviolet light has been nicely developed.

In the paper it is stated that previously the extent of voids and degree of deterioration has been determined by judgment of the person who examines the insulation. It should be noted that with this use of ultraviolet light, this is still the case. Such light reveals the condition of the insulation more clearly than ordinary light, but does not provide a quantitative measure of the degree of saturation or extent of deterioration.

Figure 6 is said to be a sample of new cable, and it is stated that some of the voids have a tree-like shape. It appears to me that the tree-like figures in this illustration are of the fine-line type that is produced by electrical discharges. They are also confined to the apex of a sector conductor where such discharges generally originate in 3-conductor cable. An attempt was made to learn more about the history of that cable shown in Figure 6, but it could not be identified in the records left by Mr. Pohnan.

About 25 years ago, ionization in void spaces was a serious problem which was impeding the use of higher-voltage cables. Now, marked improvements have been made in the manufacture of solid-type cable and thorough impregnation of the insulation with a stable oil has become common practice. Also, other types of cable have been developed in which ionization is suppressed by oil or gas under pressure. Failures in service due to deterioration of the insulation now are a small percentage of the troubles in operation, and are almost entirely in the cables that were made over 20 years ago.

Field Tests at Grand Coulee Dam on 10,000-Mva 230-Kv Low-Oil-Content Impulse Circuit Breaker

A. F. DARLAND
FELLOW AIEE

C. L. KILLGORE
MEMBER AIEE

C. J. BALENTINE
ASSOCIATE AIEE

E. B. RIETZ
ASSOCIATE AIEE

Synopsis: This paper describes field acceptance tests made on the 230-kv 10,000-mva (megavolt-ampere) impulse circuit breaker switching units furnished for the new Right Switchyard at the Grand Coulee Dam power plant. Details of the circuit breaker design are followed by a description of a successful series of line dropping and fault tests made on a single pole circuit breaker unit to observe its performance up to rating and to determine the capabilities of the circuit breaker for higher short circuit duties which will be available at this location in the near future. Line dropping tests were made up to a maximum of 300 line-miles without restrikes and, therefore, without abnormal overvoltages. Seven fault tests were made at full station capacity with short circuit duties up to 12,000 mva, with interrupting times ranging from 1.75 to 3.0 cycles, and with reclosing times of 9 cycles. The condition of the contacts and oil at the end of the test indicated that a substantial number of additional tests could have been made without replacement. There was no distress on any test and no trouble developed with any mechanical operations or breaker parts. These tests together with factory laboratory tests indicate the suitability of the 10,000 mva interrupting rating for this design of low-oil-content impulse circuit breaker and the possibility of building similar circuit breakers for higher ratings when the requirement arises.

IN the spring of 1947 a field test program was inaugurated at Grand Coulee power plant for the development of ultra-high interrupting capacity 230-kv 3-cycle 20-cycle reclosing oil circuit breakers. These tests have been described in previous papers.[1,2] The first tests were made on existing designs having a maximum interrupting rating of 3,500,000 kva. The test results exceeded expectations and demonstrated interrupting capabilities well above the nameplate rating. Manufacturers were, therefore, willing to undertake the development of 10,000,000-kva interrupting capacity circuit breakers based on existing designs.

Although, as previously reported, it was known that the maximum short-circuit duty at Grand Coulee power plant would ultimately exceed 10,000,000 kva, it was the opinion of the manufacturers that an increase in one step from 3,500,000 kva to more than three times existing interrupting ratings represented the maximum increase in capacity that should be undertaken in one development program.

Tests made in the following years provided additional experience and data for the proposed designs,[3] and helped greatly in evolving the final 10,000,000-kva circuit breaker. During this entire period, additional generating units at Grand Coulee power plant and interconnecting transmission lines of the Bonneville Power Administration were put into service thus increasing the short-circuit current available. This was made use of in the succeeding test series to place more duty on the circuit breakers under test.

This paper discusses the 230-kv field acceptance tests conducted in the fall of

Figure 1. Grand Coulee Dam and power plant will have ultimate installation in 1951 of 18 120,000-kva generators, the largest hydroelectric power installation in the world

---

Paper 51-256, recommended by the AIEE Switchgear Committee and approved by the AIEE Technical Program Committee for presentation at the AIEE Summer General Meeting, Toronto, Ont., Canada, June 25-29, 1951. Manuscript submitted March 27, 1951; made available for printing May 15, 1951.

A. F. DARLAND is with the United States Bureau of Reclamation, Coulee Dam, Wash., C. L. KILLGORE is with the United States Bureau of Reclamation, Denver, Colo., and C. J. BALENTINE and E. B. RIETZ are both with the General Electric Company, Philadelphia, Pa.

The long range planning of the engineers of the United States Bureau of Reclamation, the Bonneville Power Administration, and the General Electric Company, who made possible these high capacity field tests and the development of 10,000-mva circuit breakers, is to be commended. The assurance created by the successful experience on these several series of high capacity field tests has done more than anything else to establish high capacity circuit breakers in this most important field of power transmission.

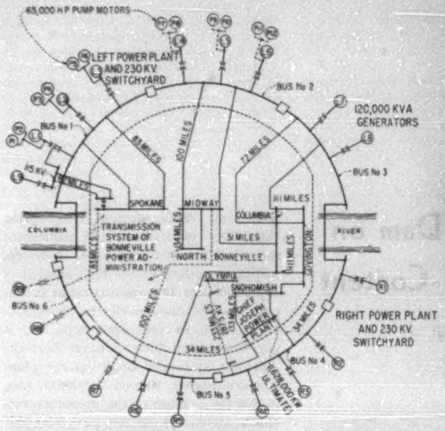
65,000 H P PUMP MOTORS
LEFT POWER PLANT AND 230 KV SWITCHYARD
BUS No 2
120,000 KVA GENERATORS
BUS No 1
BUS No 3
115 KV
83 MILES
100 MILES
72 MILES
SPOKANE
MIDWAY
141 MILES
COLUMBIA
COLUMBIA
RIVER
TRANSMISSION SYSTEM OF BONNEVILLE POWER ADMINISTRATION
134 MILES
51 MILES
NORTH
BONNEVILLE
185 MILES
111 MILES
COVINGTON
OLYMPIA
SNOHOMISH
BUS No 6
100 MILES
233 MILES 287.5 KV
133 MILES
CHIEF JOSEPH POWER PLANT
34 MILES
34 MILES
RIGHT POWER PLANT AND 230 KV SWITCHYARD
BUS No 4
BUS No 5
1,628,000 KW ULTIMATE
L1
L5
L7
L8
L9
R1
R2
R3
R4
R5
R6
R7
R8
R9

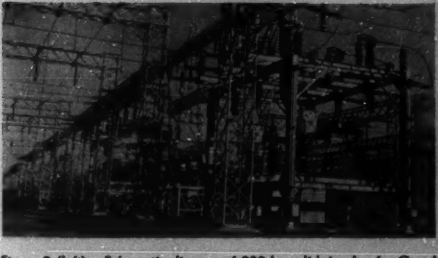

Figure 2 (left). Schematic diagram of 230-kv solid-ring bus for Grand Coulee power plants and parallel line connections to transmission system of Bonneville Power Administration

Figure 3 (above). 230-kv Right Switchyard at Grand Coulee showing 2,500,000-kva generator circuit breakers and 10,000,000-kva transmission line and bus tie low-oil-content impulse circuit breakers

1950 and describes the 10,000,000-kva interrupting capacity circuit breakers which were developed and built for the 230-kv Right Switchyard at Grand Coulee power plant. The successful performance of these circuit breakers under test have provided the system planning engineer with a new tool for use in laying out ultrahigh capacity, high voltage, generation and transmission systems. Users now are assured that ultrahigh capacity circuit breakers are feasible and from laboratory and field test data already obtained, manufacturers are confident that the 10,000,000-kva circuit breaker design can readily be extended to 15,000,000 kva.

Grand Coulee Power Plant

Grand Coulee is the largest hydroelectric power development in the world and is an integral part of the Columbia Basin Project[4] of the United States Bureau of Reclamation.

The Grand Coulee power plant consists of two identical powerhouses located on opposite sides of the Columbia River as shown in Figure 1. Each powerhouse contains nine 120,000-kva generators. The last three of the ultimate 18 generators now are being installed in the Right Powerhouse and will be placed in operation before the end of 1951. The power plant is near the electrical center of the Northwest Power Pool which now has a capability of over 5,000,000 kva. Grand Coulee is connected to the Northwest Power Pool through the transmission facilities of the Bonneville Power Administration.

A unit system wherein each generator is connected directly to its associated transformer bank, without a generator-voltage circuit breaker, and with all switching and bussing being accomplished on the high-voltage side at the 230- and 115-kv switchyards is used at Grand Coulee for the transmission system. However, six of the nine generators in the Left Powerhouse are arranged to drive the 12 65,000-horsepower irrigation pumps in the Grand Coulee pumping plant which is located adjacent to Grand Coulee Dam. Each generator will operate two pumps through a generator-voltage bus between the powerhouse and the pumping plant. Any excess generation not required for pumping will be supplied to the commercial load by operating the generators and pumps in parallel with the transmission system.

Solid 230-Kv Ring Bus

The tremendous concentration of over 2,000,000 kva at Grand Coulee presented

Figure 4. Increase in 3-phase megavolt-ampere fault capacity at Grand Coulee power plant with increased capacity and growth of Bonneville Power Administration transmission system

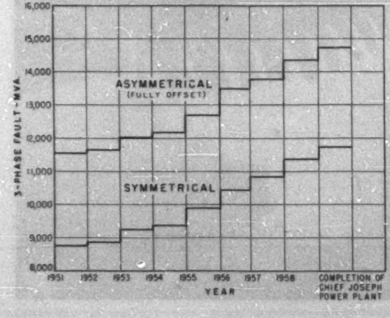

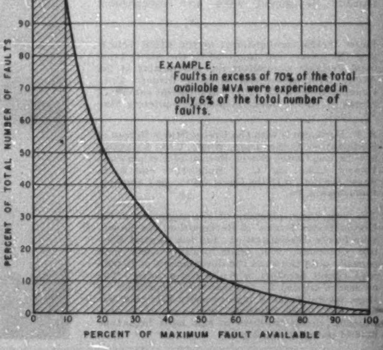

Figure 5 (right). Comparison of actual circuit breaker duty with maximum calculated fault capacity at Grand Coulee power plant from system records for years 1944 to 1951

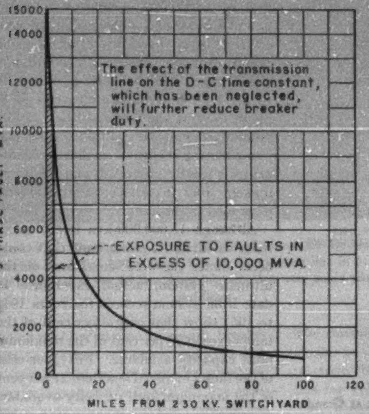

Figure 6 (left). Typical effect of line length on circuit breaker duty at Grand Coulee switchyards

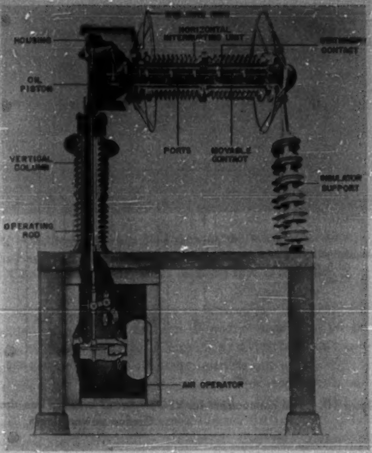

Figure 8 (right). Cross-section of complete single pole 10,000-mva 230-kv low-oil-content impulse circuit breaker showing various elements

an outstanding problem to determine the ultimate bussing arrangement for Grand Coulee power plant. Circuit breaker interrupting capacity, system stability and relaying, simplicity and operating flexibility and cost were all important factors in the final selection of a solid 230-kv ring bus. A complete discussion of this bussing arrangement was given in an earlier paper.[5] A schematic diagram of the solid 230-kv ring bus at Grand Coulee and the interconnecting transmission lines of the Bonneville Power Administration are shown in Figure 2. Selection of a solid bussing arrangement necessitated the development of ultrahigh interrupting capacity circuit breakers rated at 10,000,000 kva and 3 cycles. Because of system operating conditions the circuit breakers were specified to have no derating factor for one 20-cycle reclosure.

A low oil content impulse circuit breaker has been developed for these severe requirements and this design has been a part of the field testing program mentioned previously.

1. Tests were conducted in 1947 on an existing 3-cycle 3,500,000-kva nonreclosing impulse circuit breaker. Short circuits up to 7,000,000 kva were interrupted successfully with no signs of distress.[2,3]

2. Tests were conducted in 1948 on a 3-cycle 360-kv low oil content impulse circuit breaker designed for the 500-kv experimental Tidd Line of the American Gas and Electric system.[6] This circuit breaker was designed for high-speed reclosing and incorporated design changes for the higher interrupting ratings. Short circuits up to 8,600,000 kva were interrupted successfully and again there were no signs of distress. Instantaneous reclosing was proved feasible with successful operation up to station capacity and reclosing times of 8.5 cycles.[3]

These two series of tests were largely responsible for the successful development of the 10,000,000-kva circuit breakers now installed in the new 230-kv Right Switchyard at Grand Coulee.

230-Kv Right Switchyard

All of the 230-kv circuit breakers in the Right Switchyard are of the low oil content impulse-type as shown in Figure 3. The ultimate installation will consist of 16 10,000,000-kva circuit breakers in the

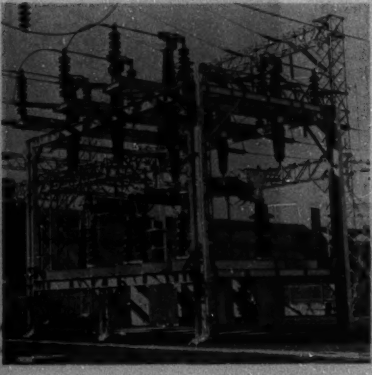

Figure 7 (left). 10,000-mva 230-kv low-oil-content impulse circuit breaker switching unit installed in the Right Switchyard at Grand Coulee Dam

Figure 9 (right). Air operator for single-pole circuit breaker unit showing operating unit, compressed air system, and control accessories

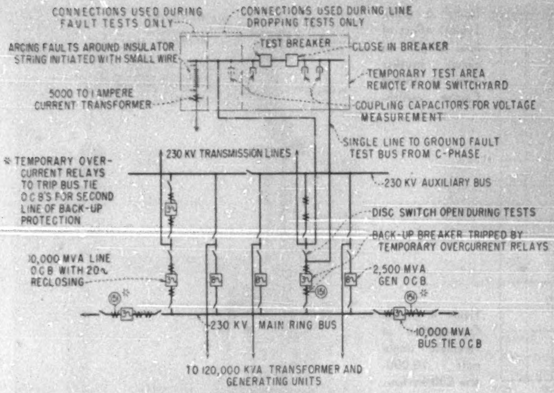
CONNECTIONS USED DURING FAULT TESTS ONLY
CONNECTIONS USED DURING LINE DROPPING TESTS ONLY
ARCING FAULTS AROUND INSULATOR STRING INITIATED WITH SMALL WIRE
TEST BREAKER
CLOSE IN BREAKER
TEMPORARY TEST AREA REMOTE FROM SWITCHYARD
5000 TO 1 AMPERE CURRENT TRANSFORMER
COUPLING CAPACITORS FOR VOLTAGE MEASUREMENT
SINGLE LINE TO GROUND FAULT TEST BUS FROM C-PHASE
230 KV TRANSMISSION LINES
* TEMPORARY OVER-CURRENT RELAYS TO TRIP BUS TIE O C B'S FOR SECOND LINE OF BACK-UP PROTECTION
230 KV AUXILIARY BUS
DISC SWITCH OPEN DURING TESTS
BACK-UP BREAKER TRIPPED BY TEMPORARY OVERCURRENT RELAYS
0,000 MVA LINE O C B WITH 20~ RECLOSING
2,500 MVA GEN O C B
3~
6~
151
230 KV MAIN RING BUS
10,000 MVA BUS TIE O C B
TO 120,000 KVA TRANSFORMER AND GENERATING UNITS

Figure 10. Test connections for 230-kv circuit breaker line-dropping and fault tests at Grand Coulee power plant

bus tie and line positions, and nine 2,500,000-kva circuit breakers in the generator positions. The low oil content impulse circuit breaker has an exceptionally fine record of interrupting performance gained over the past 15 years on a number of units installed on the Pacific coast. This includes:

1. A minimum of oil and contact deterioration resulting in reduced maintenance.
2. Interruption of line charging currents without restriking which is considered necessary to minimize overvoltages which may result under this type of operation. Low-oil-content impulse circuit breakers made it unnecessary to install an oil piping system and permanent oil handling equipment in the switchyard such as is required for 230-kv conventional dead-tank-type circuit breakers, and, therefore, considerable economies were possible in the switchyard layout.

This is the first large high-voltage switchyard with no permanent oil piping and handling facilities consisting entirely of low oil content impulse-type circuit breakers. The operating performance and maintenance record of these 25 230-kv circuit breakers will be watched with more than usual interest by the industry. This is especially true since the transmission lines from Grand Coulee are not provided with overhead ground wires and the line circuit breakers will be required to interrupt more than the usual number of faults during the lightning season with high-speed 20-cycle, or faster, reclosing operations.

Ultimate Fault Duty

As mentioned previously, the ultimate calculated fault duty as the Grand Coulee 230-kv switchyards will exceed 10,000,000 kva and will approach 15,000,000 kva. The increase in both symmetrical and asymmetrical fault capacity with installation of additional generating units at Grand Coulee and additional lines, generating capacity, and interconnections on the transmission system of the Bonneville Power Administration is shown on Figure 4. These values are based on a 3-phase fault at the Grand Coulee 230-kv switchyard bus with all generators and pump motors in operation, all transformer neutrals solidly grounded, and all transmission lines in service with maximum back-feed to the fault.

Although 15,000,000-kva is the maximum calculated 3-phase fault that could occur under the worst conditions on the ultimate system, actual experience to date from system records for years 1944 to 1951 show that only 6 per cent of the faults exceed 70 per cent of the maximum fault capacity available. Fifty per cent of the faults involved less than 21 per cent of the maximum fault capacity available. A comparison of actual circuit breaker duty with the maximum calculated fault capacity available is shown on Figure 5.

Figure 11 (left). Circuit breaker units as installed at Grand Coulee Dam switchyard for field tests. The interrupting test circuit breaker is on the left, and the closing test circuit breaker is on the right

Figure 12. The synchronous control unit used to obtain accurate timing control of both the fault application and the tripping of the test circuit breakers

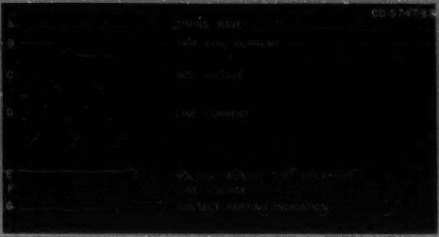

Figure 13. Oscillogram of test LD-24 showing the interruption of charging current of 300 miles of 230-kv transmission line in 1.7 cycles. This is typical of the 23 line dropping tests that were made without any restriking

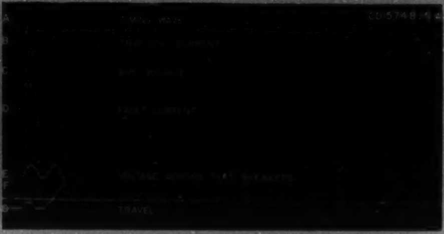

Figure 14. Oscillogram of test SF-9 showing the interruption on a reclosing duty cycle of approximately 8,500 mva with interrupting times of 1.66 and 2.67 cycles and a reclosing time of 9 cycles

The rapid reduction in circuit breaker duty as the fault is removed from the 230-kv switchyard bus out on the transmission lines is shown in Figure 6. The addition of only about 2 miles of transmission line reduces the maximum fault to 10,000,000 kva, while 1 mile reduces the fault to 12,000,000 kva. Calculations further show that for a fully offset asymmetrical wave the maximum single line-to-ground fault 1 mile from the 230-kv switchyard is less than 12,000,000 kva. The transmission lines from Grand Coulee are provided with overhead ground wires extending approximately 1 mile from the 230-kv switchyard, and there is only a remote possibility of a fault occurring in this protected area.

Therefore, there would appear to be little, if any, probability of an actual fault occurring which exceeds 12,000,000 kva, and the field tests reported herein, together with laboratory tests have demonstrated that the 10,000,000-kva circuit breakers have considerable margin above their nameplate rating.

Description of Circuit Breaker

The 10,000-mva impulse circuit breaker is part of an integrated switching unit which includes the complete 3-phase circuit breaker with current transformers, two sets of 3-pole isolating disconnecting switches and the necessary supporting structure. Figure 7 shows the circuit breaker installed in the Right Switchyard. The circuit breaker consists of three single-pole units electrically interlocked for proper co-ordination. This design is, therefore, suitable for single pole reclosing. Current transformers of the conventional bushing-type are mounted on through-type bushings which are integral with the disconnecting switches. Twelve separate bushing transformers can be accommodated on each switching unit. The bushings are of the sealed-type, similar to those widely used on tank-type oil circuit breakers. Capacitance tap outlets for voltage indication are provided. The disconnecting switches use high pressure silver-to-silver contacts and are operated manually. The structural steel framework provides a mounting for all the above mentioned parts.

The circuit breaker has the following ratings:

Interrupting	10,000 mva
	25,000 amperes at 230 kv
	26,000 amperes at 220 kv
Short time	42,000 amperes, momentary
	26,000 amperes, 4 second
Continuous	1,000 amperes
Basic impulse insulation level	900 kv
Interrupting time	3 cycles
Reclosing time	10 cycles

Although the features of the impulse-type circuit breaker have been included in previous papers, it is considered desirable to review them briefly.

Each of the single pole units, shown in Figure 8, consists of the following elements: a horizontal interrupting element, a vertical supporting column, an insulator support, and a pneumatic operating mechanism. The operating mechanism is used for closing and opening of the contacts and to charge the springs in back of the oil piston, which is instrumental in causing a flow of high dielectric insulating oil between the moving and the stationary contacts on every opening operation.

The interrupting element consists of a mechanism box and a porcelain clad assembly which houses the contacts. The contacts consist of five sets of moving and stationary contacts arranged in a series line and operated by a linkage in the mechanism box. The oil piston, located in the mechanism box and charged on every closing operation, is released as the circuit breaker starts to open and causes an oil pressure to be built up in the interrupting unit. By suitable means, this oil under pressure is directed into the arcs drawn between the moving and stationary contacts and exhausts into an expansion chamber. This positive oil flow results in early arc interruption under all conditions of operation whether de-energizing a long transmission line or interrupting fault current.

The vertical column houses the insulation operating rod connecting the linkage of the mechanism box to the air operator. This column consists of an inner paper wound tube and an outer porcelain enclosure. The entire assembly is filled with insulating oil.

In the case of both the horizontal interrupting element and the vertical column, the heavy walled impregnated

Figure 15. Oscillogram of test SF-11 showing the interruption of 9,000 mva in 2.1 cycles

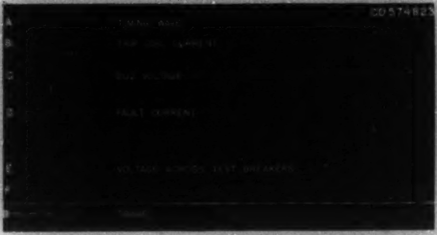

Figure 16. Oscillogram of test SF-12 showing the interruption of 12,000 mva in 1.55 cycles, a record for short circuit power interruption

paper wound tubes take all pressures and loadings incurred during the operation of the circuit breaker under no-load and short-circuit conditions. The porcelain enclosures are supported so that vibration is not transmitted directly to the porcelain, therefore, insuring adequate protection against the dangers of sudden shock loading which may result from the breaker operation.

The air operating mechanism, Figure 9, which is of the pneumatically trip-free type, is a complete operating unit in itself. Each pole unit operator has its own individual air compressor equipment and air storage tank. The operating cylinder of the mechanism is mounted directly under the vertical operating rod of the circuit breaker giving a direct straight line pull to close the circuit breaker, thus using the minimum number of moving parts and giving the most effective and economical use of the energy applied for closing.

The complete triple-pole circuit breaker uses approximately 700 gallons of oil for the various compartments of the horizontal and vertical columns. Only the oil adjacent to the contacts is subject to carbonization during circuit breaker interruptions and has to be removed for normal maintenance. When this oil, amounting to about 90 gallons per pole unit, is drained off, the contacts are accessible. This is the reason why extensive oil handling facilities are not required for the Coulee Switchyard where it is planned to use portable storage facilities when a circuit breaker inspection is required.

Field Tests

Objectives

Since the ultimate installation and 230-kv ring bus arrangement at the Grand Coulee Switchyard will present interrupting duties which may exceed 10,000 mva, the test program was set up with a twofold objective:

1. Demonstrate by full scale field tests a rating of 10,000 mva.
2. Determination of circuit breaker capabilities above rating for future needs.

Test Setup

The test setup, in general, followed that used on previous tests and is described in detail in a previous paper.[1] Figure 10 shows the test connections for the 230-kv circuit breaker line-dropping and fault tests at Grand Coulee power plant.

Two single-pole impulse circuit breaker units were installed in the test location in the Left Switchyard at Grand Coulee Dam as shown in Figure 11. These were two units destined for installation in the Right Switchyard and, therefore, were production circuit breakers. One unit was used as a closing circuit breaker to initiate the fault for opening test operations and the other unit was used to interrupt these faults. The second unit was used above for the closing-opening test operations. A single conductor test bus was connected to *C* phase of the station ring bus.

All faults were single line-to-ground on *C* phase only and were applied directly to the switchyard ground mat. Some of the tests were made with a solid ground applied directly to the test circuit breaker and others were made with an arcing ground fault obtained by flashing over a string of insulators. Pretripping of the test circuit breaker was used to obtain maximum fault current in the arc by taking advantage of the fully offset first cycle of fault current and opening the contacts during this period.

Instrumentation

An integrated set of instrumentation equipment for circuit breaker field testing was used to obtain complete information on circuit breaker performance. This equipment consisted of three magnetic oscillographs, one cathode-ray oscillograph, and the conventional recording devices for obtaining records of current, voltage, travel, arc energy, and close and trip indications. In addition to these items, two special units were used:

1. A synchronous control unit to obtain accurate timing of the fault application and the tripping of the test circuit breaker.
2. A frequency modulation radio transmitting unit to obtain records of pressure transients in the interrupting unit.

The synchronous control unit shown in Figure 12 provided closing, tripping, and

Figure 17. One of the moving contacts after the fault test series, showing only a small amount of deterioration after 14 tests

Figure 18. One of the stationary contacts after the fault test series showing the small amount of deterioration after 14 tests

Table I. Single-Phase Line Dropping Tests at Grand Coulee Dam on 10,000-Mva 230-Kv Low Oil Impulse Circuit Breaker

Test No.	Line, Miles	Charging Current, Amperes	Interrupting Time, Cycles	Arc Length, Cycles
LD-1	100	66	1.25	0.05
LD-2	100	66	1.25	0.05
LD-3	100	66	1.25	0.05
LD-4	100	68	1.45	0.03
LD-5	100	68	1.45	0.25
LD-6	100	68	1.55	0.35
LD-7	200	116	1.25	0.05
LD-8	200	115	1.35	0.15
LD-9	200	115	1.45	0.25
LD-10	200	115	1.45	0.25
LD-11	200	116	1.60	0.40
LD-12	This test was not made			
LD-13	300	164	1.30	0.15
LD-14	300	164	1.30	0.15
LD-15	300	164	1.45	0.25
LD-16	300	166	1.45	0.25
LD-17	300	164	1.45	0.25
LD-18	300	164	1.60	0.40
LD-19	300	164	1.65	0.50
LD-20	300	114	1.60	0.40
LD-21	300	164	1.60	0.40
LD-22	300	160	1.60	0.40
LD-23	300	164	1.45	0.25
LD-24	300	164	1.70	0.50
			Average 1.46	

All tests at 237 kv. No restrikes were obtained on any of the above tests.

Table II. Single-Phase Fault Tests at Grand Coulee Dam on 10,000-Mva 230-Kv Low Oil Impulse Circuit Breaker

Test No.	Bussing Arrangement	Duty Cycle	Kv	Rms Amperes Interrupted	Equiv. 3-Phase Mva	Inter., Time, Cycles	Reclosing Time, Cycles
SF-1	1 Gen.	O	237	1,570	630	1.73	
SF-2	8G & 7L	O+C	237	15,700	6,440	1.69	24
SF-3	8G & 7L	CO	235	16,400	6,660	2.11	
SF-4	8G & 7L	O	236	21,700	8,830	1.72	
SF-5†	8G & 7L	O Inst.+C†	235	13,700	5,580	1.72	10.3
SF-6A	8G & 7L	O	236	16,000	6,520	1.65	
SF-6B		Inst.+CO†	236	12,800	5,200	3.00	9.1
SF-7	13G & 7L	O+C	236	20,500	8,400	1.66	23
SF-8	13G & 7L	CO	235	20,500	8,350	2.18	
SF-9A	13G & 7L	O	236	20,500	8,400	1.66	
SF-9B		Inst.+CO†	236	21,000	8,550	2.67	9.0
SF-10*	13G & 7L	O	237	22,000	9,000	1.88	
SF-11*	13G & 7L	O	237	21,900	9,000	2.10	
SF-12*	13G & 7L	O	237	29,300	12,000	1.55	

†Fault cleared before circuit breaker reclosed.

*Tests which were pretripped: Tests No. 1, 2, 3, 4, 5, 7, and 8—arcing ground faults. Tests No. 6, 9, 10, 11, and 12—solidly grounded faults.

reclosing of the test and closing circuit breakers at accurately predetermined points. With this equipment it was possible to select points on the voltage wave to obtain the maximum offset of the fault current and to associate contact parting with current zeros. The synchronous control circuit is a 7-channel timer supplying 125 volts of direct current to the closing and tripping coils at predetermined intervals. Each channel can be set independently to fire at any desired point of any cycle of a reference voltage wave within the range of 1 to 50 cycles after the closing of the contacts which start the oscillograph motor. The desired cycle can be selected by a synchronously driven telemetering switch that picks up a new contact each cycle and the desired firing point on the cycle is selected by a 360-degree phase shifter.

The pressure measurements on the energized interrupter unit were obtained with a transient pressure recorder that provided 230-kv isolation by frequency modulation radio transmission of the pressure data from a capacitance-type gauge on the circuit breaker to the oscillograph in the control room. Mechanical peak pressure crusher-type gauges also were used.

Measurements of contact travel on the solidly grounded faults were taken with a 2,000-cycle inductive bridge-type travel recorder. Isolation of the oscillograph connections was obtained by mechanically coupling the recorder to the contacts with a long insulation rod. On the line dropping and arcing ground faults the travel recorder was replaced by a contact position indicator which transmitted the point of parting by frequency modulation radio to the oscillograph.

Voltage records were obtained with the aid of capacitance dividers and recorded on cathode-ray and magnetic oscillographs.

Current was recorded on all three magnetic oscillographs in the conventional manner using a bushing-type current transformer.

The instrumentation proved highly successful. Extensive data of a very accurate nature were obtained. In addition, the synchronous control unit gave such close control over the closing and tripping of the fault and test circuit breakers and such accurate control of the contact separation of the test circuit breaker at the time the fault was applied that every test was taken under the most severe operating conditions.

TEST PROGRAM

The test program over the week of September 17-24, 1950 was planned to cover both line dropping and fault interrupting tests. A total of 24-line dropping tests was scheduled on 100, 200, and 300 line-miles having charging currents of approximately 70, 150, and 200 amperes respectively. Twelve system fault tests were planned utilizing 1, 8, and 13 generators respectively and the seven interconnecting lines of the Bonneville Power Administration.

The line dropping tests were made on Midway Line Number 1 with it connected to the system. Tests *LD1-LD6* were made on phase *C* and represented 100 line-miles. Tests *LD7-LD12* were made on phases *B* and *C* in series and represented 200 line-miles. Tests *LD13-LD24* were made on phases *A*, *B*, and *C* in series and represented 300 line-miles.

On the fault interrupting tests, test *SF-1* was an opening test on an arcing ground fault with one generator (*L5*) on the bus. Tests *SF-2* through *SF-5* were arcing ground faults made with eight generators and seven lines and consisted of one opening test, one open-close test, one close-open test and one reclosing test with 9-cycle reclosing time. Test *SF-6* was a 9-cycle reclosing test on a solidly grounded fault with eight generators and seven lines. Tests *SF-7* and *SF-8* were made on an arcing ground fault with 13 generators and seven lines. One of these was an open-close test and the other was a close-open test. Tests *SF-9* through *SF-12* were made on a solidly grounded fault with 13 generators and seven lines. Three of these were straight opening and one was a 9-cycle reclosing test.

TEST RESULTS

The 23 line dropping tests interrupted the charging currents of from 100 to 300 miles of line. There were no restrikes on any test and the maximum interrupting time was 1.70 cycles with an average of 1.46 cycles. Arcing times varied from 0.05 to 0.50 cycle. Table I lists these results. Figure 13 is a record of test *LD-24*.

There were 14 interruptions on the fault test series listed in Table II. Two open-close tests were made with 23 cycles reclosing time primarily to check the mechanical operation of the circuit breaker on closing back in.

Arcing ground tests covered a range of 630 to 8,830 mva with interrupting times from 1.66 to 2.18 cycles. One reclosing test was made with 10.3 cycles reclosing time, and the reclosure was successful. There was a deionized time of 8.5 cycles on this test.

On the solidly grounded fault tests, 5,200- to 12,000-mva faults were interrupted with interrupting times of 1.55 to 3.0 cycles. Two reclosing tests were made with 9.0 cycles reclosing times. The last three opening tests were pretripped to obtain the maximum current in the arc. Figures 14, 15, and 16 are oscillographic records of tests *SF9*, *SF11*, and *SF12*.

All fault tests were successful with no noticeable ground shock or emission of gas or oil through the vents except on test *SF11* when there was a slight ground shock and some gas and vaporized oil emitted through the vent and the travel recorder connecting rod seal.

An inspection of the circuit breaker and contact parts made at the completion of the tests showed that no parts had been damaged. There was only slight burning on the contact surfaces which are of arc resisting material. There was slight erosion of the fiber port blocks where the oil flow had impinged the arc. The oil tested 27 kv and was somewhat darkened. Carbon deposits were noticeably absent. Figures 17 and 18 show a representative set of contacts.

SUMMARY OF TESTS

The results of the line dropping tests parallel those of previous field tests and indicated that the impulse-type circuit breaker is particularly fitted to handle the conditions when long high-voltage transmission lines have to be taken out of service. The absence of restrikes can be attributed to the large volume of oil which is passed between the moving and stationary contacts during capacitance switching. Even with extremely short-contact separation, this oil of high dielectric strength is sufficient to prevent restriking as the voltage builds up.

The performance on the fault tests indicated that the circuit breaker could handle satisfactorily short circuit conditions equal to its rating. The last seven interruptions with the full capacity of the power plant and all connected lines with fault duties of 8,350 to 12,000 mva gave the circuit breaker an opportunity to demonstrate its interrupting ability.

The fault current interrupted on the last test and representing the greatest amount of short circuit power ever interrupted resulted from pretripping to obtain maximum current in the arc. This test, together with the previous six tests under more normal conditions, would certainly permit the conclusion that the circuit breaker proved its rating. The small amount of deterioration of the contacts and oil also indicated that many more full capacity faults could have been interrupted before maintenance would have been required.

The reclosing tests added further to the information regarding the ability of the impulse circuit breaker to interrupt two successive faults with a very short time interval between them. The impulse circuit breaker had proved on previous tests that this could be done and additional confirmation was obtained on this series. There was no indication of additional severity on the second operation of a reclosing duty cycle and, in so far as the impulse circuit breaker is concerned, it would appear that no derating factors are required for this type of operation. On the arcing ground faults, special instrumentation provided by the Bonneville Power Administration gave additional data regarding the required deionizing time for instantaneous reclosing on 230-kv lines. Test *SF5* at approximately half circuit breaker rating showed that successful reclosure was obtained with approximately 8 cycles dead time.

Conclusions

1. The interrupting performance of the circuit breaker on these field tests together with a wide range of factory laboratory tests established the interrupting rating of 10,000 mva with no derating factor on 20-cycle reclosure as being well within the ability of the circuit breaker.

2. The experiences gained from these field tests added to the already known characteristics of the impulse circuit breaker indicate that short circuit duties above the circuit breaker rating could be handled with some margin of safety.

3. The low-oil-content impulse circuit breaker again proved that inherently because of its principle of interruption and its mechanical construction it is most suitable for the requirements of high-capacity high-voltage applications. Up to the present time, no line switching or interrupting requirements associated with this field have indicated the limit of circuit breaker capabilities.

4. It is believed that with a similar design, a low-oil-content impulse circuit breaker with an interrupting rating of 15,000 mva at 230 kv could be built successfully.

References

1. Field Tests for Development of 10,000 Mva 230-Kv Oil Circuit Breakers for Grand Coulee Power Plant, C. L. **Killgore**, **W. H. Clagett**. *AIEE Transactions*, volume 67, 1948, pages 271–86.

2. Unusual Performance of Standard 230-Kv Impulse and Tank-Type Oil Circuit Breakers on Field Tests, **E. B. Rietz**. *AIEE Transactions*, volume 64, 1948, pages 267–70.

3. Development and Testing of an Improved High-Voltage High-Capacity Impulse Circuit Breaker, **E. B. Rietz**. *AIEE Transactions*, volume 69, 1950, pages 15–26.

4. The Columbia Basin Project, **Alvin F. Darland**. *Electrical Engineering* (*AIEE Transactions*), volume 56, November 1937, pages 1339–45.

5. Development of the 230-Kv Ring Bus for Grand Coulee Power Plant, **N. G. Holmdahl**, **C. L. Killgore**. *AIEE Transactions*, volume 67, 1948, pages 1369–80.

6. Switchgear Equipment for Tidd High Voltage Test Line, **F. A. Lane**, **B. W. Wyman**. *AIEE Transactions*, volume 66, 1947, pages 1619–21.

7. Circuit Breaker for Boulder Dam Lines, **D. C. Prince**. *Electrical Engineering* (*AIEE Transactious*), volume 54, April 1935, pages 366–72.

8. Special Tests on Impulse Circuit Breakers. **W. F. Skeats**. *Electrical Engineering* (*AIEE Transactions*), volume 55, June 1936, pages 710–17.

Discussion

E. C. Starr (Oregon State College, Corvallis, Oreg.): Most of this discussor's comments in connection with the Darland, Clagett and Leeds' paper[1] presented at this session apply equally well to the present paper. The results of the co-operative efforts put forth by the Bureau of Reclamation, the Bonneville Power Administration, and several manufacturers have been most fruitful in improving circuit breaker excellence.

The conditions necessary for relatively light as contrasted to heavy-duty fast interruptions are clearly illustrated in Figures 14, 15, and 16 of this paper. The arcing times are short for the three interruptions shown in Figures 14 and 16. In each case contact parting occurred in the latter half of the final major loop of an offset wave with interruption following the next minor loop. The travel record indicates that in none of these three interruptions (Figures 14 and 16) was there a simultaneous occurrence of high arc current and wide contact separation. Interruptions were completed at relatively close separations, particularly in the case of Figure 16 for which the recovery voltage rate was low due to the high degree of current offset. Relatively light duties are evident.

In sharp contrast, Figure 15 records a heavy-duty interruption with much longer arcing time. Contacts parted before the crest of the last minor current loop with interruption following the next major loop. Relatively wide contact separation coincided with the crest of this major loop and the ampere-inch product was high. Visual and aural observations unquestionably confirmed the severity of this interruption and the authors state that this was the only interruption for which external evidence of stress was apparent. The oscillogram clearly shows the reason for this distinct difference, even though the interruption duty was rated at only 75 per cent of that shown in Figure 16 which was obviously actually much lighter. This is in disagreement with the author's statement that all tests were accurately timed for maximum severity. Again the need for revised rating standards and test codes is apparent.

In spite of the discrepancies allowed by our rating standards, the tests reported in this paper, as well as those reported in the paper by Darland, Clagett, and Leeds,[1] fortunately were carried far enough to obtain a few very heavy-duty interruptions and thereby to indicate the performance capabilities of these excellent breakers.

An examination of Figure 16 indicates that careful timing of fault initiation and contact parting could probably result in even heavier breaker duty at Grand Coulee than any so far reported. In a forthcoming series of tests on the Bonneville Power Administration's system, timing will be carefully controlled in an effort to obtain the maximum duties avilable at the test location.

Reference

1. Interrupting Capacity Verification of 10,000,000-Kva 230-Kv Oil Circuit Breakers for Grand Coulee Power Plant, A. F. Darland, W. H. Clagett, W. M. Leeds. *AIEE Transactions*, volume 70, part II, 1951, pages 1386–97.

Otto Naef (American Gas and Electric Service Corp., New York, N. Y.): This paper reveals an impressive increase in the interrupting rating of high-voltage circuit breakers, which for some time may be expected to satisfy most requirements. No comparable development has taken place in the field of continuous current ratings. The breaker described is still rated only 1,000 amperes.

Along with the short-circuit power the load currents of our networks increase steadily. The protective margin between actual load and circuit breaker rating becomes consequently smaller, increasing the danger of overheating as experience clearly demonstrates. While the transmitting capability of most high-voltage lines is as yet hardly approached it probably will be in the future. Snow melting requires currents of the order of 1,400 amperes already today. In any case, it is undesirable that the permissible loading of transmission lines be limited by the low continuous current rating of their circuit breakers.

I should like to know, therefore, if rated currents in excess of 1,000 or 1,200 amperes are contemplated by the manufacturer, and if so, whether radical changes in the design of the contacts are necessitated thereby.

H. Leyburn (Messrs. A Reyrolle & Co. Ltd., Hebburn Co. Durham, England): Being associated with a firm manufacturing switchgear for voltages and circuit breaking capacities of the order of those referred to in the paper under discussion, I should like to say a few words about questions that arise from the differences between the rating and proving practice in the United States and that in Great Britain. It is a pity that these differences exist and it is to be hoped that methods of rating and proving will soon be standardized internationally.

The circuit breaking capacity rating assigned to a high-speed circuit breaker in the United States is usually much higher than it would be in Britain, because the d-c component is included in the rating whereas in Britain it is not. For example, the circuit breaker under discussion would probably be rated at less than 7,500 mva in Great Britain.

In British practice, a test is included to prove the ability of a circuit breaker to interrupt asymmetrical currents corresponding to the rated symmetrical current plus a d-c component not less than 50 per cent of the peak value of the a-c component. In contrast to the implications in the paper, however, which presumably reflects American practice, such a test is not considered sufficient by itself to prove the circuit breaking capacity because, owing to asymmetry, the severity may vary considerably from test to test. For example, in Figures 14 and 16 of the paper interruption takes place after a minor current-loop; and it has been my experience that this condition is easier than that of interruption after a major current-loop or with a symmetrical current.

No mention is made in the paper of the values of the rate-of-rise of recovery voltage in the tests. The rate-of-rise may affect the ability of a circuit-breaker to clear, particularly in the case of the impulse circuit breaker, because it is of the forced-blast type.

In connection with the capacitance-current tests, it is reported that no overvoltages were observed. The ratio of line capacitance (that is the capacitance of the line being disconnected) to source capacitance, which governs the proneness of the system to generate overvoltages, is however not given. With a low value of this ratio, overvoltages are not usually produced, no matter what the circuit-breaker does.

Some of my criticisms illustrate the limitations of field tests and lead to the conclusion that many tests can be done more adequately in a powerful testing station where the test conditions can be more easily controlled.

Although I have criticized certain aspects of the paper, I do not wish to disparage the useful work done by the authors and those associated with them, of which they justly can be proud.

Interrupting Capacity Verification of 10,000,000-Kva 230-Kv Oil Circuit Breakers for Grand Coulee Power Plant

A. F. DARLAND
FELLOW AIEE

W. H. CLAGETT
MEMBER AIEE

W. M. LEEDS
FELLOW AIEE

TWELVE high-speed 230-kv oil circuit breakers rated 10,000,000 kva interrupting capacity now are installed in transmission line and bus-tie positions of the left switchyard at the Grand Coulee power plant. The development of these important pieces of protective equipment has required extensive short-circuit testing both in a manufacturer's high power laboratory and at Grand Coulee Dam. This paper covers the final stages of this development and describes in particular the field tests made in August 1950 to verify the circuit breaker interrupting capacity rating of 10,000,000 kva and to determine any possible margin above this figure.

Grand Coulee Power Plant

The engineering features of the hydroelectric development at Grand Coulee have been described in considerable detail before the Institute.[1,6] Two separate powerhouses are arranged to house nine 108,000-kva generating units each. It is expected that the last three of the 18 generators will be installed and in operation before the end of 1951. An interior view of the nearly-completed right powerhouse with six generating units running is shown in Figure 1.

Associated with the power plant development is an irrigation pumping plant consisting of 12 65,000-horsepower motors and pumps which will lift water from Lake Roosevelt into an extensive irrigation system in the Columbia Basin. Power for these pumps will be supplied at off-peak load periods from the first six generating units of the left powerhouse through 5,000-ampere 13.8-kv busses and 2,500,000-kva compressed-air circuit breakers.

230-Kv Ring Bus

All switching of main power circuits other than the pumping motors is done at high voltage by using a unit-system consisting of a generator and its associated transformer bank with bussing on the high side. Sixteen generators supply power at 230 kv, one generator supplies power at 115 kv, and one generator is connected to a 3-winding transformer with full capacity 115-kv and 230-kv high-voltage windings. The diagram of Figure 2 shows the main 230-kv ring bus and the sectionalized auxiliary bus. Circuit breakers rated 2,500,000-kva interrupting capacity at 230-kv connect to the main bus from each generating unit. However, all of the line and bus-tie circuit breakers are rated 10,000,000 kva at 230 kv with 3-cycle interrupting time. Furthermore these high interrupting capacity circuit breakers are capable of operating without any derating on 20-cycle reclosing duty. A more complete discussion of this 230-kv solid ring bus and the operating flexibility which it provides has been given in an earlier paper by Holmdahl and Killgore.[2]

230-Kv Left Switchyard

All of the 230-kv circuit breakers in the left switchyard are of the conventional dead-tank type as can be seen by the general view shown in Figure 3. Six of the 10,000,000-kva circuit breakers were rebuilt from older 3,500,000-kva circuit breakers with large 108-inch diameter tanks, while the six circuit breakers most recently installed (one of which is shown in Figure 4) are of the latest design with smaller 84-inch tanks of approximately one-half the oil volume. Two more line circuit breakers of this type are on order to fill all of the positions in the diagram of Figure 2.

The United States Bureau of Reclamation has co-operated with the circuit breaker manufacturers on several previous short circuit tests at Grand Coulee[3,4] in order to assist in the development and verification of circuit breakers of interrupting rating beyond the capacity of high power laboratories to provide direct tests. The availability of extremely high short-circuit power from 12 generators and seven transmission lines connecting to the Bonneville Power System and the Northwest Power Pool for the tests described in this paper made it seem advisable to provide a special test bay several hundred feet from the main switchyard. One of the 230-kv bus sections was isolated and connected to the test circuit breakers by a temporary single-phase transmission line as indicated in the diagram of Figure 5. One of the regular line circuit breakers in position *JY-19* served as back-up protection.

By setting up two complete test circuit breakers in what were designated as North and South positions in the test bay, it was possible to use one circuit breaker for closing in on the fault and the other to interrupt the short-circuit current. In order to separate the instrumentation and power circuit grounds as far as possible, an insulated return circuit for the fault current was brought back to a solid ground at the center of the switchyard.

Paper 51-257, recommended by the AIEE Switchgear Committee and approved by the AIEE Technical Program Committee for presentation at the AIEE Summer General Meeting, Toronto, Ont., Canada, June 25–29, 1951. Manuscript submitted March 27, 1951; made available for printing May 10, 1951.

A. F. DARLAND is with the United States Bureau of Reclamation, Coulee Dam, Wash., W. H. CLAGETT is with the United States Bureau of Reclamation, Denver, Colo., and W. M. LEEDS is with the Westinghouse Electric Corporation, East Pittsburgh, Pa.

Figure 1 (left). Right power plant at Grand Coulee with six generators in operation and the last three in process of installation. This will complete the total of 18 120,000-kva generators comprising the largest power plant in the world

Figure 3. 230-kv left switchyard at Grand Coulee showing 2,500,000-kva generator circuit breakers and 10,000,000 kva transmission line and bus tie circuit breakers

Both cathode-ray and magnetic oscillograph records were taken of the voltage across the circuit breaker and on the bus, using coupling-capacitor voltage-dividers. The heavy short-circuit currents were measured by a laboratory-type 5,000-to-1 current transformer mounted on, but insulated from, the ground lead.

Ultimate Fault Duty

As reported in previous papers[3,4] the ultimate fault duty at the Grand Coulee 230-kv switchyards will approach 15,000,000 kva. The increase in both symmetrical and asymmetrical fault capacity with installation of additional generating units at Grand Coulee and additional lines, generating capacity, and interconnections on the transmission system of the Bonneville Power Administration is shown on Figure 6. These values are based on a 3-phase fault at the Grand Coulee 230-kv switchyard bus with all generators and pump motors in operation, all transformer neutrals solidly grounded, and all transmission lines in service with maximum back feed to the fault.

Although 15,000,000 kva is the maximum calculated 3-phase fault that could occur under the worst conditions on the ultimate system, actual experience to date from system records for years 1944 to 1951 show that only 6 per cent of the faults exceeded 70 per cent of the maximum fault capacity available. About half of the faults involved less than 21 per cent of the maximum fault capacity available. A comparison of actual circuit breaker duty with the maximum calculated fault capacity available is shown on Figure 7.

The rapid reduction in circuit breaker duty as the fault is removed from the 230-kv switchyard bus out on the transmission lines is shown in Figure 8. The addition of only about 2 miles of transmission line reduces the maximum fault to 10,000,000 kva, while 1 mile reduces the fault to 12,000,000 kva. Calculations further show that for a fully offset asymmetrical wave the maximum single line-to-ground fault 1 mile from the 230-kv switchyard is less than 12,000,000 kva. The transmission lines from Grand Coulee are provided with overhead ground wires extending approximately 1 mile from the 230-kv switchyard, and there is only a remote possibility of a fault occurring in this protected area.

Therefore, there would appear to be little, if any, probability of an actual fault occurring which exceeds 12,000,000 kva, and the field tests reported herein, together with laboratory tests have demonstrated that the 10,000,000 kva circuit breakers have ample margin above their nameplate rating.

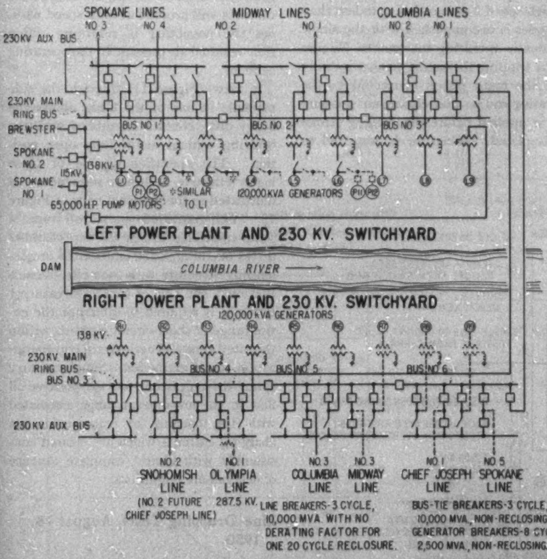

SPOKANE LINES
NO 3
NO 4
MIDWAY LINES
NO 2
NO 1
COLUMBIA LINES
NO 2
NO 1
230KV AUX BUS
230KV MAIN RING BUS
BREWSTER
SPOKANE NO. 2
SPOKANE NO 1
BUS NO 1
BUS NO 2
BUS NO 3
138KV
115KV
SIMILAR TO L1
120,000KVA GENERATORS
65,000 H.P. PUMP MOTORS
LEFT POWER PLANT AND 230 KV. SWITCHYARD
DAM
COLUMBIA RIVER
RIGHT POWER PLANT AND 230 KV. SWITCHYARD
120,000 KVA GENERATORS
138 KV
230KV MAIN RING BUS
BUS NO 3
BUS NO 4
BUS NO 5
BUS NO 6
230KV AUX BUS
NO 2 SNOHOMISH LINE
(NO. 2 FUTURE CHIEF JOSEPH LINE)
NO 1 OLYMPIA LINE
287.5 KV.
NO 3 COLUMBIA LINE
NO 3 MIDWAY LINE
NO 1 CHIEF JOSEPH LINE
NO 5 SPOKANE LINE
LINE BREAKERS-3 CYCLE, 10,000 MVA WITH NO DERATING FACTOR FOR ONE 20 CYCLE RECLOSURE.
BUS-TIE BREAKERS-3 CYCLE, 10,000 MVA, NON-RECLOSING.
GENERATOR BREAKERS-8 CYCLE, 2,500 MVA, NON-RECLOSING.

Figure 2. Single-line diagram showing physical arrangement of 230-kv main ring and auxiliary bus for Grand Coulee power plant. Maximum flexibility is obtained by operating with a solid bus in spite of added fault interrupting duty on the circuit breakers

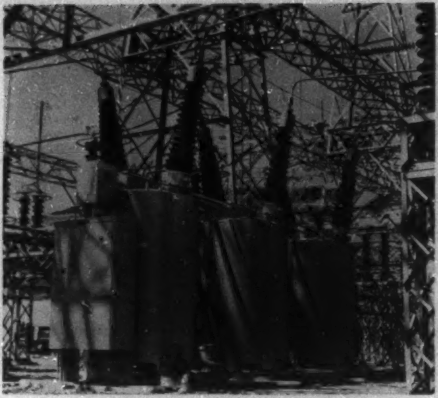

Figure 4. Tank-type 10,000,000-kva 3-cycle oil circuit breaker installed in the 230-kv left switchyard at Grand Coulee Dam. This circuit breaker is capable of 20-cycle reclosing duty at full rating

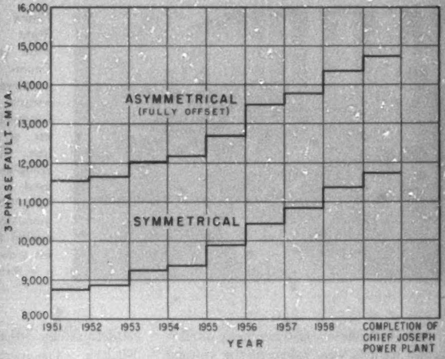

Figure 6. Increase in 3-phase megavolt-ampere fault capacity at Grand Coulee power plant with increased generating capacity and growth of Bonneville Power Administration transmission system

230-Kv 10,000,000-Kva Test Circuit Breakers

The two 3-pole tank-type 230-kv 10,000,000-kva 3-cycle test circuit breakers set up in the test bay are shown in Figure 9 illuminated by an arcing fault during a test at night. Details of the design of these new high-power circuit breakers were described in a previous paper.[5] It may be noted that the dead-tank construction not only provides mechanical ruggedness but also is inherently adapted for the use of the convenient through-type current transformers surrounding oil-impregnated and completely-sealed condenser-type bushings.

High-speed 3-pole reclosing in less than 20 cycles is accomplished with the single pneumatic-operating mechanism (Figure 10) by tripping the circuit breaker initially with the main piston connected to the operating rod so that closing air pressure can be applied before the opening stroke is completed. When air is admitted to the cylinder, the motion is reversed quickly and the contacts reclosed with a minimum of delay. If fault current is re-established and the circuit breaker tripped again, a mechanically trip-free latch, selected by a pressure-controlled transfer switch, is released so that opening of the contacts will proceed at high speed without the possibility of retarding action from residual air pressure in the operating cylinder.

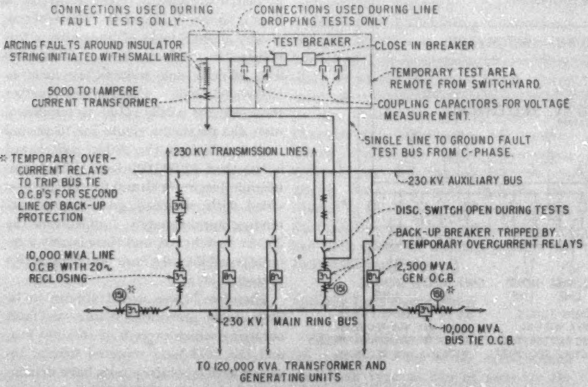
CONNECTIONS USED DURING FAULT TESTS ONLY
CONNECTIONS USED DURING LINE DROPPING TESTS ONLY
ARCING FAULTS AROUND INSULATOR STRING INITIATED WITH SMALL WIRE
TEST BREAKER
CLOSE IN BREAKER
TEMPORARY TEST AREA REMOTE FROM SWITCHYARD
5000 TO 1 AMPERE CURRENT TRANSFORMER
COUPLING CAPACITORS FOR VOLTAGE MEASUREMENT
SINGLE LINE TO GROUND FAULT TEST BUS FROM C-PHASE
230 KV TRANSMISSION LINES
* TEMPORARY OVER-CURRENT RELAYS TO TRIP BUS TIE O.C.B'S FOR SECOND LINE OF BACK-UP PROTECTION
230 KV. AUXILIARY BUS
DISC. SWITCH OPEN DURING TESTS
BACK-UP BREAKER. TRIPPED BY TEMPORARY OVERCURRENT RELAYS
10,000 MVA. LINE O.C.B. WITH 20~ RECLOSING
2,500 MVA. GEN. O.C.B.
3~
8~
151
230 KV. MAIN RING BUS
10,000 MVA. BUS TIE O.C.B.
TO 120,000 KVA. TRANSFORMER AND GENERATING UNITS

Figure 5. Diagram showing temporary connections to the special circuit breaker test bay adjoining the 230-kv left switchyard at Grand Coulee Dam

A view (Figure 11) through the side manhole in one of the tanks shows the heavy-duty contact assemblies with the bridging contact in the fully open position. The operation of one of these highly-effective multiflow interrupters is illustrated in the sectional view of Figure 12. Self-generated pressure from a series-connected arc in the top chamber drives oil through the multiorifice arc deionizing structure with such effectiveness that only one pair of contact breaks per terminal is required to interrupt the entire range of short-circuit currents within the rated time of 3 cycles from trip energization to arc extinction. Supplementary spring-driven pistons provide positive oil flow in the low-current range associated with the opening of transmission-line charging currents which are cleared consistently with almost complete absence of delayed arc reignitions.

Line-Dropping Tests, August 18, 1950

The importance of prompt extinction of the arc when de-energizing unloaded transmission lines to avoid the possibility of hazardous overvoltages is well-known, and the phenomena involved have been treated extensively in the literature. A demonstration of the ability of these large circuit breakers to handle line-charging current effectively was therefore included in the schedule of tests at Grand Coulee Dam. The single circuit carried out to the special test bay was connected to the 100-mile Midway Line number 1 with all three conductors paralleled. The North test circuit breaker picked up and dropped this line, switching approximately 150 amperes of charging current, from a section of 230-kv bus energized by one transformer bank and generator.

The interrupting time for four consecutive line-dropping tests on which oscillographic records were taken averaged 2.3 cycles, and there were no restrikes,—a "restrike" being defined as an arc reignition after a current zero pause of 0.25 cycle or more. Figure 13 shows the oscillogram of test *LD-3* which took the longest time, actually only 2.4 cycles.

The next group of tests was made opening the 66-ampere charging current of phase *C* only of the 100-mile line. Twelve consecutive line-dropping operations were recorded with the interrupting time ranging from 1.8 to 2.4 cycles. Overvoltage on the line was negligible on all tests but one, and this showed only 1.55 times normal. On about half of the tests there were harmless reignitions, representing ineffective attempts to open the circuit just after the contacts parted and before the delayed-action oil piston came into operation. The oscillogram of test *LD-12* shown in Figure 14 is typical. Table I gives the interrupting time for all of the line-dropping tests.

Table I. Grand Coulee Field Tests on 230/196-Kv 10,000,000-Kva Oil Circuit Breaker
Line Dropping Tests, August 18, 1950

Film No.	Test No.	Line Voltage, Kv	Interrupted Current, Amperes	Interrupting Time, Cycles	Overvoltage % Normal Crest (CRO)
74305-					
A	Timing			1.25	
B	Calibration				
C	LD-1	238	150	2.35	0
D	LD-2	238	150	2.25	0
E	LD-3	238	150	2.40	0
F	LD-4	238	150	2.30	0
G	Calibration				
H	LD-5	238	66	2.35	0
I	LD-6	238	66	2.40	55
J	LD-7	238	66	2.20	0
K	LD-8	238	66	2.20	0
L	LD-9	238	66	2.05	0
M	LD-10	238	66	2.15	0
N	LD-11	238	66	2.20	0
O	LD-12	238	66	2.10	0
P	LD-13	238	66	2.30	0
Q	LD-14	238	66	2.10	0
R	LD-15	238	66	2.10	0
S	LD-16	238	66	1.80	0

Table II. Grand Coulee Field Tests on 230/196-Kv 10,000,000-Kva Oil Circuit Breaker
Fault Interrupting Tests, August 20, 1950

Film No.	Test No.	Duty Cycle	Line Voltage, Kv	Interrupted Current, Amperes	Interrupting Time, Cycles	Equiv. 3-Phase Mva
74305-						
T	Timing	O			1.35	
U	Timing	OC			1.35	
V	Calibration					
W	SF-1	O	238	1,330	3.00	550
X	SF-1 R1	O	238	1,185	2.75	490
Y	Calibration					
Z	SF-2	O	237	13,000	2.60	5,350
AA	SF-3	CO	237	14,200	2.30	5,800
AB	Calibration					
AC	SF-4	CO	239	21,600	2.85	8,950
AD	SF-5	O	239	21,000	3.10	8,700
Changed to Pole #2						
AE	SF-6	O	238	23,200	2.20	9,600
AF	SF-7	O	238	25,800	2.85	10,650
AG	SF-8	O	238	19,200	2.30	7,950
18.4 cycle Reclosure		CO	238	17,100	2.80	7,050
AH	SF-9	O	238	4,600	2.20	1,900
AI	SF-10	O	238	3,100	3.00	1,280
AJ	SF-11	O	167	3,150	3.20	915
AK	SF-12	O	167	2,950	2.20	855

Figure 7 (below). Comparison of actual circuit breaker duty with maximum calculated fault capacity at Grand Coulee power plant from system records for years 1944 to 1951

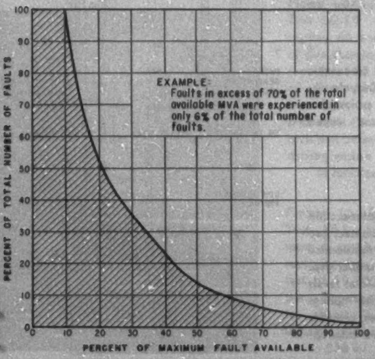

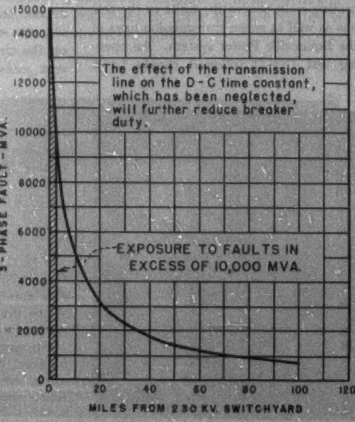

Figure 8 (right). Typical effect of line length on circuit breaker duty at Grand Coulee switchyards

Figure 9. Night view of an arcing fault interrupting test, showing the two tank-type 10,000,000-kva 3-cycle circuit breakers set up in the special test bay

Fault Tests, August 20, 1950

The short-circuit interruptions were handled by the South test circuit breaker, using the North circuit breaker for backup protection and also as the fault-establishing switch for both normal trip and pretripped opening tests. For close-open duty on the test circuit breaker, the North circuit breaker was closed before the start of test so that the South circuit breaker would initiate the short circuit when it closed.

The first two interruptions (*SF-1* and *SF-1R1*) of approximately 1,200 amperes obtained from a single generator supplying power to an isolated bus section were handled satisfactorily by pole number 1 of the South test circuit breaker in 3.0 and 2.75 cycles, see Table II. The fault power was then greatly increased by connecting eight generating units to the test bus as well as seven transmission lines of the Bonneville Power system. An opening test (*SF-2*) followed closely by a close-open test (*SF-3*) were made, interrupting 13,000 amperes in 2.6 cycles and 14,200 amperes in 2.3 cycles respectively. The operation of the test circuit breaker was quite easy with only a puff of smoke from the exhaust pipe, even though the 3-phase equivalent fault power on the latter test amounted to nearly 6,000,000 kva.

The next series of tests was made at full power with 12 generator and transformer units on the bus, and also the same seven transmission lines. A close-open test (*SF-4*) opening 21,600 amperes, equivalent to practically 9,000,000 kva 3-phase, was cleared satisfactorily in 2.85 cycles. However, the next test (*SF-5*), an opening operation, took 3.1 cycles to interrupt approximately the same amount of power. There was evidence of considerable internal pressure, and some oil was lost from the vent pipe.

The arcing time was definitely longer than expected, but since there was insufficient time for detailed inspection of the pole unit, it was decided to continue by connecting the leads to pole number 2. Under the same test conditions but with the circuit breaker pretripped by a half cycle, a fault current measuring 23,200 amperes on test *SF-6* was interrupted easily in 2.2 cycles. The equivalent 3-phase power at the line voltage of 238 kv amounts to 9,600,000 kva or practically the full rating of the circuit breaker.

The pretripping adjustment was shifted another half cycle so that the circuit breaker contacts would separate as close as possible to the crest of the first asymmetrical loop for fault current. The next test (*SF-7*) did not clear at the end of the small current loop but arced through the second large loop for a total interrupting time from energizing the trip of 2.8 cycles, see Figure 15. This was just about as severe a test as could be obtained on the circuit, the total interrupted current measuring 25,800 amperes for an equivalent 3-phase fault power of 10,650-000 kva. The circuit breaker experienced a fairly solid bump, but no oil was lost and the test was considered satisfactory.

The final high power operation was a rapid reclosing test (*SF-8*) without pretripping, the oscillogram being shown in Figure 16. The first interruption of 19,200 amperes, representing approxi-

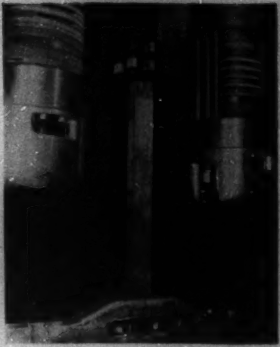

Figure 11. View through the manhole of the test circuit breaker showing the 10,000,000-kva 3-cycle multiflow interrupters with the moving contact cross arm in the full open position

Figure 10 (left). Type CASR-92 pneumatic operating mechanism used for 20-cycle reclosing duty, operating all three poles of a 230-kv 10,000,000-kva 3-cycle circuit breaker

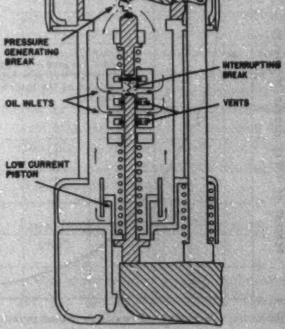

Figure 12 (right). Multiflow interrupter section view showing pressure-generating contact gap at the top driving oil into the multiorifice structure surrounding the central contact gap. Vents take gases out front and back at levels between the inlet channels. The spring-driven annular piston at the bottom provides supplementary oil flow for positive interruption of low currents

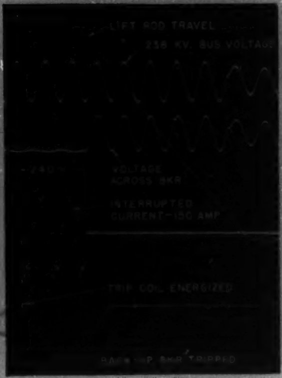

Figure 13. Test LD-3 interrupting 150 amperes of line-charging current for 300 miles of line in 2.4 cycles after energizing the circuit breaker trip coil

mately 8,000,000 kva, was cleared in 2.3 cycles. This was followed by a second interruption after an 18.4-cycle reclosing interval, interrupting 17,100 amperes in 2.8 cycles. The circuit breaker performed perfectly, there being merely two puffs of smoke from the vent pipe. This test in conjunction with laboratory tests reclosing in as short a time as 7.7 cycles, as reported in the closing discussion on the Leeds-Friedrich paper,[4] verify the ability of this circuit breaker to handle high-speed reclosing duty without derating below the 10,000,000-kva rated interrupting capacity.

Four additional tests at moderate fault power also were made successfully on the same circuit breaker pole before concluding the test program, the results being analyzed below in the section concerning out-of-phase switching.

All of the contacts in both test circuit breakers were in good condition when examined after the tests. The intermediate and lower moving contacts from both poles of the South circuit breaker subjected to the fault tests are shown in Figure 17. It is evident that there is still considerable material left on the arc tips even after duty amounting to an integrated total of almost 30,000,000 kva in pole number 1 and 40,000,000 kva in pole number 2.

The fiber plates shown in Figure 18 were taken from one of the grid stacks in pole number 2 which had the heaviest fault interruptions. Only a slight enlargement of the first two or three orifices can be noted due to cooling effect on the self-generated oil flow jets impinging on the arc from opposite sides at the various inlet levels.

Both of the aluminum and Micarta shields on the interrupter assemblies in pole number 1 were found broken after the tests. A careful examination disclosed that the grid assemblies were mounted higher on the terminals than they had been on the laboratory verification tests. This allowed the lower end of the bushing to block the opening provided at the top of the shields for release of gases expelled from the pressure chamber relief valve.

The resulting sudden rise of pressure on a fairly heavy test fractured the shields. However, the mechanical operation of the circuit breaker was not affected since the heaviest interrupting tests in pole number 2 were completed successfully after the shield damage occurred in pole number 1.

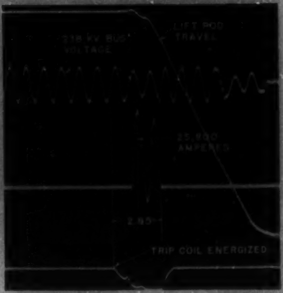

Figure 15. Test SF-7 oscillogram of the maximum fault interruption of 25,800 amperes in 2.85 cycles, corresponding to 10,650,000-kva 3-phase at the bus voltage of 238 kv

High Power Laboratory Follow-up Tests

A few weeks after the field tests a similar 230-kv 10,000,000-kva circuit breaker pole unit was set up in the High Power Laboratory, and the shield breakage duplicated with tests interrupting the same current with the same arcing time using 44 kv across a single interrupter. With this confirmation of the necessity for venting the shield more freely, the opening at the top of the metallic shields was increased appreciably, and at the same time added factor of safety was obtained by substituting high strength bronze in place of aluminum. Also the Micarta shield covers were approximately doubled in thickness. The appearance of grid assembly with the new shields is shown in Figure 19.

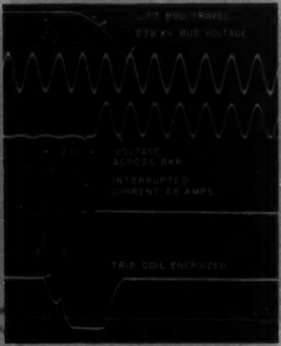

Figure 14 (left). Test LD-12 interrupting 66 amperes of line-charging current for 100 miles of line. Harmless arc reignition takes place just after contacts part before oil-driving piston starts to function

Figure 16 (right). Test SF-8 oscillogram of an 18-cycle reclosing duty cycle test of 19,200 amperes corresponding to almost 8,000,000-kva 3-phase at 238 kv

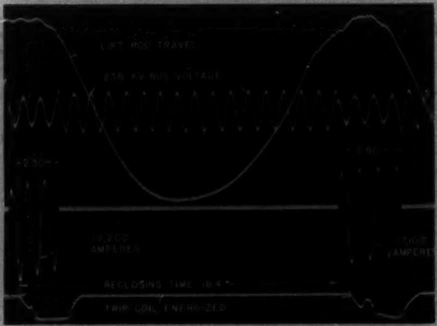

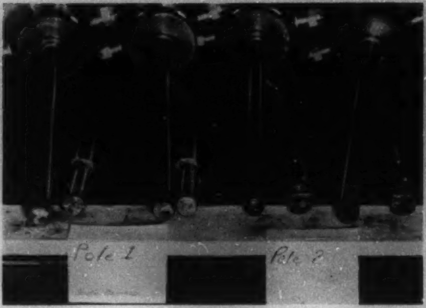

Figure 17. Contact tips from the test circuit breaker after short-circuit tests up to the 10,000,000-kva rating. The contacts were still in condition for further service even after a total integrated duty of 30,000,000 kva in pole number 1 and 40,000,000 kva in pole number 2

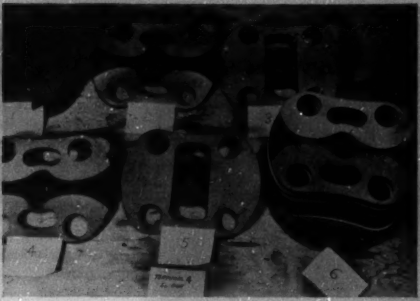

Figure 18. Fiber plates from one of the multiflow interrupters in pole number 2 of the test circuit breaker after tests to 10,650,000 kva showing the very moderate amount of burning in the orifice

Additional laboratory short-circuit tests to verify the improved design included two interruptions of 23,500 amperes, two at 26,000 amperes, one at 31,000 amperes, and an extra factor of safety test opening a single asymmetrical current loop measuring 36,300 amperes rms at the middle or 39,200 amperes rms with the envelope extended back to the point where the contacts parted close to the start of the fault, see Figure 20. The equivalent 3-phase kilovolt-amperes at 230 kv represented by 39,200 amperes is 15,600,000 kva.

Discussion of Demonstrated Interrupting Capacity

Wide differences in the severity of successive short-circuit tests of the same calculated interrupting duty have often been noted in both laboratory and field tests on large circuit breakers. The two Grand Coulee tests *SF-6* and *SF-7* were both at maximum power and offer an excellent case in point. On the first of these tests the observers were scarcely aware of any fault current being interrupted, while all agreed that there was an appreciable ground shock and muffled boom from the circuit breaker on the second test. Unless field testing is controlled to the point where the most difficult conditions that may reasonably be anticipated in service are applied to the circuit breaker, it is hardly safe to assume that the ability to handle the particular amount of short circuit power measured on any one test has really been demonstrated.

Many years of switchgear testing experience in a high power laboratory has emphasized the importance of precise control over both current asymmetry and the time at which the test circuit breaker parts its contacts with respect to the instant when the fault is initiated. The thoroughness with which all types of circuit severity was explored in the laboratory before undertaking the Grand Coulee field tests is illustrated by the data in Table III taken from nine interruptions of currents between 27,500 and 31,000, all well above the rated current-interrupting capacity of 25,000 amperes. These tests are classified in three groups,

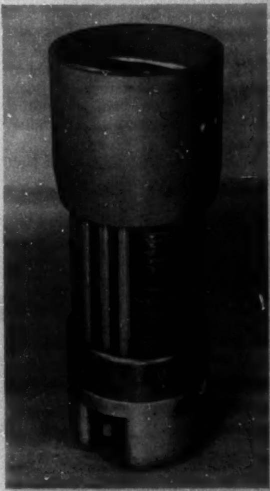

Figure 19. Photo of multiflow interrupter assembly for the 10,000,000-kva 3-cycle circuit breakers with the final design of Micarta and bronze shields

Table III. High Power Laboratory Short Circuit Tests on 230/196-Kv 10,000,000-Kva Oil Circuit Breaker with 25,000-Ampere Interrupting Capacity

44-Kv Single Phase to Ground (Across One-Half Pole Unit)

Film No.	Test No.	Interrupted Current, Amperes	Interrupting Time, Cycles	Lift Rod Travel at Interruption, Inches	First Peak Pressure, Lbs./Sq. In.	Severity Type
85784-						
AEC	2-08208	28,400	2.55	2.4	30	B
AED	09	31,000	2.60	2.5	27	B
AEE	10	1,150	2.50	2.1		
AEF	11	28,400	2.25	1.6	12	B
AEG	12	28,000	2.15	1.6	6	B
AEH	2-98213	29,500	1.90	0.9	5	A
AEI	14	29,200	2.80	2.9	93	C
AEJ	15	28,200	2.15	1.4	6	B
AEK	16	27,500	2.70	2.7	114	C
AEL	17	28,000	2.75	2.7	105	C

Note: Current measured at instant of contact parting 1.2 cycles after energizing trip coil.

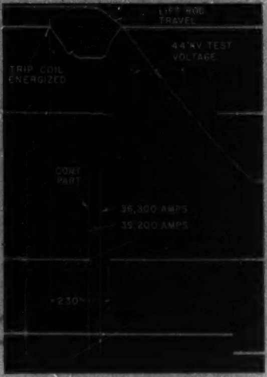

Figure 20. High Power Laboratory short circuit test with 44 kv across a half-pole unit. The current of 39,200 amperes, interrupted in 2.3 cycles, corresponds to a 3-phase fault of 15,600,000 kva at 230 kv

A, *B*, and *C*, in increasing order of severity. Only one test was of the exceptionally easy type *A*, five were of the moderate severity type *B*, while three out of the last four tests in the group belonged to the maximum severity type *C*. One current wave of each type is plotted on the same time scale in Figure 21, with zero time at the instant of energizing the trip coil. Since the degree of asymmetry was maintained constant, it is clear that the shift in timing the establishment of the fault relative to the tripping impulse was responsible for the variations in circuit breaker performance indicated approximately by the maximum pressure peak in the tank. A fault interruption ending in a small half cycle as in type *B* obviously is not particularly severe, since the amount of arc energy depends principally upon the current amplitude in the later part of the arcing period. Even when the last half cycle of arcing consists of a large current loop, this may not be a severe test unless it is known from other data that final interruption is taking place about as late in the opening stroke of the circuit breaker as it is likely to do. (Compare types *A* and *C*.)

Coulee test *SF-7* is plotted to the same current and time scale to show that this interruption, representing 10,650,000-kva 3-phase, was actually of the severe class *C* type.

Out-of-Phase Switching

During a severe case of system instability, it may happen that a circuit breaker in a tie-line position may trip out on overload just at the instant when the voltages generated on either side of the circuit breaker are in phase opposition. The dynamic recovery voltage appearing across each of the circuit breaker poles may reach from 2 to 2.5 times normal line-to-ground voltage, with high-frequency transients of uncertain amplitude superimposed to add to the difficulty of interruption. The possibility of such extreme conditions has been recognized for a long time, but the relatively few cases of circuit breaker trouble reported due to this cause have not justified insistence of operating engineers on demonstrated ability to handle these very high voltages. Experience indicates that many circuit breakers have struggled through out-of-phase operations, which usually are limited by line impedance to currents of only a fraction of the circuit breaker interrupting capacity, by continuing to arc until the separating parts of the system have swung sufficiently in phase again to permit interruption.

A very desirable characteristic for high voltage circuit breakers is the proved ability to cope with out-of-phase switching conditions. One proposal for checking a circuit breaker in the field at double voltage is to make fault tests up to approximately 25 per cent of the current-interrupting rating with one-half of interrupting units in each test pole shunted out of the circuit. This procedure is more readily justified when the half-pole assemblies are duplicates and are normally bridged by voltage-dividing resistors or capacitors. To go further and test up to

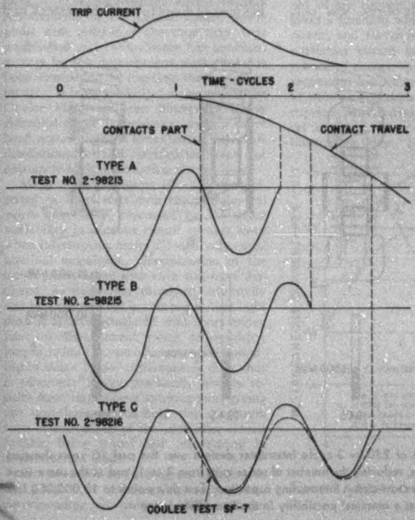

Figure 21 (left). Comparison of severity of circuit breaker duty on differently timed fault-interrupting tests with the same short-circuit current amplitude and degree of asymmetry. Types A and B are relatively easy interruptions while type C represents severe duty on the circuit breaker

Figure 22 (below). Cathode-ray oscillograph records of voltage across the circuit breaker showing the high recovery rate and voltage overshoot on test SF-11 with an isolated bus section, compared with the damped recovery voltage on duplicate test SF-11 except with 100 miles of 230-kv open-end line connected to the bus

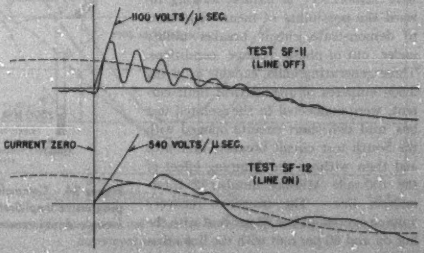

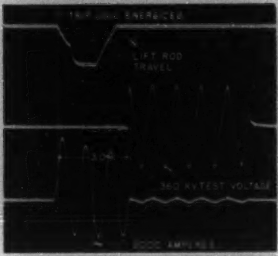

Figure 23. Out-of-phase overvoltage test of 360 kv (330-kv recovery voltage) across one pole of a 230-kv 10,000,000-kva circuit breaker, interrupting 2,000 amperes in 3.0 cycles. This laboratory test represents successful operation at more than 2½ times normal line-to-ground voltage

2.5 times normal voltage would require isolating both a test bus and generating unit, as in a high power laboratory test, and then apply to the half pole on test line-to-line voltage of suitable value obtained by controlling the generator excitation. For instance, on a 230-kv system the appropriate voltage for a half-pole test might be

$$\frac{1}{2}\times\frac{230}{\sqrt{3}}\times 2.5=166 \text{ kv}$$

which could be obtained from line-to-line voltage at 72 per cent excitation.

Unfortunately an isolated test circuit as just described would subject the test circuit breaker to an unnecessary severe condition of a relatively high frequency recovery-voltage transient overshooting to a crest perhaps 60 or 70 per cent above the 60-cycle voltage. More moderate recovery transients corresponding to actual operating conditions can be simulated by paralleling the circuit breaker with a suitable loading resistor or by connecting an open-end transmission line to the test bus.

Tests *SF-9*, *SF-10*, *SF-11*, and *SF-12* were exploratory in nature, looking toward the possibility of future field tests to demonstrate circuit breaker ability under out-of-phase voltage conditions. Three generating units, capable of giving 3,000 amperes of symmetrical fault current, were connected to the isolated test bus, and two short circuits opened with the South test circuit breaker, first with and then without the damping effect of the 100-mile Midway number 2 transmission line. The transient recovery voltage overshoot was 23 per cent with the line on and 60 per cent with the line off as measured from cathode-ray oscillograms. For the final pair of short circuit tests, the generator excitation was lowered to 70 per cent, bringing the line-to-line voltage down to 167 kv to determine whether the attenuation of the transients would be appreciably affected. For this condition the overshoot was found to be 50 per cent with the line off and 33 per cent with the line on. In addition to knocking off the transient peaks, another important effect of the transmission line on the bus was to lower the rate-of-rise of recovery voltage from approximately 1,100 volts per microsecond to only 540 volts per microsecond, see Figure 22. Additional field tests, calculations, and transient network analyzer studies are desirable to establish more definitely both the dynamic and transient voltage conditions to which circuit breakers may be subjected when interrupting transmission-line circuits during system instability. Wherever possible this should be followed up by high power laboratory circuit breaker tests.

As an indication of the ability possessed by these 10,000,000-kva circuit breakers to cope with out-of-phase voltages, the group of laboratory tests listed in Table IV may be of interest. The initial test voltages used ranged from 264 to 360 kv, representing from 2 to 2.7 times normal line-to-ground voltage on a 230-kv system. A parallel damping resistor limited the transient overshooting to about 20 per cent above the 60-cycle crest to conform with field conditions, although the high rate-of-rise was only slightly modified. On the test shown in Figure 23, 2,000 amperes at 360 kv was interrupted in 3 cycles with a transient recovery-voltage peak estimated at 560 kv, built up at a rate of approximately 750 volts per microsecond. This test is believed to represent out-of-phase voltage conditions more severe than any likely to be encountered in service.

Table IV. High Power Laboratory Short Circuit Tests on 230/196-Kv 10,000,000-Kva Oil Circuit Breaker

Out-of-Phase Voltage Interrupting Tests

Test No.	Single Phase Test Voltage, Kv	Interrupted Current, Amperes	Interrupting Time, Cycles
2-100324	330	5,050	2.5
5	330	1,800	2.9
6	330	2,050	2.8
7	360	2,250	2.7
8	360	2,000	3.0

Future 230-Kv Circuit Breaker Development

A few years ago, a circuit breaker interrupting rating of 10,000,000 kv at 230 kv looked like a definite ceiling, partly on account of limitations inherent in the momentary current-carrying capacity of butt-type contacts considered to be almost indispensable in high voltage 3-cycle circuit breakers, and partly perhaps because of vague fears of the unknown in this "stratosphere" of fault-clearing duty. Nevertheless, the prodding of necessity has opened doors to new achievement, and

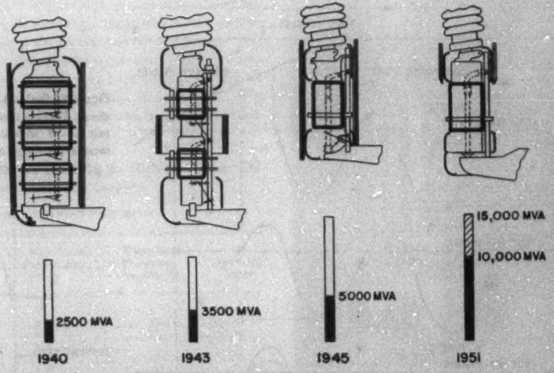

Figure 24. Comparison of 230-kv 3-cycle interrupter designs over the past 16 years showing progressive simplification, reducing the number of series units from 3 to 1, and at the same time a tremendous increase in short-circuit interrupting capacity. Test data points to 15,000,000 kva as a practical possibility in the immediate future

results already obtained with finger-contact interrupter designs for 10,000,000-kva ratings at 161 kv and 138 kv point the way to at least 15,000,000 kva at 230 kv.

Looking backward over a period of only 11 years since the first high-speed 3-cycle deion grid type of circuit interrupter was adapted from the 287-kv Hoover Dam design for installation in a 230-kv circuit breaker, a remarkable rate of development is disclosed. Figure 24 illustrates graphically the great simplification achieved, first by reducing the number of units in series per circuit breaker terminal from three to two, and then to only one. Further reduction to bare essentials without change in the 3-cycle speed of opening was accomplished by careful redesign to remove undesirable linkages and delicate adjustments. At the same time the interrupting capacity was increased four-fold from 2,500,000 kva to 10,000,000 kva, with the next step to 15,000,000 kva virtually assured.

Additional improvements of particular importance include a 50 per cent reduction in oil volume, elimination of hazardous arc restriking when opening line-charging current, and rapid-reclosing duty cycles within intervals as short as 15 cycles at practically full rated interrupting capacity. Such outstanding accomplishment in the switchgear field could hardly have been possible without the whole-hearted co-operation between system engineers and equipment designers in carrying out such valuable field tests as those described in this paper. Particular mention should be made of the helpful suggestions and active assistance of many individuals from both the engineering and operating personnel of the United States Bureau of Reclamation, Bonneville Power Administration, and the Westinghouse Electric Corporation.

Conclusions

The short circuit interrupting tests to a maximum of 10,650,000 kva made on the Grand Coulee 230-kv bus, together with a large number of high power laboratory tests of varying degrees of severity opening currents in the range from 10,000,000 kv to 15,000,000 kva at 230 kv have verified the rated interrupting capacity of this type of dead-tank circuit breaker, and with minor modifications to the contact shielding, have demonstrated the ability to interrupt successfully faults of maximum severity up to at least 12,000,000 kva. Furthermore, charging current of 100 and 300 miles of line was interrupted promptly in not over 2.4 cycles by positive oil-flow action from spring-driven pistons. Finally, laboratory tests opening currents up to 2,000 amperes at voltages as high as 360 kv across a single pole indicate factor of safety more than sufficient to handle the most severe conditions anticipated during circuit breaker operation separating parts of a system with out-of-phase voltages.

References

1. The Grand Coulee Power Development, S. M. Denton. *AIEE Transactions*, volume 67, part II, 1948, pages 899–911.

2. Development of the New 230-Kv Ring Bus for Grand Coulee Power Plant, N. G. Holmdahl, C. L. Killgore. *AIEE Transactions*, volume 67, part II, 1948, pages 1369–81.

3. 4,370,000 Kva Short-Circuit Tests on Grand Coulee 230-Kv Bus, W. H. Clagett, W. M. Leeds. *AIEE Transactions*, volume 65, 1946, pages 729–35.

4. Field Tests for Development of 10,000,000-Kva 230-Kv Oil Circuit Breakers for Grand Coulee Power Plant, C. L. Killgore, W. H. Clagett. *AIEE Transactions*, volume 67, 1948, pages 271–83.

5. High-Voltage Oil Circuit Breakers for 5,000,000 to 10,000,000-Kva Interrupting Capacity, W. M. Leeds, R. E. Friedrich. *AIEE Transactions*, volume 69, part I, 1950, pages 70–76.

6. The Columbia Basin Project, A. F. Darland. *Electrical Engineering* (*AIEE Transactions*), volume 56, November 1937, pages 1339–45.

Discussion

R. C. Starr (Oregon State College, Corvallis, Oreg.): The high-voltage circuit breaker requirements of the Grand Coulee power plant were unique at the time they were established and the industry has benefited greatly by the development work that has been carried on in meeting these requirements. It is particularly fortunate that the Coulee Plant and the Bonneville Power Administration transmission system have been made available for extensive full-scale developmental and verification tests at extremely high interrupting duty.

Many of the engineers who have participated in these tests over the past several years have been impressed by the great variability in obvious circuit breaker duty when interrupting faults of essentially equal nominal magnitude. Examination of the oscillograms taken with each test have disclosed, as frequently discussed informally and now pointed out in this paper, that light duty is always associated with short arcing time on offset current waves, or somewhat longer arcing time on offset waves terminating in minor loops. Interrupting duty that is obviously heavy practically always results from large-power interruptions giving arc durations approaching the maximum time characteristic of the particular circuit breaker being tested and terminating in major current loops.

Arc power in an interrupter is equal to the product of instantaneous current and corresponding arc voltage. This voltage, in a particular circuit breaker, is proportional to contact separation and is always influenced by pressure and interrupting medium. However, the instantaneous product of arc current and contact separation gives a function which is a measure of arc power, and therefore is a measure, in any particular circuit breaker, of the rate of release of energy in the interrupter. Consequently, low values of current appearing at wide contact separation, such as in interruptions terminating in minor loops of offset currents, involve little arc power or interrupter duty. Similarly, high currents occurring only during small contact separations involve low arc power and light interrupter duty. On the other hand, heavy currents occurring simultaneously with wide contact separation, as in maximum-length interruptions following major loops of offset current waves, result in high instantaneous products of contact separation and current, and thereby represent high arc power and heavy interrupter duty.

When contacts are parted at random on offset current waves a wide range of the above interrupting conditions can be obtained and consequently a wide range of

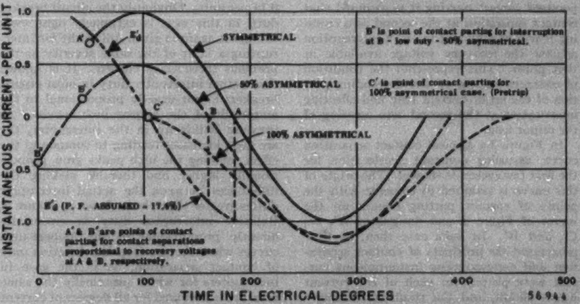

Figure 1. Fault current waves of equal total rms value for interruption within one cycle (zero decrement assumed)

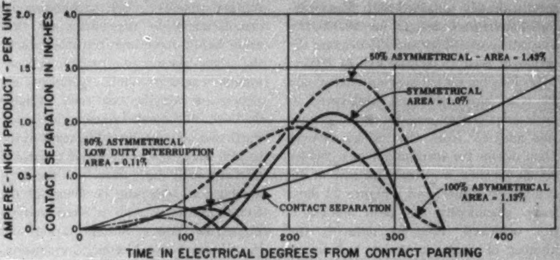

Figure 2. Relative interrupter ampere-inch curves for fault current waves of equal total rms value interruption within one cycle (zero decrement assumed)

interrupting duties can be experienced. All such interruptions in a given series, however, may be granted the same interrupting kilovolt-ampere credit when rated by the American Standards Association method of determining interrupting duty. These conditions are illustrated graphically by Figures 1 and 2 of this discussion which were selected from a number of similar graphs to be included in material to be presented before the Institute in the near future.

Figure 1 shows three different current waves, one symmetrical, the second 50 per cent asymmetrical, and the third 100 per cent asymmetrical, all having the same total rms value and with decrement neglected. Fast interruption has been assumed with contacts parting at A′ on the symmetrical wave and with interruption occurring approximately 7/8-cycle later. The transient recovery voltage appearing at the intermediate zero crossing A, as shown in relative magnitude by the dotted line between point A and the dynamic recovery voltage curve E_d', is assumed to be sufficient to barely prevent interruption at that point, necessitating an additional half cycle of arcing before actual interruption.

For the 50 per cent asymmetrical wave it is assumed that no interruption will occur at the intermediate zero crossing B if the transient recovery voltage, as designated at that point by the dotted line from B to E_d', bears the same relationship to the contact separation at that time as the recovery voltage at A bears to the contact separation at that particular moment on the symmetrical wave. This condition requires contact parting to occur at point B′ on the 50 per cent asymmetrical wave with no interruption occurring at B, and with final interruption taking place following the major loop.

For the 100 per cent asymmetrical wave it was assumed that a typical pretripped test had been made for which the contacts parted at the beginning of the completely offset wave, C′, with interruption taking place at the next zero crossing. A basis now is established for comparing the severity of interruption on the three types of waves with contacts parting at such points on the waves as to afford essentially maximum arcing times.

On the 50 per cent asymmetrical wave a 1/8-cycle earlier point of contact parting has been chosen and designated as B″. For this point of contact parting it is assumed that contact separation at the second zero crossing B will be sufficient to effect interruption against the recovery voltage available at that point. This represents the condition of contacts parting on the descending portion of the major current loop and effecting interruption at the second zero crossing of the minor loop.

In Figure 2 a typical contact separation curve, assuming constant acceleration for the first few cycles, is shown. The origin of this curve is assumed to coincide with the points of contact parting chosen on the waves of Figure 1 and designated A′, B′, C′, and B″. In each case then, as time progressed the products of contact separation and corresponding instantaneous current were plotted for each of the current waves shown, and the resulting "ampere-inch" curves are as depicted in Figure 2. It will be observed that for the symmetrical wave the ampere-inch curve has a beginning of minor amplitude, and then swings through a major amplitude reaching approximately 1.1 per unit crest value and having an area, which is some function of arc energy, equal to one per unit.

The 50 per cent asymmetrical current wave again gives a minor beginning loop and then swings into a major ampere-inch loop reaching a crest value of approximately 1.4 per unit, and having an area of 1.43 per unit.

The obvious interrupter duty on the asymmetrical interruption is considerably higher than for the symmetrical interruption even though the breaker would receive the same credit for both interruptions.

In the case of the pretripped, 100 per cent asymmetrical current wave the ampere-inch curve reaches a crest value of approximately 1.45 per unit, and has a total area of 1.13 per unit. Since the blast effect in most interrupters is a function of rate of release of arc energy, this test appears to give the least severe duty of the three cases chosen even though the rms current values are the same for all three.

Now, if it is assumed in the 50 per cent asymmetrical case that the contacts parted approximately 45 degrees earlier and thereby effected interruption at the second zero crossing of the minor loop, the ampere-inch curve resulting is that designated as the low-duty interruption and rises to a crest value of only 0.2 per unit and has an area of only 0.11 per unit. Obviously the circuit breaker duty in this case is extremely light even though it again is given full credit for interrupting a fault of the same severity as the previous three cases chosen. It is known that actual interrupter duty in most circuit breakers is not exactly proportional to the amplitude of the ampere-inch curves. As pressure builds up in the interrupter, the arc drop increases tending to compound the effect, making the high peaks grow proportionally higher and thereby making the differences between the actual interrupter duties greater than those shown in Figure 2. Relative interrupter duty is essentially directly proportional to the ampere-inch curves when the arc drop is a function only of contact separation, as is the case in interrupters for which practically the same pressure is involved for all degrees of current intensity.

Figure 2 of this discussion clearly points out the real need for an absolute rating basis rather than the American Standards Association or European bases now available. It shows also that a test code should be adopted requiring that tests of fast circuit breakers should be so conducted as to involve maximum duty for the rating given, and not to permit acceptance to be based on a minor duty test such as may be obtained if only a few interruptions are accomplished by random faulting and circuit breaker tripping, or as may be obtained by a deliberate attempt to obtain a full offset wave with pretripping to effect interruption at the end of the first major current loop or at the end of the following minor loop.

In this connection it should be pointed out that even though the American Standards Association indicated fault duty represented by Figure 20 of the paper is very high, nevertheless the arc time indicated is extremely short and contact separation was very small when final interruption took place. Interruption, of course, occurred at this point because of the high-offset character of the current wave, which resulted in relatively small recovery voltages. An ampere-inch curve plotted for this interruption showed it to be one of very modest duty as compared to some of the others taken in the laboratory and at Grand Coulee on this particular circuit breaker.

From these considerations, it is evident that high-speed circuit breakers should be rated by standards different from those now in use, and that test codes should be specific with regard to types of interruptions expected in verification tests. A proposed new basis of rating will be included in the forth-coming material.

Otto Naef (American Gas and Electric Service Corporation, New York, N. Y.): No continuous current rating is given for the circuit breaker described in this paper. Is the manufacturer prepared to build high-voltage circuit breakers for higher load currents than hitherto customary, which may be expected as the output of our generating stations steadily increases? Snow melting requires currents of the order of 1,400 amperes. It is also undesirable to limit the transmitting capability of a transmission line by the continuous current rating of its circuit breakers. Will the higher rated currents require a departure from the butt-type contacts used in present designs?

H. Leyburn (Messrs. A. Reyrolle & Co. Ltd., Hebburn, England): My remarks relating to a companion paper[1] apply also to this paper. In addition, I should like to ask the authors whether the value of current of 2,000 amperes at which the tests were done under out-of-phase switching conditions is based on scientific data or whether it is empirical.

REFERENCE

1. FIELD TESTS AT GRAND COULEE DAM ON 10,000 MVA 230-KV LOW OIL CONTENT IMPULSE CIRCUIT BREAKER, A. F. Darland, C. L. Killgore, C. J. Balentine, E. B. Rietz. *AIEE Transactions*, volume 70, part II, 1951, pages 1377–85.

W. M. Leeds: The authors appreciate E. C. Starr's excellent analysis of interrupting severity under different conditions of current asymmetry and contact separation at arc extinction. The ampere-inch basis of evaluating interrupting duty should be a useful guide where more direct data on arc energy or impulse pressure are not available. Whether or not there is a real need to change the present American Standards Association method of rating circuit breakers is a debatable question, but it is certain that verification tests to demonstrate a particular rating should include tests under a sufficient variety of conditions to make certain that the most severe duty for the rating has actually been experienced.

The asymmetrical test of Figure 20 was not intended to be conclusive proof of 15,000,000 kva interrupting capacity, but was submitted as one of the highest power tests obtainable within the limitations of High Power Laboratory facilities. Still heavier short circuit interruption must await an opportunity for further field testing at Grand Coulee Dam after all 18 generators have been installed.

In reply to Naef's question on continuous current-carrying capacity, the 230-kv 10,000,000-kva circuit breakers described in this paper are rated 1,200 amperes with not more than the allowable 30 degree rise in contact temperature. Further tests have demonstrated that these butt-type contacts will carry up to 1,400 amperes satisfactorily with less than 10-degree centigrade additional rise in temperature. No change in contact design is contemplated except for certain extra-high rupturing capacity circuit breakers where momentary ratings in excess of 40,000 amperes are required.

In answer to Mr. Leyburn: the value of 2,000 amperes for the current at which the out-of-phase switching tests were made corresponds approximately to the maximum power available in the laboratory at the test voltage of 330 to 360 kv. However, a study of a typical 230-kv system gave 1,100 amperes for the maximum current under out-of-phase conditions between generating stations 200 miles apart with a switching station at the mid-point, so the test currents of 500 to 2,000 amperes were considered quite adequate for checking the circuit breaker performance.

Operation of Bushings in Carbonized Oil

W. R. WILSON
MEMBER AIEE

L. WETHERILL
FELLOW AIEE

CIRCUIT-breaker bushings, or load-ratio control-transformer-contactor bushings, may operate with one end immersed in oil containing various concentrations of small carbon particles. Under normal conditions the presence of carbon particles suspended in the oil or deposited on the insulating surfaces of the bushings has no adverse effect.

In the presence of abnormal amounts of water, dielectric weakness might develop and it is considered good practice to avoid heavy accumulation of carbon particles adhering to the bushing insulating surface. The rate at which carbon is deposited on the bushing insulating surface may determine the frequency with which servicing is necessary. Even if the rate of carbon accumulation on the lower end of the bushing is so slow that other factors determine the desirable frequency of servicing, it is probable that further reduction or elimination of carbon accumulation constitutes improved performance.

While the problem of carbon deposition has been more or less successfully met in the past by various means, this paper presents an analysis of the facts influencing the behavior of carbon particles. From this analysis rational and reliable solutions to the problem have been derived.

General Conclusions

1. Carbon deposition is caused by the attraction of carbon particles toward concentrations in the electric field.
2. Microscopic field concentrations caused by conducting inclusions or bubbles in the glaze on the porcelain surface attract nearby carbon particles. Carbon particles thus drawn to the adjacent surface may increase field concentration and resultant attraction for additional particles.
3. The effect of macroscopic field concentration caused by configuration of bushing parts can be eliminated by avoiding sharp conducting edges near the insulator surface.
4. A carbon particle near an insulator surface of relatively high dielectric constant causes a local field concentration which attracts the particle toward the surface.
5. Carbon deposition is facilitated if insulator surface is parallel to field direction.
6. Carbon deposition can usually be substantially reduced or eliminated by one or more of the following features: homogeneous insulator surface layer, low dielectric constant insulator surface layer, insulator surface approximately normal to field direction.

Basic Test Procedure

The first problem was to establish a test procedure which would determine in a few hours the results which could be expected of a specific bushing construction after a period of months or years in severe service. After many trials the following method was adopted as most satisfactory.

Two full-size bushings, usually of 115-kv rating, were mounted in a large tank of oil and excited at normal voltage for 8 hours. Carbon particles were formed continuously by the passage of a 60-cycle current of 0.22 ampere through an arc between two tungsten electrodes spaced 0.1 inch apart in the oil below the bushings. With new oil, several days of arcing were necessary to establish suitable conditions for testing. The severity of the test conditions is indicated by power factor readings up to 95 per cent on oil samples removed from the bottom of the tank.

Because the carbon deposition process is sensitive to the condition of the oil, all conclusions have been based on bushings tested simultaneously in the same tank, and in symmetrical locations. Erroneous conclusions often would have resulted, for example, if comparisons had been made between tests run under supposedly identical conditions, but on consecutive days.

Significant changes in the characteristics of bushings under test caused large changes in the visual appearance of carbon deposited. Visual estimates of absolute weights of carbon were relatively inaccurate, but visual estimates of the relative weight of carbon on two bushings being examined simultaneously were found of adequate accuracy for practical purposes. As a check on the visual ratings the deposit was weighed. On immersing the bottom half of a bushing in a permachlor degreaser, the washing action of the fluids removed all loose nonadherent carbon and left a dry, compact, dense, black deposit which adhered firmly in characteristic pattern to the porcelain surface. The loose nonadherent carbon removed by the degreaser was the residue left from the densely carbonized oil which drained over the surface of the bushings as they were removed from the tank. The remaining adherent deposit was considered to be the important one because it contained most of the carbon and because it was actually on the surface of the porcelain under operating conditions. The adherent deposit was wiped from the bushing on weighed filter papers and the change in weight was de-

---

Paper 51-258, recommended by the AIEE Switchgear Committee and approved by the AIEE Technical Program Committee for presentation at the AIEE Summer General Meeting, Toronto, Ont., Canada, June 25–29, 1951. Manuscript submitted April 14, 1950, made available for printing May 10, 1951.

W. R. Wilson is with the General Electric Company, Philadelphia, Pa., and L. Wetherill is with the General Electric Company, Pittsfield, Mass.

The authors acknowledge with thanks the contributions made by many of their associates to the investigation described in this paper. Particular recognition is given to E. B. Rietz, E. W. Alrich, R. Meeker, and L. E. Thiess, T. R. Walters, R. P. Bass, R. D. Hawley, W. A. Keen, Jr., and W. E. Paulaski.

termined. Compensation was made for effect of changing humidity on weight of filter paper. The amount of deposit ranged from about 15 to 200 milligrams. The estimated per cent of creepage distance covered by carbon was used as a third check on comparative performance in the early stages of the investigation, but was used less in later stages when test runs with very small traces of carbon were being obtained.

Availability of this basic test procedure permitted evaluation of performance of possible modified constructions and observation of conditions occurring during carbon deposition.

Observations of Behavior of Carbon Particles in Oil

At the start of the investigation, several hypotheses to explain the mechanism of carbon deposition were investigated and rejected. It was found, for example, that the particles often carried d-c charges and that d-c fields would cause rapid deposition. However, investigation by means of a sensitive, electronic electroscope of bushings on which carbon was depositing under a-c stress revealed no d-c component. No effect on the carbon deposition rate was found on application of many hydrophobic and oleophillic surface films, or on removal of all films. None of the glazes showed serious surface irregularities when examined by means of the electron microscope. Under the optical microscope, smooth undulations were visible, but there was no correlation with carbon deposition rates.

The more obvious possible explanations of the phenomenon of carbon deposition were found to be unrelated to actual test performance. It became necessary to learn more about the nature of carbonized oil before trying to explain its behavior.

Oil carbonized by exposure to a low current a-c arc was examined under optical and electron microscopes. The particles floating in the oil were found to range in diameter from less than 0.1 micron to about 10 microns, most particles being under 0.5 micron. Myriads of particles tend to collect in lace-like patterns in which the individual particles are separated by small spaces. Chemical analysis disclosed that, in addition to carbon, the particles contained within or about themselves appreciable percentages of acids and solids representing various stages of decomposition of oil. It is probable that some of these materials form a transparent high resistance envelope surrounding a core which is largely carbon. This is suggested by the spacing observed between particles forming clusters and by evidence cited later indicating slight conductivity between particles.

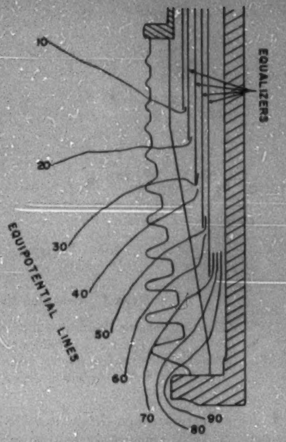

Figure 1. Electric field plot of obsolete 115-kv bushing, made on electrolytic tank

One set of simple tests was very revealing as to the fundamental behavior of carbon particles in oil under electric stress. Concentric cylinder electrodes were prepared by running an 8-mil wire down the center of a 1-inch test tube and placing a metal screen around the outside of the tube which was filled with clean oil. Then a drop of carbonized oil was inserted in the gap. On a-c voltage below 400 volts no effects were apparent. Above this voltage the particles began to line up radially like strings of beads along the flux lines and gradually moved inward toward the wire, forming a pattern like the needles on a twig of a fir tree. As the a-c voltage was raised to a higher value, turbulence was noticed at about 1,200 volts. Soon the pattern was replaced by a swirling, random cloud.

When the a-c voltage was removed after a pattern was formed at a voltage between 400 and 1,200 volts and d-c voltage of either polarity was applied in its place, the particles were quickly repelled from the inner electrode out to the glass.

Similar action was noticed when a small diameter glass tube was placed around the wire, and also when the experiment was repeated with small concentric enameled electrodes on a microscope slide. Typical action on alternating current was the gradual formation of a pattern made up of strings of particles; typical action on direct current was the destruction of patterns and a rapid swirling motion.

The probable explanation of the repelling force and turbulent motion produced by d-c voltage, or relatively high a-c voltage, is a tendency for conduction through the surface film of the particle to establish like charges on adjacent bodies. Relatively high a-c voltage was necessary to accomplish this result within a single half cycle. The small conductivity required is illustrated by the fact that glass or enamel insulation on the inner electrode did not appreciably change the observed results.

The next experiment was to put a porcelain bushing at a-c operating voltage in a glass tank of clean oil and insert a few drops of the carbonized oil near the porcelain. The particles gradually lined up, drawing a local flux plot and moving toward the porcelain. On reaching the porcelain, the particles assumed a stable flux-line pattern partly suspended in the oil. This is evidence that a d-c field was not active; if it were, this pattern would have been destroyed. More drops were inserted and the action was allowed to continue. Later when the bushing was removed from the oil, there was found a localized carbon deposit similar in pattern to that observed on large bushings under test conditions and in service. The bushing was replaced in the tank, and a-c voltage was raised to the high potential test value. Turbulence appeared in the oil and the carbon began streaming from the bushing.

It was concluded from these and similar tests that the deposition of carbon at operating voltage is a direct result of the a-c electric field surrounding the bushing.

Theoretical Analysis of Behavior of Carbon Particles in Oil

To learn more about the behavior of carbon particles in an a-c electric field it was necessary to investigate the relation between the particle and the microscopically small portion of field in its immediate vicinity. This procedure disclosed the existence of several unsuspected factors influencing the behavior of carbon particles.

While a particle in an a-c electric field is subject to a single resultant force produced by the field configuration it has been found convenient to resolve this force into a number of components caused by different types of field nonuni-

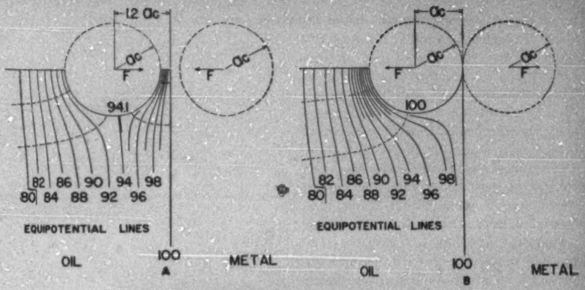

Figure 2. Field plots illustrating interparticle force F

(A). Spherical conducting particle near metal in perpendicular field showing field distortion producing attractive force

(B). Spherical conducting particle in conductive contact with metal in perpendicular field showing field distortion producing repulsive force

formity. The resultant of several component forces may apply to one particle as the result of a field which is the resultant of several component fields, each characterized by a different kind of nonuniformity. As will be seen later the resultant force is not a simple vector sum and is larger than would result from addition.

The different component forces may be conveniently catalogued as: Macroscopic nonuniformity force; interparticle force; glaze inclusion force with perpendicular field; glaze inclusion force with parallel field; and image force.

MACROSCOPIC NONUNIFORMITY FORCE

Carbon particles may be attracted by field nonuniformity on a macroscopic scale to relatively sharp configurations of metal or other conducting materials whether those edges be in contact with the oil or be separated from the oil by a thin layer of insulation. The force of attraction is determined by equation 1 derived in the Appendix.

$$\frac{F}{W}=\frac{3K_oE}{4\pi\rho gC^2}\frac{\partial E}{\partial x} \qquad (1)$$

where

$\frac{F}{W}$ = ratio electric force to gravity force
K_o = dielectric constant of oil (value 2.25)
E = volts per centimeter
ρ = grams per cubic centimeter net force of gravity on particle in oil (value 1.5)
g = 980 centimeters per second per second
C = 300 volts per statvolt
x = centimeters in direction of force on particle

Equation 1 states that the force on a carbon particle in an electric field is proportional both to the magnitude, E, of that field and to its nonuniformity, $\partial E/\partial x$. The explanation is simple and fundamental to all of the forces on carbon particles. Each of the flux lines which touches a surface element of the particle tries to pull that surface element into the oil. Therefore, in a strong but uniform field the two sides of the particle are pulled in opposite directions by forces which are precisely equal, and the net force is zero. However, if the field is nonuniform, one side of the particle experiences more pull than the other so the particle is forced in the direction of increasing field strength.

Equation 1 permits calculation of the force-weight ratio from information given by a field plot such as shown in Figure 1 for a conventional 115-kv bushing. From this plot it can be determined that at the point of maximum oil stress near the lower end of the bushing, E is about 5,000 volts per centimeter and $\partial E/\partial x$ is about 740 volts per centimeter per centimeter. This gives a force-weight ratio of 0.015 which is obviously small enough to show that the macroscopic nonuniformity force has no influence on the behavior of carbon particles in a bushing such as the one represented in Figure 1, and probably is of little consequence in any conventional bushing design.

The field plot of Figure 1 was obtained by measurement of actual voltages in and around a model bushing constructed in a conducting bath. It was found possible to obtain reasonably accurate field plots of 2-dimensional fields of rotational or translational symmetry, fully considering effects of configuration and dielectric constant of various parts. Field plots in other figures were also obtained by this procedure.

INTERPARTICLE FORCE

Each carbon particle distorts the field near itself, produces stress concentrations, and attracts neighboring particles. Equation 2 covers this force between two particles on the same flux line.

$$\frac{F}{W}=\frac{K_ob_c^3E_o^2}{2\pi\rho gm^4}\left[1+\frac{2b_c^3}{m^3}\right] \qquad (2)$$

where

b_c = microns radius of conducting spherical particle
E_o = volts per centimeter
m = microns distance between centers of particles

According to equation 2, the attractive force between two adjacent particles of 1.0-micron radius is 460 times the weight of one particle. Furthermore, the force exceeds weight for spacings between particles up to 8.7 microns on centers. The interparticle force will attract and hold a particle against the force of gravity, and if one particle is adhering to the bushing insulator surface it will attract nearby particles to it.

Figure 2(A) shows the field plot for a spherical conducting particle near a metal surface in a field perpendicular to the metal surface. In this and similar plots, equipotential lines are shown solid, and flux lines are dotted. By symmetry the field between two particles also is illustrated. The field strength between the two particles is clearly more intense than the field on the opposite side of either of the two particles and produces a net force pulling them together. The force can be calculated by graphical integration over the surface of the particle using the force per unit area as given in equation 3.

$$\frac{F}{W}=\frac{10^8K_o}{96\pi^2\rho gb_c^3}\int E^2\cos\phi\, dS \qquad (3)$$

where

ϕ = angle between normal to surface and total force
S = square centimeter surface area

For the case shown in Figure 2(A) using 1.0-micron radius particles and a field of 5,000 volts per centimeter (this stress is the maximum found in Figure 1 and will be used generally for reference purposes) the force-weight ratio as given by graphical integration of equation 3 is 280, which compares with 190 given by equation 2 for the same conditions. The discrepancy of about 50 per cent is not significant since only the order of magnitude of the force is required for analyzing the behavior of carbon particles.

If the particles make conductive con-

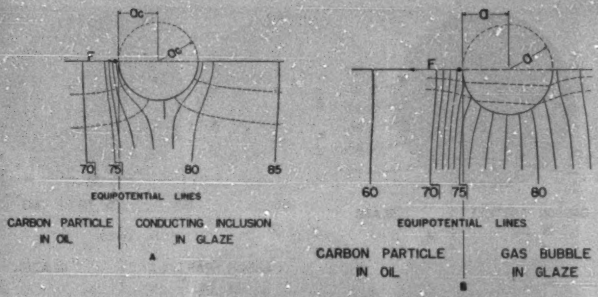

Figure 3. Field plots illustrating glaze inclusion force *F* in perpendicular field

(A). Cylindrical conducting inclusion tangent to surface of glaze in perpendicular field showing field distortion producing attractive force on carbon particle

(B). Cylindrical gas bubble inclusion tangent to surface of glaze in perpendicular field showing field distortion producing repulsive force on carbon particle

tact as in Figure 2(B) a rearrangement of charges takes place and attraction is replaced by repulsion. The repulsive force can be evaluated by graphical integration of equation 3 and is found to be 350 times the weight for 1-micron radius particles in a field of 5,000 volts per centimeter. The change from attraction to repulsion can be demonstrated physically by hanging a ball bearing near a wire at high a-c potential or by dropping bits of foil in stressed oil near a metal surface. An oscillation or dancing action, sometimes quite violent, will result.

The fact that the carbon particles line up in an electric field and form stable patterns indicates that they are covered by an insulating coating, probably products of decomposed oil. The disrupting of these patterns by turbulence in strong a-c fields could be caused either by an electric breakdown between the particles or conduction of charges through the insulating layers. The latter was indicated by an experiment in which a microscope was focused on a small point-to-plane oil gap which was in turn connected to a sensitive corona detector. Although occasional pulses of corona current were observed, they could not be correlated with the instants at which particles struck the electrode.

Glaze Inclusion Force with Perpendicular Field

A carbon particle close to a glaze which is not homogeneous will be attracted to high dielectric constant or conducting inclusions in that glaze, even if the surface is perfectly smooth, if there is an electric field perpendicular to the glaze surface. The force of attraction is given by equation 4.

$$\frac{F}{W}=\frac{K_o^2E_o^2b^4(K_g-K_p)}{\pi\rho g m^4(K_o+K_p)(K_g+2K_p)}\times\left[1+\frac{4b^2K_o(K_g-K_p)}{m^2(K_o+K_p)(K_g+2K_p)}\right] \quad (4)$$

where

K_p = dielectric constant of insulator surface layer (value 7.0)

b = microns radius of glaze inclusion (assumed value 50)

K_g = dielectric constant of glaze inclusion (∞ for conductor)

m = microns distance center of glaze inclusion to center of conducting particle in oil

The effect of a conducting inclusion is correctly represented by an infinite dielectric constant. For a 1-micron radius carbon particle adjacent to a 50-micron radius conducting inclusion tangent to the surface and in a field of 5,000 volts per centimeter, the force-weight ratio is 110. The ratio is lower than the 460 for the interparticle force but the force is effective over a much greater distance, exceeding weight at distance up to 87 microns between carbon particle center and glaze surface. If there are many conducting glaze inclusions the glaze inclusion force may be expected to attract any nearby particles.

As is shown by equation 4, if the dielectric constant K_g of the inclusion is greater than that of the surface K_p, the force is one of attraction. If the inclusion is of lower dielectric constant, such as a gas bubble, the force is negative and is one of repulsion. Either force reduces rapidly (as the fourth power) with increasing distance.

These facts concerning conducting inclusions are checked by the field plots of Figure 3 (A) and (B), which show flux distortion caused by the inclusions in a field perpendicular to the surface of the glaze. Attraction toward the surface is shown by the concentrations at the carbon particle in the plot of Figure 3(A). Repulsion, caused by a gas bubble inclusion, is illustrated in Figure 3(B).

The force on the spherical particle near the cylindrical inclusion can be evaluated from the plot by graphical differentiation. The field strength in the oil at any point is determined from the distance between equipotential lines. When field strength is plotted against distance the slope gives the value of $\partial E/\partial x$ and the force can be calculated from equation 1. For Figure 3(A), with a conducting inclusion 50 microns in radius located tangent to the glaze surface, the force-weight ratio is 150 for a cylindrical inclusion. This is satisfactory agreement with the value of

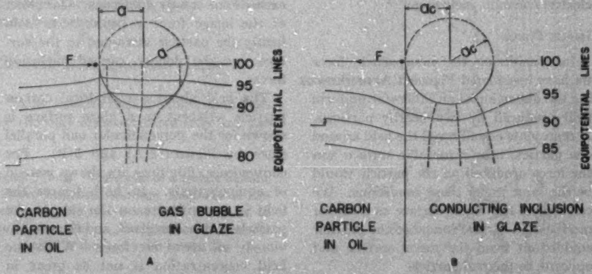

Figure 4. Field plots illustrating glaze inclusion force *F* in parallel field

(A). Cylindrical gas bubble inclusion tangent to surface of glaze in parallel field showing field distortion producing attractive force on carbon particle

(B). Cylindrical conducting inclusion tangent to surface of glaze in parallel field showing field distortion producing repulsive force on carbon particle

110 given by equation 4 for a spherical particle.

Glaze Inclusion Force with Parallel Field

A carbon particle close to a glaze which is not homogeneous will be attracted to low dielectric constant or gaseous inclusions in that glaze if there is an electric field parallel to the glaze surface. The force of attraction is given by equation 5.

$$\frac{F}{W}=\frac{K_oK_pE_o^2b^4(K_p-K_g)}{2\pi\rho gm^4(K_o+K_p)(K_g+2K_p)}\times\left[1+\frac{2b^3K_p(K_p-K_g)}{m^3(K_o+K_p)(K_g+2K_p)}\right] \quad (5)$$

For a carbon particle adjacent to a 50-micron radius spherical gaseous inclusion tangent to the surface of the glaze in an electrical field of 5,000 volts per centimeter parallel to the surface of the glaze the force-weight ratio is 58 and the range of distance over which force exceeds weight is 72 microns. The frequent occurrence of gas bubbles accounts for the relatively poor performance of many glazes as regards carbon deposition.

Equation 5 indicates that if the dielectric constant of the inclusions is raised from 1.0 the attractive force decreases, reaching zero when the dielectric constant of the inclusion equals the dielectric constant of the glaze. For still higher values of inclusion dielectric constant a force of repulsion appears on the carbon particle. Either force reduces rapidly (as the fourth power) with increasing distance.

Figure 4(A) illustrates the field concentration in the parallel field producing attraction toward the gaseous inclusion, and Figure 4(B) illustrates the repulsion that occurs with a relatively high dielectric constant inclusion.

Image Force

In considering the interparticle force we have considered Figure 2(A) as showing the distortion of an otherwise uniform field produced by two nearby particles. It represents equally well the field around one particle near a metallic surface and the force produced on the particle would be the same under these conditions. We can regard the metal surface as a mirror producing a virtual image of the particle equidistant from the metal surface and opposite to the real particle.

We are interested in forces on a particle near a glazed surface having a dielectric constant of relatively high value (about 7) as compared to oil. A surface of high dielectric constant tends to distort the field in the same manner as a conducting surface. The effect can similarly be considered to result from the presence of a virtual image behind the surface of the glaze with the strength of the image depending on the difference in dielectric constant of glaze and oil. The equation governing the image force, derived in the appendix, is as follows for a field perpendicular to glaze surface:

$$\frac{F}{W}=\frac{K_oE_o^2b_c^4(K_p-K_o)}{32\pi\rho gn^4(K_p+K_o)}\left[1+\frac{b_c^3(K_p-K_o)}{4n^3(K_p+K_o)}\right] \quad (6)$$

where

n = microns distance from center of conducting particle in oil to surface of insulator

For a 1-micron radius carbon particle this gives a force-weight ratio of 220, but the range of distance over which the ratio exceeds one is only 4 microns. One effect of the image force is probably to hold firmly the particle attracted to the surface by the longer ranged inclusion forces.

The field about a cylindrical carbon particle adjacent to a glaze surface is shown for the perpendicular and parallel cases by Figures 5(A) and 5(B). For convenience, flux lines are shown instead of equipotentials. In both figures the field is more intense on the side of the particle next to the glaze, and there is obviously an attractive force. While the field concentration is not as great in Figure 5(B) the field distortion is greater than in Figure 5(A), and forces of about equal magnitude might be expected. Graphical integration indicates the force is about 10 per cent greater for the parallel field.

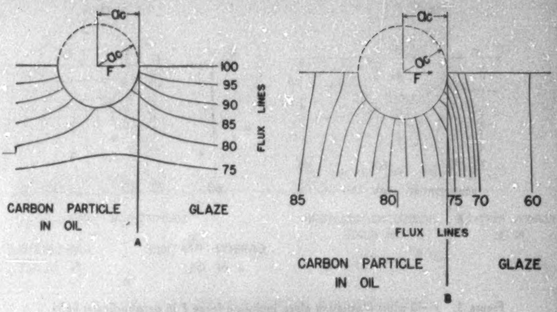

Figure 5. Field plots illustrating image force F

(A). Cylindrical carbon particle touching glaze surface in perpendicular field showing field distortion producing attractive force

(B). Cylindrical carbon particle touching glaze surface in parallel field showing field distortion producing attractive force

Whereas equation 6 is derived for a spherical particle in the perpendicular field, no equation was derived for a spherical particle in the parallel field. However, the above graphical determination of forces is sufficiently accurate and has been adequately verified in the earlier comparisons.

Effect on Design Practice

The possible effects of the five component forces are compared in Table I for various sizes of carbon particle. In each case the maximum force-weight ratio is indicated as is the range of distance over which the ratio exceeds unity. This table is calculated for the following conditions: field strength, 5,000 volts per centimeter; dielectric constant of oil, 2.25; dielectric constant of glaze, 7.0; density carbon minus oil, 1.5 grams per cubic centimeter; field nonuniformity, 740 volts per square centimeter, and radius of inclusion, 50 microns.

Table I. Comparative Effect of Component Forces on Carbon Particles

Type of Force	Radius of Carbon Particle (Microns)	Force-weight Ratio	Effective Range of Force (Microns)
Macroscopic	Any Size	0.015	
Nonuniformity Interparticle	0.1	4,600	1.6
	1.0	460	8.7
	10.0	46	49
Glaze inclusions (Perpendicular field)	Any Size	110	87
Glaze inclusions (Parallel field)	Any Size	58	72
Image	0.1	2,200	0.7
	1.0	220	4
	10.0	22	21

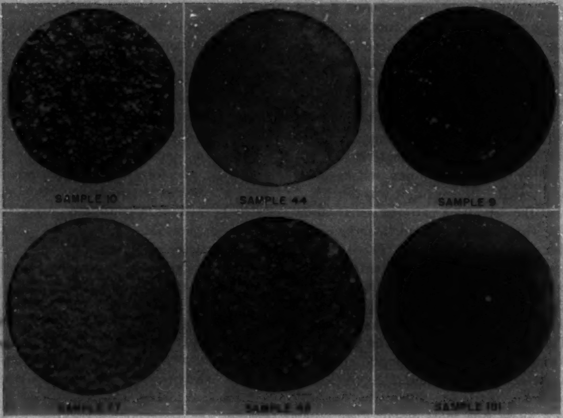

Figure 6. Appearance of sample glazes after etching (magnified 35 diameters)

Sample	Description	Performance on Carbon Deposition
10	Solid inclusion and bubbles	Poor
77	Many small bubbles	Poor
44	Medium size bubbles	Medium
45	Solid inclusions	Medium
9	Homogeneous	Good
101	Homogeneous	Good

The macroscopic nonuniformity force seems negligible. The interparticle force can be neglected if initial deposition of carbon particles from other causes can be prevented. The glaze inclusion forces and the image force require further consideration.

It should be noted that simultaneous presence of image force and glaze inclusion force produces an attractive force on carbon particles greater than the sum of the separably calculated values. While the glaze inclusion force, calculated from equation 4 or 5 depends upon the field strength E_0 that would have been present in the absence of the inclusion, it operates by increasing the local stress intensity. This increased stress intensity is then effective in producing image force on a small carbon particle near the glaze inclusion. Thus the resultant force can be much greater than the sum of the glaze inclusion force and the image force calculated separately.

Effect of Homogeneous Glaze

Table I shows that the inclusion forces are the only ones operative over any appreciable distance away from the insulator surface. If these forces draw the particles near to the surfaces where they are then held by the more intense, but short range interparticle and image forces, a substantial improvement in carbon deposition performance should result from using a homogeneous glaze substantially free from inclusions.

In many cases it is difficult to detect inclusions by direct visual examination, particularly if the glaze is opaque, or nearly so. Etching the surface with hydrofluoric acid quickly discloses the presence of such inclusions. While the significant characteristics of inclusions are dielectric constant and conductivity, they seem to correlate well with susceptibility to attack by hydrofluoric acid.

Examination of hundreds of glaze samples disclosed many inclusions of high dielectric constant or conducting particles and gas bubbles. A number of glaze samples showing correlation between glaze inclusions and carbon deposition performance are illustrated in Figure 6. Either bubbles or solid inclusions adversely affected the performance.

Glaze sample 10 (Figure 6) includes many large air bubbles signalized by characteristic dark holes surrounded by white frosty areas. In sample 77 small bubbles were visible as bright white dots. Sample 45 shows few bubbles but many minute solid inclusions. Sample 44 is marred only by a few relatively large bubbles which appear as black rings. The bubbles in samples 10 and 44 are about 50 microns in radius. In sample 44

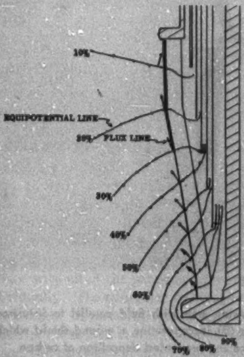

Figure 7 (left). Field plot of obsolete bushing without petticoats, showing tendency of carbon to deposit where the field is parallel to the glaze surface. The location of the deposit is shown by the heavy line

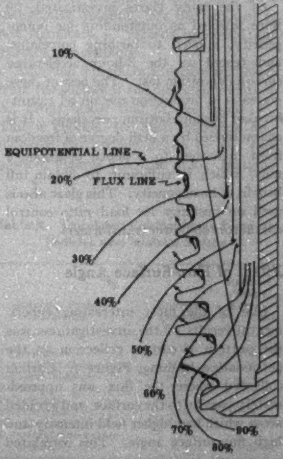

Figure 8 (right). Field plot of obsolete bushing with petticoats, showing tendency of carbon to deposit where the field is parallel to the glaze surface. The location of the deposit is shown by the heavy lines

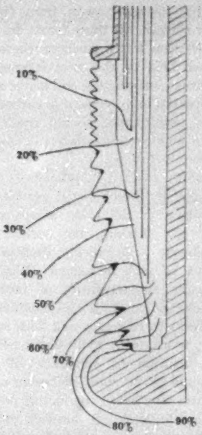

Figure 9. Field plot of special bushing to illustrate reduction of carbon deposit by minimizing areas of glaze parallel to field. As shown by the heavy lines, deposit avoids areas where the field is not parallel to the glaze surface

they are about 15 microns below the surface. In several glazes perfect cubes of magnetite (conducting) were seen close to the surface. Based on these observations, a spherical inclusion of 50 microns radius tangent to the surface was selected as suitably representative for use in Table I for both gaseous and solid inclusions.

Of the many glazes investigated, 29 were selected as outstanding for homogeneity, applied to bushing porcelains, and tested on the 8-hour accelerated carbon deposition test. The best of these glazes is in production use on oil circuit-breaker bushing bottom porcelains. It is characterized by a high degree of freedom from inclusions to a depth of about 7 mils, which is sufficient to obtain full benefit of homogeneity. This glaze also is used on bushings for load ratio control contactors on power transformers.

Effect of Flux-Surface Angle

One of the most interesting experimental results of the investigations was the pattern of carbon collection on the petticoatless bushing, Figure 7. Carbon collected where the flux was approximately parallel to the surface, and avoided areas which had higher field intensity and high flux-surface angle. This correlated with the fact, as shown in Figure 8, that much of the collection occurs against the force of gravity on the under sides of the petticoats of a bushing with standard contour where the flux is most nearly parallel to the surface.

In studying the possibility of reducing deposition by decreasing the areas over which the flux-surface angle is small, a number of special contours were designed and tested. In general, it was concluded that the deposition patterns center about the ring-shaped element at which the flux-surface angle is zero. Often the deposit consists of a series of vertically disposed hourglass patterns centered about the zero flux-surface angle region or continuous carbonized rings similarly located. The patterns usually form on a concave surface. Because the deposits grow over a surface from an initial deposit, long sweeping petticoats follow the flux-surface angle rule more closely than short choppy ones. And because carbon is brought near the dielectric surface primarily by fluid flow of oil, deep valleys between petticoats show some advantage. These principles have not been reduced to precise mathematical form, and modified constructions must be checked carefully by test. For example, some reduction in deposit was achieved by the special contour shown in Figure 9. Similarly the deposition of carbon on a 69-kv Herkolite insulated bushing, Figure 10(A), was prevented by the addition of a shield, Figure 10(B), which eliminated areas of small-flux-surface angle. This construction might have found an application except for discovery of a more convenient method for accomplishing the same result which is described later.

The apparent tendency to collect carbon in regions of zero flux-surface angle can be illuminated by consideration of the behavior of carbon particles in the adjacent oil. According to Figures 5(A) and 5(B), the force of attraction on a carbon particle is approximately the same for the 0-degree and 90-degree flux-surface angles. However, when two or more particles are present a different picture is presented. The particles will be attracted to each other by the high interparticle force and will line up like strings of beads along the flux lines. If the flux is perpendicular to the surface, the string of particles will lie perpendicular to the surface. Only the first particle in the line will touch the glaze, and this particle is held by the attraction to the next particle more strongly than to the glaze. Therefore, if this string should be carried off by oil currents, it will take the first particle with it, leaving a clean surface. This is consistent with the comparative magnitude of forces shown in Table I and has been confirmed by experiment.

If the flux-surface angle should be gradually reduced, at some stage the image force on the second particle will pull that particle to the surface. In like manner, successive particles of the string will be drawn to the surface like a rope being laid on the floor. Because each of these particles then experiences the image

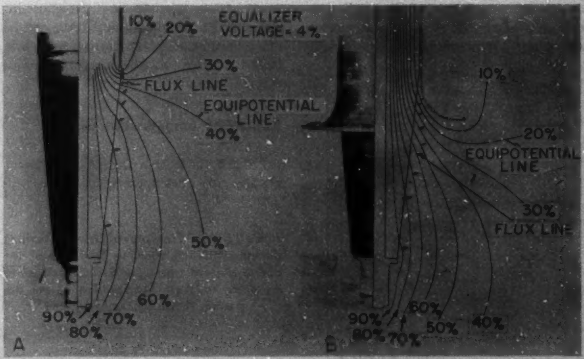

Figure 10. Field plot of experimental bushing showing area with field parallel to insulator surface (A), compared with a modified construction (B) incorporating a ground shield which limited areas with field parallel to insulator surface and prevented deposition of carbon

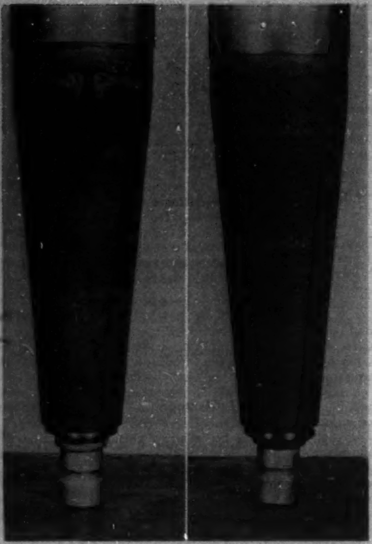

Figure 11. Bushings rated 66 kv, after accelerated test run. Bushing on the left shows a pattern of deposition such as results from the field plot pattern of Figure 10(A). Bushing on the right shows the result of a coating of varnish having dielectric constant matching oil. Deposition of carbon was eliminated

force of attraction it adheres to the glaze with sufficient tenacity to resist the effect of oil currents.

This explanation was verified by preparing a number of pieces of thin metal foil about one-eighth inch square and curled up to simulate large scale models of carbon particles. These were placed on a horizontal polystyrene shelf adjacent to a vertical glass surface in oil. A horizontal electric field (7 kv per inch) was arranged so that it could be rotated with respect to the assembly. The model carbon particles had to be made of foil to decrease their weight and thereby increase the force-weight ratio. The experiment had to be run with care: if too strong fields were used, the particles generated the turbulence previously discussed and moved out of the field.

A most interesting result occurs when seven or eight of the particles are grouped at the surface and the perpendicular field is applied. The foils quickly form a straight line perpendicular to the surface, with only one particle adhering to the surface. Agitation of the oil will pull the entire string away. If the particles are again grouped and the parallel field applied, they form a line parallel to the surface with all of the particles adhering individually. The resistance to oil agitation is high. If an additional particle is placed on the surface near a perpendicular string, the particle will often move over and join that string, pushing the other particles out one diameter. Placed near the center of a parallel string, an additional particle will separate the string and take its place in line in contact with the surface, pushing the ends of the string apart by one diameter. This may be the mechanism which accounts for the hourglass pattern of carbon deposition observed on bushings after accelerated carbon deposition test. The thin line at the center joining the two halves of the hourglass may collect particles and push them out along a flux line where they accumulate at the end of the favorable flux-surface angle area.

Effect of Dielectric Constant of Surface Layer

If the conducting parts are rounded or well insulated, and if the bushing insulator surface is homogeneous, only the image force can act to draw and hold carbon particles to the bushing surface. And, as appears from equation 6, if the dielectric constant K_p of the surface is equal to the dielectric constant K_s of the liquid, the image of the carbon particle and the force associated with it vanish, and there should be no collection of carbon.

This was first verified by wrapping a band of polyethylene sheet (dielectric constant = 2.3) around the cylindrical portion of the bushing of Figure 7. After the accelerated test run the area covered by the polyethylene was completely free of carbon; but the remaining surface showed essentially the same pattern of carbon deposition as in previous tests. This established the additional fact that deposition starting on an adjacent area will not spread over an area covered by a low dielectric constant coating. Numerous other verifications of these principles were obtained by application of varnishes (including one of polyethylene) to porcelain, herkolite, and other surfaces.

Equation 6 can be used to predict the optimum performance which any material can offer as a surface layer if it is obtained and applied without crazing, inclusions, or any kind of nonhomogeneity. In this way waste effort on basically unsatisfactory materials has been avoided. In addition, the range values from equation 6 (Image Force, Table I) indicate the approximate required thickness of the homogeneous coating for various sizes of carbon particles.

Table II lists the calculated relative force of attraction between a carbon particle and various surface materials as a function of the dielectric constant of the material. The force is expressed in per cent of the value for a conventional glaze of dielectric constant 7.

Although Table II does not include all of the materials evaluated by test, no homogeneous material has been tested which does not fit into the pattern of Table II. As is apparent from the table, and as was verified by test, changing from a conventional glaze to the lowest dielectric constant ceramic material available reduces the force of attraction by a measurable amount, but this amount is not significant as regards improved apparatus performance.

Equation 6 predicts a force of repulsion from the surface if the dielectric constant K_p drops below that of the liquid K_s. This is checked for both 90-degree and 0-degree flux-surface angles by the flux plots of Figures 3(A) and 4(B). Imagine

Table II. Calculated Relative Image Force on Particles near Insulator Surface

Insulator Surface Material	Dielectric Constant	Relative Image Force, Per Cent
Typical glaze	7.0	100
Lower limit of ceramics	3.8	50
Silicones, phenolics	3.0	28
Rubber	2.6	14
Polystyrene	2.4	6
Polyethylene	2.3	2
No. 10-C Oil	2.25	0
Polytetrafluorethylene (Teflon)	2.0	Repulsion

that the oil in the plots is replaced by a solid with an equal dielectric constant (polyethylene), and that the glaze is replaced by a liquid with a dielectric constant of 7. Then if what was the glaze inclusion is regarded as a conducting particle in the high dielectric constant liquid, close examination will reveal a slight flux concentration on the right side of the particle in each case, showing a net force of repulsion from the boundary. All that has been verified experimentally is that Teflon (dielectric constant 2.0) tested in oil (dielectric constant 2.25) does not collect carbon. Actual observation of the repelling action has not been accomplished.

Figure 11 shows the benefit obtained from a low dielectric constant coating on a Herkolite-insulated 69-kv bushing. This figure shows two bushings from the same accelerated test run. The bushing on the left had only the regular treatment formerly used and shows substantial deposition of carbon on the areas of low flux-surface angle. The bushing on the right had the protection of a low dielectric constant coating and no carbon was deposited.

The construction of the latter now is in standard production.

Appendix I. Derivation of Equations

Force on a conducting sphere[3] in oil is

$$F=K_o\alpha_c^3G\frac{\partial G}{\partial x} \tag{7}$$

G is maximum stress in any direction. To obtain equation 1 substitute E/C for G and divide by

$$W=\frac{4\pi\rho g\alpha_c^3}{3} \tag{8}$$

Charge e in region H near infinite plane boundary produces field in H which is unchanged[3] if image charge e' is placed in opposite location in region Y and material of Y is replaced by material of H.

$$e'=\frac{K_H-KY}{K_H+KY}e \tag{9}$$

A dielectric sphere in a uniform field is represented[3] by a dipole of moment M_d.

$$M_d=\frac{K_g-K_H}{K_g+2K_H}K_H\alpha^3G_o \tag{10}$$

A conducting spherical particle in region H in a field perpendicular to the interface is represented by a dipole of moment M_c with its positive axis pointing against the field direction.

$$M_c=K_H\alpha_c^3G_o \tag{11}$$

The field in region H is unchanged if image dipole M_c' is placed in opposite location in region Y and material of Y is replaced by material of H.

$$M_c'=\frac{K_Y-K_H}{K_Y+K_H}K_H\alpha_c^3G_0 \tag{12}$$

The field produced at the particle by the image is

$$P=xG_0\ \frac{M_c'\cos\theta}{K_Hr^3} \tag{13}$$

Let $\theta=0$ and differentiate twice with respect to x.

$$\frac{\partial P}{\partial x}=G=G_0+\frac{2M_c'}{K_Hx^3} \tag{14}$$

$$\frac{\partial G}{\partial x}=\frac{6M_c'}{K_Hx^4} \tag{15}$$

Substitute equation 12 in equation 14 and 15. Substitute E/C for G, E_o/C for G_o, $10^{-4}b_c$ for α_c, $2\times10^{-4}n$ for x, K_o for K_H, and K_p for K_Y. Then substitute equations 14 and 15 in equation 1 to obtain equation 6; reversing the sign for convenience.

Substitute in equation 6 $m/2$ for n, and ∞ for K_p, to obtain equation 2.

Charge e in region H near infinite plane boundary produces field in region Y which is unchanged if e is replaced by e'' and material of H is replaced by material of Y.

$$e''=\frac{2K_Y}{K_Y+K_H}e \tag{16}$$

A dielectric spherical particle in region H in a field perpendicular to the interface is represented by a dipole of moment M_d, equation 10, with its positive axis pointing against the field direction. The field in region Y is unchanged if M_d is replaced by $M_d''$and the material of H is replaced by material of Y.

$$M_d''=\frac{2\alpha^3K_HK_YG_0(K_g-K_H)}{(K_Y+K_H)(K_g+2K_H)} \tag{17}$$

The field in region Y is:

$$P=\frac{K_H}{K_Y}\ G_0x-\frac{M_d''\cos\theta}{K_Yr^3} \tag{18}$$

Let $\theta=0$ and differentiate twice with respect to x.

$$\frac{\partial P}{\partial x}=G=\frac{K_H}{K_Y}G_0+\frac{2M_d''}{K_Yx^3} \tag{19}$$

$$\frac{\partial G}{\partial x}=\frac{6M_d''}{K_Yx^4} \tag{20}$$

Substitute equation 17 in equation 19 and 20. Substitute E/C for G, K_YE_o/CK_H for G_o, $10^{-4}b$ for α, $10^{-4}m$ for x, K_o for K_Y, and K_g for K_H. Then substitute equation 19 and 20 in equation 1 to obtain equation 4, reversing the sign for convenience.

A dielectric spherical particle in region H in a field parallel to the interface is represented by a dipole of moment M_d, equation 10, with its positive axis pointing against the field direction. The field in region Y is unchanged if M_d is replaced by M_d'', equation 17, and the material of H is replaced by material of Y. The field in region Y is:

$$P=G_0y-\frac{M_d''y}{K_Y(x^2+y^2+z^2)^{3/2}} \tag{21}$$

Differentiate with respect to y, then let $y=z=0$, and differentiate with respect to x.

$$\frac{\partial P}{\partial y}=G=G_o-\frac{M_d''}{K_Yx^3} \tag{22}$$

$$\frac{\partial G}{\partial x}=-\frac{3M_d''}{K_Yx^4} \tag{23}$$

Substitute equation 17 in equation 22 and 23. Substitute E/C for G, E_o/C for G_o, $10^{-4}b$ for α, $10^{-4}m$ for x, K_o for K_Y, and K_g for K_H. Then substitute equation 22 and 23 in equation 1 to obtain equation 5, reversing the sign for convenience.

With a field of G statvolts per centimeter at the surface of a conducting particle in oil the force per square centimeter produced by the electric field on the surface is

$$F_s=\frac{K_oG^2}{8\pi} \tag{24}$$

The total force produced by the field on the particle is

$$F=\frac{K_o}{8\pi}\int G^2\cos\phi ds \tag{25}$$

Divide by equation 8, substitute E/C for G, and $10^{-4}b_c$ for α_c, to obtain equation 3.

The primary assumption of the analysis is that the particles and inclusions can be represented by the same dipoles which represent spherical inclusions perfectly in a uniform field. In the calculations of range the errors approach zero because the spheres are relatively isolated. In the maximum F/W ratio calculations, the errors may be relatively large as shown following equation 3. It has been found convenient in using the calculated forces to consider that the values are correct for radii of particles and inclusions which are slightly different from those given.

List of Symbols

α = centimeter radius of small dielectric sphere
α_c = centimeter radius of small conducting sphere
b = microns radius of dielectric sphere
b_c = microns radius of conducting sphere
C = 300 volts per statvolt
E = volts per centimeter
E_o = volts per centimeter uniform field due to charges at infinity
e = electrostatic charge
e' = electrostatic charge primary image
e'' = electrostatic charge secondary image
F = dynes
F_s = dynes per square centimeter
G = statvolts per centimeter
G_o = statvolts per centimeter uniform field due to charges at infinity
g = 980 centimeters per second per second
H = dielectric region separated from region Y by an infinite plane interface
K_g = dielectric constant of small particle or glaze inclusion
K_H = dielectric constant of region H or around a small particle
K_o = dielectric constant of oil
K_p = dielectric constant of insulator surface layer
KY = dielectric constant of region Y
M_c = moment of dipole
M_c' = moment of primary image of dipole

M_d = moment of dipole
M_d' = moment of secondary image of dipole
$m = 10^4x$
$n = 5 \cdot 10^3x$
P = statvolts
$r = (x^2+y^2+z^2)^{1/2}$
S = square centimeter surface area
W = dynes net force of gravity on particle in oil

$$\theta = \cos^{-1}\left[\frac{x}{(x^2+y^2+z^2)^{1/2}}\right]$$

x = centimeter distance in direction of force on particle or along line from real or image particle causing force to particle subject to force
Y = dielectric region separated from region H by an infinite plane interface
y = co-ordinate perpendicular to x
z = co-ordinate perpendicular to x and y
ϕ = angle between normal to surface and total force
ρ = grams per cubic centimeter net force of gravity on particle in oil.

References

1. THE MECHANISM OF THE CONTAMINATION OF PORCELAIN INSULATORS, Thompson. *Journal*, Institution of Electrical Engineers (London, England), part II, August 1944.

2. THE THEORY OF ELECTRICITY (book), G. H. Livens. Cambridge University Press, Cambridge, England, 1918, page 113.

3. ELECTRICITY AND MAGNETISM (book), J. H. Jeans. Cambridge University Press, Cambridge, England, 1933, pages 200, 229.

Discussion

O. P. McCarty (General Electric Company, Schenectady, N. Y.): Messrs. W. R. Wilson and L. Wetherill have contributed a noteworthy analysis of the various factors affecting the deposit of carbon on insulating surfaces in electric fields. This problem has been a factor in the design of load-ratio-control contactors for the past 12 years. The observance in 1939 of carbon streamers forming on insulating surfaces led to the introduction of electrostatic shielding of load-ratio-control equipment. Operating rods are shielded by cylindrical metal rings at each end, spaced out from the rods, and electrically connected to the live and grounded parts. Insulating panels are shielded by flat plates, spaced out from the panels, and also connected to the live and grounded terminals. These shields relieve the stress from a portion of the creepage path and thereby render that portion free of carbon deposits. Insulation protected in this manner will not collect carbon in continuous streamers, and will not require cleaning throughout the long life of the contractor arcing tips.

The studies of Mr. Wilson and Mr. Wetherill have resulted directly in the adoption of two important design improvements. A more homogeneous porcelain glaze is used wherever porcelain insulation is used in carbonized oil. On Herkolite panels and rods, a coating of insulating varnish with a low dielectric constant is used to reduce carbon deposits by reducing the image forces.

With all of these various factors affecting carbon deposition better understood, further design improvement may be expected which will directly benefit the power system operators by reducing maintenance and less frequent servicing of apparatus.

L. Wetherill: Mr. McCarty has brought out in his discussion the fact that of the various methods available for avoiding accumulation of carbon on an insulator surface modification of the shape of the conducting parts, either at line potential or grounded, to serve as electrostatic shields is in many cases the most convenient procedure; because it is not dependent on the application or development of new materials. Mr. McCarty also brings out the advantage of using electrostatic shielding to inhibit carbon deposition in certain areas and thus maintain a desired minimum dielectric strength.

The problem of finding a suitable solid insulating substance of dielectric constant substantially below that of insulating oil remains unsolved. Such a material would not only repel floating particles in a dielectric field but also would reduce the dielectric stress on the oil in the dielectric structure.

Operating Problems of Forced-Oil Forced-Air-Cooled Transformers

A. L. HOUGH
MEMBER AIEE

Synopsis: The adoption of forced-oil forced-air cooling for large power transformers by the electric industry has created a new problem for the operator of the equipment. The experience of this large utility has been that the supplier has not furnished a self-cooled rating for his product. The problem of determining the self-cooled rating has thus fallen upon the purchaser and the operator of the equipment. This paper discusses the operating problems caused by the partial or complete loss of auxiliary cooling equipment of this type of transformer.

THE technical press contains numerous publications on the advantages of applying forced-oil forced-air cooling to large power transformers. There is, also, a wealth of information on the operation of transformers with this type of cooling as to overload capacity with the coolers in service. The search of the technical press, as to operation with the coolers cut of service, revealed the following:

"To prevent injury to directed-flow forced-cooled transformers in case of an emergency created by an interruption of the power supply to the pumps and fans, these directed flow transformers may be designed to carry 100 per cent load for one hour or more after the pumps and fans have stopped. The temperature rise of the winding at the end of this period will not exceed the limit recommended by the AIEE Transformer Subcommittee Interim Report."[1,2]

"Transformers in large sizes, and especially those with forced-oil forced-air cooling, have been equipped with thermal relays, which function if operating temperatures are exceeded (which may result from a loss of air or oil pressure). While some advocate tripping the transformers off the line when these relays operate, in our system the alarm gives a warning signal only."[3]

It had been standard practice in our system to remove a transformer from service as soon as all fans and pumps were shut down. This general practice was adopted due to the recommendations of certain of the manufacturers regardless of whether the transformer was carrying load or excitation current only. It is not the best practice, due to customer reaction, to automatically and immediately shut down a transformer should the forced-oil forced-air cooling auxiliaries fail. It also was felt that, in certain cases, investigation as to the cause of failure could be carried out and emergency repairs effected before undesirable temperatures would be obtained.

The problem appeared to consist of several prominent aspects as follows:

1. The determination of the self-cooled rating for various banks: Field testing under service conditions; and calculations for other conditions not readily obtainable in field tests.
2. The most suitable alarm and control system for the installation.
3. Spare equipment such as fans and pumps required.

Determination of Self-Cooled Rating

It was agreed that field test data should be obtained on certain forced-oil forced-air-cooled transformers. The manufacturers were contacted to ascertain the risks and any special precautions that should be taken to carry out the proposed field tests and were invited to attend the test run on the transformer which they had supplied. The initial testing was carried out in the late fall and early winter on five representative transformers. The test runs were to be limited to a top oil temperature of 65 degrees centigrade or one and one half hours, whichever condition was reached first. The manufacturers' representatives were present for some of the test runs. In all but one set of test runs, the load was governed by operating conditions and varied throughout the test. The exception was one set of test runs in which the load was held practically constant by using a separate generator at one of our hydraulic generating stations. The test data taken consisted of readings of top oil temperature, hottest spot temperature (if the transformer was equipped with hottest spot indicators), ambient temperature and load taken at 2-minute intervals. Typical test data on two representative transformers is shown in Figures 1 and 2, which show the variation of hottest spot rise and top oil rise with time.

A study of the test results indicated that the transformers had a self-cooled rating, which was dependent upon the following: ambient air temperature, top oil temperature rise, hottest spot temperature rise, wind velocity and load conditions both prior to and after the partial or complete loss of the cooling auxiliaries.

The existing hottest spot indicators were considered to be unreliable after loss of forced oil circulation and to be reading low. This is probably due to the fact that in forced cooling the heat transfer from the winding to the oil is more effective for a given temperature rise.[4]

The test results indicated that a period of from 1/2 hour to 10 or 12 hours would be available for emergency repairs. It was decided to repeat the tests under the high ambient of summer conditions and, at the same time, secure additional test data.

Paper 51-259, recommended by the AIEE Transformers Committee and approved by the AIEE Technical Program Committee for presentation at the AIEE Summer General Meeting, Toronto, Ont., Canada, June 25-29, 1951. Manuscript submitted March 9, 1951; made available for printing May 21, 1951.

A. L. Hough is with The Shawinigan Water and Power Company, Montreal, Canada.

The author wishes to acknowledge the assistance given in the preparation of this paper by W. W. Ingram.

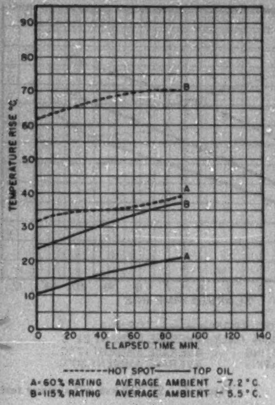

Figure 1. 20,000-kva unit winter test

The summer tests were carried out after an additional search in the technical press on cooling methods and thermal problems as they affect transformer design. Several papers on aging of insulation have been published, and it is more or less generally agreed that the rate of aging doubles for a definite temperature increment. The transformer designers approached appear to disagree on the actual increase in the gradient average winding to hottest spot, with loss of oil circulation. They indicate, however, that the gradient may increase from 50 to 150 per cent. A limit of 65 degrees centigrade was set for the top oil temperature with no coolers in service for the summer tests. Two representative transformers (also used in the winter tests) were selected for the summer tests. The test data taken consisted of ambient temperature, top oil temperature, the temperature of the transformer tank at various levels above the base, hottest spot temperature, wind velocity, load at 6-minute intervals and, at the end of the test, the average winding temperature by the direct current resistance method.

This information is shown in Table I and graphically in Figures 3, 4, 8, and 9. The load on the transformer was held practically constant for the tests shown in Figures 3 and 8, while for the tests shown in Figures 4 and 9 there was no control on the transformer load.

The variation of hottest spot rise as indicated on the hottest spot indicator, with forced oil and air circulation and thermosiphon or natural circulation of oil and air, is shown in Figure 5. It should be noted that this curve was obtained on two identical units which were in parallel on both the high- and low-voltage sides when the readings were taken.

It may be noted from Figure 4 that on the 20,000-kva unit, at 114 per cent of full load rating, the test was stopped when the hottest spot indicator reading was 85 degrees centigrade and the hottest spot rise was 65 degrees centigrade. The Transformer Standard of the American Standards Association C-57-22[5] gives the maximum allowable hottest spot rise as 65 degrees centigrade. This specification thus tends to specify the "safe temperature" at which the transformer could be operated. However, all loadings in this same publication indicate the "loss of life" that may be expected to occur if these limits are exceeded. The life of a transformer of recent manufacture is unknown and to say that one would lose a portion of this unknown period of time is rather meaningless. The operator of the equipment would much prefer to know that he is operating at a "safe temperature" which could possibly be one at which the transformers would operate for an economic life, say, of 20 to 30 years.

The data shown on Table I and Figures 3 and 4 were not readily adaptable for field use in the individual substations. It was felt that we could apply the usual exponential equations for oil rise:[5,6]

$$\theta_o=(\theta_u-\theta_i)(1-\epsilon^{-\frac{t}{\tau}})+\theta_i \tag{1}$$

$$\theta_u=\theta_{fL}[(K^2k+1)/(k+1)]^{0.8} \tag{2}$$

$$\tau_r=\frac{c\theta_{fl}}{P_{fe}} \tag{3}$$

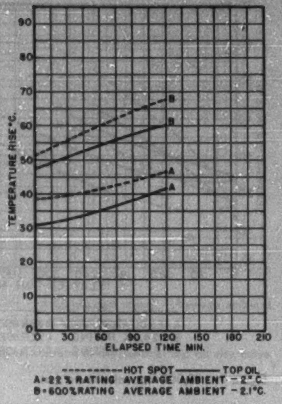

Figure 2. 50,000-kva unit winter test

$$\tau=\tau_r\left\{\left(\frac{\theta_u}{\theta_{fl}}-\frac{\theta_i}{\theta_{fl}}\right)\Big/\left[\left(\frac{\theta_u}{\theta_{fl}}\right)^{1.25}-\left(\frac{\theta_i}{\theta_{fl}}\right)^{1.25}\right]\right\} \tag{4}$$

$C=0.06$ (weight of core and coils)$+0.04$ (weight of tank)$+1.33$ (United States gallons of oil) (5)

where

θ_o = top oil rise over ambient temperature (degrees centigrade)
θ_{fl} = full load top oil rise (degrees centigrade)
θ_i = initial oil rise for $t=0$ (degrees centigrade)
θ_u = ultimate oil rise for load (degrees centigrade)
τ = thermal time constant of transformer for any load or any ratio of initial to ultimate oil temperature (hours)
τ_r = time constant for full load beginning with initial temperature rise of 0 degrees (hours)
K = ratio of load to full load
k = ratio of load loss to no load loss
$\epsilon=2.71828$
t = time load as applied in hours
P_{fe} = total loss at full load (watts)
C = thermal capacity of transformer (watt hours per degree centigrade)

In the application equation 1, the variables were not all available. The time constant τ and ultimate temperature θ_u were unknown. The graphical solution[9] to the exponential time curve was made to the 64 per cent rating curve of top oil rise for the 50,000-kva unit. This solution consists of drawing tangents to the curve and finding the temperature at which the cotangents are all equal. The temperature at which the cotangents are equal is the ultimate top oil rise and the cotangent is equal to the time constant for this particular curve. The graphical solution shown in Figure 6 gave $\tau=7.83$

Table I. Transformer Temperature Data

Unit Rating, Kva	Load	Coolers Out of Service, Hours	Top Oil	Top Oil Rise	Hottest Spot Rise	Average Winding	Ambient (Average)
50,000	Excitation only	7	67.9	41.4	36.5	63.1	26.5
50,000	25% rating	4$\frac{1}{2}$	66.2	40.7	38.5	76.1	25.5
50,000	65% rating	3$\frac{3}{4}$	66.2	42.2	52.5	76.8	24.0
20,000	Excitation only	11	61.5	39.5		43.3	22.0
20,000	64% rating	10	64.0	47.0	56.0	65.0	17.0
20,000	114% rating	4$\frac{1}{4}$	52.5	32.5	65.0	67.0	20.0

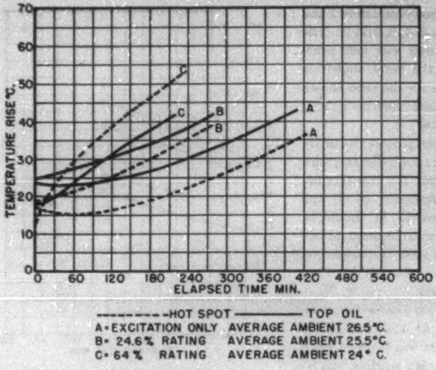

Figure 3. 50,000-kva unit summer test

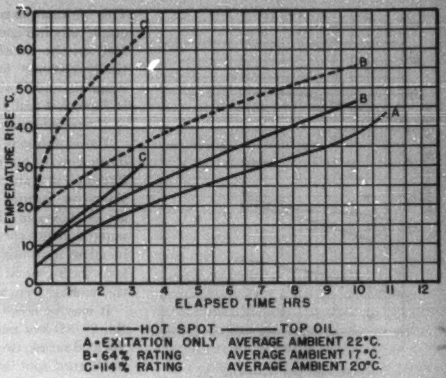

Figure 4. 20,000-kva unit summer test

hours and $\theta_u = 86.8$ degrees centigrade and $\theta_i = 18$ degrees centigrade.

The calculated temperature rises, obtained from equations 1 to 5 inclusive, as shown in Appendix I, are compared to the actual test values in Table II.

The oil rise for any load other than those shown in Table II could be calculated readily. In cases of partial loss of auxiliary cooling apparatus, the transformer would be treated as a forced-air forced-oil-cooled transformer for all loads where the total losses were less than the capacity of the coolers remaining in service. Where the load is such that the total losses are greater than the capacity of the coolers in service, the curve of top oil rise can be calculated from equations 1, 2, and 4. The main difference would be that the initial temperature θ_t in equation 1 would be in the order of 40 to 50 degrees.

A comparison of the actual test results and the calculated values, given in Appendix II, for the 20,000-kva unit is made in Table III.

In cases of partial loss of the forced-air forced-oil coolers, similar calculations could be made, as indicated for the 50,000-kva unit.

The hot spot temperature rise over top oil is given by:

$$\theta_s = \theta_g(_{fl})k^{1.6} \qquad (6)$$

where

θ_s = hot spot rise over top oil temperature (degrees centigrade)

$\theta_{g}(_{fl})$ = average copper rise over top oil at rated kilovolt-amperes plus 10 degrees centigrade

K = ratio of load to full load (7)

Equations 6 and 7 give the hot spot rise for that steady condition in which the hot spot rise above the top oil rise is constant. This condition was unobtainable in our field tests, so no further attempt was made to calculate hot spot temperature rise for either the 50,000-kva unit or the 20,000-kva unit.

Control and Alarm System

A contact-making voltmeter was included in the control circuit to protect the equipment on low voltage and to make the equipment auto-restarting upon recovery of sufficient voltage after loss of voltage.

The main problem for the alarm system was to determine the most suitable type of alarm indicators and the number required. There are transformers on this system from several manufacturers and, in general, they are equipped with one of the following types of flow indicator: a vane with a mercoid switch, a differential pressure gauge with a mercoid switch and interposing relays in the motor circuits. The alarm system ultimately selected consisted of interposing relays in the motor circuits with alarm indication for both starting and stopping the motor, a high top oil temperature alarm and a low oil level alarm. A schematic diagram of the control circuit is shown in Figure 7.

Table II. Calculated and Actual Temperature Rise, 50,000 Kva Unit

Time, Hours	Top Oil Temperature Rise, Degrees Centigrade No Load Calc.	No Load Actual	24.6 Per Cent Rating Calc.	24.6 Per Cent Rating Actual	64 Per Cent Rating Calc.	64 Per Cent Rating Actual
1	26.5	23.0	29.2	27.4	26.2	23.5
2	29.4	24.3	32.9	30.5	33.5	31.0
3	32.1	26.8	36.2	34.1	39.8	37.8
4	34.5	30.2	39.2	38.3	45.3	43.6
5	36.7	34.1				
6	38.6	38.6				

Table III. Calculated and Actual Temperature Rise, 20,000 Kva Unit

Time, Hours	Top Oil Temperature Rise, Degrees Centigrade No Load Calc.	No Load Actual	64 Per Cent Rating Calc.	64 Per Cent Rating Actual	114 Per Cent Rating Calc.	114 Per Cent Rating Actual
1	8.2	10.8	13.1	14.2	17.6	15.5
2	11.6	15.1	18.4	19.2	27.1	21.8
3	14.5	18.6	23.2	23.4	35.2	28.0
4	17.1	21.3	27.2	27.1		
5	19.4	24.0	30.8	30.5		
6	21.5	26.8	34.0	33.8		
7	23.3	29.5	36.6	37.1		
8	24.9	32.2	39.1	40.3		
9	26.3	35.0	41.2	43.7		
10	27.6	38.0	43.0	46.8		

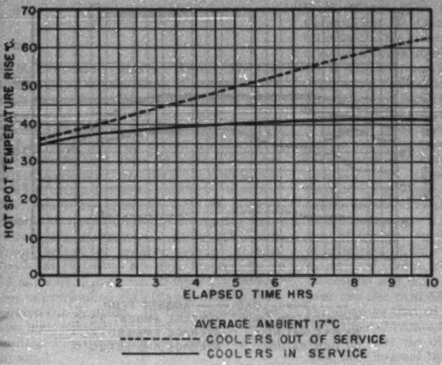

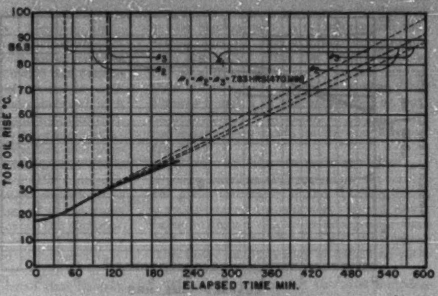

Figure 5 (left). 20,000 kva unit 64 per cent rating. Average ambient 17 degrees centigrade

Figure 6 (above). Graphical solution to 64 per cent top oil rise curve 50,000-kva unit

Spare Equipment

Transformers of the forced-oil forced-air-cooled type on this system have been supplied by five different manufacturers. It may be of interest to note that transformers of this type on this system were ordered before Canadian transformer manufacturers were supplying the coolers. The cooling equipment for these transformers has not been manufactured in any instance by the transformer supplier. The coolers, as supplied, were manufactured by three different concerns and was purchased by the operating company or the transformer manufacturer as dictated by contract. One manufacturer of coolers supplied three different types of equipment. For this particular system the question of spares such as fans, fan motors, pumps, pump motors and so on, is quite serious. It should be readily apparent that a rather large inventory of spare equipment is required. Uniformity or interchangeability of this equipment would quite obviously reduce such an inventory of spares and promote quicker restoration of service in case of trouble.

Conclusion

The field tests have indicated that it is unnecessary to remove a forced-oil forced-air-cooled transformer from service immediately after the complete loss of the auxiliary cooling equipment. The time that the transformer can remain in service after the complete loss of cooling auxiliaries is dependent in general upon the load, both prior to and after the loss of auxiliaries, the oil rise above ambient and the ambient temperature at time of the loss of cooling auxiliaries. The use of the exponential time temperature curve using constants derived from field tests appears to be a reasonably accurate method of determining the time available for emergency repairs or changes in system load distribution, to allow removal without too great a disruption to service.

The hottest spot indicators installed on the forced-oil forced-air-cooled transformers on our system appear to be unreliable when their use is most desirable. This is undoubtedly due to the change in thermal characteristics, caused by the loss of the forced-oil circulation. One solution might be to have a separate hottest spot indicator and detector for this condition.

It would appear desirable to have the supplier of transformers of the forced-oil forced-air-cooled type furnish a self-cooled rating for his product. This self-cooled rating should include the top oil rise and time constant and hottest spot rise and time constant at rated load.

The study indicated that there was no standard for the alarm system in stations

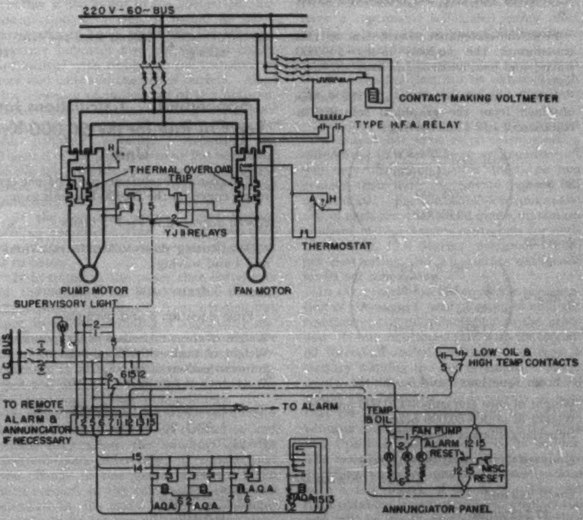
220 V - 60 ~ BUS
CONTACT MAKING VOLTMETER
TYPE H.F.A. RELAY
H
THERMAL OVERLOAD TRIP
5
2
YJ II RELAYS
A
H
THERMOSTAT
PUMP MOTOR
FAN MOTOR
SUPERVISORY LIGHT
D.C. BUS
2
1
5
2
6
15
12
7
TO REMOTE ALARM & ANNUNCIATOR IF NECESSARY
1 2 5 6 7 11 12 14 15
TO ALARM
LOW OIL & HIGH TEMP CONTACTS
TEMP & OIL
FAN PUMP
ALARM RESET
MISC RESET
12
15
6
15
14
A.Q.A.
A.Q.A.
A.Q.A.
A.Q.A.
ANNUNCIATOR PANEL

Figure 7. Typical alarm and control circuit forced-oil forced-air-cooled transformer

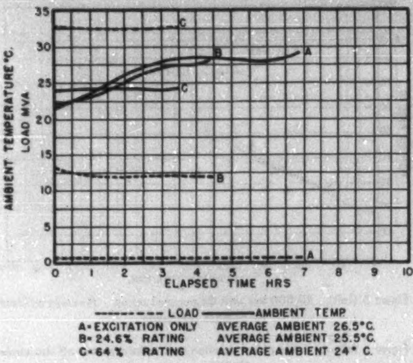

Figure 8. 50,000-kva unit summer test

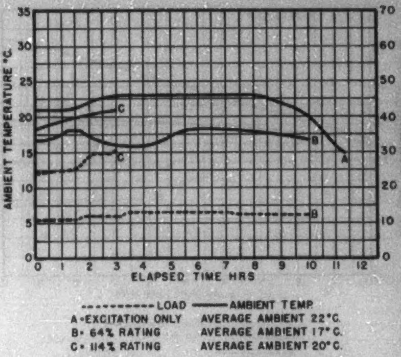

Figure 9. 20,000-kva unit summer test

where forced-oil forced-air-cooled transformers had been installed. Remedial measures are being taken to set up uniform alarm systems along the lines indicated in this paper.

The diversity of cooling auxiliaries for forced-oil forced-air-cooled transformers on our systems emphasizes the tremendous advantage to be gained by interchangeability of equipment.

Appendix I. Calculation of Top Oil Rise for the 50,000-Kva Unit

From the acceptance of test data on this transformer the no-load losses = 140,000 watts; and load losses at full load = 274,500 watts.

Substituting these values and the values obtained from the graphical solution in equations 2 and 4 and solving:

$$86.8=\theta_{fl}\left(\frac{(0.64)^2\dfrac{(274{,}500)}{(140{,}000)}+1}{\dfrac{274{,}500}{140{,}000}+1}\right)^{0.8}$$

$$\theta_{fl}=129$$

$$7.83=\tau_r\left(\frac{\dfrac{86.8}{129}-\dfrac{18}{129}}{\dfrac{(86.8)}{(129)}^{1.25}-\dfrac{(18)}{(129)}^{1.25}}\right)$$

$$\tau_r=7.72$$

From equations 3 and 5 with the:

Weight of core and coils = 170,000 pounds
Weight of tank = 60,000 pounds
Imperial gallons of oil = 9,650.

$$C=0.06(170{,}000)+0.04(60{,}000)+(1.33)(1.20)(9{,}650)$$

$$C=27{,}742 \text{ and}$$

$$\tau_r=\frac{27{,}742\times 129}{414{,}500}=8.57 \text{ hours}$$

This value of τ_r is 11.8 per cent greater than the value obtained from the graphical solution. The value obtained in the graphical solution will be used as the value τ_r was calculated from a value of θ_{fl} obtained in the graphical solution.

From equation 1 for the 64 per cent rating and with all the forced-oil forced-air cooling out of service:

$$\theta_o=(86.8-18)\left(1-\epsilon^{-\frac{t}{7.83}}\right)+18$$

$$\theta_o=68.8\left(1-\epsilon^{-\frac{t}{7.83}}\right)+18 \qquad (8)$$

The solution of equations 2 and 4 for no load and 24.6 per cent of full load gives:

$$\theta_o=31.2\left(1-\epsilon^{\frac{t}{8.66}}\right)+23 \text{ at no load} \qquad (9)$$

$$\theta_o=47\left(1-\epsilon^{-\frac{t}{8.3}}\right)+25 \text{ at 24.6 per cent rating} \qquad (10)$$

Appendix II. Calculations for Top Oil Rise for the 20,000-Kva Unit

The graphical solution to the 64 per cent rating curve for the 20,000-kva unit gave:

$\theta_u=56$ degrees and $\tau=7.5$ hours

Substituting these values in equations 2 and 4 and solving:

$\theta_{fl}=80.3$ degrees and $\tau_r=7.25$ hours

From equation 5 and with the:

Weight of core and coils = 72,000 pounds
Weight of tank = 40,000 pounds
Imperial gallons of oil = 9,875
Watts loss at full load = 178,310

$$C=0.06(72{,}000)+0.04(40{,}000)+1.33(1.20)(9{,}875)$$

$$C=21{,}700$$

From equation 3:

$$\tau_r=\frac{21{,}700\times 80.3}{178{,}310}$$

$$\tau_r=9.66 \text{ hours}$$

It may be noted that this value is 33 per cent greater than the value obtained in the graphical solution. As the test data was obtained under adverse weather conditions of rain and wind and the load varied throughout the test due to operating conditions, this error does not appear to be excessive.

Equation 2 at 64 per cent of load rating with $\theta_i=7$ from Figure 4 becomes:

$$\theta_u=49\left(1-\epsilon^{-\frac{t}{7.5}}\right)+7 \qquad (11)$$

Similarly from equations 5 and 6 and θ_i from Figure 4 at no load:

$$\theta_u=34\left(1-\epsilon^{-\frac{t}{8.8}}\right)+4.5 \qquad (12)$$

and at 114 per cent rating:

$$\theta_u=84.6\left(1-\epsilon^{-\frac{t}{7.4}}\right)+7 \qquad (13)$$

The calculated value of top oil rise from equations 11, 12, and 13, compared to the actual test values from Figure 4, is given in Table II.

References

1. Cooling Power Transformers by Forced Circulation of Cooling Medium, K. K. Palnev, L. H. Burman. *Electrical Engineering (AIEE Transactions)*, volume 62, March 1943, pages 215–21.

2. Interim Report on Guides for Overloading Transformers and Voltage Regulators, AIEE Committee Report. *Electrical Engineering (AIEE Transactions)*, volume 61, September 1942, pages 692–94.

3. Selection, Design and Operation of Power Transformers, F. A. Lane, I. W. Gross, P. S. Pugh. *AIEE Transactions*, volume 69, 1950, pages 786–95, and *Electrical Engineering*, July 1950, pages 600–04.

4. Predetermination of Self Cooled Oil Immersed Transformer Temperatures Before Conditions are Constant, W. H. Cooney. *AIEE Transactions*, volume XLIV, 1925, pages 611–18.

5. American Standards for Transformers, Regulators and Reactors. *C57, 1948*, American Standards Association (New York, N. Y.).

6. Thermal Time Constants of Dynamo-Electric Machines, A. E. Kennelly. *AIEE Transactions*, volume XLIV, 1925, pages 137–47.

Discussion

S. N. Lawrence (Canadian General Electric Company, Toronto, Ont., Canada): We wish to commend Mr. Hough on the presentation of this paper in which he has drawn attention to thermal characteristics of forced-oil forced-air cooled transformers. We believe that these characteristics are often overlooked by operating companies. We feel that a realization of the information Mr. Hough has presented will be a distinct benefit to operators when emergency conditions are encountered, as would result from the loss of auxiliary power. It also draws attention to inherent characteristics of different transformer designs that should not be overlooked when the purchase of such equipment is made. In this consideration the high thermal capacity of transil oil as indicated by its specific heat, should be kept in mind.

In attempting to establish the short time "uncooled" rating of forced-oil transformers we must take into account two things: (1) the thermal capacity of the transformer; and (2) the transfer of heat from the windings themselves into the oil. The radiating surface of the transformer tank is a very small percentage of the total required and can be neglected. Forced-oil forced-air cooled transformers have no continuous self-cooled rating.

If the transformer is so constructed that it does not depend on the oil pump to maintain a copious flow of oil through the core and windings, the flow of oil will be maintained by natural convection with the oil pump shut off. The temperature rise of the windings over the oil adjacent to the windings may be little different than when the pump is running, although there will be a larger gradient between the temperature of the oil at the top and at the bottom of the tank. If, on the other hand, the pump is relied upon to maintain the flow of cooling oil through the windings, its failure will cause a radical change in the heat dissipation characteristics of the winding. In effect, the winding becomes a solid mass of copper and insulation with only the outer surfaces radiating heat to the main volume of oil. The windings will heat up much more rapidly and critical temperatures will soon be reached which have little or no relation to the temperature of the main volume of oil and cannot be measured.

When the windings are so designed that the natural flow of oil is unimpeded when the pump is stopped, it becomes a relatively simple problem with the formulas Mr. Hough has used in his paper, to determine the transformer temperature rise versus time based on the thermal capacity of the oil, copper and steel for any kilovolt-ampere loading.

In evaluating the advantages of forced-oil-cooled transformers designed to have natural flow of oil through the windings, the benefits of forced directed flow should not be overlooked. Conservation of material and over-all reduction in the size of transformers is possible through its use. This might be of greater value than to be able to maintain continuity of service for a longer period of time during some emergency condition which might never be encountered.

V. V. Mason (The Hydro-Electric Power Commission of Ontario, Toronto, Ont., Canada): This interesting paper deals with a subject which is of great importance to the utilities and provides useful test data to corroborate the methods of calculation used. The following remarks are concerned with the hot-spot temperature and its indication.

It would be desirable to have more information on the nature of the hot-spot indicator installed in these transformers. It is assumed that these are the internal-thermal-image type which consist of a heater immersed in the top oil of the transformer to provide a point at the temperature of the winding hot spot. The theory of operation of this type of hot-spot indicator is, of course, that it is placed in the hottest oil and is so adjusted that its temperature rise over the adjacent oil will be the same as that of the hot spot. Under conditions of reduced oil flow, the temperature rise over the oil of both winding hot spot and internal-thermal-image would be expected to increase. The amount of these increases will likely be different because of the gross imperfections of the image. However, under no condition should it be possible for the hot-spot indicator to register a temperature lower than that indicated by the top-oil temperature measuring device. That this should have happened as reported in the paper means that either (1) the hot-spot indicator, temperature-measuring device is out of calibration, (2) the top-oil indicator, temperature-measuring device is out of calibration, or (3) the thermal image is not located in the hottest oil in the transformer. Allowing the transformer to cool nearly to ambient temperature would indicate which of these possibilities is nearest to the truth. If it is the third of these which holds, then immediately one must ask whether the top-oil indication is correct or whether it too is not in the hottest oil. In conjunction with this, it would be most interesting to know where the top-oil temperature indicator and the thermal image are located with respect to the transformer core and coils and the cooler outlets. Also, the accuracy of indication of the hot-spot device under normal cooling conditions might throw some light on the reasons for the behavior reported. According to Figure 3 of the paper, even at the beginning of the test, the hot-spot indicator showed a lower temperature than did the top-oil indicator.

If the test was started from normal cooling conditions, then it is obvious that one of the temperature measuring devices is to blame.

It is stated in the paper that the effects of the reduced oil flow on the thermal differential ("gradient") from winding hot spot to average winding is apparently unknown. This is entirely true but need not be of concern because the quantity of importance is not the difference between hot-spot and average winding, but between the hot-spot and top-oil temperatures. It is this latter quantity which is affected directly by the changed rate of oil circulation and which may affect the winding and the thermal image differently. It appears that the change in this quantity is not taken into account in the calculations made and checked by the tests. These calculations appear to be for top-oil temperature only. Since it is the hot-spot temperature which usually limits the operation of transformers at the higher loads, it is unfortunate that calculations of the winding temperature were not made. Since the time constant of the winding-over-oil rise is seldom greater than 15 minutes, it would appear from Figures 8 and 9 of the paper that at least an approximate calculation of this quantity could have been made for the conditions of the test.

So far as the actual hot spot to average winding differential is concerned, the present writer is of the opinion that in a well-designed transformer, this will never be more than a degree or two greater than half the top-to-bottom oil differential. This latter quantity may be measured without too much trouble.

The paper states that the tank temperatures as well as the top-oil temperatures were measured during the tests. It should therefore be possible to obtain values for the rise of the average winding over the average oil temperature as well as over the top-oil temperature. It would be most interesting to see a comparison of these figures with those obtained on the factory heat run. Even though ultimate temperatures were not reached, the winding rise over oil will have very nearly its ultimate value in the times for which the load was constant.

A. L. Hough: It is a pleasure to thank those who took part in the discussion. The reaction of the various manufacturers to the problem presented has been most gratifying.

In his discussion Mr. Lawrence has emphasized that the forced-oil forced-air-cooled transformer has no continuous self-cooled rating. The paper was concerned with the short time self-cooled rating rather than the "continuous" self-cooled rating. If the transformer were to be designed to have a continuous self-cooled rating most of the advantages of forced-oil forced-air-cooling would be lost.

Mr. Mason's discussion has emphasized the inaccuracies that can be obtained with the reflected image type of hot-spot indicator.

He has stated that in his opinion "the actual hot spot to average winding differential in a well designed transformer, will never be more than a degree or two greater than half the top to bottom oil differential." For the 50,000-kva unit at the end of each test this would give a maximum gradient of 15.5 degrees centigrade for excitation only, 13.6 degrees centigrade for 25 per cent rating and 9.5 degrees centigrade for 64 per cent rating.

In the general discussion at the presentation of the paper it was pleasing to note the reaction of the manufacturers to the problem. It was mentioned that with the forced-oil forced-air-cooled auxiliaries fed from a tertiary winding the loss of auxiliary power would be no problem as the bank itself would also be down. It is worthy of note that the auxiliary power from the tertiary winding can be lost without losing the bank and this has actually occurred in service. The tests have shown that it is possible for a utility to carry out field investigations with a fair degree of accuracy. The test data obtained is not considered confidential and will be made available to any utility interested in the problem.

Relative Performance of Normal Oils With and Without DBPC Inhibitor in Semisealed Transformers

E. D. TREANOR
FELLOW AIEE

E. L. RAAB
ASSOCIATE AIEE

IN AN earlier paper,[1] data on the performance of oil in small semisealed transformers were reported after runs of as much as 17 years under conditions approximating normal operation. Normal and inhibited oils were included and certain tentative conclusions were drawn as to factors influencing life as determined by an arbitrarily chosen end condition.

Of the inhibitors used in these tests, none seemed to have the combination of characteristics that would make its use of great value. Toward the end of these experiments, however, 2,6 ditertiary butyl para cresol, commonly known as DBPC, became available and was exploited as an inhibitor for transformer oils.[2,3] It has since come into very general use. Data on its performance in normal oil in the perspective of the earlier tests are desirable, but it is obviously impossible to obtain these data on the same basis quickly. However, the earlier tests indicated the possibility of getting information of value from accelerated runs and a different criterion for determining life. Previous runs at abnormal temperatures had shown behavior within the expected range and, by running at high temperature and comparing times for the first appearance of sludge, which can be determined fairly definitely, it was thought that this and other characteristics would offer information on the *relative* life of normal and DBPC inhibited oil in the shortest time.

On the point of what constitutes life of oil, there seems to be a wide diversity of opinion among operators. Presumably, this is based on cost considerations; that is, the amount of observation, maintenance, or reclamation, or replacement which is considered justifiable under particular conditions. One extreme view is that no sludge should be permitted. This will require meticulous knowledge and very active maintenance or reclamation program and will, of course, be based on the determination of the first appearance of sludge.

The other reasonable extreme might be that chosen in our earlier studies; that is, an amount of accumulated sludge, 1 per cent, and acid (1 milligram KOH neutralization) which has not yet affected the operating characteristics of the transformer, but which indicates the desirability of corrective action within a reasonable time.

Between these extremes, intermediate values of sludge and acid are chosen by individual operators, and there will probably continue to be some divergence of opinion. For the purpose of providing some basic data, accelerated runs have been started on small transformers with 10-C oil, 10-C plus 0.3 per cent DBPC, and 10-C plus 0.4 per cent DBPC. Data so far accumulated are being reported because of the general interest in the subject and the paucity of data from actual transformers.

Methods of Test

Power Factor of Transformers—Schering-bridge connections applied to the high-voltage bushing terminals and to the low-voltage terminals, core and tank in common. Two thousand volts, 601 cycles, were applied to the high-voltage side. Measurements were taken at room temperature.

Power Factor of Oil—In accordance with ASTM D 117-47T[4] at an applied stress of 30 volts per mil alternating current and a temperature of 100 degrees centigrade.

Resistivity of Oil—In accordance with ASTM D 117-47T at an applied stress of 5 volts per mil direct current, a temperature of 100 degrees centigrade, and a total electrification time of one minute.

Dielectric Strength of Oil—ASTM D 117-47T.

Moisture Content of Oil—In accordance with visual Karl Fischer method.

Color of Oil—ASTM D 117-47T.

Acidity of Oil—ASTM D 117-47T.

Interfacial Tension—In accordance with the method under consideration by ASTM Committee D-9, Subcommittee IV.

Bomb Oxidation Sludge of Oil—ASTM D 670-42T,[5] Method B.

Color of Bomb Oxidation Oil—Normal ASTM color taken on centrifuged oil sample after the bomb oxidation test.

Visual Condition of Oil—Oil samples withdrawn from the transformers at the operating temperature (95 degrees centigrade) and observations made for the appearance of a sludge cloud as the samples were cooled to 25 degrees centigrade.

Per Cent Unreacted DBPC—Method now under survey and subject to further modifications.

Viscosity—Saybolt viscosity taken in accordance with ASTM D 117-47T.

Four Point—ASTM D 117-47T.

Discussion of Data Obtained

Inasmuch as the purpose of this study was to obtain as accurate a comparison

---

Paper 51-260, recommended by the AIEE Transformers Committee and approved by the AIEE Technical Program Committee for presentation at the AIEE Summer General Meeting, Toronto, Ont., Canada, June 25–29, 1951. Manuscript submitted March 26, 1951; made available for printing May 10, 1951.

E. D. TREANOR and E. L. RAAB are with the General Electric Company, Pittsfield, Mass.

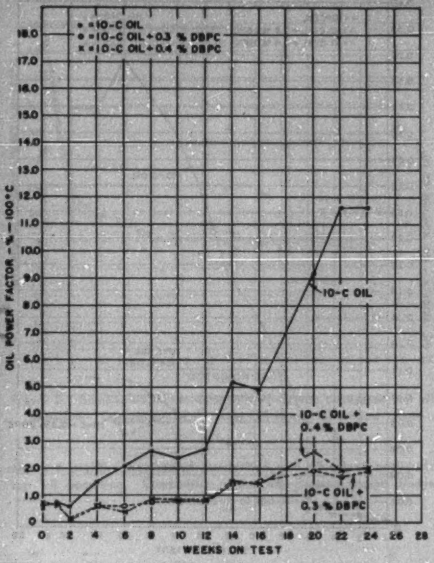

Figure 1. Semisealed transformers with 95-degree centigrade top oil operation. Comparison of oil power factors taken at 100 degrees centigrade

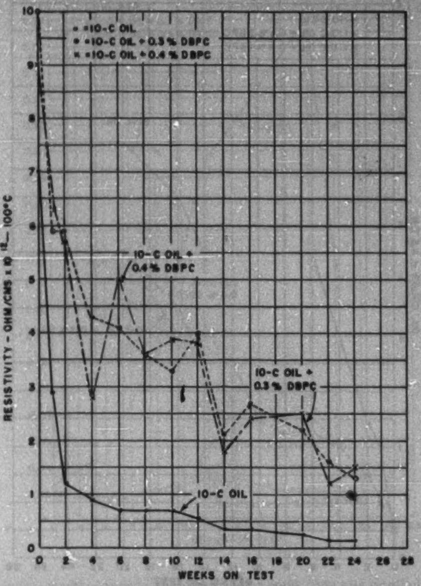

Figure 2. Semisealed transformers with 95-degree centigrade top oil operation. Comparison of d-c resistivity of the oils tested at 100 degrees centigrade

as possible of the oxidation stability characteristics under transformer operating conditions of the three oils investigated, rigid precautions were exercised to insure that the only variable present was the difference in inhibitor content. The 5-kva transformers used were identical as to design, materials, and methods of handling. The base 10-C oil for all three transformers was obtained from the same drum, the only difference in the oil used in filling the transformers being the indicated inhibitor additions to the oil prior to filling such transformers.

These transformers were not tightly sealed and can be classed as semisealed transformers, in that no special precautions were taken to exclude air. The tests were run under load conditions at a fixed ambient temperature and were accelerated by the use of a high top-oil temperature and continuous duty.

The coil temperatures were maintained at approximately 105 degrees centigrade (average) and 115 degrees centigrade (hot-spot) with a top-oil temperature of 95 degrees. Photographs were taken periodically of the core and coils, but any sludge formed was not disturbed and *the test schedule was arranged in such a fashion that no make-up oil would be required during the period of test.*

The initial condition of the oil was checked just prior to the start of the life test, as were certain electrical characteristics of the transformers. Periodic oil samples were taken *at the operating temperature of the transformer* and tested for:

Power factor—transformer
Power factor—oil
Resistivity
Dielectric strength
Moisture content
Color
Neutralization number
Interfacial tension
Bomb sludge
Bomb color
Visual condition
Unreacted inhibitor content
Viscosity
Pour point

In addition, periodic electrical tests were taken on the transformers as a unit.

While this study has not been completed as yet, it has progressed far enough to indicate a considerable improvement in oil life when the DBPC inhibitor is present and oxygen is not excluded. It is our intention that this series of tests will continue until the inhibitor has been exhausted in each case and that an additional indeterminate period of testing is then desirable in order to ascertain the behavior of the inhibited oils after the inhibitor has become exhausted. The final step in each case will consist of a measurement of the amount of sludge present following the technique previously reported.[1]

Table I. Insulation Power Factor at Room Temperature (%)

Description of Liquid Type	Weeks on Test 0	2	13	24
10-C oil	0.55	0.84	0.91	1.52
10-C oil+0.3% DBPC	0.60	0.74	0.68	0.83
10-C oil+0.4% DBPC	0.60	0.66	0.73	0.79

Power Factor of Transformers

The power factor of the transformers was measured periodically by applying the bridge connections to the high-voltage

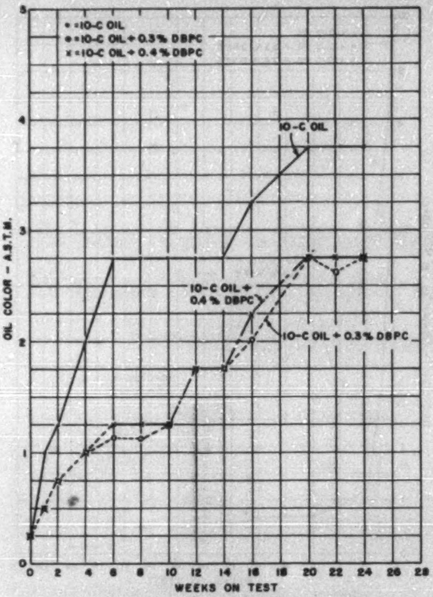

Figure 3. Semisealed transformers with 95-degree centigrade top oil operation. Comparison of the oil color change of the inhibited oils and 10-C oil

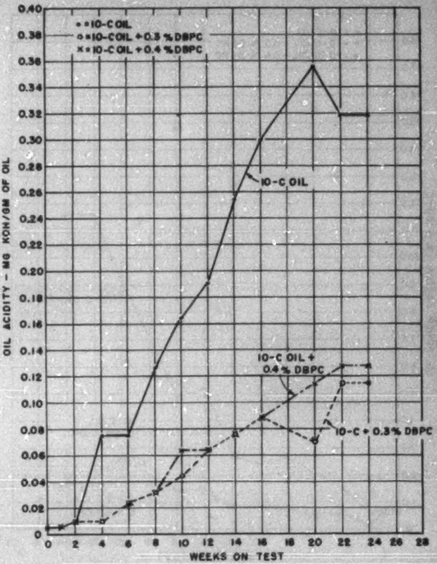

Figure 4. Semisealed transformers with 95-degree centigrade top oil operation. Comparison of the measured acidity in the inhibited oils and 10-C oil

bushing terminals and to the low-voltage terminals, core and tank in common. The results are shown in Table I.

While the increased power factor with time noted, particularly for the transformer containing the uninhibited oil, normally could not be conclusively attributed to the oil deterioration, subsequent data to be shown give some credence to the belief that the rising power factor for the 10-C oil-filled unit is primarily because of oil degradation in this instance. It is of some interest to note that the first sludge deposited out of oil solution when oil samples were cooled from operating temperature to 25 degrees centigrade was obtained after eight weeks of life for the 10-C oil. No such sludge has been obtained for either of the inhibited oils to date.

Power Factor of Oil

Figure 1, comparing the 100-degree centigrade power-factor curves of the three oils, indicates a definite inhibitor life period for the inhibited oils which has not been exceeded to date. The 10-C oil, however, has deteriorated steadily through progressive oxidation as evidenced by the steadily increasing power-factor values secured. At the end of 24 weeks of life, the power-factor values of both inhibited oils are approaching the power-factor value of the 10-C oil secured at eight weeks' life when oil insoluble sludge was first detected at 25 degrees centigrade.

It should probably be pointed out that while the power-factor test on the oil as used here where the conditions were controlled is apparently a good criterion of progressive oil deterioration, the values obtained under other aging conditions in apparatus can be influenced by moisture and soluble contaminants, as well as by the oil deterioration products. It may, however, prove to be of some value for predicting the end of the inhibitor life period for such oils.

Table II. Oil Color After Bomb-Oxidation Test

Description of Liquid Type	Weeks on Test 0	4	8	12	16	20	24
10-C oil	3¾	4	4¼	4¾		5	4¼
10-C oil + 0.3% DBPC	4¼	4¼	4	4¼	4½	4½	4
10-C oil + 0.4% DBPC	4¼	4¼	4¼	4¼	4½		4¼

Resistivity of Oil

Figure 2 illustrates the steady decline in the d-c resistivity values of all three oils, with a more rapid reduction being observed for the 10-C oil. While the inhibitor life period is not as pronounced for this property as was evidenced by oil power-factor comparisons (Figure 1), there is a definite advantage apparent for both inhibited oils.

Dielectric Strength of Oil

The dielectric strength of the oil was measured periodically at 25 degrees centigrade on samples removed at the operating temperature from the top of each transformer.

The average values secured for each sample tested exceeded 30 kv in every instance.

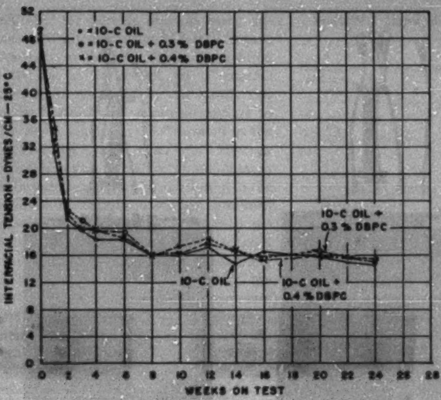

Figure 5. Semisealed transformers with 95-degree centigrade top oil operation. Comparison of the water-oil interfacial tension values

Figure 6 (right). Semisealed transformers with 95-degree centigrade top oil operation. Comparison of the high-pressure bomb sludge characteristics of the oils

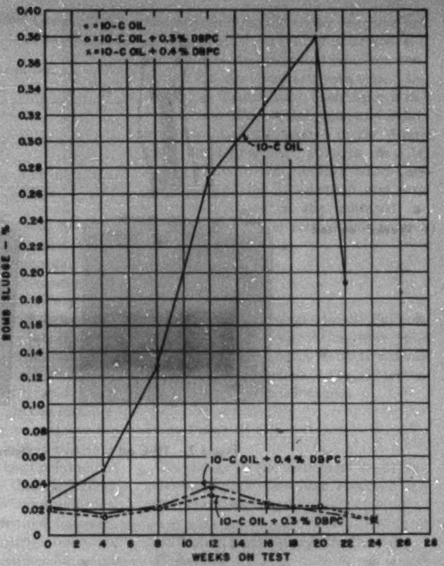

Moisture Content of Oil

During these tests the moisture content of the oils reduced from initial average values of 34 parts per million to present average values of 26 parts per million.

Color of Oil

While the color increase of an oil in service is not an infallible indicator of oxidation, in these tests it can be assumed to be of distinct value in a comparative sense, in that all other variables have been eliminated.

Figure 3 clearly indicates the beneficial effects by the inhibitor under evaluation in retarding oil deterioration, although no apparent difference between 0.3 per cent by weight of inhibitor and 0.4 per cent by weight in the oil has been found to date.

Acidity of Oil

The amount of acidic material developed as the oils oxidized and deteriorated which could react readily with potassium hydroxide is illustrated in Figure 4. Here again, a marked advantage was secured for those oils containing the inhibitor, although no practical difference has been found to exist between the two inhibited oils to date. Why there should be any definite acidic formation for the inhibited oils when other test data clearly indicate that the inhibitor present has not been exhausted, is open to some speculation. It may well be that some small acidity is developed during the normal functioning of this inhibitor with a conventional-type base oil. Another factor which may contribute to some slight acidity development is the possibility that small amounts of oil-soluble insulating materials may be present which in themselves are oxidizing to produce acidic materials, and whose deterioration is not blocked by the presence of the inhibitor. Although continued effort is being made to reduce the total amount of such oil-soluble material, which can come from any or all of the solid insulating materials used, it is obvious that a practical economic balance must be considered.

Interfacial Tension of Oil

While there is rather general recognition of the value of the interfacial-tension test as a guide in following the oxidation deterioration of oils tested under definite laboratory conditions, some controversy does exist as to its merits as the sole guide for oil life under actual service conditions. The test admittedly does not differentiate between those oil-soluble polar materials formed by oil oxidation and those dissolved in the oil from the various solid materials present.[6] As pointed out previously in the discussion of the oil-acidity development, every effort is made by the manufacturer to keep the oil-soluble polar materials from solid insulating materials at a practical minimum consistent with good economics.

Table III. Visual Conditon of Oil at 52 Degrees Centigrade

	Weeks on Test												
Description of Oil Type	0	1	2	4	6	8	10	12	14	16	20	22	24
10-C oil	Clear	Clear	Clear	Clear	Clear	Slight cloud	Slight cloud	Cloudy	Cloudy	Cloudy	Cloudy	Cloudy	Cloudy
10-C oil+0.3% DBPC	←Clear→												
10-C oil+0.4% DBPC	←Clear→												

11 Weeks' on test

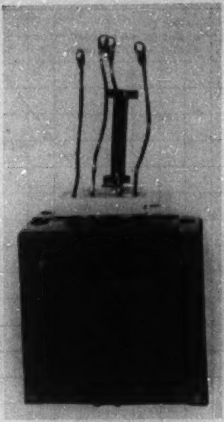
Figure 7. 10-C oil

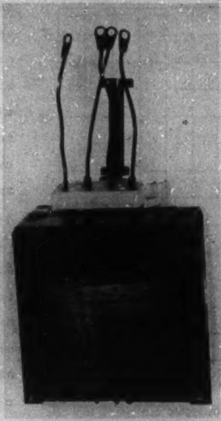
Figure 8. 10-C oil+0.3 per cent DBPC

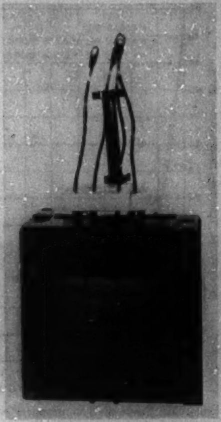
Figure 9. 10-C oil+0.4 per cent DPBC

24 Weeks' on test

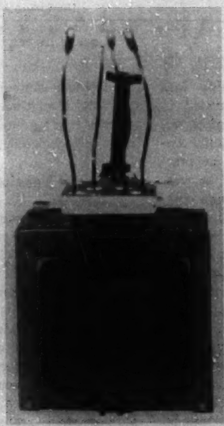
Figure 10. 10-C oil

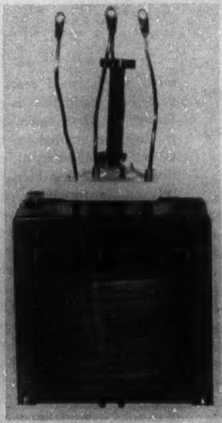
Figure 11. 10-C oil+0.3 per cent DBPC

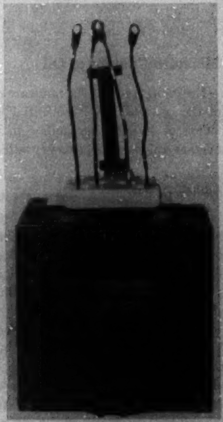
Figure 12. 10-C oil+0.4 per cent DBPC

Figure 5 indicates that all three oils yielded a rather rapid drop in interfacial-tension values to the zone (between 15 and 20 dynes per centimeter) where many operators would predict a sludging condition. Contrary to such an expectation, the inhibited oils gave no indication of any sludge formation and have not to date, although normal sludging has been taking place in the 10-C oil after eight weeks on test. This leads to some uncertainty as to the role of the interfacial tension as the sole guide for oil life in apparatus.

For these studies and others, we have never secured organic sludge when the interfacial tension exceeded 20 dynes per centimeter; however, we have found oils which have lasted a remarkably long time after the interfacial tension has been reduced to the so-called sludging zone.

Bomb Oxidation Sludge of Oil

Figure 6, comparing the high-pressure oxidation sludge characteristics of the oils under evaluation is significant in several respects. It is readily apparent from the essentially flat curves obtained for both inhibited oils that the ends of the inhibitor life periods are not being approached yet, even after 24 weeks on test. Contrary to this, the 10-C oil oxidation deterioration proceeded in a normal manner as evidenced by the steady rise in the bomb-sludge values secured up to the 20-week period. The drop-off in the bomb-sludge value after the 20-week period is not abnormal for an uninhibited oil in service and may be attributed to the removal of certain oxidation products from oil solution as sludge, thereby reducing the total amount of material available in the oil at the time of sampling subject to sludge formation under the oxidizing conditions of the high-pressure bomb-oxidation test. This same phenomenon has been noted for certain oils being evaluated by the American Society for Testing Materials under service conditions.[7]

The marked contrast between the curves secured for the inhibited oils and the one obtained for the uninhibited oil again illustrates the advantage of the inhibited oils and also points toward this test method as a possible effective tool for predicting the end of the inhibitor life period. It is interesting to note that for the uninhibited oil, sludge was first noted in the oil sample withdrawn at the operating temperature when cooled to 25 degrees centigrade after the 8-week period. This period is when the bomb-sludge value of the oil was increasing rapidly as noted in Figure 6.

Color of Bomb Oxidation Oil

Color numbers taken on the oils after the bomb-oxidation tests have been performed yield an interesting comparison, further substantiating the viewpoint that an apparent improvement in uninhibited oil may occur at an advanced stage of deterioration because of precipitation of products of deterioration. These results are given in Table II.

Visual Condition of Oil

Inasmuch as one of the primary functions of a good oil oxidation inhibitor is to retard or prevent the formation of oil sludge for a period of time, it was decided for this study to secure a direct comparison of the times required for the first appearance of sludge at 25 degrees centigrade for each oil. This could be easily done in this instance where all sample withdrawals were made at the operating temperature of the transformers and the visual oil condition observed as the samples were cooled to 25 degrees centigrade. Confirmation of an oil sludge cloud upon cooling the oil was obtained by centrifuging such oil and removing the oil by washing with precipitation naphtha. Normally the first appearance of sludge is no criterion of an oil's serviceability because some oils will sludge early in their life but have a slow rate of sludge formation thereafter, whereas other oils may exhibit sludge formation comparatively later in life but have a rapid rate of formation subsequently. In this instance, however, we were trying to evaluate the efficiency of the DBPC inhibitor in solution in 10-C oil. It has been pointed out in an earlier publication[1] that, dependent upon design and operating conditions, some sludge can be tolerated in transformers without impairing operating efficiency. Table III illustrates the visual condition of the oil samples as described.

Table IV. Unreacted DBPC Content (%)

Description of Liquid Type	Weeks on Test 0	8	12	16	20	24
10-C oil + 0.3% DBPC	0.29	0.28	0.29	0.26	0.27	0.23
10-C oil + 0.4% DBPC	0.39	0.40	0.34	0.33	0.34	0.31

While no sludge cloud has been obtained for either inhibited oil as yet, sludge was observed after eight weeks on test for the 10-C oil. Further confirmation was secured by carefully untanking the core and coils for photographing. Figures 7, 8, and 9 compare the visual appearance of the core and coils after 11 weeks on test of the 10-C oil, 10-C plus 0.3 per cent DBPC, and 10-C oil plus 0.4 per cent DBPC transformers respectively. Small amounts of sludge can be detected on the top of the iron supports and on the porcelain for the 10-C oil unit. None is apparent for either of the inhibited oil units. In addition, it is interesting to note that the color of the windings for both inhibited oil units is considerably lighter than that of the 10-C oil unit. Figures 10, 11, and 12 were taken after 24 weeks on test and are for the 10-C oil, 10-C oil plus 0.3 per cent DBPC, and 10-C oil plus 0.4 per cent DBPC units respectively. The same comparisons are again apparent, although no marked increase in the amount of sludge formed between 11 and 24 weeks is noted for the 10-C oil unit.

Per Cent Unreacted DBPC in Oil

While the method currently in use for the determination of the unreacted DBPC content of an oil is not of proven validity, the results obtained to date for the two inhibited oils under test here are of some interest. Table IV illustrates the reduction in the unreacted inhibitor content of the oils under test with time. Inasmuch as the method is based upon a determination of the cresol group and is not influenced by any changes in the ditertiary butyl groupings, changes may be taking place in the inhibitor which are not indicated by this method and any conclusions based on the indicated inhibitor consumption rate cannot as yet be substantiated.

Viscosity of Oil

No significant changes in the Saybolt universal second viscosities were obtained for any oil samples tested to date at 100 degrees Fahrenheit. The oil tested at 55 Saybolt universal seconds.

Pour Point of Oil

No change in the pour point (−57 degrees centigrade) has been observed for any oil samples tested.

Additional Laboratory Studies of Interest

At the Transmission and Distribution Committee Meeting of the Edison Electric Institute held on October 20, 1950, a discussion was presented on various aspects of the application of the DBPC inhibitor to conventional transformer oil.[2] Because of its attractive characteristics as an oxidation inhibitor, this material also has been studied with some care to see if there were any characteristics which would prove objectionable in its use in transformers. While we have found none that we regard as serious, it seems worthwhile to note some of the characteristics of the 10-C plus the DBPC inhibitor that differ from those normally accepted for 10-C oil.

For an inhibitor concentration in the range of 0.3 per cent by weight, no practical differences were observed as compared to 10-C oil for the 60-cycle or impulse-breakdown characteristics, the impulse creepage strength of oil-impregnated rag pressboard or the 60-cycle

Table V. Moisture Saturation Level of Oil at 25 Degrees Centigrade Exposed to Air at 57 Per Cent Relative Humidity

Oil Type	Moisture in Oil (ppm)
10-C oil	48
10-C oil + 0.3% DBPC	52
10-C oil + 20% DBPC	95

Table VI. Per Cent Sludge Formation at 120 Degrees Centigrade ASTM D 670-42T, Method A

Oil Type	Days on Test 0	7	14	21	28
10-C oil	0	0.15	0.25	0.29	0.28
10-C oil+0.3% DBPC	0	0.005	0.04	0.37	0.44

creepage strength of oil-impregnated rag pressboard. At higher inhibitor concentrations of the order of 20 per cent by weight, however, a definite reduction ranging from 15 to over 20 per cent was observed for the impulse strength of the oil and for the impulse creepage strength of oil-impregnated rag pressboard. This indicates that heavy concentrations should be thoroughly dispersed as a precaution before energizing equipment.

The presence of the DBPC inhibitor in 10-C oil has the effect of raising the normal saturation level of water in oil. This is shown in Table V.

For the inhibitor concentration in normal use (approximately 0.3 per cent by weight), this does not seem to be a serious fault with proper attention to maintenance and particularly where the supply or introduction of moisture is limited in transformers of modern construction.

The effectiveness of the inhibitor in oil seems to decrease at high temperature; for example, 120 degrees centigrade. This should not detract from its proven value in the usual operating range of full load and normal overload. One example of such decreased effectiveness at high temperatures is given in Table VI.

Observations and Conclusions

1. The DBPC inhibitor is an effective oxidation inhibitor as shown by the general improvement observed for the majority of the oil characteristics.
2. These transformer studies are incomplete and it is our intention to continue until after the inhibitor has been exhausted.
3. These studies do not directly form a basis for evaluation of benefits to be derived from the use of inhibited oil in transformers equipped with oil preservation means, nor do they embrace all of the criteria necessary to successful operation in other types of apparatus.
4. Certain characteristics of the inhibitor with 10-C oil have been considered, such as the decreased effectiveness at high temperature, the increased moisture saturation level, and the decrease in dielectric strength secured under certain conditions.
5. The oxidation bomb test and possibly the 100-degree centigrade oil power factor test may be useful tools for predicting the approaching end of the inhibitor life period of DBPC inhibited oil in service.
6. The first appearance of insoluble sludge as an arbitrary criterion of the end of oil life is considered to be unrealistic for uninhibited oils because it is no indicator of the rate at which sludge will be deposited from oil solution. Some operators, however, have expressed the intention of maintaining their oil so that sludge will never be formed. With such a viewpoint in mind, data on the relative periods before the first appearance of sludge in the inhibited and uninhibited oils may be of value, and such a comparison will throw light on the efficiency and inhibitor life period of this inhibitor in 10-C oil. The tests reported in this paper show that, with the exception of the interfacial tension and bomb test all other oil characteristics have now reached approximately the same levels noted for the first appearance of sludge in the uninhidited oil after eight weeks of life. The indication that the life of normal oil is extended by the order of two to three times when DBPC is added to the extent of 0.3 per cent and where oxygen is not completely excluded, may be useful in economic evaluations for the use of this inhibitor in normal oils.

References

1. Transformer Oil, E. D. Treanor, E. L. Raab. *AIEE Transactions*, volume 69, part II, 1950, pages 1060–70.

2. Minutes, 53rd Meeting Transmission and Distribution Committee. Edison Electric Institute (New York, N. Y.), discussion on Inhibited Oil, E. L. Raab, 1950.

3. New Life for Transformer Oils, R. F. Seubert, B. R. Sarchet. *Electrical World* (New York, N. Y.), volume 133, May 8, 1950, pages 84–87.

4. Standards on Insulating Materials. *D117-47T*, American Society for Testing Materials (Philadelphia, Pa.), January 1950.

5. *D670-42T*, American Society for Testing Materials (Philadelphia, Pa.).

6. Performance of Inhibited Transformer Oils, C. H. von Fuchs. *Publication 95*, American Society for Testing Materials (Philadelphia, Pa.), March 23, 1949.

7. Evaluation of Mineral Transformer Oil During Service, F. M. Clark. *Preprint Number 83*, American Society for Testing Materials (Philadelphia, Pa.), 1949.

Discussion

Frank C. Doble (Doble Engineering Company, Belmont, Mass.): This excellent paper reports on a thorough study of the effects of DBPC-inhibited oil on small semisealed transformers. The subject is most timely in view of the recent exploitation of inhibited oils by the manufacturers of distribution transformers.

The authors are careful to point out that the information contained in the paper applies only to a particular class of distribution transformer. Nevertheless, because of the lack of data on the use of DBPC-inhibited oils in power transformers, some operators will undoubtedly try to extend this information to cover the power transformer field. If this is done, some of the conclusions must be modified. For example, the conclusion is drawn from the curve in Figure 5 that interfacial tension is not a good guide for the determination of oil life. The criticism is valid for distribution transformers in which the oil is exposed to varnishes and other materials which can contaminate it. In the case of a modern, properly maintained power transformer, however, the degree of contamination is so low that the interfacial tension value can be a reliable index of oil life.

The statement that it is an extreme view to allow no sludge in a transformer may be admissible in the case of distribution transformers. It is not an extreme view in the case of power transformers, where to maintain oil free from sludge is a feasible operating practice.

The authors' conclusion that DBPC is an effective oxidation inhibitor is in agreement with our experience covering several years. The comment that DBPC loses its effectiveness at high temperatures might be amplified by including the effect of time. It should be noted that ASTM Standard D670-42T,[1] method A, calls for a maximum time of 14 days at 120 degrees centigrade. Table VI shows definitely that the inhibitor is effective during this period.

My concern that information on this important subject should be properly correlated by the Institute led me to propose that a special group be organized by the Institute for this purpose. It is encouraging to note that a subcommittee under the Transformer Committee has recently been established to deal with insulating oil as it affects transformers. An independent committee on insulating oils still seems to be indicated in view of its many other applications in the electric industry.

REFERENCE

1. See reference 5 of the paper.

T. K. Sloat (Westinghouse Electric Corporation, East Pittsburgh, Pa.): This paper has shown a very interesting phase of inhibited oil studies. If we plot acid values versus time for sealed or inert-gas protected oil in transformers we find there is very little or no change except after long periods of time. However, for inhibited oil in semisealed or free breathing transformers the increase in acid value is slower than with uninhibited oil but there is still a significant increase.

This suggests that the greatest advantage of the inhibited oil can be realized in distribution transformers which are difficult to keep sealed and where protective equipment is not feasible.

The power factor, acidity, and bomb sludge data predicts that we can expect about three times the increase in life of semisealed transformers by the use of inhibited oil.

The interfacial tension data does not differentiate between the inhibited or the uninhibited oils nor does it predict the formation of sludge. The proposed evaluation tests of inhibited oil, by those who feel that interfacial tension is the single necessary test, may be questionable.

It will be interesting to follow these tests further, particularly after the inhibitor is exhausted.

George H. von Fuchs (Consultant, Niagara Falls, N. Y.): Reference has been made in the paper to interfacial tension as a criterion of oil quality. This test found its first large scale field application by the Union Electric Company of Missouri early in 1939. Results were reported by their G. W. Gerell[1] at the Tenth Annual Doble Client Conference in January 1943. ASTM Committee D9-IV on Liquid Insulation in October 1945 formed Subcommittee T on Interfacial Tension under the chairmanship of R. G. Call. Mr. Gerell[2] as well as E. F. Walsh[3] of Narragansett Electric Company presented papers on their findings at the first ASTM Insulating Oil Symposium in October 1946 in which a definite correlation between interfacial tension and the sludging tendency of conventional oils in service was established.

When during its development stage inhibited transformer oil was first placed in a new distribution transformer, we were confronted with the fact that the interfacial tension dropped from 50 to 26 dynes and the oil lost half of its oxidation test life. We found that the oil had dissolved some of the solid insulation. Clay removed this impurity and restored both the interfacial tension and the original life expectancy of the oil. Several conclusions were drawn from this experience, namely that: Interfacial tension is a sensitive tool for detecting oil contamination; contamination indicated by a drop in interfacial tension value also causes a drop in oil life; and the solid insulation used in certain types of transformers may be the principal cause for the rapid deterioration of their oilfill. Thus the development of improved transformer oils should be accompanied by corresponding improvements in the selection and application of solid insulating materials. ASTM Method D 115-48 T on Testing Varnishes used for Electrical Insulation[4] has a chapter on "Oil Resistance." If in this test inhibited transformer oil would be used, a drop in interfacial tension of the test oil could provide a rapid and sensitive method for detecting oil-solubility of insulating varnishes.

We have learned during our development work on inhibited transformer oils, that the correlation between interfacial tension and sludge formation established in the field by Gerell and Walsh, does not always hold, since some inhibitors will form oil-insoluble oxidation products of their own, while the oil still has a high interfacial tension. Oil contaminants, which are not in true solution, are not indicated by interfacial tension measurements. For this reason, the modified *D 943* test method now under investigation by the Transformer Oil Committee of American Society for Testing Materials provides a multiple endpoint, both interfacial tension and sludge formation being considered. The failure of earlier attempts to successfully inhibit transformer oils must be attributed to the use of improper oxidation inhibitors and unsuitable laboratory test methods.

It is hoped that continued close cooperation between oil supplier, equipment manufacturer, and transformer user will permit a higher load, will reduce maintenance cost and will also appreciably lengthen the useful life of the transformer as well as that of its oil fill.

REFERENCES

1. G. W. Gerell. *Electrical World* (New York, N. Y.), May 1, 1943, page 66.

2. The Interfacial Tension Test and Its Significance in Appraising Performance of an Insulating Oil, G. W. Gerell. *Bulletin 146*, American Society for Testing Materials (Philadelphia, Pa.), May 1947, pages 92–95.

3. Application of the Interfacial Tension Test in Grading Oil in Transformers Relative to Servicability, E. F. Walsh. *Bulletin 146*, American Society for Testing Materials (Philadelphia, Pa.), May 1947, pages 95–100.

4. Testing Varnishes Used for Electrical Insulation. *D115-48T*, American Society for Testing Materials (Philadelphia, Pa.), 1948.

E. D. Treanor and E. L. Raab: The authors appreciate comments by F. C. Doble, T. K. Sloat, and G. P. von Fuchs. Mr. Sloat's comments are in general in agreement with the authors' views and thus do not seem to require further discussion.

While the authors feel that their paper has adequately covered the various points raised by Mr. F. C. Doble, some further amplification may be desirable in view of the comments made.

The distribution transformers used for these tests are of a type which has been in very general use for a number of years. No attempt at comparison with power transformers can be made, but it should be pointed out that a wide variety of materials and impregnants have been used in power transformers in the past. The validity of the interfacial tension test in the field will undoubtedly be weighed in the light of additional experience by the bodies now studying it, and what appear to be inconsistencies may be resolved. Meantime, its use should be continued to build up that experience.

The authors have pointed out in this and a preceding paper[1] the range of viewpoints as to the life of oil from the first detectable sludge to an amount which approaches an effect on operating characteristics. The basic decision will, for the present, be dictated by the particular maintenance record, desires, and economics of individual operators.

REFERENCE

1. See reference 1 of the paper.

A Portable Electronic Pile Kinetic Simulator

WALTER PAGELS
NONMEMBER AIEE

A COMPLETELY self-contained analogue computer has been designed to solve the seven simultaneous differential equations describing the operation of a nuclear reactor. Because the availability of nuclear reactors is severely limited, this analogue is found useful in demonstrating the kinetic behavior of the uranium pile. Various instruments and control systems may be tested and analyzed without the actual presence of a reactor assembly. Accompanying the intensified research on nuclear power is the problem of training engineering and scientific personnel on the theoretical and practical operation of power reactors. It is in an effort to acquaint these people with the dynamic solution of the reactor equations, that a portable pile kinetic simulator has been developed.

The manner in which the power level of a chain reacting pile will increase or decrease depends upon the past history and effective multiplication factor of the pile. A set of pile kinetic equations, describing the variation of neutron density as a function of time and reactivity, has been derived for a general power reactor.[1,2] The solving of these equations for any arbitrary change in reactivity is extremely tedious to carry out mathematically.

A procedure used in simulator design is to synthesize an electric network which follows the same equations describing the pile.[3] Each unknown in the reactor equations is represented by an equivalent voltage. The coefficients are circuit constants, and the completed terms are represented as electric currents. The sum of these currents are integrated, giving voltages representing the solutions to the equations. Potentiometers, delay networks, a current source, and a high gain d-c amplifier are the chief computing elements. External terminals allow the connection of recording instruments or automatic control devices.

Production of this instrument has shown it to be rugged, stable and easily operated. These units have few adjustments, which after initial setting, require little attention. Because of the simplicity of construction, no initial instruction is required to operate the simulator.

Reactor Equations

In the general thermal reactor, the principal source of nuclear energy is the fission of uranium induced by the absorption of slow neutrons. The uranium atom splits into two fragments and liberates a relatively high amount of energy. High velocity neutrons are ejected from the fission fragments, and begin their journey through the reactor. The neutrons speeding through the system lose energy by successive elastic collisions with the light nuclei of a moderating material. After a number of such collisions, the velocity of the neutron is reduced to such an extent that it has approximately the same average energy as the molecules in the core. It is while the neutrons are wandering about the core at thermal energies that they are most likely to be captured by other fissionable nuclei.

However, not all neutrons born in fission will be able to complete their destinies as fission incurring neutrons. Some will stray from the reactor without encountering a fissionable nucleus and be lost from the system entirely. Others will be unproductively absorbed in a nonfissionable material such as control rods within the reactor.

When the rate of neutron loss is equal to the rate of neutron production, the pile is critical and will operate at a steady neutron density. Changes in parasitic absorption or leakage can be used to control the various events in the kinetic behavior of the pile, and neutron economy is made to increase or decrease with time.

During the neutron cycle, a certain number of neutrons appear immediately after the fission process, while a smaller number are emitted much later. Each group of delayed neutrons is given off with a characteristic exponential radioactive decay. The total number of neutrons in the general assembly is the sum of the prompt plus delayed neutrons. The time dependent equations describing these events are often written in the form

$$\frac{dn}{dt}=\frac{\delta k_{eff}-\beta k_{eff}}{\tau}n+\psi\sum_{i=1}^{6}\lambda_i c_i+S \tag{1}$$

$$\frac{dc_i}{dt}=\frac{\beta_i k_{eff}}{\tau\psi}n-\lambda_i c_i \tag{2}$$

Here n is the number of thermal neutrons per cubic centimeter present in the pile. The duration of the generative cycle 1, is the average life of a neutron between emission from nuclear fission to subsequent leakage or capture by another nucleus. The reactivity or effective multiplication factor k_{eff} is the ratio between the number of neutrons produced and the number removed by absorption and leakage. The excess multiplication factor δk_{eff} is the fractional increase in the number of neutrons per cycle. Sk_{eff} also is defined as the relation $\delta_{eff}-1$. The constant β is the fraction of fission neutrons which do not come off immediately.

The probability that a neutron will remain in the pile during the slowing down process is ψ. The proportion of each type delayed neutron emitted, as compared to the total number of neutrons emitted, is denoted by $\beta_1, \beta_2 \ldots$ or, in general, by β_i.

Paper 51-262, recommended by the AIEE Nucleonics Committee and approved by the AIEE Technical Program Committee for presentation at the AIEE Summer General Meeting, Toronto, Ont., Canada, June 25–29, 1951. Manuscript submitted March 27, 1951; made available for printing May 10, 1951.

WALTER PAGELS is with the Westinghouse Electric Corporation, Pittsburgh, Pa.

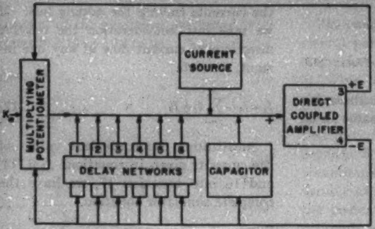

Figure 1 (left). Block diagram of the portable simulator

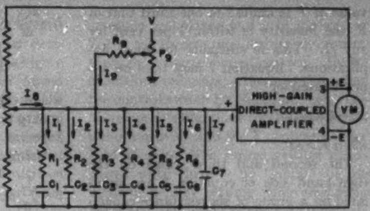

Figure 2 (right). The essential computing elements of the portable simulator

The decay constant λ_i is the probability of delayed emitter decay per second for each delayed group.[4] The variable c_i is the concentration of fission fragments of the ith kind, which emit delayed neutrons. All neutrons contributed by spontaneous fission and other independent sources are represented by the symbol S.

The first term on the right-hand side of equation 1 determines the rate of prompt neutron production, while the second term is the rate of delayed neutron contribution.

The first term on the right hand side of equation 2 represents the rate of delayed neutron formation, and the second term is the rate of radioactive decay for the ith type delayed emitter.

In general, the slowing down time from fast to thermal energies is negligible compared with the time the fission neutron spends at thermal energies. Thus, when the excess multiplication factor δk_{eff} is controlled by varying the fast leakage, the average lifetime τ of a fission neutron is relatively unaffected. However, when reactivity is varied by changing thermal leakage or parasitic absorption, neutron lifetime will vary directly as k_{eff}. This is easily understood when we consider that thermal neutrons will live longer in the reactor when the probability of thermal leakage or absorption is reduced.

A modified reproduction factor, which takes into consideration the effect of average neutron generation cycle variation, is $\delta k_{eff}/k_{eff}$, which shall hereafter be abbreviated as K_e. The average neutron lifetime τ is replaced by τ^*, the effective mean lifetime. The time constant τ^* is invariant with reactivity and is equal to τ/k_{eff}, the average neutron lifetime at critical.

Substituting these terms into equations 1 and 2, the pile equations now can be written in a form suitable for computer operation.

$$\tau^*\frac{dn}{dt}=K_e n-\beta n+\psi\tau^*\sum_{i=1}^{6}\lambda_i c_i+\tau^* S \qquad (3)$$

$$\psi\tau^*\frac{dc_i}{dt}=\beta_i n-\psi\tau^*\lambda_i c_i \qquad (4)$$

Simulator Equations

Figure 1 shows, in simplified form, a block diagram of the pile simulator. The potentiometer, delay networks, current source, and differentiating capacitor are the computing elements, corresponding to the mathematical operations performed in the kinetic equations. The voltage output of the amplifier is double ended, the positive voltage from terminal three being equal in magnitude but opposite in sign to the negative voltage from terminal four. The input grid of the amplifier is connected to the adding bus of the simulator. When the gain of the amplifier is high, any voltage on the adding bus causes the output voltage to vary in such a manner as to reduce this input voltage to zero. All dependent voltages then must vary in accordance with the mathematical operations described by the feedback circuits. The amount of amplifier regeneration is determined by the reactivity potentiometer, and the output voltage is made divergent, convergent, or critical.

Shown in Figure 2 are the essential circuit elements that perform the operations described above. The amplifier output voltage E represents ζn, where ζ is an optional proportionality constant and has the dimensions of volts per neutron.

The left-hand term of equation 3 is simulated by a capacitor which produces a current proportional to the time derivative of the voltage across it. If E represents ζn, the current is

$$I_7=C\frac{dE}{dt}=\left(\frac{\zeta C}{\tau^*}\right)\tau^*\frac{dn}{dt} \qquad (5)$$

The term enclosed in the parentheses is a scaling factor and has the dimensions of amperes per neutron.

The first term on the right-hand side of equation 3 is simulated by the circuit involving R and P. The magnitude of the current I_8 is dependent upon the setting of the potentiometer tap on P, as well as the voltage E and the ohmic values of R and P. By direct network analysis, the equation expressing the current flowing from the tap of the potentiometer is

$$I_8=\frac{D}{R\left[1+\frac{R}{P}+\frac{P}{4R}(1-D^2)\right]}E \qquad (6)$$

where D describes the proportional distance of the potentiometer tap from the center of the potentiometer, being zero at the center, +1 at the $+E$ end, and −1 at the $-E$ end. The tap remains at an essentially zero potential for any D.

When the potentiometer tap is on either extreme end of the potentiometer, I_8 is a maximum for any given E. The maximum positive current is given by equation 6 when $D=1$. If we set the ratio $K_e/K_{e\max}$ equal to $I_8/I_{8\max}$, we have

$$K_e=\frac{I_8}{I_{8\max}}K_{e\max}$$
$$=\frac{D}{1+\frac{P^2}{4R(R+P)}(1-D^2)}K_{e\max} \qquad (7)$$

Rearranging terms in equation 7, and combining the result with equation 6, we have

$$\frac{1}{R(1+R/P)}\frac{K_e}{K_{e\max}}$$
$$=\frac{D}{R\left[1+\frac{R}{P}+\frac{P}{4R}(1-D^2)\right]}=\frac{I_8}{E} \qquad (8)$$

When the voltage E represents ζn, then

$$I_8=\left[\frac{\zeta}{R\left(1+\frac{R}{P}\right)K_{e\max}}\right]K_e n \qquad (9)$$

where the term in the brackets is the scaling factor.

Because of the potentiometer loading effect, equation 7 describes K_e as a nonlinear function of D. This results in a band spread effect around the critical or mid-position of the K_e potentiometer. If, however, a strictly linear function of D is desired, the value of P should be reduced with respect to R until the desired linearity is reached. Reducing the value of P/R causes the denominator of equation 7 to approach one. When the ohmic value of P is limited to one-third that of R, the linearity is within 1 per cent for any D. This is adequate for most applications. Equation 7 may then be approximated as

$$K_e \approx DK_{e\max}$$

when $R>3P$.

The second and third terms on the right-hand side of equation 3 are simulated by a group of six resistance-capacitance delay networks. The equation describing the voltages for any ith type network is

$$E=\frac{Q_i}{C_i}+R_i\frac{dQ_i}{dt} \tag{11}$$

where Q_i is the capacitor charge in coulombs. This electrical charge is analogous to the storing of neutrons in fission fragments.

The corresponding delayed neutron equation that this circuit is to represent is equation 4, rearranged as a solution for n.

$$n=\frac{\psi\tau^*}{\beta_i}\lambda_i c_i+\frac{\psi\tau^*}{\beta_i}\frac{dc_i}{dt} \tag{4A}$$

Note that c_i does not represent capacity, which is symbolized by C_i. Matching equations 11 and 4A term by term, we find that E represents ζn when

$$Q_i=\frac{\zeta\psi\tau^*}{\beta_i R_i}c_i \qquad R_iC_i=\frac{1}{\lambda_i} \tag{12}$$

and equation 11 is like equation 4. The current contributed by each delayed group to the adding bus is given as

$$I_i=\frac{dQ_i}{dt}=\left(\frac{\zeta}{\beta_iR_i}\right)\psi\tau^*\frac{dc_i}{dt}$$
$$=\left(\frac{\zeta}{\beta_iR_i}\right)\beta_i n-\left(\frac{\zeta}{\beta_iR_i}\right)\psi\tau^*\lambda_i c_i \tag{13}$$

where the quantity in the parentheses is a scaling factor and is made the same for all i species.

Using the relation

$$\beta=\sum_{i=1}^{6}\beta_i,$$

the sum of all the delayed currents is written

$$I_1+I_2+I_3+\ldots=\sum_{i=1}^{6}I_i$$
$$=\left(\frac{\zeta}{\beta_iR_i}\right)\beta n-\left(\frac{\zeta}{\beta_iR_i}\right)\psi\tau^*\sum_{i=1}^{6}\lambda_i c_i \tag{14}$$

where $\beta_1R_1=\beta_2R_2=\beta_3R_3=\ldots=\beta_iR_i$.

The source term is simulated by introducing an independent current into the adding bus. Referring to Figure 2, if R_9 is large with respect to P_9, the current through R_9 is given as

$$I_9=\frac{D_9V}{R_9} \tag{15}$$

where D_9 is the portion of P_9 tapped off, and V is a constant voltage source. If D_9 is used to represent $S/S_{\max}$, then

$$I_9=\left(\frac{V}{R_9\tau^*S_{\max}}\right)\tau^*S \tag{16}$$

where the quantity in the parentheses is the scaling factor.

By Kirchoff's second law, the net currents entering the adding bus must equal the currents leaving the adding bus. If we take into consideration the relative directions of current flow at any one instant, we state

$$I_7=I_8-\sum_{i=1}^{6}I_i+I_9 \tag{17}$$

Substituting the equivalent values of the currents given in equations 5, 9, 14, and 16 into equation 17, we have the complete simulator equation.

$$\left[\frac{\zeta C}{\tau^*}\right]\tau^*\frac{dn}{dt}=\left[\frac{\zeta}{R\left(1+\frac{R}{P}\right)K_{e\max}}\right]K_en$$
$$-\left[\frac{\zeta}{\beta_iR_i}\right]\beta n+\left[\frac{\zeta}{\beta_iR_i}\right]\psi\tau^*\sum_{i=1}^{6}\lambda_ic_i+$$
$$\left[\frac{V}{R_9\tau^*S_{\max}}\right]\tau^*S \tag{18}$$

The scaling factors are adjusted to equal each other so that the output current of each term will be of the correct order of magnitude. If we let ζY represent the scaling factor, then

$$\zeta Y=\left[\frac{\zeta C}{\tau^*}\right]=\left[\frac{\zeta}{R\left(1+\frac{R}{P}\right)K_{e\max}}\right]$$
$$=\left[\frac{\zeta}{\beta_iR_i}\right]=\left[\frac{V}{R_9\tau^*S_{\max}}\right] \tag{19}$$

When the conditions stated in equation 19 are fulfilled, the scaling factors in equation 18 drop out, and the equation of the simulator is like that of the kinetic pile. The values for the computing com-

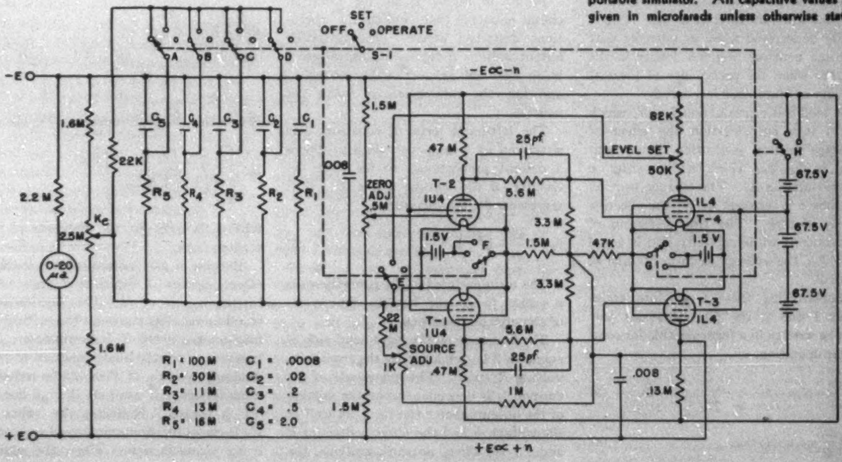

Figure 3. The complete schematic of the portable simulator. All capacitive values are given in microfarads unless otherwise stated

ponents of the simulator are found from equations 19 and 12 to be

$$C = Y\tau^* \tag{20}$$

$$\frac{P}{R(R+P)} = YK_{e\max} \tag{21}$$

$$R_i = \frac{1}{Y\beta_i} \tag{22}$$

$$R_s = \frac{V}{\zeta Y\tau^* S_{\max}} \tag{23}$$

$$C_i = \frac{Y\beta_i}{\lambda_i} \tag{24}$$

The value of Y is arbitrary and has the dimensions of admittance in mhos. The physical size of the capacitive components for the delayed neutron simulation may be made smaller, the lesser the value of Y used. However, the limiting minimum value of Y is determined to a large extent by the amount of insulation leakage, stray capacity, and ionized gas currents drawn by the input grid of the amplifier. These currents must be small compared to the currents contributed by the computing elements. For the portable simulator, Y was chosen to be 38 micromhos, which gives a maximum capacity of two microfarads for C_1.

The voltage representing n is read from a voltmeter connected across the output terminals of the amplifier.

The complete schematic for an experimental portable simulator used for demonstration purposes is shown in Figure 3. This model contains, as an added characteristic, a control switch and a level set potentiometer. The control switch disables the simulator while initial conditions are introduced. The level set potentiometer rapidly places the neutron density at any voltage level. Control of the power reactor is simulated by the manipulation of the K_e potentiometer. Step functions of reactivity are simulated by switching between "set" and "operate," with the K_e potentiometer held at the desired reactivity. The control switch is of the shorting type to prevent opening the battery circuits while switching between "set" and "operate."

In the grid circuit of *T-2* is the K_e zero adjust. This adjustment is made by initially setting the neutron density at some high value and placing the tap of the K_e potentiometer at the electrical center between $+E$ and $-E$. The zero adjust is manipulated until there is no sudden deflection or "jumping" of the neutron density while switching between "set" and "operate."

A pseudo-source term introduced by amplifier unbalance and grid current in *T-1* is set to zero by subtracting current through a source potentiometer. Initial conditions preceding adjustment are that the control switch be placed at "set," the "level set" potentiometer be turned to minimum level, and the K_e potentiometer held at zero. The source voltage is adjusted until there is no "jump" in the neutron density reading while switching between "set" and "operate." This setting gives a zero source term which is assumed when the reactor operates at a high neutron density.

Because the solution of equation 4 also can give negative values for n, it is advisable to allow a very slight positive source to remain in the simulator to prevent building up on negative neutrons. A persistent return to negative readings, with even a positive source, is often caused by excessive unbalance in the amplifier. The presence of high-frequency oscillation caused by regenerative components in the feedback current, requires phase correcting networks within the d-c amplifier. For the 2-stage amplifier in the simulator, the small amount of phase lead offered by the 25-micromicrofarad capacitors is sufficient to prohibit oscillation.

Figure 4 (below). Portable simulator

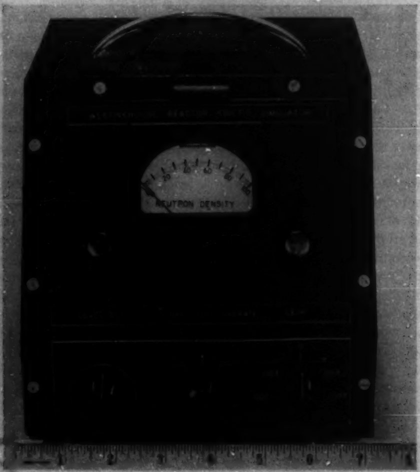

Figure 5 (right). Sample solutions given by the portable simulator for step changes in reactivity

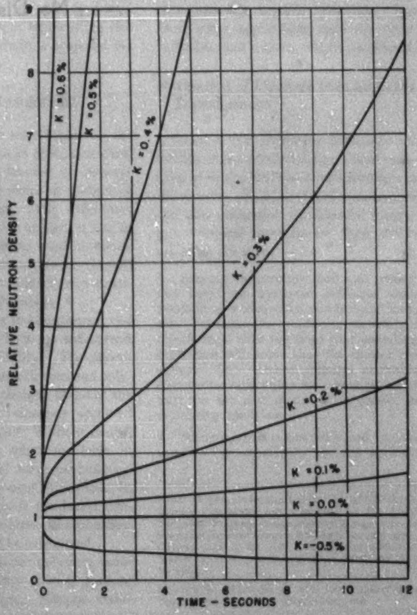

The completed simulator, shown in Figure 4, has external terminals for the connection of recording instruments. Sample runs showing step functions of reactivity are shown in Figure 5. The initial transient rise introduced by the sudden change in reactivity is caused by prompt neutron generation. If the reactivity is small enough so that the pile is not supercritical on the prompt neutrons alone, the neutron density levels off somewhat, and the slow exponential rise caused by the emergence of the delayed neutrons sets in. The fast period allows the neutron density to follow fluctuations in reactivity, while the delayed neutrons serve to limit the reactor period when K_e remains predominantly at any one value. In the case where $K_e > \beta$ the initial sharp rise is continued, leaving the delayed neutrons completely behind.

The importance of the longest delayed neutron emitter will vary and is dependent upon the nature of the problems being solved. In most cases, the very small contribution offered by this sixth group is negligible and may be safely ignored in the design of the simulator. If, however, it is desired to study the effects of large negative reactivities on neutron population, the sixth group will continue to emit neutrons long after all other delayed groups have decayed. Under these conditions, the inclusion of the longest delay emitter is essential for good accuracy.

The use of a balanced d-c amplifier tends to cancel contact potential drift and also is an effective means for obtaining phase inversion. Feedback produced by the large common cathode resistors reduces the gain of the amplifier to in-phase signals on the input grids. Because an even number of stages or equivalent phase shifts are used, it is essential that this in-phase gain be less than one, otherwise, the operational amplifier will be unstable. The differential gain, however, is made as high as practical.

During any sudden change in neutron density, the current drawn by the differentiating capacitor is sufficient to cause some unbalance in the amplifier. Symmetrical loading is maintained during these transients by the connection of a similar capacitor from the positive output terminal of the amplifier to some reference point within the d-c voltage supply. Error due to changes in gain over certain portions of the output signal will cause the critical position on the multiplying potentiometer to change with power level. This error is minimized by making the amplifier gain high and operating the tubes well within their linear range.

These simulators have been used successfully in testing period meters and automatic control devices. Because of the low wattage requirements of the battery operated elements, the simulator requires no warm-up period and can be put into service almost immediately after switching on. By being completely portable and self contained, this instrument found a maximum utility as a substitute for the actual nuclear reactor.

References

1. Elementary Pile Theory (book), H. Soodak, E. C. Campbell. John Wiley and Sons, Inc., New York, N. Y., 1950.

2. Derivation and Integration of the Pile Kinetic Equations, H. Hurwitz. *Nucleonics* (New York, N. Y.), July 1949, pages 61–67.

3. Electronic Pile Simulator, P. R. Bell, H. A. Strauss. *Review of Scientific Instruments* (Lancaster, Pa.), volume 21, August 1950, pages 760–63.

4. Delayed Neutrons from Fission of U235, D. J. Hughes, J. Dabbs, A. Cahn, D. Hall. *Physical Review* (Lancaster, Pa.), volume 73, January 15, 1948, pages 111–24.

No Discussion

The Application of Class-H Insulation to Transformers

MELVIN L. MANNING
FELLOW AIEE

THERMAL endurance of insulating materials is a major limitation of electrical equipment. For reasonable life, electric equipment is designed to keep the maximum operating temperature within the thermal limits of the insulating material. Industrial and utility engineers have long visualized an ideal dry type transformer composed of insulation which would exhibit a unique combination of balance of properties—an insulation having excellent heat stability, good electrical properties, exceptional moisture repellancy, and fire and explosion resistance. Class-*H* insulation now in volume production has reached the most important milestone yet attained by any insulating material in the realization of these ultimate objectives in sealed and ventilated dry type transformers for station auxiliary, indoor substation, and network service. Class-*H* transformers, in voltages 15 kv and below, through 3,000-kva ventilated and 1,500-kva sealed-in-nitrogen are the answer for elimination of fire and explosion hazards, exceptional resistance against moisture, reduced maintenance, overload capacity, and high ambient temperature conditions.

Seven years ago only a handful of electrical engineers and research chemists possessed a rather limited working knowledge of the unique insulating material,[1,2] now designated class-*H* by the AIEE. Only a few technical papers have been written on the application of class-*H* insulation to transformers.[3,4]

Class-*H* transformers, preferably sealed-in-nitrogen, can be installed where extreme conditions exist such as overloads, high ambient temperatures, and contamination; and where absolute safety is desired. The present extra cost for class-*H* sealed construction above the cost of class-*B* ventilated can be amortized by these advantages plus the satisfaction of eliminating fire and explosion hazards and toxic gas effects. Of prime operating importance, if nitrogen leaks occur, the transformer can continue to operate safely in air atmosphere even under high humidity conditions until the unit can be resealed in nitrogen.

This paper reviews the kinds of class-*H* insulating materials recently developed, and the evaluation of class-*H* transformers. A hottest spot temperature rise of 180 degrees centigrade is proposed for class-*H* transformers.

What Is Class-*H* Insulation?

Class-*H* insulation may consist of inorganic materials such as glass, porcelain, mica, and asbestos bonded or impregnated by the silicone resins or rubbers or by the fluorocarbons. The difference, compared with class-*B* insulation lies in the resins and varnishes used as bonds and impregnants. Exposed to air, class-*H* insulation has about 100 degrees centigrade temperature advantage.

Use of the silicones in transformer and in motor insulation is more widespread due to earlier availability. The fluorocarbons, polytetrafluoroethylene and polymonochlorotrifluoroethylene, stand at the gateway which the silicones occupied about seven years ago.[5] Without doubt, these fluorocarbons, when available in larger quantities, will serve exacting requirements for component insulation. In this paper, only class-*H* insulation consisting of the silicone-glass fiber or asbestos combinations will be considered.

Silicones are synthetic polymers composed of the elements silicon, carbon, hydrogen, and oxygen. Silicone resins and varnishes have a chemical structure similar to that found in glass, mica, and quartz. Consequently, they have proved to be natural complements to these inorganic insulating materials. Unlike organic compounds, that are based on carbon-to-carbon bonds, the silicones are built on a singularly stable molecular skeleton of alternate silicon and oxygen atoms. This inorganic skeleton gives the silicones much of the inertness and heat stability characteristic of quartz and glass. Silicones have flexibility, solubility, and ease of handling because one or more organic radicals are attached to each of the silicon atoms. Silicones can be produced as fluids, resins, varnishes, and rubbers. In all their various forms combined with Fiberglas, silicones permit operating temperatures in the range of 100 degrees centigrade above the limits of comparable organic materials. For transformer application, only the resin, varnishes, and rubbers will be considered.

Evaluation of Class-*H* Insulation for Transformers

When a new insulating material such as Class-*H* is introduced, uppermost questions in its application to transformers are the selection of a hottest spot temperature and also evaluation of dielectric properties. Several methods for their determination are open:

1. Select a temperature limit and properties based on available published data which may be somewhat obsolete and meager. Fabricate the insulating material in transformers with the hope that operating experience will prove that the choices are correct. This method requires extensive engineering supervision for a long period of time, on the part of operating people, in evaluating conditions.

2. Select a temperature limit and properties based on a carefully planned develop-

---

Paper 51-264, recommended by the AIEE Transformers Committee and approved by the AIEE Technical Program Committee for presentation at the AIEE Summer General Meeting, Toronto, Ont., Canada, June 25–29, 1951. Manuscript submitted March 21, 1951; made available for printing May 10, 1951.

Melvin L. Manning is with the Pennsylvania Transformer Company, Canonsburg, Pa.

ment program with the major suppliers of the material. In such a program lay out insulation specifications which must be met in transformers before such insulation becomes available commercially. Evaluate in the laboratory the mechanical and electrical characteristics of the new materials even to their impulse voltage strength. Conduct extensive heat aging tests up to destruction at elevated temperatures to determine the margin of dielectric strength offered above the hottest spot temperature proposed. Conduct thorough voltage creepage tests under different conditions of contamination and of humidity. Constantly keep in mind the end uses of the insulation in transformers yet utilize practical manufacturing facilities. Make exhaustive tests on transformers to duplicate extreme service conditions. This procedure requires less evaluation time in the field to determine the merits of the transformers.

The latter plan has been followed in this paper in evaluating class-*H* insulation. With major suppliers of class-*H* insulating materials organized for one common purpose, to develop required insulation, the program has been in existence for more than five years. The splendid laboratory facilities of these suppliers of insulating materials played an important part in successful culmination of effort as well as to carry on further developments. It is by such a plan of evaluation and by exhaustive tests on typical transformers that class-*H* insulation proves to be superior to other insulation for dry type transformers.

Hottest Spot Temperature

Hottest spot temperature proposed by the AIEE in 1947 for class-*H* insulating materials in rotating equipment is 180 degrees centigrade compared with 130 degrees centigrade for class-*B* and 105 degrees centigrade for class-*A* materials exposed to atmospheric conditions. Field and laboratory experience indicates, however, that silicone insulation will withstand, successfully, continuous operating temperatures of at least 220 degrees centigrade and that it will withstand much service at 250 degrees centigrade.[3,6,7,11] Composite thermal endurance data in air for class-*A*, class-*B*, and class-*H* insulation have been obtained by investigators.[7] A base of seven years (61,300 hours) was considered to represent typical life for the various classes of insulation at their respective permissible temperatures (class-*A* 105 degrees centigrade; class-*B* 130 degrees centigrade). Under such conditions a 220 degrees centigrade temperature was found to be permissible for class-*H*.

Tests on motors and on transformers, silicone insulated, verify the conclusion with wide margin that silicone insulation offers at least 10 times the life over class-*B* when compared on a basis of 220 degrees centigrade hottest spot for class-*H* and 130 degrees centigrade for class-*B*. Extensive accelerated aging at temperatures up to 310 degrees centigrade with alternate heating and humidifying cycles has established the fact that silicones follow a logarithmic relation between life and temperature. Life is halved or doubled for each 12 degrees centigrade increase or decrease in temperature in the neighborhood of 220 degrees centigrade. In nitrogen atmosphere, tests now under way indicate that silicone insulation can withstand even higher temperatures without increased aging effects.

An average temperature rise of 150 degrees centigrade with an allowable 180 degrees centigrade hottest spot temperature rise is proposed in this paper as a basis for design of class-*H* transformers. This basis of temperature rating is established not only by test on class-*H* transformers and component insulation, but also by comparing by test the 30 degrees centigrade relative margin between the average 80 degrees centigrade temperature rise and hottest spot 110 degrees centigrade rise proposed for class-*B* transformers by the AIEE. Class-*B* transformers are now rated 80 degrees centigrade average temperature rise and a 110 degrees centigrade hottest spot rise. Performance of class-*H* transformers in service demonstrates that an average temperature rise of 150 degrees centigrade with a permissible hottest spot rise of 180 degrees centigrade is feasible. Furthermore, tentative United States Navy specifications for class-*H* insulated equipment specify 150 degrees centigrade average rise.

Silicone Insulation as Applied to Newly Developed Class-*H* Transformers

To achieve the high heat stability offered by silicone insulation, it is necessary to use inorganic materials such as glass or asbestos bonded or impregnated by the silicone resins or rubbers. Cable leads should be covered by silicone rubber if glass fiber tape will not suffice. All other components used in a class-*H* transformer should consist of silicone-glass combinations capable of withstanding 180 degrees centigrade hottest spot rise. This includes glass served silicone resin bonded wire for the windings and silicone impregnating varnish. No organic materials such as cotton tape, cotton tying cord, paper or phenolic varnishes are used. This eliminates the possibility of fire, explosion, and toxic gas hazards.

See Figure 1 for construction details. The important component insulation is:

Wire—Double glass served silicone-alkyd resin bonded wire for low-voltage and high-voltage windings.

Layer Insulation—Silicone rubber-coated glass cloth combined with formable laminate.

Barriers—Core and high-to-low voltage winding insulation. Formable silicone glass cloth laminate interleaved with silicone rubber-glass cloth. Breakable glass cylinders are eliminated.

Axial Spacers—Thermosetting silicone-glass cloth or silicone-asbestos laminate.

Blocking, Interphase Barriers, Yoke and Core Insulation—Thermosetting silicone-glass cloth or silicone-asbestos laminate.

Varnish—Silicone-alkyd formulation for abrasion, scuff, and craze resistance. Vacuum impregnation is unnecessary.

Outstanding as barrier construction is the new formable silicone-glass cloth laminate. Preformed, breakable glass cylinder construction is replaced by a laminate which is strong mechanically and electrically. This laminate can be rolled from large sheets directly on the lathe during coil winding operations. At operating temperatures up to 200 degrees centigrade the dielectric strength is 300 volts per mil, 60-cycle voltage, 1-minute withstand for number 7 square wire as an electrode to a steel cylindrical mandrel as ground. For additional dielectric strength and resistance against formation of corona due to contaminating conditions, silicone rubber coated glass cloth is interleaved with the barrier.

Silicone rubber coated 0.010 inch thick (0.007 inch glass cloth plus 0.003 inch silicone rubber) glass cloth is used for layer insulation. A dielectric strength of 350 volts per mil, 60-cycle voltage, 1-minute withstand is attained. Roller type electrodes were used in evaluation tests to subject the whole surface of the material to the same test voltage.

Thermosetting silicone-glass cloth or asbestos laminate for axial spacers, blocking and core insulation provides insignificant water absorption, high heat stability, resistance to voltage creepage and high mechanical strength. A flexural strength flatwise, on a $^1/_8$-inch panel, of 22,000 pounds per square inch and a wet insulation resistance of at least 120,000 megohms is attained by following Standard American Society for Testing Materials tests.

Recently developed silicone-alkyd impregnating varnish imparts high bonding strength, abrasion resistance, and gloss to

Figure 1. Class-*H* transformer construction

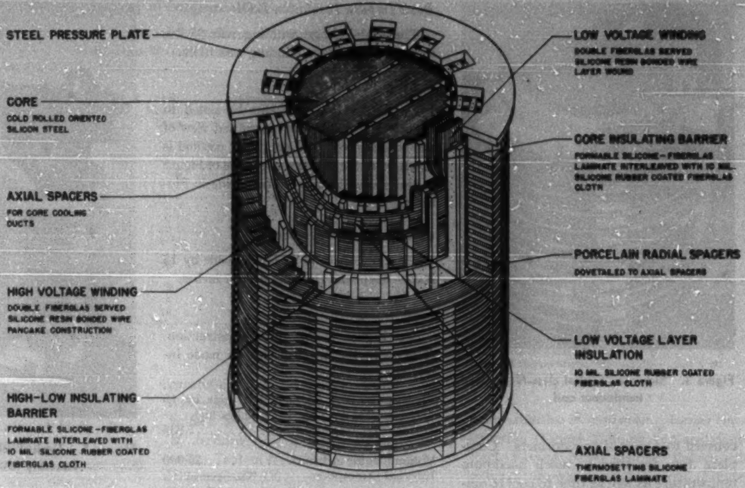
STEEL PRESSURE PLATE
CORE
COLD ROLLED ORIENTED SILICON STEEL
AXIAL SPACERS
FOR CORE COOLING DUCTS
HIGH VOLTAGE WINDING
DOUBLE FIBERGLAS SERVED SILICONE RESIN BONDED WIRE PANCAKE CONSTRUCTION
HIGH-LOW INSULATING BARRIER
FORMABLE SILICONE-FIBERGLAS LAMINATE INTERLEAVED WITH 10 MIL SILICONE RUBBER COATED FIBERGLAS CLOTH
LOW VOLTAGE WINDING
DOUBLE FIBERGLAS SERVED SILICONE RESIN BONDED WIRE LAYER WOUND
CORE INSULATING BARRIER
FORMABLE SILICONE-FIBERGLAS LAMINATE INTERLEAVED WITH 10 MIL SILICONE RUBBER COATED FIBERGLAS CLOTH
PORCELAIN RADIAL SPACERS
DOVETAILED TO AXIAL SPACERS
LOW VOLTAGE LAYER INSULATION
10 MIL SILICONE RUBBER COATED FIBERGLAS CLOTH
AXIAL SPACERS
THERMOSETTING SILICONE FIBERGLAS LAMINATE

component insulation parts of the transformer. Only 26 hours total processing time for 2-dip cycles under atmospheric pressure are required for impregnating coils compared with 76 hours and two dips under vacuum for previously used silicone varnishes. The alkyd modification to the varnish adds substantially to abrasion resistance. Heat endurance tests from 200 degrees centigrade to 250 degrees centigrade demonstrate excellent craze resistance by varnish coating aluminum panels and bending over a $^1/_8$-inch mandrel. Mechanically, a strong coil structure is obtained after this 2-dip varnishing process.

In reviewing these component insulation parts as diagrammed in Figure 1, it can be noted that only true class-*H* insulation material is considered; that is, the silicone resins and rubbers, glass cloth and porcelain to provide high temperature stability and moisture resistance. Asbestos-glass cloth silicone bonded materials now under development may be used in various combinations in class-*H* transformers of the future.

Costs

Class-*H* silicone insulation is about 20 per cent more costly at present than organic phenolic varnish bonded insulation. However, reductions in cost are being made continually and as use of silicones increases, the costs will decrease accordingly. Costs of class-*B* and of class-*H* insulated wire are now similar. Silicone-glass cloth and asbestos laminates are now under development which may decrease present costs. Due to the high-temperature stability of the silicones which result in greater possible overloads, weight saving and resistance to fire and explosion, some increased cost can be justified.

Insulation has been one of the barriers in limiting the output of a transformer. Thermal endurance of insulating materials has been the main factor. As the history of transformer construction is reviewed, the size and weight per kilovolt amperes of a transformer in a given voltage class has been reduced by improved magnetic materials, by improved cooling systems, and by progressively developing more heat stable insulating materials. Class-*H* insulation is now in the picture to dispel some of the limitations heretofore found in its predecessors.

Standardization of Design and Typical Test Data

For station auxiliary, network, and indoor substation service class-*H* insulated transformers of sealed or ventilated construction are the answer for elimination of fire and explosion hazards, high resistance against moisture, reduced maintenance, ability to carry overloads, operation in high ambient temperatures, and less weight.

With these ideas in mind, a transformer construction was agreed upon which could be standardized. For each voltage class from 1.2 kv through 15 kv, corresponding insulation clearances would be prescribed. Of most importance was improvement of insulating barriers commonly used for core and for high-to-low voltage winding insulation, interphase barriers, and axial spacers. Breakable pyrex glass cylinders, rods, and plates are not the answer to the problem. These were replaced by newly developed formable and thermosetting silicone-glass cloth laminates.

Moreover, complete temperature data for enclosures sealed with air or nitrogen and for ventilated construction under normal, up to 150 per cent, continuous loading were desired. Tests were prescribed to find basic information of most

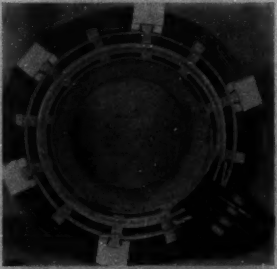

Figure 2. End view typical class-*H* insulated transformer coil

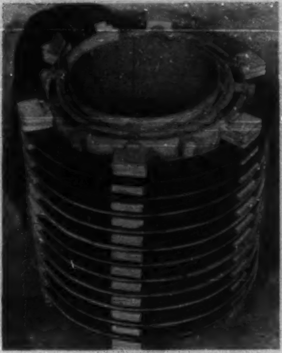

Figure 3. Side view typical class-*H* insulated transformer coil

concern to a user of transformers. Complete data for time to reach maximum temperature as well as time to cool to ambient temperature for all loadings were wanted.

RATING AND DIMENSIONS OF TYPICAL CLASS-*H* TRANSFORMERS

The data obtained for two 100-kva 2,400-120/240 volt, 5-kv class single-phase 60-cycle 150-degree-centigrade rise sealed transformer units are shown in the following. A 5-kv insulation class was chosen due to its popularity for station auxiliary equipment.

Figure 4. Typical class-*H* core and coil assembly high-voltage side

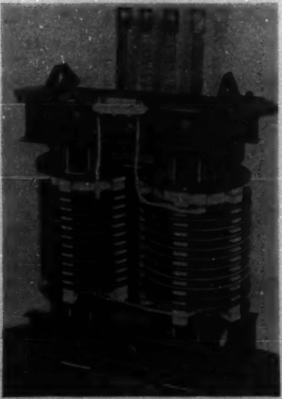

Basic Impulse Insulation Level

The high-voltage winding was 25 kv, and the low-voltage winding was 10 kv.

Coil Construction

Details of the coils can be noted in Figures 2 and 3. The assembled view of the core and coil and clamping method is given from the high-voltage side of Figure 4 and from the low-voltage side in Figure 5.

Core and Coil Dimensions

The floor space is 27 inches wide by 13 inches deep, and the height is 37 inches.

Tank

See Figure 6 for tank construction. (Normally the bracing can be made internally).

Floor space	34$^{1}/_{2}$ inches wide by 19 inches deep by 48$^{1}/_{4}$ inches high
Surface area (top and sides)	5,835 square inches
Volume, cubic inches	29,600
Internal atmosphere	(a) Nitrogen at $^{1}/_{2}$ pound gauge pressure (b) air (c) ventilated

Weight

Core steel, pounds	613
Copper, pounds	205
core and coil assembly, pounds	1,236
tank, pounds	918
bushings, pounds	21
	2,175

TEST DATA

Electrical Characteristics

Core loss at 20 degrees centigrade, watts	643.2
Core loss at 150 degrees centigrade, watts	600.0
Total loss at 75 degrees centigrade, watts	1,552.2
Total loss at 150 degrees centigrade, watts	1,856.0
Impedance 75 degrees centigrade, per cent	3.42
Impedance 150 degrees centigrade, per cent	3.54
Regulation:	
75 degrees centigrade	
100 per cent power factor	0.96
80 per cent power factor	2.72
150 degrees centigrade	
100 per cent power factor	1.3
80 per cent power factor	3.0

Insulation Resistance and Power Factor Measurements

The power factor, at beginning of heat run tests, coils had been subjected to 80–90 per cent humidity conditions for three months.

High voltage to low voltage and ground, per cent	1.1
Low voltage to high voltage and ground, per cent	1.91
High voltage and low voltage to ground, per cent	1.50

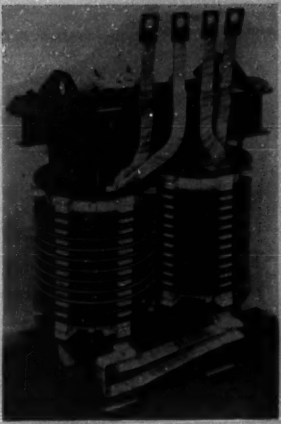

Figure 5. Typical class-*H* core and coil assembly low-voltage side

The power factor at completion of heat run tests:

High voltage to low voltage and ground, per cent	0.2
Low voltage to high voltage and ground, per cent	0.28
High voltage and low voltage to ground, per cent	0.30

The insulation resistance for all windings was infinite.

Figure 6. Class-*H* transformer sealed tank

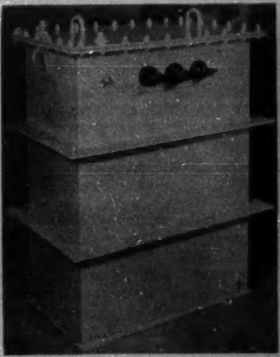

Table I. Summary of Temperature Data

Sealed Tank—Nitrogen Atmosphere at $^{1}/_{3}$ Pound Gauge Pressure 100-Kva Single-Phase 5-Kv Class, Class-*H* Transformer

Item	100 Per Cent Load	125 Per Cent Load	150 Per Cent Load	160 Per Cent Load, Loading Time Eight Hours
Average LV copper rise by resistance, °C	130.6	185.9	245.24	265.37
Duct temperature LV, °C	142.0	190.0	229.5	249
Average HV copper rise by resistance, °C	92.8	137.67	175.92	198.56
Duct temperature HV, °C	124.0	168.0	201.0	246
Maximum core temperature, °C	132.2	162.3	184.4	186
Top gas temperature, °C	90.0	114.9	132.0	142
Maximum external tank temperature, °C	52.0	60.0	61	63
Nitrogen pressure gauge, pounds	2–3	2–3	2–3	2–3
Time required to reach maximum temperature, hours	15	16	16	
Time required to cool to ambient temperature, hours	8	8	8	8
Reduction core loss, per cent	4	5	5	5
Ambient temperature, °C	26	24	15	16

LV = low voltage HV = high voltage

Table III. Summary of Temperature Data

Core and Coils Exposed to Atmosphere 100-Kva, Single-Phase, Class-*H* Transformer

Item	100 Per Cent Load	200 Per Cent Load (6 hrs.)
Average LV copper rise by resistance, °C	77.9	254.8
Duct temperature LV, °C	88.0	220.0
Average HV copper rise by resistance, °C	45.36	166.9
Duct temperature HV, °C	61.0	182.0
Maximum core temperature, °C	82.0	127.0
Top gas temperature, °C	25.7	47.8
Maximum external tank temperature, °C		
Gauge pressure, pounds		
Time required to reach maximum temperature, hours	14.0	
Time required to cool to ambient temperature	9	6
Reduction core loss, per cent	2	5
Ambient temperature, °C	21	21

Dielectric Tests

At 60-cycle voltage, the high-voltage winding, 12 kv 1 minute; and low-voltage winding, 4 kv, 1 minute.

Induced: 200 per cent voltage (400 cycles, 18 seconds).

Impulse voltage—5-kv class winding: full wave ($1^{1}/_{2}$ by 40 microseconds) 25 kv (Figure 11).

Radio Influence Voltage Tests

Tested in accordance with National Electrical Manufacturers Association NEMA) Standards 48-132 (TR-3-135 to 140 inclusive). Test voltage applied—3,180 volts. This standard for distribution apparatus specifies a maximum value of 500 microvolts. Background radio influence voltage level = 17 microvolts. Test on H_1 bushing, H_2 grounded = 215 microvolts. Test on H_2 bushing, H_1 grounded = 215 microvolts.

Table II. Summary of Temperature Data

Sealed Tank—Air Atmosphere Normal Pressure 100-Kva, Single-Phase, 5-Kv Class, Class-*H* Transformer

Item	100 Per Cent Load	125 Per Cent Load	150 Per Cent Load
Average LV copper rise by resistance, °C	154.54	201.28	252.54
Duct temperature LV, °C	156.0	195	243.0
Average HV copper rise by resistance, °C	108.89	146.86	181.77
Duct temperature HV, °C	134.0	172.2	216.0
Maximum core temperature, °C	141.3	159.8	187.5
Top gas temperature, °C	93.6	111	136.0
Maximum external tank temperature, °C	41.0	56	72
Gauge pressure, pounds	0	0	0
Time required to reach maximum temperature, hours	23	17	14
Time required to cool to ambient temperature, hours	8	8	8
Reduction core loss, per cent	4	5	5
Ambient temperature, °C	19	22	25

Audio Noise Tests

The transformer average sound level is 58.6 decibels and standard NEMA level for dry-type transformers is 66 decibels.

Thermal Characteristics

Procedure for making tests:

1. Thermocouples were located on:

   Bottom yoke of core
   Upper yoke of core
   Upper outer leg of core
   Outer lower leg of core
   Top of high-voltage coil duct
   Top of low-voltage coil duct
   Bottom tank wall
   Gas space above the core

2. Provisions were made for obtaining temperature rise by resistance on high-voltage and on low-voltage windings, to obtain time for cooling to ambient temperature after shut-down from various loadings, and to measure core loss at operating temperatures.
3. The transformer units were loaded in opposition to obtain data (summarized in Tables I, II, III) at continuous loading as follows:

Sealed construction—in nitrogen and also in air atmosphere 100 per cent, 125 per cent, 150 per cent continuous loading.

Ventilated construction—100 per cent continuous and 200 per cent loading (6 hours) was prescribed.

Fire and Water Tests

The most commonly feared enemies of insulation are fire and water. To determine the fire resistance of silicone-glass fiber insulation as used in transformer construction (Figure 1) an oxygen-acetylene torch having 5,000 degrees Fahrenheit temperature was applied to a coil (Figure 7), for the same interval of time that was required to cut 2-inch thick plate steel for a distance of several inches (Figure 8). Only two layers of the H-L silicone-glass cloth laminate were affected, and the silicone resin impregnant beaded to silica as can be noted by the white spots on the barrier surface of Figure 7.

To determine the effects of water on class-*H* insulated transformers, the coil and core was subjected to a 2-nozzle water spray for 40 minutes while the transformer was excited at 2,400 volts (Figure 9). No indication of failure was noted. Power factor and megger readings were taken before and after the spray test, see Table IV.

Table IV

Before Water Spray	Power Factor, Per Cent	Megger Reading
High to low and ground	0.2	Infinity megohms
Low to high and ground	0.28	Infinity megohms
High and low to ground	0.3	Infinity megohms

After Water Spray*	Power Factor, Per Cent	Megger Reading
High to low and ground	0.5	Infinity megohms
Low to high and ground	0.98	Infinity megohms
High and low to ground	1.24	Infinity megohms

* Water soaked for 48 hours.

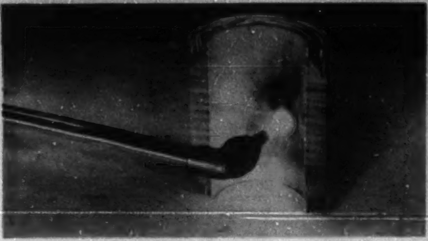

Figure 7. 5,000 degrees Fahrenheit oxygen-acetylene torch applied to class-*H* barrier insulation

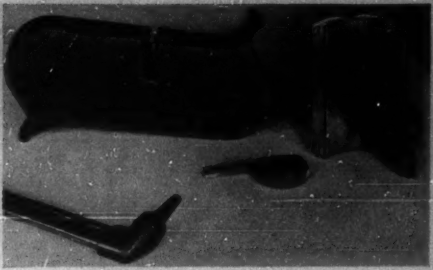

Figure 8. 5,000 degrees Fahrenheit oxygen-acetylene torch applied to 2-inch plate steel for same interval of time as to coil in Figure 7

Observations of importance in witnessing these fire and water tests were that the silicone-glass fiber insulation would not support combustion even though the tests were in air, the insulation resistance remained at infinity megohms regardless of the moisture conditions and with water allowed to remain on the insulation for almost two days the power factor increased about 1 per cent maximum measurement (high and low voltage to ground).

Short Circuit Tests

These tests were made in accordance with NEMA Standards 48-132, (TR-3-15). For two seconds 25 times rated current was circulated in the short-circuited low-voltage winding. All measurements for losses were again made besides applying the dielectric voltage tests. These tests were satisfactorily withstood and losses checked exactly with former measurements.

Impulse Voltage Tests

Standard American Standards Association (ASA) tests[9] in accordance with C57.11, Table 11.030 for dry type transformers were followed. Full wave (25 kv crest) oscillograms are given in Figures 11, 11(A).

Discussion of Temperature Test Data

Briefly summarized, the following points are of interest:

1. In nitrogen atmosphere (Table I and Figure 10), the temperature rise is lower than that for air atmosphere. Nitrogen possesses better heat transfer characteristics.

2. The time required to cool after loading to ambient temperature approximates eight hours regardless of the loading or atmosphere. The high thermal conductivity of the insulation apparently explains this fact.

3. Reduction in core loss approximates 4 per cent to 6 per cent. This reduction in core loss after quite comprehensive studies on transformer cores and Epstein samples of cold rolled oriented steels has been found to average 5 per cent for core temperatures at 150 degrees centigrade and up.[8] A beneficial aging effect takes place in the steel beginning at approximately 130 degrees centigrade.

4. The maximum external tank temperature does not exceed 72 degrees centigrade even for 150 per cent continuous loading in air atmosphere.

5. Nitrogen gauge pressure did not exceed the range of 2 to 3 pounds for an initial pressure of $^1/_2$ pound.

6. The temperature rise in the low-voltage and high-voltage coils did not exceed calculated values. Design balance for 150 degrees centigrade rise is achieved.

Conclusions

The conclusions reached concern the use of class-*H* silicone insulation to transformers of sealed-in-nitrogen atmosphere construction through at least 1,500-kva 15-kv class ratings, and of ventilated (open) construction through at least 3,000-kva 15-kv class ratings for station auxiliary, network, and indoor substation service.

The advantages of class-*H* over class-*B* insulated transformers from the user's standpoint are:

1. Fire and explosion hazards eliminated.

2. Freedom from corona at normal operating voltage and exceptional ability to withstand corona if present at high over-voltage. Ability of silicone rubber, as used in component insulation, to resist corona surpasses other insulating materials.

3. Impervious to moisture, space heaters not required.

4. Glass-like surface on coils minimizes collection of dirt and contaminants. Cleaning more easily done.

5. Greater ability to withstand overloads due to thermal conductivity of insulation.

Figure 9. Two water sprays applied to class-*H* transformer units under full excitation voltage

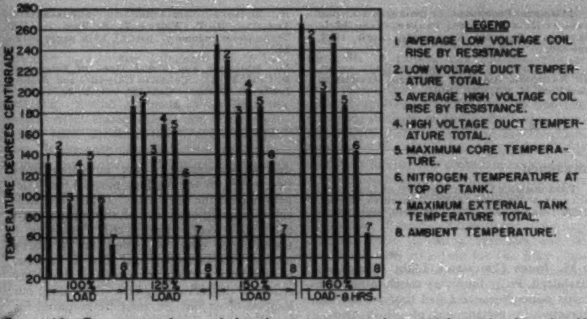

Figure 10. Temperature data, sealed tank, nitrogen atmosphere, 100-kva, 5-kv class, class-*H* transformer

6. Less weight for core and coils approximately 15 per cent as demonstrated by general designs.
7. Higher ambient temperatures permitted.

The additional advantages of sealed-in-nitrogen atmosphere construction are:

1. Less maintenance required, contaminants are not present to decrease voltage strength of cooling ducts. Clearances are more easily controlled. Transformer unit can be installed in a dirty location provided periodic checks are made of bushings and nitrogen gauge pressures.
2. Filtering equipment and valves not required as for liquid-filled transformers.
3. Can be used where flooding occurs.
4. Minimum oxidation resulting in longer life of insulation and better heat transfer characteristics as compared with air atmosphere sealed. If nitrogen leaks do occur, the transformer can continue to operate safely in air atmosphere until the unit can be resealed in nitrogen.
5. Can be used outdoors as well as indoors if proper line insulation co-ordination and protective devices are used.
6. Continual research in insulating materials and use of higher gas pressures presents the possibility of developing dry-type transformers to equal the same basic impulse levels as liquid-filled transformers.

The disadvantage for either the class-*B* or class-*H* dry-type transformer is common to both. The impulse strength is about one-half that of liquid-filled units. Eventually this disadvantage may be overcome by improved use of insulation or by higher nitrogen pressures to provide increased voltage strength. Protection by lightning arresters is required if voltage surges may occur above the limits proposed by ASA Standards[9] for dry-type transformers (C57.11, Table 11.030).

Electrical characteristics of transformers operating at elevated temperatures are satisfactory. Tests on transformers show that proper design balance is obtained for required regulation, core, and copper loss values.

Tests made by the United States Navy Department and by motor manufacturers on class-*H* silicone insulated electric equipment subjected to severe and accelerated conditions have shown that such equipment is capable of operating hundreds of times longer than conventional insulation.[4,7]

Silicone-insulated rotating equipment installed in submarines operating at 230 degrees centigrade continuous temperature does not constitute a health hazard up to 96 hours operating time submerged.[10] Surface ship ventilated installations of silicone-insulated equipment are considered to be safe from the standpoint of CO evolutions regardless of temperature.

Fire and water resistance of class-*H* insulation has been demonstrated by tests on transformers described in this paper.

An average temperature rise of 150 degrees centigrade with an allowable 180 degrees centigrade hottest spot temperature rise is proposed as a basis for the temperature rating of class-*H* transformers.

Core loss is reduced approximately 5 per cent at 200 degrees centigrade. A beneficial aging effect takes place when cold rolled oriented steels are exposed to higher temperatures.

Development of class-*H* insulation described in this paper has been achieved by keeping in mind specific design and application problems and by evaluating combinations of materials as used in transformers. Insulation development programs with suppliers of insulating materials have been most effective in obtaining results outlined.

Cost of class-*H* insulation at present is about 20 per cent greater than class *B*. The higher costs of silicones are to be expected for new materials. In this phase, the cost-volume equation as always is the great key to the future. With increasing plant production, costs are decreasing. The advantages outlined for class-*H* insulation applicable to transformers should assist in obtaining greater volume production.

It is hoped that the development work described will stimulate interest in class-*H* insulation and its application to transformers.

References

1. Silicones as Electrical Insulation Materials, A. L. Bass, M. J. Hunter, T. A. Kauppi. *Transactions*, Electrochemical Society (New York, N. Y.), volume 90, 1946.

2. Silicones, High Polymeric Substances, Shailer Bass, J. F. Hyde, E. C. Britton, R. R. McGregor. *Modern Plastics* (New York, N. Y.), volume 22, November 1944, page 124.

3. Low Voltage, Air-Cooled Transformers Designed for 225 C Operation, J. F. Dexter, M. L. Manning, H. P. Walker. *Electrical World* (New York, N. Y.), August 14, 1948.

4. Silicone Insulation as Applied to Naval Electric Equipment, H. P. Walker. *AIEE Transactions*, volume 66, 1947, pages 977–83.

5. Fluorocarbon Resins Appraised, Parts I-II, A. E. Javitz. *Electrical Manufacturing* (New York, N. Y.), August-September, 1950.

6. Organo-Silicon Compounds for Insulating Electric Machines, T. A. Kauppi, G. L. Moses.

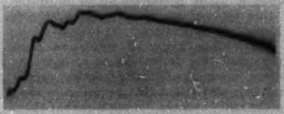

Figure 11. Neutral current, full wave impulse voltage test H_1 terminal

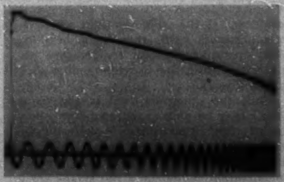

Figure 11(A). Full wave (1½ by 40 microsecond) 26-kv crest impulse voltage test H_1 terminal

Electrical Engineering (*AIEE Transactions*), volume 64, March 1945, pages 90–94.

7. Motor Tests Evaluate Thermal Endurance of Class-*H* Insulation and Silicone Varnish, **George Grant III, T. A. Kauppi, Graham Lee Moses, G. P. Gibson.** *AIEE Transactions*, volume 68, part II, 1949, pages 1133–38.

8. Magnetic Properties of Oriented Silicone Steel at High Operating Temperatures, **M. L. Manning.** *Electrical Engineering*, April 1949, page 336.

9. Standards for Transformers, Regulators, and Reactors, **American Standards Association** (New York, N. Y.), *C57*, 1948.

10. Silicone Insulation in Submarines—Toxicity, **H. P. Walker, T. E. Shea.** *AIEE Transactions*, volume 67, part II, 1948, pages 1232–35.

11. Siliconss and Their Uses in Industry, **D. C. R. Miller.** *Canadian Chemistry and Process Industries* (Toronto, Canada), volume 33, 1949.

Discussion

J. A. Elzi (Commonwealth Services Inc., Jackson, Mich.): There is a need for dry-type transformers for applications in vaults and industrial plants and for power supply to station auxiliaries in steam electric generating plants. At the present time, however, there is some reluctance in recommending dry-type transformers for these applications because of their low insulation level, their susceptibility to dirt and moisture, and the fact that serious fires have occurred with class-*B* insulation. The use of class-*H* insulation as described by the author appears to provide a means of overcoming many of the objectionable features of other types of construction. There are, however, several points which require further consideration.

It is noted that the transformer described has a 5-kv insulation class and an impulse withstand voltage of 25-kv crest. A similarly rated liquid filled transformer would have a withstand level of 60-kv crest. For general distribution service a 3-kv line-type lightning arrester would probably be used and after allowances are made for circuit gradient and lightning arrester tolerances the 25-kv level may not be adequate.[1] The paper indicates excellent 60-cycle dielectric strength for the materials used, and, if the impulse characteristics are similarly good, it would appear that these transformers could be designed for higher withstand voltages. This would be highly desirable if this type of transformer is to receive widespread application.

The various types of insulation used throughout this design appear to have excellent mechanical characteristics except that it is also noted that porcelain is used for the radial spacers. It appears that these spacers would be brittle and subject to breakage and that it would be desirable to utilize a material similar to the silicone-asbestos laminate which is used for the axial spacers.

With the wide variations in copper temperatures which will result from no load to full load operation, it appears that expansion of the copper introduces some special problems. If the coils are tight when the transformer is cold, they may be loose when operating at high temperature and might have difficulty in withstanding short circuit stresses.

While the materials used in the transformer may be able to withstand an allowable average temperature rise of 150 degrees centigrade and a hottest spot rise of 180 degrees centigrade, it appears that special consideration should be given to the bushings used in this transformer. This might require either specially designed bushings or some form of heat block between the winding terminals and the inside bushing terminals.

Reference

1. Performance Characteristics of Lightning Protective Devices, **AIEE Committee Report.** *AIEE Transactions*, volume 68, 1949, pages 1333–36.

B. M. Jones (Duquesne Light Company, Pittsburgh, Pa.): I am very much interested in this paper because I feel that we are all interested in getting rid of oil in transformers, particularly in buildings and confined places, and I believe that this is a move forward in the right direction.

We are threatened with increased fire insurance rates, due to the claims paid by some insurance companies as the result of fires in stations. Aside from the cost situation, which, of course, is important, we have a duty and an obligation to the public and to customers to take all reasonable precautions to avoid fires and explosions, particularly in places where the public congregates. I believe that the electrical industry, both operator and manufacturer, should push development vigorously towards the elimination of oil in transformers.

I was very interested in the subject of varnish insulation, where it says "vacuum impregnation is unnecessary," as I believe this will be helpful and should tend to reduce costs.

Of course, we have a problem in regulation, when the transformers are operated at a higher temperature for the same size copper conductors, but believe that such a rating used in emergency only will permit some sacrifice in voltage drop.

I raise a question relative to Item 3, of the section on Discussion of Temperature Test Data last sentence, wherein reference is made to the aging effect taking place beginning about 130 degrees centigrade. My question: why not age the steel in the factory at 130 degrees centigrade or above before assembly, thus permitting the customer to get the benefit of the aging from the time the transformers are received and put in service.

In closing, I would like to say that we do not want bigger and better transformers; we want smaller and better and ligher transformers, and of course less expensive ones!

R. H. Mertz and **E. L. Leinbach** (The Detroit Edison Company, Detroit, Mich.): The following questions are raised concerning Mr. Manning's paper:

What advantage does the value of 150-degree centigrade average winding temperature rise, as recommended in the paper, over another value, say 120 degrees centigrade? Also what is its ability to carry emergency overloads?

Following is some background information which suggests these questions to us.

We recently received some 500-kva, sealed, class-*H* insulated, network transformers with an average winding rise of 120 degrees centigrade. Our networks have two, three, or maybe four parallel feeds depending on the area load. If one feed fails the remaining one, two, or three feeds must carry the load. Under this condition a transformer may be called on to carry around 150-per-cent load for an 8-hour period with a vault temperature that may reach 50 degrees centigrade. This does not happen often but we must be prepared for it. For our oil-insulated transformers operating under this condition we install water sprays and they perform very well. Water sprays, however, probably would not be effective on class-*H* insulated transformers.

Will 150-degree centigrade average winding temperature rise, class-*H* insulated transformers meet this condition relying entirely on their overload capacity?

L. C. Whitman (General Electric Company, Pittsfield, Mass.): Engineering advances in the design of equipment are made through the use of new materials and new ideas. In the case of class-*H* insulation its efficient utilization has frequently made new and different designs possible. It is important, however, that we critically examine such designs for both advantages and disadvantages to see that our enthusiasm for them is balanced by a sense of true merit and utility.

Sealed dry-type transformers utilizing class-*B* insulation in nitrogen gas[1] as well as class-*H* insulation in air or nitrogen are growing rapidly in popularity. We have designed and built ratings through 1,250 kva and 15 kv, and duplicate orders have attested user acceptance and satisfaction. Mr. Manning's paper concerning design, construction, and performance will assist users in determining the sphere of application and design considerations pertinent to such units. The comments and questions which follow are for the purpose of further analyzing and evaluating technical details and ideas presented in this paper.

Silicone-alkyd resin is specified as the bonding resin on the wire used and as the impregnating resin. AIEE Standard Number 1[2] specifies only a minute amount of class-*A* material to be added for manufacturing purposes in class-*H* structures. What percentage alkyd resin is used in the silicone-alkyd resin specified?

A figure of 20 per cent is quoted when comparing the cost of class-*H* silicone insulation with organic phenolic varnish bonded insulation (class B). At the present time in the open market, pure silicone class-*H* insulations cost several times as much as comparable class-*B* insulations. Does the author mean this 20 per cent differential in the total cost of comparable class *B* and class *H* transformers?

In the conclusion of the paper the class-*H* transformer is quoted as having greater overload ability than a class-*B* transformer. Is this statement made on the basis of the two transformers having the same temperature rise under normal load? In this case the class-*H* transformer will have a higher first cost, and so any difference due to insulation thermal conductivity will have to be of considerable magnitude to be of importance. Radial gradients in windings of natural draft transformers[3] are small compared with air-film temperature drops. Also, in the case of sealed dry-type transformers, major thermal drops exist between the inside gas and the enclosing tank, as well as between the tank and the outside ambient. Hence, even large differences in resin conductivity will result in very minor improvement in thermal characteristics. On the other hand, if the class-*H* transformer is designed for a higher temperature than the class-*B* unit, this means that in general less copper will be used. Does not that mean that the overload ability will thereby be decreased?

The statement is made in the paper that in nitrogen atmosphere the temperature rise is less than in an air atmosphere. The tests referred to are not comparable since in the nitrogen case a positive pressure is used, which in itself has the effect of reducing thermal gradients. Natural convection varies as the square root of the absolute gas pressure.[4] This will account for some 10 per cent of the 18 per cent differential reported.

No mention is made of the evaluation in terms of cost of the higher losses in the proposed 150-degree centigrade rise sealed dry-type transformer as compared with those in a 120-degree centigrade rise transformer. The initial cost of the hotter transformer will be less, due to less material being used. However, the copper loss of such a transformer will be greater, due to the increase in the resistance of the windings at the higher temperature as well as the increase in resistance due to the lesser cross section of the copper used. Also regulation will be greater particularly at unity power factor.

Operating companies can assist manufacturers in arriving at optimum design temperatures by publishing up-to-date data that are representative of the spread in values used for capitalization of losses and regulation.

REFERENCES

1. AGING OF CLASS B INSULATION IN NITROGEN, H. C. Stewart, L. C. Whitman. *AIEE Transactions*, volume 70, part I, 1951, pages 436–39.

2. GENERAL PRINCIPLES UPON WHICH TEMPERATURE LIMITS ARE BASED IN THE RATING OF ELECTRIC MACHINES AND APPARATUS. *AIEE Standard Number 1*, 1947.

3. HOT-SPOT TEMPERATURES IN DRY-TYPE TRANSFORMER WINDINGS, H. C. Stewart, L. C. Whitman. *AIEE Transactions*, volume 63, 1944, pages 763–68.

4. HEAT TRANSMISSION, W. H. McAdams. McGraw-Hill Book Company, New York, N. Y., 1942, page 242.

M. L. Manning: Comments and questions offered are very much appreciated by the author. The main purpose of the paper is to outline the definite advantages of class-*H* insulated transformers from an operating viewpoint. It is helpful to utilize ideas of the users of transformers in developing new kinds of insulating materials and in applying them.

Mr. J. A. Elzi brings out a good point in the idea of raising the impulse voltage strength of dry-type transformers to equal that of oil-filled transformers. This is a difficult problem to solve due to the low dielectric strength of air or of nitrogen compared with materials used in combination. Impulse voltages have the habit of stressing materials having low dielectric constants in a series combination. Voltage stress varies inversely to the dielectric constant. Someday we hope to have the problem solved. Meantime, if over-voltages occur, rotating-machine type lightning arresters can be used such as 6-kv rating for the 5-kv class transformers considered. Also, additional work can be done to determine the magnitude of voltages transferred through station transformers to auxiliary transformers. Perhaps the protection problem is not as important as anticipated for many installations. Porcelain radial spacers in high-voltage coils have a good service record. The thermosetting silicone laminate possesses much greater mechanical strength but cost precludes its use at present for radial spacers. Thus far, no difficulty has been experienced by the expansion and contraction of copper in coils at 150-degree centigrade rise temperature and none is expected for the sizes of copper wire used for the transformer ratings covered in the paper. Moreover, short-circuit stresses have been withstood adequately by transformer windings after being subjected to temperatures of 265-degree centigrade rise. Provisions have been made to take care of the dissipation of heat at terminals and bushings of 150-degree centigrade rise class-*H* transformers. The problem does not appear to be difficult. Standards for switchgear, backed by corresponding research work, should be made available as development work for transformers proceeds. New ideas demand co-ordinated studies by switchgear and transformer standardizing committees.

Mr. B. M. Jones, from a safety standpoint, is interested in getting rid of oil in transformers used in buildings and confined places. We are heartily in accord with the idea of providing fire and explosion resistant class-*H* transformers for such applications. Moreover, the likelihood of increased fire insurance rates for oil-filled transformers due to fires in stations, is an item for consideration. Regulation will be somewhat higher at 150-degree centigrade rise but not excessive, since reactive voltage drop, the larger component of regulation, is independent of temperature. Regulation at low power factors (50 per cent) approximates the per cent impedance of the transformer. Beneficial aging in cold rolled steel is found at temperatures of 130 degrees centigrade and above. Since class-*H* insulated transformers permit 100-degree centigrade higher operating temperature in air over class-*B*, about 5 per cent reduction in loss is noted. Cold rolled steel is annealed at the factory at about 800-degree centigrade temperature before fabrication with windings. However, after assembly with the windings, strains are introduced in the core steel which cannot be stress relieved by annealing due to temperature limitations of the insulation on coils and associated parts. Therefore, all measures possible are taken at the factory to stress relieve the steel. And lastly as Mr. Jones infers we will continue the search for improvement of materials.

Mr. R. H. Mertz and Mr. E. L. Leinbach inquire about the advantage of proposing 150-degree centigrade temperature rise over 120 degrees centigrade, and what is the ability of transformers to carry overloads. A temperature rise of 150 degrees centigrade assists in cutting down the amount of active material, core steel and copper, which helps defray the added cost of class-*H* insulation. Adequate temperature margin exists at 150-degree centigrade rise for the thermal life of silicone insulation. The ability of class-*H* transformers to carry overloads is substantiated by tests described in Table I of the paper wherein 160 per cent load was withstood successfully for at least 8 hours.

Mr. L. C. Whitman suggests that all design factors be carefully balanced. These factors were carefully evaluated and class-*H* insulation has been found to be superior to other insulations for dry-type transformers. If nitrogen leaks occur, class-*H* transformers can continue to operate. For class-*B* insulation at similar temperatures in air, continued operation is indeed hazardous since insulation life is drastically decreased. To make the varnish impregnating cycle practical a silicone-alkyd varnish was developed. A mixture of 70 per cent silicone resin, 30 per cent alkyd constituted the formulation. This mixture polymerized to good advantage during the cure cycle and it offered good abrasion and craze resistance and high gloss with freedom from voids. The cost of a class-*H* 150-degree centigrade rise sealed-in-nitrogen transformer approximates 20 per cent more than a class-*B* 80-degree centigrade rise ventilated transformer for ratings considered. Class-*H* transformers have superior overload ability over class-*B* due mainly to the higher margin for thermal limits of the insulating material. Particularly, in nitrogen atmosphere, it appears that silicone insulation will withstand 20- to 30-degree higher temperatures over that proposed in the paper for the same aging characteristics in air. In air-sealed, compared with nitrogen-sealed transformers, temperature gradients differ. This effect is also noted in electric equipment operated at high altitudes in air atmosphere. Positive pressure did exist which reduced the thermal gradient for nitrogen-sealed units as described in the paper. In general, tests disclose that the temperature rise is less in nitrogen atmosphere as Mr. Whitman mentions.

Losses at 150-degree centigrade rise compared with 120 degrees will be somewhat higher but regulation at unity power factor, particularly for larger network and station auxiliary transformer ratings, will be affected only slightly since the reactive is greater than the resistive component. Moreover, loading conditions should be considered in designing the transformers. If peak loads occur only occasionally for sealed units the question of losses is not as important. Application data and duty cycles can assist greatly in arriving at optimum designs.

In conclusion, the author welcomes the suggestions and comments and it is hoped that this initial paper on the application of class-*H* insulation to transformers will stimulate further interest.

The Inrush of Magnetizing Current in Single-Phase Transformers

L. A. FINZI
MEMBER AIEE

W. H. MUTSCHLER, JR.
ASSOCIATE AIEE

THE inrush of abnormally high magnetizing current, that may be noted when a transformer is energized, is a familiar switching transient described by Fleming[1] some 60 years ago and treated abundantly in the literature since. In recent years, the use of improved silicon steel at high operating flux densities and also the more exacting requirements of modern fusing and relaying co-ordination have lent renewed interest to this question.[2]

A simplified and well-known treatment of the inrush transient, under the assumption of entirely negligible circuit resistance, shows that the alternating flux linked with the winding energized is displaced from symmetry by an amount that depends on the instant at which the circuit is closed and also on the residual magnetism that may be left in the core from preceding operations. Most severe displacements occur if the circuit is closed when the alternating voltage is going through zero. In such cases, the flux linked with the primary winding reaches values more than double the normal steady-state values, and enormous peaks of magnetizing current result which can be evaluated if the relationship between primary flux linkages and magnetizing current in the region of such unusually high saturation is known for the given transformer. A number of formulas, based on the above treatment with some semiempirical corrections, are available in reference books for the calculation of the first peak of inrush current.[3]

The severity of the disturbances that may be caused to the system by the switching operation considered, however, can hardly be judged on the basis of the first peak of the inrushing current only, and more complete information on the behavior of this current throughout the transient appears often desirable.

Unfortunately, attempts toward a more complete analysis meet a serious difficulty. The damping of the inrush transient is dictated by the resistance of the primary circuit, which therefore can no longer be neglected reasonably in any such studies. If resistive voltage drops are considered, the differential equation expressing Kirchoff's second law for the circuit energized assumes a nonlinear form (in view of the nonlinear relationship between flux linkages and currents in the circuit) and a straightforward integration is generally impossible. Design engineers know this difficulty and obtain semiempirical rules, to be used in connection with co-ordination problems, from actual inrush tests performed on some fairly representative transformers; however, the validity of such information is inherently limited to situations similar to those tested.

The expediency of graphical or "finite difference" methods has been suggested also,[4,5] but such procedures are lengthy and tedious and result only in particular numerical solutions, which do not yield an insight to the influence of changes of design or operating conditions. Analytical approximations also have been tried in the literature[6] under the assumption of zero initial residual flux and treatments in terms of a "broken line" representation of the magnetization curve also have been given[7,8] but, in either case, procedures and results are not simple.

It is the purpose of this paper to derive a comparatively simple formula that expresses the first as well as the subsequent peaks of inrush currents in terms of line voltage and pertinent factors of design with accuracy adequate for studies of this nature.

Method of Analysis

The differential equation of the circuit energized is written:

$$E_m \sin \omega t = Ri + \frac{d\psi}{dt} \tag{1}$$

where

E_m = crest of the applied voltage (volts)
ω = electric angular velocity (radians per second)
t = time from the instant at which the transient is initiated (in seconds)
R = a-c resistance of the circuit at rated frequency (ohms)
i = instantaneous value of the current (amperes)
ψ = corresponding total flux linked with the circuit (weber-turns)

The actual relationship between ψ and i is assumed to be known for the given transformer. (Procedures for its approximate determination from data of design are known and will be reviewed later.) In order to attempt an analytical solution of equation 1, this relationship must be approximated by some suitable analytical expression. The function chosen must meet a number of somewhat contradictory requirements as it must fit the given curve reasonably well, at least in the most interesting region of high saturations, while on the other hand, it must be continuous and simple enough to allow for further integration. An approximation of the type $i = A\psi^2 + B\psi + C$ (where A, B, and C are conveniently chosen constant coefficient) may be suitable, as the substitution of this value of i in equation (1) yields a so-called Riccati equation which, through convenient substitution of variables can be converted further into a general Mathieu equation, for which methods of solution are known.

Paper 51-266, recommended by the AIEE Transformers Committee and approved by the AIEE Technical Program Committee for presentation at the AIEE Summer General Meeting, Toronto, Ont., Canada, June 25–29, 1951. Manuscript submitted March 29, 1951; made available for printing May 9, 1951.

L. A. FINZI is with the Carnegie Institute of Technology, Pittsburgh, Pa., and W. H. MUTSCHLER, JR., is with the Allis-Chalmers Manufacturing Company, Pittsburgh, Pa.

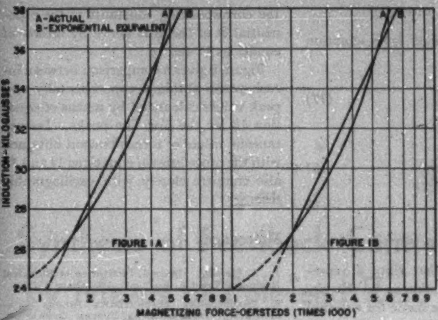

Figure 1(A). Magnetization curve 75-kva 450-volt transformer. (B). Magnetization curve 5-kva 450-volt transformer

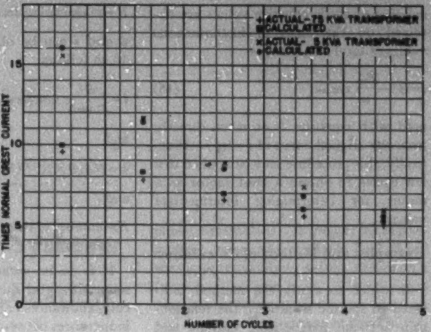

Figure 2. Inrush current crests

Easier analytical manipulations result, however, as shown later, if the given $i=f(\psi)$ relationship is approximated simply by the function

$$i=K_1\epsilon^{K_2\psi} \tag{2}$$

where K_1 and K_2 are constant coefficients and ϵ is the basis of the natural logarithm.

It may be noted at this point that neither the parabolic nor the exponential approximation suggested may be too good to represent a normal magnetization curve for all purposes, and, in fact, both functions are bound to yield more or less erroneous values of i when ψ approaches zero and reverses. However, in this transient ψ reaches abnormally high values in one direction only; and the evaluation of the integral $\int Ridt$, which determines the decay of the successive peaks of flux, is not affected by appreciable errors by a not too accurate approximation of i in those portions of the cycle in which the current happens to be small. As a matter of fact, it may be considered erroneous in principle to start from any $i=f(\psi)$ relationship obtained on the basis of normal magnetization curves, because the core material, with an initial residual, will describe a succession of asymmetrical hysteresis loops of rather unknown nature. However, in view of the above considerations applying to the inrush problem, it appears that only an approximate knowledge of the $i=f(\psi)$ relationship is needed at low values of flux density.

Solution

With the substitution

$$\psi=\psi'+\psi'' \tag{3}$$

where

$$\psi'=-\frac{E_m}{\omega}\cos\omega t \tag{4}$$

equation 1 transforms into

$$0=RK_1\epsilon^{K_2(\psi'+\psi'')}+\frac{d\psi''}{dt} \tag{5}$$

and

$$\frac{\epsilon^{-K_2\psi''}}{K_2}-\frac{\epsilon^{-K_2\psi_0''}}{K_2}=\frac{RK_1}{\omega}\int_0^{\omega t}\epsilon^{K_2\psi'}d\omega t \tag{6}$$

ψ_0'' is the value of ψ'' at the time $t=0$. At this time $\psi=\psi_R$, where ψ_R is the initial flux linkage due to residual magnetization. Therefore, from equations 3 and 4

$$\psi_0''=\frac{E_m}{\omega}+\psi_R \tag{7}$$

and

$$\epsilon^{K_2\psi''}=\frac{1}{\dfrac{RK_1K_2}{\omega}\displaystyle\int_0^{\omega t}\epsilon^{K_2\psi'}d\omega t+\epsilon^{-K_2\left(\frac{E_m}{\omega}+\psi_R\right)}} \tag{8}$$

By substituting in equation 2, the solution for the current is:

$$i=\frac{K_1\epsilon^{-K_2\frac{E_m}{\omega}\cos\omega t}}{\dfrac{RK_1K_2}{\omega}\displaystyle\int_0^{\omega t}\epsilon^{-K_2\frac{E_m}{\omega}\cos\omega t}d\omega t+\epsilon^{-K_2\left(\frac{E_m}{\omega}+\psi_R\right)}} \tag{9}$$

The integral appearing in the denominator can be evaluated by expansion of the exponential and integration of the various terms of the series obtained;[9] and, therefore, i can be calculated more or less laboriously for any instant during the transient. The first, second, third, ...nth peaks of inrush current, however, occur at approximately $\omega t=\pi,3\pi,5\pi\ldots(2n\text{-}1)\pi$ and, for such values of the limit of integration, the expression of i becomes very simple. In fact, using

$$a=\frac{K_2E_m}{\omega} \tag{10}$$

the integral becomes:

$$\int_0^{(2n-1)\pi}\epsilon^{-a\cos\omega t}d\omega t=(2n-1)\times\pi\left[1+\frac{1}{2}\cdot\frac{a^2}{2!}+\frac{1}{2}\cdot\frac{3}{4}\cdot\frac{a^4}{4!}+\frac{1}{2}\cdot\frac{3}{4}\cdot\frac{5}{6}\cdot\frac{a^6}{6!}+\ldots\right] \tag{11}$$

$$=(2n-1)b \tag{12}$$

where b, thus defined, is easily calculated. For usual values of a the series converges very rapidly and it is generally sufficient to consider only the first three terms in equation 11. (In fact b is π times the modified Bessel function of the first kind and of zero order for the parameter a.) Hence, for the current i_n at the nth peak,

$$i_n=\frac{K_1\epsilon^{a}}{(2n-1)\dfrac{2K_1K_2b}{\omega}+\epsilon^{-(K_2\psi_R+a)}} \tag{13}$$

In view of the already mentioned inadequacy of the analytical representation of equation 2 in regions of comparatively low fluxes, the validity of equation 13 decreases as the inrush peaks decay.

It may be pointed out, also, that a further determination of the effective values of the current during any cycle can be obtained approximately in many obvious ways. For example, the value of ψ_n'' at the crests can be obtained,

$$\psi_n''=\frac{1}{K_2}\log\frac{i_n}{K_1}-a \tag{14}$$

and a continuous curve can be drawn for ψ'' at intermediate times to represent approximately its decay. The instantaneous value of current needed for the calculation of cyclic effective values are obtained on the basis of instantaneous values of total flux linkages

$$\psi=\psi''-\frac{E_m}{\omega}\cos\omega t \qquad (15)$$

used with equation 2 or more directly from the original curve of $i=f(\psi)$. Practically, this procedure may be applied to a few cycles to obtain a crest factor as a means for determining intermediate values.

Examples and Method of Calculation

In order to apply the method indicated to specific situations, the relationship between magnetizing current and flux linkages must be known for the given transformer. For low values of flux densities, normal magnetization curves applied to the magnetic circuit of the core can be used with well known procedures to obtain this information. However, a most interesting portion of the $i=f(\psi)$ curve lays in a region for which the core is completely saturated. For this region, as suggested by others,[10] the relationship becomes linear and

$$B=B_{sat}+\frac{A_a+A_c}{A_c}H \qquad (16)$$

where

B = equivalent flux density (gausses)
B_{sat} = saturating flux density (usually between 19,200 and 21,200 gausses)
A_a = space between the exciting winding and the core (square centimeters)
A_c = area of the core
H = magnetizing force (oersteds)

ψ and i can be obtained from equation 16 as follows:

$$i=\frac{Hl}{0.4\pi N}\text{ (amperes)} \qquad (17)$$

and

$$\psi=NA_cB\times10^{-8}\text{ (Webers)} \qquad (18)$$

and

N = number of turns
l = length of the windings (Centimeters)

It is to be noted that since ψ represents the total flux linkages in the circuit, allowances can be made for external inductances between the source of voltage and the transformer. Figure 1 shows examples of portions of B-H curves obtained for two different transformers from equation 16. A fitting exponential function (represented as a straight line in the chosen semilog co-ordinates) is also shown for each case. Of course, some judgment is needed in any instance to find a fit that is close enough to the original curve over a wide enough range. The proper choice, however, is not too critical in terms of the final results. In any case, it is to be remembered that the original curve to be fitted unfortunately is generally assigned with a not too high degree of accuracy so that any search for refinements in the fitting operation would be deemed unwise.

As a further step, the constants K_1 and K_2 of equation 2 are obtained from the corresponding constants of the exponential fit of the B-H curve by means of equations 17 and 18.

Figure 2 gives a comparison between inrush peaks obtained experimentally and peak values calculated by means of equation 13 for the first five peaks. Instantaneous values of inrush current obtained with the procedures of equations 14 and 15 also compare closely with oscillographic tests.

References

1. **A. Fleming.** Journal, Institution of Electrical Engineers (London, England), 1892, page 677.

2. TRANSFORMER MAGNETIZING INRUSH CURRENTS AND INFLUENCE ON SYSTEM OPERATION, **L. F. Blume, G. Camilli, S. B. Fernham, H. A. Peterson.** *AIEE Transactions*, volume 63, 1944, pages 366–75.

3. TRANSMISSION AND DISTRIBUTION REFERENCE BOOK. Westinghouse Electric Corporation, East Pittsburgh, Pa., third edition, 1944, page 415.

4. TRANSIENT CURRENTS IN TRANSFORMERS, **H. M. Turner.** *Journal*, Franklin Institute (Philadelphia, Pa.), volume 211, January 1931.

5. STARTING CURRENTS OF TRANSFORMER, **T. O. Yensen.** *Bulletin 55*, University of Illinois (Urbana, Ill.), 1912.

6. QUALITATIVE THEORY OF SATURATING REACTORS, PART II, **F. Ollendorf.** *Archiv fuer Elektrotechnik* (Berlin, Germany), volume XXII, 1929, page 349.

7. INRUSH CURRENTS AND LIMITING RESISTORS, **W. Rogowski.** *Archiv fuer Elektrotechnik* (Berlin, Germany), volume 1, 1912, page 334.

8. TRANSFORMER MAGNETIZING INRUSH CURRENT, **T. R. Specht.** *AIEE Transactions*, volume 70, part I, 1951, pages 323–28.

9. TABLES OF INTEGRALS, **H. B. Dwight.** The MacMillan Company, New York, N. Y., formulas 550, 440.30, 440.50, 440.70,...1947.

10. TRANSFORMER ENGINEERING, **L. F. Blume, G. Camilli, A. Boyajian, V. M. Montsinger.** John Wiley and Sons, Inc., New York, N. Y., 1938.

No Discussion

Synthesis of Feedback Control Systems by Means of Pole and Zero Location of the Closed Loop Function

M. R. AARON
ASSOCIATE AIEE

Synopsis: In the past, feedback control systems have been designed by methods employing educated guesses, guided conception or dynamic synthesis.[1] Under the restrictive assumption that the fixed part of the system—the summing point, final control element and essential auxiliaries peculiar to the particular system—can be described by a linear differential equation with constant coefficients, a method is suggested herein whereby feedback control systems can be synthesized to prescribed performance requirements by a more direct procedure. A mathematical description of the desired frequency response, based on the location of the poles and zeros of the closed loop function, is made which insures that the specifications of velocity or acceleration error constant, bandwidth, and relative stability will be met and provides for acceptable system transient response. Algebraic manipulation yields the transfer function of main loop and subsidiary feedback loop corrective networks required to meet the specifications.

THE evolution of design techniques for feedback control systems has proceeded from the early gadgeteering methods and empirical relationships to a point where convenient illuminating means are available for a complete analysis of the most complicated system. Application of the mathematical techniques of the Laplace transform, the complex variable, and other powerful tools borrowed from a variety of fields of scientific endeavor have facilitated the study of the differential equations that describe the dynamic performance of feedback control systems. Theorems of network analysis and synthesis have been especially important in their application to problems involved in feedback control.

The most common method[1] for designing a feedback control system deals with means for shaping the locus of the open loop transfer function. A direct mathematical procedure for synthesizing a feedback control system to a desired performance has been investigated by Herr and Gerst[2] and complemented by a different analytical procedure by Travers.[3] In both of the above papers, the authors are concerned with a particular class of open loop functions, and optimum synthesis based on a minimum bandwidth design. More recently, Major Henry M. Clanton[4] has attacked the synthesis problem from the viewpoint of the system transient response to a step function in command. In the present paper, frequency analysis techniques will be employed in the synthesis procedure; however, an attempt has been made to provide a method which integrates with the transient study.

Performance Specifications

In designing a feedback control system for a particular application, it is, of course, essential that the designer have a definite goal in mind. This goal can be expressed in the form of a desired response to an arbitrary input. The most common forms are the transient response to a step function input and the response of the system to a sinusoidal input at various frequencies. In the latter case, the magnitude and phase of the ratio of response, *r*, to command, *c*, is specified as a function of frequency.

A specific transient response may be the ultimate aim of the design and may be verified experimentally with a minimum of instrumentation. However, the mathematical techniques available lend themselves quite readily to system design on a frequency response basis. The empirical correlation between frequency response and transient response mentioned in references 1, 6, and 8, and further emphasized in the main body of this paper, makes it possible to use the convenient analytic tools based on frequency response and still insure acceptable system transient performance. Further considerations of performance specifications and choice of components for feedback control systems are given in the succeeding paragraphs.

The fixed part of the system, defined as the summing point or comparing means, the final control elements and auxiliaries essential to the performance of a particular system, are either chosen or designed on the basis of the specifications. Load inertia, maximum velocity and acceleration of the load, and torque disturbances on the output shaft as well as other considerations peculiar to the type of control and medium for control determine the choice of the final control element. In addition, the practical considerations of size, weight, and space availability, as well as cost, must be included in the proper choice of the physical components that are integrated into the feedback control system.

In order to determine the required gain factors and sensitivities of the various components, the allowable steady state errors under either constant velocity or

---

Paper 51-267, recommended by the AIEE Feedback Control Systems Committee and approved by the AIEE Technical Program Committee for presentation at the AIEE Summer General Meeting, Toronto, Ont., Canada, June 25–29, 1951. Manuscript submitted November 9, 1950; made available for printing May 10, 1951.

M. R. Aaron is with Leeds and Northrup, Philadelphia, Pa.

This work was done under contract *NOrd 10625* sponsored by the United States Bureau of Ordnance, Department of the Navy. The author is indebted to Dr. C. N. Weygandt, Jr., associate professor of electrical engineering, Moore School of Electrical Engineering, University of Pennsylvania, Philadelphia, Pa., for his suggestions and advice during the course of development of the method presented herein. This paper is part of a masters thesis submitted to the faculty of the Moore School of Electrical Engineering, in partial fulfillment of the requirements for the degree of Master of Science in Electrical Engineering.

onstant acceleration input must be consulted. In roll stabilization problems, these gain factors may be determined by the maximum allowable errors at the dominant roll frequency.

System bandwidth must be limited for the following reasons:

1. Mechanical resonance of the dynamic elements in the indirectly controlled system external to the control loop must be avoided.

2. System noise must be attenuated to prevent saturation and overloading of the system components.

3. It is desirable to limit the bandwidth in order to minimize the frequency response required by the physical elements of the system.[8] For this application, the bandwidth or pass band of the system will be defined as that band of frequencies between 0 and ω_c. ω_c is the cut-off frequency of the system, the highest frequency at which $|r(j\omega)/c(j\omega)|$ is unity.

It is, of course, mandatory that the system operate with sufficient stability margin so that severe oscillations do not occur when inevitable changes in system parameters take place. It has become common practice to use the peak value of $|r(j\omega)/c(j\omega)|$ as a measure of relative stability since this magnification (M_p) determines the proximity with which the open loop locus approaches the Nyquist point, -1, $j0$ in the complex plane. Therefore, in this paper M_p will be used as a measure of the degree of system stability.

It will be shown that a mathematical description of the closed loop function can be made that will include the specification of system bandwidth, velocity or acceleration error constant, and relative stability. In addition, by the introduction of dominant or principal poles of the closed loop function, one can insure good system transient response.

In this paper, the continuous control of a linear, lumped-constant parameter feedback control system will be considered. The transfer function relating the response of such a system to its input is a proper rational algebraic fraction[7] given by the ratio of two polynomials in the Laplace transform variable, s. This transfer function will be written in factored form, thereby permitting a rapid transformation from the domain of the complex variable into the time domain by means of partial fraction expansion and the inverse Laplace transform. Therefore, the system transient response may be obtained in closed form. In order to determine transient response using the synthesis techniques commonly employed roots of high degree polynomials must be found before the transformation to the time domain can be made or tedious numerical approximations are used which do not yield the mathematical form of the response. Figures 1, 2, and 3 define some of the terminology used in this section and the succeeding sections of the paper.

The response of the system to external disturbances such as noise and load torque disturbance will not be considered.

Description of the Closed Loop Function

It has been stated in the previous section that the closed loop function relating the response, r, of the feedback control system of Figure 1 to its input, c, can be expressed as the ratio of two polynomials. Initially, for purposes of generality, it will be assumed that this system function contains p real poles, g pairs of complex conjugate poles, u real zeros, and v pairs of complex conjugate zeros, and that $p+2g>u+2v$. Furthermore, since discussion will be limited to stable systems, all of the poles will be found in the left half of the complex plane (LHP) and poles on the real frequency ($j\omega$) axis as well as zeros at the origin will not occur. The system function described above and its relation to the open loop transfer function, KG, is given in equation 1.

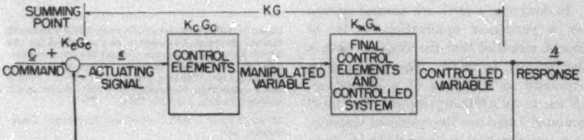

Figure 1. Block diagram of feedback control system

$$\frac{r}{c}=\frac{KG}{1+KG}=\frac{N(s)}{D(s)}$$

$$=\frac{\prod_{i=1}^{u}(sX_i+1)\prod_{i=1}^{v}\left(\frac{s^2}{\gamma_i^2}+\frac{2\alpha_i}{\gamma_i}s+1\right)}{\prod_{i=1}^{p}(sR_i+1)\prod_{i=1}^{g}\left(\frac{s^2}{\beta_i^2}+\frac{2\zeta_i}{\beta_i}s+1\right)} \quad (1)$$

where $r=r(s)$.

The X_i are the negative reciprocals of the real zeros of equation 1 and the R_i are the negative reciprocals of the real poles. α_i and ζ_i are the nondimensional damping factors of the quadratics, while γ_i and β_i are the undamped natural frequencies of the quadratics.

In order to establish a starting point for the synthesis procedure, it is obviously necessary to determine the minimum number of poles and zeros required to describe the closed loop function for a given application. The following theorem serves this purpose:

Theorem 1. The difference between the number of poles and the number of zeros of the closed loop function is greater than or equal to the difference between the number of poles, n, and the number of zeros, m, of the fixed part of the system.

This can be stated mathematically by the following inequality

$$p+2g-u-2v \geqslant n-m \quad (2)$$

The proof of equation 2 follows directly from the fact that the high-frequency asymptote of the closed loop function must be identical to the high frequency asymptote of the open loop function.

In the appendix, it is shown that the velocity or acceleration error constant can be expressed in terms of the poles and zeros of equation 1. This important result is placed in the appendix so that the resulting imposing equations do not tend to distract the reader from the practical usefulness of the synthesis procedure. Furthermore, these equations reduce to simple forms when applied to a specific problem. This fact will be further illustrated in the succeeding paragraphs.

In order to more fully explain how the location of the system poles and zeros depend on the specifications, some generality will be sacrificed for clarity. For most applications of feedback control systems, the generalized equations 1 and 2 can be reduced to

$$\frac{r}{c}=\frac{KG}{1+KG}$$

$$=\frac{\prod_{i=1}^{u}(sX_i+1)}{\prod_{i=1}^{p}(sR_i+1)\left[\frac{s^2}{\beta^2}+\frac{2\zeta}{\beta}s+1\right]}=\frac{N(s)}{D(s)} \quad (3)$$

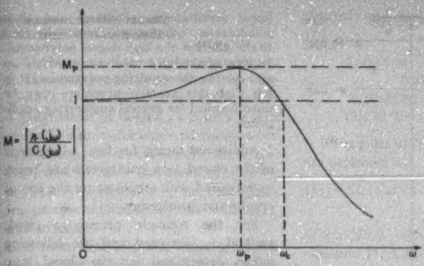

Figure 2. Typical amplitude versus frequency curve

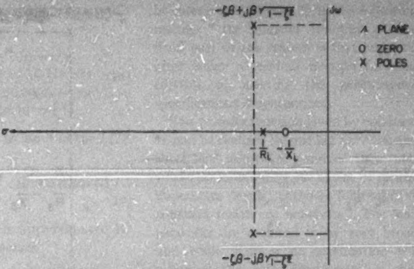
$-\zeta\beta+j\beta\sqrt{1-\zeta^2}$
$j\omega$
A PLANE
O ZERO
X POLES
σ
$-\frac{1}{R_1}$
$-\frac{1}{X_1}$
$-\zeta\beta-j\beta\sqrt{1-\zeta^2}$

Figure 3. Location of poles and zeros of system function 3

and

$$p+2-u \geqq n-m \tag{4}$$

The location of the poles and zeros of equation 3 in the s plane are shown in Figure 3.

The use of equation 3 rather than equation 1 can be justified for clarification of the procedure as well as for the following reasons. For values of $\alpha_i > 0.6$, or for values of γ_i well outside the pass band, the complex conjugate zeros of equation 1 can be adequately represented over the frequency range of interest by two real zeros. The introduction of only one pair of complex conjugate poles is of basic importance. These complex conjugate poles are the dominant poles[5] and insure that the general form of the transient response will be acceptable for most applications.

It is stated in reference 1, page 109, "Any system for which M_p does not exceed about 1.4 probably will have transient performance acceptable for most applications". This contention has been verified for some simple feedback control systems in a masters thesis[3] written at the University of Pennsylvania. Furthermore, this correlation is excellent for more complicated "well behaved systems".[4] The magnitude curve of a well-behaved system is shown in Figure 2, and it is further assumed that a well-behaved system will have a closed loop function that contains one pair of dominant complex conjugate poles in addition to its real poles and zeros.

System bandwidth and transient response are governed by the complex conjugate poles of equation 3. These are the dominant or principal poles. The remaining real poles are placed well out in the left half of the s plane (*LHP*) or adjacent to a zero so that they may give negligible contribution to either system bandwidth or general form of the transient response. The location of the secondary poles is determined from the specification of steady state error under constant velocity or constant acceleration input, or from the specification of allowable errors at the dominant roll frequencies. In addition, for cases when ζ is required to be >0.707, the adjacent poles and zeros determine the value of relative stability and to some extent system bandwidth.

As an example of the use of this method, consider the feedback control system of Figure 1. The transfer function for the final control element and controlled system K_mG_m is given by:

$$K_mG_m=\frac{K_m}{s(sT_1+1)(sT_2+1)(sT_3+1)} \tag{5}$$

This transfer function is typical of that obtained in the following physical systems:

1. A rotating magnetic amplifier (amplidyne) providing armature current for a separately excited d.c. motor driving a load consisting of inertia (J) and viscous friction (f). Shaft elastance and tooth deflection in the gearing is negligible. In this system, the magnitude of the electromagnetic time constant of the amplidyne direct axis and motor armature circuit is very much smaller than the mechanical time constant (J/f).[6]
2. A d-c generator providing armature current for a separately excited d-c motor under the same load conditions as above. However, in this system, the electromagnetic time constant must be considered in order that K_mG_m be its transfer function.

In both of the systems mentioned above it is assumed that the summing point can be represented by a gain or sensitivity factor K_s. The essential control elements in K_cG_c (preamplifier, phase sensitive detector, driving stage, and so forth) do not introduce appreciable lag in the range of control frequencies of interest.

Many other physical systems can be represented by an equivalent number of poles and zeros. One such nonelectrical final control configuration with an equivalent number of poles and zeros would consist of an axial piston hydraulic transmission whose stroke control transfer function can be represented by a simple time constant.

It is further assumed for the system of Figure 1, that the following rather difficult performance requirements determined from the specifications must be met:

Velocity error constant, $K_v=2{,}000$ sec.$^{-1}$
Bandwidth $f_c=10$ cycles per second or less.
$M_p=1.3$ or less at a frequency greater than 3.5 cycles per second.
The transient response shall have essentially one small overshoot (well-damped response).

The physical time constants of the fixed part of the system are as follows:

$T_1=0.01$ second, $T_2=0.11$ second, $T_3=0.034$ second.

From Theorem 1, the simplest form for equation 3 is

$$\frac{N(s)}{D(s)}=\frac{1}{(sR_1+1)(sR_2+1)\left[\frac{s^2}{\beta^2}+\frac{2\zeta}{\beta}s+1\right]} \tag{6}$$

From equation 32 in the appendix, the velocity error constant is

$$K_v=\frac{1}{R_1+R_2+\frac{2\zeta}{\beta}}=2{,}000 \tag{7}$$

$$\frac{1}{K_v}=5\times 10^{-4}=R_1+R_2+\frac{2\zeta}{\beta} \tag{7A}$$

R_1 and R_2 can be made small consistent with equation 7(A), but any attempt to make $2\zeta/\beta<5\times10^{-4}$ will produce a system with poor relative stability (small ζ) and/or a system with an extremely large bandwidth. Therefore, equation 6 must be modified in order to realize the desired value for the velocity error constant, and still meet the remaining performance specifications.

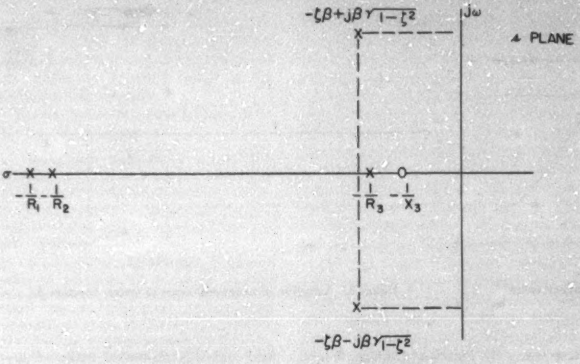

Figure 4. Location of poles and zeros of system defined by equation 10

The next simplest function for equation 3 is:

$$\frac{N(s)}{D(s)}=\frac{(sX_3+1)}{(sR_1+1)(sR_2+1)(sR_3+1)\left[\frac{s^2}{\beta^2}+\frac{2\zeta}{\beta}s+1\right]} \quad (8)$$

For this function,

$$\frac{1}{K_v}=5\times10^{-4}=R_1+R_2+R_3+\frac{2\zeta}{\beta}-X_3 \quad (9)$$

If the sum of the negative reciprocals of the real poles well out in the *LHP* is set equal to the reciprocal of the velocity error constant, then

$$R_1+R_2=\frac{1}{K_v},\ R_3+\frac{2\zeta}{\beta}-X_3=0 \quad (9A)$$

A value of $\zeta>0.707$ will be chosen in order that we have low overshoot for the system transient response and low peak for the system frequency response. With a particular value of ζ, β is determined from the value of desired bandwidth from frequency response curves of the dominant quadratic function

$$\left[1-\frac{\omega^2}{\beta^2}+j2\frac{\zeta\omega}{\beta}\right]^{-1}$$

The amplitude and phase characteristics of this function are plotted against ω/β for various values of ζ in reference 6, pages 144 and 176. Since $\zeta>0.707$, this quadratic factor will not have a peak in its frequency response curve, therefore the bandwidth will be defined as that frequency for which the quadratic is down between 1 to 3 decibels. This new definition is required because X_3 will always be greater than R_3 by an amount $2\zeta/\beta$, see equation 9(A), thereby raising the ratio $|r(j\omega)/c(j\omega)|$ by an amount,

$$\sqrt{\frac{1+\omega^2X_3^2}{1+\omega^2R_3^2}}$$

Values of $\zeta=0.8$ and $\beta=80$ were chosen in order to meet the specifications of bandwidth, relative stability, and form of transient response. If X_3 and R_3 are placed adjacent to each other and as close to the origin in the *LHP* as is consistent with equation 9(A), then the desired peak ratio (M_p) can be realized with negligible increase in bandwidth. The final adjustment of the adjacent poles and zeros as well as the adjustment of ζ and β can be accomplished by several methods, three of which are mentioned in the following:

1. Plot $|N(jw)/D(jw)|$ on a Bode diagram using the values of the poles and zeros determined from the equation K_v. Adjust the adjacent poles and zeros, and the complex conjugate poles if necessary, until the other performance requirements are met. This can be done rapidly by the method of plotting asymptotes.

2. If the poles and zeros of the closed loop function are plotted in the s plane, the closed loop frequency response can be checked rapidly by graphical means. The use of the "Spirule"[10] or transparency equivalent to it will facilitate this procedure.

3. An analytic method that eliminates graphical work can be employed by writing the equation for $|N(j\omega)/D(j\omega)|$. Choose the frequency (ω_p) at which M_p occurs and substitute this frequency and M_p into the magnitude equation. Since $M=1$ at $\omega=\omega_c$, another equation results that further restricts the closed loop parameters. With the aid of the equation for the over-all system velocity error constant, and the equations that result from the above, three closed loop parameters can be determined by the simultaneous solution of these three equations. In addition, when other specifications must be satisfied, additional equations based on the amplitude or phase characteristics of the closed loop function can be derived. The final set of equations are not linear simultaneous equations and their simultaneous solution will eventually lead to the solution of a high degree polynomial. In view of the labor involved in setting up and solving the resulting polynomial, it is felt that this analytic procedure may be uneconomical for general engineering application.

Additional means for final adjustment of the closed loop parameters are being investigated with emphasis on the use of graphs and nomograms.

For the example previously cited, method 1, was used and the following values determined for the closed loop parameters,

$\zeta=0.8$ $\quad R_1=2\times10^{-4}$ seconds

$\beta=80\dfrac{\text{rad.}}{\text{second}}$ $\quad R_2=3\times10^{-4}$ seconds

$X_3=0.08$ second $R_3=0.06$ second

When these values are substituted in equation 8, then

$$\frac{N(s)}{D(s)}=\frac{(0.08s+1)}{(3\times10^{-4}s+1)(2\times10^{-4}s+1)\times(0.06s+1)\left[\frac{s^2}{6{,}400}+0.02s+1\right]} \quad (10)$$

The poles and zeros of this function are plotted in Figure 4. The system transient response to a unit step function input is readily approximated by

$$r(t)\approx1+0.47\epsilon^{-16.67t}+2.32\epsilon^{-64t}\sin(48t-140.7°) \quad (11)$$

The poles well out in the *LHP* have been neglected in the transformation from the s domain to the time domain. These poles do not appreciably affect the transient response except in the immediate neighborhood of $t=0$. The closed loop frequency response curve and the transient response of a system described by equation 10 are plotted in Figures 5 and 6 respectively. Both of these curves indicate that the performance specifications will be met if the proper compensating networks are employed. The derivation of the transfer function of the required compensating network is the subject of the remaining sections of this paper.

Determination of Required Compensating Networks

Under the restrictive assumption of linearity and no coercive forces between components, the open loop transfer function of the single loop feedback control system of Figure 1 is the product of the transfer function of its components. If the transfer function of the fixed part of the system is denoted by $K_cK_mG_m$ and that of the compensating network by K_cG_c, then from equation 3

$$K_cG_c = \frac{N(s)}{[D(s)-N(s)]K_eK_mG_m} \qquad (12)$$

At this point of the synthesis procedure, it becomes necessary to determine the roots of $[D(s)-N(s)]$, which is in general a polynomial of degree $_\nu+2$ with b zero roots. b is unity for a zero positional error system, two for a zero velocity error system, and so on. The roots of $[D(s)-N(s)]$ may be obtained by the root squaring process of Graeffe,[7] synthetic division, and so forth.

A more desirable and rapid graphical method can be employed if the equation $[D(s)-N(s)]=0$ is written in the following form:

$$\frac{D(s)}{N(s)}-1=0 \qquad (13)$$

If $D(s)/N(s)$ is plotted against the real variable a, the real poles of equation 11 will be obtained when $D(a)/N(a)$ crosses the unity line. In addition, the "Root Locus" method[11] is directly applicable to the determination of the roots of equation 12.

In a great many cases, it will be possible to reduce the degree of $[D(s)-N(s)]$ by neglecting the poles of the closed loop function well out in the *LHP*.

After an expression in the form of the ratio of two factored polynomials is obtained for K_cG_c, a physically realizable network or networks must be derived to give the required transfer function. In simple cases, it is possible to determine the physical network by inspection of the transfer function. The recognition of simple forms is an important part of the procedure.

In recent years, the emphasis in the field of network synthesis has been on the physical realization of transfer functions encountered in the design of resistance capacitances corrective networks for feedback control systems.[11-13] The elegant, though mathematically involved, methods of network synthesis are becoming increasingly important in the design of feedback control systems and should ultimately become an integral part of the procedure discussed in this paper.

For the example previously cited,

$$[D(s)-N(s)]=5.6\times10^{-13}s[s^4+8.48\times 10^3s^3+1.79\times10^7s^2+2.48\times 10^9s+8.89\times10^8] \qquad (14)$$

and after factoring by synthetic division

$$[D(s)-N(s)]=5\times10^{-4}s[(2.78s+1)(6.72\times10^{-3}s+1)(3\times10^{-4}s+1)(2\times10^{-4}s+1) \qquad (15)$$

If the transfer function of the fixed part of the system, equation 5, is substituted into equation 12, along with 14

$$K_cG_c=\frac{2{,}000(0.08s+1)(0.01s+1)\times(0.034s+1)(0.11s+1)}{K_eK_m(2.78s+1)(0.0067s+1)\times(3\times10^{-4}s+1)(2\times10^{-4}s+1)} \qquad (16)$$

If the poles of $D(s)$ well out in the *LHP* are neglected

$$D(s)-N(s)=s^2\times1.356\times10^{-3}(0.0069s+1) \qquad (17)$$

When $[D(s)-N(s)]$ is approximated by equation 17, K_cG_c becomes

$$K_cG_c\approx\frac{740(0.08s+1)(0.01s+1)\times(0.034s+1)(0.11s+1)}{K_eK_ms(0.0069s+1)} \qquad (18)$$

Both equations 18 and 16 are equivalent over the range of control frequencies of interest, with the exception of the immediate vicinity of zero frequency. If the compensating network defined by equation 18 can be physically realized, the system will become conditionally stable, but will have zero steady state error for constant velocity inputs. The physical realization of a pure integration is difficult to achieve in practice. Therefore, if the factor 740 in the numerator of equation 18 is increased to 2,000, and the pure integration changed to $(s2{,}000/740+1)$ the following transfer function results

$$K_cG_c=\frac{2{,}000(0.08s+1)(0.01s+1)\times(0.034s+1)(0.11s+1)}{K_eK_m(2.7s+1)(0.0069s+1)} \qquad (19)$$

Again, over the frequency range of interest, equations 19, 18, and 16 are all equivalent, and must be physically realized as closely as possible to insure that the feedback control system meet the foregoing performance specifications. The resulting transfer function for K_cG_c may be interpreted physically in the following manner: the transfer function of the fixed part of the system is first removed after which a residual transfer function capable of meeting the performance specifications is synthesized.

The transfer function given by equation 16 can be realized by one lag network and three lead networks[1] provided these networks are isolated by the choice of proper impedance levels, cathode followers, or constant resistance networks. The lead networks are required to be very broad and while little or no attenuation will occur at the noise frequencies, a considerable amount of attenuation will occur at the control frequencies. In order to retain the same system velocity error constant when the common passive lead networks are employed, considerable amplification is required to make up for the high direct current attenuation of these networks. The combination of this additional gain and the fact that lead networks accentuate the noise or spurious signals with steep wave front, will cause saturation of the electronic amplifiers and rapid deterioration of system performance.

Active networks which take many different physical forms can be employed to realize the transfer function of equation 16. Further exhaustive treatment of the variety of forms taken by compensating networks is beyond the scope of this paper.

In the next section a method is suggested whereby all or a portion of the compensating function can be performed in subsidiary feedback loops. In addition to reducing the complexity of K_cG_c, this method will permit one to use only passive resistance capacitance networks for main loop compensation.

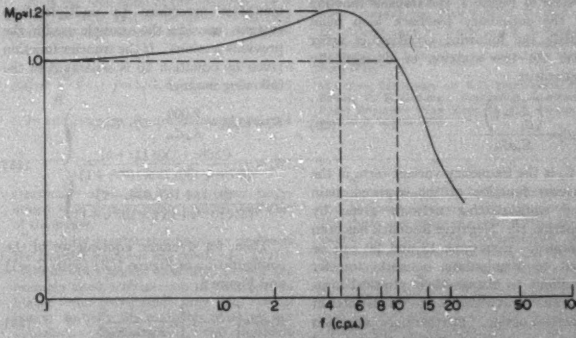

Figure 5. Frequency response for system defined by equation 10

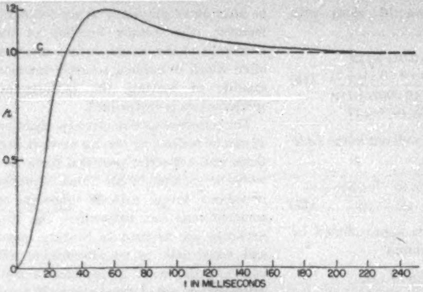

Figure 6 (above). Response of system defined by equation 10 to unit step in command

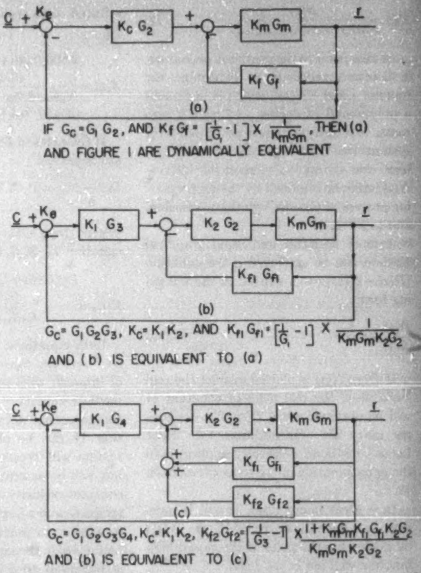
C
+
Ke
−
Kc G2
+
−
Km Gm
r
Kf Gf
(a)
IF Gc = G1 G2, AND Kf Gf = [1/G1 − 1] X 1/KmGm, THEN (a)
AND FIGURE 1 ARE DYNAMICALLY EQUIVALENT
C
+
Ke
−
K1 G3
+
−
K2 G2
KmGm
r
Kf1 Gf1
(b)
Gc = G1 G2 G3, Kc = K1 K2, AND Kf1 Gf1 = [1/G1 − 1] X 1/KmGmK2G2
AND (b) IS EQUIVALENT TO (a)
C
+
Ke
−
K1 G4
+
−
K2 G2
Km Gm
r
+
+
Kf1 Gf1
Kf2 Gf2
(c)
Gc = G1 G2 G3 G4, Kc = K1 K2, Kf2 Gf2 = [1/G3 − 1] X 1 + KmGmKf1Gf1K2G2 / KmGmK2G2
AND (b) IS EQUIVALENT TO (c)

Multiple Loop Systems

Subsidiary or internal feedback loops have long been recognized as a useful means for compensating feedback control system.[9] This type of feedback reduces the number and complexity of main loop compensating networks required, and, in addition, owes its usefulness to the following:

1. Adequate power is available at the output end of the system to drive low impedance networks in the subsidiary feedback path.
2. Feedback controllers with internal feedback are generally less sensitive to inevitable changes in system parameters and extraneous torques applied to the output end of the system.
3. Linearity of the system is generally improved.

If the open loop transfer function of a feedback control system with a subsidiary feedback loop about the fixed part of the system and no main loop compensation, is compared with that of the single loop system of Figure 1, the transfer function of the subsidiary feedback loop must satisfy the following equation in order that the two systems be dynamically equivalent

$$K_fG_f=\frac{\left(\frac{1}{G_c}-1\right)}{K_mG_m} \qquad (20)$$

G_c is the frequency variant term in the transfer function of the required main loop compensating network given by equation 12. Negative feedback has been assumed. Equations 12 and 20 can be used to manipulate network transfer functions to change their physical location and form according to the dictates of practical design. Furthermore, equation 20 can be modified so that the internal feedback loop also encloses a portion of the main loop compensating network. See Figure 7 for several possible configurations for achieving the same system dynamic performance with vastly different corrective networks. The number of different configurations is limited only by the number of factors of K_cG_c.

Figure 7 (right). Block diagram of dynamically equivalent systems

The manipulated variables (current, voltage, flow, and pressure) of the fixed part of the system and their relation to the controlled variable should be well known so that the required feedback function be performed most practically.

As an example of the extension of the synthesis procedure to multiple loop systems, consider the example used in the previous sections. If the transfer function given by equation 16 is separated in the following manner

$$\left.\begin{aligned}
&K_c=K_1K_2=\frac{2{,}000}{K_eK_m};\ G_c=G_1G_2\\
&G_1=\frac{(0.08s+1)(0.11s+1)}{(2.78s+1)(6.72\times10^{-3}s+1)}\\
&G_2=\frac{(0.01s+1)(0.034s+1)}{(3\times10^{-4}s+1)(2\times10^{-4}s+1)}
\end{aligned}\right\} \qquad (21)$$

Then, for dynamic equivalence of the configuration of Figure 7(B) (with $G_3=1$) and Figure 1,

$$K_fG_f=\left[\frac{1}{G_1}-1\right]\times\frac{1}{K_mG_mK_2G_2} \qquad (22)$$

For the values cited above

$$K_fG_f=\frac{2.6s^2(3.8\times10^{-4}s+1)}{K_2K_m(0.08s+1)} \qquad (23)$$

This feedback function can be realized by negative feedback of the first two time derivatives of the controlled variable through a high pass or derivative network. For the physical systems previously mentioned, this function can be realized by using a bridge circuit fed from the common armature circuits of the final control elements.[6]

The G_2 transfer function can be approximated by a simple active resistance-inductance-capacitance network, a symmetrical lattice made up of only resistance-capacitance components,[13] or by several other networks. The system gain factors governed by equations 21 and 23 can be adjusted consistent with practical requirements.

Conclusion

It has been shown that the synthesis of feedback control systems to prescribed performance requirements is a straightforward procedure which can be summarized in the following manner.

1. Choose the fixed part of the system from the specifications and other considerations.

2. Set up the poles and zeros of the closed loop function in accordance with

the specifications. The pair of complex conjugate poles are the dominant poles and are chosen on the basis of bandwidth and relative stability for the desired frequency response and sufficient damping in the case of transient response. The secondary poles and zeros are then adjusted to give the desired velocity or acceleration error constant with negligible increase in bandwidth.

3. After the system function is obtained, algebraic or graphical manipulation yields the transfer function, equation 12, of the required main loop compensating network. An additional expression, equation 20, can be employed to determine the transfer function of a subsidiary feedback loop equivalent to all or a portion of the main loop compensating network.

Appendix

Velocity and Acceleration Error Constants in Terms of the Poles and Zeros of the Closed Loop Function

From equation 1, the open loop transfer function of the feedback control system of Figure 1 is:

$$KG=\frac{N(s)}{D(s)-N(s)} \tag{24}$$

If equation 24 is the open loop transfer function of a system that contains only one net integration (a zero positional error system), the velocity error constant is defined as follows:

$$K_v\equiv\lim_{s\to 0} sKG(s)=\lim_{s\to 0}\frac{sN(s)}{D(s)-N(s)} \tag{25}$$

From the form of equation 1, it is readily shown that the velocity error constant is given by the reciprocal of the coefficient of s in $[D(s)-N(s)]$, and

$$K_v=\frac{1}{\sum_{i=1}^{p}R_i+\sum_{i=1}^{q}\frac{2\zeta_i}{\beta_i}-\sum_{i=1}^{u}X_i-\sum_{i=1}^{v}\frac{2\alpha_i}{\gamma_i}} \tag{26}$$

Similarly, for a system with two net integrations in the open loop transfer function, (a zero velocity error system, $K_v=\infty$) the acceleration error constant K_a, defined in equation 27 below, is given by the reciprocal of the coefficient of s^2 in $[D(s)-N(s)]$

$$K_a\equiv\lim_{s\to 0} s^2KG(s)=\lim_{s\to 0}\frac{s^2N(s)}{D(s)-N(s)} \tag{27}$$

and

$$K_a=\frac{1}{\sum_{i=1}^{q}\frac{1}{\beta_i^2}+\sum_{i=1}^{q}\frac{2\zeta_i}{\beta_i}\left(\sum_{i=1}^{p}R_i\right)+\sum_{i=1}^{p}R_i\left(\sum_{i=1}^{p}R_{i+1}\right)-\sum_{i=1}^{v}\frac{1}{\gamma_i^2}-\sum_{i=1}^{v}\frac{2\alpha_i}{\gamma_i}\times\left(\sum_{i=1}^{u}X_i\right)-\sum_{i=1}^{u}X_i\left(\sum_{i=1}^{u}X_{i+1}\right)} \tag{28}$$

In order that the result of the limit process defined in equation 27 be >0,

$$K_v=\infty\text{, or }\sum_{i=1}^{p}R_i+\sum_{i=1}^{q}\frac{2\zeta_i}{\beta_i}-\sum_{i=1}^{u}X_i-\sum_{i=1}^{v}\frac{2\alpha_i}{\gamma_i}=0 \tag{29}$$

This procedure can be extended to include systems with zero steady state error under constant acceleration, constant rate of change of acceleration inputs and so on. For this purpose, it is convenient to rewrite equation 24 in the following form:

$$KG=\frac{N(s)}{\sum_{j=1}^{n}K_js^j} \tag{30}$$

K_j is the reciprocal of the coefficient of s^j in $[D(s)-N(s)]$ and is the constant relating the steady state error to inputs of the following form:

$$c(t)=\frac{|C_j|}{j!}t^j \qquad j=1, 2, 3, \ldots n \tag{31}$$

In addition, the K_j are intimately related to the error coefficients discussed in reference 6.

If equation 3 is used to define the system transfer function, the previously developed error constants are considerably simplified and can be obtained from those previously developed by letting $g=1$ and $\gamma_i=\infty$ and by defining $\zeta=\zeta_1$ and $\beta=\beta_1$.

For example, under the above conditions, equation 26 becomes

$$K_v=\frac{1}{\sum_{i=1}^{p}R_i-\sum_{i=1}^{u}X_i+\frac{2\zeta}{\beta}} \tag{32}$$

References

1. Principles of Servomechanisms (book), G. S. Brown, D. P. Campbell. John Wiley and Sons, Inc., New York, N. Y., 1945.

2. The Analysis and an Optimum Synthesis of Linear Servomechanisms, D. Herr, I. Gerst. *AIEE Transactions*, volume 66, 1947, pages 959–70.

3. A Note on the Design of Conditionally Stable Feedback Systems, P. Travers. *AIEE Transactions*, volume 70, part I, 1951, pages 626–30.

4. Synthesis of Servomechanisms Based Upon Characteristics of the Time Response, Major Henry M. Clanton. *Doctoral Dissertation*, University of Pennsylvania (Philadelphia, Pa.).

5. The Effect of Pole and Zero Locations on the Transient Response of Linear Dynamic Systems, J. H. Mulligan, Jr. *Proceedings*, Institute of Radio Engineers (New York, N. Y.), May 1949, pages 516–29.

6. Theory of Servomechanisms (book), H. M. James, N. B. Nichols, R. S. Phillips. McGraw-Hill Book Company, New York, N. Y., 1947.

7. Transients in Linear Systems (book), M. F. Gardner, J. L. Barnes. John Wiley and Sons, Inc., New York, N. Y., volume 1, 1945.

8. Correlation of M_p Criterion with Transient Response for a Simple Servomechanism, J. F. Polifka, J. F. Johnson. *Masters Thesis*, Moore School of Electrical Engineering, University of Pennsylvania (Philadelphia, Pa.).

9. Theory of Servo Systems with Particular Reference to Stabilization, A. L. Whiteley. *Journal*, Institution of Electrical Engineers (London, England), volume 93, part II, August 1946, pages 353–67.

10. Control System Synthesis by Root Locus Method, W. R. Evans. *AIEE Transactions*, volume 69, part I, [illegible]50, pages 66–69.

11. Network Analysis and Feedback Amplifier Design (book), H. W. Bode. D. Van Nostrand Company, Inc., New York, N. Y., 1945.

12. Synthesis of RC Networks, E. A. Guillemin. *Journal of Mathematics and Physics*, Massachusetts Institute of Technology (Cambridge, Mass.), April 1949.

13. The Synthesis of R-C Networks, J. L. Bower, P. F. Ordung. *Proceedings*, Institute of Radio Engineers (New York, N. Y.), volume 38, number 3, March 1950.

Discussion

David V. Stallard (Westinghouse Electric Corporation, Pittsburgh, Pa.): Mr. Aaron's paper is commendable for its lucidity and direct method of determining a closed-loop transfer function which meets the initial specifications of velocity constant, transient overshoot, bandwidth and M_p.[1] However, a certain alternative method of finding the transfer function K_cG_c for the "control elements," after the r/c has been determined, may be more easily utilized than that of the paper.

It is quite possible that for many problems the transfer function will result in a $D(s)-N(s)$ of order higher than five, that of the example cited. Extraction of the roots of higher order polynomials may take several hours; initially the negligible roots are not apparent. Furthermore, the function K_mG_m for the "final control elements and controlled system" is often somewhat uncertain, especially for 2-phase servomotors and hydraulic systems with entrained air. For these and other reasons, it may be desirable to reduce the mathematical labor prior to designing and building the system.

An alternative method of synthesizing K_cG_c from r/c is proposed, in which the $r/c=N(j\omega)/D(j\omega)$ at various frequencies ω may be sketched as a curve on a standard chart[8] having co-ordinates $|KG|_{db}$ and $\underline{/KG}$, and loci of $|r/c|_{db}$ and $\underline{/r/c}$. From this chart a graph of the open-loop $N(j\omega)/$-

$D(j\omega)-N(j\omega)=|KG|_{db}=|K_cG_cK_eK_mG_m|_{db}$ versus log frequency is readily prepared and correspondingly a graph of $|K_cG_c|_{db}$ by subtracting $|K_eK_mG_m|_{db}$. In most cases this latter sketch can be approximated by straight-line asymptotes whose slopes are multiples of ±6. db/octave. Each intersection of asymptotes determines a "break frequency" ω_b and consequently a factor of K_cG_c, for example, $(1+s/\omega_b)$. Suitable approximations at low and high frequencies are then possible, and "recognition of simple forms" permits the selection of proper networks.

After the servomechanism is first built in theoretical accordance with this specified KG, its velocity constant and closed-loop frequency response may be tested. If unsatisfactory, the actual r/c can be sketched on the KG chart mentioned above and actual $|KG|_{db}$ versus log frequency may thus be determined. Comparison of the actual $|KG|_{db}$ with the specified $|KG|_{db}$ graph will probably suggest helpful alterations in the gain and/or "break frequencies" of the system.

REFERENCES

1. PRINCIPLES OF SERVOMECHANISMS (book), G. S. Brown, D. P. Campbell. John Wiley and Sons, New York, N. Y., 1948, page 109.

2. Ibid., page 252.

M. R. Aaron: The graphical procedure described by Mr. Stallard for determining the required main loop compensating networks after the desired performance has been specified in terms of r/c is a worthwhile addition to the paper. This alternate method, though somewhat modified in minor detail, was the first investigated by the present author for determining K_cG_c. Lack of space prevented the inclusion of the above technique, as well as other details, in the main body of the paper.

Stability of Varying-Element Servomechanisms with Polynomial Coefficients

M. J. KIRBY
MEMBER AIEE

R. M. GIULIANELLI
NONMEMBER AIEE

TIME-varying elements in servomechanisms are found in practice, for example, in systems which must operate during their warm-up periods, when the gain or the damping, or both, are changing materially. More frequently encountered, however, are cases in which a system element varies with velocity or some other dependent variable, but the program of the process is known so that the variation can be adequately represented as a function of time. An example is a speed control for a reel on which strip steel is being rolled or unrolled. The inertia changes with the amount of steel on the reel, but if either the shaft speed of the reel or the linear speed of the strip is known, the inertia can be expressed as a function of time.

When a servomechanism must be analyzed as a varying-element system, it is always desirable to represent all variations by straight lines if possible. However, the rates of variation of some elements may change radically, or the product of the values of two elements may introduce higher powers of time into the coefficients of the system equation.

This paper presents a criterion for determining the eventual stability of a servomechanism in such a case, when its elements vary as higher powers of time so that the differential equation relating output θ_o, to input θ_i, and time, t, is of the form:

$$f_n(t)\frac{d^n\theta_o}{dt^n}+f_{n-1}(t)\frac{d^{n-1}\theta_o}{dt^{n-1}}+\ldots+f_0(t)\theta_o = F(t) \quad (1)$$

where

$$f_j(t)=(a_j+b_jt+c_jt^2+\ldots+K_jt^K)$$

The right side, $F(t)$ involves θ_i, possibly its derivatives and products of these by t.

A previous paper[1] showed that when the coefficients in equation 1 contain only $(a+bt)$ terms, the stability can be determined by forming a polynomial from the "b" terms, and finding its roots. The present criterion extends this, and shows that when the coefficients in equation 1 contain higher powers of t, stability is determined by the roots of a polynomial made up of the coefficients of the highest power.

As an illustration of how an equation of the form of equation 1 is obtained, consider an elementary system in which an error actuated amplifier and motor drive a load consisting of an inertia and viscous damping; assume the elements have been found to vary thus:

inertia $=I_0+I_1t+I_2t^2$
damping $=D_0+D_1t+D_2t^2$
gain $=G_0+G_1t$

The differential equation relating output to input combines two equations stating that motor torque is the product of error times gain, and is balanced by a load torque which is the sum of a viscous damping torque plus the time rate of change of angular momentum:

$$(I_0+I_1t+I_2t^2)\frac{d^2\theta_o}{dt^2}+(D_0+I_1+D_1t+2I_2t+D_2t^2)\frac{d}{dt}\theta_o+(G_0+G_1t)\theta_o = (G_0+G_1t)\theta_i \quad (2)$$

For this system the a, b, and c coefficients of equation 1 would be:

$$\begin{array}{lll} a_2=I_0 & b_2=I_1 & c_2=I_2 \\ a_1=D_0+I_1 & b_1=D_1+2I_2 & c_1=D_2 \\ a_0=G_0 & b_0=G_1 & c_0=0 \end{array}$$

Equations for practical systems having more elements will contain a great many additional terms involving the rates of change of the elements.

The definition of stability used throughout this paper is based on the fact that equation 1 is linear, and its solution, θ_o, can be separated into a transient response or complimentary function, and a particular integral or steady state response. The transient is the solution to equation 3, which is equation 1 with the input, θ_i, equal to zero:

$$f_n(t)\frac{d^n}{dt^n}\theta_o+f_{n-1}(t)\frac{d^{n-1}}{dt^{n-1}}\theta_o+\ldots+f_0(t)\theta_o=0 \quad (3)$$

In accordance with Nyquist's widely accepted definition,[2] a servomechanism is defined as being stable if, when excited by any input or initial energy storage, the transient part of the output dies out completely as time approaches infinity. If any part of the transient persists or builds up indefinitely as time becomes infinite, the system is unstable.

A restriction on the method is that the highest power of t appearing in the coefficient of the highest derivative term, $d^n/dt^n\theta_o$ in equation 3, must be equal to or greater than the highest power of t appearing in the other derivative terms.

The Stability Criterion

It can be shown[3] that the transient response of a servomechanism described by equation 1 approaches a sum of terms of exponential form

$$\theta_o \rightarrow \sum_{j=1}^{j=n} A_j\frac{e^{\gamma_j t}}{t^{(\lambda_j+1)}} \quad (4)$$

Paper 51-268, recommended by the AIEE Feedback Control Systems Committee and approved by the AIEE Technical Program Committee for presentation at the AIEE Summer General Meeting, Toronto, Ont., Canada, June 25–29, 1951. Manuscript submitted March 14, 1951; made available for printing May 28, 1951.

M. J. Kirby and R. M. Giulianelli are with the Sperry Gyroscope Company, Great Neck, N. Y.

Nomenclature

$a_0, a_1 \ldots a_j \ldots a_n$ = constant part of coefficients in equation 1
$b_0, b_1 \ldots b_j \ldots b_n$ = coefficients of t in equation 1
$c_0, c_1 \ldots c_j \ldots c_n$ = coefficients of t^2 in equation 1
and so on

$j=\sqrt{-1}$; also used as a subscript denoting a general or typical value
k, K = when used as a coefficient or an exponent, is associated with the highest power of t in the coefficients of equation 1
n = order of equation 1
s = arbitrary complex variable
t = time
A = coefficient in equation 4
D = damping of servomechanism, equation 2
G = gain of servomechanism, equation 2
I = inertia of servomotor and load, equation 2
$P(s)$ = polynomial function of (s), equation 5
$v(s)$ = function of s in contour integral, equation 13
α = real part of γ
γ = root of $P(s)$
λ = exponent of t in equation 4
θ_i = input to servomechanism
θ_o = output of servomechanism
ω = imaginary part of γ
$\phi(s)$ = analytic function of s, equation 17

---

as $t \rightarrow \infty$. The A's are constants depending upon initial conditions and system inputs; the λ's depend on the servo system parameters, and the γ's are the zeros of the polynomial $P(s)$ formed from the coefficients of the highest power of t in equation 1, thus:

$$P(s)=K_n s^n + K_{n-1} s^{n-1} + \ldots + K_o \quad (5)$$

The s is an arbitrary complex variable.

This asymptotic form of θ_o is the basis of the stability criterion. The $\epsilon^{\gamma t}$ in each term can be written as $\epsilon^{\alpha t}\epsilon^{j\omega t}$, where α and ω are the real and imaginary parts, respectively of γ. If α is not zero, the $\epsilon^{\alpha t}$ eventually overpowers all the other elements in each term. If an α is negative, that term in the transient response approaches zero as $t \rightarrow \infty$, regardless of A or λ. If an α is positive, the term becomes infinite if A is not zero. The process of determining stability is therefore reduced to finding the γ's which are the roots of $P(s)$.

The specific steps are:

1. Express the time varying elements as polynomial functions of time, and write the differential equation relating output θ_o to input θ_i and time t in the form of equation 1.

2. Form the polynomial $P(s)$ as in equation 5.

3. Find the signs of real parts (α's) of the roots of $P(s)$ by any convenient method. If all the α's have negative signs, the system is stable. If any α has a positive sign the system is unstable. If one or more α's are zero, a special case arises which now is discussed.

Practical Considerations

A number of methods are available for finding the roots of $P(s)$. In the simpler cases, inspection and the use of rules based on the signs of the terms in $P(s)$, the presence of all terms or the absence of some, will suffice. Tables are available for finding the roots of cubic and quartic polynomials. In more complicated cases the Routh-Hurwitz criterion can be used to advantage, or a polar plot similar to a Nyquist plot may be employed. The method used will depend upon the individual and the problem at hand. Whichever method is used, the process is essentially that of finding the signs of the real parts of the roots of the characteristic equation of a system.

The steps of the preceding section do not cover the case in which $P(s)$ has one or more roots with zero real parts. The polar plot of $P(s)$ indicates this condition by passing through the origin for a finite, imaginary value of s. If the jth root of $P(s)$ has a zero real part the jth term in the eventual form of the transient,

$$A_j \frac{\epsilon^{\gamma_j t}}{t^{(\lambda_j+1)}}$$

will be an oscillation which builds up or decays as $1/t^{(\lambda_j+1)}$, since $\epsilon^{\gamma_j t}$ is simply a sine wave, equal to $\epsilon^{j\omega_j t}$ when γ_j is a pure imaginary. If any other root of $P(s)$ has a positive real part, the servomechanism is unstable. If one or more roots of $P(s)$ have zero real parts and all other roots have negative real parts, stability is determined by the $1/t^{\lambda}$ portions of these roots. When the coefficients of equation 1 are of the form $(a+bt)$, a straightforward procedure[1] is available for evaluating the λ's. When higher powers of t are present, however, the λ's are so much more difficult to determine that this is not worthwhile. In a practical situation the build-up or decay of $1/t^{\lambda+1}$ is much slower than that of an exponential term; this is more significant than the eventual stability or instability. If the system or process is to operate only a short time, such a transient might be tolerated whether stable or unstable. If the process continues for a long period this type of transient usually cannot be allowed to persist.

Rather than spend time trying to determine the eventual stability by evaluating λ therefore, it is better to recognize that such a situation exists and to remedy it by adding damping or by other physical changes.

Examples

Plots of $P(s)$ and time responses are given for two second order systems, one stable and one unstable. The time responses were obtained by means of an electronic analogue computer; the number of computing elements available limited the order of the equations and determined the form of the input. The stability could be determined in each case simply by solving the quadratic equation, $P(s)=0$, but polar plots are included to show the characteristic shapes for stable and unstable cases.

EXAMPLE 1

The system equation is:

$$(1+t+t^2)\frac{d^2}{dt^2}\theta_o+(-2+t+t^2)\frac{d\theta_o}{dt}+$$
$$(1+t+t^2)\theta_o=(1+t+t^2)\theta_i \quad (6)$$

From this, $P(s)$ is

$$P(s)=s^2+s+1 \quad (7)$$

Figure 1, the plot of $P(s)$, indicates that the system is stable; this is verified by the response to an input

$$\theta_i=\frac{1}{1+t+t^2} \quad (8)$$

which is shown in Figure 2.

EXAMPLE 2

The system equation is:

$$(1+t-0.2t^2+t^3)\frac{d^2}{dt^2}\theta_o+(0.2+t+0.1t^2-4t^3)$$
$$\frac{d}{dt}\theta_o+(1+t+0.1t^2+t^3)\theta_o$$
$$=(1+t+0.1t^2+t^3)\theta_i \quad (9)$$

$P(s)$ is made up of the coefficients of the t^3 terms

$$P(s)=s^2-4s+1 \quad (10)$$

The plot, Figure 1, indicates instability. The response, Figure 3, to the input

$$\theta_i=\frac{1}{(1+t+0.1t^2+t^3)} \quad (11)$$

shows this.

Conclusions

The criterion may appear to be of somewhat limited use because it predicts eventual stability or instability, that is, the build-up or decay of the final phase of the transient, while many servomechanisms with varying elements operate only for finite periods of time. Furthermore, the criterion tells little about the size of the early part of the transient response.

In practice, however, a transient does not necessarily require a long time to reach its "eventual" or final phase. As soon as sufficient time has elapsed for the highest power (t^k) terms in the coefficients of equation 1 to overpower the other terms, the final phase is reached. Many closed-loop systems operate long enough for their transients to progress well into this phase, even though the systems operate on programs of finite duration. The two examples in an earlier section illustrate this. In the remaining cases in which the program stops short of the final phase of the transient response, the eventual stability or instability is still important. For example, a designer would provide extra safety devices to stop a process if it were known that the system would enter a destructive oscillation if the process were to continue beyond its normal time.

The criterion states that the eventual stability depends upon the eventual rates of variation of the system elements as indicated by the coefficients of the highest power of time (t^k) in the polynomial coefficients. When $k=1$ the criterion becomes identical to that given previously[1] for systems described by equations whose coefficients vary as $(a+bt)$. When $k=0$, $P(s)$ reduces to the characteristic equation for a constant coefficient system, which is the basis for the common stability criteria for such systems.

The significance of the t^k terms suggests that stability might be determined directly by dividing each term in equation 1 by t^k, then letting t approach infinity. This procedure does not save any labor, since it arrives at the same polynomial, $P(s)$, which is written down immediately when the present criterion is used. Furthermore, this amounts to saying that the differential equation 1 approaches a constant coefficient equation as t approaches infinity, therefore, its solution approaches a sum of exponential functions. There is a tendency to extend this type of intuitive analysis to predict properties other than absolute stability, and even numerical values of the response. When such procedures cannot be rigorously justified, they may involve considerable errors.

However, since $P(s)$ has some of the properties of a characteristic equation, related to the final phase of the transient, it yields useful information as to whether the system response is satisfactory, and if not what can be done to remedy it. This will become apparent as the criterion is applied to specific servosystems; only two examples will be given here.

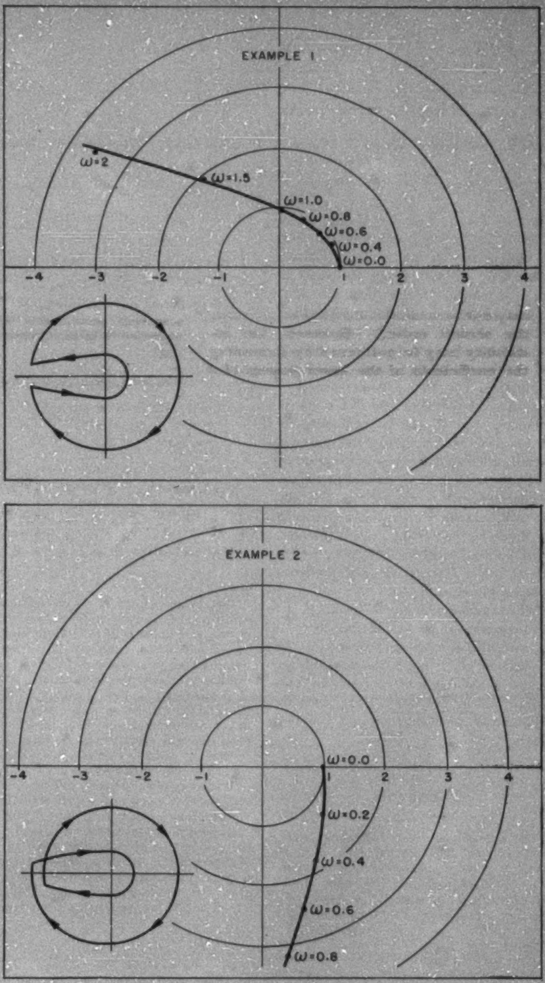

Figure 1. Plots of $P(s)$ for Examples 1 and 2

Consider a servomechanism for which all the coefficients in equation 1 vary as t^2 except one, which varies as $(a+bt)$ only. The $P(s)$ for this system will have a missing power of s, indicating a root on the imaginary axis, and the eventual response will decay or build-up slowly as a $1/t^{\lambda+1}$ term. This may be an undesirable condition; it can be remedied ideally only by changing the system so that the $(a+bt)$ coefficient varies as t^2. If this is impossible, the eventual response may sometimes be postponed or attenuated by increasing the constant (a) or first order variation (bt) term of this coefficient.

Likewise, consider a system for which all the coefficients in equation 1 vary as the same power of t, say t^2, but one of the

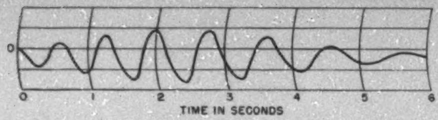

Figure 2. Response of system of Example 1 to input of form $\theta_i=1/(1+t+t^3)$

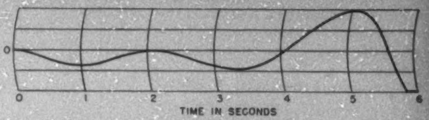

Figure 3. Response of system of Example 2 to input of form $\theta_i=1/(1+t+0.1t^2+t^3)$

terms in $P(s)$ is opposite in sign to all others. The system will eventually be unstable and can be made absolutely stable only by making all the signs in $P(s)$ the same. (This is necessary, but may not be sufficient if $P(s)$ is higher than the second order.) However, the instability may be postponed by increasing the coefficients of the lower powers of t in equation 1 so that a longer period of time must elapse before the t^K terms predominate and the transient enters its final phase. For example, if the system is second order and the damping varies, as $1+t+t^2-t^3$ while the t^3 coefficients in the inertia and gain terms are positive, the $-t^3$ will overpower the positive terms in the damping before, say $t=3$. However, if the damping term is changed to $1+t+4t^2-t^3$, the $-t^3$ term will not predominate until later, say, $t=6$.

When the polynomial coefficients in the time equation must be determined from experimental or other numerical data, the coefficients of t^K must be obtained accurately. Methods of representing empirical data by polynomials are given by Sokolnikoff[4] and Scarborough,[5] among others.

Appendix

The solution of many differential equations relating an unknown such as θ_o to time can be materially aided by introducing a new complex variable (here called s) and expressing θ_o as an integral: $\int_c f(s,t)ds$ of a function of s around a contour c in the s plane. Time, t, enters the integral only as a parameter.

The object in the present case is to show first that when the solution θ_o is assumed to be $\int_c e^{st}v(s)ds$, the function $v(s)$ and the contour, c, can be found so that equation 3 is satisfied, and, second, that this solution approaches an exponential form as $t\rightarrow\infty$.

As an example consider the time differential equation:

$$(a_2+b_2t+c_2t^2)\frac{d^2}{dt^2}\theta_o+(a_1+b_1t+c_1t^2)\frac{d\theta_o}{dt}+$$
$$(a_0+b_0t+c_0t^2)\theta_o=(a_0b_0t+c_0t^2)\theta_i \quad (12)$$

The first step is to substitute the assumed transient solution

$$\theta_o=\int_c e^{st}v(s)ds \quad (13)$$

into this equation; the result is

$$\int_c \left\{\begin{matrix}(a_2+b_2t+c_2t^2)s^2\\+(a_1+b_1t+c_1t^2)s\\+(a_0+b_0t+c_0t^2)\end{matrix}\right\} e^{st}v(s)ds=0 \quad (14)$$

Differentiation under the integral sign is assumed permissible and each term of equation 9 is next integrated by parts giving:

$$\Big[(b_2s^2+c_2ts^2-c_2ts+b_1s+c_1ts-c_1+$$
$$b_0pc_0t)e^{st}v(s)-(c_2s^2+$$
$$c_1s+c_0)e^{st}\frac{dv(s)}{ds}\Big]_c+$$
$$\int_c \left\{\begin{matrix}(a_2s^2-2b_2s+2c_2+a_1s-b_1+\\a_0)e^{st}v(s)+(-b_2s^2+4c_2s-\\b_1st+2c_1-b_0)e^{st}\dfrac{dv(s)}{ds}+\\(c_2s^2+c_1s+c_0)e^{st}\dfrac{d^2v(s)}{ds^2}\end{matrix}\right\} ds=0 \quad (15)$$

Two groups of terms, as in equation 15, result regardless of the highest power of t or of the order of the time differential equation corresponding to equation 12. The first group is the expression in brackets, to be evaluated around the contour c; products of powers of t and of s with $v(s)$ and e^{st} entering this expression. The second group, under the integral sign, contains e^{st} multiplied by a differential equation for $v(s)$ with coefficients which are powers of s, t does not enter the differential equation.

The order of this differential equation for $v(s)$ is always equal to the highest power of t in the coefficients of equation 12, and the coefficient of the highest derivative of $v(s)$ is the polynomial $P(s)$ formed from the coefficients of the highest powers of t in equation 12. The highest power of s in $P(s)$ is always s^n, where n is the order of equation 12. For the present example, equation 12

$$P(s)=c_2s^2+c_1s+c_0 \quad (16)$$

In any case, when the contour c in the s-plane is chosen so that the quantity in the brackets is identically zero when evaluated around c, and when in addition $v(s)$ satisfies the differential equation under the integral sign, then equation 15 is satisfied by the assumed form of θ_o.

A satisfactory contour begins at $-\infty$ on a line parallel to the real axis and passing through one of the γ's which are the roots of $P(s)$; the contour follows this line until it nears the γ, encircles it, and returns along the line to $-\infty$, Figure 4. A group of n such contours can be found, one for each of the n roots of $P(s)$.

In order to determine stability, it is not necessary to determine $v(s)$ completely; this would require the solution of the differential equation under the integral sign. A knowledge of some of the properties of $v(s)$ is sufficient to determine the form of θ_o as $t\rightarrow\infty$.

The γ's are the singular points of the differential equation for $v(s)$. In the neighborhood of each γ in the s-plane, say γ_K, there is one nonanalytic solution

$$v(s)=(s-\gamma_K)^{\lambda K}\phi_K(s) \quad (17)$$

where $\phi(s)$ is analytic. Each of these solutions can be put in equation 13 for θ_o and integrated around the contour which encircles the appropriate γ; this gives n solutions to equation 12. Each such integral can be divided into three parts, two along the line parallel to the real axis and the third encircling γ. By expanding $\phi(s)$ in a power series and by further steps it can be shown that as $t\rightarrow\infty$, the first two integrals approach zero and the third aproaches:

$$\frac{A_K e^{\gamma_K t}}{t^{(\lambda K+1)}}$$

The intermediate steps omitted in this summary are discussed by E. T. Ince.[3]

References

1. Stability of Servomechanisms with Linearly Varying Elements, M. J. Kirby. *AIEE Transactions*, volume 69, 1950, part II, pages 1662–68.

2. Regeneration Theory, H. Nyquist. *Bell System Technical Journal* (New York, N. Y.), volume 11, January 1932.

3. Ordinary Differential Equations (book), E. T. Ince. Dover Publishing Company, New York, N. Y., chapter 18, 1946.

4. Higher Mathematics for Engineers and Physicists, I. S. and E. S. Sokolnikoff. McGraw-Hill Book Company, New York, N. Y., 1941.

5. Numerical Mathematical Analysis, J. B. Scarborough. Johns Hopkins Press, Baltimore, Md., 1930.

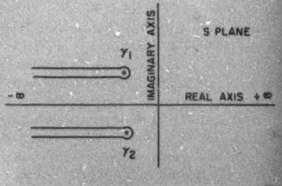

Figure 4. Contour in S plane encircling γ's used for determining $v(s)$

Discussion

W. G. Heffron (General Electric Company, Schenectady, N. Y.): The practical results of Messrs. Kirby and Giulianelli's method can be reached by another method, quite similar in actual theory, but a bit more easily visualized. By substituting particular values of time in the coefficients and then subjecting the numerical results to the Routh-Hurwitz test, the stability of the system can be predicted, with the same results for large values of time as their method gives. In addition, this method will indicate at what time the system will change from stable to unstable, if such a change does occur. For the simple Example 1 of the paper it can easily be seen that the system is stable at times greater than 1 second and is unstable from time equal zero until 1 second. In the second example, this method indicates stability from zero time up to 0.59 second, and instability thereafter. It would seem that knowledge of the periods of instability also is essential to the designer, in addition to the ever-important knowledge of stability at large values of time.

The method employed here is called by some "use of the theory of small oscillations" and by others "use of incrementalized or linearized equations." The problem discussed here is, technically, not a nonlinear one, but many types of nonlinear problems may be studied profitably in this manner. Of course, there are some problems where the nonlinearities are too complicated to make the results of a linearized study profitable: such cases are studied with an analogue computer[1] which we have available.

As the authors point out, engineering judgment must be used carefully to determine whether the results of a linearized study may be extended to predict the transient performance of the system. Nevertheless, in many instances, linearization of the equations has the important advantage of showing more clearly the functional relationships that control the system's performance, pointing out the variations in inherent gain and time constants during the operating cycle, and thus, delineating the requirements for a control. We feel that this somewhat round about method results in a superior understanding of the problem and thus in a better control system.

REFERENCE

1. A New Differential Analyzer, H. P. Kuehni, H. A. Peterson. *AIEE Transactions*, volume 63, 1944, pages 718–22.

M. J. Kirby and **R. M. Giulianelli:** Mr. Heffron's comments are quite pertinent. Linearization as he defines it is widely used in the study of varying-element systems, particularly when an analogue computer is available to check the results. Experience with particular types of systems builds up judgment as to the degree of accuracy which can be expected from the results of a linearized analysis in a particular case. The criterion in the present paper was developed not to change this procedure but to justify part of it. Absolute stability is perhaps the most important single property of a system. The present derivation provides a rigorous basis for approximating the latter part of the transient response.

Servomechanism Transient Performance from Decibel-Log Frequency Plots

H. HARRIS, JR. ASSOCIATE AIEE
M. J. KIRBY MEMBER AIEE
E. F. VON ARX NONMEMBER AIEE

SYNTHESIS of a servomechanism, like most other complex engineering synthesis, consists of a series of trial solutions based upon experience or creative insight which are then analyzed either for verification or to suggest a new and better trial solution. The reason for this is simply that the tools for analysis are more readily available than the tools for a straight-forward synthesis. This procedure is deadening to creativeness and retards the conception of original solutions if the analysis step between trials is too cumbersome or so complex that the essential factors are masked.

Any procedure intended to aid in synthesis should therefore reduce the labor of each trial analysis and at the same time present the results in a form which points the way toward a new, improved trial. The method described in this paper for obtaining the transient response of a servomechanism arose from the desire to be able to see, with almost no calculation, the characteristics of the transient response which correspond to certain characteristics of the frequency response. The method saves labor by eliminating the need for finding the roots of a polynomial of high order usually required in finding a transient response. It can be used to find the approximate response of any linear servosystem to almost any input; the resulting formulas emphasize those elements of the frequency response which contribute most to the transient, and suppress complicating nonessentials. However, the original goal was not entirely achieved, and since it may still be achievable, it seems worthwhile to discuss it briefly.

Most previous papers on servomechanisms place greatest emphasis on means for obtaining a stable and nonoscillatory closed loop response. It is assumed here that this portion of the design has already been carried out. A specification of servo performance is essentially a statement of limits placed on the error-versus-time curve as the system responds to a particular input. Present-day specifications frequently go well beyond the requirement that system simply be stable, and place limits on the peak error, time allowed to decay, et cetera. The present method is intended for use in adjusting the designs of systems which have already been stabilized, in order to meet these further requirements. In particular, it is assumed that the slope of the open loop decibel-log frequency plot is near −6 decibels per octave for a sufficiently large region on each side of the crossover (or zero decibel gain) frequency. The open loop transfer function is assumed to be a fraction, the numerator and denominator of which are products of linear or quadratic factors in "S"; the transfer function is assumed to have a low-pass characteristic roughly similar to those shown in the figures of the paper. (S is used here for the variable frequently denoted by "p".)

Conventional methods of studying the details of the shape of the transient response offer two widely divergent choices. If the inputs which the servomechanism is to follow contain velocities and accelerations which change very little within the transient time, then the error may be calculated[3] by applying steady-state velocity and acceleration constants, point by point, to the input function. This leaves the designer with some doubts as to a proper criterion to determine whether the velocity or acceleration has changed too much to allow the application of the steady-state constants. The usual alternative is a rigorous solution for the transient error as a function of time. This is a lengthy procedure which usually requires the solution of an equation of high order. The analysis to be outlined in this paper fills the gap.

The method makes use of the fact that the transfer function relating error to input in any closed loop system approaches unity at frequencies above the crossover frequency ω_c, and approaches the open loop transfer function at frequencies below ω_c. When a system has been suitably stabilized, the design problem reduces to a determination of ω_c and the shape of the open loop transfer function below ω_c. The shape of the frequency response above the crossover frequency affects the transient response of a well-stabilized servo only slightly.

Statement of the Method

The object is to find an approximate expression for $\epsilon/\theta_i(S)$ from which $\epsilon(t)$ can be computed by ordinary LaPlace Transform methods without becoming involved in finding the roots of higher order equations and without losing sight of the physical significance of the terms involved.

The exact expressions for $\epsilon/\theta_i(S)$ and its reciprocal $\theta_i/\epsilon(S)$ give the key to the approximation that will fulfill the necessary conditions.

$$\frac{\theta_i}{\epsilon}=\frac{\theta_o}{\epsilon}+1 \tag{1}$$

Since $\theta_o/\epsilon(S)$ has a low pass characteristic, θ_o/ϵ is much larger than unity at frequencies well below the unity gain crossover, ω_c, and

$$\frac{\theta_i}{\epsilon}\approx\frac{\theta_o}{\epsilon};\ \omega\ll\omega_c \tag{2}$$

Paper 51-269, recommended by the AIEE Feedback Control Systems Committee and approved by the AIEE Technical Program Committee for presentation at the AIEE Summer General Meeting, Toronto, Ont., Canada, June 25–29, 1951. Manuscript submitted November 3, 1950; made available for printing May 23, 1951.

H. HARRIS, JR., M. J. KIRBY, and E. F. VON ARX are with the Sperry Gyroscope Company, Great Neck, N. Y.

The authors wish to acknowledge the assistance of Mrs. Ellen J. Adler who set up and executed much of the electronic analogue computer work.

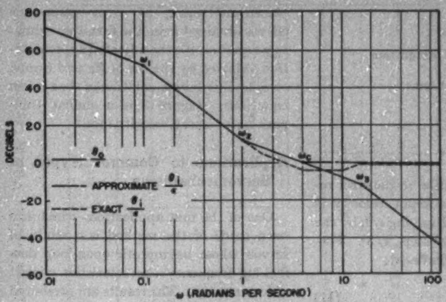

Figure 1. Decibel-log frequency plot for example in text

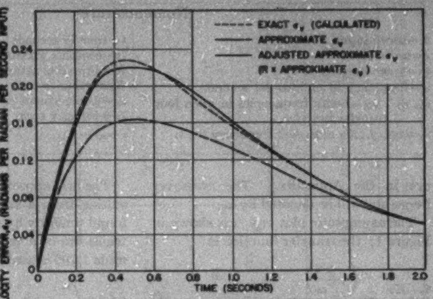

Figure 3. Error versus time for unit step of velocity input for system of Figure 1

while at frequencies considerably above ω_c, θ_o/ϵ is small and

$$\frac{\theta_i}{\epsilon} \approx 1; \quad \omega \gg \omega_c \tag{3}$$

For frequencies away from ω_c, the approximation to θ_i/ϵ is thus obtained directly in terms of readily available data; only the portion of the approximation near ω_c remains to be constructed.

If the servo is reasonably stable, as assumed, a first approximation to θ_i/ϵ is obtained by simply extending the high- and low-frequency approximations until they meet at ω_c. The resulting function is in essential agreement with the exact $\theta_i/\epsilon(S)$ except in the neighborhood of ω_c, and it has the desirable property of being in the form of a product of factors.

In the neighborhood of ω_c, the actual θ_i/ϵ lies below the approximate θ_i/ϵ (as shown by dotted curve in Figure 1); the discrepancy may amount to 6 decibels, and is usually reasonably constant between ω_2 and ω_3 which are the low- and high-frequency ends respectively, of the -6 decibels per octave region in θ_o/ϵ.

An obvious adjusting procedure is to multiply the approximate θ_i/ϵ by the absolute value of the ratio of the true θ_i/ϵ to the approximate, evaluated at ω_c. However, this would result in errors at the beginning and at the end of the time response. The method of finding $\epsilon(t)$ used throughout this paper is to form the first approximation, and use the adjustment just described in the neighborhood of ω_c only.

The step-by-step procedure for finding the error of a servomechanism as a function of time is:

1. Form the approximate θ_i/ϵ by including all the $(1+S/\omega_k)$ factors in both numerator and denominator of θ_o/ϵ* wherein ω_k is less than ω_c. Eliminate all the other $(1+S/\omega_k)$ factors and replace them by $(1+S/\omega_c)$ in the numerator. This is the "approximate θ_i/ϵ" of Figure 1.

2. The approximate ϵ/θ_i is the reciprocal of the approximate θ_i/ϵ of step 1. Multiply the approximate ϵ/θ_i by the LaPlace transform of any input θ_i which is pertinent, and find the inverse transform $\epsilon(t)$ by conventional LaPlace transform methods.[4,5]

3. Evaluate $\epsilon(t)$ for the range of time that is of interest.

4. Determine the adjusting ratio

$$R = \left| \frac{\frac{\theta_i}{\epsilon}\text{ approximate}}{\frac{\theta_i}{\epsilon}\text{ exact}} \right| \text{ evaluated at } \omega_c \tag{4}$$

5. Multiply $\epsilon(t)$ by R for $1/\omega_3 < t < 1/\omega_2$.

6. Connect the resulting curves smoothly in the regions near $t = 1/\omega_3$ and $t = 1/\omega_2$.

As an illustration, the approximate error-versus-time response to step displacement and step velocity inputs will be found for a system whose open loop transfer function consists of four regions having slopes of -6, -12, -6 and -12 decibels per octave, respectively, separated by break frequencies ω_1, ω_2, ω_3 in that order. (A more complicated example is worked

---

*θ_o/ϵ can be written as a product of factors by inspection of the open loop transfer function by well known techniques.[5,6]

Figure 2. Error versus time for unit step of displacement input for system of Figure 1

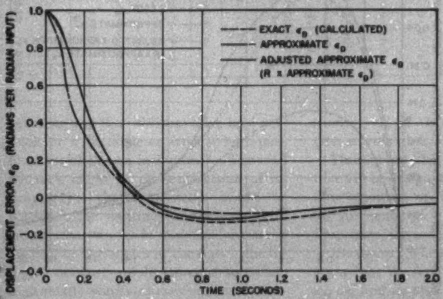

Figure 4. Decibel-log-frequency plot for example in Appendix

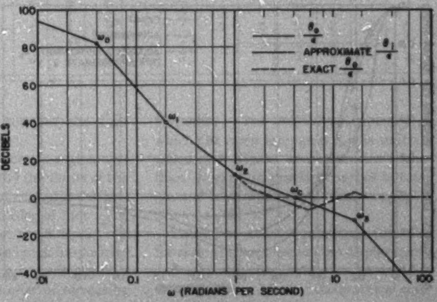

Nomenclature

θ_i = servo input
ϵ = servo error
θ_o = servo output
ω = frequency in radians per second
$\omega_1, \omega_2 \ldots \omega_k$ = break frequencies in open loop transfer function
ω_c = unity gain crossover frequency
t = time in seconds
S = complex variable of integration
R = adjusting ratio
K_V = velocity error constant
ϵ_d = displacement error
ϵ_V = velocity error
$j=\sqrt{-1}$

---

out in the Appendix.) The crossover frequency will be denoted by ω_c.

The asymptotic plot of θ_o/ϵ is shown in Figure 1; the transfer function is:

$$\frac{\theta_o}{\epsilon}=\frac{K_V}{S}\frac{\left(1+\frac{S}{\omega_2}\right)}{\left(1+\frac{S}{\omega_1}\right)\left(1+\frac{S}{\omega_3}\right)} \tag{5}$$

where

$$K_V=\frac{\omega_2\omega_c}{\omega_1} \tag{6}$$

To form the approximate θ_i/ϵ the $(1+S/\omega_3)$ factor is removed from the denominator of equation 5 and $(1+S/\omega_c)$ is inserted in the numerator:
Approximate

$$\frac{\theta_i}{\epsilon}=\frac{(S+\omega_2)(S+\omega_c)}{S(S+\omega_1)} \tag{7}$$

The LaPlace transform of the first approximation to the error response to a step of input displacement is:

$$\epsilon_d=\frac{1}{S}\times\frac{S(S+\omega_1)}{(S+\omega_2)(S+\omega_c)} \tag{8}$$

Formula 1.107 from Gardner and Barnes[4] gives the error as a function of time:

$$\epsilon_d(t)=\mathcal{L}^{-1}\frac{(S+\omega_1)}{(S+\omega_2)(S+\omega_c)} \tag{9}$$

$$\epsilon_d=\frac{(\omega_1-\omega_2)}{(\omega_c-\omega_2)}e^{-\omega_2 t}-\frac{(\omega_1-\omega_c)}{(\omega_c-\omega_2)}e^{-\omega_c t} \tag{10}$$

The first approximation to the error resulting from a step of input velocity is found similarly by multiplying ϵ/θ_i by the transform of a velocity step, $1/S^2$. Formula 1.109 is used to find $\epsilon_V(t)$:

$$\epsilon_V(t)=\mathcal{L}^{-1}\frac{S+\omega_1}{S(S+\omega_2)(S+\omega_c)} \tag{11}$$

$$\epsilon_V=\frac{\omega_1}{\omega_2\omega_c}+\frac{(\omega_1-\omega_2)}{\omega_2(\omega_2-\omega_c)}e^{-\omega_2 t}+\frac{(\omega_1-\omega_c)}{\omega_c(\omega_c-\omega_2)}e^{-\omega_c t} \tag{12}$$

The exact θ_i/ϵ is found by taking $(1+\theta_o/\epsilon)$; the adjusting ratio R is:

$$R=\left|\frac{\dfrac{S(S+\omega_1)(S+\omega_3)}{S(S+\omega_1)(S+\omega_3)+\omega_c\omega_3(S+\omega_2)}}{\dfrac{S(S+\omega_1)}{(S+\omega_2)(S+\omega_c)}}\right|_{\text{at } S=j\omega_c} \tag{13}$$

The approximate formulas for the ϵ_d and ϵ_V are equations 10 and 12 respectively, with the adjusting ratio, R, applied between the limits $1/\omega_3<t<1/\omega_2$.

For example, consider a system in which $\omega_2/\omega_1=10$, $\omega_3/\omega_2=16$, and $\omega_c/\omega_2=4$, and take $\omega_2=1$ for convenience. For these values, equation 10 gives

$$\epsilon_d=1.3e^{-4t}-0.3e^{-t} \tag{14}$$

and equation 12 gives

$$\epsilon_V=0.025-0.325e^{-4t}+0.3^{-t} \tag{15}$$

and R is 1.42.

Figure 2 is a comparison, for step displacement input, of error-versus-time curves obtained from the first approximation equation 10; the adjusted approximation obtained by the use of R; and from a completely rigorous solution of the system equations. Figure 3 is a similar comparison for a step velocity input.

Applications to Common Types of Servomechanisms

One of the first applications which has been made of the method is a study of servos whose asymptotic open loop decibel-log frequency characteristics consist of four regions. The results are presented here in condensed form, because they illustrate the use of the method, and serve as a basis for some of the statements in a subsequent section, and also because 4-region servosystems are encountered so frequently in practice that the inclusion of data concerning them is justified.

The class of servos whose open loop transfer characteristics consist of four regions includes a wide variety of systems differing in design objective, in the type of compensating network used, the kind of energy which is controlled, and in the physical form of the system elements. For example, an uncompensated servomotor and load will often have a decibel-log frequency characteristic similar to Figure 7. At very low frequencies the slope is −6 decibel per octave because of the integrating action of the motor. There is a "break" at a relatively low frequency due to the mechanical time constant (inertia/effective damping) of the motor and load, followed by a sequence of higher frequency breaks or reductions in slope due to lags in filters, motor field time constants, and mechanical resonance. The result of compensating such a system with a lead network, the effect of an integral

Figure 5. Error versus time for unit step of displacement input for system of Figure 4

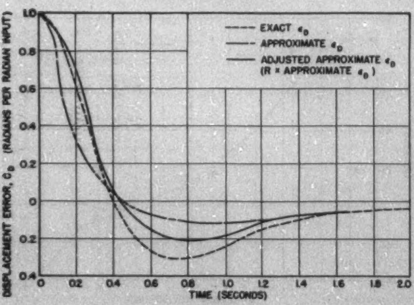

Figure 6. Error versus time for unit step of velocity input for system of Figure 4

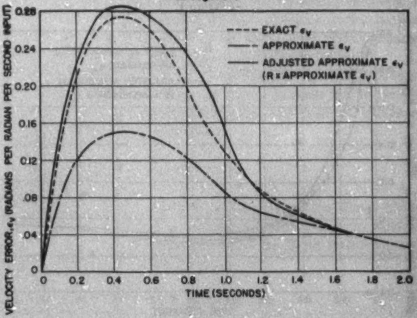

Table I. Equations* for Approximate Displacement Error, Velocity Error, and Adjusting Factor (R) for some Common Regulator, Velocity Lag, and Acceleration Lag Servos

SYSTEM	θ_o/ϵ	ϵ/θ_i (APPROX.)	ϵ_d	ϵ_v	R(ABSOLUTE VALUE AT $S = j\omega$)
−6, −6, −6, −6	$\frac{\omega_c}{S}$	$\frac{S}{S+\omega_c}$	$e^{-\omega_c t}$	$\frac{1}{\omega_c}-\frac{1}{\omega_c}e^{-\omega_c t}$	1
−6, −6, −6, −12	$\frac{\omega_c}{S(1+S/\omega_3)}$				$\frac{(S+\omega_c)(S+\omega_3)}{\omega_c\omega_3+(S+\omega_3)}$
−6, −6, −6, −18	$\frac{\omega_c}{S(1+S/\omega_3)^2}$				$\frac{(S+\omega_c)(S+\omega_3)^2}{\omega_c\omega_3^2+(S+\omega_3)^2}$
−6, −12, −6, −6	$\frac{\omega_2\omega_c(1+S/\omega_2)}{\omega_1 S(1+S/\omega_1)}$	$\frac{S(S+\omega_1)}{(S+\omega_2)(S+\omega_c)}$	$\frac{\omega_c-\omega_1}{\omega_c-\omega_2}e^{-\omega_c t}-\frac{\omega_2-\omega_1}{\omega_c-\omega_2}e^{-\omega_2 t}$	$\frac{\omega_1}{\omega_2\omega_c}+\frac{\omega_2-\omega_1}{\omega_2(\omega_c-\omega_2)}e^{-\omega_2 t}-\frac{\omega_c-\omega_1}{\omega_c(\omega_c-\omega_2)}e^{-\omega_c t}$	$\frac{(S+\omega_2)(S+\omega_c)}{\omega_c(S+\omega_2)+S(S+\omega_1)}$
−6, −12, −6, −12	$\frac{\omega_2\omega_c(1+S/\omega_2)}{\omega_1 S(1+S/\omega_1)(1+S/\omega_3)}$				$\frac{(S+\omega_2)(S+\omega_c)(S+\omega_3)}{\omega_c\omega_3(S+\omega_2)+S(S+\omega_1)(S+\omega_3)}$
−6, −12, −6, −18	$\frac{\omega_2\omega_c(1+S/\omega_2)}{\omega_1 S(1+S/\omega_1)(1+S/\omega_3)^2}$				$\frac{(S+\omega_2)(S+\omega_c)(S+\omega_3)^2}{\omega_c\omega_3^2(S+\omega_2)+S(S+\omega_1)(S+\omega_3)^2}$
−6, −18, −6, −6	$\frac{\omega_2^2\omega_c(1+S/\omega_2)^2}{\omega_1^2 S(1+S/\omega_1)^2}$	$\frac{S(S+\omega_1)^2}{(S+\omega_2)^2(S+\omega_c)}$	$\frac{(\omega_c-\omega_1)^2}{(\omega_c-\omega_2)^2}e^{-\omega_c t}+\left[\frac{(\omega_2-\omega_1)^2}{(\omega_c-\omega_2)}t-\frac{(\omega_2-\omega_1)(2\omega_c-\omega_2-\omega_1)}{(\omega_c-\omega_2)^2}\right]e^{-\omega_2 t}$	$\frac{\omega_1^2}{\omega_2^2\omega_c}-\frac{(\omega_c-\omega_1)^2}{\omega_c(\omega_c-\omega_2)^2}e^{-\omega_c t}+\left[-\frac{(\omega_2-\omega_1)^2}{\omega_2(\omega_c-\omega_2)}t+\frac{(\omega_c-2\omega_1)\omega_2^2-(\omega_c-2\omega_2)\omega_1^2}{\omega_2^2(\omega_c-\omega_2)^2}\right]e^{-\omega_2 t}$	$\frac{(S+\omega_2)^2(S+\omega_c)}{\omega_c(S+\omega_2)^2+S(S+\omega_1)^2}$
−6, −18, −6, −12	$\frac{\omega_2^2\omega_c(1+S/\omega_2)^2}{\omega_1^2 S(1+S/\omega_1)^2(1+S/\omega_3)}$				$\frac{(S+\omega_2)^2(S+\omega_c)(S+\omega_3)}{\omega_c\omega_3(S+\omega_2)^2+S(S+\omega_1)^2(S+\omega_3)}$
−6, −18, −6, −18	$\frac{\omega_2^2\omega_c(1+S/\omega_2)^2}{\omega_1^2 S(1+S/\omega_1)^2(1+S/\omega_3)^2}$				$\frac{(S+\omega_2)^2(S+\omega_c)(S+\omega_3)^2}{\omega_c\omega_3^2(S+\omega_2)^2+S(S+\omega_1)^2(S+\omega_3)^2}$
0, −6, −6, −6	$\frac{\omega_c}{\omega_2(1+S/\omega_2)}$	$\frac{S+\omega_2}{S+\omega_c}$	$\frac{\omega_2}{\omega_c}+\frac{\omega_c-\omega_2}{\omega_c}e^{-\omega_c t}$	$-\frac{\omega_c-\omega_2}{\omega_c^2}+\frac{\omega_2}{\omega_c}t-\frac{\omega_c-\omega_2}{\omega_c^2}e^{-\omega_c t}$	$\frac{S+\omega_c}{S+(\omega_2+\omega_c)}$
0, −6, −6, −12	$\frac{\omega_c}{\omega_2(1+S/\omega_2)(1+S/\omega_3)}$				$\frac{(S+\omega_c)(S+\omega_3)}{\omega_c\omega_3+(S+\omega_2)(S+\omega_3)}$
0, −6, −6, −18	$\frac{\omega_c}{\omega_2(1+S/\omega_2)(1+S/\omega_3)^2}$				$\frac{(S+\omega_c)(S+\omega_3)^2}{\omega_c\omega_3^2+(S+\omega_2)(S+\omega_3)^2}$
0, −12, −6, −6	$\frac{\omega_2\omega_c(1+S/\omega_2)}{\omega_1^2(1+S/\omega_1)^2}$	$\frac{(S+\omega_1)^2}{(S+\omega_2)(S+\omega_c)}$	$\frac{\omega_1^2}{\omega_2\omega_c}+\frac{(\omega_2-\omega_1)^2}{\omega_2(\omega_c-\omega_2)}e^{-\omega_2 t}-\frac{(\omega_c-\omega_1)^2}{\omega_c(\omega_c-\omega_2)}e^{-\omega_c t}$	$\frac{(\omega_2-\omega_1)^2}{\omega_2^2(\omega_c-\omega_2)}e^{-\omega_2 t}-\frac{(\omega_c-\omega_1)^2}{\omega_c^2(\omega_c-\omega_2)}e^{-\omega_c t}+\frac{\omega_1^2}{\omega_2\omega_c}t+\frac{2\omega_1\omega_2\omega_c-\omega_1^2(\omega_2+\omega_c)}{\omega_2^2\omega_c^2}$	$\frac{(S+\omega_2)(S+\omega_c)}{\omega_c(S+\omega_2)+(S+\omega_1)^2}$
0, −12, −6, −12	$\frac{\omega_2\omega_c(1+S/\omega_2)}{\omega_1^2(1+S/\omega_1)^2(1+S/\omega_3)}$				$\frac{(S+\omega_2)(S+\omega_c)(S+\omega_3)}{\omega_c\omega_3(S+\omega_2)+(S+\omega_1)^2(S+\omega_3)}$
0, −12, −6, −18	$\frac{\omega_2\omega_c(1+S/\omega_2)}{\omega_1^2(1+S/\omega_1)^2(1+S/\omega_3)^2}$				$\frac{(S+\omega_2)(S+\omega_c)(S+\omega_3)^2}{\omega_c\omega_3^2(S+\omega_2)+(S+\omega_1)^2(S+\omega_3)^2}$
−12, −12, −6, −6	$\frac{\omega_2\omega_c(1+S/\omega_2)}{S^2}$	$\frac{S^2}{(S+\omega_2)(S+\omega_c)}$	$\frac{\omega_c}{\omega_c-\omega_2}e^{-\omega_c t}-\frac{\omega_2}{\omega_c-\omega_2}e^{-\omega_2 t}$	$\frac{1}{(\omega_c-\omega_2)}e^{-\omega_2 t}-\frac{1}{\omega_c-\omega_2}e^{-\omega_c t}$	$\frac{(S+\omega_2)(S+\omega_c)}{\omega_c(S+\omega_2)+S^2}$
−12, −12, −6, −12	$\frac{\omega_2\omega_c(1+S/\omega_2)}{S^2(1+S/\omega_3)}$				$\frac{(S+\omega_2)(S+\omega_c)(S+\omega_3)}{\omega_c\omega_3(S+\omega_2)+S^2(S+\omega_3)}$
−12, −12, −6, −18	$\frac{\omega_2\omega_c(1+S/\omega_2)}{S^2(1+S/\omega_3)^2}$				$\frac{(S+\omega_2)(S+\omega_c)(S+\omega_3)^2}{\omega_c\omega_3^2(S+\omega_2)+S^2(S+\omega_3)^2}$
−12, −18, −6, −6	$\frac{\omega_2\omega_c(1+S/\omega_2)^2}{\omega_1 S^2(1+S/\omega_1)}$	$\frac{S^2(S+\omega_1)}{(S+\omega_2)^2(S+\omega_c)}$	$\frac{\omega_c(\omega_c-\omega_1)}{(\omega_c-\omega_2)^2}e^{-\omega_c t}+\left[\frac{\omega_2(\omega_2-\omega_1)}{\omega_c-\omega_2}t+\frac{\omega_2^2+2\omega_2\omega_c+\omega_1\omega_c}{(\omega_c-\omega_2)}\right]e^{-\omega_2 t}$	$\left[\frac{\omega_c-\omega_1}{(\omega_c-\omega_2)^2}-\frac{\omega_2-\omega_1}{\omega_c-\omega_2}t\right]e^{-\omega_2 t}$ $\frac{\omega_c-\omega_1}{(\omega_c-\omega_2)^2}e^{-\omega_c t}$	$\frac{(S+\omega_2)^2(S+\omega_c)}{\omega_c(S+\omega_2)^2+S^2(S+\omega_1)}$
−12, −18, −6, −12	$\frac{\omega_2\omega_c(1+S/\omega_2)^2}{\omega_1 S^2(1+S/\omega_1)(1+S/\omega_3)}$				$\frac{(S+\omega_2)^2(S+\omega_c)(S+\omega_3)}{\omega_c\omega_3(S+\omega_2)^2+S^2(S+\omega_1)(S+\omega_3)}$
−12, −18, −6, −18	$\frac{\omega_2\omega_c(1+S/\omega_2)^2}{\omega_1 S^2(1+S/\omega_1)(1+S/\omega_3)^2}$				$\frac{(S+\omega_2)^2(S+\omega_c)(S+\omega_3)^2}{\omega_c\omega_3^2(S+\omega_2)^2+S^2(S+\omega_1)(S+\omega_3)^2}$

network, and that of either a lag-lead network or a tachometer with a high-pass filter are all shown in Figure 7. The lead network might be chosen because of its simplicity; the tachometer would be justified when accuracy and fast response are necessary in the face of backlash in the gearing or harmonics in the data; the integral network would be used to attain high steady-state accuracy and smooth response; all of these, however, are 4-region servosystems.

Throughout this paper a 4-region system will be designated by the slopes of the four segments of its asymptotic decibel-log frequency plot in order of increasing frequency, for example, a −6, −12, −6, −18 system. The three break frequencies separating the four regions are designated ω_1, ω_2, and ω_3 also in order of increasing frequency. The crossover frequency at which the open loop gain θ_o/ϵ is unity is called ω_c. Breaks at frequencies higher than ω_3 exist in practical servos but are ignored here because of their negligible effect on ϵ/θ_i.

Table I contains approximate formulas for errors in response to step displacement and step velocity inputs for 21 4-region servosystems. Most of the practical com-

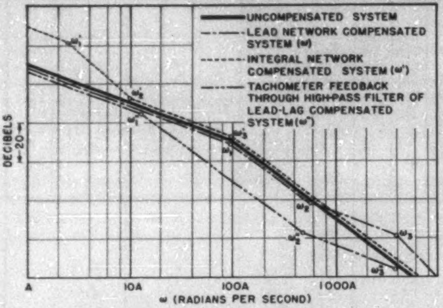

Figure 7. Open-loop transfer function of uncompensated system and system compensated by various well-known schemes

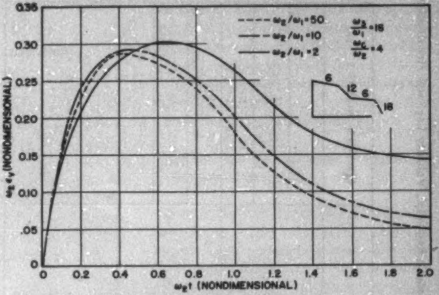

Figure 9. Velocity error versus time showing the effect of changing the ratio ω_2/ω_1 (calculated data)

binations of slopes among the four regions are included. Formulas are included for systems having 0 decibel per octave below ω_1 (displacement lag systems, or regulators), and for velocity lag systems having -6 decibels per octave, and acceleration-lag systems with slopes of -12 decibels per octave. In the region above ω_3, slopes of -6, -12, and -18 decibels per octave are included; steeper slopes are encountered in practice but at higher frequencies where θ_o/ϵ is small and ϵ/θ_i is not greatly affected. All formulas in Table I were obtained in the same manner as the example in the preceding section.

Figures 8 through 13 are error-versus-time curves for velocity-lag systems, plotted from the formulas of Table I. These show the shapes of the responses of representative velocity lag systems, and show the effect of varying those quantities which are under the control of the designer, namely:

1. The relative lengths of the segments, indicated by the ratios of the break frequencies ω_2/ω_1 and ω_3/ω_2.
2. The location of the gain crossover frequency ω_c, indicated by the ratio ω_c/ω_2.
3. The slopes of the region between ω_1 and ω_2, and the region above ω_3. (For a velocity-lag system the slope must be -6 decibels per octave in the region below ω_1, and is -6 decibels per octave between ω_2 and ω_3.)

In order to show the characteristics of a larger number of systems, Figures 14 through 17 are curves of peak overshoot in response to step displacement input and peak error in response to velocity input, as a function of location of the gain crossover ω_c/ω_2. The same quantities are allowed to vary as in Figures 8 to 13, but the range is, in general, greater. Crossover frequency location has been chosen as the independent variable because it is directly dependent on the gain of the servo. Since gain is easily adjusted intentionally and is in addition subject to undesired changes due to temperature, aging of tubes, et cetera, changes in gain are more common than are changes in the other properties of the open loop characteristic.

The curves of Figures 14 to 17 have been obtained by exact solutions on an electronic analogue computer, rather than by the approximate formulas of Table I. Thus the accuracy of the formulas can be observed by comparing the peak ordinate of any curve in Figures 8 to 13 with the corresponding point on the appropriate curve of Figures 14 to 17. In addition, the curves of Figures 14 to 17 are extended to cover systems which are not well stabilized, in order that these curves may be of help in securing initially stable systems suitable for further analysis or synthesis by the method given herein.

Conclusions

The preceding sections have shown how the synthesis of a servomechanism can be aided by a reduction of the labor involved in each repeated trial analysis. The present and final section illustrates another way in which the method explained in this paper contributes to syn-

Figure 8. Displacement error versus time showing the effect of changing the ratio ω_2/ω_1 (calculated data)

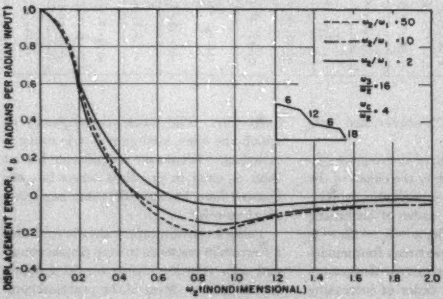

Figure 10. Displacement error versus time showing the effect of changing the ratio ω_c/ω_2 (calculated data)

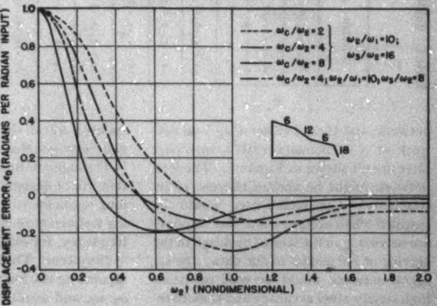

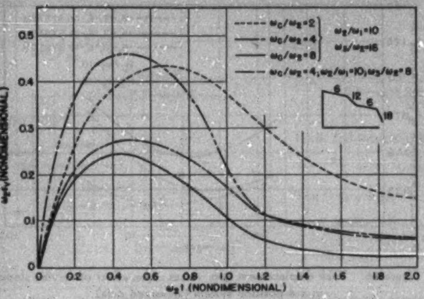

Figure 11. Velocity error versus time showing the effect of changing the ratio ω_c/ω_2 (calculated data)

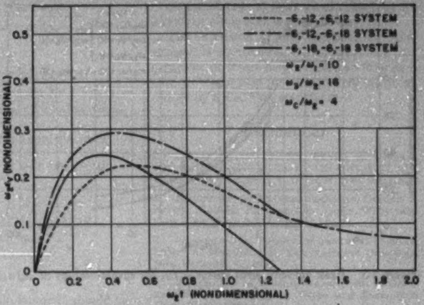

Figure 13. Velocity error versus time effect of varying slope in a 4-position system (calculated data)

thesis; the results of each trial analysis indicate in what way the trial design should be changed in order to make the next trial an improvement, thereby reducing the number of trials.

The approximate error-versus-time response includes a sum of exponential terms in which each exponent is one of the break frequencies at which the slope of the open loop transfer characteristic θ_o/ϵ increases (becomes less negative) and in addition ω_c. The coefficients of the various exponential terms are combinations of ω_c and all the break frequencies in θ_o/ϵ below ω_c. (If any such break frequency is a "multiple break", that is if the change in slope is more than 6 decibels per octave, powers of t will appear in the error response when the inverse LaPlace transform is taken.)

This points out a practical way of adjusting the shape of the error-time response of a servomechanism, since the break frequencies in the open loop transfer characteristic are directly related to the gains, time constants, and other physical quantities. The exact procedure to use will depend upon the form of the particular expression for error.

A technique which is usually helpful in adjusting the magnitudes of the various exponential terms is the following: The coefficients in the approximate formulas for error such as those of Table I will contain differences of two frequencies. For well stabilized systems, the smaller of the two frequencies may be dropped from the formula. The resulting simplification is not extremely accurate numerically but gives a useful insight into the performance of the system and shows the direction in which improvement lies.

For example, consider the group of velocity lag servos in which the slopes of the first three regions (below ω_3) are -6, -12, and -6 decibels per octave. The approximate error-versus-time curve is always built around two exponential terms, the shorter being $e^{-\omega_c t}$ and the longer-lived being $e^{-\omega_2 t}$. For a step displacement input the overshoot (which is approximately equal to the coefficient of the $e^{-\omega_2 t}$ term) is of the order of ω_2/ω_c and occurs at a time of the order of $4/\omega_c$. The peak error in the response to a step of input velocity is of the order of $1/\omega_c$ and occurs at a time of the order of $2/\omega_c$. It can be shown either from the formulas or the curves that the time is the same for the displacement error to become zero as for the velocity error to become maximum. The response of any 4-region servo system initially approaches that of a velocity lag system whose slope remains $s-6$ decibel per octave throughout the range of frequencies below ω_c; then the effect of ω_1 and ω_2 becomes apparent and the response changes its course and approaches its steady-state value, usually with the speed of $e^{-\omega_2 t}$. The principal effect of ω_1 is in determining the eventual steady state error.

Figure 12. Displacement error versus time effect of varying slope in a 4-position system (calculated data)

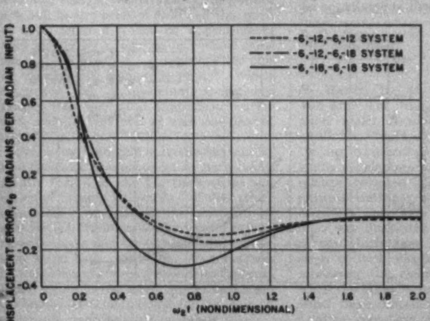

Figure 14. Peak displacement error versus ω_c/ω_2 for several values of ω_c/ω_1 (measured data)

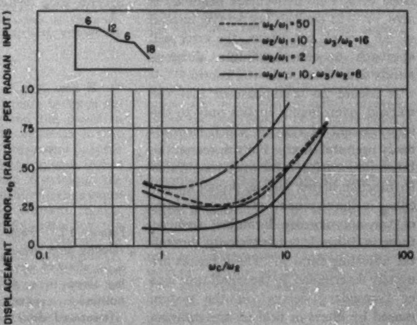

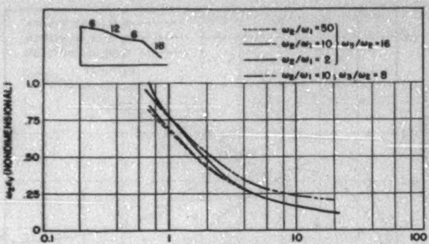

Figure 15. Peak velocity error versus ω_c/ω_2 for several values of ω_2/ω_1 (measured data)

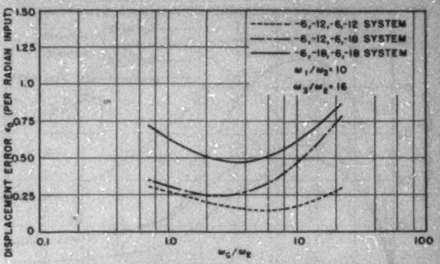

Figure 16. Peak displacement error versus ω_c/ω_2 effect of varying slope in a 4-position system (measured data)

In other words, the shape of the error-versus-time response as $t \to \infty$ is associated with the shape of the error/input transfer function ϵ/θ_i and hence the open loop transfer function θ_o/ϵ as the frequency moves from infinity toward zero. For high frequencies ϵ/θ_i is unity; the error is equal to the input at very small values of time. As the frequency is reduced past ω_c, the ϵ/θ_i response becomes that of a velocity lag system, and the error approaches that of a system whose open loop θ_o/ϵ response is -6 decibels per octave for all frequencies below ω_c. At still lower frequencies between ω_2 and ω_1 the open loop transfer function θ_o/ϵ has at least the slope of an acceleration lag system (-12 decibels per octave); at large values of time the error-versus-time curve swings away from its earlier goal and approaches zero. At the lowest frequencies, below ω_1, the system again becomes a velocity lag system (if the slope of θ_o/ϵ is -6 decibels per octave below ω_1) and the final phase of the error-time response approaches the steady state error corresponding to a velocity lag system whose open-loop, -6 decibels per octave slope passes through ω_1 and not ω_c. (If the slope of θ_o/ϵ at frequencies below ω_1 is zero, or -12 decibels per octave, instead of -6 decibels per octave, the error will approach a correspondingly different steady state value, as is well known.)

It should be re-emphasized that the method given herein applies only to the improvement of systems which have already been stabilized. For this reason the break frequencies in the open loop transfer function higher than ω_c do not appear either in the exponents or the coefficients of the approximate formulas, such as those in Table I, but enter only through the adjusting ratio *R*. These breaks are usually determined by the small time lags or "secondary delays" in the system caused by filters or field or armature inductances. They are most important in establishing the limits beyond which the accuracy and speed of the transient response cannot be improved since ω_c must be kept a reasonable distance below them to maintain stability. The designer who neglects this basic requirement will generally spend considerable time trying to improve the shape of his polar θ_o/ϵ plot near the -1 point, only to find that the plot unexpectedly swings close to the -1 point at some higher frequency resulting in the same instability in a new form.

The design of a servomechanism is usually begun by translating the customer's performance specifications into terms of major load characteristics, input-versus-time encountered, and error-versus-time responses allowed. Following this a prime mover is chosen; a control scheme is proposed. At this point an estimate of the secondary delays should be made so that the limitations which are imposed upon ω_c and ω_2 and hence upon the size and duration of the errors can be realized. If these limitations are not acceptable, the individual physical elements causing the lags must be treated separately either by cascade or feedback compensation. Several such delays will generally be of about the same length so that removing only one is not sufficient. After the system has been adequately stabilized, the approximate error/input transfer function can be obtained, and the approximate formulas such as those in Table I derived and studied to further improve the shape of the error-time response to meet the performance specifications.

Appendix

The following is an example similar to the one used in the text but the problem is more complex and it is worked out in greater detail. The problem is to find the response of the system described by the open loop transfer function of Figure 4 to a step of displacement and a step of velocity.

The open loop transfer function is:

$$\frac{\theta_o}{\epsilon} = \frac{K_V}{S} \frac{(1+S/\omega_1)}{(1+S/\omega_0)^2} \frac{(1+S/\omega_2)}{(1+S/\omega_3)^2}$$

Using the approximation shown by the dotted part of the curve and substituting

$$K_V = \frac{\omega_1\omega_2\omega_c}{\omega_0^2}$$

$$\frac{\theta_i}{\epsilon} \approx \frac{(S+\omega_1)(S+\omega_2)(S+\omega_c)}{S(S+\omega_0)^2}$$

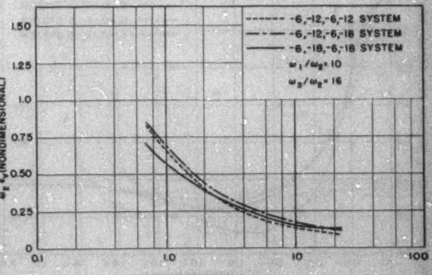

Figure 17. Peak velocity error versus ω_c/ω_2 effect of varying slope in a 4-position system (measured data)

then

$$\epsilon(t) \approx \frac{1}{2\pi i}\int_{BR}(\theta_i)\times \frac{S(S+\omega_0)^2}{(S+\omega_1)(S+\omega_2)(S+\omega_c)}e^{+st}ds$$

from which

$$\epsilon_d \approx \frac{(\omega_1-\omega_0)^2}{(\omega_2-\omega_1)(\omega_c-\omega_1)}e^{-\omega_1 t} - \frac{(\omega_2-\omega_0)^2}{(\omega_2-\omega_1)(\omega_c-\omega_2)}e^{-\omega_2 t} + \frac{(\omega_c-\omega_0)^2}{(\omega_c-\omega_1)(\omega_c-\omega_2)}e^{-\omega_c t}$$

$$\epsilon_V \approx \frac{\omega_0^2}{\omega_1\omega_2\omega_c} - \frac{(\omega_1-\omega_0)^2}{\omega_1(\omega_2-\omega_1)(\omega_c-\omega_1)}e^{-\omega_1 t} + \frac{(\omega_2-\omega_0)^2}{\omega_2(\omega_2-\omega_1)(\omega_c-\omega_2)}e^{-\omega_2 t} - \frac{(\omega_c-\omega_0)^2}{\omega_c(\omega_c-\omega_1)(\omega_c-\omega_2)}e^{-\omega_c t}$$

and

$$R = \left|\frac{(S+\omega_1)(S+\omega_2)(S+\omega_c)(S+\omega_3)^2}{S(S+\omega_0)^2(S+\omega_3)^2+\omega_c\omega_3^2\times(S+\omega_1)(S+\omega_2)}\right|_{\text{at } S=j\omega_c}$$

If the following set of constants are used

$\omega_0=0.04;\ \omega_1=0.2;\ \omega_2=1;\ \omega_c=4;\ \omega_3=16$

The time solution is

$$\epsilon_d = 0.00842e^{-0.2t} - 0.384e^{-t} + 1.375e^{-4t}$$
$$\epsilon_V = 0.02 - 0.0421e^{-0.2t} + 0.384e^{-t} - 0.3437e^{-4t}$$
$$R = 1.93$$

Here again the correction factor R should be applied only between $1/\omega_2 > t > 1/\omega_3$.

A plot of the error versus time is given in Figures 5 and 6 and as a check the time response of this system as obtained by an analogue computer is also shown.

The extension of this approach to other systems is obvious and it also is evident that any type of input may be used so long as it can be expressed or adequately approximated by a LaPlace transform.

References

1. Linear Servo Theory, Robert E. Graham. *Bell System Technical Journal* (New York, N. Y.), volume XXV, number 4, October 1946, page 616.

2. Principles of Servomechanisms, Gordon S. Brown, Donald P. Campbell. John Wiley and Sons, New York, N. Y., 1948.

3. Fundamental Theory of Servomechanisms, LeRoy A. MacColl. D. Van Nostrand Company, New York, N. Y., 1945.

4. Transients in Linear Systems, M. F. Gardner, J. L. Barnes. John Wiley and Sons, New York, N. Y., 1942.

5. Modern Operational Mathematics in Engineering, Ruel V. Churchill. McGraw-Hill Book Company, New York, N. Y., 1949.

Discussion

Emile S. Sherrard (General Electric Company, Schenectady, N. Y.): Messrs. Harris, Kirby, and von Arx give a relatively simple method for determination of the error as a function of time for representative inputs to a linear servomechanism. Figures 1 through 6 of their paper demonstrate that the method can give an excellent approximation to the exact error.

Because the method described is a straightforward one, it should prove useful to the system designer. The writer would like to inquire how the results of this method compare with results obtained by other methods. In particular, he believes a valuable comparison could be made between the results of this method and results obtained by the methods of reference 1.

The approximate expressions in this paper for ϵ/θ_i are functions of s whose poles are real negative numbers. The exact expression for ϵ/θ_i and good approximations for ϵ/θ_i may have poles for complex values of s. We see this is the case if we write

$$\frac{\epsilon}{\theta_i} = \frac{\dfrac{\theta_o}{\theta_i}}{\dfrac{\theta_o}{\epsilon}}$$

and note that, in ordinary cases, the poles of ϵ/θ_i will be the poles of θ_o/θ_i and the zeros of θ_o/ϵ. Often θ_o/ϵ can be approximated very closely by a function of s whose zeros are real and negative. However, if the plot of the absolute magnitude of θ_o/θ_i versus frequency has a maximum appreciably greater than one, good approximations for θ_o/θ_i and ϵ/θ_i will have at least one pair of complex poles.

For many high gain servomechanisms, it is difficult or uneconomical to make ω_3/ω_2 greater than 8 to 10. For the systems and errors of Figures 1 through 6 of this paper $\omega_3/\omega_2=16$. For $\omega_3/\omega_2=8$, the exact expression for ϵ/θ_i would probably have a pair of complex poles and the approximate expression would have real poles. A comparison by the authors between the exact and approximate errors for $\omega_3/\omega_2=8$, would enable an evaluation of their method for the case in which ϵ/θ_i contains complex poles.

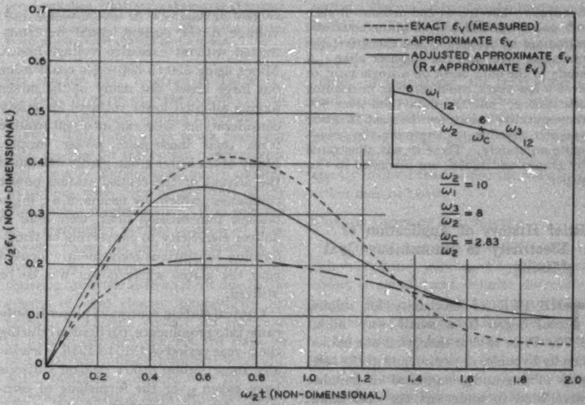

Figure 1. Error versus time for unit step of velocity input

Reference

1. Comparison of Steady-State and Transient Performance of Servomechanisms, H. Chestnut, R. W. Mayer. *AIEE Transactions*, volume 68, 1949, pages 765–77.

H. Harris, Jr., M. J. Kirby, and E. F. Von Arx: The main difference between the paper under discussion and the paper to which Mr. Sherrard makes reference is that the method described in the present paper is a way of relating transient response to frequency response without restricting the nature of the input, while the reference paper considers only step displacement inputs. This was illustrated in the paper by the curves which show the error response to steps of both displacement and velocity; moreover, the technique can be applied when the input is any function of time for which there exists or can be approximated a Laplace transform. Since the paper by Mr. Chestnut and Mr. Mayer is a tabulation of exact solutions, a comparison in the realm where the papers overlap would be no different than the comparison already given between the exact and approximate solutions. Figure 1 of this discussion shows that the agreement between exact and approximate responses is still good for ω_3/ω_2 as small as eight. As Mr. Sherrard points out, it is impossible to completely describe a function which has a complex pole by another whose poles are pure real negative numbers. When the contribution of complex poles is so large that it cannot be ignored, the transient response will contain several cycles of high-frequency oscillation of relatively large magnitude. The approximate method is not intended for systems so close to the border of instability. This limitation on the method is felt to be acceptable, since a designer who seriously contemplates using such a system would be careful to experimentally measure its performance exactly. The approximate method would still be useful to get the design to the right order of magnitude.

Analysis of Power Costs of Bituminous Coal Mines

H. P. MUSSER
MEMBER AIEE

Synopsis: The trends and amount of electric power use and cost at bituminous coal mines are of interest to the executive, the operating man, and the engineer alike. A study of the data based on a single year, or even a few years, could result in misleading conclusions; but the data from over 400 representative mines for the past 26 years make it possible to determine the trends quite accurately. These trends, illustrated by graphs and tables, are discussed in this paper.

Brief History of Application of Electricity to Bituminous Coal Mining

THE USE of electricity for mining coal began in a small way about 1879. Prior to that time, coal was hauled chiefly by mules or ponies, and at the face, pick mining and compressed air punches were used to under-cut the coal seam. Coal-cutting machines of the Breast type, first used in 1879, had increased in number to 545 by 1891, according to the first official United States Government record of the use of mining machines. Beginning about 1900 the Shortwall mining machine gradually came into general use, replacing the Breast machine.

During the two decades, from about 1880 to 1900, power plants at the coal mines furnished direct current chiefly for crude haulage locomotives, Breast cutting machines, and fan motors. In general, each mine had its own individual power plant. The mining operations were carried along as far as the relatively low-voltage direct current could be transmitted without excessive voltage losses. Mines using 550 to 600 volts could mine out large areas, but many of the mines having adopted lower voltages for safety considerations, soon ran into real trouble from their inadequate power supply. Many of the latter group gladly welcomed the advent of the central station power companies, which, by means of a-c high-tension transmission lines, were able to deliver electricity to converting or transforming substations conveniently located near the places where power was to be utilized.

Central station sources of power supply came into prominence, particularly during the 6-year period of 1910 to 1915. Gradually these public utility central stations have taken over the furnishing of electricity for the operation of coal mines, until at the present time there are very few individual or private power plants in operation at mines located in the Appalachian bituminous coal mining areas.

Records of power use and cost for mining coal were generally scanty and incomplete when private plants supplied the power requirements. In many instances no record was kept of the kilowatt-hours used, and only the powerhouse costs were known. On the other hand, as soon as the mines began to purchase electricity from the public utility companies, each month the amount of monthly kilowatt demand and energy requirements were recorded. Coal company managements became more cost conscious and more attention was directed toward the proper and efficient use of electricity for the production of coal. Nevertheless, each year the amount of electricity used for the mining of a ton of coal steadily increased. Wages have risen steadily over the years, while electricity progressively becomes cheaper, so it is natural and proper to mechanize the mining of coal and replace expensive labor with cheap electricity.

Major Trends in Power Use and Cost at Appalachian Coal Mines

This study of the use of electricity to be discussed in this paper, began in 1918 with a yearly analysis of power use and cost for a large group of mines having widely varying physical conditions and tonnage output. The scope of the analysis was enlarged and more coal companies from many Appalachian bituminous coal mining states were included in the study, until by 1923 the items of data collected and the coal companies embraced, had become stabilized and comparable data could be collected from practically the same group of mines.

For 31 years this analysis has been made, each year covering over 400 mines, principally in West Virginia, Virginia, Kentucky, Tennessee, and Pennsylvania, with a few in Maryland and Ohio.

This paper, based on these analyses gives a comprehensive representation of the amounts and trends in power use and cost in bituminous coal mining during the last 26 years. The analyses cover mines using central station power, and mines employing individual private plants. This data is given in Table I* entitled "Average Monthly Use and Cost for Coal Mines for Yearly Periods from 1923 to 1948 Inclusive." Mines using central station power are greatly in the majority. Typical of the dependence of the coal mining companies on central station power for their supply of electricity, and the disappearance of the individual private power plant from the scene, a curve has been drawn showing year by year the percentage of companies included in the annual analyses, operating their individual power plants, Figure 1. In 1923 there were 18 per cent of the coal

---

Paper 51-272, recommended by the AIEE Mining and Metal Industry Committee and approved by the AIEE Technical Program Committee for presentation at the AIEE Summer General Meeting, Toronto, Ont., Canada, June 25-29, 1951. Manuscript submitted Oct. 17, 1950; made available for printing May 10, 1951.

H. P. Musser is with the West Virginia Engineering Company, Charleston, W. Va.

*Because of their length, Tables I and II are not included in this paper. Copies of the tables are available on request to the author.

companies included in the analysis, operating their own generating plants; whereas, in 1948 this percentage had dwindled to 1.1 per cent. The opportunity of the central station to install and operate large efficient steam and electric units enabled electricity to be delivered and sold at steadily decreasing costs, but the chief handicap suffered by the independent private plant has been the steady increase in labor costs over the years.

Because of the large variation in the comparable use of power between small tonnage output mines and large ones, the mines using central station power have been divided into six monthly tonnage classes, ranging in output from the 0 to 5,000 tons per month class, to the very largest of over 60,000 tons per month. Mines of all tonnage classes using central station power, purchase it at the prevailing power rate in their locality. Usually the rates include a demand charge based on a definite time interval demand, plus an energy charge with a block price scale. The data concerning power costs for these mines do not carry any fixed charges for any investment in electric equipment used at the mines, but the demand charges are usually considered as covering the fixed charges on the generating and distributing facilities that are required to supply the power.

Tabulations for mines having their own individual private plants have been recorded so as to be as nearly comparable as is practicable to those using central station power. However, no fixed charges are included in the costs for the individual power plants for the reason that the methods of setting them up are extremely variable at the different mines. In some cases the entire powerhouse investments have been retired.

A typical and recent annual analysis, the one for 1947, is given in Table II* entitled "Analysis of Power Costs of Coal Mines for the Year Ending December 31, 1947." This table gives much pertinent data relative to the power requirements and costs of mining coal under modern conditions with over 60 per cent of the coal loaded mechanically. It is selected as a reasonably normal example of present-day power use and cost, inasmuch as there is considerable inflationary cost showing up in the 1948 analysis due to the effects of coal clauses temporarily increasing electricity costs. An electrical or mining engineer can use the data on this analysis in many practical ways and with confidence, because with its broad coverage of such a large group of mines and the yearly consistency shown by the average figures, it is authoritative for the production of coal in the Appalachian area.

Table III. Changes in Power Use and Cost

	Generation of Electricity	Coal Mining Performance*		
Year (1)	Coal Per Kilowatt-Hour, Pounds (2)	Cost Per Kilowatt-Hour, Cents (3)	Power Per Ton, Kilowatt-Hours (4)	Cost Per Ton, Cents (5)
1920	3.39	2.180	4.40	9.59
1925	2.10	2.170	3.96	8.61
1930	1.62	2.000	4.73	9.48
1935	1.46	1.830	5.41	9.88
1940	1.35	1.709	5.48	9.37
1942	1.32	1.535	6.13	9.42
1947	1.31	1.532	6.85	10.49
1948	1.30	1.595	7.54	12.03

* Averages for a group of mines in the 10,000- to 20,000-ton class.

Column 2. Source, Federal Power Commission data covering all plants contributing to public supply and Edison Electric Institute for years 1947 and 1948.

Columns 3, 4, and 5. Source, West Virginia Engineering Company, "Analyses of Power Costs for Coal Mines." Figures shown are for a large group of mines (average 45) in the 10,000- to 20,000-tons-per-month class. This group shows typical average performance because it is midway between the smallest and largest mines, and the mines in this group usually show efficient performance.

What the Long-Range Record Shows

A study of the record of the average mine in each class, for each year from 1923 to 1948 shows the following facts:

KILOWATT-HOURS REQUIRED PER TON MINED

With each succeeding year more electricity is required for each ton of coal mined (see Figure 2). Electricity is cheap and its long-term cost trend is down. Therefore, it is sound management to harness electricity for every possible task, thus giving each workman a multitude of willing slaves. Whereas, coal was loaded into mine cars by hand for the first three decades of this 20th century, the majority of coal mined now is loaded mechanically. The percentage of coal loaded mechanically is increasing rapidly. Among the group of mines included in this study, the percentage of coal loaded mechanically has increased from about 40 per cent in 1944 to over 60 per cent in 1948, Figure 3. It is cheaper to use electricity wherever it can be efficiently utilized than to use the muscles of either man or beast.

COST OF UNITS OF ELECTRICITY

The total cost of a unit of electricity (kilowatt-hour) purchased by the mines, shows a steady and definite decreasing trend, Figure 4. This trend may be attributed in part to rate reductions, in part to bettering the load factor at which the electricity is purchased, but a large portion of it has been due to the increasing use of kilowatt-hours in the lower priced brackets of the energy scale. The 1948 trend of unit cost is up, due to inflationary

Figure 1. Percentage of coal companies operating steam plants, years 1923 to 1948

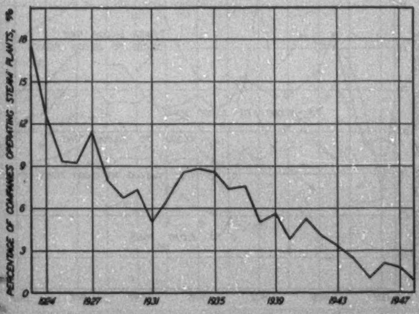

Figure 2. Kilowatt-hours required to mine a ton of coal, six tonnage classes, years 1923 to 1948

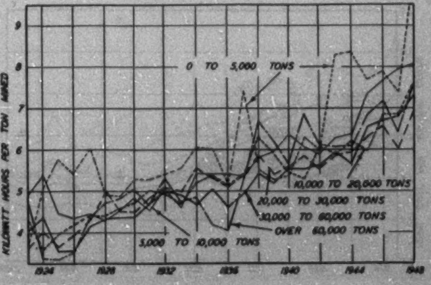

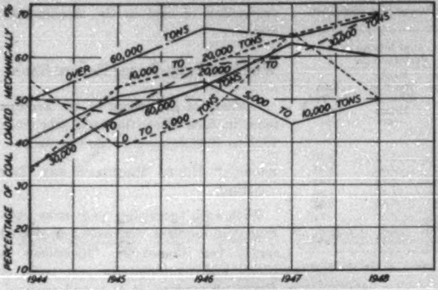

Figure 3. Percentage of coal mined mechanically, six tonnage classes, years 1944 to 1948

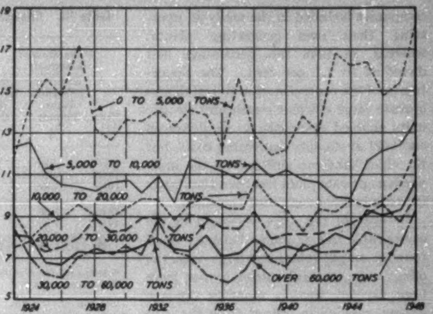

Figure 5. Power cost per ton in cents, six tonnage classes, years 1923 to 1948

prices of coal used for power generation, which increased cost of coal, acting through coal clauses in power rates, caused a temporary or intermediate upward trend in unit cost of electricity. The long-term trend is toward lower unit cost.

It is interesting to observe the extent to which central stations can generate a kilowatt-hour with less coal and reduce the unit charge for electricity, while simultaneously the coal mines use more kilowatt-hours per ton of coal mined. The net result is that the cost of power for mining a ton of coal has remained almost constant for over 25 years. In order to show the long-term trends in this respect, Table III has been prepared taking a representative group of mines, those producing 10,000 to 20,000 tons of coal per month and following the changes in power use and cost over a period of 29 years.

By referring to Table III and considering the period of 24 years from 1925 to 1948, it will be noted that the average cost of a kilowatt-hour as purchased by this group of mines dropped 26.5 per cent, or on the average slightly over 1 per cent per year; the amount of kilowatt-hours required to mine a ton of coal increased 90.5 per cent, or on the average the yearly increase was approximately 0.15 kilowatt-hour. Stated another way, the amount of power used to mine a ton of coal increased one kilowatt-hour during each 6.7 years. The increase was due to progressive mechanization, the growth in the size of the mines requiring more ventilation, pumping, longer haulage distances, and more preparation at cleaning plants. There was practically no increase in the cost of power used per ton of coal mined for this group of mines from 1925 to 1942, a period of 18 years, but the inflation during and after World War II was responsible for an increase of about 39.7 per cent in this cost. The coal clauses in power rate schedules were chiefly responsible for this increased cost of electricity. The improvements in the art of generating electricity have advanced so greatly that it required only about 38.4 per cent as much coal to generate a kilowatt-hour of electricity in 1948 as was required in 1920.

Power Costs per Ton of Coal Mined

The net result of progressively lower costs for each unit of electricity purchased, and of increased amounts of electricity used in mining each ton of coal, has been an almost constant or unchanging cost of power per ton of coal mined for all classes of mines over the period from 1923 to 1942, Figure 5. There has been an upward trend in cost of power per ton of coal mined since the beginning of World War II. Future power costs will likely follow the general trend of prices.

There is a great difference in the power requirements and costs of the different tonnage classes (see Figure 5). The mines included in the 0 to 5,000 tons per month have the highest power costs per

Figure 4. Total cost of electricity per kilowatt-hour in cents, six tonnage classes, years 1923 to 1948

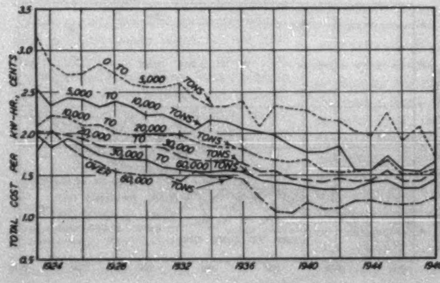

Figure 6. Load factors of electricity utilized at coal mines based on demand in percentage, six tonnage classes, years 1923 to 1948

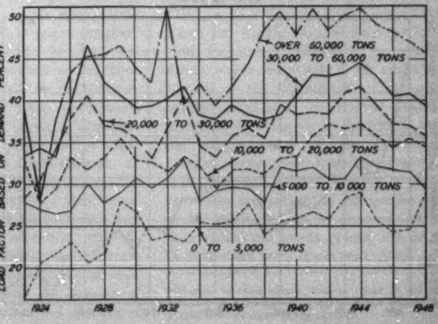

ton of coal produced. This group of mines having small monthly production includes many mines nearly worked out, in which case, pumping, ventilation, and haulage costs are high. New mines may have lightly loaded electric equipment. The power costs per ton of the group producing 0 to 5,000 tons per month are approximately twice as great as the average power costs of mines producing over 60,000 tons per month. The mines producing large monthly tonnages have many opportunities to minimize power costs, such as being able to fully load the electric equipment, purchase electricity at a high load factor, and buy most of the energy used in the low cost blocks.

Load Factor of Power Purchases

A simple definition of load factor with reference to power purchases is the relation of the average hourly rate of power use during a period of a month, to the highest rate of power use during any 15-minute or 30-minute demand interval of the same month. Power rates vary considerably in specifying the basis of maximum demand, but the term as used in this paper is simply the relation of average demand to maximum demand for a monthly period.

Load factor is extremely important because modern power rates determine the cost of electricity more on the basis of load factor than on the quantity of power purchased. For this reason, the well-managed mine usually has a high load factor, and much attention and effort are devoted to controlling or limiting maximum demand. A set of curves showing the trend of average power factors maintained by the various tonnage classes of producing mines has been prepared, Figure 6.

In general, all the groups of mines have succeeded in improving the load factor of their purchases. The large mines are able to maintain the best load factors, due to the greater diversity of their many power requirements. This is one of the reasons why power costs are proportionally less to the large tonnage mines.

To summarize, the data for the last 26 years clearly shows the increasing use of electricity in bituminous coal mining, brought about chiefly by increased mechanization; the decreased cost of electricity per kilowatt-hour, the result of both of these trends being a practically constant cost per ton. Also, the continued trend away from private steam plants to central station power is quite pronounced.

No Discussion

Metallic Rectifiers in Telephone Power Plants

D. E. TRUCKSESS
MEMBER AIEE

Synopsis: Metallic rectifiers are a comparatively new means of converting power from alternating current to direct current. Most of the component apparatus used in the Telephone Systems operates with direct current while the normal power source is alternating current. Therefore a static device without expendable parts which is obtainable in small and large current capacity lends itself as a means for power conversion in telephone power plants.

THERE ARE many uses of metallic rectifiers in telephone power plants where rectifiers are required. These applications vary from 2 to 2,500 volts and in power sizes of a few watts to 10 kw. The metallic rectifiers are used primarily for charging storage batteries. However, there are many applications where the d-c power is used directly to supply relay circuits, talking battery, plate and filament for vacuum tube amplifiers, telegraph circuits, and teletypewriters.

The principal advantage of metallic rectifiers over hot-cathode diode or triode-tube rectifiers or the mercury-pool rectifiers, in larger sizes, is that the rectifying element is not an expendable part. This feature is particularly desirable when the rectifiers are located in PBX's and small central offices where a maintenance man is not in attendance at all times and reliable operation is important. Metallic rectifiers lend themselves particularly to applications where a small amount of power is required. The rectifier can be mounted within the associated equipment in inaccessible places as it is not necessary for the maintenance personnel to have direct access to it and the equipment arrangements of the rectifier can be made to fit into the mounting arrangements of its associated equipment.

The disadvantages of metallic rectifiers are that they require in most cases more space than tube rectifiers, and they are also more sensitive to the higher ambient temperatures. However, in telephone central office applications this has not been a serious disadvantage. The metallic rectifier usually results in a higher first cost but in many cases the annual charges are less than with tube rectifiers when the cost of replacing tubes is considered. The metallic rectifiers do not lend themselves as readily to automatic regulation as thyratron rectifiers. However, with the use of saturable reactors and magnetic amplifiers to control the a-c voltage applied to the stacks a regulated metallic rectifier can be built. This combination makes it possible for regulated metallic rectifiers to compete on an annual charge basis with regulated tube rectifiers and up to approximately 10-kw sizes in the voltage range below 150 volts.

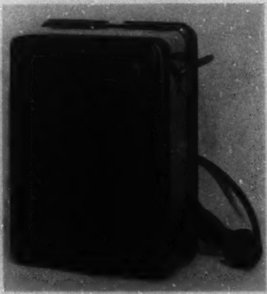

Figure 1. Copper oxide rectifier unit output, 3 volts, 0.1 ampere

This paper excludes the application of metallic rectifiers as circuit elements and does not include any description of military applications.

Copper Oxide Rectifiers

Copper oxide rectifiers first were used in the Bell System in 1927 to trickle charge PBX storage batteries. During the early 1930's a number of applications for small rectifiers were developed to supply talking battery to station wiring plans for local telephone intercommunication, to trickle charge large storage batteries and to supply 24 volts for relay operation. Figure 1 shows a copper oxide rectifier which supplies 3 volts for operating the telephone transmitter in station wiring plans and is mounted in the familiar "Bell" box. This rectifier is used on the customer's premise and is mounted on baseboards or is attached to desks. Figure 2 shows a copper oxide rectifier of a larger size for the same purpose in supplying talking battery to larger station wiring plans and key equipments. It also supplies direct current for relays, and alternating current for lighting lamps and ringing buzzers.

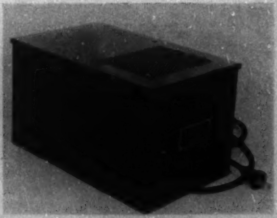

Figure 2. Copper oxide rectifier unit outputs, 18 volts, 0.5 ampere direct current for relays, 3 volts, 0.1-ampere direct current talking supply, 16 volts, 1-ampere a-c signaling

---

Paper 51-273, recommended by the AIEE Metallic Rectifiers Committee and approved by the AIEE Technical Program Committee for presentation at the AIEE Summer General Meeting, Toronto, Ont., Canada, June 25–29, 1951. Manuscript submitted March 27, 1951; made available for printing May 10, 1951.

D. E. TRUCKSESS is with the Bell Telephone Laboratories, Inc., New York, N. Y.

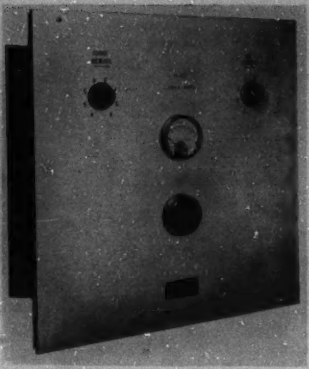

Figure 3 (left). Copper oxide rectifier unit output, 2 to 9 volts, 6 amperes

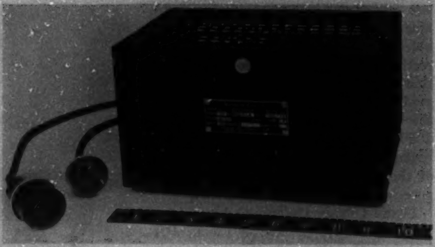

Figure 5 (right). Selenium rectifier unit, manual regulation, output, 130 volts, 0.2 ampere

Copper oxide rectifiers mounted in the same cabinet as shown in Figure 2 are used for trickle charging PBX storage batteries which range in voltage from 17 to 22 volts and provide currents up to 1.2 amperes.

Figure 3 shows the largest of the copper oxide rectifiers used in telephone power plants. It supplies 6 amperes for trickle charging 1, 2, or 4 emergency storage battery cells. These emergency cells are provided in large central offices and are connected in series with the main battery during primary power failure. They are normally not in the circuit and must be trickle charged to maintain their capacity. This rectifier is designed to mount in the power board of the telephone power plant.

Table I shows the voltage and current ratings of the principal copper oxide rectifiers in telephone power plants. All of these rectifiers use the $1^1/_2$-inch diameter copper oxide cell in series and parallel combinations. These rectifiers in 1949 required about 200,000 cells.

Selenium Rectifiers

Selenium rectifiers were first used in 1942 to supply line current and power for operating the magnets in teletypewriters. The use of selenium rectifiers from 1942 to 1945 was limited due to the war situation. After the war, selenium found an increasing application in telephone power plants. The early use was of the small

Figure 4 (below). Selenium rectifier cells annual demand

Figure 6 (upper right). Selenium rectifier unit, magnetic regulation, output, 120 volts, 1 ampere

Figure 7 (lower right). Selenium rectifier unit, magnetic regulator, output, 24 volts, 9 amperes

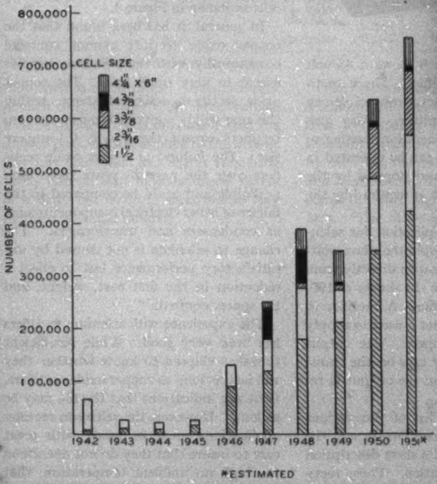

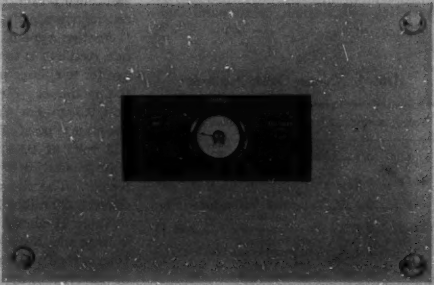

size cells from 1 inch to $4^{3}/_{8}$ inches in diameter. As larger size cells became available they were used in the higher powered rectifiers. More flexibility in the application of selenium cells was thus made available as it is always desirable to use the minimum number of cells in parallel and to select the cell size to fit the current required. But when the current capacity of the largest size cell is reached, it is necessary to operate cells in parallel.

Figure 4 shows the annual demand for the $1^{1}/_{2}$ inch, $2^{3}/_{16}$ inch, $3^{3}/_{8}$ inch, $4^{3}/_{8}$ inch and the $4^{1}/_{4}$ inch by 6 inch size cells. Notice the shift from the $4^{3}/_{8}$ inch to the larger cell.

Figure 5 shows a small selenium rectifier that mounts under the table of teletypewriter printers to supply the line current and power for the biasing winding of the line relay. This was the earliest application and continues as a large application for selenium cells. The output voltage is manually regulated with taps on the transformer. Figure 6 shows a larger selenium rectifier to supply the 19-type printer which requires approximately 1 ampere at 120 volts. This rectifier includes magnetic type of regulation.

For automatically charging 24-volt batteries in PBX's and to supply filament to repeaters, selenium rectifiers with magnetic regulation are used in several current sizes. Figure 7 shows a 24-volt 9-ampere rectifier. This rectifier is designed to mount in the relay rack associated with the telephone equipment.

Figure 8 shows a 12-volt 200-ampere regulated selenium rectifier which uses the saturable-reactor type of control to obtain regulation. The saturable reactor is driven by an electronic voltage amplifier. The electronic amplifier is required where a closely regulated voltage of ±1 per cent is needed. This rectifier floats the storage battery which is used to supply filaments in a repeater station.

In small central offices which use 24 and 48 volts, a regulated metallic selenium rectifier may be used to float the storage batteries and is built in 100- and 200-ampere sizes. Figure 9 shows a 48-volt and 100-ampere rectifier. These rectifiers use saturable reactor control driven by an electronic amplifier. They also include control equipment for starting so that several rectifiers can be operated in parallel and started and stopped by the associated power plant as required by the central office load.

Table I. Copper Oxide Rectifiers

Volts	Ampere	Applications
3	0.1	Talking battery for key equipments
2 to 9	6.0	Trickle charging 1, 2, or 4 cell battery
18	0.5	Relay and talking battery for key equipments
17 to 22	0.5	Trickle charging 8, 9, and 10 cell battery
24	1.2	Relay supply and trickle charging
130	0.125	Telegraph printer supply

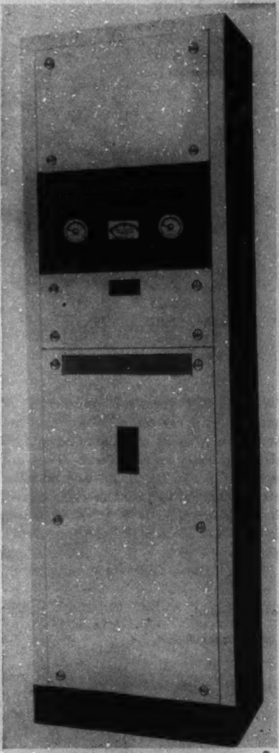

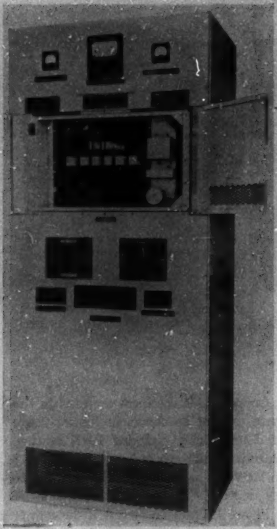

Figure 8 (left). Selenium rectifier unit, electronic regulator, output, 12 volts, 200 amperes

Figure 9 (above). Selenium rectifier unit, electronic regulator, output, 24 or 48 volts, 100 or 200 amperes

Another type of application for selenium rectifiers is to supply the plate voltage for telephone repeaters directly from the rectifiers. Figure 10 shows a 190-volt 0.5-ampere rectifier. A rectifier in the same type of cabinet is used to supply 315 volts at 0.33 ampere. The output voltage is adjusted by taps on the transformer. The ripple on the output is reduced to 20 millivolts.

Table II shows a list of the various voltage and current sizes now in use, the type of regulation and a short description of the type of application. These rectifiers have all been developed since the war and have created the demand for selenium cells as shown in Figure 4.

In general, it has been found that the copper oxide rectifier cannot compete economically with the selenium rectifier except in very small sizes. The copper oxide rectifiers described above, within this year will be converted to use selenium rectifiers except the 3-volt, 0.1-ampere size. The failures of copper oxide rectifiers over the past 23 years have been negligible and could be compared to the failure of other electrical components such as condensers and transformers. The change to selenium is not caused by unsatisfactory performance but to effect a reduction in the first cost, weight, and the space required.

The experience with selenium rectifiers has been very good. While insufficient time has elapsed to know whether they will last as long as copper oxide rectifiers, there are indications that the life may be as long. However, the selenium rectifier applications must be made with great care to insure that they do not operate in too high an ambient temperature, that

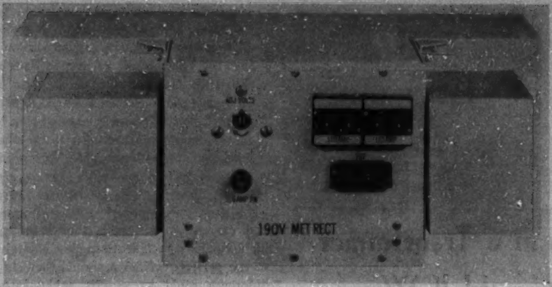

Figure 10. Selenium rectifier unit, manual regulation, output, 190 volts, 0.5 amperes

Table II. Selenium Rectifiers

Volts	Amperes	Regulation	Application
8	1	Manual	Trickle charging 4 cells
10	12	Manual	Trickle charging 1 to 4 cells
12	22	Manual	Filament supply
18	4	Manual	Trickle charging 1 to 8 cells
24	1	Manual	Relay and talking supply
48	1	Manual	Relay supply
120	0.2	Manual	Telegraph printer supply
120	0.4	Manual	Telegraph printer supply
120	0.8	Manual	Telegraph printer supply
130	0.65	Manual	Plate supply to repeaters
190	0.5	Manual	Plate supply to repeaters
250	0.25	Manual	Plate supply to repeaters
315	0.33	Manual	Plate supply to repeaters
24	1	Magnetic	Storage battery floating
24	3	Magnetic	Storage battery floating
24	9	Magnetic	Storage battery floating
48	1.5	Magnetic	Relay supply
120	1.0	Magnetic	Telegraph printer supply
120	3.0	Magnetic	Telegraph printer supply
6	15	*Electronic	Storage battery floating
12	200	Electronic	Storage battery floating
24	6	Electronic	Filament supply
24	100	Electronic	Storage battery floating
24	200	Electronic	Storage battery floating
48	100	Electronic	Storage battery floating
48	200	Electronic	Storage battery floating
53	125	Electronic	Storage battery floating
2,500	0.25	Electronic	Submarine cable supply

*Electronic amplifier driving a saturable reactor.

they operate at the proper current density in each cell, and that their rated voltage is not exceeded. It is important that the inverse peak voltage applied to the cells be carefully controlled as there is very little safety factor, and in some cases surges or a distorted 60-cycle wave shape may produce selenium failures.

The development of higher-voltage selenium cells has spurred their application by reducing the first cost of the selenium stack in low-voltage rectifiers by reducing the number of cells required and has enabled the selenium rectifier to compete with high-voltage tube rectifiers. The development of larger cell sizes to handle more current per cell has encouraged the use of selenium in higher-current rectifiers. In the 10-kw size it has been difficult for the selenium rectifiers to compete in first cost with motor generators but the higher efficiency, smaller floor space, reduced maintenance, and the absence of noise of rotating equipment have encouraged their use in some applications.

Discussion

H. G. Mah (Canadian Line Materials Ltd., Toronto, Ont., Canada): Mr. Trucksess's paper certainly shows the increasing acceptance of selenium rectifiers. There are a few points on which we would like his comments:

1. The input-output regulation requirements and how this is met by the electronic and magnetic regulated types.
2. Use of d-c marginal voltage relay controlled type for battery floating by the float-boost or 2-rate method and also by the constant voltage method using a reversible motor-driven continuously variable transformer. We find this type has higher efficiency and power factor than types using saturable reactor and result in units larger than 10 kw desirable in many applications.
3. Is 3-phase supply used in the larger electronic units?

D. E. Trucksess: The following are comments on Mr. Mah's questions:

1. The requirements of regulation are to stabilize the d-c output to ±1 per cent with changes of ±5 per cent of the a-c input voltage and load changes of no load to full load. Details of how this is accomplished will be the subject of two papers scheduled for future presentation.
2. The use of the 2-rate method of regulation is used in the Bell System only on small inexpensive batteries (20 ampere hours or less) as it definitely requires the battery to take and give a charge. This reduces the life of the battery. The motor-driven continuously varied transformer method of regulation is satisfactory and is used in the Bell System. To get the maximum battery life the voltage must be held to ±1 per cent. The power factor is higher but the efficiency need not be lower than the saturable reactor type.
3. All rectifiers larger than 2.5 kw are built for operation from a 3-phase power supply.

Transient Conditions in a Transformer Supplying Energy to a Half-Wave Rectifier Circuit

P. N. MARTIN
ASSOCIATE AIEE

HALF-WAVE rectifier circuits containing resistance, inductance, and capacitance, separately and in combination, have been analyzed and explained in several papers.[1,2,3] In general, it has been assumed that the circuit was energized from a source of negligible impedance. For most purposes this assumption is entirely satisfactory and sufficiently accurate, inasmuch as the impedance looking back into the supply circuit is usually small compared with that of the rectifier and load. In some applications of the half-wave rectifier, however, the transient conditions when the circuit is closed or opened, or in the case of a controlled rectifier, when it becomes conducting or nonconducting, are important. These transients are affected by the characteristics of the supply circuit. Also, it has been recognized that while the rectifier in the secondary circuit is conducting normally, the d-c component of the secondary current produced by the half-wave rectifier has a saturating influence on the transformer, which in turn causes the primary current to be large and to have large harmonic components, but the exact nature of this effect on the primary current is not self-evident.[4]

Purpose and Scope of the Investigation

The circuit studied in this investigation consisted of a half-wave rectifier and load fed from the secondary of a transformer, the primary of which was energized from a single-phase, sinusoidal, low-impedance a-c source. The half-wave rectifier acts like an automatic switch or valve that allows current to flow freely in one direction but blocks the flow, and in effect, opens the circuit when the voltage across it reverses polarity. Thus, even under steady-state conditions, in this type of circuit there is a discontinuity of current every cycle and the steady-state condition might be considered as a series of repeated transients. It was desired to determine just how the primary current adjusts itself to accommodate this pulsating secondary current and the effect of the transformer resistance and electromagnetic circuit on the secondary current. The effect of changes in the type of load and other parameters of the circuit, including the transformer resistances and saturation curve, and the power relationships also have been studied.

During tests on this type of circuit, it had been observed that a d-c transient voltage appeared in the primary circuit whenever the secondary circuit was closed or opened. The characteristics of these transients have been investigated, including the effect of changes in the circuit parameters and varying the time in the cycle of closing or opening the secondary circuit; also, of closing and opening the primary instead of the secondary. The results have been compared with a similar circuit except with a battery substituted for the rectifier to supply the d-c component of current.

The theoretical study has assumed the rectifier to be perfect, that is, having zero resistance to current flow in the conducting direction and infinite resistance to voltage tending to force current in the opposite direction. For the experimental work a metallic-dry-plate (copper-oxide) rectifier was used, operating at voltage and current values such that it gave highly efficient rectification, close enough to the perfect rectifier assumed that the difference could be readily taken into account by assuming a small amount of extra resistance in series with the load. The grid-controlled rectifier has not been included in the study, but the results and conclusions apply to such rectifiers also to a considerable extent, and the methods used can be extended readily to give more exact information on circuits containing grid-controlled rectifiers.

In all of this discussion the term *steady state* is used to apply when the circuit has stabilized so that successive cycles are repetitive, even though there are discontinuities in each cycle.

Summary and General Conclusions

For the first analysis a simplified equivalent circuit for the transformer has been assumed, leakage reactance and core loss being neglected. Study of this circuit shows that when the half-wave rectifier load is closed in on this energized transformer, a direct voltage component is developed in the primary caused by the pulsating load current flowing through the primary resistance. Because of this voltage drop, the net alternating voltage at the transformer exciting winding (supply voltage minus resistance drop) is not symmetrical, that is, the positive half-cycles of voltage are reduced in magnitude relative to the negative half-cycles. This, in turn, causes the magnetic flux variations in the core to be unsymmetrical and an increasing magnetic bias in one direction to develop in the core. Similarly, the exciting current develops a d-c com-

---

Paper 51-274, recommended by the AIEE Metallic Rectifiers Committee and approved by the AIEE Technical Program Committee for presentation at the AIEE Summer General Meeting, Toronto, Ont., Canada, June 25–29, 1951. Manuscript submitted July 10, 1950; made available for printing May 11, 1951.

P. N. Martin is with Union Switch and Signal Company, Swissvale, Pa.

The material presented in this paper is abstracted from a Thesis submitted to the University of Pittsburgh in partial fulfillment of the requirements for the degree of Master of Science, September, 1948. The author is indebted to Dr. P. N. Bossart for his helpful guidance in this investigation and to F. H. Krupensky who assisted in the tests with the magnetic oscillograph.

ponent whose magnitude increases on successive cycles until it is just sufficient to counterbalance the d-c component of the load current in the primary. Thus, the analysis of this transient condition leads to the explanation of the nature of the steady-state primary current. It is made up of a pulsating, unidirectional component corresponding to the load current in the secondary and the exciting current, which includes a large d-c component as well as the usual a-c exciting current. The analysis is extended to cover the complete transformer circuit and the effect of changes in the load and transformer characteristics but the same basic analysis applies and the results are modified but little.

The experimental results obtained using an oscillograph to study the voltage and current wave shapes, have verified the theoretical analysis. A method of exact mathematical analysis based on the differential equations of the circuit in a step-by-step process also is described.

In most practical applications of this type of circuit, the transformer core is highly saturated because of the d-c component. This, of course, has appreciable effect on the exciting current. Saturation does not affect the d-c component of the exciting current appreciably in the steady state, because as explained previously, that builds up just sufficiently to be equal and opposite to the d-c component of the load current on the primary side. Saturation does cause the a-c component to be increased, however, and to be unsymmetrical so that it contains large harmonic components, particularly second and other even harmonics.

It is thus apparent that the steady-state primary current will always be unsymmetrical, even without saturation in the transformer. In the usual case the transformer will be saturated and the primary current will be further complicated and its rms value increased by the harmonics in the exciting current.

Comparison of the results of the analysis of the transformer circuit having a half-wave rectifier in the secondary with a similar circuit except with a battery in series with the secondary to supply the d-c component gives some interesting results. As discussed before, the primary current in the rectifier circuit after steady-state conditions have been reached consists of discontinuous positive pulses corresponding to the current through the rectifier plus the exciting current, which has a d-c negative component equal in magnitude to the d-c average of the positive pulses, and an a-c component. This analysis accounts for the absorption of power from the a-c source to supply both the a-c and d-c power in the load circuit. With the battery substituted for the rectifier, the steady-state primary current contains only the a-c load and a-c exciting current components and the required supply voltage is much lower for the same amount of fundamental frequency current in the load.

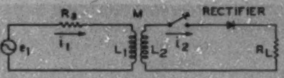

Figure 1. Basic circuit

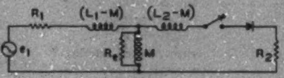

Figure 2. Equivalent circuit for that of Figure 1

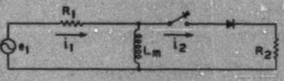

Figure 3. Simplified circuit for preliminary study

The steady-state conditions thus are different, but the transients in the primary caused by closing or opening the secondary which are superimposed on the steady-state current, are similar for these two circuits. When the secondary is closed, the primary transient consists of a positive pulse of current that rises quickly to a peak and then fades away gradually. The transient when the secondary is opened is similar except of opposite polarity. There is little difference in these transients in either type of circuit regardless of the point in the a-c cycle at which the secondary is opened or closed.

Theoretical Analysis and Experimental Verification

SIMPLIFIED CIRCUIT WITH RESISTANCE LOAD

Theoretical Analysis. Figure 1 shows the basic circuit under consideration. The load R_L is fed through the half-wave rectifier from the secondary of the transformer, which is energized from a-c source e_1 through series resistance R_s. For purpose of analysis the transformer can be replaced by its equivalent circuit as shown in Figure 2. R_1 now includes the resistance of the primary as well as R_s, and R_2 includes the resistance of the secondary and R_L. For the present analysis this circuit has been further simplified as shown in Figure 3 by substituting the single inductance L_m for the transformer windings and omitting R_e, which represented the core loss in Figure 2. This is the equivalent circuit for Figure 1 if the transformer has a one-to-one turn ratio and the leakage reactances of the windings and the core loss are neglected. In other words, the coupling coefficient is assumed to equal unity and the mutual inductance M is equal to the primary inductance L_1 and secondary inductance L_2 and is the same as the magnetizing inductance L_m. Actually this is a close approximation for an iron-core transformer of small or moderate voltage and power rating and usual design proportions.

For the first analysis it is assumed that L_m is constant, that is, the relation between magnetic flux and current is linear without saturation in the range of current involved. The following analysis follows the changes that occur after the switch is closed in the secondary circuit until the steady state is reached and successive cycles are repetitive. A general method of carrying out this solution would be to solve the differential equations for the circuit for the two conditions, one with the rectifier conducting and the second with the rectifier blocking, which is equivalent to the load circuit being open. Then, the solution would be carried on in a succession of steps of approximately a half-cycle duration each, alternating between the two conditions of the secondary circuit as its voltage alternates between positive and negative. It is more instructive, however, and more simple to use the following method, which is based on the concept of volt-seconds in an inductance corresponding to the change in flux linkages produced and to the change in current.[5] This method is very useful whenever the voltage and current do not follow simple sinusoidal patterns. It is based on the law of voltage induction by changing magnetic field that links a winding,

$$e=N\frac{d\phi}{dt}=L\frac{di}{dt}$$

(e is the applied voltage necessary to overcome the induced electromotive force so that the equations are written with positive instead of negative signs before N and L).

These equations can be rewritten in the forms,

$$\int d\phi=\frac{1}{N}\int e\,dt,\text{ and }\int di=\frac{1}{L}\int e\,dt$$

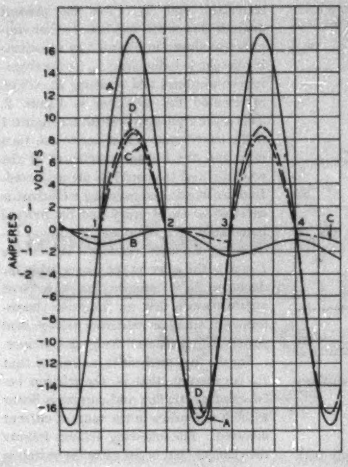

Figure 4(A) (left). Calculated conditions for circuit of Figure 3 after closing of secondary

$R_1 = 1$ ohm
$R_2 = 1$ ohm
$L_m = 0.074$ henry
Frequency = 60 cycles per second
$X_m = 28$ ohms
Switch closed during the negative half-cycle preceding time 1
Curve A—Supply voltage e_1
Curve B—Primary magnetizing current i_m
Curve C—Primary resistance voltage drop i_1R_1
Curve D—Voltage at transformer e_m (across L_m); this also is the secondary voltage

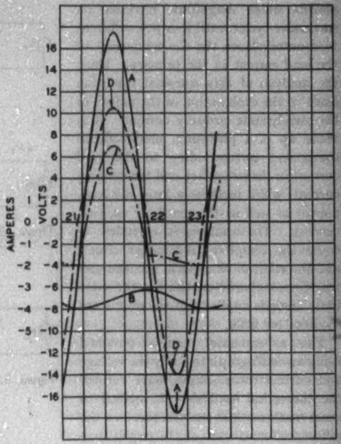

Figure 4(B) (right). Same as Figure 4(A) except several cycles later

Thus, if the value of the integral of *edt* in volt-seconds can be obtained for any interval, by usual integration methods or by measuring or estimating the area under the curve of voltage versus time, the corresponding change in flux linkages or in current is obtained directly.

Figure 4 shows the results of a calculation made in this manner for a selected set of parameters in the circuit of Figure 3. These particular values were selected in order to correspond with apparatus used in a test circuit to be described later in this paper. The value of R_1 was purposely chosen larger than it would be in most practical circuits in order to illustrate the voltage conditions in the primary circuit more clearly. It is assumed that the primary circuit has been closed sufficiently long for the steady state condition with open secondary to be established, the current i_1 having an amplitude of 0.624 ampere and lagging the applied voltage by 88 degrees. The magnetizing current i_m is the same as i_1 under this condition.

The switch in the secondary circuit is then closed at any time in the negative half-cycle prior to t_1. There is no change in conditions, the rectifier keeping the circuit effectively open, until the voltage e_m across L_m starts to go positive and the rectifier becomes conducting, and in effect, closes the secondary circuit. By estimating values of i_1 and i_2, determining the corresponding wave form for voltage e_m, then calculating the volt-seconds in this voltage wave for the positive half-cycle, the change in magnetizing current i_m during this period can be calculated. The estimated values for i_1 and i_2 are then corrected and the calculation repeated until the resulting value of i_m checks to the desired degree of accuracy with the estimated value. With judicious selection of the trial values, sufficient accuracy can be obtained usually on the first or second trial. Since the voltage applied at L_m is reduced during the conducting half-cycle because of the drop in R_1 due to the load current, the volt-seconds applied to L_m are reduced compared with the no-load condition. The change in i_m is correspondingly less so that at t_2 i_m is less than it was at the end of the preceding positive half-cycle (at -182 degrees relative to t_1).

A similar procedure is then carried out to obtain the change in i_m during the negative or blocking half-cycle, t_2 to t_3. An estimated value for i_m is used for trial, the corresponding e_m is obtained by subtracting the i_mR_1 drop from the supply voltage e_1, the volt-seconds in the e_m wave between t_2 and t_3 are calculated, and from this volt-second value, the change in i_m is obtained as explained above and checked against the trial value. A second trial is used if the first was not accurate enough. Since e_m has nearly the same amplitude during this first blocking half-cycle as before the switch was closed, the change in i_m between t_2 and t_3 is approximately the same as the difference between positive and negative peaks of i_m in the steady-state condition with open secondary. Thus, the negative change in i_m from t_2 to t_3 is larger in magnitude than the positive change between t_1 and t_2, and the value of i_m is considerably more negative at t_3 than at t_1. Thus, in succeeding cycles the average value of i_m becomes more and more negative although at a logarithmically decreasing rate in a manner typical of transient conditions in circuits containing inductance and resistance.

The reason for this development of a negative d-c component in the magnetizing current is the unbalance in the voltage e_m across the transformer winding, the positive portions of the voltage wave being smaller in amplitude and having less volt-seconds area than the negative portions. This reduction in amplitude of the positive portions of the voltage wave results from the drop of the load current pulse through the primary resistance R_1. Thus the primary iR_1 drop acts automatically to produce a negative d-c component in the magnetizing current i_m. This negative component continues to increase in magnitude until a balance is reached, that is, the volt-second integral of the positive part of the voltage wave across the transformer winding is just equal to the volt-second integral of the negative part. Succeeding cycles are then repetitive. Under this steady-state condition the average d-c voltage drop of the negative component of the exciting current in the primary resistance R_1 just counterbalances the d-c voltage drop due to the pulsating, unidirectional load current and the resulting net average in the primary circuit equals zero.

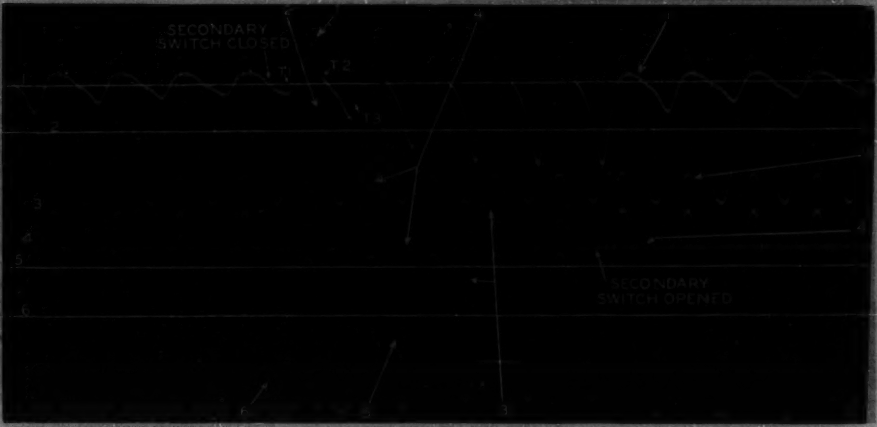

Figure 5. Oscillograph record of test on circuit similar to Figure 1. The order of traces from top to bottom is:

1. Voltage across resistor R_a in primary (shows primary current i_1)
2. Input voltage e_1 ($f=60$ cycles per second)
3. Voltage across rectifier in secondary circuit. (The trace extends below that for i_2 during the half-cycles that the rectifier is blocking current flow)
4. Voltage across load resistance R_L (shows secondary current i_2). The trace for i_2 extends above that for the rectifier voltage during the conducting half-cycles
5. Voltage across secondary of transformer
6. Voltage across primary of transformer

Figure 4(A) shows the changes in current and voltage that occur during the first two cycles after the secondary switch is closed. Figure 4(B) shows the results of a similar calculation for a cycle an appreciable time later. It is assumed that the magnetizing current i_m has reached a value of -4.0 amperes at the end of a blocking half-cycle, this time being arbitrarily designated as t_{21}. The calculation is carried out in the same manner as before. At the end of this cycle, t_{22}, i_m is found to have a value practically the same as at the beginning, t_{21}, within the limits of accuracy of the calculation. Thus, i_m is no longer tending to become further negative and succeeding cycles will be repetitive.

Test Results. Figure 5 is a set of oscillograms taken in a test circuit having substantially the same parameters as that used for the calculated curves of Figure 4. The test circuit was as shown in Figure 1 with a small transformer of suitable voltage and current rating. The voltage source for the primary was a Variac transformer of relatively large rating so that its impedance was negligible, which was energized from 115-volt 60-cycle commercial power. Low impedance a-c ammeters of the transformer type were inserted in the primary and secondary circuits, with a permanent magnet type d-c ammeter also in series in the secondary. Instead of the switch shown in the secondary circuit, a contact on an oscillating, pendulum-type circuit-interrupter was used. This opened and closed the secondary circuit six times per second so that it was alternately open and closed for intervals of approximately five cycles duration. A conventional, 6-element magnetic oscillograph with the six voltage elements connected across various parts of the circuit as indicated in Figure 5, was used. The film in the oscillograph was started at random without any particular synchronization with the circuit-interrupter.

This oscillogram has been selected for Figure 5 from several taken on the same test circuit, because the closing of the secondary happened to occur during the negative part of the cycle. The point of closing can be seen to have occurred slightly before the supply voltage reached its negative peak. The action of the circuit following this closing corresponds to the preceding theoretical analysis. There is no change during the rest of the negative half-cycle except that the secondary voltage appears as inverse voltage across the rectifier instead of across the open contact. The development of the large negative component of exciting current in i_1 after conduction starts shows up clearly. The negative peak of i_1 in the fifth cycle is only slightly different from the fourth, so that it is apparent that the steady state has been reached practically by the fifth cycle. It is apparent also that the a-c exciting component of i_1 becomes considerably larger when the switch is closed than it was with the secondary open. This results from saturation in the transformer core caused by the negative bias that develops in the exciting current and consequently in the magnetic flux.

Other effects brought out in the theoretical analysis are also apparent in Figure 5. The first load-current pulse (i_2) is somewhat smaller than the final steady-state pulses. Similarly the primary and secondary voltages at the transformer are at first unbalanced but gradually become readjusted so that the positive and negative volt-second areas for a cycle become equal. These transient conditions go along together and all the voltages have nearly reached the steady state by the fifth cycle after the contact closed.

Figure 6 shows the steady-state voltages for the same circuit as Figure 5 to a larger scale. These were carefully traced from the screen of a cathode-ray oscilloscope. The amplifier in the oscilloscope was set to a suitable sensitivity by the use of a sine-wave calibrating voltage and this setting was left unchanged so that all of the traces can be compared directly. This is not true of the traces of Figure 5 as no particular attempt was made to have the six elements of the magnetic

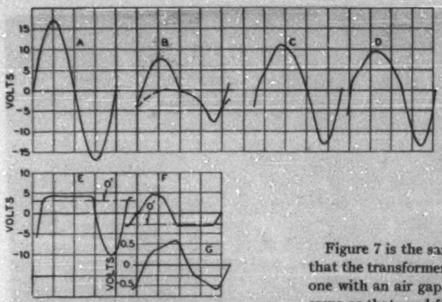

Figure 6. Steady-state voltages in same test circuit as for Figure 5, traced from screen of cathode-ray oscillograph

A—Input voltage, e_1 (12.0 volts rms)

B—Voltage across resistor R_a in primary (I_1 measured 4.85 amperes rms); dash line shows estimated magnetizing component, $i_m R_a$

C—Voltage across transformer primary (8.0 volts rms)

D—Voltage across transformer secondary (7.6 volts rms)

E—Voltage across rectifier; 0′ is corrected zero line based on reading of −3.1 volts direct-voltage component

F—Voltage across load resistance R_L (shows secondary current I_2 which measured 3.0 amperes d-c and 3.3 amperes a-c rms). 0′ is corrected zero line based on reading of 2.69 volts direct-voltage component

G—Voltage across R_a with secondary open (shows transformer no-load current, which measured 0.44 ampere rms)

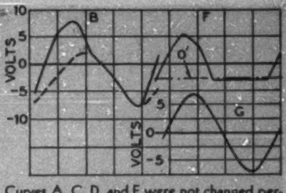

Figure 7 (right). Same as Figure 6 except with transformer replaced by one with an air gap, similar in other proportions; curve designations are the same as for Figure 6

Curves A, C, D, and E were not changed perceptibly and are not repeated

Curve B—I_1 measured 5.1 amperes rms

Curve F—Direct-voltage component measured 2.72 volts

Curve G—No-load current measured 4.55 amperes rms

oscillograph directly comparable in deflection sensitivity. Since the cathode-ray oscilloscope amplifier eliminates the d-c components and shows only the a-c components on the screen, the direct voltages shown in Figure 6 were measured separately with a voltmeter.

From the curves of Figure 6, particularly that for the drop across R_L, which is a direct indicator of the secondary current, it is apparent that conduction takes place for more than half the cycle. This also agrees with the results of the analysis of Figure 4(B). This effect is prominent in this circuit because of the relatively large value of the resistance R_a in the primary circuit. The current with the secondary open shows the typical distortion, with considerable third-harmonic content, in the exciting current for an iron-core transformer due to saturation. This core was only slightly saturated with only the a-c voltage applied, however, as the density was 5,000 gausses, a moderate value for medium quality, 0.014-inch thick, silicon steel transformer laminations.

Figure 7 is the same as Figure 6 except that the transformer has been replaced by one with an air gap, otherwise nearly the same as that used for Figure 6. The flux density in the core with the secondary open was 6,300 gausses in this circuit. The results are similar to Figure 6 except that the a-c exciting component remains sinusoidal even when the half-wave rectifier load is closed and is smaller in amplitude than with the secondary open because of the primary resistance drop, just as it was in the theoretical analysis shown in Figure 4(B). The exciting current is large compared with the load current because of the air gap.

Power Relationships. The power relationships for the steady state in a half-wave rectifier circuit with resistance load such as Figure 1 have been covered by many papers and texts, but are repeated here for completeness and to compare on the primary and secondary sides. It is assumed that the secondary current consists of a series of half-sine-wave pulses similar to that shown in Figure 7. This will be true if the primary resistance is negligible and the voltage drop through the rectifier while conducting and its leakage current while blocking are neglected. If the amplitude of the secondary current pulses is represented by A and the average value (over one or more complete cycles), which is the d-c component, is represented by I_d, then,[6]

$A = \pi I_d$
Fundamental component (rms), $I_{60} = 1.11 I_d$
Second harmonic (rms), $I_{120} = 0.472 I_d$
Third harmonic, $I_{180} = 0$
Fourth harmonic, $I_{240} = 0.094 I_d$
Higher harmonics are negligible
I_2 (rms) $= 1.57\ I_d$

The above relationships follow from a harmonic analysis of the half-sine-wave.

The following expressions will then apply for the average power of each component in the load resistance:

D-c component power $= I_d^2 R$
Fundamental component $= 1.23 I_d^2 R$
Second-harmonic component $= 0.223 I_d^2 R$
Total power $= (1.57\ I_d)^2 R = 2.46\ I_d^2 R$
$= (0.5A)^2 R$, since $A = 3.14 I_d$

As shown in the Appendix, an analysis of the power delivered by the secondary gives the same average value, confirming the results of the harmonic analysis. In a nonlinear circuit such as this, however, it is of more interest to consider the energy transfer during each part of the cycle rather than average power. The energy is delivered to the load resistor in pulses and the load does not receive any energy during the blocking part of the cycle. As shown in the second section of the Appendix, on the primary side energy also is taken from the supply in pulses (represented by a sine-squared term), which are the same as the pulses delivered to the load by the secondary, assuming the transformer winding resistances and core loss to be neglected. The expression for power on the primary side, however, also contains a sine term with amplitude proportional to the d-c component. This term represents the energy absorbed in the magnetic circuit of the transformer during the blocking half-cycles and given up again during the period that the rectifier is conducting.[7]

Thus, on the primary side the circuit absorbs energy from the source on both the conducting and blocking half-cycles. For the assumed conditions the amount of energy absorbed from the source by the transformer during the blocking half cycles and given up again during the conducting half cycles is approximately 40.5 per cent of the total energy delivered to the load. The average power expressions are the same for the primary and secondary sides, as is to be expected inasmuch as the transformer losses are neglected.

CIRCUIT WITH PRACTICAL TRANSFORMER AND RESISTANCE LOAD

The leakage reactances of the windings have the effect of series reactance in the primary and secondary circuits. With an iron-core transformer of usual proportions operated at reasonable loading, the effect of the leakage reactance will be small and can be neglected in the analysis unless great accuracy is required. The effect of inductance in the circuit is considered later. Similarly, the core loss is a minor influence in the circuit and can usually be neglected in an analysis of the currents and voltages at various parts of the circuit. In designing transformers for this service, however, the increase in core loss resulting from saturation because of the d-c component through the half-wave rectifier is important. Unless the transformer is of unusual proportions relative to the voltages and currents in the circuit, or has an air gap, saturation of the core by the d-c component will have considerable effect on the voltages and currents in the circuit, particularly their wave shapes, and the time required for steady-state conditions to be established after a change is made in the circuit. The effects of saturation are considered in the section on Effects of Saturation in the Transformer Core.

The analysis for the transformer with 1-to-1 turn ratio applies also, of course, to any turn ratio if the secondary impedances are converted to the same voltage base as the primary by multiplying them by the square of the turns ratio.

In the example in a preceding section, the primary circuit resistance R_1 was made equal to the secondary and load resistance R_2 so that the voltage drop across R_1 would be appreciable and the effect of this drop in determining the current in the primary circuit would be illustrated clearly. In a practical circuit, R_1 would usually include only the resistance of the wiring and primary winding and would be only a small fraction of R_2 in ohms, on the same voltage basis. With R_1 and R_2 in the example changed so that R_1 becomes small relative to R_2, but their total is such as to keep the final load current about the same as before, the voltage drop across R_1 at any time will, of course, be small relative to the supply voltage and the voltage e_m at the transformer winding will be more nearly the same as the supply voltage. The principal difference from the original example will be in the longer time required to reach the steady-state condition, because the difference in the i_1R_1 drop between the conducting and blocking half cycles will be less effective than before. In other words, the change in the d-c component of the exciting current is smaller per cycle, and a longer time is required to produce the same final d-c component. The action of the circuit is the same as before, however, and the voltage drop of the d-c component of the load current in the primary resistance still causes the exciting current to develop a d-c component that increases until the two just counterbalance each other.

Effects of Saturation in the Transformer Core

In a half-wave rectifier circuit involving an appreciable amount of power, the transformer feeding the rectifier usually will operate with the core saturated to a considerable degree because of the d-c component of the exciting current, which produces a d-c ampere-turn level on the core equal to that of the load current as explained above. The saturation does not change the general theory, but it does have two pronounced effects: the steady-state condition is established more rapidly after the secondary switch is closed, and in the steady-state condition, the a-c component of the exciting current will be larger and will contain large harmonics, particularly the second harmonic.

The quicker response might be considered, in a general way, to be the result of decreased inductance in the windings because of the saturation. The following analysis, in more detail, considers the changes caused by saturation compared with the simple circuit covered in a preceding section.

In the previous analysis, the results of which are shown in Figure 4, the magnetic flux ϕ in the core was assumed to be directly proportional to the magnetizing current i_m so that the curve for i_m also represents ϕ with a suitable proportionality constant. The flux thus also develops a negative unidirectional component because of the difference between the positive and negative volt-second areas of the voltage at the coupling inductance, L_m in Figure 3. The core will thus tend to become saturated on the negative swings of flux. It is still correct to use the relationship,

$$\int d\phi = \frac{1}{N}\int e_m dt$$

but it is no longer satisfactory to use the similar relationship for the integral of di_m in terms of L, e_m, and t, since i_m is no longer proportional to ϕ; in other words, L is no longer a constant. At t_3, in Figure 4, if the magnetization curve is such that ϕ is well into the saturated region (in the negative direction), i_m will swing to a large negative value. Beyond t_3, as ϕ increases in the positive direction away from the saturated state, i_m will swing back sharply to a moderate value; thus i_m will have a large negative peak of short duration in the vicinity of t_3. The i_1R_1 drop will restrain this and subsequent peaks and limit their amplitude and at the same time modify the negative voltage wave at the coupling inductance L_m, reducing its volt-second area so that ϕ will not have to swing so far in the negative direction. With the saturated core, at the steady-state condition, i_m will have the same average d-c negative component as before, just equal and opposite to the average d-c component of the pulsating load current (in the primary side). The negative swings of i_m now will have high sharp peaks, however, because of saturation, and the average value about which ϕ oscillates will still be negative but of considerably smaller magnitude than without saturation. The determination of the exact shape of the i_m curve with saturation present is not easy, but if the shape of the magnetization curve (ϕ against i_m) is known, it can be determined by a step-by-step, graphical method.[5]

Effects of saturation are seen clearly in the wave shape of the primary current i_1 in the oscillograms of Figures 5 and 6.

Closing the Secondary Circuit at Different Points in the Cycle

In the analysis of the section on Simplified Circuit with Resistance Load it was considered that the switch in the secondary circuit was closed during a period of negative secondary voltage, that is, during the part of the cycle in which the rectifier would block reverse current flow. If the switch is closed after the secondary voltage goes positive so that conduction starts immediately, the balance of this first conducting half-cycle will be different from before, but the over-all change in succeeding cycles will be similar and the final steady-state condition will be the same, but will be reached a fraction of a cycle later than for the condition in which the first conducting half-cycle is a complete one. After the switch closes, the secondary current consists of a transient and a steady-state component as in a plain a-c circuit, but the resultant current is, of course, cut off by the rectifier when it tries to go negative. In the resistance-load circuit previously discussed the time constant of the load circuit, that is, the resistance and the unavoidable reactances including the transformer leakage reactance, would be so short that the transient component would practically disappear before the end of this first conducting period. The second conducting half-cycle would then start off as in the above-mentioned analysis except that the value of flux and primary exciting current would differ by small amounts from the former values. This comparison emphasizes again that

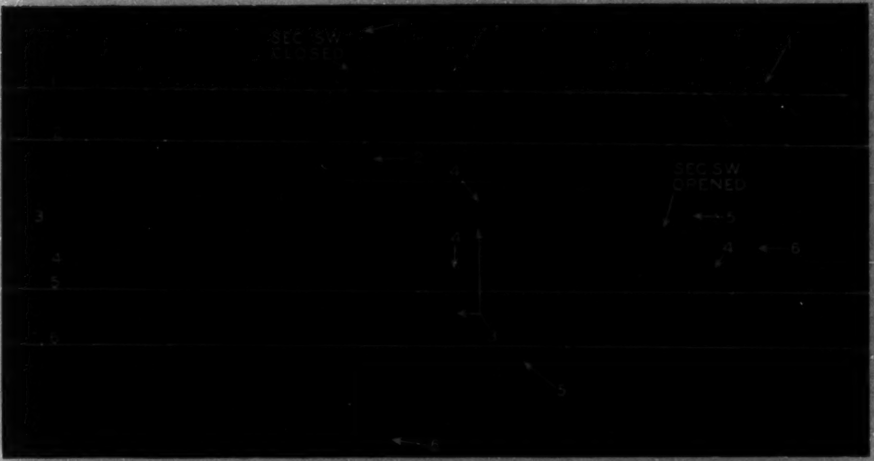

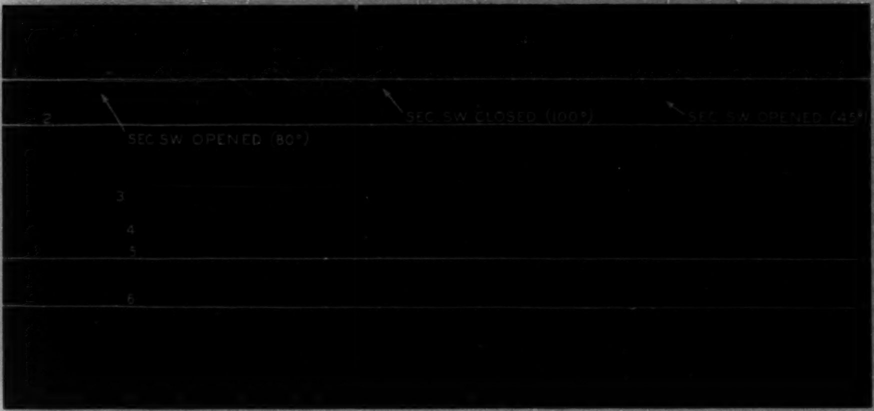

Figure 8. Same as Figure 5 except for time of closing and opening the switch in the secondary circuit. Angular values shown are electrical degrees after time that e_1 increased through zero

the time required to establish the over-all steady-state conditions in the half-wave rectifier circuit involves the magnetization of the transformer core, that is, the magnetizing inductance in addition to the smaller series inductances due to leakage flux. This time will thus usually be several cycles when the time constant of the series circuit is much shorter. The longer time is similar to that for the magnetizing transient in the same circuit when a d-c source is connected into the primary or secondary circuit with the other circuit already closed.

The oscillograms of Figure 5 and 8 show the little difference caused by closing the secondary at different parts of the cycle. For example, there is very little difference between Figure 5 after closing of the switch about 70 degrees after the voltage has gone negative, and Figure 8 after closing of the switch about 70 degrees after the voltage has gone positive. The largest differences show up in the primary current values at the end of the first conducting half-cycle. At this time, t_2 in Figure 5, the primary current i_1 has not quite decreased to zero and then in the blocking period at t_3 reaches approximately 40 per cent of its negative steady state peak value. In Figure 8, i_1 is somewhat more positive at t_2 than in Figure 5, and at t_3 it reaches only about 25 per cent of its negative steady-state peak. During this same blocking period, t_2 to t_3, the voltage across the rectifier, which is then the same as the secondary voltage, has a negative peak value approximately 6 per cent less in Figure 5 than in Figure 8. In other words, in Figure 5 there has been more progress toward the steady-state condition after a full conducting half-cycle than in Figure 8 after a conducting period that did not start until the voltage had progressed about 70 degrees past the start of its cycle. Also, in Figure 5, the steady state practically has been reached at the end of four cycles, whereas in Figure 8 there is still a measurable difference between the negative peak of i_1 at the ends of the fourth and fifth cycles.

A controlled rectifier, in which the firing point is delayed in each cycle until some predetermined time after the voltage goes positive in order to control the average d-c value, is not considered in detail here, but the first conducting cycle of Figure 8 indicates what can be expected. The general theory outlined will still apply, but, of course, the wave shapes of current and voltage will be modified because of the rectifier becoming conducting and, in effect closing the secondary circuit only during the latter part of the positive voltage periods.

Opening the Secondary Circuit

The analysis of conditions in the transformer circuit after closing the secondary circuit containing the load fed through a half-wave rectifier, showed a transient condition of relatively long duration in the primary, associated with the building up of the direct component of flux in the transformer core. A similar transient condition of opposite polarity is set up when the secondary is opened, and the study of this transient condition is of similar interest.

In a plain a-c transformer circuit when the secondary is opened, the primary current changes abruptly to the small, exciting or no-load value. A small transient will occur because of the abrupt change in current through the primary series impedance, including the primary resistance and leakage inductance. These are usually small and consequently the voltage at the primary and the resulting flux in the core will change very little when the load current is shut off by opening the secondary. If direct current produced by a direct voltage source such as a battery or generator is present in the secondary as well as the a-c load current, opening the secondary will, of course, cause a transient in the primary because of the voltage induced by the collapse of the d-c component of flux in the core. The half-wave rectifier circuit resembles this latter condition, but it is different in that the rectifier which develops the d-c component gets its energy entirely from the a-c primary supply. An interesting question for analysis is whether any transient will occur when the secondary switch is opened during a blocking half-cycle when the rectifier already has the circuit effectively opened.

The reaction that occurs upon opening of the secondary can be understood readily by considering the results shown in Figure 4 of the analysis of a circuit of this type after the secondary was closed. It is assumed that the steady-state condition, as shown by Figure 4(B), has been reached before the secondary switch is opened. It is apparent that following the opening of the switch, the primary current and the transformer flux must return to the no-load condition shown at the left of Figure 4(A), prior to t_1. In the steady-state condition of Figure 4(B) the magnetizing current i_m has been varying in a nearly sinusoidal wave about an average value of approximately −3.56 amperes, the negative sign indicating that this d-c component is in the opposite direction to the pulsating load current. In this example, the flux was assumed to be proportional to i_m so that it also has a large negative bias. After the secondary switch is opened, the load current component immediately disappears from the primary, but the induced voltage caused by the collapse of bias component of the flux tends to maintain the negative component of magnetizing current. Thus, this negative component decays in a manner similar to the transient in a series resistance-inductance circuit with a time constant determined by the total resistance and inductance of the primary circuit, including the magnetizing inductance, not just the primary-winding leakage inductance of the transformer. The cyclic variations in flux and i_m are superimposed on the d-c transient.

A more exact analysis can be made in a manner similar to that given previously for closing the circuit. If the secondary switch is opened at some point during the blocking half-cycle, that is, between t_{18} and t_{23} in Figure 4(B), there will be no change in the pattern until t_{23} since the rectifier already has the circuit effectively opened. At this time i_m has a value of −4.0 amperes which causes a voltage drop of 4.0 volts in the 1-ohm primary resistance R_1. In the positive half-cycle of voltage following t_{23}, there is no longer any positive pulse of load current, only the negative i_m, and the drop through R_1 is of polarity to cause the voltage applied at the transformer winding to be larger than the supply voltage. Thus the volt-seconds area of the positive half-cycle of voltage applied to the transformer will be increased so that the resulting change of i_m will be large in the positive direction. Similarly, in the next negative half-cycle of applied voltage, the volt-seconds will be reduced so that the change of i_m in the negative direction will be small. Thus, as long as i_m has an average value different from zero, the voltage drop through the primary resistance will set up an influence to bring i_m to zero, in a manner similar to the building up of the negative bias in i_m after the circuit was closed.

From this analysis it is apparent that the transient in the primary is caused mainly by the collapse of the d-c component of flux and will be practically the same regardless of the point in the cycle at which the secondary switch is opened. This is shown by the oscillograms of Figures 5 and 8, which include several different times of circuit opening. It will be noted in all of these that the first negative peak of primary current following the opening of the switch is much smaller in magnitude than those in the steady-state condition with the switch closed. This results from saturation in the core. In the steady-state, conducting condition the core saturated with the result that the negative swings of i_m went much larger relatively than the negative swings of flux. After the switch is opened, the bias in flux, which caused it to extend into the negative saturated region, immediately starts to disappear as explained above.

In a circuit in which the magnetizing current i_m has a larger amplitude than the average value of load current, i_m will go positive during part of the cycle as shown in the oscillogram of Figure 7 for the air-gap transformer. Even if the secondary switch is opened at a time in the cycle when i_m is positive, there will still be a transient consisting of the negative component of i_m decaying to zero. In other words, although i_m and the flux are positive at the time of opening the switch, they should be still larger in the positive direction for the no-load condition and the transient still has the same direction and corresponds to a collapse of negative magnetic flux in the transformer core.

Closing and Opening the Primary Side of the Circuit

The conditions in the circuit with the switching on the primary side instead of the load side have not been included in the detailed study, but a few conclusions are evident. Upon closing the switch, there will usually be a magnetizing transient the same as if the secondary were open, depending upon the point in the voltage cycle at which the switch is closed. This primary transient current may be very large and have either polarity and is affected by the magnetic flux density at which the core is operated, the shape of

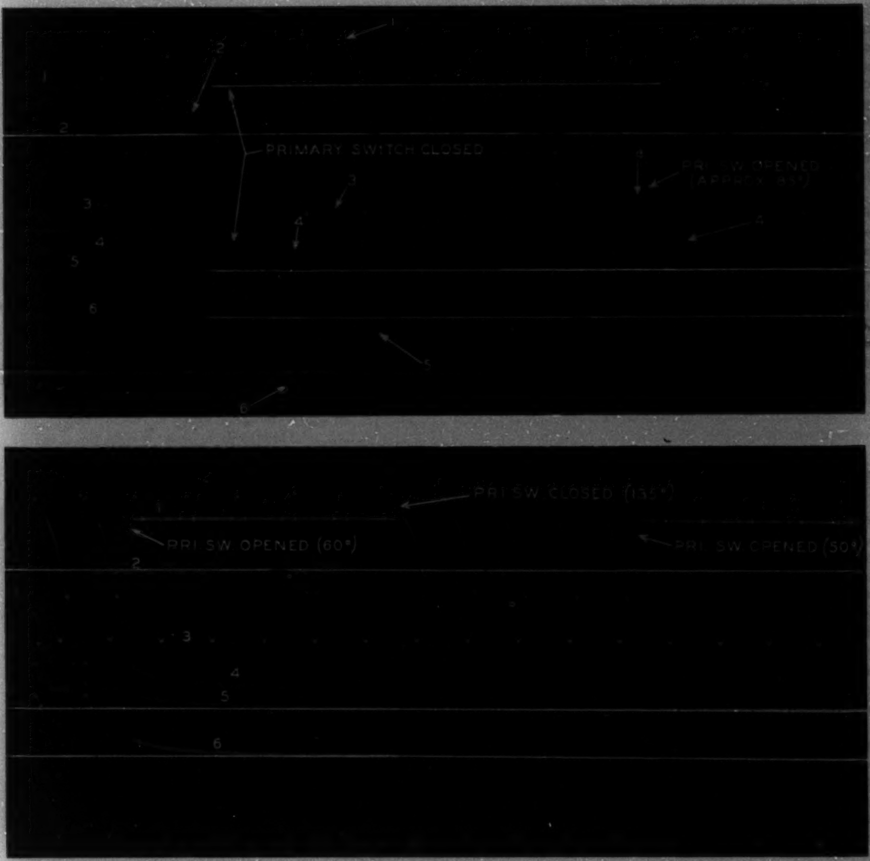

Figure 9. Oscillograph record of test circuit same as Figure 1 except with switching contact in primary circuit instead of secondary; oscillograph connections were the same as for Figure 5

the magnetization curve, and the amount and polarity of residual magnetism present. The adjustment of primary current as required to produce the pulsating current through the rectifier in the secondary circuit as previously discussed is superimposed on this magnetizing transient. The magnetizing transient will not be made more severe as it would be by direct current already existing from a battery or generator in the secondary when the switch closes at a point in the cycle requiring an initial change in flux of the same polarity as that caused by the direct current.[8]

When the primary is opened, the energy stored in the magnetic field existing in the transformer at the instant of opening the circuit normally is dissipated in a transient pulse of current from the secondary through the rectifier and load. The bias flux in the core is of the correct polarity to produce voltage to send current through the rectifier in its conducting direction when this flux collapses. In Figure 3, for example, the net current through the coupling inductance L_m has been upward (the negative magnetizing component of the total primary circuit current i_1). After the primary circuit is opened, the collapse of flux in L_m tends to induce voltage to send current in the direction shown for i_2. The amplitude of this transient will vary with the point in the cycle at which the switch is opened and will be greatest if this occurs at a negative peak of flux, that is when the voltage across L_m is increasing through zero.

It is possible for the flux to be positive at the time of opening the primary switch, so that the transient voltage produced in the secondary would tend to send current in the reverse direction through the rectifier. This would be equivalent to an open secondary and the energy would be dissipated in an arc at the switch. This could only occur in a circuit in which the magnetizing current has a large amplitude compared with the load current as with the air-gap transformer used for the oscillograms shown in Figure 7.

Figure 9 is a set of oscillograms taken in the same test set-up as Figures 5 and 8 except with the switching contact in the primary side.

General Mathematical Solution; Circuit with Inductance

The method of analysis shown in a preceding section, making use of the volt-second integral to calculate changes in magnetizing current, is correct in theory but in some circuits the calculation of the volt-second areas may be difficult to carry out accurately. For example, if the load includes inductance as well as resistance, the pulses of current from the rectifier to the load will not be parts of a sine wave in phase with the supply voltage but each current wave will increase at an increasing rate, reaching a maximum later than the voltage and continuing to lag the voltage until the current drops to zero. Conduction continues over more than 180 degrees with an inductive load. The voltage drop in the primary resistance produced by this load-current component, being nonsinusoidal, causes the voltage at the coupling inductance to be distorted also. Although the calculation of the transient change in magnetizing current may be difficult, it is apparent that it will be of the same general form as analyzed previously and will build up a negative d-c component just sufficient to counterbalance the d-c component of the load current.

In the usual practical problem it is possible to set up the circuit and obtain the transient analysis by means of an oscillograph as was done in the tests described above. This, of course, is usually the quickest and most practical method of analyzing even the more simple circuits such as that with resistance load previously discussed. The general method of mathematical analysis is always available, however, and is straightforward, provided all the circuit elements can be considered linear including the inductances; that is, saturation does not occur. The rectifier is still considered to be equivalent to an automatic switch having an open and a closed position. In the solution of the problem in which the secondary switch is closed after the primary has been energized for some time, the general basic circuit of Figure 2 can now be used, although it can be simplified with little error usually by neglecting the core loss of the transformer, that is, considering R_e to be infinite. The first step, is to solve for the steady-state primary current i_m, magnitude and phase angle, with the secondary open, and from this the voltage across the mutual inductance M. This voltage will lead the supply voltage by a small phase angle and i_m will be at its negative maximum when the voltage across M increases through zero.

This is the starting point for the transient condition, if the secondary switch has closed during this negative half-cycle. This first part of the solution is a simple a-c series-circuit, steady-state problem.

Starting from this time t_1 when e_m becomes positive, the secondary circuit will be closed and will remain so for a time longer than 180 electrical degrees until i_2 decreases to zero and starts to go negative, at which time the blocking action of the rectifier will, in effect, open the secondary circuit. During this conducting period, the problem involves the transient analysis of a simple coupled circuit containing two loops with a sine-wave voltage source in one. The rectifier is disregarded for this part of the solution. It is considered to be short circuited inasmuch as the conducting condition is now under consideration. The differential equations and their solution can be found in most texts on transient analysis.[8] The general equations for the circuit of Figure 2 with R_e neglected (infinite resistance) are as follows:

$$(L_1p+R_1)i_1-Mpi_2=E_1\sin(\omega t+\theta)$$
$$Mpi_1-(L_2p+R_2)i_2=0$$

where p indicates the derivative with respect to time.

The solutions for the primary and secondary currents will be of the form:

$$i_1=A\sin(\omega t-\beta_1)+C_1\epsilon^{-a_1t}+D_1\epsilon^{-a_2t}$$
$$i_2=B\sin(\omega t-\beta_2)+C_2\epsilon^{-a_1t}+D_2\epsilon^{-a_2t}$$

In these expressions the sine terms are the a-c steady-state currents and can be found readily by the usual calculation methods for a circuit of this type containing two meshes. It is convenient to measure time for this part of the solution from the instant that e_m increases through zero in order to simplify the exponential terms. If this is done, θ in the expression for the sine-wave supply voltage e_1 must be changed to suit. The other two terms in each expression for current are the transient terms which express the adjustment of the circuit to take care of the discrepancies between the existing values of current when the rectifier starts conducting and the values that should exist at that point in the supply voltage cycle according to the steady-state terms. The exponential coefficients a_1 and a_2 that determine the time rate of decay of these transients depend upon the resistance and inductance values. The detailed solution of the differential equations for Figure 2 results in the following values for a_1 and a_2:

$$a_1=\frac{R_1L_2+R_2L_1+\sqrt{(R_1L_2+R_2L_1)^2-4(L_1L_2-M^2)R_1R_2}}{2(L_1L_2-M^2)}$$

a_2 is the same as a_1 except with a minus sign before square root instead of plus.

The C and D coefficients are determined by the boundary conditions. C_1, D_1, C_2, and D_2 are not independent but involve only two independent quantities, the initial values of i_1 and i_2. The relation between C_1 and C_2, and D_1 and D_2 can be determined by substituting the transient parts of the solutions for i_1 and i_2 in one of the original differential equations and equating the total coefficient of ϵ^{-a_1t} to zero and that of ϵ^{-a_2t}, to zero. This can be done because the general differential equation holds good for the transient part of the solution and steady state part independently and for all values of t. The resulting relationships for the circuit under consideration are as follows:

$$C_2=\frac{C_1(L_1a_1-R_1)}{Ma_1}$$

$$D_2=\frac{D_1(L_1a_2-R_1)}{Ma_2}$$

In the rectifier circuit, the initial value of i_2, of course, is zero and the initial value of i_1 is the negative value of i_m at the close of the preceding blocking period. Substituting these initial values of i_1 and i_2 and the values of the steady-state terms for this starting instant in the equations for i_1 and i_2, with C_2 and D_2 expressed in terms of C_1 and D_1, two relationships for C_1 and D_1 are obtained which can be solved to determine these constants.

If the initial values of di_1/dt and di_2/dt are known as well as i_1 and i_2, another method of determining C_1, D_1, C_2, and D_2 is available. By differentiating the expression for i_1 and substituting the known initial values in the equations for i_1 and di_1/dt, the values of C_1 and D_1 can be determined. C_2 and D_2 would be similarly determined from the i_2 equation. This can be used here inasmuch as di_1/dt equals zero at the end of the blocking period and start of the conducting period, the voltage across the primary inductance being equal to zero at this instant. Similarly di_2/dt equals zero at the start of conduction since the voltage across the secondary inductance also equals zero at this instant, the same as the total secondary voltage.

After the mathematical expressions for i_1 and i_2, together with the constants in these equations, have been determined, the next step is to find the time when conduction stops, that is, i_2 decreases to zero. This is readily done by substituting trial values for t in the equation for i_2 until a value is found that gives $i_2=0$ within the desired limits of accuracy. The value of t must be between 180 and 360 electrical degrees, of course, depending upon the amount of inductance and resistance in the circuit. The value of i_1 is then determined for this time t_2 at which i_2 equals zero, these being the starting boundary conditions for the blocking period that follows.

For the blocking period, the circuit becomes a simple series circuit with a sine wave applied voltage and the primary resistance and inductance, the secondary being open because of the blocking action of the rectifier. The solution for such a circuit will be of the form:[8]

$$i_1=F\sin(\omega t+\theta_2)+G\epsilon^{-\frac{R_1}{L_1}t}$$

The first term of this equation, the sine term, is merely the steady-state current with the secondary open as determined previously. Again, it is convenient to start measuring time anew from t_2, and θ_2 will have to be properly correlated with t. Constant G is readily determined from the known value of i_1 at t_2 as found for the end of the conducting period. The end of the blocking period is then determined. This will occur when the voltage across the rectifier, which is the secondary voltage and also equal to the voltage across the coupling inductance M in Figure 2, becomes equal to zero and starts to go positive. For e_m to be zero, di_1/dt must equal zero, so this value of time t_3 can be found by differentiating the expression for i_1 during the blocking period and equating di_1/dt to zero. The value of i_1 will be more negative at t_3 than at t_1 as in the previous analysis for a simple resistance load.

The solution for the next conducting period, t_3 to t_4, will be the same as for t_1 to t_2 except that constants C and D will have new values because of the different value of i_1 at the starting point t_3. The angle β in the steady-state part of each expression will have to be properly correlated with the new time zero, of course.

It is apparent that this step-by-step method can be carried out until the steady state is reached. If it is desired to plot curves for i_1 and i_2, the values can be obtained from the expressions for these currents by substituting suitable intermediate values for t.

Conclusion

In a circuit energized from an a-c source through a half-wave rectifier the current flows in pulses in one direction because the rectifier blocks current from flowing in the reverse direction during the periods of reverse voltage. It has been shown that the following conditions exist when there is a transformer between the a-c source and the half-wave rectifier circuit:

1. After steady-state conditions have been reached, or when successive cycles are identically repetitive, the primary current is made up of the following components: a pulsating, unidirectional component the same as the secondary load current with the turn ratio taken into account, the alternating exciting current for the transformer, and a d-c magnetizing component, which is just equal in magnitude to the average (d-c) value of the load current in the primary and has the opposite polarity.

2. From the preceding statement it follows that there is no net direct current flowing in the primary circuit in the steady state. The alternating current, in general, will be unsymmetrical, containing even harmonic components, even when there is no appreciable saturation in the transformer core.

3. The magnetic flux in the transformer core has a bias corresponding to the d-c component of exciting current. If the core saturates as is common in this type of application, the exciting current will have a high peak value in the saturated direction on each cycle and will have large second and other even harmonic components along with the usual odd harmonics. The bias in the flux will be less when saturation occurs and will have a magnitude such that the average d-c value of the exciting current meets the conditions of conclusions 1 and 2.

4. When the secondary circuit is closed, a transient voltage appears across the resistance in the primary circuit. This causes the negative component of magnetizing current to develop and disappears as this current reaches the steady-state value. A similar transient occurs when the switch is in the primary, in addition to the usual magnetizing transient, which may be large.

5. This transient always has the same polarity and has the same general nature regardless of the point in the voltage cycle at which the switch is closed.

6. The secondary current builds up nearly to the steady-state value on the first full conducting half-cycle and is only slightly affected by transient conditions.

7. A transient voltage of opposite polarity appears in the primary when the secondary is opened, due to the collapse of the bias flux in the transformer core.

8. When there is resistance in the primary circuit, the pulses of secondary current last for longer than a half-cycle even when load has a high power factor.

The study that has been made on this type of circuit suggests the possibility of further analysis on the prediction of the duration of the transient conditions as the circuit parameters are varied. Application to a load including a capacitor in series with the rectifier also offers an interesting problem for further study. In this circuit the secondary current, becomes zero, of course, when the capacitor becomes charged to the peak secondary voltage. The general method of analysis should have other applications in analysis of circuits including rectifying elements.

Appendix I. Power Relationships

Verification that the Average Power Delivered by the Transformer is Equal to the Total Power of the Harmonic Current Components in the Load Resistance

If the peak of the load current carried by the half-wave rectifier in the circuit of Figure 1 has the value A (amperes), the amplitude of the required secondary voltage E_2 will be equal to AR_L, and the secondary voltage may be written as $E_2 \sin\theta$, in which $\theta=\omega t$. This statement applies to the steady state condition and assumes the impedance in the primary circuit to be negligible.

The secondary current equals $A\sin\theta$ from $\theta=0$ to $\theta=180$ degrees, and equals zero from $\theta=180$ to 360 degrees, for a pure resistance load.

The power delivered is thus equal to

$$\frac{1}{2\pi}\left[\int_0^\pi E_2(\sin\theta)A\sin\theta d\theta+\int_\pi^{2\pi}E_2(\sin\theta)\times 0\right]$$

$$=\frac{E_2A}{2\pi}\int_0^\pi(\sin^2\theta d\theta+0)$$

$$=\frac{E_2A}{2\pi}\left[\frac{\theta}{2}-\frac{\sin 2\theta}{4}\right]_0^\pi=\frac{E_2A}{4}$$

$$=\frac{A^2}{4}R_L\ (\text{since } E_2=AR_L)$$

This is the same expression as that in the section entitled Power Relationships based on the harmonic current components.

Verification that the Average Power Delivered to the Transformer Equals the Power Delivered to the Load, if the Transformer Losses Are Neglected

As shown in a preceding section the primary current consists of three components, the load current, which is the same as the secondary current (for a 1-to-1 turn ratio); the a-c exciting component; and a d-c component of exciting current which is equal and opposite to the d-c component of the load current. The a-c exciting component is out of phase with the voltage and can be dropped from further consideration since the transformer losses are being neglected. The power delivered to the transformer will thus be the same as the secondary power derived above except that the negative d-c component, $-I_d$, must be included. The expression for average power will then be:

$$\frac{1}{2\pi}\left[\int_0^{\pi} E_2 \sin\theta(A\sin\theta - I_d)d\theta + \int_{\pi}^{2\pi} E_2 \sin\theta(0 - I_d)d\theta\right]$$

$$=\frac{1}{2\pi}\left[\int_0^{\pi} E_2 \sin\theta(A\sin\theta)d\theta + \int_0^{2\pi} E_2(-I_d)\sin\theta d\theta\right]$$

Since the integral of the sine for a complete cycle (0 to 2π) is zero, this gives the same result as that derived for the secondary power in the preceding section of this Appendix.

References

1. Half Cycles, W. D. Cockrell. *General Electric Review* (Schenectady, N. Y.), volume 38, August 1935, pages 367–72.

2. A Graphical Analysis of the Voltage and Current Wave Forms of Controlled Rectifier Circuits, P. T. Chin, E. E. Moyer. *Electrical Engineering* (*AIEE Transactions*), volume 63, July 1944, pages 501–08.

3. Gaseous Rectifier Circuits, P. T. Chin. *Electronics* (New York, N. Y.), April 1945, pages 138–43.

4. A Nonlinear Problem, C. A. Hachemeister. *Electrical Engineering*, June 1949, page 518, and July 1949, pages 614–15.

5. Effect of Direct Current in Transformer Windings, E. L. Harder. *Electric Journal* (East Pittsburgh, Pa.), volume 27, October 1930, pages 601–07.

6. Theory and Applications of Electron Tubes (book), H. J. Reich. McGraw-Hill Book Company, New York, N. Y., 1942, page 536.

7. Track Circuit Apparatus, Paul N. Martin. United States Patent 2,465,691.

8. Introduction to Electric Transients (book), Kurtz, Corcoran. John Wiley and Sons, Inc., New York, N. Y., 1935.

No Discussion

The Scotch Plaid Raster

J. KATES
NONMEMBER AIEE

V. G. SMITH
MEMBER AIEE

Synopsis: The memory of a number of electronic computers is based on the storage of discrete charges on the inner face of a cathode ray tube. The effect of variations in the resistor network determining the location of these charges is investigated in this paper. It is shown that substantial advantages can be derived from a raster with nonuniform spacing, such a raster having somewhat the appearance of the stripes of a Scotch Plaid.

RECENTLY developed memory schemes employ the storage of a raster of discrete charges on the face of a cathode-ray tube. The individual storage areas (spots) must be sufficiently separated so that there will be no interference between adjacent areas, even in the case of the worst variations of tube and circuit parameters.

The design separation will, therefore, be the sum of two separations: (a) The minimum separation for which interference between spots is negligible; (b) An additional separation to allow for variations in the deflection voltages.

A common method of producing the raster is to relate the spot to the setting of a binary counter by means of a resistor network[1,2] as shown in Figure 1.

In this circuit the input to each resistor is at one of two discrete voltages according to the setting of the corresponding counter stage. The output voltage of this circuit is proportional to the binary number in the counter chain.

The design of this network must include the effects of resistor variations on the spot spacings. These effects are the subject of this investigation and it is shown that a very critical resistor network is required for uniform spacing, but that these requirements may be relaxed considerably by employing a nonuniform spacing.

Effect of Resistor Variations

Consider the circuit of Figure 2, using the normalized voltages 0 and 1. The output voltage of such a circuit is

$$E_0=\frac{\sum_{i=0}^{n-1}E_ig_i}{\sum_{i=0}^{n-1}g_i},\qquad E_i=0,1 \tag{1}$$

which also may be taken as the deflection on a normalized scale.

To illustrate the effect of resistor variations in this circuit, consider first the simplest case of two resistors only.

The 4-spot Raster

Consider the circuit of Figure 3(A), where $g_1=2g_0$, and each resistor is subject to ±20 per cent variation.

Figure 3(B) shows graphically the four output levels corresponding to the four possible switch settings together with the spread due to resistor variations. It will be noted that the minimum voltage difference between adjacent levels when the resistors take all possible values within the ±20 per cent limits is 0.25 volt on the outer spaces but only 0.1428 volt on the center space. Clearly it would be better to make the minimum spacing uniform rather than the mean spacing. This is done by making

$$g_1=2.3507g_0 \tag{2}$$

The resulting spacings are shown in Figure 4, where a minimum spacing of 0.2209 is evident.

This design change has therefore resulted in a 55 per cent increase in the minimum spacing for the same over-all raster size. If the original minimum separation was sufficient, the over-all linear size could be reduced to 65 per cent of that required by a uniform raster.

This elementary 4-spot raster has served to illustrate the advantages to be gained from the Scotch plaid raster. The general case now will be studied.

The General Raster Design

As in the 4-spot example, any raster based on uniform minimum spot separation rather than uniform line spacing will allow larger minimum spot separation or a smaller area or both. If both minimum separation and area are satisfactory, the nonuniform raster allows the use of larger resistor tolerances.

Table I gives the ratio of the resistor tolerances of the Scotch plaid raster to those of the uniform raster when both become vanishingly small. The same raster area and deflection voltages are assumed. The curves of Figure 5 show the values of the same ratio up to Scotch plaid resistor tolerances of 30 per cent. The table was computed from equation 25 and the

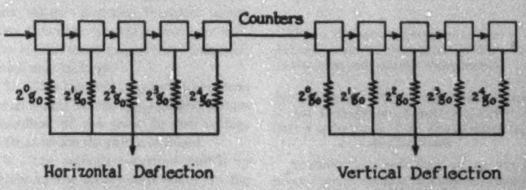

Figure 1. A deflection generator

Paper 51-276, recommended by the AIEE Computing Devices Committee and approved by the AIEE Technical Program Committee for presentation at the AIEE Summer General Meeting, Toronto, Ont., Canada, June 25-29, 1951. Manuscript submitted March 28, 1951; made available for printing May 21, 1951.

J. KATES and V. G. SMITH are with the University of Toronto, Toronto, Canada.

The authors wish to thank Professors C. C. Gotlieb and B. A. Griffith for their criticisms and suggestions during the preparation of this paper.

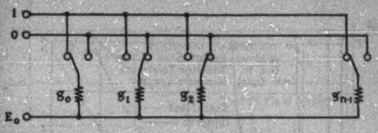

Figure 2. A generalized deflection generator

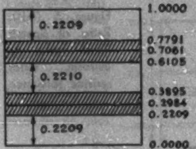

Figure 4. Spacings on a 20 per cent, 4-spot Scotch Plaid raster

curves of Figures 5 from equations 22, 23, and 24.

It will be noted that advantage of the Scotch Plaid raster over the uniform increases markedly with an increasing number of lines. As an example, suppose a 32-line, 1,024-spot raster is required. Using a Scotch Plaid raster with 6 per cent resistors gives a certain pattern size. To achieve the same size with the same minimum separation in a uniform raster 0.86 per cent resistors would have to be used.

From Figure 6, which shows the relative raster sizes, it is seen that 6 per cent resistors are quite impossible for the 32-line ($n=5$) raster.

Figure 6 is a plot of s_0/s on x and x_u as a common base, where s_0 is the spacing for ideal resistors, namely $1/(2^n-1)$. To have the same physical separation the raster size must vary inversely with respect to s.

Note the relatively slow rise in raster size with increasing resistor tolerance in the case of the Scotch Plaid raster, and the marked contrast in the case of the uniform raster. Thus for 64 lines ($n=6$, 4,096 spots) and 5 per cent resistors the size of the Scotch Plaid raster is only 1.36 times the ideal with perfect resistors, whereas for the uniform raster we should have to use 0.4 per cent resistors for the same relative size, and resistors of as little as 1.4 per cent tolerance are quite impossible.

Resistor Design

The equations for the design of the resistors of the Scotch Plaid raster are derived in Appendix I.

For a uniform raster the relative conductances are given by equation 3.

$$\frac{g_k}{g_0}=2^k \tag{3}$$

The corresponding equation for the Scotch Plaid raster is

$$\frac{g_k}{g_0}=2^k\prod_{1}^{k}\left[\frac{1+sx_{i-1}}{1-x_i+2sx_i}\right] \tag{4}$$

where s is the minimum spot separation expressed as a fraction of the total pattern size, and x_i is the fractional tolerance of the ith resistor. Note that if 2^n is the number of lines,

$$s\lesseqgtr 1/(2^n-1) \tag{5}$$

In most cases equation 4 may be approximated by

$$\frac{g_k}{g_0}=2^k\prod_{1}^{k}(1+x_i) \tag{6}$$

or even by

$$\frac{g_k}{g_0}=2^k\left(1+\sum_{1}^{k}x_i\right) \tag{7}$$

If all the resistors have the same tolerance, the preceding formulas become

$$\frac{g_k}{g_0}=2^k\left(\frac{1+sx}{1-x+2sx}\right)^k \doteq 2^k(1+x)^k \doteq 2^k(1+kx) \tag{8}$$

Care should be taken when using the approximate forms to see that the error is indeed negligible.

The Uniform Probability Raster

If a great many deflection circuits were built and aged the resistor values would be found to be grouped around their nominal values according to some frequency law, or there might be a different law for different nominal values. If this law (or laws) were known, it should be possible to design the resistor networks so that the probability of any two lines falling closer than some specified minimum spacing would be a minimum, and also to compute that probability.

Even with the assumption of normal distribution, for which there is little justification, this has proved too difficult but the problem of equalizing the probability that no two lines will be separated by less than the specified minimum has been solved for the case of normal distribution. There is some reason to believe that the raster of minimum probability would differ but little from that of uniform probability.

Only the case where all the resistors have the same standard deviations has been worked out in detail. The Scotch Plaid raster, which was designed for uniform tolerance, then turns out to be also the uniform probability raster, in which

$$\frac{g_k}{g_0}=r^k \tag{9}$$

where r is the arbitrary ratio g_1/g_0.

If equation 8 is identified with this, then

$$r=2\frac{1+sx}{1-x+2x}$$

which connects the two approaches.

As an example, suppose the resistors are nominally 1 per cent, and that after use we may expect 1 in 10,000 to be more than 5 per cent off its nominal value, either high or low. Then the probability that any two of the lines on a 64-line raster designed for 5 per cent tolerance will be less than the acceptable minimum spacing apart is about 1.8 in 10^{10}. While the normal character of the distribution is pure assumption and the 1 in 10,000 a pure guess, there is some assurance that if 1 per cent resistors are used in a deflection generator designed for 5 per cent tolerance there will be trouble only when some resistor fails completely.

Conclusions

By replacing the uniform line spacing of the uniform raster by the uniform minimum spacing of the Scotch Plaid raster, marked advantages result. These advantages should contribute materially to satisfying the stringent reliability requirements of large scale electronic computers.

The preceding analysis is for the circuit of Figure 2. Similar equations and advantages can be obtained for the circuit of Figure 7 which uses single-throw switches.

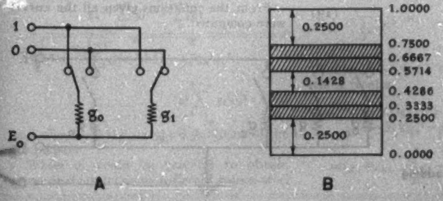

Figure 3. Spacings on a 20 per cent, 4-spot uniform raster

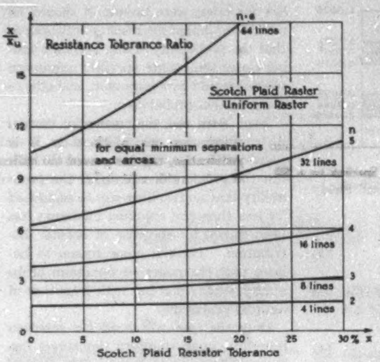

Figure 5 (left). Ratio of Scotch Plaid raster to uniform raster resistor tolerance

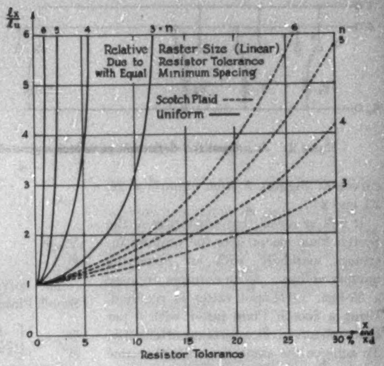

Figure 6 (right). Relative linear size of rasters with equal minimum spacing

Appendix I. Theory of the Minimum Tolerance Raster

The output of the circuit shown in Figure 2 is

$$E_0=\frac{\Sigma g_j}{\sum_{i=0}^{n-1} g_i} \tag{10}$$

where the g_j are the conductances connected to the unit potential side, and n resistors are used.

The normalized deflection where g_0 is connected to 1 and all the other conductances to zero is

$$\frac{g_0}{\sum_0^{n-1} g_i} \tag{11}$$

In this equation g_i may take any value between the tolerance limits $g_i(1+x_i)$ and $g_i(1-x_i)$. The normalized deflection will be a minimum when g_0 is a minimum and all the other conductances have their maximum values. Let x_i be the fractional tolerance of the ith conductance and s_{01} the minimum separation between lines 0 and 1. Then

$$\frac{g_0(1-x_0)}{\sum_0^{n-1} g_i(1+x_i)-2g_0x_0}=s_{01} \tag{12}$$

Similarly the separation between lines 1 and 2 is a minimum when g_1 is a minimum and all other conductances have their maximum values. Hence

Table I

Number of Resistors in Each Deflection Circuit	Number of Lines	Number of Spots	Limit of the Ratio of Resistor Tolerances for Perfect Resistors Scotch Plaid/Uniform
2	4	16	1.50
3	8	64	2.33
4	16	256	3.75
5	32	1,024	6.20
6	64	4,096	10.50

$$\frac{g_1(1-x_1)-g_0(1+x_0)}{\sum_0^{n-1} g_i(1+x_i)-2g_1x_1}=s_{12} \tag{13}$$

where s_{12} is the minimum separation of lines 1 and 2.

The minimum separation between line number (2^k-1) and line number (2^k) is

$$\frac{g_k(1-x_k)-\sum_0^{k-1} g_i(1+x_i)}{\sum_0^{n-1} g_i(1+x_i)-2g_kx_k}=s_{(2^k-1)2^k} \tag{14}$$

The Scotch Plaid raster requires that

$$s_{01}=s_{12}=\ldots.=s_{(2^k-1)2^k}=s \tag{15}$$

Putting equation 15 into equation 14 and rearranging, there results

$$s\sum_0^{n-1} g_i(1+x_i)-2sg_kx_k=g_k(1-x_k)-\sum_0^{k-1} g_i(1+x_i) \tag{16}$$

If in this $(k-1)$ be written for k and the result subtracted from equation 16, then

$$2sg_{k-1}x_{k-1}-2sg_kx_k=g_k(1-x_k)-2g_{k-1} \tag{17}$$

from which

$$\frac{g_k}{g_{k-1}}=2\frac{1+sx_{k-1}}{1-x_k+2sx_k} \tag{18}$$

and hence

$$\frac{g_k}{g_0}=2^k\prod_1^k\left[\frac{1+sx_{i-1}}{1-x_i+2sx_i}\right] \tag{19}$$

For a uniform tolerance, x, this becomes

$$\frac{g_k}{g_0}=2^k\left[\frac{1+sx}{1-x+2sx}\right]^k \tag{20}$$

Substituting equation 20 in equation 12 we obtain a relationship between s and x

$$s=\frac{1-x}{(1+x)\dfrac{2^n[(1+sx)/(1-x+2sx)]^n-1}{2[(1+sx)/(1-x+2sx)]-1}-2x} \tag{21}$$

which may be reduced to the explicit form

$$x=\frac{S_n-1}{s+S_n(1-2s)}, \tag{22}$$

where

$$S_n=\frac{1}{2}\left(\frac{1+s}{s}\right)^{\frac{1}{n}} \tag{23}$$

The corresponding formula for the uniform raster is

$$x_u=\frac{1-(2^n-1)s}{(2^n-1)-s} \tag{24}$$

where s is the specified minimum spacing and x_u is the corresponding tolerance in the resistors.

Equation (22) is plotted in Figures 8(A) and 8(B). It may be shown that

$$\lim_{s\to\frac{1}{2^n-1}}\left(\frac{x}{x_u}\right)=\frac{2^n-1}{n}, \quad x=x_u=0 \tag{25}$$

This is the tolerance ratio for very good resistors.

From the equations given all the curves were computed.

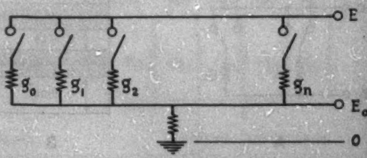

Figure 7. A current adding deflection circuit

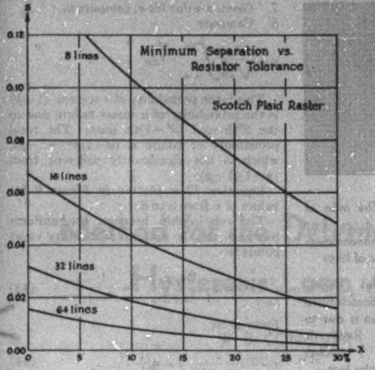

Figure 8(A, left). The minimum separation on a Scotch Plaid raster versus the resistor tolerance x, for various numbers of lines

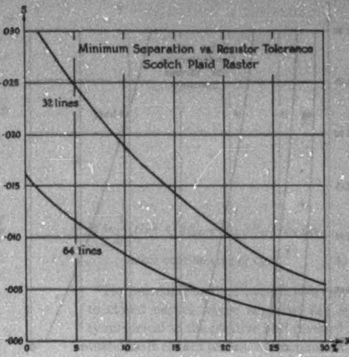

Figure 8(B, right). The same as Figure 8(A) but with a magnified s-scale

Appendix II. Theory of the Uniform Probability Raster

If it be assumed that, after being used for some time, the resistor values are distributed normally about their nominal values then the probability that no separation will be less than some acceptable minimum, s, may be found.

The separation between the (2^k-1)th line and the 2^kth line is

$$s_k=\frac{g_k-\sum_0^{k-1}g_i+g_kx_k-\sum_0^{k-1}g_ix_i}{\sum_0^{n-1}g_i+\sum_0^{n-1}g_ix_i} \tag{26}$$

where the g_i are the nominal values and the x_i, the per unit errors, are normal variables having a mean of zero.

Therefore, $s_k<s$ if, and only if,

$$(1+s)\sum_0^{k-1}g_ix_i+(s-1)g_kx_k+ s\sum_{k+1}^{n-1}g_ix_i>g_k-\sum_0^{k-1}g_i-s\sum_0^{n-1}g_i \tag{27}$$

The left-hand side of equation 27 is a normal variable having a mean value of zero. The probability that it does not exceed the right hand side is

$$p=\frac{1}{\sqrt{2\pi}}\int_{-\infty}^{u_0}\epsilon^{\frac{-u^2}{2}}du \tag{28}$$

where

$$u_0=\frac{g_k-\sum_0^{k-1}g_i-s\sum_0^{n-1}g_i}{\sqrt{(1+s)^2\sum_0^{k-1}g_i^2\sigma_i^2+(1-s)^2g_k^2\sigma_k^2+ s^2\sum_{k+1}^{n-1}g_i^2\sigma_i^2}} \tag{29}$$

and where σ_i is the standard deviation of the ith resistor.

While it would be possible to obtain numerical results using different values of σ_i for each resistor, only the case of equal deviations, $\sigma_0=\sigma_1=\ldots.\sigma_{n-1}=0$, will be discussed. Then

$$\sigma u_0=\frac{g_k-\sum_0^{k-1}g_i-s\sum_0^{n-1}g_i}{\sqrt{(1+2s)\sum_0^{k-1}g_i^2+(1-2s)g_k^2+s^2\sum_0^{n-1}g_i^2}} \tag{30}$$

The probability of failure will be equal at all points of the raster when p and u_0 are independent of k.

It is necessary, therefore, to solve the set of n simultaneous equations obtained from equation 30 by putting $k=0, 1, \ldots n-1$, for the g_i. Since only the ratios of the g_i are involved in equation 30 there will be no loss in generality in putting $g_0=1$. (The absolute values will be determined from other considerations.)

One solution of the n equations is

$$g_i=r^i \tag{31}$$

where

$$r=1+\frac{1}{K} \text{ and } K=s\sum_0^{n-1}g_i. \tag{32}$$

To prove this, write equation 30 as

$$(\sigma u_0)^2\left[(1+2s)\sum_0^{k-1}g_i^2+(1-2s)g_k^2+K_1\right] =\left[g_k-\sum_0^{k-1}g_i-K\right]^2 \tag{33}$$

where

$$K_1=s^2\sum_0^{n-1}g_i^2$$

Writing $k-1$ for k in this and subtracting, there results

$$(\sigma u_0)^2[(1+2s)g_{k-1}^2+ (1-2s)(g_k^2-g_{k-1}^2)] =(g_k-2g_{k-1})\left[g_k-2\left(\sum_0^{k-2}g_i+K\right)\right] \tag{34}$$

or

$$(\sigma u_0)^2\left[(1-2s)\frac{g_k^2}{g_{k-1}^2}+4s\right] =\left(\frac{g_k}{g_{k-1}}-2\right)\left[\frac{g_k}{g_{k-1}}-\frac{2}{g_{k-1}}\left(\sum_0^{k-2}g_i+K\right)\right] \tag{35}$$

Now put $g_k/g_{k-1}=r$, $g_0=1$, then

$$\sum_0^{k-2}g_i=1+r+\ldots.+r^{k-2}=\frac{r^{k-1}-1}{r-1} \tag{36}$$

and hence

$$\frac{2}{g_{k-1}}\left(\sum_0^{k-2}g_i+K\right)=\frac{2}{r^{k-1}}\left(\frac{r^{k-1}-1}{r-1}+K\right) \tag{37}$$

$$=2\left[\frac{1}{r-1}+\frac{1}{r^{k-1}}\left(K-\frac{1}{r-1}\right)\right] \tag{38}$$

Thus k vanishes from the equation for r if

$$K=\frac{1}{r-1} \text{ or } r=1+\frac{1}{K} \tag{39}$$

Equation 35 then becomes the cubic in r

$$(\sigma u_0^2)[(1-2s)r^2+4s]=(r-2)\left(r-\frac{2}{r-1}\right) \tag{40}$$

which gives three values for r when (σu_0) and s are given.

By plotting the two sides of equation 40, or by using Descarte's rule of signs we find that one root is less than -1, one lies between 1 and 2 and the third is greater than 2.

The negative root has no physical significance, requiring negative resistors. The root between 1 and 2 leads to an interlaced raster, the conditions for which are not part of this analysis. It follows that only the root greater than 2 is of practical importance, and this is the Scotch Plaid raster for uniform tolerance. There may, of course, be solutions of the n equations other than

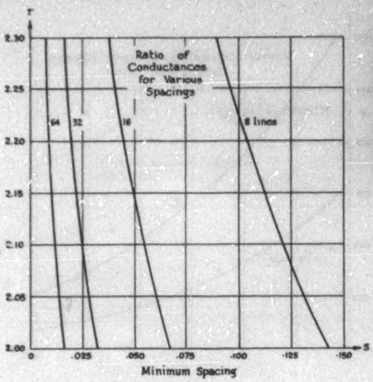

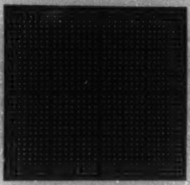

Figure 9 (left). The ratio of the conductances $g_k/g_{k-1}=r$ for the various minimum spacings and number of lines

Figure 10 (above). Photograph of an actual Scotch Plaid raster. The halation is due to reflected light. Raster is approximately 1½ inches square on the tube face

the three found but they would not give conductances in geometric ratio. No such solutions have been found.

The value of s for a given r is easily obtained from

$$K=s\sum_{0}^{n-1}g_t=s\frac{r^n-1}{r-1}=\frac{1}{r-1} \tag{41}$$

whence

$$s=\frac{1}{r^n-1} \tag{42}$$

The following design procedure can now be laid down:

1. Select a reasonable value of r (2.1, 2.2...).
2. Compute 1, $r, r^2 \ldots r^{n-1}$. $(g_0, g_1 \cdots g_{n-1})$
3. Compute

$$\sum_{0}^{n-1}g_t=\frac{r^n-1}{r-1}$$

4. Compute

$$\sum_{0}^{n-1}g_t^2=\frac{r^{2n}-1}{r^2-1}$$

5. Compute

$$s=\frac{1}{r^n-1}$$

6. Compute

$$\sigma u_0=\frac{1-s\sum_{0}^{n-1}g_t}{1-2s+s^2\sum_{0}^{n-1}g_t^2}$$

7. Given a value for σ, compute u_0.
8. Compute

$$p=\frac{1}{\sqrt{2\pi}}\int_{-\infty}^{u_0}e^{-\frac{u^2}{2}}du$$

This is the probability of a success, $(1-p)$ is the probability of a raster failure due to the 2^kth and (2^k-1)th lines. The total probability of failure is $(n-1)p^{n-2}(1-p)$, which is not significantly different from $(n-1)(1-p)$.

Equation 42 is plotted in Figure 9 for values of n from 3 to 6.

The relationship between the uniform tolerance and the uniform probability viewpoints is

$$\frac{g_k}{g_{k-1}}=r=2\frac{1+sx}{1-x+2sx}, \quad s=\frac{1}{r^n-1} \tag{43}$$

From these

$$x=\frac{r-2}{r-2rs+2s}, \quad r=\sqrt[n]{\frac{1+s}{s}} \tag{44}$$

The last is just twice the S_n of equation 23, the first of equation 44 then becomes

$$x=\frac{S_{n-1}}{s+S_n(1-2s)} \tag{45}$$

which is exactly equation 22.

References

1. A Storage System for Use with Binary Digital Computing Machines, F. C. Williams, T. Kilburn. *Proceedings*, Institution of Electrical Engineers (London, England), part II, volume 96, April 1949, pages 183–200.

2. The Test Model Deflection Generator, D. V. Anderson. *Report number 30*, University of Toronto (Toronto, Canada), August 1949.

No Discussion

Method for the Determination of Hysteresis Loop Area

W. B. CONOVER
MEMBER AIEE

A METHOD for finding the area of a hysteresis loop is described below. While somewhat less accurate than conventional methods,[1] it is more rapid and convenient, and requires no special equipment. It can be applied directly to loops on the screen of a cathode ray oscilloscope without the intervening process of photography or manual tracing.

The procedure will be referred to as the harmonic method, since its derivation is based on a consideration of the harmonic components which determine the shape of the loop.

Figure 1 shows a typical hysteresis loop for magnetic sheet steel such as may be obtained by either d-c or a-c measurements made by standard methods. It represents the values of flux density B corresponding to the magnetizing force H as the steel is taken through a complete cycle of magnetization and demagnetization. The energy loss per unit core volume per cycle is proportional to the area enclosed by the loop. The maximum flux density is B_m. The horizontal thickness of the loop is indicated by H, with a subscript indicating the value of B at which the thickness is measured. The energy loss represented by the loop can be determined by the following equation, which is derived in the Appendix:

$$W=\frac{\pi}{6}(H_0+\sqrt{3}H_{50}+H_{86.6})B_m\times10^{-8}$$

joules per cubic inch per cycle (1)

where

B_m = maximum flux density in lines per square inch, and H_0, H_{50}, $H_{86.6}$ = widths of loop in ampere-turns per inch.

If B_m and H are expressed in Gausses and Oersteds, respectively, the right-hand side of the equation must be divided by 0.4π. Using these units and expressing W in ergs per cubic centimeter per cycle, equation 1 becomes

$$W=\frac{1}{24}(H_0+\sqrt{3}H_{50}+H_{86.6})B_m$$ ergs per

cubic centimeter per cycle (1A)

The harmonic method is applicable only to closed curves whose negative half is symmetrical to the positive half reversed; therefore it cannot be used on incremental hysteresis loops.

Accuracy

The harmonic method for determining the area of a loop is based on the assumption that only the first, third, and fifth harmonics of exciting current are significant in their contribution to those loop dimensions which determine area. This assumption appears to be reasonable for most hysteresis loops encountered in practice. To test this, the areas of typical a-c and d-c loops for Deltamax, Nicaloi, and transformer grade silicon steel were measured by the harmonic method and by planimeter. Flux densities of the loops tested ranged from low densities to saturation. The disagreement between the results of the two methods ranged from +3.6 per cent to −4.7% for 17 loops, the areas as determined by the harmonic method averaging 0.7 per cent higher than the planimeter measurements.

The order of accuracy indicated by these results is believed to be sufficient for many purposes.

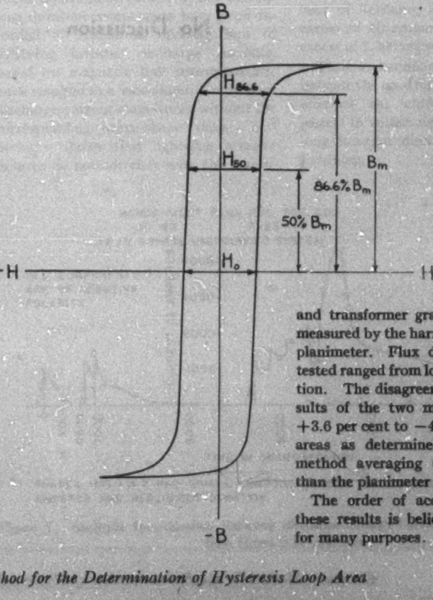

Figure 1. Typical hysteresis loop showing the three width measurements, H_0, H_{50}, and $H_{86.6}$, required to determine its area by the harmonic method

---

Paper 51-277, recommended by the AIEE Basic Sciences Committee and approved by the AIEE Technical Program Committee for presentation at the AIEE Summer General Meeting, Toronto, Ont., Canada, June 25–29, 1951. Manuscript submitted March 1, 1951; made available for printing May 11, 1951.

W. B. Conover is with the General Electric Company, Pittsfield, Mass.

Appendix. Derivation of Harmonic Method

The hysteresis loop of Figure 1 may be described by the parametric equations

$$B=B_m \sin \omega t \qquad (2)$$

$$H=H_1 \sin \omega t+H_1' \cos \omega t+H_3 \sin 3\omega t+ H_3' \cos 3\omega t+H_5 \sin 5\omega t+H_5' \cos 5\omega t+\ldots \qquad (3)$$

The absence of even harmonics follows from the stipulation that the bottom half of the loop be symmetrical to the top half reversed.[3]

The area of the loop is

$$A=\int BdH \qquad (4)$$

Finding the differential of equation 3 and substituting it, along with equation 2, in equation 4, gives

$$A=\omega B_m H_1 \int \sin \omega t \cos \omega t dt- \omega B_m H_1' \int \sin^2 \omega t dt+3\omega B_m H_3 \times \int \sin \omega t \cos 3\omega t dt-3\omega B_m H_3' \times \int \sin \omega t \sin 3\omega t dt+\ldots \qquad (5)$$

When the indicated integrations are performed between the limits of $t=0$ and $t=T$, where $T=2\pi/\omega$, all terms become zero except the second, therefore

$$A=-\omega B_m H_1' \int_0^T \sin^2 \omega t dt=-\pi B_m H_1' \qquad (6)$$

Equation 6 shows that the area of the loop is proportional to the product of B_m and H_1' (the minus sign is not significant). Therefore if H_1' can be evaluated, the area of the loop may be computed. To accomplish this, the values of H will be determined which correspond to $B=0$, $B=0.50B_m$ and $B=0.866B_m$ (The reason for this will be apparent later). From equation 2, the angles ωt at which these values occur are

$\omega t=0$ and π radians at $B=0$

$\omega t=\pi/6$ and $5\pi/6$ radians at $B=0.500B_m$

$\omega t=\pi/3$ and $2\pi/3$ radians at $B=0.866B_m$.

Designating the values of H which exist at these angles by $H_{0\pi}$, H_π, $H_{\pi/6}$, etc., the widths of the loop at $B=0$, $B=0.5B_m$, and $B=0.866B_m$ are $H_0=H_{0\pi}-H_\pi$, $H_{50}=H_{\pi/6}-H_{5\pi/6}$, and $H_{86.6}=H_{\pi/3}-H_{2\pi/3}$, respectively. Therefore, substituting the appropriate values of ωt into equation 3 gives

$$H_0=H_{0\pi}-H_\pi=H_1 \sin 0+H_1' \cos 0+ H_3 \sin 0+H_3' \cos 0+\ldots - H_1 \sin \pi-H_1' \cos \pi-H_3' \sin 3\pi- H_3' \cos 3\pi-\ldots \qquad (7)$$

Evaluating the trigonometric terms in this expression and neglecting harmonics above the fifth, yields

$$H_0=2H_1'+2H_3'+2H_5' \qquad (8)$$

Repeating this procedure for H_{50} and $H_{86.6}$.

$$H_{50}=\sqrt{3}H_1'-\sqrt{3}H_5' \qquad (9)$$

$$H_{86.6}=H_1'-2H_3'+H_5' \qquad (10)$$

The simultaneous equations 8, 9, and 10 may now be solved for H_1', with the result

$$H_1'=\frac{1}{6}(H_0+\sqrt{3}H_{50}+H_{86.6}) \qquad (11)$$

When this equation is substituted in equation 6 an expression for the area of the loop results

$$A=\frac{\pi}{6}(H_0+\sqrt{3}H_{50}+H_{86.6})B_m \qquad (12)$$

It will be noted that thus far in the derivation no units have been specified for the co-ordinates of the $B-H$ loop. Mathematically, equation 4 represents the loop area in terms of the product of whatever units happen to be represented by the scales employed for the ordinate and abscissa of the loop. For example, if a loop such as that shown in Figure 1 were to appear on an uncalibrated oscilloscope, direct measurement of the height and the appropriate widths in inches, when employed in equation 12, would give the area in square inches. On the other hand, if the oscilloscope be calibrated in terms of Gausses and Oersteds, respectively, height and thickness measurements in these units will give the loop area in Gauss-Oersteds. The relation between this area and the core loss in ergs per cubic centimeter per cycle is treated in basic texts[3] on electricity and need not be repeated here; however, it is this relation which permits the conversion of equation 12, which expresses loop area, to equation 1 or 1A, which expresses core loss.

References

1. Electric Circuits (book), **Massachusetts Institute of Technology Staff.** John Wiley and Sons, Inc., New York, N. Y., 1940, page 683.

2. Principles of Alternating Currents (book), R. R. Lawrence. McGraw-Hill Book Company, New York, N. Y., second edition, chapter IV, pages 82–84.

3. Electrical Engineering, Direct Currents (book), C. L. Dawes. McGraw-Hill Book Company (New York, N. Y.), volume I, 1937, pages 268–70.

No Discussion

Long-Duration Surge Testing of Lightning Arresters

S. B. HOWARD
MEMBER AIEE

T. J. CARPENTER
ASSOCIATE AIEE

H. SCHWARTZ
ASSOCIATE AIEE

A METHOD of long-duration surge-withstand design testing of station-type lightning arresters is proposed for consideration by the industry. The test method involves successive applications of a surge having an essentially constant magnitude and a duration measured in thousands of microseconds. This paper discusses the need for such a test, the evaluation of the test and the test-circuit arrangement required to produce the essentially rectangular current surge.

The necessity for lightning arrester surge-withstand design tests has long been recognized. Since 1944, the lightning arrester Standards have specified a 100-kiloampere 5 by 10 microsecond discharge-capacity test for station-type lightning arresters.[1,2] Although the present Standard test has been a useful design criterion, field measurements show that the test is not completely representative of lightning discharges through lightning arresters in service. Some surge-withstand test at the high-current short-duration end of the discharge current scale should be retained in the Standards, but the actual test values are presently under review by industry committees.

Furthermore, field measurements, field experience, and laboratory tests have all shown that the present type of high-current short-duration surge-withstand test has very little significance in relation to the lightning arrester's ability to withstand lower-current longer-duration discharges. Accordingly, an additional surge-withstand test, such as that discussed in this paper, is equally necessary for the low-current long-duration region of the discharge current scale.

Arrester Lightning Discharge Currents Measured in Service

Since the middle 1930's a number of direct lightning strokes with low-current long-duration components have been recorded.[3,4] Numerous investigations of lightning arrester discharge currents, based on magnetic link measurements, have resulted in a vast amount of data on discharge-current magnitudes without the corresponding wave-shape data. Experience shows that lightning arrester failures do not correlate with the magnitude of lightning arrester discharge currents. It can be implied that long-duration low-current discharges were the probable cause of most of these failures.

In the past decade, a limited number of lightning arrester discharges have been reported, in which both the current duration and magnitude were recorded. Such a record is Figure 1, reproduced from Field Investigations of Lightning by Wagner, McCann, and Beck.[5] This discharge had several components of the order of 1,000 amperes, lasting from 200 to more than 2,000 microseconds, with superimposed higher-current shorter-duration peaks. Similarly, Figure 2, reproduced from Lightning Investigation on the West Penn Power System by Bowen and Beck,[6] shows a 10-kiloampere lightning arrester discharge of 200-microsecond duration, followed by a substantially constant 150-ampere component lasting for more than 800 microseconds. The latter paper also indicates that 2 per cent of lightning arrester discharges in excess of 50 amperes have durations in excess of 1,000 microseconds.

These and similar data, though limited, indicate the need for a test which will demonstrate the ability of lightning arresters to withstand multiple low-current long-duration discharges resulting from lightning.

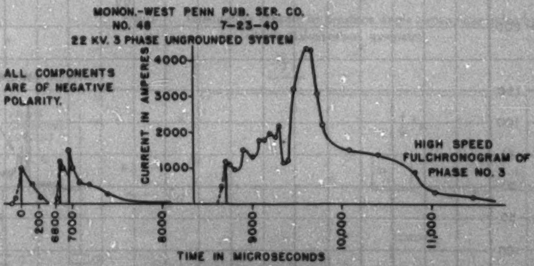

PHASES NOS. 1 & 2 HAD SINGLE COMPONENT NEGATIVE DISCHARGES OF ABOUT 300 AMPERES AND NEGLIGIBLE DURATION.

Figure 1. Multiple long-duration lightning discharge through lightning arrester (reproduced from Figure 5 of reference 5)

Paper 51-278, recommended by the AIEE Protective Devices Committee and approved by the AIEE Technical Program Committee for presentation at the AIEE Summer General Meeting, Toronto, Ont., Canada, June 25–29, 1951. Manuscript submitted March 27, 1951; made available for printing May 4, 1951.

S. B. Howard, T. J. Carpenter, and H. Schwartz are with the General Electric Company, Pittsfield, Mass.

The authors are grateful for the permission of the Niagara Mohawk Power Corporation to use the heretofore unpublished data on switching surges shown in Figure 3.

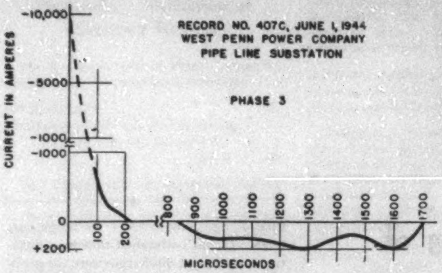

Figure 2. High-current medium-duration and low-current long-duration components of lightning discharge through lightning arrester (reproduced from Figure 5 of reference 6)

Arrester Switching-Surge Discharge Currents Measured in Service

In addition to long-duration lightning discharges, lightning arresters are frequently required to discharge surges resulting from circuit-breaker restrikes when interrupting the charging current of transmission lines or cable circuits. Investigations beginning in the early 1920's have evaluated the overvoltages resulting from switching transmission lines.[7] Many of the recorded overvoltages were of sufficient magnitude to cause lightning arrester operation.

Several years ago, some failures occurred of high-voltage station-type lightning arresters of a now-superseded design. Analysis of these cases indicated the probability that the failures had been caused by severe switching surges produced by circuit breaker restriking. Subsequently, field oscillographic measurements were made at two failure locations to determine the magnitude and duration of the actual switching surges. The results confirmed the original analysis. Figure 3 is a replot of one of the field-test oscillograms. It will be noted that four circuit breaker restrikes occurred on successive half cycles of the voltage wave. The second restrike initiated lightning arrester operation, the third and fourth restrikes occurring while the lightning arrester was still conducting. The last three restrikes each produced lightning arrester discharge currents of the order of 150 amperes and 500 microseconds duration, followed by a low-current component lasting for several thousand microseconds.

It is interesting to note that, although the indicated duty was sufficient to cause failure of the original lightning arresters at the test location, lightning arresters of a more modern design that meets the requirement of adequate long-duration discharge capacity were proof-tested at the same location with the same switching surges. These replacements have subsequently demonstrated that they are completely adequate for the service duty.

Figure 3. Lightning arrester voltage and discharge current resulting from multiple circuit-breaker restrikes during switching-surge tests on 115-kv transmission line

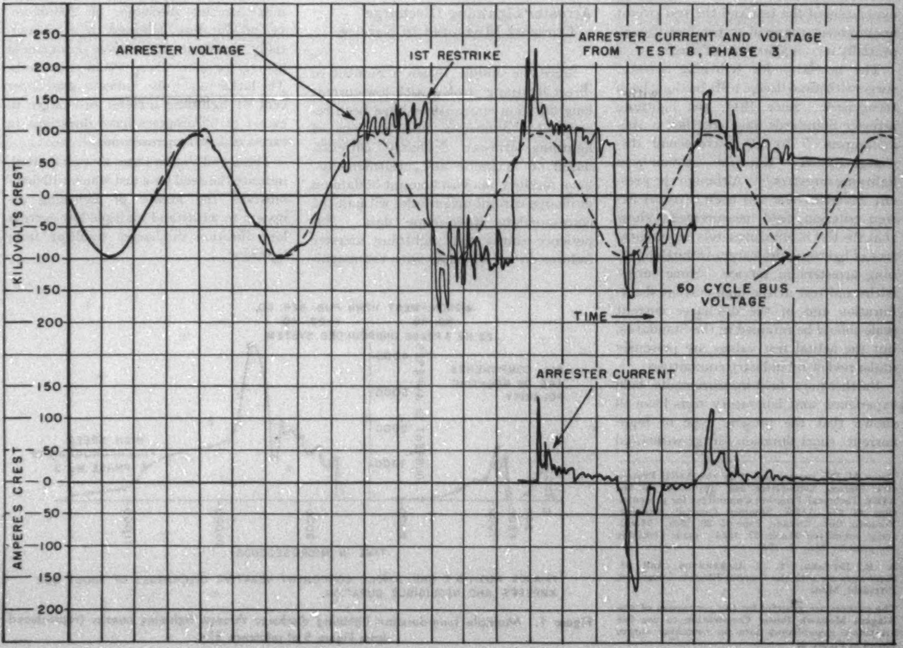

Figure 4. Oscillograms of long-duration surge-withstand test applied to 3-kv station-type lightning arrester valve element

(A) ampere-time, 1st discharge
(B) ampere-time, 20th discharge
(C) volt-time, 1st discharge
(D) volt-time, 20th discharge

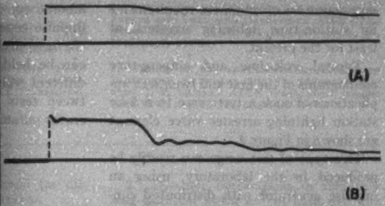

Figure 6. Oscillograms of current discharged from distributed-constant generator through station-type lightning arester valve-elements, showing effect of valve element resistance on wave shape of discharge

Initial-pulse current (I_A) and generator surge impedance (Z_G) held constant; valve-element resistance (R_A) at current I_A varied as follows: Oscillogram (A), $R_A/Z_G=58$; Oscillogram (B), $R_A/Z_G=5.4$

The field tests, experience with early lightning arrester designs and present transmission trends toward higher voltages and longer lines all point to the need for a low-current long-duration surge-withstand test for lightning arresters. Furthermore, it is important to realize that Figure 3 shows three long-duration lightning arrester discharges resulting from a single circuit breaker operation. Other circuit breaker opening tests in the same investigation produced as many as five lightning arrester discharges per operation. Although modern circuit breakers have minimized the restrike problem, power systems are not yet completely equipped with circuit breakers of modern design. Accordingly, for switching surges as well as for lightning discharges, any low-current long-duration surge-withstand test for lightning arresters must factor the probability of many successive discharges occurring in service.

Proposed Method of Long-Duration Surge-Withstand Testing

Based upon the limited field data available, a type of test which involves application of a surge having essentially rectangular wave shape and a duration of thousands of microseconds appears to be a logical approach for evaluation of the long-duration surge-withstand ability of station-type lightning arresters.

Since both the lightning and switching-surge data indicate the probability that the lightning arrester may be called upon to discharge several successive surges of this nature, the complete test should require a number of applications of the test surge. In this connection, laboratory tests have shown that a lightning arrester which will withstand 20 discharges of a given magnitude and duration would withstand a much larger number of discharges of substantially the same severity.

There is no evidence to indicate that a lightning arrester will be called upon to discharge in rapid succession more than a small number of long-duration discharges. Moreover, laboratory techniques require time between successive applications of a test surge, in order to bring the impulse generator to full charge. Thus, any proposed test method logically should permit a reasonable interval between successive applications of the test surge.

Accordingly, it is proposed that the long-duration surge-withstand test for station-type lightning arresters should consist of 20 successive applications of a surge having an essentially constant magnitude (less than 10 per cent decrement) maintained for at least 2,000 microseconds. Successive applications of the test surge should be made in five groups, each having four surges in rapid succession, with intervals between groups of not more than 15 minutes. The test might be performed on complete lightning arrester units or on prorated characteristic elements rated 3 kv or greater.

Although experience by others in the industry will undoubtedly be necessary before standard values can be adopted, it is suggested that a test surge having a magnitude of 150 amperes and a duration of 2,000 microseconds be considered as

Figure 5. Schematic diagram of distributed-constant impulse generator for production of "rectangular" surges

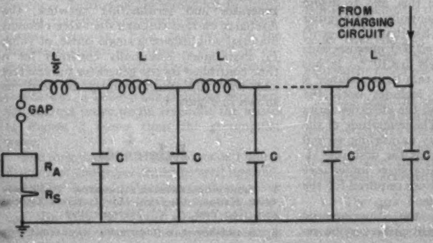

Figure 7. Terminating network to produce single rectangular pulse from distributed-constant generator

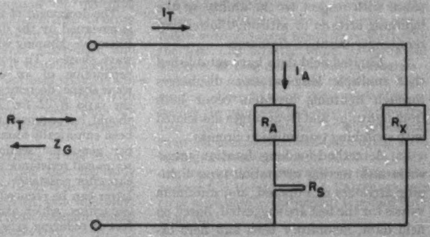

$$R_T=\frac{R_X(R_A+R_S)}{R_X+R_A+R_S}=Z_G$$

representative of minimum requirements for station-type lightning arresters, at least for the present.

Typical volt-time and ampere-time oscillograms of the first and twentieth applications of such a test surge to a 3-kv station lightning arrester valve element are shown in Figure 4.

This type of test surge can readily be produced in the laboratory, using an impulse generator with distributed constants. Details of the generator and test circuit required to insure uniform severity between tests on different valve-element materials or with different generator parameters are given in the Appendix.

Service experience over many years has been excellent with station-type lightning arresters of a modern design, which has successfully passed both the suggested long-duration surge-withstand test and the high-current short-duration test required by the present Standards. No failures of these lightning arresters have been reported to us which were traceable to lack of discharge capacity. Occasional service failures from long-duration lightning or switching surges have been experienced with lightning arresters of other than modern station-type design. Laboratory tests on these other designs indicated that they would easily pass the present Standard high-current short-duration surge-withstand test, but would not pass the suggested low-current long-duration test for station-type lightning arresters. Thus, service experience confirmed by laboratory tests both indicates the need for such a long-duration surge-withstand test and also substantiates the suggested minimum test values.

Conclusions

1. Field measurements, field experience, and laboratory tests have all shown that the present standard high-current short-duration surge-withstand test for lightning arresters has very little significance with respect to the ability of the lightning arrester to withstand lower-current longer-duration discharges.

2. Limited field data have established that multiple long-duration discharges through lightning arresters occur both from lightning and from surges associated with switching transmission circuits.

3. A method for long-duration surge-withstand testing of station-type lightning arresters is proposed, and minimum values for the test are suggested, based on field data, laboratory tests and field experience.

4. The proposed type of long-duration test surge can readily be produced in the laboratory, using a distributed-constant impulse generator. By proper design of the test circuit, the severity of the test can be held constant between tests on different valve-element materials or between tests with different impulse-generator parameters.

Appendix

Impulse Generator

The proposed type of test surge can easily be produced in the laboratory by means of a distributed-constant impulse generator, shown schematically in Figure 5.

The short circuit rectangular-wave current I produced by such an impulse generator was analyzed in 1919 by Carson.[8] His loaded-cable analysis showed that the initial pulse of short circuit current will be of the form:

$$I=\frac{E}{\sqrt{L/C}}\epsilon^{-Rt/2L}I_0[Rt/2L] \text{ amperes} \qquad (1)$$

where

E = voltage to which the generator is charged (volts)

L = inductance per section (microhenrys)

C = capacitance per section (microfarads)

R = resistance per section (ohms)

$\sqrt{L/C}$ = generator surge impedance = Z_G (ohms)

$\epsilon^{-Rt/2L}$ = damping factor (t in microseconds)

$I_0[Rt/2L]$ = Bessel function describing the superimposed oscillation on the initial current pulse

The virtual velocity per section is equal to $1/\sqrt{LC}$. This means that the duration of the initial current pulse would theoretically be:

$$T_1=2N\sqrt{LC} \text{ microseconds} \qquad (2)$$

where N is the number of generator sections.

The duration of the essentially constant portion of the initial current pulse has been found empirically to be:

$$T=2(N-1)\sqrt{LC} \text{ microseconds} \qquad (3)$$

The number of generator sections depends upon the quantity and rating of the available capacitors.

The decrement of the initial current pulse is governed by the damping factor $\epsilon^{-Rt/2L}$. Excessive damping will produce a triangular wave shape. To avoid this, and to insure production of an essentially rectangular wave shape (decrement less than 10 per cent) the ratio $R/2L$ for T = 2,000 microseconds should be approximately 5×10^{-5}. It has been empirically found that the resistance R per generator section includes both the series coil resistance and the effective series capacitor resistance. The magnitude of the latter can be reduced by paralleling several capacitors, which also has the desirable effect of reducing generator surge impedance and the number of sections required for the 2,000-microsecond surge.

The magnitude of the superimposed oscillation on the current pulse can be reduced by increasing the terminating inductance from $L/2$ to L (see Figure 5), with some resultant increase in the time-to-crest and time-to-virtual-zero of the current pulse.

Terminating Impedance

The short-circuit current output of the generator would, of course, consist of a series of rectangular current pulses of the type described but alternating in polarity. When the short circuit is replaced by a terminating impedance equal to or greater than the generator surge impedance, the current pulses will all be of the same polarity.

Typical discharges from the distributed-constant generator through station-arrester valve elements are shown in Figure 6. The percentage decrease in current from the initial pulse to the second and subsequent pulses is a function of the ratio between valve-element resistance and generator surge impedance.

It is obvious from the oscillograms of Figure 6 that different valve-element resistances can result in discharges of varying severity, assuming a constant valve-element current and constant Z_G. The higher the ratio R_A/Z_G, the smaller the drop in current between pulses and the greater the effective duration of the discharge. Constant severity for tests on different valve materials can best be assured by utilizing only the initial current pulse.

This can be accomplished by the use of an over-all terminating impedance equal to the generator surge impedance. A convenient terminating network is shown in Figure 7. Here, the terminating impedance is:

$$R_T=\frac{R_X(R_A+R_S)}{R_X+R_A+R_S}=Z_G \qquad (4)$$

where

R_A = valve-element resistance (ohms) at initial pulse current I_A (amperes)

R_S = measurement shunt resistance (ohms)

R_X = parallel loading resistance (ohms)

Solving equation 4 for R_X, we have

$$R_X=\frac{Z_G(R_A+R_S)}{R_A+R_S-Z_G} \qquad (5)$$

which enables calculations of R_X from the known valve-element characteristics and surge-generator parameters. The required generator charging voltage (volts) is:

$$E=I_T(Z_G+R_T)=2I_A(R_A+R_S) \qquad (6)$$

when I_T = total generator current (amperes, reference Figure 7).

Thus, with a properly designed surge generator and terminating network, the discharge current through the valve-element material will become a single pulse, of value I_A, maintained essentially constant for a time controlled by the generator parameters and then dropping abruptly to zero, as shown in Figure 4.

References

1. LIGHTNING ARRESTER STANDARDS. *Publication 44-89*, National Electrical Manufacturers Association (New York, N. Y.), February 1944.

2. STANDARDS FOR LIGHTNING ARRESTERS FOR

A-C Power Circuits. AIEE Number 28, May 1944; American Standards Association (New York, N. Y.), *C62.1*, 1944.

3. Lightning to the Empire State Building—II, K. B. McEachron. *AIEE Transactions*, volume 60, 1941, pages 885–90.

4. New Instruments for Recording Lightning Currents, C. F. Wagner, G. D. McCann. *AIEE Transactions*, volume 59, 1940, pages 1061–68.

5. Field Investigation of Lightning, C. F. Wagner, G. D. McCann, Edward Beck. *AIEE Transactions*, volume 60, 1941, pages 1222–30.

6. Lightning Investigation on the 25-Kv System of the West Penn Power Company, W. C. Bowen, Edward Beck. *AIEE Transactions*, volume 66, 1947, pages 831–36.

7. Power Systems Overvoltages Produced by Faults and Switching Operations, AIEE Committee Report. *AIEE Transactions*, volume 67, 1948, pages 912–21.

8. Theory of the Transient Oscillations of Electrical Networks and Transmission Systems, J. R. Carson. *AIEE Transactions*, volume XXXVIII, part I, 1919, pages 345–437.

Discussion

J. W. Kalb (Ohio Brass Company, Barberton, Ohio): Messrs. Howard, Carpenter and Schwartz are probably correct in saying that the present high current discharge capacity test of 100,000 amperes is of limited significance in judging the ability of a lightning arrester for station use to withstand service conditions. Actually, the limited field data made available on the nature of discharges through lightning arresters in stations have shown that the surges capable of damaging the lightning arresters have been of a long duration nature. Considering these data, it is somewhat surprising that some sort of long duration test has not been proposed before, and those associated with the transmission and distribution of electric power should welcome the proposal of such a test.

It is unfortunate that equipment used to measure impulse wave shapes requires the expenditure of so much money and attention compared with the simple instruments used to measure crest current only. Otherwise the nature and severity of the longer duration surges would be better known. It would seem, though, that none of the three field records presented in the paper substantiate the rectangular wave shape proposed.

The discharges shown in Figures 1, 2, and 3 of the paper might better be approximated by using test circuits of lumped rather than distributed constants. As the authors say, the distributed constant generator is easily enough constructed. For example, that of our laboratory is of 48 pi sections, and the proposed test wave (Figure 4 of the paper) was easily duplicated. However, to approximate the wave shapes of the field record shown in Figure 3, it was necessary to charge the distributed constant generator not by a conventional rectifier circuit but from the regular duty cycle testing transformer through a restriking air gap. This, of course, is nothing more than a low-voltage approximation of actual field switching conditions.

To suggest this complicated testing procedure as part of lightning arrester standards would rightly be considered impractical because of the difficulty in duplicating conditions between various laboratories. However, each half cycle of the discharge shown in Figure 3 could be approximated by discharging the lumped capacity of an impulse generator through a resistance. I believe the resulting exponential current wave would resemble the waves of Figure 3 closer than the rectangular wave.

The long duration components of Figures 1 and 2 of the paper could be well approximated by lumped inductance and resistance in series with the impulse generator capacity, and this type of circuit would also more suitably approximate the switching surge currents of Figure 3 than would the distributed constant impulse generator.

The test proposed does not include any 60-cycle power voltage. It is true that a power transformer in parallel with the lightning arrester would reduce the severity of the long duration lightning arrester current. On the other hand, the presence of the energized transformer across the lightning arrester imposes other duties perhaps equally severe. This condition rather than that of the unenergized lightning arrester probably predominates under service conditions. It has been our experience that the relative performance of different lightning arrester elements is not the same for long duration discharges with and without power frequency voltage applied. It is misleading, therefore, to base the long duration discharge strength of a lightning arrester only on its ability to withstand surges without power voltage applied. Regardless of the current magnitude and wave shape chosen for such a test, an additional test incorporating combined long duration impulse and power voltage such as that proposed in an AIEE paper by Edward Beck[1] should also be part of the standards if either such test is to have significance.

Messrs. Howard, Carpenter and Schwartz have proposed a valuable and necessary addition to present lightning arrester standards. We should be sure that full advantage is taken of this proposal, and that the result is not just another test of little more significance than the existing 100,000-ampere discharge test.

Reference

1. The Duty on Lightning Arresters for A-C Systems, Edward Beck. *AIEE Transactions*, volume 70, part II, 1950, pages 1134–48.

H. L. Rorden (Bonneville Power Administration, Portland, Oreg.): Since lightning arresters have become of increasing importance in the application of reduced insulation levels, it is desirable that the user have complete information on lightning arrester performance characteristics in order that they may be properly applied. The paper by Messrs. Howard, Carpenter, and Schwartz indicates that it would be desirable to consider revision of national standards in order that the user may request tests with surges of long duration, if such tests are equivalent to surges that may be expected in service.

It has been the experience of the Bonneville Power Administration that lightning arrester failures usually occur from dynamic overvoltages not associated with lightning. It is our belief that the most common causes of lightning arrester failures are:

1. Dynamic overvoltages of short duration but of high enough magnitude to flash over the arrester series gaps, or

2. Dynamic overvoltages of relatively long duration which do not flash over the series gaps but which result in excessive heating of the lightning arrester blocks.

In this paper a long duration test is proposed to simulate the ability of a lightning arrester to withstand switching surges. We would appreciate the authors' comments relative to probability of lightning arrester failure from dynamic transients that exceed the lightning arrester rating but are not of sufficient magnitude to flash over the series gaps. It would be helpful to the system designer to know the degree of risk involved from heating the lightning arrester blocks as well as the possibility of failure from surges of high enough magnitude to flash over the lightning arrester gaps. Would the authors perhaps be willing to advocate a test of this type also for possible inclusion in standards?

H. A. Cornelius (Public Service Company of Northern Illinois, Chicago, Ill.): Since experience and laboratory tests have shown that the 100,000 and 65,000 ampere, 5 × 10 current wave tests, applied to valve type lightning arresters as a duty cycle test, have very little significance, modification of the present standards as suggested in the paper is certainly in order. However, since lightning currents may be imposed on all types of lightning arresters, any change made in the standards, in regard to the duty cycle, should apply to line and distribution types as well as to the station type.

The use of a square 150-ampere current wave having practically a flat top for 2,000 microseconds is suggested as a new test wave which would be applied 20 times to constitute a duty cycle test. Is there any particular reason for using 150 amperes? If not, why not use the 300-crest ampere low-current surge and 2,000 microsecond full-wave duration which has been standard European test practice for some time? This would subject the nonlinear value element to a more severe test.

A point which was not covered in the paper is whether or not a 60-cycle power follow current source would be connected to the lightning arrester while the proposed low current long duration was in progress.

Also, it seems desirable to have a high-current short-duration duty cycle test as well as the proposed low-current, long-duration test. For example, a 5-microsecond front, 40-microsecond half-tail current wave having a crest current of 5,000 or 10,000 amperes would be desirable, in place of the present 5 × 10-microsecond, 100,000-ampere crest wave used in the present standard duty cycle test.

S. B. Howard: The authors wish to thank the several discussors of the paper for their interesting comments. In reply to the points raised by Mr. Kalb, we have made long-duration surge-withstand tests for several years in connection with the design tests of our lightning arresters. These earlier tests were made with the lumped-constant type of test circuit and were reasonably satisfactory as an arbitrary test in a single laboratory.

However, the difficulty of specifying the test discharge current with precision and the uneconomical use of impulse-generator capacitance makes the lumped-constant approach undesirable as a standard industry test. Similarly, while we agree that combined long-duration-impulse and power duty-cycle tests would be desirable, it does not appear practical at the present state of the art to specify such a test in a manner that would permit different laboratories to obtain equivalent results. On the other hand, Mr. Kalb mentions that our proposed rectangular 2,000 microsecond surge was easily duplicated in his laboratory.

The acid test of any proposal, of course, is service experience. As mentioned in our paper, occasional service failures from long-duration-lightning or switching surges have been experienced with arresters that would not pass the proposed long-duration surge withstand test, while no such failures have been reported on lightning arresters that would pass the proposed test.

Replying to Mr. Rorden, there is no question that lightning arresters can be damaged or destroyed by operation with higher than maximum-rated dynamic (power frequency) voltage appearing across their terminals. However, such an occurrence generally connotes incorrect lightning arrester application procedure, since the lightning arrester rating should have been chosen to match the highest dynamic voltage expected from line to ground under any condition of system operation—normal or abnormal, including faults or load rejection. Our experience indicates that, even if the dynamic overvoltage is above lightning arrester rating but below lightning arrester gap sparkover, such system overvoltages are usually accompanied by switching or lightning transients that will produce gap sparkover with consequent damage to the valve element from continued excessive power-follow current. With regard to standard tests, the lightning arrester voltage rating (which is, incidently, a *maximum* rating rather than a nominal one) is established by the power duty-cycle tests already embodied in the Standards and should not require further amplification.

Mr. Cornelius has raised a valid point in suggesting the application of a long-duration surge-withstand test to line and distribution lightning arresters as well as to station-type lightning arresters. The huge per-unit investment and importance to service continuity inherent in large station power apparatus makes it absolutely imperative that the station-type lightning arrester have the utmost reliability for all service conditions. Hence, it was logical to concentrate on the station-type lightning arrester for the first proposal in long-duration surge-withstand testing. Doubtless a similar test, scaled to the economic balance between cost and reliability suitable for line and distribution lightning arresters, will be eventually considered for inclusion in the Standards applicable to those types of arresters.

With regard to the value of crest current for the proposed 2,000-microsecond test for station-type lightning arresters, we suggested in the paper that experience by others in the industry would undoubtedly be necessary before standard values could be adopted. However, our own service experience, mentioned earlier, lends considerable support to the 150-ampere value. Incidently, the long-duration test mentioned by Mr. Cornelius as being European practice is believed to be an exponentially-shaped discharge of 300-amperes crest current, about 100 microseconds to crest and 1,000 microseconds to half value on the tail of the wave.[1] Our laboratory tests indicate this to be less severe than the 150-ampere 2,000-microsecond rectangular surge proposed in our paper.

Finally, we wish to reiterate that we believe some high-current, short-duration impulse withstand test should be retained in the lightning arrester Standards, but we are glad to note the interest of industry groups in reviewing the test values to bring them more into line with service requirements.

REFERENCE

1. ARRESTERS FOR LIGHTNING CURRENTS OF LONG DURATION. *Brown Boveri Review* (Baden, Switzerland), April-May 1950.

Transmission and Distribution Grounding in The Hydro-Electric Power Commission of Ontario

W. W. LOUCKS
NONMEMBER AIEE

W. A. R. LEMIRE
ASSOCIATE AIEE

Synopsis: Accepted grounding methods have been modified for use in areas having difficult grounding conditions. Satisfactory transmission line grounding in rocky areas is obtained economically where the improved methods are followed. Long rods are effective in reducing distribution neutral voltages to an acceptable sustained maximum of 15 volts, which introduces a negligible hazard.

Measurements taken on an air-switch installation showed the superiority, over that with rods alone, of a grounding arrangement incorporating a mat or grid. On the basis of these tests, it is proposed to use such a mat to control the potentials possible between switch handle and ground. Personnel and equipment at generating stations under construction are protected from fault currents by connecting all equipment on the ungrounded distribution system to a common metallic circuit. Ground detectors are used if this arrangement is not practical. Completed stations are safely grounded both for power-frequency system faults and lightning surges. In most instances, separate grounding arrangements are necessary for each type of installation.

THE IMPORTANCE of adequate grounding to the operation and safety of transmission and distribution systems is recognized by all utilities. Basic grounding principles have been evolved which are applied in various degrees by different organizations to meet their particular needs. Although generally accepted grounding methods are employed by The Hydro-Electric Power Commission of Ontario, special methods and techniques have been developed for use where difficult grounding conditions are encountered.

In parts of Southern Ontario good grounding conditions exist; farther north, sand and gravel predominate. In Central and Northern Ontario, high rock ridges with little or no overburden offer no convenient means for grounding. The valleys between ridges are usually sand or swamp with sand bottom. Where sand or soil does exist it is often found in isolated pockets not connected in any way with other soil areas.

Although 10-foot ground rods are used in areas having low-resistivity soil at or near ground surface, much longer rods have proved to be very effective and economical in obtaining satisfactory grounds where sand or gravel overlie material of better conductivity. Figure 1 illustrates, for some typical installations, marked reductions in resistance as rod length is increased. In some locations with deep overburden, long rods do not have resistances low enough to provide adequate grounding; in other locations, overburden is nonexistent and other means of grounding must be employed.

Transmission and distribution grounding are treated in separate sections. Air-switch and generating-station grounding require separate consideration, and are described in two shorter sections. A knowledge of materials and equipment used by the Commission is necessary for an appreciation of the grounding methods employed.

Grounding Materials and Equipment

The standard ground rod is a 10-foot length of 3/4-inch diameter medium steel having a point drawn on one end and the other end galvanized for 18 inches.

In some areas where the resistances of 10-foot rods were too high, additional 10-foot sections were welded on existing rods to produce 20-foot ground rods. Results from these units were so promising that commercially available extension rods with threaded couplings were used. Increased experience with these indicated that a harder tip on the first section would not only increase the rate of driving but also would permit penetration of hard-pan and shale to make use of underlying low-resistivity strata.

The first improvement in driving tips consisted of case-hardening the ends of standard pointed sections previously used. In using this method, two types of 10-foot rods were required, point sections threaded at one end and extension sections threaded at each end. To eliminate these two types of rods, threaded hardened steel tips approximately 5 inches in length were developed. As a result of field tests in summer and winter weather, a tip hardness of Rockwell C 30 to 40 was selected as the optimum.

Extensive field use of these rods revealed several disadvantages in threaded couplings and tips. Even with precautions it was found that corrosion of the threaded ends occurred during storage; normal shipment often resulted in damage to the threaded ends; in field use it was often necessary to clean out the threads on couplings, tips, and rods; and an appreciable delay resulted from the time consumed in connecting extension sections together.

In conjunction with the Hayes Steel Products Ltd., Merriton, Ontario, a simplified tapered coupling similar to that used for rock drills was developed for ground rods. Tests on rods applying this method of coupling showed that the joints were mechanically strong and produced better electrical contact between sections than did the threaded couplings.

Paper 51-279, recommended by the AIEE Protective Devices Committee and approved by the AIEE Technical Program Committee for presentation at the AIEE Summer General Meeting, Toronto, Ont., Canada, June 25-29, 1951. Manuscript submitted March 27, 1951; made available for printing May 14, 1951.

W. W. Loucks and W. A. R. Lemire are with The Hydro-Electric Power Commission of Ontario, Toronto, Ont., Canada.

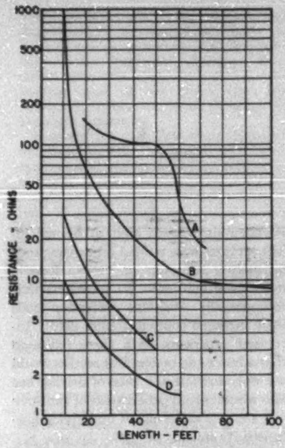

Figure 1. Reduction of measured rod resistance with increasing depth. Curves A and B are for rods in areas having poor grounding conditions. Curve A shows the effect of low-resistivity material beyond a 50-foot depth. Curves C and D illustrate the reduction in rod resistance in areas where grounding conditions are good

During the past year approximately 10,000 rods of this design were used with most satisfactory results. Figure 2 shows the present design of rod end-taper, coupling, and tip.

Recent corrosion studies of ferrous metals in Ontario soils have shown that in general, galvanizing of any part of ground rods is unnecessary. Although end-galvanizing of standard 10-foot rods has not yet been discontinued, no plating is used on extension rods, couplings, or tips.

The standard ground rod clamp is made of steel. Since the clamp should function as a low-resistance permanent connection from ground wire to rod, it is heavily galvanized. In addition, the clamping bolt has a hollow end so that pressure over the small contact area is high. Figure 3 illustrates this galvanized steel U-clamp.

Ground rods are driven both by hand and by machine, practically all distribution grounding being by hand with a pipe driver which permits convenient driving from waist height. Extension ground rods are invariably driven by mechanical means, gasoline, air, and electric hammers all having been used. Because of portability considerations, the gasoline hammer has been adopted for general use.

Counterpoise is used where ground rods cannot be driven because of extensive rock outcrops. Counterpoise conductors are of number 5 *B* and *S* soft galvanized iron. This has recently replaced copper which because of its greater value, was often pilfered. Splices in counterpoise conductors are made with compression joints.

Two types of plough were developed to facilitate the rapid laying of counterpoise. One, a modified root cutting plough, is used on cultivated land without rock or steep hills. The other is made from a bull-dozer by substituting a plough for the blade. This second type, being more rugged, is not stopped by obstacles such as small boulders and fallen logs. Figure 4 shows the larger plough in field trials.

Transmission Line Grounding

Since hydro-electric generating stations in Ontario usually are in rocky areas remote from load-centers, long transmission lines passing through districts where grounding is difficult are common. The approximate mileage of transmission lines of various voltage ratings is as follows:

230 kv	2,200 miles
115 kv	3,600 miles
90 to 13 kv	5,000 miles

Security against lightning outages depends, amongst other factors, on the ground resistance of each line structure. On more important Commission lines, satisfactory service is achieved when outages are less than 0.5 per 100 circuit miles per year.

An analysis of records for three parallel 200-mile lines illustrates the effect of ground resistance on lightning outages. These lines conveniently divide into high-resistance and low-resistance sections. Total lightning outages per 100 circuit miles per year over 20 years were 2.4 in the high-resistance section and 1.0 in the low-resistance section. A similar analysis of records for a 280-mile line traversing the same general area but having improved grounding and reduced shielding angle shows a further reduction in outages to 0.25 per 100 circuit miles per year.

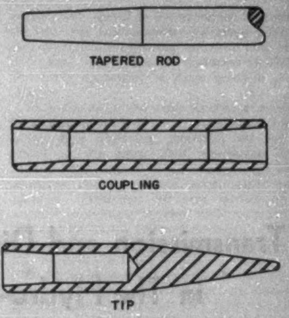

Figure 2. Coupling and hardened tip for use with sectional rod having tapered ends as shown

Outage summaries for these lines appear in Table I. Figure 5 graphically illustrates the effect of ground resistance on the frequency and location of lightning outages.

Grounding Arrangements for Lightning Protection

Transmission structure grounding for protection against lightning should make use of a ground circuit having low impedance to steep wave-front surges. Ground rods up to 100 feet in length have inductances which are negligible in their effect on lightning discharges, and thus are satisfactory if their resistances to ground are small. However, the surge impedance of a single conductor buried in soil of

Table I. Comparative Outages Due to Lightning For Two 230-Kv Lines In The Same General Lightning Areas

	Chats Falls to Leaside (3 Lines)			Beauharnois to Leaside (1 Line)
	Eastern Portion High Resistance	Western Portion Low Resistance	Complete Line	
Total lightning outages per 100 circuit miles per year	2.4	1.0	1.7	0.25
Total located lightning outages per 100 circuit miles per year	1.6	0.6	1.1	0.08
Circuit mile years of operation	5,180	6,120	11,300	2.410
Type of construction			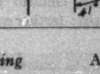	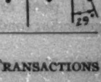

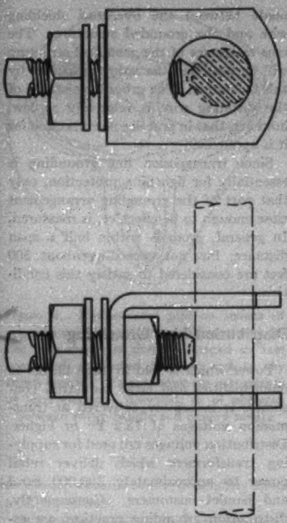

Figure 3. Ground rod clamp of galvanized steel. Hollow end clamping bolt ensures reliable electric connections

moderate to high resistivity probably lies between 150 and 300 ohms regardless of its termination. Conductor and termination effective impedance to a surge decreases from this value to the measured value, or even less, in a time which depends primarily on conductor length and secondly on soil resistivity. If the conductor length is greater than 200 feet, this impedance may decrease too slowly to prevent a flashover.

Additional conductors physically separated from, but connected at the structure to each other have a surge impedance less than that of a single conductor. Four leads will have a value of about 35 to 75 ohms. If more than four are installed, the full benefit of each is not achieved because of mutual coupling. This arrangement of four nonterminated conductors is commonly known as a crowfoot.

When a grounding conductor is terminated on a resistance greater than its surge impedance, a positive voltage reflection returns from the termination to add to that portion of the surge voltage still present, and may result in flashover of insulation. For this reason, no grounding conductor, including those of a crowfoot, is terminated except on an electrode with measured resistance less than 150 ohms.

Where no satisfactory termination for a crowfoot lead can be found before it meets that of the next structure, the leads are joined, and continuous counterpoise is the result.

Structure ground resistances of 15 ohms have resulted in line service with few lightning outages. However, no single maximum value can be defined for all line structures. It is well known that further reduction in ground resistance below a certain value requires ever increasing effort and results in ever decreasing benefits. A practical compromise occurs when a maximum resistance of 25 ohms per structure is obtained although 15 ohms or less is preferred. If the 25-ohm limit cannot be reached with rods and a crowfoot terminated on rods, continuous counterpoise is used as a last resort.

Field Methods Developed and Employed

During the summer of 1948, a 20-mile section of a 115-kv line in rugged country was experimentally grounded in accordance with the foregoing general principles. Comparative costs of the alternative methods were established. Field methods satisfying technical requirements were evolved, and fortunately the preferred sequence of steps from technical considerations was the most economical. On the basis of this preliminary study and experience, the field procedures now presented were developed.

Footing resistances of each structure are measured during line construction, and if the value is more than 15 ohms, grounding improvement is undertaken. The preferred maximum after improvement is 15 ohms, but where this cannot be obtained at acceptable cost, a practical maximum of 25 ohms is tolerated before continuous counterpoise is permitted. The sequence of steps to obtain grounding improvement is as follows:

1. Rods are driven at the structure, if this be possible. Resistance measurements taken after each section is driven indicate the rate at which the resistance is being reduced. Where 15 ohms is obtained with relative ease, driving is continued until the rate of resistance reduction levels off.

2. When a resistance below 15 ohms at the structure cannot be obtained, a search is made for a location where rods can be driven and connected to the structure with less than 200 feet of conductor. If such be found, rods are driven in accordance with

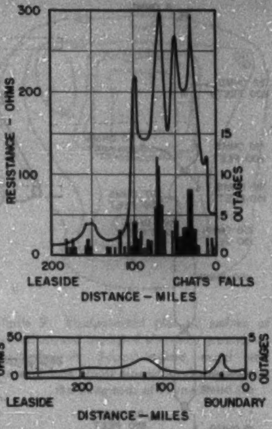

Figure 5. Effect of structure ground resistances on number and location of lightning outages for lines traversing the same general areas. Continuous curves are measured resistances. The bottom chart covers only the Ontario portion of the Beauharnois-to-Leaside line

Figure 4. Counterpoise plough used for burying grounding conductors in rough country

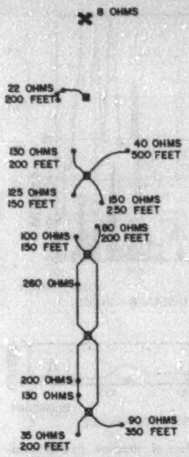

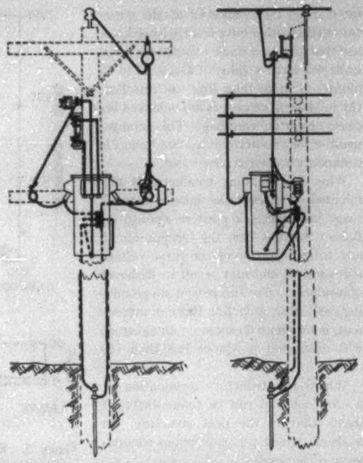

Figure 6 (left). Typical transmission line grounding arrangements in rugged country

Figure 7 (right). Standard grounding arrangement for rural transformer installation

the previous paragraph. When their combined resistance is less than 25 ohms and no further reduction in resistance can be obtained, these are connected to the structure with buried conductor. When less than 25 ohms is not obtained, a second similar location is sought, and if found, the process is repeated.

3. If a resistance of less than 25 ohms cannot be obtained within 200 feet of the structure, the possibility of installing crowfoot leads and terminations is investigated. A crowfoot consists of four conductors radiating from the structure initially at right angles to each other and subsequently kept at least 50 feet apart. Since each of these leads should terminate on an electrode of less than 150 ohms measured resistance, a search is made for possible rod locations not more than half a span distance from the structure. If such locations be found, rods are driven and their individual and combined resistances are measured. If each is below 150 ohms and the value of rods and structure combined is below 25 ohms, buried conductors are installed and connected to the structure.

4. When proper terminations for crowfoot leads cannot be obtained, resistance measurements are taken for record purposes. The leads are then connected to those of the adjoining structures to form a continuous counterpoise.

Examples of these methods of grounding as applied to lines on single structure right-of-ways are shown in Figure 6.

The success of these grounding practices depends, of course, on adequate supervision by trained and experienced personnel who can appraise the right-of-way terrain by judgment and appropriate tests and consequently can select the most likely locations for electrodes.

Extensive Application of Methods

A total of 700 miles of high-voltage transmission lines has been grounded since 1948 according to these methods. During the past year, 600 miles of counterpoise wire and 100,000 feet of sectional rod were used to ground 500 miles of line.

Structure footing resistances were high on all lines before improvement, values over 3,000 ohms being not infrequent. After improvement, 89 per cent of the structures were below 25 ohms and 54 per cent were below 15 ohms. Continuous counterpoise was used at all structures above 25 ohms. Although significant lightning outage records cannot be available for some years, it is anticipated that grounding of these lines is adequate. Cost records have confirmed the economic advantage of the preferred sequence of steps in the grounding procedures.

Resistance Measurements in Rugged Country

The "fall of potential" method of resistance measurement which is generally used to check grounds in areas having extensive overburden is not satisfactory in areas where the overburden occurs in pockets separated by rock outcrops. Instead, a series resistance measurement is made between the overhead shielding wire and the grounded structure. The true resistance of the grounded structure will be less than the value measured by this technique. The ground resistance of the shielding wire is relatively so low, however, that in practice no correction for it is applied.

Since transmission line grounding is essentially for lightning protection, only that part of the grounding arrangement close enough to be effective, is measured. In general, grounds within half a span distance, but not exceeding about 500 feet are considered to satisfy this condition.

Distribution Line Grounding

Power which is sold in large blocks to municipalities and large industrial consumers is invariably delivered at transmission voltages of 13.2 kv or higher. Distribution voltages are used for supplying transformers which deliver retail power to approximately 300,000 rural and hamlet customers. Consequently, distribution grounding practices are essentially those of a rural system.

Approximately 93 per cent of distribution line mileage makes use of a multigrounded common neutral system. The remainder has single-phase transformers connected phase-to-phase on a three-wire system, but this is gradually being replaced by the common neutral method. System voltages are 4, 8, and 12 kv, the two lower levels being used in the well-populated southern portions of Ontario.

Grounding Practices Generally Satisfactory

The distribution neutral is solidly grounded to an electrode of less than 10 ohms at small stations, or less than 2 ohms at large stations. At each bank or transformer, it is again grounded to an electrode of less than 25 ohms.

The high-voltage neutral when present, transformer tank, lightning arrester or arresters, and low-voltage neutral are connected together at transformer level on a pole-mounted "grounding plate." Two bare copper down-leads of number *6 BS* or larger connect the "grounding plate" to the ground rod whose top is at least eight inches below grade. The ground wires are covered with wood moulding guards for the full extent of the pole and cross-arm. Figure 7 illustrates the standard grounding arrangement for rural transformers.

Ground resistances are determined by means of earth testers employing either the "fall-of-potential" method or series

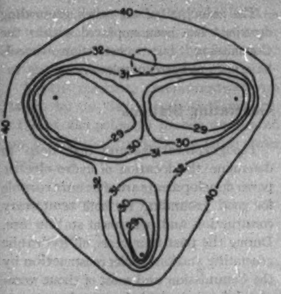

Figure 8. Equipotential plot on surface of ground around air-switch grounding-electrode. The rods shown as dots are spaced six feet apart and connected together and to the switch handle. Values shown are percentages of total electrode potential, or of potential between switch handle and ground surface

resistance measurements, depending upon local conditions.

Where the specified 25 ohms resistance cannot be obtained with one standard 10-foot rod, a second, third, or even fourth 10-foot rod is driven at least 10 feet from the first and from each other and all are interconnected. In some locations having a deep sand overburden, 20-foot rods are used.

In contrast to rules of the National Electrical Safety Code,[1] no minimum number of grounds per mile are required on the common neutral. Although the lines have an average of more than two consumers per mile, some sections are ungrounded for as much as two miles.

Grounding of low-voltage circuits and equipment connected to them is governed by rules and regulations enacted by the Provincial Legislature. These rules, although based on, do not agree in every respect with practices laid down in the Canadian Electrical Code, counterpart of the National Electrical Safety Code.

Before 1931, consumers' grounds were not connected to the neutral even on grounded neutral lines. Service boxes, conduit, and all other metallic enclosures were required to be connected to a ground rod for "safety". From 1931 to 1947, service entrance boxes were connected not only to a ground rod but also to the neutral. Thus, all metallic enclosures connected to the service entrance boxes during this period have been connected also to the common neutral, whereas those not so connected have been protected only by "safety" grounds. Since 1947, revised regulations require that all metallic enclosures be connected to both the neutral at the distribution box and a ground rod. Accidental electrocutions of livestock because of insulation failure on equipment connected only to "safety" grounds have been practically non-existent on installations grounded according to present regulations.

Although the grounding practices outlined generally produce a common neutral which remains close to ground potential, neutral voltages of hazardous magnitude can occur in areas where grounding is difficult. In such areas, this potential may be applied to livestock through the grounding conductor of a water pump or milking machine motor and metallic pipe lines, to drinking bowls or stanchions. At holiday resorts having high neutral voltages, intake pipes for private water systems may be at potentials dangerous to swimmers.

NEUTRAL VOLTAGE HAZARD

Investigations by the Commission begun in 1945 into the cause, magnitude and occurrence of neutral voltages have resulted in the following conclusions:[2]

1. Neutral currents due to normal electric loads can produce neutral potentials of 30 volts or more in areas having heavy loads and particularly difficult grounding conditions. Voltages of this magnitude are usually confined to resort areas, since in general, good farming land that creates heavy electric loads is also good for grounding.

2. High-voltage phase-to-neutral faults can produce potentials of the order of 200 volts on the neutral during a clearing time of sectionalizing devices of approximately one second.

3. Lightning surges above 40 kv can be expected once each year on the neutrals of 4 per cent of the rural transformer installations. Each installation, on the average, will experience a neutral surge of above 10 kv once every three years.

An evaluation of the hazards to which livestock will be exposed if in contact with neutral voltages involves a consideration of the time of exposure. If the voltage is sustained for periods longer than 10 or 15 minutes, 30 volts can cause death by forced muscular contraction and resultant asphyxiation. Since smaller voltages can induce distress to animals, 15 volts has been set as a satisfactory maximum. For periods up to one or two minutes, livestock can be subjected to voltages several times greater with no permanent ill effects.[3] Experiments now in progress jointly by the Commission and the Ontario Veterinary College indicate that the maximum safe voltage on cows for a 2-second application may be approximately 150 volts. This value probably will increase rapidly as the shock duration is decreased and very high voltages can be tolerated for times comparable with the duration of lightning surges.

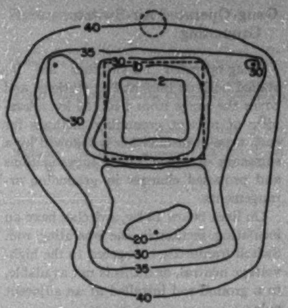

Figure 9. Equipotential plot on surface of ground around modified air-switch grounding-electrode. A 3-foot square metal grill placed 1 inch below ground level supplements the three rods of Figure 8

These have been present on barn electric systems for years without causing fatalities. Experience to date indicates that exposure to neutral potentials of less than 15 volts results in a negligible hazard to livestock.

SPECIAL INVESTIGATIONS AND GROUNDS IMPROVEMENT

In areas where neutral potentials above 15 volts are known or suspected to exist, surveys are conducted with graphic voltmeters and local improvements are undertaken. Since the increase in neutral voltage is gradual in consequence of load growth, the condition is usually disclosed by reports of cattle refusing to drink from metal bowls, or some related complaint.

Neutral voltages usually are reduced to less than 15 volts by improved grounding with sectional rods at each distribution transformer. In one summer resort area where neutral potentials above 30 volts were present, 84 long rods were driven. One rod reached 210 feet in length, but the average length of all was only 59 feet. After this improvement, neutral potentials remained less than 12 volts at all times.

In another resort area where improved grounding was virtually impossible because of rock, distribution circuits were changed from single-phase to 3-phase, thus eliminating most of the neutral current.

Gang-Operated Air-Switch Grounding

Gang-operated air-switches are installed both on lines and at stations, and cover the range from 4 to 115 kv. A review of present grounding methods for each type of installation is followed by a summary of recent safety investigations and proposed changes in grounding arrangements.

On lines below 13 kv, switches have an insulating section in the operating rod. Switch frames are connected to the high-voltage neutral, or if this is not available, to a ground rod installed at an adjacent pole.

The operating handle, which is insulated from the switch frame, is connected to a ground electrode consisting of three 10-foot ground rods placed at the vertices of an imaginary equilateral triangle having a minimum side length of six feet. These rods are so placed that the switch operator stands within the enclosed triangular area while operating the switch.

On lines above 13 kv no insulation is used in the operating rod of switches. The same interconnected 3-rod electrode is used, one rod being connected to the switch frame and the other two by separate conductors to the operating rod at a point just above the handle.

Switches at stations have an operating rod without insulation, so that the handle is electrically connected to the switch frame. One grounding conductor parallels the operating rod and connects the switch frame to the operating handle bracket and to the station ground mat or grid.

Since the neutral also connects to this grid, no additional grounding arrangement is used for the switch.

PROPOSED NEW METHOD OF GROUNDING

Several instances of electric shock while air switches without insulating operating rods were being operated led to a study of the voltage gradients to which an operator might be subjected if voltage should be applied to the operating handle. A current was passed between a typical 3-rod electrode and a remote earth connection; the resultant surface potentials were measured on a high-resistance voltmeter. The effect of a conducting layer on the surface of the ground such as might exist immediately after the start of a rain shower was also investigated. Measurements obtained were used to plot equipotential gradients on plan drawings of the installation, Figure 8 being typical. Conclusions from these tests were:

1. A person standing within the triangular area enclosed by lines connecting three ground rods and holding an operating handle connected to them may be exposed to as much as 43 per cent of the total electrode potential.

2. This potential is not due to the existence of a conducting layer on the surface of the ground.

3. At least one-third of the total voltage between electrode and true ground exists in the immediate area surrounding the individual electrode.

A steel grating 3 feet square buried 1 inch under the surface of the ground between the rods was tried as a means of reducing this potential difference between switch handle and earth. Equipotential contours obtained were similar to those of Figure 9. From these and the former tests, it was concluded that:

1. The potential to which an operator of an air-switch may be exposed is reduced by a factor of at least ten by the use of the grating.

2. The resultant potential gradient is not considered to be hazardous.

3. Conditions existing immediately after the start of a rain shower increase by about two-fold the potential to which an operator might be subjected, but it was still much less than the gradient without the mat. This was due to the formation of a conducting surface on the earth separated from the grating by the dry material.

On the basis of these tests, the Commission contemplates the use of a steel grating or mat placed on the ground surface. The operating handle, and rod if uninsulated, will be connected to this mat which, for switches remote from stations, will connect to the existing three rods, or for switches at stations, to the station ground network. With the mat at ground level, the voltage gradient possible after a rain shower is reduced, and at the same time, safe boundaries for the switch operator are well defined.

The mat proposed for use would be of galvanized welded steel fabric having number 4 ASW* wire (0.2253-inch diameter) in a 4 by 4 inch woven mesh. Fabrics such as this are commonly used for reinforcing concrete roads and structures. The 4 by 6-foot size suggested is adequate to ensure that the operator of a switch having either vertical or lateral handle motions will remain well within the boundaries. The mat will be on the surface of sand in a shallow excavation. Sand will provide for drainage from the mat, thus minimizing corrosion, and is a material which can be readily sterilized to eliminate vegetation.

The principle of air-switch grounding described has been approved within the Commission, but construction details have not yet been completed.

Generating Stations

Topographical features that help to determine the location of hydro-electric power developments are often unfavorable for good grounding for both temporary construction and permanent station use. During the past four years, all hydraulic generating stations under construction by the Commission and most of those completed have had their ground arrangements reviewed.

This involved a total of seven plants having an ultimate installed capacity of 1,026,000 kva.

CONSTRUCTION POWER GROUNDING

Construction power at developments is generally distributed by 3-phase 575- and 2,300-volt ungrounded delta systems. Experience indicates that ground electrodes of sufficiently low resistance to protect such a system adequately are difficult or impossible, to obtain. In most cases, safety is obtained by interconnecting all metallic enclosures of electric apparatus and associated ground electrodes on the same system. This interconnection is by means of a copper conductor or a structural member such as a conveyer. Where this proves impractical, monitored ground detectors are used to facilitate maintaining the system free of ground faults. One important phase of grounding is the protection of blasting crews from premature explosions during lightning storms or system faults.

PERMANENT STATION GROUNDING

For the completed station, low-resistance grounds usually must be at some distance, often as far as one mile, from the power house or switchyard. Consequently, for surge grounding it has been necessary to supplement these grounds with additional electrodes, generally of higher resistance, in the immediate vicinity of the structures. All equipment and structural steel in the dam, power house, and switchyard are connected to a common grounding bus to which both power and surge grounds also connect. Surge grounding in yards usually is obtained by means of a buried grid of copper conductor and ground rods where possible. The dam and power house make use of rods or conductor loops buried in the forebay or tailrace. In locating low-resistance electrodes for power-frequency grounding, care is taken to ensure that the earth in question is not in an isolated pocket, and that it is a part of the general overburden.

---

*American Steel and Wire Company.

When resistance measurements are taken by the "fall-of-potential" method, current and potential probes are spaced up to 4,000 feet from the electrode under test.

In some instances, telephone lines to other stations are used to bring a remote ground connection to the tester.

Experience gained in surveys for construction-power grounding is useful in establishing suitable locations for permanent grounds. Earth resistivity measurements and trial rods are used as additional determinants.

References

1. National Electrical Safety Code. National Fire Protection Association (Boston, Mass.).

2. Rural Neutral Potentials, J. H. Waghorne. *AIEE Transactions*, volume 69, part I, 1950, pages 660–63.

3. Effect of Electric Shock on the Heart, L. P. Ferris, B. G. King, P. W. Spence, H. B. Williams. *Electrical Engineering* (*AIEE Transactions*), volume 55, May 1936, pages 498–515.

No Discussion

Standardization of Ratings of Neutral Grounding Reactors

J. L. THOMASON
MEMBER AIEE

THE RATINGS of neutral grounding reactors ordered at random show a definite pattern. Consequently, it is recommended that this pattern be standardized and incorporated into the existing standards.[1] It is proposed to use the standardizing system previously presented.[2] For instance, for any voltage class the relation between ohms and amperes is nearly linear although broad banded on log-log paper. By grouping several closely associated ratings into one rating, the number of ratings is reduced from an unlimited number to a reasonable and practical number. Logical ratings established by the 60 per cent steps of preferred series of numbers are being suggested. Intermediate ratings would be available, of course, without the benefits of standardization.

After the ratings are standardized, it will only be a matter of time until the physical sizes are standardized. Then duplicates will be more frequently utilized and the resulting benefits will thus be made industry wide. This paper covers coreless, neutral grounding reactors, both air and oil immersed.

Rating Items for Standardization

Only three basic items of rating will be considered here for standardization:

Reactance. The reactance should be expressed in ohms at 60 cycles, unless the frequency is otherwise specified, and the values should be established by the 60 per cent steps of the preferred system of numbers.

Current. The current should be expressed in amperes and the values should be established by the 60 per cent steps of the preferred system of numbers.

Dielectric Test. Normally the nominal[3] circuit voltage determines the dielectric test of equipment. Here, for standardization purposes, it appears best to consider the induced potential tests as the basic rating.

By standardizing on these three items of rating, with the aid of a rating target, duplication will occur more frequently than at the present time.

Experience on Rating Sizes of Dry-Type Reactors

A review of dry-type, neutral grounding reactor designs of the last five years shows that:

1. A definite relationship exists between rated current in amperes and the reactance in ohms.
2. The above relation is the same for both the 10-second and the 1-minute time ratings.
3. Approximately 94 per cent of the designs were in the 4,160, 7,200, 12,400, and 14,400 circuit volt classes; 2 per cent were 2,400 or below; and 4 per cent above 14,400.
4. Practically all the reactors were used for ground end applications and were contained in two insulation levels—30-kv and 40-kv induced potential tests.

Items 1, 2, and 3 are clearly substantiated by Table I. Table I in Parts A, B, C, D, and E shows the ratings in which dry-type neutral grounding reactors have been furnished in the various circuit voltage classes during the last five years. Each design is tabulated in the closest proposed standard rating.

Note from AIEE Standard No. 32[1] that the induced (turn-to-turn) test for outdoor reactors is one-third greater than the values shown in column 3 of Table II. Nevertheless, outdoor reactors could be supplied from the next higher standard potential test group. Thus, 30-kv outdoor could be supplied from 40-kv indoor; 40-kv outdoor from 60-kv indoor, and so forth.

Experience on Rating Sizes of Liquid Immersed Reactors

A review of our coreless, liquid immersed neutral grounding reactor designs over the last five years shows:

1. A definite relationship between rated current in amperes and reactance in ohms.
2. The above relation is the same for all time ratings. The various time ratings and their frequency of occurrence are shown by the table below:

Time	Per Cent
10 seconds	13
1 minute	75
30 seconds	3
2 minutes	9

3. Most of the reactors were in circuit voltage classes of 33, 46, and 161 kv.
4. The potential test requirements have varied considerably. In over 50 per cent of the designs the purchasers had called for higher test values than specified by the present standard.[1] This may warrant further consideration because the present standard conservatively specifies the higher of the two values established by the circuit voltage or the reactor rated voltage.

Table III, similar to Table I, shows the designs of the liquid-immersed type tabulated in the closest proposed standard ratings. Designs for several other circuit voltage classes are not tabulated because only a few designs were made.

Rating Targets

By consolidating the data in Tables I and II, Table IV is obtained. It will cover 95 per cent of the dry-type neutral

---

Paper 51-280, recommended by the AIEE Protective Devices Committee and approved by the AIEE Technical Program Committee for presentation at the AIEE Summer General Meeting, Toronto, Ont., Canada, June 25–29, 1951. Manuscript submitted January 18, 1951; made available for printing May 7, 1951.

J. L. Thomason is with the General Electric Company, Pittsfield, Mass.

Table I. Rating Target, Neutral Grounding Reactor, Dry Type, Amperes

Part A. Experience with 2400 Circuit-Volt Class

Ohms	25	40	63	100	160	250	400	630	1,000	1,600	2,500	4,000
0.10												X/O
0.16												
0.25										O/Y		
0.40												
0.63												
1.0						O/Y						
1.6												
2.5												
4.0												
6.3												
10.0												
16.0												
25.0												
40.0												
63.0												
100.0	X/O											

Ohms	630	1,000	1,600	2,500	4,000	6,300	10,000	16,000	25,000	40,000
Part B. Experience with 4160 Circuit-Volt Class										
0.025										X/O
0.040							X/O	X/O		
0.063							X/Y	X/Y		
0.100					O/Y	O/Y	X/Y			
0.160				X/O	X/O	X/O	X/O			
0.250				X/O						
0.400			O/Y		O/Y					
Part C. Experience with 7,200 Circuit-Volt Class										
0.16						X/O	X/O	X/O		
0.25							X/Y			
0.40						O/Y				
0.63					O/Y					
1.00										
1.60	X/O		O/Y							
Part D. Experience with 12,460 Circuit-Volt Class										
0.063									X/O	
0.100								O/Y	X/O	
0.160							X/O	X/O		
0.250							O/Y	X/O		
0.400				O/Y		O/Y				
0.630				X/O						
1.00			X/O	X/O						
1.60			X/O	O/Y						
2.50				O/Y						
4.00		X/Y	O/Y							
6.30		O/Y								
10.0										
16.0	X/O									
Part E. Experience with 14,400 Circuit-Volt Class										
0.025										X/O
0.040										X/O
0.063									X/O	X/O
0.100								O/Y	X/O	X/O
0.16									X/Y	
0.25						O/Y	X/O	X/O	X/O	
0.40					O/Y	X/Y	X/Y			
0.63					X/O	X/Y	X/O			
1.0				X/O	X/Y	O/Y				
1.6				X/Y		X/O				
2.5				X/Y						
4.0				X/Y						

Note: In the symbol X/Y, the letter X shows that 10-second ratings were made, Y 1-minute ratings, and O no ratings.

Table II. Voltage Classes[1]

Circuit Voltage (Ground End Application), Kv-Rms	Circuit Voltage (Line End Application), Kv-Rms	Applied or Induced Potential Tests, Kv-Rms
1.2	1.2	12
2.5	2.5	25
5.0	5.0	30
8.7 through 34.5	8.7 through 15	40
46.0 through 345	25.0	60
	34.5	85
	46.0	115

Table III. Rating Target, Neutral Grounding Reactor, Liquid Immersed Type, Amperes

Ohms	160	250	400	630	1,000
Part A. Experience with 34,000 Circuit-Volt Class					
16					X
25					
40		X			
63		X			
100	X				

Ohms	250	400	630	1,000	1,600	2,500	4,000	6,300
Part B. Experience with 46,000 Circuit-Volt Class								
1.6							X	
2.5								X
4.0								
6.3					X	X		
10.0					X			
16.0								
25.0								
40.0								
63.0	X							
100.0								

Ohms	630	1,000	1,600
Part C. Experience with 69,000 Circuit-Volt Class			
16		X	
25		X	
40			

Ohms	160	250	400	630	1,000	1,600
Part D. Experience with 161,000 Circuit-Volt Class						
25					X	
40				X	X	
63				X		
100		X	X			
160		X				

Ohms	1,600	2,500
Part E. Experience with 230,000 Circuit-Volt Class		
25	X	
40		X

Table IV. Rating Target, Neutral Grounding Reactor, Dry Type, Amperes

Ohms	400	630	1,000	1,600	2,500	4,000	6,300	10,000	16,000	25,000	40,000
0.010											
0.016											
0.025										2	
0.040									2		
0.063								2			4
0.100					1		2			4	
0.16				1		2		3	4		
0.25			1		2		3				
0.40		1		2		3		4			
0.63	1				3		4				
1.0				3		4					
1.6			3		4						
2.5											
4.0				4							
6.3			4								
10.0		4									

Key	Induced Potential Test
1	25 Kv
2	30 Kv
3	40 Kv
4	60 Kv

grounding reactors ordinarily ordered.

By consolidating the data in Table III, Table V is obtained. Note that as the circuit voltage increases the ohms increase for the same current value. This relation is similar to that shown in the rating target for the lower voltages of the dry-type, Table IV.

By consolidating Tables IV and V into Table VI a rating target for all neutral

Table V. Rating Target, Neutral Grounding Reactor, Liquid Immersed Type, Amperes

Ohms	100	160	250	400	630	1,000	1,600	2,500	4,000	6,300
1.6									B	
2.5										B
4.0										
6.3							B	B		
10.0							B			
16.0						AC				
25.0						CD	B			
40.0				A	D	D		B		
63.0			B	A	D					
100.0		A	D	D						
160.0			D							

Key	Circuit Voltage Class	Maximum Induced Potential Test Kv
A	34,000	50
B	46,000	70
C	69,000	95
D	161,000	185
E	230,000	275

Table VI. Rating Target for Neutral Grounding Reactors, Amperes

Ohms	250	400	630	1,000	1,600	2,500	4,000	6,300	10,000	16,000	25,000
0.010											1
0.016										1	
0.025									1		2
0.040								1		2	
0.063							1		2		
0.10						1		2		3	4
0.16					1		2		3	4	
0.25				1		2		3			
0.40					2		3		4		
0.63				2		3		4			
1.0					3		4				
1.6				3		4					
2.5			3					AB			
4.0					4		AB				
6.3				4		AB	CD				
10.0			4		AB	CD	E				
16.0		4		AB	CD	EF					
25.0			AB	CD	EF						
40.0		AB	CD	EF	G						
63.0		CD	EF	G							
100.0		EF	G								
160.0	F	G									

Dry Type

Key	Induced Potential Test Kv
1	25
2	30
3	40
4	60

Liquid Type

Key	Induced Potential Test Kv
A	50
B	70
C	95
D	140
E	185
F	230
G	275

grounding reactors is obtained. For the higher circuit voltages, the induced potential tests are based on the circuit voltages and not on the rated voltages nor other specifications. The rating target of Table VI should serve:

1. As a starting point for standardizing neutral grounding reactors.
2. As a very good relationship for ohms and amperes in neutral grounding reactors.
3. As a fair relationship for induced potential tests.

Conclusions on Rating Targets

1. The ratings of the reactors in terms of reactance in ohms and current in amperes are determined logically by the preferred series of numbers.

2. The time rating (10 seconds, 30 seconds, 1 minute or 2 minutes) does not alter the current and reactance ratings.

3. Only two time ratings, 10 seconds and 1 minute, are recommended as standards to minimize the number of standard ratings and thus realize the benefits of standardization.

Advantages of Reactor Standardization

Some of the advantages of reactor standardization are:

1. Acceptance of preferred ratings should eventually result in: reduced costs, shorter delivery time, better use of material as tests and service on the same size of reactor will point to improvement.

2. The use of current and reactance ratings (as on a rating target) established by the preferred series of numbers will allow reactors to be designed and used in logical sizes.

References

1. Neutral Grounding Devices, *AIEE Standard Number 32*, 1947.

2. Standardization of Reactor Ratings, F. H. Kierstead, J. L. Thomason. *AIEE Transactions*, volume 68, part II, 1949, pages 955–58.

3. Preferred Voltage Ratings for A-C Systems and Equipment. *Report*, Joint Subcommittee of Edison Electric Institute and National Electrical Manufacturers Association (New York, N. Y.), May 1949.

Discussion

Louis E. Sauer (Westinghouse Electric Corporation, Sharon, Pa.): Mr. Thomason is to be commended for the use of preferred number values which provide a logical basis for ohmic and current standardization and can also lead to dimensional standardization. Although the 60 per cent steps (five series of preferred numbers) provide a minimum number of designs the amount of saving to be expected can hardly prevent a large number of specials. While neutral grounding reactors are usually ordered singly it is still doubtful that the lower development cost of a standard can bridge more than a 20 per cent jump. In order to encourage the use of standard ratings it would seem more practical to offer the 25 per cent steps of the ten series of preferred numbers at least for ohmic rating.

J. L. Thomason: We are grateful to Mr. Sauer for his formal commendation to add to the numerous informal commendations on the use of preferred number values for ohmic and current ratings of neutral grounding reactors. As pointed out previously, standardization of reactor ratings will be satisfactory to all concerned only if first, there are enough ratings to cover the fields of applications and if second, there are few enough ratings so that economies can be realized. The 60 per cent steps are recommended initially with the knowledge that time will determine if there be any necessity for smaller rating steps such as 25 per cent.

Electric Insect Traps

CHARLES F. DALZIEL
MEMBER AIEE

Synopsis: The electric insect trap, consisting of a filament or luminous tube light surrounded by an exposed high-voltage electrocuting grid possesses shock and fire hazards. Although little is known regarding the phenomena of insect electrocution, efficient electrocution of small insects with a reduction of these hazards to an acceptable degree may be accomplished by proper design, construction, and installation. The limited success of insect traps is attributed to fouling of the electrocuting grids by the remains of insects sticking to the electrocuting grids. Although efficiency of electrocution is important, effectiveness of the device depends upon the grids remaining in operating condition. The arc produced when the insect flies between the electrodes of the grid may puncture the insect's body and release a sufficient amount of its body fluid to cover it with a gluey liquid. As the insect falls in the vicinity of the electrodes, the electrostatic forces may cause it to impinge on one of the electrodes. If sufficient body fluid has been exuded by the time it touches an electrode it may stick in a manner similar to a fly lighting on a freshly varnished surface. Although the insect remains may or may not interfere with the electrocuting grid, or they may be consumed by the arc in a short time, it is probable that fouling is responsible for many of the unsatisfactory reports from the field. Electrocuting grids which are less subject to fouling must be devised, and two designs of improved grids are proposed by the author.

IT IS apparent to the casual observer that light exercises a powerful influence on the behavior of many insects. On warm summer evenings their irresistible attraction to light is evidenced by the number of moths and flies of many varieties that flutter around street lights, flood lights, yard and porch lights, and campers' lanterns. Years ago the lure of light was suggested as a means of control for nocturnal flying pests and annoying insects. At the present time much concern is being given to the use of light traps to combat the infestation of the European corn borer in the states of the Middle West. Various types of traps have been devised, the most satisfactory being the modern electric insect trap, the essential components of which are an electrically energized source of radiation and an associated high-voltage electrocuting grid. Although a considerable amount of scientific information is available regarding the response of insects to various frequencies in the visible or near visible (ultraviolet) spectrum, relatively little attention has been given to the effectiveness and electric shock aspects of these devices. This paper is confined to the latter problems in anticipation that safer and more efficient electric insect traps may result.

Electrical Hazards

The exposed electrocuting grid of the modern electric insect trap possesses potential electric shock and fire hazards similar to other devices having exposed electrodes, such as the electric fence, the electric stock prod, electric welding machines, the radiant heating element of the hot plate, and electrostatic spraying and dip-detearing apparatus. Reduction of the electric shock hazard of any device having exposed electrodes is a matter of serious concern.

It is obvious that the electric shock hazard of the electric insect trap could be largely eliminated by surrounding the electrocuting grid with a guard so constructed to permit insects to fly through it, but arranged to prevent accidental human contact with the energized electrodes. The disadvantages of a protective guard are: (1) increased cost, (2) increased size, (3) reduced area of effectiveness, (4) difficulty in cleaning the grids, and (5) limitation of the size of insects which can be controlled. For these and possibly other valid reasons, the use of protective guards has been opposed by both entomologists and agricultural engineers.

A more satisfactory method of controlling the electric shock hazard is by safe design, proper construction, and safe installation. In order to be specific, the electric insect traps considered in this discussion are assumed to be energized from a high reactance transformer having an output of 3,500 to 10,000 volts and 10 to 30 milliamperes. The light source, if incandescent or fluorescent, may be connected to the input terminals. If a high-voltage luminous tube is used, it may be energized from the winding also used for the electrocuting grid, or from a second winding designed especially for the light. The latter is advantageous as it permits control of the current obtainable from the electrocuting grid independent of the current requirements of the light. Since the lure is mounted inside the electrocuting grid, the electrical hazard from contact with the grid is of primary importance. The traps used in this investigation were manufactured by the Monolite Company, Berkeley, however, except for minor details of construction, they are similar to many commercial electric insect traps in general use. The chief factors affecting the electric shock hazard from the electrocuting grids of this type of device are: (1) current magnitude, (2) current pathway through the body, and (3) shock duration.

It is common knowledge that gradually increasing 60-cycle alternating currents passed through electrodes held in the hands causes tingling, warmth, muscular contractions, and pain. Pain and

---

Paper 51-282, recommended by the AIEE Safety Committee and approved by the AIEE Technical Program Committee for presentation at the AIEE Summer General Meeting, Toronto, Canada, June 25-29, 1951. Manuscript submitted June 23, 1950; made available for printing May 11, 1951.

Charles F. Dalziel is with the University of California, Berkeley, Calif.

This investigation was sponsored by the California Committee on the Relation of Electricity to Agriculture and supervised by the Division of Entomology and Parasitology in co-operation with the Division of Agricultural Engineering, College of Agriculture, and the Division of Electrical Engineering, College of Engineering, University of California. Personal acknowledgments are due J. R. Tavernetti and J. K. Ellsworth of the College of Agriculture, for participation in the experimental work and reduction of data.

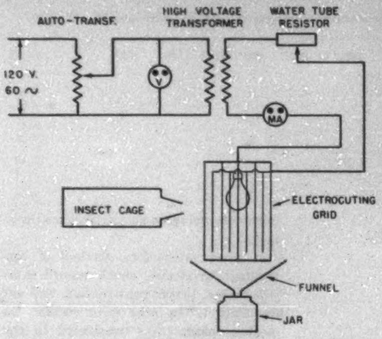

Figure 1 (left). Schematic wiring diagram of apparatus used to investigate effectiveness of electrocuting grids

Figure 3 (right). Electrocution of potato tuber moths using $^{3}/_{32}$-inch diameter grid bars spaced $^{10}/_{32}$ inch

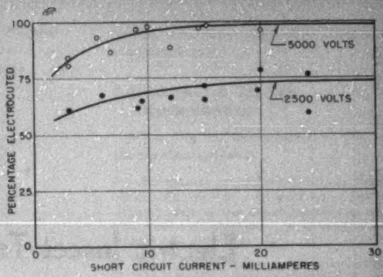

contractions increase in severity as the current is increased, and finally a current is reached where a person is unable to release his grasp of the electrodes by using muscles directly affected by the current. The maximum current which a person can just release is called his let-go current.

It is generally recognized that currents below a person's let-go current are unimportant from a safety standpoint, however, currents slightly in excess of one's let-go current may be very dangerous. About $99^{1}/_{2}$ per cent of normal men and women can release 9 or 6 milliamperes, respectively, and these values are regarded as the maximum 60-cycle current which can be considered reasonably safe for situations in which an adult can obtain a grasp of a continuously energized conductor. Currents of about 20 milliamperes, when passed across the chest, cause such strong contractions of the chest muscles that breathing is difficult if not impossible during the time the current flows. However, respiration resumes automatically upon interruption of the current, and no adverse aftereffects are to be expected due to currents of this magnitude provided such shocks are of short duration.

It is important to distinguish between the direct effects of electric shock and general shock to the nervous system, which is commonly called *shock*. Because of the wide variation in the physical condition of individuals, it is impossible to design any device having exposed electrodes which would be safe for all humans. The press contains frequent accounts of fatalities ascribed to heart failure caused by overexcitement, intense emotion, fear or shock. For such susceptible persons, it is possible that contact with any electric circuit which permits currents only slightly in excess of the threshold of sensation might result in fatality. This possibility must be recognized, and in spite of what may be done to develop a safe electric insect trap, an occasional death is to be expected from casual contact involving electric currents known to be safe for most normal individuals. Death in such cases must be considered due to shock to the nervous system, and not due to the primary effects of the electric current.

Although experimental results to be discussed presently indicate that electrocution of insects is possible with currents of the order of 6 milliamperes, the practicability of the device depends upon the electrocuting grid remaining free from fouling due to the remains of insects stocking to and short circuiting the electrocuting grid. Although the current required to consume an insect, and thus permit the trap to resume its normal operating condition depends upon the type of insect and the amount of body fluid it contains, it appears that a minimum of 10 to 20 milliamperes would be required for small insects. Since currents of this magnitude will probably be insufficient to consume the remains of large moths or beetles, should they stick on the electrocuting grid, the trap must be so constructed that the grid may be cleaned easily by an attendant. Although such a procedure would be unwise when the trap is energized, the act must be anticipated and duly considered in arriving at design requirements.

In deciding upon safety recommenda-

Figure 2. Electrocution of green-bottle flies using $^{3}/_{32}$-inch diameter grid bars spaced $^{14}/_{32}$ inch

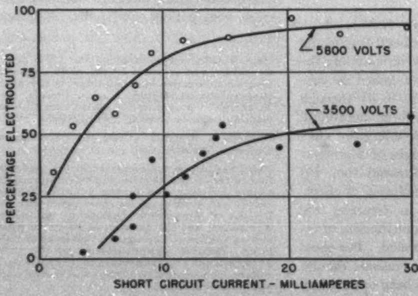

Figure 4. Maximum percentage of insects electrocuted as a function of voltage and spacing between grid bars with current limited to 30 milliamperes

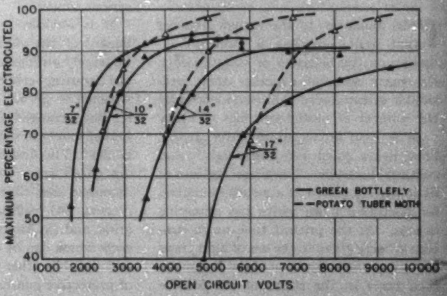

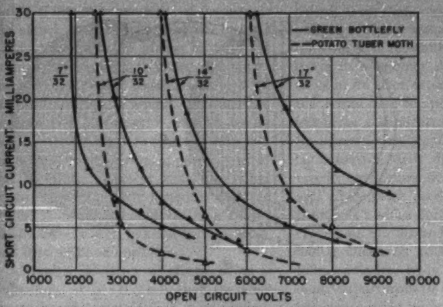

Figure 5. Current and voltage required to obtain 75 per cent electrocution for various spacings of grid bars

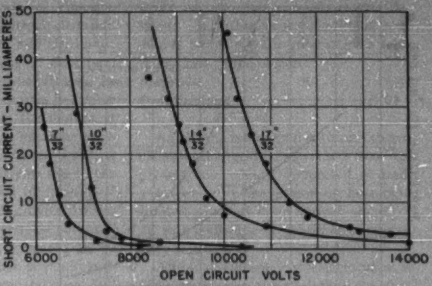

Figure 6. Voltage and current at which arcing occurs across electrocuting grids for various grid bar spacings

tions for any device one must adopt a realistic viewpoint. Safety requirements which are too restrictive would preclude the use of all devices having exposed electrodes. The hazards of electric insect traps are of the same order of magnitude as other somewhat similar devices, many of which have been *approved*.*

A very considerable degree of safety would result from installing the trap so that the bottom was at a height of at least 7½ feet above ground or floor. In this event the trap would be beyond the reach of all, including children, and it would require a deliberate act to make contact with the energized grid. The open space between the bars of the electrocuting grid should not exceed about 1/2 inch. This close spacing practically precludes securing a firm grasp of two bars of opposite polarity. Unless an energized conductor can be grasped, safety requirements based on the let-go current criterion are much too conservative. From a safety point of view, preference is given to an ungrounded high voltage circuit, however, it may be more economical to ground one point of the secondary winding. In either event, if a person touched only one of the energized grid bars when touching the housing or when standing on a grounded object, in addition to not having a firm grasp of the electrode, his position and body weight would materially assist him to free himself from the circuit.

In order to confirm the above ideas, both the writer and an associate withstood the output from a trap in which the current and voltage output was subject to control over rather wide limits. To avoid being burned by the electric arc, a 3/8-inch diameter steel rod was held in each hand and placed in contact with the electrocuting grid. Arcs were repeatedly struck and broken with the current pathway between the arms and across the chest using open circuit voltages up to 9,720 volts and currents up to 12 milliamperes. Tests with the palm of the left hand pressed against the grid were also made with voltages up to 15,750 volts and currents up to 62.5 milliamperes, the limit of the apparatus. In this case the hand, wet with water, was slapped and held firmly on the electrocuting grid, and to avoid being burned the circuit was then interrupted by an assistant. From the foregoing, it is concluded that if the maximum current between grid bars of opposite polarity, and between either grid bar and the metal housing, was limited to about 15 milliamperes, the device should be reasonably safe from high voltage shock hazards.

Safety requirements, similar to those prescribed for electric fence controllers should provide adequate protection against low-voltage shock hazards. The primary and secondary windings of the transformer should be placed on separate core legs, or otherwise separated, so that insulation failure will be to a metallic barrier, the transformer core, or housing. In addition the device must be constructed so that it will satisfactorily withstand suitable dielectric rain, and humidity tests.

For insect traps subject to rough handling in the field, it is essential that the device be equipped with a suitable length of three conductor flexible cord, and that the third or ground conductor be bonded to the core, frame and housing, and the other end connected to an effective ground. At least one standard fuse, mounted inside the waterproof housing, should be provided in the ungrounded conductor of the primary circuit. The current rating of the fuse should be as low as practicable, preferably not to exceed one ampere, in order to be sure that adequate protection is maintained during adverse grounding conditions, such as when it is necessary to use a driven ground in a location where grounding conditions are unfavorable. Although fusing and grounding the noncurrent carrying parts assures maximum safety, it is probably not feasible to incorporate these features in the somewhat smaller traps designed for use around the home or garden. It is unfortunate that proper grounding of these devices will be impracticable until 3-terminal polarized outlets come into common residential use.

During the experiments cigarettes were often lit from the arc controlled by a screw driver touching the electrocuting grid. Exposed arcs and sparks are a fire hazard, and it is important that the farmer be so informed. Insect traps are sometimes placed in storage rooms or in other enclosures. It is very important that such places be well ventilated so that there is little likelihood for the accumulation of explosive dust or gas mixtures. Traps should not be installed where a quantity of chaff might envelope the grid, such as adjacent to hay hoists and the like, and traps must not be used near highly combustible materials. Since the majority of electric insect traps are used over cultivated areas the fire hazard during ordinary operation in the field should be small, and it must be assumed that control of fire hazards is just one of the many problems associated with operating a modern mechanized farm.

Based on these considerations, an electric insect trap with an exposed elec-

---

*Approved by the Underwriters' Laboratories, Inc., United States Bureau of Standards, United States Bureau of Mines, or similar institutions of recognized standing.

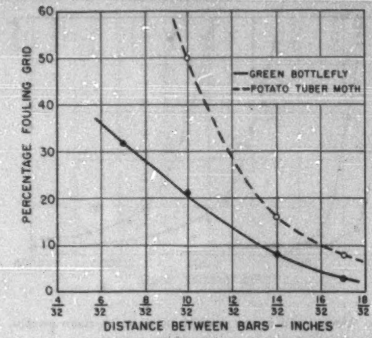

Figure 7 (left). Percentage of insects fouling electrocuting grids as a function of spacing between grid bars

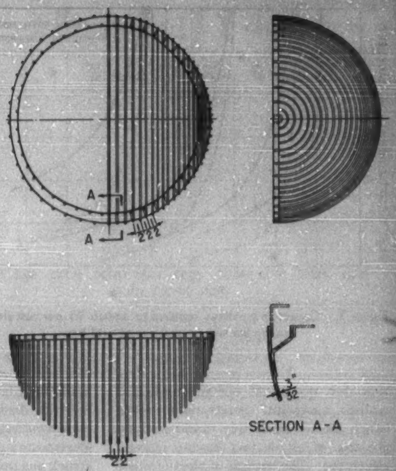

Figure 8 (right). Hemispherical electrocuting grid for insect trap

trocuting grid, constructed from approved components, supported at least 7½ feet above the ground or floor, and limited to a maximum current output of 15 rms milliamperes should be a reasonably safe device.

Effectiveness of Electrocuting Grid

The electric apparatus illustrated in Figure 1 was assembled in a darkroom and exhaustive experiments were made to determine the effectiveness of electrocuting grids. Due to time limitations, the tests were confined to the green bottlefly (Lucilia sericata), and the potato tuber moth (Phthorimoea operculella). These tests were made using readily available insects on the assumption that the results obtained would be representative, and that they might apply to other insects which are difficult to raise in the laboratory.

The curves of Figures 2 and 3 give the percentage of insects electrocuted as a function of the maximum output of the electrocuting grid for the given spacing of the grid bars. The curves are typical of the results obtained, and are sufficient to illustrate that, for a given open-circuit voltage, the grid efficiency increases up to a certain value, after which the percentage of insects electrocuted remains fairly constant regardless of the maximum current output.

The results using different electrocuting grids are shown in Figure 4 in which case the output current was limited to 30 milliamperes. For each spacing of the grid bars there was a certain voltage above which little was gained, and below this voltage, the efficiency decreased rapidly.

Values obtained from a series of curves similar to those of Figures 2 and 3 were used to obtain the curves of Figure 5. These curves show the voltampere requirements to obtain 75 per cent electrocution for various spacings of the grid bars. It is apparent that the voltage decreases rather rapidly with increased current output up to about 15 milliamperes. Based on these data, it appears that satisfactory operation for small insects should be obtained with the current output limited to a maximum of about 15 milliamperes. Although the deduction that electrocuting grids limited to 15 milliamperes should yield satisfactory results is based on tests involving only two types of insects, the fact that many commercial insect traps are limited to 10 milliamperes supports the conclusion that currents greatly in excess of these values are unnecessary as well as undesirable.

The voltage required to cause arc-over of the various grids is shown in Figure 6. Although the curves represent the maximum voltage that could be used with these particular electrocuting grids, it is concluded that the operating voltage of commercial traps should not exceed about 75 per cent of the breakdown voltage, as once flashover occurs the arc will be maintained at a somewhat lower voltage. At the higher voltages and currents, an insect would frequently initiate an arc which would fail to extinguish itself. Both visible and audible corona were produced at surface irregularities when the voltage exceeded about 5,000 volts. Problems of insulation also become costly factors at very high voltages. For these reasons it appears that the maximum practical voltage for devices of this type is about 7,500 volts.

The mechanism whereby an electric current causes death to an insect is unknown, however, considerable information was obtained from tests in which thou-

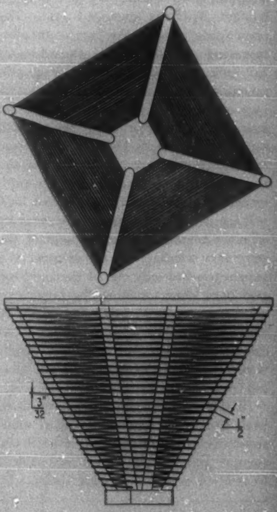

Figure 9. Conical electrocuting grid for insect trap

sands of insects were used. If the electric arc struck in the vicinity of the insect's head, it generally fell lifeless to the floor, or in a jar arranged to collect the specimens. On the other hand, if contact with the grid resulted in a light spark instead of an arc to the insect's head, it would fall lifeless to the floor, but after a few minutes it might revive, apparently without ill effect. Arcs or sparks to other parts of insect's body generally resulted in less damage, although in the majority of cases the insect was critically injured, and died within a few hours.

Although efficiency of electrocution is important, it is essential that the electrocuting grid remain free from fouling. In common with the reports of other experimenters, considerable difficulty was experienced due to insects' sticking and short circuiting the grids. Sometimes the insects stuck to the grid bars without interfering with the operation of the grid, at other times the insects were consumed by the arc and the grid automatically resumed operating condition, however, much too frequently it was necessary to clean the grid by hand before the experiment could be continued due to the remains of insects short circuiting the grid. The curves of Figure 7 show the percentage of insects sticking on the grid as a function of the spacing between the grid bars.

The chief reason insects foul the bars of the electrocuting grid is due to the electrostatic forces produced by the strong electric field. If an arc involving an insect is extinguished while the insect is in the space adjacent to, but not touching either electrode, the insect acquires an electrostatic charge. For the idealized case in which the electric field is produced by direct current, the charged insect is then attracted toward one electrode, and repelled from the electrode of opposite polarity. Upon contact with an electrode the charge is neutralized, and the insect drops in a manner similar to dust particles in an electrostatic precipitator. In the actual case the phenomena is similar but more complicated, as the motion of the insect depends upon its initial momentum, inertia, drift due to any existing breeze, convection air currents due to the arc, air currents produced by beating of the insect's wings, force of gravity, and its charge in the alternating high potential field. Often an insect appeared to be falling as a free body when it would suddenly depart from its vertical descent and impinge against an adjacent grid bar. If by this time sufficient body fluid had been exuded, it frequently adhered to an electrode, in a manner similar to a fly lighting on a freshly varnished surface.

Figures 8 and 9 were devised by the writer in an attempt to develop an electrocuting grid which would be less subject to fouling due to insects sticking on the grid bars. It is possible that the short interval of time between initiation of the arc and emergence of body fluid, may be sufficient to permit the insect to start its descent and thus fall away from the electrodes before it has exuded sufficient fluid to permit it to stick thereon. The construction of the proposed electrocuting grids is such that any vertical descent, however small a distance, will result in the insect falling away from the electrodes. In contrast, an insect causing an arc in the upper portion of the conventional vertical grid falls more or less parallel to the grid bars and within the strong electric field during its entire descent within the structure. For horizontal configurations arranged in a vertical plane, the insect's motion is transverse to the electric field, but it may strike bar after bar in its downward descent. In either case, conditions conducive to fouling are present for a relatively long period of time.

Conclusions

An electric insect trap with an exposed electrocuting grid, constructed from approved components, supported at least $7^1/_2$ feet above the ground or floor, and limited to a maximum current output of 15 rms milliamperes should be a reasonably safe device.

Although efficiency of electrocution is important, it is essential that the electrocuting grid remain free from fouling. New types of electrocuting grids must be developed which will be less subject to fouling due to insects sticking on the grid; the grids must be constructed so that they may be cleaned easily by unskilled labor in the field.

The fire hazard of electric insect traps should be recognized. Insect traps must not be used near combustible materials or in locations where there is a possibility of an explosive atmosphere.

References

1. Field Tests of the Efficacy of Colored Light in Trapping Insect Pests, W. B. Herms, J. K. Ellsworth. *Journal of Economic Entomology,* volume 27, number 5, October 1934.

2. Energy Requirements and Safety Features of Electric Insect Traps, J. R. Tavernetti, J. K. Ellsworth. *Agricultural Engineering* (St. Joseph, Mich.), volume 19, November 1938.

3. Effect of Frequency on Let-go Currents, C. F. Dalziel, Eric Ogden, C. E. Abbott. *AIEE Transactions*, volume 62, 1943, pages 745–49.

4. Dangerous Electric Currents, C. F. Dalziel. *AIEE Transactions*, volume 65, 1946, pages 579–85.

No Discussion

Operating Experience with Ground Distance Relays

M. P. OSBURN
MEMBER AIEE

P. L. DANDENO
NONMEMBER AIEE

THIS PAPER presents the results of 15 year's experience using ground distance relays as a means of protecting against faults on the 25-cycle high-voltage transmission systems of The Hydro-Electric Power Commission of Ontario. The experience obtained from this method of ground protection over this period of time has indicated that a definite field of application exists for this type of relaying.

Factors Contributing to the Use of Ground Distance Protection on the Commission's Systems

The Hydro-Electric Power Commission of Ontario made its first application of distance relaying to the 230-kv 25-cycle system which originally consisted, in 1928, of one line between the Paugan Generating Station and Leaside Transformer Station. This system expanded in four years to that shown in Figure 1, and was operated from its inception with all neutral points of Y-connected transformers solidly grounded. Ground distance relaying was employed in conjunction with phase distance protection. The principal reason for the choice of impedance relaying generally was the desire to interrupt line-to-ground faults over the same ranges as afforded by phase impedance protection. Since carrier current was not generally employed in 1928 with many schemes it was felt that the ground impedance relays could give a more consistent performance for all types of system connection, especially during light load conditions when fault currents were limited by the amount of generation on the system. Similar relay installations to those made originally in 1928, were applied to the 230-kv system as additional lines were incorporated into the network. Figures 2, 3, and 4 show the line changes up to 1949. No further additions are to be made to the 230-kv 25-cycle system. Frequency standardization was commenced in 1949 with the purpose of eventually converting most of the system shown in Figure 4 from 25-cycle to 60-cycle operation.

The original portion of the Commission's 115-kv 25-cycle system was built between 1910 and 1914. The system was only grounded at the points where a source of generation existed and originally only at Niagara Transformer Station. Resistance grounding through water boxes was initially decided upon to limit the current through the transformer neutrals and line breakers under line-to-ground fault conditions. As the sources of infeed grew in number the number of resistance grounded neutrals also increased. In the period from 1920 to 1929, Queenston Generating Station was incorporated into the high-tension system at Niagara Falls. In addition, when generation became available at the Leaside Transformer Station bus over the 230-kv network from the eastern sources, that is, Paugan, Chats Falls, Masson, and Beauharnois, a grounding source also was installed in the Toronto area.

In 1931, after 3 years' experience with ground and phase impedance relays on the 230-kv network, it was decided to install this same method of protection to the 115-kv system, in order to obtain the benefits of high speed fault clearance, since the older type of circuit breakers originally installed on this system were either being replaced or modernized. Since the amount and distribution of ground currents in the 115-kv 25-cycle network was generally governed by the value and location of the neutral grounding points, the use of induction-type ground relays was precluded.

In Figures 1 to 4 inclusive, the numbers associated with the lines are the distances in miles between bussing points. In some cases the lines are not relayed at all bussing points. The only lines considered in this paper for analysis are those shown in Figures 1 to 4 which have mileages indicated.

Furthermore, only those faults involving ground and one, two or three phases are considered; although not tabulated, the percentage of faults involving only two or three phases without ground was considered too small to be worth recording; consequently the breakdown of all faults into the three categories shown in Table I or Table II is quite indicative of the actual percentage incidence of all faults encountered.

Theoretical Considerations

The most comprehensive analysis of distance relaying and more particularly ground distance relaying has been presented by W. A. Lewis and L. S. Tippett.[1] This first treatment, written in 1931, was again brought to the attention of the profession in 1947 with a revised presentation of the original article. The aim of this paper was to provide a comprehensive means of analyzing the voltages and currents under fault conditions which may be used to operate ground distance relays on double circuit lines. The simplest and yet most preferable scheme as described by Lewis and Tippett considers the general expression for the line-to-ground voltage at a relay during a line-to-ground fault.

Paper 51-284, recommended by the AIEE Relays Committee and approved by the AIEE Technical Program Committee for presentation at the AIEE Summer General Meeting, Toronto, Ont., Canada, June 25–29, 1951. Manuscript submitted March 27, 1951; made available for printing May 10, 1951.

M. P. OSBURN and P. L. DANDENO are with The Hydro-Electric Power Commission of Ontario, Toronto, Canada.

The authors wish to acknowledge the assistance given by E. M. Wood, for his many suggestions, and to M. Nastich, who assisted in the tabulation of the operating records for this paper.

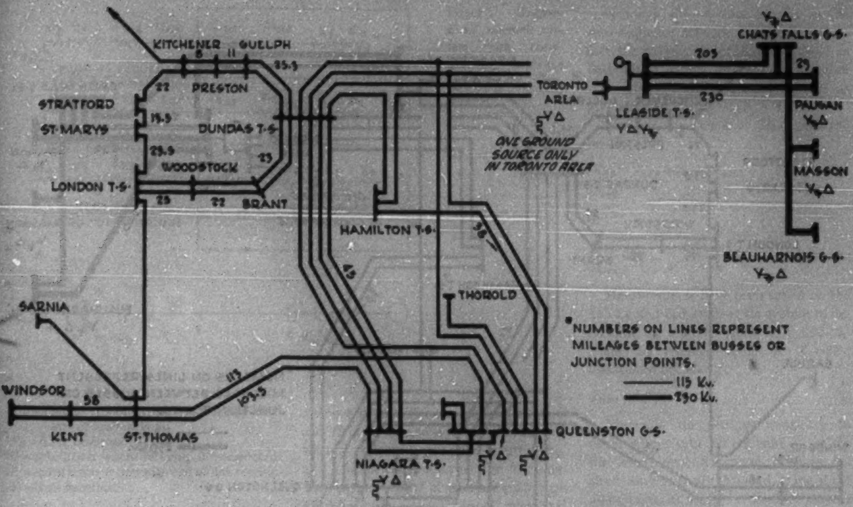
KITCHENER
GUELPH
8
11
25.3
22
PRESTON
STRATFORD
19.5
ST-MARYS
23.5
DUNDAS T-S-
23
WOODSTOCK
LONDON T-S-
25
22
BRANT
HAMILTON T-S-
38
45
TORONTO AREA
YΔ
ONE GROUND SOURCE ONLY IN TORONTO AREA
LEASIDE T-S-
YΔY
205
230
CHATS FALLS G-S-
YΔ
29
PAUGAN
YΔ
MASSON
YΔ
BEAUHARNOIS G-S-
YΔ
THOROLD
SARNIA
WINDSOR
58
KENT
ST-THOMAS
115
103.5
QUEENSTON G-S-
NIAGARA T-S-
YΔ
YΔ
YΔ
*NUMBERS ON LINES REPRESENT MILEAGES BETWEEN BUSSES OR JUNCTION POINTS.
115 Kv.
230 Kv.

Figure 1. Hydro Electric Power Commission of Ontario, 25-cycle system, 1935

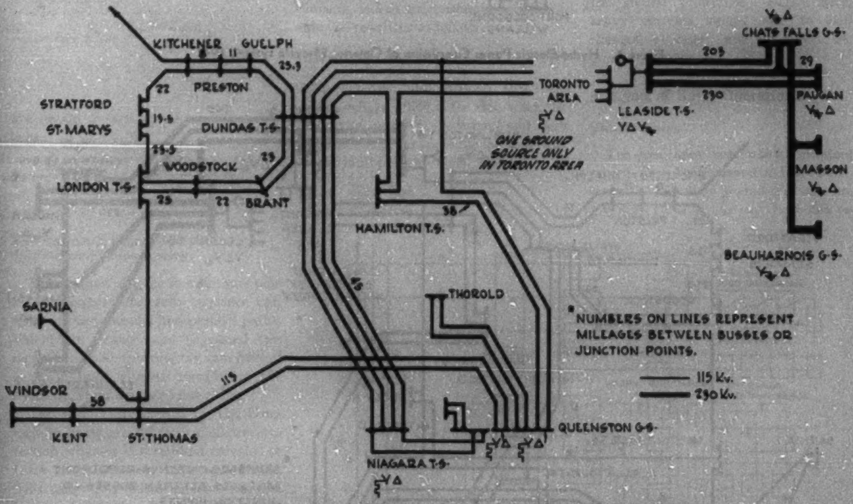
KITCHENER
GUELPH
8
11
25.3
22
PRESTON
STRATFORD
19.5
ST-MARYS
23.5
DUNDAS T-S-
23
WOODSTOCK
LONDON T-S-
25
22
BRANT
HAMILTON T-S-
38
45
TORONTO AREA
YΔ
ONE GROUND SOURCE ONLY IN TORONTO AREA
LEASIDE T-S-
YΔY
205
230
CHATS FALLS G-S-
YΔ
29
PAUGAN
YΔ
MASSON
YΔ
BEAUHARNOIS G-S-
YΔ
THOROLD
SARNIA
WINDSOR
58
KENT
ST-THOMAS
115
QUEENSTON G-S-
NIAGARA T-S-
YΔ
YΔ
YΔ
*NUMBERS ON LINES REPRESENT MILEAGES BETWEEN BUSSES OR JUNCTION POINTS.
115 Kv.
230 Kv.

Figure 2. Hydro Electric Power Commission of Ontario, 25-cycle system, 1937–1939

$$E_{aG}=mZ_{1GH}\left(I_{aGF}+I_{0GF}\frac{(Z_{0GH}-Z_{1GH})}{Z_{1GH}}+I_{0GH}\frac{M_{0GH}}{Z_{1GH}}\right)+(I_{aGF}+I_{aHF})R_G \quad (1)$$

where

E_{aG} = line-to-ground voltage, A phase at G

m = fraction of distance from G to H at which fault is assumed to occur

I_{aGF} = phase A fault current in faulted line at G

Z_{1GH} = positive-sequence impedance, station G to H

Z_{0GH} = zero-sequence impedance, station G to H

M_{0GH} = zero-sequence mutual impedance between two parallel circuits from G to H

I_{0GH} = zero-sequence fault current in parallel line

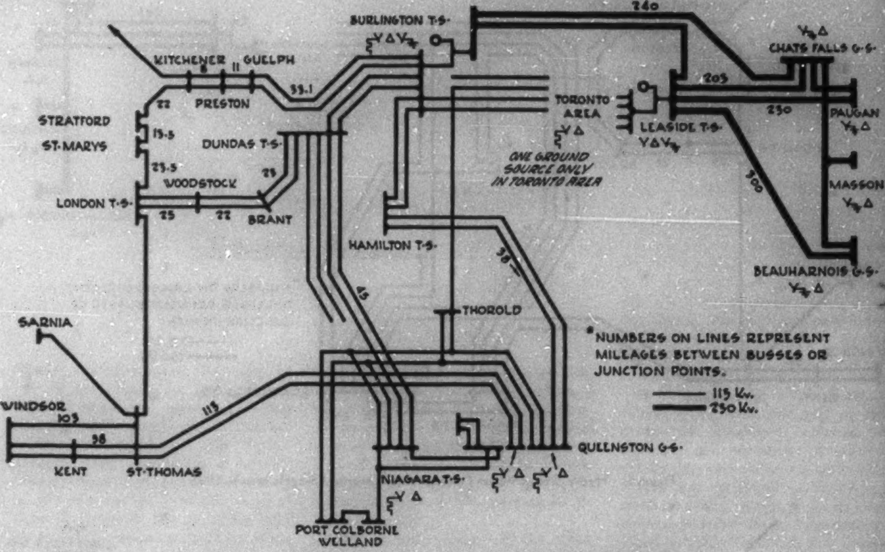
BURLINGTON T.S.
240
CHATS FALLS G.S.
KITCHENER
8
11
GUELPH
33.1
205
22
PRESTON
TORONTO AREA
STRATFORD
230
PAUGAN
13.5
LEASIDE T.S.
ST. MARYS
DUNDAS T.S.
ONE GROUND SOURCE ONLY IN TORONTO AREA
23.5
23
WOODSTOCK
300
MASSON
LONDON T.S.
25
22
BRANT
HAMILTON T.S.
38
BEAUHARNOIS G.S.
45
THOROLD
SARNIA
*NUMBERS ON LINES REPRESENT MILEAGES BETWEEN BUSSES OR JUNCTION POINTS.
115 Kv.
230 Kv.
WINDSOR
103
115
98
QUEENSTON G.S.
KENT
ST. THOMAS
NIAGARA T.S.
PORT COLBORNE
WELLAND

Figure 3. Hydro-Electric Power Commission of Ontario, 25-cycle system, 1941

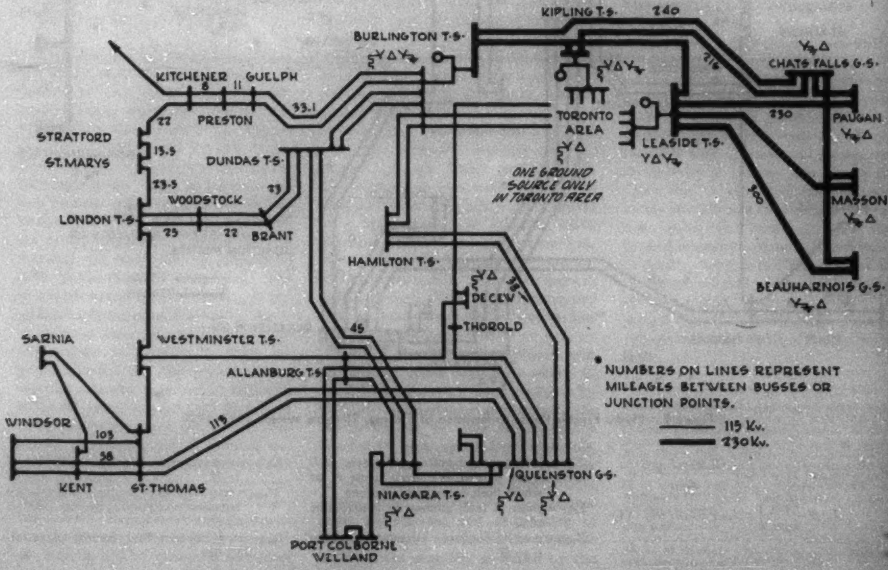
KIPLING T.S.
240
BURLINGTON T.S.
216
CHATS FALLS G.S.
KITCHENER
8
11
GUELPH
33.1
230
PAUGAN
22
PRESTON
TORONTO AREA
STRATFORD
LEASIDE T.S.
13.5
ST. MARYS
DUNDAS T.S.
ONE GROUND SOURCE ONLY IN TORONTO AREA
23.5
23
WOODSTOCK
300
MASSON
LONDON T.S.
25
22
BRANT
HAMILTON T.S.
BEAUHARNOIS G.S.
38
DECEW
45
THOROLD
SARNIA
WESTMINSTER T.S.
ALLANBURG T.S.
*NUMBERS ON LINES REPRESENT MILEAGES BETWEEN BUSSES OR JUNCTION POINTS.
115 Kv.
230 Kv.
WINDSOR
103
115
98
QUEENSTON G.S.
KENT
ST. THOMAS
NIAGARA T.S.
PORT COLBORNE
WELLAND

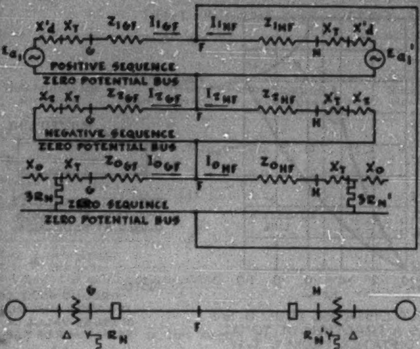
X'd
XT
Z1GF
I1GF
I1HF
Z1HF
Ea1
Ea1'
G
F
H
POSITIVE SEQUENCE
ZERO POTENTIAL BUS
X2
Z2GF
I2GF
I2HF
Z2HF
NEGATIVE SEQUENCE
ZERO POTENTIAL BUS
X0
Z0GF
I0GF
I0HF
Z0HF
3RN
3RN'
ZERO SEQUENCE
ZERO POTENTIAL BUS
Δ
Y
RN
RN'

Figure 5. Diagram of an assumed system with corresponding sequence network for line-ground fault at point F

I_{aHF} = phase A fault current from opposite end of faulted line
R_G = fault resistance
G = substation where relaying is considered
H = substation at opposite end of line section
F = fault location

If a single suitable current equal to the bracketed quantity associated with mZ_{1GH} is chosen, namely

$$I_{relay} = I_{aGF} + I_{0GF}\frac{(Z_{0GH} - Z_{1GH})}{Z_{1GH}} + I_{0GH}\frac{M_{0GH}}{Z_{1GH}} \qquad (2)$$

We obtain a very simple result, as follows:

$$Z_R = \frac{E_{aG}}{I_{relay}} = MZ_{1GH} + \frac{(I_{aGF} + I_{aHF})}{I_{relay}} R_G \qquad (3)$$

where

Z_R = impedance indicated by the relay
I_{relay} = current through relay

This method uses the line currents plus a percentage of the zero sequence currents in the protected and parallel paths. Fallou,[2] in France, also suggested this method in 1930, covering the case only of a single line, without considering the situation where a parallel line exists.

The relay current used by the Commission in its ground fault distance protection schemes is a residual current, or three times the zero sequence current. This usage of residual current was first suggested to the Commission by P. Ackerman, about 1927. The method by which it may be employed is developed in subsequent paragraphs.

Figure 5 shows an assumed line from a point G to a point H with a voltage source beyond each end of the line section. A L-G fault is assumed at F, and the corresponding sequence network connection also is shown. The transformation at G and H is connected wye on the line side with a resistance-grounded neutral R_N, and a delta connection on the low side. This is the method of grounding 25-cycle 115-kv system; the 230-kv 25-cycle system is solidly grounded.

By neglecting the presence of parallel circuits, and of arc resistance, equation 1 may be rewritten as follows:

$$E_{aG} = I_{0GF} \quad (Z_{1GF} + Z_{2GF} + Z_{0GF}) \qquad (4)$$

This equation also assumes that $I_{0GF} = I_{1GF} = I_{2GF}$, which is the case when the ratios of positive, negative, and zero sequence impedances to the left and right of the fault point are equal, that is

$$\frac{Z_{1GF}}{Z_{1HF}} = \frac{Z_{2GF}}{Z_{2HF}} \; \frac{Z_{0GF}}{Z_{0HF}}$$

Although the presence of $3R_N$ in the zero sequence network, Figure 5, will affect the magnitude of I_{0GF} (or I_{0HF}) as determined by Ea, (or Ea') the value of EA_G, the voltage to ground at G is as given in equation 4.

Dividing equation 4 by $3I_{0GF}$ gives the result

$$\frac{Ea_G}{3I_{0GF}} = \frac{Z_{1GF} + Z_{2GF} + Z_{0GF}}{3} \qquad (5)$$

or

$$\frac{Ea_G}{3I_{0GF}} = Z_{relay} = \frac{2Z_{1GF} + Z_{0GF}}{3} \qquad (6)$$

Measurements have been taken on the 115-kv and 230-kv 25-cycle system to determine the relative values of Z_0 and Z_1. Using an average value of $Z_0 = 3Z_1$, equation 6 becomes

$$Z_{relay} = 1.6Z_{1GF} \qquad (7)$$

Therefore the settings necessary to cover 80 per cent, 90 per cent, . . . of the line length depending upon the range desired, may be easily obtained. One of the advantages in using the residual current rather than line currents is that loss of potential will not cause false operation of the ground protection. Furthermore, heavy currents swings, due to load changes, et cetera will not affect the ground protection.

Analysis of Relay Operations

230-Kv Lines

The four lines from which operating records have been summarized on the 25-cycle 230-kv solidly grounded system are given in Table I. As may be noted on

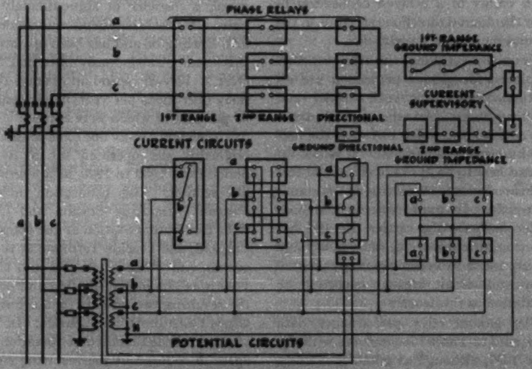
PHASE RELAYS
a
b
c
1ST RANGE
2ND RANGE
DIRECTIONAL
1ST RANGE GROUND IMPEDANCE
CURRENT SUPERVISORY
CURRENT CIRCUITS
GROUND DIRECTIONAL
2ND RANGE GROUND IMPEDANCE
a
b
c
N
POTENTIAL CIRCUITS

Figure 6. Schematic diagram showing how current and potentials are supplied to phase and ground distance relays. Current and potential circuits are shown separately, hence each impedance relay is shown twice

Figure 4, a fifth 230-kv circuit has been added to the system, but the operating record of this line has not been included. All these lines are single circuit construction, and the three original circuits from Chats Falls to Leaside, Figures 1 and 2, are on the same right-of-way, with lines 150 feet apart. The effect of mutual coupling, which was appreciable, was considered in the settings of the ground distance protection.

Figure 6 shows a typical alternating current and potential diagram which illustrates the manner in which currents and voltages are utilized by the Commission in its impedance protection schemes.

The phase currents are fed directly to the first range(instantaneous) and second range (definite time) phase impedance relays. These relays use line to line potential in conjunction with the phase currents. The phase directional relays are next shown both the current and potential diagrams. The sum of the phase currents is then passed through the first (instantaneous) range relays of the ground distance protection. Line-to-ground voltages are used along with the residual current in this relay. Two simple current relays are depicted next in the residual current circuit. One of these is used to block all relay protection in case of an accidental opening in the current circuit; the second relay has a low current setting and supervises the long range (definite time) ground protection. Residual current is next passed through the definite time ground impedance protection which also employs line-to-ground potentials.

Finally the ground directional relay is shown in the residual current circuit. This relay utilizes the voltage from the open corner of a delayed connection to give the desired directional feature to the ground impedance protection.

Generally speaking, the relay schemes employed for ground protection are essentially similar for both 115-kv and 230-kv systems. An experimental carrier trip scheme was added to two of the four 230-kv circuits considered. It is not intended here to analyze the efficacy of this additional means of clearing faults simultaneously. In most cases in the lines under analysis, the carrier trip did not function with any degree of certainty and in only one or two cases can nonsequential relay and circuit breaker operation be attributed to this feature.

The ground relay performance data presented in Table I commences with the year 1937, although as noted previously the first ground distance relays were installed on the 230-kv system along with the phase distance protection in 1928.

Figure 7. Variation in zero sequence impedance seen at terminals of faulted and unfaulted parallel lines

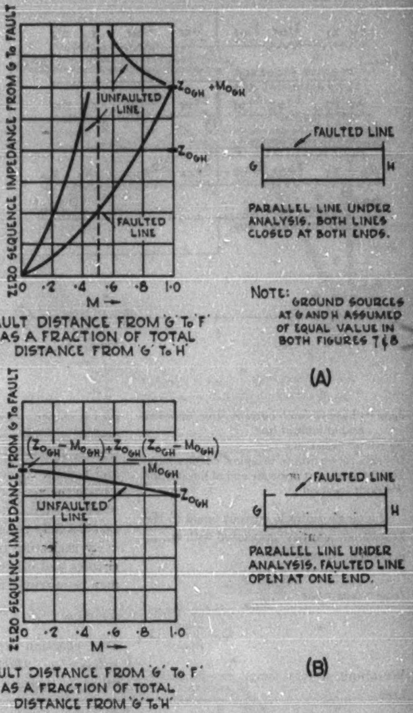

The first line to be considered, was originally connected from Chats Falls Generating Station to the Leaside Terminal, a distance of approximately 203 miles. In 1941 this circuit was connected into Burlington and has been operated in this manner continuously since that date. Over a 13-year period an average of 4.9 relay operations per year have occurred, 97 per cent of which were correct.

The second 230-kv line to be considered, originally was operated for a 10-year period from 1930 to 1940, as a 3-terminal line section. This connection involved Paugan Generating Station and Chats Falls Generating Station at the transmitting end, and Leaside Terminal at the receiving end. The single tap into Chats Falls was eliminated in 1940 and one of the resulting two circuits then connected Chats Falls directly to Leaside. In 1948 another 3-ended method of operation was again introduced at the receiving end of the line during the incorporation of the new Kipling terminal station into the system.

This record of line changes partially explains the relatively poor operating record of this section. Of the relay operations reported only 72.5 per cent are considered correct. However, during the 8-year period of 2-terminal operation when 50 per cent of these relay operations were recorded, only one was considered false giving a 96 per cent correct record, which compares favourably with the first 230-kv line considered. This circuit now is operated as a 2-terminal line connecting Chats Falls Generating Station to Kipling Terminal, see Figure 4.

The 230-mile line connecting Paugan directly to Leaside has always been operated as a 2-terminal line. Of 5.4 average ground relay operations per year recorded during the last 13 years, 98.5 per cent have been correct, with the remaining $1^1/_2$ per cent of operations unclassified as neither correct nor false. This appears to be the best record of any of the 230-kv transmission lines considered, for a comparable length of time.

The fourth and last 230-kv line under

Table I. Relay Operating Record 230-Kv Lines

Line Location and Designation	Length in Miles	No. of Years Covered	No. of Relay Operations Per Circuit Per Year	Percentage Classification Correct	False	Unclassified	Per Cent Incidence of Fault L-G	L-L-G	L-L-L-G
Chats Falls to Leaside (or Burl.)	245	13	4.9	97	3.0	0	50	41.5	8.5
Chats Falls to Leaside (or Burl.)	216	13	3.6	72.5	25.5	2	67.5	29.5	3.0
Paugan G.S. to Leaside	230	13	5.4	98.5		1.5	52	40.5	7.5
Beauharnois G.S. to Leaside	300	9	2.3	91	4.5	4.5	68.5	21	10.5
Total	991			90.0	8.0	2.0	59.5	33.1	7.4

L-G Line to ground.
L-L-G Line to line to ground.
L-L-L-G Line to line to line to ground.

analysis in Table I is the longest line operated by the Commission, extending for 300 miles from Beauharnois Generating Station (near Montreal) to Leaside Terminal (at Toronto). This line went into service in 1941. During the past 9 years, 2.3 average ground distance relay operations per year have been recorded, 91 per cent of which were correct. Two additional relay operations were actually reported over this same period but were caused by operating errors when relay potential was being transferred from one circuit breaker position to another.

Analysis of Relay Operations

115-Kv System

The lines for which operating records have been tabulated for the 115-kv resistance-grounded neutral system are summarized in Table II. The circuit miles considered for the purpose of this report total 919 miles. Reference to Figures 1 to 4 will indicate that all the 115-kv lines have not been summarized for relay performance although ground impedance protection has been applied to all of these lines exceeding approximately 15 miles in length. Pilot wire protection is the general practice for the shorter tie lines.

The longest lines in the group of Table II are those connecting Queenston Generating Station to St. Thomas Transformer Station. These lines, operated radially to St. Thomas, are 113 miles in length and carried on double circuit towers. Referring to the first of these lines it is to be noted that over a 15-year period 5.3 ground relay operations per year have taken place, 86 per cent of which were considered correct. On the second, 6.0 ground relay operations per year have occurred 97.5 per cent of which were correct. Due to the importance of these lines in supplying the Western Ontario Load centers, an analysis of probable relay performance under various fault conditions has been made on the a-c network calculator. It was shown that the effect of mutual coupling between the two circuits had not been sufficiently accounted for. Since revised settings, based on the calculator study, were placed on the relays at both ends of the line sections, in 1945, 86 per cent of the operations have been successful on the first circuit, and 100 per cent have been so far successful on the second. There is a relatively high percentage of line-to-line-to-ground faults on these circuits (Table II), although the tower footing resistances are only in the order of 5-10 ohms. No attempt has been made in the tabulated data to classify the type of fault if the relay operation was false or unclassified. Usually in such a case the fault was found to be outside the line section in which the false operation occurred and as such would be classified in the 'type of fault' column for an adjacent section.

The other line section considered, which has its source at Queenston Generating Station, is that connecting the generating station to Hamilton Transformer Station. This 38-mile section shows an average of 1.2 operations per year over a 14-year period, of which 88 per cent were considered correct, and the remainder were considered unclassifiable rather than false. This line section is one of two circuits on double circuit towers. The second circuit has been involved in a number of terminal changes at the Hamilton end and consequently was not included in this analysis.

The double circuit line between Niagara Transformer Station and Dundas Transformer Station is 45 miles long, and both lines have only a fair operating record. The first line referred to in Table II shows 75 per cent correct relay operations over a 13-year period, while on the second line, only 62.5 per cent of all relay operations were considered correct. In addition to the relative shortness of these two lines from an impedance point of view, slow circuit breaker operating times have caused the circuit breaker electrically remote from the fault on the unfaulted line section to trip on its definite time range. These slow operating times, especially at Niagara Transformer Station, have been a main contributing factor in the number of false operations. The need for revised settings of these lines to fully account for the mutual induction is under consideration at the present moment.

Reference again to Figures 1 and 2, indicates that Dundas Transformer Station was a major system connection point prior to the installation of the 230-kv terminal station at Burlington. The records of the lines between Dundas and London and between Dundas, Kitchener, and London are shown in Table II. The Dundas to London lines are of double circuit construction of a 1910 design similar to those from Niagara Transformer Station to Dundas. Woodstock and Brant Transformer Station are intermediate points in these two circuits. The lines are not normally bussed at these latter stations, one load being taken from the first circuit and the other from the second. The two lines are only relayed at London and Dundas. The inherently high zero sequence mutual coupling in these circuits has also been a factor influencing the operating record of the ground distance relays on these two lines, along with the absence of a direct ground source in the London Area. These two principal factors have accounted for only 78 per cent and 82.5 per cent correct operations over a 13-year period for these two circuits.

The Dundas to Kitchener circuits also are of a 1910 design and furthermore were connected, in 1941, to the new Burlington terminal referred to in the preceding paragraph. Consequently, the latter portion of the relay record includes the lines from Burlington through to Kitchener Transformer Station—a total distance of 52 miles. A 13-year record of relay operations for these two circuits shows 91.5 per cent correct operations and 87.8 per cent correct operations over the first and second of these circuits. Although two intermediate bussing points are shown on these two circuits it is not usual practice to bus the lines at these stations. The loads are distributed between the two line sections, and the line is only relayed at the Burlington and Kitchener end. This record, although an improvement over the Dundas to London lines, which also traverse similar territory, could probably be improved by consider-

Table II. Relay Operating Record 115-Kv Lines

Line Location and Designation	Length in Miles	No. of Years Covered	No. of Relay Operations Per Circuit Per Year	Percentage Classification Correct	False	Unclassified	Per Cent Incidence of Fault L-G	L-L-G	L-L-L-G
Queenston G.S. to St. Thomas—#1 (Q5T)	113	15	5.3	86	11.4	2.6	62	35	3
Queenston G.S. to St. Thomas—#2 (Q6T)	113	15	6.0	97.5	2.5	0	48	45	7
Queenston G.S. to Hamilton (Q9H)	38	14	1.2	88	0	12	67	33	0
Niagara T.S. to Dundas (#1) (N3D)	45	13	3.1	75	21.5	3.5	60	40	0
Niagara T.S. to Dundas (#2) (N4D)	45	13	2.8	62.5	35	2.5	65	35	0
Dundas T.S. to London (#1)	90	13	3.5	78	15.5	6.5	54	43	3
Dundas T.S. to London (#2)	90	13	3.1	82.5	14.5	3	76	21	3
Dundas (Burlington T.S.) to Kitchener (#1)	52	13	4.5	91.5	6.5	2	62	36	2
Dundas (Burlington T.S.) to Kitchener (#2)	52	13	6.3	87.8	9.8	2.4	62	34	4
Kitchener to London	62	13	3.5	78.5	21.5	0	83.3	13.9	3.8
St. Thomas T.S. to Kent T.S. (#1)	58	15	2.1	96.5	0	3.5	60	40	0
St. Thomas T.S. to Kent T.S. (#2)	58	15	2.2	82	9	9	63	37	0
St. Thomas T.S. to Windsor (T3E)	103	10	5.5	89	11	0	64	32	4
Total	919			85.0	11.4	3.6	63.6	34.3	2.1

ing the mutual coupling between the double circuits.

It would be expected that the single circuit from London through to Kitchener which is relayed only at these two stations would have an improved record over those lines which are of double circuit construction. However, the fact that only 78.5 per cent of all operations in the last 13 years have been correct indicates that some other reason than incorrect settings must be the cause of the questionable record. The ground current standby relay in this section at Kitchener is suspected of unstable operation due partially to a sticking of the contact travel arm against its stops.

The remaining 115-kv lines to be considered in this report are those commencing at St. Thomas which transmit power to the extreme western area of Ontario, of which Windsor is the principal city.

The double circuit lines from St. Thomas to Kent Transformer Station, as shown in Figures 1 to 4, were installed in 1914 and traverse a distance of 58 miles between these two points. The relay operating records on these lines are reasonably good with 96.5 per cent of relay operations correct on Number 1 line, and 82 per cent classified correct on the second line. The period covered on both lines was for 15 years.

The other circuit considered from St. Thomas westward is that connecting directly with Windsor. This is a single circuit line of 103 miles in length, completed in 1940. Out of 5.5 average relay operations per year reported on this line over a 10-year interval, 91 per cent fall in the correct category. Of the remaining 9 per cent of relay operations which were considered false, 7 per cent occurred during the first year of operation. At the beginning of 1941, new relays were installed, and since that time only one incorrect operation has been reported, thus giving 97.5 per cent correct operations excluding the first year of service.

Comments on the Effect of Mutual Coupling on Ground Distance Impedance Settings

The presence of mutual coupling[3] between three of the four 230-kv circuits considered previously has been accounted for simply by increasing the settings on the instantaneous and definite time ranges of the ground distance relays. The justification for this can be seen in considering the expression in equation 1 and rewriting it in terms of sequence quantities.

Thus

$$E_{aG}=(I_{1GF}+I_{2GF})mZ_{1GH}+ I_{0GF}.m.Z_{0GH}+I_{0GH}.m.M_{0GH} \qquad (8)$$

This equation only neglects the presence of fault resistance R_G. I_{1GF}, I_{2GF}, I_{0GF} are the sequence currents flowing in the faulted line from G to F. The term $I_{0GH}.m.M_{0GH}$ is the increased drop in the zero sequence network due to the effect of mutual coupling between the circuit considered and the adjacent parallel circuit. Thus the effect of mutual coupling is to increase the effective impedance to the point of fault. Furthermore, in considering that $I_{0GF}=I_{1GF}=I_{2GF}$, as is done in equation 4, it is also assumed that the ratios of Z_{1GF}/Z_{1HF}, Z_{2GF}/Z_{2HF}, and Z_{0GF}/Z_{0HF} are equal.

This holds approximately true in the 230-kv 25-cycle network since all step-up and step-down transformation is operated with all neutrals solidly grounded. Consequently the zero sequence impedance at the Leaside, Kipling and Burlington receiving end "bus" is of the same general magnitude as that of the Chats Falls, Paugan, Masson, and Beauharnois sending end "bus." This explains the success obtained using the type of ground distance relaying employed by the Commission, without resorting to the use of special circuits introducing a portion of zero sequence currents from the parallel lines.

The possible variations in indicated impedance due to mutual coupling also is shown in Figure 7(A). As the fault moves down the line the relays at G on the faulted line see a relative change in impedance from zero up to $Z_{0GH}+M_{0GH}$. The relays on the unfaulted line also see zero impedance at the G bus but the direction for tripping is incorrect. At the midpoint there is no current in the parallel line and impedance reached infinity. Once the midsection is passed the zero sequence impedance falls to $Z_{0GH}+M_{0GH}$ at the opposite end of the line.

In the second case considered it is assumed that the circuit breaker at the near end of the faulted line section is opened before the other circuit breaker at the far end. In this case the relays on the unfaulted line at G see a zero sequence impedance as indicated in Figure 7(B) which changes to Z_{0GH} for faults at the opposite end. Thus for certain conditions where nonsequential clearing occurs the indicated impedance on the unfaulted section may fall within the definite time range and undesired tripping will occur. This analysis presupposes as mentioned above that the zero sequence impedance from G to "neutral" and from H to "neutral" are approximately equal.

On the 115-kv 25-cycle system the ground sources are only at the infeeds of generation. As a result, many of the busses at which ground distance relaying is employed are quite remote from ground sources and there is a major difference in values of impedance from the various busses to ground. Thus it becomes increasingly difficult to compute the effect of mutual coupling; furthermore, the relation that $I_{1GF}=I_{2GF}=I_{0GH}$ becomes less and less valid. Thus accurate relay settings are difficult to ascertain, unless use is made of the a-c network calculator in determining the values of these settings.

Conclusion

The ground distance relay operation records have been presented for a representative portion of the Commission's 115-kv and 230-kv Southern Ontario 25-cycle system. The average percentage of correct operations referred to in the tables on this system does not appear to be as high as that reported on another system which also uses ground distance relay protection.[4] It is felt, however, that the ground impedance method of relaying ground faults has given reliable service during the period for which it has been installed at a low unit cost per terminal installation. The fact that the 115-kv resistance grounded system has a limited number of grounding points has discriminated against the true performance capability of this means of ground fault protection. In addition, in most applications on this 115-kv network the effect of mutual coupling has not been included in settings for the ground distance relays. This factor has probably prevented more accurate performance.

The 230-kv system performance is more accurate than that of the 115-kv network. On the former, a less pessimistic percentage than the 90 per cent average value tabulated may be obtained by omitting a portion of the operating record for the second 230-kv line from Chats Falls Generating Station to Leaside Transformer Station. This line, during this period of operation as a 2-terminal line, shows a 96 per cent correct relay operating record. The average percentage then obtained for all four 230-kv circuits is 95.6 per cent. Thus the 230-kv system ground distance protection is believed to compare very favorably with the more usual induction current application, especially so if carrier current is not used to improve performance of the latter type of protection. It is suggested that ground impedance relay protection should be seriously considered along with the more conventional solutions, when relaying requirements of comparable systems are under investigation.

References

1. FUNDAMENTAL BASIS FOR DISTANCE RELAYING ON 3-PHASE SYSTEMS, W. A. Lewis, L. S. Tippett. *Electrical Engineering*, volume 50, 1931, pages 420–422 and *AIEE Transactions*, volume 66, 1947, pages 694–708.

2. SUR L'EMPLOY DES RELAIS D'IMPEDANCE POUR LA PROTECTION DES LIGNES AERIENNES CONTRE LES MISES A LA TERRE, Jean Fallou. *Bulletin de la Societe Francaise des Electriciens* (Paris, France), series 4, volume 10, 1930, pages 82–94.

3. THE EFFECTS OF MUTUAL INDUCTION BETWEEN PARALLEL TRANSMISSION LINES ON CURRENT FLOW TO GROUND FAULTS, J. F. Holbeck, M. S. Lantz. *AIEE Transactions*, volume 62, 1943, pages 712–15 and 1002–3.

4. OPERATING EXPERIENCE WITH DISTANCE GROUND RELAYS, W. A. Wolfe. *AIEE Transactions*, volume 65, 1946, pages 455–62 and 1185–87.

Discussion

W. A. Lewis (Illinois Institute of Technology, Chicago, Ill.): High-speed relaying of ground faults on electric power systems has been a subject of considerable interest, although the importance of the quick clearing of ground faults involving only one conductor and ground is considerably less than that of clearing faults involving two or more phases, whether ground is involved or not. Several approaches to this problem have been suggested from time to time, and considerable attention has been given to various possibilities for distance relaying of ground faults during the development of high-speed relays. About the time that a comprehensive analysis of the problem was completed, as represented by reference 1 of the paper, the use of carrier-current for high-speed relaying was perfected.

Where stability considerations were of major importance, the use of carrier-current relaying was justified for clearing phase faults, and in such cases the use of distance relays for ground faults was seldom necessary. Accordingly, the use of distance relays for ground faults was not widely accepted, and relatively few installations have been made. Satisfactory operation of several installations, however, has been obtained, as indicated in particular by reference 4 of the paper.

It is gratifying at this time to have further information regarding successful application of ground distance relays, as represented by the present paper, in spite of the fact that the connections of the relays described in this paper are not in accordance with the preferred method, as outlined in reference 1. Although the data given in the present paper are insufficient to make a comprehensive analysis possible, it seems safe to say that the operating record described would undoubtedly have been substantially better in several cases if the preferred method of connections had been used.

Several comments regarding the present report appear to be pertinent. In Tables I and II of the paper the operations are classified as correct or false, without regard to whether the operations were single-line-to-ground, double-line-to-ground, or three phase. For the method of connection used, it seems probable that the most nearly correct operations would be obtained on single-line-to-ground faults, and more danger of false operation would exist on double-line-to-ground faults. If the faults were substantially balanced 3-phase faults no operation of the ground relays at all would have been expected, because of the substantial absence of zero-sequence current. Therefore, it would be particularly interesting to know whether the incorrect operations were encountered more frequently on double-line-to-ground faults, or on other types of fault.

In the tabulation, it is not indicated how the type of fault was determined. Presumably, the type of fault was classified by the record of relay targets, supplemented by examination of the line at the point of fault, and oscillographic record where it was applicable. Experience generally indicates that relay targets, alone, are not too reliable indications, because phase relays can be operated on severe ground faults, and two or more ground relays may sometimes show targets when the fault started single line to ground, and blew into a second phase only just before arc extinction. Conversely, it is sometimes possible for a fault involving two phases to operate a target on only one of the ground relays, because the shunting effect of the first target to operate limits the current in the second target coil, so that it does not operate. Further comments regarding the method of classification of the type of fault would therefore be helpful in attempting to evaluate the over-all operation of the relay system.

The use of residual current to operate the distance elements, instead of the combination current recommended by the analysis of reference 1 of the paper, opens up several possibilities for incorrect operation of the relays, but the likelihood of incorrect operation depends to a large degree upon system conditions. For example, the mutual effect between circuits can be allowed for in the setting of the relays when all circuits are in service. If, however, one of two or more parallel lines are out of service when a fault occurs, the mutual effect is reduced or is absent completely, but with the connection used there is no compensating correction in the relays. Accordingly, overreaching of the distance elements would be expected when one or more of the parallel lines are out of service. Therefore, a poorer performance would be expected if faults occurred with one or more lines out of service than if all lines were in service at the time of fault occurrence. It would be interesting to know whether any of the false operations occurred during such system conditions that false tripping could be accounted for in this way.

The analysis of reference 1 of the paper indicates several conditions under which incorrect or doubtful operation may be encountered when the fault resistance is large. The record of good performance under reasonably normal system conditions, represented by the paper, seems to indicate that the fault resistances on this system, represented by arc resistance and tower footing resistance, must have been relatively low, in comparison with the impedance of the line sections.

Although the performance record indicated in this paper is not all that might be desired in some cases, it has been shown that many of the difficulties occurred when the system conditions were such that precise settings could not be established. When allowance is made for the effects of multiterminal lines, lack of compensation for mutual effects, and the use of residual current instead of the combination current recommended in the comprehensive analysis of reference 1, the performance obtained is decidedly encouraging. It may be concluded that distance ground relaying has a definite place in the relaying picture of long and moderate length high-voltage lines, particularly when it is difficult to justify the expense of carrier-current relaying systems. The authors should be commended for calling these extensive operating results to the attention of the industry.

P. L. Dandeno: The authors appreciate the remarks of Dr. Lewis that no analysis was made for the case of double-line-to-ground faults and furthermore that of the total false operations recorded, no breakdown as to whether these were single-line-to-ground or double-line-to-ground was indicated.

It is evident that use of $3I_{0GF}$ with E_{aG} for double-line-to-ground faults gives a different result from that for the single-line-to-ground faults. Comparison with equation 4 in the paper shows that for a double-line-to-ground fault

$$E_{aG}=a^2I_{1GF}Z_{1GF}+aI_{2GF}Z_{2GF}+I_{0GF}Z_{0GF}$$

where

$$I_{1GF}=-(I_{2GF}+I_{0GF})$$

and

$$I_{2GF}=\frac{Z_{0GF}}{Z_{2GF}}.I_{0GF}$$

Then, since $Z_{2GF}=Z_{1GF}$,

$$I_{1GF}=-\left(\frac{Z_{0GF}}{Z_{1GF}}+1\right)I_{0GF}$$

and dividing the first equation by $3I_{0GF}$ gives

$$Z_R=a^2\left(\frac{Z_{0GF}+Z_{1GF}}{3}\right)+\frac{aZ_{0GF}}{3}+\frac{Z_{0GF}}{3}$$

and assuming again that

$$Z_{0GF}=3Z_{1GF}$$

$$Z_R=-\frac{7}{3}a^2Z_{1GF}=-2.333a^2Z_{1GF} \text{ for phase } B$$

$$=-2.333aZ_{1GF} \text{ for phase } C$$

as compared to $Z_R=1.6Z_{1GF}$ for a single-line-to-ground fault.

Thus the setting for single-line-to-ground faults results in a different range where double-line-to-ground faults occur. Referring to Table I for the 230 kv network analysis and noting the outages for the first circuit considered, we find that 3 per cent false operations occurred (two actual false operations). The first operation occurred under a double-line-to-ground fault condition on an adjacent circuit; the second was probably correct but not desired.

With reference to the second line considered in Table I, it is noted that during the period of 3-terminal operation (during 9 of the 13 years tabulated) that the majority of the false operations occurred. The 96 per cent correct record referred to in the conclusions during 4 years of 2-terminal operation gave only two false operations. One of these was caused by the tripping of circuit breakers in a parallel circuit with the fault falling within a definite time range of the unfaulted circuit, the possibility of which is indicated in Figure 7(B) of the paper.

On the 4th circuit considered in Table II, the correct operations were 91 per cent of the total occurring. Of the two noncorrect operations one was probably due to potential failure with the possibility of the phase relays tripping during this same instance indicated.

The method of deciding whether faults are single-line-to-ground or double-line-to-ground is

1. By relay targets.
2. Use of smoke charts or oscillographs.
3. Visual inspection.

In some cases where a single-line-to-ground fault was indicated by relay targets visual inspection with line patrol showed that two phases were involved. This difficulty in deciding whether a single-line-to-ground fault developed in a few cycles to a double-line-to-ground fault was several times evident when attempting to properly analyze the records.

On the first 115-kv circuit considered in Table II for example, which showed 11.4 per cent false operations (actual number = 9) six were double-line-to-ground faults on a parallel number 2 circuit and one occurred when the same parallel circuit was out of service. Thus the increased setting for mutual effects would extend the range of both the instantaneous and definite time features. On the second 115-kv circuit considered two actual false operations were noted and one of these occurred when the parallel number 1 line was out of service.

On the Niagara to Dundas number 1 line which showed relatively poor record (21.5 per cent false), 12 total false operations occurred of which four were attributable to double-line-to-ground faults on the parallel circuit and two could be classified as correct but not desired. These few examples indicate that a good proportion of the 115-kv false operations are also attributable to double-line-to-ground faults.

The effect of arc resistance which was neglected in computing the relay settings indicates that R_G must have been relatively low in most cases, especially on the 230-kv circuits which all show a good record. It is admitted that using only $3I_{0GF}$ has its limitations but its general simplicity and effectiveness are indicated in the 230-kv records in Table I.

Submerged Repeaters for Long Submarine Telegraph Cables

C. H. CRAMER
MEMBER AIEE

Synopsis: An experimental underwater repeater recently installed in one of The Western Union Telegraph Company's transatlantic nonloaded telegraph cables increased the operating speed of the cable from 50 words per minute to 167 words per minute. The repeater is located 170 miles at sea in a depth of 270 fathoms which places it beyond the shallow coastal waters where disturbance levels are high. The cable beyond the repeater is in deep water and free from disturbance so that signals alone are amplified and the signal-to-noise ratio at the terminal is greatly increased. The 3-stage amplifier and signal-shaping networks are mounted in a pressure-equalized steel case. Power for the repeater is supplied by rectifiers at the cable terminal. The repeater includes a switch, under control of the terminal, by means of which spare vacuum tubes can be substituted or the cable can be cut directly through for operation without repeater.

UNTIL RELATIVELY recent years, the applications of electronics to submarine cables have been limited to equipments installed at the cable terminals. During the past decade, however, there has grown an increasing awareness of the potentially great benefits to be derived from the use of intermediate submerged repeaters. The initial proposals[1] and practical applications[2,3] of such devices have been in the field of wide-band circuits involving the use of new coaxial-type cables and repeater spacings of 50 miles or less. This paper describes an experimental installation of a submerged repeater in a long transoceanic cable, the first application of such a repeater to an existing low-speed d-c or noncarrier telegraph cable.

The repeater was installed during September 1950 by the cable ship *Cyrus Field* on one of the Western Union Telegraph Company's North Atlantic cables, *1PZ*, extending from Bay Roberts, Newfoundland, to Penzance, England. This cable, 2,148 nautical miles in length, has been operated in recent years with a signal-shaping vacuum tube amplifier at the receiving terminal, the cable station at Bay Roberts. Prior to the installation of the repeater, the westward simplex or 1-way printer operating speed of the cable, limited by the interference level, was 50 words per minute. With a single repeater inserted in the cable at a point 170 miles northeast of Bay Roberts, just beyond the Newfoundland Banks and in a depth of 270 fathoms, an operating speed of 167 words per minute was obtained.

Transmission Factors of Submarine Telegraph Cables

The principal factors which determine the satisfactory maximum operating speed of a submarine telegraph cable are: (1) the signal sending level, the over-all cable attenuation, and the level of extraneous disturbance or noise at the receiving terminal—in combination the signal-to-noise ratio; (2) the inherent heavy characteristic signal distortion and the degree to which it can be equalized at the terminals, while minimizing the susceptiveness of the receiver to interference—conditions which are somewhat incompatible and call for judicious compromise; (3) on duplex-operated cables, the level of the residual duplex unbalance which adds to the interference and reduces the signal-to-noise ratio.

The signal-to-noise ratio, determined largely by the cable parameters and the specific electrical conditions surrounding the cable, can be controlled only in minor degree at the cable terminals. Characteristic distortion and duplex balance are also directly related to the cable parameters but a considerable degree of control or compensation can be applied at the cable terminals: for characteristic distortion, a receiving signal-shaping network provides a characteristic approximately the inverse of the cable characteristic; for duplex balance, an artificial line can be made to match the cable electrically to almost any desired degree of accuracy.

In the past 15 or 20 years, signal-shaping amplifiers and duplex-balance methods and networks have been developed to a point approaching a practical limit of efficiency.[4] These developments have been applied generally in the Western Union cable system. This pro-

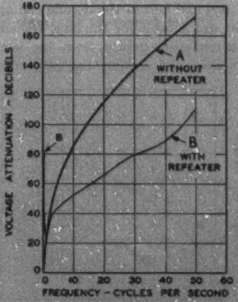

Figure 1. Attenuation of *1PZ* cable

Paper 51-286, recommended by the AIEE Wire Communications Systems Committee and approved by the AIEE Technical Program Committee for presentation at the AIEE Summer General Meeting, Toronto, Ont., Canada, July 25–29, 1951. Manuscript submitted March 27, 1951; made available for printing May 14, 1951.

C. H. CRAMER is with the Western Union Telegraph Company, New York, N. Y.

Valuable contributions to this development were made by a number of people throughout the research, engineering, and cable organizations of Western Union. The submerged repeater as a means for improving signal transmission on submarine telegraph cables was originally proposed by Harold F. Wilder. The major technical development role should be credited to Philip H. Wells, one of a small group of which the author is leader, which carried on the work through theoretical and laboratory transmission studies, design, construction, and service trials.

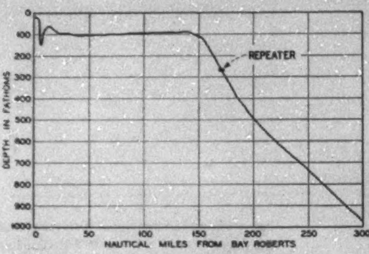

Figure 2 (left). Profile of *1PZ* cable

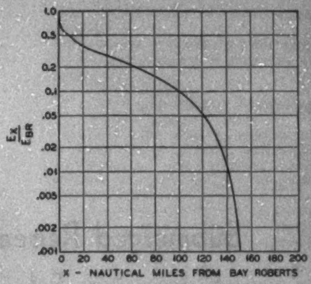

Figure 4 (right). Ratio of 20-cycle disturbance, E_X, originating beyond any point in *1PZ* X miles from Bay Roberts to total 20-cycle disturbance, E_{BR}, at Bay Roberts

gram of terminal equipment improvements brought about higher quality signal transmission at increased speeds. A significant end result was the complete conversion of Western Union's North Atlantic system from the traditional cable code operation to 5-unit code printer operation, along with a net increase in message capacity of about 30 per cent. Following completion of this program, it soon became evident that any further important improvement of transmission on the existing nonloaded cables could be obtained only through measures applied directly to the cables and departing radically from previous practices.

In the course of the developments just outlined, sending voltages had been increased to about double their original conservative values. On transatlantic nonloaded cables, the signaling frequency can be increased only 15 to 20 per cent when the sending voltage is doubled. Brief consideration of this fact eliminates increased sending voltage as a means of obtaining substantial speed increases. In such a process, a condition hazardous to the cable insulation would soon be reached and serious difficulties with sending relay contacts would be encountered.

The continuously-loaded cables, developed and laid in the decade ending in 1930, are notable for the large reduction in attenuation gained from the use of permalloy and similar magnetic alloys. Furthermore, the loaded cables have exceptionally low interference levels by reason of long bicore terminal sections in which the second core serves to carry the receiving earth to a point beyond the shallow coastal waters. The message capacities realized with the loaded cables were about four times the capacity of a typical nonloaded cable at that time.

It was perhaps inevitable that consideration would be given to the application of long receiving earths and inductive loading to the existing nonloaded cables. Although re-examined periodically, the long sea earth has remained comparatively unattractive. Large expenditures would be required to lay two new bicore end sections for each cable, since distances up to 100 miles or more are involved. Aside from the matter of costs, even though very low interference levels were obtained, a corresponding increase of signaling speed would not be possible because of conditions which limit the maximum practical gain of terminal amplifiers. These conditions include local noise from other electrical systems as well as effects inherent in high-gain amplifiers.

Inductance loading could be applied to the nonloaded cables either by substituting sections of continuously-loaded cable for nonloaded cable or by inserting loading coils at regular intervals. An investigation of coil loading indicated that the design and the effective application of submarine loading coils would be technically feasible. It also appeared that a coil-loading system would be less costly than one utilizing continuous loading. However, considerations of cost and the out-of-service periods imposed on the cables during installation of coils would dictate a program of gradual installation incidental to routine cable repair operations. At the normal rate of cable repairs, such a program would provide a substantial transmission improvement only after many years. As prospects became brighter for the development of a practical submerged repeater for low-frequency cable circuits, it soon became apparent that transmission improvements of the same order or even better than those available with coil loading could be obtained at lower cost and in a considerably shorter time.

Principles Underlying the Submerged Repeater

The following discussion of the submerged repeater will be related specifically to *1PZ* cable for the sake of directness, but the principles involved are of general application.

1PZ, one of the slowest-speed cables of the Western Union system, was laid in 1881. The original cable was of types *350/300* and *450/270* (weight of copper

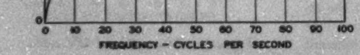

Figure 3 (left). Attenuation of sinusoidal disturbance in seawater

Figure 5 (below). Schematic diagram of repeater

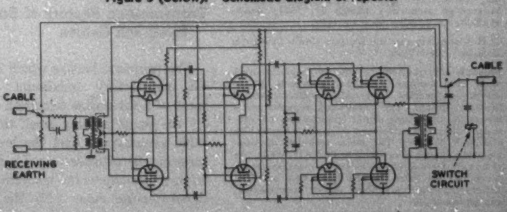

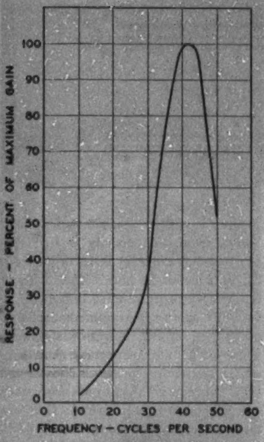

Figure 6. Frequency-response characteristic of repeater

and weight of insulation in pounds per nautical mile). Currently, original cable in the circuit is 428 nautical miles or about 17 per cent. During repairs and renewals, type *650/375* cable has been used extensively and is now the major type, about 39 per cent of the total length. The average age of the cable is 25 years. The attenuation of the cable, without repeater, is given in curve *A* of Figure 1

Figure 7. Signal power level chart for sine wave transmission on *1PZ* cable: Curve *A*, without repeater; 6.25 cycles per second, corresponding to 50 words per minute; sending battery, 90 volts. Curve *B*, with repeater; 20.83 cycles per second, corresponding to 167 words per minute; sending battery, 60 volts

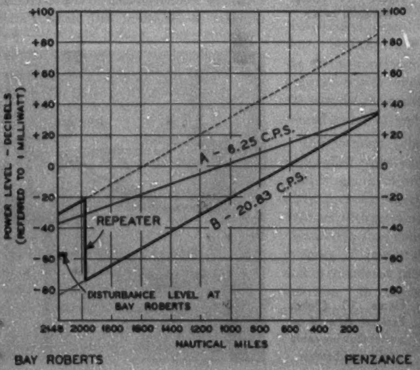

At a frequency of 6.25 cycles per second, corresponding to a speed of 50 words per minute, the attenuation is 71 decibels; while the attenuation at 20.83 cycles, corresponding to a speed of 167 words per minute, is 117 decibels.

As used in this paper, signal frequency is defined as one-half the dot frequency. In 5-unit code printer operation on Western Union cables, signal impulses of unit length are so attenuated in transmission that they are essentially missing in the received signals.[4] The receiving networks are adjusted for optimum reception of signals two units in length, and the missing dots are interpolated synchronously. With respect to cable transmission characteristics, the fundamental sinusoidal component of the signal frequency is used.

The profile of the ocean bed east from Newfoundland along the route of *1PZ* is shown in Figure 2. The cable profile is of particular significance with respect to the disturbance level on the cable. Electrical disturbances originating in the atmosphere and induced on the surface of the ocean are attenuated in propagation downward through the seawater.[5] The attenuation increases with frequency as indicated by Figure 3, which gives the magnitude of attenuation per fathom for sinusoidal disturbances through the range of cable telegraph frequencies. Thus at a depth of 250 fathoms, 20-cycle disturbance has undergone attenuation of about 80 decibels. Knowing the cable profile and assuming uniform distribution of potential on the surface of the ocean, the relative amplitude of the disturbance induced in various sections of the cable conductor can be evaluated. Summation of the sectional disturbances, taking into account the attenuation and phase characteristics of the cable, gives a relative

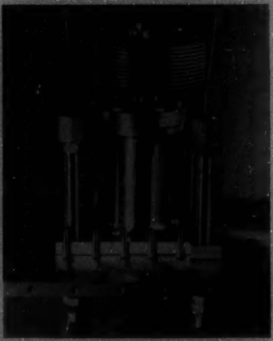

Figure 8. Pressure equalizer and cable entrance glands

amplitude of total disturbance level at the cable terminal. For *1PZ*, with Bay Roberts as the receiving terminal, the curve of Figure 4 shows the portion of 20-cycle disturbance originating in the section of the cable beyond any point *X* miles from Bay Roberts. For example, if *X* is 150 miles, then of the 20-cycle disturbance level at Bay Roberts only 0.1 per cent originates in the 2,000 miles of cable east of *X*. For distances greater than 150 miles, the residual disturbance decreases rapidly as indicated by the curve. An amplifier can be introduced in the cable 160 or more miles from Bay Roberts without appreciably increasing the terminal disturbance level.

The Repeater

Electrically, the repeater, shown schematically in Figure 5, comprises a 3-stage push-pull resistance-capacitance coupled amplifier with input and output transformers. A simple tuned signal-shaping

Figure 9. Repeater chassis with components in place

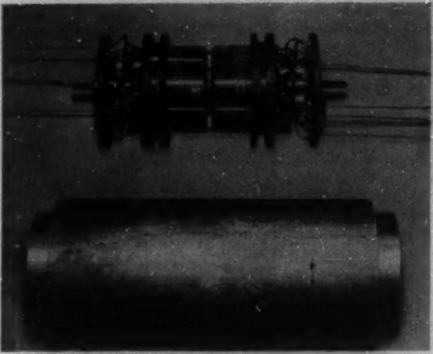

Figure 10 (left). Vacuum tube unit

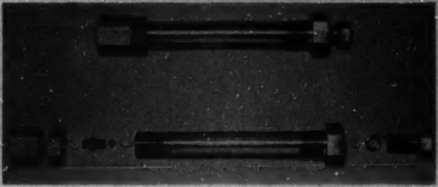

Figure 12 (above). Cable entrance gland

network precedes the input transformer. Type *5693* tubes are used in all stages, with two tubes in parallel and operated as triodes in each side of the output stage, providing theoretical undistorted output of 0.25 watt. The effect of the output transformer circuit is to reduce the net output of the repeater to somewhat less than 0.25 watt. The required signal output is determined principally by the low-frequency components of the signals.

The receiving or input-earth connection of the repeater is carried back along the cable for some distance through a bicore section and earthed on the armor wires. The repeater case and adjacent cable armor are utilized for the other earth connection. This arrangement was provided to avoid feedback troubles which might develop with an earth connection common to the input and output circuits of the repeater.

The power requirements of the repeater, 0.32 ampere at 125 volts, are supplied from Bay Roberts over the single cable conductor which also serves as the signal transmission medium. The impedance of the power supply is relatively high, including resistance of 550 ohms at the terminal and 170 miles of cable having resistance of about 295 ohms. This condition tends toward repeater instability which is heightened by the narrow range available for discrimination between power supply and the low-frequency signal components. Measures taken at the repeater to provide stable performance include a high-capacitance bypass, careful selection and matching of vacuum tubes, and utilization of negative feedback.

The frequency-response characteristic of the repeater, Figure 6, increases with frequency to a maximum at about 42 cycles per second where the gain is 67 decibels. With the repeater in circuit, the over-all frequency-attenuation characteristic of *1PZ* is as shown in curve *B* of Figure 1. The transmission benefit derived from the repeater is strikingly illustrated by the level charts of Figure 7. Curve *A* shows the circuit levels without repeater and with sending battery of 90 volts for sine wave transmission of 6.25 cycles per second (operating speed, 50 words per minute). For curve *B*, with repeater, the sending battery is 60 volts and the frequency is 20.83 cycles (operating speed, 167 words per minute). The disturbance level indicated on the chart refers to disturbance of natural origin and is the same for the two conditions. No change of disturbance level is observed at Bay Roberts when the repeater is switched into the circuit. Crossfire resulting from a crossing with another cable some distance east of the input side of the repeater was effectively reduced by a low-pass filter in the sending circuit of the offending cable. It is of interest to note that without repeater, the received level of 20.83-cycle signals would be 27 decibels below the disturbance level. On the other hand, to obtain a satisfactory receiving level at 20.83 cycles without repeater, a sending level of plus 85 decibels (316 kw) would be required. It is important that the required output level at the repeater be low because of the limitations imposed by available vacuum tubes and by the power supply. To satisfy this requirement, the repeater should be located as near to the receiving terminal as consistent with natural and

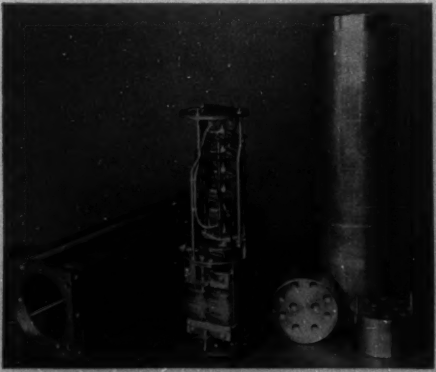

Figure 11 (left). Repeater switch

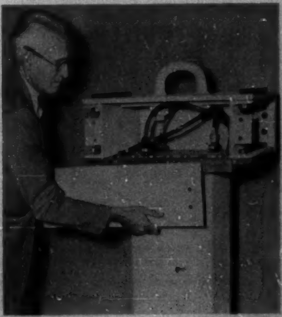

Figure 13 (right). External view of repeater showing cable entrance chamber

Figure 14. Repeater on board ship with cable attached

crossfire disturbance conditions. Aside from considerations of signal power level at the repeater, the power supply voltage imposed on the cable at the terminal increases as the repeater is moved away from the terminal by reason of the greater voltage drop in the cable.

The repeater includes a rotary ratchet-stepped switch which has two principal functions: (1) to disconnect the repeater and join the cable through for operation without repeater or for cable testing purposes; (2) to "swap" vacuum tubes in the event of a tube failure. Three complete sets of tubes are provided and can be utilized in 18 different combinations. The switch is operated as required from Bay Roberts by trains of 60-cycle sine waves. The operating winding of the switch, in series with a capacitor, is permanently connected from cable to ground at the repeater.

Mechanical Design of the Repeater

Since it was planned to install the repeater in a depth of between 200 and 300 fathoms, the major requirement to be met in the mechanical design was suitability for extended operation under hydrostatic pressures up to 750 pounds per square inch. Components for low-frequency communication equipments are inherently bulky. It thus appeared inadvisable to attempt to design a housing of the size required in which the interior would be at or near atmospheric pressure. Instead the repeater is filled with oil and a pressure equalizing bellows automatically adjusts the internal pressure to the external pressure within a few pounds per square inch. The equalizer comprises a tandem arrangement of a piston-cylinder and a bellows, Figure 8, both of corrosion-resistant metals. The outer end of the cylinder is sealed to the cover plate of the housing while the inner end opens into the bellows. A hole in the cover plate admits seawater to the outer end of the cylinder and a piston transmits the external pressure to the oil which fills the remainder of the cylinder and the bellows. In turn the bellows transmits the pressure to the oil within the housing. The equalizer has sufficient capacity to take up any small voids resulting from incomplete filling of the housing and to compensate for the relatively large volumetric temperature coefficient of the oil. At sea bottom, particularly in areas and depths involving arctic currents, the temperature may be as low as 30 degrees Fahrenheit. To minimize the change of volume and thus the capacity of the equalizer, metal filler is utilized to reduce the amount of oil required.

Since the external-internal pressure differential is small, a gasket of synthetic rubber provides an adequate seal between cover and case.

The repeater components are mounted on a rectangular chassis, Figure 9, occupying a space approximately 10 inches by 11 inches by 26 inches. Certain of the components are subjected directly to the full hydrostatic pressure. These are: (1) The capacitors which, with the exception of small bypass capacitors, are all of the oil-filled paper-foil type; (2) the inductor and the transformers which are of the wound-core type, having windings impregnated with Acme Compound; and (3) most of the resistors which are wire-wound and spiral metal-film types.

The vacuum tubes are in standard metal-shell bulbs which are not of sufficient strength to withstand the hydrostatic pressure encountered. The tubes, together with certain related resistors, are mounted in steel cylinders, six tubes to a cylinder. Figure 10 shows a tube cylinder and a completed tube chassis, ready for insertion. In completing the assembly, steel plugs are pressed into the ends of the cylinder, and fins on the plugs are soldered to corresponding fins on the cylinder. Connections are brought out through high-pressure terminals in the end plugs. Four tube cylinders are provided, one each for the first and second stages, and two for the output stage.

Figure 15. Repeater passing over bow sheaves

The rotary switch, Figure 11, also is enclosed in a cylinder identical in design with the tube containers, except that it is somewhat longer. The switch operating mechanism is balanced so that it will function in any position.

The repeater chassis is fastened to the cover plate. The two cable leads and the receiving-earth lead are brought out through glands mounted in the cover plate as shown in Figure 8. The monel metal parts of a gland and the components of a high-pressure terminal used at the inner end of the gland are shown in Figure 12. In assembling the gland, a short piece of standard polyethylene cable core is used. A "pudding" of the same insulating material is formed near one end of the stub and this enlarged section is inserted in the outer portion of the gland which is then sealed by means of a packing nut. Within the gland the cable conductor is spliced to a smaller wire which extends through the high-pressure terminal at the inner end of the gland into the repeater chassis. A rigid insulating sleeve surrounds the bare conductor in the lower part of the gland. Before sealing off the high-pressure terminal, the voids within the gland are filled with vistac.

As shown in Figure 13, a cable entrance chamber is mounted on the top of the cover plate. Holes (not shown in this

Figure 16. Ready to lower repeater and pay out cable

photograph) are provided in the end channels for the entrance of fully armored cable stubs, one in each channel. A concentric circle of small holes permits the individual armor wires to be looped back through the channel and firmly secured to the cable. The cores of the stubs are spliced to the gland cores within the entrance chamber. Side plates and a top plate complete the enclosure of the chamber, allowing entrance of seawater but protecting the unarmored cores within from mechanical damage. A heavy lowering eye on the top plate provides a means of eliminating hazardous strains on the cable at the points of attachment to the repeater. For each of the two cable stubs, a chain extends out from the eye followed by a stranded steel rope which is spliced to the cable armor about 15 feet from the repeater in a manner to allow some slack in the cable between that point and the repeater.

The repeater case proper is 12 inches wide by 11 inches deep and the corresponding dimensions of the cable entrance chamber are somewhat larger. The over-all length is about 51 inches. The complete repeater weighs 1,140 pounds.

Installation of the Repeater

At best, the operations involved in splicing a structure of the size and weight of the repeater in a submarine cable and placing it safely on the bed of the ocean depart considerably from the normal operations of cable ships. Unfavorable weather conditions introduce further complications. In one method, perhaps the least difficult, the ship would pick up the cable as in normal repair operation, heaving to at the planned repeater location with both ends of the cable on board. After completion of the splices, the repeater would be lowered. This procedure is not desirable, however, because the resulting slack cable might loop on the bottom so as to cause feedback effects in the repeater. Such effects are avoided in the method actually used. The cable was picked up at a point more than a mile east of the repeater location and the end of the eastward section was buoyed. The ship then proceeded to the repeater location, picking up the intervening cable. At that point, the cable was cut and the required splices were made. In Figure 14, the repeater is ready for laying following completion of the splices. The repeater was then lowered over the bow sheaves, Figures 15 and 16, the ship got under way and, paying out cable as in a normal repair operation, proceeded to the buoy where the final splice was made. In this method, once the repeater is free of the ship its weight is supported by the cable, except in the short sections on either side of the repeater where the load is transferred to the steel cable and chain arrangement described previously. The absence of strain on the cable adjacent to the repeater is clearly indicated in Figure 16. It is desirable that the position of the final splice be sufficiently distant from the repeater to insure that the repeater is resting on the bottom and is not in suspension during the final splicing operation. That the measures described were fully effective is confirmed by the fact that after the repeater was first lowered to the bottom, it was successfully picked up and brought on board ship. The installation was carried out under rather unfavorable weather conditions and the final result is indeed a tribute to the staff and crew of the cable ship, where skill and efficiency of a high order are traditional.

The Terminal Equipment

The receiving terminal circuit at Bay Roberts is shown schematically in Figure 17. The arrangement is similar in general to a standard duplex cable terminal, except that the bridge arms are resistors instead of capacitors. Power for the repeater is supplied by rectifiers and fed into the apex of the bridge, while a standard signal-shaping amplifier is connected across the diagonal of the bridge and functions in the usual manner. The bridge is balanced by an artificial line which simulates the section of cable between the terminal and the repeater and the impedance of the repeater to ground so that the terminal amplifier is unaffected by noise components in the power circuit. Since the current required at the repeater is 0.32 ampere, the drop in the bridge arm and cable totals approximately 275 volts and an electromotive force of about 400 volts normally is applied between apex

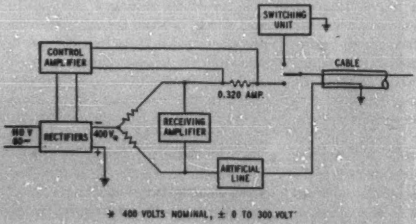

Figure 17 (left). Receiving terminal and repeater power supply circuit

Figure 18 (right). Power supply and control equipment and ground to produce 125 volts at the repeater. Automatic controls maintain the power current at a constant level despite power voltage fluctuations and in the presence of a wide range of earth potentials. When earth potentials exceed the range of the controls or if for any other reason the power current approaches a predetermined safe limit, a circuit breaker functions to protect the repeater. The rack-mounted installation of rectifiers and control equipment is shown in Figure 18.

Conclusion

Thus far only one repeater has been constructed. It was installed without having been tested previously under hydrostatic pressure because pressure-testing equipment was not immediately available and because early operating trials were desired. During the service tests, the predicted speed of 1,000 letters (167 words) per minute was obtained without difficulty and excellent performance has been obtained in traffic operation as part of a London-New York varioplex circuit. The soundness of the principles upon which the development was based has been fully confirmed, justifying plans for further development and application of the repeater. As might be expected, certain improvements of both the repeater and the terminal control equipment have been suggested by the experience with this initial installation. The most important, perhaps, is that future repeaters should be suitable for installation in greater depths. Present indications are that, on the input side of the repeater, it is desirable to avoid nearby crossings with other cables because of crossfire conditions. On congested cable routes most of the crossings occur in the two coastal areas. In general, repeaters should be located beyond the crossings at the receiving end of the cable. The crossings near the distant, sending end are unimportant from the standpoint of crossfire, since the signal level in that section of the cable is very high. On many cables, as compared with the installation on *1PZ*, such a requirement can be fulfilled only by installation in deeper water and at greater distances from the receiving terminal. The cables suited to application of repeaters are of various lengths and types so that there is a relatively wide divergence in transmission characteristics among individual cables. For this reason, repeater design cannot be standardized in all respects. For example, the optimum signaling speed of an individual cable depends upon the cable characteristics and the terminal disturbance level, and the design of the repeater network must be carefully predetermined for the chosen speed since there is no opportunity for readjustments after installation.

There is no experience upon which to base predictions of repeater life. It can be expected confidently that longer life will be realized as designs are refined and improved components become available. In any case, aside from the cost of manufacturing a repeater, the cost of an installation is little more than the cost of a routine cable repair operation. It appears, therefore, that while an ultimate life of 5 to 10 years or more is desirable and probably can be achieved, the increase in signaling speed is large enough to support renewals at intervals of two years or less.

A project now actively under way provides for installation as rapidly as practicable of nine additional repeaters in Western Union's North Atlantic cable system. Upon completion, four cables between Newfoundland and the British Isles and one New York-Newfoundland cable will be equipped for reversible high-speed operation.

References

1. THE FUTURE OF TRANSOCEANIC TELEPHONY, O. E. Buckley. *Journal*, Institution of Electrical Engineers (London, England), volume 89, part I, 1942, pages 454–61.

2. MODERN SUBMARINE CABLE TELEPHONY AND THE USE OF SUBMERGED REPEATERS, R. J. Halsey. *Journal*, Institution of Electrical Engineers (London, England), volume 91, part III, December 1944, pages 218–36.

3. A SUBMARINE TELEPHONE CABLE WITH SUBMERGED REPEATERS, J. J. Gilbert. *AIEE Transactions*, volume 70, part I, 1951, pages 564–72.

4. SOME MODERN TECHNIQUES IN OCEAN CABLE TELEGRAPHY, C. H. Cramer. *AIEE Transactions*, volume 66, 1947, page 494–500.

5. EXTRANEOUS INTERFERENCE ON SUBMARINE TELEGRAPH CABLES, J. J. Gilbert. *Bell System Technical Journal* (New York, N. Y.), volume 5, 1926, pages 404–17.

No Discussion

The Hot Spot Rise Simulator

CLARENCE F. BOOK
MEMBER AIEE

V. V. MASON
ASSOCIATE AIEE

Synopsis: The Hot Spot Rise Simulator provides a means for obtaining improved accuracy and dependability in the indication of hot-spot temperatures in electric power equipment. When used in connection with the operation of transformers, it avoids the difficulties experienced with earlier types of hot-spot indicators by restricting the apparatus mounted within the transformer to a rugged thermojunction and by limiting the remaining equipment to a thermocouple potentiometer and the Rise Simulator device itself. To insure that this method would not lead to large errors under extreme ambient temperature conditions, calculations were made of the effects of variations in top-oil temperature and load current over a wide range. The errors so calculated are less than the probable uncertainty inherent in the determination of hot-spot temperatures from heat run data.

THE NEED for accurate indication of hot-spot temperatures under both steady-state and transient conditions is well known. This applies to rotating machines and cables as well as to transformers, although the latter appear to have received most attention in this respect. In spite of the greater attention toward the transformer problem, the results generally have been unsatisfactory.

Hot-Spot Temperatures in Transformers

The hot-spot temperatures occur in the upper part of transformer coil assemblies where the oil temperature is highest and in particular at those points where the winding is least exposed to the circulating oil. The winding rise over the oil has relatively fast transient characteristics compared with the rise of the oil over the ambient air or cooling water. The former has a time constant of the order of five minutes, in a particular case, compared with over two hours for the latter. For this reason, problems involving over-all rise of the winding are most clearly understood when this rise is looked upon as the sum of the oil rise over the ambient temperature and hot-spot rise over the oil.

The steady-state top-oil rise over the cooling water in a water-cooled transformer is the sum of the following items:

1. Average temperature of ingoing and outgoing water minus the temperature of ingoing water.
2. Temperature rise from average water to cooling coil.
3. Temperature rise from cooling coil to average oil.
4. Temperature rise from average oil to top oil.

The first item 1 is subject to variation due to changes in the rate at which cooling water is supplied. Item 2 is subject to changes resulting from accumulation of lime deposits on the inside of the water passages and to changes in the velocity of the water through the tubes. Item 3 is subject to changes due to accumulations of thermal insulating material on the outer surface of the cooling coils and to changes in oil velocity and viscosity.

In an air-cooled transformer, the items 1, 2, and 3 are average temperature of the air entering and leaving the radiators minus the temperature of the entering air, temperature rise from average air to radiator, and temperature rise from radiator to average oil, respectively. In like manner, these are subject to variation from causes such as change in wind velocity or direction, rain, sleet, and oil viscosity and velocity changes. Item 4 in each case may be considered to be half the difference between the top-oil and bottom-oil temperatures.

Under normal steady-state conditions, the temperature rise of any part of the winding over the adjacent oil depends upon the current density, the copper resistance, the thermal resistance of the insulation, and the oil velocity and viscosity. Since variations in copper resistance and oil viscosity, due to temperature differences between the top and bottom of the tank are very small, the temperature rise of any part of the winding over the adjacent oil may be taken as the same for all parts of the winding for well-designed transformers, with the possible exception of transformers with graded high-voltage insulation. Calculations made on the effect of spacers indicate that they are not likely to cause local heating by more than a small fraction of a degree. On this basis, then, the hot-spot rise above top-oil temperature equals the average copper rise above the average oil temperature, and the hot-spot rise above the average copper temperature equals the top-oil rise above the average oil temperature or half the difference between the top and bottom oil temperatures.

For transformers depending upon thermal-syphon movement of oil, this difference seems to be of the order of 10 degrees centigrade as is recognized by the Canadian and American standards[1,2] in that they specify a maximum value of average copper rise 10 degrees centigrade less than that allowed for the hot-spot rise. It is probably from these standards that the present method of calculating hot-spot temperature has arisen. This addition of an arbitrary 10 degrees to the measured average copper rise at rated load to obtain the hot-spot rise is also applied to forced-oil-cooled transformers. For these, however, it is scarcely justifiable since the drop through their cooling system may be as low as 5 degrees centigrade so that the top-oil rise is only 2.5 degrees greater than that of the average oil. The British Standards[3] specifies in effect the same allowance of 10 degrees

---

Paper 51-247, recommended by the AIEE Instruments and Measurements and Transformers Committees and approved by the AIEE Technical Program Committee for presentation at the AIEE Summer General Meeting, Toronto, Ont., Canada, June 25–29, 1951. Manuscript submitted March 27, 1951, made available for printing May 9, 1951.

CLARENCE F. BOOK is with The Hydro-Electric Power Commission of Ontario, Niagara Falls, Ont., Canada, and V. V. MASON is with The Hydro-Electric Power Commission of Ontario, Toronto, Ont., Canada.

centigrade for self-cooled transformers, but only 5 degrees centigrade for those with forced-oil cooling. It is understood that it was consideration of these hot-spot matters which led the British Standards Institution to allow this higher average-copper rise with forced-oil cooling.

In view of the afore-mentioned reasoning, it is thought that it is more accurate to consider the hot-spot to be equal to the average copper temperature plus half the difference between top and bottom oil temperatures with the addition of a small allowance of the order of 2 degrees centigrade to allow for poorer exposure of the copper to the circulating oil in certain parts of the winding, rather than to be equal to the average copper temperature plus an arbitrary 10 degrees centigrade.

Since the hot-spots occur in the copper conductors, which are at high potential above ground, it is not possible to measure these temperatures directly under operating conditions. The hot-spot temperature for a particular transformer is determined on the basis of the foregoing considerations applied to the average copper rise and the oil temperature rises obtained from the heat run data taken at the time of the acceptance tests. It is usual, therefore, to employ some device which will indicate the hot-spot temperature as accurately as possible by some form of indirect measurement after the device has been adjusted to be in agreement with the calculated hot-spot values for the particular transformer.

Common Types of Hot-Spot Indicators

Most of the hot-spot indicators used on this continent are of the internal thermal image type. These are so called because they measure the temperature of a thermal image of the hot-spot mounted in the oil within the transformer. A thermometer bulb, placed in the top oil, is surrounded by a heater through which is passed a current proportional to the transformer load current. This current is obtained from a current transformer mounted in one of the bushings. To be satisfactory, such a device must meet two basic conditions. It must reach the same steady-state temperature as the hot spot, and must reach it according to the same transient law so that the indication will be correct at all times under changing load conditions. That is, the device must have the same ultimate rise and the same time constant as the hot spot above the oil for any given load on the particular transformer.

The ultimate rise of the heater over the adjacent oil is a function of its electrical resistance, the current in it, and the thermal resistance between it and the oil. Thus, the correct ultimate rise may be obtained by picking two of these variables more or less arbitrarily and choosing the third to match the particular transformer. In practice this is usually done by using a standard heater with a standard amount of thermal insulation (lagging) and adjusting the current-transformer ratio by taps to get the desired ultimate rise.

The time constant of a metallic heater surrounded by thermal insulation is the product of the thermal capacitance of the metal and the thermal resistance of the insulation. This is true for a good thermal conductor surrounded by a good thermal insulator which has negligible thermal capacitance compared to that of the metallic part. However, the thermal picture is often complicated by the practice of using a very heavy thermal lagging on the heater, and of immersing the heater assembly in an oil-filled well in the top of the transformer. This has the effect of making the thermal capacitance of the insulation anything but negligible. This in turn means that the heating curve will not be a simple one to which a single time constant can be meaningfully assigned.

In contrast with the internal image there is the external thermal image type of hot-spot indicator. This is well known in Europe. As the name implies, it attempts to reproduce a complete thermal image of the hot spot with apparatus mounted entirely outside the transformer. This requires that not only the rise of the hot spot over the top oil, but also the rise of the top oil over the ambient air, or cooling water, be reproduced artificially in the device. Even if this device were not subject to errors due to variations in conditions affecting the oil rise over the ambient air or cooling water, it would still be open to the objection that it is not the rise of the hot spot over the ambient which limits the allowable load, but the actual or total temperature which is the sum of this rise and the ambient temperature.

Difficulties With Thermal Image Indicators

To service internal thermal image indicators, the transformer must be de-energized, and with many models, the oil must be lowered. The difficulty of getting a power interruption for such work under today's loading conditions is a matter of common experience, and unfortunately, these internal thermal image devices do seem to need a considerable amount of servicing. On the other hand, the external thermal image type, and the rise simulator type of indicator to be described, do not suffer from this difficulty, and moreover, they do not require as much servicing as the internal image type. The types of internal thermal image indicators available commercially in the past have a fixed time constant which is at best only a rough approximation to that of the hot-spot rise over the oil.

The high-current low-voltage heaters frequently used in the internal image type also have given trouble. Increases in the resistance of the electrical connections to these heaters has resulted in increased burden on the current transformer with resultant error in the thermal image.

Theoretically, the internal thermal image type of indicator possesses one distinct advantage over all other types. This is in the matter of sensitivity to oil

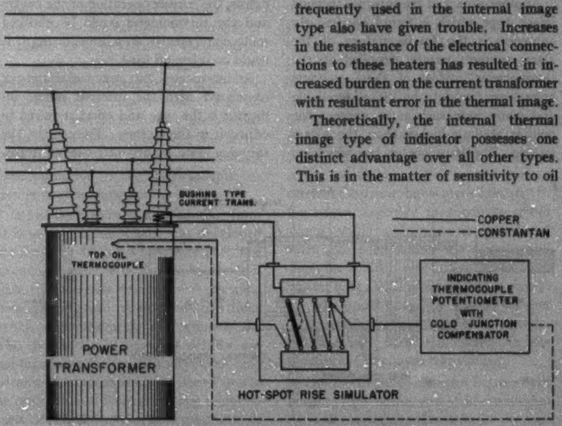

Figure 1. Schematic of typical hot-spot rise simulator installation

Figure 2 (above). The hot-spot rise simulator

Left, cover on; center, cover off, 10-minute time constant; right, cover off, 2.6-minute time constant

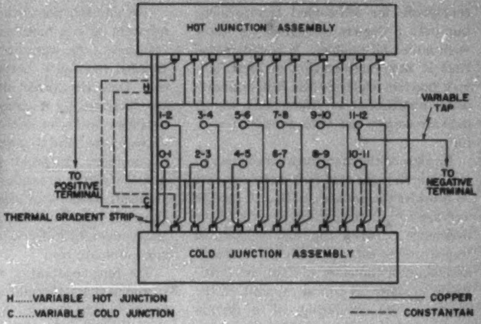

Figure 4 (right). Internal wiring of hot-spot rise simulator, showing thermocouple leads, miniature terminal board for rough adjustment of output, and thermal gradient strip for fine adjustment

velocity. If the thickness and type of thermal insulation on the internal image were the same as that of the winding and if the watts dissipated per square inch of surface were also the same, then the effect of oil viscosity and velocity should be the same for the image as for the hot spot itself. Then, if in addition, the image and the hot spot were so situated as to be exposed to the same oil velocity, they would behave identically under all conditions of oil flow. In practice, the image usually has a much heavier insulation than the winding, is usually placed in a position of very low oil velocity, and sometimes is even purposely protected from the effects of oil velocity by the use of a deflector tube. Thus it seems that although this theoretical advantage exists, it is not realizable in practice.

Another aspect of the internal thermal image type which is found particularly annoying is the fragile nature of the alarm contacts usually supplied on the thermometer. Most of these contacts have been found to be quite unreliable and many were such as to prevent the pointer reading higher than the alarm setting. The thermometers too, which are usually the vapor-pressure type, have given considerable trouble. If defective, they must be replaced as a unit and this is often very difficult in the field.

Unless special provisions are made when the transformer is manufactured, the calibration of the internal thermal image indicator cannot be accurately checked in the field. However, it was found possible to overcome this difficulty by specifying that the hot-spot indicator current transformer be provided with an auxiliary winding, the terminals of which are brought out to a junction box at ground level. This winding is specified to be such that 5 amperes in it corresponds to the rated load current of the power transformer. In addition, a thermojunction was required in the internal image to measure its temperature. With these extras, the correct operation of the heater and the thermometer could be checked quite conveniently on a transformer if it could be taken off load.

An unexpected, but very real drawback associated with the internal image indicator is the time and effort required to adjust it in the factory. Frequently, the shipping date of urgently-needed transformers has been delayed for days because of troubles in setting the indicator correctly. The extra time involved in these delays is a major annoyance to both the manufacturer and the purchaser.

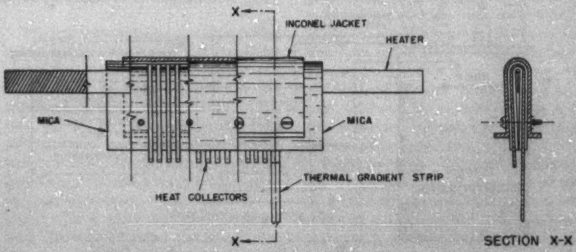

Figure 3. Construction of hot-spot rise simulator assemblies

The external thermal image indicator avoids many of the above difficulties, but suffers irremediably from two of its own particular troubles. First, it is fundamentally an indicator of rise rather than actual temperature, and second, it must incorporate two time constants, one of which has a value of several hours. These two drawbacks appear to condemn it as a practical transformer hot-spot indicator.

The Hot-Spot Rise Simulator

Although they are intended to protect expensive equipment from damage due to overheating, the transformer hot-spot indicators, normally available, leave much to be desired. Their construction, adjustment, and operating record do not inspire the confidence usually associated with protective equipment.

Realization of this state of affairs led to the development of the hot-spot rise simulator. The goal was the production of a reliable instrument which could be tested and adjusted in the field by the relay engineer in the same way that he tests and adjusts an ordinary protective relay. Work was begun in 1946, and the first installations were made early in 1947 at two stations in the Niagara Region of The Hydro-Electric Power Commission of Ontario. Subsequently, the physical form was modified slightly to make it more suitable for widespread application. All major power transformers purchased by the Commission since early 1950 are being equipped with these devices.

The hot-spot rise simulator avoids the difficulties of both the internal and ex-

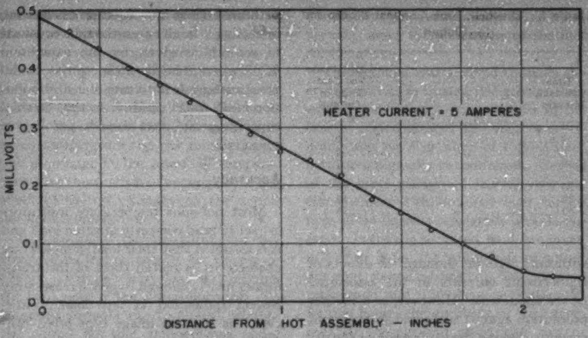

Figure 5. Typical electromotive force/distance curve for thermal gradient strip

ternal thermal image types of indicator. The only component mounted within the transformer is a rugged copper-constantan thermo-junction which requires no attention. The remainder of the equipment is external, consisting only of the rise simulator and a thermocouple potentiometer with cold junction compensator.

The external thermal image types of hot-spot indicator attempt to produce a temperature equal to that of the actual hot spot and then measure this temperature with some kind of thermometer. In contrast to this, with the rise-simulator type of indicator, some form of thermoelectric transducer is used to convert the top-oil temperature to an electrical quantity, and to this is added a similar type of electrical quantity representative of the rise of the hot spot over the top-oil. The sum of these represents the hot-spot temperature. In the rise simulator to be described, the electrical quantity used is the electromotive force produced by thermocouples. The device producing the electromotive force representative of the hot spot over top-oil simulates this temperature rise in the form of an electromotive force. Hence the name: rise simulator. The word compensator describes its action more exactly because it compensates the output of the top-oil thermojunction for the hot-spot rise over top-oil.

For this reason when the device was first developed, it was called a thermocouple hot-spot compensator, but use of this name led to confusion between the device itself and the cold junction compensator of the thermocouple potentiometer used as an indicating instrument. Accordingly, this name was dropped in favour of hot-spot rise simulator in spite of the undeserved implication of the name as something not quite as good as the real thing.

The hot-spot rise simulator works on the principle of adding to the output of a top-oil thermocouple, an electromotive force representing the temperature rise of the hot spot over the top-oil (Figure 1). Its physical form is shown in Figure 2. It derives its input from a current transformer in one of the leads from the power transformer whose hot-spot temperature is to be indicated. This current transformer is usually a ring type installed in one of the transformer bushings. The input current corresponding to rated load on the transformer usually lies between 2 and 5 amperes. The output millivoltage may be set to any value from zero to that corresponding to a hot-spot rise of 25 degrees centigrade for an input current of 2 amperes or more. The time constant is adjustable by the addition or removal of metal blocks to or from the thermojunction assemblies. The minimum time constant is 2.6 minutes and blocks are available to give time constants of 5, 10, 15, 20, 25, and 30 minutes. The output of the rise simulator is connected in series with the copper lead from the top-oil thermojunction to the thermocouple potentiometer as shown in Figure 1.

It has been learned that another form of hot-spot rise simulator was developed in Germany during World War II.[4] The essential difference in the two methods is that the German device used electrical resistance instead of electromotive force as the quantity representing temperature. The thermocouple type has definite advantages over the resistance type not only because thermocouples have been found to be preferable to resistance-type temperature detectors for electric equipment in general, but also because of the neat construction their use makes possible in the simulator.

The actual indicating device to be used with a hot-spot rise simulator and top-oil thermojunction depends somewhat upon the particular installation. A manually balanced potentiometer is usually the most desirable type of indicator for use in small stations where an operator is in attendance, but some types of direct deflection instruments can be used if these are preferred. Installation of a self-balancing potentiometer for a single transformer bank would make the cost of the rise simulator installation greater than that of an internal thermal image type, but much of this increased cost can be written off against the increased convenience and reliability. For larger stations, where one indicator is shared between several transformer banks, the cost is of the same order as for the internal image type. There also is the advantage that a simple switching arrangement allows the top oil temperature as well as that of the hot spot to be recorded in the control room on the same instrument.

Construction

The hot-spot rise simulator has no moving parts and is designed to ensure years of service without maintenance expenditures of any kind. The only materials used in the assemblies are rust-proof metals and sheet mica. The functional components consist of two physically identical assemblies placed one above the other inside a protecting metal case, Figure 2. Each assembly comprises a length of resistance ribbon about which are clamped a number of thin metal strips, Figure 3. These are insulated from each other and from the resistance ribbon by mica sheets in such a way that all parts of each assembly are in intimate thermal contact but are electrically insulated from one another. The upper assembly carries in its resistance ribbon a current proportional to the load current in the windings of the transformer. The lower assembly carries no current, but is made identical to the upper assembly to eliminate errors which would otherwise be introduced when the surrounding air temperature changes. With this construction, no matter how the air temperature is changing, the upper assembly will be warmer than the lower assembly by an amount depending only upon the current in the windings of the power transformer.

The metal strips clamped between the mica in the warm and cold assemblies serve as connecting junctions for the copper and constantan wires, Figure 4.

Thermocouples are thus formed in series proceeding from the negative output terminal towards the positive, with copper-to-constantan junctions at the lower assembly strips, and constantan-to-copper at the upper strips, ending with copper at the positive output terminal. For ease of adjustment in the field, taps are taken from each of the cool junctions to a small terminal board mounted between the assemblies and in front of them. This allows the number of thermocouples in series to be varied from 1 to 11 to provide a rough adjustment of the output.

For fine adjustment, a thermal gradient strip is provided in place of the twelfth thermocouple. This is a narrow piece of sheet brass or copper connected between the warm and cool assemblies. Two flexible leads of constantan are soldered to this strip, one from the last cool junction and the other from that hot junction which is connected to the positive output terminal by a copper lead. As the ends of these two flexible constantan leads are moved farther apart on the thermal gradient strip, a greater electromotive force is developed between them. When the lead coming from the bottom (cool assembly) is attached to the thermal gradient strip above that coming from the top (warm assembly), the electromotive force so obtained will be added to that of the coarse adjustment and vice versa. Thus this small, continuously adjustable electromotive force may be added to, or subtracted from that obtained by the coarse adjustment.

The temperature drop along this thermal gradient strip is very nearly proportional to the distance from the warm assembly, Figure 5. For the rated current of 5 amperes in the heater of the warm assembly, the electromotive force per thermocouple is approximately 0.54 millivolt. The maximum electromotive force in the thermal gradient strip is approximately 0.5 millivolt. These values are consistent enough to allow an approximate setting to be made for a given input current without an actual measurement of the output, but whenever possible, the setting is checked by measuring the output for a known current input.

The large number of thermocouples in the hot-spot rise simulator not only makes simple adjustment possible, but also, of more fundamental importance, enables the required output to be obtained with only a very small temperature difference between the two assemblies. Under normal operating conditions, only a fraction of a watt is dissipated within the device. Because the heaters operate at a low temperature, the device is able to withstand without damage the effects of short-circuit currents in the associated power apparatus. However, as a further precaution against sustained short-circuit currents causing the calibration of the device to change, in some models a saturating reactor is built into the case and connected across the current terminals. This reactor causes a negligible error at up to three-times rated current at 25 cycles per second and, of course, to even higher currents at 60 cycles per second. The low normal burden imposed upon the current transformer makes it permissible to connect this equipment in series with existing current circuits with negligible change in the performance of the other equipment.

Table I. Effect of Time Constant Blocks on Output

Time Constant, Minutes	Approximate Per Cent Drop in Output
2.6	0
5	5
10	7
15	9
20	12
25	15
30	18

Time Constant

The time constant of the rise simulator is increased by clamping blocks of metal of various sizes to the assemblies. The same size block must always be placed on both cool and warm assemblies to maintain their operation independent of changes in the air temperature surrounding the simulator. The blocks are so shaped as to minimize the effect on the ultimate output, and on the shape of the output-versus-time curve for suddenly applied loads. However, adding blocks to the assemblies inevitably increases their radiating area, and therefore decreases the millivolt output for a given current in the heater. The approximate amounts of these decreases are given in Table I.

The expression "time constant" used here is the one usual for thermal problems and is not the delay time or time to reach 90 per cent of indication used for thermal converters. As used here, time constant means the time to achieve 63.2 per cent of the change if the ultimate rise is directly proportional to the rate of heat dissipation, or, 55 to 70 per cent if the ultimate rise is proportional to a fractional power of the rate of heat dissipation; the exact value depending upon the particular characteristics of the apparatus, the initial temperature rise, the over-all temperature change and whether it is heating or cooling. In all cases, the time constant in seconds is given by the expression $\theta C/P$ where θ is the ultimate rise in degrees centigrade for a rate of heat dissipation of P watts, and C is the thermal capacitance in watt-seconds per degree centigrade.

Accuracy

Most hot-spot temperature indicators are set to read correctly at rated load and it is assumed that their load/temperature characteristics match those of the transformer nearly enough to give a reasonably correct indication at any load. However, the internal image type often cannot be set very accurately because of the large size of the smallest steps available on a tapped current transformer. With the rise simulator, on the other hand, the output may be set more accurately than the correct setting is known.

In so far as the output/load characteristic is concerned, the rise simulator obeys approximately the same law as does the transformer hot spot. The latter is usually assumed to vary as the 0.75 to 0.85 power of the copper loss whereas the former varies as the 0.85 power of the square of the input current, for the usual range of top-oil temperatures. Tests made on typical internal thermal image devices give values of the exponent of 0.86 to 1.07.

The approximate agreement in the values of the exponents for the rise simulator and hot spot could be taken as sufficient indication that the device will read correctly at all loads when adjusted to read correctly at rated load. Nevertheless, it was decided to investigate its accuracy as carefully as possible under different top-oil and load conditions, taking into account the effects of oil viscosity.

The top-oil temperature affects the accuracy of indication of the rise simulator in three ways. At low oil temperatures the actual hot spot over top-oil rise for a given load current tends to be greater than at high oil temperatures because of the greater viscosity of the oil. The same low top-oil temperatures also cause the electrical resistivity of the transformer windings to decrease and this tends to decrease the actual hot-spot rise. The former of these effects is the larger and becomes of ever-increasing importance under the very low top-oil temperatures which are encountered under the winter ambient conditions of Northern Ontario. The third effect is due to the curvature of the copper-constantan electromotive force/temperature characteristic.[6] The portion of this curve used to convert the rise simulator output from millivolts to the equivalent temperature rise is determined by the temperature of the top-oil thermocouple, since this is connected in series with the simulator output and the indicating potentiometer. The curvature of the characteristic is such that the indicated temperature rise per millivolt output is greater at the lower oil temperatures and this tends to compensate for the effect of the oil viscosity on the actual hot-spot temperature.

To determine the magnitude of the errors in indication caused by the above effects, it was necessary first to determine the behaviour of the actual hot spot. To this end a formula was developed, relating the actual hot-spot temperature under specified steady-state-load and top-oil-temperature conditions to the hot-spot temperature under the conditions of the factory heat-run. The derivation of this equation is given in the appendix. It is such that the hot spot over top-oil rise, $\theta_{s/o}$, cannot be expressed as an explicit function of the per-unit current. The per-unit current, however, can be expressed as an explicit function of the hot-spot rise. Although this is backwards in terms of cause and effect, it is convenient for calculating the accuracy as it gives the per-unit simulator current which enters directly into the calculation of the output millivolts. The simulator output is then calculated by multiplying the millivolts output at rated load by the per-unit current raised to the 0.92 power. (Its millivolt output is proportional to the rate of heat dissipation raised to the 0.92 power although in terms of equivalent temperature rise it is approximately a 0.85 power device because of the curvature of the copper-constantan characteristic.) The simulator millivolt output is added to the millivolts from the copper-constantan characteristic at the point corresponding to the top-oil temperature. The sum of the top-oil thermocouple and rise simulator millivolts is then converted back to degrees centigrade to obtain the indicated hot-spot temperature. To obtain the value of the hot-spot over top-oil rise indicated, the top-oil temperature in degrees centigrade is then subtracted from this indicated hot-spot temperature.

By comparing the actual and indicated rises calculated as above, it is possible to determine the error of indication under any condition of interest. This error and its variation with load and top-oil temperature depend upon the formula used in setting the rise simulator output. The formula found to be best is: Millivolt setting for rated current $= 0.041\theta_0[1+0.01(\theta_0-15)]$ where θ_0 is the temperature rise of the hot spot over the top oil at rated current under the conditions of the factory heat run.

This formula was selected to make the error positive (indicated rise greater than actual) for hot-spot temperatures in the critical region around 100 degrees centigrade and for the range of top-oil temperatures normally encountered. Curves of the error calculated in this way for transformers with hot-spot over top-oil rises of 15 degrees centigrade and 25 degrees centigrade at rated load are given in Figure 6 for the conditions of actual hot-spot temperatures of 105 degrees centigrade and 150 degrees centigrade. In this figure, the numbers on the curves indicate the per-unit rated load current required to produce these hot-spot temperatures at the top-oil temperatures shown. It is felt that for any realizable condition of load and ambient the error indicated by these curves is not greater than the uncertainty in the calculation of the actual hot-spot temperature.

The magnitude of the positive errors could be reduced by using a smaller multiplier for θ_0 in the foregoing equation, but this would increase the magnitude of the negative errors which can occur for very high loads at very low top-oil temperatures. As it stands, the equation makes the indications very conservative (positive error) for the more usual operating conditions.

These calculated rise simulator errors are dwarfed by the uncertainty with which the actual hot-spot rise of a transformer is known from the factory heat-run results, even at rated load. In addition to errors produced by arbitrary corrections back to shut-down of a heat run, or misinterpretation of the early readings of a cooling curve, the usual method of calculating the hot-spot temperature from a measured value of average copper temperature is open to serious question.

Hot-Spot Relay

The hot-spot rise simulator can be used as a hot-spot relay by the simple expedient of using time-constant blocks large enough to delay the indicated increase in temperature due to a sudden load increase sufficiently to allow a predetermined amount of overheating before tripping is initiated. The ultimate rise of the simulator is set to be the same as that of the hot spot so that even a small overload will produce tripping if continued for long enough to cause serious deterioration of the insulation. This avoids the undesirable band of no protection for small overloads which is characteristic of those hot-spot relays having a small time constant and an ultimate rise considerably less than that of the hot spot. Also, it allows the setting to be changed at will by the relay engineer so that it brings the field of automatic thermal-overload protection as much under his control as is the usual line and machine relaying. This is in direct contradistinc-

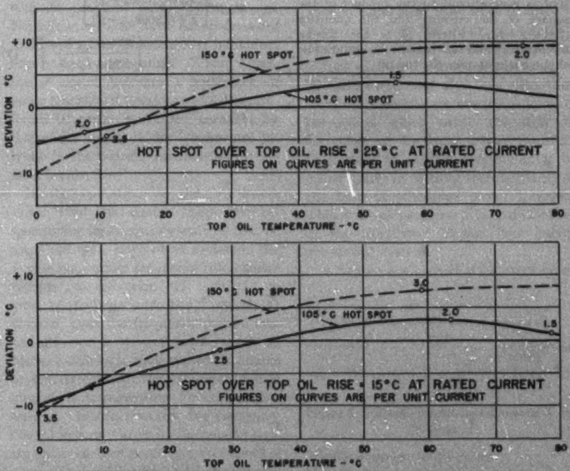

Figure 6. Calculated errors in rise simulator indication due to changing oil viscosity

tion to the more usual types of hot-spot relays which are inaccessibly immersed in the transformer oil. For this use, of course, a sensitive relay and adjustable buck-off circuit will be required in conjunction with the rise simulator.

Cables and Generators

The hot-spot rise simulator also is eminently suited for use in conjunction with other units of electric power equipment such as generators and cables. In the case of generators, the indications of a thermojunction embedded between the coil sides may be corrected for the surprisingly large discrepancy between its reading and the actual conductor temperature; or a thermocouple on the iron may be compensated to give the copper temperature. In the case of cables, a rise simulator may be adjusted to give an output corresponding to the rise of the copper over the sheath so that when it is connected in series with an indicator and a thermojunction on the hottest part of the sheath, the actual hot-spot copper temperature is indicated at all times.

Appendix

The formulas in this Appendix are derived from the information given by Montsinger.[6,7,8] The assumptions are

1. The hot-spot over top-oil temperature rise at constant oil-film temperature is proportional to the 0.8 power of the rate of heat dissipation.
2. The rate of heat dissipation at the hot spot is proportional to the product of the square of the current and the quantity $(234+T+\theta_{c/o})$ where T is the top-oil temperature and $\theta_{c/o}$ is the temperature rise of the hot spot over the top oil.
3. The hot-spot over top-oil rise for a given rate of heat dissipation is proportional to the 0.25 power of the viscosity of the oil film.
4. The temperature of the oil film is equal to that of the top oil plus one-half the temperature rise of the outer surface of the conductor insulation over the top-oil temperature.
5. For the purpose of calculating oil-film temperature, the temperature rise of the surface of the insulation at the hot spot over the top-oil temperature may be taken as proportional to the rise of the hot spot over the top oil. The constant of proportionality may be taken as equal to that derivable from Table 6-5 (page 576) of reference 6, namely 0.618.
6. The viscosity of transformer oil at a temperature T degrees may be represented by the relation:

$$\mu=3.6\times10^{6}(T+50)^{-2.9} \tag{1}$$

From the preceding assumptions, we have: The oil-film temperature $=T+[0.618/2]\theta_{c/o}=T+0.309\theta_{c/o}$. The oil-film viscosity is proportional to $(T+0.309\theta_{c/o}+50)^{-2.9}$. The effect of viscosity variations is to multiply the hot-spot over top-oil rise by

$$\left[\frac{T+0.309\theta_{c/o}+50}{T_o+0.309\theta_o+50}\right]^{-2.9\times0.25}=\left[\frac{T_o+0.309\theta_o+50}{T+0.309\theta_{c/o}+50}\right]^{+0.725} \tag{2}$$

where

T_o = top-oil temperature for factory heat-run
θ_o = rise of hot-spot over top-oil temperature at rated current under conditions of factory heat-run

Hence, the hot-spot over top-oil rise at a top-oil temperature T and current I per unit is given by:

$$\theta_{c/o}=\theta_o I^{1.6}\left[\frac{T_o+0.309\theta_o+50}{T+0.309\theta_{c/o}+50}\right]^{0.725}\times\left[\frac{234+T+\theta_{c/o}}{234+T_o+\theta_o}\right]^{0.8} \tag{3}$$

It will be noted that the required hot-spot over top-oil rise $\theta_{c/o}$ appears in the correction factors on the right-hand side of equation 3. Since the exponents of these factors are fractional, it is not possible to find a simple expression for $\theta_{c/o}$ as an explicit function of the other quantities. The equation can be rearranged, however, to give the per-unit current as an explicit function of the actual hot-spot temperature $\theta_{c/o}$ and the other variables.
The result is:

$$I=\left[\frac{\theta_{c/o}}{\theta_o}\right]^{0.625}\times\left[\frac{T+0.309\theta_{c/o}+50}{T_o+0.309\theta_o+50}\right]^{0.453}\times\left[\frac{234+T_o+\theta_o}{234+T+\theta_{c/o}}\right]^{0.5} \tag{4}$$

References

1. Standard Specifications for Power Transformers. *C88*, Canadian Standards Association (Ottawa, Canada), 1947.

2. Standards for Transformers, Regulators, and Reactors. *C57*, American Standards Association (New York, N. Y.), 1948.

3. Electrical Performance of Transformers for Power and Lighting *B.S. 171*, British Standards Association (London, England), 1936.

4. Thermal Images for Transformers, F.I.A.T. *Final Report Number 1155* (Field Information Agency, Technical, United States Group Control Council for Germany).

5. Reference Tables for Iron-Constantan and Copper-Constantan Thermocouples, W. F. Roeser, Andrew I. Dahl. *Research Paper RP 1080*, National Bureau of Standards (Washington, D. C).

6. Standard Handbook for Electrical Engineers (book), A. E. Knowlton. McGraw-Hill Book Company, New York, N. Y., *section on Thermal Characteristics of Transformers, Regulators, and Reactors*, V. M. Montsinger *et al.*, 1949, pages 569–84.

7. Transformer Engineering (book), L. F. Bloom, G. Camilli, A. Boyajian, V. M. Montsinger. John Wiley and Sons Inc., New York, N. Y., 1938.

8. Cooling of Oil-Immersed Transformer Windings After Shut-Down, V. M. Montsinger. *AIEE Transactions*, volume 36, 1917, pages 711–34.

No Discussion

Northwest Power Pool Interchange

L. B. COWGILL
NONMEMBER AIEE

IN THE Northwest Power Pool there are a multiplicity of interconnected electric systems, some forming looped circuits and others connected in series. The problem of accounting for all power and energy transactions between the various systems for purpose of settlements has been carried on by means of dispatchers' interchange logs which are described here.

Power flow from generating sources to load within any network of lines is approximately in proportion to the electrical phase angle differences of the voltages at the source of power and at the load. The division of power flows between parallel paths is approximately in inverse proportion to the impedance of each path. However, there are such a multitude of flows in various directions over lines throughout the Pool that any individual transaction for delivering power from one point to another occurs by displacement. In other words, it results in a slight shifting of power flows toward the point of load. By this displacement process there are relatively small incremental losses resulting from any one transaction, in fact the loss from the sum-total of transactions with the systems connected in the network are undoubtedly lower than they would be if each system could carry on its own operation over its own lines, disconnected from neighboring systems in the Pool.

With the network of lines it is impractical to attempt to control power flows over various interconnections. Electricity recognizes no variations in ownership and flows freely from power sources to loads. The usual devices for regulating flows over individual lines or interconnections are by the use of series capacitors or phase shifting equipment. Series capacitors cause a fixed amount of phase shift but do not have the ability to regulate for varying loads. Phase shifting equipment can be used to vary the amount of phase angle through a particular line or interconnection, thereby regulating the relative amount of power transferred through the line. However, this equipment is very costly and its accomplishment is to force power transfers by certain routes. When the number of interconnections involved in the Northwest is considered it is apparent that such equipment would add greatly to the installed cost and increase over-all losses with no practical gain. Therefore the Northwest systems have not undertaken to control power transfers over individual lines or interconnections. Where a particular circuit becomes a bottleneck in power transfers it is supplemented or reinforced to permit increased transfers by that easier route, if the incremental increase in the transfer justifies the investment involved.

In the operation of the Northwest Power Pool one system takes over responsibility for frequency control, that is, speed control. Each other system in the Pool is responsible for its net interchange receipts or deliveries. If each of the latter controls its interchange exactly as planned, then the frequency control system also will have performed exactly as planned although that system is unable to exercise control over its interchange as long as it is regulating for correct frequency. In other words, the frequency control system varies its output depending upon whether or not the Pool speed is above or below 60 cycles and depends upon the other systems to regulate interchange. Some assistance to the frequency controlling system is given if each of the other systems in the Pool sets interchange controllers with a frequency bias. This bias acts to cause some over-generation during times of low frequency and under-generation at times of high frequency.

To gain a clearer understanding of the operating procedures involved in the interchange operation, a simplified example will be taken. The following sketch is of a 2-system interconnected group, *X* system being connected to *Y* system through interconnection *r* as shown in Figure 1.

Assume that system *X* is operating to control frequency and that *Y* is controlling net interchange. If *X* and *Y* agree that *X* is to deliver 20 megawatts to *Y* for a particular hour then it is *Y*'s responsibility to maintain a 20-megawatt flow through interconnection *r*. If *Y* conscientiously tried to take 20 megawatts but actually takes only 19 megawatts after the actual meter readings are read at the end of the hour, then *Y* is assumed to be entitled to that shortage of 1 megawatt at some later time since it failed to take it during the hour in question. Therefore, if the settlement assumes that *Y* took exactly the amount scheduled, or 20 megawatts, and that any deviations from this schedule are treated as loans or borrowings which must ultimately be corrected for by later power transfers, then there is neither loss nor gain by either utility in settling their accounts on the basis of scheduled power transfers. This is the elementary principal involved in the Northwest Power Pool energy accounting system.

A further example of a 3-system group

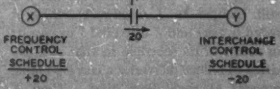

Figure 1. Simple interchange between X and Y systems

X holds frequency to 60 cycles
Y holds interchange at r to amount agreed upon or scheduled

Paper 51-287, recommended by the AIEE System Engineering Committee and approved by the AIEE Technical Program Committee for presentation at the AIEE Pacific General Meeting, Portland, Oreg., August 20–23, 1951. Manuscript submitted February 8, 1951; made available for printing August 3, 1951.

L. B. Cowgill is with Ebasco Services, Inc., Portland, Oreg.

indicated in Figure 2 will illustrate that "Net Interchange" must be the basis of setting up schedules and recording actual interchange transfers.

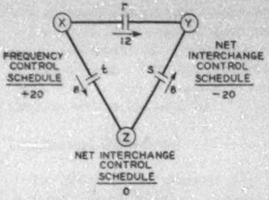
r
X
Y
12
FREQUENCY CONTROL SCHEDULE
+20
t
8
s
8
NET INTERCHANGE CONTROL SCHEDULE
−20
Z
NET INTERCHANGE CONTROL SCHEDULE
0

Figure 2. Simple interchange between three systems X, Y, and Z

Schedules

X to deliver 20 megawatts to Y
No other scheduled transactions

Actual Operation

X holds frequency at 60 cycles
Y takes in a net amount of 20 megawatts at interconnections r and s
Z takes in a net amount of 0 megawatts at interconnections t and s

This illustration covers a simplified case where X is delivering 20 megawatts to Y, X being responsible for frequency control, Z having no schedule at all. This assumes that the operation for the hour was exactly as scheduled.

The example might be developed still further with multiple schedules and actual operation deviating slightly from schedules. Refer to Figure 3 as an illustration.

The operation is for X to control frequency, Y and Z each to control net interchange. The net schedule is for Y to receive 20 plus 7 plus 4=31 mw. The net schedule for Z is to deliver 9 plus 4=13 mw. The net schedule for X is to receive 9 and deliver 20 plus 7=18 net delivery.

If X operates to hold frequency at 60 cycles then Y must operate to take 31 megawatts and Z to deliver 13 megawatts. If these two interchanges were performed exactly then X would automatically have delivered its 18 megawatts. However, the example assumes that Y actually took 28 megawatts and that Z actually delivered 14 megawatts. Under this condition Y is still entitled to 3 megawatts which it failed to take and Z delivered 1 megawatt in excess of its schedule so that it is entitled to reduce deliveries a corresponding amount at some later time. Then X must have delivered only 14 megawatts instead of the 18 scheduled so that it has a continuing responsibility to make up the 4-megawatt shortage in delivery. These variations from schedule are handled by a deviation account for each utility in the Pool. To keep proper records of the Interchange Schedules, Actual Interchange, and Deviations from Schedule, they are recorded on dispatchers' logs. On all power interchange transactions, transfers from or to other utilities are distinguished by using algebraic signs as follows:

Received = −
Interchange in = −
Delivered = +
Interchange out = +
(Actual Interchange) − (Scheduled Interchange) = (Deviation from Schedule).

A further example of multiple schedules, multiple ties, and transfer of power from one system through an intermediate system to a third system is illustrated below, referring to Figure 4.

SCHEDULE

X to deliver 20 mw to Y for storage
X to deliver 7 mw to Y for sale
Z to deliver 9 mw to X for sale
Z to deliver 4 mw to Y for sale
W to deliver 11 mw to X for redelivery to Y
V to deliver 15 mw to X for redelivery to W

ACTUAL OPERATION

X holds frequency at 60 cycles. Scheduled to deliver 18 megawatts but is unable to control deliveries while holding frequencies.

Y tries to take a net amount of 42 megawatts through interconnections at o, p, r, and s but after the hour is over finds that 39 megawatts was actually taken. This leaves +3 megawatt deviation.

Z tries to deliver a net of 13 megawatts through interconnections p, q, s, and t but after the hour is over finds that 14 megawatts was actually delivered. Deviation of +1.

W tries to take a net of 4 megawatts through interconnection m but after the hour is over finds that 7 megawatts was actually taken. Deviation of −3.

V tries to deliver a net of 15 megawatts through interconnections n and o but after the hour is over finds that 12 megawatts was actually delivered. Deviation −3.

X actually delivers 20 megawatts since all deliveries must exactly equal all receipts. Deviation is +2.

Sum of all deviations $=(+3)+(+1)+(-3)+(-3)+(+2)=0$.

It will be noted that it is quite immaterial what amount of power flows through individual interconnections of looped systems but that the algebraic sum or net of power through all interconnections of a utility's system is the measure of how close that utility approached its agreed upon schedule of operation. In this case, system Z has the same schedules as in the previous example, generates in the same manner and ends up with the same deviation. However, power flows through Z's individual interconnections are quite different. But Z's net interchange is the same since it generated 14 megawatts in excess of its own load in each case.

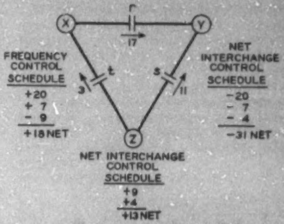
r
X
Y
17
FREQUENCY CONTROL SCHEDULE
+20
+ 7
− 9
+18 NET
t
3
s
11
NET INTERCHANGE CONTROL SCHEDULE
−20
− 7
− 4
−31 NET
Z
NET INTERCHANGE CONTROL SCHEDULE
+9
+4
+13 NET

Figure 3. Multiple schedules with actual operation deviating from schedules

Schedules

X to deliver 20 megawatts to Y for storage
X to deliver 7 megawatts to Y for sale
Z to deliver 9 megawatts to X for sale
Z to deliver 4 megawatts to Y for sale

Actual Operation

X holds frequency at 60 cycles
Y tries to take in a net amount of 31 megawatts at interconnections r and s but actually finds after the hour that he took in 28 megawatts
Z tries to deliver a net amount of 13 megawatts at interconnections s and t but actually finds that he delivered 14 megawatts, after the hour is over

These same principles can be applied with any number of participating utilities and the complexity of interconnections expanded to any degree. That is what is done in the Northwest Power Pool with 11 major utilities and many more smaller utilities tied rigidly together through a multiplicity of interconnections at all times as indicated in Figure 5.

There are no difficulties in accounting for every kilowatt-hour, but operation must be handled in a methodical manner, and any misunderstandings on amounts of schedules or classifications of energy or errors in listing must be cleared up immediately. Therefore, there is a checking system. First, the deviation for each utility for each hour is added algebraically at certain clearing points in the Pool and if the algebraic total of all of the deviations of the utilities in the Pool for any particular hour is not zero, there is an error to be found and corrected. The second checking system is that each day each utility makes copies of its interchange log, listing scheduled interchanges

Table I. Typical Dispatcher's Interchange Log for System X of Figure 4 Setup

	Est. System Operation					Scheduled Interchange								Actual Interchange						Deviations From Sched.		
Hour	Own System Load	Own System Hydro Gen.	Own System Steam Gen.	Receipts From Industrials	Surplus = + or Deficit = −	From Syst. V Steam Excess	From Syst. Z Hydro Excess	To Syst. V Transfer From Z	From Syst. Z Transfer To V	From Syst. W Hydro Excess	To Syst. Y Steam Excess	To Syst. Y For Storage	Net of All Interchange Schedules	With W at m	With V at n	With Y at r	With Z at t	With Z at q	Net of All Actual Interchange	For Hour = Net Actual − Net Sched.	Cumulative Deviation	Hour
AM	xx	xx	xx	xx	xx	xx	xx	xx	xx	xx	xx	xx	xx	xx	xx	xx	xx	xx	xx	xx	−7*	AM
12–1	150	8	0	0	−142	0	−138	+2	−2	−12	0	+8	−142	−13	−23	−12	−41	−51	−140	+2	−5	12–1
1–2	140	8	0	0	−132	0	−120	+2	−2	−20	0	+8	−132	−18	−21	−13	−32	−47	−131	+1	−4	1–2
2–3	133	8	0	0	−125	0	−106	+2	−2	−27	0	+8	−125	−25	−21	−12	−30	−36	−124	+1	−3	2–3
3–4	130	8	0	0	−122	0	−103	+2	−2	−27	0	+8	−122	−27	−22	−11	−27	−37	−124	−2	−5	3–4
4–5	131	8	0	0	−123	0	−111	+2	−2	−20	0	+8	−123	−18	−23	−14	−30	−39	−124	−1	−6	4–5
5–6	135	8	0	0	−127	0	−116	+2	−2	−19	0	+8	−127	−20	−23	−14	−29	−41	−127	0	−6	5–6
6–7	152	8	20	0	−124	0	−152	+5	−5	0	+20	+8	−124	+1	−25	−13	−38	−50	−125	−1	−7	6–7
7–8	168	36	42	0	−90	−3	−87	+7	−7	0	0	0	−90	−2	−19	−4	−27	−35	−87	+3	−4	7–8
8–9	185	66	48	2	−69	−19	−50	+7	−7	0	0	0	−69	+2	−18	+2	−20	−33	−67	+2	−2	8–9
9–10	195	79	48	3	−65	−15	−50	+7	−7	0	0	0	−65	−1	−19	−3	−13	−26	−62	+3	+1	9–10
10–11	200	85	48	3	−64	−14	−50	+7	−7	0	0	0	−64	−3	−17	+4	−18	−32	−66	−2	−1	10–11
11–12	197	81	48	3	−65	−15	−50	+7	−7	0	0	0	−65	+2	−16	+3	−18	−36	−65	0	−1	11–12
PM	xx	xx	xx	xx	xx	xx	xx	xx	xx	xx	xx	xx	xx	xx	xx	xx	xx	xx	xx	xx	xx	PM
12–1	183	55	48	2	−78	−23	−55	+7	−7	0	0	0	−78	+2	−19	−1	−25	−34	−77	+1	0	12–1
1–2	185	60	48	2	−75	−20	−55	+7	−7	0	0	0	−75	−1	−20	0	−23	−30	−74	+1	+1	1–2
2–3	186	59	48	2	−77	−22	−55	+7	−7	0	0	0	−77	−1	−17	−2	−23	−33	−76	+1	+2	2–3
3–4	182	55	48	2	−77	−22	−55	+7	−7	0	0	0	−77	−2	−17	−2	−24	−31	−76	+1	+3	3–4
4–5	186	80	48	2	−56	−1	−55	+7	−7	0	0	0	−56	+2	−15	+2	−19	−25	−56	+1	+4	4–5
5–6	195	90	48	2	−55	0	−55	+7	−7	0	0	0	−55	+2	−16	−3	−15	−23	−55	0	+4	5–6
6–7	197	94	48	0	−55	0	−55	+7	−7	0	0	0	−55	−3	−15	−4	−12	−22	−56	−1	+3	6–7
7–8	188	85	48	0	−55	0	−55	+7	−7	0	0	0	−55	+2	+14	−2	−13	−29	−56	−1	+2	7–8
8–9	180	57	48	0	−75	0	−75	+7	−7	0	0	0	−75	−3	−17	−1	−20	−35	−76	−1	+1	8–9
9–10	175	55	45	0	−75	0	−75	+7	−7	0	0	0	−75	+4	−18	+1	−21	−40	−74	+1	+2	9–10
10–11	167	52	40	0	−75	0	−75	+5	−5	0	0	0	−75	−1	−19	+1	−21	−34	−74	+1	+3	10–11
11–12	160	18	10	0	−132	0	−150	+3	−3	0	+10	+8	−132	+1	−24	−10	−41	−56	−130	+2	+5	11–12
Total For Day					−2,133	−154	−1,948	+130	−130	−125	+30	+64	−2,133	−120	−458	−108	−580	−855	−2,121	+12	xx	xx
Prev. Cumul. Total For Month					xx	−1,821	−19,982	+1,281	−1,281	−495	+104	+712	−21,432	−1,182	−5,103	−1,035	−5,935	−8,184	−21,439	−7	xx	xx
Month To Date					xx	−1,975	−21,880	+1,411	−1,411	−620	+134	+776	−23,565	−1,302	−5,561	−1,143	−6,515	−9,039	−23,560	+5	+5	xx

* From previous day.

Figures in megawatt hours.

Net Actual-Net Schedule = Deviation for Hour.
Interchange Out = +.
Interchange In = −.

by classifications, and exchanges those copies with each other utility with whom it has dealings. This provides the means of comparing understandings of amounts and classifications of schedules.

It is found that better operation can be carried on by elaborating on the above procedure somewhat. One way is for all utilities to assist the frequency controlling system in maintaining Pool speed control. This is done by setting net interchange load controllers with a frequency bias. In other words, the load controller so set, for any one utility tends to cause that utility to depart from scheduled interchange in the direction needed to maintain 60-cycle speed. If the frequency is low, and the particular utility is scheduled to receive a certain amount of power, that utility operates to receive less than its schedule. If it was scheduled to deliver power, it undertakes to deliver more than the schedule. Contrary wise, if the frequency is above 60 cycles.

Such frequency bias operation tends to cause some deviations but some are plus and some are minus so they will cancel out over a period of time. That is, if the utility's frequency meter is in correct calibration so that the controller knows when the frequency is high or low. To calibrate all frequency meters, one large utility handles frequency control each Sunday afternoon and holds as close as possible to 60 cycles between 1 and 3 p.m. Pacific Standard Time so that all others may readjust frequency meters if needed. That utility maintains its frequency meters in calibration by special equipment to adjust them to Arlington radio time signals.

A second type of operation that departs from the simplified scheduling system of energy accounting is by any two systems having an "open end" schedule. This is often extended to several pairs of systems. In this case a schedule is not fixed beforehand but left open with the amount to be filled in after each hour of operation is over. The amount of the open end schedule is fixed by some unforeseeable condition such as a receiving utility "taking all the power that it can utilize" which is often the case when a delivering utility has excess hydro capacity going to waste. Another case might be when a delivering utility has some unforeseeable part of the excess capacity from a lower cost steam plant where the schedule would be "to deliver all excess available by keeping the plant wide open." In such cases the amount of the receipt in the first case and delivery in the second case is indeterminate until the hour has passed, after which the amount

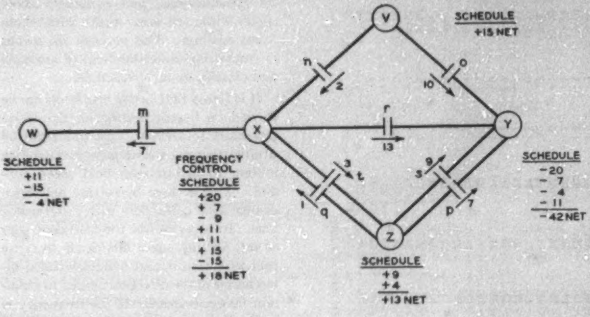
V
SCHEDULE
+15 NET
n
2
o
10
W
m
7
X
r
13
Y
SCHEDULE
+11
−15
−4 NET
FREQUENCY CONTROL
SCHEDULE
+20
+7
−9
+11
−11
+15
−15
+18 NET
3
t
1
q
9
s
p
7
SCHEDULE
−20
−7
−4
−11
−42 NET
Z
SCHEDULE
+9
+4
+13 NET

Figure 4 (above). Multiple schedules, multiple ties with transfer through an intermediate system

Schedule

X to deliver 20 megawatts to Y for storage
X to deliver 7 megawatts to Y for sale
Z to deliver 9 megawatts to X for sale
Z to deliver 4 megawatts to Y for sale
W to deliver 11 megawatts to X for redelivery to Y
V to deliver 15 megawatts to X for redelivery to W

Figure 5 (below). Northwest Power Pool, schematic diagram of interconnections

is arrived at by the utility having the restricting condition, then logged in the same amount by both of the utilities involved in the transaction. In operation with such an "open end schedule" the deviation from schedule for the limiting system must necessarily be zero because the actual interchange is the scheduled interchange.

Now let us examine the means of setting up logs for arriving at interchange schedules, recording the actual interchanges, arriving at deviations and checking deviations for errors. Table I is a sample dispatcher's log sheet on which is shown four main headings, "Estimated System Operation," "Scheduled Interchange," "Actual Interchange," and "Deviations from Schedule." Each utility has such a form, tailored to its requirements and its system.

Assuming that the *X* system on the example previously listed was using the log, the first step is to arrive at its program of carrying its estimated load for each hour of the day. This is started by estimating its Own System Load for each hour of the day. Next, its Own System Hydro Generation is listed, basing the amounts upon the water supply for hydro generation that is available or that can safely be used from reservoir storage. Own System Steam Generation is filled in on an hourly basis along with Receipts from Industrial plants connected to its own system. From these tentative estimated power supplies and estimated load the Surplus or Deficiency is arrived at. This is available for interchange delivery or needs to be received from interchange. Actually there is a considerable amount of "cut and try" adjusting between utilities in arriving at the final program of hourly operation. If lower cost power can be obtained from a neighboring utility than the cost of operating steam generation on

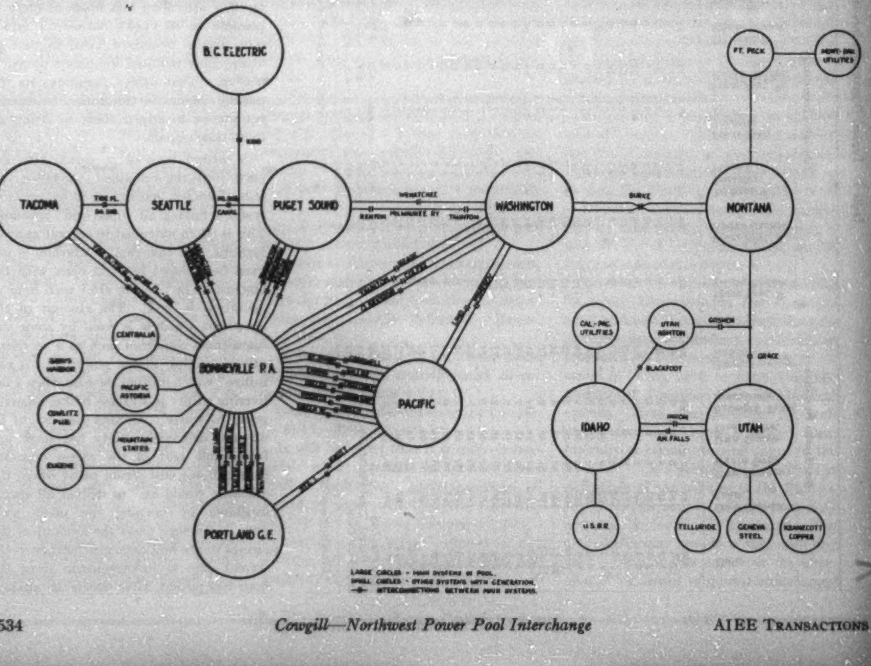
B.C. ELECTRIC
KING
TACOMA
TIDE FL.
SH. DIS.
SEATTLE
CANAL
PUGET SOUND
WENATCHEE
RENTON
MILWAUKEE RY
TAUNTON
WASHINGTON
BURKE
MONTANA
FT. PECK
MONT.-DAK. UTILITIES
CENTRALIA
GRAYS HARBOR
PACIFIC ASTORIA
COWLITZ PUD.
MOUNTAIN STATES
EUGENE
BONNEVILLE P.A.
PACIFIC
PORTLAND G.E.
CAL.-PAC. UTILITIES
UTAH ASHTON
GOSHEN
GRACE
BLACKFOOT
IDAHO
UTAH
AM. FALLS
U.S.B.R.
TELLURIDE
GENEVA STEEL
KENNECOTT COPPER
LARGE CIRCLES - MAIN SYSTEMS OF POOL.
SMALL CIRCLES - OTHER SYSTEMS WITH GENERATION.
INTERCONNECTIONS BETWEEN MAIN SYSTEMS.

X's system then a schedule is arranged for replacing the steam power with interchange purchases. Each hour is given separate consideration since the availability of power from various sources and the need for power on a utility's own system varies from hour to hour. Actually the pattern of schedules gets pretty well fixed and then adjustments are made only for shifting conditions such as seasonal changes, outages of equipment, major load shifts, et cetera.

The net result of the adjustments in schedules and planned generation by sources for each utility is agreed upon, with the Net of All Interchange Schedules being exactly equal to the Surplus of Deficit both in amount and sign, for each hour of the day. This daily program is agreed upon at least one day in advance.

Since the schedules are purchase and sale transactions they often require executive approval so the operating head of the utility is responsible for arriving at the schedules. When both the section on Estimated System Operation and on Scheduled Interchange are completely filled out with the Net of all Interchange Schedules balancing the Surplus or Deficit, the log is furnished to the dispatchers for operation during the day that it covers. His operation attempts to hold the Net of All Actual Interchange at the same amounts as the Net of All Interchange Schedules.

Of course his actual system load varies from the estimate and generation from various plants does not exactly correspond to the estimates. However, he should try not to vary from his Net of All Interchange Schedules since no other utility has agreed to furnish those variations. Own System Generation should be varied to correct for departures from the estimates unless, of course, there is a joint agreement with some other utility to change one or more schedules for this purpose.

Even then, the telemetering and load controllers will not perform so exactly that the Net of All Actual Interchange is always the same as the Net of All Interchange Schedules. To keep track of this variation and to permit correction for it, an account listed as Deviations from Schedule is kept. This is the Net of All Actual Interchange minus the Net of All Interchange Schedules. A Cumulative Deviation account is then arrived at to carry forward all past amounts of deviations with the objective of continually trying to clear this account to zero amount. Again all quantities must carry their proper algebraic signs. Deviations from Schedules should be balanced out by shifting Actual Interchange slightly above or below Scheduled Interchange. However, power at different times of the day has different value and balancing out of deviations should be under "like conditions" to those under which they were created. Also operation of a utility's generating plants should be carried on to hold deviations from schedule as close as possible to zero on a minute-by-minute basis throughout each hour.

When it is recognized that the algebraic sum of all deviations throughout the Pool must be added to or subtracted from the scheduled or agreed upon interchange of the frequency controlling system, then it is apparent that it is the duty of each other utility to diligently try to perform as scheduled or agreed upon. In fact, it is the duty of the other utilities to also assist the frequency controlling system in accelerating or decelerating the inertia of the Pool, if Pool speed should get below or above normal 60 cycles.

The final phase of the interchange power and energy accounting is billing for interchange. If the Net of All Actual Interchange was exactly equal to the Net of All Interchange Schedules for each hour then every schedule listed on the log would have been exactly met. Since the difference between these amounts is represented by the Deviations from Schedule and these deviations are merely loans or borrowings which must ultimately be balanced out, then the billing should still be upon the scheduled interchange amounts which are the agreed upon purchases and sales of power.

Each schedule for a certain class and price level of power is kept separate from all others on each log by listing it in a separate column. At the end of each day the total of each classification of power is added to the Previous Cumulative Total for the Month for the same classification. At the end of the month the power for each classification is used for billing purposes.

Since the power and energy accounting system allows complete flexibility in keeping track of any number and any kind of transaction, then the utilities are free to carry on the best operation to realize the maximum resources in the Pool. Also economy operations are set up to secure the lowest over-all cost consistent with good utility practice.

No Discussion

The Tracy Pumping Plant—Central Valley Project of California

P. E. RICHARDSON
ASSOCIATE AIEE

THE TRACY Pumping Plant is one of the important units of the Central Valley Project of California, and is the key unit in the plan to bring relatively plentiful Sacramento River water to the parched lower San Joaquin Valley. Areas in the lower San Joaquin Valley have been irrigated by pumping and by direct diversion from the river. By bringing increased areas under pumping, the water table has been lowered, especially in dry years to a point where salt water intrusion took place and many areas under cultivation had to be abandoned. Also the construction of Friant Dam and the Friant-Kern Canal contemplates diverting to the upper San Joaquin valley supplies formerly used in the lower valley.

The Tracy Pumping Plant will lift surplus water of the Sacramento River into the Delta-Mendota Canal. Water conveyed by the canal will replace water diverted by Friant Dam, provide water to areas where irrigation from wells was formerly done, restore the water table, and bring additional areas under irrigation.

To perform this purpose the Tracy Pumping Plant will raise a maximum of 4,600 cubic feet per second (cfs) of water from an average elevation of 4 feet above sea level to an average elevation of 201 feet above sea level. The installation in the plant will consist of six vertical pumping units each rated 767 cfs at a head of 197 feet. Each pumping unit will be driven by a 22,500-horsepower, 180-rpm vertical synchronous motor, making the Tracy Pumping Plant second only in size to the Grand Coulee Pumping Plant of the Bureau of Reclamation pumping installations.

The Tracy Pumping Plant is located in Alameda County, Calif., about 10 miles northeast of Tracy, Calif., for which it was named. It is located on the Delta-Mendota Canal, approximately 13,400 feet above its intake on the Old River, or old course of the San Joaquin River. Each pump discharges through a 108-inch diameter butterfly valve into a 10-foot diameter steel discharge pipe. These pipes are paired into three 15-foot diameter discharge pipes approximately 1 mile long. They discharge through a siphon structure into the Delta-Mendota Canal. Water surface at the outlet structure varies from elevation 185.5 feet to 195.8 feet. From the outlet structure, water flows approximately 117 miles through the Delta-Mendota Canal into the Mendota Pool, a storage reservoir near Mendota, Calif. Water from this pool is to be used for irrigation purposes as outlined above. In order to insure a steady and sufficient supply of fresh water to the Delta-Mendota Canal, the Delta-Cross Channel Canal is to be constructed. This canal will bring water from the Sacramento River across the Delta to the intake of the Delta-Mendota Canal.

It is expected that when the irrigation facilities are fully developed and in operation, the maximum demand for water will occur in July, and will be approximately 4,250 cfs of water. The minimum demand is expected to occur in December, and to be about 500 cfs with the yearly average demand about 2,060 cfs. To meet this varying demand it is expected that all six pumps will be operated in July and part of August, tapering down to one pump during December and January, and increasing to five pumps during April, May, and June. Pumping equipment therefore, can be serviced most of the year.

Description of Plant

The pumping plant is adjacent to the Tracy switchyard and synchronous condenser station from whence it receives its power supply. The pumps, motors, and motor-control equipment are arranged so the motors may be operated as synchronous condensers when unloaded to supplement the synchronous condenser in the station.

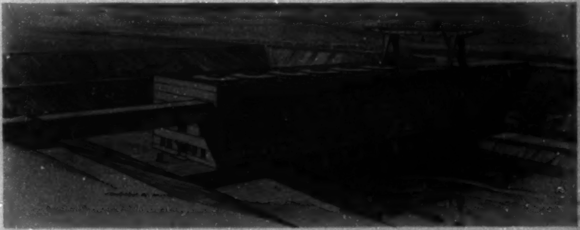

Figure 1. Artists drawing showing general view of Tracy Pumping Plant

---

Paper 51-288, recommended by the AIEE Power Generation Committee and approved by the AIEE Technical Program Committee for presentation at the AIEE Pacific General Meeting, Portland, Oreg., August 20–23, 1951. Manuscript submitted May 21, 1951; made available for printing July 6, 1951.

P. E. RICHARDSON is with the United States Bureau of Reclamation, Denver, Colo.

All engineering designs for the pumping plant are under the direction of L. N. McClellan, Chief Engineer, Branch of Design and Construction, Bureau of Reclamation, Denver, Colo. Over all planning and operation of the Central Valley Project of California is under the direction of R. L. Boke, Regional Director, Bureau of Reclamation, Sacramento, Calif. All activities of the Bureau of Reclamation are under the general charge of Michael W. Straus, Commissioner, Washington, D. C.

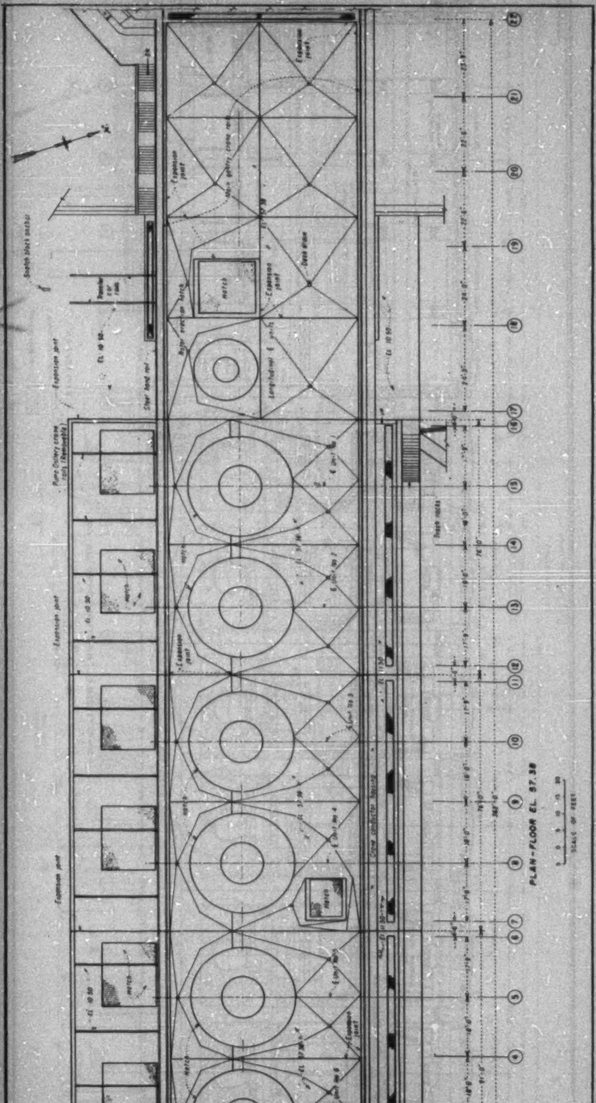

Figure 2. Tracy Pumping Plant roof slab

Figure 1 is an artist's conception of the plant viewing the intake side. The plant has an over-all length of 362 feet and an over-all width of 96 feet. The pumping plant is a reinforced concrete structure of the semioutdoor type. It may be roughly divided into two parts, one consisting of the six main pump bays at left in the figure, having a length of 243 feet, and the service bay, having a length of 119 feet. The roof deck supports a 100-ton gantry crane for handling the equipment. A cable bridge and tunnel connects the plant to the switchyard. Referring to Figure 2, there is a circular hatch, approximately 27 feet in diameter, in the roof deck centered over each pumping unit to facilitate handling by the gantry crane. There is also one smaller hatch in the main unit part of the building roof and two in the service bay area.

Due to poor foundation conditions, the plant is supported on timber piles, as shown in Figure 7. The foundation is at an elevation of approximately 30 feet below sea level. To continue with a brief description of the main unit bays, the pump inlet structures are similar in design to turbine draft tubes. The centerline of the scroll case of the pumps and of the butterfly valves in the discharge lines and of the discharge lines as they leave the plant are at elevation 0 (sea level). The pump inlets are protected by trash racks extending from elevation −17.75 to elevation 11.50. On the intake side there is an exposed deck at elevation 11.50 for servicing the trash racks and stop logs.

On the discharge side of the plant, at elevation −12.00, a gallery is provided for access to the pump scroll cases, space for the installation of the butterfly valves, the valve operating mechanisms, by-pass lines, air vents, and other appurtenances. Above the butterfly valves is a roof deck through which is a hatch to provide for crane service to the valves.

Referring to Figure 6, the pump scroll-cases are embedded in concrete. On the intake side of the main bays is a pipe gallery at elevation −3.25. In it are air, oil, and water piping, and the unit cooling water pumps.

The main pump floor shown on Figure 5 is at elevation 10.50. This is the main operating floor of the plant. On the intake side on this floor are located the hydraulic gage and unit control boards, unit auxiliary boards, heating and ventilating boards, and d-c boards. In the center of this floor, along the center line of units are access stairways to the

Figure 3. Longitudinal section through center-line of units

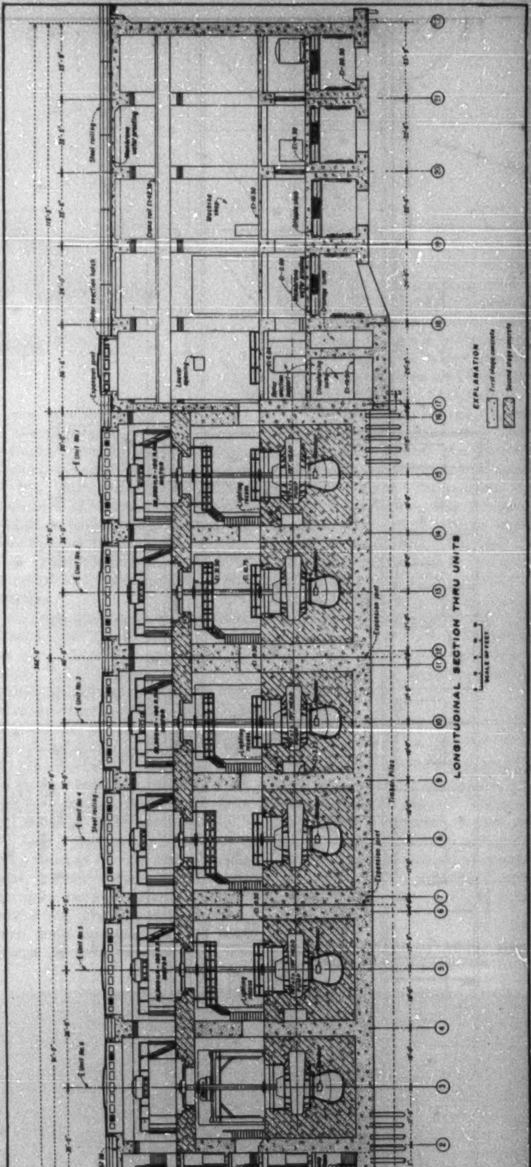

pump crown plates, and along the transverse walls are located the motor voltage regulating rotating amplifiers. On the upstream side and outside at this elevation is a deck over the butterfly valves with hatches to each valve. There is a 22-foot wide door at each unit at this elevation with gantry crane tracks extending over the outside deck to beyond the center line of units, transversely of the building. On these tracks operates a special gantry crane designed to remove the rotating parts of the pumps while leaving the motor rotors in place. The outdoor portions of these tracks are accessible to the main gantry crane, so as to rehandle pump parts as well as to move the special gantry crane from one bay to another and to handle the butterfly valves.

On the downstream side of the plant at elevation 23.63, there is a cable gallery used primarily for routing control cables, both inside the plant and connecting to the cable tunnel to the switchyard. In this gallery also is located a double-ended unit substation for station service power.

The main motor floor, shown in Figure 4, is at elevation 38.63. On this floor, in addition to the six main motors are located the motor-neutral grounding reactors, the rotating machine protective equipment and instrument transformers, and heating and ventilating equipment. From this level the cable bridge and tunnel lead to the switchyard.

In the service bay, there is a partial floor at elevation 19.50 feet below sea level containing the unwatering sump. There are full floors at elevations 4.50 feet below sea level and 10.50 feet above sea level. On the lower of these two floors, see Figure 6, are located cooling water pumps for the synchronous condenser in the switchyard, domestic water pumps, unwatering pumps sump pump, air compressors and receivers, oil purifier, oil storage tanks, oil pumps, and water-softening equipment, and suitable operating boards for the above equipment. At elevation 10.50, as shown in Figure 5, are located a machine shop and an equipment handling area including a rotor erection base. This area is served by a 20-ton inside crane. A door is provided on the south side of the service building at this elevation complete with transfer tracks and a transfer car for handling turbine and butterfly valve parts. A door also is provided on the north side for truck entrance to the service area.

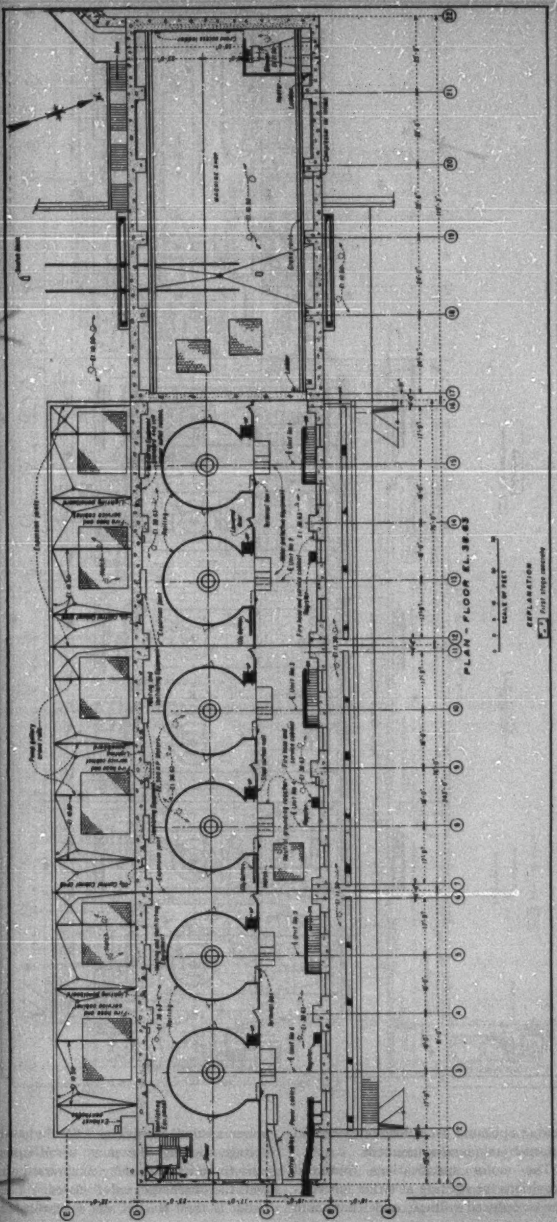

Figure 4. Plan of motor floor

The location of the plant in an earthquake area is reflected in heavy concrete sections shown in Figure 3. This figure also shows the stair well section on the east end of the building.

Pumping Units

Pumps

The main pumps are of the vertical-shaft single-impeller, single-suction, centrifugal type. They were manufactured by the Worthington Pump and Machinery Corporation and are designated as 84-inch vertical volute pumps of the closed-type impeller design. The pumps were specified to deliver 767 cfs when operating at 180 rpm under a total dynamic head of 197 feet. The specifications further required that the pumps have stable operation under all heads within the range of 174 to 204 feet, with the maximum input to the pump not exceeding 22,500 horsepower over the entire operating range. Rotation is counterclockwise.

Prior to beginning manufacture of the pumps, a prototype pump was constructed and tested at the manufacturer's plant. These tests indicated the following expected performance of the pumps:

Capacity at design point (197 feet head)	785 cfs
Efficiency at design point	89.3 per cent
Maximum input in operating range	21,000 horsepower

At this writing actual tests on the pumps have not been conducted.

The pumps are designed so that the entire internal assembly can be removed from above without disturbing the pump casing, discharge piping, et cetera. Each pump is equipped with a guide bearing located above the main stuffing box. The guide bearing is lubricated by means of motor-driven oil circulating pumps. The lubrication system is provided with indicating and alarm devices. The pump shaft is made in two sections to facilitate assembly and disassembly. The shafts are furnished with integral couplings for bolting to each other and to the motor shaft. The pump casings are of cast iron, and were made in four sections, bolted together. The average diameter of the scroll case is 18 feet. The impellers are of 1-piece cast bronze having a diameter of 145 inches. Provision is made in the pump designs to permit the units to operate as synchronous condensers with the water depressed in the suction tube and the impeller operating in air.

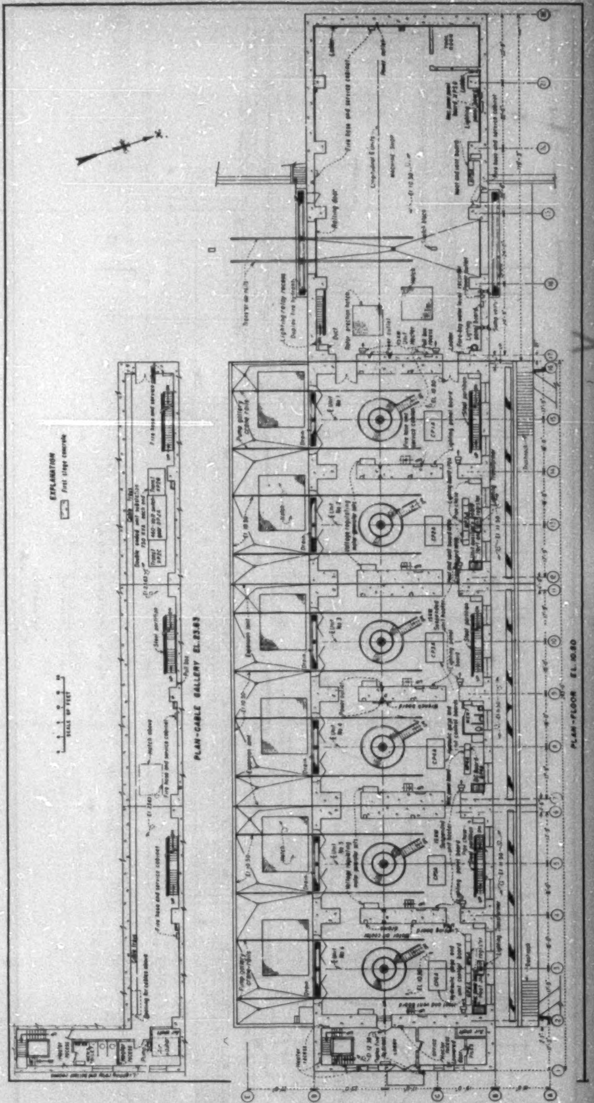

Figure 5. Plan of pump floor and cable gallery

Motors

The six main motors were manufactured by the Allis-Chalmers Manufacturing Company. Each of the motors is rated 22,500 horsepower, 13,600 volts, 0.95 leading power factor, 3 phase, 60 cycle, 180 rpm. The motors are of the synchronous, vertical-shaft type, with the thrust bearing and upper guide bearing located above the rotor, and a lower guide bearing below the rotor. The entire weight of the rotating parts of the motor, main exciter and pump, together with the unbalanced hydraulic thrust of the pump is carried by the motor thrust bearing.

The motors are totally enclosed and are air cooled with four surface air coolers symmetrically spaced around the stator frame.

Rated output may be delivered with one air cooler out of service without exceeding the 40-degree-centigrade temperature limit for cooling air entering the motor. The motor housings are sufficiently airtight to insure proper operation of the carbon dioxide fire extinguishing system. This equipment releases carbon dioxide into the motor upon operation of the motor differential relays or whenever temperature within the air housing reaches a predetermined level.

The armature windings are wye connected with the neutral grounded through a reactor. Current transformers are installed in the main and neutral leads for differential protection of the windings. The rotor spider is built up from fabricated steel. The calculated rotor WR^2 is 3,500,000 pounds at a radius of 1 foot. This high value was required to improve stability of operation and obviate the necessity of surge tanks in the motor discharge lines. The rotors are equipped with amortisseur windings. The motors have an over-all diameter over the air housings of 25 feet, 6 inches. The weight of one complete motor and exciter is approximately 286,000 pounds. The motors were shipped dismantled and erected at the site of the work. The motors are equipped with combination brakes and jacks, including a provision for lifting the rotors prior to starting, following an extended shutdown, in order to establish an oil film on the thrust bearing to reduce break-away torque requirements, and afford protection to the thrust bearing. Also furnished with the motors was field-application equipment including motor-field circuit breakers, and automatic field application relays of the polarized type designed to automatically apply the field at optimum conditions of speed and rotorpole angular displacement.

The motor specifications contained provisions for starting at either full voltage or reduced voltage, under minimum power system conditions. For reduced voltage starting, the pump scroll cases were to be unwatered by compressed air and the discharge valve closed. The motor is then started and synchronized

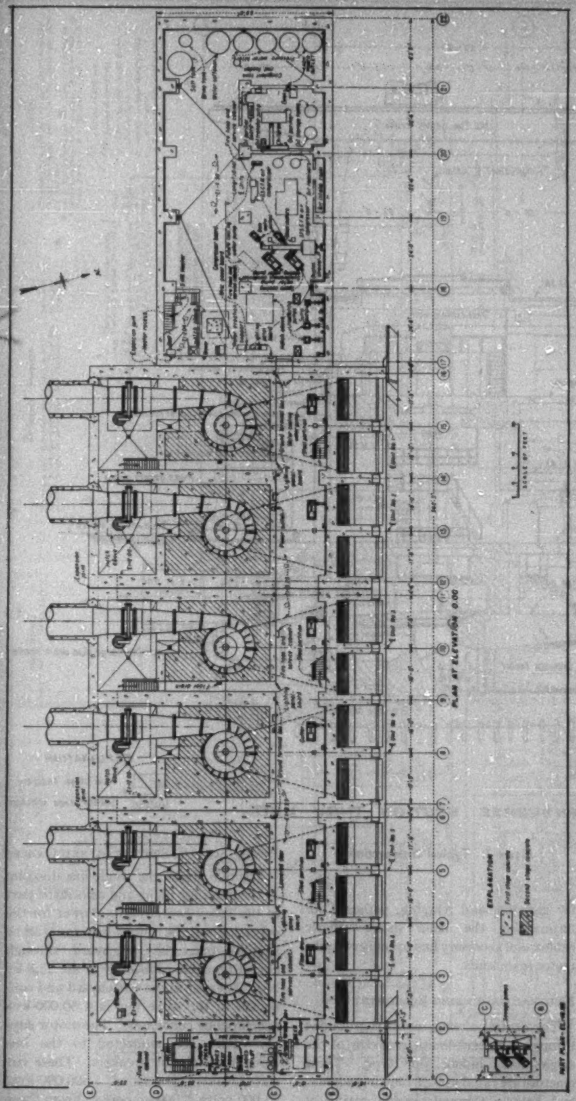

Figure 6. Plan at centerline of scrollcases

at reduced voltage, and then full voltage applied to the motor. Water is then admitted to the pump, and the discharge valve gradually opened. For the alternate method of starting, the scroll case is filled with water, with the discharge valve closed. Full voltage is applied, the motor started and synchronized. The discharge valve is then gradually opened. Since the motors have a relatively low locked-rotor current, approximately 375 per cent, and the system to which it is connected is relatively stiff, it was determined that the reduced-voltage method of starting could be omitted. The provision for unwatering the pump is used for synchronous condenser operation and may be used in connection with full-voltage starting.

Each motor is designed to operate as a synchronous condenser with the pump impeller operating in air as described previously. Each motor, when operating at full rated voltage, has a synchronous condenser capacity of 8,250-kva leading and 17,900-kva lagging.

Calculations indicate that a maximum reverse speed of 235 rpm (130 per cent of normal) may be expected due to unrestricted return flow of water in the discharge pipe following shutdown. The motors are designed to safely withstand this overspeed.

Excitation

The excitation equipment for each motor consists of a direct-connected vertical shaft, shunt-wound, 150-kw 230-volt main exciter mounted above the thrust bearing and a rotating amplifier or "Regulex" exciter set driven by a 10-horsepower, 1,750-rpm induction motor. The main exciter is designed to operate self-excited either with or without the rotating amplifier. The "Regulex" generator has the equivalent of two complete d-c windings and operates as a 2-stage amplifier, the second stage having an output of 5-kw at 250-volts. The "Regulex" generator is connected in the main exciter field circuit in series with the motor-operated rheostat and can operate to either buck or boost the exciter field.

Voltage Regulation

Provision is made for either manual or automatic voltage regulation and power factor control by switching the "Regulex" set in or out of service. Manual regulation is accomplished by operation of the motor-operated main exciter field rheostat, with the main exciter operating self-excited. During starting this type of regulation is employed. Automatic voltage regulation is obtained through the operation of "Regulex" control equipment. In addition to the rotating amplifier this equipment consists of a cubicle assembly containing a comparison network, a voltage control powerstat, current compensators and related equipment. The comparison network is energized by

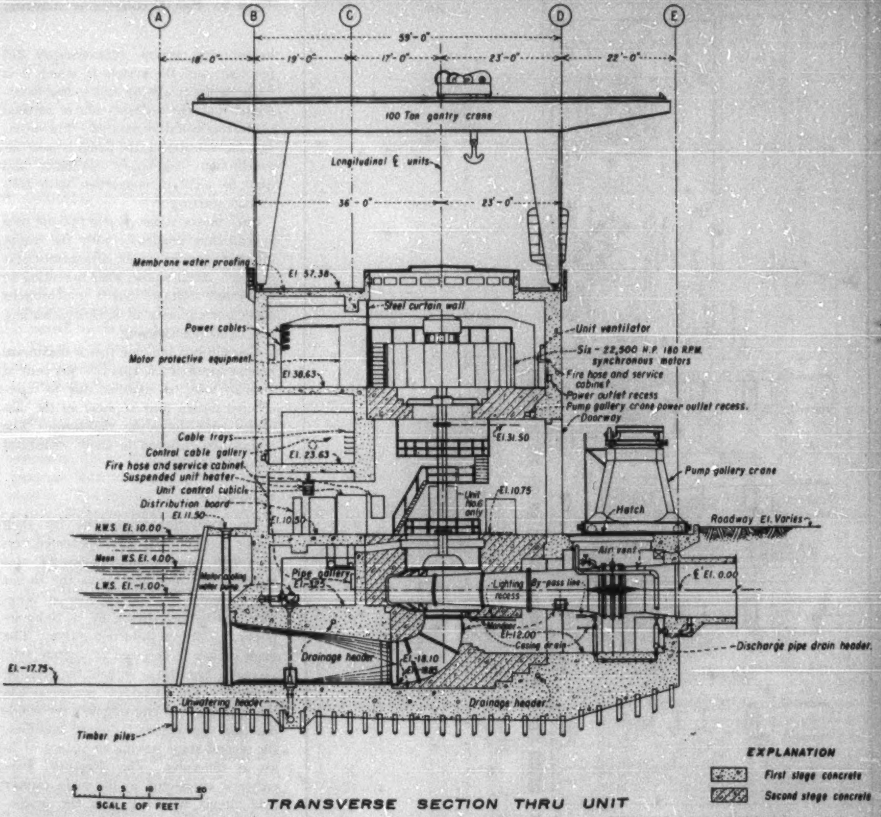
A
B
C
D
E
59'-0"
18'-0"
19'-0"
17'-0"
23'-0"
22'-0"
100 Ton gantry crane
Longitudinal ℄ units
36'-0"
23'-0"
Membrane water proofing
El 57.38
Steel curtain wall
Power cables
Motor protective equipment
El 38.63
Unit ventilator
Six - 22,500 H.P. 180 RPM synchronous motors
Fire hose and service cabinet
Power outlet recess
Pump gallery crane power outlet recess.
Doorway
El. 31.50
Cable trays
Control cable gallery
El. 23.63
Fire hose and service cabinet
Suspended unit heater
Unit control cubicle
Distribution board
El. 11.50
El. 10.50
Unit No.6 only
El. 10.75
Pump gallery crane
Hatch
Roadway El. Varies
H.W.S. El. 10.00
Mean W.S. El. 4.00
L.W.S. El. -1.00
Motor cooling water pump
Pipe gallery El. -3.25
Air vent
℄ El. 0.00
Lighting recess
By-pass line
Manhole
El. -12.00
Casing drain
Discharge pipe drain header.
El. -17.75
Drainage header
El. -18.10
El. -18.85
Unwatering header
Drainage header
Timber piles
EXPLANATION
First stage concrete
Second stage concrete
5 0 5 10 20
SCALE OF FEET
TRANSVERSE SECTION THRU UNIT

Figure 7. Typical cross section

instrument transformers in the motor leads. The desired terminal voltage is selected by adjusting the powerstat and essentially the equipment operates to maintain this voltage from signals received from the comparison network. It is designed to maintain voltage within 0.5 per cent of the setting.

Auxiliary Equipment

Motor Protective Equipment

Each motor is provided with surge protective equipment consisting of heavy duty station-type lightning arresters and surge-protective capacitors. This equipment is connected to the main motor leads and is mounted in a cubicle installed adjacent to the motor. Also included in this cubicle are instrument transformers for metering and relaying, potheads for terminating the main motor supply cables, and necessary bus to connect to the motor main leads.

Neutral Grounding Equipment

The neutral of each motor is grounded through a current-limiting reactor of the single-phase, indoor, dry type. These reactors are rated at 0.37-ohm impedance, and have a thermal current rating of 7,500 amperes for 1 minute. Each reactor is enclosed in a metal housing and installed adjacent to its respective motor. This equipment and that described in the preceeding paragraph was furnished by the General Electric Company.

Power Supply, Switching, and Cables

Figure 8 shows the single-line diagram of the pumping plant and associated part of the Tracy Switchyard. Power for the operation of the pump motors will be supplied from the switchyard, through circuit breakers connected to the 13.8-kv bus. Located in the switchyard and connected to the same bus is a 50,000-kva synchronous condenser. The motor supply cables are connected to the bus through oil circuit breakers. These circuit breakers are rated 1,500,000-kva, 15,000 volts, 2,000 amperes. From these circuit breakers, insulated cables lead through a tunnel and bridge to the individual motors, an average run of approximately 1,000 feet. There is one cable per phase. The cables are 1,250,000-circular mil, single-conductor, solid-type,

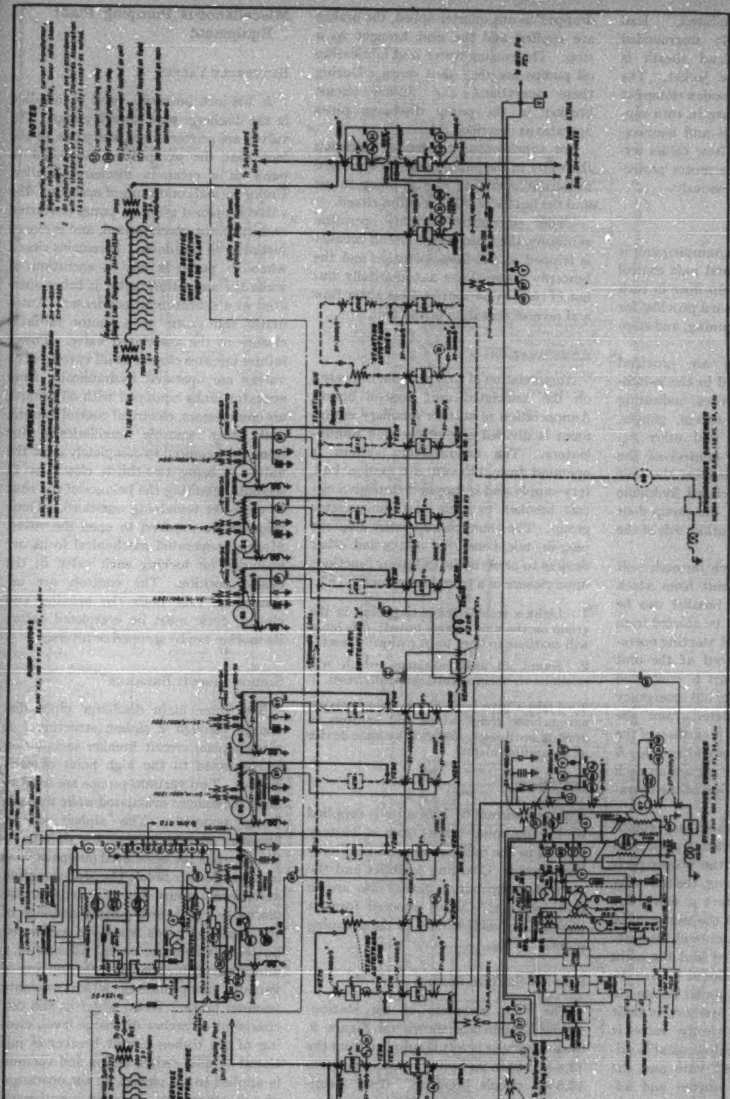

NOTES
REFERENCE DRAWINGS
PUMP MOTORS
STARTING BUS
SYNCHRONOUS CONDENSER

Figure 8. Tracy Pumping Plant single-line diagram

impregnated paper-insulated, lead sheathed for 15,000-volt ungrounded neutral service. The lead sheath is covered with a neoprene jacket. The cables are supported on wooden clamps at 30-inch intervals, which are in turn supported on a suitable steel and nonmagnetic metal structure. These cables terminate in potheads at the motor protective cubicles described previously.

CONTROL

Normal control of each pumping unit is centralized in its associated unit control board located on the pump floor in each main unit bay. A unit board provides for normal pump starting, running, and stopping.

Limited controls also are provided at the main control board in the switchyard. The control switches, indicating instruments, protective relays, gauges, annunciator equipment, and other devices necessary for the control of the pumping units are located on the unit control boards and associated hydraulic gauge boards located on the pump floor in each main bay on the intake side of the plant.

A master control switch on each unit board determines the point from which the main motor circuit breaker can be closed. The unit cannot be started from the switchyard until most starting operations have been completed at the unit board. Normal shutdown is controlled only from the unit boards, but emergency shutdown can be initiated from the switchyard control board regardless of the position of the master control switch. A motor-condenser transfer switch on each unit board permits selection of the operation desired.

Assuming main and auxiliary equipment in normal and operating conditions and control switches in the proper position preparatory to starting, the following procedure is used to start a motor for pumping operation from the unit control board: The cooling water and lubricating oil pumps are started and the main motor circuit breaker is closed. After the motor has synchronized under automatic control and scroll-case pressure is built up to normal, the butterfly valve is opened. The exciter field rheostat is adjusted to obtain desired vars and the "Regulex" exciter set started and adjusted to zero output and then placed in voltage control operation.

Normal shutdown procedure consists in closing the butterfly valve; adjusting the voltage regulator to zero output and taking it out of service; and tripping the main circuit breaker. After the speed has dropped to one-quarter speed, the brakes are applied and the unit brought to a stop. The cooling water and lubricating oil pumps are then shut down. During these operations, the siphon circuit breaker in the pump discharge pipes operates as described later.

For synchronous condenser operation the water in the pump casing is depressed to permit operation of the pump in air and the butterfly valve remains closed.

Under emergency or relay operation shutdown the main motor circuit breaker is tripped as the first operation and the butterfly valve closes automatically but not in time to prevent reverse water flow and reverse operation of the unit.

ANNUNCIATION

Annunciation of unit trouble is located on the associated unit control board. Annunciation of station auxiliary equipment is divided among the unit annunciators. The annunciation system is operated from 125-volt d-c station battery supply and is supplied through a circuit breaker to each unit annunciator group. The annunciator system employs plug-in, telephone-type relays and other devices to perform the following functions upon closure of a trouble contract:

1. Light a trouble indicating lamp in the group on the unit control board; this lamp will continue to burn until manually reset.
2. Sound an audible alarm, which will continue to operate until manually reset.
3. Light a pilot lamp above the associated annunciator group, which will continue to operate until reset. Reset is by same device as for audible alarm.

D-C SYSTEM

Direct current at 125 volts is supplied to the pumping plant from a battery located in the control house in the Tracy Switchyard. Charging facilities and the main d-c distribution board also are in that location. Cables proceed from it through the cable tunnel to the pumping plant.

STATION-SERVICE SYSTEM

The main elements of the station-service system are shown on Figure 9. Station-service power is supplied from the 13.8-kv bus in the switchyard through two 13.8-kv circuit breakers. Two 3-conductor number 6 cables lead from these circuit breakers in the switchyard through the cable tunnel terminating in a double-ended, 1,500/1,874-kva, 3-phase 14,400- to 480-volt load center unit substation, located in the cable gallery on the downstream side of the plant.

Miscellaneous Pumping Plant Equipment

BUTTERFLY VALVES

A 108-inch butterfly valve is installed in the discharge pipe of each pump. The valves are primarily necessary due to the fact that the pumps are connected in pairs to a common discharge header. Under normal conditions of operation, the valve is opened after its pump is started and its motor synchronized, and is closed just prior to shutdown. It remains closed when its pump is not in operation or while the associated motor is being operated as a synchronous condenser. Automatic shut-down of a motor initiates closure of the associated valve. Power failure initiates closure of all valves. The valves are operated hydraulically from actuator tanks equipped with oil pumps, air compressors, electrical control system, and other suitable auxiliaries. One minute is required to completely close the valve, it being two-thirds closed in 14 seconds, requiring the balance of the time to close the remaining one-third. Three minutes are required to open the valve. Manually-operated mechanical locks are provided for locking each valve in the closed position. The controls are arranged so that both the opening and closing cycle must be completed before its motion can be stopped or reversed.

SIPHON CIRCUIT BREAKER

The three main discharge pipes discharge through a siphon structure. A single-siphon circuit breaker installation is connected to the high point of each siphon. Two vacuum pumps are used to keep the siphons evacuated while water is being pumped. The siphon circuit breakers operate to vent the siphons to the air when the associated pumps are not in operation to break the siphon action and prevent return flow of water from the discharge canal, and permit draining of the discharge pipes when the associated butterfly valves are open. Closing of a motor circuit breaker initiates starting of vacuum pump motors which evacuate vacuum tanks. When water in the discharge pipe reaches discharge level, closing of the siphon circuit breaker is initiated by float switch action and vacuum is applied to the siphon by the operation of suitable valves. Vacuum is automatically maintained in the tanks between 16 and 24 inches of mercury by the operation of pressure switches. A siphon circuit breaker opens when the last pump of an associated pair is shut down through auxiliary contacts on the motor circuit

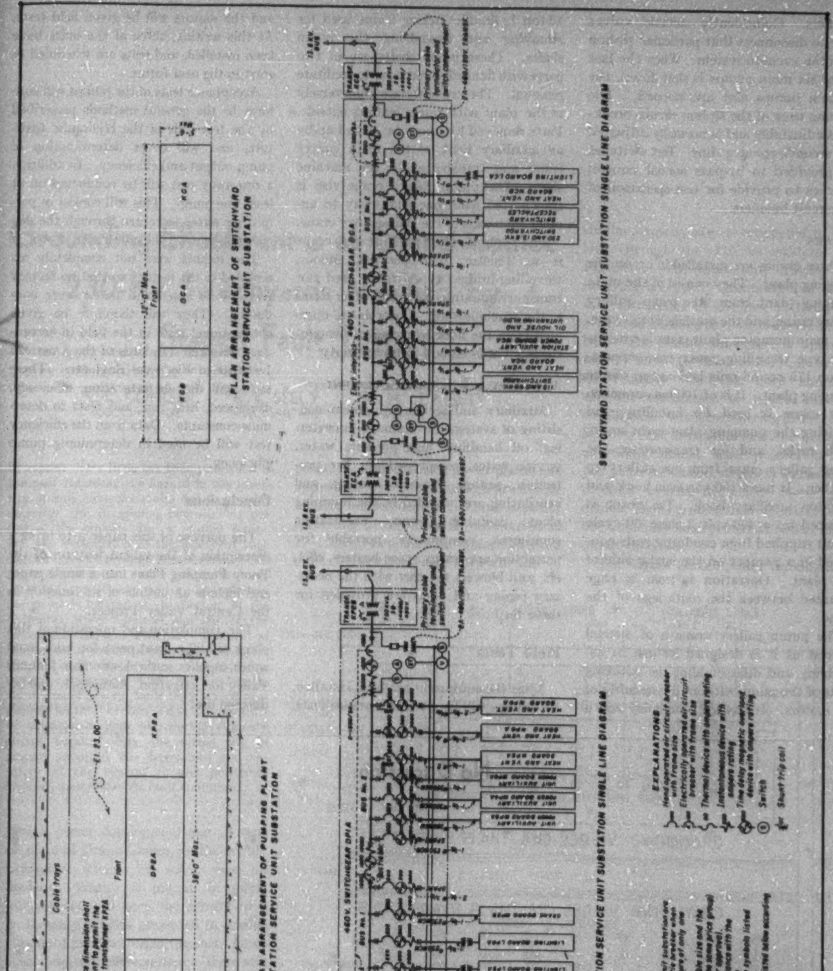
PLAN ARRANGEMENT OF SWITCHYARD STATION SERVICE UNIT SUBSTATION
SWITCHYARD STATION SERVICE UNIT SUBSTATION SINGLE LINE DIAGRAM
460V. SWITCHGEAR OGA
PLAN ARRANGEMENT OF PUMPING PLANT STATION SERVICE UNIT SUBSTATION
PUMPING PLANT STATION SERVICE UNIT SUBSTATION SINGLE LINE DIAGRAM
460V. SWITCHGEAR DPIA
EXPLANATIONS
NOTES

Figure 9. Station-service system single-line diagram

breakers. Coincidently suitable valves close to disconnect that particular siphon from the vacuum system. When the last of the six main pumps is shut down, the vacuum pumps also are stopped. The opening time of the siphon circuit breakers is adjustable and is normally adjusted to 2 seconds opening time. Test switches are provided to by-pass normal control switches to provide for test operation of the circuit breakers.

CRANES

Three cranes are installed in or on the pumping plant. They consist of the main pumping plant crane, the pump gallery gantry crane, and the machine shop crane. The main pumping plant crane is an outdoor type, travelling, gantry crane operating on 175 pound rails laid on top of the pumping plant. It is of 100-ton capacity. This crane is used for installing and servicing the pumping plant main units, trash racks, and for transporting the pump gallery crane from one gallery to another. It has a 100-ton main hook and a 20-ton auxiliary hook. The crane is operated on a 440-volt 3-phase 60-cycle circuit supplied from conductor rails concealed in a parapet on the intake side of the plant. Operation is from a cage mounted between the south legs of the crane.

The pump gallery crane is of special interest as it is designed for use in assembling and disassembling the rotating parts of the pump without disassembly of the motors. It has a 21-ton hoist and a 40-ton hydraulic jacking frame used for removing and assembling the pump shafts. These pump shafts are in two parts with flanged connections to facilitate removal. The crane travels transversely of the plant with tracks leading outside. Parts removed by it may be picked up by an auxiliary hook of the main gantry crane and transported to the machine shop. The pump gallery crane also is transported from one pump bay to another by means of the main gantry crane.

The pumping plant machine shop crane is a 3-motor floor-operated, indoor, travelling-bridge type crane used for transporting pump parts and other items in the machine shop. Controls are operated from the floor by means of pendant cords. The hoist is of 25-ton capacity.

AUXILIARY AND SERVICE EQUIPMENT

Auxiliary and service equipment consisting of systems for drainage, unwatering, oil handling, high pressure water, service water, compressed air, fire protection, sewage disposal, heating, and ventilating are provided in the pumping plant. Suitable pumps, purification equipment, compressors, portable fire protection apparatus, space heaters, coolers, and blowers together with the necessary piping and ducts are provided for these facilities.

Field Tests

After the equipment has been installed, the pumps will be given acceptance tests, and the motors will be given field tests. At this writing, three of the units have been installed, and tests are scheduled to start in the near future.

Acceptance tests of the pumps will conform to the general methods prescribed by the test code of the Hydraulic Institute, and will cover determination of pump output and efficiency. In addition a run-away test will be conducted on at least one pump. This will consist of permitting water to return through the discharge pipe with the motor shut down.

The motors were not completely assembled in the factory so that no factory tests of an assembled motor were conducted. They will therefore be given conventional tests in the field in accordance with the standards of the American Institute of Electrical Engineers. These tests will include saturation, efficiency, overspeed, heat run, and tests to determine constants. Data from the efficiency test will be used in determining pump efficiency.

Conclusions

The purpose of this paper is to bring a description of the salient features of the Tracy Pumping Plant into a single paper and include an outline of its function in the Central Valley Project.

The completion and operation of this plant will fill a great need for additional water supplies in the lower San Joaquin Valley for irrigation, municipal, and industrial use.

No Discussion

Grounding Effectiveness at Grand Coulee 230-Kv Switchyards Verified by Staged Fault Tests

A. C. CONGER
ASSOCIATE AIEE

R. K. SEELY
ASSOCIATE AIEE

W. H. CLAGETT
MEMBER AIEE

Synopsis: Very little has been published in the past regarding the hazard to the integrity of long control circuits due to possible excessive rise in ground potential at one end of the circuits during station faults; and the verification of the safety of such control circuits through actual tests. This paper describes the rather unique arrangement at Grand Coulee power plant wherein the plant is located at the bottom of the Columbia River Channel and one of the associated 230-kv switching stations is located on a rocky plateau approximately 600 feet higher in elevation, thus requiring control cables over 4,000 feet in length. By means of several fault tests staged specifically for this purpose, and as a by-product of subsequent high-interrupting capacity circuit breaker tests, the actual rise in ground potential was determined and the safety of the control circuits positively verified, under 60-cycle fault conditions.

THE power development and physical plant at Grand Coulee, on the mighty Columbia River, 93 miles west of Spokane, Wash., is unique in many features and has been the subject of a great many articles presented in a wide variety of publications in the past. However, despite such prominence, there still remains many interesting and important engineering aspects of this great project which have been inadequately covered.

From the electrical engineer's viewpoint, the Grand Coulee power plants and appurtenant switching stations are unique in that unprecedented machine capacity consisting of an ultimate installation of 17 120,000-kva units is connected to a single 230-kv bus, and an 18th unit of similar capacity also is connected to this bus through the 115 kv system, see Figure 1. All main unit transformer neutrals are solidly grounded and there are no reactors in the bus to limit the available short-circuit current values to below the possible maximum of approximately 15,000,000 kva, which is, however, theoretically attainable only under a certain combination of several adverse conditions. When considering probability factors, such as routine machine outages, overhead ground wire protection adjacent to the station, degree of asymmetry of fault current, decrement factor, and others, faults greater than about 12,000,000 kva may be expected at rather infrequent intervals.

The Grand Coulee power development

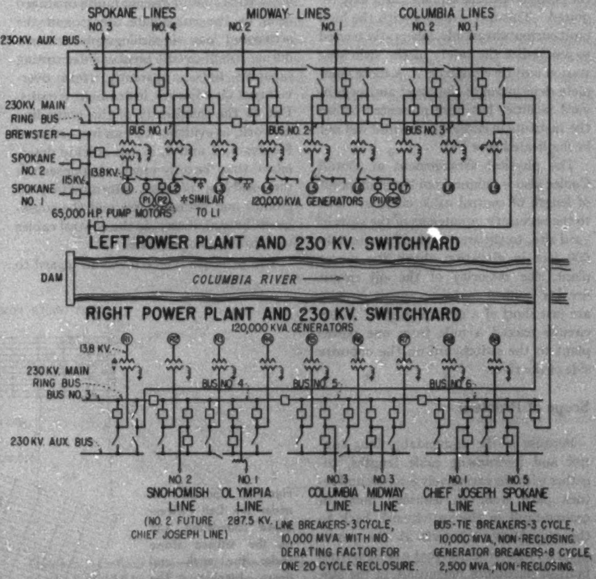
SPOKANE LINES
NO. 3
NO. 4
MIDWAY LINES
NO. 2
NO. 1
COLUMBIA LINES
NO. 2
NO. 1
230KV. AUX. BUS
230KV. MAIN RING BUS
BUS NO. 1
BUS NO. 2
BUS NO. 3
BREWSTER
SPOKANE NO. 2
115KV.
SPOKANE NO. 1
13.8KV.
L1
L2
L3
L4
L5
L6
L7
L8
L9
P1
P2
P11
P12
*SIMILAR TO L1
120,000 KVA. GENERATORS
65,000 H.P. PUMP MOTORS
LEFT POWER PLANT AND 230 KV. SWITCHYARD
DAM
COLUMBIA RIVER
RIGHT POWER PLANT AND 230 KV. SWITCHYARD
120,000 KVA. GENERATORS
R1
R2
R3
R4
R5
R6
R7
R8
R9
13.8 KV.
230 KV. MAIN RING BUS
BUS NO. 3
BUS NO. 4
BUS NO. 5
BUS NO. 6
230 KV. AUX. BUS
NO. 2 SNOHOMISH LINE
(NO. 2 FUTURE CHIEF JOSEPH LINE)
NO. 1 OLYMPIA LINE
287.5 KV.
NO. 3 COLUMBIA LINE
NO. 3 MIDWAY LINE
NO. 1 CHIEF JOSEPH LINE
NO. 5 SPOKANE LINE
LINE BREAKERS-3 CYCLE, 10,000 MVA. WITH NO DERATING FACTOR FOR ONE 20 CYCLE RECLOSURE.
BUS-TIE BREAKERS-3 CYCLE, 10,000 MVA., NON-RECLOSING.
GENERATOR BREAKERS-8 CYCLE, 2,500 MVA., NON-RECLOSING.

Figure 1. Single-line diagram of the Grand Coulee 230-kv ring bus, with 18 120,000-kw generators, 12 ultimate 230-kv transmission lines and the lesser important 115-kv installation

---

Paper 51-290, recommended by the AIEE Protective Devices Committee and approved by the AIEE Technical Program Committee for presentation at the AIEE Pacific General Meeting, Portland, Oreg., August 20-23, 1951. Manuscript submitted May 21, 1951; made available for printing July 11, 1951.

A. C. CONGER, R. K. SEELY, and W. H. CLAGETT are all with the United States Bureau of Reclamation at Bismarck, N. D., Coulee Dam, Wash., and Denver, Colo., respectively.

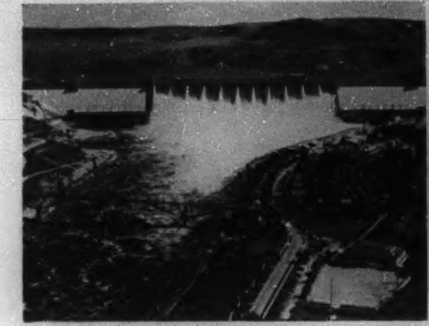

Figure 2. Aerial view of the 4,300-foot Grand Coulee Dam, with duplicate power plants on either end of the 1,650-foot spillway

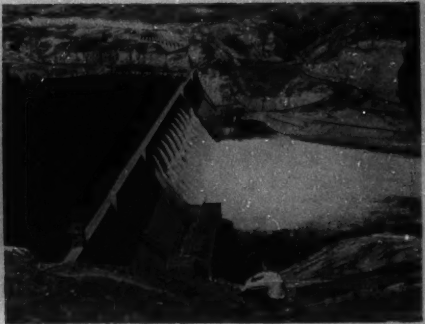

Figure 3. View of the Right Powerhouse in the foreground, Left Powerhouse in the center background, and the Left Switchyard at the extreme top

also is rather unique in that, as in the case of the Hoover power plant, the high-voltage switching facilities on the west bank of the river are located on a relatively high rocky plateau with inherently poor ground resistance characteristics, see Figure 3. Because of the proximity of well-drained bedrock, driven ground rods were infeasible, and long ground leads to the powerhouse and tailrace mats were required. This fact, coupled with the high fault currents available, inherently tended to jeopardize the safety of the switching station and its equipment. A more complete description of the plant and switchyard facilities has been presented before the Institute in earlier papers and will not be duplicated here.[1,2,3]

The physical arrangement at Grand Coulee also is unique from the standpoint of length of control cable circuits. Due to the necessary remoteness of the switchyard site, to the west and approximately 600 feet in elevation above the power plant, the majority of the oil circuit breaker control and instrument circuits are just short of a mile in length. A few circuits exceed a mile from one power plant to the switchyard on the opposite side of the river.

Scope of Problem

Because of the unavoidably long control and instrument cable lengths, together with the excessively long ground return path from an assumed point of ground-fault in the switchyard, back to the transformer neutrals at the power plant, it was conceived that a solid ground fault of maximum magnitude in the station might cause an impedance drop in this ground return of sufficient magnitude to raise the whole switchyard ground potential to a point which would threaten the insulation on the control cables or the associated equipment wiring. Also, of considerable concern were the occurrence of several unexplained trip-outs of circuit breakers during system trouble; the undesirable but unavoidable ringing of local subscriber's telephone bells simultaneously with system ground faults or staged tests in the immediate area; and the occasional loss of oscillograph elements during recent circuit breaker interrupting capacity tests, apparently from overvoltages on adjacent instrument circuits. Due to the complexity of the grounding network, as evidenced by an inspection of Figures 4, 5, and 6, it was quickly determined that the only practical approach to the problem of the determination of ground mat potential rise and the consequent hazard, if any, to the control cables was through staged tests.

The principal concern was in regard to heavy 60-cycle fault currents of possibly several cycles duration, for which ground-return impedance values were not available. With reference to steep-front lightning surges, the surge impedance of the bus is reduced to a relatively low value due to the multiplicity of 17 transformer circuits, 2 trans-river tie circuits and 12 outgoing lines, all terminating on the Coulee 230-kv ring bus. A lightning arrester is located at each power transformer at the termination of each of the 17 transformer circuits. Difficulties from overvoltages from lightning surges are not anticipated; however, if a flashover should occur in the switchyard, the surge current and associated voltage would tend to quickly dissipate through multiple paths, such as the double ground wires over each of the above 230-kv circuits, as well as into the station ground. As a matter of fact, since the addition of several new 230-kv outgoing lines and transformer circuits in recent years,

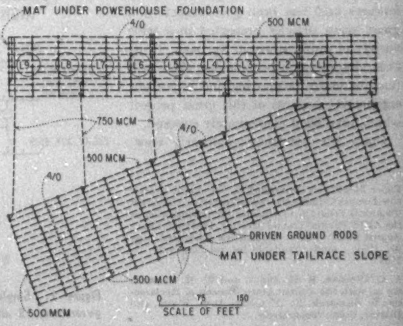

Figure 4. Ground mat under the Left Powerhouse foundation and on the tailrace slope under the earth and riprap blanket. The Right Powerhouse mat is of similar construction

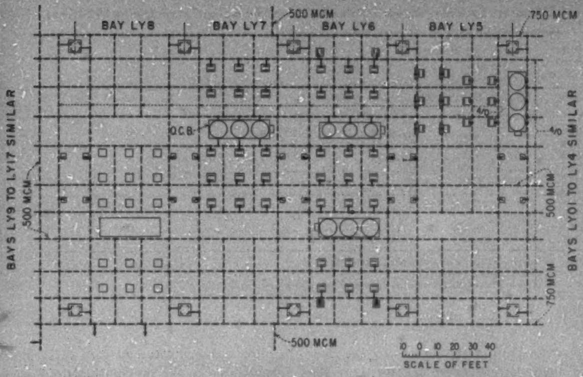

Figure 5. Typical section showing grounding details in four of the nineteen 230-kv bays of the Left Switchyard

lightning arrester operations as recorded on special counters, have actually decreased markedly. Therefore, as stated above, this paper will deal only with the investigation of possible overvoltage hazards incidental to 60-cycle ground faults within the 230-kv switchyards.

Test Objectives

The principal test objective was to determine through staged faults the ground mat potential rise at several representative points on the grounding system, as shown in Figures 6 and 8, using a main-unit generator isolated from the system. In an attempt to ascertain the worst possible condition, and as a cross-check between tests, faults were applied at several locations. Also, for the same reason, generators in both power plants were utilized as a source of fault current. Examination of the resulting data then revealed the most unfavorable set of conditions and permitted the extrapolation of the test potentials to values corresponding to that which would have been obtained, had the full compliment of 18 main unit generators and interconnection with the power system been used. From these values, direct comparisons with the control cable and equipment wiring insulation level then made the degree of hazard quite evident. All control and instrument cable at Grand Coulee is rated 600 volts, and is given a 1-minute high-potential test at 1,500 volts, direct current, after installation and splicing.

From a purely academic viewpoint, and because of the relative ease of determination, a secondary objective of the test was to determine the relative proportion of fault current returning to the transformer neutral via the transformer circuit counterpoise route, as indicated in Figure 6, as compared with that portion returning through the more direct route and through other parallel paths. Also, such information indicated the apparent effectiveness of a solid connection at this point between these two ground returns, with reference to the limiting of the potential rise of the switchyard ground mat.

Test Outline

Point of Fault Application

In general, to assure test data as conclusive as possible, consistent with the limited number of tests available, the test program included ground faults in both the Right and Left Switchyards, using generators in both the Right and Left Powerhouses. The initial test series performed on June 7, 1950, consisted of three faults with an arrangement as shown in Figure 8(A), as follows: (a) Single generator in the Left Powerhouse supplying fault current to a bolted fault in the Left Switchyard, (b) single generator in the Right Powerhouse supplying fault current to a ground in the Left Switchyard, on the opposite side of the river, and (c) a single generator in the Right Powerhouse supplying fault current to a ground in the Right Switchyard. The second test series conducted on the following weekend, June 15, 1950, Figure 8(B), consisted of a single fault with an arrangement similar to (a) above, except that all instrumentation was moved from the Left Switchyard to the Left Powerhouse, as a verification test for possible inductive pickup effects in the instrument leads. Spare lead-covered control cables in an underground cable tunnel were used for the potential circuits, with the exception of the circuit between powerhouses, through Grand Coulee Dam. Rubber-covered nonshielded cable was the only

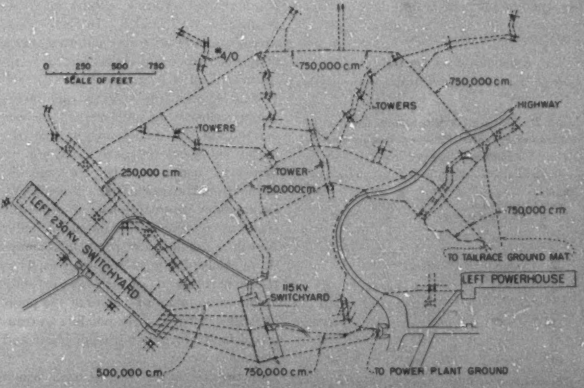

Figure 6. General grounding plan on the West bank of the Columbia River, for the Left Powerhouse, Left 115-kv and 230-kv Switchyards, and for the tower footings on the ten 115-kv and 230-kv generator circuits. This paper is principally concerned with the difference in ground potentials between the mats shown on this drawing

Table I. Summary of Test Values of Potential Differences Between Various Points on Coulee Grounding System During 1950 Tests

Test No.	Reference Fig. No.	Fault Current Source	Ground Fault Location	Fault Current Rms Sym Component, Amperes	Rms Symmetrical Component of Ground Mat Potentials—Volts*											
					E_1	E_2	E_3	E_4	E_5	E_6	E_7	E_8	E_9	E_{10}	E_{11}	E_{12}
1	8(A)	Left Powerhouse**	LSY-LY8	731			1.82	0.00	1.84	1.76	0.43					
2	8(A)	Right Powerhouse**	LSY-LY14	728	1.78	0.05	1.31	1.85	1.36	1.08		0.42				
3	8(A)	Right Powerhouse**	RSY-X1	760	4.35	0.00	0.00	4.36	0.00	4.05		0.00				
4†	8(B)	Left Powerhouse**	LSY-LY8	724		0.00	2.09		2.01				6.50			
5	8(C)	Left Powerhouse**	LSY-LY10	411	1.94	1.64										
6	8(C)	Left Powerhouse**	LSY-LY10	413	2.4	2.3										53.9
7	8(C)	8 Gen on system	LSY-LY10	5,280	15.6	22.6								22.9	6.8	512.0
8	8(C)	8 Gen on system	LSY-LY10	5,280	14.0	21.7								21.3	6.8	505.0
9	8(C)	12 Gen on system	LSY-LY10	7,000	18.9	29.2								27.9	8.5	687.0
10	8(C)	12 Gen on system	LSY-LY10	7,000	17.9	28.3								22.9	8.5	‡

* See reference Figure 8 for location of potentials obtained between various points on grounding system.

** Fault current supplied by single 120,000-kva generator isolated from the system.

† Instrumentation located at left powerhouse on Test 4. On all other tests, instrumentation was at left 230-kv switchyard.

‡ Measurement discontinued for safety of instrument circuits.

type of cable available for these circuits. Single generators were utilized as the power source for the above tests for operating reasons, and to facilitate the interpretation of the results, as related to the ultimate 18-unit plant development.

A third test series was performed on August 20, 1950, Figure 8(C), by taking advantage of an opportunity afforded by the high interrupting capacity circuit breaker tests, recently reported before the Institute.[3] However, due to the multiplicity of generators in both plants, together with fault current feedback from several connected transmission lines, on Tests Number 7 to 10, inclusive, the interpretation of these results in relation to what would be expected of the ultimate 18-unit plant is a little more obscure. These final higher-current tests were not without value, however, as they did furnish general verification of the results obtained on previous tests.

POTENTIAL MEASUREMENTS

The impedance potential drops, or change in relative elevations of potentials between ground mats, due to the flow of fault current, were measured at the various points indicated in Figures 8(A), 8(B), and 8(C). It is to be noted that in the first four tests, and more particularly during the subsequent high-current circuit breaker tests, several local measurements were obtained within the Left Switchyard and the area immediately adjacent to the test circuit breaker. This special study, aside from the principal problem, was prompted by a history of unexplained losses of oscillograph elements during earlier circuit breaker tests, apparently from stray overvoltages on the grounded instrument leads.

Table II. Theoretical Maximum Differential in Ground Potential Between Coulee Switchyards and Power Plants*

Reference Test No.	Reference Figure No.	Volts E_1	Volts E_3	Volts E_{10}
1	8(A)		94.6	
2	8(A)	92.9	68.4	
3	8(A)	217.5	0.0	
4	8(B)		109.7	
5	8(C)	179.4		
6	8(C)	221.8		
7	8(C)	112.3		164.8
8	8(C)	100.7		153.3
9	8(C)	102.6		151.5
10	8(C)	97.2		124.3

* Corresponds to faults involving ultimate plant and system capacity, as estimated by applying the ratio of ultimate fault current to test current, to applicable test potentials E_1, E_3, and E_{10} of Figure 8 and Table I. Due to fault current path configuration, above ratio not applicable to other test potentials.

RELAYING AND INSTRUMENTATION

All tests were conducted with normal voltage on the 230-kv bus and the single-line-to-ground faults were applied by closing a 230-kv oil circuit breaker into a solidly-bolted ground, except in Tests Number 5, 6, 7, and 8. In these cases, arcing-ground faults were initiated over a string of suspension insulators, as a requirement of the circuit breaker tests. For the isolated June 1950 tests, Numbers 1 to 4, inclusive, an overcurrent relay was set to clear the staged fault in approximately 28 cycles (60-cycle basis) and all values of current and voltage were obtained from the oscillograms immediately before fault interruption, and represent the rms symmetrical component only. As will be noted below, in the final analysis a multiplying factor was used to translate these single-unit steady-state values into maximum values at the point of fault initiation, corresponding to computed fault currents with full plant and system capacity.

In the case of the August tests, which were conducted principally as circuit breaker performance tests, the faults were cleared by fast relay operation in less than 3 cycles. Here again, the symmetrical component only was read from the oscillograms, due to the random nature of the degree of offset; and as the initial increase due to transient and subtransient machine reactance had largely disappeared at the time of fault clearing, on these particular tests, the same multiplier was considered sufficiently accurate for this purpose.

Test Results

The test results are summarized in Figures 8(A), 8(B), and 8(C) and Tables I, II, and III. Tests 1 to 6, inclusive, were performed with only one source of generation and therefore the resulting tabulated ground mat potentials, when referenced back to the transformer neutral point at the powerhouse, are truly representative of the impedance drop in the composite cable and earth ground return, due to the flow of fault current between the switchyard ground mat and the transformer neutral at the powerhouse ground mat. It therefore follows that, except for a negligible amount of inductive coupling in the paralleling control circuits, the difference in ground and associated equipment frame potentials at the two reference locations will appear as voltage stress on the interconnecting control cables and equipment wiring.

In contrast with the single-unit tests, the remaining Tests 7 to 10, inclusive,

Table III. Calculated Ground Return Neutral Impedance

Test No.	60-Cycle Impedance Calculated between	Z = E/I Ohms
1	Left Switchyard and Left Powerhouse	0.00248
2	Left Switchyard and Right Powerhouse	0.00254
3	Right Switchyard and Right Powerhouse	0.00572
4	Left Switchyard and Left Powerhouse	0.00288

Figure 7. Left 230-kv Switchyard located on rock outcropping approximately 600 feet above the powerhouse

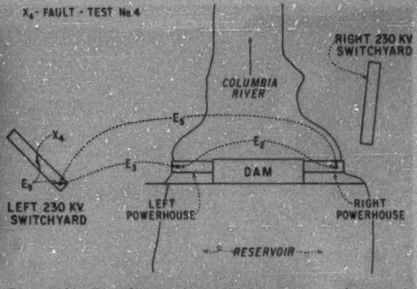
X₄ - FAULT - TEST No.4
RIGHT 230 KV SWITCHYARD
COLUMBIA RIVER
E₅
X₄
E₂
E₃
E₉
DAM
LEFT 230 KV SWITCHYARD
LEFT POWERHOUSE
RIGHT POWERHOUSE
RESERVOIR

Figure 8(A). Identification of potential measurements with respect to the various ground mats, as summarized in Tables I and II, obtained during the June 7, 1950 tests

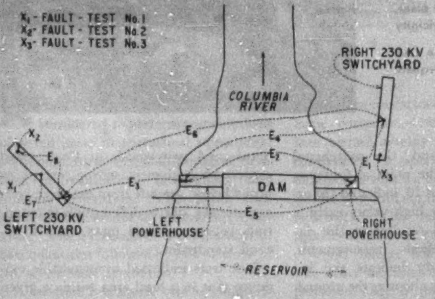
X₁ - FAULT - TEST No.1
X₂ - FAULT - TEST No.2
X₃ - FAULT - TEST No.3
RIGHT 230 KV SWITCHYARD
COLUMBIA RIVER
E₆
E₄
E₂
E₈
X₂
X₁
E₇
E₃
E₁
X₃
DAM
E₅
LEFT 230 KV SWITCHYARD
LEFT POWERHOUSE
RIGHT POWERHOUSE
RESERVOIR

Figure 8(B). Identification of potential measurements as summarized in Tables I and II, obtained during the June 15, 1950 tests

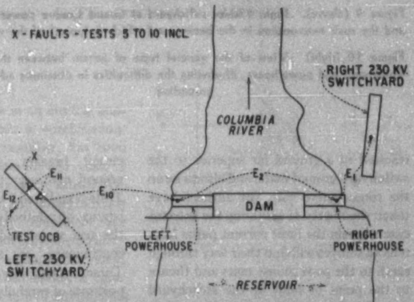
X - FAULTS - TESTS 5 TO 10 INCL.
RIGHT 230 KV. SWITCHYARD
COLUMBIA RIVER
X
E₁₁
E₁₂
E₁₀
E₂
E₁
DAM
TEST OCB
LEFT 230 KV. SWITCHYARD
LEFT POWERHOUSE
RIGHT POWERHOUSE
RESERVOIR

Figure 8(C). Identification of potential measurements as summarized in Tables I and II, obtained during the August 20, 1950 circuit breaker performance tests

performed on the Northwest Power Pool System, included a rather indeterminate contribution of fault current from remote grounded-Y transformer banks which did not result in a proportionate increase in the impedance potential difference between the powerhouse and switchyard ground mats. Therefore these tests are looked upon for general confirmation of previous isolated tests, at the higher currents otherwise unattainable by other means.

Consideration was given to possible errors in instrumentation due to inductive coupling between the excessively long oscillograph circuits and the fault current path. Lead covered, twisted, spare control cables were utilized wherever possible for instrument leads. Inasmuch as the primary single-phase fault current formed a closed loop from the main-unit transformer at the powerhouse via one of the 230-kv transformer circuits to the point of fault in the switchyard, and returned partially through the continuous copper path, Figure 6, and partially through earth; and inasmuch as the potential tap instrument circuit bridged the loop from one extreme end to the other, the induced voltages from the fault current flowing in opposite directions would tend to cancel in the instrument circuit. It was recognized, however, that the instrument circuit was somewhat more closely coupled with the ground return path than the line conductor, but due to the physical remoteness of both, any possible effects were considered negligible.

As stated previously, the currents and potentials shown in Table I are actual test values of rms symmetrical components only, as scaled from the oscillograms. Table II contains the same data except that the values of potential rise have been multiplied by the ratio of computed maximum ultimate fault current, divided by the actual test current, to obtain the maximum potentials possible under the condition of full plant and system capacity. The values thus obtained for the first half-cycle of fault current, properly represents the maximum possible voltage stress on the control circuits.

By way of further explanation, in extrapolating the data for the single-unit test condition to that which would be expected for the ultimate plant and connected system development, computation of the theoretical voltage rise resulting from a bus fault with contribution from all 18 units is a relatively simple matter from the basic test data available, but the additional portion of the voltage rise of the switchyard ground mat above the powerhouse mat, attributable to fault contribution from remote sources, is not readily computable without adequate information on the distribution of this return current. Lacking such information, and at the same time recognizing that the continuously submerged power plant and tailrace ground mats, Figure 4, and the miles of intricate and extensive mesh of 12-inch copper water-stop and grout-stop between the blocks in Grand Coulee Dam

Figure 9 (above). Right 230-kv switchyard at Grand Coulee power plant, and the rock outcropping in the background which is typical of the vicinity

Figure 10 (right). View of the general type of terrain between the Left Switchyard and powerhouse, illustrating the difficulties in obtaining adequate grounding

resulted in a ground far superior to the switchyard ground mats, and also to be on the conservative side, the authors have taken the liberty of assuming the extreme case wherein the fault current paths from remote sources will find their way through earth to the powerhouse mats and thence to the point of fault at the switchyard through the copper counterpoise and buried grounding circuits. Such fault current contribution from other large generating sources such as Chief Joseph Dam would, under this assumption, add directly to the impedance drop between the two mats in question. Such an assumption is admittedly rather extreme, but from the control circuit safety viewpoint as related to the basic purpose of this investigation, a more severe situation is not forseeable. The data presented in Table II was therefore prepared on this basis.

The measurement of the fault current flow from the Left Switchyard ground mat into the transformer circuit counterprise mat for Test Number 1 indicated that 41 per cent of the total fault current returned to the transformer neutral via this route; and Test Number 2 indicated 58 per cent returned via this route. The fault current source for Test Number 1 was a single unit in the Left Powerhouse and for Test Number 2 a single unit in the Right Powerhouse.

The difference in ground potential in the local area between the grounded test circuit breaker, and the switchyard ground mat near the point of fault, on Tests Numbered 5 to 10, indicated the existance of relatively high values early in the test series and resulted in the discontinuance of these measurements. These results clearly indicate the importance of carefully choosing the grounding point for oscillograph and instrument circuits during high-current fault tests, and the probability of relatively high potentials between adjacent circuits originating at different locations.

Conclusions

In conclusion, it has been demonstrated that the method of verifying the effectiveness of the grounding systems at the remotely located 230-kv switchyards at Grand Coulee, with respect to 60-cycle fault currents, by means of staged fault tests, is both feasible and convenient. The multi-unit and multi-line, heavy-current tests, utilizing the power system capacity, would not have necessarily been required as a part of the test, but the data obtained assisted in further substantiating earlier test results. The basic method of analysis presented in this paper is not, of course, applicable to investigations for lightning protection but may be indicative of conditions during a power-follow fault after flashover has occurred.

It may be safely concluded that the station control circuits between power plants and switchyards at Coulee, and associated equipment wiring, except as noted below, are safe from excessive voltage stresses, due to differentials in potentials between ground mats, from a 60-cycle standpoint.

The tests indicated unmistakable evidence that in a local area within a given switchyard, or within a specific area such as immediately adjacent to the special test circuit breaker during the August 1950 tests, undesirably high overvoltages do occur which may jeopardize the control circuits to that individual piece of equipment. This evidence appears to explain the loss of oscillograph elements on earlier high-capacity circuit breaker tests when instrument circuits were not all grounded at the same point.

References

1. Development of the 230-Kv Ring Bus for Grand Coulee Power Plant, C. L. Killgore, N. G. Holmdahl. *AIEE Transactions*, volume 67, 1948, pages 1369–78.

2. Interrupting Capacity Verification of 10,000,000-Kva, 230-Kv Oil Circuit Breakers for Grand Coulee Power Plant, A. F. Darland, W. H. Clagett, W. M. Leeds. *AIEE Transactions*, volume 70, 1951, pages 1386–97.

3. Field Tests at Grand Coulee Dam on 10,000-Mva, 230-Kv Low Oil Content Impulse Circuit Breaker, A. F. Darland, C. L. Killgore, E. B. Rietz, C. J. Balentine. *AIEE Transactions*, volume 70, 1951, pages 1377–85.

No Discussion

The Use of High-Speed Relays in Electric Analogue Computers

R. R. BENNETT
ASSOCIATE MEMBER AIEE

A. S. FULTON
NONMEMBER AIEE

ANALOGUE computers are usually considered to perform combinations of seven basic mathematical operations: addition, subtraction, multiplication, division, differentiation, integration, and function generation. This paper considers applications of a "comparison operation" which consists of a comparison of two quantities followed by one or more of the seven basic operations.

A selection is a simple type of comparison operation. For example, a system may operate such that when the output is positive, input A is selected; when the output is negative, input B is selected. Such an operation may be represented as comparison of the output with zero and addition of either A or B to the input, depending upon whether the output is greater than or less than zero.

Comparison operations, or operations involving logical choice, are quite familiar to digital computers. In fact, by addition of the comparison operation to the repertoire of an analogue computer the latter may be made to perform digital computations. In a sense then, an analogue computer so equipped is a more general instrument than its digital brother. It is capable of manipulating either continuous or discrete quantities.

A high-speed relay, driven by a high gain d-c amplifier, may be used to effect comparison operations in an electric analogue computer. Such a combination, here termed a relay amplifier, has been constructed to operate in less than 1 millisecond with an operating sensitivity, (limited by drift, hum, and noise) of a few millivolts. The relay amplifiers are polarity sensitive in that only one polarity of input voltage will operate the relay. The relay amplifier then makes a comparison of its input (or sum of inputs) and zero. The relay contacts effect the subsequent computing operations.

An interesting use of such relay amplifiers is for providing storage in an analogue computer. For example, one relay may be used to maintain a capacitor at a voltage $f(t)$. The disconnection of this relay from the capacitor at time t_0 stores $f(t_0)$ until some arbitrary later time when a second relay may be used to pick off $f(t_0)$. Such a scheme may be used in automatically computing an autocorrelation function for a continuously available noise source. In reality, storage is a special case of addition in that it consists of continuously adding the quantity zero to the stored variable.

The remainder of this paper considers the utilization of relay amplifiers to provide computer circuits whose output-

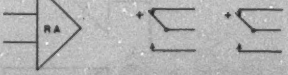

Figure 1. Symbol for a relay amplifier. Relay contacts connected as shown when the sum of the inputs is positive

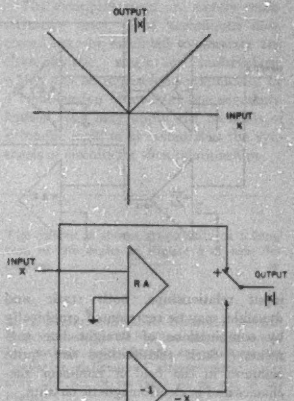

Figure 2. Circuit for generating the absolute value of an input

Figure 3. Circuit for simulating a limit stop

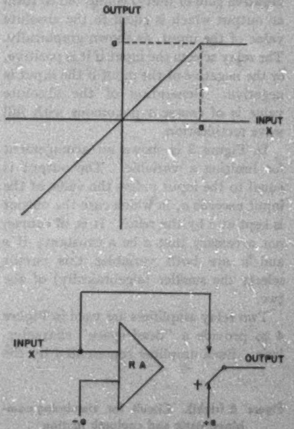

Paper 51-291, recommended by the AIEE Computing Devices Committee and approved by the AIEE Technical Program Committee for presentation at the AIEE Pacific General Meeting, Portland, Oreg., August 20–23, 1951. Manuscript submitted April 19, 1951; made available for printing July 11, 1951.

R. R. BENNETT and A. S. FULTON are with the Hughes Aircraft Company, Culver City, Calif.

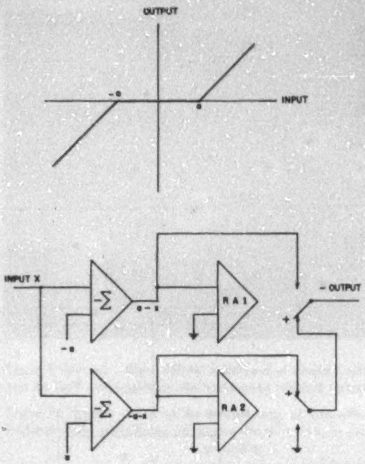
OUTPUT
-a
INPUT
a
INPUT X
-Σ
a-x
RA1
- OUTPUT
+
-a
-Σ
-a-x
RA2
+
a

Figure 4 (left). Circuit for simulating dead space

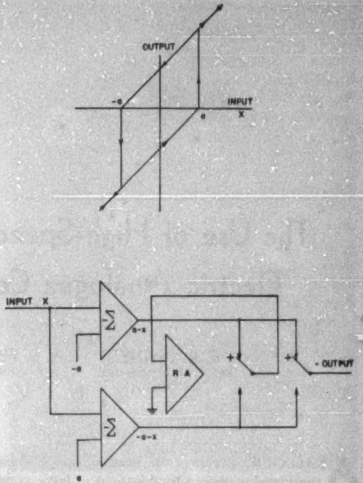
OUTPUT
-a
INPUT
X
a
INPUT X
-Σ
a-x
-a
RA
+
+
- OUTPUT
-Σ
-a-x
a

Figure 5 (right). Circuit for simulating "negative deficiency"

input relationships, both static and dynamic, may be represented graphically by combinations of straight line segments. Such relationships are quite common in the field of nonlinear mechanics and in electromagnetic circuits.

The symbol used here for a relay amplifier is shown in Figure 1. The relay armatures are in the position shown when the sum of the amplifier inputs is positive. The armatures switch to the opposite terminals when the sum of the amplifier inputs is negative.

Figure 2 shows a relay amplifier and inverting amplifier (an amplifier having a negative gain of unity) connected to form an output which is equal to the absolute value of the input, as shown graphically. The relay selects the input if it is positive, or the negative of the input if the input is negative. Generation of the absolute value is of course synonomous with full wave rectification.

In Figure 3 is shown an arrangement for limiting a variable. The output is equal to the input unless the value of the input exceeds a, in which case the output is kept at a by the relay. It is, of course, not necessary that a be a constant; if x and a are both variables this circuit selects the smaller (algebraically) of the two.

Two relay amplifiers are used in Figure 4 to provide a "dead space" characteristic. Each amplifier represented by the symbol $-\Sigma$ provides an output equal to the negative of the sum of its inputs. (Such amplifiers are common in analogue computers.) In the region $-a<x<a$ the relays select ground or zero output.

A characteristic sometimes called "negative deficiency" is shown graphically in Figure 5. It is a double-valued function in the region $-a<x<a$, and the jumps occur in traversing the loop in the direction shown. The accompanying circuit holds $x+a$ as the output whenever it

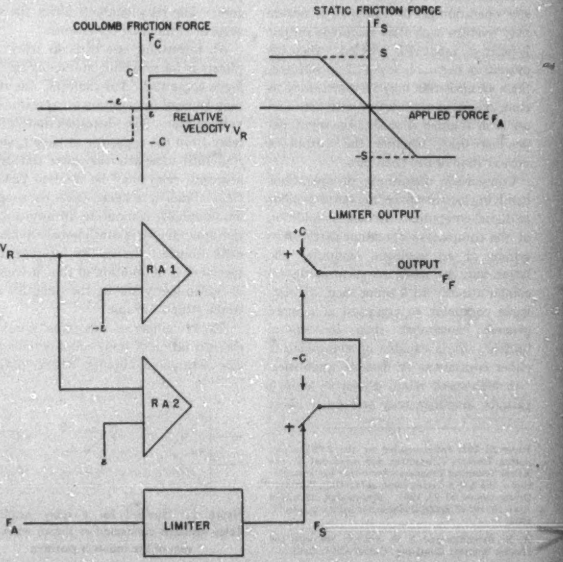
COULOMB FRICTION FORCE
F_C
C
-ε
ε
RELATIVE VELOCITY V_R
-C
STATIC FRICTION FORCE
F_S
S
APPLIED FORCE F_A
-S
LIMITER OUTPUT
+C
+
OUTPUT F_F
V_R
RA1
-ε
RA2
ε
-C
+
F_A
LIMITER
F_S

Figure 6 (right). Circuit for simulating combined static and coulomb friction

Vol. 1951

is positive and switches to $x-a$ when $x+a$ becomes negative ($x-a$ is held as long as it is negative).

It is sometimes necessary, in studies involving sliding surfaces, to include both static and Coulomb friction effects. The phenomenon of chattering, for instance, requires such inclusion. By way of example, consider the friction force between a surface and a block resting (or sliding in one dimensional translation) thereon. When the block is stationary with respect to the surface, the static friction force, F_S, (see Figure 6) is equal and opposite to the sum, F_A, of the other forces applied to the block. (In the case where both sides of the interface are in motion, F_A may include an inertial force). When F_A exceeds, in absolute magnitude, the threshold, S, corresponding to static friction, the block will begin to slide. While the block is sliding, the Coulomb friction force, F_C, is $\pm C$, the sign depending on the direction of the relative velocity between the block and the surface. C, the magnitude of the Coulomb friction force, is less than S. C and S are here assumed constant. Whenever V_R, the relative velocity is not zero, the relays in the circuit of Figure 6 select $\pm C$ for the friction force, F_F, (ϵ represents a small voltage chosen to be slightly greater than the drift and noise at the relay amplifier input). When V_R is zero, (strictly, when $\epsilon < V_R < \epsilon$) the output, F_S, of a limiter circuit is chosen for F_F. The limiter is shown, for simplicity, as a single circuit element rather than a collection of relay amplifiers or diode limiters.

Many of the foregoing transfer characteristics, and others, can be simulated very simply by using diodes. However, the "softness" of diodes makes them unsatisfactory for many computer applications.

The relay is a "hard" device, and its delay time is negligible when considered in relation to the upper frequencies of interest in computations on a slow speed analogue computer such as an electronic differential analyzer.

The examples given are merely representative ones. The techniques illustrated may be extended to simulate any characteristic, single or multivalued, which can be represented graphically by a combination of straight line segments. Indeed, one may apply the methods of symbolic logic in systematizing the synthesis of circuits for such relationships.

Discussion

Adam G. Kegel (Westinghouse Electric Corporation, Pittsburgh, Pa.): The use of relays to give a comparison operation in analogue computers is a valuable concept, well presented in this paper.

A circuit which produces the "negative deficiency" effect, using a relay amplifier which requires only one set of contacts, is shown in Figure 1 of this discussion.

For the position of RA shown, $a-x>0$, which means that $x<a$, and the negative of the output is $-y=a-x$, or the output is $y=x-a$. This output will be maintained until $a-x<0$, which will put RA in the up position. RA will remain in the up position as long as $-a-x<0$, which means that $x>-a$, and the negative of the output is $-y=-a-x$, or the output is $y=x+a$.

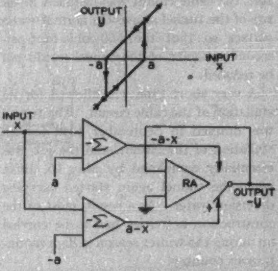

Figure 1. Circuit for simulating "negative deficiency"

The output is shown graphically as a function of the input in Figure 1 of this discussion.

A. S. Fulton and R. R. Bennett: As Mr. Kegel points out in his discussion, it would be entirely satisfactory to produce the "negative deficiency" characteristic using only one set of contacts as shown in his Figure 1.

This obvious simplification of the circuit was neglected by us due mainly to the terminal arrangements on the computer with which the circuit was used. In particular, it is easier to use two sets of contacts rather than make multiple connections to one set of contacts. The relay amplifiers were constructed having two sets of contacts in each, as was shown in Figure 1 of the paper.

Cable Through Tunnel Under Continental Divide Links Power Systems

F. M. WILSON
MEMBER AIEE

R. A. NELSON
ASSOCIATE MEMBER AIEE

IT IS the purpose of this paper to discuss the salient features of the 69-kv gas-filled pipe-type cable circuit which was recently installed by the United States Bureau of Reclamation through the 13.1-mile-long Alva B. Adams Tunnel under the Great Divide. This tunnel, which pierces the backbone of the continent, is a major link in the vast Colorado-Big Thompson Project in northern Colorado and was constructed to carry diversion water from the western slope of the Rocky Mountains to the eastern slope for purposes of irrigation and power development.

The cable installation is an integral part of the transmission circuit between the Estes Power Plant and the Granby Pumping Plant. This circuit connects the power systems on the eastern and western slopes of the Rocky Mountains and carries eastern slope power for operation of the Granby Pumping Plant. Two means of providing this circuit were considered. One was a transmission line over the mountains which would have skirted the Rocky Mountain National Park and crossed 11,850-foot-high Buchanan Pass; the other consisted of transmission lines on each side of the Divide connecting to a high-voltage cable circuit at the tunnel portals. The circuit including the cable installation through the tunnel was selected on an economic basis as a result of competitive bids for furnishing and installing the two types of circuits.

When the tunnel was built no special provisions were made to accommodate this cable circuit, because at that time it could not be definitely determined that a cable installation through the tunnel was the most economical method of providing this transmountain transmission circuit. Also, at that time the pipe-type cable systems did not have the experience backgrounds which they now enjoy. As a result, the cable circuit was installed in the top of the tunnel above the normal water surface so that the 550-cubic-foot-per-second capacity of the tunnel would not be reduced.

A very short time was allowed for installation of the cable circuit. The tunnel was drained in September 1949 for installation of the circuit, and the job was essentially completed by May 15, 1950, when the tunnel again started carrying diversion water. As a result, most of the construction activities had to be carried on during the winter season in high mountainous country.

Figure 1 is a plan and profile of the Adams Tunnel showing the east and west portal areas and the depth and slope of the tunnel.

Circuit Description

Figure 2 shows the termination of the cable circuit at the west portal of the tunnel. The termination at the east portal is essentially the same.

The circuit consists of three single-conductor cables housed in a $5^9/_{16}$-inch outside diameter steel pipe supported from the top of the 9.75-foot diameter tunnel. The pipe is brought out of the tunnel at each end through a shaft to a cable spreader which is connected by copper tubes to single-conductor potheads where the cables are terminated. The potheads are connected to lightning arresters and then through gang-operated horn-gap switches to the overhead transmission lines. The sections of cable at each end of the tunnel and extending into the tunnel approximately 925 feet to the first splice and semistop joint have a 300,000-circular mil conductor size. The remainder of the cable circuit inside the tunnel consists of size 3/0 conductor. Different conductor sizes were required in the circuit to carry the maximum load of 30,000-kva because of the higher ambient temperatures outside the tunnel and near the portals.

The pipe is filled with dry nitrogen gas at an average pressure of 200 pounds per square inch.

From a mechanical standpoint, the installation is unique because the pipe is anchored and prestressed so that stresses due to wide variations in temperatures are taken by the pipe without movement. The pipe is anchored at about 1,000-foot intervals and supported at approximately 20-foot intervals throughout the length of the tunnel.

Semistop joints are provided in the pipe approximately 925 feet from each end of the horizontal pipe run inside the tunnel and at intervals of about 2,686 feet thereafter. The cable splices are made at these semistop joints in the pipe.

Provision was made in the design to use the cable circuit for carrier-current communications. The initial installation will include two communication channels over the phase *A* conductor at frequencies of 31.5 and 60 kc. One future channel over the phase *C* conductor is planned.

The cable circuit has a capacitive reactance equivalent to approximately 275 miles of overhead 69-kv transmission line and a series impedance equivalent to about 5 miles of 69-kv overhead line.

Pipe and Coating

Electric welded steel pipe conforming to the Standards of the American Petroleum Institute was used for this job and was pressure tested at the factory at 1,000 pounds per square inch. The pipe, which has an outside diameter of $5^9/_{16}$

Paper 51-293, recommended by the AIEE Insulated Conductors Committee and approved by the AIEE Technical Power Committee for presentation at the AIEE Pacific General Meeting, Portland, Oreg., August 20–23, 1951. Manuscript submitted May 18, 1951; made available for printing July 6, 1951.

F. M. Wilson and R. A. Nelson are with the United States Bureau of Reclamation, Denver, Colo.

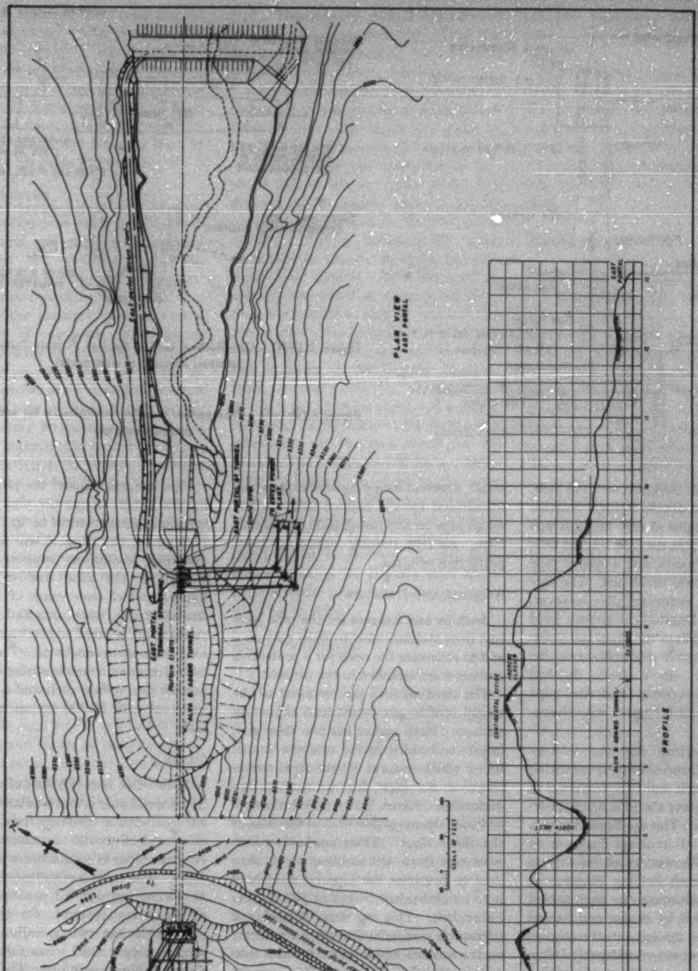
PLAN VIEW
EAST PORTAL
PLAN VIEW
WEST PORTAL
PROFILE
GRAND LAKE
TUNNEL INTAKE STRUCTURE
WEST PORTAL TERMINAL STRUCTURE
WEST PORTAL GATE HOUSE
TO GRANBY PUMPING PLANT
EAST PORTAL TERMINAL STRUCTURE
ALVA B. ADAMS TUNNEL
EAST PORTAL OF TUNNEL
TO ESTES POWER PLANT
SCALE OF FEET
CONTINENTAL DIVIDE
ANDREWS GLACIER
WEST PORTAL
EAST PORTAL
ALVA B. ADAMS TUNNEL
ELEVATION
MILES

Figure 1. Plan and profile of Adams Tunnel showing portal areas and depth and slope of tunnel

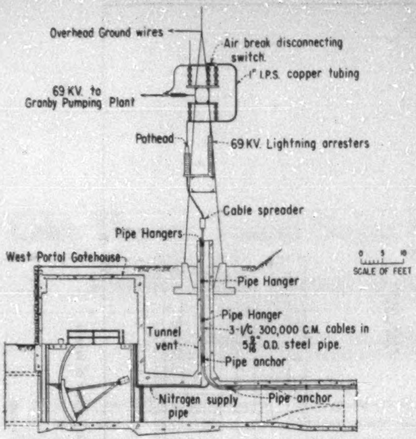
Overhead Ground wires
Air break disconnecting switch
1" I.P.S. copper tubing
69 KV. to Granby Pumping Plant
Pothead
69 KV. Lightning arresters
Cable spreader
Pipe Hangers
West Portal Gatehouse
0 5 10
SCALE OF FEET
Pipe Hanger
Pipe Hanger
Tunnel vent
3-1/C 300,000 C.M. cables in 5 9/16" O.D. steel pipe.
Pipe anchor
Nitrogen supply pipe
Pipe anchor

Figure 2 (left). Longitudinal section through Adams Tunnel showing terminal structure at west portal

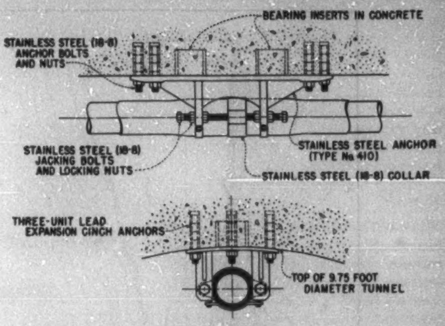
BEARING INSERTS IN CONCRETE
STAINLESS STEEL (18-8) ANCHOR BOLTS AND NUTS
STAINLESS STEEL (18-8) JACKING BOLTS AND LOCKING NUTS
STAINLESS STEEL ANCHOR (TYPE No. 410)
STAINLESS STEEL (18-8) COLLAR
THREE-UNIT LEAD EXPANSION CINCH ANCHORS
TOP OF 9.75 FOOT DIAMETER TUNNEL

Figure 3 (above). Pipe anchor showing arrangement for anchoring and prestressing pipe

inches and a wall thickness of 0.156 inch, was furnished in double random lengths. To limit the number of field welds, it was first planned to join the pipe lengths with bell and spigot joints, and a special pipe belling machine was developed. The pipe would not bell symmetrically, however, because of the longitudinal factory weld running the length of the pipe, and a few splits also occurred in this weld during the belling process. As a result, the bell joints were abandoned and the pipe lengths were welded together with sleeve-type joints.

After sandblasting, the pipe sections were given a submarine coating consisting of coal-tar enamels and two wrappings of fiberglass to protect the pipe against corrosion in service. This application gave a minimum over-all coating thickness of 5/32 inch, which was tested for defects with a wire brush holiday detector at 12,500 volts. Although the shop-coated pipe was handled by cranes and hauled into the tunnel throughout the winter, often at temperatures considerably below freezing, there was no evidence of cracking or disbonding due to normal flexure and handling.

It was originally planned to have the first pipe wrap of fiberglass and the second wrap of bonded asbestos felt. However, when this application was tried on several sections of pipe, the 500-degree Fahrenheit temperature of the coal-tar enamel resulted in release of volatiles from the felt which formed an abnormal amount of large gas pockets under the felt and many pinholes in the coal-tar enamel on both sides of it. As a result, a second wrapping of fiberglass was substituted for the bonded asbestos felt for all pipe on this installation, and a uniform, gas-free coating affording more protection resulted.

ANCHORS AND HANGERS

Anchors and hangers for the pipe were cast from stainless steel to resist corrosion and to eliminate the need for a protective coating when installed in the tunnel.

The rigid anchors are mounted to the tunnel roof by six 3-unit lead expansion anchors. Each anchor has two shear ring inserts embedded in the concrete tunnel lining which prevent longitudinal movement of the pipe due to temperature variations. Grout was applied through threaded openings provided at the base of the shear rings. These anchors, which were cast from 410 stainless steel, were used to prestress the pipe by stretching it to its equivalent length at 103 degrees Fahrenheit. This was done by means of adjustable stud bolts through the brackets on the anchors which were threaded into collars welded to the pipe. This arrangement required extreme accuracy in locating the collars welded to the pipe so that they came within the anchor brackets in the proper position. The anchors have a maximum design stress of 31,300 pounds per square inch, a minimum yield point of 70,000 pounds per square inch, and a minimum tensile strength of 95,000 pounds per square inch. A total of 71 of these anchors were used in the installation. Figure 3 shows an anchor with the pipe in place and the stud bolts threaded into the pipe collar.

Pipe hangers support the pipe containing the cable. Since the pipe will be in tension at temperatures up to 103 degrees Fahrenheit, the hangers will under most operating conditions support only the weight of the pipe and cable. The hangers, which were made of 18-8 stainless steel and were annealed to relieve stresses, are secured to the tunnel roof by lead expansion anchors. The hangers have a minimum tensile strength of 70,000 pounds per square inch and a minimum yield point of 30,000 pounds per square inch.

CABLE

Each cable has 480 mils of oil-impregnated wood pulp paper insulation which is covered with a moisture-resistant jacket composed of several aluminum and polyethylene tapes in combination with copper tapes. The cable has sufficient insulation to permit ungrounded neutral operation of the power system. On the outside, each cable has two spirally wound D-shaped copper skid wires for protection during pulling operations. The 3/0 standard strand cable has a diameter of 1.461 inches over the skid wire, and the 300,000 circular mil compact round cable has an over-all diameter of 1.561 inches.

The cable was given thorough electrical and mechanical tests at the factory. These tests included a high-voltage test at 103.7 kv to ground for 15 minutes on each cable length and high-voltage time tests at voltages up to 282 kv on representative samples of the cable.

The reels on which the cable was shipped were sealed inside the lagging to prevent free moisture from collecting on the cable surfaces. After sealing with sealing paper, the reels were purged and shipped under a slight nitrogen pressure. Several bags of silica-gel were shipped inside each reel. Reels were protected from direct rain or snow at all times and were placed in a heated reel house at least 24 hours before the cable was pulled.

PRESSURE SYSTEM

Consideration was given to the use of either nitrogen gas or oil as the pressure medium for this cable circuit. The simpler pressure-regulating facilities required to take care of expansion and contraction of the pressure medium over a wide range of operating temperatures were the basis for the selection of nitrogen gas for this purpose. The use of gas allows an approximately constant pressure on the cable over its entire length for any given operating temperature. If oil had been used, there would have been a considerable variation in pressure between the two tunnel portals due to the 110-foot difference in elevation. Small oil leaks in the system would have been easier to detect than gas leaks, but contamination of the diversion water by oil, even in minute quantities, would have been objectionable.

The gas pressure system comprises 69,058 feet of pipe through the tunnel, terminating at cable spreaders at each end and connected by copper tubing to the pressure-regulating equipment. The regulating equipment is located in the gatehouse at the west portal and in the pressure equipment house at the east portal. The equipment at each portal includes six high-pressure nitrogen gas cylinders connected through a manifold header to the pipe, with the necessary valves, pressure reducing regulators, and pressure gages. Additional spare nitrogen cylinders are stored at each portal.

The pipe run is divided by 26 semistop joints into sections, each approximately 2,686 feet long, except for the shorter section at each end. The semistop joints provide for restricted flow of gas from one pipe section to another through by-pass piping under normal operating conditions, but are equipped with shut-off valves permitting isolation between adjacent sections in case of a rupture or leak in the pipe.

The gas pressure system is arranged so that it can be operated either as a closed system or with the connected gas cylinders floating on the system. Normally the system is operated with the manifold header valves closed, which isolates the terminal regulating equipment from the pipe. This requires manual operation of the terminal equipment to adjust for pressure changes resulting from seasonal temperature variations or leakage.

A maximum-minimum pressure relay is connected to the system at each portal. Each pressure relay is set to initiate an alarm when the pressure in the pipe falls below 185 pounds per square inch or rises above 225 pounds per square inch. Gas pressure alarm signals initiated by the pressure relay located in the west portal gatehouse will be automatically transmitted to the Granby Pumping Plant by supervisory control. This is done by utilizing one position of the supervisory control equipment used to operate the west portal gates from Granby Pumping Plant. Both visual and audible alarm will be given in the Granby Pumping Plant control room for abnormal gas pressures. The alarm signal will continue until shut off manually at the west portal gatehouse. At the east portal the gas pressure alarm signals will be automatically transmitted by radio to the Estes Power Plant. A frequency-modulated transmitter having a distinctive modulating tone is used for this purpose. The alarm signal is received at the Estes Power Plant on the power system maintenance radio system at a frequency of 40.02 megacycles.

RELAY PROTECTION

The cable circuit is protected as a part of the transmission link between Estes Power Plant and Granby Pumping Plant. Since the circuit is supplied from the Estes Switchyard through a delta-delta transformer bank, a grounding transformer is connected to the line at the Estes end to prevent excessive 60-cycle and transient overvoltages on the cable during 69-kv system line-to-ground faults, and to supply ground fault current at the Estes end of the 69-kv system to permit relatively simple, reliable, and fast clearing of ground faults.

At both ends of the transmission link, high-speed relaying is provided to clear the circuit on phase faults as well as faults involving ground. A combination of distance impedance phase and ground relays, as well as other directional and nondirectional ground relays are used to provide instantaneous trip for faults in zones including the cable section and time delay trip for coordination with relays on other lines and for back-up protection. Overvoltage relays are provided at the Granby end to protect against excessive voltages resulting from the charging requirements of the cable when disconnected from the Estes Switchyard. The relaying scheme provides maximum flexibility for the various possible connections of the 69-kv system.

High-speed relaying is provided on the circuit to minimize the possible damage due to burning in case of a fault in the cable section. Automatic reclosing was omitted to eliminate the possibility of additional damage resulting from re-energizing the circuit with a permanent cable fault.

Installation

ANCHOR AND HANGER LOCATION

The first field operation in the circuit installation was to make a survey through the tunnel to spot very accurately the locations for the pipe anchors and hangers. The concrete lining in the roof of the tunnel was then drilled for the anchor and hanger inserts using templates to give maximum accuracy. The anchors and hangers were then attached in place to the top of the tunnel by lead expansion anchors and bolts. Since the performance of the anchors depends to a large extent on proper bearing of the inserts or shear rings on the concrete, particular care was given to grouting around these shear rings to prevent voids and undue shrinkage.

TUNNEL VENTILATION

Ventilation in the tunnel during construction activities was by natural air circulation. About 90 per cent of the time the air circulation was from west to east and the air velocity averaged about 3 miles per hour. The use of combustion equipment in the tunnel was limited by the amount of air contamination.

TUNNEL ACCESS

Access to the tunnel through the gatehouse at the west portal was difficult and was limited to the entrance of men and small tools and equipment. This required that construction activities be carried on primarily by access through the east portal of the tunnel.

Workmen were transported in the tunnel by means of jeeps, which were equipped with special tires to run on the rounded walls of the tunnel. Since the jeeps could not be turned around inside the tunnel it was necessary to back them in one direction of travel.

All operations inside the tunnel required very careful coordination because of the limited space for working and for transporting men, materials, and equipment in and out of the tunnel. This limited space and the difficulty of access made it necessary that as much work as possible be done outside the tunnel. An

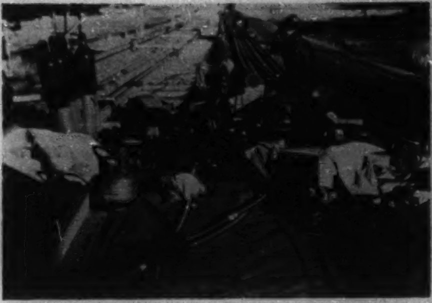

Figure 4. Work area below tunnel portal showing cables protruding from pipe section after pulling operation

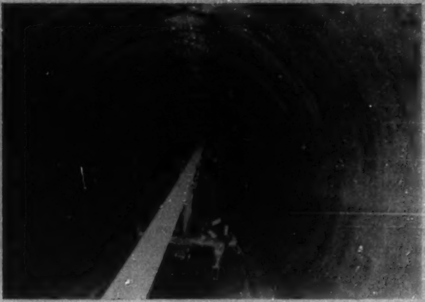

Figure 5. Section of pipe being wedged upward into position in top of tunnel

oiled road approaching the east portal of the tunnel was selected as the working area for welding the pipe into approximately 1/2-mile-long sections and for pulling the cable into these sections.

Pipe Welding

The pipe sections to be welded were placed on rubber rollers to facilitate turning the pipe during the welding operations. After a 1/2-mile-long section of pipe was welded, the flanged end casings which formed a part of the semistop joints were welded to each end and a test plate was gasketed and bolted to the flange at one end, the other end being left open. A compressor-drier was then connected to the pipe section and the pipe was flushed with dry air until the air at the far end showed a dryness test of at least minus 20 degrees Fahrenheit when tested with a dewpoint potentiometer. A test plate was then bolted to the other end of the pipe section and the pressure was raised to 400 pounds per square inch. All welded joints were then tested for leaks by means of a water bath which completely surrounded and covered the welds. After a pipe section successfully passed the leakage tests the pressure was reduced to 100 pounds per square inch. The welds on only a few sections of pipe were coated outside the tunnel since the onset of cold weather made this impracticable for the remainder of the pipe. As a result it was necessary to coat most of the welds after the pipe had been installed in the tunnel.

Cable Pulling

Prior to pulling the cable, the pressure in the pipe was reduced to atmospheric by removing the test plates. If the dewpoint tested minus 20 degrees Fahrenheit or lower the section was considered satisfactory for pulling. Cable guide tubes were then bolted to the pipe end casings to prevent possible injury to the cable in pulling over sharp edges.

The pulling bolts of each cable were attached to a pulling yoke and the three cables were pulled into the pipe simultaneously by a gasoline-engine-driven winch. The pulling line attached to the winch was drawn into the pipe by first blowing a fish line through the pipe by compressed air. The cable was pulled into the 1/2-mile sections of pipe at the rate of about 25 feet per minute. The working area was such, that the pipe sloped with the grade of the road and the operations were arranged so that the cable was pulled downhill. While the cables were being pulled they were lubricated by uniformly feeding 5 gallons of oil into the pipe section. After the cable was pulled the ends were cut so that $4^1/_2$ feet protruded beyond each end of the pipe section. Figure 4 shows the work area below the tunnel portal just after the cables had been pulled into a section of pipe. A ferrule plate was then threaded over the cable ends and gasketed and rigidly fastened to the flanged end casing of the pipe. Next a rubber tube was pulled over each protruding length of cable and clamped to the ferrules, sealing the cable from all contact with the outside air. A vacuum was then drawn on the pipe for 24 hours, after which the pipe was filled with nitrogen gas.

Only the end sections of cable, including risers to the terminal structures, were pulled after the pipe sections were installed.

Installation of Pipe Sections

The installation started from the west portal and the steel terminal structure there was erected before any pipe or cable was installed in the tunnel. When ready to be hauled into the tunnel, the pipe section containing the cable was loaded on rubber-wheeled dollies which were spaced at about 40-foot intervals. The dollies were designed to follow along the curved surface of the tunnel and rubber tires were provided to protect the tunnel lining against injury. The winding route from the assembly area to the tunnel portal required wooden tracks and guides in many places.

After the 1/2-mile length of pipe was hauled into the tunnel to its location by a diesel tractor, the west end was raised to the tunnel arch and secured. By means of a system of rubber rollers mounted on top of the tractor and on a rolling frame pushed about 40 feet ahead of the tractor, the pipe was wedged upward into place and laid on rubber-covered rollers hung at about 40-foot intervals from the stainless steel hangers. Figure 5 shows a section of pipe being raised into position in the top of the tunnel.

After a 6- to 24-hour wait to allow the pipe section to assume the tunnel temperature, the air temperature about the pipe was taken. Measurements were then

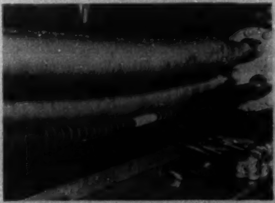

Figure 6. Comparison of stepped-down insulation and completed insulation at cable splice

Figure 7. Boiling out completed splice assembly prior to slipping 10-inch diameter sleeve in place

Figure 8. Sleeve in place over splice assembly ready for welding

made between the semistop joint flange previously installed and the flange of the new section, and between the center of each anchor and its matching pipe collar. Computations were then completed to determine where each collar should be located in relation to its anchor to simulate the condition of the pipe if warmed up to a temperature of 103 degrees Fahrenheit. When it was determined that all pipe collars fitted properly within the anchor brackets, the pipe section was adjusted so that the semistop flanges were the designed distance apart. This adjustment was accomplished by jacking at the first anchor east of the semistop joint.

Cable Splicing

The ends of the pipe at the splice were then lowered to the working position in the canvas-enclosed splicing platform, which was mounted on wheels. Next, the ferrule plates were removed and the armor skid wires were unwound back to the ends of the pipe where several closely spaced turns were made which were then soldered together. The next step involved soldering copper braid to the armor wire of each cable. Rubber tubing was then pulled over the cable ends so that it extended into the pipe, and this was bound to the cables with wire for a distance of 2 inches. The ferrule plates were then gasketed and fastened to the flanged end casing of the pipe after bringing the copper braid and the rubber tubing through each ferrule. Each rubber tube was next folded back over its ferrule as far as it would go and bound in place with wire for a distance of 2 inches. The cables were then measured and cut to the proper length for joining and the insulation was removed to the conductor where the connectors fit. The conductors were joined by connectors, which were compressed at a pressure of 4,000 pounds per square inch by a hydraulic press. The insulation on each side of the connectors was then stepped back and each step was wrapped with yarn. At this stage and at intervals throughout the splicing operation the insulation was flushed with oil at a temperature of 110 degrees centigrade to remove impurities and moisture. Crepe paper tape was next applied to build up the stress cone until the diameter became $3^3/_{16}$ inches. Over this the copper braid shielding tape lapped 1/16 inch was wrapped. The turns of braid were soldered together along a lengthwise line at the top of the shielded reinforcement and then a ground braid connecting the ferrule plates was soldered to the shielding tapes.

Figure 6 shows a comparison between the penciled insulation on one cable and the completed stress cone including the copper braid shielding on the other two cables. Varnished cambric tape applied over the cable at each ferrule and fastened with hose clamps provided, along with the rubber tubing, the semistop for the gas and in addition a means of preventing the cable from creeping in the slight grade in the tunnel.

Figure 7 shows a completed splice being boiled out with hot oil prior to slipping the 10-inch diameter pipe sleeve over it. Wooden blocks fastened to the splices by twine hold the assembly from the sides of the pipe sleeve. Figure 8 shows a 10-inch sleeve ready for welding in place over a splice. After a pipe sleeve was welded to the flanged end casings of the pipe, a vacuum was applied and maintained for 15 minutes, after which the joint was filled with nitrogen gas to a pressure of 40 pounds per square inch. The pipe at the splice was then raised to position in the top of the tunnel and the section of pipe was prestressed by stretching to its equivalent length at 103 degrees Fahrenheit.

Cable Termination

At each terminal of the circuit the pipe was welded to the semistop plate of the cable spreader. From the spreader casing each cable went through a separate spreader tube to a single-conductor pothead. At each pothead termination the cable insulation was penciled and a taped stress cone was built up. When the pothead connections at the east portal were completed, the pressure system was filled with nitrogen at a pressure of 200 pounds per square inch.

Field Tests

High-Voltage Test

After the installation was completed a 3-phase 60-cycle 120.75-kv test for 4 hours was made on the three cables simultaneously. The voltage was supplied by generating facilities at the Estes Power Plant and was transmitted to the cable circuit over approximately 6 miles of overhead transmission line, of which 1 mile is rated at 115 kv, and 5 miles are rated at 69 kv. This was a reduced voltage test considering the insulation thickness of the cable, but it was maximum voltage to which the facilities at Estes were desired to be subjected.

Two of the Estes generators rated at 16,667 kva were connected in parallel to supply the cable charging requirement of 22 000 kva at 120.75 kv. To supply the charging current of 105 amperes under these conditions it was necessary to operate the generators with the excitation reduced to 16 per cent of that required for rated output, resulting in greatly reduced synchronizing torques. Excitation of the two-unit exciters during the test was provided by an external battery connected in a bridge circuit. The two exciter fields were connected in series to provide smooth control of the exciters of the two units from zero to maximum excitation.

Reversal of the polarity in the bridge circuit permitted a reversal of exciter field current to neutralize the residual magnetism in the field poles.

To prevent the possibility of one unit tripping off the line and leaving the remaining unit to supply the entire charging requirements of the cable circuit, a condition which would result in unstable operation of the remaining generator, the control circuits of both units were modified to parallel the tripping circuits of the unit circuit breakers on each generator.

Attenuation Tests

Attenuation tests were performed on the cable circuit at carrier frequencies between 30 and 90 kc. The tests were made by applying signal voltages at carrier frequencies to the circuit at the west portal terminal and measuring the signal voltages at the west portal terminal and the east portal terminal. The signal generator was connected to the circuit through an impedance matching transformer and inductance-capacitance network adjusted for optimum transfer of signal power. It was assumed that the characteristic impedance of the cable was essentially pure resistance and the attenuation measurements were made with the receiving end terminated with a shunt resistance equal to the characteristic impedance. This was determined by adjusting the shunt resistance to give a receiving end voltage equal to one-half the open circuit voltage. Under these conditions, the attenuation can be determined from the following:

$$A = 20 \log_{10} \frac{V_S}{V_R}$$

where

A = attenuation loss in decibels
V_S = sending end voltage
V_R = receiving end voltage

In addition to the above test, the input impedance of the cable circuit alone was measured at carrier frequencies with the receiving end both open circuited and short circuited. These values were found to be essentially equal and also the same as the characteristic impedance of the cable.

The attenuation loss of the cable circuit measured from the potheads at the west portal to the potheads at the east portal was found by the tests, which were conducted by the contractor, to be 27.2 decibels on the A phase to ground and 27.4 decibels on the B phase to ground at 50 kc. The characteristic impedance of the cable was calculated from the test data to be approximately 35.5 ohms at 50 kc.

Provision was made in the design for the addition of carrier current by-pass and line tuning equipment to be installed at the terminals if necessary to reduce the junction loss and improve the communication characteristics of the entire circuit.

Discussion

Victor Siegfried (American Steel and Wire Company, Worcester, Mass.): The authors are to be complimented on an interesting and attractive presentation of a splendid bit of pioneering in cable applications.

Two questions on which engineering decisions were based in the decision regarding type and size of cable bear further elaboration as a guide to other similar applications and are to be inferred only from the introduction regarding "competitive bids" furnishing "an economic basis" for choice.

One of the proposals was for rubber-insulated cable of the submarine type, necessarily at a lower voltage and with parallel circuits. While it is appreciated that suspension might have been more involved, the advantages of having cable which could withstand immersion are worthy of consideration. The authors are requested to compare the economics of paper- versus rubber-insulated cable as they entered into this decision.

The current-carrying-capacity of these cables in close proximity to cool, moving water should furnish a lower ambient than usually figured into such underground designs. What factors were allowed, or were considered for ambient conditions in such an installation, where heat dissipation is about as favorable as ever could be found short of total immersion?

The choice of cable in this instance is undoubtedly a good one and very practical. Further discussion of these points would aid later engineering of other such projects.

A. R. Lee (General Electric Company, Schenectady, N. Y.): The authors of this paper are to be congratulated on their fine description of the installation of pipe-type cable through the Adams Tunnel and I think the paper is a worthwhile addition to the literature on cable systems. The writer was associated with this project during its formative and design states and in connection with the installation. A few additional points may therefore be of interest.

The first point is in connection with the maximum load rating assigned to this circuit. The authors have stated the maximum load to be 30,000 kva. This is a conservative application and is based on a maximum copper operating temperature of 60 degrees centigrade. Industry standards for this class and voltage of cable allow a maximum copper operating temperature of 75 degrees centigrade which has been proved by test and years of experience to be an entirely safe value. The cable circuit may therefore be operated safely with an additional 25 per cent load in case system operating conditions require it. This additional loading will, of course, have a direct bearing on the mechanical operation of the pipe itself. When the operating temperature exceeds 60 degrees centigrade, the pipe temperature will, of course, exceed 39.5 degrees centigrade (103 degrees Fahrenheit) and the pipe will go into compression. However, it is possible, I believe, to operate with the pipe in compression in this system. This can be checked by calculation and, if a sufficient mechanical margin of safety remains, continuous operation at 75 degrees centigrade copper temperature with a consequent 25 per cent additional load carrying ability would be entirely feasible.

In regard to the cable construction, a point of interest is in connection with the 3/0 American wire gauge conductor. From the standpoint of economics, it was advisable to keep the number of splices to a minimum. It was felt that 1/2-mile cable sections would provide a good economical figure if the small conductor could take the pulling strains. Medium-hard drawn copper strands were therefore used in the conductor to allow pulling the 1/2-mile section and still not stretch the copper to the point that damage would occur. Field experience showed this to be the case. The average coefficient of pulling friction of the cables in the pipes was 0.275 with a range from 0.25 to 0.28.

The authors have discussed the simplicity of gas-filled cable from a pressure maintenance standpoint and have pointed out its attractiveness. It should also be noted that the winter temperatures at the portals of the tunnel are such that the use of oil pumping and storage equipment would have been impractical. The temperatures may reach −40 degrees Fahrenheit for a number of days and the pour point of the insulating oil usually used in pipe cables is −5 degrees Fahrenheit. Expensive heating equipment would have been necessary at the portals to maintain oil pumping equipment in operating condition. Further, under no-load conditions, with voltage on the line, the dielectric heating in the cables in the exposed risers and spreader tubes would not be sufficient to keep the oil in a fluid state. Consequently, shrinkage voids could form in the potheads and risers and lead to ionization troubles.

This paper describes the most interesting cable job to be installed in many years and the authors are to be complimented on a fine over-all job.

F. M. Wilson and R. A. Nelson: The authors wish to thank the discussers of this paper for the additional information given and for the pertinent questions which were raised.

In connection with Mr. Siegfried's discussion, it should be pointed out that operating voltages of from 115-kv down to 13.8-kv. were considered for this cable circuit. It was determined that operation at 69-kv would provide the most economical cable circuit having both suitable electrical characteristics and the desired capacity of 30,000 kva. Therefore, only the 69-kv cable circuit was included in the competitive bidding, although the use of rubber-insulated submarine-type cable at lower voltages was considered earlier and found to be impracticable for this particular installation because of the electrical characteristics and limitations. The use of rubber-insulated cable would have required transformer banks at each end of the cable circuit to tie to the connecting overhead higher voltage transmission lines and would have materially increased the reactance of the transmission link between the Estes Power Plant and the Granby Pumping Plant. One disadvantage of this arrangement would have been the increased voltage dip at Granby when starting the motors with power supplied over this transmission link.

As noted by Mr. Siegfried, the heat dissipation from the cable will be very good when water is flowing in the tunnel due to the low ambient temperature of the air surrounding the pipe. The circuit was designed however, to operate at full capacity with the tunnel unwatered. Under these conditions the temperature in the tunnel may be as high as 68 degrees Fahrenheit depending on how long the tunnel is unwatered.

Mr. Lee in his discussion has indicated that the cable circuit was designed to carry a load of 30,000 kva with a maximum copper temperature of 60 degrees centigrade even though the industry standards for this type cable permit a maximum copper operating temperature of 75 degrees centigrade. This limitation on maximum copper temperature was made for mechanical reasons. Since the pipe is prestressed and anchored so that stresses due to temperature variations are taken by the pipe without movement, it was desired to limit as much as feasible the temperature range and resultant stresses to which the pipe would be subjected.

Incremental Method for Sag-Tension Calculations

MAURICE LANDAU
MEMBER AIEE

Synopsis: This paper presents an analytical method for calculating sags, tensions, and lengths of overhead cables. The method is applicable to both level and non-level spans; self contained, not requiring the use of precalculated data or functions; and adaptable to both cables with constant modulus of elasticity, such as steel or copper, and cables such as steel reinforced aluminum cable where stress-strain curves must be resorted to. Included in the method is a direct calculation of the horizontal component of tension in a span where the tension at either support is known. Increments of length of cable are calculated rather than total lengths, thus permitting adequate accuracy to be had using a 10-inch slide rule.

THE methods of sag and tension calculations described in this paper were developed for use in the design of the transmission lines of the Department of Water and Power of the City of Los Angeles. They have been used in the design of the 287.5-kv Boulder transmission lines which extend 266 miles from Hoover Dam to Los Angeles, the 138-kv belt line in and adjacent to Los Angeles, and the 230-kv transmission line from the Owens River Gorge, 260 miles from Los Angeles, to Los Angeles. The Boulder line conductors are 512,000 circular mil, type HH copper, the belt line conductors 500,000 circular mil stranded copper, and the Owens Gorge line 954,000 circular mil steel reinforced aluminum cable 54/7. All of the lines have 1/2-inch high strength stranded steel overhead ground wires.

General

In general the problems of sag and tension calculations for overhead suspended cable are to determine sag, tensions, and lengths of overhead cable between fixed supports at stringing temperatures and conditions of maximum sag such that under the most severe loading conditions the maximum tension in the cable will not exceed a predetermined allowable maximum.

For the purpose of calculations, the weight of the cable itself and the superimposed ice and wind loads are assumed to be uniformly distributed along the line of the cable. Under these conditions, the cable takes the curvature of the catenary.

Expressed as a series the equations of the catenary for a level span are:

$$y=\frac{L^2}{8a}\left[1+\frac{L^2}{48a^2}+\frac{L^4}{5,760a^4}+\ldots\right] \qquad (1)$$

$$S=L\left[1+\frac{L^2}{24a^2}+\frac{L^4}{1920a^4}+\ldots\right] \qquad (2)$$

If the weight of the cable and superimposed ice and wind loads are assumed to be uniformly distributed along the horizontal projection of the cable, the curve taken by the cable is that of the parabola. The equations of the parabola are:

$$y=\frac{L^2}{8a} \qquad (3)$$

$$S=L\left[1+\frac{L^2}{24a^2}-\frac{L^4}{640a^4}+\ldots\right] \qquad (4)$$

Comparing equations 1 and 3, the first terms of each equation are identical. The same is true of the first two terms of equations 2 and 4. Thus for spans where L is small with respect to a, the catenary and parabola are for practical purposes identical. This is the basis for the so-called parabolic methods.

Sag and Tension Calculations

Essentially sag and tension calculations of overhead cables consist of the following:

1. Determine the stressed length of the cable between supports under the assumed maximum tension and maximum loading conditions.

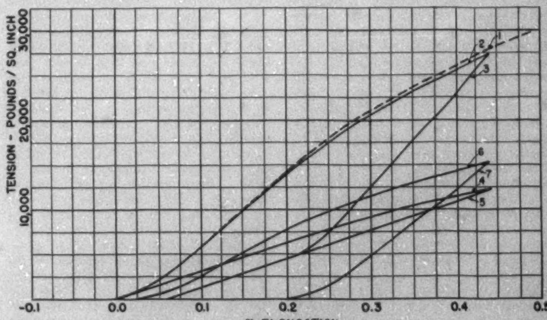

Figure 1. Stress-strain curves

795,000 circular mil ACSR; 54×0.1214 inch aluminum; 7×0.1214 inch steel

---

Paper 51-294, recommended by the AIEE Transmission and Distribution Committee and approved by the Technical Program Committee for presentation at the AIEE Pacific General Meeting, Portland, Oreg., August 20–23, 1951. Manuscript submitted May 17, 1951; made available for printing July 6, 1951.

MAURICE LANDAU is with the Department of Water and Power, Los Angeles, Calif.

2. Remove all load (weight) from the cable and determine the length of the unstressed length of cable.

3. Determine the change in unstressed length of wire due to change in temperature.

4. Place the desired load (weight) on the cable at the new temperature and determine the stressed length.

5. Calculate the sag and tension characteristics corresponding to the stressed length at the new temperature.

Published Methods of Calculation

A method developed by James S. Martin,[1] using tabulated precalculated functions of a level span of unit length is widely used for sag and tension calculations. Methods of solution using the level span data are resorted to for calculation of nonlevel spans. The method requires the use of seven or eight significant figures in calculation, and also interpolation of the tabulated data for particular solutions.

In the aluminum steel reinforced cables, (ACSR) both the aluminum and steel are stressed. Steel has a constant modulus of elasticity. Aluminum has a variable modulus of elasticity in the working range and is subject to considerable permanent stretch. Accuracy of calculation requires the use of stress-strain curves rather than an assumed constant modulus of elasticity except in cases where the ratio of aluminum to steel is small. The methods of calculation using Martin's Tables do not lend themselves to the use of stress-strain curves.

Calculations of sags and tensions of ACSR are usually made by the method described in ACSR Graphic Method for Sag-Tension Calculations.[2] Briefly this method consists of the following:

1. Preparation of stress-strain curves for the cable based upon data obtained by stressing samples of the cable in a testing machine. Figure 1 is illustrative of these curves.

2. Preparing stress-strain curves for various temperatures to the required maximum tension from the stress-strain curve obtained by test. Figure 2 is illustrative of these curves.

3. Preparing curves which give the variations in sag and tension of a particular span corresponding to the same change of arc length as those given in the stress-strain curves and then superimposing the stress-strain curves for the various temperatures upon such sag-tension curves.

Figure 1 is a set of stress-strain curves for 795,000 circular mil ACSR at 60 degrees Fahrenheit. Per cent elongation is plotted as abscissae, and tension in pounds per square inch of cable as ordinates. The curves are from the ACSR Method.

Curve 2 on Figure 1 shows the behavior of the complete cable upon the first application of load, while Curve 3 shows the effect of releasing the load. Curve 4 is the initial application of load for the steel core while Curve 5 is the release of the load. Curves 6 and 7 give corresponding data for the aluminum portion and are obtained from Curves 2, 3, 4, and 5. The dotted Curve 1 is the elongation produced immediately after the application of load. Curve 2 is the result after stretching has practically ceased (that is, after holding the final load for approximately one hour).

Figure 2 is a set of stress-strain curves for various temperatures derived from the

Units and Notations

L = span length, feet
D = difference in elevation of supports, feet
L_c = straight line distance between supports, feet
S = stressed length of conductor, feet
x, y = co-ordinate of any point on the conductor, feet
x_1 = horizontal distance between low point to upper support, feet
x_2 = horizontal distance between low point to lower support, feet
y_1 = vertical distance between low point to upper support, feet
y_2 = vertical distance between low point to lower support, feet
W = weight of conductor per unit length, pounds per foot
T = tension of conductor at point x, y, pounds
T_1 = tension of conductor at point x_1, y_1, pounds
T_2 = tension of conductor at point x_2, y_2, pounds
T_{avg} = effective or average tension of conductor, pounds
$T_{as} = T_{avg}/A$, pounds per square inch
H = horizontal component of tension, pounds
$a = H/W$, feet
$a_1 = T_1/W$, feet
$Z = L/2a$, a pure number
A = area of cross-section of conductor, square inches
E = modulus of elasticity, pounds per square inches
α = coefficient of linear expansion, feet per foot per degree Fahrenheit
t = temperature, degree Fahrenheit
$\delta = (2a_1 - D)L_c$, a pure number

$$Q = \sqrt{\frac{1+\left(\frac{D}{L}\right)^2}{1+\left(\frac{D}{L}\right)^2\left(\frac{Z}{\sinh Z}\right)^2}} \quad \text{A pure number}$$

$$P = \left[\frac{\sinh^{-1}\frac{D}{L}\left(1-\frac{Z^2}{6}\right)}{\frac{D}{L}\left(1-\frac{Z^2}{6}\right)}\right] \quad \text{A pure number}$$

Figure 2 (below). Stress-strain curves

795,000 circular mil ACSR 54/7, maximum tension 12,750 pounds per square inch at 0 degree Fahrenheit

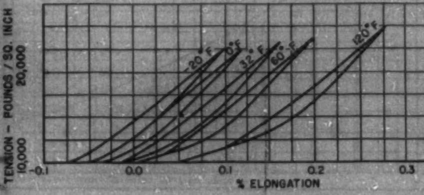

Figure 3 (right). Z, temperature chart, Example 1

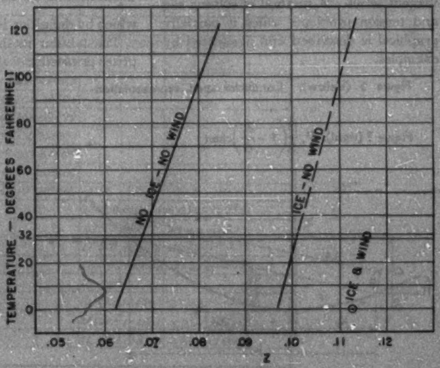

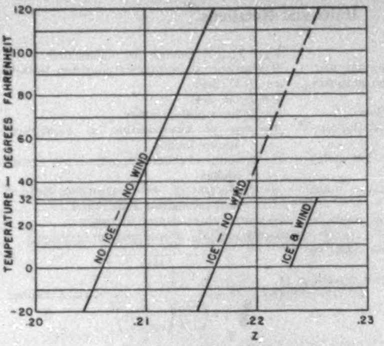

Figure 4. Z, temperature chart, Example 2

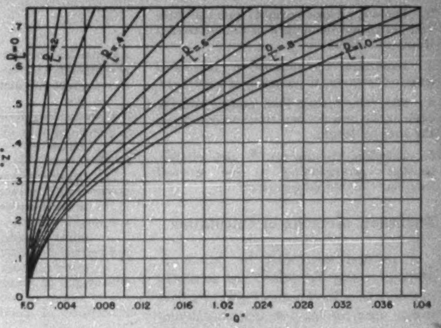

Figure 6. Z, Q chart

stress-strain curves, Figure 1. The curves are maximum tension of 12,750 pounds per square inch at 0 degree Fahrenheit temperature. In deriving these curves, the coefficient of expansion of aluminum was taken as 1.28×10^{-5} and for steel 6.4×10^{-6}.

H. W. Eales and E. Ettlinger[3] derive the general equation of the length of a suspended cable in terms of the span length, the difference in elevation of supports, and the catenary constant. Using this equation, the authors develop a method of calculation of sags and tensions equally applicable to either level or nonlevel spans. The method, while accurate, lacks simplicity and requires the use of seven and eight significant figures in calculation.

Mr. D. O. Ehrenburg[4] derives the general equation of length previously derived by Eales and Ettlinger, and also additional equations for stretch, sag, and tension of suspended cables. These equations are then expanded into convergent series. A method of solving sag and tension problems which is partially graphical is described and illustrated by examples.

In a comment to Ehrenburg's paper, Mr. H. J. McCracken[5] suggests a tabular method of calculation using the equations derived by Mr. Ehrenburg. Both the method of Mr. Ehrenburg and that proposed by Mr. McCracken require the use of precalculated tabulated functions.

The Incremental Sag-Tension Calculation Method is a further development of those included in Mr. Ehrenburg's paper and the comment by Mr. McCracken.

Incremental Sag-Tension Calculation Method

The incremental sag-tension method is set forth on two calculation forms titled Form 1 and Form 2, respectively. Form 1 is for use where a constant modulus of elasticity may be assumed. Form 2 is adapted for use with stress-strain curves. The calculations are in terms of the function

$$\frac{\text{Span}\times\text{Weight}}{2\times\text{Horizontal Tension}}=\frac{LW}{2H}$$

which by definition is designated Z.

The tabular method of Form 1 comprises primarily:

1. Determining the initial value of Z for the particular span, tension, and maximum loading conditions.
2. Selecting various values of Z for the loaded conditions and unloaded (that is, cable only) and calculating the temperatures corresponding to such values of Z.
3. Preparing curves for various loading conditions with Z as abscissae and temperature as ordinates.
4. Calculating sags and tensions for selected values of temperature from the corresponding value of Z as determined from the Z-temperature curves.

The tabular method using Form 2 is similar to that of Form 1, differing only in operation 2 above. Stress-strain curves plotted for particular temperatures, values of Z corresponding to such temperatures are calculated.

Forms 1 and 2 each consist of 25 items arranged vertically, a series of columns being provided for tabulating data and calculations. Except for Items 12 to 16, inclusive, Forms 1 and 2 are identical.

Examples of Sag Calculations

To illustrate the incremental method two examples for each of the two forms

Figure 5 (below). Conductor span representation

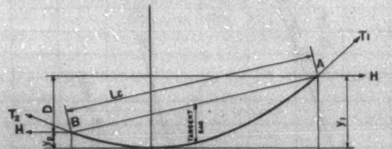

Figure 7 (right). P, $\frac{D}{L}\left(1-\frac{Z^2}{6}\right)$ chart

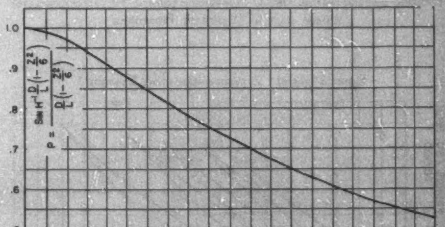

Cable 5/8" High Strength 30% Cond. Copper Weld
Maximum Tension 5670 lbs. @ 0°F; ½" Ice, 8# Wind
Project
Computed by M.L. Date

SAG AND TENSION CALCULATIONS
FORM NO. I

EXAMPLE I

Cable Weight W=.322#/ft; W÷AE=[illegible] x10^-6
Cable Weight plus Ice W=.871#/ft; W÷AE=[illegible] x10^-6
Wind W=____#/ft.
Max. Result. Load at 0°F, W=1.269#/ft; W÷AE=[illegible] x10^-6
Area of Cross Section, A=.0901 sq. in.
Diameter of Cable, inches
Modulus of Elasticity, E=23 x 10^6
Coefficient of Linear Expansion α = 7.2 x10^-6

Form Number 1

Example 1

		Cable + Ice + Wind	Cable + Ice			Cable Only				Cable + Ice	Cable Only		
1	L = Span Length	1000											
2	D = Difference in Elevation	0											
3	$L_e = L + d;\ d = D^2/(2L + d)$	1000											
4	$6\,L_e/L^2$	.006											
5	T_1 = Maximum Tension	5670											
6	W	1.269	.871	.871	.871	.322	.322	.322	.322	.871	.322	.322	.322
7	$a_1 = T_1/W$	4468.1											
8	$\partial = (2a_1 - D)/L_e$	8.936											
9	$Z = 1/(\partial - Z/2)$	.1126	.1126	.100	.105	.06	.08	.07	.075	.1010	.0676	.0731	.0838
10	Slack $= (Z^2/\underline{4})(1 + Z^2/20)$	2.113	2.113	1.667	1.840	.600	1.067	.817	.937				
11	S_0	999.4	999.4	999.4	999.4	999.4	999.4	999.4	999.4				
12	$W/AE \times 10^6$	.6124	.4203	.4203	.4203	.1551	.1551	.1551	.1551				
13	Stretch $= (W/AE)(S_0^2/2Z)$	2.720	1.865	2.099	1.998	1.293	.971	1.109	1.035				
14	$(S_0 - L_e) = \underline{10} - \underline{13}$	-.607	+.248	-.432	-.158	-.693	.096	-.292	-.098				
15	$\Delta S = \Delta\,\underline{14}$	0	.855	.175	.499	-.086	.703	.315	.509				
16	$\Delta t = \Delta S/(S_0\alpha)$	0	118.9°	24.35°	62.5°	-11.95°	97.7°	43.8°	70.8°				
17	$t = t_0 + \Delta t$	0°F	118.9°	24.35°	62.5°	-11.95°	97.7°	43.8°	70.8°	32°	30°	60°	120°
18	$a = L/2Z$	4440								4350	7396	6840	5967
19	$(Da/L)(1 - Z^2/6)$	0								0	0	0	0
20	$X_2 = L/2 - \underline{19}$	500								500	500	500	500
21	$Y_2 = (x_2^2/2a)(1 + x_2^2/12a^2)$	28.15								26.25	16.90	18.28	20.95
22	Tangent Sag $= (L_eZ/4)(1 + Z^2/12)$	28.15								26.25	16.90	18.28	20.95
23	$a_1 = a + D + y_2$	4468								4375	7413	6858	5987
24	$H = Wa$	5635								4311	2382	2202	1921
25	$T_1 = Wa_1$	5670								4333	2387	2208	1928

Underlined numerals refer to item numbers

Cable 318,000 C.M. A.C.S.R.
24×.1151 Aluminum
43× Various Size Steel
Maximum Tension 33,000 lbs. @ 0°F, ½" Radial Ice, 8 lb. Wind
Project
Computed by M.L. Date

SAG AND TENSION CALCULATIONS
FORM NO. I

EXAMPLE 2

Cable Weight W=1.684#/ft; W÷AE=.14204x10^-6
Cable Weight plus Ice W=2.623#/ft; W÷AE=.22124x10^-6
Wind W=____#/ft.
Max. Result. Load at 0°F, W=3.322#/ft; W÷AE=.28020x10^-6
Area of Cross Section, A=.3952 sq. in.
Diameter of Cable, inches
Modulus of Elasticity, E=30 x 10^6
Coefficient of Linear Expansion α =6.62 x10^-6

Form Number 1

Example 2

		Cable + Ice + Wind		Cable + Ice		Cable Only			Cable + Ice	Cable Only			
1	L = Span Length	4279											
2	D = Difference in Elevation	185.5											
3	$L_e = L + d;\ d = D^2/(2L + d)$	4283											
4	$6\,L_e/L^2$	.0014035											
5	T_1 = Maximum Tension	33,000											
6	W	3.322	3.322	2.623	2.623	1.684	1.684	1.684	2.623	1.684	1.684	1.684	
7	$a_1 = T_1/W$	9933.8											
8	$\partial = (2a_1 - D)/L_e$	4.5954											
9	$Z = 1/(\partial - Z/2)$	.22302	.22500	.218	.215	.205	.210	.215	.2187	.2085	.2128	.2162	
10	Slack $= (Z^2/\underline{4})(1 + Z^2/20)$	35.5266	36.1618	33.9415	33.0116	30.0069	31.4907	33.0116					
11	S_0	4306.9	4306.9	4306.9	4306.9	4306.9	4306.9	4306.9					
12	$W/AE \times 10^6$	.28020	.28020	.22124	.22124	.14204	.14204	.14204					
13	Stretch $= (W/AE)(S_0^2/2Z)$	11.6537	11.5511	9.4134	9.5447	6.4268	6.2749	6.1279					
14	$(S_0 - L_e) = \underline{10} - \underline{13}$	23.8729	24.6107	24.5281	23.4669	23.5791	25.2158	26.8837					
15	$\Delta S = \Delta\,\underline{14}$	0	.7378	.6552	-.4060	-.2938	1.3429	3.0108					
16	$\Delta t = \Delta S/(S_0\alpha)$	0	25.88°	22.98°	-14.24°	-10.30°	47.10°	105.60°					
17	$t = t_0 + \Delta t$	0°F.	25.88°	22.98°	-14.24°	-10.30°	47.10°	105.60°	32°F.	32°F.	80°F.	120°F.	
18	$a = L/2Z$	9593.3							9782.8	10,261.4	10,054.1	9895.9	
19	$(Da/L)(1 - Z^2/6)$	302.7							420.7	443.2	434.2	425.57	
20	$X_2 = L/2 - \underline{19}$	1836.8							1718.8	1696.3	1706.5	1713.9	
21	$Y_2 = (x_2^2/2a)(1 + x_2^2/12a^2)$	140.79							151.38	143.44	147.65	148.79	
22	Tangent Sag $= (L_eZ/4)(1 + Z^2/12)$												
23	$a_1 = a + D + y_2$	9919.8							10,119.7	10,596.3	10,387.2	10,230.2	
24	$H = Wa$	31,869							25,660.3	17,280.2	16,931.1	16,664.7	
25	$T_1 = Wa_1$	32,954							26,544.6	17,834.1	17,492.6	17,228.7	

Underlined numerals refer to item numbers

Form Number 2

Example 3

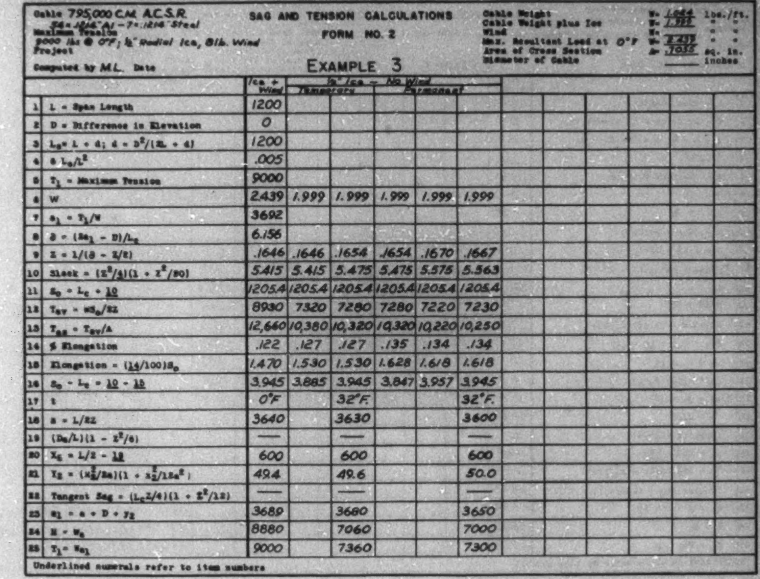

Cable 795,000 C.M. A.C.S.R.
54×.1216" Al – 7×.1214" Steel
Maximum Tension
9000 lbs @ 0°F; ½" Radial Ice, 8lb. Wind
Project
Computed by M.L. Date

SAG AND TENSION CALCULATIONS
FORM NO. 2

EXAMPLE 3

Cable Weight W= 1.024 lbs./ft.
Cable Weight plus Ice W= 1.999 " "
Wind W= " "
Max. Resultant Load at 0°F W= 2.439 " "
Area of Cross Section A= .7053 sq. in.
Diameter of Cable ______ inches

		Ice + Wind	½" Ice — No Wind										
			Temporary		Permanent								
1	L = Span Length	1200											
2	D = Difference in Elevation	0											
3	$L_c = L + d;\ d = D^2/(2L + d)$	1200											
4	$6\ L_c/L^2$	.005											
5	T_1 = Maximum Tension	9000											
6	W	2.439	1.999	1.999	1.999	1.999	1.999						
7	$a_1 = T_1/W$	3692											
8	$\partial = (2a_1 - D)/L_c$	6.156											
9	$Z = 1/(\partial - Z/2)$	.1646	.1646	.1654	.1654	.1670	.1667						
10	Slack = $(Z^2/4)(1 + Z^2/20)$	5.415	5.415	5.475	5.475	5.575	5.563						
11	$S_0 = L_c + \underline{10}$	1205.4	1205.4	1205.4	1205.4	1205.4	1205.4						
12	$T_{av} = WS_0/2Z$	8930	7320	7280	7280	7220	7230						
13	$T_{as} = T_{av}/A$	12,660	10,380	10,320	10,320	10,220	10,250						
14	% Elongation	.122	.127	.127	.135	.134	.134						
15	Elongation = $(\underline{14}/100)S_0$	1.470	1.530	1.530	1.628	1.618	1.618						
16	$S_0 - L_c = \underline{10} - \underline{15}$	3.945	3.885	3.945	3.847	3.957	3.945						
17	t	0°F		32°F.			32°F.						
18	$a = L/2Z$	3640		3630			3600						
19	$(D_a/L)(1 - Z^2/6)$	—		—			—						
20	$X_2 = L/2 - \underline{19}$	600		600			600						
21	$Y_2 = (X_2^2/2a)(1 + X_2^2/12a^2)$	49.4		49.6			50.0						
22	Tangent Sag = $(L_c Z/4)(1 + Z^2/12)$	—		—			—						
23	$a_1 = a + D + Y_2$	3689		3680			3650						
24	$H = Wa$	8880		7060			7000						
25	$T_1 = Wa_1$	9000		7360			7300						

Underlined numerals refer to item numbers

Form Number 2

Example 4

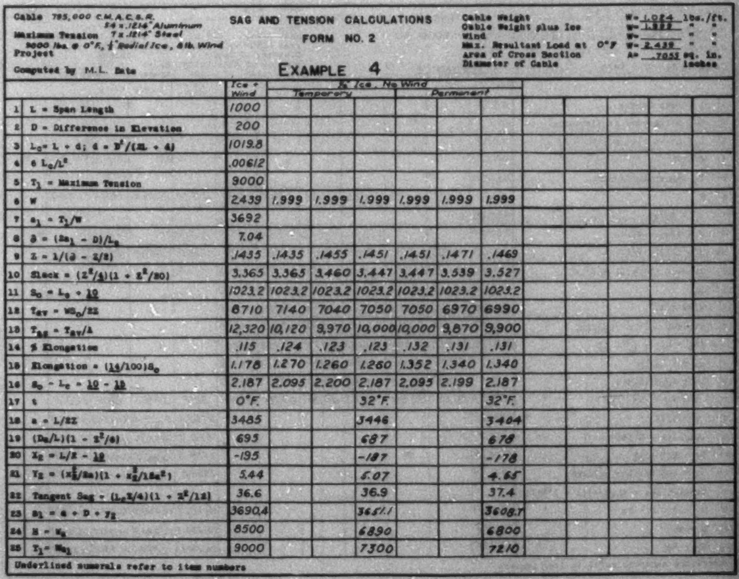

Cable 795,000 C.M. A.C.S.R.
54×.1214" Aluminum
Maximum Tension 7×.1214" Steel
9000 lbs. @ 0°F., ½" Radial Ice, 8lb. Wind
Project
Computed by M.L. Date

SAG AND TENSION CALCULATIONS
FORM NO. 2

EXAMPLE 4

Cable Weight W= 1.024 lbs./ft.
Cable Weight plus Ice W= 1.999 " "
Wind W= ______ " "
Max. Resultant Load at 0°F W= 2.439 " "
Area of Cross Section A= .7053 sq. in.
Diameter of Cable inches

		Ice + Wind	½" Ice, No Wind										
			Temporary			Permanent							
1	L = Span Length	1000											
2	D = Difference in Elevation	200											
3	$L_c = L + d;\ d = D^2/(2L + d)$	1019.8											
4	$6\ L_c/L^2$	.00612											
5	T_1 = Maximum Tension	9000											
6	W	2.439	1.999	1.999	1.999	1.999	1.999	1.999					
7	$a_1 = T_1/W$	3692											
8	$\partial = (2a_1 - D)/L_c$	7.04											
9	$Z = 1/(\partial - Z/2)$	.1435	.1435	.1455	.1451	.1451	.1471	.1469					
10	Slack = $(Z^2/4)(1 + Z^2/20)$	3.365	3.365	3.460	3.447	3.447	3.539	3.527					
11	$S_0 = L_c + \underline{10}$	1023.2	1023.2	1023.2	1023.2	1023.2	1023.2	1023.2					
12	$T_{av} = WS_0/2Z$	8710	7140	7040	7050	7050	6970	6990					
13	$T_{as} = T_{av}/A$	12,320	10,120	9,970	10,000	10,000	9,870	9,900					
14	% Elongation	.115	.124	.123	.123	.132	.131	.131					
15	Elongation = $(\underline{14}/100)S_0$	1.178	1.270	1.260	1.260	1.352	1.340	1.340					
16	$S_0 - L_c = \underline{10} - \underline{15}$	2.187	2.095	2.200	2.187	2.095	2.199	2.187					
17	t	0°F.			32°F.			32°F.					
18	$a = L/2Z$	3485			3446			3404					
19	$(D_a/L)(1 - Z^2/6)$	695			687			678					
20	$X_2 = L/2 - \underline{19}$	-195			-187			-178					
21	$Y_2 = (X_2^2/2a)(1 + X_2^2/12a^2)$	5.44			5.07			4.65					
22	Tangent Sag = $(L_c Z/4)(1 + Z^2/12)$	36.6			36.9			37.4					
23	$a_1 = a + D + Y_2$	3690.4			3651.1			3608.7					
24	$H = Wa$	8500			6890			6800					
25	$T_1 = Wa_1$	9000			7300			7210					

Underlined numerals refer to item numbers are included: one for level spans and one for nonlevel spans. For this purpose, previously published examples are used so that a comparison with current methods of calculation may be had. In each case the cable characteristics and maximum loading conditions are stated in the heading of the form.

EXAMPLE NUMBER 1. CALCULATED ON FORM NUMBER 1, WITH 1,000-FOOT LEVEL SPAN[1] AND CONSTANT MODULUS OF ELASTICITY

The calculations are set forth in columnar arrangement, the first column being for the condition of maximum tension at 0 degree Fahrenheit and maximum loading.

Columns 2 to 8, inclusive, are calculations of temperatures corresponding to various assumed values of Z, from which "Z-temperature" curves Figure 3 are prepared.

Columns 9 to 12, inclusive, contain calculations of sags and tensions for various selected temperatures, the values of Z being obtained from the "Z-temperature" curves, Figure 3.

In detail the calculations are as follows, the underlined numerals in all cases referring to item numbers. For column 1, in sequential order:

1. L $=1{,}000$ Span length
2. D $=0$ Level span
3. L_c $=1{,}000$ $D=0$; therefore $L_c=L$
4. $6L_c/L^3$ $=0.006$ $6\times1{,}000/1{,}000^3=0.006$
5. T_1 $=5{,}670$ Maximum tension
6. W $=1.269$ Weight per foot at maximum loading conditions
7. $a_1=T_1/W$ $=4{,}468.1$ $5{,}670/1.269=4{,}468.1$
8. $\partial=\frac{2a_1-D}{L_c}$ $=8.936$ $\frac{(2\times4{,}468.1-0)}{1{,}000}=8.936$
9. $Z=\frac{1}{\partial-\frac{Z}{2}}$ $=0.1126$ $\frac{1}{\partial}=0.112$; $Z=\frac{1}{8.936-0.112/2}=0.1126$
10. $\text{Slack}=\frac{Z^2}{\underline{4}}\left(1+\frac{Z^2}{20}\right)$ $=2.113$ $\frac{0.1126^2}{0.006}\left(1+\frac{0.1126^2}{20}\right)=2.113$
12. $\frac{W}{AE}\times10^6$ $=0.6124$ $\frac{W}{AE}$ for maximum loading $=0.6124\times10^{-6}$

11 & 13.

$\text{Stretch}=\frac{W}{AE}\,\frac{S_0^2}{2Z}$

Assume $S_0=L_c+\text{slack}=1{,}000+2.1=1{,}002.1$

Then stretch $=0.6124\times10^{-6}\times\frac{1{,}002.1^2}{2\times0.1126}=2.735$

11. $S_0=L_c+\text{slack}-\text{stretch}$ $=999.4$ $1{,}000+2.1-2.7=999.4$
13. $\text{Stretch}=\frac{W}{AE}\,\frac{S_0^2}{2Z}$ $=2.720$ $\frac{0.6124\times10^{-6}=999.4^2}{2\times0.1126}=2.720$
14. $(S_0-L_c)=10\text{–}13$ $=-0.607$ $2.113\text{–}2.720=-0.607$
15. ΔS $=0$ ΔS is the change in length due to change in temperature. This being the initial temperature, there is no change in length
16. $\Delta t=\Delta S/(S_0\,\alpha)$ $=0$ $0/(S_0\,\alpha)=0$
17. t $=0°\text{F}$ Initial temperature
18. $a=\frac{L}{2Z}$ $=4{,}440$ $1{,}000/2\times0.1126=4{,}440$
19. $\frac{Da}{L}\left(1-\frac{Z^2}{6}\right)$ $=0$ $D=0$, therefore $\underline{19}=0$
20. $x_2=\frac{L}{2}-\underline{19}$ $=500$ $\frac{1{,}000}{2}-0=500$
21. $\text{Sag } y_2=\frac{x_2^2}{2a}\left(1+\frac{x_2^2}{12a^2}\right)$ $=28.15$ $\frac{500^2}{2\times4{,}440}\left(1+\frac{500^2}{12\times4{,}440^2}\right)=28.15$
22. Tangent sag* $=\frac{L_cZ}{4}\left(1+\frac{Z^2}{12}\right)$ $=28.15$ $\frac{1{,}000\times0.1126}{4}\left(1+\frac{0.1126^2}{12}\right)=28.15$
23. $a_1=a+D+y_2$ $=4{,}468$ $(4{,}440+0+28)=4{,}468$
24. $H=Wa$ $=5{,}635$ $4{,}440\times1.269=5{,}635$
25. $T_1=Wa_1$ $=5{,}670$ $4{,}468\times1.269=5{,}670$

The next steps are to calculate temperatures corresponding to arbitrarily assumed values of Z. Columns 2, 3, and 4 are such calculations for $W=0.871$ (cable + ice loading) while columns 5 to 8, inclusive, are for $W=0.322$ (cable only).

In sequential order the calculations of column 2 are:

6. W $=0.871$
7. Z $=0.1126$ Arbitrarily assumed value
10. $\text{Slack}=\frac{Z^2}{\underline{4}}\left(1+\frac{Z^2}{20}\right)$ $=2.113$
11. S_0 $=999.4$ Unstressed length of cable at 0 degree Fahrenheit
12. $\frac{W}{AE}\times10^6$ $=0.4203$ Value corresponding to $W=0.817$
13. $\text{Stretch } \frac{W}{AE}\left(\frac{S_0^2}{2Z}\right)$ $=1.865$ $0.4203\times10^{-6}\times\frac{999.4^2}{2\times0.1126}=1.865$
14. $(S_0-L_c)=\underline{11}-\underline{13}$ $=+0.248$ $2.113-1.865=+0.248$
15. $\Delta S=(\underline{14}\text{ Column 2})-(\underline{14}\text{ Column 1})$ $=0.855$ $0.248-(-0.607)=0.855$
16. $\Delta t=\Delta S/(S_0\,\alpha)$ $=118.9°$ $\frac{0.855}{999.4\times7.2\times10^{-6}}=118.9°$
17. $t=t_0+\Delta t$ $=118.9°$ Since $t_0=0$ degree Fahrenheit; $t_0+\Delta t=118.9°$

Columns 9 to 12, inclusive, are calculations of sags and tensions for particular temperature and loading conditions. In each case the value of Z for the particular temperature is obtained from the "Z-temperature" curve, Figure 3. Calculations of items 18 to 25, inclusive, are then made in Column 1.

---

* This being a level span, the sag y_2 and the tangent sag are identical.

NOTE. Item 23 should equal item 7, and item 25 should equal item 5.

Example Number 2. Calculated on Form Number 1 with 4,279-Foot Nonlevel Span[3] and Constant Modulus of Elasticity

These calculations are similar to those in Example Number 1. Due to the difference in elevation, the straight line distance between supports, L_c is greater than the span length L; also the tangent sag and sag y_1 have different values. Figure 4 is the "Z-temperature" curve for this example.

Example Number 3. Calculated on Form Number 2 with 1,200-Foot Level Span[2] and Variable Modulus of Elasticity

This calculation makes use of the stress-strain curves, Figure 3.

As in the solution of problems, Example Number 1 and Example Number 2, calculations at maximum tension and loading conditions are made in column 1.

Sequentially the calculations of items 1 to 10, inclusive, are similar to those described previously.

The operations in items 11 to 17, inclusive, are

11.	$S_0=L_c+\underline{10}$	$=1205.4$	$1{,}200+5.4=1{,}205.4$
12.	$T_{avg}=\dfrac{WS_0}{2Z}$	$=8{,}930$	$\dfrac{2.439\times1{,}205.4}{2\times0.1646}=8{,}930$
13.	$T_{as}=\dfrac{T_{avg}}{A}$	$=12{,}660$	$\dfrac{8{,}930}{0.2055}=12{,}660$
14.	Per cent elongation	$=0.122$	From 0° Fahrenheit, curve Figure 3 for $T_{as}=12{,}660$
15.	Elongation $(\underline{14}\div100)S_0$	$=1.470$	$0.122/100\times1{,}205.4=1.470$
16.	$S_0-L_c=\underline{10}-\underline{15}$	$=3.945$	$5.415-1.470=3.945$
17.	t	$=0°$ F	Temperature at maximum tension and loading

Calculation of items 18 to 25, inclusive, are similar to those previously explained in Example Number 1.

Columns 2, et cetera, indicate the calculations of "Temporary" and "Permanent" sags and tension at 32 degrees Fahrenheit, 1/2-inch ice, no wind. Under these conditions $W=1.999$.

A method of successive approximations is used. Referring to column 2, a value of $Z=0.1646$ is assumed; calculating items 9 to 16, inclusive, in a similar manner to that indicated in column 1, we have item $\underline{16}$, $(S_0-L_c)=\underline{10}-\underline{15}=3.885$.

The value of $\underline{16}$ should be 3.945

The difference of these to values is	0.060
Adding slack, column 2	5.415
	5.475

for slack $=5.475$, we calculate the value of $Z=0.1654$ completing calculation of items 12 to 16, inclusive; in column 3 we get item 16, $S_0-L_c=3.945$, therefore, for the temporary condition (cable not prestretched) at 32 degrees Fahrenheit, $Z=0.1654$. Proceeding down column 3, items 18 to 25, inclusive, are calculated as in column 1.

Columns 4, 5, and 6 give the calculations for the "Permanent" condition (cable prestretched) at 32 degrees Fahrenheit, 1/2-inch ice, no wind.

Example Number 4. Calculated on Form Number 2 with 1,200-Foot Nonlevel Span with Variable Modulus of Elasticity

The calculations of Example 4 are similar to those for Example Number 3.

Appendix. Derivation of Formulas

Let the conductor be represented by the Curve A-B, Figure 5.

The fundamental formulas of the catenary referred to the point where it has a horizontal tangent are:

$$y=a\left(\cosh\frac{x}{a}-1\right) \tag{5}$$

$$s=a\sinh\frac{x}{a} \tag{6}$$

The horizontal component of tension at any point on the suspended conductor is:

$$H=Wa \tag{7}$$

The tension at any point on the suspended conductor is

$$T=Wy+H=W(y+a) \tag{8}$$

The following equations are derived in "Transmission Line Catenary Calculations."[4]

$$Z=\frac{L}{2a}\quad\text{(by definition)} \tag{9}$$

$$\partial=\frac{2T_1-WD}{WL_c} \tag{10}$$

$$\text{Slack}=S-L_c=\frac{L^2}{6L_c}Z^2\left(1+\frac{Z^2}{20}\right)+\dots \tag{11}$$

$$\text{Tangent sag}=\frac{L_cZ}{4}+\frac{3L^2-2D^2}{144L_c^2}Z^3+\dots$$

$$=\frac{L_cZ}{4}\left(1+\frac{Z^2}{12}\right)+\dots \tag{12}$$

$$\text{Stretch}=\frac{T_{avg}S}{AE} \tag{13}$$

$$T_{avg}=\frac{WS}{2Z}+\dots \tag{14}$$

$$\text{Coth } Z=\frac{2T_1-WD}{WS} \tag{15}$$

$$x=\frac{L}{2}\pm a\sinh^{-1}\left[\frac{D}{L}\frac{Z}{\sinh Z}\right] \tag{16}$$

From the foregoing equations by substitution, transposition, et cetera:
Let

$$a_1=\frac{T_1}{W}\quad\text{(by definition)} \tag{17}$$

Substituting equation 17 in equation 10

$$\partial=\frac{2a_1-D}{L_c} \tag{18}$$

Combining equations 10 and 15

$$\frac{\text{Cosh } z}{z}=\partial Q \tag{19}$$

where

$$Q=\sqrt{\frac{1+\left(\dfrac{D}{L}\right)^2}{1+\left(\dfrac{D}{L}\right)^2\left(\dfrac{Z}{\sinh Z}\right)^2}} \tag{20}$$

Transforming and simplifying equation 19

$$Z=\frac{1}{\partial Q-\dfrac{Z}{2}}+\dots \tag{21}$$

Figure 6 shows the relationship between Q and Z for various values of D/L. It is evident that Q may be generally considered to be unity without loss of accuracy.
Expanding $(z/\sinh z)$ as a series

$$\frac{Z}{\sinh Z}=\left(1-\frac{Z^2}{6}\right)+\dots \tag{22}$$

Substituting equation 22 in equation 16

$$x=\frac{L}{2}\pm a\sinh^{-1}\left[\frac{D}{L}\left(1-\frac{Z^2}{6}+\dots\right)\right] \tag{23}$$

Let

$$P=\frac{\sinh^{-1}\left[\dfrac{D}{L}\left(1-\dfrac{Z^2}{6}\right)\right]}{\left[\dfrac{D}{L}\left(1-\dfrac{Z^2}{6}\right)\right]} \tag{24}$$

Substituting equation 24 in equation 23

$$x=\frac{L}{2}\pm P\left[\frac{aD}{L}\left(1-\frac{Z^2}{6}\right)\right] \tag{25}$$

Values of P are plotted on Figure 7. It can be seen that for ordinary values of D/L, P may be considered to be unity. Expanding equation 6 as a series

$$y=\frac{x^2}{2a}\left[1+\frac{x^2}{12a^2}+\ldots\right] \tag{26}$$

Neglecting terms beyond the 2nd as negligible

$$y=\frac{x^2}{2a}\left[1+\left(\frac{x^2}{2a}\right)\left(\frac{1}{6a}\right)\right] \tag{27}$$

The equation of the straight line distance between supports is

$$Lc=\sqrt{L^2+D^2} \tag{28}$$

Let

$$L_e=L+d \tag{29}$$

then

$$d=\frac{D^2}{2L+d} \tag{30}$$

Summarizing the foregoing equations and rearranging their order

$$L_e=L+d; \text{ where } d=\frac{D^2}{2L+d} \tag{A}$$

$$a_1=\frac{T_1}{W} \tag{B}$$

$$\partial=\frac{2a_1-D}{L_e} \tag{C}$$

$$Z=\frac{1}{\partial Q-\frac{Z}{2}} \tag{D}$$

$$\text{Slack}=\frac{Z^2}{\left(\frac{6L_e}{L^2}\right)}\left(1+\frac{Z^2}{20}\right) \tag{E}$$

$$\text{Stretch}=\frac{T_{avg}S}{AE} \tag{F}$$

$$T_{avg}=\frac{WS}{2Z} \tag{G}$$

$$\text{Tangent sag}=\frac{L_eZ}{4}\left(1+\frac{Z^2}{12}\right) \tag{H}$$

$$a=\frac{L}{2Z} \tag{I}$$

$$H=Wa \tag{J}$$

$$x_2=\frac{L}{2}-P\left[\frac{Da}{L}\left(1-\frac{Z^2}{6}\right)\right] \tag{K}$$

$$y_2=\frac{x_2^2}{2a}\left[1+\left(\frac{x_2^2}{2a}\right)\left(\frac{1}{6a}\right)\right] \tag{L}$$

References

1. SAG CALCULATIONS BY THE USE OF MARTIN'S TABLE (book), James S. Martin. Copperweld Steel Company, Glassport, Pa., 1931.

2. ACSR GRAPHIC METHOD FOR SAG CALCULATIONS (book). Aluminum Company of America, Pittsburgh, Pa., 1927.

3. MISSISSIPPI RIVER CROSSING OF CRYSTAL CITY TRANSMISSION LINE, H. W. Eales, E. Ettlinger. *AIEE Transactions*, volume 44, 1925, pages 387–97.

4. TRANSMISSION LINE CATENARY CALCULATIONS, D. O. Ehrenburg. *Electrical Engineering* (*AIEE Transactions*), volume 54, July 1935, pages 719–27.

5. TRANSMISSION LINE CATENARY CALCULATIONS, (letter), H. J. McCracken. *AIEE Transactions*, volume 54, August 1935, page 910.

6. BROKEN CONDUCTOR EFFECT ON SAGS IN SUSPENSION SPANS, Alfio Bissiri, Maurice Landau. *AIEE Transactions*, volume 66, 1947, pages 1181–88.

No Discussion

Steady-State Characteristics of Carbon-Pile Voltage Regulators

D. G. SCORGIE
ASSOCIATE AIEE

D. H. SCHAEFER
ASSOCIATE AIEE

ATTEMPTS to measure the steady-state characteristics of carbon-pile voltage regulators have repeatedly been made and have ended in failure. The straight-forward method of measuring carbon-pile resistance versus operating coil voltage is to connect the operating coil of a regulator in series with a source of current and a variable resistance. This method fails, though, because upon increasing the voltage applied to the operating coil a point is reached where the carbon-pile resistance can no longer be controlled by manual adjustments.

It is not sufficient to attribute this result to a lack of sensitivity in controlling the voltage. Instead, the measurements reported upon here indicate that there exists an operating voltage above which the carbon-pile resistance jumps discontinuously to a high value. An electronic measuring circuit (see Appendix I) which controls pile resistance directly has been used to circumvent this difficulty. With its use steady-state carbon-pile resistance versus operating coil voltage hysteresis loops have been obtained under several conditions with constant current flowing through the carbon pile. The first case uses carbon-pile currents of the order of milliamperes, and hence eliminates most of the heating effects within the pile. The other cases use current of the same order of magnitude as that which actually flows through a carbon pile in operation.

In an effort to evaluate the effects due to heating, hysteresis loops were taken at an elevated ambient temperature and low pile current, then again at room ambient temperature and high pile current. It was hoped to separate the effects caused by: (a) expansion due to heating of the metallic parts of the regulator, and (b) resistance and pressure changes due to extremely high local temperatures within the carbon stack.

Measurement Technique

The electronic measuring circuit is reproduced in Figure 1. It consists essentially of a d-c amplifier with a cathode-follower matching stage to supply the large current for the regulator operating coil.

For the measurements in which small constant carbon-pile current flows, the input to the d-c amplifier is connected across the series combination of the regulator carbon pile and the variable resistor, R_s. For measurements using high pile currents the Helipots and carbon-pile supply of Figure 1(A) are replaced by the arrangement shown in Figure 1(B). In both cases a closed, stable loop is formed which acts automatically to control the magnitude of the pile resistance. The operation of this circuit is described in Appendix I.

Linear Theory of Regulator Operation

The dotted curves of Figure 2 are several force-versus-displacement curves for the regulator magnet at constant operating coil ampere-turns. The voltage across the operating coil circuit is R_cI where R_c is the total circuit resistance. Hysteresis is ignored in these curves but will be discussed later. Two additional curves are superimposed on the magnet curves in Figure 2. The first is the force-versus-deflection characteristic of the spring. The second, although misnamed, is called the carbon-pile characteristic,[1] and is constructed by adding the carbon pile and spring forces at each deflection. Therefore the net force on the carbon pile is given by the difference between the latter two curves, and a deflection to the left corresponds to an increase of carbon-pile resistance. Loosening the pile screw corresponds graphically to moving the origin of the carbon-pile characteristic to the right along the spring curve. Figure 2(B) shows a carbon-pile characteristic for a regulator with its pile screw further out than Figure 2(A).

Provided system stability criteria are satisfied,[2] the only requirement for a regulator to operate at a specific point is that the algebraic sum of the spring, magnet, and carbon-pile forces be zero. Any point of intersection of a magnet and carbon-pile characteristic satisfies this condition, and the operating voltage will be determined by which magnet curve is selected. It can be seen from Figure 2(A) that for low carbon-pile resistances the armature must be far to the right and the carbon-pile characteristic intersects a low NI magnet curve. As the resistance is increased, points of equilibrium are found at higher NI magnet curves until the curve marked NI_2 is intersected. From then on, points of equilibrium for still higher resistances are found at lower NI magnet curves. In other words, it would be expected that for increasing carbon-pile resistance the operating coil voltage would increase to a maximum of R_cI_2 then decrease. Both the ascending and descending portions of curve A of Figure 8 show such a situation. Similar arguments applied to Figure 2(B) show that no maximum voltage would be expected. Curve B of Figure 8 was measured on the same regulator as curve A, but with the pile screw loosened.

According to linear theory, perfect regulation would be afforded by parallelism between the magnet and carbon-pile characteristic curves. Linear sta-

---

Paper 51-295, recommended by the AIEE Air Transportation Committee and approved by the AIEE Technical Program Committee for presentation at the AIEE Pacific General Meeting, Portland, Oreg., August 20–23, 1951. Manuscript submitted May 18, 1951; made available for printing July 11, 1951.

D. G. Scorgie and D. H. Schaefer are with the Naval Research Laboratory, Washington, D. C.

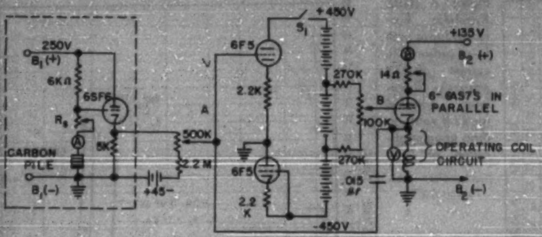

Figure 1(A). Schematic diagram of regulator test circuit

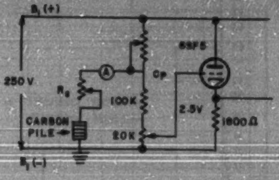

Figure 1(B). Test circuit modification for high pile current

bility criteria demand, however, that the magnitude of the slope of the carbon-pile curve be greater than that of the magnet curve at a point of stable operation. This is equivalent to saying that generator terminal voltage must drop with load for any stable regulated generator. Since we know this to be false, in practice nonlinearities must exist, and their nature has been experimentally investigated in the section which follows.

Experimental Results

The experiments performed were intended to determine the manner in which performance differs from the idealized picture given above. A standard 28-volt d-c regulator with disk-type spring was used for all measurements. The various adjustments of the regulator are noted on the graphs.

Constant Temperature Data

For the series of tests in Figures 3, 4, and 5, the temperatures in the regulator were held constant during the measurement of each loop. All were run with less than 0.1 watt power dissipation in the carbon pile, so that the variable heating was all due to operating coil current and thus very nearly constant. Figure 3 shows major hysteresis loops, A, B, C, and D for which the maximum carbon pile resistances were infinity, 50 ohms, 30 ohms, and 10 ohms, respectively. If, after each loop, the voltage is lowered to the neighborhood of 15 volts the rising portion of the loop can then be reproduced very accurately. If however, the base carbon-pile resistance was never reached, the rising portion of the next loop was in some cases not reproduced. This effect is shown in Figure 4, curve A, the descending portion of which is identical with curve A of Figure 3. From the graphs it can be seen that hysteresis alone can account for variations of up to 1.5 volts in the operating coil voltage for a given resistance.

Further constant temperature curves were taken but this time at elevated ambient temperatures. Carbon-pile current remained of the order of milliamperes and the ambient temperature was raised. As a result, operating coil voltages were higher than before, as shown in Figure 5. Only the rising portions of the curves are reproduced, and are compared in Figure 5 with the corresponding curves at room ambient temperature.

High Pile Current Data

The remainder of the tests were run with pile currents of either 1, 2, or 3 amperes. The ambient temperature was regulated in such a manner as to hold resistance of the operating coil circuit at a constant value for all tests. Figure 6 shows rising portions of four curves taken on a regulator adjusted for no drop upon application of full generator load. Figure 7 shows the same four curves measured on a regulator adjusted for a half-volt drop upon application of full load. It can be seen that larger currents in the pile lower the operating coil voltage for a given resistance in Figure 6 while the opposite effect is shown for the lower parts of the 2- and 3-ampere curves of Figure 7.

Effect of Regulator Adjustment

Figure 8 shows experimental results obtained from the regulator under two conditions of adjustment. For curve A the regulator was adjusted for zero regulation at 27.7 volts. The conditions in curve B were the same except for a readjustment to obtain a $^1/_2$-volt regulation upon application of full rated load to the 200-ampere generator. Each curve was measured while a constant current of 1 ampere was flowing in the carbon pile. For resistance values higher than those plotted, the pile current was decreased and the value of pile resistance raised to infinity.

Discussion of Experimental Results

Hysteresis

Multivalued curves such as those given in Figures 3 and 4 can only be explained on the basis of hysteresis since temperature was held constant. Two kinds are present in the regulator, namely magnetic and carbon-pile hysteresis. The latter is recognized by the pile manufacturers, who publish pressure-resistance hysteresis loops in their catalogues. Their loops indicate that for the same force on

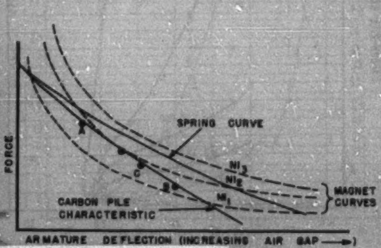

Figure 2(A) (left). Force-deflection characteristics with pile screw tightened

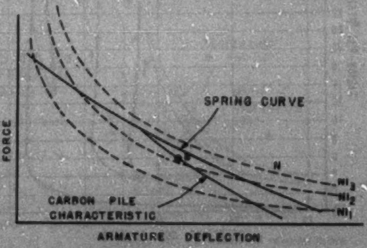

Figure 2(B) (right). Force-deflection characteristics with pile screw loosened

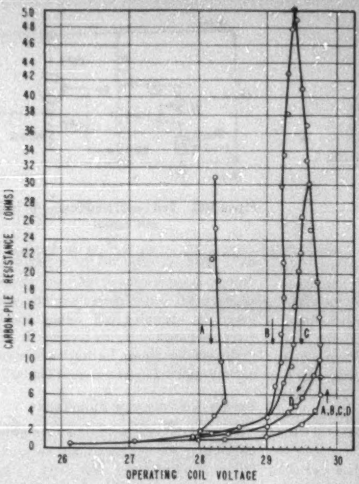

Figure 3 (left). Regulator hysteresis loops with low carbon-pile current (0.033 ampere). Regulator adjusted for 27.8 volts, no drop upon application of load

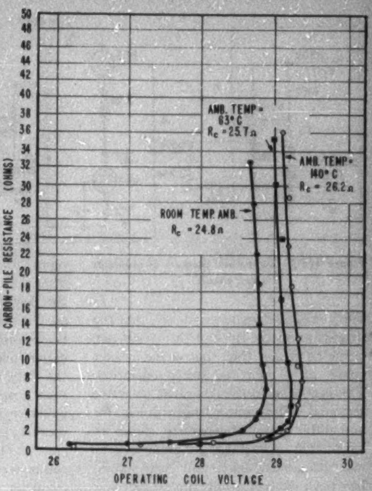

Figure 5 (right). Ascending portions of loops for various ambient temperatures, 21-milliampere pile current. Regulator adjusted for 27.35 volts no drop upon application of load

the carbon pile the resistance will be greater upon compression than upon decompression. If no other hysteresis were present this would mean that the diagrams in Figure 2 must be valid. Therefore, in Figure 3, the descending portion would cover the identical voltage range as the ascending portion, but for every voltage the resistance would be higher. The result would be a curve such as shown in Figure 9, which was calculated from the manufacturer's curves for the particular pile. For all practical purposes, Figure 9 shows the effect of carbon-pile hysteresis to be negligible.

Figures 3 and 4 must then be explained on the basis of magnetic hysteresis. In all cases the pull of the magnet is proportional to the square of the flux across the air gap; and, of course, the flux-versus-H_t relationship of the iron has a certain small amount of hysteresis. We are directly concerned, however, not with the ϕ-versus-H_t relationship but with the relationship between flux, ϕ, and total ampere-turns, NI. H_t is a function of both ampere-turns and air gap, and since the air gap varies inversely with flux, the relative width of the loop ϕ versus NI will be enormously greater than that of ϕ versus H_t. The clearest generality which can be made is that armature motion toward the pole piece always in-

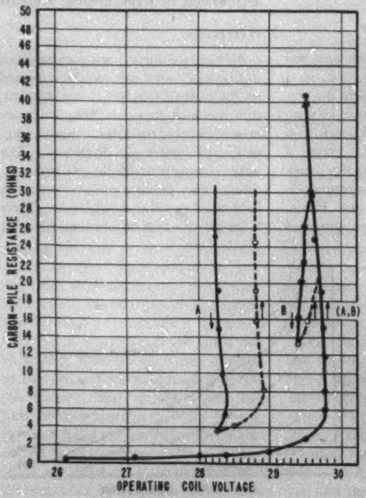

Figure 4 (left). Minor hysteresis loops with low carbon-pile current (0.033 ampere). Regulator adjusted for 27.8 volts, no drop upon application of load

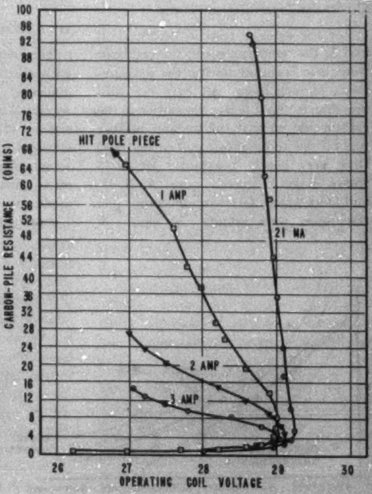

Figure 6 (right). Ascending portions of loops with various pile currents. Regulator adjusted for 27.3 volts. Zero drop upon application of load. Operating coil resistance≅25.8 ohms

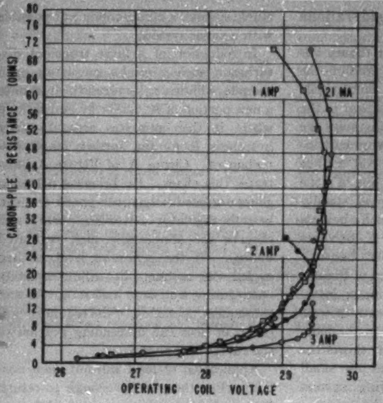

Figure 7 (left). Ascending portions of loops with various pile currents. Regulator adjusted for 27.3 volts. Half-volt drop upon application of load. Operating coil resistance ≅ 25.9 ohms

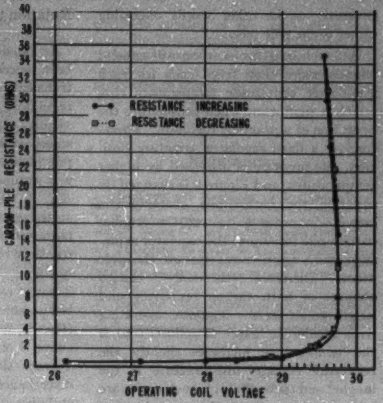

Figure 9 (right). Effect of carbon-pile hysteresis

dicates an increase of flux. Therefore, flux and carbon-pile resistance increase together and decrease together. As a result, a single constant *NI* curve (Figure 2) will move to a region of greater magnet force (therefore flux) for a given pile resistance when the resistance is being decreased. It is not particularly necessary to know whether it is an air-gap change or a current change which is determining the hysteresis. However, the hysteresis effect due to change of air gap is held responsible for the regulator behavior near the peaks in Figure 3, because the coil current is decreasing monotonically through this region.

Let us think of the magnet curves of Figure 2 as representing, at each point, the force on the armature while approaching the pole piece. They will then represent the minimum force on the armature for a given current. The hysteresis effect indicates that for displacements away from the pole piece each magnet force curve will be higher for a given current. In other words for displacements away from the pole piece less current is needed for the same magnet force. In terms of carbon-pile resistance this means that less operating coil current is required for a given resistance when the resistance is decreasing.

Heating Effects

In Figure 5 the increase in terminal voltage observed upon raising the ambient temperature was only one-third as great as the increase that would be caused only by a change in resistance of the operating coil circuit. This can be explained by the fact that the regulator under test has temperature compensators that alter the magnetic circuit. Here these compensators balanced out the effect of two-thirds of the operating coil resistance change.

The data shown in Figures 6 and 7 were taken with ambient temperature held such that the operating coil resistance was approximately the same for all runs. This was done primarily to eliminate the effect of changes in the magnetic compensator during the tests. Since the magnetic compensator and the operating coil occupy the same physical region, their temperatures probably remain constant if the operating coil resistance is constant.

High current in the carbon pile has two results, namely a thermal expansion of the carbon, and a decrease in its resistivity. Measurements with a thermocouple placed in the space at the center of a carbon pile indicate that the temperature rises about 200 degrees centigrade under normal operation. Temperatures in the pile itself must increase a great deal more. The resulting decrease in the resistivity of the carbon must be compensated for by lowering the pile

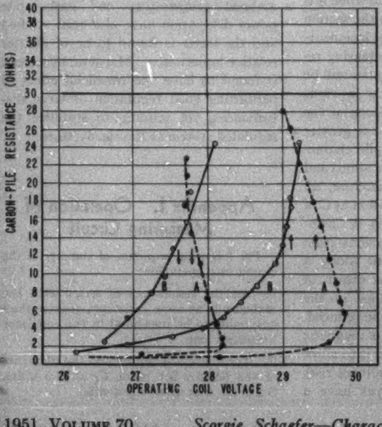

Figure 8 (left). Effect of regulator adjustment

Curve A—Adjustment for zero regulation

Curve B—Adjustment for 1/2-volt regulation

Regulator adjusted for 27.7 volts—no load

One-ampere carbon-pile current

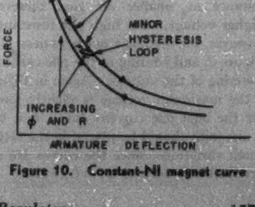

Figure 10. Constant-NI magnet curve

pressure, or in other words operating closer to the pole piece.

A 2-inch length of carbon will expand slightly more than 0.001 inch for each 100-degree centigrade temperature rise, which is significant when considering the operation of a practical regulator. Therefore for a fixed regulator armature position, pile pressure is increased by higher temperatures, and Figure 2 is changed by lowering the carbon-pile characteristic curve. In order to restore the original carbon-pile resistance the regulator armature must again move toward the pole piece. Therefore thermally caused changes of both carbon resistivity and length result in the regulator operating with smaller air gap. It follows that if the temperature increases slightly the regulated voltage will decrease if the magnet and carbon pile characteristics are related as at point A, Figure 2(A), and will increase if they are related as at point B, Figures 2(A) and 2(B).

Examine Figures 6 and 7 in the light of the preceding two paragraphs. The data of Figure 6 were taken with the regulator adjusted for zero drop with load, corresponding to a point near C of Figure 2. As pile power dissipation increases, the changes of carbon resistivity and length make it necessary to operate at smaller air gap in order to obtain the same resistance, so that the operation moves to the vicinity of point A, Figure 2, which is a region of decreasing voltage. This change in operating point for the same resistance is well illustrated in Figure 6 where, on the 1-ampere curve, the regulator armature struck the pole piece. With low power dissipation the resistance was raised to 100 ohms without the armature striking the pole piece. With 1-ampere pile current, however, the armature struck the pole piece at 70 ohms. A general lowering of the carbon pile characteristic results from pile heat, as mentioned above, and this effect manifests itself in a slightly smaller maximum voltage for the high current curves.

Data for Figure 7 were taken with an adjustment for 1/2-volt regulation, corresponding at low pile resistances to a region near B of Figure 2. In this instance pile heating causes operation for a given resistance at smaller air gap, therefore higher voltage. For high pile resistance, however, the regulator operates near A of Figure 2, and heating of the pile causes a lowering of the voltage. Again in Figure 7 the maximum voltage is slightly lower for the high pile current data. Not too much faith should be placed in the latter small variations, since the curves are reproducible to only about ±0.1 volt.

Relation to Transient Considerations

In previous papers[2,3] linear theory has been successfully used to predict the transient characteristics of carbon pile regulators. It will be recalled that in the vicinity of some initial operating point the steady-state relationship between carbon-pile resistance and operating coil voltage was assumed to be a straight line of slope K_r. In the linear theory good steady-state regulation depends upon K_r being a large positive number, but if K_r becomes too large or negative the system becomes unstable. The upward portion of Figures 3 and 4 seems to show regions of instability according to the above criteria (that is, negative K_r). The minor loop, curve B of Figure 4, however, shows the average slope angle decreases for small disturbances, thereby allowing system stability.

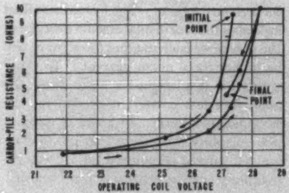

Figure 11. Simulated regulator performance upon application of load (carbon-pile current 1 ampere)

This can be explained in terms of a force-deflection diagram. Figure 10 shows the position of one constant-*NI* magnet curve both when the carbon-pile resistance is being increased and when it is being decreased. As stated in the section of hysteresis effects, for displacements away from the pole piece (decreasing resistances) each such magnet curve will be higher. From the results of the previous paper[3] it follows that if the slope of the magnet curve is nearly as great or greater than the slope of the carbon-pile characteristic, then K_r is very large or minus and the system is unstable. Therefore, all points to the left of such a position as C of Figure 2(A) should be points of instability. However, small excursions from an operating point will occur along a minor hysteresis loop such as drawn in Figure 10. The effective slope of the magnet curve is thus seen to be reduced, allowing stability. The effect of magnetic hysteresis in the regulator then is to allow perfect regulation and even voltage rises for large disturbances and yet have a stable system, a combination not possible with a linear system.

Introduction of a large transient disturbance, such as might completely open the pile, will drive the regulator iron onto a new portion of its major hysteresis loop where it then operates around minor hysteresis loops for further small disturbances. Curve A of Figure 4 illustrates this effect. By bringing a loaded generator gradually up to speed one can keep the regulator on its rising portion and observe the abnormally high regulated voltage. If the generator load is then cycled the carbon pile will completely open during transient load removals and subsequent operation of the regulator will be on or near the descending portion of the curves of Figure 8.

Application of load will not then normally close the pile far enough to return the regulator to the region of high regulated voltage. Figure 11 serves to illustrate this point. There the hysteresis loops are those followed in an actual case by the regulator controlling a generator to which full load was applied. The regulator was adjusted to give 1/2-volt drop with load. However, heating effects were not taken into account, as a constant carbon-pile current of 1 ampere was used in obtaining the hysteresis measurements.

Summary

The use of a feed-back electronic control circuit permits measurement of steady-state carbon-pile regulator characteristics throughout the complete operating range. Measurements obtained using such a circuit reveal the part played by magnetic hysteresis in determining regulator performance. The effects of ambient temperature and carbon-pile power dissipation have also been studied and the latter is found to be of greater relative importance. Magnetic hysteresis is found to have the beneficial effect of permitting good regulation of large disturbances, yet tending to stabilize the regulated system in the steady state.

Appendix I. Operation of Measuring Circuit

The following sequence of steps puts the circuit into operation:

1. Set the resistances in series with the carbon pile at some resistance greater than any value to be measured in the regulator hysteresis loop.
2. Turn on the *B* supply and the filaments of the *6SF5*. Set point C_P at 2.5 volts. Set point *A* at ground potential.

3. Heat the *6F5* filaments. Close switch S_1 and set point B at ground potential.

4. Heat the *6AS7* filaments. Turn on the B_2 supply and allow a voltage of less than 10 volts to be impressed across the operating coil circuit of the regulator.

5. Rebalance the whole circuit. Warm for an hour. Rebalance again.

The circuit now is ready for use. Up to a point just below the operating range of the regulator the operating coil voltage can be adjusted by varying the *6AS7* plate supply, and the circuit balanced by varying the series resistor (R_s in Figures 1(A) and 1(B)). Above that point, however, the regulator becomes extremely sensitive to voltage changes. Therefore from that point on the *6AS7* plate supply is left at a constant value while the series resistors are further decreased, allowing the electronic circuit automatically to increase the carbon-pile resistance. This eliminates minor hysteresis loops and assures control over the direction of each carbon-pile resistance change. During this time the circuit will become unbalanced, but the fluctuations in current through the carbon pile during each loop measurement are less than 5 per cent. All resistances are calculated from ammeter and voltmeter readings.

When it is desired to extend the hysteresis loop to infinite pile resistance values, the pile resistance is first increased to the highest plotted value by the technique described above. Then, in parallel with the pile, a 70-ohm rheostat is connected, the resistance of which is slowly decreased. The action of the feed-back loop is such that the carbon-pile resistance goes to infinity. Manually increasing the *6AS7* plate supply assures complete opening of the pile. From the time the 70-ohm rheostat is connected the carbon-pile current is of course not held constant. All of these operations are done in reverse to obtain the decreasing portion of the hysteresis loop.

References

1. ANALYSIS AND REDESIGN OF A CARBON-PILE VOLTAGE REGULATOR FOR AIRCRAFT GENERATORS, W. B. Kouwenhoven, G. H. Thaler. *AIEE Transactions*, volume 67, part II, 1948, pages 1197–1203.

2. TRANSIENT ANALYSIS OF VOLTAGE-REGULATED AIRCRAFT D-C SYSTEMS, Donald G. Scorgie. *AIEE Transactions*, volume 69, part II, 1950, pages 1318–23.

3. DYNAMIC CHARACTERISTICS OF CARBON-PILE VOLTAGE REGULATORS, R. L. Mills. *AIEE Transactions*, volume 69, part II, 1951, pages 1347–52.

No Discussion

Design of Permanent-Magnet Alternators

ROBERT M. SAUNDERS
MEMBER AIEE

ROBERT H. WEAKLEY
ASSOCIATE MEMBER AIEE

Synopsis: Permanent-magnet alternators offer a substantial reduction in weight and space for aircraft and portable applications and are therefore becoming more attractive. In this paper qualitative remarks are made on the major electrical factors to be considered in beginning the design of this class of machines; these are: voltage regulation, magnet stabilization, rotor design, subtransient reactance, negative sequence reactance, heating, and efficiency.

PERMANENT-magnet alternators have been used for many years in small sized units such as tachometer generators, governor frequency sources, and magnetos, but until recently have not been adopted widely as primary sources of power. With the development of dispersion-hardening alloys typified by the Alnico family and their application to rotating machinery, the permanent magnet alternator has assumed a more important role for power applications. In some ratings these machines weigh less, consume less space, and cost less than d-c excited alternators. The saving in weight and space is accomplished chiefly by the elimination of the d-c exciter. When the exciter is absent, commutation problems are eliminated. Hence, these machines are assuming an important role for portable and aircraft applications.

Since the literature pertaining directly to permanent-magnet synchronous machines is largely descriptive and not very extensive in the design field, it is the object of this paper to outline in a rather general and qualitative manner the procedures and factors that must be considered in the design of permanent-magnet alternators. Future papers will consider the individual problems in more complete fashion than is feasible here.

Throughout the paper the term "standard machine" is used. The authors wish to define a standard machine for the purposes of this paper as one which has a d-c excited field, approximately 40 per cent regulation, and is used with an external voltage regulator.

In beginning the design of a permanent-magnet synchronous machine the designer is faced with several problems and factors which are different from those encountered in the design of standard machines; they are (1) a consideration of the behavior of magnetic circuits employing permanent-magnet materials, (2) the effects of demagnetizing forces upon the permanent-magnet materials, (3) the means to be employed for magnetizing the machine, (4) the type of magnet stabilization to be utilized, (5) methods for reducing the voltage regulation, and (6) methods for reducing the transient and negative-sequence reactances.

These aspects now will be considered in detail.

Permanent Magnets With Demagnetizing Forces

While it will be assumed that the reader is familiar with the general principles pertaining to magnetic circuits containing permanent magnets,[1-4] for clarity it is necessary to set forth a few maxims and comments:

1. For a magnetic circuit of specified area and length and having a specified flux, the volume of magnetic material is least when the energy product is a maximum.[3,5]

2. If a permanent magnet is partially demagnetized by the application of a certain magnetomotive force, then it will not be demagnetized further by magnetomotive forces of smaller magnitude than the original demagnetizing magnetomotive force.[6,7]

3. When the permanent magnet material is subjected to a magnetizing or demagnetizing force, the change in the molecular structure is essentially instantaneous.

4. The magnetizing magnetomotive force (mmf) should be of the order of five times the product of the coercive force (H_c) and the magnet length.[4]

As a consequence of (1), for minimum volume of magnetic material, the operating line *OR*, Figure 1, should intersect the demagnetization curve B_rH_c at *Q*. Note that the operating line *OR* is a curve in general rather than a straight line; this is especially true in synchronous machines that are heavily saturated in the armature teeth.

Maxim (2) is a very important property and is known as the stabilization condition. Each permanent magnet must be stabilized by subjecting it to a demagnetizing force greater than any expected in service. A permanent magnet may be considered as a source of mmf possessing a reluctance which is a function not only of the flux density but also of its previous magnetic history. The relation between the flux density associated with a magnet and the mmf available for use in the external circuit is the demagnetization curve, B_r, *Q*, H_c, Figure 1. If *OR* represents the function describing the relationship between the external mmf and flux density, the point of stable operation of the permanent magnet with the magnetic circuit will be at *Q*. If the magnet is now subjected to an external demagnetizing force, F_A, the stable operating point with this demagnetizing mmf is *Q'*. When F_A is removed, the magnet will not recover to *Q* but rather along the minor-hysteresis loop back to *OR*. This minor hysteresis loop may be thought of as a straight line parallel to the slope of the major loop at B_r. Any subsequent demagnetization mmf less than or equal to F_A will result in operation along the minor loop line *Q'A*. In the synchronous machine, the maximum possible mmf, and hence the maximum possible demagnetizing effect, exists when the machine has been suddenly short-circuited. The magnitude of the armature mmf is limited

---

Paper 51-296, recommended by the AIEE Rotating Machinery Committee and approved by the AIEE Technical Program Committee for presentation at the AIEE Pacific General Meeting, Portland, Oreg., August 20-23, 1951. Manuscript submitted April 19, 1951; made available for printing July 16, 1951.

ROBERT M. SAUNDERS is with the University of California, Berkeley, Calif. and ROBERT H. WEAKLEY is with the U. S. Electrical Motors, Inc., Los Angeles, Calif.

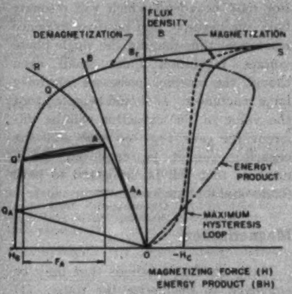

Figure 1. Magnetization, demagnetization, and energy product curves for a permanent magnet material. Note that for positive magnetizing forces a reduced scale is employed

mainly by the subtransient reactance and may be 5 to 8 times the no-load mmf. If short circuits are unlikely, the maximum mmf encountered is the steady-state direct axis armature mmf whose order of magnitude is the same as the no-load main field mmf. At zero power factor lagging as a generator, the armature reaction mmf lies in direct opposition to the main field mmf and thereby represents the worst steady-state condition. In a machine with a permanent magnet rotor, these mmfs might well demagnetize the poles to such an extent that the resultant output voltage would be in the neighborhood of 10 per cent of rated voltage. However, there are steps that may be taken in the design of the machine to reduce these demagnetizing mmfs to such an extent that they are not harmful. Sometimes it also is possible to remagnetize the poles rather easily while the machine is operating, thus restoring the residual mmf to the desired operating value.

Armature Design

Once the magnets have been stabilized, the operating characteristics of a permanent magnet alternator are virtually the same as a standard alternator operating at a constant field current. Since low-voltage regulation is generally necessary, departure must be made from the armature design employed for standard machines utilizing a voltage regulator. There are three possibilities: (1) use a "close-regulated" design, (2) use series capacitors, and (3) use interpolar shunts. In a "close-regulated" machine, one approach is to make the armature reaction mmf small with respect to the rotor mmf, the direct-axis reactance which is proportional to the armature mmf thus being small. This results in a lower I_aX_d drop and less regulation. To reduce the armature reaction mmf and direct-axis reactance, the armature turns must be reduced, which requires that the total air gap flux must be increased to generate the proper voltage. This practice will tend to increase the volume of the machine, but, at the same time, the inherent voltage regulation will be decreased. It is not uncommon for the short-circuit ratio to be in the neighborhood of 2.0 to 3.0 as compared to 1.0 for the standard machine. The disadvantage of this approach is that the machine size is increased over that for a standard machine.

Resonating the adjusted synchronous reactance with a capacitor offers another solution. It would appear on the surface that this would produce essentially zero regulation for all types of loads, but such is not the case. In the machine the adjusted synchronous reactance will tend to increase with leading power factor loads and decrease with lagging power factor loads; thus the resonating capacitor will be too large for the lagging and too small for the leading power factor conditions. In general this variation is not excessive, and regulations well within 10 per cent can be expected with the proper choice of capacitors. To summarize, the advantages of series capacitors are that for a given voltage regulation the over-all size and weight will be less than for a close regulated machine. The disadvantage is that in larger ratings the physical size and cost of the capacitor becomes prohibitively large.

The third possibility lies in use of interpolar shunts. In this scheme, the armature reaction mmf is encouraged to establish its flux in a magnetic shunt between the poles. This procedure means that a large percentage of the armature mmf is consumed in establishing the flux through the shunts and little remains to oppose the direct-axis magnet mmf. In the authors' experience, this method holds little promise unless the power factor of the load remains at or near unity. As an example a machine with 13.5 per cent regulation on a unity power factor load had a regulation of 5.0 per cent with interpolar shunts in the quadrature axis, but when the power factor was 0.8 lag the regulation was 35.7 per cent without shunts and 46.5 per cent with shunts. To summarize, interpolar shunts are an advantage when unity power factor loads are encountered and permit the permanent magnet machine to be of a comparable physical size to the standard machine. It may have an advantage over the capacitor-compensated machine mentioned above in the ratings where the capacitor is prohibitively large. Interpolar shunts have not been found to be feasible for lagging-power factor loads.

Irrespective of the type of armature design, there will result from the calculations of the armature winding and magnetic circuit a required mmf that the permanent magnet will have to deliver. The next section considers some factors involved in the manner of computing this mmf.

Rotor Design

The type of permanent magnet alloy and whether one uses an integrally cast 1-piece rotor or separate poles as shown in Figure 2 will depend upon mechanical, economic, and other factors which are beyond the scope of this paper. The procedures developed herein will apply to 1-piece rotors but are specifically developed for the separate pole type.

The first decision to be reached is that

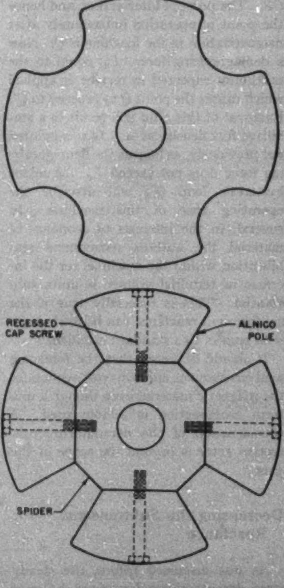

Figure 2. Two possible forms that a permanent magnet alternator rotor can assume. The upper is an integrally cast unit employed on small machines, while the lower is an assembled unit for larger machines

of the stabilization method. In this application the magnets may be stabilized in air or in the machine. Stabilization in air is desirable in case magnetization can not be easily effected in the machine but has the disadvantage of making relatively poor use of the permanent-magnet material. Stabilization within the machine permits operation on the best minor loop in the sense of the highest energy product available for the demagnetizing force encountered.

For air stabilization one may make a flux plot for the magnet configuration employed while the rotor is removed from the machine. From this flux plot the average permeance of the external air can be computed and the slope of the line OQ_A determined, Figure 1. The point Q_A represents the operating point while the rotor is in air. Placing the rotor in the machine will cause the flux density to increase along the minor hysteresis loop to A_A, which lies on the B versus H function for the machine.

For stabilization within the machine, the B versus H function for the magnetic circuit (excepting the magnet) is computed in usual fashion and plotted as OR. The point of intersection, and hence the point of operation immediately after magnetization in the machine is Q. Now a demagnetizing force, F_A, equal to the maximum expected in service is applied which causes the point Q to proceed to Q'. Removal of this mmf will result in a stabilized flux density at A. As was pointed out previously, as long as the demagnetizing force does not exceed F_A, the minor hysteresis loop Q'_A will describe the operating zone of this machine. In general, in the interests of economy of material the authors recommend stabilization within the machine, for the increase in terminal voltage is quite substantial. This is especially true if the subtransient reactance can be made large with respect to a standard machine.

It should be noted that the foregoing analysis assumes uniform cross-section for the magnetic material even though a uniform cross-section is seldom used. A consideration of the nonuniform cross-section rotor is beyond the scope of this paper.

Decreasing the Subtransient Reactance

As was discussed before, the steady-state demagnetizing forces can be minimized by keeping the armature mmfs to a minimum. In the case of the steady-state armature mmfs, this meant a decrease in the ratio of the armature mmf to the rotor mmf. This will not give lower armature mmfs on short-circuit; in fact, just the opposite will be true. Low synchronous and leakage reactances tend to result in large armature mmfs on short-circuit. When the cage and field windings are both absent, this transient-armature mmf must be balanced by an equal and opposite mmf in the poles alone. This represents a very serious demagnetization of the poles. By placing a heavy cage winding in the poles, a counter mmf will be established opposing the transient-armature mmf. If this cage is sufficiently large and well coupled, the net demagnetizing mmf to which the poles will be subjected may be well below the stabilization mmf and thus result in no net reduction of the pole strength. Two approaches may be employed to accomplish this objective.

Casting the entire rotor in aluminum is one solution. This, in effect, places an infinite bar cage winding on the rotor. The aluminum thickness over the pole shoe cannot be great, however, because it increases the effective air gap. Too thin an aluminum casting will be subject to mechanical damage. Where air gaps are small, the use of a copper plated pole may be of value. This method has had considerable success in shielding permanent-magnets of watthour meters from transient demagnetizing mmfs due to surge currents passing close to the meter.[13] This plating method involves covering all of the pole surfaces except the surface in contact with the spider. This method is considered superior to the cast aluminum cage, for the copper can be made thinner over the pole face thus retaining the optimum air gap. A further decrease in subtransient reactance can be achieved by filling in the space between poles with a copper sheet or other material which is carefully bonded to the poles.

Decreasing the Negative Sequence Reactance

This reactance is important in single-phase machines for the steady-state voltage regulation will be effected adversely by large negative-sequence reactances. Under single-phase conditions the negative is in series with the positive sequence reactance and the terminal voltage will be the induced voltage less the drop across each reactance. Fortunately, any steps taken to decrease the subtransient reactance also will decrease the negative-sequence reactance. Hence the addition of an aluminum ring or the plating of the poles will be of assistance in reducing the negative-sequence reactance.

As for the 3-phase case, a series capacitor may be added which will resonate both the negative and positive sequence reactances thus making the single-phase voltage regulation quite small even though the machine possesses relatively large reactances. It should be noted that the value of the capacitor will be different for each type of load and one capacitor cannot be employed for a machine that will be subjected to both single- and 3-phase loads.

Magnetization

There are four methods that may be employed to magnetize the rotor: (1) coils around the poles, (2) direct current in the armature, (3) leading power factor loads, and (4) magnetizing jig (for outside-the-machine magnetizing only). The first three methods were employed by the authors. Method (1) has the disadvantage that it requires a special winding of a few turns around each pole. Method (2) seems to be the most suitable but requires orientation of the field with respect to the armature before energizing the armature. This may be done by passing a small direct current through the armature first, and then passing a relatively large value. Method (3) works on the principle that leading power factor currents produce mmfs which aid the main field mmf. This would tend to magnetize a machine, but would be limited to rather small machines for the capacitor banks become prohibitively large for machines of large rating. The authors favor method (2) as the most direct and expeditious for most installations. In order to assure complete saturation the magnetizing mmf must be approximately five times the product of H_c and magnet length.[4]

Miscellany

Many electromagnetic synchronous machines are limited in rating largely by the ability of the field to dissipate the heat loss associated with the windings. In the permanent magnet alternator, the armature will be the limiting factor since the field winding is absent. The operation of the armature windings at the limiting temperature for the class of insulation will effect economies in size for those machines whose limitation has heretofore lain in the field winding.

Similarly the absence of a field winding reduces the losses associated with a given machine thus increasing the efficiency. A 15-kva 220-volt, 3/60, 1,200-rpm machine has an efficiency of 82.5 per cent with the electromagnet field while it shows an efficiency of 90.9 per cent with a permanent magnet field under the same load conditions.

References

1. Alnico Materials for Small Motor and General Fields, F. W. Merrill. *Electrical Manufacturing* (New York, N. Y.), volume 39, March 1947, pages 78–83, 180–190.

2. Magnetic Circuits and Transformers (book), Staff, Massachusetts Institute of Technology. John Wiley and Sons, New York, N. Y., 1945, pages 98–117.

3. Electromagnetic Devices (book), Herbert C. Roters. John Wiley and Sons, New York, N. Y., 1941, pages 44–47, 106–11.

4. Permanent Magnets (monograph), Raymond Sanford. *C448*, National Bureau of Standards (Washington, D. C.), August 10, 1944.

5. Permanent Magnets in Theory and Practice, S. Evershed. *Journal*, Institution of Electrical Engineers (London, England), volume 58, 1919–1920, pages 780–837.

6. Stabilized Permanent Magnets, P. P. Cioffi. *AIEE Transactions*, volume 67, 1948, pages 1540–43.

7. The Output and Optimum Design of Permanent Magnets Subjected to Demagnetizing Forces, A. J. Hornfeck, R. F. Edgar. *AIEE Transactions*, volume 59, 1940, pages 1017–24.

8. Designing Stabilized Permanent Magnets, E. M. Underhill. *Electronics* (New York, N. Y.), volume 17, January 1944, pages 118–21.

9. Permanent Magnets, and the Relation of Their Properties to the Constitution of Magnet Steels, E. A. Watson. *Journal*, Institution of Electrical Engineers (London, England), volume 61, 1922–1923, pages 641–60.

10. The Design and Performance of Permanent Magnet Rotors, C. T. Thomas, J. R. Ireland. *Electrical Manufacturing* (New York, N. Y.), volume 40, 1947, pages 110–13, 170–72.

11. The Use of Modern Steels for Permanent Magnets, A. Th. van Urk. *Phillips Technical Review* (Eindhoven, Holland), volume 5, February 1940, pages 29–35.

12. The Shielding of Permanent Magnets from Transient Magnetic Fields, George J. Wey. *AIEE Transactions*, volume 60, 1941, pages 875–77.

No Discussion

Servomechanism Characteristics of D-C Motor Driven by Controlled Rectifiers

L. DALE HARRIS
MEMBER AIEE

THERE IS a significant number of applications of d-c motors in which either the armature power, field excitation, or both, is supplied by one or more controlled rectifiers. In one type of servomechanism system, the speed of the motor is controlled through the armature power by a controlled rectifier; in another type, the motor speed is controlled by the action of a controlled rectifier upon the field excitation. Previous papers[1,2] have been written wherein an analysis is made of the case where the armature power is supplied by a controlled rectifier under steady state conditions.

This paper presents an analysis of each of the following situations:

1. Steady-state condition where the armature power is controlled with a rectifier. This is the basis of some of the other situations to follow, and it is shown how the graphical and successive approximations presented by Puchlowski and Vedder[1,3] are not always necessary. Supporting experimental data are presented also.

2. Transient conditions with a controlled rectifier at the armature leading to a servomechanism transfer function.

3. Steady-state condition where the field excitation is controlled by a rectifier.

4. Transient conditions with a controlled rectifier at the field leading to another transfer function.

By transient conditions is meant conditions arising from change in respect to time of the control quantity (tube breakdown angle) and motor speed.

In this paper the term controlled rectifier shall refer to the ignitron or thyratron types of rectifiers where the a-c applied voltage is constant and the tube-breakdown point is controlled. Furthermore, all analytical and empirical efforts described in this paper are limited to the case of the single-phase, full-wave rectifier; however, the concepts herein developed may be applied to the more general situation. This paper discusses only the linear approximation to the actual situation that exists.

Figure 1 shows one type of electrical connection under consideration. In this case the armature is driven by a controlled rectifier and the field is excited with a constant voltage. The situation wherein the field is driven by a controlled rectifier is considered also.

Armature Power Supplied by Rectifier

Steady-State Discontinuous Conduction

When the armature power to a d-c motor is supplied by a controlled rectifier, the armature current may be in the form of discontinuous pulses or the flow may be continuous from one pulse to another. Figure 2 shows an example of discontinuous current flow in the armature; Figure 7 shows an example of continuous flow in the field. The situation where the flow is discontinuous is the more typical for the armature circuit and is discussed first.

The analysis that follows is based on the assumption that the generated counter electromotive force of the motor does not change a significant amount within any one cycle. The instantaneous torque changes radically within a particular cycle, but the polar moment of inertia of the rotor in the great majority of cases is so large that the speed can be considered constant within one particular cycle.

Equation 1 is the differential equation for the d-c motor relating the armature current to the applied voltage during that part of the cycle while one of the tubes allows current to flow.

$$e=E_m \sin(\omega t+\beta)=L_a\frac{di}{dt}+IR_a+E_b \qquad (1)$$

where tube breakdown is at time equal to zero, L_a is the combined inductance of the armature of the motor and leakage inductance of the source transformer, R_a is the total resistance of the same circuit, E_b is the sum of the motor counter electromotive force and the tube drop (E_b is assumed constant within any one cycle), i is the instantaneous value of the armature current, and β is the angle of tube breakdown.

Figure 2 is an oscillogram of armature voltage and current for a typical case where a controlled rectifier is supplying armature power. From common circuit theory we know the particular integral part of the solution to equation 1, and we also know the form of the complimentary function, so that we are able to write

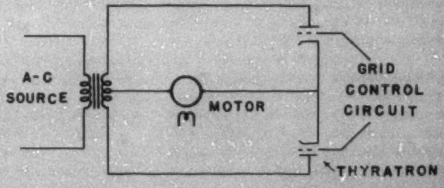

Figure 1. The armature power of a d-c motor is supplied by a grid controlled rectifier. The field is excited by a steady d-c source

---

Paper 51-297, recommended by the AIEE Feedback Control Systems Committee and approved by the AIEE Technical Program Committee for presentation at the AIEE Pacific General Meeting, Portland, Oreg., August 20–23, 1951. Manuscript submitted May 21, 1951; made available for printing July 6, 1951.

L. Dale Harris is with the University of Utah, Salt Lake City, Utah.

This paper is a portion of a Doctor of Philosophy thesis written under the direction of the staff of the School of Electrical Engineering, Purdue University, Lafayette, Ind.

Figure 2. Armature voltage, v(t), and armature current, i(t), for a d-c, shunt, 3/4-horsepower 115-volt 7-ampere motor with a controlled rectifier at the armature and steady d-c excitation. Discontinuous conduction as shown by the current wave. Relatively flat portion of the voltage wave shows the motor counter electromotive while the current is zero

$$i=-\frac{E_b}{R_a}+\frac{E_m}{Z_a}\sin(\omega t+\beta+\theta_a)+C\epsilon^{-\frac{\omega t}{\Gamma_a}} \qquad (2)$$

where

$$\theta_a=-\tan^{-1}\Gamma_a,\ \Gamma_a=\frac{\omega L_a}{R_a},\ Z_a=\sqrt{R_a^2+\omega^2L_a^2}$$

and C is the arbitrary constant. Because the current is zero at time equal to zero, we may evaluate the arbitrary constant. Equation 2 now becomes

$$i=-\frac{E_b}{R_a}+\frac{E_m}{Z_a}\sin(\omega t+\beta+\theta_a)+\left(\frac{E_b}{R_a}-\frac{E_m}{Z_a}\sin(\beta+\theta_a)\right)\epsilon^{-\frac{\omega t}{\Gamma_a}} \qquad (3)$$

Equation 3 is the equation of the armature current for $0 \leqslant \omega t \leqslant \gamma$ where γ is the angle at which the current returns to zero and the tube "cuts off". Significant information is obtained by equating the right-hand side of equation 3 to zero when ωt is γ.

$$\frac{E_m}{Z_a}\left(\sin(\beta+\theta_a+\gamma)-\epsilon^{-\frac{\gamma}{\Gamma_a}}\sin(\beta+\theta_a)\right)+\frac{E_b}{R_a}\left(\epsilon^{-\frac{\gamma}{\Gamma_a}}-1\right)=0 \qquad (4)$$

From equation 4 comes equation 5.

$$S_f=\frac{E_b}{E_m}=\cos\theta_a\times\left[\frac{\sin(\beta+\theta_a+\gamma)-\epsilon^{-\frac{\gamma}{\Gamma_a}}\sin(\beta+\theta_a)}{1-\epsilon^{-\frac{\gamma}{\Gamma_a}}}\right] \qquad (5)$$

where S_f is the speed factor and is a measure of the actual motor speed as is indicated in equation 6. In equation 6, S is the motor speed in radians per second, and K_s is the speed constant of the motor that gives the generated volts per radian per second of speed.

$$S=\frac{E_mS_f-E_t}{K_s} \qquad (6)$$

Because Γ_a in equation 5 is equal to $-\tan\theta_a$, S_f is fixed exclusively by three angles: β, θ_a, and γ. Or it may be more proper to say that for a given motor, a given speed factor, and a given breakdown angle, the cut-off angle, γ, is fixed.

Another equation in addition to equation 5 is needed in order to predict the performance of the motor. Useful information comes from dividing equation 1 through by the factor π and integrating between the limits of zero and γ.

$$\frac{1}{\pi}\int_0^\gamma E_m\sin(\omega t+\beta)d(\omega t)=\frac{L_a}{\pi}\times\int_0^\gamma\frac{di}{dt}d(\omega t)+R_a\int_0^\gamma\frac{id(\omega t)}{\pi}+\frac{E_b}{\pi}\int_0^\gamma d(\omega t) \qquad (7)$$

The first term on the right-hand side of the equation reduces to zero as shown.

$$\int_0^\gamma\frac{di}{dt}d(\omega t)=\omega\int_0^0 di=0$$

The second term on the right-hand side of equation 7 yields the average value of the armature current such that

$$\frac{E_m}{\pi}(\cos\beta-\cos(\beta+\gamma))=IR_a+\frac{E_b\gamma}{\pi} \qquad (8)$$

Or

$$T_f=\cos\beta-\cos(\beta+\gamma)-S_f\gamma \qquad (9)$$

where T_f, the torque factor, is given by

$$T_f=\frac{IR_a\pi}{E_m} \qquad (10)$$

From equations 5 and 9 one can predict the curves of speed factor against torque factor or speed against average armature current for various values of the controlled angle of breakdown, β. Puchlowski and Vedder[1,2] chose to solve an equation of the type of equation 5 for the cut-off angle γ by a combination of graphics and successive approximations after the angle β and the speed factor had been selected. These graphics and successive approximation methods seem unnecessary for many purposes. One may consider equations 5 and 9 as the parametric equations relating S_f to T_f through the parameter γ. In order to compute one point on the curve of speed against average armature current for a given value of breakdown angle, arbitrarily select the cut-off angle. From this selection, through the use of equation 5, one can compute the corresponding value of the speed factor, S_f. Then the corresponding torque factor T_f is computed by the use of equation 9 to yield the co-ordinates for one point on curve of speed factor against torque factor.

A particular numerical example of this type of computation is here illustrated. This computation is based on data on the particular motor: 3/4 horsepower, 115 volts, shunt, 3,100–900 rpm. The closed armature circuit had the following constants: $R_a=7.9$ ohms, $\omega L_a=20.6$ ohms, $Z_a=22$ ohms, and $\theta_a=69$ degrees. The applied voltage was such that: $E_m=318$ volts and $\beta=90$ degrees. The motor excitation was set such that the motor generated a counter electromotive force of 5.07×10^{-2} volts per unit of rpm. The tube drop was found to be 12 volts. By selecting γ as 122 degrees, the speed factor is computed through the use of equation 5 to be 2.82×10^{-1} and the speed, 1,530 rpm. Equation 9 gives $T_f=2.43\times10^{-1}$, and in turn, $I_{av}=3.09$ amperes. The speed of 1,530 rpm and the current of 3.09 amperes are the co-ordinates of one point on curve B of Figure 3. An adjacent point on the same curve may be computed by selecting a modified value of the cut-off angle, γ.

Figure 3 shows a family of curves that give the relationship of speed to average armature current for various conditions. The circular points plotted on this figure were calculated as illustrated in the preceding paragraph, and the cross points were observed directly by running the motor under load to measure the speed and current directly. These plotted points show a rather close correspondence between computed and observed data. Figure 4 represents the same type of plotted data but in a different co-ordinate system.

Boundaries Between Regions of Continuous Current and Discontinuous Current, Between Regions of Control, and No Control

Figure 4 shows three regions: A discontinuous current flow, B continuous current flow, and C region of no control. The previous analysis is applicable only to the case where the armature current flow is discontinuous ($\gamma \leqslant \pi$). The boundary between regions A and B is found by examining equation 5 when γ is allowed to approach the limiting value of π.

$$S_f=-\cos\theta_a\sin(\beta+\theta_a)\frac{1+\epsilon^{-\pi/\Gamma_a}}{1-\epsilon^{-\pi/\Gamma_a}} \qquad (11)$$

The boundary between the regions of control and no control is fixed by the fact that the tube cannot conduct unless the a-c applied voltage is equal to or greater than E_b. This fact leads us to equation 12

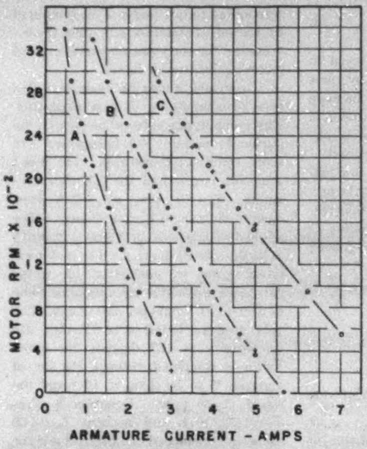

Figure 3. Curves showing measured and computed values of speed as a function of average value of armature current. Circular points show computed values; cross points show measured values. Curves for three different breakdown angles, β: A for $\beta=108$ degrees, B for $\beta=90$ degrees, and C for $\beta=70$ degrees. Peak value of a-c applied voltage was 318 volts. Same motor as caption of Figure 2

which defines the boundary between the regions of control and no control.

$$S_f=\sin\beta \tag{12}$$

When equations 11 and 12 are plotted on one set of co-ordinates, these various regions are defined as shown in Figure 5. The two sine functions that define the boundaries between these various regions of control are fixed exclusively by the angle θ_a as shown in equations 11 and 12.

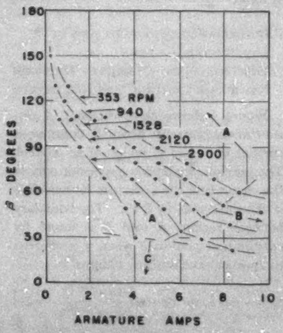

Figure 4. Curves showing how the breakdown angle, β, must be adjusted as a function of average value of the armature current in order to keep the speed constant. A different co-ordinate system of the data of Figure 3

Steady State Continuous Conduction

Figure 5 illustrates the fact that the speed factor and the control angle may be of such a combination that the current flow will not go to zero but will continue to flow in one tube until the next tube is allowed to conduct so that the flow is continuous. It is assumed in this discussion that the time required for the current to commutate from one tube to the other is negligible.

Equation 1 is still applicable, and it is significant to integrate this equation between the limits of zero and π.

$$\frac{E_m}{\pi}\int_0^\pi \sin(\omega t+\beta)d(\omega t)=\frac{L_a}{\pi}\int_0^\pi\frac{di}{dt}\,d(\omega t)+R_a\int_0^\pi\frac{id(\omega t)}{\pi}+E_b \tag{13}$$

In the steady-state condition, the integral involving the time rate of change of current reduces to zero because the current at time equal to zero is equal to the current at the end of the cycle.

$$\int_0^\pi\frac{di}{dt}\,d(\omega t)=\omega\int_{i(0)}^{i(\pi)}di=0 \tag{14}$$

out of equation 13 and the indicated operation, comes an expression that relates the speed and torque factors where these terms are as previously defined.

$$T_f=2\cos\beta-\pi S_f \tag{15}$$

Equation 15 yields a family of torque factor against speed factor curves that are straight parallel lines.

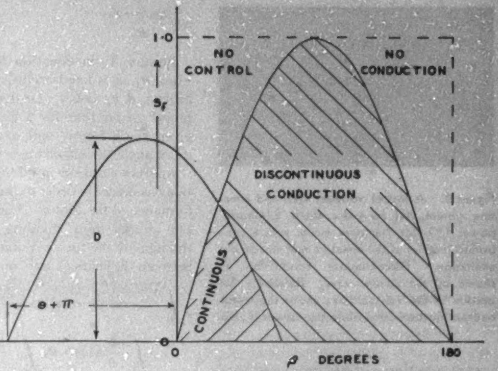

Figure 5. Cross hatched areas show region where grid control of armature current is possible. In one of these regions, the current flow is continuous; in the other the flow is discontinuous. D is defined by equation 11 of the text

Transient Discontinuous Conduction

It is significant to determine the transient response of the armature current to a sudden displacement of the control angle, β. In the case where the armature current is discontinuous, there is no delaying effect of the armature inductance upon the armature current response, because in each cycle the armature current must start at zero and end at zero. The current as a function of time in any one cycle is completely independent of the previous cycle assuming speed is constant and the flow discontinuous. However, since the effect of a change in the control angle is felt only at the beginning of a current cycle, there is an inherent maximum possible time delay of one-half of one cycle of the applied a-c power. This delay, however, is due to the discontinuous nature of the method of control, is independent of the inductive time constant of the armature circuit, and is assumed negligible throughout this discussion. The oscillogram of Figure 6 shows the sudden response of the armature current to a sudden displacement of the control angle.

Servomechanism Constants for Discontinuous Conduction

The d-c motor and controlled rectifier combination is used as the prime mover in some of the automatic, closed loop, speed control systems. It is the objective of this section to present an analysis of the motor and rectifier combination of this type of

Figure 6. Oscillogram showing transient armature current and voltage with a grid-controlled rectifier at the armature and with steady d-c excitation. The control angle, β, is suddenly changed from approximately 110 degrees to approximately 80 degrees. Adjacent current pulses are dissimilar because of dissimilar characteristics of the two tubes in the rectifier

speed servo system where it is desired to regulate the speed to a constant value. The approach is very similar to the one used in vacuum tube analysis where the tube parameters are considered constant about a given operating point, and the instantaneous departures of the driving force and response quantities are sufficiently small such that significant parameters can be assumed constant.

Let the operating point be fixed by the combination of β_0, S_0, and T_0, where the control angle, β_0, produces a steady state torque, T_0, at a steady state speed, S_0. The effect of a small change of the control angle, $\Delta\beta$, upon the change of speed, ΔS, is now considered.

The torque required by the load over and above that required to accelerate the moment of inertia, J, is represented by T_L and is given by equation 16.

$$T_L=T_0+\frac{\partial T_L}{\partial S}\Delta S \tag{16}$$

It is assumed, of course, that the change of speed is small enough such that T_L as a function of speed in the region of the operating point may be considered as a straight line. As has been shown, the developed torque, T, is a function of both β and S. This leads us to equation 17.

$$T=T_0+\frac{\partial T}{\partial S}\Delta S+\frac{\partial T}{\partial \beta}\Delta\beta \tag{17}$$

By equating the total torque required by the load (including that required for acceleration) to the developed torque, equation 18 results.

$$J\frac{d(\Delta S)}{dt}+\left(\frac{\partial T_L}{\partial S}-\frac{\partial T}{\partial S}\right)\Delta S=\frac{\partial T}{\partial \beta}\Delta\beta \tag{18}$$

The partial, $\partial T_L/\partial S$ is fixed exclusively by the nature of the load and the other two partials are fixed by the characteristics of the rectifier motor combination.

The partials, $\partial T/\partial S$ and $\partial T/\partial \beta$, could be determined directly by graphical methods from families of curves such as those of Figures 3 and 4 wherever the proper families of curves were available. It is more direct to determine these partials through the use of some explicit expressions for them. The development of these expressions follow.

Equations 5 and 9 were developed from the steady state point of view but are applicable to the transient case (β is variable) as well, because there is no delay in armature current response to a change in β. We may find the partial of the torque factor in respect to the speed factor by the use of equation 9. One must remember, however, that γ is a function of both the speed factor and β.

$$\frac{\partial T_f}{\partial S_f}=\frac{\partial \gamma}{\partial S_f}(\sin(\beta+\gamma)-S_f)-\gamma \tag{19}$$

where β is constant. In order to evaluate the partial of γ in respect to S_f, we use equation 5.

$$\frac{\partial \gamma}{\partial S_f}=\frac{1-\epsilon^{-\gamma/\Gamma_a}}{\cos\theta_a\left[\cos(\beta+\theta_a+\gamma)+\dfrac{\epsilon^{-\gamma/\Gamma_a}}{\Gamma_a}\left(\sin(\beta+\theta_a)-\dfrac{S_f}{\cos\theta_a}\right)\right]} \tag{20}$$

where β is constant.

The combination of equations 19 and 20 can be used to determine the factor, $\partial T_f/\partial S_f$, after choosing the angles β, γ, and S_f corresponding to the desired operating point.

The partial of torque factor in respect the control angle can be determined by taking the partial of T_f in respect to β from equation 9 and the partial of γ in respect to β from equation 5.

$$\frac{\partial T_f}{\partial \beta}=-\sin\beta+\sin(\beta+\gamma)+(\sin(\beta+\gamma)-S_f)\frac{\partial \gamma}{\partial \beta} \tag{21}$$

where S_f is constant.

$$\frac{\partial \gamma}{\partial \beta}=\frac{\epsilon^{-\gamma/\Gamma_a}\cos(\beta+\theta_a)-\cos(\beta+\theta_a+\gamma)}{\cos(\beta+\theta_a+\gamma)+\dfrac{\epsilon^{-\gamma/\Gamma_a}}{\Gamma_a}\left(\sin(\beta+\theta_a)-\dfrac{S_f}{\cos\theta_a}\right)} \tag{22}$$

where S_f is constant.

The combination of equations 21 and 22 can be used to determine the factor $\partial T_f/\partial \beta$. In order to convert the partials of T_f in respect to S_f and β, to the corresponding partials of T in respect to S_f and β, we use equations 6, 10, and 23.

$$T=K_tI \tag{23}$$

where K_t is another excitation constant equal to pound-feet of torque per ampere of armature current.

$$\frac{\partial T}{\partial S}=\frac{K_tK_s}{R_T}\frac{\partial T_f}{\partial S_f} \tag{24}$$

and

$$\frac{\partial T}{\partial \beta}=\frac{K_tE_m}{R_T}\frac{\partial T_f}{\partial \beta} \tag{25}$$

A numerical computation of a value of $\partial T/\partial S$ and of $\partial T/\partial \beta$ seems significant.

Out of the same data that was used as the previous numerical illustration, comes the operating point: $\beta=1.57$ radians (90 degrees); $\gamma=2.13$ radians (122 degrees); and $S_f=2.82\times10^{-1}$ (1,528 rpm). When these data are inserted into equations 19 to 22 inclusive, it is found that

$$\frac{\partial T_f}{\partial S_f}=-0.68$$

and

$$\frac{\partial T_f}{\partial \beta}=-0.40$$

From equations 24 and 25, values of $\partial T/\partial S$ and $\partial T/\partial \beta$ are found as shown below.

$$\frac{\partial T}{\partial S}=-K_t\times1.32\times10^{-1}\ \frac{\text{pound-feet}}{\text{radians per second}}$$

$$\frac{\partial T}{\partial \beta}=-K_t\times5.12\ \frac{\text{pound-feet}}{\text{radians}}$$

As was previously mentioned, the values of these partials can be determined directly from families of curves of the type plotted in Figures 3 and 4. When the slope of the $\beta=90$ degrees curve is taken at 1,528 rpm, the value of $\partial T/\partial S$ is found to be as indicated below.

$$\frac{\partial T}{\partial S}=-K_t\times1.29\times10^{-1}\ \frac{\text{pound-feet}}{\text{radians per second}}$$

In a similar manner by taking the slope of the 1,528 rpm curve of Figure 4 at

Figure 7. Oscillogram of steady-state field voltage, $e(t)$, and field current, (It), with controlled rectifier at the field and with a steady d-c source at the armature. The current shows continuous conduction with a rather large average value compared to the ripple component

$\beta=90$ degrees, the following value for $\partial T/\partial\beta$ is found.

$$\frac{\partial T}{\partial\beta}=-K_t\times 5.06\ \frac{\text{pound-feet}}{\text{radians}}$$

In the preceding paragraphs, these two servo constants in the form of partial derivatives have been determined by two different approaches, and a reasonable correlation between the results from the two different approaches is indicated. For most purposes, the direct approach through the use of formulas 19 to 25 inclusive seems the more desirable.

The servo coefficients appearing as partial derivatives in equation 18 are functions of the variables, S and β. However, over a limited range of operation one may assume for practical purposes that they are constant. It is not the purpose of this paper to present an analysis of errors introduced when these coefficients are assumed constant and the system is operated with large variations in β and S. Certainly the treatment of these coefficients as constants, for many purposes, yields an adequate tool for servomechanism synthesis.

Servomechanism Transfer Function for Discontinuous Conduction

Equation 18 is rewritten in terms of S and β as shown in equation 26. It is understood that each of these variables, S and β, represent a small variation above or below the corresponding operating point value.

$$J\frac{dS}{dt}+\left(\frac{\partial T_L}{\partial S}-\frac{\partial T}{\partial S}\right)S=\frac{\partial T}{\partial\beta}\beta \qquad (26)$$

By substituting $j\omega$ for the operator d/dt in equation 26, equation 27 gives the transfer function in the angular velocity domain.

$$\frac{\boldsymbol{S}}{\boldsymbol{\beta}}=\frac{\partial T/\partial\beta}{\dfrac{\partial T_L}{\partial S}-\dfrac{\partial T}{\partial S}+j\omega J} \qquad (27)$$

In equation 27, $\boldsymbol{S}$ and β are the complex sinusoidal values of speed and control angle respectively, and ω is the angular velocity of the sinusoidal variation in both $\boldsymbol{S}$ and β. Equation 27 gives the complex ratio of the response of the system, $\boldsymbol{S}$ to the complex driving force, β. This ratio is useful in predicting the performance of any closed loop control system that uses the rectifier-motor as the prime mover.

Servomechanism Transfer Function for Continuous Conduction

The transfer function between the control angle and the motor speed when the controlled rectifier supplies armature current that is continuous is not specifically developed here. However, all of the basic concepts relative to this problem are outlined within the bounds of this paper. The situation of continuous current in the armature is quite parallel to the one where the controlled rectifier supplies the field excitation to control the speed of the motor and the current flow in the field is continuous. The analysis of the transfer function for field control with continuous flow of current is detailed in the remaining part of this paper and can be modified rather simply to apply to the armature circuit. Equation 15 or its equivalent plus some concepts basic to the development of equation 44 enter into the development of the transfer function for continuous current conduction in the armature circuit.

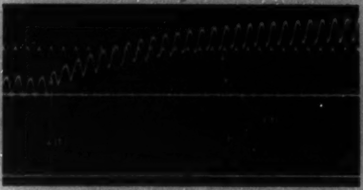

Figure 8. Oscillogram showing transient field current and voltage with a grid-controlled rectifier at the field and with a steady d-c voltage at the armature. The control angle is suddenly changed from approximately 80 degrees to approximately 20 degrees

Controlled Excitation Supplied by Rectifier

Where a limited range of control is needed in a closed loop system, it may be more economical to control the speed through the field excitation rather than through the armature power. In the following paragraphs an analysis is made of the operation of the d-c motor where the field excitation is supplied and controlled by a grid controlled rectifier and the armature power is supplied by a constant d-c voltage source. As was the case of the rectifier at the armature, the circuit parameters are assumed to be constant.

Steady State Continuous Conduction of Field Current

With a controlled rectifier supplying the field excitation, the current flow in the field may be continuous or discontinuous, but the case of continuous current flow is much more important, for the average value of the field current is too small to be practical for most cases when the flow is discontinuous. A typical steady state situation is shown in the oscillogram of Figure 7. It should be noted that the a-c component of the field current is considerably smaller than the average value.

When the current flow is continuous, the field current commutates from one tube to the other over a finite period of time depending on the leakage reactance of the supply transformer. In this analysis, this commutating time is neglected; Figure 7 shows it to be small compared to a period of the current wave.

Equation 28 is the differential equation of the field current, and equation 29 is the solution to equation 28.

$$E_m\sin(\omega t+\beta)=L_f\frac{di}{dt}+iR_f+E_t \qquad (28)$$

$$i=-\frac{E_t}{R_f}+\frac{E_m}{Z_f}\sin(\omega t+\beta+\theta_f)+C\epsilon^{-\frac{\omega t}{\Gamma_f}} \qquad (29)$$

Of course, the constants R_f, L_f, Z_f, Γ_f, and θ_f are now the parameters of the closed field circuit including the supply transformer, whereas, similar symbols applied to the closed armature circuit in the same manner in the previous parts of this discussion. The symbol E_t is the tube drop. After the circuit has reached a steady-state condition such that each current cycle repeats the previous one, we know that the current at the beginning of any cycle is equal to the current at the end of the same cycle ($\omega_t=\pi$). This allows one to evaluate the arbitrary constant, C.

$$C=\frac{-2E_m\sin(\beta+\theta_f)}{Z_f(1-\epsilon^{-\pi/\Gamma_f})} \qquad (30)$$

Equation 31 results from the combination of equations 29 and 30, and gives the field current in any one cycle for steady state conditions and for continuous flow.

$$i=-\frac{E_t}{R_f}+\frac{E_m}{Z_f}\sin(\omega t+\beta+\theta_f)-\frac{2E_m\sin(\beta+\theta_f)}{Z_f(1-\epsilon^{-\pi/\Gamma_f})}\epsilon^{-\frac{\omega t}{\Gamma_f}} \qquad (31)$$

There is special significance in the average value of the field current, and this average value can be obtained more readily by integrating equation 28 than by integrating equation 29. The indicated integration of equation 32 leads one to equation 33.

$$\frac{E_m}{\pi}\int_0^{\pi}\sin(\omega t+\beta)d(\omega t)=\frac{\omega L_f}{\pi}\int_{i(0)}^{i(\pi)}di+R_fI+E_t \qquad (32)$$

$$I=-\frac{E_t}{R_f}+\frac{2E_m}{R_f\pi}\cos\beta \tag{33}$$

In equation 33 is found a rather simple relationship between the value of the control angle and the average value of the field current, I. It should be remembered, however, that this equation is only applicable to values of control angle, β, that yield continuous current flow.

In order to find that critical value of β that separates the region of continuous flow from the region of discontinuous flow, it is only necessary to set the value of the current in equation 31 to zero at $\omega t=0$; equation 34 follows.

$$\beta_c=-\theta_f+\sin^{-1}\frac{E_tZ}{R_fE_m}\left(\frac{\epsilon^{-\pi/\Gamma_f}-1}{\epsilon^{-\pi/\Gamma_f}+1}\right) \tag{34}$$

For many field circuits, Γ_f is considerably greater than π. It is not difficult to show that as the ratio, Γ_f/π, approaches infinity, equation 34 reduces to equation 35.

$$\beta_c=-\theta_f-\sin^{-1}\frac{\pi E_t}{2E_m} \tag{35}$$

Furthermore, E_m will be, for many cases, more than twenty times the magnitude of E_t making β_c approximately equal to the negative of θ_f. For the motor relative to which numerical data has previously been applied in this paper, Γ_f/π is approximately equal to 8.0; E_m, 318 volts; and E_t, 12 volts. Using this data in equation 34, β_c is calculated as follows:

$$\beta_c=87.7^\circ-\sin^{-1}0.058=84.3^\circ$$

When β_c is computed by the use of equation 35, using this same data, there is no slide-rule difference between the two results. For this particular example, the current flow will be continuous when $0<\beta<84.3$ degrees, and equation 33 is applicable in this range only. For β greater than β_c, the flow is discontinuous. The corresponding formulas developed for discontinuous flow in the armature circuit are applicable to the field circuit where E_b is equal to E_t, a constant.

TRANSIENT CONTINUOUS CONDUCTION OF FIELD CURRENT

It seems significant to analyze the proposition where the driving force, β, is suddenly changed from one value, β_1, to another value, β_2. This condition is illustrated in the oscillogram of Figure 8 where β is suddenly decreased from approximately 80 degrees to approximately 20 degrees. One should note that the current rises in a delayed manner in contrast to the sudden rise of current when the flow is discontinuous. It is now intended to make an analysis of this rise.

Immediately after the control angle has been changed from β_1 to β_2, the total voltage applied to the field circuit, e_2, can be written as shown in equation 36.

$$e_2=\frac{2E_m\cos\beta_2}{\pi}+e_{a\text{-}c}(t)_2 \tag{36}$$

In equation 36, $e_{a-c}(t)_2$ has the meaning of the total applied voltage less the average or d-c value,

$$\frac{2E_m\cos\beta_2}{\pi}$$

It is important to think of $e_{a-c}(t)_2$ as the equation of the a-c component of the applied voltage over an indefinite number of cycles and not restricted to just one cycle. From this point of view, the differential equation of the current in the field circuit is as shown in equation 37.

$$\frac{2E_m\cos\beta_2}{\pi}+e_{a\text{-}c}(t)_2=E_t+L_f\frac{di}{dt}+iR_f \tag{37}$$

The solution to equation 37 can be written as equation 38.

$$i=\frac{2E_m\cos\beta_2}{R_f\pi}-\frac{E_t}{R_f}+i_{a\text{-}c}(t)_2+C\epsilon^{-\frac{\omega t}{\Gamma_f}} \tag{38}$$

In equation 38, $i_{a-c}(t)_2$ has the meaning of the steady-state component of current due to $e_{a-c}(t)_2$ alone. It is not necessary to determine this a-c component of current, since it has no significant effect upon the speed of the motor. The symbol $i_{a-c}(t)_2$ represents the equation of the ripple component of the field current.

In order to find the arbitrary constant, one may make use of the facts that the total current has reached a steady state while the control angle is still equal to β_1 and that the current is unchanged immediately after the control angle changes to the new value, β_2.

$$\begin{aligned}i(0)_1&=\frac{2E_m\cos\beta_1}{R_f\pi}-\frac{E_t}{R_f}+i_{a\text{-}c}(0)_1=i(0)_2\\&=\frac{2E_m\cos\beta_2}{R_f\pi}-\frac{E_t}{R_f}+i_{a\text{-}c}(0)_2+C\end{aligned} \tag{39}$$

From equation 39, the value of the arbitrary constant is found as shown in equation 40.

$$C=\frac{2E_m}{R_f\pi}(\cos\beta_1-\cos\beta_2)+i_{a\text{-}c}(0)_1-i_{a\text{-}c}(0)_2 \tag{40}$$

The a-c component of the current is not significant to the problem, so when it is dropped from equation 38 and equation 40 is used, equation 41 follows.

$$\begin{aligned}I(t)=-\frac{E_t}{R_f}+\frac{2E_m}{R_f\pi}\Big[\cos\beta_2+(\cos\beta_1-{}&\\ \cos\beta_2)\epsilon^{-\frac{\omega t}{\Gamma_f}}\Big]+(i_{a\text{-}c}(0)_1-i_{a\text{-}c}(0)_2)\epsilon^{-\frac{\omega t}{\Gamma_f}}&\end{aligned} \tag{41}$$

In equation 41, $I(t)$ represents the equation of the current less the a-c component. It is significant to note that this transient d-c current changes suddenly at time equal to zero because of the difference between the two a-c components evaluated at time equal to zero. Each of the two currents, $i_{a-c}(0)_1$ and $i_{a-c}(0)_2$ can be found by the use of equations 31, 33, and 42 where $i(0)$ is the value of current at time equal to zero from equation 31.

$$i_{a\text{-}c}(0)=i(0)-I(0) \tag{42}$$

When β_1 is equal to 70 degrees and β_2 is equal to 20 degrees and the other previously applied numerical data are substituted in equation 42, it is found that: $i_{a-c}(0)_1-i_{a-c}(0)_2=-2.4/R_f$ and that $I_1-I_2=-122/R$. For this example, it is seen that the exponential term in equation 41 due to the difference between a-c components is negligible compared to the exponential term due to the difference between d-c components. Wherever the first exponential term can be neglected, equation 41 simplifies to equation 43.

$$\begin{aligned}I(t)=-\frac{E_t}{R_f}+\frac{2E_m}{R_f\pi}\Big[\cos\beta_2+(\cos\beta_1-\cos\beta_2)\times&\\ \epsilon^{-\frac{\omega t}{\Gamma_f}}\Big]&\end{aligned} \tag{43}$$

Equation 43 is the solution to equation 44, the differential equation that relates, the average value of the field current to the driving force, β.

$$\frac{2E_m\cos\beta}{\pi}-E_t=L_f\frac{dI(t)}{dt}+R_fI(t) \tag{44}$$

Equation 44 might be considered as a good approximation whenever the a-c component of the field current is small compared to the d-c component.

In the case where the breakdown angle, β, is controlled by a d-c grid signal, E_c, that is superimpressed upon an a-c grid signal that is in turn displaced 90 degrees from the a-c anode voltage, and the tube is assumed to breakdown when the net grid voltage is equal to zero, then $E_c=E_{mg}\cos\beta$ where E_{mg} is the maximum value of a-c component of the grid signal. Under these assumptions, equation 44 yields the sinusoidal transfer function of the field circuit as shown in equation 45.

$$\frac{I}{E_c}=\frac{2E_m}{\pi E_{mg}(R_f+j\omega L_f)} \tag{45}$$

TRANSFER FUNCTION WITH CONTINUOUS CONDUCTION

It is the purpose of this section to find the approximate linear transfer function of the d-c motor and controlled rectifier combination when the rectifier controls the field excitation to control the motor speed. The situation is analyzed wherein the change of driving force and response are small variations about a fixed operating point.

$$V=E_g+I_aR_a+L_a\frac{dI_a}{dt} \tag{46}$$

where V is the applied armature voltage, E_g is the motor generated voltage, I_a is the armature current, I_f is the field current, and other terms are as previously defined. Since V is constant, equation 47 comes from equation 46.

$$\Delta E_g+R_a\Delta I_a+L_a\frac{d(\Delta I_a)}{dt}=0 \tag{47}$$

Using other previously defined nomenclature, equations 48 to 50 can be written.

$$\Delta E_g=\frac{\partial E_g}{\partial S}\Delta S+\frac{\partial E_g}{\partial I_f}\Delta I_f \tag{48}$$

$$\Delta T=\frac{\partial T}{\partial I_f}\Delta I_f+\frac{\partial T}{\partial I_a}\Delta I_a \tag{49}$$

$$J\frac{d\Delta S}{dt}+\frac{\partial T_L}{\partial S}\Delta S=\Delta T \tag{50}$$

By proper elimination of variables among equations 47 to 50 inclusive and by changing from the time to the frequency domain, equation 51 is developed.

$$\frac{S}{I_f}=\frac{R_a\frac{\partial T}{\partial I_f}-\frac{\partial T}{\partial I_a}\frac{\partial E_g}{\partial I_f}+j\omega L_a\frac{\partial T}{\partial I_f}}{\left(\frac{\partial T_L}{\partial S}+j\omega J\right)(R_a+j\omega L_a)+\frac{\partial T}{\partial I_a}\frac{\partial E_g}{\partial S}} \tag{51}$$

Upon examining each one of the partial derivatives in equation 51, one would expect each to be rather constant over a limited range of operation with the possible exception of $\partial T/\partial I_f$. This partial derivative is proportional to I_a, and I_a will normally make a rather large change for a relatively small change in the field current. Of course, it should be remembered that equation 51 is applicable in the strictest sense only when the variations about the operating point are infinitesimally small. Thus equation 51 is a linear differential equation giving the relationship of the speed of the motor to the field current accurate only for small variations in the significant variables.

When I_f is eliminated between equations 45 and 51, equation 52 follows.

$$\frac{S}{E_c}=\frac{2E_m\left[R_a\frac{\partial T}{\partial I_f}-\frac{\partial T}{\partial I_a}\frac{\partial E_g}{\partial I_f}+j\omega L_a\frac{\partial T}{\partial I_f}\right]}{\pi E_{mg}(R_f+j\omega L_f)\left[\left(\frac{\partial T_L}{\partial S}+j\omega J\right)\times(R_a+j\omega L_a)+\frac{\partial T}{\partial I_a}\frac{\partial E_g}{\partial S}\right]} \tag{52}$$

Equation 52 is the transfer function between the d-c control voltage, the driving force and the motor speed, the response, when the controlled rectifier controls the field excitation and a constant voltage is applied to the armature circuit. In order to avoid nonlinearities, a number of approximations have been made in the development of this equation as are discussed in the body of the text. Equation 52 should be considered as the small signal transfer function and therefore can be used as a guide in synthesizing a servo system using the d-c motor with controlled excitation to achieve speed control.

Conclusion

Steady state and transient characteristics of the controlled rectifier and d-c motor combination have been analyzed for both armature and field control. Consideration of some of these characteristics lead to two different servomechanism transfer functions in the frequency domain. Approximations were made in the analysis such that the pertinent differential equations were linear.

The transfer function for the case of continuous current in the armature circuit may have more practical significance than is suggested by this paper. The analysis of this case was eliminated from this paper for the sake of brevity.

References

1. Theory of Rectifier—D-C Motor Drive, E. H. Vedder, K. P. Puchlowski. *AIEE Transactions*, volume 62, 1943, pages 863–70.

2. Voltage and Current Relations for Controlled Rectification with Inductive and Generative Loads, K. P. Puchlowski. *Electrical Engineering* (*AIEE Transactions*), volume 64, May 1945, pages 255–60.

3. Behavior Factors of Rectifier-Driven D-C Motors, Victor Siegfried. *Electrical Engineering* (*AIEE Transactions*), volume 63, July 1944, pages 530–32.

4. Operation of Large D-C Motors from Controlled Rectifiers, A. Schmidt, W. P. Smith. *AIEE Transactions*, volume 67, part I, 1948, pages 679–83.

No Discussion

Audio Noise of Power Transformers in Residential Areas

ARMAND V. LAMBERT
ASSOCIATE MEMBER AIEE

HEAVY load growth and economics necessitate the construction of large outdoor substations close to load centers. This brings humming electric equipment near dwellings and makes people more noise conscious. At the same time, manufacturers endeavor to build smaller and more economical transformers by using oriented cold rolled steel. Although the magnetostriction of this steel is less for a given flux density than that of the hot rolled steel, economics dictates the adoption of higher densities thereby offsetting the magnetostrictive advantages. Magnetostriction is the minute elongation of the steel when submitted to magnetization. It is recognized as the main source of transformer noise. The vibrations of the core set up by the 60 cycles per second (cps) alternating flux produce an audio noise composed of a fundamental frequency of 120 cps and its harmonics 240, 360, 480, 600 cps, ... The noise spectrum is the representation of these frequencies with their relative intensities. The subject of transformer noise deals mainly with the frequencies below 600 cps. For most power transformers, 120, 240, and 360 cps are found to be predominant. Any means that will reduce the magnetostriction or the intensity of the audio frequencies will bring us nearer a satisfactory solution.

The purpose of this paper is to trace some of the many and varied engineering aspects of the transformer noise problem and to present a few suggestions which might be beneficial to both the power engineer and the manufacturer.

It is suggested that the references mentioned at the end of this paper be read if more specific information is desired.

Corrective Measures

Briefly, the present means that could be used to attenuate the noise around distribution substations may be grouped as follows:

INSIDE AND ON THE POWER TRANSFORMER

The Core

1. Use of special steel with little magnetostriction.
2. Reduce flux density to retain the advantages of low magnetostriction steel.
3. Careful design and construction of the core and coils to avoid resonances and vibration of parts.

Between the Core and the Tank Walls

1. Insulating the core from the tank by paddings to avoid the transmission of vibrations to the tank walls.
2. Use of acoustical impedances or noise barriers in the oil.

The Tank

1. Design and build tank to avoid resonances.
2. Sound insulation of the tank.

Fittings and Auxiliaries

1. Mount them on resilient cushions and avoid resonances.

OUTSIDE THE POWER TRANSFORMER

1. Building sound barriers or enclosure around the transformer.
2. Adequate distance between the transformer and the nearest dwelling.

At the present time, there is not one satisfactory general solution. According to the importance of a noise problem, one or a combination of the means enumerated above can be applied. Economics, then, determines the solution to be adopted, as Mr. Fahnoe[1] wrote in 1942:

"Transformer noise is troublesome in relatively few cases, but none lend themselves to a general solution. Each is an economic problem, to balance the additional cost of a quiet transformer against the cost of providing a suitable enclosure or locating the transformer far enough away for the noise not to be objectionable."

The only thing that has changed in this statement is that the number of cases of transformer noise complaints have increased. Thus, each case should be studied individually and the most adequate solution, for noise and economics, should be adopted. A lower noise level transformer obtained by reducing the flux densities in the core requires more iron, more copper, more insulation, a larger tank, and more oil. This results in an increase in cost sometimes as high as 25 per cent for a noise reduction which cannot be, in most cases, accurately determined because of some unexplained behavior of the cold rolled steel. The hot rolled steel, however, lends itself to more accurate and predictable noise reduction. It is realized that the cost of all transformers should not be increased in order to obtain the low noise level required for special installations. This indicates some of the problems involved in adopting new noise level standards. On the other hand, there might be some possibilities of noise reduction in the transformer itself, without excessive increase of the cost. They will be reviewed at the end of this paper.

Suggestions for the Utility Engineers

When complaints arise about an existing substation, the utility engineer has a choice of two solutions: Replace the existing transformer with a quieter one, or, build an enclosure. When he is planning to build a new substation, he has one more solution: install it on a large lot.

Paper 51-299, recommended by the AIEE Transformers Committee and approved by the AIEE Technical Program Committee for presentation at the AIEE Pacific General Meeting, Portland, Oreg., August 20-23, 1951. Manuscript submitted May 21, 1951; made available for printing July 9, 1951.

ARMAND V. LAMBERT is with the Portland General Electric Company, Portland, Oreg.

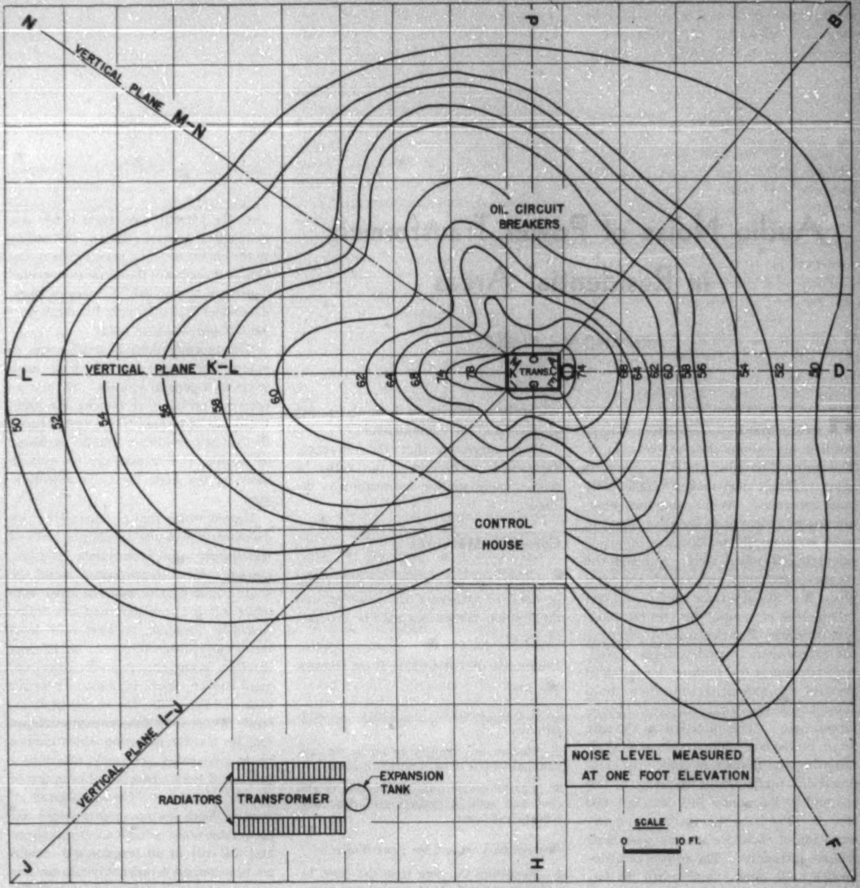
N
VERTICAL PLANE M-N
P
B
OIL CIRCUIT BREAKERS
L
VERTICAL PLANE K-L
D
50
52
54
56
58
60
62
64
68
74
78
TRANS
74
68
64
62
60
58
56
54
52
50
CONTROL HOUSE
VERTICAL PLANE I-J
RADIATORS
TRANSFORMER
EXPANSION TANK
NOISE LEVEL MEASURED AT ONE FOOT ELEVATION
SCALE
0
10 FT.
J
H
F

Figure 1. Equal noise level curves in a horizontal plane at 1-foot elevation around a 3,000-kva 57-12.5-kv 3-phase transformer

In both cases, the problem is one of economics; technically, it can be condensed in three questions:

1. What should be the nonobjectionable noise level at the nearest dwelling?
2. What should be the minimum distance between the transformer and the nearest dwelling to obtain the nonobjectionable noise level?
3. What should be the noise level around the transformer?

NONOBJECTIONABLE NOISE LEVEL

In the present state of the art, there are two things that can be measured in a noise:

1. The total noise level expressed in decibels as measured by the noise level meter.
2. The frequency spectrum, which represents the relative intensity of all the frequencies contained in a complex noise, traced by means of a frequency analyzer.

To be comparable, two noises must have the same level and a similar frequency spectrum. Consequently, the noise at the dwelling would be nonobjectionable if it had the same level and frequency spectrum as a reference noise considered to be nonobjectionable. Such comparison would certainly be difficult to make for many reasons, the major one being the determination of a standard nonobjectionable noise, since it is well known that the same noise may have various effects on different individuals. The following procedure is suggested to determine whether a noise is nonobjectionable. Since transformer noise is most troublesome at night, the ambient noise level and the harmonic index should be measured after all traffic has ceased and at a point far enough away from the substation so that the transformer hum is not audible. The noise level measured with the *A* (or 40 decibels) weighting of the noise meter would give the total ambient noise level in decibels (NEMA Standards for transformer noise are given for weighting *A*). The harmonic[3] index ($h_i = DB$) flat $- DB_{40}$ would be an indication only of the frequencies contained in the noise. Any noise that would have the same level and the same harmonic index as the one measured could be considered as nonobjectionable. The advantages of such procedure are twofold: measurements are kept to a minimum and only require a noise level meter. When a new substation has to be built, the level in decibels on weighting *A* and the h_i could thus be measured at the nearest dwelling before the construction starts. These two figures would be the references that the engineer would attempt to maintain. Needless to say that, with our present means, this would be a difficult, if not impossible task, especially in a quiet residential section. However, these references could serve as an accepted guide. As an example of the noise level in a quiet suburban area, an ambient as low as 26 decibels has been measured.

In order to find data for questions 2 and 3, field readings were taken around one 3-phase 3,000-kva 57−12.5-kv transformer remote from all buildings that could reflect the sound. Curves of equal noise level in horizontal planes were traced around the transformer at 1-foot, 6-foot, and 16-foot elevations. Figure 1 shows these curves for a 1-foot elevation. The odd shape of the noise level pattern obtained is caused by the transformer itself and the sound reflection from the control house, the circuit breakers, and the structure. Patterns traced for 6-foot and 16-foot elevations were similar. It is interesting to notice that the noise level decreases less rapidly in the direction perpendicular to the side of the transformer without radiators or expansion tank. The dampening effect of the radiators and expansion tank on the right-hand side is apparent. Such a pattern, if available, could help in locating the transformer and the equipment in a substation with respect to neighboring dwellings.

Curves of equal noise level in vertical planes also were traced with the data from the preceding curves. The general pattern was as shown in Figure 4. Near the transformer, the noise level was much higher at 1 foot than at 16 feet. This might be explained by the fact that the core rests solidly on the bottom of the tank and that the ground is reflecting the noise. At a distance from the transformer, the noise level was the same at any height; this distance varied with the direction of the vertical plane. Beyond this point the noise level was higher at 16 feet than at 1 foot. As a consequence, the noise would be more troublesome to the occupants of a 2-story house, and a sound barrier of adequate height should be built preferably as close as possible to the transformer.

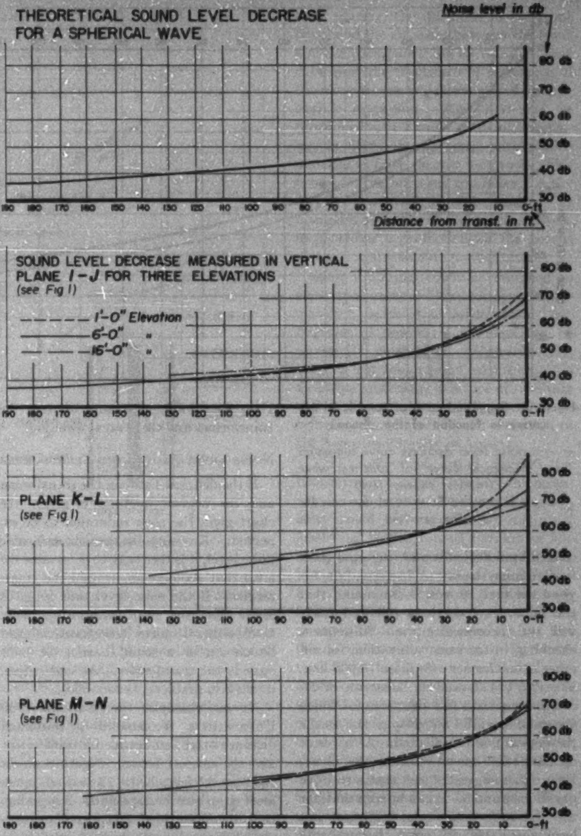

Figure 2. Noise level decrease in function of the distance for three elevations in different vertical planes

Finally, using the same data, curves representing the decrease in the noise level as a function of the distance were traced for different vertical planes and elevations, see Figure 2.

The 16-foot elevation curves indicate that near the transformer, the noise level at 16-foot elevation was lower than at 1-foot or 6-foot elevation, but decreased less rapidly with the distance. The curves in the vertical plane *I-J*, Figure 2, show that the noise level was approximately 70 decibels near the transformer and 36 decibels at 200 feet from the transformer. These curves were compared with the upper left curve which represents the theoretical sound level decrease for a spherical wave. The intensity of spherical wave varies inversely as the square of the distance from the source, or the sound level decreases 6 decibels each time the distance is doubled. Within the first 10 feet from the transformer, interferences,

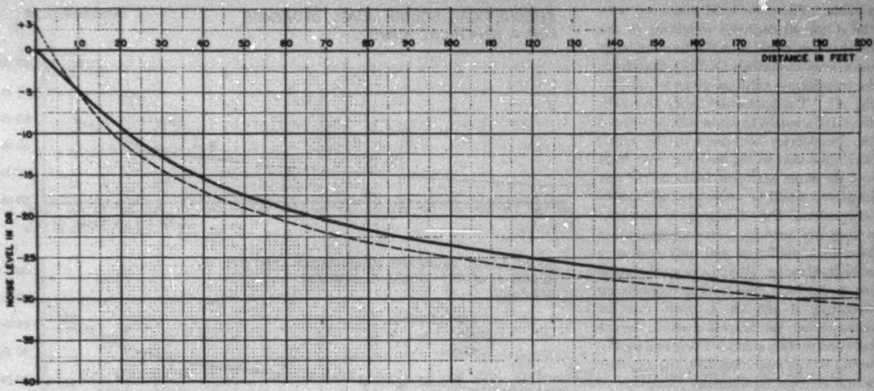

Figure 3. Suggested curve of noise level decrease in function of the distance

——— noise level decrease curve suggested
– – – theoretical curve for spherical wave (inverse square law)
------- field checked noise level decrease for the first ten feet

caused by reflected sound, were too great to determine the law of decrease, but, beyond the first 10 feet, it was found that the noise level decrease followed fairly well the theoretical curve. Subsequent checking, in the same substation, for another transformer (3-phase 6,000-kva, 57−12.5-kv) showed the same rate of decrease except in a few directions for which the noise level did not drop as fast as the theoretical curve indicated. As a result of these field measurements the chart, Figure 3, is suggested as a means to solve questions 2 and 3. It can be seen that, for the first 40 feet, the noise level drop has been purposely flattened, because the noise level of a transformer always represents the arithmetic mean of several readings taken around the transformer. In using this curve it is believed that the calculated noise level at a distant point would be higher than the measured. It is suggested that this curve be checked in as many installations as possible. Discrepancies must be expected because of interferences, particularly when the equipment is located in the vicinity of buildings. Consequently, this curve should not be used for heavily built-up areas; in any case, it should be used only as an indicator.

Minimum Distance

Knowing the noise level of a transformer and the nonobjectionable noise level to be attained, Figure 3, readily gives the minimum distance between the transformer and the nearest dwelling.

Noise Level Around the Transformer

If the distance between the transformer and the nearest dwelling is given, the chart gives the noise reduction to be expected. Knowing the nonobjectionable noise level, it is then easy to determine the level that should exist around the transformer. If the noise level thus found is lower than the given transformer noise level, either a quieter transformer should be chosen or a sound barrier be built outside the transformer. As said before, it will be a problem of economics.

As an example, the National Fire Underwriters recommend a minimum distance of 32 feet between a transformer and the nearest house. Figure 3 shows that for 32 feet, 14 to 17 decibels noise level drop can be expected. Supposing, that the noise level considered as nonobjectionable be 30 decibels, the noise level of the transformer should be between 44 and 47 decibels.

Sound Barrier

Two types of sound barrier are being built at the present time. They are:

1. Partial barrier, which reduces the noise in one or two directions.

2. Enclosure partly roofed or not.

Both types make use of sound absorbing materials which are not always suitable for outdoor installations. Partial sound barriers have been made of frames faced on both sides with transite and filled with sound absorbing material such as rock wool. Some were made of rigid 1- or 2-inch thick sheets of absorbing material called "sonotherm" with the outside face covered with stucco. Hollow concrete blocks filled with sand have been used to build enclosures around transformers. The references give many examples of such constructions.

There are a few points that should be kept in mind when building a sound barrier. The barrier should be built as close to the transformer as ventilation permits. This is especially important when the barrier is partial; in this case, sound deflectors on both sides and on the top of the barrier should be built, see Figure 6. An enclosure, with adequate sound absorbing material, built around and very close to the transformer would help to eliminate interferences and thereby noisy spots.

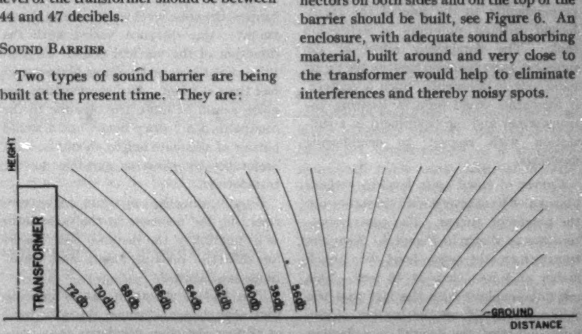

Figure 4. Pattern of equal noise level curves in a vertical plane

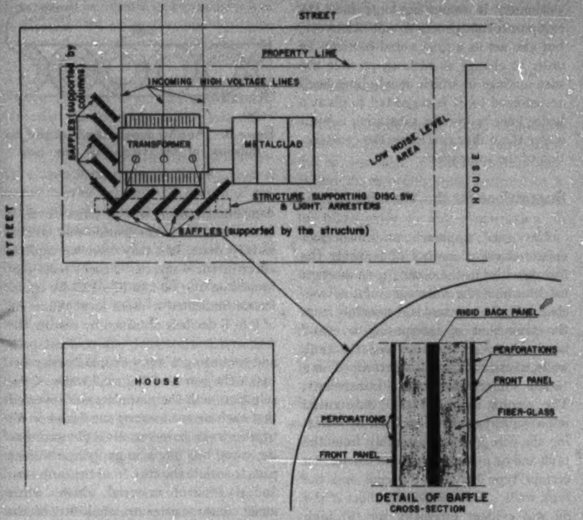
STREET
PROPERTY LINE
INCOMING HIGH VOLTAGE LINES
BAFFLES (supported by columns)
TRANSFORMER
METALCLAD
LOW NOISE LEVEL AREA
HOUSE
STRUCTURE SUPPORTING DISC. SW. & LIGHT. ARRESTERS
BAFFLES (supported by the structure)
STREET
HOUSE
RIGID BACK PANEL
PERFORATIONS
FRONT PANEL
FIBER-GLASS
PERFORATIONS
FRONT PANEL
DETAIL OF BAFFLE
CROSS-SECTION

Figure 5. Partial sound barrier built with sound-absorbing baffles

It would create a more uniform noise pattern outside the enclosure which is favorable to a better noise reduction with the distance. It would also reduce noise spilling over the barrier. Finally, if the enclosure itself is compared to a spherical source of noise, the sound intensity may vary as the second power of its linear dimensions. (See discussion of Mr. S. Bennon, reference 3.)

The structure and material used should be such that most high frequencies are attenuated by the barrier since the ear is more sensitive to the high frequencies. Here again, the harmonic index (h_t) may be used to evaluate the efficacy of a sound barrier. A higher h_t, measured after the sound barrier has been built, would indicate a shifting of the predominant frequencies toward lower frequencies. It also should be remembered that sound attenuation through a barrier is caused by viscous losses within a porous material of sufficient thickness, or, may be accomplished by a rigid impervious heavy wall. In most cases, both porous and impervious material are required to make a satisfactory sound barrier. It has been found, for instance, that a wall built with pumice blocks, which have good absorption characteristics, was a better sound barrier if backed by an impervious lay of plaster.[4] A perfect sound barrier would thus consist of a space where sound energy would be dissipated, and sound reflexion greatly reduced, backed by an impervious material which would stop the remaining sound energy. The space where sound dissipation would take place would certainly require a large quantity of porous material and thus would make the cost of the barrier prohibitive.

It is believed, however, that this difficulty could be overcome by using a type of sound-absorbing structure, successfully used in radio-broadcasting studios, which applies the principle of the Helmholtz Resonators or resonant cavities.[5] Briefly, this type of sound-absorbing structure is composed of a perforated front panel and a solid impervious back panel, separated by an air space. The perforations in the front panel can be round holes or slots. The dimensions of these perforations, their spacing, the thickness of the front panel and the air space between the front and the back panels are all variables that determine the frequency of resonance of the air space for which the sound absorption is maximum. The latter can be broadened over a wider range of frequencies in filling the air space with porous material as fiber glass or rockwool. This type of structure thus combines the absorptive qualities of such material as fiberglass with that of the structure itself, in providing a protection for the porous material against weather conditions.

Such structures could be designed to work as acoustical filters for specific frequencies, since the predominant frequencies of power transformers can be accurately determined. Unfortunately, there is not much practical information available concerning this type of structure and their calculation. The author is bringing this subject to the attention of the Acoustical Society of America.

The problem of sound barriers for transformers is complicated by the necessity for adequate ventilation. This difficulty could be overcome by mounting absorbing baffles (sound barriers of the same type just described mounted back to back) around the transformer. Figure 5 shows one possible way to locate such baffles. The sound energy would decrease after each reflexion against the panels and would come out of the acoustical filter thus formed, considerably reduced. Besides, no sound over-pressure would be created as in the case of the conventional enclosure. The baffles could be of light construction since most of the absorbing effect would be obtained by their resonance property. Finally, they could be arranged in order to form an attractive architectural ensemble with the structure supporting the switching equipment.

Mounting the transformer on wood, cork, rubber pads, or on a separate foundation also should be investigated because vibrations may be transmitted through the foundation and the ground and set the

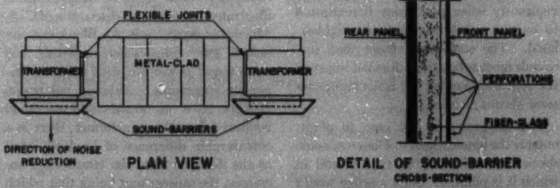
FLEXIBLE JOINTS
TRANSFORMER
METAL-CLAD
TRANSFORMER
SOUND-BARRIERS
DIRECTION OF NOISE REDUCTION
PLAN VIEW
REAR PANEL
FRONT PANEL
PERFORATIONS
FIBER-GLASS
DETAIL OF SOUND-BARRIER
CROSS-SECTION

Figure 6. Another type of partial sound barrier consisting of a sound-absorbing panel mounted on one side of the transformer

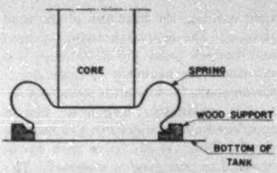

Figure 7. Test performed with the core of a 15-kva distribution transformer mounted on two springs. Test showed a noise reduction by isolating the core from the tank with springs

switchgear housing, structure and adjacent buildings in vibration, thus increasing the noise. It is suggested that the transition throats of unit-substations be attached to the transformers by means of flexible joints in order to prevent vibration transmission from transformer to metal-clad. If the metal-clad is not set in vibration, it will act as a noise filter because of the many partitions; furthermore, the transition throats and the partitions could be lined with sound-absorbing material. With this arrangement the sound barrier or the absorbing baffles would have to be built on one, two, or three sides of the transformer only according to the location of adjacent dwellings. In some cases, a partial sound-barrier would be adequate and would consist of a small screen built as close as possible to the transformer. Figure 6 shows another type of partial sound-barrier built on one side of the transformer.

In conjunction with the construction of a sound barrier, the esthetic value of the installation must be considered. It has been found, in many cases, that complaints from people living in the neighborhood of a substation also were based on the nonattractiveness of the installation. Streamlining the equipment does not seem to help in the matter, especially if a structure gives the appearance of a steel plant shipping yard. People, definitely, do not like to have such an installation in their sight and they protest vigorously when permission is requested to build a substation in their neighborhood. The steel mesh fence that surrounds most substations does not improve the appearance either if it is not hidden by some shrubs or trees.

It is suggested in this case, to plant, outside the fence, a hedge of laurel of some species according to the type of soil in which it is planted. Such a hedge would probably cost less than shrubs and would grow faster to any desired height and thickness; it would not only hide the equipment that people do not like to see, but also act as a final sound barrier. In order to change as little as possible the surroundings in which people have been accustomed to, it is suggested to plant a hedge long before the substation is built where the utility can forsee the construction of the substation.

Suggestions for the Manufacturers

The usual approach to transformer noise reduction consists of reducing the flux densities in the core. In an attempt to determine the value of isolating mechanically the core and coil assembly from the tank and of interposing a sound barrier between the core and the tank walls, a series of tests was performed on a 15-kva distribution-type transformer. The results indicated that substantial improvement could be realized by isolating the core and coil assembly from the tank and by mounting a sound barrier of a certain type between the core and the tank walls. The dampening effect of the oil was evident especially for the high frequencies, although similar tests performed by some manufacturers indicated that the oil had no dampening effect at all and consequently, isolating the core from the tank would have no beneficial effect. It may be of some interest, however, to recall the analogy between mediums oil-air and conductors of different impedances (see Appendix). The acoustical impedance of the oil is in the order of 10,000 centimeter-gram-seconds while that of the air is 40 centimeter-gram-seconds which makes the sound energy transmission from the oil to the air very inefficient. It is true that the equations at the boundary of two conductors of different impedances, written in the Appendix, are only valid for two infinite conductors, or, for mediums of great dimensions compared to the wave length of the sound.

In the case of a transformer, these equations would be valid only for the high frequencies. It is, however, worthwhile to dampen the high frequencies as much as possible, as E. A. Blomqvist has illustrated so well in his discussion of C. S. Murray's paper.[3] E. A. Blomqvist assumed four transformers emitting the same sound power but with different frequency spectrums. Although all transformers have an equal loudness level measured near the transformer, there is a considerable difference of loudness level as the distance from the transformer increases, the quieter unit being that which has the lowest predominant frequency. Thus, it may appear that the oil has no dampening effect if the noise level is measured close to the transformer, as it is usually done, but may have an audible effect in the distance. Recent tests performed on a 3,000-kva 57−12.5-kv transformer indicated a noise level reduction of 8 to 9 decibels obtained by resting the core and coil assembly on resilient pads and mounting a very simple barrier between the core and the tank walls. Consultation with the manufacturer revealed that such means was not successful on all transformers, however. It is obvious that the stumbling block in applying resilient pads to isolate the core from the tank is to find a resilient material which, when under constant pressure, would still retain its elasticity and not contaminate the oil. Subsequent and periodic tests will determine whether the material used as resilient pads in the mentioned transformer is suitable. One possible solution to this problem was indicated by a test performed on the core of a 15-kva distribution-type transformer resting on two steel springs, as shown in Figure 7 in place of rubber pads. The average reduction of noise level, in this test, was approximately 7 decibels (without sound-barrier). Unfortunately, the frequency analyzer was not available at the time the test was performed and the noise spectrum could not be traced. Other types of pads could be developed. For instance, rubber-like thick wall cylinders could be used as shown in Figure 8. The same thick wall rubber cylinders could be used for bracing

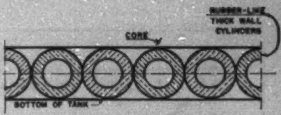

Figure 8. Another type of resilient pad for isolation of the core from the tank

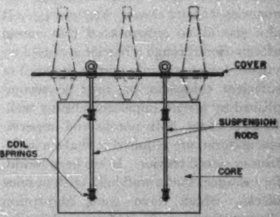

Figure 9. Another way to isolate the core from the tank, by suspending the core from the cover

the core. They would be inexpensive and easily installed. The core could also be suspended from the cover. This could be accomplished by the use of heavy steel rods and coil springs as suggested in Figure 9. This is an old type of construction that could be readily adaptable for vibration dampening.

The tests on the 15-kva distribution-type transformer also indicated that a sound barrier between the core and the tank walls would reduce the noise transmission through the oil. The ordinary kind of sound-absorbing material, used in building construction, could not be installed in transformer oil because any porous material would become saturated with oil.

In this case, the noise reduction would be accomplished through the use of alternate layers of mediums having different acoustical impedances, such as oil and air, where sound energy would be lost at each boundary. The electrical analogy to this is found at the boundary of two electrical lines or circuits of different impedances where energy transfer is inefficient if matching impedances are not used. Such an air sound barrier could be made of two parallel sheets of metal, or any other material impervious to oil, separated by 1/2 inch to 1 inch air space and hermetically sealed. One or two of these barriers could be mounted between the core and the tank walls, thus providing the desired air layers. Again, this type of sound barrier would be more effective for high frequencies than low frequencies and its effect may not be apparent when noise level readings are taken near the transformer.

Outside the tank many possibilities for sound reduction exist, for example, metal cabinets, fittings and fans could be mounted on rubber cushions. Advantage could be taken of the fact that radiators have some sound absorbing effect as shown in the first part of this paper. This is more pronounced with flat-type radiators than with tube type. Radiators could be designed to have the greatest possible sound absorbing effect. Also, to avoid transmission of the vibrations, they could be mounted on rubber-like gaskets or supported by resilient pads. For especially quiet installations, the radiators could even be separated from the transformer. The tank would then be enclosed in a soundproof enclosure and all rigid connections between the tank and the radiators would be avoided.[6] By this method, British constructors claim to have reduced the 100-cycle component by 12 decibels and the 300-cycle component by 16 decibels (European frequency is 50 cycles per second). In this case, radiators also could be used as partical sound-barriers or acoustical filters.

Conclusions

The present noise level standards should be revised for power transformers to be installed in urban substations. Where an especially quiet installation is indispensable, noise measurements should be taken prior to any construction, in order to set the requirements. An economical study should then be made to determine the solution to be adopted. Finally, the substation itself should be very carefully laid out in order to take every possible advantage of the type of equipment purchased. It is felt that it is possible for the utility engineer to be more definite in his specifications for transformer noise and in the planning of quieter, as well as, more appealing substations.

Appendix

Reflection and Refraction in an Electric Transmission Line

In a transmission line, when a current meets a boundary between two conductors of different impedances the current divides into two currents: a reflected current and a refracted current.

Let us consider two infinite lines on both sides of the boundary *M*:

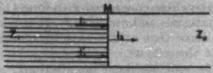

The characteristic impedance of the line at left is Z_1 and at right Z_2.

i_1 = the current flowing from left to right in the line at left.

i_2 = the transmitted (or refracted) current at right which is different than i_1.

The actual current at *M* can be considered as the resultant of two superposed currents which are: the incoming current i_1 and the reflected current i_1'. We can write: $i_1+i_1'=i_2$. To i_1 corresponds a voltage e_1, and to i_1' corresponds a voltage e_1'. Since i_1 flows from left to right (positive) we can write: $e_1=Z_1\times i_1$, and since i_1' is flowing from right to left (negative) we must write: $e_1'=-Z_1\times i_1'$ and also: $e_2=Z_2\times i_2$.

Thus, the equations at the boundary of two infinite lines with different characteristic impedances will be:

$$i_1+i_1'=i_2 \qquad (1)$$

and

$$e_1+e_1'=e_2$$

or

$$Z_1\times(i_1-i_1')=Z_2\times i_2 \qquad (2)$$

From equations 1 and 2 we deduce:

$$i_1'=i_1\times\frac{Z_1-Z_2}{Z_1+Z_2} \qquad i_2=i_1\times\frac{2Z_1}{Z_1+Z_2}$$

$$e_1'=-Z_1\times i_1'=-Z_1\times i_1\times\frac{Z_1-Z_2}{Z_1+Z_2}$$

$$=-e_1\times\frac{Z_1-Z_2}{Z_1+Z_2}$$

$$e_2=Z_2\times i_2=i_1\times\frac{2Z_1\times Z_2}{Z_1+Z_2}=e_1\times\frac{2Z_2}{Z_1+Z_2}$$

The reflection coefficient is

$$r=\frac{i_1'}{i_1}=\frac{Z_1-Z_2}{Z_1+Z_2}=-\frac{e_1'}{e_1}$$

The incoming power is

$$\frac{Z_1\times I_1^2}{2}\ (I_1=\text{maximum of } i_1)$$

The transmitted power is

$$\frac{Z_2\times I_2^2}{2}$$

The efficiency in power transmitted is

$$n=\frac{Z_2-I_2^2}{Z_1+I_1^2}=1-r^2$$

Reflection and Refraction of a Plane Sound Wave

Application of the equations at the boundary of two mediums with different acoustical impedances.

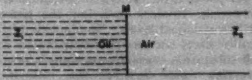

Let us suppose that the medium at left is oil; its acoustical impedance is $Z_1=10\times10^4$ centimeter-gram-seconds (this value is assumed, for it could not be found in any available literature; the actual value may be higher but it will not affect the final result), and the medium at right is air for which the acoustical impedance is:

$Z_2=40=0.004\times10^4$ centimeter-gram-seconds

We will have:

1. Reflected particle velocity (analogous to the current in the foregoing equations)

$$i_1'=i_1\times\frac{Z_1-Z_2}{Z_1+Z_2}=i_1\times\frac{10-0.004}{10+0.004}\sim i_1$$

where i_1' is positive. This means that i_1' is in phase with i_1. The reflection coefficient is $r=i_1'/i_1$ (very close to 1).

2. Reflected pressure (analogous to the voltage):

$$e_1'=-Z_1\times i_1'$$

where the pressure of the incoming wave is $e_1=Z_1\times i_1$ and e_1' is very close to $-e_1$.

3. Transmitted velocity:

$$i_2 = i_1 \times \frac{2Z_1}{Z_1+Z_2} = 2i_1 \times \frac{10}{10+0.004} \sim 2i_1$$

4. Transmitted pressure:

$$e_2 = e_1 \times \frac{2Z_2}{Z_1+Z_2} = e_1 \times \frac{0.008}{10.004} = 8.10^{-4} \times e_1$$

5. The transmitted power $Z_2 \times i_2^2$ is very small and the efficiency is

$$\eta = \frac{Z_2 \times i_2^2}{Z_1 \times i_1^2} = \frac{0.004 \times 4 \times i_1^2}{10 \times i_1^2} = \frac{0.016}{10} = 0.0016$$

which represents a loss in power transmitted equal to 28 decibels (assuming infinite mediums).

For transformers in which the oil space between the core and the tank walls is relatively small, there may be some loss of sound energy affecting only the higher frequencies.

References

1. Transformers Are Loud—Only If You Hear Them, H. Fahnoe. *Westinghouse Engineer* (East Pittsburgh, Pa.), May 1942.

2. Harmonic Index—A Tool for Transformer Audio Noise Investigation, W. H. Mutschler, Jr., T. F. Madden. *AIEE Transactions*, volume 69, part I, 1950, pages 115–20.

3. Transformer Audio Noise Problems on an Electric Power System, C. S. Murray. *AIEE Transactions*, volume 68, part I, 1949, pages 740–51.

4. Cinder Block: Sound Transmission, R. H. Ealing, E. R. Bascom. *Progressive Architecture*, (New York, N. Y.), August 1950.

5. The Application of Helmholtz Resonators to Sound-Absorbing Structures, Vilheim L. Jordon. *Journal*, Acoustical Society of America (New York, N. Y.), volume 19, number 6, November 1947.

6. Reduction of Noise in Power Transformers, E. T. Norris. *Review*, Ferranti Ltd., (England), October 1938.

7. The Audio Noise of Transformers, W. C. Sealey. *Electrical Engineering* (*AIEE Transactions*), volume 60, 1941, pages 109–12.

8. A Study of Sound Levels of Transformers, H. Fahnoe. *Electrical Engineering* (*AIEE Transactions*), volume 60, 1941, pages 277–83.

9. Hipersil, a New Magnetic Steel and its Use in Transformers, J. K. Hodnette, C. C. Horstman. *Westinghouse Engineer* (East Pittsburgh, Pa.), August 1941.

10. Audible Noise of Power Transformers, T. D. Gordy. *AIEE Transactions*, volume 69, part I, 1950, pages 45–53.

11. Audio Noise in Transformers in Residential and Commercial Areas, C. E. Baugh. *AIEE Transactions*, volume 69, part I, 1950, pages 121–27.

Discussion

C. S. Murray (Consolidated Edison Company of New York, Inc., New York, N. Y.): The author outlines various means of attenuating the noise around distribution substations and it is agreed that there is no single satisfactory solution to the problem at the present time.

I feel that the ultimate solution to the transformer noise problem will be to decrease the noise at its source. Up until two or three years ago transformer designers had stated that it was not practical to build the larger power transformers for a reduction of more than 10 decibels below the present NEMA specified levels. In the case of the smaller sizes, such as the distribution and unit substation types, it was stated that the reduction would be even less. However, during the last few years the manufacturers have built low noise level transformers with reductions exceeding the 10-decibel figure and these transformers are not the immense giants that were previously prophesied by the manufacturers. Some of these transformers represent the first attempts by these manufacturers to supply low noise level transformers. Further investigations by the manufacturers and an adoption of some of the methods outlined by the author may permit even greater reductions to be achieved economically.

In regard to the placing of barriers between the core and main tank, this had been tried abroad but to my knowledge it has not been applied in this country. Mr. Forrest[1] describes a 20,000-kva transformer in which the core was placed in a steel tank and this entire assembly was then placed in another steel tank which was resiliently isolated from the first. A reduction of 10 decibels was claimed due to this construction. There was no data published as to the change in loudness of the noise at a remote point from the transformer. It will be interesting to note the reaction of the transformer designers as regards the suggestions of the author to install barriers within the tank.

In his discussion of nonobjectionable noise the author states that any noise with the same level and harmonic index as the noise without the transformer energized can be considered as unobjectionable noise. This cannot be used as a hard and fast rule. Under certain conditions of ambient and transformer noise levels, at points remote from the transformer, the transformer noise will not add materially to the sound level meter indication. Yet the transformer noise will be audible and may be objectionable. If one wishes to compare noises at a given location before and after the transformer is energized, it would be much better for him to obtain the sound level of the various components of the noise with a sound analyzer.

The author discusses barriers which apply the principle of the Helmholtz Resonator. Some time ago I suggested that the application of resonant cavities should be considered by those concerned with sound absorbent materials and methods.[2] It is gratifying to know that others have become interested in the subject. In applying this principle to out-of-doors installations, some means must be provided to prevent the accumulation of foreign debris and water within the cavity that may change the frequency characteristics of the filter.

I agree with the author that the present specified sound level values should be revised not only for transformers to be installed in urban substations, as he suggests, but for all transformers. Manufacturers can design and build transformers with noise levels somewhat below the present standard without cost to anyone.

Ultimately, a transformer noise standard would specify the permissible amount of noise that a transformer can emit which is founded on factual evidence showing that this is the requirement for the general case. This factual evidence would be collected by a standardizing body such as the American Standards Association. Such information would be extremely valuable to those of us dealing with the noise problem.

References

1. Quantitative Survey of Noise Characteristics of Large Transformers, J. S. Forrest. *Beama Journal* (London, England), volume 44, number 20, February 1930, pages 51–54.

2. See reference 3 of the paper.

Theodore R. Specht (Westinghouse Electric Corporation, Sharon, Pa.): Mr. Lambert has covered the problem of transformer noise quite thoroughly in his paper. The curve he suggests for the decrease of noise level with distance is one for which there has been a need for some time, and it would certainly be desirable for various people to make similar measurement and see if the results agree with the curve. In his curve though, he has not taken into account the size of the transformer, so strictly speaking the curve would only apply approximately to the range of sizes he tested, which was 3,000 to 6,000 kva. For small transformers, about 15 kva, the inverse square law should apply quite closely; and for larger transformers, over 30,000 kva, the attenuation would be about 3 decibels less than given by the curve beyond 30 feet, and proportionately less closer to the transformer.

The partial sound barriers described in the paper would certainly be quite desirable as they would allow normal ventilation of the transformer. Does the author know what the attenuation of barriers like this would be? Corbett McLean, in a recent article,[1] described a roofless enclosure which was provided with small ventilating openings in the walls. He said it was necessary to complete the entire enclosure before appreciable noise reduction was achieved, that is with the ventilating openings closed. At 35 feet from the transformer, he found the attenuation was doubled with the ventilating openings closed. The basic idea of using ventilating openings lined with acoustic material to reduce the transmission of sound through the openings is practical and methods for calculating the attenuation are available.[2] An approximate calculation would give about 3 or 4 decibels attenuation directly outside the baffles in the overlapped pattern shown in Figure 5. It would seem doubtful whether a 3-sided enclosure, spaced three or four feet from the transformer, would appreciably reduce the rating of the transformer. In most cases, it should be practical to use a 3-sided enclosure from a noise standpoint. But where 4-sided enclosures must be used, ventilating openings lined with acoustic material may be desirable.

Mr. Lambert has secured favorable results by mounting the core and coils on springs and vibration dampeners. We have made tests with a transformer setting normally in its tank and then repeated the tests with the core and coils held by a crane so the core and coils were still in the tank but not touching the tank. We were unable to find any significant difference in the sound levels. Experience has shown that with the core and coils properly assembled in a tank, the addition of spring or resilient mountings and vibration absorbers does not give any appreciable reduction in noise. It also has been determined that with an improper assembly of core and coils, these devices may show moderate to very high reductions in noise. If there are loose laminations in the core, there is a definite dampening effect by the oil on the vibration of these laminations. The oil tends to dampen out these high-frequency buzzes.

The use of sound barriers inside the transformer has definite possibilities, but there are many considerations. The barriers should not prevent the circulation of the oil and cooling of the transformer to any large extent.

This may mean that there will be sufficient paths for the sound to by-pass the barrier. Also the barrier must be able to stand the oil pressure and the vacuum treatment of the transformer, and must withstand varying operating pressures and temperatures as well as the effect of the oil on the barrier over the life of the transformer. The pressure and vacuum will make it very difficult to use the barrier consisting of two parallel sheets of metal separated by an air space such as is suggested. It is entirely possible that the cost of such internal barriers may exceed the cost of external barriers to achieve the same noise reduction.

The use of vibration absorbers between the transformer and cabinets on the transformers may be desirable. We have made tests on transformers with large banks of radiators to use flexible couplings between the transformer and radiators, but no improvement resulted. It is doubtful if much vibration from the tank wall is transmitted to the radiator bank, as the bank is so heavy and is filled with oil. The case would be different with switchgear cubicles and it is possible that flexible couplings between the transformers and cubicles may help in some cases.

REFERENCES

1. TRANSFORMER NOISE AND ITS CONFINEMENT, **Corbett McClean.** *AIEE Transactions*, volume 69, 1950, pages 1409–16.

2. ACOUSTICAL DESIGNING IN ARCHITECTURE, **V. O. Knudsen, C. M. Harris.** J. Wiley and Sons, Inc., New York, N. Y., 1950, page 286.

W. H. Mutschler, Jr., and T. F. Madden (Allis-Chalmers Manufacturing Company, Pittsburgh, Pa.): Mr. Lambert has succeeded in presenting some of the numerous engineering aspects of the transformer noise problem. His concise and complete list of corrective measures which can be applied to transformer noise serves as a useful guide for both the user and the manufacturer of transformers.

Before discussing the various corrective measures listed, it should be noted that where noise is a problem, the reduction in noise level required to remove possible objections is usually on the order of 15 to 20 decibels. Reductions of this magnitude cannot be accomplished by design alone as the result of limitations imposed by existing materials. However, careful design and construction to avoid all resonance serves to reduce the noise level generated by a given unit but usually not more than 6 decibels. Further reductions below the noise levels normally obtained in economical designs can best be achieved by recourse to the modification of standard designs by means of the devices suggested by Mr. Lambert in the section on corrective measures.

The isolation of the core and coil assembly from the tank proper has been investigated with varying degrees of success. In some cases the noise level has been actually increased by isolating the core and coil assembly.

The effectiveness of core and coil isolation can only be determined when considered in conjunction with the noise transmitted through the oil and the modes of vibration caused by the transmittal of noise through these two media. A study of a typical transformer assembly will show that the vibrational amplitudes transmitted through the oil to the tank wall are 180 degrees out of phase with the vibrational amplitudes in the tank wall caused by vibration of the bottom of the tank.

Since oil has a high acoustical impedance, the vibrational amplitudes are transmitted to the tank wall through the oil with little attenuation. These vibrational amplitudes may then be either larger or smaller than the vibrational amplitudes in the tank caused by vibration of the tank bottom. If the vibrational amplitudes through the oil are larger, isolating the core and coil assembly will increase the total vibrational amplitude and the transformer noise level. If they are smaller, isolating the core and coil assembly will decrease the total vibrational amplitude and the transformer noise level. Thus to build an effectively quiet transformer it is necessary to decrease the vibrational amplitudes in the tank wall by sound barriers in the oil as well as by core isolation.

Sound barriers, to be located inside the transformer tank, must fulfill certain requirements before they can even be considered as economically justifiable. They must not interfere with the normal circulation of oil for cooling. They must not alter the insulating characteristics of the oil. They must be effective over the range of frequencies normally present in the transformer noise spectrum. Their characteristics should not be influenced by the presence of oil or, if so, means must be provided for isolating the sound barrier from the oil.

Although the noise is attenuated from the core to the tank, experience has shown that this attenuation does not approach the theoretical value of 28 decibels as shown in the Appendix of Mr. Lambert's paper, but rather approaches a value of 10 decibels over the range of frequencies present in transformer noise.

Armand V. Lambert: Originally, I was inclined to feel, as Mr. Murray does, that the ultimate solution to the transformer noise problem would be to decrease the noise at its source. After study and discussion with transformer design engineers, it appears that unless radically new designs are used, noise level reductions, as required in residential areas, will be difficult to accomplish in the transformer alone. However, I feel that the noise level of the present-day transformers can be substantially reduced without greatly increasing the cost. If especially quiet installations require further noise reduction, a sound barrier is in order. In any event, close co-operation between the manufacturers and the utility engineers may be beneficial in laying out substations.

I agree with Mr. Murray that a frequency analyzer would be much more adequate for the tracing of a complete frequency spectrum.

However, because this instrument, as it now exists, does not lend itself to field work, the harmonic index method was suggested. Needless to say, a frequency analyzer designed for this type of work would be more than welcome. It may be that an octave-band analyzer is the answer, but my lack of experience with this instrument prevents me from giving any opinion. Finally, the cost of this equipment is another factor that has to be considered. A utility engineer may justify the acquisition of a noise-level meter, but may not be able to justify the additional cost of a frequency analyzer. Consequently, the harmonic index is a quick and nonexpensive way to obtain an indication of the frequencies present in the noise, but is not suggested as an accurate method.

The Portland General Electric Company now is experimenting with scale models to obtain more data on resonant cavities and to investigate the possibility of applying them in sound barriers.

It is right, as Mr. Specht remarks, that the curve suggested for the noise level decrease, as a function of the distance, applies for transformers of 6,000 kva or smaller. It is felt that if a larger transformer has to be located in a residential area, it should be installed in a total enclosure or building, else serious noise complaints will develop. In this case, the curve no longer applies. Mr. Specht, and other transformer design engineers have found that isolating the core from the tank would not reduce the noise level of the transformer. However, in one of our 3,000-kva 69-kv class power transformers a noise reduction has been achieved by this means and at a moderate cost. It may be that in most cases this method does not give the expected amount of noise reduction, but a combination of inexpensive means to cut a few decibels here and there may prove to be a practical solution. It is felt that there is no one clear-cut method in reducing transformer noise. Isolating the core from the tank is suggested only as one of many ways to cut down the present noise levels. As Mr. Murray says, there have been improvements already, probably due partly to improving some construction details.

I agree with Messrs. Mutschler and Madden that where a reduction of 15 to 20 decibels is required, it can not be accomplished in the transformer alone, at least with the present conventional design. As stated before, such a large reduction must be achieved by close co-operation between the manufacturer and the utility engineer. The theoretical value of 28 decibels shown in the Appendix of the paper was not intended to prove that it would be possible to achieve or even approach such reduction. Instead, the

Appendix was intended to draw attention to the fact that the difference in the acoustical impedance of air and oil is a contributing factor to the reduction in the intensity level of the high frequencies.

It might be of some interest to mention that the magnetostrictive phenomena is not only responsible for transformer noise, but also for the deterioration of transformer oil in power transformers.

This chemical change of the oil is produced by the vibrations in the sonic and ultrasonic ranges emitted by the laminations.

It is my pleasure to thank Messrs. Murray, Specht, Mutchler, and Madden for their contribution to this paper. Their points of view are of great value to all engineers interested in this problem.

Some Methods of Obtaining Correct Line Drop Compensation on Single-Phase Voltage Regulators Used on 3-Phase Systems

H. L. PRESCOTT
MEMBER AIEE

MANY OF the feeder voltage regulators used on distribution circuits are equipped with line-drop compensators to permit adjusting the regulator control to maintain constant voltage at a point some distance from the regulator installation. The smaller sizes of regulators, particularly the pole mounting types, are single-phase devices. When single-phase regulators are used on 3-phase systems, the phase-angle relationships between the voltages and currents in the regulators must be observed and correlated if proper line-drop compensation is to be obtained.

This paper outlines three of the ways by which this correlation may be accomplished.

1. By auxiliary current transformers.
2. By phase-shifting networks.
3. By modified compensator settings.

The Line-Drop Compensator

Consider a line from a regulator to a load center, as shown in Figure 1. Let

E_L = voltage at the load
I = line current
$R+jX$ = line impedance
  R = line resistance
  X = line reactance
E_R = voltage output at the regulator

The voltage drop in the line is the product of the line current and the line impedance, or

$$IZ = IR + jIX \tag{1}$$

Starting at the load and adding voltages,

$$E_L + (IR + jIX) = E_R \tag{2}$$

In the vector diagram the current is illustrated as lagging the voltage by the angle θ as observed at the regulator.

At the voltage regulator, the voltage E_R is applied to the control circuits through a potential transformer. The current I is applied to the line-drop compensator through a current transformer. The R and X elements of the compensator produce the voltages IR and IX, and subtract them from E_R so that the voltage applied to the voltage regulating relay is $E_R - IR - jIX$ which equals E_L.

3-Phase Voltages and Currents

The vector relations of currents and voltages for a 3-phase system are shown by Figure 2 where the voltages E_{OA}, E_{OB}, E_{OC} are line-to-neutral voltages; E_{AB}, E_{BC}, E_{CA} are line-to-line voltages; and I_A, I_B, I_C are line currents as indicated in the figure. This figure is drawn with the same phase angle, θ, between line-to-neutral voltage and line current as between I and E_R of Figure 1.

Table I. Voltages and Currents in Delta-Connected Regulators

	Figure 4(A)		Figure 4(B)	
Regulator	Voltage	Current	Voltage	Current
1	E_{AB}	I_B	E_{BA}	I_A
2	E_{BC}	I_C	E_{CB}	I_B
3	E_{CA}	I_A	E_{AC}	I_C

Y Connection

When three single-phase regulators are Y connected on a 3-phase system, as shown in Figure 3, the voltage and current relationships in each regulator are the same as for the single-phase case of Figure 1. This may be seen by comparing Figures 2 and 3 with Figure 1. Regulator 1 is excited by voltage E_{OA} and has line current I_A. Regulator 2 is excited by voltage E_{OB} and has line current I_B. Regulator 3 is excited by voltage E_{OC} and has line current I_C. In each case, the phase relation between the voltage and the current is exactly the same as between E_R and I of Figure 1.

Therefore, single-phase voltage regulators may be Y connected on a 3-phase system, and the line-drop compensation will function in the normal manner, and no special connections are required.

Delta Connection

The two delta connections for single-phase voltage regulators on 3-phase systems are shown in Figures 4(A) and 4(B). The voltages and currents in each regulator are shown in Table I.

In Figure 5, the vectors from Figure 2 are redrawn to show more clearly the voltage and currents of Figure 4. The dotted lines represent the phase positions of the voltages E_{OA}, E_{OB}, and E_{OC}. From Figure 5, the phase-angle relations between the voltages and the currents can be determined by inspection, as tabulated in Table II. For each case, the positive direction of the angle is counterclockwise from the voltage to the current.

Thus, each regulator in the delta connection has its voltage and current phase angle changed by 30 degrees from the conditions which would exist if the regulators were Y connected. It, there-

---

Paper 51-300, recommended by the AIEE Transmission and Distribution Committee and approved by the AIEE Technical Program Committee for presentation at the AIEE Pacific General Meeting, Portland, Oreg., August 20–23, 1951. Manuscript submitted May 18, 1951; made available for printing July 18, 1951.

H. L. Prescott is with Westinghouse Electric Corporation, Sharon, Pa.

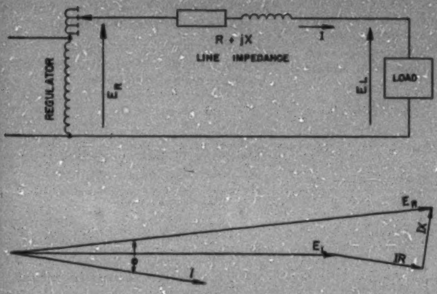

Figure 1. Schematic and vector diagrams of a typical line with voltage regulator

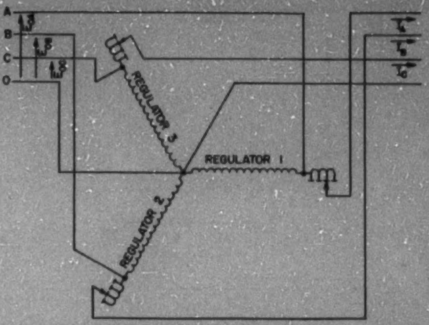

Figure 3. Y-connected single-phase voltage regulators on a 3-phase system

fore, follows that in order to obtain correct line-drop compensation on delta-connected regulators, some means of compensating for this 30-degree phase shift must be provided.

Open-Delta Connection

The connections for open-delta operations are shown in Figure 6. For purposes of illustration, the regulators are shown connected in lines *A* and *C*. The voltages, currents, and phase angles are given in Table III. Regulator 1 in Figure 6 is subject to identically the same voltage and current conditions as regulator 1 of Figure 4(B), while regulator 2 in Figure 6 is subject to the same conditions as regulator 2 of Figure 4(A).

Thus, open-delta operation also requires some means of compensating for a ±30-degree shift between regulator voltage and regulator current.

Methods of Phase Shifting

One method of compensating for the phase shift introduced by delta or open-delta operation of regulators is to interconnect the secondaries of current transformers in each of two lines to obtain a current which is in phase with the regulator excitation voltage. A second method is to use impedance networks in the control circuits to shift the phase angles within the control devices. A third method is to modify the settings of the line-drop compensator dials to correlate the regulator operation with the actual line conditions. The remainder of this paper is devoted to describing each of these methods.

Cross-Current Connections

Figure 7 shows the connection and vector diagram of current transformer secondaries for current transformers in lines *A* and *B*. At the point *P*, the currents I_B and I_A combine to form the current $I_B - I_A$ which flows through the primary winding of the auxiliary current transformer. The vector addition shows that the resultant current $(I_B - I_A)$ is displaced from I_B by the angle, −30 degrees. In Figure 4(A), it was found that regulator 1 has current I_B which leads the excitation voltage, E_{AB}, by +30 degrees $-\theta$. Therefore, if the current $I_B - I_A$ is substituted for I_B in regulator 1 of Figure 4, the correct phase relations for line drop compensation will be obtained.

The vector diagram of Figure 7 shows that the addition of I_B and $-I_A$ produces a current which not only is shifted in phase angle from I_A and I_B, but also is increased in magnitude by $\sqrt{3}$ as compared with I_A or I_B. The auxiliary current transformer has a ratio $\sqrt{3}$ to 1 and is for the purpose of reducing $(I_B - I_A)$ to be equal in magnitude to I_A and I_B. The combination of interconnected current transformer secondaries with an auxiliary $\sqrt{3}$ to 1 ratio current transformer, therefore, makes possible line-drop compensation which is correct in both phase angle and magnitude on regulators having the compensator circuit designed for single-phase operation.

The current transformer interconnections required for all regulators of Figures 4(A), 4(B), and 6 are shown in Table IV. Figure 8 shows, schematically, the complete current circuits for the regulators of Figures 4 and 6.

Each single-phase voltage regulator equipped with a line-drop compensator is supplied with one line-current transformer. The three regulators for delta connection, therefore, provide all the necessary line-current transformers.

For the open-delta connection of Figure 6, there will be only two regulators and

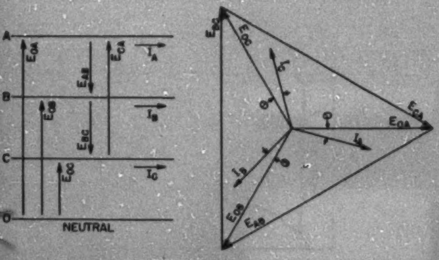

Figure 2. Diagram of 3-phase voltages and currents

Table II. Phase Angles in Delta-Connected Regulators

Regulator	Figure 4(A)	Figure 4(B)
1	$+30° - \theta$	$-30° - \theta$
2	$+30° - \theta$	$-30° - \theta$
3	$+30° - \theta$	$-30° - \theta$

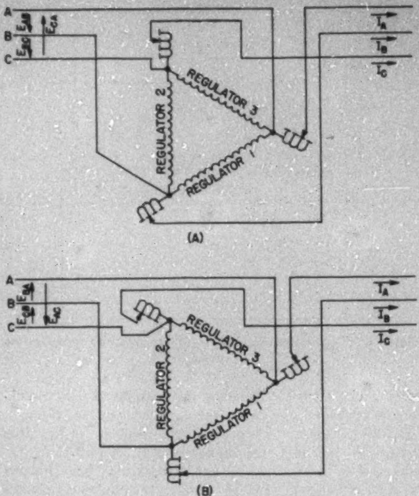

Figure 4. Delta-connected single-phase voltage regulators on a 3-phase system

(A). Connections with current leading voltage in each regulator; (B). Connections with current lagging voltage in each regulator

therefore only two line-current transformers. The need for the third line-current transformer can be eliminated by using a 3-winding auxiliary current transformer in each regulator, connected as shown in Figure 9. The turns ratio of the auxiliary transformer is in the proportion 100:50:86.6 for windings 1, 2, and 3 respectively. From Figure 9, the current equations can be written

$86.6\ I_{\text{Reg}}\ 1 = 100I_A + 50I_C$ or

$$I_{\text{Reg}}\ 1 = \frac{1}{0.866}(I_A + 0.5I_C) \qquad (3)$$

$86.6\ I_{\text{Reg}}\ 2 = 100I_C + 50I_A$ or

$$I_{\text{Reg}}\ 2 = \frac{1}{0.866}(I_C + 0.5\ I_A) \qquad (4)$$

Figure 9 also shows the vector diagram for this addition.

Table III. Voltage, Current, Phase Angle in Open Delta-Connected Regulators

Regulator	Voltage	Current	Phase Angle
1	E_{BA}	I_A	$-30° - \theta$
2	E_{BC}	I_C	$+30° - \theta$

The proof of this connection is most easily shown mathematically.

$$I_A = I\epsilon^{-j\theta} = I[\cos\theta - j\ \sin\theta] \qquad (5)$$

$$I_C = I\epsilon^{j(120-\theta)} = I[\cos(120-\theta) + j\sin(120-\theta)] \qquad (6)$$

By the equation derived from Figure 9:

$$I_{\text{Reg}}\ 1 = \frac{I}{0.866}[\cos\theta - j\ \sin\theta + 0.5\cos(120-\theta) + j\ 0.5\ \sin(120-\theta)] \qquad (7)$$

$$= I[0.866\ \cos\theta + 0.5\sin\theta + j(0.5\cos\theta - 0.866\sin\theta)] \qquad (8)$$

$$= I[\cos(30-\theta) + j\ \sin(30-\theta)] = I\epsilon^{j(30-\theta)} \qquad (9)$$

Since the voltage of regulator 1 is E_{BA}, which from Figure 5 is $\sqrt{3}E\epsilon^{j30}$, this shows that the current is shifted in phase so that it bears the same relation to the voltage as for the single-phase case for which the line-drop compensator is calibrated.

In a similar manner

$$I_{\text{Reg}}\ 2 = \frac{I}{0.866}[\cos(120-\theta) + j\sin(120-\theta) + 0.5\cos\theta - j0.5\sin\theta] \qquad (10)$$

$$= I[(0)(\cos\theta) + (1)(\sin\theta) + j(1)(\cos\theta) - (0)(\sin\theta)] \qquad (11)$$

$$= I[\cos(90-\theta) + j\ \sin(90-\theta)] = I\epsilon^{j(90-\theta)} \qquad (12)$$

Since the voltage of regulator 2 is E_{BC}, which from Figure 5 is $\sqrt{3}E\epsilon^{j90}$, this shows that the current is shifted in phase so that it bears the same relation to the voltage as for the single-phase case for which the line-drop compensator is calibrated.

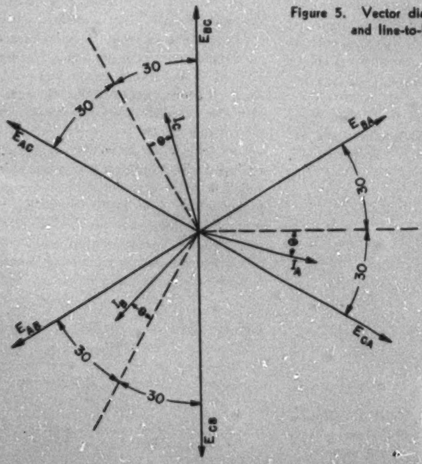

Figure 5. Vector diagram of line currents and line-to-line voltages

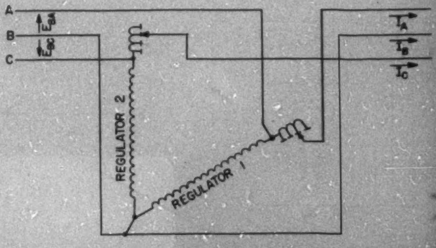

Figure 6 (below). Open delta-connected single-phase voltage regulators on a 3-phase system

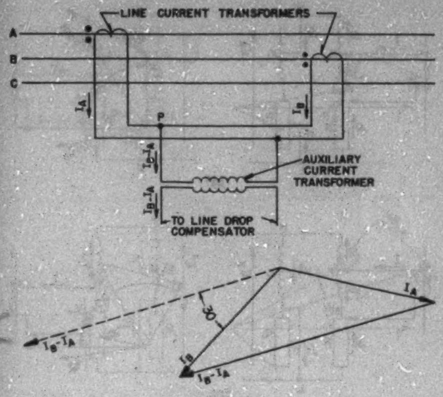

Figure 7 (left). Schematic and vector diagrams of cross-current connection

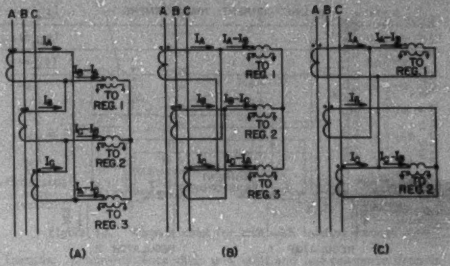

Figure 8. 3-phase schematic diagrams of control cross connections for delta and open-delta operation

(A). For regulators connected as shown in Figure 4(A); (B). For regulators connected as shown in Figure 4(B); (C). For regulators connected as shown in Figure 6

In these relations the voltage expression includes the multiplier $\sqrt{3}$, while the current expression does not. This is as it should be. In the derivations E is considered as line-to-neutral voltage; that is, $E_{OA} = E\epsilon^{j\theta}$. But the open delta-connected regulator is excited at $\sqrt{3} \times E$ volts. Therefore, $\sqrt{3} \times E$ is the rated voltage of the single-phase regulator required for this application. In the manufacture of the regulator, the line-drop compensator calibration is related to the regulator's rated voltage. Therefore, as far as the compensator is concerned, the base voltage on which compensation is based is $\sqrt{3} \times E$. For this reason, the multiplier, $\sqrt{3}$, appears in the voltage equation only.

Phase Shifting Networks

In a series circuit of resistive and reactive or capacitive components, the voltage drops in the circuit are in phase, leading by 90 degrees or lagging by 90 degrees, respectively, with relation to the current flowing in the circuit. Similarly, in a parallel circuit of resistive and reactive or capacitive components the currents are in phase, lagging by 90 degrees or leading by 90 degrees espectively, with relation to the voltage applied to the circuit. Because of these relationships, the currents and voltages in parts of circuits may have phase angles different from the applied current or voltage.

A line-drop compensator consists essentially of a resistive element which has a voltage drop in phase with the applied current and a reactive element which has a voltage drop 90 degrees leading the applied current. This is shown schematically in Figure 10, where a current transformer load consists of a resistance R and a reactor X, and voltages from these elements are applied in the voltage regulating relay circuit. The voltage $\boldsymbol{E}_K$, applied to the voltage regulating relay circuit, may be any magnitude and phase angle, depending upon the tap settings on R and X. Once these settings are made, the voltage $\boldsymbol{E}_K$ will remain constant in phase angle relative to $\boldsymbol{I}$, but will vary in magnitude in direct proportion to $\boldsymbol{I}$. Thus, the voltage $\boldsymbol{E}_K$ can be made to be in proportion to the voltage drop in the line on which the regulator is applied.

To provide for changing the phase relationship between voltage $\boldsymbol{E}_K$ and current $\boldsymbol{I}$, to compensate for the 30-degree phase shift of open delta or delta operation, phase-shifting networks may be used in combination with R and X. Such phase-shifting networks may be designed using a wide range of circuits and circuit components. The detail derivation of these circuit constants and connections is beyond the scope of this paper, which is a survey of methods rather than a detailed discussion of any one method. However, the principle involved can be illustrated by the simplified circuit and vector diagrams of Figures 11 and 12.

In Figures 11 and 12, a resistance-reactance circuit is connected in parallel with the compensator resistance and reactance of Figure 10. Connectors permit making the parallel circuit normal, as in Figures 11(A) and 12(A), highly reactive as in Figures 11(B) and 12(B), or highly resistive as in Figures 11(C) and 12(C). The current $\boldsymbol{I}$ from the current transformer divides into two components, $\boldsymbol{I}_K$ and $\boldsymbol{I}_O$, which follow the parallel paths as shown in the figures. In Figure 11, the voltage $\boldsymbol{E}_K$ applied to the voltage regulating relay circuit is the summation of the voltages $\boldsymbol{E}_{LM}$ caused by current $\boldsymbol{I}_O$ in resistor R and $\boldsymbol{E}_{MN}$ caused by currents $\boldsymbol{I}_K$ and $\boldsymbol{I}_O$ in the reactor X. In Figure 12, the voltage $\boldsymbol{E}_K$ applied to the voltage regulating relay circuit is the summation of the voltages $\boldsymbol{E}_{LP}$ caused by current $\boldsymbol{I}_O$ in that portion of R between L and P, $\boldsymbol{E}_{PN}$ caused by current $\boldsymbol{I}_K$ in that portion of R between P and M, and $\boldsymbol{E}_{MN}$ caused by current $\boldsymbol{I}_O$ in reactor X. The vector diagrams show these additions. As the vector diagrams show, changing the parallel circuit from its normal condition to a highly reactive circuit advances the voltage $\boldsymbol{E}_K$, while changing to a highly resistive circuit retards the voltage $\boldsymbol{E}_K$.

A phase-shifting network can, therefore, be used to permit applying single-phase regulators on 3-phase circuits in delta or open-delta connection. It should be recognized that the addition of the phase-shifting device connects additional components in the circuit and therefore tends to reduce the over-all accuracy of the circuit, and this fact must be considered in the selection and design of the circuit components. The important advantage of this method, that no control interconnections are required between units, makes it a common method of building phase-shift adjustment into single-phase regulators.

Table IV. Current Transformer Interconnections

Regulator	Figure 4(A)	Figure 4(B)	Figure 6
1	I_B-I_A	I_A-I_B	I_A-I_B
2	I_C-I_B	I_B-I_C	I_C-I_B
3	I_A-I_C	I_C-I_A	

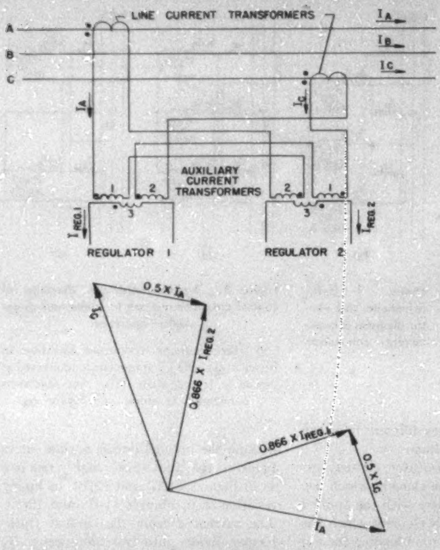

Figure 9. Schematic and vector diagrams of phase shifting transformer connections

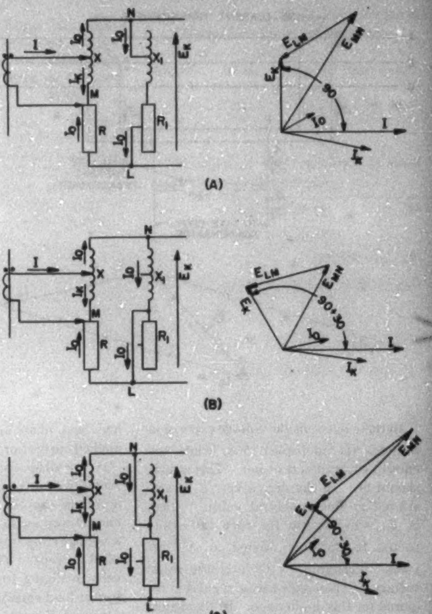

Figure 11. Schematic and vector diagrams for reactance compensation current phase shift networks

(A). Zero phase shift; (B). 30-degree phase advance; (C). 30-degree phase lag

MODIFIED COMPENSATOR SETTINGS

The method of modified compensator settings, often called the "Wagner Method" in honor of Charles F. Wagner who patented the scheme in 1934, obtains correct line-drop compensation for single-phase regulators in delta or open-delta connection by applying a 30-degree phase shift to the settings of the line-drop compensator. A chart for determining the revised settings is shown in Figures 13 and 14 for the unit with 30-degree leading current and the unit with 30-degree lagging current, respectively. To permit using this method, the resistance and the reactance elements of the line drop compensator must both be reversible so that either positive or negative settings may be obtained.

The derivation and proof of this method is most easily shown mathematically. Let $R+jX=Z\epsilon^{j\phi}$ be the line impedance; $I\epsilon^{j\theta}$ be the line current.

Then the impedance drop in the line is

$$I\epsilon^{j\theta}\times Z\epsilon^{j\phi}=IZ\epsilon^{j(\theta+\phi)} \tag{13}$$

In a delta or open-delta connection, as has already been shown, the voltage and current in the regulator are displaced by 30 degrees. Therefore, if equation 13 is expressed in terms of regulator quantities instead of line quantities, a 30-degree phase shift must be added. Thus, the line impedance drop, in terms of regulator quantities, is

$$I\times Z\epsilon^{j(\theta+\phi\pm 30^\circ)} \tag{14}$$

The line-drop compensator settings are modified by multiplying the line values by the quantity $\epsilon^{j\mp 30^\circ}$ giving revised settings on line-drop compensator, of

$$Z\epsilon^{j(\phi\mp 30^\circ)} \tag{15}$$

Substituting this compensator setting in expression 14 for the line-drop compensator voltage gives

$$I\times Z\epsilon^{j(\theta+\phi\pm 30^\circ\mp 30^\circ)}=I\times Z\epsilon^{j(\theta+\phi)} \tag{16}$$

Equation 16 shows that using line-drop compensator settings modified by the factor $\epsilon^{j\mp 30^\circ}$ gives line voltage drops in terms of regulator quantities which are identical with the actual line drops of equation 13.

For convenience in use, the operator $\epsilon^{j\mp 30^\circ}$ is expressed in the form

$$\cos 30^\circ\mp j\sin 30^\circ \tag{17}$$

Using the line drop in the form: $R+jX$, the revised compensator dial settings are $(R+jX)$ $(\cos 30^\circ-j\sin 30^\circ)$ for the regulator with leading current, and $(R+jx)$ $(\cos 30^\circ+j\sin 30^\circ)$ for the regulator with lagging current.

These expressions can be simplified to:

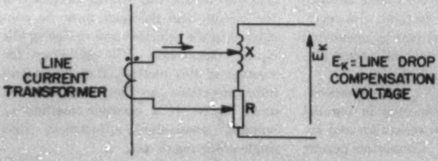

Figure 10. Schematic diagram of basic elements of a line-drop compensator

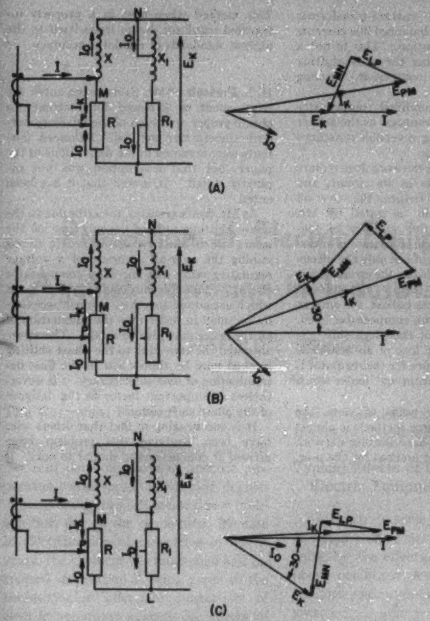

Figure 12. Schematic and vector diagrams for resistance compensation with current phase shift networks

(A). Zero phase shift; (B). 30-degree phase advance; (C). 30-degree phase lag

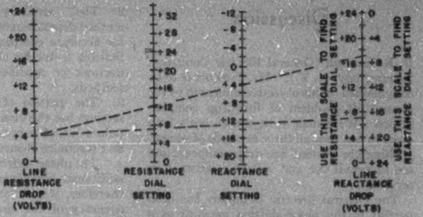

Figure 13. Wagner chart for unit with leading current

Example: If line-resistance drop is 4 volts and line-reactance drop is 7 volts, set resistance dial on +7 and reactance dial on +4

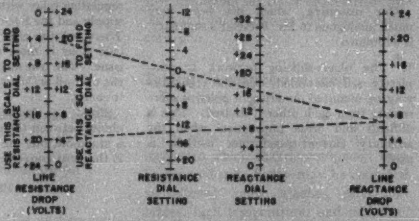

Figure 14. Wagner chart for unit with lagging current

Example: If line-resistance drop is 4 volts and line-reactance drop is 7 volts, set resistance dial on 0 and reactance dial on 8

$(0.866R+0.5X)+j(0.866X-0.5R)$ for the leading current unit; and $(0.866R-0.5X)+j(0.866X+0.5R)$ for the lagging current unit.

Letting R_w and X_w be the new dial settings, this gives: for unit with leading current

$$R_w=0.866R+0.5X \quad (18)$$

$$X_w=0.866X-0.5R \quad (19)$$

for unit with lagging current

$$R_w=0.866R-0.5X \quad (20)$$

$$X_w=0.866X+0.5R \quad (21)$$

Figures 13 and 14 are a convenient representation of these four relations.

The modified compensator setting scheme of obtaining correct line drop compensation for delta or open-delta connected single-phase voltage regulators gives correct results for any load power factor and may be adjusted for any line resistance and reactance ratio. It requires that the line-drop compensator elements be reversible. Since it requires no interconnecting control wires and has no extra equipment to add size and weight to the apparatus, it is particularly suitable for pole mounted feeder voltage regulators.

It should be noted that, for some cases, the dial settings required may be larger than either the resistance or the reactance line drops. This is shown by equations 18 and 21 and by Figures 13 and 14. Therefore, when voltage regulators will be used on systems having large line drops, this limitation must be considered to make sure that the dial settings required will not exceed the range available on the line-drop compensator.

Conclusion

When single-phase voltage regulators with line-drop compensators are installed in delta or open-delta connection on 3-phase power systems, the voltage applied to the voltage regulating relay and the current applied to the line-drop compensator are displaced from each other by 30 degrees. This may be overcome by using auxiliary current transformers to shift the phase of the current applied to the line drop compensator, by using phase-shifting networks within the compensator to shift the phase angle of the compensation voltage relative to the applied current, or by adjusting the dial settings of the line-drop compensator to represent a 30-degree phase shift in the line impedance.

The auxiliary current transformer method gives accurate performance with no loss of available range and with no special features in the line-drop compensator. It requires the use of auxiliary current transformers and it requires interconnections between units.

The phase-shifting network method is completely self-contained in each unit. It does not reduce the available range. But because of the difficulty of obtaining and mounting circuit components to give accurate response, the use of this method is largely limited to compensators designed specifically for this application.

The dial setting adjustment method gives accurate performance with no interconnections between units and with no special equipment, except that both the resistance and the reactance elements of the compensator must be reversible. Its application is sometimes limited by the range available in the compensator.

All three methods are in actual use and are giving satisfactory service.

Discussion

D. R. Samson (General Electric Company, Schenectady, N. Y.): Mr. Prescott is to be commended on his objective approach to the phase-shift problem of line-drop compensators. We concur with the author's final observation that all three methods of accomplishing the desired line-drop compensation are in actual use and will give satisfactory service.

The General Electric Company has been partial to the phase-shifting network as a method of obtaining the desired line-drop compensation, and we have provided a convenient phase-shifting plug arrangement on all of our single-phase regulators for many years.

Our reasoning, which has been very much analogous to Mr. Prescott's summary, is as follows:

1. The phase-shifting network is completely self contained, and the regulators may be mounted on adjacent poles or more remote from each other if desired. This is difficult and often impractical when the auxiliary current-transformer method is used.
2. The auxiliary current-transformer method depends upon balanced line currents for accurate compensation. This is not a limiting factor for either the phase-shifting network or modified compensator setting methods.
3. The method of modified compensator settings has the disadvantage, as the author points out, of requiring reversible resistance and reactance elements.
4. The phase-shifting network does require additional components in its circuit, and therefore, tends to reduce the over-all accuracy of the circuit as stated by Mr. Prescott. However, the accuracy of control devices for voltage regulators is measured in terms of errors of not only the phase-shift circuit but in addition the errors occurring in the potential supply, the voltage-regulating relay with its ballast, the current supply and the line-drop compensator itself. Therefore, the error of the phase-shift circuit alone is more or less of an academic issue. The true measure for the regulator is the over-all or "class accuracy" under which it comes.

From an idealistic point of view, the choice between the three methods is almost a stand-off, but the phase-shifting network is the most convenient method for the user. This method when used in a properly integrated regulator design lends itself to the highest standards of regulator accuracy.

H. L. Prescott: Mr. Samson has noted the requirement of balanced line currents to obtain proper operation of the auxiliary current transformer method. Balanced currents were assumed in the derivations in the paper, but that assumption was not explicitly stated. It is well that it has been noted.

As Mr. Samson states, the error due to the phase shifting method is only one of the errors which must be considered in determining the over-all accuracy of a voltage regulating relay and line drop compensator circuit. Since it is only one of several items which are added together, it must necessarily be small in order that the summation of all the items may also be small. Therefore, although the error due to the phase shifting method may be almost lost in the final determination of over-all accuracy, it is nevertheless an important factor to the designer of the phase shift circuit.

It is encouraging to find that others who have been studying this problem have arrived at conclusions so similar to ours.

Protection of Electric Equipment Against Corrosion in Industrial Plants

HAROLD E. SPRINGER
MEMBER AIEE

The Corrosion Problem

CORROSION of mechanical and current carrying parts of electric apparatus works havoc in varying degrees in many industries. It is not a new problem but, due to the tremendous increase in electrification of industries in recent years, the problem has multiplied and increased recognition is being given to the necessity for adequate protection of electric apparatus against the effects of even mildly corrosive atmospheric conditions, if reasonable length of service and reliability are to be expected.

Corrosive conditions are likely to be encountered in most any plant which manufactures or uses chemicals of various kinds, whether they be in liquid, gaseous, or dust form. This includes such industries as pulp and paper mills, cement plants, and chemical plants. They are also to be found around salt water, in mining operations, in steam plants which burn coal or hogged fuel, and even in wood cut up mills particularly where hemlock is handled.

It is the purpose of this paper to discuss in some measure various corrosive agents which are encountered in industry and some of the protective measures which may be taken to guard against their effects.

In a large majority of industries only very mildly undesirable atmospheric conditions are to be found, and it is not necessary to take any extensive measures to guard against anything except dirt and high temperature. However, in some of the types of industries mentioned previously, atmospheric conditions exist which may vary from quite favorable to extremely severe, and in these industries the protection of electric equipment against corrosion is a necessity to provide trouble-free operation.

Typical Effects of Corrosion on Electric Equipment

To illustrate some of the various ways in which electric devices are made unreliable by the effects of corrosive atmospheric conditions, some of the numerous troubles encountered are listed as follows:

1. Overheating of contacts on starters, fuses, and circuit breakers.
2. Disintegrating of braided or twisted shunts, connection studs, and terminal screws.
3. Open circuits in fine wires of operating coils on relays and contactors.
4. Sticking of relays, meters, instruments, control buttons, rheostats, solenoids, and controllers.
5. Rusting away of apparatus enclosures, conduits, motor frames, ball bearings, transformer cases, and line hardware.
6. Failure of power circuit breakers to trip or close.
7. Grooving and burning of commutators and collector rings.
8. Insulation failures on motor windings and coils of various types.
9. Flashovers of porcelain bushings.

These are some of the common effects, to which might be added many less common ones, some of which tax the electrical trouble shooter to the utmost and very often at times when production is at a standstill. From this list it is not difficult to see that corrosion has detrimental effects on electric apparatus.

If, in addition to the high operating and maintenance costs of such effects, we consider the safety hazards which result when rotating apparatus cannot be stopped or started at the right time, or switches cannot be depended upon to safely de-energize a circuit when required to do so, we can readily understand how necessary it is to protect all types of electrical apparatus from conditions that might cause corrosion.

Typical Corrosives and their Reactions

The most commonly encountered corrosives to which electric equipment may be exposed in industry may be classified as follows: acids, alkalies, salts and brines, high temperature, and moisture.

The corrosive action of some acids proceeds slowly if no free oxygen is available, but is greatly accelerated if air is present to furnish oxygen. Thus some materials which may be suitable for use in handling acids are nevertheless subject to corrosion when out in an atmosphere where moisture, acid fumes and air are present. In many instances corrosive action of acids is greatly accelerated by high temperature while relatively slow at room temperatures.

Alkaline solutions are in general not as widely corrosive to metals as acids but, like acids, they are likely to attack fabrics and insulating materials, and since many caustic solutions are used in industrial processes they are a prolific source of insulation troubles if not kept away from motor windings and controls.

Salts are corrosive to some metals and, being good conductors, can also be a source of insulation failures. Electric machinery and apparatus located close to salt water is exposed to corrosive effects from salt spray and fog, and in some tide flat areas to a variety of marsh gas. These are particularly severe on steel and cast iron. Salt deposits on high-voltage

---

Paper 51-301, recommended by the AIEE General Industry Applications Committee and approved by the AIEE Technical Program Committee, for presentation at the AIEE Pacific General Meeting, Portland, Oreg., August 20–23, 1951. Manuscript submitted May 18, 1951; made available for printing July 11, 1951.

HAROLD E. SPRINGER is with Rayonier, Inc., Port Angeles, Wash.

Figure 1. 2,300-volt bus gutter showing corrosion of steel, aluminum, and copper from exposure to traces of chlorine gas and moisture

Figure 3. Lead cable sheath crystallized possibly from stress or vibration and exposure to air

porcelain insulators also provide a ready path for flashovers.

Excessive temperature causes rapid oxidation of copper contacts and connections and, due to the fact that copper oxide is a poor conductor, a high resistance connection develops. This causes further heating of the joint and the effect being accumulative, the temperature may become high enough to melt the metal. High temperature also greatly accelerates the action of some corrosive agents.

Moisture, when present, nearly always contains more or less chemical content and may be quite corrosive in its action on metals. Very often it attacks the varnish on coils of various types and on motor windings, eating it away and eventually penetrating the insulation and causing electrical failure. Dry chemical fumes are a potential corrosive, because many of them become active when moisture is present. The combination of moisture and fumes reacts to form acid or alkaline solutions which are corrosive, whereas most chemical fumes are relatively noncorrosive to metals when dry.

Many forms of dust may be regarded as merely abrasive or as a dirt nuisance, but they also may contain chemicals which react with moisture to have highly corrosive action. Among these are hogged fuel soot particularly from hemlock fuel, sawdust from hemlock, salt cake, lime, and many others. Thus moisture may be detrimental both by direct action on materials and through reacting with chemical fumes to form corrosive solutions.

Of the metals commonly used in electric equipment, copper, cast iron, and steel predominate. Copper is corroded to some degree by most acids if moisture and oxygen are present, while corrosion by most alkaline solutions is slow. Some salts have very little effect on copper except to tarnish the surface, while others are highly corrosive to it. High temperature and other copper corrosives are extremely detrimental to commutators and collector rings. Very slight traces of sulphur dioxide or chlorine gas will react immediately on commutators, and on copper, bronze or brass collector rings, to cause grooving and burning and collecting of copper in brush faces.

Steel is corroded rapidly by most acids and salts, but not by alkalies. Chromium is corroded by acids that are not strongly oxidizing, but otherwise is immune to many corrosives. This makes some varieties of stainless steel very good for enclosures and mechanical parts for electrical devices.

Cast iron is widely used for motor frames and motor control enclosures and parts, and of the materials commonly used in electric equipment it is much more resistant to most corrosives than many others. However, it is subject to surface pitting by many acids and corrodes some-

Figure 2. 480-volt open rack type capacitor showing corrosion of steel and copper parts from exposure to traces of chlorine gas and moisture

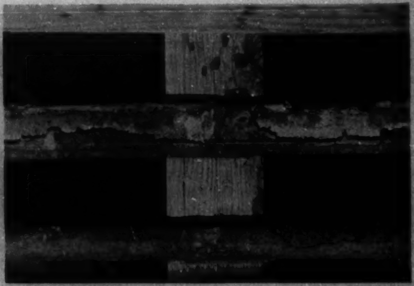

Figure 4. Steel conduit corroded through by action of sulphur dust and rain

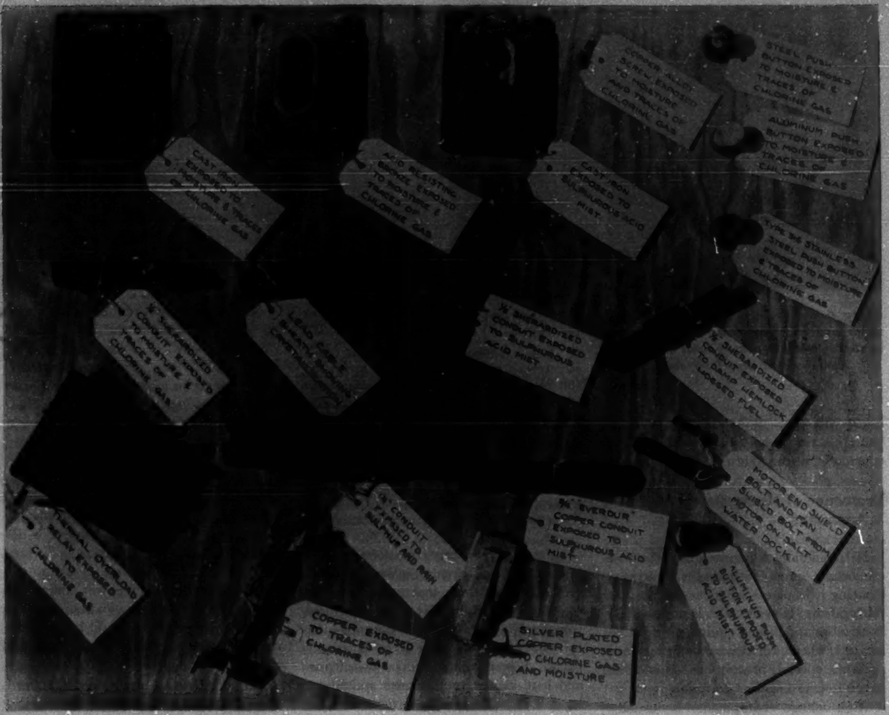
COPPER ALLOY SCREW EXPOSED TO MOISTURE AND TRACES OF CHLORINE GAS
STEEL PUSH BUTTON EXPOSED TO MOISTURE & TRACES OF CHLORINE GAS
ALUMINUM PUSH BUTTON EXPOSED TO MOISTURE & TRACES OF CHLORINE GAS
CAST IRON EXPOSED TO MOISTURE & TRACES OF CHLORINE GAS
ACID RESISTING BRONZE EXPOSED TO MOISTURE & TRACES OF CHLORINE GAS
CAST IRON EXPOSED TO SULPHUROUS ACID MIST
TYPE 316 STAINLESS STEEL PUSH BUTTON EXPOSED TO MOISTURE & TRACES OF CHLORINE GAS
½" SHERARDIZED CONDUIT EXPOSED TO MOISTURE & TRACES OF CHLORINE GAS
LEAD CABLE SHEATH SHOWING CRYSTALLIZATION
½" SHERARDIZED CONDUIT EXPOSED TO SULPHUROUS ACID MIST
½" SHERARDIZED CONDUIT EXPOSED TO DAMP HEMLOCK HOGGED FUEL
MOTOR END SHIELD BOLT AND FAN SHIELD BOLT FROM MOTOR ON SALT WATER DOCK
THERMAL OVERLOAD RELAY EXPOSED TO CHLORINE GAS
½" CONDUIT EXPOSED TO SULPHUR AND RAIN
¾" "EVERDUR" COPPER CONDUIT EXPOSED TO SULPHUROUS ACID MIST
ALUMINUM PUSH BUTTON EXPOSED TO SULPHUROUS ACID MIST
COPPER EXPOSED TO TRACES OF CHLORINE GAS
SILVER PLATED COPPER EXPOSED TO CHLORINE GAS AND MOISTURE

Figure 5. Effects of different corrosive agents on some materials used in electrical installations. Overload relay is totally inoperative from corrosion. Corrosion of steel conduit from sulphurous acid mist has been from surface inward, reducing original 7/8 inch outside diameter to 5/8 inch. Damp hemlock sawdust, also sulphur and rain have had the same effect. Everdur copper conduit is very little affected by the sulphurous acid mist. Chlorine gas has disintegrated the steel conduit and caused it to fall apart

what rapidly from exposure to salt water.

Aluminum is corroded by caustics very rapidly and by some acids. Zinc is corroded rapidly by most acids and alkalies and galvanizing treatment is not satisfactory around most corrosive atmospheres unless concentration is very mild. Cadmium seems to be quite resistant to corrosion from alkalies but not quite so resistant to the effects of acids. However, cadmium plating of parts on motor control apparatus has proven of inestimable value toward keeping parts working which otherwise might be unreliable in corrosive places.

Lead is considered quite highly resistant to corrosion from most chemicals and is quite impervious to action from most acids. However, hydrochloric, acetic and nitric acids will attack it to some extent, and some experiments indicate that it becomes brittle under stress, vibration, and exposure to oxygen. This might account for many cases of the type of lead cable sheath deterioration illustrated in Figure 3. For this reason circulation of air through conduits containing lead sheathed cables should be prevented.

Silver is somewhat immune to many corrosives, but is attacked by chlorine gas and moisture. Tin is also subject to corrosion under some conditions.

The varied effects of these undesirable atmospheric conditions make the use of most standard types of switchgear, control, and rotating apparatus very unsatisfactory in locations where such conditions are present in any appreciable degree.

In general there are two means of protecting electrical equipment from these corrosive effects:

1. To remove the equipment from the offending atmosphere.
2. To use equipment designed for operation in the atmosphere as it is.

The first alternate involves either providing suitable air conditioned enclosures, or locating apparatus at a distance from the bad conditions. The second involves making a careful study of the corrosive conditions in order to select materials and apparatus to resist them.

Since it is desirable to locate apparatus as close as possible to the usage area in most applications, the practice of providing protection for the equipment in the midst of bad operating conditions seems to offer the best solution, and is becoming

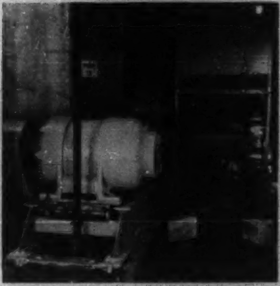

Figure 6. A totally enclosed fan-cooled motor and an open motor with sheet-steel hood side by side. Open motor is protected only against drip from above

quite common. Some of the methods being used in present-day practice will be considered in the following paragraphs.

Protection of Heavy Power Apparatus

It is generally recognized that the cost of heavy power apparatus warrants locating it in places where conditions are fairly ideal. However this is not possible in all cases and if such equipment must be located where corrosive conditions are present, special precautions should be taken to guard against corrosion.

High-voltage equipment is usually located outdoors, in which case there are three particular precautions which can be taken, as follows:

1. Bushing-type transformers and switchgear can be equipped with over rated insulators to provide extra creepage distance. For instance, a 66-kv transformer or circuit breaker can be equipped with 73-kv porcelains which provide quite a safety factor where conducting films are liable to be deposited on the porcelain surfaces.

The number of high-voltage insulators on switching tower structures can be kept to a bare minimum, thus minimizing chances of flashovers and reducing cleaning maintenance.

2. Apparatus can be given extra durable paint finishes by the manufacturer. Some manufacturers offer what are known as "subway" finishes, which include better priming protection than the standard finishes. These are well worth the added cost in the corrosive places, including those near salt water. Equipment finishes should always be gone over after installation to cover up shipping and installation abrasions.

3. Line hardware, copper bus and tower structures can be painted with any good corrosion resistant paint to better preserve the metal. A very effective means of protecting outdoor copper bus work, line hardware, high-voltage disconnecting switches, and steel work is to coat heavily with General Electric Company outdoor Glyptal or equal of other manufacture. This type of finish is extremely durable and resistant to corrosion of most types and has been successfully applied to many such installations.

In general, dry-type transformers and high-voltage air circuit breakers are not satisfactory for use in locations where any corrosive atmosphere is present, unless completely air conditioned because of the corrosive effects on inside air passages and parts. Lower-voltage indoor switchgear and load center transformers should be located in air conditioned rooms. This applies even up to 13,000-volt primary distribution apparatus which is available in complete metal clad form for safe indoor installations.

Liquid filled switchgear and transformers are inherently protected on the inside by the cooling medium, and the protection of the exterior only need be considered.

Careful maintenance and painting schedules should be established to guard against the development of spots where corrosion may start or to prevent conducting films from forming in excess on insulators. Chemical dusts or liquids depositing on porcelain insulators during dry weather may become highly conductive when the first rain or fog hits them and are a possible source of flashover. Where such conditions are present insulators should be cleaned frequently.

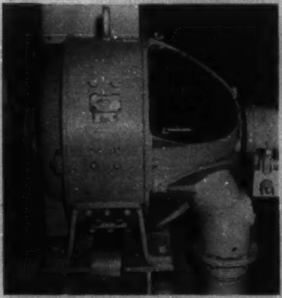

Figure 7. Totally enclosed force ventilated d-c motor. Plexiglass cover is to facilitate visual inspection of commutator and brushes

Protection of Control Equipment

Motor control equipment and small control apparatus in general must very often be located close to the equipment to be controlled and the selection of locations removed from undesirable atmospheric conditions is not as easy as in the case of heavier power equipment. The use of enclosed air conditioned control rooms into which apparatus may be grouped is very desirable. This affords good protection and allows the use of standard control apparatus with attendant relatively low initial cost of equipment.

Where a source of clean air is available, control rooms may be pressurized by forced ventilation. In some cases the air may be filtered and washed to remove moderate dirt or gas content. Where no good outside air is available the room may be sealed tight and the air circulated through a surface cooling and filtering unit. Usually the concentration of corrosive agents in a room thus conditioned may be kept very low if no outside air is admitted. If a small amount of relatively clean air is available it may be introduced to pressurize the room. A cooling and filtering unit may be used to recirculate the main volume of air in the room where normally a large volume of outside air would be required from a source not desirable for the entire purpose. Surface cooling units must be large enough to absorb all heat losses of power equipment located in rooms so conditioned. In general, the humidity should be kept low to prevent equipment from sweating when shut down and cold.

In rooms thus air conditioned, standard apparatus will give good reliable service. Maintenance is reduced to a minimum, paint jobs last longer, temperatures are easily controlled, and workmen take more interest in proper upkeep of equipment. Dirt, another enemy of electric apparatus, does not accumulate so rapidly and what does enter is more likely to be removed by maintenance men. Even the improved

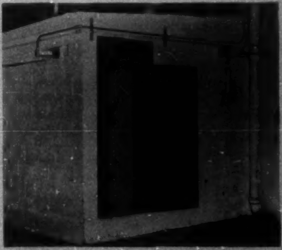

Figure 8. An air conditioned concrete block vault within a building and for protecting motor control cubicles from gas and moisture

Figure 9. An enclosed pressurized balcony within a building and protecting load center transformers and switchgear from heat and moisture

Figure 10. An enclosed pressurized balcony protecting motor control cubicles

morale among operators and maintenance men resulting from these better conditions is not to be overlooked.

Enclosures for this purpose may be constructed of wood, steel and transite, concrete, brick, concrete blocks, or other suitable materials which meet fire underwriters requirements for the location and class of apparatus to be housed. They may be either inside or outside of main buildings, but the important thing is to provide a clean air supply and to exclude all corrosive agents. Figures 8, 9, 10, 11, and 12 illustrate some typical types of enclosure construction. The means of air conditioning may vary to meet conditions. Sometimes the air must be washed and filtered. Often it must be heated or cooled. Again, a surface cooling unit is the best arrangement. Many existing plants are carrying on modernizing programs which include this class of protective work even where relocation and grouping of apparatus are necessary.

Where it is necessary for apparatus such as push buttons, rheostats, controllers, instruments and similar devices to be in the open, they should be of water and dust-tight construction. There are many types of these devices to select from but careful consideration should be given to the class of corrosive agent to which they will be exposed, bearing in mind that not all materials are affected in the same degree, and that very often a number of different corrosive agents may be present. Hence the necessity for considering each application separately.

As mentioned before, cadmium plating of copper and other vital parts has been used with some success and has offered protection against some corrosives where the expense of air conditioned enclosures is not warranted. It also has been found very advantageous in exposed installations in relatively mild corrosive locations to heavily coat all metal work including copper busses, steel enclosures, and control devices with Glyptal type paint. The inside parts of the equipment in particular should be coated heavily, since it is very difficult to get at these parts to recondition them without excessive time outages after corrosion has started.

Bus compartments of metal-clad switchgear and motor control cubicles should be given particular attention and treatment if they are to be exposed to even a mildly corrosive atmosphere, since inspections are usually infrequent after they are placed in operation and reconditioning later is usually a major operation. In some applications cadmium-tinned bus is used, and very often bus work is heavily taped and painted to exclude air. Around moist locations it is very desirable to support busses and disconnecting switches above 600 volts on porcelain since most other types of insulation such as ebony asbestos, fiber, and plastics are subject to moisture absorption and possible breakdown of insulation resistance. Surface leakage is a very common failure on ebony asbestos and other similar materials even in 440-volt service where moisture is present. Where bare bus is supported at a number of points by such materials which have been exposed to moisture, it is often impossible to get a satisfactory insulation resistance test on the bus.

In summary, experience is proving that for most installations where the best of conditions are not to be had, all possible effort should be made to group main control equipment together in enclosed air conditioned rooms, and to carefully select the proper type of materials and type of construction for all other apparatus which must be exposed.

Protection of Rotating Apparatus

Of necessity, many drive motors must be located in some of the worst places in a plant. Before the totally enclosed fan-

Figure 11 (right). A recent installation of load centers, lighting transformers, motor-generator sets, and motor control cubicles in an air conditioned room for serving a pulp mill wood chipping plant

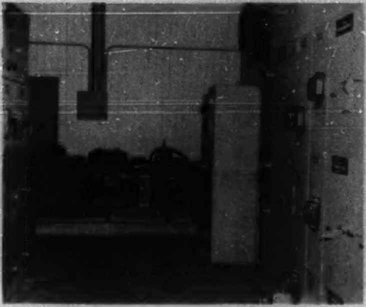

Figure 12 (left). Another view of room in Figure 11 showing variety of apparatus in one room

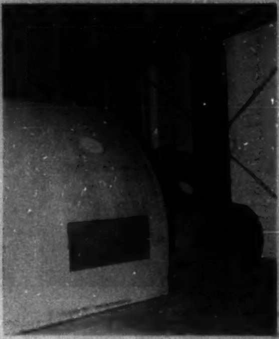

Figure 13 (right). A pressurized enclosure protecting an 800-horsepower wound rotor log chipper motor

cooled motor was developed, the most common means of protecting motors was to cover them with sheet metal hoods. This afforded protection only from dirt or water falling on them and not from splash, vapor, or dirt being drawn into the windings. A typical example of this type of protection is illustrated in Figure 6. In fact, the way that open motors have stood up in past years on some applications is nothing less than phenomenal.

The other side of the story, however, is that they do not all stand the abuse equally well, and present-day installations and production schedules place more exacting demands on the motive power equipment than in the past. To meet these demands the manufacturers have constantly been striving to make rotating apparatus more reliable for all conditions of operation, and one outstanding development has been the totally enclosed fan-cooled motor. Variations of this, namely, the totally enclosed force ventilated, the totally enclosed nonventilated, the totally enclosed surface cooler cooled, the air tube cooled, and the water tube cooled motors have been developed, but all toward the same purpose—protection of vital parts against moisture, dirt and corrosion. For drives up as high as 1,000 horsepower totally enclosed fan-cooled motors are available, and are the best answer to the motor protection problem in many industries. In this class of motors the bearings are all sealed and the windings, the most vital part of any motor, are completely sealed from the outside. They are occasionally equipped with weep holes or breathers to prevent moisture accumulation within the motor when temperature changes cause excessive breathing of moist air.

Dripproof and splashproof motors are widely used, but they will not protect the windings against corrosive gases, vapors, moisture or dirt when the motor is running. These agents are more or less free to enter the motor by means of the suction action of the rotor fans and are plastered around the windings in the same manner that they would be in an open motor. When they are down and cold, condensation may take place even on the inside of the motor particularly following a sudden rise in air temperature and humidity. No perfect impregnating treatment has yet been developed that will withstand the ravages of corrosive agents on motor windings and frequent reconditioning is required, unless motor windings are shielded completely from all these conditions.

The totally enclosed motor accomplishes this, and its use is becoming increasingly widespread in many industries including many steam power stations where greater reliability is needed on feed pumps, draft fans and fire pumps. A typical example of a standard totally enclosed fan-cooled motor is shown in Figure 6.

Most totally enclosed motors of standard design are built with cast-iron frames and are quite satisfactory in nearly all corrosive atmospheres. This is due, as mentioned before, to the reasonably high resistance of cast iron to many corrosives and, possibly, somewhat due to the thickness of metal usually involved. Some of the later totally enclosed motors have pressed steel frame parts, and while it appears to many users that the cast iron is preferable, the specially treated heavy steel construction has withstood some very rigorous tests.

Motor manufacturers have recently developed a class of totally enclosed motor which is designed particularly for use in corrosive atmospheres and known as the chemical motor by one manufacturer. The smaller sizes of these are made of heavy pressed steel construction bonderized and treated in various ways to make them highly resistant to most corrosives. In the larger sizes they are still made of cast-iron frame construction with special features to make them corrosion resisting. It appears that the development of this new chemical motor is an improvement in corrosion-resistant motor construction, and, though experience to date has pointed to the cast-iron frame as being quite satisfactory for most applications, the motor especially built for corrosive applications should warrant attention.

The cost of large sized totally enclosed fan-cooled motors is relatively quite high, as compared to open motors, and for drives above 500 horsepower the use of other means of protection may sometimes be more economical. Some of those other means include using totally enclosed force ventilated motors where clean air is available; building an enclosure around an open motor and pressurizing it with clean external air, as shown in Figure 13; or building a sealed enclosure around an open motor and conditioning the enclosure with a surface cooling unit. The investment in motors of this size is sufficient to warrant the use of surface cooling units and enclosed rooms to reduce maintenance and insure reliability. Starting at about 1,000 horsepower there is considerable merit in going to closed air systems similar to those used on turbogenerator units with surface cooler built into the foundation under the motor. In many applications a motor of this size is equally as important to plant operation as a turbogenerator and warrants the same protection. Large pumps, fans, grinders, and log chipper drives are typical examples worthy of this class of winding protection.

Motor generator sets are very often located in air conditioned control rooms along with load centers and other control equipment. Direct current motors may be protected in the same way as induction motors. Totally enclosed nonventilated d-c motors are serving in many severe applications and doing well as long as outside air is excluded completely. Totally enclosed fan-cooled d-c motors are widely used. Likewise totally enclosed force ventilated d-c motors such as shown in Figure 7 exclude undesirable elements from vital parts very effectively. In fact, the performance of totally enclosed motors of all types has been so satisfactory for most applications that some users specify them exclusively, regardless of the application.

Protection of Wiring Systems

In treating of corrosion problems, the protection of distribution circuits and motor and control circuits is not to be overlooked. Many failures result from moisture or corrosive gases circulating through conduits and rusting through the conduit or eating away the insulation and even the wire. All conduits in any corrosive location should be completely sealed against air circulation. This should also apply when a conduit leaves a warm area and emerges into a cold area. Naturally air circulates from the high-pressure areas to the low-pressure areas, and if the circulation is through a conduit from a warm portion to a cold portion, condensation takes place with resulting possible damage to the inside of the conduit and the wires. The use of Everdur copper conduit has been very effective in locations where corrosives that attack steel, but not so readily copper are present. Black or galvanized conduits are not satisfactory in corrosive places unless kept heavily painted.

Sherardized conduits are much better but must also be kept well painted in most bad locations. There are available conduits with specially treated surfaces over the sherardizing which improve the corrosion resistance, and experience has proven that the original cost of these materials is small compared to frequent replacement.

The importance of good paint and frequent painting for conduits and fittings exposed to corrosion cannot be overemphasized. Corrosion of unprotected metallic conduits may be extremely rapid under some conditions, and when conduits are eaten away and wires left exposed to mechanical injury they present a potential hazard to personnel and to continuity of electrical service.

Neither can the importance of high-grade wire be overemphasized under such conditions, to minimize the chances of damage to wires when water enters a conduit, and to protect them mechanically when the conduit rusts away.

Some plants are even using direct burial types of wire in conduit installations above ground to insure reliable performance. The various makes and classes of neoprene jacketed wires are gaining recognition in many industries for use under the most severe conditions due to their moisture, corrosion and heat resisting properties, and their ease of handling. The use of preassembled aerial cable is becoming quite common and this type of cable is now available with plastic type coatings on the messenger cable and bandings to protect them against corrosion.

Conclusions

It is only fair to mention that the statements and observations presented in this paper are the results of actual experience and research in pulp and paper mills of one company in northwestern Washington, and of exchanging ideas and observations made by other similar industries in the same area. Due credit should be given to the fact that there may be some industries whose experiences do not agree entirely with those set forth herein, and that perhaps much could be added to make a paper on this subject more complete by taking a larger field into account.

However, many interesting incidents and experiments could be cited to corroborate some of the statements made in the preceding paragraphs and they would all point to these conclusions:

1. Heat, moisture, and chemicals are inseparable from many industries.
2. Electric equipment does not perform reliably in corrosive atmospheres resulting from them.
3. Something can be done about it.

This paper deals with a subject which is largely of a practical nature. It involves no mathematical data, unless it might be that which expresses the action of acids, alkalies, salts, and so forth, on metals and on insulating materials. It presents no specific figures showing dollars and cents savings to lay before management when talking in terms of spending money to save money.

We might look at the proposition of corrosion protective measures for electrical apparatus the same as if we were purchasing a new automobile and trying to decide whether to build a garage to keep it in or let it stand outside, whether to wash and wax it occasionally or let the mud and rust accumulate, and then try to determine how much more or less money we could sell or trade it for in a few years. Or, to put it stronger, if we are building a plant of any sort should we select good equipment and take good care of it, or should we neglect and abuse it.

These are easy questions to answer but hard to evaluate in dollars and cents. Sometimes the equipment failures and lost production speak for themselves and sell the idea of proper protection against corrosion, but often the only selling point one can present in support of a protection program is the improvement in general appearance, safety, employee morale, stability of operation, product, and general reputation of the plant and its operators, and then we should ask this question—Are neatness, cleanliness, orderliness, employee morale, safety, and respect for machinery important to plant operating costs?

If a plant is to operate on a solid foundation and remain stable over a long period of years, they are very important; and the proper protection of equipment vital to production plays an essential part in establishing and perpetuating these conditions.

Discussion

Herbert A. Rose (Westinghouse Electric Corporation, Seattle, Wash.): Mr. Springer should be commended for his valuable paper in which he gives so many bases of approach to the problems of what "to do about corrosion." The paper deserves careful reading by both manufacturers and industrial users of all forms of electric apparatus. He indicates the best solutions to a problem may very well rest with the manufacturer and user alike. Unless this point is fully appreciated by both, an unsatisfactory installation can easily result.

The author justifiably uses the word "corrosion" in a broad sense to cover the effects of contamination which may be responsible for equipment failure, regardless of whether the agents of corrosion are present or not. A motor installed where it can become plugged with pulp will fail just as surely as one located in an adjacent room contaminated with wet chlorine fume. In this connection I believe that many poor installations of individual pieces of electric apparatus could be eliminated by joint consideration of the contamination problems by the plant layout engineers and the electrical maintenance superintendent.

The superior protection afforded by totally enclosed fan-cooled motors against many forms of contamination and corrosion can hardly be overstressed. These motors cost about 40 per cent more than the usual open drip-proof motor. The cost of making a single "rewind" will usually pay for the initial price difference without considering the costs assignable to lost production and emergency repair crews. It is somewhat difficult to understand why open-type motors are tolerated in many of our modern pulp and paper mills.

Where bad corrosion and contamination problems are involved, serious consideration should be given in layout of new plants and the rehabilitation of old ones to placing groups of electric apparatus in protected rooms.

Particularly is this advisable for the primary power switchgear, load centers, low-voltage switchgear, motor control centers, rectifiers, motor generators, and special control equipment. It would appear to be far more economical to protect standard low-cost apparatus by such means than to continually replace and repair it under unprotected conditions, or to purchase special apparatus to withstand the corrosion. The heat losses can be easily and economically removed from the room by water to air heat exchanger or by piping a clean source of filtered air to the room.

Harold E. Springer: In his discussion on this paper, Mr. Rose has emphasized the joint responsibility of the manufacturer and user alike in working out solutions to the corrosion problems.

Many unsatisfactory installations of electric apparatus in contaminated atmospheric conditions result from lack of information or experience on the part of both manufacturer and user relative to the application.

Too often, competitive pricing and low initial cost govern the layout of new installations or rehabilitation work. Occasionally, over zealous efforts to promote the sale of a new product which might not be properly applied will result in an unsatisfactory installation.

Much credit is due the manufacturers for continually striving to develop apparatus better able to withstand severe operating environment and the recognition which Mr. Rose has given to the dual responsibility in being alert to the corrosion problem is commendable.

Handling Logs by Electric Motocylinders

H. A. ROSE
MEMBER AIEE

SAWMILLS and log breakdown plants have for years employed various forms of specialized machinery to produce reciprocating and oscillating forms of motion for moving the logs, cants, and boards during the breakdown process. The vast majority of these operations have been performed by steam, air or water cylinders with piston connected directly to the mechanism. These cylinder and piston type operators have been well suited to the applications, being simple in construction, fast acting, powerful in small size, of low cost and readily manufactured in rugged forms required for the service.

Their disadvantages which in the past were of little if any consequence are today gaining considerable economic importance in the industry, namely:

1. Wasteful of steam (air) when total losses incident to its generation, transmission, and utilization are included.

2. Maintenance of the over-all system is high, including problems and cost of cylinder lubrication.

3. Presents problems of freezing in localities subject to low temperatures.

4. Investment and operational costs of the steam generating plant are high if mill could otherwise be designed so as to essentially eliminate its need. This factor becomes of prime importance for small sawmills and isolated wood mills where purchased power can be had at attractive rates.

The Motocylinder

Of recent years a new type of electric motor thrustor operator[1] called the "Motocylinder" is receiving increased consideration and application in the industry. The name is a contraction of its mode of operation and the name of the device for which it substitutes. Its principal advantage accrues from the fact that only electric power is required for its complete operation, the factor which has become of major economic importance in the selection of types of mill drives.

The motocylinder is essentially a gearmotor with a short powerful crank mounted on its output shaft, as shown in Figure 1. The crank is connected to the device to receive reciprocating motion by a connecting rod. Electric limit switches associated directly with the crank cause the motor to stop at definite stroke positions as determined by an electric motor-mounted brake. Operation is by push or foot button, electric eye, or control switch. The units are powered by standard 3-phase high torque induction motors capable of producing the required pounds lift at the crank pin. The gear ratio of the unit is chosen to give the operating time required for the thrust motion. The retrieve time equals essentially the thrust time.

Motocylinders of the type described, having the crank associated directly with the unit are called true motocylinders. True motocylinders are used mostly for applications requiring normal values of thrust, speed of operation and crank throw.

Offset Motocylinder

For applications involving higher than normal thrust, slow speeds of operation, abnormally long stroke or unusually heavy shock conditions, it often becomes desirable to set the crank apart from the unit and provide a chain sprocket drive between them. The drive unit for such an arrangement is called an "Offset Motocylinder." The chain sprocket ratio will range from 1/1 to 5/1, the order of 3/1 being most common.

Applications

Motocylinders have been applied to most of the thrust-motion applications of woodworking plants. It is believed that all applications can be successfully handled by them with the possible exception of the "nigger" for the log carriage. Table I gives typical motocylinder applications and the normal range of requirements for this class of service. The values given are subject to considerable variation dependent on specific requirements. To properly establish the type and size of the drive a detail study of each application should be made, including a kinematic scale drawing of the entire loaded mechanism in its various positions of motion. The drawing is of considerable aid in establishing the magnitude of forces involved.

Figure 1. 3-horsepower true motocylinder
Note: Compact construction of unit, motor mounted brake, limit switches and adjustable operating cams, heavily constructed nonadjustable base. Upper half of gear case removable for inspection without disassembling unit

---

Paper 51-302, recommended by the AIEE General Industry Applications Committee and approved by the AIEE Technical Program Committee for presentation at the AIEE Pacific General Meeting, Portland, Oreg., August 20–23, 1951. Manuscript submitted May 18, 1951; made available for printing July 11, 1951.

H. A. Rose is with the Westinghouse Electric Corporation, Seattle, Wash.

The author wishes to give credit and express his appreciation to Mr. Paul Jones for valuable consultation and assistance leading to the preparation of the material for this paper.

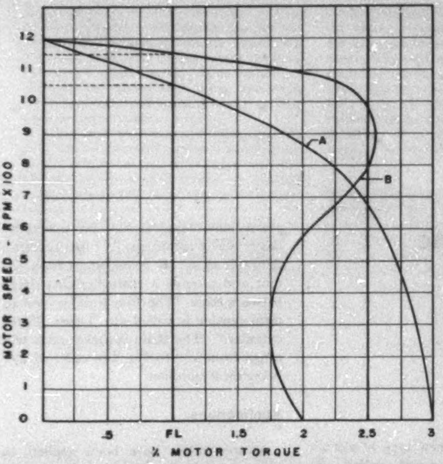

Figure 2. Curve A, speed torque characteristic of high torque, high slip, 1,050 rpm, 1/4 hour 55 degrees centigrade rise hoist type induction motor used to drive motocylinders. Curve B, conventional high torque NEMA design C for comparison

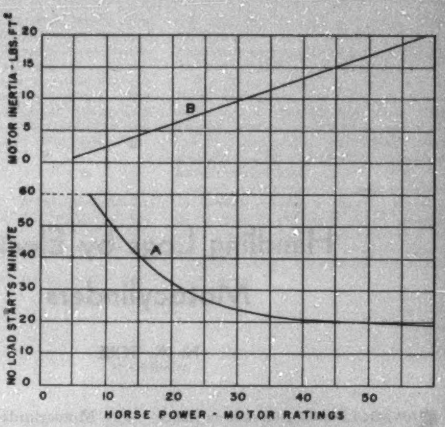

Figure 3. Curve A, permissible starting frequency of hoist type motors of Figure 1, accelerating rotor inertia only. Curve B, rotor inertia of hoist type motors of Figure 1, pounds squared feet

Motocylinder Ratings

Motocylinders are given designation numbers for convenience in defining their characteristics—horsepower, output speed in revolutions per minute, and inches of stroke. For example, a 15-horsepower 41-rpm motocylinder having an 18-inch crank throw would be designated as MC-15-41-18.

Although practically any range of requirements can be met, Table II gives standardized ratings using the preceding method of designation. Most sawmill applications of true motocylinders can be satisfied from this table. It might be thought that a 41-rpm unit would be too slow for some operations. Experience shows for example that a MC-15-60-18 unit, having approximately 0.5-second stroke time, to be very fast acting, in fact too fast for many applications. High speeds are to be avoided when not needed, as the cost of the unit is adversely affected and the higher inertia forces which always result cause unnecessary wear and tear to the entire mechanism and building supports.

Table I. Typical Motocylinder Data for Sawmills and Wood Mills

Motocylinder Application	See Fig. Number	Type of Motocylinder Drive**	Typical Stroke Time, Seconds†	Typical Range of Hp Ratings	Length of Stroke in Inches, Typical‡
Log haul unloader, heavy duty	9	O	0.75–1.0	15–50	18
Log haul unloader, moderate duty	9*	M-O	0.75–1.0	10–25	18
Roll case unloaders, general purpose	9*	M	0.75–1.0	7.5–20	18
Log kickers, heavy duty	10	O	0.75–1.0	20–50	34
Log kickers, moderate duty	10*	M-O	0.75–1.0	10–20	34
Deck stop and loaders	11–13	M-O	0.5–1.0	7.5–20	90° Rot.
Pin stops	12	M	0.5–1.0	3–7.5	18
Lift skids	14	M	0.5–1.5	3–7.5	18
Skid lifts	16	M	0.5–1.5	3–7.5	18
Lumber sweeps "Swedes"	15	M	0.5–.75	3–5	24
Lumber stops	18	M	0.5–.75	1–3	8
Cant unloaders	17	M	0.5–.75	5–15	12
Barker loader	20	M-O	0.5–1.0	7.5–20	24
Barker unloader	20	O	0.75–1.5	15–75	48
Chipper loader		O	1.5–3.0	7.5–15	26
Cutoff saw	19	O	Variable	0.3–10	60
Log carriage loader	11	M-O	0.5–1.0	7.5–15	90° Rot.

* Except driven by true motocylinder.

** (M = true motocylinder) (O = offset motocylinder).

† Stroke time faster than 0.75 second should be avoided unless necessary to meet operational requirements. Those faster than 0.5 second are generally impractical.

‡ Values given are subject to considerable variation depending on layout of the specific mechanism.

Drive Motor Characteristics

Most motocylinder applications require motors having high starting and pull-up torque characteristics to rapidly accelerate a moderate amount of inertia or to start against a heavy dead weight load, or both. They must also be capable of frequent starting without overheating. Intermittently rated high torque hoist-type

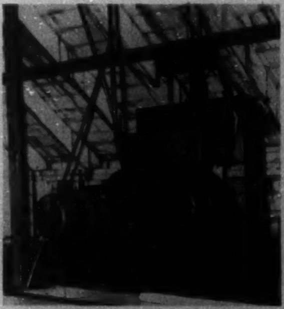

Figure 4. 5-horsepower motocylinder operating heavy duty pin stops on spudding deck, details in Figure 12

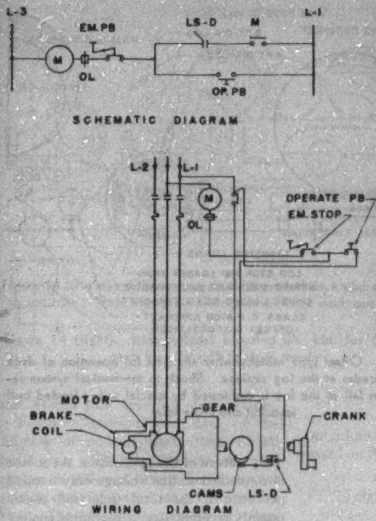

Figure 5 (left). Typical control diagrams for motocylinder operated log-slip unloader, see Figure 9

Figure 6 (right). 20 - horsepower, heavy duty motocylinder roll case unloader. Note safety guard for crank and connecting rod

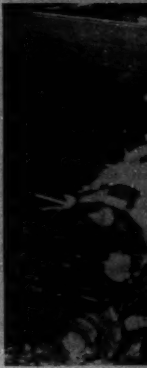

Figure 7. Automatic motocylinder operated roll case unloader transferring log to deck chains. Operation initiated by farthest end of log breaking light beam of electric eye control

induction motors with National Electrical Manufacturers Association (NEMA) design D characteristics[7] meet these requirements, either as totally enclosed nonventilated (TENV) or protected drip-proof types. Hoist-type motors are intentionally designed for frequent starting, a requirement of most motocylinder applications.

Figure 2, curve *A*, is typical of the speed-torque characteristics of hoist-type motors. The starting torque is the maximum torque and is approximately 300 per cent of the full load value. Curve *B* is typical of a general purpose class-C motor and is shown for comparison, particularly as regards differences in starting torques. The thrust rating of the motocylinder is taken at 250 per cent of the motor rating which allows sufficient reserve torque to assure positive acceleration of the maximum loads. In making an application it is therefore the maximum load which sets the required rating of the

Figure 8. $7^1/_2$-horsepower motocylinder operating jump skids. Similar to Figure 14. Note heavy construction of parts and shock absorbing spring at top end of connecting rod

Table II. Standard Motocylinder Ratings

Inches Stroke Equipment Number	8	12	16	18	20	24
	Maximum Pounds Thrust Capacities					
MC-1-41-*	900	600	450	400	350	300
MC-2-41-*	1,800	1,200	850	800	700	600
MC-3-41-*	3,000	1,800	1,500	1,300	1,200	900
MC-5-41-*	5,000	3,000	2,500	2,250	1,800	1,500
MC-7.5-41-*	7,500	5,000	3,500	3,300	3,000	2,500
MC-10-41-*		6,000	4,500	4,000	3,500	3,000
MC-15-41-*		9,000	6,500	6,000	5,000	4,500
MC-20-41-*		11,000	8,500	7,500	6,500	5,500
MC-1-22-*	1,800	1,200	900	800	700	600
MC-2-22-*	3,400	2,300	1,800	1,500	1,800	1,100
MC-3-22-*	6,200	4,200	3,200	2,800	2,400	2,000
MC-5-22-*		6,500	4,500	4,200	3,800	3,100
MC-7.5-22-*		9,500	7,000	6,400	5,800	4,200
MC-10-22-*		11,500	8,500	7,800	7,000	5,800
MC-15-22-*		15,000	11,500	10,000	9,000	7,500
MC-20-22-*			Off Set Types			

* Add stroke length to complete motocylinder number.

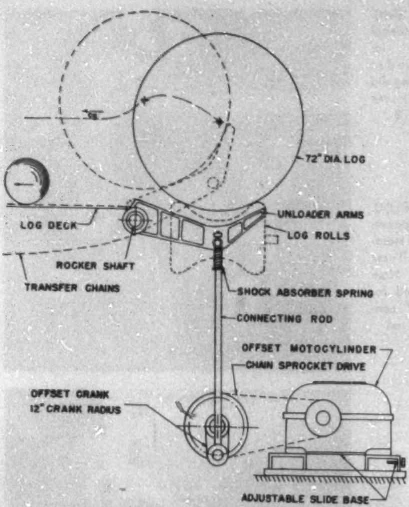
72" DIA. LOG
LOG DECK
UNLOADER ARMS
LOG ROLLS
ROCKER SHAFT
TRANSFER CHAINS
SHOCK ABSORBER SPRING
CONNECTING ROD
OFFSET MOTOCYLINDER
CHAIN SPROCKET DRIVE
OFFSET CRANK
12" CRANK RADIUS
ADJUSTABLE SLIDE BASE

Figure 9. Heavy duty offset type motocylinder operated log-slip unloader. Logs weighing from 15 to 25,000 pounds, after being cut to length, can be handled by this type drive

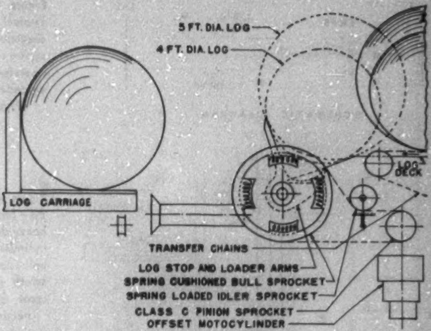
5 FT. DIA. LOG
4 FT. DIA. LOG
LOG CARRIAGE
LOG DECK
TRANSFER CHAINS
LOG STOP AND LOADER ARMS
SPRING CUSHIONED BULL SPROCKET
SPRING LOADED IDLER SPROCKET
CLASS C PINION SPROCKET
OFFSET MOTOCYLINDER

Figure 11. Offset type motocylinder arranged for operation of deck stop and loader at the log carriage. Shock to mechanical system resulting from fall of the log is cushioned by special spring loaded bull sprocket and chain idler

drive. For the usual application the percentage of maximum weight logs will be low. It is therefore usually permissible to apply the motocylinder near the limit of its capacity for the largest sizes, knowing that the smaller ones will be handled considerably faster.

By nature of the application the motor is connected to line voltage only a small per cent of the total time and consequently receives almost negligible cooling effect from rotation. Its losses, however, for the stroking periods are comparatively high on account of accelerating the inertia of the loaded system. There is therefore a limit to the number of starting operations or accelerations that a motor can make under such a duty cycle, and

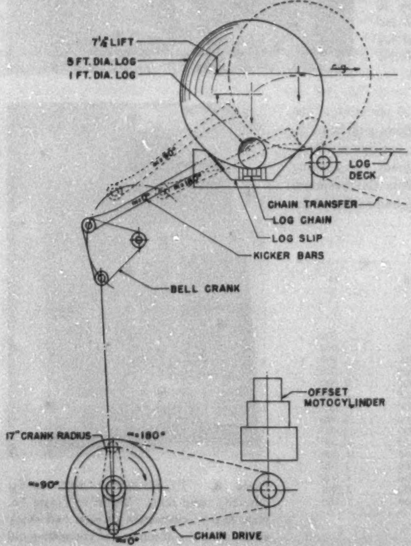
7½" LIFT
5 FT. DIA. LOG
1 FT. DIA. LOG
LOG DECK
CHAIN TRANSFER
LOG CHAIN
LOG SLIP
KICKER BARS
BELL CRANK
OFFSET MOTOCYLINDER
17" CRANK RADIUS
=180°
=90°
=0°
CHAIN DRIVE

Figure 10. Offset motocylinder log kicker for transferring logs from log slip to log deck. Also suitable for roll case unloading

Figure 12. Motocylinder operated pin stops between log storage and spudding decks. Shock absorbers similar to Figure 16 are desirable if large logs are passed over decks

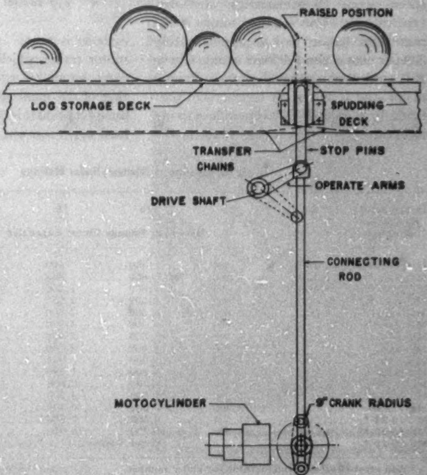
RAISED POSITION
LOG STORAGE DECK
SPUDDING DECK
TRANSFER CHAINS
STOP PINS
OPERATE ARMS
DRIVE SHAFT
CONNECTING ROD
MOTOCYLINDER
9" CRANK RADIUS

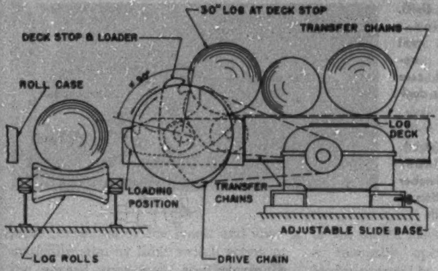
30" LOG AT DECK STOP
DECK STOP & LOADER
TRANSFER CHAINS
ROLL CASE
LOG DECK
LOADING POSITION
TRANSFER CHAINS
ADJUSTABLE SLIDE BASE
LOG ROLLS
DRIVE CHAIN

Figure 13 (above). Offset motocylinder operated deck stop and loader to roll case. Note adjustable slide base to keep slack out of chain

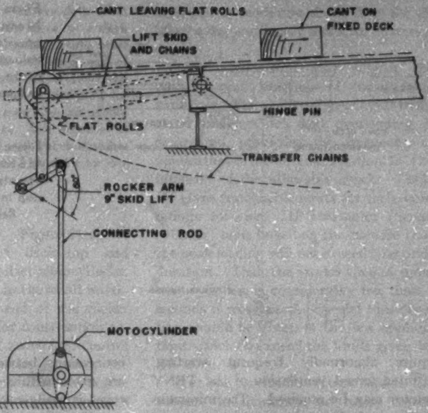
CANT LEAVING FLAT ROLLS
CANT ON FIXED DECK
LIFT SKID AND CHAINS
HINGE PIN
FLAT ROLLS
TRANSFER CHAINS
ROCKER ARM 9" SKID LIFT
60°
CONNECTING ROD
MOTOCYLINDER

Figure 14 (right). Motocylinder operated lift skids for transferring cants from flat rolls to chain transfers

not exceed safe operating temperature.

Figure 3 gives typical data of the number of no-load starts that TENV hoist type, 1,200 rpm, 60-cycle induction motors of different ratings can make per minute and not exceed rated temperature rise. The starting frequency as taken from this curve applies for accelerating the inertia of the motor rotor only. The inertia of the load including the motocylinder gearing and brake increases both the rotor and stator losses, and consequently reduces the number of allowable accelerations essentially in inverse proportion to the net total inertia of the system. A simple generalization that can be made is that an external WK^2 equivalent to that of the rotor, when referred to the motor shaft, halves the values shown by the curve. For instance a 20-horsepower unit connected ~~to an~~ external inertia of 6.35 pounds feet squared foot equivalent, would result in a permissible number of starts of 16 per minute instead of 32.

The following formula gives the approximate number of starting operations per minute allowable for a loaded system based on the curve values of Figure 3.

$$N = n\frac{WK_m^2}{\Sigma WK_{ex}^2 + WK_m^2}$$

where

N = allowable operations/minute for loaded system

n = allowable operations/minute as given by Figure 3

WK_m^2 = motor rotor inertia as given by Figure 3

ΣWK_{ex}^2 = summation of all other inertias referred to the motor shaft (inversely as the square of the torque ratio)

Figure 13 shows a reversing type of offset motocylinder drive, a type of control which normally requires two starts of the motor per cycle of operation and in some cases plug reversing of the drive for nudging the logs. This same log handling operation when performed by unidirectional rotation with different type of loader-arms approximately halves the number of starting operations required. This application when handled by true motocylinder, also requires about half the number of motor starts. It is therefore important in selecting the type of drive that consideration be given to the starting frequency that will be required as related to the capabilities of the motor.

Motor Enclosures

Usual service subjects the unit to conditions of water, moisture-laden sawdust and wet bark. These, if allowed to come in contact with the windings will cause trouble and eventual failure of the motor. Tannic acids from barks such as hemlock is particularly detrimental to insulation. Modern methods of hydraulic barking of logs[3] results in fine mist spray from the working nozzles which can be carried into the windings of any nearby open type motors.

For such motocylinder applications TENV motors usually make ideal drive units. For those few cases which may re-

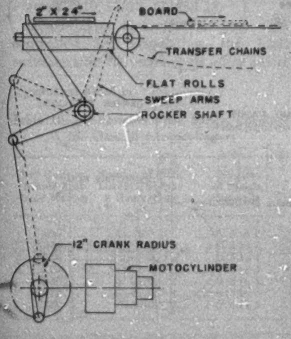
2" X 24"
BOARD
TRANSFER CHAINS
FLAT ROLLS
SWEEP ARMS
ROCKER SHAFT
12" CRANK RADIUS
MOTOCYLINDER

Figure 15 (left). Motocylinder operated lumber sweep (Swede) for transferring lumber from flat rolls to chain transfer. These drives are usually fast acting—1 to 1.5 seconds complete cycle time required

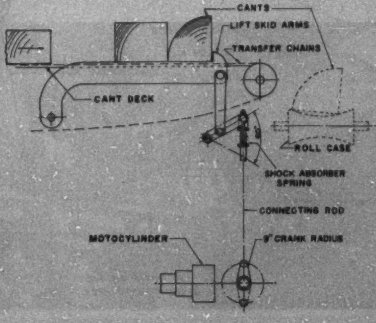
CANTS
LIFT SKID ARMS
TRANSFER CHAINS
CANT DECK
ROLL CASE
SHOCK ABSORBER SPRING
CONNECTING ROD
MOTOCYLINDER
9" CRANK RADIUS

Figure 16 (right). Motocylinder operated lift skid and cant stop ahead of roll case. Shock absorbers in connecting rod not usually required for these slow speed lifts

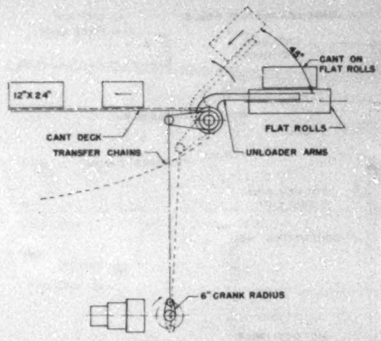
12"X24"
CANT ON FLAT ROLLS
CANT DECK
TRANSFER CHAINS
UNLOADER ARMS
FLAT ROLLS
6" CRANK RADIUS

Figure 17 (left). Motocylinder operated cant unloader between roll case and transfer deck

Figure 18 (right). Motocylinder operated lumber stop in section of flat rolls

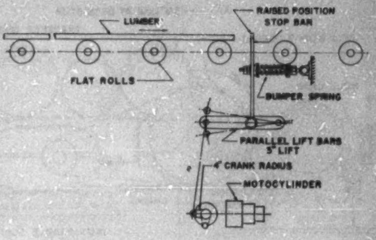
LUMBER
RAISED POSITION STOP BAR
FLAT ROLLS
BUMPER SPRING
PARALLEL LIFT BARS 5" LIFT
4" CRANK RADIUS
MOTOCYLINDER

quire abnormally frequent starting, limited forced ventilation of the TENV motor may be required. The minimum amount of clean air necessary to carry away the heat losses should be passed through the unit, thereby avoiding unnecessary contamination of the interior parts.

Figures 4 and 6 show the water-tight construction and compact assembly of the unit including the integrally-mounted weather-proof electric brake. Electrical connections between brake and motor are made within the unit. The brake cover is easily removed for maintenance or adjustment. Figure 4 shows a usual case of water drippage and presence of moisture-laden debris.

Where large quantities of dry sawdust are present, TENV motors should be used to avoid plugging of the air gaps and windings, even if some forced air cooling may be required on account of the frequency of the duty cycle.

Controls

One of the principal advantages of the motocylinder is in the simplicity and flexibility of its control. It can be automatized to any degree required and conveniently interlocked with other electrically controlled machines or mechanisms. Figure 5 shows a simple control system for a true motocylinder type of log-slip unloader. The unloader is controlled by two remotely located push buttons. One is for normal operation of the unit, the other for safety as an emergency lockout feature. Momentarily depressing the operate button causes the motocylinder to start, make one com-

Figure 19. Motocylinder with wound rotor type motor arranged to operate cutoff saw. Control provides for speed control and reversing of the drive in any position of the stroke

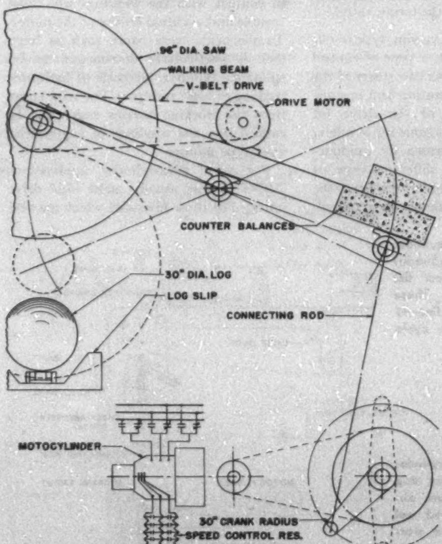
96" DIA. SAW
WALKING BEAM
V-BELT DRIVE
DRIVE MOTOR
COUNTER BALANCES
30" DIA. LOG
LOG SLIP
CONNECTING ROD
MOTOCYLINDER
30" CRANK RADIUS
SPEED CONTROL RES.

Figure 20. (1). Heavy duty offset motocylinder for driving unloader mechanism of Bellingham hydraulic barker. (2). Direct acting motocylinder operated deck stop and loader to Bellingham barker

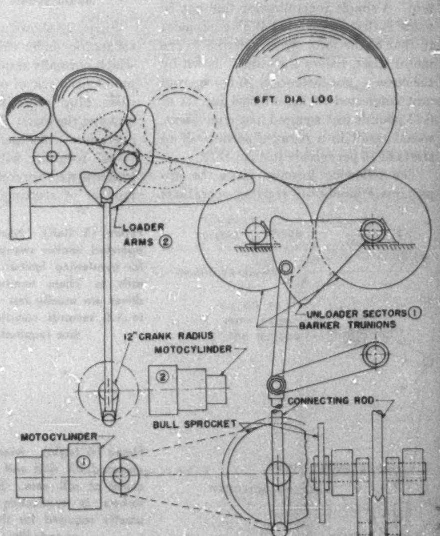
6FT. DIA. LOG
LOADER ARMS ②
UNLOADER SECTORS ①
BARKER TRUNIONS
12" CRANK RADIUS
MOTOCYLINDER
②
CONNECTING ROD
BULL SPROCKET
MOTOCYLINDER
①

Figure 21. Heavy duty offset motocylinder drive for a deck stop and loader. Note small limit switch cabinet at end of loader shaft. Chain is covered by safety guard designed for slack take-up by adjustable slide base. Bull sprocket is equipped with shock absorber springs, see Figure 13 for details

plete revolution of the crank and automatically stop by limit switch action at the normal arms-down position of the unloader. The application is similar to that shown by Figure 9.

Thermal overload relays forming part of the motor starter protect the unit against possible prolonged stalled conditions with the motor energized.

The electric brake coil is connected across one phase of the motor terminals, which upon energization of the motor, results in simultaneous brake release and starting of the motor. The events are reversed when the unit is stopped. The brake is a-c operated and the circuit is the simplest type possible.

Motocylinders result in very efficient log and cant handling operation when controlled by electric eye. Controls of this type may be had in many different forms either full or semiautomatic. For semiautomatic operation the control can be transferred to and from the electric eye at will, thus conserving the time of the inspector for other duties. Figures 6 and 7 are examples of this type of control applied to a direct acting roll case unloader. Figure 7 is an action photograph showing a log being lifted from the roll case, the action having been initiated by the far end of the log breaking the light beam of the electric eye control.

Other operations which may, depending on mill layout, be effectively controlled by electric eye are illustrated by Figures 9, 10, 14, 15, 17, and 18.

Offset type motocylinders are best controlled by associating the limit switches with the crank shaft, or as a part of the driven machine. Figure 21 shows a manually operated deck-stop and loader powered by an offset motocylinder. The limit switches are in the small waterproof cabinet at the end of the rocker shaft. See Figure 13 for construction details. Reversing type automatic control initiated by push button is used, the loader shaft making only about 90-degree angular motion. The limit switches stop and reverse the motor in both extremes of travel. If the operate button is held down, rocking motion of the loader arms is obtained. If the button is released the arms automatically return to the normal "up" position. Forward and reverse "inch" buttons form part of the control for nudging logs into position. An emergency stop button also is provided.

Table III. Allowable Peak Shock Loadings for Class III Motocylinders

Per Cent of Motor Full Load Rating	Number of Peak Loads/Hour for 8 Hours/Day	Duration of Shock, Seconds
400	4.0	0.5 to 5
375	5.0	0.5 to 5
350	7.0	0.5 to 5
325	12.0	0.5 to 5
300	20.0	0.5 to 5
275	45.0	0.5 to 5
250	100.0	0.5 to 5

Gear Unit and Crank

The gear unit of motocylinders is subjected to heavy duty since it couples the inertia of the high torque motor to the dead weight and inertia of the load. Frequent starting and stopping by brake action subjects the gearing and shafts to repeated shock and stress reversals. On account of the general severity of the service which prevails for almost any application, the gear units for all standard motocylinders should be capable of meeting the requirements of American Gear Manufacturers Association class III service designation for gearmotors,[4] characterized as moderate shock duty for 24 hours a day and heavy shock for 8 hours a day.

Some applications may subject the unit to peak loadings of considerable variation. The ability of gearing to withstand heavy shock and overloading is recognized, providing the frequency of application is in inverse relation to the intensity of the allowable shock. Table III gives permissible limits for these conditions for class III gearmotor (motocylinder) units based on the premise that the peak loading will not exceed 5-seconds duration. That the stroke time of most motocylinders is considerably less than 5 seconds is recognized. Special consideration should be given to the few applications which do exceed the limits given by the table.

True motocylinder drives which are subject to moderate or heavy shock should be equipped with shock absorbing devices in the linkage system to limit the peak values. These absorbers are usually short powerful springs associated with the connecting rod or lever system such as illustrated by Figures 9 and 16. The heavy spring can be seen at the top of the connecting rod in Figure 8.

Offset motocylinder drives are particularly desirable where a stalled condition of the load mechanism can be had with the crank at angles near top or bottom limits of throw. Simple analysis will show that forces of extreme magnitude can result to the crank, connecting rod and driven mechanism in this case. Stress relieving springs should be provided in the connecting linkages of these drives to limit the forces to safe design values. The offset motocylinder fully protects the drive unit in these cases since the crank and connecting rod which are subject to the forces are removed from it.

Offset motocylinders should always be provided with adjustable slide bases so that slack can be kept out of the chain.

Figure 22. Factory view showing motocylinders undergoing test

Abnormal chain slack can result in unnecessarily severe shock forces being applied against the entire system and will eventually result in failure at some point. Figure 9 shows a typical offset motocylinder drive with shock absorbing devices.

Type B drive sprockets should always be used on offset motocylinders. These sprockets locate the chain as close to the gear case as possible, thus minimizing the moment of the overhung load. The drive sprocket should have a pitch diameter of at least three times the diameter of the output shaft.

Offset motocylinder drives are sometimes preferred over true motocylinders for applications where changes in speed or torque are anticipated. Considerable variation in these characteristics can be inexpensively made at later date by change in sprocket ratio. Ample power in the drive unit should be provided to cover the future consideration.

In the preceding discussion considerable emphasis is placed on the importance of minimizing shock. This is important for any type of drive if minimum destructiveness and lowest maintenance expense is to be expected. In this connection it is important to note that motocylinder drives as a class give a smooth sinusoidal form of motion and acceleration of the load which minimizes much of the shock and noise of operation so common to cylinder type operators. The ease with which a motocylinder performs its task, regardless of size of load, appears almost effortless and is indeed a pleasure to watch.

Power Requirements

The energy required for operation of any motocylinder is practically nil. This is because the unit including its electric brake is energized only during the operate period. In some applications regeneration takes place during the deceleration period at the upper limit of stroke, tending to still further reduce energy consumption.

The power supply for motocylinders should be from the same sources used to supply the other 440-volt mill motors. It is seldom that the size of the power center transformer need be increased in capacity on account of the motocylinder loads.

A large motocylinder in the order of 100-horsepower capacity should be supplied from a power source that will not suffer more than 10 per cent voltage drop at the moment the unit is energized. The locked kilovolt amperes per horsepower may be taken as five for such calculations.

Conclusions

The motocylinder makes possible new and effective methods for powering log and lumber handling machinery. It is simple in operation and a versatile tool that can be inexpensively applied to practically any operation requiring reciprocating or oscillating forms of motion. Its power consumption and stand-by losses are practically nil. It is constructed in rugged form capable of withstanding the rigors of sawmill service. The absence of steam and water leaks tend toward a dryer cleaner mill which is conductive to lower general maintenance and clean up expenses.

A considerable number of installations have been made in the mills of the Pacific Coast area. With the rapidly decreasing availability of steam power from sawmill waste, considerable increased use of motocylinder drives is forecast, both for new mills and in the rehabilitation of old ones.

It is expected that the operators of eastern mills may also find the motocylinder an economic solution to many of their material handling problems. It should also be found useful in other industries where readily controllable thrust motion is required.

References

1. ELECTRIC LIFTING DEVICE, F. W. Horstkotte. United States Patent number *2304360*, December 8, 1942.

2. STANDARDS FOR MOTORS AND GENERATORS, National Electrical Manufacturers Association (New York, N. Y.), *MG1-1.7*, 1949.

3. THE BELLINGHAM HYDRAULIC LOG BARKER, V. C. Haner, H. A. Rose. *AIEE Transactions*, volume 67, part II, 1948, pages 1068–74.

4. STANDARDS FOR GEARMOTORS. American Gear Manufacturers Association (Pittsburgh, Pa.), *AGMA 462.01*, March 1948.

Discussion

H. E. Springer (Rayonier Incorporated, Port Angeles, Wash.): For some years the forest industries have been seeking ways of handling logs, cants, and lumber more efficiently than has been done in the past by the various steam, air, and hydraulic devices.

Of widespread interest alike to designers, operators, and maintenance personnel of sawmills and other wood cut up plants, the motocylinder is a valuable contribution to the forest industries in many ways. Some of the more important economic advantages are outlined in the paper.

In addition to those listed, might be added the elimination of the steam, water, and oil vapor nuisance which contributes substantially to dirt accumulation and to damage of motor windings; wiring systems, and control apparatus in plants where the steam or hydraulic cylinders have been used.

Leaks in the steam, water, or oil systems are difficult to completely eliminate and oil and water soaked dirt or steam and oil vapor seem almost inseparable from the older wood cut up industries. Elimination of these is immediately manifested in much cleaner appearance of the plant and lower maintenance costs.

Power supply to the wood handling device also is simplified by use of the motocylinder.

Very often the cylinder and piston type of device requires air, water, oil, or steam for the main cylinder and an additional supply of a-c or d-c power to operate a solenoid valve to control the prime power flow to the cylinder.

The motocylinder requires only one source of power, normally 440 volt, 60 cycle, 3 phase and the control can be adapted to a wide variety of schemes for initiating the operation of the device.

All things considered the motocylinder is demonstrating its value in a number of recent installations on the Pacific Coast and while the proving ground of actual service has exposed a few defects, these have been minor and have been eliminated to a point where the motocylinder has made a place for itself in industry and is worthy of more widespread use.

H. A. Rose: The ideas introduced by Mr. Springer are very much appreciated. They represent the kind of advantages possessed by motocylinders from the operator's and maintenance man's points of view. The points which he has raised could very well have been given more attention in the paper. Improved cleanliness by eliminating water and grease is conducive to a cleaner, safer, and more orderly mill, and should reflect in higher production and improved operating conditions for the workmen.

Although the motocylinder has to date been used practically entirely in the wood industries of the Pacific Coast, it should be given serious consideration by operators and plant engineers of other industries and sections of the country. It has particular value in climates subject to extreme cold where freezing of water and steam lines and congealing of lubrication and hydraulic systems are encountered.

A 24,000-Kilovar Series Capacitor in a 230-Kv Transmission Line

R. E. MARBURY
FELLOW AIEE

F. D. JOHNSON
MEMBER AIEE

Synopsis: The necessity for long distance transmission of electric power has grown rapidly during recent years. Line reactance becomes a problem of increasing importance when transmission distances continue to increase. Long lines cannot be loaded sufficiently for maximum over-all economy because of limitations imposed by transient stability and kilovar requirements. The most important alternative to reduction in equivalent line impedance by further increase in transmission voltage, is the use of line reactance compensation. Such compensation can best be obtained through the use of capacitors operating in series with the line conductors. To permit the use of series capacitors rated on the basis of normal load conditions, it is necessary to protect them effectively during line fault conditions. To make maximum use of line reactance compensation with capacitors it is necessary to by-pass and protect them only during line fault condition and reinsert them with minimum delay after the line fault is cleared. Lack of means for accomplishing the latter has prevented the use of capacitors for line reactance compensation where the primary objective is increasing power transmission. While protective devices have been developed which are adequate for use with series capacitors when used to improve voltage regulation, they are by far too slow in operation to meet the requirements when series capacitors are used to increase power transmission. A protective means has now been developed which meets these requirements, and a 24,000-kilovar series capacitor has been installed by the Bonneville Power Administration in a 230-kv line at their Chehalis substation, for the purpose of compensating line reactance and increasing the power limits of this line. This is the first installation of this type, and the first time a series capacitor has been used in a high-voltage transmission line in the United States. The purpose of this paper is to describe this equipment and its method of operation.

THE USE of series capacitors for line reactance compensation has been recognized for many years as a means of improving regulation and eliminating voltage dips caused by sudden changes in load. Such an installation on a 66-kv line was described in a paper by Johnson, Marbury and Arthur.[1] Many other and smaller series capacitors have been installed for this same purpose during the last 15 years. In these applications stability was not a problem and it was not necessary therefore to reinsert the series capacitor instantly following the clearing of a line fault. Failure to do so merely introduces a short period of operation where voltage dips and lamp flicker are present but can be tolerated. This fact permitted the use of a by-pass switch to transfer the current from the gap circuit to a switch circuit, such that the opening of the switch restores the series capacitor to service. In applications where the series capacitor is used to increase the power that can be transmitted, the time required for these operations is far too great to permit of effective use because the system usually becomes unstable unless the series capacitor is restored promptly after the isolation of the fault on the line.

In some cases the series capacitor may be used merely for impedance matching purposes, to control the division of current through parallel circuits. In such cases it may be possible to de-energize the circuit containing the series capacitor when a fault occurs on that portion of the circuit. In such applications a protective gap may be used to protect the capacitor and this gap will recover its insulation during the period while the line is de-energized. However, tests have shown that in the case of relatively large series capacitors the period of de-energization required for satisfactory de-ionization of gaps is longer than can be tolerated in most cases. Also, if the gap restrikes when the line is re-energized it becomes necessary to extinguish the arc by the closing of a by-pass switch, thus removing the series capacitor from service during a period when it may be badly needed. In view of these facts there has been a need for a more satisfactory device, not only for the application where stability is involved but even for those where it is possible to de-energize the line for a brief period following each fault.

The protective device should not only protect the series capacitor while the line current is excessive but should restore it to service at the instant the fault is removed. In the case where the line is de-energized, the protective device should not function when the line is re-energized, even though the line is de-energized for only a few cycles. Such a protective device permits the use of capacitor units having a voltage rating based on the maximum continuous load current, and also permits of a relatively close protection level. This close protection level may be used since the operation of the protective device does not create risks as to system stability. Operation of the protective device takes place only during the actual periods of excessive

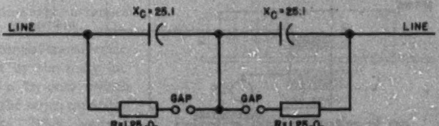

Figure 1. Simplified schematic diagram of series capacitors

Paper 51-304, recommended by the AIEE Transmission and Distribution Committee and approved by the AIEE Technical Program Committee for presentation at the AIEE Pacific General Meeting, Portland, Oreg., August 20–23, 1951. Manuscript submitted May 17, 1951; made available for printing July 9, 1951.

R. E. Marbury and F. D. Johnson are with Westinghouse Electric Corporation, East Pittsburgh, Pa.

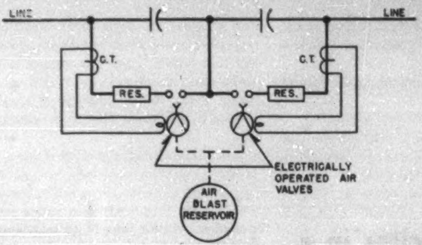
LINE
LINE
C.T.
C.T.
RES.
RES.
ELECTRICALLY OPERATED AIR VALVES
AIR BLAST RESERVOIR

Figure 2. Schematic diagram showing air blast gap arrangement

currents. It is expected that since these requirements have now been met the series capacitor will become a practical means of increasing the power capacity of existing transmission lines, and permit the use of longer lines.

Rating of Series Capacitors

Five basic factors go to determine the rating of a series capacitor as follows:

1. Reactance.
2. Maximum continuous line current.
3. Maximum momentary line current.
4. Maximum fault current and duration.
5. Line voltage.

Reactance

The reactance of each phase of a series capacitor is determined by the line reactance and the degree of compensation necessary to meet the objectives. It is not the purpose of this paper to discuss the factors which influence a decision as to the amount of line reactance to be compensated by the series capacitor in a particular case.

Maximum Continuous Line Current

The line current is determined by line requirements and is the maximum continuous current expected to be present in the circuit in which the capacitor is installed. The above line current when multiplied by the reactance gives the rated voltage. The product of the current squared and reactance gives rated kilovar per phase. The number of capacitor units required per phase may be determined by simply dividing this kilovar by the rated kilovar of the standard capacitor units to be used. If the voltage obtained from the load current and capacitor ohms is close to a standard shunt capacitor unit rating such as 4,160, 7,200 or 7,960, then the standard shunt capacitor units may be used. If this voltage is a multiple of standard ratings, the standard units may also be used by means of series groups. For example each phase of a series capacitor may be made up of two groups of 7,960-volt standard capacitor units. Units with standard kilovar ratings and special voltage ratings are sometimes required where the use of standard voltage units involves too much sacrifice due to the fact that the working voltage is too far below their rated voltage.

Maximum Momentary Line Current

This is the maximum expected line current associated with load fluctuations such as motor starting. This value should not exceed 150 per cent of the maximum continuous working current and no operation of the gaps should occur under these conditions.

Maximum Fault Current and Duration

The expected fault current magnitude and duration affect the design of the by-pass gap, and particularly the current limiting resistor which is used in conjunction with the by-pass gap.

First Transmission Line Installation

The first installation of a series capacitor in a transmission line for the purpose of increasing the transmission of power was energized February 23, 1951. This capacitor is located on the Bonneville Power System at the Chehalis substation, and is installed in a 230-kv line

Figure 3. Schematic diagram showing by-pass switch arrangement

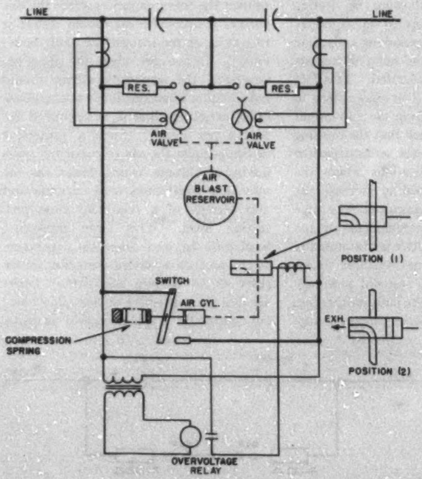
LINE
LINE
RES.
RES.
AIR VALVE
AIR VALVE
AIR BLAST RESERVOIR
SWITCH
AIR CYL.
COMPRESSION SPRING
POSITION (1)
EXH.
POSITION (2)
OVERVOLTAGE RELAY

Figure 4. Schematic diagram showing means of detecting individual fuse operation

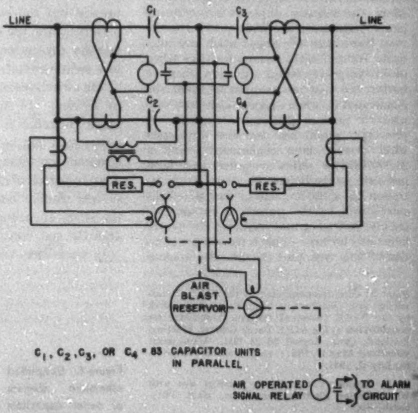
LINE
LINE
C1
C3
C2
C4
RES.
RES.
AIR BLAST RESERVOIR
C1, C2, C3, OR C4 = 83 CAPACITOR UNITS IN PARALLEL
AIR OPERATED SIGNAL RELAY
TO ALARM CIRCUIT

Figure 5 (left). One phase of Chehalis series capacitor during installation, showing the two housed groups, insulated from ground

Figure 6 (right). Chehalis series capacitor installation showing circuit connections

leading to the Longview Substation. The rating of the initial installation was as follows:

1. Reactance 51 ohms.
2. Continuous working current 312 amperes.
3. Momentary working current 468 amperes.
4. Fault current 3,200 amperes; duration 15-cycle maximum.
5. Line voltage 230 kv.

The housings provide additional space for adding capacitor units to bring the reactance to 31.84 ohms, for a working current of 500 amperes and a 3-phase kilovar rating of 23,800 kilovars.

General Requirements

FAULT CURRENT PROTECTION

Since a tenfold increase in voltage on the capacitor is expected corresponding to a line fault of 3,200 amperes, it was necessary to protect the capacitors from voltages in excess of a predetermined amount. This was accomplished by shunting the capacitor with a gap and resistor. The gap shown in Figure 1 breaks down when the voltage across the capacitor exceeds $2^{1}/_{2}$ times the capacitor continuous rated voltage. The resistor in series with the gap is nominally $1^{1}/_{4}$ ohms and is used to limit the capacitor discharge current when the gap breaks down. This permits repetitive discharges to occur for duration of the line fault without harm to the capacitors.

After the fault current no longer exists and the current in the line is again normal, the resistor must be permanently disconnected. This is accomplished by the use of a special gap designed in a manner to permit the use of a constant blast of air during the period current flows. The volume of air is made sufficiently large to render the arc unstable so that it clears at each current zero. Thus the gap restrikes on each half cycle, and is extinguished at each current zero so long as the line current exceeds 250 per cent of normal. As soon as the system short is removed (by high speed relays and circuit breakers), and the line current is again near normal the gap will cease to break down and the resistor will no longer be connected in parallel with the capacitor.

The flow of air through the gap chamber is initiated by gap current. Termination of gap current de-energizes the solenoid operated air valves and allows them to close. A time delay inherent in the design of these air valves allows the air to continue to flow and complete the deionization of the gap and fully restore the gap insulation value. The gap circuit connections are shown in Figure 2.

The operation is the same whether system relays and circuit breakers function or if the fault is self clearing.

OVERLOAD PROTECTION

Since the capacitor units must not be operated continuously above a predetermined voltage for thermal reasons it was considered necessary to provide overload protection. The capacitors may be operated continuously at the rated current of 312 amperes plus 5 per cent corresponding to standard practice for shunt capacitors. They may be operated for periods of 30 minutes at 135 per cent and 5 minutes at 150 per cent voltage. Means were provided to prevent operation of the series capacitor in excess of these established limits. This was accomplished by the use of an inverse time relay arranged to detect overvoltage across the series capacitor through a potential transformer. Completion of contact by the relay initiates the closing of a by-pass switch which then shorts out the series capacitor until manually reset. This by-pass switch is a 15-kv indoor single-pole switch, arranged to remain closed by spring pressure, and to be opened by air pressure. The normal supply of air in the air blast reservoir keeps the switch normally in the open position. The switch is caused to close by shutting off the air from the switch operating cylinder and dumping the air from this cylinder. The previously mentioned operation of the inverse time relay performs this function. Voltmeters are also provided to permit reading the voltage across the series capacitor. These are mounted so they can be read from the ground. See Figure 3 for general arrangement of switches.

FUSE INDICATION

If several capacitor units are disconnected from the group due to fuse operation the impedance of this group in-

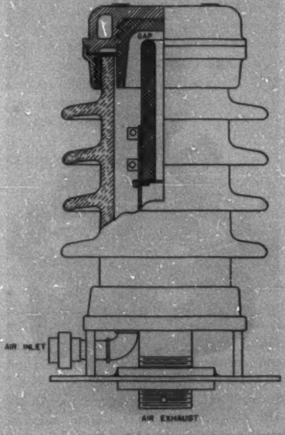

Figure 7. Detail construction of gap

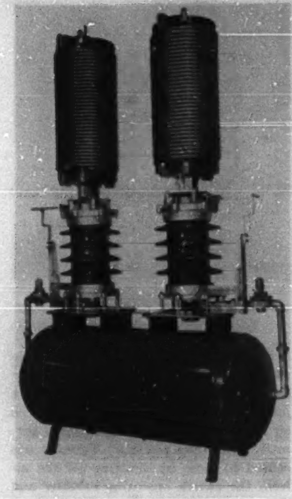

Figure 8. Gap and air tank assembly

creases, and the remaining capacitors in the group operate at a higher voltage for the same current flowing in the line. Since the series capacitor is insulated from ground, it is not possible to inspect the fuses conveniently as with a shunt capacitor, so it was felt desirable to provide some indicating means to enable the operator to determine if some fuses had operated before such a condition reached a point where the operation of the capacitors was seriously affected with respect to working voltage.

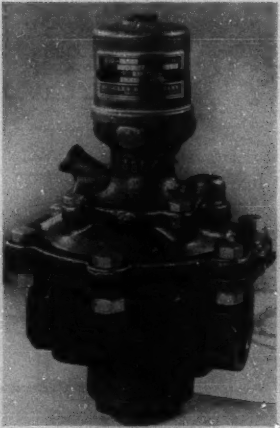

Figure 9. Air blast valve

This is accomplished by dividing the capacitor into two equal branches as shown in Figure 4 and providing relays to compare the current in these branches. Operation of these relays operates an air valve which in turn closes the by-pass switch.

The closed position of the by-pass switch is indicated at ground level by means of a pneumatically operated relay located in the compressor station.

General Construction

The capacitor units are single bushing, 7,960-volt 15-kilovar outdoor units. One-half of the total quantity of capacitors are standard shunt capacitor units. The other half are of special design with approximately 20 per cent added dielectric to gain field experience in the event mortality rate should prove to be high with standard units. Subsequent experience however indicates that the protective equipment will adequately protect standard capacitor units.

Each unit is connected to the bus through a fuse especially designed to interrupt the stored energy in the large number of adjacent units. No fault current interruption problem exists, but the stored energy is quite large.

One hundred and sixty-six of the 15-kilovar units are assembled in an outdoor steel housing and arranged in two groups of 83 units each as shown in Figure 4 with a current transformer to compare the current in each group of 83 units. These housings have space for 288 capacitor units to provide for later change in the rating of the series capacitor to 23,000-kilovars and 520 amperes line current.

Two of these housings are mounted on a platform $12^{1}/_{2}$ feet wide and 80 feet long, which is in turn supported on 24 columns of insulators. On a platform between the two housings is located a tank for gap air supply, two gaps and two resistors.

Figure 5 shows the two metal enclosures during installation, with the compressed air supply tank, two gaps and resistors in the center between the housings. The two housed groups shown are operated in series to give the rating of 51 ohms for 312 amperes, or the contemplated rating of 31.84 ohms for 500 amperes, in which case each group is protected by a gap and resistor, with one compressed air supply for the two gaps. The two groups may be reconnected for parallel operation, giving one-fourth the reactance and twice the rated working current. When so operated one gap is disconnected.

The 3-phase legs are placed side by side as shown in Figure 6, on 25 foot centers. The three phases of the series capacitor equipment are located within a fenced enclosure 100 feet wide and 135 feet long. Another larger fence encloses associated equipment consisting of by-pass disconnects and air supply equipment. This outside fence encloses an area 125 feet wide and approximately 260 feet long.

The Compressed Air Gap

The gap consists of an inverted cup electrode of special graphite, a cylindrical porcelain insulator, and a second graphite electrode located along the axis of the porcelain tube. The central electrode forms a gap in the cavity of this inverted electrode, see Figure 7.

When a flow of current through the gap is initiated by the breakdown of the gap, air is supplied to the bottom chamber from which it flows into the porcelain tubular insulating body. The only outlet for this air is down through the hole in the center electrode, from which it may escape to the outside air.

The two portions of each phase leg of the series capacitor are each protected by a gap as described above, with a resistor connected in series with each gap. One tank supplies the air to these two gaps, see Figure 8.

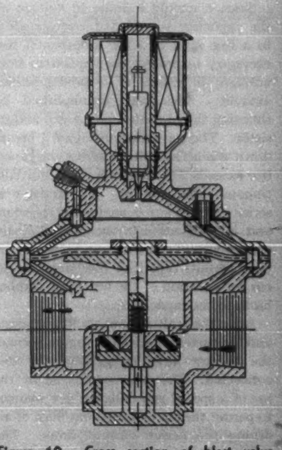

Figure 10. Cross section of blast valve

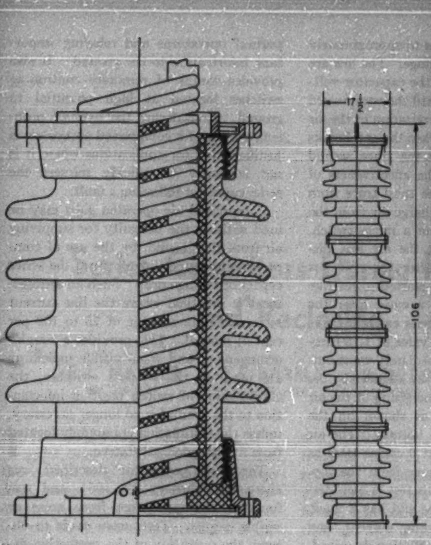

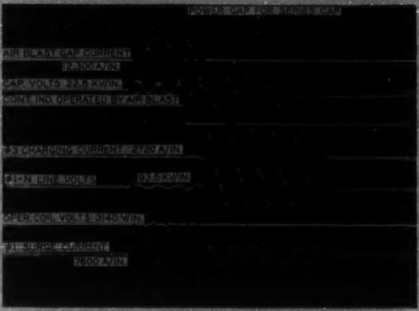

Figure 11 (left.) Air column

Figure 12 (above.) Oscillogram of gap operation

Air Blast Valves

One of the most important detail pieces of equipment is the air blast valves. These may be seen on either side of the assembly shown in Figure 8. These rather large air valves ($1^1/_4$-inch pipe size) must be operated from a current transformer. The current corresponding to low load current in the line and even light load currents, if diverted through the gap must pick up these air valves so as to quench the arc if initiated by a surge. In addition, the valve solenoids must not suffer any damage on the fault current of 3,200 amperes through the gap. This wide range of requirements was met by the use of a saturating current transformer and surge damping resistor, with the solenoid coil designed for very low voltage.

In addition to these requirements it was necessary to use a valve which would open in about 2 cycles after the solenoid is energized, and close with a delayed action to insure thorough removal of ionized gases following termination of the arc in the gap.

It was also felt necessary to provide a type of valve that would not foul up and stick if it remains in one position for long periods of time.

The valve shown in Figure 9 is a modified form of a standard air valve. The detail construction of this valve is shown in Figure 10, and may be seen to consist of a large valve operated by a diaphragm. The use of a diaphragm eliminates any problem of lubrication as would be the case with a piston. The solenoid lifts a magnetic member which has a slideable relation to a needle valve stem. The impact of this magnetic member against the stop on this valve pin jerks the seat open and admits air to the chamber above the diaphragm. Air enters this chamber faster than it can escape through the calibrated vent to the discharge side of the valve, consequently the pressure on the diaphragm opens the main valve.

When the current stops flowing in the solenoid the needle valve closes. The air pressure on the diaphragm then dies down at a rate governed by the escape path, thus closing the main valve with a time delay. The time delay used is 7 to 10 cycles.

Insulating Air Column

In this series capacitor installation it was considered desirable to locate the compressor at ground potential and operate it from a local 230-volt power supply. Also it was considered desirable to be able to reset the by-pass switches to the open position from the ground, and to provide an indicating means to show whether the by-pass switches, not visible from the ground, were in the closed or open position.

These requirements necessitated an insulated air column, containing three air lines: one to supply air to the gap reservoirs, one to reset the by-pass switches, and one to operate a pneumatic relay to show whether the by-pass switches were in the open or closed position.

All three of these hose lines are assembled in a porcelain stack as shown in Figure 11. This stack has ample wet and dry flashover to withstand the line to ground voltage. Three outlets are provided at the bottom and top castings for continuing these three air lines. The bottom connections go to the compressor house, while the top connections go to the air tank and proper air valves. Each hose line consists of a 3/8 inside diameter ×3/4 outside diameter special high-pressure synthetic rubber hose 57 feet long giving a stress of about 2,300 volts per foot. The hose is coiled on a core approximately 8-feet long, and compounded into the porcelain column. Activated Alumina dryers are provided at the compressor location to eliminate moisture condensation in this hose line and maintain high level of insulation in the hose itself. The complete assembly was given a 485-kv, 1-minute 60-cycle test.

Compressor House

Only one compressor is required for the complete series capacitor installation. This compressor supplies air to a reservoir located in the compressor house. From this reservoir air flows through a filter, and pressure regulator and dryer. The latter regulates the air supply to the gap air supply tanks. Three air pushbuttons are also located in the compressor house, for resetting the by-pass switches previously mentioned. Interlocks are provided to prevent resetting these by-pass switches unless the main by-pass disconnect is operated first to remove voltage from the series capacitor. The three air operated signal relays are also located in the compressor house. These indicate when operation of by-pass switches has occurred.

Other Protective Features

In addition, provisions were made to automatically close the by-pass switch in the event of loss of air in the reservoirs, or prolonged arcing of the gaps due to inadequate air supply or failure of air valve to open. Also to close the switch in the event of flashover the auxiliary back-up gaps.

A ground switch is provided for grounding the platforms of the series capacitor and thus avoid the collection of static charges on the large housings and platforms.

Operation of Protective Gap

Figure 12 shows an oscillogram of a laboratory test which illustrates the operation of the compressed air protective device. In this test a $3^{1}/_{2}$ ohm series capacitor was connected in a circuit which would produce a large current through the capacitor, and a current which would develop a voltage across the capacitor many times the breakdown setting of the gap, which was $2^{1}/_{2}$ times the continuous voltage rating of the series capacitor. The bottom trace shows the fault current which was allowed to flow for $3^{1}/_{2}$ cycles, and then reduced to the normal continuous current rating of this capacitor which is 1,150 amperes.

The voltage across the capacitor is shown on the trace second from the top. When the fault was applied to the capacitor the gap broke down and limited the voltage on the capacitor to approximately $2^{1}/_{2}$ times its rated voltage. The low arc drop of the gap holds the capacitor voltage down thereafter until the compressed air comes on. The energization of the air blast solenoid occurs when the gap breaks down as indicated by the trace second from the bottom. The effectiveness of the air is shown by the third trace from the top where the discharge air from the gap is made to operate a micro-switch. It will be noted that the air was discharging $2^{1}/_{2}$ cycles after the coil was energized, and the gap started to restrike at this time. About a cycle later the current through the series capacitor was reduced to the normal value of 1,150 amperes and the arc immediately went out. The termination of the arc is shown by the top trace and the de-energizing of the air blast valve solenoid as shown on the second trace from the bottom. The air actually shut off about 9 cycles later as shown on the third trace from the top. The model used for this test is considerably lower in reactance and has a much higher continuous working current than the series capacitor installation described, making the gap working conditions considerably more severe. Actual tests on the Chehalis installation are covered by an unpublished AIEE paper by C. C. Diamond, E. J. Harrington, and J. R. Curtin.

Conclusions

The use of compressed air makes possible a very effective type of self clearing gap. With this type of gap the series capacitor will be by-passed only during the period of the fault, or when there is sufficient current to break down the gap on each half cycle. Compressed air also provides a means of performing other important operations and relaying important information to the ground. It also provides means of remotely controlling switches located at high potential to ground. Considering the over-all problem, the use of a compressed air system is justified even for applications where it is not necessary to quickly reinsert the series capacitor following a fault.

Compressed air operated gaps may be used without the necessity for supplying air from the ground, by the use of compressors operated directly from the series capacitor voltage drop. Such an arrangement is practical where the line current remains within a range of 25 to 100 per cent of normal. This provides a simpler arrangement and when visible indicators are used on the by-pass switches, the transmission of switch position information to the ground is no longer necessary, unless the installation is remotely located from an attended substation.

The series capacitor described was energized February 23, 1951, and was found to be quite free from noise or visible corona. Tests were made to observe the operation of the protective devices by placing faults on the circuit or associated circuits and observing the operation of the gaps. The gap protection operated in a manner quite similar to the laboratory test, Figure 12. The speed with which air became effective at the gap was such as to insure fast re-insertion of the series capacitor even in the case of faults that are cleared in very short periods such as 3 cycles.

Reference

1. DESIGN AND PROTECTION OF 10,000-KVA SERIES CAPACITOR FOR 66-KV TRANSMISSION LINE, A. A. Johnson, R. E. Marbury, J. M. Arthur. *AIEE Transactions*, volume 67, part I, 1948, pages 363–68.

Discussion

E. J. Harrington (Bonneville Power Administration, Portland, Oreg.): Since its installation this series capacitor has not been subjected to line faults other than those during the staged tests. It has been and is still being operated with the capacitor groups in parallel.

We hope to soon fill the housings to the full 24,000-kvar capacity and operate the groups in series thereby obtaining approximately 24 ohms of capacitive reactance compensation.

Operation so far has been trouble free with one exception. This was a failure of one of the air columns. This failure resulted in a fire in the column which ultimately caused the capacitor protective equipment to function. This resulted in by-passing of the capacitors and their removal from the circuit without interruption of load in the 230-kv circuit.

I would like to suggest that the authors describe their air column failure, its cause and the measures they have taken to insure against similar failures in future equipment.

R. E. Marbury and **F. D. Johnson**: Mr. Harrington has mentioned a case of trouble with this series capacitor installation involving the air column used to maintain air pressure in the reservoirs mounted on the insulated platforms. The leakage current through one of the air columns became excessive and resulted in a failure in one air line. The air line burned open at one point permitting a low current arc which ignited the compound in which the hose was embedded. The escape of air at this point released pressure sufficient to rupture the porcelain casing.

At first this condition was attributed to excessive accumulation of moisture in the air line, but final analysis disclosed that the trouble was entirely due to defective hose material. The hose material receiving engineering approval contained only small traces of free carbon and measured well over 50,000 megohms per foot, while the material actually used was found to contain up to 50 per cent of free carbon and measured 10 to 40 megohms per foot. The resulting accumulation of heat resulted in excessive heating of the hose and the failure in service.

The rebuilt air columns were entirely satisfactory on leakage and overvoltage tests, with or without the presence of condensate.

In view of the above there is no reason to expect future trouble and the design is entirely adequate when manufactured as intended. Steps have been taken to rigidly control the manufacture in the future, and the physical and electrical properties of the hose itself.

Series Capacitors During Faults and Reclosing

E. L. HARDER
FELLOW AIEE

J. E. BARKLE
MEMBER AIEE

R. W. FERGUSON
ASSOCIATE MEMBER AIEE

THE FUNDAMENTAL purpose of a series capacitor is to compensate for the voltage drop, or part of the voltage drop, caused by current through the inductive reactance of a circuit. This effect can be viewed as compensation of the positive inductive reactance of the circuit by the negative capacitive reactance of the series capacitor. Transmission line inductive reactance has an important influence on voltage regulation and steady-state and transient stability; thus, the series capacitor can have an important bearing on the solution of power transmission problems.[1,2,3,4]

Transmission ties operating near the steady-state or transient stability limit can be made more stable by series compensation; likewise, the power-transfer ability of the tie can be increased. Used in this manner, series capacitors can delay the need for additional transmission lines to handle increasing power-transfer requirements and can economically justify proposed tie lines by reducing transmission line requirements. For a given loading condition, series capacitors can be used to improve voltage regulation and power factor. Another possible use for series compensation is in effecting a desirable division of load between parallel circuits of different capacity.

A 230-kv series capacitor has already been installed at the Bonneville Power Administration's Chehalis Substation and subjected to system tests to determine its effect on system operation and relaying. A number of installations on 230-kv systems are planned for the near future, and consideration is being given their use with circuit voltages above 230 kv. Series compensation introduces several application problems not ordinarily encountered in transmission system design. The effect on system operation has already been discussed in the literature,[1,2,3,4] but there has been little discussion of the effect of series compensation on system relaying and of the transients introduced into series-compensated systems during faults and switching.

Series Capacitor Protection

The application of series capacitors for the purposes described above has been made practical by the development of suitable protective equipment.[5] The principal component of the protective equipment is a gap that flashes over to protect the capacitor form being stressed with too high a voltage. To provide the maximum benefit to system transient stability, it is important that the capacitor by-pass circuit be opened immediately after the capacitor voltage is reduced below the critical value.[5]

A typical series capacitor protective by-pass circuit is shown in Figure 1. The breakdown voltage of the by-pass gap is adjusted in the range of 2.5 to 3.0 times the rated voltage of the capacitor, which is considered satisfactory from the standpoint of protection of the capacitor against damage due to high overvoltage. Additional relay equipment is provided to protect against moderate overvoltages of longer duration. Sufficient resistance is provided in series with the gap to limit the capacitor discharge current to a safe value and to avoid oscillations in the discharge circuit when the gap fires. Higher values of resistance were considered in some cases to retain as much as possible the benefit of the compensation during transient swings. Flow of current in the gap circuit causes operation of the electrically-operated air valves and the air-blast reservoir discharges a stream of air into the gap conducting area. After establishment of sufficient air flow, the arc in the gap space is quenched at each current zero, and gap flashover occurs again on the next half-cycle of high voltage. Thus, when the cause of the capacitor overvoltage is removed, the gap arc is quenched at the first current zero thereafter and no restrike occurs. The capacitor is fully reinserted in the transmission circuit within one-half cycle after the overvoltage condition is removed.

The time required to establish sufficient air flow to cause quenching of the arc after the initial gap breakdown is in the

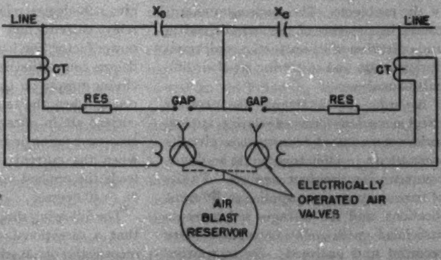

Figure 1. Protective by-pass circuit for a series capacitor

Paper 51-305, recommended by the AIEE Transmission and Distribution Committee and approved by the AIEE Technical Program Committee for presentation at the AIEE Pacific General Meeting, Portland, Oreg., August 20-23, 1951. Manuscript submitted May 22, 1951; made available for printing July 9, 1951.

E. L. Harder, J. E. Barkle, and R. W. Ferguson are all with Westinghouse Electric Corporation, East Pittsburgh, Pa.

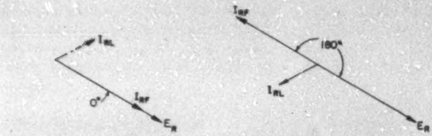

(A) - CURRENTS IN TRIPPING DIRECTION. 60° INDUCTIVE LINE BETWEEN RELAY AND FAULT

(B) - CURRENTS IN NONTRIPPING DIRECTION. 60° INDUCTIVE LINE BETWEEN RELAY AND FAULT

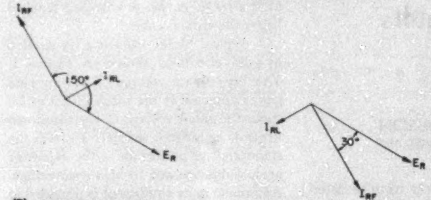

(C) CURRENTS IN TRIPPING DIRECTION. 90° CAPACITIVE CIRCUIT BETWEEN RELAY AND FAULT

(D) - CURRENTS IN NONTRIPPING DIRECTION. 90° CAPACITIVE CIRCUIT BETWEEN RELAY AND FAULT

I_{RL} = UNITY POWER FACTOR LOAD CURRENT APPLIED TO RELAY
I_{RF} = FAULT CURRENT APPLIED TO RELAY
E_R = VOLTAGE APPLIED TO RELAY

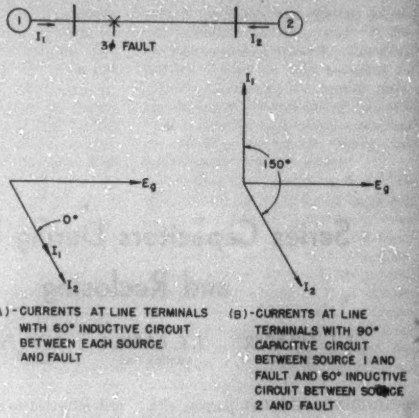

(A) - CURRENTS AT LINE TERMINALS WITH 60° INDUCTIVE CIRCUIT BETWEEN EACH SOURCE AND FAULT

(B) - CURRENTS AT LINE TERMINALS WITH 90° CAPACITIVE CIRCUIT BETWEEN SOURCE 1 AND FAULT AND 60° INDUCTIVE CIRCUIT BETWEEN SOURCE 2 AND FAULT

Figure 2 (left). Relay quantities for a directional element with 60-degree connection during internal and external faults

Figure 3 (above). Phase-comparison relay quantities during an internal 3-phase fault

range of 1.5 to 3 cycles. After this time, the gap arc extinguishes and restrikes each half-cycle until termination of the overvoltage condition.

Application Problems

The relaying of series-compensated transmission lines is complicated by the fact that the circuit impedance is changed abruptly when the capacitor is short-circuited by its protective equipment upon the occurrence of a short circuit. Bypassing the series capacitor causes an increase in the circuit impedance, which causes a reduction in short-circuit current. Thus, the impedance measured by a distance relay changes when the by-pass gap fires. There are problems concerning directional element operation and phase comparison relaying that are difficult to analyze because of the transient nature of the problems. The system transients caused by presence of the series capacitor and operation of its protective equipment during faults and switching are also difficult to analyze.

In order to determine the possible effect on various forms of relaying, typical series-compensated transmission circuits were set up in miniature on the analogue computer for transient analysis. Faults of various types were applied at different locations, and the voltages and currents associated with relay operation were recorded and analyzed. By comparing the results with the voltages and currents obtained on conventional circuits where it is known that correct relay operation takes place, it is possible to predict the correct or incorrect functioning of the relay protection on the series-compensated system. Of primary interest is the operation of single-phase high-speed directional elements of the type used in directional-distance relaying and directional-comparison carrier relaying.

The directional element connections most used with high-speed directional elements are the 60-degree and 90-degree connections. The 60-degree connection utilizes a delta current and a line-to-line voltage such that the relay current leads the relay voltage by 60 degrees with unity power factor load current on the line. In the 90-degree connection, a phase current and a line-to-line voltage are used to give a 90-degree relationship between the relay current and voltage with unity power factor line loading. When the 60-degree connection is used, the maximum closing torque on the directional element occurs when the relay voltage and relay current are in phase, while on the 90-degree connection maximum torque occurs when the current applied to the relay leads the applied voltage by an angle of 35 to 40 degrees.

The following simple illustration proves that a directional element can operate incorrectly on a series-compensated circuit under specific steady-state conditions. Figure 2 shows vector diagrams of the voltage and current applied to a 60-degree directional element. The relay is assumed to be connected to the line on one side of the series capacitor when a 3-phase fault occurs on the opposite side of the capacitor. Figures 2(C) and (D) show the resulting relay voltages and currents for the conditions of a fault in a

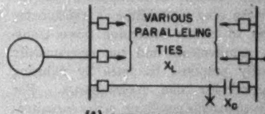

(A) SINGLE SOURCE SYSTEM

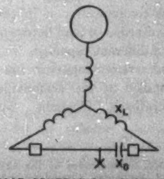

(B) IN-PHASE GENERATION. SYSTEM EXCEPT FOR SERIES COMPENSATED LINE REPRESENTED BY EQUIVALENT STAR

Figure 4. System arrangements in which phase comparison relaying is not applicable if X_C exceeds X_L

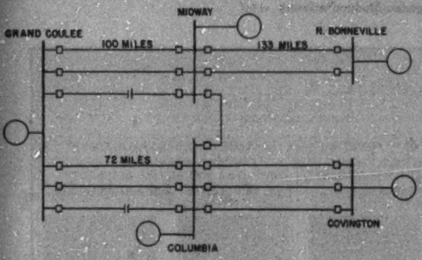

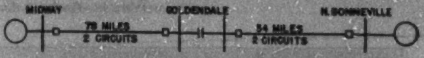

Figure 5 (left). 230-kv grid of Bonneville Power Administration

Figure 6 (above). Midway–North Bonneville system

location where the relay should close and where closing should not take place. In each case the capacitor is between the relay and the fault. Figures 2(A) and (B) show the relay quantities for the same conditions, except with a 60-degree inductive line between the relay and the fault. In Figure 2(A) the relay closing torque is maximum because the voltage and current are in phase, while in Figure 2(B) the torque is maximum in the opening direction. By comparing Figures 2(C) and (D) with (A) and (B), it is easily concluded that the directional relay indicates direction incorrectly when the circuit is capacitive between the relay and the fault.

One factor that can prevent false directional indication in a series-compensated circuit is the fact that the series capacitor is protected by a set of gaps that are adjusted to sparkover and divert current from the capacitor when the current through the capacitor exceeds $2\frac{1}{2}$ times normal. With the capacitor short-circuited, the circuit between the relay and the point of fault which was originally capacitive may now appear inductive. The speed with which the capacitor is short circuited is important, therefore, in determining correct relay operation.

The transient studies on the analogue computer were made to determine whether the operation of the gap is fast enough to cause correct relay operation, and also to study types of faults other than three phase. A large number of conditions were studied with many variables to enable an intelligent interpretation of the resulting data in terms of a prediction of the relay operation. The variables included the type of fault, the point on the voltage wave at which the fault occurs, the load current, the point of sparkover of the protective gaps, and system configuration.

A similar simple steady-state condition can be set up to show incorrect operation of phase comparison relays. If the fault is assumed to be internal on the protected line and if the reactance to one source is assumed to be capacitive and that to the other source inductive, the currents applied to the phase comparison relays at the line terminals are such that tripping does not occur. The vector diagrams of Figure 3 illustrate this condition. During normal system operation the generator internal voltages are assumed to be in phase, and if the voltages remain in the same relative phase position during the initial stages of the fault, the current to the fault through the inductive source is lagging the voltage, while the current to the fault through the capacitive source is leading the voltage. Therefore, the currents at the terminals of the line appear to the relay to be out of phase and the relay does not trip.

A similar condition arises for a line with single power source if the capacitive reactance exceeds the inductive reactance of the paralleling circuits, Figure 4(A). A more general representation applicable in the case of all generator voltages in phase is that shown in Figure 4(B), in which the entire system external to the series-compensated line is represented as an equivalent star. The branches are generally inductive. An internal fault at X will draw currents approaching 180 degrees out of phase from the two ends if the capacitive reactance, X_C, exceeds the inductive reactance, X_L, to the star point.

Similar analyses will show that the relay operates correctly for an external fault, but may not cause tripping for an internal fault. The possibility of having a capacitive circuit between the fault and one source of generation (or to the star point) is rather remote since compensation of this magnitude would seldom be encountered; therefore, it might be concluded that phase comparison relaying would in general operate correctly provided the transient conditions do not cause incorrect operation. To analyze this, records were made of the transient conditions affecting phase comparison relaying to determine the relay operation.

In addition to these relay considerations, the transients caused by operation of the capacitor by-pass equipment might affect the operation of the series-compensated system. A reinsertion transient occurs when the by-pass circuit opens and the capacitor is reinserted in the line. If the function of the capacitor is to improve transient stability, this reinsertion transient should not cause firing of the gaps to short-circuit the capacitor again. Reinsertion transients under various conditions were studied to determine the likelihood of gap firing after clearing of a fault and to determine whether the gap firing would interfere with the effectiveness of the capacitor in aiding stability.

High-speed reclosing is being applied on many high-voltage transmission lines, and it is likely that series compensation might also be used on these lines. Again it is important to know the transients caused by reclosing the series-compensated circuit and whether these transients will cause gap firing to short-circuit the capacitor. If this occurs it may cause system instability. Also, if the fault should not be cleared, the closing transients will have an effect on the system relaying.

ANALOGUE COMPUTER STUDIES

Investigations were made on the analogue computer of three possible locations of series capacitors on the 230-kv grid of the Bonneville Power Administration, Figure 5, for the purpose of studying transient phenomena occurring on systems with series compensation, and the effect of series capacitors on system relaying. The details of these studies are discussed in the following sections and in Tables I through VIII. The systems studied were represented in miniature by 3-phase 4-wire networks. The neutral impedances in the lines and at the busses were adjusted to give a correct representation of the zero-sequence impedances of the system.

The first study was made on the part of the system shown in Figure 6 in which

Table I. Analogue Computer Study—Reclosing

A. RECLOSING AFTER A SINGLE LINE-TO-GROUND FAULT WITH MAXIMUM CHARGE ON φA CAPACITOR AND ZERO CHARGE ON φB AND φC CAPACITORS. TERMINAL VOLTAGES ARE ASSUMED TO HAVE AN ANGULAR DISPLACEMENT THAT WILL GIVE A STEADY STATE CURRENT AFTER RECLOSING OF TWICE NORMAL CAPACITOR CURRENT

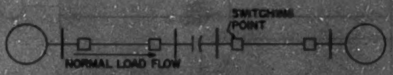

A.1-BREAKER CLOSED AT ZERO OF VOLTAGE ACROSS φA BREAKER

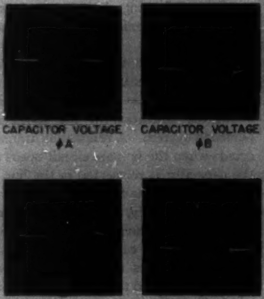

CAPACITOR VOLTAGE φA · CAPACITOR VOLTAGE φB

CAPACITOR VOLTAGE φC · φA CURRENT

VOLTAGE ACROSS φA BREAKER

A.1(a)-SAME AS A.1 WITH GAPS PERMITTED TO FIRE AT 2-1/2 TO 3 TIMES NORMAL GAP VOLTAGE. GAPS OPEN AT FIRST CURRENT ZERO AND DO NOT FIRE AGAIN. 25 OHMS IN SERIES WITH GAPS

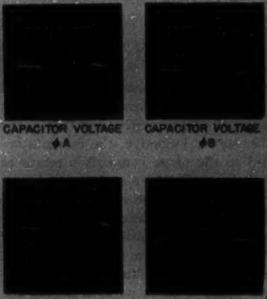

CAPACITOR VOLTAGE φA · CAPACITOR VOLTAGE φB

CAPACITOR VOLTAGE φC · φA CURRENT

A.1(b)-SAME CONDITIONS AS 1(a) EXCEPT A SECOND GAP OPERATION IS PERMITTED. GAPS IN φA AND φC FIRE AGAIN BUT φB GAP DOES NOT FIRE A SECOND TIME.

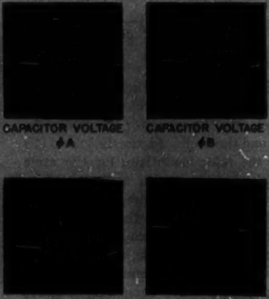

CAPACITOR VOLTAGE φA · CAPACITOR VOLTAGE φB

CAPACITOR VOLTAGE φC · φA CURRENT

A.2-BREAKER CLOSED AT CREST OF VOLTAGE ACROSS φA BREAKER CONTACTS

CAPACITOR VOLTAGE φA · CAPACITOR VOLTAGE φB · CAPACITOR VOLTAGE φC · φA CURRENT · VOLTAGE ACROSS φA BREAKER

A.2(a)-SAME CONDITIONS AS A.2 EXCEPT ONE GAP OPERATION PERMITTED IN EACH PHASE. (20-Ω IN SERIES WITH EACH GAP)

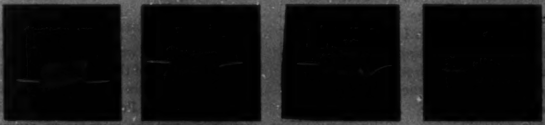

CAPACITOR VOLTAGE φA · CAPACITOR VOLTAGE φB · CAPACITOR VOLTAGE φC · φA CURRENT

A.2(b) SAME CONDITIONS AS A.2(a) EXCEPT φC GAP OPERATION NOT PERMITTED UNTIL SECOND HALF CYCLE AFTER RECLOSING.

CAPACITOR VOLTAGE φA · CAPACITOR VOLTAGE φB

A.2(c) SAME CONDITION AS A.2 WITH TWO GAP OPERATIONS PERMITTED IN EACH PHASE. ONLY ONE GAP OPERATION WAS NECESSARY IN φB

CAPACITOR VOLTAGE φA · CAPACITOR VOLTAGE φB · CAPACITOR VOLTAGE φC · φA CURRENT

CAPACITOR VOLTAGE φC

Table II. Analogue Computer Study—Reclosing and Reinsertion

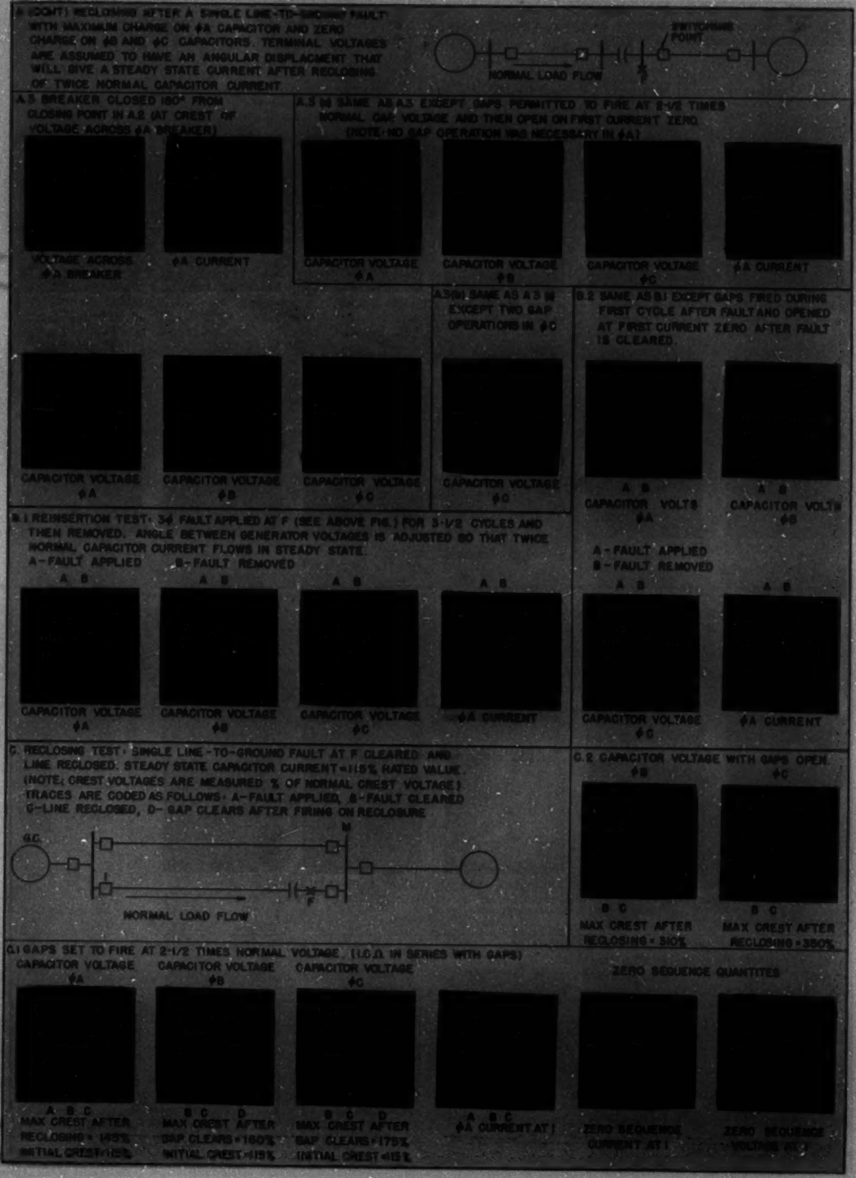

A (CONT.) RECLOSING AFTER A SINGLE LINE-TO-GROUND FAULT WITH MAXIMUM CHARGE ON ϕA CAPACITOR AND ZERO CHARGE ON ϕB AND ϕC CAPACITORS. TERMINAL VOLTAGES ARE ASSUMED TO HAVE AN ANGULAR DISPLACMENT THAT WILL GIVE A STEADY STATE CURRENT AFTER RECLOSING OF TWICE NORMAL CAPACITOR CURRENT

A.3 BREAKER CLOSED 180° FROM CLOSING POINT IN A.2 (AT CREST OF VOLTAGE ACROSS ϕA BREAKER)

A.3 (a) SAME AS A.3 EXCEPT GAPS PERMITTED TO FIRE AT 2-1/2 TIMES NORMAL GAP VOLTAGE AND THEN OPEN ON FIRST CURRENT ZERO. (NOTE: NO GAP OPERATION WAS NECESSARY IN ϕA)

A.3(b) SAME AS A.3 (a) EXCEPT TWO GAP OPERATIONS IN ϕC

B.1 REINSERTION TEST: 3ϕ FAULT APPLIED AT F (SEE ABOVE FIG.) FOR 3-1/2 CYCLES AND THEN REMOVED. ANGLE BETWEEN GENERATOR VOLTAGES IS ADJUSTED SO THAT TWICE NORMAL CAPACITOR CURRENT FLOWS IN STEADY STATE.

A–FAULT APPLIED B–FAULT REMOVED

B.2 SAME AS B.1 EXCEPT GAPS FIRED DURING FIRST CYCLE AFTER FAULT AND OPENED AT FIRST CURRENT ZERO AFTER FAULT IS CLEARED.

A–FAULT APPLIED
B–FAULT REMOVED

C. RECLOSING TEST: SINGLE LINE-TO-GROUND FAULT AT F CLEARED AND LINE RECLOSED. STEADY STATE CAPACITOR CURRENT=115% RATED VALUE. (NOTE: CREST VOLTAGES ARE MEASURED % OF NORMAL CREST VOLTAGE) TRACES ARE CODED AS FOLLOWS: A–FAULT APPLIED, B–FAULT CLEARED C–LINE RECLOSED, D–GAP CLEARS AFTER FIRING ON RECLOSURE

C.1 GAPS SET TO FIRE AT 2-1/2 TIMES NORMAL VOLTAGE. (1.6 Ω IN SERIES WITH GAPS)

C.2 CAPACITOR VOLTAGE WITH GAPS OPEN.

SWITCHING POINT
NORMAL LOAD FLOW
F
VOLTAGE ACROSS ϕA BREAKER
ϕA CURRENT
CAPACITOR VOLTAGE ϕA
CAPACITOR VOLTAGE ϕB
CAPACITOR VOLTAGE ϕC
ϕA CURRENT
CAPACITOR VOLTAGE ϕA
CAPACITOR VOLTAGE ϕB
CAPACITOR VOLTAGE ϕC
CAPACITOR VOLTAGE ϕC
A B
CAPACITOR VOLTS ϕA
A B
CAPACITOR VOLTS ϕB
A B
CAPACITOR VOLTAGE ϕA
A B
CAPACITOR VOLTAGE ϕB
A B
CAPACITOR VOLTAGE ϕC
A B
ϕA CURRENT
A B
CAPACITOR VOLTAGE ϕC
A B
ϕA CURRENT
G.C.
M
I
F
NORMAL LOAD FLOW
ϕB
B C
MAX CREST AFTER RECLOSING = 310%
ϕC
B C
MAX CREST AFTER RECLOSING = 350%
CAPACITOR VOLTAGE ϕA
A B C
MAX CREST AFTER RECLOSING = 145%
INITIAL CREST=115%
CAPACITOR VOLTAGE ϕB
B C D
MAX CREST AFTER GAP CLEARS = 160%
INITIAL CREST=115%
CAPACITOR VOLTAGE ϕC
B C D
MAX CREST AFTER GAP CLEARS = 175%
INITIAL CREST=115%
A B C
ϕA CURRENT AT I
ZERO SEQUENCE QUANTITES
ZERO SEQUENCE CURRENT AT I
ZERO SEQUENCE VOLTAGE AT I

Table III. Analogue Computer Study—Line-to-Line, Double-Line-to-Ground and 3-Phase Faults

D. 60° CONNECTION DIRECTIONAL ELEMENT QUANTITIES, $I_A - I_B$ (SMALL TRACE BEFORE THE FAULT) E_{AC}, FOR A FAULT AT HB AND RELAYS AT GL.

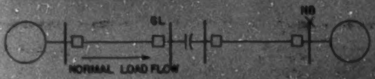

3φ FAULT NO GAPS	3φ FAULT 6 OHMS IN SERIES WITH GAPS	LINE-TO-LINE FAULT 18 OHMS IN SERIES WITH GAPS

RELAY DOES NOT GIVE A POSITIVE INDICATION OF FAULT LOCATION	RELAY CORRECTLY INDICATES AN EXTERNAL FAULT	RELAY CORRECTLY INDICATES AN EXTERNAL FAULT

LINE-TO-LINE FAULT NO GAPS	DOUBLE LINE-TO-GROUND FAULT. 25 OHMS IN SERIES WITH GAPS

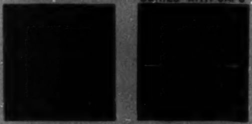

RELAY CORRECTLY INDICATES AN EXTERNAL FAULT IN BOTH OF THE ABOVE CASES.

E. 60° CONNECTION DIRECTIONAL ELEMENT QUANITIES, $I_A - I_B$ (SMALL TRACE BEFORE THE FAULT) AND E_{AC}, FOR A FAULT AT GL AND RELAYS AT GR

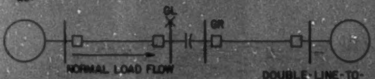

3φ FAULT 25 OHMS IN SERIES WITH GAPS	3φ FAULT 32 OHMS IN SERIES WITH GAPS	DOUBLE LINE-TO-GROUND FAULT. 25 OHMS IN SERIES WITH GAPS

RELAY ELEMENTS INCORRECTLY INDICATE AN INTERNAL FAULT

RELAY CORRECTLY INDICATES AN EXTERNAL FAULT

F. 60° CONNECTION DIRECTIONAL ELEMENT QUANTITIES, $I_A - I_B$ (SMALL TRACE BEFORE THE FAULT) AND E_{AC}, FOR A FAULT AT GR AND RELAY AT GL.

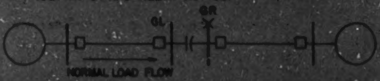

3φ FAULT AT CREST OF E NO GAPS	3φ FAULT AT ZERO OF E NO GAPS	3φ FAULT 6 OHMS IN SERIES WITH GAPS*

RELAY INCORRECTLY INDICATES AN INTERNAL FAULT

RELAY INDICATION IS INDEFINITE

* φA GAP FIRES ON SECOND HALF CYCLE AFTER FAULT.

DOUBLE LINE-TO-GROUND FAULT 25 OHMS IN SERIES WITH GAPS	LINE-TO-LINE FAULT NO GAPS	LINE-TO-LINE FAULT 18 OHMS IN SERIES WITH GAPS.

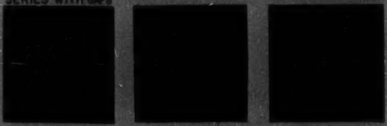

RELAY CORRECTLY INDICATES AN EXTERNAL FAULT IN THE ABOVE THREE CASES.

G. 60° CONNECTION DIRECTIONAL ELEMENT QUANTIES, $I_A - I_B$ (SMALL TRACE BEFORE THE FAULT) AND E_{AC}, FOR A FAULT AT M AND RELAYS AT GR

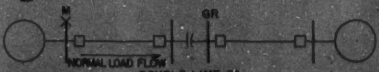

3φ FAULT 25 OHMS IN SERIES WITH GAPS	DOUBLE LINE-TO GROUND FAULT 25 OHMS IN SERIES WITH GAPS

RELAY ELEMENTS CORRECTLY INDICATE AN EXTERNAL FAULT

H. 60° CONNECTION DIRECTIONAL ELEMENT QUANTITIES, $I_A - I_B$ (SMALL TRACE BEFORE THE FAULT) AND E_{AC}, FOR A LINE TO LINE FAULT AT GR AND RELAYS AT M.

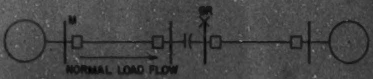

(NOTE: A FAULT AT GR SHOULD APPEAR TO BE AN INTERNAL FAULT TO RELAYS AT M)

FAULT AT ZERO OF E_{AB} 18 OHMS IN SERIES WITH GAPS	FAULT AT CREST OF E_{AB} ZERO OHMS IN SERIES WITH GAPS	FAULT AT CREST OF E_{AB} ZERO OHMS IN SERIES WITH GAPS

RELAY ELEMENTS CORRECTLY INDICATE AN INTERNAL FAULT

Table IV. Analogue Computer Study—3-Phase and Single-Line-to-Ground Faults

I. 3ϕ AND SINGLE LINE-TO-GROUND FAULTS WITH CAPACITOR IN THE CENTER OF THE COMPENSATED LINE. GAPS ARE SET TO FIRE AT 2-1/2 TIMES RATED CREST CAPACITOR VOLTAGE. CAPACITOR CURRENT BEFORE THE FAULT IS EQUAL TO RATED CURRENT.
(1.6 OHMS IN SERIES WITH CAPACITOR GAPS)

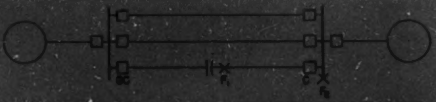

I.1 3ϕ FAULT A F_1. FAULT AT CREST OF ϕA VOLTAGE.

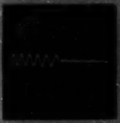
CAPACITOR VOLTAGE ϕA

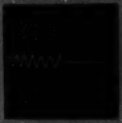
CAPACITOR VOLTAGE ϕB

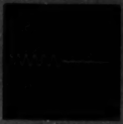
CAPACITOR VOLTAGE ϕC

NOTE THAT GAPS FLASH IN LESS THAN 1/4 CYCLE

RELAY IMPEDANCE ELEMENT-VOLTAGES AND CURRENTS AT GC.
(CURRENT IS SMALL TRACE BEFORE THE FAULT)

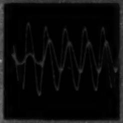
PHASE AB RELAY E_{AB} AND $I_A - I_B$

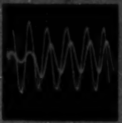
PHASE BC RELAY E_{BC} AND $I_B - I_C$

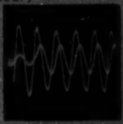
PHASE CA RELAY E_{CA} AND $I_C - I_A$

RELAY IMPEDANCE ELEMENTS WILL OPERATE CORRECTLY FOR THIS FAULT.

RELAY DIRECTIONAL ELEMENT-VOLTAGES AND CURRENTS AT GC. (60° CONNECTION)
(CURRENT IS THE SMALL TRACE BEFORE THE FAULT.)

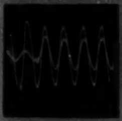
PHASE AB RELAY E_{AC} AND $I_A - I_B$

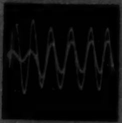
PHASE BC RELAY E_{BA} AND $I_B - I_C$

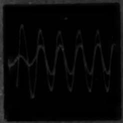
PHASE CA RELAY E_{CB} AND $I_C - I_A$

RELAY DIRECTIONAL ELEMENTS CORRECTLY INDICATE AN INTERNAL FAULT.

PHASE COMPARISON RELAY QUANTITIES PHASE A CURRENT AT GC AND C

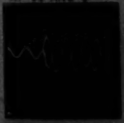
CURRENT AT GC IS POSITIVE DURING THE FIRST CYCLE AFTER FAULT. RELAY CORRECTLY INDICATES AN INTERNAL FAULT

RESIDUAL OR ZERO SEQUENCE CURRENT AT GC BUS

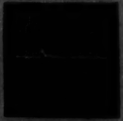
MAGNITUDE OF PULSE OF CURRENT IS APPROX 1% OF 3ϕ FAULT CURRENT CREST

I.2 3ϕ FAULT AT F_2. FAULT AT CREST OF ϕA VOLTAGE.

RELAY IMPEDANCE ELEMENT-VOLTAGES AND CURRENTS AT GC.

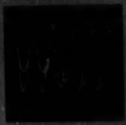
PHASE AB RELAY E_{AB} AND $I_A - I_B$

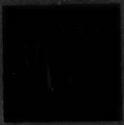
PHASE BC RELAY E_{BC} AND $I_B - I_C$

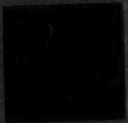
PHASE CA RELAY E_{CA} AND $I_C - I_A$

(CURRENT IS THE SMALL TRACE BEFORE THE FAULT)
RELAY IMPEDANCE ELEMENTS OPERATE CORRECTLY FOR THIS FAULT.

RELAY DIRECTIONAL ELEMENTS - VOLTAGES AND CURRENTS AT GC. (60° CONNECTION)
(CURRENT IS SMALL TRACE BEFORE THE FAULT)

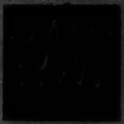
PHASE AB RELAY E_{AC} AND $I_A - I_B$

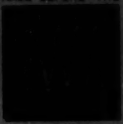
PHASE BC RELAY E_{BA} AND $I_B - I_C$

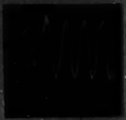
PHASE CA RELAY E_{CB} AND $I_C - I_A$

RELAY DIRECTIONAL ELEMENTS CORRECTLY INDICATE A FAULT IN THE CONTACT CLOSING DIRECTION.

PHASE COMPARISON RELAY QUANTITIES ϕA CURRENT AT GC AND C

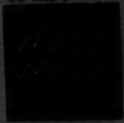
UPPER TRACE IS GC CURRENT.
RELAY CORRECTLY INDICATES AN EXTERNAL FAULT

I.3 SINGLE LINE-TO-GROUND FAULT AT F_1. FAULT AT CREST OF ϕA VOLTAGE

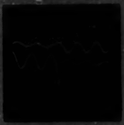
TOP-ϕA CURRENT AT GC.
BOTTOM ϕA CAPACITOR VOLTAGE. (TRACE IS INVERTED)

PHASE COMPARISON

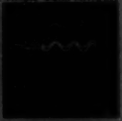
TOP: I_0 AT C
BOTTOM: I_0 AT GC
(TRACE INVERTED)
RELAY INDICATES AN INTERNAL FAULT

I.4 SINGLE LINE-TO-GROUND FAULT AT F_2 FAULT AT CREST OF ϕA VOLTAGE

TOP-I_A AT GC
BOTTOM: ϕA CAPACITOR VOLTAGE (TRACE IS INVERTED)

PHASE COMPARISON RELAY QUANTITIES

TOP-I_A AT GC
BOTTOM-I_A AT C
RELAY INDICATES AN EXTERNAL FAULT

Table V. Analogue Computer Study—3-Phase and Single-Line-to-Ground Faults

J. 3-PHASE AND SINGLE LINE-TO-GROUND FAULTS WITH THE CAPACITOR IN THE CENTER OF THE COMPENSATED LINE. CAPACITOR CURRENT BEFORE THE FAULT IS EQUAL TO RATED CURRENT. (1.6 OHMS IN SERIES WITH GAPS)

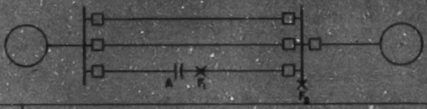

J.1 SINGLE LINE-TO-GROUND FAULT AT F_1. GAPS SET TO FIRE AT 2-1/2 TIMES RATED VOLTAGE. ANGLE OF FAULT INITIATION IS VARIED. (BOTH VOLTAGE AND CURRENT ARE ϕA QUANTITIES)

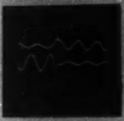

FAULT AT 0° ON PHASE A VOLTAGE
TOP: I_A AT A.
BOTTOM CAPACITOR VOLTAGE (INVERTED)

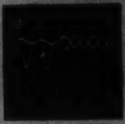

FAULT AT 45° ON PHASE A VOLTAGE

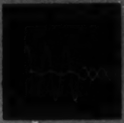

FAULT AT 225° ON PHASE A VOLTAGE

SMALL TRACE BEFORE FAULT IS I_A AT A. LARGE TRACE IS THE CAPACITOR VOLTAGE (INVERTED)

J.2 THREE PHASE FAULT AT F_2. FAULT AT CREST OF PHASE A VOLTAGE. GAP SETTING IS VARIED.

GAP FIRES AT 1-1/4 TIMES NORMAL CREST.
TOP: I_A AT A
BOTTOM: ϕA CAP. VOLTAGE (INVERTED)
GAP FIRES IN 1/4 CYCLE

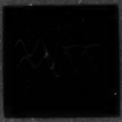

GAP FIRES AT 3-3/4 TIMES NORMAL CREST.
TOP ϕA CAPACITOR VOLTAGE (INVERTED)
BOTTOM: I_A AT A
GAP FIRES IN 0.9 CYCLE

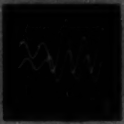

NO GAP
TOP: ϕA CAPACITOR VOLTAGE (INVERTED)
BOTTOM: I_A AT A

K. THREE PHASE FAULT AT F WITH CAPACITOR AT THE END OF THE COMPENSATED LINE. CAPACITOR CURRENT BEFORE THE FAULT IS AT RATED VALUE. RELAY QUANTITIES ARE MEASURED AT C ON AN UNCOMPENSATED LINE.

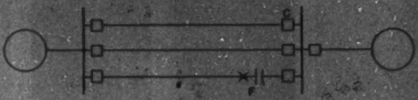

K.1 GAPS ARE NOT ALLOWED TO FIRE.

ϕA CAPACITOR VOLTAGE

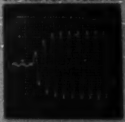

VOLTAGE RISES TO 25 TIMES NORMAL

A-B RELAY DIRECTIONAL ELEMENTS

TOP: $I_A - I_B$
BOTTOM: E_{AC}

NOTE: THE EQUIVALENT SYSTEM LOOKING TOWARD THE CAP. FROM F IS NEAR SERIES RESONANCE. THE DIRECTIONAL ELEMENT AT C INCORRECTLY INDICATES AN INTERNAL FAULT.

K.2 GAPS SET TO FIRE AT 2-1/2 TIMES NORMAL CREST CAPACITOR VOLTAGE.

DIRECTIONAL A-B RELAY

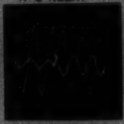

CURRENT $I_A - I_B$
VOLTAGE E_{AC}

ELEMENTS B-C RELAY

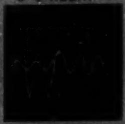

CURRENT $I_B - I_C$
VOLTAGE E_{BA}

DIRECTIONAL ELEMENTS CORRECTLY INDICATE AN EXTERNAL FAULT.

IMPEDANCE A-B RELAY

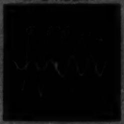

CURRENT $I_A - I_B$
VOLTAGE E_{AB}

ELEMENTS B-C RELAY

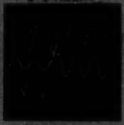

CURRENT $I_B - I_C$
VOLTAGE E_{BC}

IMPEDANCE ELEMENTS OPERATE CORRECTLY TO INDICATE A FAULT.

CURRENT IS THE SMALL TRACE BEFORE THE FAULT AND LARGE TRACE AFTER THE FAULT.

L. GAP FIRING DURING A TRANSIENT SWING. THE ANGULAR POSITION OF THE TWO GENERATORS IS ADJUSTED TO GIVE 2-1/2 TIMES NORMAL CAPACITOR CURRENT. ϕA CAPACITOR GAP WAS THEN SHORTED AT 0.866 OF CREST VOLTAGE ACROSS THE CAPACITOR.

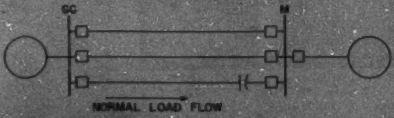

NEUTRAL OR RESIDUAL CURRENT IN THE COMPENSATED LINE

STEADY STATE VALUE IS 23% OF NORMAL CAPACITOR CURRENT

Table VI. Analogue Computer Study—3-Phase Faults

M. 3φ FAULT AT F AT MINIMUM SYSTEM CONDITION
FAULT AT CREST OF φA VOLTAGE.
1.6 OHMS IN SERIES WITH GAPS.

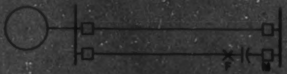

M.1 NO GAP OPERATIONS PERMITTED

CAPACITOR VOLTAGE

MAXIMUM VOLTAGE IS GIVEN IN PERCENT OF CREST OF RATED CAPACITOR VOLTAGE.

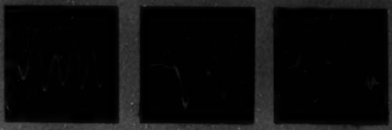

φA MAX VOLTS = 267%

φB MAX VOLTS = 333%

φC MAX VOLTS = 269%

RELAY DIRECTIONAL ELEMENTS – 60° CONNECTION (RELAY AT M)

TOP: $I_A - I_B$ BOTTOM: E_{AC}

TOP: $I_B - I_C$ BOTTOM: E_{BA}

TOP: $I_C - I_A$ BOTTOM: E_{CB}

DIRECTIONAL ELEMENTS INCORRECTLY INDICATE AN EXTERNAL FAULT.

M.2 φB GAP FIRES AT 2-1/2 TIMES NORMAL CAPACITOR VOLTAGE.

CAPACITOR VOLTAGE

MAXIMUM VOLTAGE IS GIVEN IN PERCENT OF CREST OF RATED CAPACITOR VOLTAGE.

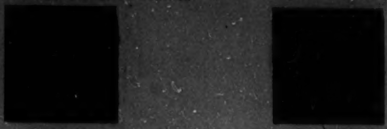

φA MAX VOLTS = 244%

φC MAX VOLTS = 378%

NOTE THAT THE MAXIMUM φC VOLTAGE AFTER ONE GAP (φB) HAS OPERATED IS GREATER THAN THE VOLTAGE WITH NO GAP OPERATIONS.

RELAY DIRECTIONAL ELEMENTS 60° CONNECTION (RELAY AT M)

TOP: $I_A - I_B$ BOTTOM: E_{AC}

TOP: $I_B - I_C$ BOTTOM: E_{BA}

TOP: $I_C - I_A$ BOTTOM: E_{CB}

DIRECTIONAL ELEMENTS INCORRECTLY INDICATE AN EXTERNAL FAULT.

RELAY DIRECTIONAL ELEMENTS 90° CONNECTION (RELAY AT M)

TOP: I_A BOTTOM: E_{BC}

TOP: I_B BOTTOM: E_{CA}

TOP: I_C BOTTOM: E_{AB}

I_A AND I_C ELEMENTS INDICATE AN EXTERNAL FAULT WHILE THE I_B ELEMENT CORRECTLY INDICATES AN INTERNAL FAULT.

NEUTRAL CURRENT

STEADY STATE I_N = 4.8 TIMES RATED CAPACITOR CURRENT.

M.3 φB GAP AND THEN φC GAP FIRE AT 2-1/2 TIMES CREST OF RATED CAPACITOR VOLTAGE.

RELAY DIRECTIONAL ELEMENTS 60° CONNECTION (RELAY AT M)

TOP: $I_A - I_B$ BOTTOM: E_{AC}

TOP: $I_B - I_C$ BOTTOM: E_{BA}

TOP: $I_C - I_A$ BOTTOM: E_{CB}

THE $I_A - I_B$ ELEMENT DOES NOT GIVE A POSITIVE INDICATION OF FAULT DIRECTION WHILE THE $I_B - I_C$ ELEMENT CORRECTLY INDICATES AN INTERNAL FAULT AND THE $I_C - I_A$ ELEMENT INCORRECTLY INDICATES AN EXTERNAL FAULT.

RELAY DIRECTIONAL ELEMENT 90° CONNECTION (RELAY AT M)

TOP: I_A BOTTOM: E_{BC}

TOP: I_B BOTTOM: E_{CA}

TOP: I_C BOTTOM: E_{AB}

I_A ELEMENT INCORRECTLY INDICATES AN EXTERNAL FAULT WHILE I_B AND I_C ELEMENTS INDICATE AN INTERNAL FAULT.

NEUTRAL CURRENT

STEADY STATE I_N = 2.95 TIMES RATED CAPACITOR CURRENT.

Table VII. Analogue Computer Study—3-Phase Faults

N.3ϕ FAULT AT F AT MINIMUM SYSTEM CONDITION. FAULT AT ZERO [illegible]
ϕA VOLTAGE. 1.6 OHMS IN SERIES WITH GAPS.

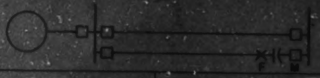

N.1 NO GAPS OPERATE

CAPACITOR VOLTAGE

RATED CREST CAPACITOR VOLTAGES = 1.0 PU

RELAY DIRECTIONAL ELEMENTS – 60° CONNECTION
(RELAY AT M)

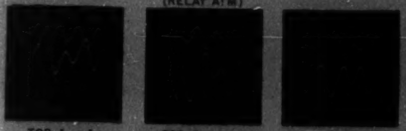

RELAY ELEMENTS INCORRECTLY INDICATE AN EXTERNAL FAULT

RELAY DIRECTIONAL ELEMENTS – 90° CONNECTION
(RELAY AT M)

RELAY ELEMENTS INCORRECTLY INDICATE AN EXTERNAL FAULT

N.3 ϕA GAP AND LATER ϕB GAP FIRE AT 2-1/2 TIMES RATED CAPACITOR VOLTAGE

CAPACITOR VOLTAGE

RATED CREST CAPACITOR VOLTAGE = 1.0 PU

ϕC VOLTAGE IN THIS TEST IS GREATER THAN ϕC VOLTAGE WHEN ONLY ONE GAP, ϕA, HAS FIRED (SEE TEST A.2)

RELAY DIRECTIONAL VOLTAGE – 60° CONNECTION
(RELAY AT M)

$I_A - I_B$ ELEMENT INCORRECTLY INDICATES AN EXTERNAL FAULT. $I_B - I_C$ ELEMENT CORRECTLY INDICATES AN INTERNAL FAULT. $I_C - I_A$ ELEMENT DOES NOT GIVE A POSITIVE INDICATION OF FAULT DIRECTION.

RELAY DIRECTIONAL ELEMENTS – 90° CONNECTION
(RELAY AT M)

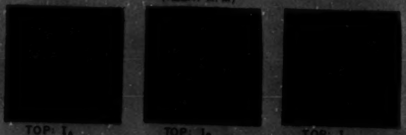

RELAY ELEMENTS INCORRECTLY INDICATE AN EXTERNAL FAULT

NEUTRAL CURRENT

THIS CURRENT IS CAUSED BY NONSIMULTANEOUS SHORTING OF THE PHASES WHEN THE 3 PHASE FAULT IS APPLIED TO THE SYSTEM

N.2 ϕA GAP FIRES AT 2-1/2 TIMES RATED CAPACITOR VOLTAGE

CAPACITOR VOLTAGE

RATED CREST CAPACITOR VOLTAGE = 1.0 PU. ϕB VOLTAGE FOR THIS TEST IS GREATER THAN ϕB VOLTAGE IN TEST A1. (NO GAPS FIRING.) ϕC VOLTAGE IS LESS THAN ϕC VOLTAGE IN TEST A1.

NEUTRAL CURRENT

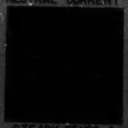

STEADY STATE I_N = 5.15 TIMES RATED CAPACITOR CURRENT

NEUTRAL CURRENT

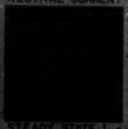

STEADY STATE I_N = 2.94 TIMES RATED CAPACITOR CURRENT

Table VIII. Analogue Computer Study—3-Phase Faults and Reclosing

O. 3φ FAULT AT F WITH REDUCED GENERATION AT B. FAULT AT 90° ON φA VOLTAGE. NO GAPS FIRE.

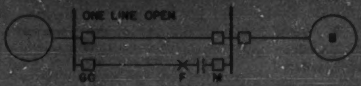

VOLTAGE ACROSS CAPACITORS

MAXIMUM VOLTAGE IS GIVEN IN % OF RATED CREST CAPACITOR VOLTAGE.

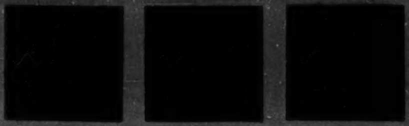

φA MAX = 278 %

φB MAX = 333 %

φC MAX = 333 %

FOR THE PURPOSES OF THIS TEST IT WAS ASSUMED THAT THE GAPS DID NOT FIRE.

RELAY DIRECTIONAL ELEMENTS 90° CONNECTION
(RELAYS AT M)

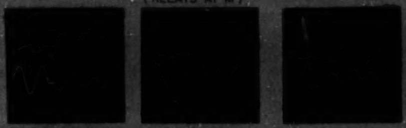

TOP: I_A BOTTOM: E_{BC}

TOP: I_B BOTTOM: E_{CA}

TOP: I_C BOTTOM: E_{AB}

RELAYS INCORRECTLY INDICATE AN EXTERNAL FAULT.

RELAY DIRECTIONAL ELEMENTS 60° CONNECTION
(RELAYS AT M)

TOP: $I_A - I_B$ BOTTOM: E_{AC}

TOP: $I_B - I_C$ BOTTOM: E_{BA}

TOP: $I_C - I_A$ BOTTOM: E_{CB}

RELAYS INCORRECTLY INDICATE AN EXTERNAL FAULT

RELAY IMPEDANCE ELEMENT
(RELAYS AT M)

TOP: $I_A - I_B$ BOTTOM: E_{AB}

TOP: $I_B - I_C$ BOTTOM: E_{BC}

TOP: $I_C - I_A$ BOTTOM: E_{CA}

RELAY CORRECTLY MEASURES THE IMPEDANCE OF THE SERIES CAPACITOR

PHASE COMPARISON RELAY

TOP: I_A AT GC
BOTTOM: I_A AT M

RELAY CORRECTLY INDICATES AN INTERNAL FAULT

P. RECLOSING ON A 3φ FAULT AT F. BREAKER AT GC CLOSES AT CREST OF φA VOLTAGE. GAPS FIRE AND THEN OPEN ON FIRST CURRENT ZERO.

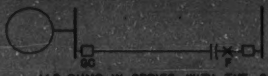

(1.6 OHMS IN SERIES WITH THE GAPS)

CAPACITOR VOLTAGES AND GAP CURRENTS.

PEAK GAP CURRENT IS GIVEN IN PER UNIT OF THE CREST OF RATED CAPACITOR CURRENT.

φA TOP: GAP CURRENT 20.6 P.U.
BOTTOM: CAP VOLTS

φB CAPACITOR VOLTAGE

φC TOP: CAP VOLTS
BOTTOM: GAP CURRENT = 22 P.U.

RELAY DIRECTIONAL ELEMENTS - 90° CONNECTION
(RELAYS AT GC)

TOP: I_A BOTTOM: E_{BC}

TOP: I_B BOTTOM: E_{CA}

TOP: I_C BOTTOM: E_{AB}

ALL ELEMENTS CORRECTLY INDICATE AN INTERNAL FAULT

RELAY DIRECTIONAL ELEMENTS 60° CONNECTION
(RELAYS AT GC)

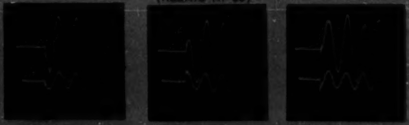

TOP: $I_A - I_B$ BOTTOM: E_{AC}

TOP: $I_B - I_C$ BOTTOM: E_{BA}

TOP: $I_C - I_A$ BOTTOM: E_{CB}

ALL ELEMENTS CORRECTLY INDICATE AN INTERNAL FAULT

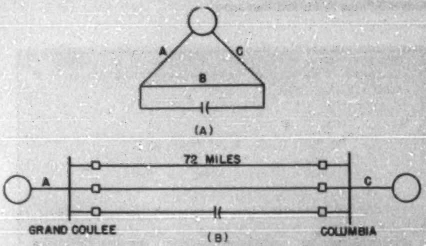

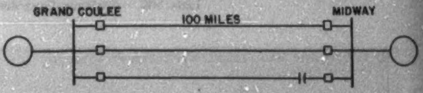

Figure 7 (left). Grand Coulee–Columbia system

Figure 8 (above). Grand Coulee–Midway system

a series capacitor was considered at Goldendale near the center of the double-circuit line between Midway and North Bonneville. The capacitor was adjusted to give approximately 50 per cent compensation of the Midway to North Bonneville lines. Consequently, the circuit from the left Goldendale bus to North Bonneville is capacitive while the circuit from the right Goldendale bus to Midway is inductive. With fixed system constants studies were made for various locations and types of faults as well as various locations of relays. Reclosing and capacitor reinsertion phenomena were also studied on this system. The latter phenomenon occurs when the capacitor has been shorted by gaps during a fault. The gaps open after the fault is cleared and reinsert the capacitor in the line.

The second capacitor location studied was in one of the lines between Grand Coulee and Columbia, Figure 7. This line has a larger conductivity than the other two lines between these points; therefore, a series capacitor is to be installed in the line to reduce its reactance and cause it to carry a share of the total load current proportionate to its capability. The system studied on the computer was derived from the actual power system of Figure 5 by representing all the power system exclusive of compensated Grand Coulee to Columbia line by an equivalent delta, Figure 7(A). The impedances *A* and *C* then represented the system equivalent impedances to the Grand Coulee and Columbia busses with the three Coulee to Columbia lines open. *B* represented the two uncompensated Coulee to Columbia lines. This is shown in Figure 7(B). Studies were made on this system with the capacitor located at the Columbia bus as well as in the center of the compensated line as shown in Figure 7(B). In both cases the capacitor was adjusted to compensate for 36 per cent of the total inductance of the Grand Coulee to Columbia line.

The third series capacitor location studied was in one of the Grand Coulee to Midway lines. As in the above case, a capacitor is to be placed in the line to cause proper division of load current between the three parallel lines. In this study, it was assumed that the Columbia to Midway line was open, thereby isolating the top half of the 230-kv grid in Figure 5. A single-line diagram of the system studied is shown in Figure 8. In addition to studying the system shown in Figure 8, one of the uncompensated Grand Coulee–Midway lines was considered open and the generation connected to the Midway bus was reduced or removed in certain of the studies to represent minimum system conditions. In all cases the capacitor compensated for 40 per cent of the inductance of the compensated Grand Coulee to Midway line

In all of the above studies provision was made for measuring directly the voltages and currents applied to the relays as well as capacitor and system voltages and currents. These measurements were recorded by photographing the oscilloscope traces of the various currents and voltages. These photographs together with a brief description of the test and analysis of the results are given in Tables I through VIII. When analyzing the photographs of relaying quantities, the following facts should be kept in mind.

1. Sixty-degree connection directional elements receive maximum closing torque when the relay voltage and current are in phase.

2. Ninety-degree connection directional elements receive maximum closing torque when the relay current leads the relay voltage by 35 to 40 degrees.

3. Phase comparison relays receive maximum contact-closing torque when the relay currents are 180 degrees out of phase. Tripping will take place when the currents are more than approximately 50 degrees out of phase. The currents used with phase comparison relays are weighted combinations of the positive, negative, and zero sequence currents at the two ends of the protected lines. However, in the computer studies the phase *A* current at the two ends of the protected line was used to determine the performance of the phase comparison relays. This gave a correct indication of the actual relay currents since the positive, negative, and zero sequence currents are in phase with the phase *A* current for 3-phase faults and single-line-to-ground faults on phase *A*.

4. In the tables the directional and phase-comparison relays are said to indicate an internal fault when they produce contact-closing torque in accordance with the above statements.

5. In certain studies it was necessary to invert, that is turn upside down, one of the traces to prevent shorting the analogue through the recording circuit. Where this is the case, it has been noted in the tables. When analyzing a photograph of this type, the phase relations for maximum closing torque discussed in 1, 2, and 3 should be increased by 180 degrees.

Results of the Analogue Computer Studies

The studies made on the analogue computer are completely covered in Tables I through VIII. These tables give a diagram of the system studied, the specific conditions investigated in the tests, and photographs of the measured quantities. In conjunction with the photographs, some of the important results are briefly pointed out in the tables. The following discussion describes some of the major points studied; however, the reader should refer to the tables for the details of the computer studies.

Tables I and II give the results of the reclosing and reinsertion tests on the Midway–North Bonneville and Coulee–Columbia systems. The purpose of these tests was to show the form of the transient voltage across the capacitor when it was reinserted in the line or when the line was reclosed after a fault. Tests A and C show that the transient following reclosing of the line may cause the voltage across the capacitor to exceed $2^{1}/_{2}$ times normal and consequently cause the gaps to fire. However, the transient voltage across the capacitor following clearing of the gaps will not cause the gaps to fire a second time; therefore, only one gap operation will usually occur following reclosure of the line.

The tests in Table III show the effect of the series capacitor in the Midway to North Bonneville line on a relay directional element with a 60-degree connection during 3-phase, double-line-to-ground, and line-to-line faults. The relay operation is correct for all of the double-line-to-ground and line-to-line faults and for the 3-phase faults when the circuit between the relay and the fault is inductive. In Tests D, E, and F the circuit between the relay and the fault was capacitive. Without gaps the relay operation was incorrect. However, the use of gaps with low series resistance tended to correct the operation of the relays for these cases.

Tests I through K in Tables IV and V, applying to the Grand Coulee–Columbia compensated line, show the relay operation for 3-phase and single-line-to-ground faults with a low resistance in series with the capacitor gaps. In Tests I and K the gaps fire in less than 1/4 cycle and the relay operation is correct. The angle of fault initiation and the firing voltage of the gaps were varied in Test J. The latter test showed that with the gaps set to fire at $3^3/_4$ times normal crest capacitor voltage, the gaps failed to fire until the second half cycle of fault voltage with a 3-phase fault. This delay in gap firing might affect the relay operation in cases where the gaps must fire to insure correct relay performance. Such cases did not occur in this test.

Since the firing of the protective gaps is controlled solely by the voltage across the protected capacitor, they may fire in an unsymmetrical fashion; that is, one or two of the gaps may fire while the remaining gap stays open. When this occurs during faults not involving ground or during a transient swing of the system, negative and zero sequence currents are introduced into the system, causing possible misoperation of ground relays. Test L, Table V, shows the zero-sequence current introduced into the system when one gap fires during a transient swing of the system. This test was made on the Grand Coulee–Midway compensated system.

Continuing the study of relay operation during abnormal operation of the protective gaps, Tables VI and VII contain tests made at minimum system condition of the Grand Coulee–Midway compensated system. During this condition the 3-phase fault currents are low; therefore, any number of gaps might fire during a 3-phase fault. These tests show that if one gap fires, the voltage is increased on one of the remaining gaps, and if this gap fires the voltage is increased on the last gap. Thus, there is a tendency for all three gaps to fire if one gap fires for this system condition. These tests also provide a comparison of the results obtained by applying a fault at the zero of the phase *A* voltage with those obtained for a fault at the crest of the phase *A* voltage.

The incorrect operation of directional elements of the phase relays when the impedance between the relay and a 3-phase fault is capacitive is demonstrated in Test O, Table VIII. In this test it is assumed that none of the protective gaps fire.

Test P on the same table shows correct operation of the directional elements when the source is reclosed on a 3-phase fault. Air is assumed to be flowing in the gap when the line is reclosed; therefore the gap opens on the first current zero after it fires. Both of Tests O and P were run on the Grand Coulee–Midway compensated system.

Effect of Series Compensation on Protective Relay Performance

The protective-relay application problems introduced by series compensation and by the operation of the associated protecting gaps have already been outlined. The computer studies covering the various critical situations have been described and the action in each individual case detailed in the Tables I through VIII. It is the purpose of this section to review and interpret these individual findings as they apply to the various types of line-protective relays in common use.

PHASE COMPARISON CARRIER RELAYS

These relays compare the phase of the currents at the two ends of a transmission line via a carrier (or equivalent pilot) circuit and trip if the currents are of fault magnitude and are more than approximately 50-degrees apart. Normal-load currents entering one end and leaving the other are in phase except for line-charging current.

For all through-fault conditions in which the fault is external to the series-compensated line, no appreciable phase differences were expected or observed. Thus phase-comparison relays may be used on the series-compensated line or on adjacent lines without any hazard of misoperation for faults external to the series-compensated line. This is without regard to the amount of compensation or to the nature of gap operation, and includes consideration of faults, load swings, and reclosing. Typical computer results demonstrating this condition are given in Tests I.2 and I.4, Table IV.

For internal faults on the compensated line, correct operation is indicated for phase-comparison relays on all adjacent lines. However, a failure to trip for the internal fault may occur if the compensation results in net capacitive reactance from the fault to one of the sources, or to the equivalent-system star point, as outlined in the introduction.

For small amounts of compensation such as used for equalizing line loading, this possibility can usually be ruled out by a quick inspection of the impedance diagram. In fact, with the capacitor in the middle of the line and of less than 50 per cent of line reactance, there is no fault location for which the impedance is capacitive from fault to either line terminal, and hence it cannot be capacitive to a source or star point. Test O, Table VIII, and Tests I.1 and I.3, Table IV, are illustrative cases of correct internal fault operation of phase-comparison relays when the compensation leaves both sources inductive for all internal faults.

It is important to note that if this single condition is met (reactance to both sources inductive for all fault locations) then the series compensation introduces no restrictions whatever on the use of phase-comparison relays, either on the compensated line or on neighboring lines.

The condition must be tested for both positive and zero sequence currents as the phase-comparison relays respond to positive-sequence currents for 3-phase faults and largely to zero-sequence currents for single-line-to-ground fault.

REACTANCE TO A SOURCE OR STAR POINT CAPACITIVE

When one path for fault current flow is inductive and the other capacitive, the relative phases of currents at the two ends of the line for an internal fault is approximately the same as obtained for an external fault. The phase-comparison relay then fails to trip for the internal fault unless some further influence comes into play. The capacitor protective gap may operate removing temporarily the series compensation and permitting normal operation of the relays. To prove safe operation in this mode, it is necessary to check that for all fault locations, either on the compensated line or its neighbors, where the impedance to one source may be capacitive, and if phase-comparison relays are depended on to trip for that fault, that sufficiently fast gap operation will be obtained to meet the relaying needs at the currents corresponding to the relay settings. It must further be checked that the gap resistances are sufficiently low that the currents are more than 50* degrees out of phase after gap operation (calling through-fault currents in phase). The check must be made independently for phase faults and ground faults since the fault area in which the reactance to one source may be negative will differ for the two types of faults.

---

*Check value for individual relay.

Thus the gap operation may result in satisfactory phase-comparison relay operation even in some cases where the reactance to one source or the star point is capacitive.

DIRECTIONAL COMPARISON CARRIER RELAYING

This type of relaying depends for its operation on comparison of the measured fault current directions at the two ends of the line. It usually requires also the operation of fault detectors which rule out tripping on low magnitude currents or high impedances. The effects of series compensation of lines to be considered are therefore of three general varieties.

1. Wrong indications given to directional elements due to having capacitive reactance from a bus to a fault.
2. Circulating currents due to the series unbalance occasioned by unsymmetrical gap operation.
3. The shifting line impedance as the gaps cut in or out, and its effect on distance relay setting co-ordination.

For directional-comparison relays to be entirely in the clear, it is necessary to demonstrate their substantial immunity, in the particular application, to these three phenomena. Not only relays on the compensated line, but also on neighboring lines may be affected and should be checked for these three possible influences. Applications will now be considered with respect to these three problems, in order.

Most serious is the possible wrong indication to directional elements. This occurs for the phase relays if the reactance from the relay to the fault is capacitive. It occurs for residual relays if the reactance from the relay to the source is capacitive. Relay directions are all based on these reactances being inductive, and this relationship must be retained since most of the circuits will be inductive even when a few capacitive circuits are introduced into the system.

This problem is completely eliminated in those cases where the capacitor is located in the middle of the line and compensates less than 50 per cent of the line reactance. For then the impedance from any relay to any fault or to any source is inductive. Test I, Table IV, shows illustrative cases of successful directional element functioning under this condition.

The next possibility is that even though a capacitive circuit exists from a relay to a fault (or to the source for residual relays), gap operation will occur with sufficient rapidity to prevent any misoperations. The first and simplest thing to investigate is the possibility of a fault for which no gap operation is obtained. If such is likely for conditions under which the tripping of the wrong lines would not be permissible, a change must be made either in the relaying or capacitor application, and it would be worthless to go further into gap operation for this case.

For phase relays the worst condition will be a minimum fault, possibly under an emergency or test condition which results in currents too low to operate the gaps. For residual relays a ground fault, with resistance reducing the current to the minimum trip of the relays, might be considered. The gap voltage can then be calculated from the resulting line currents. If this voltage exceeds the gap operating voltage by a reasonable margin, the computer studies indicate correct directional indications. This is further predicated on the resistance in series with the gap being low enough so that the circuit becomes definitely inductive when the gap operates.

Correct directional operations dependent on gap operation are shown in Test K, Table V. Incorrect directional operation in event of no gap operation or partial gap operation is shown in Test K.1 of Table V, VI, and VII, and Test O of Table VIII. Cases of incorrect directional operation even with gaps, but due to too high series gap resistance are shown in Tests D, E, and F of Table III.

SERIES UNBALANCE AND CIRCULATING CURRENT

The adverse effects of circulating residual current induced from another line, or introduced by a series unbalance are quite well known. When residual current simply flows through a line to a fault, the polarizing and line current directions are respectively "up and in" at the sending, "up and out" at the receiving end, the latter "pointing out" and giving a correct blocking signal.

The circulating residual current, however, is "up and in" at one end, "down and out" at the other. Both ends "point in" and there is no blocking action. If the current is large enough a faulty trip results.

The simplest example of this action for a series-compensated line is when but one gap operates for a heavy load swing or a remote 3-phase fault. This introduces a series source of residual voltage on the line and results in circulating current both in the compensated line and in parallel lines. The directions are such as to cause a faulty tripping. Correct discrimination therefore depends purely on magnitude of the resulting circulating current. For the case studied the circulating current in the compensated line amounted to 23 per cent of the capacitor full-load current and is shown in Test L of Table V. This was taken for the largest swing that might result in operating only one gap. If more gaps operate, the residual current is reduced. Currents in the parallel lines are much less than in the compensated line; the proportion can be readily estimated from the zero-sequence diagram.

A residual current of the same order of magnitude but of very short duration is obtained due to the sequential operation of gaps even for very high 3-phase currents. Such a case is shown in Test I of Table IV.

Thus assurance of correct operation from the standpoint of circulating current requires that the residual relays have current settings above the maximum circulating current that can be occasioned by operation of a single gap. This in turn occurs for a 3-phase current that results in a capacitor voltage just equal to the gap setting. A suitable margin must of course be allowed.

LINE IMPEDANCE CHANGES

This phenomenon is quite obvious and mainly requires that the fault detectors have sufficient reach even with the compensation nullified by gap operation. In the case of the first-zone distance elements, if their settings are based on the compensated line impedance, their reach will be foreshortened when the gaps operate. However, if dependence is placed on gap operation and the first-zone elements set for the uncompensated value, then study must be given to the possible overtripping in event of minimum system conditions that do not operate the gaps.

OTHER RELAYS

The phenomena described for phase-comparison relays may also occur in connection with any differential relays whose protective zone includes the series capacitors. Such might include differential protection around the capacitor itself, or pilot wire relays of the current differential type.

Two of the three phenomena discussed in connection with directional-comparison carrier relays, namely possible directional element misoperation, and change in reach of distance elements, apply equally well to directional and distance elements not involving carrier or equivalent pilot channels.

Conclusions

The economy of series compensation and the benefits to be obtained have been demonstrated in prior studies. This critical examination of the transient conditions, coupled with tests which have now been completed on the Chehalis unit of the Bonneville Power Administration, show that correct operation will be obtained during faults and reclosing provided proper consideration is given to the following points. This list does not include the usual application considerations such as voltage rating, current rating, and gap settings.

1. *Is the capacitive reactance less than the inductive reactance to a source (or the equivalent system star point)?*

If so, phase-comparison relays will trip correctly for internal faults on the series compensated line.

If not, they may fail to trip if internal faults can occur for which X_C exceeds X_L and the capacitor protective gaps do not operate.

Control is by capacitor location, gap settings, or type of relaying.

2. *Is the reactance capacitive from a system bus to any fault location? This will always occur if the capacitor is at the bus but may be avoided if the capacitor is in the middle of the line and the compensation less than 50 per cent of the line.*

If the bus-to-fault reactance may be capacitive, there is a possibility of misoperation of all directional elements of relays at that bus whether voltage or current polarized, and whether associated with the compensated line or others. The worst case is a capacitor adjacent to the bus, a 3-phase fault just beyond, and fault current too low to operate the gaps. The bus voltage is reversed to its usual phase for fault in the same location but inductive reactance between bus and fault. If the bus-to-fault reactance is always inductive, this relay problem does not exist.

Between these two simple limits are many intermediate cases in which the success hinges on gap operation, relay characteristics, and type of fault, which are treated in detail in the paper.

It is important to note that phase-comparison relaying is immune to this difficulty.

3. *Is the circulating zero-sequence current occasioned by single-phase gap operation sufficient to trip residual relays falsely?*

A severe case is a system swing or remote 3-phase fault that operates one gap but not the other two. This will circulate residual currents in directions to trip in the compensated and also in paralleling circuits. The magnitude is calculable and must be checked against the residual relay settings.

Intermediate cases are discussed in the paper and hinge on type of fault, system impedances, relay time characteristics, and nature of gap operation.

Heavy phase fault current causing gap operation in all faulted phases may cause a "flick" of residual current due to the difference in gap operating times. Usually the combined magnitude and duration is too small to cause operation of relays. The magnitudes encountered in the computer study being from 1 to 5 per cent of the 3-phase fault current for a severe case.

4. *Has due account been taken of the change in impedance measured by distance relays with the capacitor shorted out or in circuit?*

Carrier distance elements must reach through the section for both conditions. First zone elements must have settings based on the reduced or compensated impedance unless there is positive assurance of fault gap operation for all first zone faults. Even then a slight delay may be necessary depending on the relay and system characteristics.

5. *Is the zero-sequence impedance capacitive from any bus to its source?*

If so, the possible misoperation of residual directional relays must be checked, since zero-sequence voltage is the drop from bus to the source rather than from bus to the fault. Such a condition may generally be ruled out by quick inspection of the impedance diagram and is mentioned here mainly for completeness.

6. *Will the gaps clear after a reclosure under heavy load swings?*

The steady capacitor voltage is never reached without passing through a higher value. This gave concern lest re-energizing during a swing would cause gap operation, arc extinction, reignition, and so forth. The computer studies showed that this did not occur for quite high swing loads, in fact for the highest that could be encountered over the comparatively long lines in question. The gaps always cleared on the reclosure, even though a gap firing occurred due to the reclosing transient.

References

1. Series Capacitor for Transmission Circuits, E. C. Starr, R. D. Evans. *AIEE Transactions*, volume 61, 1942, pages 963–73.

2. Characteristics of 400-Mile 230-Kv Series-Capacitor-Compensated Transmission System. B. V. Hoard. *AIEE Transactions*, volume 65, 1946, pages 1102–14.

3. Steady-State and Transient Stability Analysis of Series Capacitors in Long Transmission Lines, J. W. Butler, J. E. Paul, T. W. Schroeder. *Electrical Engineering (AIEE Transactions)*, volume 62, February 1943, pages 58–65.

4. Fundamental Effects of Series Capacitors in High-Voltage Transmission Lines, A. A. Johnson, J. E. Barkle, D. J. Povejsil. *AIEE Transactions*, volume 70, part I, 1951, pages 526–36.

5. A 24,000-Kilovar Series Capacitor in a 230-Kv Transmission Line, R. E. Marbury, F. D. Johnson. *AIEE Transactions*, volume 70, part II, 1951, pages 1621–26.

Discussion

J. R. Curtin and **C. C. Diemond** (Bonneville Power Administration, Portland, Oreg.): We were very pleased to notice the close agreement between conclusions reached through these analogue studies and those reached by system tests.

We appreciate the magnitude of the problem undertaken by Messrs. Harder, Barkle, and Ferguson in analyzing system and relay performance for a series-compensated system.

We believe that the authors will agree that, in general, analogue studies of this type will lack conclusiveness because of the multiplicity of parameters and the difficulty of duplicating performance of the actual system elements. Potential devices with their tuned circuits, the magnetizing characteristics of transformer and corona effects are examples of nonlinear system elements difficult of representation. In the final analysis, analogue studies can give only an indication. The final answer must come from actual operation and tests of the equipment in service.

As an additional example, the performance of protective relays with their inertia and resulting time delays are difficult to predict. We believe that, in general, the effect of relay inertia will be in the direction to improve operation during transients in a series-compensated circuit. The time delay will provide a means of at least partially bridging the transient periods. Electronic or inertialess relays would have some disadvantages in this respect.

We question the implication that relaying will not be a problem where compensation approaches 50 per cent for any transmission circuit of appreciable length. For these circuits fault magnitudes will tend to be below gap flash-over values for the end-of-line regions. With much more than 30 per cent compensation, the use of high speed distance relays may be unduly limited and with 50 per cent compensation the first zone instantaneous elements would need to be set to cover not more than 40 per cent of the line inductive impedance, or else risks of improper relaying must be accepted. We base these conclusions on the lack of assurance of gap flash-over for faults on the entire line.

The magnification of the negative reactance of the capacitors as seen by remote (as well as near) line terminals which supply a portion of the total fault current also should be considered. While we believe that the Bonneville Power Administration tests of the Chehalis installation show that this consideration is of no consequence when gap operation is assured, it may be of much greater importance in case gap settings are increased, for any reason, or in case the gap flash-over voltage level rises above intended settings.

We have the feeling that the problem associated with the circulating zero sequence current occasioned by single-phase gap operation is not of too great importance, except in cases as typified by single tie lines between major systems. We agree that the condition should be considered in analyzing any series capacitor installation.

These analogue studies and the general conclusions drawn from them will be valuable guides to anyone contemplating a series capacitor installation. However, it will bear repeating that final verification of the success of any design can be made only by system tests and operational experience.

E. L. Harder, J. E. Barkle, and **R. W. Ferguson:** Messrs. Curtin and Diemond have called attention to the close agreement between the conclusions derived from the analogue computer studies described in this paper and the conclusions reached as a result of system tests. They also state that "analogue studies of this type will lack conclusiveness." We believe that the close agreement between the computer studies and the system tests proves the value and reliability of the analogue computer in predicting system performance under conditions similar to those studied. It is true that there are many parameters and complicated circuit elements involved, but these can be restricted in number and complexity by profit in knowledge from previous studies of a similar nature.

The analogue computer is like all similar computing devices in that it depends on correct set-up of the problem and correct analysis of the results in yielding a correct answer. Circuit elements such as potential devices with their tuned circuits, the magnetizing characteristics of transformers, and corona affects are not difficult of representation on the analogue computer and each has been set up at one time or another to determine its affect on a specific problem. For example, the effect of the transient performance of coupling capacitor potential devices on relay operation has been studied on the computer and the results verified by full-scale tests, so the effect of this variable in the present problem can be evaluated. The same is true of many other parameters that might be mentioned. Thus, an almost insurmountable task is made relatively easy by eliminating those circuit elements whose effect can be predicted once certain other conditions are known. The problem of handling a large number of circuit parameters is reduced by choosing a particular system case and varying certain parameters during the course of the study to determine their effects.

The authors, therefore, are of the opinion that the results of the analogue computer studies bear a large degree of conclusiveness when properly interpreted. The results are the equivalents of mathematical solutions of the cases studied and as such represent a very considerable saving in time and manpower.

The great value of the computer is in proving the validity of an application, but of course, the long-time effect of system operation on the equipment involved can only be proved by actual operation. Of equal importance, is the fact that the flexibility of the computer is far greater than that of an actual system and a far greater range of conditions can be covered. System tests of a similar nature are usually difficult or impossible to make.

The conclusions stated in the paper are based on the popular forms of electromechanical relaying presently in use and as described in the paper.

It is impossible by mathematical analysis to predict the operation of these relays for given electrical conditions including the effects of inertia.

This is merely a matter of taking into proper account the various forces operating within the relay. However, the authors are of the opinion that for the relay operating times involved, the effects of inertia in the present problem can be neglected. The development of electronic or inertialess relays would require further study if their operating times were considerably shorter than those now considered standard for electromechanical relays.

We understand that the discussors' reference to compensation of 50 per cent is in connection with the second conclusion of the paper, which states that the circuit between the bus and the fault will never be capacitive if the capacitor is in the center of the line and the compensation is less than 50 per cent. Misoperation of directional elements can occur when the circuit between the relay and fault is capacitive. The effect of the degree of compensation on impedance element settings is covered in conclusion 4. Actually, with directional-comparison carrier relaying, the compensation can approach 50 per cent provided the user is willing to rely on tripping through the second impedance element and carrier, reducing the reach of the first element or entirely eliminating it. However, one should not overlook the fact that location of the capacitor adjacent to the bus is hazardous from the standpoint of directional element operation if protective gap operation does not occur.

Magnification of the capacitive reactance as mentioned by the discussors must be considered in applying impedance relays in the same light as any impedance under similar conditions. The effect may be critical for some relay locations and require modification of the relay setting.

The information and conclusions derived from these analogue computer studies have inspired a great deal of confidence in the soundness of series compensation so far as transient and relaying effects are concerned. System tests on a somewhat restricted basis have thus far supported these conclusions, and it is the authors' conviction that operation over a long period of time will add further support. Without the benefit of these studies, it is conceivable that the use of high-voltage series compensation might have been delayed for quite some time.

Development of Corona Measurements and Their Relation to the Dielectric Strength of Capacitors

R. J. HOPKINS
ASSOCIATE MEMBER AIEE

T. R. WALTERS
MEMBER AIEE

M. E. SCOVILLE
FELLOW AIEE

Synopsis: Development and evaluation of corona measurements have contributed greatly toward solution of the problem of determining satisfactory voltage stress levels in capacitors. Until recent years, short-time voltage breakdown tests were the only quick means of determining required dielectric thicknesses. However, practical operating voltage stress levels were established more by service experience than by short-time measurements. The time consumed in obtaining the service experience on new materials or designs made advances in design practice slow and uncertain. During the last 15 years it has become evident how closely the life of a capacitor in service is linked with the ionization voltage level of its dielectric. New measurement techniques have been developed, by means of which insulation ionization levels can be quickly and quantitatively established. Results of ionization tests have been correlated with long-time life tests and service experience. As a result, it now is possible to use the ionization test as a valuable guide in selecting improved dielectric materials, and in designing to meet new operating conditions. While this paper refers specifically to the very thin dielectrics used in capacitors, the techniques described can be applied also to evaluate electrical insulations for other devices.

Need for New Techniques in Establishing Voltage Stress Levels

QUALITY of dielectric materials is of vastly greater importance in a capacitor than in resistive or inductive devices. The size and cost of the latter depend largely on the properties of the conductor and magnetic materials, whereas the size and cost of a capacitor vary almost inversely with the square of the voltage strength of the dielectric between its conductors. Because this is true of capacitors, economic necessity dictates that the voltage strength and uniformity of the dielectric be the highest obtainable, so that a minimum thickness can be used. Consequently, as the capacitor industry has grown to major proportions, very extensive research and development programs have been carried on to improve capacitor dielectrics and their application.

The dielectric materials, such as glass, petroleum wax, and oil-saturated papers, first used in capacitors, were those already developed for other applications. The voltage strength of such materials was determined by short-time breakdown tests, with either power frequency or direct voltage applied. Much work of this type was done under the able direction of F. M. Clark.[1–4] Such test data were used in investigating new materials and processes of manufacture. Life tests of three to five years duration and experience with capacitors in service provided a basis for selection of operating voltage stress levels. Advance in capacitor design was slow but successful during the early 1930's.

At that time some important conclusions were reached:

1. Rapidly applied breakdown data as a criterion of adequate life in service are unreliable and frequently misleading as such breakdown voltage values are six to ten times the safe operating voltage level in service.

2. Service experience as a means of establishing safe operating voltage stress levels in capacitors is satisfactory, but too slow to permit reasonably rapid introduction of new materials, or to obtain design data for new voltage conditions.

Early insulation breakdown studies had included small glass-covered samples energized in a dark room which permitted observation of corona discharge as light spots at the electrode edges. The voltage levels which produced visible corona discharge were found also to cause permanent markings on the insulation samples adjacent to the electrode surface. The literature contains reports of work done by Whitehead,[5] Dawes,[6] Shanklin[7] and many others using dielectric power factor measurements as a very successful indication of ionization damage in cables. However in capacitors, the amount of damage done to the dielectric, before detection by power factor increase is possible, is so great as to eliminate this method from our consideration.

The authors of this paper, together with several other interested engineers and researchers, recognized these important considerations in the early 1930's and began to investigate improved test methods to meet the need for a more accurate means of determining practical voltage strength levels.

Development of Test Techniques in Measuring Voltage Ionization Levels

Thus, when in 1935 a general laboratory study of dielectric phenomena instigated by K. K. Paluev[8,9] was placed under the direction of one of the authors, it was quickly found desirable to devise a sensitive means of actually measuring, rather than just visually observing, the corona

---

Paper 51-306, recommended by the AIEE Transmission and Distribution Committee and approved by the AIEE Technical Program Committee for presentation at the AIEE Pacific General Meeting, Portland, Oreg., August 20–23, 1951. Manuscript submitted April 25, 1951; made available for printing July 9, 1951.

T. R. WALTERS is with the General Electric Company, Pittsfield, Mass. R. J. HOPKINS and M. E. SCOVILLE are with the General Electric Company, Hudson Falls, N. Y.

The authors acknowledge with thanks the contributions made by many of their associates to the investigation described in this paper. Particular recognition is given to G. C. Nonken, B. H. Colby, W. R. Wilson, and J. R. Nye, all of the Electrical Research Section, who successively contributed to the development and application of the method described.

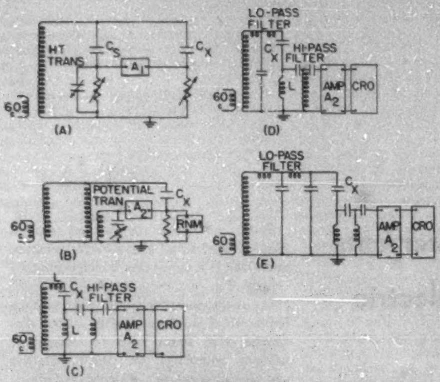

Figure 1 (above). Schematic circuit diagrams of stages of developments in test equipments for measuring ionization voltage stress levels in capacitor samples. C_s = standard air capacitor; C_x = test sample; A_1 and A_2 = resistance-capacitance coupled amplifiers input to magnetic oscillograph and cathode-ray oscillograph, R_{nm} = radio noise meter

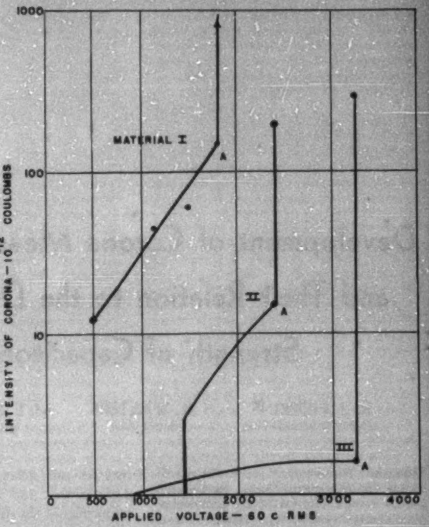

Figure 3 (right). Comparison of ionization intensities versus voltage for three typical dielectric samples

starting voltage. A reasonable first approach to this measurement problem seemed to be one of balancing out the normal 60-cycle charging current, and observing what was left. As a result, an available Schering bridge was used, with its output at the detector terminals fed through a broad-band amplifier into a standard magnetic type oscillograph. See Figure 1(A). Although this work was done independently, it was soon learned that others[10,11] had developed much the same method.

During the next five years, several improvements were made in the method. The Schering bridge circuit was modified, a better broad-band amplifier built, and a cathode-ray oscilloscope substituted for the magnetic oscillograph. A radio-noise meter was sometimes used as a detector. See Figure 1(B). At this stage, corona currents in the order of 6×10^{-6} amperes could readily be measured. Chokes were added to smooth the applied voltage wave and a high-pass filter added to the measuring circuit. See Figure 1(C). Later the choke coil was changed to a low-pass filter, Figure 1(D). The final step was to add a high-voltage capacitor in parallel with the sample capacitor and series measuring inductance. This is a refinement of the resonant circuit described by Quinn[12] in 1940. See Figure 1(E) and Figure 2.

This latest circuit proved to be from 200 to 600 times more sensitive than either the early oscilloscopic or the radio noise method. With its use a new type of ionization disturbance, extremely small, was found to exist in certain capacitors at voltages much below visible and even below ionization starting voltages indicated by earlier methods. Thus it became evident that the intensity of ionization had to be evaluated numerically, or the corona starting voltages would be considered primarily a function of the sensitivity of the equipment.

Figure 2. Test equipment rated 7 kv, 60 cycle for measurement of ionization voltage levels in capacitors and insulation samples

Each pulse of ionization current independently produces an instantaneous voltage ΔE between the electrodes of the test sample, the most severe pulses producing the greatest voltages. Intensity of ionization (I) was defined as the product of the greatest value of ΔE multiplied by the capacitance C of the test sample.

$$I = 10^{12} C \Delta E \qquad (1)$$

where

I = intensity of ionization in micromicrocoulombs
C = capacitance between test electrodes in farads
E = change of voltage on capacitor C caused by a single pulse of ionization. This must be measured on a ballistic basis; that is, the change ΔE must be completed before appreciable charge flows to the capacitor from the external circuit.

Means of calibration were necessary, so a device was developed including a d-c microvolter to introduce a known charge into the measuring circuit. This charge produced a vertical line on the oscilloscope screen, the same as those caused by ionization pulses. Although the pulse is actually a high-frequency transient, the horizontal sweep frequency of the cathode-ray oscilloscope is so slow relatively that the transient wave is compressed to a

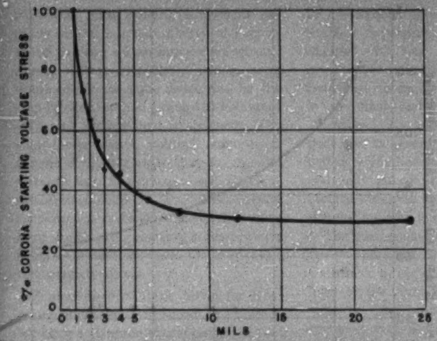

Figure 4 (above). Average 60-cycle corona starting voltage stress versus dielectric thickness for typical diphenyl chloride impregnated kraft paper capacitor dielectric

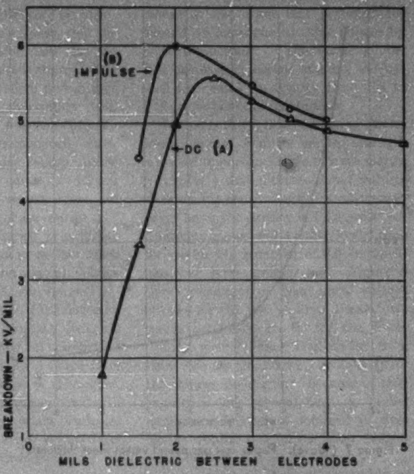

Figure 5 (right). Average direct voltage breakdown versus dielectric thickness for typical capacitor dielectric samples of diphenyl chloride impregnated 0.5 mil sheets of kraft paper. (A) Direct voltage increased to breakdown in 100-volt steps with voltage held 10 seconds at each step. (B) Impulse voltage applied with front of wave breakdown in about 5 microseconds

single vertical retraced line of height ΔE. The magnitude of the known pulse is varied until it produces the same deflection on the cathode-ray screen as the ionization pulse. The ΔE of the known pulse then equals the ΔE of the ionization pulse; the capacitance C of the sample can be readily measured on any capacitance bridge and the intensity (I) calculated from equation 1.

This improved technique permits measuring ionization intensity independently of all circuit constants. This is in marked contrast to the commonly used radio noise microvolt unit which depends as much upon capacitance of the test sample and other circuit constants as upon the amount of ionization produced in the sample. Test results are reproducible on a given sample, making it possible to obtain comparative measurements with variation of temperature, pressure, voltage wave shape, and all other pertinent variables which may affect quantitative values. Aging and the effect of time, with repeated measurements on a given sample give particularly valuable technical information.

About a year after the new intensity unit and calibrating device were put into use, Austen and Hackett[13] proposed the use of the micromicrocoulomb as the unit of ionization intensity. They did not show a means of calibrating their equipment, which was not as sensitive as that described here. In fact, the equipment used here had reached the "optimum practical conditions" that they predicted from a theoretical analysis of the factors limiting sensitivity.

Originally the capacitance of test samples was limited by practical circuit constants to a value below 0.1 microfarad. With the increased sensitivity in the latest test equipment samples up to 0.5 microfarad are tested. The sample rating inherently affects the sensitivity as the higher capacitance absorbs the ionization energy making the signal to the detecting amplifier weaker. It is desirable to be able to measure a completed 15-kvar or 25-kvar capacitor, but such is beyond present capabilities.

Measurements made on a given sample may include ionization intensities for a range of applied voltages. Plotted in these two parameters characteristics as

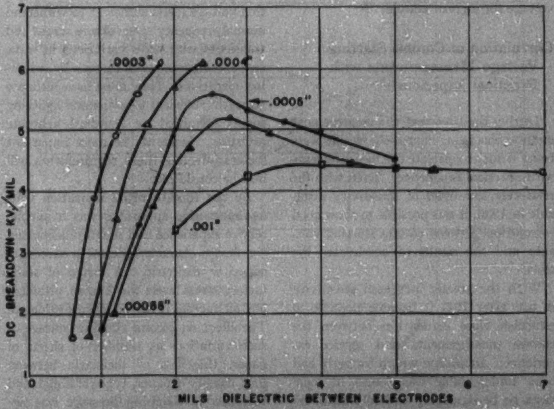

Figure 6. Average direct voltage breakdown strength for typical capacitor dielectric pads built up with five different capacitor paper thicknesses showing effects of varying the number of paper sheets between electrodes

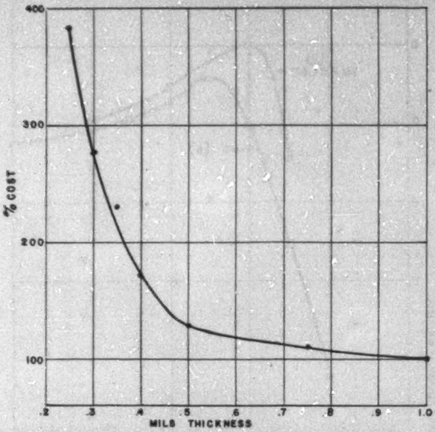

Figure 7 (above). Paper cost per pound versus sheet thickness

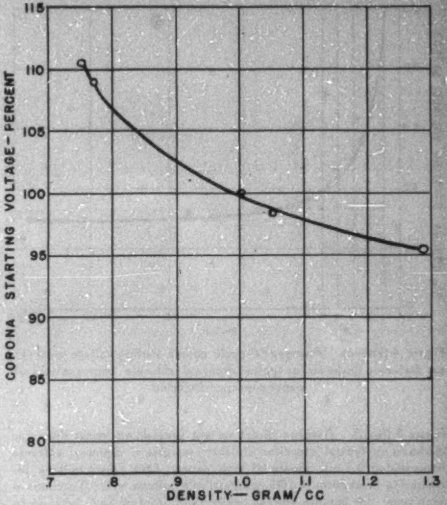

Figure 8 (right). Corona starting voltage versus paper density (dry apparent density before impregnation) for a typical capacitor dielectric of diphenyl chloride impregnated kraft paper 4.0 mils thick

shown in Figure 3 are obtained for three different dielectric materials. One characteristic is common to all curves, at some voltage value the intensity increases very rapidly. This break-point ("A" on curves Figure 3) indicates a condition of continuing contagious ionization in the sample, and the voltage at which it occurs has been defined as the corona starting voltage for a given sample.

Correlation of Corona Starting Voltage Measurements with Practical Experience

During the time that the measurement method was being improved, studies were being made to correlate the measurements with practical experience. Even with the relatively low order of sensitivity available in 1936, it was possible to show good correlation between corona starting voltages and the results of accelerated life tests.

With the greatly increased sensitivity in use after 1941 it became possible to establish close correlation between the corona measurements and service experience. Ionization which formerly had been undetectable was found in some cases to be damaging and to lead to reduced life. The effect of very short applications of voltage, from a fraction of a cycle up to hours and longer, could be determined, and thus voltage limits for a wide variety of capacitor applications could be intelligently specified.

Influence of Corona Starting Voltage Measurement on Dielectric Design

Capacitor dielectrics must have ionization voltage levels sufficient to withstand normal frequency overvoltage surges and transients with wide variations in wave shape, such as imposed thereon by switching operations. They must have ultimate strengths sufficient to withstand lightning surges permitted by standard lightning arresters. Some of the more important factors affecting these requirements will now be considered.

By the time accurate ionization voltage measuring apparatus was available, service experience had roughly delineated the design characteristics of a successful capacitor dielectric. A range of satisfactory stress levels was known, although not all factors involved were evaluated. The effect on corona starting voltage of such variations as number of sheets of paper, thickness of dielectric between foils, density of paper, types of liquid, and variation in clamping pressure was unknown. However, these variables were known to have an important effect on the initial dielectric strength of the dielectric. Even more important is the effect of time and temperature on the voltage strength of the dielectric.

The dielectric samples used for the tests reported in the following discussion were constructed as nearly like commercial designs of capacitors as possible. The capacitances of the sample rolls were in the range of 0.2 to 0.5 microfarad, which is less than is used in large size standard units. Unless otherwise specified, the samples were wound with standard kraft papers, impregnated with pentachlor diphenyl and tested under conditions of normal room temperature (20–30 degrees centigrade) and pressure (29 in. Hg).

Tests show that for a given thickness of dielectric between foils the ionization voltage is independent of the number of sheets of paper within the limits of two to ten sheets. The average corona starting voltage stress decreases as the thickness of dielectric between electrodes is increased, as shown in Figure 4. It is apparent from this curve that the highest ionization voltage level can be realized by the use of very thin dielectric pads between foils. If necessary for total voltage strength the pads can be connected in series. However, impulse strength must also be considered. Curves of impulse and direct voltage strength are shown in Figure 5. The impulse breakdowns were all on either front or crest of wave, with four to five microseconds time to breakdown. Shorter times to breakdown are difficult to obtain with existing equipment because of the inherent ability of capacitance to slope off an impulse wavefront. Direct voltage breakdown stresses were obtained for the same dielectrics, by the step-by-step method (using 100-volt steps with each voltage held 10 seconds). The short time direct voltage strength in general is slightly lower than the impulse strength but the variation with numbers of sheets is similar. Since direct voltage data are more easily taken, they have been used as representing a conservative impulse breakdown level for most practical considerations.

Similar direct voltage curves for other paper thicknesses are shown in Figure 6. All have a common characteristic in that maximum strength in volts per mil is obtained or approached with five or six sheets of paper between electrodes. In general, the highest breakdown stress is obtained with the thinnest papers. The reduction, with increasing sheet thickness, is not serious, however, for the commonly used paper thicknesses.

As previously stated, the 60-cycle corona starting voltage level for a given dielectric thickness is independent of the number of sheets of paper. This is not true of direct voltage breakdown which is markedly influenced by the number of sheets of paper, below about 5 mils, as shown in Figure 6.

The design of a dielectric is thus influenced by the ionization voltage data, which indicate that as thin a dielectric as possible be used, and by the direct voltage breakdown data, which indicate that for maximum strength this dielectric should be made up of four or more sheets of paper. Thus, for a given total dielectric structure for a given voltage it would be possible to use a number of very thin dielectric pads, each with an optimum number of sheets, connected in series. Such a dielectric structure would have a very high ionization voltage compared to one made up of thicker pads, but would have only slightly higher breakdown strength as far as impulse is concerned. The cost of such a dielectric structure would be high because the cost of the thinner papers is high as shown by a typical paper price level curve, Figure 7. It may be concluded that the use of more sheets of thinner paper is economically justified only where unusually high voltage surges are expected.

For normal high-voltage 60-cycle service, pad thicknesses of 2.5 to 3.5 mils have a satisfactory ionization level and direct voltage breakdown and make use of thicker, less costly papers. A 4-sheet dielectric, although exhibiting a satisfactory breakdown strength, may be undesirable. Experience has shown that dielectrics with four sheets and less are more erratic as to dielectric strength and contribute to higher failure percentages in the final factory overvoltage test. Therefore, 3- and 4-sheet dielectric pads are, in general, economically justified only for low-voltage ratings (below 600 volts alternating current). Higher factory losses at final electrical test are justified for such low voltage ratings.

The component materials in a dielectric pad have individual properties which contribute to the corona starting voltage level of the composite impregnated insulation. Such properties of the dielectric materials as dielectric constant, dielectric loss, and permanent chemical stability do effect the corona starting voltage level but are beyond the scope of this paper. The following discussion is concerned with some of the other important variables affecting the corona starting voltage level for a given composite dielectric pad.

Effect of Solid-Liquid Relationship

The density of the paper and consequently the ratio of fibrous material to impregnating liquid affects the corona starting voltage level. If a lower density paper is used, then the relative amount of liquid is higher. A change in dry apparent paper density[14] from 0.7 to 1.1 grams per cubic centimeter causes about 8 per cent decrease in corona starting voltage level, as shown in Figure 8. This change is less than that reported for mineral oil impregnated cable papers by J. B. Whitehead[15–17] who shows 11 per cent decrease in corona starting voltage level for change in density from .85 to 1.12 grams per cubic centimeter.

However, there is an offsetting factor where impulse or direct voltage strength is also of importance. Tests have shown conclusively that ultimate direct voltage strength for pentachlor diphenyl treated paper having a density of 0.75 gram per cubic centimeter will average lower than for one having a density of 0.9, in thicknesses of three mils or less. Figure 9 shows comparative breakdown voltage stresses for the two papers. Breakdown results are more erratic for the lower density paper, which contributes to a lower average breakdown, particularly for the thinner dielectrics. Because of this, experience has shown that a higher number of failures is obtained in final factory voltage test for the lower density paper dielectrics.

In practical winding and assembly of capacitor rolls, adjacent sheets of paper and foil have some free space between them which is later filled with the impregnating pentachlor diphenyl. This free space is variable, depending on the clamping pressure applied during assembly of a roll pack. It is commonly called "per cent film" and is based on the nominal paper thickness. Increasing the per cent film increases the corona starting voltage level, as shown by Figure 10, giving the same effect as reducing the

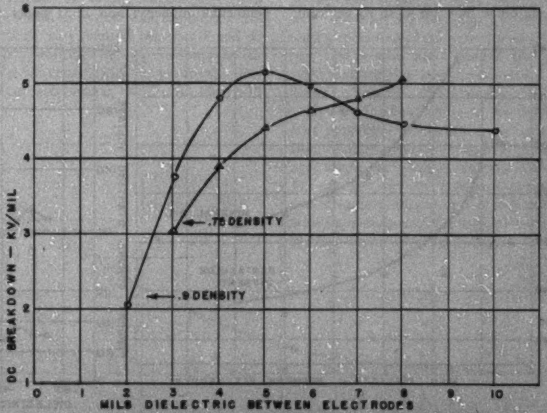

Figure 9. Average direct voltage breakdown strength versus dielectric thickness between electrodes for a typical capacitor dielectric of diphenyl chloride and kraft paper of two different densities

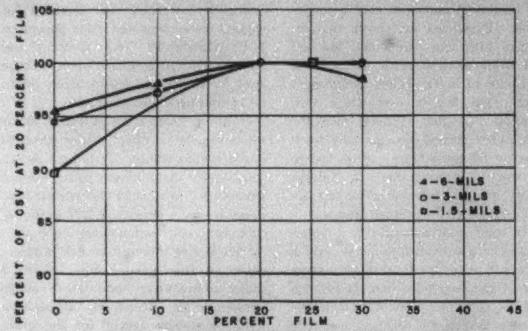

Figure 10. Corona starting voltage versus per cent film for typical capacitor dielectrics of three thicknesses

paper density. The effect of film variation is greater for dielectrics of two mils thickness and below. Practically any film from 10 to 30 per cent is satisfactory, and this factor is varied in practice to aid in standardization of paper thicknesses and sizes of containers.

Effect of Impregnant

The impregnating liquid can have considerable effect on the corona starting voltage level of the composite dielectric pad. Pentachlor diphenyl has superseded mineral oil since 1931 as a more suitable kraft paper impregnant for most a-c capacitor applications. However, it is surprising to compare their corona starting voltage levels. Figure 11 shows mineral oil to have an 83 to 96 per cent higher level than pentachlor diphenyl. On the basis of this comparison alone it appears that oil would have an advantage even to the extent of permitting a higher voltage rating. This could offset a 33 per cent lower dielectric constant for oil and permit a higher kilovar rating per-unit volume. But these data are misleading, as there is another important factor to be considered. This high corona starting voltage level for mineral oil is the initial value before any continuous operation comparable to life in service.

Mineral oil is not stable with time in service and the initial high corona starting voltage level decreases quite rapidly. It has been well established that the long time and even relatively short time 60-cycle breakdown voltage strength of pentachlor diphenyl and kraft paper is somewhat higher than that of mineral oil and kraft paper. For example, specially designed capacitors were built and hermetically sealed in metal cases, with individual rolls connected to separate bushings so that measurements could be made on each roll. Half of these identical capacitors were impregnated and filled with pentachlor diphenyl and half with mineral oil. The capacitors were placed on a-c life test at a 50 per cent overvoltage in an ambient temperature equivalent to the maximum expected in service. Corona starting voltage measurements were taken before life test and at intervals during life test. After one week, the ionization voltage of the oil impregnated samples had dropped to a range of 12 to 50 per cent of the initial values. Some of the values were below life test voltage and these samples failed shortly thereafter. All oil impregnated samples failed within 28 days. In contrast, no failures of pentachlor diphenyl impregnated samples occurred within one year of life test and at the end of one year the corona starting voltage levels were unchanged from the original values.

These tests illustrate one of the reasons why mineral oil has been generally unsatisfactory for use in power factor improvement capacitors, unless operated at lower voltage stresses than the more stable chlorinated diphenyls. These test results also illustrate that while good initial characteristics are important in a dielectric, maintenance of good characteristics under service conditions is more important and is a controlling factor in the selection of materials. It is concluded that measurement of corona starting

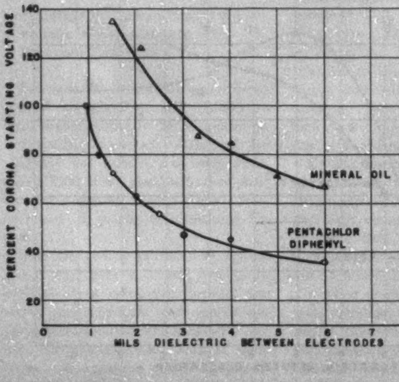

Figure 11. Comparison of average corona starting voltage versus dielectric thickness for two impregnating liquids with kraft paper in typical capacitor dielectrics

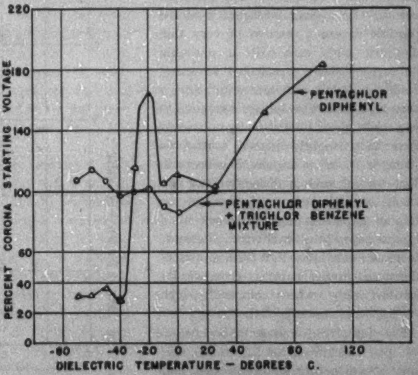

Figure 12. Average corona starting voltage versus dielectric temperature for two impregnating liquids with kraft paper in typical capacitor dielectrics of 3.3 mils thickness

voltage levels during life test can well be added to other measurements as a test of the ability of materials to withstand the required service and remain stable.

Effect of Temperature

Capacitors for installation on power circuits out-of-doors may be subjected to ambient temperatures ranging from −40 to +40 degrees centigrade. If the capacitors are automatically switched, dielectric temperatures may reach the lower value while de-energized.[18] It is essential for reliable service that the dielectric operation be satisfactory for such temperature ranges. Some of the common capacitor impregnants are solids at the lower temperatures and may crack or form shrinkage voids. Figure 12 shows a typical variation of corona starting voltage over a temperature range of −70 to 100 degrees centigrade for pentachlor diphenyl impregnated kraft paper dielectrics. A satisfactory corona starting voltage level exists over the temperature range of −30 to +100 degrees centigrade. Below −30 degrees the ionization voltage drops sharply so that at −40 degrees centigrade it may be below normal operating voltage. Figure 12 also gives the ionization voltage characteristics for dielectrics impregnated with a special low temperature liquid. With this liquid a satisfactory corona starting voltage level exists to temperatures as low as −70 degrees centigrade. These data are confirmed by field experience which has shown that some random failures have occurred when pentachlor diphenyl impregnated capacitors have been energized at temperatures below about −26 degrees centigrade, whereas no such failures have occurred with capacitors impregnated with the new liquid.

Thus it can be seen that the measurement of corona starting voltage level over the expected operating range of temperature is of value during the development of any new dielectric. Otherwise serious difficulties may arise in service due to unforeseen reductions in ionization voltage at temperatures other than room temperatures, where measurements are usually made.

Short-time Overvoltage Considerations for Shunt and Series Capacitor Applications

Shunt capacitors have a nominal voltage rating consistent with the continuous operating voltage level of the circuit to which they are connected. During normal service, transient overvoltages in excess of rating are also expected. The corona starting voltage level of shunt capacitors has been, in general, inherently high enough to withstand transient overvoltages of short duration as normally encountered in service. However, the actual limits for the transient overvoltages caused by various switching operations were not definitely known. Neither was the ability of the capacitor to withstand such transients known with any great accuracy. The practice, evolved out of experience, is to use a final factory overvoltage test of not less than two times nominal rating at power frequencies.

Shunt capacitors have been well standardized in a few voltage ratings to meet application needs. On the other hand, the application of capacitors connected in series with power circuits has been intermittent, very limited in volume and so widely varying in requirements as to make standardization impractical. Recently established National Electrical Manufacturers Association and AIEE Standards on series capacitors have included shunt capacitor ratings where practical. Since series capacitors are also subjected to overvoltages, in this case during short circuit faults or overloads on the circuit, the overvoltage limit is again an important consideration and is usually fixed by protective gaps. In the past the protective level was limited to two times nominal rating which was in agreement with shunt capacitor standards. Where protective limits greater than twice nominal were required due to system characteristics, the capacitors were designed accordingly.

However, recent developments in the field of series capacitors for high voltage transmission lines have made it desirable to re-examine the earlier position. Some applications have required protective equipment settings of 2.5 to 3 times the rated capacitor voltage. Even higher short-time voltage ratings have shown economic promise from theoretical system studies. The question naturally raised was whether or not dielectrics could be operated for periods of a few cycles per year at voltages above their corona starting voltage level without being permanently damaged.

Typical results of an investigation along these lines are shown in Figure 13. This figure gives the maximum safe voltage that can be applied to a 2.75-mil pentachlor diphenyl impregnated dielectric for one application of voltage as a function of time of application of voltage based on the continuous 60-cycle corona starting voltage level as 100 per cent. These data were obtained by stepping up voltage until a reduction of 60-cycle corona starting voltage level was observed immediately following a single application of higher voltage of specific duration.

Figure 13 is interesting in the light of past practice which required that capacitors should never be subjected to voltages above their corona starting voltage. For example, the curve shows that for 15 cycles, almost 200 per cent of the corona starting voltage can be applied without damage (reduction in subsequent corona

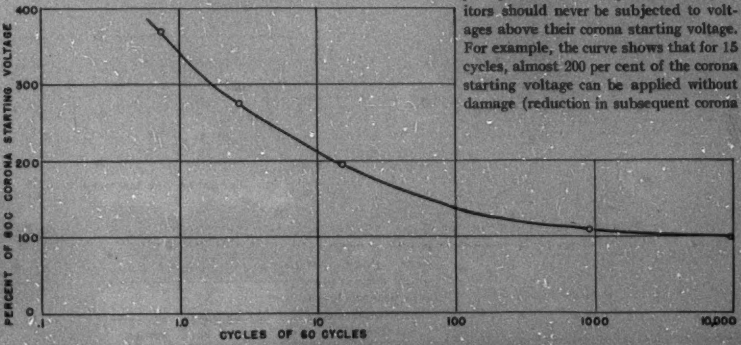

Figure 13. Typical safe maximum 60-cycle voltage limit versus duration in cycles for single applications to a typical capacitor dielectric of diphenyl chloride and kraft paper 2.75 mils thick

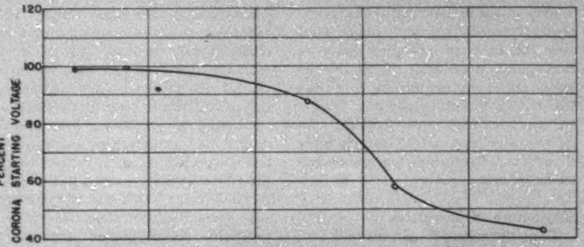

Figure 14. Per cent corona starting voltage versus frequency for a typical capacitor dielectric of diphenyl chloride impregnated kraft paper of 3.3 mils thickness

starting voltage). For a 1-cycle voltage application, 345 per cent of 60-cycle corona starting voltage can be applied.

This investigation yielded other interesting data on the effect of repeated overvoltages on dielectrics. Frequently-repeated application of voltages somewhat below those given in Figure 13 results in a measurable reduction in corona starting voltage and ultimately reduces the useful life of a capacitor. Also repeated applications at close intervals will result in less damage than one application for a number of cycles equal to the sum of the cycles for the repeated applications. Both of these conclusions are illustrated by Table I for the same dielectric.

These data indicate some recovery of the dielectric between repeated short applications of voltage which is not present in the case of the 1500-cycle application.

Another illustration of the cumulative effect of repeated applications of voltage is given in Table II for the same dielectric. The voltage applied was 170 per cent of the corona starting voltage level, for a time of 15 cycles. This voltage is below the one application safe voltage of 195 per cent but above the 100 application safe voltage of 146 per cent. The cumulative damage is expressed as a percentage reduction in the continuous 60-cycle corona starting voltage level.

A logical question is whether or not dielectrics which have been damaged, as shown by a reduction of corona starting voltage, will recover if allowed to rest. Tests have shown that a specific dielectric, which has been damaged to the extent of approximately 15 per cent or less reduction in corona starting voltage, will recover to its initial value after one week rest with no voltage applied. Sufficient data are not available to permit general conclusions but limited data indicate that damage to the extent of a 30–40 per cent reduction in corona starting voltage level will never be restored by rest. In normal service a rest period without voltage is unlikely as normal voltage operation will usually follow a transient overvoltage, which minimizes the practical value of corona starting voltage level recovery after damage.

These questions of effect of short time overvoltage and recovery are old ones. In 1925, Clark[1] and Montsinger[2] discussed them chiefly in relation to their effect on relatively short time breakdown, that is, up to 15 minutes. The corona starting voltage method of detecting damage is so much more sensitive than the older method, that damage which would not cause failure in less than a year in service, can be detected.

Effects of Frequency and Voltage Wave Shape

Increasing frequency from 60 cycles to 500,000 cycles decreases the corona starting voltage level as shown in Figure 14. Continuous 60-cycle corona starting voltage measurements have been used as a reference base for comparison. Although test measurements have not been made, it is believed that the characteristic shown in Figure 13 would also apply for higher frequencies.

In some capacitor applications a thorough analysis of all conditions of operation reveals that a number of variations in voltage wave shape are applied to the dielectric. Power circuit capacitors encounter transient voltages of many wave shapes usually superimposed on the normal frequency wave. It is generally assumed that energy storage with welders, surge generators, et cetera are d-c applications of capacitors but the wave shape associated with the discharge of the energy of the capacitors may cause corona starting voltage levels to be a design limitation.

A number of variations in voltage wave shape have been studied for effect on corona starting voltage level. Typical wave shapes are shown in Figure 15. Innovations in test equipment arrangement were necessary to obtain corona starting voltage measurements on nonrepetitive voltage waves and to generate repetitive nonsinusoidal waves. The few wave shapes studied do not permit rigorous detailed conclusions. However, in general, there is a correlation to show that

Table I

Time of Application	Safe Voltage, Per Cent of Corona Starting Voltage
15 cycles—one application	195
15 cycles—100 applications at one minute intervals	146
1,500 cycles—one application	107

Table II

Number of Applications	Per Cent Reduction in Corona Starting Voltage
1	0
100	14
200	20
250	34

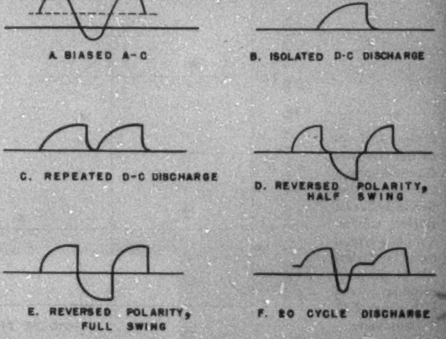
A. BIASED A-C
B. ISOLATED D-C DISCHARGE
C. REPEATED D-C DISCHARGE
D. REVERSED POLARITY, HALF SWING
E. REVERSED POLARITY, FULL SWING
F. 20 CYCLE DISCHARGE

Figure 15. Variations in voltage wave shape for which corona starting voltage levels have been determined

corona starting voltage levels are dependent on at least three variables, as follows:

1. The total change in voltage during one cycle.

The total voltage swing for the waves shown in Figure 15 has about the same effect as the peak-to-peak value of a sinusoidal wave of the same repetition rate, disregarding the position of the voltage swing with regard to the zero axis.

2. Time required for the voltage change.

The time required for the voltage swing to take place affects the corona starting voltage level in the same order of magnitude as increased frequency (Figure 14) for sinusoidal waves.

3. Length of rest periods between voltage changes.

The interval, or rest period, between voltage changes affects the corona starting voltage level but has not been evaluated specifically.

Conclusions

1. A highly refined test method has been developed in the laboratory to measure ionization voltage levels in liquid impregnated paper dielectrics.

2. Ionization test data obtained on dielectric samples, as a means of determining damaging effects of high-voltage stress, correlate with life tests and long time service experience on capacitors.

3. Safe operating voltage stress levels can be established in a few days by corona starting voltage measurements on capacitor dielectrics as compared to years required for accelerated life test results and service experience, provided chemical stability has been established.

4. Development and evaluation of new dielectric materials and design features can now be done with dispatch thus accelerating sound design.

5. Safe short-time overvoltage limits consistent with expected service life can be established by corona starting voltage measurements.

6. The effects of operating variables such as temperature, voltage wave shape, frequency and overvoltage duty cycle, on dielectric stress limits can be studied in advance under controlled laboratory conditions.

7. Both better quality and lower cost capacitors are made available to the user with known factors of safety to allow for overvoltage conditions.

References

1. Dielectric Properties of Fibrous Insulation as Affected by Repeated Voltage Applications, F. M. Clark. *AIEE Journal*, volume 44, 1925, pages 628–38.

2. Dielectric Strength—Thickness Relation in Fibrous Insulation, F. M. Clark, V. M. Montsinger. *General Electric Review* (Schenectady, N. Y.), volume 28, 1925, pages 286–90.

3. Research—Brings Remarkable New Liquid Insulation, F. M. Clark. *Electrical World* (New York, N. Y.), volume 100, 1932, pages 373–74.

4. The Electric Breakdown of Liquid Dielectrics, F. M. Clark. *Journal*, Franklin Institute (Philadelphia, Pa.), volume 216, 1933, pages 429–39.

5. The Influence of Residual Air and Moisture in Impregnated Paper Insulation, J. B. Whitehead, F. Hamburger, Jr. *AIEE Transactions*, volume 47, January section, 1928, pages 314–33.

6. Ionization Studies in Paper Insulated Cables III, C. L. Dawes, P. H. Humphries. *AIEE Transactions*, volume 49, April section, 1930, pages 766–75.

7. Progress in High-Tension Underground Cable Research and Development, G. B. Shanklin, G. M. J. Mackay. *AIEE Transactions*, volume 48, April section, 1929, pages 338–72.

8. Transient Voltage Stresses in Power Transformers, K. K. Paluev. *The Engineer* (London, England), volume 153, 1932, pages 480, 495, 518, and 551.

9. Power Transformers with Concentric Windings, K. K. Paluev. *Electrical Engineering* (*AIEE Transactions*), volume 55, June 1936, pages 649–59.

10. Oscillations Due to Ionization in Dielectrics and Their Methods of Detection, J. T. Tykociner, H. A. Brown, E. B. Paine. *Bulletin 259*, University of Illinois Engineering Experiment Station (Urbana, Ill.), 1933.

11. The Measurement of Discharges in Dielectrics, A. N. Arman, A. T. Starr. *Journal*, Institution of Electrical Engineers (London, England), volume 79, 1936, page 67.

12. A Method for Detecting the Ionization Point on Electrical Apparatus, G. E. Quinn. *Electrical Engineering* (*AIEE Transactions*), volume 59, December 1940, pages 680–82.

13. Internal Discharges in Dielectrics: Their Observation and Analysis, A. E. W. Austen, Miss W. Hackett. *Journal*, Institution of Electrical Engineers (London, England), volume 91, 1944, pages 298–322.

14. Standards on Electrical Insulating Papers. *D-202-48*, American Society for Testing Materials (Philadelphia, Pa.), section 9.

15. The Dielectric Strength and Life of Impregnated-Papers Insulation, II, J. B. Whitehead. *Electrical Engineering* (*AIEE Transactions*), volume 59, December 1940, pages 660–63.

16. The Dielectric Strength and Life of Impregnated-Paper Insulation, III, J. B. Whitehead. *Electrical Engineering* (*AIEE Transactions*), volume 61, August 1942, pages 618–22.

17. The Dielectric Strength and Life of Impregnated-Paper Insulation, IV, J. B. Whitehead, J. M. Kopper. *Electrical Engineering* (*AIEE Transactions*), volume 64, April 1945, pages 171–77.

18. The Why of a 25-Kvar Capacitor, M. E. Scoville. *General Electric Review* (Schenectady, N. Y.), volume 52, May 1949, pages 19–28.

Discussion

Bror Hansson (Aktiebolaget Liljeholmens Kabelfabrik, Stockholm, Sweden): As another capacitor maker I want to say that this corona bridge must be a wonderful tool when you should decide on the design, the foil and paper thickness, the impregnating liquid et cetera of a capacitor. I would like to know what plans the authors have of developing this instrument to a production tool—a tool for the tracing of production faults in full-size commercial capacitor units. Such faults usually cover a smaller area than 10 square millimeters. Considering an insulation thickness of 0.1 millimeter and that the volume of one of your standard capacitor units is more than 10,000,000 cubic millimeters a "sensitivity" of one in 10,000,000 would be needed.

It is mentioned in this paper that every test takes some of the life out of the insulation. That would mean that the corona-voltage is time dependent. That would also mean that the reading you obtain is dependent of the time it takes to obtain this reading. I am herewith especially referring to Figure 8 of the paper and to Figure 1 of a paper entitled The Design of Capacitor Units for Series Connection.[1] Figure 8 shows that dense paper has lower corona voltage than porous paper, while Figure 1 of reference 1 indicates that at times shorter than 1 second, the a-c strength is higher for dense than for porous paper. Our opinions would correspond if it takes more than 1 second to take the corona readings.

Reference

1. The Design of Capacitor Units for Series Connection, Bror O. N. Hansson. *AIEE Transactions*, volume 70, part II, 1951, pages 1824–28.

R. J. Hopkins, T. R. Walters, and M. E. Scoville: There seems little reason to expect that this technique can be developed to the point of making it a practical test for production capacitor units of large capacitance. Also, Mr. Hansson's method of considering "sensitivity" based on relative volumes seems less realistic than the method described in the paper.

In the paper where the development of the measuring technique was described and discussed, a formula (1) defined the ionization intensity in terms of $C\Delta E$. It can be shown by test as well as calculation that the value of C is critical, while volume as such is not. Since this is so, it can be further shown[1] that there is a theoretical limit to the sensitivity attainable by this method. This is the basis for our statement that our measurements are limited to about 0.5 microfarad, and that while it is admittedly desirable to measure a completed 15-kvar or 25-kvar capacitor it is beyond present capabilities.

Mr. Hansson states that it is mentioned in the paper that every test takes some of the life out of the insulation. This should be qualified, as it was in the paper, by tying the statement in with the effect of over-voltages. Unless the sample is deliberately overstressed, there is no damage done by this type of measurement. This is because its extreme sensitivity enables us to detect corona at intensities below those that cause damage. This is the region below point A of the curves shown as Figure 3 of our paper. Thus, while the time consumed in making a measurement is generally longer than 1 second, it need have no effect on the measured value. Also, we would not expect any close correlation between corona-starting voltage and short time breakdown. This was brought out in the paper.

Reference

1. See reference 13 of the paper.

A Magnetic Fluid Dynamometer

DWIGHT W. BREDE
ASSOCIATE AIEE

Synopsis: The magnetic fluid formed by mixing finely divided iron and oil has been used extensively for clutch service and to a lesser extent for brake service. This paper describes the use of the magnetic fluid in an absorption dynamometer. Design data are derived and a mechanical power indicating instrument is proposed.

SINCE the announcement of the magnetic fluid by J. Rabinow[1] in 1948, several manufacturers have been producing magnetic fluid clutches for use primarily in servomechanisms. Though some manufacturers have also produced a design for braking service, the author knows of no instance where the magnetic fluid has been used for absorption dynamometer applications. The smoothness of control and the possibility of simple water cooling make this use very attractive, particularly where one is required to run load tests on larger motors. The purpose of this paper is to discuss the design criteria and performance characteristics of a magnetic fluid dynamometer. A magnetic fluid factor is defined and derived for the dynamometer design presented. Further, the use of the dynamometer as a torque element in a mechanical power indicating instrument is proposed and discussed.

Design of the Dynamometer

The following design data were set up as the goal for the design of the dynamometer:

Power	10 horsepower
Speed	400 rpm
Torque	125 foot-pounds
Water rate	3 gallons per minute
Gaps	1/16 inch

Proration of a design suggested by Rabinow[1] was used as a starting point and resulted in the dynamometer whose cross section is shown in Figure 1. The power and speed values were taken as design criteria as they determine the maximum torque required of the dynamometer. The torque value required was then calculated from the horsepower and speed values assumed. The water rate was calculated on the basis of 10-degree centigrade temperature rise in the cooling water and represents a minimum rate of flow for maximum horsepower absorbed. The choice of 1/16 inch for the gap length is a compromise between the reduction in magnetomotive force required and the increase in the viscous torque resulting in a decrease in gap length. The coil was wound with 1,252 turns of number 18 copper magnet wire. The total weight of the dynamometer was 70 pounds.

Testing and Results

The dynamometer of Figure 1 is shown in Figure 2 in the test arrangement. The motor used was a 10-horsepower d-c machine capable of delivering 128-foot pounds maximum torque and having a speed range from 600 to 1,800 rpm. The dynamometer was mounted on the motor shaft as shown in the figure. Operation consists solely of provision for varying the excitation which can be readily accomplished with the usual potentiometer circuit. Torque measurements are made with a suitable torque arm. The torque characteristic is shown in Figure 3. This curve has the same general shape as a typical saturation curve of any electromagnetic machine. No variation of torque with speed was observed between the speeds of 400 and 1,200 rpm. A slight decrease in the torque was observed above 1,200 rpm which may be caused by turbulence in the fluid. The torque characteristic repeats consistently though after standing for any length of time the iron particles tend to settle out of the mixture and the torque is higher than normal until the iron and oil are remixed. This period of remixing may be eliminated by the use of any of several thixotropic agents such as Antaron R-210. The addition of a thixotropic agent produces a fluid which jells in the static condition and supports the iron particles and which liquifies with shearing action.

The power absorbed by the dynamometer varied from eight horsepower at 400 rpm to 22 horsepower at 1,800 rpm. The power absorbed at 400 rpm corresponds to 1.7 amperes or 130 per cent of rated current in the exciting coil. The power absorbed at 1,800 rpm corresponds to 0.3 ampere in the exciting coil. This value would be about 36 horsepower at 1.7 amperes but the drive motor used was unable to deliver the necessary power. Since the dynamometer torque is essentially independent of speed and since the horsepower increases directly with speed, the critical point in the design of the dynamometer is the horsepower at 400 rpm which is 20 per cent low with respect to the desired design.

The temperature rise was observed by placing thermocouples at strategic spots in the dynamometer. Referring to Figure 1, the temperature rise of the outer surface of the gap was about 70 degrees centigrade above an ambient temperature of 22 degrees centigrade when absorbing 10 horsepower. The temperature rise of the inner surface of the gap was about 80 degrees centigrade. The cooling water temperature rise from inlet to outlet was about 15 degrees centigrade for a water rate of 1.5 gallons per minute. These temperatures indicate that the cooling was sufficient to absorb 10 horsepower

---

Paper 51-307, recommended by the AIEE Instruments and Measurements Committee and approved by the AIEE Technical Program Committee for presentation at the AIEE Pacific General Meeting, Portland, Oreg., August 20–23, 1951. Manuscript submitted May 21, 1951; made available for printing July 10, 1951.

Dwight W. Brede is with the University of California, Berkeley, Calif.

The author wishes to express his appreciation to H. Vanzolini for his contribution to the study of the flux variation in the dynamometer described herein, and to R. M. Saunders for his assistance in preparing the manuscript.

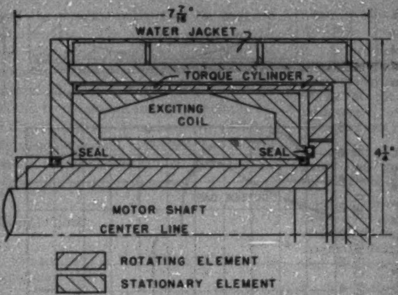

Figure 1 (above). Cross section of the dynamometer tested. The cooling water connections and the coil leads are not shown

Figure 2 (right). The testing arrangement showing the relative sizes of the dynamometer and a 10-horsepower d-c motor

though the inner surface of the gap requires more cooling.

The Magnetic Fluid

The dynamometer was tested with several mixtures of magnetic fluid ranging from iron filings in SAE 30 motor oil to carbonyl E and silicone fluid. The carbonyl E particles range from six to ten microns in diameter and were the smallest particle size used. The silicone fluid has a viscosity of 20 centistokes at 75 degrees Fahrenheit and was the fluid of least viscosity used. The iron filings used are about 2,000 microns in diameter and the SAE motor oil has a viscosity of 250 centistokes at 75 degrees Fahrenheit. It was found that the torque increased with the amount of iron in the gaps which was increased by increasing the ratio of iron to oil in the mixture. This increase in the ratio is limited by saturation of the iron in oil mixture. When saturation occurs the mixture is very stiff and the residual torque caused by the viscosity effect of the mixture is high. This is undesirable and as saturation occurs at a ratio of 8-to-1 for carbonyl E and silicone oil, a ratio slightly lower than this was used. For the design of Figure 1 the residual torque was found to be about 5 foot-pounds which includes the friction of the bearings and seals as well as the viscosity effect of the mixture. Some manufacturers of magnetic fluid clutches have used a dry mixture of iron and graphite or the iron alone. These mixtures have not been tested in the dynamometer but it is believed that the use of such mixtures would have the following effects:

1. The elimination of the oil in the mixture would eliminate any pressure in the magnetic fluid. With the allowed expansion volume this pressure is about 10 pounds per square inch.

2. The use of the dry mixture[3] would decrease the thermal conductivity in the gaps and result in higher temperatures. This would increase the possibility of oxidation of the iron particles. Any oxidation would decrease the magnetic effect of the fluid. With proper cooling this increase in gap temperature would not effect the exciting coil.

Sealing the Magnetic Fluid

In testing the unit it was observed that the magnetic fluid expands with increase in temperature and that the iron particles have a strong abrasive effect. The expansion results in high pressures in the magnetic fluid which puts considerable stress on the seals. The seals are further subjected to rapid wear caused by the abrasive effect of the fluid. Several schemes to provide an expansion reservoir were tested with the conclusion that the expansion could best be provided for by filling the unit only 90 per cent full. Several seals were tested in the unit resulting in the design shown in Figure 1. This design consists of two neoprene O-rings between the magnetic fluid and the first bearing. An iron guard ring (not shown) serves to trap the iron particles and keep them out of the seal. A third O-ring after the second bearing maintains a positive lubricating oil pressure on the second O-ring to help prevent leakage of the magnetic fluid to the first bearing. When the torque cylinder is rotating there is sufficient centrifugal force to throw the iron particles away from the axis of rotation. Several relief holes are drilled in the torque cylinder support just above the guard rings to allow some of the magnetic fluid to pass to the outer gap. The centrifugal effect minimizes the effect of decreased amounts of iron in the mixture and tends to increase the torque.

Torque as a Function of Flux Density

The relation between the torque and the average flux density existing in the gaps was determined from measurements described below and is shown in Figure 4. This curve is extremely interesting in that it is a straight line, whereas the torque in an eddy current dynamometer is proportional to the square of the flux density. From this curve an expression for the torque as a function of the flux density can be written as:

$$T = C + KB$$

where

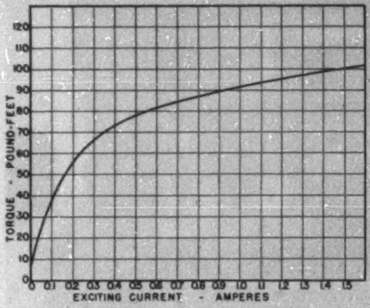

Figure 3 (left). Torque versus exciting current characteristic of the dynamometer

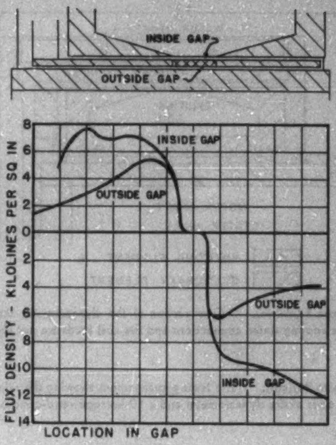

Figure 5 (right). The flux density variation in the gaps of the dynamometer. The gaps are identified as either outside or inside of the torque cylinder. Correlation between the flux density at any location and the location is provided by the cross section shown above the curves

T = the total torque
C = the torque caused by the viscosity and frictional effects
B = the average flux density
K = the slope of the curve

The term *KB* is the torque contributed by the magnetic fluid and the flux. Assuming that this torque is proportional to the effective area of the torque cylinder surface and the average radius to that surface, the following expression is written:

$$T' = K'RAB$$

where

T' = KB in the previous expression
R = the average radius of the torque cylinder
A = the effective area of the torque cylinder
K' = the force per flux line

The value of K' for the dynamometer of Figure 1 is 0.24 pound per kiloline. This factor depends on the magnetic fluid and provides a basis for future design of magnetic fluid machinery.

The average flux density used above was determined by measuring the flux density distribution in the gaps of a section of the dynamometer. A flux meter and a 100-turn exploring coil were used to measure the flux existing within the exploring coil for various values of exciting current. These measurements were made and the flux density calculated for 29 points in the gaps. Figure 5 is one of a family of flux density curves plotted from this data. The orientation of the exploring coil in the gap was such that only the component of the flux normal to the gap was measured. Other measurements have shown that it is only this component that produces the torque observed. The average flux densities were determined by measurement of the area under each set of curves of the family of curves of which Figure 5 is typical. This area was then divided by the active length of the torque cylinder surface to calculate the average flux density for a particular value of exciting current. The torque corresponding to the particular value of exciting current was then taken from Figure 3. Corresponding values of average flux density and torque were plotted as Figure 4.

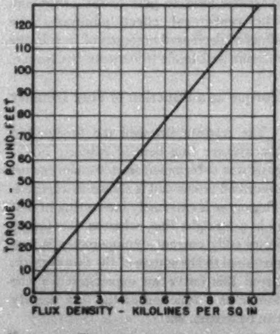

Figure 4. The torque versus average flux density characteristic of the dynamometer shown in Figure 1

The irregularity of the flux distribution indicates in addition an inefficient utilization of the exciting magnetomotive force. This irregularity is apparently due to poor design of the iron shape around the coil and to the shunting of some of the flux through the magnetic fluid and the torque cylinder. This effect was anticipated in the design and to reduce the shunting effect of the torque cylinder the center section was made of brass while the end pieces were made of iron to decrease the magnetomotive force required along the desired flux path. The lack of symmetry in the curves of Figure 5 is caused by the lack of symmetry in the reluctance of the magnetic circuit at either end of the dynamometer. Consequently the amount of leakage flux varies which results in the lack of symmetry observed.

Use of the Dynamometer, A Mechanical Power Instrument

When a given dynamometer has been calibrated for the torque-exciting current characteristic, the unit can be firmly fastened to the foundation and the torque read from the calibration curve or an ammeter may be calibrated directly in values of torque. The linear portion of the torque characteristic curve (Figure 3) may be extended by using an iron of higher permeability than that used in the test dynamometer. This also may be accomplished by using the present iron and increasing the dimensions. The linear characteristic thus achieved and the linear characteristic of the conventional electric tachometer may then be combined in an electrodynamometer-type indicating instrument. The meter reading will now be proportional to the product of a speed and a torque indication. These indications can be the indication of torque and speed for a motor under test and the reading would then be proportional to the mechanical output of the motor.

This reading could be calibrated in terms of horsepower or watts output of the motor. In addition the tachometer and the dynamometer may be designed as one unit. The voltage generated by the tachometer would be applied to the potential coil of a conventional wattmeter and current coil of the wattmeter would be connected in series with the exciting coil of the dynamometer. Such a dynamometer and indicating instrument would be very useful in testing motors for inspection or other purposes.

Conclusions

As a result of this investigation, it is concluded that:

1. A magnetic fluid dynamometer is definitely feasible and can be a useful engineering tool.

2. A mechanical power indicating instrument can be made by using an iron of greater permeability or increased dimensions in the design of the dynamometer, an electric tachometer, and a conventional electrodynamometer instrument.

3. Neoprene O-rings combined with iron guard rings provide a satisfactory seal for the magnetic fluid.

4. A mixture of seven parts by weight of carbonyl E and one part by weight of silicone oil, 20 centistokes viscosity provides a magnetic fluid of low residual torque and high magnetic fluid torque.

5. The factor, K', of the magnetic fluid is about 0.24 pound per kiloline.

6. Further study needs to be made of the factor, K', of the magnetic fluid.

7. The tendency of the iron particles to settle out of the mixture may be reduced by adding a thixotropic agent.

References

1. MAGNETIC FLUID CLUTCH, J. Rabinow. *Technical News Bulletin*, United States Bureau of Standards (Washington, D. C.), volume 32, 1948, pages 54–60.

2. THE MAGNETIC FLUID CLUTCH, Jacob Rabinow. *AIEE Transactions*, volume 67, part II, 1948, pages 1308–15 and *Electrical Engineering*, volume 67, December 1948, page 1167.

3. MAGNETIC POWDER CLUTCH SERVO, S. Wald. *Radio and Television News* (Chicago, Ill.), September 1950, pages 12A and 26A.

No Discussion

The Accuracy of Current Transformers Adjacent to High-Current Busses

R. A. PFUNTNER
ASSOCIATE MEMBER AIEE

CURRENT transformers normally have excellent accuracy when applied correctly under conditions for which they were designed. While the common operating conditions affecting accuracy are usually recognized and properly considered, there is one factor, the importance of which is frequently underestimated or even overlooked entirely. This is the effect of stray flux produced by high-current busses adjacent to the transformer.

When current transformers are applied in the vicinity of busses carrying large currents, the transformer accuracy may be very seriously affected. This is particularly true on systems which normally carry over 2,000 amperes and may carry 10 or 20 times this current during faults. A current transformer designed to operate protective relays during such a fault may be rendered completely useless by improper installation. For instance, Figure 10 gives the accuracy of a certain current transformer with the primary return conductor at various spacings. If a burden of 0.190 ohm were used, and a return spacing of 12 inches, saturation would occur at about 10,000 amperes. However, with the same burden and a return spacing of 6 inches, saturation would occur at only 6,000 amperes. This could mean the difference between relays operating properly and relays not operating at all. Because such operating conditions are difficult to reproduce in test, it is usually necessary to rely on calculated rather than tested accuracy when such a situation is encountered.

There has been a certain amount of published information[1-3] on the effect of stray fields on current transformer accuracy. However, in general, such information has been qualitative rather than quantitative; and, as a result, designers have considerable difficulty in predicting performance if the conditions are somewhat unusual. An investigation has been undertaken of both the theoretical and practical aspects of this problem. This investigation is divided into three sections as follows:

1. Theoretical analysis (basis of tests).
2. Flux pick-up factors (empirical data).
3. Accuracy calculations and tests (use of data).

While the theoretical study is applicable to any type of current transformer, empirical pick-up factors were determined primarily for bushing transformers because other types take an almost prohibitive number of shapes and designs. However, with a little care, the data presented can be applied to almost any design with sufficient accuracy to permit reasonable estimates of performance.

Theoretical Analysis

In a perfect current transformer, the ampere-turns produced in the secondary would be exactly equal to the ampere-turns applied to the primary. Practically, this condition is never attained because the core material is not perfect and, therefore, uses some of the primary ampere-turns in maintaining magnetic flux in the core. Since these exciting ampere-turns are used in the core, they cannot be reproduced in the secondary, and an error results. The core flux may be considered to be made up of two components; first, the mutual or burden flux which links both the primary and secondary windings and is necessary to produce the required secondary voltage; and second, the leakage or stray flux which may exist in some sections of the core due either to the leakage reactance of the primary and secondary coils themselves or to other current carrying conductors in the immediate vicinity.

The effect of stray flux produced by internal transformer leakage has been understood for many years. Since leakage flux (produced either by the coils themselves or by external conductors) will change the flux density in certain sections of the core, the errors will be affected. This fact is just as true in a bushing transformer with a uniformly distributed winding as in any other type of transformer, although this has not always been generally understood.

In the theoretical study of the effect of stray flux on current transformer accuracy, two conditions were analyzed as being representative of the general problem. The first considered an annular core transformer with uniformly distributed secondary winding, and the second an annular core transformer with the secondary concentrated on two small sections of the core. In both cases, a bar type (single turn) primary was assumed since nearly all high-current transformers have a single turn primary.

RING CORE WITH DISTRIBUTED SECONDARY WINDING AND SINGLE BAR PRIMARY

The following assumptions were made:

1. Transformer completely symmetrical above and below a plane taken through the primary conductor and the adjacent conductor.
2. Primary bar perfectly centered in core.
3. Secondary winding evenly distributed around core.
4. Stray flux enters at one point of core. In practice, other flux entering at other points would act in a similar manner since the point of entry is general.

Paper 51-308, recommended by the AIEE Instruments and Measurements Committee and approved by the AIEE Technical Program Committee for presentation at the AIEE Pacific General Meeting, Portland, Oreg., August 20–23, 1951. Manuscript submitted May 21, 1951, made available for printing July 9, 1951.

R. A. PFUNTNER is with the General Electric Company, West Lynn, Mass.

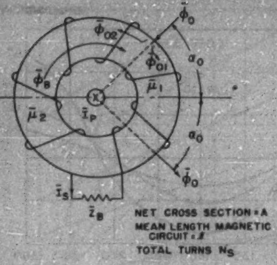

Figure 1 (left). Ring core with distributed winding

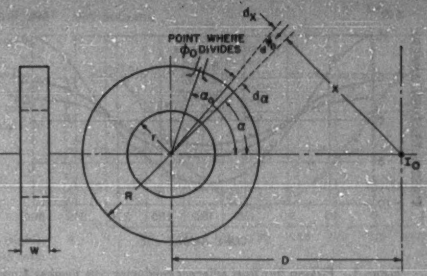

Figure 2 (right). Ring core with adjacent conductor

Referring to Figure 1, three equations may be written as follows:

The total voltage across the burden must equal the voltage induced by the flux linking the windings

$$I_sZ_B=\frac{\alpha_0}{\pi}N_s(\phi_B+\phi_{01})+\left(1-\frac{\alpha_0}{\pi}\right)N_s(\phi_B-\phi_{02}) \quad (1)$$

The total primary ampere turns minus the total secondary ampere turns must equal the magnetizing ampere turns of the core

$$I_p-I_sN_s=\frac{\frac{\alpha_0}{\pi}l}{A\mu_1}(\phi_B+\phi_{01})+\frac{\left(1-\frac{\alpha_0}{\pi}\right)l}{A\mu_2}\times(\phi_B-\phi_{02}) \quad (2)$$

The stray flux in the core must equal the flux entering the core

$$\phi_{01}+\phi_{02}=\phi_0 \quad (3)$$

Eliminating ϕ_{01}, ϕ_{02}, ϕ_B from equations 1, 2, and 3 gives

$$I_p-I_sN_s=\frac{\frac{\alpha_0}{\pi}l}{A\mu_1}\left[\frac{I_sZ_B}{N_s}+\left(1-\frac{\alpha_0}{\pi}\right)\phi_0\right]+\frac{\left(1-\frac{\alpha_0}{\pi}\right)l}{A\mu_2}\left[\frac{I_sZ_B}{N_s}-\frac{\alpha_0}{\pi}\phi_0\right] \quad (4)$$

While equation 4 may be solved for I_s, it is most conveniently used in its present form.

It should be noted that equation 4 is in exactly the same form as equation 2 and, therefore,

$$\phi_B=\frac{I_sZ_B}{N_s},\quad \phi_{01}=\left(1-\frac{\alpha_0}{\pi}\right)\phi_0,\quad \phi_{02}=\frac{\alpha_0}{\pi}\phi_0$$

Since, in the above equation, ϕ_B produces all the required burden voltage, no voltage is induced by ϕ_0. The voltage induced by ϕ_{01} is exactly equal and opposite to that induced by ϕ_{02}. This flux condition is independent of the permeabilities in the two sides of the core. However, if the primary current is reduced to zero, secondary current will flow due to the action of ϕ_0 unless the permeabilities are equal.

From a practical point of view, equation 4 indicates the basic method of test or calculation. From the above definitions, ϕ_B, ϕ_{01}, and ϕ_{02} may be calculated directly at any value of secondary current I_s if ϕ_0 and α_0 are known. Once the flux is determined, known data on the core material will give the permeabilities, μ_1 and μ_2, and I_p can be calculated from equation 4.

To show that ϕ_0 can always be assumed to divide such that ϕ_{01} and ϕ_{02} induce equal and opposite voltages in the secondary winding, a nonuniformly wound secondary is considered.

Ring Core with Two Concentrated Secondary Winding and Single Bar Primary

The assumptions were the same as for the distributed winding calculation except that the secondary is wound in two sections, one on either side of the core at the central horizontal plane.

The analysis is the same except for equation 1 which becomes

$$I_sZ_B=\frac{N_s}{2}(\phi_B+\phi_{01})+\frac{N_s}{2}(\phi_B-\phi_{02}) \quad (5)$$

The same solution as before gives the following result

$$I_p-I_sN_s=\frac{\frac{\alpha_0}{\pi}l}{A\mu_1}\left[\frac{I_sZ_B}{N_s}+\frac{\phi_0}{2}\right]+\frac{\left(1-\frac{\alpha_0}{\pi}\right)l}{A\mu_2}\left[\frac{I_sZ_B}{N_s}-\frac{\phi_0}{2}\right] \quad (6)$$

This is basically the same as equation 4 for the distributed winding. The same discussion holds, and the only point to be made is that again the assumed ϕ_0 split should be made such as to induce no voltage in the winding. In this case, this means that $\phi_{01}=\phi_{02}$ regardless of the entry point of ϕ_0 if it is between the two coils.

In a practical case, the stray flux does not enter the core at one point but rather at all points on the core. However, the same assumption of no apparent induced

Nomenclature

I_p = primary current (rms amperes)
I_0 = adjacent conductor current (rms amperes)
I_s = secondary current (rms amperes)
E_s = secondary voltage (rms volts)
ϕ_B = circulating flux in core (rms volts/turn)
ϕ_0 = total stray flux entering core from adjacent conductor (rms volts/turn)
ϕ_{01} = portion of ϕ_0 which follows core side 1 (rms volts/turn)
ϕ_{02} = portion of ϕ_0 which follows core side 2 (rms volts/turn)
ϕ_{0a} = stray flux at any point (a) in core (rms volts/turn)
H = magnetic intensity at any point in core (rms ampere turns/inch)
μ_1 = permeability of core side 1 (rms volts/turn square inch/rms ampere turns/inch)
μ_2 = permeability of core side 2 (rms volts/turn square inch/rms ampere turns/inch)
α = angle around core to point where $d\phi_0$ enters core, radians
α_0 = angle around core to point where ϕ_0 divides, radians
R_s = secondary resistance, ohms
Z_B = total secondary burden including R_s, ohms
N_s = total secondary turns
A = net cross section of core, square inches
l = mean length of magnetic circuit, inches
R = outside radius of core, inches
r = inside radius of core, inches
W = width of core, inches
D = distance from center of primary conductor to center of adjacent conductor, inches
x = distance from adjacent conductor to point where $d\phi_0$ enters core, inches
k = core pick-up factor (ratio of the flux entering a magnetic core to the flux entering a nonmagnetic core of the same dimensions when placed in a magnetic field)

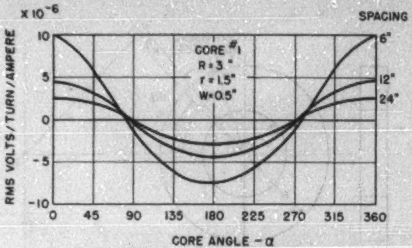

Figure 3. Pick-up flux from adjacent conductor core number 1

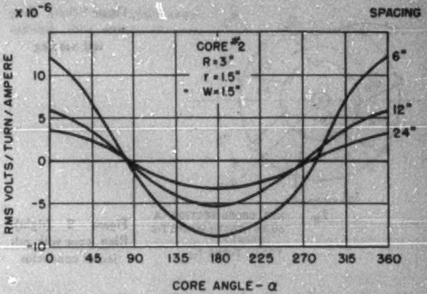

Figure 4. Pick-up flux from adjacent conductor core number 2

voltage may be used to determine how ϕ_0 divides.

Flux Pick-Up Factor of Ring Cores

The other question to be given some theoretical consideration is involved in the amount of stray flux picked up by a magnetic core located in the field of a current-carrying conductor. The core will be considered to have a rectangular cross section but annular in shape, similar to the usual bushing transformer core.

The following assumptions were made:

1. Core completely symmetrical above and below the plane through the axis of the core and the adjacent conductor.
2. Adjacent conductor straight and infinite in length.
3. Permeability of core large compared to air.
4. Path of flux from adjacent conductor can be considered a complete circle around conductor. Empirical pickup factors include the effect of shortening of air path by magnetic core.
5. Pick-up factor uniform over core (not strictly true, but gives sufficient accuracy for most purposes).

Referring to Figure 2, the flux $d\phi_0$ entering the core over an incremental distance dx at a distance x from the adjacent conductor (neglecting the effect of the core in shortening the air path) is

$$d\phi_0 = k\frac{3.2\times 1.414 I_0}{2\pi x}Wdx\frac{1}{4.44\times 60\times 10^{-8}}$$

$$= 1.92\times 10^{-6}kWI_0\frac{dx}{x}\ \text{volts/turn at 60 Cycles} \qquad (7)$$

Table I

Transformer Number	R, Inches	r, Inches	W, Inches	N_s	R_s, Ohms
1	3	1.5	0.5	183	0.139
2	3	1.5	1.5	165	0.174
3	3	2.5	1.5	209	0.157

Writing x in terms of the angle α around the core

$$x = [(D - R\cos\alpha)^2 + (R\sin\alpha)^2]^{1/2} \qquad (8)$$

$$x = [D^2 - 2RD\cos\alpha + R^2]^{1/2} \qquad (9)$$

$$dx = \frac{RD\sin\alpha d\alpha}{[D^2 - 2RD\cos\alpha + R^2]^{1/2}} \qquad (10)$$

Substituting equations 9 and 10 in equation 7

$$d\phi_0 = 1.92\times 10^{-6}kWDRI_0\frac{\sin\alpha d\alpha}{D^2 - 2RD\cos\alpha + R^2} \qquad (11)$$

Equation 11 is an expression for the flux entering the core through the differential angle $d\alpha$ at any point on the core described by the angle α. The flux in any section of the core may be found by integrating equation 11 from the point where the flux divides, α_0, to that section. However, equations 4 and 6 stated that α_0 must be taken such that no voltage is induced in the windings. This condition involves an integration which becomes very difficult to perform.

In order to avoid this integration, it is better to numerically integrate equation 11 for the particular core involved. By carrying on this integration from $\alpha = 0$ toward α_0 and $\alpha = \pi$ toward α_0 simultaneously, α_0 may be found for the condition of zero induced voltage.

The total flux picked up by the core may be found directly by integrating equation 11 from $\alpha = 0$ to $\alpha = \pi$.

$$\phi_0 = 1.92\times 10^{-6}kWDRI_0\times \int_0^\pi \frac{\sin\alpha d\alpha}{D^2 - 2RD\cos\alpha + R^2} \qquad (12)$$

$$\phi_0 = 1.92\times 10^{-6}kWDRI_0\times \left[\frac{1}{2RD}\log_n(D^2 - 2RD\cos\alpha + R^2)\right]_0^\pi \qquad (13)$$

$$\phi_0 = 1.92\times 10^{-6}kWI_0\log_n\frac{D+R}{D-R} \qquad (14)$$

The only unknown factor involved in equation 14 is the pick-up factor k. Considerable data has been taken in order to evaluate k empirically.

Flux Pick-Up Test

For the purpose of evaluating k for ring cores, three experimental transformers were made up of mumetal. A 20-turn search coil was placed each $22^1/_2$ degrees around the cores before winding the evenly distributed secondary. Table I gives the dimensions, secondary turns, and secondary resistance of each.

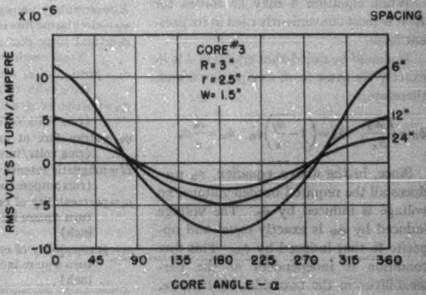

Figure 5. Pick-up flux from adjacent conductor core number 3

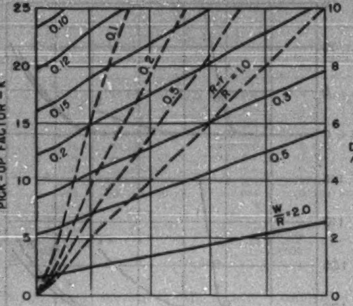

Figure 6 (left). Core pick-up factor—enter with D/R, horizontally to (R—r)/R, vertically to W/R, horizontally to k

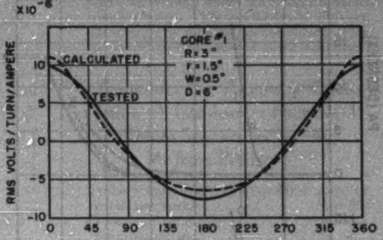

Figure 7 (right). Pick-up flux from adjacent conductor core number 1

These transformers were placed in a test fixture in such a manner that the bar primary passed through the core and returned at distances of 6, 12 or 24 inches, as desired. The secondary was short-circuited and search-coil voltages measured for known values of primary current. That component of search-coil voltage which was 90 degrees out-of-phase with the primary current, was assumed to be due to the adjacent conductor. The in-phase component was constant around the core and corresponded to the resistance load of the secondary winding. Figures 3, 4, and 5 give the results in terms of volts/turn/primary ampere at 60 cycles.

The total flux picked up by these three cores at the three spacings was substituted into equation 14 and the pick-up factor, k, calculated in Table II. The dimensionless ratios D/R, W/R, and $(R-r)/R$, also are included in Table II.

Figure 6 is a plot of pick-up factor versus the dimensionless ratios given in Table II. While there was insufficient data taken to accurately determine the exact functions involved, the curves fit the ranges of dimensions covered by test and are sufficiently accurate for practical purposes.

While these curves were made for ring cores, sufficient checks have been made against rectangular cores to show that estimated radii of rectangular cores can be used to obtain the pick-up factor in the above range of dimensions.

The calculated flux distribution in the cores was found to agree quite well with the tested values. As might be expected, the pick-up factor was smaller on the side of the core which was close to the return. This tended to make the calculated α_0 smaller than the tested α_0, and the calculated flux in the side of the core next to the return larger than the tested value. Figure 7 is a comparison of the tested curve for a 6-inch spacing on core number 1 (see curve 3) against a numerically integrated curve (equation 11) for the same conditions. This integration is given in Appendix I.

Accuracy Calculations and Tests

A current transformer which is being subjected to interference flux from an adjacent conductor presents the same problem of accuracy calculation as a transformer with internal leakage. The general method is to divide the core into several sections, estimate the flux density in each section, find the exciting ampere turns necessary to produce this density in each section, and vectorially add these exciting ampere turns to give the total exciting ampere turns from which ratio and phase angle errors may be found. This type of calculation has been discussed in previous papers, so it will not be considered further here. Appendix II gives a sample calculation for one of the above transformers.

The three bushing-type transformers were tested at two burdens and three return conductor spacings. The accuracy curves are presented on Figure 8, 9, and 10. Several calculated points are included to give an idea of the comparison between calculated and tested results.

It should be noted that when calculations are made in the region where the core iron is saturating, very small errors in density produce very large changes in calculated accuracy. This means that calculated accuracy cannot be expected to check tested accuracy closely if the transformer errors are large. Usually the point where the errors start to increase rapidly can be calculated with reason-

Table II

Transformer Number	$\frac{R-r}{R}$	$\frac{W}{R}$	D=6 inch D/R	 k	D=12 inch D/R	 k	D=24 inch D/R	 k
1	0.5	0.167	2	16.6	4	18.7	8	22.8
2	0.5	0.5	2	6.60	4	7.59	8	10.4
3	0.167	0.5	2	6.15	4	7.00	8	8.16

Table III

α	$d\phi_a$	$Nd\phi_a$	E_s	$a=\alpha-5$ ϕ_{oa}	α	$d\phi_a$	$Nd\phi_a$	$-E_s$	$a=\alpha+5$ ϕ_{oa}
5	0.47	0.24	0.24	11.05	175	0.05	0.03	0.03	6.44
15	1.26	1.89	2.13	10.58	165	0.16	0.24	0.27	6.39
25	1.71	4.27	6.40	9.32	155	0.27	0.68	0.95	6.23
35	1.85	6.48	12.88	7.61	145	0.38	1.34	2.29	5.96
45	1.81	8.15	21.03	5.76	135	0.50	2.26	4.55	5.58
55	1.67	9.21	30.24	3.95	125	0.62	3.42	7.97	5.08
65	1.52	9.86	40.10	2.28	115	0.75	4.89	12.86	4.46
56% of 75	0.76	5.71	45.81	0.76	105	0.89	6.66	19.52	3.71
	11.05				95	1.03	8.75	28.27	2.82
					85	1.19	11.28	39.55	1.79
					44% of 75	0.60	6.25	45.80	0.60
						6.44			

$d\phi_a = 7.96\frac{\sin\alpha d\alpha}{1.25-\cos\alpha}$

Figure 7 is a plot of ϕ_{oa} versus α
$\alpha_0 = 75.6$ $(\Sigma E_s = 0)$

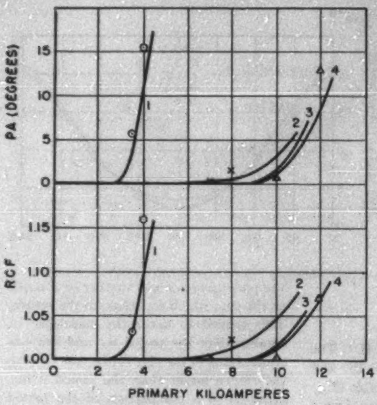

Figure 8 (left). Overcurrent accuracy of transformer number 1

Tested Curve	Calculated Points	Connected Burden	Return Spacing, Inches
1	⊙	0.766+j0	6
2	×	0.166+j0	6
3		0.166+j0	12
4	△	0.166+j0	24

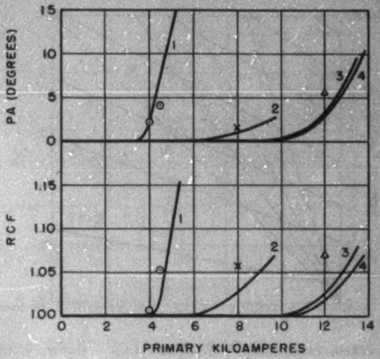

Figure 10 (right). Overcurrent accuracy of transformer number 3

Tested Curve	Calculated Points	Connected Burden	Return Spacing, Inches
1	⊙	0.790+j0	6
2	×	0.190+j0	6
3	△	0.190+j0	12
4		0.190+j0	24

able accuracy, but no attempt is made to carry the curve further.

In the practical case, it is usually unnecessary to go through the complete accuracy calculation in order to determine whether or not a given installation will be satisfactory. Referring to Table III, Appendix II, it may be noted that nearly all of the error is caused by saturation in section 1, which is the section of the core closest to the return conductor. This means that the transformer accuracy will be good for primary current up to the point where section 1 starts to saturate. By estimating the flux density in this section, the maximum safe operating current may be obtained. The burden flux ϕ_B, and the stray flux ϕ_{01} will be assumed to be in phase since this represents the worst possible condition. By definition, the burden flux, ϕ_B, is given by

$$\phi_B=\frac{I_sZ_B}{N_s}=\frac{I_pZ_B}{N_s^2} \text{ volts/turn} \qquad (15)$$

for a transformer with a single-turn primary. If the only stray flux to be considered is that produced by an adjacent conductor (no internal leakage), equation 14 may be used to find the total flux picked up by the core.

$$\phi_0=1.92\times10^{-6}kWI_0 \log_e \frac{D+R}{D-R} \qquad (14)$$

From the curves of Figure 3, 4, and 5, it may be assumed that ϕ_{01} = 60 per cent of ϕ_0, that is 60 per cent of the flux picked up by the core passes through the section nearest the return conductor so

$$\phi_{01}=1.15\times10^{-6}kWI_0 \log_e \frac{D+R}{D-R} \qquad (16)$$

For the transformer calculated in Appendix II

$$\phi_B=\frac{I_p\times0.305}{(183)^2}=9.1\times10^{-6}I_p \text{ volts/turn}$$

$$\phi_{01}=1.15\times10^{-6}\times0.5\times I_0 \log_e \frac{6+3}{6-3}$$
$$=10.5\times10^{-6} \text{ volts/turn}$$

In this case, the adjacent conductor is the primary return so that $I_p=I_0$ and the total flux in section 1 is

$$\phi_B+\phi_{01}=(9.1+10.5)10^{-6}I_p=19.6\times10^{-6}I_p$$

Figure 9. Overcurrent accuracy of transformer number 2

Tested Curve	Calculated Points	Connected Burden	Return Spacing, Inches
1	⊙	0.750+j0	6
2	×	0.150+j0	6
3		0.150+j0	12

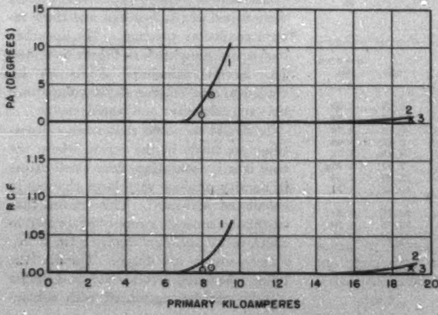

Figure 11. Allegheny mumetal 0.025-inch thick ring punchings transformer numbers 1, 2, 3 at 60 cycles

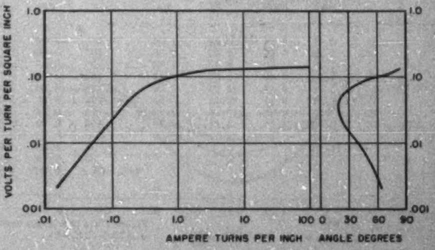

Table IV

Section	Section l	ϕ_B/A	ϕ_{oa}/A	$\frac{\phi_B+\phi_{oa}}{A}$	H	Hl section
1	0.88	0.103+j0	0+j0.109	$0.150\underline{/+46}$	$180\underline{/-87}$	120−j 104
2	0.88	0.103+j0	+j0.103	0.145 +45	100 −87	66−j 58
3	1.76	0.103+j0	+j0.084	0.133 +39	18 −83	23−j 22
4	1.76	0.103+j0	+j0.046	0.113 +24	1 −73	1−j 2
5	1.76	0.103+j0	+j0.006	0.103 + 3	1 −63	1−j 2
6	1.76	0.103+j0	−j0.026	0.106 −15	1 −67	0−j 2
7	1.76	0.103+j0	−j0.056	0.117 −29	2 −76	−1−j 4
8	1.76	0.103+j0	−j0.074	0.127 −36	6 −81	−5−j 10
9	1.76	0.103+j0	−j0.082	0.132 −39	16 −83	−15−j 24
	$\Sigma l=14.1$					190−j 228

$RCF=1+\frac{190}{8{,}000}=1.024$ $\qquad PA=-57.3\frac{-228}{8{,}000}=+1.6°$

The core cross section is 0.71 square inch, so the flux density is

$$\frac{\phi_B+\phi_{oa}}{A}=\frac{19.6\times10^{-6}I_p}{0.71}$$
$$=27.6\times10^{-6}I_p \text{ volts/turn/square inch}$$

From Figure 11, core saturation will occur at about 0.14 volt per turn per square inch, so the limiting primary current for good accuracy is approximately

$$I_p=\frac{0.14}{27.6\times10^{-6}}=5{,}100 \text{ amperes}$$

From Figure 8, this is seen to be somewhat conservative, but nevertheless, a very good guide in determining whether or not a given installation is satisfactory.

Conclusions

1. A practical method of estimating the flux in a transformer core under the influence of an adjacent current-carrying bus has been investigated. It has been shown that by assuming a fixed secondary current, the stray flux in the core may be assumed to divide in such a manner as to induce no voltage in the secondary winding.

2. Empirical data is given for estimating the pick-up factor of a ring core in such a field. This may be applied with reasonable accuracy to rectangular cores by using the estimated equivalent radii of the rectangular core.

3. The use of this data in calculating current transformer accuracy is discussed and verified by test results.

4. A simplified method of calculating the approximate maximum current at which good accuracy can be expected is demonstrated.

Appendix I

Numerical calculation of equation 11:

$$d\phi_0=1.92\times10^{-6}kWDRI_0\frac{\sin\alpha d\alpha}{D^2-2RD\cos\alpha+R^2} \qquad (11)$$

For transformer number 1 with 6 inch return:

$W=0.5,\ D=6,\ R=3\ \ I_0=1$ ampere

k from Figure 6 is found to be 16.6. Substituting the constants in equation 11 gives

$$d\phi_0=7.96\frac{\sin\alpha d\alpha}{1.25-\cos\alpha} \text{ microvolts/turn}$$

$d\alpha$ is taken as 10 degrees for the numerical integration. Referring to Table III, $d\phi_0$ is calculated for various values of α starting simultaneously from $\alpha=0$ and $\alpha=180$ degrees. $Nd\phi_0$ is taken as the number of sections through which $d\phi_0$ passes times $d\phi_0$ since the turns per section is a constant. E_s is the sum of the $Nd\phi_0$ terms up to α. This integration is carried on until the point, α_0, is found where the voltage is equal from both sides. The actual flux in the core ϕ_{oa} is found by totaling $d\phi_0$ and substracting the amount which entered at each section.

Appendix II. Accuracy Calculation of Transformer Number 1 Return Spaced Six Inches from Primary

Primary current....$I_p=I_s=8{,}000$ amperes
Secondary turns................$N_s=183$
Secondary resistance.....$R_s=0.139$ ohms
Net cross section
of core..................$A=0.71$ inch^2
Mean length of magnetic
circuit of core...........$l=14.1$ inches
External burden.........$=0.166+j0$ ohms
Secondary burden.....$Z_B=0.305+j0$ ohms
Core material.................Mumetal
(See Figure 11 for data)

The core is divided into 18 sections; 14 sections are $22^1/_2$ degrees and the other 4 are $11^1/_4$ degrees. The smaller sections are taken next to the return conductor because the density changes rapidly in this area. Since the core is symmetrical above and below the plane of the primary and return, the top and bottom half may be combined to give seven sections of 45 degrees and two sections of $22^1/_2$ degrees.

The procedure is conventional in that the density, magnetic intensity from Figure 11, and exciting ampere-turns are found for each section and then added to give the total exciting ampere turns. The error in terms of ratio correction factor and phase angle are calculated from the in-phase and in-quadrature components of the ampere turns necessary to maintain the flux in the core. Table IV gives the calculations for this example.

References

1. LEAKAGE PHENOMENA IN RING-TYPE CURRENT TRANSFORMERS, A. H. M. Arnold. *Journal, Institution of Electrical Engineers* (London, England), volume 74, May 1934, pages 413–23.

2. INFLUENCE OF LEAKAGE FLUX UNDER VARIOUS CONDITIONS, H. R. Forest. *Electrical Review* (London, England), volume 143, July 9, 1948, pages 51–54.

3. COMPUTATION OF ACCURACY OF CURRENT TRANSFORMERS, A. T. Sinks. *Electrical Engineering (AIEE Transactions)*, volume 59, December 1940, pages 663–68.

Discussion

E. C. Wentz (Westinghouse Electric Corporation, Sharon, Pa.): Mr. Pfuntner is to be congratulated on a most workmanlike and practical solution of a most difficult yet important problem. The importance of stray fields from high current busses in affecting nearby current transformers is not generally realized.

Even when this effect has been understood to exist, no good method for calculation of the effect has been published. Any exact method of calculation is entirely too complicated for practical use, and any practical methods have been not much better than rules of thumb.

Stray fields due to current limiting reactors also are known to affect current transformers. I would like to know whether any simple adaptation of this method can be used to deal with this problem.

The usual installation has three current transformers side by side in a 3-phase bus. The outside transformers are exposed to the fields from the other two phases. Presumably the flux would have to be calculated for each bus and added vectorially.

The principal utility of this method is in number 4 of the author's conclusions—the calculation of the saturation point of the transformer. At densities below saturation the leakage fluxes flowing in opposite direction in the opposite parts of the core tend to cancel their effects, but when one part of the core begins to saturate the transformer rapidly becomes useless. Therefore the method is not usually necessary for calculation of metering accuracy over the range of current up to 100 per cent current, but will often be of value in determining the operation of relays at high currents.

The method is of value in determining the performance of existing installations, or proposed installations with existing designs. It will possibly be of interest to describe how we have designed transformers for some 20 years to overcome the effect of return busses or stray fields so that it is not necessary to perform any special calculations to insure good accuracy. The construction we have

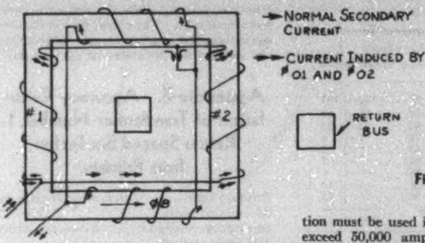

Figure 1

used is shown in Figure 1 of this discussion. Inspection of this figure will show that coils number 1–2 will supply approximately equal currents as they are effectively connected in parallel with respect to the flux ϕ_B, but they are effectively short circuited against each other with respect to the leakage fluxes ϕ_{01} and ϕ_{02} and current flows around the number 1–2 coil circuit which opposes the leakage flux. Inasmuch as there is relatively little leakage current magnetomotive force developed across the space occupied by the current transformer, the leakage flux is readily diverted from the transformer into the space around the transformer and the core is effectively free of leakage flux.

A rule of thumb which has been generally successful is that this series parallel connection must be used if the fault current is to exceed 50,000 amperes with 20-inch bus spacing. Supposing a typical transformer to have constants $W=2$, $R=5$, $r=4$ with 1.8 square inch core section, 50,000 amperes produces, by the author's method about 7,500 gausses, or more than one-third the effective "saturation" density, showing that the rule of thumb should be reasonably successful. It is always encouraging to get scientific confirmation of a rule of thumb. In this case, as in many others, the scientific confirmation shows where the rule of thumb may get us into trouble. It appears, however, that the series parallel connection must still be used when the calculation according to Mr. Pfuntner's method shows too high a leakage flux density.

A parallel connection scheme, used in wound-type current transformers to eliminate leakage flux, has been patented.

R. A. Pfuntner: I would like to express my appreciation for the interesting comments and discussion presented by Mr. Wentz. While, as Mr. Wentz says, it is always encouraging to get scientific confirmation of a rule of thumb, it is likewise very encouraging to have one's scientific data confirmed by a rule of thumb developed through years of operating experience.

With respect to the effect of current limiting reactors on current transformer accuracy, I have had no occasion to work on this problem, but I see no reason why the pick-up factors obtained in the paper could not be applied quite easily.

It is true that in a polyphase installation it is necessary to vectorially add the flux produced by each bus. While under normal operating conditions with balanced phase currents there is usually some cancellation effect, under fault conditions this may not be true. The interference problem is most serious during faults when currents are very high. These bus currents may be widely unbalanced depending on the type of fault encountered.

Generally the short calculation of the saturation point is all that is required. In most cases this will show that a given installation is either well within the safe operating range or seriously in trouble. Occasionally installations are found where it is desirable to make a more exact check in order to be sure that the operation will be satisfactory under all conditions.

Economic Aspects of Series Capacitors in High-Voltage Transmission

R. S. SEYMOUR
ASSOCIATE MEMBER AIEE

E. C. STARR
FELLOW AIEE

THE TECHNICAL aspects of series-capacitor compensation of high-voltage transmission lines have been covered rather fully in the technical literature.[1,2,3] The economic aspects of series capacitors, however, have not been very thoroughly explored, particularly in the light of recent cost, and technical developments.

It is the purpose of this paper to report the results of detailed studies of the economic aspects of certain segments of the series capacitor problem.

Previous studies have emphasized the economic importance of adequate circuit loading and of proper load distribution among the several circuits of a transmission system. Series capacitors afford an excellent means of increasing the power capability of long lines to their economic maximum, and of adjusting the distribution of load in various parts of multiple networks to achieve best economy.

The present paper treats the compensation of single and 2-circuit sectionalized lines of various lengths and voltages. Three-conductor sizes were studied and the influences of load factor and relative loss cost were included.

Basic Assumptions

The several component costs involved in transmission facilities were analyzed very carefully on both the public and private financing bases and relative cost levels were established. It was found that the ratio of costs of losses to annual fixed costs for comparable facilities was essentially the same for both public and private financing in all of the several systems studied. This made possible the establishment of relative base costs both for peaking capacity and for energy transmission to which the costs of all examples studied could be compared. This base was taken to be the annual cost of a 230-kv single-circuit line, 100 miles long, using aluminum cable steel-reinforced (ACSR) conductors of 500,000 circular mil copper equivalent. The loading base was surge impedance value, approximately 125,000 kw, and the annual load factor was taken to be 75 per cent. Sending and receiving-end circuit breaker positions were included and the operating voltage ratio, sending to receiving, was taken to be 230 kv to 220 kv.

Table I lists the components of this base, evaluated in percentage, for which the total annual cost per peak kilowatt is taken to be 100 per cent. Likewise, the total transmission cost per kilowatt-hour of the base facility was taken to be 100 per cent and the four principal components were evaluated and tabulated. All other annual costs in the study were related to these base costs in terms of percentages or per unit. This tabulation also contains comparative data for the same line operating at 50 per cent load factor, surge-impedance load, and at the load of maximum economy, 75 per cent load factor and 50 per cent load factor. It is shown that the annual cost per peak-kilowatt of the base facility is 88 per cent of the base total when the loading is increased to that of maximum economy and that a change of load factor makes a significant change in the annual cost per peak-kilowatt. The cost of energy transmission or cost per kilowatt-hour is shown to be affected to a greater degree by load factor and likewise to be reduced by increasing the peak load to that of maximum economy.

The annual cost of facilities is given in terms of its ratio to the annual transmission cost per peak-kilowatt of the above-mentioned base condition. The cost in dollars would be the product of the given ratio and the dollars per peak-kilowatt for the base condition. The following is a list of the assumptions used in making the calculations:

Reactive Supply

The cost of supplying the line reactive requirements at the receiving-end, as a function of equipment rating, is shown in Figure 1. The costs are based on one-third of the reactive being supplied by synchronous condensers and two-thirds by shunt capacitors.

It was assumed that the sending-end generators were 95 per cent power factor machines. No charge for sending-end reactive was made for power factors of 95 per cent and above. For sending-end power factors under 95 per cent, charges were made at the rate shown in Figure 1 for all reactive in excess of the reactive that could be obtained from the 90 per cent power factor machines, without overloading.

Where sending-end generators are unity power factor machines some charge would have to be made for all reactive supplied the sending-end of the transmission line. For this case series compensation would prove to be more favorable since the amount of reactive supplied to the sending-end of the line is reduced by series capacitors.

For lines originating at substations in a transmission grid system, remote from generating stations, full charge for supplying the line reactive requirements should be made and also credit be given to any line supplying reactive to the sending-end substation. The use of series capacitors in such lines would be more

---

Paper 51-309, recommended by the AIEE Transmission and Distribution Committee for presentation at the AIEE Pacific General Meeting, Portland, Oreg., August 20–23, 1951. Manuscript submitted May 23, 1951; made available for printing July 10, 1951.

R. S. Seymour is with the Bonneville Power Administration, Portland, Oreg., and E. C. Starr is with Oregon State College, Portland, Oreg.

The authors wish to express their appreciation to their colleagues for contributions to this paper and especially to acknowledge the assistance given by A. K. Johnson and R. H. Rankin in making the calculations.

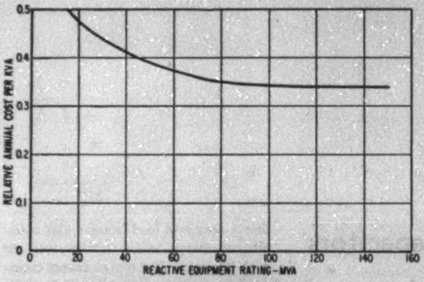

Figure 1. Annual cost of reactive. One-third supplied by synchronous condensers, two-thirds by shunt capacitors

Relative annual cost base: annual cost per peak kilowatt of 230-kv, 500,000 circular mil copper equivalent, 100-mile transmission at surge impedance loading, 75 per cent load factor

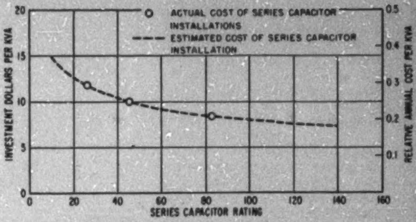

Figure 2. Estimated and actual cost of high-voltage series capacitors

Relative annual cost base: annual cost per peak kilowatt of 230-kv, 500,000 circular mil copper equivalent, 100-mile transmission at surge impedance loading, 75 per cent load factor

favorable than shown in the analysis presented in this paper.

Series Capacitors

Figure 2 shows the estimated and actual installed cost in dollars and the annual cost ratio for high-voltage series capacitors. The actual cost of three 230-kv series capacitor installations is indicated on the curve.

Autotransformers

For 287-kv and 345-kv transmission, autotransformers were used for transformation between line and sending-end and receiving-end 230-kv busses. In all analyses, costs and power capability, the autotransformers were considered as part of the transmission lines. The autotransformer impedances assumed were 3.5 per cent for 287 kv and 6.5 per cent for 345 kv. Figure 3 shows the estimated annual cost ratios for 230/287-kv and 230/345-kv autotransformers.

Line

Table II lists the cost per mile of average single-circuit construction for the transmission voltages and conductor sizes considered. Also included in the tabulation is the approximate loading required to prevent the formation of ice on the conductors under sleeting conditions.

Method of Calculation

The electrical characteristics were determined by long-line power-circle diagrams. An example of a power-circle diagram is shown in Figure 4. This figure illustrates the characteristics of a compensated line as compared with an uncompensated line. It can be seen how the power capability is increased by compensation by the comparison of the voltage angles indicated on the circles for the two lines.

Table I. Annual Transmission Cost Ratios

Per Cent of Base Total Annual Transmission Cost 230-Kv Line, 100 Miles, 500,000 Circular Mil Copper Equivalent Conductor

	Annual Transmission Cost per Peak Kw				Transmission Cost per Kw-Hr			
	At Surge Impedance Loading, Per Cent, Load Factor		At Maximum Economy, Lowest Annual Cost,* Per Cent, Load Factor		At Surge Impedance Loading, Per Cent, Load Factor		At Maximum Economy, Lowest Annual Cost,* Per Cent, Load Factor	
	75**	50	75	50	75**	50	75	50
Fixed Charges								
Line, Per Cent	62	62	40	40	62	93	40	60
Circuit Breakers	19	19	12	12	19	29	12	18
Power Losses	17†	14‡	28†	22‡	17§	20¶	28§	33¶
Reactive Supply	2	2	8	8	2	3	8	12
Total, Per Cent	100	97	88	82	100	145	88	123

* Loading at Maximum Economy—200,000 kw.

** Base condition.

† Charged at 5.45 per unit of base cost per peak kilowatt loss.

‡ Charged at 4.40 per unit of base cost per peak kilowatt loss.

§ Charged at 6.96 per unit of base cost per kilowatt-hour total loss.

¶ Charged at 11.00 per unit of base cost per kilowatt-hour total loss.

Power Capability

A voltage angle of 40 degrees between 230-kv sending-end and receiving-end busses was used as the criterion of maximum power capability, but the 30-degree angle points are indicated also for use when the reactances of the terminal systems are higher than those necessary to effectuate the 40-degree criterion.

Series Capacitor Applications

The application of series capacitors to lines and feeders supplying fluctuating low-power-factor loads to prevent voltage flicker has been well explored previously and the conditions necessary for economical application have been pointed out.[3] This application is not discussed in the present paper.

The division of load between circuits of various lengths and current capacity operating essentially in parallel in an integrated network can be controlled by series capacitors to bring about the most economical over-all operation. The curves and data presented in this paper make possible the choice of loadings of

Table II. Transmission Line Cost and Ice-Prevention Loading

Line, Kv	Conductor, Thousand Circular Mil Copper Equivalent ACSR, Unexpanded	Approximate Ice Prevention Loading, Mva	Cost per Mile of Average Single-Circuit Construction (Late 1950 Costs)
230	500	150*	$39,400
	800	220	45,900
	1,240	300	55,000
287	800	275	46,800
	1,240	375	56,200
345	1,240	450	58,200

* Actual experience value in Pacific Northwest.

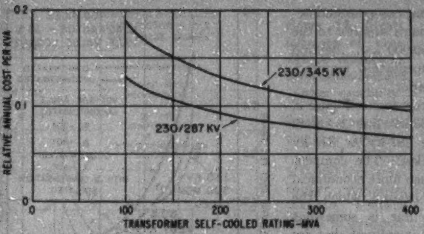

Figure 3. Annual cost of 230/287-kv and 230/345-kv autotransformers

Relative annual cost base: annual cost per peak kilowatt of 230-kv, 500,000 circular mil copper equivalent, 100-mile transmission at surge impedance loading, 75 per cent load factor

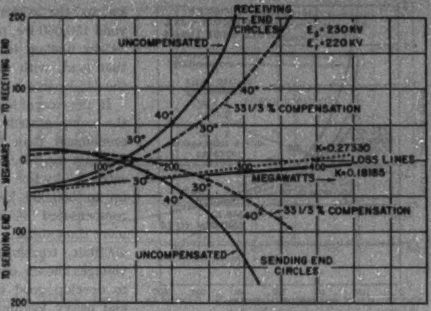

Figure 4. Power circle diagrams. 200 miles, 230-kv, 800,000 circular mil ACSR copper equivalent conductor

circuits of various lengths, voltages and conductor sizes to effect the best over-all economy. The necessary load division can then be adjusted by compensating part of the reactance of the underloaded circuits to raise their loads to the desired levels.

Perhaps the most important application of series capacitors in wide-spread networks or in interconnected systems is for the purpose of increasing the maximum power capability of long tie lines and main trunk circuits. This is the application treated in detail in the present report.

Low Load Factor Tie Lines

Long inter-system or inter-regional tie lines are vital units in integrated operations and are used both for peaking purposes and to exchange blocks of energy. It is usually necessary that they have high peaking capacity and low annual operating cost. The line investment must necessarily be kept low and the cost of losses, due to possible surplus conditions in certain areas, may be low.

The curves of Figure 5 give the relative transmission costs for lines of several lengths operating at low load factor without intermediate loads and generation, as a function of peak load transmitted. Uncompensated costs are given for loadings up to those values required to give an over-all line-voltage angle of 40 degrees, and compensation is included in those cases where it is necessary in order to carry the loadings up to the values required to develop maximum economy. Both 30-degree and the 40-degree line-angle operating points are indicated, and the cost of compensated operation for loads above the values required to give these angles uncompensated are based essentially on amounts of compensation required to obtain the specific loadings at an angle between 35 and 40 degrees. It will be observed that in some of the later curves overlap is shown between compensated and uncompensated operation and that the costs do not differ greatly between the two types of operation up to an uncompensated line angle of approximately 30 degrees. This condition is brought about by the reduction in necessary station reactive capacity due to the reactive kilovolt-amperes supplied by the series capacitors.

It is shown that for distances up to approximately 200 miles between low-impedance busses, the load of maximum economy can be transmitted at 230 kv over 500,000 circular mil copper equivalent conductors without series compensation; however, the peaking capacity can be improved considerably by the use of some degree of compensation without increasing the transmission cost to any substantial degree. For the longer, 300-, 400-, and 500-mile lines, considerable compensation is necessary to obtain peaking capacity in the range of the loads of maximum economy. In the cases of these long tie lines where high peaking capacity is required and where energy is to be transmitted at a relatively low load factor, compensation effects very substantial savings.

Figures 6 and 7 give relative transmission cost data on lines 200 miles long operating at low load factor and at three voltages. The cost of losses in Figure 6 was placed at the full value indicated in Table I, and in Figure 7 the loss cost was placed at 50 per cent of this value. The conductors chosen were considered minimum size, unexpanded ACSR for the various voltages as indicated on the curves. It will be observed that with losses at full value the 230-kv line gives minimum costs up to 180,000 kw; the 287-kv line is minimum between 180,000 and 320,000 kw, and the 345-kv line is lowest between 320,000 and 500,000 kw. The upper values stated in each case represent the approximate loads of maximum economy for the respective voltages. It is apparent that high loading is necessary for best economy.

When loss costs are reduced as might be the case in surplus power transmission between integrated systems, the points of cross-over between the curves for the various voltages increase considerably and the total transmission cost in any case is decreased appreciably. Some degree of compensation is required to obtain the

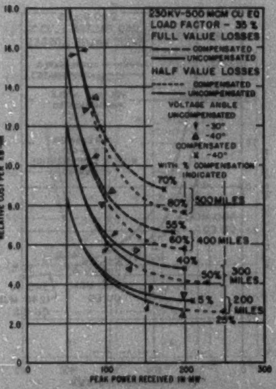

Figure 5. Influence of transmission distance and peak load on low load factor transmission cost

Relative cost base: cost per kilowatt-hour of 230-kv, 500,000 circular mil copper equivalent 100-mile transmission at surge impedance loading, 75 per cent load factor

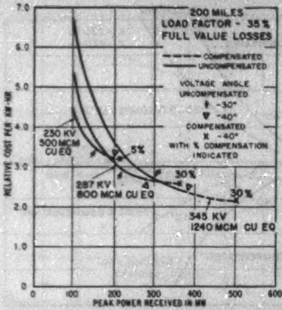

Figure 6. Influence of transmission voltage and peak load on low load factor transmission cost, full-value loss

Relative cost base: cost per kilowatt-hour of 230-kv, 500,000 circular mil copper equivalent 100-mile transmission at surge impedance loading, 75 per cent load factor

loadings of maximum economy with the two higher voltages.

The situations explored in Figures 6 and 7 for 200-mile low-load-factor transmission are repeated in Figures 8 and 9 for 400-mile low-load-factor transmission. When losses are taken at full value, Figure 8, there is little economic choice between 230-kv and 287-kv transmission with the respective conductor sizes chosen, even with loads of only 125,000 kw, and the 287-kv line, compensated beyond 150,000 kw, remains superior to the 345-kv line up to 250,000 kw. Beyond that load, with compensation required, the 345-kv line is superior.

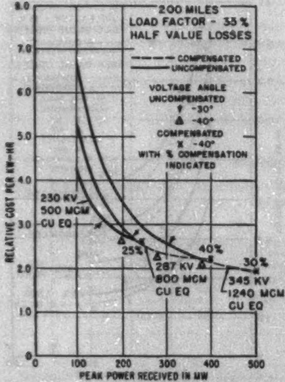

Figure 7. Influence of transmission voltage and peak load on low load factor transmission cost, half-value loss

Relative cost base: cost per kilowatt-hour of 230-kv, 500,000 circular mil copper equivalent 100-mile transmission at surge impedance loading, 75 per cent load factor

In the case of low cost losses, Figure 9, the compensated 230-kv line is more economical than the 287-kv or 345-kv lines up to 180,000 kw. The compensated 287-kv line is then more economical up to 300,000 kw, beyond which the compensated 345-kv line is somewhat more economical. It is evident that for 400-mile transmission at any of the voltages chosen, compensation is required to develop good transmission economy, and heavy loadings are again advantageous.

High Load Factor Trunk Transmission Lines

Cost of 230-kv transmission at high-load factor as functions of peak power and length of line, single circuit, are shown in Figure 10. No compensation is required to attain the load of maximum economy at 200 miles with low-impedance terminals, but under the basic assumptions chosen a small amount of compensation improves the economy slightly in the vicinity of 200,000 kw and can be used to increase the power capability of the line by a substantial factor.

At 300 miles, compensation is required for loadings, under good terminal conditions, above approximately 140,000 kw, and the best economy is attained with compensation at approximately 200,000 kw. Here again the peak capability can be extended beyond 200,000 kw by suitable compensation.

The 400-mile line requires compensation for loads above 105,000 kw and a substantial improvement in economy can be effected by compensating and loading to 180,000 kw.

A 500-mile line requires compensation above 85,000 kw and the economy can be greatly improved by compensating and loading up to approximately 180,000 kw.

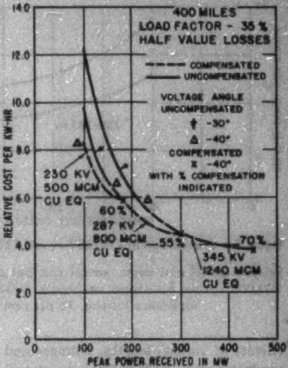

Figure 8. Influence of transmission voltage and peak load on low load factor transmission cost, full-value loss

Relative cost base: cost per kilowatt-hour of 230-kv, 500,000 circular mil copper equivalent 100-mile transmission at surge impedance loading, 75 per cent load factor

Each point on the curves for compensated operation includes only the amount of compensation necessary to attain the loading indicated with a sending-to-receiving voltage angle of 35 to 40 degrees. This is considered to be the maximum angle for satisfactory stable operation in most practical cases. Under compensated operation the total transmission cost at a particular loading is not affected appreciably by a rather wide range of compensation, that is, compensation somewhat above the amount necessary for power capability considerations does not appreciably increase the transmission cost. This condition arises from the fact that increased compensation results in reduced reactive requirements at the line

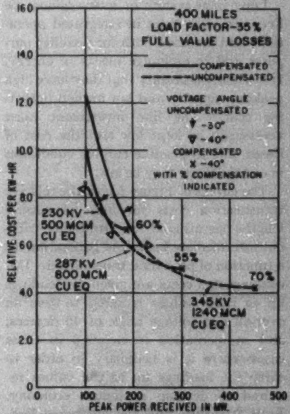

Figure 9. Influence of transmission voltage and peak load on low load factor transmission cost, half-value loss

Relative cost base: cost per kilowatt-hour of 230-kv, 500,000 circular mil copper equivalent 100-mile transmission at surge impedance loading, 75 per cent load factor

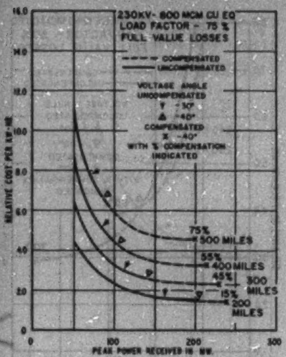

Figure 10. Influence of transmission distance and peak load on high load factor transmission cost

Relative cost base: cost per kilowatt-hour of 230-kv, 500,000 circular mil copper eqivalent 100-mile transmission at surge impedance loading, 75 per cent load factor

terminals and also in somewhat reduced losses. The savings in the latter more or less offset the increased cost of the former.

The effect of reduced load factor in increasing transmission costs for the same lines as those considered in Figure 10 is shown by Figure 11 which was computed for a medium load factor of 50 per cent. The same facilities are involved in corresponding situations under either load factor, and the total annual costs are reduced by only a relatively small saving in annual losses at the lower load factor. The over-all energy transmission costs are therefore substantially increased in approximately inverse proportion to the load factor.

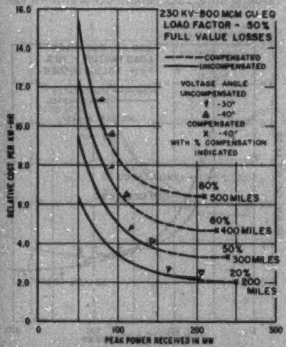

Figure 11. Influence of transmission distance and peak load on medium load factor transmission cost

Relative cost base: cost per kilowatt-hour of 230-kv, 500,000 circular mil copper equivalent 100-mile transmission at surge impedance loading, 75 per cent load factor

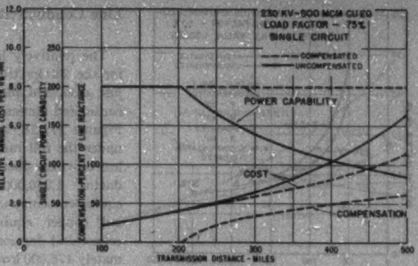

Figure 12 (right). Influence of transmission distance on transmission cost and power capability

Relative cost base: cost per kilowatt-hour of 230-kv, 500,000 circular mil copper equivalent 100-mile transmission at surge impedance loading, 75 per cent load factor

The influence of transmission distance on total single-circuit transmission cost is shown in Figure 12. Two sets of curves are given, one for uncompensated operation and the other for compensated operation. Single-circuit 230-kv lines are assumed with 800,000 circular mil copper equivalent conductors and operating at 75 per cent load factor. The uncompensated power capability is taken to be the load of maximum economy or that which gives a sending-to-receiving voltage angle of 40 degrees. The uncompensated costs shown are for maximum economy below 200 miles and for maximum capability above 200 miles. The curve of compensation indicates the degree of reactance compensation necessary to obtain a transmission capability, at line-voltage angle of 40 degrees, equal to the load of maximum economy. The relative cost curve for the compensated line gives the minimum cost obtainable when the line is compensated as indicated and operated at the load of maximum economy. No appreciable economy for compensation is indicated below 200 miles as loadings are not required to exceed the value for maximum economy. For distances above 200 miles compensation improves the economy and has a major influence above 250 miles.

Higher Transmission Voltages

The influence of higher voltages on 200-mile trunk transmission costs is shown in Figures 13 and 14. The same conductor was used in each case and it was chosen to be of sufficient size unexpanded, to give satisfactory corona and radio influence performance at the highest voltage considered.[8] For load factors of both 50 per cent and 75 per cent, 230-kv compensated above 200,000 kw, gave more economic performance than either 287.5 kv or 345 kv up to approximately 300,000 kw. For further increased loadings, up to 400,000 and 500,000 kw, the economy improved as the voltage was increased. To avoid confusion, the 287.5-kv curves were omitted from both figures since they lie approximately midway between the 230-kv and 345-kv curves and all intersect at approximately the same peak load.

When the transmission distance is increased to 400 miles and the same large conductor is employed, the cost curves for the compensated 230-kv and the 345-kv lines intersect at around 250,000 kw as shown by Figures 15 and 16. The 287.5-kv curves again lie between the two shown and were omitted. It is evident that if

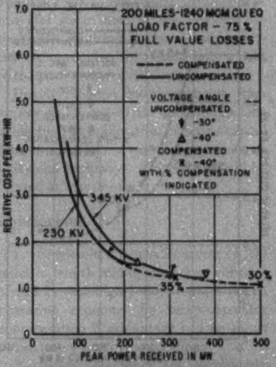

Figure 13. Influence of transmission voltage and peak load on high load factor transmission cost

Relative cost base: cost per kilowatt-hour of 230-kv, 500,000 circular mil copper equivalent 100-mile transmission at surge impedance loading, 75 per cent load factor

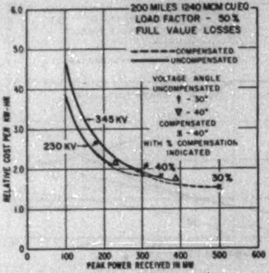

Figure 14. Influence of transmission voltage and peak load on medium load factor transmission cost

Relative cost base: cost per kilowatt-hour of 230-kv, 500,000 circular mil copper equivalent 100-mile transmission at surge impedance loading, 75 per cent load factor

the peak loading, even at this distance, is not to exceed approximately 200,000 kw, compensated 230 kv gives the best economy. However, if the line is so situated with respect to other system or intersystem facilities as to obtain loadings of the order of 300,000 to 400,000 kw, compensated 345 kv gives the best economy at either 50 per cent or 75 per cent load factor.

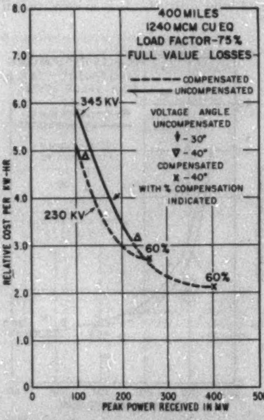

Figure 15. Influence of transmission voltage and peak load on high load factor transmission cost

Relative cost base: cost per kilowatt hour of 230-kv, 500,000 circular mil copper equivalent 100-mile transmission at surge impedance loading, 75 per cent load factor

Line Conductivity

The relatively large conductor chosen for the 230-kv transmission in the cases just discussed may at first thought be considered unreasonable but reference to Figures 17, 18, and 19 will show that under the full range of load factors and loss costs considered, the very large conductor, 1,240,000 circular mil copper equivalent compared to 500,000 circular mil copper equivalent becomes more economical for loadings above approximately 175,000 kw when the transmission distance is of the order of 200 miles. Calculations have shown that the same relationship exists for a transmission distance of 400 miles. Figure 17 indicates that the large conductor at 75 per cent load factor shows excellent economy at approximately 33 per cent compensation when peak loading is between 250,000 and 300,000 kw. The improvement here is quite substantial in comparison with the 500,000 circular mil copper equivalent conductor at its load of maximum economy which is approximately 190,000 kw.

The difference in favor of the large conductor at the higher peak loadings is even more pronounced at lower load factors as indicated by Figure 18; however, the transmission cost of any line is again shown to be very much higher at the low than at the high-load factors.

The influence of low-loss costs under low-load-factor operation is brought out by a comparison between Figures 18 and 19. The smaller conductor shows a very substantial improvement when the loss costs are reduced but the larger conductor, because of the relatively small influences of losses on its total cost, is affected very little in over-all economy by loss cost.

Intermediate sizes of conductors between 500,000 and 1,240,000 circular mil copper equivalent give cost curves lying between the two groups of curves shown on each of the figures just discussed. It must be emphasized, however, that the improved economies available through the use of larger conductors can be realized only through relatively heavy loading of the circuits.

When trunk circuits or other network components can be heavily loaded there is an obvious economy in employing what may be considered to be abnormally large conductors. If the distance involved is of the order of 200 miles or more, the loadings necessary to realize large-conductor economies can be obtained by the use of series-capacitor compensation.

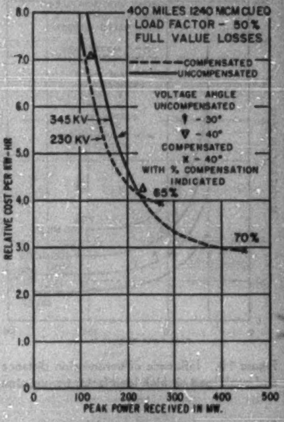

Figure 16. Influence of transmission voltage and peak load on medium load factor transmission cost

Relative cost base: cost per kilowatt-hour of 230-kv, 500,000 circular mil copper equivalent 100-mile transmission at surge impedance loading, 75 per cent load factor

In many geographical regions, ice melting or prevention becomes a major factor in the choice of conductor size or conductivity. Table II lists the approximate loads necessary at the voltages and with the conductors considered to prevent the formation of ice under heavy sleet conditions. The 230-kv, 500,000 circular mil copper equivalent ACSR value is an actual experience value in the

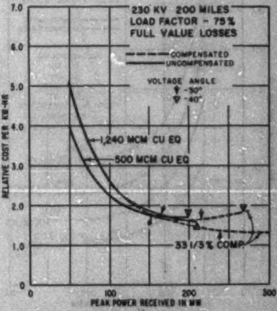

Figure 17. Influence of conductor size and peak load on high load factor transmission cost

Relative cost base: cost per kilowatt-hour of 230-kv, 500,000 circular mil copper equivalent 100-mile transmission at surge impedance loading, 75 per cent load factor

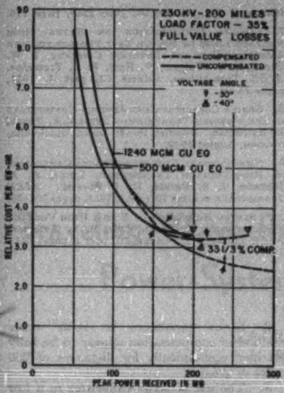

Figure 18. Influence of conductor size and peak load on low load factor transmission cost, full-value loss

Relative cost base: cost per kilowatt-hour of 230-kv, 500,000 circular mil copper equivalent 100-mile transmission at surge impedance loading, 75 per cent load factor

Northwest. It is considered by some to be conservative. The other values are based on the generation of an equal amount of conductor heat per unit of conductor surface area. The values thus computed are of the same order as the loadings of maximum economy for the conductors and voltages tabulated. If provision is made system wise for obtaining these loadings during critical icing periods, no difficulties should be experienced. Further experimental data are desirable however.

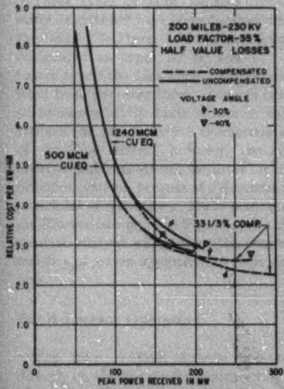

Figure 19. Influence of conductor size and peak load on low load factor transmission cost, half-value loss

Relative cost base: cost per kilowatt-hour of 230-kv, 500,000 circular mil copper equivalent 100-mile transmission at surge impedance loading, 75 per cent load factor

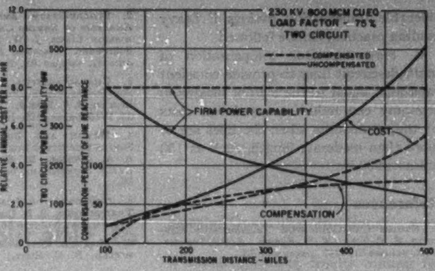

Figure 20 (right). Influence of transmission distance on 2-circuit firm-power transmission cost and power capacity

Relative cost base: cost per kilowatt-hour of 230-kv, 500,000 circular mil copper equivalent 100-mile transmission at surge impedance loading, 75 per cent load factor

Two-Circuit Lines with Sectionalizing Stations

Where firm transmission capability is required, multiple-circuit lines are necessary and the loadings during critical periods must be held down to values which will not result in instability when any one section is faulted and isolated or faulted, isolated, and quickly reclosed. Double-circuit or 2-circuit 230-kv lines, operating effectively in multiple and sectionalized or practical intervals, cannot be loaded safely to their economic maximum for distances in excess of 150 miles. However, by incorporating suitable series capacitors in common relation to both circuits at the sectionalizing stations, as proposed in a previous paper,[1] it is possible to maintain the transient capability of a sectionalized 2-circuit line at its economic maximum for any distance presently considered. Figure 20 presents the capability and transmission cost performance of a 2-circuit transmission line as a function of distance for both compensated and uncompensated operation. Fast relaying and circuit breakers are necessary and assumed. It is shown that the transmission costs, when suitable amounts of compensation are employed, are less by major amounts than for uncompensated operation.

The attractiveness of this application of compensation may be further enhanced by taking advantage of the short-time overvoltage capability of capacitors. If the over-load on any section produced by isolating a parallel faulted section can be limited to time intervals of the order of 30 minutes or less, this scheme would involve switching certain segments of the capacitor banks to effect the same degree of reactance compensation with one section out as with the line unfaulted. If the full original line load were maintained during such outages the remaining or active section of the capacitor would be overstressed with respect to its normal rating but not beyond its capability for short lengths of time. Such a plan would reduce the total investment necessary in series capacitors, and would lessen the transient swing of terminal synchronous equipment at the time of dropping a faulted section if the change in compensation were made essentially simultaneously with the isolating of the faulted section.

Full overload duty on the remaining section after one section of a double-circuit line is isolated occurs only when the double-circuit facility is the only connecting link between a generating system and its load. The usual arrangement provides some more or less devious bypass path resulting in the remaining circuit being required to assume only a part of the power lost by the faulted section.

Heavily loaded multiple-circuit lines appear to be one of the most important fields for the application of series capacitors to improve over-all system capability and economy. This subject will be treated at length in a future report.

Conclusions

1. Single-circuit lines in excess of 200 miles in length and operating at voltages of 230 kv and higher can be improved in operating economy by series-capacitor compensation if advantage can be taken of the heavy loading capabilities.

2. Series capacitors are particularly useful in providing high emergency overload capabilities in tie lines and integrated system transmission circuits.

3. The combination of series capacitors and increased conductor sizes in long high-voltage transmission lines makes possible the realization of con-

siderable transmission savings if heavy loading practices can be followed.

4. Series-capacitor compensation of multiple-circuit lines to provide transient capability equal to the load of maximum economy can reduce transmission costs by major amounts when the lines are of more than moderate length, such as 150 miles at 230 kv.

References

1. Series Capacitor for Transmission Circuits, E. C. Starr, R. D. Evans. *AIEE Transactions*, volume 61, 1942, pages 963–73.

2. Steady-State and Transient Stability Analysis of Series Capacitors in Long Transmission Lines, J. W. Butler, J. E. Paul, T. W. Schroeder. *Electrical Engineering* (*AIEE Transactions*), volume 62, February 1943, pages 58–65.

3. Characteristics of a 400-Mile 230-Kv Series-Capacitor-Compensated Transmission System, B. V. Hoard. *AIEE Transactions*, volume 65, 1946, pages 1102–14.

4. Design and Protection of 10,000-Kva Series Capacitor for 66-Kv Transmission Line, A. A. Johnson, R. E. Marbury, J. M. Arthur. *AIEE Transactions*, volume 67, 1948, pages 363–68.

5. Economics of Long-Distance A-C Power Transmission, S. B. Crary, I. B. Johnson. *AIEE Transactions*, volume 66, 1947, pages 1092–1102.

6. Minimize Cost Per Kilowatt Hour Transmitted, E. C. Starr. *Electric Light and Power* (Chicago, Ill.), volume 26, June 1948, page 116.

7. Corona Investigation on Extra High Voltage Lines of 500-Kv Test Project for the American Gas and Electric Company, I. W. Gross, C. F. Wagner, O. Naef, R. L. Tremaine. *AIEE Transactions*, volume 70, part I, 1951, pages 75–94.

8. Series Capacitors and Double Conductors in the Swedish Transmission System, A. Rusck, Bo Rathsman. Swedish Power Board, Stockholm, Sweden, August 1949.

9. Fundamental Effects of Series Capacitors in High-Voltage Transmission Lines, A. A. Johnson, J. E. Barkle, D. J. Povejsil. *AIEE Transactions*, volume 70, part I, 1951, pages 526–36.

10. System Economies of Extra High Voltage Transmission, H. P. St. Clair, E. L. Peterson. *AIEE Transactions*, volume 70, part I, pages 841–51.

Discussion

S. B. Crary (General Electric Company, Schenectady, N. Y.): Series capacitors for transmission systems have been considered for many years as a possible method for decreasing the cost of transmission, particularly long-distance transmission of large blocks of power at high voltage. The 230-kv American installation at Chehalis and the Swedish installation at Alfta are noteworthy steps in reducing to practice the theoretical possibilities. It is particularly encouraging that the technical and economic aspects of the use of series capacitors are being given close attention. Series capacitors may now be purchased from the manufacturers to meet rational system requirements and have become a full-fledged tool for the transmission engineer. Studies we have made are in agreement with Starr and Seymour:

1. Our studies indicate that intermediate switching stations are needed to reduce the cost of transmission with or without series capacitors, provided such expediencies as suddenly changing the system load or generation by the application of braking resistors or disconnection of loaded generators are not resorted to. Such practices are generally undesirable in large interconnected systems having interconnecting ties to other systems.

2. Series capacitors or some other method of compensation appear to be fully justified economically for distances of 250 miles or greater.

3. The use of series capacitors in a low resistance line to reduce system losses when paralleled with higher resistance lines appears to be quite marginal in economic benefit.

4. Quick reinsertion means appear to have the greatest future application in this country in contrast to the Swedish installation (which does not have a rapid means for reinsertion) as it reduces appreciably the kilovars required to affect an increase in stability limit.

Traveling Wave Relations Applicable to Power-System Fault Locators

LAUREL J. LEWIS
MEMBER AIEE

FAULT locators employing traveling waves to measure distance have a response dependent on the propagation characteristics of multivelocity components of a surge, and the type of fault. Analysis of wave characteristics leads to a method for determining the response with different types of discontinuities.

Sectionalizing and switching of lines and the proper repair of facilities requires rapid and accurate location of faults on power systems; thus the development of automatic fault locators is an important activity for improving service continuity.

Three types of fault locators, previously described[1,2] have been developed by the Bonneville Power Administration and designated as types *A*, *B*, and *C*. A fourth type,[3] the Linascope, differs somewhat from the other three. In each case, performance of the fault locator is conditioned on the transient characteristics of traveling waves; however, the significant problems are not the same for the different systems, because of differences in principles of operation. These principles are illustrated simply in Figure 1; a subsequent analysis will present the characteristics of waves applicable to each system.

Fault Locator Operation

The type *A* fault locator operates directly on the line surges generated by a fault. An initial surge travels to the end of the line where the locator is situated and is used to trigger the sweep of a cathode-ray oscillograph. The initial surge experiences a reflection on the transmission line, and the reflected wave traveling back toward the fault again experiences a reflection at the fault, which on return to the locator is recorded as a "pip" on the cathode-ray trace. The round-trip distance from locator to fault is measured by comparison with marker "pips" superimposed on the horizontal sweep.

The type *B* fault locator also bases recording on the fault-generated surges, but utilizes only the initial waves arriving at the two ends of the line. One wave reaches the far end of the line, where it is picked up and transmitted back to the fault locator over a microwave communication channel, and used to start an electronic timer. The other traveling wave, reaching the fault locator directly over the transmission line actuates a delay system, which after a controlled time turns off the timer. Calibration of the controlled delay permits direct reading of the distance between fault and locator, and the result is indicated on a mechanical printer.

In the type *C* fault locator, the fault-generated surge is utilized only to initiate a sequence of operations, and is not recorded directly. After a controlled time delay of three cycles, a surge obtained from a charged capacitor is applied to the faulted conductor and also used to initiate a sweep on a cathode-ray oscillograph. The reflected surge returning from the fault appears as a "pip" on the cathode-ray sweep.

The Linascope makes no use of the fault-generated surges, but instead is used to detect sustained faults. A periodic sequence of pulses is applied to the transmission line, and the resulting echoes are displayed on a cathode-ray tube, the sweep being synchronized at the pulse repetition rate. Tests and measurements have been made using both unidirectional pulses and modulated radio-frequency pulses.

Special Operating Problems

Actual operating results contain features not indicated by the foregoing simple explanation. The type *A* locator depends on wave travel between fault and locator; there is, however, a wave traveling from the fault to the far end of the line and there being reflected. It was initially expected that the low fault-impedance would act to confine the far-end wave to that section and prevent its transmission back toward the fault locator. Experience has shown this conclusion to be incorrect; noticeable reflections have been recorded from the far end of a line with a fault at midpoint. An extra "pip" appears on the record, making interpretation difficult.

The type *C* locator was initially tested[3] to determine the nature of reflections under different fault conditions. It was concluded from these tests that controlled surges had to be applied to the conductor of one of the phases involved in the fault to assure reflection from the fault itself. The reasons for the types of behavior were not fully determined.

The type *B* locator involves only initial surges arriving at the two ends of a line, and so avoids difficulties due to multiple reflections. The system requires, however, as do the others, the use of a coupling system for obtaining pulses from the transmission line. The characteristics of the traveling waves are of importance in the design of a coupling system. Likewise the speed of wave travel is of importance in all systems, since time measurements are to be translated into distances.

In the following sections an analytical

Paper 51-312, recommended by the AIEE Transmission and Distribution Committee and approved by the AIEE Technical Program Committee for presentation at the AIEE Pacific General Meeting, Portland, Oreg., August 20–23, 1951. Manuscript submitted May 22, 1951; made available for printing July 10, 1951.

LAUREL J. LEWIS is Associate Professor of Electrical Engineering at the University of Washington, Seattle, Wash., and Consulting Engineer with the Bonneville Power Administration.

The assistance of Howard King of the Bonneville Power Administration in obtaining test data is gratefully acknowledged.

method is presented to explain some of the results not previously understood.

Mathematical Approximations

Since a complete mathematical analysis of traveling waves on a physical system is impossible, various approximate procedures are resorted to; a number of these will be reviewed to indicate the general results and to emphasize the limitations.

The simplest case is that of a 2-wire line isolated in space, with losses neglected. These assumptions permit the use of inductive and capacitive coefficients and lead to the classical "wave" equation, a partial differential equation relating voltages (or currents), distance, and time. Propagation is at the velocity of light, without distortion of wave shape.

The case of a single-wire line with ground return can be treated by the same method as for the 2-wire line, when the line is at a uniform height above ground and losses in the ground are neglected. Results are again of the same general form.

Efforts to include the effects of losses lead first to the introduction of series resistances and shunt conductances as line parameters. With an isolated 2-wire line or a single-wire with ground return, and earth losses neglected, the mathematical formulation results in the "telegraphers' equation," the solution of which was obtained by Heaviside. A special case arises, of the so-called "distortionless" line, in which the signal velocity is the velocity of light; surges are also attenuated with distance, but do not change shape. For all other cases, however, it is impossible to speak of a single velocity, for if the initial surge is considered in terms of frequency components, each component travels at a different velocity, and with the highest frequency components approaching the velocity of light. Modification of shape is evident by lengthening of the tail of a traveling surge.[4] It is also significant that the nature of the traveling wave depends on the nature of its origin, that is, whether it is initiated by release of bound charge on the conductors or by application of a surge at a single point on the line.

That losses in line conductors are not truly represented by resistance parameters is evident when account is taken of conductor skin effect. The effect in an isolated conductor can be calculated in terms of Bessel functions[5] for a fixed frequency. The result, however, cannot be conveniently included in analysis of traveling surges, since strictly speaking the concepts of inductive and capacitive coefficients lose their validity under such conditions. The only rational approach is through the basic Maxwell equations.

One of the poorest approximations involved in the preceding methods is the assumption of perfect conduction in the earth. The situation is similar to that of skin effect in a wire. The effect for the steady state has been calculated by Carson.[6] Again the result is not one that can be included in a wave equation. Perhaps a way to include the effect would be to analyze a surge first into frequency components, and to include the effect for each component separately, and then to superimpose the results. The end result for the general case could only be expressed in terms of integral equations, which would yield little practical data.

The problem of 3-phase transmission has been extensively studied; with losses neglected, waves propagate at the velocity of light. It has been shown[7] that if a surge is applied to one conductor of a uniformly transposed system, an induced surge will exist on the other two conductors, the value being determined by the potential of the point in space at which the conductor is situated. Complete reflection of the direct surge at a discontinuity results also in cancellation of the induced surges.

One of the first proposals for explaining the nature of wave distortion on 3-phase lines was made by Bewley,[8] who suggested a multivelocity theory of wave travel. That waves do separate into components which travel at different velocities was convincingly demonstrated by oscillograms.[9] To explain the nature of multivelocity components, Bewley based an analysis on a "lossless" system, with no resistance terms included specifically in the analysis, by considering that the capacitive coefficients were determined by the ground plane, and the inductive coefficients were determined by a zero plane located at a significant distance below the ground surface. That such a procedure has a basis in fact can not be denied, for the effect of finite conductivity in the earth is to result in penetration of the earth current below the surface. However, the procedure contains no basis for determining the subsurface zero plane, nor does it account for attenuation of waves.

The fact that the use of a separate zero plane leads to terms involving two velocities of propagation tends to obscure the fundamental factors responsible for traveling wave behavior. It needs to be pointed out that the existence of multivelocities does not depend upon such an approach, but is an inherent property of the 3-phase system when losses are in-

Table I. Surge Components for Specified Conditions

Case	Initial Conditions			A_1	B_1	A_0
I	E_A	E_B	E_C	$\frac{1}{3}(2E_A-E_B-E_C)$	$\frac{1}{3}(-E_A+2E_B-E_C)$	$\frac{1}{3}(E_A+E_B+E_C)$
II	I_A	I_B	I_C	$\frac{Z_1}{3}(2I_A-I_B-I_C)$	$\frac{Z_1}{3}(-I_A+2I_B-I_C)$	$\frac{Z_0}{3}(I_A+I_B+I_C)$
III	E_A	E_B	I_C	$\frac{1}{1+2r}[(1+r)E_A-rE_B-Z_0I_C]$	$\frac{1}{1+2r}[-rE_A+(1+r)E_B-Z_0I_C]$	$\frac{r}{1+2r}[E_A+E_B+Z_1I_C]$
IV	E_A	I_B	I_C	$\frac{1}{2+r}[2E_A-Z_0I_B-Z_0I_C]$	$\frac{1}{2+r}[-E_A+(1+r)Z_1I_B-Z_1I_C]$	$\frac{1}{2+r}[rE_A+Z_0I_B+Z_0I_C]$
V	E_{AB}	E_{BC}	E_{CA}	$\frac{1}{3}(2E_{AB}+E_{BC})$	$\frac{1}{3}(2E_{BC}+E_{CA})$	0
VI	E_{AB}	I_{AB}	I_C	$\frac{1}{2}E_{AB}+\frac{1}{6}Z_1I_{AB}-\frac{1}{3}Z_1I_C$	$-\frac{1}{2}E_{AB}+\frac{1}{6}Z_1I_{AB}-\frac{1}{3}Z_1I_C$	$\frac{1}{3}Z_0(I_{AB}+I_C)$
VII	E_{AB}	I_{AB}	E_C	$\frac{1}{2}E_{AB}-\frac{1}{2+r}E_C+\frac{1}{4+2r}Z_0I_{AB}$	$-\frac{1}{2}E_{AB}-\frac{1}{2+r}E_C+\frac{1}{4+2r}Z_0I_{AB}$	$\frac{1}{2+r}[rE_C+Z_0I_{AB}]$

$E_{AB}=E_A-E_B$ $I_{AB}=I_A+I_B$ $r=Z_0/Z_1$

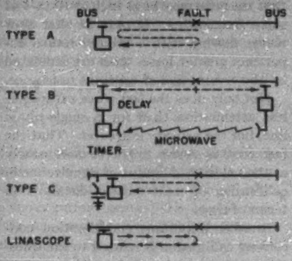

Figure 1. Fault locator operation

cluded. It has already been shown,[10] that for the steady state, with operation at a single frequency, and even assuming a perfect earth, there are two phase velocities for a 3-wire system, when conductor losses are included.

The 3-phase traveling-wave system has an analogy in coupled-circuit theory. When two or more identical lumped circuits containing losses are coupled symmetrically, the system has two resonant frequencies, one higher and one lower than that of the individual mesh. A double-humped frequency response occurs for coupling larger than a critical value. The transient response contains two natural angular velocities, with one frequency higher and one lower, and with one damping factor higher and one lower, than that of the single mesh. Translated into terms of the traveling wave case, this corresponds to two velocity terms and two attenuation factors, for each frequency component traveling in each direction. From the analysis in the Appendix, the attenuation is shown to be higher for the wave traveling at the slower speed.

As for the isolated 2-wire line with losses included, in a 3-wire system it is again not appropriate to speak of a velocity of propagation of a surge, although it may be permissible to refer to the speed of travel of the maximum of energy distribution. It is significant that there are two such maxima traveling at different speeds. The faster wave moves at a speed higher than that on a single-phase line having the same losses, but with less attenuation and distortion. The highest frequency components in the fast wave have velocities approaching the velocity of light. The slower wave experiences more attenuation, with the crest moving at a lower speed, although again the higher frequency components have a speed approaching that of light. The effect is a more rapid reduction in crest value and a much greater reduction in the slope of the wave front.

The Components of the Multivelocity Waves

The resolution of a surge into slow and fast components is accompanied by a special disposition of the currents and voltages among the three conductors. The voltages to ground of the three conductors and the three line currents may be expressed by the equations:

$$\begin{aligned} e_1(x,t) &= A_1f_1(x,t,\alpha_1,v_1)+A_2f_2(x,t,\alpha_2,v_2)\\ e_2(x,t) &= B_1f_1(x,t,\alpha_1,v_1)+B_2f_2(x,t,\alpha_2,v_2)\\ e_3(x,t) &= C_1f_1(x,t,\alpha_1,v_1)+C_2f_2(x,t,\alpha_2,v_2) \end{aligned} \qquad (1)$$

$$\begin{aligned} i_1(x,t) &= D_1f_1(x,t,\alpha_1,v_1)+D_2f_2(x,t,\alpha_2,v_2)\\ i_2(x,t) &= E_1f_1(x,t,\alpha_1,v_1)+E_2f_2(x,t,\alpha_2,v_2)\\ i_3(x,t) &= F_1f_1(x,t,\alpha_1,v_1)+F_2f_2(x,t,\alpha_2,v_2) \end{aligned}$$

These are merely symbolical expressions indicating the dependence of the voltage and current variations on separate velocity and attenuation coefficients. These coefficients themselves are not constants, but are functions of the frequency components contained in the initial wave. (A more explicit form could be used, employing Fourier integrals and the corresponding transforms.)

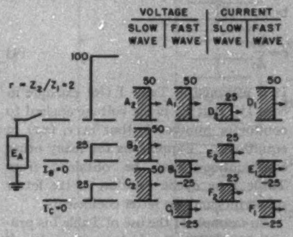

Figure 2. Surge components

Of particular importance are the values of the coefficients $A_1, A_2, B_1, B_2, \ldots$.

These may be functions of time, but in the simplest cases are merely numbers which determine the relative magnitudes of the individual components necessary to satisfy the initial boundary conditions. In the notation to be used:

A_1 = initial value of the fast component of $e_1(x,t)$

A_2 = initial value of the slow component of $e_1(x,t)$

D_1 = initial value of the fast component of $i_1(x,t)$

D_2 = initial value of the slow component of $i_1(x,t)$

with similar designations for the other components.

In what is to follow, a completely rigorous approach is not possible. The position taken is therefore that the losses are to be considered small, and that they can be approximated by resistance and conductance coefficients. It also will be assumed that the inductive and capacitive coefficients are to be calculated with the ground surface as the zero plane. The mathematical relations take the form of a set of equations similar to the "telegraphers' equation," but including coupling terms.

From the basic nature of the system, assuming uniformity of distributed constants and transposition of conductors, it follows, as shown in the Appendix, that:

$$\begin{aligned} &A_1+B_1+C_1=0\\ &A_2=B_2=C_2\\ &D_1+E_1+F_1=0\\ &D_2=E_2=F_2 \end{aligned} \qquad (2)$$

A similarity is to be noted between these relations and those involving symmetrical components. For example, the relation involving the slow components of current is equivalent to current flow on the three wires in parallel, with ground return, analogous to the zero sequence. The fast components of current satisfy the relations between instantaneous values in an isolated 3-phase system, analogous to the sum of the positive and the negative sequences.

The relations of equation 2 are equivalent to those obtained by Bewley,[8] but are in a sense more general, since they apply independently of the manner in which account is taken of losses. The relations hold for each frequency com-

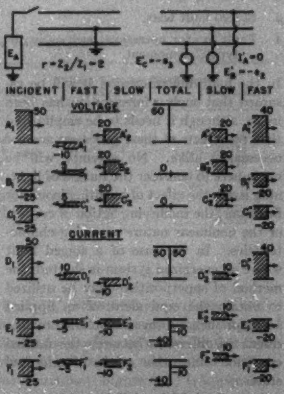

Figure 3. Wave components

ponent and therefore to the composite.

The effect of the assumption of low loss is to make the velocities nearly independent of the losses and to make the initial ratios of slow and fast components primarily a function of the inductance and capacitance coefficients.

The slow and fast waves are each separate solutions of the differential equations. For any particular frequency component, therefore, a certain ratio exists between the voltage and current waves. This is similar to the characteristic impedance of a single-phase line. The assumption of low loss amounts to making the two characteristic impedances essentially pure resistances, and with the same essential value for each frequency component in the waves. The characteristic impedance of the fast wave is lower and that of the slow wave is higher than for a single-phase line of the same height and conductor size.

Separation of a Wave Into Components

For fault locator considerations, the important problems are the determination of the manner in which an initial surge is resolved into separate waves, the nature of their propagation, and the effect of discontinuities in the system on the transmission and reflection at these discontinuities.

The first step requires a mathematical formulation of the original surge itself. This will depend on the origin of the surge, which may result from any one of the following processes:

1. Lightning.
2. Switching operations.
3. Staged fault tests.
4. Fault locator operation, such as in the type C equipment.

In the following discussion it will be assumed that such a formulation has been made, although it needs to be emphasized that the effects of these processes are not necessarily alike. No attempt will be made here to consider the nature of lightning itself, the effect of resulting insulator flashover, the modifying action of corona, or the nonlinear nature of arcing characteristics. In the case of a staged fault where an energized system is shorted, the method of superposition may be utilized to obtain the equivalent of an applied surge, of such a form and polarity to represent the difference between the faulted condition and the original unfaulted state.

Once the initial conditions are stated, the separation of the wave into components requires the evaluation of the coefficients in equation 1. For the 12 coefficients, six relations are provided by equation 2. In addition, each fast wave of voltage is related to the fast wave of current by a characteristic impedance, and the slow waves are similarly related, as shown by equation 3:

$$Z_1 = \frac{A_1}{D_1} = \frac{B_1}{E_1} = \frac{C_1}{F_1} \tag{3}$$

$$Z_2 = \frac{A_2}{D_2} = \frac{B_2}{E_2} = \frac{C_2}{F_2}$$

Thus three initial conditions are necessary to determine the complete set of coefficients.

A large number of combinations of the six variables are possible. Solutions for the coefficients A_1, A_2, and B_1 are given in Table I for seven of the most important cases. The other nine coefficients can be derived from these by the relations of equations 2 and 3. In Table I, the ratio of characteristic impedances is expressed by:

$$r = \frac{Z_2}{Z_1} \tag{4}$$

It is assumed in Table I (for example in case IV) that E_1 is the voltage applied to conductor number 1, that is, $e_1\ (x,t)$ in equation 1. Expressions for many other combinations may be obtained from Table I by cyclic rotation of the letter subscripts and the letter coefficients.

An example of the use of Table I is provided by Figure 2, which has been drawn for a step wave applied to conductor number 1, computed with the value of r equal to 2. A positive voltage is applied to conductor number 1, and voltages are induced on the other two conductors. The separate components satisfy the six relations of equation 2 and also the terminal conditions.

The Propagation of the Components

From the relations derived in the Appendix, it has been determined that the surge components not only travel at different speeds, but that the slow wave is attenuated more than the fast wave. When the attenuation is multiplied by a large distance, the effect is to make the slow wave magnitude very small in comparison to the fast component. It is concluded that in cases involving multiple reflections, the effect of the slow wave is usually negligible.

From the equations, a ratio of less than 2-to-1 might be expected for the attenuation terms in a line of usual dimensions. Actual tests on carrier systems[10] indicate that the ratio may be as high as 10-to-1 at some frequencies. It may be that slow waves flowing with a ground return experience greater losses than are indicated by the assumption of constant resistance.

Not only does the fast wave experience less attenuation than for a single-phase line, but the velocity is greater. That the fast wave is shown to travel more nearly at the velocity of light is of significance in calibration of fault locator distances in terms of time.

Another important consideration concerning calibration is related to the question of the actual path by which a wave travels, taking account of conductor sag and irregular terrain. Although no direct evidence is available from the analysis, it is tempting to speculate that since the fast-wave current flow is confined to the metallic conductors, there may be reason to believe that the distance of travel is determined primarily by the physical length of the conductor and only secondarily affected by the changing height.

The Effect of Discontinuities

Calculation of the effect of a short circuit, or other type of discontinuity can be most conveniently made by a method employing superposition. Thus, the effect of the arrival of a voltage at a short circuit can be simulated by the application of an equivalent generator, having a voltage equal and opposite to that of the arriving surge. The superposition of the original waves and those of the equivalent generator will represent the resultant conditions on both sides of the fault.

The nature of the equivalent generators to be employed to simulate a discontinuity depends on the nature of the arriving wave and the boundary conditions imposed by the discontinuity. Table I can be used to provide the relations at the equivalent generator in most cases.

An example is provided by Figure 3, illustrating a case where a surge, originally applied to phase A, as initiated in Figure 2, arrives at a fault, after sufficient travel so that the slow component has become negligible. The fault is between B and C phases and ground.

In calculating the reflected waves (denoted by primes), it is necessary to consider that the characteristic impedances are negative quantities for waves traveling in the negative direction. This is consistent with designation of positive current as a current flowing in the direction of the incident wave.

In the case of Figure 3, the continuity conditions require that the resultant conditions on the two sides of the discontinuity satisfy the following relations between transmitted waves (designated by double primes), the incident waves, and the reflected waves:

$$e_{\text{left}}=e_{\text{right}}=e+e'=e''$$
$$i_{\text{left}}=i+i' \qquad (5)$$
$$i_{\text{right}}=i''=i-i'$$

These relations apply when shunt generators are used. Analogous but somewhat different relations are required when a series current-generator is used to simulate an open circuit. The relations are determined by the principle of superposition.

It is convenient to designate as transfer characteristics, the fractions of fast waves which are reflected and transmitted at a discontinuity. The voltage characteristics, for a 3-phase system, unlike those for a single-phase system, are functions not only of the type of discontinuity, but also of the disposition of the incident waves.

The number of possible combinations is almost without limit. However, some of the most important cases are illustrated in Table II. The values in Case 4 are those applicable to Figure 3. Although general expressions are possible in terms of the parameter r, Table II has been prepared for a value of r equal to 2, which is probably a representative value.

Table II. Fast-Wave Voltage Transfer Coefficients*

Case	Applied Surge	System	Generators Case	Generators Data	Voltage Transfer Coefficients Phase	Voltage Transfer Coefficients Reflection	Voltage Transfer Coefficients Transmission
1	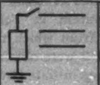	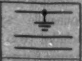	IV	E_A	A	−0.5	0.5
				$I_B=0$	B	−0.5	0.5
				$I_C=0$	C	−0.5	0.5
2		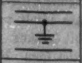	IV	E_B	A	−0.125	0.875
				$I_A=0$	B	−0.5	0.5
				$I_C=0$	C	0.25	1.25
3		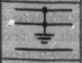	III	E_A	A	−0.8	0.2
				E_B	B	−1.4	−0.4
				$I_C=0$	C	−0.2	0.8
4		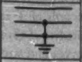	III	E_B	A	−0.2	0.8
				E_C	B	−0.2	0.8
				$I_A=0$	C	−0.2	0.8
5		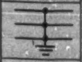	I	E_A	A	−1.0	0
				E_B	B	−1.0	0
				E_C	C	−1.0	0
6		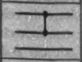	VI	E_{AB}	A	−0.75	0.25
				$I_{AB}=0$	B	−1.5	−0.5
				$I_C=0$	C	0	1.0
7		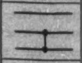	VI	E_{BC}	A	0	1.0
				$I_{BC}=0$	B	0	1.0
				$I_A=0$	C	0	1.0
8		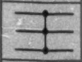	V	E_{AB}	A	−1.0	0
				E_{BC}	B	−1.0	0
				E_{CA}	C	−1.0	0
9		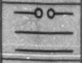	II	I_A	A	0.8	0.2
				$I_B=0$	B	0.8	0.2
				$I_C=0$	C	0.8	0.2
10		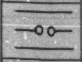	II	I_B	A	0.2	0.8
				$I_A=0$	B	0.8	0.2
				$I_C=0$	C	−0.4	1.4
11		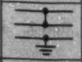	VII	E_{AB}	A	−0.875	0.125
				$I_{AB}=0$	B	−1.25	0.25
				E_C	C	−0.5	0.5
12	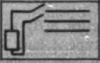	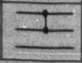	VI	E_{AB}	A	−1.0	0
				$I_{AB}=0$	B	−1.0	0
				$I_C=0$	C	−1.0	0

*Computed for $r=Z_0/Z_1=2$.

Table III. Fast-Wave Voltage Transfer Coefficients*

Applied Surge	System	Phase	Voltage Transfer Coefficients Reflection	Voltage Transfer Coefficients Transmission
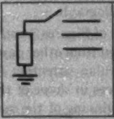	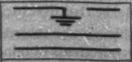	A	−0.474	0.316
		B	−0.474	0.316
		C	−0.474	0.316
	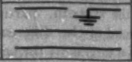	A	0.790	0.316
		B	0.790	0.316
		C	0.790	0.316

*Computed for $r=Z_0/Z_1=2$.

Special Cases

Certain special cases are of importance which require a special treatment not covered by the foregoing analysis.

The first of these is one involving dissymmetry with respect to the two directions at the fault. Two examples are illustrated in Figure 4. Neither of these are included in Table I. The analysis involves simultaneous solutions for two transmission systems having common boundary conditions, involving equal and opposite currents in the ungrounded conductors. Details of the analysis will be omitted, but the transfer characteristics are given in Table III (for $r=2$), assuming an incident fast wave such as that originating in Figure 2. The fault conditions differ very little in practical form, but differ widely with respect to fault-locator considerations. Both systems transmit the same fast waves beyond the discontinuity, but the fast-wave reflections from the case in Figure 4(B) are nearly twice those in Figure 4(A).

Another special case is that where the ground fault impedance is not zero. Figure 5 illustrates the form that must be assumed for the equivalent generator. The situation requires simultaneous solution of the line equations and the following equation at the generator:

$$e_1'=E_A-2i_1'R_f \qquad (6)$$

The ratio of e_1' and i_1' can be determined by calculation from Case IV in Table I.

A third special case is illustrated in Figure 6, where the ungrounded conductors have significant lumped capacitances to ground, as would be the case where a fault occurs adjacent to a large bus structure. Figure 6(A) is applicable to the initial surge, when one conductor is suddenly grounded; Figure 6(B) is the

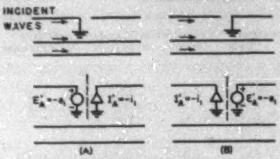

Figure 4. Fault representation

equivalent system for simulating the effect on arrival of a surge. In these situations, the conductors act initially as though grounded, but after a time, they behave as though ungrounded. These are cases where the coefficient $A_1, A_2, \ldots$ are not constants, but are functions of time. Details will not be included, but the solutions can be considered as transitions between two states, involving a certain time constant.

Comparison with Test Results

The validity of the proposed procedure is supported by test results obtained under three widely different conditions.

Figure 7 shows a series of oscillograms previously reported by Spaulding and Diemond,[2] obtained from operation of the type *C* fault locator, and reproduced here for illustration. Also indicated are calculations of the relative sizes of the reflections to be expected. The tests shown were all made on the Ross-Longview 230-kv line of the Bonneville Power Administration, with the line de-energized. Surges were applied at the Ross end, with faults connected at a distance of 32 miles, and with the line open at Longview, at a distance of 51 miles. These are all cases represented by Cases 1 through 8 in Table II. Some of the results show reflections obtained from the fault and from the far end, while others show reflections from the fault only and others from the far end only. Reflections indicated at 62 miles are reflections obtained from the fault after two round trips. Considering that any reflections obtained from the far end must traverse the fault position twice, once in each direction, it is necessary to multiply the incident wave twice by the transmission coefficient in order to obtain comparative results. Since the fault-locator response is dependent on the steepness of the wave front, which changes due to attenuation, a direct comparison between reflections obtained at the fault and at the far end is not applicable. If it be assumed that the steepness of the wave is diminished approximately in proportion to distance traveled, and proper allowance made, the results obtained are almost exactly those which are indicated by Table II, within the limits of recording accuracy.

Another series of tests, made on the Bonneville system in February 1951, included two from which the records in Figures 8 and 9 were obtained. In each case, a fault was initiated by closing a circuit breaker at Chehalis substation, 87 miles from Ross substation, where the records were obtained. For Figure 8, the fault was from *A* to *B* phase, and for Figure 9, from *B* phase to ground. The records of Figure 8(A) and 9(A) are indicative of the true nature of the traveling waves, and were obtained by recording the voltage on *B* phase at Ross through a coupling system consisting of a high-voltage carrier coupling capacitor and a voltage divider network. The coupling system introduced a long time constant of about 450 microseconds, about half the length of the record, which modified the long-time average but did not materially modify the short-time variations. The records in Figure 8(B) and 9(B) were taken on the type *A* fault locator equipment (but with some modifications not of significance here). The input to the fault locator was obtained from an antenna-type coupler, with a very short time constant, located under the main station bus. The effect of the short time constant is to make the response essentially proportional to the rate of change of the input recorded by the first oscillograph.

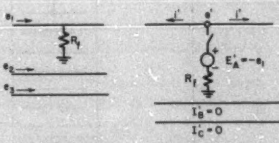

Figure 5. Fault with ground resistance

Although the records of Figures 8 and 9 show reflections obtained from other parts of the system, particular attention is directed to the differences in shape of the initial surges at the beginning of the records, and the magnitudes of the reflections at the 87-mile point (the range markers are at 10-mile intervals). A line-to-ground fault initiates a wave consisting of both slow and fast components; in the present instance, the initial surge was modified by the effect of a large capacitance to ground on the unfaulted conductors, such as was discussed in connection with Figure 6. The initial wave rises to a maximum and then actually decreases, with a time constant determined by the bus capacitance and the line impedances (the effect is somewhat obscured, however, because of the capacitance of the bus structure at the receiving end). In the line-to-line fault, only a fast-wave component is produced; since no voltage change occurs on the unfaulted conductor, its capacitance to ground has no effect. The difference between reflected waves at the 87-mile point is the result of two factors: first, the line-to-line fault produces an initial fast wave of larger value, and second, the reflection characteristics are different in the two cases. For the line-to-line fault, the reflection coefficient is 100 per cent; for the line-to-ground fault, the reflection coefficient would be 100 per cent at the initial instant because of the capacitance, but if the bus capacitance were not considered, the coefficient would be only 50 per cent. The actual results correspond to a value somewhere between. It is to be expected that after the wave front of a surge has become less steep due to attenuation, the modifying action of the bus capacitance will become less pronounced.

A third set of data for comparison is provided by an interesting series of oscillograms published by Rudge[11] in 1930. These were obtained for different types of discontinuities and recording conditions by application of surges to phase *A* and measurements of voltage on phase *B* at points approximately 5 miles away. These are examples in which the slow waves are of significant magnitude, but the differences in velocity have resulted in the separation of components. Although the information available does not permit quantitative analysis, the application of the principles discussed here give predictions of wave shape in full agreement with test results. Account must be taken not only of the velocity differences, but also of the reduction in slope of the slow wave.

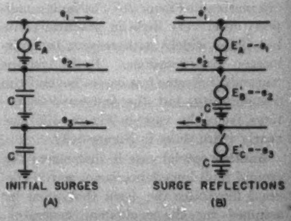

Figure 6. Fault with capacitance to ground

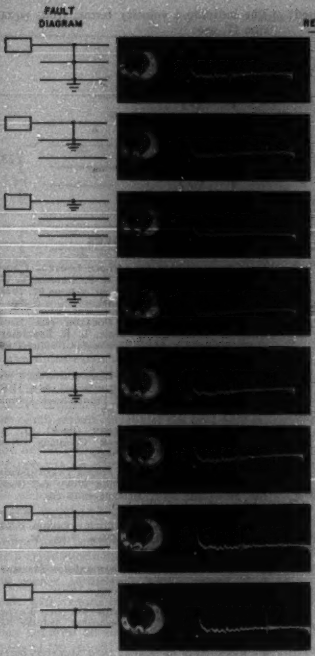

CALCULATED RELATIVE REFLECTIONS	
FROM FAULT	FROM FAR END
1.0	0
0.8	0.04
0.5	0.25
0.125	0.765
0.2	0.64
1.0	0
0.75	0.062
0	1.0

Figure 7 (left). Type C dead line tests

Conclusions

An appraisal of the response possibilities for the different fault locators can be made in terms of the foregoing analysis. From the standpoint of the initial waves, the type *C* and the Linascope are the simplest systems, since the surges are controlled and of the same character each time. Because of the relative unimportance of the slow wave, an applied-surge system is effective only to the extent of the fast wave produced, and only if the fast wave is such as to produce reflections for all types of faults to be recorded. Applying a single voltage always to the same conductor does not insure reflections. The selective switching arrangement of the type *C* system does assure reflections; an alternate arrangement would be the application of unequal voltages simultaneously between each of two conductors and ground. In the latter arrangement, by the proper choice of the voltages it would be possible to establish fast wave voltages between each conductor and ground and between each pair of conductors, so that reflections would be obtained from both line-to-ground and line-to-line faults.

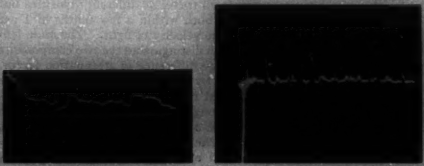

Figure 8. Fault from A to B phase. Records taken at 87 miles

(A) (below). Voltage on B phase
(B) (right). Fault locator

In the type *A* and *B* systems, the initial surge will have a character determined by the nature of the fault. Particularly in the case of lightning strokes, it would appear most probable that a fault would be initially from one line to ground. For the type A system, a subsequent reflection from the fault might involve surges of a different nature than the original, particularly if the initial fault condition has progressed to a multiline fault. At least the original faulted phase would still be involved in the discontinuity. There is reason to believe that some of the conditions possible in staged tests would be unlikely to occur with lightning strokes.

A major concern in all systems is the type of coupling used to record traveling waves. The coupling system should have a response with as little variability as possible. With recording dependent on fast waves, the possible combinations of received voltage are the same as the possible combinations of instantaneous voltage in a 3-phase system. Thus, coupling to a single conductor alone does not assure a response. The most effective system would be one which would respond to the largest of the three voltages which could exist on any one of the three conductors at any one instant.

Mathematical Appendix

The voltage and current variations for a 3-wire transmission line may be considered as represented by:

$$
\begin{aligned}
-\frac{\partial e_1}{\partial x} &= L_{11}\frac{\partial i_1}{\partial t}+R_{11}i_1+L_{12}\frac{\partial i_2}{\partial t}+L_{13}\frac{\partial i_3}{\partial t}\\
-\frac{\partial e_2}{\partial x} &= L_{21}\frac{\partial i_1}{\partial t}+L_{22}\frac{\partial i_2}{\partial t}+R_{22}i_2+L_{23}\frac{\partial i_3}{\partial t} \qquad (7)\\
-\frac{\partial e_3}{\partial x} &= L_{31}\frac{\partial i_1}{\partial t}+L_{32}\frac{\partial i_2}{\partial t}+L_{33}\frac{\partial i_3}{\partial t}+R_{33}i_3
\end{aligned}
$$

$$
\begin{aligned}
-\frac{\partial i_1}{\partial x} &= C_{11}\frac{\partial e_1}{\partial t}+G_{11}e_1+C_{12}\frac{\partial e_2}{\partial t}+C_{13}\frac{\partial e_3}{\partial t}\\
-\frac{\partial i_2}{\partial x} &= C_{21}\frac{\partial e_1}{\partial t}+C_{22}\frac{\partial e_2}{\partial t}+G_{22}e_2+C_{23}\frac{\partial e_3}{\partial t} \qquad (8)\\
-\frac{\partial i_3}{\partial x} &= C_{31}\frac{\partial e_1}{\partial t}+C_{32}\frac{\partial e_2}{\partial t}+C_{33}\frac{\partial e_3}{\partial t}+G_{33}e_3
\end{aligned}
$$

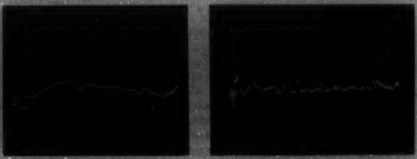

Figure 9. Fault from B phase to ground

(A) (left). Voltage on B phase
(B) (below). Fault locator

Symmetry conditions will be assumed, as a result of uniformity of coefficients and transpositions. Inductive and capacitive coefficients may be evaluated in accordance with methods previously described.[12] It will be assumed that the ground surface is the zero plane.

Using $E_1(x,s)$, or simply E_1, as the Laplace transform of $e_1(x,t)$, and similar notation for the other terms, and neglecting initial conditions for simplicity, the set of equations may be written as:

$$-\frac{\partial E_n}{\partial x}=\sum_{r=1}^{3}J_{nr}(s)I_r \tag{9}$$

$$-\frac{\partial I_n}{\partial x}=\sum_{r=1}^{3}K_{nr}(s)E_r \tag{10}$$

where

$$J_{nn}(s)=J=sL_{nn}+R_{nn}=sL+R$$
$$J_{nm}(s)=J'=sL_{nm}=sL'$$
$$K_{nn}(s)=K=sC_{nn}+G_{nn}=sC+G$$
$$K_{nm}(s)=K'=sC_{nm}=sC'$$

Differentiating equation 9 and substituting from equation 10, there results:

$$\frac{\partial^2 E_n}{\partial x^2}=\sum_{r=1}^{3}M_{nr}(s)E_r \tag{11}$$

and similarly:

$$\frac{\partial^2 I_n}{\partial x^2}=\sum_{r=1}^{3}M_{nr}(s)I_r \tag{12}$$

where $M_{nr}(s)=\sum_{r=1}^{3}\sum_{q=1}^{3}J_{nr}(s)K_{rq}(s)$

which will be designated briefly by:

$$M_{nn}(s)=M$$
$$M_{nm}(s)=M'$$

Denoting $\partial^2E_n/\partial x^2$ by p^2E_n, the solution for the complex propagation coefficients $p_n=\alpha_n(s)+\beta_n(s)$ depends on the roots of the characteristic equation:

$$\begin{vmatrix}[p^2-M] & -M' & -M' \\ -M' & [p^2-M] & -M' \\ -M' & -M' & [p^2-M]\end{vmatrix}=0 \tag{13}$$

which also can be expressed as:

$$[p^2-(M-M')]^2[p^2-(M+2M')]=0$$

or alternately as

$$[p^2-(K-K')(J-J')]^2\times[p^2-(K+2K')(J+2J')]=0$$

Of the four propagation coefficients, two apply to the wave moving in the positive direction. Solutions of equation 11 for the positive wave are:

$$E_n(s,x)=F_{n1}(s)\epsilon^{\alpha_1(s)x}\epsilon^{\beta_1(s)x}+F_{n2}(s)\epsilon^{\alpha_2(s)x}\epsilon^{\beta_2(s)x} \tag{14}$$

The expressions for $F_{n1}(s)$ and $F_{n2}(s)$ are transforms of time functions which are to be evaluated for conditions existing at $x=0$, and in many cases will have the same form as $E_n(s,0)$ except for arbitrary constants.

Solutions to equations 1 are then obtained by taking the inverse Laplace transforms of equation 14. The results are expressed symbolically as:

$$\begin{aligned}e_1(x,t)&=A_1f_1(x,t,\alpha_1,v_1)+A_2f_2(x,t,\alpha_2,v_2)\\ e_2(x,t)&=B_1f_1(x,t,\alpha_1,v_1)+B_2f_2(x,t,\alpha_2,v_2)\\ e_3(x,t)&=C_1f_1(x,t,\alpha_1,v_1)+C_2f_2(x,t,\alpha_2,v_2)\end{aligned} \tag{15}$$

Similar expressions for the currents are:

$$\begin{aligned}i_1(x,t)&=D_1f_1(x,t,\alpha_1,v_1)+D_2f_2(x,t,\alpha_2,v_2)\\ i_2(x,t)&=E_1f_1(x,t,\alpha_1,v_1)+E_2f_2(x,t,\alpha_2,v_2)\\ i_3(x,t)&=F_1f_1(x,t,\alpha_1,v_1)+F_2f_2(x,t,\alpha_2,v_2)\end{aligned} \tag{16}$$

An alternate view to equations 9 through 14 is obtained through comparison of the Laplace transform with the related Fourier transform. Thus, by writing $(j\omega)$ in place of (s) in equation 14 there is obtained a relationship applicable to each value of frequency in the frequency spectrum of the traveling wave. The phase characteristic at each frequency is related to the phase velocity by:

$$v(\omega)=\frac{\omega}{\beta(\omega)} \tag{17}$$

Equations 15 and 16 can likewise be considered as summations through Fourier integrals of the frequency components of equation 13.

Substituting equations 15 in equations 11, and equations 16 in equations 12, and treating each velocity term separately, using the relations of equation 13, there results:

$$\begin{aligned}&A_1+B_1+C_1=0\\ &A_2=B_2=C_2\\ &D_1+E_1+F_1=0\\ &D_2=E_2=F_2\end{aligned} \tag{18}$$

In terms of the frequency variable, there is obtained by equations 11 and 18:

$$\begin{aligned}A_1[\alpha_1(\omega)+j\beta_1(\omega)&=D_1[J(j\omega)-J'(j\omega)]\\ A_2[\alpha_2(\omega)+j\beta_2(\omega)]&=D_2[J(j\omega)+2J'(j\omega)]\end{aligned} \tag{19}$$

To the extent that the losses are small, approximate expressions may be obtained for the ratios in equation 19:

$$Z_1=\frac{A_1}{D_1}\approx v_1(L-L')$$

$$Z_2=\frac{A_2}{D_2}\approx v_2(L+2L') \tag{20}$$

Values of the complex propagation coefficients are obtained from equation 13, and with the higher order terms neglected, may be expressed in the form:

$$p(s)=\sqrt{\beta_0{}^2s^2\left[1+\frac{a}{s}\right]} \tag{21}$$

where $\beta_0=1/c$ and $c=$ velocity of light, or in terms of frequency components, as

$$p(j\omega)=\alpha(\omega)+j\beta(\omega)$$
$$\approx\frac{a_n}{2}\beta_0+j\omega\beta_0\sqrt{1+\left(\frac{a_n}{\omega}\right)^2}$$

For the individual terms, the attenuation parameters become:

$$a_1=\frac{R}{L-L'}+\frac{G}{C-C'}$$

$$a_2=\frac{R}{L+2L'}+\frac{G}{C+2C'} \tag{22}$$

The individual velocity terms, from equation 17, are:

$$v_1\approx\frac{c}{\sqrt{1+\left(\frac{a_1}{\omega}\right)^2}}$$

$$v_2\approx\frac{c}{\sqrt{1+\left(\frac{a_2}{\omega}\right)^2}} \tag{23}$$

References

1. A Transmission Line Fault Locator Using Fault Generated Surges, R. F. Stevens, T. W. Stringfield. *AIEE Transactions*, volume 67, 1948, part II, pages 1168–78.

2. A Transient Fault Locator for High Voltage Transmission Lines, L. R. Spaulding, C. C. Diemond. *AIEE Transactions*, volume 68, 1949, part II, pages 1005–10.

3. The "Linascope"—An Echo Ranging Type Fault Locator for High Voltage Lines, J. R. Leslie, K. H. Kidd. *AIEE Transactions*, volume 67, 1948, part II, pages 1162–67.

4. Electromagnetic Theory (book), J. A. Stratton. McGraw-Hill Book Company, New York, N. Y., 1941, pages 297–309.

5. Principles of Electric Power Transmission (book), L. R. Woodruff. John Wiley and Sons, Inc., New York, N. Y., 1925, pages 78–86.

6. Wave Propagation in Overhead Wires with Ground Return, J. R. Carson. *Bell System Technical Journal* (New York, N. Y.), October 1926, page 539.

7. Traveling Waves on Transmission Systems, L. V. Bewley. *AIEE Transactions*, volume 50, June section, 1931, pages 532–50.

8. Attenuation and Distortion of Waves, L. V. Bewley. *AIEE Transactions*, volume 53, 1934, pages 1749–57.

9. Resolution of Surges Into Multivelocity Components, L. V. Bewley. *Electrical Engineering* (*AIEE Transactions*), volume 54, November 1935, pages 1199–1203.

10. Propagation of High-Frequency Waves Along a Symmetrical Three-phase Line, A. Chevalier. *Revue Generale de L'Electricité* (Paris, France), January 1945.

11. *Discussion* by W. J. Rudge of Traveling Waves on Transmission Lines with Artificial Lightning Surges, K. B. Mc Eachron, J. G. Hemstreet, W. J. Rudge. *AIEE Transactions*, volume 49, July section, 1930, pages 932–33.

12. Critique of Ground Wire Theory, L. V. Bewley. *AIEE Transactions*, volume 50, March section, 1931, pages 1–22.

Discussion

K. H. Kidd (The Hydro Electric Power Commission of Ontario, Toronto, Ont.): The analysis of waves on 3-phase systems is certainly facilitated by the two component concept. It is unfortunate however that these are referred to as slow and fast components. It is true that the two components do travel at different velocities but they are both within a few tenths of 1 per cent of the velocity of light. The main feature which distinguishes the two components is the large difference in attenuation factor. As noted by the author the slow waves are attenuated rapidly. This fact is not illustrated though by equations 22 in which the slow wave attenuation factor a_2 is actually less than the fast wave attenuation factor a_1. The rapid attenuation of the second com-

Table I

	Applied Voltage Total	Applied Voltage 1st Comp.	Reflected Voltage Total	Reflected Voltage 1st Comp.	Arrival Voltage Total
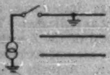	1.0	0.5	−0.5	−0.4	−0.8
	0	−0.25	+0.1	+0.2	+0.4
	0	−0.25	+0.1	+0.2	+0.4
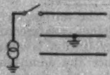	1.0	0.5	−0.05	−0.1	−0.2
	0	−0.25	+0.25	+0.2	+0.4
	0	−0.25	−0.05	−0.1	−0.2

ponent is only accounted for when the effect of the finite earth resistance is considered. The current and voltage waves of the first kind add to zero, and are analogous to positive sequence symmetrical components. The earth return current of the first kind is the sum of the 3-phase currents of the first kind and is zero. Hence the finite earth resistance has no effect on the component of the first kind. However, the component of the second kind produces an earth return current equal to three times the individual phase currents, similar to a zero sequence symmetrical component. Hence the finite earth resistance acts to attenuate this component very rapidly.

Some interesting observations can be made with regard to Table I of the paper. In case I and II if the same voltage is applied between all three phases and ground, waves of the second or "slow" kind only are generated and the attenuation is very rapid. This checks with Spaulding's and our tests.

If the pulse E_A is applied to one phase only, with the other two phases left open circuited (Case IV, $I_B=I_C=0$, $r=2$) the waves of the first and second kind are equal and are $E_A/2$. If the pulse E_A is applied to one phase only and the other two phases are grounded (Case I $E_B=E_C=0$) the wave of the first kind is $2/3 E_A$ and that of the second kind is $2/3\ E_A$. This agrees with experience with the linascope when locating sustained faults when better transmission is noted if the two adjacent phases are grounded.

As indicated in Figure 4, the reflected wave also consists of the two components even though the incident wave is of the first kind only. Thus only the first component of the reflected wave would travel back to the test terminal. This consideration casts doubt on the reflection coefficients calculated in Case 1, Table II. Since the reflected voltages are indicated to be equal on the three phases there would be no first component of the reflected wave and hence the attenuation would be rapid. I have calculated the reflected voltages for Case 1 and get −0.5, +0.1, and +0.1 for the three phases and not −0.5 on all phases as shown by the author.

On returning to the point of application the reflected wave would again be altered by the terminal impedance. Thus there are four steps to a complete solution:

1. Assume applied voltage. Calculate component of first kind from Table I of paper.
2. Assume fault characteristic. Calculate total reflected wave from Table II.
3. Calculate first component of total reflected wave again referring to Table I of paper.
4. Calculate magnitude of arrival wave at test terminal by again referring to Table II with assumed values of terminal impedances.

Typical examples of this complete solution are shown in the Table I of this discussion, where the generator is assumed to have a high internal impedance, so that the returning echoes are doubled in voltage.

Appendix

1. Reflection at a single-phase ground fault, following the method of Bewley.[1]

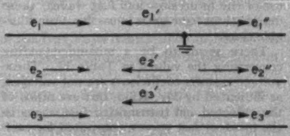

Voltage relations at the fault.

$$e_1+e_1'=e_1''=0$$
$$e_2+e_2'=e_2''$$
$$e_3+e_3'=e_3''$$

Current relations at the fault.
Phase 2.

$$Y_M(e_1-e_1')+Y_0(e_2-e_2')+Y_M(e_3-e_3') = Y_Me_1''+Y_0e_2''+Y_Me_3''$$

Phase 3.

$$Y_M(e_1-e_1')+Y_M(e_2-e_2')+Y_0(e_3-e_3') = Y_Me_1''+Y_Me_2''+Y_0e_3''$$

Solving for the reflected waves.

$$e_1'=-e_1$$
$$e_2'=e_3'=\frac{Y_M}{Y_0+Y_M}e_1$$

On a typical 230-kv circuit, 795,000 circular mil steel reinforced aluminum cable, horizontal spacing 25 feet, height above ground 60 feet.

$Z_0=1/Y_0=470$ ohms
$Z_M=1/Y_M=95$ ohms

Hence

$$e_1'=-e_1$$
$$e_2'=e_3'=+0.2_{e1}$$

The incident voltage on phase 1 is completely reflected. The reflected voltages on phases 2 and 3 are functions of the incident voltage on the faulted phase only.

Referring to Table I of the paper, Case 1, the components of the first kind are -0.8_{e1}, $+0.4_{e1}$, $+0.4_{e1}$.

2. Calculation of fast and slow component velocities. Taking values for a typical 230-kv circuit and calculating the resistance at 1 megacycle.

$R=10^{-3}$ ohms/foot
$G=0$
$L=0.5$ microhenrys/foot
$L'=0.1$ microhenrys/foot
$A_1=2.5\times10^3$
$A_2=1.4\times10^3$

Attenuation coefficients in decibels per mile are therefore:

$\alpha_1=0.06$ decibel per mile and $\alpha_2=0.034$ decibel per mile

The velocities are given by

$$V_1=\frac{C}{\sqrt{1+\left(\frac{2.5\times10^3}{6.28\times10^6}\right)^2}}\simeq C$$

and

$$V_2=\frac{C}{\sqrt{1+\left(\frac{1.4\times10^3}{6.28\times10^6}\right)^2}}\simeq C$$

3. Effect of finite earth resistance. The difference in attenuation of the two components is much more pronounced when the effect of finite earth resistance is considered. Let earth have finite resistance R_e. This adds the following terms to equations 1.

$$R_e(i_1+i_2+i_3)$$

The expressions for $J_{nn}(s)$ $J_{nm}(s)$ become

$$J_{nn}(s)=sL+R+R_e$$
$$J_{nm}(s)=sL'+R_e$$

Solving for A_1 and A_2

$$A_1=\frac{R}{L-L'}+\frac{G}{C-C'}\text{ as in equation 16}$$

$$A_2=\frac{R+3R_e}{L+2L'}+\frac{G}{C+2C'}\text{ increased over equation 16}$$

The effective earth resistance at high frequencies is given by

$$R_e=\frac{\sqrt{2}}{h}\sqrt{\rho f\times10^{-9}}\text{ ohm per centimeter}$$

where ρ = the earth resistivity = 10,000 say
h = the conductor height
f = the frequency

Hence R_e = 75 milliohms per foot and α_2 becomes 7.6 decibels per mile. The attenuation would be somewhat lower than this, if there were an overhead ground wire.

Reference

1. Traveling Waves on Transmission Systems, (book) L. V. Bewley. John Wiley and Sons, Inc., New York, N. Y.

L. R. Spaulding (Bonneville Power Administration, Portland, Oreg.) and **C. C. Diemond** (Bonneville Power Administration, Vancouver, Wash.): Dr. Lewis' paper presents a very creditable explanation of the experimental data reported earlier in connection with the type-C fault locator.[1] In the light of this work, we are studying the possibility of eliminating the phase selecting relays from the type-C fault locator design. These relays represent a substantial portion of the cost of this device.

It is suggested that in describing the initiation of the type-C fault locator, the terminology be clarified. The type-C locator is initiated by operation of fault detecting relays. These respond to 60-cycle-per-second quantities present during the fault and not to the initial fault-generated surge which is taken to mean, in fault locating terminology, the steep wave front at the start of the fault.

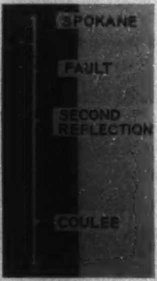

Figure 1

We would like to take this opportunity to report the first successful operation of the type-C fault locator using an electronic counter to give a direct indication of fault distance, independent of photographic processes. The first outage on the Coulee-Spokane 230-kv lines during the 1951 lightning season occurred on July 1, 1951. At 4:02 p.m., Pacific Standard Time, the Coulee-Spokane Line number 3 was hit by lightning, cleared and reclosed. The type-C fault locator operated and its electronic counter registered 227 microseconds, which indicated a distance of 21 miles from Spokane. This point falls between towers 316 and 317. The line patrolman dispatched to this point reported that flashover and conductor burns were found at towers 317 and 318. The film showing the cathode-ray trace from the type-C fault locator was later developed and showed a reflection of 21 miles, which verified the counter reading. This verifying trace is shown in Figure 1 of this discussion.

Reference

1. See reference 2 of the paper.

Laurel J. Lewis: The discussion by K. H. Kidd, indicating a method for including specifically the effects of ground resistance on the wave components is a significant contribution. The original equations showed definitely the relation between attenuation and velocity and the fact that a wave which experiences greater attenuation necessarily travels at a reduced speed. While experience had been relied upon primarily as the basis for disregarding the propagation of the wave with ground return over long distances, it is valuable to have the effects more completely represented in the equations. It must be recognized, however, that the complete relations depend upon all the frequency components in the initial surge, and that calculations at a single frequency are informative but do not indicate the full effect on the wave shape and velocity of the surge. When wave travel involves only short distances, the differences in velocity of the components are clearly evident.[1] There seems to be no fundamental objection to the use of the terms slow and fast waves; these designations have been in use for a considerable time.

There seems to be a misunderstanding concerning the values in Table II. These voltage transfer coefficients are not voltages, as indicated by Mr. Kidd, but are ratios of the reflected and transmitted fast waves to the incident fast waves, computed for each phase separately. The fact that the coefficients may be equal on the three phases does not mean that the voltages are equal, but only that the relative values are the same as in the incident waves.

Mr. Kidd's calculations for Case 1 and Case 2, Table II, do not agree with those in the paper. In the first place, the incident waves were determined from the equations in Table I, for the case where $r=2$, and agree with the values used by the author. For the reflected waves, however, the computation is based on the physical dimensions of a line which (using Kidd's values) corresponds to a value of $r=1.76$. Finally, although the voltage and current equations in Mr. Kidd's Appendix 1 are correct, the relations between surge impedance and surge admittance are not as indicated. The Y matrix is the reciprocal of the Z matrix, but the individual terms are not reciprocals of each other, as shown. Actually Y_M is negative, although Z_M is positive.

The method used by the author for determining reflected voltages, using equivalent generators and superposition, is actually an easier approach, since the admittances need not be calculated. One can use directly the equations in Table I of the paper, once r has been found from the values in equation 20. An alternate procedure is to use:

$$Z_1=Z_0-Z_M$$
$$Z_3=Z_0+2Z_M$$

with values determined from:

$$Z_0=138\log_{10}\frac{2h}{\rho}$$

$$Z_M=138\log_{10}\frac{2h}{D}$$

where:

h = equivalent conductor height
ρ = conductor radius
D = equivalent conductor spacing

Spaulding's and Diemond's discussion indicates the importance of developments continuing with the type-C fault locator. It seems reasonable to expect an increasing interest in the applied-pulse type of system, especially because its operation does not depend on the availability of a communication circuit such as a microwave system. A particular topic requiring further investigation is the study of the pulse system itself, especially where the pulses are applied through one of a group of coupling capacitors, and where auxiliary equipment consisting of carrier-coupling units and wave traps may remain connected to the other phases. The physical arrangements influence the form of initial surges and the received voltages, and are much more complicated than has generally been considered.

Reference

1. See reference 9 of the paper.

Resistance Effect on 230-Kv Fault Values Relating to Circuit Breaker Application at Grand Coulee

A. C. CONGER
ASSOCIATE MEMBER AIEE

EARLY studies and calculations[1,2] concerning the bussing at 230 kv of the generators at the Grand Coulee Power Plant and the lines emanating therefrom indicated that the asymmetrical fault currents to be encountered as the Coulee installation grew would increase very rapidly and the development of ultrahigh interrupting capacity circuit breakers, as well as means of limiting the fault current were investigated thoroughly. The Grand Coulee generators have a low subtransient reactance of 16 per cent and, therefore, contribute considerable d-c component to the total fault current for faults close to the 230-kv switchyard. Actual field tests show that the affect factor is 1.4 for faults supplied entirely by the Coulee generators. Since a few ohms resistance results in a small (fast) d-c time constant which acts to reduce a large proportion of the fault current which comes from the generators, an investigation was made to determine the possibility of using resistance in the two river-crossing circuits interconnecting the two Coulee switchyards to reduce the asymmetrical portion of the total fault current.

Grand Coulee Power Plant

The Grand Coulee Power Plant is located on the Columbia River near the geographical center of the State of Washington. The two powerhouses, one located at either end of the dam, generate the largest concentration of hydroelectric power in the world and are solidly bussed at 230 kv. This power is transmitted to the Northwest Power Pool through the transmission lines of the Bonneville Power Administration. The nine generators installed in the Left Powerhouse and the nine for the ultimate installation in the Right Powerhouse will provide a rated capacity of 1,944,000 kw with a peaking capability of approximately 2,340,000 kw. The total rated generating capability of the pool exceeds 5,000,000 kva at present.

The generator voltage of the units in the power plant is 13.8 kv with single-phase transformers stepping the voltage of the Left Powerhouse units to 230 kv on seven generators, to 115 kv on one, and on another to both 115 kv and 230 kv through a 3-winding bank which constitutes the tie between the 115-kv and 230-kv switchyards. The nine generators of the Right Powerhouse will connect to the 230-kv switchyards. The bussing is accomplished in the two 230-kv switchyards with the ultimate installation of 12 lines emanating therefrom. The switchyard busses constitute a closed ring, Figure 3, electrically connecting the 12 lines and 17 generators at 230 kv. The solid ring bus is comprised of six sections connected by 10,000,000-kva bus sectionalizing circuit breakers with two river-crossing circuits interconnecting the two switchyards. The line and bus-tie circuit breakers are rated 10,000,000 kva at 3-cycle interrupting time with 20-cycle reclosing on the line circuit breakers.

Purpose of Tests

The resistance tests were proposed to verify computations of the effect that resistance would have on the fault current as well as a means of checking the calculated value of resistance required to limit the fault current at circuit breaker interruption to the desired value. Consideration was given to the placing of resistor banks in each tie circuit or the installing of resistance conductors in the two tie circuits. The resistance conductors appeared the more feasible and investigations were made into the usage of a copper alloy conductor with approximately 1-ohm resistance per phase per circuit and it was mainly with this in view that these tests were made.

Test and Switching Arrangement

These resistance tests pertain directly to the effect that added resistance has on the resultant fault current as its transient d-c component is affected, thereby reducing the fault current that the circuit breakers would be interrupting. The tests were made with one generator, a small section of transmission line and a variable resistance with the object of simulating as near as possible the equivalent conditions that would actually exist with a bus fault with resistance in the bus and the ultimate generator installation. To simulate these conditions, 4,388 feet of transmission line would be required between the switchyard bus and the point of fault to represent one half the length of one tie circuit. This arrangement with one generator required approximately 7-ohms resistance in the fault circuit to obtain an L over R time constant of the circuit comparable to that of the nine generators of one powerhouse operating in parallel through high-resistance tie-circuit conductors under fault conditions. In order to accomplish this the faults were applied on the 230-kv Coulee-Midway number 1 line at a tower 4,153 feet from the switchyard bus. This

---

Paper 51-313, recommended by the AIEE Switchgear Committee and approved by the AIEE Technical Program Committee for presentation at the AIEE Pacific General Meeting, Portland, Oreg., August 20-23, 1951. Manuscript submitted May 21, 1951; made available for printing July 9, 1951.

A. C. CONGER is with the United States Bureau of Reclamation, Bismarck, N. D.

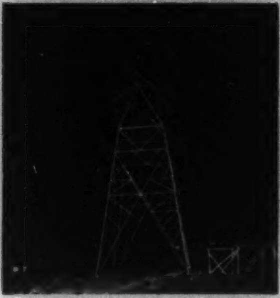

Figure 1. Midway line number 1 transmission tower Number 1151 showing variable resistance nichrome wire connected to line for test number 3

Figure 2. Nichrome resistance wire and support staging for variable resistance of 10 ohms per phase

distance being chosen due to the accessibility of the line at a tower near the desired distance.

Existing equipment and installations were utilized for the test including a General Electric impulse-type 230-kv 3,500,000-kva 3-cycle-interrupting-time oil circuit breaker (*JY20*); about one mile of Midway line Number 1 adjacent to the left Switchyard with the related relaying; and one of the main unit generators (*L-6*) manufactured by Westinghouse which has a connected amortisseur winding and is rated at 108,000 kw, 13.8 kv and 120 rpm. A 13.6/230-kv transformer bank connected delta-star with solidly grounded neutral is connected between the generator and the switchyard bus and was in the test circuit. The existing line metering circuits were utilized for obtaining the currents and voltages recorded by a magnetic oscillograph at the powerhouse.

The main unit generator was isolated

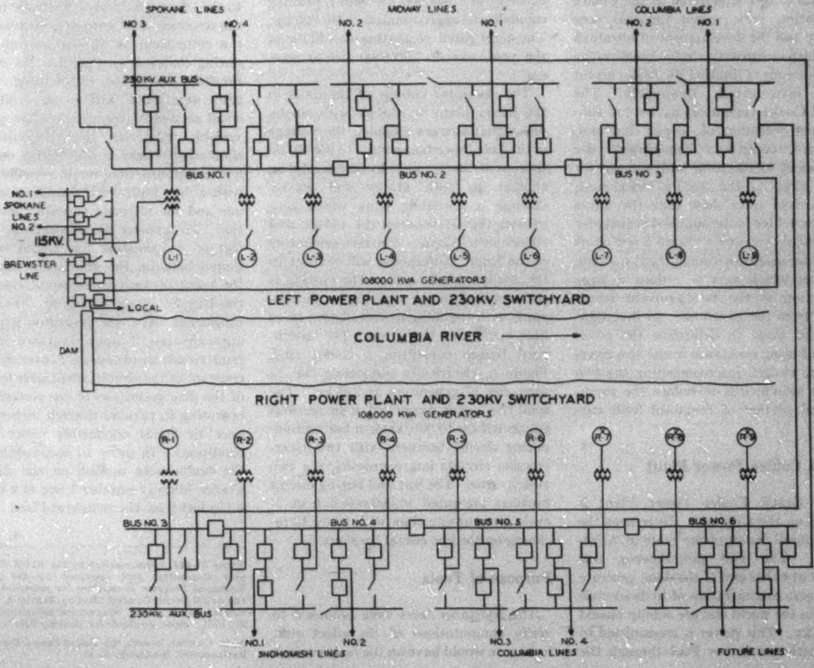

Figure 3. Grand Coulee 230-kv ring bus and switchyard arrangement (ultimate)

SPOKANE LINES
NO 3
NO. 4
MIDWAY LINES
NO. 2
NO. 1
COLUMBIA LINES
NO. 2
NO 1
230 KV AUX BUS
BUS NO. 1
BUS NO. 2
BUS NO 3
NO. 1
SPOKANE LINES
NO. 2
115KV.
BREWSTER LINE
LOCAL
L-1
L-2
L-3
L-4
L-5
L-6
L-7
L-8
L-9
108000 KVA GENERATORS
LEFT POWER PLANT AND 230KV. SWITCHYARD
DAM
COLUMBIA RIVER
RIGHT POWER PLANT AND 230KV. SWITCHYARD
108000 KVA GENERATORS
R-1
R-2
R-3
R-4
R-5
R-6
R-7
R-8
R-9
BUS NO. 3
BUS NO. 4
BUS NO. 5
BUS NO. 6
230KV. AUX. BUS
NO. 1
NO. 2
SNOHOMISH LINES
NO. 3
NO. 4
COLUMBIA LINES
FUTURE LINES

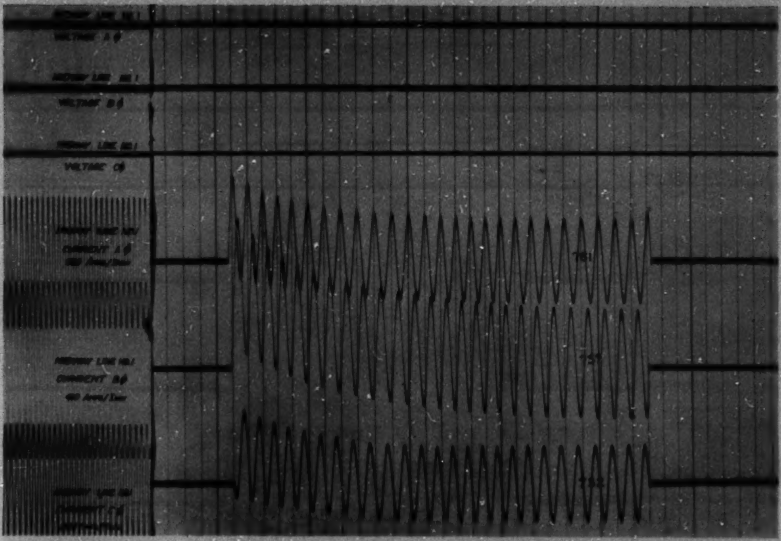

Figure 4. Oscillogram of test number 1, 3-phase solid ground to Y point at switchyard bus

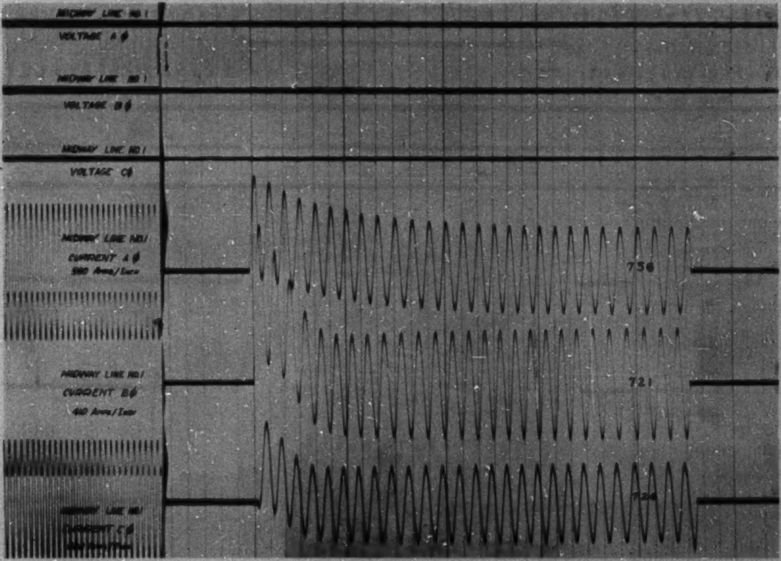

Figure 5. Oscillogram of test number 1-R1, 3-phase solid ground to Y point at switchyard bus

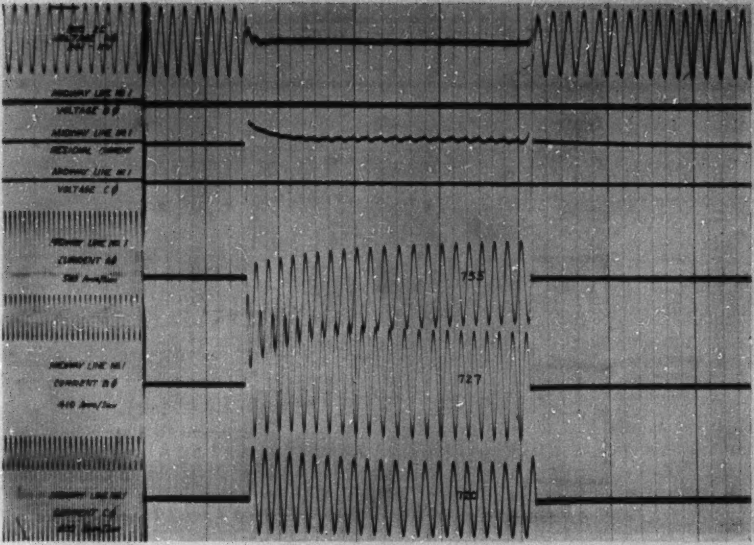

Figure 6. Oscillogram of test number 2, 3-phase solid ground at tower, no resistance added

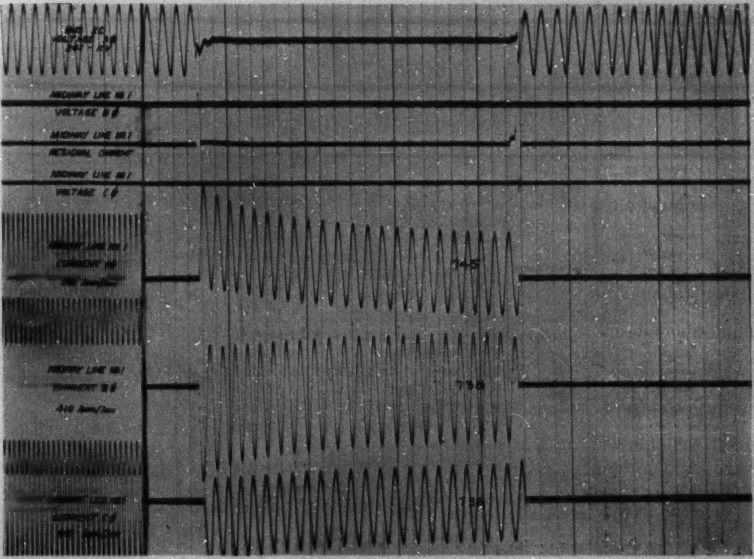

Figure 7. Oscillogram of test number 2-R1, 3-phase solid ground at tower, no resistance added

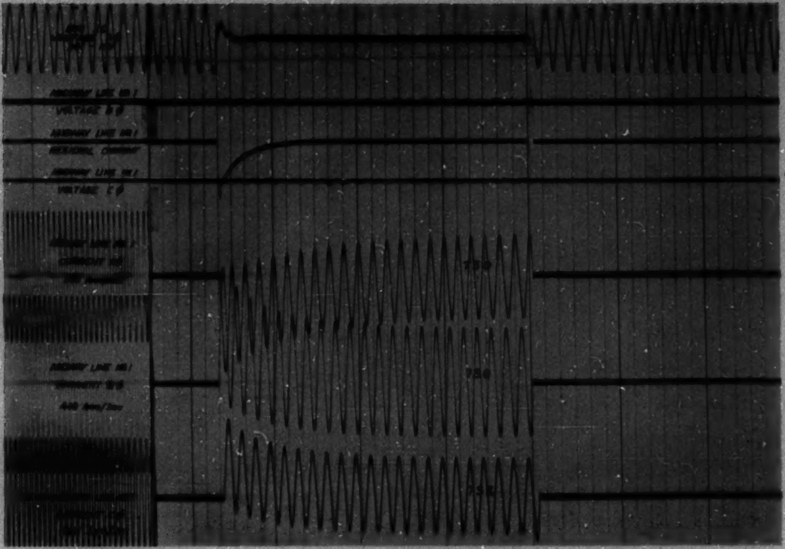

Figure 8. Oscillogram of test number 3, 3-phase fault to ground at tower, 2 ohms added per phase

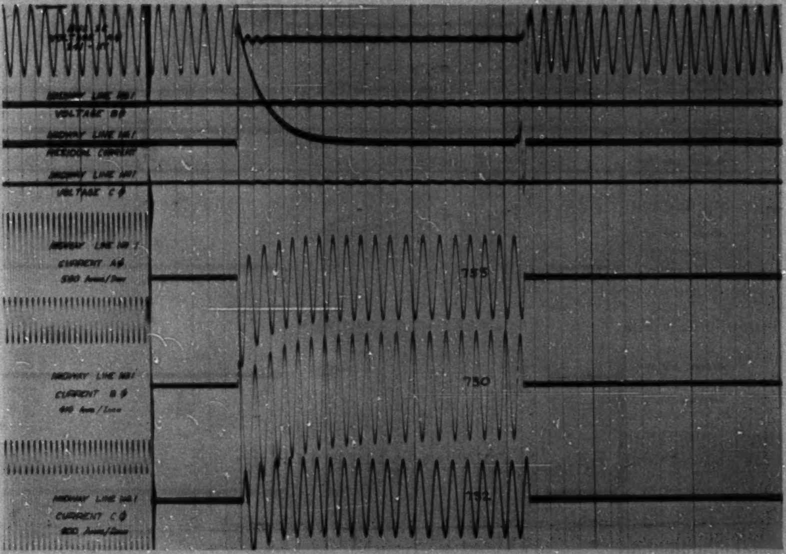

Figure 9. Oscillogram of test number 3-R1, 3-phase fault to ground at tower, 2 ohms added per phase

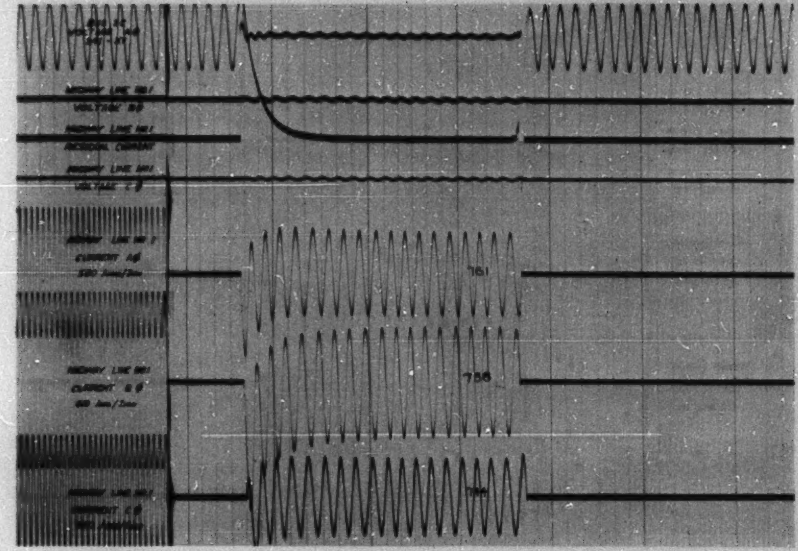

Figure 10. Oscillogram of test number 4, 3-phase fault to ground at tower, 5 ohms added per phase

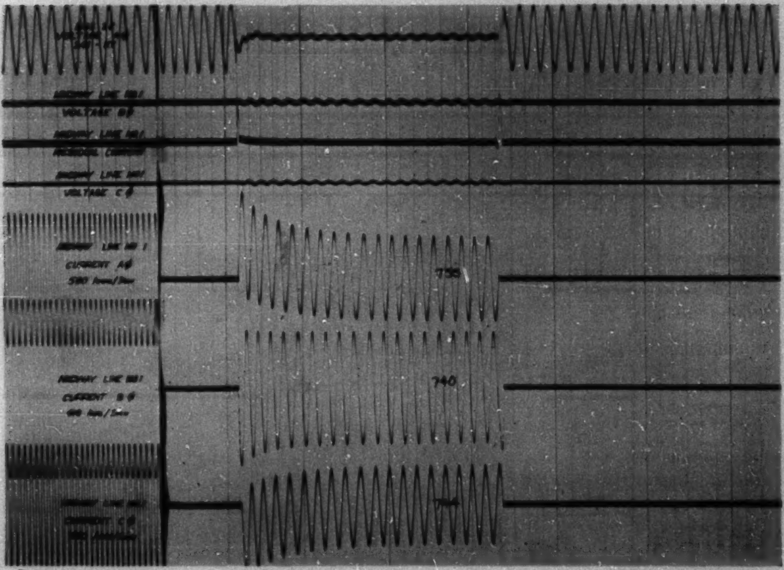

Figure 11. Oscillogram of test number 4-R1, 3-phase fault to ground at tower, 5 ohms added per phase

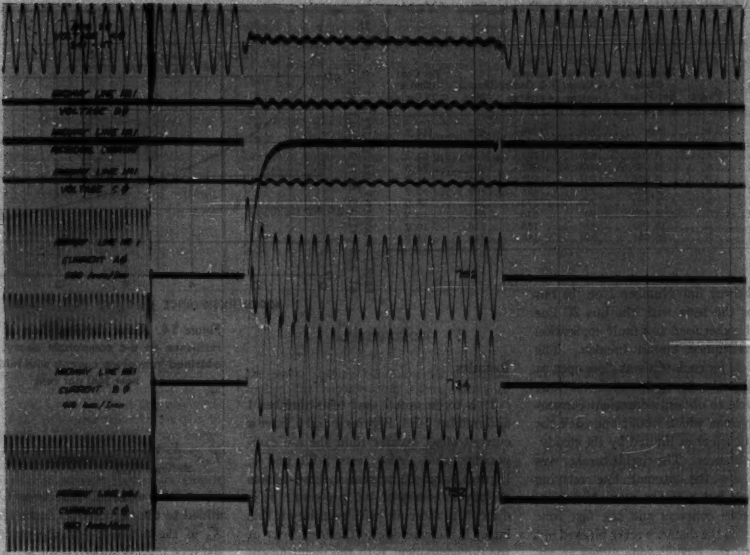

Figure 12. Oscillogram of test number 5, 3-phase fault to ground at tower, 10 ohms added per phase

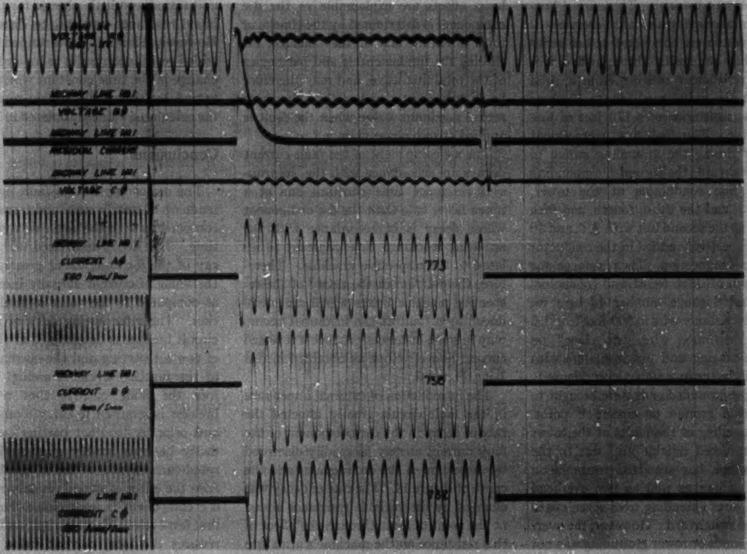

Figure 13. Oscillogram of test number 5-R1, 3-phase fault to ground at tower, 10 ohms added per phase

Table I. Calculated Values of Fault Currents Showing Effect of Variable Circuit Resistance

Test No.	Phase	Resistance, Ohms per Phase	Fault Current A-C Comp, Amperes	Fault Current D-C Comp, Amperes	Asymm. Mva	Per Cent Offset at 2.25 Cycles
1	B	Bus	808	1288	633	114.2
1-R1	B	Bus	717	1015	515	100.0
2	A	0.092	840	713	474	63.8
2-R1	A	0.092	828	872	502	74.5
3	B	2.092	807	522	402	44.9
3-R1	B	2.092	795	498	392	40.7
4	B	5.092	799	372	368	33.6
4-R1	C	5.092	800	435	381	40.3
5	B	10.092	816	185	340	16.2
5-R1	B	10.092	820	180	342	15.8

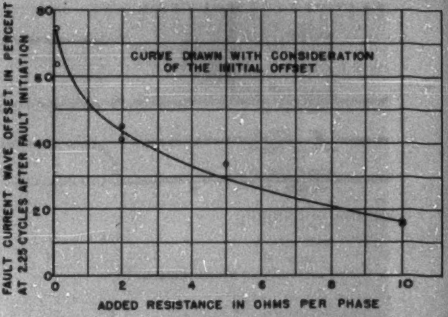

Figure 14. Curve showing effect of variable resistance on d-c component decay. Points obtained from phase currents with initial offset near 100 per cent

with Midway line Number 1 on the bus (*2C*) for the tests with the bus *2C* line circuit breaker used as a fault application and interruption circuit breaker. The duty cycle for each test was close-open at approximately 20 cycles with the long duty cycle to obtain a transient current-flow envelope which would approach the value of current as limited by the steady-state reactances. The circuit breaker was tripped by the normal line relaying equipment but with the ground relay instantaneous contacts and the first zone contacts on the distance relay blocked out and with the second zone timed at approximately 20 cycles. The coil of an over-current relay was placed in the *A* phase current circuit for back-up tripping of the circuit breaker. The normal bus-differential relaying also was in service.

The tests were completed in one series consisting of faults through five different resistances ranging from a solid fault at the switchyard bus to 10 ohms plus the resistance of 4,170 feet of line conductor. The first test arrangement was by closing the grounding switch in the switchyard, the second by grounding of the line conductors at the tower, Figure 1, and the third, fourth, and fifth similar to the second but with 2, 5, and 10 ohms respectively added in the conductor to ground connection. The resistance was comprised of three ten-strand conductors of B and S gauge number 14 bare nichrome resistance wire in 600-foot lengths.

The resistance wire was placed on wooden staging and pin insulators with each conductor in a single loop, Figure 2. The three grounded ends were brought to a common ground or circuit Y point. The grounding of the faults at the tower was considered reliable and was to the tower which has standard transmission line grounding as well as two overhead ground wires extending over seven spans from the switchyard. However, the overhead grounds or tower grounding was not directly connected to the switchyard grounding system at that time.

Results

It is to be noted that tests number 1 and number 1-R1, Figures 4 and 5, have a current offset greater than the a-c component value. Also tests 3-R1 and 4, Figures 9 and 10, appear to have offsets slightly in excess of 100 per cent. It is difficult to ascertain with certainty if this latter is the case due to the fast decay of the d-c component with the resulting envelope on the oscillograms. However, it does appear likely in view of the offsets obtained on the first two tests. These large offsets are explainable as the d-c component is determined by the change in total armature flux of the machine, including the fundamentals and harmonics of the total flux wave, and may therefore be slightly greater or less than the theoretical maximum value when the fault is applied at zero phase voltage.[3]

The a-c component of the fault current decays in accordance with the subtransient-reactance time constant and at a much faster rate than the d-c component whose decay is in accordance with the armature reactance time constant as related to the respective machine. Therefore, this relation in the decay of the respective machine fluxes which are introduced by a fault at the instant it occurs may in some instances produce a reversed current-flow envelope as obtained in test 1-R1, Figure 5.

The introduction of external impedance in the fault circuit greatly affected the rate of decay in the d-c component of the fault current as may be readily discerned by inspection of the oscillograms and the curve of Figure 14. The rate of decay was changed by the variable resistance added at the point of fault through the effect of this resistance on the machine's armature constants. This effect is shown in the expression[4]

$$T_a \times \frac{X_2+X_{ext}}{2\pi f(r_a+r_{ext})} \text{ in seconds}$$

where the external reactance (X_{ext}) is added to the negative-sequence reactance X_2 of the machine and the external resistance (r_{ext}) is added to the armature resistance of the machine (r_a) to obtain the armature time constant (T_a). The external reactance of the test circuit was low and introduced little change for the combined reactance and can be disregarded. However, it is readily ascertained that the added resistance results in an appreciable change in the time constant which is confirmed by the oscillographic results and the calculated values tabulated in Table 1.

Conclusions

The a-c component of fault current is made up of steady-state and transient a-c components with the latter decaying with time. This decay associated with the decay of the d-c component greatly affects the value of current actually interrupted as compared to the value at fault initiation. The interrupting duty rating of a circuit breaker is determined at the point of contact parting and the current rating at the first half-cycle of arcing. Therefore the fault current that a circuit breaker is required to carry momentarily and prior to "contact parting" will normally be considerably greater than the rated current value of the circuit breaker. Also the effect of added resistance on the d-c component is appreciable during the first few cycles of fault current and further reduces the total current value by the time the contacts part.

The relaying time and circuit breaker

contact parting time at Coulee total about 2.25 cycles. The tests with the faults at the tower show a d-c component decay after 2.25 cycles of fault current of approximately 30, 57, 65, and 84 per cent respectively for added resistance of zero, 2, 5, and 10 ohms per phase. This relation confirms the expected reduction in the fault current value at circuit breaker interruption and would very appreciably reduce the required rating of circuit breakers on the Coulee bus. On this basis, bus resistors could be utilized that would satisfactorily reduce the asymmetrical fault that the circuit breakers would be required to interrupt. However, it was found that the characteristics of the copper alloy conductor would prevent its usage in this instance in that the conductor temperature would be prohibitive under heavy load conditions and the presently installed 10,000,000-kva circuit breakers are considered adequate for the Grand Coulee Power Plant.

References

1. Development of the Transmission System from the Grand Coulee Power Plant, B. V. Hoard, E. E. Helwith. *AIEE Transactions*, volume 67, 1948, pages 1095–1100.

2. Development of the 230-Kv Ring Bus for Grand Coulee Power Plant, N. G. Holmdahl, C. L. Killgore. *AIEE Transactions*, volume 67, 1948, pages 1369–80.

3. Reactance of Synchronous Machines and Its Applications, R. E. Doherty, O. E. Shirley. *AIEE Transactions*, volume 37, part II, 1918, pages 1209–97.

4. Circuit Analysis of A-C Power Systems, Edith Clarke. Chapter I. John Wiley and Sons, Inc., New York, N. Y., 1943.

5. Electrical Transmission and Distribution Reference Book. Westinghouse Electric Corporation (East Pittsburgh, Pa.), page 156.

6. Fundamentals of AC Circuit Interruption, Dr. Erwin Salzer. Allis-Chalmers Manufacturing Company (Milwaukee, Wis.), 1950.

Discussion

M. J. Lantz (Bonneville Power Administration, Portland, Oreg.): The author of the discussion notes with interest the test verification of the generator offset factor of 1.40 at 2.25 cycles. This exact value was calculated and used in 1945 for the effect of asymmetry for the Coulee generators.

The limitation of fault current for circuit breaker duty reduction discussed by the author would be effective for both 3-phase and single-phase-to-ground faults; however, it should be kept in mind that if the resistance is placed in the powerhouse tie lines, less than 35 per cent of the total fault current is limited by the affected decrement. The balance of current comes from transmission lines and the powerhouse adjacent to the fault. It might be of interest to note the effect of normal fault resistance on the reduction of large magnitude single-phase-to-ground faults near Coulee.

For the maximum future faults expected at Coulee, in the neighborhood of 12,500 megavolt-amperes for 3-phase and 14,000 megavolt-amperes for single-phase-to-ground, the positive sequence system reactance is approximately 4.2 ohms and the zero sequence system reactance is approximately 3.2 ohms or the total system reactance to a single-phase-to-ground fault would be approximately 11.6 ohms. Since the fault resistance, namely the tower footing resistance, is multiplied by three, normally low footing resistance will have a pronounced effect on the system fault impedance. One mile of transmission line neglecting fault resistance and the overhead ground wires would decrease the maximum fault by about 26 per cent. Beyond that point, the full value of tower footing resistance would become effective in reducing the fault magnitude. Within the ground wire area, the tower footing resistance value would be paralleled with the resistance of the two overhead ground wires back to the essentially zero ground mat resistance. The average resistance of the ground wire is approximately 1.7 ohms per mile per conductor. This would effectively short circuit the tower footing resistance for a ground fault. The average tower footing resistance near Coulee based on past measurements is approximately 10 ohms for steel tower and 15 ohms for wood pole structures.

It is suggested that the ground wire be insulated from the towers except for the dead end structure at the end of ground wire. This would not affect the station protection provided the insulation value is coordinated but would permit the tower footing resistance to very effectively limit the ground fault current within the area for all conditions of fault not flashing the ground wire insulator.

Table I of this discussion shows the approximate ground fault reductions due to tower footing resistances. It should be kept in mind that no effect will be had on phase fault magnitudes.

Past system experience shows all ground faults that have occurred within the ground wire area have been nonlightning caused. The foregoing proposal would effectively reduce the circuit breaker duty for these faults.

This is a limited solution to the problem but should merit consideration as a method for reduction of circuit breaker duty for a large percentage of the single-phase-to-ground faults that may occur between the station bus and the end of the ground wire area.

Table I. Effect of Fault Resistance on Fault Mva for Single-Line-to-Ground Fault at Coulee Based on 14,000-Mva Total

Tower Footing Resistance, Ohms	Per cent of Total Single-Line-to-Ground Fault
0	100
2	89
4*	72
5	61
10	36

* The 4-ohm value reduces the fault to the circuit breaker rating or 10,000 mva.

A. C. Conger: The discussion by M. J. Lantz is appreciated as is his interest in the system fault capabilities at Grand Coulee.

The method presented by Mr. Lantz for limiting the asymmetrical fault current appears to be feasible in that the fault current could actually be reduced prior to contact parting of the interrupting circuit breaker by a relatively simple procedure. However the physical aspects encountered would require alteration of the tower peaks in order to obtain adequate isolation of the continuous overhead ground wires. On a comparative cost basis this could involve approximately the same expense as resistors, due to the several lines emanating from the Coulee busses.

Another consideration would be that all lightning striking the overhead wires would then be routed directly to the switchyard ground mats. It is possible that these heavy discharges could cause a serious ground mat potential difference. The existing grounding is considered adequate for system faults.[1] However, lightning could cause larger potential differences, and this would be given consideration before insulating the overhead ground wires from the numerous tower grounding points.

The overhead ground wires were recently connected permanently to the switchyard steel, thereby extending the counterpoise system. This was done to obtain the added capacitance effect, as well as to obtain more adequate grounding of the overhead wires. The isolation of the steel transmission line towers, with their individual counterpoise, would appreciably reduce the capacitance effect of the Coulee grounding system and defeat the purpose of the recent connection in this respect.

Reference

1. Grounding Effectiveness at Grand Coulee 230-Kv Switchyards Verified by Staged Fault Tests, A. C. Conger, R. K. Seely, W. H. Clagett. *AIEE Transactions*, volume 70, part II, 1951, pages 1547–52.

New Design Oil Circuit Breakers for 7,500,000-Kva 230-Kv Service

F. BICE JOHNSON
MEMBER AIEE

R. E. FRIEDRICH
ASSOCIATE AIEE

Synopsis: As a logical step in the trend toward achieving a minimum oil content but still retaining the advantages of the time-proved dead-tank construction a new 230-kv circuit breaker built around a novel design of tank has been developed. The extra volume of oil which contributes nothing to the insulation nor to the efficiency of the circuit breaker in interrupting performance has been eliminated and the required amount of oil reduced to the point where simplified methods of oil handling and maintenance procedures are possible. Design tests on the circuit breaker prove its adequacy in meeting design standards and extensive High Power Laboratory tests reveal a superior performance in interrupting fault and line-charging currents. The quantity of oil used and the design of the contacts is such as to permit a number of fault interruptions without maintenance operations.

EVERYONE familiar with the use of high-voltage switching equipment is familiar with the tremendous strides that have been made over the last few years in reliability, speed of operation, and interrupting ability of large outdoor oil circuit breakers. Also well-known, but perhaps not so widely publicized is the fact that this tremendous improvement in operating characteristics has been accompanied by a very startling reduction in the amount of oil required in the circuit breakers. This reduction of quantity of oil required is most noticeable in the highest voltage circuit breakers. The over-all effect of these development trends is an increase in efficiency in the use of the oil, and a reduction in maintenance effort, the extent of which can be appreciated by considering the kilovolt-amperes interrupted per gallon of oil which, in the 230-kv class has increased by a ratio of 11-to-1 in a period of 10 years. This accomplishment is graphically illustrated in Figure 1.

The first step in this tremendous improvement was made approximately ten years ago with the development of the multiflow deion grid which made possible the reduction in tank size for a 230-kv circuit breaker with 196-kv insulation from 108 inches to 78 inches at the same time that the interrupting capacity was raised from 2,500,000 to 3,500,000 kva. Further improvement in these deion grids to meet the demand for more interrupting ability has resulted in a design capable of interrupting 7,500,000 and even 10,000,000 kva in this size tank.

The second step was the development of the circuit breaker described in this paper which has gone further in reducing the amount of dead space oil by a radical redesign of the tank. This takes a shape roughly resembling that of a watch case.

The more conventional round tank, of course, represents close to the ultimate in mechanical strength but considering a cross section of such a circuit breaker it is obvious that a considerable volume is occupied by oil which serves no purpose from the standpoint of insulation or aiding in the interruption process. A tank with an elliptical cross section and straight vertical sides eliminates some of this useless space but is inherently weaker and still contains a considerable amount of excess oil.

To improve the strength of the elliptical tank and effect a further reduction in oil the new design was developed. The first design of the new tank consisted of a bottom section made up of two formed domes welded together to form a watch case-shaped container. One edge of the container was cut off and an oval cross-sectioned extension attached to form the

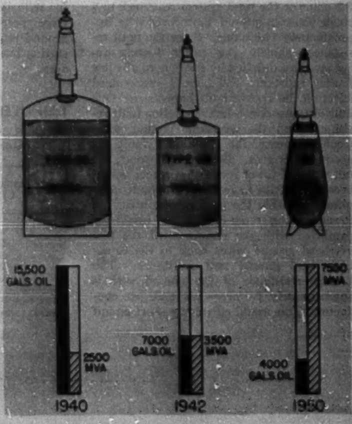

Figure 1. Comparison of 230-kv oil circuit breaker tank sizes over the past 10 years showing the reduction in oil content with increase in interrupting rating

---

Paper 51-314, recommended by the AIEE Switchgear Committee and approved by the AIEE Technical Program Committee for presentation at the AIEE Pacific General Meeting, Portland, Oreg., August 20-23, 1951. Manuscript submitted May 22, 1951; made available for printing July 9, 1951.

F. BICE JOHNSON and R. E. FRIEDRICH are with the Westinghouse Electric Corporation, East Pittsburgh, Pa.

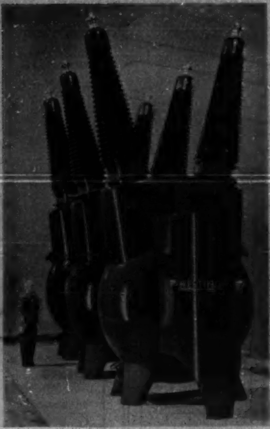

Figure 2. Model of early design of new tank shape

upper part of the assembly, providing a base for the condenser bushings, current transformers, and pole unit levers.

A scale model, Figure 2, of a modification of this form was made and studied from the standpoint of appearance and ease of manufacture. As a result of this study a further modification was made resulting in the present form as shown in Figure 3. This consists essentially of a bottom section formed by welding together two halves of a single dome and attaching thereto a conical-shaped member of elliptical cross section which tapers upward to enclose the bushing current transformers, pole unit levers, et cetera, with a minimum of waste space. This design obtains mechanical strength from the inherent stiffness of the dome sections comprising the bottom, and from a slight increase in thickness of the steel and readily withstands, without deformation, the same hydrostatic pressure test of 150 pounds per square inch that is made on conventional design tanks.

Figure 4 shows the new tank superimposed on the equivalent round tank and gives a good idea of the amount of excess volume that was eliminated. The quantity of oil required in the new design has been reduced to the point that oil maintenance and handling equipment can take the form of truck-mounted portable equipment, whereas formerly permanent storage and handling facilities were required at each location.

It is obvious that the new tank form reduced the amount of space available for workmen to assemble and adjust the contacts. In this voltage rating, however, there remains sufficient room for this operation and a removable wooden floor provides a stable platform on which workmen can operate. However, this condition does impose a practical limitation on the minimum size of circuit breaker to which this general design may be applied, experience showing that the present application represents about the lower limit. Preliminary design work has been done to apply this development to higher voltage circuit breakers.

Laboratory and field development tests on high interrupting capacity circuit breakers emphasized the necessity for adequate initial contact acceleration during the opening stroke. The required accelerating forces are provided by a conventional accelerating spring operating on the horizontal pull rod, individual springs located in the pole unit lever mechanisms and contact loading and similar springs in the deion grids. The total of these forces imposes a considerable load on the operating mechanism which is taken care of by building into the operating linkage a sufficient mechanical advantage to overcome this load. This is accomplished in the pole unit lever system and in the bell crank shown in Figure 5, which are both of somewhat novel design. By providing a considerable portion of this mechanical advantage, especially at the closed position, in the bell crank and by keeping to a minimum the mass of parts at this point, fullest advantage of the opening accelerating forces is obtained. The efficiency of this combined system is indicated by the lift rod travel obtained three cycles after energizing the trip coil which is 10 to 20 per cent more than that found to be required by interrupting tests.

Figure 3. New design 230-kv 7,500,000-kva oil circuit breaker set up for standard shop verification tests

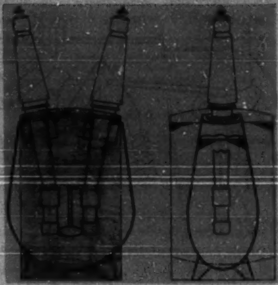

Figure 4. New design 230-kv 7,500,000-kva oil circuit breaker superposed on round-tank circuit breaker of comparable rating showing regions of excess oil eliminated

Electrical clearances in the first circuit breakers manufactured were designed to meet a special 825-kv impulse level, which is lower than the 900-kv level generally accepted as the standard for general application on a solidly-grounded 230-kv system. Voltage tests, both 60-cycle and impulse, were satisfactorily completed with an indication that with little modification other than a change in bushings the 60-cycle and impulse-withstand voltages corresponding to the 900-kv level can be met.

The circuit breaker is equipped with the latest refinement of the multiflow deion grid similar to that used in the 10,000,000-kva circuit breakers installed at Grand Coulee and described in detail in other Institute papers, specifically the Leeds-Friedrich paper[1] and the Darland-Clagett-Leeds[2] paper presented at the 1951 Summer General meeting. A cross section of the grid is shown in Figure 6.

The operating mechanism is a standard pneumatic device designed to give 3-cycle interrupting performance under all operating conditions and also to provide the ultimate in reclosing speed. Figure 7 is a timing test showing reclosing in 13.6 cycles. When specified, the control can be arranged to provide adjustment in the reclosing time between 15 cycles and 40 cycles.

Other new features worthy of note are an oil conserving dash pot which permits tripping the circuit breaker without oil in the tanks, a new compression seal where the current transformer secondary leads

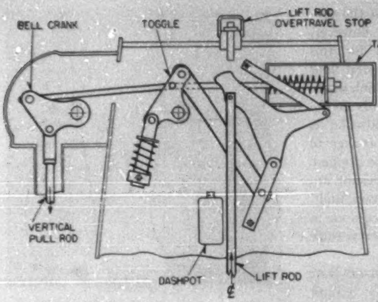

Figure 5 (above). Section view through top portion of new design circuit breaker showing bell crank, accelerating spring and straight-line pole unit lever system

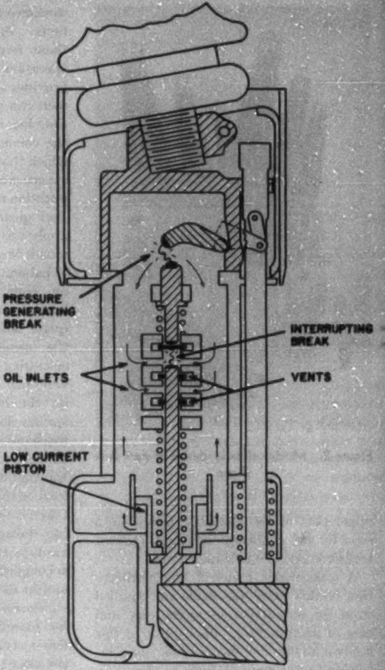

Figure 6 (right). Section view of multiflow interrupter showing pressure-generating gap at top driving oil into the orifice structure surrounding the interrupting break. Vents pass gases out front and back at levels between the inlet channels. At the bottom a spring driven annular piston provides supplementary oil flow for positive interruption of low currents

come out of the tanks, Figure 8, and right- and left-hand thread adjustment of the horizontal pull rods between poles for ease of adjustment.

Satisfactory results were obtained in design tests made to conform to the requirements of recognized standards.[8] These tests included the 60-cycle and impulse overvoltage tests previously referred to, a temperature test at rated current which showed that the reduction in oil volume had not impaired the current-carrying ability, an extensive life test, and a thorough check of interrupting ability in the High Power Laboratory. Well over 2,000 operations were made during the life test which included the following:

1. Timing tests under all conceivable types of operation.
2. One hundred fifty operations with high-speed reclosing.
3. One hundred fifty trip-free operations with full air pressure and the tripping impulse timed to coincide with the making of the circuit breaker contacts.
4. One hundred fifty additional trip-free operations with full air pressure and the tripping impulse initiated when the circuit breaker lift rods were three-quarters of an inch from making the contacts.

Numerous timing tests were made at various times during the life test to verify the consistent performance of the breaker.

High Power Laboratory Interrupting Tests

Several extensive series of fault interrupting tests were made to demonstrate the ability of the circuit breaker to perform in a completely satisfactory manner comparable with the more conventional round-tank type of circuit breaker. A complete 3-pole circuit breaker assembly was set up in the High Power Laboratory at East Pittsburgh as shown in Figure 9 to verify the excellent performance previously shown by a single pole unit of practically identical construction during development tests. Data from these tests are summarized in Tables I to IV.

Practically restrike-free performance was obtained on capacitor switching tests simulating the interruption of line charging current which is typical for the multiflow deion grid. As shown in Figure 6 the oil-driving pump at the lower end of the interrupter serves to augment flow from the pressure generating break on such relatively low current.

Pole number 1 of the 3-pole circuit breaker was tested to the maximum capacity of the laboratory with the full line-to-neutral voltage of 132 kv applied to the terminals. Following several relatively low current and three duty cycle interrupting tests at currents from 2,170 to 8,590 amperes, a high power test at 132 kv was made with the interrupted current measuring 12,100 amperes. This value of current was obtained by setting for maximum asymmetry of the current wave and tripping the test circuit breaker prior to fault initiation to cause the instant of contact parting to occur during the first cycle of short circuit current. The oscillogram of this test, in which the interrupting time was 2.60 cycles, is shown in Figure 10(A). The power interrupted is the equivalent of that involved in a 3-phase fault of 4,800,000 kva at 230 kv. The interrupting rating of the circuit breaker was verified by applying the full power of the laboratory at approximately one-half normal line-to-ground voltage across the half-pole unit. Pole number 2 was tested with one interrupting unit shunted out of the circuit and 66-kv-to-ground applied to the other unit. Duty cycle tests were made with symmetrical short-circuit currents up to a maximum of 13,900 amperes. By pretripping the circuit breaker and making the current wave asymmetrical, 21,250 amperes, Figure 10(B), were interrupted in a total time of 2.30 cycles. This is the equivalent of a 3-phase fault of 8,500,000 kva at 230 kv or 13 per cent above the circuit breaker rating.

To demonstrate the mechanical adequacy of the tank shape under shock loading accompanying the interruption of ex-

Table I. Heavy Duty High Power Laboratory Interrupting Tests on Three-Pole Circuit Breaker

Test No.	Duty	Interrupted Current, Rms Amperes	Interrupting Time, Cycles	Equivalent 3 Phase, Mva
132-Kv Line—Ground—Pole #1				
1	0+30 seconds	250	2.15	100
2	CO	378	2.25	150
3	O+Inst.	267	2.50	105
	CO	267	2.80	105
4	0+30 seconds	777	2.05	310
5	O	785	2.55	315
6	0+30 seconds	2,170	2.40	865
7	CO	2,690	2.75	1,050
8	0+30 seconds	6,300	2.40	2,500
9	CO	6,300	2.90	2,500
10	0+30 seconds	8,590	2.25	3,400
11	CO	6,650	2.95	2,650
12	O	12,100	2.60	4,800
66-Kv Line—Ground—Half Pole #2—#3 Terminal				
1	O	568	2.45	225
2	0+30 seconds	830	2.55	330
3	CO	830	2.65	330
4	0+30 seconds	10,200	2.35	4,050
5	CO	10,000	2.60	4,000
6	0+30 seconds	13,900	2.85	5,550
7	CO	13,750	2.70	5,500
8	O	21,250	2.30	8,500
44-Kv Line—Ground—Half Pole #2—#3 Terminal				
1	0+instantaneous	820	2.45	325
	CO	1,100	2.90	440
2	0+instantaneous	18,600	2.95	7,400
	CO	17,900	2.90	7,100
3	O	28,900	2.25	11,500

tremely high fault currents, an asymmetrical pretripped test with 44 kv applied to half the pole unit was made interrupting 28,900 amperes in 2.25 cycles corresponding to a 3-phase fault of 11,500,000 kva or more than 50 per cent above the circuit breaker rating. This oscillogram is shown in Figure 10(C). Justification of testing at two-thirds normal line-to-ground voltage under laboratory conditions of high rates of rise of transient recovery voltage and with overshooting of this transient to values comparable to those obtained under field conditions has been explained previously in the paper by Leeds-Friedrich.[1] The results of this test conform with those obtained earlier on the single-pole unit which was subjected to the mechanical shock accompanying the interruption of more than 30,000 amperes at 44 kv on a single interrupter. On this test the interrupting time was 2.7 cycles. The accompanying liberated arc energy represents very nearly the maximum to be expected at these currents with the type of interrupter unit with which this circuit breaker is equipped. Careful measurement of the stresses set up in the tank walls indicated values only a fraction of the safe limits for the material. The external demonstration accompanying such high power tests appeared to be somewhat less than that experienced with round-tank circuit breakers under similar test conditions, the only evidence of the tremendous power handled being swinging of the cables and a moderate ground shock. This is further borne out by the fact that on the test involving more than 30,000 amperes several 0.5-inch diameter bolts varying in length from 1 to 3 inches placed on end on the top of the tank remained standing throughout the circuit breaker operation. There is some reason to believe that the shape of the bottom of this tank is conducive to minimizing the effect of the downward traveling pressure shock wave produced in the oil by the rapid liberation of arc energy.

Table II. 198-Kv Factor-of-Safety Tests

Test No.	Interrupted Current Rms Amperes	Interrupting Time Cycles
1	170	2.3
2	170	2.6
3	170	2.5
4	510	2.5
5	525	3.0
6	540	2.7
7	1,080	3.0
8	1,080	2.6
9	1,100	3.0
10	2,670	3.0
11	2,580	2.8
12	2,700	2.9
13	4,460	2.7
14	4,510	2.6
15	4,410	2.7

Table III. Overvoltage Tests—Half Pole Number 2—Number 4 Terminal

Test No.	Test Voltage, Kv	Interrupted Current, Rms Amperes	Interrupting Time, Cycles
1	132	140	2.45
2	167	179	2.45
3	176	1,990	2.90
4	176	4,050	2.85
5	176	5,490	2.65

Measurements indicated that notwithstanding the reduced volume of air above the oil available as expansion space for the oil displaced by the rapidly growing gas bubble, the instantaneous pressures in the oil accompanying interruption are comparable with those experienced in the round-tank circuit breaker of similar rating but of much greater air space.

Several high-speed reclosing tests were made at both 66 and 44 kv on one-half of Pole number 2. One test at 44 kv involved currents of 18,600 and 17,900 amperes with a reclosing time interval of 14.2 cycles. As indicated in Figure 11 both symmetrical fault currents were nearly 100 per cent of the standard duty interrupting capacity indicating a comfortable margin over that required by the standards.[3] Table I presents the data obtained on the 3-pole circuit breaker on the 132-, 66-, and 44-kv tests.

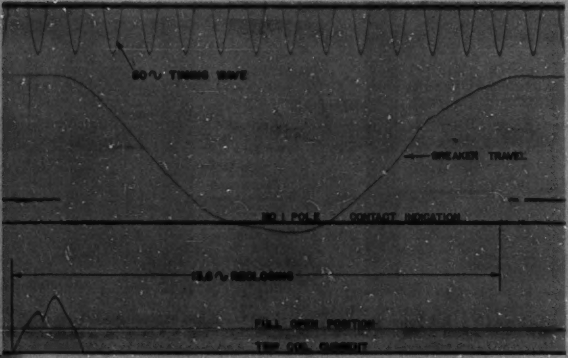

Figure 7. Oscillogram showing 13.6-cycle reclosing timing test

Table IV. 230-Kv 3-Phase Ungrounded Fault Tests

Test No.		Interrupted Current, Rms Amperes	Interrupting Time, Cycles	Interrupted Mva
1	φ1	2,790	2.90	1,150
	φ2	2,600	2.90	
	φ3	1,990	2.65	
2		5,010	2.80	1,995
		4,500	2.60	
		3,880	2.80	
3		6,900	2.75	2,750
		5,760	2.95	
		4,550	2.95	

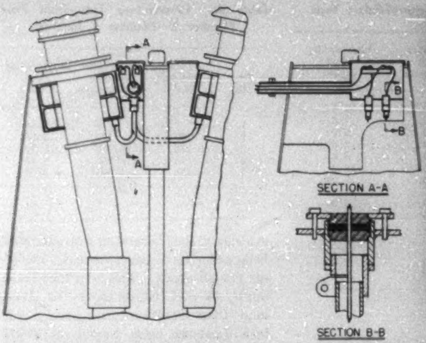

Figure 8. Section view through top portion of new design oil circuit breaker showing location of current transformer and details of connection of leads

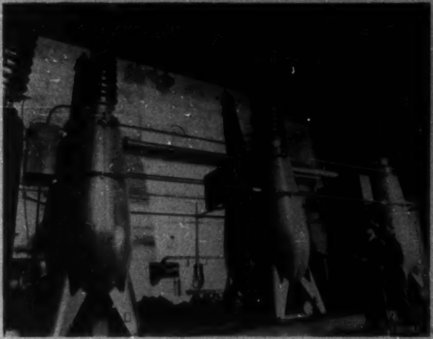

Figure 9. New design 230-kv 7,500,000 kva-oil circuit breaker set up for fault interrupting tests in the High Power Laboratory

Following this run of high-power tests on one-half of pole number 2 another advantage of the reduced oil content was demonstrated, namely: The rapidity with which the oil can be removed and contact parts inspected. This entire operation required approximately 25 minutes to complete.

The condition of the single interrupter involved in the tests at 66 and 44 kv totaling over 67,000,000 kva is shown in several photographs made after the tests were completed. Considering the appearance of the contacts and plate assembly, it is evident that a considerably greater integrated power could be handled by the unit before replacement of parts subject to erosion would be necessary. Measurements indicated a loss of approximately 15 per cent of the contact arcing material due to burning. The appearance of the lower tip of the intermediate and the lower contact is shown in Figure 12. Figure 13 presents the condition of the fiber plates removed from the section surrounding the main interrupting gap. Likewise, depreciation of the oil following this series of heavy current tests due to carbonization by the arc had not progressed sufficiently to require rehabilitation or to impair the operating performance of the breaker.

Factor of Safety Tests

A series of interrupting tests were made with 198 kv applied across the terminals of a single pole to determine not only the performance of the circuit breaker under 3-phase fault conditions in which the first phase to clear is subjected to 87 per cent of line-to-line voltage but to check the effect of the gas bubble on the insulation of the circuit breaker. This data is submitted in Table II. Currents ranging in value from 170 to 4,510 amperes were interrupted in 3.0 cycles or less in all cases. The recovery voltage following each of these tests was not removed from the circuit breaker until 5 seconds after interruption occurred, thus demonstrating the clearances found in this form-fitting tank to be entirely adequate during the period in which the gas bubble accompanying interruption is located in the electrostatic field between live parts and ground. Further proof of this fact was obtained for currents up to the current rating of the circuit breaker by a special test connection in which 132-kv-to-ground was applied to the circuit breaker for several seconds immediately following an extremely high-current interruption at reduced voltage.

Overvoltage Interrupting Tests

Increased interest among system-operating people in the problem of out-of-step switching led to the series of tests given in Table III. Calculations of dynamic voltage appearing across a tie circuit breaker under the most unfavorable conditions have indicated maximum values appre-

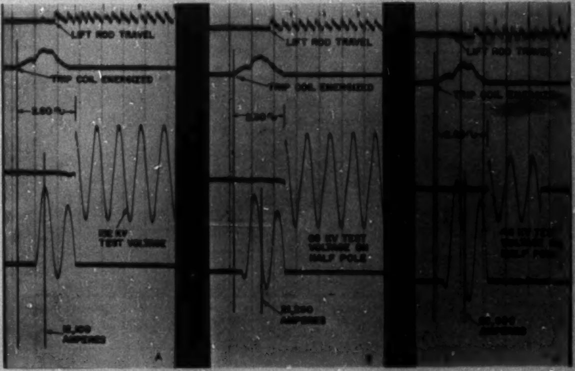

Figure 10. High Power Laboratory tests on 230-kv 7,500,000-kva circuit breaker

(A) 132-kv 12,100 amperes single-pole equivalent to 3-phase 230-kv, 4,800,000 kva
(B) 66-kv 21,250 amperes half pole equivalent to 3-phase 230-kv 8,500,000 kva
(C) 44-kv 28,900 amperes half pole equivalent to 3-phase 230-kv 11,500,000 kva

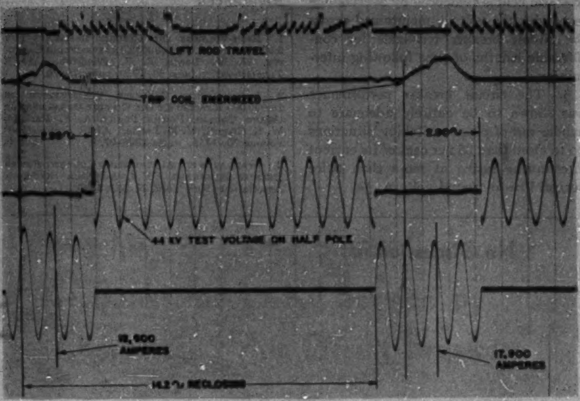

Figure 11. Oscillogram of 14.2-cycle reclosing duty test on 230-kv, 7,500,000-kva circuit breaker opening 18,600 amperes at 44 kv across a half-pole unit equivalent to a 3-phase fault of 7,400,000 kva at 230 kv

ciably above the generally accepted two times normal even for solidly-grounded systems. Voltages as high as 176 kv-to-ground were applied to the half of pole number 2 previously shunted out of the circuit. This voltage represented over two and one-half times the normal voltage for a single interrupting unit equivalent to 352 kv across a full pole. To simulate field conditions, the circuit was partially damped with parallel resistance to limit overshooting of the recovery transient to approximately 20 per cent. Following a check test at 132 kv and 140 amperes, currents of 179 to 5,490 amperes were interrupted within three cycles after tripping. These interruptions were made at approximately 30 per cent of the current rating of the circuit breaker. On the highest power test the maximum crest voltage was 288 kv, representing 21 per cent overshoot above the peak of the 168 kv (rms) normal frequency recovery voltage. Even under this extreme condition, equivalent to a recovery voltage peak of 576 kv across a single pole the circuit breaker cleared the circuit in only 2.6 cycles.

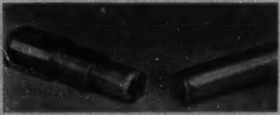

Figure 12. View of contacts removed from interrupter after series of fault interrupting tests totaling over 67,000,000 kva showing excellent condition of arcing tips

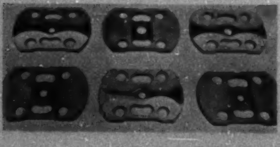

Figure 13. View of fiber plates removed from interrupter after series of fault interrupting tests totaling over 67,000,000 kva showing the minimum amount of erosion of the orifice plates

Three-Phase Tests

It seemed desirable to utilize this unusual opportunity to make 3-phase tests at 230 kv up to the full power available. Accordingly, a number of 3-phase ungrounded fault interruptions were made. The data from the oscillograms given in Table IV shows that a maximum of 2,750,000 kva was interrupted in 2.9 cycles with a current of 6,900 amperes measured in Phase 1, Figure 14. This is believed to be the highest power 3-phase test ever made on a 230-kv circuit breaker in either the laboratory or field.

Inspection of the interrupting units made subsequent to these tests showed them to be in excellent condition and capable of additional fault interruptions.

Conclusions

1. A novel form of high-speed, high-voltage, dead-tank type of oil circuit breaker has been developed culminating a period of intensive development over the past ten years. An increase in the ratio of interrupting rating to oil volume of more than 11-to-1 has accompanied this development. This has been accomplished not only by considerable improvements in the interrupter unit itself described in previous papers[1–3] to the Institute but also by the new form-fitting shape of the tank so designed as to eliminate regions of excess oil, particularly around the bushing flange and at the sides and below the interrupters.

2. The minimum clearances of the round tank are maintained so that the new form passes successfully all voltage tests required of the more conventional shape. Likewise, the circuit breaker performed satisfactorily on all standard design tests including temperature rise at rated current in a manner comparable with the more conventional round-tank type.

3. The 7,500,000 kva interrupting capacity of this oil circuit breaker was demonstrated with considerable margin by 3-phase tests at 230 kv to 2,750,000 kva, single phase tests at normal line-to-ground voltage of 132 kv to the 3-phase equivalent of 4,800,000 kva, by half-pole tests at 66 kv to 8,500,000 kva, and by factor-of-safety half-pole tests at 44 kv to a maximum fault current corresponding to 11,500,000 kva.

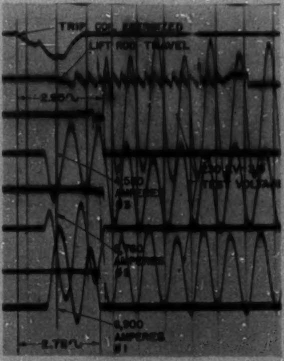

Figure 14. Oscillogram of 230-kv 3-phase ungrounded fault test on 230-kv 7,500,000-kva circuit breaker opening a maximum of 2,750,000 kva with a current of 6,900 amperes measured in phase one

4. It has been shown that the closely-fitting tank shape is entirely adequate to sustain the pressure shocks accompanying interruption of currents well above the rating of the circuit breaker and possibly serves to reduce the external demonstration by virtue of the curvature of the tank bottom.

5. Adequate insulation even during the period in which the gas bubble resulting from the arc is located in the electrostatic field is evidenced by overvoltage tests with the voltage maintained across the circuit breaker terminals for considerable lengths of time following interruption.

6. The circuit breaker performance was shown to be entirely adequate to handle out-of-phase switching situations up to more than 25 per cent of its current interrupting rating at more than twice normal line-to-ground voltage.

References

1. High-Voltage Oil Circuit Breakers for 5,000,000 to 10,000,000 Kva Interrupting Capacity, W. M. Leeds, R. E. Friedrich. *AIEE Transactions*, volume 69, 1950, pages 70–76.

2. Interrupting Capacity Verification of 10,000,000 Kva 230 Kv Oil Circuit Breakers for Grand Coulee Power Plant, A. F. Darland, W. H. Clagett, W. M. Leeds. *AIEE Transactions*, volume 70, 1951, pages 1386–97.

3. Standards for Alternating Current Power Circuit Breakers. *C37.4*, American Standards Association (New York, N. Y.), 1945.

No Discussion

Switching of Large Shunt Capacitor Banks for 15-Kv Service by Compressed Air Circuit Breakers

B. P. BAKER
FELLOW AIEE

ECONOMICAL operation of large power systems, emphasizes the importance of reducing to a minimum the generation and transmission of reactive power. Currently, this is being accomplished by using capacitor banks, up to 25,000 kilovars at voltage up to 34.5 kv. These may be applied either direct to low-voltage systems or to high-voltage systems through a tertiary winding of a high-voltage power transformer. The normal variation in system power requirements, usually results in switching the larger capacitor banks on and off the line several times per day. In addition to the frequency of operation which is often necessary, the unusual switching requirements have developed a demand for circuit breakers with operating performance which is generally not found in standard powerhouse circuit breakers.

Circuit Breaker Requirements

Circuit breakers for the large capacitor banks should not only be capable of performing many thousand switching operations with low maintenance, but they must be capable of developing dielectric strength across the arcing space very rapidly once the interrupting process has started. Also they must be capable of withstanding sudden surges of current, that is, sudden changes in current after the contacts are parted on opening and before they are closed on the closing stroke.

Circuit Breaker Performance

In order to switch these capacitors without producing overvoltages which might cause overstressing or breakdown of system insulation, the circuit breakers are required to interrupt leading currents over the entire range and under all kinds of circumstances without restrikes and with only a limited number of reignitions. Reignitions are defined as the initiation of current flow after the arc has been extinguished for a period of 1/4 cycle or less of the fundamental frequency. These re-establishments of current produce no overvoltages or damaging effect on the circuit breaker or connected apparatus. Restrikes are defined as the initiation of current flow after the arc has been extinguished 1/4 cycle or more. These re-establishments may produce unnecessary and damaging overvoltages as will be discussed later.

When a circuit breaker interrupts the flow of current through a circuit, the success of the arc extinction process depends upon a race between the rate at which the interrupter can develop dielectric strength between its contacts and the rate at which the constants of the circuit permit voltage to reappear across the contacts. On single-phase circuits containing inductance only, the maximum voltage of approximately twice crest of the fundamental wave is applied in a matter of microseconds. In many breakers this results in re-establishment of the arc following the first one or two current zeros. Conditions following each re-establishment repeat rather faithfully and are not affected by previous re-establishments, so that ultimately the arc is extinguished with overvoltages which are almost entirely a function of the circuit, at least almost independent of the struggle the circuit breaker has had in accomplishing interruption.

In the case of a leading current, the initial arc extinction is exceedingly easy in that the maximum restored voltage is not reached until 1/2 cycle later. However, if the restored voltage produces re-establishment of the current after it has been zero for more than 1/4 cycle, the voltages begin to exceed normal and each succeeding restrike tends to become worse due to the residual effect of preceding reignitions.

The following are some of the factors which affect restrikes and reignitions:

Circuit breaker characteristics

1. Dielectric strength of arc path at time of current zero.
2. Rate of development of dielectric strength of arc path, following current zero.

If the interrupting effort is incapable of developing dielectric strength very rapidly

Figure 1. Simple single phase circuit showing power source circuit breaker C_2 load capacitor bank, C_1 line capacitor bank and circuit inductance

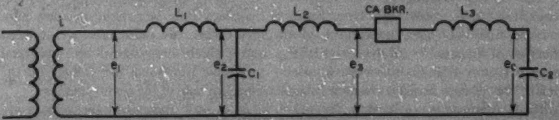

Paper 51-316, recommended by the AIEE Switchgear Committee and approved by the AIEE Technical Program Committee for presentation at the AIEE Pacific General Meeting, Portland, Oreg., August 20-23, 1951. Manuscript submitted May 22, 1951; made available for printing July 10, 1951.

B. P. BAKER is with the Westinghouse Electric Corporation, East Pittsburgh, Pa.

The author wishes to acknowledge the helpful assistance rendered in the preparation of this paper by E. J. Harrington of the Bonneville Power Administration, Portland, Oreg., and R. C. Van Sickle of the Westinghouse Electric Corporation, East Pittsburgh, Pa.

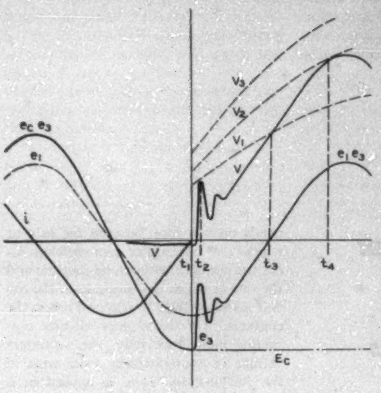

Figure 2 (left). Circuit interruption with no reignition or no restrike

V = Voltage across circuit breaker

E_c = Voltage on load capacitor bank after interruption

V_1, V_2, V_3, indicate several possible rates of recovery of dielectric strength across the interrupter following arc extinction

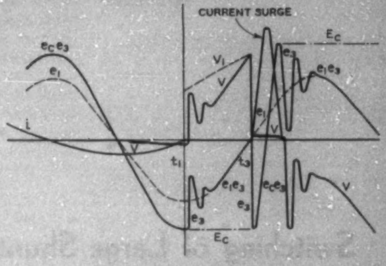

Figure 3(B). Reignition at t_3 on Figure 2. Followed by interruption after 1/2 cycle oscillatory frequency

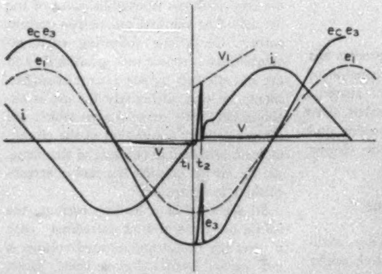

Figure 3(A)(left). Reignition at t_2 on Figure 2. Not followed by an immediate interruption

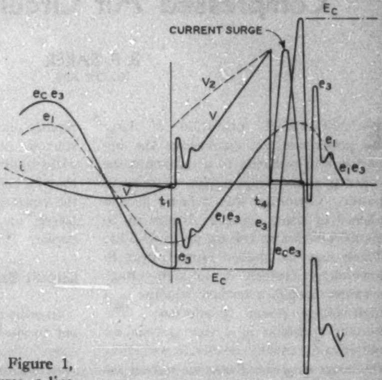

Figure 3(C). Restrike at t_4 Figure 2. Followed by interruption after 1/2 cycle of oscillatory frequency

following the first current zero, methods must be devised to obtain only slight effort at the current zero. Likewise, if an interrupter develops appreciable effort quickly, it must follow through with rapidly increasing effort. Thus any re-establishment of current after a given zero will result in an early reignition rather than a delayed restrike. Contact speed and the control of deionizing agents in the interrupter are the determining factors.

Circuit characteristics

1. Operating voltage.
2. Size of capacitor load bank.
3. Size of capacitor line bank.
4. Inductance and its distribution in the circuit.
5. Short circuit kilovolt-ampere capacity.

Capacitor Switching Theory

The theory relating to switching of capacitor bank, cables and long transmission lines has been the subject of a number of papers.[1,2,3] However, a brief review seems desirable in order to correlate the circuit breaker characteristics with its requirements. Assume for simplicity, a circuit as shown in Figure 1, consisting of a single phase source, a line inductance L_1, a line capacitance C_1, which may be either a capacitor bank, bus cable or transmission line, an additional inductance L_2, the circuit breaker, another inductance L_3 and the load bank C_2 which is to be switched. Normally C_1 will be small and L_1 will constitute most of the circuit impedance, so that, before i in Figure 2 is interrupted, the voltage e_3 at the bank C_2 will be greater than the voltage e_1, at the source, by the rise in voltage due to the leading current flowing in the inductance L_1 and L_2. As soon as i ceases to flow at time t_1 this voltage difference disappears and e_3 collapses toward e_1 with a transient whose frequency is determined by C_1 and L_1. Generally this is very fast having a frequency in the order of 10 kc. However, if C_1 is a capacitor bank, comparable in size to C_2 this frequency may be reduced to a few hundred cycles. In either case e_3 is reduced and e_c which before current zero was equal to e_3 now represents the voltage on the capacitor side of the circuit breaker.

As is well understood the voltage appearing across the circuit breaker is the difference between the voltage left on the bank C_2 and the instantaneous values of voltage represented by e_3 as controlled by the source and circuit constants. It is therefore apparent that the voltage across the circuit breaker terminals on a single phase circuit increases rather rapidly at first during the first half cycle of the oscillation frequency then more slowly and finally reaches a maximum of ap-

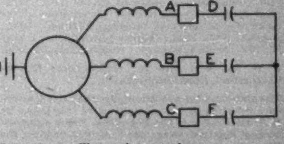

Figure 4. Three-phase schematic system

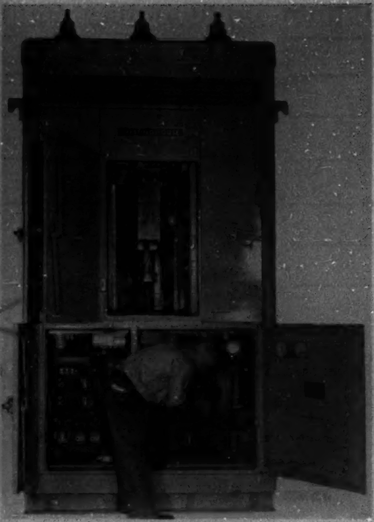

Figure 5 (left). Switching unit with air supply and 15-kv, 1,000 megavolt ampere 1,200 - ampere compressed air circuit breaker

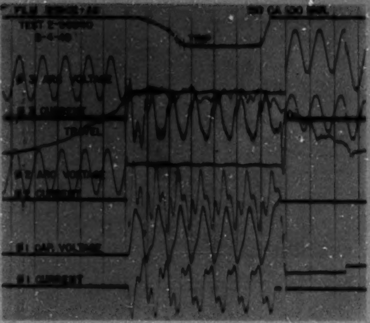

Figure 6 (right). Oscillogram of close - open operation on laboratory test at 15.5-kv, 19,100 kilovar, 110 pounds per square inch operating pressure, showing one reignition

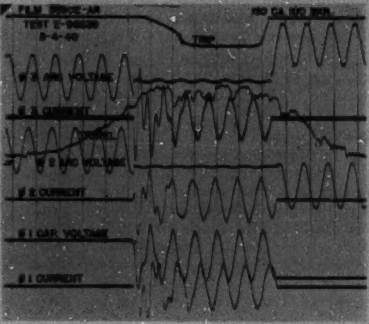

Figure 7 (right). Oscillogram of close - open operation on laboratory test at 15.5-kv, 19,100-kilovar, 127 pounds per square inch operating pressure

proximately twice the source voltage, 1/2 cycle of the system frequency after arc extinction. The course of this recovery voltage is affected very little by the circuit breaker characteristics, but is almost entirely a function of the circuit characteristics.

On the other hand the rate at which the arcing space recovers its dielectric strength is almost entirely a circuit breaker function. If this rate is represented by V_1 in Figure 2, it is apparent that the voltage may exceed the dielectric strength either at t_2 on the transient or at t_3 on the fundamental. The former as shown in Figure 3(A) would constitute an unnoticed and harmless reignition. The latter would be a reignition with a 1/4 cycle current pause which would be generally harmless, and if interrupted in 1/2 cycle of the oscillatory frequency as shown in Figure 3(B), would leave no extra charge on the capacitor except it would have its polarity reversed. If the dielectric recovery rate is represented by V_2 Figure 2, a restrike would occur at t_4 as shown in Figure 3(C). In this case prompt interruption following the restrike would leave a higher charge on the bank C_2. This type of reignition results in a tendency toward voltage pyramiding and sometimes in insulation failure. If the dielectric recovery rate follows line V_3 Figure 2, the operation is normal, satisfactory and contains neither reignitions or restrikes. If fast dielectric development is difficult to obtain following the first current zero or small contact separation it is desirable to have the first interruption result in a prompt reignition some time between t_1 and t_2. This will depend on the amplitude and frequency of the transient. This in turn depends on the following:

1. If C_1 the line capacitance is increased, the frequency of the oscillation is decreased and the correspondingly lower initial rate of rise of the recovery voltage may cause the arc to remain extinguished for a short period and to reignite before the crest of the voltage of system frequency is reached.

2. Even though the presence of a line capacitance makes early reignitions less likely and thus increases the tendency to restrike, the restrikes generally produce less overvoltages because the equalization of the capacitor voltages reduces the amplitude of the following voltage transient.

3. The amplitude of the transient varies directly with the source inductance and the time to the peak of the transient varies as the square root of the inductance, consequently the average rate of rise of voltage varies directly with the square root of the source inductance. Therefore, the smaller the inductance the less the tendency to reignite the arc on the initial rise of the recovery transient and the greater the tendency to restrike later. This emphasizes that demonstrations on capacitor switching ability of circuit breakers should be made on circuits having short circuit kilovolt-amperage, at least as large as expected in service.

Three-Phase Switching

In the preceding discussion and in Figure 2 it was pointed out that single-phase capacitor switching without restriking resulted in double crest voltage across the circuit breaker contacts in 1/2 cycle after arc extinction.

Three-phase restrike-free switching is similar except for slightly different voltage shifts. In the usual circuit as shown in Figure 4 with the source neutral grounded and the bank neutral ungrounded, the first phase to clear (*A*) causes a voltage of 2.5 times line-to-ground crest voltage to appear across the breaker terminals *A-D*, 1/2 cycle after *A* clears. Assuming that *B* and *C* clear 1/4 cycle later, the voltage across the circuit

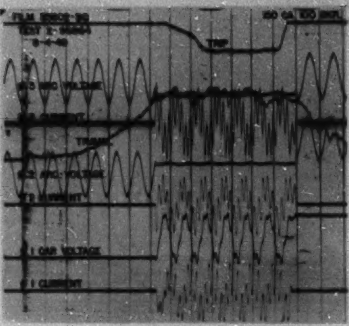

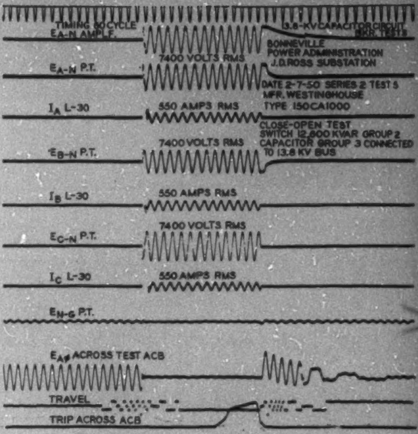

Figure 8 (above). Oscillogram of close-open operation on laboratory test at 15.5-kv, 19,100-kilovar, 110 pounds per square inch operating pressure. Circuit adjusted to give large fifth harmonic

Figure 9 (left). Oscillogram of close-open operation on field test where one 12,600-kilovar load bank was switched against a 15,300-kilovar line bank at 13.8 kv

breaker terminals *B-E* and *C-F* reaches 1.87 times line-to-ground crest in 2/3 and 5/6 cycles respectively after *A* clears, depending upon phase rotation. If, however, an improbable situation exists and *A* opens and *B* opens 1/4 cycle later and for some reason *C* remains conducting, *AD* will reach 4.12 times line-to-neutral crest in 7/12 cycles after *A* clears and *BE* will reach 3.46 times line-to-neutral crest in 3/4 cycles after *A* clears.

All other circuit conditions fall within this range.

High Current Surges

Capacitor switching not only produces wide swings in voltage but also sudden surges in current which may constitute the greater of the two hazards. If these sudden current changes occur when the contacts are closed, no harm is done, but if the current suddenly increases in an arc gap which is confined by an incompressible medium, large and disrupting forces may result. Oil circuit breakers using confined arcing spaces have been known to be damaged before the sudden release of energy can open normal venting channels, while in air circuit breakers the arcing chamber is partially surrounded by compressible material or at least provided with air-filled vents capable of instantaneous pressure release.

When de-energizing a bank there are no appreciable current surges unless there is a restrike or reignition, in which case the equalizing current between the two banks through a relatively small inductance can reach a value comparable to the power source faults, with rates of current rise approximately a hundred times greater than that of a power fault. With such a restrike the rate of current rise is not only great but it may occur 1/2 cycle after a short arcing period, when the contacts are separated relatively far, during which, in the case of the oil breaker there would be a very small gas bubble available in the interrupter to absorb the explosive impact.

15-Kv, 1,000-Megavolt Ampere, 1,200-Ampere Compressed Air Circuit Breaker

Figure 5 shows a switching unit which has been giving very satisfactory performance on large capacitor banks. It consists essentially of an indoor compressed air circuit breaker and its air supply system housed in a weatherproof metal enclosure. The enclosure is equipped with condenser bushings and current transformers which make it a complete switching package. The front of the unit as shown has five weatherproof doors. The three upper doors open into the three separate phase compartments which house the interrupters, contacts and all parts operating at high potential. The two lower doors when open expose the operating mechanism, air valves, control panel and all parts operating at ground potential. In the rear of the unit there are two doors which open into the compartment housing the air supply system consisting of a small compressor and an auxiliary air storage reservoir.

The circuit breaker itself is essentially a standard 1,000-megavolt ampere 15-kv, 1,200-ampere compressed air circuit breaker[4] except that the air inlet to the operating mechanism was enlarged to increase the opening speed of the contacts from about 12 to 16 feet per second and another shock absorber was added to decelerate the contacts to minimize shock for highly repetitive service. The design of the circuit breaker followed conventional lines which has been proven to be very satisfactory, that is, the air reservoir, operating mechanism, blast valves, control panel and all parts operating at ground potential are located in the lower compartment. Above that and in separate compartments are all parts which are at line potential, such as the blast tube, contacts, all current-carrying parts, operating rods and the interrupters. Above this is an expansion chamber for receiving all the exhaust gases from the interrupters, before they are harmlessly released into the atmosphere. The straight line flow of air from the bottom to the top, that is, from the reservoir through the blast valve, blast tube, interrupter, coolers and into the expansion chamber has been found to be satisfactory. Also there appeared to be no need for increasing the operating pressure above its normal 150 pounds per square inch or for adding shunting resistors as is sometimes done with circuit breakers which restrike.

The operating mechanism consists of a single cylinder and piston, somewhat directly connected to an operating shaft. To this shaft are connected the three contact operating rods, the three blast valves, shock absorbers and indicating devices.

Air for operating the mechanism is controlled by electropneumatic pilot valves and pneumatic relay valves, one set for applying opening air to the top of the cylinder and one set for applying air to the bottom of the cylinder for closing. Dump valves and interlocks permit normal speed opening operations, immediately following closing.

The moving contacts are hinged at the lower end and rock back and forth into and out of engagement with finger-type stationary contacts. The arc is drawn across the upper end of the air blast tube, substantially perpendicular to the plane of the fiber splitters. Here the arc is caught between the air blast and the insulating splitters which permits rapid deionization of the arc space immediately following current zero and consequently development of dielectric strength faster than the circuit can apply voltage to the circuit breaker terminals. The rapid increase in dielectric strength is the result of: (1) enhanced de-ionization resulting from air turbulence; (2) rapidly increasing contact separation due to high contact speed; (3) elevated dielectric strength of deionized air due to blast air pressure.

Laboratory Tests

As final verification, one of these switching units was set up at the High Power Laboratory and subjected to a series of 63 tests. All tests were on a 3-phase basis with line-to-line voltage varied between 13.8 and 15.5 kv and leading currents ranging from 210 to over 710 amperes, giving a maximum 3-phase power equivalent of 19,000 kilovars. The tests were all close-open operations and generally made in groups of three. At the beginning of each group of three tests the circuit breaker air reservoir was raised to 150 pounds per square inch, and the valve between it and the compressor reservoir closed. The first test generally dropped the pressure to 130 pounds per square inch and the second to approximately 112 pounds per square inch. Although the circuit breaker was designed for only two operations per reservoir of air, it was given a third operation as a factor of safety test. Usually there was an appreciable time interval between groups of tests but very little time between tests in the same group. Therefore, the capacitor bank was generally discharged for the first close-open operation but for the other two operations the circuit breaker closed into a charged bank of capacitors. During the first 42 tests the power supply came through a transformer with a grounded Y with external impedance sufficient to limit the fault current to 5,000 amperes at 13.8 kv. For the remainder of the tests, the transformer was connected in delta with the current limited to 13,200 amperes at 13.8 kv. With this circuit there was no connection to ground potential except through capacity dividers used for potential measurements.

During the first 51 tests at 13.8 kv and currents between 210 and 625 amperes, there were no restrikes or reignitions. The remainder of twelve operations were made at overvoltages up to 15.5 kv and currents up to 710 amperes corresponding to 19,000 kilovars. During one of these tests at 15.5 kv, the oscillogram of which is shown in Figure 6, there was one reignition on one phase where the current re-established after an outage of almost 1/4 cycle. Although recognized capacitor switching specifications permit two reignitions per operation, it is believed that this one is not entirely random, but associated with the 12 per cent overvoltage and the diminished rate of development of dielectric strength caused by subnormal reservoir pressure which decreases the rate of contact separation and air pressure between the contacts. It may be noted that two and one-half cycles after the final interruption there is a shift in the recording elements. This is due to a flashover on one of the capacitor elements which had been working at double its voltage rating. Figure 7 is an oscillogram of a typical operation on a system consisting of a grounded Y power source and an ungrounded Y-connected capacitor bank.

Figure 8 is an oscillogram of a typical operation on a system consisting of an ungrounded delta power source and an ungrounded Y-connected capacitor bank where the ratio of the kilovars of the bank to the kilovolt amperes of the system was

Figure 10. Oscillogram of close-open operation on field test switching a 25,260-kilovar bank at 13.8 kv. On this test there was one reignition

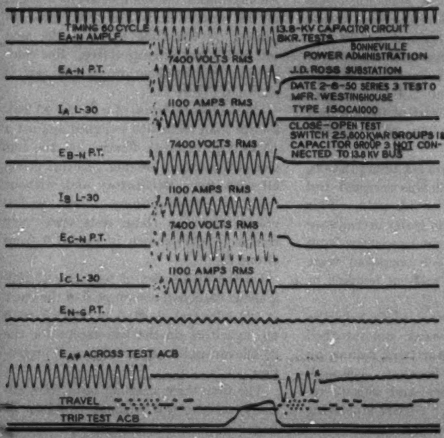

Figure 11. Oscillogram of close-open operation on field test switching a 25,260-kilovar bank at 13.8 kv, without reignitions

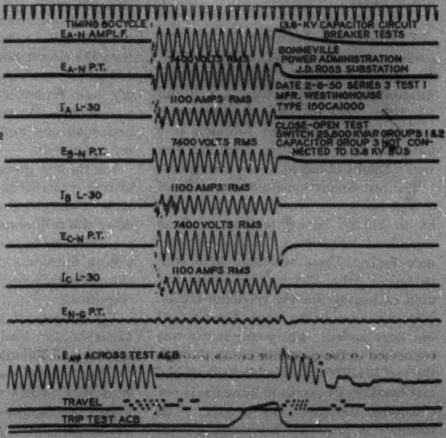

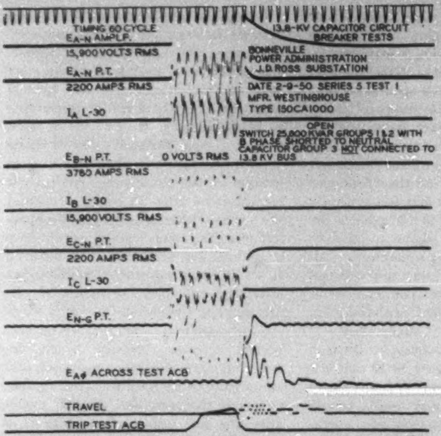

Figure 12. Oscillogram of opening operation on field test switching a 25,260-kilovar bank at 13.8 kv with one phase of the bank shorted to neutral

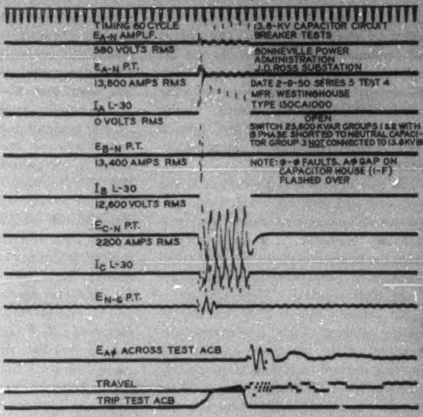

Figure 13. Oscillogram of opening operation on field tests switching a 25,260-kilovar bank at 13.8 kv with one phase of the bank shorted to neutral. On this test the protective gap in parallel with an unshorted phase flashed on the closing surge, resulting in a phase-to-phase fault with the third phase connected through the bank

such as to cause considerable fifth harmonic current to flow. Since the amplitude of this harmonic was an appreciable percentage of the fundamental, the frequency with which the current passed through zero was increased several times. Consequently, opportunities for arc extinction were offered more frequently at very short contact separations. During these tests the current was interrupted many times on current zeros not corresponding to the fundamental zero.

Field Tests

A rather comprehensive set of tests was made on this circuit breaker at the J. D. Ross Substation of the Bonneville Power Administration on February 7, 8, 9 and 10, 1950. The purpose of these tests was to prove the circuit breaker's performance under operating conditions and verify results obtained in the laboratory.

The test circuit consisted essentially of a 3-phase power transformer bank 230 kv to 115 kv having tertiary windings capable of delivering a 750-megavolt ampere fault. These windings were connected in delta 13.8 kv line-to-line and used exclusively for the capacitor banks. The capacitor banks were Y-connected but ungrounded. The power source was connected to the capacitor banks through the test breaker and suitable back-up circuit breakers by overhead bus circuits not exceeding 200 feet total length. The distance is probably somewhat greater than would normally be encountered in most installations.

The amount of instrumentation and recording apparatus is indicated by the traces on the oscillograms (Figures 9, 10, 11, 12 and 13). The tests were scheduled in groups of six close-open (energizing and de-energizing) operations each. Each group consisted of one operation as a check to see that all records were correct and then the five remaining tests were made without air replacement by the compressor. At the beginning of the five tests the circuit breaker reservoir was at 150 pounds per square inch and the supply unit reservoir at 250 pounds per square inch. At the end of the fifth test both reservoirs were down to 150 pounds per square inch.

For the first group of six tests a 12,600-kilovar capacitor bank was energized and then de-energized after 14 cycles. This delay was deliberate in order to eliminate any effect due to harmonics resulting from closing transients. All operations were entirely satisfactory without restrikes or reignitions.

For the second group of six tests the 12,600-kilovar load bank was switched against a 15,300-kilovar bank floating on the bus side of the breaker. Again all tests were satisfactory and without restrikes or reignition. Figure 9 showing the last test of this group is typical.

On the third group of tests where a 25,260-kilovar bank was switched, the oscillogram as shown in Figure 10 indicated that the first operation Test 0 had one reignition with a current outage of almost 1/4 cycle on phase *C*. There was no external evidence of this reignition and the restored voltage across phase *A* of the circuit breaker shows only a little more than the normal displacement. Actually the maximum voltage reached as a result of this reignition is less than that appearing on the same phase of the next test which was reignition free. For comparison, the oscillogram of this test is shown in Figure 11.

On the fourth group of tests the 25,260-kilovar load bank was switched against a 15,300-kilovar bank floating on the bus side of the circuit breaker. In this group all tests were satisfactory and without restrikes or reignitions. The oscillograms taken on these tests were very similar to that shown in Figure 9 from Group 2.

On the fifth series of tests the 25,260-kilovars bank had one phase *B* of the bank (8,420 kilovars) shorted to neutral, with no capacitors on the bus except for the 25-kilovar units for transformer protection.

The first three opening tests were entirely satisfactory without restrikes or reignitions, even though the voltage across and circuit breaker in *A* phase rose to 3.5 times the line-to-neutral voltage and the currents increased from 1,100 amperes for the balanced system to 2,200, 3,780, and 2,200 amperes respectively as shown in Figure 12.

Figure 13 is an oscillogram of the fourth test in this series. On this test the protective gap in parallel with *A* phase of the bank, flashed on the closing surge. This placed a phase-to-phase fault on the circuit breaker with the third phase *C* connected through the bank. The current through these phases rose to 13,400 and 13,800 amperes respectively, which was cleared by the test circuit breaker without incident.

Following these scheduled tests it was decided to make 71 more close-open operations on the normal 25,260-kilovar bank without oscillograms to bring the total to 100. From external appearances these tests seemed to be entirely satisfactory. Following these, two more tests were made with oscillograms for comparison with those taken earlier but no change in circuit breaker performance could be detected.

An examination of the circuit breaker, its interrupter and contacts showed no deterioration and indicated that the circuit breaker was in excellent condition to go into service.

A number of these switching units have now been in service for over a year, and are giving satisfactory performance.

References

1. Capacitor Switching Phenomena, R. C. Van Sickle, John Zaborszky. *AIEE Transactions*, volume 70, part 1, 1951, pages 151–59.

2. The Interruption of Charging Current at High Voltage, Dr. W. M. Leeds, R. C. Van Sickle. *AIEE Transactions*, volume 66, 1947, pages 373–82.

3. Tests and Analysis of Circuit Breaker Performance When Switching Large Capacitor Banks, T. W. Schroeder, E. W. Boehne, J. W. Butler. *Electrical Engineering* (*AIEE Transactions*), volume 61, November 1942, pages 821–30.

4. A 2,500,000 Kva Compressed Air Powerhouse Breaker, L. R. Ludwig, H. M. Wilcox, B. P. Baker. *Electrical Engineering* (*AIEE Transactions*), volume 61, May 1942, pages 235–41.

Discussion

E. J. Harrington (Bonneville Power Administration, Portland, Oreg.): As mentioned by the author this circuit breaker was tested at one of the substations of the Bonneville Power Administration. Since that time nine of these circuit breakers have been placed in service and 11 more will soon be installed. Field performance has been very satisfactory so far and maintenance is very low.

As a result of this field experience and the above mentioned tests this discusser would not hesitate to switch capacitor banks of 30,000 kilovars with this circuit breaker. It is believed that it is entirely capable of switching even larger banks, say up to 50,000 kilovars, if its current rating would so permit.

In general, our experience indicates that air-blast circuit breakers such as this are more satisfactory for capacitor switching duty than oil circuit breakers of present design.

In an oil circuit breaker a prestrike on closing if accompanied by a heavy surge of current, generates pressure in an incompressible medium which transmits this pressure to the interrupting chambers and can result in damage to these members. On opening, a restrike, if it occurs, is generally in a gaseous medium which tends to absorb the shock, but if additional capacitor banks are connected to the same bus, the current inrush to the switched bank can generate pressure at such a rate that the gas cushion cannot prevent severe damage to the interrupting chambers and possible explosion of the circuit breaker. We have had several instances of such damage on our system.

In the case of circuit breakers such as described by the author, prestrikes and restrikes, if they should occur, have very little chance of producing pressures that would result in damage to the circuit breaker mechanism.

B. P. Baker: The author appreciates Mr. Harrington's frank and complimentary discussion.

We concur with his belief that the circuit breaker is capable of switching capacitor banks up to 50,000 kilovars. In this case the current would exceed the normal rating of the contacts by about 75 per cent, which is more than can be expected from a most conservative rating. However, an increase in current carrying capacity can be obtained without sacrificing interrupting integrity.

The liberal extrapolation from 25,000 to 50,000 kilovars, which Mr. Harrington made, does not appear to be hazardous in that high-frequency current surges of great amplitude cannot build up damaging pressure waves in an open-type air-filled interrupter.

Electrostatic Radiation Monitors

J. R. BRADBURN
MEMBER AIEE

A. A. LAHTI
NONMEMBER AIEE

THE rapid developments in the military and civilian use of atomic energy have resulted in a large scale demand for instrumentation to measure radiation of a radioactive nature resulting from atomic explosions or being inherent in laboratory or manufacturing operations.

Much has been written about the effects of radioactive radiation on persons and structures. Since this type of radiation cannot be detected by the human senses, potential hazards of great magnitudes may exist. Proper instrumentation can greatly reduce the exposure to these hazards.

It is not the purpose here to discuss all the possible types of instruments required. Instead, consideration will be limited to those instruments which will be required in considerable quantities by large numbers of individuals who might be exposed to radiation in either military or civilian capacity. For instance, those required to enter a contaminated area for rescue or maintenance work must have a ready indication of exposure to radioactive radiation. Since magnitudes of allowable exposures have been established, it is possible for personnel to work maximum periods without deleterious effects.

The instruments previously developed for laboratory use are too large, expensive and complicated for widespread personal use, and furthermore they are more accurate than necessary. Consequently attention has been given to the design of an inexpensive device for such application which can be used repeatedly without being consumed and provides a visual direct reading.

The instrumentation for monitoring radioactive radiation falls into two functional classes, namely:

1. Instruments for measuring accumulated doses, these instruments frequently being referred to as dosimeters.
2. Instruments for measuring instantaneous rates or intensities of radiation.

The following discusses the various considerations involved in the design of two dosimeters of vastly different sensitivities.

In the design of a dosimeter to fit civil defense and large scale military requirements many factors have to be taken into account. The instrument should be:

1. Simple to operate.
2. Reliable.
3. Small and lightweight.
4. Inexpensive.
5. Readily readable at low light levels.
6. Able to withstand severe environmental conditions of temperature, humidity and altitude.
7. Capable of being stored indefinitely without deterioration.
8. Independent of wave length or energy of gamma radiation.
9. Self-contained without requiring accessory equipment for charging or reading.
10. Made of materials which will not become unpredictable sources of radioactivity if subjected to high rates of radiation.

Intensity of radiation at any given time or the total amount received over a period of time, is determined by measuring the amount by ionization produced in free air. This method of measurement is so fundamental that it is the basis for the definition of the *R*, or Roentgen unit. In general terms an *R* is that amount of radiation which will cause unit ionization of a unit volume of air. This ionization can be measured by decrement of charge of a capacitive system.

The method chosen to measure the decrement of charge and still meet the practical requirements mentioned above is based upon the fundamental design of an electroscope. To review briefly the theory of such a device, consider an electrometer as a variable capacitor with a mechanical torque system included tending to maintain the system at a minimum capacity. At any deflected position, θ, the mechanical and electrostatic torques must be in equilibrium, or

$$M_t = K\theta = \frac{\partial U}{\partial \theta}$$

where

M_t = torque moment
K = spring constant
θ = angular deflection of spring
U = energy in capacitive system

The electric energy in a capacitive system is:

$$U = {}^1/_2 CV^2 = {}^1/_2 \frac{Q^2}{C}$$

where

C = capacity
V = voltage
Q = charge

By differentiating and combining terms

$$\theta = \frac{1}{2K}\, V^2 \frac{\partial C}{\partial \theta} = \frac{1}{2K}\, \frac{Q^2}{C^2}\frac{\partial C}{\partial \theta}$$

An examination of this equation will disclose the fundamental parameters of design of an electrometer of suitable sensitivity. For high sensitivity it is apparent that the spring employed be soft, that the total capacity be minimized and that the rate of change of capacity be maximized. For low sensitivity it is not practical to increase the stiffness of the spring since this would result in too great a voltage increase. However, capacity can be readily increased to produce lowered charge sensitivity.

If the capacitive electrometer is suitably enclosed it becomes an integrating ionization chamber of dosimeter. After

---

Paper 51-318, recommended by the AIEE Instruments and Measurements and Nucleonics Committees and approved by the AIEE Technical Program Committee for presentation at the AIEE Pacific General Meeting, Portland, Oreg., August 20-23, 1951. Manuscript submitted May 21, 1951; made available for printing July 10, 1951.

J. R. Bradburn and A. A. Lahti are with the Consolidated Engineering Corporation, Pasadena, Calif.

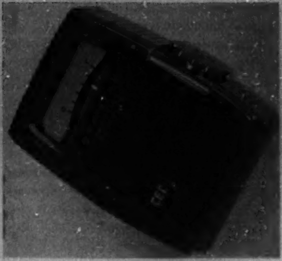

Figure 1. Exterior view, 200-milliroentgen dosimeter

this system is initially charged and is subjected to radiation the system is discharged by ionization of the contained air. Thus the electrometer indicates radiation.

There are many means of establishing the initial charge in the electrometer system, but here the choice is greatly limited by the design requirements already covered. A simple friction charger appears to meet these requirements in the most satisfactory manner. Through the selection of materials which have high triboelectric potential differences and good physical characteristics, it is possible to produce a sufficient charge with very little mechanical effort.

An embodiment of the previous discussion pertaining to a high sensitivity instrument is shown in Figure 1 showing an instrument based on a fundamental design of Dr. Charles Lauritsen of the California Institute of Technology. It is a high sensitivity dosimeter with a full scale range of 250 milliroentgens. It is small, being the size of a package of cigarettes. It is lightweight, weighing about $1^1/_4$ ounces.

It is charged by pulling out the knob and operating as if winding a watch. The charge is indicated by a pointer and scale visible through the window.

Figure 2 depicts the same instrument with the cover removed and placed upside down. The case, including cover, is dyed, injection molded polystyrene. This material has been chosen for four reasons:

1. It is a very low loss material electrically, thus making possible insulators integral with the case.

2. It is inexpensive, easy to mold and dimensionally stable.

3. It contains nothing but hydrogen and carbon atoms, thus making it least likely to become a source of radioactivity if subjected to high neutron bombardment.

4. It can easily be sealed, thus making possible hermetic enclosure.

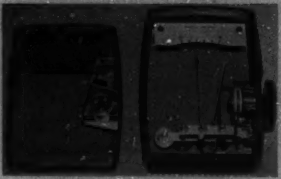

Figure 2. Interior views, 200-milliroentgen dosimeter

The inside of the case, including cover, is coated with colloidal carbon for the following reasons:

1. To form one electrode of the capacitive system.

2. To prevent the retention of residual charges on the inside surfaces.

The window is clear polystyrene coated on the inside with a molecular film of gold or beryllium. This coating is again used to prevent residual charges from accumulating.

The pointer assembly consists of a lightweight pointer mounted on a staff rotating on jeweled bearings. Two opposed hairsprings are used to reduce the effect of temperature. The jewels are mounted in wells used to contain high viscosity silicone oil for damping purposes. A stop prevents the pointer from touching the attractor plate and thereby discharging the movement.

This attractor plate is attached to the desiccant holder on the cover, while the repeller, also made of aluminum, is attached to the movement. The repeller is therefore at the same potential as the needle at all times.

On the right side is the charging mechanism shown with the winding knob pulled out for charging purposes. About a full turn completely charges the mechanism a little beyond the "zero" on the scale. An "0" ring serves as a seal on the shaft to prohibit the entrance of moisture or dirt. When the knob is pushed in the charging mechanism is grounded and its charge is lost, thereby reducing total charge in the system. This causes the needle to drop back to zero reading. The instrument now is ready to be discharged through ionization as a result of radiation to which it might be subjected.

A trimmer capacitor attached to the indicating mechanism mount is provided to permit adjustment of sensitivity at the time of manufacture. This assures equal sensitivity range of instruments.

Largely through the use of polystyrene, cleanliness in manufacture, and the use of a desiccant, the instrument has an extremely low leakage of less than 10 per cent of full scale in 24 hours. This corresponds a leakage resistance of about 10^{19} ohms. Linearity of the device is extremely good.

In order to make a low sensitivity instrument of around 150 Roentgens, several basic changes have to be made. As previously mentioned, lower charge sensitivity can be attained most readily by the addition of fixed capacity. Thus it requires more ionization, hence radiation, to cancel out the same percentage of full scale charge. Assistance in the same direction can be secured by reducing the ionization volume, thereby effectively diminishing the amount of ionization from equal radiation.

Figure 3 shows a 150-Roentgen unit with cover removed. The pointer assembly is identical with that used on the 250-milliroentgen unit, but it is hidden from view by carbon-coated polystyrene baffles used to reduce effective ionization volume. A 0.0025-microfarad capacitor can be seen mounted on the repeller. It is an extremely low loss component, having a leakage resistance of approximately 10^{16} ohms.

Figure 3. Interior view, 150-Roentgen dosimeter

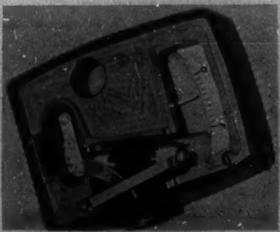

Figure 4. Exterior view, charging mechanism

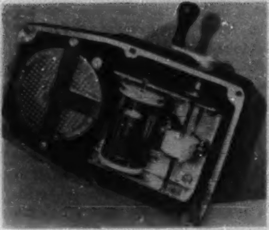

Figure 5. Interior view, charging mechanism

Figure 6. 150-Roentgen dosimeter being charged

Because of the charge requirements of this system the simple charger used in the 250-milliroentgen unit is no longer adequate. Hence, an accessory charger must be used which is coupled to the dosimeter by means of a coaxial connector. This connector is designed to preclude the inadvertent discharge of the instrument.

The charger for the above-described unit is also an electrostatic device in order to provide a unit with unlimited shelf life. Figure 4 shows the assembled unit, and Figure 5 the unit with the base removed. The charger has a connector which matches the dosimeter and will fully charge the instrument in 5 seconds by turning the handle at a moderate rate. Figure 6 shows the dosimeter and charger engaged.

In order to understand the principle of operation, reference is made to Figure 7.

A friction generator (1) applies a charge to a stator plate (2). This in turn induces a charge on the rotor plate at (3), this charge being drawn from system ground. As the rotor rotates clockwise, this ground connection is broken while the rotor plate is still meshed with the stator, hence the charge remains on the rotor. When this rotor plate reaches the output brush (4) the charge will be transferred to the load, the amount of charge transferred following standard capacitive distribution laws.

In the case of a counterclockwise rotation, the charged rotor plate is discharged at (5) before reaching the collecting position.

When this uncharged plate reaches the collector, it will be at zero charge and hence will draw charge from the load. Hence, we have accomplished a system capable of both incrementally charging and discharging a capacitive load.

This unit will provide energy at approximately 200 microwatts, enough to keep a *NE-51* bulb lighted. The voltage is limited only by the load. The charger is hermetically sealed and contains a desiccant. Consequently, it has an unlimited shelf life.

Rate meters premised on similar principles to those used in these dosimeters can be developed. The technique of measurement, and therefore the mechanics of the "rate" system are, however, somewhat more complex.

To review, the definition of the Roentgen unit states that a unit rate (R per second) obtains when the ionization in a unit volume of air causes a unit current. Thus if we devise a method of measuring the ion current in a known volume, we will have an indication of radiation rate.

Consider the system diagrammed in Figure 8. The functions are blocked for convenience. These functional blocks exist in ionization-chamber-type rate meters already in use. The innovations suggested here are in the detail methods proposed for making possible a self-contained unit of unlimited shelf life.

The ionization chamber employed is an enclosed volume with two electrodes for collecting the ions. The indicator is an electrostatic voltmeter which is used to measure the voltage drop across a current metering resistor. The voltage source is an extremely low loss "tank" capacitor (C-1) energized periodically by an electrostatic generator (E-1) of the type previously shown in Figure 7.

Figure 7. Schematic diagram, electrostatic generator

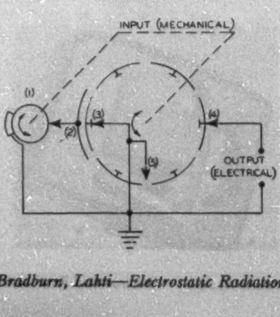

As the system irradiated, ion currents will flow across C-2 (ionization chamber) and M-1 (electrostatic voltmeter). Assuming for the moment that the entire system is at uniform pressure, and composed of similar materials, these currents will be proportional to the effective volumes of C-2 and M-1 and to the rate of radiation. As these currents flow in the same direction, their difference is the current flowing through R-1. Hence the voltage drop (V_r) across R-1 is:

$$V_r = I_r R = (I_c - I_m)R = K\rho(\text{Vol}_c - \text{Vol}_m)R$$

or

$$\rho = \frac{V_r}{KR(\text{Vol}_c - \text{Vol}_m)}$$

where

ρ = radiation rate
V_r = voltage across R-1 (and therefore M-1)
K = an ionization constant dependent upon materials and geometry
R = resistance of R-1
Vol_c = effective volume of ionization chamber
Vol_m = effective volume of electrostatic voltmeter

The fundamental parameters are rather obvious. For radiation sensitivity to be high the voltage sensitivity of the electrostatic voltmeter also must be high, the metering resistor must be of high ohmage, the effective equivalent volume of the ionization chamber must be large and that of the electrostatic voltmeter must be small.

As a wide range is desired in one instrument, consideration has been given to the use of an electrostatic voltmeter with non-linear voltage response, that is, high sensitivity at low voltages and vice versa. This obviates to a degree the

Figure 8. Schematic diagram, radiation rate meter

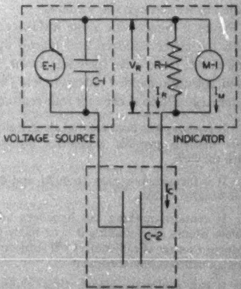

disparity in reading error inherent in a linear scale.

The instruments described do not exhaust the field of radiation monitors. The sensitivities mentioned are not limiting. Of course certain compromises between great sensitivity and small volume must be made.

There are undoubtedly other equally interesting practical applications of electrostatic devices. The systems outlined are merely isolated examples of the potential utility of this branch of applied physics.

No Discussion

Magnetic Amplifiers of the Balance Detector Type—Their Basic Principles, Characteristics, and Applications

W. A. GEYGER
MEMBER AIEE

Synopsis: At first two special problems concerning magnetic amplifiers for self-balancing d-c potentiometers and d-c bridge networks are specified. Numerous basic circuits of simple magnetic amplifiers preferably utilizing feedback effects are classified and explained. Then different push-pull circuits of the balance detector type are described systematically. Some figures for single-stage and multistage amplifiers are quoted to indicate the performance obtained. Speed of response in magnetic amplifiers, the possibility of providing derivative feedback, and design procedure with respect to time lag are briefly considered.

IT IS a well known fact that the most important progress made in electrical engineering during the past 30 years is due to a large extent to the successful use of electronic amplifiers, especially in communication circuits and control equipments. The introduction of electronic amplifiers in the field of electrical measurements and control problems made possible an efficient amplification of very small direct voltages such as produced by photoelectric cells, thermocouples, and radiation pyrometers. High-speed recording potentiometers using electronic servoamplifiers have been constructed.[1-3] Various kinds of electronic devices have been used for military purposes, for example: in gun control servomechanisms, in automatic aircraft pilots, and as radio aids to air and marine navigation. The Navy, especially, has numerous technical problems in which electronic amplifiers represent a very important part.

However, two serious disadvantages of electronic amplifiers must be considered in practical applications. First, the life of vacuum tubes used in electronic equipment is limited, and second, shocks or vibrations are dangerous to such tubes. Indeed, perfect operation of important military equipment can be hindered by the sudden failure of a vacuum tube, consequently, jeopardizing the success of a respective action.

Furthermore, it is significant that in the field of d-c amplifier problems the electronic amplifier tube represents a d-c measuring instrument of a very high resistance, especially fitted for the measurement or amplification of direct voltages in the order of 0.1 to several volts. This method, however, is unsuitable when only very small direct voltages of about 1 to 10 millivolts are available. Therefore, in such cases, especially in high-speed electronic recording potentiometers[1-3] the direct millivoltage created by a thermocouple or a radiation pyrometer is changed to an alternating voltage of proportional magnitude in a mechanical converter acting as a chopper or modulator. This alternating voltage may readily be amplified by an ordinary a-c amplifier. As an a-c amplifier is inherently more stable than a d-c amplifier, it is comparatively easy to maintain a very constant adjustment of the system if a converter is used.

In order to maintain the various advantages introduced by suitable use of electronic amplifiers and to avoid, on the other hand, the serious disadvantages mentioned above, a tubeless amplifier has been developed in different countries: the magnetic amplifier, also called d-c controlled reactor, saturable reactor, and transductor. This amplifier consists of electric and saturable magnetic circuits so interlinked that a direct current controls the reactance of an a-c circuit. The magnetic amplifier, being a real d-c amplifier containing no moving parts and not requiring any servicing, will be of great importance in future development of numerous technical fields offering rough working conditions. This amplifier will undoubtedly have extensive use chiefly in the electrical control of military equipment, in commerce, and for control of various manufacturing processes and automatic devices for private use.

Special Problems for Measuring and Control Technique

The author's research activity in the field of magnetic amplifiers has been conducted toward the use of such amplifiers in the operation of self-balancing d-c potentiometers and d-c bridge networks, especially high-speed recording potentiometers making a permanent record of very small direct voltages created for instance by thermocouples, photoelectric cells, or radiation pyrometers. The general aim of this research work was replacing the mechanical converter and the electronic a-c amplifier used in such high-speed recording potentiometers[1-3] by a special magnetic amplifier having polarized characteristics, high d-c sensitivity, and a great power gain. Therefore the main problem consisted in developing a "magnetic amplifier of the balance detector type" having an extremely small drift rate and an output power sufficient for the control of a small reversing motor, which can be either a separately excited a-c motor of the induction-meter type or a d-c motor of the moving coil meter type.

According to different special problems concerning d-c potentiometers or d-c bridge networks making available different d-c input power values corre-

---

Paper 50-93, recommended by the AIEE Electronics Committee and approved by the AIEE Technical Program Committee for presentation at the AIEE Winter General Meeting, New York, N. Y., January 30-February 3, 1950 and at the Fall General Meeting, Cleveland, Ohio, October 22–26, 1951. Manuscript submitted October 31, 1949; made available for printing September 5, 1951.

W. A. Geyger is with the United States Naval Ordnance Laboratory, Silver Spring, Maryland.

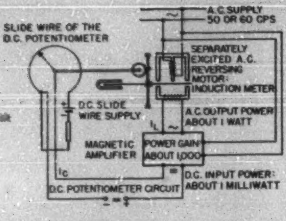

Figure 1. Self-balancing d-c potentiometer with a separately excited a-c reversing motor of the induction-meter type being controlled by a magnetic amplifier. This amplifier of the balance detector type must have a d-c input power of about 1 milliwatt, an a-c output power of about 1 watt, and a power gain of about 1,000 (first problem)

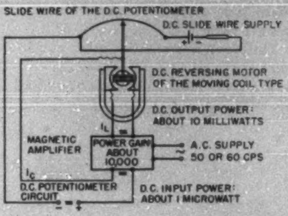

Figure 2. Self-balancing d-c potentiometer with a d-c reversing motor of the moving coil-meter type being controlled by a magnetic amplifier. This amplifier of the balance detector type must have a d-c input power of about 1 microwatt, a d-c output power of about 10 milliwatts, and a power gain of about 10,000 (second problem)

sponding to full scale deflection of the recording mechanism two types of magnetic amplifiers must be developed, including the following fundamental problems.

First Problem (Figure 1): A magnetic amplifier of the balance detector type operated from an a-c source of 50 or 60 cycles per second, to be used for the control of a separately excited a-c motor of the induction-meter type. This amplifier must have a d-c input power of about 1 milliwatt, an a-c output power of about 1 watt, and a power gain of about 1,000.

Second Problem (Figure 2): A magnetic amplifier of the balance detector type operated from an a-c source of 50 or 60 cycles per second, to be used for the control of a d-c motor of the moving coil-meter type. This amplifier must have a d-c input power of about 1 microwatt, a d-c output power of about 10 milliwatts, and a power gain of about 10,000.

This paper gives a treatise on the basic principles, characteristics, and applications of these two types of magnetic amplifiers based upon the use of special push-pull circuits.

Basic Circuits of Magnetic Amplifiers

These d-c controlled magnetic core reactor circuits[4–13] represent the basic arrangements of several magnetic amplifiers of the push-pull type containing two balanced reactor systems preferably utilizing feedback effects.

CIRCUITS WITHOUT FEEDBACK

Circuits Without Bias

The series circuit (Figure 3) consists of two separate and equally rated transformer-like structures, preferably of the nickel-iron alloy ring core type, having series aiding connected load windings N_L and series opposing connected control windings N_C, so that no induced voltage of the fundamental of the supply frequency can appear at the input terminals. The load windings N_L are shown connected in series to a bridge rectifier across which is a load resistor R_L.

Some typical characteristics representing results of measurements on small Orthonol[14]-core reactors[15] are shown in Figure 4 and Figure 5. The actual or measurable current I_L flowing in the load resistor R_L is the resultant of two components: the exciting current component I_{L0} which is practically independent of the control current I_C and the load component I_{LC} flowing in response to changes in control current I_C. Equal increments in control ampere-turns I_CN_C produce approximately equal increments in load component ampere-turns $I_{LC}N_L$ in the linear region of the characteristics. Thus, as I_{L0} can normally be made very small compared with I_{LC} the following equation holds to a good degree of accuracy:

$$I_{LC}N_L = I_LN_L = I_CN_C \qquad (1A)$$

or

$$I_L/I_C = N_C/N_L \qquad (1B)$$

There is a linear relationship between I_L and I_C. Over certain ranges changes in applied alternating voltage E and changes in load resistance R_L have no appreciable effect upon the current gain I_L/I_C, which depends only on the ratio of d-c to a-c turns. However, the characteristics described above are true only when the load current I_L measured is expressed in mean values over one half-cycle. Therefore it is essential that a moving coil instrument with a rectifier must be used. Instruments measuring rms values will not give same results.

These very interesting facts can be used as a basic principle for the design of a so-called d-c instrument transductor[16] to be especially applicated for the measurement of very large d-c values in the range from 100 to 10,000 amperes, preferably employing a bar-type transformer construction.

The Parallel Circuit: Alternatively, the a-c windings of the two reactor elements may be connected in parallel as shown in Figure 6. The voltage across each element is then the supply voltage, and the number of turns N_L has had to be doubled. Here the ratio between load current I_L and control current I_C is given by the equation:

$$I_L/I_C = 2 \times N_C/N_L \qquad (2)$$

In practice the arrangement with a-c windings in series (Figure 3) is preferable for magnetic amplifiers because it has a lower time lag. But in special cases, for instance in the design of so-called direct voltage transductors[17] for the measurement of high direct voltages the parallel circuit has some advantages.

Circuits with Bias

Considering Figure 5, it is important to notice that the characteristics are symmetrical about the I_LN_L-axis so that the polarity of the d-c terminals—the direction of current flow in the d-c control windings N_C—will have no influence upon the operation of a simple saturable core reactor as shown in Figure 3 and in Figure 6. Such an arrangement, therefore, represents a "nonpolarized" magnetic amplifier which is unable to discriminate between positive and negative control currents I_C in the d-c circuit.

However, in practice it is necessary to obtain a "polarized" magnetic amplifier

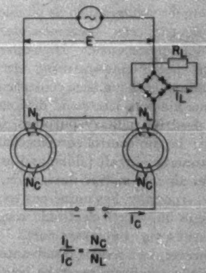

Figure 3. The series circuit

being influenced by changes in direction of the control current I_C. Such an operation can be realized by using an additional d-c magnetization, a bias, of a preferable constant value. This bias-magnetization may be produced either by an additional direct current flowing in d-c windings or by a permanent magnet creating an additional d-c magnetization in the cores of the reactor elements.[18] In special cases the use of permanent magnets for biasing purposes may have some advantages.[19]

Circuit with an Additional Bias Winding: Figure 7 shows the circuit connections of a polarized magnetic amplifier having an additional bias-winding supplied by a full-wave rectifier with an a-c series resistor R_{ac} and a d-c series resistor R_{dc}. The polarizing or bias current $I_B = \text{const} \times E$ produces an additional d-c magnetization, which is independent of the d-c control magnetization produced by the control current I_C having a variable direction of current flow in the control windings N_C.

Circuit Without an Additional Bias-Winding: Moreover it is possible to apply the bias current I_B directly to a simple common d-c winding acting simultaneously as a bias-winding and as an ordinary control winding, as shown in Figure 8. In this case, however, the d-c series resistor R_{dc} shunting the common d-c winding must be rated as to have a sufficiently high resistance value in order to avoid a considerable decrease of the control current action.

Figure 9 representing a typical response characteristic of such an arrangement shows the load current I_L as a function of control current I_C having either "positive" or "negative" direction of current flow in the control windings N_C. The characteristic curve itself remains unchanged and is shifted in a certain amount by the bias effect of the additional constant d-c magnetization.

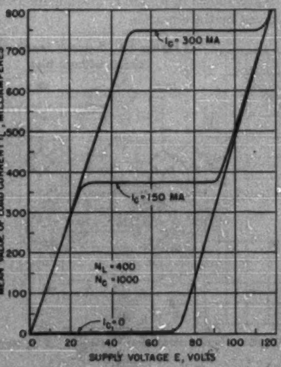

Figure 4 (left). Mean value of load current I_L as a function of supply voltage E with the control current I_C as a parameter ($N_L = 400$, $N_C = 1{,}000$)

CIRCUITS WITH FEEDBACK

It is possible to alter materially the response characteristics of a magnetic amplifier through the use of feedback or similar equivalent effects. This is accomplished by combining a portion of the output power with the input power: Using dry disk rectifiers an additional d-c magnetization, proportional to the alternating load current, will be produced, and also a respective additional d-c control action. According to the use of feedback effects in the field of vacuum tube amplifiers this additional input control-action of the output current I_L may be either aiding or opposing to the control action of the input current I_C. If aiding control conditions are used, the feedback is "positive" or "regenerative." However, if opposing control conditions are used, the feedback is "negative" or "degenerative." These feedback effects produced either by "external feedback" or by "self-feedback" (also called "self-saturation" and "self-excitation") of the d-c controlled magnetic core reactor elements will be illustrated by the following considerations.

There are different kinds of external feedback circuits and self-excitation circuits. But in principle in all cases dry disk rectifiers are used for producing an additional d-c magnetization, proportional to the alternating load current, and a corresponding positive or negative feedback effect.

External Feedback Circuits (Full-Wave Type)

Circuits Without Bias: Figure 10 shows the series circuit of the external feedback type having special feedback windings N_F supplied by a full-wave rectifier and producing an additional d-c magnetization, which is proportional to the feedback current I_F representing the converted load current I_L. It is to be noted that the direction of direct current flow I_F and of the respective additional d-c magnetization is always the same and especially not dependent upon the direction of direct current flow I_C. This is true during both half-cycles.

However, the resultant d-c control action will be greatly influenced by changes in direction of the control current I_C, the additional control action of the feedback current I_F being either aiding or opposing to the control action of I_C and consequently producing either positive (regenerative) or negative (degenerative) feedback. Therefore such an arrangement represents a polarized magnetic amplifier, as its operation will be influenced by changes in direction of the control current.

Considering positive feedback and assuming an ideal rectifier, the d-c ampere-turns assisting those provided by the control circuit will be

$$I_F N_F = I_L N_F \qquad (3)$$

and the total d-c ampere-turns AT_{dc}, due to a control current I_C in the control windings N_C will be

$$AT_{dc} = I_C N_C + I_L N_F \qquad (4)$$

Substituting this for $I_C N_C$ in equation 1A and neglecting the very small exciting current component I_{LO} as before, we get

$$I_L N_L = I_C N_C + I_L N_F \qquad (5)$$

Therefore

$$I_L / I_C = \frac{N_C}{N_L} \times \frac{1}{1 - N_F/N_L} \qquad (6)$$

The current gain I_L/I_C has been increased in the ratio $1/(1 - N_F/N_L)$.

In the case of negative feedback, however, the d-c feedback ampere-turns $I_L N_F$ oppose to the d-c control ampere-turns $I_C N_C$, and we get

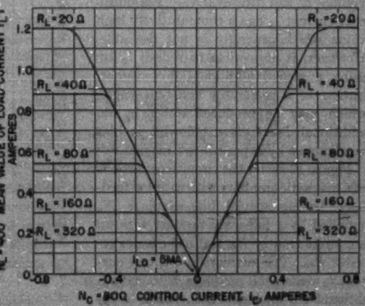

Figure 5 (right). Mean value of load current I_L as a function of control current I_C with load resistance R_L as a parameter ($N_L = 400$, $N_C = 800$)

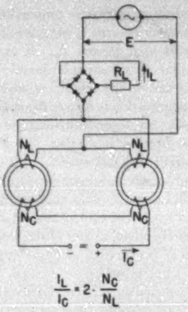

Figure 6. The parallel circuit

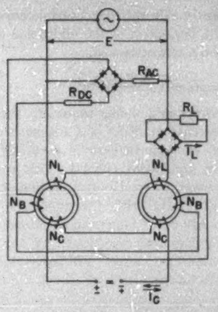

Figure 7. Circuit connections of a polarized magnetic amplifier with additional bias windings

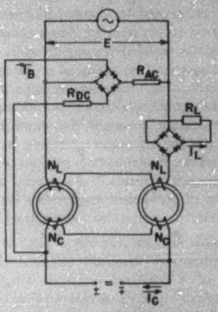

Figure 8. Circuit connections of a polarized magnetic amplifier without additional bias windings

$$I_L/I_C=\frac{N_C}{N_L}\times\frac{1}{1+N_F/N_L} \qquad (7)$$

The current gain I_L/I_C is therefore reduced in the ratio $1/(1+N_F/N_L)$.

In general, the effects of exciting current I_{LO} on the characteristics are not negligible. When $I_C=0$ the residual current in the a-c load circuit produces direct current in the feedback windings N_F, which results in the load current being considerably greater than in the nonfeedback amplifier (Figure 3) when $I_C=0$. Figure 11 represents a typical response characteristic of a magnetic amplifier with external feedback as shown in Figure 10.

Circuit with Bias: Referring to Figure 11 it is evident that with $I_C=0$ the load current I_L has a certain value I_Q, which may be called the "quiescent current value" or "Q-current." This value corresponds to the "quiescent point" or "operating point Q" of a 3-element vacuum tube. The magnitude of the quiescent current I_Q is dependent upon the size of the saturable core reactor, magnetic properties of the core material, magnitude of the applied alternating voltage E, and ratio N_F/N_L. The quiescent current I_Q has a comparatively high value which generally is not desirable. However, it is possible to reduce I_Q by using a second additional d-c magnetization of a preferably constant value, which may be produced either by an additional direct current flowing in bias windings or by a permanent magnet.[18,19]

Figure 12 shows the circuit connections of a magnetic amplifier with external feedback having special bias-windings N_B supplied by a full-wave rectifier with an a-c series resistor R_{ac} and a d-c series resistor R_{dc}. The auxiliary d-c circuit current $I_B=\text{const}\times E$ produces a second additional d-c magnetization, which is opposing to the d-c magnetization produced by the feedback windings N_F and independent of the d-c control magnetization. Figure 13 shows the response characteristic of such a biased feedback amplifier having a comparatively small quiescent current value I_Q.

Self-Excitation Circuits (Half-Wave Type)

Circuits with Additional D-C Windings: The basic circuit shown in Figure 14 involving two half-wave dry disk rectifiers to provide the desired feedback effects produced by a special kind of self-saturation represents a polarized magnetic amplifier of the half-wave type. There are two pulsating direct currents both producing d-c magnetization of the two reactor elements, which is proportional to the average value of the load current I_L. It is to be noted that the additional control action of the d-c components of these two pulsating currents will be either aiding or opposing to the control action of I_C and consequently producing either positive or negative feedback effect. The magnitude of this feedback effect depends upon the number of turns of the load windings N_A and of the additional d-c windings N_F. Here the current gain I_L/I_C is given by the equation

$$I_L/I_C=2\times\frac{N_C}{N_A}\times\frac{1}{1\mp\dfrac{N_A-2N_F}{N_A}} \qquad (8)$$

Figure 15 and Figure 16 show modifications of this self-excitation circuit. The number of turns N_F of the additional d-c windings determine the current gain I_L/I_C according to equation 8, but N_F has no influence upon the magnitude of the alternating voltage E which can be applied to the arrangement.

Circuits with Additional A-C Windings: The current gain I_L/I_C of the self-excitation circuits with additional a-c windings N_D as shown in Figure 17 and Figure 18 is given by the equation

Figure 9. Response characteristic of a biased magnetic amplifier: $I_L=f(I_C)$ with $N_L=400$ and $N_C=800$

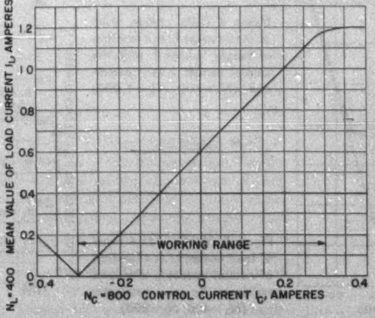

Figure 10. External feedback circuit without bias

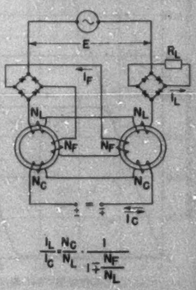

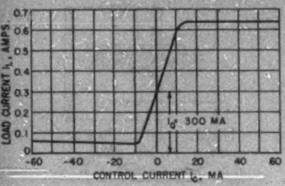

Figure 11. Response characteristic of an external feedback circuit without bias: $I_L = f(I_C)$ with $I_Q = 300$ milliamperes

$$I_L/I_C = \frac{2N_C}{N_A+2N_D} \times \frac{1}{1 \mp \frac{N_A}{N_A+2N_D}} \qquad (9)$$

The number of turns N_D of the additional a-c series windings has a certain influence upon the magnitude of the alternating voltage E which can be applied.

Figures 19, 20, and 21 show further modifications of these circuits having additional cross-connected a-c windings N_E. Here the current gain is

$$I_L/I_C = \frac{2N_C}{N_A+N_E} \times \frac{1}{1 \mp \frac{N_A-N_E}{N_A+N_E}} \qquad (10)$$

The number of turns N_E of the additional a-c windings has a certain influence upon the magnitude of the alternating voltage E which can be applied.

It is interesting to note that response characteristics of self-excitation circuits as shown in Figures 14 to 21 are in principle equivalent to corresponding response characteristics of the external feedback series circuit shown in Figure 10. Therefore it will be possible to use a bias current (Figure 12: I_B) supplying bias windings in order to reduce the magnitude of the quiescent current I_Q without changing the characteristic itself (Figure 13).

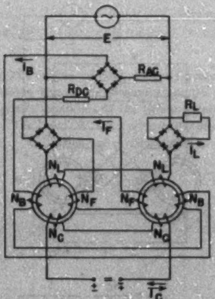

Figure 12. External feedback circuit with bias

Push-Pull Circuits of Magnetic Amplifiers

General

According to the two special problems described in the section on Special Problems for Measuring and Control Technique and illustrated in Figure 1 and Figure 2, a "magnetic amplifier of the balance detector type" must have response characteristics of a real balance detector, as used in connection with self-balancing d-c potentiometers and d-c bridge networks. Therefore the output current of such a device must correspond to the input current following balance detector response characteristics.

Figure 22 illustrates three typical response characteristics being especially interesting in the field of magnetic amplifiers of the balance detector type:

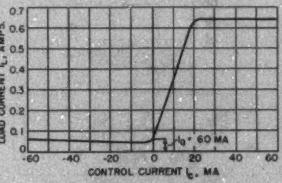

Figure 13. Response characteristic of an external feedback circuit with bias: $I_L = f(I_C)$ with $I_Q = 60$ milliamperes

"A" shows a linear characteristic curve, the output current $\pm I_L$ being exactly proportional to the input current $\pm I_C$.

"B" shows a nonlinear characteristic curve following a nearly linear law with low values of input current $\pm I_C$, but having considerable deviations with higher input current values.

"C" shows another nonlinear characteristic curve having diminished steepness with low values of input current $\pm I_C$, but following a nearly linear law with higher input current values.

It is to be noted that response characteristics, as illustrated in Figure 22 "A" and "B" are very practicable, but that characteristics corresponding to "C" are generally unsuitable. In principle, sensitivity of a balance detector must be especially high with low values of input current and may be diminished with higher input current values. Therefore a characteristic curve, as shown in "C" must be considered as not practicable.

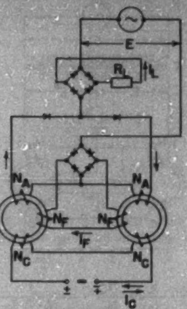

$$\frac{I_L}{I_C} = 2 \cdot \frac{N_C}{N_A} \cdot \frac{1}{1 \mp \frac{N_A-2N_F}{N_A}}$$

Figure 14. Self-excitation circuit with additional d-c windings, type I

Referring to the treatise of the basic circuits it is evident that these simple circuits, although having "polarized" response characteristics, cannot be used in connection with reversing motors as a balance detector amplifier. For with no control current ($I_C = 0$) the quiescent current I_Q flows through the motor which will run at a certain speed. In fact a real balance detector amplifier must have a characteristic curve corresponding to the working conditions: $I_L = 0$ if $I_C = 0$, as shown in Figure 22.

In order to obtain magnetic amplifiers having such response characteristics the author[20-24] devised some special types of symmetrical push-pull circuits which con-

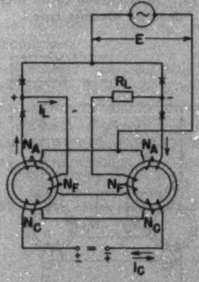

$$\frac{I_L}{I_C} = 2 \cdot \frac{N_C}{N_A} \cdot \frac{1}{1 \mp \frac{N_A-2N_F}{N_A}}$$

Figure 15. Self-excitation circuit with additional d-c windings, type II

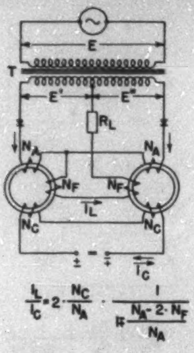

$$\frac{I_L}{I_C}=2\cdot\frac{N_C}{N_A}\cdot\frac{1}{1\mp\frac{N_A-2\cdot N_F}{N_A}}$$

Figure 16. Self-excitation circuit with additional d-c windings, type III

tain two balanced saturable core reactor systems, both utilizing positive and negative feedback. According to the two special problems previously described, the output current will be used for the control of a small reversing motor, which can be either a separately excited a-c motor of the induction-meter type (Figure 1) or a d-c motor of the moving coil meter type (Figure 2).

DIFFERENTIAL OUTPUT CIRCUITS FOR MAGNETIC AMPLIFIERS OF THE PUSH-PULL BALANCE DETECTOR TYPE

Circuits for an A-C Load

Circuit with Supply Transformer: Figure 23 shows the equivalent circuit of a magnetic amplifier containing two equal d-c controlled saturable core reactor systems connected in push-pull and a supply transformer T_s with center tapped secondary. This type of network that frequently arises in either power or communication circuits is that of two a-c generators—voltages E_1 and E_2—feeding a common load Z_L, the impedances Z_1 and Z_2 representing the actual impedance values of these two reactor systems, which are functions of the control current I_C. With $I_C=0$ the impedances Z_1 and Z_2 will be equal, and the alternating load current will be zero. But with a "positive" or "negative" control current I_C, an alternating load current $I_L=I_L'-I_L''$ will flow according to the response characteristics of the two reactor systems:

$$I_L=E\times\frac{Z_2-Z_1}{Z_1Z_2+(Z_1+Z_2)\times Z_L} \tag{11}$$

Figure 17. Self-excitation circuit with additional a-c windings, type I

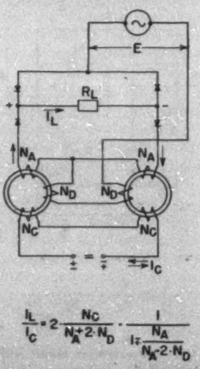

$$\frac{I_L}{I_C}=2\cdot\frac{N_C}{N_A+2\cdot N_D}\cdot\frac{1}{1\mp\frac{N_A}{N_A-2\cdot N_D}}$$

Circuit with Load Transformer: Figure 24 shows the equivalent circuit of a magnetic amplifier containing two equal d-c controlled saturable core reactor systems connected in push-pull and a load transformer T_L with center tapped primary. This differential transformer feeds the load impedance Z_L with a secondary current I_L corresponding to the difference of the two primary currents:

$$I_L=\text{const}\times(I_L'-I_L'') \tag{12}$$

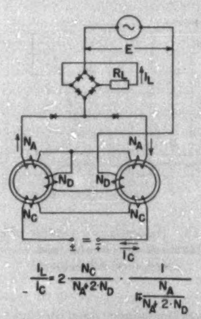

$$\frac{I_L}{I_C}=2\cdot\frac{N_C}{N_A+2\cdot N_D}\cdot\frac{1}{1\mp\frac{N_A}{N_A+2\cdot N_D}}$$

Figure 18. Self-excitation circuit with additional a-c windings, type II

Circuits for a D-C Load

In magnetic amplifiers of the balance detector type corresponding to the second problem (Figure 2) the effects of two direct output currents I_L' and I_L'' are superimposed in a differential arrangement, and the direct output current $I_L=I_L'-L_L''$ or $I_L=\text{const}\times(I_L'-I_L'')$ flowing through the d-c load corresponds to the control current I_C with regard to magnitude as well as to direction of current flow. Therefore the resultant output current is duo-directional and is zero at zero input control current I_C. This principle is especially interesting, when several magnetic amplifier stages are to be connected in cascade. There are three types of differential output circuits and three corresponding methods for coupling push-pull multistage amplifiers.

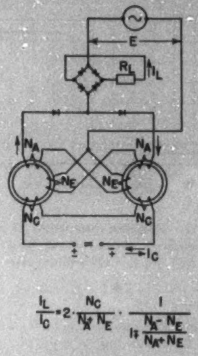

$$\frac{I_L}{I_C}=2\cdot\frac{N_C}{N_A+N_E}\cdot\frac{1}{1\pm\frac{N_A-N_E}{N_A+N_E}}$$

Figure 19. Self-excitation circuit with additional a-c windings, type III

Series Mixing Circuit: Referring to Figure 25 the first method is superposition of voltage drops E_S' and E_S'' in series resistors R_S proportional to direct output currents I' and I''. In order to find the direct load current components I_L' and I_L'' flowing through the load resistor R_L according to superposition theorem each load current component will be considered separately:

$$I_L'=I'\times\frac{R_S}{2R_S+R_L} \tag{13}$$

Figure 20. Self-excitation circuit with additional a-c windings, type IV

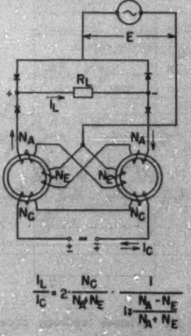

$$\frac{I_L}{I_C}=2\cdot\frac{N_C}{N_A+N_E}\cdot\frac{1}{1\pm\frac{N_A-N_E}{N_A+N_E}}$$

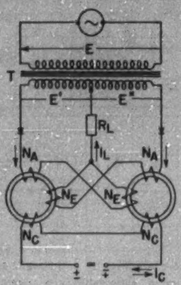

$$\frac{I_L}{I_C} = 2 \cdot \frac{N_C}{N_A + N_E} \cdot \frac{1}{1 \mp \frac{N_A - N_E}{N_A + N_E}}$$

Figure 21. Self-excitation circuit with additional a-c windings, type V

$$I_L'' = I'' \times \frac{R_S}{2R_S + R_L} \qquad (14)$$

$$I_L = I_L' - I_L'' = (I' - I'') \times \frac{R_S}{2R_S + R_L} \qquad (15)$$

Therefore the output power is

$$P_L = I_L^2 \times R_L = (I' - I'')^2 \times \frac{R_S^2 \times R_L}{(2R_S + R_L)^2} \qquad (16)$$

Differentiating this equation with respect to R_L we obtain the condition for a maximum that

$$R_L = 2 \times R_S \qquad (17)$$

and

$$I_L = {}^1/_4 \times (I' - I'') \qquad (18)$$

However, even when optimal rating of this mixing resistor network is realized, a considerable loss of power occurs, as I_L is only 1/4 of $(I' - I'')$. The series mixing circuit is suitable only for d-c loads having high resistance values.

Parallel Mixing Circuit: Referring to Figure 26 the second method is superposition of direct currents I_B' and I_B'' representing converted alternating output currents, so that I_B' and I_B'' are in opposition in the load resistor R_L. For proper operation, ballast resistors R_P of resistance about three times that of the load resistance R_L are needed in series with the rectifier outputs to prevent one rectifier by-passing part of the load current. Here a considerable loss of power is caused by the two ballast resistors $R_P = 3R_L$. The parallel mixing circuit is suitable especially for d-c loads having very low resistance values.[20,23,24]

Figure 22. Three typical response characteristics being especially interesting in the field of magnetic amplifiers of the balance detector type: "A" and "B" are very practicable, but "C" is generally unsuitable

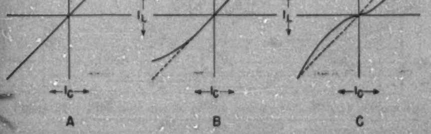

Twin Load Circuit: The third method (Figure 27) is using a differential type load having two equal separate load resistors R_L' and R_L'', in example: two equal separate d-c input control windings of the next amplifier stage (Figure 28). This method is based upon the superposition of d-c magnetizations produced by two separate load resistors (Figure 28: two d-c windings) acting in opposite directions as a differential type device. The twin load circuit involves no loss of power, as no mixing resistor network is needed, and this method should be used if convenient.

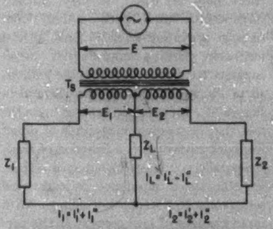

Figure 23. Differential output circuit for an a-c load with supply transformer

PUSH-PULL CIRCUITS OF THE BIAS-EXCITATION TYPE

Circuits Without Feedback

Circuit with Additional Bias Windings (Figure 29): This push-pull circuit contains two equal polarized d-c controlled magnetic core reactor systems as shown in Figure 7, utilizing no feedback effects. These two systems are combined by means of a supply transformer T_S having two separate secondaries (voltages E' and E''). The bias currents I_B' and I_B'' produce additional d-c magnetizations, which are independent on the d-c control magnetization produced by the control current I_C having a variable direction of current flow. According to the response characteristics shown in Figure 30 a positive control current I_C causes the output current I' to decrease, and the output current I'' to increase. If I_C is very large, the output current I' begins to increase again. Because of this the arrangement must be so designed that the maximum value of I_C does never lie outside the working range marked in Figure 30 by dotted lines. Voltage drops E_R' and E_R'' in series resistors R_S being proportional to direct output currents I' and I'' are superimposed (Figure 25), and the direct output current I_L flowing through load resistor R_L is reversing in direction with change in direction of control current I_C. Perfect balance of the two reactor systems can be easily accomplished by means of the slide-wire resistor R_O at zero control current.

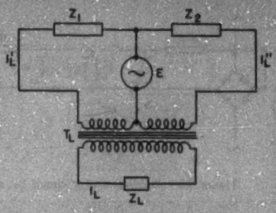

Figure 24. Differential output circuit for an a-c load with load transformer

Circuit Without Additional Bias Windings (Figure 31): It is possible to apply the bias currents I_B' and I_B'' directly to simple common d-c windings acting simultaneously as bias windings and as ordinary control windings (see Figure 8).

Figure 25. Series mixing circuit for a d-c load

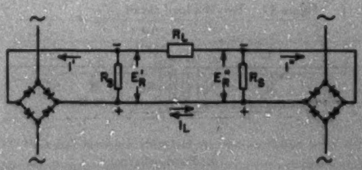

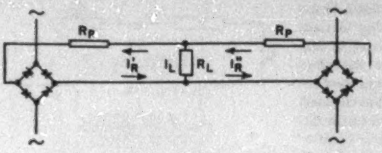

Figure 26. Parallel mixing circuit for a d-c load

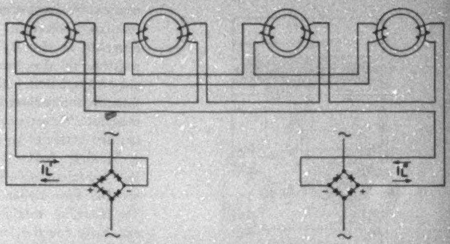

Figure 28. Two equal separate d-c windings of a magnetic amplifier acting in opposite directions as a differential-type device (twin windings)

In this case, however, the d-c series resistors R_{dc}' and R_{dc}'' shunting the common d-c windings must be rated as to have sufficiently high values in order to avoid a considerable decrease of the control current action. Here too, a slide-wire resistor R_0 is provided, so that the two reactor systems can be easily balanced at zero control current.

Circuits with Feedback

The power amplification of the bias-excitation type circuits, as shown in Figure 29 and Figure 31, is comparatively low and not sufficient for the most practical purposes. However, it is possible to obtain sufficiently high power amplification by providing special feedback windings producing additional d-c magnetizations, which are proportional to the actual direct load current $I_L = \text{const} \times (I' - I'')$, and corresponding positive (regenerative) feedback effects. This method has been introduced by the author,[20,22,24] and may be called "differential feedback method", as the feedback current effect is proportional to the difference of the two direct output currents I' and I''.

Circuits Without Derivative Feedback: In the circuit shown in Figure 32 the differential output current I_L flowing through the d-c load resistor R_L is fed back through special feedback windings N_F, which aid the control windings N_C. Using this circuit power amplification of the same order as for self-excitation can be obtained. As the additional d-c magnetization produced by the feedback windings N_F is proportional to the actual difference of the direct output currents I' and I'', these windings may be replaced in special cases by two equal feedback windings carrying the output currents I' and I'' separately, and acting as differential twin windings, Figure 28.

Circuits with Derivative Feedback: In order to reduce the response time of the magnetic amplifier a derivative feedback effect may be used. A very efficient method introduced by the author[22] consists in providing an additional special feedback circuit containing a large-capacity condenser C_F across the load resistor R_L, as shown in Figure 33 and in Figure 34. This method is based upon the fact that here actual magnitude of direct feedback current I_F is a function of time, the parallel condenser C_F acting as a time-variable series impedance on additional series connected feedback windings. With rapid changes of load current I_L the current I_F flowing through these feedback windings is relatively large, but later on before reaching steady conditions the current I_F will slowly decrease up to its normal value corresponding to steady conditions. Using this method it is possible to reduce the time of response to about 1/5 of its original value.

PUSH-PULL CIRCUITS OF THE SELF-EXCITATION TYPE

Full-Wave Type Circuits

Circuit Without Bias-Network (Figure 35): The two reactor systems of the external feedback type are combined by means of a d-c load device having two equal separate load resistors R_L' and R_L'', acting as differential windings (Figures 27 and 28). It is to be noted that with a "positive" control current, $+I_C$, flowing through the series connected control windings, in the first reactor system the d-c magnetization produced by I_C and the d-c magnetization produced by I_F' will have the same direction, and that in the second reactor system the d-c magnetization produced by I_C and I_F'' will be opposite in direction. Therefore, while first load current I_L' is increasing, second load current I_L'' is decreasing, and the effect of differential load windings R_L' and R_L'' will be proportional to $I_L' - I_L''$. But with a "negative" control current, $-I_C$, flowing through the control windings, this effect will be proportional to $I_L'' - I_L'$.

Figure 29 (right). Push-pull circuit of the bias-excitation type with additional bias windings

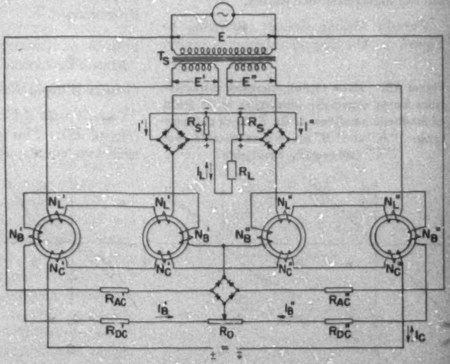

Figure 27. Twin d-c load circuit

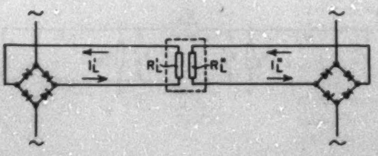

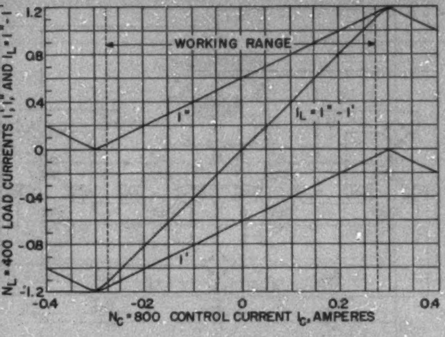

Figure 30. Response characteristics of a push-pull circuit of the bias excitation type: $I_L = I'' - I' = f(I_C)$ with $N_L = 400$ and $N_C = 800$

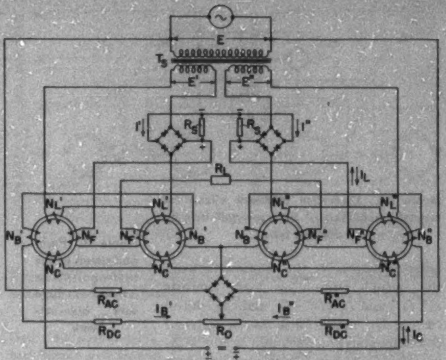

Figure 32. Push-pull feedback circuit of the bias-excitation type without derivative feedback

Circuit with Bias-Network (*Figure 36*): This push-pull circuit contains two reactor systems of the external feedback type (Figure 12), a differential load transformer T_L (Figure 24), and a complete bias-network reducing the quiescent current values of the two alternating output currents I_L' and I_L'' at zero control current I_C. The actual alternating load current I_L corresponds to $I_L' - I_L''$ with $+I_C$, and to $I_L'' - I_L'$ with $-I_C$, respectively.

Half-Wave Type Circuits

Circuit Without Bias-Network (*Figure 37*): The two reactor systems of the self-saturation type (Figure 17) are combined by means of a supply transformer T_S having a center-tapped secondary—voltages E' and E''—, and the alternating current I_L flowing through the load resistor R_L is proportional to $I_L' - I_L''$ with $+I_C$, and to $I_L'' - I_L'$ with $-I_C$, respectively.

Circuit with Bias-Network (*Figure 38*): This push-pull circuit contains two reactor systems of the self-saturation type (Figure 20), a supply transformer T_S having two separate secondaries (voltages E' and E''), series mixing resistors R_S', R_S'' (Figure 25), and a complete bias-network reducing the quiescent current values of the two direct output currents I_L' and I_L'' at zero control current I_C. The actual direct load current I_L corresponds to $I_L' - I_L''$ with $+I_C$, and to $I_L'' - I_L'$ with $-I_C$, respectively.

PERFORMANCE OF MAGNETIC AMPLIFIERS OF THE BALANCE DETECTOR TYPE

Response Characteristics of Push-Pull Circuits

Characteristics Without Biasing: The behavior of push-pull circuits can be determined with the aid of a load line plotted on composite curves, as shown in Figure 39. To obtain these composite curves, the I_C-I_L curves of the individual reactor systems are placed back to back, and the composite curves are then derived by considering the load current values I_L' and I_L'' corresponding to the same control current I_C: $I_L = I_L' - I_L''$. The resulting derived response charac-

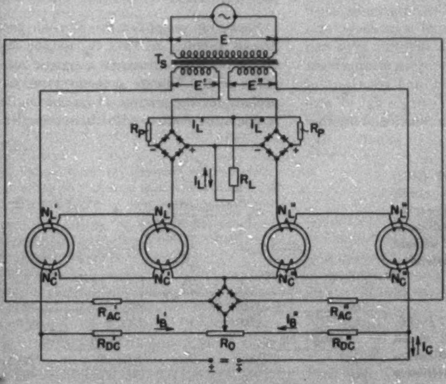

Figure 31. Push-pull circuit of the bias-excitation type without additional bias windings

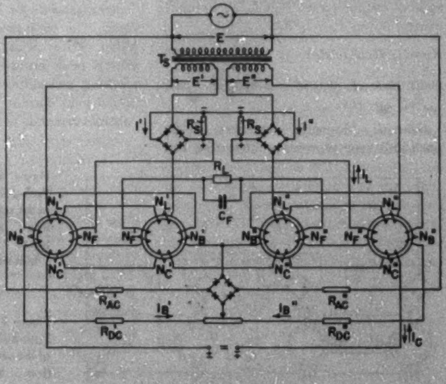

Figure 33. Push-pull feedback circuit of the bias-excitation type with derivative feedback

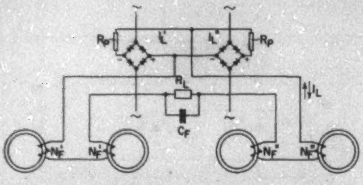

Figure 34. Derivative feedback circuit for magnetic amplifiers of the push-pull balance detector type

teristics represents the relation between the actual alternating load currents I_L', I_L'', and $I_L=I_L'-I_L''$ and the control current I_C. Figure 39 shows the response characteristics of a push-pull circuit without biasing having a comparatively high quiescent current value I_Q.

Characteristics with Biasing (Figure 40): Here the quiescent current value I_Q is considerably reduced, in order to obtain a very small drift rate.

Amplification Factors of Magnetic Amplifier Push-Pull Circuits

The current gain K_I is the ratio between output current I_L and control current I_C:

$$K_I=I_L/I_C \tag{19}$$

The voltage gain K_E is the ratio between output voltage $E_L=I_LR_L$ and input voltage $E_C=I_CR_C$:

$$K_E=(I_LR_L)/(I_CR_C) \tag{20}$$

where R_C is actual total resistance of either series or parallel connected d-c control windings of the two equally rated magnetic core reactor systems.

The power gain K_P is defined as the ratio of output power $P_L=I_L^2R_L$ to input control power $P_C=I_C^2R_C$:

$$K_P=(I_L^2R_L)/(I_C^2R_C) \tag{21}$$

Drift Rate of Magnetic Amplifier Push-Pull Circuits

General: Magnetic amplifiers of the push-pull type represent differential circuits operating on bridge network balance conditions: Load current $I_L=0$, if the control current I_C is zero. In practice it is required that fulfilment of this condition must be mostly independent upon changes in voltage, frequency, and waveshape of the a-c supply, change in temperature, etc. The performance of such devices will be illustrated in a subsequent section entitled Practical Results, where some performance data of different magnetic amplifiers of the balance detector type will be given.

In order to secure complete fulfilment of balance condition: $I_L=0$ if $I_C=0$ the ratio between the actual impedance values of the two reactor systems can be changed by means of a slide-wire resistor R_0 (see Figures 29, 31, 32, 33, 36, and 38) easily allowing a change of the ratio I_B'/I_B''. Thus it is possible to annihilate any effects caused by unsymmetrical magnetic core and dry disk rectifier characteristics.

Arrangements for Determining the Drift Rate: The drift rate of a magnetic amplifier of the balance detector type can exactly be determined by an arrangement allowing measurement and recording of actual load current $I_L=I_L'-I_L''$ at zero control current I_C as a function of another variable quantity, as supply voltage, supply frequency or room temperature. With d-c load amplifiers corresponding to the second problem (Figure 2) a very simple arrangement, as shown in Figure 41, consisting of a d-c milliammeter and a d-c recorder having respective high sensitivity both of the moving coil type, may be used, for exact measurement and recording of direct load current $I_L=\text{const}\times(I_L'-I_L'')$ under various working conditions of the amplifier.

However, with magnetic amplifiers corresponding to the first problem (Figure 1) the alternating load current $I_L=I_L'-I_L''$ will be exactly measured and recorded by means of a phase selective dry disk rectifier device of the "ring-modulator" full-wave type (Figure 42) containing two center-tapped transformers, an ordinary d-c milliammeter and a d-c recorder, both of the moving coil type.

Practical Results

Push-Pull Amplifier for 50-Cycle-per-Second Supply: In 1942 the author developed a high-sensitivity magnetic amplifier of the balance detector type, especially for the purpose of an automatic temperature control with thermocouples.

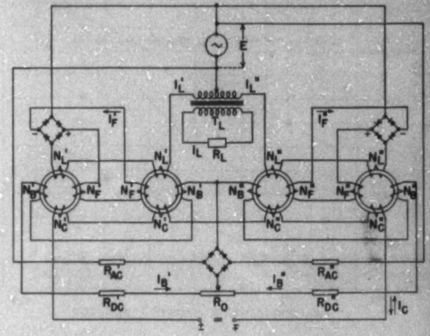

Figure 36. Push-pull circuit of the self-excitation full-wave type with bias-network

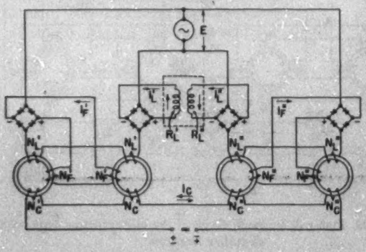

Figure 35 (left). Push-pull circuit of the self-excitation full-wave type without bias-network

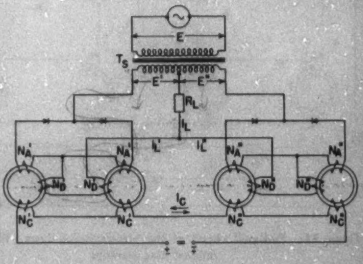

Figure 37 (right). Push-pull circuit of the self-excitation half-wave type without bias-network

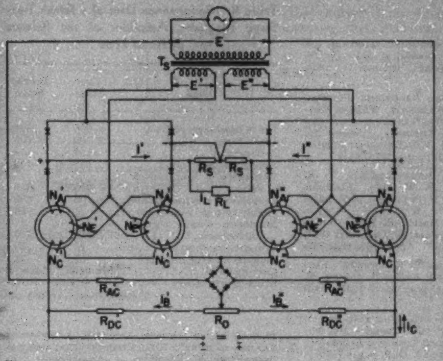

Figure 38. Push-pull circuit of the self-excitation half-wave type with bias-network

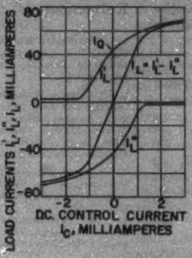

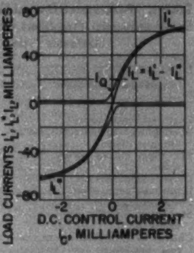

Figure 39 (above, left). Response characteristics of push-pull feedback circuits without biasing: $I_L = I_L' - I_L'' = f(I_C)$ with $I_Q = 45$ milliamperes

Figure 40 (above, right). Response characteristics of push-pull feedback circuits with biasing: $I_L = I_L' - I_L'' = f(I_C)$ with $I_Q = 10$ milliamperes

This push-pull amplifier[22] having only one stage of amplification (Figure 33), which operates from a 50-cycle-per-second supply had the following characteristics:

1. Resistance of control windings: $R_C = 15$ ohms.

2. Magnitude of control current corresponding to a change in temperature of 1 degree centigrade: $I_C = 1.13$ microamperes.

3. Magnitude of input voltage corresponding to a change in temperature of 1 degree centigrade: $E_C = I_C R_C = 17$ microvolts.

4. Magnitude of input power corresponding to a change in temperature of 1 degree centigrade: $P_C = I_C^2 R_C = 1.9 \times 10^{-11}$ watts.

5. Total ampere-turns of control windings ($N_C = 300$) corresponding to a change in temperature of 1 degree centigrade: $I_C N_C = 3.4 \times 10^{-4}$.

6. Ampere-turns/centimeter of control windings (mean length of the magnetic circuit of the Mumetal-core type = 17 centimeters) corresponding to a change in temperature of 1 degree centigrade: 2×10^{-5}.

7. Magnitude of d-c output power corresponding to a change in temperature of 1 degree centigrade: $P_L = I_L^2 R_L = 10^{-7}$ watts.

8. Power gain corresponding to a change in temperature of 1 degree centigrade: $K_P = P_L/P_C = (10^{-7}$ watts$)/(1.9 \times 10^{-11}$ watts$) = 5{,}300$.

9. Magnitude of control current corresponding to a change in temperature of 100 degrees centigrade: $I_C = 0.113$ milliamperes.

10. Magnitude of input voltage corresponding to a change in temperature of 100 degrees centigrade: $E_C = I_C R_C = 1.7$ millivolts.

11. Magnitude of input power corresponding to a change in temperature of 100 degrees centigrade: $P_C = I_C^2 R_C = 0.19$ microwatts.

12. Magnitude of d-c output power corresponding to a change in temperature of 100 degrees centigrade: 10^{-3} watts.

13. Power gain corresponding to a change in temperature of 100 degrees centigrade: $K_P = P_L/P_C = (10^{-3}$ watts$)/(1.9 \times 10^{-7}$ watts$) = 5{,}300$.

14. Drift rate, due to ordinary changes in supply voltage, in room temperature et cetera: each about ±1 degree centigrade (being ±1 per cent of the 100 degrees centigrade—range over a period of eight hours).

Push-Pull Amplifiers for 500-Cycles-per-Second Supply: In Table I figures for two typical single-stage magnetic amplifiers, which have been developed in Germany during the 1939–1945 War, are quoted to indicate the performance obtained.[9] These amplifiers were designed to operate at ambient temperatures between +70 and −60 degrees centigrade for supply voltage and frequency ranges of 30 to 40 volts and 400 to 600 cycles per second. The core material used was of the Permalloy type.

Multistage Amplifiers of the Balance Detector Type

General: Magnetic amplifiers involving two or three stages of the push-pull type give very high power gain values. Using a multistage amplifier having two equal stages a total power gain

$$K_{\text{total}} = \frac{\text{Output power of the output stage}}{\text{Input power of the input stage}} \tag{22}$$

of 1,000,000 has been obtained as a result of the author's research work. In such arrangements the entire design revolves around the essential problem that fulfilment of balance condition: $I_L = 0$ if $I_C = 0$, must be mostly independent upon changes in voltage and frequency of the a-c supply, changes in room temperature, etc.

Push-Pull Two-Stage Amplifier for 400-Cycle-per-Second Supply: In Table II figures for a British 2-stage magnetic amplifier of the push-pull type[9] are quoted to indicate the performance obtained. This amplifier for 400-cycle-per-second supply has been successfully designed to operate a sensitive polarized relay for an input power of 0.004 microwatt (±2 microamperes in 1,000 ohms). The power required to operate the relay was about 600 microwatts, and therefore the power amplification required was 1.5×10^5. Obviously the time lag of a single stage design would have been excessive. Therefore a 2-stage arrangement (Table II) was constructed. Self-excitation was used in both stages, and the output mixing circuit for each stage was of the type shown in Figure 25 (series resistor mixing circuit). Two special points of interest[9] are the reduced self-excitation of the first stage in order to ensure good zero stability, and the lower maximum output of this stage in order that the final stage could not be swamped by an excessive input signal and its output reduced below the level required to operate the relay.

Speed of Response in Magnetic Amplifiers

General: In principle, magnetic amplifier circuits containing a large amount of inductance have an inherent slow response time, and there is a certain time lag between the application of the input signal and the attainment of the full output load current. In certain practical applications this sluggishness of response due to "magnetic inertia" is not an im-

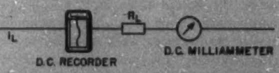

Figure 41. Arrangement for determining the drift rate of d-c load amplifiers

Table I. Performance Data of German Single-Stage Magnetic Amplifiers of the Balance Detector Type

Magnetic Amplifier	Type A	Type B
Load resistance, ohms	400	25
Maximum load current, milliamperes (linear)	2.5	200
Maximum output power, milliwatts	2.5	1,000
Current amplification	100	250
Input resistance, ohms	2,000	1,000
Power amplification	2,000	1,560
Maximum input power, microwatts	1.25	640
Change in input current to correct maximum zero wander, microamperes	3	16
Zero wander expressed as input power, microwatts	0.018	0.256
(Zero wander)/(Maximum input power) expressed in per cent	1.44	0.04
Time-constant (approx.), seconds		0.15
Weight, pound	$^{3}/_{4}$	$1^{3}/_{4}$

portant drawback. But in other applications, especially for high-performance servomechanisms and some other types of automatic control and instrument work, a very short response time is of paramount importance.

As the minimum time delay will be of the order of one cycle of the a-c supply frequency, an obvious method to reduce the response time is increasing the supply frequency (up to about 2,000 cycles per second). Another efficient method consists in providing derivative feedback, as described in the section on Circuits with Derivative Feedback. Using this method in connection with a 400-cycle-per-second supply it would be possible, to achieve a response time of about 10 milliseconds or less.

Design Procedure with Respect to Time Lag: The ratio K_P/T between power amplification K_P and time-constant T is increased by the application of positive (regenerative) feedback or similar effects. Furthermore the time-constant of a magnetic amplifier increases in direct proportion to the power amplification. When two or three stages of amplification are connected in cascade, the over-all power amplification is the product of the stage amplifications, whereas the total time-constant is roughly the sum of the individual time-constants. It follows that as the number of stages is increased there is an increase of the ratio of amplification to time-constant K_P/T. Therefore, in order to obtain a high value of this ratio, the design procedure[9] will be in many applications to connect in cascade two or three stages, each stage having a comparatively low power amplification and yet using the maximum positive feedback that is consistent with the required stability of the amplifier.

References

1. High-Speed Recording Potentiometer for Small D-C Voltages. *Journal of Scientific Instruments* (London, England), volume 11, 1934, pages 400–01.

2. A Simple High-Speed Recording Potentiometer for D-C Measurements, **Wilhelm Geyger.** *Wissenschaftliche Veroffentlichungen aus den Siemens-Werken* (Berlin, Germany), volume 15, 1936, pages 109–15 and *VDI-Zeitschrift* (Berlin, Germany), volume 81, 1937, pages 577–78.

3. A Self-Balancing Potentiometer, **T. R. Harrison, W. P. Wills, F. W. Side.** *Electronic Industries* (New York, N. Y.), volume 2, 1943, pages 68, 153–57.

4. The Transductor, **Harold B. Rex.** *Instruments* (Pittsburgh, Pa.), volume 20, December 1947, pages 1102–09 and volume 21, April 1948, page 332.

5. Magnetic Amplifiers, **S. E. Tweedy.** *Electronic Engineering* (London, England), volume 20, February 1948, pages 38–43 and March 1948, pages 84–88.

6. Saturable Reactor and Magnetic Amplifier Circuits, **Frank G. Logan.** *Magnetic Materials Symposium*, Naval Ordnance Laboratory (Washington, D. C.), June 15, 1948, pages 7–20.

7. Transductor Fundamentals, **Sven-Eric Hedstroem, Lennart F. Borg.** *Electronics* (New York, N. Y.), September 1948, pages 88–93.

8. Saturable Reactors and Magnetic Amplifiers, **Frank G. Logan.** *Electronics* (New York, N. Y.), October 1948, pages 104–09.

9. Magnetic Amplifiers, **A. G. Milnes.** *Proceedings*, Institution of Electrical Engineers (London, England), volume 96, part I, number 99, May 1949, pages 89–98.

10. A Theoretical and Experimental Study of the Series-Connected Magnetic Amplifier, **H. M. Gale, P. D. Atkinson.** *Proceedings*, Institution of Electrical Engineers (London, England), volume 96, part I, number 99, May 1949, pages 99–114.

11. An Analysis of Magnetic Amplifiers with Feedback, **D. W. VerPlanck, M. Fishman, D. C. Beaumariage.** *Proceedings*, Institute of Radio Engineers (New York, N. Y.), volume 37, August 1949, pages 862–66.

12. An Analysis of Interlinked Electric and Magnetic Networks with Application to Magnetic Amplifiers, **D. W. VerPlanck, M. Fishman.** *Proceedings*, Institute of Radio Engineers (New York, N. Y.), volume 37, September 1949, pages 1021–27.

13. Self-Saturation in Magnetic Amplifiers, **W. J. Dornhoefer.** *AIEE Transactions*, volume 68, part II, 1949, pages 835–50 and *Electrical Engineering*, volume 68, November 1949, page 988.

14. Special Magnetic Alloys and Applications, **G. W. Elmen, E. A. Gaugler.** *Electrical Engineering*, volume 67, September 1948, pages 843–45.

15. Processing of Magnetic Materials at the Naval Ordnance Laboratory, **E. A. Gaugler.** *Magnetic Materials Symposium*, Naval Ordnance Laboratory (Washington, D. C.), June 15, 1948, pages 49–56.

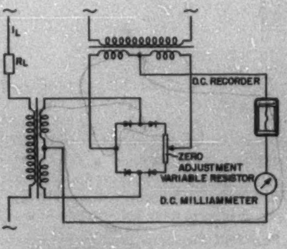

Figure 42. Arrangement for determining the drift rate of a-c load amplifiers

Table II. Performance Data of a British Two-Stage Magnetic Amplifier of the Balance Detector Type

Detail	First Stage	Second Stage
Input resistance, ohms	1,000	600
Input turns	2,700	2,200
A-c turns	150	150
Self-excitation turns	135	150
Resistance of load resistor, ohms	330	330
Overall load resistance, ohms	600	680
Supply voltage, volts (rms)	8	16
Maximum output current, milliamperes	3.5	7.0
Current amplification	15	30
Lamination type number	21	21
Core material	Mumetal	Mumetal
Stack depth, inches	$^{5}/_{16}$	$^{5}/_{16}$

16. A Simple Direct Current Instrument Transductor with Real Current Transformer Properties, **W. Kraemer.** *Elektrotechnische Zeitschrift* (Berlin, Germany), volume 58, 1937, pages 1309–13.

17. A New Direct Voltage Instrument Transductor for the Measurement of High Direct Voltages, **W. Kraemer.** *Elektrotechnische Zeitschrift* (Berlin, Germany), volume 59, 1938, pages 1295–98.

18. Electrical Translating Apparatus, **Philip H. Dowling.** United States Patent 1,739,579, December 17, 1929.

19. The Theory of Magnetic Amplifiers and Some Recent Developments, **E. H. Frost-Smith.** *Journal of Scientific Instruments* (London, England), volume 25, August 1948, pages 268–72.

20. Fundamentals of Magnetic Amplifiers for the Techniques of Measurement and Control, **Wilhelm Geyger.** *Wissenschaftliche Veroffentlichungen aus den Siemens-Werken* (Berlin, Germany), volume 19, 1940, pages 4–47.

21. Experimental Investigations on Magnetic Amplifiers for the Techniques of Measurement and Control, **Wilhelm Geyger.** *Wissenschaftliche Veroffentlichungen aus den Siemens-Werken* (Berlin, Germany), volume 20, 1942, pages 33–47.

22. A Very Sensitive Magnetic Amplifier of the Balance Detector Type to be Used in the Techniques of Measurement and Control, **Wilhelm Geyger.** *Wissenschaftliche Veroffentlichungen aus den Siemens-Werken* (Berlin, Germany), volume 22, 1943, pages 47–57.

23. Magnetic Amplifiers for the Techniques of Measurement and Control, **Wilhelm Geyger.** *Elektrotechnische Zeitschrift* (Berlin, Germany), volume 62, 1941, pages 849–53 and 891–98.

24. Magnetic Amplifier of the Balance Detector Type, **Wilhelm Geyger.** German Patent 702,082, January 3, 1939.

Discussion

William F. Horton (Westinghouse Electric Corporation, East Pittsburgh, Pa.): Dr. Geyger discusses two types of mixing circuits for a balanced magnetic amplifier with d-c output. The conditions for maximum power output to the load are developed for series and parallel mixing circuits. In the case of the series mixing circuit the condition for maximum power output is obtained as: $R_L = 2R_S$ (equation 16).

It can be shown (see Appendix to this discussion) that the condition for maximum power output for balanced magnetic amplifiers with series or parallel mixing circuits is dependent not only on the constants of the mixing circuit but on the saturated imped-

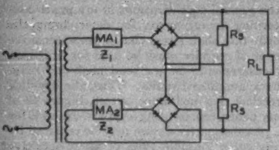

Figure 1. Balanced magnetic amplifier with series mixing circuit

ance of the amplifiers. If the saturated impedance of the amplifier of one side of the balanced circuit is taken to be Z_{1S} (see Figure 29) then for maximum power output:

For series mixing circuit

$$R_L=2Z_{1S}$$

$$R_S=\sqrt{2}Z_{1S} \text{ and } R_L=\sqrt{2}R_S$$

For parallel mixing circuit

$$R_L=Z_{1S/2}$$

$$R_P=Z_{1S/\sqrt{2}} \text{ and } R_L=R_P/\sqrt{2}$$

The efficiency of these mixing circuits with respect to the efficiency of the twin load circuit can then be determined.

APPENDIX

Series Mixing Circuit

In the case of the series mixing circuit, equation 16 is differentiated with respect to R_L.

$$P_L=I_L^2R_L=(I'-I'')^2\frac{R_SR_L}{(2R_S+R_L)^2} \qquad (16)$$

$$\frac{dP_L}{dR_L}=(I'-I'')^2\frac{d}{dR_L}\frac{R_SR_L}{(2R_S+R_L)^2}+\frac{R_SR_L}{(2R_S+R_L)^2}\frac{d}{dR_L}(I'-I'')^2$$

$$=(I'-I'')^2\frac{2R_S-R_L}{2R_S+R_L}+2R_L(I'-I'')\frac{d}{dR_L}(I'-I'')$$

This is set equal to zero to obtain R_L for maximum P_L. If

$$\frac{d}{dR_L}(I'-I'')=0$$

then $R_L=2R_S$ is the condition for maximum P_L, however for maximum P_L

$$\frac{d}{dR_L}(I'-I'')\neq 0$$

Consider the balanced magnetic amplifier circuit as shown with series mixing circuit in Figure 1 of this discussion. The mode of operation is that the control is acting in opposite directions in the amplifiers MA_1 and MA_2; when Z_1 is a minimum, Z_2 is a maximum. Let the saturated impedance of MA_1 be Z_{1S}. When $Z_1=Z_{1S}$, Z_2 is at its maximum value which can be assumed to be infinite with respect to any other impedance in the circuit. Then the circuit to be considered to determine the conditions of maximum power output is simply one side of the balance amplifier, the circuit of MA_1.

The equivalent circuit is shown in Figure 2 of this discussion. The conditions for maximum P_L are:

$$Z_a=Z_{1S}$$

$$Z_b=R_L$$

$$Z_a=\frac{R_S(R_S+R_L)}{R_L+2R_S}=Z_{1S}$$

$$Z_b=R_S+\frac{R_SZ_{1S}}{R_S+Z_{1S}}=R_L$$

Eliminating Z_{1S}:

$$R_L=R_S+\frac{R_S(R_S+R_L)}{R_L+2R_S+R_S+R_L}$$

$$2R_L^2=4R_S^2$$

$$R_L=\sqrt{2}R_S$$

in terms of Z_{1S}:

$$R_L=2Z_{1S}$$

$$R_S=\sqrt{2}Z_{1S}$$

The efficiency of the balanced magnetic amplifier circuit with series mixing circuit with respect to the efficiency of the twin load circuit can then be determined. With the matched loads in both cases:

$$E=\left[\frac{Z_{1S}}{(2+\sqrt{2})Z_{1S}}\right]^2\left(\frac{2Z_{1S}}{Z_{1S}}\right)=\frac{2}{(2+\sqrt{2})^2}=17.1\%$$

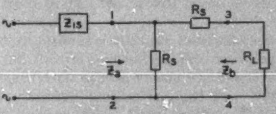

Figure 2. Equivalent circuit with MA_1 saturated

Z_a = impedance looking from terminals 1, 2
Z_b = impedance looking from terminals 3, 4 source short circuited

Parallel Mixing Circuit

Similarly, for the parallel mixing it can be shown that the conditions for maximum power output are:

$$R_L=R_P/\sqrt{2}$$

$$R_L=Z_{1S}/2$$

$$R_P=Z_{1S}/\sqrt{2}$$

The efficiency of the parallel mixing circuit with respect to the twin load circuit is 17.1 per cent as before.

S. E. Tweedy (Queensburg, Edgware, England): Mr. Geyger's paper is a useful summary of the essential properties of a number of magnetic amplifier circuits that are today in common use. I should, however, like to point out that his analysis of the series mixing circuit requires comment. I am referring to the differentiation of equation 16, in which he has assumed that $(I'-I'')$ is independent of the load resistance. This is not in practice true. An analysis in which this fact is taken into account gives the interesting result that as high a percentage as desired of the power that the amplifiers are capable of giving can be delivered into the load, but at the expense of taking more power from the a-c supply, and wasting it in the series mixing resistors.

Mr. Geyger also states that "the time constant increases in direct proportion to the power amplification." Paradoxically, this statement is at the same time true and untrue. If circuit conditions are varied in such a way that the power amplification is altered, but the ampere-turn amplification is kept constant, then the statement is true. If, on the other hand, the power amplification is varied by altering the degree of self-excitation or feedback, then the statement is untrue, and in fact the time constant becomes proportional to the square root of the power amplification.

In Figure 42, Mr. Geyger shows an arrangement for recording the zero drift of a magnetic amplifier with a-c output, employing a ring modulator. This will clearly only be accurate provided that the drift of the ring modulator is small compared with the amplifier drift, and I would like to ask Mr. Geyger if he has in fact found this to be the case.

W. A. Geyger: The analysis of the series mixing circuit in my paper is based upon the assumption that the actual impedance values of the two magnetic amplifier elements are very large in comparison with the actual resistance values R_S and R_L of the mixing circuit so that $(I'-I'')$ is substantially independent of these resistance values. Of course, this will be only true if bias effects are applied in such a way that the quiescent currents (the output currents with no-signal condition) are reduced to have very small magnitudes, and if the difference between the actual impedance values of the two magnetic amplifier elements is small, corresponding to minor excursions in the vicinity of null.

I am grateful to W. F. Horton and S. E. Tweedy for stressing that, in general, the condition for maximum power output for balanced magnetic amplifiers with series or parallel mixing circuits is dependent not only on the constants of the mixing circuit but on the saturated impedance of the amplifiers. Mr. Horton's complete analysis shows the actual conditions for large excursions without making the aforementioned assumption.

Referring to the general considerations in my paper concerning the design procedure with respect to time lag, it is to be noted that the ratio K_P/T between power gain K_P and time-constant T can be increased by the application of positive (regenerative) feedback, as defined by the feedback multiplier[1] $A=1/(1-N_F/N_L)$. The power gain K_P with positive feedback will be A^2 times the power gain without feedback ($A=0$). On the other hand, the time-constant T increases linearly with the feedback multiplier A.

According to common practice, the speed of response of the conventional types of magnetic amplifiers utilizing external or internal feedback can be increased with an attendant proportional decrease of power gain by placing an additional resistor (sometimes called "forcing resistor") in series with the control windings. By increasing the total resistance R_C of the control circuit to A times its previous value, the increase of time constant T due to positive feedback can be eliminated and the power gain K_P is reduced from A^2 to A. Hence, for increasing control voltages, the magnetic amplifier with positive feedback can be made with the same speed of response (with the same time-constant T) as the one without feedback and yet have a power gain of A times the power gain of the magnetic amplifier without feedback. Thus, K_P/T will be approximately proportional to the actual value of feedback multiplier $A = 1/(1-N_P/N_L)$. Similar results will be obtained, when "internal" feedback (self-saturation) is provided instead of "external" feedback (using separate feedback windings N_P).

With regard to Mr. Tweedy's question, whether the drift of a ring modulator arrangement, as shown in Figure 42 of my paper, is small compared with the drift of the push-pull a-c load type magnetic amplifier, I would like to stress that in practice the variable quantities, as supply voltage, supply frequency, room temperature, et cetera, will only be applied to the magnetic amplifier itself. However, the phase-sensitive ring modulator circuit containing four dry-disk rectifier elements can be arranged to operate under substantially constant conditions:

1. The synchronous reference (polarizing) voltage may be provided by means of a constant-voltage device, preferably a saturating core type of constant-voltage transformer, to eliminate differences in voltage-current characteristics of the rectifier elements.

2. The dry-disk rectifier elements of the ring modulator circuit may be arranged in a box having automatic temperature control, to eliminate undesired effects of changes in ambient temperature.

Additionally, any drift of the ring modulator circuit itself can easily be detected and completely eliminated by recording the output current of the ring modulator circuit both with and without input current (I_L) of this circuit. In this case, the moving-coil type recorder will trace two separate curves, and the actual differences between these curves will show the pure drift of the magnetic amplifier.

Moreover, I should like to point out that the general considerations in my paper concerning arrangements for determining the drift rate shall stress that a phase-sensitive type of rectifier must be used for drift rate measurements on a-c load push-pull magnetic amplifier circuits. Thus, the dry-disk rectifier ring modulator circuit, Figure 42 of my paper, representing a typical example for a phase-sensitive device may be replaced by any other suitable type of phase-sensitive rectifier arrangement, preferably by a mechanical rectifier using either an oscillating or a rotating contact device. For example, the "contact rectifier," as developed by Mr. F. Koppelmann,[2] has proved to be very useful for such investigations, particularly for input-stage circuits having a comparatively small output power of a few milliwatts only.

REFERENCES

1. MAGNETIC AMPLIFIERS WITH ORTHONOL TAPE CORES, W. A. Geyger. *Proceedings*, National Electronics Conference (New York, N. Y.), volume 6, September 1950, page 62.

2. THE "VECTOR-METER"—A NEW ELECTRICAL MEASURING INSTRUMENT, F. Koppelmann. *The Engineers' Digest* (New York, N. Y.), volume 12, August 1951, pages 248–50, also *Elektrotechnik und Maschinenbau* (Vienna, Austria), volume 68, number 2, January 1951, pages 27–30 and number 9, May 1951, pages 225–29.

A Simple New Resistance Type A-C Load Flow Board

WALDO E. ENNS
MEMBER AIEE

IT HAS become quite common practice for system planning engineers of many of the larger electric power distributors to obtain an advance check of their major transmission and distribution system developments by setting up and studying the operating characteristics of a number of alternate plans on an a-c board. By so doing, it is possible to choose a development plan which will do the best job in the most economical manner for the particular system being analyzed. Even though recognition has been given to the advantages of the a-c boards in quickly solving complicated a-c network problems, it appears that the many engineers who do not have the constant use of these devices must do a great deal of computational work. This could be done better and much more quickly on one of the conventional type, or one of the new resistance type of a-c boards.

In a previous paper[1] the writer described a new simple type of a-c calculator using resistance circuits. The basic principles set forth therein were used in the design and construction of the new load flow a-c board now in successful operation. Certain modifications were made in the original design which made it possible to concentrate all of the control functions within easy reach of a small operating desk, so that all of the balancing and reading of the instruments is done by a single operator sitting at this desk.

Following the publication of the previous paper in 1943 there was a definite interest aroused in the development of such a device, both in this country, and abroad, as indicated by inquiries the writer received at that time. On the other hand, some very competent engineers, familiar with load flow analysis, expressed their doubts as to whether an a-c board built upon the principle of this one could be adjusted into balance fast enough to make it a really useful tool. Because of these very reasonable doubts which were expressed, the writer did not make any further claims for the device until they could be based on actual operating experience.

In September 1949 the Portland General Electric Company put into operation a resistance type a-c board which now is in constant use making load flow and voltage studies. These studies will be used for determining the system additions which will provide for the short-term requirements, and at the same time fit into a long-term program of system development to economically serve a growing load.

In addition to explaining the present design this paper will indicate how it can be modified to provide a board which will not only read real and reactive power and voltages for load flow studies, but will provide the means of setting up the sequence networks for short circuit studies as well. This modification should make it a useful tool for the system engineers of either large or small electric power distributors.

Description of A-C Board

Figure 1 shows a front view of the new a-c board. The over-all dimensions of the cabinet section of the device are 66 by 82 by 18 inches, and the desk top is 44 by 20 inches. The present capacity of the board is 92 circuits and 60 busses. Of the 60 busses, ten will connect a maximum of eight circuits, and 50 will connect a maximum of four circuits. At present the requirements for setting up the company system and associated interconnections is less than 40 busses and 60 circuits, so that the board has adequate capacity for increases in the size of the network. The design is such that more circuits and busses may be added later if required.

Referring to Figure 1, in the left-hand cabinet, plugging panels provide the means of setting up the network being studied. The section above the instruments and underneath the desk of the center and right-hand cabinets provides plugging panels for the *M* and *N* circuit constants, the significance of which will be explained in the mathematical basis for load flow measurements. The *M* and *N* resistors are multitapped and provide a range of 0 to $109^2/_3$ per cent in 1/3-per cent steps. Each panel also has additional 100 per cent fixed resistors which may be plugged in to obtain values above $109^2/_3$ per cent. Figure 2 is a back view of the interior of the right-hand cabinet, and it shows the mounting of the resistors as well as the fixed wiring between them and the jacks of the plugging panels.

The instruments shown in Figure 1 consist of the following: the small white faced instrument which reads the base voltage being used for the study; the center instrument, a 2-element wattmeter, which reads per cent megawatts and megavars; and the right-hand instrument, a 2-element wattmeter, which reads per cent bus volts. This latter instrument is not being used because in recording the studies the bus voltage and phase angle is desirable. This is quickly obtained on a slide rule from the values of E_p and E_q set up at each bus when the network is balanced and read. To the right of the per cent volts instrument is the dial of a variable autotransformer which is used to adjust the base voltage of the board.

Referring again to Figure 1, notice that

Paper 50-172, recommended by the AIEE Computing Devices and System Engineering Committee and approved by the AIEE Technical Program Committee for presentation at the AIEE Summer and Pacific General Meeting, Pasadena, Calif., June 12-16, 1950 and at the AIEE Fall General Meeting, Cleveland, Ohio, October 22-26, 1951. Manuscript submitted March 13, 1950; made available for printing August 29, 1951.

WALDO E. ENNS is with the Portland General Electric Company, Portland, Oreg.

Figure 1 (left). New resistance type a-c load flow board

Figure 2 (right). Rear interior view of analyzer, showing tapped resistors and wiring

all of the control functions of the board are conveniently located in the desk top and the voltage plugging panels just above the desk top. In the desk top are 60 lever switches, one for each bus. Busses 1 to 30 are located on the left side and busses 31 to 60 are located on the right side. In the center portion of the desk there are nine push buttons. One marked "*Bus*" is used to read loading or generation at any bus selected to read. The other eight marked "*A*" to "*H*", inclusive, are used to select and read the flow in the individual circuits connected to the bus being read. For example, let bus 1 have the following six circuits connected to it: *A11, C3, D5, E1, F2,* and *H3*. By throwing forward bus 1 lever switch, then depressing the "*Bus*" push button, the six circuit relays *A11* to *H3*, inclusive, are picked up, and the total load or generation at bus 1 may be read on the wattmeter. Continuing with bus 1 lever switch forward and releasing "*Bus*" push button, the load flow in the six individual circuits may be read in turn by depressing the circuit push buttons *A, C, D, E, F,* and *H*. Similar readings of load flow in per cent megawatts and megavars may be made at all busses.

There are no generator or load units used for this type of board because simulated generation or load can be obtained at any bus in the network by adjusting the two voltage components at each bus. These components are marked E_p and E_q and their significance will be made clear in the explanation of the mathematical basis of the board. Figure 1 shows the writer plugging in bus 15 E_p voltage cord at plus $8^2/_3$ per cent above reference voltage. The section of the voltage plugging panel just above the desk top provides taps minus with respect to the reference voltage. Located between the minus and plus voltage plugging sections are the bus jacks. One red and one black jack adjacent to each other are provided for each bus. The red jack and an associated red cord with red plugs are used to connect E_p to the particular bus. The black jack and an associated black cord with black plugs are used to connect E_q to the particular bus. Bus jacks for busses 1 to 30 are located in the left-hand plugging panel and those for busses 31 to 60 are located in the right-hand panel. This grouping conforms exactly to the grouping of the bus lever switches in the desk top. The voltage plugging section is supplied from one main multitapped autotransformer. This provides a voltage range of $9^2/_3$ per cent above and $9^2/_3$ per cent below the E_p and E_q reference voltage in 1/3-per cent steps. Where greater range than the $\pm 9^2/_3$ per cent is required there are separate boost or buck coils on the main transformer. These are connected to jacks located at the ends of the instrument section. Experience with this board indicates the desirability of reducing the size of the 1/3-per cent steps to about 1/4-per cent steps. This would provide a finer adjustment when the busses are connected by circuits which have very low values for *M* and *N*.

Speed of Operation

Although the operating experience has been brief, it is adequate to indicate that the time required to set up, balance, and record complicated network load flow studies on the resistance type board is quite comparable to that required to make the same studies on the conventional type a-c board.

When the new board was first used the errors in the design showed up, the worst one being in the use of instrument current transformers with too high burden to give accurate bus readings. In December 1949 this condition was corrected, and since that time the studies have been completed at an ever increasing pace, as the operator gained experience. Whereas, at first the time required to balance and record a load flow study ranged from two to ten days, now the time is reduced to several hours for studies of the same complexity. The operator is an intelligent young electrical engineer with a sound basic knowledge of electrical circuit theory but without previous experience in network analysis. Now a second operator is working the board, and in two weeks' time he has become almost as proficient as the first one because of the training given him by the first operator.

As is the case with any load flow study on any type of analyzer or calculator, the greater part of the time is used in deciding what to study and the preparation of the network data necessary to set up the study. After the plugging diagram and circuit constants have been prepared it only requires three to four hours to set up the network and its circuit constants including the check-back to be sure that the plugging is correct.

Figure 3 shows the 1-line diagram and the recorded results of a study typical of those being made on the board. Therefore, the speed of setting up, balancing, and recording referred to previously are for studies of this complexity. For larger problems the time required would be greater and for smaller problems the time would be less.

Computational Check of Network Problem, Figure 3

Referring to Figure 3, the loop circuit formed by the lines between busses 1, 32, and 40 were checked by computation so that a comparison with the readings taken on the a-c board could be shown. The comparison is given in Table I.

A computational check of real and reactive power losses was made for the 57.75-kv portion of the a-c board study recorded in Figure 3, the comparison with indicated board losses is noted below:

1. Computed losses were 15.4 megawatts and 37.7 reactive megavolt amperes.
2. Indicated losses from a-c board study obtained by deducting total of bus loads from total bus inputs was 11 megawatts and 38 reactive megavolt amperes.

Mathematical Basis for Load Flow Measurements on New Board

Assuming the use of a common megavolt-ampere base and a common reference voltage with all values expressed in per cent, the following equations illustrate the mathematical basis for measuring load flow in real and reactive power when using four resistances to simulate an impedance circuit.

With current components (I_p+jI_q) flowing through a circuit of impedance $(R+jX)$ voltage drop components (V_p+jV_q) will exist between the circuit terminals.

Where conductance $G=(R/Z^2)$ and susceptance $B=(X/Z^2)$ then $I_p=(GV_p+BV_q)$ and $I_q=(GV_q-BV_p)$.

If the voltage at one terminal of the circuit is (E_p+jE_q) then the equations for real and reactive power flow in the circuit at this terminal are:

$$P=E_pI_p+E_qI_q=E_p(GV_p+BV_q)+E_q(GV_q-BV_p)$$

$$Q=-E_pI_q+E_qI_p=-E_p(GV_q-BV_p)+E_q(GV_p+BV_q)$$

To convert these equations to the form useful to the resistance type a-c board, let $M=(1/G)$, $N=(1/B)$.

$$P=E_p(V_p/M+V_q/N)+E_q(V_q/M-V_p/N) \quad (1)$$

$$Q=-E_p(V_q/M-V_p/N)+E_q(V_p/M+V_q/N) \quad (2)$$

If a number of circuits are terminated at a common bus then the total real and reactive power flow into the bus as load, or away from the bus as input or generation, will be the algebraic sum of the P flow and the Q flow in all of the circuits and may be expressed as follows:

$$P=E_p(\Sigma V_p/M+\Sigma V_q/N)+E_q(\Sigma V_q/M-\Sigma V_p/N) \quad (3)$$

$$Q=-E_p(\Sigma V_q/M-\Sigma V_p/N)+E_q(\Sigma V_p/M+\Sigma V_q/N) \quad (4)$$

Referring to equation 1 it may be seen that by setting up two M and two N resistors to represent a single impedance circuit and by setting up different values of E_p and E_q at the two terminals of the circuit so represented so that V_p, the difference in level of the E_p values, is impressed across one M and one N resistor, and also so that V_q, the difference in level of the E_q values, is impressed across a second M and a second N resistor, then currents equal to V_p/M, V_p/N, V_q/M, and V_q/N will flow through these resistors. If the currents V_p/M and V_q/N are carried through separate primary windings of a current transformer then a secondary current $(V_p/M+V_q/N)$ is obtained. Likewise if currents V_q/M and V_p/N are carried through separate primary windings of a second current transformer with V_p/N connected for reversed polarity, then a secondary current equal to $(V_q/M-V_p/N)$ is obtained. Now if the secondary current $(V_p/M+V_q/N)$ flows through the current coil of the first element of a 2-element wattmeter, and the voltage E_p at one end of the circuit is connected to the potential coil of this first element the measured product $E_p(V_p/M+V_q/N)$ is obtained. Likewise by using secondary current $(V_q/M-V_p/N)$ and voltage E_q for the second element of the wattmeter the measured product $E_q(V_q/M-V_p/N)$ is obtained. The total resulting torque on the 2-element wattmeter will be the sum of those on the separate elements, and thereby the instrument will solve equation 1 for real power flow in the circuit at the terminal where E_p and E_q are picked up.

Referring to equation 2, it will be seen that the reactive power equation contains the same components of current and voltage as the real power equation 1, but in a different combination for the products. To measure Q on the instrument requires that voltage E_p be transferred and reversed in polarity to connect to the second element, and that voltage E_q be transferred from the second element to the first.

When reading the load or generation at a bus with a number of circuits connected to it the a-c board has a bus push button which is used to pick up and close all of the circuits connected to the bus being read. This causes the V_p/M, V_p/N, V_q/M, and V_q/N currents in the connected circuits to combine algebraically to give $\Sigma V_p/M$, $\Sigma V_p/N$, $\Sigma V_q/M$, and $\Sigma V_q/N$ currents. These go through their respective current transformer primary windings in the manner described for a single circuit measurement. Consequently the 2-element wattmeter may be used to solve equations 3 and 4 for the real and reactive power load or input at the bus being read.

The 2-element wattmeter for measuring real and reactive power flow has a 0–100 scale. A throw-over switch marked "*P-Q*" provides the means of choosing the P or Q reading. Another throw-over switch marked "*In-Out*" provides the means of obtaining a positive reading on the instrument scale and indicates the direction of flow with respect to the bus being read. Using the generally accepted convention, "*In*" indicates flow into the bus and "*Out*" indicates flow out from the bus. When reading a bus, "*P-In*" indicates power load and "*Q-In*" indicates inductive reactive load on the bus. "*P-Out*" and "*Q-Out*" indicate real and reactive power input to the bus from generation.

Table I

Bus No.	Circuit Bus to Bus	A-C Board Readings Power Flow	A-C Board Readings Voltage	Computed Values Power Flow	Computed Values Voltage
1	1–32	54 in, (7) out	60.8/3.10°	54 in, (7) out	60.8/3.10°
1	1–40	2 in, (8) out	60.8/3.10°	2 in, (8) out	60.8/3.10°
32	32–1	55 out, (1) in	61.6/10.26°	55.5 out, (0)	61.75/10.56°
32	32–40	59 out, (1) out	61.6/10.26°	59.6 out, (1.4) out	61.7/10.5°
40	40–1	2 out, (8) in	60.6/3.29°	2 out, (8) in	60.6/3.27°
40	40–32	58 in, (6) out	60.6/3.29°	58 in, (6) out	60.6/3.27°

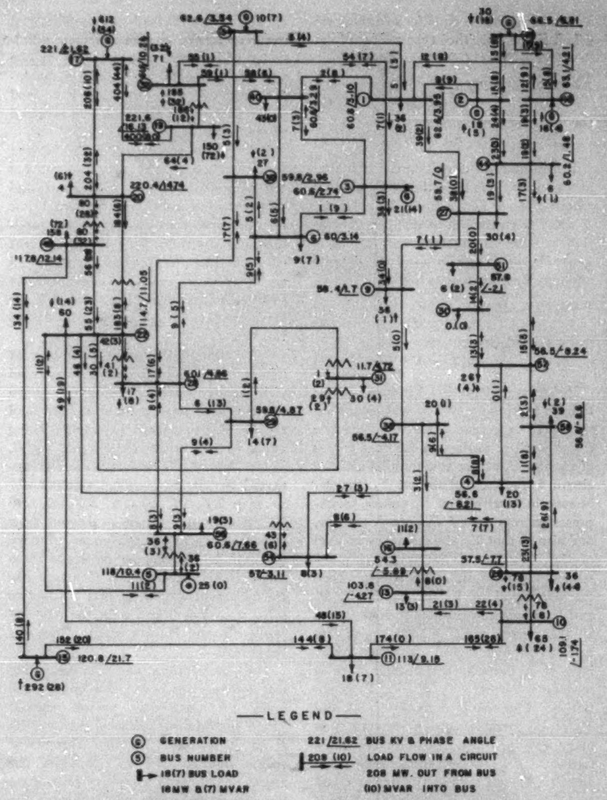

Figure 3. Typical load flow problem solved on new type resistance board

Balancing the Board

After experimenting with the procedure of balancing a load flow study on the a-c board, the quickest method discovered to date is as follows:

1. Starting at points of heavy input to the system either from generating stations or interconnection points, set up the approximate E_p and E_q components which should exist at these busses. Since in the usual transmission circuit or transformer the flow of power will be influenced primarily by difference in E_q voltage level and the flow of reactive will be influenced primarily by the difference in E_p voltage level, go through the network and set up estimated E_p and E_q components at all busses. This means that the E_p and E_q voltages at load busses remote from sources will be at lower voltage levels, and those closer to the source points will be at higher voltage levels.

2. Assuming that little is known about the load flow in the network being studied, usually the voltage at the generating stations is to be held at some particular level. Maintain the voltage at these points and adjust the E_p and E_q voltages at the next adjacent busses until the desired output is obtained from each source. Knowing that circuits set up with large values of M and N will not change their flow much with large changes in voltage level, a mark can be placed through these circuits on the reading diagram and thereby form smaller network subdivisions. Going back to the busses adjacent to the major source, each bus is read and its E_p and E_q voltage adjusted until the loading is approximately correct. This reading and adjusting can be done quickly and after going from bus to bus in the loops of the smaller subdivision an approximation of the loading is obtained in several times around. The same procedure is then followed in the other subdivisions of the network until they all have an approximate balance. Then working the busses in the fringe areas of the subdivisions will bring the entire network into approximate balance. After this has been accomplished it is usually necessary to run through the entire network and make minor adjustments to bring the network loading into a close balance.

It must be emphasized that this type of board is not brought into balance quickly by carefully reasoning out each step in the voltage adjustments. The board can be balanced quickly if the simple procedure of reading and adjusting each bus in turn is followed without hesitation.

After a few studies have been completed on a particular network, even though major changes in connections or loadings are involved, time for balancing may be reduced by first setting up the E_p and E_q voltages of the previous study which is most similar to the new study.

Limitations of A-C Board

As previously noted the present a-c board illustrated by Figures 1 and 2 is designed to make load flow and voltage studies of the type illustrated by Figure 3, but it does not provide for making short circuit or transient stability studies. The limitation was purposely built into the device because the company has a d-c board for short circuit work, and it is expected that both boards would be in almost constant use making their respective types of studies. Also it was believed desirable to use a minimum number of resistors of large wattage in the a-c board so that the base currents would be high enough to actuate a conventional type of wattmeter without amplifying the currents. This was done, but because of it the amount of fixed wiring and the number of plugging panels was much greater than it would have been if individual small rheostats and vacuum tube amplifiers had been used. Since the 1943 paper[1] described how the number of resistors could be kept to a minimum by using the same resistors over and over again in setting up a load flow study, this discussion will not be repeated here.

Another limitation which has shown up in the operation of the board is that of the range of the E_p and E_q voltage plugging board. At the time the design was worked out line and transformer loadings were much lighter and, therefore, the phase angle differences between the voltages at the extreme ends of the system were much less. Under the design conditions the $\pm 9^{3}/_{8}$ per cent range for the E_p and E_q voltages would take care of almost all of the required bus voltage components. It was expected that only a few E_q components would require the use of the buck or boost voltages which are available on the board. Actual experience shows that there are enough E_q voltages requiring more than the $\pm 9^3/_4$ per cent range, that the board would be easier and faster to operate if this range were doubled.

Another limitation which preliminary design computations did not indicate was the fact that 1/3 per cent voltage steps are too large to give a close adjustment on the bus loadings, when the busses are connected together through very low impedance circuits. Therefore, in some cases it is necessary to be satisfied with bus loadings approximating the desired values and make the total load on the several busses closely linked together equal to the total desired. This condition has little effect on the over-all accuracy of the network study, but it would be better if the voltage steps were reduced to 1/4 or 1/5 per cent instead of the 1/3 per cent on this board.

The present board has no provision for inserting buck or boost autotransformers in loop circuits where several transformers in the loop circuit may be set on different ratios. This feature could be added. It is not essential, because the effect of buck or boost is readily available on the present board if two busses are set up to represent one and the voltage components on the two busses are always adjusted together, taking into account the amount of buck or boost desired. This procedure requires the reading of the two busses separately and adding them together to obtain total loading on the bus being simulated. This limitation has not slowed down the operation of the board.

Although it should not be called a limitation, because the design is adequate for the needs, the present board will not set up more than eight circuits on any one bus. If this requirement is exceeded it will call for the use of more than one bus to simulate the larger bus and the separate readings added together to give total bus loading.

An oversight in design, but not a limitation insofar as board operation is concerned, is indicated by the way the component parts were grouped. Both the amount of fixed wiring and the labor of installing could have been reduced greatly if the board had been designed with eight identical circuit units complete with associated relays and plugging panels. In the present board the circuit resistor plugging panels are grouped, the network plugging panels are grouped, and the circuit relays are grouped, which requires a very large amount of inter-cabinet wiring. This could have been eliminated if the unitized design had been used.

Modified Design of Resistance Type A-C Board

The limitations of this first board have been explained and now a discussion of a modified design is presented.

It has been shown that the resistance type board accurately solves the real and reactive power equations for network circuits and bus loadings, providing the proper E_p and E_q voltage components are established at all busses or junction points in the network. If, as in the case of short circuit studies, a source of voltage is set up behind the M and N constants of the synchronous machines, and a single load is placed at the point of fault on the network, the current flow through the M and N resistors will be accurate if the X/R ratio of all circuits is the same. The flow will be only approximate if the X/R ratios are different. Computational checks indicate that in most networks the X/R ratios vary enough so that setting up Z values instead of M and N constants will give more accurate distribution and values of short-circuit megavolt amperes.

The modification required to make the load flow board useful for short-circuit studies is not great. In a new preliminary design the size of the unit would be no larger than the present board. The cost of the component parts would be about the same, but the labor of construction would be reduced.

The principal points of change in the modified design are:

The large wattage resistor units with associated circuit M and N plugging panels would be eliminated and replaced with 25-watt rheostats grouped into four identical sections. These sections would also provide for the associated network plugging. For example, if the design is for 100 load flow circuits, each of the sections would contain 100 rheostats, a total of 400 rheostats. Also if the board design had 60 load flow busses, each section would contain 60 busses, a total of 240 busses. The 400 rheostats and the 240 busses could be used for setting up the sequence networks for short-circuit studies.

Instead of using bus lever switches which function to impress E_p voltage component on one M and one N network and simultaneously impress E_q voltage component on the second M and second N network, bus relays would be used. Two relays are required per bus with one for E_p and the other for E_q voltages. Each bus would be limited to four circuit positions. With the modified design it is possible to group as many busses together as required to set up larger busses and to read them as one bus. Each bus would have one bus push button, which when depressed would pick up the two relays associated with the bus. In addition to the bus push buttons, five additional buttons would provide the selection of total bus reading and the four circuits available at each bus. For short-circuit studies selectivity for reading any one of the 400 circuits is obtained by means of four push buttons and four relays per section, a total of 16 short-circuit push buttons for the board. A double-throw transfer switch would energize the source side of the push buttons and in one position it would be for load flow operation and in the other position it would be for short circuit studies.

The foregoing modification does make the board completely flexible. For load flow studies the operation of the load flow push buttons pick up all of the necessary relays to provide either bus or circuit load flow readings as selected. For short-circuit studies the individual circuits, in each of the four board sections, can be selected and read by operating the short-circuit push buttons.

In the modified design the current capacity of the circuit resistances is reduced. Thus the burden imposed on the circuits by the instrumentation must also be reduced by the use of two vacuum tube amplifiers to produce adequate I_p and I_q currents for the 2-element wattmeter. The wattmeter will serve better than the usual ammeter for short circuit studies because of the uniformity of its scale. Therefore, no changes are contemplated in the instruments other than eliminating the wattmeter used as a voltmeter. Instead use a second wattmeter with an associated *"In-Out"* switch for measuring per cent megavars so that both real and reactive power can be read simultaneously. This change will further speed up balancing the board when making load flow studies.

In connection with instruments, the "load flow"-"short circuit" transfer switch must provide separate contacts to connect E_p and E_q potentials to the P and Q wattmeter elements, when in the "load flow" position. In the "short circuit" position E_q would be disconnected from the P wattmeter and E_p connected to both elements of this instrument. To make the Q wattmeter inactive E_p and E_q would be disconnected from its potential coils.

Modified Design, Voltage Set Up for Short Circuit Studies

Since the procedure would be similar to that used for short-circuit studies on the conventional d-c board only a brief explanation will be given showing how the board voltage can be selected and set up.

The board wattmeter will read per cent megavolt-amperes by solving the equation $E_p(V_p/Z)$ in which $V_p = E_p$ so that per cent megavolt-amperes $= E_p^2/Z$.

As an example assume that the circuit impedance values are set up on a 100-megavolt-ampere base and the maximum range desired is 2,500 megavolt-amperes (2,500 per cent). Therefore, 100 per cent on the wattmeter is to be equal to 2,500 megavolt-amperes. At 100 per cent voltage the equivalent system impedance to the 2,500 per cent fault is $(100)^2/2{,}500 = 4$ per cent. To read 2,500 per cent on the 100 per cent scale of the wattmeter will require a reduction in base voltage to 20 per cent because with this voltage per cent megavolt-ampere $= (20)^2/4 = 100$ per cent.

For line-to-ground faults, if Z_1 and Z_2 are considered set up at one-half value on the rheostats for Z_1 and Z_0 is also set up at one-half value, then with the d-c board and its reading ammeter the voltage would be increased to 1.5 times the base voltage used for 3-phase faults. However, due to the use of a wattmeter the reading increases as the square of the voltage so that on this board if 20 per cent is used for 3-phase faults the board voltage would be increased to $\sqrt{1.5 \times 20} = 24.5$ per cent for line-to-ground faults.

Conclusions

The new type resistance board described in this paper is small, relatively inexpensive, and will solve complex network load flow studies quickly and accurately. These facts are based upon actual operating experience with the resistance type load flow board.

Although the resistance type a-c board now in operation does not have facilities for making short-circuit studies, the writer has devised a design which will make short-circuit studies as well as load flow studies without increasing size or cost.

A-c boards of this type should adequately fill in the wide gap now existing between the d-c boards and the conventional a-c analyzers and calculators. The cost of units of this type should be about that of a mile or two of 60-kv wood pole line. Certainly the advantage of having such a device at hand to quickly and accurately check on planning procedure should pay off its cost in a short time.

References

1. A New Simple Calculator of Load Flow in A-C Networks, Waldo E. Enns. *Electrical Engineering (AIEE Transactions)*, volume 62, December 1943, pages 786–90.

2. Network Analyzer, Waldo E. Enns. United States Patent 2,491,095.

3. Apparatus for A-C Network Analysis, Waldo E. Enns. United States Patent 2,323,588, July 6, 1943.

Discussion

Glenn W. Bills (Bonneville Power Administration, Portland, Oreg.): It is pleasing to read that this a-c board has fulfilled the promise it offered when it was still in the paper stage. Particularly impressive is the comparison of computed values with actual board readings. It indicates that the accuracy of the board is on par with the more expensive standard a-c calculating board.

It would appear that this a-c board would require a greater time for making a plugging diagram, setting up the board and balancing than would the conventional a-c analyzer. However, for utilities that normally study only their own system, this objection is not serious since the system being analyzed would be the same except for gradual changes.

A question that arises concerns the effect the metering had on the values of power being read since direct reading meters are used. Is it better to keep metering simple and possibly introduce slight errors under same conditions or should amplifiers be used in conjunction with meters to give greater accuracy?

Many utilities should find this simple a-c board perfectly fitted to their needs since it can be so constructed as to be suitable for both short-circuit and load-flow studies and will cost but one tenth that of a standard a-c network analyzer.

Waldo E. Enns: The discussion by Glenn W. Bills indicates that he believes that a-c calculating boards of the type described in the paper could provide many utilities with a low cost means of making their own load flow and short circuit studies. The experience that has been gained on this type of board by the Portland General Electric Company engineers substantiates this belief.

In comparing the relative speed of setting up and balancing the resistance type board with the conventional type a-c board, it is necessary to consider several factors. The author believes that the resistance type can be set up as fast, or faster, than the conventional type because there are no load units to connect and adjust, also there are no generators to connect. In the range of network studies which might be classified as relatively simple to moderately complex it is believed that the resistance type requires less man-hours than the conventional type. One reason for this belief is that this board is controlled entirely with one operator at the desk whereas with the conventional type it is usual to have several assistants to make adjustments to loads and generators remote from the desk. For studies of load flow in large and very complex networks with large phase angle differences between various sections of the network there can be little doubt that the conventional type of a-c board can be balanced faster than with this board. However, even in such cases, the man-hour requirements may be quite comparable because of the group of operators required to balance the conventional type. In these very complex studies the operator of the resistance board must be very alert and experienced in its operation in order to obtain a balance comparable in time with that which can be made with the conventional type.

Mr. Bills raises the question as to the use of direct reading instruments as compared to amplifier fed instruments. At this time, the author is not qualified to judge which is the better method. The use of amplifiers would permit the use of smaller resistors or rheostats and would reduce the size of the board but they would increase the maintenance problem somewhat. On the basis of tests made with the present board plus further analysis of the instrumentation problem it has been determined that accuracy quite comparable to that obtainable with high quality amplifier fed instrument could be obtained by elimination of the multiwinding current transformers from the current circuits. To do this, it will be necessary to use a 4-element wattmeter or electrically separate E_p and E_q voltages by the use of two voltage component transformers instead of one. The use of amplifier fed instruments would make it possible to use separate watt and var instruments without having excessive burden and also it would be possible to have a wider range of scales. Both of these features are desirable.

Insulation Co-ordination and a New Line of Oil Insulated Potential Transformers

F. J. VOGEL
FELLOW AIEE

D. R. LAIB
NONMEMBER AIEE

General Considerations

THE development of a new line of potential transformers, featuring lightweight and small space requirements, while incorporating all the necessary operating characteristics, demands the consideration of factors, other than the minimum published standards. The new line, described here, gives considerations given to various features by the designer.

In the design of oil-immersed equipment it is necessary to build in the apparatus the ability to perform over and above the minimum recognized requirements. In the distant past the requirement of a certain voltage test to ground was made. This 1-minute low-frequency test, demonstrated certain insulation strength but told very little about the ability of the design to stand steady stress, impulse disturbance, or ordinary continuous service.

An intensive study was made of insulation assemblies to determine the highest 60-cycle dielectric strength to ground, at the same time obtaining the best impulse characteristics and the ability to withstand steady 60-cycle voltage.

Discussion of Design

In previous papers, the shapes of the impulse voltage characteristics of insulation assemblies have been given. For a given 60-cycle strength some representative values are shown in the curves of Figure 1.

Considering these various curves on Figure 1, curve 3 would give the minimum clearance for a given 60-cycle 1-minute test. This curve applies to some conditions in a transformer, but the arrangements giving results as shown in curves 1 and 5 give the 60-cycle test clearances generally used and are most representative.

Curve 1 in Figure 1 is merely representative and it can have less turn-up for the short times. A study was made so that the best characteristics were obtained. The results of a barrier test, where the tests were made with steep front and full $1^1/_2$-40 waves, and at 60 cycles are shown in Figure 2. Insulation assemblies giving this shape of time lag curve are desirable.

One reason why this type of insulation was considered desirable was because of its ability to withstand steady stress. Figure 3 shows some of the possibilities of insulation assemblies to stand such stress. There are two reasons why insulation may not stand long continued stress. One is because corona is formed adjacent to the insulating materials. Trees result and progress until failure occurs. The other is because heat is formed due to dielectric losses and eventually burns up the insulation. In the construction of curves 1, 2, 3, and 5 of Figure 1, it was assumed that clearances avoiding corona would be used. There is, incidentally, no requirement that such construction be used. Figure 3, then, considers only the case of heat failure. In order to approach the values shown for curves 1, 2, 4, and 5, it is necessary that the space be broken up into ducts, and that no great mass of solid material be used. Heat failure can then be avoided.

Another reason why it is desirable to break the space into ducts, is that in operation the power factor of the oil and material may increase. If the insulation is solid, and the power factor increases, heat failure will result at a lower voltage. If the insulation is broken up into ducts, the increased power factor will have little effect. The shape of curve 3 in Figure 3 indicates why the power factor of cable insulation should be very important. In assemblies having the characteristics shown in curves 1, 2, 4, and 5 of Figure 3, the voltage stress is largely in the oil or oil ducts, and hence the dielectric strength varies very little with temperature, but assemblies similar to that shown by curve 3 would be greatly affected by temperature.

Although it was stated before that Figure 3 had in mind only the case of "heat" failure, it is somewhat similar to that obtained by extreme conditions as affected by corona. The upper curve would be that for no corona present at test voltage. With corona present, failure from treeing would result after different times depending on the voltage. Such failures have occurred a month or so after being in service in spite of meeting specified 60-cycle 1-minute tests.

It is obvious that both the insulation to

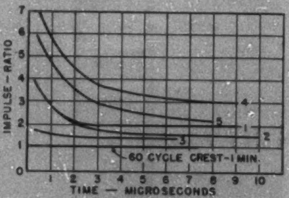

Figure 1. Time lag curves of typical insulation assemblies

1. Square corners well insulated
2. Square corners with no insulation
3. Solid insulation of some types
4. Oil gaps and ducts
5. Square corners with slight insulation

Paper 51-81, recommended by the AIEE Transformers Committee and approved by the AIEE Technical Program Committee for presentation at the AIEE Winter General Meeting, New York, N. Y., January 22–26, 1951 and at the Fall General Meeting, Cleveland, Ohio, October 22–26, 1951. Manuscript submitted October 13, 1950; made available for printing September 4, 1951.

F. J. Vogel is with Allis-Chalmers Manufacturing Company, Milwaukee, Wis., and D. R. Laib is with Allis-Chalmers Manufacturing Company, Pittsburgh, Pa.

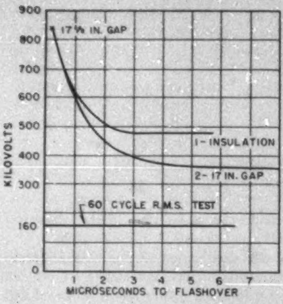

Figure 2. Time lag curve of typical barrier. Comparison of gap and insulation curves

1. Insulation barrier tested with 17½-inch gap
2. Typical time lag curve for 17-inch gap

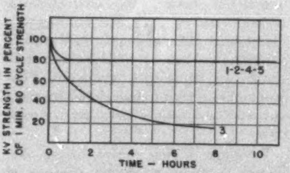

Figure 3. Ability of insulations to stand continuous stress. Curve numbers refer to the same conditions of Figure 1. Curve 3 varies greatly, depending on power factor, temperature and thickness of insulation

ground and the insulation within the windings are nearly independent. It was estimated that the use of four coils would give a very good voltage distribution within the winding. The insulation between layers has characteristics similar to curve 3 of Figure 1, so it was necessary to determine this on the basis of the highest surge voltage to be expected. Referring to curve 1 of Figure 1, if at 1,000 kv per microsecond the impulse ratio of the insulation to ground was four, the insulation between layers as a whole was made to withstand this impulse voltage rather than the 60-cycle or induced 120-cycle voltage. In general, the layer insulation and coil-to-coil clearance are determined in this way. The amount to be gained by reducing this to American Standards Association levels does not appear to be worthwhile, and the coil insulation was made slightly stronger than that to ground, even allowing for the excess stress if the transformer were excited.

With the foregoing general design conditions in mind, tentative dimensions were set up, the windings were calculated, and the ratio and phase angle also were calculated. The design of the coil insulation was made up to provide a maximum of ventilation consistent with minimum dimensions. To assist in this, special formed pieces of insulation were developed and the design made especially rugged mechanically. Figure 4 shows how the formed parts interleave to hold the coils together, and still provide ventilation. Figure 5 shows a typical coil assembly.

Another consideration was the tank and bushing assembly. The tank was made round to fit close to the coil assembly, in order to reduce weight and amount of oil. The porcelains were made to meet the 60-cycle wet and dry tests specified by standards of the American Standards Association and in particular to exceed the full wave standards by an adequate margin. It is extremely undesirable to barely meet this latter if impulse tests are required. Nothing is more frustrating than to try to make full wave tests on transformers and have bushing flashovers.

Four sizes of these units were made—25, 34.5, 46, and 69 kv ratings. Quite comprehensive insulation tests were made on the 34.5 kv and 69 kv ratings, and these results and other performance results follow.

Insulation Test Data

Tests on 69-Kv Unit

According to the American Standards Association rules, these transformers should withstand 140 kv for one minute, 350 kv full wave impulse voltage, and 400 kv chopped wave after three microseconds. Referring to Figure 2, and ratioing the values down, the core and coil structure should then stand 140 kv for one minute, about 420 kv full wave or chopped wave to 3 microseconds duration. Correspondingly, it should also be protected by a 14-inch gap for steep front surges with rates of rise of 1,000 kv per microsecond at about 700 kv.

Actually, the design allowed for a factor of safety for commercial work, and three 60-cycle tests of 165 kv were applied for one minute without any sign of failure. These same units were then given impulse tests at 350 kv full wave, and 400 kv chopped wave, and also steep

Figure 4. Typical coil assembly section

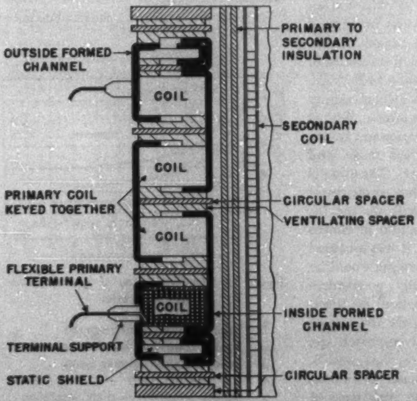
OUTSIDE FORMED CHANNEL
PRIMARY TO SECONDARY INSULATION
COIL
SECONDARY COIL
COIL
PRIMARY COIL KEYED TOGETHER
CIRCULAR SPACER
VENTILATING SPACER
COIL
FLEXIBLE PRIMARY TERMINAL
COIL
INSIDE FORMED CHANNEL
TERMINAL SUPPORT
STATIC SHIELD
CIRCULAR SPACER

Figure 5. Assembled core and coils, 69 kv unit

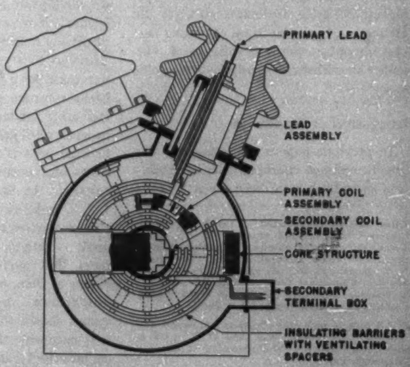
PRIMARY LEAD
LEAD ASSEMBLY
PRIMARY COIL ASSEMBLY
SECONDARY COIL ASSEMBLY
CORE STRUCTURE
SECONDARY TERMINAL BOX
INSULATING BARRIERS WITH VENTILATING SPACERS

front tests at over 700 kv were applied with a rate of rise of 1,000 kv per microsecond or more and a 14-inch rod gap.

One of these transformers then was tested and a time lag curve of the porcelain lead was obtained, for both positive and negative waves. These are shown on Figure 6. It will be seen that the porcelain leads have a satisfactory margin for full waves over the 350 kv value required, and still flash over well below the actual transformer strength.

The unit was then given steep front wave tests using from 14.5 inch up to 19.5-inch rod gaps at voltages up to 867 kv. Twenty-five shots were given at each gap setting to insure that failures due to "deterioration" did not occur.

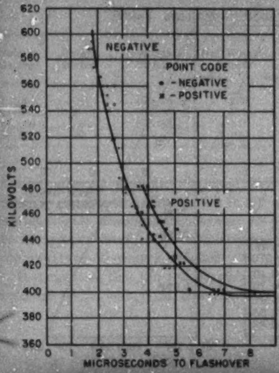

Figure 6 (left). Time lag curve, lead assembly

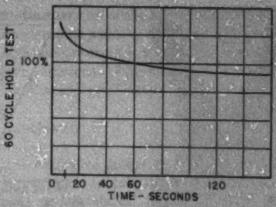

Figure 8 (above). Variation of 60-cycle strength of insulation with time

Figure 7. Typical oscillograms of impulse tests—69-kv unit

Oscillogram 4648—Steep front test with 14½-inch rod gap
Oscillogram 4380—Chopped wave test
Oscillogram 4384—Full wave test
Oscillogram 4650—Steep front test with 20-inch rod gap
Oscillogram 4292—Full wave tests
Oscillogram 4412—Lead flashovers

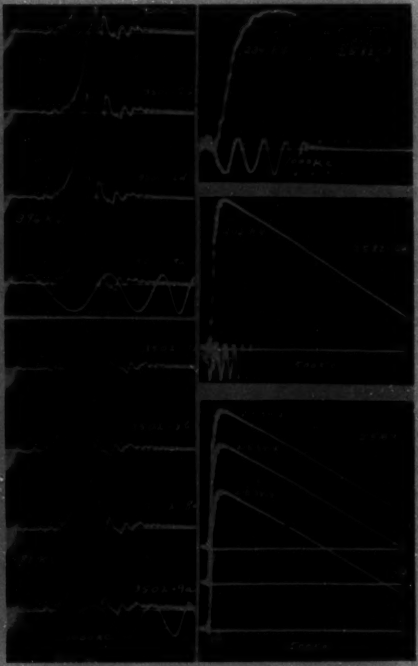

Figure 9. Typical oscillograms of impulse tests—34.5-kv unit

Oscillogram 3501—Steep front test 7-inch rod gap
Oscillogram 2582-3—Chopped wave tests
Oscillogram 2582-6d—Full wave tests
Oscillogram 3502—Steep front test 9-inch rod gap
Oscillogram 2583—Full wave tests

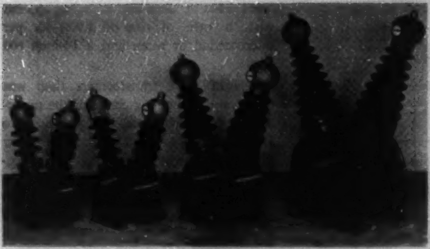

Figure 10. Potential transformers designed for insulation co-ordination. Primary voltage ratings—24,000, 34,500, 46,000, and 69,000

Figure 12 (right). Typical performance of 69,000-115 volt potential transformer for 0.3 accuracy class

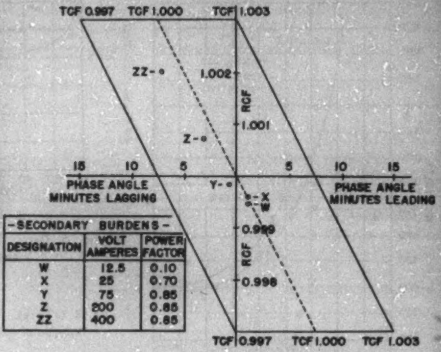

-SECONDARY BURDENS-		
DESIGNATION	VOLT AMPERES	POWER FACTOR
W	12.5	0.10
X	25	0.70
Y	75	0.85
Z	200	0.85
ZZ	400	0.85

Oscillograms taken during the progress of these tests are shown on Figure 7.

If the data on Figure 3 were correct, it should be possible as far as the insulation is concerned to operate it at about 130 kv continuously. Actually, due to the flux density used, it was not possible to exceed 90 kv excited at 60 cycles with one terminal grounded. Operation at 90 kv with one terminal grounded for a period of one month indicates that there was neither deterioration from corona, or from heating at that voltage. Even this, however, indicates that there can be plenty of margin so far as ability to stand steady stress to ground is concerned on a 69-kv line, even with one terminal grounded.

The specified 60-cycle 1-minute hold tests and 10-second wet hold tests for bushings do not exactly apply, since the outlet leads really are a part of the transformer and can not be tested separately. Nevertheless, it has been shown that the time-voltage curve for this type of insulation is about as shown on Figure 8. Consequently, for 10 seconds it should hold about 20 per cent higher voltage than for one minute, or about 195 kv. Therefore, the wet 10-second hold for the porcelain lead could be and was made with the transformer completely assembled, at 145 kv.

Tests on the 34.5-Kv Transformer

The tests on the 34.5-kv transformer were made similarly. The details of the design were similar. The units withstood 90 kv for one minute. Full wave tests were in excess of the 200 kv and 230 kv required as shown by the oscillograms, Figure 9. Steep front tests using 1,000 kv per microsecond fronts were made with gaps up to 9 inches and 486 kv, also shown on Figure 9.

The 34.5-kv unit was excited for two weeks at 50 kv with one terminal grounded, with no sign of distress. In this case the ground terminal was connected to the case through a radio frequency choke, and the voltage across the choke applied to a cathode-ray oscillograph with a high gain to show that no corona existed.

Similarly, wet hold tests at 60 cycles for 10 seconds were made to show that these requirements were met.

Discussion of the Insulation Tests

The tests indicate that the impulse and 1-minute hold tests do not necessarily bear any fixed relation, and that the 60-cycle 1-minute test will not necessarily insure insulation which will withstand continuous voltages. However, it is believed that the structures having properties close to curves 1 and 5 of Figure 1 give reasonably small dimensions, and in addition can be ventilated so that high continuous stresses can be withstood.

Figure 11. End view of transformer before attaching porcelain leads and sealing case

Dry-type units with solid insulation or even oil-insulated units and bushings with solid insulation, may be subject to heating and heat failure, and this must be considered if operation occurs at overvoltage for long times and in high temperatures.

Electrical Characteristics

The ratio and phase angle performance of the line was calculated by well known methods which require no discussion. The performance of these transformers is listed as 0.3W, 0.3X, 0.3Y, and 0.3Z as defined in publication C-57 of the American Standard Association.[1] The output, not exceeding a 55-degree centigrade rise, varies from 3 kva in the 24,000-volt transformer to 6 kva in the 69,000-volt transformer.

Figure 12 illustrates the average performance of transformers of the 69,000-volt class. The best accuracy specified for potential transformers for metering purposes is defined as the 0.3 class. The 69-kv design has performance characteristics well within the limits, even when extended to include a secondary burden of 400-volt amperes.

Mechanical Construction

Figure 10 illustrates four transformers of a line with primary ratings of 24,000, 34,500, 46,000, and 69,000 volts for 60-cycle operation. Figure 11 is an end view of the element and case before final sealing. At this stage of construction the transformer is subjected to a drying process which is continued until an insulation power factor reading of less than 1 per cent is obtained. The end plate is then welded in place and the porcelain leads assembled. A completely sealed unit is obtained by pressure plates bearing

Table I

Voltage Rating	Height, Inches	Floor Space, Inches	Net Weight, Pounds
24,000	37	15×26	252
34,500	39	17×27	310
46,000	49	19×35	615
69,000	61	24×43	1,050

against oilproof gaskets, contained by carefully machined surfaces. Oil is admitted into the transformer under vacuum to the proper level. One magnetically operated type oil gauge is supplied.

It is essential that the transformers be installed on a horizontal base for the proper operation of the oil gauge and to insure equal oil levels in the porcelain leads with pressure changes, caused by temperature variations. Physical dimensions of transformers are shown in Table I.

Conclusion

A method of design and co-ordination of insulation in primary leads, primary coils, and insulation to grounded parts has been described. Test results have been given, proving that the designs are equally able to withstand standard full wave and steep front impulse tests, have ample coil insulation and 60-cycle insulation characteristics. Ventilation of insulation parts is provided and it has been shown by test that the assembly can withstand continuous excitation at 30 per cent over the line voltage to ground.

The core and coils are housed so as to give a light weight assembly occupying small space while developing operating characteristics well within the best metering accuracy specified by present standards.

Reference

1. Transformers, Regulators and Reactors. C57.1, American Standards Association (New York, N. Y.), 1948.

Discussion

R. C. Wentz (Westinghouse Electric Corporation, Sharon, Pa.): The oil-poor type of construction described in Mr. Vogel's and Mr. Laib's paper is not entirely new, as the paper states, but the transformer described in the paper has many new features which indicate a fresh approach to the design problem. The test results indicate that it has produced a satisfactory result.

The Germans pioneered this oil-poor type of design more than 20 years ago presumably because the low material and oil content of this sort of design was particularly attractive to them. It was not particularly attractive to American manufacturers because of its high hand-labor content, but was adopted by one American manufacturer about 1943. Its popularity with operators was astonishing; apparently the small size and weight were particularly attractive to them.

It was because of this popularity that we worked out an oil-poor design which resembled the European design only superficially but actually represented an entirely new approach to the insulation design problem to avoid the high hand labor content.

Now Mr. Vogel and Mr. Laib present what seems to be an even more independently American design, embodying still different approaches to the insulation design problem.

But, as the paper states, the transformer itself is secondary to the insulation theory. The paper makes the point that because of the ventilation of the insulation, it can operate at higher continuous 60-cycle stress.

Mr. Vogel's background of insulation development is probably as extensive as that of any insulation engineer in America, and I should like to ask him if the 60-cycle test was not originally considered to be a test to show, among other things, that heat failure would not occur at normal voltage. Admittedly we now know that it is not always effective, but my impression is that this was part of the original philosophy. Certainly it is true that if the dielectric losses are really high, failure can occur during the 60-cycle test.

Our experience is that if potential transformer insulation is adequately dried and impregnated, the insulation dryness being adequately checked, the measured values of dielectric loss are much too small to produce any cumulative heat failure regardless of whether the insulation is ventilated or not.

The 60-cycle test was also believed to be a check against corona failure; that is, if sufficient corona did not occur at test voltage to cause failure in the short test time, it was hoped that no destructive corona existed at normal voltage. Nowadays we consider that corona should not be perceptible even during impulse tests so that we should hardly be too concerned about corona at normal voltage.

The fact that solid cable insulation worked at stresses much higher than those used in transformers have served successfully for many years confirms the value of solid insulation.

The conclusion which can be drawn from the paper and this discussion is that corona and heat failure are not quite such a problem as the paper would lead us to believe, but it is true that a ventilated construction permits better cooling if this is necessary to the design. We see nothing to necessitate its use in voltage transformers if the insulation used has inherently low power factor and is adequately dried.

Eric T. B. Gross (Illinois Institute of Technology, Chicago): Some of the discussers mentioned that low-oil-content apparatus were introduced in Europe as late as 15 years ago in order to save material, especially oil. Such reasons have been given in the American press repeatedly; but they are, nevertheless, not the real reasons.

Low-oil-content instrument transformers were available commercially in Germany in the early twenties, nearly 30 years ago, and I believe that these types had been developed in Berlin by Dr. George Keinath and his associates.

The real reason for developing low-oil-content apparatus in Europe in the early twenties was the recognition of the fact that oil may lead to fires and that large oil quantities increase greatly the damage resulting from such fires. Oil was available at that time from nearby oil fields at reasonable cost and in unlimited quantities. The need for designs without oil, or with low oil content, was recognized by a number of engineers who had enough foresight to try and change the trend in a direction which is now appreciated all over the world. The results of their systematic planning were the low-oil-content instrument transformers of Keinath, and the air-blast circuit breaker of Biermanns and Ruppel. However, there were no economic reasons involved since oil was cheap and plentiful.

I am certain that Mr. Vogel remembers these early developments, and I am wondering if he would care to comment on the fact that we in this country have started not more than a few years ago to develop these new improved instrument transformers with greatly reduced oil content.

G. Camilli (General Electric Company, Pittsfield, Mass.): It is very gratifying that the trend in design initiated by the General Electric Company is being followed by other manufacturers. In 1943 with our

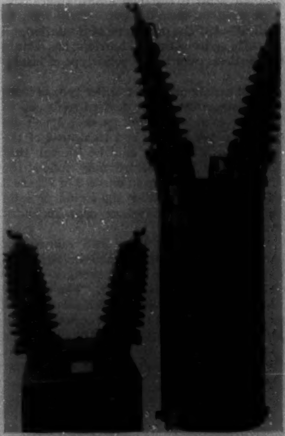

Figure 1. Comparison between new and old General Electric 69-kv potential transformers

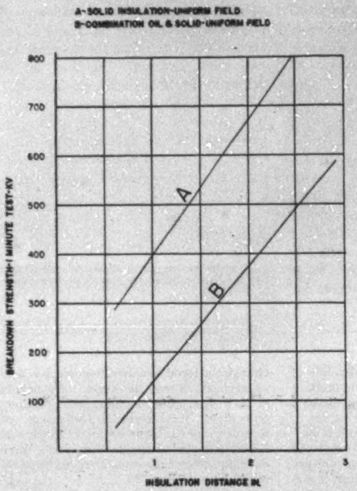

Figure 2. Relative dielectric strength of oil impregnated solid insulation and combined insulation, solid and free oil ducts in series

type *E-236* a new line of potential transformers was introduced[1] in which the arrangement of parts was designed to permit the maximum utilization of insulation copper and iron. These transformers, see Figure 1 of this discussion, have but a fraction of the size and weight of the older designs which followed the design practice of small power transformers. The weights, volumes, and floor space of the transformers described in the paper by Messrs. Vogel and Laib appear to be comparable with those of our early development.

The authors have devoted a good portion of their paper to the type of insulation structure used in their designs. They wish to indicate that the open type of insulation, oil ducts in series with solid barriers, has certain advantages over the all solid type of insulation.

Test arrangements for either type of insulating structure can be devised to fit any of the curves shown in the paper. Much depends on the history and treatment of the insulation. Thus it can be shown that either type of structure may follow the characteristics shown in curve 3 of Figure 3 of their paper if either the liquid or solid has been contaminated or contains moisture.

In 1924 Messrs. Vogel and Montsinger published the results of their investigation on the effect of time on the strength of insulation.[2,3] They found that, "The effect of time on the strength of solid insulation and oil in series is about the same as for solid insulation alone until the oil distance exceeds the solid insulation thickness after which it begins to be the same as for oil without barriers."

For a given spacing and electrode configuration the 1-minute (60-cycle) dielectric strength of solid insulation is much higher than that of an insulating structure of the same total spacing and electrode configuration and in which the spacing is broken up with one or several oil ducts. This is shown in Figure 2 of this discussion which shows the results of tests made on several thicknesses of crepe paper impregnated with Number 10-C oil using round electrodes.

As has been pointed out by Messrs. Vogel and Laib, the results shown in curve 3 of Figure 3 of their paper depend on the power factor, temperature, and thickness of insulation. By the use of carefully controlled materials, modern methods of treating the insulation, and all-welded construction, a very flat power factor temperature curve is obtained and the all-solid type of insulation is electrically stronger than the open-type.

The excellent performance of modern oil-filled paper-insulated high voltage cables demonstrates the validity of these statements.

Instrument transformers in which solid insulation has been used, similar to the type described by Messrs. Vogel and Laib, have been built by the General Electric Company for the past ten years, and their service record has been excellent.

REFERENCES

1. NEW DEVELOPMENTS IN POTENTIAL-TRANSFORMER DESIGN, G. Camilli. *Electrical Engineering (AIEE Transactions)*, volume 62, July, 1943, pages 483–487.

2. EFFECTS OF TIME AND FREQUENCY ON INSULATION TEST OF TRANSFORMERS, V. M. Montsinger. *AIEE Transactions*, volume 43, 1924, pages 337–347.

3. INSULATION TESTS OF TRANSFORMERS AS INFLUENCED BY TIME AND FREQUENCY, F. J. Vogel. *AIEE Transactions*, volume 43, 1924, pages 348–354.

F. J. Vogel, D. R. Laib: It is interesting that both Mr. Wentz and Mr. Gross called attention to the fact that the low oil content transformers were brought out in Europe long before those described by Mr. Camilli. These European designs, as I recollect it, did not seem to us to be sturdy enough for American service then.

At that time impulse testing had not been established and there was no satisfactory standard. In 1940 or thereabouts, the art had progressed to the point in this country where the oil poor design promised to be entirely adequate, and could be proved by test. I believe that is the explanation as to why this type of design was not used earlier.

With respect to Mr. Wentz's question about the origin of the 60-cycle test, I cannot give a complete answer. At the risk of not being entirely accurate, I believe the first equipment built did not meet any specified tests, and of course did not always stand up too well. I believe that the AIEE established the rule of two times plus 1,000 volts for apparatus in general, excluding protective equipment. This applied to rotating equipment and transformers, whether dry type or oil insulated. At that time, the effects of time and temperature were not known. I would think that the 60-cycle test value was chosen in hope that it would provide a margin for all service conditions, switching included, based entirely on judgment. Designers have never designed equipment to meet this test alone or plus a fixed margin, but rather have often times exceeded it to better meet service conditions. This point of view seems to be entirely forgotten now.

Both Mr. Wentz and Mr. Camilli agree that corona and thermal instability are not problems in their designs, but nevertheless the present standards of the American Standards Association caution against operation of potential transformers with displaced neutral, probably unnecessarily for oil insulated units. Also, neither furnish any test data to prove their point.

Mr. Camilli furnishes Figure 2 to indicate the high strength of solid material for 1-minute tests, but does not supply information regarding the relative ability to withstand continuous stress for long periods of time. It is of interest that the voltage stress which can be held for a long time is greatly reduced for solid insulation as can be found in several articles and texts, and is also greatly affected by the power factor. Ventilation greatly reduces the effect of power factor in lowering the long time strength.

The great effect of heat, power factor, and time are well recognized by cable engineers, and their care to keep within the limits imposed by these factors, determined by test, explains their good service records. Transformers, however, are relatively much less affected by these factors because they are better ventilated.

Report on Transformer Magnetizing Current and Its Effect on Relaying and Air Switch Operation

AIEE COMMITTEE REPORT

WHEN the Subcommittee was first suggested it was assigned the task of finding out whether representative values of magnetizing current could be established, for both normal and inrush conditions, and also whether there was any consistent difference between cold-rolled and hot-rolled steel. When the membership of the Subcommittee was being selected the chairman suggested that the work would be of much greater benefit to the industry if the effect of transformer magnetizing current on relaying and air switch operation were also examined.

Accordingly, three working groups were set up within the Subcommittee: one group to study the magnetizing current characteristics of transformers, one group to study its effect on relaying, and one to study its effect on air switch operation. Each group has prepared its report and the three together form the report of the Subcommittee.

Part I. Magnetization Characteristics of Transformers

AIEE Working Group*

The effect of magnetization characteristics of transformers on relaying and air break switches has been a topic of discussion for several years. One difficulty which retarded the establishment of representative magnetization characteristics of transformers was variations of these characteristics that exist between designs of the same rating. A Working Group was established to study this problem and accumulate pertinent data. It was hoped that such a study would result in a group of representative magnetization characteristics, or if such representative characteristics could not be arrived at, findings with reasons for their variations would be made available.

The Working Group has segregated its findings into normal magnetizing current and inrush magnetizing current sections. A third related subject on the calculation of short-circuit currents in transformers when a small portion of the winding becomes short circuited is included in this report.

Normal Magnetizing Current

There is a tendency in transformer design toward the use of cold-rolled core steel. Transformers built of cold-rolled steel show smaller normal magnetizing currents than do comparable units using hot-rolled steel. Since cold-rolled steel is the newer steel, values for cold-rolled steel apply to newer designs; hot-rolled values apply to older and possibly some newer designs.

Representative average values of magnetizing current of single- and 3-phase designs are given in Table I of Part I of this report. These average values have variations for specific designs of from −50 per cent to +90 per cent, with a mean deviation of ±40 per cent of the tabulated values. Specific values for particular transformers should be obtained from the manufacturer.

Inrush Magnetizing Current

REPRESENTATIVE AVERAGE VALUES

Transformers built of cold-rolled steel have larger inrush currents than those built of hot-rolled steel. For interleaved designs, low-voltage inrush current is practically equal to that of the high-voltage, while for the usual concentric design, low-voltage and high-voltage inrush currents are different. Most concentric designs have high-voltage windings outside of the low-voltage windings; hence, a larger air core inductance of the high-voltage winding than of the low-voltage winding. For this reason, most concentric designs have higher inrush currents when excited from the low-voltage winding than when excited from the high-voltage winding.

Representative average values of inrush magnetizing current are given in Table II of Part I. Values in this table are expressed as (crest inrush current)/(crest full load current). Table II applies mostly to concentric designs; values for interleaved designs are approximately equal for high-voltage and low-voltage windings and fall within the ranges of values of Table II.

Table I. Representative Average Values of Normal Magnetizing Current for Single- and 3-Phase Transformers

Kva	Per Cent Exciting Current Cold-Rolled Steel	 Hot-Rolled Steel
500	2.5	2.7
1,000	2.2	2.7
5,000	1.5	2.5
10,000	1.3	2.3
50,000	1.0	1.8

Paper 51-113, recommended by the AIEE Transformer Committee and approved by the AIEE Technical Program Committee for presentation at the AIEE Winter General Meeting, New York, N. Y., January 22–26, 1951 and at the Fall General Meeting, Cleveland, Ohio, October 22–26, 1951. Manuscript submitted November 28, 1950; made available for printing August 29, 1951.

Personnel of the AIEE Subcommittee on Magnetizing Characteristics of Transformers: J. E. Clem, *Chairman;* J. A. Elzi, T. G. Gordy, S. C. Killian, J. H. Kinghorn, A. J. Maslin, W. E. Marter, W. W. Perry, A. H. Powell, R. J. Salsbury, W. C. Sealey, H. T. Seeley, W. K. Sonneman, D. W. Taylor, J. M. Wallace.

* Members of this group are: T. D. Gordy, *Sponsor:* J. H. Kinghorn, A. J. Maslin, R. J. Salsbury, and W. C. Sealey.

Table II. Representative Average Values of Inrush Magnetizing Current for Single- and 3-Phase Transformers

	Crest Inrush Current—Times Crest Full Load Current			
	Cold-Rolled Steel		Hot-Rolled Steel	
Kva	HV	LV	HV	LV
500	11	16	6.0	9.4
1,000	8.4	14	4.8	7.0
5,000	6.0	10	3.9	5.7
10,000	5.0	10	3.2	3.2
50,000	4.5	9	2.5	2.5

These average values have variations for specific designs of from −60 per cent to +100 per cent, with a mean deviation of ±50 per cent. Data given in the tabulation are based upon the following assumptions and conditions:

1. Maximum residual flux exists in the transformer core at the time the transformer is switched on the line.
2. Transformer is switched on a bus having 100 per cent rated voltage maintained.
3. Resistance of transformer winding has negligible effect on the first crest of inrush current.
4. Transformer is switched on to the line at the worst possible point on the voltage wave; that is, at the zero point of the voltage wave.
5. Polarity of the residual flux is such that it is added to the alternating-current flux required by the applied alternating-current voltage.
6. Crest inrush current is expressed as times crest rated load current.
7. No load is on the transformer.

INRUSH CURRENT DECREMENT

It is difficult to isolate the transformer from the system to such an extent that decrement of transformer inrush current can be determined under the conditions for which Table II inrush values are tabulated. As a result, little data on decrement of inrush current is available. From data that are available and to serve as a guide, the decrements shown in Table III of inrush currents may be expected for most conventional designs.

Table III

Kva	Cycles to Reach 50 Per Cent of First Crest Inrush Value
500–1,000	Maximum from 8 to 10 depending upon transformer design
1,667–10,000	Maximum from 10 to 60 depending upon transformer design
10,000–Larger	Maximum from 60 to 3,600 depending upon transformer design

EFFECT OF SYSTEM CONDITIONS ON INRUSH CURRENT

To determine the approximate inrush current considering system impedance, the following procedure may be followed:

1. Determine transformer inrush current, assuming an infinite bus, or with zero reactance in the system. Let this current be I_{inf} and the transformer terminal voltage be V_t.
2. Assume I_{inf} to flow through the system to the transformer and determine the voltage at the transformer terminals. Let this terminal voltage be V_t'.
3. Inrush current taking into account system impedance is then

$$I = I_{\text{inf}}\left(\frac{V_t'}{V_t}\right)$$

If it is desired to determine inrush current for under- or over-excitation, or when load ratio control under- or over-excites the transformer, the relation of step "C" may be used by letting V_t' be the known applied voltage. Voltage V_t' will be smaller than rated voltage V_t for underexcitation, larger than V_t for overexcitation.

Calculation of Short-Circuit Currents in Transformers When A Small Portion of the Winding Becomes Short Circuited

Such short-circuit currents are dependent upon certain conditions in, and characteristics of, the transformer, such as:

1. Type of coil design.
2. Ratio of number of turns shorted to number of turns in the winding.
3. Location of shorted turns in the winding; that is, in one end, in the stack center, in one group or section, et cetera.
4. Effective reactance limiting current in the shorted section.

For many transformers, the fault current in the supply line due to a single turn fault in the winding will be less than 10 per cent of full load current, and will seldom exceed full load current.

Conclusions

Magnetization characteristics of transformers vary over wide ranges for a given transformer rating, and vary with the rating of the transformer. These variations are caused by differences in design and steels used in the core. Representative average values together with their variations have been obtained. Variations from the average are so large that if magnetization characteristics of a transformer are of importance, characteristics of that transformer should be obtained from the manufacturer.

Calculations of short-circuit currents in transformers when a small portion of the winding becomes short circuited is a complex problem not having a simple general solution at this time. Calculations can, however, be made using established formulas for self and mutual inductance.[1]

Reference

1. MECHANICAL FORCES IN TRANSFORMERS, J. E. Clem. *AIEE Transactions*, volume 46, 1927, pages 577–80.

Part II. Relaying Problems Associated with Excitation Current of Transformers

AIEE Working Group*

Nature of Problem

Normal magnetizing current of transformers is far below the pickup current of transformer protective relays and therefore presents no problems in their application. Inrush magnetizing current, however, may be well above pickup of overcurrent and differential relays. Overcurrent relays are normally of the time-delay type and the time-delay setting required to provide selectivity with other overcurrent protective equipment is almost always well in excess of the duration of the magnetizing inrush current. The principal problem therefore lies in the effect of inrush magnetizing current on differential relays.

Transformer differential protection is based on the principle that the vector sum of the ampere turns in the various windings must equal the magnetizing ampere turns of the transformer. The steady state magnetizing current of a transformer is such a small percentage of its full load rating as to be neglected and for practical purposes the vector sum of the ampere turns is considered to be zero. Differential relays measure the current in the various transformer windings and, with due regard to the turn ratio of the windings, use the vector sum, or differential current, to furnish operating torque for the relay. Any transformer short circuit will produce a torque in the operating direction, the magnitude of which will depend on the nature of the short circuit and its location in the transformer.

---

* Members of this group are: J. H. Kinghorn, T. D. Gordy, J. A. Elzi, W. E. Marter, H. T. Seeley, and W. J. Sonneman.

There are two general types of relays employed. The first is the earlier simple induction overcurrent type which is operated by the differential current of the transformer bank. This type of relay is readily adjustable in pickup and operating time. The second is the percentage unbalance type which also is operated by the differential current, but has additional restraining windings operated by the current in the individual transformer windings. This type is usually adjustable to a limited extent as to pickup and operating time and can be set more sensitively than the simple overcurrent relay.

The magnetizing inrush current which can occur when a transformer is energized flows only in the winding to which the voltage has been applied and therefore appears as differential current. Its magnitude and duration depend on the total circuit impedance, which includes both the transformer bank and the system, on the point in the voltage wave at which the circuit is energized, and on the magnitude and polarity of the residual magnetism in the transformer iron.[1]

Transformer design has changed over the years, taking advantage of improved materials and methods. This has unfortunately brought with it increases in magnetizing inrush current in many cases. Modern transformers may have crest inrush current from five to 16 times normal crest full load current while the older designs seldom exceeded eight times full load when energized from a system of negligible impedance. Current of this magnitude is far above the pickup normally employed for differential relays and will therefore cause them to operate if it exists for a sufficient length of time. The time constant of the inrush may be as much as ten times as great for the second as for the first of a pair of transformers switched in successively at a substation fed through a line with appreciable resistance.[2] Also the d-c voltage drop in the line causes a considerable inrush in the running transformer when the incoming is switched in.

There are a number of methods employed for avoiding false tripping which will be described briefly together with their advantages and disadvantages.

Relays with Inverse Time Characteristics

Probably the most common practice in the past has been to increase the relay operating time or pickup or a combination of both so as to make the total operating time exceed the duration of the magnetizing inrush. Obviously the pickup cannot be raised as high as the maximum value of the inrush current and still retain a reasonable degree of sensitivity for detecting transformer short circuits, and the inverse time characteristics of the relay must be depended upon to provide sufficient delay to prevent tripping. For simple inverse time overcurrent relays considerations of unbalance current which exists during external short circuits usually determine relay pickup and time settings which are adequate to prevent tripping by magnetizing inrush.

For percentage unbalance relays this is not the case since external short circuits produce a restraining force ample to overcome any operating torque normally encountered even with fairly sensitive settings. Normally such relays have a pickup of 40 to 80 per cent of bank full load current and with an operating time of 0.1 to 0.2 seconds at ten times pickup do not give false tripping on energizing. There is some indication that the wave shape of the inrush current alters the relay characteristics in a direction to reduce the danger of false tripping but there is no data available at present for evaluating this effect. When unusual cases are encountered where inrush current is higher, the pickup is sometimes doubled and the time increased a few cycles.

Such settings are usually determined by trial since data for calculating magnitude and duration of inrush current and for correlating with relay characteristics is seldom available. They mean decreased sensitivity and increased operating time on actual short circuits, both of which lessen the value of the protection. If still higher current is encountered on newer transformers further increase in time setting appears to be more effective than any except rather large increase in pickup.

Some Relays Using Characteristic Wave Shape of Inrush

A percentage unbalance relay has been developed which takes advantage of the high content of harmonics in magnetizing inrush.[3] The harmonics are filtered out and passed through an additional restraining coil. The restraining force so obtained is adjusted to have a higher value than the operating force for the percentage of harmonics normally encountered. To make sure that it will not be improperly restrained by harmonics which might occur due to current transformer saturation during a very severe transformer short circuit an instantaneous element without any restraining windings is included in the turned operating circuit which has a pickup above the maximum magnetizing inrush which can occur. This relay can be set sensitively in pickup and short in time. It could conceivably be slow in operating on a low current fault existing when the bank is energized since there might not be enough operating torque until the harmonics in the inrush had diminished but for all other conditions it provides fast and sensitive protection.

A characteristic of inrush current is that the half waves of current are much greater on one side of the zero line than on the other. A percentage unbalance relay has been developed the contacts of which vibrate with these alternate half cycles but remain continuously closed with normal symmetrical current.[4] The contacts operate an auxiliary relay with sufficient time delay to prevent operation during the vibrating action. The relay can be set about as sensitively as the percentage unbalance relays previously described and has an operating time of 0.1 to 0.15 second. It is delayed in operating when the fault current contains enough direct current to produce vibrating action. The delay in this case will usually be short since the direct current need delay only enough to produce half cycles of current equal to the relay sensitivity to produce tripping.

Another relay which takes advantage of the characteristic offset of inrush current uses two polarized elements in the differential circuit operating on opposite halves of the current wave.[5] Both elements must be picked up to produce tripping. The relay trips in about one cycle on symmetrical short circuits but is delayed in action with a completely offset short circuit current. It has a pickup of about 40 per cent of transformer bank full load current. Since the relay is not of the percentage unbalance type, current transformer ratios must be matched closely to prevent incorrect operation during through short circuits. To avoid incorrect action due to saturation of current transformers during magnetizing inrush it is desensitized approximately two cycles after the transformer is energized to about double its sensitive pickup setting. Short circuits existing when a transformer is energized are thus tripped in one cycle with the sensitive setting provided they are not completely offset. If not tripped in two cycles the pickup is doubled and a correspondingly longer time is required for sufficient current to develop in both halves of the cycle to produce tripping.

Special Current Transformer Connections

Differential protection of individual windings can be accomplished by locating current transformers at each end of the winding and connecting them differentially. This eliminates the effect of magnetizing inrush entirely and the relay can be set sensitively and fast. It requires more relays and current transformers for the complete protection of a transformer bank than is the case with the more conventional arrangements. It is not readily applicable to 3-phase transformers and cannot be made to include bushings and connected leads on delta-connected windings. It will not detect short circuited turns or winding sections, which constitute a majority of faults described in a recent report.[6]

A modification of individual winding protection is sometimes used with Y-grounded connected windings by adding the 3-phase currents and balancing them against a single current transformer in the connection from neutral to ground. This also is immune to the effect of magnetizing inrush but will be affected by current transformer inaccuracy on phase-to-phase faults. It requires only a single relay for a 3-phase winding. It will not detect short-circuited turns or short circuits between phases.

Desensitizing Methods

Various methods of desensitizing percentage unbalance relays or making the tripping circuit inoperative have been employed. Some are based on the assumption that transformer short circuits produce a greater voltage dip than magnetizing inrush and employ voltage relays connected to the transformer leads or to the energizing source to determine the conditions.

One of these, which operate on the trip circuit, permits direct tripping whenever the voltage relay is dropped out and starts a timer which completes the trip circuit through the differential relay contacts after a time delay when the voltage relay picks up. Thus on energizing a sound transformer the voltage relay picks up and the timer allows enough time to permit the magnetizing inrush to disappear and the differential contacts to reset before completing the trip circuit. If the transformer is faulty the voltage relay does not pick up and tripping is immediate. If the fault is a low current one the voltage relay may pick up anyhow and tripping is delayed until the timer has operated. The differential relay can be set sensitively in pickup and short in time and for all other conditions will provide fast and sensitive protection.

Another control arrangement uses a time delay voltage relay to desensitize the differential relay. When de-energized it connects a resistance shunt across one restraining coil and the operating coil of the differential relay. On energizing the bank this shunt circuit is opened after a time delay sufficiently long to permit the magnetizing inrush to disappear. The resistance shunt is usually adjusted to increase the pickup to two or three times its normal value. Since this still may be below possible magnetizing inrush the differential relay must be one with inverse time characteristics to prevent incorrect tripping, having an operating time in the order of 0.1 second at ten times pickup. If a low current fault occurs when the bank is energized, tripping will be delayed for the time setting of the voltage relay. Higher short-circuit currents will cause operation even in the desensitized condition although perhaps not quite as fast as when the relay pickup is normal because of its inverse time characteristics. If this arrangement is to protect against false tripping due to voltage recovery after clearance of a fault, it must also be controlled by voltage relays on each of the three phases. In this case the voltage relay dropout value must be such that it will not desensitize the differential relay for short circuit currents below the desensitized pickup but will still handle the recovery inrush. When making settings of the desensitizing shunt all parallel banks should be in service, and the bank under test should be unloaded.

Voltage-operated desensitizing arrangements on the running transformer will not respond when another transformer is switched in, so special settings or connections may be necessary in order to avoid false tripping, whenever the d-c voltage drop is large enough to cause difficulty otherwise. Under such circumstances types of relays that do not need voltage operated desensitizing equipment are free from this limitation.

Pressure Sensitive Relays

These relays[6,7,8] are operated by a pressure wave and are so located in the transformer as to detect transformer faults. Since they do not measure electrical quantities they are unaffected by magnetizing inrush so long as it does not produce pressure waves through vibration. They will detect short circuits between turns and from turns to ground equally well but cannot detect transformer bushing faults which are external to the tank. No data is available to correlate the magnitude of current and generated pressure during a short circuit and the sensitivity cannot be stated in electrical terms. Since pressure change is transmitted almost instantaneously the relay is fast in operation. The pressure setting must be sufficiently high to avoid false operation either from shocks caused by through short circuits and external vibrations or from static pressure changes caused by temperature change. At the same time it must not be so high as to be rendered ineffective by pressure relief devices on the transformer.

Conclusion

Differential relays can be desensitized permanently so that they will not operate on magnetizing inrush but only at the sacrifice of sensitive protection. They can be desensitized only during the existence of magnetizing inrush by either employing auxiliary devices or the characteristic harmonic or offset of the inrush current wave. This sacrifices sensitive protection only when energizing the bank. There is no information available by which inrush characteristics and relay characteristics can be correlated to determine the degree of desensitizing required and settings are therefore determined by trial. Availability of pressure sensitive and gas detector relays makes the magnetizing inrush problem less critical because they provide sensitive protection for low current faults and so permit desensitizing the differential relays.

References

1. Transformer Magnetizing Inrush Currents and Influence on System Operation, **L. F. Blume, G. Camille, S. B. Farnham, H. A. Peterson.** *AIEE Transactions*, volume 63, 1944, pages 366-74.

2. Prolonged Inrush Currents with Parallel Transformers Affect Differential Relaying, **C. D. Hayward.** *AIEE Transactions*, volume 60, 1941, pages 1096–1101.

3. Harmonic-Current-Restrained Relays for Transformer Differential Protection, **C. D. Hayward.** *AIEE Transactions*, volume 60, 1941, pages 377–82.

4. Enhanced Transformer Protection Through Inrush-Proof Ratio Differential, **G. Bertola.** *Brown Boveri Review* (Baden, Switzerland), volume 32, 1945, pages 129–33.

5. Rectifier Relay for Transformer Protection, **E. L. Michelson.** *Electrical Engineering* (*AIEE Transactions*), volume 64, May 1945, pages 252–54.

6. Typical Transformer Faults and Gas Detector Relay Protection, **J. T. Madill.** *AIEE Transactions*, volume 66, 1947, pages 1052–60.

7. Relay Protection of Power Transformers. **AIEE Committee Report.** *AIEE Transactions*, volume 66, 1947, pages 911–16.

8. Report of Subcommittee on Gas Detector Relays. Canadian Electrical Association (Montreal, Canada), December 26, 1946.

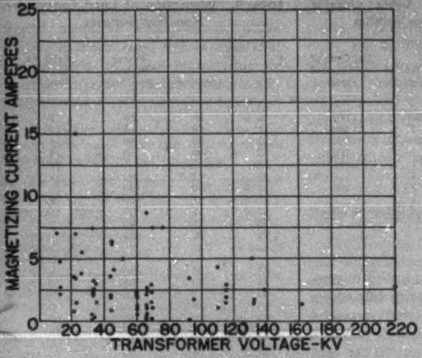

Figure 1. Interruption of transformer magnetizing current by horn gap switch—all operations successful

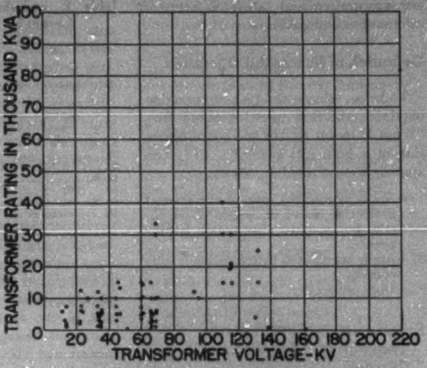

Figure 2. Interruption of transformer magnetizing current by horn gap switch—all operations successful

Part III. Survey of Air Switch Practice

AIEE Working Group*

The interrupting ability of horn gap switches has long been a subject of discussion. Although no ratings have been assigned by any standardizing organization it has been widely recognized that horn gap switches are able to interrupt small currents. Since there are many variables involved in the use of these switches it has been impossible to find any basic approach which would permit the assignment of interrupting ratings. However, they are widely used for the disconnection of power transformers, isolation of circuits and cables, and the interruption of small load currents.

In 1948 the Technical Committee on Transformers appointed a Subcommittee to study the effect of magnetization characteristics of transformers on various operating problems. One of these was the problem of the use of air switches to interrupt the magnetizing current of the transformer. A Working Group, designated to study this problem, decided that the only practical approach would be a survey of present-day practice. From the survey it was hoped that conclusions could be drawn.

The Working Group prepared a questionnaire which was sent to approximately 250 utilities in April 1949. Fifty-nine replies were received and the results

---

*Members of this group are: J. M. Wallace, *Sponsor;* S. C. Killian, W. W. Perry, A. H. Powell, R. J. Salsbury, and D. W. Taylor.

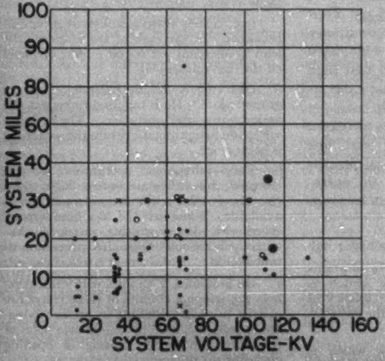

Figure 3. Interruption of overhead line charging current by horn gap switch

•—signifies 100 per cent successful operation
○—signifies 90 to 99 per cent successful operation
×—signifies 75 to 80 per cent successful operation
⊙—signifies 50 per cent successful operation

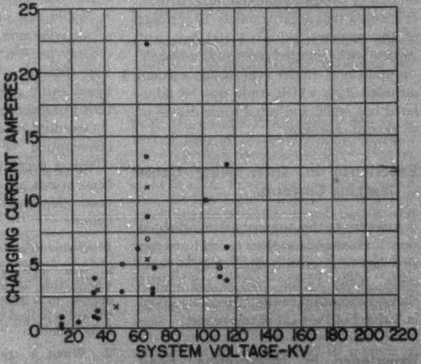

Figure 4. Interruption of overhead line charging current by horn gap switch

•—signifies 100 per cent successful operation
○—signifies 90 to 99 per cent successful operation
×—signifies 75 to 80 per cent successful operation

are summarized and tabulated here for information and guidance.

Definition of Successful Operation

To help evaluate the type of operation obtained, the first question asked was, "What is meant by the successful operation of a horn gap switch?" Fifty-two answers were divided as follows:

13—Arc is interrupted without operation of protective relays or system short circuit, but perhaps after switch is fully opened.

37—Arc is interrupted before switch is fully opened.

2—Does not matter.

Experience in Interrupting Transformer Magnetizing Current

The data in Figures 1 and 2 show experience in interruption of transformer magnetizing currents. All points on the chart represent at least three operations per year. Over 95 per cent of the replies indicated all 100 per cent successful operations. On the basis of these replies, the Working Group concluded that the transformer magnetization characteristics had no observable effect on the ability of the switch to interrupt a given current.

Experience in Interrupting Line Charging Current

Additional data for possible future investigation are given in Figures 3 and 4 which show experience with the interruption of overhead line charging current. It is noted that approximately 70 per cent of the answers indicated 100 per cent success with a limited range of line length. An additional 15 per cent of the answers included data which could not be tabulated but which indicated some degree of successful operation.

Experience in Interrupting Cable Charging Currents

Answers to the questionnaire indicated very limited and cautious use of horn gap switches to interrupt cable charging currents. Only 14 per cent of the replies showed successful results, which are given in Table I of Part III of this report.

Experience in Interrupting Load Currents

Replies to the questionnaire indicated a much wider range of practice and results with the interruption of load currents by horn gap switches. Table II of Part III of this report indicates present-day practice. Approximately 40 per cent of the answers showed successful operations throughout limited range of current and voltage values, 20 per cent showed partial success and 40 per cent no experience.

Table I. Interruption of Cable Charging Currents by Horn Gap Switches

Kv	Amperes	Miles	Total No. of Oper. Per Yr.	Per Cent of Successful Oper.
11	500	3	20	100
13.8	0.99	0.5	2	100
23	1.5	0.5	150	100
33		0.5	1	100
33	0.144	0.045	1	100
34.5		7.1	1	
66	200	5	3	100
66	34	4.8	1	

No experience or not accepted practice—all others.

Circuit Conditions and Comments

Seventeen per cent of the replies indicated that the values in the previous tabulations were the maximum in voltage, current, transformer size, or line length, on the systems reporting, and 76 per cent of the replies stated the values in question were not their maxima.

Data from the questionnaire indicated that 32 per cent of those replying did not use horn gap switches for the maximum conditions of voltage, current, or transformer size, because of adverse experience or poor performance. Sixty eight per cent gave other reasons, the most common one being that power circuit breakers were available and preferably used for interrupting the maximum circuit conditions.

Sixty per cent of the replies indicated that those answering believed that high speed switch operation increased the interrupting ability of the switch.

One-third of those reporting successful interruption of magnetizing and line charging current told of special precautions which are taken during the operation. Representative comments are given below:

1. Switches are not opened in a high wind.

2. We "inch" switches open in locations where this is indicated. The switch is opened to a 2-inch gap and the quality of the arc is judged quickly before the switch is fully opened.

3. When a transformer bank which is normally supplied from the 138-kv transmission system is to be switched out of service, the lower voltage bus (13.8 kv or 45 kv) is tied to an adjacent bus supplied from another transformer. Under these conditions the horizontally mounted 138-kv disconnecting switches are opened followed by the opening of the lower voltage oil circuit breaker. The voltage difference is probably less than 1,000 volts and the current is very small.

Table II. Interruption of Load Currents by Horn Gap Switches

Kv	Amperes	Power Factor, Per Cent	Total No. of Oper. Per Yr.
4.8	75	90	2
11	50	85	15
11	30	80	4
12	100	50	20
13	Up to 200		50
13	32.5	80	3
13.8	200	90	10
13.8	75	70	8
13.8	17	80	80% Successful
22	75	86	2
22	40	85	
22 and 46	20	80	50% Successful (10 oper./year)
23	35	90	1
33	52	85	10
33	15	80	35
33	20	95	0.5
33	10	80	10
33	Up to 80		30
33	8.5	80	3
34.5	10	80	80% Successful
34.5	16.8	85	80% Successful
34.5	70	85	90% Successful (3 oper./year)
34.5	25	85	10
34.5	84	85	4
44	50	90	11
44	50	Good	1.2
44	80	85	20
46	37.7	85	60% Successful
46	12.6	85	80% Successful
50	10	80	12
66	50	70	8
66	Up to 50		5
66	4.4	85	
66	100–150	90	90% Successful
66	60	80	6
66	80	80	4
110	50	Good	1
110	10	80	80% Successful
115	60	90	5

No experience or not accepted practice—all others.

4. (a). Open the switch quickly at the start.

(b). Shield the operator's eyes from a possible arc.

(c). Load is always broken by oil circuit breakers. In the case of transformers the load is disconnected by oil circuit breakers on the low-voltage side.

5. Operator is on an insulated stool or ground plate. He is required to inspect the arcing horns after operation. The reclosers are made nonautomatic while the switching is being done.

6. Very infrequent operations are attempted, but when necessary high speed opening is used when manual operation is available. Some trouble has been experienced with slow operating motor mechanisms. Wind conditions also are an important factor.

7. On grounded Y circuits with neutral relays the tripping circuits of these relays are opened prior to switching to prevent possible operation caused by one or two poles of the horn gap switch closing or opening ahead of the others.

8. We regularly interrupt successfully with air break switches current in an open line to be cleared from the system, by first paralleling a second line with the line to be cleared and reducing the current in the line to be cleared to a minimum value before opening the air break switch.

Over 25 per cent of the replies told of special mounting arrangements, phase spacing, et cetera, used with switches that are intended to open magnetizing or charging current. Typical comments pertaining to this subject are given below:

1. Use wider phase spacing. Generally mount switches so that the arc cannot rise into other conductors or equipment.
2. Increase the spacing and overhead clearance beyond standard—say 25 per cent.
3. Standard spacing for pole installations:
   13.2 kv 44 inches
   33.0 kv 56 inches
4. Vertical break switches are the only type that are opened for the more severe service.
5. Positively ground the operating mechanism and the operating mechanism handle.
6. Phase spacing on 69-kv equipment, 7 feet. Operating mechanism to be a type that will allow the blades to open quickly; not the gear reduction type of mechanism.

Conclusions

From the data compiled it seems apparent that the magnetization characteristics of a transformer have little or no effect upon the ability of a horn gap switch to interrupt the magnetizing current. The Working Group felt that it was not justified in drawing any further conclusions. However, data are herein presented which show present-day use of air switches and should enable system operators to compare individual system procedure with a large number of other systems.

Acknowledgment

The Working Group wishes to acknowledge the assistance of the following companies who answered the questionnaire. In addition there were 11 companies who answered the questionnaire but wished that their names be withheld:

Alabama Power Company
Boston Edison Company
Buffalo Niagara Electric Corporation
California Electric Power Company
Cambridge Electric Light Company
Central New York Power Corporation
Concord Electric Company
Danbury and Bethel Gas and Electric Light Company
Dayton Power and Light Company
Duquesne Light Company
Eastern Kansas Utilities Inc.
Eastern Shore Public Service Company
Exeter and Hampton Electric Company
Fitchburg Gas and Electric Company
Florida Power and Light Company
Georgia Power Company
Iowa-Illinois Gas and Electric Company
Louisiana Power Company
Minnesota Power and Light Company
Montana Power Company
Mountain States Power Company
New Jersey Power and Light Company
New Orleans Public Service Company
New York Power and Light Corporation
New York State Electric and Gas Corporation
Northwestern Public Service Company
Ohio Public Service Company
Orange and Rockland Electric Company
Pacific Power and Light Company
Peoples Gas and Electric Company
Philadelphia Electric Company
Potomac Electric Power Company
Public Service Company of Colorado
Public Service Company of Oklahoma
Rochester Gas and Electric Corporation
Rockland Light and Power Company
Southern California Edison Company
Staten Island Edison Corporation
Superior Water, Light and Power Company
Texas Electric Service Company
Toledo Edison Company
Union Electric Company of Missouri
United States Bureau of Reclamation
Utah Power and Light Company
Westchester Lighting Company

Discussion

Eric T. B. Gross (Illinois Institute of Technology, Chicago, Ill.): It appears that the Subcommittee neglected to take into consideration the very valuable information contained in the paper "Interrupting Ability of Horn Gap Switches," which was presented at the Pasadena Meeting and made available[1] to the membership of the Institute long before this report was submitted. Anyone interested in this phase of the report will find the answer to his questions in a comprehensive paper[1] by Andrews, Janes, and Andersson.

In Part II of the report, which deals with relaying problems, there is a short reference to pressure relays in the section on Pressure Sensitive Relays, but the even more important "gas detector" relays[2] are mentioned only by this same word in the Conclusion of the paper.

It may be worthwhile to repeat some of the recommendations of the relay engineers who summarized in the latest "AIEE Committee Report on Relay Protection of Power Transformers" that:[3]

"The value of gas accumulator relays for detecting incipient faults has been underestimated generally in the United States.

"1. Substantial experience in Canada has demonstrated the value of gas accumulator relays to detect conditions such as turn-to-turn faults, core insulation failures, and defective joints.

"2. Objections commonly raised to the gas accumulator method of detecting faults can be overcome largely by suitable application and proper interpretation of relay indications.

"3. The present commercially developed gas detector relays are limited in application to conservator type transformers. Experimental installations indicate that devices may be developed for extending gas detection principles to other types of transformers."

The magnetizing inrush current necessitates a reduction of sensitivity and/or a complication of differential schemes if false operation is to be prevented. The fact that new solutions to overcome these inherent difficulties of differential schemes have been announced in periodic intervals during the last decade produces an element of doubt as to the effectiveness of these newer and better solutions. It has been stated that none of these solutions is entirely satisfactory.[6]

Since gas and pressure-relays are not influenced by any inrush currents, they seem to indicate a real and ideal solution to this problem. It should be kept in mind, however, that the gas element has been found[4] to be the more valuable component of this type of protection since it indicates faults in their incipient stages, thereby reducing otherwise possible damage and simplifying as well as speeding up repair work.

REFERENCES

1. INTERRUPTING ABILITY OF HORN GAP SWITCHES, F. E. Andrews, L. R. Janes, M. A. Andersson. *AIEE Transactions*, volume 69, 1950, pages 1016–27 and *Electrical Engineering*, volume 70, February 1951, page 136.
2. SIMPLICITY IN TRANSFORMER PROTECTION, Eric T. B. Gross. *Electrical Engineering*, volume 66, 1947, pages 564–69.
3. RELAY PROTECTION OF POWER TRANSFORMERS, AIEE Committee Report. *Electrical Engineering*, volume 66, 1947, pages 964–68 and *AIEE Transactions*, volume 66, 1947, pages 911–17.
4. TYPICAL TRANSFORMER FAULTS AND GAS DETECTOR RELAY PROTECTION, J. T. Madill. *AIEE Transactions*, volume 66, 1947, pages 1052–60.
5. *Discussions* by A. M. Doyle, E. E. George, F. L. Lawton to Reference 3, pages 915–16.
6. *Discussion* by B. C. Hicks of reference 3, page 915.
7. GAS DETECTOR RELAYS, A. L. Hough. *Report*, 57th Annual Convention of the Canadian Electrical Association (Montreal, Canada), Engineering Section, 1947, pages 56–69.

L. R. Janes and **F. E. Andrews** (Public Service Company of Northern Illinois, Chicago, Ill.): This is a discussion of the section on Survey of Air Switch Practice. The statement is made in this section of the report that "it has been impossible to find any basic approach which would permit the assignment of interrupting ratings" which might be applied to horn-gap switches used for interruption of small currents. The committee which prepared this report apparently did not utilize the information in the paper by Andrews, Janes, and Andersson.[1]

In this paper "reach" was used as a measure of the arc spread to provide a criterion for safe operation related to switch clearances. Arc reach was defined as the distance from a point midway between the arc extremities and the most remote point of the arc at the time of its maximum length. Figure 10 was a plot of the test data. It showed a curve representing the limit of probable reach in terms of feet per kilovolt of open switch voltage. Probable reach for currents less than 100 amperes was shown as $0.0165 \times kv \times I$. Figure 16 was a graph showing arc reach for small currents at various line voltages from 12 kv to 132 kv and was applicable to transformer magnetizing currents.

On the last page of the committee report is shown phase spacings of standard air break switches for different voltages. From the formula in our paper,[1] the current may be calculated which will produce a maximum reach equal to the switch clearance. This value should be reduced somewhat to prevent the arc from contacting another part of the switch. Referring to Figure 1 of the report, the magnetizing currents which may be opened for standard switches of the various voltages are lower than those calculated from our formula. Therefore, it is not surprising that the operations were successful.

The report makes reference to interrupting line charging current. Figures 13 and 14 of our paper show the data from 132-kv line charging current tests. It was pointed out in the text that currents of 7 amperes were interrupted with reaches which appeared to be safe for the 16-foot horizontal phase spacing used, and that currents of 10, 13, and 20 amperes also were interrupted with reaches greater than the phase spacing. These interruptions were successful because of favorable oblique wind. It was stated that, because of the trapped charge and stored energy in the capacitive circuit, the voltage used in calculating reach for interrupting line charging current should probably be twice the actual voltage.

The report makes reference to interruption of load currents. Our paper covered this phase of the subject largely from the standpoint of opening a switch in a closed transmission system loop. Such operation depends on the current through the switch before opening and the open switch voltage across the gap after opening. This voltage can usually be obtained by multiplying the current through the switch by the equivalent impedance of the loop opened. Figure 17 of our paper presented a graph applicable to this case.

REFERENCE

1. See reference 1 of preceding discussion.

An Electromechanical A-C Line Voltage Stabilizer

D. M. MURRAY
MEMBER AIEE

N. L. KUSTERS
NONMEMBER AIEE

THERE are several advantages of a controlled autotransformer-type stabilizer[1,2] over the magnetic saturation- and electronic-type stabilizers.[3,4] These include less wave form distortion, less transient error for given load variations and higher efficiency since heavy current is only drawn when there is an error in output voltage. When there is integration in the regulating loop, the over-all accuracy is good and there is no need for voltage or load current compensation. There is, however, one inherent disadvantage to this type of stabilizer or regulator. The slow speed of response due to the inertia of the driving unit has in the past rendered this type unsuitable for instrumentation or electronic applications, since step changes in input voltage still affected the equipment.

This paper describes an electromechanical stabilizer having a fast recovery time that compares favorably with some of the commercial electronic stabilizers.

In attaining this feature two points of design received special attention: the choice or a low inertia driving unit that could be easily controlled and, the development of a control circuit that would produce the best response.

Driving Unit

A d-c driving motor was chosen for this application because of its versatility in control circuits and its good torque characteristics. The disadvantages of gears and commutators were overcome by using a 270-degree type of meter movement especially adapted as the driving motor. The allowable rotation of the motor corresponds to that of the brush arm on the toroidal-type variable autotransformer. This type of movement can be designed for very low inertia since it needs no moving iron in the armature.

Figure 1 shows the magnetic circuit of this driving unit. The flux density in the air gap is low compared to other d-c machines because of the long air gap and the narrow cross section of iron feeding the flux to the center field pole. This flux can be increased only at the loss of range of rotation for the armature and corresponding increase in the width of iron in the outer loop of magnetic circuit.

The inertia of the armature was kept to a minimum by dipping and baking the coil so that no form was needed to support the armature when assembled. Other design details of the driving unit were directed at convenience of assembly and compactness as shown in Figure 2.

The size of the unit was arrived at arbitrarily since there are several factors to be considered. Most of the load is brush friction in the autotransformer and since there is considerable static friction, the load characteristic with speed is not linear. Therefore in order to get the best performance, the rated torque is considerably in excess of the maximum friction torque value. The static friction can be minimized, however, by an alternating signal large enough to keep the brush vibrating slightly, but the rating of the armature has to be great enough to absorb this steady power. This power is about twice that required to overcome the static friction.

Another consideration from the development point of view is that in synthesizing the control circuit, it was necessary to take the frequency response characteristic to check the transfer function. In order to get an amplitude large enough to give a good frequency response curve it is necessary to draw considerable power. For these reasons a design value of rated torque was chosen equal to ten times friction torque which was satisfactory from all considerations. A practical operating value, however, would be about five times the friction torque. Also regarding the physical size of the unit, considerable reduction in the amount of iron could be obtained by using laminated steel which would operate with twice the flux density.

Control Circuit

The necessary components of the control circuit are: detector, phase inverter, and driving circuit. With this general arrangement it is necessary to have high enough sensitivity to overcome static friction for errors of 0.1 volt on the line. It also is necessary to have good stability. Stability considerations were taken up after the components of the main block diagram were chosen and a transfer function obtained from each.

One of the better detectors of a-c line voltage variations is the temperature-limited diode used in a bridge circuit. It has very high gain and may be considered linear over a fairly wide range. The characteristic of one such tube, Sorensen *2AS15*, is indicated in Figure 3. The bridge circuit is shown in Figure 4. The transfer function of this block is

$$\frac{\text{D-c volts}}{\text{Line voltage}}=\frac{14}{(0.04S+1)}$$

One difficulty with the diode detector is the large second harmonic ripple voltage in the output. This ripple is too large to be handled by the succeeding amplifiers and therefore has to be reduced, preferably without increasing the time

---

Paper 51-271, recommended by the AIEE Feedback Control Systems Committee and approved by the AIEE Technical Program Committee for presentation at the AIEE Summer General Meeting, Toronto, Ont., Canada, June 25–29, 1951 and at the Fall General Meeting, Cleveland, Ohio, October 22–26, 1951. Manuscript submitted October 27, 1950; made available for printing September 5, 1951.

D. M. MURRAY and N. L. KUSTERS are with the National Research Council, Ottawa, Canada.

The driving motor shown in Figure 2 of this paper was designed by A. R. Morse of the National Research Council.

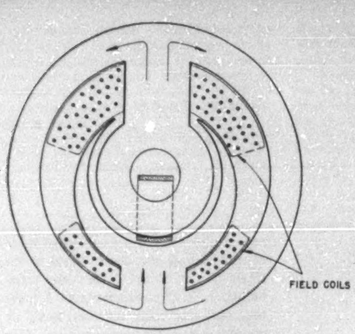

Figure 1. Magnetic circuit of driving unit

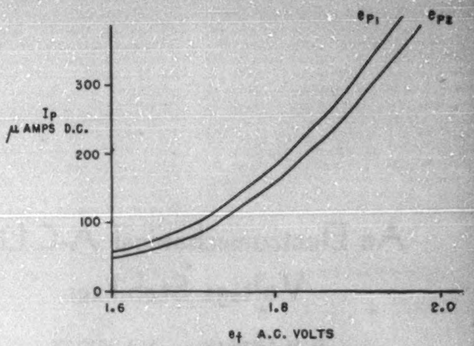

Figure 3. Characteristic of diode detector

constant of the combination. This is accomplished by introducing a voltage from the power supply rectifier output in an appropriate part of the detector bridge in such a way that the ripple was reduced to the fourth harmonic at 5 per cent of the previous amplitude. The bucking voltage was obtained without using a tube and the transfer function was not affected.

With a d-c output voltage from the detector circuit, the simplest control of the thyratrons is the d-c control voltage with fixed a-c bias. Since two thyratrons have to be controlled, it is necessary to have the d-c control voltage increasing on the grid of one thyratron and decreasing at the same time on the other. Thus some form of phase inversion is necessary after the detector stage and since the thyratrons both must use the same d-c reference level on their cathodes, separate plate windings are necessary.

These requirements led to the adoption of a circuit similar to that of J. P. Rogers.[5]

A cathode coupled phase inverter[4] was used with the input taken directly from the detector bridge. The thyratron grids were fed from each inverter plate respectively and the thyratron bias level was set by a voltage divider across the plate supply. The gain in the phase inverter using a *6SN7* tube was six. The phase inverter and thyratron circuit are shown in Figure 5.

In the case of the thyratron circuit, the thyratron grid return circuit was made through the center tap of a resistor across the armature. The fixed a-c bias on the thyratrons was introduced in series with the d-c bias by means of a phase shift circuit and transformer coupling. There is no interference in the control due to the plate voltage on the opposite thyratron since each thyratron only fires on alternate half cycles and in this application the steady state condition is such that the firing angle of each thyratron is only 10 degrees or so. However, with inductive load such as the armature used here and with only one thyratron firing, the voltage across the armature becomes negative and the time constant is such that there

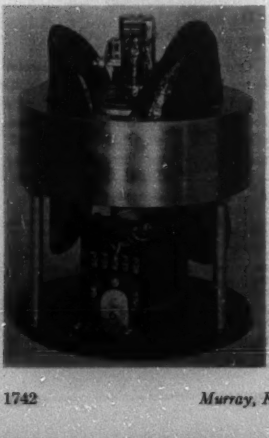

Figure 2 (left). Driving unit

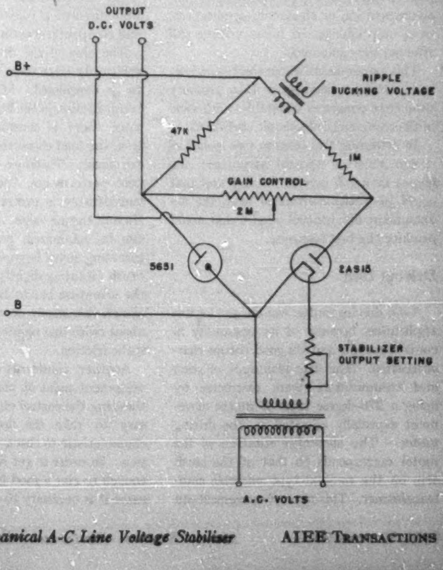

Figure 4 (right). Detector bridge circuit

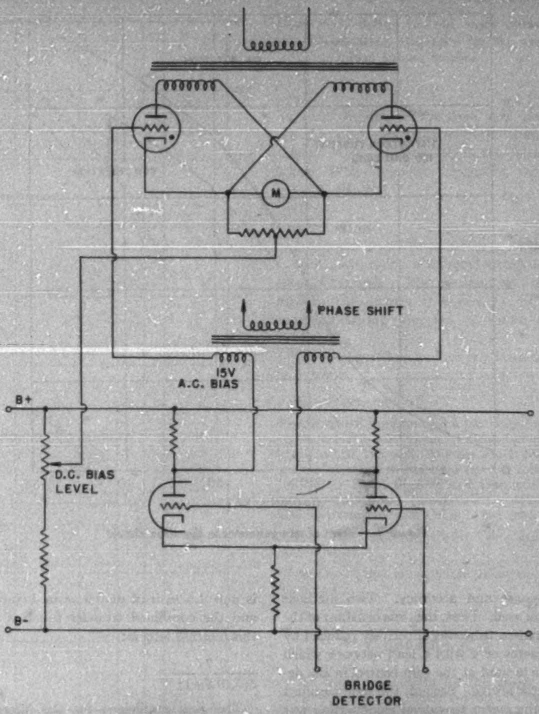

Figure 5. Phase inverter and thyratron circuits

is still an appreciable negative voltage at the start of the next firing cycle.[7] This negative portion is, in effect, positive feedback, which results in erratic behavior around the null. This is overcome by using rectifiers at the cathode of each thyratron which clip the negative voltage and keep this effect out of the thyratron grid circuit.

Another effect which occurs in the thyratron circuit is the negative feedback due to the back electromotive force of the motor. This back electromotive force is halved and applied to the thyratron grid circuit. The effect of the back electromotive force of the motor with respect to the thyratron plate voltage is negligible compared to the feedback in the grid circuit. The block diagram and transfer function of this feedback loop are shown in Figure 6. The basis for the motor transfer function is given in Appendix I.

The regulator loop is closed by the variable autotransformer and series transformer. The combination gives a ratio of 4 volts alternating current per radian of rotation.

Accuracy and Stability

It now is possible from the description of the main components to construct the complete block diagram and transfer function of the regulator so this will be considered for accuracy and stability conditions. The complete transfer function is

$$KG=\frac{14}{(1+0.04S)}\times K_e\times 6\times \frac{1}{S}\,\frac{1.67}{(0.023S+1)}\times 4 \quad (1)$$

A synthesis[8] of this transfer function to find the gain and resonant frequency for normal stability gave these results:

$M_p=1.5$
$K_v=20$
$\omega_R=16$ radians per second
Speed of response ≈ 0.7 second

The speed of response is much slower than the 0.1 second desired. Another point to be considered from these results is whether the velocity constant necessary for stability is high enough to give the required accuracy. The maximum possible accuracy of the regulator is the variation in output voltage for a brush movement of one wire on the variable autotransformer. Neglecting commutation by the brush, the accuracy is 0.08 volt for this regulator. Considering the brush friction and the motor constants, the stiffness of the control circuit to achieve the maximum sensitivity is 0.31 ampere per line volt in the armature of the motor. See Appendix II for constants and calculations. With the velocity constant of $K_v=20$ the gain setting K_e equation 1 is 0.035. To obtain the desired accuracy the setting of K_e should be 0.24.

The preceding results show that the transfer function would have to be altered considerably in order to give the required

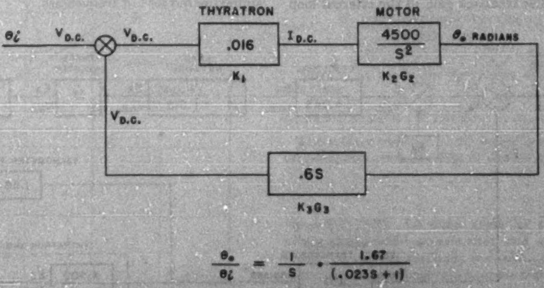

Figure 6. Block diagram and transfer function of motor loop

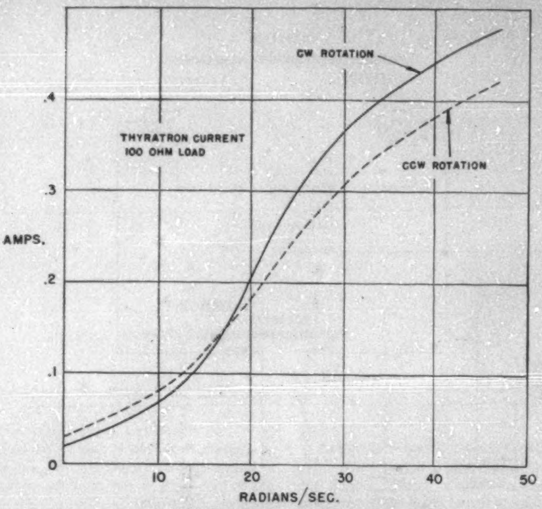

Figure 7. Effect of rate generator in thyratron circuit

response and accuracy. Two methods were used. First, the time constant of the Sorensen tube was effectively reduced by a factor of 4 with a lead network which was located at the gain control in the detector bridge. Second, the time constant of the motor thyratron combination was reduced by velocity feedback from a rate generator attached to the motor shaft. The feedback voltage after amplification was coupled in proper phase with the other a-c voltages on the thyratrons. The effect of the rate generator on the thyratron circuit is shown in Figure 7. This characteristic is not very linear but the approximate slope was used for calculations.

The feedback gain of the internal loop is now 1.5 instead of 0.6 as in Figure 6 and the combined transfer function for this internal loop is:

$$\frac{0.7}{S(0.01S+1)}$$

The gain coefficient for the internal loop was reduced by the additional feedback and this, combined with the attenuation in the lead network, made it necessary to go to a higher gain tube in the phase inverter. Due to the lead network there was an increase in noise level from the detector circuit. Since most of this noise consisted of 240 cycles, a parallel-T filter was used to eliminate it. The transfer function for the filter was approximated for low frequencies.

The complete block diagram of the regulator is shown in Figure 8. A reference block E_r has been shown to indicate that the control circuit produces a correction only when there is an error E between the output voltage E_o and the reference voltage. The correction to E_o is accomplished by the variation of voltage E_s in the series buck boost transformer output E_s.

The open loop transfer function is as follows:

$$KG(S)=\frac{E_s}{E}=\frac{14}{1+0.04S}\times\frac{1}{14}\times\frac{1+0.04S}{1+0.01S}\times 21\times\frac{1}{1+0.003S}\times\frac{0.7}{S(1+0.01S)}\times 4$$

The closed loop operation was calculated using log modulus and phase curves[3] with the following results:

$M_p=1.5$
$K_v=50$
$\omega_R=47$

The experimental results were obtained with the gain set to the calculated value. This gave an M_p of 1.75 and a ω_R of 40. The plot of experimental and calculated curves is shown in Figure 9. The stiffness of the control circuit at this gain setting is 0.39 ampere per line volt which is better than the design value of 0.31 ampere per line volt to obtain the required accuracy.

The response time to a step function at these settings was obtained from the analogue computer. With damping factor $\cong 0.3$ the recovery time was 0.18 second. In the actual test on the regulator for step input and step load the friction and nonlinear effect of the diodes at the thyratron cathodes produced beneficial results, the damping factor becoming $\cong 0.8$ and the recovery time 0.15 second. Transient tests were made with a voltage sensitive bridge having a fast response. The results were recorded by a Brush oscillograph and are shown in Figure 10, for both input and load steps. In these recordings

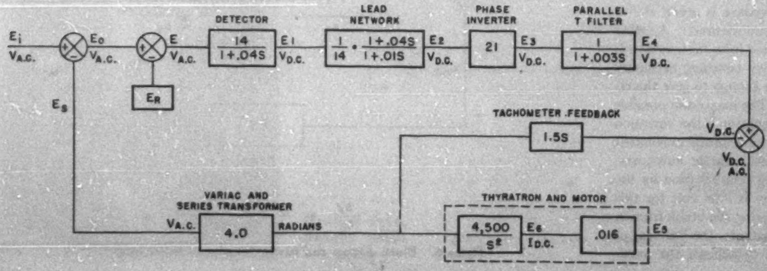

Figure 8. Complete block diagram

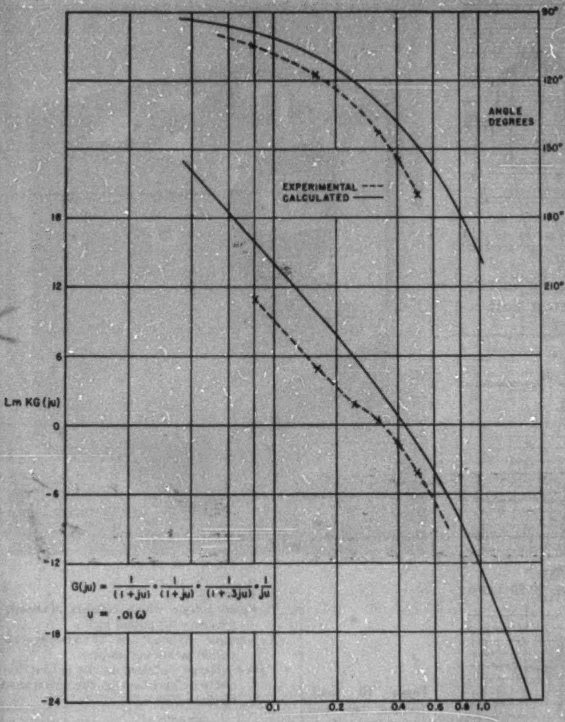

Figure 9(A) (left). *Lm* **and angle plotted with dimensionless frequency for the open loop transfer function**

for each division of the time axis there are 2.5 cycles of the 60-cycle timing signal. Also in Figure 10 is the record taken of the regulator operation compared to the line.

Construction

This instrument was constructed for laboratory use. Photographs of the regulator are shown in Figure 11. The complete wiring diagram is shown in Figure 12.

The specifications for this regulator are as follows:

Power—3 kva.

Regulation—0.1 per cent for input volts 105–125 on the 115-volt range. The output can be set at 110, 115, and 120 volts which gives an over-all range of input voltage 100 volts–130 volts. Load current and load power factor do not affect the accuracy. Allowable frequency variation is ±15 per cent.

Recovery time—0.15 second for a step input up to 5 volts.

Distortion—There is negligible distortion of the output.

Appendix I

The transfer functions for the blocks in the internal loop of Figure 6 are as follows:

In the case of the motor operating on thyratrons, acceleration would continue until the back electromotive force almost reached the peak value of the thyratron plate voltage. Since the maximum speed of the directly coupled one turn motor is such that the back electromotive force is negligible compared to the plate voltage, then the transfer function of the motor is characterized by an acceleration constant.

$$K_2G_2 = \frac{K_2}{S^2}$$

$$\text{and } K_2 = \frac{K_T}{J} = \frac{\text{12 pound inches per ampere}}{\text{0.0027 slug in}^2} = 4{,}500$$

There is no lag in the thyratrons so for this block

$K_1 = 0.016$ amperes per volt d-c

The voltage constant of the motor armature obtained from the flux in the air gap

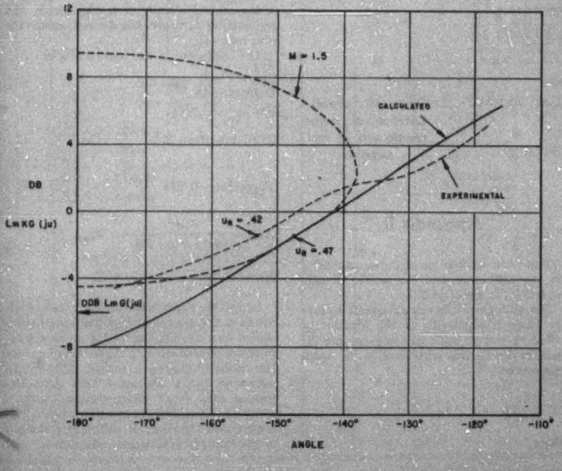

Figure 9(B) (left). *Lm* **versus angle for calculating the closed loop gain when used with a chart[8] of constant amplitude and angle contours. The experimental results for the closed loop operation were changed to the open loop by means of the same chart**

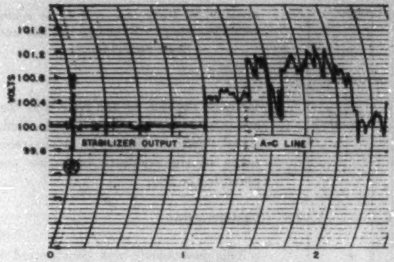

COMPARISON OF VARIATIONS IN OUTPUT VOLTAGE AND LINE VOLTAGE UNDER CONSTANT LOAD

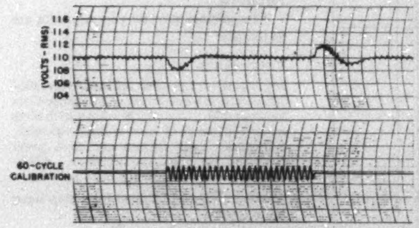

OUTPUT VOLTAGE VARIATION DUE TO 6-AMPERE NON-INDUCTIVE STEP LOAD

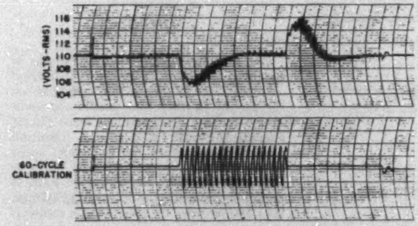

OUTPUT VOLTAGE VARIATION DUE TO 5-VOLT STEP CHANGE IN LINE VOLTAGE

A-C LINE VOLTAGE STABILIZER

Figure 10 (left). Transient tests and operation on the a-c line

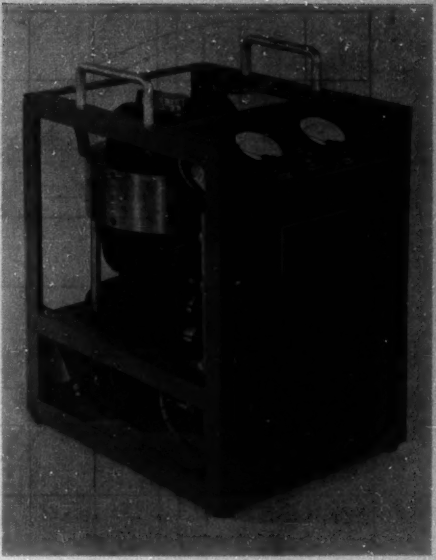

Figure 11 (above). Location of major components in final assembly

and the armature turns is 1.2 volts per radian per second. Since the divider across the armature applies half the voltage to the thyratron grid circuit

Then $K_3=0.6$
$G_3=S$

These blocks were combined to give one transfer function for the loop.

$$\frac{\theta_o}{\theta_i}=\frac{K_1K_2G_2}{1+K_1K_2G_2.K_3G_3}$$

$$\frac{\theta_o}{\theta_i}=\frac{1.67}{S(0.023S+1)}$$

Appendix II

This is the calculation of the sensitivity of the control circuit and the setting of gain control K_o in equation 1.

The stiffness of the control circuit to give the desired sensitivity is the amount of armature current necessary to overcome the load torque for one wire error in the autotransformer.

$$S=\frac{T_L}{K_T\times V}$$

where

S = stiffness
T_L = load torque which consists of brush friction = 0.3 pound inches
K_T = torque constant of the motor = 12 pound inches per ampere
V = a-c voltage variation in the output for one wire variation on the autotransformer = 0.08 volt

$$\therefore S=0.31\ \frac{\text{ampere}}{\text{line volt}}$$

Since S is the product of the coefficients in the control circuit up to this block, the gain setting K_o to give the desired sensitivity is as follows:

The coefficient of the known blocks

Detector—14 $\frac{\text{volts d-c}}{\text{line volt}}$

6SN7 Inverter—5.7 $\frac{\text{volts d-c}}{\text{volts d-c}}$

Thyratron—0.016 $\frac{\text{amps d-c}}{\text{volts d-c}}$

$$\therefore K_o=\frac{0.31}{14\times 5.7\times 0.016}=0.24$$

Note

Since this paper was originally prepared, filters in the control circuit have been redesigned and the driving motor armature redesigned to operate at a higher temperature rise when producing a torque sufficient to overcome brush friction. This gave improved step input characteristics with a speed of response of the regulator being 4 to 5 cycles on the 60-cycle calibration instead of the 8 to 10 cycles previously shown.

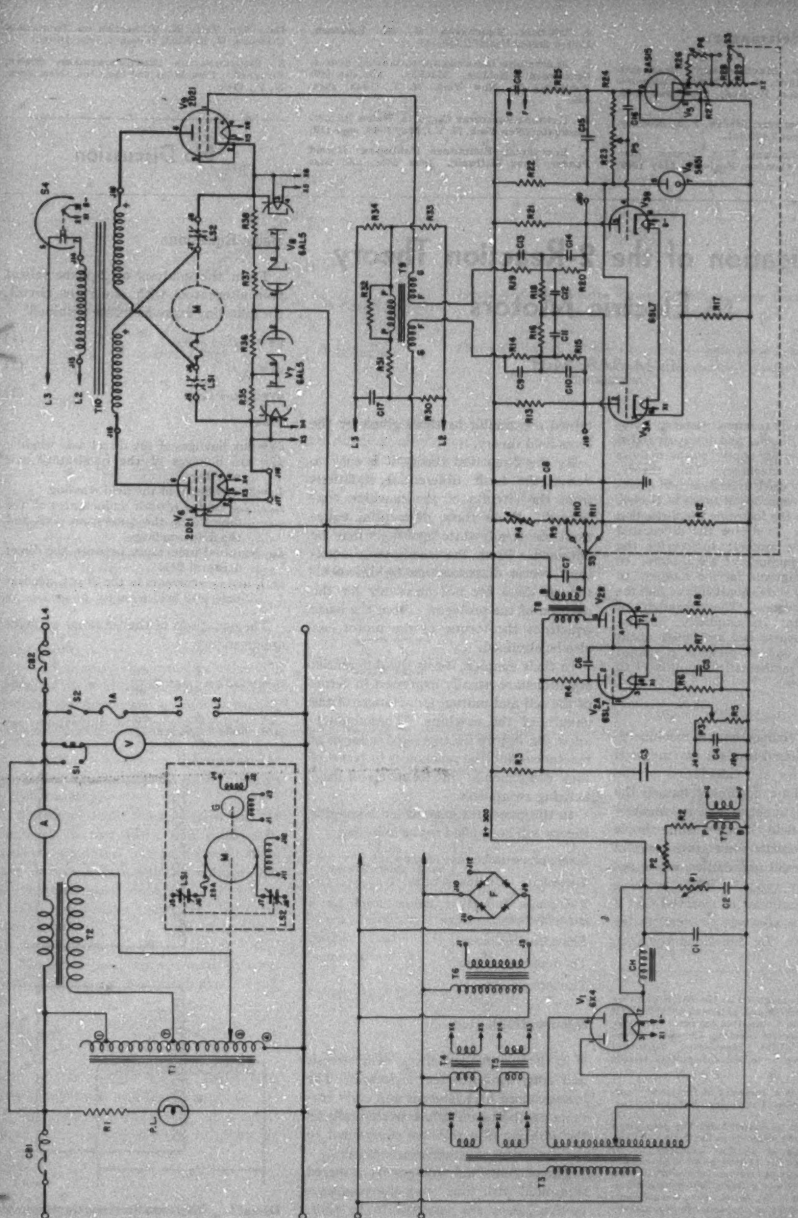

L1
L2
L3
L4
CB1
CB2
S1
S2
1A
A
V
T1
T2
R1
P.L.
M
G
LS1
LS2
T3
T4
T5
T6
F
V1
5X4
CH
C1
C2
P1
P2
R2
T7
B+ 300
R3
C3
C4
P3
R5
V2A
6SL7
V2B
C5
C6
R4
R6
R7
R8
T8
C7
S3
P4
R9
R10
R11
R12
C8
R13
R14
R15
R16
R17
R18
R19
R20
R21
R22
R23
R24
R25
R26
R27
R28
R29
C9
C10
C11
C12
C13
C14
C15
C16
C18
V3A
V3B
6SL7
V4
5651
V5
2A55
P5
P6
T9
R30
R31
R32
R33
R34
C17
R35
R36
R37
R38
V6
2D21
V7
6AL5
V8
6AL5
V9
2D21
T10
S4

Figure 12. Wiring diagram

P1 = Ripple bucking circuit phase adjustment
P2 = Ripple bucking circuit amplitude adjustment

P3 = Damping adjustment
P4 = Overlap adjustment
P5 = Gain setting

P6 = Regulator voltage adjustment
S3 = Regulator voltage setting and overlap correction

References

1. An Electro Mechanically Stabilized Mains Supply Unit, A. E. Maine. *Electronic Engineering* (London, England), September 1949, pages 319–21.

2. Voltage Regulator System, F. L. Moseley. United States Patent 2,453,451.

3. Voltage Stabilizers, F. A. Benson. *Electronic Engineering* (London, England), May 1949.

4. Voltage Regulator, E. M. Sorensen. United States Patent 2,455,143.

5. Electronic Instruments Radiation Series, Greenwood, Holdam, MacRae. McGraw-Hill Publishing Co., New York, N. Y., 1948. Page 469.

6. Cathode Follower Circuits, Walter Richter. *Electronics* (New York, N. Y.), May 1943, page 112.

7. Electrical Engineers Handbook, Harold Pender, Knox McIlwain. John Wiley and Sons Inc., New York, N. Y., section on Thyratron Circuits, W. R. Kind, volume 5, page 16–03.

8. Principles of Servomechanisms, Brown, Campbell. John Wiley and Sons Inc., New York, N. Y., 1948.

No Discussion

Application of the 2-Reaction Theory to Electric Motors

E. M. SABBAGH
MEMBER AIEE

Synopsis: The 2-reaction theory, introduced first by Blondel and later expanded by others, is generally applied to the analysis of synchronous machines. This theory, however, can be used to analyze and calculate the performance of all types of electric machinery. In the following the 2-reaction theory is used: to derive the differential equations of a-c motors; to develop the steady state equations of a-c motors; to draw vector diagrams for a-c motors; to solve the steady state equations and find the currents and torques. The advantages of this method are: its simplicity; the exclusion of vagueness and ambiguity about certain signs; and it presents a unified method for the mathematical analysis of all electric machines.

In teaching courses on a-c machinery, the writer found that the two methods usually used for the calculation of the performance of a-c machinery, namely the method of symmetrical components[1,2] and the cross field theory[3,4] while simple and straight forward for certain types of machines, present difficulties when applied to other types.[1] While working with Parks equations[5] he observed that if the quadrature axis was assumed to lag the direct axis, the equations thus obtained are similar to those given by the cross-field theory.

By the 2-reaction theory it is easy to derive the basic differential equations from the circuits of the machine considered. From these differential equations the steady-state equations may be obtained. From the steady-state equations vector diagrams can be drawn although these are not necessary for the solution of the problem. From the basic equations the torque of the motor can also be obtained.

In their simplest forms the differential equations are usually expressed in terms of the self and mutual inductances of the circuits of the machine. These inductances can in turn be expressed in terms of reactances and the reactances in terms of their components: the leakage and magnetizing reactances.

In this paper the generalized 2-reaction theory will be applied to the following:

Single-phase induction motor.
Two-phase induction motor.
Two-phase induction motor used as a capacitor motor.
The capacitor motor.
The repulsion motor.
The series motor.

Assumptions

In the analysis the effects of hysteresis and eddy currents are neglected. The losses caused by hysteresis and eddy currents can be taken into consideration by the addition of a resistive component to the equivalent magnetizing reactance.

The currents and voltages are assumed sinusoidal with time, and the magnetomotive forces are assumed to be sinusoidally distributed in space.

Basic Equations

From the analysis of 2-phase salient pole alternators with one rotor circuit, the following expressions are obtained:

$$\psi_d = L_{dd}i_d + L_{df}i_f \tag{1}$$

$$\psi_q = L_{qq}i_q \tag{2}$$

$$\psi_f = L_{ff}i_f + L_{df}i_d \tag{3}$$

where

ψ_d = flux linkages of the direct axis winding
ψ_q = flux linkages of the quadrature axis winding
ψ_f = flux linkages of the field winding
L_{dd}, L_{qq} and L_{ff} = self inductances of the direct axis, the quadrature axis and the field windings
L_{df} = mutual inductance between the direct axis and field
i_d, i_q and i_f = currents in the direct, quadrature, and field circuits

The equations of the terminal voltages are given by:

$$v_d = -i_dR_d - \frac{d}{dt}\psi_d - \psi_q\frac{d\alpha}{dt} \tag{4}$$

$$v_q = -i_qR_q - \frac{d}{dt}\psi_q + \psi_d\frac{d\alpha}{dt} \tag{5}$$

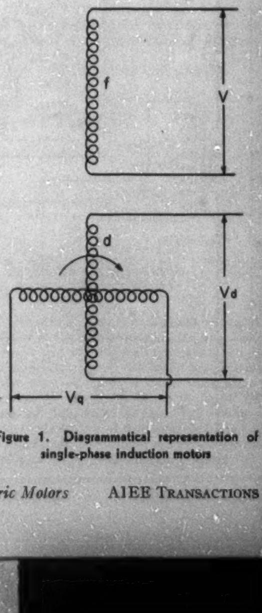

Figure 1. Diagrammatical representation of single-phase induction motors

---

Paper 51-319, recommended by the AIEE Rotating Machinery Committee and approved by the AIEE Technical Program Committee for presentation at the AIEE Fall General Meeting, Cleveland, Ohio, October 22–26, 1951. Manuscript submitted April 19, 1951; made available for printing August 6, 1951.

E. M. Sabbagh is a Professor of Electrical Engineering with Purdue University, Lafayette, Ind.

The writer wishes to acknowledge the help given him by the graduate students in the School of Electrical Engineering at Purdue University. The problems contained herein were given to his class in advanced machinery as exercises for the application of the 2-reaction theory to asynchronous machines. R. S. Carlson and L. W. Anania gave the solutions for the 2-phase motor as a capacitor motor, and the capacitor motor. Richard K. W. Cheng gave the solutions of the repulsion and series motors.

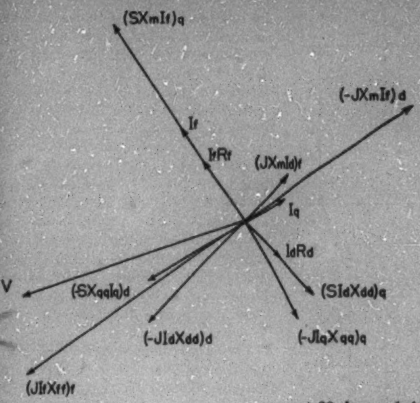

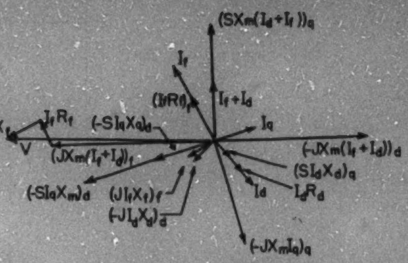

Figure 2 (left). Vector diagram of single-phase induction motors in terms of self and mutual reactances

Figure 3 (above). Vector diagram of single-phase induction motors in terms of leakage and magnetizing reactances

$$v_f = i_fR_f + \frac{d}{dt}\psi_f \tag{6}$$

where

v_d, v_q and v_f = the terminal voltages of the direct axis winding, the quadrature axis windings and the field winding.
R_d, R_q and R_f = the resistances of the three circuits.
$d\alpha/dt$ = the angular velocity of the rotor.

In the analysis giving these equations, the so-called armature reaction is helping the field, namely the armature current is assumed to lead the generated voltage. Hence, the direct axis current is leading the quadrature axis current by 90 degrees.

Equations 4 and 5 are the equation of generator circuits while equation 5 has an applied voltage.

Equations 4 and 5 clearly show how the voltages in the direct and quadrature axis are produced. In each circuit there are an induced transformer voltage, and a generated speed voltage.

The transformer voltage in the direct axis circuit is given by $-d\psi_d/dt$ and that in the quadrature axis by $-d\psi_q/dt$.

The generated voltage, caused by rotation is given, in the direct axis circuit, by

$$-\frac{N_d\psi_q}{N_q}\frac{d\alpha}{dt}$$

and is 180 degrees out of phase with the quadrature axis flux linkages ψ_q.

The generated voltage in the quadrature axis, due to motion, is given by

$$\frac{N_q\psi_d}{N_d}\frac{d\alpha}{dt}$$

and is in phase with ψ_d. This is always true in motors if the quadrature axis is put 90 degrees behind the direct axis in the direction of rotation.

The mechanical power given by the expression

$$p_m = -\frac{1}{2}\sum_n\sum_m i_ni_m\frac{dL_{nm}}{dt} \tag{7}$$

yields the torque equation

$$\tau = p_m\frac{dt}{d\alpha} \tag{8}$$

$$= -\frac{1}{2}\sum_n\sum_m i_ni_m\frac{dL_{nm}}{d\alpha} \tag{9}$$

where

τ = instantaneous torque
p_m = instantaneous power

After substitution equation 9 becomes

$$\tau = \frac{N_q}{N_d}\psi_di_q - \frac{N_d}{N_q}\psi_qi_d \text{ synchronous watts} \tag{10}$$

$$= \frac{7.04}{\text{synchronous speed}}\left[\frac{N_q}{N_d}\psi_di_q - \frac{N_d}{N_q}\psi_qi_d\right] \text{ pound feet} \tag{11}$$

When the effective values of currents are used in equation 11, 1, and 2 the average torque T is

$$T = \omega\left[\frac{N_q}{N_d}\psi_d\cdot\mathbf{I}_q - \frac{N_d}{N_q}\psi_q\cdot\mathbf{I}_d\right] \text{ synchronous watts} \tag{12}$$

The applications of these equations to a-c motors now will be undertaken.

Single-Phase Induction Motor

Under running condition, this induction motor can be represented by the diagram shown in Figure 1.

Voltage V is applied to the stator. The rotor is represented by two windings in quadrature with each other. The direct axis winding d is in space phase with the stator. The quadrature axis winding q is in phase quadrature with the stator. As these two windings are short circuited $v_d = v_q = 0$ and

$$0 = -i_dR_d - \frac{d}{dt}\psi_d - \psi_q\frac{d\alpha}{dt} \tag{13}$$

$$0 = -i_qR_q - \frac{d}{dt}\psi_q + \psi_d\frac{d\alpha}{dt} \tag{14}$$

When the values of ψ_d and ψ_q given in equations 1 and 2 are substituted in equations 13 and 14, we get

$$0 = -i_dR_d - \frac{d}{dt}(L_{df}i_f + L_{dd}i_d) - L_{qq}i_q\frac{d\alpha}{dt} \tag{15}$$

$$0 = -i_qR_q - L_{qq}\frac{di_q}{dt} + (L_{df}i_f + L_{dd}i_d)\frac{d\alpha}{dt} \tag{16}$$

$$v = i_fR_f + L_{ff}\frac{di_f}{dt} + L_{df}\frac{di_d}{dt} \tag{17}$$

The steady-state equations now are obtained from 15, 16, and 17, and are

$$0 = -\mathbf{I}_d(R_d + jX_{dd}) - jX_m\mathbf{I}_f - SX_{qq}\mathbf{I}_q \tag{18}$$

$$0 = -\mathbf{I}_q(R_q + jX_{qq}) + SX_m\mathbf{I}_f + SX_{dd}\mathbf{I}_d \tag{19}$$

$$V = \mathbf{I}_f(R_f + jX_{ff}) + jX_m\mathbf{I}_d \tag{20}$$

where

$X_{dd} = \omega L_{dd}$

$X_m = \omega L_{fd}$

$X_{qq} = \omega L_{qq}$

$$S = \frac{\frac{d\alpha}{dt}}{\omega} = \frac{\omega_s}{\omega}$$

ω = the angular velocity of the applied voltage
ω_s = the angular velocity of the rotor

The solution of equations 18, 19, and 20 yields

$$\mathbf{I}_f=\frac{\mathbf{V}}{\mathbf{D}}[R_dR_q-X_{dd}X_{qq}(1-S^2)+ j(R_dX_{qq}+R_qX_{dd})] \quad (21)$$

$$\mathbf{I}_d=\frac{\mathbf{V}}{\mathbf{D}}[X_mX_{qq}(1-S^2)-jX_mR_q] \quad (22)$$

$$\mathbf{I}_q=\frac{\mathbf{V}}{\mathbf{D}}(SX_mR_d) \quad (23)$$

where

$$\mathbf{D}=R_dR_qR_f-R_dX_{qq}X_{ff}- R_q(X_{dd}X_{ff}-X_m^2)+ R_fX_{dd}X_{qq}(1-S^2)+j[X_{dd}R_qR_f- X_{qq}(X_{dd}X_{ff}-X_m^2)(1-S^2)+ R_dR_qX_{ff}+R_dR_fX_{qq}]$$

The torque equation is given by

$$T=\omega[(L_{df}\mathbf{I}_f+L_{dd}\mathbf{I}_d)\cdot\mathbf{I}_q-L_{qq}I_q\cdot\mathbf{I}_d] \quad (24)$$

For a constant gap $X_{dd}=X_{qq}$ and $R_d=R_q$ then

$$T=X_m\mathbf{I}_f\cdot\mathbf{I}_q \quad (25)$$

$$=\frac{V^2}{|D|^2}SX_m^2R_d[R_d^2-X_{dd}^2(1-S^2)] \quad (26)$$

where

$$|D|^2=[R_d^2R_f-R_dX_{dd}X_{ff}-R_d(X_{dd}X_{ff}- X_m^2)+R_fX_{dd}^2(1-S^2)]^2+ [X_{dd}R_dR_f-X_{dd}(X_{dd}X_{ff}- X_m^2)(1-S^2)+R_d^2X_{ff}+R_dR_fX_{dd}]^2 \quad (27)$$

From equations 18, 19, and 20 a vector diagram of the currents and voltages may be drawn as shown in Figure 2. The subscript put at the end of each bracket encircling the voltage quantity is added for convenience only to show to what circuit the voltage belongs. Thus the voltage $(-jI_dX_{dd})d$, for example, is induced in the direct axis circuit d, while $(SI_dX_{dd})q$ signifies that this speed voltage is generated in the quadrature axis q.

The vector diagrams in this paper are not drawn to scale. Equation 18 states that the sum of the voltages induced, generated and applied in the direct axis is equal to the ohmic voltage drop.

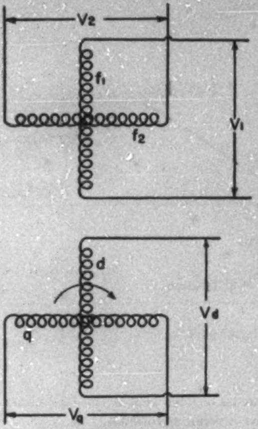

Figure 4. Diagrammatical representation of a 2-phase induction motor

Equations 19 and 20 make similar statements for the quadrature and field circuits.

If the self reactances in equations 18, 19, and 20 are replaced by their equivalent value of leakage and magnetizing reactances, the following equations are obtained.

$$\mathbf{I}_dR_d=-j\mathbf{I}_dX_d-jX_m(\mathbf{I}_f+\mathbf{I}_d)-SX_q\mathbf{I}_q- SX_m\mathbf{I}_q \quad (28)$$

$$\mathbf{I}_qR_q=S(\mathbf{I}_d+\mathbf{I}_f)X_m+S\mathbf{I}_dX_d-jX_q\mathbf{I}_q-j\mathbf{I}_qX_m \quad (29)$$

$$\mathbf{V}=j(\mathbf{I}_d+\mathbf{I}_f)X_m+\mathbf{I}_fR_f+j\mathbf{I}_fX_f \quad (30)$$

where X_d, X_q, and X_f are respectively the leakage reactance of the direct axis winding, the quadrature axis winding and the field winding, and X_m is the magnetizing reactance of the field. The quantity I_f+I_d is the magnetizing current. The term $-jX_m(I_f+I_d)$ is the transformer voltage induced by the field flux in the direct axis winding. The quantity $-SI_qX_m$ is the speed voltage generated by the quadrature flux in the direct axis winding. The term $-SI_qX_q$ is the speed voltage generated by the quadrature leakage flux in the direct axis winding, and $-jI_dX_d$ is the transformer voltage induced in the direct axis winding by the direct axis leakage flux. Equation 28 refers to the direct axis winding, equation 29 to the quadrature axis, and equation 30 to the field axis.

The vector diagram corresponding to equations 28, 29, and 30 is given in Figure 3. Subscripts d, q, and f have been added to denote the windings to which the voltage belongs.

Application to 2-Phase Motor:

In the 2-phase motor there are two windings f_1 and f_2 on the stator as shown diagrammatically in Figure 4. Winding f_1 contributes flux which links with the direct axis winding on the rotor. Winding f_2 sets up flux which links with the quadrature axis on the rotor. The flux linkages of the q axis winding now become

$$\psi_q=L_{qq}i_q+M_{qf2}i_{f2} \quad (31)$$

The quadrature axis winding on the other hand contributes flux linkages to the stator winding f_2, so that the flux linkages of this winding are

$$\psi_{f2}=L_{ff}i_{f2}+i_qM_{qf2} \quad (32)$$

The flux linkages of the f_1 winding are

$$\psi_{f1}=L_{ff}i_{f1}+L_{df1}i_d$$

and those of the direct axis are given by

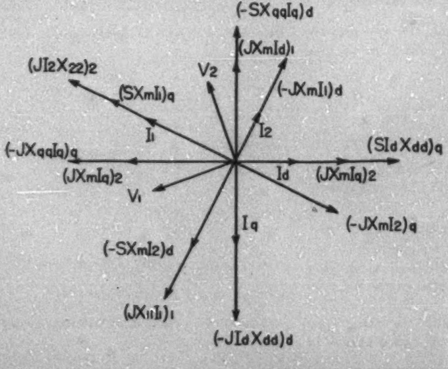

Figure 5 (left). Vector diagram of a two-phase induction motor in terms of self and mutual reactances

Figure 6 (below). Equivalent circuit diagram of a 2-phase induction motor

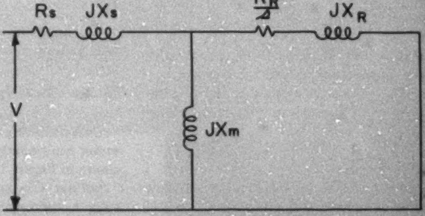

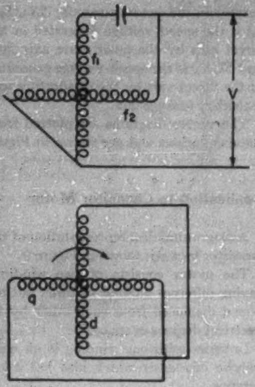

Figure 7(A) (left). Diagrammatical representation of a 2-phase induction motor as a capacitor motor

Figure 7(B) (right). Vector diagram of a 2-phase induction motor as a capacitor motor in terms of self and mutual reactances

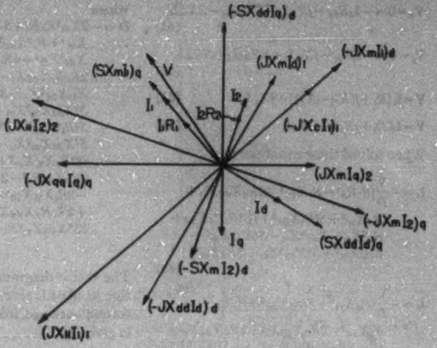

$\psi_q = L_{qq}i_q + L_{qf2}i_{f2}$

The differential equations of the motor can now be written as

$$v_d = -i_dR_d - \frac{d\psi_d}{dt} - \psi_q\frac{d\alpha}{dt} \qquad (33)$$

$$v_q = -i_qR_q - \frac{d\psi_q}{dt} + \psi_d\frac{d\alpha}{dt} \qquad (34)$$

$$v_{f1} = i_{f1}R_{f1} + \frac{d\psi_{f1}}{dt} \qquad (35)$$

$$v_{f2} = i_{f2}R_{f2} + \frac{d\psi_{f2}}{dt} \qquad (36)$$

For the 2-phase motor with constant gap

$$M_{qf2} = L_{df1} = M \qquad (37)$$

$$R_{f1} = R_{f2} = R_f \qquad (38)$$

$$X_{ff1} = X_{ff2} = X_{ff} \qquad (39)$$

under balanced condition of applied voltage

$$\mathbf{V}_{f2} = -j\mathbf{V}_{f1} = -j\mathbf{V} \qquad (40)$$

Substitution of equations 37 to 40 in equations 23 to 26 gives the following differential equations:

$$v_d = -i_dR_d - L_{dd}\frac{di_d}{dt} - M\frac{di_1}{dt} - L_{qq}i_q\frac{d\alpha}{dt} - Mi_2\frac{d\alpha}{dt} \qquad (41)$$

$$v_q = -i_qR_q - L_{qq}\frac{di_q}{dt} - M\frac{di_2}{dt} + L_{dd}i_d\frac{d\alpha}{dt} + Mi_1\frac{d\alpha}{dt} \qquad (42)$$

$$v_{f1} = i_1R_f + L_{ff}\frac{di_1}{dt} + M\frac{di_d}{dt} \qquad (43)$$

$$v_{f2} = i_2R_f + L_{ff}\frac{di_2}{dt} + M\frac{di_q}{dt} \qquad (44)$$

i_1 and i_2 are used for i_{f1} and i_{f2}.

When converted to the steady-state condition these equations become, with the rotor short circuited

$$0 = -\mathbf{I}_d\mathbf{Z}_{dd} - jX_m\mathbf{I}_1 - SX_{qq}\mathbf{I}_q - SX_m\mathbf{I}_2 \qquad (45)$$

$$0 = -\mathbf{I}_q\mathbf{Z}_{qq} - jX_m\mathbf{I}_2 + SX_{dd}\mathbf{I}_d + SX_m\mathbf{I}_1 \qquad (46)$$

$$\mathbf{V} = \mathbf{I}_1\mathbf{Z}_{11} + jX_m\mathbf{I}_d \qquad (47)$$

$$-j\mathbf{V} = \mathbf{I}_2\mathbf{Z}_{22} + jX_m\mathbf{I}_q \qquad (48)$$

When solved these equations yield

$$\mathbf{I}_1 = \mathbf{V}\frac{R_d + jX_{dd} - jSX_{qq}}{R_fR_d - X_{ff}X_{dd} + X_m^2(1-S^2) + SX_{qq}X_{ff} + j[X_{ff}R_d + X_{dd}R_f - SX_{qq}R_f]} \qquad (49)$$

$$\mathbf{I}_2 = -j\mathbf{I}_1 \qquad (50)$$

$$\mathbf{I}_d = \mathbf{V}\frac{-jX_m(1-S)}{R_fR_d - X_{ff}X_{dd} + X_m^2(1-S^2) + SX_{qq}X_{ff} + j[X_{ff}R_d + X_{dd}R_f - SX_{qq}R_f]} \qquad (51)$$

$$\mathbf{I}_q = -j\mathbf{I}_d \qquad (52)$$

The torque is given by

$$T = \omega M[\mathbf{I}_1 \cdot \mathbf{I}_q - \mathbf{I}_2 \cdot \mathbf{I}_d] \text{ synchronous watts} \qquad (53)$$

$$= \frac{v^2[R_dX_m(1-S) + R_dX_m(1-S)]X_m}{[R_fR_d - X_{ff}X_{dd} + X_m^2(1-S^2) + SX_{qq}X_{ff}]^2 + [X_{ff}R_d + X_{dd}R_f - SX_{qq}R_f]^2}$$

$$= \frac{2v^2R_dX_m^2(1-S)}{[R_fR_d - X_{ff}X_{dd} + X_m^2(1-S^2) + SX_{qq}X_{ff}]^2 + [X_{ff}R_d + X_{dd}R_f - SX_{qq}R_f]^2} \qquad (54)$$

The vector diagram given in Figure 5 and representing equations 45 to 48 stands for the 2-phase motor and is similar to the one given in Figure 2 for the single-phase motor. Here the subscripts modifying the voltage terms indicate the circuit to which this voltage belongs.

If it is desired to find the value of the currents in terms of the leakage reactances the magnetizing reactance and the slip, substitute in equations 45 to 48 the values given below

$$Z_{dd} = Z_{qq} = R_R + jX_R + jX_m \qquad (55)$$

$$Z_{ff} = R_S + jX_S + jX_m \qquad (56)$$

$$S = 1 - s \qquad (57)$$

The value of $\mathbf{I}_1$ is then found to be

$$\mathbf{I}_1 = \mathbf{V}\frac{R_R + js(X_R + X_m)}{(R_S + jX_S)[R_R + j(X_R + X_m)s] + jX_m(R_R + jsX_R)} \qquad (58)$$

or

$$\frac{\mathbf{V}}{\mathbf{I}_1} = R_S + jX_S + \frac{\left(\frac{R_R}{s} + jX_R\right)jX_m}{\frac{R_R}{s} + j(X_R + X_m)} \qquad (59)$$

From equation 59 the classical equivalent circuit of a polyphase induction motor on a per phase basis is obtained.

By substituting equations 55 to 57 in equation 54 the torque equation in terms of leakage and magnetizing reactance is obtained as

$$T = \frac{2V^2X_m^2\frac{R_R}{s}}{\left[R_S\frac{R_R}{s} - X_SX_R - X_SX_m - X_RX_m\right]^2 + \left[X_S\frac{R_R}{s} + X_m\frac{R_R}{s} + R_S(X_R + X_m)\right]^2} \qquad (60)$$

This agrees with the value of torque obtained from the equivalent circuit.

Two-Phase Motor as a Capacitor Motor

The diagrammatic circuit of a 2-phase motor used as a capacitor motor is shown in Figure 7(A). The four differential equations when translated to steady state give the following:

$$\mathbf{V}_d=0=-\mathbf{I}_dZ_{dd}-jX_m\mathbf{I}_1-SX_{dd}\mathbf{I}_q-SX_m\mathbf{I}_2 \quad (61)$$

$$\mathbf{V}_q=0=-\mathbf{I}_qZ_{qq}-jX_m\mathbf{I}_2+SX_{dd}\mathbf{I}_d+SX_m\mathbf{I}_1 \quad (62)$$

$$\mathbf{V}=\mathbf{I}_1[R_1+j(X_{11}-X_c)]+jX_m\mathbf{I}_d \quad (63)$$

$$\mathbf{V}=\mathbf{I}_2(R_1+jX_{11})+jX_m\mathbf{I}_q \quad (64)$$

When solved these equations give

$$\mathbf{I}_1=-\frac{\mathbf{V}}{D}[R_1R_d^2-R_1X_{dd}^2-2R_dX_{dd}X_{11}+R_dX_m^2+S^2R_1X_{dd}^2+j\{2R_1R_dX_{dd}+R_d^2X_{11}-X_{dd}^2X_{11}-S^2X_{dd}X_m^2+X_{dd}X_m^2+S^2X_{dd}^2X_{11}+SR_dX_m^2\}] \quad (65)$$

$$\mathbf{I}_2=-\frac{\mathbf{V}}{D}[R_dX_m^2+S^2R_1X_{dd}^2+R_1R_d-R_1X_{dd}^2-2R_dX_{dd}X_{11}+2R_dX_{dd}X_c+j\{-SR_dX_m^2+X_{dd}X_m^2+S^2X_{dd}^2X_{11}-S^2X_{dd}^2X_c-S^2X_{dd}X_m^2+2R_dX_{dd}R_1+R_d^2X_{11}-X_{dd}^2X_{11}-R_d^2X_c+X_{dd}^2X_c\}] \quad (66)$$

$$\mathbf{I}_d=\frac{\mathbf{V}}{\mathbf{D}}[-X_mR_1X_{dd}-X_mR_dX_{11}+S^2R_1X_{dd}X_m+SX_mR_dR_1+j\{X_mR_dR_1-X_mX_{dd}X_{11}-S^2X_m+X_m^2+S^2X_{dd}X_mX_{11}+SX_mR_dX_{11}-SX_mR_dX_c\}] \quad (67)$$

$$\mathbf{I}_q=\frac{\mathbf{V}}{\mathbf{D}}[-SX_mR_dR_1+S^2X_mX_{dd}R_1-X_mR_dX_{11}+X_mR_dX_c-X_mR_1X_{dd}+j\{-SX_mX_{11}R_d+X_m^2+S^2X_mX_{dd}X_{11}-S^2X_mX_{dd}X_c-S^2X_m^2+X_mR_dR_1-X_mX_{dd}X_{11}+X_mX_{dd}X_c\}] \quad (68)$$

where

$$\mathbf{D}=-2X_m^2R_dR_1+2X_m^2X_{dd}X_{11}-X_m^4+R_1^2X_{dd}^2+R_d^2X_{11}^2-R_d^2R_1^2-X_{dd}^2X_{11}^2+4R_dR_1X_{dd}X_1-2R_dR_1X_{dd}X_c-R_d^2X_{11}X_c+X_{11}X_{dd}^2X_c-X_{dd}X_m^2X_c+S^2X_m^4-S^2X_{dd}X_m^2X_{11}-S^2X_{dd}X_m^2X_{11}-S^2R_1^2X_{dd}^2+S^2X_{11}^2X_{dd}^2+S^2X_{dd}X_m^2X_c-S^2X_{dd}^2X_{11}X_c+j[2R_dX_{11}X_m^2+2R_1X_{dd}X_m^2+2R_dX_{dd}R_1^2-2R_dX_{dd}X_{11}^2+2R_d^2R_1X_{11}-2R_1X_{11}X_{dd}^2-X_cR_d^2R_1+X_cX_{dd}^2R_1+2X_cR_dX_{dd}X_{11}-X_cX_m^2R_d-2S^2X_{dd}X_m^2R_1+2S^2R_1X_{11}X_{dd}^2-S^2X_cX_{dd}^2R_1] \quad (69)$$

The vector diagram obtained from equation 61 to 64 is given in Figure 7(B). The torque obtained from equations 65 to 69 is given by

$$\tau=X_m(\mathbf{I}_1\cdot\mathbf{I}_q-\mathbf{I}_2\cdot\mathbf{I}_d) \quad (70)$$

In terms of leakage reactances and magnetizing reactances equations 61 to 64 give

$$0=-\mathbf{I}_dR_R-j\mathbf{I}_dX_R-jX_R(\mathbf{I}_1+\mathbf{I}_d)-\mathbf{I}_qSX_R-SX_m(\mathbf{I}_2+\mathbf{I}_q) \quad (71)$$

$$0=-\mathbf{I}_qR_R-j\mathbf{I}_qX_R-jX_m(\mathbf{I}_2+\mathbf{I}_q)+\mathbf{I}_dSX_R+SX_m(\mathbf{I}_1+\mathbf{I}_d) \quad (72)$$

$$\mathbf{V}=\mathbf{I}_1R_S+j\mathbf{I}_1(X_S-X_c)+jX_m(\mathbf{I}_1+\mathbf{I}_d) \quad (73)$$

$$\mathbf{V}=\mathbf{I}_2R_S+j\mathbf{I}_2X_S+jX_m(\mathbf{I}_q+\mathbf{I}_2) \quad (74)$$

Equation 71 gives the voltage equations in the direct axis. The quantity $\mathbf{I}_1+\mathbf{I}_d$ is the magnetizing current in the direct axis; $jX_m(\mathbf{I}_1+\mathbf{I}_d)$ is the transformer voltage induced in the direct axis by the direct axis flux; $\mathbf{I}_2+\mathbf{I}_q$ is the magnetizing current in the quadrature axis; $SX_m(\mathbf{I}_2+\mathbf{I}_q)$ is the speed voltage generated in the direct axis by the quadrature axis flux; and $S\mathbf{I}_qX_R$ is the speed voltage generated in the direct axis by the quadrature axis secondary leakage flux.

The vector diagrams are plotted from these equations and are shown in Figure 8.

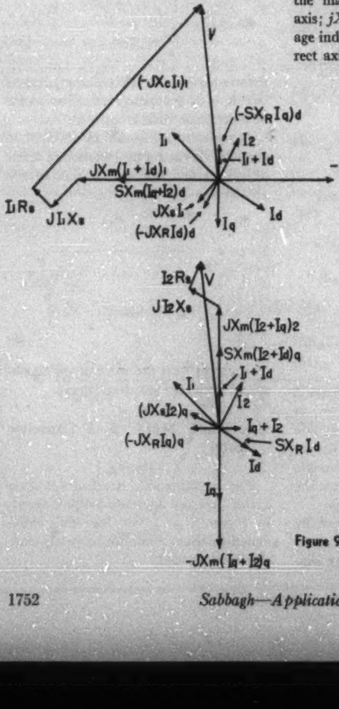

Figure 8 (left). Vector diagram of a 2-phase induction motor as a capacitor motor in terms of leakage and magnetizing reactances

Application to Capacitor Motor

A diagrammatical representation of the capacitor motor is shown in Figure 9.

The motor consists of two windings having different number of turns but assumed displaced from each other by 90 electrical degrees in space.

In series with one winding is an electrolytic condenser which also has a resistance.

The rotor is usually of the squirrel cage type. Let the winding with the condenser be called the *S* winding and the other the *R* winding.

The differential equations for this motor are

$$v_d=-i_dR_d-\frac{d}{dt}\psi_d-\psi_q\frac{d\alpha}{dt} \quad (75)$$

$$v_q=-i_qR_q-\frac{d}{dt}\psi_q+\psi_d\frac{d\alpha}{dt} \quad (76)$$

$$v_S=i_SR_S+\frac{d}{dt}\psi_S \quad (77)$$

$$v_R=i_RR_R+\frac{d}{dt}\psi_R \quad (78)$$

and

$$\psi_d=i_dL_{dd}+i_SM_{dS} \quad (79)$$

$$\psi_q=i_qL_{qq}+i_RM_{qR} \quad (80)$$

$$\psi_S=i_SL_{SS}+i_dM_{dS} \quad (81)$$

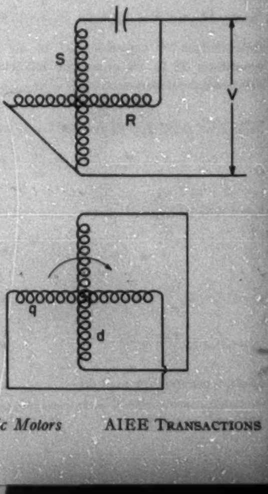

Figure 9 (right). Diagrammatical representation of a capacitor motor

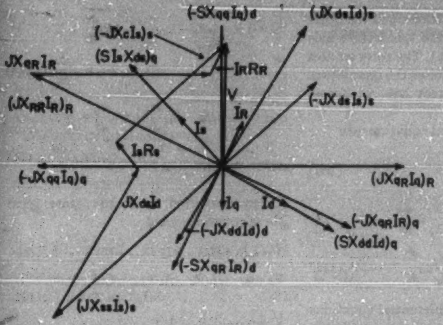

Figure 10. Vector diagram of a capacitor motor in terms of self and mutual reactances

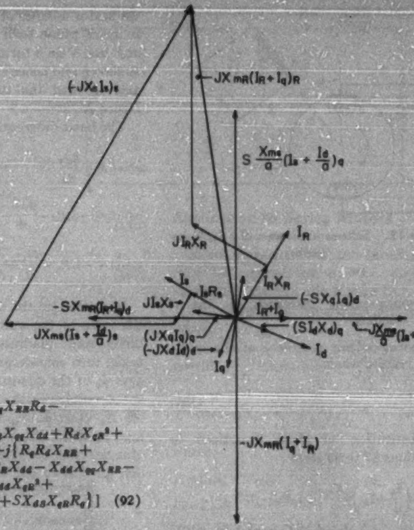

Figure 11. Vector diagram of a capacitor motor in terms of leakage and magnetizing reactances

$$\psi_R = i_R L_{RR} + i_q M_{qR} \tag{82}$$

By substitution the differential equations become

$$v_d = -i_d R_d - L_{dd}\frac{di_d}{dt} - M_{dS}\frac{di_S}{dt} - L_{qq} i_q \frac{d\alpha}{dt} - M_{qR} i_R \frac{d\alpha}{dt} \tag{83}$$

$$v_q = -i_q R_q - L_{qq}\frac{di_q}{dt} - M_{qR}\frac{di_R}{dt} + L_{dd} i_d \frac{d\alpha}{dt} + M_{dS} i_S \frac{d\alpha}{dt} \tag{84}$$

$$v_S = i_S R_S + L_{SS}\frac{di_S}{dt} + M_{dS}\frac{di_d}{dt} \tag{85}$$

$$v_R = i_R R_R + L_{RR}\frac{di_R}{dt} + M_{qR}\frac{di_q}{dt} \tag{86}$$

In the steady state these equations give

$$0 = -\mathbf{I}_d(R_d + jX_{dd}) - \mathbf{I}_S jX_{dS} - \mathbf{I}_q SX_{qq} - \mathbf{I}_R SX_{qR} \tag{87}$$

$$0 = S\mathbf{I}_d X_{dd} + S\mathbf{I}_S X_{dS} - \mathbf{I}_q(R_q + jX_{qq}) - \mathbf{I}_R jX_{qR} \tag{88}$$

$$\mathbf{V} = \mathbf{I}_d jX_{dS} + \mathbf{I}_S(R_S + j(X_{SS} - X_c)) \tag{89}$$

$$\mathbf{V} = \mathbf{I}_q jX_{qR} + \mathbf{I}_R(R_R + jX_{RR}) \tag{90}$$

The resistance R_S is the sum of the resistance of the *S* winding and the resistance of the condenser.

The vector diagram for these equations is given in Figure 10 and except for scale is similar to that given for the 2-phase induction motor used as capacitor motor.

When solved equations 87 to 90 give the following results.

$$\mathbf{I}_d = \frac{\mathbf{V}}{\mathbf{D}}[-X_{qq}X_{dS}X_R - X_{RR}X_{dS}R_q + S^2X_{qq}X_{dS}R_R + SX_{qR}R_qR_R + j\{-X_{qq}X_{RR}X_{dS} - S^2X_{dS}X_{qR}^2 + X_{dS}X_{qR}^2 + S^2X_{qq}X_{dS}X_{RR} + RR_RX_{dS} + SX_{qR}R_qX_{SS} - SR_qX_{qR}X_c\}] \tag{91}$$

$$\mathbf{I}_S = -\frac{\mathbf{V}}{\mathbf{D}}[R_dR_qR_R - X_{qq}X_{RR}R_d - R_qX_{RR}X_{dd} - R_RX_{qq}X_{dd} + R_dX_{qR}^2 + S^2X_{dd}X_{qq}X_{RR} + j\{R_qR_dX_{RR} + R_dR_RX_{qq} + R_qR_RX_{dd} - X_{dd}X_{qq}X_{RR} - S^2X_{dd}X_{qR}^2 + X_{dd}X_{qR}^2 + S^2X_{dd}X_{qq}X_{RR} + SX_{dS}X_{qR}R_q\}] \tag{92}$$

$$\mathbf{I}_q = \frac{\mathbf{V}}{\mathbf{D}}[-SR_dR_RX_{dS} - R_SX_{dd}X_{qR}(1-S^2) - R_dX_{SS}X_{qR} + R_dX_cX_{qR} + j\{-SR_dX_{RR}X_{dS} + X_{dS}^2X_{qR}(1-S^2) - X_{dd}X_{SS}X_{qR}(1-S^2) + X_{dd}X_cX_{qR}(1-S^2) + R_dR_SX_{qR}\}] \tag{93}$$

$$\mathbf{I}_R = \frac{\mathbf{V}}{\mathbf{D}}[-X_{dS}^2R_q - S^2X_{dd}X_{qq}R_S - R_dR_qR_S + X_{dd}X_{qq}R_S + X_{dd}R_qX_{SS} + X_{qq}X_{SS}R_d - X_{dd}R_qX_c - X_{qq}R_dX_c + j\{SX_{qR}X_{dS}R_d - X_{dS}^2X_{qq} - S^2X_{dd}X_{qq}X_{SS} + S^2X_{dd}X_{qq}X_c + S^2X_{qq}X_{dS}^2 - X_{dd}R_qR_S - X_{qq}R_dR_S - R_dR_qX_{SS} + X_{dd}X_{qq}X_{SS} + R_dR_qX_c - X_{dd}X_{qq}X_c\}] \tag{94}$$

with **D** given by

$$\begin{aligned}\mathbf{D} = {} & -R_dR_SX_{qR}^2 + X_{dd}X_{SS}X_{qR}^2(1-S^2) - X_{dd}X_cX_{qR}^2(1-S^2) - X_{dS}^2X_{qR}^2(1-S^2) - R_RR_qX_{dS}^2 + R_dR_RX_{qq}(X_S - X_c) + \\ & R_RR_SX_{dd}X_{qq}(1-S^2) - R_dR_qR_RR_S + R_RR_qX_{dd}(X_{SS} - X_c) + R_dR_SX_{qq}X_{RR} - X_{dd}X_{qq}X_{RR}(X_{SS} - X_c)(1-S^2) + \\ & R_dR_qX_{RR}(X_{SS} - X_c) + R_qR_SX_{dd}X_{RR} + X_{qq}X_{RR}X_{dS}^2(1-S^2) + j\{-R_dX_{qR}^2(X_{SS} - X_c) - R_SX_{dd}X_{qR}^2(1-S^2) - \\ & R_RR_dR_SX_{qq} + R_RX_{dd}X_{qq}(X_{SS} - X_c)(1-S^2) - R_dR_RR_q(X_{SS} - X_c) - R_qR_SR_RX_{dd} - R_qX_{RR}X_{dR}^2 + \\ & R_dX_{qq}X_{RR}(X_{SS} - X_c) + R_SX_{dd}X_{qq}X_{RR}(1-S^2) - R_dR_qR_SX_{RR} + R_qX_{dd}X_{RR}(X_{SS} - X_c) - R_RX_{qq}X_{dS}^2(1-S^2)\}\end{aligned} \tag{95}$$

The torque equation now becomes

$$T = X_{dd}\mathbf{I}_d \cdot \mathbf{I}_q + X_{dS}\mathbf{I}_S \cdot \mathbf{I}_q - X_{qq}\mathbf{I}_q \cdot \mathbf{I}_d - X_{qR}\mathbf{I}_R \cdot \mathbf{I}_d \tag{96}$$

Equations 87 to 90 may be written in terms of leakage and magnetizing reactance. The following substitutions should be used.

$$X_{dd} = X_d + X_{dm} \tag{97}$$

$$= X_d + \frac{X_{dS}}{a} \tag{98}$$

$$= X_d + \frac{X_{mS}}{a^2} \tag{99}$$

where

X_d = leakage reactance of the direct axis winding

X_{dm} = magnetizing reactance of the direct axis winding

X_{mS} = magnetizing reactance of the *S* winding

$$X_{SS} = X_S + X_{mS} \tag{100}$$

$$X_{RR} = X_R + X_{mR} \tag{101}$$

$$X_{qq} = X_q + X_{qm} \tag{102}$$

$$= X_q + X_{qR}$$

$$= X_q + X_{mR} \tag{103}$$

The quadrature axis constants are measured from the *R* winding and hence the ratio of turns of the *R* winding and the *q* winding is assumed 1-to-1. Where

X_q = leakage reactance of the quadrature winding

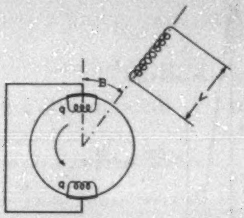

Figure 12. Schematic diagram of a repulsion motor

X_{mR} = magnetizing reactance of the R winding

X_{qm} = magnetizing reactance of the quadrature winding

$$a=\frac{N_S}{N_R} \qquad (104)$$

Substitution of these equations in equations 87 to 90 gives

$$0=-\left(\frac{\mathbf{I}_d}{a}+\mathbf{I}_S\right)j\frac{X_{mS}}{a}-\mathbf{I}_dR_d-j\mathbf{I}_dX_d-(\mathbf{I}_R+\mathbf{I}_q)SX_{mR}-\mathbf{I}_qSX_q \qquad (105)$$

$$0=\mathbf{I}_dSX_d+\left(\mathbf{I}_S+\frac{\mathbf{I}_d}{a}\right)S\frac{X_{mS}}{a}-\mathbf{I}_qR_q-j\mathbf{I}_qX_q-(\mathbf{I}_R+\mathbf{I}_q)jX_{mR} \qquad (106)$$

$$\mathbf{V}=\mathbf{I}_SR_S+\mathbf{I}_Sj(X_S-X_c)+\left(\mathbf{I}_S+\frac{\mathbf{I}_d}{a}\right)jX_{mS} \qquad (107)$$

$$\mathbf{V}=\mathbf{I}_RR_R+\mathbf{I}_RjX_R+(\mathbf{I}_R+\mathbf{I}_q)jX_{mR} \qquad (108)$$

where X_R and X_s are the leakage reactance of the R and the S windings respectively.

From the foregoing equations the vector diagram shown in Figure 11 is drawn. The equations 105 to 108 and the vector diagram are exactly similar to those obtained by the cross-field theory.

Application to the Repulsion Motor

In its simplest form the repulsion motor may be represented by the diagram of Figure 12.

The rotor is short circuited by brushes. The brush axis is set at an angle β with the stator axis. Some of the rotor conductors are locally short circuited by the brushes which cover them. These conductors constitute the quadrature axis and local current i_q flows through them. The rest of the rotor turns are in series and as such are short circuited by the brushes, and constitute the direct axis circuit.

The stator could be divided into two circuits, one in space phase with the direct axis and has $N\cos\beta$ turns, N being the stator number of turns, and the other in space phase with the quadrature axis and has $N\sin\beta$ turns. The rotor rotates as shown and hence causes the quadrature axis to lead the direct axis in space. Hence $d\alpha/dt=-\omega_s$.

The basic differential equations are

$$v_1=i_1R_1+\frac{d\psi_1}{dt} \qquad (109)$$

$$v_d=0=-i_dR_d-\frac{d\psi_d}{dt}-\frac{N_d}{N_q}\psi_q\frac{d\alpha}{dt} \qquad (110)$$

$$v_q=0=-i_qR_q-\frac{d\psi_q}{dt}+\frac{N_q}{N_d}\psi_d\frac{d\alpha}{dt} \qquad (111)$$

In setting up the differential equations the ratio of the number of turns in the direct and quadrature axis should be taken into consideration. The flux linkages ψ_q of the quadrature axis generate a speed voltage in the direct axis of value $N_d/N_q/\psi_q d\alpha/dt$. Similarly the flux linkages ψ_d of the direct axis generate a speed voltage in the quadrature axis given by $N_q/N_d\psi_d d\alpha/dt$, where N_d is the number of turns on direct axis and N_q is the number of turns on quadrature axis. Here also because of the direction of rotation

$$\frac{d\alpha}{dt}=-\omega_S=-S\omega \qquad (112)$$

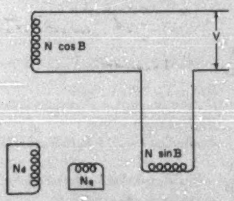

Figure 13. Diagrammatical representation of a repulsion motor

The flux linkages are given by

$$\psi_1=L_{11}i_1+M_{d1}i_d+M_{q1}i_q \qquad (113)$$

$$\psi_d=L_{dd}i_d+M_{d1}i_1 \qquad (114)$$

$$\psi_q=L_{qq}i_q+M_{q1}i_1 \qquad (115)$$

Let

$$a=\frac{N_d}{N_q} \qquad (116)$$

and substitute equations 113 to 116 in equations 109 to 111. The following equations will result:

$$v_1=i_1R_1+L_{11}\frac{di_1}{dt}+M_{d1}\frac{di_d}{dt}+M_{q1}\frac{di_q}{dt} \qquad (117)$$

$$v_d=0=-i_dR_d-L_{dd}\frac{di_d}{dt}-M_{1d}\frac{di_1}{dt}-a(i_qL_{qq}+i_1M_{1q})\frac{d\alpha}{dt} \qquad (118)$$

$$v_q=0=-i_qR_q-L_{qq}\frac{di_q}{dt}-M_{1q}\frac{di_1}{dt}+\frac{1}{a}(i_dL_{dd}+i_1M_{1d})\frac{d\alpha}{dt} \qquad (119)$$

When converted to steady state form these equations yield

$$\mathbf{V}=\mathbf{I}_1R_1+j\mathbf{I}_1X_{11}+\mathbf{I}_d\,jX_{1d}+\mathbf{I}_q\,jX_{1q} \qquad (120)$$

$$\mathbf{V}_d=0=-\mathbf{I}_dR_d-j\mathbf{I}_dX_{dd}-j\mathbf{I}_1X_{1d}+Sa\mathbf{I}_qX_{qq}+Sa\mathbf{I}_1X_{1q} \qquad (121)$$

$$\mathbf{V}_q=0=-\mathbf{I}_qR_q-j\mathbf{I}_qX_{qq}-j\mathbf{I}_1X_{1q}-\frac{S}{a}\mathbf{I}_dX_{dd}-\frac{S}{a}\mathbf{I}_1X_{1d} \qquad (122)$$

The solution of these equations for $\mathbf{I}_1$, $\mathbf{I}_d$, and $\mathbf{I}_q$ gives the following results:

$$\mathbf{I}_1=\frac{\mathbf{V}}{\mathbf{D}}[R_dR_q-X_{dd}X_{qq}(1-S^2)+j(R_dX_{qq}+R_qX_{dd})] \qquad (123)$$

$$\mathbf{I}_d=\frac{\mathbf{V}}{\mathbf{D}}[X_{1d}X_{qq}(1-S^2)+SaR_qX_{1q}-jR_qX_{1d}] \qquad (124)$$

$$\mathbf{I}_q=\frac{\mathbf{V}}{\mathbf{D}}[X_{1q}X_{dd}(1-S^2)+\frac{S}{a}R_dX_{1d}-jR_dX_{1q}] \qquad (125)$$

where

$$\begin{aligned}\mathbf{D}=&R_1R_dR_q-R_1X_{dd}X_{qq}(1-S^2)-\\&X_{11}X_{qq}R_d-R_qX_{11}X_{dd}+R_dX_{1q}^2+\\&R_qX_{1d}^2+j\{R_1R_dX_{qq}+R_1R_qX_{dd}+\\&R_dR_qX_{11}-X_{11}X_{dd}X_{qq}(1-S^2)+\\&X_{1q}^2X_{dd}(1-S^2)+X_{1d}^2X_{qq}(1-S^2)-\\&\frac{S}{a}X_{1d}X_{1q}R_d+SaX_{1q}X_{1d}R_q\}\end{aligned} \qquad (126)$$

The torque equation is given by

$$T=\omega\left(\psi_d\frac{N_q}{N_d}\mathbf{I}_q\cdot-\psi_q\frac{N_d}{N_q}\cdot\mathbf{I}_d\right) \qquad (127)$$

$$=X_m\cos\alpha\mathbf{I}_1\times\mathbf{I}_q'-X_m\sin\alpha\mathbf{I}_1\times\mathbf{I}_d' \qquad (128)$$

where

X_m is the magnetizing reactance of the stator winding

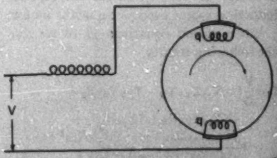

Figure 14. Schematic diagram of a series motor

$$\mathbf{I}_q' = \mathbf{I}_q \frac{N_q}{N_1} \tag{129}$$

$$\mathbf{I}_d' = \mathbf{I}_d \frac{N_d}{N_1} \tag{130}$$

Analysis in Terms of Leakage and Magnetizing Reactances

The values for self and mutual reactances are given by

$$L_{11} = L_1 + M_1 \tag{131}$$

$$M_{d_1} = M_1 \frac{N_d}{N_1} \cos \beta \tag{132}$$

$$M_{q1} = M_1 \frac{N_q}{N_1} \sin \beta \tag{133}$$

$$L_{dd} = L_d + M_1 \left(\frac{N_d}{N_1}\right)^2 \tag{134}$$

$$L_{qq} = L_q + M_1 \left(\frac{N_q}{N_1}\right)^2 \tag{135}$$

If equations 131 to 135 are substituted in equations 117 to 119, the following results will be obtained for the steady-state condition:

$$\mathbf{V} = \mathbf{I}_1[R_1 + j(X_1 + X_m)] + \mathbf{I}_d \frac{N_d}{N_1} jX_m \cos \beta + \mathbf{I}_q \frac{N_q}{N_1} jX_m \sin \beta \tag{136}$$

$$0 = -\mathbf{I}_1 \frac{N_d}{N_1} [jX_m \cos \beta - SX_m \sin \beta] - \mathbf{I}_d \left[R_d + jX_d + jX_m \left(\frac{N_d}{N_1}\right)^2\right] + \mathbf{I}_q \frac{N_d}{N_q} S \left[X_q + X_m \left(\frac{N_q}{N_1}\right)^2\right] \tag{137}$$

$$0 = -\mathbf{I}_1 \frac{N_q}{N_1} [jX_m \sin \beta + SX_m \cos \beta] - \mathbf{I}_d \frac{N_q}{N_d} \left[SX_d + SX_m \left(\frac{N_d}{N_1}\right)^2\right] - \mathbf{I}_q \left[R_q + jX_q + jX_m \left(\frac{N_q}{N_1}\right)^2\right] \tag{138}$$

where X_1, X_d, and X_q are leakage reactances of the stator winding, the direct axis winding, and the quadrature axis winding. X_m is the magnetizing reactance of the stator. Let

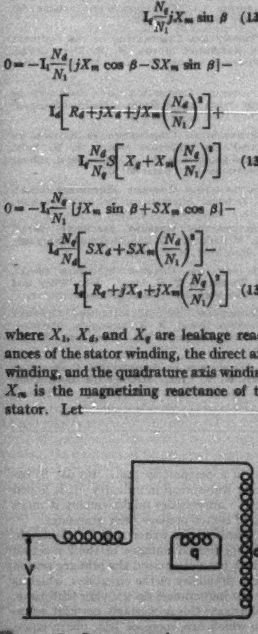

Figure 15. Diagrammatical representation of a series motor

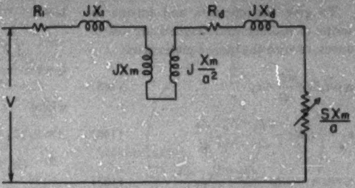

Figure 16. Equivalent circuit diagram of a series motor

$$\mathbf{I}_d' = \mathbf{I}_d \frac{N_d}{N_1} \tag{139}$$

$$\mathbf{I}_q' = \mathbf{I}_q \frac{N_q}{N_1} \tag{140}$$

$$R_d' = R_d \left(\frac{N_1}{N_d}\right)^2 \tag{141}$$

$$R_q' = R_q \left(\frac{N_1}{N_q}\right)^2 \tag{142}$$

$$X_q' = X_q \left(\frac{N_1}{N_q}\right)^2 \text{ and } X_d' = X_d \left(\frac{N_1}{N_d}\right)^2 \tag{143}$$

When equations 139 to 143 are substituted in equations 136 to 137, the following equations will be obtained:

$$\mathbf{V} = \mathbf{I}_1[R_1 + jX_1 + jX_m] + \mathbf{I}_d' jX_m \cos \beta + \mathbf{I}_q' jX_m \sin \beta \tag{144}$$

$$0 = -\mathbf{I}_1[jX_m \cos \beta - SX_m \sin \beta] - \mathbf{I}_d'[R_d' + j(X_d' + X_m)] + \mathbf{I}_q' S(X_q' + X_m) \tag{145}$$

$$0 = -\mathbf{I}_1[jX_m \sin \beta + SX_m \cos \beta] - \mathbf{I}_d' S(X_d' + X_m) - \mathbf{I}_q'[R_q' + j(X_q' + X_m)] \tag{146}$$

The solution of these equations for the currents gives

$$\mathbf{I}_1 = \frac{\mathbf{V}}{\mathbf{D}}[R_d'R_q' - X^2(1 - S^2) + j(R_d' + R_q')X] \tag{147}$$

$$\mathbf{I}_d' = \frac{\mathbf{V}}{\mathbf{D}}[X_m X(1 - S^2) \cos \beta + SR_q'X_m \sin \beta - jR_q'X_m \cos \beta] \tag{148}$$

$$\mathbf{I}_q' = \frac{\mathbf{V}}{\mathbf{D}}[X_m X(1 - S^2) \sin \beta - SR_d'X_m \cos \beta - jR_d'X_m \sin \beta] \tag{149}$$

where

$$X = X_d' + X_m = X_q' + X_m \tag{150}$$

$$\begin{aligned}\mathbf{D} = {} & R_1R_d'R_q' - R_1X^2(1 - S^2) - (R_d' + R_q')(X_1 + X_m)X + X_m^2[R_d' \sin^2 \beta + R_q' \cos^2 \beta] + \\ & j[R_1(R_d' + R_q')X + R_d'R_q'(X_1 + X_m) - (X_1 + X_m)X^2(1 - S^2) + X_m^2X(1 - S^2) + SX_m^2(R_q' - R_d') \sin \beta \cos \beta]\end{aligned} \tag{151}$$

The torque equation then becomes

$$T = \frac{V^2X_m^2}{|D|^2}[-S(R_d' \cos^2 \beta + R_q' \sin^2 \beta)(R_d'R_q' - X^2(1 - S^2)) - (R_d' + R_q') \times (R_d' - R_q') \sin \beta \cos \beta] \tag{152}$$

Application to Series Motors

In its simplest form the series motor may be represented by the diagrams shown in Figure 14 and Figure 15.

The differential equations are as follow:

$$v_1 = i_1R_1 + \frac{d\psi_1}{dt} + i_1R_d + \frac{d\psi_d}{dt} + \frac{N_d}{N_q}\psi_q \frac{d\alpha}{dt} \tag{153}$$

$$v_q = 0 = -i_qR_q - \frac{d\psi_q}{dt} + \frac{N_q}{N_d}\psi_d \frac{d\alpha}{dt} \tag{154}$$

where

$$\psi_1 = L_{11}i_1 + M_{q1}i_q \tag{155}$$

$$\psi_d = L_{dd}i_1 \tag{156}$$

$$\psi_q = L_{qq}i_q + M_{q1}i_1 \tag{157}$$

Substitution and transformation into steady state give

$$\mathbf{V}_1 = \mathbf{I}_1R_1 + jX_{11}\mathbf{I}_1 + jX_{q1}\mathbf{I}_q + \mathbf{I}_1R_d + jX_{dd}\mathbf{I}_1 + SX_{qq}\frac{N_d}{N_q}\mathbf{I}_q + SX_{q1}\frac{N_d}{N_1}\mathbf{I}_1 \tag{158}$$

$$0 = -\mathbf{I}_qR_q - jX_{qq}\mathbf{I}_q - jX_{q1}\mathbf{I}_1 + S\frac{N_q}{N_d}X_{dd}\mathbf{I}_1 \tag{159}$$

Solution for $\mathbf{I}_1$ and $\mathbf{I}_q$ gives

$$\mathbf{I}_1 = \frac{\mathbf{V}}{\mathbf{D}}[-R_q + jX_{qq}] \tag{160}$$

$$\mathbf{I}_q = \frac{\mathbf{V}}{\mathbf{D}}\left[S\frac{N_q}{N_d}X_{dd} - jX_{q1}\right] \tag{161}$$

where

$$\mathbf{D} = -\left[R_q\left(R_1 + R_d + SX_{q1}\frac{N_d}{N_1}\right) - X_{qq}(X_{11} + X_{dd}) + S^2X_{dd}X_{qq} + X_{q1}^2 + j\left\{X_{qq}\left(R_1 + R_d + SX_{q1}\frac{N_d}{N_1}\right) + R_q(X_{11} + X_{dd}) + X_{q1}S \times \left(\frac{N_q}{N_d}X_{dd} - \frac{N_d}{N_q}X_{qq}\right)\right\}\right] \tag{162}$$

The torque equation is given by

$$T = \omega\left(\frac{N_q}{N_d}\psi_d \cdot \mathbf{I}_q - \frac{N_d}{N_q}\psi_q \cdot I_d\right)$$

$$= \frac{N_d}{N_q}X_{q1}\mathbf{I}_1 \cdot \mathbf{I}_1 \tag{163}$$

$$= \frac{V^2}{|D|^2}[R_q^2 + X_{qq}^2]X_{q1}\frac{N_d}{N_q} \text{ synchronous watts} \tag{164}$$

To give the currents and torque in terms of leakage and magnetizing reactances, rewrite the basic equations as

$$v_1 = i_1R_1 + \frac{d\psi_1}{dt} - v_d \tag{165}$$

$$v_d = -i_dR_d - \frac{d\psi_d}{dt} - \frac{N_d}{N_q}\psi_q\frac{d\alpha}{dt} \tag{166}$$

$$v_q = 0 = -i_qR_q - \frac{d\psi_q}{dt} + \frac{N_q}{N_d}\psi_d\frac{d\alpha}{dt} \tag{167}$$

But

$$M_{1q} = \frac{N_q}{N_1}M_1 \tag{168}$$

$$M_d = \left(\frac{N_d}{N_1}\right)^2 M_1 \tag{169}$$

$$M_q = \left(\frac{N_q}{N_1}\right)^2 M_1 \tag{170}$$

$$\frac{L_d}{L_q} = \left(\frac{N_d}{N_q}\right)^2 \tag{171}$$

$$\psi_1 = i_1(L_1 + M_1) + i_qM_{q1} \tag{172}$$

$$\psi_d = i_1(L_d + M_d) \tag{173}$$

$$\psi_q = i_q(L_q + M_q) + M_{q1}i_1 \tag{174}$$

Let

$$i_q' = \frac{N_q}{N_1}i_q \tag{175}$$

$$R_q' = R_q\left(\frac{N_1}{N_q}\right)^2 \tag{176}$$

$$a = \frac{N_1}{N_d} \tag{177}$$

The steady-state equations may be found to be

$$\mathbf{V} = \mathbf{I}_1[R_1 + jX_1 + jX_m] + \mathbf{I}_q'jX_m - V_d \tag{178}$$

$$\mathbf{V}_d = -\mathbf{I}_1\left[R_d + jX_d + j\frac{X_m}{a^2} + S\frac{X_m}{a}\right] + \mathbf{I}_q'S\left(aX_d + \frac{X_m}{a}\right) \tag{179}$$

$$0 = \mathbf{I}_1\left(SaX_d + \frac{SX_m}{a} - jX_m\right) - \mathbf{I}_q'[R_q' + ja^2X_d + jX_m] \tag{180}$$

These equations give

$$\mathbf{I}_1 = \mathbf{V}\frac{R_q' + j(a^2X_d + X_m)}{A + jB} \tag{181}$$

$$\mathbf{I}_d = \mathbf{I}_1 \tag{182}$$

$$\mathbf{I}_q = \mathbf{V}\frac{aS\left(X_d + \frac{X_m}{a^2}\right) - jX_m}{A + jB} \tag{183}$$

where

$$A = R_q'(R_1 + R_d) - X_1X_m - a^2X_d \times (X_1 + X_m) + \frac{S}{a}R_q'X_m - a^2 \times \left(X_d + \frac{X_m}{a^2}\right)^2(1 - S^2) \tag{184}$$

$$B = R_q'(X_1 + X_m) + a^2R_1\left(X_d + \frac{X_m}{a^2}\right) + aSX_m\left(X_d + \frac{X_m}{a^2}\right) + (R_q' + a^2R_d)\left(X_d + \frac{X_m}{a^2}\right) \tag{185}$$

The torque equation is given by

$$T = \omega|I_1|^2\frac{M_1}{a} \tag{186}$$

$$= V^2\frac{X_m}{a}\,\frac{(R_q')^2 + (a^2X_d + X_m)^2}{A^2 + B^2} \quad \text{synchronous watts} \tag{187}$$

Equation 181 could be written

$$\mathbf{I}_1 = \frac{\dfrac{\mathbf{V}}{A + jB}}{R_q' + j(a^2X_d + X_m)} \tag{188}$$

$$= \frac{\mathbf{V}}{R_1 + R_d + \dfrac{SX_m}{a} + j\left(X_1 + X_d + X_m \times \left(1 + \dfrac{1}{a^2}\right)\right) + \dfrac{a^2S^2\left(X_d + \frac{X_m}{a^2}\right)^2 + X_m^2}{R_q' + ja^2\left(X_d + \frac{X_m}{a^2}\right)}} \tag{189}$$

If R_q' is infinite, the equivalent circuit of the motor becomes as shown in Figure 16.

The component SX_m/a the only component variable with speed represents the developed power or power output, since

$$T = \frac{X_m}{a}|I_1|^2$$

and

$$\text{Power output} = ST = \frac{SX_m}{a}|I_1|^2 \tag{190}$$

This result could be predicted from physical reasoning.

$\mathbf{I}_1SX_m/a$ is the speed generated voltage or back electromotive force of the motor. When this is multiplied by the armature current the developed power results.

Conclusion

The basic equations derived from the 2-reaction theory are applied for the analysis of asynchronous motors. When the self and mutual reactances are replaced by their equivalent values of leakage and magnetizing reactances, the equations thus obtained are those of the so-called cross field theory. No vector diagram is necessary for the establishment of these equations.

References

1. Two-Reaction Theory of Synchronous Machines, **R. H. Park.** *AIEE Transactions*, volume 48, July section, 1929, pages 716–30.

2. The Cross-Field Theory of the Capacitor Motor, **A. F. Puchstein, T. C. Lloyd.** *Electrical Engineering* (*AIEE Transactions*), volume 60, February 1941, pages 58–62.

3. Theory and Calculation of the Squirrel Cage Repulsion Motor, **H. R. West.** *AIEE Transactions*, volume 43, June 1924, pages 1048–57.

4. Physical Conception of Single-Phase Motor Operation, **R. Beach.** *Electrical Engineering*, July 1924, pages 1048–55.

5. Symmetrical Components as Applied to Single-Phase Induction Motor, **F. W. Suhr.** *Electrical Engineering* (*AIEE Transactions*), volume 64, September 1945, pages 651–56.

6. Alternating Current Machinery (book), **J. G. Tarboux.** International Textbook Company, Scranton, Pa., 1947.

7. Alternating Current Machines (book), **T. C. McFarland.** D. Van Nostrand Company, Inc., New York, N. Y., 1948.

8. Alternating Current Machines (book), **A. F. Puchstein, T. C. Lloyd.** John Wiley and Sons, New York, N. Y., 1942, 655 pages.

9. Principles of Alternating Current Machinery (book), **R. R. Lawrence.** McGraw-Hill Book Company, Inc., New York, N. Y., 1937.

10. Application of Symmetrical Components (book), **W. V. Lyon.** McGraw-Hill Book Company, Inc., New York, N. Y., 1937.

Discussion

W. G. Heffron (General Electric Company, Schenectady, N. Y.): Dr. Sabbagh's demonstration of the wide applicability of the 2-reaction theory is very interesting. The fact that graduate students of Purdue University worked up the solutions is not only to their credit but to Dr. Sabbagh's, for it is a sign of his unusual ability as a teacher to inspire his students to greater efforts.

Gabriel Kron has written[1] the general equation of all rotating machines as the tensor equation

$$\boldsymbol{e} = \boldsymbol{Ri} + p\boldsymbol{\psi} + \gamma\boldsymbol{\psi}p\delta \tag{1}$$

where γ is ±1 depending on whether, in this case, the *d or q* axis is considered. Thus Dr. Sabbagh's paper is chiefly interesting in its application to vector diagrams. Kron gives equivalent circuits for these motors in references 1 and 2 of this discussion which would be useful in developing the vector diagrams, et cetera.

It is disappointing not to see the equations in a per-unit system. Its use is becoming widespread in industry; it is hoped that the universities might employ it more fully to better prepare their graduates.

It seems to the writer that Dr. Sabbagh, in listing the advantages of the 2-reaction method, has not stressed the primary reason for the simplicity of the equations, which is that the inductances do *not* vary with time. To illustrate this advantage, per-unit equations which are, more or less, phase equations of the single-phase and 2-phase motors are given below. The writer objects some-

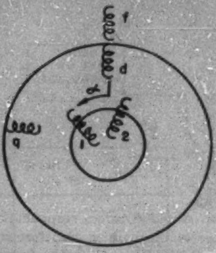

Figure 1. Single-phase induction motor

what to the use of the d and q notation for, as used by Park,[3] such a notation refers to equivalent circuits that rotate with the rotor, whereas Dr. Sabbagh's system has the equivalent circuits fixed in space in a modified form of the α, β, 0 system popularized by Clarke[4] and most recently used by Concordia.[5] In this matter, as well as whether the q axis leads the d, or vice versa, it appears to be every man for himself and an ensuing confusion of the reader. A suggestion that the notations mean what they mean in the so-called "classical" papers is hereby made by the writer.

SINGLE-PHASE INDUCTION MOTOR

For the coil locations shown in Figure 1 of this discussion the phase equations are

$$\psi_1 = X_1 i_1 + X_{1f} i_f \cos\alpha \tag{2}$$

$$\psi_2 = X_2 i_2 + X_{2f} i_f \sin\alpha \tag{3}$$

$$\psi_f = X_{ff} i_f + X_{1f} i_1 \cos\alpha + X_{2f} i_2 \sin\alpha \tag{4}$$

$$V_f = R_f i_f + p\psi_f \tag{5}$$

$$V_1 = 0 = -R i_1 - p\psi_1 \tag{6}$$

$$V_2 = 0 = -R i_2 - p\psi_2 \tag{7}$$

The general transformations are

$$K_d = K_1 \cos\alpha + K_2 \sin\alpha \tag{8}$$

$$K_q = K_1 \sin\alpha - K_2 \cos\alpha \tag{9}$$

Investigating the application of equations 7 and 8 to equation 3 we see that if $X_{1f} = X_{2f}$ equation 3 becomes

$$\psi_f = X_{ff} i_f + X_{1f} i_d \tag{10}$$

Such an equality is indicated in this case because of the nature of the rotor. But if the motor were an unusual design (say a single-phase reluctance motor) so that $x_{1f} \neq x_{2f}$, this type of transformation would not be applicable. As a matter of fact there is no transformation which will eliminate trigonometric coefficients where both the rotor and the stator exhibit saliency. If the motor we are considering was salient in the rotor and smooth in the stator the desirable transformation would be one that gives equivalent circuits rotating with the rotor and positioned with the centerlines of the two dissimilar rotor circuits. Conversely, the transformation used here is still applicable if the stator is salient and the rotor smooth. In such a case X_1 and X_2 would contain a constant and a cos 2α term and a new reactance X_{12} which also is a sin 2α term would be created by the saliency. Chapter 2 of reference 3 of this discussion has a treatment of a similar case which shows that the magnitude of the variable part of X_1 and X_2 approximately equals the magnitude of X_{12}.

If it is true that $X_{1f} = X_{2f}$ it follows that $X_1 = X_2$ and the transformation to give ψ_d follows very simply. It is of interest to show the transform which gives e_d.

$$e_d = 0 = -R_1 i_1 \cos\alpha - R_2 i_2 \sin\alpha - \cos\alpha p\psi_1 - \sin\alpha p\psi_2 \tag{11}$$

We now find that $R_1 = R_2$ is a necessary condition for this transformation to be useful, and not a particular case as Dr. Sabbagh insinuates. With this satisfied,

$$e_d = -R_1 i_d - \cos\alpha p\psi_1 - \psi_1 p \cos\alpha + \psi_1 p \cos\alpha - \sin\alpha p\psi_2 - \psi_2 p \sin\alpha + \psi_2 p \sin\alpha \tag{12}$$

$$e_d = -R_1 i_d - p[\psi_1 \cos\alpha + \psi_2 \sin\alpha] - [\psi_1 \sin\alpha - \psi_2 \cos\alpha] p\alpha \tag{13}$$

$$e_d = -R_1 i_d - p\psi_d - \psi_q p \tag{14}$$

TWO-PHASE INDUCTION MOTOR

Again the applicability of the transform depends upon the two rotor circuits being identical except for the phase relationships (that is, $R_1 = R_2$, $X_{r1f1(\max)} = X_{r2f2(\max)}$, etc.). With these satisfied, and a constant air gap, the equations for the circuits of Figure 2 are

$$\psi_{f1} = X_{f1} i_{f1} + X_{r1f1} i_{r1} \cos\alpha + X_{r2f1} i_{r2} \sin\alpha \tag{15}$$

$$\psi_{f2} = X_{f2} + i_{f2} + X_{r1f2} i_{r1} \sin\alpha - X_{r2f2} i_{r2} \cos\alpha \tag{16}$$

$$\psi_{r1} = X i_{r1} + X_{r1f1} i_{f1} \cos\alpha + X_{r1f2} i_{f2} \sin\alpha \tag{17}$$

$$\psi_{r2} = X i_{r2} + X_{r2f1} i_{f1} \sin\alpha - X_{r2f2} i_{f2} \cos\alpha \tag{18}$$

$$V_{f1} = R_{f1} i_{f1} + p\psi_{f1} \tag{19}$$

$$V_{f2} = R_{f2} i_{f2} + p\psi_{f2} \tag{20}$$

$$V_1 = 0 = -R i_{r1} - p\psi_{r1} \tag{21}$$

$$V_2 = 0 = -R i_{r2} - p\psi_{r2} \tag{22}$$

Using essentially the same transform as before

$$\psi_d = X i_{r1} \cos\alpha + X i_{r2} \sin\alpha + X_{r1f1} i_{f1} \cos^2\alpha + X_{r2f1} i_{f1} \sin^2\alpha + X_{r1f1} i_{f2} \sin\alpha \cos\alpha - X_{r2f2} i_{f2} \cos\alpha \sin\alpha \tag{23}$$

$$\psi_d = X i_d + X_{r1f1} i_{f1} = X_{dd} i_d + X_{df1} i_{f1} \tag{24}$$

Similarly, we obtain

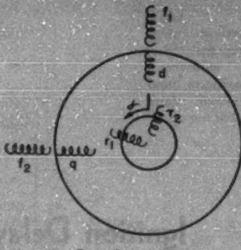

Figure 2. Two-phase induction motor

$$\psi_q = X i_q + X_{r2f2} i_{f2} = X_{qq} i_q + X_{qf2} i_{f2} \tag{25}$$

The other equations, of course, follow by the same routine. Note, however, that it is not necessary to restrict the equations by the relationships given in equations 37, 38, and 39 of the paper. Thus this same analysis may be easily extended to cover the "two-phase induction motor used as a capacitor motor" and "the capacitor motor."

REFERENCES

1. A SHORT COURSE IN TENSOR ANALYSIS, Gabriel Kron. John Wiley & Sons, New York, N. Y., 1941.

2. EQUIVALENT CIRCUITS OF ELECTRIC MACHINERY, Gabriel Kron. John Wiley & Sons, New York, N. Y., 1951.

3. See reference 3 of the paper.

4. PROBLEMS SOLVED BY MODIFIED SYMMETRICAL COMPONENTS, Edith Clarke. *General Electric Review* (Schenectady, N. Y.), volume 41, 1938, pages 488–95 and 545–49.

5. SYNCHRONOUS MACHINES, THEORY AND PERFORMANCE, Charles Concordia. John Wiley and Sons, New York, N. Y., 1951.

E. M. Sabbagh: I would like to thank Mr. Heffron for his interesting discussion of the above paper. His kind words are a source of encouragement and are greatly appreciated.

With regard to the d and q notations, I still feel that they are the correct ones to use. In Park's paper the armature is stationary and the field is rotating. This is usually the case with large synchronous machines. On the other hand if, as is sometimes the case with small synchronous machines, the field is the stator and the armature is the rotor, the d and q windings equivalent to the armature will be stationary in space and rotating with respect to the rotor. The d winding is along the same axis as the field winding and the q winding is in quadrature with the d winding or along the interpoles. This is exactly what has been assumed in the paper. The saliency in this case is on the stator and the equations developed are to cover this case. This assumption is indeed fortunate as the armatures of asynchronous machines are the rotors and the fields, the stators.

Ignition Delay in Oil Burners

FERDINAND HAMBURGER, JR.
FELLOW AIEE

DURING the fall of 1949 an oil burner installation in an apartment house development failed to give satisfactory performance. Within a very short time "puffs" of considerable magnitude occurred in eight out of 14 burner locations with repetition of this difficulty as many as six times for a single burner. The burners involved were gun type domestic oil burners burning from five to fifteen gallons of oil per hour. The difficulty was traced to ignition delay, and this paper reports a program of test that has been conducted to investigate the delay phenomenon. The delay referred to is the time delay occurring between the application of voltage to the primary of the ignition transformer and the initiation of the spark discharge in the spark gap. This paper reports the results of this test program, and indicates the direction to be taken in further investigation of the delay phenomenon.

Test Arrangement

A standard domestic oil burner has been used in all tests, without oil. The electrodes used are commercial nichrome electrodes of 1/8-inch diameter adjusted for a 1/8-inch spacing. The power supply to the burner has been arranged so that the starting of the blower motor has no effect upon the voltage supplied to the ignition transformer primary.

A special timer was constructed to automatically cycle the oil burner for any desired on-off period, and to simultaneously control a 2-pen Brush Oscillograph used to measure the delay. (This oscillograph was modified by the installation of a relay to permit automatic starting and stopping.) One pen of the oscillograph records the instant of application of voltage to the ignition transformer primary, while the second pen records the incidence of the spark discharge. Measurement of the time difference between the start of the traces of the two pens gives the time-delay, that is, the time between application of voltage to the ignition transformer primary, and the beginning of the spark discharge across the spark gap.

For most of the tests, the ignition transformer was mounted external to the oil burner in order to enable monitoring and measuring of the secondary voltage. A check showed that this arrangement caused no significant difference in delay time from runs made with the transformer mounted on the oil burner.

A schematic of the test arrangement is shown in Figure 1. It will be observed that one of the Brush Amplifiers measures the voltage across the ignition transformer primary, while the other, connected across a very low resistance shunt in series with the ignition transformer primary, indicates by the increase in transformer primary current the existence of the spark across the spark gap. The cycle of operation is as follows: timer contact *K*1 closes and operates relay *K*3 to start the record paper in the Brush Oscillograph. One second later, timer contact *K*2 closes operating *K*4, *K*5 and the main relay *K*6 which applies voltage simultaneously to the blower motor and ignition transformer primary.

The timer is so arranged that the Brush Oscillograph is disconnected after about ten seconds (or any desired interval) independently of the "on-time" of the cycle. The center pole of the relay *K*6 operates a simple counter showing the number of cycles of operation. The several capacitors shown and the resistors *R*1 were required to prevent the operation of the several relays from false-triggering the timer.

Test Program

Preliminary investigations indicated that with a given spark duration, followed by an off-period before reapplication of voltage to the ignition transformer primary, the length of the off-period was a factor in the delay time. Subsequent careful measurements showed this assumption to be erroneous as will be shown later. However, for a given test condition, a series of 100 applications of voltage for varying off-periods was made for many runs before it became evident that this was unnecessary.

Test data have been obtained for many conditions of operation, but in the interest of brevity, only a portion is reported here. The test data can best be interpreted by noting the following:

1. No attempt was made to control such factors as temperature, humidity or barometric pressure since it was desired to determine the delay time that might be experienced in actual practice. The test runs reported in this paper were made through the period from November 1949, to September 1950, during which time the usual range of barometric, humidity and temperature conditions was encountered.

2. The test technique consisted of applying voltage simultaneously to the blower motor and ignition transformer primary, and then removing the voltage at the end of one minute—this has been referred to as a one-minute "on-time."

3. A waiting period of varying length (as noted previously) was introduced between successive applications of voltage, and is called the "off-time." Arbitrary off-times of one minute, $2^{1}/_{4}$ minutes, $4^{1}/_{2}$ minutes, 9 minutes, 14 minutes, and 29 minutes have been used.

4. The blower, when operating at normal speed, produced an air velocity of approxi-

---

Paper 51-320, recommended by the AIEE Domestic and Commercial Applications Committee and approved by the AIEE Technical Program Committee for presentation at the AIEE Fall General Meeting, Cleveland, Ohio, October 22-26, 1951. Manuscript submitted October 16, 1950; made available for printing August 13, 1951.

Ferdinand Hamburger, Jr. is with The Johns Hopkins University, Baltimore, Md.

The author wishes to express his appreciation to the C. Hoffberger Company of Baltimore, Md., for their co-operation in providing the oil burner and accessories; to R. G. Roush of the Institute for Cooperative Research of the Johns Hopkins University for the design and construction of the versatile electronic timer, without which the data reported in this paper could not have been obtained; to Dr. J. M. Kopper of the Johns Hopkins University for his assistance in the early phases of the investigation.

Vol. 7
1951

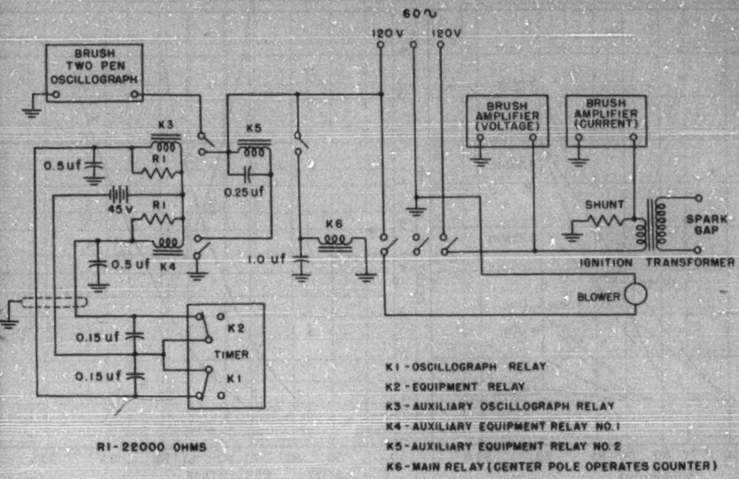
60∿
120V
120V
BRUSH TWO PEN OSCILLOGRAPH
K3
K5
R1
0.5uf
45V
R1
0.25uf
K6
0.5 uf
K4
1.0 uf
BRUSH AMPLIFIER (VOLTAGE)
BRUSH AMPLIFIER (CURRENT)
SHUNT
SPARK GAP
IGNITION TRANSFORMER
BLOWER
K2
TIMER
K1
0.15 uf
0.15 uf
R1-22000 OHMS
K1 - OSCILLOGRAPH RELAY
K2 - EQUIPMENT RELAY
K3 - AUXILIARY OSCILLOGRAPH RELAY
K4 - AUXILIARY EQUIPMENT RELAY NO. 1
K5 - AUXILIARY EQUIPMENT RELAY NO. 2
K6 - MAIN RELAY (CENTER POLE OPERATES COUNTER)

Figure 1. Schematic diagram of test arrangement. Connections from Brush amplifiers to Brush oscillograph are not shown

mately 50 feet per second. The electrodes in all cases were normally mounted in the draft tube, the spark occurring in the vertical plane, and spacing was maintained at 1/8 inch, although it could be checked only at the beginning and end of each run of 100 trials. The spacing was controlled by using a new 1/4-inch drill as a feeler gauge. The electrode tips were rounded with a radius of roughly 1/16 inch.

5. The variation in the surface condition of the electrodes is difficult to control since it is not possible to polish or treat them between successive applications of voltage. Some evidence is presented later indicating the possible extent of this effect.

6. Figure 2 shows two typical records, *A* shows zero delay and *B* a 3-second delay.

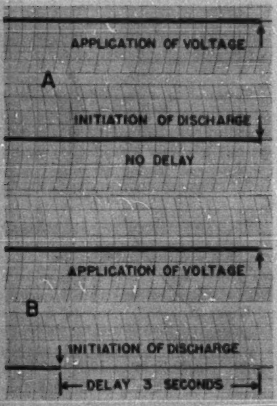
APPLICATION OF VOLTAGE
A
INITIATION OF DISCHARGE
NO DELAY
APPLICATION OF VOLTAGE
B
INITIATION OF DISCHARGE
DELAY 3 SECONDS

Figure 2. Typical delay record. *A*-zero delay; *B*-3-second delay

Test Results

Effect of "Off-Time"

Since initial investigation indicated that off-time was possibly significant, many runs were made using various off-times. The typical data plotted in Figure 3 seem to show that the off-time is not significant since the spread for repeated runs at a fixed off-time is as great as the spread between runs for various off-times. The data, for convenience, are plotted on probability paper using delay-time as ordinate and cumulative per cent as abscissa. Thus, for example, the percentage of the delays occurring between zero and three seconds is given by the abscissa at the intersection of the curve and the 3-second line.

The evidence of Figure 3 makes it possible to accumulate all the data without regard to off-time, and present a composite picture of delay, representing in this case the results of 900 applications of voltage. This is curve *A* of Figure 4.

In order not to be extravagant in the use of recorder paper, the recorder operating time for each operation was generally about ten seconds. Thus, any delay in excess of slightly over nine seconds could not be measured. In all the plotted data, therefore, all delays in excess of nine seconds are grouped, and the exact length of these delays is unknown.

Effect of Voltage

A comparison of curves *A* and *B* of Figure 4 shows the results of reducing the ignition transformer secondary peak voltage from 14,661 volts for curve *A* to 12,579 volts for curve *B*. Observe, for example, that with the transformer operating at a secondary peak voltage of 14,661, in 98 per cent of the cases the delay was five seconds or less; but when the voltage is reduced to 12,579, in only 86 per cent of the cases was the delay five seconds or less. Also note that for 14,661 peak volts, in 99.6 per cent of the cases the delay was eight seconds or less; but for 12,579 volts, the delay was eight seconds or less in only 93.5 per cent of the cases.

An even more striking result of changing the applied voltage can be seen by a comparison of Figures 5 and 6. The two curves shown here represent the most carefully controlled set of data obtained to date, and show clearly that an approximate 50 per cent increase in voltage applied to the spark gap results in a 10-fold decrease in delay.

Effect of Electrode Surface Condition

In an effort to determine the significance of electrode surface condition, several series of data of one hundred points each were taken following careful polishing of the electrode surfaces. Successive

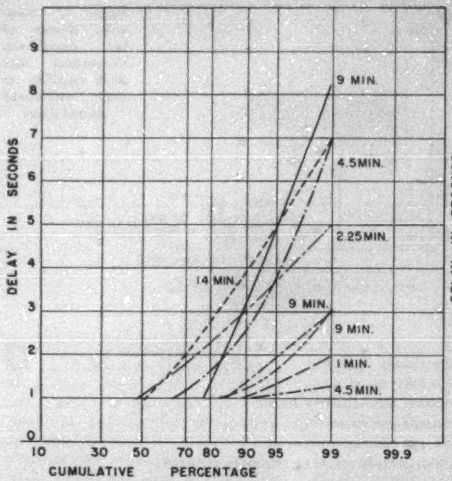

Figure 3. Effect of "off-time" on delay. Transformer A secondary peak volts 14,661. Data of April 3 to April 19, 1950

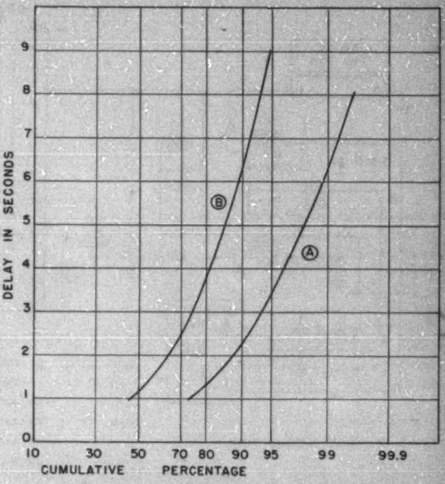

Figure 4. (A). Transformer A, delay for secondary peak voltage of 14,661. (Summation of data of Figure 3). (B). Transformer A, delay for secondary peak voltage of 12,579. Data of January 27 to February 24, 1950

firing caused the surface to gradually change from an initial mirror-like condition to a condition of marked grayness and quite noticeable pitting. Such a series of data are shown in Figure 7 which are actually the data from which Figure 5 was plotted. Figure 7 represents data taken in the order of numbering of the curves. Prior to run number one, the electrodes were carefully polished to a mirror-like appearance by the use of number three zero metallographic dry emery paper as the final polishing agent and microscopic observation at a magnification of approximately thirty times. Between runs one and six, in each case the electrodes remained untouched, but were observed by the microscope.

An examination of the figure seems to indicate that the delay is progressively worse as the electrodes are fired, but after a time, the delay becomes less and may even improve over the initial polished condition. The data are quite fragmentary, and there has been some evidence that this effect does not always appear. This is not surprising in light of the many other possible variables.

SUMMARY OF DATA

Figure 8 presents a summary of a portion of the available data. It covers measurements from June 28 to November 25, 1950. All data were obtained with Transformer *B* at a secondary peak voltage of 14,661 volts. The curve shows the tremendous range of possible delay. It also shows an apparent contradiction of the effect of polishing the electrodes; curve (14a) before polishing shows longer delays than curve (14b) after polishing, but curve (15a) before polishing shows shorter delays than curve (15b) after polishing. In addition, these data indicate that there is no noticeable effect of the spark orientation, that is, whether the spark occurs in the horizontal or vertical plane.

EFFECT OF IRRADIATION

It seemed obvious that the ignition delay could be greatly reduced by irradiation of the gap, and this was investigated during some preliminary studies using a 3/16-inch gap. Experiments showed that delays could readily be reduced from a range of several seconds to well below one second. Under the particular conditions of this test, for example, without irradiation 25 per cent of the delays exceeded two seconds; whereas with irradiation, under otherwise identical conditions, no delays exceeded 3/4 of a second. The irradiation was from a neutron source producing in the region of the spark gap approximately 500,000 ion pairs per cubic centimeter per second, per atmosphere.

Field Study

As was stated in the Introduction, the tests described above were carried out as a

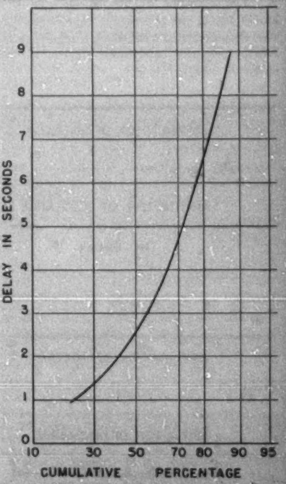

Figure 5. Transformer B, delay for secondary peak voltage of 14,661 volts. Data of July 12 to July 21, 1950

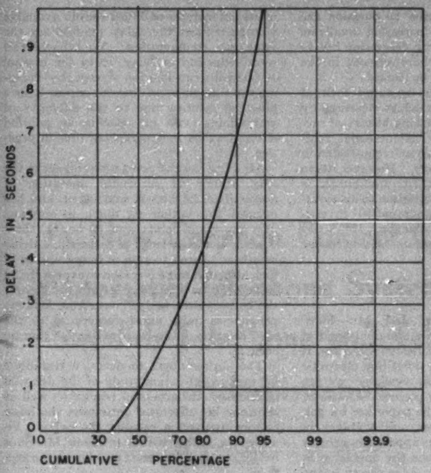

Figure 6. Transformer *B*, delay for secondary peak voltage of 22,403 volts. Data of August 2 to August 8, 1950

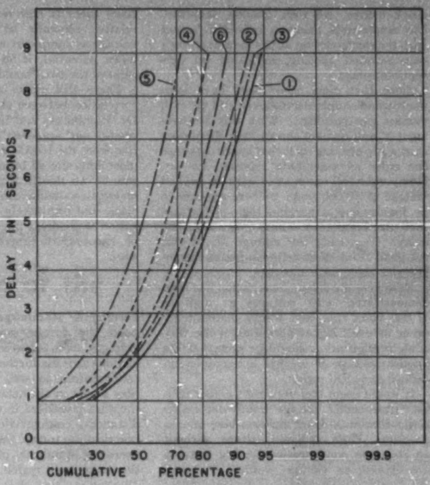

Figure 7. Effect of electrode surface condition on delay. Data or Figure 5.

result of a series of "puffs" that occurred in a number of oil burner installations. These burners were using from five to fifteen gallons of oil per hour. A study of the phenomenon in the field forced the conclusion that ignition delay was responsible. This conclusion is emphasized by the following facts.

Plans were made to install a series relay in the ignition transformer primary, and this relay, operated only upon ignition, then energized the motor driving blower and pump. Thus it would not be possible to have an explosive mixture in the boiler before ignition was present.

To date, 142 such relay installations have been made, the first on October 29, 1949, and the great majority during the months of December 1949, and January 1950. All of the burners thus equipped have functioned entirely satisfactorily.

Conclusions

The tests reported here show that long ignition delays are possible with the commonly used ignition system of gun type oil burners. The delay could be effectively reduced either by arranging for adequate irradiation of the gap, or by a 50 per cent increase in secondary voltage of the ignition transformer.

The basic factors causing the long delays have not yet been discovered, but a program of investigation is anticipated. It is the intention to study the phenomenon by use of a simulated oil burner system to permit control of all possible variables. It would be valuable to have available data as to the maximum permissible delay for various rates of fuel consumption. It should be remembered that a delay of short duration may not be the cause of a serious "puff," but may be responsible for excessive noise and vibration.

Discussion

M. W. Sims (General Electric Company, Fort Wayne, Ind.): After Dr. Hamburger's first disclosure of investigations indicating

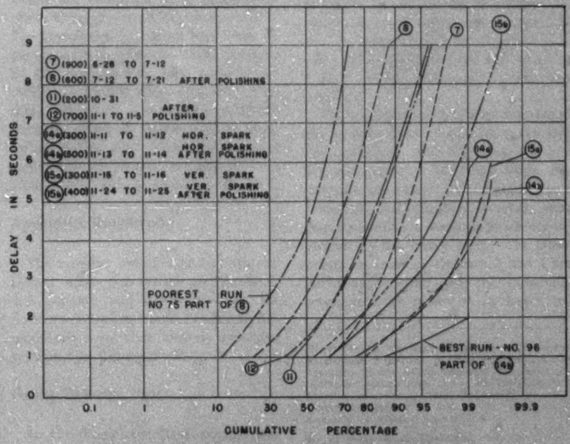

Figure 8. Summary of data from June 28 to November 25, 1950. Transformer *B*, secondary peak volts 14,661

spark delays, we were frankly skeptical. Our simple tests, using an unfired oil burner with the electrodes set at the manufacturer's recommended spacing, indicated no perceptible delays.

Since that time other tests have been made using simple electrodes in still air with various gap spacings. With this arrangement it was quickly shown that there does exist a gap spacing such that spark delays of the order of magnitude reported by Dr. Hamburger will occur, even with an applied voltage of 10,000 volts. There appears to be, for any gap, a marginal band of voltages such that breakdown occurs only after some delay. Increasing the voltage above this marginal band effectively eliminates the delay—for that particular gap.

However, the delay phenomenon has been demonstrated with voltages as high as 17,000 volts rms, and would undoubtedly occur at even higher potentials if the electrode configuration should be such that the applied voltage is in this not-completely-defined marginal region.

It would seem therefore that higher ignition transformer voltage would not necessarily eliminate spark delay where it is a problem. High available voltage, without an electrode configuration having suitably low breakdown voltage, would be wasted. Also, there is real reason to question the relative economy of increasing available voltage as compared with decreasing breakdown potential, if an improvement in the ratio of the two should be needed.

There still exists an apparent lack of correlation between the delays measured by Dr. Hamburger and the long history of successful, and apparently instantaneous, ignition from the 10,000-volt source provided in most domestic oil burners. However, there can be no doubt that Dr. Hamburger is making a valuable contribution in his systematic and completely unprejudiced investigation of the delay phenomenon. He should be encouraged to continue this excellent work.

Ferdinand Hamburger, Jr.: Mr. Sims' point, that for any gap a marginal band of voltages exists for which delays will occur, is obvious as is his further point that electrode configuration as well as available voltage play a part in the delay picture. However, the data presented in the paper are for gap distances, configurations and voltages in practical use today, thus apparently present operating standards place the operation in the "marginal" region. As is shown in the paper, an increase of 50 per cent in available voltage reduces the delay ten-fold for the same gap configuration. To achieve this same reduction in delay, using the normal 10,000 volts rms ignition voltage, by changing gap configuration does not appear to be a practical solution due to the difficulty of maintaining close gap spacings or pointed electrodes over long periods of time in practice.

Mr. Sims' second point with respect to the long history of successful operation of domestic oil burners is well taken, and has puzzled the author as much as anyone. The important points seem to be, (1) there is no actual knowledge of permissible delay length as related to rate of consumption of fuel, although there is reason to expect that a given delay will be more serious the greater the burning rate, and (2) data from field experience is quite unsatisfactory as to the identification of the cause of "puffs" that do occur.

The author hopes to devise a technique for making an actual study of the delay of ignition of oil burners in service as well as continue his efforts to determine the basic factors involved in causing the delay. Finally, the author wishes to thank Mr. Sims for his continued interest and his encouragement.

A New Common Control Crossbar Automatic Telephone System of the Swedish Telephone and Telegraph Administration

H. F. ROST
MEMBER AIEE

G. MODEE*
NONMEMBER AIEE

F. EK*
NONMEMBER AIEE

H. STRANDLUND*
NONMEMBER AIEE

IN 1926 the first crossbar automatic telephone office was placed in operation in Sweden at Sundsvall for 3,500 subscribers by the Swedish Telephone and Telegraph Administration.[1] Today there are about 1,750 crossbar telephone offices in Sweden serving 260,000 subscribers. The crossbar system used in these installations is known as the Standard 41 System of the direct dial controlled type and the links used for connections are progressively selected as in a step-by-step system.[2] The maintenance required to obtain reliable service in this system was so low that most of the small offices were left unattended. However, the first cost of the system was rather high. Therefore, an effort was made to design a new crossbar system which would have low first cost, low maintenance and improved traffic facilities.

This effort has materialized in a new common control crossbar system denominated *A-204*. This system is based on ideas proposed in 1912 by Betulander and Palmgren,† but for some reason their ideas were at the time not practically utilized.

When information, however, was obtained about the advantages of the American marker crossbar system, work was resumed to design a similar Swedish system. New telephone offices according to this common control crossbar system have been constructed in Sweden and others are being projected.

Application of the New Common Control Crossbar System

The new common control crossbar system can be used for all sizes of offices from 100 numbers up to the largest plants which are composed of a plurality of offices generally of 10,000 numbers each. The description presented here refers in particular to an office size about the same as the Slottsstaden office recently installed in Malmö City, Sweden. This office will have a capacity of over 20,000 numbers of which 10,000 will be ready for service in 1951. The first 5,000 of these were cut over in February 1950. A view of this office is shown in Figure 1.

Apparatus Employed

The crossbar switches and relays employed in this new system are the standard switches and relays used by the Swedish Telephone and Telegraph Administration in their various switching systems,[3] see Figures 2 and 3.

Group Selector Unit

In the direct controlled crossbar system,[1] each crossbar switch is used to carry only one connection at a time. A 100 point crossbar switch was used to reach one of 100 outputs. The outputs were multipled between switches as in the step-by-step system. Switches used in this manner with access to ten groups of ten outputs would require an average of 220 crosspoints per Erlang (36 unit calls) submitted. An average of 350 crosspoints per Erlang submitted would be required if 200 point switches with ten groups of 20 outputs were used. A feature of the new system is that the crossbar switches are used more efficiently in a link arrangement. An average of only 85 crosspoints per Erlang submitted is required. In the direct controlled Standard 41 System[1] all verticals of a crossbar switch were multipled together to give the switch a single input which could be connected to any of the 100 or 200 outputs. In the new common controlled link system each vertical unit is used as a separate 10 point switching device. Units of four 100 point crossbar switches are arranged in selector stages to give ten inputs access to ten groups of 20 outputs. Associated with each ten inputs is a common controller which serves to set up connection in the stage for one call at a time. As many as ten simultaneous connections may be successively established in each unit. Thus trafficwise one unit acts like a shelf of ten 200 point step-by-step selectors.

Figure 4 shows a simplified diagram of the crossbar switch connections of a unit of ten selectors. This diagram is the same for each selector switching stage employed in the system. The squares 1 to 4 represent four crossbar switches, each provided with ten verticals which are indicated by the heavy lines. The crosspoints on crossbar switches 3 and 4 are individually wired and the individual crosspoints are indicated by heavy tri-

---

* Coinventors of the automatic telephone system described in this paper.

† Swedish patent number 38,514.

Paper 51-321, recommended by the AIEE Communication Switching Systems Committee and approved by the AIEE Technical Program Committee for presentation at the AIEE Fall General Meeting, Cleveland, Ohio, October 22–26, 1951. Manuscript submitted October 20, 1950; made available for printing August 18, 1951.

H. F. Rost is at Djursholm, Sweden, and G. Modee, F. Ek, and H. Strandlund are all with the Swedish Telephone and Telegraph Administration, Stockholm, Sweden.

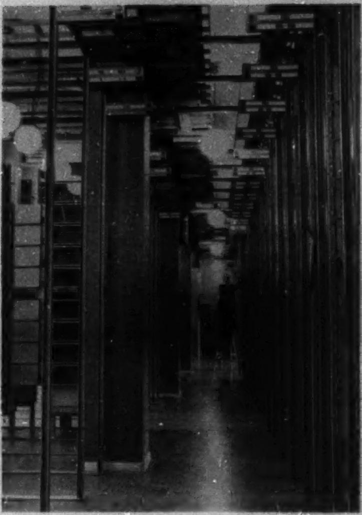

Figure 1 (left). General view of racks at Slottsstaden office in Malmö, Sweden

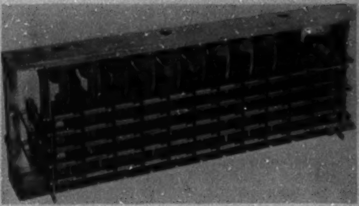

Figure 2 (right). Modern swedish crossbar switch

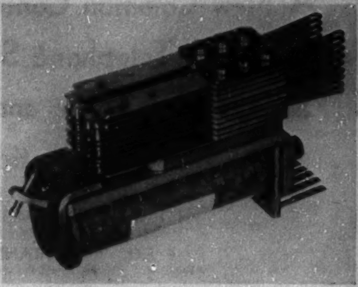

Figure 3 (right). Modern swedish general purpose relay

angles. Switches 1 and 2 are multipled horizontally. Each horizontal level is indicated by a fine horizontal line crossing the heavy lines.

Ten junctors, *F1* to *F10*, arrive at crossbar switches 1 and 2. Each junctor is multipled to two crossbar switch verticals, one in crossbar switch 1 and one in crossbar switch 2. These verticals act together as a 20 point switching device. Thus switches 1 and 2 act as ten 20 point switches, one for each incoming junctor.

The crosspoints of these 20 point selectors are horizontally multipled and connected to 20 links, *L1-L20*. Each link is connected to a vertical unit of crossbar switches 3 or 4. Each of the crosspoints of the verticals on switches 3 and 4 is connected to a junctor to the next stage. Thus each unit of selectors may reach a maximum of 200 outputs. These outputs are grouped so that the outputs connected to a single horizontal level form half of one group, the other half group coming from the corresponding horizontal level on the other switch. An example of an established connection through a group selector unit is indicated by heavy lines from junctor input *F1* over the closed crosspoint and crossbar switch 2 over link *L11* and through the operated crosspoint switch 4 to outlet 11 in group *D0*.

A call coming in over a junctor to a selector unit when the other nine junctors are idle can be connected to any one of the outputs in a group over one of twenty links. Each call makes busy one of the links, and when a call has been set up there are only 19 idle links for the next call so that in each of the other groups there is one outlet blocked in the selector unit. If nine calls are already set up in the unit, a tenth call arriving over the remaining idle junctor can reach outlets only through one of the 11 idle links. In a selector switching stage provided with units of this type lower output usage is obtained than that ordinarily obtained by step-by-step selectors hunting over groups of 20 outputs but is higher than that obtained when step-by-step selectors hunt over groups of ten outputs. Figure 5 shows an illustration of a rack of first selectors including their common controller.

Trunk Diagram

The arrangement of the switching stages to form the new system is shown in outline form in Figure 6. The selecting system is made up on a decimal basis, four stages being provided for offices having a capacity of up to 90,000 numbers. The subscriber lines terminate in a combined line switch-final selector stage. Line appearances on switches in this stage are used for both originating and terminating calls.

The system of this size is generally provided with senders and the figure shows a simple crossbar sender link with its associated controller. The junctors incoming to the first selectors are connected to a relay unit *GVR.* These relays serve to supervise the originating end of each connection and to enable the call to be switched to the register during the dialing period. Junctors incoming to the last selector switching stage are connected to another group of relays which provide talking battery supply and ring the called line and provide busy tone on calls to busy lines. Besides the junctors between the last selector and the line switch-final selector switching stages there are separate operating circuits between the controllers for these stages.

The vertical units of the crossbar switch use four make contacts at each crosspoint except in the last selector units and in the line switch-final selector units where four or five contacts per crosspoint are used. Each crosspoint is used for only one possible connection.

Twenty junctors are outgoing from each line switch-final selector unit to the first selectors and 20 junctors are incoming to the unit from the last selector switching stage. The output junctors from several line switch-final selector units are multipled together to achieve a greater concentration of traffic. The junctors between each selector stage are multipled and distributing frames may be provided for grading this multiple. Junctors between the third selector switching stage and the line switch-final selector

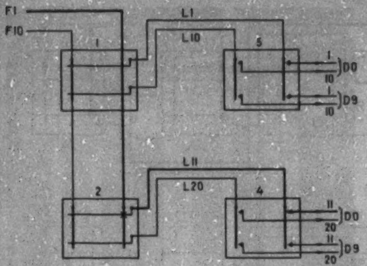

Figure 4 (left). Simplified diagram of a selector

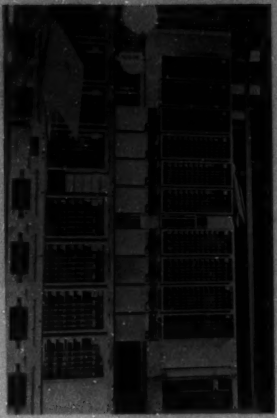

Figure 5 (right). Racks of first selectors

stage are not graded. Junctors from all third selector units serving a certain hundreds numerical digit are directly connected to the proper line switch-final selector unit.

Brief Description of Circuit Operation

Referring again to Figure 6, the following is a short description of the switching operations. When calling, subscriber *A* removes his receiver from the switchhook, his line relay is actuated, and the origination of a call is noted by the line relay unit and in the controller for line switch-final selector unit on which his line appears. The controller recognizes the origination of a call and hunts for an idle junctor to a first selector stage which has an idle controller. When such a junctor has been found a connection is set up in the line switch-final selector stage to the junctor. Through the controller for the first selector a connection is established to a sender link. Each first selector controller has access to two links to a sender selector. The sender selector controller actuates its crossbar switch to hunt for an idle sender. Once the sender selector controller is connected a signal is sent back to the *GVR* relay unit associated with the first selector junctor. This signal causes the operation of a holding relay in the *GVR* unit and operates the cut-off relay associated with the calling line. Thereafter the controllers of the line switch-final selector stage and the first selector stage are released and the sender selector hunts for an idle sender. When an idle sender is found the connection is established between the line and the sender and the sender selector controller is released. The subscriber now can dial the desired number. Two connections through a first selector controller to senders may be established at any one time. Thereafter the first selector controller is made to look busy so that its junctors will not be chosen by the line switch-final selectors originating calls. Figure 7 shows a rack of senders.

After sufficient digits are received by the sender it prepares to send (pulse) the information out to the various controllers to set up the call. The controller for the first selector stage through which the call is passed is called in again and the first numerical digit is pulsed to it. The first selector controller then tests to find an idle junctor associated with an idle controller to the desired second selector group. When such a junctor has been found, the connection is established through the first selector and the controller for the second selector is called in. The first selector controller is then released.

The second numerical digit is pulsed from the sender and received in the controller for the second selector. The second selector controller then hunts over the output junctors on its stage for an idle

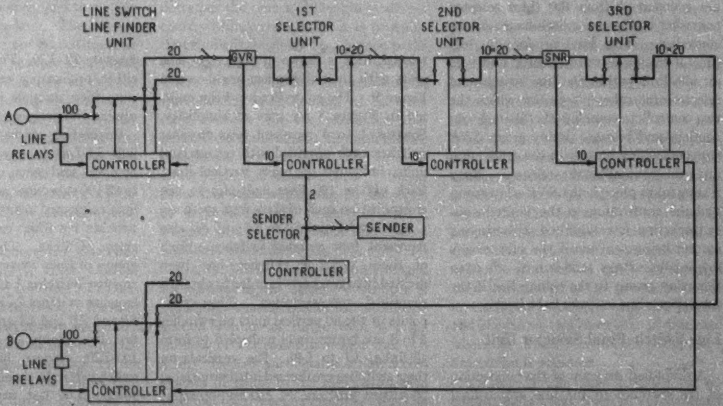

Figure 6. Diagram of internal routes of an office having a maximum capacity of 90,000 lines

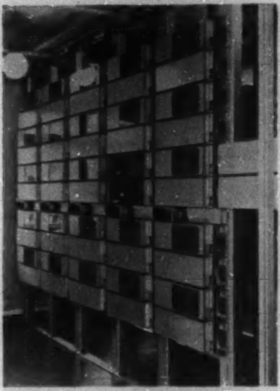

Figure 7. Rack of senders. Covers of one sender removed

junctor associated with an idle controller to the desired group in the third selector stage. When such a junctor is found the second selector controller may be released after setting up the desired connection.

The last three digits of the numbers are now sent to and registered by the third selector controller after which the sender and sender selector are released. Using the hundreds digit the controller of the third selector is connected over operating circuits to the controller for the desired hundreds group line switch-final selector. If the desired line switch-final selector controller is busy the third selector controller waits its turn. When the controllers are connected together the last two digits of the subscriber's number, that is, the tens and units numerical digits are transferred from the third selector controller to the line switch-final selector controller. The hunting for an idle junctor from the third selector unit and an idle link within the line switch-final selector unit takes place after which the two controllers establish the desired connections and release. Relay group *SNR* supplies talking battery to the connection after the controllers are released. Busy testing takes place in the *SNR* relay group and the connection to the desired subscriber's line is established with ringing current being sent out if the subscriber's line is idle. Busy tone is sent out from this relay group to the calling line if the subscriber's line is found to be busy.

Line Switch-Final Selector Unit

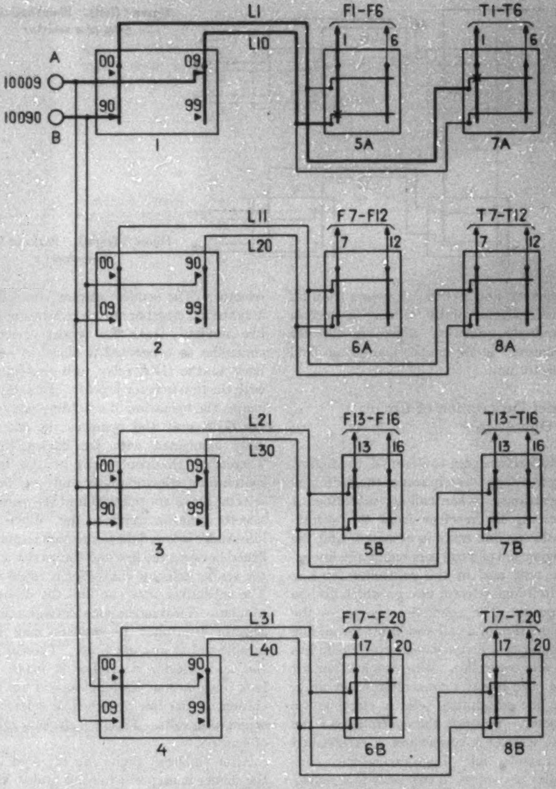

Figure 8. Simplified diagram of a line switch-final selector

A simplified diagram of the connection of the switches in the line switch-final selector unit is shown in Figure 8. The units with their controllers are shown in Figure 9. The controller has been omitted in Figure 8 for sake of simplicity. Squares 1 to 4 represent four crossbar switches each provided with ten vertical units, indicated by heavy vertical lines. Each of the 100 lines multiples to one crosspoint on each of these four switches.

Squares *5A* and *5B* to *8A* and *8B* also represent four crossbar switches. Each of these crossbar switches has been divided into two parts in order to obtain a simplified representation. The crosspoints of the 40 vertical units on switches 5 to 8 are horizontally multipled to form 40 links, *L1* to *L40*. The verticals on these switches are divided into two groups; 20 output junctors, *F1-F20* and 20 input junctors *T1-T20*. The links are used for either originating or terminating calls since they multiple before both the incoming and outgoing junctors.

Connection can be obtained over each link *L1-L40* to any of ten subscriber numbers, and connection can be obtained to all 100 subscriber numbers over the ten links connected to any one of the crossbar switches 1–4 which can be said to form a group of links. There are four such groups of links connected respectively to crossbar switches 1 to 4 and to parts of crossbar switches *5A* and *7A*, *6A* and *8A*, *5B* and *7B* and *6A* and *8B*. Each of the first two groups of links, *L1-L10* and *L11-L20*, appear before 12 crossbar switch verticals, six incoming and six outgoing. The last two groups of links,

Figure 9 (left). Racks of line switch, final selector

Figure 10 (right). Trouble recorder for recording out-of-order conditions

L21-L30 and *L31-L40*, appear before eight verticals each, four incoming and four outgoing.

Before a connection is established in the line switch-final selector unit, hunting takes place for idle links within the unit and idle junctors to the first selector or from the third selector. This hunting is in a fixed order beginning in the first group of links, then going to the second, third and fourth link groups in order. To carry the highest possible traffic load, the groups of links chosen first are provided with the greater number of outgoing junctors and incoming junctors than groups of links chosen later. The junctors to the first selectors are graded together with corresponding junctors from other line switch-final selector units so that ten line switch-final selector units comprising 1,000 subscriber numbers are normally provided with 50 to 70 junctors to first selectors. The 20 incoming junctors from the third selector units are directly connected to the group outputs of all the third selector units in the same thousands numerical group.

The subscriber numbers are associated with the crosspoints of these crossbar switches as indicated in Figure 8 by numbers at the crosspoints (00-99). The lines are connected in crossbar switches 1 and 3 in such a manner that those having the same units digit are connected to the crosspoint multiple of a certain vertical unit. The lines are further connected to crossbar switches 2 and 4 in such a manner that lines having the same tens digit are connected to the crosspoint multiple in a certain vertical unit.

The sequence of selection for each call takes place in such a manner that a link wired to a vertical unit for a units digit is selected alternately with a link connected to a vertical unit for the tens digit. The manner of connection of subscriber lines in the line switch-final selector unit thus forms a pattern whereby a grading here called "alternate sequence grading" is obtained. The alternate sequence grading decreases the chance of blocking calls because within certain limits it is probable that traffic is distributed by chance to the verticals which are successively selected. There is a gain in this arrangement, in spite of the small amount of material used, because, for the permitted congestion, the traffic density through the line switch-final selector unit can be relatively high, and because that particular subscriber lines will hardly be subjected to abnormally high congestion with a number of by chance unsuitably placed high duty subscriber lines.

Mr. G. Modée has furnished methods for calculating the necessary number of switching elements needed for handling a certain volume of traffic with a given number of lost calls in the new link system.[4] He has particularly studied congestion of traffic in the line switch-final selector unit when subscriber lines of heavy traffic are by chance connected to such a unit.[5] The line switch-final selector unit is engineered on the basis of a normal load of 6.7 Erlangs (240 unit calls) with one call lost for every 500 handled (P = 0.002), but an amount of traffic of about 10–12 Erlangs can in fact be reached at this loss.

In Figure 8 heavy lines indicate talking paths set up in the line switch-final selector unit, one for incoming and one for an outgoing call. The outgoing call originates at subscriber *A* over a vertical unit crossbar switch 1 through link *L10* and over an operated crosspoint in crossbar switch *5A* to junctor *F1*. The incoming call is shown arriving over junctor *T1* through a crosspoint on crossbar switch 7 and over link *L10* through crossbar switch 1 to subscriber *B*.

When a line such as *A* originates a call its line relay in the *LR* unit is operated. If the controller associated with this line switch-final selector unit is idle, the line's tens and units digit, 0 and 9, are indicated by the line relay circuits. From these circuits the proper select bars on each of the crossbar switches 1 to 4 and *5A* to *8B* are operated and the four links *L10*, *L11*, *L30*, and *L31* which can be used to connect the subscriber's line to a junctor are tested. The operation of a relay for each group with idle links connects the test wires for the outgoing junctors to the controller which starts the testing operation. When an idle junctor, is found, for example *F1*, the connection is set up by the operation of the magnet connected with junctor *F1* and thereafter the magnet connected with link *L10* on switch 1 operates. A call start signal is then transmitted to the controller of the first selector associated with this junctor and thereafter this controller is dismissed when the cut-off relay of the subscriber's line circuit is operated.

Testing of idle links suitable for incoming calls takes place in substantially the same manner as for outgoing calls. A call from the third selector is preceded by testing to determine if the controller for the desired line switch-final selector unit is idle. Only one third selector unit may obtain access to the line switch-final selector unit at a time. Precedence is obtained by means of a lockout circuit.

After the line switch-final selector controller is seized, the tens and units digits are transmitted from the third group of selector controller unit. The tens and units numerical digits of the called subscriber are used in the line switch-final selector unit to operate the proper select magnets of the switches. Four links, for example *L1*, *L20*, *L21*, and *L40*, are the only ones which can be used to establish a connection to line *B*. The links are tested successively as before and if in this case *L1* tests idle, idle indications are sent to the third selector controller for those of junctors *T1* to *T6* that are idle. When an idle junctor has been found by the third selector controller the connection is established in the third selector and the line switch-final selector unit proceeds to set up the call from this junctor to the called line. The hold magnets associated with junctor *T1* and link *L1* are operated and the connection is established from the *SNR* relay circuit to the desired subscriber B. The controllers are released after the connection has been set up. Busy test is made by the *SNR* relay circuit which remains as a part of the established connection.

Group Selector Controller

The controllers of the different selector switching stages shown in Figure 6 are not entirely alike, but all controllers contain a crossbar switch connecting the incoming junctors to the respective controllers and progressively hunting for idle output junctors and relays for receiving numerical pulses. The controller for the line switch-final selector stage does not contain a crossbar switch, since it is comprised of nothing but relays.

Switching operations are of the simplest kind in the second selector unit. A junctor from the first selector unit is thus connected to a pulse receiving relay unit in the second selector controller over a vertical of the crossbar switch in the controller. Relays are provided in the controller for receiving numerical pulses over the tip and ring wires and a third wire of the junctor from the sender through the previously set stages. When the numerical pulses have been received, hunting is started for an idle link which has access to an idle junctor to the next stage in the desired group. When an idle junctor has been found the connection is established and the controller in the next stage is called in. When the controller in the next stage is connected a signal is sent back over the junctor to the controller in the second selector stage. As soon as this signal has been received the second selector controller is released. As long as the second selector controller is busy the other idle junctors to this unit cannot be called since they are artificially made busy.

The controllers of the other switching stages perform other functions in addition to the principal one just described. The controller for the first selector has access to two different sender selectors. Two calls can be simultaneously connected through the controller to senders. When the sender is ready to set up a connection the pulse receiving relays in the first selector controller are connected to the path from the sender during the time needed for operation of the first selectors.

As mentioned earlier the controller for the third selector receives three numerical digits. The tens and units digits are passed over twenty wires directly to the select magnets of the final selectors over a hundred group connector in the third selector controller. This connector is operated in accordance with the hundreds numerical digit to pick the required line switch-final selector unit.

Pulse Methods, Supervision, and Trouble Recording

Two types of controllers have been designed for the selector units, one receiving dial pulse and another for code pulsing. (Code pulsing is much like the panel call indicator pulsing used in the panel and crossbar systems in the United States.) The new common control link system can, therefore, without the addition of senders, interconnect with other systems where the selections may be made by dial pulses. Within larger offices of this system with senders code pulsing is used whereby connections are set up more rapidly. Small rural offices employ controllers which receive dial pulse directly and therefore need no senders. In such systems the selector controllers are still common to ten input junctors.

In order to reduce maintenance effort and maintenance cost many self-checking and trouble detecting features are included in the controllers. Thus, before a controller is released, it assures itself that the controller in the succeeding switching stage has received the call correctly. If trouble does occur the first controller engages a trouble recorder, and a record is made. The trouble recorder will automatically record a succession of troubles on a paper tape. Figure 10 is an illustration of the trouble recorder. It is expected that the cost of maintenance of the new common control system will be substantially less than that for the previous direct control system because the new system has very simple circuits, very few marginal adjusting requirements of relays, and the ease of locating trouble due to the availability of the previously mentioned trouble recorder.

Although economically suitable for large size offices, this new system is particularly well adapted for plants which need decentralization of offices because, according to experiences in Sweden, crossbar offices can be left unattended for long periods without any inconvenience.[6,7]

References

1. The Swedish Telegraph Administration's Crossbar Switch System, Standard 41, S. Vigren, A. Finström. *Tekn. Meddelanden fran Kungl. Telegrafstyrelsen* (Stockholm, Sweden), number 1–3 and 6–7, 1944.

2. Fundamentals, Strowger Dial Systems, Automatic Electric Company (Chicago, Ill.), *Bulletin 301.*

3. The Crossbar Switch—Its Design and Manufacture, E. I. Wiberg. *Ericsson Review* (Stockholm, Sweden), number 2, 1949, page 52.

4. Blocking Calculations for the Link System of the Telegraph Administration, G. Modée. *Tekn. Meddelanden fran Kungl. Telegrafstyrelsen* (Stockholm, Sweden), number 1, 1948, pages 9–22.

5. Blocking in Line Switch—Final Selector Unit Upon Random Connection of a Number of Subscribers with Heavy Traffic, G. Modée. *TELE* (Stockholm, Sweden), number 3, 1949.

6. Telecommunications in Sweden—Present and Future, H. Sterky. *TELE* (Stockholm, Sweden), number 1, 1949.

7. Considerations Regarding Most Convenient Size of Dial Offices in Large Local Systems, G. Modée. *Tekn. Meddelanden fran Kungl. Telegrafstyrelsen* (Stockholm, Sweden), number 1, 1945.

8. Blocking in Line Switch—Final Selector Unit in the Link System of the Swedish Telegraph Administration, G. Modée. *TELE* (Stockholm, Sweden), number 3, 1950.

No Discussion

A Heavy Duty Slip Regulator For Steel Mill Service

W. SCHAELCHLIN
MEMBER AIEE

G. E. MATHIAS
ASSOCIATE MEMBER AIEE

SLIP REGULATORS have been used as early as 1913 in connection with steel mill applications. They have been successfully applied for blooming mills where the heavy impact load peaks of the mill motors would result in excessive power surges.

Figure 1 illustrates a typical installation of this type consisting of a motor-generator set driven by a wound rotor induction motor. The secondary of this motor is connected to a slip regulator which automatically increases its resistance in case of heavy load peaks, thereby permitting the motor-generator set to slow down and give up part of its stored kinetic energy. In this manner it is possible to supply high momentary load peaks to the mill motor with a practically constant power demand from the a-c supply.

Old Design of Slip Regulator

The slip regulator that has been successfully used for many years is illustrated in Figure 2. It consists of a relatively large steel tank which contains the electrolyte, the cooling coils which are arranged around the tank wall to transfer the heat from the electrolyte to the cooling water, and three cylindrical insulating tiles. Each tile surrounds a pair of electrodes, one movable and one stationary, forming an adjustable 3-phase secondary resistor.

The moving system is partially balanced by means of a suitable counterweight and is operated from a direct connected torque motor which in turn receives its energy from a current transformer measuring motor input. If the motor load exceeds a certain value, the torque motor develops sufficient excess torque to separate the electrodes and thereby introduce secondary resistance.

New Type of Slip Regulator

In developing a new design slip regulator for steel mill service, emphasis was laid on the following features:

1. More compact design and reduction of weight.
2. Higher electrode efficiency.
3. Higher efficiency and more flexibility of the cooling system.
4. Improved operation and simplification of the regulating system.
5. Better accessibility and lower maintenance.

With these considerations in mind, a design of slip regulator illustrated in Figure 3 was established. This unit is completely self-contained and includes the heat exchanger to form a completely

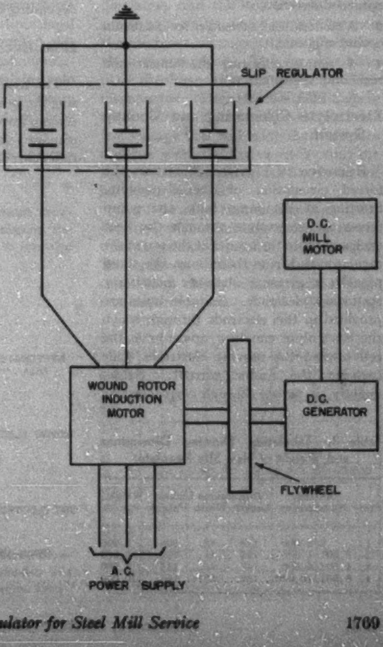

Figure 1. General arrangement of a blooming mill with slip regulator for a-c motor

---

Paper 51-322, recommended by the AIEE Mining and Metal Industry Committee and approved by the AIEE Technical Program Committee for presentation at the AIEE Fall General Meeting, Cleveland, Ohio, October 22-26, 1951. Manuscript submitted March 28, 1951; made available for printing August 28, 1951.

W. Schaelchlin and G. E. Mathias are with the Westinghouse Electric Corporation, Buffalo, N. Y.

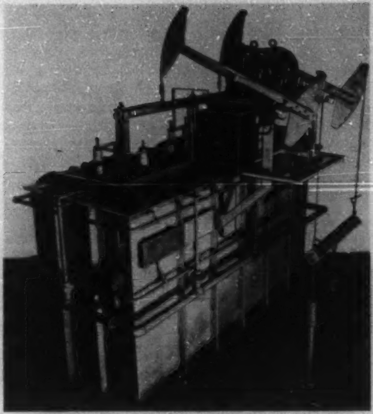

Figure 2 (left). Old type slip regulator for a 6,000 - horsepower blooming mill. Outline dimensions: 211-inch long × 134-inch wide × 192-inch high. Weight 23,000 pounds net

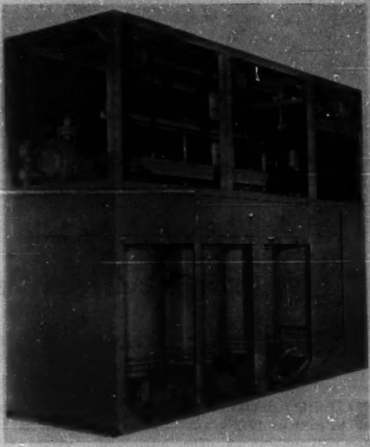

Figure 3 (right). New type heavy-duty slip regulator

closed circulating system. The dimensions and weights of the various ratings up to 10,000 horsepower are shown in Table I.

The outstanding new features of this new design are as follows:

1. Three separate cell assemblies insulated from each other.
2. Forced electrolyte circulation instead of natural convection.
3. A modern heat exchanger for maximum cooling efficiency.
4. A simple operating mechanism and regulating system.

Electrolyte Circulating and Cooling System

Reference to Figure 4 illustrates the forced circulation of the electrolyte. Starting at the sump tank, the pump forces the electrolyte through the heat exchanger into the header at the top of the regulator and from there down the stand pipe to a pressure chamber below the stationary electrode. Suitable holes are provided in this electrode through which the electrolyte can flow upwards in the cell toward the moving electrode while carrying the motor current. Subsequently, it passes through corresponding openings in the moving electrode and then rises to the top of the cell where it overflows and returns to the sump tank. This method of circulation insures a positive removal of the heat between the electrodes and thereby will permit a greater current density and a higher regulator load as compared to a system depending on natural convection.

Table I. Tabulation Showing Dimensions and Weight of New Slip Regulator

Size	Rating, Horsepower	Dimensions Inches, Length	Width	Height,	Weight, Pounds
1	0–2,000	118	38	105	5,000
2	2,001–4,000	132	41	110	6,000
3	4,001–6,500	147	45	115	8,000
4	6,501–10,000	162	50	125	10,000

Heat Exchanger

The heat exchanger used for transferring the heat from the electrolyte into the cooling water is shown in Figure 5. It is of standard design and contains a bundle of tubes carrying the cooling water. Special stainless steel is used for these tubes to give maximum resistance to mechanical wear as well as corrosion due to impurities in the cooling water. The tube bundle can readily be removed for inspection by unbolting one end plate as shown.

Cell Arrangement

The insulating cells are made of heavy asbestos cement, vacuum dried and impregnated with tung oil under heavy pressure. This insures a high grade insulation with no danger whatsoever of electrical breakdown so that the slip regulator can be safely applied to large motors with high secondary voltages.

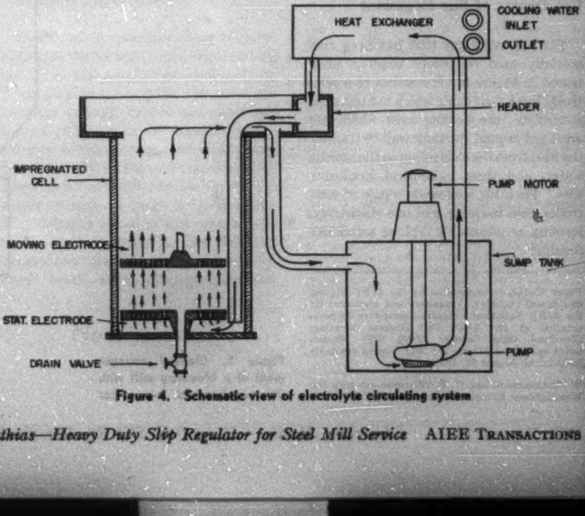

Figure 4. Schematic view of electrolyte circulating system

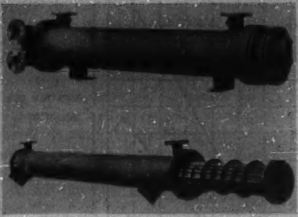

Figure 5 (left). Heat exchanger showing assembly of stainless steel tubes

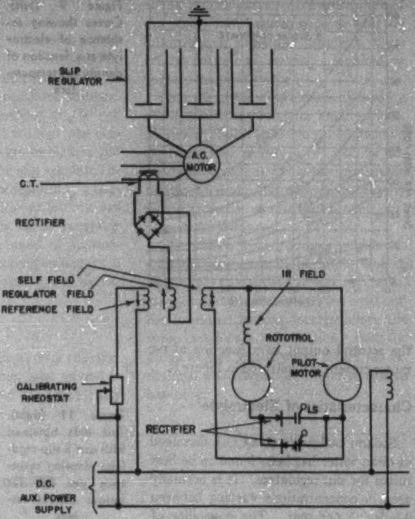

Figure 7 (right). Schematic diagram of regulating system

An additional feature of interest consists in the method of clamping the electrode to the bottom of the cell and fastening the cell to the top structure. Reference to Figure 6 shows that this is accomplished by laying a split ring into a circular groove in the cell and then clamping the electrode to a pressure ring provided with a 45-degree pressure surface. Experience has shown that this type of mounting for the electrode is very reliable and insures a tight seal without causing excessive stresses in the cell material.

Operating Mechanism

Reference to Figure 3 shows that the operating mechanism consists of a pilot motor driving the electrode shaft through a self-contained and grease lubricated worm gear. A counter-weight is provided to balance the moving system so that approximately equal motor torque is required in the raise and lowering directions.

Attached to the drive shaft is also a cam type limit switch for stopping the pilot motor at each end of the travel and for other miscellaneous purposes such as pilot lights, or interlocks, and so forth.

The simplicity of the electrical system is illustrated in Figure 7. It shows that the pilot motor is energized from a Rototrol, the output of which is proportional to the difference between a fixed reference field and a regulating field measuring motor current. A self-energizing field of the shunt type also is included to insure the necessary over-all amplification of the system.

At normal load, the reference and regulating fields are balanced and the Rototrol output therefore is zero. If, on the other hand, the motor load exceeds this value, the regulating field excitation predominates and the Rototrol will supply power to the pilot motor so as to increase the electrode distance, thereby reducing the a-c motor load. The opposite takes place of course, after the power peak has disappeared. The reference field ampere turns now are higher and produce a rototrol voltage that will bring the electrodes together until the limit switch stops the travel when the electrodes have reached minimum distance.

It will be noted that each limit switch is provided with a suitable rectifier to obtain directional selectivity of operation. This is necessary for systems that have a closed loop circuit without including directional contactors. A curve illustrating

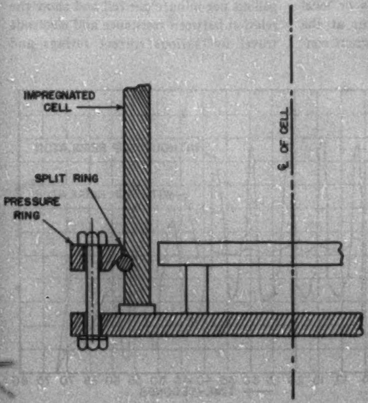

Figure 6 (left). Sketch showing method of clamping stationary electrode to insulated cell

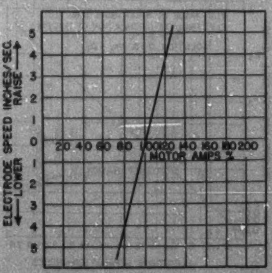

Figure 8 (right). Curve showing speed of electrodes as a function of a-c motor load

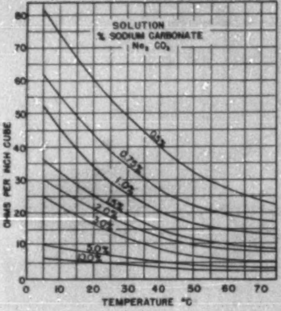

Figure 9 (left). Curves showing resistance of electrolyte as a function of density and temperature

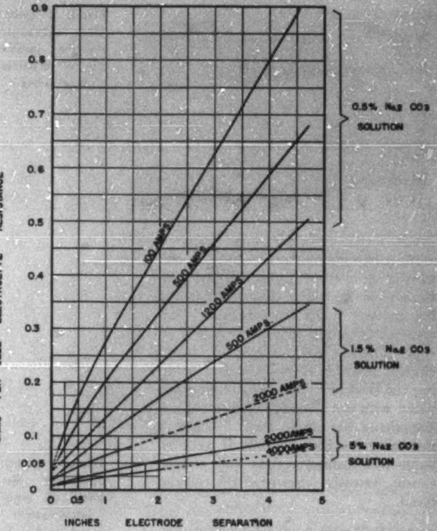

Figure 11 (right). Test data obtained with size 3 slip regulator showing resistance per cell for various current ratings

the rototrol output as a function of a-c motor current is illustrated in Figure 8.

Characteristics of Electrolyte

Sodium carbonate (Na_2CO_3), dissolved in clean water has been found to be best suited for slip regulators. It is normally used in concentrations varying between 0.5 and 5 per cent. The possibility of varying its density makes the application of slip regulators very flexible because it provides a means of readily changing their resistance to suit certain operating conditions and motor characteristics. A chart showing the relation between electrolyte density and resistance per cubic inch is shown in Figure 9.

These curves also indicate that the temperature affects the resistance to a considerable extent. It decreases with increasing temperature which, as is well known, is due to the increased ionization of the electrolyte. At 100 degrees centigrade steam bubbles are generated which tend to increase the resistance due to a reduction in cross section and which will also cause erratic operation of the slip regulator.

It is the usual practice to keep the electrolyte temperature below 70 degrees centigrade in order to avoid the formation of steam vapor.

Current Density of Electrolyte

The permissible current density of electrolyte and electrodes has been the subject of considerable discussion. However, it can be stated that it is primarily a function of heating, that is, the loss generated per cubic inch electrolyte and the rate at which the heat is carried away.

Thus, it readily can be seen that a good electrolyte circulating system is very desirable to avoid hot pockets or local steaming which is apt to occur at the electrodes because of higher current concentrations. It has been found that with the forced circulating system the current density can be raised up to 15 amperes per square inch without distress of any kind. To insure sufficient margin, however, it is recommended to operate the regulator between 6 and 10 amperes per square inch electrode surface.

Figures 10 and 11 show some interesting test results obtained with a slip regulator having an inside cell diameter of 20 inches and an active electrode surface of 250 square inches. These tests were made with a fixed electrolyte circulation of 30 gallons per minute per cell and show the relation between resistance and electrode travel for various current ratings and

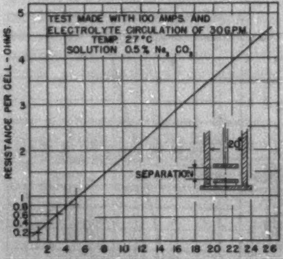

Figure 10 (left). Test data obtained with size 3 slip regulator showing resistance per cell for 100-ampere load

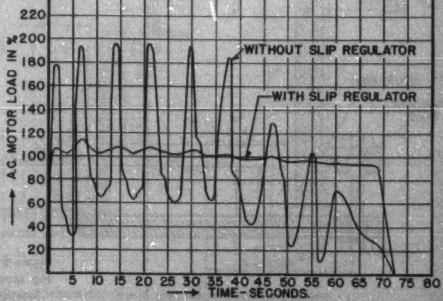

Figure 12 (right). Performance of a 6,000 - horsepower blooming mill showing power surges of a-c motor during a complete rolling cycle with and without slip regulator electrolyte densities. In all cases, the temperature of the incoming electrolyte was 27 degrees centigrade. It is to be noted that basically the electrolyte resistance is independent of current. The fact, however, that these test results show a decreasing resistance with increasing current is caused by the higher losses resulting in increased temperature of the electrolyte.

It was interesting to note that regardless of current and electrolyte density, boiling of the electrolyte started when the loss per cell reached about 400 kw. Of additional interest is also the fact that for zero electrode distance (electrodes not touching) the resistance does not decrease below a certain minimum value. This effect appears to be the result of a contact resistance which is independent of current and is proportional to the electrolyte resistance.

Operation

A typical operating cycle of a 6,000 horsepower blooming mill is illustrated in Figure 12. It shows the performance of the drive with the slip regulator adjusted to have zero rototrol output at 100 per cent load. Note that without the regulator the power peaks are as high as 130 per cent, while with the slip regulator in operation the surges are reduced to a negligible value. Of additional interest are the speed changes of the motor generator indicating a minimum speed of approximately 90 per cent corresponding to a maximum electrode travel of $3^1/_8$ inches.

Maintenance

In designing the new type of slip regulator, special attention was given to ease of maintenance and the accessibility of the various parts. All bearings are of the sealed ball bearing type so that no lubrication is needed. Moreover, there are no contactors or relays required to operate the pilot motor.

Long life of the electrodes is assured by the special alloy used for their surface. Moreover, both stationary and moving electrodes are readily accessible for inspection because it is a relatively simple matter to drain the respective cells by means of the valve provided for this purpose at the lower end.

The electrolyte pump, which is mounted submersed in the sump tank so as to avoid trouble due to leaking glands, is equipped with a stainless steel shaft and has its thrust bearing located above the sump tank for ready inspection. Both the pump as well as the pump motor are individual unit assemblies to insure ease of handling.

No Discussion

A Polyphase Thermal Kilovolt-Ampere Demand Meter

A. J. PETZINGER
MEMBER AIEE

Synopsis: In the past decade, the use of thermal meters has increased rapidly for the measurement of demand. The measurement of kilovolt-ampere demand by thermal means has been an objective of the metering industry for years. A few years ago, a polyphase thermal-ampere demand meter was developed. Using such a meter as a basis, voltage compensation has been added. The result is a combination polyphase watthour and thermal kilovolt-ampere demand meter as described in this paper.

THE COST of supplying electric service to a consumer is dependent on many factors. One of the major items of this cost is the relatively high investment which the utility must make. Generally, the cost of producing the energy consumed is less than the investment cost involved in making the service available.

The manner in which the consumer uses a given amount of energy also has a great effect on the investment required. A constant load requires relatively little investment in generation, transmission, and distribution facilities compared to an installation which draws large amounts of power at infrequent intervals.

These conditions have given rise to numerous rate schedules,[1] which endeavor to distribute the utility's cost equitably among its consumers. For many classes of service, the rate involves the measurement of energy and demand. Demand measurement may take the form of kilowatt demand, kilovolt-ampere demand, kilovar demand, or a combination of these, depending on the rate schedule.

In recent years, the emphasis in demand metering has been on reduction of maintenance. The use of thermal demand meters[2,3] has been of great value in attaining this objective. Reduction in maintenance has resulted in two principal benefits:

1. Reduction in the total cost of demand metering.
2. The extension of demand metering to loads on which such metering could not previously be justified on an economic basis.

Summary of Practical Methods of Measuring Kilovolt-Ampere Demand

As mentioned above, one form of demand rate which is commonly used is kilovolt-ampere demand. Many principles have been used to measure kilovolt-ampere demand with more or less accuracy and each has had its peculiar merits and drawbacks. Relatively few are in widespread use at the present time.

Most frequently used is probably the meter with kilowatt and kilovar elements and a ball mechanism which adds the two components vectorially. These meters can be used with demand registers or recorders to read true kilovolt-ampere demand. While the measurement is accurate for all variations encountered in service, the initial cost and maintenance expense are relatively high. This has limited the application of these meters to larger loads.

Another fundamental method commonly used is the use of phase-shifting transformers in conjunction with a standard watthour meter and demand register or with a thermal meter. Ideally, the potential applied to the meter is shifted by the same angle as the load current lags the voltage at maximum demand. In practice, several selected angles of shift are provided, and one of these is chosen and assumed to be reasonably close to the actual power factor angle. As long as these conditions hold, the results are reasonably good.

Thermal ampere demand meters are also used for kilovolt-ampere demand measurement by assuming a constant voltage. The accuracy is therefore proportional to the constancy of the voltage. Recently, a singlephase meter was developed with compensation for voltage variation.[4]

Review of Polyphase Thermal Ammeter Principles

Previous to 1946, thermal-ampere demand meters were confined to singlephase circuits. A thermal-ampere de-

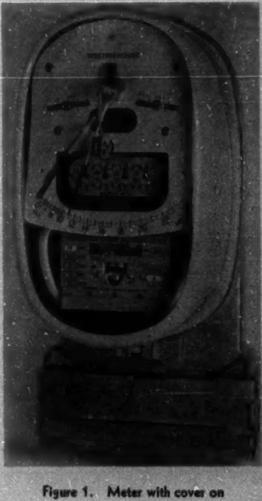

Figure 1. Meter with cover on

Paper 51-323, recommended by the AIEE Instruments and Measurements Committee and approved by the AIEE Technical Program Committee for presentation at the AIEE Fall General Meeting, Cleveland, Ohio, October 22–26, 1951. Manuscript submitted October 25, 1950; made available for printing August 28, 1951.

A. J. Petzinger is with the Westinghouse Electric Corporation, Newark, N. J.

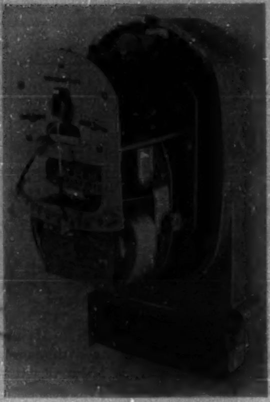

Figure 2. Meter with cover off

mand meter was then introduced which extended the thermal-ampere demand meter to polyphase circuits as well.[5,6,7] The meter described in this paper, shown in Figures 1 and 2, is a modification of the polyphase thermal ampere demand meter. A brief review of the principles and circuits of the polyphase thermal ampere demand meter will be helpful in obtaining a complete understanding of the new device.

In symmetrical component terminology,[8] all the current circuits are essentially positive-sequence networks, though this term is not ordinarily applied to unsymmetrical systems such as the 3-wire network or 3-phase 4-wire delta circuit.

The object is to produce a single current, the magnitude of which represents the kilovolt-ampere load of the circuit. To do this, it is necessary to:

1. Employ a method of properly shifting the phase of voltages derived from the individual currents (voltages proportional in magnitude to the magnitude of the currents).
2. Obtain their vector sum.
3. Apply this sum to a demand device.

No combination of the algebraic sums or differences of the currents will accomplish this. Figure 3 shows the basic circuit for 3-phase 3-wire services. Current transformers, a mutual reactance and a resistance are the circuit elements which develop the required voltage across the current element heaters. Similar circuits are used for 3-wire network, 3-phase, 4-wire delta and 3-phase 4-wire Y services. Figure 4 shows a typical wiring diagram for a complete meter.

Voltage Compensation

The kilovolt-ampere demand unit, Figure 5, is comprised of two distinct elements—current and voltage. Separate thermal elements respond to current and voltage changes in the circuit. The current element consists of two opposing bimetallic springs enclosed in separate chambers of a molded insulating box. The rear spring is heated by two heaters, one on each side, connected in series across the voltage e of Figure 3. The front bimetallic spring serves only for ambient temperature compensation.

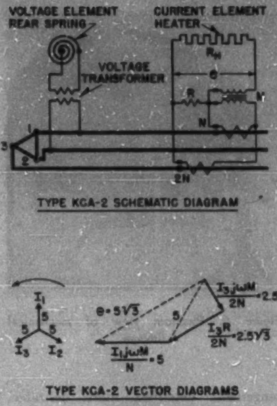
VOLTAGE ELEMENT REAR SPRING
CURRENT ELEMENT HEATER
R_H
VOLTAGE TRANSFORMER
e
R
M
N
1
2
3
2N
TYPE KCA-2 SCHEMATIC DIAGRAM
I_1
I_2
I_3
5
5
5
$e = 5\sqrt{3}$
5
$\frac{I_3 j\omega M}{2N} = 2.5$
$\frac{I_3 R}{2N} = 2.5\sqrt{3}$
$\frac{I_1 j\omega M}{N} = 5$
TYPE KCA-2 VECTOR DIAGRAMS

Figure 3. Schematic and vector diagram

In order to minimize the heat generated in the meter, the voltage demand unit, Figure 4, uses a directly heated bimetallic spring. A small transformer has its primary connected across one of the phases and its secondary connected directly to one of the bimetallic springs on the shaft assembly. An arm on this shaft is coupled to an arm on the current element shaft by a movable link. A phantom view of the mechanism is shown in Figure 6.

The current and voltage thermal units are arranged in an inverted V and the indicating pointer is geared to the current element shaft by 1-to-1 gearing. Actually, the current element shaft could serve as the pointer shaft, but space considerations in this meter make the ar-

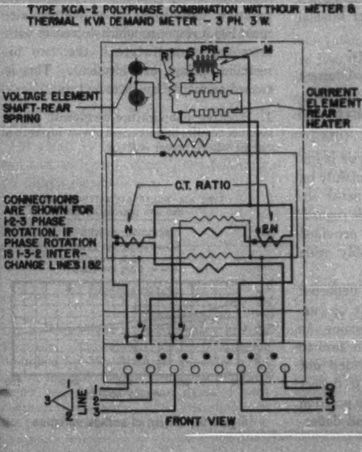
TYPE KCA-2 POLYPHASE COMBINATION WATTHOUR METER & THERMAL KVA DEMAND METER – 3 PH. 3 W.
VOLTAGE ELEMENT SHAFT-REAR SPRING
R
S
PRI.
F
M
S
F
CURRENT ELEMENT REAR HEATER
C.T. RATIO
N
2N
CONNECTIONS ARE SHOWN FOR 1-2-3 PHASE ROTATION. IF PHASE ROTATION IS 1-3-2 INTERCHANGE LINES 1 & 2
1
2
3
LINE
1
2
3
LOAD
FRONT VIEW

Figure 4 (left). Wiring diagram, 3-phase 3-wire meter

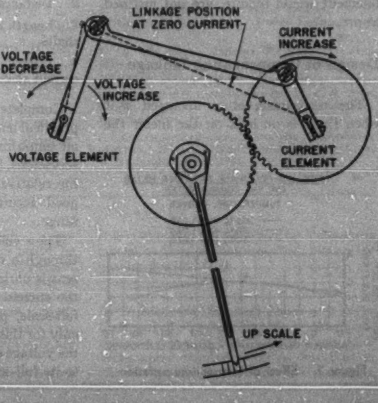
LINKAGE POSITION AT ZERO CURRENT
CURRENT INCREASE
VOLTAGE DECREASE
VOLTAGE INCREASE
VOLTAGE ELEMENT
CURRENT ELEMENT
UP SCALE

Figure 5 (right). Pointer mechanism

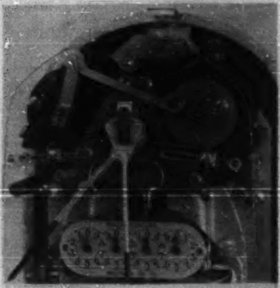

Figure 6. Phantom view of mechanical linkage

rangement described more desirable. The meter is basically a polyphase-ampere demand meter whose reading is modified by voltage changes, acting through the voltage element, to give kilovolt amperage.

The meter takes into account individual magnitude and phase variations of the currents, but assumes that the voltages are balanced, as it measures the voltage variations of only one of the phases. Balanced voltage is an assumption common to 3-wire single-phase watthour meters, 2-element 4-wire watthour meters, and all polyphase kilovar metering. Unbalance in voltage could also be taken into account by a positive sequence filter in the potential circuit. However, polyphase systems are usually rather well balanced in voltage and the errors of the meter described are smaller than those of the common form of phase-shifting transformers used for kilovar metering.[7] Increases in size and cost, which further refinement would require, are not justified at present.

Design of Compensating Linkage

The mechanism is so arranged that when there is no load on the meter the link and the arm on the current element shaft are in line. Therefore, under these conditions voltage variations do not cause any motion of the pointer. As deflection of the current element increases, however, the influence of the voltage element increases proportionally due to the angular relation. The two thermal units and the linkage mechanism are designed to give a correct indication of kilovolt amperage over a wide variation of voltage and currents. Since the two elements are electrically independent, they are obviously not affected by changes in power factor.

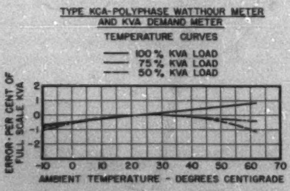

Figure 7. Effect of temperature variation

Figure 5 shows a schematic diagram of the linkages between the voltage and current units. When the linkage is adjusted as described previously, the voltage element is exercising a slight restraint on the current element over the operating range.

The voltage compensation action is very similar to that of the common type of full-scale adjuster used on most thermal meters. At zero current, changes in voltage have no effect on the reading, as the link is under slight tension and is in line with the current arm. As the current increases, the position of the current arm makes the voltage element increasingly effective in its influence on the pointer deflection.

The object is to have the pointer deflection change the same amount for a given percentage change in voltage as for the same percentage change in current and to accomplish this with the greatest possible efficiency.

A number of factors are involved in attaining this goal:

1. Torque, temperature, and deflection characteristics of the two sets of bimetal springs.
2. Distance between shaft centers.
3. Length of arms on voltage and current shafts.
4. Length of link between voltage and current shaft arms.

Complete mathematical analysis is impractical and development was mainly on an empirical basis. A few general observations, however, can be made regarding relative values which have provided good accuracy over a reasonably wide range.

The voltage element is deflected through a relatively small angle as current is varied from zero to full-scale. As the current element moves from zero to full-scale, power must be provided not only for this deflection, but also to deflect the voltage element from its zero position to its full-scale position. A small deflection of the voltage element over this range therefore minimizes the power required in the current circuit.

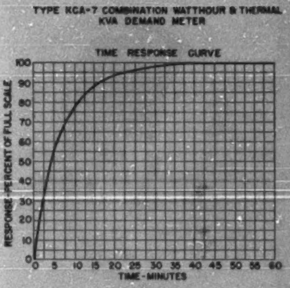

Figure 8. Time response curve

The angle between the link and the voltage element arm remains relatively close to 90 degrees at all times. This assures effective utilization of the torque of the voltage element as the voltage changes.

The angle between the link and the current element arm is close to 90 degrees at full scale. This assures maximum effect of the voltage element on the current element at full scale as the voltage changes.

Design of Temperature Compensation

The design of the current element is practically the same as that of the ampere-demand meters referred to above,[8] and the current element is therefore substantially independent of ambient temperature variations. The voltage element has a response which decreases with increasing temperature if the two bimetallic springs are identical. This is caused primarily by three factors:

1. Positive temperature coefficient of resistance results in decreased power input in a circuit where power $= E^2/R$.

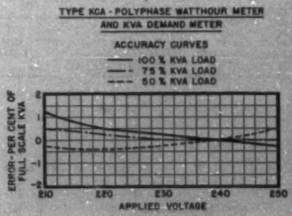

Figure 9. Effect of voltage variation

2. The temperature-deflection curve of the bimetal is not completely linear.

3. At higher temperatures the radiation of heat from the insulating chamber of the hotter of the two springs increases more than that of the compensating spring.

Accuracy over the operating range is attained by the use of unequal width bimetallic springs for the potential element, the heated spring having greater torque than the compensating spring. This, of course, would make the device inaccurate for ambient temperature variations at zero and very low voltages, but these are not operating conditions, and are therefore of no consequence.

The compensation of both the current and voltage elements for ambient temperature variation results in performance of the complete meter as shown in Figure 7.

Calibration and Adjustment

As in all commercial measuring devices, means must be provided to adjust the meter for various conditions. Since the watthour meter and thermal meter are independent, they may be calibrated in whatever order is more convenient. The watthour meter adjustments are the same as those of the corresponding watthour meters.

The adjustments of the thermal meter consist of:

1. Phase-balance adjustment.
2. Adjustment of the linkage.
3. Zero adjustment.
4. Full-scale adjustment.

Phase balance is adjusted by moving a sliding keeper above the air gap in the mutual inductance. This assures that the meter will read correctly on any single-phase load or combination of singlephase and polyphase loads. It is most easily checked by vacuum-tube voltmeter readings taken across the heater element with the same current applied to successive phases.

At about 10 per cent above rated voltage and with zero current, the following conditions should be true:

1. The pointer should be on zero.
2. The link should be directly in line with the current element arm.
3. The voltage arm should be exercising practically no force on the link.

The arms on both the current and voltage element shafts are locked in position by screws which can be loosened to obtain these conditions.

Zero is adjusted by a vernier screw which moves a helical spring to change tension on the tail of the indicating pusher pointer. It is so positioned that the spring has no effect at full-scale.

Full-scale is adjusted on a balanced polyphase load in the same manner as zero, except that the pointer is not affected at zero.

Meter Construction

The meter includes a standard polyphase kilowatthour meter in addition to the kilovolt-ampere demand unit described previously. The thermal unit and the watthour meter unit are independent. This is one of the advantages of using thermal means to measure demand. Ordinarily, kilowatt hours must be measured to satisfy the rate requirements. Relatively seldom is it necessary to measure kilovolt-ampere hours or kilovar hours. The elimination of this unnecessary information permits the two desired quantities to be measured by a single device which occupies a minimum of space. All the meters described are mounted in the same base as a standard 3-element watthour meter and use standard connections.

Performance

Like all thermal demand meters, this meter is defined as a class 3 lagged-demand meter in accordance with the Code for Electricity Meters.[9] The demand interval is considered to be the time required for the meter to indicate 90 per cent of the full value of a constant load suddenly applied. A curve of time response is shown in Figure 8.

The meter has a squared scale since the power generated in the current element heaters is proportional to the square of the current and likewise, the power generated in the voltage element is proportional to the square of the voltage.

The accuracy at different scale points for various ambient temperatures is shown in Figure 7. The errors at all points, from −10 degrees centigrade to 60 degrees centigrade are less than one per cent of full-scale. Figure 9 shows the accuracy for given kilovolt-ampere values at various applied voltages. Over the operating range of 210 to 250 volts, errors are seen to be less than 2 per cent of full-scale value. It will be noted that accuracy at low voltages has been emphasized in the design, since this condition is more likely than extremely high voltages, particularly at the time when maximum demand is established.

Conclusion

The development of a polyphase combination thermal kilovolt-ampere demand and watthour meter completes the line of thermal meters so that they can be used for all types of demand metering. The range of loads on which kilovolt-ampere demand can be metered economically, both as to initial cost and maintenance, has been extended greatly thereby.

References

1. Rates and Rate Making, P. M. Lincoln. *AIEE Transactions*, volume 34, 1915, part II, pages 2279–2318.

2. The Character of the Thermal Storage Demand Meter, P. M. Lincoln. *AIEE Transactions*, volume 37, 1918, part 1, pages 180–210.

3. The Case for the Thermal Meter, A. J. Petzinger. *Electrical World* (New York, N.Y.), volume 129, June 19, 1948, pages 82–83.

4. A New Thermal Volt-Ampere Demand Meter, M. E. Douglass, W. H. Morong. *AIEE Transactions*, volume 68, part I, 1949, pages 79–83.

5. Phase Sequence Device, A. J. Petzinger. United States Patent *2,513,890*.

6 Volt Ampere Responsive Device, A. J. Petzinger, B. E. Lenehan. United States Patent *2,513,891*.

7. A Polyphase Thermal Ampere Demand Meter, A. J. Petzinger. *AIEE Transactions* volume 66, 1947, pages 167–74.

8. Symmetrical Components (book). C. F. Wagner, R. D. Evans. McGraw-Hill Book Company, Inc., New York, N.Y., 1933.

9. American Standard Code for Electricity Meters. Edison Electric Institute, New York, N. Y., fourth edition, 1941.

Discussion

G. B. Schleicher (Philadelphia Electric Company, Philadelphia, Pa.): The meter described by Mr. Petzinger provides a desirable simplification in measuring kilowatt-hours and kilovolt-ampere demand with commercial accuracy. The description in the paper is confined to the indicating form of demand meter. Fundamentally, it appears that the same mechanism could be adapted also to a graphic chart instrument if sufficient torque is available. Thus it would be possible to use this relatively simple meter in place of the more complicated kilovolt-ampere demand meters that measure also quantities that frequently are not needed.

The question is raised, therefore, whether it is contemplated to produce an instrument along the lines of that described, but in the graphic demand form.

G. D. Stobbart (Missouri Power and Light Company, Jefferson City, Mo.): The combination kilowatt-hour and thermal kilovolt-ampere demand meter as described in Mr. Petzinger's paper should fill the existing need for a relatively low-cost meter to accurately measure energy and kilovolt-ampere demand of polyphase loads.

Based upon catalog information, this new meter has a favorable initial cost when compared to present types of meters. Maintenance costs for the new meter should also be favorable in comparison to presently available meters, as the new meter has a minimum of complex mechanisms that are a part of present meters.

The new meter being compact and contained in one case also presents installation advantages. The amount of accessory equipment, such as test switches, wiring and size of meter enclosures may be reduced with a saving in material costs and installation labor. The new meter, because of its size and standard connections, could ordinarily be placed in existing installations with little or no change in the physical make-up of the installation.

The demand unit of the new meter is of the indicating type with an additional pointer to indicate maximum demand and this type of indication is satisfactory for a majority of polyphase loads. However, there are some installations where a chart record of a customer's demand is helpful, particularly for load analyses. It is realized that the addition of mechanisms for chart drive and recording would increase the cost and size of the meter, but the thought is advanced for consideration by meter designers.

Perry A. Borden (The Bristol Company, Waterbury, Conn.): In designating the instrument a "thermal kilovolt-ampere demand meter, the title of Mr. Petzinger's paper agrees with the nameplate as shown in the illustrations; but nothing in the description would justify the liberty which has thus been taken with the definition. The device appears to embody little more than an improvement, in the form of a voltage compensation, over that described in the same author's A.I.E.E. paper of 1947.[1] While the earlier instrument is referred to as a "polyphase thermal ampere demand indicator," the author would seem to imply that compensation effected in the manner shown qualifies the present device as responsive to volt-amperes, rather than amperes. This is most misleading; and, whatever the merits of the instrument, it should be presented for what it really is and not for what the author would like it to be. Though the Institute is hardly in a position to dictate how the manufacturer shall mark the nameplate of his instrument, and though the reviewers have passed the paper for publication, I would urge that in the interest of correct terminology the author be asked to alter its title to be more correctly descriptive of the apparatus to which it is directed.

Considering the difficulties which have been encountered in incorporating such relatively simple concepts as demand and power-factor in commercial rates, it would be interesting to learn the reaction of the nontechnical commercial customer to a contract involving the intangible magnitude which this instrument purports to measure.

Reference

1. See reference 7 of the paper.

A. J. Petzinger: Mr. Schleicher and Mr. Stobbart have indicated the desirability of developing a combination kilowatthour and graphic thermal kilovolt-ampere demand meter. Such a development would be entirely practical from a technical viewpoint since adequate torque is available. However, it should be kept in mind that a graphic thermal meter would reintroduce a number of factors such as pen, ink, paper chart and motor, which are partly responsible for relatively high maintenance costs of present recording kilovolt-ampere demand meters.

If in the future there are indications that there is a considerable market for such a device its development would naturally follow.

Mr. Borden has criticized the designation of the meter as a kilovolt-ampere demand meter. Since the meter indicates kilovolt-ampere demand with good accuracy over the commercial range of all variables, it would seem obvious that it should be called a kilovolt-ampere demand meter. It is independent of load balance. It does assume voltage balance—an assumption which is common to single phase 3-wire meters; 2-element, 3-phase, 4-wire, Y or delta meters; and all polyphase kilovar and kilovolt-ampere meters. The designation of such meters has not been questioned because of this assumption.

If Mr. Borden is questioning the method of compensation, because it does not follow a fundamental law over an unlimited range of voltage, it should merely be necessary to call attention to the fact that almost all commercial meters and instruments are accurate over a limited range of some variable. As an extreme example, synchronous clocks are accurate only at rated frequency. Many instruments and meters have vanes or pole pieces of a shape which follows no mathematical law but causes the device to be accurate over the desired range of variables.

Sampled-Data Control Systems Studied Through Comparison of Sampling with Amplitude Modulation

WILLIAM K. LINVILL
NONMEMBER AIEE

SAMPLING of a signal is compared to amplitude modulation by the signal of a carrier of regularly recurring unit impulses. The frequency spectrum of the sampled signal is periodic including the spectrum of the pure signal plus some complementary or ripple signals. Smoothing of sampled data is simply filtering to remove the ripple. With this point of view both sampled and unsampled data may be analyzed by the conventional frequency domain analysis familiar to engineers. A system containing some parts operating on sampled data and some parts operating on continuous data can be handled entirely by a simple extension of conventional frequency analysis. By this technique a given feedback system can be analyzed for stability and the exact nature of its output as a continuous time function can be predicted. The analysis is simple enough so that the design of a sampled-data servo system is as direct as the design of a conventional system. The prediction of the effect of cascaded filters and compensating networks on system performance proceeds in much the same way as it is done in the conventional studies of continuous-data systems.

What Is a Sampled-Data Control System and What Unique Problem Does Its Analysis Present?

A sampled-data control system is one wherein the signal supplied to one or more parts of the system is not given continuously in time, but is supplied at discrete values of the time variable, t. In such a system, the part of the system being fed intermittently might, for example, have an input signal applied to it at $t=0$, T, $2T$, $3T$, . . . (where T is the length of time between samplings) with no data at all supplied in the intervals separating these sampling instants. A control system makes use of sampled data when it is impossible to supply continuous data to all its parts. For example, if digital computers are used in control systems, the data output from the computer must be supplied intermittently, hence the data supplied the remainder of the control system from the computer will be sampled. In radar tracking of moving targets, the information on the position of a given target is supplied intermittently, at instants separated by the scanning period. In all cases wherein pulsed detectors are used on amplitude-modulated signals, the output of the detector is intermittent, being sampled at carrier frequency for a half-wave detector or at twice carrier frequency for a full-wave detector. In all pulse-modulation systems, the data supplied by the pulsed signal is intermittent, being given only at the instants when the pulse occurs.

If the sampling frequency in a system being supplied intermittent data is high enough compared to the signal frequency and to the critical frequencies of the system, then the fact that the data are not supplied continuously has no important implications and the whole system behaves essentially as a continuous system.

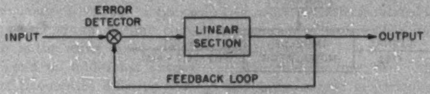

(A) SERVO WITH CONTINUOUS SIGNALS THROUGHOUT

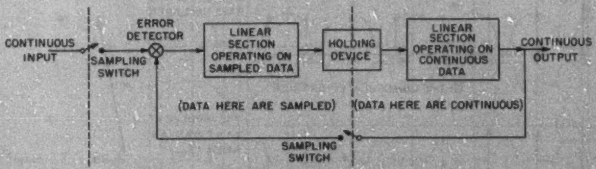

(B) SERVO HAVING SAMPLED DATA IN ONE PART OF THE SYSTEM AND CONTINUOUS DATA IN THE REST

Figure 1. A conventional servo and one having a sampled-data section

---

Paper 51-324, recommended by the AIEE Feedback Control Systems Committee and approved by the AIEE Technical Program Committee for presentation at the AIEE Fall General Meeting, Cleveland, Ohio, October 22–26, 1951. Manuscript submitted March 28, 1951; made available for printing August 28, 1951.

WILLIAM K. LINVILL is with the Massachusetts Institute of Technology, Cambridge, Mass.

The research described in this paper was part of a doctoral research program done in 1949 in the Servomechanisms Laboratory at Massachusetts Institute of Technology under Navy Contract *N5ori60*. The author wishes to acknowledge his indebtedness to Professors E. A. Guillemin, M. F. Gardner, and G. S. Brown, and to his colleagues on Project Whirlwind for their valuable assistance in carrying out the research and in the preparation of this paper.

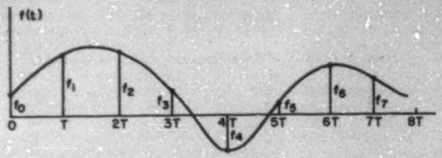

Figure 2. An example of sampled data

When the sampling frequency cannot be made high enough for this to be true, quite clearly the system will not behave as a continuous system.

Sampling of data often occurs in high-accuracy systems employing feedback. The basic objective in the use of feedback in any control is to allow a high-gain, or high-power controller of very low accuracy to be monitored by a low-power high-accuracy measuring system placed in the feedback loop. Such a system must employ a sensitive error detector. As is well-known, when the gain of the feed-forward section is increased, the over-all accuracy of the system is increased, but the problem of stability becomes critical. The system may become unstable when the gain is increased; for example, if there is too much difference in phase between the error signal and the resulting output. If the error signal is sampled instead of continuous, the stability problem becomes more acute and also harder to investigate. It is certainly possible to have a system which is perfectly stable and satisfactory when the error data are supplied continuously but which becomes unstable when the error is sampled.

Though the point of view presented in this paper is applicable to many types of sampled-data control systems which do not use feedback, the main emphasis will be placed on a study of a feedback control system with sampled error. A simple servo without and with error sampling is shown in Figure 1. The basic difficulty in describing sampled-data servomechanisms arises because part of the system operates on sampled data and part of it operates on continuous data. For that part which operates on continuous data, conventional analysis in the frequency domain is the best tool to use in the study of system behavior. For that part of the system which receives, operates on, and transmits sampled data, the use of sequences and linear difference equations is a very useful analytical approach. For a single system having a part operating on continuous data and a part operating on sampled data, the analysis would be greatly facilitated by a single technique which would work conveniently on both the continuous-data part of the system and on the sampled-data part. The two obvious approaches to this problem are: (1) the extension of the analytical method of sequences to the continuous part, (2) the extension of the conventional methods using the frequency domain to the sampled part. The first method has been exploited, as will be reviewed in the next paragraph. The second method is introduced in this paper.

Stibitz, Shannon, Hurewicz, and others have studied sampled-data control systems by use of sinusoidal sequences and linear difference equations. Essentially the approach they use is to describe the signal in terms of sequences rather than continuous time functions even in those parts of the system receiving, operating on, and transmitting continuous data. Such a procedure describes the whole system in terms of one kind of data and allows a thoroughgoing study of system stability, but it is so cumbersome that almost nothing more than stability can be studied. There are two serious shortcomings in this point of departure: (1) in much of the system continuous signals are received and transmitted so that many of the elements of the system could be properly and very conveniently described by conventional transfer functions, and (2) the output is continuous and should be expressed as a continuous function of time, rather than as a sequence. One needs a more complete picture than is given by knowledge of the output only at the sampling instants, but such information is hard to get from the difference equation approach.

This paper presents a procedure whereby the whole system, sampled-data or not, can be described in terms of continuous time functions. The resulting study of sampled-data systems becomes as easy and direct as the study of continuous-data systems. There are two types of junctures in a sampled-data control system which require special attention: (1) points where continuous data are sampled, and (2) points where the sampled data are smoothed and fed to a continuous-data part. Once the phenomena at these junctures are properly examined, one has merely to study the continuous-data part by conventional procedures and to formulate some analogous

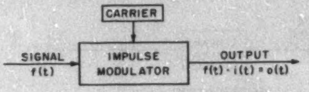

(A) THE DEVICE

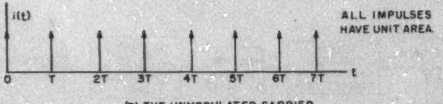

(B) THE UNMODULATED CARRIER

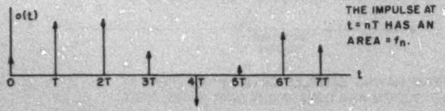

(C) THE MODULATED CARRIER

Figure 3 (left). How an impulse modulator effectively samples the continuous time function of Figure 2

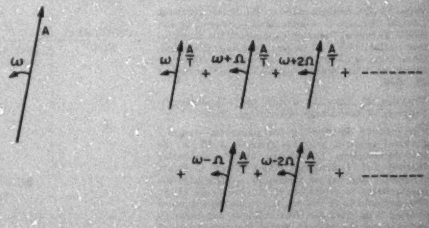

INPUT

OUTPUT OF IMPULSE MODULATOR

Figure 4 (below). Vectors describing a single exponential input to the impulse modulator and the resulting output

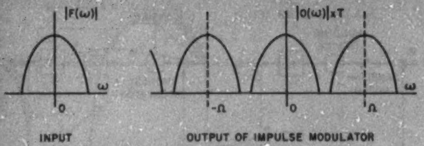

Figure 5 (above). Amplitude spectrum of an input to the impulse modulator and of the resulting output

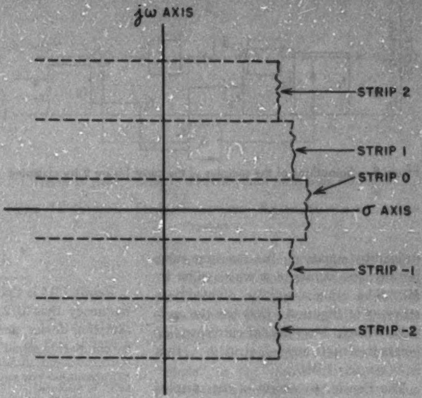

Figure 6 (right). Because of periodicity, O(s) has the same values at corresponding points in any two strips of the s-plane

procedure for studying the sampled-data part. Before this formulation is presented here, the nature of events at the indicated junctures will be investigated more closely.

Sampling Analogous to Impulse Modulation

The first problem of this paper is to describe sampled data in a form which is familiar to engineers and which allows it to be treated by conventional Fourier analysis. In Figure 2, $f(t)$ is a continuous time function which is sampled at regularly spaced instants. In describing only the sampled data, the continuous function $f(t)$ is replaced by the sequence $f_0, f_1, f_2, \ldots$. To avoid the use of sequences in describing sampled data, a fictitious analogous situation will be invented wherein the data have precisely the same information as that implied by the sequence but wherein the data are described by time functions rather than by sequences. Suppose that the time function, $f(t)$, is used to modulate a carrier made up of a string of unit impulses. Call the time function describing the unmodulated impulse wave $i(t)$. The output of the impulse modulator would then be $i(t)\times f(t)$, or a string of impulses whose successive areas bear a 1-to-1 correspondence with the sequence $f_0, f_1, f_2, \ldots$. A picture of the fictitious situation described above is given in Figure 3. In short, the process of sampling is entirely analogous to the process of impulse modulation. The great advantage of the latter point of view is that it allows the use of conventional Fourier analysis.

Consider now the response of the impulse modulator to a single exponential input $f(t)=Ae^{st}$. A Fourier analysis may be made of the impulse train, $i(t)$. The form of the exponential Fourier series will be:

$$i(t)=\sum_{n=-\infty}^{\infty}\alpha_n e^{jn\Omega t} \qquad (1)$$

where $\Omega=2\pi/T$, the sampling frequency, and α_n's are the Fourier coefficients. By performing the Fourier analysis it follows

$$\alpha_n=\frac{1}{T}\int_{-T/2}^{T/2} i(t)e^{-jn\Omega t}dt=\frac{1}{T} \qquad (2)$$

The impulse modulator output $o(t)$ is

$$o(t)=f(t)\times i(t)=Ae^{st}\sum_{n=-\infty}^{\infty}\frac{1}{T}e^{jn\Omega t} \qquad (3)$$

Carrying out the multiplication term by term, it follows

$$o(t)=\frac{A}{T}\sum_{n=-\infty}^{\infty}e^{(s+jn\Omega)t} \qquad (4)$$

Thus application of an input signal of complex frequency s to the impulse modulator results in an output component which is the exact input multiplied by $1/T$, and an additional output component of frequencies differing from s by integral multiples of sampling frequency $j\Omega$. For $s=j\omega$, the situation may be pictured graphically as in Figure 4.

Since responses of the modulator are additive, each signal component is handled independently. If a signal having an amplitude spectrum, $F(\omega)$, as shown in Figure 5, is applied at the input of the impulse modulator, the modulator output, $O(\omega)$, will be as indicated. The Fourier transform of the output is related to the transform of the input by:

$$O(\omega)=\frac{1}{T}\sum_{n=-\infty}^{\infty}F(\omega+n\Omega) \qquad (5)$$

It is impossible to describe the operation of the modulator by a transfer function because the transform $F(s)$ cannot be multiplied by any function of s independent of $F(s)$ which will yield the transform $O(s)$, since the latter is related to $F(s)$ by a summation or convolution and not by a multiplication.

Note that the transform of the impulse modulator output is periodic. $O(\omega)$ as

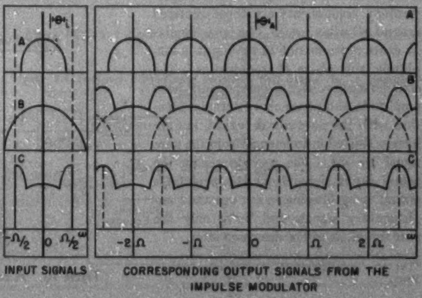

Figure 7. High-frequency input signals are lost in the impulse modulator. Three input signals and corresponding outputs

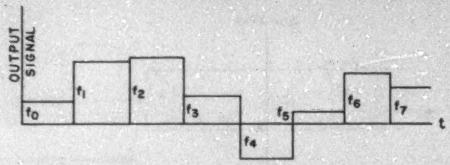

Figure 8. Smoothing of the samples of the curve Figure 2 by clamping

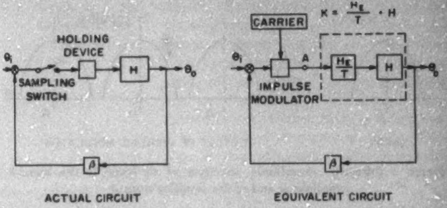
θ_i
HOLDING DEVICE
H
θ_o
SAMPLING SWITCH
β
ACTUAL CIRCUIT
CARRIER
$K = \frac{H_E}{T} \cdot H$
θ_i
A
$\frac{H_E}{T}$
H
θ_o
IMPULSE MODULATOR
β
EQUIVALENT CIRCUIT

Figure 9. A closed-loop servo system with error sampling and its equivalent circuit

defined by equation 5 has the same value for any two values of ω which differ by $k\Omega$. The s-plane can be divided into strips as in Figure 6. $O(s)$ has the same value in strip 1 as it has at corresponding points in strip 0, strip -1, strip -2, . . . that is, $O(s) = O(s+jk\Omega)$.

The Fourier transform of the sampled data should be expected to be periodic. Recall that the Fourier transformation of a periodic time function yields a Fourier series which is represented by a set of samples (impulses) in the frequency domain. The Fourier transformation of a set of samples in the time domain should accordingly be expected to yield a periodic frequency function.

The impulse modulator has two fundamental characteristics which are seen directly from its description in the frequency domain:

1. The impulse modulator output contains the exact replica of the input as well as unwanted or complementary* signals.

2. Any input signals of frequency greater than $\Omega/2 = \pi/T$ get mixed up with complementary signals and can never be regained.

Figure 7 gives the amplitude spectra of the input and output of the impulse modulator for three different signals. For result (1) consider signal A. The output signal of the modulator can be divided into two kinds, pure and complementary signals. The pure signal is the one component of the output which is centered around zero frequency. The complementary components are those centered around $n\Omega$ when $n \neq 0$. The pure signal is an exact reproduction of the input in amplitude and phase characteristics. The complementary signal components have amplitude and phase characteristics identical with the pure signal output, but are merely shifted in frequency from the pure signal by $n\Omega$. The way to regain the actual input signal from the modulator output is by filtering to cut out the complementary signals and leave only the pure signal, as will be discussed later.

Result (2)* is that no signal of higher frequency than $\Omega/2$ is transmitted by a sampling device, and it can be observed by comparing signal A to signals B and C in Figure 7. There would be no confusion as to what was pure signal and what was complementary signal in the case of the output to signal A. However, for input signal B and signal C, which themselves are radically different, the impulse modu-

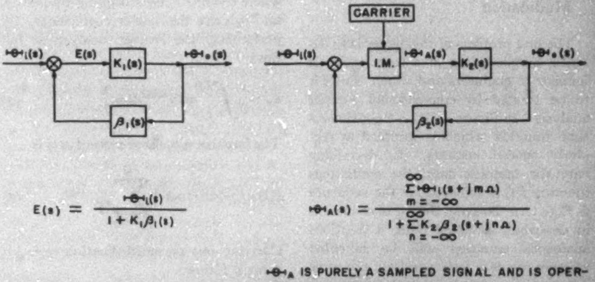
$\theta_i(s)$
E(s)
$K_1(s)$
$\theta_o(s)$
$\beta_1(s)$
CARRIER
$\theta_i(s)$
I.M.
$\theta_A(s)$
$K_2(s)$
$\theta_o(s)$
$\beta_2(s)$
$E(s) = \frac{\theta_i(s)}{1+K_1\beta_1(s)}$
$\theta_A(s) = \frac{\sum_{m=-\infty}^{\infty} \theta_i(s+jm\Omega)}{1+\sum_{n=-\infty}^{\infty} K_2\beta_2(s+jn\Omega)}$
θ_A IS PURELY A SAMPLED SIGNAL AND IS OPERATED ON BY THE LOOP AS IF THE LOOP DEALT ONLY WITH SAMPLED SIGNALS.
(A) EQUIVALENT CIRCUITS OF THE TWO SYSTEMS.
$\theta_i(s)$
CONTINUOUS INPUT
$\frac{1}{1+K_1\beta_1(s)}$
E(s)
CONTINUOUS ERROR
CARRIER
$\theta_i(s)$
I.M.
$\sum_{m=-\infty}^{\infty} \theta_i(s+jm\Omega)$
SAMPLED INPUT
$\frac{1}{1+\Sigma K_2\beta_2}$
$\theta_A(s)$
SAMPLED ERROR
CONTINUOUS INPUT
CONTINUOUS DATA
SAMPLED DATA
PERIODIC SYSTEM FUNCTION OPERATING ON SAMPLED INPUT TO YIELD SAMPLED ERROR.
(b) EQUIVALENT CASCADED SYSTEMS RELATING ERROR TO INPUT.
$\theta_i(s)$
$\frac{1}{1+K_1\beta_1}$
E(s)
K_1
$\theta_o(s)$
CARRIER
$\theta_i(s)$
I.M.
$\frac{1}{1+\Sigma K_2\beta_2}$
$\theta_A(s)$
$K_2(s)$
$\theta_o(s)$
CONTINUOUS DATA
SAMPLED DATA
CONTINUOUS DATA
SAMPLED DATA ARE SMOOTHED BY THE TRANSFER FUNCTION $K_2(s)$ BECAUSE IT IS NOT PERIODIC.
(c) EQUIVALENT CASCADED OVERALL SYSTEMS.

Figure 10. A comparison between a sampled-data control and a conventional type

---

*The term "complementary" was suggested by T. F. Jones.

*This result has been stated as a sampling theorem by C. E. Shannon.

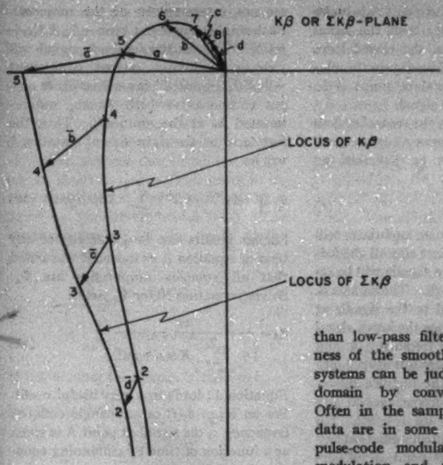

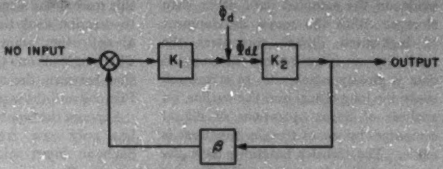

Figure 11 (left). Steps in obtaining ΣKβ locus from Kβ locus

Figure 13 (above). Feedback monitors the output in a continuous system

lator outputs are identical. When frequencies of pure and complementary signals overlap, the pure and complementary signals cannot be unscrambled, therefore signals of frequency Ω/2 or greater just cannot be transmitted by the sampling device. Thus, a fixed sampling rate imposes a limit on the frequency band of the signals that can be transmitted, and for signals of higher frequencies it is necessary to increase the sampling rate.

Smoothing of Sampled Data Is Linear Filtering

When sampled data are fed into a continuous-data section of a control system the problem of smoothing the data is important. From the preceding frequency analysis of sampled data, the problem of smoothing is seen to be nothing more than low-pass filtering. The effectiveness of the smoothing of two different systems can be judged in the frequency domain by conventional procedures. Often in the sampled-data section, the data are in some coded form, such as pulse-code modulation, or pulse-width modulation and the conversion from sampled data to continuous data involves some conversion operation in addition to filtering. One very popular type of filtering used in conjunction with such a conversion device is called clamping. When a converter output is clamped the procedure is to hold the latest sample until a new sample is supplied. Figure 8 shows how the sequence of samples of the curve of Figure 2 could be reconverted to continuous data by clamping. If the successive samples have little relative change, the clamping can be used successfully. If successive samples are very different, the use of a clamper is ineffective because it "remembers stale data." Study of the clamper in the frequency domain is very simple and enlightening. The purpose of the clamper is merely filtering the complementary signals out of the pure signals. Use of a clamper is the equivalent of applying the impulse-modulated data into a filter having an impulse response which is a pulse of unit height and length T. The transfer function of such a filter is $1/s(1-\epsilon^{-sT})$. This is a low-pass-filter characteristic with a slow cutoff. The proportion of complementary signal passed by the filter determines the amount of "ripple" in the smoothed output. In general, the specification of the smoothing filter is a typical filter problem which can be handled by conventional procedures. Theoretically, at least, if good smoothing is wanted, the lags which are inherent in a low-pass filter must be tolerated. Since the characteristics of both pure and complementary signals are known, the Wiener-Lee method for specifying optimum linear filtering is applicable.

Analysis of Sampled-Error-Data Servo Systems

With the description of the operation at the two important junctures in a sampled-data control system, the analysis problem would be well in hand if a description could be made of the operation on the signal by the continuous-data part of the system and the operation on the signal by the sampled-data part of the system. The operation of the continuous-data part is readily described by conventional transfer functions. Many sampled-data control systems have no operation on sampled data except storage, so this paper will be confined to cases wherein no operation is

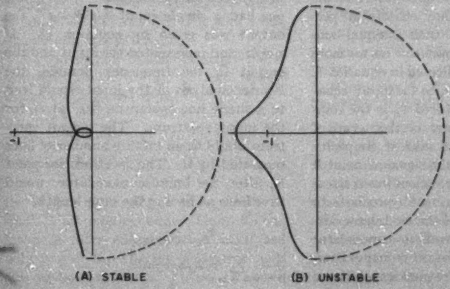

Figure 12 (left). Loci of ΣKβ for a stable and an unstable system

Figure 14 (below). Feedback monitors the output in a sampled-error-data system

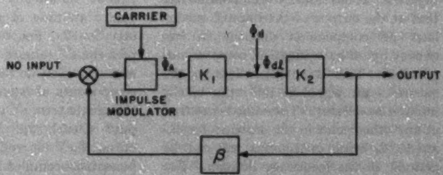

made on the sampled data other than storage. With the recent development of high-speed digital computers the feasibility of operating on the sampled data is greatly enhanced. In a research study by John Salzer and the author, an analysis of linear operations of digital computers by use of transfer functions is made. The transfer functions have the same periodic character as the Fourier transforms of sampled data. The point of view which describes sampled data as the equivalent of a modulated wave of unit impulses makes it possible to describe all parts of a sampled data control system by frequency analysis. The only restriction on the system is that it operate on the data in a linear fashion.

The present section will treat the analysis of a sampled-error-data servomechanism which has no dynamic elements operating on the data while it is in sampled form. Figure 9 shows such a system along with its equivalent circuit. The combination of sampling switch and holding device is replaced by the combination of impulse modulator and filter. The effect of the impulse modulator is indicated in equation 5, but the $1/T$ factor is now transferred to the filter. This arbitrary transfer makes the pure component of the modulator output equal to its input and will facilitate further analysis. The holding filter has low-pass characteristics, as defined by its transfer function $H_B(s)$, which is the transform of its unit impulse response. For reasons stated above, $H_B(s)$ is changed to $H_B(s)/T$ and can be combined with the rest of the feed-forward section $H(s)$. The product $H\times(H_B/T)$ is called $K(s)$ and considered a single transfer function.

APPLICATION OF THE EQUIVALENT CIRCUIT TO THE STUDY OF A SAMPLED-ERROR-DATA SERVO SYSTEM

The one interesting phenomenon which makes a sampled-error-data servomechanism somewhat harder to analyze than a conventional servomechanism is the fact that complementary output signals are fed back and enter as error signals into the sampling device where they contribute to the pure output. Refer to the output of the impulse modulator (point A) in Figure 9. It has already been pointed out that at the output of the impulse modulator all components differing in frequency by $n\Omega$ have identical complex amplitudes. This is so regardless of the nature of the signal at the input of the impulse modulator. The same is not true at any other point in the system; for example, θ_o being continuous will not be periodic in the frequency domain. For this reason, the signal at point A is easier to describe analytically than the signal at any other point in the closed loop. This fact leads one to investigate the relation between the signal at point A in Figure 9 and the input signal.

Suppose the input to the control system has only one frequency component. Such an input might be described by equation 6,

$$\theta_i(t)=\Phi_i\epsilon^{s_1t} \tag{6}$$

The input to the impulse modulator will contain not only $\theta_i(t)$ but also all the fed-back signals. All these signals will be related to the value of θ_o. The signals θ_o are all linearly related to the signals at point A, Figure 9. Since the input signal $\theta_i(t)$ has only a single frequency s_1, and since new frequencies are introduced into the system only by the impulse modulator, the permissible frequencies at any point in the system are $s_1+jn\Omega$. No signal of any other frequency exists at any point; furthermore, at point A all permissible signals exist and have equal complex amplitudes. Call this complex amplitude Φ_A; then signal at A is given by

$$\begin{aligned}\theta_A(t)=\Phi_A\epsilon^{s_1t}+\Phi_A\epsilon^{(s+j\Omega)t}+\Phi_A\epsilon^{(s_1+j2\Omega)t}+\\ \Phi_A\epsilon^{(s+jn\Omega)t}+\ldots+\Phi_A\epsilon^{(s_1-j\Omega)t}+\\ \Phi_A\epsilon^{(s_1-j2\Omega)t}+\Phi_A\epsilon^{(s_1-j3\Omega)t}+\ldots\end{aligned} \tag{7}$$

If the fed-back signal was known, Φ_A could be found. The fed-back signal may be found in terms of Φ_A and $K\beta$. Call the fed-back signal $\theta_{fb}(t)$; then

$$\begin{aligned}\theta_{fb}(t)=-\Phi_A[K\beta(s_1)\epsilon^{s_1t}+\\ K\beta(s_1+j\Omega)\epsilon^{(s_1+j\Omega)t}+\\ K\beta(s_1+j2\Omega)\times\epsilon^{(s_1+j2\Omega)t}+\\ K\beta(s_1-j\Omega)\epsilon^{(s_1-j\Omega)t}+\\ K\beta(s_1+j2\Omega)\epsilon^{(s_1+jn\Omega)t}+]\end{aligned} \tag{8}$$

The signal input to the impulse modulator is

$$\theta_i+\theta_{fb}=\Phi_i\epsilon^{s_1t}-\Phi_A\sum_{n=-\infty}^{\infty}K\beta\times(s_1+jn\Omega)\epsilon^{(s_1+jn\Omega)t} \tag{9}$$

Equation 9 shows that the input to the impulse modulator may contain all permissible frequencies with unequal amplitudes, yet its output can be no more complicated than indicated in equation 7. It remains to relate Φ_A to the input, equation 9. As already noted Φ_A is the complex amplitude of any of the terms of equation 7. For the sake of simplicity pick the ϵ^{s_1t} term of the signal at point A and ask: How do the various input signal components of equation 9 contribute to this single term ϵ^{s_1t} of the modulator output? Clearly $\Phi_i\epsilon^{s_1t}$ leads to a modulator output $\Phi_i\epsilon^{s_1t}$ (as well as other output components of complex frequencies which we are not interested in at the moment). Each single component term $-\Phi_AK\beta(s_1+jn\Omega)\epsilon^{(s_1+jn\Omega)t}$ of the fed-back signal will yield a modulator output component $-\Phi_AK\beta(s_1+jn\Omega)\epsilon^{s_1t}$ (as well as other output components which we are not interested in at the moment). Thus the first term on the right side of equation 7 will be

$$\Phi_A\epsilon^{s_1t}=\Phi_i\epsilon^{s_1t}-\Phi_A\epsilon^{s_1t}\sum_{n=-\infty}^{\infty}K\beta(s+jn\Omega) \tag{10}$$

Similar results can be obtained for any term of equation 7, as indeed it was noted that all complex amplitudes are Φ_A. Solving equation 10 for Φ_A yields

$$\Phi_A=\frac{\Phi_i}{1+\sum_{n=-\infty}^{\infty}K\beta(s_1+jn\Omega)} \tag{11}$$

Equation 11 leads to a very useful result. For an input $\theta_i(t)$ of any single complex frequency s_1 the signal at point A is given as a function of time by combining equations 7 and 11; that is,

$$\theta_A(t)=\sum_{m=-\infty}^{\infty}\frac{\Phi_i\epsilon^{(s_1+jm\Omega)t}}{1+\sum_{n=-\infty}^{\infty}K\beta(s_1+jn\Omega)} \tag{12}$$

Since the coupling between point A and the servo output is made by a purely conventional linear element, the complex output signal is Φ_A multiplied by the conventional transfer function. Thus the amplitude of the output component having frequency $(s_1+jm\Omega)$ is $\Phi_AK(s+jm\Omega)$. Summing the output components and using equation 11 one obtains the output time function,

$$\theta_o(t)=\sum_{m=-\infty}^{\infty}\frac{\Phi_iK(s_1+jm\Omega)\epsilon^{(s_1+jm\Omega)t}}{1+\sum_{n=-\infty}^{\infty}K\beta(s+jn\Omega)} \tag{13}$$

Because of the fact that a sampled-data control system is a linear device, one can superpose responses and relate the Fourier transform of the output of such a system to the Fourier transform of the input by merely extending Equation 13. Where one had a simple input $\theta_i(t)=\Phi_i\epsilon^{s_1t}$, the output was given by equation 13. If $s_1=j\omega_1$ and represented the input and the output in the frequency domain, the Fourier analysis of the input would lead to a single line spectrum, $|\Phi_i|$, at ω_1 for the input spectrum. The output spectrum would be an infinite number of lines separated by Ω. The spectrum for point A, after the impulse modulator, would have lines all having the same length,

$$\left|\frac{\Phi_i}{1+\sum_{n=-\infty}^{\infty}K\beta(j\omega_1+jn\Omega)}\right|$$

At the output the same frequencies would be present as were present at A, but the respective amplitudes would be different because of the filtering properties of the feed-forward section after the impulse modulator.

The preceding discussion is nothing more than an interpretation of equation 13. Now, suppose that instead of applying an input having a single term in its Fourier transform, one applied an input having a Fourier transform $\Theta_i(s)$. The Fourier transform of the signal at the point A would be

$$\Theta_A(s)=\frac{\sum_{m=-\infty}^{\infty}\Theta_i(s+jm\Omega)}{1+\sum_{n=-\infty}^{\infty}K\beta(s+jn\Omega)} \qquad (14)$$

It follows that the output transform is

$$\Theta_o(s)=K(s)\Theta_A(s)$$

$$=\frac{\sum_{m=-\infty}^{\infty}\Theta_i(s+jm\Omega)}{1+\sum_{n=-\infty}^{\infty}K\beta(s+jn\Omega)}K(s) \qquad (15)$$

So far as the quantitative description of the system characteristics of a sampled-error-data servomechanism is concerned, equation 15 gives a complete story. Its physical significance now will be explored.

A sampled-error-data servomechanism has so much in common with a conventional continuous-error-data type that a comparison of the two is enlightening. Figure 10 pictures such a comparison. Parts (A) and (B) of this figure draw an analogy between the error signal $E(s)$ of a continuous-data system and the sampled-error signal Θ_A of a sampled-data system. In spite of the fact that the servo loop enclosing the impulse modulator has a major section which receives and transmits continuous data, the loop signal, Θ_A, at the output of the impulse modulator has characteristics entirely like the output of a system operating entirely on sampled data. The error, though sampled, is smoothed by the filter K_1, which has nonperiodic characteristics.

A good picture of the operation of the sampled-data-control system can be obtained by plotting the locus of

$$\frac{K}{1+\sum_{n=-\infty}^{\infty}K\beta(s+jn\Omega)}$$

for $s=j\omega$. This plot is very simple to make in all practical cases. Since $K\beta$ has low-pass filter characteristics $\Sigma K\beta$ has only two or three terms of large enough size to be important. Figure 11 shows the steps in obtaining a $\Sigma K\beta$ from the $K\beta$ locus. First lay out the $K\beta$ locus and mark off on it the ω-values. For the locus shown, the sampling frequency is 10 radians per second. Because the value of $K\beta$ is small for $\omega>10$, only the two low-frequency terms of $K\beta$ need be considered. As an example, to find $\Sigma K\beta$ for $\omega=4$, add $K\beta(j4)+K\beta(j14)+K\beta(j24)+\ldots+K\beta(-j6)+K\beta(-j16)+\ldots$. All terms except $K\beta(j4)$ and $K\beta(-j6)$ are negligibly small. The addition of these two terms is indicated by the vectors $K\beta(j4)$ and $\bar{b}=K\beta(-j6)$ in Figure 11. The process is repeated for $\omega=5$, 3, 2, et cetera. If it is wished to form $\Sigma K\beta$ for $\omega=6$, it would be found to be the same as $\Sigma K\beta$ for $\omega=6-10=-4$ which is the conjugate of $\Sigma K\beta$ for $\omega=4$. Once the $\Sigma K\beta$ locus is found, the system function $K/1+\Sigma K\beta$, is found exactly as in the conventional case. When the engineer has the necessary loci for a given system, what further problems does he face? Essentially there remain three questions:

1. What is the stability of the system?
2. How well are the complementary signals filtered out at the output?
3. How effective is the feedback link in monitoring the output?

INVESTIGATION OF STABILITY

In the study of linear continuous-data systems two avenues for determining stability are available: (1) the location of the roots of the characteristic equation obtained from the differential equation describing the system, and (2) the location in the s-plane of the poles of the system function. In the case of conventional linear systems operating on continuous data, both procedures are usable and results agree, but for linear systems operating on both sampled and continuous data, only the second method, essentially that of Fourier or Laplace transformation, is usable because differential equations cannot be used directly with sampled signals.

Recall that the use of Fourier or Laplace transformations to analyze a superposable system has three steps,

1. Transformation of the input.
2. Relation of the input and output transforms.
3. Composition of the frequency components of the output into a time function.

Even if the system is unstable, as shown by system function poles in the right half-plane, the output of the system is still described by its Laplace transform. The inverse transformation (step 3) is still unique with the abscissa of absolute convergence of the resulting output function moved to the right of all the poles. It is well to note that the conventional inverse Fourier transformation breaks down on the problem of composition of output components into a time function output when the system is unstable. The inverse Laplace transformation is still valid because the transformation integral is not evaluated along the imaginary axis in the s-plane as the inverse Fourier integral is, but along a vertical line to the right of all singularities, and hence the growing exponentials in the resulting time function are adequately handled.

With the assurance that the Laplace transform approach is valid even for unstable systems, one now passes to the application of it to test stability. One could say that a system is stable if its response to any bounded input has no growing exponentials; that is, the transform of the output has no poles in the right half s-plane. Reference to equation 15 indicates that the right half-plane poles of $\Theta_o(s)$, the transform of the output, can only come from the denominator of equation 15, because neither the transform of the input nor $K(s)$ will have poles in the right half-plane. The sufficient condition for stability of the system is that the 0's of $1+\Sigma K\beta$ be in the left half-plane. This condition is equivalent to saying that the -1's of $\Sigma K\beta$ lie in left half s-plane. Since $\Sigma K\beta$ is periodic in s of period $j\Omega$, all its -1's come in groups. If there be one -1 of $\Sigma K\beta$ in right half-plane there will be an infinite number of -1's each separated by multiples of $j\Omega$ from all the rest. The Nyquist plot is still a valid and convenient way to test for the presence of -1's in the right half s-plane. Figure 12 shows $\Sigma K\beta$ loci of a stable and an unstable system.

PRESENCE OF COMPLEMENTARY SIGNALS IN THE OUTPUT

Since the output of the impulse modulator has pure and complementary signals of equal size the only factor which suppresses complementary signals (those for $m\neq0$) before they get to the output is the smallness of $K(s+jm\Omega)$ compared to $K(s)$. In short, to suppress complementary signals, K must be made to have low-pass filter characteristics. The fact that feedback is present does not reduce at all the proportion of pure to complementary signals. As a matter of fact, this proportion is always the same for the output of an impulse modulator no matter where it is located. If any nonlinearity exists in the output member, such as would result from motor saturation, it is possible to have mixing of the pure and complementary signals in the nonlinear elements. This mixing is most troublesome when the input signal spectrum extends to frequencies near $\Omega/2$. The difference-frequency signals arising from the intermodulation could be very troublesome because they are of low frequencies and the natural low-pass filter characteristics of the output member would favor these purely noise signals over the higher frequency pure signals. The only cure for this trouble is to remove saturation effects from the nonlinear elements or if this is impossible to filter out complementary signals from the impulse modulator before they reach the nonlinear element.

EFFECTIVENESS OF OUTPUT MONITORING BY SAMPLED ERROR

The essential objective in the use of feedback in any control system is to monitor a high-power low-accuracy output element with a sensitive measuring device in a feedback loop. If a disturbance causes an output not called for at the input, an error signal goes down the feed-forward path to improve the situation. The effects of inaccuracies in the output member can be represented by disturbance signals applied at the input of the output members. Figure 13 shows such a representation. Assume for simplicity that the input is zero and that the disturbance is a single exponential of complex amplitude Φ_d and frequency s_2. The loop signal resulting from the disturbance can be called Φ_{dl}. It is smaller than it would be without feedback if the fed-back signal subtracts from Φ_d.

$$\Phi_{dl}=\Phi_d-K_1(s_2)K_2(s_2)\beta(s_2)\Phi_{dl} \qquad (16)$$

$$\Phi_{dl}=\Phi_d\frac{1}{1+K_1(s_2)K_2(s_2)\beta(s_2)}=\Phi_d\left(1-\frac{K_1(s_2)K_2(s_2)\beta(s_2)}{1+K_1(s_2)K_2(s_2)\beta(s_2)}\right)$$

The size of Φ_{dl} will be much smaller than Φ_d only if

$$1-\frac{K_1K_2\beta}{1+K_1K_2\beta}$$

is much smaller than unity. This will be true so long as

$$\frac{K_1K_2\beta}{1+K_1K_2\beta}$$

is nearly unity.

The use of feedback in a sampled-error-data system has the same objective as the use of feedback in a continuous-data system except for the fact that the monitoring is done on a "periodic check-up" basis rather than continuously. Figure 14 shows a possible representation of a disturbance in a sampled-error-data system. Sampling introduces two effects on monitoring. First the correcting signal, which is the output of the impulse modulator, will contain pure and complementary components with equal complex amplitudes Φ_A. The pure component is able to counteract the disturbance if it subtracts from Φ_d, but the complementary components are merely ripple and have no beneficial effect on the system output. The second consequence of sampling is that the size of the pure correcting signal depends on the sizes of both pure and complementary fed-back signals. Thus the amplitude of the pure component of the correcting signal at the output of the impulse modulator can be found by

$$\Phi_A=-\Phi_dK_2(s_2)\beta(s_2)-\Phi_A\sum_{n=-\infty}^{\infty}\times K_1(s_2+jn\Omega)K_2(s_2+jn\Omega)\beta(s_2+jn\Omega) \qquad (17)$$

Call the amplitude of the pure loop signal Φ_{dl}. Then,

$$\Phi_{dl}=\Phi_d+\Phi_AK_1(s_2) \qquad (18)$$

Combining equations 17 and 18 yields

$$\Phi_{dl}=\Phi_d\times\left[1-\frac{K_1(s_2)K_2(s_2)\beta(s_2)}{1+\sum_{n=-\infty}^{\infty}K_1(s_2+jn\Omega)K_2(s_2+jn\Omega)\beta(s_2+jn\Omega)}\right] \qquad (19)$$

The nearness of

$$\frac{K_1K_2\beta}{1+\Sigma K_1K_2\beta}$$

in equation 19 to a value of one is a measure of how well the sampled-error-data feedback system suppresses a disturbing signal of frequency s_2.

The correcting signal contains both pure and complementary signals. There are two aspects of this fact which deserve particular attention. First, if the disturbing signal frequency is less than $\Omega/2$, the frequency of the complementary components of the correcting signal all lie above $\Omega/2$ and can be filtered out by the feed-forward section, K_1K_2. Second, if the frequency of the disturbing signal is greater than $\Omega/2$, the frequency of some complementary component of the correcting signal lies below $\Omega/2$ and it causes a high-amplitude low-frequency output disturbance at the output which is more objectionable than the disturbance that initiates it. The feedback in this case makes matters worse than they would be without it. In short, the section between any high-frequency-disturbance inputs and the input to the impulse modulator must contain very good low-pass filters. In the above example $K_2\beta$ must be a low-pass filter. Furthermore, since feedback cannot reduce the corruption of the output due to a high-frequency disturbance, it is necessary to make K_2 by itself a good low-pass filter because it is the only obstacle standing between the actual disturbing signal and the output.

Summary of Analysis and Consequent Design Objectives

Treating the process of sampling as impulse modulation allows one to analyze a sampled-error-data system by conventional methods. The analysis is direct and the effects of changes in design appear as changes in K or β. In turn it is very easy to evaluate the effect of changes in K or β on the system performance. Having developed an analysis procedure one can now turn to a study of design objectives.

In any of the common control systems the objective in design is to obtain a system which will cause the output quantity described by the variable $\theta_o(t)$ to assume values as close as possible to those dictated by the input quantity, $\theta_i(t)$. At the outset it should be made clear that there exists no single, universal criterion of "goodness" of a control system. Below are three basic design conditions which are among the most important in sampled-data-control system design. No claim is made that they are *the criteria*, but they are at least worthy of consideration in a majority of practical cases.

1. The feedback monitoring must be effective; therefore, the value of $K\beta/1+\Sigma K\beta$ shall be kept close to unity for as much of the fundamental frequency range (from $-\Omega/2$ to $\Omega/2$) as possible.
2. The system response must be satisfactory; therefore the value of $K/1+\Sigma K\beta$ shall have, insofar as possible, an acceptable amplitude and phase characteristic up to the frequency $\Omega/2$.
3. Output ripple, produced by sampling, must be suppressed; therefore the transfer function $K(s)$ of the feed-forward element should cut off as sharply as practicable at $\Omega/2$.

Having reduced the analysis of sampled-data-systems to one similar to the analysis of conventional servomechanisms and having laid out design objectives, one can now design sampled-data control systems by conventional techniques.

References

1. FUNDAMENTAL THEORY OF SERVOMECHANISMS (book), L. A. MacColl. D. Van Nostrand Company, New York, N. Y., Chapter X, 1945.
2. THEORY OF SERVOMECHANISMS (book), James, Nichols, Phillips. McGraw Hill Book Company, New York, N. Y., Chapter V, 1947.
3. ANALYSIS AND DESIGN OF SAMPLED DATA CONTROL SYSTEMS (thesis), W. K. Linvill. *Project Whirlwind Report R-170*, Massachusetts Institute of Technology (Cambridge, Mass.), 1949.

Discussion

John R. Ragazzini and **L. A. Zadeh** (Columbia University, New York, N. Y.): There are several interesting results in this paper which correlate with some of the work done by the discussors in connection with the so-called z-transform method of analysis and synthesis of sampled-data control systems.

The z-transform of a function $f(t)$ is essentially the Laplace transform of the product $f(t)\delta_T(t)$ (where $\delta_T(t)$ represents a train of unit impulses with period T) expressed in terms of an auxiliary variable $z=\epsilon^{-sT}$ instead of s. The z-transform approach is closely related to the so-called "generating function" method of solution of difference equations which dates back to Laplace.[1] Other closely related methods are those due to Jordan,[2] Samuelson,[3] Tuttle,[4] and Stone.[5] The z-transform method as such and, in particular, its application to servomechanisms and pulsed filters is treated in two standard tests on servomechanisms[6–7] and, in somewhat greater detail, in a paper by Raymond.[8] Various extensions of the z-transform approach and its reduction to engineering practice now are under way and will be presented in forthcoming papers.

The connecting link between Dr. Linvill's and z-transform methods is placed in evidence by expressing the Laplace transform of a sampled function $f(t)\delta_T(t)$ in two different ways.

Thus, employing complex convolution, one can write

$$\mathcal{L}\{\delta_T(t)f(t)\}=\frac{1}{2\pi j}\int_{c-j\infty}^{c+j\infty}\Delta_T(x)F(s-x)dx \tag{1}$$

where $\Delta_T(s)$ and $F(s)$ are the Laplace transforms of $\delta_T(t)$ and $f(t)$ respectively. Substituting the expression for $\Delta_T(s)$.

$$\Delta_T(s)=\frac{1}{1-\epsilon^{-Ts}} \tag{2}$$

in equation 1 and performing the contour integration yields:

$$\mathcal{L}\{\delta_T(t)f(t)\}=\frac{1}{2\pi j}\int_{c-j\infty}^{c+j\infty}\frac{F(s-x)}{1-\epsilon^{-Tx}}dx$$

$$=\sum_{n=-\infty}^{\infty}F(s+jn\Omega),\quad \Omega=\frac{2\pi}{T} \tag{3}$$

Alternatively, interchanging the functions $\delta_T(t)$ and $f(t)$ yields:

$$\mathcal{L}\{\delta_T(t)f(t)\}=\frac{1}{2\pi j}\int_{c-j\infty}^{c+j\infty}\frac{F(x)dx}{1-\epsilon^{-T(s-x)}}$$

$$=F^*(\epsilon^{-sT})=F^*(z),\ z=\epsilon^{-sT} \tag{4}$$

where $F^*(z)$ is the z-transform of $f(t)$, as defined in references 6 and 7. Consequently, the connecting link between an infinite summation of the form 3 and the corresponding z-transform is

$$\sum_{n=-\infty}^{\infty}F(s+jn\Omega)=F^*(z) \tag{5}$$

which is equivalent to equation 65 of reference 6. It is of historical interest to note that the identity expressed by equation 5 was discovered more than a century ago by Poisson and is known as the Poisson summation rule.

The point which is being made here is that the infinite summations used by the author may be expressed in closed and generally simple form by using the z-transform formulation. As a matter of fact, the Nyquist plot of the function

$$\sum_{n=-\infty}^{\infty}K\beta(s+jn\Omega)$$

which is used by the author for the investigation of stability, can be constructed without any recourse to approximation by plotting the associated z-transform $K\beta^*(z)$ as z traverses the unit circle in the z-plane. This approach results in a considerable saving in time and effort.

From the standpoint of z-transform method, the input-output relation given by the author's equation 15 may be regarded as stemming from the expression for the z-transform of the error

$$e^*(z)=\frac{\theta_i^*(z)}{1+K\beta^*(z)} \tag{6}$$

Thus, multiplying this expression by the forward gain function $K(s)$ one obtains

$$\theta_0(s)=\frac{\theta^*(z)K(s)}{1+K\beta^*(z)},\quad z=\epsilon^{-sT} \tag{7}$$

which is equivalent to the author's result, equation 15.

In the past, the applications of z-transform technique in the field of servomechanisms have centered chiefly around the investigation of stability of sampled-data control systems. However, work now in progress indicates that the z-transform method also can be used advantageously for the design of such systems by shaping the loop transmission function $K\beta^*(z)$ in much the same manner as in the case of continuous control systems.

In conclusion, it is believed that the z-transform method has much promise as a tool in the analysis and design of sampled-data control systems, although the frequency analysis technique developed by Dr. Linvill is frequently more practicable and has the unquestioned advantage of being more easily applied by the engineer familiar with the conventional techniques of handling continuous control systems.

REFERENCES

1. DU CALCUL DES FONCTIONS GENERATRICES, PART I OF THEORIE ANALYTIQUE DES PROBABILITES (book), P. S. Laplace. Paris, France, 1812.

2. CALCULUS OF FINITE DIFFERENCES (book), C. Jordan. Chelsea Publishing Company, New York, N. Y., 1946.

3. FOUNDATIONS OF ECONOMIC ANALYSIS (book), P. A. Samuelson. Harvard University Press, Cambridge, Mass., 1947.

4. TRANSIENTS IN LINEAR SYSTEMS (book), M. F. Gardner, J. L. Barnes. John Wiley and Sons, Inc., New York, N. Y., chapter 9, 1942.

5. A LIST OF GENERALIZED LAPLACE TRANSFORMS W. M. Stone. *Journal of Science*, Iowa State College, Ames, Iowa, volume 22, April 1948, pages 215–25.

6. See reference 1 of the paper.

7. See reference 2 of the paper.

8. ANALYSIS OF DISCONTINUOUS SERVOMECHANISMS, F. H. Raymond. *Annales de Telecommunication* (Paris, France), volume 4, 1949, pages 250–56, 307–14, 347–57.

William K. Linvill: As indicated by the discussors, all common results of the z-transform approach and the approach of this paper agree. The essential difference between the z-transform approach and the approach of this paper is that the z-transform approach describes all signals in the system by sequences of samples whereas this paper describes all signals by continuous time functions and their transforms. With the z-transform approach, a continuous signal is described only by its value at the sampling instants and no data on the signal is given at other values of time. With the approach of this paper, a continuous signal is described in the conventional fashion and a sampled signal is described as the limiting case of a continuous signal. A look at the characteristics of the impulse modulator illustrates this point. The modulation of a string of impulses by the signal to be sampled may be viewed as the limiting case of the modulation of a string of smooth pulses by the signal as the pulses become sharper and sharper. The modulator output corresponding to a carrier of smooth pulses is a continuous time function. As the pulses become sharper and sharper the modulator output approaches an instantaneously sampled signal. The Fourier transform of the continuous output signal is aperiodic. As the carrier pulses become sharper, the transform of the modulator output becomes more nearly periodic until finally the transform of the sampled signal is periodic and consequently is a rational function of ϵ^{-sT} (or z). Thus the signals in a control system whether sampled or not can be handled by the conventional frequency approach. The control system components whether continuous-type or sampled-type can all be handled by transfer functions. The components which receive and transmit sampled data are described naturally by transfer functions which are periodic in the frequency domain (rational functions of ϵ^{-sT}); those components delivering continuous output signals are described by conventional transfer functions which are aperiodic (rational functions of s).

The fact that all parts of the system are described in conventional terms makes the handling of mixed systems very convenient.

The root of the difficulty in handling sampled-error-data servomechanisms is that the whole closed loop behaves like a sampled data device, although it is made up of continuous-data components. This fact is illustrated by Figure 10 of the paper. Using the frequency domain approach one can handle this type of system as a conventional system except that he must account for the complementary signals which cause $K\beta(s)$ to be replaced by

$$\sum_{n=-\infty}^{\infty}K\beta(s+jn\Omega)$$

Figure 11 shows an approximate graphical procedure to evaluate

$$\sum_{n=-\infty}^{\infty}K\beta(s+jn\Omega)$$

Though the paper neglected to mention it, this summation can always be obtained analytically in closed form by making a partial fraction expansion of $K\beta(s)$ and then performing the infinite summation on each term of the partial fraction expansion. The infinite summation on each term always exists in closed form and agrees with the $K\beta^*(z)$ mentioned by the discussors. Though the $K\beta^*(z)$ described by the discussors above equation 6 of their discussion exists in closed form it is unnecessary to go to the *z*-transform formulation to obtain closed form for the summation. While the final form of $K\beta^*(z)$ is simple enough, the process for obtaining it from the characteristics of the servo loop components by the *z*-transform approach is tortuous. Suppose one were given a servo system with the characteristics of all the loop components given and he wished to investigate quickly the effect on the system performance of introducing a lead network into the system. This investigation would be hard by the *z*-transform approach and easy by the procedure of this paper. One could not obtain the new $K\beta^*(z)$ directly from the old one; however, the new $K\beta(s)$ is found easily from the old one by merely multiplying the old $K\beta(s)$ by the transfer function of the lead network. A very good approximation of the new $\Sigma K\beta$ can be easily obtained from the new $K\beta(s)$ by the graphical procedure of Figure 11. While the graphical summation is approximate, it is a very good approximation and is very easy to get. It is an excellent vehicle for the cut-and-try process which is often useful in system design.

Summarizing: all common results between the *z*-transform approach and the approach of this paper agree. The difference between the two is that one describes all signals by sequences of samples, while the other describes all signals as if they were continuous; the approach of this paper seems particularly advantageous on mixed systems, for example, the exact characterization of a sampled-error-data system is possible by both methods but a convenient approximate characterization also can be made from the approach of this paper.

The Thermal Conductivity of Moist Soil

A. S. MICKLEY
MEMBER AIEE

MOIST soil consists of three component materials: solid soil particles, air, and water. It is the composite heat transfer properties of these three items which make up what is apparent as the thermal conductivity of moist soil. This apparent thermal conductivity is of great importance to electrical engineers in the calculation of ampere load ratings of underground cable lines and also in other problems of underground heat transfer, such as the calculation of buried steam line losses and the design of heat pump ground coils.

The purpose of this paper is fourfold:

1. To build up the theory of thermal conduction in the composite soil, air, and water body.
2. To present laboratory data on the thermal conductivity of various combinations of these three components to illustrate the application of the theory.
3. To present field data showing the behavior of a soil in situ over the seasons, illustrating the thermal conductivity effects of variations of moisture content brought about by rainfall and soil water movement under thermal gradients.
4. To show how the theory and data can be applied to a practical problem.

Theory

A unit volume of soil in situ consists of the following:

1. A fixed volume of solid material.
2. Water, which occupies some of the volume not occupied by the solid material.
3. Air (or vapor), which occupies that part of the remaining volume, if any, which is not occupied by either solid material or water.

Under the usual conditions the solid material is, of course, broken up into tiny soil particles, with water and air occupying the pore spaces between the particles.

For the purpose of the development of this theory, it will be considered that, in a unit volume of soil, the solid material is monolithic, rather than broken into many particles. The limitations of this assumption will be taken up later.

The monolith assumed is illustrated in Figures 1(A) and 1(B) for the case of completely dry soil. This form, fitted into a unit cube, has the following properties for each set of parallel faces of the cube:

1. There is a column of air space extending from face to face of length 1 and area a^2.
2. There is a column of solid material extending from face to face of length 1 and area $(1-a)^2$.
3. There are two columns between the cube faces consisting of solid material in series with air space. The area of each column is $a(1-a)$ with a solid length of $(1-a)$ in series with an air space of length a.

The conductivity of this composite figure between two faces consists of the summation of the parallel conductivities of each of the above four columns.

$$k=k\,(\text{air})+k\,(\text{solid})+2k\times(\text{air space in series with solid}) \qquad (1)$$

This assumes that the soil is dry, so that the pore space is occupied entirely by air. The per-unit conductivities of the material are taken as follows:

air $=k_a$
solid $=k_s$

The composite conductivity from face to face is then:

$$k=k_a\frac{a^2}{1}+k_s\frac{(1-a)^2}{1}+2\frac{1}{\dfrac{a}{k_a(a)(1-a)}+\dfrac{(1-a)}{k_s(a)(1-a)}}$$

or

$$k=k_aa^2+k_s(1-a)^2+\frac{k_sk_a(2a-2a^2)}{k_s(a)+k_a(1-a)} \qquad (2)$$

If the soil is completely saturated, so that the pore space is occupied entirely by water, then, assuming that the unit conductivity of water is k_w, the composite conductivity becomes:

$$k=k_wa^2+k_s(1-a)^2+\frac{k_sk_w(2a-2a^2)}{k_s(a)+k_w(1-a)} \qquad (3)$$

For the intermediate case, in which both water and air are present, it is assumed that the water lies in a uniform layer of thickness b on the six surfaces of the solid which are inside the cube. This is illustrated in Figure 1(C). In this case, the conductivity is:

$$k=k_a(a-b)^2+k_s(1-a)^2+k_wb^2+2\frac{1}{\dfrac{a-b}{k_a(b)(a-b)}+\dfrac{1-a+b}{k_w(b)(a-b)}}+2\frac{1}{\dfrac{a-b}{k_a(a-b)(1-a)}+\dfrac{b}{k_w(a-b)(1-a)}+\dfrac{1-a}{k_s(a-b)(1-a)}}+2\frac{1}{\dfrac{a}{k_w(b)(1-a)}+\dfrac{1-a}{k_s(b)(1-a)}} \qquad (4)$$

Unfortunately, these equations do not hold for very porous soil or for dry or nearly dry soil. The actual conductivity in these cases is lower than indicated by the formulas, since they do not account for the point contact between the angular soil particles. Under higher moisture content conditions, this point contact between soil particles is enlarged by the sealing action of the soil moisture, in which case the above formulas hold quite well. However, the conditions under which the formulas do not apply are usually confined to artificial or laboratory cases, since soil in situ is generally well packed and fairly moist.

Paper 51-326, recommended by the AIEE Insulated Conductors Committee and approved by the AIEE Technical Program Committee for presentation at the AIEE Fall General Meeting, Cleveland, Ohio, October 22-26, 1951. Manuscript submitted June 8, 1951; made available for printing August 31, 1951.

A. S. Mickley is with the Philadelphia Electric Company, Philadelphia, Pa.

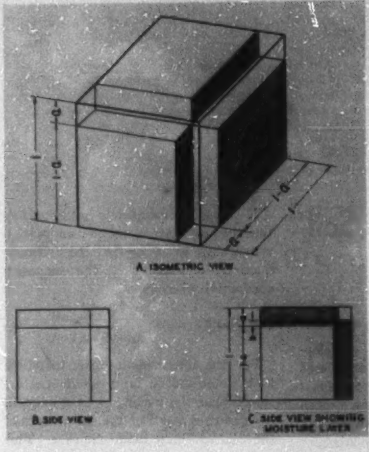

Figure 1 (left). Theoretical unit soil structure containing solid monolith

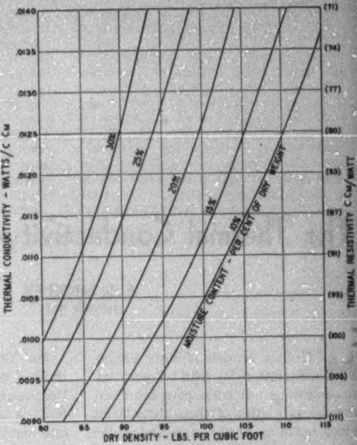

Figure 2 (right). Thermal conductivity of clay-loam soils by equation 4

Evaluation of Constants

The density of packing of the solid material in a soil is commonly indicated through the use of the term dry density, which is the density of the dry soil structure. This is, of course, less than the density of the solid material itself which, for ordinary soils, can be taken at 168 pounds per cubic foot.

For the usual clay-loam type soils encountered in the construction of underground structures, the following thermal conductivity constants apply:

$k_s = 0.0272$ watt per degree centigrade centimeters (reference 1)
$k_w = 0.00585$ watt per degree centigrade centimeters (reference 2)
$k_a = 0.000238$ watt per degree centigrade centimeters (reference 1)

These constants may be substituted in equation 4, assuming values of a and b. Each value of a and b determines the proportion of solid and of liquid occupying the unit volume, which in turn corresponds to the dry density and moisture content. A series of curves in terms of the latter parameters is shown in Figure 2 for clay-loam soils.

It is sometimes of interest to study the characteristics of sand or cinders. Sand appears to have a higher conductivity than the solid material in clay-loam types, the component k_s being in the order of 0.0350 watts per degree centigrade centimeters. This checks with the conductivity value given by Hudson[2] for marble. Cinders, on the other hand, appear to have a lower conductivity than the clay-loam solid material, being in the order of 0.0150 watts per degree centigrade centimeters.

In applying equation 4 to sand or cinders, the density value of 168 pounds per cubic foot may be used for the solid material in sand, but it is not applicable to the solid material in cinders. A density value of 125 pounds per cubic foot should be used in the latter case.

Laboratory Tests

Thermal conductivity tests were made in the laboratory on a number of soil samples using the method of Shannon and Wells.[3] According to this method, a soil sample packed in a cylinder with a 2-to-1 ratio of height to diameter is chilled suddenly from room temperature by immersion in a bath of ice water. The resulting curve of temperature decrease with time at the center of the cylinder indicates the thermal diffusivity of the soil, or ratio of thermal conductivity to thermal capacity. The thermal capacity is the heat storage of a unit volume for a 1-degree rise in temperature. This value is easily calculated from their weights of materials present and the values of

Table I. Thermal Conductivity of Clay-Loam Soils, Philadelphia Electric Company Tests

Location	Description of Soil	Dry Density (Lbs/Ft^3)	Moisture Content (Per Cent of Dry Weight)	Measured Conductivity (Watts/C Cm)	Calculated Conductivity (by Eq. 4) (Watts/C Cm)	Conductivity Ratio (Calculated to Measured)
Sphere —1 (Allegheny Ave.)	Yellow clay loam	63.1	48.7	0.00975	0.00840	0.86
Sphere —2 (Wister Street)	Micaceous loam	97.6	17.4	0.0101	0.0110	1.09
Sphere —3 (Wister Street)	Micaceous loam	81.4	21.1	0.00815	0.00907	1.11
		81.4	31.8	0.0108	0.0107	0.99
Delaware Station	Coarse sandy loam	104.5	14.2	0.0170	0.0121	0.71
Oxford Circle	Clay loam	86.9	26.0	0.0112	0.0106	0.94
		86.9	29.2	0.0126	0.0112	0.88
Holmesburg Substation	Clay loam	83.3	20.0	0.00795	0.00914	1.15
		83.3	29.2	0.0114	0.0104	0.91
		98.0	22.3	0.0148	0.0128	0.86
		98.0	23.6	0.0152	0.0128	0.85
Luzerne Street and Rising Sun Avenue	Micaceous loam	98.9	15.5	0.0107	0.0114	1.07
		98.9	21.8	0.0126	0.0128	1.01
Erie Avenue & 20th St	Micaceous loam	94.0	12.1	0.00917	0.00972	1.06
		94.0	23.7	0.0137	0.0121	0.89

Table II. Thermal Conductivity of Clay-Loam Soils—Other Investigators' Tests

Name of Investigator	Description or Location of Soil	Density, Lbs/Ft³	Moisture Content (Per Cent of Dry Weight)	Measured Conductivity Investigators' Units	Measured Conductivity (Watts/C Cm)	Calculated Conductivity (by Eq. 4) (Watts/C Cm)	Conductivity Ratio (Calculated to Measured)
Miles S. Kersten[10]	Fairbanks silt loam	100.9 (dry)	9.0	6.57 $\frac{\text{Btu in}}{\text{ft}^2\text{ hr F}}$	0.00948	0.0105	1.11
Miles S. Kersten[10]	Fairbanks silt loam	94.4 (dry)	18.8	6.66 $\frac{\text{Btu in}}{\text{ft}^2\text{ hr F}}$	0.00961	0.0100	1.04
Miles S. Kersten[10]	Healy clay	94.0 (dry)	17.0	8.28 $\frac{\text{Btu in}}{\text{ft}^2\text{ hr F}}$	0.0119	0.0105	0.88
Miles S. Kersten[10]	Healy clay	108.2 (dry)	15.5	11.30 $\frac{\text{Btu in}}{\text{ft}^2\text{ hr F}}$	0.0163	0.0133	0.82
W. O. Smith[7]	Barnes loam Horizon C	1.74 gm/cm³ (wet)	25.2	12.91 $\frac{\text{cal}\times 10^4}{\text{cm sec C}}$	0.00541	0.0105	1.95
Charles H. Coogan, Jr.[11]	Storrs, Conn.	107.0 (wet)	18.5	0.551 $\frac{\text{Btu}}{\text{ft hr F}}$	0.00955	0.0101	1.06
W. A. Hadley[12]	Lima, Ohio	116.1 (wet)	15.8	0.611 $\frac{\text{Btu}}{\text{ft hr F}}$	0.0106	0.0114	1.08
W. A. Hadley[12]	Lima, Ohio	123.7 (wet)	22.8	0.764 $\frac{\text{Btu}}{\text{ft hr F}}$	0.0132	0.0133	1.01
W. A. Hadley[12]	Chicago, Ill.	115.5 (wet)	16.6	0.616 $\frac{\text{Btu}}{\text{ft hr F}}$	0.0107	0.0123	1.15
W. A. Hadley[12]	Chicago, Ill.	119.2 (wet)	29.4	0.759 $\frac{\text{Btu}}{\text{ft hr F}}$	0.0131	0.0129	0.99

specific heat which preferably are measured, but which may be assumed. For the tests made by the author, the specific heats have been assumed as follows:

Water—1.0
Solid matter—0.2

Thermal conductivity is then easily obtained, since it is equal to the product of thermal diffusivity and thermal capacity.

Table I indicates that the laboratory tests check equation 4 with a reasonable degree of accuracy in virtually all cases. Data which was gathered by other investigators was then introduced into equation 4. Table II gives a comparison of published conductivity test results against the conductivity indicated by the application of equation 4. This table indicates that the calculated values check other investigators' data with a satisfactory degree of accuracy in most cases.

Table III compares calculated sand conductivities with measured conductivities by the author and other investigators. Table IV gives samples of the author's work with cinders.

Field Tests

Tests were made in the field through the use of a sphere, 8 inches in diameter, as shown in Figure 3, buried to a depth of 4 feet. A constant heat input was placed within this sphere and the resulting temperature rise measured. A simple calculation based on the geometry of the installation gives the unit thermal conductivity directly. The proper equation is given by Neher's[5] equation 4, which can be written:

$$\Delta T = Q_s \frac{1}{4\pi k}\left(\frac{1}{d}-\frac{1}{d'}\right) \qquad (5)$$

where

ΔT = temperature rise in degrees centigrade
Q_s = heat dissipation in watts
d = sphere radius in centimeters
d' = twice the buried depth in centimeters
k = soil thermal conductivity in watts per degree centigrade centimeters

In the attempt to duplicate conditions as frequently met under high loading on electric cable conduit and pipe lines, sufficient heat input was employed to maintain the sphere surface temperature between 50 and 55 degrees centigrade.

Spheres number 1 and number 2 were placed under unpaved, open ground and gave results as shown in Figures 4 and 5. These indicated sustained conductivities of 0.016 and 0.011 respectively, subject

Table III. Thermal Conductivity of Sand

Name of Investigator	Description or Location of Soil	Dry Density (Lbs/Ft³)	Moisture Content (Per Cent of Dry Weight)	Measured Conductivity Investigators' Units	Measured Conductivity (Watts/C Cm)	Calculated Conductivity (by Eq. 4) (Watts/C Cm)	Conductivity Ratio (Calculated to Measured)
Philadelphia Electric Co.	Thompson and Lewis Sts.	103.0	8.2	0.0131 Watts/C Cm	0.0131	0.0134	1.02
		103.0	13.4	0.0160 Watts/C Cm	0.0160	0.0145	0.91
		103.0	18.5	0.0183 Watts/C Cm	0.0183	0.0158	0.87
Shannon and Wells[3]	Lowell sand	101.0	20.9	1.00 $\frac{\text{Btu}}{\text{Ft Hr F}}$	0.0173	0.0158	0.91
		106.5	16.4	1.025 $\frac{\text{Btu}}{\text{Ft Hr F}}$	0.0177	0.0163	0.92
Shannon and Wells[3]	Bangor sand and gravel	127.0	9.3	1.13 $\frac{\text{Btu}}{\text{Ft Hr F}}$	0.0196	0.0202	1.03
Hooper and Lepper[9]	Sand	100.0	8.8	11.0 $\frac{\text{Btu in}}{\text{Ft}^2\text{ Hr F}}$	0.0159	0.0128	0.81

Table IV. Thermal Conductivity of Cinders—Philadelphia Electric Company Tests

Location	Dry Density (Lbs/ft³)	Moisture Content (Per Cent of Dry Weight)	Measured Conductivity (Watts/C Cm)	Calculated Conductivity (by Eq. 4) (Watts/C Cm)	Conductivity Ratio (Calculated to Measured)
Schuylkill Station	62.9	30.0	0.00600	0.00616	1.03
	75.2	16.3	0.00630	0.00686	1.09
Oregon Avenue	62.9	18.9	0.00467	0.00532	1.14
	62.9	34.7	0.00734	0.00653	0.89
Natrona Street	67.4	33.8	0.00806	0.00836	1.04

only to slight variation due either to changes in soil moisture or to experimental error. These compare with calculated conductivities of 0.015 and 0.010, based on the dry density and moisture content found at the time of the installation of the spheres.

Sphere number 3 on Wister Street is an example of a sphere placed under paving. Based on the dry density and moisture content of the soil found on excavation, the calculated conductivity was 0.0095. As may be seen in the plot in Figure 5 resulting from two years of observation, the initial conductivity checked this very well, being on the order of 0.0099. After a few months of operation, however, the thermal conductivity decreased from time to time to approximately 0.0078 and remained near this figure. Superimposed on this trend was a considerable month to month variation, presumably caused by seasonal changes in the amount of ground moisture present.

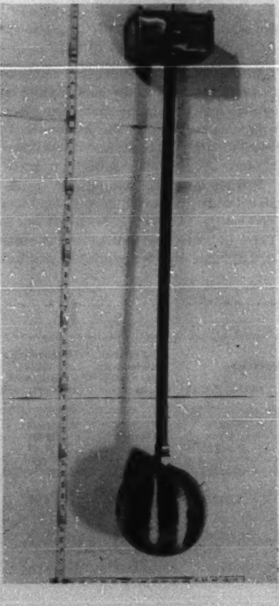

Figure 3 (right). Cast bronze sphere used to determine earth thermal conductivity in situ

Moisture Migration

There has been much awareness of the existence of moisture migration away from a hot buried structure. Little has been done, however, in the way of evaluating the specific effects under various conditions. The phenomenon was discussed in reference 4 and certain laboratory data were presented. Reference 5 applied the available data to problems of buried structures in the attempt to evaluate the effects. The above sphere tests provided an excellent opportunity to observe the migration phenomenon in the field under the dynamic conditions of evaporation, vapor transfer, and moisture replenishment from rainfall.

It was predicted in reference 4 that little, if any, migration would be observed under conditions of either fairly high or fairly low moisture content. This was apparently the case for spheres number 1 and 2, since no migration was observed. In the case of sphere number 3, however, there was a definite long time decrease in conductivity. The fact that the migration did not take place as quickly as predicted in reference 4 may be due to either of two possibilities: (1). The critical moisture content was not present at the start of the experiment, or (2). A long time vapor transfer effect may have been present. The latter condition was not observed in short time laboratory experiments.

Whatever the explanation, it is interesting to observe the magnitude of migration actually observed under paving against the magnitude which would have been predicted by previous theory. Neher[4] presents his equation 41 for the temperature rise of a sphere with moisture migration. As shown in Appendix I, this equation can be used to state the relationship of the initial conductivity and the conductivity apparent after migration has taken place. For sphere number 3 at Wister, the experimental data indicates the relationship:

$$k_{ap} = k_1(0.79) \qquad (6)$$

Solving Neher's equation 41 in this case gives $B = 140$, and $K_M = 0.001$. K_M is the basic constant for the conductivity change due to migration. According to Neher's theory, this constant may be used to determine the migration effect with any geometry, whether with a spherical body or a cylindrical one. Neher had assumed a maximum K_M of 0.002, which is twice the value actually found under the Wister Street paving.

In a previous paper[4] the author described an experience with a so-called "runaway" sphere, in which the migration phenomenon occurred very quickly, as observed by a recorder. These data have been analyzed for K_M, which was found to be about 30 per cent lower than observed for sphere number 3.

Predetermination of Natural Moisture Content

In construction work in the field, it is often desirable to have a foreknowledge of probable thermal conductivity. This may be done by means of equation 4 if the dry density and natural moisture content are known. The dry density is easily measured by excavating, drying, and weighing a known volume of the soil in its natural packed state.

The natural moisture content of the soil, on the other hand, is not so easily obtained. A test of moisture content can

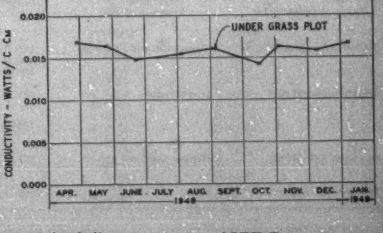

Figure 4 (left). Thermal conductivity of sphere number 1

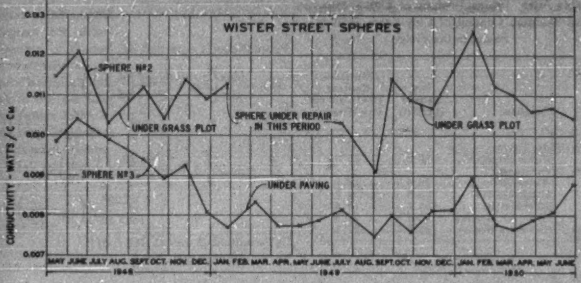

Figure 5. Thermal conductivity of sphere numbers 2 and 3

be made from a field sample, but it is well known that the moisture will vary considerably over the seasons at a given location. What an investigator usually desires to know is the minimum moisture content to which the soil is likely to drain in a dry season. For soil not immediately at the surface, this seems to be a fairly predictable figure, for a guide has been developed through the use of the tension table of Leamer and Shaw.[4] In this table, shown in Figure 6, a sample of water saturated soil is placed under the suction power of a 60-centimeter column of water. The soil is kept under this suction pressure until the moisture content has been reduced to a stable level. The resulting moisture content is largely capillary water, or water which does not normally take part in gravitational percolation. It is the minimum moisture which will, therefore, normally be available for thermal conduction unless taken away by plant root action or by movement under local thermal gradients.

The tension table, therefore, is an excellent tool to predetermine the minimum moisture holding property of a soil. The soil at Wister Street was at a high and well drained elevation, so that the minimum value would presumably be present. The actual values obtained are given in Table V. The average tension table moisture content was about 20.1 per cent. Under the grass plot in an undisturbed state, the soil was found to have a moisture content of 18.8 per cent. The ratio of field to laboratory observations was, therefore, 0.93, which is rather close, considering the difficulty of reproducing exactly the dry density in the laboratory.

It should be noted that the moisture content under the paving was found to be lower than under the grass plot, presumably due to the greater unavailability of rain water. The particular location of sphere number 3 was under the paving in the middle of a large, 6-point street intersection, and was approximately 75 feet from the nearest large plot of unpaved ground. It may be that the 60-centimeter height, which has been used by the United States Forest Service as being generally correct, is applicable only to unpaved areas, and that some height greater than 60 centimeters should be used in tests for soils under paving.

Collecting Field Data

In cases where it is desired to make more elaborate checks of thermal conductivity, or to measure conductivity through the seasons, it is possible to make a permanent installation of a buried sphere similar to the ones mentioned in this paper. Care must be taken to keep the temperature rise of a sphere relatively low, however, since the theory indicates that small diameter spheres have a tendency to produce more moisture migration than the buried cylinders to which the data will most likely be applied. A representative limit would be a 25-degree centigrade rise.

Table V. Tension Table Tests on Soil at Wister Street

	Sphere #2 (Under Grass Plot)	Sphere #3 (Under Paving)
As Found		
Dry density (Lbs/Ft^3)	88.6	89.3
Moisture Content (Per Cent)	18.8	15.9
Tension Table Test		
Dry density (Lbs/Ft^3)	85.1	84.8
Moisture Content (Per Cent)	20.2	20.0

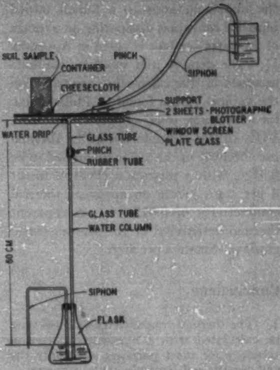

Figure 6. Tension table of Leamer and Shaw[4]

An instrument which shows promise and which seems to have less of a tendency to produce moisture migration is the one recently presented by Hooper and Lepper,[9] which observes the transient temperature rise of suddenly applied constant heat flow from a line source.

Application

This paper presents four tools for determining the effective thermal conductivity of the earth. The results may be applied to thermal calculations for buried structures while these structures are still under construction, or contemplated. The four tools and the test methods required for the necessary data on the particular soil involved are given in Table VI.

A sample problem on the application of

Table VI

Tool	Data Obtained By
Dry density of the soil in situ	Excavating, drying, and weighing a sample of known volume
Predetermination of minimum soil moisture content	Tension table test on soil sample packed to field density
Determination of initial soil thermal conductivity	Calculation by equation 4 or reference to Figure 2 using the dry density and the tension table moisture content
Determination of moisture migration	No apparatus for field data at present. One method is to use Neher's[3] equation 37 for buried cylinders, with K_M between 0.002 proposed by Neher and 0.001 measured under paving

the above methods to a 6-inch buried pipe line for cables dissipating an average of 25 watts per foot is given in Appendix II. The density and moisture contents assumed in this calculation are based on the typical values found in Philadelphia for clay-loam soils, as given in Table VII. In this example, the initial thermal conductivity of the soil is calculated to be 0.0126, with a migration effect of about 3 per cent, giving an apparent thermal conductivity of 0.0122, or an apparent thermal resistivity of 82 degrees centigrade centimeters per watt.

Conclusions

1. The thermal conductivity of a soil may be calculated with a reasonable degree of accuracy for most purposes with only the dry density and moisture content known.

2. The minimum probable moisture content of a soil in situ may be obtained in the laboratory through the use of a tension table with a 60-centimeter water column for soils not under paving. For soils under paving, a higher column may be necessary.

3. The moisture migration calculation method proposed by Neher[5] on somewhat meager data appears to have been sustained by field tests. Neher, however, proposed the use of a constant, K_M, of 0.002. The highest value found in the field by this investigation was 0.001. It may be that the value of 0.002 is too high for practical use.

4. The basic theory of thermal conductivity of soils indicates that it may be of value to replace the water and air volume in a soil with some insoluble chemical of good thermal conductivity. Soil might be impregnated with this chemical as a liquid, which would solidify and thereby not be subject to drainage or thermal migration.

Appendix I. Calculation of Moisture Migration After Neher[5]

Sphere temperature rise without moisture migration

$$\Delta T=\frac{Q_s}{4\pi k_t}\left(\frac{1}{d}-\frac{1}{d'}\right) \tag{7}$$

where k_t is the conductivity of undisturbed soil. Sphere temperature rise with moisture migration

$$\Delta T=\frac{Q_s}{4\pi k_t}\left[\left(\frac{1}{d}-\frac{1}{d'}\right)+\frac{B}{12}\left(\frac{1}{d^3}-\frac{1}{d'^3}\right)+\frac{B^2}{40}\left(\frac{1}{d^5}-\frac{1}{d'^5}\right)+\ldots\right] \tag{8}$$

where

$$B=\frac{Q_sK_M}{\pi k_t^3} \tag{9}$$

and K_M = migration constant. The apparent soil conductivity after migration is therefore:

Table VII. Typical Values of Dry Density and Moisture Content of Clay-Loam Soils as Found in the Field

Location	Dry Density (Lb/Ft³)	Moisture Content (Per Cent of Dry Weight)
(A) Under Paving		
Wister Street	89.3	15.9
(B) Open Ground		
Wister Street	88.6	18.8
Allegheny Ave	98.5	29.6
Whitemarsh	105.5	19.4
Plymouth Meeting	100.7	26.3
Richmond Station	102.0	27.1

$$k_{ap}=k_t\times\frac{\left(\frac{1}{d}-\frac{1}{d'}\right)}{\left(\frac{1}{d}-\frac{1}{d'}\right)+\frac{B}{12}\left(\frac{1}{d^3}-\frac{1}{d'^3}\right)+\frac{B^2}{40}\left(\frac{1}{d^5}-\frac{1}{d'^5}\right)} \tag{10}$$

In the case of sphere number 3 at Wister:

$$k_{ap}=k_t\left(\frac{0.78}{0.99}\right)=k_t(0.79) \tag{11}$$

and $d=10.2$ centimeters
$d'=244$ centimeters

Solving equation 10 for B gives

$B=140$ approximately

Solving for K_M in equation 9 where $Q_s=37$ watts (approximately) and $k_t=0.0099$ gives $K_M=0.0011$.

Appendix II. Sample Problem

Assume a 6-inch cable pipe line is to be buried 36 inches deep, dissipating 25 watts per foot average.

It is desired to determine the effective thermal resistivity of the earth (or conductivity). The following field data is obtained:

Dry density: 100 pounds per cubic foot
Tension Table Moisture Content: 20 per cent of dry weight
K_M: 0.001 (assume)

The initial conductivity is obtained from Figure 2 which, for the above values of dry density and moisture content, indicates:

$k_t=0.0126$ watts per degree centigrade centimeters

or in terms of thermal resistivity:

$\rho_t=79.4$ degrees centigrade centimeters per watt

Applying Neher's equation 1 for the case without moisture migration:

$$\Delta T_P=\frac{Q_e\rho_t}{2\pi}\log_\epsilon\frac{d'}{d}$$

$$=\frac{\frac{25}{12\times(2.54)}(79.4)}{2\pi}\left[\log_\epsilon\frac{72''}{3''}\right]$$

$$\Delta T_P=10.35\log_\epsilon 24=10.35(3.18)=32.9$$

$$A=\frac{2}{\pi}\rho_t^2Q_eK_m \text{ (Neher's equation 36)}$$

$$A=\frac{2}{\pi}(79.4^2)(0.82)(0.001)=3.29$$

From Neher's equation 37:

$$\Delta T_P=\frac{Q_e\rho_t}{2\pi}\left[\log_\epsilon\frac{d'}{d}+\frac{A}{4}\left(\frac{1}{d}-\frac{1}{d'}\right)+\frac{A^2}{16}\left(\frac{1}{d^2}-\frac{1}{d'^2}\right)\right]$$

$$=10.35\left[3.18+\frac{3.29}{4(2.54)}\left(\frac{1}{3}-\frac{1}{72}\right)+\frac{3.29^2}{16(2.54^2)}\left(\frac{1}{3^2}-\frac{1}{72^2}\right)\right]$$

$$\Delta T_P=10.35[3.18+0.10+0.01]$$
$$=10.35[3.29]=34.0$$

$$\rho_{ap}=79.4\times\left(\frac{34.0}{32.9}\right)=82 \text{ degrees centigrade centimeters per watt}$$

References

1. The Thermal Conductivity of Dry Soil, W. O. Smith. *Soil Science* (Morgantown, W. Va.), volume 53, 1942, page 448.

2. The Engineers' Manual, R. G. Hudson. John Wiley and Sons, Inc., New York, N. Y., second edition, page 317.

3. Tests for Thermal Diffusivity of Granular Materials, William L. Shannon, Winthrop A. Wells. *Proceedings*, American Society for Testing Materials (Philadelphia, Pa.), volume 47, 1947, page 1044.

4. The Thermal Movement of Moisture in Soil, A. S. Mickley. *AIEE Transactions*, volume 68, part I, 1949, pages 330-34.

5. The Temperature Rise of Buried Cables and Pipes, J. H. Neher. *AIEE Transactions*, volume 68, part I, 1949, pages 9-20.

6. A Simple Apparatus for Measuring Noncapillary Porosity on an Extensive Scale, Ross W. Leamer, Byron Shaw. *Journal*, American Society of Agronomy (Geneva, N. Y.), volume 33, 1941, page 1003.

7. Thermal Conductivities in Moist Soils, W. O. Smith. *Proceedings*, Soil Science Society of American (Morgantown, W. Va.), volume 4, 1939, page 32.

8. Laboratory Research for the Determination of the Thermal Properties of Soils, Miles S. Kersten. *Bulletin 28*, Engineering Experiment Station, University of Minnesota (Minneapolis, Minn.).

9. Transient Heat Flow Apparatus for the Determination of Thermal Conductivities, F. C. Hooper, F. R. Lepper. *Heating, Piping, and Air Conditioning* (New York, N. Y.), volume 22, 1950, page 129.

10. Determination of Thermal Properties of Soils for Investigation of Airfield Construction in Arctic and Subarctic Regions. *Report*, Department of the Army, Corps of Engineers, St. Paul, Minn., January 1948.

11. The Residential Heat Pump in New England, Charles H. Coogan, Jr. *Booklet*, The Connecticut Light and Power Company, Waterbury, Conn., August 1948.

12. Operating Characteristics of Heat Pump Ground Coils, W. A. Hadley. *Bulletin*, Edison Electric Institute (New York, N. Y.), volume 17, December 1949, page 457.

Discussion

Miles S. Kersten (University of Minnesota, Minneapolis, Minn.): As pointed out by Mr. Mickley, a knowledge of the thermal

Figure 1. Minnesota diagram for determination of thermal conductivity of silt and clay soils. Values in Btu per hour per square foot per unit thermal gradient in degrees Fahrenheit per inch

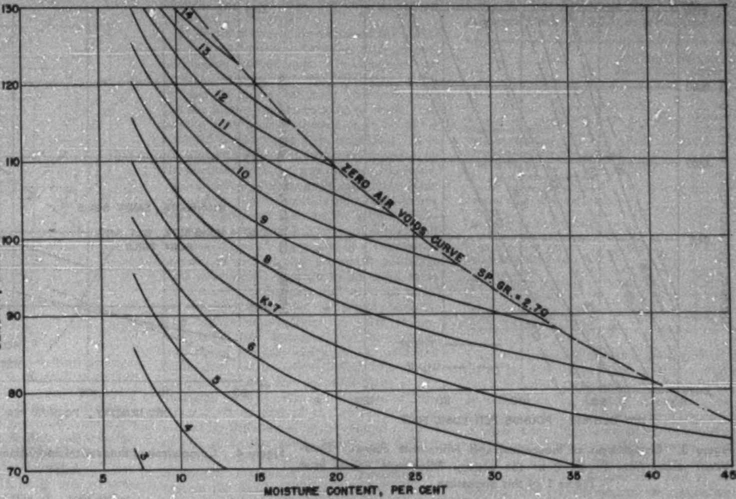

conductivity of soils is useful in many types of engineering problems. A recent study at the University of Minnesota[1] for the Corps of Engineers was for the purpose of obtaining constants to be used in design of structures in regions of permafrost. Calculations of depth and rate of frost and thaw penetration below field structures (pavements and buildings) with these constants have shown the test values to be reasonably accurate. It is of much interest and value to find that a theoretical equation has been developed which checks, at least in a substantial range of soil conditions, actual thermal conductivity determinations of numerous investigators. In this discussion a further comparison is made between the theoretical equation of Mr. Mickley and some of the Minnesota results, and some possible limitations of the theoretical equation are pointed out.

The Minnesota tests included about a 1,000 laboratory determinations of the thermal conductivity of 19 different soils at a variety of moisture content and density conditions. On the basis of these tests a series of empirical curves for the determination of the thermal conductivity on the basis of soil texture, density, and moisture content were evolved. In setting up these curves it was found necessary to separate the fine-grained soils, such as silts and clays, from the sand type soils, since at a given moisture content and density, sandy or coarse-textured soils had definitely higher conductivities than fine-textured soils. This difference would not be taken into account by the theoretical expression given in the paper, although it can be handled by the use of a higher value of k_s for the sandy soils, as has been done by Mr. Mickley. It would appear that conductivity is dependent not only upon the volume of solid material in a given unit volume, but also upon the number of grain-to-grain crossings which must be made during a traverse through the unit cube. In the fine-textured soils, the number of such crossings is greater than in a coarse-textured soil, and consequently the conductivity is less.

The equations as given, particularly equation 4, are in a very cumbersome form to solve, particularly if the soils information is in the usual terms of density in pounds per cubic foot and moisture content in per cent of the dry weight. Presentation in a curve such as Figure 2 of the paper is the best form for practical use.

Figures 1 and 2 of this discussion represent the curves developed from Minnesota tests for prediction of thermal conductivity. In these curves k is the thermal conductivity expressed in British thermal units (Btu) per hour per square foot per unit thermal gradient in degrees Fahrenheit per inch. Such values should be multiplied by 0.00144 to change to watts per square centimeter per unit thermal gradient in degrees centigrade per centimeter. It will be noted that the values of k on Figure 2 of this discussion, for sandy soils, are greater than those of Figure 1 (this discussion) which is for silt and clay soils. The equations for these curves are: Figure 1

$$k = [0.9 \log (\text{moisture content}) - 0.2] 10^{0.01d}$$

Figure 2

$$k = [0.7 \log (\text{moisture content}) - 0.4] 10^{0.01d}$$

with k in units as previously noted, the moisture content a per cent of the dry weight, with d the dry soil density in pounds per cubic foot.

Figure 3 of this discussion is a reproduction of Mr. Mickley's Figure 2 with the superimposed curves from the Minnesota data as calculated from Figure 1. Although

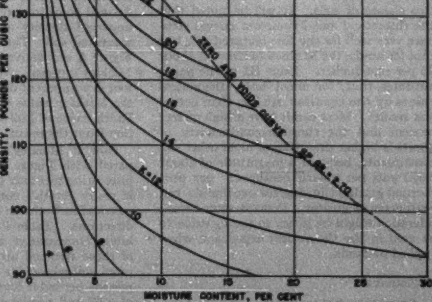

Figure 2. Minnesota diagram for determination of thermal conductivity of sandy soils. Values in Btu per hour per square foot per unit thermal gradient in degrees Fahrenheit per inch

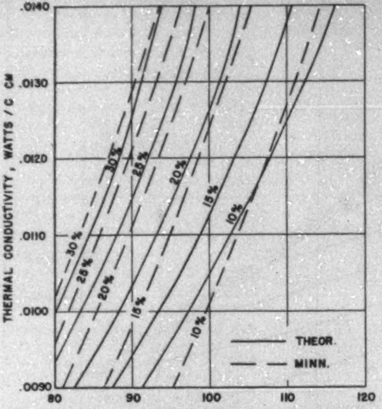

Figure 3. Comparison of theoretical and Minnesota curves. Theoretical values from Figure 2 of the paper; Minnesota values from Figure 1 of this discussion

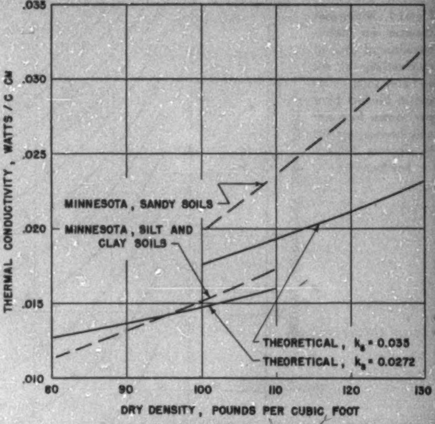

Figure 4. Comparison of theoretical and Minnesota values for saturated soils

the Minnesota curves give somewhat higher values, the similarity of form and general agreement is considered quite remarkable, since Mr. Mickley's are based on theoretical considerations and the Minnesota curves are entirely empirical and based on test values.

In certain field work done in areas of permafrost, the conductivity of saturated soils is important. It is of interest, therefore, to compare the theoretical expression for such soils (equation 3 of paper) with the empirical results of Minnesota tests. Figure 4 of this discussion is presented for this comparison. Two theoretical curves are plotted—one for fine-textured soils using $k_s = 0.0272$ watt per square centimeter per unit thermal gradient in degrees centigrade per centimeter, and one for sand using $k_s = 0.035$ watt per square centimeter per unit thermal gradient in degrees centigrade per centimeter.

The sand curve is shown for a higher range of densities since such soils may exist in such a condition. The curves from the Minnesota report also are shown for the two classes of soils. It will be noted that the theoretical and Minnesota curves compare very well for the fine-textured soil, but that for sands, the Minnesota curve is about 25 per cent higher. Table III of the paper indicates that, for most tests, theoretical values by the equation are less than actual test results. Most sands have a high quartz content and the thermal conductivity of quartz is higher than that of most other soil constituents, being of a magnitude of about 0.070 watt per square centimeter per unit thermal gradient in degrees centigrade per centimeter or greater. Perhaps some reconsideration might be given to the k_s value to be used in the theoretical expression when applied to sands.

Reference

1. See reference 8 of the paper.

William Parkerson (Middle West Service Company, Chicago, Ill.): The author and his associate, J H. Neher, are to be congratulated for their straightforward treatment of the subject in hand. It is believed that this is the first successful attempt to predict, by mathematical means, the thermal conductivity of soil at an intermediate stage between bone dry and saturated. It is further believed that there has not previously appeared a mathematical evaluation of moisture migration.

It is a fact, as can be demonstrated mathematically, that W. O. Smith in his several papers, which have appeared in "Soil Science," had in mind a soil whose particle arrangement was not identical in the horizontal and vertical directions. Nevertheless, it is interesting to note that Mickely's theory and Smith's theory[1] produce results not far apart for saturated soil, as shown by Figure 5 of this discussion. Using Smith's maximum value of S, the uppermost of the solid lines on Figure 5 was derived. Using Smith's minimum value of S, the solid line, third from the top, was derived to express relationship between dry apparent density and the conductivity of saturated soil. The dotted curve drawn on Figure 5 was derived from the equations in Mickley's paper. At 100 pounds per cubic foot dry apparent density, the range is from the Mickley value of 0.89 to the maximum Smith value of 1.02–only 6.8 per cent variation from the mean.

Now if Mickley's Figure 1(A) be compared with Figure 6 of this discussion an interesting fact may be developed. Figure 6 is really Smith's configuration made symmetrical in both the horizontal and vertical directions. Table I of this discussion exhibits comparative thermal characteristics of these two soil arrangements for a saturated soil whose dry apparent density is 84 pounds per cubic foot, assuming the density of solid soil particles to be 168 pounds per cubic foot. It will be noticed that k_s in the last line of the table does not agree exactly with Mickley's value 0.0272 watt per degree centigrade centimeter whose equivalent would be 1.57 Btu per foot per hour per degrees Fahrenheit. However, for comparative purposes, it was necessary to use the same value of k_s in computing the resultant thermal characteristics for Figure 1(A), as had been used for calculating those for Figure 5 of this discussion. Now when the determined resultant value of k_s namely, 0.7003 is plotted on Figure 5 of this discussion (as indicated by the cross mark), it becomes evident that though the structural arrangement of Figure 6 is as symmetrical as, perhaps even more so than that of Figure 1(A), the conductivity values do not agree any more closely than do Mickley's and those which result from Smith's theory.

Figure 5. Thermal characteristics of saturated soil for maximum, minimum, and weighted average value of soil factor (S)

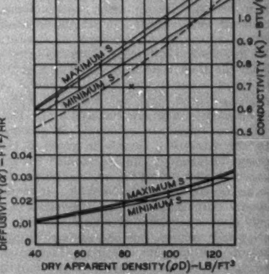

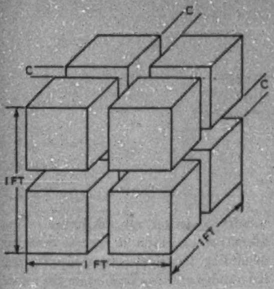

Figure 6. Idealized soil structure

That is to say, the cross mark is no closer to the dotted curve, than the dotted curve is to the solid curves. From this it would appear that the disagreement between Mickley's and Smith's theory is not only a function of the dissymmetry of Smith's soil arrangements and the symmetry of Mickley's, but is also a function of the imagined soil particle arrangement itself, be it ever so symmetrical.

Perhaps a more faithful representation of soil particle arrangement might be a system of touching spheres, such as ball bearings in a can. But the mathematics involved in finding the thermal conductivity of such a configuration of thermal particles would be very difficult.

REFERENCE

1. See reference 1 of the paper.

A. S. Mickley: The curves of conductivity furnished by Professor Kersten are based on the results of his numerous laboratory tests. Since these curves are entirely empirical, they can form an excellent check against the basically theoretical curves presented in the paper.

Professor Kersten has discussed the variation of conductivity between fine grained and coarse grained soils. He mentions two possible reasons: (a) the difference in the number of grain to grain contacts, and (b) the higher quartz content of sand. He implies that both of these factors could be reflected in the value of k_s employed. It is the author's intention, however, to use k_s as the conductivity of the grain material itself, without allowance for grain contacts. This is based on the supposition that they do not form a significant part of the whole in determining total conductivity of a wet soil because of the sealing action of a very small amount of moisture at the point contacts. This assumption appears to be valid since the data checks for clay and silt soils without consideration of the number of contacts. The higher conductivity of sand is undoubtedly due, however, to the greater content of quartz which is an excellent conductor. It is believed that this is the principal reason for the difference. The variation between the sand results of Professor Kersten and of the author may be caused by differences in the quartz content of the particular sands tested. A further refinement of the theoretical method would, of course, involve a definite classification system for sandy soils to be used in conjunction with the application of the theory.

Parkerson's analysis of the differences between the theory proposed by Smith in reference 1 and the theory proposed in this paper is most interesting. As Parkerson points out, it appears that Smith was particularly interested in undisturbed soil, which, because of a particular particle arrangement, might have a difference in conductivity between the vertical and the horizontal directions. This paper is intended to deal with soil which has been disturbed in the course of construction so as to upset the particle arrangement of the virgin soil. With regard to the differences in the theoretical arrangements of the soil particles, it may be seen from Parkerson's Figure 6 that no soil particles are touching.

Table I. For Saturated Soil Whose Dry Apparent Density Is 84 Pounds Per Cubic Foot

	Mickley's Figure 1(A)	Parkerson's Figure 6
a	0.5	
c		0.2063
Volume of solid	0.5	0.5
Volume of water	0.5	0.5
Area of uninterrupted solid material path	0.25	0
Length of uninterrupted solid material path	1	0
Area of uninterrupted water path	0.25	0.37
Length of uninterrupted water path	1	1
Area of mixed path	0.5	0.63
Solid material length in mixed path	0.5	0.7937
Water length in mixed path	0.5	0.2063
k	0.7755	0.7008
kw	0.337	0.337
ks	1.646	1.646

This extension of Smith's arrangement is quite in contrast to the author's Figure 1(A), in which there is an unbroken column of solid material in any direction. As a matter of fact, neither arrangement expresses the actual situation completely. Smith's is in error by the omission of the effect of direct contact between soil particles. Smith recognized this fact in mentioning that point contacts do exist between particles, but that this did not appear to be an important factor in the completely dry soils with which he was dealing. The author's assumption is in error by virtue of the fact that there is only a so-called point contact, and not a general contact area as Figure 1(A) would imply. This limitation was recognized in the text, however, by the statement that for fairly moist soil, these point contacts were considerably enlarged by water films and did not act as a significant limitation on heat flow for this condition. It would appear then that either theoretical figure is workable, each within its own limited sphere. As Parkerson indicates, a theoretical figure to cover all situations would involve very complicated mathematics.

Forced-Air Cooling for Station Cables

R. W. BURRELL
MEMBER AIEE

A. J. FALCONE
MEMBER AIEE

W. J. ROBERTS
ASSOCIATE MEMBER AIEE

Introduction

NEW generating capacity required to keep pace with system load growth has been provided by utilities through the years by modernization of older existing stations as well as by the construction of new plants. Improvements in the design of component equipment have made possible replacement of older units with more efficient units of considerably greater capacity. To increase the generator outlet capacity proportionately, the station designer has a choice of adding ducts, changing size, type and number of cables, or using metal-clad bus. Usually, economics will govern the final choice among conventional installation alternatives. There may be some cases, however, where the cost of obtaining the required outlet capacity appears to be disproportionate and where, as an expedient, the use of forced-air cooling may be justified as a means of increasing capacity well beyond the self-cooled rating.

In the modernization of older stations of the Consolidated Edison System, there have been a number of cases where increased generator outlet capacity has been obtained at relatively low cost by the installation of forced-ventilation systems supplying sufficient cooling air through the cable ducts to absorb appreciably higher cable losses than could be dissipated by natural means. The installations discussed in this paper, which are applied to single conductor cable circuits installed one per duct, are designed on a practical basis governed by general thermal principles. No claim is made for refinement of basic thermal design. Such refinement, it is felt, is precluded by the nature of the problem.

General Design and Application

The elements of a forced-air system for cooling cables, as applied in the Consolidated Edison System stations, are shown in Figure 1. Cooling air is drawn from the outside through filters, or an air cleaner, by a blower which in turn discharges through suitable duct work into a header feeding individual ducts. The connections from the header to the ducts in this case are made by means of flexible rubber hose terminating in sheet copper nozzles, one form of which is shown in detail in Figure 1. Sealing compound is used to make the inlet end airtight. The duct air discharges freely at the exit end into the electrical galleries.

The blower is generally a centrifugal-type direct connected to a constant speed induction motor. Air flow requirements vary from 100 to 250 cubic feet per minute (*CFM*) per duct, and blowers rated as high as 3,000 cfm have been installed for banks of nine ducts.

Cooling systems of this type have been applied, in recent years, on some 15 generator units at various plants of the Consolidated Edison System. In addition, a number of installations have been made on bus-tie circuits, station runs of tie feeders and various other circuits where it appeared that the cables were operating above their prescribed temperature limits. One installation has been applied recently to an underground run in a generating station yard where hot-spot conditions were found to prevail.

These installations have been applied to circuits installed, generally, prior to 1940. With present-day changes in loading conditions, the self-cooled ratings of these circuits no longer are adequate. Consideration was given, in specific cases, to rebuilding the duct systems, changing the number or type of cables, or the use of metal-clad bus. By far, the most economical solution was to install forced-air cooling systems.

Figure 2 shows an application, in a somewhat different form, as installed on a portion of the leads of generator number 4 at Waterside number 2 Station. In this case the cooling air is fed into a sealed gallery compartment near the center of the duct run between the generator terminal chamber and the reactor compartment. Figures 3(A), (B), and (C) show the filtered air intake, inlet duct, blower and compartment inlet header. Other installations, while generally similar, are easily adapted to varying existing conditions.

The effectiveness of the cooling system is indicated by the data of Table I, which shows a comparison of averaged cable sheath temperatures before and after application of forced air. The temperatures, observed by means of thermocouples attached to the lead sheath of the cables, are adjusted to full load on the generators and a 40-degree centigrade outdoor air ambient.

Location number 1 was a hot-spot location with a high external ambient. With forced-air cooling, the effect of the local ambient is appreciably suppressed.

Determination of Air Requirements

To increase current carrying capacity above self-cooled limits, cooling air must

Table I. Effectiveness of Forced-Air Cooling Installation

Thermocouple	Location	Sheath Temperatures, °C	
		Without Forced Air	With Forced Air
TC-1	10 ft. from generator end	84	50
TC-2	10 ft. from disconnect switch end	61	47
TC-3	1½ ft. from reactor end	61	49

Paper 51-327, recommended by the AIEE Insulated Conductors Committee and approved by the AIEE Technical Program Committee for presentation at the AIEE Fall General Meeting, Cleveland, Ohio, October 22-26, 1951. Manuscript submitted June 22, 1951; made available for printing September 12, 1951.

R. W. Burrell, A. J. Falcone, and W. J. Roberts all are with the Consolidated Edison Company of New York, Inc., New York, N. Y.

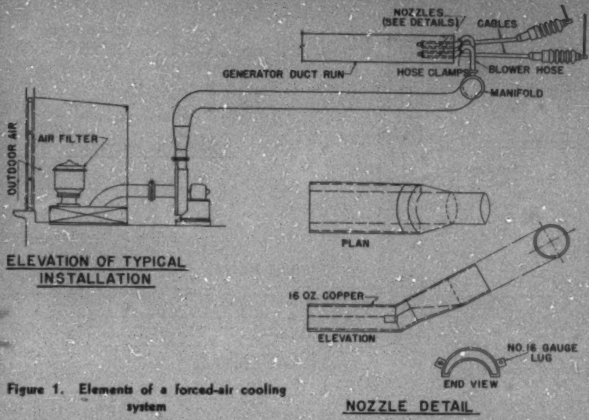

Figure 1. Elements of a forced-air cooling system

be supplied to the cable system at a rate sufficient to absorb at least the excess heat loss over and above that dissipated by natural means. The design of the system involves, however, a combination of electrical, physical, and mechanical considerations such that close accuracy is neither realizable nor necessary. In view of the approximations required, it has been considered reasonable to design on the more conservative basis of absorbing the total heat loss dissipated at the desired current carrying capacity.

The problem of heat transfer from a cable to moving air (and to the duct system) is discussed in further detail in Appendix I. It is concluded in this Appendix that the rate of air supply required to absorb the total heat loss can usually be estimated with sufficient accuracy using the heat balance equation commonly used for determining cooling air requirements for enclosed generators[1] or for transformers,[2] namely:

$$CFM = K_a WL/(T_e - T_i) \qquad (1)$$

Cooling Air Temperature Limits

The temperature of the air supplied to the duct system will be increased above source ambient by the compression rise in the blower. This rise may be appreciable in some cases but in many applications can be limited to the order of 5 degrees centigrade or less by proper design. Further discussion of the blower rise will be given under Duct Inlet Air Temperature.

Assuming a uniform duct bank ambient, the temperature of the cooling air will rise progressively along the path of flow and maximum duct air temperature will occur, for practical purposes, at the end of the run. The exit air temperature must be held below the maximum allowable sheath temperature at least by an amount sufficient to provide the driving force (temperature differential) required for transferring the total cable heat loss to the air stream. The governing equation may be written:

$$T_{cu} = T_e + W(R_{cs} + R_{sa}) \text{ degrees centigrade} \qquad (2)$$

or, for determination of maximum allowable exit air temperature,

$$T_e = T_{cu} - W(R_{cs} + R_{sa}) \text{ degrees centigrade} \qquad (2A)$$

The thermal resistance from copper to sheath, R_{cs}, is determined by conventional means.[3]

The determination of R_{sa}, the thermal resistance between the cable sheath and longitudinally flowing air moving at velocities of 20 to 50 feet per second can be made with even less accuracy than for the case of cable in duct with still air.[4] In Appendix I, a formula for R_{sa} is developed which takes the form, for air at an average temperature of 50 degrees centigrade, of

$$R_{sa} = 6.0(D_e/CFM)^{0.8} \text{ degrees centigrade per watt per foot} \qquad (3)$$

where

$$D_e = (D_2^2 - D_1^2)/D_1 \text{ inches} \qquad (3A)$$

Using equation 3, the minimum temperature differential to be maintained between cable sheath and the exit air has been found, in a number of cases to be of the order of 5 degrees centigrade. Consequently, the determination of the maximum allowable exit air temperature, T_e, generally is not seriously affected by lack of accuracy in determining R_{sa}. Using equations 3 and 2A, the values of T_e can be established for a range of air flow values and, by trial and error, using equation 1, the approximate air requirements can be established for any given duct inlet air temperature. A typical curve is shown in Figure 4(A).

Duct Inlet Air Temperature

The temperature rise in the blower is a function of the head it develops and hence of the air flow. The pressure required to move some hundred of cubic feet of air per minute through the restrictions of the piping and duct system may range up to 20 inches of water, or more.

The calculation of pressure drops in the piping and duct systems is discussed in Appendix II, treating these systems as a simple equivalent piping load on the

---

Nomenclature

C_p = specific heat at constant pressure, Btu per pound per degree Fahrenheit
CFM = air flow, cubic feet per minute
D = inside diameter, inches
D_1 = cable outside diameter, inches
D_2 = duct inside diameter, inches
D_e = equivalent diameter, 4× net air flow area/heat transfer perimeter, inches
G = mass velocity, pounds per hour per square foot of cross section
K_a = a constant depending on the air density, varying from about 1.88 at 40 degrees centigrade to 2.11 at 80 degrees centigrade. Can be taken as approximately 1.93 for an average duct air temperature of 50 degrees centigrade
L = length of cable run, feet
Δp = pressure drop, inches of water
R_{ad} = thermal resistance from air stream to duct inside wall, degrees centigrade per watt per foot
R_b = thermal resistance from duct inside wall to duct bank external ambient, degrees centigrade per watt per foot
R_{cs} = thermal resistance from conductor to cable sheath, degrees centigrade per watt per foot
R_{sa} = thermal resistance from cable sheath to air stream, degrees centigrade per watt per foot
T_a = duct bank external ambient temperature, degrees centigrade
T_{cu} = conductor (copper) temperature, degrees centigrade
T_e = duct exit air temperature, degrees centigrade
T_i = duct inlet air temperature, degrees centigrade
V = average air velocity, feet per minute
W = cable loss, watts per foot

blower. The temperature rise in the blower is a function mainly of the differential pressure across the blower and of the blower efficiency. A typical curve of blower rise versus differential pressure, based on test results of several installations, is shown in Figure 4(B).

The differential head of the blower can be related to *CFM* if the resistance of the proposed ventilating system is known (see Appendix II). A curve of blower temperature rise as a function of air flow, based on the data of Figure 4(B), is shown in Figure 4(C). Although the blower temperature rise will depend also on such blower design factors as internal losses and radiating surface, for practical purposes the blower rise can be taken to be proportional to the square of the air flow, for any given system.

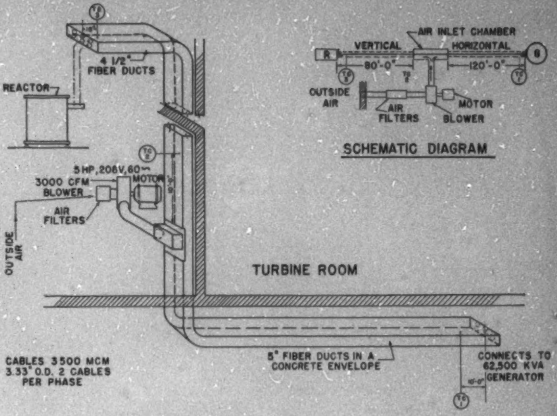

Figure 2. Forced-air cooling system as applied on generator number 4, Waterside Number 2 Station

Operating Range

By adding the maximum expected source ambient temperature to the blower rise scale of Figure 4(C), a curve of *CFM* air delivery at various blower output, or duct inlet air, temperatures is obtained. This is shown as the lower curve in Figure 4(D). Superposed, as the upper curve in this figure, is shown the air requirement characteristic, reproduced from Figure 4(A). The shaded area enclosed between the requirement characteristic and the delivery characteristic curves in Figure 4(D) represents the safe operating range within which the temperature of the air supplied by the blower plus the rise along the duct bank produces an exit air temperature below the limit imposed by copper temperature requirements.

Theoretically, the optimum operating point is the air flow corresponding to the maximum differential ordinate in the shaded area of Figure 4(D).

Although the graphical procedure outlined above provides the information required for application, a more realistic understanding of the effect of varying the air flow is obtained by plotting calculated copper (or sheath) temperatures against *CFM*. A typical curve of copper temperature, corresponding to the data of Figures 4(A), (B), (C), (D), is shown in Figure 5. The optimum operating point, producing minimum copper temperature, is seen to correspond to the above mentioned maximum differential ordinate of Figure 4(D). The data for Figure 5 are obtained, for various *CFM* values, as follows:

1. Inlet air temperature, from Figure 4(D), curve A.
2. Exit air temperature, from $T_e - T_i$ obtained using equation 1.
3. Copper temperature, from equation 2; R_{sa} is obtained employing equation 3.

It will be noted that the curve is relatively flat over a considerable range of air flow which, fortunately, allows an appreciable margin for error.

Effect of High Duct Bank Ambient

The rise calculated using a simple formula of the form of equation 1 neglects heat transfer across the duct bank structure. The transfer may vary in direction, depending on relative air temperatures inside and outside the duct bank, and the magnitude will be dependent also on the thermal resistance of the duct structure. A more accurate solution of the heat balance along a duct run may be justified where high duct bank ambients are prevalent.

Table II. Effect of Duct Bank Ambient on Exit Air Temperature

Duct Bank Ambient, °C	Conditions Inlet Air Temperature, °C	Flow, CFM	Calculated Exit Air Temperature, °C Using Equation 1	Using Equation 4, R_b, Duct Bank Thermal Ohms Per Duct Per Foot of Run 2.5	5.0	7.5
45	45	100	64.3	58.5	61.0	62.0
60	45	100	64.3	66.5	65.8	65.0

Boiler room ambients may, in the summer, reach 60 degrees centigrade, or even higher at hot spot points. At the cooling air inlet end, with an ambient of 60 degrees centigrade surrounding the duct structure and with an air temperature somewhat above 40 degrees centigrade inside the ducts, there will be heat transfer inward through the duct structure. The amount of such heat transfer will gradually decrease along the duct run and will reverse in direction beyond the point where the air temperature inside the duct begins to exceed 60 degrees centigrade.

A formula for the calculation of the temperature rise along the duct structure, which takes into account heat transfer across the duct structure, is developed in Appendix III. A differential equation set up for the heat balance at any point in the duct run leads to a solution in the form

$$T_e - T_i = (T_a - T_i + W.R_b)(1 - \epsilon^{-PL}) \quad \text{degrees centigrade} \quad (4)$$

where P has the value $1.93/(CFM.R_b)$.

The determination of R_b, the thermal resistance from the air stream through the duct structure to external ambient, is outside the scope of this paper. An approach to the calculation of the component of R_b due to the duct structure is presented in an AIEE paper by J. H. Neher.[5] As used here, R_b includes a "film resistance" from the air stream to inside duct wall based on equations 7(A) and 8 of Appendix I.

For average ambient conditions of the

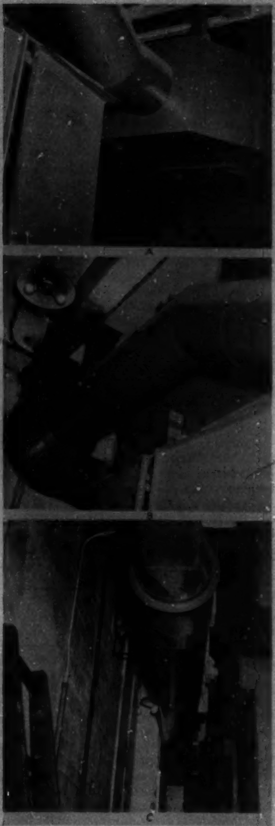

Figure 3. Forced-air cooling system installed on generator number 4, Waterside Station Number 2

A) Air supply intake, filter and duct
(B) Inlet duct and blower
(C) Blower discharge duct and plenum chamber

order of 40–50 degrees centigrade, with duct structures of high thermal resistance such as are generally found to be responsible for "bottled" self-cooled ratings, use of equation 1 ordinarily does not produce serious error in determining air supply requirements, especially if the design is applied liberally to take care of inherent limitations.

Some measure of the effect of duct bank ambient is indicated by the data of Table II, which compares exit air temperatures, calculated for a specific case, using equations 1 and 4.

It will be noted that the use of equation 1 results in exit air temperatures on the high side for the case of the lower duct ambient value, as compared with the results using equation 4, whereas for the case of the higher duct ambient, the reverse result is obtained.

A number of cases studied with ambients as high as 65 degrees centigrade indicated that in extreme cases the use of equation 1 resulted in underestimating air requirements by 10 to 35 per cent, which is within the range of the "over-design" usually applied.

Mechanical Design Considerations

Based on the characteristic shape of Figure 5, it has been the policy in our applications to specify blowers producing flows appreciably in excess of the optimum values to compensate for gradual clogging of the ducts with dirt, variations in duct resistances, and errors in pressure loss calculations.

Two general methods for introducing the air into the cable ducts have been used. One is the use of crescent-shaped nozzles (see detail of Figure 1) which fit in the space between the cable and the duct, the nozzles being connected to a header by means of flexible rubber hose. A second method is the use of a plenum chamber around the cables where they enter the duct bank, into which chamber the blower discharges. Either method is considered satisfactory, the choice between them being based principally on constructional convenience, although theoretically the nozzle design is better suited to the higher velocities.

In some installations of forced cooling it is advantageous to use induced draft fans on the exhaust side, thus avoiding the effect of blower compression temperature rise. In the particular installations so far made on the Consolidated Edison System, practical disadvantages of this method have made its use inadvisable. It would be necessary to install additional piping and filters between the outside air and the inlet of the cable ducts to avoid using the warmer gallery air as a cooling medium and to avoid rapid clogging of the cable ducts with dust. Also, the blowers would be somewhat less efficient at reduced inlet pressures.

It has been found generally advisable to break up the forced air system into duct runs of not more than 100 to 200 feet, depending on duct friction. Where longer runs and high pressure drops are unavoidable, an after-cooler may be economically justifiable.

Conclusions

1. The adaptation of forced-air cooling principles to station cables in ducts is an expedient which, while not generally applied in connection with new construction where adequate current carrying capacity

Figure 4. (A) Variation of air-flow requirements with duct inlet air temperature

(B) Blower temperature rise characteristic. Blower rise as a function of differential pressure, test results

(C) Variation of blower temperature rise with delivered air-flow

(D) Superposition of air-flow requirement and air-flow delivery characteristic curves

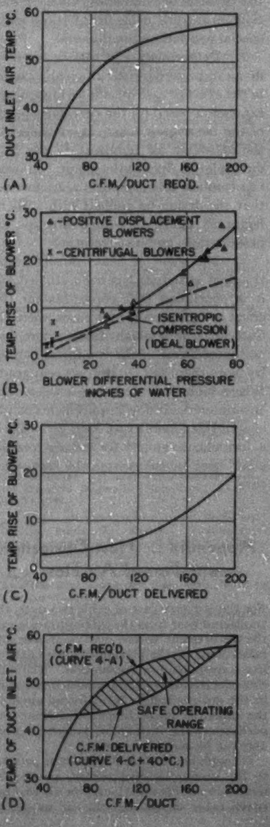

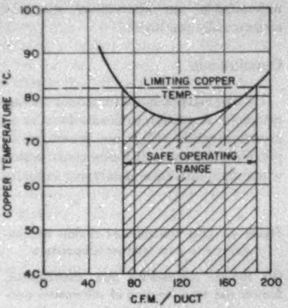

Figure 5 (left). Copper temperature characteristic curve

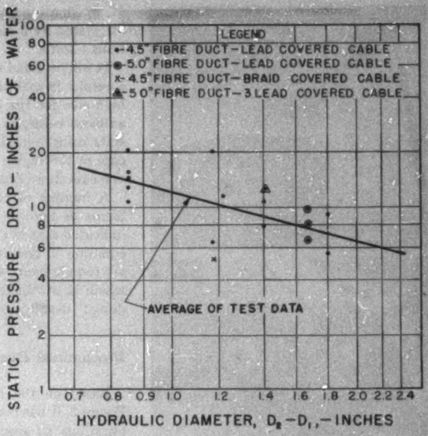

Figure 6 (right). Summary of test data on duct pressure drop characteristics.

Friction loss for 100 feet of duct with average air velocity of 3,000 feet per minute

can be obtained with conventional self-cooled systems, often does offer, however, an economical and practical solution to the problem of eliminating rating limitations in existing cable installations where special restrictions are imposed.

2. Determination of the required air flow can be made with sufficient accuracy in the average case by employing a simple expression based on the thermal capacity of the moving air mass, as controlled by the allowable air temperature rise from duct inlet to duct outlet point. In order to be on the safe side, it is recommended that the design be applied with a liberal factor of safety to compensate for approximations and uncertainties.

3. The effect of heat transfer across the duct structure has been studied and it is concluded that correction for this effect is not necessary for cases where the duct structure ambient temperature does not exceed that of the cooling air supply by more than, say, 10 degrees centigrade. Where high duct structure ambients are encountered, air flow requirements can be checked on a more exact basis by means of a formula developed for taking into account heat transfer across the duct structure.

Appendix I. Heat Dissipation with Forced Air Flow

For the ordinary case of cable in a duct, the transfer of heat from the cable surface across the air crescent to the duct wall normally takes place by the phenomena of radiation, free convection, and conduction. The relative effectiveness of these modes is generally in the order given.[3] With forced air flow, the radiation effect becomes of lesser importance, while the conduction effect probably can be neglected entirely.

In applying a forced-ventilation system to the cooling of duct cables, a sufficient temperature differential must be allowed between cable sheath and the air stream to ensure dissipation of the cable losses from the cable surface. The thermal balance at the controlling point at the end of the duct run, assuming a uniform external ambient, is given by equation 2 or equation 2A in which this temperature drop is expressed by $(W.R_{sa})$.

In determining R_{sa}, we are concerned with heat transfer at the inner wall of an eccentric annulus for the condition of turbulent air flow. Although a number of investigators have studied the problem of heat transfer in concentric annuli, the experimental data do not cover the conditions with which we are here concerned. The formulas quoted in the literature relating film co-efficients to fluid properties and apparatus dimensions have taken many forms[6] but Davis[7] indicates that the problem of determining the proper equation for use in calculating heat transfer in concentric annuli has not yet been adequately resolved. For the eccentric annulus, it can be said that the problem is even less resolved.

Neglecting the effect of eccentricity, calculations made using various equations indicated that even with the more conservative expressions the temperature differential required between cable sheath and the airstream is not large. To be on the conservative side, therefore, in order to compensate somewhat for the uncertain effect of eccentricity of the cable in the duct, an expression by McAdams[8] was used as a basis for determining R_{sa}. From the correlation of available data for the flow of common gases in hot tubes, McAdams gives the expression

$$h = 0.0144 C_p \frac{G^{0.8}}{D^{0.2}} \text{ Btu per hour per square foot per degree Fahrenheit} \quad (5)$$

For air flow, equation 5 becomes

$$h = 0.015 C_p \frac{G^{0.8}}{D^{0.2}} \text{ Btu per hour per square foot per degree Fahrenheit} \quad (6)$$

Equations 5 and 6 hold for turbulent flow with Reynolds numbers in the range 2,100 to 100,000. For these applications the Reynolds number will be well within the turbulent range.

For flow in an annulus, equation 6 was adapted by substituting for D the equivalent diameter, D_e, taken as four times the flow area over the heated diameter so that

$$D_e = (D_2^2 - D_1^2)/D_1 \text{ inches} \quad (7)$$

For heat transfer from the air stream to the duct bank, the heated perimeter is taken as that of the duct inside wall, and the corresponding equation used for D_e in evaluating R_{ad} becomes

$$D_e = (D_2^2 - D_1^2)/D_2 \text{ inches} \quad (7A)$$

In the absence of more specific data, it has seemed reasonable to assume that for the case with which we are concerned, equations 5 and 6 are sufficiently valid to establish a reasonably correct basis for evaluating the temperature drop from cable sheath to air stream. Our experience confirms this belief. McAdams gives an expression for heat transfer with gas or fluid flow in annular spaces but indicates that equation 5 is preferable.

For our purpose we are interested in R_{sa}, the reciprocal of h as given in equation 6. Substituting common cable rating units and reducing, we obtain

$$R_{sa} = 6.0(D_e/CFM)^{0.8} \text{ degree centigrade per watt per foot} \quad (8)$$

Appendix II. Pressure Drops in Forced-Air Cooling Systems

Successful design of the mechanical components of the forced-air cooling system requires a satisfactory estimate of the total flow resistance offered by the system. The total pressure necessary to produce the desired air flow is determined by the resistance of the blower inlet, air filter, exhaust piping, and the cable-duct system.

The pressure losses in the inlet filter, blower piping and nozzles may be determined by means of standard references on heating and ventilation[9,10] and will not be discussed in further detail here.

With respect to the cable-duct system, limited data are available in the literature on the pressure drop in eccentric annuli with turbulent flow.[11] Axiomatically, it can be said that it is best to obtain actual test data on the resistance of the cable-duct systems involved at a rate of air flow in the required range. On earlier applications on our system, flow resistances were determined by a number of such tests. With data thus accumulated, pressure drops are now estimated with sufficient accuracy using the hydraulic diameter[6–8,11–14], D_2-D_1, as a basis for comparison, see Figure 6. The hydraulic (equivalent) diameter, D_2-D_1, which is equal to four times the flow area over the wetted perimeter, is defined as the diameter of an equivalent circular pipe of equal theoretical flow resistance.

Although the hydraulic diameter concept has been used in connection with Figure 6, there is reason to believe that some modification may be necessary for satisfactory correlation of pressure drop data in annuli;[14] however, in the absence of a generally accepted procedure, the treatment used here is considered to be sufficiently adequate.

Figure 6 is a graphical summary of test data obtained from actual installations. In this figure the pressure loss for a 100 foot length of duct having an air velocity of 3,000 feet per minute is plotted against D_2-D_1 for each duct surveyed. Each plotted point represents an average of approximately six duct measurements.

Although there is considerable dispersion, a curve can be drawn which will give a general trend. In a group of six ducts of apparently identical physical dimensions and construction, it is common to have a range of flow values varying ±30 per cent from the average. The variations encountered in ordinary pipe and ventilating duct friction losses are considerably increased in these installations due to a number of factors such as accumulation of cable grease in the duct, especially around bends, snaking of the cable, leakage in cracked ducts, and rough joints. Accurate testing is difficult because of the crescent shaped outlet openings and the widely varying velocity distribution. Frequently, the locations are such that access to the discharge areas is difficult.

The tests shown in Figure 6 were for fiber ducts of 4.5 and 5 inch inside diameter and for cables having either lead sheath or braid covering. Apparently, the differences in friction loss due to a limited range of duct and cable sizes and surfaces are not appreciable as compared with variations due to factors such as those listed above.

Based on the average of the test data given in Figure 6, the pressure loss in a 100-foot length of duct with an air velocity of 3,000 feet per minute may be expressed by the following empirical equation:

$$\Delta p = 12.0/(D_2-D_1)^{0.88} \text{ inches of water} \qquad (9)$$

The pressure loss data obtained from our tests are presented in the form of Figure 6 for practical use. It is not considered that the data are sufficiently accurate, consistent or complete to allow presentation in the usual form of roughness index, friction factor and Reynold's number.

The pressure loss values given in Figure 6 and in the empirical equation 9 may be computed for other lengths and velocities by assuming the flow resistance to be proportional to length and approximately proportional to the square of the air velocity. These relations are supported by test measurements within the limits of expected experimental error. A general empirical equation can be written, then, as

$$\Delta p = 13.3\times 10^{-9} L V^2/(D_2-D_1)^{0.88} \text{ inches of water} \qquad (10)$$

The velocity head at the entrance to the cable-duct may conservatively be considered to be completely lost and should be added to the duct friction drop.

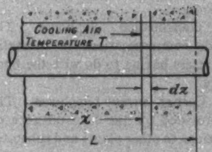

Figure 7. Differential section of duct for heat balance setup

Appendix III. Temperature Rise of Duct Cooling Air, Taking Into Account Heat Transfer Across the Duct Structure

For an incremental length of duct, dX, as shown in Figure 7 we can write the heat balance equation, algebraically, as

$$dW = dW_1 + dW_2 \qquad (11)$$

where

$$dW = W.dX$$

$$dW_1 = \frac{(CFM)}{(1.93)} dT$$

$$dW_2 = \frac{(T-T_a)}{(R_b)} dX$$

then

$$W.dX = \frac{(CFM)}{(1.93)} dT + \frac{(T-T_a)}{(R_b)} dX \qquad (12)$$

where

W = watts generated in the cable

W_1 = watts absorbed by moving air

W_2 = watts transferred across the duct structure

T = mean temperature of the moving air at any point X

T_a = the external ambient of the duct structure; assumed to be uniform along the duct run

Collecting terms, integrating and substituting limits, we get

$$T_o - T_i = [T_a - T_i + (W.R_b)](1-\epsilon^{-PL}) \qquad (13)$$

where P has the value $1.93/(CFM.R_b)$.

Equation 13 is identical with equation 4 given in the text.

References

1. **Standard Handbook for Electrical Engineers.** McGraw-Hill Book Company, New York, N. Y., section 7, paragraph 124, equation 28, 1941.

2. **A Method for Estimating Requirements of Transformer Cooling Air, Tyler G. Hicks.** *Electrical World* (New York, N. Y.), April 10, 1950, page 120.

3. **Current Carrying Capacity of Impregnated Paper, Rubber and Varnished Cambric Insulated Cables.** *Publication P-29-226*, Insulated Power Cable Engineers Association (New York, N. Y.), December 1943.

4. **The Thermal Resistance Between Cables and a Surrounding Pipe or Duct Wall, F. H. Buller, J. H. Neher.** *AIEE Transactions*, volume 69, part 1, 1950, pages 342–49.

5. **The Temperature Rise of Cables in a Duct Bank, J. H. Neher.** *AIEE Transactions*, volume 68, 1949, pages 540–48.

6. **Heat Transfer and Pressure Drop in Annuli, Elmer S. Davis.** *Transactions*, American Society of Mechanical Engineers (New York, N. Y.), volume 65, 1943, pages 755–59.

7. **Heat Transfer and Friction of Water in an Annular Space, F. G. Carpenter, A. P. Colburn, E. M. Schoenborn, A. Wurster.** *Transactions*, American Institute of Chemical Engineers (New York, N. Y.), volume 42, 1946.

8. **Heat Transmission (book), W. H. McAdams.** McGraw-Hill Book Company, New York, N. Y., 1942, equation 4K, page 174.

9. **Heating, Ventilating, Air Conditioning Guide (book).** American Society of Heating and Ventilating Engineers (New York, N. Y.).

10. **Heating, Ventilating and Air Conditioning (book), Harding, Willard.** John Wiley and Sons, New York, N. Y., 1932.

11. **Transfer Processes in Annuli, J. H. Wiegand, E. M. Baker.** *Transactions*, American Institute of Chemical Engineers (New York, N. Y.), volume 38, 1942.

12. **A Study of the Data on the Flow of Fluids in Pipes, E. Kemler.** *Transactions*, American Society of Mechanical Engineers (New York, N. Y.), volume 55, 1933.

13. **Fluid Mechanics (book), Dodge, Thompson.** McGraw-Hill Book Company, New York, N. Y., 1937, chapter VIII-IX.

14. **Velocity Distribution and Fluid Friction in Smooth Concentric Annuli, R. R. Rothfus, C. C. Monrad, V. E. Senecal.** *Industrial and Engineering Chemistry* (New York, N. Y.), volume 42, December 1950.

No Discussion

Public Address Systems in Generating Plants

S. C. BARTLETT
MEMBER AIEE

THE USE of public address systems in generating plants is a special application of the device and has not been particularly well covered in the technical literature to date. It differs from other public address applications in several important respects and it is the intent of this paper to give the basic requirements and considerations leading to the design of a truly practical system. Trials in practical plants over the past 15 years provide a basis for selecting components most suitable.

The expression "public address" is a misnomer in this case in that the device is specifically not used for entertainment or group talks but is confined to many brief uses for paging, co-ordination of activities and emergency warnings. It would be better known as an "amplifier system" or "loud-speaker system."

Other Communication Facilities

First, it is necessary to consider what other devices for communication may be at the disposal of plant operators. Any or all of the following may be found:

1. Leased telephone lines. These circuits handle all normal business functions from the plant to the local central office and to long distance phones.
2. Intercommunicating telephones. These take care of person-to-person conversations within the plant and may or may not be tied through a *PAX* or *PBX* to external trunks.
3. Code calling. This is for paging key men throughout the plant and is usually a part of the intercommunicating telephone system.
4. Test telephone. This is a system of complete simplicity being generally no more than a pair of conductors running throughout the plant with arrangements for plugging in handsets at any desired location.
5. Transmission telephones. These provide communications to substations for matters having to do with the flow of energy.
6. Carrier current telephones. These are provided for the long distance conversations to other plants and substations on the main transmission system and are used almost entirely for system operating functions.
7. Radio. Where provided, this is used primarily for dispatching line maintenance crews and sometimes serves for directing switching at remote, unattended substations.

Need for Public Address Systems

With all of the foregoing facilities there is still need for some means of paging all plant personnel either individually or in groups, a means of conveying orders to groups of people simultaneously, a means of communication from any one of these individuals to the entire group, and a means of notifying all personnel in cases of emergency. This is capably disposed of by means of a properly designed public address (P.A.) system.

Modern plants with the multiplicity of devices provided to obtain high efficiency introduce problems of co-ordination of all personnel, the observations which they make, the readings of instruments and, in turn, the orders regarding control and adjustment. This is important during periods of start-up, synchronizing, load change, boiler blowdown and shut down of units and is especially necessary during emergencies or unexpected conditions requiring immediate changes to be made.

The present-day trend in plant design is in the direction of unit construction, in which case a separate P.A. system should be provided for each unit. These may be readily consolidated at one or more points for simultaneous control as in the case of fire or other emergencies involving the entire plant.

History of Development

Early attempts to apply this equipment involved installations made by the manufacturer who, it often developed, was not fully cognizant of the problem, considering the noise levels involved, temperatures, humidity, and vibration. The equipment, therefore, was not properly adapted to the service and performance was poor. Such devices as crystal microphones with their inherent fragility would not today be considered for such an application. Similarly, microphones of low output level would not be considered except possibly by using a preamplifier at each microphone to reduce the susceptibility of the microphone circuit to pick-up from the many power conductors. Amplifiers attained a maximum rating of about 50 watts. Where additional power was required it was obtained only by using more 50-watt amplifiers. Thus, if 250 watts output was required the tube complement of all amplifiers totaled something in the order of 50 to 60 tubes.

Another early error of judgment resulted from the attempt to cover entirely too much area with the result that reverberations from the building destroyed intelligibility at any appreciable distance from the loud speakers. These early attempts, however, were not entirely wasted

---

Paper 51-329, recommended by the AIEE Special Communications Applications Committee and approved by the AIEE Technical Program Committee for presentation at the AIEE Fall General Meeting, Cleveland, Ohio, October 22–26, 1951. Manuscript submitted March 23, 1951; made available for printing September 5, 1951.

S. C. Bartlett is with The American Gas and Electric Service Corporation, New York, N. Y.

The writer desires to express appreciation to both R. S. Tucker and J. L. Lindner of the Bell Telephone Laboratories for advice and assistance in making the measurements of noise levels.

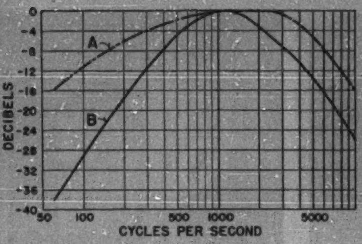

Figure 1 (left). Amplifier response characteristic

Figure 3 (right). Relation between articulation and energy distribution of speech

A—Relative importance for intelligibility
B—Energy distribution

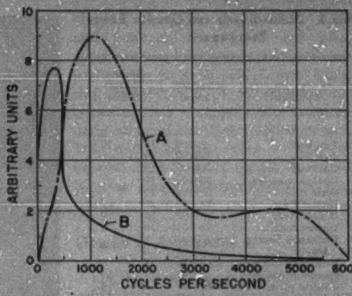

since they demonstrated that many useful purposes could be served by a properly designed system.

Statement of the Problem

The problem, then, is to provide:

1. A system capable of paging simultaneously throughout the entire plant.
2. A system providing speech coverage in all operating areas.
3. A means of reply or break-in from any operating position.
4. A simple means for adjusting audio power level for any background noise level from that of office areas to that of fan floors.

Basic Considerations

Knowledge of noise levels and reverberation characteristics coupled with an understanding of the manner in which a plant is operated leads to the premise that it is unnecessary and in fact improper to attempt to cover all plant areas except possibly for paging. The essential requirement is met by selecting and locating speakers to cover only observation and control areas where personnel are normally stationed. The speakers may then be supplemented by a means of conveying detailed information without error. High reliability must be achieved through selecting components designed to withstand extremes of temperature, humidity, dirt, and mechanical abuse. Consideration must be given to the great lengths of microphone and speaker cable, their selection and installation as a matter of minimizing susceptibility to magnetic and electric fields. The method of operation at each control point must be as simple as possible. The circuits employed must be held to basic simplicity to avoid becoming future sources of trouble and so maintenance work may be done without the necessity of calling in people with special skills or equipment.

Figure 2. Effect on syllable articulation of removing portions of the speech frequency range[4]

A—All frequencies below the indicated frequencies transmitted
B—All frequencies above the indicated frequencies transmitted

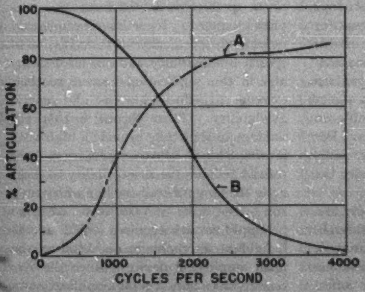

Reverberation Characteristics

Assuming that it is impractical to provide acoustic treatment of any areas other than offices or control room, it is necessary to adapt speakers to the plant as it stands. If, for instance, it were attempted to cover an entire turbine room floor from a single speaker, it would be found impossible regardless of the sound power employed because the large ceiling, wall and floor areas cause reverberation sufficient to completely destroy intelligibility. Illustrative of this was an early attempt to use an extremely high power horn speaker at one end of a turbine room floor. This device operated on the principle of modulating a flow of air from a compressor and produced sound volumes comparable to 500 watts of audio power with good intelligibility. With this device located at one end of the turbine room floor, high sound levels were produced throughout the entire 60 by 225 foot area. However, beyond about 60 feet from the source, words were completely unintelligible and the only thing heard was substantially a monotone determined by the reverberation characteristics of the room itself. If the entire area must be covered, the solution here is through the use of many small units. Actually we find that a practical solution results from the use of a single speaker at the turbine control panel or at the control end of each unit to concentrate all sound energy in those areas where operators are normally on duty. Similar logic applies to the application on the fan floor or other places where large wall areas may reasonably be expected to give trouble. Throughout the remainder of the plant the space is very largely broken up by pipes, tanks,

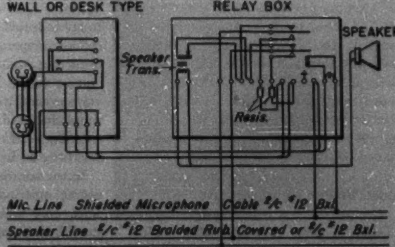
MONOPHONE STAND
WALL OR DESK TYPE
RELAY BOX
SPEAKER
Speaker Trans.
Resis.
Mic. Line Shielded Microphone Cable 2/c #12 Bxl.
Speaker Line 2/c #12 Braided Rub. Covered or 2/c #12 Bxl.

Figure 4. Circuit for relay control box, handset, and hookswitch

Table I. Noise Levels and Speaker Power Requirements

	Location	Decibel Level	Speaker Power, Watts	
			A	B
1.	Fan floor	95–120	20	20
2.	Fan floor	95–120	20	
3.	Coal conveyor	92– 97	20	
4.	Coal pulverizers	96–103	10	
5.	Scale floor	95–105	10	
6.	Heater floor	92– 97	20	
7.	Burner deck	93–101	10	10
8.	Burner deck	93–101	10	10
9.	Utiliscope (water level)	95	5	
10.	Utiliscope (burners)	95	5	
11.	Evaporator floor	93– 95	10	10
12.	Control room	70– 91	5	5
13.	Turbine room	93–107	20	20
14.	Turbine control panel	90–105	10	10
15.	Steam driven exciter	100–103	10	
16.	Boiler control panel	93–103	10	10
17.	Boiler room basement	100	20	20
18.	Boiler room basement	100	20	20
19.	Turbine room basement	90–107	20	20
20.	Feedwater pump	102–105	20	20
21.	Condenser pit	95–103	20	20
22.	Circulating pump	91–104	10	10
23.	Pump panel	98–105	10	10
24.	Condensate panel	102	10	
25.	Hotwell pumps	99	10	
26.	Machine shop	75– 85	10	10
27.	Elevator	81– 96	*	*
28.	Superintendent's office	67– 75	0.5	0.5
29.	Watch engineer's office	74– 81	0.5	0.5
30.	Electrician's office	74– 81	0.5	0.5
31.	Storeroom	83	5	5
32.	Amplifier room	75– 85	0.5	0.5
33.	Electric gallery	84– 91	5	
34.	Chem. laboratory	78	1	
35.	Results department	82	1	
36.	Lobby	82	5	
37.	Hallway	77– 91	1	
38.	Screen house	93	10	10
39.	Transformer yard	91– 96	10	
40.	Outside, near plant	75– 95	10	
41.	Outdoor substation	71– 82	10	
42.	Gate house	73	1	
Total power			406	242
Number of speakers			41	22
Average power			9.9	11.0

Column A—Complete coverage
Column B—Minimum requirements
* Handset but no speaker provided

columns, and machinery such that reverberation is not a problem.

Noise Levels

Many observations were made in both old and new plants using Western Electric Company sound level meter type *700-A*. These readings are tabulated in Table I, the values being in decibels above the threshold of hearing, which is taken as zero level, or 10^{-16} watts per square centimeter. Noise levels indicated are generally between 80 and 120 decibels with a few exceptions as in soundproofed offices and control rooms.

Audio Power Requirement

Table I gives average noise levels based on observations in practical plants.

Figure 5 (above). Typical monophone station mounted on relay control box

Figure 6 (right). Amplifier cabinet—rear

The final column indicating loudspeaker watts for each location has been determined by experience. This is not directly related to the noise level since there is an additional factor of the area to be covered. Note that the average for an entire plant is in the order of 10 watts per speaker and the total requirement for a single unit plant is in the order of 250 watts.

Loud Speakers

In the production plant itself and outdoor areas, all speakers should be of the horn-type using either straight trumpets or re-entrant horns. For our purposes, the smallest horns manufactured are entirely suitable. Specifically, a horn providing $2^1/_2$ to $3^1/_2$ foot air column with a bell diameter of 12 inches will pass everything from 150 to 5,000 cycles essentially without distortion. Inasmuch as the intent is to cover only selected areas, these horns should be chosen with not more than 40 degrees spread at 1,000 cycles. Drivers of the permanent-magnet type attained a high degree of development for military applications and are available today in forms which are largely impervious to temperature, humidity, vibration or dirt, as would be encountered in a generating plant. These are available in various sizes from 5 to 25 watts. For simplicity and interchangeability, it is recommended that just one type, say the 25-watt size, be provided.

In the control room a ceiling type 360-degree unit may be employed although, since only a low power is required, a small 5 inch cone speaker mounted in one control panel is adequate. For office areas the sloping panel type speaker mounted at the junction of wall and ceiling is quite satisfactory. In large offices where only certain of the employees are directly concerned with operation of the physical plant, it is convenient to use one or more small desk speakers in plastic housings such as are commonly employed for interoffice communicating systems.

Microphones

Having in mind the over-all response characteristic indicated in Figure 1 and discussed in the paragraph under Amplifier Characteristics, it is apparent that any modern microphone will provide adequate fidelity. Crystal microphones should be definitely avoided because of their fragility and the fact that they are subject to damage from temperature and humidity. Dynamic microphones would be quite suitable but in general involve more expense than necessary. The real practical solution appears to be through the use of a conventional carbon microphone, preferably in the form of a telephone handset. These have been highly developed, specifically for transmission of speech intelligibility and are most desirable in this application because of their extreme ruggedness, low cost and general availability. There is one further advantage in that they provide a high-level low-impedance source which very materially reduces the susceptibility to pick-up in the long microphone line which may run to the order of 1,000 feet. Also, no preamplifiers are required either at the individual microphones or ahead of the main amplifying device. Since the system involves only a total amplification in

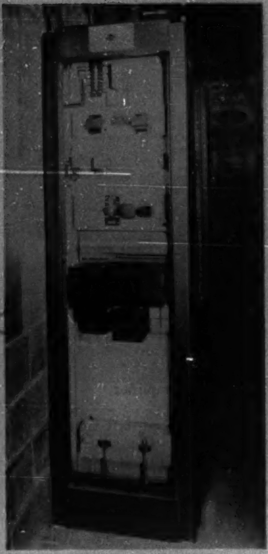

Figure 7. Same as Figure 6—covers removed

Top panel—Master Switch
2nd panel—48-volt rectifier
3rd panel—Monitor
4th panel—Control
5th panel—250-watt amplifier
6th panel—Blank
7th panel—Terminal

the order of 60 decibels, the matter of microphone hiss is not a problem.

In levels of extremely high noise, intelligibility of sound coming from loud speakers is limited to simple words, names or phrases. For anything more detailed, it is necessary to listen to a telephone receiver and, where the room noises are particularly bad, to have the additional protection of a soundproof booth. The conventional monophone suggested above serves very well for this additional function.

Microphone Supply

Considering the necessity of controlling plate voltage and the need to cut off local loud speakers, the simplest means is through the use of microphone current for control. Thus the microphone supply must not only be adequately filtered but should have high enough voltage to operate two relays in series with the microphone. Assuming that 600-ohm telephone relays and a conventional carbon microphone are used, this requires a 48-volt supply which is available in any of a number of forms, for instance, as a power supply for use in small telephone exchanges or as a part of a carrier current telephone set or a radio transmitter. This arrangement also has the advantage that no additional conductors are required for control.

Amplifier Characteristics

The first thought is normally for a means of designing or selecting high fidelity equipment. However, we must realize that in this application there is no intent to use the device for entertainment or reproduction of music. Not only is capability along these lines unnecessary, but for our purposes would be actually detrimental. In a power plant the background noise, although high, does tend to concentrate at either end of the audio spectrum. Thus we have many rumble noises as from crushers, fans, and hum from motors and transformers. At the upper end of the spectrum we have the characteristic screaming of turbine blades and feedwater pumps.

Figure 2 indicates the effect on syllable articulation of removing portions of the speech frequency range.[4] Note that no substantial improvement results from extending this range either below 400 cycles or above 3,000 cycles and adequate intelligibility will be attained by concentrating all audio energy within this range.

Consider further Figure 3 which indicates the relation between articulation and energy distribution of speech. Note that about one-half of the total energy is confined to the frequencies below 500 cycles but these frequencies contribute only 5 per cent to the intelligibility. By eliminating most of these and concentrating everything in the 400- to 3,000-cycle range, a given size of amplifier and number of speakers will provide far better performance.

What would be called a high quality amplifier for voice might have an over-all fidelity characteristic as indicated by curve A of Figure 1, which is flat from 1,000 cycles to 2,500 cycles and down 6 decibels at 200 cycles and 5,000 cycles. Even this is far more linear than required and an amplifier with characteristics as indicated in curve B would be quite satisfactory. This peaks at about 1,000 cycles and is down 6 decibels at 500 cycles and 2,500 cycles. In a power plant there is much opportunity for magnetic pickup into the microphone circuits of 60-, 120-, and 180-cycle frequencies and here, again, the amplifier response to these low frequencies must be held down. Thus, continuing curve B, the roll off below 500 cycles and above 2,500 cycles could be designed for about 12 decibels per octave. This, and in fact the entire shape of the over-all characteristic, may be obtained by very simple resistance-capacity networks.

Design of Amplifiers

For this type of work where the equipment will operate continuously under conditions of temperature variations, humidity and vibration, carefully planned mechanical design, along with simplicity of electrical components, is essential. By proper design the number of tubes should be minimized and any critical circuits should be carefully avoided. High impedance circuits characteristic of resistance coupled amplifiers and phase inverters should be avoided by using transformer coupling throughout.

A simple and practical arrangement would be through the use of a single triode, say type *6J5*, or a pair in push-pull for the input stage followed by a pair of triodes, say type *6A3*, in push-pull as a driver stage, these all being operated in class A, and followed by a final stage consisting of a pair of *805*'s in push-pull

Figure 8. Same as Figure 6—front view

operating as either class AB or class B. A pair of *866A* tubes would suffice as plate supply for the final stage using a bleeder to feed input and driver stages. If desired, the input and driver stages could be supplied from a low-voltage rectifier which might include microphone supply mentioned before. Thus the entire amplifier, including rectifiers, totals only seven or eight tubes.

The audio range should be limited at the input to conform to either curve "A" or "B" indicated in Figure 1. As mentioned previously, total output power requirements will be in the order of 250 watts. If we assume an input power in the order of 25 milliwatts, the entire gain comes out to be 60 decibels. Both microphone and speaker lines could conveniently be designed for 60 ohms.

Degenerative feedback for final stages using beam power tubes is conventional and can be introduced with little difficulty to reduce distortion, noise and instability caused by voltage fluctuation and, at the same time, improve output regulation of the amplifier.

Assuming class AB or B is used in the final stage, a power supply of good regulation is required. This is readily accomplished through the use of mercury rectifier tubes with choke input filter. Considering the comparatively low gain of the amplifier, there will be no trouble from rectifier tube noise if a conventional hash filter is employed.

The transformers themselves must be designed with due consideration for such factors as saturation of core material, symmetry of windings, avoidance of resonance, low loss, adequate shielding against hum pickup from chokes and other transformers. Many well designed transformers are available.

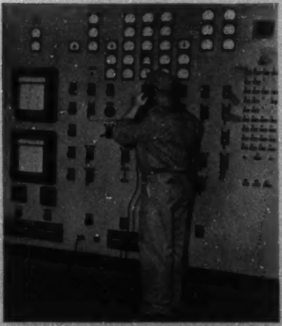

Figure 9. Control room showing operator using portable monophone (Note speaker in upper right corner of panel)

Choice of Tubes

The basis for choice of tetrodes or triodes may be argued. However, either may be employed to produce an amplifier of adequate fidelity. Our own choice for audio work of this nature is the triode since there is some reason to believe it is more capable of retaining its original characteristics throughout its life and is somewhat less subject to failure from "hot shorts." Considering the comparatively low total gain, separate cathodes are not required except possibly in the first stage. Conventional receiving type tubes are available in many types for the input and driver stages and many transmitter tubes, such as types *211*, *805*, *811*, *838*, *845*, are available for use in the final stage.

Table II

Ohms	Total Watts	Watts in Receiver
2,200	3.36	0.0452
3,300	2.25	0.0203
4,700	1.58	0.0100
6,800	1.10	0.00483
10,000	0.749	0.00224
22,000	0.340	0.000463
33,000	0.227	0.000206
47,000	0.160	0.000102
68,000	0.110	0.0000485
100,000	0.075	0.0000225

Plate Voltage Control

Since amplifying systems of this type are in use for only a very few per cent of the total time, it is advisable to disconnect the plate supply during the idle periods. This is a very simple matter and will result in material extension of tube life and, at the same time, will reduce temperatures of all other components of the amplifiers, thus similarly extending their lives. A thermal relay should be incorporated in the plate supply as a matter of protecting the rectifier tubes whenever the supply voltage may be interrupted and restored.

Amplifier Mounting

For convenience and simplicity, all equipment should be mounted in a cabinet with: the 48-volt relay/microphone supply; a panel containing speaker and monophone for local operation; a control chassis carrying equipment for plate supply control; the main amplifier; and terminal boards for the microphone, speaker, and power connections. In plants where a separate room is available for communication equipment, a relay rack will provide excellent mounting.

Figure 10. Control room with operator using desk set

Location of Amplifier

In a power plant there are many possible locations. If a separate room is provided for the telephone switchboard, carrier current equipment or other electronic devices, it would be ideal. Otherwise, there may be space in the control room or one of the offices. If none of these is practical, an amplifier designed along the lines indicated above can be located almost anywhere as long as the ambient temperature does not exceed about 90 degrees Fahrenheit and the equipment will not be subjected to excessive vibration or direct spatter of liquids.

Handset Volume Level

The standard desk set cords and handset cords are not available as shielded conductors or even with the microphone lead shielded. It is therefore important to reduce the level of the speaker line to handset level before bringing it into proximity to the microphone lead. Thus the speaker line in the control box goes immediately to the relay and then through resistances to the flexible cord. The value of these resistors may be changed to produce any desired receiver volume depending on the background noise level. Using resistors in pairs to maintain balance and assuming a 122.5-volt speaker line (250-watt amplifier, 60-ohm line) and handset receivers of 60 ohms each, the receiver power levels shown in Table II will be produced.

Handset Mountings

The conventional wall mounting hookswitch is suitable for all locations except in telephone booths and in offices where the

Figure 11. Machine shop showing loud speaker, control box, and soundproof booth for handset. (Booth also used for intercommunicating telephone)

desk set is preferred. No dial, ringer, capacitor, or induction coil is required. One make contact of the hook switch is used to control microphone current.

Speaker Transformers

These matching transformers serve the purpose of matching the impedance of all speakers in parallel to whatever impedance it is desired to operate the speaker line. Thus the individual speakers are set for impedances considerably above that of the line itself. For instance, if a line is operated at 60 ohms, the impedance to be used to obtain any desired speaker power is given in Table III.

For simplicity it is suggested that all horn speakers be equipped with 25-watt adjustable transformers to cover the impedance range from 600 to 3,000 ohms. Transformers for all other speakers could be 5 watts rating with input impedances from 3,000 to 30,000 ohms.

For example, if we took the installation suggested in Table I under condition B, there are seven 20-watt speakers, nine 10-watt speakers, two 5-watt speakers, and four 1/2-watt speakers. Using transformer input impedances as indicated above, we get the following figures:

7 units, each 750 ohms in parallel = 107 ohms
9 units, each 1,500 ohms in parallel = 167 ohms
2 units, each 3,000 ohms in parallel = 1,500 ohms
4 units, each 30,000 ohms in parallel = 7,500 ohms

$$\text{Total } Z = \frac{1}{1/107 + 1/167 + 1/1{,}500 + 1/7{,}500} = 62$$

$$\text{Total power} = \frac{(122.5)^2}{62} = 242 \text{ watts}$$

Cables

For both microphone and speaker lines there are many practical choices. We would suggest that these be restricted to the types generally to be found in plant stocks for which fittings are immediately available and with which the plant personnel are thoroughly familiar. For instance, the speaker line could consist of either *BX* or number 12 weatherproof wire in conduits. For the microphone line type *BXL* would be excellent. The characteristic impedance of these lines is not a factor since for the highest frequency handled, say 3,000 cycles, we have a wave length of approximately 62 miles compared with a length of the longest run of cable in the order of 1,000 feet.

It is advisable, wherever possible, to keep microphone and speaker leads in separate conduits. The microphone circuit may be carried in the same conduits with other signaling circuits if desired.

Table III

Speaker Power, Watts	Transformer Z, Ohms
25	600
20	750
15	1,000
10	1,500
5	3,000
2.5	6,000
1	15,000
0.5	30,000

Control Room Switchboard

In addition to the loud speaker and the desk set the control room should have jacks in the panels such that an operator may use a portable monophone while working at the panels, reading instruments, and making adjustments. A conventional double telephone jack located every alternate panel will be adequate. The operator uses a standard monophone with 4-wire cord and double plug. Plugging in the portable monophone accomplishes the same thing as picking up the desk set monophone in that the local speaker is cut off.

Control Boxes

To eliminate acoustic feedback it is necessary to provide a relay at each control point to cut off the local speaker when its associated monophone is off the hook. For convenience, this is mounted in a 12 inch by 12 inch by 4 inch steel box, Figure 4, with a 10-microfarad capacitor by-passing the relay coil, a pair of fixed resistors to apply a low level signal to the handset receiver and, an adjustable speaker transformer. The steel box is well adapted to welding or bolting to steel structures throughout the plant and is of ample size to accommodate *BX*, *BXL* or conduit. For office areas, the same components in smaller size may all be built into a standard telephone ringer box.

Over-all Performance

As it normally functions, the system is put into operation by lifting any monophone which, in turn, applies plate voltage and the call is received by all speakers. Assuming that a certain person is called, when he picks up the monophone at some other point, a high quality telephone channel is established with receivers at each end adjusted in amplitude depending upon local noise levels. It would then be a simple matter to cut off all loud speakers. However, experience indicates that it is better to leave them in operation. Thus, all personnel are fully informed of any contemplated changes being discussed and may prepare to make such adjustments as necessary on the equipment under their control.

In general, the sound power being concentrated in that part of the frequency range conveying maximum intelligibility, the over-all performance is very good. However, it must be recognized that in the extremely high noise level areas, the best that can be expected from loud speakers is ability to understand simple words or phrases. "It is common ex-

Figure 12. Office showing desk speaker and monophone

perience that when any sound is impressed upon the ear, it reduces the ability of the ear to sense other sounds."[4] Each tone tends to mask those near and above it in frequency. As would be expected, masking by complex sounds is the composite masking of each individual tone. In these areas the P.A. system serves for paging only, after which the transmission of intelligence is accomplished by the local monophone with the protection of a soundproof booth.

The cost is an extremely variable factor but in no case should exceed 1/20th of 1 per cent of the plant value and is readily recovered by improved personnel efficiency, plant performance, and reduction of damage during emergencies.

Maintenance

Equipment as indicated above requires very little maintenance. The circuits are simple and straightforward and very few tubes are used. There is very little reason for duplicate equipment, and maintenance can be handled by anyone with average understanding of audio circuits equipped with basic tools and a volt-ohmmeter. A tube tester is hardly essential since conventional types will handle only the receiver tubes used on the input and driver stages. For most work, all that needs to be done is to check tubes by interchanging with new tubes, observing the resultant values of tube voltages and currents. The power output level may be checked approximately by observing the voltage across the speaker circuit, using voice or whistle as an input to the microphone circuit. If it is desired to be more precise, an audio oscillator should be provided. With this instrument, it will be possible at any time to restore the full original characteristics of the amplifier through the ability to observe the actual gain at any frequency. Speakers are seldom a source of trouble. Handsets are subject to some damage and it is reasonable to expect to replace handset cords from time to time. It would be advisable to stock spare tubes, filter condensers, handsets and handset cords.

Conclusions

It is felt that by adhering rigidly to practical considerations as detailed herein a device may be produced using commercially available components in circuits of basic simplicity, attaining high performance characteristics at low cost to provide a service not possible by other communication devices either separately or in combination.

References

1. Elements of Acoustical Engineering (book), H. F. Olson. D. Van Nostrand Company, Inc., New York, N. Y., 1947.

2. Applied Acoustics (book), Olson, Massa. The Blakiston Company, Philadelphia, Pa., 1939.

3. Manual of Sound Systems, L. B. Cooke. Bell Telephone Laboratories (New York, N. Y.), 1939.

4. Speech and Hearing (book), Harvey Fletcher. D. Van Nostrand Company, Inc., New York, N. Y., 1929.

No Discussion

Bell System Cable Sheath Problems and Designs

F. W. HORN
NONMEMBER AIEE

R. B. RAMSEY
ASSOCIATE MEMBER AIEE

THE wide variety of hazards to which Bell Telephone System cable sheaths are subjected impose many design problems. The nature of these hazards and their effect on cable sheaths engineering are discussed. The currently used cable sheath designs are described.

The sheaths of telephone cables play a most important role in the Bell System. These sheaths provide the first line of defense against the whims of nature and of man for 70,000,000 circuit miles, or 90 per cent of the Bell System's communication network. These 70,000,000 miles of circuit are covered with over 300,000 miles of cable sheath. The growth in the number of miles of cable and in the Bell System's investment in cable during the past 40 years, see Figure 1, are testimony to the importance of the cable sheath itself. The dependability of service to its customers and the protection of its investment go hand-in-hand in causing the Bell System to pay particular attention to cable sheath. The engineering of each cable installation is a complex problem in economics involving a satisfactory balance between costs and the quality of the service required of the circuits inside the sheath.

Recent developments in sheath design have tended to complicate the terminology concerning cable sheath. For this reason the following definition is given and is used throughout this paper: Everything outside the cable core is considered to be part of the cable sheath and consists of a basic sheath only, or a basic sheath and various protective coverings that may be applied over the basic sheath for the purpose of further safeguarding it. The sheath types that now are considered to be basic are shown in Figure 2.

Approximately 75 per cent of all Bell System cables are located in exchange areas and are covered only with a basic type of sheath. Protective coverings are applied over the basic sheath of all submarine cables, a substantial part of all toll cables, and some exchange area cables.

The worst enemy of paper insulated cable is water. Particular care is employed at the factory to insure that the cable core of insulated conductors is dry before the basic sheath is applied. If the paper is allowed to absorb moisture the shunt conductance rises rapidly and the increase in attenuation that results can eventually put the circuit out of service.

General Requirements

There are several requirements which cable sheath must meet prior to installation. All cable sheath, for instance, must have sufficient flexibility and tensile strength to permit the cable to be placed on and removed from a reel of reasonable diameter several times without injury. Such rereeling is required when cable is being armored or corrosion protected and when stock cable is to be shipped on orders for less than full reel lengths. Upon arrival at location the cable must then endure removal from the reel and the process of installation. From then on it must withstand the damaging influences that are peculiar to its particular location. An accurate evaluation and understanding of the hazards which beset every cable installation are mandatory if an average Bell System cable life of 30 to 40 years is to be achieved. The requirements placed upon a cable by its environment are very much dependent upon whether the cable is placed underground, on the ground, under water, or in the air. Underground cables may either be buried or placed in ducts.

The requirements placed upon cable sheaths by environment may be classed as mechanical, electrical, and corrosional. The mechanical requirements include tensile strength, resistance to abrasion, creep, bruising, and to fatigue caused by vibration and temperature changes. The electrical requirements are necessitated by lightning and the inductive interference effects of power lines. The corrosional requirements result from stray currents from electrified railway lines, earth currents, or from corrosive soil and duct conditions.

Cable Sheath Problems

The rest of this paper is divided into two parts. The first part sets forth the background and explanation of the various mechanical, electrical, and corrosional problems on the basis that they must always be considered. The last part is devoted to a description of the current Bell System cable sheath designs along with their fields of use and capabilities.

Mechanical Problem

The mechanical requirements of buried cable sheath would be rather severe if it were not for the fact that most buried telephone cables are covered with approximately 30 inches of earth. This depth protects the cable from severe and sudden changes in temperature and is sufficient to prevent wholesale damage by plows and small hand tools. Erosion in hilly terrain, however, can materially reduce the cable depth and, in some cases, will completely expose the sheath. In locations of this sort the sheath is subject to abrasion by rock movements caused by freezing and thawing and to bruising by rock-falls and slides. Also,

---

Paper 51-330, recommended by the AIEE Wire Communications System Committee and approved by the AIEE Technical Program Committee for presentation at the AIEE Fall General Meeting, Cleveland, Ohio, October 22-26, 1951. Manuscript submitted January 11, 1951; made available for printing August 31, 1951.

F. W. Horn is with the Bell Telephone Laboratories Inc. at Kearny, N. J. and R. B. Ramsey is with the Bell Telephone Laboratories Inc. at Baltimore, Md.

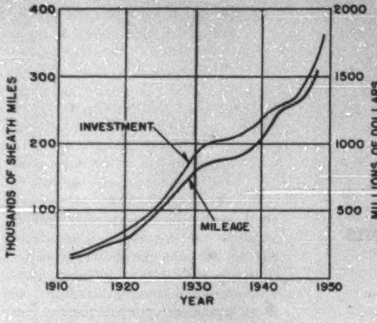

Figure 1 (left). Bell Telephone System cable plant mileage and investment

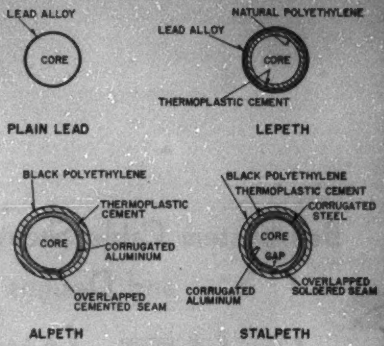

Figure 2 (right). Basic sheath designs

some sections of the United States, notably the north central part, are inhabited by gophers. These rodents have caused so much damage to cable sheath that special measures are taken against them.

Cable that is laid on the ground in gullies and dry washes must have sufficient tensile strength and sturdiness in its sheath to resist the drag and pounding which it will receive during flash floods. Some cables must be installed in rocky and rugged terrain that is inaccessible for normal installation equipment. In those cases the cable must be snaked into position with a wire rope; the sheaths involved must not only have considerable tensile strength but also must resist serious abrading and cutting forces during installation.

The mechanical requirements of duct cable sheath are usually simple in that they only involve installation. The cable sheaths are well lubricated as they enter the ducts and except under adverse duct conditions are subjected to only minor abrasion during the pulling-in process. The sheath, however, must be able to withstand the rather severe bending and twisting incidental to splicing and racking in manholes.

Where aerial cable sheath is involved the mechanical requirements are focused mainly upon fatigue. Wind and temperature changes cause the cable to swing and bow. The basic sheath materials, therefore, must be sufficiently proof against fatigue from these sources. Damage to aerial cable occasionally results from stray bullets from small arms, flying stones from blasting operations, and objects cast by small boys. Even the lowly fishhook has taken its toll.

The list of mechanical requirements for submarine cables includes tensile strength abrasion resistance and stiffness. Great tensile strength is required because irregularities in submarine topography may leave long spans of cable unsupported and because large dragging forces are created by tides and, now and then, by anchors of ships. Vibration fatigue is important where fast tides cause the cable to be in almost constant motion.

THE LIGHTNING PROBLEM

The damaging aspects of lightning to cable take two forms in that the current can burn holes in the sheath and can arc from the sheath to the inside of the cable. Holes in the sheath can cause eventual circuit failure by allowing the ingress of water, the carbonized products of burned insulation can produce immediate outages, and in severe cases of damage actual fusing of the conductors may occur.

Extensive studies and measurements of natural lightning have been made by engineers of the Bell Telephone Laboratories and these studies have produced much factual information and have led to the development of a strong theoretical background for designing a plant less susceptible to lightning damage.

The important characteristics of lightning itself include the current amplitude and wave shape of the stroke, and its frequency of occurrence. The current[1] of the average stroke has been found to reach its crest value in 5 to 10 microseconds and to drop to half of its maximum value in 70 microseconds. The possibility of damage to a cable depends upon the magnitude of the peak current; the severity of the damage is related to the energy content in the wave following the peak. The crest currents of lightning discharges vary over a wide range, see Figure 3. The number of thunderstorm days per year varies extensively throughout the United States and is shown in Figure 4.[1] Field studies extending over a number of years have shown that the number of strokes to earth per square mile per thunderstorm day ranges from 0.28 in northern to 0.43 in some southern parts of the country.

An aerial cable will attract all the strokes along a zone whose width is about seven[2] times the height of the cable above the ground, and hence the average number of strokes per year to an aerial cable can be readily computed. For a buried cable the width of the zone of attraction in feet ranges from 1.4 to 2.4 times the square root of the earth resistivity in meter-ohms. The 1.4 applies for resistivities in excess of 1,000 meter-ohms and the 2.4 is for resistivities less than 100 meter-ohms. From these figures it can be seen that an aerial cable 25 feet high will collect four times as many strokes as a buried cable where the soil resistivity is 1,000 meter-ohms. The presence of trees, power lines, buildings or water towers along the cable route cause a marked reduction in the effective width of the lightning zone of an aerial cable, but has little effect on that of buried cable. However, buried and duct cable are given considerable protection by water pipes and other conducting structures along the line of the cable.

After the number of strokes per year to a cable has been estimated the next step is to determine the number of those strokes that will have sufficient peak cur-

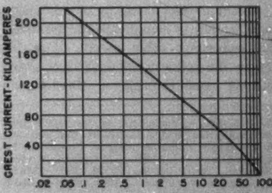

Figure 3. Percentage of lightning strokes to buried structures in which current exceeds ordinate

rent to damage the cable. For buried cable this maximum allowable crest current, I_m, in kiloamperes is approximately equal to

$$I_m = \frac{0.31\,V_e}{R\sqrt{\rho}}$$

where

V_e = impulse rating in kilovolts of core-to-sheath dielectric
R = d-c resistance of sheath in ohms per mile
ρ = earth resistivity in meter-ohms

The number of faults per year, N, on the length, l, of buried cable now can be obtained from

$$N = \frac{an}{100}$$

where

a = per cent obtained from Figure 3 using I_m for the ordinate value
n = probable number of strokes collected by buried cable in one year.

The situation is more complicated for aerial cables[3] because the current can flash over to ground at guy wires, pole protection wires, et cetera.

From the foregoing it can be seen that the resistance of the cable sheath and the impulse breakdown voltage of the core-to-sheath insulation are the only controllable features which are an integral part of the cable itself.

Induction from Power Lines

This section outlines the various forms of the power line induction problem and sets forth the part that the cable sheath plays in its solution.

There are two aspects to the induction problem—one concerns the normal operating condition of the power line while the other is associated with the abnormally large currents when a fault occurs. Both of these aspects are fundamentally the same although they manifest themselves in rather different ways in their effect on Bell System cable circuits. Under normal operating conditions noise can be introduced into the cable circuits by the fundamental and harmonics of the power frequency. When sufficiently high, induced voltages can render signaling circuits inoperative and noise can impair the intelligibility of talking circuits. Fault currents induce voltages from conductor to sheath, sheath to ground, and across the ends of an opened conductor which may be dangerous to personnel working on the cable. In addition, these high induced voltages can cause protectors on the cable conductors to operate and thereby ground the conductors either momentarily or permanently.

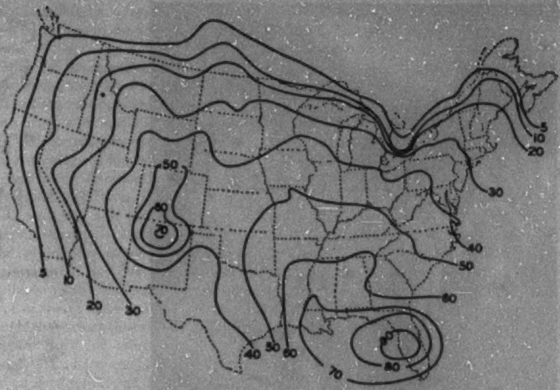

Figure 4. Map showing the average number of thunderstorm days per year

The layer of metal in all basic cable sheath provides an almost perfect shield against electric fields and reduces the deleterious effect of magnetic fields. The magnetic shielding comes about because the power line current induces voltage in the metallic shield. The resulting current sets up a magnetic field of its own in opposition to that of the power line current. The d-c resistance of the sheath, therefore, plays a predominant part in the determination of the magnetic shielding and should be as low as practicable. This requirement is in entire agreement with that presented by the lightning problem.

Other variables involved in the amount of magnetic shielding are frequency, the impedance of ground connections, the earth resistivity, or the leakance of the sheath to earth. When magnetic materials such as steel tapes are used as part of the sheath the shielding depends, in addition to the above, upon the amount of induced current in the shield and the permeability, diameter, number, thickness, width, angle of spiral, and air gap between turns of the steel tapes.

The Corrosion Problem

The corrosion problem results from the various electrochemical phenomena that can be present when:

1. Dissimilar metals are conductively connected together and immersed in an electrolyte.
2. A given metal is immersed in dissimilar electrolytes that are conductively connected.
3. Stray currents from d-c systems enter or leave the sheath via an electrolyte.
4. The electrolyte is chemically active with regard to the metal.

The currents involved may be man-made (such as stray trolley currents) or may be caused by self-generated voltages that are established in accordance with the electromotive series and the nature of the electrolyte.

Duct and buried cables are far more subject to corrosion than are aerial cables. Normal atmospheric conditions usually keep aerial cables dry. Duct and buried cables, however, are frequently exposed to at least one or more of the outlined conditions.

The part that the cable sheath can play in the reduction of corrosion is to minimize the reaction of its metallic parts with electrolytes and metallic structures. From the corrosion problem standpoint the insulation resistance of the sheath to ground should be high enough to limit current densities to safe values.

Cable Sheath Designs

This section first gives attention to the three basic sheath designs and then deals with the various protective coverings and armors.

Basic Sheath Design

Plain Lead: As its name implies it is simply a sheathing of lead which is extruded over the cable core. While the sheath is broadly referred to in most cases as lead it is in reality a lead alloy. Pure lead has been found to be inferior to some of the alloys from a fatigue standpoint and is therefore not recommended for aerial use. Small or fractional percentages of tin, calcium, silver, and zinc have been alloyed with lead with reasonable success but for all around service 1 per cent antimony alloyed with 99 per cent lead is now most generally used.

Lead sheath alone provides sufficient

Figure 5 (above). Alpeth cable production lines at Western Electric Company Kearny Works

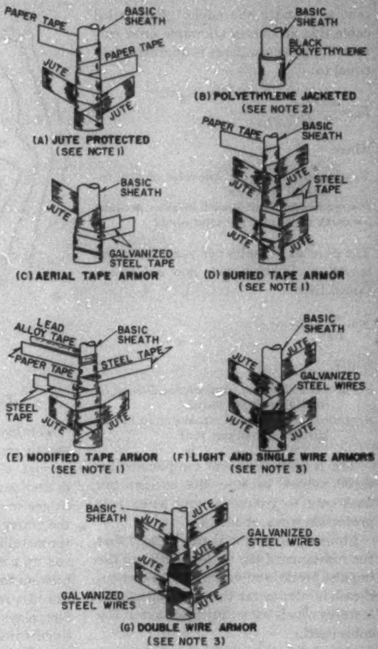
PAPER TAPE
BASIC SHEATH
PAPER TAPE
JUTE
JUTE
(A) JUTE PROTECTED (SEE NOTE 1)
BASIC SHEATH
BLACK POLYETHYLENE
(B) POLYETHYLENE JACKETED (SEE NOTE 2)
BASIC SHEATH
JUTE
GALVANIZED STEEL TAPE
(C) AERIAL TAPE ARMOR
PAPER TAPE
BASIC SHEATH
JUTE
JUTE
STEEL TAPE
JUTE
JUTE
(D) BURIED TAPE ARMOR (SEE NOTE 1)
LEAD ALLOY TAPE
BASIC SHEATH
PAPER TAPE
STEEL TAPE
STEEL TAPE
JUTE
JUTE
(E) MODIFIED TAPE ARMOR (SEE NOTE 1)
BASIC SHEATH
JUTE
JUTE
GALVANIZED STEEL WIRES
JUTE
JUTE
(F) LIGHT AND SINGLE WIRE ARMORS (SEE NOTE 3)
BASIC SHEATH
JUTE
JUTE
GALVANIZED STEEL WIRES
JUTE
JUTE
GALVANIZED STEEL WIRES
JUTE
(G) DOUBLE WIRE ARMOR (SEE NOTE 3)

Figure 7 (right). Protective covering designs

NOTES:

1. BASIC SHEATH AND EACH LAYER FLOODED WITH ASPHALT COMPOUND. COATING OF WHITING APPLIED TO FINISHED CABLE.
2. BASIC SHEATH FLOODED WITH THERMOPLASTIC CEMENT.
3. EACH LAYER PROTECTION FLOODED WITH ASPHALT COMPOUND. COATING OF WHITING APPLIED TO FINISHED CABLE.

mechanical protection for most aerial and duct installations and is likewise an effective moisture barrier. Its conductivity in combination with the dielectric strength provided by the conductor insulation and core wrap is sufficient to prevent excessive lightning failures in most duct installations and in aerial installations except where very small cables are involved in areas where lightning storms are prevalent. From the standpoint of low frequency induction the lead sheath when properly grounded is reasonably effective as a shield and of substantial benefit in reducing noise in the telephone circuits. From the corrosion standpoint lead is satisfactory in dry surroundings but susceptible to corrosion in a wet environment if stray electrical currents or corrosive soil conditions exist.

In addition to the primary conditions noted above lead is very adaptable to forming during the installation operations. Also, the sheath integrity is made continuous across a splice by hot-wiping a lead sleeve directly to the lead sheath.

Alpeth and Stalpeth Sheath: Alpeth sheath which is shown in Figure 2 consists of an 0.008-inch aluminum tape applied longitudinally with overlap and an extruded polyethylene outer jacket. The seam in the aluminum is filled with a polyisobutylene cement, and a flooding of rubber thermoplastic cement applied over the aluminum forms a bond between the aluminum and polyethylene. The manufacturing equipment for this design is shown in Figure 5.

This sheath is a postwar development. The scarcity of lead, lead controls, and high lead price all pointed out the importance of having a substitute sheath available, and if possible a more economical one. The problem was not an easy one, however, as all materials used would have to be in plentiful supply and at a reasonable cost. Also any sheath developed would have to fulfill to a reasonable degree all the obligations previously discussed for lead sheath.

Investigation of materials and application techniques indicated that metals or metal alloys were not particularly promising. Development of plastics during the war years, however, had proceeded at a rapid rate and there were several that showed promise. Plastics, in contrast to metals, permit passage of moisture and in this respect polyethylene appeared to be the most logical choice since its diffusion constant is lower than other commercially available plastics. The mechanical characteristics of polyethylene are

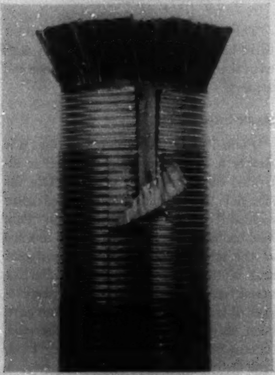

Figure 6. Stalpeth cable

likewise excellent. It is tough and abrasion resistant and can be readily extruded at temperatures in the range of 300 to 500 degrees Fahrenheit. It does not become brittle until temperatures well below those normally encountered in the field are reached and continued flexing or vibration does not appear to produce the fatigue effect found in metals.

These characteristics are all excellent, but degradation of the polymer will take place if it is exposed to sunlight. Bell Telephone Laboratories' chemists found, however, that very great improvement in aging characteristics could be achieved by thoroughly dispersing 2 per cent finely divided carbon black in the polyethylene.[3] An antioxidant is also added to the compound to protect it during processing and to improve its aging characteristics.

The polyethylene, however, could not alone fulfill all of the requirements of a sheath as the amount of moisture which would diffuse through any jacket of reasonable thickness would be intolerable and the cable would have essentially no protection against lightning or inductive interference. A metal was, therefore, needed, and the field was readily narrowed to copper and aluminum with aluminum being chosen because of lower cost.

The thickness of the tape decided upon was 8 mils which represents a compromise between electrical and mechanical considerations. To obtain the most moisture-proof seam and maximum longitudinal conductivity the tape was applied longitudinally with an overlapped seam which could be sealed with cement. Such a tube, however, is not sufficiently flexible except for core diameters below approximately 0.60 inch, so a means of adding flexibility to this structure for the larger cables was needed. This was accomplished by precorrugating the aluminum tape at right angles to its length before forming. With approximately sine wave shape and ten corrugations per inch, sufficient material is stored up to give excellent flexibility to the completed sheath. To further improve the moisture resisting properties, the aluminum envelope is flooded with thermoplastic cement which also adheres to the polyethylene outer jacket.

The completed alpeth sheath provides good mechanical protection and its lightning protective and inductive shielding qualities are adequate for most situations. In fatigue it is better than lead and the polyethylene jacket is a corrosion resistant covering. The lighter weight of alpeth sheath permits the use of longer spans. From a moisture barrier standpoint it is inferior to lead in service but even in this regard the life should be adequate.

It is not the intention to replace lead sheath completely by a composite sheath, but rather to use substantial quantities of both types when conditions permit. In case of shortages, restrictions or drastic price revisions production can then be shifted in one direction or the other, as circumstances dictate.

As with any new product there were many problems. As explained previously, lead splicing sleeves can be readily wiped to lead cable but obviously cannot as easily be joined to alpeth. An effective type of sheath splice has been developed but at the present time this joint must be accomplished by using adhesive materials and a fairly complicated technique which increases the cost of the splice.

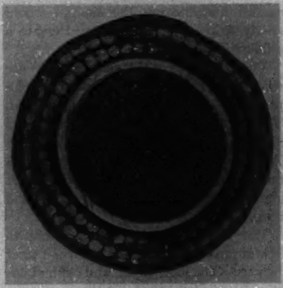

Figure 8. Cross-sectional view of double wire armored cable

Many minor problems were encountered and solved but a major trouble also developed which threatened the very life of alpeth cable. About six months after production began, field reports started coming in to the effect that the polyethylene sheath had cracked near the splice or that cracks had been found after removing a cable which would not hold gas. The first reaction was that the failures were due to structural weakness of the polyethylene and test cables were subjected to all manner of extreme handling, which only emphasized the toughness and strength of the jacket.

After many blind alleys had been explored it was found that certain agents, which will be referred to as contaminants, would cause polyethylene to crack under reasonably mild strain conditions.[4] Among the most active of these surface contaminants are detergents and soaps. Since splices are often pressurized and tested for gas leaks with a liquid soap solution and a compound consisting largely of soap was used in certain areas as a duct lubricant, it is not surprising that failures were reported from the field.

All known contaminants were immediately banned, and new types of pressure testing solutions and duct lubricants were developed and put into use. The most important goal was, however, to obtain a polyethylene which is crack proof. This project has not been completed but great improvement has already been obtained mainly through increasing the average molecular weight of the polymer. Laboratory tests now indicate that the most active contaminants will not crack the present alpeth jacket even at strains far beyond any to be found in the field.

The Western Electric Company and Bell Telephone Laboratories engineers then attacked the problem of improving the moisture resistance and lowering the high splicing cost inherent with the present type splice used for alpeth cable. The result is a modification of alpeth sheath and is called stalpeth. In this construction, which is shown schematically in Figure 2 and as a photograph in Figure 6, there is a corrugated 0.008-inch aluminum tape applied longitudinally with slight gap. There is then a corrugated 0.005-inch terne-coated steel tape applied longitudinally with a soldered overlap. The steel is flooded with thermoplastic cement and over this is applied a polyethylene jacket.

Soldering is the critical operation in producing this design. A flat solder strip is fed into the overlap in the corrugated steel just after forming, and immediately thereafter the cable passes underneath the work coil of an induction heater. With steel, soldering can be accomplished with 4 to 5 kva with a line speed of 50 feet per minute.

Stalpeth, which in time will replace alpeth, is essentially moisture proof. The initial cost is roughly the same as alpeth since it is practicable to reduce the thickness of the polyethylene jacket, and splicing costs should be considerably lower since the steel jacket furnishes a surface to which lead sleeves can be joined by the wiping technique. Although for the time being stalpeth will only be applied at the plants manufacturing exchange area cable, there is no basic reason why this type of sheath could not be used for toll cable, except where lightning is a problem, if the relative supply or price of polyethylene with respect to lead made this desirable.

Lepeth Sheath: The basic sheath design for lightning protection is called "lepeth" sheath. This design, as shown in Figure 2, consists of a 75-mil layer of polyethylene surrounded by a layer of lead. A flooding of thermoplastic cement is applied between the polyethylene and lead layers.

The 75-mil layer of polyethylene is tested at the factory for 3 seconds at 20,000 volts of direct current and has an impulse voltage breakdown rating of 30,000 volts. This high impulse voltage rating and the low resistance of the lead covering provide excellent electrical protection against lightning. For example, a buried lepeth cable with a core diameter of 1.57 inches has a sheath resistance of approximately 1.5 ohms per mile. When installed in soil that has a resistivity equal to or less than 1,800 meter-ohms the sheath will be electrically immune to strokes that place less than 150,000 amperes on the sheath. In localities where the number of thunderstorm days per year does not exceed 50, the probability of failure due to lightning would be approximately one or less failure per year per 1,000 miles of sheath.

PROTECTIVE COVERINGS FOR BASIC CABLE SHEATH

This section describes the protective coverings which are applied, when necessary, over the basic sheaths that have already been described. These protective coverings have, to date, only been applied to the plain lead and lepeth basic types. Protective coverings could be applied over stalpeth or alpeth sheath if desired. Figure 7 gives a pictorial description of the various protective coverings.

Jute Protected: Buried cables with plain lead or lepeth basic sheaths may be "jute protected." This design, Figure 7(A), is relatively inexpensive and provides good protection against the hazards of the plowing-in operation. It is used where corrosion, power line interference, gophers, and mechanical damage risks do not present special problems. The paper, asphalt, and jute covering over the basic sheath do not offer any protection against lightning in addition to that provided by the basic sheath.

Polyethylene Jacketed: The polyethylene jacket type of protective covering is used at present only in duct installations where corrosion problems are present. This design, Figure 7(B), gives excellent corrosion protection to the lead under the polyethylene because the resistivity of polyethylene is very high even when immersed. The polyethylene covering is tough and is scuff resistant; its smooth surface allows the cable to be pulled into ducts with ease.

Steel Tape Armored: Aerial and buried cables with plain lead or lepeth basic sheath may be "tape armored". The aerial design, Figure 7(C), consists of a layer of jute and two layers of galvanized steel tapes. The buried design, Figure 7(D), is made up of a layer of paper over the basic sheath, two layers of jute, two layers of steel tape, and two more layers of jute; the basic sheath and each layer of protection are flooded with an asphalt compound and a coating of whiting is applied to the finished cable. No asphalt compound is used in the aerial design because corrosion protection is usually not needed and because the asphalt would slowly drip from the cable and create a public nuisance.

These designs are intended for use where the increased inductive shielding provided by the steel tapes is desired. They also are used where the moderate amount of mechanical protection inherent in the steel tapes is advantageous. This mechanical protection is effective against gophers and against injury by small hand tools.

The buried design is susceptible to lightning damage in a way that is rather curious. The jute, paper, and asphalt applied between the lead and the steel tapes act as an insulator between them. Lightning currents may, therefore, arc from the steel tapes through this insulation to the lead. The explosion products produced by this arc create a high pressure gas pocket between the lead and the steel tapes which can collapse or flatten the cable at the point of entry of the stroke. This problem is especially serious where the essentially hollow tubes of coaxials are involved.

In order to circumvent this lightning problem a modified form of tape armor was developed for buried cables. This design, see Figure 7(E), consists of a layer of alternate lead alloy and paper tapes, three layers of steel tape, and two layers of jute. The basic sheath and each layer of protection are flooded with an asphalt compound and a coating of whiting is applied to the finished cable.

This modified design of tape armor replaced the design previously described for all buried toll cables exposed to lightning, and derives its advantage from the fact that the lead tape allows lightning and rent to travel from the steel tapes to the lead sheath without arcing.

Light Wire Armored: The tensile strength and abrasion resistance of the armor wires used by this design, Figure 7(F), allow it to be used in a variety of places. Light wire armored cable can be laid over rocky terrain that is not plowable, and can be snaked into locations, such as swamps and very rugged terrain, that are inaccessible to cable installation equipment. It also can be used as buried cable across gulleys or other places where erosion is likely to expose the cable and leave unsupported lengths. This protective design also is employed for crossings of reservoirs, shallow lakes and streams where navigation is restricted to canoes, rowboats, and launches.

Single and Double Wire Armored: The single wire armored design employs heavier armor wires and thicker lead sheath than the light wire armored design; these are the only differences between the two. The double wire armored design is shown in Figures 7(G) and 8.

Both of these designs are intended for submarine use. Single wire armored cables are employed in deep lakes, across navigable streams and in coastal waters, including estuaries, bays, and inlets. Double wire armoring is for use under unusually severe submarine conditions such as locations having fast tides and rocky irregular bottoms.

The cable sheath designs described herein are those currently used by the Bell System as the practical solution to the many problems involved. Some designs are old; others are new. The developments of new materials and manufacturing techniques are continually offering unexplored possibilities.

References

1. LIGHTNING PROTECTION OF BURIED TOLL CABLE, E. D. Sunde. *Bell System Tech. Journal* (New York, N. Y.), volume 24, April 1945.

2. EARTH CONDUCTION EFFECTS IN TRANSMISSION SYSTEMS, E. D. Sunde. D. Van Nostrand Company, Inc., New York, N. Y., 1949.

3. WEATHERING STUDIES ON POLYETHYLENE FOR WIRE AND CABLE APPLICATIONS, V. T. Wallder, W. J. Clark, J. B. DeCoste, J. B. Howard. *Industrial and Engineering Chemistry* (Easton, Pa.), volume 42, November 1950, page 2320.

4. CRACKING OF STRESSED POLYETHYLENE—EFFECT OF CHEMICAL ENVIRONMENT, J. B. DeCoste, F. S. Malm, V. T. Wallder. *Industrial and Engineering Chemistry* (Easton, Pa.), volume 43, January 1951, page 117.

No Discussion

Analyses of Subsequent Faults

HOWARD K. AMCHIN
ASSOCIATE MEMBER AIEE

ERIC T. B. GROSS
FELLOW AIEE

Synopsis: Renewed interest in resonant neutral grounding makes it important to have available methods for predicting accurately voltages and currents under abnormal system conditions. In this paper are discussed solutions of subsequent faults on power systems, often called simultaneous faults; included are systems so grounded that a single line-to-ground fault is not a short circuit. Based on a general selection of line locations to be faulted, analyses are made by component methods and 3-phase methods. Each analysis treats representation of the system, unbalance, and measurements. It is concluded that the component methods are more applicable to large systems, while small systems are more satisfactorily studied by the 3-phase methods. Advantages and shortcomings of the various solutions are indicated.

GROUNDING the neutrals of power systems plays no part in the actual transfer of power from the generating stations to the consumers if the system is without a fault. Therefore, in the early days of power transmission, it was natural to operate systems with the neutral isolated. Furthermore, several inherent features of delta systems[*] which favor continuity of service made it desirable to retain a type of system in which a ground fault is not a short circuit.

Extensive load growth, the need for system interconnections, and the advantages of diversity in system peaks soon brought higher voltages and longer transmission lines. The resulting system expansions manifested themselves in an unexpected epidemic of trouble due to single line-to-ground faults. Investigations indicated that the main problem was the elimination of arcing grounds. An associated difficulty was the subsequent[**] fault, caused by full system voltage stresses (line-to-line) to ground at weak points on the system during sustained single line-to-ground faults.

The problem of arcing grounds has been condensed to the choice between two solutions of seemingly opposite character, effective (solid or low reactance) grounding of the neutral, and resonant neutral grounding. With effective neutral grounding, each single line-to-ground fault becomes a short circuit and is relayed; this answer has been used in the United States extensively since the first trouble occurred on large delta systems. Resonant neutral grounding avoids short circuits by making arcing grounds self-extinguishing. During sustained ground faults, however, the voltages-to-ground on the two unfaulted phases rise to line-to-line magnitude.

A resonant grounded system, therefore, has many of the advantageous characteristics of a small delta system with negligible capacitance-to-ground, since single line-to-ground faults do not directly produce short circuits. However, the voltage triangle is shifted for a continuous line-to-ground fault; both systems are subject to subsequent faults.

In many countries abroad, and especially in Europe, both underground cable and overhead line systems have operated for many years with resonant neutral grounding. The number of installations of Petersen coils in this country has slowly but steadily increased, indicating renewed interest in this grounding method.[1,2] As a result, it is important to have available methods for accurately predicting voltages and currents under abnormal system conditions.

Subsequent fault solutions have been treated by many authors; because of the popular practice in the United States of grounding solidly or through low reactance, most analyses have been confined to such systems. It is the purpose of this paper to review and extend these solutions to subsequent faults on power systems where a single line-to-ground fault is not a short circuit.

Networks may be solved by two basically different methods: the network analyzer method and the algebraic method.

Network analyzer methods are preferred because of the rapidity and ease with which they are obtained. As numerous a-c network analyzers are available, the solutions will be discussed from this viewpoint.

Faults will be imposed on two short sections of line at x and y as shown in Figure 1, with the conductors at x indicated by A, B, C, and those at y by a, b, c. This selection is intended to be general, in that it places no restrictions whatsoever on the location of the chosen line sections. The sections may be portions of radial feeders at opposite ends of a general network. They may be portions of lines connecting two general networks in any manner, as shown by Vaage,[3] or may be any of the simpler and more familiar configurations. A and a are of the first phase, B and b of the second phase, and C and c of the third phase in the order of their normal phase sequence. Let E_{AG}, E_{BG}, E_{CG}, and E_{aG}, E_{bG}, E_{cG}, indicate the voltages-to-ground of conductors A, B, C, at x and a, b, c, at y, respectively.

Corresponding currents flowing from the conductors into the faults are to be indicated by I_{AG}, I_{BG}, I_{CG}, and I_{aG}, I_{bG}, I_{cG}, respectively. Phase A will be chosen as reference and faulted to ground at x, and phase b so faulted at y.

---

[*] A delta system is one with no metallic connection to ground; it is an ungrounded system.

[**] Ground faults at different locations on a system and on different phases are known as subsequent faults.

Paper 51-331, recommended by the AIEE Transmission and Distribution Committee and approved by the AIEE Technical Program Committee for presentation at the AIEE Fall General Meeting, Cleveland, Ohio, October 22–26, 1951. Manuscript submitted May 31, 1951; made available for printing August 31, 1931.

HOWARD K. AMCHIN is with the American Gas and Electric Service Corporation, New York, N. Y. and ERIC T. B. GROSS is with the Illinois Institute of Technology, Chicago, Ill.

This paper is based on a thesis submitted to the Graduate School of Illinois, Institute of Technology, Chicago, Ill., by Howard K. Amchin, in partial fulfillment of the requirements for an MS. Degree.

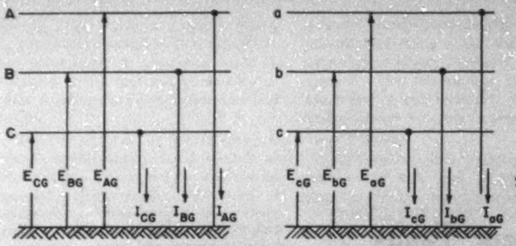

Figure 1 (above). Subsequent faults at locations x (left) and y (right) of a symmetrical 3-phase system

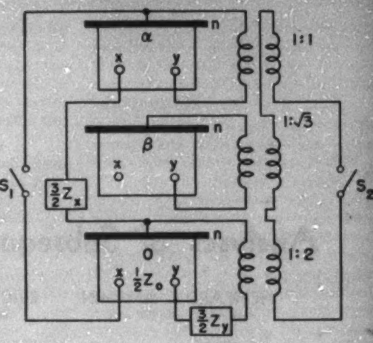

Figure 3 (right). Clarke component network connections for subsequent AG-bG faults

Analyses by Component Methods

The method of symmetrical components has been applied to the solution of a multitude of problems involving unbalanced system disturbances. For the more common problems (single line-to-ground faults, line-to-line faults, and so forth), solutions have been discussed and compiled. Several methods utilizing symmetrical component principles for the solution of subsequent faults will be discussed in the following.

SEQUENCE NETWORK CONNECTION METHOD

Representation of System. This general method,[4-6] most familiar to power systems engineers, is based entirely upon symmetrical components. It requires that all three sequence networks be set up at the same time. However, no special restrictions are placed on the values of system sequence impedances and all loads and sources of generation may be included.

For most purposes, short circuit studies assume zero fault impedance as maximum values of short circuit current are usually required. In relay application, however, this impedance may play an important role in the determination of relay operating characteristics. Fault impedance appears only in the zero sequence network at its proper system location with a value of three times its positive sequence impedance. In the resonant grounded system, where representation of the grounding impedance (Petersen coil) is required, an adjustment of the zero sequence network is made which is similar to that for fault impedance.

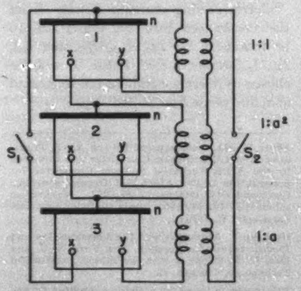

Figure 2. Sequence network connections for subsequent AG-bG faults

Representation of Unbalance. The conditions imposed by the symmetrical component equations for a fault on phase *A* at *x* are satisfied by a series connection of the left-hand terminals of the positive (1), negative (2), and zero (0) sequence networks, as illustrated by Figure 2.

In general, not more than one conductive interconnection between networks to represent unbalances can be permitted. Voltage restrictions are introduced which may not be true restrictions and, in addition, there is no assurance that proper current division will occur at each junction. Therefore, it is necessary to represent a second unbalance by connecting the networks through transformers.

For the line-to-ground fault at *y*, dissymmetry of the fault with respect to the reference phase (*b*) leads to further restrictions on the sequence currents and voltages in the form of 120-degree phase shifts, which may be produced by a phase converter, or by phase shifting networks. Complete sequence connections are given by Figure 2; both switches are closed during the fault.

Measurements. Once properly connected, the sequence networks may be metered for component currents and voltages at any system location. Actual phase currents and voltages are obtained from the formulas for converting sequence quantities.

NETWORK CONNECTION MODIFIED BY CLARKE COMPONENTS

A set of three voltage or current phasors pertaining to the phases of a 3-phase system can be replaced by any of a number of different sets of component phasors. The system of symmetrical components is one such set. Another is the system of Clarke components.[7] The use of Clarke components for the solution of system unbalances offers in many cases distinct advantages, as will be illustrated by their application to the present problem.

Representation of System. Transmission lines and static apparatus of a symmetrical 3-phase power system have the same impedances in Clarke component networks as in the positive (Z_1), negative (Z_2), and zero (Z_0) sequence networks. In terms of complete self (Z_{aap}) and mutual (Z_{abp}) phase impedances, the line impedances are

$$Z_\alpha = Z_\beta = Z_1 = Z_2 = Z_{aap} - Z_{abp}$$
$$Z_0 = Z_{aap} + 2Z_{abp}$$

Generator sequence impedance representation is also the same for cylindrical rotor machines. For salient pole machines the equivalent circuit contains a nonreciprocal mutual impedance between the α and β networks.[8] This quantity depends upon the difference between the direct and quadrature axis reactances which, for a modern machine with connected dampers, are approximately equal. The mutual impedance is, therefore, very small. Its effect is further minimized by the impedances of the lines and equipment between the faults and the gener-

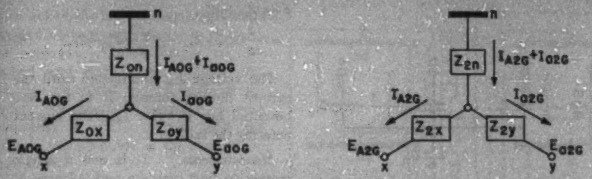

Figure 4 (above). Equivalent Y to replace the zero sequence network (left) and to replace the negative sequence network (right) between points x and y and the zero potential bus

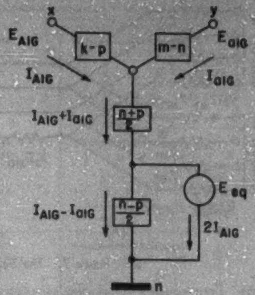

Figure 5 (right). Equivalent circuit to replace faults at x and y in the positive sequence network

ators. Thus, the nonreciprocal mutual impedance may be neglected without adversely affecting the results of the study.

All generator sequence impedances are then represented in terms of direct and quadrature axis reactances as follows

$$Z_\alpha = Z_\beta = \frac{3X_d + X_q}{4}$$

Z_0 = zero sequence impedance

For balanced voltages in a symmetrical 3-phase system, generated α voltages are positive sequence voltages. The β network includes generated voltages which are positive sequence voltages advanced through 270 degrees, and the zero-network has no source electromotive forces.

Thus, the complete α network and zero network are the same as the positive and zero sequence network, while the β network differs only by its generated voltages from the negative sequence network.

Representation of Unbalance. The constraints imposed by a fault at x on phase A through fault impedance Z_x are satisfied by connecting the α and zero networks in series and dividing all zero network impedances by two. The β network is not involved in this fault. The left-hand terminals of Figure 3 illustrate the connections. The right-hand terminals of this figure, using coupling transformers, are connected to satisfy the conditions imposed by the fault at y on phase b through fault impedance Zy. Note the odd ratio coupling transformers, and the values of fault impedance used in the networks.

Measurements. Sequence current and voltage distributions throughout the system are obtained on the network analyzer, and phase quantities computed by recombination of Clarke Components. Both switches are closed during the fault.

SUPERPOSITION PRINCIPLE APPLIED TO THE NETWORK CONNECTION METHODS

In general, the interconnections for any particular system unbalance can be introduced by closing or opening a switch in the component networks. The procedure to be discussed employs the principle of superposition in conjunction with sequence network connections and was suggested by J. R. Mortlock.[9]

Representation of System. Sequence networks for either power system are connected as discussed for the sequence network connection methods. It is necessary, however, to make provision for switching faults on and off the system. Figures 2 and 3 show the switches in open positions.

Representation of Unbalance and Measurements. The procedure employed is:

1. With switch S_2 open, close switch S_1 which controls the direct interconnections. The sequence networks now represent the system with phase A connected to ground at x.
2. Meter the networks where system quantities are desired and determine the voltage across S_2. In this manner, the current and voltage distributions as affected by the first fault are obtained. It may be pointed out that this fault does not produce a short circuit if the system is high-impedance grounded.
3. The current or voltage distribution due only to grounding the system at y is now found by an operation equivalent to closing S_2, that is, by applying across its terminals with all system generation short circuited a voltage equal and opposite to that determined from the operation of S_1.
4. The actual current or voltage distribution for the subsequent faults is simply the vector sum of the distributions due to the closing of S_1 and S_2. Phase currents and voltages are given by the usual equations relating sequence components and system quantities.

EQUIVALENT Y

Solutions for subsequent faults as previously discussed require some means of providing phase shift, or coupling transformers with "odd" turn ratios. While it is sometimes possible to provide this equipment, a more suitable circuit may be derived by following a procedure developed by Edith Clarke.[10,11]

Ten equations are written in terms of the unknown positive, negative, and zero sequence currents and voltages, and of the known negative and zero sequence impedances. There will be twelve unknowns, three voltages and three currents for each point of fault. Six of the equations pertain to the unbalanced and four to the balanced portion of the network (two each for the negative and zero sequence networks). The ten equations are then reduced to two in terms of positive sequence voltages and currents, and the known impedances. From these two equations, an equivalent circuit is derived which represents conditions at the point of fault and it is inserted in the positive sequence network. The network analyzer may now be used to obtain volt-

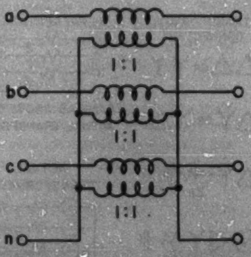

Figure 6. Connection of forcing transformers for use in the 3-phase and neutral method

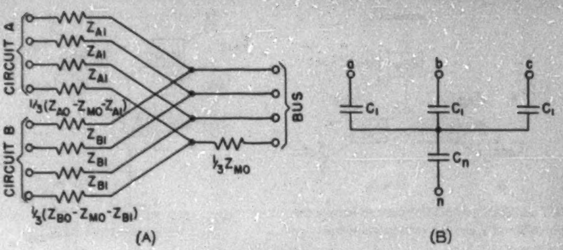

Figure 7. The 3-phase and neutral method

(A). Zero sequence mutual impedance representation. (B). Shunt capacitance representation

ages and currents at any location in this circuit.

The fault acts as a generator of negative and zero sequence voltages. Data obtained from the positive sequence network, and the four equations relating to the balanced portion of the system determine these generated voltages. The two passive sequence networks, after being properly energized at the fault points, are metered at any location for sequence quantities. Finally, all three sequence voltages or currents at each desired location are combined to give phase values.

Representation of System and Unbalance. The positive, negative, and zero sequence networks of the system are completely set up on the network analyzer. For each subsequent fault condition to be studied, an equivalent Y between the faulted points and neutral of the negative and zero sequence network is determined (see Figure 4). These circuit constants are then combined into an equivalent circuit, shown in Figure 5, which is inserted into the positive sequence network between the fault points and the neutral bus.

For the delta system, the constants of the equivalent circuit are:

k = sum of negative and zero sequence impedances as viewed from x with no fault at y

$$=Z_{2n}+Z_{2x}+Z_{0x} \tag{1}$$

m = sum of negative and zero sequence impedances as viewed from y with no fault at x

$$=Z_{2n}+Z_{2y}+Z_{0y} \tag{2}$$

$$n=aZ_{2n}=-\frac{1}{2}Z_{2n}+j\frac{\sqrt{3}}{2}Z_{2n} \tag{3}$$

$$p=a^2Z_{2n}=-\frac{1}{2}Z_{2n}-j\frac{\sqrt{3}}{2}Z_{2n} \tag{4}$$

The constants for the resonant grounded system equivalent circuit are:

$$k=Z_{2n}+Z_{2x}+Z_{0n}+Z_{0x} \tag{5}$$

$$m=Z_{2n}+Z_{2y}+Z_{0n}+Z_{0y} \tag{6}$$

$$n=aZ_{2n}+a^2Z_{0n}$$

$$=-\frac{1}{2}(Z_{2n}+Z_{0n})+j\frac{\sqrt{3}}{2}(Z_{2n}-Z_{0n}) \tag{7}$$

$$p=a^2Z_{2n}+aZ_{0n}$$

$$=-\frac{1}{2}(Z_{2n}+Z_{0n})-j\frac{\sqrt{3}}{2}(Z_{2n}-Z_{0n}) \tag{8}$$

The voltage E_{eq} is adjusted until the current flowing through it to the zero potential bus is twice I_{A1G}, the current entering the fault at x.

Measurements. It is now a simple matter to find currents and voltages at any system location. In the positive sequence network, conditions at the fault points have been represented by the equivalent circuit of Figure 5 and sequence quantities are therefore easily obtained. Equations 9, 10, 11, and 12 for the delta system, and equations 11, 12, 13, and 14 for the resonant grounded system, determine the generated negative and zero sequence fault voltage.

Delta system:

$$E_{A0G}=-Z_{0x}I_{A0G} \tag{9}$$

$$E_{a0G}=-Z_{0y}I_{a0G} \tag{10}$$

$$E_{A2G}=-(Z_{2n}+Z_{2x})I_{A2G}-Z_{2n}I_{a2G} \tag{11}$$

$$E_{a2G}=-Z_{2n}I_{A2G}-(Z_{2n}+Z_{2y})I_{a2G} \tag{12}$$

Resonant grounded system:

$$E_{A0G}=-(Z_{0x}+Z_{0n})I_{A0G}-Z_{0n}I_{a0G} \tag{13}$$

$$E_{a0G}=-Z_{0n}I_{A0G}-(Z_{0y}+Z_{0n})I_{a0G} \tag{14}$$

Positive sequence fault currents, I_{A1G} and I_{a1G}, are known from readings previously taken. Operating on these currents to find the negative and zero sequence components of fault current and substituting the new calculated values in

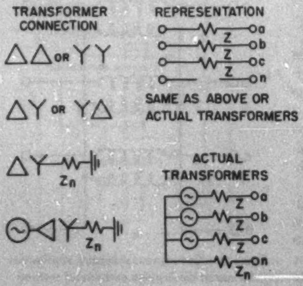

Figure 8 (left). Transformer bank representation in the 3-phase and neutral method

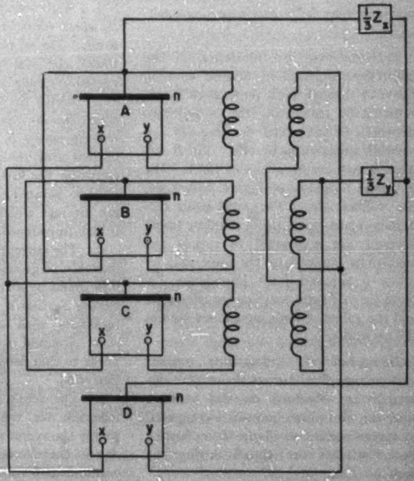

Figure 9 (right). Three-phase and zero sequence network connections for subsequent AG-bG Faults. All three transformers 1:1

either set of the four equations gives the required voltage components in the passive networks. These voltages are now applied and current and voltage distribution measured by the network analyzer. All quantities necessary for the evaluation of phase voltages and line currents at any point of the system are now known.

Modified Equivalent Y

Suggested by W. V. Lyon,[12] this method is very similar to Clarke's except that each fault is represented by a single impedance connected in parallel with the positive sequence network at the point of fault. The impedance of each shunt depends not only upon the impedance of each sequence network but also upon a ratio of the pre-fault positive sequence voltages at the fault points.

The basic steps, that is, determination of an equivalent Y for the negative and zero sequence networks, are identical to those used in the equivalent Y. However, as the shunt impedances are functions of the impedances of all three sequence networks, the equivalent process must also be extended to the positive sequence network. Shunt impedances at x and y, Z_{x1} and Z_{y1}, respectively, in terms of the sequence impedances and positive sequence prefault voltages are[13]

$$Z_{x1}=k-n\frac{A(p+Z_{1n})-(k+Z_{1x}+Z_{1n})}{A(m+Z_{1y}+Z_{1n})-(n+Z_{1n})} \qquad (15)$$

$$Z_{y1}=m-n\frac{A(m+Z_{1y}+Z_{1n})-(n+Z_{1n})}{A(p+Z_{1n})-(k+Z_{1x}+Z_{1n})} \qquad (16)$$

where

$$A=\frac{E_{A1G}'}{E_{a1G}'} \qquad (17)$$

After these impedances are inserted in the positive sequence network, the remainder of the solution is identical to the equivalent Y.

Analyses by 3-Phase Methods

Although it has been general practice to use the method of symmetrical components for fault studies of a 3-phase power system, it is often possible and sometimes more practical to use either phase quantities directly or variables other than symmetrical components.[14] The discussion of Clarke components illustrates the use of a modified component system. In the following sections, three solutions utilizing 3-phase methods are described. Two of them require the assumption that the positive and negative sequence networks are identical, generated voltages excepted, but no restriction is placed on the zero sequence network. As previously pointed out, this assumption is not unreasonable and does not adversely affect the unbalance study.

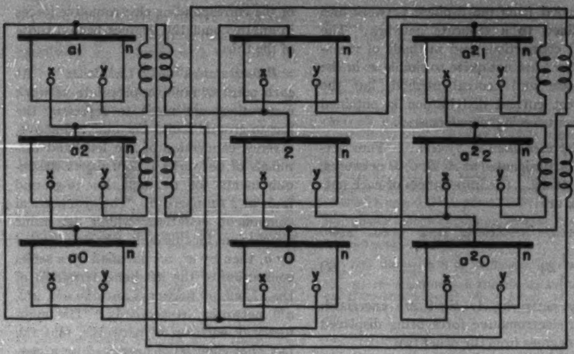

Figure 10. Triple sequence network connections for subsequent AG-bG faults. All four transformers 1:1

Three-Phase and Neutral Method

This method was independently devised and used on the calculating boards at Westinghouse Electric Corporation and at the Massachusetts Institute of Technology.

Representation of System. A 3-phase 4-wire circuit is used to represent the power system. The 3-line conductors of each system branch are set up with impedances equal to the branch positive sequence impedance. The impedance of the neutral conductor, Z_n, is given by

$$Z_n=\frac{1}{3}(Z_0-Z_1) \qquad (18)$$

Since positive and negative sequence current components flow only in the line conductors, they produce the correct voltage drops in the line-to-neutral voltage. Zero sequence currents, when present, produce a line-to-neutral voltage drop of

$$I_{a0}Z_1+3I_{a0}\left[\frac{1}{3}(Z_0-Z_1)\right]=I_{a0}Z_0 \qquad (19)$$

which is correct if $3I_{a0}$ returns in the neutral conductor. This requirement is, of course, automatically satisfied in all radial branches but will not be satisfied, in general, for closed loops. However, the current may be forced to satisfy this requirement by the use of "forcing transformers" in series with one or more branches as shown in Figure 6. The best procedure, when in doubt as to whether the current distribution in a branch is satisfied, is to check line and neutral currents without the forcing transformers. If the agreement is not satisfactory, forcing transformers should be inserted and readings again taken.

For both systems under consideration, the effect of shunt capacitance is represented by the connections of Figure 7(B). C_1 and C_0 are positive and zero sequence capacitance and C_n is given by

$$C_n=\frac{3C_0C_1}{C_1-C_0} \qquad (20)$$

The Petersen coil is connected at its proper system location to neutral with an impedance equal to its impedance.

Power transformer banks may be represented on the network analyzer by actual transformer banks or, in some cases, by simple series impedances (see Figure 8); phase shift is not necessary.

Finally, generator voltages are represented by balanced 3-phase electromotive forces.

Representation of Unbalance. Faults are imposed by making the actual fault connections; connections to ground are made to the corresponding point of the neutral conductor.

Measurements. The following quantities can be measured directly: line currents, residual current (in neutral), line-to-line voltages, and line-to-ground voltages (measured line-to-neutral).

Three-Phase and Zero Sequence Method

This method, due to E. W. Kimbark,[14] differs from the preceding one in that the zero sequence current and voltage are excluded from the 3-phase network and confined to a separate network. The fault connections and methods of measurement are not quite so simple as in the 3-phase and neutral method, but the correct current distribution is obtained without forcing transformers.

Representation of System. Four networks, designated as *A, B, C, D* networks, are set up. The impedances of each network are:

$$Z_A = Z_B = Z_C = Z_1 = Z_2 \qquad (21)$$

$$Z_D = \frac{1}{3} Z_0 \qquad (22)$$

Only networks *A, B, C* are energized, each electromotive force being displaced 120 degrees from the other two.

Representation of Unbalance. Conditions for a line-to-ground fault at x on phase A through fault impedance Z_x are given by

$$I_{BG} = I_{CG} = 0 \qquad (23)$$

$$E_{AG} = I_{AG} Z_x \qquad (24)$$

Similarly, the following equations give conditions for a line-to-ground fault at y on phase b through fault impedance Z_y.

$$I_{aG} = I_{cG} = 0 \qquad (25)$$

$$E_{bG} = I_{bG} Z_y \qquad (26)$$

These equations, when resolved into *A, B, C, D* components, determine the constraints on sequence network connections. All conditions are satisfied by the connections shown in Figure 9.

Measurements. Directly measured may be: line-to-line voltages between corresponding points of networks *A, B, C;* line-to-ground voltages between corresponding points of networks *A, B, C,* and network *D;* residual current in network *D;* zero sequence voltage in *D.* For phase currents, connect the primary of a 3:1 current transformer in network *D* and the secondary in parallel with the corresponding branch of the phase network.

TRIPLE CONNECTION METHOD

As this method[14] combines 3-phase and symmetrical component representation, it could be classified as either a symmetrical component method or 3-phase method.

Representation of System. Each sequence network is set up in triplicate. The three negative and zero sequence networks are identical, but the positive sequence networks differ from one another in that the electromotive forces in any one of them are 120 degrees ahead of the corresponding electromotive forces in another and 120 degrees behind those of the third.

Representation of Unbalance. At each point of fault, appropriate network connections are made to represent the line-to-ground fault. As analyzed above, a series connection of the left-hand terminals of networks 1, 2, 0 meets the requirements for a single line-to-ground fault at x on phase A. The symmetrical component equations which determine connections for this fault, when multiplied by a, then by a^2, are satisfied by a series connection of the left-hand terminals of the $a1$, $a2$, $a0$ networks and the a^21, a^22, a^20 networks, respectively. The symmetry of each set of networks, plus the fact that each set is energized by a generator 120 degrees ahead of another and 120 degrees behind the third, insures the 120-degree difference in distribution of currents and voltages of each complete set of networks.

Circuit restrictions imposed by the ground fault at y are satisfied by a series connection of the right-hand terminals of the 1, a^22, $a0$ networks. If the constraint equations are multiplied by a and a^2, respectively, it may be seen that the right-hand terminals of the $a1$, 2, a^20, and a^21, $a2$, 0 sequence networks are also to be connected in series. In making this connection, the usual restrictions necessitating coupling transformers must be observed, and in this particular case at least four of these transformers must be used. The completed sequence connection diagram is shown in Figure 10.

Measurements. As in all solutions, sequence currents and voltages are read in any branch. Zero sequence quantities are read in the 0 network, positive and negative sequence quantities in networks 1 and 2, respectively, and combined by the usual relations to obtain phase quantities. It is also possible to read a or a^2 times a sequence quantity in either the a or a^2 networks, thus saving some work in determining phase voltages and currents. Furthermore, by simple switching and combination of proper components through current and potential transformers, phase quantities may be read directly.

A simplification in setting up the networks may be realized if only three networks are completely set up and the other six in reduced form.

Conclusions

The choice of a particular method of solution is almost immediately dictated by the size of the power system under consideration.

COMPONENT METHODS

1. In general, the symmetrical component methods are more applicable to larger systems. However, they are more time-consuming for system quantities are all obtained by calculation, and not by direct readings, as is the case for the 3-phase methods.
2. The sequence network connection method has the disadvantage of requiring a 120-degree phase shift. Apparatus to provide this shift is not standard equipment on calculating boards, and, therefore, this method cannot be too widely used. Adjustment of circuit elements is "cut-and-dry" and usually time-consuming.
3. Problems of phase shift are obviated by the use of Clarke components.
4. Application of the superposition principle has the particular advantage of retaining the physical significance of the faults. In addition, distributions of currents and voltages due to each fault are readily determined. This method has, of course, the disadvantages attributed to the symmetrical component and Clarke component methods. Furthermore, the computations required to obtain the final results inherently double the time as compared to the sequence connection and Clarke component methods.
5. Edith Clarke's equivalent Y stands out as the most desirable method of solution. No phase-shifting devices or coupling transformers are required, and the determination of equivalent negative and zero sequence circuits is rapid and simple. Only one sequence network need be set up at one time, permitting the study of a large, complex system.
6. The modified equivalent Y is also a desirable method if the positive sequence shunt impedances remain constant. It has been pointed out that these impedances are functions of the open circuit pre-fault positive sequence voltages. As a result, the shunts are affected by swinging of generators if the open circuit voltages are affected thereby, as is generally the case.

THREE-PHASE METHODS

The 3-phase and neutral method, 3-phase and zero sequence method, and the triple connection method are to be preferred, in general, over all other methods, for they have the very desirable advantage of direct reading of phase quantities.

1. The first two methods require 4-board impedance units to represent one

power system impedance, while the triple-connection method requires 9-board impedances to represent one system impedance.* Many of today's network analyzers average 60 impedance units, so that all three methods are suited only to small or medium-sized systems.

2. Switching and measurement problems incurred by the 3-phase and zero-sequence method, and in the "reduced" triple-connection method make the 3-phase and neutral method appear as the most desirable of all 3-phase methods.

3. Forcing transformers to insure correct current distribution are required by the 3-phase and neutral method. Furthermore, other coupling transformers are usually needed to represent actual transformer banks. The number of coupling transformers, therefore, on any network analyzer further limits the application of this method.

4. The best field of application of the 3-phase and neutral method is to networks of small or medium size and principally at one voltage, with only one or two equivalent generators. On these systems, it is admirably suited to problems (such as relay studies) in which phase quantities are required.

---

*The maximum number of required network analyzer impedance units is reduced slightly when a portion of the system does not have a zero sequence representation for the study.

References

1. Application of Resonant Grounding in Power Systems in the United States, E. T. B. Gross, E. W. Atherton. *AIEE Transactions*, volume 70, part I, 1951, pages 389–97; *Electrical Engineering*, volume 70, September 1951, page 808.

2. Trends in Transmission Systems Grounding Practice, E. T. B. Gross. *Proceedings*, Midwest Power Conference (Chicago, Ill.), volume 13, 1951, pages 389–95.

3. A Solution for Faults at Two Locations in 3-Phase Power Systems, E. F. Vaage. *The Bell System Technical Journal* (New York, N. Y.), volume 19, 1940, pages 290–305.

4. Double Ground Faults on a Single Circuit Line Fed from Two Points, G. Oberdorfer. *Wissenschaftliche Veroeffentlichungen aus dem Siemens Konzern* (Berlin, Germany), volume 9, 1930.

5. Experimental Analysis of Double Unbalances, E. W. Kimbark. *Electrical Engineering* (*AIEE Transactions*), volume 54, February 1935, pages 159–65.

6. Sequence Network Connections for Unbalanced Load and Fault Conditions, E. L. Harder. *The Electric Journal* (East Pittsburgh, Pa.), volume 34, 1937, pages 481–88.

7. Problems Solved by Modified Symmetrical Components, Edith Clarke. *General Electric Review* (Schenectady, N. Y.), volume 41, 1938, pages 488–94, pages 545–49.

8. Analysis of Synchronous Machine Short Circuits, R. D. Camburn, E. T. B. Gross. *AIEE Transactions*, volume 69, part II, 1950, pages 671–79.

9. The Evaluation of Simultaneous Faults on 3-Phase Systems, J. R. Mortlock. *Journal*, Institution of Electrical Engineers (London, England), volume 94, part II, 1947, pages 166–90.

10. Simultaneous Faults on 3-Phase Systems, Edith Clarke. *AIEE Transactions*, volume 50, September 1931, pages 919–41.

11. *Ibid*, discussion of H. W. Bibber, page 943.

12. Applications of the Method of Symmetrical Components (book), W. V. Lyon. McGraw-Hill Book Company, New York, N. Y., 1937, page 525.

13. *Ibid*, page 527.

14. Network-Analyzer Solution of Multiple Unbalances, E. W. Kimbark. *Electrical Engineering* (*AIEE Transactions*), volume 56, December 1937, pages 1476–82.

15. A-C Calculating Board Methods for the Solution of Consequent Faults, H. K. Amchin. *Thesis*, Illinois Institute of Technology (Chicago, Ill.), 1949.

16. Transient Analysis of 3-Phase Power Systems—I, E. T. B. Gross, Leonard Rabins. *Journal*, Franklin Institute (Philadelphia, Pa.), volume 251, 1951, pages 333–41.

Discussion

R. D. Goodrich, Jr. (Bureau of Reclamation, Denver, Colo.): This paper presents a very interesting application of the A. C. Network Analyzer. It is unfortunate that modern systems have grown so large that the simple, complete 3-phase representation cannot be used in most cases. Indeed it is often difficult to find enough units to set up the positive sequence network alone. With the ideas presented here, however, any system can be set up, one phase sequence at a time if necessary.

Perhaps the concept of equivalent circuits to represent outlying portions of the system should be considered, particularly in the case of a resonant-grounded system interconnected with a solidly-grounded system. The points of interconnection will include isolating transformers which curtail the extent of the zero-sequence network as seen from the resonant-grounded system. Therefore, if the resonant-grounded system is not too extensive, its 3 sequence networks may be set up completely, utilizing equivalent circuits for the positive and negative phase sequence networks of the solidly-grounded system. No equivalent of the zero-phase sequence network would be required.

It would be interesting to know if a satisfactory equivalent circuit can be worked out for parts of a system when the 3-phase and neutral method is used.

I should like to ask the authors if they have considered whether or not alternate sets of approximations can be added profitably to the methods presented, if the results are to be used exclusively for fault studies or for system stability studies. For fault studies, for instance, use of an unloaded system without line resistance or capacitance may suffice.

H. K. Amchin and Eric T. B. Gross: As Mr. Goodrich has pointed out, today's power systems are so large that it is often difficult to completely represent the positive sequence network for a load study, to say nothing of making a fault study with all three sequence networks or with a 3-phase representation. Common use is made of equivalent circuits to represent outlying portions of a system which are of no interest or have little effect on the problem. These equivalents often make a different method of analysis possible, as suggested in the discussion, thereby shortening the time required to obtain the desired result.

Because of the limitation imposed by the number of available generators on the average network analyzer, it is unlikely that more than one or two equivalents can be used in the 3-phase and neutral method. In the simpler cases, for example, radial feeders and single points of interconnection to another system, the usual four terminal equivalent with six impedances, three to neutral and three between phases, and three emf's, from each phase to neutral, will be satisfactory.

An equivalent for two interconnection points to another system or for a loop will in general require too many analyzer units to be of practical use.

The use of approximations depends, of course, upon the acceptable degree of accuracy. When the various methods are applied to circuit breaker and relay studies, it is generally satisfactory to neglect line resistance, especially if the conductors have an X/R ratio equal to or greater than two, and line capacitance, and use an unloaded system. For delta or resonant grounded systems, however, representation of line resistance, capacitance, and loads may all be required for special relay applications.

Stability studies will tend to be more pessimistic when line resistance and capacitance are neglected. An analysis of each individual problem should be made to check more exactly the effect of these assumptions.

We are indeed glad that Mr. Goodrich's remarks gave us the opportunity to clarify these points, and we wish to express our thanks for his contribution.

The Design of Capacitor Units for Series Connection

BROR O. N. HANSSON
MEMBER AIEE

Synopsis: The fundamental possibilities of adapting the design of capacitors to meet the special stresses encountered in series capacitors are reviewed. The design of the Allmänna Svenska Elektriska Aktiebolaget units in the Swedish State Power Board's series capacitor at Alfta and of a new 50,000-kva bank now under production is described. Possibilities of future improvements are outlined.

A CAPACITOR as used for series installation is fundamentally an extremely simple apparatus constructed of only three components, the electrodes, the paper, and the impregnating liquid.

It would, however, be a tremendous task to completely treat the question of how these three components should be selected and treated to make a good capacitor, as the possibilities of varying the qualities of those components are unlimited.

It is possible to so adapt the quality of the components and the design as to obtain a capacitor which is exceptionally resistant to the especially high short-time stresses and discharges a series capacitor is exposed to. Some unusual measures which have been taken in the design of the Alfta capacitors will be listed here. They will be illustrated by a life curve which comprises not only the a-c strength versus time, but in addition curves or points for d-c and impulse strength. Such a complete life curve is shown in Figure 1.

Knowledge of the left-hand part of this curve (impulse strength versus time) is still incomplete. This field has only been explored during the last decade, while the right-hand part, the long time a-c strength, is very well known. That part has been the scope of much research ever since paper cables were introduced, more than 50 years ago. The d-c part is of special interest for d-c cables and capacitors and for the d-c testing of capacitors and cables.

The part of the a-c curve which extends towards very short times is still fairly unknown. It is, however, that part which is most interesting for the design of series capacitors.

First of all it should be stated that the right-hand part of the complete curve in Figure 1 (long time a-c breakdown) entirely depends on the dielectric losses and the ability of the design to dissipate those losses. Long time breakdowns are thermal breakdowns and show a burnt structure.

A-c breakdowns which occur after a shorter time also may be thermal breakdowns, but during this short time the heat is not dissipated. It is absorbed by the heat capacity of the dielectric and the armatures.

A-c breakdowns for very short time, impulse and d-c breakdowns resemble more mechanical rupture than thermal destruction. The shorter the breakdown time, the smoother and more clean cut the puncture appears. Let us first see how some variations in the components affect the life curve.

The Electrodes

It might be expected that the choice of another metal other than aluminum might influence the ionization voltage. For the present we are limited to the use of aluminium foils. Aluminium with its oxidized surface is chemically indifferent and is a good conductor of heat and electricity. Greater thickness of the foils would give more heat capacity and better heat dissipation and would raise the whole a-c part of the life curve. At very short times however this raise seems negligible.

Paper Density

A dense paper represents a more difficult obstacle for the impulse and d-c breakdowns, but on the other hand a dense paper means more cellulose content in the insulation and therefore higher losses and thus reduced strength against such a-c stresses as cause thermal breakdown. Increased paper density tilts the complete life curve, increasing strength for impulse, direct current and short time alternating current but lowering the strength for long time alternating current. Dense paper should obviously be used in series capacitors if the design can afford the increased temperature at rated voltage, Figure 1.

Oil Viscosity

The viscosity of the oil seems to have a similar influence on the dielectric strength

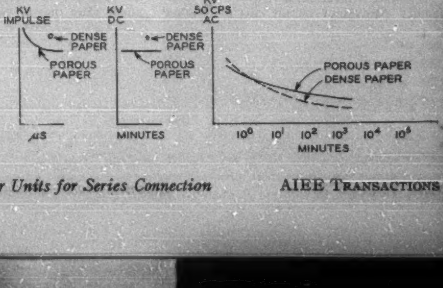

Figure 1. Influence of the denseness of the paper on dielectric strength

---

Paper 51-332, recommended by the AIEE Transmission and Distribution Committee and approved by the AIEE Technical Program Committee for presentation at the AIEE Fall General Meeting, Cleveland, Ohio, October 22-26, 1951. Manuscript submitted June 29, 1951, made available for printing August 30, 1951.

Bror O. N. Hansson is with the Aktiebolaget Liljeholmens Kabelfabrik (ASEA Cable Works), Stockholm, Sweden.

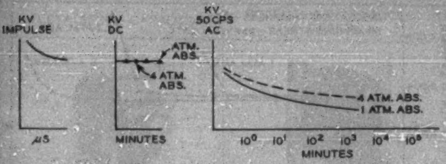

Figure 2 (left). Influence of oil pressure on dielectric strength

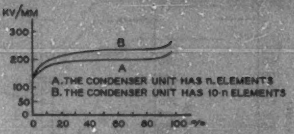

Figure 4. Strength of the different elements in a capacitor unit arranged consecutively

A. The capacitor unit has *n* elements
B. The condenser unit has 10.*n* elements

as the paper density. It must be remembered, however, that it is difficult to prove this definitely as oils with different viscosities differ chemically.

The fact is that a more viscous oil will give higher impulse and d-c strength, but it also may give higher losses and therefore impart a lower long time a-c strength to the impregnated paper than a thin oil. In the Alfta capacitor an oil thicker than transformer oil was used.

Influence of Cooling

We do not refer to the relatively small increase in impulse and d-c strength obtained because of the increased viscosity of the oil at very low temperatures, but to the influence of the thermal design of the capacitor on its dielectric strength.

The heat capacity determines the short time a-c breakdown and the heat dissipation the long time breakdown. A design which gives better cooling and lower temperature in the insulation lifts the right part (=long time a-c part) of the life curve upwards. We refer to what has been earlier said about the thickness of the aluminium foils, and to the "foil cooled" design as used in the Alfta capacitor, (see Figures 3 and 8).

Destructive, Elimination Testing as a Method for Improving Dielectric Strength

A very interesting and effective way to improve dielectric strength is to test the material until breakdown occurs and then disconnect or repair the faulty pieces.

This method is probably now used by all capacitor manufacturers. The capacitors are divided up into many small sections and those which break down for the test voltage are disconnected.

In Figure 4 the strengths of the different sections of such a capacitor are consecutively arranged. If 5 per cent of the elements are punctured and disconnected, the total dielectric strength of the capacitor is increased from 130 kilovolts per millimeter to 150 kilovolts per millimeter, that is, by 15 per cent. If the number of elements was to be increased tenfold (as in curve *B*, Figure 4) then an elimination test which punctures 5 per cent of the windings would increase the strength from 130 kilovolts per millimeter to 170, that is by 30 per cent.

For this sorting out of the weak parts of the insulation only direct current may be used, because a-c tests may cause thermal deterioration not only of the punctured windings but also of those which are nearly as weak as the punctured ones. This method improves only the impulse, the direct current and perhaps the short time a-c strength of the capacitor, but no guarantee is given, that the long time a-c strength is also improved because that strength is highly influenced by spots or sections which have high losses. Further attention will be given to these facts later in this paper.

If each section has its separate fuse, however, this will, regardless of the time it takes, disconnect any section which does not hold for all the separate or combined over-voltages the capacitor may meet during its life. If each element is tested with direct current and has its own fuse, both the impulse, the d-c and the a-c strength will be improved, Figure 5.

Oil Pressure

It is commonly accepted that an increased oil pressure improves the a-c dielectric strength of the impregnated paper but that it has no influence on the direct current and the impulse strength, Figure 2.

Much research on this question, not only in connection with our pressure capacitors but also the 380-kv paper cable, recently installed at Harspranget in northern Sweden, has revealed that the above statement is not quite true. At the same time the nature of the different breakdowns has been made quite clear, and it will be of interest to deal with this question at some length.

Capacitor insulation consists of interleaved layers of paper and oil films. (Actually the paper itself has a very complicated structure—fibers, fibriles, mizelles, and molecules—but this can be disregarded for the present.)

The dielectric constant of cellulose is 5.6 and that of oil is 2.3. With alternating current the main stress would therefore occur over the oil component.

With direct current on the other hand, the stresses on dielectrics connected in series distribute themselves proportional to the insulation resistances. For cellulose and oil these resistances are such that with direct current the cellulose component would take the highest stress.

This working hypothesis has proved of great value when judging the stresses in a series capacitor at the unusual load it is exposed to in service and during tests. It might be of interest to review some recent indirect evidence that the hypothesis is true.

A glance at Figure 6 shows better than many words what the writer wants to express. As regards impulse and direct current we formerly were of the opinion that the strength of impregnated paper was independent of the pressure, in

Figure 3. How the cooling influences the dielectric strength

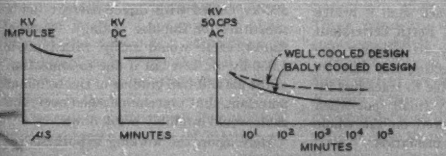

Figure 5. How sorting out tests and fuses improve the dielectric strength of a condenser

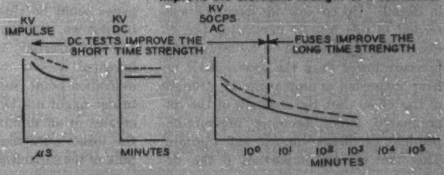

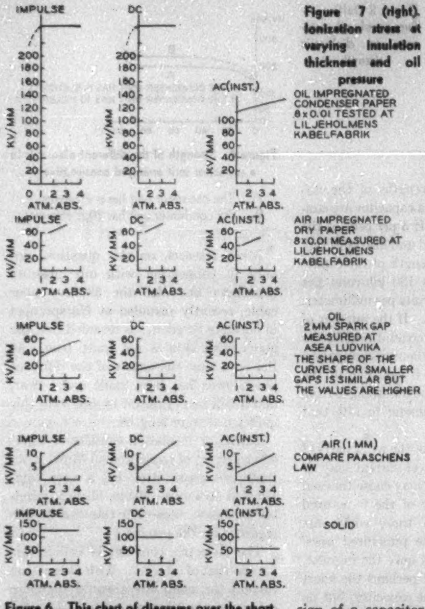

Figure 6. This chart of diagrams over the short time dielectric strengths versus pressure illustrates the nature of breakdown in different materials. For oil impregnated paper as used in cables (with thicker insulation and oil pockets between papers) the impulse and d.c strength appears to be more pressure dependent than capacitor insulation

Figure 7 (right). Ionization stress at varying insulation thickness and oil pressure

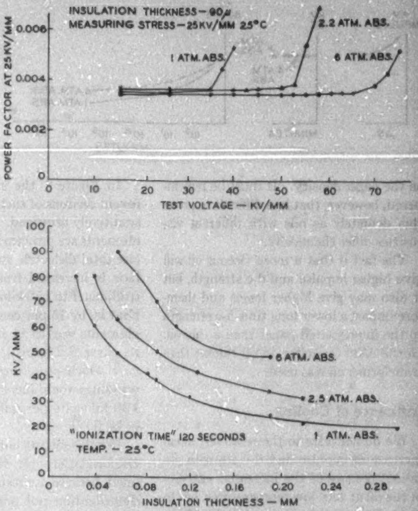

spite of the fact that the strength of the oil is highly dependent on pressure. Towards direct current and impulse voltage, impregnated paper behaved like a solid.

Would it not be possible by using an oil or other liquid of poor dielectric strength or with very good insulation resistance to cause the breakdown to start in the impregnant and thus make the direct current and impulse breakdowns dependent on pressure? If we could find an impregnating liquid which at some temperatures had higher and at other temperatures lower insulation resistance than cellulose, then it ought to be possible to study the nature of the breakdown in detail. Up to now we have not succeeded in this but by decreasing the dielectric strength of the oil by means of a pressure lower than the atmospheric we have succeeded in decreasing the strength of the oil so that the strength of the impregnated paper becomes pressure-dependent at direct current and impulse. This fact is very important if the design of a capacitor is such that due to contraction of the oil the pressure at low temperature may fall below atmospheric. As a matter of fact it caused quite some anxiety when during the d-c tests at Alfta the temperature was −15 degrees centigrade. At low temperatures we have, however, a compensation for this decreased strength in the increased strength due to increased oil viscosity. For alternating current the low temperature itself means protection when the breakdown is of a thermal nature.

Ionization

For several decades gas ionization in voids has been recognized as the cause for the deterioration and breakdown of solid cables. For some time it was believed that oil-filled cables and capacitors properly impregnated with thin oil were free from such ionization. Improved technique, however, developed the ionization bridge by the means of which increased losses could be traced at stresses below breakdown. When once such a bridge was out of order, Mr. Bertil Zetterstedt invented a new way to discover the ionization point, suspecting also that the bridge might not be able to trace loss increases in an infinitely small spot when the losses were measured on the whole bulk of the capacitor's insulation.

He tested a capacitor step by step with increasing voltage during 2 minutes. After each step at high-test voltage he loaded the capacitor for 5 hours with the rated voltage and then measured the losses. The test voltage at which the losses started to increase he named the ionization point.

From Figure 7 it can be seen that high oil pressure and thin insulation should be used to give a high ionization point.

It remains to be seen if the ionization point thus obtained is a true ionization point or if it just indicates the stress at which decomposition of the insulation has started. In the latter case the ionization point should be time-dependent. It also might be a combination of both. This test method is, however, a very valuable tool for tracing a "decomposition curve" below the life curve, above which the capacitor never should be used or tested.

Experience with the Swedish discharge test for coupling capacitors and with capacitors for surge generators and for discharge welding has been rather discouraging. Capacitors are rather sensitive to discharge. Similar experience has recently been gained from the testing of 220-kv cables with direct current (as a substitute for impulse testing). Such a 220-kv cable would easily withstand a 1,050-kv d-c test but if due to ionization of the air and bad grading of the terminal porcelain, that porcelain flashed over, the cable would infallibly break down.

Here again the working hypothesis re-

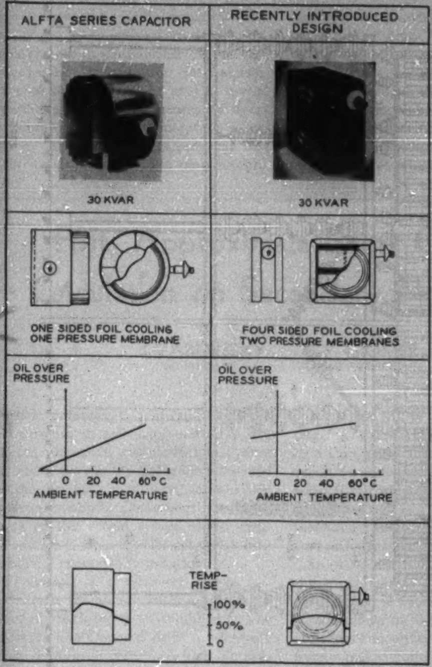

Figure 8 (left). Comparison between the design of Alfta units and new capacitor units

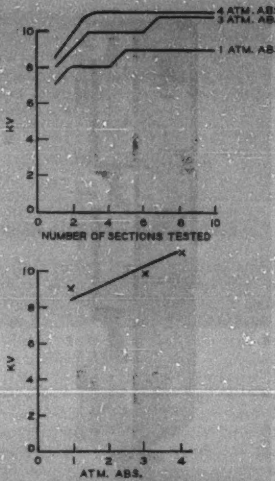

Figure 9 (right). Discharge strength of capacitors

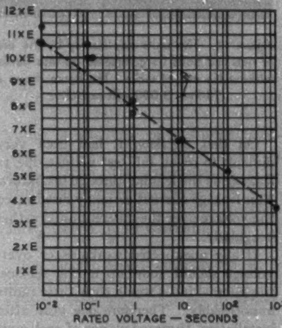

Figure 10 (below, right). 50 cycles per second strength of capacitor units for Alfta at very short time. Each circle represents one unit. The voltage was step by step increased when the capacitor was given voltage shots of the duration indicated on the diagram

ferred to previously comes in useful. When the d-c voltage is on, the main stress is over the paper, but when the a-c discharge starts, the main stress shifts over to the oil which simply breaks down. The stress is too high. If this theory is right, an increased oil pressure should raise the "discharge strength" of a capacitor. Ample proof is given by the test results plotted in Figure 9.

The fundamental theories behind the design of the series capacitor for Alfta have now been recapitulated and in the following, a description of the construction of the units will be given, Figure 8.

The capacitor units are "foil cooled." One of the two aluminium foils which protrudes out of the winding is tightly pressed against the wall of the capacitor tank. On the outside this wall has cooling fins. Direct metallical conduction of the losses from the interior of the capacitor windings to the surrounding atmosphere is thus established. The other foil is connected to a leading-through insulator soldered to the tank.

The wall opposite the cooling wall is a steel diaphragm, capable of exerting an overpressure of up to 3 – 4 atmospheres on the oil and capable of taking care of the heat expansion of the oil.

In the Alfta capacitor such a unit was divided up into seven windings, each one equipped with its own fuse. No series connection was allowed inside the tank. Many units were in the final arrangement connected in parallel. These groups of many parallel-connected units were then connected in series with similar groups. If a breakdown should occur in one small winding, the short circuit current would be limited by the series-connected capacity. The capacity in parallel contains a suitable quantity of energy to blow the fuse when it is discharged through the faulty winding.

What have we now achieved at the Alfta installation? How strong is the installation? What is the safety margin? Those questions are very difficult to answer accurately.

In the factory all units were tested with direct current, six times the rated voltage, *E*, with a few units failing. We may therefore be sure that among all the 600 units at Alfta there must be one unit that just escaped failure and has no safety margin for a d-c voltage of 6 × *E*. We also know that quite a number of units were successfully tested with three consecutive discharges from 5 × *E* (followed by the rated voltage and loss measurements) but we do not know whether the remaining units would have escaped safely from that test. We did not want to test all units that way as the high-frequency discharge might impair the life of the capacitor. At the final tests after construction the total bank was charged with direct current and then discharged through the spark gap that was set at 4.2 *E*. A total of seven units failed. Besides real weaknesses caused perhaps by transport and handling, bad weather conditions during one of the days may have caused these failures.

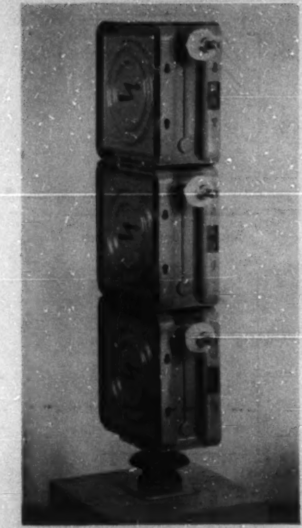

Figure 11. The units may merely by the use of nuts and bolts be connected up into banks without the use of racks. The figure shows a 75-kva, 3,000-volt capacitor

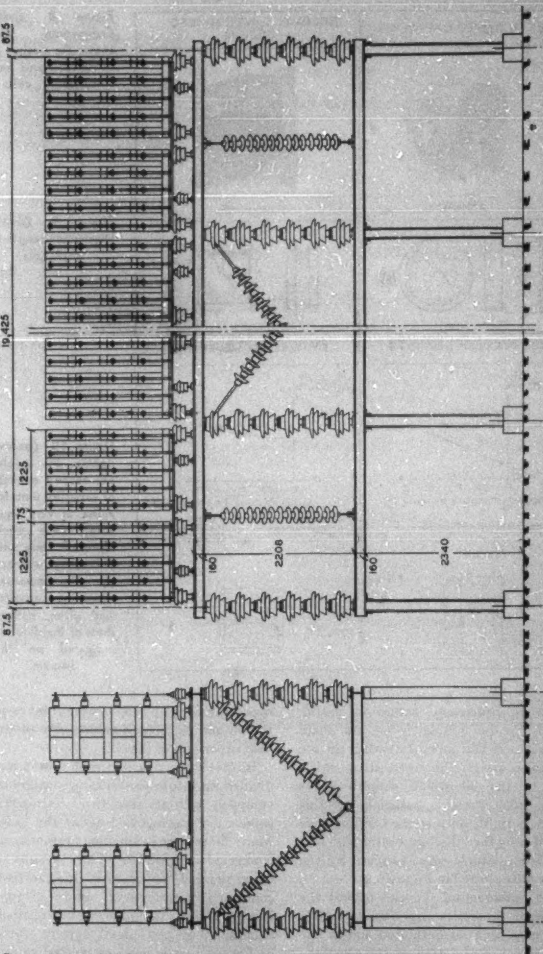

Figure 12. 50,000-kva series capacitor, composed of 30-kva capacitor units. This design is proposed for 220 kv. A similar 50,000-kva bank for 30 kv is under production

On that occasion it had been very difficult to reach full test voltage due to leakage on the leading-through insulators. This leakage current certainly distributed the voltage over the different units rather irregularly.

If any unexpected weakness or over-voltage should show up during service, the internal fuses would clear these faults unnoticeably. Therefore one year after installation, the capacitance of each unit in the installation was checked. All units were found to be intact. Recently, new tests were carried out with the purpose of obtaining for full size units, the break-down strength, (the a-c life curve) for very short time.

The result is in the shape of a life curve given in Figure 10. In each test, 3-capacitor units were tested. Each unit was given many shots with gradually increased voltage before the break-down voltage was found, Figure 10.

In future tests each shot will be followed by 24 hours of rated voltage and by a check of the dielectric losses in order to find the voltage (the "ionization point") at which destruction of the insulation starts.

For the design of future series capacitors, confidence and knowledge has been gained from severe tests and service records and therefore the design of series capacitors most probably need not be limited by stipulations that the units in case of failure should be suitable as shunt capacitors. There are possibilities of producing a series capacitor that is specially suited for this service, when we know fully the stresses to which the capacitor may be exposed during its life.

One and a half year's perfect service has proved the reliability of the design used for the Alfta capacitor. From the foregoing it may, however, be seen that even that design has its limitation.

For a new 50,000-kva series capacitor now in production we have improved the Alfta design considerably, see Figure 8.

A more compact interior design of this unit gives reduced oil volume and thus less oil expansion. This coupled with the use of two steel-membranes makes possible the use of a still higher oil pressure which is less dependent on the temperature of the unit. Even at the lowest possible ambient temperatures an overpressure of about one atmosphere is ensured. In these units not only one but four "cooling" walls are in metallic contact with the aluminium foils protruding out of the windings.

This 4-sided foil cooling would be superfluous for a series capacitor, but also in this case the bank had to be arranged in such a way that it possibly might be used as shunt capacitor.

A special feature of the new unit is the cooling flanges which are arranged as 4-sided mounting flanges. Units may be connected up to huge banks without racks, merely by nuts and bolts, see Figure 11. The arrangement of a 50,000-kva series capacitor with these units is shown in Figure 12.

No Discussion

Fast, Approximate Short Circuit Calculation on Secondary Networks

J. ZABORSZKY
MEMBER AIEE

C. F. CROMER
STUDENT MEMBER AIEE

THE determination of short circuit currents in secondary networks by means other than with network analyzers is inherently lengthy and tedious because of the very large number of branches and sources involved. Consequently a miniature of the actual system under consideration is often used for network study and fault current determination.

Following is a relatively simple approximate calculation which agrees satisfactorily with the results supplied by the network analyzer and yields a relatively easy solution in cases for which a-c network analyzers with large dimensions would otherwise be needed.

The Secondary Network Distribution System

Figure 1 shows in a single line diagram the usual construction of a secondary network distribution system. The secondary network forms a solidly connected uniform low voltage grid, with uniformly distributed loads along the mains. The grid is fed through uniformly distributed transformers from a radial high-voltage feeder system.

Equivalent of the Secondary Mains

Actually the complete uniformity of the secondary grid is only an approximation of the actual conditions. Here this approximation will be carried one step further. The uniform grid will be replaced by a thin conducting plate (I in Figure 2) which is equivalent to the grid in the sense that corresponding sections of grid and plate have equal impedances, except possibly for such differences as result from the sectionalized nature of the grid.

In order to make the plate equivalent to the grid in this sense, a square section of it such as is contained within lines *ab*, *bc*, *cd*, and *da* in Figure 1 should have an impedance in either of the lateral directions which is equal to the impedance of one section of the main, z_m. In the sense that resistance equals resistivity × length/area, this will be the case if:

$$\rho_1 \frac{l}{d_1 l} = z_m \qquad (1)$$

Nomenclature

z_m = impedance of secondary main
z_t = impedance of transformer
l = length of one section of the mains
d_1 = thickness of equivalent plate I in Figure 2
d_2 = thickness of equivalent plate II in Figure 2
ρ_1 = resistivity of plate I in Figure 2
ρ_2 = resistivity of plate II in Figure 2
i_t = contribution to the 3-phase short circuit current by the local transformer
i_n = contribution to the 3-phase short circuit current by the network
e = voltage above neutral in general
$e(x)$ = voltage of the secondary network above neutral at distance x from the fault
E = feeder voltage above neutral referred to the secondary
v = voltage drop in the secondary grid
$I_0(s)$ = modified Bessel function of the first kind zero order
$K_0(s)$ = modified Bessel function of the second kind zero order
$K_1(s)$ = modified Bessel function of the second kind first order

Equivalent of the Transformers

In a similar manner the transformers may be equivalently represented in Figure 2 by plate II. This latter plate must be homogeneous but nonisotropic. It is uniform but conducts current in the vertical direction only. If a physical picture of this situation is desired plate II may be visualized as consisting of very thin insulated vertical wires packed solidly together. To make plate II equivalent to the actual transformers the impedance of one transformer should be distributed over the area which it is normally feeding. This would be the area of square, *abcd*, in Figure 1 if a transformer is connected to each node of the grid. This means that:

$$\rho_2 \frac{d_2}{l^2} = z_t \qquad (2)$$

Values of $\rho_2 d_2/l^2$ for various other transformer distributions are shown in Figure 3 along with other quantities (a, z, k) which will be explained later.

The Short-Circuit Current

For short circuit calculations it is usually possible to assume that the network is very large (infinite) in extent,

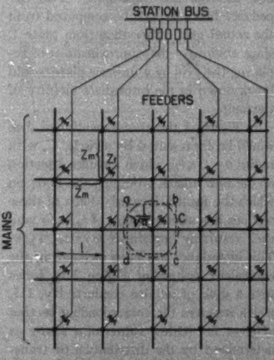

Figure 1. Simplified diagram of secondary network distribution system

---

Paper 51-333, recommended by the AIEE Transmission and Distribution Committee and approved by the AIEE Technical Program Committee for presentation at the AIEE Fall General Meeting, Cleveland, Ohio, October 22–26, 1951. Manuscript submitted June 20, 1951; made available for printing August 30, 1951.

J. ZABORSZKY is with the University of Missouri, School of Mines and Metallurgy, Rolla, Mo. C. F. CROMER is with Westinghouse Electric Corporation, East Pittsburgh, Pa.

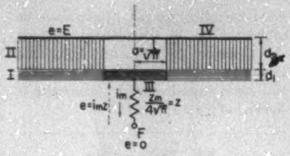

Figure 2 (left). Equivalent of the secondary network distribution system

Resistive plates I and II represent the secondary grid and the transformers respectively. Ideally conductive plate IV represents the feeder network. The void above the ideally conductive electrode III eliminates the contribution of the local transformer to the short circuit current

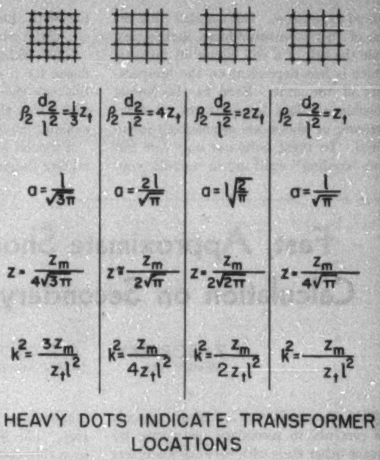

Figure 3 (right). Values of ρ_2, a, z, and k^2 for various transformer distributions

since the contribution to the short circuit current by the various parts of the network decreases rapidly with the distance of the contributing part from the fault.

The value of the short circuit current will depend upon the location of the fault and reaches its maximum if the short circuit is located at one of the nodes. This maximum short circuit current consists of two components: That contributed by the local transformer:

$$i_t = \frac{E}{z_t} \tag{3}$$

and that contributed by the remainder of the network; i_n.

Completing the Equivalent System

It is customary to handle the two portions of the short circuit current separately. Accordingly a disk of unit area (radius, $a = l/\sqrt{\pi}$) has been omitted from plate II around the point of short circuit, F, in the equivalent system, (Figure 2). This eliminates the contribution of the local transformer, to the short circuit current.

The section of the grid (plate I) which falls within the area of the above mentioned disc will have a certain impedance. The short circuit currents which are contributed by the network actually have to flow through this impedance. This impedance however will be computed from the actual grid rather than from plate I, since obviously the approximation of replacing the grid by a uniform plate would break down in the immediate vicinity of the fault.

In Figure 1 the above mentioned disk would be represented by a circle, C, with radius $a = l/\sqrt{\pi}$, which includes a section of the four mains adjoining the node on which the fault is located. Each of these sections has an impedance of $z_m/\sqrt{\pi}$, and their resulting impedance is $z = z_m/4\sqrt{\pi}$. This impedance has been included in the equivalent system of Figure 2 in series with a disk of infinite conductivity, III, which replaces the corresponding section of plate I. (Other values of a and z as determined by the distribution of transformers are shown in Figure 3.)

The influence of the network load on the short circuit currents is relatively small and consequently the loads are neglected although the method could easily be generalized to include them.

The voltage at the primary terminals of the transformers can be considered to be unaffected by the short circuit and to be equal for all the transformers. This is accounted for in the equivalent system, Figure 2, by electrode IV, a conductive plate with a constant voltage $e = E$.

Because of the short circuit the voltage at the fault, F, will be zero.

Short Circuit Current Calculation

The differential equation of the equivalent system is

$$\frac{d^2e}{dx^2} + \frac{1}{x}\frac{de}{dx} - k^2e = -k^2E \text{ (Appendix I)} \tag{4}$$

where k is as shown in Figure 3. Its solution after evaluating the constants

$$\frac{i_n}{i_t} = \frac{z_t}{s}\frac{K_1(s)}{K_1(s) + \dfrac{z_m}{2\pi s z}K_0(s)} \text{ (Appendix II)} \tag{5}$$

where

$$s = k\,a = \sqrt{\frac{z_m}{\pi z_t}} \tag{6}$$

for all transformer distributions, and z is given in Figure 3. Approximate values of $K_0(s)$ and $K_1(s)$ can be taken from Figure 4(a). ($\sigma = 0$ curve if s is real). More exact values are available in tables of functions and the literature of Bessel functions.[1]

There have been published in the literature[4] results of d-c network analyzer studies of the short circuit currents in secondary networks when the ratio z_m/z_t is a real number. The comparison of these data with those calculated by equation 5 shows quite satisfactory agreement, Figure 5.

Actually both z_m and z_t are complex impedances and their respective phase angles are markedly different in most cases, $z_m = |z_m|\underline{/\beta_m}$ being predominantly resistive and $z_t = |z_t|\underline{/\beta_t}$ being predominantly inductive. Consequently s is a complex number.

$$s = |s|\underline{/-\sigma} \tag{7}$$

where both $|s|$ and σ are determined by equation 6.

Equation 5 also applies for complex z_m and z_t, since a review of the above derivation reveals that it is not necessary to restrict it to real values for z_m and z_t.

The basic assumption of the method is that the secondary grid and the transformers which are actually periodically repeated, lumped, electric circuits, are equivalently replaced by suitable continua (Plates I and II). In a mathematical sense such replacement is possible whether the line and transformer impedances are real or complex. The only difference is that in the latter case ρ_1 and ρ_2, as defined by equations 1 and 2, will be complex numbers. Now it is true that complex resistivity does not actually exist as a physical characteristic but this only means that it is not possible to build a physical model for the equivalent system of Figure 2 for complex values.

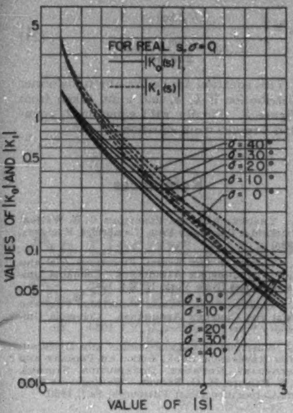

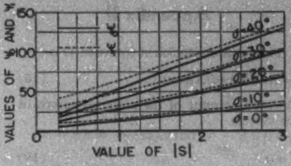

Figure 4(A) (left). Chart showing magnitude of $K_0(s)$ and $K_1(s)$ for complex $s=|s|\underline{/-\sigma}$

Figure 4(B) (right). Chart showing angle of $K_0(s)$ and $K_1(s)$ for complex $s=|s|\underline{/-\sigma}$

For purposes of calculation however this equivalent system is equally valid for either real or complex impedances; consequently equation 5 also applies for complex s, z_t, z_m, and z. $K_0(s)$ and $K_1(s)$ can be calculated for complex arguments with the following expressions:

$$K_0(s)=|K_0(s)|\underline{/\psi_0(s)}$$

$$K_1(s)=|K_1(s)|\underline{/\psi_1(s)} \qquad (8)$$

Approximate values of K_0, K_1, ψ_0, and ψ_1 can be taken from Figure 4 for some specific values of σ. Tables for more exact values are available.[2,3] If these tables are used

$$K_0(s)=\frac{\pi}{2}j[J_0(\rho e^{j\varphi})+jY_0(\rho e^{j\varphi})]$$

$$K_1(s)=-\frac{\pi}{2}[J_1(\rho e^{j\varphi})+jY_1(\rho e^{j\varphi})] \qquad (9)$$

where $\rho=|s|$ and $\varphi=-\sigma+90$ degrees.

Sample Calculation

To illustrate the use of the method let it be assumed that

$z_t=0.015\underline{/85^\circ}$ ohms and $z_m=0.015\underline{/25^\circ}$ ohms

From equation 6

$s=0.565\underline{/-30^\circ}$ or $|s|=0.565$ and $\sigma=30^\circ$

Taking the magnitudes from Figure 4(A) and the angles from Figure 4(B)

$K_0(s)=0.91\underline{/27^\circ}$ and $K_1(s)=1.52\underline{/38^\circ}$

and with Figure 3 and the assumption of one transformer being located at each corner

$z=0.00212\underline{/25^\circ}$ ohm

Finally from equation 5

$$\frac{i_n}{i_t}=3.28\underline{/49.7^\circ}$$

From Figure 5 $i_n/i_t=3.25$ (which is nearly equal to the above value) for an impedance ratio having a magnitude equal to that in the above example ($|z_m/z_t|=1$) but involving real impedances. This means that the difference in $|i_n/i_t|$ for real or complex impedances is not very large at an impedance ratio of 1. However while i_n and i_t are in phase with each other (i_n/i_t is real) in the case of real impedances, in case of complex impedances the power factor angle of i_n is smaller than that of i_t (by 49.7 degrees in the example) as could be expected since the mains have a much smaller impedance angle (β_m) than do the transformers (β_t).

If $|z_m/z_t|$ becomes much larger than 1 the difference between the magnitudes of i_n/i_t for real versus complex impedances becomes much more pronounced.

Conclusions

A novel method is introduced for fast approximate calculation of short circuit currents on secondary networks. Simplicity of the calculation is achieved by representing the secondary grid and the transformers by suitable continuous conductors. Local irregularities of the actual secondary network are not considered, but even so the accuracy will suffice for many purposes. On account of its simplicity and the small amount of work required by its use the method appears to be particularly well suited to supply data for preliminary design where a large number of systems with different components are considered.

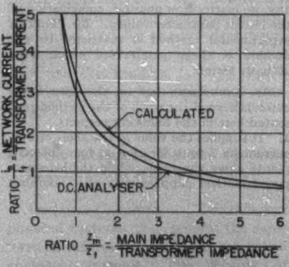

Figure 5. Comparison of calculated data with those from the d-c analyzer, in the case of purely real impedances

Appendix I

Since no charge is accumulating in any part of the system, the sum of the currents flowing into any arbitrary section is zero. This statement will be applied to a ring with a radius x and thickness Δx which is located in plate I around the point of the short circuit, F, Figure 6.

$$-i(x)+i(x+\Delta x)+\Delta i=0 \qquad (10)$$

but with Ohms law

$$\Delta i=-[E-e(x)]\frac{2\pi x\,\Delta x}{\rho_2 d_2} \qquad (11)$$

And since the current density is equal to negative voltage gradient times conductivity

$$i(x)=-2\pi x d_1\frac{1}{\rho_1}\frac{d}{dx}e(x) \qquad (12)$$

Similarly

$$\begin{aligned}i(x+\Delta x)&=-2\pi(x+\Delta x)d_1\frac{1}{\rho_1}\frac{d}{dx}e(x+\Delta x)\\&\cong-2\pi(x+\Delta x)d_1\frac{1}{\rho_1}\times\\&\qquad\left(\frac{d}{dx}e(x)+\Delta x\frac{d^2}{dx^2}e(x)\right)\end{aligned} \qquad (13)$$

because $f(x+\Delta x)\cong f(x)+\Delta x\,df/dx$ and becomes an equality in the limit when $\Delta x\rightarrow 0$. Substituting equations 11, 12, and 13 into equation 10

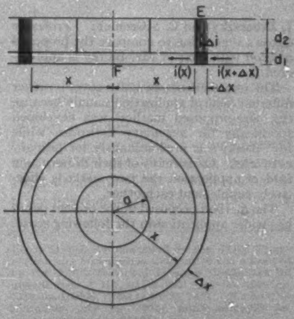

Figure 6. Illustration of the system for which the differential equations were written

$$x\,\Delta x\,\frac{d^2}{dx^2}e(x)+\Delta x^2\frac{d^2}{dx^2}e(x)+\Delta x\frac{d}{dx}e(x)+$$

$$x[E-e(x)]\,\Delta x\,\frac{\rho_1}{\rho_2}\,\frac{1}{d_1d_2}=0$$

Finally letting $\Delta x \rightarrow 0$ and substituting from equations 1 and 2

$$\frac{d^2}{dx^2}e(x)+\frac{1}{x}\,\frac{d}{dx}e(x)-k^2e(x)=-k^2E \qquad (14)$$

where

$$k^2=\frac{z_m}{z_tl^2} \qquad (15)$$

if transformers are located at each corner, otherwise see Figure 3. Introducing the voltage drop

$$v(x)=E-e(x) \qquad (16)$$

Substituting into equation 14:

$$\frac{d^2v}{dx^2}+\frac{1}{x}\,\frac{dv}{dx}-k^2v=0 \qquad (17)$$

Appendix II

The general solution of equation 17 is

$$v=AI_0(kx)+BK_0(kx) \qquad (18)$$

Since on account of the physical nature of the system

$v \rightarrow 0$ if $x \rightarrow \infty$, but $I_0(kx) \rightarrow \infty$ if $x \rightarrow \infty$

$$A=0 \qquad (19)$$

and with equation 16

$$e(x)=E-BK_0(kx) \qquad (20)$$

or with equation 12

$$i(x)=2\pi xBkK_1(kx) \qquad (21)$$

The total contribution of the network to the short circuit current $i(a)=i_n$ is the current entering the periphery of electrode III, Figure 2, where $x=a$ and

$$e(a)=i_ns \qquad (22)$$

substituting this into equations 20 and 21 and eliminating B

$$i_n=\frac{E}{s}\,\frac{K_1(ka)}{K_1(ka)+\dfrac{z_m}{2\pi kas}K_0(ka)} \qquad (23)$$

This equation applies for any transformer distribution if k, a, and s are taken from Figure 3. Finally with equation 3, equation 5 results from equation 23.

References

1. Theory of Bessel Functions, G. N. Watson. Cambridge University Press (Cambridge, England), 1945.

2. Tables of the Bessel Functions $J_0(z)$ and $J_1(z)$ for Complex Arguments. Columbia University Press (New York, N. Y.), 1943.

3. Tables of the Bessel Functions $Y_0(z)$ and $Y_1(z)$ for Complex Arguments. Columbia University Press (New York, N. Y.), 1950.

4. Westinghouse Transmission and Distribution Reference Book, section on Primary and Secondary Network Distribution Systems, J. S. Parsons, H. G. Barnett. Westinghouse Electric Corporation (East Pittsburgh, Pa.), 1950.

Discussion

Eric T. B. Gross (Illinois Institute of Technology, Chicago, Ill.): A systematic study of short circuit currents in secondary distribution networks was undertaken on our a-c network analyzer some time ago by one of our graduate students,[1] and an abstract of his thesis was later published.[2] It may be worthwhile to compare the results of this paper with the data[2] received from our network analyzer study; it resulted in a number of curves which make possible a quick estimate of short circuit currents in such systems.

References

1. Coordination of Fuses with Circuit Breakers in Primary Networks, J. N. Banky. *Thesis*, Illinois Institute of Technology, Chicago, Ill., 1947.

2. Fault Currents Estimated from Curves. J. N. Banky. *Electrical World* (New York, N. Y.), volume 129, March 13, 1948, pages 108–09.

J. Zaborszky and **C. F. Cromer**: Professor Gross's suggestion to compare the proposed method with that of Mr. Banky is appreciated.

The two methods actually cover a rather different field of application mainly because the here-proposed method was developed specifically for secondary networks, while Mr. Banky's is predominantly for primary networks. On account of their difference in field of application the two methods effectively supplement each other.

The method proposed in the present paper has wider application in the following sense:

1. It considers the actual impedance angle of the line and the transformer, where Mr. Banky's method is based on the assumption of one specific value for these angles ($\beta_m=65$ degrees and $\beta_t=90$ degrees in the notations of the present paper.)
2. It yields the magnitude *and* phase angle of the short circuit current, where Mr. Banky's method yields only the magnitude.
3. It is applicable to any transformer distribution; Mr. Banky's method applies only to the case when a transformer is connected to each corner of the grid.
4. Being mathematical it is applicable to any, no matter how unusual, combination of the circuit parameter values. Mr. Banky's experimental method is restricted to the domain of these parameters which were actually tested.

Table I

Present	Banky	Present equation 5	Banky Curve C
$\left\lvert\frac{Z_m}{Z_t}\right\rvert$	$\frac{X_L}{X_T}=\left\lvert\frac{Z_m}{Z_t}\right\rvert\sin 65°$	$\frac{i_m}{i_t}$ per unit	$\frac{i_n}{i_t}$ %
1	0.91	3.42	3×10
5	4.55	0.86	75
10	9.1	0.45	40
15	13.6	0.32	30

Mr. Banky's method on the other hand extends beyond the reach of the method presented here in the following respects.

1. It supplies the value of the short circuit current for a fault location at four different points along the main, while the here-proposed method supplies only the maximum short circuit current for a fault location on or close to the transformer terminals.
2. It is applicable to a small-size network even down to the case when the "network" consists of only one loop fed by four transformers. The here-proposed method applies only to large networks including a large number of transformers and mains. The a-c secondary network is always large in this sense.

Nevertheless in spite of these differences there is an overlapping area between the two methods, where it is possible to compare the numerical values yielded by them. The fact that only a small portion of the respective areas of application overlap for the two methods makes such a comparison even more desirable, since satisfactory agreement in the overlapping region would bolster the confidence in the reliability of either method, in cases where only one is applicable.

Curve (C) of Figure 3 in Mr. Banky's paper can be compared with equation 5 of this paper (assuming $\beta_t=90$ degrees and $\beta_m=65$ degrees). One hundred per cent has to be subtracted from the values taken from Mr. Banky's curve (C) to compare with equation 5 because curve (C) gives the total short circuit current in per cent of the contribution of the local transformer and equation 5 gives the contribution of the network in per-unit of the contribution of the local transformer.

The comparison of four values covering the length of curve (C) is given in Table I of this discussion.

The agreement is apparently as good as the accuracy with which curve (C) can be read.

An Electric Analogue Method for the Direct Determination of Power System Stability Swing Curves

W. B. BOAST
MEMBER AIEE

J. D. RECTOR
ASSOCIATE MEMBER AIEE

THE FUNDAMENTAL relationships from which stability evaluations can be made for electric power systems have been well established during the past 30 years. The mathematical equations from which solutions must be obtained are in themselves relatively simple and easily expressed even for complex networks involving several machines. However, the direct solution of the simultaneous equations involved cannot be accomplished except by machine methods.

Step-by-step methods have been developed, which, with the use of network analyzers for steady-state intermediate steps, permit solution of the simultaneous differential equations by a rather laborious and slow process. This paper presents a fundamental analogue method for obtaining directly on calibrated d-c cathode-ray oscilloscopes the swing curves for power systems during disturbance conditions.

Fundamental Relationships

The simplest a-c power system for which stability is of interest consists of a synchronous machine connected to an infinite bus of voltage E_b through an inductive reactance X. The electric power output of the machine is given by

$$P=\frac{E_gE_b}{X}\sin\delta \qquad (1)$$

where E_g is the electromotive force of the machine behind the proper total reactance X and δ is the relative electrical displacement angle between rotors. The angle is positive when E_g leads E_b in time phase.

During a short disturbance caused by a change in X, the air-gap power P_i of the electric generator is usually assumed constant. The acceleration equation[1] for the simple system then is

$$M\frac{d^2\delta}{dt^2}=P_i-\frac{E_gE_b}{X}\sin\delta \qquad (2)$$

where M is the angular momentum of the generator and its prime mover.

If the impedance between the machine and the infinite bus contains resistance as well as inductive reactance, and if the damping action of the mechanical system is considered, the acceleration equation becomes

$$M\frac{d^2\delta}{dt^2}=P_i-E_g^2Y_{gb}\cos\theta_{gb}-$$
$$E_gE_bY_{gb}\cos(\theta_{gb}-\delta)-D\frac{d\delta}{dt} \qquad (3)$$

where Y_{gb} and θ_{gb} are the magnitude and angle, respectively, of the transfer admittance between the generator and the infinite bus, and D is an equivalent damping constant[2] of the machine. If D is zero and the complex form of Y_{gb} is $(1/X)\underline{/-90°}$, equation 3 reduces to equation 2.

Electric Analogue Method for One Machine and an Infinite Bus

Analogous Quantities. Two different physical systems that possess the same form of differential equations are called analogous systems. The network of Figure 1 constitutes an electrical system that is analogous to the 2-machine system described by equation 3. The voltage drop of the capacitor can by proper choice be made negligible with respect to the other voltage drops in the circuit. The remaining voltage equation then is

$$L\frac{d^2q}{dt^2}=V-K\cos(\theta-aq)-R\frac{dq}{dt} \qquad (4)$$

The application of Buckingham's π theorem[3] to this system as a model of the 2-machine system establishes the fact that three arbitrary constants can be assigned. These will be called a, b, and c in the following relations:

$$aq=\delta \qquad (5)$$

$$bV=P \qquad (6)$$

$$ct=t_m \qquad (7)$$

where a is the scale factor that multiplies the charge in coulombs to obtain electrical degrees of relative rotor position, b is the scale factor that multiplies any voltage in volts to obtain power in per-unit power values, and c is the scale factor that multiplies electrical time in seconds to obtain mechanical time in the same unit.

From these arbitrary constants, the other scale factors can be established by applying well-known dimensional-analysis procedures[4] as

$$\frac{bc^2}{a}L=M \qquad (8)$$

and

$$\frac{bc}{a}R=D \qquad (9)$$

An Analogue Computer. The function of the dependent variable $K\cos(\theta-aq)$ is obtained from an arbitrary function device called a photoformer.[5] The photoformer is a device that provides an output voltage which is an arbitrary function of the input voltage. Its

---

Paper 51-338, recommended by the AIEE Transmission and Distribution Committee and approved by the AIEE Technical Program Committee for presentation at the AIEE Fall General Meeting, Cleveland, Ohio, October 22–26, 1951. Manuscript submitted July 13, 1951; made available for printing September 5, 1951.

W. B. Boast is with the Iowa State College, Ames, Iowa, and J. D. Rector is with the Consolidated-Vultee Aircraft Corp., Fort Worth, Tex.

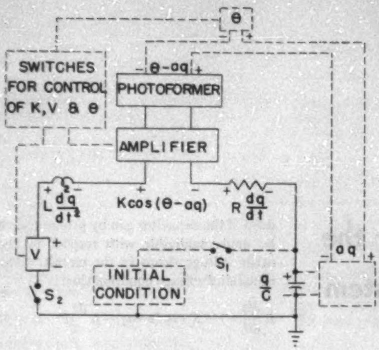
θ
SWITCHES FOR CONTROL OF K,V & θ
θ-aq
PHOTOFORMER
AMPLIFIER
$L\frac{d^2q}{dt^2}$
$K\cos(\theta-aq)$
$R\frac{dq}{dt}$
V
S_1
aq
INITIAL CONDITION
$\frac{q}{C}$
S_2

Figure 1 (left). Electric analogue of one machine and an infinite bus

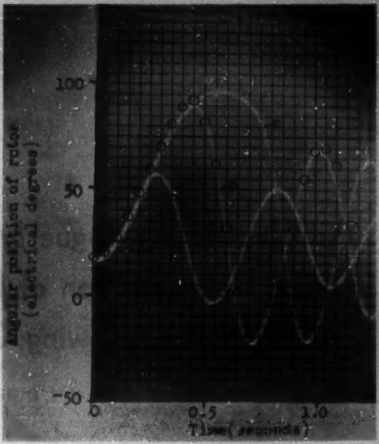

Figure 2 (right). Swing curves of example for clearing times of a, 0.2 second; b, 0.4 second; c, 0.55 second

input voltage is obtained from the difference of the displacement (charge) measuring system and the θ system as shown by the dashed lines of Figure 1. This input signal provides the horizontal or X-axis deflecting voltage. The phototube and amplifiers of the photoformer force the output voltage to be a cosine function of the input by means of a trigonometric mask. The output stage is a low-impedance cathode follower which incorporates the voltage V needed in the analogue. The gain control of the output provides a means for setting the magnitude of the function $K \cos (\theta - aq)$. All amplifiers used in the analogue must be capable of amplifying d-c as well as a-c signals.

In order to simulate power system disturbances, the coefficient K and the voltages V and θ must be changed instantly one or more times during the period of the disturbance. For example, a fault on a lossless line may be simulated by an instantaneous reduction in the value K and the following fault clearing may be simulated by another instantaneous change of the value K. (No change in V or θ is required for a lossless line.) These changes of K are obtained by the timed operation of switches in sequence that change the gain of the photoformer output amplifier from one preset value to another. Both the preset values of K (and of V or θ when necessary) and the timing of the switch operations must be controlled easily.

The remaining elements of the computing circuit consisting of inductance and resistance are essentially the same as those of the conventional linear electric analogue.

The quantity θ of the term $(\theta - aq)$ may be obtained by positioning the mask along the X-axis of the photoformer instead of inserting the fixed voltage corresponding to θ as shown in Figure 1, if this procedure is more advantageous.

Swing curves are observed on the screen of a conventional calibrated d-c oscilloscope which obtains its vertical deflecting voltage from the charge measuring circuit. A switch provides repetitive solutions at a rate sufficient to establish a steady image of the swing curve on the oscilloscope. Switch (S_1) applies the desired initial charge during the "off period" of the repetitive solution and switch (S_2) closes the computing circuit during the disturbance period.

All switch operations of the computer must be synchronized and relatively timed. In the original investigation, a system of ganged synchronous switches was used.

The original computer for this investigation was assembled from laboratory equipment and shop-made devices.

Experimental Results. A stability problem representing a faulted 2-machine system (or one equivalent machine and an infinite bus) was used in checking the performance of the original computer. This problem, a modification of an example from Kimbark,[8] is represented by the following data and swing equations.

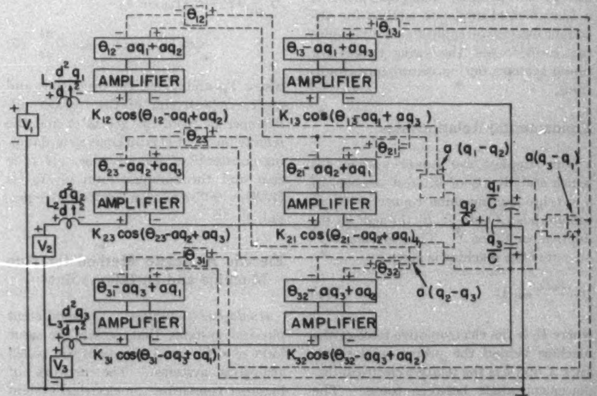
θ_{12}
$\theta_{12}-aq_1+aq_2$
AMPLIFIER
$L_1\frac{d^2q_1}{dt^2}$
V_1
$K_{12}\cos(\theta_{12}-aq_1+aq_2)$
θ_{13}
$\theta_{13}-aq_1+aq_3$
AMPLIFIER
$K_{13}\cos(\theta_{13}-aq_1+aq_3)$
θ_{23}
$\theta_{23}-aq_2+aq_3$
AMPLIFIER
$L_2\frac{d^2q_2}{dt^2}$
V_2
$K_{23}\cos(\theta_{23}-aq_2+aq_3)$
θ_{21}
$\theta_{21}-aq_2+aq_1$
AMPLIFIER
$K_{21}\cos(\theta_{21}-aq_2+aq_1)$
$a(q_1-q_2)$
$a(q_3-q_1)$
$\frac{q_1}{C}$
$\frac{q_2}{C}$
$\frac{q_3}{C}$
θ_{31}
$\theta_{31}-aq_3+aq_1$
AMPLIFIER
$L_3\frac{d^2q_3}{dt^2}$
V_3
$K_{31}\cos(\theta_{31}-aq_3+aq_1)$
θ_{32}
$\theta_{32}-aq_3+aq_2$
AMPLIFIER
$K_{32}\cos(\theta_{32}-aq_3+aq_2)$
$a(q_2-q_3)$

Figure 3. Electric analogue of a 3-machine system with damping neglected

$P_t = 0.8$ per-unit power

$\theta_{gb} = 90°$

$\delta_0 = 18.1°$ and $(d\delta/dt_m)_0 = 0$

$M = 0.01465$ unit power second² per electrical radian (or 2.56×10^{-4} unit power second² per electrical degree)

$C_1 = E_g E_b Y_{gb}$ (during fault) $= 0.936$ per-unit power

$C_2 = E_g E_b Y_{gb}$ (after clearing) $= 2.06$ per-unit power

$D = 0.0143$ unit power second per electrical radian

$d^2\delta$

During the fault, $(0 < t_m < 0.4)$

$$0.01465 \frac{d^2\delta}{dt_m^2} = 0.8 - 0.936 \cos (90° - \delta) - 0.0143 d\delta/dt_m$$

After clearance of the fault $(0.4 < t_m)$

$$0.01465 \frac{d^2\delta}{dt_m^2} = 0.8 - 2.06 \cos (90° - \delta) - 0.0143 d\delta/dt_m$$

The three allowable selections of analogous constants are made on the basis of physical capability of the computer and for convenience of using a certain fixed inductor. By the use of equations 5 through 9, the following relations exist between the analogous quantities of the prototype and analogue:

$$c = \frac{t_m}{t} = 100$$

$$b = \frac{P_t}{V} = 0.1$$

$$K_1 = \frac{C_1}{b} = \frac{0.936}{0.1} = 9.36 \ (0 < t_m < 0.4)$$

$$K_2 = \frac{C_2}{b} = \frac{2.06}{0.1} = 20.6 \ (0.4 < t_m)$$

$$\frac{bc^2}{a} = \frac{M}{L} = \frac{0.01465}{0.863}, \text{ or } a = 59 \times 10^3$$

$$R = \frac{a}{bc} D = \frac{59 \times 10^3}{0.1 \times 100} \times 0.0143 = 84.5$$

Figure 2, which is a direct photograph of the oscilloscope, illustrates swing curves for three fault clearing times—0.2, 0.4, and 0.55 second. The data of a point-by-point[7] solution for 0.4-second clearing are plotted as circles on the photograph. The two methods of solution compare favorably.

The output impedance of the photoformer amplifier presents one limitation that should be considered. Because this impedance is a part of the total resistance of the analogue computing circuit, there is a definite minimum limit of the damping factor D of equation 3 which a given computer can handle. The coefficient of 0.0143 on the damping term was chosen to conform to this minimum possibility on the present computer.

Application of the Method to Multimachine Systems

When three or more machines are interconnected, several swing equations must be solved simultaneously.[1] The acceleration equations, neglecting damping, are of the form

$$M_1 \frac{d^2\delta_1}{dt^2} = P_{t1} - E_1^2 Y_{11} \cos \theta_{11} - E_1 E_2 Y_{12} \cos (\theta_{12} - \delta_1 + \delta_2) - \ldots - E_1 E_n Y_{1n} \cos (\theta_{1n} - \delta_1 + \delta_n)$$

$$M_2 \frac{d^2\delta_2}{dt^2} = P_{t2} - E_2^2 Y_{22} \cos \theta_{22} - E_2 E_1 Y_{21} \cos (\theta_{21} - \delta_2 + \delta_1) - \ldots - E_2 E_n Y_{2n} \cos (\theta_{2n} - \delta_2 + \delta_n)$$

$$M_n \frac{d^2\delta_n}{dt^2} = P_{tn} - E_n^2 Y_{nn} \cos \theta_{nn} - E_n E_1 Y_{n1} \cos (\theta_{n1} - \delta_n + \delta_1) - \ldots - E_n E_{n-1} Y_{n(n-1)} \cos (\theta_{n(n-1)} - \delta_n + \delta_{n-1}) \quad (10)$$

where $Y_{11}, Y_{22}, \ldots Y_{nn}$ are the magnitudes of the driving-point admittances from the viewpoint of the respective electromotive forces, $Y_{12}, \ldots Y_{1n}$ are the magnitudes of the respective transfer admittances, and the θ's are the angles of the corresponding admittances where the order of subscripts is immaterial.

Figure 3 illustrates an electric analogue for a 3-machine system. No switching circuits are shown. The voltages labeled V with the respective subscripts represent the terms of the form $P_{tn} - E_n^2 Y_{nn} \cos \theta_{nn}$. These voltages are fixed during an interval of the swing curve.

The differences of the angular displacements appearing in equation 10 are obtained in the analogue from the differences of the voltages of the capacitors as shown in Figure 3. Each of these differences of voltage is used twice in the analogue as is required by the equations.

For each equation in an n-machine system, n-1 photoformers and amplifiers are connected in series with the respective L, V, and C elements forming one branch of the n-branch network. Therefore, $n(n$-1) photoformers and amplifiers are necessary for the general case. If the transfer admittances in the original power network contain no conductive components, all of the transfer admittance angles are 90 degrees and only one half as many photoformers are required. However, $n(n$-1) amplifiers are still required.

The damping for the multimachine system is considered negligible, because damping introduces derivatives of the differences of the displacements and cannot be represented in the analogue by simple resistance in each branch circuit. Methods can be devised, however, to bring in the other displacement effects by supplementary amplifiers. In the form as shown, the output resistance of the amplifiers must produce negligible voltage drops with respect to the other voltages in the branch to faithfully reproduce the case for no machine damping.

References

1. POWER SYSTEM STABILITY (book), Edward W. Kimbark. John Wiley and Sons, Inc., New York, N. Y., volume I, 1948, page 28.

2. ELECTRIC POWER CIRCUITS (book), O. G. C. Dahl. McGraw-Hill Book Company, New York, N. Y., volume II, 1938, pages 647–83.

3. MATHEMATICAL AND PHYSICAL PRINCIPLES OF ENGINEERING ANALYSIS, Walter C. Johnson. McGraw-Hill Book Company, New York, N. Y., 1944, page 219.

4. SIMILITUDE IN ENGINEERING (book), Glenn Murphy. Ronald Press, New York, N. Y., 1950, pages 235–47.

5. THE PHOTOFORMER IN ANACOM CALCULATIONS, H. W. Schultz, J. F. Calvert, R. L. Buell. *Proceedings*, The National Electronics Conference, volume 5, 1949, pages 40–47.

6. Kimbark, *op. cit.*, page 44.

7. Kimbark, *op. cit.*, page 36.

Discussion

Alexander Kusko (Massachusetts Institute of Technology, Cambridge, Mass.): Engineers who use the step-by-step method for solving transient-stability problems are well aware that the procedure is time consuming and tedious, in spite of the ease with which system-power-flow data can be obtained at each step from a network analyzer. For this reason, a paper such as this one should be highly regarded as a step in the right direction, that is, to apply machine methods to the solution of transient-stability problems.

To be sure, solutions have been carried out on the differential analyzer, which can solve the electromechanical system equation directly; and the job also can be done on a digital computer. However, this necessitates first measuring system parameters from a network-analyzer representation and then transferring this information to the computer.

Another means of handling this problem was given in a paper by R. Roberts in 1950.[1] The scheme described by Mr. Roberts is one using small machines connected to a miniature 3-phase system. Model theory is applied to the scaling-down process and the proper time constants in the model alternators are obtained by use of a feedback arrangement in the field circuits of the machines. System transients are then observed on an oscilloscope with fault application and switching carried out cyclically.

Here, again, the device for solving the transient-stability problem is not a working network analyzer suitable for day-in and day-out power-system studies.

At the Massachusetts Institute of Technology, we have been building a network-analyzer phase shifter equipped with a feedback loop relating shaft position with electrical power output. This feedback loop contains computing elements so that if the power output of the phase shifter is disturbed through a change in other sources or loads in the network to which it is connected, or through a fault applied to the network, the phase shifter in question will attempt to restore its initial power output by a change in shaft angle. The computing elements will be so designed and set that the mechanical transient which the phase shifter undergoes will simulate the transient undergone by a large machine which it is chosen to represent in the system. With all of the phase shifters feeding a common network so equipped, and with the instantaneous angles of each recorded on a common paper strip, the resulting record will be a set of system swing curves. The time scale for the operation will be so expanded, for example, one second on the system equals five minutes on the computer, that the fault application and subsequent switching can be done manually. Damping, governor action, and exciter response also can be introduced easily.

The implication conveyed by these phase shifters is that it will be possible to take a static system representation on the network analyzer, switch it into a dynamic representation for a transient-stability solution, and then back again in little time to the original representation. But the implications are even deeper.

Having a network analyzer where the phase shifters are responsive to signals, we can now feed information to the phase shifters from some sort of a central computing device and perhaps start solving problems having to do with allocation of generation, tie-line control, incremental-loss studies, and so on, where the central computing device can vary the phase shifter outputs to seek out some optimum condition such as minimum system losses or some other predetermined criterion.

To extend our thinking further, we can perhaps visualize such a network analyzer and central computer directly controlling a complete power system with the computer using the network analyzer to find optimum operating solutions before transmitting commands to the actual system. This could be done continuously, or at time intervals, with the computer receiving information from all key points in the system and retransmitting operating instructions.

REFERENCE

1. MODEL MACHINES AND MODEL SYSTEMS: STUDY OF TRANSIENT-STABILITY PROBLEMS BY THE USE OF ELECTROMECHANICAL MODELS RESEMBLING THE EXISTING MACHINES AND SYSTEM, R. Roberts. *Paper Number 338*, International Conference on Large High-Voltage Electric Systems (Paris, France), 1950.

Vol. 1951

Transposition of High-Voltage Overhead Lines and Elimination of Electrostatic Unbalance to Ground

ERIC T. B. GROSS
FELLOW AIEE

ANDREW H. WESTON
ASSOCIATE MEMBER AIEE

Synopsis: Improvements and new developments in both the communications and power fields have, for the most part, eliminated the need for transposing high-voltage power lines at close intervals. In many systems transpositions are made only at switchyards and substations. Geometric unbalance of untransposed power lines leads to residual ground currents in solidly grounded systems. Methods of reducing the residual ground currents to tolerable levels are investigated in this paper.

IN THE early years of high-voltage power transmission and until about 20 years ago the problem of transposing the conductors of transmission lines was of great importance. Transpositions influence the electromagnetic coupling between power and communication open-wire circuits. Power lines were transposed primarily in order to eliminate or reduce disturbances in the communication circuits produced by the geometric unbalance of power lines that were operating under balanced conditions of voltage and of load current. A by-product of transposing each and every power line section was the geometric balancing of such circuits between terminals, which assured balanced conditions at every point of the power transmission system.

Developments in both the communications and power fields have greatly reduced the reasons for transposition of the power lines. Increasing use is made of underground cables or otherwise shielded circuits for communication purposes and the communication equipment itself has become less susceptible to noise. The reduction of mutual interference of metallic, carrier and other communication circuits to a minimum might eliminate any need of further attention to residuals. Separate rights of way are often used for new power and communication circuits. Improved design of rotating machines and transformers has led to a reduction of harmonics in the power circuits.

Experience has shown that many disturbances on high-voltage lines occur on transposition towers; records indicate that in some power systems or transmission line sections at least one of four outages is physically associated with a transposition. Many high-voltage systems have been built in the last few years without the use of transposition structures, and such structures have also been eliminated in some of the older systems. The practice in many systems has been changed so that "transpositions" are made only in or near the switchyards by rearranging phases.

Leaving off transpositions between stations enlarges the effects of geometric unbalances of the conductor arrangement on the power system itself. It is, therefore, important to analyze and evaluate the resulting dissymmetries in order to predict their magnitudes and their effects. The available literature contains little material dealing with this subject and applied to conductor configurations of present-day practice in a thorough analytical and still practical manner. Therefore, it appears desirable to develop a quantitative method for the evaluation of unbalances which are due to the elimination of transpositions on line sections.

The effects of geometric unbalance of power lines are electrostatic and electromagnetic. Electrostatic effects occur under all conditions of operation and are essentially independent of the load currents in the phase wires. Electromagnetic effects depend upon the currents in the wires and are negligible on open circuit. Since electrostatic effects also influence the no-load conditions of power transmission, they appear to be of prime importance. This investigation deals with the study of these electrostatic effects. Particular emphasis is placed on high-voltage systems (70-kv and above) since such systems contain long sections between stations or switchyards. With few exceptions, systems operating in this country at such voltages are "solidly grounded." Therefore, it will be assumed in the following that the neutrals of power transformers are so grounded.

Unbalanced Current and Ground-Displacement Voltage

The charging current of a transmission line can be resolved into two components, one is due to the "capacitance between conductors" and the other is due to the "capacitance to ground". Capacitances

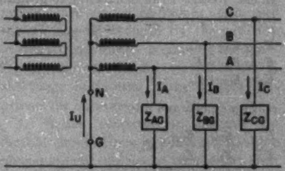

Figure 1. Solidly grounded system

Paper 51-339, recommended by the AIEE Transmission and Distribution Committee and approved by the AIEE Technical Program Committee for presentation at the AIEE Fall General Meeting, Cleveland, Ohio, October 22–26, 1951. Manuscript submitted June 22, 1951; made available for printing August 31, 1951.

Eric T. B. Gross is with the Illinois Institute of Technology, Chicago, Ill., and Andrew H. Weston is with the Commonwealth Edison Company, Chicago, Ill.

The authors are indebted to Mr. A. E. Davison, Toronto, for encouragement in this work.

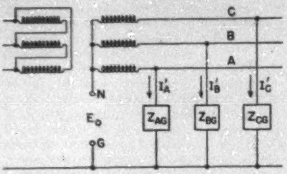

Figure 2. Ungrounded system

between conductors, as well as other shunt loads, do not directly influence currents and voltages to ground and may be omitted. With these simplifications a system may be represented as shown in Figure 1, in which the impedances Z_{AG}, Z_{BG}, and Z_{CG} are the capacitive impedances to ground of the line section to be considered. The current I_u in the transformer neutral is the unbalanced (residual) current of the section, and its value is $I_u = I_A + I_B + I_C$, or

$$I_u = \frac{E_{AN}}{Z_{AG}} + \frac{E_{BN}}{Z_{BG}} + \frac{E_{CN}}{Z_{CG}} \tag{1}$$

where E_{AN}, E_{BN}, and E_{CN} are the phasors of the phase-voltages which are related by the phasor-equation

$$E_{AN} + E_{BN} + E_{CN} = 0 \tag{2}$$

If the line is balanced to ground electrostatically, $Z_{AG} = Z_{BG} = Z_{CG}$ and $I_u = 0$.

The resistive component of the impedances to ground is usually negligible so that the impedances Z may be replaced by the capacitive reactances X_{AG}, X_{BG}, and X_{CG}, or expressed by the capacitances C_{AG}, C_{BG}, and C_{CG}.

Assuming for a moment that the line is not solidly grounded through the neutral of a power transformer, and referring to Figure 2, the phasor equation:

$$I_A' + I_B' + I_C' = 0 \tag{3}$$

will relate the three currents to each other. If E_A, E_B, and E_C denote the phasor voltages to ground of the three phases, equation 3 may be written:

$$\frac{E_A}{Z_{AG}} + \frac{E_B}{Z_{BG}} + \frac{E_C}{Z_{CG}} = 0 \tag{4}$$

If the voltage from neutral N to ground G is called E_o, the relations

$$\begin{aligned} E_A &= E_{AN} + E_o \\ E_B &= E_{BN} + E_o \\ E_C &= E_{CN} + E_o \end{aligned} \tag{5}$$

change equation 4 into

$$\frac{E_{AN}}{Z_{AG}} + \frac{E_{BN}}{Z_{BG}} + \frac{E_{CN}}{Z_{CG}} + E_o \cdot \left[\frac{1}{Z_{AG}} + \frac{1}{Z_{BG}} + \frac{1}{Z_{CG}}\right] = 0 \tag{6}$$

which may be written

$$I_u + E_o \frac{1}{Z_G} = 0 \tag{7}$$

if

$$\frac{1}{Z_{AG}} + \frac{1}{Z_{BG}} + \frac{1}{Z_{CG}} = \frac{1}{Z_G} \tag{8}$$

Introducing E_{ph}, any one of the phase-voltages of the system, gives

$$I_u + \frac{E_o}{E_{ph}} \frac{E_p}{Z_G} = 0 \tag{9}$$

in which $E_{ph}/Z_G = I_G$, the ground fault current (that is, the capacitive current between the faulted phase and ground) in the ungrounded (delta) system of Figure 2.

Finally, changing equation 9 into a scalar equation gives

$$\frac{|I_u|}{|I_G|} = \frac{|E_o|}{|E_{ph}|} = d_o \tag{10}$$

I_G can be computed from the zero sequence capacitive reactance X_o', or it may be estimated, for example from the equation

$$I_G = \frac{\text{kv (line-to-line) times miles}}{160} \text{ amperes} \tag{11}$$

for a single circuit overhead line. Therefore, I_u may be found if d_o is known.

The ratio d_o, the "ground displacement" in per unit of phase voltage, is known for many configurations of lines operating at moderately high voltages from early investigations which were made when the inductive interference between power and communication circuits was first studied thoroughly. The most complete data are contained in a study by L. P. Ferris that was made in 1916.[1] However, this investigation did not consider any lines equipped with overhead ground wires (static wires or shield wires), as is now accepted practice on most lines at the voltages under discussion. In the next section of this paper are summarized some of the results of a study concerning the effects of ground wires.

The ground fault current I_G is proportional to the length of the line, but d_o depends only on the average heights above ground and the geometric configuration of the phase and overhead ground wires on the towers. Therefore I_u will increase directly with the length of the line. Since too large a value of I_u may influence the correct operation of sensitive ground relay elements, in addition to introducing stray losses in earth and in ground wires, it may be desirable to reduce d_o of a long section in order to limit I_u to a certain permissible value.

For example, for a 200-mile section (between two switchyards) of a single-circuit 230-kv line, I_G will be approximately 300 amperes. With an assumed value of $d_o = 5$ per cent, I_u becomes 15 amperes. This current would circulate through the neutrals of the power transformers (Figure 1) and cause additional losses. It may be helpful to the industry to have data available which indicate how d_o can be reduced, without transposition structures on the line, but with phase transpositions in or near switchyards.

Results of Analysis

The accurate evaluation of d_o is a very lengthy and laborious task since the capacitances to ground of all conductors for a unit length of line have to be computed. Each conductor adds one equation to a system of linear equations[2] with the charges and voltages of each conductor as variables. For example, the computation of the ground displacement d_o of a single-circuit line with the phase wires in a horizontal plane (H-frame towers) and with two overhead ground wires reduces to the problem of solving five simultaneous linear equations with five unknowns. However, symmetrical arrangements of some of the conductors lead to simplifications.

In this analysis the so-called "Doolittle method" of solving[3] such systems of linear equations has been used throughout. This practical method has many advantages over the rigorous method using determinants and it enables easy check of errors. All computations were made on a standard slide rule. In a few cases lines without ground wires were also considered and the results checked very well with the data given in Ferris' report.[1]

PHASE CONDUCTORS IN HORIZONTAL CONFIGURATION

Since many new lines now are designed as single-circuit lines with all

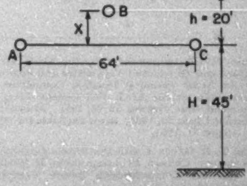

Figure 3. Single-circuit line with raised middle conductor

three conductors on the same level above ground, this arrangement was studied in a number of variations.

Three conductors, spaced 32 feet between the middle and outer conductors, each at an average height of 45 feet above ground were assumed. The conductors are 1,272,000 circular mil steel reinforced aluminum cable. The capacitances to ground for this 230-kv line in micromicrofarads per mile are:

$C_{AG}=C_{CG}=10{,}080$
$C_{BG}=9{,}170$

These values lead (equations 1 and 10) to the unbalance $d_o=3.12$ per cent.

The addition of two ground wires, each of 1/2-inch diameter, reduces the unbalance of 2.60 per cent. Following a suggestion of A. E. Davison, the middle conductor of the 3-phase wires was raised and the new unbalances computed. The results of these changes are shown in Table I (Figure 3).

There are high-voltage lines in operation in this country on which the middle conductor is somewhat raised, however, this was done for other reasons than because of a consideration of d_o. If the ground wires are nearer to each other, the unbalance is reduced, for example d_o becomes smaller.

In general, the computations have shown that d_o is reduced by the addition of ground wires on lines with horizontal phase relationship and also by an increase of the ratio "horizontal spacing between phase wires to their average height above ground." The practical conclusion of these results is that d_o decreases with increasing voltage. The influence of the horizontal spacing between the conductors on d_o is much greater than a change in the height of the conductors above ground.

Balancing of a configuration of three conductors on the same horizontal level without ground wires can be done by raising or by lowering the middle conductor.

Lowering has a greater effect on d_o than raising. In general, it would be necessary to raise the middle conductor more than is practically feasible in order to achieve complete balance. For example, a configuration as indicated in Figure 4, but without overhead ground wires, and with conductors of 0.528-inch diameter leads to $C_{AG}=C_{CG}=7{,}860$ micromicrofarads, $C_{BG}=7{,}040$ micromicrofarads and $d_o=3.66$ per cent. It is evident that a change of the C_{BG} to C_{AG} ratio will influence d_o, and lowering of the middle conductor will increase C_{BG} and reduce the unbalance. Some data about such balancing are contained in Ferris' report.[1]

Table I

Middle Conductor Raised by x	4′6″	6′9″	0′0″
$C_{AG}=C_{CG}=\mu\mu f$	11,110	11,120	11,110
$C_{BG}=\mu\mu f$	10,180	10,210	10,270
$d_o=\%$	2.81	2.81	2.60

Raising the middle conductor to a good height on lines without ground wires will greatly expose this conductor to lightning strokes and it will act as a shield wire for the other conductors. Such reduction of the unbalance should be recommended only for medium-high-voltage subtransmission systems (35 kv) that are resonant grounded, since arcing grounds produced by flashovers on the raised middle conductors are made harmless through self-extinction of the arc.

The influence of ground wires on the electrostatic unbalance is shown in Figure 4. Two ground wires, if arranged as indicated in the configuration of Figure 4, reduce the unbalance since the computation gives $C_{AG}=C_{CG}=9{,}360$ micromicrofarads and $C_{BG}=8{,}780$ micromicrofarads, hence $d_o=2.09$ per cent. The ground wires were assumed here to have the same diameter (0.528 inch) as the phase conductors.

Phase Conductors in Vertical Configuration

Vertical arrangement of the phase conductors also produces relatively large unbalances. For the configuration of Figure 5, without and with ground wire (7) the capacitances given in Table II were computed. All conductors have 0.528 inch diameter and the values are in micromicrofarads per mile.

Without ground wires, good balance can be achieved by interchanging only the two lower phase wires B and C since their average is not greatly different from the capacitance of the uppermost conductor A. An overhead ground wire, (7) in Figure 5, changes the picture completely. The lowest and highest conductors again have the maximum and minimum values of capacitance, but in reversed relation, and an interchange of the middle and highest phase wire would now reduce the unbalance. The knowledge of these facts and data is of practical importance for the effective interchanging of phase positions in switchyards.

Table II

	Without Overhead Ground Wire	With Overhead Ground Wire
C_{AG}	7,110	8,480
C_{BG}	6,620	7,250
C_{CG}	7,800	8,190
d_o %	4.82	4.68

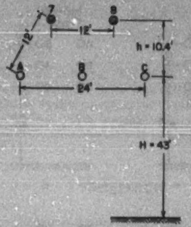

Figure 4 (left). Single-circuit line with conductors in horizontal configuration

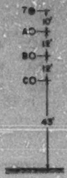

Figure 5 (right). Single-circuit line with conductors in vertical configuration

Similar improvement can be brought about in double-circuit lines as indicated in Figure 6(A). The phase (B) which has the middle position on one circuit (to the left) should be in the lowest position on the other circuit (right) and vice versa. Again, ground wires, Figures 6(B), 6(C), and 6(D) may reverse the picture.

As a general rule it is worthwhile mentioning that d_o will be smallest in double-circuit lines if the arrangement of the phases on both sides of the towers is not symmetrical relative to the tower. The values found for the capacitances in the four cases considered in Figure 6 are given in Table III. Again all conductors are assumed to have a diameter of 0.528 inch, and the capacitances are in micromicrofarads per mile.

Conclusions

1. Elimination of transpositions on line sections increases circulating residual ground currents in solidly grounded systems.
2. These circulating currents may be reduced by appropriate arrangements of phase and ground wires.
3. The electrostatic unbalance of power lines using H-frame poles and towers may be reduced by the addition of two ground wires. Increasing the spacing between the conductors which are in the same horizontal plane further improves the balance.
4. Better electrostatic balance on double circuit lines is achieved if some phases are not carried by conductors that are symmetrical on both sides of the tower, Figure 6.

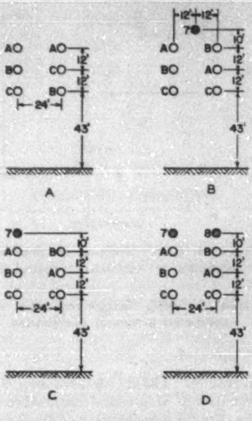

Figure 6. Double-circuit lines

Appendix I. The Doolittle Method for Solving Systems of Linear Equations

The classical approach to the solution of a system of linear equations by means of determinants involves a great amount of work, and in spite of this, numerical errors can not be easily detected. The Doolittle method, which is a modification of one due to Gauss, is characterized by the systematic elimination of unknowns through elementary processes. An important feature of this method is that every step can be checked. The sum of the coefficients of all unknowns on the left side of one equation and of its right-hand member is called the "check sum." This number is changed in the same way as all the coefficients of the equation under consideration. For example, if the equation is divided by a number, the check sum of the new equation is equal to the check sum of the previous one divided by this same number; if two equations are added, the new check sum is the sum of the two previous check sums. The method will be illustrated by applying it to the following three equations:

$$1.02x+2.11y+0.98z=3.23 \qquad \text{(A)}$$

$$1.89x+1.05y+1.07z=6.85 \qquad \text{(B)}$$

Table III

Configuration as Figure 6	A	B	C	D
C_{AG} μμf	18,390	11,730	12,000	13,010
C_{BG} μμf	10,930	$=C_{AG}$	11,410	$=C_{AG}$
C_{CG} μμf	$=C_{BG}$	12,930	12,870	13,600
d_o %	1.76	3.33	3.39	1.44

Table IV

Equation	Coefficients of x	y	z	Right Member	S	S_1
A	1.02	2.11	0.98	3.23	7.34	
A′	1.00	2.07	0.96	3.17	7.20	7.20
B	1.89	1.05	1.07	6.85	10.86	
$B_1=-1.89\,A'$	−1.89	−3.91	−1.81	−5.99	−13.60	−13.60
$B_2=B+B_1$	0	−2.86	−0.74	0.86	−2.74	−2.74
B′	0	1.00	0.26	−0.30	0.96	0.96
C	3.14	2.91	−4.17	2.25	4.13	
$C_1=-3.14\,A'$	−3.14	−6.51	−3.02	−9.95	−22.62	−22.61
$C_2=C+C_1$	0	−3.60	−7.19	−7.70	−18.49	−18.48
$C_3=3.6\,B'$	0	3.60	0.94	−1.08	3.46	3.46
$C_4=C_2+C_3$	0	0	−6.25	−8.78	−15.03	−15.02
C′	0	0	1.00	1.40	2.40	2.40

$$3.14x+2.91y-4.17z=2.25 \qquad \text{(C)}$$

The solution is given in Table IV. The check-sum by horizontal addition is called *S*; the one by division or addition is called S_1. *S* and S_1 should be equal. All operations are carried to two decimal places (same as the original equations). It is believed that the various steps need little explanation.

It is evident that A′ is found by dividing A by the coefficient of *x*; similarly B′ by dividing B_2 by the coefficient of *y*, and so on.

From equation C′ follows immediately $z=1.4$, from equation B′ the value $y=-0.66$, and finally from A′ the value $x=3.19$. In order to check these values, a substitution in C (which was not used directly for the evaluation of *x* and *y*) gives 2.24 on the left, which is close enough to the 2.25 on the right side of the same equation.

Appendix II. Single Circuit Line with One Overhead Ground Wire

Figure 7 shows the line configuration under consideration. The average conductor height above ground is $36^1/_2$ feet, the three conductors are 336,400 steel reinforced aluminum cable, and the ground wire is 5/16-inch diameter steel. From these data follows $r_1=r_2=r_3=0.3605$ inch, $r_7=0.1562$ inch, $d_{12}=d_{23}=144$ inches, $d_{13}=288$ inches, $d_{17}=d_{27}=183.6$ inches, $d_{37}=274.1$ inches, $D_{11}=D_{22}=D_{33}=876$ inches, $D_{77}=1{,}214$ inches, $D_{12}=D_{23}=890$ inches, $D_{13}=923$ inches, $D_{17}=D_{27}=1{,}048$ inches and $D_{37}=1{,}068$ inches.

The relations between the charges on the conductors and the voltages impressed are given by the following equations:

$$\left.\begin{array}{ll} P_{11}Q_1+P_{12}Q_2+P_{13}Q_3+P_{17}Q_7=V_1 & \text{(A)}\\ P_{12}Q_1+P_{22}Q_2+P_{23}Q_3+P_{27}Q_7=V_2 & \text{(B)}\\ P_{13}Q_1+P_{23}Q_2+P_{33}Q_3+P_{37}Q_7=V_3 & \text{(C)}\\ P_{17}Q_1+P_{27}Q_2+P_{37}Q_3+P_{77}Q_7=V_7 & \text{(D)} \end{array}\right\} \quad (12)$$

In these equations are the potential coefficients P_{ik} given by the expressions:

$$P_{11}=P_{22}=P_{33}=\log D_{11}/r_1=3.386, \qquad P_{77}=\log D_{77}/r_7=3.891$$

$$P_{12}=P_{23}=\log D_{12}/d_{12}=0.792, \qquad P_{13}=\log D_{13}/d_{13}=0.506$$

$$P_{17}=P_{27}=\log D_{17}/d_{17}=0.756, \qquad P_{37}=\log D_{37}/d_{37}=0.590$$

In our particular case, equations 12 become:

$$\left.\begin{array}{l} 3.386Q_1+0.792Q_2+0.506Q_3+0.756Q_7=V_1\ \text{(A)}\\ 0.792Q_1+3.386Q_2+0.792Q_3+0.756Q_7=V_2\ \text{(B)}\\ 0.506Q_1+0.792Q_2+3.386Q_3+0.590Q_7=V_3\ \text{(C)}\\ 0.756Q_1+0.756Q_2+0.590Q_3+3.891Q_7=V_7\ \text{(D)} \end{array}\right\} \quad (13)$$

The relations between charges and potentials also can be expressed in the following form:

$$\left.\begin{array}{l} Q_1=\quad C_{11}V_1-C_{12}V_2-C_{13}V_3-C_{17}V_7\ \text{(E)}\\ Q_2=-C_{12}V_1+C_{22}V_2-C_{23}V_3-C_{27}V_7\ \text{(F)}\\ Q_3=-C_{13}V_1-C_{23}V_2+C_{33}V_3-C_{37}V_7\ \text{(G)}\\ Q_7=-C_{17}V_1-C_{27}V_2-C_{37}V_3+C_{77}V_7\ \text{(H)} \end{array}\right\} \quad (14)$$

The equations contain altogether ten unknown Maxwell coefficients, the capacitances C_{ik}.

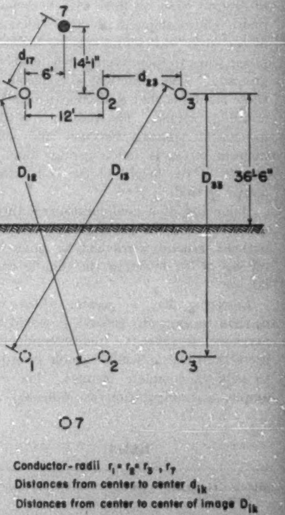
7
d17
6'
14'-1"
d23
O1
O2
O3
12'
D12
D13
D33
36'-6"
O1
O2
O3
O7
Conductor-radii r1 = r2 = r3 , r7
Distances from center to center dik
Distances from center to center of image Dik

Figure 7. Single-circuit line with one overhead ground wire

Equations 13 can be solved for Q_i if values of potential V_k are specified. Substituting these values of Q_i and the same specified voltages in equations 14 leads to the values of the unknown C_{ik}. Since equations 13 are valid for any values of V_k, we may select specific values which will simplify the solution of equations 14.

In the first step, we select $V_1=1$, $V_2=V_3=V_7=0$. With these values, the Doolittle method gives the solution of equations 13 as:

$$Q_1=0.324,\quad Q_2=-0.058,\quad Q_3=-0.027 \text{ and } Q_7=-0.0475$$

Applying these values to equation 14 gives:

$$C_{11}=Q_1=0.324,\quad C_{12}=-Q_2=0.058,\quad C_{13}=-Q_3=0.027 \text{ and } C_{17}=-Q_7=0.047$$

In the next step, we select $V_2=1$, $V_1=V_3=V_7=0$. The new value Q_1' follows from equation (14E) as $Q_1'=-C_{12}=Q_2=-0.058$. The other values are found by the Doolittle method from the remaining three equations (B), (C), and (D) (equation 13) as $Q_2'=0.333$, $Q_3'=-0.061$, $Q_7'=-0.044$, and with the new V-values as selected:

$$C_{22}=Q_2'=0.333,\quad C_{23}=-Q_3'=0.061,\quad C_{27}=-Q_7'=0.044$$

In the next step, we select $V_3=1$, $V_1=V_2=V_7=0$, find Q_1'' and Q_2'' immediately from equations (E) and (F), as $Q_1''=-C_{13}=-0.027$ and $Q_2''=-C_{23}=-0.061$. The remaining two equations (C-13, D-13) give $Q_3''=0.319$ and $Q_7''=-0.031$ from which $C_{33}=Q_3''=0.319$ and $C_{37}=-Q_7''=0.031$. The capacitances to ground are therefore:

$$C_{1G}=C_{11}-C_{12}-C_{13}=0.238$$
$$C_{2G}=C_{22}-C_{12}-C_{23}=0.213$$
$$C_{3G}=C_{33}-C_{13}-C_{23}=0.231$$

From equations 8 and 1, we have

$$C_0=C_{1G}+C_{2G}+C_{3G}, \text{ and } I_u=\omega E_{AN}(C_{1G}+a^2C_{2G}+aC_{3G})$$

therefore

$$d_o=100\frac{|C_{1G}+a^2C_{2G}+aC_{3G}|}{C_{1G}+C_{2G}+C_{3G}}=3.20\%$$

If the C-values are desired in micromicrofarads per mile, the values given above should be multiplied by 38,830. For this example:

$$C_{1G}=9{,}270\ \mu\mu\text{f/mile},\quad C_{2G}=8{,}290\ \mu\mu\text{f/mile},\quad C_{3G}=8{,}970\ \mu\mu\text{f/mile}$$

The same configuration also was used in a calculation for an average conductor height above ground of 50 feet 7 inches, with all other data unchanged. This modification gave

$$C_{AG}=8{,}720\ \mu\mu\text{f/mile},\quad C_{BG}=7{,}790\ \mu\mu\text{f/mile},\quad C_{CG}=8{,}380\ \mu\mu\text{f/mile}$$

$$d_o=3.29\%$$

The result indicates that d_o does not change greatly when the same conductors, in equal relative spacings, are raised from $36^1/_2$ feet to 50 feet. The capacitances to ground, however, are decreased by about 6 per cent.

References

1. Technical Report Number 51. Joint Committee on Inductive Interference, Railroad Commission of the State of California, California State Printing Office (Sacramento, Calif.), 1919, pages 266–351.

2. Circuit Analysis of Power Systems (book), **Edith Clarke.** John Wiley and Sons, New York, N. Y., volume 1, chapter XII, 1942, pages 434–89.

3. Methods of Correlation Analysis (book), **M. J. B. Ezekiel.** John Wiley and Sons, New York, N. Y., chapter 12, page 200 and appendix I, page 464.

4. Co-ordination of Power and Communication Circuits for Low-Frequency Induction, **J. O'R. Coleman, H. M. Trueblood.** *AIEE Transactions*, volume 59, 1940, pages 403–12.

5. Report on Survey of Unbalanced Charging Currents, **AIEE Committee Report.** *AIEE Transactions*, volume 68, 1949, pages 1328–29.

6. Ground Faults in High Voltage Systems (book), **R. Willheim.** Julius Springer Publishers, Berlin, Germany, 1936.

Discussion

J. A. Rawls (Virginia Electric and Power Company, Richmond, Va.): The subject paper by Messrs. Gross and Weston presented the problem in an excellent manner. The information in this paper is very interesting and valuable and should be of material help to transmission engineers and designers.

I have been fortunate in being connected with transmission work for over 20 years. During this period we have constructed approximately 1,000 miles of 110- and 132-kv transmission lines. The majority of these lines have been of wood H-frame construction, many of them with two overhead ground wires. Some steel tower lines have been constructed using one and two overhead ground wires and vertical configuration with provision for two circuits.

Prior to 1926, high-voltage lines on our system used steel towers with vertical configuration. On these lines no transpositions were made except where the line changed to horizontal configuration at stations. In most cases a roll was made at each station which changed the configuration of the conductors for each line section.

In 1926 we changed to construction with wood H-frame horizontal configuration. These early lines had transpositions in them depending on the requirements of the local communication companies. Our experience with these early transpositions in wood H-frame lines was not satisfactory. In order to get proper phase clearance on these structures it was necessary to add additional guys which made the structures very weak electrically and we have had considerable trouble due to lightning splitting the poles and cross arms at these transposition points. These original wood lines did not have overhead ground wires. In 1930 we commended building wood H-frame lines with two overhead ground wires. We found that it would be quite difficult to place transpositions in these lines due to the presence of these overhead ground wires. After encountering this trouble we tried to lay out our new lines so as not to have close parallels with communication circuits. We have found over the period of the last 20 years that these lines operated satisfactorily without transpositions and we have not had difficulty with the communication companies even though they now have lines which are near our lines for considerable distances.

On one old steel tower line where transpositions were made by installing long arms on the towers we have recently removed all of these transpositions so as to increase the mechanical strength of the tower and secure additional phase clearance. On a new double-circuit steel-tower line that we have recently constructed we were careful not to have the phases on the two circuits opposite each other. On the double circuit wood H-frame line which we are planning we are considering making the phases on the adjacent conductors of the two circuits the same.

I am of the opinion that too many transpositions have been used on high-voltage transmission lines in the past and from my experience a much more reliable line can be built if the transpositions are eliminated. The communication companies, whereas they preferred transpositions, now find that they can take care of their circuits so as not to require transpositions.

W. W. Woodruff (Tennessee Valley Authority, Chattanooga, Tenn.): We do not transpose our 161-kv circuits. The majority are of flat configuration; however, at the terminal stations double circuit deadend towers, with perhaps one or two additional double circuit towers, are used to conserve space. There is no deliberate transposing of conductors, and any that may occur is accidental to the transition from horizontal to vertical configuration or vice-versa.

At present our longest line is slightly over 100 miles. The average length would probably be about 50 miles. With lines of this average length and the voltage level of 161 kv, we have experienced no difficulties from the lack of transposing.

Our subtransmission voltages are 69 kv and 46 kv. On none of the lines constructed by Tennessee Valley Authority have transpositions been used. These lines are relatively short and have given no trouble from unbalanced voltages.

A. E. Davison (The Hydro Electric Power Commission of Ontario, Toronto, Ont., Canada): Professor Gross observed a need for clarification and amplification of the technical features of a distinct trend away from frequent transpositions in power systems especially those at higher voltages.

The suggestion was made that this information which had evidently been worked out at some earlier date should be published.

Later, it was suggested that an example of application of the formula and information should also be recorded, so as to be reasonably certain that interpreters and users of the method could think along the same lines as the authors and use their nomenclature and units. This now has all been done concisely in the author's paper.

Engineers responsible for the continuity of electrical service over great distances are always seeking ways and means of eliminating discontinuities of which transpositions are the best example. Others are change of route, dead-ending of conductors, taps, sectionalization facilities, and various types of discontinuities that may be introduced at the request of other types of utilities when being crossed-over such as railways, communication circuits and the more important highways.

Until recently, transpositions have been most prominent at these discontinuities which statistically appear to account for at least one out of every four outages on important high-voltage transmission systems. An electrical disturbance seems to travel some distance along a standard type of construction until some discontinuity is reached.

The authors of this paper have been careful in introducing and summarizing the subject in the early part of their paper. This is wise since two groups of interested engineers are always quite concerned about keeping residual ground currents and other disturbances within tolerable limits. Included in these groups are all engineers responsible for commercial and other types of communication and relay engineers within an electrical utility.

A case involving major elimination of existing transpositions came up in the United Kingdom during and shortly after World War II. Interruptions to service because of bombing and enemy attack were frequently not restored for some time because of the difficulties which operating men had in finding correct phase relationships at a fault which, in the interest of all concerned, should be restored quickly. The communication interests and the operators of the British Grid, in each case publicly owned, soon found that the service continuity of each group might be improved by a liberal elimination of power transpositions. This was done. However, insofar as the writer knows it was found advisable for the communication interest to ask for the restoration of a comparatively small number of transpositions in the various high voltage systems of that country. This, we understand was done and it is evident that close co-operation can be arranged thereby improving the service of two types of utilities.

There is another general statement in this connection that should be recognized by all engineers concerned. It is almost axiomatic that if all internal noises, inconvenience and interference of a communication system are cleared up to a point where the services are commercially operative, then there is little left by way of transpositions in controlling emanations from extraneous sources such as power transmission lines with the possible exception of those close parallels where there are both physical and inductive hazards.

This paper has two authors, associated in one case with a technical institute and secondly with a large electrical utility. It is observed that it is a habit of Professor Gross when appearing before the technical sessions of the AIEE to associate some student or interested operating engineer with his writing. This practice is commended.

Discussing briefly the relative merits of the so-called "rolling" and the "dead-ending" types of transpositions the practice of one fairly large utility over 40 years has been to use first the rolling transpositions. They soon found troubles accumulating with this type of transposition largely used at lower voltages. After about ten years, a change was made because of these experiences to dead-ending. Presently the troubles associated with rolling transposition were forgotten because of their elimination and because of the incidence of faults at dead-ending transpositions which became unbearable to the point where there was a distinct movement back to rolling transpositions. This trend is now observable as a 20-year cycle to a point as in the United Kingdom and Europe where all interested parties are agreeing as stated by Professor Gross that transpositions be kept to a minimum.

A. W. Adams (Bonneville Power Administration, Portland, Oreg.): The authors of this paper are to be complimented on a thorough study of this problem, which is of great interest to power utilities.

The Bonneville Power Administration has recently been giving very careful study to the question of whether or not line transpositions should continue to be used and we appreciate very much the information in this paper. Our study of the unbalances agrees in general with the results reported by Messrs. Gross and Weston. The practice of the Bonneville Power Administration system is to make the transposition at a single tower by means of jumpers. If the tower where the transposition is to be made is a dead-end tower, the additional cost for the transposition is nominal. However, if it is necessary to use a special tower where otherwise a light type of tangent tower would be suitable, the cost of the transposition is increased by a ratio of 5 or 6 to one. We are considering allowing leeway in the location of the transpositions so that very few special towers will be necessary. This leeway will be about 15 per cent of the line length and transpositions will be eliminated entirely from lines under 40 miles in length.

It appears that the unbalance shown in the paper for vertical configurations of conductors (A) and (B) in Fig. 6 would be satisfactory. Transpositions on vertical configurations of these two types could be limited to reversing the position of only two of the conductors, as indicated in the paper.

The authors mention that the circulating ground current will cause additional losses. Our calculations indicate that the additional losses in the conductors due to the unbalanced currents are enough to influence the design. For example, the additional losses on a 100-mile 230-kv line using "Pheasant" type conductor and a loading of 600 amperes are 19 kw. The cost of transposing the line, if no special structures are required, is approximately half the capitalized value of these additional losses.

W. A. Morgan (United States Bureau of Reclamation, Denver, Colo.): Investigations by the Bureau of Reclamation were made as to why a transposition barrel is required at all, and there were three reasons found: (1) telephone line interference in paralleling telephone circuits; (2) unbalanced voltages; and, (3) continuous residual current flow in the circuit.

After a thorough check with telephone engineers, it was found that transpositions are of value for reason number one only where a close parallel of many miles is involved. In most cases, parallels with telephone circuits are only a few miles long. The main concern of telephone engineers is the high residual current that flows when a fault to ground occurs on the transmission line, and this causes an induced voltage in the paralleling telephone circuit whether or not the power transmission line is transposed because the zero sequence current flows equally in all three phases. Therefore, telephone interference was eliminated as a reason for requiring transpositions in nearly all of the Bureau's transmission lines.

Reason number two, unbalance of the 3-phase voltages, was not considered serious in view of the equalizing effect of the 3-phase transformer banks and synchronous machinery at various points on the system.

That left reason number three, continuous residual current flow, as the main item whose magnitude we must study so that relay pickup setting could be determined to prevent the possibility of causing undesirable tripping of ground current relays as pointed out in the paper. We did not investigate the importance of system losses due to residual current flow. On many of the Bureau's long transmission lines it is necessary to set these ground relays on their most sensitive setting of 0.5 ampere, in order to protect for remote faults for minimum conditions of generation connected.

Then, there arose the problem of how to calculate the value of this residual current in an untransposed transmission line. A review showed that the text books used in college courses all assume a balanced, fully transposed line for the basic assumptions in deriving the equations. A more advanced book gave a partial solution, but did not consider both electrostatic and electromagnetic effects simultaneously. A solution for simultaneous equations which we derived in using this advanced book was not obtainable.

Tennessee Valley Authority had reported no difficulty on their system with no transpositions. However, TVA's system is made up of shorter line sections and lower voltages than the 230-kv grids the Bureau is building in California, Arizona, and in the Missouri River Basin. Therefore, we were unwilling to make a major change in design practice without knowing the magnitude of these residual currents that would flow with untransposed transmission lines.

Thus, when Dr. Gross came to us in July 1950 for work during the summer vacation period at his college, the question of "what is that maximum length transposition barrel we can use from a technical standpoint" was put up to him as one of the special problems we wanted his assistance on while we took care of the heavy backlog of routine design problems. Dr. Gross came up with a solution and, considering probable relay settings, current transformer ratios, working margin, and other factors, he recommended 200 miles as the maximum length of untransposed transmission line.

After study the Bureau of Reclamation has adopted the practice of 125–150 miles as the maximum length line without transpositions until field measurements may be

Vol. 7
1951

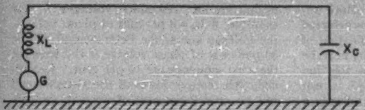

Figure 1

made of the amount of residual current. This practice is being followed in the 230-kv and 115-kv transmission lines consisting of many hundreds of miles of circuit now being built in the Missouri River Basin system for transmission of power from Garrison and Fort Randall power plants in North and South Dakota.

The procedure we follow is equivalent to transposing at the main switching points. We lay out the network approximately geographically with the mileages on the various line sections. Then we designate the phasing of the various line sections as *ABC*, *BCA*, and *CAB*, with no untransposed section more than about 125–150 miles long, and try to equalize the system so that the total amount of each of the three configurations is about equal. Also, we check to see whether the resulting unbalance at any breaker or switching point is within the limit of 125–150 miles when one or more are out of service. As soon as some of this system is completed we plan to make accurate measurements of the residual currents on these untransposed lines and will report to the Institute if it appears worthwhile. This may have a bearing on the desirability from a practical standpoint of elevating the middle conductor of a horizontal configuration transmission line purely from the standpoint of reducing residual currents, as brought out in the paper.

Again, I want to congratulate the authors on a fine paper. It is possible that combined efforts on this problem may see the relegation of transposition tower to the status of a curiosity of the past.

R. F. Lawrence and **D. J. Povejsil** (Westinghouse Electric Corporation, E. Pittsburgh, Pa.): The authors are to be congratulated on their exposition of some of the important characteristics of untransposed transmission lines. The experience of the discussors has revealed considerable current interest in the subject of transpositions which make additions to the scant literature on this topic very welcome.

In this paper, the authors have discussed the communication interference problem which might be caused by eliminating transpositions. Actually, noise problems are seldom caused by fundamental frequency residual currents. Rather, they are caused by harmonic currents and transposition affects only the induction problem associated with the nontriple series of harmonics. This, of course, results from the fact that, by definition, the residual or zero-sequence components in the several conductors are of identical magnitude and phase and, therefore, their resultant electric and magnetic fields are not affected by power circuit transpositions. Fundamental frequency currents are more important from the standpoint of induced voltages on communication circuits. However, this type of low frequency co-ordination generally is determined by residual currents, under faulted conditions, since these residual currents are much larger than those caused by electrostatic or electromagnetic unbalance.

However, residual currents due to the elimination of transpositions might be important from other reasons. Among these is the possible misoperation of sensitive ground relays. In this respect, an accurate method of calculating residual currents is very desirable.

The authors have confined their study to an analysis of the effects of electrostatic unbalance of untransposed lines. It is stated that electromagnetic effects are secondary since they are negligible at light load. However, many long lines are operated at heavy loadings for extended periods of time and our knowledge indicates that the residual currents caused by electromagnetic unbalance at these loadings are comparable to those caused by the electrostatic effects. Therefore, it would appear that a complete analysis must, of necessity, include both electromagnetic and electrostatic effects especially for the shorter line lengths. Since such an analysis is extremely complicated, we would appreciate any comments which the authors might have on these points.

We are in accord with the authors' conclusion that in many cases it is impractical to manipulate line configuration to reduce residual current flow in an untransposed line. However, the authors have shown several common configurations which yield relatively low residual current due to electrostatic unbalance. The question naturally arises as to whether such configurations also reduce the electromagnetic unbalance which exists under loaded conditions.

One obvious application of the information contained in this paper is found in the calculation of the zero-sequence currents which would flow in an untransposed transmission line which is operated as part of a resonant grounded system. As shown in Figure 1 of this discussion, the zero-sequence voltage which is generated by the capacitive unbalance is in series with the series resonant combination of the zero-sequence capacitance and the Petersen coil. The result of this connection is that a relatively small zero-sequence voltage is capable of producing a high voltage across the Petersen coil with the result that the system neutral is displaced and abnormal heating takes place in the Petersen coil.

REFERENCES

1. ELECTRICAL TRANSMISSION AND DISTRIBUTION REFERENCE BOOK. Westinghouse Electric Corporation, East Pittsburgh, Pa., fourth edition, 1950.

2. THE ELECTROSTATIC UNBALANCE OF TRANSMISSION LINES AND ITS EFFECT ON THE APPLICATION OF PETERSEN COILS, J. A. M. Lyon. *Electrical Engineering (AIEE Transactions)*, volume 58, March, 1939, pages 107–112.

Eric T. B. Gross: It is gratifying that this paper seems to be of interest to many operating engineers, and there appears to be general agreement as to the validity of our conclusions.

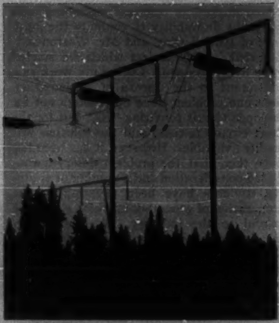

Figure 2. Transposition of Swedish 230-kv single-circuit double-conductor line. (Courtesy Swedish State Power Board)

I am certain that we all are familiar with the transposition structures generally used in this country. However, a different and unique type of transposition, widely used in Sweden for about 30 years, is shown in Figure 2 of this discussion. The circuit is one of the recently built 230-kv lines with double conductors (buendle conductors). It appears that such arrangement is particularly well suited for transpositions at dead-end structures and near switchyards.

The experiences of Messrs. Rawls and Woodruff are of particular interest since they refer to large high-voltage systems. Mr. Davison's kind remarks are greatly appreciated. The practice in the United Kingdom on their 132-kv grid, referred to by Mr. Davison, has its equivalent in this country where all lines in the systems of one very large company, operating thousands of miles of sections at voltages of 132 kv and below, have been designed and built for many years without transpositions; however, transpositions are later added if the operation indicates that inductive co-ordination makes them desirable. It must be added that the number of such transpositions has been remarkably small.

Mr. Adams is quite correct in stating that the losses due to unbalanced currents are increased if transpositions are made at longer intervals, but the saving is really a differential and may be compared with the variations in copper losses because of small changes in temperature. As pointed out in the text and emphasized by Messrs. Davison and Rawls, the advantages brought about by the elimination of transposition structures are manifold and it is felt that our recommendations are in line with the over-all balance of all factors which should be considered.

Mr. Morgan adds most welcome comments relative to the general problem. The study of this problem was undertaken many years ago in connection with a question concerning resonant neutral grounding of power systems in which the voltage between system neutral and ground is of importance. Very satisfactory over-all balance to ground can be achieved by appropriate transpositions in switchyards,[1] in spite of unbalances (E_0) on each of the line sections as such. Renewed interest in resonant grounding indicated the desirability to evaluate the influence of ground wires and Mr. Weston participated in this project which we started some five years ago. During my work as a consultant to the Bureau of Reclamation, the same problem came up (though not for the open circuit condition "E_0," but for the short circuit I_s-case) and the solution was readily available. However, it has been felt since then that the problem deserves continued consideration and a number of graduate students have been assisting in the preparation of general data which should be helpful to the industry. We have been using various means to find the ground displacement d_0. Different methods can be used to derive expressions for d_0, analytical methods using either the C_{ik} (as in the example of the Appendix) or the potential coefficients P_{ik}, but we have also used our a-c network calculator to solve the equations.

The network analyzer has been helpful for circuits without symmetries, since the solution of a large number of equations becomes otherwise very lengthy and laborious.

Messrs. Lawrence and Povejsil point out that both electric and magnetic unbalances deserve consideration and their comments are in line with our own thinking. Both unbalances are included in our studies referred to, and we hope that some simplification of the extremely complicated analysis may be forthcoming. It is known that the solution which is best electromagnetically[2] is not necessarily best electrostatically and only a compromise solution will give optimum results. As for their reference to the production of "high voltages across the Petersen coil" in resonant grounded systems, a few clarifying remarks may be in order:

1. The unbalance E_0 of any and each line section must not be mixed up with the unbalance of the whole system. Transpositions in stations do as well in resonant grounded systems as in any other system, and most systems do not[3] require new transpositions when resonant grounding is introduced.

2. The circuit drawn by Messrs. Lawrence and Povejsil is incomplete since the losses in X_L and X_G have been neglected, which is not permissible when tuned conditions are considered. Furthermore, a properly designed Petersen coil will saturate at or near phase voltage and thereby introduce self-detuning of the circuit. High voltages will then never be produced. The inclusion of the important effects of the losses leads to Jonas' equation[4] which enables easy evaluation of "resonance voltages."[5] For example, if $E_0 = 3$ per cent of phase voltage, the voltage across the Petersen coil will be 30 per cent of phase voltage if the losses in the zero sequence are 10 per cent. Accordingly, the copper losses of the Petersen coil will be only 9 per cent of normal, and the total losses still smaller.

We wish to thank all discussers for their valuable and most interesting contributions.

REFERENCES

1. *Discussion* by **Eric T. B. Gross** of REPORT ON SURVEY OF UNBALANCED CHARGING CURRENTS, **AIEE Committee Report.** *AIEE Transactions,* volume 68, part 2, 1949, pages 1328–30. (See also reference 6 of the paper.)

2. REDUCING INDUCTANCE ON ADJACENT TRANSMISSION CIRCUITS, **H. B. Dwight.** *Electrical World* (New York, N. Y.), volume 83, 1924, page 89–90.

3. APPLICATION OF RESONANT GROUNDING IN POWER SYSTEMS IN THE UNITED STATES, **Eric T. B. Gross, E. W. Atherton.** *AIEE Transactions,* volume 70, 1951, pages 389–96.

4. PROTECTION OF HIGH VOLTAGE SYSTEMS WHICH ARE ELECTROSTATICALLY UNBALANCED WITH RESPECT TO GROUND, **J. Jonas.** *Elektrotechnik und Maschinenbau* (Vienna, Austria), volume 38, 1920, pages 453–60.

5. PRACTICAL EXPERIENCE WITH RESONANT GROUNDING IN A LARGE 34, 5-KV SYSTEM, **H. H. Brown, Eric T. B. Gross.** *AIEE Transactions,* volume 69, part 2, 1950, Appendix Fig. 16 and equation (19), pages 1400–05.

Overvoltages in Saturable Series Devices

A. BOYAJIAN
FELLOW AIEE

G. CAMILLI
FELLOW AIEE

SATURATION leads to high current peaks in shunt devices and to high voltage peaks in series devices. Of particular importance among the latter are current transformers. They are generally designed with magnetizing currents less than 1 per cent of their rated full load currents; and if their secondaries become accidentally open circuited the entire current becomes magnetizing current, causing high saturation and peaked voltages in them. Another case is the sensitive high-impedance relay coils in the current-transformer secondaries of differential-protection systems. Normally no current flows in these relays, but in case of a fault within the protected apparatus a current of saturating magnitude may be forced through them.

Saturation is frequently thought of as limiting the voltage drop across a reactor, but this is true primarily of the effective value of the voltage. A substantial reduction in the crest voltage also takes place, but not as much as in the effective value and not enough to remove all concern over the matter, inasmuch as the peak voltage need not be as high as 100 times normal to require attention. Ten times normal voltage also may be serious.

It is desirable therefore to predict these voltages when the circuit constants are known, and to be able to determine them experimentally with reasonable convenience and without endangering the apparatus.

Accordingly, a theoretical analysis is made in subsequent paragraphs, providing both a formula and an insight into the physics of the phenomena, and then a convenient and safe test method is described.

Analysis

The solution of engineering problems generally requires both physics and mathematics. Adequate use of physical analysis generally provides better insight into the phenomena and greatly reduces the mathematical burden. Although our present problem involves recurrent transient phenomena in a nonlinear system, physical analysis shows them to be of the simplest kind with a well-known solution, obviating resort to differential equations or the like. The mathematical burden will be primarily simplifying clumsy expressions by appropriate approximations.

The strategy underlying the attack on the problem will be that outlined in detail in an earlier article,[1] the essentials of which are as follows.

Ordinary circuit theory can be applied to a nonlinear circuit in two steps when the characteristic curve of the circuit can be approximated with two straight lines. Considering the well-known hysteresis loop of an iron-core reactor, Figure 1, the rising or falling unsaturated zone can be represented by a straight line; and the upper or lower saturated zone, by another straight line.

In a nonlinear device two kinds of impedances are distinguished: (1) the ordinary one, based on the rms current and voltage drop in the device, and (2) the incremental one, based on the slope of the curve. In the unsaturated zone, these two values are roughly equal; but in the saturated zone, the incremental reactance is much lower than the ordinary reactance for flux densities alternating between the plus and minus saturation values. Capital X will be used for the unsaturated and x for the saturated incremental reactance.

Following the arrow along the lower portion of the hysteresis loop, the reactance will be the low value x until the critical current i_k' is reached. Past i_k', the reactance will change to the high value (X) and will remain so until the second critical current i_k is reached. Past this current, the reactance drops back to x. The rest of the loop repeats a similar process. The critical current i_k' is so close to zero that, for simplicity, it may be assumed as zero, within the accuracy of many other complexities and uncertainties of saturation phenomena.

The a-c hysteresis loop differs from the

Nomenclature

i_k = instantaneous value of current at which the core saturates on a rising current, Figure 1
i_k' = instantaneous value of current at which the core de-saturates on a falling current, Figure 1
I_m = crest value of line current, Figure 3
i = instantaneous current in the branch indicated by subscript
X = unsaturated magnetizing reactance of winding, exclusive of eddy currents, Figure 2(A)
x = saturated incremental reactance exclusive of eddy currents, Figure 2(B)
Z = complex value of the impedance of R, r, and X in series with each other, Figure 2(A)
Z_s = absolute value of Z
$R' = R + r$, Figure 2(A)
R = equivalent shunt resistance representing the eddy current loss
r = equivalent series resistance representing the hysteresis loss, Figure 2(A)
θ = time in radians, 2π feet
ϕ = angle between the line current and the true magnetizing component of the current (that is, exclusive of the eddies)

Paper 51-340, recommended by the AIEE Basic Sciences and Transformers Committees and approved by the AIEE Technical Program Committee for presentation at the AIEE Fall General Meeting, Cleveland, Ohio, October 22–26, 1951. Manuscript submitted June 19, 1951; made available for printing September 17, 1951.

A. BOYAJIAN and G. CAMILLI are with the General Electric Company, Pittsfield, Mass.

The authors are indebted for the experimental work to Walter Piazza and J. A. Edward. Mr. Piazza started the experimental work at Pittsfield and continued it at Massachusetts Institute of Technology for a master's thesis. Mr. Edward continued the work to conclusion.

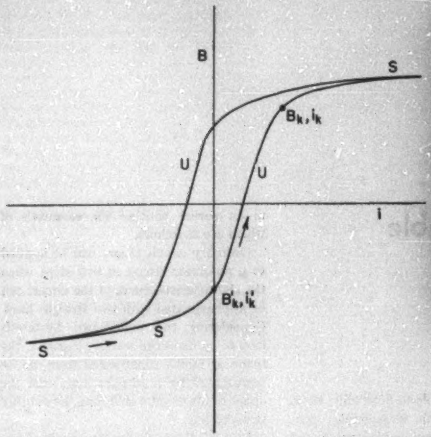

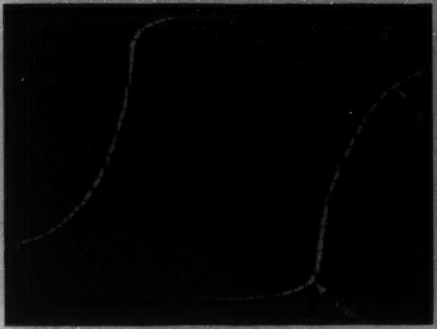

Figure 1(A) (left). Hysteresis loop of an iron core reactor. (U) Unsaturated zone. (S) Saturated zone

Figure 1(B) (above). Hysteresis loop of an iron core reactor operating at very high flux density. Loop enlarged in the (H) axis. Critical currents i_k and i_k of Figure 3 are shown in the oscillogram

d-c loop because of induced eddy currents. The eddy current paths constitute a concealed secondary circuit around the core and are therefore a shunt load on the reactive device as a transformer. So, a current transformer with open-circuited secondary does still have a closed high-resistance secondary in its eddy current paths. The equivalent circuit of the reactive device for our purposes will then be those shown in Figure 2.

Figure 2(A) represents the unsaturated condition, and 2(B) the saturated condition, r representing the effective resistance of the hysteresis loss, and R that of the eddy current loss. The conductor resistance r', Figure 2(B), is left out of Figure 2(A) because it is very small compared with the other resistances shown.

The relative magnitudes of these impedances may be visualized by the indicated values taken from a commercial current transformer. They will be helpful in making approximations to simplify long expressions. The ratio of r to X is the ratio of the hysteresis watts to the wattless magnetizing volt-amperes (exclusive of the eddy currents) in the unsaturated zone. This may mean a fraction between 0.5 and 1.0. The ratio of X to R is the ratio of the wattless magnetizing volt-amperes to the eddy loss watts. For the 14-mil steels this ratio may be 0.5–0.2. Then R may be two to ten times r. The ratio of the conductor resistance r' to r may be less than 2 per cent.

The hysteresis-loss constant (r) is assigned to the unsaturated zone, Figure 2(A), because Figure 1 shows that moving to the right beyond i_k and coming back to it does not enclose an appreciable hysteresis loss area. This conclusion follows also from the consideration that the hysteresis loss has to be in the iron, not in space, and as the flux in the iron itself does not change a great deal in the saturated zone, no considerable hysteresis loss need be expected there.

During most of the cycle the device will be saturated and Figure 2(B) will apply; practically all of the current will be flowing through x with negligible voltage drop. As the current approaches zero, dipping below i_k', Figure 1(C) the device will desaturate, Figure 2(B) changing to Figure 2(A) and the line current will be diverted to the eddy current path R until the i_k' trapped in X dies out and the saturating current i_k is built up in it. As the circuit saturates past this point and its voltage drop becomes negligible, the maximum voltage drop will be the resistance drop in R at the instant that i_k is reached in X.

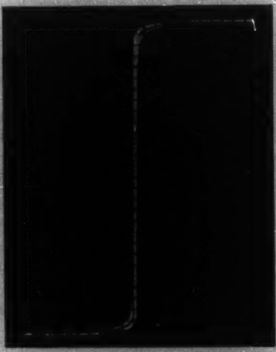

Figure 1(C). Actual hysteresis loop of an iron core reactor operating at very high flux density

As is shown in Appendix I, after various approximations this voltage is estimated to be:

$$e_R = Ri_R \approx 1.4\sqrt{I_m E_k R} \tag{14}$$

as larger loops generally have steeper unsaturated zones and therefore higher values of X. This formula may underestimate the voltage 10–20 per cent.

A more rigorous formula is given in Appendix II.

Application to Relay Coils

A current transformer with a relay coil across its secondary may be considered as having the relay impedance in parallel with R in Figure 2(A). As relay coils are saturable as well as current transformers, the application of the foregoing analysis to such a system requires that we consider in what sequence they may saturate.

RELAY SATURATES FIRST

If the relay coil tends to saturate first, Figure 2(A) applies to the relay coil itself directly in its unsaturated condition, and maximum voltage associated with this unsaturated condition of the relay coil may be calculated by equation 14 in which I_m now is the maximum value of

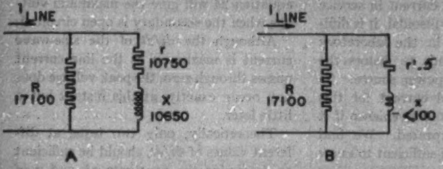

Figure 2(A). Equivalent circuit of the reactor, unsaturated conditions, where R = equivalent shunt resistance due to eddy loss, r = equivalent series resistance due to hysteresis loss, X = unsaturated magnetizing reactance of winding

(B) Equivalent circuit of the reactor, saturated conditions, where x = saturated incremental reactance of winding

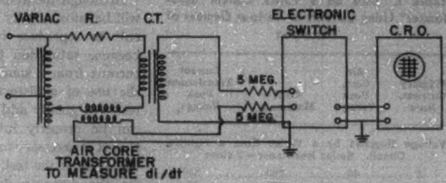

Figure 4. Schematic diagram for obtaining simultaneous values of current-transformer and air-core transformer secondary voltages

the secondary current of the transformer unsaturated, E_k is the relay coil voltage (crest) at the knee of its saturation curve, and R the effective shunt resistance of the eddy currents in the magnetic circuit of the relay coil. The winding resistance can be added to r in Figure 2(A).

After the Relay Saturates

After the relay core saturates, the voltage will drop off very rapidly. The question may arise whether a large RI voltage drop can later be built up across the relay coil as the line current rises to its maximum. This is verified easily by multiplying the effective resistance of the relay coil with I_m. If this is dangerously high, then we have to determine whether the current transformer will saturate before this voltage is reached. If it will, then the maximum voltage will be that point of the RI wave at which the current transformer saturates.

Current Transformer Saturates First

In this case the unsaturated voltage wave of the relay coil will apply up to the instant when the current transformer saturates, and therefore the instantaneous value of the relay coil voltage at the instant when the current transformer saturates will be the maximum voltage we are looking for.

Experimental Checks on Formulas

Check on the Approximate Formula 14

Data obtained on the current transformer of Figure 5 were as follows:

The voltage corresponding to the flux density at the knee of the excitation curve was 450 volts rms (645 volts peak) across the 5-ampere winding, hence,

$E_k = 645$
Rated $I_m = 5\times 1.41 = 7.05$ ampere crest

By means of a "separation" test, the eddy loss at 270 volts rms (nonsaturating voltage) was found to be 4.28 watts, the hysteresis loss 3.4 watts, the reactive volt-amperes 3.38 all at a line current of 0.031 ampere rms. Hence,

$$R = \frac{270^2}{4.28} = 17{,}100 \text{ ohms}$$

Putting these constants in formula 14,

$$e_R = 1.4(645\times 7.05\times 17{,}100)^{1/2}$$
$$= 12{,}300 \text{ volts}$$

The tested value from Figure 5 was about 14,000 volts.

Check on the More Exact Formulas 20-23

The complete circuit parameters required by the more exact method are those shown in Figure 2. Because some of these data are variable and uncertain and difficult to determine, how these particular ones were determined will be indicated here in detail.

The following quantities were measured and calculated for Figure 2(A) the unsaturated condition of the circuit:

$E = 270$ volts, 60 cycles
Exciting current rms $= 0.031$
Total watts $= 7.68$
Hysteresis loss $= 3.4$
Reactive volt-amperes $= 3.38$

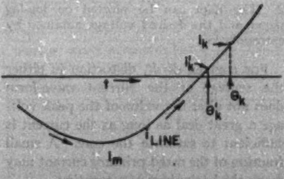

Figure 3. Tracing of line current: i_k corresponds to the value at which the core desaturates on a falling current and i_k at which core saturates on a rising current

Eddy loss $= 4.28$
$(v\text{-}a)_{rX} = (3.4^2 + 3.38^2)^{1/2} = 4.8$
$i_{rX} = 4.8/270 = 0.0178$
$r = 3.4/0.0178^2 = 10{,}750$
$R = 270^2/4.28 = 17{,}100$
$R' = r + R = 27{,}850$
$X = 3.38/0.0178^2 = 10{,}650$
$Z = r + R + jX = 27{,}850 + j10{,}650$
$Z_0 = (27{,}850^2 + 10{,}650^2)^{1/2} = 30{,}000$
$\phi = \tan^{-1}(X/R') = \tan^{-1}(10{,}650/27{,}850)$
$= 0.383$ radian
$R'/X = 27{,}850/10{,}650 = 2.61$
$R/Z_0 = 0.57$

From the oscillograms, Figure 1(B) and (C),

$i_k' = I_m \sin\theta_k'$
$= 0.0195$

therefore

$\theta_k' = 0.00276$ radian
$i_k = E_k/X = 645/10{,}650 = 0.06$

The determination of i_k may need some comments.

In the magnified loop Figure 1(B), the point i_k' is reasonably definite, and the value of the incremental x in the preceding zone clearly low enough to be negligible. In the approximate formula, the product i_kX was replaced by E_k as a single number because E_k could be obtained with considerable accuracy and ease, but the more exact formula calls for i_k and X separately and these are difficult to obtain separately. Having obtained X above in the manner indicated, however, the value of i_k was then determined to make their product check E_k.

We determine θ_k, corresponding to i_k, by plotting a curve of various values of i_k against assumed values of θ_k, and interpolating the θ for the pertinent value of i_k.

With this done, the θ_k for $i_k = 0.06$ was found to be about 0.12 radian. Then,

$i_{\text{line}} = 7.05\times\sin 0.12 = 0.845$
$i_R = 0.845 - 0.06 = 0.78$
$e_R = Ri_R = 17{,}100\times 0.78 = 13{,}300$
Measured value 14,000

It must not be inferred, however, that results as good as this can always be depended on.

Table I. Data on a 15-Kv Current Transformer* Using Currents of Various Degrees of Distortion

Primary Current, Rms	Air Core, Peak Voltage	di/dt Maximum	Current Transformer Peak Voltage
Voltage Supplied by a Variac from a Lighting Circuit. Series Resistance = 7 ohms			
3	60	760	330
4	65	820	365
5	75	950	520
6	100	1,260	660
7	145	1,830	780
8	190	2,400	950
9	265	3,350	1,040
10	305	3,850	1,140
11	350	4,430	1,240
12	390	4,930	1,340
13	440	5,560	1,440
14	480	6,070	1,500
15	520	6,580	1,550
Voltage Supplied Directly by a Generator. Series Resistance = 7 Ohms			
15	360	4,550	1,440
17.5	450	5,700	1,620
20	570	7,200	1,810
22	680	8,600	1,900
25	775	9,800	2,030
30	960	12,100	2,280
Voltage Supplied by a Variac from a Lighting Circuit. Series Resistance = 11 Ohms			
3	60	760	226
4	80	1,010	364
5	90	1,140	540
6	110	1,390	720
7	160	2,020	920
8	190	2,400	1,000
9	246	3,100	1,020
10	300	3,800	1,150
11	360	4,550	1,250
12	410	5,200	1,350
Voltage Supplied by a Variac from a Lighting Circuit. Series Resistance = 22 Ohms			
2	45	570	80
3	60	760	210
4	75	950	360
5	100	1,260	560
6	128	1,620	770
7	165	2,080	870
8	210	2,650	900
9	250	3,160	950
Voltage Supplied by a Variac from a Lighting Circuit. Series Resistance = 44 Ohms			
2	45	570	96
3	63	800	225
4	85	1,070	380
5	100	1,260	560
(The following data were obtained using a very large generator. In this case the di/dt values were not measured directly and the estimated values are not reliable)			
210		112,000	7,500
357		191,000	9,800
667		356,000	13,250
858		458,000	14,750
1575		842,000	19,750

*General Electric Type KF-305.

A Convenient and Nondestructive Test Method to Determine the Peak Voltages

Direct measurement of the peak voltage actually induced by the full load current in an open-circuited current transformer is in general difficult and expensive, and may also be dangerous. So a convenient and nondestructive equivalent test method is highly desirable.

Although the actual current in service will be substantially sinusoidal, it is difficult to reproduce it in the laboratory because saturation tends to distort the current from a small power source. So the use of a distorted current for this test will greatly add to convenience if it can be properly interpreted. We find that it is necessary and sufficient to know the *di/dt* of the test current, so a means for the accurate determination of the *di/dt* of the current makes distorted currents and reduced values of *di/dt* serviceable for this purpose.

Experiments confirm the mathematical result that under open-circuit conditions when the primary current is ample to saturate the core, the peak voltage e_m is related to the maximum *di/dt* of the primary current in the following manner,

$$e_m = aL(di/dt)^n \qquad (24)$$

and is relatively independent of the magnitude and shape of the primary current during the remaining portion of the cycle. In this equation a, L, and n are constants for a given transformer. The proposed test method then consists of determining these constants by measuring e_m and *di/dt* at conveniently obtained values of primary current, and then calculating the value of e_m for the *di/dt* expected at the rated loading, Figure 4.

To measure the *di/dt* of the test current, an air-core transformer is connected in series with the current transformer under test. The voltage across this air-core transformer is a measure of the *di/dt*. This voltage and that across the current transformer under test are measured simultaneously, either by a dual-beam cathode-ray oscilloscope, or, a single-beam oscilloscope in conjunction with an electronic switch.

Measurements are made at different supply voltages, and the results are used in either one of the following methods:

1. By direct substitution in equation 24, the constants aL and n can be evaluated, and the expected voltage for any other value of *di/dt* calculated.
2. The data can be plotted on log-log paper and the desired voltage obtained by extrapolation.

For a given *di/dt*, distortion in either the voltage or the current wave-form does not alter the value of the peak voltage a great deal as long as the current is sufficient to saturate the core. A small fraction of the rated primary current may mark the beginnings of saturation.

Substitution of the maximum value of the *di/dt* of the expected sine-wave current, that is, substitution of $2\pi f I_m$ in equation 24 will give the maximum voltage when the secondary is open circuited.

Although the *di/dt* of the sine-wave current is maximum as the line current passes through zero, the peak voltage does not occur exactly at this instant but a little later.

Theoretically, only two tests, at different values of *di/dt*, should be sufficient to determine the constants aL and n of equation 24. But as this method is an empirical approximation, more reliable results will be achieved if the two values of *di/dt* are considerably different from each other, and one of them is as large as can be had conveniently. Subsequent data also will show the wisdom of taking more than two readings.

Data

Complete readings taken on one of the current transformers tested is given in Table I and plotted in Figure 5 on log-log paper. Similar plots for two other transformers are shown in Figures 6 and 7.

Figure 5 covers a *di/dt* range of 1,000:1, and Figure 6, 100:1. The close alignment of the various points along a straight line over such a wide range was unexpectedly good for an approximation method. The deviation of the few points at the lower ends of these curves is explained as due to the insufficiency of the currents to saturate the core. The alignment of the data along a straight line is not quite as good in Figure 7 as in Figures 5 and 6, and it suggests the wisdom of taking one or more readings at as high values of *di/dt* as convenient. The width of the band that includes all the data in these plots shows that more than two readings should be taken, at as wide a range of *di/dt* as convenient.

Of course, in all cases, the *di/dt* should be determined by measurement, and not taken for granted, as if the current were sine wave without a good basis for such belief.

The values of n for these transformers were found to be 0.546 in Figure 5, 0.715 in Figure 6, and 0.52 + in Figure 7. In the last case, n would have been greater than 0.52 if the graph had been drawn to include the upper block of four points.

According to the approximate theoretical analysis given above, n would have been 0.5, and the values observed on two of the transformers, namely, 0.546 and 0.52, could have been considered as pretty good checks on theory; but the third one, 0.715, may be a warning against banking altogether too much on an approximate formula in a saturable circuit. As these three series of tests were made by dif-

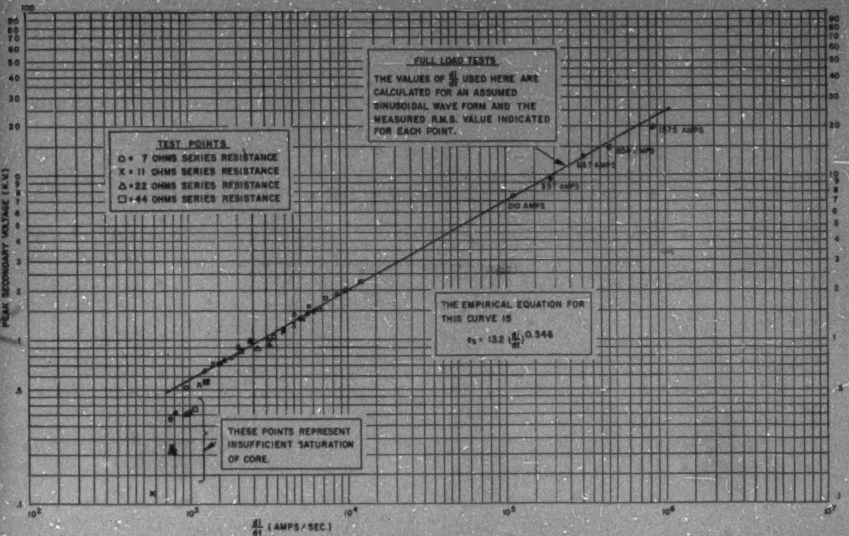

Figure 5. Relation between *di/dt* and peak secondary open circuit voltages. Results of tests made on a 15-kv current transformer using currents of various degrees of distortion

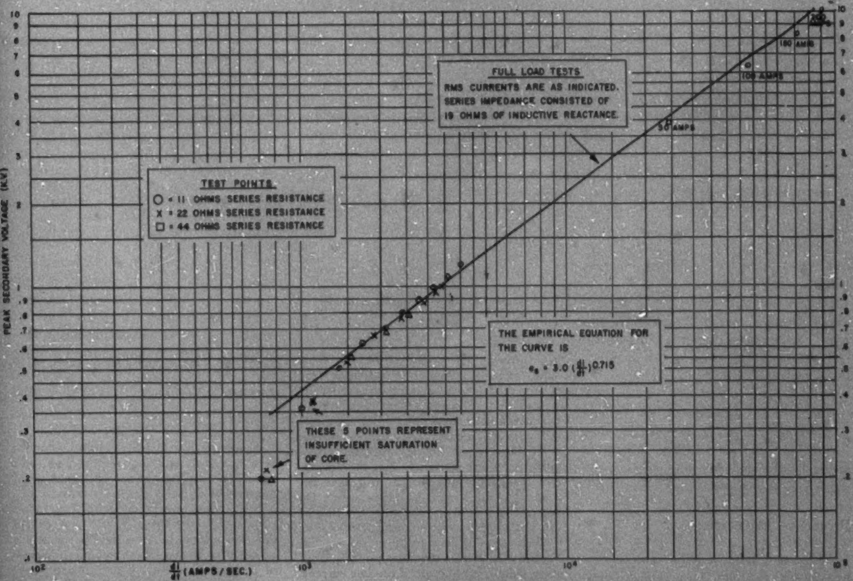

Figure 6. Relation between *di/dt* and peak secondary open circuit voltages. Results of tests made on 69-kv current transformer using currents of various degrees of distortion

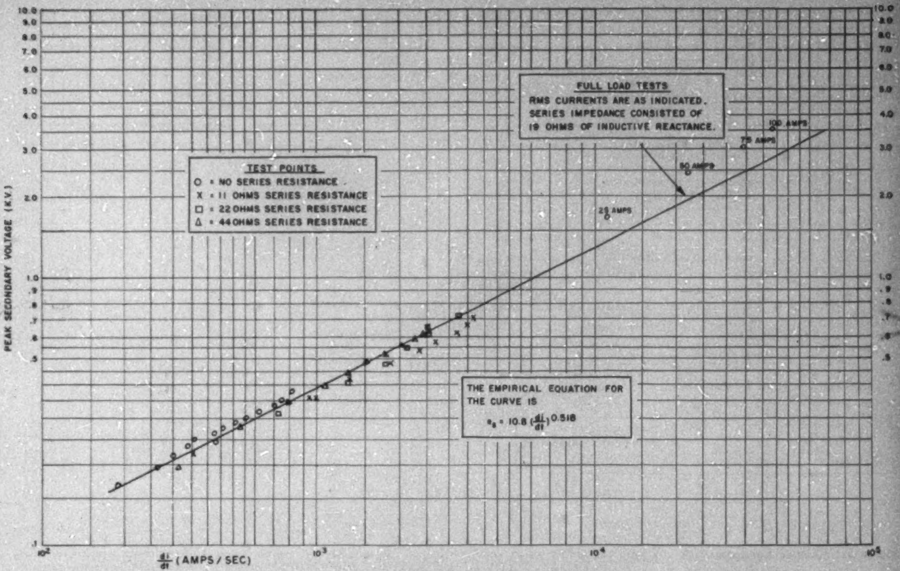

Figure 7. Relation between *di/dt* and peak secondary open circuit voltages. Results of tests made on a toroidal transformer

ferent individuals at different times and places, on three different transformers, it was not practicable for the present authors to undertake to repeat the tests to run down the source of the difference.

Obviously the foregoing test method is equally applicable to relay coils, either using equation 24 or plotting the data and extrapolating. According to C. R. Mason of the General Electric Company, the experimental value of n for a relay circuit was of the order of 0.5. The relay can be tested alone or in combination with its current transformer.

In cases where the relay coil saturates long before the current transformer, the relay may be tested by itself. If the relay coils and current transformer saturate about the same time, they must be tested together.

Two typical oscillograms of current, peak voltage and *di/dt* are reproduced in Figure 8(A) and 8(B). The *di/dt* corresponding to the peak voltage has to be taken from such a record.

Protective Measures

As the magnetizing inductance of ferromagnetic reactors is generally very high, even a high resistance shunt resistor is likely to lower the peak voltages. If the shunt resistor is of the constant-resistance type, the larger the protection it affords, the greater will be the impairment of the current transformer accuracy or the relay sensitivity. But the "Thyrite" type resistors, being highly variable with voltage, afford excellent protection under overvoltage conditions, with practically no reduction in the current transformer accuracy under normal conditions. These have been in successful use for a number of years.[3]

Appendix I. Approximate Solution

Assuming a line current with a crest value many times i_k, Figure 3, it follows that during most of the cycle the core will be saturated, and Figure 2(B) will apply to it. Let us trace the phenomena along the arrow in Figure 3. All along the negative portion of the line current shown, the circuit will be saturated until we reach time θ_k'—nearly zero—when the line current will have become i_k', which also is nearly zero. On account of the relatively long duration of this zone, we shall assume that, by the time θ_k' is reached, the current in the circuit, Figure 2(B) will be the appropriate steady-state value, and that all of the line current, assumed sinusoidal,

$$i_{\text{line}} = I_m \sin\theta \tag{1}$$

will be flowing through the inductive branch of Figure 2(B)

At the instant θ_k'

$$i_x = I_m \sin\theta_k' = i_k' \approx 0 \tag{2}$$

Just past this point, the circuit will change to Figure 2(A). As the actual current in X cannot change suddenly, it will be the same value now as at the moment before, that is, zero. But this is not the steady-state current of the new circuit for that instant.

Considering the current as complex numbers, the effective value of the steady-state current in X will be

$$I_X = I_{\text{line}} \frac{R}{R+r+jX} = I_{\text{line}}(R/Z) \tag{3}$$

The corresponding equation for the steady-state instantaneous currents will be

$$i_{X(\text{steady state})} = I_m(R/Z_0) \sin(\theta - \phi) \tag{4}$$

$$\phi = \tan^{-1}(X/R') \tag{5}$$

$$R' = R + r \tag{6}$$

As the actual current at this instant is zero, not as in equation 4, there must be a transient component of current equal to the negative of equation 4, so as to cancel it.

This transient component of the current circulates in the loop, R, r, X: it cannot flow in the lines because the line current is assumed to be fixed as a sine-wave current of a specified value. The transient component of the reactor current will then decay exponentially in the indicated loop based on its constants, and the complete equation of

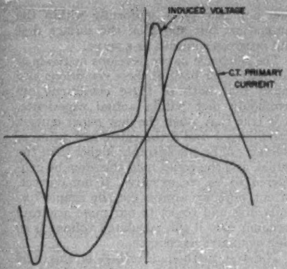

Figure 8(A) (left). Wave shapes of current and secondary induced voltage

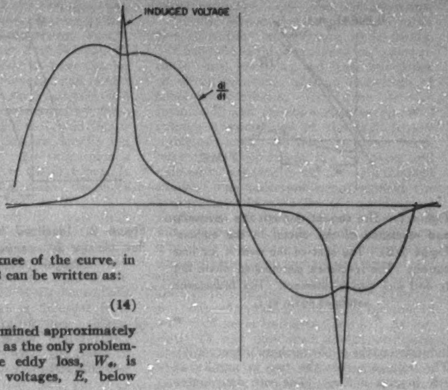

Figure 8(B) (right). Wave shapes of *di/dt* and induced voltage

this instantaneous current in X, from 0 to θ_k, will be

$$i_{X(\text{total})}=I_m(R/Z_0)[\sin(\theta-\phi)+\sin\theta\,\epsilon^{-(R'/X)\theta}] \quad (7)$$

This expression can be further simplified by expanding the terms in the brackets, and remembering that for small values of θ, $\sin\theta$ equals θ:

$$\sin(\theta-\phi)=\sin\phi(\sin\theta\cot\phi-1) \quad (7A)$$
$$=\sin\phi(\theta R'/X-1) \quad (7B)$$

and

$$\epsilon^{-(R'/X)\theta}\approx 1-(R'/X)\theta+(R'/X)^2\theta^2/2 \quad (8)$$

Substituting these in equation 6,

$$i_{X(\text{total})}=I_m(R/Z_0)\sin\phi[(\theta R'/X)-1+1-(R'/X)\theta+(R'/X)^2\theta^2/2]$$
$$=I_m(R/Z_0)\sin\phi(R'/X)^2\theta^2/2 \quad (9A)$$

Recognizing that $\sin\phi$ is X/Z_0, and R'/Z_0 is of the order of unity, equation 9A reduces to

$$i_{X(\text{total})}=I_mR\theta^2/2X \quad (9B)$$

At the time θ_k, $i_X=i_k$. Substituting this into equation 9B and solving for θ_k,

$$\theta_k\approx 1.4\sqrt{i_k(X/R)/I_m} \quad (10)$$

At this time, the line current is

$$i_{\text{line}}=I_m\sin\theta_k\approx I_m\theta_k\approx 1.4\sqrt{I_mi_kX/R} \quad (11)$$

The current in the shunt resistance R is,

$$i_R=i_{\text{line}}-i_k\approx i_{\text{line}} \quad (12)$$

Then, at time θ_k,

$$e_R=Ri_R\approx 1.4\sqrt{I_mi_kXR} \quad (13)$$

Since, after θ_k, X drops to a very low value, x which may be one per cent of X, we may recognize this change as practically short circuiting R. The maximum voltage that will appear across R (and hence across the terminals of the inductive device) will be the e_R at time θ_k, as defined in equation 13. This then is the peak voltage we are looking for.

In equation 13, i_k and X are somewhat problematic quantities, because the loop of Figure 1(A) is rather idealized, and the bend at i_k may not be as sharp as indicated and X not as constant as implied. However, the product of i_kX can be interpreted as the crest voltage E_k corresponding to a sinusoidal flux density having its maximum equal to that at the knee of the curve, in which case equation 13 can be written as:

$$e_R\approx 1.4\sqrt{I_mE_kR} \quad (14)$$

E_k could then be determined approximately by a-c tests, leaving R as the only problematic quantity. If the eddy loss, W_e, is determined at some voltages, E, below saturation,

$$R=E^2/W_e$$

But it is not always easy to separate the eddy losses from the hysteresis loss. The well-known separation tests, equation 5, made at different frequencies, may not be consistent.

Appendix II. Closer Approximation

When i_k' cannot be assumed zero, Figure 1(B), and r, R, and X do not lend themselves to much simplification, the equations take the following forms. Even though i_k' may not be zero, the voltage drop across x may still be considered negligible until i_k' is reached. The maximum voltage that builds up after that will depend on the line current at time θ_k when i_k is reached. So, as before, our major problem is to determine θ_k. Since

$$i_k'=I_m\sin\theta_k'\approx I_m\theta_k' \quad (15)$$

$$\theta_k'\approx i_k'/I_m \quad (16)$$

Past this instant, the steady-state component of current in X will be

$$i_{X(\text{steady state})}=I_m(R/Z_0)\sin(\theta-\phi) \quad (17)$$

The difference between this for θ_k' and the actual current i_k' is the transient component of i_X at time θ_k', decaying exponentially:

$$i_{X(\text{transient})}=\{i_k'-I_m(R/Z_0)\sin(\theta_k'-\phi)\}\times\epsilon^{-(R'/X)(\theta-\theta_k')} \quad (18)$$

The resultant current in X, during the interval θ_k' to θ_k, will accordingly be,

$$i_X=I_m(R/Z_0)[\sin(\theta-\phi)+\{(i_k'Z_0/I_mR)-\sin(\theta_k'-\phi)\}\epsilon^{-(R'/X)(\theta-\theta_k')}] \quad (19)$$

At time θ_k (to be determined), this current is i_k:

$$i_k=I_m(R/Z_0)[\sin(\theta_k-\phi)+\{(i_k'Z_0/I_mR)-\sin(\theta_k'-\phi)\}\epsilon^{-(R'/X)(\theta_k-\theta_k')}] \quad (20)$$

As θ_k is the only unknown in this equation, plotting i_k as the dependent variable for several assumed values of θ_k yields a curve with the help of which the θ_k corresponding to the pertinent i_k can be determined. Then, as before,

$$i_{\text{line}}=I_m\sin\theta_k\approx I_m\theta_k \quad (21)$$

$$i_R=i_{\text{line}}-i_k\approx I_m\theta_k \quad (22)$$

$$e_{R\,\max}\approx RI_m\theta_k \quad (23)$$

References

1. MATHEMATICAL ANALYSIS OF NONLINEAR CIRCUITS, A. Boyajian. *General Electric Review* (Schenectady, N. Y.), September and December 1931, pages 531–37 and 745–51.

2. OVERVOLTAGE PROTECTION OF CURRENT TRANSFORMER SECONDARIES, R. H. Kaufman, G. Camilli. *Electrical Engineering* (*AIEE Transactions*), volume 62, July 1943, pages 467–72.

3. PEAK VOLTAGES INDUCED BY ACCELERATED FLUX REVERSAL IN REACTOR CORES OPERATING ABOVE SATURATION DENSITY, Theodore Specht, E. C. Wentz. *Electrical Engineering* (*AIEE Transactions*), volume 65, May 1946, pages 254–62.

4. MAGNETIC CIRCUITS AND TRANSFORMERS (book), Staff, Massachusetts Institute of Technology. John Wiley and Sons, New York, N. Y., pages 151–54.

Discussion

E. C. Wentz and T. R. Specht (Westinghouse Electric Corporation, Sharon, Pa.): The authors of this paper seem to believe that the shape of the hysteresis loop has an important bearing on the magnitude of the peak voltage. The current i_R that flows in R in the authors' Figure 2(B) is usually much larger than the current i_X that flows in X at the instant the core saturates and under this condition the shape of the hysteresis loop has no effect on the crest voltage. Referring to Figure 1 of this discussion the line current is shown as a straight line as it goes through zero with an equation $i_{\text{line}}=I_m\sin\omega t\cong I_m\omega t$. This current divides between the resistance and

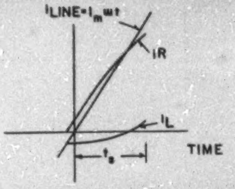

Figure 1. The current through the resistance and reactance of the circuit in the authors' Figure 2(B). The sum of the two is the line current. The reactance desaturates where the i_L and i_{line} curves intersect. The inductance saturates again at t_s

inductive paths of the authors' Figure 2(B). The voltage across the two in parallel at any instant is $R\,i_R$. The core desaturates where i_L intersects the i_{line} curve, and the two must, of course, be equal at that instant. Also then at this instant $i_R=0$ and the voltage is zero. As time progresses, i_R increases.

This voltage is applied to the inductance and the change in flux in the core is proportional to the integral of $R\,i_R\,dt$. From the hysteresis loop, the corresponding value for i_L could be found. The peak voltage will occur when the inductance saturates, but by this time i_R will be much larger than i_L, and for all practical purposes will be equal to i_{line} at this instant. This was also concluded by the authors in their equation 12. Also, the current through the resistance is equal to the line current during the transient for all practical purposes.

The volt-seconds the inductance can develop is,

$$\int edt=\int_{-\phi_S}^{+\phi_S} N\frac{d\phi}{dt}10^{-8}\,dt=N2\phi_S10^{-8}$$

where ϕ_S is the saturation flux in the core. The quantity ϕ_S can be found from E_k, the peak of the sinusoidal voltage that can be developed by a sinusoidal flux with a peak value ϕ_S:

$$E_k=\phi_S\omega N10^{-8}$$

Then the integral of edt is:

$$\int edt=\frac{2E_k}{\omega}$$

The integral of the voltage across the resistance to time t_s is:

$$\int_0^{t_s} edt=\int_0^{t_s} R\,i_R\,dt=\int_0^{t_s} R\,I_m\omega t dt$$
$$=\frac{R\,I_m\omega t_s^2}{2}$$

Equating these two:

$$\frac{2E_k}{\omega}=\frac{R\,I_m\omega t_s^2}{2}$$

$$t_s=\frac{2}{\omega}\sqrt{\frac{E_k}{RI_m}}$$

The peak voltage across R is then:

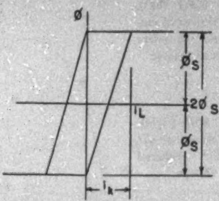

Figure 2. Idealized hysteresis curve. The flux change $2\phi_s$ corresponds to the current change i_k, hence $i_kX=2E_k$

$$E_R=R\,i_R=R\,I_m\omega\left(\frac{2}{\omega}\sqrt{\frac{E_k}{RI_m}}\right)$$
$$=2\sqrt{E_kRI_m}$$

This should be the same as the authors' equation 14, but the above is larger by a factor of $\sqrt{2}$. This discrepancy is due to the authors' statement in Appendix I just before equation 14: "However the product of i_kX can be interpreted as the crest voltage E_k corresponding to a sinusoidal flux density having its maximum equal to that at the knee of the curve . . ." Actually $i_kX=2E_k$. This can be shown as follows. In Figure 2 of this discussion is shown a hysteresis loop, rather idealized. For this loop, $I_k'\cong 0$ as is assumed by the authors (equation 2). Since X, the unsaturated reactance is assumed constant during the unsaturated periods, the sloping portions of the hysteresis loop are straight lines. It then follows:

$$L\frac{\Delta i_L}{\Delta t}=N\frac{\Delta\phi}{\Delta t}10^{-8}$$

$$L=\frac{N\Delta\phi10^{-8}}{\Delta i_L}=\frac{N2\phi_S10^{-8}}{i_k}$$

But,

$$E_k=\omega N\phi_S10^{-8}$$

$$L=\frac{2E_k}{\omega i_k};\quad i_k\omega L=i_kX=2E_k$$

If this value of i_kX is substituted in the authors' equation 13, it will give the same peak voltage secured above, $2\sqrt{E_kR\,I_m}$. With this correction, the formulas for crest voltage developed in the paper are correct and useful within the limits of the approximations stated in the paper. The corrected formula 14 agrees with formula 23, of reference 4 in the authors' bibliography, because the method of derivation and the assumptions made are essentially the same in both this new paper and the old one.

However, the new paper goes only this far, and is of limited usefulness on this account. Reference 4, a paper written in 1946 by the authors of this discussion, considers two conditions of fundamental importance which are not considered in this new paper:

Condition 1. The source voltage is sufficiently low that the current is not maintained sinusoidal.

Condition 2. The current is sufficiently high that the flux reversal is so rapid that it does not take place uniformly within the lamination, but starts on the surface first and progresses inward as a wave.

The reference paper develops methods of calculation for both of these conditions and shows that both of these conditions are commonly met within actual experience. It is true that when the new paper ignores Conditions 1 and 2 the calculated value of voltage will be considerably higher than the actual, and the result may therefore be considered to be conservative, if not correct. In our work we always use the simple formula first and resort to our more accurate formulas only if the calculated voltage is so high as to give us concern.

The test method described in this new paper is new, interesting, and again is useful within its limitations. However, in assuming that $e_m=aL(di/dt)^n$, equation 24, it ignores Condition 2 stated before, with the result that the open circuit voltage will be measured to be much higher than it really is.

The paper discusses the case of a saturating relay coil. The application of equation 14, corrected, to a current transformer with the secondary open will ordinarily be quite accurate as the primary current usually will be sufficient to saturate the transformer in a short time and the unsaturated reactance of the transformer X is in the same order of magnitude as the eddy loss resistance R. With a relay, these conditions may not be met, and the value of peak voltage given by equation 14 corrected will be too pessimistic. For the case where the current transformer does not saturate and the relay does saturate, if the product of the current through the relay times the unsaturated impedance of the relay is more than four times the maximum voltage the relay can develop without saturating equation 14, corrected, will give the correct answer if the unsaturated reactance X is not too small compared to the eddy current resistance R. It is necessary that the current through X be small compared to the current through R. This current ratio will be larger for longer times to saturate, lower inductance X, and lower values of current through the relay. Again the authors' reference 4, gives general formulas that take care of all cases.

For the case where the current transformer saturates first, equation 14, corrected will give the correct answer if the value of E_k is for the current transformer, and if R is the parallel resistance of the eddy resistances of the current transformer and the relay. The problem of the relay unsaturated reactance again enters and should be considered if it is materially less than R; this consideration is also fully discussed in the paper reference 4.

A. Boyajian and **G. Camilli:** Knowing the interest of Messrs. Specht and Wentz in our subject, very early we had sent them a copy of our manuscript, expressing the hope that they might wish to discuss the matter. So we welcome their discussion at this time. A point made by them is that our development is limited to sine wave currents. That is true neither of the experimental method we have described nor of the mathematical development. In fact, our experimental method, developed first, was for the very purpose of making measurements with any available distorted current, and to extrapolate to high currents, having any specified maximum *di/dt*. Our mathematical treatment, developed later, was similarly oriented. It was based on the unsaturated X_L of the circuit and the slope of the current as it crossed zero. Our frequent references to sine-wave currents were for a double reason. Sine-wave currents lead to higher voltages and are likely to be pretty well approximated in large systems, so that the sine wave constitutes the proper base for such calculations. It also helps visualization and improves the intelligibility of the presentation. As we said in the conference edition of our paper, "For a given *di/dt*, distortion in either the voltage or the current wave-form does not alter the value of the peak voltage a great deal. . . . Substitution of the maximum value of the *di/dt* of the expected sine-wave current, that is, substitution of $2\pi f/I_m$ in formula 24, will give maximum voltage. . ." Thus, when the current is distorted, I_m in our formulas is the crest value of that equivalent sine-wave current that has the same slope as the contemplated current in the neighborhood of zero.

Another comment regarding our analysis is that we have ignored the increased skin effect that results from the rapid recovery of the reactance. That raises two questions: (1) How much difference does that factor make in the end? and (2) If it is to be taken into account, may it not be better to take care of it by inserting the appropriate values of L and R in the equations? To get a line on the answer to the first question, we may compare the two alternative formulas 23 and 63 offered by Messrs. Specht and Wentz (see reference 3 of the paper). The latter formula is said to take the increased skin effect into account and is said to be more accurate. An inspection will show that the voltages calculated by these two formulas differ as 2.5 to 1, and this is confirmed explicitly by Messrs. Specht and Wentz in their paper. As they offer a correction factor of 0.85 to the first formula based on experience, that makes the more rigorous formula (63) 2-to-1 too low.

In their discussion on the relay coil, Messrs. Specht and Wentz give the impression that they have treated the relay coil taking into account the differences between a relay coil and a current transformer. We fail to find in their work an explicit solution for relays that is different from that for a current transformer. Theoretically, a perfect formula would apply equally well no matter what the name of the saturating device may be, but with the bold approximations that are generally made in saturation problems, and the important differences between relays and transformers—such as, a large air gap in the relays, together with the fringing of the flux across the face of the laminations near the poles—for use with relays, we would not want to put a lot of confidence on a formula that has been justified experimentally only for transformers.

Finally, Messrs. Specht and Wentz make the point that our formula 14 is wrong. We had offered this formula as an "approximate" one, involving the least knowledge of circuit constants and no knowledge of loop characteristics. Our more rigorous formula 13 and the most rigorous one (23) require a knowledge of the high-density hysteresis loop. No issue has been taken with these two, except the sine-wave and skin-effect arguments that were explained above. The objection raised against the approximate formula 14 is regarding its coefficient, and is based on a hysteresis loop selected by Messrs. Specht and Wentz. The loop does have an important effect, and a different loop would have given a still different coefficient. We stated in the text that as high-density loops will have steeper portions than unsaturated loops, formula 14 will yield lower voltages than 13. As formula 13 was developed along pessimistic assumptions, it does not appear unreasonable to make an optimistic simplification in an admittedly "approximate" formula like (14). In any case, we believe that, if a large number of data be taken, they will be found scattered between our formulas 13 and 14. We might reiterate here our belief that calculations involving saturation phenomena must not be counted on much beyond the order of magnitude of the quantity desired.

Evaluation of Energy Differences in the Economic Comparison of Alternative Facilities

A. P. FUGILL
MEMBER AIEE

THE TREATMENT of the various factors involved in comparing the cost of two or more methods for accomplishing a desired result in the planning of an electric power system deserves serious consideration. Because the subject is so broad that it could not be treated effectively otherwise, this paper and three companion papers[1,2,3] were presented to cover several phases of the general problem. Since there is not complete agreement on this whole subject, this paper is written in a provocative rather than a dogmatic vein, with the hope that the thoughts expressed will induce additional discussion which will eventually lead to a clarification of the whole problem.

In this paper, a method is given for determining the amount of energy involved in the different schemes being compared, and the money value of that energy. Although the emphasis is placed on the problem of energy loss and particularly that type of loss problem in which the whole electrical system is an important factor in the solution, the general principles set forth are equally applicable to the problem of evaluating the differences in installed generating capacity which may exist from time to time for the several alternatives being considered. These differences, for the years in which they exist, should be evaluated on the basis of their present worth, as covered by another paper[3] in this group.

The first responsibility of the planning engineer is to design a system which will give satisfactory performance under all normal and reasonable emergency operating conditions. Since it is possible to do this in several ways, his second responsibility is to select the method which will result in the lowest over-all cost. Although differences in losses among the several schemes may not be the deciding factor, some value for them should be introduced into the over-all economic comparison. Since the purpose of this group of papers is to point out the factors to be considered and outline general methods of approach to the problem, no effort will be made to present specific examples nor to assign specific values to the quantities involved. Because conditions will vary among power systems, each company must assign its own values. The general principles in this paper should be applicable to any type of system, even though the procedures outlined were developed for a large metropolitan system with steam generation.

Fundamental Principle

In the evaluation of energy differences in the economic comparison of alternative facilities, the fundamental principle underlying any method should be to determine as accurately as possible the actual cost which will accrue to the company during the life of the piece of equipment, substation, or power plant in question because of the difference in losses in the various schemes. To approach this ideal, even moderately close, it is necessary to examine each type of problem individually, to be sure that all factors are correctly evaluated. It would not be sufficient, for instance, to use one value for a unit of transformer loss regardless of the function of the transformer because the actual cost will vary considerably with the manner in which the transformer is used. Probably most engineers will agree in theory with this principle, but the objection will be that it is impracticable to apply because a rigorous solution involves far too much work, or the fundamental data on which the solution must be based are not available with sufficient accuracy. In considering the validity of this objection, it should be remembered that all planning is based on an estimate of what will happen in the future. No matter how carefully such a prediction is made, it is inevitably subject to considerable error. A high degree of accuracy in method of solution is not necessary in other planning problems, nor should it be considered necessary in the loss evaluation problem. Simplifying assumptions can usually be made to reduce the work without destroying the validity of the result. In most cases, the necessary data are available to the planning engineer or can be obtained for a particular system rather easily. To show how this principle can be applied, three types of problems will be analyzed.

Choice of Power Plant Site

For the first example, a new power plant is to be added to a system at one of two possible locations. Satisfactory performance can be obtained for either location, and the electrical system required for the plant at each location to give satisfactory performance has been determined. The system losses, however, are different for the two locations, and the evaluation of those differential losses is needed to complete the economic comparison.

Although it is necessary to determine the cost for the entire life of the plant, it is best to study the problem a year at a time. The usual data needed for system

---

Paper 51-341, recommended by the AIEE System Engineering Committee and approved by the AIEE Technical Program Committee for presentation at the AIEE Fall General Meeting, Cleveland, Ohio, October 22–26, 1951. Manuscript submitted June 18, 1951; made available for printing August 30, 1951.

A. P. Fugill is with The Detroit Edison Company, Detroit, Mich.

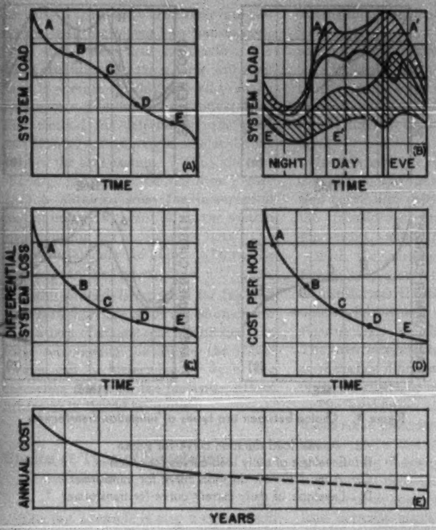

Figure 1. Choice between two power plant sites

A. Annual load duration curve for system

B. Envelope of daily load curves for system

C. Differential annual loss duration curve for system

D. Differential annual cost duration curve

E. Annual cost for life of plant

planning are available. Particularly, it is necessary to know the expected peak load for the year being considered, the distribution and power factor of load on the system for different times of day and seasons of the year, the distribution of generation throughout the complete annual load cycle, the electrical system required for each plant location, the annual load duration curve for the system, and the envelope of the daily load curves for the system.

Figure 1(A) is the load duration curve for the system which shows how many hours each year the system operates at each load from peak to minimum. It is relatively simple, particularly if a network calculator is available, to determine the system loss for a given system for one distribution of load and generation. The current division is usually known from studies made for other planning problems, and the calculation of losses, branch by branch, is not a long process with most systems. If the loss were constant for a given load, it could be determined readily for each plant location for a number of points, such as A, B, C, D, and E on the load duration curve. The loss duration curve for the difference in loss between the two cases could then be determined and plotted as in Figure 1(C).

However, the load duration curve of Figure 1(A) does not indicate at what time of day or at what season of the year each load occurs. Usually this will make a difference in the system loss because different load distribution and power factor result in different current division within the system network. In the case being studied, the loss is affected by the time of day. That is, the system loss depends on whether the load occurs during the day when power load predominates, during the evening when the lighting load is heavy, or during the night. It also depends upon whether the load occurs on a week day, from Monday through Friday, or over the week end on Saturday or Sunday. This effect can be taken into account by using the envelope of daily load curves given in Figure 1(B). The upper band includes all the loads which occur on week days; the lower band, those occurring on week ends. For this purpose, it can be assumed that all magnitudes of loads are equally distributed within these bands. Within one time area—that is, night, day or evening—the losses can be considered to vary only with load and not with time of day or season. On week ends, the day load is considered similar in loss characteristics to the evening load. In using these curves, it should be remembered that the week day band represents two and one-half times as much time as the week-end band.

In general, it will be necessary to calculate the loss for each time area and use the weighted averages in plotting the curve of Figure 1(C). For example, to determine the loss corresponding to load A, it would be necessary to calculate loss for both day loads and evening loads. From Figure 1(B), it is evident that of all the loads having a magnitude A, about two-thirds occur in the day and one-third in the evening and they all occur on a week day. Therefore, the loss corresponding to point A on the load duration curve, would be the average of the system loss for a day load and that for an evening load with the day loss being given twice the weight of the evening loss. Loads of magnitude E, on the other hand, occur only during week ends, about two-thirds at night and one-third during the day when the distribution is similar to that in the evening of a week day. Hence the loss would be determined at this load for the night and week-end day conditions and the night value given twice the weight of the day value.

If the loss is calculated for a few points on the load duration curve, as at points A, B, C, D, and E, for each location of plant, the difference in loss for each point provides the basis for the curve of Figure 1(C). This is an annual loss duration curve showing the number of hours duration during the year for each value of loss. The integration of the area under the curve is the total annual energy due to the difference in losses between the two locations of power plant.

The more difficult problem is the determination of the actual cost of this energy. The natural tendency is to use the cost of energy generated in the new plant, the average cost of energy for the system, or some intermediate value determined somewhat arbitrarily. The more accurate approach is to follow the principle established for the determination of the total differential energy; that is, to predict, for the year being considered, the actual cost of that energy for the generator operating schedule most likely to be used at that time. In all steam systems, the more efficient generation units will be loaded whenever possible in preference to the less efficient ones. Thus at load A, when most of the units are already well loaded, the incremental losses will have to be supplied by rather inefficient ones. At load E, even the best units on the system are probably not fully loaded, so the incremental losses can be supplied by them at a lesser cost. The problem is to determine the incremental cost of energy at a number of load points, A, B, C, D, and E, as for loss determination. Generally, this information is readily available from studies made for other planning and operating problems. In most steam systems, this incremental cost of energy is a function solely of mag-

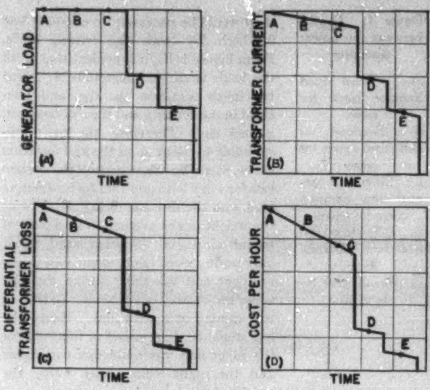

Figure 2. Choice between two types of generator transformers

A. Annual load duration curve for generator
B. Annual current duration curve for transformer
C. Differential annual loss duration curve for transformer
D. Differential annual cost duration curve

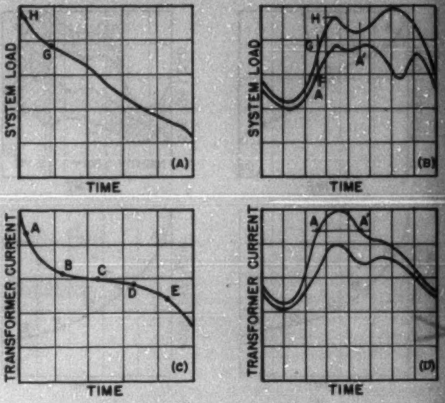

Figure 3. Choice between two types of substation transformers

A. Annual load duration curve for system
B. Envelope of daily load curves for system
C. Annual current duration curve for transformer
D. Envelope of daily current curve for transformer

nitude of load and is little affected by the load distribution; that is, the effect of time of day and season of the year can be ignored. If those factors are important, their effect can be included by a weighting process similar to that used for loss determination.

From the loss at point *A* on the loss duration curve, and the incremental unit cost of energy at point *A* on the load duration curve, the cost per hour can be determined and plotted as point *A* on an annual cost duration curve as shown in Figure 1(D). Completing similar calculations for points *B*, *C*, *D*, and *E*, will give the complete curve which shows the number of hours duration for each value of unit cost. The integration of the area under this curve is the total annual cost of energy attributable to the difference in losses for the two locations of power plant for the year.

Since the period under consideration for such problems is of the order of 20 or 30 years, it is necessary to estimate the present value of money to be spent several years hence. Certainly a dollar spent today cannot be considered to have the same value as a dollar to be spent 20 years from now. Since this phase of the problem is thoroughly discussed in another paper of the group,[8] no specific method need be included in this paper. It is sufficient to point out that after the cost of energy losses for each year of the life of the facility has been determined, some factor should be applied for each year to take account of the present worth of future costs.

This weighted cost for each year, then, can be plotted as in Figure 1(E) and the total cost obtained by integrating the area under the curve. As a rule, it is not necessary to calculate the result for every year, but only at intervals of three to five years or whenever a major change in system is expected. There is little need for making calculations beyond ten years, since the pattern of annual cost is usually well established by that time and valid results can be obtained by extrapolation.

Choice of Type of Generator Transformer

The second example is a comparison between two types of generator transformers with different losses. The transformer is in series with the generator so its power load is directly controlled by the load on the generating unit but the reactive load and the cost of the differential energy are influenced by system conditions. The choice is to be made between a self-cooled transformer and a forced-oil, water-cooled transformer with higher full load losses. Constant voltage will be assumed on the transformer so that the total loss at any load is the sum of a constant core loss and a copper loss which varies with the square of the current.

Again the problem will be solved by a year by year study of the probable operation of this transformer throughout its life. The load duration curve for the system is the one given in Figure 1(A). For the year under study, this generator will be loaded as indicated by the generator load duration curve in Figure 2(A). The generating unit operates at full load for high system loads, at reduced load for light system loads, and at no load for a short period to provide for inspection and maintenance outage time. From studies made for other planning problems, the variation in power factor on the generator is known, so that a current duration curve for the transformer can be plotted as in Figure 2(B). With the current known, the total loss in each type of transformer can be calculated for several points, say *A*, *B*, *C*, *D*, and *E*, and the difference in loss plotted as in Figure 2(C) to give a differential loss duration curve for the two types of transformers. As in the first problem, the total energy can be obtained by integrating the area under the curve.

The cost of this energy will depend on the method of operation. If the unit is operated at base load as measured on the generator terminals, the incremental loss in the transformer, due to the higher loss design, will not be supplied by the generating unit in question but by the rest of the system. In other words, for a given output from the generator, there will be less output from the transformer into the system with the higher loss transformer. Since the system load is constant, the other generators on the system will then have to operate at a higher load to make up for this additional transformer loss. The method for determining the total cost of energy, then, can be similar to that used in the first example. Thus, the cost of energy for differential loss *A* on Figure 2(C) is obtained from the incremental cost of energy at point *A* on the system load duration curve of Figure 1(A). The cost duration curve of Figure 2(D) can be plotted as in the first example.

If this process is repeated for the first few years of the life of the transformer and the pattern of annual cost established, the total cost during the life of the transformer can be determined. Again the correction factor for the present worth of future costs should be applied.

Choice of Type of Substation Transformer

The last example is also a comparison between two types of transformers and is included to emphasize the fact that the treatment and results depend upon the application as well as the type of equipment.

In other words, all transformer loss problems should not be treated alike just because they deal with losses in transformers, since the type of service for which the transformer is used may have an important effect on the result. In this case, the problem is to decide between two types of step-down power transformers used on the system to supply load at substations. The comparison is between a straight self-cooled transformer and a transformer equipped with supplementary cooling to give a continuous rating equal to the self-cooled unit. The full load loss in the latter is higher but the no load loss may be less.

It is assumed that this transformer is used on a system with the load duration curve and daily load curves of Figures 1(A) and 1(B), which are reproduced in part in Figures 3(A) and 3(B). For simplicity, the week-end daily load curve will be eliminated from consideration. The loss in the transformer is dependent on the current in the transformer, not the load on the system, so it is necessary to have the current duration curve and the envelope of the daily current curves for the transformer under consideration. If this transformer is to be purchased for use anywhere on the system, these curves may be quite different. A transformer serving industrial load may have its peak load during the day while a transformer serving residential load is more likely to have its peak load in the evening. If the transformer is to be used for general application on the system, a weighting factor for the different types of service should be used.

In this example, the type of service is known so that the annual current duration curve and daily current curves for the transformer are those shown in Figures 3(C) and 3(D).

With the current duration curve of Figure 3(C) known, the loss for each type of transformer is easily calculated, and a differential loss curve similar to those of Figures 1(C) and 2(C) can be plotted. The area integration gives the total annual energy difference for the two types of transformers, as before.

The evaluation of this energy introduces some difficulties. As in the earlier examples, the cost of the differential loss is a function of system load and hence the transformer daily current curve must be correlated in some way with the system load duration curve. This can be done without too much effort by using the curves in Figure 3. Referring to Figures 3(C) and 3(D), the current at point *A* on the current duration curve of Figure 3(C) occurs between the times *A* and *A'* on the daily current curve of Figure 3(D). From Figures 3(D) and 3(B), it is evident that at this time of day, the system load is between *F* and *H* with most of the loads between *G* and *H*. It is safe to conclude that most of the transformer currents of magnitude *A* will occur when the system load is between *G* and *H* on the load duration curve. The cost of energy for loss *A* on the loss duration curve, therefore, can be obtained by averaging the incremental cost of energy on the system at loads *G* and *H*. Following this procedure, a cost duration curve can be plotted similar to those in Figures 1(D) and 2(D) and the total annual cost obtained by integration. By similar calculation for subsequent years, with the present worth factor included, the total cost of the differential energy during the life of the transformer can be determined for the two types of units.

Conclusions

These three examples are typical of the multitude of problems which arise in system planning in which the general method outlined can be used. Although it may appear that considerable work is involved, improvements and simplification in method will develop as each problem is considered, which will lessen the work. In many cases, certain variants will make little difference in the final result and can be neglected. After a few problems of one type have been worked out rather completely for a given system, a set of values for many of the quantities will be obtained which often can be used to make subsequent solutions much simpler.

It is well to emphasize that the procedures have been outlined in each case because that was believed to be the best way to point out the factors to be considered in such problems. These factors will vary in importance with the type of problem, the type of power system, and methods of operation. In some cases, the accounting practices of the particular company will have an important bearing on the procedure. In every case, however, the planning engineer should be able to determine, within the accuracy obtainable in most planning problems, the cost which will accrue to the company over the years for the different ways of accomplishing the desired result. To do so, he must study each case carefully, not as an isolated problem, but as a problem which affects the system as a whole. It is not a simple problem to evaluate these energy differentials, but it is a soluble one. A planning engineer is certainly not justified in assuming in an economic comparison of alternate facilities, even in a particular system, that a unit of energy is worth a given amount of money regardless of the manner in which that unit of energy enters into the situation.

References

1. Carrying Charges as Related to the Economic Comparison of Alternative Facilities, P. H. Jeynes. *AIEE Transactions*, volume 70, 1951, pages 1942–53.

2. Operating and Maintenance Costs for Use in the Economic Comparison of Alternative Facilities, W. E. Slemmer. *AIEE Transactions*, volume 70, 1951, pages 1954–55.

3. Present Worth or the Time Cost of Money as a Factor in the Economic Comparison of Alternative Facilities, P. H. Jeynes. *AIEE Transactions*, volume 70, 1951, pages 1956–62.

Discussion

A. E. Knowlton (Electrical World, New York, N. Y.): From the papers presented at this session one could as likely draw confusions as to draw conclusions. It is evident that there is reasonable agreement on the major premises but comparatively little unanimity on the interpretation of the details. This is quite to be expected when engineers begin to delve actively in a realm previously reserved largely for the actuaries, accountants, and rate specialists.

There is ample excuse for us engineers to examine our respective methods of determining comparative costs for alternative ways of meeting a given engineering problem. Nor is there any reason why they should follow the prescribed techniques of accountants. Their task is to evaluate present worth of some engagement that may stand as a commitment for 20, 30, 50, or even 100 years.

It is extremely desirable that the various procedures exemplified by the papers be resolved toward uniformity. There are three good reasons for a degree of standardization.

1. It is due to investors in the enterprise that their money be spent as wisely and as advantageously as possible. The equipments purchased and system configurations decided should be based on as sound a technical-economic basis as possible.
2. It is due to the manufacturers to know how the criteria for competitive selection of apparatus on an economic worth basis differ from company to company, or better yet, the degree of uniformity in establishing these criteria.
3. It is due to the rate-payers and regulatory authorities to have uniformity in judgment on the part of the regulated utilities in making expenditures that have to stand the test of prudence. Otherwise the least "prudent" utility (the one with the dullest pencil) may find itself paying a penalty because the criterion for decision on prudence may follow the pattern set by utilities that use the sharpest pencils.

In brief there is ample urge to prosecute what this symposium has initiated toward exploration of engineering-economic theories. Whether the accountants concur in the prospective conclusions is beside the point. At least the engineers will have made their decisions sound by clarification and unification. The expenditures will thus have been prudent at the source.

W. E. Slemmer (Ebasco Services Inc., New York, N. Y.): Mr. Fugill has presented an excellent paper showing how to determine the quantity of the difference in energy loss between two plans and how to determine the incremental cost of producing that quantity of energy from a particular group of generators. The paper is intended to consider only the energy component so that no discussion of power or capacity component is included, although determination of over-all cost difference is not complete without adequate allowance for this component, which may be greater in magnitude than the energy component. A true determination of the number of dollars associated with the energy component as production cost requires consideration of the capacity component since the two must be co-ordinated.

The literature includes many discussions of the evaluation of this capacity or demand component proposing several methods to be used for its evaluation. Each method is based upon the fact that sometime, additional investment must be made in generating equipment to supply this portion of system load. Then there is generating capacity on the system that would not be there if the loss differential were not present. This generating capacity is available not only to supply the capacity component but also to generate the necessary energy. The cost of the energy and demand components should be based on the same generating capacity installation. The cost analysis proposed by Mr. Fugill would apply in those cases in which no capacity charge is required or in which the capacity charge is based on capacity having higher production cost than other sources available to the system.

H. B. Dwight (Massachusetts Institute of Technology, Cambridge, Mass.): The problem of how much additional money should be paid for a transformer that has 1 kw less copper loss at rated load than another, other things being equal, arises when a large transformer is purchased. There are two solutions. The first may be called the solution for a generating system; the second, the solution for an energy-purchasing system.

According to the first solution, 1 kw of unnecessary copper loss at full load renders useless 1 kw of generating capacity, which usually has cost $100 or more, and it uses up fuel besides. For a numerical example, a steam station may be taken which uses 0.9 lb of coal per kilowatt-hour, with coal at $10 per ton. The "loss factor" may be taken as 0.2, that is, the number of kilowatt-hours per year is 8,760 × 0.2 = 1,752. The loss factor is the ratio of the kilowatt-hours to the number there would be if there were full load all the time. The loss factor is less than the load factor except in the case when they are unity. The fuel cost per year in this example is then 1,752×0.9×10.00/2,000 = 1,752×0.0045 = $7.90.

To have 1 kilowatt of generating capacity year after year entails an annual cost equal to the first cost multiplied by the ratio of fixed charges, the latter representing interest, depreciation, taxes, and insurance. Taking this to be 15 per cent, the annual cost is 15.00+7.90 = $22.90. The solution of the transformer problem then is 22.90/0.15 = $153.00.

An advantage of giving a numerical example of this kind is that the computation described is definitely shown. A disadvantage is that some readers and discussers are likely to concentrate their attention on whether the illustrative cost values are before inflation or after inflation, to the exclusion of the main problem.

The second solution, to be used for energy purchasers where there is no demand charge, is obtained by multiplying the number of kilowatt-hours by the cost per kilowatt-hour.

This solution should give at least as large a cost as the other. The cost of the energy would then be 22.90/1,752 = 0.0131 dollars per kilowatt-hour, or more.

The core loss of the transformer is treated in the same way as the copper loss, except that the loss factor is practically unity.

The second solution has often been given in books on electric transmission and distribution as the method for any type of company and there have been many serious differences of opinion as to what numerical value of dollars per kilowatt-hour should be used. It would seem that the way to settle this question would be to compute the first solution and then make the second solution agree with it, as has just been done in the example. This, however, is awkward and unnecessarily indirect. It may be noted that the energy lost in line conductors has exactly the same characteristics as the energy of copper loss in a transformer winding with which the conductors are in series.

The figure of 0.0131 dollars per kilowatt-hour is not the incremental cost. Incremental cost is a well-known term and is the part of the cost of electric energy which varies with the kilowatt-hours. It is the same as incremental production cost. For a steam station it has almost the same numerical value as the fuel cost, namely, 0.0045 dollars per kilowatt-hour in the example given. Incremental cost is used in deciding which generating station in a city should be given an increase in load. The fixed charges for the generating capacity go on, regardless of load, and of the generating stations which are built and in operation, the one should be given an increase in load which has the lowest fuel cost, or "incremental cost." It is well known that if some offpeak energy is sold at a low rate based on the incremental cost, such a rate should not be used for normal cases, or for the bulk of the sales, as it is too low. It would not be possible at this date to assign a new and different definition for the term "incremental cost of energy."

Mr. Fugill seems to have used the incremental cost of energy for the transformer problem, and has omitted the term of the first solution for cost of generating capacity, which results in an answer for the transformer problem which is about one-third as large as it should be in this example for copper loss. He states in all three of his problems that incremental cost is used.

His problem of choice of power plant site is plainly one where the company owns the generating plants, and the problems of choice between a self-cooled and a water-cooled transformer and of choice between two types of substation transformer are apparently not those of a company which buys energy at a certain rate per kilowatt-hour without demand charge. The sentence in his second paragraph about differences in installed generating capacity does not describe the generating-capacity term of the first solution described in this discussion.

A general statement should be given that 1 kw of copper loss (or core loss) at rated load or peak load renders useless 1 kw of generating capacity, and the cost of this capacity constitutes the first component of the cost of the copper loss.

A numerical example should be solved in Mr. Fugill's paper. There is currently a debate[1] among engineers, resulting in distinctly different numerical results for the transformer problem described. A numerical example would show almost unmistakably on which side of the debate Mr. Fugill is. In the example in this discussion, the only difference between the two transformers is the difference in energy of copper loss. In the second paragraph of the paper it is announced that a method is given for determining..."the money value of that energy." The paper should show in numbers, which are the engineer's language, just what that method is, for when it is described in words it may be doubtful.

An important question that can change the value of the second component of the cost of transformer loss by a large ratio is as follows: One is faced with the alternative whether to buy an expensive transformer with low losses, or a cheaper transformer with higher losses. The difference in price of the two transformers should cover the two components of cost of losses. If one buys the cheaper transformer, part of the money saved compensates the company for the generating capacity rendered useless, which the company has already paid for. The question may be asked, should the remainder be large enough to be invested in stocks or bonds, paying perhaps 5 per cent interest which can pay for the additional fuel in the years to come, or should this fuel cost be capitalized at the carrying-charge percentage, of about 15 per cent? This would represent a large difference in the valuation of the energy loss. The better method seems to be to compute first the annual cost for the alternatives. This is quite different from using present worth based on 5 or 6 per cent compound interest.

If the apparatus producing the copper loss is a line conductor, the amount of money which the company should be willing to pay to provide extra copper is, in the notation very clearly described in a paper by P. H. Jeynes,[2] equal to $G+E$, where G is the capital cost of the generating capacity saved, and E is the value of the fuel loss or incremental loss saved, capitalized by dividing by the carrying-charge rate of about 0.10 or 0.15.

REFERENCES

1. STANDARD HANDBOOK FOR ELECTRICAL ENGINEERS, A. E. Knowlton. McGraw-Hill Book Company, New York, N. Y., section 14, paragraph 347, 1949.

2. See reference 3 of the paper.

G. D. Floyd (The Hydro-Electric Power Commission of Ontario, Toronto, Ont., Canada): The prime consideration when evaluating energy differences is to make an assignment of the cost of these differences, and this has not been treated in the paper, except to point out one method whereby the incremental cost of supplying the losses for various values of loads is used as the basis. Now there are many other bases, and while the author's suggestion is probably as good as any other where steam plants are concerned, it might give a misleading answer in the case of hydraulic plants. In the latter, the incremental cost is more likely to be the cost of the next development, if costs are to be derived at values close to the system peak. If values are desired at smaller system loads, the cost might be that of providing additional storage and at still lighter loads, the cost might approach zero, as the incremental losses could be supplied from surplus water.

In the purely hydraulic system, the situation is somewhat different to that prevailing to the purely thermal system. The fuel (in this case water) does not effect the costs nearly as much as in a thermal station, and therefore energy differences may not be as important as differences in peak capacity. Any evaluation of energy differences or peak capacity differences should, in my opinion, take account of this situation, and the paper therefore, while treating the matter of energy differences very effectively, has not presented the complete picture. It therefore lacks completeness in this respect. The treatment of this problem as applied to hydro systems might very well form the subject for another paper, and cannot very well be treated, even very briefly, in the scope of discussion of this nature.

In a combined hydraulic and steam system where hydraulic resources predominate, it would appear to be correct to use the incremental cost of steam generation for loads greater than those which can be supplied from hydraulic resources. There are so many variable costs that it will often be a matter of judgment which to apply, and quite different conclusions may be drawn, depending on the dollar value assigned to the losses.

The value of this paper would have been enhanced, in my opinion, if the author had indicated what proportion the cost of the losses was to the total expenditure, in the general case. I would expect that the proportion would vary widely. Is it possible to determine in many cases by inspection, whether the cost of the losses is of such magnitude that they are unlikely to overcome the savings effected by the plan involving less capital expenditure, and so avoid what appears to be tedious, if not complicated, calculations.

Lester B. LeVesconte (Sargent & Lundy, Chicago, Ill.): This paper together with the three companion papers[1] constitutes the beginning of a much needed field of investigation and study. They indicate the wide variations that exist today in this field. While this wide variation is often blamed on engineers, we suspect that the basic trouble is the lack of co-ordination between the engineers and the accountants. As has been pointed out in a previous discussion[2] the final choice of the equipment is often determined by accounting procedures rather than by engineering considerations.

It would seem that this whole program has started out correctly with an exploration of all of the factors involved as has been done in this set of papers. A review indicates 50 or more factors that should be given consideration. The next step would be to determine reasonable limits for actual values of all of the factors. Then a study of these actual values would indicate that many of them can be combined into relatively simple rules. By this means it is hoped that the entire procedure can be simplified and standardized sufficiently to make it practical to apply this analysis more generally. At the present time it is rarely possible for all of the factors listed in these papers to be given serious consideration for any except the largest projects and many of them are usually overlooked entirely.

A somewhat similar process of simplification was accomplished in the method for calculating short circuit currents. Fifteen years ago the correct determination[3] involved the initial and sustained values of subtransient, transient and synchronous internal voltages; direct axis subtransient, transient, and synchronous reactance; resistance in armature and external connections; and the d-c, open circuit and short circuit transient and subtransient time constants. The answer could be further modified by considering the change in excitation. All of this complication has been simplified to a few rules and multipliers using only two of the above factors and it is agreed that the answers have sufficient accuracy for practically all of the problems involved.

It is recognized that standard percentages cannot be applied to all cases. Different companies will have different interest rates, taxes, and operating costs which must be given consideration. However, it should be possible to agree on a more uniform method of using these values. While accuracy is of the greatest importance in accounting procedures it should be recognized that the problem discussed in these papers involves estimates into the future where extreme accuracy is impossible and many compromises and approximations can be used without affecting the decisions that are based on the analysis. In most cases the answer is not one of fine degree but rather a choice between the two or three methods of accomplishing the same result and the accuracy of the analysis is adequate if it does not change the choice of equipment.

REFERENCES

1. See references 1, 2, and 3 of the paper.

2. *Discussion* by L. B. LeVesconte of THE CHOICE OF MAIN POWER TRANSFORMERS FOR GENERATING STATIONS, N. E. Dillow, J. W. Butler. *AIEE Transactions*, volume 69, 1950, page 785.

3. WESTINGHOUSE APPLICATION DATA SECTION 33-116 (East Pittsburgh, Pa.), February 1936.

L. K. Kirchmayer (General Electric Company, Schenectady, N. Y.): The author has presented important considerations relative to the choice of alternative facilities. With reference to the information on the choice of plant sites, this writer has the following comments.

In widespread systems it is necessary for optimum system operation to schedule generation co-ordinating the effects of both incremental fuel costs and incremental transmission losses. Hence, the scheduling of generation of a given plant at a given site is dependent upon its thermal characteristics, the cost of the fuel at the site, and the electrical location in the network. In order to compare the system operation for a given plant located at either of two different sites it is necessary to determine the optimum operation of the system for each alternative plant location. One manner in which the difference in optimum operation of the two alternatives can be determined is as follows:

1. Determine a transmission loss formula for the transmission system with both the proposed and existing plant sites as variables in the loss formula.[1]
2. By methods available for co-ordinating incremental fuel costs and incremental transmission losses determine generation schedules for various total loads with the new plant located at first one and then the other site.[2]
3. Determine the transmission losses for the generation schedules obtained for the alternative plant sites by application of the transmission loss formula.
4. Calculate the total fuel input for all the plants in the system in dollars per hour as a function of received load for both alternatives.
5. Subtract the two fuel inputs in Step 4 and obtain a curve of dollars per hour saved as a function of received load.
6. The information in Step 5 may then be used in a manner similar to that described in the paper.

REFERENCES

1. ANALYSIS OF TOTAL AND INCREMENTAL LOSSES IN TRANSMISSION SYSTEMS, L. K. Kirchmayer,

G. W. Stagg. *AIEE Transactions*, volume 70, 1951, pages 1197–1205.

2. EVALUATION OF METHODS OF CO-ORDINATING INCREMENTAL FUEL COSTS AND INCREMENTAL TRANSMISSION LOSSES, L. K. Kirchmayer, G. W. Stagg. *AIEE Transactions*, volume 71, 1952 (*Proceedings T2-112*).

A. P. Fugill: The amount and quality of the discussion on this paper, and on others in the symposium, indicate an intense interest in this subject of economic comparisons. The author concurs with the conclusion in several of the discussions that complete unanimity of opinion on the subject has not yet been reached in the industry. In fact, one of the objects of the symposium was to bring such differences into the open for frank discussion as a prelude to later agreement, at least on general principles, if not on detailed procedures. It seems that the symposium has accomplished that purpose and may be the incentive for future efforts toward standardization.

Some of the criticism of this paper in the written discussion seems to stem from a misunderstanding of the basic rules under which this paper and others in the symposium were written. It was agreed, because of the widespread differences in conditions which exist throughout the industry, that only general principles would be included in these papers. The assignment of specific values, or even the presentation of exact procedures was not considered desirable because they might differ for each company. Furthermore, in this particular paper, the capacity component of the cost of energy differences was deliberately excluded because it will be covered in another paper which was originally scheduled for this meeting but was postponed until a later meeting. With this in mind, certain of the discussion needs no comment.

Mr. Knowlton makes the point that there is considerable lack of unanimity on the subject, particularly as to interpretation of details, and that a degree of standardization is definitely needed. There certainly can be no disagreement with this statement. There may, in fact, be more fundamental agreement on this subject already than appears from a superficial review of surface disagreements.

Mr. Slemmer has correctly concluded that the paper was not intended to include the capacity component. On the other hand, that omission should not be interpreted as an indication that the capacity component of cost should be ignored in an economic comparison. Obviously, in any actual comparison, that component would be included.

Much of Mr. Dwight's criticism of the paper revolves about the omission of the capacity component and numerical examples, and requires no comment as stated earlier. He is right in assuming that the author had in mind a system with its own generating plant, although the general principles could be applied just as well to one which purchased its power, since this merely determines more easily the cost of a unit of energy. The term "incremental cost" as used in the paper is not significantly different from the definition Mr. Dwight gives for that term. It is, in the paper, essentially the fuel cost of an additional unit of energy at the particular load existing at the time that the additional unit of energy is supplied. It does not include fixed charges, although it should include operating costs other than fuel. The point that is important, however, is that this incremental cost is not a fixed quantity for a given generator, plant, or system, but depends upon the load at which the unit is operating at the moment. Mr. Floyd's discussion indicates quite clearly why it was undesirable to include specific procedures in this paper. As he points out, in a hydraulic system, the treatment might be quite different than in a steam system. Within the framework of the general principles stated in the paper the techniques should be suited to the particular system. That can be done most accurately by the planning engineer for the particular system. A universal mold will not fit all systems. Although it would be highly desirable to set up a yardstock to tell when the cost of losses is so insignificant that it can be neglected, it is not possible to state a general rule. Usually, however each engineer in dealing with his own system, will be able to determine this by a few simple calculations in each case.

Mr. LeVesconte, in common with others, states that engineers and accountants vary widely in their approach to the problem. Here again, the difference may be more superficial than fundamental. After all, they are both interested in obtaining the actual cost to the company of the alternative methods under study and should be able to agree on a method to obtain it. Mr. LeVesconte suggests that a simple, unified method may eventually evolve which will be entirely satisfactory, in view of the fact that a high degree of accuracy in the result is not necessary. With that view, the author concurs.

Mr. Kirchmayer brings out the point that transmission losses also should be included, and proposes a method for doing this. This is certainly true and the proposed method offers considerable promise of being able to do this with a minimum of effort.

Synthesis of Paralleled 3-Terminal R-C Networks to Provide Complex Zeros in the Transfer Function

P. F. ORDUNG ASSOCIATE MEMBER AIEE
G. S. AXELBY MEMBER AIEE
H. L. KRAUSS ASSOCIATE MEMBER AIEE
W. P. YETTER STUDENT MEMBER AIEE

Synopsis: A method is given whereby a transfer ratio that contains complex zeros can be realized by means of R-C (resistance-capacitance) ladder networks connected in parallel. It is an improvement on the method previously given by Guillemin in that fewer paralleled networks are required and the level of the transfer ratio is greater.

The general procedure is (1) to convert the desired transfer ratio into the sum of several transfer ratios, each of which can be realized with a single ladder network, (2) to develop the theory of paralleling ladders, and (3) to develop the method of synthesis of the individual ladder networks in terms of a common driving-point admittance function.

THE design of resistance-capacitance networks for the realization of a specified transfer ratio (ratio of open-circuit output voltage to input voltage) has been treated in a number of papers.[1–4] Transfer ratio functions containing complex zeros have been synthesized with R-C networks in the form of lattices, bridged-T's, and paralleled 3-terminal structures. The purpose of this paper is to demonstrate how the latter form can be used, but with fewer networks and elements than in the method given by Guillemin,[1] where each term in the numerator polynomial of the transfer ratio is represented by a 3-terminal network.

The method for realization of a specific transfer ratio with an R-C network involves three steps. First, the general requirements for a transfer ratio that can be realized with an R-C network must be satisfied. Second, a suitable topological form must be selected for the network; and finally, the synthesis must be made to determine the parameter values.

Requirements for Transfer Ratios to Be Realized with R-C Networks

The transfer ratio $H(p)$ of the R-C network symbolized by Figure 1 can be expressed as the ratio of two polynomials in the complex frequency $p=\alpha+j\omega$. This ratio can be identified with the ratio of two cofactors of the network determinant (obtained on a mesh basis) by the use of Thevenin's Theorem.

$$H(p)=\frac{E_{out}}{E_{in}}=\frac{h(p)}{g(p)}=$$

$$\frac{a_0+a_1p+a_2p^2+\ldots a_rp^r}{b_0b_1+b_1p+b_2p^2+\ldots b_sp^s}=\frac{Y_{12}}{Y_{22}}=\frac{\dfrac{\Delta_{12}}{\Delta}}{\dfrac{\Delta_{22}}{\Delta}} \qquad (1)$$

where $h(p)$ and $g(p)$ are polynomials in p, Y_{12} and Y_{22} are the short-circuit transfer and driving-point admittances, Δ is the network determinant obtained by mesh analysis, and Δ_{12} and Δ_{22} are cofactors of Δ. Through a study of transients in R-C networks, Δ_{22} can be shown to have zeros only at real negative values of p. The residue criterion for such networks[5] may be used to show that any zeros of multiplicity r in Δ_{22} must appear with multiplicity r or r-1 in Δ_{12}, Δ_{11}, and Δ. Thus the transfer ratio must have poles that are simple, and that occur at negative real values of p. Since bridge networks that balance at imaginary or complex values of p can be constructed, it follows that the zeros of $H(p)$ may be real or complex. Complex zeros must occur in conjugate pairs, however, since the coefficients in $h(p)$ are real. Finally, the magnitude of $H(p)$ must be finite at all "real" frequencies ($p=j\omega$), otherwise some resistor would receive infinite power—an obvious impossibility. Any transfer ratio that fulfills the foregoing three conditions can be realized with R-C networks.

The topological considerations in the realization of a transfer ratio are much more subtle than the foregoing considerations of existence. This is true because the topology of the network is inherently involved in the synthesis process, as will be evident from the following discussion. The procedure for the realization of a transfer ratio is to synthesize the driving-point admittance Y_{22} in such a way that the transfer admittance Y_{12} also is realized. This is done by selecting a polynomial $f(p)$ to correspond to the network determinant Δ, so that the transfer and driving-point admittances can be identified as

$$Y_{12}=\frac{h(p)}{f(p)}$$

and (2)

$$Y_{22}=\frac{g(p)}{f(p)}$$

For the realization of Y_{22} in the form of an R-C network, a great variety of choices may be made for $f(p)$ as long as the function satisfies the requirements that its roots be negative, real, and simple, and that they alternate with the roots of $g(p)$. For any $f(p)$ that satisfies the above requirements, the residue criterion[4] may be used to show the existence of an R-C network that realizes the desired Y_{12}, as well as Y_{22}. However, the topological form of the network that will realize both Y_{12} and Y_{22} for arbitrarily selected $f(p)$ is not known; that is, the number of

---

Paper 51-342, recommended by the AIEE Basic Sciences Committee and approved by the AIEE Technical Program Committee for presentation at the AIEE Fall General Meeting, Cleveland, Ohio, October 22–26, 1951. Manuscript submitted April 1, 1951; made available for printing October 1, 1951.

P. F. ORDUNG and H. L. KRAUSS are Associate Professors, Department of Electrical Engineering Yale University, New Haven, Conn. G. S. AXELBY is with Westinghouse Electric Corp., Baltimore, Md., and W. P. YETTER is with North American Aviation, Downey, Calif.

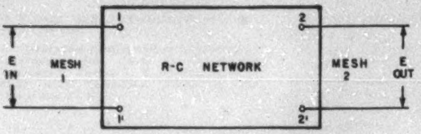

Figure 1 (above). General resistance-capacitance network

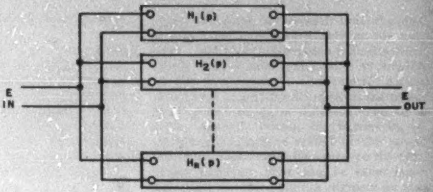

Figure 2 (right). Paralleled ladder networks

meshes and their arrangement is not determinable from $f(p)$. A previous paper[2] has shown that a network of lattice form can realize the desired $H(p)$ for any choice of $f(p)$ that allows Y_{22} to be synthesized. In the case of a 3-terminal network, however, there are definite restrictions on the location of the zeros of $f(p)$ and these restrictions can be stated only after the topological form of the network has been chosen.

Synthesis with Paralleled Ladder Networks

The topological form employed for the realization of a transfer ratio with complex zeros will be chosen as a set of ladder networks connected in parallel at their input and output terminals as shown in Figure 2.

Each of the ladder networks used in Figure 2 can be used to realize a transfer ratio of the form

$$H_1(p)=\frac{h_1(p)}{g(p)} \tag{3}$$

where $H_1(p)$ has

(1) simple poles that are negative and real (2) simple or multiple zeros that are negative and real (3) a finite magnitude of the transfer ratio for all values of ω.

The first step in the synthesis is to express the $h(p)$ in equation 1 as the sum of polynomials

$$h(p)=h_1(p)+h_2(p)+\ldots+h_r(p) \tag{4}$$

where each of the $h_r(p)$ has zeros at negative real values of p. (See Appendix). Then the transfer ratio $H(p)$ can be expressed as

$$H(p)=\sum_{n=1}^{r}\frac{h_n(p)}{g(p)}=\sum_{n=1}^{r}H_n(p) \tag{5}$$

where each term in equation 5 can be realized as the transfer ratio of an R-C ladder network by a method analogous to one described by Ordung and Fleck.[3]

If the network that realizes $H_1(p)$ is synthesized with the driving-point-admittance

$$Y_{22(1)}=\frac{a_1}{A}\frac{g(p)}{f(p)}$$

the network that realizes $H_2(p)$ is synthesized with the driving-point admittance

$$Y_{22(2)}=\frac{a_2}{A}\frac{g(p)}{f(p)}$$

and so forth, where the factors a_n/A are admittance-level adjusting constants, the parallel combination of the ladders will realize $H(p)$ to within a constant of proportionality. A polynomial $f(p)$ must be chosen in such a way that $Y_{22}=g(p)/f(p)$ can be realized with resistances and capacitances. For the realization of the transfer ratio of the nth ladder structure, it is necessary that that ladder be developed from $Y_{22(n)}$ in such a way that its short circuit transfer admittance is obtained as

$$Y_{12(n)}=r_n\frac{h_n(p)}{f(p)} \tag{6}$$

wherein the constant r_n is a value that can be computed only after the network has been synthesized. When the ladders are paralleled the over-all short-circuit transfer admittance obtained should be proportional to the value of Y_{12} given by equation 2. In order for this to be accomplished it is necessary that the component admittances in each of the ladders be scaled in such a way that the corresponding short-circuit transfer admittances are realized as

$$Y_{12(1)}=\frac{a_1}{A}r_1\frac{h_1(p)}{f(p)}$$

$$Y_{12(2)}=\frac{a_2}{A}r_2\frac{h_2(p)}{f(p)} \tag{7}$$

$$Y_{12(n)}=\frac{a_nr_n}{A}\frac{h_n(p)}{f(p)}$$

where

$$a_1r_1=a_2r_2=a_3r_3=\ldots a_nr_n=1 \tag{8}$$

and where

$$A=a_1+a_2+a_3+\ldots \tag{9}$$

The transfer ratio that results when these ladders are paralleled is

$$H(p)=\frac{\frac{1}{A}\left(\frac{h_1(p)}{f(p)}+\frac{h_2(p)}{f(p)}+\ldots\right)}{\left(\frac{a_1}{A}Y_{22}+\frac{a_2}{A}Y_{22}+\ldots\right)=Y_{22}}=\frac{1}{A}\frac{h(p)}{g(p)} \tag{10}$$

Thus $1/A$ is the level of the transfer ratio actually achieved.

This section has shown how a transfer function that contains complex zeros may be represented by a sum of transfer functions that contain only real zeros, and that can be realized with R-C ladder networks. The next section will discuss the method of synthesis of one of the ladders.

Synthesis of a Ladder Network to [illegible]

In the [illegible] of the paralleled ladders [illegible] $f(p)$) will [illegible] each of the individual ladders represented in Figure 2 or equation 7 can be synthesized to yield the

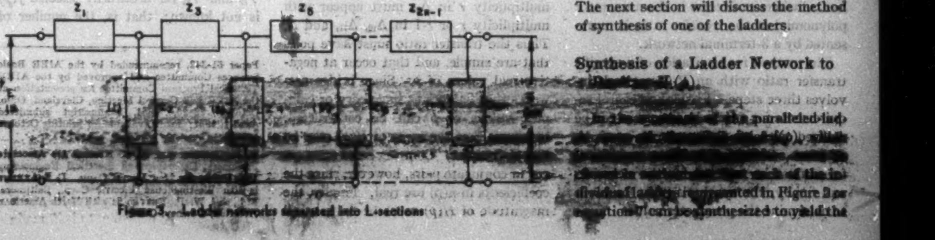

Figure 3. Ladder networks separated into L-sections

Vol. 7
1951

desired transfer function. The determination of $f(p)$ for a single ladder network that has the transfer ratio $H_1(p)$ given by equation 3 will be considered first. The ladder network of Figure 3 has been drawn in such a way as to separate the L-sections of which it is composed. If loading effects were ignored (which could be done if a vacuum tube were placed between each section) the transfer ratio of the rth section would be

$$H_{(p)}^{(r)}=\frac{Z_{2r}}{Z_{2r-1}+Z_{2r}} \tag{11}$$

and the over-all transfer ratio would be the product of the transfer ratios of the individual sections.

$$H_1(p)=H_1^{(1)}(p)\times H_1^{(2)}(p)\times\ldots\times H_1^{(n)}(p) \tag{12}$$

By ignoring the loading effects, a network configuration that will permit the introduction of the zeros and poles of $H_1(p)$ may be chosen, and its transfer ratio is approximated by equation 12. Then an $f(p)$ is chosen to give a Y_{22} that is realizeable. This Y_{22} is synthesized in the configuration previously determined, with the element values proportioned so as to introduce the desired zeros and poles of $H_1(p)$.

Figures 4 and 5 show typical L-sections, and indicate their transfer ratios, zero-pole groupings, and asymptotic plots of the transfer ratios. The procedure for designing a ladder network of the form of Figure 3 to provide the transfer ratio given by equation 12, is to choose from Figures 4 and 5 the L-sections that would permit $H_1^{(1)}(p)$, $H_1^{(2)}(p)$, and so forth, to be realized if loading were ignored. In other words, $H_1(p)$ is factored, and groups of factors are chosen to correspond to $H_1^{(1)}(p)$, $H_1^{(2)}(p)$, and so forth, where $H_1^{(r)}(p)$ contains the factors in the transfer ratio of the rth section. Note that the sections in Figure 4 give unity transfer ratio at zero frequency, whereas the sections of Figure 5 give unity transfer ratio at infinite frequency. Since any ladder is likely to be constructed of both kinds of sections, it follows that the over-all transfer ratio will generally be less than unity at all frequencies. The zeros and poles of $H_1(p)$ may generally be grouped in a number of different ways, each yielding a different configuration of L-sections to form the network. The configuration that yields maximum over-all transfer ratio should be chosen from consideration of the multiplying [illegible] of the transfer ra[illegible] (Several configurations may be possible to [illegible] give the same transfer level.) [illegible]

After the appropriate types of L-sec[illegible]

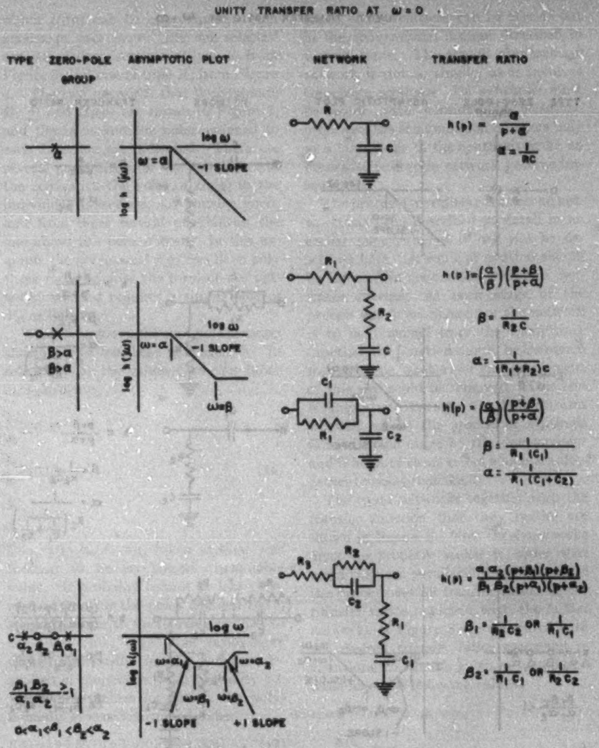

Figure 4. Typical L-sections

Resistance in shunt with C_1 can be provided with a slight reduction in h

tions have been chosen from Figures 4 and 5, they may be cascaded in an arbitrary order to form the ladder network. If the impedance level is scaled up progressively in going from the first to the nth section, see Figure 3, the value of the output driving-point admittance Y_{22} will be determined primarily by the values of Z_{2n} and Z_{2n-1} in the nth (output) section. Going back from the output terminals, each successive section ($n-1$, $n-2$, ... 1) will have a lower impedance level and a relatively smaller effect on the value of Y_{22}. This require[illegible] order of the L-sections in the ladder [illegible]

been chosen, the zeros may be plotted on the p-plane as shown in Figure 5, with each zero identified with the number, from Figure 3, of the section with which it is associated. The poles of Y_{22} (roots of $f(p)$) must then alternate with the zeros, as is indicated by the dotted crosses in Figure 5. The value of Y_{22} at some frequency ω_a is determined by the product of the vectors drawn from its zero to ω_a divided by the product of the vectors drawn from its poles to ω_a.[9] Therefore, if the locations of the poles are chosen so that

[illegible] (13)

[illegible] distances indicated by the [illegible] which were indicated in Figure 5, the desired impedance scaling will be accom-

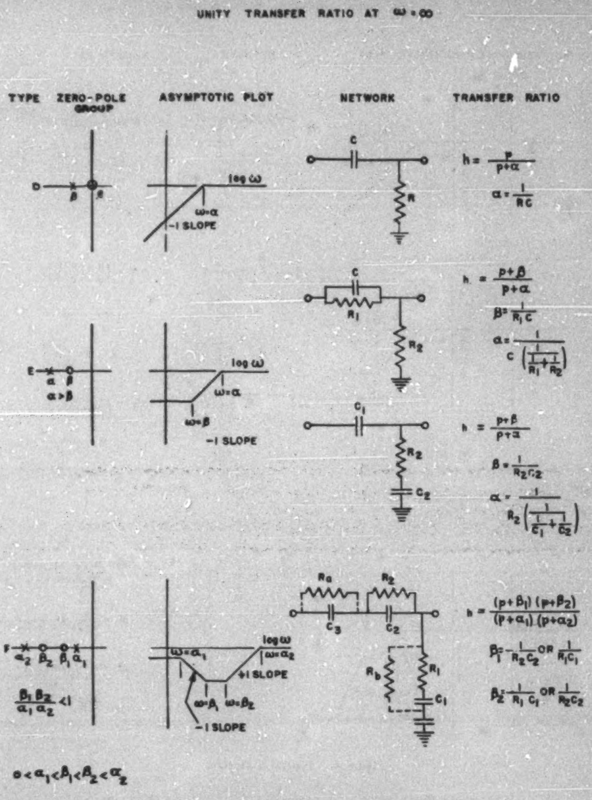

Figure 5. Typical L-sections

The capacitors C_1 and C_3 can be provided with shunt resistors R_a and R_b without reduction in h provided $1/R_aC_3$ is sufficiently near zero. The pole in the series arm $1/R_aC_3$ must then also be a pole of the shunt arm of the L-section

plished. Equation 13 is discussed in detail by Fleck and Ordung in reference 3. Generally the value of each of the ratios in expression 13 is adjusted to be some fraction of the ratio that precedes it; that is

$$\frac{b_n}{d_n}=\frac{1}{10}\,\frac{b_{n-1}}{d_{n-1}};\quad \frac{b_{n-1}}{d_{n-1}}=\frac{1}{10}\,\frac{b_{n-2}}{d_{n-2}}\ldots$$

The fraction need not be the same for all of the inequalities, and its value must be adjusted to fit the particular problem. In general, if the fraction is made too large the loading effects become great enough to prevent the realization of the given Y_{22} in the form of the network that has been chosen to yield $H_1(p)$. As the value of the fraction is decreased, the chances of obtaining a realizable network increase, but the change in impedance level from one end of the network to the other may become excessive, as illustrated by the example that follows. The only known way to test the validity of the choice of locations for the poles of Y_{22} is to try to synthesize the network in the predetermined form. If the process fails, that is, if negative resistances or capacitances are encountered, the only recourse is to shift the poles of Y_{22} closer to the zeros, thus decreasing the loading effects and try again.

Synthesis of Several Ladders in Parallel

Each of the paralleled ladders is synthesized by the method given in the preceding section. However, since all of the ladders must have the same Y_{22}, the poles of Y_{22} chosen for the first ladder must be common to all the ladders. This requires further that the zero (s) of Y_{22} associated with the nth L-section of the first ladder network must also be associated with the nth L-section of all the other ladders.

Therefore, after appropriate L-sections have been chosen to realize the desired transfer ratio of each of the ladders, the L-sections must be arranged in the same order with respect to zeros of Y_{22} that they introduce, in all the ladder networks. This is a necessary requirement to make the impedance level increase properly from section to section in each of the ladders.

After the individual ladders have been synthesized, their impedance levels must be properly scaled so that when all the ladders are paralleled, the over-all transfer ratio will have the desired form. This is done in the following manner. The transfer ratio of each ladder network must be evaluated at any convenient frequency. The result will come out in the form

$$H_1(p)=r_1\frac{h_1(p)}{g(p)}$$

where $h_{1(p)}/g(p)$ is the value of $H_1(p)$ initially chosen, and r_1 is a constant multiplier determined by the parameter values of the network. Since this is the factor r appearing in equations 7, the values of $a_1 \ldots a_n$ may be chosen to satisfy equation 8. The factors a/A that are used to adjust the relative impedance and transfer ratio levels according to equation 10 may then be determined by the use of equation 9.

Summary of the Synthesis Procedure

The steps in the synthesis procedure may now be summarized as follows:

1. Separate the polynomial $h(p)$ which has complex zeros into a sum of polynomials which have only real zeros in the manner of equation 4. From this process obtain the set of transfer ratios for the component ladders that will ultimately be paralleled to realize $H(p)$.

2. Express the transfer ratio $H_r(p)$ of each of the component ladder structures in a factored form so that its zeros and poles are evident. Then for each $H_r(p)$, group the zeros and poles into sets which can be assigned to L-sections selected from Figures

4 and 5. The only groupings that should be considered are those for which the transfer ratio is a maximum.

3. Plot the zeros of $g(p)$ on the p-plane. Number these zeros in correspondence with the order in which the L-sections are cascaded in the network. Note that the order of the zeros of $g(p)$ for each of the ladders must be the same.

4. Pick the poles of Y_{22} [zeros of $f(p)$] such that the poles separate the zeros of Y_{22} [zeros of $g(p)$] and such that the locations of the zeros and poles satisfy the loading considerations expressed in relation 13.

5. Synthesize each of the component ladders by removing elements in such a way that the forms established in step 3 are realized.

6. Calculate the short-circuit transfer admittance of each ladder from equation 7.

7. Determine from equations 8 and 9 the scaling factors to be applied to each of the ladders.

8. Scale the ladders accordingly and then parallel them.

9. In the final structure, scale all impedances to suitable sizes.

EXAMPLE

An example has been chosen to illustrate the method of synthesis and to convey some concept of the variety of the ways for synthesizing the network.

Given

$$H(p)=\frac{p^4+124p^3+11.37\times10^4p^2+6.63\times10^6p+9.5\times10^7}{p^4+38\times10^2p^3+5.39\times10^6p^2+3.382\times10^9p+7.920\times10^{11}}\tag{14}$$

$$=\frac{h(p)}{g(p)}=$$

$$\frac{(p+32.1+j328)(p+32.1-j328)\times(p+36.1)(p+24.1)}{(p+800)(p+900)(p+1{,}000)(p+1{,}100)}$$

There are a variety of ways in which the $h(p)$ may be separated into the form of equation 4. In this example, the separation has been accomplished by making the identifications as follows:

$$H_1(p)=\frac{h_1(p)}{g(p)}=\frac{p^4}{(p+800)(p+900)(p+1{,}000)(p+1{,}100)}\tag{15}$$

$$H_2(p)=\frac{h_2(p)}{g(p)}=\frac{124(p+23.64)(p+855.5)(p+37.86)}{(p+800)(p+900)(p+1{,}000)(p+1{,}100)}$$

$H_1(p)$ can be approximated with four sections of type-D chosen from Figure 5; hence $H_1(p)$ can be realized with one of the canonic forms of driving-point R-C admittances. Of the many networks with which $H_2(p)$ can be approximated with maximum gain factor, the one selected consists of three sections of type-E, from Figure 5, and one of type-A, from Figure 4. The two networks that approximate $H_1(p)$ and $H_2(p)$ are shown in Figure 7, and the zeros and the poles assigned to each L-section are indicated. There are several possibilities for the correlation of the zeros with the poles of $H_2(p)$ in the individual L-sections, all equally good, and from these several possibilities the one above has been chosen. In this example the polynomial $f(p)$ can have only three roots because the form of the networks selected requires a simple pole of Y_{22} at infinity.

With these roots, the zero-pole diagram shown above has been constructed. In selecting $f(p)$, the values taken for b_3/d_3, $b_2/d_2, b_1/d_1$ are

$$\frac{b_3}{d_3}\cong0.05$$

$$\frac{b_2}{d_2}\cong0.03\tag{16}$$

$$\frac{b_1}{d_1}\cong0.01$$

The ratio b_n/d_n was taken at what was thought to be its largest permissible value. It probably cannot be larger because otherwise the poles denoted by b_3 would be closer to the fourth zero than to the third zero. The other ratios were chosen arbitrarily in the manner described in connection with inequality 13. With these values for ratios, the polynomial $f(p)$ was determined to be

$$f(p)=(p+860)(p+970)(p+1{,}090)\tag{17}$$

Hence Y_{22} is

$$Y_{22}=\frac{g(p)}{f(p)}=\frac{(p+800)(p+900)(p+1{,}000)(p+1{,}100)}{(p+860)(p+970)(p+1{,}090)}\tag{18}$$

The first approximate network is a canonic form of driving-point admittance, so its synthesis can be carried out in the conventional fashion described in various texts. The second approximate network is not so simple, as it involves composite sections. Its synthesis must be made with considerable accuracy, otherwise the accumulation of errors may at a later stage in the synthesis make an otherwise realizable network become unrealizable.

The process for realizing the second network has been described in detail in an earlier paper;[3] hence it will not be described here. A word of caution should be injected in connection with this synthesis process. At each stage of the process where an element of the network is to be removed from the admittance function, the function should be examined to determine whether or not an element of this size could be removed. This test is important because it demonstrates whether or not the process of synthesis fails at some stage of the development and it helps to catch errors which are altogether too easy to make.

The exact networks together with the transfer function that they realize are shown in Figure 8. Now these networks must be properly scaled in order that when they are paralleled they will realize the proper over-all transfer ratio. If the transfer ratios achieved with the ladder networks of Figure 8 are compared with the desired transfer ratios expressed in equations 15, the r's given in equation 6 must have the following values:

$$r_1=1$$

$$r_2=\frac{878}{124}=7.06\tag{19}$$

Thus according to equation 8, the a's are chosen as

$$a_1=1$$

$$a_2=\frac{124}{878}=0.141\tag{20}$$

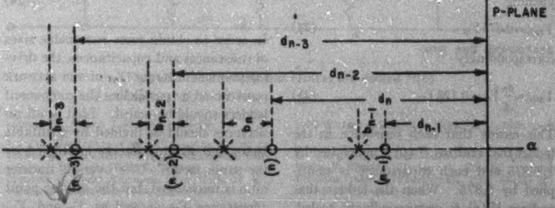

Figure 6. A possible arrangement of the zeros of Y_{22} numbered in correspondence with the L-sections with which they are associated. Possible locations of the poles of Y_{22} (zeros of $f(p)$ are shown by the dotted crosses)

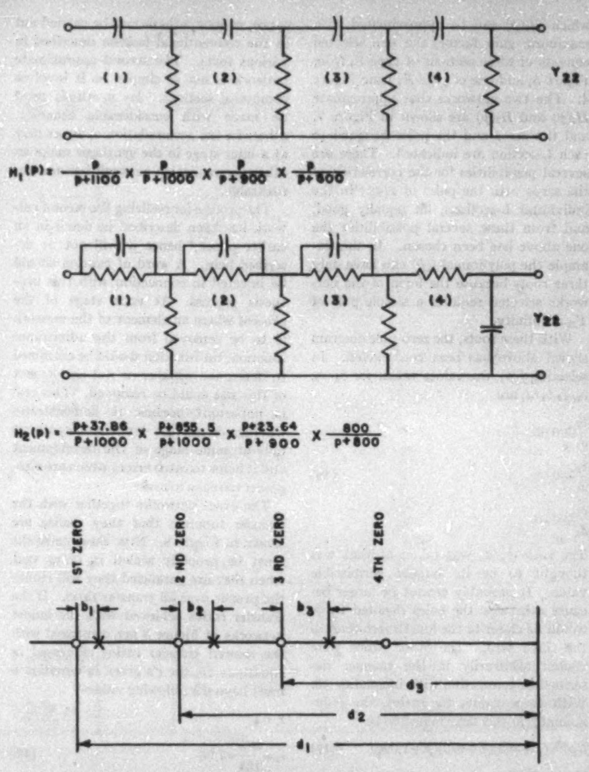
(1)
(2)
(3)
(4)
Y22
H1(P) = p/(p+1100) × p/(p+1000) × p/(p+900) × p/(p+800)
(1)
(2)
(3)
(4)
Y22
H2(P) = (p+37.86)/(p+1000) × (p+855.5)/(p+1000) × (p+23.64)/(p+900) × 800/(p+800)
1 ST ZERO
2 ND ZERO
3 RD ZERO
4TH ZERO
b1
b2
b3
d3
d2
d1

Figure 7. The approximate networks for realizing H₁(p) and H₂(p) and the zero-pole diagram of Y_{22} in the manner of Figure 5

And from equation 9

$$A = a_1 + a_2 = 1.141 \tag{21}$$

Thus according to equation 10 the driving-point admittance of the network that realizes $H_1(p)$ is scaled by $a_1/A = 0.875$ yielding

$$Y_{22(1)} = 0.875\, Y_{22} \tag{22}$$

correspondingly

$$Y_{22(2)} = \frac{a_2}{A}\, Y_{22} = 0.123\, Y_{22} \tag{23}$$

This means that each resistance in the ladder that realizes $H_1(p)$ is multiplied by 1/0.875 and each capacitance is multiplied by 0.875. When the ladder that realizes $H_2(p)$ is correspondingly scaled, the paralleled combination shown in Figure 9 has the driving-point admittance Y_{22} and the transfer ratio

$$H(p) = \frac{1}{A}\,\frac{h(p)}{g(p)} = \frac{1}{1.141} \times \frac{p^4 + 124p^3 + 11.37 \times 10^4 p^2 + 6.63 \times 10^6 p + 9.5 \times 10^7}{p^4 + 3{,}800p^3 + 5.39 \times 10^6 p^2 + 3.382 \times 10^9 p + 7.92 \times 10^{11}} \tag{24}$$

In order to obtain more reasonable sizes of resistances and capacitances, the driving-point admittance Y_{22} of the network constructed by paralleling the component ladders should be scaled. That is, all resistances should be divided by a suitable factor and all capacitances multiplied by the same factor. The over-all transfer ratio is unchanged, but the driving-point admittance Y_{22}, as well as Y_{12} and Y_{11}, are multiplied by a scaling factor. In obtaining the networks shown in Figure 9, the individual ladders that realized $H_1(p)$ and $H_2(p)$ were respectively scaled and then all resistances were further divided by 2×10^{-8} and all capacitances were further multiplied by 2×10^{-8}.

Conclusions

The synthesis procedure described in this paper produces a network that contains fewer paralleled ladders and much smaller aggregate capacitance than an analogous method previously described by Guillemin. The reduction in the number of paralleled ladders results in less loading on each individual ladder. Consequently, a higher possible transfer level is attained for both the individual ladders and the over-all network. In the foregoing example the transfer ratio must be limited to a maximum value of unity at infinite frequency. The transfer ratio of the network of Figure 9 is 1/1.141 at infinite frequency, or 87.5 per cent of the optimum value.

On the other hand, it would seem from the example selected that unduly large range of parameter values is involved. This is characteristic of the particular example and not necessarily characteristic of the method. In the example chosen, the large range of parameter values is a direct consequence of the fact that the zeros of Y_{22} are closely grouped, and that the group is at a considerable distance from the origin of the p-plane. Thus, in order to place poles between the zeros, the percent of loading assumed must be small. For the same distribution of zeros, any of the Cauer ladder forms will have a similar range of parameter values. This means that the Guillemin realization of this particular transfer ratio will have a range of parameter values comparable to that in the example.

The concluding observation may be made that when the poles of a transfer ratio are necessarily closely grouped and far from the origin, it is probably better from the standpoint of range of parameter values to factor the transfer ratio into the product of two or more component transfer ratios and to realize these as networks coupled together by vacuum tubes in order to avoid the excessive range of part sizes.

Appendix I

The reduction of a polynomial containing complex zeros into a sum of polynomials containing only real zeros can be accomplished in a variety of ways, the extent of the variety depending upon the particular polynomial which is to be reduced. It is unfortunate that in so far as the authors have been able to determine there is no criterion for determining the least number of polynomials with which equation 4 can be accomplished. Some of the ways in which the breakup can be accomplished will be illustrated. Let

$$h(p)=(p+\alpha_1)\ldots(p+\alpha_n+jp_n)\times(p+\alpha_n-j_n) \quad (25)$$

where the roots may be real or complex provided the complex roots occur in conjugate pairs. One method is that due to Guillemin, in which $h(p)$ is written in the form

$$h(p)=a_rp^r+a_{r-1}p^{r-1}+\ldots+a_1p+a_0 \quad (26)$$

and in which the following identifications are made:

$$\begin{aligned} h_r(p)&=a_rp^r\\ h_{r-1}(p)&=a_{r1-}p^{r-1} \quad (27)\\ h_{(0)}(p)&=a_0 \end{aligned}$$

For an rth degree polynomial $h(p)$ this gives $r+1$ polynomials, each with zeros at the origin, and the synthesis requires $r+1$ paralleled ladder networks.

Another way is to let

$$\begin{aligned} h_q(p)&=a_rp^r+a_{r-1}p^{r-1} \quad (28)\\ h_{q-1}(p)&=a_{r-2}p^{r-2}+a_{r-3}p^{r-3} \end{aligned}$$

thus yielding in general a number of ladders given by the first integer $\geq r+1/2$. This method involves approximately half as many ladders. In general, the more terms of $h(p)$ that can be included in a given polynomial $h_q(p)$ subject to the requirement that $h_q(p)$ has real negative zeros, the fewer will be the number of the polynomials and the fewer will be the number of ladder structures involved in the synthesis process.

Another method which deserves mention is that in which the transfer ratio

$$H(p)=\frac{h(p)}{g(p)} \quad (29)$$

may be expressed as

$$H(p)=h_0+\frac{h'(p)}{g(p)} \quad (30)$$

where $h'(p)$ has real positive coefficients. In turn $h'(p)/g(p)$ may be realized by the methods of this paper. In the final network the constant h_0 in the transfer ratio is realized by connecting between the input and output terminals, an appropriately scale 2-terminal admittance kY_{22} where k is the scaling factor.

As the designer becomes familiar with the process, other methods for breaking $h(p)$ will become evident. The virtues associated with the variety of methods for reducing $h(p)$ is that for each way of reducing $h(p)$ a particular network exists; hence the extent of the variety of ways of reducing $h(p)$ is the extent of the variety of networks that will have the same transfer ratio.

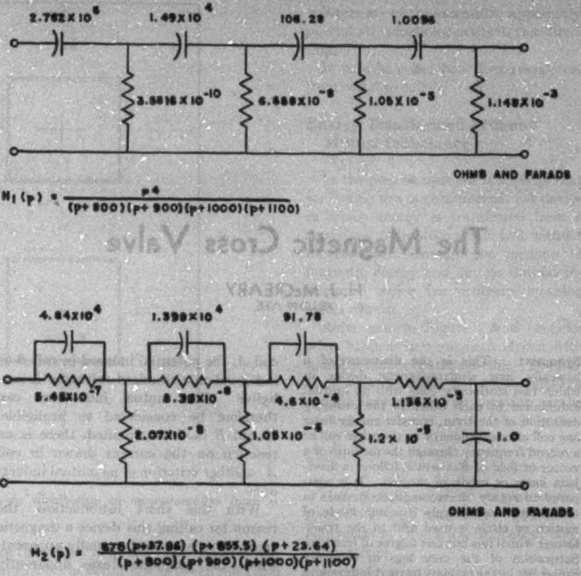
2.762X10^5
1.49X10^4
106.28
1.0096
3.5816X10^-10
6.888X10^-8
1.05X10^-5
1.148X10^-3
OHMS AND FARADS
H1(p) = p4 / (p+800)(p+900)(p+1000)(p+1100)
4.84X10^4
1.399X10^4
91.78
5.45X10^-7
8.35X10^-8
4.6X10^-4
1.136X10^-3
2.07X10^-8
1.05X10^-5
1.2X10^-5
1.0
OHMS AND FARADS
H2(p) = 878(p+37.86) (p+855.5) (p+23.64) / (p+800)(p+900)(p+1000)(p+1100)

Figure 8. Ladder networks that realize $H_1(p)$ and $H_2(p)$

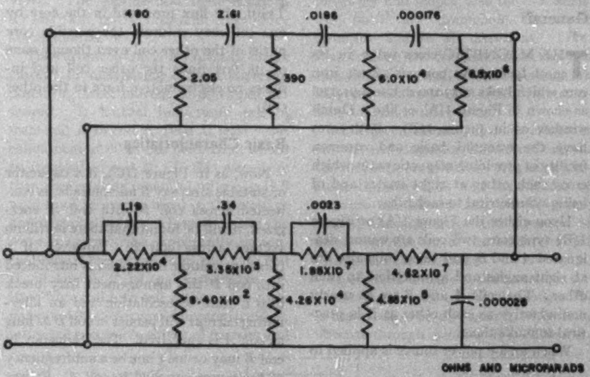
480
2.61
.0186
.000176
2.05
390
6.0X10^4
6.5X10^6
1.19
.34
.0023
2.22X10^4
3.35X10^3
1.86X10^7
4.62X10^7
8.40X10^2
4.26X10^4
4.86X10^5
.000026
OHMS AND MICROFARADS

Figure 9. The network that realizes the desired H(p)

References

1. Synthesis of R-C Networks, E. A. Guillemin. *Journal of Mathematics and Physics* (Cambridge, Mass.), volume XXVIII, number 1, April 1949, pages 22–42.

2. The Synthesis of Resistor-Capacitor Networks, J. L. Bower, Philip F. Ordung. *Proceedings*, Institute of Radio Engineers (New York, N. Y.), volume 38, March 1950, pages 263–69.

3. The Realization of a Transfer Ratio by Means of a Resistor-Capacitor Ladder Network, J. T. Fleck, Philip F. Ordung. *Proceedings*, Institute of Radio Engineers (New York, N. Y.), volume 39, September 1951, pages 1069–74.

4. The Synthesis of Resistor-Capacitor Networks, J. L. Bower, J. T. Fleck, Philip F. Ordung. General Electric Company (Schenectady, N. Y.), August 1948.

5. Communication Networks, E. A. Guillemin. John Wiley and Sons, New York, N. Y., 1935, pages 216–19.

6. Frequency Coordinate Vector Diagram, Philip F. Ordung, Herbert L. Krauss. *Journal*, Franklin Institute (Philadelphia, Pa.), volume 251, March 1951, pages 343–50.

No Discussion

The Magnetic Cross Valve

H. J. McCREARY
FELLOW AIEE

Synopsis: This is the discussion of a basically new electromagnetic device in which two stationary coils with no mutual inductance to each other in the ordinary definition of the term, transfer energy from one coil at one frequency to the other coil at a second frequency through the medium of a vector or field of flux which follows a lissajous locus or mode of motion. It is compared to rotary electromagnetic devices in which the more simple lissajous mode of motion or circle is used and to the transformer which has but one degree of freedom. Saturation of the core legs in sequence causes an instantaneous mutual inductance to become active, and alternating at a frequency different than the power source.

General

THE MAGNETIC cross valve in its most basic form consists of an iron core which looks very much like a pretzel as shown in Figure 1(A) or like a Dutch window as in Figure 1(B). Both cores have the essential basic and common facility of providing magnetic paths which cross each other at right angles and of being symmetrical to each other.

Upon either the Figure 1(A) or Figure 1(B) type core, two coils are wound, designated *A* and *B*, and these coils also are at right angles and symmetrical to each other. The coils *A* and *B* are as nearly noninductive to each other as it is practical to make them.

When an a-c power source is applied to coil *A*, the potential induced in coil *B* as indicated on a standard voltmeter is negligible. The mutual inductance can therefore be considered as negligible. If coil *B* is short circuited, there is no reaction on the current drawn in coil *A*, another criterion of no mutual inductance.

With this short introduction, the reason for calling this device a magnetic cross valve is at least partially apparent. First, the magnetic fluxes apparently cross and are symmetrical. Second, the magnetomotive forces of the two coils cross symmetrically at right angles. Third, the flux produced in the core by one coil may saturate the possible core paths of the other coil even though none of its flux links the other coil and induces no electromotive force in the other coil.

Basic Characteristics

Now, as in Figure 1(C), if a capacitor of suitable size, say 6 microfarads, is connected across coil *B* with coil *A* energized, it will be found that there is still no voltage across coil *B*. However, if a transient voltage or impulse is introduced into coil *B* this arrangement may break into a state of oscillation and an alternating current will persist in coil *B* as long as coil *A* is energized. The frequency in coil *B* may or may not be a subfrequency of the power supplied to coil *A*. It was found that if a continuous d-c magnetomotive force is superimposed on the magnetic circuit of coil *A* as in Figure 1(D) or Figure 1(E), there is a tendency for an even subharmonic to appear in coil *B*, (that is, with 60 cycles applied to coil *A* with d-c superimposed) either 30 cycles or 15 cycles may be obtained from coil *B*.

If the current in the output coil of Figure 1(C) is of such a value as to cause a degree of saturation, then an odd subharmonic may be generated in the output coil. The technique and design of equipment for starting and generating an odd subharmonic will be described later, but for the present only the generation of even subharmonics will be discussed.

It has been noted that there was a negligible mutual inductance between coil *A* when *A* was energized and *B* was open or short circuited.

Actually, in a model in which no particular pains were taken to obtain a perfect balance with 110 volts 60 cycles on coil *A*, of 400 turns, a voltage of less than 0.25 volt was measured with a vacuum tube voltmeter of high impedance (about 1,000,000 ohms) across coil *B* of 1,100 turns. This shows that less than 0.83 per cent of the flux through coil *A* passes through coil *B*. Rebalancing the legs by changing the laminations, this was further reduced to 0.02 volt or 0.006 per cent of flux in coil *A* passing through coil *B*. Such an insignificant amount of mutual

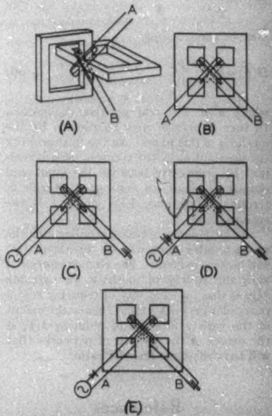

Figure 1(A). Magnetic cross valve first type. **(B).** Magnetic cross valve second type. **(C).** Cross valve with no inherent mutual inductance. **(D).** Even subharmonic cross valve using battery. **(E).** Even subharmonic cross valve using rectifier

---

Paper 51-343, recommended by the AIEE Basic Sciences Committee and approved by the AIEE Technical Program Committee for presentation at the AIEE Fall General Meeting, Cleveland, Ohio, October 22–26, 1951. Manuscript submitted December 21, 1950; made available for printing September 11, 1951.

H. J. McCreary is with the Automatic Electric Company, Chicago, Ill.

Some portions of this paper are entirely new, some parts of it have been taken from a paper by the author in Proceedings of the National Electronics Conference 1949, volume 5 and some parts are taken from his Thesis presented to the University of Nebraska, Lincoln, Nebr., June 1, 1950.

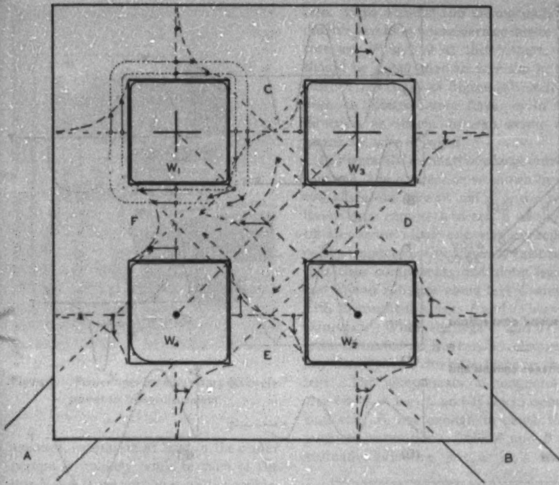

Figure 2. Magnetic cross valve showing varying distribution of magnetomotive force

inductance cannot account for what takes place and in so far as this device is concerned can be neglected and assumed to be zero. At such a fine value of balance a higher frequency of induced potential was noted which was probably caused by the Barkhausen effect. This fine degree of balance did not seem to affect noticeably the ability of the unit to start in the two cases mentioned previously.

Now consider the case when 30-cycle power is produced in coil *B* and coil *A* is energized by 60-cycle power. Is there negligible mutual inductance between coil *A* and coil *B*? First consider the AIEE American Standard definition of mutual inductance:[1]

> "Mutual Inductance is the common property of two associated electric circuits which determines, for a given rate of change of current in one of the circuits, the electromotive force induced in the other."

Now from this definition it is clear that, in order to have mutual inductance, what takes place in circuit number 1 must have mathematical relationship with what takes place in circuit number 2. Specifically the potential in the primary coil 1, or at least some component of it, must be equal to a constant *M* multiplied by the rate of change of current in the secondary. Likewise the potential in the secondary coil 2 or at least some component of it must be equal to this same constant *M* multiplied by the rate of change with respect to time of the current in the primary circuit. The relations just stated in the definition, between coil 1 and coil 2, apparently do not exist between coil *A* and coil *B* of the magnetic cross valve. The reasons that these relations do not exist in the magnetic cross valve are as follows.

The current in coil *A* is pulsating direct current or alternating current superimposed on direct current of 60 cycles per second. If mutual inductance existed from coil *A* to coil *B*, then at least some component at 60 cycles per second would be induced in coil *B*. If this were true then the resulting potential wave of coil *B* would not be symmetrical in the positive and negative halves. However, since the wave is symmetrical, apparently no mutual inductance exists from coil *A* to coil *B*. Likewise if mutual inductance existed from coil *B* to coil *A* then some component of 30 cycles would appear in coil *A*, but since successive waves of current and voltages are of the same size, apparently no mutual inductance exists in this direction.

It may be asked how does energy get from coil *A* to coil *B*?

Energy Transformed Without Mutual Inductance

In the present instance it appears that something new is encountered. A device in which energy is transferred from a single coil to another single coil without moving parts through the medium of magnetic energy and yet no mutual inductance under the ordinary meaning seems to exist.

Refer now to Figure 2 and consider what happens in a magnetic circuit with multiple parallel paths possible. In practical work, constant μ (permeability) is usually assumed and an equation can be used as:

$$\phi = \frac{F}{R}$$

Here flux is equal to magnetomotive force divided by reluctance. This is the equivalent of Ohm's law applied to magnetic circuits.

However, μ (permeability) is not a constant, and the flux does not always follow the same pathway. The magnetomotive forces per unit length, also the flux densities, both vary throughout the whole structure and in all directions. Likewise because the frequencies of the two coils are different, all of these relations are different with respect to time. First consider magnetomotive force.

At a given instant, specific values of current and magnetomotive force exist in the magnetic cross valve. At such an instant the directions and magnitudes of currents are known and curves representing the magnitude and direction of magnetomotive forces can be determined throughout the structure.

In Figure 2, as shown, the current in the conducting copper of coil *B* window W_1 is assumed to be downward, while it is upward through window W_3. The cur-

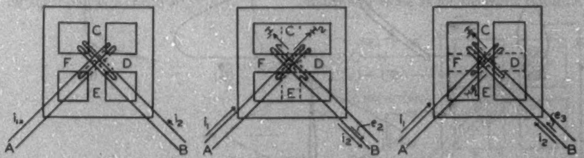

(A) (B) (C)

Figure 3. Magnetic cross valve. (A). No inherent mutual inductance. (B). Currents in coils so that horizontal legs only are effective. (C). Currents in coils so that vertical legs only are effective

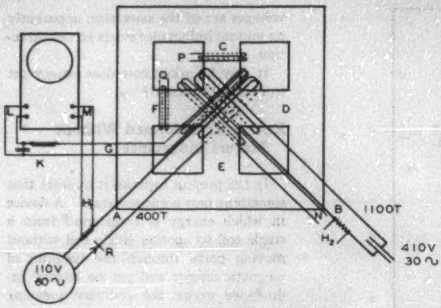

Figure 4 (above). Magnetic cross valve with oscilloscope connections

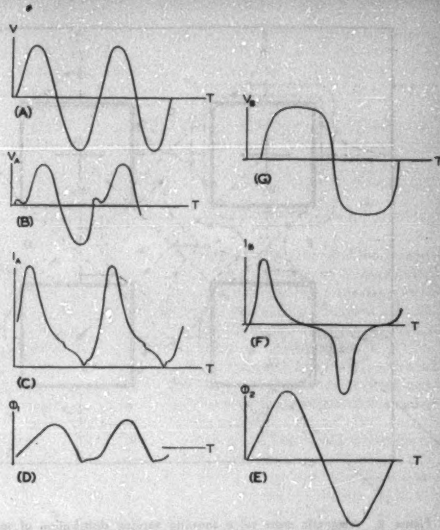

Figure 6 (right). Oscillograms of input and output voltages currents and magnetic fluxes

rent in the conducting copper of coil *A* window W_3 is assumed to be downward, while in window W_4 the same current is upward. The foregoing fact is indicated schematically by the crosses denoting the tails of the arrow, and the dot the point of the arrow.

When curves of magnetomotive force are superimposed on the core of Figure 2 it is clear that the summation of *H* (magnetomotive force per centimeter) about the magnetic circuit gives an over-all magnetomotive force which is most concentrated near the conducting copper.

It is observed that the iron immediately adjacent to the conducting copper will experience a magnetomotive force which is almost a direct function of the current in the adjacent copper, but the magnetomotive force back in the iron core is a compromise between it and the other conductor.

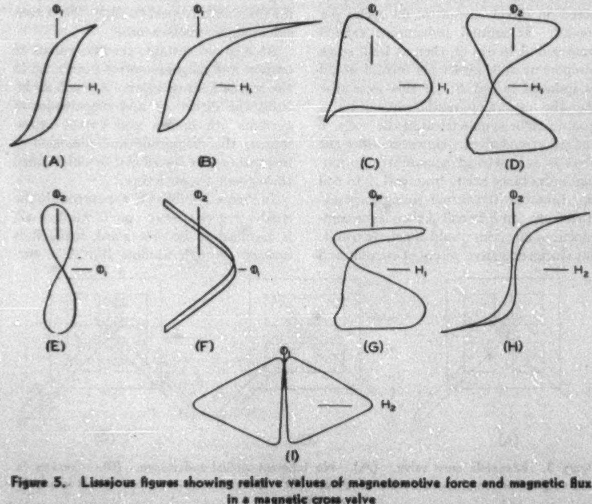

Figure 5. Lissajous figures showing relative values of magnetomotive force and magnetic flux in a magnetic cross valve

The path of least reluctance for the magnetic flux is the shortest path about the conducting copper. These two factors combine to cause the resulting flux normally to be most intense in close proximity to the conducting copper.

This is not the whole story, however, because the reluctance in iron is not a constant, and when the iron next to the copper becomes saturated, the flux then takes the next more favorable path which is just a short distance back in the iron away from the conducting copper.

In this way, magnetic saturation may exist in close proximity to the copper, and yet not exist back in the core away from the copper. As the magnetomotive force increases, the magnetic flux and the magnetic saturation may expand outward from one conducting copper, until it is common to the magnetic flux and magnetic saturation of one of the other conducting coppers.

Referring now to one of the old masters of the electrical art, A. E. Kennelly:[3]

> "When one realizes, from such observation as these here reported, that not only the alternating flux density, but also alternating flux wave form is different at each and every radial belt, the entire phenomenon of a-c magnetic conduction in ring laminae takes an altered aspect."

This fact has been checked using exploring coils.

In each of the legs designated *C* and *E* of Figure 2, since the magnetomotive forces are in opposition, at the instant

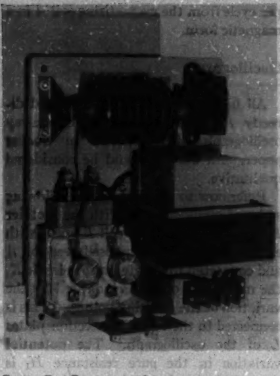

Figure 7. Poweringer for converting 60-cycle power to 30-cycle power

assumed, saturation at least in the center portion is unlikely while in each of the legs *F* and *D*, saturation is quite possible. Therefore in such a case instantaneous mutual inductance between coil *A* and coil *B* might be said to exist. At such an instant it is clear that the instantaneous potential induced in coil *B* is equal to the instantaneous mutual inductance from *A* to *B* times the rate of change of current in coil *A* with respect to time and vice versa.

In order to more clearly illustrate the operation of the magnetic cross valve and the alternating mutual inductance refer to the illustrations Figures 3(A), (B), and (C).

In Figure 3(A) a relatively low value of flux density is active in any part of core due to the magnetomotive force of coil *A*, coil *B*, or their combination. This results in a zero mutual inductance at this instant because none of the iron is saturated and no electromotive force is induced in coil *A* by coil *B*.

In Figure 3(B) a relatively large current i_1, in coil *A* in a direction as shown by arrow along one wire of coil *A* and a relatively large current i_2 in coil *B* as shown by the arrow along one wire of coil *B* causes magnetomotive forces to exist such that their components add along legs *C* and *E* and subtract along legs *F* and *D*, with the result that legs *C* and *E* become saturated. When the legs *C* and *E* are saturated no further flux change of any consequence can take place in these legs. The components of magnetomotive force along legs *F* and *D* subtract from each other therefore the magnetomotive forces in legs *F* and *D* are not enough to cause magnetic saturation. Coils *A* and *B* now are mutually inductive just as in a transformer due to the core legs *F* and *D* at this instant. It should be noted that an increase in the current i_1 of coil *A* of Figure 3(B) will induce an electromotive force, e_2 in the direction as shown by the arrow adjacent one wire of coil *B*.

In Figure 3(C) a relatively large current i_1 in coil *A* in a direction as shown by arrow along one wire of coil *A* and a relatively large current i_2 in coil *B* as shown by the arrow along one wire of coil *B* causes magnetomotive forces to exist such that their components add along legs *F* and *D* and subtract along legs *C* and *E* with the result that legs *F* and *D* become saturated. When the legs *F* and *D* become saturated no further flux change of any consequence can take place in these legs. The components of magnetomotive forces in legs *C* and *E* are in opposition and are not enough to cause their magnetic saturation. Coils *A* and *B* are mutually inductive just as in a transformer due to the core legs *C* and *E* at this instant. It should be noted that an increase in the current i_1 in coil *A* of Figure 3(C) will induce an electromotive force, e_2 in the direction as shown by the arrow adjacent one wire of coil *B*.

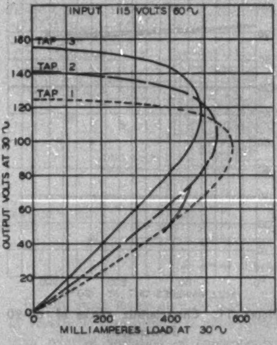

Figure 8. Characteristic curves of 60-30 Poweringer

It should further be noted comparing Figure 3(B) and Figure 3(C) that an increase in current in coil *A* induces a potential e_2 down on one wire of coil *B* under conditions of Figure 3(B) but the same current change induces a potential e_2 up in the same wire under conditions of Figure 3(C) so that the mutual induction relations have been reversed.

Now if the current in coil *A* is direct current with alternating current superimposed it is clear that the mutual inductance relationship can be reversed only by the current in coil *B* since the magnetomotive force due to coil *A* is always in the same direction.

The legs *F* and *D* may saturate with legs *C* and *E* not saturated at one instant; the legs *C* and *E* may saturate with legs *F* and *D* not saturated the next instant. In this case it is clear that *m* will be reversed. From this it now becomes clear that mutual inductance does not exist between the two fixed coils as in a transformer, but a variable mutual inductance exists very much like that between a rotor and stator of a rotating electromagnetic device, and this variable mutual inductance can and does reverse itself. In the 60-30 magnetic cross valve the average value of *m* is zero. The direction and value of the instantaneous mutual inductance is determined by the relative currents in coils *A* and *B* and the structure and material of the core.

Now refer to another of the old masters of the electrical art, Charles Fortescue,[3] when he said:

> "We can no longer express the electromotive force induced in a given circuit due to a current flowing in another by $M_{12}di_2/dt$ as in a simple network but must use instead $d/dt(M_{12}i_2)$."

Both the current and the mutual inductance may vary with respect to ti me Take the statement of C. Fortescue

$$e_1 = \frac{d}{dt}(M_{12}i_2)$$

but adopt the more formal notation of small m_{12} instead of large M_{12} for a variable function and use large M_{12} for the maximum value as for the usual notation

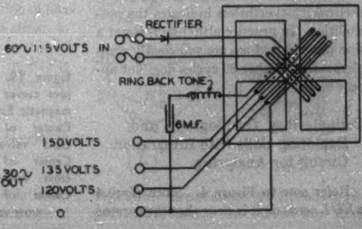

Figure 9. Circuit of 60-30 Poweringer

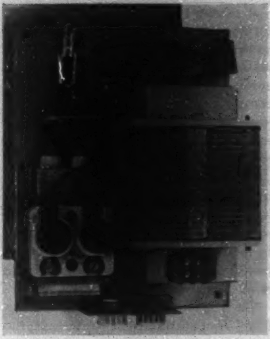

Figure 10. Poweringer 60-20 cycles

of current or voltage. Then the relation is

$$e_1=\frac{d}{dt}(m_{12}i_2)$$

Now let

$$m_{12}=M_{12}\sin\omega t$$
$$i_2=I_2\sin(\omega t+a)$$

assuming that i_2 is the same frequency as m_{12} but with a phase displacement a. Then

$$i_2m_2=I_2M_{12}\sin\omega t\sin(a+\omega t)$$

And

$$e_1=\frac{d}{dt}(i_2m_{12})=I_2M_{12}\omega[\sin\omega t\cos(a+\omega t)+\sin(a+\omega t)\cos\omega t]$$

But from trigonometry

$$\sin(A+B)=\sin A\cos B+\cos A\sin B$$

So that the above reduces to

$$e_1=\frac{d}{dt}(i_2m_{12})=I_2M_{12}\omega\sin(a+2\omega t)$$

If $\omega=2\pi f$ and $f=30$ cycles per second then it is obvious that: e_1 is varying at 60 cycles per second; i_2 is varying at 30 cycles per second; m_2 is varying at 30 cycles per second.

Although the assumed case is hypothetical it nevertheless indicates the possibilities. In practice although i_2 is not a sine wave, i_2 and m_{12} are sufficiently complementary so that 30 cycles does not appear in coil 1.

Cathode-Ray Oscillograph and Exploring Coils with Integration Circuit for Analyzing

Refer now to Figure 4. Since $H=0.4\pi Ni/L$ oersteds it is clear that the current is directly proportional to the magnetomotive force per centimeter for any given magnetizing coil. Therefore, if a very small pure resistance is placed in series with the coil the resulting electrical potential across this resistance is proportional to the current flowing through it and in phase with that current, and therefore proportional to H and in phase with H.

Since $e=-Nd\phi/dt10^{-8}$ for an exploring coil when it is placed about a section of iron which is being magnetized, we will obtain an electromotive force which is proportional to the rate of change of the flux through the iron and the turns of the coil encircling it. If the exploring coil G is connected through an integration circuit with respect to time K and then applied to an amplifier a potential will be obtained at L which varies in magnitude and time with the magnetic flux through the exploring coil G.

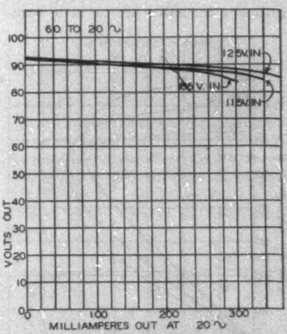

Figure 11. Characteristic curves of 60-20 Poweringer

If the voltage representing H is applied to the horizontal scan M and the voltage representing B or ϕ of coil G is applied to the vertical scan L a hysteresis curve results, and its area represents energy lost per cycle from the magnetizing coil A in a magnetic form.

Oscillograms

All figures in Figure 5 were traced directly from the face of a cathode-ray oscillograph with a pencil on tracing paper. All curves should be considered qualitative.

Refer now to Figure 4 for the following series of oscillograms. With the rectifier R short circuited, with coil B open, with exploring coil G superimposed over coil A and connected to an integration circuit K, the magnitude of flux is indicated by the variation of the resulting voltage. This is connected to the vertical deflection plates L of the oscillograph. The potential variation in the pure resistance H_1 is connected to the horizontal deflection plates M where it indicates current. The result is the hysteresis curve shown in Figure 5(A).

When the short circuit is removed from the rectifier R thus superimposing a d-c component, the hysteresis curve is distorted into the curve as shown in Figure 5(B).

If now the 6-microfarad capacitor is connected into the secondary circuit, the hysteresis curve suddenly becomes larger to form the greatly increased area ϕ_1-H_1 or $B-H$ curve shown in Figure 5(C). This curve indicates larger magnetic energy losses, caused by the absorption of the magnetic energy by coil B into its magnetic and electric circuit.

Now since energy was lost from coil A and apparently it was absorbed by coil B, disconnect the integration circuit from exploring coil G superimposed on coil A, and connect it to an exploring coil N superimposed on coil B. This shows in Figure 5(D) the variation of magnetic flux through coil B as the magnetomotive force varies in coil A. It looks somewhat like the curve of Figure 5(C) plus a mirror reflection of itself. It is interesting to note that a planimeter

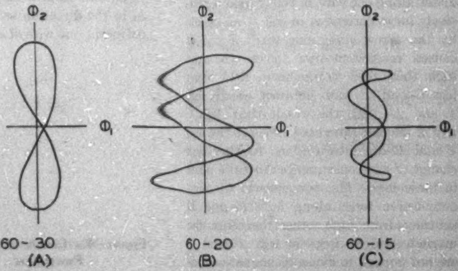

Figure 12. Lissajous curves of the magnetic flux. (A). Center of 60-30 cross valve. (B). Center of 60-20 cross valve. (C). Center of 60-15 cross valve

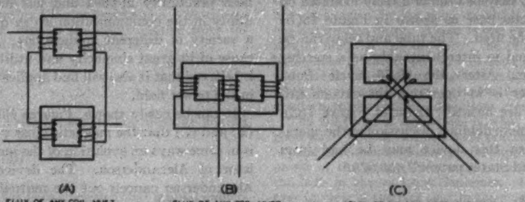

(A)	(B)	(C)
FLUX OF ANY COIL MUST LINK ANOTHER COIL	FLUX OF ANY COIL MUST LINK ANOTHER COIL	FLUX OF ANY COIL NEED NOT LINK ANOTHER COIL
MUTUAL INDUCTANCE EXISTS BUT INDUCED EMF'S CANCEL	MUTUAL INDUCTANCE EXISTS BUT INDUCED EMF'S OR MMF'S CANCEL	NO MUTUAL INDUCTANCE LOCALIZED CORESATURATION OF PAT. 2,324,634 ONLY IN C
	MORE EFFICIENT THAN A	MORE EFFICIENT THAN B
4 COILS 2 MAGNETIC CIRCUITS	3 COILS 3 MAGNETIC CIRCUITS	2 COILS 4 MAGNETIC CIRCUITS
		CENTERS OF MMF. SUPERIMPOSED AND CROSSED ONLY IN C

ALL ARE SYMMETRICAL ELECTRICALLY & MAGNETICALLY

ALL CAN BE USED AS: FREQUENCY MULTIPLIER, FREQUENCY DIVIDER, MODULATOR, AMPLIFIER, RELAY.

Figure 13

applied to this figure will indicate that it has a zero area while that of Figure 5(C) has a real area.

By placing integration circuits on both exploring coils *G* and *N* of Figure 4, a curve is produced showing how the resulting flux varies in direction and time at the center of the core. This is shown in Figures 5(E) and (F) for two different values of impressed primary voltage. It is quite clear from Figure 5(E) how a single vector of flux can vary through two cycles along one axis and yet in the same time period only one cycle along the other axis and in so doing convert 60 cycles to 30 cycles. It might be here noted that the tendency towards subsynchronism between the even subharmonic and the power source with direct current superimposed is so strong that the capacitance can be varied from 10 to 90 microfarads on some models without disrupting the operation or changing the output frequency.

Following the $B-H$ curves further, an exploring coil *Q* can be placed about the core leg *F* to discover how this flux varies as the magnetomotive force H_1 is applied. The curve shown in Figure 5(G) is the result. In this case the planimeter indicates a real area. A curve identical to that found in the leg *F* exists in leg *C*, but if the two exploring coils *P* and *Q* are connected in series aiding, a curve identical to Figure 5(C) results when passed through the integration circuit. If the exploring coils *P* and *Q* on legs *F* and *C* are reversed with respect to each other, the resulting induced voltage when passed through the integration circuit produces a curve identical to Figure 5(D).

If the current flowing in coil *B* is used as the magnetomotive force H_2 for comparison, and an exploring coil *N* with integration circuit *K* used to indicate the magnitude of flux through coil *B* then the hysteresis curve of Figure 5(H) results.

If the current in coil *B* is used as the magnetizing force H_1 and an exploring coil *G* with integration circuit used to indicate the flux through coil *A*, the curve shown in Figure 5(I) results.

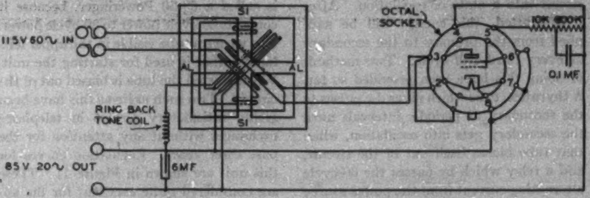

Figure 14. Circuit of 60-20 Poweringer

Finally since many may be interested in variations with respect to time rather than relative variation of components: in 6(A) is shown the wave shape of the power supply voltage which is almost a perfect sine wave with respect to time; in (B) is shown the variation of voltage across the terminals of coil *A* with respect to time; in (C) is shown the variation of input current to coil *A* with time; in (D) is shown the variation of flux through coil *A* with respect to time; in (E) is shown the variation of flux through coil *B* with respect to time; in (F) is shown the variation of current in coil *B* with respect to time; in (G) is shown the variation of voltage across coil *B* with respect to time.

Summary of Fundamentals for 60-30 Frequency Conversion

To summarize fundamentals, it is believed that this is a basically new type of static apparatus in which energy is transferred from one single coil to another single coil by magnetic energy and furthermore, that it does not have mutual inductance *M*, according to the ordinary definition of this term. The results might be explained mathematically, if it is assumed that an instantaneous mutual inductance *m* exists which varies cyclically with time, and which may be pulsating or reversing and positive or negative. Mechanical analogues have been found useful in analyzing and predicting results in the magnetic cross valve.

In Figure 12(A) is shown the locus of the vector of flux for 60- to 30-cycle frequency conversion; in Figure (B) is shown the locus of the vector of flux for 60- to 20-cycle frequency conversion; in Figure (C) is shown the locus of the vector of flux for 60- to 15-cycle frequency conversion.

The cathode-ray oscillograph with integration circuits has been found useful to display the relationships of magnetomotive force and resulting fluxes from instant to instant. It is believed and hoped that the magnetic cross valve will find economic significance somewhere between the motor generator and the transformer, because, though it has the structure of a transformer, and can under the right conditions act like one, yet, without moving parts, it can change frequencies like the motor-generator.

Its inherent simplicity of structure indicates its very basic natures. It is be-

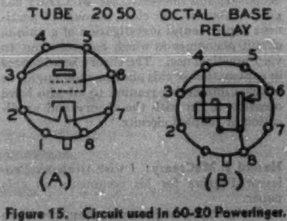

Figure 15. Circuit used in 60-20 Poweringer. (A). 2050 tube. (B). Octal base relay

lieved that this is the first time two stationary coils have been linked together by a balanced cyclical mutual inductance in a static device.

It also is believed that this is the first time that a vector or field of flux which oscillates in a Lissajous mode more complex than a single loop (that is, a circle, ellipse or straight line) has ever been used to couple or transfer power.

The Magnetic Cross Valve for 60-20 Frequency Conversion

In order to generate the third subharmonic, it is apparent that the magnetic cross valve should be so designed that the primary coil is thrown into mutual induction relationship with the secondary coil in every third half cycle only.

Since there is no mutual inductance between the primary and secondary coils of the 60-20 Poweringer produced by the primary coils, some means must be provided to get the secondary into oscillation. In other words, starting means must be provided to get the secondary circuit into a state of oscillation. After it is started, this energy will be supplied from the primary to the secondary at every third half cycle. Two methods of doing this have been provided so far. A thyratron tube which gives d-c pulses to the secondary at periodic intervals until the secondary gets into oscillation, when that tube biases itself out of the circuit, and a relay which by-passes the 60-cycle alternating current from the power source to the secondary circuit until it gets into oscillation when it disconnects the power source from the secondary.

The starting circuit means are shown in Figure 14.

A standard *2050* thyratron tube, Figure 15(A) may be used or a relay mounted on an octal base as shown in Figure 15(B) may be used. The tube and relay can be plugged in interchangeably as a starting means. After the 60-20 cycle Poweringer is in operation the circuits utilized are basically those of Figure 1(C).

A more detailed discussion of the operation of this device may be had from United States patent 2,455,078.[4]

Practical Embodiments of the Cross Valve for Frequency Division

In Figure 7 is shown a unit employing the magnetic cross-valve fundamental. It has been called a Poweringer. Such a unit has been in use in a telephone exchange for the past 5 years for a proving-in test and the service organization has not touched it in that time. In Figure 8 is shown some regulation curves of the device of output volts against output current from the three different output taps provided. In Figure 9 is shown the actual circuit of the 60-30 Poweringer. In Figure 10 is shown another unit employing the magnetic cross valve fundamental. This is called a 60-20 Poweringer, because it converts 60-cycle power to 20-cycle power. The vacuum tube visible in the upper left-hand corner is used for starting the unit. When started the tube is biased out of the circuit. Two such units as this have been giving satisfactory service in telephone exchanges without any attention for the past three years. Regulation curves for this unit are shown in Figure 11. These are considered quite excellent for the applications in which they are used.

Conclusion

In so far as now known, this is a basically new inductive phenomenon, it has been practically applied and has found utility in the communication art in quite a variety of different applications. Because of its great simplicity and utility it is believed that it also will find application in the power field.

It can be easily shown, Figures 13(A), (B) and (C) that the magnetic cross valve is in some ways an evolution of the modulator of Alexanderson. The device of Alexanderson cancels out the mutual inductance with two opposing balanced coils. In the magnetic cross valve the mutual inductance is zero to start with.

References

1. AMERICAN STANDARD DEFINITIONS OF ELECTRICAL TERMS. AIEE, section 05,20,175, 1941.

2. MAGNETIC FLUX DISTRIBUTION IN ANNULAR STEEL LAMINAE, **A. E. Kennelly, P. L. Alger.** *AIEE Transactions*, volume 36, 1917, page 1147.

3. *Discussion* by **C. Fortescue** of NO-LOAD CONDITIONS OF SINGLE-PHASE INDUCTION MOTORS AND PHASE CONVERTERS, **R. E. Hellmund.** *AIEE Transactions*, volume 37, part I, 1918, pages 663–68.

4. FREQUENCY CHANGER, **Harold J. McCreary.** United States Patent number 2,455,078, November 30, 1948.

5. GYROMAGNETIC AND ELECTRON-INERTIA EFFECTS, **S. J. Barnett.** *Reviews of Modern Physics* (New York, N. Y.), volume 7, April 1935, pages 129–66.

6. MAGNETIC CORE MATERIALS PRACTICE, **Research and Engineering Staffs**, Allegheny Steel Company (Brackenridge, Pa.), 1937.

7. MAGNETIZATION IN PERPENDICULARLY SUPERPOSED DIRECT AND ALTERNATING FIELDS, **E. J. Beck, J. M. Kelly.** *Journal of Applied Physics* (New York, N. Y.), volume 19, June 1948, pages 551–62.

8. *Discussion* by **H. J. McCreary** of a 60-CYCLE HYSTERESIS LOOP TRACER FOR SMALL SAMPLES OF LOW-PERMEABILITY MATERIAL, **D. E. Wiegand, W. W. Hansen.** *AIEE Transactions*, volume 66, 1947, pages 131–32.

9. ELECTRIC AND MAGNETIC FIELDS (book), **Steven S. Attwood.** John Wiley and Sons, Inc., New York, N. Y., second edition, 1941, *Law of Biot and Savart*, page 233; *Mutual Relations*, page 314; *Flux Lines Which Cross*, page 404.

10. ELECTRICITY AND MAGNETISM (book), **S. G. Starling.** Longmans, Green and Company, London, England, second edition, 1921, page 428.

Discussion

Thomas J. Higgins (University of Wisconsin, Madison, Wisconsin): I find this paper of considerable interest. Mr. McCreary has given a concise, but clear, account of pertinent experimental investigation of a unique circuit phenomenon which has been put to very practical use. The theory he advances in explanation of this phenomenon ought to provide interesting reading to all who have occasion to do with the theory and application of coupled circuits.

Harold J. McCreary: I wish to thank Professor Higgins for his comments on this paper.

The question of just what happens when magnetic fields apparently cross was an experimental investigation that was being made when the magnetic cross valve was invented or discovered. No proof has yet been found that the magnetic flux lines, tubes of force, stresses or strains in the ether or whatever you wish to call them either do or do not cross each other. All that can be determined experimentally is the resultants at specific points, and of course these never cross although the elemental components of which they are composed might do so.

Some writers seem to feel that the magnetic field is merely fictional and that it is the result of the orthogonal motional component of the electric field, which is the real thing. Others like Felix Ehrenhaft feel that the magnetic field is very real and that the magnetic poles can even be isolated.

The field equations of Maxwell, alone stand unbroken where linear constants apply, but so far as I know even the Maxwell equations have never been rigorously applied to non-linear phenomena without a lot of simplifying assumptions which eliminate rigorous accuracy from the results. "Ferro-inductance as a variable element" is discussed by J. D. Ryder[1] and the gudermanian function is applied. Although this is apparently the nearest to an exact solution, even this does not take account of hysteresis.

The coefficient *M* is just one of the many so-called constants of the electrical art just like *R*, *C*, and *L*, any one of which may vary as a function of temperature, time, voltage, and current but in general they are assumed to be constant.

The implication of the usual definitions of mutual inductance is that *M* is constant [illegible]

$e_2 = M\frac{di}{}$ [illegible]

otherwise this expression has no meaning. Requoting Charles Fortescue. "We can no longer express the electromotive force induced in a given current by

$$M_{12}\frac{di_2}{dt}$$

as in a simple network but must use instead

$$\frac{d}{dt}(M_{12}i_2)$$

It has been suggested that mutual inductance exists but is self cancelling, so that the net result is zero mutual inductance. If this is so then the flux lines must cross each other, and whether the magnetic flux lines do or do not cross each other is a point on which various authorities differ. There is one experimental fact that we do know, the mutual inductance is effectively zero to start with and also its algebraic average value is zero, when the cross valve is in operation, because it alternates in opposite directions equally.

The final test of my device is what is it good for. This device has been practically applied in telephone exchanges for supplying power of the proper frequency for ringing the bells in the various telephones. However in view of the fact that in the small 60 watt unit the efficiency of power conversion is better than 70 per cent it is quite probable that this device will prove valuable where small reliable power supplies of different frequencies are required. This device can efficiently multiply the frequency. It makes a good magnetic amplifier.

Applications for patents have been filed in 21 or more countries on the magnetic cross valve device and at least 25 patents have been issued. Thus far not a single reference has been found disclosing a device of this type.

REFERENCE

1. FERROINDUCTANCE AS A VARIABLE ELECTRIC-CIRCUIT ELEMENT, J. D. Ryder. *Electrical Engineering (AIEE Transactions)*, volume 64, 1945, pages 671–78.

The Requirements and Design for a D-C Null Detector

FREDERICK L. MALTBY
MEMBER AIEE

MODERN instrumentation requires the measurement of many variables that are most readily expressed as d-c voltages. These may be rapidly and accurately measured with a potentiometer in which the unbalance potential (or "error signal") is inverted into a more readily amplified alternating voltage. This alternating voltage is amplified and used in the operation of a reversing motor to restore the potentiometer balance.

In the apparatus described herein, a reversing synchronous contactor is used to invert the error signal into an alternating potential of the power frequency. This alternating potential is in turn amplified and impressed upon the control winding of a 2-phase motor which has its reference winding continuously energized at the power frequency. Such a system is shown in the block diagram, Figure 1.

The early use of mechanical inverters in conjunction with d-c measuring networks is exemplified in a patent granted to H. F. Porter in 1920.[1] This patent shows the inversion of a thermocouple current into pulsating current which is amplified and measured. The idea of modulating the unbalance current in a null-type measuring circuit for the purpose of actuating a balancing motor appears first to have been shown in an article in *Instruments* in 1933.[2] The work covered by this article culminated in a patent issued to A. J. Williams, Jr.[3] In this patent the unbalance current is inverted with a synchronously driven microphone while a contemporary development by Parker and Aceves[4] shows inversion with a synchronous commutator. The first reference to inversion by a vibrating contact in a null-type circuit seems to be a patent by W. S. MacDonald in 1940.[5]

While it is evident that the combination of any periodically varying impedance and an amplifier will provide a result of the form desired, optimum functioning requires that each circuit element be designed for the specific use.

The present paper analyzes the requirements for the circuit elements and describes the design of a circuit based upon these requirements.

The d-c networks of such instruments are subject to inductive or resistive coupling with the power lines whereby alternating voltages of the power frequency are superimposed upon the circuit, tending to produce malfunctioning in the apparatus. The merit of an unbalance detector for a network of this class lies in its ability to discriminate between the d-c potentials, which represent the true unbalance conditions in the circuit, and stray alternating potentials of the power frequency which may be superimposed upon them. By suitable design it is possible to build a detector that inherently provides a high degree of discrimination.

The two factors which determine the degree of discrimination are:

1. The degree of symmetry of the inverter.
2. The frequency response of the amplifier.

By proper co-ordination of these factors a detector system has been developed which will tolerate a stray a-c voltage whose effective value is 2,000 times the d-c voltage required for operation of the motor.

Transmission Characteristics of a Reversing Switch

There are three ways in which stray voltages of the power frequency can interfere with the performance of the instrument.

1. Error in the reading due to the presence at the motor terminals of voltage of the power frequency and driving phase as a result of the stray voltages.
2. Broadening of the neutral zone due to overloading of the amplifier by quadrature voltage. (The neutral zone is the range through which the input voltage may be changed without producing rotation of the rebalance motor.)
3. Broadening of the neutral zone due to overloading of the amplifier by harmonics of the operating frequency.

The first two of these interfering effects can be eliminated by a symmetrical reversing switch. The following analysis of the output voltage from a reversing switch when a voltage is impressed on the input will show the effect of the degree of symmetry.

The switching pattern is illustrated in Figure 2. This may be considered as an operator acting upon the input voltage. This operator has three values only, 0, +1, and −1. The intervals in which the operator is zero may be either of two conditions, depending upon the switch design. In the case of make before break contact action, the intervals are the times during which both contacts are closed. If the action is break before make, the intervals are the times during which neither contact is closed. Note that if intervals k and k_1 are equal, the switching action is symmetrical.

If a d-c voltage is applied to the switch input, the output has the same wave form as the switch transmission of Figure 2. For simplicity a peak amplitude of 1 volt may be assumed. Representing the re-

---

Paper 51-344, recommended by the AIEE Instruments and Measurements Committee and approved by the AIEE Technical Program Committee for presentation at the AIEE Fall General Meeting, Cleveland, Ohio, October 22–26, 1951. Manuscript submitted July 5, 1951; made available for printing September 4, 1951.

FREDERICK L. MALTBY is with The Bristol Company, Waterbury, Conn.

The author wishes to acknowledge the contributions of P. A. Borden, A. W. Jacobson, and J. I. Johnson who have provided technical or editorial assistance and to J. L. Russell who was responsible for the development and design of the reversing switch.

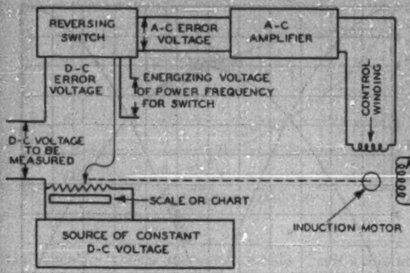

Figure 1. Potentiometer system

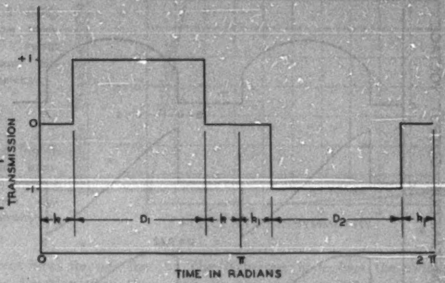

Figure 2. Switch transmission

sulting voltage as a Fourier series, we can show the power frequency components of the output to be

$$a_1 \cos \omega t + b_1 \sin \omega t \tag{1}$$

where

$$a_1 = 0$$

$$b_1 = \frac{2}{\pi} (\cos k + \cos k_1) \tag{2}$$

Thus the output voltage contains a power frequency component in phase with the switch action. If k and k_1 are equal to zero, the amplitude of this component will be equal to $4/\pi$ or 1.27 times the d-c voltage impressed. Small values of k and k_1 will have little effect upon this amplitude. For example, if k and k_1 are each 0.1 radian, the amplitude will be reduced by 0.5 per cent.

A useful concept is that of per cent dissymmetry which may be defined as the difference between the dwell time on alternate contacts expressed as a percentage of a complete cycle.

$$\text{Per cent dissymmetry} = \frac{D_1 - D_2}{2\pi} \times 100 \tag{3}$$

$$\text{or } \frac{k_1 - k}{\pi} \times 100 \tag{4}$$

There are several ways in which k and k_1 may vary from their design values, that is, one may increase as the other decreases, one stay fixed while the other increases or decreases, et cetera. However, the results for dissymmetrics of a few per cent are so nearly identical for the various ways that the results of one only will be shown; k will be made equal to zero and k_1 will be varied.

If an alternating voltage of the power frequency

$$e = E_m \sin (\omega t + \theta) \tag{5}$$

is present at the input terminals of the reversing switch, the voltage at the output terminals of the switch has a wave form as shown in Figure 3. θ is the phase angle between the switch action and the impressed voltage. (For simplicity a peak amplitude of 1 volt may be assumed.) Representing the resulting voltage as a Fourier series, the power frequency components of the output can be shown to be:

$$a_1 \cos \omega t + b_1 \sin \omega t \tag{6}$$

where

$$a_1 = \frac{\sin \theta}{2\pi} [2(k - k_1) + \sin 2k - \sin 2k_1] \tag{7}$$

and

$$b_1 = \frac{\cos \theta}{2\pi} [2(k - k_1) - \sin 2k + \sin 2k_1] \tag{8}$$

As an example, let

$$k = 0 \text{ and } k_1 = \frac{\pi}{200} \text{ radians}$$

$$\text{Per cent dissymmetry} = \frac{\frac{\pi}{200} - 0}{\pi} \times 100 = \frac{1}{2} \tag{9}$$

$$a_1 = \frac{\sin \theta}{2\pi} \left[-\frac{\pi}{100} - \sin \frac{\pi}{100} \right] \tag{10}$$

$$a_1 = \sin \theta [-1.0 \times 10^{-2}] \tag{11}$$

$$b_1 = \frac{\cos \theta}{2\pi} \left[-\frac{\pi}{100} + \sin \frac{\pi}{100} \right] \tag{12}$$

$$b_1 = \cos \theta [-8.0 \times 10^{-7}] \tag{13}$$

The transmission for 1/2 per cent dissymmetry and values of θ from $\pi/2$ radians lag to $\pi/2$ radians lead is shown in Figure 4.

If θ is allowed to assume any value, the coefficient of $\cos \theta$ in equation 8 represents the maximum transmission in phase with the contact action while the coefficient of $\sin \theta$ in equation 7 represents the maximum transmission of voltage in quadrature phase relation. These coefficients are plotted against per cent dissymmetry in Figures 5 and 6.

Because of the extremely small transmission of the inphase component it may for practical purposes be assumed that only quadrature voltages are transmitted.

In addition to overloading the amplifier this quadrature voltage will produce a driving component at the motor unless there exists an ideal phase relation between the voltage impressed on the motor control winding and the reference winding.

The production of harmonics of the power frequency is affected to a negligible degree by variations in the symmetry of inversion.

The maximum values of harmonic voltages occur for the phase position illustrated in Figure 3(B) and for values of k and k_1 of zero.

A Fourier analysis of this wave form yields

$$\frac{8}{3\pi} \sin 2\omega t + \frac{16}{15\pi} \sin 4\omega t \ldots \tag{14}$$

Thus in the worst phase position the output contains a component of twice the power frequency having an amplitude of 85 per cent of the input amplitude. It also contains a fourth harmonic of 35 per cent and successively smaller values of all even harmonics.

Required Detector Characteristics

The relative ability of the detector to tolerate stray voltages of the power frequency will be determined by

1. The symmetry of the reversing switch.
2. The attenuation in the amplifier of even harmonics of the operating frequency.
3. The accuracy of phasing of the reversing switch, amplifier, and motor.

A convenient method for stating this ability is the discrimination ratio. This is defined as the ratio between the rms value

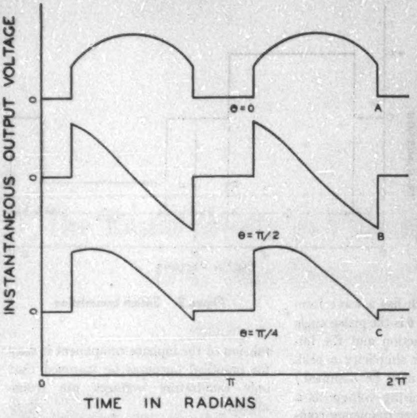

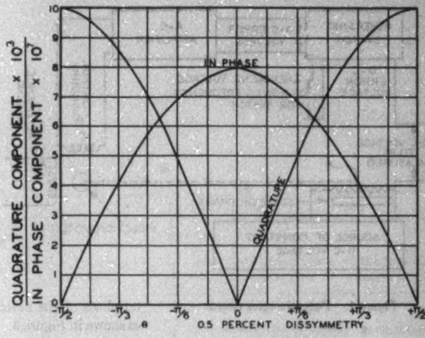

Figure 3 (left). Output voltage with power frequency input voltage

Figure 4 (above). Transmission versus phase

of the alternating voltage that is just sufficient to produce measurable effects and the d-c voltage necessary to start the motor.

Because of unavoidable friction present in all motors a definite amount of power is required to operate the motor. With a *6V6* power amplifier the maximum a-c power output is approximately 5 watts. This power will be delivered when the output voltage is approximately 20 times that required to operate the motor. Thus a voltage of 20 times that required to produce motor operation will overload the amplifier and lower the detector sensitivity regardless of the frequency.

If a discrimination ratio of 2,000/1 is desired the following four conditions must be met:

1. Dissymmetry must be 0.5 per cent or less to prevent overloading due to quadrature voltage.
2. The second harmonic amplification must not exceed 1 per cent of the amplification for the fundamental to prevent overloading due to the second harmonic.
3. The fourth harmonic amplification must not exceed 3 per cent of the amplification for the fundamental to prevent overloading due to the fourth harmonic.
4. The total phase shift must be held within 3 degrees to prevent the quadrature voltage from producing a component sufficient to start the motor. A phase displacement of 6 degrees would be necessary to produce an error of 0.1 per cent with a stray a-c voltage of the worst phase position and an effective value equal to the recorder full-scale voltage.

Detector Design

The detector system that was developed to meet these conditions is shown in Figures 7 and 8. In Figure 8 the switch is located on the right of the amplifier and the input transformer on the left.

The switch is hermetically sealed to insure against any possible effects from corrosive atmospheres because this detector is required to operate under all industrial plant conditions. The input transformer isolates the d-c measuring circuit from the amplifier ground. This is required because many sensing elements, such as thermocouples, are subject to grounding.

This detector meets the four above requirements as follows:

Dissymmetry

The experience with semiresonant reed inverters shows that they probably cannot be made to hold a dissymmetry as low as 0.5 per cent. The fundamental reason is that, for symmetry, inverters of this class depend upon making a contact at a consistent position. Thus the symmetry is subject to variation with wear or any mechanical bias.

A principle by which the dissymmetry may be held within this value is that of timing the action to the zero transitions of the supply line voltage. If the line voltage has only odd harmonics, the zero transition points are evenly spaced. (The condition of no even harmonics is effectively met in most commercial power supplies as the percentage of second harmonic is usually less than 0.2 per cent.) If the contact position is reversed at these zero transition points or at points in consistent relation to them the contact action will be symmetrical.

In the switch, shown in Figures 9 and 10, this action is produced in the following manner. The moving armature is mounted between two laminated pole pieces. These pole pieces are polarized by means of a permanent magnet which is not visible in Figures 9 and 10. The armature is energized by alternating current having a peak value approximately ten times that necessary to produce magnetic saturation of the armature. This results in a substantially square wave reversing force on the armature. This force reverses at effectively the zero current point.

The armature is approximately 0.007 inch thick by 3/32-inch wide by 3/8-inch long. Thus its mass is small compared to the switching force of 10 grams. This results in an acceleration of the armature tip of approximately 200 g (acceleration of gravity). To shorten the switching time and thus more definitely fix the reversal point, the spacing between the stationary contacts is reduced to allow a free travel of the armature of 5/10,000 of an inch. This small gap restricts the time for contact acceleration and thus limits the maximum velocity of the moving contact. The reed has no tendency to resonate at any frequency near the operating range. The high force to mass ratio and small travel produce an armature motion which follows the force pattern with a negligible lag.

Using this principle the production version of the switch is held to an average dissymmetry of 0.2 per cent and a maximum of 0.5 per cent. Because the operation depends essentially upon timing rather than position, the change in spacing that unavoidably occurs with contact wear produces only second order changes

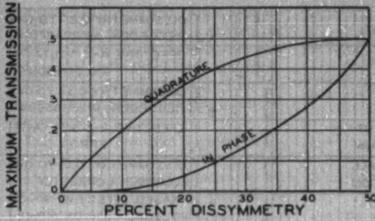

Figure 5 (left). Maximum transmission versus per cent dissymmetry

Figure 6 (right). Maximum transmission versus per cent dissymmetry

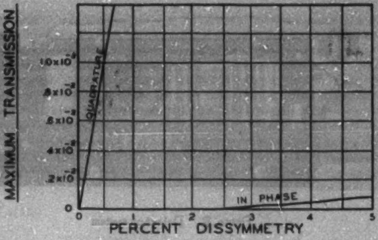

in symmetry. Thus the switch retains its symmetry essentially unchanged throughout its operating life.

Second Harmonic Attenuation

To provide the necessary discrimination between fundamental and the second harmonic, a parallel-T filter is used to attenuate the harmonic. In this filter, components are held to within 5 per cent of the design values. A compensating resistor R_{24} is selected by test to trim the network to minimum transmission for the harmonic voltage. This allows a transmission for the fundamental voltages of 30 times that of the harmonic voltage. The additional attenuation is provided by the tuned input transformer T_1, and the low pass networks (R_{16} and C_{11}, R_{17} and C_{12}, R_{19} and C_{14}) in the amplifier.

Fourth Harmonic Attenuation

The fourth harmonic is attenuated by the tuned input transformer and the low pass networks. Harmonics higher than the fourth have smaller initial amplitudes and are more attenuated by these filters. Thus, these elements also eliminate any possibility of amplifier over-loading due to higher harmonics.

Phasing

The necessary phase tolerance requires that no elements be sharply tuned at the operating frequency. This is the reason for using the multiple filter sections rather than a single parallel *T* as a degenerative feedback network. Any such sharply tuned element would cause a comparatively large phase shift with change in a component value or in operating frequency.

Measurement of Dissymmetry

The average per cent dissymmetry of a contactor may be determined to a high degree of precision by the use of the circuits shown in Figure 11, that at A being adaptable to a single pole, and that at B to a double-pole contactor. In this circuit a constant current flows through the galvanometer in one direction when the switch is in one position and in the opposite direction when the switch is reversed. The galvanometer deflection thus is a measure of the difference in dwells.

The technique is to bias the switch with d-c energization on its operating coil to one of its extreme positions. This corresponds to a condition of 100 per cent dissymmetry. The variable voltage source is then connected as shown in Figure 11 and its voltage is adjusted to

RESISTORS

R_1 - 15 OHMS (10 WATTS)
R_2 - 4.7 MEGOHMS
R_3 - 470,000 OHMS
R_4 - 220,000 OHMS
R_5 - 2 MEGOHMS
R_6 - NOT USED
R_7 - 470,000 OHMS
R_8 - 1 MEGOHM
R_9 - 470,000 OHMS
R_{10} - 470,000 OHMS
R_{11} - 2200 OHMS (±10%)
R_{12} - 1000 OHMS (10 WATTS)
R_{13} - 50,000 OHMS (10 WATTS)
R_{14} - 680,000 OHMS
R_{15} - 39,000 OHMS (±5%)
R_{16} - 47,000 OHMS
R_{17} - 150,000 OHMS
R_{18} - 2200 OHMS
R_{19} - 47,000 OHMS
R_{20} - 1 MEGOHM
R_{21} - 470,000 OHMS
R_{22} - 20,000 OHMS (10 WATTS)
R_{23} - NOT USED
R_{24} - CALIBRATING RESISTOR
R_{25} - 240,000 OHMS (±5%)
R_{26} - 75,000 OHMS (±5%)
R_{27} - 300.000 OHMS (±5%)

CONDENSERS

C_1 - .0015 MICROFARAD
C_2 - .1 MICROFARAD
C_3 - .01 MICROFARAD
C_4 - 10 MICROFARADS
C_5 - 10 MICROFARADS
C_6 - 10 MICROFARADS
C_7 - .01 MICROFARAD
C_8 - NOT USED
C_9 - .1 MICROFARAD
C_{10} - NOT USED
C_{11} - .05 MICROFARAD
C_{12} - .01 MICROFARAD
C_{13} - .01 MICROFARAD
C_{14} - .05 MICROFARAD
C_{15} - NOT USED
C_{16} - .0062 MICROFARAD (±5%)
C_{17} - .0062 " "
C_{18} - .0062 " "

TRANSFORMERS

T_1 - INPUT TRANSFORMER
T_2 - POWER TRANSFORMER

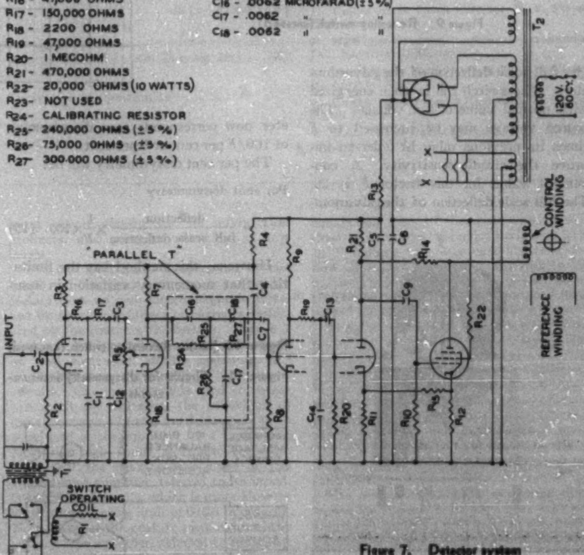

Figure 7. Detector system

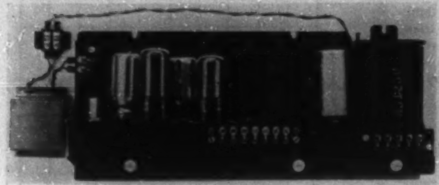

Figure 8. Detector system

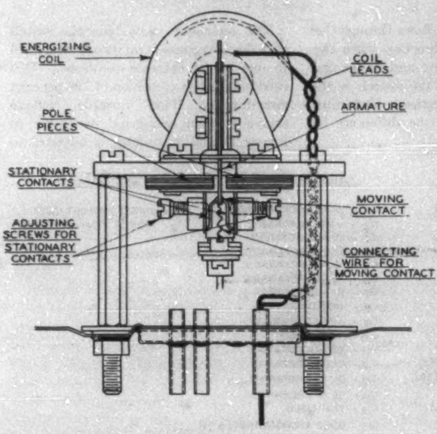
ENERGIZING COIL
COIL LEADS
ARMATURE
POLE PIECES
STATIONARY CONTACTS
MOVING CONTACT
ADJUSTING SCREWS FOR STATIONARY CONTACTS
CONNECTING WIRE FOR MOVING CONTACT

Figure 9. Reversing switch (uncased)

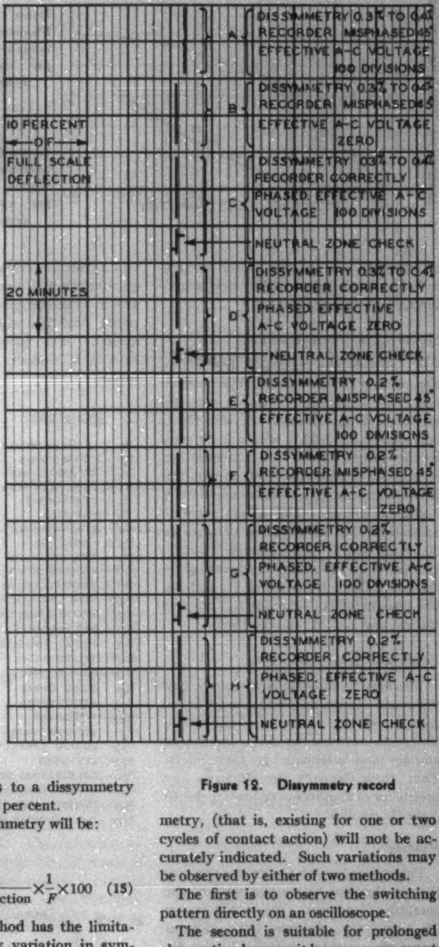

Figure 12. Dissymmetry record

give full scale deflection of the galvanometer. The switch coil is then energized with normal value of a-c voltage. The source voltage may be increased to *F* times its previous value in order to improve the circuit sensitivity. A convenient value for this factor *F* is 20. The full scale deflection of the galvanometer now corresponds to a dissymmetry of 100/*F* per cent or 5 per cent.

The per cent dissymmetry will be:

Per cent dissymmetry

$$=\frac{\text{deflection}}{\text{full scale deflection}}\times\frac{1}{F}\times 100 \quad (15)$$

However, this method has the limitation that momentary variation in symmetry, (that is, existing for one or two cycles of contact action) will not be accurately indicated. Such variations may be observed by either of two methods.

The first is to observe the switching pattern directly on an oscilloscope.

The second is suitable for prolonged observation because it leaves a permanent record of any variations in symmetry. It consists of using the switch in a high speed recording potentiometer wherein the phase of the voltage which is continuously applied to the motor reference winding has been deliberately displaced by 45 degrees. On the input is applied an a-c voltage having an effective value equal to the full scale of the recorder and a phase 90 degrees leading or lagging the switch action. This phase position gives the maximum transmission through the switch. With the recorder misphased in this manner, the quadrature voltage

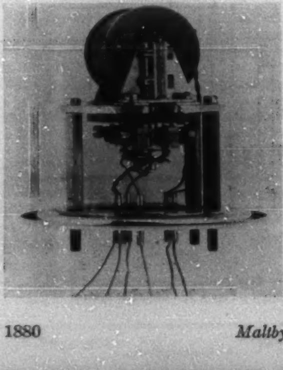

Figure 10 (left). Reversing switch (uncased)

Figure 11. Circuits for dissymmetry measurements

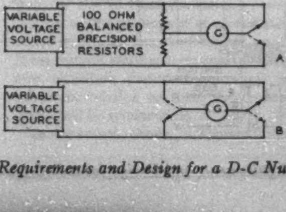
VARIABLE VOLTAGE SOURCE
100 OHM BALANCED PRECISION RESISTORS
G
A
VARIABLE VOLTAGE SOURCE
G
B

transmitted through the switch is as effective as the error signal in driving the motor. Note in Figure 6 that a 1 per cent dissymmetry will allow a 2 per cent transmission of quadrature voltage. Thus the reading changes by 2 per cent of the recorder scale.

This method provides a record readable to 0.1 per cent dissymmetry, either momentary or sustained. Such a record as shown in Figure 12 is of inestimable value in evaluating the performance of a synchronous reversing switch.

Referring to Figure 12, records *A*, *B*, *E*, and *F* show the results with the recorder misphased 45 degrees in order to measure the dissymmetry. Records *C*, *D*, *G*, and *H* show the results of the same systems with correct phasing. The sensitivity checks were made by manually forcing the motor off balance and allowing it to return. As the records show, this was done in both directions to check the neutral zone.

Appendix

Derivation of equation 2

$f(x)=0$
$-\pi<x<-(\pi-k)$
$f(x)=-1$
$-(\pi-k)<x<-k$
$f(x)=0$
$-k<x<k_1$
$f(x)=+1$
$k_1<x<(\pi-K_1)$
$f(x)=0$
$(\pi-k_1)<x<\pi$

$$a_n=\frac{1}{\pi}\int_{-\pi}^{+\pi}f(x)\cos nxdx$$

$$a_1=\frac{1}{\pi}\left[-\int_{k-\pi}^{-k}\cos xdx+\int_{k_1}^{\pi-k_1}\cos xdx\right]$$

$$a_1=0$$

$$b_n=\frac{1}{\pi}\int_{-\pi}^{+\pi}f(x)\sin nxdx$$

$$b_1=\frac{1}{\pi}\left[-\int_{k-\pi}^{-k}\sin xdx+\int_{k_1}^{\pi-k_1}\sin xdx\right]$$

$$b_1=\frac{2}{\pi}[\cos k+\cos k_1] \qquad (2)$$

Equation 4:

$$\text{Per cent dissymmetry}=\frac{D_1-D_2}{2\pi}\times 100$$

$D_1=\pi-2k$
$D_2=\pi-2k_1$

$$\text{Per cent dissymmetry}=\frac{\pi-2k-\pi+2k_1}{2\pi}\times 100$$

$$=\frac{k_1-k}{\pi}\times 100 \qquad (4)$$

Derivation of equations 7 and 8:

$f(x)=-\sin(x+\theta)$
$-(\pi-k)<x<-k$
$f(x)=\sin(x+\theta)$
$k_1<x<(\pi-k_1)$

$$a_1=\frac{1}{\pi}\left[-\int_{k-\pi}^{-k}\sin(x+\theta)\cos xdx+\int_{k_1}^{\pi-k_1}\sin(x+\theta)\cos xdx\right]$$

$$a_1=\frac{\sin\theta}{2\pi}[2(k-k_1)+\sin 2k-\sin 2k_1] \qquad (7)$$

$$b_1=\frac{1}{\pi}\left[-\int_{k-\pi}^{-k}\sin(x+\theta)\sin xdx+\int_{k_1}^{\pi-k_1}\sin(x+\theta)\sin xdx\right]$$

$$b_1=\frac{\cos\theta}{2\pi}[2(k-k_1)-\sin 2k+\sin 2k_1] \qquad (8)$$

Derivation of equation 14

$f(x)=-\cos x$
$-\pi<x<0$
$f(x)=\cos x$
$0<x<\pi$

The function is odd, therefore $a_n=0$

$$b_n=\frac{1}{\pi}\int_{-\pi}^{+\pi}f(x)\sin nxdx$$

$$b_n=\frac{1}{\pi}\left[-\int_{-\pi}^{0}\cos x\sin nxdx+\int_{0}^{\pi}\cos x\sin nxdx\right]$$

$$\underset{n\neq 1}{b_n}=\frac{1}{2\pi}\left[\frac{2-2\cos(\pi+n\pi)}{n+1}+\frac{2-2\cos(\pi-n\pi)}{n-1}\right]$$

$$\underset{n=3,5,7\ldots}{b_n}=\frac{1}{2\pi}\left[\frac{0}{n+1}+\frac{0}{n-1}\right]=0$$

$$\underset{n=2,4,6\ldots}{b_n}=\frac{4\pi}{(n+1)(n-1)\pi}$$

$$b_2=\frac{8}{3\pi}$$

$$b_4=\frac{16}{5\times 3\pi}=\frac{16}{15\pi}$$

As shown under derivation for equation 8, if $k=k_1=0$, then $b_1=0$ and

$$f(x)=\frac{8}{3\pi}\sin 2\omega t+\frac{16}{15\pi}\sin 4\omega t+\ldots+\frac{4n}{(n+1)(n-1)\pi}\sin n\omega t \qquad (14)$$

where $n=2N\ (N=1,2,3,\ldots)$

References

1. United States Patent 1,363,267, H. F. Porter, December 28, 1920.

2. New Instruments, *Instruments* (Pittsburgh, Pa.), November 1933, page 211.

3. United States Patent 2,113,164, A. J. Williams, Jr., April 5, 1938.

4. United States Patent 2,150,006, H. F. Parker, March 7, 1939.

5. United States Patent 2,203,689, W. S. McDonald, June 11, 1940.

Discussion

R. E. Tarpley (Leeds and Northrup Company, Philadelphia, Pa.): The author has an interesting approach to the design of a d-c null-detector. His detector circuit, consisting of a converter and an amplifier, is designed to accommodate large a-c pickup voltages directly across its terminals. For some applications this characteristic is undoubtedly quite useful.

However, Leeds and Northrup has approached the problem somewhat differently, in that they place a resistor-capacitor filter in the input circuit ahead of the detector. The input circuit and its components, including the converter, are designed to give negligible pickup from stray fields. This method places no severe symmetry requirements on the converter, protects all stages of the amplifier from overload arising from input circuit pickup and its modulation products, and permits operation at low levels.

The low level limit of operation of the Leeds and Northrup converter is not set by pickup from its own electromagnetic drive, but by spurious voltages or currents generated by the contacts themselves. Figure 1 of this discussion shows results of tests made on two somewhat similar instruments[1,2] employing these converters in their input circuits. One instrument is used to measure small d-c voltages, the other, small direct currents. In this particular case both were used as preamplifiers for a Leeds and Northrup high speed electronic recorder. Note that the peak-to-peak noise of the voltage-type amplifier, referred to its input, is only 0.1 microvolt, which is quite close to its theoretical noise limit of 0.073 microvolt. Note also that the peak-to-peak noise of the current type amplifier, referred to its input, equals only 0.8×10^{-13} ampere which also is close to its theoretical noise limit of 0.65×10^{-13} ampere. In each case the resulting zero-offsets, which are partially due to the spurious voltages or currents generated by the converter, are of the same order of magnitude as the peak-to-peak noise.

The above amplifiers use converters of the so-called "semiresonant reed" type, the specifications for which contain no severe symmetry requirements. The curves of Figure 2 of this discussion however, show that the variation in "dissymmetry" of a test converter amounted to only 1 per cent over a period of approximately three years.

It would be of interest to know the lowest level at which the author's detector has satisfactorily performed.

The author states that the method illustrated by Figure 11 of his paper will not accurately indicate variations in symmetry existing for one or two cycles, but that such

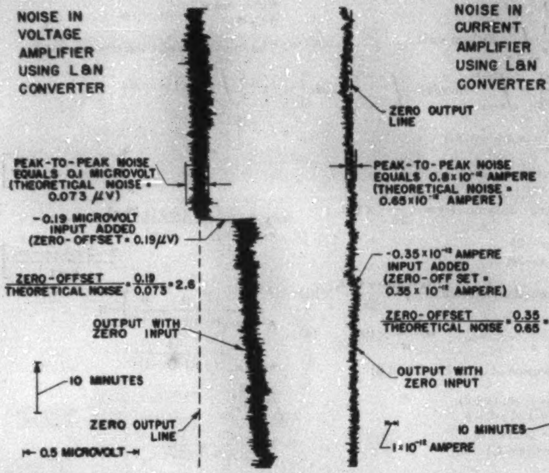

Figure 1. Noise and zero offset

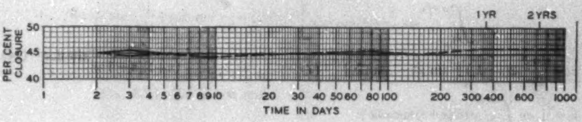

Figure 2. Symmetry data on one converter on life test

variations may be observed by using the converter in a high speed recording potentiometer under certain conditions which he describes. If it is assumed that the galvanometer of Figure 11 and the recording potentiometer have the same time response, say one half second, it would seem that both should show variations in symmetry equally well, excepting that one would indicate while the other would record.

REFERENCES

1. D-C AMPLIFIER STABILIZED FOR ZERO AND GAIN, A. J. Williams, Jr., R. E. Tarpley, W. R. Clark. *AIEE Transactions*, volume 67, 1948, pages 47–57.

2. A MULTIPURPOSE D-C AMPLIFIER WITH REDUCED ZERO-OFFSET, Will McAdam, R. E. Tarpley, A. J. Williams, Jr. *Proceedings*, National Electronics Conference (Chicago, Ill.), 1950.

F. L. Maltby: There are two ways of approaching the problem of reducing the effects of stray pickup of power frequency in d-c detectors. These are:

1. To design the detector so that it does not respond to stray voltages.
2. To design the detector without adequate pickup tolerance and then add filters to overcome this limitation.

This paper considers the careful design of the detector to be preferable. In this approach the filter becomes an optional feature which may be used if its characteristics are desirable while in the second approach filters are required.

Mr. Tarpley in his discussion claims three advantages for the second approach.

1. Places no severe symmetry requirements on the converter.
2. Protects all stages of the amplifier from overload arising from input circuit pickup and its modulation products.
3. Permits operation at low levels.

Let us consider these points individually.

SYMMETRY

Mr. Tarpley refers to 0.5 per cent as a "severe symmetry requirement." While 0.5 per cent maximum dissymmetry is a severe requirement for a semiresonant reed converter, it presents no particular problem for a converter based upon the zero switching principle.

To provide a comparison for the 3-year record of a single converter shown by Mr. Tarpley, the figures shown in Table I of this discussion have been selected from a 3-year run of 40 production-type switches. Eight switches (A through H) have been selected as representative of the complete results. In this table, eight switches have been arranged according to their degree of symmetry and the per cent dissymmetry for each has been tabulated as a function of time.

It is a point of interest in regard to the implication of symmetry by Mr. Tarpley that the circuits shown in his first reference (for example Figure 6 of this reference), would make no use of even a moderate degree of symmetry. The most important factor is the lack of any appreciable second harmonic attenuation. Because voltage at power frequency is converted to a second harmonic component 85 per cent as large as the original voltage even in a converter having zero dissymmetry, a small stray voltage present at the detector input terminals will cause the amplifier to overload regardless of the symmetry or lack of it in the converter.

OVERLOAD

It is a requirement that none of the stages of the detector-amplifier be overloaded if the detector is to be unaffected by the stray pickup. In the detector circuit described in my paper, overloading of any stage is prevented by discriminating against the harmonics of the power frequency at an early stage in the amplifier, before they are amplified sufficiently to produce overloading.

LOW LEVEL OPERATION

With regard to "permitting operation at low levels" it would seem that the inclusion of the filter in the d-c circuit in itself imposes the limitation on such operation. Tarpley's first reference gives a good analysis of this limitation. It shows the noise figure of 0.073 microvolt to be generated primarily in the input filter resistance and describes attempts to lower this without losing the filtering.

A few quotations from this reference will serve to illustrate the point.

"Since the noise-making resistance of Figure 10 was principally in the input filter and since it was desired to retain the same 60-cycle-per-second filtering for certain applications, the 2,000-ohm filter resistors were increased to 2,500 ohms and then shunted experimentally with inductors of 22 henrys and 41 ohms d-c resistance. . . ."

"The noise-making resistor has been further reduced in other set-ups by dispensing with the filter and by using an input transformer of greater step-up and lower primary impedance."

In other words, in order to provide minimum thermal noise for low level operations, the pickup tolerance must be eliminated when it is most necessary.

The paper under discussion made no mention of low level operation. We have not had time to explore thoroughly the low level operation of this detector. This will be the subject of a further paper.

Tentative results, however, indicate that the thermal offset is of a lower order of magnitude than 0.1 microvolt. The primary reason for this will be seen upon examination of the switching circuit. The

Table I

	A	B	C	D	E	F	G	H
Start	0.2	0.1	0.2	0.3	0.2	0.3	0.3	0.5
6-months	0.1	0.3	0.3	0.2	0.1	0.5	0.6	0.6
1-year	0.1	0.2	0.2	0.4	0.4	0.4	0.2	0.4
2-years	0.1	0.2	0.2	0.3	0.4	0.6	0.3	0.7
3-years	0.1	0.2	0.2	0.2	0.3	0.5	0.2	0.5

use of a double pole reversing switch opposes the thermals generated at the two armature contacts. Thus we are concerned only with the difference between the thermal electromotive forces at the two armatures rather than their individual values. The difference is small because the two armatures and the associated contacts are symmetrically disposed with respect to the coil which is the only source of heat within the switch enclosure. These two factors tend to reduce the thermal effects to a very low order of magnitude.

Also the fact that no filter is required reduces the order of magnitude of the thermal noise.

In regard to Mr. Tarpley's remarks on the measurement of dissymmetry, he is correct in all but emphasis. The galvanometer would show variations equally well as the recorder, if an observer were present when the variation occurred. Each single recorder makes available the equivalent of over three alert, full-time observers. As we are both vitally concerned with recording instruments, I appeal to Mr. Tarpley not to sell short their inherent advantages.

A Short-Haul Radio Communication Link Channelized by Time Division

E. M. MORTENSON
ASSOCIATE MEMBER AIEE

C. B. YOUNG
NONMEMBER AIEE

Synopsis: A microwave radio system channelized by pulse amplitude modulation (PAM) has been developed to fulfill a need for a short-haul, low-cost communications link having a moderate traffic capacity. For such short-range operation the microwave equipment has been greatly simplified, eliminating many of the refinements necessary for trunk-line workings. The PAM multiplex terminal subdivides the 100-kc information band into eight 3,000-cycle voice bands, employing a 3-element binary counter as the time division distributor.

WESTERN UNION has had in operation for several years a number of microwave repeater circuits carrying telegraph traffic over paths several hundred miles long. These have proved very satisfactory and much has been learned and written about them.[1-5] It is foreseen that, in the extension of these circuits into a nationwide radio beam network, there would be a definite need for a means to tie in and drop out blocks of traffic to localities off the main trunk route. Also, there are adjacent localities where telegraph traffic is sufficiently heavy or intervening terrain makes maintenance of cable circuits costly enough to warrant the installation of a single-hop microwave circuit.

For such short-range operation the equipment can be greatly simplified, eliminating such complexities as repeater relays, diversity receivers, and fault-locating circuits. In addition the use of relatively simple, low-cost channelizing techniques is possible. When this project was initiated in the early part of 1948, a study of different modulation systems[6] indicated that a pulse amplitude modulated (PAM) multiplex terminal which frequency modulates a radio frequency carrier is a satisfactory combination for this type of service. These factors prompted the development of a short-range microwave relay with time division multiplex. The radio has a high-quality 100-kc modulation band which is subdivided by the time division equipment to provide eight 3,000-cycle voice bands. These voice bands are suitable for carrier telegraph, telephone, or facsimile operation and can accommodate as many as 160 duplex teleprinter circuits.

The Microwave Equipment

Figure 1 shows the complete radio transmitter and receiver consisting of four panels: transmitter, receiver radio-frequency chassis; receiver intermediate- and video-frequency chassis; and a power supply. The power requirement is only 285 watts from a 115-volt a-c line. Line voltage stabilizers are not required, as all the high-voltage supplies include regulator circuits.

Each chassis has a cover panel which may be easily removed, giving access to various voltage regulator and gain controls. The meters and operating controls are mounted on hinged subpanels and protrude through holes in the cover panels. Although the equipment has been simplified to very nearly a practical minimum, extensive metering has been provided to facilitate maintenance.

The *2K56* Reflex Klystron was chosen for both transmitter oscillator and receiver local oscillator. This tube requires a beam voltage of only 300 volts at 30 milliamperes, keeping power supply size to a minimum. Its 200 milliwatts output in the range from 3,900 to 4,200 megacycles is probe-coupled into waveguide for efficient transmission to the antenna. A disk-dipole antenna with a 30-inch parabolic reflector, having a gain of 28 decibels, has proved satisfactory for optical paths of 20 miles.

The Klystron is frequency modulated by applying the intelligence signal to the repeller. The repeller voltage, klystron cavity tuning, and waveguide matching stub may be adjusted for maximum power output as indicated by a crystal detector coupled into the waveguide.

A small amount of the energy in the waveguide is coupled into two variable-tuned cavities which form a microwave discriminator. The d-c output from this is amplified and used to vary the repeller voltage, providing automatic frequency control.

The receiver has waveguide feed from the antenna through a preselector cavity to a waveguide crystal mixer where it combines with the local oscillator signal to produce a 32-megacycle intermediate frequency. A Wallman low-noise preamplifier is followed by a 4-stage intermediate-frequency amplifier and two limiter stages having a 4-megacycle bandwidth. The discriminator is a modified Foster-Seely circuit with a bifilar-wound transformer. A reference voltage obtained from the discriminator is used to change the repeller voltage of the local oscillator to maintain a constant intermediate frequency.

The modulation recovered by the discriminator is amplified by one stage and passes through a cathode follower into a 75-ohm cable to the PAM equipment.

The PAM Multiplex Terminal

The 100-kc information band provided by this microwave circuit is a transmission medium of sufficiently high quality to

---

Paper 51-346, recommended by the AIEE Radio Communications Systems Committee and approved by the AIEE Technical Program Committee for presentation at the AIEE Fall General Meeting, Cleveland, Ohio, October 22–26, 1951. Manuscript submitted June 22, 1951, made available for printing September 5, 1951.

E. M. MORTENSON and C. B. YOUNG are with the Western Union Telegraph Company, New York, N. Y.

The authors gratefully acknowledge the advice and counsel offered them in the preparation of this paper by the several engineers and associates concerned with the development of the system.

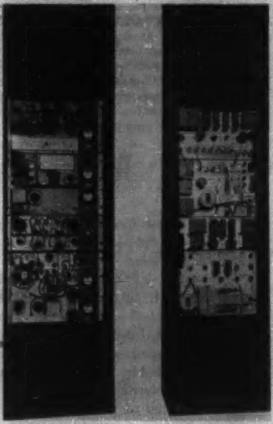

Figure 1. Microwave terminal equipment, front and rear views

permit the application of time division multiplexing. The PAM method was chosen for this purpose, as previously mentioned, principally because of its relative simplicity. In keeping with the low-cost nature of the system, the multiplexing portion is constructed entirely of common, readily available commercial components.

ELECTRONIC DISTRIBUTOR

In discussing any time division system, principal attention is naturally focused upon the type of "switch" or distributor employed, since it is this feature which defines the character of the system.

The electronic distributor developed for this system is based on the principle of the binary code. A binary code having n units will give 2^n combinations or distinctive code groups, so that for eight combinations a 3-unit code is required ($2^3=8$). The three units employed in this arrangement are square waves of frequencies 32, 16, and 8 kc derived from a 64-kc crystal oscillator and a series of 2:1 frequency dividers connected in tandem. Figure 2 is a schematic diagram of this circuit.

For purposes of illustration, only voice bands A and E are shown. They enter the distributor via triodes V_a and V_e respectively. The cathode of V_a is paralleled with the cathodes of three switching tubes V_a32, V_a16, and V_a8, so that when one or more switching tubes are conducting the resulting current flowing through cathode resistor R_a biases V_a beyond cutoff. This isolates voice band A from the distributor output load resistor R_L. If these three switching tube grids are made simultaneously negative so as to prevent the flow of switching tube current through R_a, V_a becomes a normal self-biased amplifier and the signals on its grid appear at the distributor output. The switching tubes are controlled by the frequency dividers. Each divider has two outputs 180 degrees apart in push-pull fashion, designated as $\phi1$ and $\phi2$. Figure 3 illustrates the time and phase relationship of the number 1 and number 2 phases.

Note that there is only one interval during a revolution of the distributor where all three number 1 phases are simultaneously negative.

Observing in Figure 2 that the switching tubes associated with V_a are each connected to a $\phi1$ output, it follows that V_a will become conducting only during this interval "A" to allow a sample of the intelligence on band A to appear at R_L. At all other intervals at least one of the three number 1 phases is positive, thus maintaining V_a biased beyond cutoff.

Figure 2. Sending distributor, theory

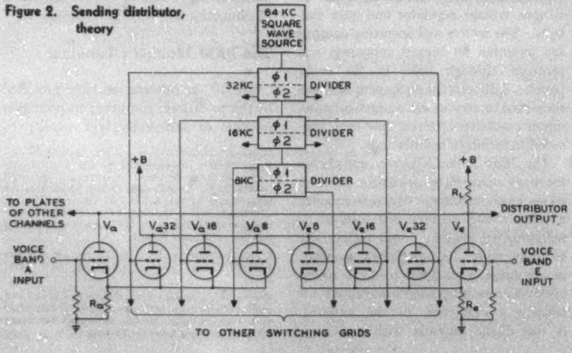

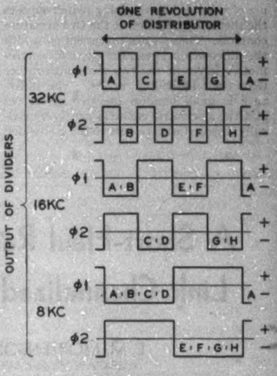

Figure 3. Output of frequency dividers

Note: Letters designate portion of time cycle devoted to each channel

Voice band E operates in a similar fashion through triode V_e in conjunction with switching tubes V_e32, V_e16, and V_e8. But in this case a different "code combination" is set up on the switching tubes in that V_e8 is controlled by the number 2 phase output of the 8-kc divider. As a result, it is only during interval "E" of Figure 3 that all three tubes are cut off allowing a sample of the signal on channel E to appear at the output. Similarly, by using the proper combinations of number 1 and number 2 phases all eight voice bands can be sampled one at a time in logical sequence. Figure 4 is an oscilloscope picture of the distributor output covering about one revolution with band D modulated by speech and band E carrying a 1,000-cycle tone.

The receiving distributor employs the same principle of operation, as shown in Figure 5. Here the switching elements are crystal rectifiers instead of triodes but they perform the same function. The incoming samples arriving at the signal input appear on all eight grids simultaneously, but since only one triode at a time is conducting, only the voice band associated with that triode receives the signal. Thus, when the A voice band sample enters the distributor, only V_a is in a conducting condition to pass the sample to the A voice band output, and similarly for all other voice bands.

PULSE GENERATOR AND TRANSMITTER

The driving frequency for this system is derived from a 64-kc crystal oscillator

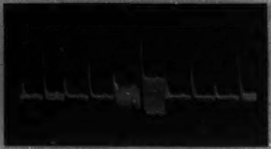

Figure 4. Sending distributor output showing two bands modulated

in the transmitter, the output of which is amplified and clipped to produce a square wave. Observing Figure 6, which is a functional block diagram of the system, it can be seen that this frequency is used to drive a series of four cascaded 2:1 frequency dividers producing square waves of 32, 16, 8, and 4 kc. The output of the 4-kc divider is passed through a narrow-band filter and applied to the input of channel *A* to provide a register signal. Since this tone is above the response range of the channel, it may be sent along with the channel intelligence without causing interference. The 32, 16, and 8-kc dividers produce the switching frequencies used to drive the electronic distributor as previously explained.

SYNCHRONOUS GATE

The pulses, as they leave the sending distributor, are not suitable for transmission. First, the pulses are too wide so that in being sent through a transmission medium of restricted bandwidth they would be further broadened and excessive pulse overlap would result, with corresponding crosstalk. Secondly, all of the pulses do not have the same shape, and thus they may be differently modified by the transmission medium. For this reason, the pulses are passed through a synchronous gate which operates at 64 kc. The gate selects a small portion toward the end of each pulse for transmission. The portion selected is shown in Figure 4 by the two small pips or notches appearing on each pulse. The gate, at the same time, introduces a small amount of the 64 kc into the signal. The 64-kc component is transmitted along with the signal frequencies and is used to drive the distributor at the receiving end. Referring to Figure 7, the distributor output is applied to the grid of V_1. A 64-kc keying wave of large amplitude and proper phase is applied to the grid of V_2. The keying wave is so controlling that its amplitude, when positive, is sufficiently large to cause the cathode current of V_2 to bias V_1 beyond cutoff; and when negative, to permit V_1 to perform as a normal amplifier. The outputs of V_1 and V_2 are as shown at *C* and *D*, and being 180 degrees out-of-phase they can be subtracted to control the magnitude of the 64-kc component in the output signal. Rheostat *R* is provided for this purpose.

The pulse train now consists of short, separated pulses of uniform shape and duration, together with the required amount of 64 kc as shown at *E*. High-frequency switching components are also in evidence, and as they convey no essential intelligence, are removed by a 64-kc, low-pass filter to give the waveform shown in Figure 8. The pulses now have a more sinusoidal shape, and after amplification are ready for transmission. In the illustration shown, channel *D* is being modulated by voice, and channel *E* is carrying a single frequency. Channel *A* can be identified by the 4-kc registration signal on its pulse.

RECEIVING TERMINAL

Referring again to Figure 6, it is seen that at the receiving terminal the incoming pulses are amplified and again filtered by a 64-kc low-pass network. This is to remove any high-frequency noise components which may be present in the transmission medium. Inspection of Figure 9 shows that the incoming signal pulses have been further broadened in traversing this filter and considerable overlap is evidenced which, if left uncorrected, would cause crosstalk between adjacent channels. For this reason, and also because the transmission medium may have introduced some modification of the pulses, a means for reshaping and reconditioning them must be inserted before they reach the receiving distributor. This is accomplished by means of an adjustable signal-shaping amplifier which consists essentially of a phase shifter and a differentiating circuit. By varying the time constants of these circuits, it is possible to compensate the effects of phase distortion introduced by the transmission medium and line filters.

Next it is necessary to recover the 64-kc component introduced at the transmitter for driving the receiving terminal. This is accomplished by passing a portion of the incoming signal through a phase shifter and a 64-kc crystal filter. The filter has an extremely narrow passband, and removes all components of the received signal except the 64 kc. After amplification this 64-kc component is clipped to produce the required square wave for driving the 32, 16, and 8-kc frequency dividers which in turn control the receiving distributor. Now back to the intelligence signal.

The reshaped pulses enter the synchronous gate which operates similarly to that at the sending terminal. Here however, the gate functions to select a small portion at the pulse center. Figure 10 shows the pulses as they appear at the output of the pulse shaping amplifier. The small notches occurring at the center of the pulses indicate the time at which the synchronous gate operates; and since this occurs at the point of greatest amplitude, it affords the best margin against interference. The timing of the gate operation in relation to the incoming pulses is determined by the phase control

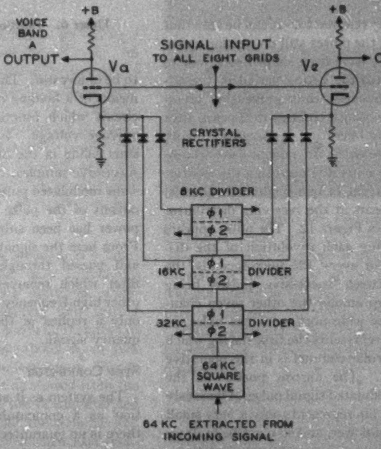

Figure 5. Receiving distributor, theory

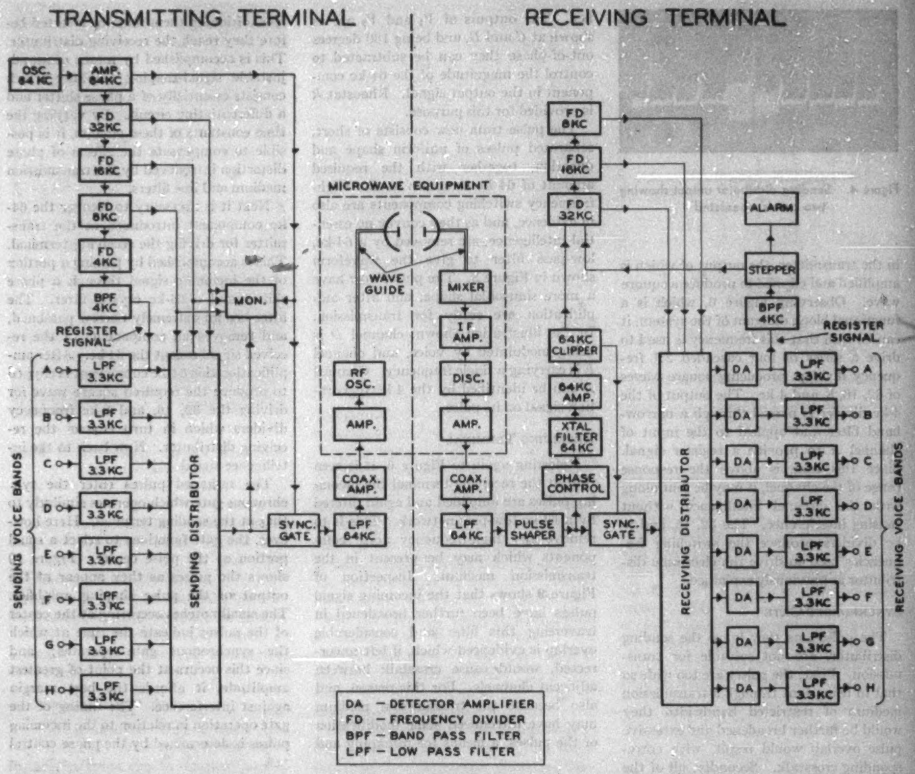
TRANSMITTING TERMINAL
RECEIVING TERMINAL
OSC. 64 KC
AMP. 64KC
FD 32KC
FD 16KC
FD 8KC
FD 4KC
BPF 4KC
MON.
REGISTER SIGNAL
A
B
C
D
E
F
G
H
LPF 3.3KC
SENDING VOICE BANDS
SENDING DISTRIBUTOR
SYNC. GATE
MICROWAVE EQUIPMENT
WAVE GUIDE
RF OSC.
AMP.
COAX. AMP.
LPF 64KC
MIXER
I F AMP.
DISC.
AMP.
COAX. AMP.
LPF 64KC
PULSE SHAPER
SYNC. GATE
PHASE CONTROL
XTAL FILTER 64KC
64KC AMP.
64KC CLIPPER
FD 32KC
FD 16KC
FD 8KC
ALARM
STEPPER
BPF 4KC
REGISTER SIGNAL
RECEIVING DISTRIBUTOR
DA
LPF 3.3KC
RECEIVING VOICE BANDS
DA — DETECTOR AMPLIFIER
FD — FREQUENCY DIVIDER
BPF — BAND PASS FILTER
LPF — LOW PASS FILTER

Figure 6. Functional block diagram

previously referred to. It can be seen that although the pulses still do overlap somewhat they have been shaped so as not to extend into the gating period of the adjacent channels, thus preventing crosstalk. The pulse train as it appears after the gating operation is shown in Figure 11. These pulses are now properly conditioned to enter the receiving distributor.

The output of one modulated channel as it appears at the receiving distributor is shown in Figure 12. The pulse appears once during each revolution of the distributor, or every 125 microseconds, the time between successive pulses being divided up among the other seven channels. The wide portion of the pulse, or pedestal, represents the time during which the particular channel is in the operative condition. The narrow portion is the actual modulated signal pulse. Obviously this little pip represents only a very small amount of power, and so must be built up to be of any use. This is accomplished by means of a holding or "pulse stretching" circuit which functions to increase the average voltage. It is thus possible to start filling in the blank spaces between successive samples. Figure 13 shows the same modulated pulse as it appears at the output of the pulse stretcher where the power has been substantially increased. From here the signal is further amplified and passed through a 3.3-kc low-pass filter which removes all switching and other high-frequency components, leaving only a replica of the original voice-frequency signal.

Step Corrector

The system as it stands now will function as a communications circuit, but there is no guarantee that a signal entering voice band *A* at the sending terminal will appear at the *A* band jack at the receiving terminal. It is therefore necessary to provide a means for correcting the channel alignment of the two terminals. It will be remembered that an identifying tone (4 kc) was superimposed on the *A* band at the sending terminal, and this is used to control the operation of a multivibrator. This multivibrator operates at about 100 cycles per second and introduces a sharp kick at the input of the 32-kc frequency divider at each reversal, causing an extra operation of the divider which advances the receiving distributor one segment or channel. The receiving distributor will thus advance channel by channel at a 100-cycle rate until proper registration of the distributors is reached. The channels are now momentarily in alignment so that the 4-kc registration frequency will appear at the output of the 4-kc band-pass filter associated with the

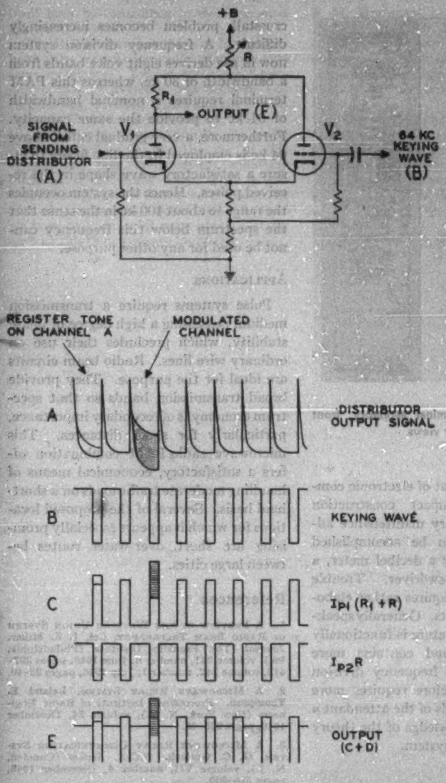

Figure 7. Synchronous gate, theory

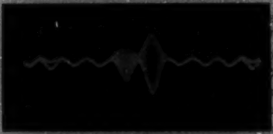

Figure 8 (right). Pulse train as transmitted

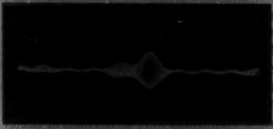

Figure 9 (right). Received pulses, before reshaping

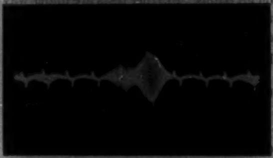

Figure 10 (right). Reshaped pulses

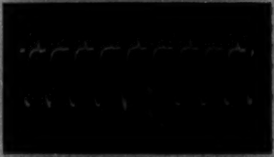

Figure 11 (right). Pulse train after gating

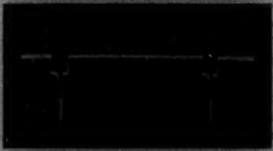

Figure 12 (right). Receiving distributor output of one voice band

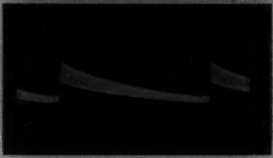

Figure 13 (below, right). Output of stretcher pulse

receiving side of band *A*. This tone is amplified and detected to apply a negative bias to the multivibrator, thereby halting its operation and leaving the terminals in registration. The entire scanning operation requires less than one tenth of a second. Inasmuch as registration will be maintained only when the 4-kc tone is present on the output of band *A*, the same negative bias is also used to prevent the operation of audible and visual alarms. Thus loss of registration for any reason will immediately be called to the attention of operating personnel.

Channel Monitor

A monitor is provided at the transmitting terminal for use in checking the output of the sending distributor. The circuit employed corresponds to one channel of the receiving distributor, including a stretcher amplifier and output filter. An eight-position switch connects the grids of three switching triodes to various combinations of the 32, 16, and 8-kc frequency dividers corresponding to bands *A* to *H*. The operation of the monitor can thus be adjusted to coincide with the operation of any particular channel and permits monitoring of the traffic thereon.

Terminal Assembly

The finished PAM terminal is a completely self-contained unit embodying sending and receiving multiplex units, power supply, monitoring and testing facilities, and failure alarm all mounted in a single cabinet rack about seven feet high and less than two feet square. Figure 14 shows this cabinet as viewed from the front and rear. The use of miniaturized components throughout the terminal and the adoption of other construction techniques have resulted in a very substantial saving in space over our present frequency division systems of equal traffic capacity. The original prototype model was completed in October 1949, and has been undergoing tests since that date. Certain refinements and improvements have resulted, but all have been of a minor character.

Performance

Several of these terminals have been constructed to date and they have been substantially uniform in performance. With the sending and receiving terminals on a back-to-back basis, noise and crosstalk are down at least 50 decibels (rms multichannel signal to rms noise) on all channels. Preliminary tests conducted over the short-range radio beam circuit between New York and Newark have given satisfactory results. These tests were made using only one PAM terminal located in New York and with the Newark radio terminal on a looped-back basis to form a one-repeater radio relay link. The signal-to-noise ratios obtained under these conditions were 40 decibels or better on all bands. Further tests are under way to check the life expectancy of the various components and to aid in formulating a preventive maintenance routine.

Conclusions

While it is not practical at this early date to form any conclusive opinions as to the relative merits of the pulse amplitude modulation method of time division multiplexing, certain general comparisons with frequency division systems are in order.

Cost

A savings in initial cost of about 50 per cent and a reduction in size and weight of about 75 per cent can be realized over frequency division systems presently installed in the telegraph plant. These savings are due in large measure to the use of miniaturized components and the application of new construction techniques. Even when compared on an equal footing, however, the PAM system should still show an appreciable savings due to a reduction in the number of filters required.

Maintenance

The substitution of electronic components for filters, while reducing the initial cost, creates a more expensive maintenance problem because the stability and useful life of passive networks are far superior to that of electronic components. The compact construction facilitates the ordinary maintenance adjustments which can be accomplished simply by using only a decibel meter, a handset, and a screwdriver. Trouble shooting, however, requires rather elaborate testing instruments. Generally speaking a system of this nature is functionally more complicated and contains more critical factors than frequency division equipment. It therefore requires more attention and demands of the attendant a more specialized knowledge of the theory and operation of the system.

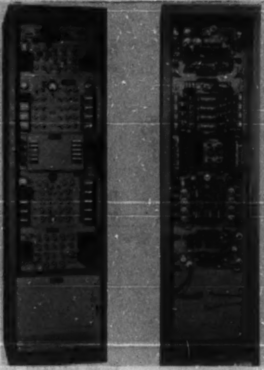

Figure 14. PAM terminal assembly, front and rear views

Spectrum Economy

The transmission bandwidth required for a pulse system of this type depends upon the amount of pulse overlap which can be readily corrected to prevent interchannel crosstalk. In practice this works out to be about twice the spectrum interval required for an equivalent frequency division system. If pulse transmission is confined to a narrower bandwidth, the crosstalk problem becomes increasingly difficult. A frequency division system now in use derives eight voice bands from a bandwidth of 30 kc, whereas this PAM terminal requires a nominal bandwidth of 64 kc to provide the same capacity. Furthermore, a very gradual cutoff above 64 kc is employed in the line filters to insure a satisfactory wave shape in the received pulses. Hence the system occupies the range to about 100 kc in the sense that the spectrum below this frequency cannot be used for any other purpose.

Applications

Pulse systems require a transmission medium possessing a high degree of phase stability, which precludes their use on ordinary wire lines. Radio beam circuits are ideal for the purpose. They provide broad transmission bands so that spectrum economy is of secondary importance, particularly for short distances. This microwave radio-PAM combination offers a satisfactory, economical means of handling moderate traffic loads on a short-haul basis. Several of the proposed locations for which it appears especially promising are short, over-water routes between large cities.

References

1. A Preview of the Western Union System of Radio Beam Telegraphy, Col. J. Z. Millar. *Journal*, The Franklin Institute (Philadelphia, Pa.), volume 241, number 6, June 1946, pages 397–413, volume 242, number 1, July 1946, pages 23–40.

2. A Microwave Relay System, Leland E. Thompson. *Proceedings*, Institute of Radio Engineers (New York, N. Y.), volume 34, December 1946, pages 936–42.

3. A Microwave Relay Communication System, G. C. Gerlach. *R.C.A. Review* (Camden, N. J.), volume VII, number 4, December 1946, pages 576–600.

4. A 150-Kc Carrier System for Radio Relay Applications, J. E. Boughtwood. *Western Union Technical Review* (New York, N. Y.), volume 2, April 1948, pages 57–65.

5. Frequency-Modulated Carrier Telegraph System, F. B. Bramhall, J. E. Boughtwood. *Electrical Engineering* (*AIEE Transactions*), volume 61, January 1942, pages 36–39.

6. Theoretical Analysis of Various Systems of Multiplex Transmission, V. D. Landon. *R.C.A. Review* (Camden, N. J.), volume IX, number 2, June 1948, pages 287–351; number 3, September 1948, pages 433–82.

Discussion

L. G. Abraham (Bell Telephone Laboratories Inc., Murray Hill, N. J.): This was an interesting paper and we are generally in agreement with the ideas expressed in the paper. We agree that this sort of system seems practically limited to use over microwave radio today because of the large amount of frequency space required as compared to amplitude modulated systems.

The pulse shaping treatment in the paper is interesting. It probably should be emphasized that this sort of pulse shaping takes care of systematic and fixed characteristics only. Interference from random or variable factors cannot be helped by such shaping and such interference may at times be very serious.

We agree, in general, with the feeling about reduced terminal size possible with pulse modulated systems, except that perhaps the estimates in the paper are too conservative. It is the feeling of some of our people that substantial reductions in size of pulse modulated system terminals should be possible even as compared to miniaturized *N* carrier systems based on frequency division.

Of course, we all know that the cost of the actual terminal discussed here may be a small part of the total cost of providing the facilities and whether this equipment is cheaper may not be the controlling factor in deciding upon a system. Buildings, power plant, towers, et cetera, tend to be a very large part of the cost of small circuit groups and the cost of the intermediate line facility itself may be controlling in deciding on a particular system.

The Bell System has three or four short-haul pulse modulation radio telephone systems in service. Two of these are 8-telephone channel systems, one between Los Angeles and Catalina Island and the second between Hyannis and Nantucket. A third is a 16-telephone channel system also in the California area. So far the use of this system has been confined to temporary facilities or to cases where geographical barriers such as intervening water makes the cost of wire facilities quite high. In time we hope to know a lot more about systems such as this than we have found out to date.

E. M. Mortenson and C. B. Young: It is gratifying to note from Mr. Abraham's comments that there exists such a wide area of general agreement on this subject. Especially so in the light of the Bell System's experience with similar systems in operational service.

In connection with the pulse-shaping technique, it should be mentioned that other methods for crosstalk correction can be used, but whatever the method, any change in the transmission medium which alters the received pulse shape will require a compensating adjustment of the correcting circuits.

It is possible to devise automatic methods for crosstalk compensation, but the consequent increase in circuit complexity was not considered worthwhile particularly for this short-range application.

We agree that our estimates of the saving in space to be gained over frequency division systems are conservative. The Telegraph Company is interested in miniaturization insofar as it makes for more efficient use of space and reduces equipment costs, but not to the point where reliability or ease of maintenance are sacrificed to any appreciable degree.

The authors wish to thank Mr. Abraham for his interest and his enlightening discussion.

Transfer Function for a 2-Phase Induction Servo Motor

LLOYD O. BROWN, JR.
ASSOCIATE MEMBER AIEE

THE usual analysis[1] of a 2-phase servo induction motor based on its steady state speed torque characteristics results in a LaPlace transfer function of the form

$$KG(s)=\frac{H}{s(s+\omega_1)} \quad (1)$$

In a paper on stabilization of servos using 2-phase motors, Andrew Sobczyk[2] has reproduced a differential equation developed by N. B. Nichols for the induction motor. From this equation, it is shown that the motor can be represented by a demodulator followed by a d-c motor. While a transfer function for the motor alone is not obtained, an extension of the work of Mr. Sobczyk would result in a function of the above type.

The frequency response of such a system will have a phase shift of 90 degrees at low frequencies and will increase toward, but not beyond, 180 degrees as the frequency increases. The amplitude of the function will decrease with increasing frequency, being asymptotic to a slope of −20 decibels per decade at low frequencies and approaching a slope of −40 decibels per decade at high frequencies.

If the frequency response of a 2-phase motor is measured experimentally, the response to low frequencies will very nearly match those given by equation 1. At high frequencies (servowise) however, the phase shift will be found to increase beyond 180 degrees. Such a system cannot be represented as simply as the given expression, but must contain at least one more time constant. A more probable transfer function for the system would take the form

$$KG(s)=\frac{H}{s(s+\omega_1)(s+\omega_2)} \quad (2)$$

The presence of a second time constant is further borne out by the fact that high gain 2-phase servo systems employing an amplifier exhibiting no dynamic characteristics will have a tendency to be unstable.

In this paper, an analysis is made of a 2-phase servo induction motor which results in a transfer function having two time constants. A method for determining the magnitudes of these time constants from a knowledge of the inertia and friction of the motor and the load plus the steady state speed-torque characteristic also is given.

General Approach

The approach used in obtaining the transfer function of the motor is that of applying a voltage of rated magnitude and frequency to the reference phase of the machine. After the transient current in this phase has subsided, a voltage of rated magnitude and frequency, but having a 90-degree phase relation with that of the reference phase, is applied to the control field. The transient velocity of the rotor and load is then obtained. By integrating this function with respect to time to obtain the rotor position, transforming to a function of frequency by means of the LaPlace operational methods, and dividing the resultant frequency function by the transform of the input step function, the transfer function may be had. Since the time integration can be performed after the transformation by dividing the transformed results by s, and since the division by the input step function is accomplished by multiplying the transformed function by s, the results of these two operations cancel each other. Therefore, the transfer function can then be obtained by transforming the velocity function directly.

In order to find the transient velocity, the magnetic fields due to the magnetizing currents of the stator are defined as function of both time and position relative to a reference line rotating at the instantaneous rotor velocity. The voltage generated in a given rotor element and the resultant element current may then be found. The instantaneous torque produced on the element will be the product of the instantaneous element current and the flux density in which the element is lying. The total torque will be the sum of the torques on each rotor element. By equating the total torque to the requirements of the rotor and load, the transient velocity of the system may be evaluated.

Assumptions

The analysis is based on the following simplifying assumptions: the magnetic material of the paths within the machine has a constant permeability so that the magnetizing currents are proportional to the applied voltages; the currents of both the rotor and the stator are distributed over the entire surface instead of being confined to discrete slots; the current density of a single phase of the stator varies sinusoidally with angular displacement around the stator, the point of maximum current density for one phase being displaced by 90 degrees from the point of maximum current density of the other phase; and the self impedances of

---

Paper 51-347, recommended by the AIEE Feedback Control Systems Committee and approved by the AIEE Technical Program Committee for presentation at the AIEE Fall General Meeting, Cleveland, Ohio, October 22–26, 1951. Manuscript submitted February 16, 1951; made available for printing September 18, 1951.

L. O. Brown is with the Electrical Engineering Department of the University of Illinois, Urbana, Ill.

The author wishes to express his gratitude to Dr. G. H. Fett of the Electrical Engineering Department, University of Illinois, for his suggestions and guidance in the study of this problem and the preparation of this manuscript. The author also acknowledges the permission granted by the Graduate College of the University of Illinois to utilize material included in a thesis submitted under the title, "Transfer Function of a 2-Phase Servo Motor" in partial fulfillment of the requirements for the degree of Master of Science.

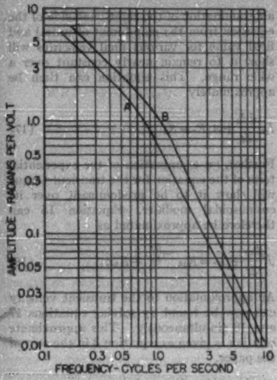

Figure 1. Transfer function amplitude versus frequency for a 2-phase servo induction motor

Curve A, response calculated from the derived expression evaluated for a Diehl FPE25-11 motor driving a tachometer generator. Curve B, experimentally obtained response of the same system

the stator windings are negligible when compared to the magnetizing impedances of the machine.

Further, since the transfer function of the motor can be interpreted as the steady state magnitude and phase response to a sinusoidally modulated input signal, the initial conditions under which the system is set into operation will not affect the results. Therefore, the voltages applied to the phases of the machine will be taken in such a way that the simplest expressions will result throughout the analysis.

Results of Analysis

Since both the magnitude and frequency of the rotor current changes as the motor accelerates, the analysis leads to three nonlinear differential equations which must be solved simultaneously to find the transient velocity. (See Appendix I). An approximate solution for these three equations leads to an expression for the transient velocity in the form

$$\omega_r = M_1 + M_2\epsilon^{\frac{-f}{J}t} + M_3\epsilon^{\frac{-R_r}{L_r}t} \tag{3}$$

From the initial conditions of zero acceleration and velocity, the coefficients of the exponentials can be evaluated in terms of the constant M_1. Further, M_1 must be the final value of the velocity and can be expressed as the steady state torque divided by the coefficient of friction for the system.

By applying the LaPlace transformation termwise to the transient velocity, and collecting terms over a common denominator, the transfer function of the system becomes

$$KG(s) = \frac{\theta_0}{V_2} = \frac{M_1\omega_1\omega_2}{V_2} \times \frac{1}{s(s+\omega_1)(s+\omega_2)} \tag{4}$$

Evaluation of the Transfer Function

The methods used to find the transient velocity also may be used to derive an expression for the steady-state torque of the motor in terms of its final velocity. This expression may be obtained for the condition of unequal voltages applied to the two fields as easily as for the case of equal voltages. Under these conditions, the expression will be (see Appendix II)

$$T_{ss} = \frac{338.2r_r}{N_s}\left[\frac{(V_2+V_1)^2\frac{\omega-\omega_{ss}}{\omega}}{r_r^2+\left(\frac{\omega-\omega_{ss}}{\omega}\right)^2 x_r^2} - \frac{(V_2-V_1)^2\frac{\omega+\omega_{ss}}{\omega}}{r_r^2+\left(\frac{\omega+\omega_{ss}}{\omega}\right)^2 x_r^2}\right] \tag{5}$$

the torque being given in the units of ounce inches. If equal voltages are applied to each field, this equation will reduce to

$$T_{ss} = \frac{338.2r_r}{N_s} \times \frac{2V^2\left(\frac{\omega-\omega_{ss}}{\omega}\right)}{r_r^2+\left(\frac{\omega-\omega_{ss}}{\omega}\right)^2 x_r^2} \tag{6}$$

The last relation now may be used to evaluate the ratio of the rotor resistance to the rotor reactance, if the no-load torque speed curve for a given motor run under the conditions of rated voltage on each field is available. Such curves, whether published by the manufacturer of the motor or obtained experimentally, must usually be corrected for the friction of the bearings. This can be done with sufficient accuracy by assuming the bearing friction to be viscous. The speed-torque curve can then be extended beyond the zero torque axis into the negative region until it crosses the ordinate corresponding to the synchronous speed of the motor. At this point the torque produced by the machine will be zero, so that the negative torque indicated by the curve will be equal to that torque required to overcome friction of the bearings. A proportionate amount now may be added at each speed to give a curve of the internal torque of the motor. By substituting the magnitude of internal torque at a given speed into equation 6, an equation involving only rotor resistance and reactance will result. This can be done at a second speed and this equation solved simultaneously with the first to find rotor resistance and reactance. By putting these values into equation 6, the resulting curve will be found to match the internal torque-speed curve very closely. Further, the calculated values of rotor resistance and reactance may be put into equation 5 and a series of curves representing the steady-state conditions of unbalanced voltages may be obtained.

By drawing the curve of frictional requirements of the motor and load on the same sheet with the speed-torque characteristic of the motor, the constant of the transfer function can be evaluated at the point of intersection of these two curves.

Experimental Confirmation

This procedure was carried out for a Diehl *FPE25-11*, 2-phase 60-cycle 115-volt servo induction motor from the torque-speed curves published by the manufacturer. The rotor constants found were as follows: rotor resistance, 538 ohms; rotor reactance, 443 ohms; ratio of rotor resistance to rotor inductance, 457 radians per second.

For the purpose of confirming the developed transfer function, a motor of the above-mentioned type was geared to a tachometer generator. The reference field of the motor was excited from a source of voltage of rated magnitude and frequency. The control phase winding was excited from a suppressed carrier source, modulated with a low-frequency variable voltage. The carrier, although suppressed, was adjusted to be 90 degrees out of phase with the voltage applied to the reference field. Further, an arrangement was made whereby the phase shift between the modulation signal and the response of the motor could be measured.

The total moment of inertia of the system was 0.156 ounce-inch-squared and the coefficient of viscous friction was 0.0019 ounce inch per radian per second. A series of speed torque curves was calculated for various magnitudes of voltage applied to the control field, and the transfer function multiplier was calculated for a control voltage of 40 volts. Under these conditions, the calculated transfer function of the system is

$$KG(s) = \frac{14{,}920}{s(s+4.71)(s+457)} \tag{7}$$

A comparison of the calculated transfer function in both magnitude and phase with one which was experimentally obtained is shown in Figures 1 and 2.

Conclusions

A comparison of the experimental and calculated curves in Figure 1 and Figure 2 will show the following: the amplitude curves follow the same general trend but differ in magnitude; the phase shift curves are alike within the accuracy to which phase shift may be measured with any oscilloscope. The difference in amplitude may be explained by examining the final speed the system will attain for various voltages applied to the control field. In doing this, it will be found that the speed will approximately double with an increase in voltage from 10 volts to 40 volts. Since the constant multiplier of the transfer function is proportional to the final speed divided by the applied voltage, lower voltages would give rise to larger transfer function amplitudes. For example, if the constant multiplier is calculated for a control voltage of 40 volts, the amplitude of the transfer function of the motor tested is 1.84 radians per volt at a frequency of 0.5 cycle per second. If, however, the multiplier had been calculated for a control voltage of 10 volts, the transfer function would have an amplitude of 3.32 radians per volt at this same frequency. Further decreases in voltage will result in only small changes in the amplitude. Since in high-gain servo systems, the voltage applied to the control winding of the motor will be small, a more accurate analysis of the system will be made if the multiplier is calculated for 10 per cent rated voltage or less.

The near match between the calculated and experimental transfer function does not prove conclusively the validity of the derived expression, since data have been obtained on only one motor. The use of the derived transfer function including the additional time constant will lead to greater accuracy in predicting the performance of a high gain servo using this type of motor.

Appendix I

By expressing the voltage applied to the two fields of the machine as

$$V_c=0,\ t<0$$

$$V_c=V\sin\left(\omega t+\tan^{-1}\frac{\omega L_m}{R_m}\right),\ t>0 \qquad (8)$$

$$V_{re}=V\cos\left(\omega t+\tan^{-1}\frac{\omega L_m}{R_m}\right) \qquad (9)$$

the magnetic flux density of the machine as a function of position and time referred to a single differential rotor element will be

$$\beta(t,\theta_r)=-\frac{P_cI_s}{2}\sin(\omega t-\alpha-\theta_r) \qquad (10)$$

The instantaneous voltage in any given rotor element will be proportional to magnetic flux cutting that element and the relative velocity between the element and the field. Since the current in the element under consideration will be of the same frequency as the voltage of the element, but shifted in phase due to the rotor inductance, it may be expressed as

$$i_r=C\epsilon^{-\frac{R_r}{L_r}t}+A_1\sin(\omega t-\alpha-\theta_r)+A_2\cos(\omega t-\alpha-\theta_r) \qquad (11)$$

where A_1 and A_2 are functions of time and may be defined by the relations

$$L_r\frac{dA_1}{dt}-A_2(\omega-\omega_r)L_r+A_1R_r=-\frac{P_cI_s}{2}(\omega-\omega_r) \qquad (12)$$

$$L_r\frac{dA_2}{dt}+A_1(\omega-\omega_r)L_r+A_2R_r=0 \qquad (13)$$

The constant C can be evaluated from the initial conditions of the problem.

The element torque as a function of time will be proportional to the product of the element current and the flux density. The total torque of the rotor will be the sum of the torques on each element and will therefore be the integral from 0 to 2π of the element torque with respect to θ_r.

$$T_r=K_1\epsilon^{-\frac{R_r}{L_r}t}\cos(\omega t-\alpha)+K_2A_1 \qquad (14)$$

The total torque can then be equated to the mechanical requirements of the motor and load.

$$J\frac{d\omega_r}{dt}+f\omega_r=K_1\epsilon^{-\frac{R_r}{L_r}t}\cos(\omega t-\alpha)+K_2A_1 \qquad (15)$$

The transient velocity of the system now can be found by solving equations 12, 13, and 15 simultaneously. Since these equations exhibit nonlinearities, a solution cannot be found without further approximations. By rewriting equation 12 as

$$L_r\frac{dA_1}{dt}+A_1R_r=\left(A_2L_r-\frac{P_cI_s}{2}\right)(\omega-\omega_r) \qquad (16)$$

an examination of the right-hand side of the equation from the standpoint of initial and final value for various final velocities will show it to remain nearly constant over a wide range. This equation can then be approximately

$$L_r\frac{dA_1}{dt}+A_1R_r=K_3 \qquad (17)$$

Further, an examination of the exponential term of the equation for the transient torque will show it to be predominant over its cosinusoidal modifier. Equation 15 can therefore be approximated as

$$J\frac{d\omega_r}{dt}+f\omega_r=K_1\epsilon^{-\frac{R_r}{L_r}t}+K_2A_1 \qquad (18)$$

An approximation to the transient velocity can now be found by solving equations 17 and 18 simultaneously. This approximate solution is given as equation 3 in the text of the paper.

Appendix II

The steady-state torque of a 2-phase induction servo motor may be evaluated for the condition of unequal voltages applied to the phases in a manner similar to that used to find the transient torque in Appendix I. By expressing the voltages to the phases as

$$V_c=V_2\sin\left(\omega t+\tan^{-1}\frac{\omega L_m}{R_m}\right) \qquad (19)$$

$$V_{re}=V_1\cos\left(\omega t+\tan^{-1}\frac{\omega L_m}{R_m}\right) \qquad (20)$$

the magnetic flux density as a function of position and time referred to a single differential rotor element will be

$$\beta(t,\theta_r)=-P\left(\frac{V_2+V_1}{2}\right)\sin(\omega t-\omega_{ss}t-\theta_r)+P\left(\frac{V_2-V_1}{2}\right)\sin(\omega t+\omega_{ss}t+\theta_r) \qquad (21)$$

The instantaneous voltage generated in any rotor element is the product of the constant velocity, the magnetic flux cutting the element, and the element length. Since steady-state conditions of velocity exist in this analysis, the current in a rotor element can be found directly as the rotor voltage divided by the rotor impedance, and is

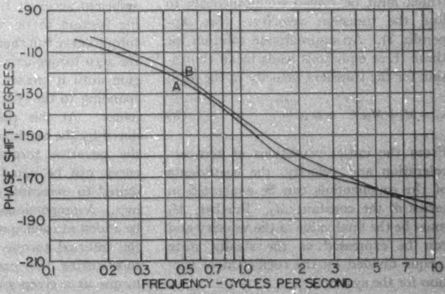

Figure 2. Phase shift of transfer function versus frequency for a 2-phase servo induction motor

Curve A, calculated
Curve B, measured

$$i_r = -\frac{Pl(V_2+V_1)(\omega-\omega_{ss})R_r}{2(R_r^2+(\omega-\omega_{ss})^2L_r^2)}\times \sin((\omega-\omega_{ss})t-\theta_r) + \frac{Pl(V_2+V_1)(\omega-\omega_{ss})^2L_r}{2(R_r^2+(\omega-\omega_{ss})^2L_r^2)}\times \cos((\omega-\omega_{ss})t-\theta_r) + \frac{Pl(V_2-V_1)(\omega+\omega_{ss})R_r}{2(R_r^2+(\omega+\omega_{ss})^2L_r^2)}\times \sin((\omega+\omega_{ss})t+\theta_r) - \frac{Pl(V_2-V_1)(\omega+\omega_{ss})^2L_r}{2(R_r^2+(\omega+\omega_{ss})^2L_r^2)}\times \cos((\omega+\omega_{ss})t+\theta_r) \qquad (22)$$

The instantaneous element torque is the product of the element length, the flux density in which the element is lying, and the element current. The total rotor torque is the sum of the element torques, or the integral from 0 to 2π of the element torque with respect to θ_r. By performing the integration, the time element is removed from the relation and the steady state rotor torque is

$$T_{ss} = \frac{P^2l^2\pi(V_2+V_1)^2(\omega-\omega_{ss})R_r}{8(R_r^2+(\omega-\omega_{ss})^2L_r^2)} - \frac{P^2l^2\pi(V_2-V_1)^2(\omega+\omega_{ss})R_r}{8(R_r^2+(\omega+\omega_{ss})^2L_r^2)} \qquad (23)$$

By using the concept of transformer action within an induction motor, the constants of the torque relation can be referred to the stator and a constant multiplier evaluated. When this is done, equation 5 results.

Appendix III. Symbols and Definitions

A_1 = amplitude of the in-phase component of the rotor current as a function of instantaneous rotor velocity

A_2 = amplitude of the quadrature component of the rotor current as a function of instantaneous rotor velocity

f = viscous friction of the rotor and the load

H = transfer function gain constant

I_s = magnitude of the magnetizing current in either stator field

i_r = rotor current as a function of position and time

J = inertia of the rotor and load

$KG(s)$ = standard notation for the transfer function of a servo component

K_1, K_2, K_3 = constants used in expressing the final forms of the rotor current and torque equations

l = active length of a rotor element

L_m = inductance of the motor magnetizing circuit

L_r = inductance of a single element of the rotor

M_1, M_2, M_3 = constants used in the final form of the transfer function

N_s = synchronous speed of the motor

P = proportionality constant between stator voltage and flux density

P_c = proportionality constant between stator current and flux density

R_m = resistance of the motor magnetizing circuit

R_r = resistance of a single element of the rotor

r_r = effective rotor resistance referred to the stator by transformer action

s = the LaPlace variable

T_r = total rotor torque as a function of instantaneous rotor velocity

T_{ss} = steady-state rotor torque

V_c = instantaneous voltage as a function of time applied to the control phase of the motor

V_{re} = instantaneous voltage as a function of time applied to the reference phase of the motor

V = magnitude of the voltage applied to either phase

V_1 = magnitude of the voltage applied to the reference field under steady-state conditions

V_2 = magnitude of the voltage applied to the control field under steady-state conditions

x_r = effective rotor reactance referred to the stator by transformer action

α = angle between the stator and rotor reference lines as a function of time

$\beta(t,\theta_r)$ = flux density as a function of position and time with respect to the rotor

θ_0 = shaft position as a function of time

θ_r = angle between an element of the rotor and the reference line of the rotor

ω_1 = reciprocal of the mechanical time constant of the system

ω_2 = reciprocal of the electrical rotor time constant

ω_r = angular velocity of the rotor as a function of time

ω_{ss} = steady-state angular velocity of the rotor

ω = angular frequency of the applied voltage

References

1. PRINCIPLES OF SERVOMECHANISMS (book), G. S. Brown, D. P. Campbell. John Wiley and Sons, Inc., New York, N. Y., 1948.

2. STABILIZATION OF CARRIER FREQUENCY SERVOMECHANISMS, A. Sobczyk. *Journal, Franklin Institute* (Philadelphia, Pa.), volume 246, 1948.

3. OPERATING CHARACTERISTICS OF 2-PHASE SERVOMOTORS, R. J. W. Koopman. *AIEE Transactions*, volume 68, 1949, pages 319–28.

4. SERVOMECHANISMS FUNDAMENTALS (book), H. Lauer, R. Lesnick, L. E. Matson. McGraw-Hill Book Company, New York, N. Y., 1947.

5. PRINCIPLES OF ALTERNATING CURRENT MACHINERY (book), R. R. Lawrence. McGraw-Hill Book Company, New York, N. Y., 1940.

No Discussion

Analysis of The Drag-Cup A-C Tachometer by Means of 2-Phase Symmetrical Components

R. H. FRAZIER
FELLOW AIEE

THE DRAG-CUP a-c tachometer is a 2-phase induction generator designed so that when one phase of the stator is energized from a constant-amplitude constant-frequency voltage source the other stator phase gives a voltage of amplitude closely proportional to the speed at which the cup is driven and phase nearly fixed with respect to the supply voltage over a substantial speed range. The parts of one design of such a tachometer are shown in Figure 1. The laminated core on the right carries both windings, concentrated alternately in eight slots to form a 4-pole machine. The cup in the center slips into the housing on the left (the central portion of which carries laminations) and the core and windings slip inside the cup. The housing completes the magnetic circuit and the cup is free to rotate between it and the core. Other such tachometers are manufactured that use cup, disk, or squirrel-cage rotors, and though their design details differ, the basic principles are the same. These types of tachometers have very important uses as velocity feedback elements in computing machines, automatic pilots for planes and missiles, automatic fire-control mechanisms, directing mechanisms for radar antennas, and in numerous other military or industrial control applications. Since some of these applications require high accuracy, a knowledge of basic principles must be supplemented by a thorough analysis of all the details that influence errors or departures from ideal performance.

Analysis of the steady-state performance of such tachometers has been made by Vickers[1] by means of crossed-field theory. Another convenient approach utilizes 2-phase symmetrical components. The basic steady-state relations and an equivalent circuit have been developed by this approach by A. E. Fitzgerald and C. Kingsley and the basic transient relations have been developed by W. V. Lyon in unpublished manuscripts, though the extension of Fortescue's methods to include transients was developed over 25 years ago by Bekku.[2,3] The details of application of these basic relations in the manner presented in this paper are based on study of tachometers used in the computer section of the Massachusetts Institute of Technology Flight Simulator in the Dynamic Analysis and Control Laboratory. The analysis first is limited by the assumption of sinusoidal space distribution of flux density in the air gap, and then is extended to apply to the case of concentrated stator windings. These general analyses are examined to show how parameters of a tachometer can be obtained by measurement and how they influence the ratio of output voltage to supply voltage and the phase angle between them, and to study the errors that arise as functions of supply voltage and frequency, speed, acceleration, temperature, and dissymmetry and inhomogeneity of parts. The results are the equations themselves. They reduce to relatively simple and usable forms for design studies and for check of design by measurement; they thus indicate important factors that influence errors and lead to schemes for minimizing them.

Basic Steady-State Relations

This analysis considers only the fundamental space components of air-gap flux density, assumes the stator and drag-cup structures to be entirely symmetrical and homogeneous except that the two stator windings though symmetrically arranged in space so as to be electromagnetically in quadrature need not be identical windings, and ignores time harmonics in the voltages and currents. The last restric-

Figure 1. Parts of ARMA Corporation type 1B400 tachometer

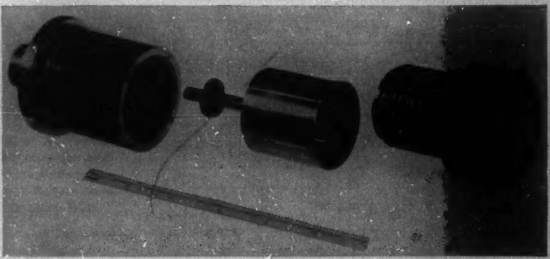

Paper 51-348, recommended by the AIEE Computing Devices and Feedback Control Systems Committees and approved by the AIEE Technical Program Committee for presentation at the AIEE Fall General Meeting, Cleveland, Ohio, October 22-26, 1951. Manuscript submitted April 30, 1951; made available for printing September 5, 1951.

R. H. Frazier is with the Massachusetts Institute of Technology, Cambridge, Mass.

The writer expresses most sincere appreciation to Miss Constance D. Boyd for editorial assistance in preparation of the manuscript.

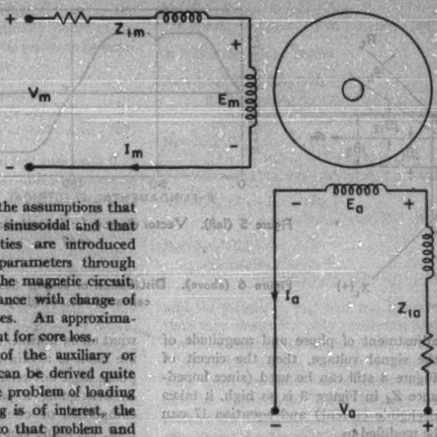

Figure 2. Schematic representation of 2-phase machine

tion is equivalent to the assumptions that the supply source is sinusoidal and that negligible nonlinearities are introduced into the electrical parameters through presence of iron in the magnetic circuit, change of cup resistance with change of speed, or other causes. An approximation is used to account for core loss.

The special case of the auxiliary or signal winding open can be derived quite simply, but since the problem of loading the auxiliary winding is of interest, the solution is directed to that problem and the special case of open auxiliary winding can be checked by allowing the load impedance to become infinite. In the derivations, the subscripts *m* and *a* apply, respectively, to main-winding and auxiliary-winding quantities, the subscripts 1 and 2 apply, respectively, to stator and rotor quantities, and the subscripts *f* and *b* apply, respectively, to the forward and backward sets of symmetrical components. The machine is shown schematically in Figure 2. The equations that express the balance of impressed voltages V_m and V_a with impedance drops I_mZ_{1m} and I_aZ_{1a} and electromotive forces E_m and E_a generated by the resultant air-gap fluxes in the respective windings are

$$V_m=I_mZ_{1m}+E_m \tag{1}$$

$$V_a=I_aZ_{1a}+E_a \tag{2}$$

In these equations Z_{1m} is the leakage impedance of the main winding with respect to the rotor plus any series impedance connected externally to the main winding; likewise, Z_{1a} is the leakage impedance of the auxiliary winding with respect to the rotor plus any series impedance connected externally to the auxiliary winding. By application of symmetrical components, the process of which is omitted here, the equivalent circuit shown in Figure 3 is obtained. In it

$$I_{mf}=(I_m-j\alpha I_a)/2 \tag{3}$$

$$I_{mb}=(I_m+j\alpha I_a)/2 \tag{4}$$

$$V_{mf}=(V_m-jV_a/\alpha)/2 \tag{5}$$

$$V_{mb}=(V_m+jV_a/\alpha)/2 \tag{6}$$

$$N_a/N_m\equiv\alpha \tag{7}$$

$$Z_d\equiv(Z_{1a}/\alpha^2-Z_{1m})/2 \tag{8}$$

A similar equivalent circuit has been developed by Gabriel Kron[4,5] by means of tensor analysis. The use of the ratio of the turns N_a of the auxiliary winding to the turns N_m of the main winding refers all auxiliary-winding quantities to the main winding, and the magnetizing reactance x_ϕ, the rotor resistance r_2, and the leakage reactance x_2 of the rotor with respect to either stator winding are assumed to be referred to the main winding. Core loss is neglected in the analysis at this point but its effect is considered ultimately because it is of appreciable importance. Its effect can be simulated reasonably well in a rather simple way when desirable by introduction of resistance r_c shown dotted in Figure 3, but introduction of it at the outset merely aggravates the complicated algebraic situation that develops in the solution of the circuit relations pertaining to Figure 3 without adding to the understanding of the basic theory.

In solution of the circuit the condensations

$$Z_o\equiv(Z_{1a}/\alpha^2+Z_{1m})/2 \tag{9}$$

$$x_{22}\equiv x_\phi+x_2 \tag{10}$$

$$Z_f\equiv jx_\phi(r_2/s+jx_2)/(jx_\phi+r_2/s+jx_2)$$
$$=jx_\phi[r_2+j(1-n)x_2]/[r_2+j(1-n)x_{22}] \tag{11}$$

$$Z_b\equiv jx_\phi[r_2/(2-s)+jx_2]/[jx_\phi+r_2/(2-s)+jx_2]=jx_\phi[r_2+j(1+n)x_2]/[r_2+j(1+n)x_{22}] \tag{12}$$

are used. Here *s* is the per-unit slip and *n* is the per-unit speed based on synchronous speed. In terms of the condensed symbols

$$I_a=j(I_{mf}-I_{mb})/\alpha=j[(V_{mf}-V_{mb})\times(Z_o-Z_d)+V_{mf}Z_b-V_{mb}Z_f]/\alpha[(Z_o+Z_f)(Z_o+Z_b)-Z_d^2] \tag{13}$$

and for the conditions of zero voltage impressed on the auxiliary winding and load impedance Z_L connected across its terminals,

$$V_{mf}=V_{mb}=V_m/2 \tag{14}$$

$$I_a=-jV_m(Z_f-Z_b)/2\alpha[(Z_o+Z_f)(Z_o+Z_b)-Z_d^2] \tag{15}$$

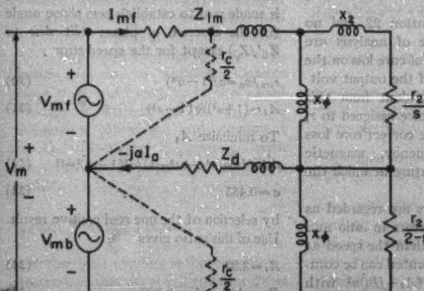

Figure 3 (left). Equivalent circuit of 2-phase induction machine

Figure 4 (below). Equivalent circuit of Figure 3 reduced to special case of signal winding open

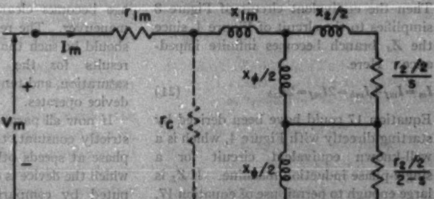

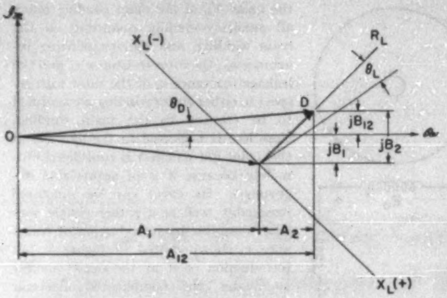

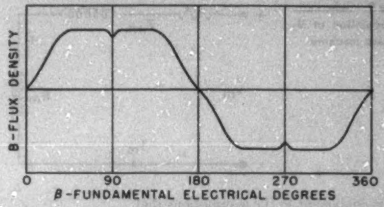

Figure 5 (left). Vector diagram for denominator of equations 22, 38' or 67

Figure 6 (above). Distribution of air-gap flux density due to concentrated stator windings

If now a signal voltage $\boldsymbol{V_L'}$ is picked off a portion $\boldsymbol{Z_L'}$ of $\boldsymbol{Z_L}$

$$\boldsymbol{V_L'}=\boldsymbol{I_a Z_L'}=-j\boldsymbol{V_m Z_L'}(\boldsymbol{Z_f}-\boldsymbol{Z_b})/2\alpha[(\boldsymbol{Z_o}+\boldsymbol{Z_f})(\boldsymbol{Z_o}+\boldsymbol{Z_b})-\boldsymbol{Z_d}^2] \quad (16)$$

Signal Winding Open

In condensed form the expression for $\boldsymbol{V_L'}$ is very simple; $\boldsymbol{Z_L}$ is supposed to be contained in $\boldsymbol{Z_{1a}}$ and, consequently, in $\boldsymbol{Z_d}$ and $\boldsymbol{Z_o}$, but when equation 16 is expanded to display the details of the components of each impedance involved, it becomes very lengthy and hence the expansion is omitted. Inspection of the complete expansion shows that most of the algebraic complexity arises from the presence of $\boldsymbol{Z_L}$, so that by allowing $\boldsymbol{Z_L}$ to approach infinity, equation 16 approaches

$$\boldsymbol{V_L}/\boldsymbol{V_M}=\alpha n/\{(b-a^2b)x_{11}+2abr_{1m}+a+j[2abx_{11}-(b-a^2b)r_{1m}-1]+(a^2bx_{11}-a)n^2-ja^2br_{1m}n^2\} \quad (17)$$

in which

$$a\equiv x_{22}/r_2 \quad (18)$$

$$b\equiv r_2/x_\phi^2 \quad (19)$$

$$x_{11}\equiv x_\phi+x_{1m} \quad (20)$$

and is expressed in terms of two ratios, x_{22}/r_2 and r_2/x_ϕ^2, the self-resistance, r_{1m}, and the self-reactance, x_{11}, of the main winding that (apart from core loss and transformation ratio) completely determine the performance of the device. Then the equivalent circuit of Figure 3 simplifies to the circuit of Figure 4, since the $\boldsymbol{Z_d}$ branch becomes infinite impedance. Here

$$\boldsymbol{I_m}=\boldsymbol{I_{mf}}+\boldsymbol{I_{mb}}=2\boldsymbol{I_{mf}}=2\boldsymbol{I_{mb}} \quad (21)$$

Equation 17 could have been derived by starting directly with Figure 4, which is a well-known equivalent circuit for a single-phase induction machine. If $\boldsymbol{Z_L}$ is large enough to permit use of equation 17, but not so large that it is unstable or impractical to arrange in parts as a means of adjustment of phase and magnitude of the signal voltage, then the circuit of Figure 4 still can be used (since impedance $\boldsymbol{Z_d}$ in Figure 3 is so high, it takes negligible current) and equation 17 can be modified to

$$\boldsymbol{V_L'}/\boldsymbol{V_m}=\boldsymbol{Z_L'}\alpha n/\boldsymbol{Z_L}[A_1+jB_1+(A_2-jB_2)n^2] \quad (22)$$

Here the constants in the denominator of equation 17 have been condensed into A_1, B_1, A_2, and B_2.

Core loss cannot be represented rigorously by any scheme of incorporating linear elements into the circuit. However, study of the construction and operation of a few of the devices and of core-loss measurements made on them indicates that the use of a resistance r_c, shown dotted in Figures 3 and 4, is quite logical and gives a very good approximation. Furthermore, insertion of r_c does not upset the scheme of analysis already developed into a rather simple form for the circuit in which core loss is neglected. By application of Thévenin's theorem, $\mathbf{V_m}$ and r_{1m} can be replaced, respectively, by

$$\boldsymbol{V_m'}=r_c\boldsymbol{V_m}/(r_{1m}+r_c) \quad (23)$$

$$R_{1m}=r_{1m}r_c/(r_{1m}+r_c) \quad (24)$$

in equation 17 or equation 22, and no changes in the scheme of analysis are needed. The influence of core loss on the magnitude and phase of the output voltage becomes clearly evident from this maneuver. The resistance assigned to r_c should be such that the correct core loss results for the frequency, magnetic saturation, and temperature at which the device operates.

If now all parameters are regarded as strictly constant, the errors in ratio and phase at speeds other than the speed at which the device is calibrated can be computed by comparing $(A_2-jB_2)n^2$ with (A_1+jB_1) over the operating range of n. The size of these errors depends somewhat on the manner in which adjustments are made to attain the desired ratio and phase angle between $\boldsymbol{V_L}$ (or $\boldsymbol{V_L'}$) and $\boldsymbol{V_m}$. In attempting a particular design, this comparison of course can be made by trial, the result can be observed, and the design then can be modified to change the parameters as may be necessary to reduce the error. However, to see the problem more broadly than a cut-and-try process permits, some idealization may be helpful. Study of equation 17 indicates that for reduction of A_2 and B_2, the ratios x_2/x_ϕ, x_{1m}/x_ϕ, and r_{1m}/r_2 should be made small. If the leakage reactances could be eliminated completely,

$$A_2=x_{22}^2(x_{1m}+x_\phi)/r_2x_\phi^2-x_{22}/r_2=x_\phi/r_2-x_\phi/r_2=0 \quad (25)$$

$$B_2=x_{22}^2r_{1m}/r_2x_\phi^2=r_{1m}/r_2 \quad (26)$$

Under these circumstances

$$A_1=r_2/x_\phi+2r_{1m}/x_\phi \quad (27)$$

$$B_1=1-r_{1m}(r_2/x_\phi^2-1/r_2) \quad (28)$$

$$a=x_\phi/r_2 \quad (29)$$

Now presumably as high a voltage ratio $\boldsymbol{V_L}/\boldsymbol{V_m}$ as possible without excessive speed is desirable. Hence B_1 should be made zero and A_1 should be minimized. If B_1 is made zero to establish zero phase angle (in the absence of phase shift due to $\boldsymbol{Z_L'}/\boldsymbol{Z_L}$) except for the speed error

$$r_{1m}/x_\phi=a/(1-a^2) \quad (30)$$

$$A_1=(1+a^2)/a(1-a^2) \quad (31)$$

To minimize A_1

$$dA_1/da=(a^4+4a^2-1)/a^2(1-a^2)^2=0 \quad (32)$$

$$a=0.485 \quad (33)$$

by selection of the one real positive result. Use of this ratio gives

$$A_1=3.33 \quad (34)$$

$$B_2=a^2/(1-a^2)=0.308 \quad (35)$$

$$\boldsymbol{V_L'}/\boldsymbol{V_m}=\boldsymbol{Z_L'}\alpha n/\boldsymbol{Z_L}(3.33-j0.308n^2) \quad (36)$$

Since A_3 has been reduced to zero, the speed error has practically no effect on the ratio V_L'/V_m. The phase-angle error can be computed from

$$|\Delta\phi| = B_3 n^3/A_1 = 0.308n^3/3.33 = (0.308)(0.25)^3/3.33 = 0.00578 \text{ radian or 0.33 degree} \quad (37)$$

with V_L' leading V_m, if full speed n_f is 0.25 (for example) and no shift of phase is made through use of Z_L'/Z_L. The magnitude of the extreme error depends on the speed at which calibration is made. If a slight phase shift is introduced through Z_L'/Z_L, or by slight reduction of r_{1m} so that B_1 is given a small positive value, the phase can be set at zero for any desired speed within the range of operation. If a certain portion of the speed range is utilized largely to the exclusion of the extremes, calibration should be made at a speed in the commonly used portion of the range. If calibration is made at low speed, the maximum error occurs at full speed, and V_L' leads V_m. If calibration is made at full speed, the maximum error occurs at low speed (theoretically zero speed) and V_L' lags V_m. If the entire range (0 to 0.25 per unit, for example) is used, then calibration should be made at $n_f/\sqrt{2}$ to distribute the errors equally at both ends of the range. For such calibration, the maximum phase errors, at the extremes of the range, are half the error computed in equation 37, namely, 0.00289 radian or 0.17 degree; V_L' leads V_m at speeds above 0.707 n_f and lags at speeds below 0.707 n_f.

In practice, x_2 and x_{1m}, of course, cannot be made zero within the machine, so that A_3 cannot be made zero by tachometer design alone. Hence, to keep the speed errors down, increase of A_1 may be advantageous at the sacrifice of ratio. The ratio, of course, is subject also to control through α to the extent that space limitations and practical range of wire size permit. Speed errors might be reduced further by allowing B_1 to have substantial magnitude. Theoretically, if $A_1/A_3 = B_1/B_3$, no phase error could appear, but B_1 would have to be negative. Correct phase then would have to be established through adjustment of Z_L'/Z_L. The problems of calibration and adjustment are discussed further in connection with the conditions for the output winding loaded.

Signal Winding Loaded

If the signal winding is loaded with resistance, so that $Z_L = R_L$, equation 22 is replaced by a similar expression that contains additional terms in the denominator

$$V_L'/V_m = R_L'\alpha n/R_L\{A_1+A_2+j(B_1+B_2)+[A_3+A_4-j(B_3+B_4)]n^2\} \quad (38)$$

in which the added terms

$$A_2 \equiv A_1 r_{1a}'/R_L - B_1 x_{1a}'/R_L + [(1+x_2/x_\phi)(r_2/x_m - x_2/r_2)r_{1m} - x_{1m} - 2x_2x_{11}/x_\phi]\alpha^2/R_L \quad (39)$$

$$B_2 \equiv B_1 r_{1a}'/R_L + A_1 x_{1a}'/R_L + [(1+2x_2/x_\phi)r_{1m} + (1+x_2/x_\phi)(r_2/x_m - x_2/x_\phi)x_{1m} + r_2 - x_2^2/r_2]\alpha^2/R_L \quad (40)$$

$$A_4 \equiv A_3 r_{1a}'/R_L + B_3 x_{1a}'/R_L + [(1+x_2/x_\phi)x_2 r_{1m}/r_2]\alpha^2/R_L \quad (41)$$

$$B_4 \equiv B_3 r_{1a}'/R_L - A_3 x_{1a}'/R_L - [(1+x_2/x_\phi)x_2x_{11}/r_2 - (x_2/x_\phi)(x_\phi^2/r_2)]\alpha^2/R_L \quad (42)$$

and the primes on r_{1a}' and x_{1a}' indicate that they designate only resistance and reactance internal to the machine.

As for the simpler conditions with Z_L very large, the influence of speed errors can be appreciated more broadly by making the idealizations of zero leakage reactance than by making computations by trial for specific design figures. If x_2, x_{1m}, and x_{1a}' are each zero, then the terms in the denominator of equation 38 reduce to

$$A_1+A_2 \equiv A_{12} = (r_2/x_\phi + 2r_{1m}/x_\phi)\times(1+r_{1a}'/R_L) + (r_2r_{1m}/x_\phi)\alpha^2/R_L \quad (43)$$

$$B_1+B_2 \equiv B_{12} = [1-(r_2/x_\phi^2 - 1/r_2)r_{1m}]\times(1+r_{1a}'/R_L) + (r_{1m}+r_2)\alpha^2/R_L \quad (44)$$

$$A_3+A_4 \equiv A_{34} = 0 \quad (45)$$

$$B_3+B_4 \equiv B_{34} = (r_{1m}/r_2)(1+r_{1a}'/R_L) \quad (46)$$

If phasing is accomplished by reducing B_{12} to zero,

$$r_{1m}/x_\phi = a(1+r_{1a}'/R_L+\alpha^2 r_2/R_L)/[(1-a^2)(1+r_{1a}'/R_L) - a^2\alpha^2 r_2/R_L] = a(h+k)/[(1-a^2)h - a^2k] \quad (47)$$

in which

$$h \equiv 1+r_{1a}'/R_L \quad (48)$$

$$k \equiv \alpha^2 r_2/R_L \quad (49)$$

Equations 43 and 46 then become

$$A_{12} = h[1+a^2(1+k/h)^2]/a[1-a^2(1+k/h)] \quad (50)$$

$$B_{34} = ha^2(1+k/h)/[1-a^2(1+k/h)] \quad (51)$$

Equations 50 and 51 are in forms for ready comparison with equations 31 and 35, respectively. The phase-angle error is

$$|\Delta\phi| = B_{34}n^3/A_{12} = a^2(1+k/h)\times n^3/[1+a^2(1+k/h)^2] = a^2yn^3/(1+a^2y^2) \quad (52)$$

Even with the idealizations made, the algebraic complexity of determining a, h, and k to minimize A_{12} is considerable if such conditions exist, and hence the investigation is omitted here. If equation 52 is differentiated partially with respect to y and equated to zero

$$\partial|\Delta\phi|/\partial y = a^2n^3(1-a^2y^2)/(1+a^2y^2)^2 = 0 \quad (53)$$

and

$$y = 1+k/h = 1/a \quad (54)$$

$$|\Delta\phi| = a^2n^3/2 \quad (55)$$

$$A_{12} = 2h/a(1-a) \quad (56)$$

for minimum $|\Delta\phi|$ with a fixed. Partial differentiation of equation 56 with respect to a and equating the result to zero gives

$$\partial A_{12}/\partial a = 2h(2a-1)/a^2(1-a^2) = 0 \quad (57)$$

$$a = 0.50 \quad (58)$$

$$y = 2.0 \quad (59)$$

$$h = k = \alpha^2 r_2/R_L = 1+r_{1a}'/R_L \quad (60)$$

$$A_{12} = 8h \quad (61)$$

$$r_{1m} = r_2 \quad (62)$$

If full-speed n_f is 0.25, and since $h>1$

$$|\Delta\phi| = (0.5)^2(0.25)^3/2 = 0.0078 \text{ radian or 0.44 degree} \quad (63)$$

$$A_{12} > 8 \quad (64)$$

The phase-angle error (which can be halved to 0.22 degree by calibration at $0.707n_f$) is essentially the same as computed for the idealized conditions with the signal winding open, but for the same turns ratio the signal voltage of the loaded machine is, of course, inevitably lower than the signal voltage from an open winding under the conditions assumed. The turns ratio and resistances are forced into definite relation as a result of equations 60 and 62, so that

$$\alpha^2 r_2 = R_L + r_{1a}' = r_{1a} = \alpha^2 r_{1m} \quad (65)$$

$$V_L'/V_m = R_L'\alpha n/8R_Lh = R_L'n/8\alpha r_2 = R_L'n/8\sqrt{r_{1a}r_{1m}} \quad (66)$$

The various forms of equation 66 must be used with full recognition of the restrictions imposed.

If the signal winding is loaded with pure reactance, so that $Z_L = jX_L$, the equation for voltage ratio retains the same form as equation 38

$$V_L'/V_m = X_L'\alpha n/X_L\{A_1+A_2'+j(B_1-B_2')+[A_3-A_4'-j(B_3+B_4')]n^2\} \quad (67)$$

in which the primed terms in the denominator are

$$A_2' \equiv B_1 r_{1a}'/X_L + A_1 x_{1a}'/X_L + [(1+2x_2/x_\phi)r_{1m} + (1+x_2/x_\phi)(r_2/x_m - x_2/r_2)x_{1m} + r_2 - x_2^2/r_2]\alpha^2/X_L \quad (68)$$

$$B_2' \equiv A_1 r_{1a}'/X_L - B_1 x_{1a}'/X_L + [(1+x_2/x_\phi)(r_2/x_m - x_2/r_2)r_{1m} - x_{1m} - 2x_2x_{11}/x_\phi]\alpha^2/X_L \quad (69)$$

$$A_4' \equiv B_3 r_{1a}'/X_L - A_3 x_{1a}'/X_L - [(1+x_2/x_\phi)x_2x_{11}/r_2 - (x_2/x_\phi)\times(x_\phi^2/r_2)]\alpha^2/X_L \quad (70)$$

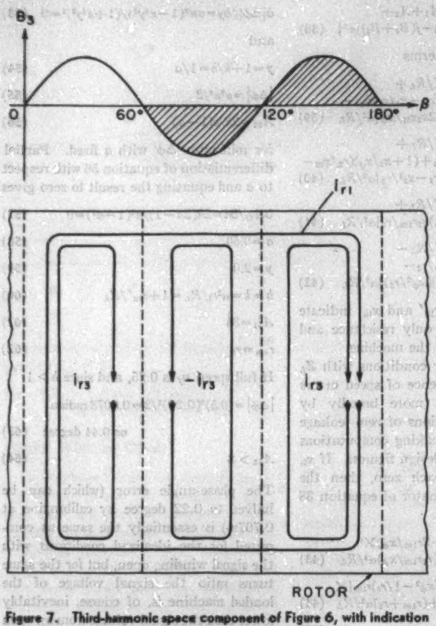
B_3
0
60°
120°
180°
β
I_{r1}
I_{r3}
$-I_{r3}$
I_{r3}
ROTOR

Figure 7. Third-harmonic space component of Figure 6, with indication of associated rotor currents

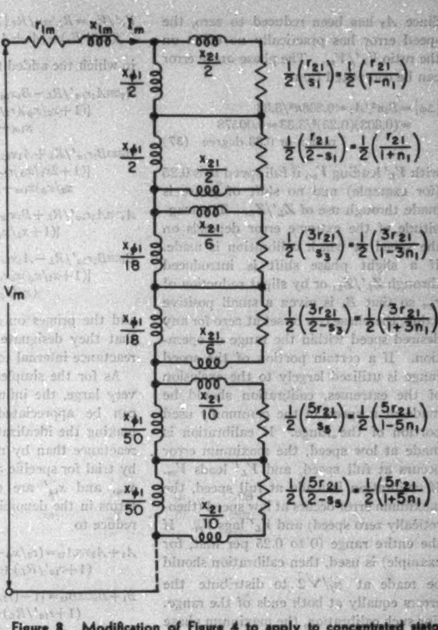
r_{1m}
x_{1m}
I_m
V_m
$\frac{x_{\phi1}}{2}$
$\frac{x_{21}}{2}$
$\frac{1}{2}\left(\frac{r_{21}}{s_1}\right)=\frac{1}{2}\left(\frac{r_{21}}{1-n_1}\right)$
$\frac{x_{\phi1}}{2}$
$\frac{x_{21}}{2}$
$\frac{1}{2}\left(\frac{r_{21}}{2-s_1}\right)=\frac{1}{2}\left(\frac{r_{21}}{1+n_1}\right)$
$\frac{x_{\phi1}}{18}$
$\frac{x_{21}}{6}$
$\frac{1}{2}\left(\frac{3r_{21}}{s_3}\right)=\frac{1}{2}\left(\frac{3r_{21}}{1-3n_1}\right)$
$\frac{x_{\phi1}}{18}$
$\frac{x_{21}}{6}$
$\frac{1}{2}\left(\frac{3r_{21}}{2-s_3}\right)=\frac{1}{2}\left(\frac{3r_{21}}{1+3n_1}\right)$
$\frac{x_{\phi1}}{50}$
$\frac{x_{21}}{10}$
$\frac{1}{2}\left(\frac{5r_{21}}{s_5}\right)=\frac{1}{2}\left(\frac{5r_{21}}{1-5n_1}\right)$
$\frac{x_{\phi1}}{50}$
$\frac{x_{21}}{10}$
$\frac{1}{2}\left(\frac{5r_{21}}{2-s_5}\right)=\frac{1}{2}\left(\frac{5r_{21}}{1+5n_1}\right)$

Figure 8. Modification of Figure 4 to apply to concentrated stator windings

$$B_4' \equiv A_3 r_{1a}'/X_L + B_3 x_{1a}'/X_L + [(1+x_2/x_\phi)x_2 r_{1m}/r_2]\alpha^2/X_L \quad (71)$$

If now x_2, x_{1m}, and x_{1a}' are zero, as before, the terms in the denominator of equation 67 reduce to

$$A_1+A_2' \equiv A_{12}' = r_2/x_\phi + 2r_{1m}/x_\phi + [1-(r_2/x_\phi^2 - 1/r_2)r_{1m}]r_{1a}'/X_L + (r_{1m}+r_2)\alpha^2/X_L \quad (72)$$

$$B_1-B_2' \equiv B_{12}' = -(r_2/x_\phi + 2r_{1m}/x_\phi)r_{1a}'/X_L + 1-(r_2/x_\phi^2 - 1/r_2)r_{1m} - (r_2 r_{1m}/x_\phi)\alpha^2/X_L \quad (73)$$

$$A_3-A_4' \equiv A_{34}' = -(r_{1m}/r_2)r_{1a}'/X_L \quad (74)$$

$$B_3+B_4' \equiv B_{34}' = r_{1m}/r_2 \quad (75)$$

If phasing is accomplished by reducing B_{12}' to zero,

$$r_{1m}/x_\phi = (1-r_{1a}'/aX_L)/[2r_{1a}'/X_L + 1/a - a + \alpha^2 r_2/X_L] = (a-m)/[1+a(2m+p-a)] \quad (76)$$

in which

$$m \equiv r_{1a}'/X_L \quad (77)$$

$$p \equiv \alpha^2 r_2/X_L \quad (78)$$

Then

$$A_{12}' = [(1/a+m+p)^2 + (a-m)^2/a^2]/[(1/a+m+p)-(a-m)] \quad (79)$$

$$A_{34}' = m(a-m)/[(1/a+m+p)-(a-m)] \quad (80)$$

$$B_{34}' = (a-m)/[(1/a+m+p)-(a-m)] \quad (81)$$

The phase-angle error and the per-unit error in ratio are, respectively

$$|\Delta\phi| = B_{34}'n^2/A_{12}' = (a-m)n^2/[(1/a+m+p)^2+(a-m)^2/a^2] \quad (82)$$

$$A_{34}'n^2/A_{12}' = mB_{34}'n^2/A_{12}' \quad (83)$$

Here also the algebraic complexity of determining a, m, and p to minimize A_{12}' is considerable, if such conditions exist, and hence the investigation is omitted. But for inductive X_L (for which m and p are positive) the ratio and phase errors theoretically can be made zero by fixing a and m so that a-m is zero. Then,

$$r_{1m} = 0 \quad (84)$$

$$p = a\alpha^2 r_2/r_{1a}' \quad (85)$$

$$A_{12}' = 1/a + a + p = 1/a + a(1+\alpha^2 r_2/r_{1a}') \quad (86)$$

To minimize A_{12}' with fixed $\alpha^2 r_2/r_{1a}'$

$$\partial A_{12}'/\partial a = -1/a^2 + 1 + \alpha^2 r_2/r_{1a}' = 0 \quad (87)$$

$$a = \sqrt{r_{1a}'/(r_{1a}'+\alpha^2 r_2)} \quad (88)$$

For example, if $\alpha^2 r_2/r_{1a}'$ is 8.0, a reasonable value, a is 0.33 and A_{12}' is 6.0, intermediate between A_1 for the unloaded signal winding and A_{12} for the resistance-loaded signal winding.

For capacitive loading the ratio and phase errors cannot be made zero. The conditions for such loading can be examined merely by considering X_L to be negative. Even if capacitive loading is undesirable, its effect may require investigation, owing to the capacitance associated with instruments or amplifiers fed by the signal winding. Though the speed errors for capacitive loading are relatively large, relatively small A_{12}' is attainable. This condition is illustrated graphically in Figure 5, which generalizes the possibilities.

The equivalent of the idealized conditions of zero leakage reactance can be approached rather closely in practice if desirable. The leakage reactance x_2 can be made relatively small by design, and leakage reactances x_{1m}' and x_{1a}' can be canceled by use of series capacitance. Also, winding resistance r_{1m}' can be kept relatively small. However, for the actual device, many conditions of loading other than pure resistance or pure reactance can be investigated. Phasing of V_L' with V_m may not be required, and minimizing A_1, A_{12}, or A_{12}' may not be necessary. Figure 5 is a generalized vector diagram for the denominator D of equations 22, 38, or 67, aside from the speed-dependent terms. If the output winding is not loaded, phasing is accomplished by reducing B_1 to zero. For resistance loading, phasing is accomplished by reducing B_{12} to zero. As is evident from the derivations, A_2 and B_2 are largely functions of A_1 and B_1. For a tachometer of fixed design, A_2+jB_2 can be increased indefinitely from zero (when the output winding is open) along the line marked R_L as R_L is decreased from infinity. If the load is pure reactance, then $A_2'-jB_2'$, which also is a function largely of A_1 and B_1, may be increased indefinitely from zero along the line marked $X_L(+)$ or along the line marked $X_L(-)$, for positive or negative reactance, respectively. In the 180-degree span from $X_L(+)$ through R_L to $X_L(-)$ an infinite variety of other possibilities exists. As Z_L changes from pure resistance through intermediate stages to pure reactance, the line along which the component of D that is dependent on Z_L adds to A_1+jB_1 departs from the line R_L by θ_L, the angle of Z_L. Evidently, then, phasing can be accomplished, in general, merely by making the angle of Z_L'/Z_L the same as θ_D, the angle of D. For example, if Z_L' is pure resistance,

$$V_L'/V_m=(\alpha n R_L'/Z_L\underline{/\theta_L})/D\underline{/\theta_D} \quad (89)$$

$$-\theta_L=\theta_D \quad (90)$$

to place V_L' in phase with V_m. For a specific application, the manner and accuracy of adjustment of ratio and phase depend upon the requirements of the situation.

Measurement of Parameters

The form in which the equations for V_L'/V_m have been cast not only enables the design and adjustment of the device to be visualized for study in terms of a few parameters and ratios, but also is convenient from the point of view of measurement. Whereas the reactances x_{1m}', x_{1a}', x_2, and x_ϕ, and resistance r_2 cannot be measured separately, the ratios a and b, resistances r_{1m}', r_{1a}', and r_c, reactances x_{11} and $x_{1a}'+\alpha^2x_\phi$, and the transformation ratio α can be measured. For the unloaded tachometer only a, b, r_{1m}', r_c, x_{11}, and α are needed. Since favorable design requires x_2 to be relatively small, neglect of it where it appears in equations 39 through 42 or 68 through 71 is not serious; in fact, use of assumed ratios x_2/x_ϕ with the measured quantities permits computation of all the stray terms needed for A_2, B_2, A_4, B_4, or A_2', B_2', A_4', B_4'. The procedure can be systematized by progressing along the following column headings

$$\frac{x_2}{x_\phi}\quad x_\phi\quad x_{1m}\quad x_{1a}\quad r_2\quad \frac{x_2}{r_2}\quad \frac{x_2^2}{r_2}\quad \frac{x_{1a}'}{R_L}\ \text{or}\ \frac{x_{1a}'}{X_L}$$

Whether or not the actual ratio x_2/x_ϕ makes these stray terms important can be found by trial use of several sets of data inserted in the suggested tabulation. Neglect of x_2 or substitution of assumed data, where x_2 appears separately means not that such assumption has been made throughout, but only insofar as it influences certain stray terms that appear when the tachometer is loaded.

If the cup is removed from the tachometer, measurement of impedance at the input terminals gives

$$r_{1m}'+r_{cs}+jX_s=r_{1m}'+jr_c\times \\ (x_{1m}'+x_\phi)/[r_c+j(x_{1m}'+x_\phi)] \quad (91)$$

in which r_{cs} is the equivalent series core-loss resistance and X_s is the equivalent series reactance. The winding resistance r_{1m}' can be determined by a d-c measurement, the sum $r_{1m}'+r_{cs}$ can be determined by an a-c measurement at the desired frequency, and X_s can be determined directly or from measurement of the magnitude of the impedance at the desired frequency. With r_{cs} and X_s known separately

$$r_{cs}+jX_s=r_c(x_{1m}'+x_\phi)^2/[r_c^2+(x_{1m}'+x_\phi)^2]+ \\ jr_c^2(x_{1m}'+x_\phi)/[r_c^2+(x_{1m}'+x_\phi)^2] \quad (92)$$

whence,

$$r_c^2(x_{1m}'+x_\phi)/[r_c^2+(x_{1m}'+x_\phi)^2] \\ =X_s\approx x_{1m}'+x_\phi \quad (93)$$

because $X_s \gg r_{cs}$ means $r_c \gg (x_{1m}'+x_\phi)$; also

$$[r_c^2+(x_{1m}'+x_\phi)^2]/r_c(x_{1m}'+x_\phi)^2 \\ =1/r_{cs}\approx r_c/(x_{1m}'+x_\phi)^2\approx r_c/X_s^2 \quad (94)$$

$$r_c\approx X_s^2/r_{cs} \quad (95)$$

Similar measurements made at the output terminals give r_{1a}', $x_{1a}'+\alpha^2x_\phi$, and the core-loss resistance from the point of view of the output winding.

With the cup replaced but stationary, measurement of impedance at the input terminals gives

$$r_{1m}'+r_{cs}+R_i+jX_i=r_{1m}'+r_{cs}+ \\ j[x_{1m}'+x_\phi(r_2+jx_2)/(r_2+jx_{22})] \quad (96)$$

or

$$R_i+jX_i=j[x_{11}'-x_\phi+(r_2^2x_\phi+x_\phi x_2x_{22}- \\ jr_2x_\phi^2)/(r_2^2+x_{22}^2)]=r_2x_\phi^2/(r_2^2+x_{22}^2)- \\ jx_{22}x_\phi^2/r_2^2+x_{22}^2+jx_{11}' \quad (97)$$

whence

$$R_i=r_2x_\phi^2/(r_2^2+x_{22}^2) \quad (98)$$

$$X_i'=x_{11}'-X_i=x_{22}x_\phi^2/(r_2^2+x_{22}^2) \quad (99)$$

$$a=x_{22}/r_2=X_i'/R_i \quad (100)$$

$$b=r_2/x_\phi^2=1/(1+a^2)R_i=a/(1+a^2)X_i' \quad (101)$$

Similar measurements made at the output terminals give

$$R_o=\alpha^2r_2x_\phi^2/(r_2^2+x_{22}^2) \quad (102)$$

$$X_o'=\alpha^2x_{22}x_\phi^2/(r_2^2+x_{22}^2) \quad (103)$$

$$a=X_o'/R_o \quad (104)$$

$$b=\alpha^2/(1+a^2)R_o=\alpha^2a/(1+a^2)X_o' \quad (105)$$

$$\alpha^2=R_o/R_i=X_o'/X_i' \quad (106)$$

Because X_i' and X_o' result from differences of separately measured reactances that are the same order of magnitude, the accuracy of equations 99 and 103 is not high unless very careful measurements are made. Another approach that gives better accuracy and at the same time gives some indication of possible variation of r_2 with frequency and gives a check against the measurement of x_{11}' is as follows. Measurements of R_i+jX_i are made at two frequencies, for example, 400-cycles per second and 800-cycles per second for a 400-cycle-per-second tachometer. Then

$$R_{i1}+jX_{i1}=j[x_{1m}'+ \\ x_\phi(r_2+jx_2)/(r_2+jx_{22})] \quad (107)$$

$$R_{i2}+jX_{i2}=j[2x_{1m}'+ \\ 2x_\phi(r_2+j2x_2)/(r_2+j2x_{22})] \quad (108)$$

whence,

$$(R_{i1}r_2-X_{i1}x_{22})+j(R_{i1}x_{22}+X_{i1}r_2) \\ =-(x_{1m}'x_{22}+x_\phi x_2)+j(x_{1m}'r_2+x_\phi r_2) \quad (109)$$

$$(R_{i2}r_2-2X_{i2}x_{22})+j(2R_{i2}x_{22}+X_{i2}r_2) \\ =-(4x_{1m}'x_{22}+4x_\phi x_2)+ \\ j(2x_{1m}'r_2+2x_\phi r_2) \quad (110)$$

Subtraction of the real part of equation 110 from four times the real part of equation 109 gives

$$(4R_{i1}-R_{i2})r_2+(2X_{i2}-4X_{i1})x_{22}=0 \quad (111)$$

$$a=x_{22}/r_2=(4R_{i1}-R_{i2})/(4X_{i1}-2X_{i2}) \quad (112)$$

Subtraction of the imaginary part of equation 110 from twice the imaginary part of equation 109 gives

$$(2R_{i1}-2R_{i2})x_{22}+(2X_{i1}-X_{i2})r_2=0 \quad (113)$$

$$a=(2X_{i1}-X_{i2})/2(R_{i2}-R_{i1}) \quad (114)$$

For consistent data, equations 114 and 112 should check. Likewise equation 101 should give check results for b, but instead X_{i1}' now can be computed from

$$X_{i1}'=x_{22}x_\phi^2/(r_2^2+x_{22}^2)=a/(1+a^2)b \quad (115)$$

after b has been computed from the part of equation 101 that depends on R_t. Furthermore

$$X_{t1}'=8a/[1+(2a)^2]b \qquad (116)$$

$$b=1/[1+(2a)^2]R_{t1} \qquad (117)$$

$$x_{11}'=X_{t1}+X_{t1}' \qquad (118)$$

$$2x_{11}'=X_{t1}+X_{t1}' \qquad (119)$$

give additional checks. As final checks, the 400-cycle-per-second and 800-cycle-per-second measurements can be repeated at the output terminals.

To obtain consistent measurements considerable care must be exercised to have as nearly the same conditions of frequency, magnetic-flux density, and temperature for all measurements as reasonably feasible. Furthermore, to make computations for specified operating conditions, and to make corrections for inevitable discrepancies in the conditions, the frequency, magnetic-flux density, and temperature (or equivalent information) at which measurements are made must be known. Various schemes may be used for making the actual measurements, and, unless high accuracy is desired, no difficulties of any consequence arise. A pure sine source is desirable, and means should be provided for distinguishing harmonics in the output from residual voltage of fundamental frequency. When high accuracy is demanded, the technique of measurement and the adjustment of results to correspond to operating conditions are in themselves problems, discussion of which is omitted here. Such techniques have been developed which, with the aid of second-order correction formulas utilizing the first approximation of a, give parameter values that make possible computation of r_{1m} within about 1 part in 400 of the resistance required for phasing and computation of V_L'/V_m within about 3 parts in 500, as compared with the results of direct adjustment of phase and ratio. Hence the theory can be checked quite accurately by measurements.

Effect of Concentrated Stator Windings

In the tachometer shown in Figure 1 the windings are relatively concentrated in eight slots so that coil sides of the input and output windings occupy alternate slots separated by 45-degrees mechanically or 90-degrees electrically. The machine hence has four poles formed by four relatively concentrated coils of the input winding. For the purpose of this analysis the output winding is considered to be open, so that it produces no magnetic effect.

If the input coils could be considered ideally as completely concentrated, the magnetomotive forces of these coils would form a rectangular space wave along a development of the air gap. Furthermore, if the air gap could be considered as completely smooth and uniform, the flux-density distribution in the air gap for the component of air-gap flux that is caused by the magnetomotive force of the input coils also would be rectangular. For linear parameters and for input voltage sinusoidal with time, the height of the rectangular space wave of flux density would vary sinusoidally with time; for nonsinusoidal input voltage, the height of the space wave of flux density would contain the same time harmonics (though in different proportions) as the input voltage. In this analysis the time variation of the height of the space wave of flux density is assumed to be sinusoidal.

For the ideal condition of a rectangular space wave of flux density, the Fourier series is

$$B=B_1 \sin \beta+(B_1/3) \sin 3\beta+ (B_1/5) \sin 5\beta+(B_1/7) \sin 7\beta+\ldots \qquad (120)$$

in which B is the flux density at electrical angle β measured on the fundamental scale beginning at a coil side. For the stator core as actually constructed, owing to presence of slots and absence of perfect winding concentration, the distribution of flux density along the air gap probably is similar to Figure 6 rather than rectangular. The sharp corners are removed by the presence of the slots that contain the input winding and by the distribution of the conductors in the slots, and the dips in the centers of the waves are caused by the presence of the intermediate slots occupied by the output winding. This space wave should contain all the odd-harmonic space components shown in equation 120 for the rectangular wave, but in different proportions; probably the higher harmonics would be substantially reduced for the wave of Figure 6 as compared with the harmonic content of the rectangular wave. However, for the purpose of analysis, equation 120 is used. The result should be reliable enough to indicate the order of magnitude of the effects involved.

If for the fundamental space component of flux density a machine has p poles and synchronous speed n_{s1}, for the third harmonic it has $3p$ poles and synchronous speed $n_{s1}/3$, for the fifth harmonic it has $5p$ poles and synchronous speed $n_{s1}/5$, and so on, for the other space harmonics. For the purpose of analysis, attention may be directed to one space harmonic such as the third. This harmonic is sketched in Figure 7 for the 180-electrical degrees under one input coil, and the corresponding portion of the rotor is developed below it.

A rough indication of the paths for rotor currents i_{r3} induced by the third-harmonic space component of flux density is shown in contrast with the path for rotor current i_{r1}, induced by the fundamental space component of flux density with the rotor at standstill. The amplitude of the third-harmonic space component of flux density (or of any other space harmonic) varies at the fundamental frequency in time as do the corresponding rotor-current components with the rotor stationary or when referred to the input winding. For the third-harmonic space component of flux density, the voltage induced in the input winding is

$$e_{m3}=N_m(d\phi_{m3}/dt-d\phi_{rm3}/dt) \qquad (121)$$

in which ϕ_{m3} is the total third-harmonic flux represented by one loop of Figure 7 (all of which is supposed to link the rotor), ϕ_{rm3} is the portion of the flux set up by one current i_{r3} that links the input winding. The effects of the flux of two loops of Figure 7 (for example the loops shown crosshatched) neutralize each other with respect to induction of voltage of the input winding, as do the fluxes set up by adjacent rotor currents i_{r3} and $-i_{r3}$. The voltage induced in one of the i_{r3} loops is

$$\begin{aligned} e_{r3}=d\phi_{m3}/dt&=r_{33}'i_{r3}+d\phi_{r3}/dt \\ &=r_{33}'i_{r3}+d\phi_{rm3}/dt+d\phi_{rl3}/dt \qquad (122)\end{aligned}$$

in which r_{33}' is the resistance of an i_{r3} path, ϕ_{r3} is the total flux of i_{r3}, and ϕ_{rl3} is the portion of it that does not link the input winding. Hence,

$$e_{m3}=N_m(r_{33}'i_{r3}+d\phi_{rl3}/dt) \qquad (123)$$

or in complex notation

$$E_{m3}=N_m(r_{33}'+jx_{33}')I_{r3} \qquad (124)$$

Now roughly, as an approximation, the resistance of an i_{r3} path can be taken as three times the resistance of an i_{r1} path, since for the vertical (axial) parts of the paths the cross-sectional areas are in the ratio 1:3. Likewise the leakage reactance of an i_{r3} path with respect to the input winding can be taken as one third the leakage reactance of an i_{r1} path, since the reluctances for the respective flux paths are in the ratio 3:1. To refer r_{33}', x_{33}', and I_{r3} to the input winding, equation 124 may be multiplied and divided by N_m

$$\begin{aligned} E_{m3}&=N_m^2(r_{33}+jx_{33})I_{r3}/N_m \\ &=(N_m^2r_{33}'+jN_m^2x_{33}')I_{m3} \\ &=(3r_{11}+jx_{11}/3)I_{m3} \qquad (125)\end{aligned}$$

whence

$$E_{m3}/I_{m3}=3r_{21}+jx_{21}/3 \qquad (126)$$

the equivalent rotor resistance and leakage reactance seen from the input winding at standstill, due to the third-harmonic space component of flux density in the air gap.

The equivalent rotor parameters for other space harmonics can be computed similarly.

The magnetizing reactance that should be attributed to the third-harmonic space component of flux density can be deduced from equation 121 by allowing the rotor currents to be zero (rotor removed) so that ϕ_{rm3} is zero. Then

$$e_{m3}=N_m d\phi_{m3}/dt \qquad (127)$$

$$E_{m3}=jx_{\phi3}I_m=j(x_{\phi1}/9)I_m \qquad (128)$$

since the magnetic flux included in one loop of Figure 7 is one ninth of the fundamental space component of flux. The leakage reactance of the input winding with respect to the rotor, which arises from flux that leaks across the tips of the slots and at the end connections of the coils, is unaffected by the space distribution of the flux that crosses the air gap.

Consideration of the analysis given in the two preceding paragraphs gives the equivalent circuit of Figure 8 for the output winding open.

The quantities actually measured now can be interpreted on the basis of Figure 8, which is correct in form but only approximate with respect to the relative magnitudes of the parameters of the successive portions of the network that apply to the respective space harmonics because of the assumption of rectangular distribution of flux density and because of the approximations made in estimating rotor resistance and leakage reactance for the various harmonics. With the cup removed

$$\begin{aligned}x_{11}&=x_{1m}+x_{\phi1}(1+1/9+1/25+1/49+\ldots)\\&=x_{1m}+x_{\phi1}\pi^2/8=x_{1m}+1.234x_{\phi1} \qquad (129)\end{aligned}$$

With the cup in place, but stationary

$$\begin{aligned}R_t+jX_t={}&jx_{1m}+jx_{\phi1}(r_{21}+jx_{21})/\\&[r_{21}+j(x_{\phi1}+x_{21})]+j(x_{\phi1}/9)(3r_{21}+\\&jx_{21}/3)/[3r_{21}+j(x_{\phi1}/9+x_{21}/3)]+\\&j(x_{\phi1}/25)(5r_{21}+jx_{21}/5)/\\&[5r_{21}+j(x_{\phi1}/25+x_{21}/5)]+\ldots\\&=jx_{1m}+jx_{\phi1}(r_{21}+jx_{21})/(r_{21}+jx_{m1})+\\&jx_{\phi1}(r_{21}+jx_{21}/9)/9(r_{21}+jx_{m3})+\\&jx_{\phi1}(r_{21}+jx_{21}/25)/25(r_{21}+jx_{m5})+\ldots \qquad (130)\end{aligned}$$

in which

$$x_{m1}\equiv x_{\phi1}+x_{21} \qquad (131)$$

$$x_{m3}\equiv x_{\phi1}/27+x_{21}/9 \qquad (132)$$

$$x_{m5}\equiv x_{\phi1}/125+x_{21}/25 \qquad (133)$$

and so on. Equation 130 now can be modified to

$$\begin{aligned}R_t+jX_t={}&j(x_{11}-x_{\phi1}\pi^2/8)+\\&jx_{\phi1}(r_{21}+jx_{21})(r_{21}-jx_{m1})/(r_{21}^2+x_{m1}^2)+\\&j(x_{\phi1}/9)(r_{21}+jx_{21}/9)(r_{21}-jx_{m3})/\\&(r_{21}^2+x_{m3}^2)+j(x_{\phi1}/25)(r_{21}+jx_{21}/25)\times\\&(r_{21}-jx_{m5})/(r_{21}^2+x_{m5}^2)+\ldots \qquad (134)\end{aligned}$$

whence,

$$\begin{aligned}R_t={}&x_{\phi1}^2r_{21}/(r_{21}^2+x_{m1}^2)+x_{\phi1}^2r_{21}/243\times\\&(r_{21}^2+x_{m3}^2)+x_{\phi1}^2r_{21}/3125(r_{21}^2+x_{m5}^2)+\ldots\\&\approx x_{\phi1}^2r_{21}[1/(r_{21}^2+x_{m1}^2)+1/243r_{21}^2+\\&1/3125r_{21}^2] \qquad (135)\end{aligned}$$

within a fraction of a per cent, since for x_{m1}/r_{21} of the order of 0.5, as required by favorable design

$$x_{m1}^2/r_{21}^2\approx0.25 \qquad (136)$$

$$x_{m3}^2/r_{21}^2\approx0.0004 \qquad (137)$$

$$x_{m5}^2/r_{21}^2\approx0.000016 \qquad (138)$$

likewise

$$\begin{aligned}x_{11}-X_t={}&x_{\phi1}\pi^2/8-(x_{\phi1}r_{21}^2+x_{\phi1}x_{m1}^2-\\&x_{\phi1}^2x_{m1})/(r_{21}^2+x_{m1}^2)-(x_{\phi1}r_{21}^2+\\&x_{\phi1}x_{m3}x_{21}/9)/9(r_{21}^2+x_{m3}^2)-(x_{\phi1}r_{21}^2+\\&x_{\phi1}x_{m5}x_{21}/25)/25(r_{21}^2+x_{m5}^2)-\ldots\\&\approx x_{\phi1}\pi^2/8-(x_{\phi1}r_{21}^2+x_{\phi1}x_{m1}^2-\\&x_{\phi1}^2x_{m1})/(r_{21}^2+x_{m1}^2)-x_{\phi1}(1/9+\\&1/25+\ldots)\\&\approx x_{\phi1}-(x_{\phi1}r_{21}^2+x_{\phi1}x_{m1}^2-x_{\phi1}^2x_{m1})/\\&(r_{21}^2+x_{m1}^2)=x_{\phi1}^2x_{m1}/(r_{21}^2+x_{m1}^2) \qquad (139)\end{aligned}$$

since

$$\begin{aligned}&x_{\phi1}x_{m3}x_{21}/9x_{\phi1}r_{21}^2\\&=x_{m3}x_{21}/9r_{21}^2\approx0.0014 \qquad (140)\end{aligned}$$

$$x_{m5}x_{21}/25r_{21}^2\approx0.0000012 \qquad (141)$$

if $x_{21}/x_{\phi1}<10$, and in view of the ratios given in equations 136 to 138. Hence in measurements interpreted in accordance with Figure 8, the leakage reactance of the input winding with respect to the rotor appears practically as

$$x_{1m}+(\pi^2/8-1)x_{\phi1} \qquad (142)$$

the true leakage reactance plus a portion of the exciting reactance. If the last two terms within the brackets of equation 135 are omitted, the error is less than 0.5 per cent, so that equations 135 and 139 should give essentially the same ratio for x_{m1}/r_{21} as obtained for x_{22}/r_2 from equations 98 and 99.

On the basis of Figure 8, the equation for the output voltage is

$$\begin{aligned}V_L={}&j\alpha V_m[(Z_{f1}-Z_{b1})-(Z_{f3}-Z_{b3})+\\&(Z_{f5}-Z_{b5})-\ldots]/[2Z_{1m}+Z_{f1}+\\&Z_{b1}+Z_{f3}+Z_{b3}+Z_{f5}+Z_{b5}+\ldots] \qquad (143)\end{aligned}$$

The alternation of signs between the pairs of forward and backward impedances can be checked by remembering that for the fundamental the input and output windings are separated by ±90 degrees electrically, for the third harmonic by ±270 degrees, for the fifth harmonic by ±450 degrees, and so on. The individual forward and backward impedances are

$$Z_{f1}=jx_{\phi1}[r_{21}+j(1-n_1)x_{21}]/[r_{21}+j(1-n_1)x_{m1}] \qquad (144)$$

$$Z_{b1}=jx_{\phi1}[r_{21}+j(1+n_1)x_{21}]/[r_{21}+j(1+n_1)x_{m1}] \qquad (145)$$

$$Z_{f3}=jx_{\phi1}[r_{21}+j(1-3n_1)x_{21}/9]/9[r_{21}+j(1-3n_1)x_{m3}] \qquad (146)$$

$$Z_{b3}=jx_{\phi1}[r_{21}+j(1+3n_1)x_{21}/9]/9[r_{21}+j(1+3n_1)x_{m3}] \qquad (147)$$

$$Z_{f5}=jx_{\phi1}[r_{21}+j(1-5n_1)x_{21}/25]/25[r_{21}+j(1-5n_1)x_{m5}] \qquad (148)$$

$$Z_{b5}=jx_{\phi1}[r_{21}+j(1+5n_1)x_{21}/25]/25[r_{21}+j(1+5n_1)x_{m5}] \qquad (149)$$

and so on. When n_1 traverses the operating range 0 to 0.25, for example, the order of magnitude of the impedances of equations 144 to 149 does not change, so that the same approximations as indicated in equations 135 to 141 are valid in determining the denominator of equation 143 as

$$\begin{aligned}2Z_{1m}+Z_{f1}+Z_{b1}+2(\pi^2/8-1)x_{\phi1}={}&2r_{1m}+\\Z_{f1}+Z_{b1}+j2[x_{1m}+(\pi^2/8-1)x_{\phi1}]& \qquad (150)\end{aligned}$$

but for determining the numerator the individual differences in each pair of forward and backward impedances must be investigated

$$\begin{aligned}Z_{f1}-Z_{b1}={}&-2x_{\phi1}^2r_{21}n_1/[r_{21}+j(1-n_1)x_{m1}]\times\\&[r_{21}+j(1+n_1)x_{m1}] \qquad (151)\end{aligned}$$

$$\begin{aligned}Z_{f3}-Z_{b3}={}&-2x_{\phi1}^2r_{21}n_1/81[r_{21}+\\&j(1-3n_1)x_{m3}][r_{21}+j(1+3n_1)x_{m3}] \qquad (152)\end{aligned}$$

$$\begin{aligned}Z_{f5}-Z_{b5}={}&-2x_{\phi1}^2r_{21}n_1/625[r_{21}+\\&j(1-5n_1)x_{m5}][r_{21}+j(1+5n_1)x_{m5}] \qquad (153)\end{aligned}$$

and so on. Since the denominators of equations 151 to 153 are of the same order of magnitude except for the numerical coefficients, equation 143 can be rewritten as

$$\begin{aligned}V_L/V_m\approx{}&-j(0.99)(x_{\phi1}^2r_{21})\alpha n_1/[r_{1m}+j(x_{1m}+\\&0.234x_{\phi1})+(Z_{f1}+Z_{b1})/2] \qquad (154)\end{aligned}$$

The 0.99 coefficient arises from adding the differences of the forward and backward impedances for the harmonic terms to the difference for the fundamental as if they added in the same line, whereas actually the differences of phase angles of the various pairs of impedances introduce a slight effect on the magnitude and phase of the numerator. If numerator and denominator are divided through by $x_{\phi1}^2r_{21}$ and the denominator is expressed in terms of ratios a and b and parameters r_{1m} and x_{11} where now

$$a\equiv x_{m1}/r_{21} \qquad (155)$$

$$b\equiv r_{21}/x_{\phi1}^2 \qquad (156)$$

$$x_{11}\equiv x_{1m}+x_{\phi1}\pi^2/8 \qquad (157)$$

the form is identical with equation 17 except for the 0.99 coefficient. Furthermore, if a as defined by equation 155 is computed from equations 135 and 139, it is about 0.5 per cent larger than x_{22}/r_2 as computed from equations 98 and 99, and as a consequence b is about 0.25 per cent smaller than r_2/x_ϕ^2 as computed from equation 101. Hence, use of equation 154 gives a result about 0.5 per cent higher than equation 17 for r_{1m} necessary to phase and gives for the real part of the denominator of equation 154 a result about 0.5 per cent higher than obtained in equation 17 which makes the ratio about 1.5 per cent smaller than obtained from equation 17.

The analysis for rectangular flux-density distribution makes quite evident the fact that $x_{\phi 1}$, x_{2m}, and r_{21} are quite different, respectively, from x_ϕ, x_{22}, and r_2, for sinusoidal flux-density distribution, but the ratios involved are essentially the same. Furthermore, the apparent leakage reactance $x_{1m}+0.234x_{\phi 1}$ obviously is quite different from x_{1m}, but it does not appear separately (except in certain correction terms when the output winding is loaded) and x_{11} and r_{1m} have the same interpretation in both analyses.

Errors Due to Fluctuation of Source Voltage, Frequency, or Temperature

Since in the analysis presented all parameters are regarded as linear, the equations for V_L'/V_m are independent of V_m, or, in other words, V_L' changes only in proportion to change in V_m. Actually both ratio and phase are influenced by fluctuation in V_m, because the reactances and the equivalent core-loss resistance are affected by the saturation of the magnetic materials. If the amount by which these parameters are affected by departure from normal saturation can be estimated, the resulting changes in ratio and phase can be estimated by means of the equations for V_L'/V_m. For small voltage fluctuations in the vicinity of rated voltage, the change in ratio can be held within a few thousandths of a per cent per volt and the change in phase can be held within a few thousandths of a degree per volt by careful design. For large swings of supply voltage the change in ratio and phase per volt may become substantially larger than the figures given. Change in supply voltage produces also secondary effects through change in self-heating in the machine and change in speed errors.

The primary effects of change in frequency can be estimated by examining the consequences of change of reactance in the equations for V_L'/V_m. For small changes of frequency in the vicinity of rated frequency, change in equivalent core-loss resistance should be considerably less important than change in reactances, and change in other resistances should be relatively negligible. For small frequency fluctuations in the vicinity of rated frequency, the change in ratio may be of the order of a few hundredths of a per cent per cycle per second and the change in phase may be of the order of a few tenths of a degree per cycle per second, depending on the design proportions of the machine. Change in frequency also produces secondary effects through change in self-heating in the machine and change in speed errors. If the source is a rotating machine, the voltage changes directly with frequency, so that the errors due to fluctuation of voltage and frequency then superpose.

Inspection of equations 17, 39, 40, 68, and 69 indicates that both ratio and phase are quite sensitive to change of resistances r_{1m} and r_2, and in general are somewhat less sensitive to change in resistance r_{1a}' and other resistance in the signal-winding circuit when it is loaded. The phasing resistance is, in effect, composed of r_{1m}', r_c, and such external resistance as required. Unless the cup and the stator winding can be made of substantially zero-temperature-coefficient material, the errors that are due to change of resistance through self-heating and change of ambient temperature may be considerable. External resistors, of course, readily can be made of very-low-temperature-coefficient wire, and the change in internal resistance can be compensated to some extent by use of a negative-temperature-coefficient resistor in association with the external resistors, but the use of only one such correcting resistor cannot compensate perfectly for all the internal changes, though the ratio error thus can be reduced to the order of several thousandths of a per cent per degree centigrade and the phase error can be reduced to the order of several thousandths of a degree per degree centigrade in the allowable temperature range for the machine. Use of very-low-temperature-coefficient materials wherever feasible of course reduces the difficulty of compensation. Change in temperature also produces secondary effects through change in speed errors and especially through emphasis of errors caused by dissymmetries and inhomogeneities of parts, which are considered separately in a following section.

For highly accurate results, close control of frequency is of primary importance, voltage must be controlled only moderately or very closely, depending upon whether only V_L'/V_m or V_L' itself is of interest, and ambient temperature must be controlled within a few degrees.

Minimizing Speed Errors—Calibrating Procedures

Various networks may be utilized at the input or output terminals, or both, for adjustment of ratio and phase. For a particular application a tachometer can be designed to give the desired ratio and phase when energized at specified voltage and frequency; for high accuracy some kind of adjustments must be made on individual machines, and such adjustments may be made more conveniently outside than inside. Furthermore, these external networks make possible adaptation of the machine to other than the rated supply voltage and frequency for special uses, and some of them can minimize or eliminate errors that cannot be eliminated through design of the machine itself.

Probably the simplest way of adjusting ratio and phase is by means of a series and a shunt resistor, as shown in Figure 9(A), with Thévenin equivalent in Figure 9(B). Since adjustment of either R_a or R_b affects both ratio and phase, the procedure should be systematized by adjusting one or both resistors to establish phase only, though the actual signal voltage V_{ab} with the tachometer phased should be noted. Then for desired ratio ρ and desired phase (not necessarily zero),

$$R_aR_b/(R_a+R_b)=R \tag{158}$$

$$V_L/V_{ab}=V_m/V=R_b/(R_a+R_b) \tag{159}$$

$$\rho=V_L/V \tag{160}$$

$$R_a=RV_{ab}/V_L=RV_{ab}/\rho V \tag{161}$$

$$R_b=R_a/(V_{ab}/\rho V-1) \tag{162}$$

in which V_L is the desired signal voltage for source voltage V at the speed chosen for calibration. The adjustment should be made at speed $n_f/\sqrt{2}$ if the full speed range is used, or at speed $\sqrt{(n_1^2+n_2^2)/2}$ if the speed range is between speeds n_1 and n_2. Equations 161 and 162 permit quick computation of nearly correct R_a and R_b from which refined adjustments can be made by trial. The scheme is workable for the signal winding open or loaded, provided that $R>0$ and $V_{ab}>V_L$. With the signal winding open and in the absence of C, whatever speed errors are inherent to to the design of the machine with associated input resistors must be accepted. If with the signal winding open, C is adjusted so that

$$\mathfrak{Im}[r_c(r_{1m}'+jX_c)/(r_c+r_{1m}'+jX_c)+ j(x_{1m}+x_\phi x_2/x_{22})]=0 \tag{163}$$

$$X_c = -1/\omega C \qquad (164)$$

the ratio error is theoretically zero. A close approximation of the desired setting of C can be obtained by estimating r_c, x_{1m}, x_ϕ, and x_2 for use in equation 163, and the setting then can be improved by trial. The first term in equation 163 appears because the X_c cannot in effect be placed directly in series with x_{1m}; a junction of r_c is between them. The term $x_\phi x_2/x_m$ appears because in practice x_2 cannot be made zero.

If the signal winding is loaded with resistance R_L, (Figure 9(C)), R_b is unnecessary. The desired phase then can be established by adjusting R_a and the desired ratio can be obtained by selection of R_L', provided that $R_a > 0$, $R_L' < R_L$. Equations 17, 41, and 42 indicate that use of C reduces the speed error for ratio and use of C' in addition can eliminate it, but that the phase error is increased by the presence of the capacitance. To interpret equations 41 and 42, the terminals of the signal winding may be imagined to be the terminals of R_L and x_{1m} and x_{1a}' may be imagined to be modified by the presence of C and C', respectively.

Though the ideal conditions $r_{1m}' = 0$, $x_2 = 0$ for complete elimination of speed errors with inductive loading cannot be met, use of C and C', Figure 9(D), nevertheless permits reduction of either A_{34}' or B_{34}' to zero, and the one not zero can be made exceedingly small. Close approximations to the desired settings of C and C' can be obtained from

$$A_{34}' \approx [r_{1m}'r_{1a}' - (x_{1m}' + X_c)(x_{1a}' + X_c' + X_L)]x_m^2/r_2x_\phi^2X_L \approx 0 \qquad (165)$$

$$B_{34}' \approx [(x_{1m}' + X_c)r_{1a}' + (x_{1a}' + X_c + X_L)r_{1m}']x_m^2/r_2x_\phi^2X_L \approx 0 \qquad (166)$$

Here the terminals of the signal winding may be imagined to be the terminals of L, and the impedance of the auxiliary path $1-2$ may be considered high enough to have little influence. Final setting of C and C' can be obtained by trial. The desired phase can be obtained by adjusting r_L and the desired ratio can be obtained by tapping the necessary fraction of r_L. The vector relations are illustrated in Figure 10. The phase angle of branch $1-2$ is

$$\theta' = \theta_L - \phi = \tan^{-1}(1/\omega C_L r_L) \qquad (167)$$

which suggests that if adjustment can be made so that $\phi = \theta_L$, C_L can be eliminated. Such adjustment can be made by adding resistance in series with C for $\phi < \theta_L$ or by adding resistance in series with L for $\phi > \theta_L$. Addition of external resistance gives opportunity for compensation for change of internal resistance due to temperature change, but tends to increase the speed errors.

The illustrations given are but a few of many similar schemes that can be invented for adjusting ratio and phase and minimizing speed errors. The feasibility and appropriateness of any particular scheme depend on the electrical proportions of the machine and the conditions of its application. In this analysis, the impedance of the source, including transformer if any, is considered negligible. If such impedance is not negligible, reference voltage V_m then is not constant in magnitude or phase, tachometers supplied from the same source may interact slightly, and harmonics of voltage or current may be unnecessarily introduced. Furthermore, in any terminal networks used, the resistors, capacitors, and inductors should be very stable. With careful design, computations and tests indicate that over an operating range up to $n_f \approx 0.25$, speed errors can be reduced to about 0.01 per cent for ratio, and to about 0.01 degree for phase.

Acceleration Error

The equations and equivalent circuits used thus far are strictly for steady-state conditions and give no indication of the delay in signal-voltage response subsequent to change in speed. Examination of transient conditions must start from the differential equations for the actual stator and rotor voltages and currents or the equivalent; for example, the equations may be written in terms of actual stator voltages and currents and the voltages and currents of a 2-phase rotor

$$v_{1m} = (r_{1m} + L_{11m}D)i_{1m} + L_\phi D[i_{2m}\cos\theta + i_{2a}\cos(\theta + 90°)] \qquad (168)$$

$$v_{1a} = (r_{1a} + L_{11a}D)i_{1a} + L_\phi D[i_{2a}\cos\theta + i_{2m}\cos(\theta - 90°)] \qquad (169)$$

$$v_{2m} = (r_{2m} + L_{22m}D)i_{2m} + L_\phi D[i_{1m}\cos\theta + i_{1a}\cos(\theta - 90°)] \qquad (170)$$

$$v_{2a} = (r_{2a} + L_{22a}D)i_{2a} + L_\phi D[i_{1a}\cos\theta + i_{1m}\cos(\theta + 90°)] \qquad (171)$$

in terms of the resistances, self- and mutual inductances of the various windings. Here subscripts m and a are carried over to designate the respective equivalent

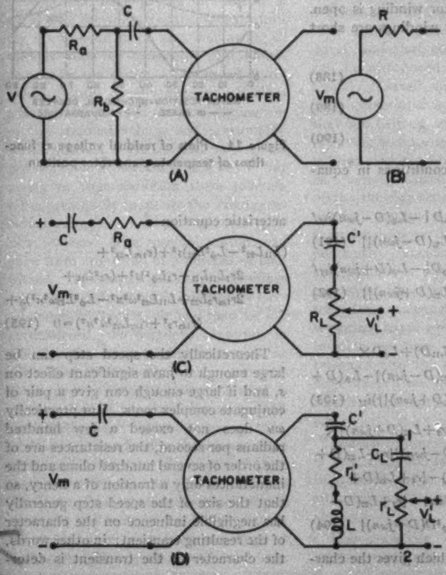

Figure 9 (left). Various auxiliary calibrating networks

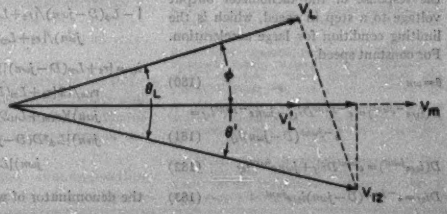

Figure 10 (below). Vector diagram to illustrate phasing for circuit of Figure 9(D)

rotor windings that correspond to the stator windings; all quantities are referred to the main (m) stator winding and D means d/dt. The equations for the 2-phase machine are especially simple because the stator phases are not coupled and the rotor phases are not coupled. If the distribution of flux density in the air gap is sinusoidal, the mutual inductance between a stator phase and a rotor phase varies as the cosine of the electrical angle between them. If the electrical angle between correspondingly designated phases is θ, the angle between the stator phase and the other rotor phase is $\theta \pm (\pi/2)$. The mutual inductances are, therefore, $L_\phi \cos \theta$ and $L_\phi \cos(\theta \pm 90°)$. For a 2-pole machine, θ is the actual angular displacement of the corresponding phases and ωn is the actual angular speed of the rotor; otherwise the mechanical angle must be multiplied by the number of pairs of poles to obtain the electrical angle. Use of exponential expressions for the cosines, and the relations

$$v_{1m}=v_{1f}+v_{1b} \qquad (172)$$

$$i_{1m}=i_{1f}+i_{1b} \qquad (173)$$

$$v_{1a}=-jv_{1f}+jv_{1b} \qquad (174)$$

$$i_{1a}=-ji_{1f}+ji_{1b} \qquad (175)$$

(with similar relations for the rotor currents) give the basic equations for stator and rotor of a symmetrical machine in terms of symmetrical components

$$v_{1f}=(r_{1m}+L_{11}D)i_{1f}+L_\phi D(i_{2f}e^{j\theta}) \qquad (176)$$

$$v_{1b}=(r_{1m}+L_{11}D)i_{1b}+L_\phi D(i_{2b}e^{-j\theta}) \qquad (177)$$

$$v_{2f}=(r_2+L_{22}D)i_{2f}+L_\phi D(i_{1f}e^{-j\theta}) \qquad (178)$$

$$v_{2b}=(r_2+L_{22}D)i_{2b}+L_\phi D(i_{1b}e^{j\theta}) \qquad (179)$$

If the rotor is stationary, θ is constant and the solution of equations 176 to 179 is simple. If the rotor is of squirrel-cage or cup design, θ can be taken as zero at standstill. If the rotor is in motion, the solution is in general very complex and may be attainable only approximately or by machine methods. However, for constant angular speed the differential equations again become linear with constant coefficients and are readily solved. This condition can be imposed to determine the response of the tachometer output voltage to a step in speed, which is the limiting condition for large acceleration. For constant speed,

$$\theta=\omega n \qquad (180)$$

$$D(i_{1f}e^{-j\omega nt})=e^{-j\omega nt}Di_{1f}-j\omega n e^{-j\omega nt}i_{1f}= e^{-j\omega nt}(D-j\omega n)i_{1f} \qquad (181)$$

$$D(i_{2f}e^{j\omega nt})=e^{j\omega nt}Di_{2f}+j\omega n e^{j\omega nt}i_{2f} \qquad (182)$$

$$Di_{2f}=e^{-j\omega nt}(D-j\omega n)i_{2f}e^{j\omega nt} \qquad (183)$$

Substitution of equations 181 and 183 into equation 178 and multiplication by $e^{j\omega nt}$, and a similar maneuver with equation 179 modify the basic equations 176 to 179 to

$$v_{1f}=(r_{1m}+L_{11}D)i_{1f}+L_\phi D(i_{2f}e^{j\omega nt}) \qquad (184)$$

$$v_{1b}=(r_{1m}+L_{11}D)i_{1b}+L_\phi D(i_{2b}e^{-j\omega nt}) \qquad (185)$$

$$v_{2f}e^{j\omega nt}=[r_2+L_{22}(D-j\omega n)]i_{2f}e^{j\omega nt}+ L_\phi(D-j\omega n)i_{1f} \qquad (186)$$

$$v_{2b}e^{-j\omega nt}=[r_2+L_{22}(D+j\omega n)]i_{2b}e^{-j\omega nt}+ L_\phi(D+j\omega n)i_{1b} \qquad (187)$$

which may be taken as the starting point for the condition of constant ωn.

For symmetrical conditions, the negative-sequence equations are the conjugates of the positive-sequence equations, so that only the positive-sequence pair needs to be considered. The characteristic equation derived from them is a quadratic, the roots of which are readily obtained. The characteristic equation derived from the negative-sequence pair is the conjugate of the characteristic equation derived from the positive-sequence pair, and the full characteristic equation is a fourth-degree equation, the product of the two quadratics.

For unsymmetrical conditions, both the positive- and negative-sequence equations must be used. The conditions for the problem at hand are unsymmetrical, since the auxiliary (a) stator winding is open. The equivalent rotor windings are short circuited. Then

$$-ji_{1f}+ji_{1b}=0 \qquad (188)$$

$$v_{2f}=0 \qquad (189)$$

$$v_{2b}=0 \qquad (190)$$

Utilization of these conditions in equations 184 to 187 gives

$$v_{1f}=(r_{1m}+L_{11}D)i_{1f}+L_\phi D\{-L_\phi(D-j\omega n)i_{1f}/ [r_2+L_{22}(D-j\omega n)]\} \qquad (191)$$

$$v_{1b}=(r_{1m}+L_{11}D)i_{1}f+L_\phi D\{-L_\phi(D+j\omega n)i_{1f}/ [r_2+L_{22}(D+j\omega n)]\} \qquad (192)$$

whence

$$v_{1m}=v_{1f}+v_{1b}=(2(r_{1m}+L_{11}D)+L_\phi D\times \{-L_\phi(D-j\omega n)/[r_2+L_{22}(D-j\omega n)]-L_\phi(D+ j\omega n)/[r_2+L_{22}(D+j\omega n)]\})i_{1f} \qquad (193)$$

$$i_{1f}=[r_2+L_{22}(D-j\omega n)][r_2+L_{22}(D+j\omega n)]\times v_{1m}/\{2[r_2+L_{22}(D-j\omega n)][r_2+L_{22}(D+ j\omega n)](r_{1m}+L_{11}D)-[r_2+L_{22}(D+ j\omega n)]L_\phi^2D(D-j\omega n)-[r_2+L_{22}(D- j\omega n)]L_\phi^2D(D+j\omega n)\} \qquad (194)$$

the denominator of which gives the characteristic equation

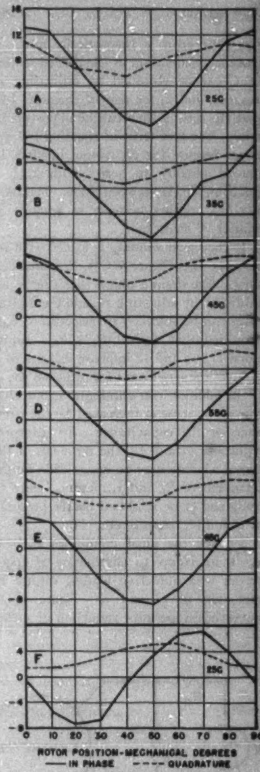

Figure 11. Plots of residual voltage as functions of temperature and rotor position

$$(L_{11}L_{22}^2-L_\phi^2L_{22})s^3+(r_{1m}L_{22}^2+ 2r_2L_{11}L_{22}-r_2L_\phi^2)s^2+(r_2^2L_{11}+ 2r_{1m}r_2L_{22}+L_{11}L_{22}^2\omega^2n^2-L_\phi^2L_{22}\omega^2n^2)s+ (r_{1m}r_2^2+r_{1m}L_{22}^2\omega^2n^2)=0 \qquad (195)$$

Theoretically the speed step can be large enough to have significant effect on s, and if large enough can give a pair of conjugate complex roots. But practically ωn does not exceed a few hundred radians per second, the resistances are of the order of several hundred ohms and the inductances only a fraction of a henry, so that the size of the speed step generally has negligible influence on the character of the resulting transient; in other words, the character of the transient is determined essentially by the electrical parameters of the system. For example, if the tachometer illustrated in Figure 1 is adjusted for ratio and phase by means of a series and a shunt resistor, as shown in Figure 9(A), and subjected to a speed step of 300 radians per second,

$$s = -1{,}840,\ -5{,}490,\ -17{,}590 \text{ second}^{-1} \tag{196}$$

but if the speed step is cut in half,

$$s_1 = -1{,}830,\ -5{,}450,\ -17{,}510 \text{ second}^{-1} \tag{197}$$

If the capacitance is used, as shown in Figure 9(A), equation 168 must be modified by the addition of i_m/CD, and equations 176 and 177 consequently acquire additional terms i_{1f}/CD and i_{1b}/CD, respectively. Then

$$s = -817,\ -17{,}760,\ -3{,}120 \pm j2{,}040 \text{ second}^{-1} \tag{198}$$

though if the tachometer used for the illustration had been designed with such scheme of adjustment in mind, its electrical proportions probably would be different and hence give different transient response than computed here. However, the analysis shows that acceleration errors need not be significant.

Errors Due to Dissymmetry or Inhomogeneity of Parts

When the rotor of the tachometer is stationary the voltage of the output winding is supposed to be zero, but owing to various lacks of symmetry and homogeneity in the device a zero-speed or residual voltage usually appears. Various schemes are directed towards elimination of this residual voltage and presumably would succeed if the residual voltage did not vary with position of the rotor, but owing to that variation these schemes serve principally to reduce the average residual voltage with respect to rotor position to zero. The residual voltage can arise from any or all of a number of conditions. The input and output windings may not be effectively in quadrature electromagnetically, the air gap may be unsymmetrical, the magnetic materials in the structure may be unsymmetrical in disposition or inhomogeneous in composition, the cup may be unsymmetrical in position, not of circular form, of nonuniform thickness, or inhomogeneous in composition. An extensive theory has been developed to examine the effects of these various conditions, and possible remedies for them, but since application of the theory is tied more or less to the manner of construction of a particular type of tachometer, the details are omitted here.

In brief, the direct effects of dissymmetry and inhomogeneity in the stator structure can be compensated by means of adjustable assymmetries deliberately introduced into a part of the stator structure, or by means of compensating windings, but the variation of residual voltage caused by dissymmetry or inhomogeneity in the rotor structure can be reduced only by means of some modification of the rotor.

For example, by means of core adjustment, and if necessary by use of an auxiliary winding in the same slots as the output winding supplied with current in correct magnitude and phase to induce the desired compensating voltage in the output winding, the residual voltage can be made zero for any one position of the rotor. But for other positions of the rotor the residual voltage is not compensated. The variation of residual voltage substantially repeats itself in each 180 electrical degrees of rotor position (90 mechanical degrees for a 4-pole machine), as shown in Figure 11. When the machine is running, therefore, the residual voltage is amplitude modulated at a frequency proportional to the speed of the machine. No adjustment of the core has any important effect on the amount by which the residual voltage varies with rotor position but merely changes the level about which it varies and shifts its position with respect to rotor angle. The performance suggests that as a first approximation the rotor acts as a perfect rotor with a bump on it, and that compensation therefore can be introduced by deposition or removal of small quantities of material. Such procedures actually are used, but they are tedious, so that the importance of having homogeneous rotor material and holding close machining tolerances cannot be overemphasized. For a rotor that carries the core structure, the variation of residual voltage is likely to be greater than for cups or disks that rotate independently. Incidentally, in calibrating the tachometer and later in mounting it, care should be exercised to keep it away from large pieces of iron, such as large wrenches, angle iron of a mounting rack, or other machines. The dissymmetry introduced into the magnetic circuit by a large wrench touching the case can make considerable change in the residual voltage.

The distribution of current in the rotor is very complex, both geometrically and in time phase, as is the distribution of eddy currents in the various parts of the stator.

Dissymmetries and inhomogeneities in the materials cause dissymmetries in the current distributions which depend also upon the reactions of these currents on each other. When temperature changes, the current distributions change, owing to changes in resistance, permeability, and dimensions. Thus when a tachometer is favorably adjusted for a low level of residual voltage at one temperature it may have a relatively high level of residual voltage at another temperature. Figure 11 is illustrative of an unadjusted tachometer, having relatively high residual voltage, subjected to successively higher ambient temperatures, (A) to (E), and (F) shows the best results that could be had by core adjustment alone at normal ambient temperature. These results are practically uninfluenced by the presence of a negative-temperature-coefficient resistor external to the tachometer. Hence even if compensation can be introduced to offset the changes of r_{1m} and r_2 with change of temperature, insofar as ratio and phase are affected, or if those resistances can be made of essentially zero-temperature-coefficient materials, the residual voltage may change with change in temperature due to change in resistance of stator iron and change in dimensions and, therefore, control of ambient temperature may be important.

Conclusions

By careful design and with the use of auxiliary networks, the drag-cup a-c tachometer can be developed to have ratio error of about 0.01 per cent and phase error of about 0.01 degree over a range from zero to about 25 per cent synchronous speed. To make available such accuracy requires close control of supply voltage and frequency, and of ambient temperature. The symmetry and homogeneity of the cup is of special importance to minimize the variation of residual voltage.

References

1. AN INDUCTION GENERATOR USED WITH THE ALL-ELECTRIC AUTOMATIC PILOT FOR AIRPLANES, **Herbert Vickers.** *AIEE Transactions*, volume 67, part I, 1948, pages 182–85.

2. THEORETICAL RESEARCHES ON THE TRANSMISSION LINE PROBLEMS WITH SPECIAL REFERENCE TO THE ARC SUPPRESSING REACTOR, **Sadatoshi Bekku.** Researches of the Electrotechnical Laboratory (Tokyo, Japan), number 129, April 1923, pages 33–38.

3. SUDDEN SHORT-CIRCUIT OF ALTERNATOR, **Sadatoshi Bekku.** Researches of the Electrotechnical Laboratory (Tokyo, Japan), number 203, June 1927, pages 1–4.

4. EQUIVALENT CIRCUIT OF THE CAPACITOR MOTOR, **Gabriel Kron.** *General Electric Review* (Schenectady, N. Y.), volume 44, 1941, pages 511–13.

5. STEADY-STATE EQUIVALENT CIRCUITS OF SYNCHRONOUS AND INDUCTION MACHINES, **Gabriel Kron.** *AIEE Transactions*, volume 67, part I, 1948, pages 175–81.

Discussion

George C. Newton, Jr. (Massachusetts Institute of Technology, Cambridge, Mass.): Professor Frazier is to be congratulated for the most comprehensive and scholarly treatment of the drag-cup a-c tachometer presented to date. My discussion is devoted to additional comment rather than criticism of his excellent paper.

In most computer and automatic control applications of a-c tachometers the output signal is ultimately demodulated to provide a noncarrier representation of the speed information. In such cases the performance of the tachometer should be appraised in conjunction with the demodulation process. For example, the possibility exists for partial compensation of the tachometer's deviation from linearity by suitable offsetting of the phase of the demodulator reference voltage relative to the phase of the tachometer excitation. Also the effective transient performance of the tachometer can be appreciably affected by the demodulation process which follows. In other words, in situations where the tachometer's signal is demodulated, it is highly desirable to consider the tachometer and demodulator as a system.

A somewhat different approach to the transient performance of the tachometer (and demodulator) can be obtained through frequency response methods. Both analytically and experimentally the response of the tachometer system to sinusoidal speed fluctuations gives valuable information on the transient behavior. The analytical methods are similar to those used by H. C. Stanley in his analysis of the induction machine subjected to pulsating loads.[1]

Finally, a very important figure of merit for tachometers used in automatic control applications is the ratio of the speed voltage sensitivity to the maximum variation of residual, in-phase, position voltage. It is this ratio rather than the absolute level of position voltage that determines the ultimate usefulness of the tachometer in feedback control applications. Unfortunately, this index of usefulness cannot be very readily predicted in design and the principal method of keeping it within bounds is production control once a suitable prototype has been constructed by semi-empirical means. This explains why tachometers for precision use are expensive.

Reference

1. An Analysis of the Induction Machine, H. C. Stanley. *AIEE Transactions*, volume 57, 1938, pages 751–57.

Peter Kennedy (Westinghouse Electric Corporation, Baltimore, Md.): Prof. Frazier's paper is a most interesting contribution to the literature on components of computing devices. However, this reader would have appreciated more detail relating to the derivation of the equivalent circuit of the machine by symmetrical components. This was only hinted at, but presumably it would be beside the main purpose of the present work. Further report of the confirmation of the theory by laboratory measurements would have been of interest.

As a side-light, it may be remarked that it is interesting to observe how the very up-to-date science of electronic computation can profitably draw upon concepts originated long before electronic computers were visualized. For example, the method of symmetrical components was advanced first more than 30 years ago. Indeed, the action of the machine as a tachometer is basically similar to the action of the induction machine as a phase balancer, which was among the things prompting Fortesque's work. For another example, consider the measurement technique suggested by equations 107 and 108 in which the measurement of an impedance is made at two different frequencies to check calculation of reactance and to show the variation, if any, of resistance with frequency. This procedure was first employed around the turn of the century in connection with the classic Epstein core loss method.

R. H. Frazier: Professor Newton's comments relative to the desirability of considering the tachometer and the demodulator as a system, with the possibility of studying the transient response of the system by frequency-response methods, and his observations concerning the importance of minimizing the variation of residual voltage with rotor position, are valuable supplements to the paper.

The author would have been glad to oblige Mr. Kennedy (and others who have made similar comment) by including full details of the application of the method of symmetrical components to reach the equivalent circuits. These maneuvers (and miscellaneous other intermediate algebraic steps) were omitted largely in the interest of saving space, and because, as Mr. Kennedy intimates, the procedure really is quite straightforward and is in itself somewhat beside the main objectives of the paper. The unpublished work of Fitzgerald and Kingsley, mentioned near the beginning of the paper, is scheduled to be published in May 1952 by the McGraw-Hill Book Company, Incorporated, under the title, "Electric Machinery." The application of the method of symmetrical components to transients is quite analogous to the steady-state application, but apparently no published general treatment exists. Likewise, considerable data could have been included on measurements, had space permitted. For accuracies of the order of several per cent, various conventional measuring techniques may suffice, but for accuracies of the order of 0.5 per cent or less, methods that devote special attention to numerous details are necessary, the presentation and discussion of which, with the inclusion of numerical data, would require a full-length paper.

Relay Counting Chains, Codes, and Translations in Dial Pulse Register Circuits

R. M. M. OBERMAN
NONMEMBER AIEE

SPEECH is transmitted electrically by subscriber's lines, which are numbered systematically to permit simple interconnection of the lines. When this interconnection is performed by means of automatic switching equipment, a counting system is introduced which can be handled by subscribers. The subscribers phone is provided with a dial to operate the counting system in the automatic exchange.

This dial interrupts the subscriber's line loop as many times as indicated by the digits of the dialed number. The number of the current interruptions of each series is counted and the automatic equipment is positioned accordingly.

This paper deals with the counting of series of dial pulses by means of relay chains. It is the author's object to give a logical review of some types of counting chains, leading to more systematic solutions and their use in dial pulse register circuits. It is necessary to count up to ten pulses. The use of all possible operating conditions of the relays of the counting chain leads to rather complicated and unsystematic diagrams with an inconveniently arranged sequence of the operating combinations. Counting chains of this type are practically of no importance for telephone switching systems.

The way generally used to build up counting chains is to connect in series a number of counting pairs of relays. There are two principal types of counting chains.

Homogeneous Linear Relay Counting Chains

The main problem in designing counting chains is to use the least possible number of relays and contacts having a clear registration code. This code is of great importance because a clear code facilitates the design of the telephone switching system and permits easy maintenance and fault location. The practical solution of this problem will be found between the two extremes, that is, a relay chain using ten pairs of relays and a chain using all possible operating conditions of five relays. There is no single solution but a number of solutions depending on the requirements of the switching system in which the counting chain will be applied and the construction of the relays of the system.

Counting chains built up of sections with equal diagrams are called homogeneous. These chains are linear when no combinations of the operating conditions of the sections or relay-pairs are used, or when these combinations are limited to a double use of the chain. The principle of a counting chain of this type, used for many years in the Bell *7A2* Rotary System,[1] is shown in Figure 1. This chain consists of ten pairs of relays (six pairs shown), each releasing the preceding pair when being operated. After ten pulses the tenth relay-pair only remains operated. This counting chain produces an entirely systematic but expensive registration in a one out of ten code on groups of ten register relays per digit.

A linear counting chain with ten pairs of relays and ten register relays per digit offers no practical solution of the problem. The *7A2* Bell Rotary System (Bell Telephone Manufacturing Company, Antwerp, Belgium) solved this problem by making a double use of the first four pairs of a relay chain of six pairs as is shown in Figure 1. As may be seen in the sequence diagram of Figure 2, the counting chain of Figure 1 counts as follows. Relay *A* is magnetized by the first pulse on the pulse relay *IR*, relay *B* is magnetized in series with relay *A* in the pause after the first

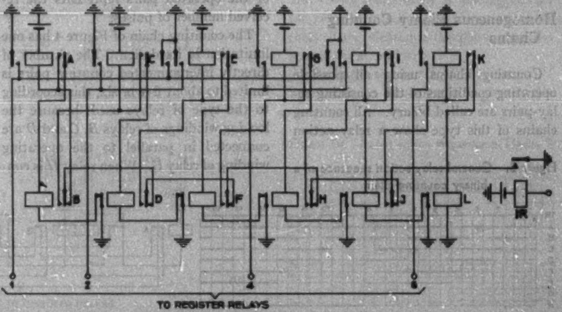

Figure 1. Homogeneous linear counting chain

Paper 51-350, recommended by the AIEE Communications Switching Systems Committee and approved by the AIEE Technical Program Committee for presentation at the AIEE Fall General Meeting, Cleveland, Ohio, October 22–26, 1951. Manuscript submitted September 1, 1950; made available for printing September 5, 1951.

R. M. M. Oberman is with the Netherlands Postal and Telecommunications Laboratories, The Hague, Netherlands.

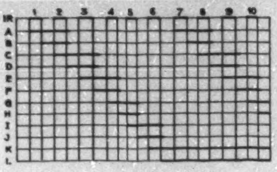

Figure 2. Relay action sequence of Figure 1

pulse, and so on. The sixth pulse magnetizes relay *K*, and relay *L* is magnetized in series with relay *K* in the pause after the sixth pulse. The second relay of each pair breaks with its left-hand contact the holding circuit of the preceding pair. Relay-pair *I/J* releases in the pause after the sixth pulse. This again connects the pulse contact to the first relay-pair. Relay-pair *K/L* remains operated. The seventh pulse now operates pair *A/B* and so on till the tenth pulse operates pair *G/H*.

In this system the digits are not registered on groups of six relays, but on groups of four relays, which is the minimum possible number. The relays of such a group have the systematic value of one, two, four, and six. The sum of the values of the operated relays of a register group represents the received digit. As seen in Figure 1, the code translation from counting chain code into register relay code is easily performed by means of a small number (eight) of contacts on the counting relays.

This rather elegant solution lacks constancy in code. It may be regarded as an important requirement for a good register that the code of the receiving chain, the register relays and the sending counting chain in a register are the same.

The double use of the relay-pairs in the linear counting chain may be extended further, degenerating this type, but this leads to nonpractical solutions as far as they do not reach the binary stage.

Homogeneous Binary Counting Chains

Counting chains using all possible operating conditions of the consisting relay-pairs are called binary. All counting chains of this type show a relay action sequence as is given in Figure 3. A chain of four pairs of relays counts up to 15 pulses. The diagram of a very useful chain is shown in Figure 4. Relay *A* is operated on the first pulse, relay *B* is operated in series with relay *A* in the pause after the first pulse. The second pulse closes a holding circuit for a second winding of relay *B* and operates relay *C*. The left-hand contact of relay *C* breaks the holding circuit of relay *A* and the first winding of relay *B*. Relay *A* releases. Relay *B* remains operated via the second winding as long as the contact of the pulse relay *IR* is closed on the second pulse. Relay *D* is operated in series with relay *C* in the pause after the second pulse when relay *B* also releases.

After two pulses relays *C* and *D* are operated and relays *A* and *B* are then nonoperated. The pulse lead is again connected to the first pair of relays. Relay-pair *A/B* is reoperated on the third pulse and pulse pause. This connects the pulse lead to the third pair of relays *E/F*. The fourth pulse operates this pair and releases pairs *A/B* and *C/D*, and so on. All possible operating combinations of the pairs are passed systematically. The number of received pulses can be counted easily by giving the values 1, 2, 4 and 8 to the pairs. The sum of the values of the operated pairs represents the received number of pulses.

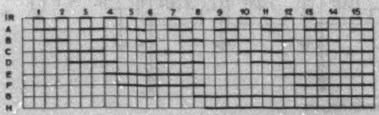

Figure 3. General relay action sequence of a binary counting chain

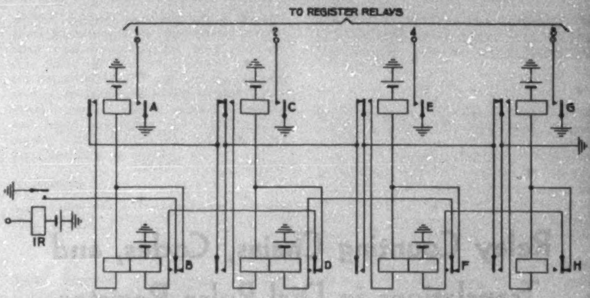

Figure 4. Binary counting chain

The counting chain of Figure 4 has one limitation in its design. The number of directly interconnected counting pairs is limited to about five or six, this according to the type of relays used, because the locking windings of relays *B*, *C* and *D* are connected in parallel to the operating winding of relay *G*. When relay *H* is connected in series with relay *G* in the pause after the eighth pulse, the locking windings of relays *B*, *C* and *D* remain connected in parallel to the winding of relay *G* during a short time. This reduces the holding current of relay *G*, which may go so far with an unsuitable design that it releases. For normal counting chains going up to 15 pulses this limitation is of no importance.

The advantage of the binary counting chain in register circuits is that no code translation is necessary. The received combination of the four pairs of the counting chains can be transferred to groups of four register relays without change in code. The chain itself is very simple, using only one transfer and one make contact on each relay, or in total ten springs per pair. The linear counting chain of Figure 1 has 11 springs on pair *E/F* as a maximum.

The binary counting chain may be adapted easily to the 1-,2-,4-,6-code of the Bell Rotary System. The pulse contact is then connected with the fourth relay-pair having the value "six" when the sixth pulse will be received. This 1-,2-,4-,6-code was used when no practical binary counting chains existed, but now this code seems to be overtaken by the binary code.

Homogeneous Single Relay Counting Chains

The diagram of a single relay counting chain is shown in Figure 5. The relay

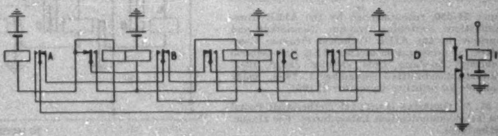

Figure 5. Single relay counting chain

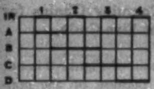

Figure 6. Relay action sequence of single relay counting chain

action sequence of this chain is given in Figure 6. The chain is controlled by means of a continuity transfer contact of the pulse relay *IR*. The circuit of relay *A* is closed on the first pulse via the break-sides of the left-hand transfer contacts of the relays. In the pause after the first pulse relay *B* is operated in series with relay *A* via a second pulse wire leading via the right-hand transfer contacts of the relays.

The first pulse wire via the left-hand transfer contacts is connected by the left-hand transfer contact of relay *B* to the second section of the diagram consisting of a second winding of relay *B* and a first winding of relay *C*. The second pulse closes the circuit of the first pulse wire and breaks that of the second pulse wire. This locks relay *B* on the second winding and breaks the circuit of the winding of relay *A* and the first winding of relay *B*. Relay *A* releases. Relay *C* is operated via a first winding and the second pulse wire in series with the second winding of relay *B*. The left-hand transfer contact of relay *C* connects the first pulse wire to the third section of the diagram, and so on. A counting chain of this type needs $n+1$ relays for n pulses.

A more systematic use of this counting chain can be made by reversing the position of the pulse contact. Relay *A* is then already operated in the rest condition of the counting chain, relay *B* is the only one operated after the first pulse, relay *C* is the only one operated after the second pulse, and so on.

Figure 7. Nonhomogeneous counting chain in one, two, four, six code

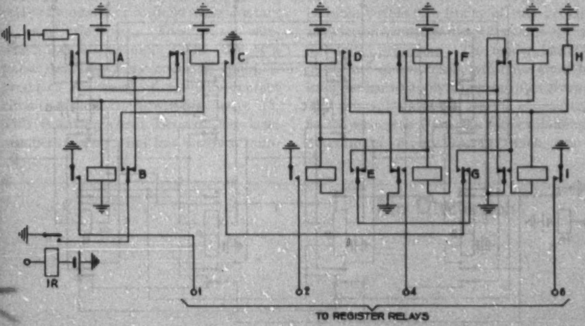

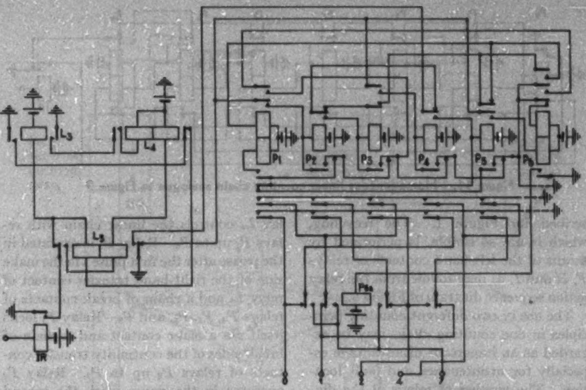

Nonhomogeneous Counting Chains

It is possible to design counting chains with different types of diagrams of the sections. Figure 7 shows a chain with a binary working start section followed by a double used linear chain. Counting chains of this type are called nonhomogeneous. The object of the design of counting chains of this type is not always clear as may follow from the example after the next one.

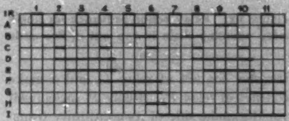

Figure 8. Relay action sequence of Figure 7

The counting chain of Figure 7 is designed under the requirements that relays with one winding and two transfer contacts only may be used, and that it can co-operate with groups of four register relays with the 1,2,4,6 operating code. This problem may be solved, to some extent satisfactorily, by means of a single stage of a binary counting chain (relays *A*, *B* and *C*) followed by a double used linear counting chain consisting of three sections (*D*/*E*, *F*/*G*, and *H*/*I*). The relay action sequence of this diagram is shown in Figure 8. The binary section (*A*, *B* and *C*) is working under the direct control of the contact of the pulse relay *IR*, the linear sections are working under the control of the right-hand make contact of relay *C*. On the first pulse relay *IR* closes an operating circuit for relay *A*. Relay *B* is magnetized in series with relay *A* in the pause after the first pulse. The second pulse operates relay *C* via the right-hand transfer contact of relay *B*. The break side of the left-hand transfer contact of relay *A* then releases relay *A* and closes temporarily a holding circuit for relay *B*. Relay *C* and consequently relay *B* are released in the pause after the second pulse, and so on.

Figure 9. Nonhomogeneous two out of five code counting chain

The linear sections *D*/*E*, *F*/*G* and *H*/*I* operate in the same way as is already de-

Figure 10. Relay action sequence of Figure 9

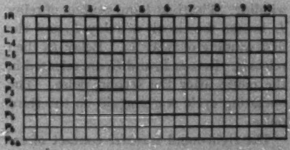

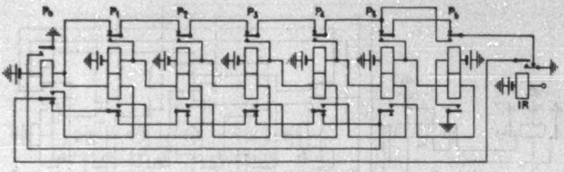

Figure 11. Homogeneous linear counting chain analogue to Figure 9

scribed for Figure 1. The recycling, which is not so simple, is performed by means of the left-hand contacts of relays *F*, *H* and *I*, as may follow from the relay action sequence diagram of Figure 8.

The use of two different counting principles in one counting chain may be regarded as an important disadvantage especially for maintenance and fault location. The number of relays of the diagram of Figure 7 can be reduced to six in a rather appreciable diagram, when the linear counting chain of Figure 5 is used instead of that of Figure 1. That diagram does not fulfill the above given requirements.

A nonhomogeneous counting chain, which has drawn much attention and which seems to be applied on a big scale, is shown in Figure 9.[3] The relay action sequence is given in Figure 10. The counting chain consists of a single binary section with three relays (L_3, L_4 and L_5), followed by a double used linear chain (P_1 up to P_6) and an auxiliary relay P_{6a}. These linear sections count as follows: P_1, P_2, P_3, P_4, P_5, P_5+P_6, P_1+P_6, P_2+P_6, P_3+P_6, P_4+P_6. The relays of the binary working start section only play an auxiliary role. The operating conditions of the relays of the linear sections are transferred to groups of five register relays. The receiving code is translated meanwhile into another code in which two relays are always operated—the "two out of five" code. The five register relays of the group have the values 0, 1, 2, 4, and 7. The sum of the values of the operated relays equals the received number, except for 0(ten), which is "four plus seven."

The contact of the pulse relay *IR* operates relay L_3 on the first pulse. In the pause after the first pulse relay L_5 is magnetized on a first winding in series with relay L_3. The second pulse operates relay L_4 and locks relay L_5 on a second winding. The right-hand contact of relay L_4 breaks the circuit of relay L_3 and the first winding of relay L_5. Relay L_3 then releases. Relays L_4 and L_5 are released in the pause after the second pulse. The operating cycle starts again on the third pulse.

The right-hand transfer contact of relay L_5 controls the linear chain with relays P_1 up to P_6. Relay P_1 is operated in the pause after the first pulse via the make side of the right-hand transfer contact of relay L_5 and a chain of break contacts of relays P_4, P_2, P_3, and P_5. Relay P_1 locks itself via a make contact and a chain of break sides of the continuity transfer contacts of relays P_2 up to P_5. Relay P_2 operates in the pause after the second pulse via the break side of the right-hand transfer contact of relay L_4 and a make contact of relay P_1. Relay P_1 locks itself via the make side of its continuity transfer contact, which breaks the holding circuit of relay P_1 and so on. Relay P_6 operates in the pause after the sixth pulse. The upper contact of this relay closes the pulse wire to relay P_1, which is again operated in the pause after the seventh pulse. Relay P_1 now releases relay P_5.

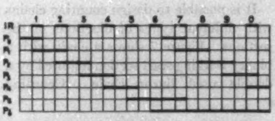

Figure 12. Relay action sequence for single relay counting chain in two out of five code

Homogeneous Counting Chains for the Two Out of Five Code

The counting chain of Figure 9 is not logically designed because of the nonhomogeneous character and the code translation. Two questions arise from this, namely is it possible to design a homogeneous relay chain counting in the same code as the counting chain of Figure 9, and is it possible to design a homogeneous counting chain already counting in the given two out of five code, thus approximating the logical counting ideal.

A counting chain counting in the same code as the *L* and *P* relays of Figure 9 may be readily designed by means of the linear principle given in Figure 5. The diagram is given in Figure 11, and the relay action sequence in Figure 12. As this chain counts exactly in the same code, the contacts translating the receiving code into the register code are omitted in the diagram.

The disadvantage of the continuity transfer pulse contact is probably of no importance in this case. After the aforesaid about the diagram of Figure 5, the working of the chain of Figure 11 may be clear from the relay action sequence shown in Figure 12. The chain consists of six counting relays P_1 up to P_6, having the values one to six respectively and an auxiliary relay P_0, which plays a role in the starting and the recycling of the chain. The balance between the counting parts of both diagrams results in nine relays with 53 springs and 31 contacts (Figure 9) against seven relays with 39 springs and 25 contacts (Figure 11), which is favorable for the logical solution of the problem. The diagram of Figure 11 moreover, offers the

Figure 13. Homogeneous two out of five code counting chain

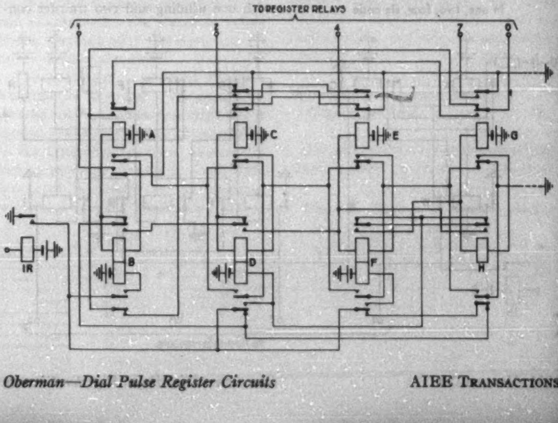

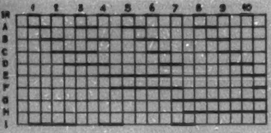

Figure 14. Relay action sequence of Figure 13

advantage that all seven relays can be made equal without difficulty.

The counting chain of Figure 11 gives no satisfaction from the viewpoint of the still necessary code translation. An investigation of the two out of five code, shows that it comes close to the code of the binary counting chains. The difference is principally incorporated in the fact that the relay-pair with the values "eight" in the binary code has a value of only "seven" in the two out of five code. In the groups of register relays a fifth with the value "zero" has been added, which has no meaning in the problem of the counting chain. This "zero" unit has to be produced artificially.

A relay counting chain in the 1-,2-,4-,7-code, derived from the binary counting chain of Figure 4, is shown in Figure 13, the relay action sequence is given in Figure 14. The chain works binary up to six pulses exactly in the same way as described for Figure 4. The pulse wire is switched over to the fourth relay-pair *G/H*. The seventh pulse operates this pair. After that the first three relay-pairs work as a linear counting chain, the first two pairs being operated via the normal pulse wire, the third pair on the tenth pulse via the auxiliary control wire via the upper transfer contacts of relays *F* and *H*. In this way the relay counting chain works in the 1-,2-,4-,7-code. This code can be transferred without any translation to groups of register relays by means of a single make contact of each relay-pair. The "zero" wire, which has no meaning in the case of a pulse receiving relay counting chain, is produced by means of a simple contact circuit, which is shown in Figure 13. This counting chain has not the least number of relays, but has the least number of springs and contacts, which is of importance for a reliable working.

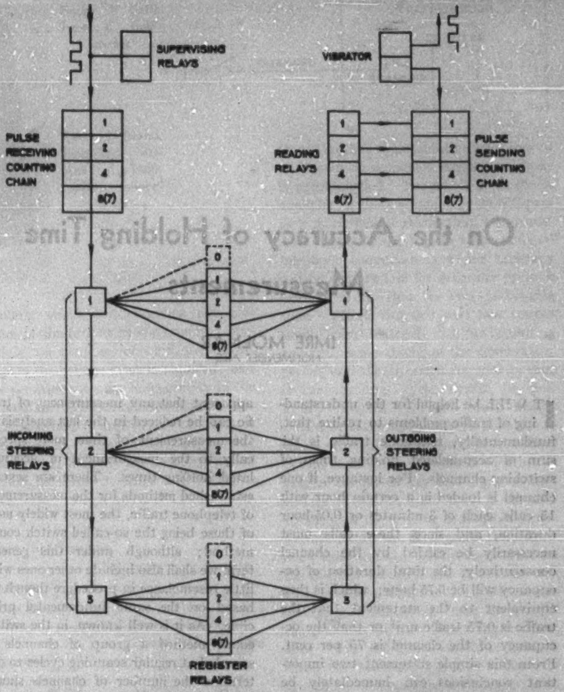

Figure 15. General diagram of pulse register

Conclusion

No attention was paid in the preceding paragraphs to the switching systems, in which the register circuits have to be applied. These systems are so large in number and differ so much that it is impossible within the limits of this article to describe a number of applications of the developed principles. The reader, skilled in the art of switching, will have enough information to apply the principles given. The principles are of a general character, as may be seen from the self explaining diagram of Figure 15, in which symbolically a complete pulse register is shown having no code translation. The receiving counting chain is shown on one side, the sending counting chain on the other side, the register relays between both counting chains, and the registration code going straight through this diagram.

References

1. THE 7A2 ROTARY AUTOMATIC TELEPHONE SYSTEM, L. Schreiber, W. Hatton. *Electrical Communication* (New York, N. Y.), volume 12, October 1933, page 131.

2. CODES AND TRANSLATIONS, Oscar Myers. *AIEE Transactions*, volume 68, part 1, 1949, pages 592–97.

No Discussion

On the Accuracy of Holding Time Measurements

IMRE MOLNAR
NONMEMBER AIEE

IT WILL be helpful for the understanding of traffic problems to realize that, fundamentally, telephone traffic is the sum of accumulated holding times of switching channels. For instance, if one channel is loaded in a certain hour with 15 calls, each of 3 minutes or 0.05-hour duration, and since these calls must necessarily be carried by the channel consecutively, the total duration of occupancy will be 0.75 hour; which is then equivalent to the statement that the traffic is 0.75 traffic unit or that the occupancy of the channel is 75 per cent. From this simple statement two important conclusions can immediately be drawn. First, that telephone traffic is completely equivalent to the length of occupancy of the switching channels; that it may be expressed in any convenient unit of time; and that the same traffic or occupancy can be made up by many calls of short holding times each, or a few calls of long holding times each, or in any conceivable mixture of these as long as the sum of the individual holding times add up to the total length of occupancy. Second, since a channel naturally cannot be occupied for more than one hour in any single hour, the traffic carried per channel in one hour cannot exceed one traffic unit. These considerations apply equally to a single channel, or to any one channel in any arbitrary grouping of channels, or to the average traffic per channel in a group.

From what we have said up to now, it is apparent that any measurement of traffic can be reduced in the last analysis to the measurement of time, more specifically to the measurement of accumulated holding times. There are several established methods for the measurement of telephone traffic, the most widely used of these being the so-called switch count method; although under this generic term we shall also include other ones with little resemblance in procedure though all based on the same fundamental principle. As it is well known, in the switch count method a group of channels is sampled at regular scanning cycles to determine the number of channels simultaneously occupied at a certain instant. If these simultaneous occupancies are totalized for, say, one hour and the total divided by the number of scans, the average number of simultaneously occupied channels during that hour will be obtained. It can be demonstrated that this average number of occupied channels, neglecting some fine points, is numerically equal to the traffic carried by the group during that hour (or traffic density), expressed in traffic units. The agreement can be made very close if certain rules in the technique of switch counts and in the method of sampling are observed, and the present paper will deal with some of the refinements in the accuracy of traffic observations.

The scanning during the switch count process can be carried out either by visual inspection of the number of cord circuits plugged in, or of the number of switches in use, or of the number of circuit busy lamps lit, or it can be entirely mechanized by an automatic scanning device such as one of the several types of Trafficorders.[1] Figure 1 shows a picture of the Automatic Electric Company's type *C* Trafficorder.

Whichever of the methods are to be used, the basic rules of sampling, as particularly adapted for switch count methods, apply.

From the preceding it will be understood that the switch count process is a particular method of time measurement by sampling, and its accuracy can be appraised by comparison with direct measurement of time, for instance, by a clock, where the latter term is used in its broadest possible interpretation. We also have seen that the amount of traffic is equal to the accumulated holding times of individual calls; therefore, if in addition to measuring the traffic, the number of calls carried by the group of channels under observation are simultaneously counted, the average holding time of a call can be determined by dividing the traffic by the total number of calls. Conversely, if by some means we have obtained the average holding time of a call and the total number of calls, the product of the two will give us the total amount of traffic; though the former procedure is the one more commonly occurring in practice, that is, where the traffic and the number of calls are measured, and the holding time then is directly determined. If the laws governing the accuracy of peg count methods and holding time measurements are determined, we have the necessary tools available by which the accuracy of traffic measurements can be appraised. The former was recently studied and published by the author,[2] who found that the commonly used peg counting methods provide an exactness well within that required for traffic measurements.

In 1941 Roger I. Wilkinson of the Bell Telephone Laboratories published an outstanding paper[3] using methods of mathematical statistics, on the reliability of holding time measurements, which can be considered as the fundamental work for all problems related to switch count methods. This in conjunction with the paper quoted in the last paragraph, provides sufficient material to appraise the accuracy obtainable with switch count programs occurring in practice. Mr. Wilkinson reduced his theory into a series of equations, and then developed a

---

Paper 51-351, recommended by the AIEE Communication Switching Systems Committee and approved by the AIEE Technical Program Committee for presentation at the AIEE Fall General Meeting, Cleveland, Ohio, October 22–26, 1951. Manuscript submitted July 11, 1951; made available for printing September 21, 1951.

IMRE MOLNAR is with the Automatic Electric Company, Chicago, Ill.

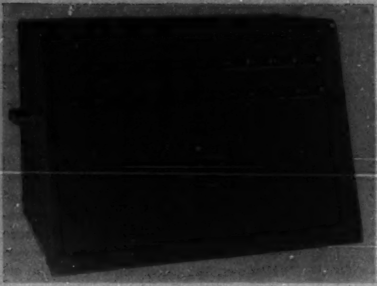

Figure 1 (left). Type C Trafficorder

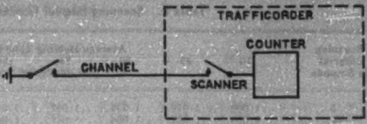

Figure 2 (right). Simplified diagram of Trafficorder connections

number of graphs to assist the traffic engineer in devising working schedules for the sampling of holding times.

As in all sampling processes of homogeneous populations the accuracy improves with an increasing number of samples taken. However, a point of diminishing returns will be reached, beyond which the improvement in accuracy becomes so slight that it would not justify the expense of further sampling; particularly when one considers the mechanical limitations of the sampling procedure, the purpose for which the knowledge of the holding time is required, and the persistence in the homogeneity of the population. There are a few simple rules which can help to improve the accuracy of the program. First, other things being equal, the longest observation period should be selected, consistent with the view that enough periods must be included so that representative sampling of all known or suspected major variations is accomplished. Second, if a choice is available, a short scanning cycle will produce more reliable results than a long one. As a result, for the holding times of usual telephone conversations a fair accuracy can be obtained if the scanning cycle is one-half or less than the average holding time. Third, the first and last counts should coincide closely with the beginning and end, respectively, of the observation period, and the intermediate counts, that is the scanning cycle, should be uniformly spaced. Fourth, each count should be taken as quickly as possible, so that a substantially instantaneous reading of calls in progress is obtained. Fifth, the graphs computed for this purpose are, strictly speaking, valid only if the distribution of the holding times around the average follow the exponential law; however, they are not greatly dependent on the form of holding time distribution as long as the average call length covers several scanning cycles, and the graphs can probably be used with a slight allowance. For relatively constant holding times the accuracy can be further improved by choosing the scanning cycle so that it will be contained in the average holding time approximately a whole number of times. A high accuracy can be obtained with relatively few observations if the scanning cycle is exactly equal to the constant holding time.

Table I. Accuracy of Holding Time Sampling

Number of Samples (n)	Confidence (P) 0.50	0.80	0.90	0.95	0.99	0.999
	Per Cent Error (e)					
30	12.315	23.407	30.034	35.786	47.033	60.087
35	11.401	21.670	27.805	33.130	43.542	55.627
40	10.664	20.269	26.008	30.988	40.727	52.031
45	10.055	19.111	24.523	29.218	38.401	49.060
50	9.529	18.111	23.240	27.690	36.392	46.494
55	9.095	17.287	22.181	26.429	34.735	44.376
60	8.708	16.551	21.237	25.304	33.257	42.488
65	8.366	15.901	20.403	24.310	31.951	40.819
70	8.061	15.321	19.660	23.424	30.786	39.331
80	7.541	14.333	18.391	21.913	28.800	36.794
90	7.110	13.514	17.340	20.660	27.154	34.691
100	6.745	12.820	16.450	19.600	25.760	32.910
125	6.033	11.467	14.714	17.531	23.041	29.436
150	5.507	10.467	13.431	16.003	21.032	26.870
175	5.099	9.692	12.436	14.817	19.474	24.879
200	4.769	9.064	11.631	13.858	18.213	23.269
230	4.447	8.452	10.846	12.922	16.984	21.698
260	4.183	7.950	10.202	12.155	15.975	20.410
300	3.894	7.401	9.497	11.315	14.872	18.999
350	3.605	6.852	8.792	10.476	13.768	17.589
400	3.373	6.410	8.225	9.800	12.880	16.455
450	3.180	6.044	7.756	9.241	12.145	15.516
500	3.016	5.732	7.356	8.764	11.518	14.716
550	2.876	5.466	7.014	8.357	10.984	14.032
600	2.754	5.234	6.717	8.003	10.518	13.437
650	2.646	5.029	6.453	7.689	10.105	12.910
700	2.549	4.845	6.217	7.407	9.735	12.437
800	2.385	4.533	5.817	6.930	9.109	11.637
900	2.248	4.273	5.483	6.532	8.585	10.968
1,000	2.133	4.054	5.202	6.198	8.146	10.407
1,250	1.908	3.626	4.653	5.544	7.287	9.309
1,500	1.742	3.311	4.248	5.062	6.653	8.500
1,750	1.612	3.064	3.931	4.684	6.156	7.865
2,000	1.508	2.866	3.678	4.382	5.759	7.358
2,300	1.406	2.672	3.429	4.086	5.370	6.860
2,600	1.323	2.515	3.227	3.844	5.053	6.455
3,000	1.231	2.340	3.002	3.577	4.701	6.011
3,500	1.140	2.167	2.780	3.313	4.354	5.562
4,000	1.066	2.026	2.600	3.098	4.071	5.201
4,500	1.005	1.910	2.451	2.920	3.838	4.904
5,000	0.954	1.813	2.327	2.772	3.643	4.655
5,500	0.909	1.728	2.217	2.641	3.472	4.435
6,000	0.871	1.655	2.124	2.531	3.326	4.250
6,500	0.837	1.591	2.041	2.432	3.197	4.084
7,000	0.806	1.532	1.966	2.342	3.078	3.933
8,000	0.754	1.433	1.839	2.191	2.880	3.679
9,000	0.711	1.351	1.734	2.066	2.715	3.469
10,000	0.675	1.282	1.645	1.960	2.576	3.291

According to Mr. Wilkinson, neglecting a few minor causes, there are three principal sources affecting the accuracy of the measurement.

1. The homogeneity of sampling processes in general, that is, the samples which have been drawn at random represent the characteristics of the population. This accuracy, of course, can be improved by increasing the number of samples.
2. Errors at the beginning and at the end of the observation period, due to observations of calls being included at the beginning from the preceding period, and at the end which will project into the next period.
3. Errors due to the nature of the method itself, that is by counting switches in definite cycles; therefore an exact measurement of the holding time of any one call will practically never be made.

When the average holding time is evaluated from the results of the switch count process, the best estimate for the aver-

Table II. Scanning Interval Corrections

Scanning Interval in Seconds	Average Holding Time in Seconds: 10	25	50	75	100	125	150	200
	Multiplier (k)							
5	1.035	1.019	1.031	1.047	1.060	1.075	1.086	1.112
10	1.089	1.032	1.034	1.049	1.061	1.076	1.088	1.114
15	1.170	1.050	1.039	1.051	1.063	1.077	1.089	1.115
20	1.280	1.075	1.046	1.052	1.065	1.078	1.090	1.116
30		1.140	1.065	1.062	1.071	1.081	1.092	1.118
40		1.220	1.091	1.076	1.078	1.086	1.098	1.121
50		1.310	1.122	1.091	1.088	1.092	1.102	1.124
60		1.420	1.160	1.111	1.100	1.102	1.110	1.130
70			1.202	1.132	1.115	1.112	1.117	1.135
80			1.246	1.157	1.131	1.123	1.125	1.140
90			1.293	1.181	1.146	1.135	1.134	1.147
100			1.340	1.210	1.163	1.147	1.143	1.152
110			1.390	1.239	1.182	1.161	1.154	1.159
120				1.270	1.204	1.176	1.164	1.166
130				1.301	1.225	1.191	1.178	1.175
140				1.338	1.248	1.209	1.190	1.182
150				1.371	1.271	1.225	1.202	1.192
160				1.405	1.297	1.242	1.208	1.201
170					1.321	1.262	1.232	1.211
180					1.348	1.282	1.249	1.221
190					1.373	1.302	1.263	1.231
200					1.401	1.323	1.280	1.242
210						1.345	1.299	1.255
220						1.367	1.315	1.268
230						1.389	1.332	1.280
240							1.350	1.292

(1) Obtain per cent error *e* from Table I for number of calls *n* included in one observation period and for selected confidence *P*.

(2) Obtain multiplier *k* to *e* from this table for length of scanning interval and anticipated average holding time.

(3) Obtain number of observation periods *N* required from Table III for *ke* and for selected over-all per cent error *E*.

age holding time of the population will be this result; however, there is a certain amount of uncertainty inherent to this value due to the above three causes. As a result of Mr. Wilkinson's work this uncertainty can be estimated, and by extending the program to include many observation periods any specified degree of accuracy is obtainable.

Tables I, II, and III were calculated from Mr. Wilkinson's equations. Table I represents the limits *e* of the percentage of error in the average holding time which can be expected with a given confidence *P* if *n* samples are drawn in one observation period from an exponentially distributed holding time population, and is equally valid whether the holding times of the samples are exactly measured by a clock method, or obtained by a switch count process. Table II gives the multiplier to the per cent error *e* obtained from Table I, due to causes (*1*) and (*2*) above and which are peculiar to switch count methods. Table III specifies the number of observation periods required for any desired limit in the percentage over-all error if the single period error *e* is obtained from Table I, and multiplied by *k* of Table II. The basis of Table III is the central limit law, according to which (provided that certain conditions are satisfied as they are in this problem) the averages derived from groups of *n* samples have a tendency to be normally distributed with increasing number *N* of such groups.

As an example for the use of this table let us assume that we devise a switch count schedule in which approximately 1,000 samples are to be observed in one period, that the scanning cycle is 10 seconds, and that from some preliminary information we know that the average holding time is in the order of 125 seconds. We wish to know from this program the average holding time, so that we may have a confidence *P* of 0.95 that the result will be accurate within ±1 per cent. From Table I we find opposite 1,000 in the column for 0.95 an error *e* of 6.198. In Table II we find opposite 10 seconds scanning cycle and in the column for 125-second holding time the multiplier 1.076. ($6.198 \times 1.076 = 6.67$). From Table III opposite 6.5 and in the column for 1 per cent, we find that 42.3 observation periods are required. Interpolating between 6.5 and 7.0 single period error we conclude that about 45 or 46 observation periods would provide the desired degree of accuracy. Had we been satisfied with, say, 5 per cent accuracy, Table III tells us that two observation periods would have sufficed.

In his paper Mr. Wilkinson compares his theoretical conclusions with a series of observations taken in New Jersey between the two. The tables of this paper were applied in several traffic studies made by W. A. Alden and D. E. Klang of the Automatic Electric Company Laboratories with Trafficorder equipment and the resulting accuracy was likewise confirmed as long as the holding times were in the usual telephone conversation range. However, the convenience, ease, and accuracy of Trafficorder measurement encouraged us to measure several special types of equipment which had holding times much below that of telephone conversations, and there some discrepancy was noticeable. For instance, we attempted to determine with a Trafficorder having a 10-second scanning cycle the average holding time of translators used in a Director system. By preliminary calculations from the individual operating times of the circuit components, the holding time was estimated to be about 400 milliseconds; the results, however, of the Trafficorder observation showed a greater discrepancy than could have been reasonably expected from the accuracy of the preliminary estimate. The same translator holding time was then measured with the aid of the delay register[4] to a fairly high degree of precision, and found to be approximately 100 milliseconds less than the holding time obtained from the Trafficorder process Furthermore, by making comparison of the two methods on various types of equipment and in a holding time range from 300 to 600 milliseconds, the same discrepancy, that is about 100 milliseconds, was obtained regardless of the length of the holding time or the function of the circuit. By a mathematical analysis and subsequent experimental confirmation, it was discovered that there is an additional source of error inherent to switch count methods not disclosed by previous studies, and in order to understand this more clearly we must first

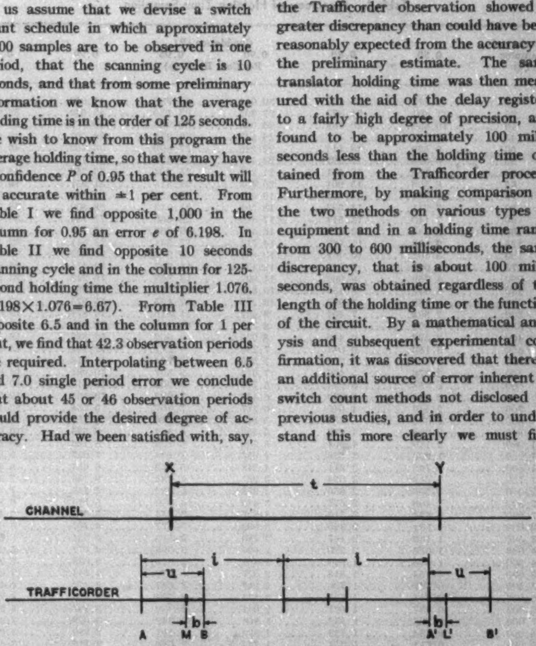

Figure 3. Generalized sequence diagram for Trafficorder measurements

Table III. Number of Observation Periods Required

% Error Single Observation Period (ke)	Per Cent Over-All Error (E) 0.5	1	2	3	4	5	6	8	10	15	25
	Number of Observation Periods Required (N)										
0.8	2.56	0.640	0.160	0.071	0.040	0.026	0.018	0.010	0.006	0.003	0.001
0.9	3.24	0.810	0.203	0.090	0.051	0.032	0.023	0.013	0.008	0.004	0.001
1.0	4.00	1.00	0.250	0.111	0.063	0.040	0.028	0.016	0.010	0.004	0.002
1.2	4.84	1.44	0.360	0.160	0.090	0.048	0.040	0.023	0.014	0.006	0.002
1.4	7.84	1.96	0.490	0.218	0.123	0.078	0.054	0.031	0.020	0.009	0.003
1.6	10.2	2.56	0.640	0.284	0.160	0.102	0.071	0.040	0.026	0.011	0.004
1.8	13.0	3.24	0.810	0.360	0.203	0.130	0.090	0.051	0.032	0.014	0.005
2.0	16.0	4.00	1.00	0.444	0.250	0.160	0.111	0.063	0.040	0.018	0.006
2.2	19.4	4.84	1.21	0.538	0.303	0.194	0.134	0.076	0.048	0.022	0.008
2.4	23.0	5.76	1.44	0.640	0.360	0.230	0.160	0.090	0.058	0.026	0.009
2.6	27.0	6.76	1.69	0.751	0.423	0.270	0.188	0.106	0.068	0.030	0.011
2.8	31.4	7.84	1.96	0.871	0.490	0.314	0.218	0.123	0.078	0.035	0.013
3.0	36.0	9.00	2.25	1.00	0.563	0.360	0.250	0.141	0.090	0.040	0.014
3.3	43.6	10.9	2.72	1.21	0.681	0.436	0.303	0.170	0.109	0.048	0.017
3.6	51.8	13.0	3.24	1.44	0.810	0.518	0.360	0.203	0.130	0.058	0.021
4.0	64.0	16.0	4.00	1.78	1.00	0.640	0.444	0.250	0.160	0.071	0.026
4.5	81.0	20.3	5.06	2.25	1.27	0.810	0.563	0.316	0.203	0.090	0.032
5.0	100	25.0	6.25	2.78	1.56	1.00	0.694	0.391	0.250	0.111	0.040
5.5	121	30.3	7.56	3.36	1.89	1.21	0.840	0.473	0.303	0.134	0.048
6.0	144	36.0	9.00	4.00	2.25	1.44	1.00	0.563	0.360	0.160	0.058
6.5	169	42.3	10.6	4.69	2.64	1.69	1.17	0.660	0.423	0.188	0.068
7.0	196	49.0	12.3	5.44	3.06	1.96	1.36	0.766	0.490	0.218	0.078
7.5	225	56.3	14.1	6.25	3.52	2.25	1.56	0.879	0.563	0.250	0.090
8.0	256	64.0	16.0	7.11	4.00	2.56	1.78	1.00	0.640	0.284	0.102
8.5	289	72.3	18.1	8.03	4.52	2.89	2.01	1.13	0.723	0.321	0.116
9.0	324	81.0	20.3	9.00	5.06	3.24	2.25	1.27	0.810	0.360	0.130
10.0	400	100	25.0	11.1	6.25	4.00	2.78	1.56	1.00	0.444	0.160
12.0	484	144	36.0	16.0	9.00	4.84	4.00	2.25	1.44	0.640	0.230
14.0	784	196	49.0	21.8	12.3	7.84	5.44	3.06	1.96	0.871	0.314
16.0	1,024	256	64.0	28.4	16.0	10.2	7.11	4.00	2.56	1.14	0.410
18.0	1,296	324	81.0	36.0	20.3	13.0	9.00	5.06	3.24	1.44	0.518
20.0	1,600	400	100	44.4	25.0	16.0	11.1	6.25	4.00	1.78	0.640
22.0	1,936	484	121	53.8	30.3	19.4	13.4	7.56	4.84	2.15	0.774
24.0	2,304	576	144	64.0	36.0	23.0	16.0	9.00	5.76	2.56	0.922
26.0	2,704	676	169	75.1	42.3	27.0	18.8	10.6	6.76	3.00	1.08
28.0	3,136	784	196	87.1	49.0	31.4	21.8	12.3	7.84	3.48	1.25
30.0	3,600	900	225	100	56.3	36.0	25.0	14.1	9.00	4.00	1.44
33.0	4,356	1,089	272	121	68.1	43.6	30.3	17.0	10.9	4.84	1.74
36.0	5,184	1,296	324	144	81.0	51.8	36.0	20.3	13.0	5.76	2.07
40.0	6,400	1,600	400	178	100	64.0	44.4	25.0	16.0	7.11	2.56
45.0	8,100	2,025	506	225	127	81.0	56.3	31.6	20.3	9.00	3.24
50.0	10,000	2,500	625	278	156	100	69.4	39.1	25.0	11.1	4.00
55.0	12,100	3,025	756	336	189	121	84.0	47.3	30.3	13.4	4.84
60.0	14,400	3,600	900	400	225	144	100	56.3	36.0	16.0	5.76
65.0	16,900	4,225	1,056	469	264	169	117	66.0	42.3	18.8	6.76
70.0	19,600	4,900	1,225	544	306	196	136	76.6	49.0	21.8	7.84

take a closer look at the conditions under which switch counts, either by visual or mechanical means, are performed.

Figure 3 shows the occupancy of a channel in parallel with the scanning process of the Trafficorder. In this example the holding time of a call extends approximately over two scanning cycles and may, of course, start and end at any time. For our problem we assume that it starts at the point X which is somewhere within the scanning interval A-B, but it did not exist at the instant A, which we will assume for our present discussion to be the reference point: that is, only calls in existence at A should be counted.

We now see that calls originating between A and M will be actually registered by the Trafficorder though they were to be excluded under the premises of switch counts and will therefore cause positive errors in the average holding time resulting from the observation program. A call originating between M and B will not be counted since there is insufficient time left for the counter to register.

In addition to this positive error there also will be a negative error. In our present example the call extends beyond the point A', and it should therefore be included in the scanning interval $A'-B'$. The point Y indicates the termination of the call, which will be properly registered if the point Y falls anywhere to the right of the point L'. If, however, Y falls in the interval $A'-L'$ it will not register, because the call will not be long enough for the counter to respond, and, therefore, would not be included in the switch count, causing a negative error in the average holding time.

It should be noted that these two errors are over and above any others occurring in sampling or because of other peculiarities of switch count methods, and are only due to the necessity of allowing a sufficiently long scanning interval u for the counter to respond reliably. We may be inclined to correlate this error with those arising by the fact that switches are counted at finite intervals so that an exact measurement of the holding time t of any one call cannot be made since the points X and Y will fall somewhere within the scanning cycle i. The latter error has been completely accounted for by Mr. Wilkinson in section IV-c of his paper,[3] and our present problem represents an error in excess and practically independent of those caused by the inaccuracy in measuring each call, since the latter will always be present regardless whether the scanning interval u is finite or infinitely short. (u represents the time during which the counter is connected to the circuit to be measured, and b represents the time required by the counter to respond.) By extending the switch count program, the magnitude of such error can be reduced, and by taking sufficient number of observations we can arrive at the true average holding time as closely as we wish to. On the other hand, as we shall see, the magnitude of our present error is for all practical applications independent of the number of samples taken and represents an error of a definite magnitude which cannot be eliminated, however far the sampling process is extended. Therefore the best approach is to treat these two sources of error independently from each other: the one due to measuring each call in finite intervals in conformance with Mr. Wilkinson's

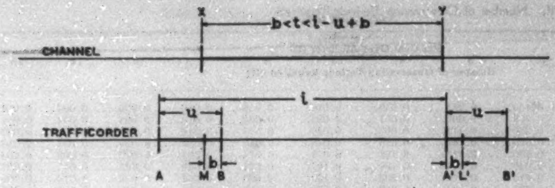

Figure 4. Sequence diagram for Step 2

work, by assuming infinitely short scanning interval; and applying independently for the other a correction according to our presently discussed method.

We now shall make the assumption that calls originate at random, which is customary in most telephone traffic problems, and also, for the time being, that the holding times t are exponentially distributed about their average. The latter condition is sufficient to insure that the probability for a call to terminate is asymptotically proportional to the length of the time interval under consideration and is independent of the time when that call has originated; that is, the probability of termination of a call is independent of the length of time it has already been in progress. These assumptions are considered generally true for telephone conversations. It might be mentioned here that some advanced studies indicate that these are not necessary conditions for a Poisson process to take place, but, because they are usually satisfied in telephone traffic, they are very helpful to simplify demonstrations.

Since calls originate at random, the probability that it originates between the points A and M, if it does originate within the scanning cycle i, is simply $(u-b)/i$. If this has taken place we have added i to the true holding time of this particular call, therefore the average positive error on all calls will be $i(u-b)/i=(u-b)$. Since according to our second assumption this call may terminate at any moment independently of the time it has already been in progress, the probability for a call to terminate in the interval $A'-L'$, if it does terminate during a scanning cycle i, will be b/i and the resulting negative error will be $ib/i=b$.

The occurrences of positive and negative errors are represented by two random variables, therefore the expectation of an error will be the sum of their expectation, with due regard to the sign. Combining the positive and negative errors will give us a total error, $u-2b$.

As we now see, this error is independent of the holding time t or the length of the scanning cycle i, and is completely determined by the length of the scanning interval u and the counter response b. Furthermore, it shows that it will completely disappear if the scanning interval is made equal to twice the response time of the counter.

We may now extend our problem to the constant holding time case, where all calls have the same length. Here calls still originate at random as before; however, their termination is no longer independent of the time already elapsed. On the contrary, by knowing that the call has originated at the point X we definitely also know that it must end at the point Y, which is t (the constant holding time) apart from X by hypothesis.

The problem of constant holding times can be broken down into five separate steps.

Step 1: t is less than b. In this case the Trafficorder will not respond at all, but it is of no interest since, naturally, there would be no attempt made to measure holding times less than the minimum response time inherent to the measuring apparatus.

Step 2: t is greater than b but less than $i-u+b$. This case is illustrated in Figure 4. If X falls between points $A-M$ there will be a positive error $u-b$ recorded and there will be no negative error. If point Y falls between $A'-L'$ there will be a negative error b recorded. Since these two cases are mutually exclusive the total error will be $u-2b$.

Step 3: t is greater than $i-u+b$ but less than $i-u+2b$. This case is illustrated in Figure 5. If the point X falls beyond point A, a positive error will be obtained as long as the point Y of the same call is to the left side of point A'. The probability of such an event is $(i-t)/i$. A negative error will be recorded if the point X falls between $M-B$ and the point Y of the same call falls between points $A'-L'$, with a probability of $(i+b-t-u+b)/i$. For any other point of origin there will be no error recorded, since the positive errors occurring will compensate for the negative one of the same call. Since the probabilities of the positive and negative errors are mutually exclusive, the net error will be equal $u-2b$ as before.

Step 4: t is greater than $i-u+2b$ but less than i. This case is illustrated in Figure 6. If the point X is to the right of A and the point Y of the same call is to the left side of point A' there will be a positive error recorded with a probability $(i-t)/i$. If the point X falls to the left of point M and the point Y of the same call to the right of point L' a positive error will likewise be recorded with a probability of $(t+u-b-i-b)/i$. In all other cases, that is, if Y falls between points $A'-L'$, the positive and negative errors compensate each other. The total error will therefore be $u-2b$ as in all the other cases.

Step 5: t is greater than i. The previous considerations can readily be extended to the case if t is between i and $i+b$, that is, a positive error $u-2b$ will be registered only if a call begins to the left of point M and terminates to the right of L, with a probability of $(u-2b)/i$. If t covers more than one scanning period i it can be considered as made up by two parts: one which covers exactly one or several scanning

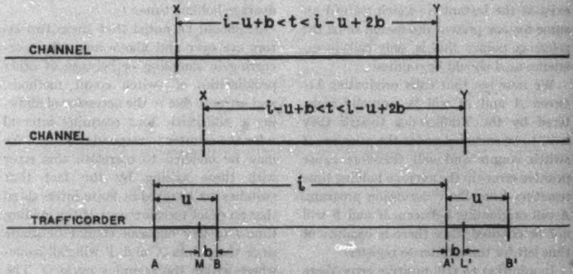

Figure 5. Sequence diagram for Step 3

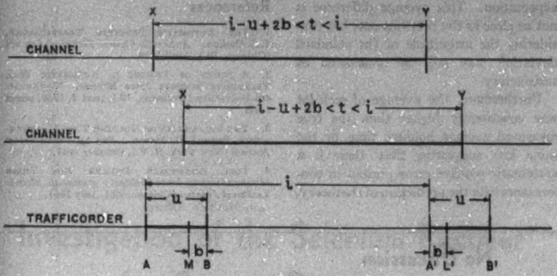

Figure 6. Sequence diagram for Step 4

cycles for which, of course, the correct number of counts will be obtained, and the second consisting of a fraction of a scanning cycle which will cause the same amount of errors as those enumerated in the preceding three cases.

The foregoing analysis indicates that the magnitude of the error will be $u-2b$, regardless whether the holding times are exponentially distributed or constant. These two represent extreme cases of holding time distributions, therefore it may perhaps be justified to conclude without further analysis that we are facing here an error term which is independent of the scanning cycle of the traffic recording process, of the magnitude of the holding time to be measured, and of their distribution about the average, since an arbitrary distribution could be considered as a step function subdivided into extremely narrow widths, and for each such subdivision the holding time t is constant, with an error term independent of t.

It is however, dependent on the length of the scanning interval u and the response time of the counting device b, and can be minimized by choosing the scanning interval to be approximately twice the counter response time. The error $u-2b$ should be deducted from the average holding time as obtained from the switch count process, and the net value should be considered as the best estimate for the average holding time.

This error also appears as a variable in the sampling process, and the true amount of error can only be obtained after a sufficiently large number of samples have been observed. Actually, it can be represented by a three valued variable, which is observed either as $-i$ or 0 or $+i$. Their respective probabilities for instance in the constant holding time case, step 2, are: b/i, $1-(u/i)$, and $(u-b)/i$. The standard deviation of each variable is:

$$\sigma_b=\sqrt{iu-(u-2b)^2}$$

The standard deviation for the other steps can be estimated similarly; for instance for step 5 the probability of an error $-i$ is 0, and for $+i$ is $(u-2b)/i$: thus $\sigma_b=\sqrt{(u-2b)(i-u+2b)}$. However considering the magnitudes of the various intervals of Trafficorders, step 2 or its "harmonics" will be most frequently encountered.

For the exponential case the probabilities for $-i$ and $+i$ are about the same as in step 2, except that allowance would have to be made for those calls where the positive and negative errors cancel out each other. Such calls will start at a point x between 0 and $u-b$, and terminate between $i-x$ and $i-x+b$, or between $2i-x$ and $2i-x+b$, etc. later. The probability for such call lengths is:

$$\begin{aligned}P_r=&(e^{-(i-x)/t}-e^{-(i-x+b)/t})+\\&(e^{-(2i-x)/t}-e^{-(2i-x+b)/t})+\dots\\&=e^{(x-i)/t}(1-e^{-(b/t)})/(1-e^{-(i/t)})\end{aligned}$$

The probability for the errors to cancel out each other will thus be:

$$\begin{aligned}\int_0^{u-b}P_r dx/i=&(t/i)(e^{(u-b)/t}-1)\times\\&(1-e^{-(b/t)})/(e^{i/t}-1)\end{aligned}$$

For the computation of the standard deviation this probability should be subtracted from b/i, as well as from $(u-b)/i$. However, b/t is usually a small fraction, on the order of at least 1/20, and $(u-b)/t$ is likewise small: thus the above correction can be disregarded for most applications, the positive and negative errors considered as essentially uncorrelated, and the standard deviation will be about the same as for step 2 in the constant holding time case.

The correct procedure would be now to enter the above expressions for the standard deviation into Mr. Wilkinson's equations 40 or 42, and use the new values to recalculate Table II. However, considering the magnitude of u and b for Trafficorders, the value for σb is about 0.23. Since, because of the other sources or errors, holding time measurement always includes at least several hundred samples, the accuracy in the holding time will be within 10 milliseconds due to using the expectation $u-2b$ for the constant error term and neglecting its own fluctuation in sampling.

It now remains to verify our theoretical considerations by factual evidence. The type *C* Trafficorder, which was used in these investigations, has a scanning interval u of 167 milliseconds and a response time b of 25 milliseconds. Therefore we may expect that the average holding time, as measured by the Trafficorder, will be $u-2b=117$ milliseconds too long. As it will be recalled, actual observations on working equipment indicated a discrepancy of about 100 milliseconds.

For further experimental verification the trafficorder was subjected to a series of tests, in which it was connected to a source of artificial traffic of constant holding time. In each test about 1000 holding times were measured and varied between tests from approximately 0.5 second up to 15 seconds. Simultaneously, the holding times of the same calls were measured to the required degree of accuracy by a delay register. The average difference between the holding times obtained by the Trafficorder and the delay register, respectively, 118 milliseconds. The minimum observed difference was 101 milliseconds and the maximum 140 milliseconds. The standard deviation of the average differences of each test was 12.8 milliseconds while the expected standard deviation of the same averages from the foregoing formula alone is 7.3 milliseconds and 9.0 milliseconds if the errors in measuring each call as well as end effect errors are also included. The average standard deviation derived from subsets of 100 calls each was 39 milliseconds, while the expectation for such subsets, including the various sources of errors, is 29 milliseconds.

To check further the validity of the theory, the scanning interval u was reduced to 100 milliseconds; thus a difference of 50 milliseconds was expected. From a similar series of tests the average difference was 51 milliseconds.

A series of tests were made, with 1,800 artificial random calls of exponential distribution about an average holding time of 3.76 seconds, using again 167 milliseconds scanning interval. The average difference was 124 milliseconds compared with 117 milliseconds expectation; and the standard deviation of the average differences in each test was 10 milliseconds compared with 12 milliseconds expectation.

Finally, the holding times of 340 telephone calls, subdivided into five lots, were found to have a measured average holding time of 60.5 seconds. The average difference was 96 milliseconds compared with 117 milliseconds expectation; and the standard deviation 26 milliseconds compared with 28 milliseconds expectation. This average difference is not as close as the previous one, but considering the magnitude of the standard deviation may still be considered as satisfactory.

Furthermore, the average of each lot was consistently higher than the true measured average holding time of the same lot, suggesting that there is a systematic positive error present in conformance with the prediction of the theory.

References

1. THE AUTOMATIC ELECTRIC TRAFFICORDER, J. E. Ostline. *Automatic Electric Technical Journal* (Chicago, Ill.), April 1948.

2. A STUDY OF TRAFFIC IN AUTOMATIC TOLL TELEPHONE SYSTEMS, Imre Molnar. Northwestern University (Evanston, Ill.), part 2, 1950, pages 2–27.

3. THE RELIABILITY OF HOLDING TIME MEASUREMENTS, Roger I. Wilkinson. *Bell System Technical Journal* (New York, N. Y.), October 1941.

4. TOLL ANSWERING DELAYS AND THEIR MEASUREMENTS, Imre Molnar. *Automatic Electric Technical Journal* (Chicago, Ill.), July 1951.

No Discussion

Investigation of the Selenium Rectifier for Contact Protection

H. F. HERBIG
MEMBER AIEE

J. D. WINTERS
NONMEMBER AIEE

A VOLTAGE surge suppressor is described comprising selenium rectifier cells connected in series (in opposed relation) whereby the resulting resistance is high at low voltages and low at high voltages.

This combination of rectifiers when used for electrical contact protection results in an excellent arc suppressing device which does not materially affect the release time of the shunted electromagnet.

The history of selenium rectifiers is well known and has been published in its various aspects in a number of articles.[1] The primary use of selenium rectifiers has been in the rectification of alternating current for power applications. Among the special applications, particularly in the telephone field, selenium rectifiers have been used as contact protectors.

This paper deals with an application of the selenium rectifier for contact protection in such a manner as to overcome the defect of excessive slow release of shunted electromagnets. This is accomplished by shunting the electromagnet with a novel arrangement of selenium rectifier cells. It deals also with the peak voltage developed across contacts controlling electromagnets when shunted by such a unit, with the condition of the contacts after many millions of such operations, and with the time of release of the electromagnet after the controlling contacts have opened.

Need for Contact Protection

The operation of a modern telephone office depends upon the positive operation of millions of electrical contacts. "A 10,000-line office may handle an average of 50,000 calls daily, which runs the number of yearly contact operations into the billions. The operation for the bulk of the contacts vary from 50,000 to 15,000,000 annually."[2]

Contact erosion is the cause of many circuit failures in telephone offices and in many systems using relays and switches for controlling electrical circuits. Erosion is due to arcing between a pair of contacts and usually results in the loss of material from one contact and the distribution of the lost material on or adjacent to the other contacts. A badly-eroded contact often causes snagging and sometimes mechanical locking. This results in circuit failures which are reflected in higher maintenance cost and inferior service. The control of contact erosion is a major problem for the telephone companies in extending contact life. This control of erosion is accomplished by the use of a suitable contact protector.[2]

The criterion of a good spark suppressor is that it affects the operation of the associated circuit to a minimum degree while giving good protection to the controlling contacts at the same time. In the case of contacts controlling electromagnets, the spark suppressing device should have little effect on the release time of the controlled electromagnet and should extend the dependable life of the contact many times at the lowest possible cost. The suppressor circuit components should be dependable and free from attention over extended periods.

At the same time, ease of replacement and low cost also are important factors.

At present, the most generally accepted method of contact protection is the use of a suitable capacitor and resistor in series, this combination being either in parallel with the coil or the contacts. However, their initial cost and installation make their extensive use prohibitive and such protection is provided only for critical cases. The modern trend is toward the development of an inexpensive protector of small size that may be used extensively. The nearest approach to this now is being carried out in Sweden where the Telephone Administration is going "all out" for complete contact protection.

Methods of Using Selenium Rectifiers for Contact Protection

The conventional method of using the selenium rectifier as a spark suppressor is shown in Figure 1. When contact "A" is closed, there will be little current flowing through the rectifier due to its high reverse resistance. When contact "A" is opened, the induced electromotive force

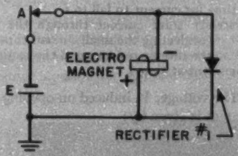

Figure 1. Conventional method of using the selenium rectifier as a spark suppressor

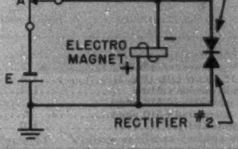

Figure 2. Method of improving the release time by adding rectifier number two

---

Paper 51-352, recommended by the AIEE Communication Switching Systems Committee and approved by the Technical Program Committee for presentation at the AIEE Fall General Meeting, Cleveland, Ohio, October 22–26, 1951. Manuscript submitted June 21, 1951; made available for printing September 10, 1951.

H. F. Herbig and J. D. Winters are both with the Federal Telecommunication Laboratories, Inc., Nutley, N. J.

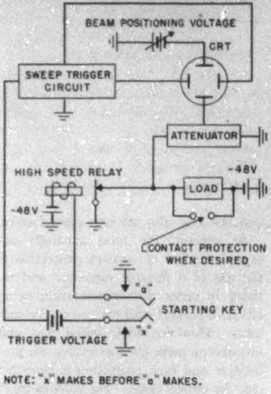

will maintain the current flow through the coil in the same direction, and the open contact will be shunted by the low forward resistance of the rectifier. This low resistance shunt will eliminate arcing at the contact but has the effect of prolonging the release time of the electromagnet. After contact "A" opens, and assuming that arcing does not occur, it is known that the time for the current in the coil to fall to a percentage of its initial value is given by the following equation:

$$t = -\frac{L}{R_L + r} \log_\epsilon \frac{i}{I}$$

where

R_L = coil resistance
r = forward resistance of rectifier
L = coil inductance
t = time for current to fall to i
I = steady state current through the coil (neglecting the small current through the reverse resistance of the rectifier)
i = current at time t

The voltage, V, induced on opening the contact is given by:

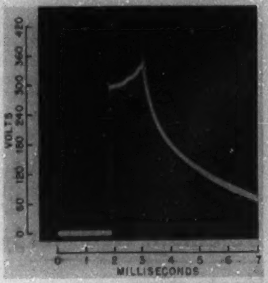

Figure 3 (left). Method of determining voltage at relay contacts

Figure 4 (above). Voltage at unprotected relay contacts controlling a clutch magnet

$$V = -L\frac{di}{dt} = (R_L + r) I \epsilon^{-\frac{R_L + r}{L} t}$$

The maximum value of V occurs at the instant the contact opens, or when $t = 0$ and is given by the following equation:

$$V_{\max} = I(R_L + r) = E + Ir$$

where E = supply voltage as shown in Figure 1.

The increase of the voltage across the contact is directly proportional to the rectifier resistance. An increase in rectifier resistance will reduce the release time but will increase arcing.

This conflict between arc suppression and required release time may be resolved by the introduction of a voltage dependent resistance. If the resistance is low at high voltage, arcing will be eliminated; if the resistance is high at low voltage, improved release time will result. Such an element is obtained when rectifier number two is added to the circuit as shown in Figure 2.

It may be seen from Figure 2, that when contact "A" is closed, rectifier number one blocks the current flow from battery "E" and forces practically all of the current through the electromagnet. When contact "A" is opened, the self-induction of the electromagnet causes a reversal of current flow through the rectifiers, and rectifier number two blocks the current flow resulting from the collapsing field of the electromagnet. However, the reverse resistance of rectifier number two is greatly reduced as the voltage rises and the peak voltage at the open contact does not rise to the ionizing potential.

Observation of Arcing at Relay Contacts and Methods of Arc Suppression

The voltage at the contact versus the time of collapse of the magnetic field was observed oscillographically by means of the circuit shown in Figure 3. The transient was photographed with and without contact protection using inductive loads typical of those existing in telephone central offices. Peak voltages and release times are tabulated in Table I.

Sparking at an unprotected relay contact controlling a clutch magnet may be seen in Figure 4. The horizontal line indicates closed contacts. The steep vertical rise occurs at the instant the contacts separate. It may be noted that the voltage rises almost instantly to a value of 300 volts at which value sparking starts. The gradual upward sloping line indicates the duration of the glow. The sharp vertical rise at the end of this sparking line indicates the instant at which the glow extinguishes due to the increased separation of the contacts. From this

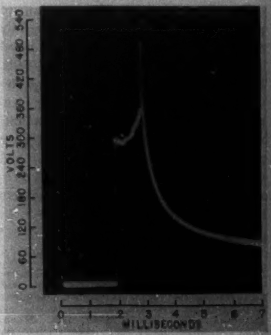

Figure 5. Voltage at unprotected relay contacts controlling a telephone relay

Table I. Peak Voltages and Release Times for Electromagnets with Different Types of Contact Protection

Contact Protection	Telephone Clutch Magnet* Release Time, Milliseconds	Telephone Clutch Magnet* Peak Voltage at Contact, Volts	Telephone Clutch Magnet* Figure Number	Telephone Relay** Release Time, Milliseconds	Telephone Relay** Peak Voltage at Contact, Volts	Telephone Relay** Figure Number
(3) $^5/_{16}$" diameter cells (Fig. 1)	4.0	83		55.0	57	8
(2) $^5/_{16}$" diameter cells (Fig. 2)	1.3	180	6	12.0	150	7
(3) 1" square cells (Fig. 2)	1.3	192		10.9	169	
Silicon-carbide varistor	1.3	210		12.8	140	11
0.5 microfarad+510 ohms		arcing		10.9	160	9
0.1 microfarad+510 ohms		arcing		7.9	250	10
Unprotected	1.0	400 to 900	4	7.6	450 to 750	5

*L = 0.485 henry
R = 164 ohms
I = 0.293 ampere

**L = 3.45 henrys
R = 1,650 ohms
I = 0.029 ampere

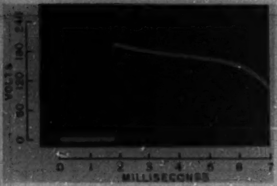

Figure 6. Voltage at rectifier-protected relay contacts controlling a clutch magnet. (Protection as shown in Figure 2)

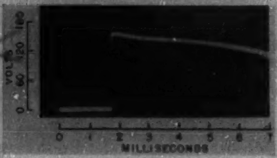

Figure 7. Voltage at rectifier-protected contacts controlling a telephone relay. (Protection as shown in Figure 2)

peak value, the voltage falls exponentially to the supply potential.

Figure 5 shows the curve for contacts controlling a telephone relay and is similar to Figure 4 with the exception that there is less stored energy in the relay as represented by the shorter duration of the glow.

The selenium rectifiers used for protection of relay contacts are basically combinations of 9/32-inch diameter cells. The arrangement used consists of two groups of two cells connected in opposition as shown in Figure 2. Therefore, the reverse resistance of two cells is in series with the forward resistance of the other two cells. The voltage at the contact versus the time of collapse of the magnetic field is shown in Figure 6 for the clutch magnet, and in Figure 7 for the telephone relay.

The effect of the spark suppressor unit on voltage is to limit the peak voltage to approximately 180 volts in the case of the clutch magnet, and to 150 volts for the telephone relay.

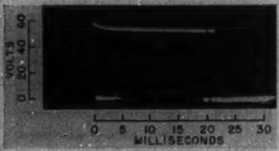

Figure 8. Voltage at rectifier-protected contacts controlling a telephone relay. (Protection as shown in Figure 1)

Figure 8 shows the results obtained with three 9/32-inch diameter cells connected across the load, as shown in Figure 1. The voltage rise is limited to approximately 60 volts with the telephone relay, but the release time is extended six times.

The results obtained by using resistor-capacitor spark suppressor units may be seen in Figure 9 and Figure 10. When capacitors are used, it is necessary to provide a suitable series resistance to limit the charge and discharge currents that occur during the switching operations. Otherwise, contact burning can occur on initial closure and on immediate reclosure that might result from contact bounce. This is not a problem where selenium rectifiers or silicon carbide varistors are used because they offer very high resistance to current flow at voltages of 50 volts or less. On closure the contacts are firmly engaged before the current can build up through the coil to the steady state value.

The effect on the voltage at the contact when a silicon-carbide varistor is used may be seen in Figure 11. Silicon-carbide varistor protection gives rise to a transient of a type similar to that shown in Figures 6 and 7 which are for selenium rectifier protection.

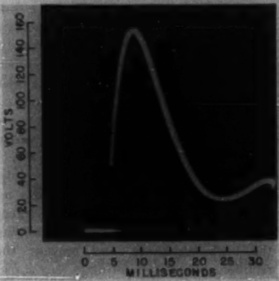

Figure 9. Voltage at resistor-capacitor protected contacts controlling a telephone relay. (510 ohms and 0.5 microfarad)

Reverse Resistance Characteristics of Selenium Rectifiers

The reverse resistance versus voltage characteristic of the 9/32-inch diameter cells is of considerable interest, particularly at voltages that exceed the direct current rating of the cells. In order to simulate load conditions, the rectifiers were stressed with a voltage lasting 8 milliseconds. A circuit such as shown in Figure 12 is convenient for such measurements. The time constant may be adjusted for the desired duration of the voltage.

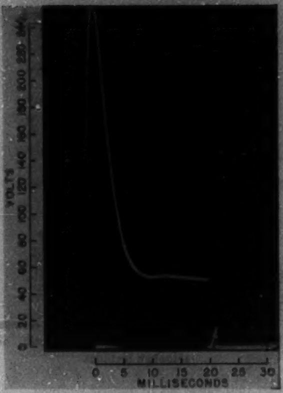

Figure 10. Voltage at resistor-capacitor protected contacts controlling a telephone relay. (510 ohms and 0.1 microfarad)

Relays and clutch magnets typical of the inductive loads found in telephone central offices were operated with combinations of back-to-back selenium rectifiers as spark suppressors. Life tests were conducted in order to determine the effect on the electrical characteristics of the rectifiers, and to evaluate the degree of protection afforded the contacts. Figure 13 shows life test operating conditions.

Figure 14 illustrates a family of these reverse resistance-voltage characteristics. For voltages greater than 50 volts, readings were taken with an oscilloscope with voltage applied for approximately eight

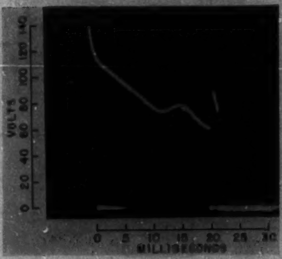

Figure 11. Voltage at silicon-carbide varistor protected contacts controlling a telephone relay

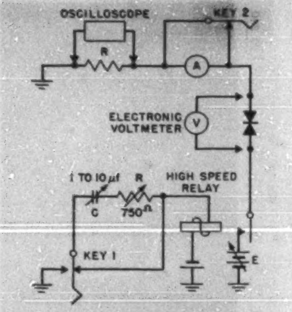

Figure 12. Method of obtaining reverse resistance versus voltage characteristic of selenium rectifiers

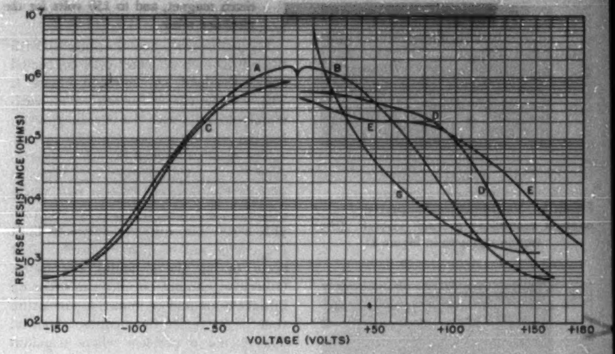

Figure 14. Family of reverse resistance versus voltage characteristics of spark suppression units

milliseconds. For voltages lower than 50 volts, the voltage was applied long enough to read a moving coil instrument.

The reverse resistance versus voltage characteristics for typical two-cell units, shown in Figure 13, were measured according to Figure 12 and the results plotted in Figure 14. Curves A and B are typical for unaged 2-cell units of 9/32-inch diameter. Curve A corresponds to the characteristic for rectifier number one and curve B for rectifier number two. Reference to Figure 13 shows that rectifier number one normally blocks the supply voltage.

Curves C, D, and E represent the characteristics for 2-cell units of this type after 50,000,000 operations over a period of six months. Curve C represents the typical decrease of reverse resistance with aging which is a well known characteristic of selenium rectifiers.

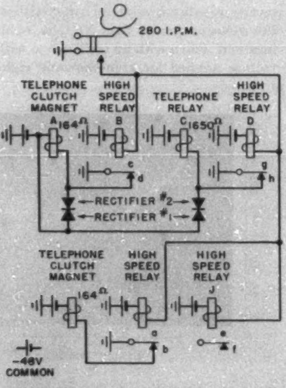

Figure 13. Circuit for life testing spark suppression units and contacts

Curve E represents the characteristic of rectifier number two with a clutch magnet as the load as shown in Figure 13. The resistance drops at a slower rate. The effect of this is to decrease the release time of the load magnet, but the peak voltage at the contacts rises correspondingly. However, this does not materially affect the unit as a spark suppressor. The peak voltage is still held well below 200 volts.

Curve D shows a similar effect as curve E but to a lesser degree due to a relay load instead of a clutch magnet.

The increase in reverse resistance described above in curves D and E is related to the forming process. Higher reverse voltages have the effect of raising the back resistance, and prevent the rectifiers from deteriorating as they sometimes do when the current flows in one direction only.

Curve G is the characteristic for a silicon-carbide varistor. This varistor is one chosen as being suitable for contact protection with telephone relays, and is shown for direct comparison with the rectifier combination. It should be noted that for voltages greater than 50 volts, the change of resistance is less than for the rectifier combination. It should also be noted that the silicon-carbide varistor has a lower resistance at 50 volts which means greater current drain and increased power dissipation. The fact that the silicon-carbide characteristic is concave upwards as opposed to the rectifier combination is obviously less desirable from the point of view of maintaining favorable release times consistent with good spark protection.

Mechanism of Rectifier Breakdown

Rectifier breakdown, that is the tendency for the forward and reverse resistance to equalize, is always associated with excessive temperature. If the high voltage stress is not applied long enough for the temperature to rise excessively, and the duty cycle is not excessive, the rectifier will not be injured. The maximum period for which the rectifier can stand an excessive electrical stress is dependent upon the effective heat capacity of the cell and the ambient temperature. This period must be determined empirically for the particular application, since efforts to generalize these relationships have not been successful.

Photomicrographs of Relay Contacts After Life Test

Reference to Figure 13 will show the circuit conditions under which the contacts shown in the photomicrographs were operated. The contact metal is 99 per cent palladium. The physical dimensions of the contact are shown in Figure 15.

The contacts shown in Figure 16

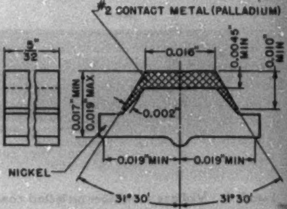

Figure 15. Structure of relay contact

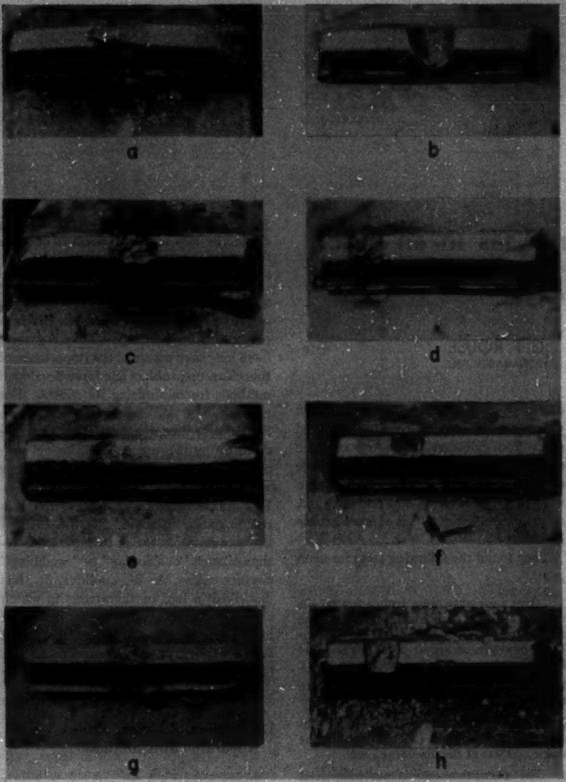

Figure 16 (a and b). Unprotected contacts after 1,300,000 operations. (Clutch magnet as load.) (c and d) rectifier-protected contacts after 50,000,000 operations. (Clutch magnet as load.) (e and f) mechanical wear of contacts after 50,000,000 operations (no current). (g and h) rectifier-protected contacts after 50,000,000 operations. (Telephone relay as load)

(a and b) were unprotected with the clutch magnet as a load. After 1,300,000 operations, the back contact had eroded through to the relay spring. In this case the armature "a" was positive with respect to the back contact "b", and the transfer of metal was from negative to positive. Figure 16 (c to h) show rectifier-protected contacts that were operated with the clutch magnet and the telephone relay respectively as loads. The total number of operations was 50,000,000. The improvement over the unprotected case is of the order of 100-to-1. It is interesting to observe that the back contact and armature contact are eroded to the same extent. The transfer of metal from one contact to the other is not in evidence.

In order to judge how much of the erosion is due to mechanical wear alone, see contacts "e" and "f" in Figure 16. These contacts were operated 50,000,000 times but interrupted no current.

Dimensions and Mountings

For applications where 50-volt d-c power supplies are used, and the loads are of the same order as discussed above, the 9/32-inch cells are satisfactory. Their small size and light weight enable them to be mounted directly across coil terminals. Drillings and mountings are not required because the lead out wires are sufficiently strong to support the unit. They may be mounted in the same manner as the familiar radio type resistor. The physical dimensions may be seen in Figure 17. The weight is approximately 0.09 ounce (2.6 grams).

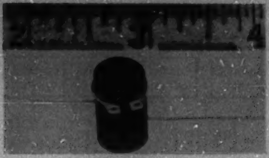

Figure 17. Physical dimensions of rectifier contact protector

Conclusions

Contact erosion in the sense that metal is lost from one contact and deposited on the mating contact seems to be eliminated. This is important from the standpoint of reducing snagging. When contacts retain their original shape, minimum readjustment is necessary.

Satisfactory release time or rate of decay of current is obtained by the addition of rectifier number two as shown in Figure 2. The rectifier combination compares very favorably with other known methods of contact protection with respect to peak voltage and timing characteristics.

Selenium rectifiers are inexpensive and are known to have an almost indefinite life. The contact protection units are simple to mount and, furthermore, it is not necessary to observe polarity when wiring. This, together with their dependability over extended periods without attention, makes them most desirable circuit elements.

Power consumption is small when it is desired to connect the unit in parallel with the contacts to be protected.

The use of selenium rectifiers as voltage surge suppressors is not limited to telephone applications. Cells ranging in area from a quarter of a square inch to thirty square inches may be arranged in series-parallel combinations as the application warrants.

References

1. Metal Rectifiers (book), H. K. Henisch. Oxford University Press, London, England, 1949, pages 131–155.

2. Contacts, P. W. Swenson. *Bell Laboratories Record* (New York, N. Y.), volume 27, February 1949, pages 50–53.

No Discussion

Clean-Up of Helium Gas in an Arc Discharge

M. J. REDDAN
NONMEMBER AIEE

G. F. ROUSE
NONMEMBER AIEE

GAS clean-up, or the gradual disappearance of the filler gas in an electrical discharge, has been observed by many investigators. From a paper by E. Pietsch[1] published in 1936 and listing 169 references we can draw some interesting conclusions regarding work performed before that date. In evaluating the data, several facts should be recalled: most of the articles were published before the announcement of Langmuir's probe theory; most of the work was carried out in chemically active gases; and finally, much of the work was performed with poor vacuum techniques. Nevertheless, several areas of agreement may be noted:

1. It was generally agreed that cathode sputtering strongly influences clean-up. In many cases clean-up and the onset of sputtering were found to appear at the same critical potential.
2. Practically no absorption into the anode was observed.
3. Noble gases are absorbed far less readily than are molecular gases.
4. Gas absorption was sometimes explained by recourse to the supposition that various unstable chemical compounds were formed. Even "helides" were reported.
5. Absorption into the envelope of the discharge tube was reported, and it was frequently claimed that the amount absorbed was not dependent on the type of gas, wall material, or wall potential.

Since this earlier work was done under a wide range of experimental conditions, the failure to deduce from it any consistent explanation of gas absorption is not surprising.

About 1936, a great deal of information was contained in a series of papers published in Germany by Alterthum, Lompe, and Seeliger.[2,3] Their work was simplified by being restricted to the noble gases. They worked with an a-c glow discharge in cylindrical glass tubes in which the electrodes were open-ended sheet iron cylinders. The use of open cylindrical electrodes gives the advantage of almost constant cathode fall over a wide range of currents and pressures. A summary of their results is of considerable interest.

They found the following facts for neon gas:

1. Over a pressure range from a few tenths of a millimeter to about 3 millimeters, the absorption rate is independent of the pressure; however, at higher pressures the rate falls off.
2. The absorption rate is proportional to the discharge current.
3. At the current employed (100 milliamperes) the rate is independent of the shape and size of the discharge tube.
4. The absorption rate is not influenced even by excessive sputtering.

By conducting separate experiments with a d-c glow discharge, it was found that absorption was taking place in the cathode. Recovery of about 30 per cent of the trapped gas was accomplished by inductively heating the cathode. An important observation was that by creating a high cathode fall either through operation at low pressures (below 0.2 millimeter), or through the use of closed-end electrodes, the absorption rate was increased by a factor of four. This leads to the attractive explanation that absorption results from the fact that ions are driven into the cathode under the accelerating field of the cathode fall. A direct estimate of the dependence of such clean-up on ion energy cannot, however, be obtained from these data for the following reasons:

1. The energy of the ions cannot be determined since multiple collisions take place in the cathode-fall region.
2. The proportion of current at the cathode carried by ions must be known in order to determine the number of ions striking.

It now is generally thought that clean-up can result from the bombardment of negatively charged electrodes by ions present in the discharge. Tube engineers have long been aware of the importance of this clean-up problem and have developed methods for minimizing its effects. For example, D. V. Edwards and E. K. Smith[4] described a method of minimizing clean-up by the use of "cushioning" circuits which permit deionization to occur while the inverse anode voltage is low. D. E. Marshall and C. L. Shackelford in a recent paper[5] discussed the influence of the commutation factor rating on the design of such "cushioning" or "snubbing" circuits. Also, A. W. Coolidge, Jr., has described[6] a line of thyratrons in which close spacing of the electrodes permits a high filling pressure, and a well-shielded anode exposes a minimum area to ion bombardment during inverse voltage conditions.

Description of Experimental Apparatus and Methods

Experimental equipment was designed to obtain data on controlled clean-up which results from the bombardment of a tantalum surface by positive helium ions. Since there was reason to believe that other important clean-up effects would be present, it was necessary to carry out the experiment in a manner which made the required correction possible.

The problem of obtaining pure gas received particular attention. Spectro-

---

Paper 51-353, recommended by the AIEE Electronics Committee and approved by the AIEE Technical Program Committee for presentation at the AIEE Fall General Meeting, Cleveland, Ohio, October 22–26, 1951. Manuscript submitted June 19, 1950; made available for printing September 5, 1951.

M. J. Reddan and G. F. Rouse are with the National Bureau of Standards, Washington, D. C.

This is an interim report on the gas clean-up program initiated at the National Bureau of Standards by Dr. J. B. White, to whom the authors express appreciation for many valuable discussions and suggestions. The primary object of these studies is the discovery of information on gas clean-up which will be of value to tube designers.

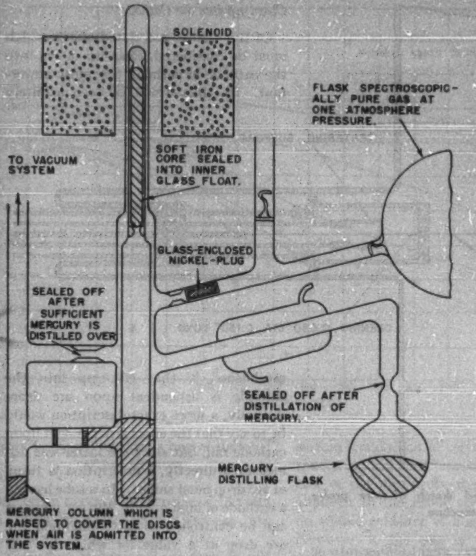
SOLENOID
FLASK SPECTROSCOPICALLY PURE GAS AT ONE ATMOSPHERE PRESSURE.
SOFT IRON CORE SEALED INTO INNER GLASS FLOAT.
TO VACUUM SYSTEM
GLASS-ENCLOSED NICKEL-PLUG
SEALED OFF AFTER SUFFICIENT MERCURY IS DISTILLED OVER
SEALED OFF AFTER DISTILLATION OF MERCURY.
MERCURY DISTILLING FLASK
MERCURY COLUMN WHICH IS RAISED TO COVER THE DISCS WHEN AIR IS ADMITTED INTO THE SYSTEM.

Figure 1 (left). Apparatus for admitting gas to vacuum system

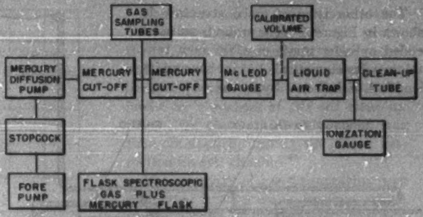
GAS SAMPLING TUBES
CALIBRATED VOLUME
MERCURY DIFFUSION PUMP
MERCURY CUT-OFF
MERCURY CUT-OFF
McLEOD GAUGE
LIQUID AIR TRAP
CLEAN-UP TUBE
STOPCOCK
IONIZATION GAUGE
FORE PUMP
FLASK SPECTROSCOPIC GAS PLUS MERCURY FLASK

Figure 2 (above). Block diagram of experimental system

scopically pure gas was obtained from commercial sources. To attain even greater purity, a gettering device was employed during the initial work. This consisted of strands of zirconium and tantalum wire which were heated in the presence of the gas to remove from the gas any minute traces of non-noble gases. It was subsequently discovered that the very small amounts of impurity present in the unopened flask of pure gas were not sufficient to affect the experimental results. In later work, a check on the gas purity was achieved by sealing off small samples for mass-spectrometer analysis. This was supplemented by a continuous visual observation of the arc spectrum in a spectroscope.

To assure that the original purity was maintained during admission of filling gas to the tube, several schemes were tried. A device for introducing gas which avoids entirely the use of stopcocks was finally developed. A detailed view of this is shown in Figure 1. When this device is first attached to the vacuum system, the seal-off constriction is open, the gas flask is unopened and the mercury shown at the right of the fritted disks is still in the distillation flask. All parts of the structure, other than the distilling flask, can then be thoroughly outgassed by baking at about 425 degrees centigrade. When the baking is completed, mercury is distilled over slowly until the right fritted disk is completely covered. The seal-off constriction directly above the fritted disks is then closed, the mercury flask is sealed off the system and the gas flask is opened. Gas now can be admitted to the system by raising the float and uncovering a small portion of the fritted disk. In order to maintain the purity of the gas when it becomes necessary to admit air to the vacuum system, the mercury column at the extreme left of the figure is raised to cover the fritted disk on the left.

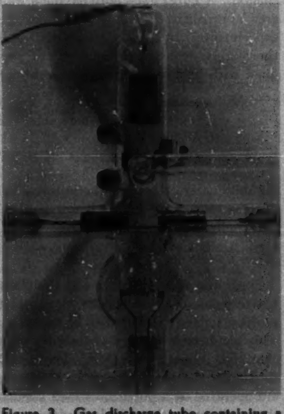

Figure 3. Gas discharge tube containing a wire probe

A block diagram of the vacuum system employed is shown in Figure 2. No stopcocks were used in that portion of the system in which clean-up takes place. Instead, barometrically operated cut-offs were employed.

Data have been obtained on discharge tubes of two types, the essential difference between them being in the design of the probe structure. The features of the cathode and anode structures common to both types are shown in Figure 3. The oxide cathode, a commercial one having a nickel mesh base, has an area of approximately 30 square centimeters. The hollow cylindrical anode is made of grade *A* nickel. Figure 3 also pictures one type of probe structure the details of which are shown in Figure 4.

In this structure the probe is a tantalum wire, 0.010 inch diameter, mounted so that current can be passed through it for purposes of outgassing. Its tension is maintained by a tantalum-tungsten alloy ribbon-type spring (0.002 inch by 0.150 inch). The action of this spring, in conjunction with the centering action of the molybdenum spacers, maintains an accurate positioning of the wire. Even at temperatures in excess of 2,000 degrees centigrade, the positioning is satisfactory. The nickel shields allow only a chosen fraction of the probe wire to be exposed to the discharge plasma. The cylindrical openings in the ends of the shields through which the probe wire passes are 0.050 inch in diameter and 0.150 inch long. The opening between the wire and the shield is thus so small as to reduce to a negligible amount the migration of ions toward shielded parts of the probe. The shields are readily outgassed by inductive heating.

The other type of probe structure is shown in Figure 5. The probe is an open ended cylinder made of 0.005 inch tantalum. Its diameter is 1.55 inches and its length 1.55 inches. By means of a magnetically controlled mechanism, not shown in the illustration, the probe cylinder can be placed in either of the two positions indicated in the figure. In the lower (#2) position the cylinder rests on tungsten wire supports through which electrical connection is made. The clearance between the probe cylinder and the wall of the glass envelope is small enough (approximately 1 millimeter) to prevent migration of ions behind the probe. When the probe is in the #1 position it can be heated to a very high temperature without endangering the glass envelope.

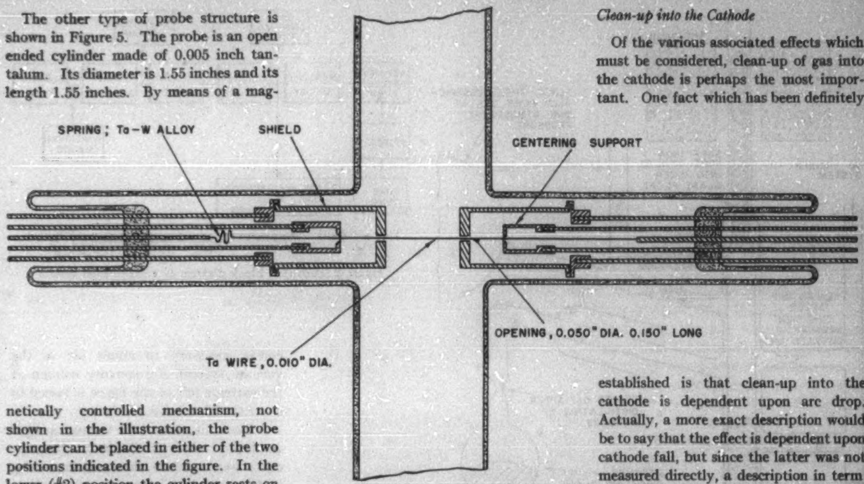

Figure 4. Detailed sketch of wire probe structure

Excessive heating of the probe wire or the probe cylinder by ion bombardment was avoided by applying negative pulses of about 10-milliseconds duration with a repetition rate of ten per second.

The calculation of the number of disappearing helium atoms is based on measurements of a pressure drop occurring in the known volume of the system. This volume is determined by observing pressure drops which occur when the system is opened to an accurately-calibrated standard volume.

Associated Sources of Gas Disappearance

In an experimental study of the conditions governing clean-up into a probe, it would naturally be desirable to eliminate all other sources of clean-up. Since their complete elimination was not possible, these effects were reduced in magnitude and proper allowance made for them:

Leakage Through the Tube Wall

It was realized that a loss of gas might occur which would be completely independent of the presence of a discharge in the tube. Neutral atoms of gas having only thermal energy might diffuse into or through the glass wall of the tube. Data exist[7] which make it possible to calculate the drop in pressure to be expected as a result of helium diffusion through the Pyrex envelope. Assuming the envelope temperature to be 250 degrees centigrade, and the helium pressure as 0.2 millimeter mercury the calculated pressure drop in a system having an approximate volume of 2.0 liters is 6×10^{-3} micron per hour. A simple test was made to check this conclusion. A Pyrex glass bulb having a wall area approximately equal to that of the experimental tube was evacuated and thoroughly degassed, after which it was filled with helium to a pressure of about 0.2 millimeter. Heating the bulb to 350 degrees centigrade for 22 hours resulted in a negligible change in pressure.

Clean-up into the Anode or Shields

Since the anode acquires the highest positive potential in the tube, clean-up of positive ions into it is not to be expected. This has been confirmed repeatedly by a thorough inductive heating. The nickel shields in the wire-type probe structure are operated at a potential which assures that current to the shields is almost entirely due to electrons.

Clean-up into the Cathode

Of the various associated effects which must be considered, clean-up of gas into the cathode is perhaps the most important. One fact which has been definitely established is that clean-up into the cathode is dependent upon arc drop. Actually, a more exact description would be to say that the effect is dependent upon cathode fall, but since the latter was not measured directly, a description in term of arc drop must suffice. In a tube having a cathode of high quality, the gas pressure can be controlled so as to maintain the arc drop at a value for which the self clean-up rate is approximately 10^{-3} micron per minute. Anything which causes the arc drop to rise, as for instance too great a drop in pressure or poisoning of the cathode, causes an increase in the self clean-up rate. For example, it was deduced from a series of observations

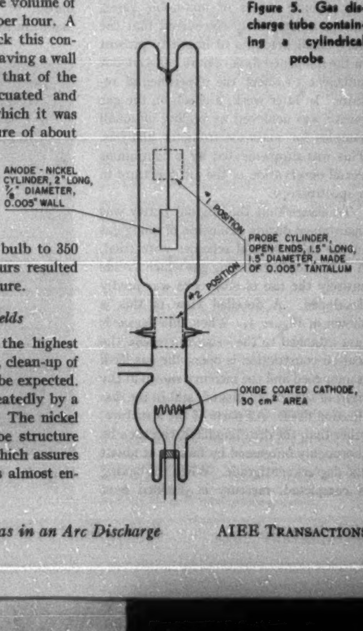
ANODE - NICKEL CYLINDER, 2" LONG, 7/8" DIAMETER, 0.005" WALL
#1 POSITION
PROBE CYLINDER, OPEN ENDS, 1.5" LONG, 1.5" DIAMETER, MADE OF 0.005" TANTALUM
#2 POSITION
OXIDE COATED CATHODE, 30 cm² AREA

Figure 5. Gas discharge tube containing a cylindrical probe

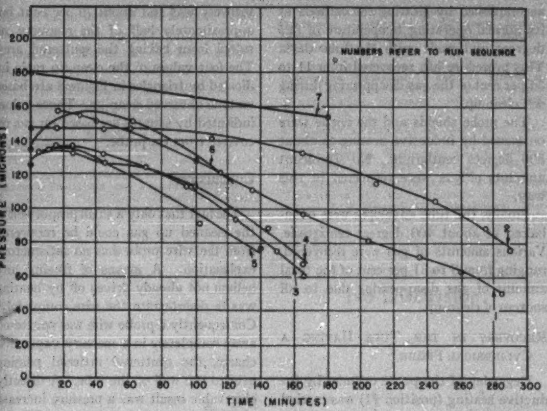

Figure 6. Data illustrating a case of abnormal cathode clean-up

that on an average an increase of 13 volts in arc drop increases the self clean-up rate by a factor of approximately 100.

The effect of increased arc drop on self clean-up is strikingly illustrated by data taken on a tube in which the cathode had low emission and which operated with an arc drop about 15 volts higher than that in a similar tube having a good cathode. These data are plotted in Figure 6. During the initial run, to which curve 1 applies, the pressure dropped from 158 microns to 50 microns. Since it was thought best not to operate the tube at a pressure below 50 microns, fresh gas was added. The data from which curve 2 was plotted were then taken. This procedure was repeated a total of seven times. It is interesting to note that the total gas absorbed in about 22 hours is approximately equivalent to that in a liter flask at 600 microns pressure. It also is interesting to note that there is little indication that the process was approaching saturation. The initial rise which appears in some of the curves is accounted for by an increase in tube temperature.

The self clean-up rates just mentioned contrast markedly with the almost complete lack of clean-up exhibited by many commercial tubes which operate with a much lower arc drop and which do not contain helium gas.

Clean-up into a Sputtered Deposit

Comments made in the introduction to this paper emphasize that a wide divergence of opinion exists as to the role played by sputtering in gas clean-up. Under certain conditions a certain amount of sputtering has been unavoidable. In the case of the wire probe the glass surfaces adjacent to the probe structure showed no visible evidence of a sputtered layer. However, in the case of the cylindrical probe a band of sputtered material appeared on the glass near each end of the probe after several hours operation at negative probe voltages in the range of 400 to 600 volts. Some data on the effects produced by these sputtered bands will appear in the section dealing with recovery of gas.

Determination of Probe Clean-up

The first step in a determination of probe clean-up was to clean and degas the tantalum probe thoroughly. This was accomplished by maintaining its temperature at approximately 2,000 degrees centigrade for several minutes in a vacuum of about 10^{-4} millimeters of mercury. Following this the tube was filled with helium to a desired pressure.

Since all the associated clean-up effects discussed in the previous section may be unavoidably present during operation of the tube, some method of correcting for them was necessary. A correction factor was determined by observing the rate of clean-up when the conditions of operation limited the ion probe current to a negligible value. This rate of clean-up will be referred to as self clean-up. Probe clean-up always occurred at a rate at least ten times as great as that for self clean-up. Therefore errors existing in measured values of self clean-up did not have an unduly large effect upon the corrected values of probe clean-up.

The tube was then operated with a pulsed negative potential on the probe, that is, with an ion current to the probe, and the new rate of clean-up was established. In most instances this was followed by a recheck of the self clean-up rate. Net clean-up into the probe was then obtained by making the proper correction for self clean-up.

The quantity of gas disappearing was calculated from pressure readings which were recorded at the beginning and end of a test when all parts of the tube were at room temperature.

It is of great practical interest to know what fraction of the ions which strike the probe surface at a given voltage are trapped. This information is plotted in Figures 7 and 8. The numerator of the ratio plotted as ordinate was derived from the net pressure change due to probe clean-up, while the denominator was derived from conversion of values of peak probe current to fundamental charge units. The latter calculation does not take into account that part of the probe current due to electrons ejected from the probe by ion impact. Direct experimental data which might be used to correct the probe current for this effect are not available. An indication of the probable magnitude of the correction might be obtained by using data for impact of helium ions on molybdenum.[8,9] However, from an application view-point, the data are probably of greater interest in the form presented.

Although the points plotted in Figure 7 may appear to be randomly distributed over the voltage range, it is possible to attach significance to the position of each point. This may be done by selecting as a parameter the ratio, R, of ionic mean free path to sheath thickness around the probe wire. The first of these can be calculated by means of simple kinetic theory formulas and the sheath thickness is obtained by use of the appropriate space charge formula. The fraction of positive ions which pass through the sheath without collision is given by $\epsilon^{-1/R}$. Average values for this fraction, expressed in per cent, appear in Figures 7 and 8 adjacent to the plotted points.

In the case of the wire probe (Figure 7) the percentage values vary from about 40 to 85 per cent. Dash lines have been drawn to suggest groupings of the points. It becomes evident from a study of Figure 7 that the number of ions cleaned up is a strong function of probe voltage. However, it also is evident that this number is dependent upon other factors which determine the fraction of ions passing through the sheath without collision.

In the case of the cylindrical probe (Figure 8) the percentage values vary from about 4 to 40 per cent. It will be observed that the number of ions cleaned up depends upon voltage in a manner quite similar to that shown in Figure 7. A striking feature of these data is that the clean-up rate is essentially the same for both probes even though the number of ions reaching the cylindrical probe without suffering collision in the sheath is relatively very small.

Recovery of Cleaned-up Gas

The fact that a clean-up of gas is associated with the flow of positive ions to a negatively charged metal surface has been definitely established. Although this effect is well supported by experimental data, it was considered worthwhile to attempt a reversal of the clean-up process and in this way obtain evidence that gas trapped in the probes is primarily responsible for a pressure decrease.

Recovery in the Tube Having a Wire Probe

The wire was heated by Joule heat to 2,000 degrees centigrade. In four recent tubes this has yielded percentages of recovery ranging from 5 to 22 per cent of the net probe clean-up.

Recovery from the cathode has been accomplished by glowing the cathode at its normal operating temperature of 825 degrees centigrade with the tube dark. This procedure has recovered from 11 to 54 per cent of the gas disappearing during self clean-up.

The probe shields and the anode were outgassed by inductive heating to about 800 degrees centigrade. No significant amounts of gas were recovered in this way.

Finally, the tube envelopes were oven-baked at about 400 degrees centigrade. Various amounts of gas were recovered, ranging from 8 to 31 per cent of the total amount of gas disappearing due to all sources of clean-up.

Recovery in the Tube Having a Cylindrical Probe

Degassing of the probe cylinder by inductive heating (position #1) was carried out after each clean-up run. While the tube was relatively new and free from any sputtered desposit, degassing the cylinder accounted for 70 per cent or more of the cleaned-up gas. As the sputtered bands near the ends of the probe cylinder became increasingly opaque percentage recovery from the probe declined.

Following each of the last four runs recorded, the sputtered region of the envelope was baked for several hours at 350 degrees centigrade. In these cases total recovery was still about 70 per cent but approximately half of the recovery resulted from baking the sputtered area. The four values of the clean-up ratio indicated by triangles in Figure 8 are based on total observed clean-up. Those values indicated by squares are based on gas recovered from the probe.

Conclusion

The fact that only a small proportion of the cleaned up gas could be recovered from the wire probe has no satisfactory explanation. A means of freeing any helium not already driven off by heating was to disintegrate the wire completely. Consequently a probe wire was sputtered away completely in a mercury vapor discharge, the sputtered material passing over to the wall of the tube. A directly observable result was a pressure increase of one micron. Assuming that the gas which disappears during a probe clean-up is held in the wire, the 1-micron increase in pressure is only a small fraction of that which might have been expected.

It has been assumed in the preceding work that clean-up occurs only during the initial impact of an ion with the surface. However, in view of the significant amounts of gas recoverable from the area of the tube wall on which metal is sputtered, it may be that rebounding atoms

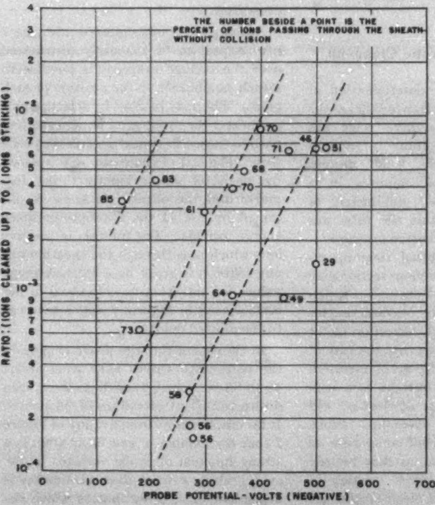

Figure 7. Dependence of clean-up upon the number and energy of impacting ions: wire probe

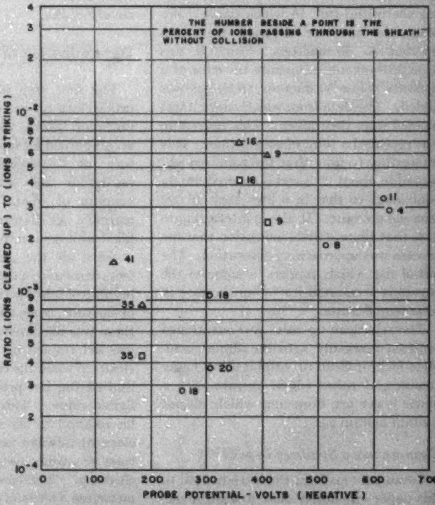

Figure 8. Dependence of clean-up upon the number and energy of impacting ions: cylindrical probe

play an important role. It is conceivable that some of the impacting ions are reflected as neutral atoms which in turn are trapped as they strike some nearby surface. An effort will be made to check this possibility in future work.

References

1. Gas Absorption Under the Influence of an Electric Discharge and Related Phenomena, E. Pietsch. *Physikalische Zeitschrift* (Leipsig, Germany), volume 37, December 1936, page 214.

2. The Absorption of Noble Gases in the Electrical Discharge I, Alterthum, Lompe, Seeliger. Julius Springer, Berlin, Germany, 1936, pages 833–38.

3. The Absorption of Noble Gases in the Electrical Discharge II and III, Alterthum, Lompe, Seeliger. *Zeitschrift für Technische Physik* (Leipsig, Germany), volume 19, 1938, pages 113–18.

4. Circuit Cushioning of Gas-Filled Grid-Controlled Rectifiers, D. V. Edwards, E. K. Smith. *Electrical Engineering* (*AIEE Transactions*), volume 65, October 1946, pages 640–43.

5. Commutation Factor Rating of Inert Gas Thyratrons and Its Influence on Circuit Design, D. E. Marshall, C. L. Shackelford. *Electrical Engineering*, volume 69, 1950, page 255.

6. A New Line of Thyratrons, A. W. Coolidge, Jr. *Electrical Engineering*, volume 67, 1948, page 435.

7. Diffusion in and Through Solids (book), R. M. Barrer. Cambridge University Press, Cambridge, England, 1941, page 136.

8. Liberation of Electrons From Metal Surfaces by Positive Ions, M. L. E. Oliphant, P. B. Moon. *Proceedings*, Royal Society of London (London, England), volume 127, 1930, page 373.

9. The Emmission of Secondary Electrons Under High Energy Positive Ion Bombardment, Hill, Buechner, Clark, Fisk. *Physical Review* (New York, N. Y.), volume 55, 1939, page 463.

No Discussion

Basis for Dielectric Tests for Rectifier Equipment

C. C. HERSKIND
FELLOW AIEE

THE POOL cathode mercury-arc power converter has developed progressively through several different types, beginning with multianode glass tubes and pumped metal tanks and continuing to the single anode metal tanks and tubes, such as the ignitron and excitron. The structural arrangement has taken a variety of forms, ranging from the field-assembled unit to a factory-built assembly. The mounting and construction of the auxiliaries also has varied widely in such items as grounded or insulated heat exchangers and frame or separately mounted auxiliary devices. The advent of the single anode tank or tube has increased the variety of circuits and equipment arrangements which may be employed. Recent applications using the double-way circuit do not include the rectifier transformer as a part of the rectifier unit.

This variety of tube types and equipment arrangement of the rectifier units, together with the growing application of phase control, necessitated a drastic revision of the rules for determining dielectric test voltages. The test code, set forth in the new American Standards for Pool Cathode Mercury-Arc Power Converters,[1] was devised to provide a sound and uniform basis for testing rectifier units embodying a large variety of tube types, equipment arrangement, and service conditions.

The purpose of this report is to review the principal factors which were considered in formulating the rules for dielectric tests, and to outline the general basis for these tests.

In order to determine the values of test voltage to be applied to a rectifier unit, the following steps must be taken:

1. Definition of the terminals or points of potential difference to which the test voltage shall be applied.
2. Determination of the circuit conditions which establish the voltage stress in normal sustained operation.
3. Evaluation of the crest working voltage.
4. Calculation of test voltage.

Each of these steps is discussed below:

Points of Potential Differences

A rectifier unit is defined as an operative assembly consisting of the rectifier(s), the rectifier auxiliaries, the rectifier transformer equipment, and the essential switchgear. The part of the unit comprising the rectifier and its auxiliaries is usually connected to two main power systems, namely, the a-c system at the terminals of the rectifier transformer d-c windings and the d-c system at the cathode terminal, and to one auxiliary power system at the terminals of the auxiliary devices used for excitation, evacuation, and temperature regulation. The main power terminals of the rectifiers are the anodes and cathode (or cathodes) of the rectifier tanks or tubes, which connect to the a-c and d-c power systems in the main power circuit. These terminals have a potential difference with respect to each other and with respect to ground. In the multianode metal tank rectifiers, the vacuum envelope operates at a potential differing slightly from that of the cathode, but for purposes of making dielectric tests, the two are assumed to have the same potential.

The rectifier auxiliaries are usually energized from a low-voltage a-c auxiliary source. Some of the auxiliaries are conductively connected to a power terminal of the rectifier, either directly or through the auxiliary electrodes and the arc discharge. Others are mounted on a frame member which is at power terminal potential, such as the cathode. Auxiliaries which are so connected or mounted may operate with voltage stresses arising from both power and auxiliary circuit potentials.

Examples of some of the more usual circuit arrangements are shown in the illustrations. Figure 1 shows a rectifier with its auxiliaries mounted on the frame at cathode potential and supplied with auxiliary power from an insulated source. In the arrangement shown in Figure 2, the auxiliary devices, while also mounted on the frame, must provide insulation in themselves between the power and auxiliary circuits. An arrangement with auxiliaries mounted at ground potential is shown in Figure 3. Figure 4 illustrates the complexity of the double-way circuit with auxiliaries mounted at several different potentials.

Rectifier Circuits

The crest working voltage between anodes, between cathodes and between anodes and cathodes is established by the rectifier circuits employed and is equal to the peak inverse voltage for rectifier operation and peak forward voltage for inverter operation. Values of the peak inverse voltage for some circuits is given in Table IV of reference I. The crest working voltage between anodes and ground and between cathodes and ground is established by both the rectifier circuit employed and the ground point. When no ground point is provided or specified a ground is assumed at the point which requires the highest test voltage, that is, either the positive or negative d-c bus.

The peak inverse voltage is the maxi-

Paper 51-354, recommended by the AIEE Electronic Power Converters Committee and approved by the AIEE Technical Program Committee for presentation at the AIEE Fall General Meeting, Cleveland, Ohio, October 22-26, 1951. Manuscript submitted March 28, 1951; made available for printing September 25, 1951.

C. C. Herskind is with the General Electric Company, Schenectady, N. Y.

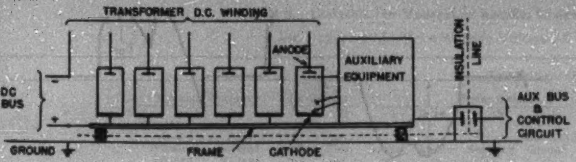
TRANSFORMER D.C. WINDING
ANODE
AUXILIARY EQUIPMENT
INSULATION LINE
DC BUS
AUX BUS & CONTROL CIRCUIT
GROUND
FRAME
CATHODE

Figure 1. Rectifier with auxiliaries mounted at frame (cathode) potential

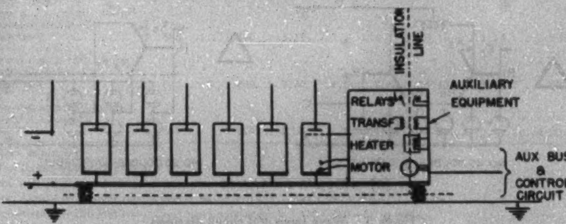
INSULATION LINE
AUXILIARY EQUIPMENT
RELAYS
TRANSF
HEATER
MOTOR
AUX BUS & CONTROL CIRCUIT

Figure 2. Rectifier with frame mounted auxiliaries and insulation line through devices

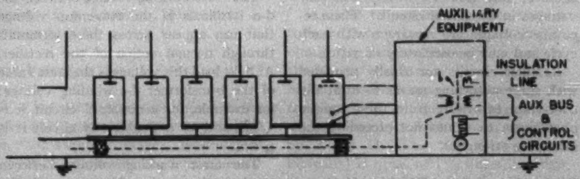
AUXILIARY EQUIPMENT
INSULATION LINE
AUX BUS & CONTROL CIRCUITS

Figure 3. Rectifier with auxiliaries mounted at ground potential and insulation line through devices

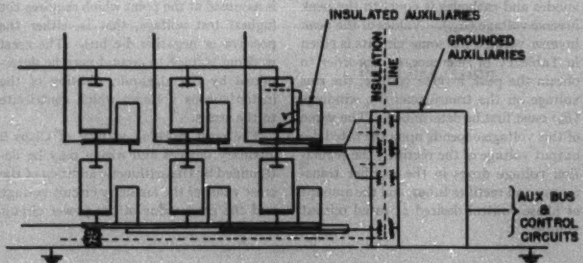
INSULATED AUXILIARIES
INSULATION LINE
GROUNDED AUXILIARIES
AUX BUS & CONTROL CIRCUITS

Figure 4. Double-way rectifier with auxiliaries mounted at four potentials

mum instantaneous voltage between the anodes and cathodes of a rectifying element during the inverse period. The value of peak inverse voltage used for determining test voltages is the peak inverse voltage obtained when operating as a power rectifier, at no load, with no phase control, and with rated a-c voltage on the d-c windings of the rectifier transformer.

The wave forms and circuit diagrams for two widely used circuits are shown on Figure 5. The values of crest working voltage for these circuits are given in Table I.

Insulation Line

The voltage between power circuit terminals and ground and between power circuit terminals and auxiliary circuit terminals on the rectifier assembly results in a stress on specific insulating members. These members may be said to define the insulation line.

In the simple arrangement shown in Figure 1, the base insulators under the rectifier, and the insulating transformers in the auxiliary power circuit, form the insulation line. The primary function of these devices is to provide insulation. In the more complex arrangement shown in Figure 2, the insulation line passes through some of the auxiliary devices and the insulation in these devices is called on to act in a dual insulating capacity, that is, it must insulate for both the usual voltage stresses of the auxiliary power circuit and the additional stress arising from the rectifier power circuit.

For purposes of testing auxiliary circuits of rectifier sections (assemblies), two classes of auxiliaries are defined:

Class 1

Auxiliary devices and wiring so mounted and connected that they are subjected to voltage stresses arising only from auxiliary circuit voltages. (For example, devices mounted at ground potential and connected to a grounded or insulated circuit, and devices mounted at cathode or anode potential and connected to an insulated circuit.)

Class 2

Auxiliary devices and wiring so mounted and connected that they are subjected to voltage stresses resulting from both auxiliary circuit and power circuit voltages. (For example, auxiliary devices mounted at cathode or anode potential and connected to a grounded circuit, or auxiliary devices mounted at ground potential and connected to cathode or anode or to a device mounted at cathode or anode potential.)

Devices mounted on the rectifier frame to meet Class 2 requirements must either be made special to withstand the added voltage stress or be selected from standard devices of higher voltage ratings. Added insulation may be provided between conducting elements, such as windings, and contacts or the device may be mounted on an insulated sub-base.

Unusual Service Conditions

The crest working voltage has been determined on the basis of the conditions

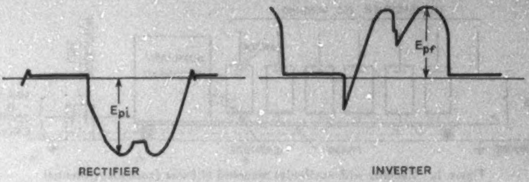

(A) ANODE TO CATHODE VOLTAGE WAVE FORMS

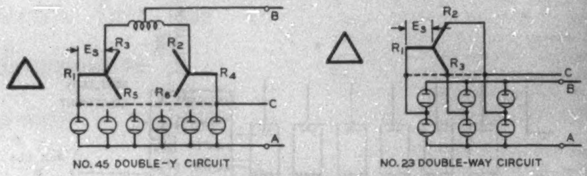

(B) CIRCUIT DIAGRAMS

Figure 5. Wave forms and circuit diagrams

incurred during sustained operation in normal service. Actually the stress imposed on the rectifier may exceed this value under a variety of conditions frequently encountered in service. Some of the conditions under which over-voltages may be obtained are listed below:

1. System over-voltages resulting from overspeed of generators in the a-c system or over-voltage on unfaulted phases of 3-phase impedance grounded systems with one phase faulted.
2. D-c over-voltages occurring when keying a phase-controlled rectifier, or arising from an over-running d-c load.
3. Over-voltages due to switching.
4. Over-voltages occurring during fault interruption.

No attempt is made to accurately evaluate the insulation requirements for these abnormal conditions. Experience has shown that insulation can withstand high-voltage stresses for short intervals. The value of the test voltage is selected so as to assure the use of insulation having adequate strength to meet these abnormal conditions to the extent that they are usually encountered in service.

Rectifier Over-Voltages

Over-voltages also may be produced in the rectifier circuit from three phenomena which are unique in rectifier operation.

1. *Arc Extinction.* When the arc-back current in a rectifier decays to zero under unfavorable conditions, a very rapid decay of current may be obtained at a substantial current value, when the cathode spot on the anode surfaces goes out. The magnetic energy in the transformer core at the beginning of extinction is transformed into electrostatic energy in the distributed capacity associated with the transformer windings. Since this value of capacity is small, the resulting voltage may be many times rated voltage.

2. *Arc Starvation.* When a rectifier is operated at high current and low temperature, the voltage across the arc discharge may vary rapidly from the normal value to several times the normal value. This voltage fluctuation is an arc phenomena resulting from a deficiency of positive ions incurred at low vapor densities and high current flow. It may produce substantial voltage surges in the rectifier power circuit.

3. *Recurrent Recovery Phenomena.* When a rectifier is operating with a large amount of phase control, a high initial inverse voltage is obtained at the end of conduction. This voltage, acting upon the distributed capacity and leakage reactance, may give rise to high recovery voltages in the power circuit. These recovery voltages are recurrent with each cycle and may be oscillatory in nature.

Rectifier circuits are usually provided with surge absorbing means to limit the over-voltages arising from these unique phenomena to values not exceeding the insulation strength.

Evaluation of Crest Working Voltage

The crest working voltage between anodes, between cathodes, and between anodes and cathodes is equal to the peak inverse voltage (E_{pi}). Values of the peak inverse voltage for some circuits is given in Table IV of reference 1. In order to obtain the peak inverse voltage, the rms voltage on the transformer d-c windings (E_s) must first be determined. The value of this voltage depends upon the rated d-c output voltage of the rectifier, the regulation voltage drops in the rectifier transformer and rectifier tubes, and the amount of phase control desired at rated output voltage.

The crest working voltage between the d-c terminals is the maximum voltage that can appear across these terminals through normal action of the rectifier. At light load this voltage is the crest value of the transformer d-c winding voltage; for example, for a double-Y circuit it is $\sqrt{2}E_s$ and for a double-way circuit it is $\sqrt{6}E_s$.

The crest working voltage between anodes and ground, and between cathodes and ground, is established by the rectifier circuit and the ground point. Where no ground is provided or specified, a ground is assumed at the point which requires the highest test voltage, that is, either the positive or negative d-c bus. The crest working voltage to ground may be determined by the algebraic addition of the instantaneous voltages which contribute to the stress.

The crest working voltage of Class 2 auxiliary devices and wiring may be determined by the arithmetic addition of the crest value of the auxiliary circuit voltage and the crest value of the power circuit voltage.

Table I. Table of Voltages

Circuit	Peak Inverse Voltage	Crest Working Voltage Anode to Anode	Anode to Cath.	Bus A to B	Anode to Bus A	Anode to Bus B
# 45 Double-Y	$\sqrt{6}E_s = \frac{2\pi}{3} E_{do}$	$\sqrt{6}E_s$	$\sqrt{6}E_s$	$\sqrt{2}E_s$	$\sqrt{6}E_s$	$\sqrt{2}E_s$
# 23 Double-way	$\sqrt{6}E_s = \frac{\pi}{3} E_s$	$\sqrt{6}E_s$	$\sqrt{6}E_s$	$\sqrt{6}E_s$	$\sqrt{6}E_s$	$\sqrt{6}E_s$

Table II. Dielectric Test Voltages for Rectifier Equipment

Test Voltage = 1.5 × Crest Working Voltage + K

	Working Voltages		Test Voltages (Rms Kilovolts)										
			Tubes (or Tanks)		Power Circuit					Auxiliary Circuit (Aux. Devices & Wiring)			
			1	2	3	4	5	6	7	8 Class 1	9 Class 2	10 Class 2	11 Class 2
Example	Transformer D-C Winding Voltage E_s	Peak Inverse Voltage E_{pi}	Anode to Cath.	Aux. Elec. to Cath.	Anode to Anode	Anode to Cath.	Between D-C Term.	Bus C to Ground at Bus A	Bus C to Ground at Bus B	Conductor to Mount	D-C Term. to Ground at Other	Bus C to Ground at Bus A	Bus C to Ground at Bus B
Value of K			3	1*	3	3	1	3	1**	1	1	3	3
#1 600-v d-c with no phase control, circuit 45 double-Y	585	1,430	5.15	1.5	5.15	5.15	3.14	5.15	2.24	1.5†	3.00‡	5.61§	4.71‡
#2 600-v d-c with 15% phase control, circuit 45 double-Y	655	1,605	5.40	1.5	5.40	5.40	3.41	5.40	2.39	1.5	3.00	5.87	4.85
#3 600-v d-c with 15% phase control, circuit 23 double-way	330	810	4.20	1.5	4.20	4.20	2.21	4.20	4.20	1.5	3.00	4.68	4.68

*1.5-kv minimum

**For double-way circuit k = 3.

†Aux. voltage assumed to be 220 volt rms.

‡Aux. voltage is 220-volt rms; Crest working voltage is 1.41 × 585 + 310 = 1,140 volts.

§Aux. voltage is 220-volt rms; Crest working voltage is 1,430 + 310 = 1,740 volts.

These two components of the crest working voltage should be taken with respect to a terminal point that is common to both.

Test Voltages

The test voltages are determined on the basis of the general rule that they shall be twice the working voltage. Inasmuch as it is more convenient to determine the working voltage on the rectifier in terms of its crest, the rms test voltages are taken as $1^1/_2$ times the crest working voltage. Using this rule, the crest value of the test voltage will be approximately twice that of the crest working voltage.

In order to provide adequate voltage tests for lower voltage equipment, and to obtain the margins necessary in parts of the circuit which may be subjected to higher stresses than are indicated by the crest working voltage, the test voltages are increased by a fixed amount as shown by Table II. The test voltage (rms kilovolts) is equal to $1^1/_2$ times the crest working voltage (kilovolts) plus the fixed voltage (K in kilovolts) given in the Table. Test voltages are given in the Table for three typical examples.

Conclusions

It is hoped that this review of the factors bearing on the determination of dielectric test voltages will prove helpful in the understanding and application of the rules established by the standards.

References

1. AMERICAN STANDARD FOR POOL CATHODE MERCURY-ARC POWER CONVERTERS. *C34.1—1949*, American Standards Association (New York, N. Y.), 1949.

2. REPORT ON GUIDING PRINCIPLES FOR DIELECTRIC TESTS. AIEE Report Number 51, September 1949.

No Discussion

The Design of High Power Vacuum Tubes for Industrial Heating Applications

H. D. DOOLITTLE
NONMEMBER AIEE

Synopsis: Analysis of tube failures from industrial application has pointed up three principal sources of failure: (1) copper-glass seals are not strong enough to withstand handling by industrial maintenance people; (2) filament structures of the spring-tensioned type are not too reliable; (3) thin-walled copper anodes will not stand occasional overloads. Tubes have been designed which greatly increase tube life by eliminating failures of the above types. The use of thick kovar metal in glass seals will withstand about ten times the torsion of the conventional copper seals commonly used in transmitter tubes. A self-supporting filament structure not only eliminates the failures caused by filaments sticking in guides and annealing of the spring material, but maintains uniform tube characteristics throughout life. Data on a type *ML-5658* 20-kw tube shows less than 2 per cent change in static data after 10,000 hours of life. The use of copper anodes from four to eight times thicker than customary permits nearly 100 per cent increase in plate dissipation ratings without additional water flow. For use at normal plate dissipation, the anode temperature runs lower and scaling of the anode, with resultant anode puncture, is eliminated.

Failure of tubes due to excessive cathode temperature cannot be reduced since evaporation of the cathode material is a physical reality which cannot be compromised. Instead of running a tube above ratings, a larger tube with greater cathode area must be used.

THE ATTITUDE of a plant foreman and a radio station chief engineer towards vacuum tube equipment is naturally quite different. In general, a plant foreman knows very little, and cares very little about the details of operation of the radio-frequency generator he is using. His main interest is that it shall cause him no trouble and do the job. A radio station chief engineer, however, takes considerable pride in the equipment on its own behalf and, in many cases, spends hours of labor improving the operation or tending tubes to get the maximum possible life.

On a recent trip to an industrial establishment which uses the *ML-5619* tube, it was surprising to find that all water flow switches had been disconnected. The foreman's explanation was that every time a certain machine in the next room drew a few gallons of water, all his heaters cut off in the middle of the job. He found that by disconnecting the switch which cut off power in the radio-frequency heaters, if the water flow fell below 5 gallons per minute, he was no longer bothered. The only trouble encountered was that the rubber gaskets in the tube water jacket had to be replaced about every 1,000 hours. This incident contrasts a foreman's attitude with that of a radio station engineer.

It is not possible to make a vacuum tube which will be as rugged as a forging die; however, considerable improvement can be made over the conventional type broadcasting tube. A vacuum tube involves glass or ceramic for insulation, high refractory metals such as tungsten operating at 2,000 degrees centigrade or higher, and pressure of the order of 1/1,000,000,000 of atmospheric pressure. Besides these extreme conditions, the tube is expected to operate for 5,000 hours.

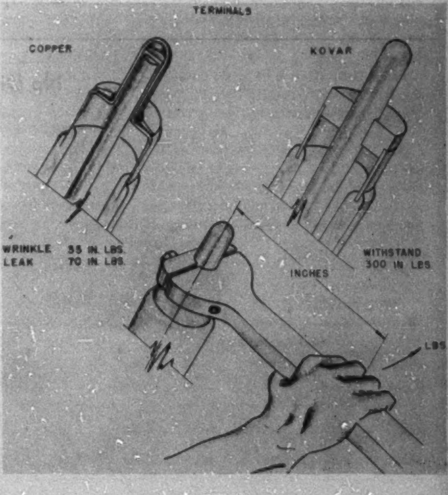

Figure 1. Comparison of torsion strength of copper and kovar glass-to-metal seals

---

Paper 51-355, recommended by the AIEE Electronics Committee and approved by the AIEE Technical Program Committee for presentation at the AIEE Fall General Meeting, Cleveland, Ohio, October 22-26, 1951. Manuscript submitted March 15, 1951; made available for printing September 11, 1951.

H. D. DOOLITTLE is with the Machlett Laboratories, Inc., Springdale, Conn.

Figure 2 (left). Test equipment for evaluation of metal-to-glass seal strength

Table I. Static Test Data on ML-5658 20-kw Tube Before and After 9,700 Hours of Life

Test	Prior to Shipment	After 9,714 Hours of Service
Filament current.....	321.6 ..	313.0 amperes, alternating current
Grid biased 200 volts negative with plate current 2 amperes, plate voltage, (E_{b1}) = ...	7.25..	7.25 kv, direct current
Grid at zero potential with plate current of 2 amperes, plate voltage = ...	3.0 ..	3.05 kv, direct current
Amplification factor..	21.2 ..	21.0
Plate voltage at 10 kv, grid cut-off voltage = ...	−530.0 ..	−540.0 volts, direct current

Comparing life to that of an automobile, the latter would have to operate in excess of 100,000 miles with no internal repairs in accumulating such mileage.

In analyzing vacuum tube failures it is obvious that the principal troubles are (1) seal breakage; (2) shorting grid cathode due to weak seals or warping of the high temperature filament; (3) excessive filament temperature causing rapid evaporation of cathode material; (4) overheated anodes with heavy scale formation and premature failure due to anode puncture; (5) excessive grid dissipation resulting in grid distortion; (6) gassiness due to momentary overload. Fortunately, most of these evils can be rather easily corrected. There is, however, no cure for excessive filament temperature except getting a tube with sufficient cathode emission to do the job.

Machlett Laboratories has redesigned existing tubes, or designed new tubes to cover the power range from 5 to 100 kw output power. These tubes follow the same general pattern. The best possible techniques are used to provide strong

Figure 3. Tube ML-5604, weighing 48 pounds, suspended from a single grid terminal

Figure 4 (below). Comparison of older spring tensioned filament and recent design free-hung filament

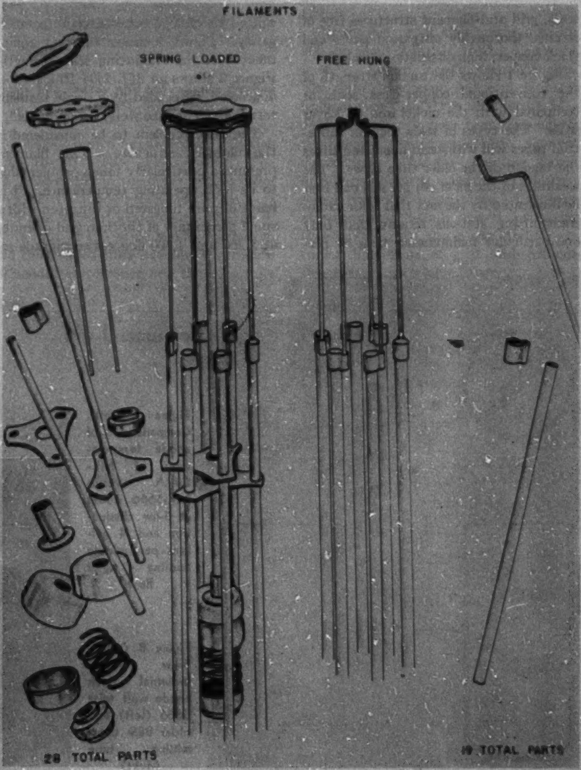

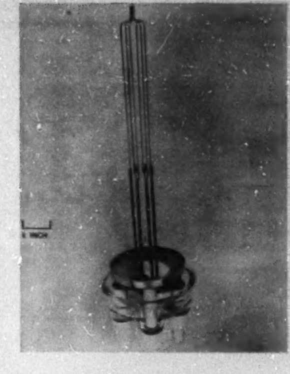

Figure 5. Filament structure of ML-5666 tube mounted on glass dish

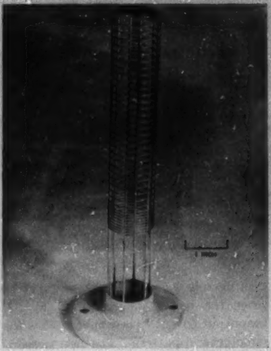

Figure 6. Grid structure of ML-5666 tube

seals, grid and filament structures free of strains, thoroughly outgassed parts and thick copper, high dissipation anodes.

Figure 1 shows the torsion strength of the conventional copper-glass seals as compared with the nickel-iron or kovar seals. The types of seals used on industrial tubes will withstand about ten times the torsion of the older tube types. The weakness of the older copper seal can best be illustrated by the fact that some radio-transmitting stations require that only one particular maintenance man be permitted to change tubes except in emergency. Figure 2 shows the test equipment used in evaluating seal strength. Figure 3 shows an *ML-5604* 10-kw tube, air-cooled, suspended by a single filament terminal. The tube weighs 48 pounds.

The next problem to be considered is the filament structure. The filament presents a particularly tough problem due to its high operating temperature. It is made of pure tungsten or tungsten with a small percentage of thorium and operates at 2,200 and 1,600 degrees centigrade respectively; for good life and proper emission its temperature cannot vary by more than ±20 degrees centigrade in any particular tube. At these temperatures it has a strength comparable with annealed copper at room temperature. As the filament heats up it will expand about 1/8 inch for a 4-inch length, and hence provision must be made for free expansion to prevent bowing with resultant grid cathode shorting. It has been common practice to tension the filament structure to keep it straight. We have found, however, that all attempts to tension a filament with a spring leads to excessive short life failures due to binding, warping of the support structures, et cetera. Figure 4 compares a conventional spring-loaded structure. Figure 5 shows a filament structure mounted on the tube base for an *ML-5666* (5-kw tube). The acid test of freedom from bowing is the static test data which defines the relative position of cathode, grid and anode. Table I shows such data taken on a 20-kw *ML-5658* tube at zero hours and after nearly 10,000 hours of service. A shift of 1 kv in the E_M test is equivalent to a change of 0.015 inch in the grid cathode spacing. This tube has maintained its filament stability for nearly 10,000 hours to within a few mils. The filament current has fallen from 321.6 amperes to 313.0 amperes due to tungsten evaporation.

Figure 6 shows the type of grid structure used in the *ML-5666* tube, 5 kw. Large wire diameters are used and the grid is carefully etched to cool efficiently by radiation.

The next problem to be considered is anode dissipation. The usual transmitter tube anode has about 0.060 inch wall thickness. In our ruggedized tubes from 1/4-inch to 1/2-inch anode thickness is used. The reason for the increased anode

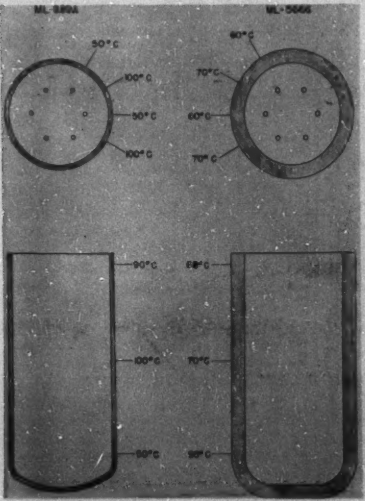

Figure 7 (left). Comparison of anode temperatures of ML-889A versus ML-5666 tubes at 5-kw dissipation and 4 gallons-per-minute cooling-water flow

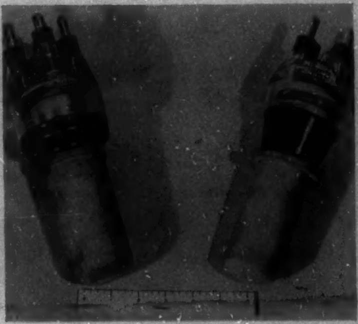

Figure 8 (right). 5-kw tubes. Industrial thick anode wall tube 5666 (left) and older 889 transmitting tube (right)

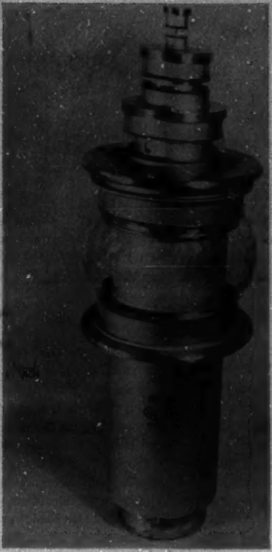

Figure 9. ML-5682 tube for 300-kw input

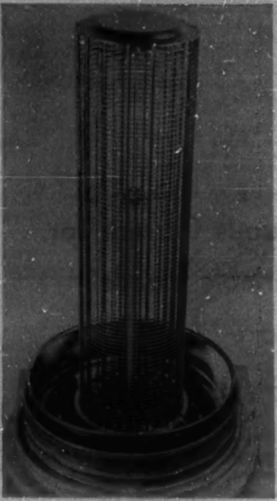

Figure 10. Sturdy grid and cathode structure of ML-5682

thickness is to improve the anode dissipation. There is always some focusing of electrons by the vertical grid support stays. This leads to the heat distribution shown for the conventional *889* tube in Figure 7. Temperature distribution in the heavy-walled counterpart of this tube, the *ML-5666*, also is shown. The six small circles in the upper cross-section view of the anode represent the six vertical grid support stays seen in Figure 6. Note that at the same anode dissipation the thin-walled tube has 2-to-1 variation in anode temperature and that the tube runs at the hotter spots considerably hotter than the heavy-walled tube. The lower temperature as achieved by the latter anode helps in many ways. First of all, a 50 to 100 per cent overload can be taken without permanently damaging the tube. Secondly, the lower temperature in normal operation greatly reduces scale formation. This is particularly advantageous where water may have a relatively high mineral content. A third advantage is reduction in flash arcs, since localized heating is reduced. Figure 8 shows two 5-kw tubes, the *889* and *ML-5666*. The *889* tube has the spring-tensioned filament structure, see Figure 4, and an anode wall 0.060 inch thick. The *ML-5666* has a free-hung filament structure, anode wall 0.25-inch thick and strong kovar seals. These two tubes are interchangeable electrically, but the *ML-5666* has higher ratings and will give much better service due to its more rugged construction and greater safety factors.

Figure 9 shows a high power tube for 300-kw input, the *ML-5682*. This tube includes further design improvements. The small diameter grid and filament leads of the "dish" type used in the *ML-5666*, see Figure 5, have been replaced by two large-diameter concentric filament connections. The grid structure shown in Figure 10 also is mounted on a sturdy 8-inch diameter copper plate. This type of structure is ideally suited for cavity type circuits, but also is essential for accurate alignment of grid and cathode structures in such large tubes.

No Discussion

Equivalent Continuous Current for Groups of Variable Loads

W. K. BOICE
MEMBER AIEE

THE current rating of most electric equipment is a selected value of continuous current which will not cause excessive temperature rise. For d-c equipment it is a constant current. For a-c equipment it is usually a sinusoidal current with the same rms value for every cycle. In most cases, a variable load will not cause excessive temperature rise if its rms value does not exceed the rated current. This procedure is satisfactory if this rms value of the variable load is applicable to a time interval roughly comparable to the time for full temperature rise to be reached, and further, overloads during this interval are of relatively short duration.

Often each variable load repeatedly follows a fairly definite pattern of short duration. Examples include resistance welders, arc welders, looms, presses, and elevators. For such cases, the rms current for each load can be evaluated over one typical repetition of the complete load pattern. Each such rms current may be called the equivalent continuous current for the individual variable load.

When a group of such loads operate independently but are supplied from a common power source, the required rating of power supply equipment, such as transformers or feeder cables, is dependent upon the total current to the group. The equivalent continuous total current to such a group of variable loads is not equal to the sum of the equivalent continuous currents for the individual loads. This paper shows how the equivalent continuous value for the total current can be calculated from data for the individual loads.

Methods previously presented[1,2] apply only to loads with simple and identical load patterns. The method of this paper may be used for groups of loads with diverse magnitudes and load patterns.

Some examples are presented. These are all concerned with resistance welders, but the procedures they illustrate can be applied to other types of loads.

Individual Loads

Procedures for calculating the equivalent continuous current for an individual load are well known. A typical procedure for an a-c load is as follows:

1. Find the squares of all the rms a-c values during a typical load pattern.
2. Multiply each square by the duration of its occurrence.
3. Add all the products, of current-squared times time.
4. Divide by the total time, including any time of zero current.
5. Take the square root.

For simple load patterns, simpler procedures are possible. For example, consider a resistance welder having a single value of rms demand current during the weld time, and zero current until the beginning of the next weld. In this case the equivalent continuous current is the demand current multiplied by the square root of the duty cycle. The duty cycle in this case is defined as the ratio of weld time to total time. Suppose the current to the welder is expressed in kilovolt-amperes, the demand being 200 kva, and the duty cycle is 25 per cent. The equivalent continuous load for this machine is 200 times the square root of 0.25 or $200\times 0.5=100$ kva.

Groups of Loads

The equivalent continuous total current to a group of variable loads is less than the sum of equivalent currents for the individual loads, if these loads operate independently. It would equal this sum if all the loads had similar patterns and operated exactly together. The chance that this will happen with independent loads is ordinarily quite negligible. Occasionally it does happen, but this condition does not last long enough to affect the rating required of power supply equipment.

If overlapping of load currents is prevented, as when intermittent loads are interlocked, the equivalent continuous total current is equal to the square root of the sum of the squares of the equivalent currents of the individual loads.

When loads operate independently, without interlocking, their load patterns will coincide only occasionally. The equivalent continuous total current will then be less than the sum, but more than the square root of the sum of the squares, of the individual currents. Its value will depend upon the probabilities of all possible total current values. Fortunately it is not necessary to calculate these probabilities. Instead, relatively simple procedures are presented, which make use of the concept of standard deviation, taken from probability theory.

This paper includes a number of statements which are based upon fundamental probability theory. Justification for these statements may be found in reference 3.

Standard Deviation

The standard deviation is[3] the root mean square of all random deviations from the average load. It is analogous to a radius of gyration. Any equivalent continuous load also is a rms value, which is analogous to a radius of gyration about

---

Paper 51-356, recommended by the AIEE Electric Welding Committee and approved by the AIEE Technical Program Committee for presentation at the AIEE Fall General Meeting, Cleveland, Ohio, October 22–26, 1951. Manuscript submitted March 29, 1951; made available for printing September 4, 1951.

W. K. Boice is with the General Electric Company, New Haven, Conn.

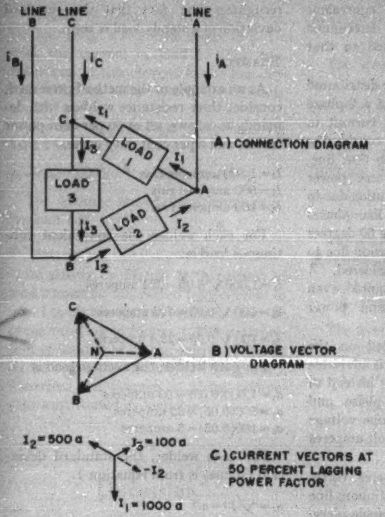

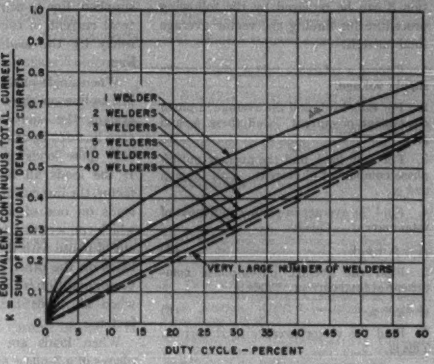

Figure 1 (left). Distribution of single-phase line-to-line loads on a 3-phase system

Figure 2 (above). Equivalent continuous total current for a group of resistance welders. (All welders alike) Single-phase welders supplied from a single-phase system

the axis of zero current. The displacement between the axes of these two radii of gyration is equal to the average load.

The most probable[3] value for the standard deviation for the total load is equal to the square root of the sum of the squares of the standard deviations of the individual loads, if they operate independently.

Average Load

The average load is[3] the average of variations which may occur independently. For an a-c load it is the average of all rms a-c values, rather than the average of instantaneous values.

As an illustration of average current, consider a resistance welder with a demand of 1,000 rms amperes and a duty cycle of 10 per cent. For this simple load pattern, the average current is the product of demand times duty cycle. Hence the average load is 100 amperes.

The average total current is[3] the sum of the average currents of the individual loads.

Repetitions of Load Pattern

In any selected time interval, the rms total current may not exactly equal the equivalent continuous total current. However if each load repeats its load pattern many times during the time interval, the equivalent current will[3] very probably be quite closely approached. Consequently the method presented is most applicable when the time for each complete load pattern is much less than the time for full temperature rise to be reached by the power supply equipment. It is not necessary for the number of loads to be large.

Procedure for Groups of Loads

The following procedure can be used to calculate the equivalent continuous total current to a group of independent d-c loads or a group of independent a-c loads whose power factors can be assumed to be constant and alike.

1. Calculate the equivalent continuous current for each load. Call these values i_1 and i_2, ... for the various loads.

2. Calculate the average current for each load. (For a-c loads this is the average of rms values.) Call the average currents a_1 and a_2 ...

3. For each load calculate the standard deviation. By analogy with the relationship[4] between radii of gyration, the following formula may be used[3] for finding the standard deviation (sigma) for an individual load current.

$$\sigma_1=\sqrt{i_1^2-a_1^2} \tag{1}$$

4. Calculate the standard deviation for the total current to the group of loads, using the following[3] formula:

$$\sigma_T=\sqrt{\sigma_1^2+\sigma_2^2+\ldots} \tag{2}$$

5. Calculate the average total current. This is

$$a_T=a_1+a_2+\ldots. \tag{3}$$

6. Calculate the equivalent continuous total[3] current, as follows:

$$i_T=\sqrt{\sigma_T^2+a_T^2} \tag{4}$$

Loads with Different Power Factors

When the power factors of individual a-c loads are not all alike, equation 3 for the total average current is not valid. Instead the vector sum of the average currents should be used.

When the power factor of an individual a-c load varies with time, its average current, designated by a_1 in equations 1 and 3, should be the vector average. This vector average is obtained by adding vectorially the products of current times duration of occurrence, before dividing by total time to obtain the average. When power factor varies with time, the vector average is less than the arithmetic average in the same way that the resultant of two vectors can be less than their arithmetic sum.

To facilitate vector additions, it is convenient to consider separately components which are at right angles to each other. Probability relationships analogous to equations 1 to 4 then apply[3] to each of these components. Since the resultant of such components is the square root of the sum of their squares, the equations 1, 2, and 4 can be expressed in terms of summations of squares of components, and consequently, they are applicable to vector resultant currents, if vector average currents are used. Equation 3 can be replaced by the following procedure for finding the vector average total current.

1. Choose a reference vector, such as the supply voltage.

2. For each load, find the average in-phase component of current. Call these p_1 and $p_2 \ldots$

3. For each load, find the average out-of-phase component of current. Call these q_1 and $q_2 \ldots$

4. Find the average in-phase component of total current. This is

$$p_T = p_1 + p_2 + \ldots \qquad (5)$$

5. Find the average out-of-phase component of total current. This is

$$q_T = q_1 + q_2 + \ldots \qquad (6)$$

6. Find the vector average total current. This is

$$a_T = \sqrt{p_T^2 + q_T^2} \qquad (7)$$

Power and Reactive Kilovolt-Amperes

The line voltage of a single-phase system and a line-to-neutral voltage of a 3-phase system are convenient reference vectors. When one of these is used, the in-phase component of the corresponding line current is proportional to power, while the out-of-phase component is proportional to reactive kilovolt-amperes.

Sign of Components

Any of the components described in the preceding discussion can have[3] a positive or negative sign.

An in-phase component is customarily considered as positive if it corresponds to power input to a load. Sometimes a load such as a loom can return power to the supply during part of its load pattern. The in-phase component of current corresponding to the returning power should bear a negative sign to permit correct calculation of the average in-phase component.

Positive reactive kilovolt-amperes can be designated as that corresponding to the out-of-phase component of current to a load of lagging power factor. The current to a load with a leading power factor then has an out-of-phase component with a negative sign.

Number of Phases

The procedures which have been described apply to single-phase loads on a single-phase system, 3-phase loads on a 3-phase system, and single-phase loads all on one line-to-line phase of a 3-phase system. When single-phase loads are supplied line-to-neutral, the equivalent total current in each line is determined solely by the loads connected to that line.

When single-phase loads are distributed line-to-line on three phases of a 3-phase system, the equivalent total current in each line can be calculated by considering only those loads connected to that line. If the loads all have the same power factor, the line current contribution due to loads on one of the line-to-line phases which connect to a line will be 60 degrees out of phase with the contribution due to loads on the other phase considered. A vector addition is therefore required, even when all loads have the same power factor.

When loads are distributed on the phases of a 3-phase system, it is advisable to express current in amperes instead of kilovolt-amperes, because 3-phase and single-phase circuits of the same voltage have different values of kilovolt-amperes per ampere.

The 3-phase kilovolt-amperes corresponding to the equivalent continuous line current to a group of similar single-phase loads distributed evenly among three line-to-line phases is slightly greater than the equivalent continuous kilovolt-amperes for these same loads connected to a single-phase supply. When the loads cannot be evenly distributed, a still greater equivalent kilovolt-ampere is required of a 3-phase system. When the number of variable loads is very large, however, the required single-phase and 3-phase kilovolt-amperes values approach each other.

Similar Loads

When all loads are alike, it is possible to plot the equivalent continuous total current as affected by number of loads. Figure 2 shows how the number of machines and the duty cycle of a group of resistance welders affect the equivalent continuous total current.

Steady Loads

If a group of variable loads is combined with a steady load, such as an industrial heating load, the resulting equivalent continuous current will be less than the sum of the steady load plus the equivalent current for the group of variable loads.

A precise result can be obtained by adding the steady current, vectorially, to the average total current of the variable loads, and then following the procedures already described. This merely recognizes the fact that the standard deviation of a steady load is zero.

EXAMPLE

As an example of the method presented, consider three resistance welders with demands as follows, all at 50 per cent power factor, and 5 per cent duty cycle.

$I_1 = 1{,}000$ amperes rms
$I_2 = 500$ amperes rms
$I_3 = 100$ amperes rms

For each welder the equivalent continuous load is:

$$i_1 = 1{,}000\sqrt{0.05} = 224 \text{ amperes}$$

$$i_2 = 500\sqrt{0.05} = 112 \text{ amperes}$$

$$i_3 = 100\sqrt{0.05} = 22.4 \text{ amperes}$$

For each welder, the average load is

$a_1 = 1{,}000(0.05) = 50$ amperes
$a_2 = 500(0.05) = 25$ amperes
$a_3 = 100(0.05) = 5$ amperes

For each welder, the standard deviation (sigma) is from equation 1.

$$\sigma_1 = \sqrt{i_1^2 - a_1^2}$$
$$= \sqrt{(224)^2 - (50)^2} = 218 \text{ amperes}$$

$$\sigma_2 = \sqrt{(112)^2 - (25)^2} = 109 \text{ amperes}$$

$$\sigma_3 = \sqrt{(22.4)^2 - (5)^2} = 21.8 \text{ amperes}$$

The standard deviation for the total current is, from equation 2.

$$\sigma_T = \sqrt{\sigma_1^2 + \sigma_2^2 + \sigma_3^2}$$
$$= \sqrt{(218)^2 + (109)^2 + (21.8)^2} = 245 \text{ amperes}$$

If the welders are connected to a single-phase supply, the average total current is, from equation 3.

$$a_T = a_1 + a_2 + a_3$$
$$= 50 + 25 + 5 = 80 \text{ amperes}$$

For this case, the equivalent continuous total load is, from equation 4.

$$i_T = \sqrt{\sigma_T^2 + a_T^2}$$
$$= \sqrt{(245)^2 + (80)^2} = 258 \text{ amperes}$$

For a 440-volt single-phase circuit, this is 113 kva.

If the three welders had been connected to a 3-phase system, each to a different line-to-line phase, the maximum equivalent continuous line current would be that for the line to which the two larger machines connect (since all machines have the same duty cycle). If we call this line A, as in Figure 1, the deviation of its current is, from equation 2

$$\sigma_A = \sqrt{\sigma_1^2 + \sigma_2^2}$$
$$= \sqrt{(224)^2 + (112)^2} = 244 \text{ amperes}$$

In order to obtain the average current, we may select a reference vector in phase with the current in load 1. The contributions of this current to the line current will then be as follows (for d = duty cycle).

The average in-phase component for load 1 is

$$p_1 = I_1 d_1 = 1{,}000(0.05) = 50 \text{ amperes}$$

The average out-of-phase component, for load 1 is

$$q_1 = 0$$

As shown by Figure 1(A), current of load 2 must be subtracted from current of load 1 to obtain current in line A. For the phase rotation of Figure 1, the contribution of load 2 leads the reference vector by 60 degrees as shown by Figure 1(C). Therefore the average in-phase component contributed by load 2 is

$$p_2 = I_2 d_2 \cos 60° = 500(0.05)(0.500) = 12.5 \text{ amperes}$$

The average out-of-phase component is

$$q_2 = -I_2 d_2 \sin 60° = -500(0.05)(0.866) = -21.6 \text{ amperes}$$

The average in-phase total current is from equation 5

$$p_T = p_1 + p_2 = 50 + 12.5 = 62.5 \text{ amperes}$$

The average out-of-phase total current is, from equation 6

$$q_T = q_1 + q_2 = 0 - 21.6 = -21.6 \text{ amperes}$$

The average total current of line A is, from equation 7

$$a_T = \sqrt{p_T^2 + q_T^2} = \sqrt{(62.5)^2 + (-21.6)^2} = 66.2 \text{ amperes}$$

The equivalent continuous total current of line A is, from equation 4

$$i_A = \sqrt{\sigma_T^2 + a_T^2} = \sqrt{(244)^2 + (66.2)^2} = 252 \text{ amperes}$$

For a 440-volt 3-phase circuit, this corresponds to 193 kva.

References

1. L'Application du Calcul des Probabilities aux Reseaux de Distribution D'energie Electrique ou de Fluides, C. Volff. *Revue Generale de l'Electricite* (Paris, France), volume LIV, April 1945, pages 122–24.

2. The Design of Low-Voltage Welding Power Distribution, C. A. Adams, J. R. Fetcher, A. C. Johnson. *AIEE Transactions*, volume 63, 1944, pages 1180–90.

3. Introduction to Mathematical Probability, Uspensky. McGraw Hill Book Company, New York, N. Y., 1937.

4. Handbook of Engineering Fundamentals, Eschbach. John Wiley and Sons, New York, N. Y., 1936.

Discussion

Myron Zucker (Myron Zucker Engineering Co., Detroit, Mich.): The method presented in Mr. Boice's paper is applicable to a-c only when harmonics are negligible. Can the method be extended to include consideration of harmonics? In the resistance welding field, harmonics can be appreciable in some cases. Harmonics are introduced at reduced heat settings when electronic heat control is used. Harmonics appear in the a-c line current to frequency-changer welders. Harmonics also appear in the current to flash welders during flashing. Arc welding currents contain harmonics.

W. K. Boice: The method of my paper can be extended to include the effect of harmonics. It is usually necessary to have advance knowledge of the nature and probable magnitudes of the harmonics associated with each variable load. Each expected harmonic frequency should be considered separately and treated in exactly the same manner as the fundamental currents, thus obtaining the equivalent continuous total value for each harmonic. The squares of such values for all harmonics can be added to the square of the corresponding fundamental current to obtain the square of the total equivalent current. If the wave shape of all loads is constant and alike, the proportion of total current contributed by harmonics will be the same as for the individual loads. In many cases, harmonics can be safely neglected.

Annual Carrying Charges in Economic Comparisons of Alternative Facilities

PAUL H. JEYNES
MEMBER AIEE

THE EXPRESSION economic comparison of alternative facilities means an estimate of the effect on future revenue requirements of adopting one plan of action instead of some alternative. The economic choice is the plan which will result in minimum revenue requirements–that is, the minimum compensatory selling price–after all costs have been covered, including an adequate return to owners of the business.

It is admittedly difficult to anticipate future variations in some of the essential factors in an economic study–factors such as future costs of money, tax rates, and average lives–just as it is difficult for the engineer designing transmission lines to anticipate future peak loads, load factors, and power factors. But in either case, the final result associated with a given set of initial assumptions is definite and factual; the arithmetic of economic comparisons is just as clear-cut and rigorous as Ohm's law.

The present paper deals with the appropriate treatment of four annual costs often inaccurately referred to as "fixed charges," namely:

1. Return on the investment.
2. Depreciation.
3. Taxes.
4. Insurance.

Other basic considerations involved in economic comparisons, including the estimate of investment costs and operation and maintenance expense, as well as the evaluation of energy and capacity differentials, are discussed in companion papers.[1,2,3]

Return on the Investment

In view of the large amount of confusing literature dealing with costs of money, it seems advisable to stress the precise definition of the estimate of return on the investment. The objective is an estimate of the total dollars available for interest and dividends that the enterprise would earn in each future year under each of the various alternative plans.

By "interest" is meant the annual return paid on bonded indebtedness. In the long run, annual return is substantially interest on bonds plus dividends on stock, but earnings in excess of dividends actually paid should be included, as indicated. The resultant percentage is established by what investors have demanded and will require in order to attract capital to the enterprise.

Although the ultimate objective is an estimate of the return in dollars for each separate year of the study, ordinarily the investigator must be content to predict a single level average rate for the whole period of comparison. The desired rate for any given year may be specifically defined as the ratio a/b, where:

a = interest paid plus earnings available for dividends in the given year
b = net capital originally obtained by the utility from issuance of all securities outstanding in that year

Clearly this rate is not, as sometimes erroneously concluded, the return on the particular securities issued at the time the project is contemplated. Nor is it the rate of return on current market price of the utility's securities.

The question sometimes raised whether the rate of return should be regarded as compounded annually or at shorter intervals is rather academic quantitatively. If quantity a is taken to represent the single annual total without part-year compounding of interim payments, then annual compounding is the consistent assumption in all other applications.

Sound judgment as to the probable future rate of return has its foundation in a survey of past and present earnings of the company, attitudes of regulatory authorities, and trends in the money market. Reflecting the relatively steady and prolonged decline in interest rates over more than a decade, the survey of past experience will usually show a downward trend. A projection of that trend is then called for, since the objective is an estimate of the rate applicable over the future period of comparison.

A convenient alternative to this rather involved research project is to base the estimate, instead, on the stream of commission and court orders specifying permissible rates of return on the rate base. Although the long-term trend of the adjudicated return has been downward, the range of post-war values has been fairly narrow. A "fair rate" below 5 per cent or above 7 per cent is rather extraordinary.

Frequently the fair rate of return adjudged applicable to the rate base is substantially less than the actual rate of return applicable to first cost. In one recent important and well-documented case, the allowed return of 5.7 per cent on the rate base corresponded to an actual return of more than 7 per cent on first cost. A thorough explanation of this difference is beyond the scope of this paper; the two major reasons for it will be discussed briefly.

First is the effect of rising price levels. In many jurisdictions, consideration is given to effects of reproduction cost in arriving at the rate base. The effect on rate of return is obvious; having arrived at the rate believed appropriate for application to the rate base, it is necessary to multiply by the ratio of (rate base)/(original investment cost) to obtain the proper rate for application to the original cost.

Paper 51-358, recommended by the AIEE System Engineering Committee and approved by the AIEE Technical Program Committee for presentation at the AIEE Fall General Meeting, Cleveland, Ohio, October 22–26, 1951. Manuscript submitted May 24, 1951; made available for printing August 30, 1951.

PAUL H. JEYNES is with Public Service Electric and Gas Company, Newark, N. J.

Table I. Computation of Annual Cost of Depreciation

6 Per Cent Present-Worth Method, Group Basis, Yielding the Weighted Average Annual Rate = d%. 30-Year Average Life; Iowa Type R_1 Dispersion

Columns						
1 Year	2 Jan. 1 Survivors	3 Mean Survivors	4 Annual Return, Per Cent	5 Present Worth Factors	6 Present Worth of Annual Return, Per Cent	7 Present Worth of Annual Cost of Depreciation, Per Cent
1	1.0000	0.9956	6.0000	0.9434	5.6604	0.9392d
2	0.9913	0.9867	5.9478	0.8900	5.2935	0.8782d
3	0.9821	0.9774	5.8926	0.8396	4.9474	0.8206d
4	0.9726	0.9676	5.8356	0.7921	4.6224	0.7664d
etc.	etc.	etc.	etc.	etc.	etc.	etc.
57	0.0103	0.0082	0.0618	0.0361	0.0022	0.0003d
58	0.0061	0.0045	0.0366	0.0341	0.0012	0.0002d
59	0.0029	0.0015	0.0174	0.0321	0.0006	0.0000d
60	0.0001	0.0000	0.0006	0.0303	0.0000	0.0000d
	Totals	30.0000			76.3645	12.6099d

Explanation

Column 2:	Survivors at the beginning of each year for 30-year life, type R_1 dispersion, from *Bulletin 156*, Iowa Engineering Experiment Station, Iowa State College, Ames, Iowa.
Column 3:	Mean survivors computed as the arithmetic mean of successive January 1 values for Column 2. The total of Column 3 equals average life.
Column 4:	Annual return at 6 per cent of January 1 survivors (= 0.06 × Col. 2).
Column 5:	Present-worth factor at 6 per cent = $^1/_{1.06^n}$, where n = number of years per Col. 1. Obtainable from standard interest tables.
Column 6:	Col. 4 × Col. 5.
Column 7:	Annual depreciation at d% of mean survivors multiplied by present-worth factor (= Col. 3 × Col. 5 × d%).

Solution for d%

Since the present worth of future annual costs for depreciation plus return throughout life is always 100% (of first cost):

$$76.3645\% + 12.6099d\% = 100.0000\%$$
$$d = 1.874\%$$

This is the depreciation annuity if net salvage is zero. If net salvage is s% (of first cost, installed), the adjusted annuity is $d(100-s)/100$.

A second factor which makes the rate base greater than the original investment cost is the manner of treating depreciation reserves when establishing the rate base. Simply deducting 100 per cent of the reserves amounts to recognizing that by reinvesting these funds in the business the company avoids issuing a corresponding amount of securities on which a return would have to be paid, with consequent savings in annual costs.

Such reinvestment in the enterprise involves a risk which could be avoided by investing the reserves, instead, in securities suitable for trust funds. Regulatory authorities recognize that this course, while giving the investor greater security, also would increase rates, because these "riskless" securities earn perhaps 50 per cent less than an equal investment in the utility itself. Accordingly, management is induced to reinvest reserves in the property by being allowed a moderate increase in the rate of return commensurate with the greater risk.

Some commissions, as in Missouri and Louisiana, accomplish their purpose by stipulating a "gross plant" rate base (that is, the depreciation reserve is not deducted from total plant investment), and a return on the reserves is computed at a lower rate than the stipulated rate of return. This is equivalent to deducting less than 100 per cent of the reserve and allowing the higher rate of return on the resultant rate base, which is a familiar alternative.

In order to reflect the effect of such procedures on annual costs, some writers compute the depreciation annuity by assuming that the rate of return on reinvested reserves is less than the rate of return on original capital investment. This approach in economic studies should be discouraged for several reasons, as follows:

1. It is not a faithful version of the actual cost behavior. Reinvested reserves take the place of security issues in the amount of the reserve, which would earn the same return as that applicable to original investment. The whole purpose of these rate-base procedures is to justify a higher rate of return on original investment than if reserves were not reinvested.

2. Because it underestimates the true rate of return, it introduces an error into the estimate of taxes.

3. It complicates present-worth calculations, which are an essential part of most studies. Present worths must be computed at the true annual cost of money, not at the rate of return on the rate base.

As an index to the magnitude of this effect (that is, the increase in rate of return resulting from reinvestment of the reserve with its associated risks), a rate of 6 per cent applicable to the rate base might approach 6.7 per cent of first cost, from this cause alone. The method of estimating the true rate of return on original investment, given the rate applicable to the rate base obtained by treating the reserve as described, is outlined in the Appendix.

Depreciation

The appropriate method of calculating annual costs of depreciation is not a matter of opinion; the proper arithmetic is perfectly clear and precise. Annual cost of depreciation is a function of:

1. Average life in years.

2. The type of dispersion (that is, the manner in which individual retirements are scattered about average life).

3. Net salvage when finally retired.

4. The rate of return on investment.

Such considerations as obsolescence, inadequacy, wear and tear, action of the elements, requirements of civil authorities, maintenance standards, et cetera, are completely irrelevant except as they may help to establish average life or type of dispersion. The company's method of accounting for depreciation, whether it may be "straight-line," compound interest, sinking fund, percentage of sales, is of no moment whatever; the level annual cost of depreciation is entirely independent of such matters.[3]

The common method of applying the "straight-line" procedure, estimating an-

Table II. Short-Cut Computation of Annual Cost of Depreciation

6% Present-Worth Method, Group Basis Yielding the Weighted Average Annual Rate = d%. 30-Year Average Life; Iowa Type R_1 Dispersion

Column			
1 Year	2 Mean Survivors	3 Present Worth Factors at 6%	4 Present Worth of Mean Survivors Col. 2 × Col. 3
1	0.9956	0.9434	0.9392
2	0.9867	0.8900	0.8782
3	0.9774	0.8396	0.8206
4	0.9676	0.7921	0.7664
etc.	etc.	etc.	etc.
57	0.0082	0.0361	0.0003
58	0.0045	0.0341	0.0002
59	0.0015	0.0321	0.0000
60	0.0000	0.0303	0.0000
		Total	12.6099

$$d = \left(\frac{100}{\text{Total Col. 4}} - \text{Percentage return}\right) \Big/ \left(1 + \frac{\text{Percentage return}}{200}\right)$$

$$= \left(\frac{100}{12.6099} - 6.00\right)/1.03$$

$$= 1.874 \text{ per cent}$$

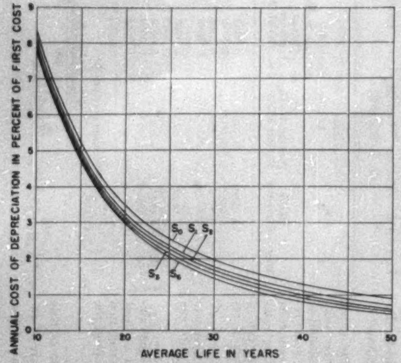

Figure 1. Depreciation annuities, Iowa Type S dispersions at 5 per cent return

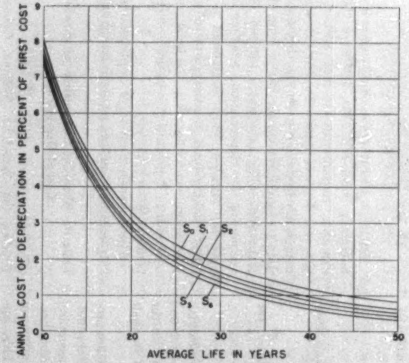

Figure 2. Depreciation annuities, Iowa Type S dispersions at 6 per cent return

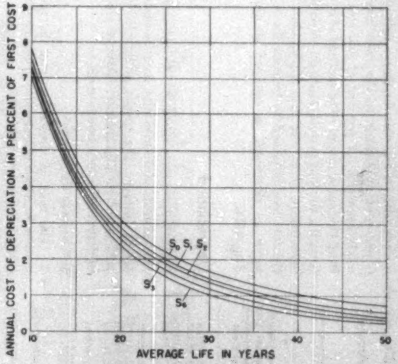

Figure 3. Depreciation annuities, Iowa Type S dispersions at 7 per cent return

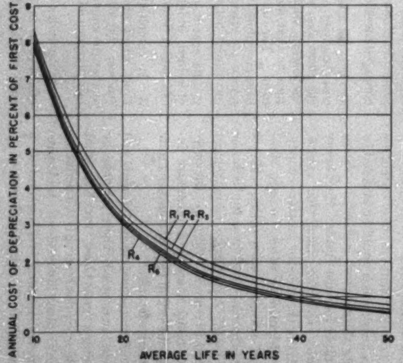

Figure 4. Depreciation annuities, Iowa Type R dispersions at 5 per cent return

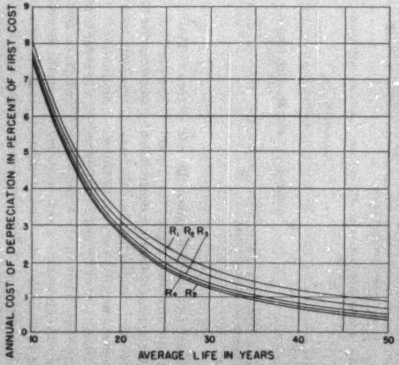

Figure 5. Depreciation annuities, Iowa Type R dispersions at 6 per cent return

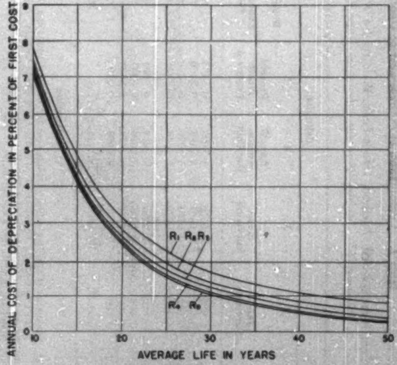

Figure 6. Depreciation annuities, Iowa Type R dispersions at 7 per cent return

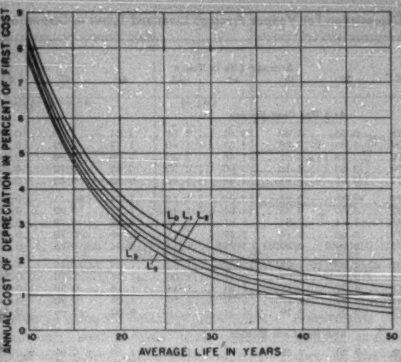

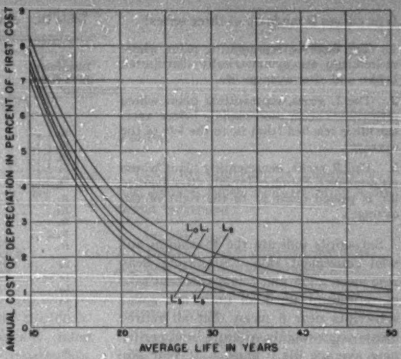

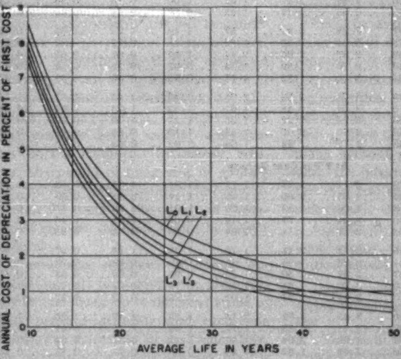

Figure 7 (above, left). Depreciation annuities, Iowa Type L dispersions at 5 per cent return

Figure 8 (left). Depreciation annuities, Iowa Type L dispersions at 6 per cent return

Figure 9 (above, right). Depreciation annuities, Iowa Type L dispersions at 7 per cent return

nual cost of depreciation as the reciprocal of average life applied to original investment, is a gross error in arithmetic; it does not reflect the cost behavior that results from the accountant's "straight-line" bookkeeping. The assumption that "straight-line" depreciation must be associated with average interest (that is, the full rate of return in the first year only, declining in each year to zero at the end of life) also is an incorrect version of actual cost behavior although sometimes proposed as a rough approximation.

Table I, which is self-explanatory, describes the computation of the level annual cost of depreciation. This procedure is known as the "present-worth method, group basis"; it yields the percentage which, applied to the original cost of survivors in each year, will exactly recoup the first cost of plant in its lifetime. A less obvious but equally rigorous method of computation appears in Table II; it reduces the number of calculations by 50 per cent, once mean survivors have been established.

Computations were actually made in the manner of Table II for average lives of 10, 20, 30, 40, and 50 years, with return at 5, 6, and 7 per cent, and for 15 types of dispersion. Figures 1 to 9, inclusive, were then prepared, and values were read from the plotted curves for lives of 15, 25, 35, and 45 years to complete Table III.

As in most economic problems, there is no question as to the correct depreciation arithmetic; the major difficulty lies in the selection of reasonable starting assumptions, particularly as to average life and type of dispersion. Both of these items, being estimates of future behavior which will not necessarily duplicate past performance, are matters for fully informed judgment based on a survey of actual experience to date.

Within the past decade, great advances have been made in the art of estimating the life of physical plant. Although these developments have been largely the work of engineers, they may have escaped the attention of the profession because their sponsors have usually been accountants.

Choice of a statistical method for making life studies depends upon the nature of the records available, but the so-called "simulation" methods are most useful because:

1. They utilize data ordinarily available from the books of account.
2. They reveal not only average life but the type of dispersion.
3. They provide means for testing the trustworthiness of the estimate.[4,5,6]

A thorough discussion of life estimates is beyond the scope of this paper, but a few words appear necessary on the perhaps unfamiliar subject of retirement dispersion. As in the case of human mortality, some units in every group have longer lives, some shorter, than the average. Plotting survivors, in per cent of the original group, against age in years, produces the "survivor curve". As Table III demonstrates, the shape of the survivor curve has an important bearing on the costs of depreciation. For example, a change in type of dispersion from R_1 to R_5 may have approximately the same effect as a change of 10 years in estimated life, as shown in Table IV.

Authoritative contributions on this subject have been made by several groups and individuals.[7–13] A codified system for classifying types of dispersion has been developed by the Iowa Engineering Experiment Station, Iowa State College.[14,15,16] Commonly referred to as the "Iowa Type Curves," this system has become widely accepted, and is used in the present paper.

Briefly described, the Iowa family of 18 type curves is made up of three series:

1. The S series, representing plant whose retirements are symmetrically distributed before and after average life.
2. The L series, representing plant whose retirements occur more rapidly before average life is reached (that is, to the left of the average).
3. The R series, representing plant whose retirements occur more rapidly after average life is passed (that is, to the right of the average).

Table III. Annual Cost of Depreciation For Various Average Lives and Types of Dispersion

Dispersion (Iowa Type)	10	15	20	25	30	35	40	45	50
				Average Life in Years					
				At 5 Per Cent Return					
S_0	8.33	5.28	3.51	2.58	2.01	1.59	1.31	1.10	0.93
S_1	8.14	5.04	3.32	2.38	1.81	1.40	1.13	0.92	0.75
S_2	8.00	4.86	3.18	2.27	1.68	1.30	1.00	0.80	0.64
S_3	7.91	4.82	3.09	2.16	1.60	1.20	0.92	0.72	0.57
S_6	7.78	4.77	3.03	2.07	1.48	1.09	0.82	0.64	0.48
R_1	8.32	5.27	3.51	2.56	2.00	1.58	1.34	1.11	0.96
R_2	8.11	5.03	3.30	2.38	1.81	1.42	1.13	0.92	0.76
R_3	7.96	4.85	3.14	2.21	1.65	1.25	0.98	0.78	0.62
R_4	7.87	4.77	3.06	2.14	1.58	1.18	0.90	0.70	0.55
R_5	7.81	4.75	2.99	2.07	1.51	1.12	0.84	0.65	0.50
L_0	8.74	5.62	3.90	2.95	2.36	1.93	1.63	1.40	1.22
L_1	8.43	5.28	3.59	2.67	2.11	1.68	1.37	1.15	0.96
L_2	8.20	5.11	3.37	2.42	1.85	1.44	1.15	0.93	0.77
L_3	8.03	4.91	3.20	2.27	1.70	1.30	1.01	0.80	0.64
L_5	7.83	4.77	3.01	2.10	1.52	1.13	0.86	0.66	0.51
				At 6 Per Cent Return					
S_0	8.05	4.92	3.30	2.39	1.85	1.45	1.19	0.99	0.84
S_1	7.82	4.77	3.10	2.18	1.62	1.24	0.98	0.78	0.64
S_2	7.65	4.57	2.88	2.04	1.47	1.12	0.84	0.67	0.51
S_3	7.55	4.50	2.80	1.91	1.37	1.00	0.75	0.56	0.44
S_6	7.39	4.33	2.66	1.77	1.25	0.87	0.64	0.45	0.34
R_1	8.04	4.97	3.28	2.41	1.87	1.49	1.23	1.05	0.89
R_2	7.79	4.75	3.05	2.20	1.62	1.28	0.99	0.82	0.66
R_3	7.61	4.59	2.87	2.00	1.44	1.07	0.82	0.65	0.50
R_4	7.50	4.49	2.76	1.89	1.34	0.97	0.72	0.55	0.42
R_5	7.43	4.38	2.69	1.82	1.27	0.92	0.66	0.49	0.36
L_0	8.53	5.49	3.75	2.82	2.25	1.83	1.55	1.32	1.15
L_1	8.16	5.10	3.39	2.48	1.91	1.52	1.23	1.04	0.86
L_2	7.90	4.86	3.13	2.22	1.66	1.26	1.00	0.80	0.65
L_3	7.69	4.68	2.93	2.05	1.48	1.10	0.84	0.66	0.51
L_5	7.45	4.42	2.71	1.83	1.29	0.92	0.68	0.50	0.37
				At 7 Per Cent Return					
S_0	7.78	4.79	3.11	2.22	1.71	1.31	1.09	0.88	0.76
S_1	7.52	4.54	2.85	2.00	1.46	1.11	0.86	0.69	0.55
S_2	7.33	4.33	2.66	1.89	1.29	1.01	0.70	0.57	0.41
S_3	7.20	4.20	2.54	1.71	1.18	0.85	0.61	0.45	0.34
S_6	7.02	4.03	2.37	1.54	1.04	0.70	0.50	0.35	0.25
R_1	7.78	4.85	3.13	2.28	1.75	1.38	1.15	0.97	0.83
R_2	7.48	4.51	2.83	1.99	1.46	1.10	0.88	0.70	0.58
R_3	7.27	4.27	2.62	1.80	1.26	0.93	0.69	0.53	0.41
R_4	7.15	4.19	2.50	1.65	1.14	0.79	0.59	0.42	0.32
R_5	7.06	4.10	2.41	1.57	1.07	0.73	0.52	0.37	0.27
L_0	8.35	5.40	3.62	2.72	2.15	1.73	1.47	1.25	1.09
L_1	7.92	4.92	3.21	2.33	1.77	1.39	1.13	0.91	0.75
L_2	7.60	4.60	2.90	2.04	1.49	1.12	0.87	0.69	0.55
L_3	7.36	4.40	2.68	1.82	1.29	0.93	0.71	0.53	0.41
L_5	7.09	4.10	2.44	1.62	1.15	0.77	0.54	0.40	0.28

*In per cent of first cost of investment, before adjustment for salvage.

Subscripts indicate the maximum annual retirement rate. Subscripts near zero mean a low and nearly constant rate of retirement until all units are gone; subscripts near 6 mean that all retirements occur rapidly within a brief period near average life. Thus, a 30-year life with Type S_0 dispersion means that retirements begin at an early age and continue at a nearly constant rate for 60 years, the rate being a maximum at age 30. On the other hand, a 30-year life with Type R_5 dispersion means that few retirements occur before age 20, after which retirements increase rapidly to a maximum rate near age 31, the last unit being retired at about age 40. Note that this is simply a generalized system of classifying curve shapes; it is not to be inferred that a given type curve is invariably associated with any specific class of plant or any particular industry.

It is usually discovered, on reviewing a company's experience, that many classes of plant do have a predictable dispersion type, well described by one of the Iowa type curves. Even when it can be demonstrated that past experience has not been entirely consistent, such surveys provide the basis for judgment in estimating the future.

Experience of different companies varies, of course, but for electrical plant, types approaching S_0 to S_2, and R_1 to R_3, appear to be most frequently encountered. Referring to Table III, it will be seen that this limits the estimate of depreciation expense within a quite narrow range; lacking any factual basis for estimate, it may be assumed that the dispersion type is of that order. Such an approach, though arbitrary, provides a more rational estimate than the usual alternative, that is, making the assumption that all units are retired exactly at average life, a phenomenon that virtually never occurs.

Even when estimating annual costs of a single unit of property, which obviously must be retired all at once, it is necessary to make allowance for dispersion of retirements. The explanation is that each individual unit must be regarded as conforming to the average behavior for the group to which it belongs; there is no statistical justification for any other treatment of the average-life estimate.

This also applies when the individual unit is the only one of its kind, so that the estimate represents probable, rather than average, life. For example, when the estimator places probable life at 30 years, he reasons somewhat as follows:

> "Less than 15 or more than 45 years is possible, but most unlikely. In fact, it will be rather disappointing if it lasts less than 20 years, and gratifying if it serves for 40. So, if I must commit myself to one most probable figure, the estimate is 30 years."

This is a good description of the normal curve of probability, with a mode at 30 and limits near 15 and 45 years. However, the most probable annuity is not that corresponding to 30-year life, with no dispersion. It is the annuity for 30-year life and the dispersion type whose frequency curve answers the quoted description—approximately Type S_3. Accordingly, it is recommended that Iowa Type S_3 be assumed to apply in estimating depreciation costs for a single unit when its group behavior is not determinate.

Table I indicates the manner of adjusting the depreciation annuity for net salvage; for example, if net salvage is expected to be 10 per cent of first cost, installed, then the adjusted annuity is 90 per cent of the unadjusted rate.

The allowance for salvage is usually small but reasonably predictable for many types of plant. For example, almost all utilities realize appreciable net salvage on retirement of transformers, overhead conductors, underground cable, and automobiles. Removal costs usually exceed

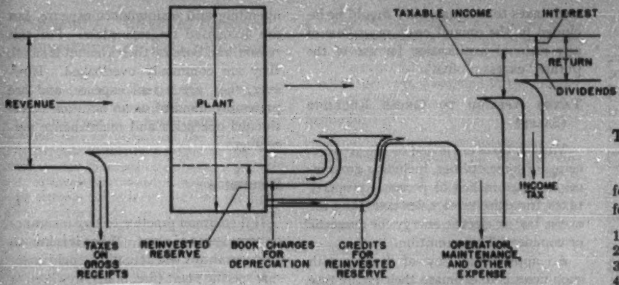
TAXABLE INCOME
INTEREST
RETURN
DIVIDENDS
REVENUE
PLANT
INCOME TAX
TAXES ON GROSS RECEIPTS
REINVESTED RESERVE
BOOK CHARGES FOR DEPRECIATION
CREDITS FOR REINVESTED RESERVE
OPERATION, MAINTENANCE, AND OTHER EXPENSE

Figure 10. Flow chart of annual costs

gross scrap value for buildings, generating equipment, switchboards and control equipment, poles, and towers; in such case, the salvage adjustment increases the depreciation annuity.

Land is customarily treated as nondepreciable for purposes of financial statements. Nevertheless, if the period of ownership is anything less than infinite, the annual costs of ownership do actually include the equivalent of depreciation costs, perhaps better called "amortization" in this instance. Ordinarily, however, the period of ownership is so long and "salvage" values so high that any allowance for costs in the nature of depreciation expense on land would be rather academic.

In preparing estimates of annual depreciation costs for a composite property, that is, one made up of different kinds of plant, perhaps including land, each type of property should be treated separately. The estimate of a single average life for the composite property introduces extremely complicated problems without any compensating advantages. If possible, the several types of plant should be grouped according to the standard classification of accounts, which is the usual convenient basis for statistical analyses of life experience.

In view of the fact that the great majority of textbooks seem to indorse the "straight-line" estimate of depreciation, it appears desirable to comment on the shortcomings of that procedure in economy studies.

Its outstanding defect is that the "straight-line" method does not result in a constant annual percentage. In the first year of life, the annual cost is equal to the bookkeeper's entry, which is the first cost divided by average life. (For convenience, zero net salvage is here assumed.) But in subsequent years, the bookkeeper divides average life into annual survivors (existing plant per the books), which are less than the original investment. In other words, the bookkeeping procedure automatically takes care of the dispersion of retirements, which fact must be recognized in the cost analysis.

Also, in every subsequent year, the accumulated reserve is reinvested in the property; it is not ordinarily returned to the investors, nor used to retire outstanding securities. Consequently, it does not reduce the return on original investment. But it does serve to acquire additional plant without issuing additional securities; the return on these avoided securities is a real saving, and it represents a reduction in the cost of depreciation.

Accordingly, under "straight-line" bookkeeping, the annual costs of depreciation consist of two components:

1. The bookkeeper's entry, equal to surviving investment divided by average life, less
2. The credit for return on security issues avoided by reinvestment (that is, the result of deducting reserves in obtaining the rate base).

The net result is a relatively high percentage cost in the early years, which decreases with age. The level weighted average of these nonuniform annual costs is exactly equal, to the penny, to the "present-worth method, group-basis" annuity described in this paper.

Computation of the true "straight-line" costs, year by year, is extremely laborious; the application of such a nonuniform rate to practical problems is awkward; precisely the same final answer to the economic comparison is obtained by use of the simpler approach here described.

On the rare occasions when reserves are actually invested in securities, it must be recognized that costs of depreciation are greater than if reinvested in utility's own plant. Present-worth computations, in such cases, require special consideration. A suggested treatment is outlined in the Appendix.

Taxes

Taxes are conveniently classified into four general types, each requiring a different treatment:

1. Income taxes.
2. Taxes applied to gross receipts (sales).
3. Real-estate and capital-stock taxes.
4. Payroll taxes.

INCOME TAXES

Income-tax laws may vary from time to time, with respect to both the tax rate and the statutory definition of taxable income. The present federal tax rate is 45 per cent; taxable income is substantially revenues less all operating and maintenance expenses, interest on bonded indebtedness including amortization of debt discount and expense, and taxes other than federal income tax. Depreciation allowance deductible is permissibly computed as the reciprocal of average life. In other words, income taxes are a function of the return on investment, but taxable income is not identical with annual return nor with net income.

It is, of course, impossible to anticipate with assurance either the future tax rate, or continuance of the present statutory basis for its computation; the estimator has no recourse except to rely on his fully informed judgment. However, to illustrate the proposed approach, let it be assumed that a weighted average future rate has been estimated at 40 per cent, and that taxable income will continue to be defined as at present.

$$\text{Taxable income} = (i+d-100/L)\times(1-Bb/i)+\text{Federal Income Tax}$$

where

i = annual rate of return, in per cent of investment
d = level depreciation annuity, in per cent of investment
L = average life, in years
B = ratio of bonds to total capitalization
b = rate of interest on bonds

Table IV. Annual Cost of Depreciation

From Table III: Return at 6 Per Cent

Average Life, Years	Type of Dispersion	Annual Cost of Depreciation
30	R_1	1.87
30	R_5	1.27
40	R_1	1.23

Then:

$$\text{Federal income tax} = \text{Statutory rate} \times \text{taxable income} = 0.40[(i+d-100/L) \times (1-Bb/i) + \text{Federal Income Tax}]$$

For example, if:

$i = 6.00$ per cent
$d = 1.90$ per cent
$L = 30$ years; $100/L = 3.33$ per cent
$B = 50$ per cent
$b = 4$ per cent

$$\text{Federal Income Tax} = 0.40[(6.00 + 1.90 - 3.33)(1 - 2.00/6.00) + \text{Federal Income Tax}] = 2.03 \text{ per cent of investment}$$

Two common errors with respect to income-tax estimates deserve attention. First is the opinion that they should be omitted entirely because they are a function of revenue rather than investment. Such reasoning overlooks the basic objective of the whole economic study—to estimate the difference in revenues arising from alternative installations.

Second is the view that maintenance costs constitute a source of income-tax savings. That is, an additional dollar of maintenance expense reduces taxable income, and hence reduces income taxes accordingly.

Reference to Figure 10 reveals the flaws in both conclusions. Annual revenues, coming in from the left, supply the annual costs tapped off at the right. The book charge to depreciation is the only item not actually disbursed to others; being plowed back into plant, as indicated, its net effect is found by subtracting credits for earnings on reinvested reserves. After deduction of all expenses, the remainder is available for return on the investment, partly tax-exempt interest. Income tax is applied to the taxable return.

Since it is annual return, and not revenue, that is a fixed percentage of investment under any alternative, the tax is obviously a function of the investment. Also an increase of one dollar in maintenance expense obviously increases the revenue requirement accordingly.

Many states levy income taxes. In such cases, it is necessary to ascertain the statutory definition of taxable income, particularly as to whether federal income tax is deductible. The computation is then performed in the same general manner as for the federal tax, above.

In the light of current attitudes of taxing bodies with respect to the definition of excess profits, it is probable that no provision should be made for excess profits taxes. However, should a statutory pattern evolve in the future which relates such taxes to earnings, they should be included in the annual costs regardless of any rational justification for use of the phrase "excess profits".

TAXES APPLIED TO GROSS RECEIPTS (SALES)

Various taxes are levied on the gross receipts of some utilities, including gross receipts taxes in lieu of personal property taxes, franchise taxes, sales taxes, and the excise tax on electric energy for domestic or commercial consumption.

An appropriate way of dealing with such taxes is to estimate their future rate in "per cent of gross receipts before gross receipts taxes"; the total of annual costs other than gross receipts taxes is then to be increased by that percentage.

The estimated tax rate, as a per cent of gross receipts, is readily converted into a percentage of first cost as follows, if desired.

Let:

T_g = tax rate in per cent of investment cost
G = tax rate in per cent of gross receipts
a = total annual costs, in per cent of investment costs, exclusive of gross receipts taxes

Then

$$T_g = G(a + T_g) = aG/(1-G)$$

As before, G is the weighted average rate anticipated throughout the period of comparison, which is not necessarily the same as the current rate.

REAL-ESTATE AND CAPITAL-STOCK TAXES

Little need be said concerning real-estate and capital-stock taxes beyond emphasizing the nature of the ultimate objective, that is, an estimate of the annual dollars actually payable under the alternative plans. As an annual rate, they are to be expressed as a percentage of investment cost. Thus, in the case of real-estate taxes, it is obviously incorrect to use the stated tax rate applicable to assessed value.

If future changes in the tax rate are predictable, the equivalent average rate throughout the period of comparison can be obtained by means of present-worth calculations discussed in a companion paper.[3]

PAYROLL TAXES

The so-called "payroll taxes" (federal old age benefits tax, federal unemployment insurance tax, state unemployment insurance tax) are assessed as a percentage of labor costs entering into operating and maintenance expense. They are not ordinarily included in book figures for operating and maintenance expense, but are accounted for separately. For this reason, and because their amount is small, they are commonly overlooked. However, they are a real expense, and are preferably handled as an addition to estimated operation and maintenance percentages.

Insurance

It is common practice to buy insurance on some types of plant. When it is known that premiums will actually be paid to insure specific plant (fire, boiler, flywheel, or plate glass insurance), the appropriate percentage to be included in annual charges for that particular plant is obtained by dividing the annual premium by the investment involved. The result is ordinarily substantially less than the stated premium rate, since the value insured is commonly considerably less than the first cost, and also decreases with age according to some arbitrary rule. The experience of the company in this regard, together with application of present-worth arithmetic, is the source of the appropriate percentage for the present application.

Other types of insurance quite unaffected by the choice of alternative installations, for example, public liability insurance, fidelity bonding, and the great bulk of self-insurance, should be ignored for the present purpose.

Conclusion

The phrase "annual carrying charges" is used herein to mean annual return on investment, depreciation, taxes, and insurance. These costs are most conveniently estimated and applied as a level annual percentage of first cost of the investment, the percentage being different for different types of plant. Also, changing economic conditions necessitate periodic reviews of such estimates; despite the familiar use of the term "fixed charges" to describe them, they do not necessarily remain a fixed percentage of first cost.

The ultimate objective of economic comparisons is to forecast the annual dollars of revenue that must be forthcoming in order to cover the costs involved in alternative plans, in other words, differential annual costs.

A sharp distinction must be observed between the rate-making process, which undertakes to allocate current costs on a nondiscriminatory basis, and actual cost behavior. The present paper describes and discusses appropriate methods of estimate.

Appendix. Effect of Reserve Reinvestment on Rate of Return

As noted in the text, it is the practice of some writers to estimate the return on reinvested reserves at a lower rate than the nominal rate of return on the rate base. The purpose of this is to reflect in the cost estimate the increased rate of return on first cost of investment which is associated with reinvestment of reserves in the utility's plant rather than in trust funds. An equivalent procedure is to apply the nominal rate of return to a rate base computed by deducting less than 100 per cent of reserves from total plant, instead of applying it to actual first cost.

The preferred procedure in economic comparisons, for the reasons noted, is to derive the actual rate of return on the investment, which also is the actual rate of return on reinvested reserves, and to ignore the nominal rate of return on the rate base. One important reason for this recommendation is the resultant simplification of present-worth calculations, which enter into almost all economic comparisons. The following section of this Appendix indicates how the actual rate of return on investment may be derived from an estimate of the nominal rate of return plus hypothetical depreciation, assuming reinvestment of reserves at the lower rate.

DERIVATION OF THE ACTUAL RATE OF RETURN ON INVESTMENT FROM THE RATE OF RETURN ON THE RATE BASE PLUS THE DEPRECIATION ANNUITY WHICH ASSUMES THAT THE RESERVE EARNS A LOWER RATE OF RETURN

Given:

i' = nominal rate of return (return on rate base) = 6.0 per cent

d' = depreciation annuity for reserve reinvested at 3.0 per cent (assume 30-year life, Iowa type S_0 dispersion, zero net salvage)
= 2.41 per cent, computed in the manner of Table I

Required:

i = actual rate of return on investment

d = depreciation annuity for reserve reinvested at i per cent (assume, as above, 30-year life, Iowa type S_0 dispersion, zero net salvage)

Solution:

$i' = 6.00\%$
$d' = 2.41$
$i' + d' = 8.41\% = i + d$

From Table III

If $i = 6.00\%$, $d = 1.85\%$ and $i + d = 7.85\%$
If $i = 7.00\%$, $d = 1.71\%$ and $i + d = 8.71\%$
Interpolating for $i + d = i' + d' = 8.41\%$:

$$\frac{8.41-7.85}{8.71-7.85}=\frac{0.56}{0.86}=0.65;$$

$$i = 6.00 + 0.65 = 6.65\%$$

$$0.65(1.85-1.71)=0.09;$$

$$d = 1.85 - 0.09 = \underline{1.76}$$

$$i + d = 8.41\%$$

CONCLUSION:

The actual rate of return on investment (= 6.65 per cent) should be used in compiling annual costs, in estimating income taxes, in present-worth calculations, and in other economic studies.

References

1. OPERATION AND MAINTENANCE COSTS FOR USE IN THE ECONOMIC COMPARISON OF ALTERNATIVE FACILITIES, W. E. Siemmer. *AIEE Transactions*, volume 70, part II, 1951, pages 1954–55.

2. EVALUATION OF ENERGY DIFFERENCES IN THE ECONOMIC COMPARISON OF ALTERNATIVE FACILITIES, A. P. Fugill. *AIEE Transactions*, volume 70, part II, 1951, pages 1854–60.

3. PRESENT WORTH, OR THE TIME COST OF MONEY, AS A FACTOR IN THE ECONOMIC COMPARISON OF ALTERNATIVE FACILITIES, P. H. Jeynes. *AIEE Transactions*, volume 70, part II, 1951, pages 1956–62.

4. METHODS OF ESTIMATING UTILITY PLANT LIFE, 1950. *Report*, Engineering Subcommittee, Depreciation Accounting Committee, Edison Electric Institute (New York, N. Y.).

5. LIFE ANALYSIS OF UTILITY PLANT FOR DEPRECIATION ACCOUNTING PURPOSES BY THE SIMULATED PLANT-RECORD METHOD, Alex. E. Bauhan. *Proceedings*, National Conference of Electric and Gas Utility Accountants, 1947.

6. SIMULATED PLANT-RECORD METHOD OF LIFE ANALYSIS OF UTILITY PLANT FOR DEPRECIATION-ACCOUNTING PURPOSES, Alex E. Bauhan. *Land Economics* (Madison, Wis.), May 1948.

7. AN APPRAISAL OF METHODS FOR ESTIMATING SERVICE LIVES OF UTILITY PROPERTIES, 1942. *Report*, Cooperating Committees on Depreciation of the American Gas Association and Edison Electric Institute (New York, N. Y.).

8. REPORT OF SPECIAL COMMITTEE ON DEPRECIATION, 1938. National Association of Railroad and Utilities Commissioners (New York, N. Y.).

9. REPORT OF COMMITTEE ON DEPRECIATION 1943. National Association of Railroad and Utilities Commissioners (New York, N. Y.).

10. LIFE EXPECTANCY OF PHYSICAL PROPERTY BASED ON MORTALITY LAWS, E. B. Kurtz. Ronald Press (New York, N. Y.), 1930.

11. THE SCIENCE OF VALUATION AND DEPRECIATION, E. B. Kurtz. Ronald Press (New York, N. Y.), 1937.

12. A SYSTEM OF LIFE TABLES, B. T. Kimball. *Econometrica* (Chicago, Ill.), October 1947.

13. ESTIMATES OF AVERAGE SERVICE LIFE, J. B. Jeming. *Econometrica* (Chicago, Ill.), April 1943.

14. STATISTICAL ANALYSES OF INDUSTRIAL PROPERTY RETIREMENTS, R. Winfrey. *Bulletin 125*, Iowa Engineering Experiment Station, Iowa State College (Ames, Iowa), 1939.

15. DEPRECIATION OF GROUP PROPERTIES, R. Winfrey. *Bulletin 155*, Iowa Engineering Experiment Station, Iowa State College (Ames, Iowa), 1942.

16. CONDITION-PERCENT TABLES FOR DEPRECIATION OF UNIT AND GROUP PROPERTIES, R. Winfrey. *Bulletin 156*, Iowa Engineering Experiment Station, Iowa State College (Ames, Iowa), 1942.

Discussion

M. J. Steinberg (Consolidated Edison Company of New York, Inc., New York, N. Y.): This paper discusses methods for calculating those items which are generally grouped to constitute the "annual carrying charges" or "annual fixed charge rates" which are applicable to investments and which must be established to permit the economic evaluation of alternate proposals. Because of the excellence of the paper it is hoped that it will induce the constructive discussion which it merits.

In order to confine this discussion within reasonable limits, comments only on the author's methods of calculating the annual return on the investment and the annual cost of depreciation will be offered. The paper describes a method of approach applicable to a group of property units having a specific survivorship dispersal. With respect to depreciation, a method is described which "yields the percentage which, applied to the original cost of survivors in each year, will exactly recoup the first cost of plant in its lifetime." It is pertinent to note that this percentage is not applied to the first cost of plant or to total initial investment, but to the original cost in each year proportionate to the survivors. The effect is a nonuniform annual cost of depreciation. This, it is believed, differs from the customary practice of developing a depreciation rate which applied to the total initial investment will result in an equivalent uniform annual cost.

The annual cost of depreciation combined with the annual return on investment has been defined as the annual recovery of capital with a return, more commonly referred to as "capital recovery," which is fixed in value by the period for amortization and the rate of interest on money.

The application of capital recovery factors to present worth values permits conversion of nonuniform annual values to equivalent uniform values. Applied to the present worth value of the annual cost of depreciation as determined from Table I of the paper, assuming a 60-year amortization period and 6 per cent interest rate, gives,

$$(100\% - 76.3645\%)(0.06188) = 1.4626\%$$

A similar application to the present worth value of the annual return, gives,

$$76.3645\% \times 0.06188 = 4.7254\%$$

The above values applied to the initial total investment would give uniform annual values for the cost of depreciation and return, respectively, equivalent to the nonuniform values shown in Table I of the paper, and would in this case be the appropriate values to use in determination of the total annual fixed charge rate.

It is pertinent to note that for the purpose of establishing the fixed charge rate for return and depreciation there is no need for the computation shown as Column 7 of Table I, since the present worth of the annual costs of depreciation can be obtained by differences. Thus

Capital recovery rate = 6.1880% of initial investment
Return = 4.7254
Depreciation = 1.4626%

If the method of Table II is employed, the fixed charge rates can be obtained as follows, Present worth of depreciation $= 12.6099 \times 1.874\% = 23.6355\%$

Fixed charge rate for depreciation $= 23.6355 \times 0.06188 = 1.4626\%$

Fixed charge rate for return $= 6.1880\% - 1.4626\% = 4.7254\%$

Referring to Table I of the paper it is noted that the annual returns (Column 4) are expressed in per cent of January 1 survivors, while the annual costs of depreciation are expressed in per cent of mean survivors for each year. While it is recognized that for statistical purposes the use of mean survivorship is quite common in practice, it seems inconsistent not to use the same basis with respect to the annual return.

With reference to Table III of the paper, the tabular values can serve as helpful data for determination of the nonuniform annual costs of depreciation. It is our opinion that the corresponding present worth values or preferably the corresponding fixed charge rates derived as indicated in this discussion, would be very useful.

The short cut method for computing the annual costs of depreciation shown in Table II is a handy tool. It is suggested that the author supply the derivation of the equation, shown at the bottom of this table, in his written closure for the benefit of interested readers.

In conclusion, we wish to compliment the author for the excellent quality of his paper. Our purpose is not to be critical but rather to offer some supplementary thoughts on a subject which does not enjoy unanimity of opinion. It is our position that studies leading to the publication of recommended practices under Institute sponsorship would be very beneficial in resolving such differences of opinion.

Maurice R. Scharff (Consulting Engineer, New York, N. Y.): As in his companion paper[1] the author has performed an outstanding service in presenting so clearly the application of the concept of the present worth or the time cost of money to the treatment of annual carrying charges in economic comparisons of alternative facilities. In particular, his demonstration of the error of omitting income taxes from consideration in economic comparisons and of the equivalence of the income tax to an additional fixed charge on investment, particularly in the public utility industry, is of major importance. The writer can testify from his own experience both as to the controlling effect which this factor may have in drawing sound conclusions from economic comparisons and as to the frequency with which it is left out of account even by experienced engineers.

The author's presentation also provides occasion for calling attention to the effect of prevailing high corporate income tax rates in confiscating a large proportion of savings in expenses that can be accomplished by substituting modern efficient equipment for obsolete inefficient equipment and in thus discouraging replacements and improvements in efficiency.

A word of caution should perhaps be said against any conclusion, which the writer is sure the author did not intend, that because he made use of the extremely valuable dispersion curves developed by the Iowa Engineering Experiment Station in certain of his examples, these curves are superior or more generally applicable than those contributed by the other groups and individuals to which reference is made in references 7 to 13 inclusive of the paper. To these references it might be helpful to add the groups of standard dispersion and reserve requirement curves developed from time to time by the staff of the New York Public Service Commission, of which the current series known as the H-type curves have been widely used by the staff of that Commission and the public utility companies operating in New York State.

REFERENCE

1. See reference 3 of the paper.

John E. Girard and **Hubert M. Langlois** (Department of Water and Power, Los Angeles, Calif.): As a prelude to presentation of points of comment, and for discussion, we emphasize the fact that the purpose of depreciation accounting is solely to recover original investment, and no more and no less. Such recovery involves the determination of annual costs, and regardless of the methods utilized, the allocation of the costs across the years of usable life. Depreciation lives inherently involve two component aspects, namely, one which is determined by structural or so-called physical depreciation, and another which is determined by functional depreciation. The physical life aspect is more readily estimated, based on patterns of past experience, than is functional life. Yet, even the former is subject to variations resulting from changes in practices or conditions during the use of the equipment, and is inter-related with changes made in the program and practices of maintenance and partial replacements, and it is also subject to changes in the art which provide new methods for extension of the lives of existing equipments. On the other hand, the inflationary times through which we are going may either extend or shorten the functional lives of equipment, dependent upon change in the economic factors, as may be affected by inflationary investment versus inflationary operation costs. Numerous authorities have indicated that functional depreciation is apt to, and is likely to, exceed in many instances, the effects customarily related to physical life, factors consisting of wear, tear, or decay.

An examination of the subject paper, by no means detailed by us because of time limitation, nevertheless resulted in general reactions which may be summarized as follows:

1. The over-all tenor of the presentations, particularly with respect to depreciation costs, but also true of other items, is to imply that such costs may be reduced to a mathematical preciseness covering fairly long periods of time on the basis of various elements which in themselves involve estimates relative to the future. The possibility should be recognized that the comparative results of the over-all summations may be completely reversed if only fairly small errors are involved in the basic assumptions as to proper rates of return, direct operation and maintenance expenses, and other elements of costs, particularly those which are influenced through the estimates of depreciation lives. Unless the comparative results are conclusively in favor of one plan or the other by a fairly wide margin (which certainly will not always be the case), then no great deal of reliance can justifiably be placed upon the comparison. Sound engineering management judgment, after all, is a highly important element in such studies with respect to depreciation studies, it would be a marked aid to final judgment if there were not used a single estimate of probable life, but lower and higher values within reasonable limits of deviation in order to produce in the studies alternative effects covering a range of possible error.

2. In arriving at what is stated as an "annual cost of depreciation," it has been assumed that such cost is a function, among other things of "rate of return on investment." This conclusion is at variance with a fair segment of regulatory thinking. It ignores the fact that funds from depreciation reserve accruals over a long period of time often must wait the completion of plans and the starting of construction before "plowing back" or "reinvesting" such recovered capital in the enterprise; to this extent depreciation money takes on in part the character of short-term funds commanding somewhat lower interest earning rates than fixed utility investments as a whole.

The foregoing factor, coupled with the fact that "fair rates of return" in an over-all sense for utility operation are never firm or assured over long periods of time, forms the principal basis for using, in sinking fund depreciation accounting, interest rates which should not be higher than the general levels of over-all "rates of earned return," and in no event lower than the going rate of interest on long-term debt; rational choice related to specific utilities usually results in a choice of interest rate for depreciation reserves (sinking fund basis) somewhat lower than the "rates of earned return."

3. For purposes of the paper, computation examples were set up in terms of estimated dispersion of retirements in accordance with certain typical form curves developed by the Engineering Department of Iowa State College. While, for purposes of long-term alternative economic studies, the treatment is probably satisfactory theoretically, it should be clearly recognized that in the end result for long-term economic studies it is subject to limitations of accuracy respecting costs and estimates, upon which comment has previously been made.

However, one should not conclude that use of factors of "Survivors," "Mean Survivors" and calculations predicated thereon (see Table I) and embodying inherently a "remaining-life" concept, is necessarily appropriate or even acceptable in actual practice for depreciation accounting. Such method has been suggested for application in certain recent cases under California Utilities Commission jurisdiction but to date has been rejected for a variety of reasons. Among these reasons are the complexities and confusion which would be introduced into the handling of ordinary depreciation accounting; in addition, the method would involve practically annual and continuing review of plant records and depreciation scheduling with the concomitant increase in actual expenses thus adding to the burden of costs necessarily borne by the rate payer.

No particular advantages have been demonstrated in the methods proposed.

4. Relative to rates of return, there is a

reference to the term "rate base," and there is a failure to recognize, or at least clearly state, the fundamental element of distinction between the terms "rate base" and "investment in plant." Regulatory jurisdictions, in determining a rate base upon which return can be appropriately predicated, customarily recognize, in addition to plant investment, important allowances for working capital, including appropriate amounts necessary for maintaining materials and supplies needed to carry on operations. Inasmuch as the term "rate base" has been used in the paper, it seems essential that specific mention be made of the distinction and that the two terms are by no means identical.

While discussing the aspect of depreciation costs in economic studies, the paper implies that the computation of depreciation annuities (sinking fund) assuming return on reinvested reserves to be less than the ordinary over-all return on original invested capital is in effect "not a faithful version of utility cost behavior." Specifically, it is stated that "the whole purpose of these rate base procedures is to justify a higher rate of return on original investment..." An almost exactly contrary conclusion is indicated by the record and evidence of many regulatory jurisdictions, and in particular by that of the California Commission.

5. Economic studies of alternative prospective investments warrant a distinction being made as between those investments which are of more or less routine character and of continuing type of addition, such as poles, meters, distribution transformers, small substations, et cetera, and those which are of major magnitude, such as for large power sources, and occurring at periodic but irregular intervals in a utility's history. The very nature of the routine and continuing additions is such as to give the utility a wealth of experience in service lives of such facilities and in their dispersion patterns, and which are subject to precise mathematical treatment. However, such records relate to the *past*, and those results relative to the *future* are subject to changes in the art. In the continuing type of routine additions, new developments or methods may be readily tried out by the utility on a relatively small scale, and the experiences of other utilities and the estimated value of new methods may be judged with much less effect on the utility's operations. On the other hand, projects of major magnitude, such as a major power source installation, comprising a 10 to 15 per cent or even greater expansion in the utility's total plant investment, require extremely careful considerations relative to the impact of the installation on the financial and operating requirements, and of immediate effect on rates.

6. These observations are not intended to negate in any way stimulation to thinking by engineers and others on the subject afforded by the papers submitted by Mr. Jeynes, nor are they intended to negate the desirability of having recourse to all of the past experiences, to tabulations of service lives, (inclusive of dispersion patterns), and to mathematical analyses thereof, but to emphasize that they are not to be relied upon as sole criteria for estimating the future.

As indicated hereinbefore, judgment considerations are involved, and the interrelationship of many factors; also such judgment considerations are highly important, and may be required in greater degree in one type of investment consideration as against another.

F. L. Lawton (Aluminum Laboratories, Ltd., Montreal, Canada): The author has presented an excellent and very lucid treatment of that aspect of economic comparison of alternative facilities concerned with annual carrying charges; the paper should help clarify the thinking of engineers concerned with economic evaluations of alternative facilities.

The author's opening paragraph to the effect "...economic comparison of alternative facilities means an estimate of the effect on future revenue requirements by adopting one plan of action instead of some alternative. The economic choice is the plan which will result in minimum revenue requirements...that is, the minimum compensatory selling price...after all costs have been covered, including an adequate return to owners of the business...." is excellent. However, there are other criteria, such as a comparison of optimum net earnings, which would involve a comparison of present worths of the probable future net earnings.

It should be recognized that the general subject of this group of papers is not confined to the regulated public utilities, which constitute a special aspect of the over-all problem of economic comparison of alternative facilities.

When considering the trend of the future rate of return and the factors influencing such, attention should be given to those influencing factors such as governmental policy, political trends, state of international affairs, rate of technological improvement, and availability of capital. Other aspects of this phase of the author's presentation warranting consideration are rising price levels versus decreasing price levels. Recognition must be given to the over-all fluctuations experienced during the ordinary life of most production facilities.

The effect of reinvestment of depreciation reserves must be studied in line with the premise that ensures the optimum net earnings for the investment. At times it will pay to reinvest in the business. On other occasions, withdrawal of capital or investment in outside facilities may be warranted.

Depreciation is a function of obsolesence, inadequacy, wear and tear, action of the elements, requirements of civil authorities, maintenance standards, et cetera. However, in the true sense, depreciation should reflect the annual loss of service value of the facility. Prediction of the annual cost of depreciation is difficult because of the influences stemming from governmental and financial origins, irrespective of the exactness of mathematical determinations. It is very doubtful if many facilities have been written off in accordance with any one method, due to such factors as change of management, change of ownership, effect of accelerated write-offs during war, or depressions. Influence of these factors must be recognized, with the knowledge that any one plan is not likely to achieve universal acceptance. That is, each enterprise and each unit thereof must be treated in accordance with the particular circumstances concerning it.

Herbert B. Reynolds (J. G. White Engineering Corporation, New York, N. Y.): As pointed out by Mr. Jeynes, the life of equipment is a major factor in estimating the annual carrying charges in making economic studies. However, the determination of the life of equipment is generally based on guesses backed by judgment.

In order to have data available which at least could be a guide in estimating the life of equipment, it has often occurred to me that it would be worth while for some of the technical organizations which collect statistics, such as the Edison Electric Institute, to collect data from users giving the life history of their major pieces of equipment whenever such equipment is retired from service. For example, in the case of a turbine such information should include date of installation, date of retirement from service, size of unit, steam conditions, output of unit during each year of its life, et cetera.

The collection and compilation of such data over a period of years should result in very useful information and would be equivalent to the information which the life insurance companies collect relating to the life of the human being and which is essential in establishing premium rates.

A. E. Knowlton (Eelctrical World, New York, N. Y.): From the papers presented at this session, one could as likely draw confusions as to draw conclusions. It is evident that there is reasonable agreement on the major premises but comparatively little unanimity on the interpretation of the details. This is quite to be expected when engineers begin to delve actively in a realm previously reserved largely for the actuaries, accountants and rate specialists.

There is ample excuse for us engineers to examine our respective methods of determining comparative costs for alternative ways of meeting a given engineering problem. Nor is there any reason why they should follow the prescribed techniques of accountants. Their task is to evaluate present worth of some engagement that may stand as a commitment for 20, 30, 50, or even 100 years.

It is extremely desirable that the various procedures exemplified by the papers be resolved toward uniformity. There are three good reasons for a degree of standardization:

1. It is due to investors in the enterprise that their money be spent as wisely and as advantageously as possible. The equipments purchased and system configurations decided should be based on as sound a technical-economic basis as possible.
2. It is due to the manufacturers to know how the criteria for competitive selection of apparatus on an economic worth basis differ from company to company, or better yet, the degree of uniformity in establishing these criteria.
3. It is due to the rate-payers and regulatory authorities to have uniformity in judgment on the part of the regulated utilities in making expenditures that have to stand the test of prudence. Otherwise the least "prudent" utility (the one with the dullest pencil) may find itself paying a penalty because the criterion for decision on prudence may follow the pattern set by utilities that use the sharpest pencils.

In brief there is ample urge to prosecute what this symposium has initiated toward exploration of engineering-economic theories. Whether the accountants concur in the prospective conclusions is beside the point. At least the engineers will have made their decisions sound by clarification and unification. The expenditures will thus have been prudent at the source.

William Parkerson (Middle West Service Company, Chicago, Ill.): The paper by the author and an unpublished Conference Paper by F. L. Lawton presented at the same time cover the subject in a very comprehensive manner, but the urgent plea for standardization of procedure in such comparisons is not answered. There is a noticeable lack of community of thought among the authors.

Mr. Lawton's paper fails to recognize the very impressive discussion of dispersion in Mr. Jeynes paper. The equation given by Mr. Lawton for "uniform annual rate of depreciation," namely $i \div [(1+i)^n - 1]$, holds only for zero dispersion, or for *S6* at best, conditions which Mr. Jeynes paper considers to be highly improbable in practical experience.

Both papers recommend and endorse the use of the "uniform system of accounts" in comparing the relative economics of alternate facilities and this would seem to be an obvious and important step in the direction of standardization of method.

Paul H. Jeynes: Mr. Steinberg correctly observes that the depreciation percentage described in this paper (a constant percentage in every year) when applied to the original cost of survivors (which is a diminishing amount in each year) results in a gradually decreasing annual cost in dollars. He points out, also quite accurately, that this departs from the customary practice of estimating the equivalent uniform annual cost of the whole original investment, and gives an example of that alternative treatment.

The reason for preferring the author's approach is that it is universally applicable. The usual alternative, described by Mr. Steinberg, applies in just one special case, that being when replacements of the original installation have (a) the same first cost as the original units they replace, and (b) the same average life, dispersion type, and net salvage as the original units. Unless both of these requirements are met, then annual cost of the project changes every time a replacement is made.

For textbook purposes, it simplifies the explanation to assume that future replacements will have the same first cost as the original units, as well as the same life. In practical applications, however, it is important to recognize that total annual costs of a project in any future year are actually the sum of two components, which may have different percentage annual costs and therefore require separate calculation. The two components are:

1. Annual costs of survivors of original units.
2. Annual costs of survivors of replacements of original units (and replacements of replacements).

This distinction may be of no consequence in comparing costs of two contemplated alternatives if both installations have the same expected life. On the other hand, this may be the essential factor in problems of economic replacement where the replacement is known to have different costs and is expected to have a longer life than the old plant. Accordingly, in a rigorous general approach, which this paper purports to be, it is necessary that the actual situation be recognized.

Of course, if it can be reasonably assumed that all replacements will have the same first cost and average life as the original units, then the percentages described in this paper, when applied to the initial capital cost of the project, will yield the level annual cost of the project in the usual textbook manner.

Mr. Steinberg's proposed use of January 1 survivors as the basis for both return and depreciation would be an acceptable approximation, though use of mean survivors for calculating depreciation costs is believed to be nearer to the actual facts. That is, the whole objective of the economic study is an estimate of equivalent annual costs as at the end of each year, which costs can be converted to a "present worth" by application of standard present-worth factors based on year-end payments. Now, the investor receives a return on his total investment until the original amount is repaid. Thus, in any year, he receives a return on his January 1 investment until part is repaid on December 31st via depreciation expense. Most utilities base depreciation charges on monthly plant balances, that is, mean survivors. Hence the proposed basis for Tables I and II.

Accounting practices of individual companies may vary in such minor details. In any particular case where the facts are definitely otherwise, the small adjustment factor can be determined and applied to all Table III values, if that refinement is felt to be justified. Perhaps it is worth pointing out that the sum of mean survivors equals average life; the sum of January 1 survivors equals average life plus 1/2 year.

Present-worth factors, for conversion of annual costs throughout one life cycle to a single equivalent present worth, may be computed as $1/(i+d)$, where i = rate of return on the investment, and d = depreciation annuity per Table III.

Appendix I of this discussion, entitled "Depreciation Annuity Calculations" presents the analytical derivation of the shortcut method of Table II from the self-explanatory method of Table I, requested by Mr. Steinberg.

Mr. Scharff calls deserved attention to the h-type curves of the New York Public Service Commission, which are believed to have some advantages over the Iowa series. The author preferred the latter only because they have been more widely known for many years, and because tables of survivors at all ages are more readily available in the bulletins of the Iowa Engineering Experiment Station.

Mr. Scharff modestly fails to mention his own numerous and outstanding contributions to the present subject. One of them, the book Depreciation of Public Utility Property, by Scharff, Leerburger, and Jeming,[1] deserves particular mention.

The author has been asked whether depreciation annuities have been calculated for the so-called *GC* type of dispersion; that is, for the survivor curves representing a uniform retirement rate at all ages. Table I of this discussion entitled "Depreciation Annuities; Type GC Dispersion," presents these data in the manner of Table III of the paper.

In their opening paragraph, and again in Item 5 of their discussion, Messrs. Girard and Langlois emphasize the importance of functional depreciation as a determinant of service life. They also stress the fact that the progress of functional depreciation is subject to change as times and circumstances change.

Presumably none of their comments are intended as criticism of the approach described in this paper, which devotes only four sentences to the subject of life estimates for two compelling reasons:

1. That subject not only lies outside the scope of the present paper, but would require much more space for an adequate presentation than was available.
2. The authoritative references suggested, particularly the 85-page Edison Electric Institute report "Methods of Estimating Utility Plant Life,"[2] provide a comprehensive treatment fundamentally in accord with the approach described in this paper and, it is believed, with the views of the discussors.

The admitted importance of functional depreciation must not be permitted to obscure the fact that it influences the economic comparison only through its effect on the life estimate.

It is true that this paper emphasizes the clear-cut and rigorous nature of the arithmetic involved in economic comparisons. But any intimation that it disparages the need for sound judgment would be an unwarranted perversion of its tenor. The first part of the paper deals with "Sound judgment as to the probable future rate of return," and the section entitled "Depreciation," states that "the major difficulty lies in the selection of reasonable starting assumptions, particularly as to the average life and type of dispersion. Both of these, being estimates of future behavior which will not necessarily duplicate past performance, are matters for fully informed judgment." The section on "Taxes" says of income taxes, "the estimator has no recourse except to rely on fully informed judgment."

The point is that while sound judgment is the essential ingredient, it is futile to pretend that sound judgment can be exercised by anyone unfamiliar with the correct arithmetic. Before simplified practical procedures can be developed, it is necessary to understand what is to be simplified.

In their discussion of the appropriate interest rate on reinvested reserves, Messrs. Girard and Langlois regard the author's views as "at variance with a fair segment of regulatory thinking" in that (they say) it ignores the possibility of a lower rate of return on reserves and the reason therefor. But the paper does not ignore that possibility. It is specifically treated in the first two sections, and in the Appendix I.

The discussors advance two reasons for assuming a lower rate of return on reserves: (1) delays in reinvesting available reserve funds, and (2) lack of assurance of a sustained "fair rate of return." It is the author's conclusion that, so far as economy studies are concerned, the first factor is of negligible importance; the second would seem to have no validity at all.

That is, in order for the first factor to have

Table I. Annual Cost of Depreciation For Various Average Lives, Type GC Dispersion*

	Average Life								
	10	15	20	25	30	35	40	45	50
5% return	8.62	5.48	3.83	2.92	2.33	1.91	1.64	1.42	1.25
6% return	8.41	5.35	3.68	2.81	2.24	1.85	1.57	1.36	1.20
7% return	8.21	5.13	3.56	2.70	2.16	1.78	1.53	1.31	1.17

*In per cent of first cost of investment, before adjustment for salvage.

appreciable significance, it would be necessary to have a substantial portion of the total reserve permanently represented by idle cash in excess of needs for working capital, a situation that would constitute a serious indictment of managerial and regulatory competence. Occasional short-term delays may be anticipated, but ordinarily such delay has unimportant effect on long-term average return, being an occasional postponement of a small fraction of the total reserve, which has a relatively long period of reinvestment (equal to remaining life of the plant concerned).

As for the lack of assurance of a sustained "fair rate of return," that possibility would seem to apply in exactly the same measure to return on original investment as to return on reinvestment in the same enterprise. Neither factor mentioned is the important reason for recognizing a lower rate of return on the reserve which is discussed in Section 1 of the paper. The effect of reinvesting reserves in securities, rather than in the business, is also described in the paper.

In reply to the statement that use of the Iowa type curves necessarily implies use of the "remaining-life" method of accounting for depreciation, the author has no option but a categorical and emphatic contradiction. The use of survivor curves is simply a convenient device for describing the manner in which individual retirements are scattered about average life, just as individual human deaths occur before and after the average man's expectancy of 65-year life. Use of type curves does not presuppose any particular method of accounting for depreciation. Economic comparisons are not concerned with the advantages or disadvantages, from bookkeeping or regulatory standpoints, of depreciation accounting methods.

Were this paper devoted to regulatory problems or development of rates, a definition and explanation of "rate base" would be in order. However, for purposes of economy studies, that seems immaterial and irrelevant. It is not at all essential that the reader understand the nature of the rate base in order to profit from the remarks in the first section of the paper.

All the estimator wants to know is how to go about establishing what percentage return he should use. The paper warns him not to adopt uncritically the percentage, usually available, adjudged applicable to the "rate base" (whatever that may be). It then explains how to proceed from the percentage applicable to the undefined rate base to the rate applicable to first cost, which he is seeking.

Messrs. Girard and Langlois also object to the statement that assuming a lower return on reserves (when reinvested in plant) is not a faithful version of actual cost behavior, and to the view that "the whole purpose of these rate-base procedures is to justify a higher rate of return on original investment than if reserves were not reinvested."

Possibly they have missed the point illustrated in the Appendix of the paper. This is simply a matter of arithmetic, not a conclusion to be drawn from regulatory experience. As for commission understanding of the situation, see Docket Number 4271 of the Louisiana Public Service Commission, dated July 29, 1946,[3] or General Order Number 38-A of the Missouri Commission, dated December 28, 1945.[4]

Mr. Lawton is technically correct in observing that in nonregulated industry a suitable criterion of the economic choice may be the comparison of optimum net earnings. However, three comments are pertinent:

1. In any case, the criterion described in this paper (the comparison of present worths of future revenue requirements) correctly identifies the economic choice. The comparison of optimum net earnings may improve the quantitative estimate of differential savings in those cases where it is applicable.
2. As a practical matter, it is important to be warned against comparisons of optimum net earnings in situations where that approach is not appropriate. It is a favorite means for obtaining wrong answers in utility practice, where it is almost always based on unrealistic assumptions. Commonest error is the assumption that revenues would be the same in any event, and that all savings would serve to increase the cost of money.
3. The comparison of optimum net earnings is a difficult operation, because many costs (particularly depreciation and taxes) are a function of the rate of return, which is the unknown quantity in that approach.

Depreciation, in the sense of loss in value, is a function of obsolescence, inadequacy, wear and tear, action of the elements, requirements of civil authorities, maintenance standards, et cetera, as Mr. Lawton states. But the only influence these matters have on the economic choice is by way of their effect on service life, as noted before. Whether depreciation accrues at a uniform or variable rate, rapidly or slowly or irregularly, need be given no consideration in economy studies except as that may help to estimate probable life.

The importance of functional depreciation in making life estimates has been stressed by several commentators. The effect of functional depreciation is not only variable from time to time, but from one enterprise to another, as Mr. Lawton observes. No doubt that fact accounts in part for the lukewarm attitude of many engineers toward compilation of life data in the manner proposed by Mr. Reynolds.

Appendix I. Depreciation Annuity Calculations

Demonstration of the identity of $d\%$ calculated as in Table I and Table II, respectively, of the paper.

Let

P_x = present-worth factor, payment due at end of year x
S_x = survivors at end of year x
S_{x-1} = survivors at beginning of year x
M_x = mean survivors, year $x = \dfrac{S_x+S_{x-1}}{2}$

Year	S_{x-1}	S_x	P_x
1	1	S_1	$1/(1+i)$
2	S_1	S_2	$1/(1+i)^2$
3	S_2	S_3	$1/(1+i)^3$
4	S_3	S_4	$1/(1+i)^4$

$$\Sigma P_x S_{x-1} = 1\times 1/(1+i) + S_1 \times 1/(1+i)^2 + S_2\times 1/(1+i)^3 + \ldots$$

$$(1+i)\Sigma P_x S_{x-1} = 1\times 1 + S_1\times 1/(1+i) + S_2 \times 1/(1+i)^2 + \ldots$$

$$\Sigma P_x S_x = S_1\times 1/(1+i) + S_2\times 1/(1+i)^2 + \ldots$$

therefore

$$\Sigma P_x S_x = (1+i)\Sigma P_x S_{x-1} - 1 \tag{1}$$

also

$$\Sigma P_x M_x = \frac{\Sigma P_x S_{x-1} + \Sigma P_x S_x}{2}$$

therefore

$$\Sigma P_x S_{x-1} = 2\Sigma P_x M_x - \Sigma P_x S_x \tag{2}$$

Substituting equation 1 in equation 2:

$$\Sigma P_x S_{x-1} = 2\Sigma P_x M_x - (1+i)\Sigma P_x S_{x-1} + 1$$

$$\Sigma P_x S_{x-1} = 2\Sigma P_x M_x - \Sigma P_x S_{x-1} - i\Sigma P_x S_{x-1} + 1$$

$$2\Sigma P_x S_{x-1} + i\Sigma P_x S_{x-1} = 2\Sigma P_x M_x + 1$$

Collecting terms and dividing by 2:

$$(1+i/2)\Sigma P_x S_{x-1} = \tfrac{1}{2} + \Sigma P_x M_x$$

or

$$\Sigma P_x S_{x-1} = \frac{\tfrac{1}{2} + \Sigma P_x M_x}{(1+i/2)} \tag{3}$$

Per Table I:

$$d = \frac{1 - i\Sigma P_x S_{x-1}}{\Sigma P_x M_x}$$

Substituting equation 3:

$$= \frac{1 - \dfrac{i/2 + i\Sigma P_x M_x}{1+i/2}}{\Sigma P_x M_x}$$

$$= \frac{1 + i/2 - i/2 - i\Sigma P_x M_x}{(1+i/2)\Sigma P_x M_x}$$

$$= \frac{1 - i\Sigma P_x M_x}{(1+i/2)\Sigma P_x M_x} = d\text{, per Table II}$$

References

1. Depreciation of Public Utility Property, Scharff, Leerburger, Jeming. Burstein and Chappe, New York, N. Y., 1940.

2. See reference 4 of the paper.

3. *Docket Number 4271*, Louisiana Public Service Commission, July 29, Public Utilities Reports (Washington, D. C.), 1946

4. *General Order 38-A*, Missouri Public Service Commission, December 28, Public Utilities Reports (Washington, D. C.), 1945.

Operating and Maintenance Costs for Use in the Economic Comparison of Alternative Facilities

W. E. SLEMMER
MEMBER AIEE

Synopsis: In making economic comparisons of alternative facilities, decisions are required as to what operating and maintenance cost items are to be included in the comparisons. This paper suggests a criterion for making these decisions and lists several cost items that should be considered. Three companion papers treat other related cost problems.[1,2,3]

IN SETTING up operating and maintenance costs for economic comparisons, decision as to what costs to include is based on their effect on the comparison. If aggregate cost differences will be the same whether or not a particular cost item is included that item may as well be omitted. However, if a cost item will change the aggregate cost difference then it must be included if it is an actual cost.

This statement of principle may be modified, as a practical matter, to require the effect to be substantial. There are many uncertainties in cost estimates so that absolute accuracy is impossible. If the effect of a particular cost item is small as compared to these contingencies it is probably not worth the time and effort to include it. In general, economic comparisons serve only as aids to judgment and the accuracy required is that which will lead to sound decisions. Based on this general principle the following are examples of costs that should be included if they are significant.

Material Cost

Cost of material required for operation and maintenance should be included. This cost should include the following items unless they are otherwise included in the comparison:

Purchase price.
Cost of handling and storing, including maintenance of equipment and cost of money invested in equipment and material stored.
Taxes resulting from procurement of material.
Cost of purchasing, inspecting, and accounting for materials.
Allowance for shrinkage.

Labor Cost

Cost of operating and maintenance labor should include the following items:

Direct payroll cost.
Taxes based on payroll, such as Social Security taxes.
Provisions for vacations, sickness, and so forth.
Employee benefits such as pension plans, insurance paid for by employer and similar items.
Transportation if furnished by employer.
Travel time.
Living expense paid by employer.
Tools and work equipment.
Overheads including general supervision and accounting expense.

Other Cost

In addition to cost of labor and material there are other cost items that are sometimes involved. Among these are the following:

Power and energy for driving equipment or for losses.
Crop damage, tree trimming, and so forth.
Loss of revenue when equipment is out of service for maintenance.
Cost of purchased power and energy.
Rents.
Cost of special insurance.

Co-ordination of Costs

Costs for operation and maintenance used in economic comparisons should be co-ordinated with other costs used in the comparison. For example, in comparisons involving a steam-electric station, the heat rate should be based upon the same design as the investment estimates. Similarly if the investment estimate includes automatic controls to reduce operating labor the resulting reduction should be reflected in the operating labor cost, and appropriate maintenance costs for the added equipment should be included.

If investment estimates of transmission system components include items to reduce maintenance such as shield wires, this should be reflected in maintenance costs. On the other hand, if investment cost is based on a design using high-unit stresses that increase the probability of storm damage, this should be reflected in the maintenance cost.

Similarly in determining cost of power and energy obtained from the system for electric drives or for losses, co-ordination is required. If the power cost or demand charge is based upon cost of efficient installations, this efficiency should be reflected in the energy cost.

Effect on Existing Costs

It is usually not enough to include operating and maintenance costs of new equipment only but effect on operating and maintenance costs already existing must also be considered. Perhaps the

---

Paper 51-359, recommended by the AIEE System Engineering Committee and approved by the AIEE Technical Program Committee for presentation at the AIEE Fall General Meeting, Cleveland, Ohio, October 22-26, 1951. Manuscript submitted June 13, 1951; made available for printing August 30, 1951.

W. E. Slemmer is with Ebasco Services, Inc., New York, N. Y.

outstanding example of this is the reduction in load factor on existing generating equipment when a new generating unit having a low production cost is put in service. The same principle applies in other situations, for example, addition of a second transformer in a substation may facilitate removal of equipment for maintenance and permit a reduction in maintenance cost of existing equipment. On the other hand, addition of a large generating unit in an existing station may result in increased labor cost above additional men by causing an increase in rate for other employees in the station.

Future Costs

Economic comparisons of alternative facilities are usually made as a guide to making an investment which will have an economic life of many years. The objective is to determine which facilities will give the lower over-all cost throughout the life of the facilities to be installed. To determine this these future costs should be estimated. This, of course, makes the task more difficult but only future costs have any meaning in relation to investments yet to be made. In using present or historical costs careful consideration should be given to any factors that will tend to change those costs in the future, bearing in mind of course that a dollar saved several years in the future is not worth a dollar today.

As an example, new generating capacity when added to a system often has a lower production cost than existing equipment and therefore operates at a high load factor. However, in making economic comparisons of such an installation allowance should be made for probable future installations having still lower production costs. These future installations will in turn take the base load position and reduce the load factor on the facilities under consideration. The load factor used for economic comparisons should recognize this probability.

Unless comparisons are to be made for a specific period, future cost estimates should include allowance for major maintenance items which occur infrequently. Examples of such items are rewinding of generators or transformers or retubing steam condensers. In evaluating such items the period of time before these costs will be incurred should be considered.

Conclusion

While several items have been mentioned that should be considered in setting up operation and maintenance costs for economic comparisons, it is not considered feasible to make a complete list that will fit all cases. Each problem will have some circumstances peculiar unto itself. The only safe guide is whether or not a particular item of cost will change the resulting differential significantly.

References

1. Annual Carrying Charges in the Economic Comparison of Alternative Facilities, P. H. Jeynes. *AIEE Transactions*, volume 70, part II, 1951, pages 1942–53.

2. Evaluation of Energy Differences in the Economic Comparison of Alternative Facilities, A. P. Fugill. *AIEE Transactions*, volume 70, part II, 1951, pages 1854–60.

3. Present Worth, or the Time Cost of Money, as a Factor in the Economic Comparison of Alternative Facilities, P. H. Jeynes. *AIEE Transactions*, volume 70, part II, 1951, pages 1956–62.

Discussion

A. E. Knowlton (Electrical World, New York, N.Y.): From the papers presented at this session one could as likely draw confusions as to draw conclusions. It is evident that there is reasonable agreement on the major premises but comparatively little unanimity on the interpretation of the details. This is quite to be expected when engineers begin to delve actively in a realm previously reserved largely for the actuaries, accountants and rate specialists.

There is ample excuse for us engineers to examine our respective methods of determining comparative costs for alternative ways of meeting a given engineering problem. Nor is there any reason why they should follow the prescribed techniques of accountants. Their task is to evaluate present worth of some engagement that may stand as a commitment for 20, 30, 50, or even 100 years.

It is extremely desirable that the various procedures exemplified by the papers be resolved toward uniformity. There are three good reasons for a degree of standardization:

1. It is due to investors in the enterprise that their money be spent as wisely and as advantageously as possible. The equipments purchased and system configurations decided should be based on as sound a technical-economic basis as possible.

2. It is due to the manufacturers to know how the criteria for competitive selection of apparatus on an economic worth basis differ from company to company, or better yet, the degree of uniformity in establishing these criteria.

3. It is due to the rate-payers regulatory authorities to have uniformity in judgment on the part of the regulated utilities in making expenditures that have to stand the test of prudence. Otherwise the least "prudent" utility (the one with the dullest pencil) may find itself paying a penalty because the criterion for decision on prudence may follow the pattern set by utilities that use the sharpest pencils.

In brief there is ample urge to prosecute what this symposium has initiated toward exploration of engineering-economic theories. Whether the accountants concur in the prospective conclusions is beside the point. At least the engineers will have made their decisions sound by clarification and unification. The expenditures will thus have been prudent at the source.

Paul H. Jeynes (Public Service Electric and Gas Company, Newark, N.J.): Mr. Slemmer makes one point that is particularly important, though frequently overlooked, which is worth repeating. That is, the only purpose of an economic comparison is to estimate the difference in costs of alternative facilities. Therefore, any items of cost that are the same in either case may well be omitted. It is essential that only real differentials be included.

It is easy to produce examples to illustrate this thesis, and some of them create awkward problems. One of the most awkward is the appropriate treatment of "overheads, including general supervision and accounting expense," which Mr. Slemmer includes under Labor Cost.

For example, suppose the alternative facilities are shunt capacitors versus synchronous condensers. One involves trifling charges for operation or maintenance; the alternative involves very substantial operation and maintenance expense.

Now, the percentage for overheads is no small figure. In some cases, total overheads may exceed 80 per cent of total direct charges for maintenance. If the direct charges for operation and maintenance for both alternatives are increased by 80 per cent, it means that adoption of synchronous condensers is estimated to cause a substantial increase in costs of general supervision, superintendence, accounting expense, and other clerical costs.

Obviously, that is an absurd conclusion. At the same time, it is difficult to justify omitting the overheads altogether. But if they are estimated as a percentage of direct expense, there is this real danger of foolish estimates, as above. And it is equally easy to show that the same danger lies in estimating these overheads as a percentage of first cost.

A more detailed discussion of appropriate means for dealing with this problem would be very helpful.

Present Worth, or the Time Cost of Money, as a Factor in the Economic Comparison of Alternative Facilities

PAUL H. JEYNES
MEMBER AIEE

THE objective of economic comparisons is to estimate in advance the financial effect of adopting one particular plan of action instead of some alternative. One of the major factors in such studies is the return on investment,[1] representing the annual rental paid for money.

In a regulated industry, it can ordinarily be anticipated that the rate of return on investment will be independent of the choice of plan. In such case, the cheapest plan, or "economic choice," is the one which, for the given rate of return, will result in minimum revenue requirements, that is, the minimum cost of product. In nonregulated industry, it is sometimes assumed that the selling price will remain fixed in any event, in which case the economic choice is the plan that will result in the highest rate of return. The same plan will be identified as the economic choice, whichever method is used.

In any case, the fact that money does command an annual rental is implicit in the whole approach, and never questioned. If the rate of return is 6 per cent, an initial investment of \$100 earns \$6 by the end of the first year, making a total of \$106 available for investment throughout the second year. At the end of the second year, without further capital additions, the total amount will stand at $106 \times 1.06 = \$112.36$. This is the familiar law of accumulations at compound interest:

> The amount of \$1 placed at interest, compounded annually at i per cent for n years, equals $(1+i/100)^n$.

The present-worth factor is simply the reciprocal of the foregoing compounding factor. That is, if P dollars (=present worth) invested today at i per cent compounded annually amounts to \$1 in n years:

$$P(1+i/100)^n = 1$$

then

$$P = 1/(1+i/100)^n$$

It is inescapable that if we provide for a return we must also discount all future costs; the two operations are simply alternative ways of expressing the same phenomenon. Yet this simple fact is frequently ignored in engineering literature, very often leading to unsound conclusions in the selection of alternative facilities.

Note particularly that the phrase "present worth" does not imply an appraisal of property in terms of present-day reproduction costs. It means specifically the arithmetical result of discounting future payments for interim interest.

The Basic Cost Comparison

Textbooks suggest several methods for making economic comparisons of alternative facilities, including "capitalized" costs, the "pay-off period" procedure, and others. Correctly performed, all give identical answers; but there is little excuse for using any but the direct approach, which is simplest, most readily comprehended, least vulnerable to errors of omission, and is universally applicable. That is the comparison of present worths of future revenue requirements. By revenue requirements is meant the annual gross receipts that must be obtained in order to recover all annual costs, including a return on the investment.

A simple example will illustrate this method, as well as the error that would be committed by failing to discount future costs. Suppose annual costs of alternative Plans A and B are as shown in Table I, including return at 6 per cent, over a 5-year period, after which costs are expected to be identical in either case (or else not affected by the present choice).

It might be carelessly concluded that the two proposals are a stand-off. But actually, Plan A is \$980.35 cheaper, as is revealed by comparing present worths as of January 1, 1952, as shown in Table II.

Tables of present-worth factors at various interest rates are conveniently available in engineering handbooks and textbooks dealing with financial mathematics; it is no great chore to compile tables for any odd interest rate, using the formulas given in this paper. Three companion papers discuss the preparation of annual cost estimates.[1,2,3]

A Practical Application

Table III presents a typical application of present-worth arithmetic to a practical problem.

Table I. An Example of Comparative Annual Costs

Year	Annual Revenue Requirements Plan A	Plan B
1952	\$ 1,000	\$ 5,000
1953	2,000	4,000
1954	3,000	3,000
1955	4,000	2,000
1956	5,000	1,000
Totals	\$15,000	\$15,000
Arithmetical average	\$ 3,000	\$3,000

Paper 51-360, recommended by the AIEE System Engineering Committee and approved by the AIEE Technical Program Committee for presentation at the AIEE Fall General Meeting, Cleveland, Ohio, October 22–26, 1951. Manuscript submitted May 16, 1951; made available for printing August 30, 1951.

PAUL H. JEYNES is with the Public Service Electric and Gas Company, Newark, N. J.

A piece of land desired for a generating-station site in 1962 is available in 1952 at an attractive price ($\$P$). If the purchase is postponed until 1962, what could we then afford to pay for it ($\$p$), in order to break even? Annual costs are estimated as follows:

	Per Cent
Return on investment	6.00
Federal income taxes	3.45
State income taxes	0.38
Real-estate taxes	2.00
Other expense (1952–1961 only, if purchased in 1952)	0.05
Total annual costs, 1952–1961 =	11.88
Annual costs after 1961, in either event =	11.83

Note that no allowance is made for depreciation, the life of land being conveniently estimated as infinite.[1] Annual costs are tabulated in two parts: (1) 1952 to 1961, inclusive, and (2) after 1961, see Table III.

Accordingly, the present worth (January 1, 1952) of future annual costs may be summarized as follows:

A. If purchased in $1952 = \$0.8744P + 1.1010P$

B. If purchased in $1962 = \$0.00 + 1.1010p$

Equating, and solving for p:

$$1.1010p = 1.9754P$$
$$p = 1.7942P$$

Weighted Average Annual Costs

It is usually discovered that annual costs of a given plan are not a constant amount in each year. This might result, for example, from a decreasing annual capacity factor, from major maintenance jobs at infrequent intervals, from replacements at rising price levels, et cetera. In some such cases it is desired to find the weighted average of those nonuniform costs. An example of the application of present-worth arithmetic to this situation appears in Tables IV and V.

Table IV shows the calculation of annual costs of return plus depreciation, using the "straight-line" method, for plant having 20-year life and 6 per cent return. For simplicity, salvage is assumed to be zero, and there is no dispersion of retirements; that is, all of the property is retired at once at age 20. Annual costs amount to 11 per cent in Year 1, diminishing gradually to 5.3 per cent in Year 20. Such nonuniform annual costs are characteristic of the misnamed "straight-line" method.

The corresponding level weighted average rate is derived in Table V. This corresponds to the partial-payment factor, or the amount that would be paid annually in 20 equal installments to recover first cost, assuming interest at 6 per cent. Three observations with respect to Table V are pertinent:

1. "Return plus average interest," sometimes proposed as the appropriate "straight-line" arithmetic, is only a rough approximation (=8.15 per cent instead of 8.72 per cent).

2. Regardless of relative merits of various depreciation methods for accounting or rate-base purposes, for a given life and percentage return all methods yield exactly the same weighted average rate, which is all that is needed in economic comparisons.

3. The present worth of future annual costs of return plus depreciation, throughout total life, is exactly equal to first cost.

The last observation provides a test for correctness of depreciation arithmetic. For example, it is a very common error to assume that "straight-line" depreciation for 20-year life is 5 per cent annually, which together with 6 per cent return would equal 11 per cent per year. The absurdity of this assumption is revealed by finding the present worth of 11 per cent annually for 20 years:

$$11.469921 \times 11 \text{ per cent} = 126.17 \text{ per cent}$$

In other words, this would be equivalent to assuming that present worth brand new equals 126 per cent of present worth brand new.

Another familiar application of this same arithmetic is the development of a weighted average tax rate, or weighted average maintenance costs, when the percentage is expected to increase at a predictable rate throughout life.

In this connection, it is to be noted that the weighting process may allow not only for the increasing percentage annual cost, but also for the decreasing number of plant units. For example, the annual maintenance cost of meters may increase with age, but the total annual dollars may at the same time decrease with time as the ranks of old meters are depleted by retirements, replacements being equipment of an improved type requiring smaller maintenance expenditures. The net effect is fortunately to emphasize the importance of costs in the immediate future, and to discount heavily the importance of more remote costs which are difficult to estimate with equal assurance.

Table II. Present Worth of Table I Annual Costs

Year	Present-Worth Factors at 6 Per Cent	Present Worth of Annual Costs	
		Plan A	Plan B
1	0.943 396	$ 943.40	$ 4,716.98
2	0.889 996	1,779.99	3,559.98
3	0.839 619	2,518.86	2,518.86
4	0.792 094	3,168.38	1,584.19
5	0.747 258	3,736.29	747.26
Present worth, 1/1/52		$12,146.92	$13,127.27
Advantage of Plan A = 13,127.27 − 12,146.92 = $980.35			

Economic Criteria

The fundamental criterion of economy–minimum revenue requirements associated with a given rate of return–is an annual cost phenomenon. But usually the study involves capital costs (investment in alternative facilities) as well as differences in annual costs (operating expense, maintenance, et cetera), and it is necessary to reduce all items to a common basis before they can be summated and compared.

This operation is preferably performed by estimating the annual costs which result from the capital investment, readily accomplished by applying the appropriate carrying-charge percentage to the capital dollars. By the same token, annual costs such as operating and maintenance expense can be "capitalized" by dividing by the appropriate percentage. The comparison in terms of capitalized costs, when properly carried out, yields figures identical with the recommended "present worth of annual costs" basis.

Table III. Break-Even Cost of Land, $P in 1952 Versus $p in 1962

Year	Present Worth Factors	Land Purchased in 1952		Land Purchased in 1962	
		Annual Costs	Present Worth of Annual Costs	Annual Costs	Present Worth of Annual Costs
(1) Annual Costs, 1952–1961, Inclusive					
1952	0.9434	0.1188P	0.1121P	0	0
1953	0.8900	0.1188P	0.1057P	0	0
etc.	etc.	etc.	etc.	etc.	etc.
1960	0.5919	0.1188P	0.0703P	0	0
1961	0.5584	0.1188P	0.0663P	0	0
Present worth, 1/1/52, of Annual Costs			$0.8744P		$0.00
(2) Annual Costs After 1961					
After 1961	9.3066*	0.1183P	1.1010P	0.1183p	1.1010p

* Present worth on 1/1/62 of $1 annually forever is $\frac{1.00}{0.06} = \$16.6667$

Present worth on 1/1/52 of $16.6667 due on 1/1/62 is $16.6667 \times 0.558\,395 = 9.3066$

Nevertheless, the latter approach is virtually always to be preferred. There are several practical reasons for this recommendation; space limitations permit discussing only a few.

Estimating annual costs resulting from a given capital cost is a familiar, readily-comprehended process; determination of the proper percentage for capitalizing annual expense is less obvious and is very commonly done wrong. To illustrate, consider the familiar problem of balancing the cost of larger conductors against the saving in generating costs.

Let

C = capital cost of larger conductors
c = annual carrying-charge percentage for conductors
G = capital cost of incremental generating capacity
g = annual carrying-charge percentage for generating stations
e = incremental energy costs per year

Then the break-even equation is, in terms of annual costs:

$$Cc = Gg + e$$

In terms of "capitalized" costs, it might be written:

$$C = G + E,$$

where E is the capitalized energy cost, obtained by dividing e by the appropriate percentage.

What is that appropriate percentage? Is it simply the rate of return? Is it the carrying-charge rate applicable to generating stations $(=g)$? Or is it the carrying-charge rate applicable to conductors $(=c)$?

None of these is correct, and it is obvious that many writers do not know the correct answer, $=(Cc-Gg)/(C-G)$.

Yet the proper annual-cost approach is obvious and never questioned.

In some problems, particularly those involving alternatives which do not have the same life or in studies of economic replacements, it is necessary to consider not only alternative initial installations, but perpetual future replacements. This also is the case if allowance is to be made for future price rises.

The replacement function, which is involved if the "capitalized cost" basis is adopted, is complicated, unfamiliar to most engineers, and not conveniently available for various average lives, types of dispersion, and rates of return. The corresponding annual cost (that is, annual cost of depreciation) is conveniently available[1] and better, if imperfectly, understood by most engineers.

As a matter of practical experience, errors of omission are encountered much less frequently in studies made on the annual-cost basis. A familiar example is the presentation of cost comparisons on the basis of first cost per kilovolt-ampere of the several alternatives. In a large percentage of cases, the most economic plan does not have minimum first cost per kilovolt-ampere, for reasons which become apparent when the comparison is set up properly on the basis of total annual revenue requirements.

The safest, simplest, most rigorous procedure is to tabulate annual costs over the appropriate period of comparison, and compare their present worth.

Table IV. Annual Costs of Return Plus Depreciation

"Straight-Line" Method; 20-Year Life, No Dispersion, Zero Net Salvage; 6 Per Cent Return

Columns						
1 Year	2 Annual Return at 6%	3 Book Charge for Depreciation at 5%	4 Accrued Reserve (Σ Col. 3)	5 Credits for Reinvested Reserve (6% of Col. 4)	6 Net Cost of Depreciation (Col. 3 − Col. 5)	7 Total Annual Costs (Col. 2 + Col. 6)
1	6.00%	5.00%	0.00%	0.00%	5.00%	11.00%
2	6.00	5.00	5.00	0.30	4.70	10.70
3	6.00	5.00	10.00	0.60	4.40	10.40
4	6.00	5.00	15.00	0.90	4.10	10.10
5	6.00	5.00	20.00	1.20	3.80	9.80
etc	etc.	etc.	etc.	etc.	etc.	etc.
16	6.00	5.00	75.00	4.50	0.50	6.50
17	6.00	5.00	80.00	4.80	0.20	6.20
18	6.00	5.00	85.00	5.10	−0.10	5.90
19	6.00	5.00	90.00	5.40	−0.40	5.60
20	6.00	5.00	95.00	5.70	−0.70	5.30

Arithmetic mean of annual costs for return plus depreciation = 163.00 ÷ 20 = 8.15%.* Total 163.00%

*This is the same as the "depreciation plus average return," sometimes proposed, as follows:

Return in year 1 = 6.00%
Return in year 20 = 6.00(1.00 − 0.95) = 0.30%

$$\text{Average return} = \frac{6.00+0.30}{2} = 3.15\%$$

Depreciation plus average return = 5.00 + 3.15 = 8.15%

This is not only a rough approximation of the proper arithmetic, but an inaccurate version of actual cost behavior.

Table V. Weighted Average Costs of Return Plus Depreciation

"Straight-Line" Method; 20-Year Life, No Dispersion, Zero Net Salvage; 6 % Return

Year	Annual Costs of Return plus Depreciation (Table IV)	Present-Worth Factors At 6%	Present Worth of Annual Costs of Return plus Depreciation
1	11.00%	0.9434	10.38%
2	10.70	0.8900	9.52
3	10.40	0.8396	8.73
4	10.10	0.7921	8.00
5	9.80	0.7473	7.32
etc.	etc.	etc.	etc.
16	6.50	0.3936	2.56
17	6.20	0.3714	2.30
18	5.90	0.3503	2.07
19	5.60	0.3305	1.85
20	5.30	0.3118	1.65
Totals	163.00%	11.4700	100.00%

Weighted average annual costs,* return plus depreciation $= \frac{100.00}{11.47} = 8.718\%$

Annual cost of depreciation (level weighted average) = 8.718 − 6.000 = 2.718%

*This same weighted average is obtained no matter what method of depreciation accounting may be used—"straight line," sinking fund, compound interest, present worth, retirement accounting, or any other.

Term of the Cost Comparison

The economic comparison involves all future annual costs of the enterprise that are affected by the choice of plan; annual costs are to be compared from the date of installation to perpetuity. This may appear excessively academic, in view of the great difficulty of anticipating events beyond the immediate future, but actually the inevitable effects of present-worth arithmetic operate to facilitate a practical solution.

For example, if annual costs of two alternatives differ by $100 per year 50 years from now, the present worth of that difference, at 6 per cent return, is only $5.43 per year. The present worth of $100 per year 100 years from now is only 29¢ per year. Since most types of plant have average lives of 30 years or thereabouts, which means that the last survivors may serve 60 years or more, it is rarely necessary to extend the comparison beyond the history of one generation – perhaps 50 or 60 years.

Problems in economic replacement involve a comparison of annual costs under the two alternatives:

Plan A: If the existing equipment were retired and replaced immediately, versus

Plan B: If the existing equipment were retained to serve out its normally-expected life.

In such problems, the appropriate period may be the remaining life of the existing equipment per Plan B, because thereafter annual costs would be the same (= annual costs of new replacements, and successors, to perpetuity) whichever plan is now adopted. Of course, this convenient solution must be modified if continued price rises can be predicted, because replacements under Plan A would then cost more than under Plan B, coming as they would at later dates.

In the great majority of published solutions, whether in technical papers or textbook examples, no year-by-year tabulation is presented. Instead, there appears a single statement of annual costs for each alternative. The implication is that these same annual costs will be repeated in each future year.

This assumption is understandable, in the interests of simplification, in an elementary exposition of principles involved. It occasionally represents the reasonable expectations in an actual situation. But strictly speaking, such situations are rather special cases, and not generally typical. They are encountered only when three conditions are met:

1. Average lives of the alternative facilities are identical.
2. Capacity supplied by both alternatives is identical.
3. Neither plan prejudices the nature of future additions; or else both commit the utility in the same manner.

If requisite number 1 is not met, future replacements will be needed as of different dates, and price rises will therefore affect the alternatives differently in the future. If the capacity supplied is not identical, additions necessary to supply load growth will be required as of different dates, which will change relative annual costs in the future. If the two plans prejudice future additions differently, replacements may have different costs, and affect future annual costs correspondingly.

Accordingly, when annual costs are stated as a single figure, it must not be overlooked that this figure represents an estimate of the amount that would appear in each year of the year-by-year tabulation in perpetuity, or at least throughout the appropriate period of comparison. In brief, the appropriate period is ordinarily established by one of two considerations:

1. The date after which annual costs will be identical whichever alternative is selected.
2. The date which is so far in the future (say 50 or 60 years) that annual cost differences thereafter have insignificant present worth.

Evading this issue on the plea that future costs are too uncertain for long-term estimates amounts to deliberately assuming zero cost difference when a differential is acknowledged to exist but is difficult to estimate. Judgment must be used in deciding how much refinement is economically justified, but judgment is worthless unless based on a sound understanding of the correct arithmetic, in order to gauge the quantitative effects of refinements on the estimate. Details that appeal to the uninitiated as unjustifiable refinements may prove to be glaring omissions. Attempting shortcuts by comparing "capitalized" costs or first costs per kilovolt-ampere, and ignoring annual costs, is very apt to conceal difficulties without solving them.

Effect of Changing Price Levels

Although the disastrous effects of inflation have become fully recognized, and governmental measures have been taken to control prices, there is a real possibility of continued price rises in the future. Whether that possibility can be firmly predicted or not, it is often desirable to anticipate what the effect would be on the economic comparison if a stipulated price rise were to occur. Mention has been made at several points in this paper of the special measures that are called for in such estimates; in general, the appropriate procedure is as follows:

1. Tabulate for each year of the comparison the number of retirements and survivors of the original installation, per the appropriate survivor curve.
2. Price the replacements (=number of retirements) in each year per the assumed price increase.
3. Compute separately the annual costs of: (a) Survivors of the original installation, and (b) Survivors of each year's replacements. This must be done year by year because each original group decreases in size each year, and a new group of different size and cost is added each year. Rising costs of operation and maintenance, in dollars per year, must also be estimated.
4. Determine the present worth of the foregoing annual costs.

The effect of price rises is apt to be less than might be imagined except in problems of economic replacement when:

1. The equipment involved has a very long life.
2. The choice between retaining versus replacing must be made at a relatively early age.
3. Rapid price rises are predicted.

The general effect of anticipated price increases, in such problems, is to reduce the maintenance expenditure that is justified as an alternative to replacement.

Having prepared estimates of the investment costs and expenses associated with the several alternative plans, the relative economics of the various proposals is desirably expressed as a comparison of their respective revenue requirements, or cost of product. This is preferably done by tabulating annual costs (=revenue requirements) over the appropriate period of comparison, and comparing their respective present worths. This same present-worth arithmetic is indispensable in several parts of the estimating process, some of which are discussed in this paper.

References

1. ANNUAL CARRYING CHARGES IN THE ECONOMIC COMPARISON OF ALTERNATIVE FACILITIES, P. H. Jeynes. *AIEE Transactions*, volume 70, part II, 1951, pages 1942–53.

2. EVALUATION OF ENERGY DIFFERENCES IN THE ECONOMIC COMPARISON OF ALTERNATIVE FACILITIES, A. P. Fugill. *AIEE Transactions*, volume 70, part II, 1951, pages 1854–60.

3. OPERATING AND MAINTENANCE COSTS FOR USE IN THE ECONOMIC COMPARISON OF ALTERNATIVE FACILITIES, W. E. Slemmer. *AIEE Transactions*, volume 70, part II, 1951, pages 1954–55.

Discussion

Wm. R. Brownlee (Southern Services, Inc., Birmingham, Ala.): Especially in periods of rising costs, a keen appreciation of all of the economic factors is of vital importance in the planning of additions to power supply systems. All too often the basic concept of the present worth of future carrying charges, so well illustrated in Mr. Jeynes' paper, has not been given sufficient weight.

A thorough theoretical knowledge of exact "timing arithmetic" is valuable, even though based on rather unprecise assumptions or generalizations on the cost of money and life of equipment. It must be recognized that less precision is available in evaluating the other side of the equation. For example, the author's illustration shows that (on a given basis) one can afford to pay ten years from now a price equal to 1.7942 times the present-day price for a station site, whereas few would care to predict even to two significant figures what the cost of such a site might be ten years from now.

The illustration of the calculation of economic conductor size poses a difficult problem in evaluating the "Capital Cost of the Incremental Generating Capacity." If this be considered to be the unit cost (with a reserve component included) of the next system capacity addition, it might be either the first unit of a new plant with corresponding site development items involving a high cost per kilowatt or the addition of a second generating unit in a previously provided 2-unit building, giving a materially lower cost.

Another concept of incremental capacity might be the differential cost of increasing the size of a proposed generating unit and dividing the added cost in dollars by the added capacity in kilowatts. Such a computation might show a unit cost per kilowatt from one-half to two-thirds of the unit cost of a complete generating installation. Opposed to this concept is the hypothesis that the maximum size of the unit has already been determined by considerations, such as the size of the power system, relative reserve requirements, interconnections, or even the largest unit considered to have adequate service reliability as now designed. Still another basis would hold that if energy cost is based on the higher cost units in operation at various representative time periods, then it would not be proper to select any new (and therefore efficient) unit as a basis for capacity cost.

The author's reaction to these various concepts and an explanation of his preferred basis would be appreciated.

William Parkerson (Middle West Service Company, Chicago, Ill.): After all of the first costs and all of the annual expenses enumerated by all of the papers, have been compiled and tabulated by years, according to the Uniform System of Accounts, the task of comparing the relative economics still remains. To accomplish this all-important function, Mr. Jeynes paper presents irresistable arguments for the "present worth method" which appears to be more surefooted in its progress, and more practical in its results, than any other method developed, especially since it minimizes the effect of distant estimates.

It is hoped that the Committee can continue the study of this highly important subject to the end that they will be able to present and recommend to the AIEE a standard approach or procedure for economic comparison of alternate facilities, even perhaps including working forms and convenient tables such as compound interest, dispersion factors, et cetera. It seems obvious that such a report, so constituted would be invaluable to all engineers.

Maurice R. Scharff (Consulting Engineer, New York, N. Y.): The author performs an important service in emphasizing the necessity and in explaining so clearly the correct method of giving effect to the present worth or the time cost of money in economic comparisons of alternative facilities. The writer can confirm from his own experience that this necessity, which ought to be self evident, is too frequently ignored even in engineering reports by experienced engineers.

It may be of interest to call attention to the fact that the method of analysis, suggested by the author and illustrated by examples, utilizing a "level weighted average depreciation" cost, related to investment service life and rate of return, is equally applicable to calculations utilizing a "level weighted average" depreciation or depletion per unit of output. Such an approach might have application to economic comparisons of power plants, for example, utilizing a weighted average cost per kilowatt-hour; or of investments in wasting natural resources, such as oil, natural gas or minerals, utilizing a weighted average depletion cost per unit of output. The writer discussed one aspect of this suggestion, with an example based upon what he there referred to as "Compound Interest Depletion," published in 1947.[1]

REFERENCE

1. COMPOUND INTEREST DEPLETION. Maurice R. Scharff. *Technical Valuation*, New York, N. Y., volume 8, number 2, July 1947, page 9.

M. J. Steinberg (Consolidated Edison Company of New York, Inc., New York, N. Y.): This paper stresses the importance of the present worth concept as a calculating tool for evaluation of alternative investments when annual values are not uniform. It is claimed in the paper that a comparison of present worths of future revenue requirements is a direct approach which is simplest and most readily comprehended. The three most common methods of evaluation are by comparison of annual costs, capitalized annual costs, and present worths of annual costs. By proper application of compound interest formulas comparable results can be obtained. Under specific circumstances one method may be preferable to the others. Generally, however, the choice will be one of personal taste.

Where nonuniform annual values are involved, a comparison of present worths is perhaps the most direct. It is pertinent to note, however, that there is a strong preference for indicating comparative results in terms of annual values, and where nonuniform annual values are involved, the corresponding present worth can be converted into equivalent uniform values. Reduction to present worth then becomes an intermediate step.

Our thoughts on the matter are best presented by reference to the examples in the paper. In this connection it is relevant to stress the distinction between equal and equivalent values. Thus in Table I, it is shown that by arithmetic averaging, the annual revenue requirements are equal. By converting to present worth values as shown in Table II, it is shown, however, that the equal average annual values are not however equivalent. The equivalent uniform annual values are obtained by applying the appropriate capital recovery factor as follows:

Plan B	$\$13{,}127.27\,\dfrac{(0.06(1.06)^5)}{((1.06)^5-1)}=$ $\$13{,}127.27\ (0.237\,396)=$	$3,116.36
Plan A	$=12{,}146.92\ (0.237\,396)=$	2,883.63
Difference Plan B – Plan A	$ 980.35 (0.237 396)	$ 232.73

Similarly, for the "break-even" example illustrated by Table III of the paper an equally direct solution can be obtained without recourse to the use of present worth values. Let P = price paid if purchased in 1952, and p = price paid if purchased in 1961 Then with annual fixed charges at 11.88 per cent and 11.83 per cent as indicated in the paper, to break even, savings from 1952 through 1961 = increased costs subsequent to 1961 or

$$0.1188P\left(\frac{(1.06)^{10}-1}{0.06}\right)=\frac{0.1183(p-P)}{0.06}$$

$$0.1188(13.181)P=1.9717(p-P)$$

solving gives

$$p=1.7942P$$

which is identical with the results derived in the paper.

With reference to Table V of the paper, it should be noted that recourse to tabular values as shown in the table is not necessary, since identical results are obtained from tables of capital recovery rates. In this case, the capital recovery factor is

$$CRF=\left(\frac{i(1+i)^n}{(1+i)^n-1}\right)=\frac{0.06(1.06)^{20}}{(1.06)^{20}-1}=0.08718$$

or

	8.718%
Equivalent uniform annual return	6.000
Equivalent uniform annual depreciation	2.718%

The fundamental principle that is illustrated by Tables IV and V of the paper is the fact that all methods of depreciation are equivalent although not equal, and that by proper application of appropriate compound interest formulas, it is possible to convert nonuniform rates for annual return and annual costs of depreciation into equivalent uniform annual rates. For the purpose of this conversion use of present worth values becomes an important tool.

A. E. Knowlton (*Electrical World*, New York, N. Y.): From the papers presented at this session one could as likely draw confusions as to draw conclusions. It is evident that there is reasonable agreement on the major premises but comparatively little unanimity on the interpretation of the details. This is quite to be expected when engineers begin to delve actively in a realm previously reserved largely for the actuaries, accountants and rate specialists.

There is ample excuse for us engineers to examine our respective methods of determining comparative costs for alternative ways of meeting a given engineering problem. Nor is there any reason why they should follow the prescribed techniques of accountants. Their task is to evaluate present worth of some engagement that may stand as a commitment for 20, 30, 50, or even 100 years.

It is extremely desirable that the various procedures exemplified by the papers be resolved toward uniformity. There are three good reasons for a degree of standardization:

1. It is due to investors in the enterprise that their money be spent as wisely and as advantageously as possible. The equipments purchased and system configurations decided should be based on as sound a technical-economic basis as possible.

2. It is due to the manufacturers to know how the criteria for competitive selection of apparatus on an economic worth basis differ from company to company, or better yet, the degree of uniformity in establishing these criteria.

3. It is due to the rate-payers and regulatory authorities to have uniformity in judgment on the part of the regulated utili-

ties in making expenditures that have to stand the test of prudence. Otherwise the least "prudent" utility (the one with the dullest pencil) may find itself paying a penalty because the criterion for decision on prudence may follow the pattern set by utilities that use the sharpest pencils.

In brief there is ample urge to prosecute what this symposium has initiated toward exploration of engineering-economic theories. Whether the accountants concur in the prospective conclusions is beside the point. At least the engineers will have made their decisions sound by clarification and unification. The expenditures will thus have been prudent at the source.

John E. Girard and **Hubert M. Langlois** (Department of Water and Power, Los Angeles, Calif.): The paper, in considering the matter of economic comparisons, carries a suggestion that all methods of accounting for depreciation "yield exactly the same weighted average rate," presumably leading to the same end result. That this holds true as an equivalence throughout the life of the property is seriously debatable. In any case, the implications of the concept, particularly as affecting individual years of operation of a utility, are not likely to be accepted by certain regulatory jurisdictions as being fully equivalent.

It may be observed that under the method used in computing the "annual costs" of depreciation in Table IV, the straight line annuity has been reduced year by year in the amount of a return on the accumulated reserve, at the same rate as predicated for return on investment in its ordinarily understood sense. Such treatment essentially presumes that depreciation funds as a source of investment money should be entitled to the same rate of return as the fixed and established investment in utility plant; this concept is not universally supported by regulatory authorities, and certainly is not held by the California Utilities Commission.

Hamilton Treadway (Bureau of Yards and Docks, Department of the Navy, Ashton, Md.): This and the companion papers[1] are timely. They focus attention on that phase of engineering, namely economics, which differentiates management from the other fields in the profession. In a period, during which the expenditures for military and other defense purposes are constantly increasing and the amount which the available funds will purchase is ever decreasing, the principles outlined in these papers are of utmost importance if we are to get the maximum defense value from that portion of our economy which we now propose to devote to this effort. While the authors have limited their presentation primarily to the public utility field generally and the electric power industry in particular, the principles expounded are adaptable to almost any problem in engineering economics. They are especially useful in the planning and management of utility systems for military shore establishments.

The use and advocacy of the present worth theory is, of course, sound. It can be, however, over-emphasized. It is well to keep in mind that, as cost of money decreases, its present worth increases, for example. $1.00 of annual costs per year for ten years has a present worth of $8.9796 at 2 per cent, while at 6 per cent the present worth is $7.3602. Lower cost money reduces the spread between the several plans for accomplishing a project. This is shown in Table I of this discussion by a comparison of plans A and B of Tables I and II of Mr. Jeynes' paper, using 2 per cent and 6 per cent money. Instead of plan A being $980.00 more favorable than plan B, it is only $374.00 better at the lower rate. This change in the relative economics may result in other factors controlling the final selection.

Table I

Plan	Present Worth at 6 Per Cent	Present Worth at 2 Per Cent
A	$12,146.92	$13,953.40
B	13,127.27	14,327.00
Net in favor of plan A	980.35	373.60

Lower cost money does not mean the abandonment of the present worth concept. It does, however, reduce its value in the short term comparisons which must often be made in selecting facilities or in evaluating relative economy when planning shore developments for military requirements. The permanency of the installation and the duration of the period during which the added facilities will be used dictate the interval of comparison in these cases. The three conditions precedent to the use of a single statement of annual costs, as outlined by Mr. Jeynes, are at present warranting this simplification of the problem. It is, however, difficult to establish general criteria for determining when the present worth method may be dispensed with. It is always safe to make the detailed calculations involved in its use, although not always necessary to the exercise of sound judgment.

One of the common problems encountered in providing utility services for military installations involves the choice of alternate sources of providing for both expanded heating and electric power needs, where a boiler plant already exists with or without by-product electric generation. The problem usually involves many facets. Often in working out the detailed calculations for the various possible solutions, it is found that many of the items of annual cost are the same in each case. It is not considered advisable to omit these from the detail of the study. Mr. Jeynes' illustration in Tables I and II of his paper on present worth shows one of the pitfalls of omitting items of cost because they appear to set off each other. Most items of annual operation, maintenance, and replacement are found to vary widely with the type of equipment selected and in any long range problem a detailed estimate is required year by year. Items such as turbine and boiler maintenance provide good examples of the variables encountered in annual maintenance. Only a detailed year-by-year estimate of these expenses based on operating experience will give a true picture of the annual cost and present worth.

Mr. Jeynes advocacy of the present worth method of treating depreciation will surely provoke discussion. Here the problem is to reconcile the differences between sound engineering economics and accounting practice in a manner which may be clearly understood by those who must make the final decision. His remarks concerning life estimates and retirement dispersion provide a brief but clear picture of the survivor life method. His suggestion to use the Iowa Type S_2 dispersion in estimating depreciation costs for a single unit when its group behavior is not determinate has been found to give satisfactory results in most cases.

The problem of estimating salvage has become increasingly difficult in recent years. With shortages and rising prices plant items normally abandoned a few years ago may be salvaged now at values which are sometimes even higher than original cost. This factor like all of those affected by inflationary trends is not given to scientific treatment. The estimate must be based largely on judgment but salvage should be given a higher value in many instances today than was normally considered sound a few years ago. This is particularly true in short term estimates.

The cost of money is important when selecting from several types of equipment. Low cost of money warrants larger investment to reduce fixed items of annual cost, such as, core losses in transformers. In considering such an item independent of the other variables of annual cost care must be taken to assure that other items are not materially affected by the changes necessary to reduce the fixed annual item. In considering this aspect of the problem the present worth of the annual item under consideration should be evaluated in comparison with the present worth of the added investment. One must be careful not to confuse the present worth and capitalization methods in considering this phase of the problem. Either one or the other method must be used throughout in order that all comparisons will be on the same basis.

REFERENCE

1. See references 1, 2, 3, and 4 of the paper.

Paul H. Jeynes: Mr. Brownlee comments on the futility of computing break-even costs to four decimal places in Table III when it is impossible to predict future prices to one decimal with any assurance. The author is heartily in accord with that viewpoint. As a practical matter, an estimate of 1.8 per cent would be just as useful as, and a great deal less amateurish than, the estimate of 1.7942 per cent developed in the paper. At the same time, the latter version was adopted deliberately for the following reason.

The use of several unnecessary decimal places emphasizes the fact that there is nothing subjective about the correct arithmetic. Given the same starting assumptions, any two estimators must inevitably arrive at precisely the same final answer. Too often it is assumed that the arithmetic of economic comparisons differs from ordinary engineering calculations in that there is no single "correct" answer, but a number of defensible solutions depending upon the estimator's viewpoint with respect to the validity of present-worth calculations, his acceptance of some particular theory of depreciation, or his preference for comparisons of "capitalized" costs rather than annual costs, et cetera. The facts are quite otherwise.

One of the major objectives of the present symposium is to promote the idea that the arithmetic of economic comparisons is just as definitive and rigorous as Ohm's Law. The fact that sound judgment is essential, or that approximations and short-cuts are acceptable in practical applications, should not be allowed to obscure this fundamental truth, as it does in much of the literature.

A complete reply to Mr. Brownlee's penetrating inquiry concerning incremental capital cost of generating capacity cannot be undertaken here. That is the subject of a proposed technical paper under the title of "Evaluation of Capacity Differences in the Economic Comparison of Alternative Facilities," planned as a future contribution to the present symposium.

Briefly, the additional investment in generating stations over a period of years may not grow in direct proportion to the increased peak loads supplied. Most utilities, on plotting year-end plant investment against the corresponding peak loads for 20 years or more, discover that the investment has increased much more slowly than the peak loads, despite rising price levels.

In other words, experience in the recent past frequently demonstrates that the incremental investment per kilowatt of peak load is substantially less than the average cost per kilowatt. It is possible that the reverse may be predictable in some cases. But in any event, it is necessary to recognize that the incremental cost, which is the figure required for the economic comparison, may differ appreciably from the average cost. Accordingly, the meticulously correct phraseology was used in the example without explaining the rather involved details of its estimate.

The discussions presented by Messrs. Parkerson, Scharff, and Steinberg attest the practical nature of present-worth arithmetic. Mr. Steinberg is quite correct in his view that the year-by-year tabulation of annual charges per Table V is unnecessary, being equivalent to a single application of the capital-recovery factor. Again, that tabulation of annual charges was adopted deliberately, in order to emphasize the fact that use of the capital-recovery factor is not abstract theory, but a faithful version of the book entries actually made by the accountant as a result of the transaction.

Mr. Knowlton's comment on a lack of unanimity in interpreting the details of economic comparisons is mildly puzzling. A more specific indication of the particular details that appear to him to be confusing or lacking in uniformity would be helpful as a guide in future discussions on this subject.

Possibly Mr. Knowlton feels that this symposium is confusing because it differs in several details with generally-accepted practice in engineering economics. It is true that these papers do find serious shortcomings in a number of techniques commonly used in economic studies and frequently encountered in the literature. The very fact that so much in common practice is bad practice is, of course, a major reason for undertaking this symposium on preferred methods.

However, the symposium is not adequately described as "an exploration of engineering-economic theories," unconcerned over possible lack of concurrence by accountants. On the contrary, it is devoted to presenting sound practical methods of evaluating in advance the same situation which would be revealed after the fact by orthodox cost accounting.

The familiar assumption that cost behavior necessarily signifies something different to engineers and to accountants, respectively, is responsible for much of the confused thinking in this field. It is believed to be unlikely that accountants will differ seriously with any views expressed in these papers. On the other hand, it is more probable that they will feel it is high time the engineering profession recognized the factual nature of cost phenomena (as apposed to economic theory) that is emphasized in this symposium.

Messrs. Girard and Langlois are not convinced that all methods of accounting for depreciation "yield exactly the same weighted average rate," and lead to the same answer to the economic comparison. The reason for their objection is not apparent; it must be based on some misunderstanding. The notion that assuming some particular method of accounting for depreciation makes a difference in the economic comparison is one of the most widespread and harmful fallacies of the business world.

It is obviously true that costs in individual years would be different, depending upon the method of depreciation accounting used, which is an important consideration in rate-making. But the weighted average of the resultant annual costs remains the same in any case, and it is only this weighted average that is of importance in economic comparisons. This instance provides a good example of the urgent need to distinguish between desirable rate procedures and techniques suitable for making economic comparisons.

Messrs. Girard and Langlois also call attention to the California practice of computing a return on reinvested reserves at a lower rate than on the initial investment; but their comment again appears to confuse regulatory matters with the making of economic comparisons. For the latter purpose, the enlightened California procedure can be converted into a rate of return (i) on the investment, plus a depreciation annuity (d) based on reinvestment at that same rate i, the sum of which ($=i+d$) equals the allowed return (i') on the rate base plus the depreciation annuity (d') based on reinvestment at the stipulated rate which is less than i'. The reasons for this recommendation, as well as the reasons for that regulatory practice, are discussed in a companion paper.[1]

Mr. Treadway's remarks illustrate the sort of conclusions which the author hoped would be drawn from this paper. That is, a thorough understanding of the meticulously correct arithmetic facilitates development of reasonable approximations and acceptable short cuts, as well as the over-all exercise of truly sound judgment in practical applications.

REFERENCE

1. See reference 1 of the paper.

Steady-State and Transient Synthesis of 3-Phase Reluctance Motors (Synchronous Motors Without Field Excitation)

MOSTAFA E. TALAAT
ASSOCIATE MEMBER AIEE

Synopsis: In this paper the 2-reaction theory of synchronous machine analysis has been extended to obtain a synthesis procedure for 3-phase reluctance motors. Experiments were made on a motor with a rotor especially designed and constructed to conform with the assumptions of the generalized 2-reaction theory. Results of a differential analyzer investigation formed the basis for a method for simultaneous steady-state and optimum transient synthesis.

In the synthesis procedure presented, the assumption is made that the desirable pull-out torque, load torque to be pulled into synchronism, load inertia, supply voltage, supply frequency, and desired motor speed are specified. Certain stator laminations are assumed to be available. The maximum flux density in the stator teeth and the maximum current density in the stator conductors also are specified. The synthesis procedure then aims at obtaining the optimum design using the available stator laminations.

UP TO the present, literature on reluctance motors[1,2] has been very scarce. Their limited use in the past made the extensive study of the theory of their performance or design seem not worth the effort from a practical viewpoint. However, the recent increasing needs for small synchronous motors and also the requirement that such motors should pull-in certain load torques at certain load inertias, has increased the importance of the problem and has made the study of the transient performance of reluctance motors desirable.

In this paper the methods of analysis presented in the 2-reaction theory of synchronous machines by R. H. Park[3,4,5] has been developed and transformed to forms which are most suitable for a desirable synthesis procedure. The transformed equations used give the desired performance of the reluctance motor in terms of its dimensions and physical constants. A motor with a special rotor shape constructed to verify certain assumptions was used as an example. An intensive study was made on the differential analyzer which led to the pull-in criterion for reluctance motors. This pull-in criterion was verified quantitatively and qualitatively in different ways.

Discussions and Conclusions

The synthesis procedure presented here is based on a stator magnetic circuit of fixed contour. It makes use of the two families of curves, T_{po}/A (Figure 1), and T_{pi}/A together with the universal curve T_{pio}/A (Figure 2). When the pull-out torque, and load torque to be pulled in at a certain inertia are prescribed, then a direct solution for optimum pull-in performance may be obtained for the following quantities:

1. The ratio of minimum to maximum equivalent air gap.
2. The equivalent length of stack.
3. The rotor resistance.
4. The minimum equivalent air gap.
5. The number of stator conductors per phase.

Such a desirable optimum synthesis has become possible through the use of the universal curve T_{pio}/A (Figure 2) to obtain a solution for y as indicated by equation 35. In using this universal curve only significant values of y should be considered. For instance, for the given numerical example the flux plots given in Figure 3 show that y cannot be greater than about 0.06, otherwise assumption 12 becomes invalid. This means that solutions for y of equation 35 less than 0.06 will not be significant. The method may show that it is impossible to obtain a positive real y greater than 0.06, which will satisfy the given prescribed performance. This would mean that the size of laminations tried is too small and that a larger size should be used.

The use of the special rotor shape (Appendix I) to satisfy assumptions 4 to 6 inclusive has also led to the expressions for x_{ad}, X_{a1d}, x_{aq}, and X_{a1q} in terms of dimensions and geometry of the machine as given by equations 9 and 10. Figure 4 shows a comparison of calculated and measured values of the synchronous reactance as a function of rotor position. This comparison was made for a motor with a solid Armco iron rotor constructed as outlined in Appendix I. The figure shows that the greatest discrepancy from sinusoidal variation of self-inductance is about 10 per cent.

The pull-in criterion as presented by equation 64, and the expression for pull-in torque in its synthesis form as given by equation 16 together with its presentation by the family of curves shown in Figure 2 is believed to be original. This pull-in criterion was derived through an intensive study made on the differential analyzer. A comparison of results obtained from analyzer runs with results calculated using criterion is given in Figure 5. Figure 6 gives a comparison of calculated values of slip S_0 using equation 62 and values observed during analyzer runs. The criterion was also tested by varying the

---

Paper 51-361, recommended by the AIEE Rotating Machinery Committee and approved by the AIEE Technical Program Committee for presentation at the AIEE Fall General Meeting, Cleveland, Ohio, October 22–26, 1951. Manuscript submitted March 19, 1951; made available for printing September 12, 1951.

Mostafa E. Talaat is with University of Pennsylvania, Philadelphia, Pa.

The author wishes to express his gratitude to Dr. C. N. Weygandt of the University of Pennsylvania for his advise, interest, and encouragement in the carrying out of this work.

Nomenclature*

A = see equation 17
a = see equation 18
A_b = area of rotor bar
A_r = area of rotor end ring
A_s = area of stator slot
B_{cr} = maximum flux density in rotor core
B_{cs} = maximum flux density in stator core
B_m = maximum flux density in air gap
B_{tr} = maximum flux density in rotor teeth
B_{ts} = maximum flux density in stator teeth
b_{or} = equivalent rotor slot opening at the air gap
b_{os} = equivalent stator slot opening at air gap
c = see equation 20
D_r = approximate average diameter of rotor end ring
D_s = stator core bore
d_i = density of lamination iron
e_m = peak terminal voltage per phase
e_{ma} = peak air gap voltage per phase
f = supply frequency
g = equivalent air gap at any point
g' = physical air gap at any point
g_d = equivalent minimum air gap
g_d' = physical minimum air gap
g_i = air gap equivalent to effect of finite permeability of iron
g_q = equivalent maximum air gap
g_q' = physical maximum air gap
i_a, i_b, i_c = instantaneous currents in phases a, b, c
i_{mm} = maximum allowable current per phase
J_L = load inertia
J_r = rotor inertia
J = total inertia
J_m = maximum allowable current density in the stator conductors
$k = 0.18$, $p > 2$; $k = 0.36$, $p = 2$ in equation 31
k_c = Carter coefficient at any point on the stator periphery; see equation 48
k_{d1} = stator distribution factor for fundamental
k_{h1} = stator winding factor for all harmonics (see reference 6)
k_{h2} = rotor winding factor for all harmonics (see reference 6)
k_{p1} = stator pitch factor for fundamental
k_s = stator slot factor
k_{w1} = stator winding factor for fundamental components
L_e = length of end winding $= L_{e1} + L_{e2}$ (see reference 6)
L_b = length of rotor bar
L_r = length of rotor end ring
L_o = see equation 7
L_s = length of stack

$$M = \frac{8\omega^2 x_d J}{3_p{}^2 e_m{}^2}$$

N = number of stator turns per phase
N_s = number of stator conductors per slot
n = motor speed in rpm
p = number of poles
Q_2 = number of rotor slots or bars
Q_s = number of stator slots
R_{1d} = rotor resistance in the direct-axis
R_{1q} = rotor resistance in the quadrature-axis
r = stator resistance per phase
r_1 = see equation 25
r_{1d} = see equation 15 and 29
s_0 = slip speed at beginning of synchronizing periods in radians per second
t = time in seconds
T_L = load torque

$$T_{Lu} = \frac{4\omega x_d}{3pe_m{}^2} T_L$$

T_{pi} = pull-in torque
T_{pio} = optimum pull-in torque
T_{po} = pull-out torque
T_{st} = starting torque
V = line to line supply voltage (rms)
x_d = direct-axis synchronous reactance
x_q = quadrature-axis synchronous reactance
X_{11d} = direct-axis self-reactance of rotor referred to stator
X_{11q} = quadrature-axis self-reactance of rotor referred to stator
x_{Ld} = direct-axis leakage reactance per phase
x_{Lq} = quadrature-axis leakage reactance per phase
x_1 = see equation 26 and 30
X_{L1d} = direct-axis leakage reactance of rotor referred to stator
X_{L1q} = quadrature-axis leakage reactance of rotor referred to stator
x_{1d} = see equation 27 and 31
x_{ad} = direct-axis armature reaction synchronous reactance
x_{aq} = quadrature-axis armature reaction synchronous reactance
x_d'', x_q'' = direct- and quadrature-axis subtransient reactance
X_{a1d} = magnitude of mutual reactance between a phase winding and the direct-axis rotor winding referred to stator side
X_{a1q} = magnitude of mutual reactance between a phase winding and the quadrature-axis rotor winding referred to stator side
$y = g_d/g_q$
$\alpha_d = \omega R_{1d}/X_{11d}$
$\alpha_q = \omega R_{1q}/X_{11q}$
β = see equation 19
γ = angle in electrical radians between magnetic axis of phase a and any point on the stator surface
δ = angle in electrical radians between magnetic axis of phase a and rotor direct-axis
$\delta'(0)$ = motor speed in electrical radians per second at the initial instant
$\theta = \omega t + \delta$
λ_{cr} = length of magnetic flux path in rotor core
λ_{cs} = length of magnetic flux path in stator core
λ_{tr} = length of magnetic flux path in rotor teeth
λ_{ts} = length of magnetic flux path in stator teeth
$\mu_0\lambda_{sr}$ = rotor slot permeance (reference 6)
$\mu_0\lambda_{ss}$ = stator slot permeance (reference 6)
$\mu_0\lambda_{ttr}$ = rotor tooth top permeance (reference 6)
$\mu_0\lambda_{tts}$ = stator tooth top permeance (reference 6)
μ_0 = permeability in air $= 4\pi \times 10^{-7}$ henry/meter (meter kilogram second)
μ_{cr} = magnetic permeability of rotor core
μ_{cs} = magnetic permeability of stator core
μ_{tr} = magnetic permeability of rotor teeth
μ_{ts} = magnetic permeability of stator teeth
ρ_r = resistivity of rotor conductor
ρ_s = resistivity of stator conductor
σ = see equation 21
τ_{sgr} = rotor slot pitch at the air gap
τ_{sgs} = stator slot pitch at the air gap
ϕ_{1aa} = fundamental armature reaction flux in phase a due to i_a
ϕ_{1ab} = fundamental armature reaction flux in phase a due to i_b
ϕ_{1a1d} = fundamental armature reaction flux in direct axis rotor circuit due to i_a

machine constants and observing their effect on the pull-in torque. Analyzer runs made in that respect showed close agreements with predicted values when calculated using the pull-in torque as given by equation 64. Table I gives a summary of results obtained for a fixed total inertia of three times the self inertia of the sample motor. It also was observed from analyzer runs that different angular positions of rotor direct-axis with respect to the magnetic axis of phase a at the initial instant affects only the time taken by the motor to pull-in but has no effect on the criterion. Figure 7 gives typical analyzer runs for pull-in case, nonpull-in case, and critical case. In Figure 8 is given a typical oscillograph for three similar cases for the sake of qualitative comparison. The comparison of analyzer results with criterion results given in Figure 5 and Table I also shows that the criterion is a little on the pessimistic side. This, however, is more desirable if any factor of safety is to be considered.

It also must be remembered that in order to obtain a certain prescribed performance and at the same time achieve a reasonable length of stack, the appropriate size of laminations must first be selected. In order to readily make this selection from many laminations of different sizes, it is suggested that this synthesis procedure be applied in a routine study of existing laminations for standard ratings. If this were done, it would be possible to formulate rules for the selection of lamination sizes for standard ratings.

It should be mentioned that there is a minimum limit on r_{1d} which is governed by the fact that the starting torque must be greater than the load torque to be pulled in, otherwise the motor would never start. Therefore, if the value of r_{1d} determined by the synthesis procedure cannot satisfy this condition, then a different size lamination has to be tried in

---

*All units are in meter-kilogram seconds.

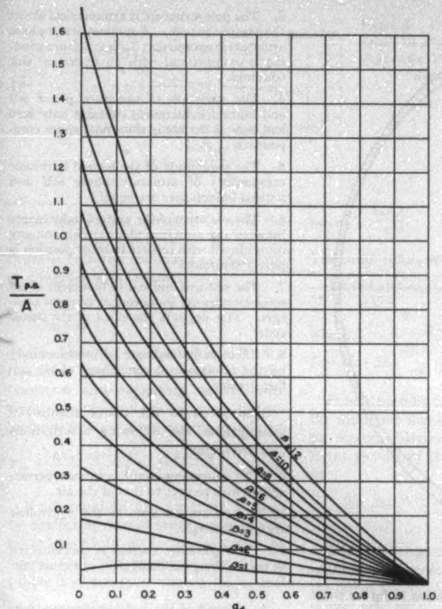

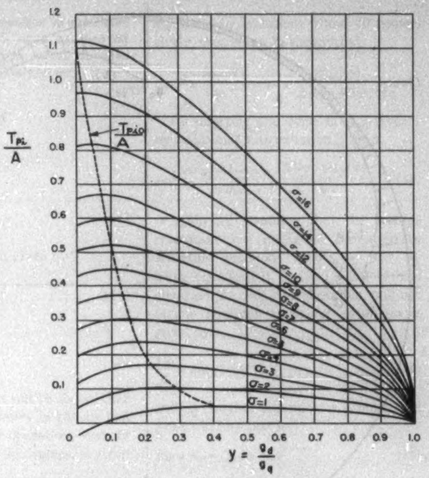

Figure 1 (left). Pull-out torque family of curves

Figure 2 (above). Pull-in torque family of curves. Dotted line is the universal curve of optimum pull-in torque

order to obtain the prescribed performance of the 3-phase reluctance motor.

It is necessary to point out that the method of synthesis presented here aims at obtaining an optimum pull-in torque at a given inertia from laminations of a certain size. In other words it is best applicable to cases where it is important to design for a high value of pull-in torque at a prescribed inertia. This point of view has been the primary interest of this paper because it represents one of the most difficult problems in the design of 3-phase reluctance motors. However, for cases where other factors are more important the steps previously outlined may not yield the best solution and therefore should not be followed. For instance, in cases where the main problem is to obtain the highest pull-out torque from laminations of a certain size, it is clear from the nature of the family of curves presented in Figure 1 and the expressions for A and β given by equations 17 and 19 respectively that the best choice of y is the minimum realizable y, namely $y=0.06$ in the given numerical example.

On the other hand, for cases where obtaining the highest efficiency of maximum load is of primary importance, a different problem arises. However, if expressions for iron losses, friction and windage losses can be developed in terms of the machine dimensions and physical constants, then a similar method of attack could be used and an expression for efficiency may be obtained, which would depend on y and other parameters. Curves similar to those presented in Figure 2 could then be

Table I

Case	1	2	3	4	5	6
$\frac{x_q}{x_d}$	0.472	0.556	0.417	0.472	0.472	0.472
$\frac{x_d''}{x_d}$	0.176	0.176	0.176	0.176	0.10	0.10
$\frac{x_q''}{x_d}$	0.176	0.176	0.176	0.176	0.10	0.10
$\frac{r}{x_d}$	0.0784	0.0784	0.0784	0.0784	0.0784	0.125
$\frac{\alpha_d}{\omega}$	0.25	0.25	0.25	0.20	0.20	0.20
$\frac{\alpha_q}{\omega}$	0.375	0.375	0.375	0.20	0.20	0.20
T_{pi} by equation 64	0.87	0.82	0.077	0.176	0.226	0.196
T_{pi} by analyzer	0.100	$0.075 < T_{pi} < 0.1$	$0.075 < T_{pi} < 0.1$	$0.2 < T_{pi} < 0.225$	$0.225 < T_{pi} < 0.25$	$0.175 < T_{pi} < 0.225$

Note: Values of T_{pi} in this table are referred to a base torque $= 3pe_m^2/4\omega x_d$.

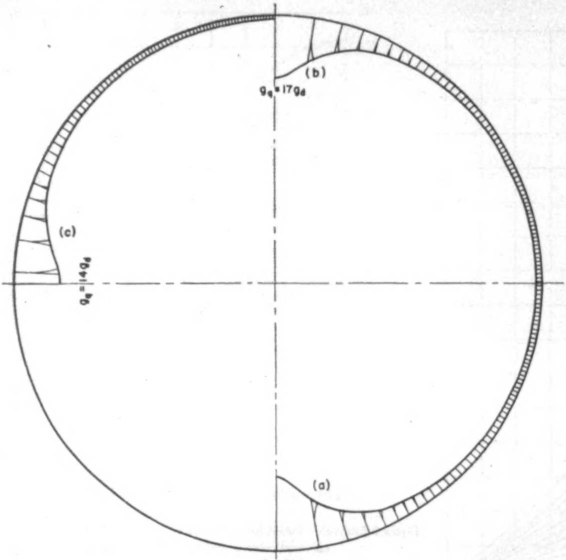

Figure 3. Flux plots for obtaining the minimum limit on y to satisfy assumption 12 for the given laminations

plotted for efficiency instead of pull-in torque. A universal curve of optimum efficiency as a function of y only may result. The synthesis method could then be adapted to obtain the simultaneous solution for y and L_s to yield a certain prescribed pull-out torque and maximum efficiency.

General Theory

In this paper the analysis equations which are developed and transformed to the desirable synthesis forms are based on the generalized 2-reaction theory of synchronous machines, in which the following assumptions are made:

ASSUMPTIONS

1. Saturation, hysteresis and eddy currents in all magnetic circuits are neglected. This linearizes the machine. Eddy currents in electric circuits and charging currents between electric circuits or parts of circuits also are ignored.

2. Each armature phase winding is sinusoidally distributed. In other words a sinusoidal space distribution of magnetomotive force is considered.

3. The pole structure is symmetrical about the axis of the pole. A symmetrical 3-phase armature is assumed. Each armature winding is symmetrical with no fractional slot windings.

4. The variation of armature phase self and mutual inductances contains only zero and second harmonic sinusoidal space components.

5. The magnitude of the second harmonic components of armature phase self and mutual inductances are equal.

6. The variation of the mutual inductances between any armature phase circuit and any rotor circuit with respect to rotor position is purely sinusoidal.

7. The self and mutual inductances of all rotor circuits are independent of rotor position. This neglects the effect of the stator slots.

8. Effective flux linkages are produced only by the fundamental component of air gap flux density.

Subsequent to the above mentioned assumptions, the following assumptions also are made:

9. The equivalent iron has infinite permeability with respect to that of the air.

10. There are no slots in the equivalent armature surface.

11. The armature current is concentrated at points along the equivalent armature surface.

As a result of the last two assumptions the armature magnetomotive force becomes equivalent to a distribution of magnetic potential along the armature surface.

12. The length of the magnetic flux path from the stator surface to the rotor surface is equal to the radial length of the equivalent air gap from a point on the stator surface to the point of intersection of the line connecting this stator point with the center and the equivalent rotor surface.

ANALYSIS EQUATIONS

By neglecting resistance in Park's voltage equations for the unexcited synchronous machine, and assuming opti-

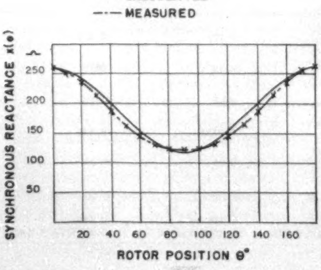

Figure 4 (left). Comparison between calculated and measured values of the synchronous reactance as a function of rotor position θ

Figure 5 (right). Comparison of results obtained from the differential analyzer runs with results calculated using the pull-in criterion

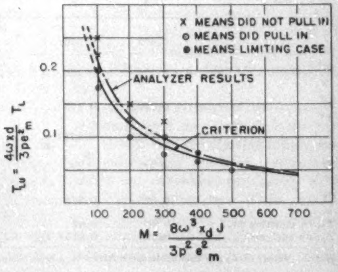

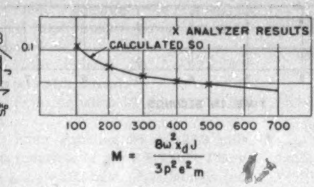

Figure 6. Comparison of calculated values of slip S_0 using equation 62 Appendix II with values observed during analyzer runs

mum steady-state operation to be in the vicinity of zero power factor and $2\delta=90$ degrees, then the maximum possible current is given approximately by

$$i_{mm}=\frac{2e_m}{x_d+x_q} \tag{1}$$

Also from the manipulation of Park's equations under steady-state balanced operation and neglecting second order terms in r, the pull-out torque of the reluctance motor is given approximately by

$$T_{po}=\frac{3pe_m^2}{8\omega x_d}\,\frac{x_d-x_q}{x_q}\left(1-\frac{r}{x_d}\,\frac{x_d-x_q}{x_q}\right) \tag{2}$$

From equation 64, Appendix II, and by neglecting second order terms in r in equations 55 to 59 inclusive it can be shown that the expression for pull-in torque is given approximately by

$$T_{pi}=\frac{3pe_m^2}{8\omega x_d}\left[\frac{2}{\pi}\left(\frac{3p^2e_m^2\,(x_d-x_q)}{2\omega^3Jx_dx_q}\right)^{0.5}\times\left(\frac{x_dX_{a1q}^2}{x_q^2R_{1q}}+\frac{X_{a1d}^2}{2x_dR_{1d}}\right)-\frac{r}{x_d}\left(\frac{x_d-x_q}{x_q}\right)^2\right] \tag{3}$$

Also from the manipulation of Park's equations at starting, then it can be shown that the starting torque equation is given by

$$T_{st}=\frac{pe_m^2}{4\omega}\left[\frac{R_{1d}}{\left(\frac{2}{3}r+R_{1d}\right)^2+\left(\frac{2}{3}x_{Ld}+X_{L1d}\right)^2}+\frac{R_{1q}}{\left(\frac{2}{3}r+R_{1q}\right)^2+\left(\frac{2}{3}x_{Lq}+X_{L1q}\right)^2}\right] \tag{4}$$

TRANSFORMATION OF ANALYSIS EQUATIONS

From the standpoint of allowable current density J_m it follows that

$$i_{mm}=J_m\,\frac{k_sA_sQ_s}{6N} \tag{5}$$

The stator resistance is given by

$$r=\frac{12N^2(L_o+L_s)\rho_s}{Q_sk_sA_s} \tag{6}$$

where

$$L_o=2L_s+2k_{p1}\,\frac{D_s}{p} \tag{7}$$

From Appendix I, it can be shown that the maximum flux density in the air gap for limiting balanced operation, namely in the vicinity of $2\delta=90$ degrees, is given by

$$B_m=\frac{3\mu_0}{\pi}\,\frac{2k_{w1}N}{p}\,\frac{(5+6y+5y^2)^{0.5}}{4g_d}\,i_{mm} \tag{8}$$

Also, from Appendix I, the armature reaction synchronous reactances in both the direct and quadrature axes are given respectively by

$$x_{ad}=\frac{3}{2}X_{a1d}=3\omega\frac{\mu_0}{\pi}\left(\frac{2k_{w1}N}{p}\right)^2D_sL_s\,\frac{3+y}{4g_d} \tag{9}$$

$$x_{aq}=\frac{3}{2}X_{a1q}=3\omega\,\frac{\mu_0}{\pi}\left(\frac{2k_{w1}N}{p}\right)^2D_sL_s\,\frac{1+3y}{4g_d} \tag{10}$$

Now by inserting the value of i_{mm} given by equation 1 into equation 8 and neglecting leakage reactances as compared to armature reaction reactances, that is assuming

$$x_d=x_{ad}\text{ and }x_q=x_{aq} \tag{11}$$

and then using the expressions for x_{ad} and x_{aq} given by equations 9 and 10 respectively, then it can be shown that

$$e_{ma}=\omega\,\frac{2k_{w1}N}{p}\,D_sL_sB_m\,\frac{2(1+y)}{(5+6y+5y^2)^{0.5}} \tag{12}$$

By inserting the value of i_{mm} given by equation 5 into equation 8, then

$$g_d=\frac{\mu_0J_mk_{w1}k_sA_sQ_s}{\pi pB_m}\,\frac{(5+6y+5y^2)^{0.5}}{4} \tag{13}$$

Again by assuming that the leakage reactances are negligible compared to armature reaction reactances, and by using equations 6, 9, 10, 12 and 13 into equation 2, then the desirable pull-out torque equation form for synthesis is given by

$$\frac{T_{po}}{A}=\beta f_1(y)-f_2(y) \tag{14}$$

and by further assuming a symmetrical rotor winding that is

$$R_{1d}=R_{1q}=(k_{w1}N)^2r_{1d} \tag{15}$$

then the desirable expression for the pull-in torque from a synthesis standpoint is given by

$$\frac{T_{pi}}{A}=\sigma f_3(y)-f_2(y) \tag{16}$$

where

$$A=a(L_o+L_s) \tag{17}$$

$$a=2pk_sA_sQ_s\frac{\rho_s}{\omega}\,J_m^2 \tag{18}$$

$$\beta=\frac{cL_s}{A} \tag{19}$$

$$c=k_{w1}D_sB_mk_sA_sQ_sJ_m \tag{20}$$

$$\sigma=\frac{8\omega}{\pi r_{1d}\rho_s(L_o+L_s)}\left(\frac{k_{w1}(D_sL_sB_m)^3}{k_sA_sQ_sJ(pJ_m)^3}\right)^{0.5} \tag{21}$$

$$f_1(y)=\frac{(1-y)(1+y)^2}{(1+3y)(3+y)(5+6y+5y^2)^{0.5}} \tag{22}$$

$$f_2(y)=\left[\frac{(1-y)(1+y)}{(1+3y)(3+y)}\right]^2 \tag{23}$$

Figure 7. Typical differential analyzer runs

Case	$\delta'(0)$	T_{Lu}	M	$\frac{\alpha_d}{\omega}$	$\frac{\alpha_q}{\omega}$	$\frac{x_d}{x_d}$	$\frac{x_q}{x_d}$	$\frac{x_d''}{x_d}$	$\frac{x_q''}{x_d}$	$\frac{r}{x_d}$
a	-1.0	0.225	300	0.2	0.2	1.0	0.472	0.1	0.1	0.0784
b	-1.0	0.25	300	0.2	0.2	1.0	0.472	0.1	0.1	0.0784
c	-1.0	0.1	300	0.25	0.375	1.0	0.555	0.176	0.176	0.0784

a. PULL-IN CASE
b. NON PULL-IN CASE
c. CRITICAL CASE

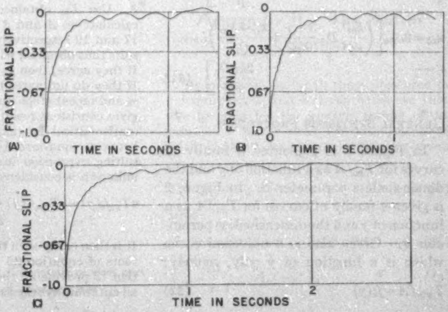

Case	$\dot{\delta}(0)$	T_{Lu}	M	$\frac{\alpha_d}{\omega}$	$\frac{\alpha_q}{\omega}$	$\frac{x_d}{x_d}$	$\frac{x_q}{x_d}$	$\frac{x_d''}{x_d}$	$\frac{x_q''}{x_d}$	$\frac{r}{x_d}$
a	-1.0	0.47	560	0.07	0.14	1.0	0.472	0.105	0.105	0.0784
b	-1.0	0.47	630	0.07	0.14	1.0	0.472	0.105	0.105	0.0784
c	-1.0	0.47	570	0.07	0.14	1.0	0.472	0.105	0.105	0.0784

a. PULL IN CASE
b. NON PULL-IN CASE
c CRITICAL CASE

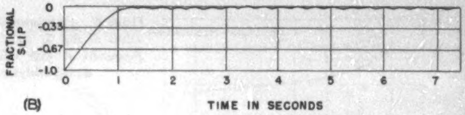

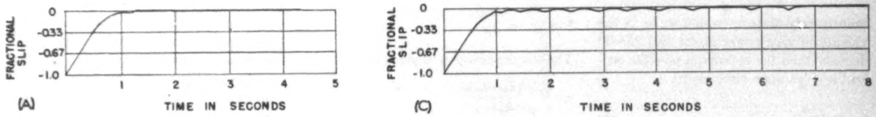

Figure 8. Typical oscillograph pictures

$$f_2(y)=\frac{(1+y)^3}{(5+6y+5y^2)^{1.25}}\left[\frac{1-y}{(1+3y)(3+y)}\right]^{0.5} \tag{24}$$

By using the following definitions in equation 4

$$\frac{2}{3}r=r_1N^2 \tag{25}$$

$$\frac{2}{3}x_{Ld}=x_1N^2 \tag{26}$$

$$X'_{L1d}=x_{1d}(k_{w1}N)^2 \tag{27}$$

then, the expression for the starting torque in synthesis form is given by

$$T_{st}=\frac{2\omega(k_{w1}D_sL_sB_m)^2}{p}\times \frac{k_{w1}{}^2r_{1d}}{(r_1+k_{w1}{}^2r_{1d})^2+(x_1+k_{w1}{}^2x_{1d})^2}\,\frac{4(1+y)^2}{5+6y+5y^2} \tag{28}$$

where, from reference 6

$$r_{1d}=8\rho_r\left(\frac{L_b}{A_bQ_2}+\frac{2L_r}{\pi^2p^2A_r}\right) \tag{29}$$

$$x_1=8\omega\mu_0\left[\left(\frac{k_{h1}{}^2}{\pi p^2}D_s\,\frac{3+y}{4g_d}+\frac{\lambda_{ss}+\lambda_{tts}}{Q_s}\right)L_s+\frac{0.4k_{w1}L_e}{p}\right] \tag{30}$$

$$x_{1d}=8\omega\mu_0\left[\left(\frac{k_{h2}{}^2}{\pi p^2}D_s\,\frac{3+y}{4g_d}+\frac{\lambda_{sr}+\lambda_{ttr}}{Q_2}\right)L_b+\frac{2k\pi D_r}{9p^2}\right] \tag{31}$$

GENERAL SYNTHESIS PROCEDURE

In Figure 1 is presented a family of curves for T_{po}/A as a function of y and the dimensionless parameter β. In Figure 2 is given a family of curves for T_{pi}/A as a function of y and the dimensionless parameter σ. Given also is a universal curve which is a function of y only, namely:

$$T_{pio}/A=f_0(y) \tag{32}$$

Now, the pull-out torque, load torque to be pulled into synchronism, load inertia, supply voltage, supply frequency and desired motor speed are assumed known. The maximum flux density in the stator teeth and the maximum current density in the stator conductors also are prescribed. The suggested synthesis procedure is then outlined in the following steps from the point of view of a manufacturer who already has stator laminations of different sizes and who desires to use such laminations to obtain for each size the optimum design for 3-phase reluctance motors.

1. Calculate p from

$$p=120f/n \tag{33}$$

2. Enter T_{pio}/A at $0.06\leq y\leq 0.3$ and use the corresponding value of $f_0(y_1)$ together with the specified T_{pi} to determine an A_1. The corresponding value of σ_1 is also noted.

3. Use specified T_{po}, determined A_1 and chosen y_1 to obtain β_1 from Figure 1.

4. Form the product β_1A_1 and solve for a tentative L_{s1} from

$$L_{s1}=\frac{\beta_1A_1}{k_{w1}k_sA_sQ_sD_sB_mJ_m} \tag{34}$$

5. Use L_{s1} obtained by equation 34 to calculate an A and β as given by equations 17 and 19 respectively and compare the results thus obtained with the previous values. If they agree, then y_1 is the correct solution. If they do not agree then try another value y_2 and repeat steps until y is obtained which gives consistent results. This is clarified by mathematical language if L_s is eliminated between equations 14 and 32 and the resulting expression involving y as the only unknown is considered

$$aT_{po}f_0(y)-cT_{pio}f_1(y)+aT_{pio}f_2(y)+acL_of_0(y)f_1(y)=0 \tag{35}$$

It is then easily seen that all the real positive roots of equation 35 which satisfy assumption 12 provide all the possible solutions for an optimum synthesis.

6. Use final value of L_s to determine the approximate value of rotor inertia

$$J_r=\frac{\pi}{16}D_s{}^4L_sd_i \tag{36}$$

7. Use L_s and the corresponding σ to obtain r_{1d} from equation 21.

8. Use y to determine g_d from equation 13.

9. Also use y, L_s, and r_{1d} in equation 28 to solve for x_{1d} if a starting torque is specified. If not, then check for $T_{st}>T_L$, after the design is completed.

10. From formulas similar to equations 29 and 31 choose the number of rotor slots, their size and shape and the end ring dimensions to satisfy the values obtained for r_{1d} and x_{1d}.

11. Use y and L_s in equation 12 to determine the number of stator conductors per phase and their size.

NUMERICAL EXAMPLE

Prescribed. Pull-out power = 1/40 horsepower, pull-in power 1/50 horsepower, $J_L=3.6\times10^{-4}$ watts × cubic second, $V=115$ volts, $f=60$ cycles per second, $n=3{,}600$ rpm. Stator laminations: core diameter = 3.808 inches, $D_s=2.043$ inches, $Q_s=24$, $A_s=0.118$ square inch. Take: $k_s=0.2$, $J_m=4.5\times10^6$ amperes per square meter, $B_{ts}=0.8$ weber per square meter, winding throw = 3/4 resulting in $k_{p1}=0.923$.

Results. From equation 33 $p=2$, therefore $k_{d1}=0.958$ and $k_{w1}=0.885$. For $V=115$ volts take $2L_e=2$ inches, then $L_o=3.9$ inches.

1. Assume iron + friction + windage losses = 9.4 watts. Therefore, $T_{po}=28/\omega$ watts × second. $T_{pi}=24.3/\omega$ watts × second. Try $y_1=0.15$: $T_{pio}/A=0.30$ (Figure 2), therefore $A_1=81/\omega$ and $\sigma=5$.

2. $T_{po}/A_1=0.35$ therefore $\beta_1=4$ (Figure 1).

3. From equation 34 $L_{s1}=1.5$ inches.

4. From equation 17 $A=81/\omega$ (checks), and from equation 19 $\beta=4$ (checks).

5. From equation 36 $J_r=1.2\times10^{-4}$ watts per cubic second.

6. From equation 21 $r_{1d}=5.02\times10^{-6}$ ohm.

7. From equation 24 $g_d=23.3$ mils. From equation 51 $g_i=3.8$ mils. Therefore, $g_d'k_{cd}=19.5$ mils. $b_{os}=90$ mils (obtained by experiment or flux plotting for type of slot used).

8. From equations 6 and 25: $r_1=6.03\times10^{-6}$ ohm (for copper). From equations 30 and 31 and curves in reference 6: $x_1=2.7\times10^{-5}$ ohm, and $x_{1d}=2.6\times10^{-5}$ ohm (see step 9 for dimensions of rotor). Therefore, $2\omega T_{st}/p=110$ watts>24.3 watts per pull-in power.

9. Use aluminum for rotor bars. Assume $Q_2=18$, $L_b=L_s=1.5$ inches. Take rotor slot of shape and dimensions as shown in Figure 9. Therefore, $A_b=0.034$ square inch, $r_{1b}=2.07\times10^{-6}$ ohm. Now estimate: $b_{or}=108$ mils, $\tau_{sgr}=350$ mils, then from equation 48 $g_d'=12.5$ mils. Also $L_r=4.85$ inches, $r_{1r}=r_{1d}-r_{1b}=2.95\times10^{-6}$ ohm, giving $A_r=0.07$ square inch. Therefore, end ring thickness $=0.14$ inch.

10. $e_m=94$ volts. Since leakage $=6$ per cent, then $e_{ma}=88$ volts. From equation 12 $N=472$ turns, therefore, $N_s=118$ conductors and wire size $=k_sA_s/N_s$ gives B and S number 26.

Experiments made on a 3-phase reluctance motor of approximately the size and dimensions calculated yielded the following results which are given here for comparison: Pull-out power $=22$ watts>18.6 watts as specified. Pull-in power at $J=4.8\times10^{-4}$ watts × cubic second $=15.4$ watts>14.3 watts as specified. $2\omega T_{st}/p=129$ watts>110 watts as calculated in step 8.

Appendix I. Rotor Shape to Satisfy Assumptions 4, 5 and 6

The fundamental component of the magnetomotive force due to armature phase currents i_a, i_b, i_c at any point A on the stator surface is given by [3,4]

$$F_1(\gamma)=\frac{2}{\pi}\,\frac{2k_{w1}N}{p}[i_a\cos\gamma+i_b\cos(\gamma-120)+i_c\cos(\gamma+120)] \quad (37)$$

Now let the permeance at point A be defined by*

$$P(\gamma,\theta)=\frac{\mu_0}{g(\gamma-\theta)} \quad (38)$$

$$\frac{1}{g(\theta)}=\frac{1}{2g_d}[(1+y)+(1-y)\cos 2\theta] \quad (39)$$

Therefore, the armature reaction flux density $B(\gamma,\theta)$ at A is then given by

$$B(\gamma,\theta)=F_1(\gamma)P(\gamma,\theta) \quad (40)$$

By expanding equation 39 and gathering only fundamental terms in γ, then the fundamental space component of flux density is given by

$$B_1(\gamma,\theta)=\frac{2}{\pi}\,\frac{2k_{w1}N}{p}\,\frac{\mu_0}{2g_d}\Big[(1+y)\{i_a\cos\gamma+i_b\cos(\gamma-120)+i_c\cos(\gamma+120)\}+\frac{1}{2}(1-y)\{i_a\cos(\gamma-2\theta)+i_b\cos(\gamma-2\theta+120)+i_c\cos(\gamma-2\theta-120)\}\Big] \quad (41)$$

Consequently, the total fundamental armature reaction flux in phase a is given by

$$\phi_{1a}(\theta)=\int_{\pi/2-}^{\pi/2}B_1(\gamma,\theta)L_s\frac{D_s}{2}\,d\left(\frac{2}{p}\gamma\right) \quad (42)$$

It can then be shown from equations 41 and 42, and basic principles that the armature reaction self-inductance of phase a is given by

$$L_{aa}(\theta)=\frac{k_{w1}N\phi_{1aa}(\theta)}{i_a}=\frac{\mu_0}{\pi}\left(\frac{2k_{w1}N}{p}\right)^2\frac{D_sL_s}{g_d}\times[(1+y)+0.5(1-y)\cos 2\theta] \quad (43)$$

Also that the armature reaction mutual inductance between phases a and b is given by:

$$L_{ab}(\theta)=\frac{k_{w1}N\phi_{bab}(\theta)}{i_b}=\frac{\mu_0}{\pi}\left(\frac{2k_{w1}N}{p}\right)^2\frac{D_sL_s}{g_d}\times[-0.5(1+y)+0.5(1-y)\cos 2\theta] \quad (44)$$

From equations 43 and 44 it is readily seen that an equivalent air gap given by equation 39 satisfies assumptions 4 and 5.

Again from equation 41, the fundamental armature reaction flux in the direct-axis amortisseur winding is given by

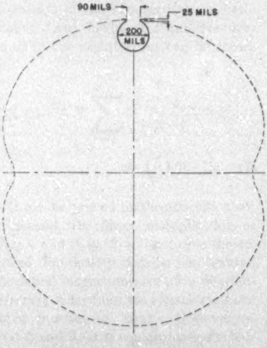

Figure 9. Shape and dimensions of slots and general shape of rotor contour

$$\phi_{11d}(\theta)=\int_{-\pi/2+\theta}^{\pi/2+\theta}B_1(\gamma,\theta)L_s\frac{D_s}{2}\,d\left(\frac{2}{p}\gamma\right) \quad (45)$$

Consequently the armature reaction mutual-inductance between phase a and direct-axis rotor circuit is given by

$$L_{a1d}(\theta)=\frac{k_{w1}N\phi_{a1d}(\theta)}{i_a}=\frac{2\mu_0}{\pi}\times\left(\frac{2}{p}k_{w1}N\right)^2D_sL_s\frac{3+y}{4g_d}\cos\theta \quad (46)$$

Similarly it can be shown that the armature reaction mutual-inductance between phase a and quadrature-axis rotor circuit is given by

$$L_{a1q}(\theta)=-\frac{2\mu_0}{\pi}\left(\frac{2}{p}k_{w1}N\right)^2D_sL_s\frac{1+3y}{4g_d}\sin\theta \quad (47)$$

From equations 46 and 47 it also is readily seen that an equivalent air gap given by equation 39 satisfies assumption 6.

Now from reference 6 and assuming that the stator inner radius is large compared with the air gap at any point, then the equivalent air gap at any point is given by

$$g=k_cg'=\frac{\tau_{sgs}(5g'+b_{os})}{\tau_{sgs}(5g+b_{os})-b_{os}^2}\times\frac{\tau_{sgr}(5g'+b_{or})}{\tau_{sgr}(5g'+b_{or})-b_{or}^2}g' \quad (48)$$

If the equivalent air gap at both direct- and quadrature-axis are known, the equivalent air gap at definite angles could be found and the physical air gap at the same definite angles be calculated from equation 48. The required rotor dimensions to satisfy assumptions 4, 5, and 6 can thus be obtained. To take account of iron and saturation it was found appropriate toreplacer $(3+y)/4g_d$ and $(1+3y)/4g_d$ in equations 46 and 47 respectively by

$$\frac{1}{G_d}=\frac{1}{g_d}\left[\frac{3+y}{4+2y_i+2yy_i}-\frac{y_i-yy_i}{(2+y_i+yy_i)^2}\right] \quad (49)$$

$$\frac{1}{G_q}=\frac{1}{g_q}\left[\frac{1+3y}{4+2y_i+2yy_i}+\frac{y(y_i-yy_i)}{(2+y_i+yy_i)^2}\right] \quad (50)$$

where

$$y_i=\frac{\mu_0}{B_mg_d}\left[\frac{B_{ts}\lambda_{ts}}{\mu_{ts}}+\frac{B_{cs}\lambda_{cs}}{\mu_{cs}}+\frac{B_{tr}\lambda_{tr}}{\mu_{tr}}+\frac{B_{cr}\lambda_{cr}}{\mu_{cr}}\right] \quad (51)$$

Appendix II. The Pull-in Criterion

By methods similar to those presented in references 5, 7, and 8 it can be shown that the formula for the electric torque of the reluctance motor near synchronous speed with armature resistance included is given by

$$T_e=T_{es}+T_{ea} \quad (52)$$

where

$$T_{es}=k_{s2}\sin 2\delta+k_{ro}-k_{r2}\cos 2\delta \quad (53)$$

$$T_{ea}=\frac{d\delta}{dt}(k_{a0}+k_{a2}\cos 2\delta) \quad (54)$$

---

*After writing this paper it was discovered that substantially the same assumption was made in Patent Number 1,915,069 issued to W. J. Morril and W. A. Pringle, June 20, 1933.

$$k_{s2}=\frac{\dfrac{3pe_m^2}{8\omega x_d}\;\dfrac{x_d-x_q}{x_q}}{\left(1+\dfrac{r}{x_d}\dfrac{r}{x_q}\right)^2}\left(1-\frac{r}{x_d}\frac{r}{x_q}\right) \tag{55}$$

$$k_{r0}=k_{s2}\frac{\dfrac{r}{x_d}\;\dfrac{x_d-x_q}{x_q}}{1-\dfrac{r}{x_d}\dfrac{r}{x_q}} \tag{56}$$

$$k_{r2}=k_{r0}\frac{x_d+x_q}{x_d-x_q} \tag{57}$$

$$k_{a0}=\frac{\dfrac{3pe_m^2}{8\omega x_d}}{\left(1+\dfrac{r}{x_d}\dfrac{r}{x_q}\right)^2}\left[\frac{x_d}{x_q}\,\frac{x_q-x_q''}{\alpha_q x_q}\left(1+\frac{r^2}{x_d^2}\right)+\frac{x_d-x_d''}{\alpha_d x_d}\left(1+\frac{r^2}{x_q^2}\right)\right] \tag{58}$$

$$k_{a2}=\frac{\dfrac{3pe_m^2}{8\omega x_d}}{\left(1+\dfrac{r}{x_d}\dfrac{r}{x_2}\right)^2}\left[\frac{x_d}{x_q}\,\frac{x_q-x_q''}{\alpha_q x_q}\left(1+\frac{r^2}{x_d^2}\right)-\frac{x_d-x_d''}{\alpha_d x_d}\left(1+\frac{r^2}{x_q^2}\right)\right] \tag{59}$$

Based on observations made on many differential analyzer runs the following assumptions are made:

1. The motor has already reached a slip speed $-S_0$ in electrical radians per second through the induction motor action, when the synchronizing period begins.

2. The synchronizing period begins at $\delta_1=0$ (or $-\pi$) with the direct axis in line with the magnetic axis of phase *a* and ends at $\delta_2=-\pi/2$ (or $-3\pi/2$) with the quadrature-axis in line with the magnetic axis of phase *a*.

3. During the synchronizing period the slip speed varies according to the formula obtained from the solution for $d\delta/dt$ obtained from the following differential equation

$$\frac{2}{p}J\frac{d^2\delta}{dt^2}=-k_{s2}\sin 2\delta \tag{60}$$

namely

$$\frac{d\delta}{dt}=-S_0\cos\delta$$

$$0\leqq\delta\leqq-\frac{\pi}{2}\left(\text{or }-\pi\leqq\delta\leqq-\frac{3}{2}\pi\right) \tag{61}$$

where

$$S_0=(pk_{s2}/J)^{1/2} \tag{62}$$

Accordingly, by integrating the equation of motion as given by

$$\frac{2}{p}J\frac{d^2\delta}{dt^2}=-T_e-T_L \tag{63}$$

between limits: $0\leqq\delta\leqq-\pi/2$ (or $-\pi\leqq\delta\leqq-3\pi/2$) and using equations 52, 53, 54, and 61, there results the following criterion for pull-in torque.

$$T_L=\frac{2}{\pi}S_0(k_{a0}+k_{a2}/3)-k_{r0} \tag{64}$$

References

1. PERFORMANCE CALCULATIONS ON POLYPHASE RELUCTANCE MOTORS (SYNCHRONOUS MOTORS WITHOUT FIELD EXCITATION), P. H. Trickey. *Electrical Engineering* (*AIEE Transactions*), volume 65, April 1946, pages 191–93.

2. SMALL SYNCHRONOUS MOTORS WITHOUT EXCITERS, P. H. Trickey. *Electric Journal* (Pittsburgh, Pa.), volume 30, April 1933, pages 160–62.

3. DEFINITION OF AN IDEAL SYNCHRONOUS MACHINE AND FORMULA FOR THE ARMATURE FLUX LINKAGES, R. H. Park. *General Electric Review* (Schenectady, N. Y.), volume 31, June 1928, pages 332–34.

4. TWO-REACTION THEORY OF SYNCHRONOUS MACHINES, PART I, GENERALIZED METHOD OF ANALYSIS, R. H. Park. *AIEE Transactions*, volume 48, July 1929, pages 716–30.

5. TWO-REACTION THEORY OF SYNCHRONOUS MACHINES, PART II, R. H. Park. *AIEE Transactions*, volume 52, June 1933, pages 352–55.

6. ELECTRIC MACHINERY, M. Liwschitz-Garik, C. C. Whipple. D. Van Nostrand Company, Inc. (New York, N. Y.), volumes I and II, 1946.

7. SYNCHRONOUS MACHINES, PART III, TORQUE-ANGLE CHARACTERISTICS UNDER TRANSIENT CONDITIONS, R. E. Doherty, C. A. Nickle. *AIEE Transactions*, volume 46, 1927, pages 1–18.

8. PULL-IN CHARACTERISTIC OF SYNCHRONOUS MOTORS, D. R. Shoults, S. B. Crary, A. H. Lauder. *Electrical Engineering* (*AIEE Transactions*), volume 54, December 1935, pages 1385–95.

No Discussion

Characteristics of Reluctance Machines

CHI-YUNG LIN
STUDENT MEMBER AIEE

ALTHOUGH thousands of reluctance motors have been used in domestic appliances, laboratories, and in industrial plants, a review of the literature on reluctance machines[1-13] has revealed the need for an improved but simplified method of analyzing their performances. Such a method may be found by the application of equivalent circuits developed by the author in a companion paper.[14] Two alternative circuits of fundamental frequency are used in this paper to illustrate the usefulness of equivalent circuits in studying the operation of reluctance machines.

The application of these circuits not only will simplify materially the complete performance calculations, but also will make possible the direct calculations of pull-out characteristics, and characteristics with the known mechanical power output without resorting to the trial and error method, mentioned by Trickey.[13]

Since a clear picture of the nature of reluctance torque may be important in understanding the behavior of reluctance machines, a fundamental analysis of this torque is also presented, and the factors influencing it investigated.

The following assumptions have been made.

1. The eddy current and hysteresis losses, and the saturation effect can be neglected.

2. The distribution of air gap permeance per unit area is independent of the order of magnetomotive force harmonic, and has a space period τ_s (see Appendix III for explanation of all symbols). With respect to the symmetrical axis of winding a, it can be expressed as

$$\mathcal{P}(x,t)=\mathcal{P}_0+\sum_{n=1}^{\infty}\mathcal{P}_{vn}\cos(2\pi/\tau_s)n(x-\alpha') \tag{1}$$

3. In expressing the symmetrical magnetomotive force distribution having the positive area equal to the negative one, the ampere conductors in each slot are considered as concentrated in the center line of the slot.

Flux Distribution Around Air Gap

In equation 1, if it is assumed that the air gap is uniform at effective lengths δ_1 and δ_2, and that the permeance at every point is inversely proportional to the air gap length at that point, the Fourier series expression of the permeance curve shows that

$$\mathcal{P}_0=K\left[\frac{1}{\delta_2}+\varphi\left(\frac{1}{\delta_1}-\frac{1}{\delta_2}\right)\right]$$

$$\mathcal{P}_{v_n}=\mathcal{P}_v\frac{\sin(n\varphi\pi)}{n}=$$

$$\frac{2K}{\pi}\left(\frac{1}{\delta_1}-\frac{1}{\delta_2}\right)\frac{\sin(n\varphi\pi)}{n} \tag{2}$$

Although the further development will be carried on the preceding relations, the results obtained can be applied to any machine if the values of $\mathcal{P}_0$ and $\mathcal{P}_{vn}$ found for that machine are properly substituted.

Consider that only the winding a is on the armature surface. The Fourier series expression of the symmetrical magnetomotive force having the positive area equal to the negative one can be shown as

$$\mathfrak{F}_a(x,t)=\frac{2n_as_a}{\pi}i_a\sum_{r=1}^{\infty}\frac{(-1)^{r-1}k_{a(2r-1)}}{2r-1}\times$$

$$\cos\left(\frac{\pi}{\tau}\right)(2r-1)x \tag{3}$$

It can be proved mathematically that, in general, the direct multiplication of $\mathcal{P}(x,t)$ and $\mathfrak{F}_a(x,t)$ will not give the required flux density distribution, because the actual magnetomotive force distribution may differ from the symmetrical one by a function of time. However, if $\mathcal{P}(x,t)$ and $\mathfrak{F}_a(x,t)$ contain no space harmonics of the same order, as found in a machine having $\tau=q\tau_s$, for which the space permeance wave will contain only zero and even harmonics while the space magnetomotive force will contain only odd harmonics, the above manipulation will give the correct result. Therefore, under the preceding condition[16]

$$B_a(x,t)=\mathcal{P}(x,t)\mathfrak{F}_a(x,t)$$

$$=G_a^0i_a\sum_{r=1}^{\infty}\frac{(-1)^{r-1}k_{a(2r-1)}}{2r-1}\times$$

$$\cos\frac{p}{2}(2r-1)x+G_a^vi_a\sum_{n=1}^{\infty}\sum_{r=1}^{\infty}\times$$

$$\frac{(-1)^{r-1}k_{a(2r-1)}\sin(n\varphi\pi)}{n(2r-1)}\times$$

$$\left\{\cos\frac{p}{2}[(2qn-2r+1)x-2qn\alpha']+\right.$$

$$\left.\cos\frac{p}{2}[(2qn+2r-1)x-2qn\alpha']\right\} \tag{4}$$

In a similar manner, the flux density distribution due to any additional armature winding carrying current can be found. For example, that due to the current i_b in winding b spaced θ' mechanical radians from the winding a in the direction of rotation will be

$B_b(x,t)$ = equation 4 with changes of α' to $(\alpha'-\theta')$, x to $(x-\theta')$, and the subscript a to b (5)

General Torque Equations

Consider first a single-phase reluctance machine. From previous assumptions and the Bli rule, the force acting on arma-

---

Paper 51-362, recommended by the AIEE Rotating Machinery Committee and approved by the AIEE Technical Program Committee for presentation at the AIEE Fall General Meeting, Cleveland, Ohio, October 22-26, 1951. Manuscript submitted October 23, 1950; made available for printing August 30, 1951.

CHI-YUNG LIN was at the University of Illinois, Urbana, Ill. at the time this paper was written.

The author wishes to express his sincere gratitude to Professors M. A. Faucett, C. A. Keener, G. H. Fett, V. P. Hessler, and K. Fong of the Electrical Engineering Department, University of Illinois, for their suggestions and discussions. He is indebted to P. H. Trickey, chief engineer of the Vickers Electric Division, for supplying the experimental data on reluctance machines. He also acknowledges the permission granted by the Graduate College of the University of Illinois to utilize the material included in the author's Doctor of Philosophy thesis in writing this and the companion paper.[14]

ture conductors in each slot can be found by multiplying $(n_a s_a l)$ and the value of the flux density at the center of that particular slot. Summing up these forces over the conductors in all slots will give the resultant force. As the armature is stationary, the rotor will experience an equal and opposite force, giving rise to the mechanical torque equal to the negative expression of the resultant force, if the flux density is expressed in webers per inch-mechanical radian of area. Furthermore, if each space flux density harmonic of equation 4 is resolved into its cosinusoidal and sinusoidal components, then as the cosinusoidal component will not contribute to the resultant torque, the torque due to any space flux density harmonic can be found conveniently by multiplying the value of its sinusoidal component at $x=\tau/2$ with $(pn_a s_a l)$ and the winding factor with respect to the corresponding space harmonic concerned. The final instantaneous torque equation will be

$$T_{aa}=-G_a^{v}(ps_a n_a l)i_a^2\sum_{n=1}^{\infty}\sum_{r=1}^{\infty}\times \frac{k_{a(2r-1)}\sin(n\varphi\pi)}{n(2r-1)}\times [(-1)^{qn-1}k_{a(2qn-2r+1)}+(-1)^{qn}k_{a(2qn+2r-1)}]\sin(pqn\alpha') \quad (6)$$

The case of cylindrical machines is realized by setting $\delta_1=\delta_2$, or $\varphi=1$, or $\varphi=0$. The reluctance torque for these machines will be zero since $G_a^{v}=0$, or $\sin(n\varphi\pi)=0$.

Equation 6 permits the investigation of reluctance torque with respect to any time harmonic currents. In particular, if the product of the instantaneous expressions of m_1th and m_2th harmonic currents is substituted for i_a^2, the following equation can be shown at a speed of v' mechanical radians per second.

$$T_{aa}=-G_a^{v}(ps_a n_a l)(I_{am1}I_{am2})\times \sum_{n=1}^{\infty}\sum_{r=1}^{\infty}\frac{k_{a(2r-1)}\sin(n\varphi\pi)}{2n(2r-1)}\times [(-1)^{qn-1}k_{a(2qn-2r+1)}+(-1)^{qn}k_{a(2qn+2r-1)}](\sin\{[pqnv'+(m_1+m_2)\omega]t+(\alpha_{m1}+\alpha_{m2})+pqn\alpha_0'\}+\sin\{[pqnv'-(m_1+m_2)\omega]t-(\alpha_{m1}+\alpha_{m2})+pqn\alpha_0'\}+\sin\{[pqnv'+(m_1-m_2)\omega]t+(\alpha_{m1}-\alpha_{m2})+pqn\alpha_0'\}+\sin\{[pqnv'-(m_1-m_2)\omega]t-(\alpha_{m1}-\alpha_{m2})+pqn\alpha_0'\}) \quad (7)$$

An investigation of this equation shows that the time average torque will be zero unless

$$v=pv'/2=\pm(m_1\pm m_2)\omega/2qn \quad (8)$$

and the corresponding operating angle $\pm(\alpha_{m1}\pm\alpha_{m2})+pqn\alpha_0'$ does not vanish. For a given rotor speed, equation 8 specifies the time order of harmonic currents and the space order of harmonic permeance, which may yield the time average component torque by their interaction. Each component torque, if present, will have contributions from all space current density harmonics.

Since the time harmonic currents in an ordinary reluctance machine are of the odd order, equation 8 shows that as the right-hand side may yield any submultiple of (ω/q), a single-phase reluctance motor can possibly stay at any submultiple of the speed (ω/q). However, unless for a special design,[3] the time average torque at the speed (ω/q) will be the greatest.

For machines having the same number of poles in salient rotor and in armature winding, that is, $q=1$, and running at synchronous speed, the most important component of the time average torque, contributed by the fundamental current and second harmonic permeance, can be obtained from equation 7 by setting $m_1=m_2=1$ and $n=1$.

$$\mathbf{T}=-\frac{1}{2}G_a^{v}(ps_a n_a l)I_{a1}^2\sum_{r=1}^{\infty}\frac{k_{a(2r-1)}}{2r-1}\times [k_{a(3-2r)}-k_{a(2r+1)}]\sin\varphi\pi\sin 2\alpha \text{ Newton-meters} \quad (9)$$

In the preceding equation, the operating angle α is recognized as the angle between one of salient pole axes and the axis of fundamental positive rotating magnetomotive force. For the convention used in this paper, $\mathbf{T}$ is positive for a motor torque and negative for a generator torque. Therefore, α must be negative for the motor operation, and positive for the generator operation. The numerical value of α will lie between 0 and $\pi/2$. When $\alpha=0$ or $\pi/2$, $\mathbf{T}$ is zero because of the symmetry of magnetic circuit with respect to the position of magnetomotive force wave. Maximum torque under constant current operation is reached when $\alpha=\pi/4$. The optimum value of φ under constant current operation is seen to be equal to 0.5, which is not the value under constant voltage operation, as will be discussed later.

Consider an unsymmetrical 2-phase reluctance machine. There are four component torques due to the interaction of current in one winding and the flux set up by the currents in the same and also in the other winding. These component torques can be found in the same manner as discussed above. In particular, if the two armature windings are in space quadrature electrically, and have the same number of slots per pole so that their winding factors are the same, the expression of the resultant torque can be found as

$$T_t=\frac{-2plK}{\pi^2}\left(\frac{1}{\delta_1}-\frac{1}{\delta_2}\right)\sum_{n=1}^{\infty}\sum_{r=1}^{\infty}[(s_a n_a i_a)^2+(-1)^{qn}(s_b n_b i_b)^2]\times \frac{(-1)^{qn-1}k_{a(2r-1)}\sin(n\varphi\pi)}{n(2r-1)}\times [k_{a(2qn-2r+1)}-k_{a(2qn+2r-1)}]\sin(pqn\alpha')-\frac{2plK(s_a n_a s_b n_b)}{\pi^2}\left(\frac{1}{\delta_1}-\frac{1}{\delta_2}\right)i_a i_b\times \sum_{n=1}^{\infty}\sum_{r=1}^{\infty}\times \frac{(-1)^{qn+r-1}k_{a(2r-1)}\sin(n\varphi\pi)}{n(2r-1)}\times [k_{a(2qn-2r+1)}+k_{a(2qn+2r-1)}]\times [1+(-1)^{qn-1}]\cos(pqn\alpha') \quad (10)$$

In equation 10, the second term of mutual torque is identically equal to zero for all even qn. If the machine is a symmetrical one operated from the balanced sinusoidal current supply, the first term of self torque will average zero for all even qn. Since qn is even when n is even, the above relations, together with the study of equation 8, show that a symmetrical 2-phase reluctance motor operated from balanced sinusoidal current supply cannot stay at even submultiple of (ω/q), since no time average torque is developed to maintain its running. Analogous conclusions can be drawn for any polyphase reluctance motor operated from the balanced sinusoidal current supply.

If the symmetrical 2-phase reluctance motor, operated from the balanced sinusoidal current supply, runs synchronously, the time average torque can be shown as

$$\mathbf{T}_t=-\frac{3.19\times 10^{-8}}{\pi^2}(s_a n_a)^2 pld\left(\frac{1}{\delta_1}-\frac{1}{\delta_2}\right)I_{a1}^2\times \sin(\varphi\pi)\sin 2\alpha\sum_{r=1}^{\infty}\frac{k_{a(2r-1)}}{2r-1}\times \{k_{a(3-2r)}[1-(-1)^r]-k_{a(2r+1)}[1+(-1)^r]\}\text{ Newton-meters} \quad (11)$$

As shown in equations 9 and 11, under the conditions of same machine dimensions, same total number of armature slots and conductors per slot, same effective conductor current, and same operating angle, the ratio of the time average torque of a balanced 2-phase machine to that of a single-phase machine depends on the winding factors. For ideal condition of sinusoidal distribution of conductors, the ratio is 2. On the other hand, if there are 8 slots per pole, the ratio is 1.62. This indicates the desirability of having a 2-phase motor or a single-phase one in split-phase operation.

Flux Linkage Equations

To find the flux linkages on winding a of an unsymmetrical 2-phase reluctance machine, resolve the air gap flux density distribution of equations 4 and 5 into sinusoidal and cosinusoidal components and note that the sinusoidal components will contribute no resultant flux linkages. The flux linkages on winding a are, therefore, due to cosinusoidal components of air gap flux only, and are found by multiplying the space integrals of their distributions from $(-\tau/2)$ to $(\tau/2)$ with the factors $(pn_a s_a l)/2$. If the flux linkages due to leakage fluxes are added, and if the notations given in the nomenclature are introduced, the following expression of the total flux linkages on winding a can be shown for a machine having $q=1$.

$$\lambda_{at}=\left\{L_a^0+\sum_{n=1}^{\infty} L_{an}\cos(pn\alpha')\right\}i_a+\left\{M_{ab}^0+\sum_{n=1}^{\infty}[M_{abn}^c\cos(pn\alpha')+M_{abn}^s\sin(pn\alpha')]\right\}i_b \quad (12A)$$

The expression of total flux linkages on winding b can be derived more conveniently from equation 12A by changing θ' to $(-\theta')$, α' to $(\alpha'-\theta')$ and the interchange of subscripts a and b.

$$\lambda_{bt}=\left\{L_b^0+\sum_{n=1}^{\infty} L_{bn}\cos pn(\alpha'-\theta')\right\}i_b+\left\{M_{ab}^0+\sum_{n=1}^{\infty}[M_{ban}^c\cos pn(\alpha'-\theta')-M_{ban}^s\sin pn(\alpha'-\theta')]\right\}i_a \quad (12B)$$

As for the flux linkage equation of a single-phase reluctance machine, it is derived from equation 12A by neglecting the second term involving i_b.

A study of the flux linkage equations 12 shows that for a fixed rotor position α', the machine impedance is dead, and the voltages and currents will have the same wave form. Under running condition, as α' is a function of time, the situation is different. Even when the applied voltages are sinusoidal, the currents will contain an infinite number of components having frequencies different from the frequency of the source supply. Consider, in particular, only the presence of zero and second harmonic air gap permeances. It can be shown from equations 12 that the flux linkages, and hence the voltages, of one angular velocity are not only related to the current of the same angular velocity but also related to currents having angular velocities $2v$ above and $2v$ below at an asynchronous speed v. This is the fundamental fact that will be utilized in developing equivalent circuits in the companion paper.[14]

Equivalent Circuit Study

In the companion paper equivalent circuits have been developed under the consideration of having closed rotor circuits. The case with no closed rotor circuits is only a particular one having infinite rotor circuit resistances and zero mutual inductances between the armature and the rotor. Formulas for calculating various machine inductances are given in the nomenclature.

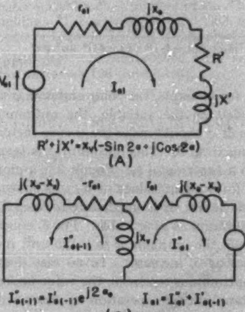

Figure 1. Two alternative equivalent circuits of fundamental frequency for reluctance machines

It has been shown that under synchronous operation, the equivalent circuits of fundamental frequency are of the same form of Figure 1, which is the reproduction of Figure 6 in the companion paper with $Z_0(j\omega)=0$, for single-phase and balanced polyphase reluctance machines. The circuits can be used, therefore, for the further discussions of the characteristics of reluctance machine without regard to whether it is a single-phase one or a balanced polyphase one.

Consider the equivalent circuit of Figure 1(A). The operating angle α will be regarded as the parameter. For any assumed α, the circuit impedance is calculated, and the series circuit is solved for the input current and hence other performance characteristics. As seen from this circuit, the mechanical load on the shaft is converted into a fictitious resistance $R'=-x_v\sin(2\alpha)$ in the electric circuit. The neglect of this equivalent load resistance will inevitably lead to errors in final results as given by Jasse.[4] For the motor operation, as α is negative, R' will be positive, and the power is consumed on the electrical side. For the generator operation, as α is positive, R' becomes negative, and the power is delivered on the electrical side. These facts are in agreement with the physical behavior of the machine.

It will be shown in the next section and also in the numerical examples of Appendix I that this circuit can be used for the direct calculations of pull-out characteristics, and characteristics when the mechanical power output is given.

For a complete set of performance calculations, the numerical steps will be reduced if the alternate circuit of Figure 1(B) is used. Under constant applied voltages, the "characteristic currents" are first solved from this 2-mesh circuit as

$$I_{a1}''=\frac{V_{a1}(r_{a1}-jx_0)}{r_{a1}^2+x_0^2-x_v^2},\qquad I_{a(-1)}''=\frac{jx_vV_{a1}}{r_{a1}^2+x_0^2-x_v^2} \quad (13)$$

At any assumed initial angle α_0, the input current is calculated by

$$I_{a1}=I_{a1}''+I_{a(-1)}^{*''}e^{j2\alpha_0} \quad (14)$$

Numerical examples on performance calculations are illustrated in Appendix I on an educational reluctance motor used by Trickey in his investigation.[12] The performance characteristics are given in Figure 2 as compared with the test results.

Pull-Out Characteristics

Refer to the equivalent circuit of Figure 1(A). As the torque corresponding to the core loss, the frictional and windage losses is approximately constant, the pull-out conditions will reach when the mechanical torque developed or the power consumed in R' is the maximum. The mechanical torque developed per phase can be expressed by the relation

$$\mathrm{T}=\frac{p}{2\omega}I_{a1}^2(-x_v\sin 2\alpha)=\frac{p}{2\omega}\times\frac{V_{a1}^2(-x_v\sin 2\alpha)}{(r_{a1}-x_v\sin 2\alpha)^2+(x_0+x_v\cos 2\alpha)^2} \quad (15)$$

Setting $d\mathrm{T}/d\alpha=0$, and simplifying yield

$$(r_{a1}^2+x_0^2+x_v^2)\cos 2\alpha+2x_0x_v=0$$

from which the operating angle α at the pull-out condition is

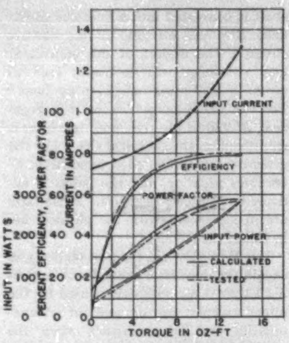

Figure 2. Performance characteristics of 1/4-horsepower 220-volt 60-cycle 3-phase 1,800 rpm synchronous reluctance motor

$$\alpha_M = \frac{1}{2}\cos^{-1}\left(\frac{-2x_0x_v}{r_{a1}^2+x_0^2+x_v^2}\right) \qquad (16)$$

The maximum developed torque per phase can be found by substituting equation 16 for α in equation 15. Simplifying gives

$$\mathbf{T}_M = \frac{pV_{a1}^2}{2\omega}\times \frac{x_v\sqrt{[r_{a1}^2+(x_0+x_v)^2][r_{a1}^2+(x_0-x_v)^2]}}{(r_{a1}^2+x_0^2+x_v^2)^2+2x_v\left\{r_{a1}\sqrt{r_{a1}^2+(x_0+x_v)^2][r_{a1}^2+(x_0-x_v)^2]}-2x_0^2x_v\right\}}$$

Newton-meters per phase (17)

If the resistance is neglected, equation 17 is reduced to

$$\mathbf{T}_M = \frac{pV_{a1}^2}{2\omega}\left(\frac{x_v}{(x_0^2-x_v^2)}\right)\times$$

Newton-meters per phase (17A)

To study the factors affecting the pull-out torque, consider, in particular, a balanced 2-phase reluctance motor, for which the following approximate expression of x_0 and x_v can be shown.

$$x_0 = 2\omega l(s_a n_a)k_{a1}^2G_a^0 = \frac{4K\omega l(k_{a1}s_a n_a)^2}{\pi\delta_1}\times [\delta_r+\varphi(1-\delta_r)] \qquad (18A)$$

$$x_v = 2\omega l(s_a n_a)k_{a1}^2G_a^v = \frac{4K\omega l(k_{a1}s_a n_a)^2}{\pi^2\delta_1}\times [(1-\delta_r)\sin(\varphi\pi)] \qquad (18B)$$

with

$$\delta_r = \delta_1/\delta_2 \qquad (18C)$$

The substitution of equations 18 in equation 17A gives

$$\mathbf{T}_M = pV_{a1}^2\delta_1\pi^2F/8K\omega^2l(k_{a1}s_a n_a)^2 \qquad (17B)$$

where the torque factor

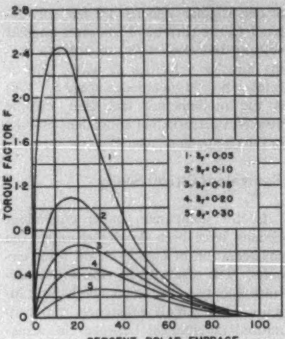

Figure 3. Effect of polar embrace on the pull-out torque of polyphase reluctance machines

$$F = \frac{(1-\delta_r)\sin(\varphi\pi)}{\pi^2[\delta_r+\varphi(1-\delta_r)]^2-(1-\delta_r)^2\sin^2\varphi\pi} \qquad (19)$$

If, for example, the polar embrace φ is regarded as the variable, the optimum value of φ should make the torque factor F a maximum. This optimum φ is seen to be a function of δ_r. Figure 3 is a plot of F for various values of δ_r. As shown in this figure, it is important to keep δ_r as minimum as practicable. For δ_r equal to 0.05, the optimum φ is 0.125 and increases as δ_r increases. In no case does the optimum φ reach 0.5, the value under constant current operation as discussed before.*

It can be shown that the torque factor F given in equation 19 is the same for all balanced polyphase reluctance machines. Therefore, the above conclusions are true for all balanced polyphase reluctance machines. A similar relation may be derived for single-phase reluctance machines. The optimum φ is even smaller than that for balanced polyphase reluctance machines for the same δ_r. However, a reluctance machine using the above indicated optimum φ does not necessarily mean a good design. A comparison of two designs using respectively the optimum φ under constant voltage and constant current operations is made in Appendix II.

Circle Diagrams of Reluctance Machines

The development of circle diagrams of reluctance machines has been discussed in several papers.[6,7,9] It will be shown here that the circle diagram can be derived readily from a study of the equivalent circuit. By referring to the equivalent circuit of Figure 1(B) and equations 13 and 14, the circular loci of $\boldsymbol{I}_{a1}$ are readily recognized, since $\boldsymbol{I}_{a1}''$ fixes the center of the circle, and $\boldsymbol{I}_{a(-1)}''$ gives the radius of the circle.

A direct construction of the current circle is also possible by considering the equivalent circuit of Figure 1(A). As shown in Figure 4, the conjugate impedance circle is first drawn with the center at 0′ (r_a, $-jx_0$) and radius equal to x_v. Draw the line 00′ to intersect the above circle at points z_1 and z_6. Find the geometric inversion points i_1 and i_6 with respect to the inversion circle of the radius equal to V_{a1}. Bisect i_1i_6 at 0″ and draw the required current circle with 0″ as the center and 0″i_1 as the radius. All quantities found from the equivalent circuits of Figures 1 can also be obtained graphically from the above circle diagram. To illustrate this fact, consider the operating conditions at the operating angle α_5. The corresponding initial angle α_{o5} happens to be equal to (−90) degrees. It is easily seen that the operating point i_5 on the current circle and z_5 on the impedance circle must lie on the opposite side of the inversion circle, and either point will fix the other point. When the current phasor is fixed, the input power factor angle can be found, and the power factor calculated. As the machine is operated under constant applied voltage, the in-phase component of the current phasor, that is, i_5p_5, will represent the input power. As seen from the equivalent circuit of Figure 1(A), this input power is divided into the mechanical power developed and the $I_{a1}^2r_{a1}$ loss in the ratio of $(-x_v \sin 2\alpha_5)$ to r_{a1}. To find the division point, drop the perpendicular line z_5p_5' to intersect the line $0'z_7$ at d_5'. The point of intersection of the lines od_5' and i_5p_5 will give the required division point d_5. The loci of these division points give the loss curve.

For single-phase reluctance machines, it may be desirable to know the effective value of harmonic currents at each load. As has been shown[14] that the ratio of two consecutive harmonic currents is constant, the ratio of the effective value of harmonic currents to the fundamental one will be constant. The harmonic current content line is so drawn that its slope with respect to the vertical line is equal to this last ratio. For the effective value of the fundamental current equal to the magnitude of the phasor i_5, the effective value of harmonic currents will be represented by the length I_5.

---

*See also the end of Appendix II.

Since for the motor operation, α is negative and may have any value between 0 degree and (−90) degrees, the right half of the impedance circle will correspond to the motor operating range. The line i_2i_7, obtained by connecting the geometric inversion points z_2 and z_7, will divide the current circle into two parts corresponding to the motor and generator operating ranges. In the part i_2i_0, however, there is still no electrical power output. Both the mechanical and the electrical power inputs are used to supply losses of the machine. Braking action thus appears in this operating range.

If the loss curve is moved parallel to itself, until it is tangent to the current circle, the point of tangency will fix the pull-out operating point. Beyond this point, the machine is in an unstable operation. It can be shown mathematically that for practical reluctance machines, the operation at the maximum input point is, in general, in the unstable operating range.

It is also seen from Figure 4 that the condition of maximum power factor is reached when the current vector is tangent to the current circle. From the graphical construction, it can be shown that the current vector under this condition is tangent to the impedance circle also. Referring again to Figure 4, one can obtain

$$\text{Maximum power factor} = \cos\beta' = \cos(\beta'+\gamma'-\gamma') = \cos(\beta'+\gamma')\times \cos\gamma' + \sin(\beta'+\gamma')\sin\gamma' = \frac{x_0x_v + r_{a1}\sqrt{x_0^2+r_{a1}^2-x_v^2}}{x_0^2+r_{a1}^2} \tag{20}$$

If the resistance is neglected, equation 20 is reduced to

$$\text{Maximum power factor} = \cos\beta' = x_v/x_0 \tag{20A}$$

Since x_v/x_0 is ordinarily around 0.33 for a single-phase reluctance machine having no damper windings, and 0.58 for a polyphase one, the power factor of reluctance machines is fairly low. However, as they are simple in construction, constant in speed, and reliable in operation, they find their wide application as small motor drives in laboratories and in industrial plants.

Conclusions

The reluctance torque of single-phase and balanced polyphase machines under both the constant current and the constant voltage operation has been analyzed and the factors affecting this torque investigated. Equivalent circuits have been applied to facilitate (a) the complete performance calculations, (b) the direct calculations of pull-out conditions, (c) the direct calculations of performance characteristics with the known mechanical power output, (d) the design of reluctance machines. Numerical examples have been found in agreement with the test results.

Appendix I. Examples of Performance Calculations

Consider the educational reluctance motor used by Trickey in his investigation.[12] The known data are: 1/4 horsepower, 220 volts, 3-phase, 60-cycle, 4-pole, Y-connected, 1,800 rpm synchronous reluctance educational motor. The dimensions of the machine are:

Stator: Length = 2 inches, diameter, outer = 6 inches, inner = 3.526 inches, total number of slots = 36, Carter coefficient = 1.217, number of conductors per slot = 76.

Rotor: Length = 2 inches, diameter, outer = 3.502 inches, number of slots before milling = 47, Carter coefficient = 1.05, actual polar embrace in per cent of pole pitch = 0.5.

Air gap: Actual = 0.012 inch, saturation factor = 1.126 (calculated).

Calculation of Machine Constants:

$\delta_1 = 0.012\times1.126\times1.05\times1.127 = 0.01722$ inch

$\delta_2 = 0.3$ (assumed)
$s_a = 3$, $n_a = 76$, effective polar embrace = 0.52
$G_a^0 = 2.61\times10^{-4}$, $G_a^v = 1.43\times10^{-4}$
Slot and end winding leakage reactance = 5 ohms
Resistance per phase = 6.76 ohms

$$x_0 = 3\omega l n_a s_a G_a^0\left(k_{a1}^2+\frac{k_{a5}^2}{25}+\frac{k_{a7}^2}{49}+\ldots\right)+5 = 114.5 \text{ ohms}$$

$$x_v = 3\omega l n_a s_a G_a^v \sin(\varphi\pi)\left(k_{a1}^2+\frac{2}{35}k_{a5}k_{a7}+\ldots\right) = 60.4 \text{ ohms}$$

Complete Performance Calculations: It is more convenient to use the equivalent circuit of Figure 1(B). The characteristic currents solved from this circuit are

$$I_{a1}'' = I_{a1}' = \frac{127(6.76-j114.5)}{(114.5)^2-(60.4)^2+(6.75)^2} = 0.0902-j1.528$$

$$I_{a(-1)}'' = j127\times60.4/9{,}506 = j0.805$$

Assume that the performance characteristics at $\alpha_0 = -95$ degrees are to be found. Then the input current is equal to

$$I_a = I_{a1}' + I_{a(-1)}{}^{*\prime\prime}\epsilon^{j2\alpha_0} = 0.2299-j0.737$$

Therefore, $I_{a1} = 0.771$ ampere:

Input power factor = 0.298
Input watts = 3×127×0.2299 = 87.5
Frictional and windage watts = 5.8 (measured)
Core loss in watts = 21.7 (measured)
Copper loss in watts = 12
Mechanical power output in watts = 48
Torque in ounces-feet = 112.7×48/1,800 = 3
Efficiency = 48/87.5 = 0.549

The characteristics corresponding to other assumed α_0 can be found in the same way. They are plotted in Figure 2 as compared with the tested results.

Calculation of Pull-Out Power and Torque: By referring to the equivalent circuit of

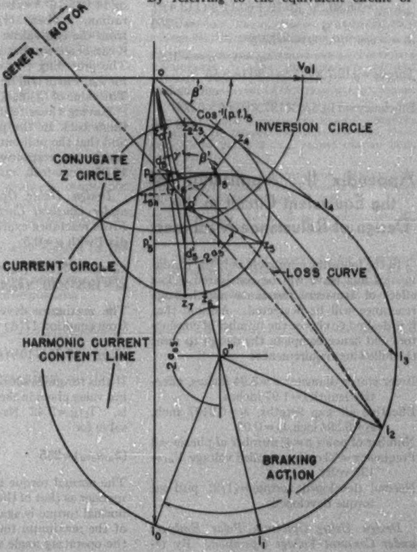

Figure 4. Circle diagram of reluctance machines

Figure 1(A) and equation 16, the operating angle α corresponding to the pull-out condition is found as equal to $\alpha_M = -72.7$ degrees. The total maximum power calculated is $P_{max} = 285$ watts. The pull-out torque is therefore equal to $112.7(285-27.5)/1800 = 16.1$ ounces-feet.

Performance Calculation with the Known Mechanical Power Output: Assume the known mechanical power output = 141.5 watts. Then the power developed across the fictitious load resistance

$$R' = -x_v \sin(2\alpha) \text{ is } (141.5+27.5)/3 = 56.3 \text{ watts per phase}$$

Referring to Figure 1(A), one can see that

$$-x_v \sin(2\alpha) = 56.3/I_{a1}^2$$

therefore,

$$x_v \cos(2\alpha) = \pm\sqrt{(60.4I_{a1}^2)^2 + (56.3)^2}/I_{a1}^2$$

Since

$$I_{a1}^2 = V_{a1}^2/[(6.76 - x_v \sin(2\alpha))^2 + (x_0 + x_v \cos(2\alpha))^2]$$

the above two relations can always be combined into a fourth order equation with even powers of I_{a1}

$$1{,}754I_{a1}^4 - 9{,}855I_{a1}^2 + 7{,}666 = 0$$

Solving, $I_{a1} = 0.966$ ampere or 2.17 amperes. The first value corresponds to the normal operation while the other value corresponds to the operation in the unstable region as seen from the circle diagram. Under normal operation, α is solved from the above relation as equal to -45.5 degrees.

Power factor

$$= 66.86/\sqrt{[(6.76+60.1)^2 + (113.4)^2]} = 0.509$$

$$\alpha_1 = -\cos^{-1}(0.509) = -59.5°, \quad \alpha_0 = \alpha_1 + \alpha = -105°$$

$$\text{Torque} = 112.7 \times 141.5/1{,}800 = 8.85 \text{ ounces-feet}$$

$$\text{Efficiency} = 114.5/3 \times 127 \times 0.966 \times 0.508 = 0.755$$

Appendix II. Application of the Equivalent Circuit to the Design of Reluctance Machines

In the following approach, only the fundamental flux wave will be considered. The effect of armature resistance and leakage reactance will be neglected. Assume that it is desired to choose the number of conductors and hence complete the design to meet the following requirements:

Inner stator diameter $d = 3.94$ inches, effective length $l = 1.97$ inches
Effective air gap lengths, $\delta_1 = 0.0197$ inch, $\delta_2 = 0.394$ inch, $\delta_r = 0.05$
Number of poles $p = 4$, number of phases = 3
Frequency = 50 cycles, applied voltage $V_{a1} = 127$ volts
Normal developed torque = (1/2) pull-out torque developed

Design Using Optimum Polar Embrace under Constant Voltage Operation: By referring to Figure 3, it is seen that for $\delta_r = 0.05$, the optimum value of polar embrace φ is 0.125. The corresponding torque factor F is 2.45. The total pull-out developed torque for a 3-phase machine can be obtained from equation 17(A) and the expressions of x_0 and x_v given in Appendix I with harmonic winding factors and leakage reactance neglected; thus

$$x_v = 4.375 \times 10^{-4}(k_{a1}n_as_a)^2$$
$$x_0 = 6.38 \times 10^{-4}(k_{a1}n_as_a)^2$$
$$(T_t)_M = \frac{3V_{a1}^2\pi^2p\delta_1}{12K\omega^2l(n_as_ak_{a1})^2} = \frac{62.7 \times 10^4}{(n_as_ak_{a1})^2}$$

Under normal operating condition having the operating angle α, the developed torque is found conveniently from the power consumed in the resistance R' in Fig. 1(A). If this torque is set equal to one-half the pull-out torque, it can be shown that

$$31.35 = -70.35 \sin 2\alpha / \times [(1.458 + \cos 2\alpha)^2 + \sin^2 2\alpha]$$

from which, $\alpha = -55.3$ degrees.

Since α denotes the relative angular position of the fundamental magnetomotive force wave with respect to one of salient pole axes, and since $|\alpha| = 55.3$ degrees is greater than one-half of the polar embrace in degrees, that is, 11.25 degrees, the point of maximum flux density will occur at the edge of the pole. The flux density there is given by

$$B_M = 3\sqrt{2}K(k_{a1}n_as_a)I_{a1} \times \cos(55.3 - 11.25)/0.0197\pi$$

The substitution of numerical values gives

$$B_M = 3.01 \times 10^{-6}(k_{a1}n_as_a)I_{a1}$$

Assume $B_M = 60$ kilolines per square inch, or 11.82×10^{-4} webers per inch–mechanical radian. Then $(k_{a1}n_as_a)I_{a1} = 393$. Now from the equivalent circuit of Figure 1(A), it can be shown that $I_{a1} = 20 \times 10^4/(k_{a1}n_as_a)^2$. The preceding two relations can be solved for I_{a1}, which will be equal to 0.772 ampere. The value of $(k_{a1}n_as_a)$ will be 509.5.

Having these results, one can substitute them back in the previous equations and find that the pull-out torque and the normal torque are respectively equal to 28.7 and 14.35 ounce-feet.

Design Using Optimum Polar Embrace under Constant Current Operation, $\varphi = 0.5$: From reactance expressions given in Appendix I with $\varphi = 0.5$

$$x_v = 11.42 \times 10^{-4}(k_{a1}n_as_a)^2$$
$$x_0 = 19.85 \times 10^{-4}(k_{a1}n_as_a)^2$$

The maximum developed torque obtained from equation 17(A) will be

$$(T_t)_M = 13.35 \times 10^4/(k_{a1}n_as_a)^2$$

If this torque is set equal to the corresponding value given in the preceding section, that is, $(T_t)_M = 2.42$ Newton-meters, one can solve for

$$(k_{a1}n_as_a) = 235$$

The normal torque is obtained in the same manner as that of the previous case. If this normal torque is again set equal to one-half of the maximum torque, one can solve for the operating angle which is found as equal to -44.77 degrees. The flux density distribution will have its maximum value at the point very near the pole tip. This maximum flux density is found as $B_M = 10.13I_{a1} \times 10^{-4}$. The normal current I_{a1} obtained from the equivalent circuit of Figure 1(A) is equal to 1.002 ampere. Therefore, $B_M = 10.15 \times 10^{-4}$ webers per inch–mechanical radian. The total effective ampere conductors per pole per phase will be $(k_{a1}n_as_a)I_{a1} = 235 \times 1.002 = 235.5$.

Comparing the above two designs, one can see that the first design requires less iron since the polar embrace is the smaller. Furthermore, as it has higher ratio of x_v/x_0, the power factor in the operating range is, in general, higher if there is no saturation effect. Under normal operation, the power factor is equal to 0.645 as against 0.5 of the second design. However, the presence of saturation effect and hence the increase in magnetizing current tend to reduce the power factor. Also as the first design requires 67% more effective ampere conductors, it will result in a machine using more copper. The fact of higher electric loading and higher magnetic loading (that is, larger B_M) makes the machine of the first design, in general, one of greater loss and less efficiency. Hence, the machine of the first design may not be a favorable one. In addition, if the machine is to be designed for self-starting, too small a polar embrace may lead to the difficulty of designing and installing the damper windings. From this point of view, the value of polar embrace φ around 0.5 is probably the most efficient.

Furthermore, the question arises on the theoretical value of polar embrace of around 15 per cent of the pole pitch derived for constant voltage operation. The optimum value might be affected by the saturation effect. The consideration of the leakage reactance of the primary, however, will not make much difference on this conclusion, since it is only a small percentage of the reactances x_0 and x_v. Nor the change of figure of merit from F to $(F\delta_1/d)$ will alter the theoretical optimum polar embrace, since δ_1 can only affect the magnitude of the pull-out torque but not the variation of pull-out torque with polar embrace. In small nonself-starting reluctance motors, the polar embrace of around 15 per cent of the pole pitch has been used in practice.[4] For reluctance machines of moderate size, this value might be impractical.

Appendix III. Nomenclature

$\alpha = \alpha_0 - \alpha_1$ = operating angle, α_M = pull-out operating angle
α_s, α' = instantaneous angular position from the axis of rotor symmetry (for example, one of the salient pole axes) to the axis of winding a in electrical radians, and in mechanical radians
α_0 = initial angular position of the rotor with respect to same references in electrical radians
α_1 = phase angle of I_{a1} at $t = 0$
α_{m1}, α_{m2} = phase angle of I_{am1} and I_{am2} at $t = 0$
δ_1, δ_2 = effective uniform air gap lengths in inches under poles, and in the interpolar spaces
$\delta_r = \delta_1/\delta_2$

θ, θ' = angular displacement of winding *b* from winding *a* in the direction of rotation in electrical radians, and in mechanical radians

τ, τ_s = pole pitch of armature windings and salient rotor in mechanical radians

φ = polar embrace in the fraction of a pole pitch

ω = fundamental angular velocity of applied voltages

$\mathfrak{F}_a(x,t)$ = Symmetrical magnetomotive force distribution of winding *a* with respect to its own axis

$\mathcal{P}_0$, $\mathcal{P}_{vn}$ = magnitude of zero and *n*th harmonic permeance per unit area with respect to the period of permeance variation. For uniform air gap lengths δ_1 and δ_2, $\mathcal{P}_0$ and $\mathcal{P}_{vn}$ are expressed in equations 2

$\mathcal{P}(x,t)$ = distribution of air gap permeance per unit area with respect to the symmetrical axis of winding *a*

If the following quantities are defined with respect to winding *a*, the quantities with respect to winding *b* can be defined in the same manner by the interchange of subscripts *a* and *b*.

B, B_M = air gap flux density and its maximum value in webers per inch-mechanical radian of area.

$B_a(x,t)$ = flux density distribution around the air gap due to current in winding *a* with respect to the axis of winding *a*

d = armature diameter in inches

F = torque factor defined in equation 19

$G_a^0 = 2n_as_a\mathcal{P}_0/\pi$, $G_a^v = n_as_a\mathcal{P}_v/\pi^2$

$I_{a1} = I_{a1}e^{j\alpha_1}$ = input current phasor $= I_{a1}' + I_{a(-1)}^{*\prime} = I_{a1}'' + I_{a(-1)}^{*\prime\prime}e^{j2\alpha_1}$

I_{a1}'', $I_{a(-1)}''$ = mesh current phasors in the equivalent circuit of Figure 1(B)

$I_{a(-1)}^{*\prime}$, $I_{a(-1)}^{*\prime\prime}$ = conjugate current phasors of $I_{a(-1)}'$ and $I_{a(-1)}''$

i_a = instantaneous current in winding *a*

$K = 1.596\times 10^{-8}d$

$k_{a(2qn-2r+1)}$ = phase *a* winding factor with respect to space $(2qn-2r+1)$th harmonic

$$L_a^0 = 2(s_an_al)G_a^0\sum_{r=1}^{\infty}\frac{k_{a(2r-1)}^2}{(2r-1)^2} + S_a$$

$$L_{an} = 2(s_an_al)G_a^v\sum_{r=1}^{\infty}\frac{(-1)^{n-1}k_{a(2r-1)}}{n(2r-1)}\times$$

$$\left[\frac{k_{a(2n-2r+1)}}{2n-2r+1} - \frac{k_{a(2n+2r-1)}}{2n+2r-1}\right]\sin(n\varphi\pi)$$

l = effective length of armature conductor in inches

$$M_{ab}^0 = M_{ba}^0 = 2(s_an_al)G_b^0\sum_{r=1}^{\infty}\times$$

$$\frac{k_{a(2r-1)}k_{b(2r-1)}}{(2r-1)^2}\cos\frac{p}{2}(2r-1)\theta' + S_{ab}$$

$$M_{abn}^c = 2(s_an_al)G_b^v\sum_{r=1}^{\infty}\times$$

$$\frac{(-1)^{n-1}k_{b(2r-1)}\sin(n\varphi\pi)}{n(2r-1)}$$

$$\left[\frac{k_{a(2n-2r+1)}}{2n-2r+1} - \frac{k_{a(2n+2r-1)}}{2n+2r-1}\right]\cos\frac{p}{2}(2r-1)\theta'$$

$$M_{abn}^s = 2(s_an_al)G_b^v\sum_{r=1}^{\infty}\times$$

$$\frac{(-1)^{n-1}k_{b(2r-1)}\sin(n\varphi\pi)}{n(2r-1)}$$

$$\left[\frac{k_{a(2n-2r+1)}}{2n-2r+1} + \frac{k_{a(2n+2r-1)}}{2n+2r-1}\right]\sin\frac{p}{2}(2r-1)\theta'$$

m_1, m_2 = time order of current harmonics

n = space order of permeance harmonics with respect to the period of τ_s

n_a = number of conductors per slot of winding *a*

P_M = total maximum power in watts

p = number of poles of armature winding $= 2\pi/\tau$

q = ratio of pole pitch of armature winding to that of salient rotor

$R' = -x_v \sin(2\alpha)$ = effective resistance corresponding to the shaft load

r_{a1} = armature resistance in ohms at the fundamental frequency

$2r-1$ = space order of magnetomotive force harmonic with respect to the fundamental wave having *p* poles

S_a, S_{ab} = self leakage inductance of winding *a*, and mutual leakage inductance of winding *a* with respect to winding *b*

s_a = number of slots per pole of winding *a*

T_{aa}, T_t = instantaneous reluctance torque due to current in winding *a* only, and the total instantaneous torque in Newton-meters

T, T_t, T_M = time average torque per phase, total time average torque, and the maximum time average torque per phase in Newton-meters

V_{a1} = fundamental applied voltage phasor on winding *a*

x = position co-ordinate with respect to the symmetrical axis of winding *a*

x_0 = magnitude of machine reactance independent of the rotor position

x_v = magnitude of machine reactance of saliency due to the presence of harmonic permeance

$X' = x_v\cos(2\alpha)$ = effective reactance of saliency at the operating angle α

References

1. Synchronous Torque of an Unexcited Salient Pole Motor, R. D. Ball. *Electrical Engineering*, volume 52, February 1933, pages 136–37.

2. Drehfeldmaschinen mit veraenderlicher Reaktanz, R. Bruederlin. *Archiv fuer Elektrotechnik* (Berlin, Germany), volume 13, 1924, pages 12–29.

3. Ueber den Einphasen-Magnetmotor und seine Moeglichkeiten mit mehreren synchronen Drehzahlen laufen zu koennen, T. Buchhold. *Elektrotechnische Zeitschrift* (Berlin, Germany), volume 61, 1940, pages 7–10.

4. Ueber Synchronmotoren ohne Erregung, E. Jasse. *Archiv fuer Elektrotechnik* (Berlin, Germany), volume 2, 1913, pages 27–48.

5. Die synchrone Drehfeld-Reaktions Maschine, J. Kucera. *Elektrotechnik und Maschinenbau* (Vienna, Austria), volume 56, 1938, pages 173–78.

6. Consideration sur les proprieties particulieres des machines a poles salliants, M. P.-G. Laurent. *Revue Generale de l'Electricite* (Paris, France), volume 53, 1944, pages 113–19.

7. The Reaction-Type Synchronous Motor, H. Lundkvist. *ASEA Journal* (Vasteras, Sweden), volume 9, 1932, pages 142–45.

8. Das Drehmoment der synchronen Drehfeld-Reaktionsmaschine, K. Schaffer. *Elektrotechnik und Maschinenbau* (Vienna, Austria), volume 55, 1937, pages 99–102.

9. Die Ortskurve der synchronen Drehfeld-Reaktionsmaschine, K. Schaffer. *Elektrotechnik und Maschinenbau* (Vienna, Austria), volume 55, 1937, pages 629–33.

10. Theory and Calculations of Electrical Apparatus (book), C. P. Steinmetz. McGraw-Hill Book Company, New York, N. Y., 1917, pages 260–73.

11. The Non-Excited Synchronous Motor, P. H. Trickey *Electric Journal* (Pittsburgh, Pa.), volume 30, 1933, pages 160–62.

12. Performance Calculations on Polyphase Reluctance Motors (Synchronous Motors without Field Excitation), P. H. Trickey. *Electrical Engineering* (*AIEE Transactions*), volume 65, April 1946, pages 191–98.

13. Fractional Horsepower Electric Motors (book), C. G. Veinott. McGraw-Hill Book Company (New York, N. Y.), second edition, 1948, pages 356–61.

14. Equivalent Circuits of Reluctance Machines, C. Y. Lin. *AIEE Transactions*, volume 71, part I, 1952 (*Proceedings T1-363*).

15. Induction Motor Slot Combinations, G. Kron. *AIEE Transactions*, volume 50, June 1931, pages 757–68.

16. Synchronous Machines I—An Extension of Blondell's Two-Reaction Theory, R. E. Doherty, C. A. Nickle. *AIEE Transactions*, volume 45, June 1926, pages 912–26.

No Discussion

An Analysis of Unexcited Synchronous Capacitor Motors

S. S. L. CHANG
ASSOCIATE AIEE

RELUCTANCE type capacitor motors are widely used in smaller frame sizes. Compared with other types of single-phase synchronous motors of the same physical size, these motors are most efficient, and powerful in terms of either synchronous pull out torque or torque angle. The noise or pulsating torque also is lower in these motors than in plain single-phase reluctance motors. With the rapid improvements of the a-c capacitors, these motors are gaining popularity in the synchronous motor field.

Little comprehensive theoretical work has been published about these motors. A designer has to meet the widely diversified performance requirements with no other means than trial and error. However, with all the theoretical work on capacitor motors, and polyphase and single-phase reluctance motors in its background, a comprehensive analysis of the capacitor reluctance motor can be readily made.

In this paper, an equivalent circuit for the capacitor reluctance motor at synchronous speed is constructed based on the double revolving field theory. The equivalent circuit can be used to calculate the motor performance at synchronous speed, and to find favorable winding ratios as well as capacitor values. An equation for the starting torque which accounts for both the induction motor torque and "cogging" is derived from the cross-field theory. This equation also shows how "cogging" in a reluctance motor can be eliminated.

Synchronous Condition, Revolving Field Theory Equivalent Circuit

At synchronous speed, the voltages, and currents can be resolved into positive and negative sequence components. The positive sequence components are locked into synchronism with the rotor, while the negative sequence components rotate in the opposite direction at twice synchronous speed, referring to the rotor. Throughout this analysis, the magnetizing reactances are considered as part of the rotor circuit. The ratio of the positive sequence air gap electromotive force to the positive sequence stator current is defined as $\boldsymbol{Z}_+$. Similarly, the ratio of the negative sequence air gap electromotive force to the negative sequence stator current is defined as $\boldsymbol{Z}_-$. The impedance $\boldsymbol{Z}_+$ depends on the torque angle, but not on the rotor resistance, while $\boldsymbol{Z}_-$ depends on the rotor resistance, but not on the torque angle. The explicit expressions of $\boldsymbol{Z}_+$ and $\boldsymbol{Z}_-$ will be derived later. The voltage and current equations are, by definition

$$E_+ = Z_+ I_+ \tag{1}$$

$$E_- = Z_- I_- \tag{2}$$

$$E_m = I_m Z_{lm} + \frac{1}{\sqrt{2}}(E_+ + E_-) \tag{3}$$

$$E_s = I_s(Z_{ls} + Z_c) + \frac{ja}{\sqrt{2}}(E_+ - E_-) \tag{4}$$

$$I_m = \frac{1}{\sqrt{2}}(I_+ + I_-) \tag{5}$$

$$aI_s = \frac{j}{\sqrt{2}}(I_+ - I_-) \tag{6}$$

Substitute equations 1, 2, 5, 6 into equations 3, 4 and we have

$$\sqrt{2}E_m = (Z_{lm} + Z_+)I_+ + (Z_{lm} + Z_-)I_- \tag{7}$$

$$-\frac{j\sqrt{2}E_s}{a} = \left(\frac{Z_{ls}+Z_c}{a^2} + Z_+\right)I_+ - \left(\frac{Z_{ls}+Z_c}{a^2} + Z_-\right)I_- \tag{8}$$

Taking the sum and difference of equations 7 and 8:

$$\frac{1}{\sqrt{2}}\left(E_m - \frac{jE_s}{a}\right) = \left(\frac{Z_{lm}}{2} + \frac{Z_{ls}+Z_c}{2a^2} + Z_+\right) \times I_+ - \left(\frac{Z_{ls}+Z_c}{2a^2} - \frac{Z_{lm}}{2}\right)I_- \tag{9}$$

$$\frac{1}{\sqrt{2}}\left(E_m + \frac{jE_s}{a}\right) = \left(\frac{Z_{ls}+Z_c}{2a^2} + \frac{Z_{lm}}{2} + Z_-\right) \times I_- - \left(\frac{Z_{ls}+Z_c}{2a^2} - \frac{Z_{lm}}{2}\right)I_+ \tag{10}$$

Equations 9 and 10 are the mesh equations for the equivalent circuit of Figure 1.

An expression of $\boldsymbol{Z}_+$ can be derived from the 2-reaction theory. Let δ be the electrical angle by which the direct axis lags behind the positive sequence air gap flux. The vector diagram of $\boldsymbol{E}_+$, $\boldsymbol{I}_+$ and their components in the direct and quadrature axes are shown in Figure 2. Referring to the diagram:

$$I_+ = I_{q+} - jI_{d+} \tag{11}$$

$$E_+ = I_{d+}X_d + jI_{q+}X_q \tag{12}$$

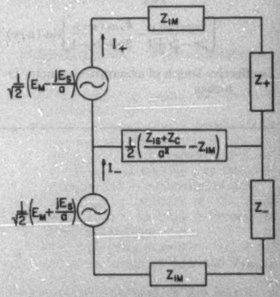
Z_{lM}
I_+
$\frac{1}{\sqrt{2}}\left(E_M - \frac{jE_s}{a}\right)$
Z_+
$\frac{1}{2}\left(\frac{Z_{ls}+Z_c}{a^2} - Z_{lM}\right)$
I_-
$\frac{1}{\sqrt{2}}\left(E_M + \frac{jE_s}{a}\right)$
Z_-
Z_{lM}

Figure 1. The revolving field theory equivalent circuit of a single-phase motor

---

Paper 51-364, recommended by the AIEE Rotating Machinery Committee and approved by the AIEE Technical Program Committee for presentation at the AIEE Fall General Meeting, Cleveland, Ohio, October 22-26, 1951. Manuscript submitted April 2, 1951; made available for printing September 12, 1951.

S. S. L. Chang is with Robbins & Myers, Incorporated, Springfield, Ohio.

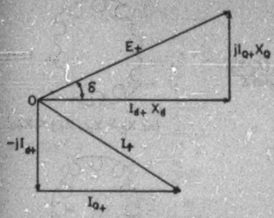

Figure 2. Vector diagram of the positive sequence voltages and currents

$$I_{d+}X_d = I_{q+}X_q \cot \delta \qquad (13)$$

From the above equations, we find:

$$\frac{1}{\mathbf{Z}_+} = \frac{\mathbf{I}_+}{\mathbf{E}_+} = \frac{\left(1 - j\frac{X_q}{X_d}\cot \delta\right)}{X_q(\cot \delta + j)} \qquad (14)$$

Equation 14 can be simplified by eliminating δ from the numerator. It becomes:

$$\frac{1}{\mathbf{Z}_+} = \frac{1}{jX_d} + \frac{1}{\frac{X_dX_q}{X_d - X_q}\cot \delta + j\,\frac{X_dX_q}{X_d - X_q}} \qquad (15)$$

Equation 15 leads to the equivalent circuit of Figure 3(A). Alternatively equation 14 also can be written as

$$\mathbf{Z}_+ = jX_q + \frac{1}{\frac{1}{j(X_d - X_q)} + \frac{X_d \tan \delta}{X_q(X_d - X_q)}} \qquad (16)$$

Equation 16 leads to another form of $\mathbf{Z}_+$, as shown in Figure 3(B). The power dissipated in the equivalent load resistances R_a and R_b are equal to the output mechanical power, or the torque in synchronous watts.

The negative sequence flux slips past the direct and quadrature axes at twice synchronous speed. The impedance $\mathbf{Z}_-$ can be calculated as the average value of the apparent rotor impedances of the *d*- and *q*-axes for a slip of 2. It is

$$\mathbf{Z}_- = R_- + jX_- = \frac{1}{2}\left\{\frac{jX_d\left(\frac{R_{2d}}{2} + jX_{2d}\right)}{\frac{R_{2d}}{2} + j(X_d + X_{2d})} + \frac{Xj_q\left(\frac{R_{2q}}{2} + jX_{2q}\right)}{\frac{R_{2q}}{2} + j(X_q + X_{2q})}\right\} \qquad (17)$$

In most motors, the rotor cage impedances are much smaller compared to X_d and X_q, and approximate expressions can be used:

$$R_- = \frac{1}{4}(R_{ed} + R_{eq}),\; X_- = \frac{1}{2}(X_{ed} + X_{eq})$$

The constants R_{ed}, X_{ed} . . . are defined in the nomenclature. The torque due to the negative sequence flux is $-R_-I_-^2$ synchronous watts.

In actual motors, $\mathbf{E}_s = \mathbf{E}_m = V$, and $X_{lm} = X_{ls}/a^2$. Substituting the equivalent circuits for $\mathbf{Z}_+$ and $\mathbf{Z}_-$ in Figure 1, we obtain the equivalent circuit for a capacitor reluctance motor as shown in Figure 4. In this equivalent circuit, R_b is the only variable component as the angle δ varies with load. The motor performance at synchronous speed is fully represented by this two mesh circuit.

Balanced Operation, Maximum Torque, Torque Angle

The capacitor reluctance motor can be so designed that $\mathbf{I}_- = 0$ for one value of the torque angle. At this load point, the motor behaves the same as a polyphase motor. The condition for balance can be obtained by equating $\mathbf{I}_- = 0$ and eliminating $\mathbf{I}_+$ from equations 7 and 8, it is:

$$\mathbf{Z}_{lm} + \mathbf{Z}_+ = ja\left(\frac{\mathbf{Z}_{ls}}{a^2} + \mathbf{Z}_+\right) \qquad (18)$$

Separating equation 18 into real and imaginary parts, expressions of a and X_c can be obtained. They are:

$$a = \frac{X_+ + X_{lm}}{\frac{R_{ls}}{a^2} + R_+} \qquad (19)$$

$$X_c = a^2(X_+ + X_{lm}) + a(R_+ + R_{lm}) \qquad (20)$$

For given δ, X_+, and R_+ can be readily calculated from Figure 3(B). As R_{ls}/a^2 is independent of the turn ratio with fixed copper cross-section area, the turn ratio a can be calculated from equation 19.

In a reluctance motor, the value of primary copper loss is usually relatively high. The peak efficiency occurs approximately at a point for which R_+ is maximum. Under this condition:

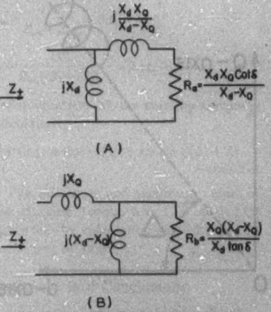
j X_d X_Q / X_d - X_Q
Z+
jX_d
R_a = X_d X_Q Cot δ / X_d - X_Q
(A)
jX_Q
Z+
j(X_d - X_Q)
R_b = X_Q(X_d - X_Q) / X_d tan δ
(B)

Figure 3. Equivalent circuits for the positive sequence impedance Z+

$$\left.\begin{aligned} \tan \delta &= \frac{X_q}{X_d} \\ R_+ &= \frac{1}{2}(X_d - X_q) \\ X_+ &= \frac{1}{2}(X_d + X_q) \end{aligned}\right\} \qquad (21)$$

If this point is chosen as the balanced point, equations 19 and 20 become:

$$a = \frac{X_{lm} + \frac{1}{2}(X_d + X_q)}{\frac{R_{ls}}{a^2} + \frac{1}{2}(X_d - X_q)} \qquad (22)$$

$$X_c = a^2\left(X_{lm} + \frac{X_d}{2} + \frac{X_q}{2}\right) + a\left(R_{lm} + \frac{X_d}{2} - \frac{X_q}{2}\right) \qquad (23)$$

The maximum torque can be calculated from the equivalent circuit with the aid of Thevenin's Theorem. At the maximum torque point, the negative sequence torque is usually small. It can be neglected or treated as a correction to the positive sequence torque. Let I_t be the short circuit current if a short is placed across R_b, and let Z_t be the impedance measured at the two terminals of R_b, with R_b disconnected and the voltage sources replaced by short circuits. Let θ_t be the power factor angle of Z_t. For the maximum synchronous torque point, $R_b = \mathbf{Z}_t$, and the torque in synchronous watts is:

$$T_{\max} = \frac{I_t^2 Z_t}{4 \cos^2 \frac{\theta_t}{2}} - \text{friction and windage} \qquad (24)$$

Another consideration besides the maximum torque is the stiffness or torque per radian of the angle δ. Under light load or no load conditions

$$T = \frac{I_t^2 Z_t^2}{R_b} = \frac{I_t^2 Z_t^2 X_d \tan \delta}{X_q(X_d - X_q)} \qquad (25)$$

Differentiating equation 25 we obtain an expression for stiffness. Near $\delta = 0$, $\sec^2 \delta = 1$ and

$$\frac{dT}{d\delta} = \frac{I_t^2 Z_t^2 X_d}{(X_d - X_q)X_q} \qquad (26)$$

Although equation 26 is derived for no-load condition, it is found to be correct approximately for light load up to about one-fourth of the maximum torque.

An Analytical Expression of the Starting Torque, Cross-Field Theory

Single-phase reluctance motors are noted for "cogging" at locked rotor condition. This is a very disagreeable effect and is recognized as some form of reluctance torque. The following analysis will give a quantitative account of both the induction motor torque and the reluctance torque at locked rotor condition.

Referring to Figure 5, the stator currents can be resolved along the two rotor axes *d* and *q*:

$$I_d = I_m \cos \Delta - aI_s \sin \Delta \quad (27)$$

$$I_q = I_m \sin \Delta + aI_s \cos \Delta \quad (28)$$

From the cross-field theory, the starting torque can be expressed as:

$$T = E_q I_d \sin (E_q, I_d) - E_d I_q \sin (E_d, I_q) \quad (29)$$

Since $\mathbf{E}_d = \mathbf{I}_d \mathbf{Z}_{ed}, \mathbf{E}_q = \mathbf{I}_q \mathbf{Z}_{eq}$ equation 29 can be written as:

$$T = I_q I_d Z_{eq} \sin (\theta + \theta_q) - I_d I_q Z_{ed} \sin (\theta_d - \theta) \quad (30)$$

Note that $Z_{eq} \sin \theta_q = X_{eq}, \ldots .$, equation 30 becomes:

$$T = I_d I_q \sin \theta (R_{ed} + R_{eq}) + I_d I_q \cos \theta (X_{eq} - X_{ed}) \quad (31)$$

$I_d I_q \sin \theta$ and $I_d I_q \cos \theta$ are the imaginary and real components of I_q conj. I_d. From equations 27 and 28, these are readily found to be:

$$I_q I_d \sin \theta = aI_m I_s \sin \theta_{sm} \quad (32)$$

$$I_q I_d \cos \theta = \frac{1}{2}(I_m^2 - a^2 I_s^2) \sin 2\Delta + aI_s I_m \cos \theta_{sm} \cos 2\Delta \quad (33)$$

Equation 33 will be put into a simpler form. Let I_k and Δ_k be defined by the following equations:

$$I_k^4 = \frac{1}{4}(I_m^2 - a^2 I_s^2)^2 + a^2 I_s^2 I_m^2 \cos^2 \theta_{sm} \quad (34)$$

Equation 33 becomes:

$$I_q I_d \cos \theta = I_k^2 \sin 2(\Delta_k + \Delta),$$

$$\tan 2\Delta_k = \frac{2aI_s I_m \cos \theta_{sm}}{I_m^2 - a^2 I_s^2} \quad (35)$$

Substitute equations 32 and 35 into equation 31, it is

$$T = aI_m I_s \sin \theta_{sm}(R_{ed} + R_{eq}) + I_k^2 \sin 2(\Delta_k + \Delta)(X_{eq} - X_{ed}) \quad (36)$$

The first term represents the induction motor torque and is independent of the rotor position. The second term represents the reluctance motor torque and varies sinusoidally with the rotor position.

Equation 34 shows $I_k = 0$ if $I_m = aI_s$ and $\theta_{sm} = 90$ degrees, as in the case of a polyphase reluctance motor, and that I_k is large if I_m and aI_s, are widely different, or if θ_{sm} is small as in the cases of permanent capacitor motor and split-phase motors. Correspondingly, the reluctance motor torque or cogging is rarely noted in polyphase reluctance motors, but is very pronounced in reluctance motors of the permanent capacitor and split-phase types.

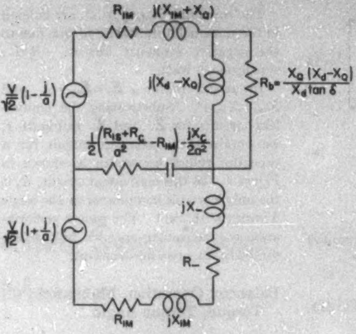
R_{1M}
$j(X_{1M} + X_a)$
$j(X_d - X_a)$
$R_b = \frac{X_a (X_d - X_a)}{X_d \tan \delta}$
$\frac{V}{\sqrt{2}}\left(1 - \frac{j}{a}\right)$
$\frac{1}{2}\left(\frac{R_{1S}+R_c}{a^2} - R_{1M}\right) - \frac{jX_c}{2a^2}$
jX_-
$\frac{V}{\sqrt{2}}\left(1 + \frac{j}{a}\right)$
R_-
R_{1M}
jX_{1M}

Figure 4. An equivalent circuit for the capacitor reluctance motor

The slots containing the *d*-axis rotor winding are located around the *q*-axis, and the slots containing the *q*-axis rotor winding are located around the *d*-axis. In a typical reluctance motor, the air gap of the *q*-axis is increased by cutting off all or part of the rotor teeth around the *q*-axis as shown in Figure 6(A). The slot and zig-zag leakage reactances for the *d*-axis rotor winding are greatly diminished by this process, and X_{ed} is smaller than X_{eq} as a result. A simple experiment was carried out to prove the effect. Direct current was passed through the main winding of a reluctance motor at first, and it was observed that the rotor turned until the direct axis was lined up with the main winding axis. Then the direct current was disconnected and an alternating current was passed through the main winding. It was noted that the rotor turned 90 electrical degrees until the quadrature axis was lined up with the main winding axis.

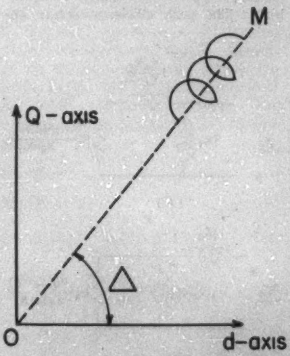

Figure 5. Diagram showing positions of stator and rotor axes at standstill

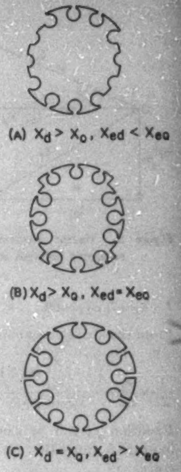

(A) $X_d > X_a$, $X_{ed} < X_{ea}$

(B) $X_d > X_a$, $X_{ed} = X_{ea}$

(C) $X_d = X_a$, $X_{ed} > X_{ea}$

Figure 6. Three different types of rotor laminations

The above experiment clearly indicates that though X_d is larger than X_q, X_{ed} is usually smaller than X_{eq}.

The above theory can be utilized to eliminate the cogging in a reluctance motor, by using a lamination as shown in Figure 6(B). The slot leakage reactance of the *d*-axis rotor winding is increased so that X_{ed} is equal to X_{eq}. On the other hand, a rotor lamination as shown in Figure 6(C) would not provide reluctance torque at synchronous speed, but causes much cogging at standstill.

An Example of Performance Calculation

To illustrate the application of the theory, the starting and running performance of a 4-pole 1/8-horsepower reluctance motor is calculated and compared with test results. The values of X_d and X_q are calculated by a method derived in the Appendix. Other motor constants are calculated by well known methods and checked approximately by test.

The motor constants are:

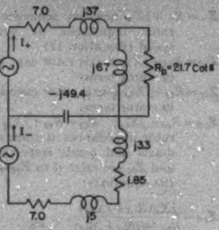

Figure 7. Equivalent circuit for a 1/8-horsepower 4-pole capacitor reluctance motor

$a=1.76$
$R_{1m}=7.0$ $R_{1s}=18.7$
$X_{1m}=5.0$ $X_{1s}=15.5$
$X_d=99$ $X_q=32$
$X_{2d}=2.4$ $X_{2q}=4.2$
$R_{2d}=4.3$ $R_{2q}=4.3$
$\mathbf{Z}_c=3-j306$ (running)
$\mathbf{Z}_c=-j68$ (starting)
Iron loss = 24 watts
Friction and windage loss = 10 watts

The circuit constants of Figure 4 are calculated as below:

$$\mathbf{Z}_{rd}=4.1+j2.5$$
$$\mathbf{Z}_{rq}=3.3+j4.1$$

$$\mathbf{Z}_-=\frac{1}{4}(4.1+3.3)+j\frac{1}{2}(2.5+4.1)=1.85+j3.3$$

$$\frac{1}{2}\left(\frac{R_{1s}+R_c}{a^2}-R_{1m}\right)=0$$

$$\frac{X_c}{2a^2}=49.4$$

$$X_q(X_d-X_q)/X_d=21.7$$

Substituting these values in Figure 4, we obtain the equivalent circuit for this 1/8-horsepower motor as shown in Figure 7. Take as an example of calculation from the equivalent circuit, the load point $\delta=14$ degrees:

$$R_b=21.7\cot 14°=87.1$$

$$\frac{j67\times 87.1}{87.1+j67}=32.4+j42$$

The mesh equations from the equivalent circuit are:

$$93.4\underline{/-29.6°}=(39.4+j29.6)I_+ +j49.4I_-$$
$$93.4\underline{/29.6°}=(8.85-j41.1)I_- +j49.4I_+$$

From these equations, I_+ and I_- are solved to be:

$$I_+ =1.86\underline{/-63.1°}=0.84-j1.66$$
$$I_- =0.12\underline{/-170.5°}=-0.12+j0.02$$

$$I_m=\frac{1}{\sqrt{2}}(I_+ +I_-)=0.51-j1.16$$

$$I_s=\frac{j}{1.76\sqrt{2}}(I_+ -I_-)=0.675+j0.386$$

The iron loss consists of two parts: the yoke and teeth iron loss which should be added to the electrical input, and the tooth pulsation loss which should be deduced from the mechanical output. As an approximation, one-half of the total iron loss is assigned to each part. The friction and windage loss is deduced from the mechanical output.

$$\text{Output}=1.86^2\times 32.4-0.12^2\times 1.85-12-10=90 \text{ watts}$$

$$\text{Line Current}=I_m+I_s+\frac{12}{115}=1.29-j0.774=1.51\underline{/31°}$$

Input = 1.29 × 115 = 149 watts
Efficiency = 90/149 = 60.3%
Power Factor = cos 31° = 85.6%

Similar calculations are made for various values of δ, and the calculated results are compared with measured values in Figure 8.

To calculate the maximum torque and the torque angle ratio, Z_t and I_t are calculated from the equivalent circuit. They are:

$$Z_t=28.7\underline{/76.4°} \text{ ohms, } I_t=3.86 \text{ amperes}$$

Hence, from equations 24 and 26:

$$T_{\max}=\frac{3.86^2\times 28.7}{4\cos^2 38.2°}-22$$
$$=150 \text{ synchronous-watts}=9.4 \text{ ounce feet}$$

$$\frac{dT}{d\delta}=\frac{3.86^2\times 28.7^2}{21.7}=565 \text{ synchronous-watts/radian}=0.61 \text{ ounce feet/degree}$$

Measured values for the maximum torque and torque angle ratio are 8.8 ounce feet and 0.56 ounce feet per degree respectively.

Apparently, the starting currents depend on the rotor position. As a first approximation, the average value of the rotor impedance is used to calculate these currents.

$$\mathbf{Z}_{\text{avg}}=\frac{1}{2}(\mathbf{Z}_{rd}+\mathbf{Z}_{rq})=3.7+j3.3$$

$$I_m=\frac{115}{\mathbf{Z}_{1m}+\mathbf{Z}_{\text{avg}}}=8.5\underline{/-37.8°}$$

$$I_s=\frac{115}{\mathbf{Z}_{1s}+\mathbf{Z}_c+a^2\mathbf{Z}_{\text{avg}}}=2.14\underline{/51.8°}$$

From equation 36, the starting torque is calculated:

$$\text{Starting torque}=14.8+2.9\sin 2(\Delta_k+\Delta) \text{ ounce feet}$$

The minimum and maximum values of the starting torque are 11.9 and 17.7 ounce feet by calculation and 10.2 and 16 ounce feet by test.

Summary and Conclusions

1. An equivalent circuit for the capacitor reluctance motor is derived, based on the double revolving field theory, Figure 4.

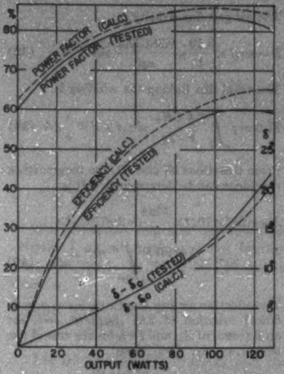

Figure 8. Performance curves for a 1/8-horsepower 4-pole capacitor reluctance motor

2. The mechanical output is represented as power dissipated in a load resistance in the equivalent circuit. The value of the load resistance depends only on X_d and X_q and the torque angle.

3. From the equivalent circuit, the torque angle, efficiency, and power factor for various load points, as well as the maximum torque can be calculated.

4. The starting torque, as calculated by the cross-field theory, equation 36, consists of a constant term and a sinusoidally varying term, depending on the rotor position. The sinusoidal term is undesirable, as it creates low values of the starting torque.

5. The sinusoidal term of the starting torque can be eliminated by either of two alternative means: By making $I_m=aI_s$, and $\theta_{ms}=90$ degrees, and by increasing the slot leakage reactance of the slots located below the large air gap, so that $X_{sd}=X_{sq}$.

6. The starting and running performance of a 1/8-horsepower 4-pole capacitor reluctance motor is calculated. The results agree reasonably well with test values.

Appendix

For calculations of X_d and X_q:

C = total conductors
K_w = winding factor
q = number of poles
l = effective length of air gap
w = length of stack
λ = pole pitch
I = winding current
B = flux density in the air gap
A = position angle, in electrical degrees

It is assumed that the windings are sinusoidally distributed. The magnetomotive force is:

$$mmf=\frac{4}{\pi}\frac{CK_wI}{2q}\sin A \qquad (37)$$

The air gap flux density is:

$$B=mmf\times\frac{3.19}{l}=\frac{6.38CK_wI}{\pi ql}\sin A \qquad (38)$$

The total flux linking the winding is:

$$\text{Flux}=q\int_0^\pi \frac{4}{\pi}\,\frac{CK_w}{2q}\sin A\times BW\frac{\lambda}{\pi}\,dA \qquad (39)$$

From equations 38 and 39, the magnetizing reactance can be determined. It is:

$$X_m=2\pi f\times 10^{-8}\times\frac{\text{Flux}}{I}=2\pi fC^2K_w^2\times$$
$$10^{-8}\times\frac{0.411W\lambda}{q}\int_0^\pi \frac{\sin^2 A}{l}\,dA \qquad (40)$$

The effective air gap length varies as a periodical function of 2A. Suppose $l=l_1$ for an interval of A_1, and $l=l_2$ for the rest of the period, $\pi-A_1$; $l_1>l_2$, then:

$$X_d=2\pi fc^2K_w^2\times 10^{-8}\times\frac{0.411W\lambda}{q}\times$$
$$\left[\frac{A_1-\sin A_1}{2l_1}+\frac{\pi-A_1+\sin A_1}{2l_2}\right] \qquad (41)$$

Similarly

$$X_q=2\pi fC^2K_w^2\times 10^{-8}\times\frac{0.411W\lambda}{q}\times$$
$$\left[\frac{\pi-A_1-\sin A_1}{2l_2}+\frac{A_1+\sin A_1}{2l_1}\right] \qquad (42)$$

For the motor cited in the example:

Small air gap = 0.0145 inch
Saturation factor = 1.15
Air gap constant = 1.3
$l_2=0.0145\times 1.15\times 1.3=0.0216$ inch
Large air gap = 0.200 inch
$C=1{,}168$
$K_w=0.821$
$\lambda=3.04$ inches
$W=1.50$ inches
$q=4$
$A_1=\frac{\pi}{2}$

The values of X_d and X_q as calculated from equations 41 and 42 are 99 and 32 respectively.

Nomenclature

a = effective turn ratio
E_m = main winding voltage
E_s = auxiliary winding voltage
E_+ = positive sequence, air gap electromotive force
E_- = negative sequence, air gap electromotive force
E_d = d-axis, air gap electromotive force
E_q = q-axis, air gap electromotive force
I_m = main winding current
I_s = auxiliary winding current
I_+ = positive sequence current
I_- = negative sequence current
I_d, I_q = direct and quadrature axis stator currents, at locked rotor condition
I_{d+}, I_{q+} = positive sequence direct and quadrature axis stator currents, at synchronous speed
I_k = cogging current, defined by equation 34
I_t = short circuit current of R_b in Figure 4
X_d, X_q = d-axis and q-axis magnetizing reactances
$Z_{lm}=R_{lm}+jX_{lm}$ main winding local impedance
$Z_{ls}=R_{ls}+jX_{ls}$ capacitor and auxiliary winding local impedance
$Z_+=R_++jX_+$ positive sequence apparent rotor impedance, at synchronous speed (Figure 3)
$Z_-=R_-+jX_-$ negative sequence apparent rotor impedance at synchronous speed (Equation 17)
$Z_{2d}=R_{2d}+jX_{2d}$ d-axis rotor cage impedance in stator terms
$Z_{2q}=R_{2q}+jX_{2q}$ q-axis rotor cage impedance in stator terms
$Z_{ed}=R_{ed}+jX_{ed}$, $Z_{eq}=R_{eq}+jX_{eq}$ effective rotor impedances at standstill of the d-axis and q-axis respectively. Z_{2d} and Z_{2q} are related to Z_{ed} and Z_{eq} by the equations:

$$Z_{ed}=\frac{jX_d(R_{2d}+jX_{2d})}{R_{2d}+j(X_d+X_{2d})},\qquad Z_{eq}=\frac{jX_q(R_{2q}+jX_{2q})}{R_{2q}+j(X_q+X_{2q})}$$

δ = torque angle, defined in Figure 2
Δ = angle between main winding axis and d-axis, defined in Figure 5
Δ_k = defined by equation 34
θ = angle between I_q and I_d
θ_d, θ_q = power factor angles of Z_{ed} and Z_{eq} respectively
θ_{sm} = angle between I_s and I_m

References

1. PERFORMANCE CALCULATIONS ON POLYPHASE RELUCTANCE MOTORS, P. H. Trickey. *Electrical Engineering* (*AIEE Transactions*), volume 65, April 1946, pages 190–93.

2. A DESIGN METHOD FOR POLYPHASE RELUCTANCE SYNCHRONOUS MOTORS, C. H. Crouse. *AIEE Transactions*, volume 70, part I, 1951, pages 957–62.

3. THE CROSS-FIELD THEORY OF THE CAPACITOR MOTORS, A. F. Puchstein, T. C. Lloyd. *Electrical Engineering* (*AIEE Transactions*), volume 60, February 1941, pages 58–62.

4. STEADY-STATE EQUIVALENT CIRCUITS OF SYNCHRONOUS AND INDUCTION MACHINES, Gabriel Kron. *AIEE Transactions*, volume 67, part I, 1948, pages 175–81.

No Discussion

Single-Phase Motor Synthesis

T. C. LLOYD
MEMBER AIEE

IN DESIGNING a single-phase motor, no method has been shown whereby it is possible to start with a desired maximum torque, and solve for the winding and length of lamination stack.

By assuming a stack and a desired maximum torque, it has been shown to be possible to solve directly for the stator winding.[1] This method, however, depends upon the judgment of the designer in making his choice of stack for initiating the design. If his selection is a poor one, the design may result in too high a flux density or be wasteful in steel.

The present paper shows a method whereby, on a single-phase motor, the designer can select a value of maximum torque (which fixes the horsepower through National Electrical Manufacturers Association (NEMA) standards), select a desired flux density in the magnetic circuit, and solve simultaneously for both the number of conductors in the winding and the length of stacking in inches. The method is somewhat similar to that shown for polyphase motors,[2] based on the little known fact that the maximum torque of an actual motor is a function of two fictitious motors. One has no end coils and is all stacking and embedded conductors; the other has no stacking, but is made up only of end coils and end rings.

By this artificial separation, we are able to deal with resistance and reactance components either independent of stack or "per inch of stack." The simultaneous solution of conductors and stacking is thereby achieved.

The Maximum Torque

Since the horsepower rating of single-phase motor is defined in terms of maximum torque, this offers an important and logical value by which to initiate a design.

Expressions for the maximum torque of a single-phase motor have always been unwieldy, partly due to the fact that they are not independent of rotor resistance. However, a new equation is available, based on the reduction of Dr. Chang's equivalent circuit for the capacitor motor[3] to the plain single-phase case. A partial derivation is given in Appendix I, resulting in this working formula:

$$T_m = \frac{112.6}{\text{Syn. rpm}}\left[\frac{V^2}{X}\beta' - F - F_c\right] \text{ ounce-feet} \quad (1)$$

The important factor β' is read from Figure 1 as a function of the leakage factor K_r and the resistance–reactance ratio α:

$$\frac{0.55R_2}{X} + \frac{K_r R_1}{X} = \alpha$$

The friction loss (F) in watts, and the cross-axis core loss (F_c) in watts, must be subtracted as shown, to yield a net torque. For convenience, the designs will be made for gross torque, greater than T_m by these losses. Then

$$T_g = \frac{112.6}{\text{Syn. rpm}}\frac{V^2}{X}\beta' \text{ ounce-feet} \quad (2)$$

Friction loss must be obtained from previously known or estimated data on the motor. Cross-axis core loss can be estimated in watts as:

100×horsepower	Below 0.5 horsepower
50×horsepower	0.5 to 1.5 horsepower

For instance, on a 1/3-horsepower 1,725 rpm motor having a friction loss of 40 watts and a cross-axis core loss of 33 watts, the net maximum torque should be 40.5 ounce feet. Obviously the gross torque

$$T_g = 40.5 + \frac{112.6}{1{,}725} \times 73 \text{ or } 45.27 \text{ ounce-feet}$$

Nomenclature

T_m = the net maximum or breakdown torque in ounce-feet

T_g = the gross value of breakdown torque

T_{ms} = the breakdown torque of a "stack" motor

T_{me} = the breakdown torque of an "end" motor

F = friction loss in watts

F_c = cross-axis core loss in watts

R_1 = the stator winding resistance

R_2 = the rotor resistance in stator terms

R_{1s} = the resistance of the stator "stack" winding (embedded)

R_{1e} = the resistance of the stator "end" winding (end coils)

X = the total leakage reactance

X_e = the leakage reactance of the "end" motor

X_{ss} = the leakage reactance of the "stack" motor

X_0 = the total reactance from leakage and mutual fluxes

n = number of phases (2 for single-phase)

C = the series conductors of the stator winding

C_0 = a function of conductors and stack length

L = inches of stack of laminations

L_0 = apparent, uncorrected, stack length

l_c = average length of one stator conductor in inches ($^1/_2$ turn)

l_e = that part of l_c which is not embedded

U = the decimal fraction of the slot cross-section which is filled with copper

S' = the effective number of full slots, for calculating resistance. If all slots were equally full, $S' = S_1$

K_1 = a factor, greater than unity, for obtaining apparent air gap length

K_e = a constant for end ring leakage governed by end ring contour

$S.F.$ = saturation factor. This times the air-gap ampere-turns equals the total ampere-turns for gap and complete mutual flux path at the flux density used. Assume 1.2

Paper 51-365, recommended by the AIEE Rotating Machinery Committee and approved by the AIEE Technical Program Committee for presentation at the AIEE Fall General Meeting, Cleveland, Ohio, October 22–26, 1951. Manuscript submitted March 26, 1951; made available for printing August 30, 1951.

T. C. Lloyd is with Robbins and Myers, Inc., Springfield, Ohio.

Of the several solutions for the quadratic equation, giving the simultaneous solution for stack and conductors, an investigation by Dr. S. S. L. Chang resulted in the final form presented here. The fundamental expression for maximum torque of the single phase motor also resulted from his work.

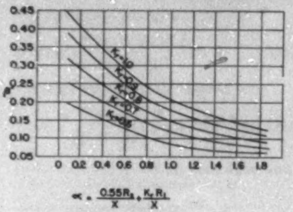

Figure 1. The breakdown torque factor as a function of resistance-reactance ratios

Although this maximum torque equation involves simplifying approximations, comparisons with more complicated equations and with actual tests, indicate a high degree of working accuracy.

Stack and End Motors

Of the three components of leakage reactance used here, slot and zigzag vary directly with the length of stack. End leakage is independent. The resistances of the end coils, and the end rings, are independent of stack.

A stack motor will be concerned with a value of β'' depending upon

$$\frac{0.55R_2}{X}(\text{stack})+\frac{K_rR_1}{X}(\text{stack})$$

One problem will be to set up a method for calculating these values as well as similar values for the "end" motor. We will then have two values of β'' to deal with; β_s'' for the stack motor and β_e'' for the end motor. In general:

$$T_g=\frac{T_{gs}\times T_{ge}}{T_{gs}+T_{ge}} \tag{3}$$

and

$$T_{gs}=\frac{112.6}{\text{Syn. rpm}}\,\frac{V^2}{X_{sz}}\,\beta_s'' \quad \text{for the stack motor} \tag{4}$$

$$T_{ge}=\frac{112.6}{\text{Syn. rpm}}\,\frac{V^2}{X_e}\beta_e'' \text{ for the end motor} \tag{5}$$

Equations 4 and 5 should be substituted in equation 3, but not before some further expansions are made.

Leakage Reactance and Reactance Ratios

Leakage reactance components used are:

$$X=2\pi fC^2\mathcal{P}_snL10^{-8} \tag{6}$$

where $\mathcal{P}_s$ = the slot permeance per inch of stack.

$$X=2\pi fC^2\mathcal{P}_znL10^{-8} \tag{7}$$

where $\mathcal{P}_z$ = the zigzag permeance per inch of stack.

$$X=2\pi fC^2\mathcal{P}_en10^{-8} \tag{8}$$

where $\mathcal{P}_e$ = the end permeance.

The permeances involve the usual formulas:
Slot:

$$\mathcal{P}_s=3.60\left(\frac{K_s'}{S_1}+\frac{K_s''}{S_2}\right)K \text{ per inch} \tag{9}$$

Zigzag:

$$\mathcal{P}_z=\frac{8.5D}{\Delta S_1S_2}\left(\frac{T_e'+T_e''}{\lambda'+\lambda''}-0.5\right)^2K \text{ per inch} \tag{10}$$

End:

$$\mathcal{P}_e=\frac{\lambda}{P}K_eK \tag{11}$$

The correction for winding distribution (K) is read from Figure 2.

Resistances

The average length of one stator conductor is l_c. (This is one conductor or a half turn.) If the length of stack is L, then the average length of the end conductor is:

$$l_e=l_c-L \tag{12}$$

The resistance of the stator winding for the stack motor is:

$$R_{1s}=\frac{LC^2}{A_sUS'} \tag{13}$$

For the end motor:

$$R_{1e}=\frac{l_eC^2}{A_sUS'} \tag{14}$$

The resistance of the rotor bars is:

$$R_{2s}=\frac{Lk_bC^2K_w^2n}{A_bS_2} \tag{15}$$

The resistance of the end rings is:

$$R_{2e}=\frac{2D_rk_rK_4C^2K_w^2n}{\pi P^2Ar} \tag{16}$$

Combining these ratios, for the "stack" motor:

$$\frac{R_1}{X}\text{ stack}=\frac{10^8}{A_sUS'2\pi f\mathcal{P}_{sz}n} \tag{17}$$

where

$$\mathcal{P}_{sz}=\mathcal{P}_s+\mathcal{P}_z \tag{18}$$

See equations 9 and 10.

$$\frac{R_2}{X}\text{ stack}=\frac{k_bK_w^210^8}{A_bS_22\pi f\mathcal{P}_{sz}} \tag{19}$$

For the "end" motor:

$$\frac{R_1}{X}\text{ end}=\frac{l_e10^8}{A_sUS'2\pi f\mathcal{P}_en} \tag{20}$$

$$\frac{R_2}{X}\text{ end}=\frac{2D_rk_rK_4K_w^210^8}{\pi P^2A_r2\pi f\mathcal{P}_e} \tag{21}$$

The flux factor

$$K_r=\frac{X_0-X}{X_0} \tag{22}$$

Or, in terms of permeances:

$$K_r=\frac{\mathcal{P}_O-\mathcal{P}_L}{\mathcal{P}_O} \tag{23}$$

wherein

$$\mathcal{P}_O=\frac{0.322\lambda LK_w^2}{P\Delta K_1(S.F.)}+\frac{\mathcal{P}_L}{2} \tag{24}$$

$$\mathcal{P}_L=\mathcal{P}_{sz}L+\mathcal{P}_e \tag{25}$$

To evaluate equation 23, it is necessary to know the stack, L. But, if any reasonable value such as 2 or 4 inches is assumed for L (for this calculation only) the results will not be affected appreciably.

Derivation of Final Equations

Equations 3 will now be expanded by equations 4, 5, 6, 7, and 8.

$$T_g\left(\frac{\beta_s''}{L\mathcal{P}_{sz}}+\frac{\beta_e''}{\mathcal{P}_e}\right)=\frac{112.6}{\text{Syn.}}\,\frac{V^2}{2\pi fC^2n10^{-8}}\,\frac{\beta_s''\beta_e''}{L\mathcal{P}_{sz}\mathcal{P}_e} \tag{26}$$

This equation involves both conductors in the stator winding (C) and stack length (L), but it does not tie together the two in terms of flux density.

We will use the maximum flux density in kilolines in the stator teeth as a measure of magnetic loading. Then by usual magnetic circuit calculations:

$$C=\frac{1}{L}\left[\frac{VP}{B_tf}\,\frac{70.9\times10^3}{S_1atwK_w}\right] \tag{27}$$

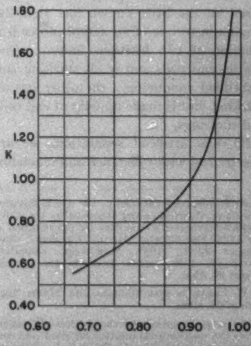

Figure 2. Effect of winding factor on the leakage reactance

Let the expression in brackets be C_0.

$$C=\frac{C_0}{L} \qquad (28)$$

Substitute for C in 26 and transpose:

$$2\pi fC_0^2n10^{-8}\left[\frac{\mathcal{P}_e\beta_s''}{L^2}+\frac{\mathcal{P}_{sz}\beta_e''}{L}\right]=\frac{112.6V^2\beta_s''\beta_e''}{\text{Syn. }T_g} \qquad (29)$$

This is a quadratic equation for which one solution for L can take the form:

$$L=\frac{L_0}{\sec\theta-1}\text{ (See Figure 3)} \qquad (30)$$

$$L_0=2\frac{\mathcal{P}_e\beta_s''}{\beta_e''\mathcal{P}_{sz}} \qquad (31)$$

The secant of θ is calculated from the relationship:

$$\tan\theta=7.74\sqrt{\frac{\mathcal{P}_eP}{nT_g\beta_e''}\,\frac{\beta_s''}{1}\,\frac{V\times10^8}{fC_0\mathcal{P}_{sz}}} \qquad (32)$$

Using these equations to solve for the required stacking, we then determine that the series conductors needed in the stator winding are:

$$C=\frac{C_0}{L} \qquad (33)$$

This winding and stack then give the required maximum torque in ounce-feet and result in the desired flux density.

EXAMPLE

A motor rated at 1/3 horsepower, 1,725 rpm is to be designed in NEMA frame 56. As an aid in showing the procedure, the data will be tabulated. It is assumed that the laminations are known and such items as slot constants, slot areas, et cetera, can be copied directly from the master lamination sheets.
The data needed are:

Stator slot constant $K_s'=1.366$
Rotor slot constant $K_s''=1.483$
Number of stator slots $S_1=36$
Number of rotor slots $S_2=48$
Inside diameter of stator, inches $D=3.875$
Axial air-gap length, inch $\Delta=0.015$
Stator slot area, circular mils $A_s=186{,}000$
Slot fullness $U=0.35$
Rotor bar area, circular mils $A_b=20{,}820$
Stator tooth width, inch $a.t.w.=0.125$
Stator tooth face, inch $T'=0.246$
Rotor tooth face, inch $T''=0.185$
Corrected stator tooth face, inch $T_c'=0.2855$
Corrected rotor tooth face, inch $T_c''=0.2175$
Stator tooth pitch, inch $\lambda'=0.339$
Rotor tooth pitch, inch $\lambda''=0.250$
Corrected gap length multiplier $K_1=1.36$

As soon as the end ring section of the rotor is selected, the following additional data can be calculated:

End ring size, inches $^1/_8\times1.00$
End ring area, circular mils $A_r=150{,}000$
Diameter across bar centers, inches $D_r=3.600$
Inside diameter of ring, inches $D_i=1.845$
Ratio: $D_i/D_r=0.511$
Correction for current distribution $K_R''=1.13$
End ring permeance constant $K_e=0.65$

The factor K_R'' follows Trickey[4] in correcting the apparent resistance of the end ring through uneven current distribution.

The constant K_e is used as shown because the end ring has a comparatively great radial depth.

The winding distribution will be selected, using 100 per cent as the fullest slot. Then:

Slot	Per Cent Conductors
1	100
2	88.4
3	65.5
4	
5	
6	
7	65.5
8	88.4
9	100

With the distribution selected, the following values can be calculated:

Winding factor $K_w=0.857$
Leakage correction $K=0.825$ (See Figure 2)
Length of end conductor, inches $=3.14$
Equivalent number of full slots $S'=20.32$
Pole pitch, inches $\lambda=3.05$

Calculation of Permeances and Ratios

From equation 9 $\mathcal{P}_s=0.206$ per inch
From equation 10 $\mathcal{P}_z=0.134$ per inch
Sum: $\mathcal{P}_{sz}=0.340$
From equation 11 $\mathcal{P}_e=0.405$
Sum: $\mathcal{P}_L=0.745$ complete motor 1-inch stack
From equation 24 $\mathcal{P}_O=22.85$ assume 3-inch of stack
From equation 23 $K_r=0.94$ for any stack of about 3 inches

For the "stack" motor

$R_1/X=0.294$ Equation 17
$R_2/X=0.571$ Equation 19
$K_rR_1/X+0.55R_2/X=0.583$ "stack"

For the "end" motor

$R_1/X=0.77$ Equation 20
$R_2/X=0.488$ Equation 21
$K_rR_1/X+0.55R_2/X=0.975$ "end"

From Figure 1

$\beta_s''=0.265$ $\beta_e''=0.193$

A flux density in the stator teeth of 69.5 kilolines will be accepted as a reasonable measure of magnetic loading. Then, from equation 27: $C_0=1{,}670$ and, from equation 31: $L_0=3.28$ inches.

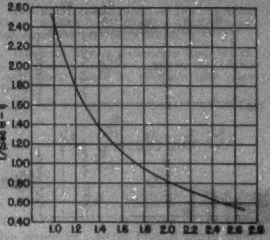

Figure 3. Correction for apparent stack length

Bear in mind that the "apparent stack" L_0 is a constant for these laminations, with this winding distribution, and rotor end rings, regardless of the number of conductors, stacking or flux density used.

The maximum torque desired for this 1/3-horsepower motor is 40.5 ounce-feet, representing the top of the NEMA torque band. The gross torque is then 45.27 ounce-feet.

$\tan\theta=2.10$ from Equation 32
$\sec\theta-1=1.33$

The correct stack is then:

$$L=\frac{L_1}{\sec\theta-1}\text{ or 2.46 inches}$$

This is "rounded off" to 2.50 inches. The series conductors will then be:

$$C=\frac{C_0}{L}\text{ or 668}$$

Proportionate Designs for Fast Estimating

Examination of the terms making up equation 31 reveals an interesting fact. For a given set of laminations, any windings using the same winding distribution and slot fullness, will display a constant value of L_0, regardless of the stack. In short, L_0 is a function of the magnetic contour, winding distribution and end rings of the rotor, as previously mentioned.

Assume that one design has been made by this method so that L_0 is known. Other ratings with the same number of poles can be estimated quickly by simple proportion. Thus, for a difference in gross maximum torque:

$$\text{new }\tan\theta=\frac{1}{\sqrt{\dfrac{\text{new }T_g}{\text{old }T_g}}}(\text{old }\tan\theta) \qquad (34)$$

If the flux density in the new design is to be different than in the old:

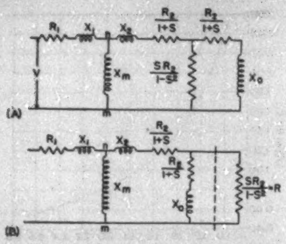

Figure 4. The Chang equivalent circuit for the capacitor motor is shown in (A) with the capacitor branch removed. The circuit is rearranged in (B) and is exactly equivalent to other forms of the equivalent circuit with core loss neglected

$$\text{new } \tan\theta = \frac{B_t \text{ new}}{B_t \text{ old}} (\text{old } \tan\theta) \qquad (35)$$

In this latter case, C_0 varies also, so that:

$$\text{new } C_0 = \text{old } C_0 \frac{\text{old } B_t}{\text{new } B_t} \qquad (36)$$

Example of Proportion

A 1/2-horsepower 4-pole motor displays the following values:

$L_0 = 3.41$ inches $C_0 = 1310$ $B_t = 69.5$ kilolines

$\tan\theta = 2.21$ $T_g = 70$ ounce-feet

In Figure 3, $\tan\theta$ is plotted against $1/\sec\theta - 1$ for convenience in calculation. For $\tan\theta = 2.21$, the correction for stack is read as 0.718. Then:

$L = 3.41 \times 0.718$ or 2.45 inches of stack

The series conductors required are:

$$C = \frac{C_0}{L} = \frac{1{,}310}{2.45} \text{ or } 532$$

The design was actually built with 2.5 inches of stack and 528 series conductors.

The problem is to investigate a 3/4-horsepower rating in this same lamination. Higher flux densities will be used and the gross maximum torque desired is 109 ounce-feet. Assume that 74.0 kilolines in the teeth will not be excessive. The new $\tan\theta$ is then:

$$\text{new } \tan\theta = \frac{1}{\sqrt{\dfrac{109}{70}}} \times \frac{74}{69.5} \times 2.21 \text{ or } 1.88 \quad \text{(From equation 35)}$$

From the curve, the stack multiplier is 0.88. The required stack

$L = 3.41 \times 0.88$ or 3.0 inches

The new C_0 is:

$$1{,}310 \times \frac{69.5}{74} \text{ or } 1{,}230$$

The series conductors needed are:

$$C = \frac{1{,}230}{3.0} \text{ or } 410$$

The design, made in the usual way, had used 3.0 inches of stack and 412 series conductors.

Appendix I

It is assumed that the reader is familiar with the usual equivalent circuits for the single-phase motor by the cross-field theory, including that developed by Dr. Chang[3] for the permanent-split capacitor type. The latter reduces to that shown in Figure 4 when the "capacitor branch" is omitted.

The maximum torque developed by the plain single-phase motor occurs when the power absorbed by the "load" resistance R is a maximum. This is a function of speed and so are the two resistances $R_2/(1+S)$. For the time being, these two resistances will be considered as fixed, but of unknown value.

From Thevenin's theorem the circuit to the left of the dotted line is equivalent to a voltage source V_e in series with an impedance Z_e. V_e is the open circuit voltage appearing at the two terminals of R if R is removed. Z_e is the impedance measured at the two terminals with R removed, and with the lines at the voltage source V short circuited.

Then the maximum power absorbed by R is:

$$\frac{V_e^2}{2[R_e + \sqrt{R_e^2 + X_e^2}]}$$

where: $R_e + jX_e = Z_e$

Since V_e is the open circuit voltage with R removed, it differs from V by the small voltage drop in the series impedance, caused by the magnetizing currents through X_m and X_0.

The impedances of these series elements are much less than X_m or X_0 and their resistances cause a shift in the position of V_e with little effect on its magnitude. Our interest is in the latter, and hence the resistances will be neglected.

Since

$K_p = X_m/X_0$

x_1 or x_2 or $X/2 = (1-K_p)X_0$

The combined reactance of X_m in parallel with $X_0 + X/2$ is:

$$\frac{K_pX_0(2-K_p)X_0}{K_pX_0 + (2-K_p)X_0} = \frac{K_p}{2}(2-K_p)X_0$$

The voltage across X_m is, therefore:

$$V_m = V \frac{\dfrac{K_p}{2}(2-K_p)X_0}{(1-K_p)X_0 + \dfrac{K_p}{2}(2-K_p)X_0}$$

$$= \frac{K_pV(2-K_p)}{2-K_r}$$

The voltage V_e is:

$$V_e = V_m \frac{X_0}{(1-K_p)X_0 + X_0}$$

Combining:

$$V_e = V \frac{K_p}{2-K_r}$$

Although the resistances could be neglected in determining V_e, they are large enough with respect to x_1 or x_2 so that they should be considered in calculating Z_e.

The resistances $R_2/(1+S)$ have been considered as though they were not functions of speed. We now wish to assign them an average value. On the assumption that the usual speed at which the maximum torque is likely to occur is 82 per cent of synchronism:

$$\frac{R_2}{1+S} = 0.55R_2$$

Now the impedance Z_e can be considered as being made up of two parallel impedances, shown on Figure 5 as (A) and (B).

For Figure 5(A) the impedance is: $0.55R_2 + jX_0$. By the simplification of the flux factors, for Figure 5(B) the impedance is: $0.55R_2 + K_rR_1 + jX$.

Then:

$$Z_e = \frac{1}{2-K_r}(0.55R_2 + K_rR_1 + jX) \quad \text{approximately}$$

The maximum torque in synchronous watts is then:

$$T_m = \frac{V^2}{2X}\frac{K_r}{2-K_r} \times \frac{1}{\dfrac{0.55R_2 + K_rR_1}{X} + \sqrt{1 + \left(\dfrac{0.55R_2 + K_rR_1}{X}\right)^2}}$$

To save repetitive work, terms can be combined in this manner:

$$\alpha = \frac{0.55R_2}{X} + \frac{K_rR_1}{X}$$

$$\beta_0 = \frac{1}{\alpha + \sqrt{1+\alpha^2}}$$

$$\beta'' = \frac{0.5K_r}{2-K_r}\beta_0$$

Converting to ounce-feet and subtracting the friction and cross-field core losses:

$$T_m = \frac{112.6}{\text{Syn. rpm}}\left[\frac{V^2}{X}\beta'' - F - F_s\right]$$

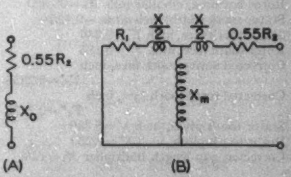

Figure 5. Equivalent components of the circuit

The various values of β'' are plotted in Figure 1.

The assumption made for the speed at which maximum torque occurs (whereby $R_3/(1+S)$ became a fixed value) has little effect on the accuracy of the final results.

For instance, if R_3/X is 0.5, S may vary from 0.7 to 0.9 with only a change of 0.017 added to α in the former case. The net effect on the calculated torque is very small.

References

1. SINGLE-PHASE INDUCTION-MOTOR PERFORMANCE, A. F. Puchstein, T. C. Lloyd. *Electrical Engineering* (*AIEE Transactions*), volume 56, October 1937, pages 1277–84.

2. SOME ASPECTS OF ELECTRIC MOTOR DESIGN—POLYPHASE INDUCTION MOTOR DESIGN TO MEET FIXED SPECIFICATIONS, T. C. Lloyd. *Electrical Engineering* (*AIEE Transactions*), volume 63, January 1944, pages 14–20.

3. THE EQUIVALENT CIRCUIT OF THE CAPACITOR MOTOR, Sheldon S. L. Chang. *AIEE Transactions*, volume 66, 1947, pages 631–40.

4. INDUCTION MOTOR RESISTANCE RING WIDTH, P. H. Trickey. *Electrical Engineering* (*AIEE Transactions*), volume 55, February 1936, pages 144–50.

No Discussion

2-Phase A-C Servo Motor Operation for Varying Phase Angle of the Control Winding Applied Voltage

MARK A. STEINHACKER
ASSOCIATE MEMBER AIEE

WILBUR E. MESERVE
MEMBER AIEE

THE 2-phase induction motor is used extensively in a-c servo systems. As ordinarily used one phase is supplied with constant voltage from a single-phase source through a phase shifting capacitor and the pertinent control information is carried in the form of the magnitude variation of the voltage impressed on the second or control winding. This voltage is maintained displaced at 90 degrees with respect to the main winding voltage.

The work here presented is the outgrowth of a proposal to design a servo system employing such a motor but with the control information carried in the form of a varying phase angle of a constant magnitude control voltage.

Servo systems using voltage magnitude control are subject to interference appearing in the control channel as a false signal or "noise."

Both the signal and the noise are of an amplitude nature and consequently if the noise is of an appreciable amount, the operation of the system may be affected adversely. With the information transmitted in the form of a varying angle of constant voltage, in cases where the control signal is small, the noise would have little or no effect. For the conventional system the noise voltage might be an appreciable portion of the total voltage under conditions of small control signal. Thus in terms of noise there is certain similarity between the two systems and those of phase modulated and amplitude modulated telephony.

Motor Torque Characteristic

The types of induction motors used for servo work have very high rotor resistance and hence very low operating efficiencies.

The reason for this design is that the motor torque characteristic must be fairly linear so as to accurately reproduce the input, and also single-phase operation must not occur for any value of excitation. As shown in Figure 1 (which illustrates single-phase operation) the motors tend to develop negative torque with respect to rotation of the rotor. For sine wave 2-phase excitation, only twice the upper half of Figure 1 is present and the motor will develop torque as a function of control.

In order to point the direction of the analysis of the motor, an experimental steady-state study of torque curves were first determined. Reference to the positive sequence part of Figure 1 will show that over the normal operating range of the motor (positive slip) the slope of the torque-speed curve is uniform. The 2-phase motors available for test purposes were low wattage types built by Diehl Manufacturing Company. The pertinent data for these motors are shown in Table I.

Discussion of Torque Coefficients

Since the motors are of the 2-phase type, they are very sensitive to harmonics in the applied voltage wave. Especially noticeable is the effect of the third harmonic in reducing the net torque output. In the light of this condition, all the voltage sources used for test purposes must be as nearly sinusoidal as possible in order to accurately determine the motor characteristics.

A 20-volt source of 2-phase sine wave voltage with the time phase angle easily and accurately adjustable was used to supply motor number *FP25-3*. A complete set of speed-torque curves were obtained under voltage and phase angle control. The results of these tests are plotted in Figures 2 and 3. Adjustable 2-phase sine wave voltages of the order of magnitude of 75 to 115 volts were not readily available and hence only the blocked torque curves were obtained for motor *FPE 25-11*. The characteristics of both motors, however, are similar.

Under normal positional servo operation two conditions can be defined. Zeroing, or operation about the balance point (the desired output), occurs most of the time in a high performance system, since the output must accurately reproduce the

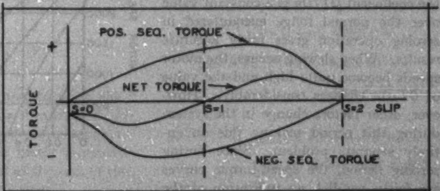

Figure 1. Two-phase motor torque speed curve

Paper 51-366, recommended by the AIEE Rotating Machinery Committee and approved by the AIEE Technical Program Committee for presentation at the AIEE Fall General Meeting, Cleveland, Ohio, October 22–26, 1951. Manuscript submitted June 14, 1951; made available for printing August 30, 1951.

MARK A. STEINHACKER is with the Arma Corporation, Brooklyn, N. Y., and WILBUR E. MESERVE is with Cornell University, Ithaca, N. Y.

This work is a portion of a Thesis submitted by Mark A. Steinhacker in partial fulfillment of the requirements for the Degree of Master of Electrical Engineering, Cornell University.

Table I. Motor Information*

	Motor A†	Motor B†
Style number	FP 25-3	FPE 25-11**
Outline	1-A-357	4-A-369
Watts output	2.5	5/25
Poles	2	2
Frequency, cycles per second	60	60
Volts per phase	20	115/75
Performance curve	ED 4037	ED 3780
Locked torque in ounces	2.5	5/2.5
Motor rating	Continuous	Continuous
Temp. rise, centigrade (55° Ambient)	65	65

*Source—Diehl Servo Motor Catalog.

†Motors develop 63 per cent locked torque at 55 per cent of rated speed.

**Stator—8 slots; 3-slot coil pitch.

Rotor—11 slots (squirrel cage), 5/8 inch diameter, $1^1/_2$ inch long, 60-degree skew.

Terminals—Phase 1, 1,3; Phase 2, 2,4.

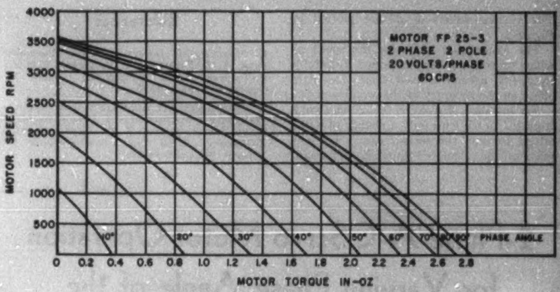

Figure 2. Speed torque curves, phase control

input. Slewing, on the other hand, occurs when a large step input is applied to the system and there is a definite time before the output can regain correspondence with respect to the input. During normal zeroing operation, the motor speed generally does not exceed one half full motor speed, while during slewing periods, top motor speed is approached. There are then two conditions to investigate when interpreting the speed-torque curves.

The end result of these curves is an expression of motor torque which can be used in servo system equations. A general expression[1] for the curve shown in Figures 2 and 3 is as follows:

$$T=\frac{\partial T}{\partial n}n+\frac{\partial T}{\partial \psi}\psi \tag{1}$$

where n = motor speed and ψ = control quantity.

The use of equation 1 involves the determination of the coefficients $\partial T/\partial n$ in the neighborhood of the operating speed, n, and $\partial T/\partial \psi$ in the neighborhood of the operation control position. Observation of Figures 2 and 3 shows that for speeds below 2,000 rpm the speed-torque curves are of fairly constant slope. No change is noted in the shape of the curves for the phase control set as compared with the voltage control set. While not entirely correct, the assumption that the coefficient $\partial T/\partial n$ is a constant value over the normal range encountered in zeroing operation gives fairly accurate results. When slewing occurs, the motor speeds become quite high and the value of $\partial T/\partial n$ changes considerably. However, other factors change in the system during this period making this an entirely separate problem. Since during zeroing period, the speed-torque curves are fairly parallel, an indication of the value $\partial T/\partial \psi$ can be obtained by using the blocked or zero speed values. A curve of torque versus control for zero speed is plotted in Figure 4 for motor *FP 25-3* and in Figure 5 for motor *FP 25-11*. A comparison of voltage control and phase control is shown in Figure 4.

The results plotted in Figure 4 show the main difference between the torque functions of motors operated with voltage and with phase control. The curve for the voltage controlled system approaches a fairly straight line (B), giving a constant for the value of $\partial T/\partial \psi$. Thus linear differential equations with constant coefficients can be written for the voltage controlled case. The phase controlled system on the other hand has a characteristic that approaches a sine function of the control (dotted curve). The results of tests on motor *FPE 25-11* shown in Figure 5 more nearly approach the ideal sine curve. Therefore the value of $\partial T/\partial \psi$ for the phase controlled case is a sine function rather than a constant. As will be shown later, this gives an equation that is nonlinear and as such has at the present no formal solution.

The motor torque equations can be written as follows. For voltage control:

$$T=-K\frac{d\theta_0}{dt}+K_A\epsilon \tag{2}$$

For phase control:

$$T=-K\frac{d\theta_0}{dt}+K_B\sin\epsilon \tag{3}$$

where

$-K$ = slope of the speed-torque curves below 2,000 rpm

$\frac{d\theta_0}{dt}$ = motor output speed

K_A = value $\left.\frac{\partial T}{\partial \psi}\right|_{d\theta_0/dt=0}$

K_B = maximum blocked motor torque

ϵ = control quantity in proper units

Another factor to be noted is that in the voltage control system, saturation alone limits the maximum motor torque, since it is possible for the control phase voltage to rise above rated value (with great increases in motor heating). The phase controlled system on the other hand has an upper limit at rated value, since any

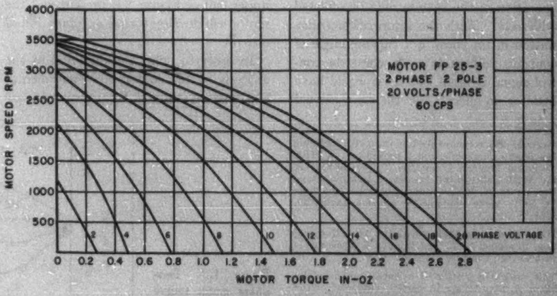

Figure 3. Speed torque curves, voltage control

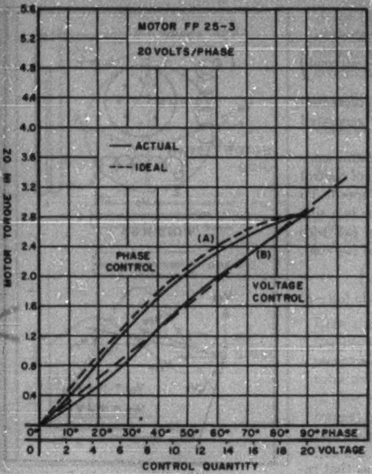

Figure 4 (left). Torque - control quantity curves

Figure 5 (right). Torque - control angle curves

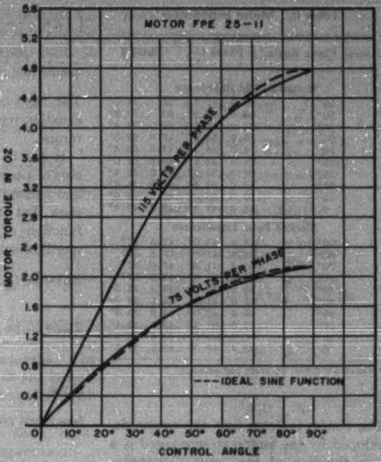

further increase of the time phase angle beyond 90 degrees will decrease the motor torque along the sine curve. This feature protects the motor from high exciting currents with resultant heating.

The motor impedances are given in Table II. Observation of the running light and blocked rotor impedances show that the exciting impedance is low in comparison with the rotor impedance. This checks the form of the speed-torque curves which indicate a high rotor resistance. The shape of the curve contributes the term $-K(d\theta/dt)$ which can be called a damping term since it opposes the motor generated torque in the equation of the curves. This inherent damping is an aid in stabilizing servo systems.

It must be stated at this point that the torque-speed curves and equations developed thus far are for relatively steady state conditions. That is, the control function must change at a rate that is slow compared to the carrier or exciting frequency. Under balanced 2-phase conditions the field in the motor can be considered as rotating at a constant speed with a constant magnitude generating a uniform torque. As either the phase or the magnitude of one of the vector phase voltages is varied, the rotating field locus becomes elliptical in shape, rotating with a varying velocity. When the vector phase voltage becomes zero, or in phase with the other phase voltage, the motor field merely pulsates. Thus the average torque varies from maximum to zero. If the control quantity changes at a rate that approaches the synchronous flux speed, the experimentally determined curves do not give the true facts. For this reason higher excitation frequencies than 60 cycles are often used to increase the information carrying ability of an a-c servo system.

Analytical Proof of Torque Characteristic

The experimental results can be verified analytically in several ways. The most direct means is by the method of symmetrical components. If values are defined as shown in Figure 6, then

$$V_m = V_{m1} + V_{m2};\quad V_c = V_{c1} + V_{c2} \qquad (4)$$

and for a 2-phase component system

$$V_{c1} = -jV_{m1};\quad V_{c2} = jV_{m2}$$

Substituting these values in equation 4

$$V_m = V_{m1} + V_{m2};\quad V_c = -jV_{m1} + jV_{m2};\quad jV_c = -V_{m2} + V_{m1} \qquad (5)$$

Adding and subtracting equations 4 and 5

$$2V_{m1} = V_m + jV_c \qquad (4)+(5)$$

$$2V_{m2} = V_m - jV_c \qquad (4)-(5)$$

Solving

$$V_{m1} = \frac{V_m + jV_c}{2};\quad V_{m2} = \frac{V_m - jV_c}{2}$$

Since the sequence quantities are noninteracting, they may be treated as though representing separate motors acting in opposition. The motor generated torque can be expressed as the sum of the positive and negative torques

$$T = K_d(|I_1^2|R_2/s - |I_2^2|R_2/2-s) = K_d(|I_1^2|/s - |I_2^2|/2-s)$$

where s = slip. For zero speed

$$T = K_d(|I_1^2| - |I_2^2|) = K_d\left[\left(\frac{|V_{m1}|}{Z_1}\right)^2 - \left(\frac{|V_{m2}|}{Z_2}\right)^2\right] = K_e[(V_{m1})^2 - (V_{m2})^2] \qquad (6)$$

For a phase controlled system with equal phase voltages:

$$V_c = V_m[\cos K\,90° - j \sin K\,90°]$$

where K is the control factor, therefore: $(-1 < K < +1)$

$$V_{m1} = \frac{V_m + jV_m[\cos K\,90° - j\sin K\,90°]}{2};$$

$$V_{m2} = \frac{V_m - jV_m[\cos K\,90° - j\sin K\,90°]}{2}$$

$$V_{m1} = (V_m/2)(1 + \sin K\,90° + j\cos K\,90°);$$
$$V_{m2} = (V_m/2)\times(1 - \sin K\,90° - j\cos K\,90°)$$

$$|V_{m1}^2| = (V_m^2/4)([1 + \sin K\,90°]^2 + [\cos K\,90°]^2);\quad |V_{m2}^2| = (V_m^2/4)([1 - \sin K\,90°]^2 + [\cos K\,90°])^2$$

Now $T_{\text{blocked}} = K_s V_m^2$ and substituting the sequence voltages in the torque equation

$$T = \frac{T_{\text{blocked}}}{V_m^2}\left\{\frac{V_m^2}{4}[([1+\sin K\,90°]^2 + [\cos K\,90°]^2) - ([1 - \sin K\,90°]^2 + [\cos K\,90°])^2]\right\}$$

$$= \frac{T_{\text{blocked}}}{4}[1 + 2\sin K\,90° + \sin^2 K\,90° - 1 + 2\sin K\,90° - \sin^2 K\,90°]$$

$$= T_{\text{blocked}} \sin K\,90°$$

Table II. Motor Impedances*

Control Phase Angle	Phase 1		Phase 2	
Running Light Impedance				
90°	59.6	71.7°	54	74.4°
80°	66.6	67.5°	50	73.3°
70°	74.0	61.2°	46.5	72.4°
60°	76.9	54.0°	43.6	69.6°
50°	74.0	45.1°	41.6	65.4°
40°	71.5	38.6°	40.6	62.0°
30°	62.5	34.2°	40.0	56.4°
20°	55.6	33.5°	40.0	51.4°
10°	50.0	35.6°	41.4	43.8°
0	45.5	42.4°	43.6	40.4°
Blocked Rotor Impedances				
90°	44.4	41.0°	42.5	37°
80°	44.4	41.0°	42.3	37°
70°	44.4	41.8°	42.6	37°
60°	44.4	41.0°	43.2	37°
50°	46.0	40.5°	43.5	38.5°
40°	45.0	41.5°	44.0	38.5°
30°	45.4	42.0°	44.0	38.5°
20°	45.6	42.5°	43.5	38.4°
10°	46.0	42.5°	43.6	38.5°
0	45.4	42.5°	43.5	38.5°

*Motor FP-25-3, 20 volts per phase.

The results indicate that the torque developed by the motor at zero speed is a sine function of the control quantity. The experimental results confirm this. Again it must be mentioned that the result is for essentially steady state or very slowly changing control conditions. In a servo system using a 60-cycle excitation frequency, a maximum signal frequency of 10 cycles per second is within the above assumptions. The loss of information in a low excitation frequency system is felt in the response to transients which generally contain higher frequencies.

The conclusions reached by the method of symmetrical components can be arrived at by a study of the actual motor magnetomotive forces. This equation is presented in the literature as taken without derivation from the Notes of Mr. N. B. Nichols.[3] It is (after linearization) as follows:

$$T_m\frac{d^2\theta_0}{dt^2}+\frac{d\theta_0}{dt} = \left[2\omega_0 B(t)\sin\omega_0 t+\frac{dB(t)}{dt}\cos\omega_0 t\right]$$

where

T_m = motor time constant
$B(t)$ = arbitrary control voltage (the other phase voltage is given by $\cos\omega_0 t$)

Rewriting the equation in terms of motor torque:

$$J_m\frac{d^2\theta_0}{dt^2}=2f_m\times\left[\omega_0 B(t)\sin\omega_0 t+\frac{dB(t)}{dt}\cos\omega_0 t\right]-f_m\frac{d\theta_0}{dt}$$

where

J_m = motor inertia
$f_m=\partial T/\partial n$ = motor viscous friction coefficient

$$\left(T_m=\frac{J_m}{f_m}=\frac{\text{pound foot second}^2}{\text{pound foot per radian per second}}=\text{second}\right)$$

The right-hand side of the differential equation represents the motor generated torque.

It can be seen that the equation consists of a term that is a function of control and a term that is a function of speed. To show that the generated torque is a sine function of the phase angle (at zero speed), assume $B(t)$ equal to $\cos(\omega_0 t-\phi)$.

$$B(t)=\cos(\omega_0 t-\phi);\quad (d/dt)B(t)=-\omega_0\sin(\omega_0 t-\phi)$$

$$\begin{aligned}T_{sin}&=2f_m[\omega_0\cos(\omega_0 t-\phi)\sin\omega_0 t-\omega_0\sin(\omega_0 t-\phi)\cos\omega_0 t]\\&=2f_m\omega_0\sin[\omega_0 t-(\omega_0 t-\phi)]=KT_m\sin\phi\end{aligned}$$

since

$$f_m\omega_0=\text{foot pound/radian per second}\times\text{radian/second}=\text{constant}$$

This conclusion is the same as that recorded for the derivation using symmetrical component theory.

In order to more accurately determine the conditions under which the above relation can be applied the following derivation has been developed. Figure 7 shows the relation of the stator magnetomotive forces acting in a 2-phase motor. The stator magnetomotive force can be expressed as follows;

Magnetomotive force 1

$N_s B(t)\sin\alpha$ ampere turns

Magnetomotive force 2

$N_s A\cos\omega_0 t(-\cos\alpha)$ ampere turns

These expressions can be assumed to represent the air gap net magnetomotive force if the reaction of rotor currents is neglected and the primary voltage drop as a result of leakage impedance is assumed to remain constant. These two assumptions are consistent with respect to each other since the effect of rotor current is being neglected compared to the exciting current. The impedance tabulated in Table II along with the fact that the rotor is known to be of high resistance, makes the above assumption valid. Inspection of the torque versus control curves (Figures 4 and 5) indicates that the motors do not operate in the saturated region since the curves closely fit the ideal case. Therefore under the assumption of constant permeability the motor flux can be written as

$$\phi=KN_s(B(t)\sin\alpha-A\cos\omega_0 t\cos\alpha)$$

lines where K = lines per ampere turns

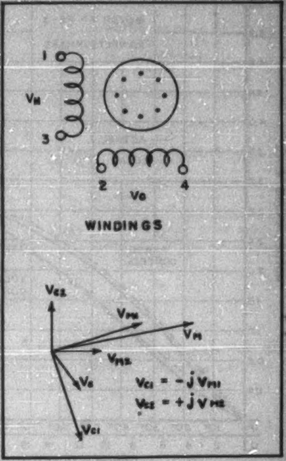

Figure 6. Symmetrical component voltages for the two windings of a 2-phase motor

The expression for the motor flux is seen to be a general equation of a rotating field (rotation being dependent on the phase of $B(t)$). There will therefore be two components of voltage acting around a shorted turn aa' of the squirrel cage rotor (Figure 7), consisting of speed voltage and a transformer voltage

$$e_T=-d\phi/dt\times10^{-8}\text{ volts};\quad e_V=BLV\times10^{-8}\text{ volts}$$

and since the density B is changing with respect to the incremental area considered

$$e_V=L(d\phi/dA)V\times10^{-8}=\frac{L}{Ld\alpha}d\phi(r\omega_{rotor})10^{-8}=r\omega_{rotor}(d\phi/d\alpha)\times10^{-8}\text{ volts}$$

Now if the units of length are redefined so that r inches is equal to one unit, then:

$$e_0=\omega_{rotor}(d\phi/d\alpha)10^{-8}\text{ volts}$$

Therefore the rotor circuit voltage per bar as a function of position (α) is,

$$e_{rotor}=\left[\left(\frac{d\theta_0}{dt}\right)\times\left(\frac{d\phi}{d\alpha}\right)-\frac{d\phi}{dt}\right]10^{-8}\text{ volts}$$

where $d\theta_0/dt=\omega_{rotor}$

Note that when the actual rotor speed, $d\theta_0/dt$ equals the stator magnetomotive force synchronous speed, $d\alpha/dt$, the expression shows that there is no net rotor voltage to cause current flow.

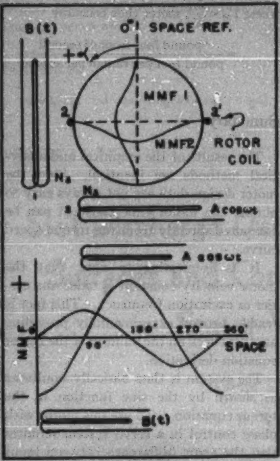

Figure 7. Space diagram for windings of 2-phase motor

$$\frac{d\phi}{dt}=KN_s\left[\omega_0 A\cos\alpha\sin\omega_0 t+\frac{d}{dt}B(t)\sin\alpha\right]$$

$$\frac{d\phi}{d\alpha}=KN_s[A\sin\alpha\cos\omega_0 t+B(t)\cos\alpha]$$

Of interest is the fact that the differentiation of the equation for flux automatically takes into account the quadrature position of the component of flux generating the speed voltage with respect to the axis of the component of transformer flux.

The rotor bar current now can be found:

$$Ri+L\frac{di}{dt}=e_{\text{bar}}=KN_s10^{-8}\left\{\frac{d\theta_0}{dt}\times (A\sin\alpha\cos\omega_0 t+B(t)\cos\alpha)-\left(\omega_0 A\cos\alpha\sin\omega_0 t+\frac{dB(t)}{dt}\sin\alpha\right)\right\}$$

This equation does not have a usable solution but can be simplified if the rotor inductance is neglected. This assumption is valid since the rotor resistance is high. Actually it is the rotor inductance that causes the slight curvature in speed torque characteristic. Therefore, the designer of the induction motor should strive for negligible rotor leakage flux in order to make the motor a more linear device.

Neglecting rotor inductance

$$i_{\text{rotor bar}}=\frac{KN_s10^{-8}}{R_{\text{bar}}}\left\{\frac{d\theta_0}{dt}\times (A\sin\alpha\cos\omega_0 t+B(t)\cos\alpha)-\left(\omega_0 A\cos\alpha\sin\omega_0 t+\frac{dB(t)}{dt}\sin\alpha\right)\right\}$$

If the number of rotor bars is large the instantaneous motor torque as a function of position with respect to the stator is given by:

$dT=c\phi Id\alpha$ foot pounds

where c = foot pounds per line ampere.

$$dT=\frac{c(KN_s)^2 10^{-8}}{R}[-A\cos(\alpha-\pi/2)\times \cos\omega_0 t+B(t)\sin(\alpha-\pi/2)]$$

$$\left[\frac{d\theta_0}{dt}(A\sin\alpha\cos\omega_0 t+B(t)\cos\alpha)-\left(\omega_0 A\cos\alpha\sin\omega_0 t+\frac{dB(t)}{dt}\sin\alpha\right)\right]d\alpha$$

Here the reference for the flux equation has been shifted so that the current element will act in the correct field. The total motor torque acting at one instant of time will be the summation of dT with respect to position α.

Simplifying parts of the above equation and integrating with respect to α:

PART I

$$dT_V=\frac{c(KN_s)^2 10^{-8}}{R}\frac{d\theta_0}{dt}\left[-A^2\cos^2\omega_0 t\times \cos\left(\alpha-\frac{\pi}{2}\right)\sin\alpha+AB(t)\cos\alpha\times \cos\omega_0 t\cos\left(\alpha-\frac{\pi}{2}\right)+AB(t)(\cos\omega_0 t)\times \sin\alpha\sin\left(\alpha-\frac{\pi}{2}\right)+B^2(t)\times \cos\alpha\sin\left(\alpha-\frac{\pi}{2}\right)\right]d\alpha$$

$$dT_V=\frac{c(KN_s)^2 10^{-8}}{R}\frac{d\theta_0}{dt}\left[-A^2\cos^2\omega_0 t\sin^2\alpha- AB(t)\frac{\sin(2\alpha)}{2}\cos\omega_0 t-AB(t)\times \frac{\sin(2\alpha)}{2}\cos\omega_0 t-B^2(t)\cos^2\alpha\right]d\alpha$$

$$T_V=\frac{-2c(KN_s)^2 10^{-8}}{R}\frac{d\theta_0}{dt}\int_0^\pi\left[A^2\cos^2\omega_0 t\times \sin^2\alpha+AB(t)\cos\omega_0 t\frac{\sin(2\alpha)}{2}+ AB(t)\cos\omega_0 t\frac{\sin(2\alpha)}{2}+ B^2(t)\cos^2\alpha\right]d\alpha=\frac{-2c(KN_s)^2 10^{-8}}{R}\times \frac{d\theta_0}{dt}\left\{\left[\frac{\alpha}{2}-\frac{\sin 2\alpha}{4}\right]_0^\pi A^2\cos^2\omega_0 t+ \left[\frac{\alpha}{2}+\frac{\sin(2\alpha)}{4}\right]_0^\pi B^2(t)+\frac{B(t)}{2}\cos\omega_0 t\times \left[\cos(2\alpha)\right]_0^\pi\right\}=\frac{-c(KN_s)^2 10^{-8}\pi}{R}\times \frac{d\theta_0}{dt}[A^2\cos^2\omega_0 t+B^2(t)]$$

PART II

$$dT_T=\frac{c(KN_s)^2 10^{-8}}{R}\left[A^2\omega_0\cos\alpha\times \cos\left(\alpha-\frac{\pi}{2}\right)\frac{\sin(2\omega_0 t)}{2}+ A\frac{d}{dt}B(t)\sin\alpha\cos\left(\alpha-\frac{\pi}{2}\right)\times \cos\omega_0 t-\omega_0 AB(t)\cos\alpha\sin \left(\alpha-\frac{\pi}{2}\right)\sin\omega_0 t-B(t)\frac{d}{dt}\times B(t)\sin\alpha\sin\left(\alpha-\frac{\pi}{2}\right)\right]d\alpha$$

$$=\frac{c(KN_s)^2 10^{-8}}{R}\left[A^2\omega_0\left(\frac{\sin 2\alpha}{2}\right)\times \frac{\sin(2\omega_0 t)}{2}+A\frac{d}{dt}B(t)\sin^2\alpha\cos\omega_0 t+ \omega_0 AB(t)\sin\omega_0 t\cos^2\alpha+ B(t)\frac{d}{dt}B(t)\frac{\sin(2\alpha)}{2}\right]d\alpha$$

$$T_T=\frac{2c(KN_s)^2 10^{-8}}{R}\int_0^\pi\left[\frac{A^2\omega_0}{4}\sin(2\alpha)\times \sin(2\omega_0 t)+A\frac{d}{dt}B(t)\sin^2\alpha\cos\omega_0 t+ \omega_0 AB(t)\sin\omega_0 t\cos^2\alpha+ B(t)\frac{d}{dt}B(t)\frac{\sin(2\alpha)}{2}\right]d\alpha=$$

$$\frac{2c(KN_s)^2 10^{-8}}{R}\int_0^\pi\left\{\left[\frac{A^2\omega_0}{4}\times \sin(2\omega_0 t)+ \frac{B(t)\frac{d}{dt}B(t)}{2}\right]\sin(2\alpha)+A\frac{d}{dt}B(t)\times \sin^2\alpha\cos\omega_0 t+\omega_0 AB(t)\sin\omega_0 t\times \cos^2\alpha\right\}d\alpha=\frac{2c(KN_s)^2 10^{-8}}{R}\left\{\left[\frac{A^2\omega_0}{4}\times \sin(2\omega_0 t)+\frac{B(t)\frac{d}{dt}B(t)}{2}\right]\times \left(\frac{-\cos(2\alpha)}{2}\right)_0^\pi+A\frac{d}{dt}B(t)\cos\omega_0 t\times \left[\frac{\alpha}{2}-\frac{\sin(2\alpha)}{4}\right]_0^\pi+\omega_0 AB(t)\sin\omega_0 t\times \left[\frac{\alpha}{2}+\frac{\sin(2\alpha)}{4}\right]_0^\pi\right\}=\frac{2c(KN_s)^2 10^{-8}\pi}{R}\times \left[A\frac{dB(t)}{dt}\cos\omega_0 t+\omega_0 AB(t)\sin\omega_0 t\right]$$

The total torque is

$$T=\frac{c(KN_s)^2\pi 10^8}{R}\left\{\left[\frac{dB(t)}{dt}\cos\omega_0 t+ \omega_0 B(t)\sin\omega_0 t\right]2A-\frac{d\theta_0}{dt}[(A\cos\omega_0 t)^2+ B^2(t)]\right\}\text{foot pounds}$$

A dimensional check of this equation can be made as follows:
Consider the constants

c = foot pounds per line ampere, line of flux
K = line per ampere turn
N_s = stator turns
R = rotor ohms = volts/amperes = lines per second/ampere
π = radians (numeric)
10^{-8} = numeric

$$\frac{c(KN_s)^2\pi 10^{-8}}{R} = \text{foot pound/line ampere} \times [\text{line/ampere turn} \times \text{turn}]^2 \frac{1}{\dfrac{\text{Lines per second}}{\text{ampere}}} \pi 10^{-8} = \text{foot pound second per ampere}^2 \text{ (modified units of length)}$$

The dimensions of the entire bracketed term can be seen to be (amperes)^2 (radians per second).

$$T = \text{foot pound second per ampere}^2 [(\text{amperes})^2(\text{radians per second})] = \text{foot pound}$$

The total motor equation now can be written:

$$J_m \frac{d^2\theta_0}{dt^2} + f_m \frac{d\theta_0}{dt} = D\left\{\left[\frac{dB(t)}{dt}\cos\omega_0 t + \omega_0 B(t)\sin\omega_0 t\right]2A - \frac{d\theta_0}{dt} \times [(A\cos\omega_0 t)^2 + B^2(t)]\right\}$$

where

$$D = \frac{c(KN_s)^2\pi 10^{-8}}{R}$$

J_m = motor inertia, pound foot second^2
f_m = motor viscous mechanical friction, pound foot per radian per second

The general practice in dealing with the mechanical viscous friction is to neglect it since it is small compared to the internal motor damping term. This assumption gives:

$$J_m \frac{d^2\theta_0}{dt^2} + D[(A\cos\omega_0 t)^2 + B^2(t)]\frac{d\theta_0}{dt} = 2AD\left[\omega_0 B(t) + \frac{dB(t)}{dt}\cos\omega_0 t\right]$$

$$J_m \frac{d^2\theta_0}{dt^2} + \frac{D}{2}[A^2 + A^2\cos 2\omega_0 t + 2B^2(t)]\frac{d\theta_0}{dt} = 2AD\left[\omega_0 B(t)\sin\omega_0 t + \frac{dB(t)}{dt}\cos\omega_0 t\right]$$

$$\frac{2J_m}{DA^2}\frac{d^2\theta_0}{dt^2} + \left[1 + \cos 2\omega_0 t + \frac{2}{A^2}B^2(t)\right]\frac{d\theta_0}{dt} = \frac{4}{A}\left[\omega_0 B(t)\sin\omega_0 t + \frac{dB(t)}{dt}\cos\omega_0 t\right]$$

Under the statements of the derivation, only the exciting current was assumed to be flowing in the stator. If the exciting impedance is large compared to the stator leakage impedance (a fairly valid assumption for these motors) the exciting currents can be redefined in terms of the terminal voltages.

For the phase controlled case define $B(t)$ equal to $A\cos(\omega_0 t - \phi)$

$$\frac{dB(t)}{dt} = -\omega_0 A\sin(\omega_0 t - \phi)$$

Substituting this in the relation

$$\frac{2J_m}{DA^2}\frac{d^2\theta_0}{dt^2} + [1 + \cos 2\omega_0 t + 2\cos^2(\omega_0 t - \phi)] \times \frac{d\theta_0}{dt} = \frac{4}{A}[\omega_0 A\cos(\omega_0 t - \phi)\sin\omega_0 t - \omega_0 A\sin(\omega_0 t - \phi)\cos\omega_0 t]$$

$$\frac{2J_m}{DA^2}\frac{d^2\theta_0}{dt^2} + [2 + \cos 2\omega_0 t + \cos 2(\omega_0 t - \phi)] \times \frac{d\theta_0}{dt} = 4\omega_0 \sin\phi$$

which represents the total motor equation for a phase controlled system.

The solution of the above equation can be readily obtained if the double frequency terms in the coefficient of $d\theta/dt$ are neglected. This linearization of the equation is valid since the period of θ_0 is much greater than that of $2\omega_0 t$. Hence, these terms have an effective average value of zero. The equation becomes:

$$T_m \frac{d^2\theta_0}{dt^2} + \frac{d\theta_0}{dt} = K_v \sin\phi$$

$$= \frac{\text{pound foot second}^2}{(\text{pound foot second/ampere}^2)\ \text{amperes}^2}$$

$$= \text{second}$$

where $T_m = J_m/DA^2$ the motor time constant

$K_V = 2\omega_0$ radian per second

Using the empirical equation 1 and again neglecting mechanical viscous friction

$$J_m \frac{d^2\theta_0}{dt^2} = \frac{\delta T}{\delta n}\frac{d\theta_0}{dt} + \frac{\delta T}{\delta\psi}\psi$$

$$J_m \frac{d^2\theta_0}{dt} - \frac{\delta T}{\delta n}\frac{d\theta_0}{dt} = \frac{\delta T}{\delta\psi}\psi$$

For the phase control equation 3, there results

$$\frac{J_m}{K}\frac{d^2\theta_0}{dt^2} + \frac{d\theta_0}{dt} = \frac{K_2}{K}\sin\phi$$

$$T_m \frac{d^2\theta_0}{dt^2} + \frac{d\theta_0}{dt} = K_V \sin\phi$$

$K_V = \dfrac{K_2}{K}$ motor velocity constant

$$= \frac{\text{pound foot}}{\text{pound foot per radian per second}}$$

$$= \text{radian per second}$$

where $T_m = \dfrac{J_m}{K}$, motor time constant

$$= \frac{\text{pound foot second}^2\ \text{second}}{\text{pound foot per radian per second}}$$

Summary

The results of the empirical and analytical methods are identical. Since the motor design data are not always easy to obtain, the motor time constant can be computed directly from the torque speed curve.

It is interesting to note that the motor velocity constant is twice the carrier or excitation frequency. This fact is readily proved experimentally providing another check on the validity of the motor equation derivation.

The system is thus basically nonlinear as shown by the sine function in the torque equation. To use this motor with phase control in a servo system requires that the error (difference between input and output of closed loop system) be transferred into a directly proportional amplified phase shift. The signal then applied to the motor must be of the form $\sin K_1(\theta_{\text{input}} - \theta_{\text{output}})$ giving:

$$T_s \frac{d^2\theta_0}{dt^2} + \frac{d\theta_0}{dt} = K_s \sin K_1(\theta_{\text{input}} - \theta_{\text{output}})$$

where T_s is the over-all system time constant and K_s is system velocity constant.

In a practical system employing phase shift control some means will have to be employed to cause the motor to exert maximum torque (90-degree phase shift) even when the quantity $K_1(\theta_i - \theta_o)$ is greater than 90 degrees. This is necessary in order to prevent false zeroes since the motor torque decreases when the phase shift across its terminals is greater than 90 degrees.

This is probably one of the principal disadvantages of a system employing phase shift control. Another disadvantage of the system is that full voltage is applied to both motor windings at all times regardless of the value of the error signal, thus producing more motor heating than when employing voltage control.

The nonlinearities have been found not to cause trouble in an actual system. The major difficulty, however, is to obtain a stabilized transducing element. Another problem is that of power supply frequency shift changing phase shifts present in the servo loop.

It is felt that because of the inherent noise suppression characteristics of this method of operation, phase controlled induction motors will find application in instrument servo work.

References

1. PRINCIPLES OF SERVOMECHANISMS (book), Brown, Campbell. John Wiley and Sons, New York, N. Y., 1948.

2. STABILIZATION OF CARRIER FREQUENCY SERVOMECHANISMS, A. Sobczyk. *Journal*, Franklin Institute (Philadelphia, Pa.), volume 246, July 1948, pages 36–39.

3. AN EXPERIMENTAL ANALYSIS OF A PHASE CONTROLLED TWO-PHASE A-C SERVO SYSTEM, Mark A. Steinhacker. Thesis, Cornell University, Ithaca, N. Y.

No Discussion

Slot Discharge Detection Between Coil Surfaces and Core of High-Voltage Stator Windings

JOHN S. JOHNSON
MEMBER AIEE

Synopsis: Basic studies in connection with the nature and method of detection of slot discharge phenomena in high-voltage stator windings are presented. Discharging is seen to result from a loss of electrical contact between conducting coil surfaces in the slot portions and the core. This gives rise to a relatively high energy capacitive discharge which may seriously degrade basic insulation if it continues unchecked. The several possible methods for detection and location of discharge in stator windings were studied. The development of the slot discharge analyzer is described. This is useful as a maintenance tool for the detection and location of slot surface discharging on high-voltage machine stator windings.

THE phenomenon of surface discharging between conducting coil surfaces and core has been observed on several high-voltage stator windings in the past five years. This phenomenon is distinctly different from surface corona which may be present in high-voltage end windings or internal void ionizations which exists to a greater or less extent in the internal structure of high-voltage machine insulation. There are several cases on record where surface discharging has in time led to serious degradation and eventual failure of the stator coil ground insulation.

It is the purpose of this paper to describe the nature of the basic phenomena and to report studies in connection with the development of detection equipment. It is important to detect discharging if it exists during routine generator maintenance inspections because corrective measures if made in time are usually simple, inexpensive and are not time consuming. The discharge analyzer described in this paper has been used extensively in connection with the generator maintenance inspection program of the manufacturer. It is a relatively simple test requiring only a source of a-c test voltage of sufficient capacity to charge the stator winding under test to its normal operating voltage stress. Reported separately in a companion paper by the author and Mead Warren of the Aluminum Company of America are studies made in an effort to further simplify the detection problem.[1]

Basic Phenomena

Modern practice in connection with the insulation of high-voltage stator windings includes the use of a conducting surface coating on the slot portions of the stator coil insulation. This conducting material is applied to the coil finish tape which may be either of fiber glass or some other inorganic textile. The intended function of the conducting surface treatment is to relieve the voltage stress on unavoidable air gaps which exist between the coil surface and core. Without coil surface conducting treatments these gaps ionize at normal operating voltages with resultant corona formation which is generally undesirable. Insulated coils are built slightly smaller than the finished slot size. As coils are wound into the stator, mica plate (usually in the range of 0.020 to 0.030 inch thick) is driven down one side of the coil. This coil tightening operation makes for a tighter coil fit than would otherwise be possible and forces the other coil side into good contact with the slot. This construction is believed to be advantageous in that coils may be wound with less likelihood of damage and a better mechanical fit in the slot is assured. It does, however, place the entire burden of draining the coil charging current on the bottom and one side face in the case of bottom coil sides. Where an insulating filler strip between top and bottom coil sides is used, the entire charging current of the top coil side must be handled by one side face.

If for any reason electrical contact is completely lost between the conducting coil surfaces and core, a seriously destructive capacitive discharge results. For coil surface resistivities less than several hundred thousand ohms per unit area no discharge is possible if the resistive coating is continuous and the coil surface makes contact at any point along the length of the slot. Complete loss of electrical contact with the core is necessary to give rise to a surface discharge.

The frequency of occurrence of this phenomenon has been low. The first case of difficulty was reported after 17 years of trouble-free experience since the introduction of conducting coil finishes. The first such experience naturally brings on a re-examination of insulation practices with the objective of preventing similar occurrences on future designs. Design and manufacturing changes result which take care of the future. In this case a conducting coil filler strip was developed for use between top and bottom coil sides. This provides an additional grounding path for top coil sides. No difficulty has been encountered due to discharges on bottom coil sides. Other changes included the development of a new varnish type conducting compound

---

Paper 51-367, recommended by the AIEE Rotating Machinery Committee and approved by the AIEE Technical Program Committee for presentation at the AIEE Fall General Meeting, Cleveland, Ohio, October 22–26, 1951. Manuscript submitted June 21, 1951; made available for printing August 31, 1951.

JOHN S. JOHNSON is with Westinghouse Electric Corporation, East Pittsburgh, Pa.

The author gratefully acknowledges the assistance of C. D. Fahrnkopf of the Westinghouse Engineering Laboratories in the engineering investigation which led to the development of the slot discharge analyzer.

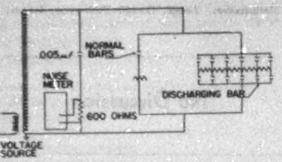

Figure 1. Connections for conducted radio noise measurements

and improved methods of applying the surface treatment. Also developed were improved methods for checking uniformity of coil tightening operations. As a final step in this problem detection equipment was developed which made it possible to make a rather simple test on machines in service to determine the adequacy of the coil surface grounding.

In the few cases where surface discharging has been found by this test corrective measures needed to suppress the discharge have been minor in scope. However, uncorrected this phenomena in time can be severely destructive to the major coil insulation.

Development of Discharge Analyzer

Detection of discharges which result from partial breakdown in nonhomogenous dielectric materials (such as the combination of gaseous voids in a solid dielectric) is possible because of electrical oscillations which result in the circuit comprising the materials under stress and the voltage source.

In the case of high-voltage machine insulation voids normally exist within the internal structure of the insulation. For slot discharge detection purposes, it is therefore necessary to distinguish between electric oscillations which result from internal voids and those which result from the surface discharge. The oscillations resulting from these two phenomena would be expected to be distinguishable, because the discharge energies involved are of an entirely different order of magnitude. In the case of the slot discharge, the energy would be that resulting from all or a substantial part of the entire coil side capacitance. In the case of the internal voids only the capacitance of an extremely small area would be involved. The energy in the discharge varies as the square of the voltage across the gap and directly as the effective capacitance at the point of breakdown.

Electric oscillations which result from the gaseous voids in solid insulation are detectable over a wide range in frequencies. University of Illinois Experimental Station Bulletins[2] report the results of extensive studies on ionization detection in cable insulation. For cables with ionizable voids, they report that oscillations resulting from ionization of this type have two components as follows:

1. Oscillations in the audio-frequency range which follow the successive breakdown and build-up of voltage across the voids or air gap. These have the nature of a wave train which is repetitive with alternations of the applied voltage. The frequency and amplitude of these are stated to be principally a function of void size, chemical and physical factors.

2. Superimposed on the audio-frequency oscillations are damped oscillations in the radio-frequency range. The frequency and magnitude of this component are reported to depend principally on the constants of the test circuit.

In the development of the discharge detector the relative discriminations between surface discharging and internal void ionization were studied with both radio- and audio-frequency detection schemes. It was found that the relative discrimination was inherently better at audio frequencies. It was further found that in the audio-frequency range, internal ionization and surface discharging had maximum energies at different frequency ranges. Accordingly, the use of a circuit resonant in the frequency range where energy from surface discharging was high, resulted in corresponding poor sensitivity to oscillations resulting from internal ionization.

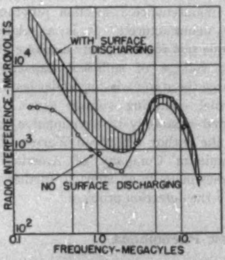

Figure 2. Noise frequency characteristic, radio-frequency measurements

Tests

Tests were made in the laboratory using test bars wound into a core model. It was possible in these tests to make a comprehensive study of the merits of the several detection schemes. Test bars were prepared having low, medium, and high surface resistivity. Some were prepared with poor fill and others with good fill of conducting material in the coil binder tape. Bars were wound into the model according to standard practice except that their tightness in the slot was varied. Bars were studied which were tight, loose, and clear of the slot wall on the contact face.

It was found that when there was an air gap between coil surface and slot wall discharging would occur. When the gap was 0.010 inch, discharging occurred at test voltages as low as 3 kv.

Since it was possible to produce or eliminate discharging at will by the removal or application of a ground at one point on the coil surfaces, all the bars were finally wound in the core with slot mica on one side and an air gap of approximately 0.010 inch on the contact side. Foil electrodes to which a ground could be applied, were wrapped around the bar, just outside of the core. As a further refinement, a micrometer gap was connected from the grounding foil to core. With this gap, the effect of very small gaps between the test bar surfaces and coil could be studied. Also in studying the frequency sensitivity of the various audio frequency circuits under consideration a continuous frequency voltage from an audio oscillator was impressed across this gap instead of an actual discharge. This simulated discharge voltage was more controllable than the actual discharge and consequently facilitated the evaluation of the characteristics of the circuits investigated.

Radio-Frequency Studies

A standard radio noise meter was used for all tests in the radio-frequency range. The instrument used was a standard

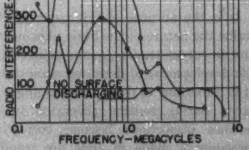

Figure 3. Noise frequency characteristic, radio-frequency loop antenna measurements

measuring instrument of high sensitivity, indicating values as low as 1 microvolt when used as a voltmeter or 1 microvolt per meter when measuring field strength. The noise meter was used in two ways:

Loop Antenna

By using the noise meter with a special type loop antenna the field generated by discharges within the machine can be detected and measured. An elongated loop was designed which could be inserted in the air gap and positioned over the slots of the stator windings. The intent of this method was to survey the stator coils of a wound machine without having to make a physical contact with the conducting coil surface.

Conducted Noise Measurements

Conducted noise measurements were made by coupling the noise meter directly to the high-voltage line. As shown in Figure 1, a 0.005-microfarad capacitor with a 600-ohm resistance in series on the ground side, was connected directly across the high-voltage line. The noise meter was used to measure the high-frequency drop across the resistor.

With either of the above methods, it was found that the energy of the field due to ionization of voids within the insulation was picked up as well as the surface discharges. The curve of Figure 2 shows the variation of conducted noise measured at frequencies from 0.16 to 18 megacycles of low surface resistance bar in the core model. The lower curve is for a test bar well tightened in the slot and the upper envelope is for the same bar loose and discharging to core. For bars having higher surface resistance there was correspondingly less difference in measured noise between the arcing and grounded conditions at any frequency. Even with the low surface resistance bar, at frequencies above 3 megacycles, the ionization of internal voids completely masks the surface discharging. As shown at 160 kc (the lowest frequency at which radio noise measurements could be made with available equipment), the measured noise under arcing conditions is approximately 10 to 20 times greater than that measured when the bar is not discharging.

With the elongated loop antenna placed above the slot containing a test bar, similar measurements over the frequency range were made. The field picked up in this manner is a combination of the radiated magnetic and electrostatic fields due to the radio-frequency currents within and at the test bar surface. Results similar to the conducted measurements of Figure 2 were obtained using the loop pick-up for low surface resistance test bars. Figure 3 illustrates the noise frequency characteristic determined with loop antenna pickup. As was true for the conducted measurements bars with surface resistivities of the order of 100,000 ohms per square or higher showed only small differences in noise when measured "arcing" and well grounded.

Audio-Frequency Circuits

Probe Measurement

Slot discharging was found to be most readily detectable with a circuit involving the use of a probe which was made to contact the conducting surface of the coil sides. Figure 4 is a schematic diagram of the circuit used. As shown, the pickup circuit consists of a probe, a capacitor, and an inductance. All are connected in series and one side of the inductance is grounded. Connected across the inductance are the input terminals of a high pass filter (used for blocking 60-cycle voltage). A conventional cathode-ray oscilloscope is connected across the output terminals of the filter. With the circuit constants used, the pickup circuit is in series resonance at 2,000 cycles. The 60-cycle impedance of the pickup circuit is 1.3 megohms. The selection of a suitable value of capacitance for the series capacitor is determined by two considerations.

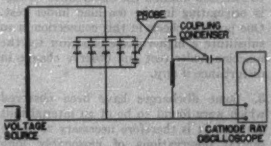

Figure 4. Connections for audio-frequency probe measurements

1. Values of capacitance as small as 0.00005 microfarad (corresponding to series resonant frequency of 10,000 cycles) had adequate sensitivity for detecting discharges in the model set up. However, the sensitivity increased with increasing value of series capacitance.

2. Capacitance values greater than 0.005 microfarad (corresponding to a resonant frequency of 1,000 cycles) reduced the 60-cycle impedance of the pickup circuit to the point where it tended to suppress the discharging.

To check a machine for slot discharging by this method, it is necessary to contact the conducting coating of the individual coil sides of the machine. This usually involves removing end bell covers to get to the winding. It also involves the use of a suitable probe. Conducting areas within the slot are accessible at the vent ducts. On the machines tested to date, it has been possible to contact the coil surface at vent ducts near the top of the winding. In general, only top coil sides of a machine are accessible. This is probably not a serious limitation since no evidence of discharging has been found on bottom coil sides.

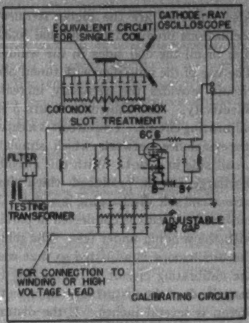

Figure 5. Schematic diagram of slot discharge analyzer showing connections for making over-all tests on a generator stator winding

Complete Winding Measurements

Figure 5 shows the circuit used for detection of slot discharging in which test connections are made to the machine terminals. In this case, the constants of the pickup circuit are the same as for the probe method. The capacitor instead of being connected to a probe is connected to a machine terminal. As shown, a stage of amplification with a tuned parallel resonant plate circuit is inserted between the output terminals of the 60-cycle filter and the input to the oscilloscope. The plate circuit is tuned to the same frequency (2,000 cycles) as the pickup circuit. This additional filtering improves the relative sensitivity between surface discharging and internal ionization.

The detection of surface discharges by coupling through capacitance to machine terminals is more difficult because the detectable discharge voltage is reduced in the ratio of the coils which are discharging to those which are in good contact. In the case of a generator with one coil side out of 800 discharging, the detectable discharge voltage at the machine terminals is reduced by 800 times. It is therefore necessary to provide more amplification to detect the discharge voltage.

Also amplified are the higher frequency oscillations produced by internal ionization of all the coil sides in the winding. The use of the amplifier with tuned plate circuit provides the necessary increased selectivity. Also shown in Figure 5 is a calibrating circuit. The circuit is a capacitor-resistance network which simulates a coil side in a slot. With this circuit a discharge can be produced which simulates a coil side discharging in a slot. The calibrating circuit is connected in parallel with the winding under test. The gain of the oscilloscope is adjusted so that when the calibrating circuit is discharging the magnitude of the disturbance trace on the screen is several inches. If the disturbance trace substantially disappears when the discharge from the calibrating circuit is stopped it is concluded that no coil sides in the machine are discharging.

Test Experience

When used for complete winding checks the analyzer is limited in the following respects:

1. The discharge voltage at the machine terminals in general is a fraction of a volt. Considering that the applied voltage is of the order of 8 kv it is apparent that the disturbance voltage is a small percentage of the applied voltage. The presence of high harmonics in the test source which limit the sensitivity of the device is possible. This effect can be minimized by the use of a suitable line filter.

2. While it is possible to build a filter which is effective for steady-state disturbances, it is very difficult to filter out high-frequency transient disturbances, which arise in connection with the operation of bell alarms, welders, et cetera. It therefore is essential to ascertain whether the disturbance voltage is originating in the machine under test. One possible check in this connection is to substitute a high-voltage capacitor for the machine under test and observe change in disturbance if any.

3. Some discharges have been observed which were found to be of an intermittent nature. It is therefore necessary to make several observations of reasonably long duration.

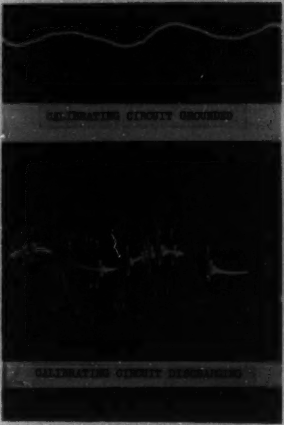

Figure 6. Results of a slot discharge detection test on a turbine generator stator. Test voltage 8 kv

Techniques and equipment have been developed which have overcome these limitations. Complete winding tests give dependable indication of the presence or absence of discharge phenomena. Probe tests should be necessary only for location of affected coil sides when the complete winding test indicates the presence of discharging. An improved line filter has been developed and has proved satisfactory. In making tests in the field it has been found that local conditions vary and are somewhat unpredictable. Also it is not always practical or necessary to completely isolate the winding under test. In making field tests, when disturbance voltage is detected, check measurements should be made to definitely establish that the machine insulation is responsible for the disturbance. It has been found helpful in this connection to substitute a high voltage capacitor (0.5 microfarad) for the machine insulation under test. If the disturbance disappears the machine insulation or associated wiring and equipment (potential transformers, leads to potential transformers, or lightning arresters), should be investigated.

When the analyzer is used for making probe tests, the only limitation appears to be the problem of contacting the conducting coil surface with a suitable probe. In this connection a low-voltage ohmmeter is useful for checking to be certain that the probe is actually contacting the conducting material. The ohmmeter checks are made before test voltage is applied to the winding.

Figure 6 shows a typical oscilloscope trace obtained during a test on a large stator winding. As shown the trace with the calibrating circuit not discharging is small compared to that obtained with the calibrating circuit discharging. In general when the trace obtained under normal

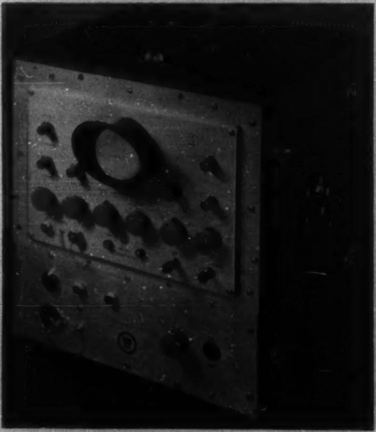

Figure 7 (left). Slot discharge analyzer

Figure 8 (right). Slot discharge test on a turbine generator stator

conditions is 30 per cent or less than with the calibrating circuit discharging, the winding is considered to be discharge free. This residual trace is that conducted in from the source of test voltage. The magnitude of this residual is the principal limitation to the sensitivity of the analyzer. Figures 7 and 8 are the analyzer and equipment being used to test a large hydrogen cooled stator winding.

Summary

A sound preventive maintenance program for any type of electric equipment is most effectively achieved when there is an understanding of the potential sources of trouble which may be in need of adjustment, repair, or replacement. Knowledge of the potential trouble sources is gained by experience and intelligent analysis of the performance record of the equipment involved. In the case of high voltage generators the exceptionally fine performance record makes it necessary to examine the performance of relatively large numbers of machines to get a good perspective to the potentialities for distress.

In a complex piece of equipment such as a large generator, it is seldom if ever possible to develop a single test which gives a complete and accurate picture of the insulation conditions of the various components. It has been found possible, however, to further the cause of diagnostic testing on these machines by developing several tests each of which are directed toward detecting particular types of trouble which experience has shown are possible. Slot discharge detection techniques are an example of this particular type of test. It is a single purpose instrument designed specifically for use in detection and location of discharging between conducting coil surfaces and slots in high-voltage stator windings.

References

1. Detection of Slot Discharges in High-Voltage Stator Windings During Operation, John S. Johnson, Mead Warren. *AIEE Transactions*, volume 70, part II, 1951, pages 1998–2000.

2. Discharge Detection Bridge for Cable Ionization Measurements. *Experimental Station Bulletins 259 and 260*, H. A. Brown, E. B. Paine, J. T. Tykociner. University of Illinois (Urbana, Ill.), August 1933.

3. A Method for Detecting the Ionization Point on Apparatus, G. E. Quinn. *AIEE Transactions*, volume 59, 1940, pages 680–82.

4. A Maintenance Inspection Program for Large Rotating Machines, J. S. Johnson. *AIEE Transactions*, volume 70, part I, 1951, pages 749–55.

No Discussion

Detection of Slot Discharges in High-Voltage Stator Windings During Operation

JOHN S. JOHNSON
MEMBER AIEE

MEAD WARREN
MEMBER AIEE

Synopsis: A modified slot discharge detection method, which permits tests without shutting down the machine or using auxiliary high-voltage test equipment, was investigated. The method involves connection of frequency sensitive equipment across all or part of the neutral impedance. Tests on eight vertical water wheel generators in the range of 20,000- to 40,000-kva capacity indicate that the method is generally applicable when there is a current transformer or some other impedance in the generator neutral.

Review

SLOT discharge is a result of poor contact between the conducting surface on a generator coil and the stator iron. Discharges of this nature can be very severe because of the high current involved and can cause serious damage to the coil insulation. If permitted to continue, small pin holes or craters will develop in the insulation because of the dehydration of the mica. Eventually this will result in failure of the coil.

Basic work on slot discharge detection has shown that this disturbance is most readily detectable in the audio-frequency range. Fundamentally the problem is one of discriminating between the disturbance created by the surface discharging and that created by other effects such as internal void ionization, end winding surface corona on the machine under test, and residual harmonics or other disturbance existing in the test voltage. The sensitivity of any detection scheme is limited by the level of residual disturbance and the ability to isolate the discharge disturbance from the residual.

In the use of the slot discharge analyzer either for probing or detection, the test voltage is supplied from an external source. The testing transformer usually is effective in filtering out much of the residual source disturbance. When this is not the case, it is always possible to use a line filter to accomplish this objective.

The purpose of the present work is an attempt to further simplify the detection problem. It was believed that on those machines having current transformers or some other impedance in the generator neutral there exists the possibility of detecting slot discharging by connecting frequency sensitive circuits across generator neutral impedance. With this method it was recognized that it is not possible to separate source harmonics (which in this case is the generator itself) from the disturbance due to surface discharging.

Machine Harmonics

In the range of magnitudes of interest (extremely small values), machine harmonics may be the result of a number of factors difficult to calculate or control. The principal harmonic of interest is the slot harmonic.

The order of this harmonic is approximately equal to the number of slots per pair of poles. Harmonics of this slot frequency are also possible. Other harmonics are possible because of the interaction between the stator slots and the damper winding. Also, the accuracy of field pole spacing and other causes may influence the machine harmonics.

In the design of machines, the principal concern in connection with these higher harmonic frequencies is to meet or come well within telephone interference or influence factor limits. This factor is the ratio of the square root of the sum of the squares of the weighted values of harmonic components to the rms value of the wave. When the machines meet these limits, the exact magnitude and frequencies of these very small harmonics have not received much attention.

Sensitivity Determination

The only alternative in connection with this method of slot discharge detection is to explore the frequency spectrum and find a frequency or frequency band where residual harmonics are small compared to the disturbance caused by surface discharging.

For an effective test, it is believed that the residual should be in the range of 1/5 to 1/10 of the smallest possible disturbance caused by slot discharging. This minimum disturbance would be that resulting from one discharging coil side in the machine winding.

In order to check the sensitivity or discrimination of the various filters in the test, it was necessary to produce a calibrating signal equal in magnitude to the minimum discharge disturbance. Insulated test bars simulating coils were used for this purpose. The bars were 54 inches long. The central 30 inches of the bars were prepared with a conducting surface finish similar to that used on high-voltage stator coils. The several bars were prepared with resistivities in the normal, moderately high, and extremely high range of surface resistivities. Sheet metal cells 26 inches long simulating stator coil slots were made. The test

---

Paper 51-368, recommended by the AIEE Rotating Machinery Committee and approved by the AIEE Technical Program Committee for presentation at the AIEE Fall General Meeting, Cleveland, Ohio, October 22-26, 1951. Manuscript submitted June 22, 1951; made available for printing September 20, 1951.

JOHN S. JOHNSON is with Westinghouse Electric Corporation, East Pittsburgh, Pa., and MEAD WARREN is with Aluminum Company of America, Alcoa, Tenn.

Figure 1 (left). Test set-up for producing calibrating signal

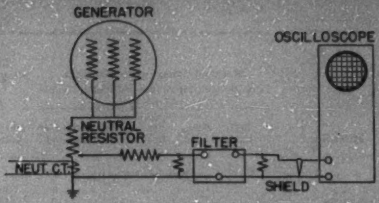

Figure 2. Discharge detection circuit filters used: 1,046-cycle single frequency; 1,568-cycle single frequency; 2,349-cycle single frequency; 3,520-cycle single frequency; 2,500-cycle high pass; 2,500–4,000-cycle band pass; 4,000 – 10,000-cycle band pass

bars were assembled in the cells but insulated from the cells so that a small air gap existed between the conducting coil surface and the grounded metal cell (simulating conditions which give rise of slot discharging). A small adjustable gap was connected between conducting coil surface and the grounded cell. When this gap opening was made small (0.001 to 0.005 inch), the discharge voltage from coil surface to ground was limited to approximately the minimum sparking potential.

Closing the gap entirely grounded the coil surface and suppressed the discharging. The test bars were successively connected to a machine terminal, depending on the coil surface resistivity desired. So connected, the bar producing the calibrating signal was at the greatest possible distance from the detection point (the neutral). It was therefore possible to reproduce discharge disturbance smaller than would be produced by a single coil side (coil side slot portions were generally longer than the test bars) having either normal or high surface resistance. The test set up for producing the calibrating signal is illustrated in Figure 1.

Detection Circuits

The detection circuits studied consisted of a series of single frequency, high-pass and band-pass filters used in combination with a cathode ray oscilloscope. Figure 2 is a diagram of test connections and also lists and characteristics of the filters used. As shown, the input terminals of the filters were connected across a portion of the impedance plus 1/8 or 1/9 of the neutral resistance. For the machine studies, the neutral resistance was in the range of 40 to 80 ohms. Tests were also made by connecting only across the primary of the neutral current transformer. The output of the filters was observed with a cathode-ray oscilloscope. Output and input resistances of the filters were 500,000 and 1,000 ohms respectively. The input level of the filters was 8 volts. The voltage gain of the filters was approximately 15 decibels in the pass band or at the tuned frequency in the case of the single-frequency filters. The cutoff for all the filters was relatively sharp, being 45 decibels per 0.5 octave.

Tests

Of the eight machines tested, three were 40,000-kva 13.8-cv 150-rpm vertical water wheel generators at one location; 37,500 kva, 6.6 kv, 164 rpm at another; and four 20,000-kva 13.8-kv $171^{1}/_{3}$-rpm machines at another powerhouse. Residual harmonics were measured with each of the filters. Tests were made with the machines on the line under various conditions of loading from no load to full load on each machine type. Tests also were made with all filters on machines of each type running but not connected to the line. The residual was measured on each machine with the 4 to 10–kc band-pass filter. The relative sensitivity of the filters to residual harmonics and the slot discharge calibrating signal was observed. The relative sensitivity as a function of normal and moderately high coil surface resistance and for a strong and very minute discharge was determined on each machine type using all filter combinations.

Results

The results of the tests are outlined in Tables I and II. Briefly these may be summarized as follows:

1. It was found that the residual disturbance when the machine was on the line was high for any filter and that the surface discharge was undetectable under these conditions. One curious condition noted in this connection was that while the big jump in residual occurs when the machine was connected to the line, a further increase of between 3 and 5 to 1 occurred in going from no load to full load. The reason for this change with load is not apparent. To further explore this, two machines were paralleled (not connected to the line) and loaded up to rating with leading and lagging kilovolt amperes respectively. In this case there was no

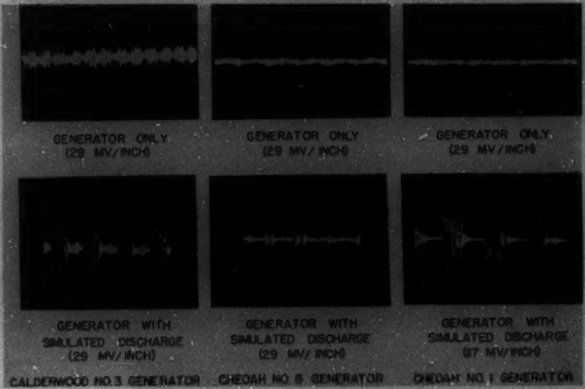

Figure 3. Sensitivity tests of discharge detection circuits

Table I

Filter Used	Residual Voltage—No Discharge Filter Output, Maximum Millivolts, Double Amplitude					Discharge—Disturbance Filter Output, Maximum Millivolts, Double Amplitude, Generator Isolated			
						Low Surface Resistance		High Surface Resistance	
	Full Load	Half Load	Quarter Load	No Load	Generator Isolated	Milli-volts	Per Cent Residual Discharge	Milli-volts	Per Cent Residual Discharge
Number 3 Generator, Calderwood									
1,046 cycles					348.0	380	91.0		
1,568 cycles					81.0	163	50.0		
2,349 cycles					81.0	130	62.0		
3,520 cycles					12.2	40	30.0		
2.5-kc high pass					174.0	522	33.0		
2.5 to 4-kc band pass					174.0	290	62.0		
4 to 10-kc band pass	580	425	275	185	12.6	146	8.6	87	14.5
Number 5 Generator, Cheoah									
1,046 cycles					58	64	91.0		
1,568 cycles					29	44	67.0		
2,349 cycles					14	46	30.0		
3,520 cycles					5	26	21.0		
2.5-kv high pass					26	130	21.0		
2.5 to 4-kc band pass					23	102	23.0		
4 to 10-kc band pass	240	208	160	96	5	107	4.7	93	5.4
Number 1 Generator, Cheoah									
1,046 cycles					32.0	50	67.0		
1,568 cycles					23.0	93	25.0		
2,349 cycles					14.5	102	14.0		
3,520 cycles					3.0	90	3.0		
2.5-kc high pass					14.5	960	1.5		
2.5 to 4-kc band pass					11.6	240	4.8		
4 to 10-kc band pass	382	313	313	290	6.0	348	1.7	230	2.6

difference in residual with change in stator amperes.

2. When the machines were off the line, the residual harmonics were found to be small compared to the calibrating signal for several of the filters. The 4 to 10–kc band-pass filter was found to be most effective. For this filter, the residual was in the range of 2 to 10 per cent of the discharge calibrating signal for the machine tested. Figure 3 illustrates the difference in disturbance between the residual and the discharge signal for the three machine types using the 4 to 10–kc band pass filter. In comparing these pictures consideration should be given to the difference in oscilloscope deflection sensitivity for the two conditions of test.

3. As would be expected, coil surface resistivities and the magnitude of the discharge voltage have an effect on the magnitude of the detectable discharge signal. Discharges were found to be definitely detectable for normal and moderately high surface resistivities with very minute discharge potentials. Based on the tests, it is estimated the discharging with surface resistivities up to several hundred thousand ohms per square would be detectable.

Summary

Slot discharge, if permitted to continue, will eventually damage insulation to the point where failure will occur. A simple method of detecting slot discharge with the unit running normally is desirable.

Table II. Residuals Measured for All Generators with 4- to 10–Kc Band-Pass Filter

Generator		Full Load, Millivolts	No Load, Millivolts	Generator Isolated, Millivolts
Calderwood	1			9
	2			35
	3	580	185	13
Cehoah	1	382	174	6
	2			6
	3			5
	4			4
	5	240	96	6

Based on the studies made on these machines, the following conclusions are believed to be justified:

1. The tests made have demonstrated the feasibility of detecting the existence of surface discharging by test from the neutral for the machines studied. It was necessary, however, to make these measurements with the generator isolated from the line because of an unusual amount of noise on the line at time of tests.

2. The 4 to 10–kc band-pass filter was shown to have the greatest sensitivity for discharge detection by this method.

3. It is believed that this method is generally applicable to machines which are not solidly grounded at the neutral. It was found that the disturbance was detectable by connecting across the primary of the neutral current transformers.

4. Where applicable, this method represents a definite test simplification since it is not necessary to shut the machine down or provide an external source of test voltage. Another possible advantage is that normal machine vibrations incident with machine operation are present during the test.

No Discussion

Network Analysis of A-C Machine Conductors

D. S. BABB
ASSOCIATE MEMBER AIEE

J. E. WILLIAMS
ASSOCIATE MEMBER AIEE

IN A previous paper,[1] the authors explained the use of equivalent transmission line circuits to represent the impedance of a-c machine conductors and pointed out that such equivalent circuits lend themselves to a quick solution by measurements on a network analyzer. Extensive and tedious calculations for determination of conductor impedances, especially when these conductors are of odd shapes, are thereby avoided. A recent paper by John F. H. Douglas,[2] also suggests the use of similar equivalent circuits.

In this paper it is shown that the impedance-frequency characteristics of complicated conductor and slot shapes can be determined with acceptable accuracy using a relatively simple network. The accuracy of the network method is tested on rectangular, T- and I-shaped conductors because a good analytical solution is known for these shapes.

The Elementary Network Section

A special type of elementary network section, Figure 1, is chosen since it gives exact values of inductance and resistance as the frequency approaches zero. A tee circuit or a Pi circuit might also be used. The tee circuit, however, yields high values of d-c inductance and the Pi circuit yields low values of d-c inductance. All three types of circuits will give exact values of d-c resistance. Table I gives the equivalent inductance when the equivalent circuit is divided into a number of elementary sections:

The elementary network section of Figure 1 may be used to represent an increment of the rotor conductor and slot. The R of the network section is equal to the resistance of 1-foot length of the conductor increment and the L of the elementary network is equal to $4\pi \times 10^{-9}$ henrys times the permeance across the slot increment per foot length of slot. Example calculations of L and R are given in the determination of the equivalent networks for the various bar shapes.

Network Solution for a Rectangular Conductor

Analytical solutions and network measurements are compared for a rectangular aluminum bar 1.5-inches deep and 0.3-inch wide. A resistivity of 21.2 ohms per circular mil foot is used for the aluminum. It is assumed that the conductor completely fills the slot. The total inductance of the slot is equal to the inductance of a small wire at the bottom of the slot, thus

$$L_1 = \frac{4\pi}{10^9} \times \frac{d_1}{W_1} \text{ henry per centimeter of stack length}$$

or

$$L_1 = \frac{4\pi}{10^9} \times \frac{1.5}{0.3} \times 2.54 \times 12 = 1.918 \times 10^{-6} \text{ henrys/foot length}$$

The resistance of the bar is

$$R_1 = 21.2 \times \frac{1}{1{,}500 \times 300 \times 4/\pi} = 37.0 \times 10^{-6} \text{ ohms/foot length}$$

For network measurements, circuit components of the above small magnitudes are not readily available. Therefore, both L and R are multiplied by 10^7 for convenience in arranging the network. Since the Q of the inductor units is better at higher frequencies, measurements are made with frequency $\times 10$ and inductance $L \times 0.1$. After these multiplying factors have been included the constants for the network are,

$R_{1n} = 370$ ohms
$L_{1n} = 1{,}918$ millihenrys

The network sections used correspond to Figure 1. Test data are obtained for an elementary network of 1, 2, 3, and 4 sections over a test frequency range of 50 to 3,000 cycles. This corresponds to the frequency-impedance characteristics of the conductor over a frequency range of 5 to 300 cycles per second. The test data is compared with calculated values in Figure 2 and Figure 3. The calculated values are determined from the equation

$$Z = \frac{1}{Y_1} \sqrt{Y_1 Z_1} \operatorname{ctnh} \sqrt{Y_1 Z_1} \qquad (1)$$

where

$$Y_1 = \frac{1}{R_1} = \frac{10^6}{37} \underline{/0^\circ} \text{ mho/foot}$$

$$Z_1 = j2\pi f L_1 = 12.03 f \times 10^{-6} \underline{/90^\circ} \text{ ohm/foot}$$

$$\sqrt{Y_1 Z_1} = \sqrt{0.325 f} \underline{/45^\circ}$$

Solutions for a T-Shaped Conductor

Analytical solutions and network measurements are compared for a T-bar composed of a rectangular bottom section 0.3-inch wide and 1.5-inches deep and a rectangular top section 0.1-inch wide and 0.4-inch deep. Since the bottom section is the same as the rectangular bar discussed

Table I

Type of Section	Equivalent Inductance 1 Section	 2 Sections	 3 Sections	 4 Sections
Tee	0.500 L	0.750 L	1.055 L	1.375 L
Pi	0.250 L	0.624 L	0.973 L	1.318 L
Figure 1	0.333 L	0.667 L	1.000 L	1.333 L
Correct L	0.333 L	0.667 L	1.000 L	1.333 L

Paper 51-369, recommended by the AIEE Rotating Machinery Committee and approved by the AIEE Technical Program Committee for presentation at the AIEE Fall General Meeting, Cleveland, Ohio, October 22–26, 1951. Manuscript submitted June 22, 1951; made available for printing September 12, 1951.

D. S. BABB and J. E. WILLIAMS are both with the University of Illinois, Urbana, Ill.

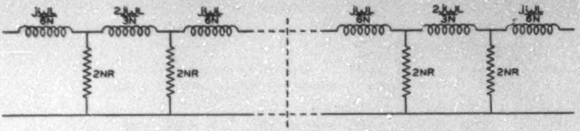

Figure 1. Elementary network sections. *N* is the number of sections

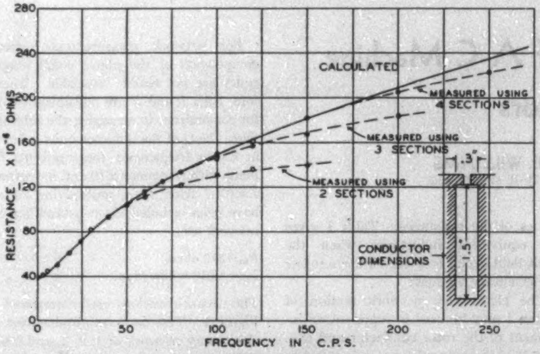

Figure 2. Comparison of measured with calculated resistance for a rectangular conductor using 2, 3, and 4 network sections

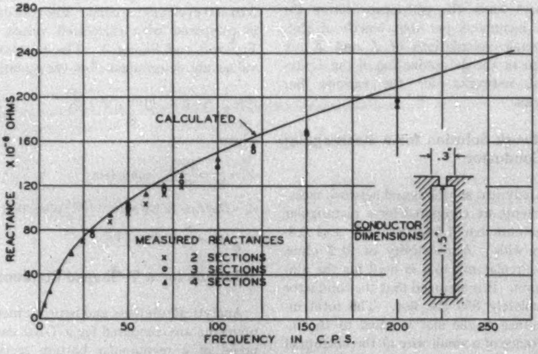

Figure 3. Comparison of measured with calculated reactance for a rectangular conductor using 2, 3, and 4 network sections

in the preceding paragraph, the network for that part will again be arranged using *R* of 370 ohms and *L* of 1,918 millihenrys. The total inductance of the top section of the slot

$$L_2=\frac{4\pi}{10^9}\times\frac{d_2}{W_2} \text{ henry per centimeter length of stack}$$

or

$$L_2=\frac{4\pi}{10^9}\times\frac{0.4}{0.1}\times 2.54\times 12=1.534\times 10^{-6} \text{ henry/foot length}$$

and the resistance of the top section is

$$R_2=21.2\times\frac{1}{100\times 400\times 4/\pi}=416\times 10^{-6} \text{ ohm/foot length}$$

Using the multipliers for *R*, *L*, and frequency as in the previous case for the rectangular conductor, the constants for the network which represent the top portion of the T-section are,

$R_{2n}=4{,}160$ ohms
$L_{2n}=1{,}534$ millihenrys

Four elementary network sections of the type shown in Figure 1 were used to represent the top part of the T-bar. The bottom part of the T-bar was represented by two elementary network sections. These six network sections required 12 decade inductors and 12 decade resistors. The settings of these circuit components starting with the meter end of the circuit are listed in Table II.

The input impedance-frequency characteristic of this circuit is measured over a frequency range of 50 to 3,000 cycles per second. This corresponds to the impedance-frequency characteristic of the T-bar over the frequency range of 5 to 300 cycles per second. The measured values of T-bar resistance and reactance from this data are plotted as a function of frequency in Figure 4.

Calculations of the T-bar resistance and reactance for various values of frequency are made by the method of reference 1. A transmission line representing the top section is terminated by the impedance of the bottom section. Then in the transmission line equations

$$E_R=I_RZ_A \tag{2}$$

where Z_A is the impedance of the bottom section.

$$E_S=I_R\left[Z_A\cosh\sqrt{Y_2Z_2}+\sqrt{\frac{Z_2}{Y_2}}\sinh\sqrt{Y_2Z_2}\right] \tag{3}$$

$$I_S=I_R\left[\cosh\sqrt{Y_2Z_2}+\sqrt{\frac{Y_2}{Z_2}}Z_A\sinh\sqrt{Y_2Z_2}\right] \tag{4}$$

The input impedance, Z_B, of the T-bar is then equal to

$$Z_B=\frac{E_S}{I_S}$$

$$=\frac{Z_A\cosh\sqrt{Y_2Z_2}+\sqrt{Z_2/Y_2}\sinh\sqrt{Y_2Z_2}}{\cosh\sqrt{Y_2Z_2}+\sqrt{Y_2/Z_2}\,Z_A\sinh\sqrt{Y_2Z_2}} \tag{5}$$

Dividing both numerator and denominator by $\cosh\sqrt{Y_2Z_2}$ gives

$$Z_B=\frac{Z_A+\sqrt{Z_2/Y_2}\tanh\sqrt{Y_2Z_2}}{1+Z_A\sqrt{Y_2/Z_2}\tanh\sqrt{Y_2Z_2}} \tag{6}$$

The calculated values of resistance and reactance as plotted in Figure 4 are a re-

Table II. Inductor and Resistor Settings for a T-Bar and an I-Bar

Unit No.	T-Bar Inductance, Millihenrys	T-Bar Resistance, Ohms	I-Bar Inductance, Millihenrys	I-Bar Resistance, Ohms
1			24	22,200
2			96	22,200
3			48	22,200
4			96	22,200
5	64	33,280	88	33,280
6	256	33,280	256	33,280
7	128	33,280	128	33,280
8	256	33,280	256	33,280
9	128	33,280	128	33,280
10	256	33,280	256	33,280
11	128	33,280	128	33,280
12	256	33,280	256	33,280
13	224	1,480	224	1,480
14	639	1,480	639	1,480
15	319	1,480	319	1,480
16	639	1,480	639	1,480

sult of application of the above method as calculated for numerous values of frequency.

Although each elementary network section has three inductor units, as shown in Figure 1, the tabulation shown in Table II combines the last inductance of a given section with the first inductance of the following section. For example, Unit 7 for the T-Bar is 64 plus 64 or 128 millihenrys; or Unit 13 is 64 plus 159.5 or 224 millihenrys.

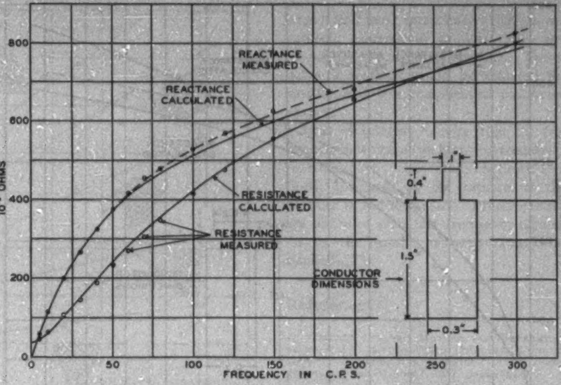

Figure 4. Resistance and reactance characteristics for a T-shaped conductor

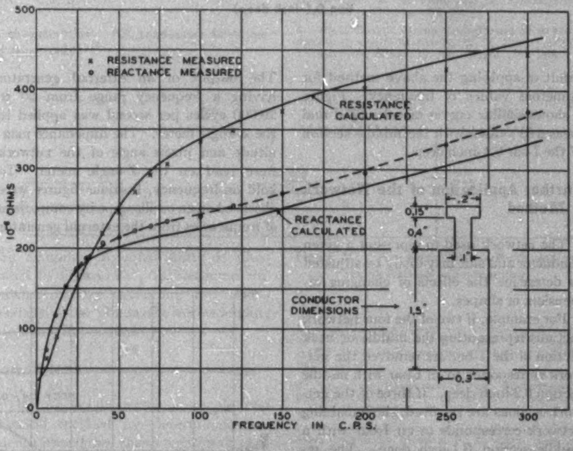

Figure 5. Resistance and reactance characteristics for an I-shaped conductor (middle section 0.4-inch deep)

Solutions for an I-Shaped Conductor

Addition of another rectangular section on the T-shaped bar gives an I-shaped bar. The new section used at the top of the I-bar has a width of .2-inch and a depth of 0.15-inch. The total inductance of the added section is

$$L_3=\frac{4\pi}{10^9}\times\frac{d_3}{W_3}\text{ henry per centimeter length of stack}$$

or

$$L_3=\frac{4\pi}{10^9}\times\frac{0.15}{0.20}\times 2.54\times 12=0.2875\times 10^{-6}\text{ henry/foot}$$

and the resistance of the added section is

$$R_3=21.2\times\frac{1}{150\times 200\times 4/\pi}=555\times 10^{-6}\text{ ohms/foot}$$

Using the same multipliers on R, L, and frequency as in the two previous cases the constants for the network representing the top section of the I-bar are,

$R_{3n}=5{,}550$ ohms
$L_{3n}=287.5$ millihenrys

Two elementary sections were used to represent the top part of the I-bar. Four decade inductors and four decade resistors are needed in addition to those used for the T-bar. The settings of the decade inductors and resistors for the I-bar network are included in Table II where they may be compared with the settings for the T-bar. Measured results for this network are plotted in Figure 5.

Calculations of the I-bar resistance and reactance for numerous values of frequency are made by an extension of the method used on the T-bar. The impedance, Z_I, of the I-bar may be computed with the use of the equation

$$Z_I=\frac{Z_B+\sqrt{Z_3/Y_3}\tanh\sqrt{Y_3Z_3}}{1+Z_B\sqrt{Y_3/Z_3}\tanh\sqrt{Y_3Z_3}} \qquad (7)$$

where Z_B is the T-bar impedance at the particular frequency, and

$$Y_3=\frac{1}{R_3}\underline{/0^\circ}$$

$$Z_3=2\pi fL_3\underline{/90^\circ}$$

The calculated curves of Figure 5 are a

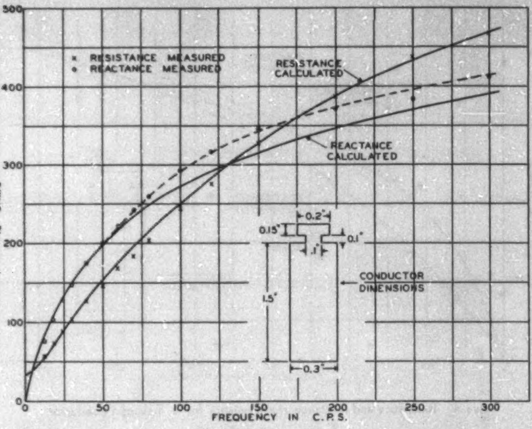

Figure 6. Resistance and reactance characteristics for an I-shaped conductor (middle section 0.1-inch deep)

result of applying the above method for numerous values of frequency. Figure 6 shows similar curves of calculated and measured values with the middle section of the I-bar 0.1-inch deep.

Further Application of the Network Method

The network used to represent a given conductor and slot may easily be adjusted to determine the effects of changing dimensions or shapes.

For example, if two of the four network sections representing the middle or neck section of the I-bar are removed the network corresponds to an I-bar with middle section 0.2-inch deep. If three of the network sections are removed, the remaining network corresponds to an I-bar with a middle section 0.1-inch deep. The resistance versus frequency curves plotted on Figure 7 were determined from measurements on the corresponding networks.

Figure 8 is a group of resistance-frequency curves determined from network measurements for conductors of various shapes. All conductors shown have the same area as the rectangular bar of Figure 2.

Measurement Method

The block diagram of Figure 9 indicates the method used to measure the impedance of the various networks discussed in previous sections of this paper. The output of an external generator having a frequency range from 20 to 20,000 cycles per second was applied to the Z-angle meter. The impedance magnitude and phase angle of the network were read on the Z-angle meter. To hold on-frequency, lissajous figures were observed on an oscilloscope by comparison of frequencies from the external generator and a standard 1,000-cycle-per-second oscillator.

Refinements in the Application of the Network Method

In the solution of all the conductor shapes discussed in this paper it was assumed that lines of force are parallel across the slot and that the conductor may be represented by a number of rectangular parts. The authors believe these assumptions satisfactory for T- and I-shapes and also for trapezoids with a small angle of taper.

Professor Douglas has shown in reference 2 that the above assumptions lead to considerable error for some conductor shapes such as circular shapes and trapezoidal conductors with a large angle of taper, and suggests that greater accuracy is obtained by subdividing the slot into areas bounded by lines of force which may be obtained originally by field mapping. The network method of this paper may be applied on the basis of Professor Douglas' division of the slot. The L and R of the various network sections may be chosen on the basis of the Douglas slot divisions and impedance-frequency characteristics of the conductor determined by measurements on the network.

An Alternate Network Arrangement

An alternate network arrangement consisting of resistors and capacitors

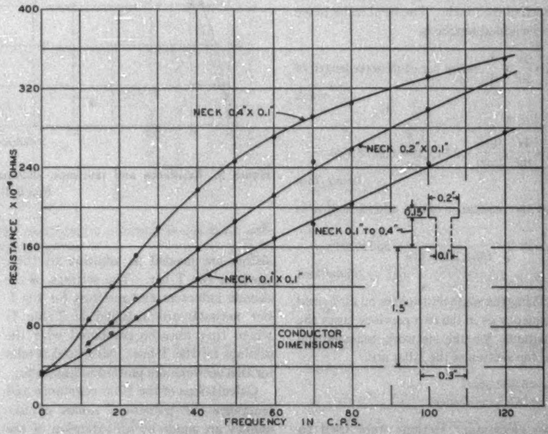

Figure 7. Effect of depth of middle section on resistance characteristics of an I-shaped conductor

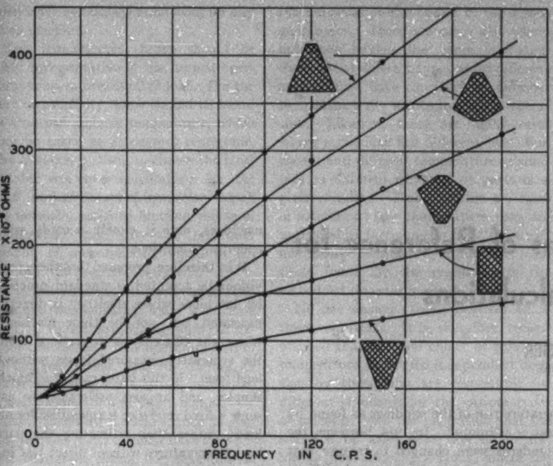

Figure 8. Effect of conductor shape on resistance characteristics. All conductors have the same area (measured values only)

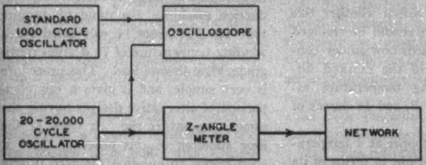

Figure 9. Block diagram of measuring circuit

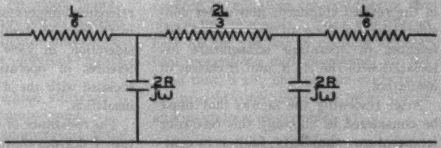

Figure 10. An elementary network section using resistors and capacitors

could be used instead of the one applied in this paper. Near perfect capacitors are more easily realized than near perfect inductors. To convert the network section of Figure 1 to one of resistors and capacitors, multiply the original circuit elements by $1/j\omega$ which permits the use of resistors in place of inductors and capacitors in place of resistors. This conversion assuming N equal unity is illustrated in Figure 10. All measured impedances on the circuit are then multiplied by $j\omega$ to obtain the corresponding conductor impedance.

Conclusions

This paper illustrates a simple and practical method for determining frequency-impedance characteristics of various conductor sizes and shapes. The largest and most complicated shape is accurately represented to 300 cycles per second by ten network sections. Fewer network sections would be required for smaller and less complicated conductor shapes.

It is of interest to note that the frequency to which a conductor is accurately represented by elementary network sections, increases as the square of the number of sections used. Precise results are obtained near zero frequency regardless of the number of network sections applied.

References

1. Circuit Analysis Method for Determination of A-C Impedances of Machine Conductors, D. S. Babb, J. E. Williams. *AIEE Transactions*, volume 70, part I, 1951, pages 661–66.

2. A Contribution to the Theory of the Deep-Bar Induction Motor, John F. H. Douglas. *AIEE Transactions*, volume 70, part I, 1951, pages 867–73.

3. Eddy Currents in Large Slot-Wound Conductors, A. B. Field. *AIEE Transactions*, volume 24, 1905, pages 761–88.

4. Heat Losses in the Conductors of Alternating-Current Machines, W. V. Lyon. *AIEE Transactions*, volume 40, 1921, pages 1361–1409.

5. The Calculation of the Armature Reactance of Synchronous Machines, P. L. Alger. *AIEE Transactions*, volume 47, February 1928, pages 493–513.

6. Starting Performance of Synchronous Motors, H. V. Putnam. *AIEE Transactions*, volume 46, 1927, pages 39–59.

7. The Development of Low-Starting Current Induction Motors, P. L. Alger. *General Electric Review* (Schenectady, N. Y.), volume 26, July 1925, pages 499–508.

Discussion

John F. H. Douglas (Marquette University, Milwaukee, Wis.): In securing high starting torques with low locked rotor currents, the rotor bar shown in Figure 5 of the paper seems to offer superior characteristics, in that the resistance is larger than the reactance. Thus it appears that a given starting performance can be secured with a less volume of active material.

Figure 8 of the paper conclusively proves the trapezoidal bar with the narrow section near the surface is superior to the coffin-bar, or the rectangular bar. Attention should be called to the fact (not shown in the paper) that the reactance of this bar is larger than its resistance at starting. Thus while an excellent bar shape, its use might require some extra stacking of laminations.

Standard Temperatures of Reference for Efficiency Calculations

P. L. ALGER
FELLOW AIEE

PRESENT AIEE and American Standards Association standards require that in calculating the efficiency of electric machines and transformers the I^2R losses shall be calculated for a winding temperature of 75 degrees centigrade. The question has arisen whether this reference temperature should be changed in the revised standards now under consideration, in view of the marked differences in operating temperature associated with the *A*, *B*, and *H* classes of insulation.

After reviewing the factors that must be considered in choosing this reference temperature—simplicity, fairness in comparing alternative designs, and true representation of operating conditions—the conclusion is reached that the standards should be revised; making the reference temperature for efficiency calculations 75, 100, and 140 degrees centigrade for typical Class-*A*, Class-*B*, and Class-*H* insulated machines, respectively. As an alternative, it is proposed that the reference temperature for efficiency calculations be 20 degrees centigrade plus the guaranteed temperature rise by the resistance or embedded detector method. This agrees with the above for normal Class-*B* and Class-*H* insulated machines.

It is proposed to retain the present provision in the Test Code for Polyphase Induction Machines,[1] that the reference temperature for the windings of machines whose efficiency is directly measured, as for small motors, shall be equal to 25 degrees centigrade plus the observed temperature rise.

As early as 1908, AIEE standards required that the calculated efficiency values for electric machines and transformers be based on a normal ambient of 25 degrees centigrade plus the actual temperature rise of the windings as found by test or estimated. In 1914, however, the standards were changed to require that all temperatures for efficiency calculations be corrected to 75 degrees centigrade winding temperature, and this provision has been in effect ever since.

The question has arisen whether this reference temperature should be changed in the revised standards now under consideration, in view of the marked differences in operating temperature associated with the *A*, *B*, and *H* classes of insulation.

The resistance of copper at a temperature *T* degrees centigrade, in terms of its value at 25 degrees centigrade, is:

$$R_T = [(234.5+T)/(234.5+25)]R_{25}$$

For example, if R_{25} is taken as unity, the resistance at 75 degrees centigrade is 1.19, at 100 degrees is 1.29, and at 140 degrees is 1.44.

There are three factors to be considered in choosing the reference temperature: simplicity, fairness in comparing alternative designs, and true representation of operating conditions.

The present AIEE Test Code for Polyphase Induction Machines provides that, when the efficiency is directly measured, the test efficiency be corrected to a standard ambient temperature of 25 degrees centigrade. It also implies that the same procedure be followed for machines whose efficiency is calculated from separately measured losses, even though the actual temperature rise of the winding is not determined by test. These rules make the reference temperature of the windings equal to 25 degrees centigrade, plus the observed temperature rise, which is different at each load. This procedure gives truly comparable values for different machines, and it closely accords with operating conditions.

It is, therefore, proposed that these provisions be accepted as standard practice for machines whose efficiency is directly measured, but not for those machines where the efficiency is determined from the separately measured losses without load tests. In this latter case, it is much simpler, and appears preferable, to assume a fixed reference temperature for all loads, rather than estimating the part load temperatures without direct test information.

Where the efficiency is calculated from separately measured losses, as for transformers and all large machines except induction machines, the standards require that the I^2R losses be calculated for a winding temperature of 75 degrees centigrade, regardless of load. This procedure is very simple, and it gives a fair comparison of alternative designs having the same temperature rise. In view of the long standing of this practice, there is good reason to question the need of any change. When the losses are separately stated, it is a simple matter to calculate the change in copper loss due to any difference between the expected and the reference temperature; and for these cases the 75-degree centigrade value may well be retained.

However, when the efficiency or the total losses are given as a single number, the use of 75-degree centigrade reference temperature does not give a fair comparison between machines with widely different temperature rises, nor does it accurately represent operating conditions for high temperature machines. It is proposed, therefore, that a higher reference temperature be adopted for those machines having a considerably higher than usual temperature rise, as machines with Class-*H* insulation, and that the

---

Paper 51-370, recommended by the AIEE Rotating Machinery Committee and approved by the AIEE Technical Program Committee for presentation at the AIEE Fall General Meeting, Cleveland, Ohio, October 22–26, 1951. Manuscript submitted June 20, 1951; made available for printing September 6, 1951.

P. L. Alger is with the General Electric Company, Schenectady, N. Y.

same value be retained at all loads for any given machine.

The temperatures chosen should be fairly representative of the normal operating temperatures at rated load. For the sake of simplicity, these should be based on a normal ambient temperature, which may be taken as 25 degrees centigrade. The question is, then, to choose the most suitable reference temperatures for the *A*, *B*, and *H* classes of insulation, which are normally assigned limiting values of temperature rise (by the resistance method of measurement) equal to 60, 80, and 120 degrees centigrade.

Typical machines will have actual temperature rises somewhat lower than these limiting values, say 50, 75, and 115 degrees centigrade. A temperature rise of 50 degrees, rather than 55 degrees, is taken as normal for Class-*A* insulation, in recognition of the large numbers of Class-*A* insulated machines, such as general-purpose motors, which have a 40-degree centigrade rating, corresponding to 50-degree rise by resistance. This leads to the conclusion that the most suitable reference temperatures are equal to the normal ambient, 25 degrees, plus these typical rises, or 20 degrees plus the guaranteed temperature rise. That is: 75 degrees for Class-*A* insulation, 100 for Class-*B* insulation, and 140 for Class-*H* insulation.

There will be cases where a machine is designed for a Class-*A* temperature rise, even though it is built with Class-*B* insulation; and the question thus arises whether the reference temperature in the standards should be fixed by the insulation class alone, as above indicated, or by the temperature rise stated in the design guarantees. There are cases also where machines having the same insulation class, but of different types or for different applications, have considerably different temperature rise values in normal operation. Likewise, there are many cases where a machine has different insulation classes and different temperature guarantees on different windings or parts of a given winding. Finally, there are cases of machines whose temperature rises are measured by thermometer only, these values being considerably different from those found by the resistance or the embedded detector method.

No one answer can be best for all of these conditions. It is, therefore, recommended that the final choice of reference temperature be left for independent decision by those who are responsible for different standards for the various types of machine, with the suggestion that the selection be made from one of the following five alternative plans, where the reference copper temperature to be assumed in making efficiency calculations shall be:

I. For machines whose efficiency is directly measured, as for small motors, the reference temperature of the windings shall be 25 degrees centigrade plus the observed temperature rise (different for each load).

II. For machines whose efficiency is calculated from the separate losses:

(1). The reference temperature of the windings shall be 75 degrees centigrade.

This is the present rule. It is recommended for all machines designed for a temperature rise at the rating of 65 degrees centigrade by resistance or less. It also may continue to be used for those machines for which the losses are separately tabulated, enabling the correction for a change in copper temperature to be readily made.

(2). The reference temperature of the windings shall be 100 degrees centigrade.

This rule is recommended for all machines designed for a temperature rise at the rating of more than 65 degrees centigrade, up to and including 90 degrees centigrade, by the resistance or the embedded detector method.

(3). The reference temperature of the windings shall be 140 degrees centigrade.

This rule is recommended for all machines designed for a temperature rise at the rating of more than 90 degrees centigrade by the resistance or the embedded detector method.

(4). The reference temperature of the windings shall be 20 degrees centigrade plus the guaranteed temperature rise at the rating.

This rule is an alternative to 2 and 3 above. It agrees with them for the usually specified Class-*B* and Class-*H* temperature rises.

It is believed that all of the requirements for the standards for rotating electric machines and transformers will be covered by adopting one or other of the above five proposals. They are offered here for the purpose of eliciting alternative suggestions and discussion, in the hope that, if any changes are made from the present rules, they will be as simple and as uniform as possible.

Reference

1. Test Code for Polyphase Induction Machines. AIEE Standard Number 500, August 1937.

No Discussion

Selection of the Electric Motors for Oil Well Beam Pumping

J. N. POORE
NONMEMBER AIEE

IT IS a well-known fact that sometime during the producing life of an oil well, it is necessary to apply artificial means of lifting the oil from the well. There are many ways in which artificial lift is applied to produce oil from the well, but there are five methods generally in use today. These are:

1. Beam pumping of individual wells.
2. Central power pumping of the wells in groups.
3. Gas lift.
4. Centrifugal bottom hole pumping.
5. Hydraulic bottom hole pumping.

Beam pumping of individual wells is used in about 90 per cent of the cases where artificial lift is applied. It is the purpose of this paper to:

1. Describe the action of beam pumping.
2. Discuss the conditions affecting the application of electric power to beam pumping.
3. Describe the types of motors available for this type of service.
4. Introduce a formula for estimating the necessary electrical horsepower required to produce oil by beam pumping methods.
5. Discuss the characteristics of the various types of electric motors applied to this method of pumping.
6. Describe tests conducted with the various types of motors used for beam pumping.

Description of Beam or Sucker Rod Pumping

The beam or sucker rod method of pumping consists of a single-acting reciprocating pump located at the bottom of the well and actuated by means of a string of sucker rods which are raised and lowered by some external means at the surface. The surface means may be a walking beam actuated by a connecting rod connected to a crank on a gear reduction unit. The gear reduction unit is usually connected by a V-belt drive to the prime mover whether it be an electric motor or an engine.

Pumping speeds vary widely. In most cases they range from 15 to 25 strokes per minute. Pumping units operating in this range or higher normally use a double reduction gear unit on the pump itself. When the pumping speed is under 10 to 12 strokes per minute, it is usually called slow motion pumping and usually a single reduction gear unit is utilized on such pumping units.

In those wells where it is necessary to pump considerable quantities of water along with the oil, it is often necessary to pump at high speeds up to 35 strokes per minute.

Figure 1 shows a typical beam pumping installation with an electric motor providing the motive power to drive the pumping unit.

Electric Motors for Beam Pumping

It is common practice today to utilize the squirrel-cage induction motor to drive a beam pumping unit. This motor offers the simplest, most inexpensive type of electric motor. The motor is used with a cross-the-line starter and, therefore, the simplicity of the squirrel cage motor and its control and the high operating efficiency of such equipment has resulted in its being almost exclusively used in the single-rated single-speed type.

It is necessary that the electric motor have sufficient starting torque to break away the load and accelerate it. The motor must be of such mechanical construction that it may be safely utilized outdoors with adequate protection from the weather. It must have sufficient horsepower capacity to pump continuously the peculiar cyclic pumping load. The squirrel-cage induction motor well meets these requirements.

Because it is possible to automatically control the pumping period by means of a time switch, it is doubly important that a motor have sufficient torque to break away and accelerate the load. The automatic feature obtained by means of a time switch on oil well pumping means that the unit will be started and stopped and restarted at predetermined periods of time on a repeat cycle without any pumper being available to perform the actual starting and stopping of the motor. This automatic operation must be possible in all types of weather conditions and under the starting loads imposed by the particular well with which it is used.

With double reduction pumping units the most widely used motor is the 6-pole 1,200-rpm motor. This speed motor is easily adapted through the proper application of the sheave on the motor shaft to provide pumping speeds in the range of 15 to 25 or 30 strokes per minute with a

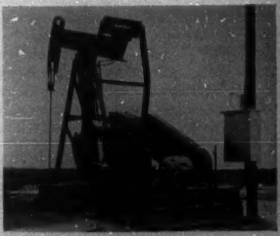

Figure 1. Typical electrified oil well beam pumping installation

---

Paper 51-372, recommended by the AIEE Rotating Machinery Committee and approved by the AIEE Technical Program Committee for presentation at the AIEE Fall General Meeting, October 22–26, 1951. Manuscript submitted August 2, 1950; made available for printing September 10, 1951.

J. N. Poore is with the General Electric Company, Dallas, Tex.

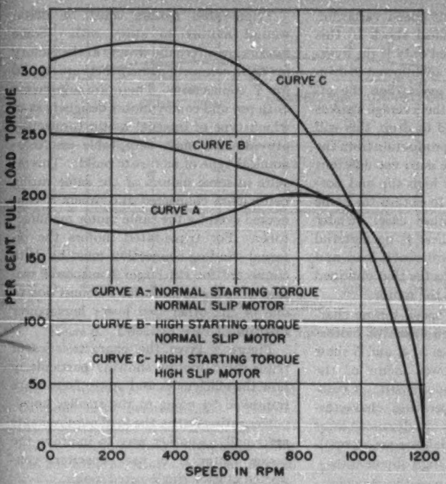

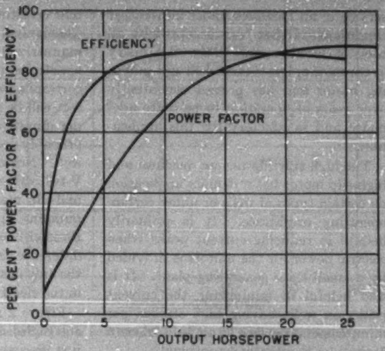

Figure 2 (left). Speed-torque characteristics of three types of motors used for oil well beam pumping

Figure 4 (above). Estimated characteristics for medium-slip (5 to 8 per cent) high starting torque motor used for oil well beam pumping

double reduction unit. If a single reduction unit is utilized, it is often necessary to resort to a lower speed motor, usually the 8-pole 900-rpm motor.

Types of Electric Motors

There are three types of squirrel-cage motors normally considered for oil well pumping.

These three types, well defined as to torque and current characteristics by the National Electrical Manufacturers Association (NEMA), are

1. Normal starting torque, normal-slip motor, NEMA classification Design B.
2. High starting torque, normal-slip motor, NEMA classification Design C.
3. High starting torque, medium and high-slip motors, NEMA classification Design D.

The normal starting torque motor is rarely used today on most oil well pumping applications involving an automatic control. The prime reason for its not being used is that the starting torque usually is only of the order of 150 per cent of full load torque. This per cent of starting torque is rather small to provide absolute assurance that the motor will start the load and accelerate it under all conditions. This motor might be used where the motor is manually started by an operator each time so that if it were necessary to "rock" the pumping unit in order to get it started because of the lack of sufficient starting torque, the operator would be available to perform this function. Since the advent of automatic operation where motors start and stop without operator attendance, it is not usually advisable to use the normal starting torque motor for this type of service. Normal starting torque motors are used in locations such as California, where there is no cyclic pumping and somewhat oversized motors are used because of changing well conditions.

The high starting torque, normal-slip motors are by far the most widely used for oil well pumping applications. The high starting torque, normal-slip motor has a starting torque of approximately 250 per cent of full-load torque and has proven adequate to start motors on pumping

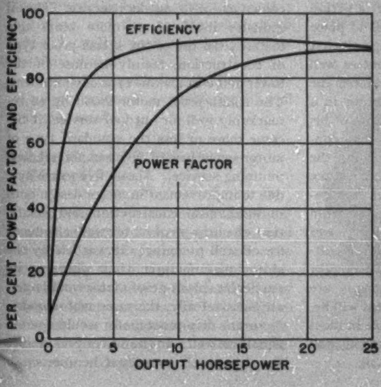

Figure 3 (left). Estimated characteristics for normal-slip (3 per cent) high starting torque motor used for oil well beam pumping

Figure 5 (right). Estimated characteristics for high-slip (8 to 13 per cent) high starting torque motor used for oil well beam pumping

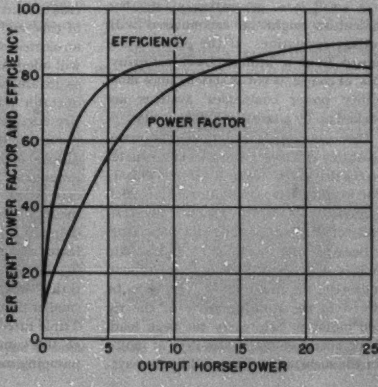

service in all localities under all weather conditions. It has been accepted by all users of electric motors in the oil industry as the more or less standard oil well pumping motor and has proved consistently over years of operation to be quite adequate and satisfactory for this application.

The high starting torque, medium and high-slip motor has a definite application on certain types of wells or under certain operating conditions. It is primarily helpful in reducing current peaks when electric power for the motors is provided by a small lease generating plant. It is also helpful in minimizing the current peaks on wells having high strokes per minute operation such as on wells where a high water to oil ratio is prevalent.

There exists today somewhat of a misunderstanding as to what constitutes a high-slip motor. There are in existence today two motors normally termed high slip by NEMA classification. These two high-slip type motors are one having a slip of from 5 to 8 per cent and the other having a slip of from 8 to 13 per cent. In order to differentiate between these two types of motors, the author has termed the 5 to 8 per cent as a medium-slip motor and the 8 to 13 per cent slip motor as a high-slip motor. (In NEMA standards, any motor with more than 5 per cent slip is termed a high-slip motor, Design D.)

On the normal duty cycle of a beam pumping unit, there are two power peaks on each pumping stroke, one when the rods and oil are lifted and the other when the counterweights are lifted. It is possible, unless certain precautions are taken, for the power peaks on a number of wells on a particular lease to sometimes coincide. The result is an extremely high power demand from the power source. As mentioned before, if this power source is a small lease generating plant, then difficulties might be encountered with voltage regulation. If the power is obtained from a utility power company, this, of course, is not as serious since most utility power companies' systems are backed up by a large system capacity.

One common method applied by many operators is to vary the sheave diameter on the driving motor by a very small fraction for the various wells on a lease. Such a practice considerably reduces the possibility of all motor power peaks coinciding.

Because the medium and high-slip motors slow down some as the peak load comes on, the motor allows energy to be stored in the rotating parts of the rig and motor to help carry the peak load. Some operators desire this type of motor for the cushioning effect on the power system resulting from this speed variation. Cushioning of mechanical shock in this manner will be obtained only if the average strokes per minute are allowed to drop correspondingly, and even then the effect will be small. If the average strokes per minute are allowed to drop, this will probably decrease the production from the well. Normal practice is to use different V-belt drive ratios for high-slip and normal-slip motors so as to obtain the same pumping speed in either case. Under these circumstances there is no material difference in mechanical-shock load and the only cushioning effect is that obtained in the electric input to the motor.

Figure 2 shows the speed-torque characteristics of the three types of motors just discussed. Figures 3, 4, and 5 show the efficiency and power factor of the three types of motors discussed. A comparison of actual operating characteristics from actual tests are discussed later in the article for the high-torque, normal-slip, medium-slip, and high-slip motors.

Triple-Rated Motors

In a great many of our oil fields today, the gradual encroachment of water into the oil producing zone, with the consequent necessity for lifting large volumes of water in order to obtain maximum oil production, has brought about the consideration and use of triple-rated motors in some instances. The triple-rated motor gets its name from the fact that the internal connections of the motor windings are brought out through the terminal box so that they may be externally connected in one of three different ways to obtain a high, a middle, or a low horsepower rating at a single speed. The triple-rated motor is advantageous primarily where it is known and anticipated that water encroachment will be gradual over a period of time and the operator desires to place an electric motor on his pumping unit that will adequately serve his present as well as future needs. In some instances the operator would purchase the motor in a size that would normally take care of his requirements during maximum load conditions and would reconnect it for the lower or middle horsepower rating to take care of his present horsepower requirements. The advantage he gains from doing so is primarily an increase in power factor and efficiency for the motor operating on the lower or middle horsepower rating when the load requirements are smaller than the final requirement will be. Triple-rated motors are available in most of the commonly-used sizes of oil well pumping motors.

Triple-rated motors must be delta-wound motors to start with. Some motors are internally wound at the factory for delta connection and others are wound for Y connection. There are arguments both pro and con by motor designers as to which type of internal motor connection provides the most acceptable and economical type of motors to build. This results in some motors of the same rating being delta connected and others Y connected even by the same motor manufacturer. For triple-rated motors the internal winding connection must be delta connected for the larger horsepower ratings in order to allow for reconnection to one of the other two lower horsepower ratings.

Figure 6 gives the characteristics of triple-rated motors showing particularly how the efficiencies and power factors are improved by going to the smaller horsepower ratings when the load requirements are small. Another way to improve the power factor is to use capacitors connected at each single-rated motor.

Motor Enclosures

There are three types of motor enclosures available for oil well pumping service. The three types of motor enclosures are:

1. Open drip-proof, 40-degree centigrade temperature rise motor.
2. Splash-proof, 50-degree centigrade temperature rise motor.
3. Totally enclosed-fan-cooled, 55-degree centigrade rise motor.

Practically all oil well pumping equipment is operated out of doors without protection from the weather. It was and still is common practice for manufacturers to recommend the totally enclosed-fan-cooled motor for outdoor service. The oil industry itself, 15 or more years ago, fostered the use of the splash-proof type of construction, mainly because of the lower first cost for this type of equipment. The splash-proof motor stood up so remarkably well for outdoor service, it became more or less the standard type of motor enclosure to be used for oil well pumping service. About five years ago, due to improvement in motor design both in mechanical construction and insulation, the drip-proof motor was introduced for oil well pumping. It was felt by the motor manufacturer that wherever its particular splash-proof motor would operate satisfactorily, the same motor manufacturer's drip-proof motor would operate equally as well. In the 5-year period since the drip-proof motor first became avail-

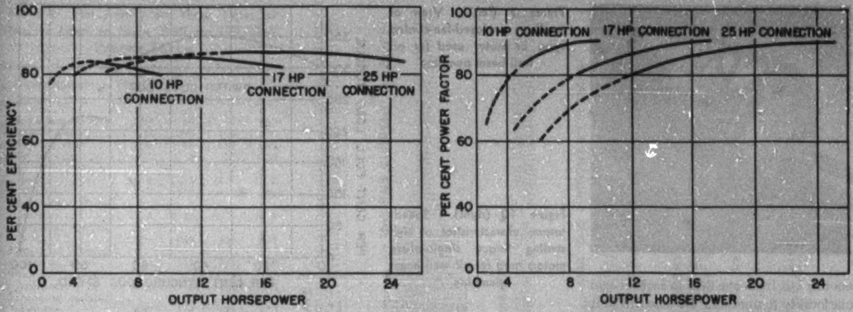

Figure 6. Estimated characteristics of a triple-rated high starting torque normal-slip (3 per cent) motor used for oil well beam pumping

able for oil well pumping service, several thousand have been installed. The reliable performance of this motor has justified the manufacturer's confidence in it and has led other motor manufacturers to introduce their drip-proof motors for this type of service.

The open drip-proof type motor has been used only in those areas and localities where the splash-proof motor has proven satisfactory in the past. In those areas, particularly along the Gulf Coast where salt-laden air is injurious to motor windings, the totally enclosed-fan-cooled motor has become somewhat the standard.

In areas where heavy snows introduce severe weather hazards, totally enclosed-fan-cooled motors outdoors or drip-proof motors in "dog houses" are sometimes used.

In practically no instance has it been necessary to resort to the totally enclosed-fan-cooled explosion-proof type of motor for oil well pumping service primarily because the well is capped when the motor is operating, and the motor is shut down when the well is open and the gas might possibly escape.

Figures 7, 8, and 9 show the three types of motor enclosures available for oil well pumping service.

Single Phase Oil Well Pumping Motors

It is normally recommended that whenever possible the 3-phase motor be used for oil well pumping service. Because the oil producer does not select the site of his oil well to coincide with the availability of 3-phase electric power, it is sometimes necessary for the producer to use single-phase power, usually from a Rural Electrification Administration system. In such instances, it is necessary to use single phase motors. Since most single-phase power systems are designed primarily for lighting and fractional horsepower motor service, the capacity of the single phase line usually limits the size of the single phase motors to a maximum size of $7^1/_2$ horsepower. Most Rural Electrification Administration systems will not allow motors larger than 5 horsepower to be installed on their systems without special consent.

Single-phase high starting torque, 440-volt or 220-volt motors in either the drip-proof, splash-proof, or totally enclosed-fan-cooled construction are available for this type of service. The same conditions with regard to break-away torque and accelerating torque that were true for 3-phase motors equally apply to single-phase motors.

Single-phase motors for the same horsepower size naturally carry a higher current than the corresponding 3-phase motor, and consequently larger control equipment is necessary. Also, the single-phase motor of the same horsepower rating as its 3-phase counterpart is considerably more expensive in first cost.

Single-phase motors of the capacitor-start, induction-run type are normally applied for oil well pumping service. A centrifugal-type switch or voltage responsive relay in the motor provides for cutting out the capacitor and starting winding when the motor reaches full speed. Figure 10 shows typical characteristics of the single-phase motor.

Determination of Motor Horsepower

The conditions which govern the horsepower required to pump a well are many and varied. A few of the more important factors are as follows:

1. Amount of fluid to be lifted.
2. Length of pumping period in hours.
3. Depth of pump in well.
4. Specific gravity and viscosity of fluid.
5. Size of pump.
6. Length of stroke and strokes per minute.
7. Weight of rods.
8. Existence of paraffin.
9. Possible water encroachment.

No two oil wells are exactly alike. Well conditions not only vary from one well to

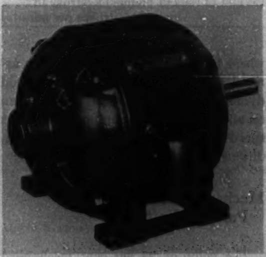

Figure 7. View of drip-proof type of motor used for oil well beam pumping

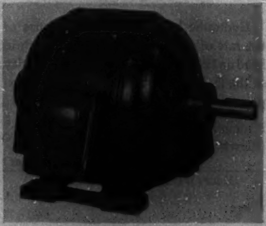

Figure 8. View of splash-proof type of motor used for oil well beam pumping

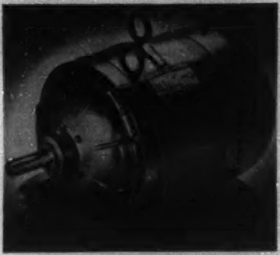

Figure 9 (left). View of totally enclosed-fan-cooled type of motor used for oil well beam pumping

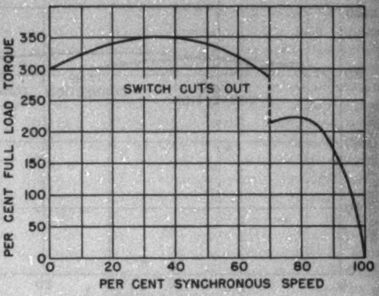

Figure 10 (right). Speed-torque characteristics of high starting torque single-phase motors used for oil well beam pumping

another but from one field to another and one locality to another. Because this fact is true, each well and local condition surrounding it must be taken into account in arriving at the necessary horsepower required to pump it.

Calculating the horsepower required is at best a rough approximation which must be substantiated by tests at the polished rod or at the motor as soon as possible.

The motor horsepower required to pump an oil well is composed of three main components. These components are:

1. Hydraulic horsepower.
2. Friction horsepower.
3. Motor heating factor.

To arrive at the estimated motor horsepower rating, the following formula is suggested:

$$\text{Motor horsepower rating} = \frac{(\text{Hydraulic horsepower}) + (\text{friction horsepower at polished rod})}{\text{Mechanical efficiency of pumping unit} \times \text{motor heating factor}}$$

Other formulas for estimating the motor horsepower rating are also in use, but any formula must recognize all of the factors shown in the above formula. A discussion of the components of the preceding formula will help to understand better the evolution of the formula.

Hydraulic Horsepower

Hydraulic horsepower is a measure of the rate of fluid production, the net fluid head on the pump, and the specific gravity of the fluid in the tubing. It may be expressed as follows:

$$\text{Hydraulic horsepower} = \frac{(\text{Barrels per day}) \times 42 \times 8.33 \times \text{specific gravity} \times (\text{depth in feet})}{(\text{Hours pumped daily}) \times 60 \times 33{,}000}$$

where:

42 = gallons per barrel
8.33 = pounds per gallon of water
60 = minutes per hour
33,000 = feet-pounds per minute per horsepower
Specific gravity = 1.0 for pure water and somewhat less for mixture of oil and water (0.95 is a good average value)

Barrels per day of fluid may be calculated as follows:

$$\text{Barrels per day} = \frac{3.1416 \times R^2 \times L \times S \times (\text{hours pumped daily}) \times 60 \times 0.75}{231 \times 42}$$

where:

R = radius of pump plunger in inches
L = effective length of stroke in inches
S = strokes per minute
60 = minutes per hour
0.75 = assumed volumetric efficiency of the pump
231 = cubic inches per gallon
42 = gallons per barrel

Friction Horsepower at Polished Rod

This component of the rated motor horsepower represents the work required to lift the weight of rods plus any friction of the pump itself. A suggested formula for estimating this friction horsepower is as follows:

$$\text{Friction horsepower at polished rod} = \frac{(\text{weight of rods in pounds}) \times (\text{stroke in inches}) \times (\text{strokes per minute})}{1{,}600{,}000}$$

where 1,600,000 is an empirical factor arrived at from hundreds of polished rod dynamometer cards which were taken on all types of wells, pumping at various speeds and under varying subsurface conditions.

Mechanical Efficiency of Pumping Unit

The value of 93 per cent mechanical efficiency of the pumping unit is based on a 3 per cent loss in the V-belts between the motor and the pumping unit, 2 per cent loss in the walking beam, pitman and sampson post and 2 per cent loss in the double reduction gears. These various losses are representative of modern designed pumping units and are an improvement over older designs.

Motor Heating Factor

The rating of an electric motor is based on a permissible temperature rise. The temperature rise is a function of the losses. The current-resistance losses are an important part of the motor losses. These losses in a motor vary as the square of the current. Motor heating is, therefore, a function of the rms value of the motor current.

The peculiar cyclic variation of motor current on an oil well beam pump is due to the up and down strokes of the rods and counterweights. The current value of the motor will hit a peak value twice during one complete pumping cycle. These peak values of current as well as the current values over the complete pumping cycle must be taken into account in calculating the rms or heating value of the motor current.

The pumping load carried by the motor is proportional to the average motor line current. In order to compensate for the higher rms heating current obtained because of the cyclic current peaks a motor heating factor is used. This motor heating factor will be slightly different for normal-slip motors as compared to medium or high-slip motors since the peak current values in the latter motors are somewhat less.

For normal-slip motors a motor heating factor of 0.7 is used for splash-proof and totally-enclosed motors and a factor of 0.8 is used for drip-proof motors. The drip-proof motor is a 40-degree temperature rise motor, and therefore has 15 per cent additional thermal capacity in it as

Table I. Test Results on Three Types of Motors Used on Same Well for Oil Well Pumping Service

Test Number	1	2	3	4
Motor horsepower	10	10	10	10
No load speed	1,200	1,200	1,200	1,200
Full load speed	1,160	1,140	1,080	1,080
Slip, per cent	3.33	5	10	10
Rated full load amperes	14.3	13.5	13.2	13.2
Voltage	440	440	440	440
Maximum starting current	77.5	72.45	69.9	72.9
Maximum starting voltage	450	450	456	456
Length of starting periods, cycles	119	147	127	156
Peak rms running current	36.8	27.8	24.8	28.45
Minimum running voltage	480	474	486	468
Rms peak amperes to full load amperes, per cent	257	206	189	216
Wattmeter maximum peak	5.64	4.8	4.50	
Wattmeter true peak	6.48	6.00	6.00	
Calculated effective rms heating amperes	11.61	8.83	8.03	
Effective rms heating amperes to full load amperes, per cent	81.2	65.4	60.8	
Kilowatts from watthour meter	2.332	3.54	2.545	2.88
Length of one complete stroke in cycles	174	187	191	179
Length of one complete stroke in seconds	2.9	3.12	3.183	2.985
Strokes per minute calculated from tests	20.7	19.25	18.84	20.1
Barrels fluid produced per day	327	304.5	298	318
Kilowatt hours per barrel fluid	0.171	0.279	0.205	0.217

a. Test number 3 made with 12-inch sheave on motor.

b. Test number 4 made with 13-inch sheave on motor to get well strokes/minute and fluid production approximately equal to other test motors.

compared to the other two types. The 0.8 factor for drip-proof motors takes into account the additional thermal capacity available.

The suggested formula for estimating the rated motor horsepower is, of course, subject to variation due to peculiar conditions of a particular well. Judgment and experience must be depended upon to supplement the calculations and to interpret them in terms of probable future conditions.

After an electric motor has been applied to a pumping unit, it is possible to quite accurately check the actual horsepower requirement. A watthour meter affords an accurate determination of the average motor horsepower provided the well is properly counterbalanced to eliminate any periods of power regeneration. The following formula can be used to determine the rated horsepower if the kilowatt-hours are known

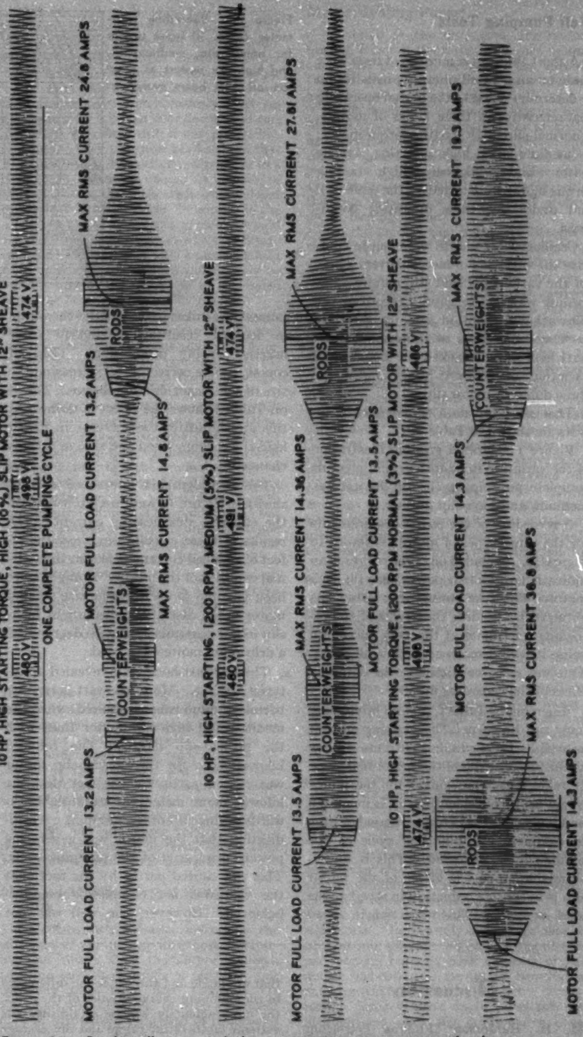

Figure 11. Graphic illustration of the variation in motor current and voltage over one complete pumping cycle for normal-slip medium-slip and high-slip motor as used on oil well beam pumping

$$\text{Motor horsepower rating} = \frac{\text{Kilowatt-hours consumed} \times 1.1}{\text{Hours of test} \times \text{motor heating factor}}$$

where motor heating factor = 0.7 for splash-proof and totally-enclosed fan-cooled motors, and 0.8 for drip-proof motors.

There 1.1 factor converts the average input kilowatts to average horsepower assuming 82 per cent motor efficiency.

Well Pumping Tests

A short time ago a number of tests were made on an oil well pumping installation to determine some of the actual operating characteristics of three types of motors. A normal-slip, high starting torque motor; a medium-slip, high starting torque motor; and a high-slip, high starting torque motor were tested on the same well and under the same operating conditions.

Oscillographic charts were run to compare the variation in motor current peaks for the various per cent slip motors. Recording wattmeters gave a record of the kilowatt consumption and its variation for the three types of motors. A kilowatt-hour meter checked the amount and variation of kilowatt-hours under the three different motor slips.

The tabulated data taken from these tests are shown in Table I.

Figure 11 shows a graphic illustration of the variation in motor current over one complete pumping cycle for the normal, medium, and high-slip motors.

A recording of the power requirements for the three types of motors is shown in Figure 12. Included on these curves is an indication of the true power peak for each motor. The true power peak value was obtained by holding the stylus of the recording wattmeter at the very maximum value it would reach at each peak point. This was done to eliminate the damping effect of the recording meter.

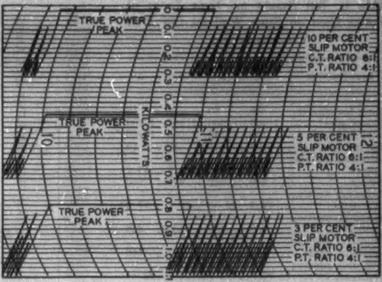

Figure 12. Recording wattmeter curves of input power for normal-slip, medium-slip, and high-slip motors as used on oil well beam pumping

Referring to Table I, several interesting facts can be seen. The starting current as well as peak running currents decline as the per cent slip of the motor increases. It takes somewhat longer for the motor to get up to speed as the slip is increased and it also requires a longer period of time to complete one pumping cycle as the motor slip is increased. This is understandable since one effect of the motor slip is to cause a reduction in speed as the load increases. This reduction in speed causes the strokes per minute of the pump to decrease resulting in slightly lower barrels per-day production. This, of course, can be corrected by increasing the size of the motor driving sheave. Test 4 on Table I shows the effect of doing just this and indicates the increase in motor load that occurs when the sheave ratio is changed.

The oscillographic curves of current shown in Figure 11 were used to calculate the effective rms heating current. The results of these calculations show the effect of reduced current peaks on the thermal capacity of the motor. It might have been possible to use a frame size smaller motor in the case of the medium or high-slip motor particularly if a 40-degree rise, a drip-proof motor were used.

The kilowatt-hour tests revealed an interesting fact. More kilowatt-hours per barrel of fluid were required with the medium and high-slip motor than with the normal-slip motor. The reduced kilowatt-hour for the normal-slip motor was caused partly by the fact that the kilowatt-hour meter was rotating backwards during part of the pumping cycle indicating that the motor was generating power during part of the pumping cycle. This was caused partly by the fact that the well was not completely counterbalanced. However, the well was not completely counterbalanced when the medium and high-slip tests were made either as can be seen from the power curves shown in Figure 12.

Some revisions in kilowatt hours consumption would have occurred had the well been completely counterbalanced in each test. It might be added, however, that the results obtained probably more truly depict actual operating conditions. It is very difficult to counterbalance completely a well and expect it to remain in balance over a long period of time. Well conditions vary too much from day to day and sometimes even from hour to hour.

If we accept the fact that the normal-slip motor does result in lower kilowatt-hours per barrel of fluid, then the saving in the cost of purchased power would shortly offset the reduction in first cost of a frame size smaller medium or high-slip motor.

References

1. Oil Production by Electric Power, W. G. Taylor. *AIEE Transactions*, volume 67, part II, 1948, pages 977–88.

2. Electrified Oil Well Pumping (Bulletin). Westinghouse Electric Corporation (East Pittsburgh, Pa.), April 1950.

3. Oil Field Electrification (Manual). General Electric Company (Schenectady, N.Y.), May 1947.

Discussion

M. H. Halderson (Phillips Petroleum Company, Bartlesville, Okla.): The load versus time relationship on a beam pumping installation is influenced by many factors and is different for each installation. For this reason, reaching general conclusions regarding horsepower requirement, pumping unit efficiency, electric motor load carrying capacity, and similar items requires that tests be made on many installations. As tests are made on greater numbers of installations, these various items are found to vary over a range of values. The more tests that are made and the wider the differences in the pumping characteristics of the wells, the more definitely will be established the extreme limits of the range and the average value of the items being checked.

Thirty-eight tests have been made in the Smackover Field in Arkansas to determine pumping unit efficiency, motor derating factors (also called heating factor or cyclic load factor), and power factor. The conclusions from these tests are different in a number of respects from those presented in the subject paper. These differences will be mentioned with the hope that other operators will be encouraged to make and report properly conducted tests.

Mechanical Efficiency of Pumping Units

The efficiency of a pumping unit on a given well is found by taking a polished rod dynamometer card and simultaneously measuring average motor input and motor rms current. Average motor output is calculated with the aid of the performance curves of the motor, and the efficiency of the pumping unit is found by dividing polished rod horsepower by average motor output.

Using the above method, pumping unit efficiencies on heavily loaded pumping units with double reduction gears have been found to range from 67 to 80 per cent. Efficiency will be less on lightly loaded pumping units and efficiencies have been found to be as low as 42 per cent. According to these results, a pumping unit efficiency of 93 per cent is higher than normally can be expected.

Motor Heat Factor (Derating Factor)

From ten tests of normal slip motors operating in the Smackover Field, the highest heating factor found was 0.70, the lowest 0.51. For six of the motors where rms current was within 20 per cent of rated current the highest heating factor was 0.65, the lowest 0.51. These factors are the ratio of actual average motor output on pumping service to the output that the motor would develop on a steady load at measured rms current.

These tests show that the use of a motor heating factor of 0.70 for normal slip motors would result in many such motors being undersized.

The data given in Table I of the paper shows that the heating factor for the normal slip motor on this particular test was only 0.33. The motor kilowatt input is shown to be 2.33. For an estimated motor efficiency of 85 per cent, the average motor output was 2.65 horsepower or 26.5 per cent of rated. The rms current was 81 per cent of rated, giving an approximate heating factor of $0.265/0.81 = 0.33$. If the data is reliable, this establishes a new low for the heating factor for normal slip motors. However, there are some questions on the data.

Tests in the Smackover Field of 11.5- to 8-per cent slip motors that were loaded within 20 per cent of rated rms current gave heating factors ranging from 0.68 to 0.91, or 34 to 40 per cent higher than found for normal slip motors. Hence, there is definitely more than a slight difference in the heating factor for the two types of motors.

The subject paper states that a watthour meter offers an accurate means of determining average power input to a motor driving a pumping unit, provided the well is properly counterbalanced to eliminate any period of power regeneration. A pumping unit is properly counterbalanced when the peak load on the rise of the sucker rods is equal to the peak load on the rise of the counterbalance weights. When the condition exists, there are many installations where there will be regeneration at the top and bottom of the stroke. On such wells, no position or counterweights can be found that will eliminate regeneration. A comment on why a watthour meter will not give average input if regeneration is present would be desirable, it being assumed that the watthour meter is not equipped with a ratchet that prevents reversal of disk rotation.

Well Pumping Tests

There are some questions regarding the data presented in Table I.

Difficult to reconcile is the fact that when a change was made from a motor with 3.33 per cent slip to a motor with 5 per cent slip, the kilowatt motor input increased 52 per cent while the rms current decreased 24 per cent. That such a great increase in kilowatt input could have simultaneously been accompanied by a 24 per cent decrease in rms current is very doubtful, if not impossible.

Another very questionable result is that a change from a 3.33 per cent slip motor to a 5 per cent slip motor caused an increase of 62 per cent in the kilowatt-hours used per barrel of fluid lifted. The differences in the efficiency of the two types of motors would not be more than three to five percentage points on a steady load. On a pumping load the difference in efficiencies would likely be less because of the reduction in rms when using the 5- to 8-per cent slip motor.

Some possible causes for the excessively great increase in kilowatt-hours per barrel are: (1) changing well conditions; (2) dragging of the brake on the pumping unit; (3) tightened stuffing box on the well, or (4) error in measuring kilowatt motor input.

Oral discussion of the paper at the 1950 General Fall meeting of the AIEE at Oklahoma City brought out the fact that the fluid production rate was measured on Test number 1 and then the producing rates on the remaining tests were found by assuming that production rate varied directly with strokes per minute. This procedure is not accurate enough where tests are being made to determine kilowatt-hours per barrel for different types of motors. Well conditions may change from one test to another and field tests have shown that for a given stroke and strokes per minute, producing rate changes with changes in the polished rod velocity versus time relationship.

J. N. Poore: Oil wells, by their nature, are extremely difficult to predict. No two wells are alike, and no well necessarily stays the same over extended periods. Because of this, a wide range of test results can be expected as the discussor has pointed out. It was not the intent of the author to draw specific conclusions from the one set of tests described, but rather to report results of one such test and add these results to many more tests that must be made before even good general conclusions can be drawn.

Mechanical Efficiency of Pumping Units

The discussor's remarks concerning the efficiency of pumping units is both interesting and timely. To the author's knowledge, no published results of pumping unit efficiency tests have been available. It would be very desirable to have additional data of this nature published as it becomes available.

Motor Heating Factor

As stated in the discussion, the motor heating factor is the ratio of average motor output on pumping service to the output that the motor would develop on a steady load at measured rms current.

In the discussion, the motor heating factor is arrived at by comparing the percentage horsepower output with the percentage rms current. This method does not take into account the power factor. The average horsepower should be compared with the rms horsepower to give the proper motor heating factor.

For the normal slip motor, on this particular test, the rms current and the average current was calculated from oscillograph recordings. This resulted in an rms current of 11.6 amperes and an average current of 7.17 amperes. Referring to a motor characteristic curve for the normal slip motor, it develops that at 11.6 rms amperes the rms motor horsepower would be 8.2. At 7.17 amperes average current the average motor horsepower output is 4.5. The ratio of average motor output to rms motor output then becomes 55 per cent for the normal slip motor. This is contrasted to the 33 per cent approximate heating factor arrived at in the discussion. The above ratio is arrived at by direct comparison of horsepower values applying for the average and rms currents. It disregards the motor kilowatt input measure with the watthour meter. This kilowatt reading is subject to error since the meter was observed to rotate backwards during the pumping cycle due to unbalanced conditions of the well.

It is admitted that the motor heating factor of a normal slip motor will be somewhat higher than for a medium slip or high slip motor. This is off-set to a great extent, however, by the fact that a 40-degree-centigrade rise normal slip motor has a 15 per cent service factor while the same medium or high slip motor has no service factor. This is in accordance with NEMA (National Electrical Manufacturers Association) recommendations. In a medium or high slip motor, the high resistance rotor introduces more inaccuracies in heating at a given load and hence a greater design margin is needed and the temperature rise is greater for a given increase in load due to higher rotor I^2R.

It is the conclusion of the author that only under very favorable conditions can a smaller medium or high slip motor be used, as compared to a normal slip motor, to offset the higher cost of the medium or high slip motor. In general, this motor should be used only where its higher starting torque per ampere, reduced peak currents or reduced rms currents, results in benefits to the user which will justify the extra investment. Some definite applications for the medium and high slip motor have been pointed out in the paper.

Turbogenerator for Use in Short-Circuit Testing

STERLING BECKWITH
FELLOW AIEE

LARGE short-circuit testing generators in this country, have in the past been built with speeds comparable to those of synchronous condensers, that is, they have been salient pole machines with from 10 to 16 poles.

It has long been recognized that the inherent reactance of a 2-pole machine is far below that of machines with salient poles, and consequently that 2-pole machines are the most logical for short-circuit testing if they can be made to withstand this heavy service.

The low reactance is essentially the consequence of using a forged and slotted cylindrical rotor construction which permits higher peripheral speed and therefore longer pole pitch.

Since the design and bracing of coils on large turbogenerators has been most satisfactory, in spite of the low reactance and consequent high currents and mechanical forces, the building of a 2-pole short circuit generator was considered feasible and one such machine has recently been completed, tested, and put in commercial service. This unit is shown in Figure 1.

Generator Design

The nameplate rating of this particular generator was arbitrarily taken as 21,500 kva as this corresponded with the physical size of the machine and served to maintain perspective when calculating reactances, losses, and other performance characteristics. On this rated base, a subtransient reactance of 2.9 per cent was calculated neglecting saturation, and the actual saturated value was well below 2 per cent.

The size of the machine was set by the requirement that 260,000-kva rms symmetrical single phase be developed at the end of one cycle on the secondary side of the test transformer which was supplied with the generator and which permitted testing at 69 kv, 46 kv, 34.5 kv, and 23 kv. However, the machine at its terminal voltage of 15 kv, 8.66 kv, 7.5 kv, or 4.33 kv, has a zero-time equivalent 3-phase rating of 1,280,000-kva rms asymmetrical. A typical short-circuit oscillogram is shown in Figure 4.

The duty cycle of the machine is such that it is suitable for operation at full voltage for two minutes out of ten during which period it is subject to two full voltage short circuits. The direct-connected slip-type induction motor is suitable for reaccelerating the generator after each short circuit as well as for starting duty.

The generator differs from the electrical proportions of an ordinary turbogenerator in two major respects. The first of these major differences is in the flux density, which in this machine is comparable to that which would exist in an ordinary turbogenerator if it were possible to raise the terminal voltage to 160 or 180 per cent of normal. The coil end forces increase as the square of the current and, as the current goes up in proportion to the voltage, this means that the mechanical forces on the winding have been increased by a factor of three because of the increased flux in the machine.

The second major difference is the increase in the short-circuit capacity obtained by reducing the cross section of copper in the stator coils, thus making the stator slot depth less than half of normal. This was permissible since the duration of the short circuit is not great enough to cause undue heating. The reduction in slot depth to half of normal means that the reactance was decreased to between one-half and two-thirds of its value with normal slot depth; thus, an additional factor of three was introduced in the magnitude of mechanical forces on the stator winding. Combination of these two factors, that is, a factor of three because of the slot depth and a factor of three because of the flux density means that the mechanical forces to be encountered were about nine times those that would have existed if the machine had had normal electrical proportions. Since a normal 2-pole machine is more difficult to brace than any other speed machine because of its long coil ends and inherently low reactance, the bracing problem was of considerable magnitude.

Figure 1. Two-pole 3,600-rpm generator capable of supplying a zero-time equivalent 3-phase short circuit current of 1,280,000 kva rms asymmetrical

---

Paper 51-373, recommended by the AIEE Rotating Machinery Committee and approved by the AIEE Technical Program Committee for presentation at the AIEE Fall General Meeting, Cleveland, Ohio, October 22–26, 1951. Manuscript submitted November 10, 1950; made available for printing September 4, 1951.

STERLING BECKWITH is with the Allis-Chalmers Manufacturing Company, Milwaukee, Wis.

Stator Coil Bracing

The bracing of the stator coil ends is similar to, but more complete, than on a normal turbogenerator as shown in Figure 2. However, a major difference from normal machines exists in the construction of the ends of the coils themselves as they were made of solid hard drawn copper bars instead of stranded copper.

Stator coils are of the conventional double-layer diamond-type construction used in all turbine generators built in this country. They are single turn coils made in halves. Series connections between coils are silver brazed. The stranding, which of course is transposed, is terminated near the end of the core. Use of such construction is permissible because the end zone fluxes are kept to a minimum by the use of nonmagnetic rotor coil support rings. (This material is the usual fully annealed nickel manganese chrome molybdenum material with which many years of successful experience are available on the largest turbine generators.)

Support of the stator coils up to the end of the stator core is obtained by the use of the usual slot wedges. The combination of the nonmagnetic stator coil support rings, plus the use of a patented slot in the stator end teeth, made it unnecessary to step back the end core parcels to avoid stray losses.

Support of the straight coil extension beyond the core is by means of heavy Bakelite linings inserted into machined spaces in the coil end finger plates. These finger plates are of the sectional nonmagnetic type which are standard for large turbogenerators and for which ample precedent was available.

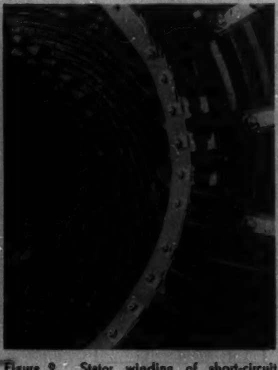

Figure 2. Stator winding of short-circuit test generator

Figure 3. Rotor and damper winding construction

Support of the diamond or diagonal portion of the coil ends is by means of the usual blocking and cording. The unsupported span between blocking is kept well below the calculated maximum safe span at every point. This span also was adhered to in designing the coil supports behind the coil ends.

The exceedingly high localized pressure on the mica at points of maximum pressure loading was carefully calculated and studied in the design of the blocking and supporting member.

The adequacy of the stator coil bracing was investigated by means of high speed moving pictures. It was found that very small motions could be accurately seen and analyzed, and some minor changes in the stator coil end blocking were made as a result of these studies.

Stator leads are brought out at both ends of the stator since twelve leads are required to permit external switching for 15,000-, 8,660-, 7,500-, and 4,330-volt operation. Leads from the stator coils to the machine terminals are of the usual solid strap construction with Bakelite lined metal clamps spaced relatively closer than normal.

End Turn Reactances

End turn reactance is of far more importance in this machine than in normal machines. A careful investigation was consequently made, and new methods were used to check available formulas. It is interesting to note that the transient value of end turn reactance differs considerably from the subtransient value, for the following reason:

End turn leakage fluxes are set up by continuous ampere-turn (or magnetic equipotential) surfaces, one edge of which terminates on the stator current and the other edge of which terminates on the rotor current. Consider the simplified case where the stator has one full pitch coil only and the rotor field winding consists only of one coil. Also consider that there is no damper winding. Under these conditions, the subtransient magnetic equipotential surfaces will extend from the stator coil end to the portion of the rotor body where the subtransient end currents are flowing in the solid forging. However, the transient magnetic equipotential surfaces will extend only from the stator coil end to the rotor coil end, and thus on the rotor will terminate considerably before they reach the subtransient current paths in the solid forging. Under extreme conditions, the span of these stator end turn to rotor end turn equipotential surfaces may differ $1^{1}/_{2}$ to one or more, thus accounting for the difference between the transient and subtransient values of end turn reactance.

Damper Winding

As the particular application required single-phase testing, an ample and rugged damper winding was necessary. Several types of damper windings were considered and past satisfactory experience with 2-pole synchronous motor windings, as well as past experience with machines which had been subjected to damaging single-phase currents or prolonged operation out of synchronism, were evaluated.

The damper winding chosen was one which was placed below the rotor slot wedges, but which was in direct metallic contact with the wedges and also with the rotor coil support rings. The winding was uniformly distributed around the periphery by the use of shallow slots in the pole centers as shown in Figure 3. The end windings were made effectively solid

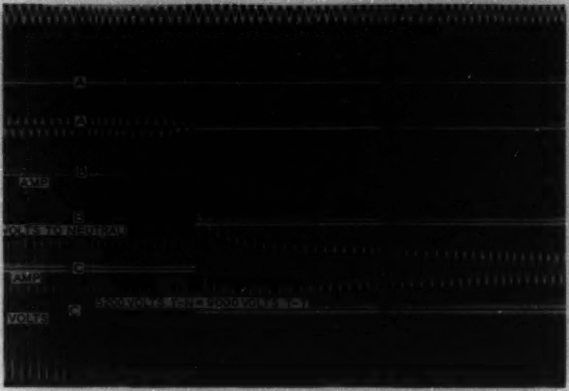

Figure 4. Typical single-phase short-circuit oscillogram from 60 per cent voltage

by choosing the proper angle for the "diamond" or angle portion at each end and also by appropriate choice of coil pitch.[1] Thus, the two layers of the damper winding were under high pressure metal-to-metal contact over substantially the entire area under the coil retaining rings. In addition to this, the upper and lower layers were brazed together at the ends to form the usual double layer diamond type, single turn winding of long pitch, but instead of being connected in series, each coil was short circuited on itself. The damper winding would undoubtedly have been satisfactorily connected by the large metal-to-metal contact area between layers on the end, but brazing was used in addition so that the damping would be about 96 per cent effective even if zero damping currents flowed between the contact areas.

Contact burning from currents flowing in the rotor slot wedges was avoided, since the damper winding was in direct high pressure contact with the wedges, thus very effectively short circuiting the joints between the individual wedges and between the wedges and the rotor coil retaining rings. Use of rotor slot wedges of higher resistance material also served to reduce wedge currents. Undoubtedly, some subtransient currents will flow in the solid rotor teeth as the damper winding is below the slot wedges and thus would be cut only by fluxes which would penetrate to that depth. Effectiveness of the above measures is shown by the fact that evidence of damping currents could be detected only where a few minute burrs had caused localized contact.

Flexible Mounting

Since the machine is to be short circuited single phase, the pulsating torque during the short circuit has to be absorbed by means of a flexible mounting. This type of mounting is not particularly new, but the magnitudes of the forces encountered were far greater than any others previously provided for with a flexible mounting. The mounting consisted of a special heavy H-beam along each side of the generator. The ends of the beam were supported from the foundation and the generator was fastened to the beam at two intermediate points selected to give the desired critical speed. Resonance with the fundamental single phase torque pulsation, or any of its harmonics was avoided. Figure 1 shows the general proportions.

Possible Synchronous Condenser Application

A machine of the type described might possibly have some usefulness for maintaining voltage at the middle of a long transmission line under transient conditions. The low inherent reactance permits the flow of large transient currents with relatively small voltage fluctuations at times of sudden load changes. It is not suitable for the combined function of continuously generating kilovars plus supplying high transient currents, but if continuous kilovar generation can be taken over by the usual static or rotating condensers, then the supplying of high transient currents can be performed by the special 2-pole machine considerably better than it can be done by the usual rotating condenser of the same nominal rating or physical size.

The Starting and Driving Motor

The generator is started and driven by a direct-connected 2-pole wound rotor induction motor which can be seen in Figure 1. Resistance is inserted in the rotor just prior to the short circuit so that the current drawn from the power supply will not be excessive. Typical power requirement curves are shown in Figure 5.

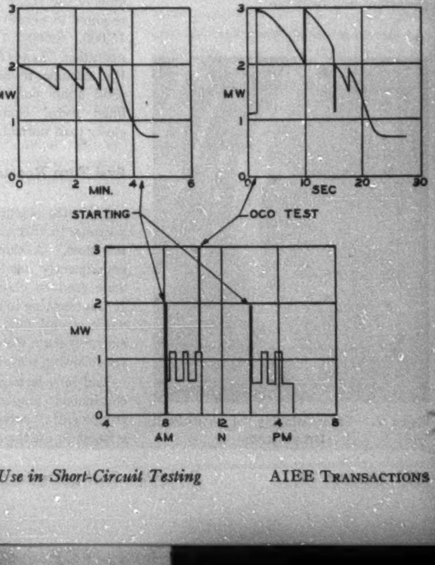

Figure 5. Typical power requirements for short-circuit test generator

An appreciable portion of the short-circuit torques are, of course, transmitted to the induction motor because of its mechanical inertia and may be amplified because of their transient nature combined with the flexibility of the drive shaft. During a single-phase short circuit under the worst conditions, the entire unit was calculated to slow down from its normal operating speed of 59.2 cycles to a speed of about 52 cycles in ten cycles. The maximum rate of deceleration at the peak of the pulsating torque is about 47,000 rpm per second. A torque limiting coupling was used between the induction motor and the generator in order to limit the torsional forces on the induction motor and in order to avoid possible build-up of these forces due to resonance.

Reference

1. The Development of Turbo-Generators of Brown Boveri Design, J. Prevost. *Brown Boveri Review* (Baden Switzerland), November 1941, page 367.

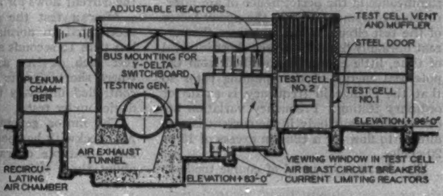
ADJUSTABLE REACTORS
TEST CELL VENT AND MUFFLER
STEEL DOOR
BUS MOUNTING FOR Y-DELTA SWITCHBOARD
TESTING GEN.
PLENUM CHAMBER
TEST CELL NO. 2
TEST CELL NO. 1
ELEVATION + 96'-0"
AIR EXHAUST TUNNEL
RECIRCULATING AIR CHAMBER
ELEVATION + 83'-0"
VIEWING WINDOW IN TEST CELL
AIR BLAST CIRCUIT BREAKERS
CURRENT LIMITING REACTORS

Figure 1 (left). Exterior view of building

Figure 2 (above). Cross section of generator foundation

Discussion

George H. Manke (Line Material Company, Milwaukee, Wis.): Mr. Beckwith has pointed out in his paper some of the design problems and some of the electrical advantages of a high speed generator over a slower speed generator for short circuit testing. To the user there are a number of other advantages besides those discussed by Mr. Beckwith which are of equal importance to the electrical features.

To the user one of the important advantages is the reduced weight of a high speed generator over a slower speed unit. The generator described by Mr. Beckwith weighs approximately one half that of a 900 or 720 rpm generator. This reduction in weight results in considerable savings to the user in that the first cost of the unit is reduced, the building in which it is housed and the foundation to support it can be much lighter in construction, and the moving of the equipment during installation or during possible repairs is not the problem that it would be with a heavier unit.

The generator described by Mr. Beckwith is housed in a relatively small building; the floor dimensions of the generator room are only 36 by 48 feet; although the equipment is arranged compactly into the room there is adequate space for dismantling any piece of equipment.

The relatively small weight of the generator makes it practical to move the various parts without the aid of an overhead crane. This means a large saving in building construction and results in a considerable saving in the first cost of such an installation.

The clearances required for lifting the various dust covers and other parts off the generator are small so that a relatively low ceiling is adequate. Adding these savings to the lower cost of the machine itself means that the economic balance is strongly in favor of the high speed generator over the slower speed design.

Figure 1 of this discussion shows the exterior view of the building, which is small and relatively simple in construction. Figure 2 shows a cross section of the generator foundation and again shows the simplicity of the building. The floor plan of

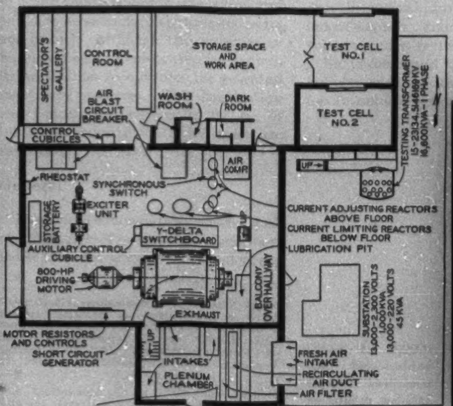
SPECTATOR'S GALLERY
CONTROL ROOM
STORAGE SPACE AND WORK AREA
TEST CELL NO. 1
TEST CELL NO. 2
AIR BLAST CIRCUIT BREAKER
WASH ROOM
DARK ROOM
CONTROL CUBICLES
TESTING TRANSFORMER 15-23134.5146169 KV 16,600 KVA-1 PHASE
UP
AIR COMPR.
RHEOSTAT
SYNCHRONOUS SWITCH
STORAGE BATTERY
EXCITER UNIT
CURRENT ADJUSTING REACTORS ABOVE FLOOR
CURRENT LIMITING REACTORS BELOW FLOOR
Y-DELTA SWITCHBOARD
AUXILIARY CONTROL CUBICLE
LUBRICATION PIT
800-HP DRIVING MOTOR
BALCONY OVER HALLWAY
SUBSTATION 13,000-2,300 VOLTS 1,000 KVA 13,000-220 VOLTS 45 KVA
EXHAUST
MOTOR RESISTORS AND CONTROLS
SHORT CIRCUIT GENERATOR
INTAKES
PLENUM CHAMBER
FRESH AIR INTAKE
RECIRCULATING AIR DUCT
AIR FILTER

Figure 3 (left). Floor plan of laboratory

Figure 4 (below). Size of various machines

the laboratory seen in Figure 3 of this discussion shows the compact arrangement of the equipment. Although the floor appears congested, there is adequate room to dismantle any piece of equipment for repairs, and Figure 4 shows the physical size of the various machines in the generator room.

The decrease in speed of the generator during the testing interval has proved to be of little consequence in practical testing even though the mass of the machine is not large and though it is essentially coasting during the test. Experience has proved that a slight change in frequency is of little significance in the performance of arc interrupting equipment. Since the power factor of the test circuit is low and since the current normally flows for a very short interval of time, little energy is absorbed from the potential energy of the spinning rotor so that the change in frequency is small for ordinary testing. Frequency variation becomes important only if the current is permitted to flow for a time in excess of 15 or 20 cycles.

The decrease in speed of course tends to lower the generated voltage. The voltage also is reduced by the decay of flux in the generator rotor as current is drawn in the test circuit. These characteristics are largely neutralized by "forcing" the field. This means that some resistance is removed from the d-c field circuit at the instant that the test circuit is closed. The increase of field current then tends to compensate for the decay of flux in the rotor and the speed reduction, thus holding the voltage essentially constant during the duration of the test. "Forcing" the field is especially effective in maintaining the voltage when the current flows for longer than 8 cycles.

After a test the generator can be reaccelerated to normal operating speed in less than 15 seconds so that it is possible to test such devices as oil circuit breakers where short circuits must be repeated at controlled intervals to properly prove the device under test.

The motor generator set described by Mr. Beckwith has been in very satisfactory and profitable operation for a matter of about three years. The modern machine together with modern controls and measuring equipment has proven to be very very flexible, yet simple to operate. Aside from the analysis of the oscillograms and other data only two men are required to keep the station in full scale operation.

All in all, this installation has proved that the 3,600-rpm turbo type of generator is a practical source of short circuit currents.

Sterling Beckwith: Mr. Manke has pointed out some of the advantages of the small 2-pole machine, from the user's viewpoint, as compared to the large slow-speed units formerly employed for short circuit testing.

The compact arrangement of equipment and ingenious design of the laboratory are clearly shown in Mr. Manke's illustrations. The system of control and the protective devices employed are equally outstanding.

Both Mr. Manke and R. H. Earle of the Line Material Company are to be congratulated for achieving, through foresight and careful planning, a major forward step in short circuit laboratory design.

Evaluation of Butyl Insulation for Outdoor Instrument Transformers

J. A. McDONNELL
MEMBER AIEE

H. E. CRABTREE
NONMEMBER AIEE

ADVANCES in electrical insulation development often result in progress in instrument transformer design. These two advances take place concurrently because one of the primary functions of an instrument transformer is that of an insulator. Regardless of whether a high voltage or a high current is to be measured, the end device must be insulated from the circuit voltage, which is normally of a dangerously high value.

Two years ago, an outstanding advance in instrument transformer design was made possible by the introduction of a special transformer butyl compound. Molded butyl compound made possible an entirely new concept in a device as old as the use of alternating current. Another step in the progress of measurements now has been made. This same molded butyl insulation has been successfully applied to a new transformer for use indoors and outdoors on secondary circuits (600 volts and below). Although the properties of butyl pertinent to indoor use were known, its application to outdoor use presented many new problems. The investigation and conclusions concerning the use of butyl compound in outdoor service are described in this paper.

General

It has been common practice among all manufacturers of instrument transformers to use two general types of insulation, determined by the operating voltage involved. Up to about 15,000 volts, a dry type or compound impregnated construction is employed. Above that voltage, liquid-filled designs are used. For outdoor service, it has been common design practice to place the insulated transformer in a waterproof metal casing with porcelain bushings.

With the development of a molded butyl insulation, a new dry type material was added to those available to design engineers.[1] This synthetic elastomer possesses many outstanding advantages over other dry type insulations and is being used successfully and to an increasing extent on a line of 5,000-volt indoor metering transformers.[1] This transformer is illustrated in Figure 1.

The use of this molded butyl compound has now been extended to include outdoor, as well as indoor, service. The first indoor-outdoor transformer, for low-voltage service, is illustrated in Figure 2.

Butyl compound has several outstanding characteristics that make it suitable for an outdoor insulation: low-moisture absorption, good corona and sunlight resistance, excellent adhesion to copper, very low-power factor, and good resistance to mechanical damage.

By the use of butyl compound, large expensive cases of metal and porcelain are no longer necessary on low-voltage outdoor transformers. In addition, the compact designs made possible by molded insulation result in a universal low-voltage transformer, small enough to meet the standardized mounting dimensions for indoor service and completely waterproof for outdoor service. Figure 3 compares the new butyl design with the conventional outdoor metal-porcelain construction and a typical indoor transformer with asphalt-impregnated insulation. Indoor-outdoor designs offer definite possibilities for standardization to both the user and the manufacturer.

Butyl gum is a synthetic elastomer (GRI) developed just prior to and during World War II. The gum for electrical usage is composed 97 to 99 per cent of polyisobutylene, plus 1 to 3 per cent of isoprene necessary for vulcanization. The polyisobutylene molecule, since it has no double valence bonds, is in an exceedingly stable molecular condition.[3,4,5] This results in unusually good chemical stability and resistance to oxidation.

The major use of butyl gum at present is in inner tubes, since it is extremely impervious to air. Special compounds with excellent electric properties are being widely used as cable insulation.

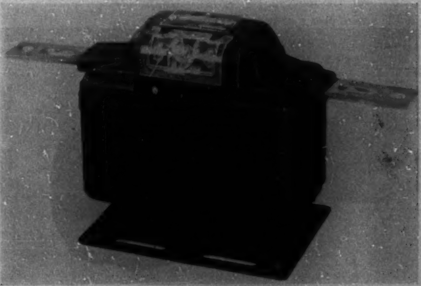

Figure 1. 5,000-volt butyl-molded current transformer for indoor metering service

---

Paper 51-374, recommended by the AIEE Transformers Committee and approved by the AIEE Technical Program Committee for presentation at the AIEE Fall General Meeting, Cleveland, Ohio, October 22-26, 1951. Manuscript submitted June 22, 1951; made available for printing September 7, 1951.

J. A. McDonnell and H. E. Crabtree are both with the General Electric Company, West Lynn, Mass.

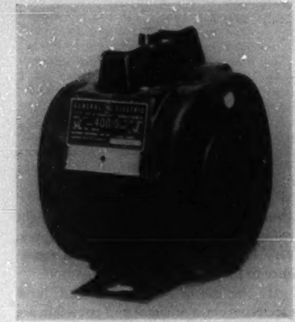

Figure 2. Butyl-molded current transformer for indoor and outdoor metering service

To make the gum suitable for molded transformer insulation, it is mixed with several other ingredients. These fillers, plasticizers, and vulcanizing agents make up about 60 per cent of the final compound.

In the molding process, the uncured compound is forced into a heated mold, which forms the outside contours of the transformer and also locates the core with windings, terminals, and mounting base. Figure 4 illustrates the insert ready for molding. When filled, the loaded mold is heated under closely controlled conditions to cure or vulcanize the butyl into a solid, homogeneous mass, possessing excellent insulation properties.

When cured, the transformer is removed practically complete, needing only to have excess molding flash removed and the secondary hardware and nameplate installed to make it ready for final test and shipment.

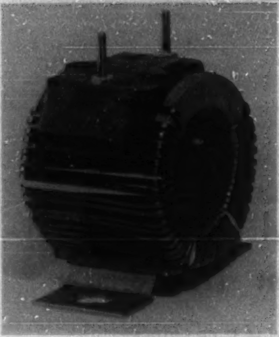

Figure 4. Indoor-outdoor transformer insert ready for butyl molding

Properties of Butyl Insulation

Once butyl had been proved as an indoor transformer insulation, the next consideration was its suitability for outdoor use as well. To determine the possibilities, its properties were evaluated in terms of the performance required and the various conditions that such an insulation would be required to meet.

Specifications for a suitable outdoor insulation were drawn up. Tests were then made to determine whether the material met these specifications.

Test Results and Conclusions

Summary of Results

The properties of butyl compound required for outdoor use were determined by test. It was found that molded butyl is excellent for certain outdoor applications.

An effective waterproof casing made of butyl molded as an integral part of the transformer has been developed. The butyl casing is sealed to the terminals and other metal parts during molding to provide watertight seals for outdoor usage. The result is a butyl casing that performs all of the functions of an outdoor housing made of metal and porcelain.

Figure 3. Butyl-molded current transformer for indoor and outdoor metering service shown with the conventional asphalt-paper porcelain-steel outdoor type and the conventional asphalt-paper indoor type

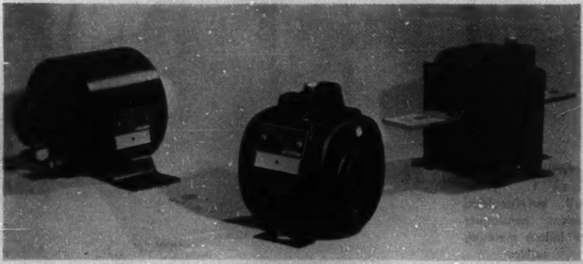

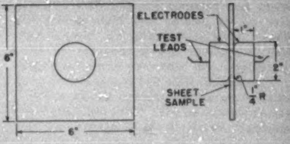

Figure 5. Water penetration sheet sample. Samples were immersed in water for aging, then tested in air for capacitance and power factor

Results—Detailed Discussion

Resistance to Water Penetration: The resistance of butyl to the penetration of moisture was determined by the use of water-immersed samples of various known thicknesses. Molded and sheet samples were used as shown in Figures 5 and 6. The molded samples contained wire-mesh electrodes, so that any moisture that penetrated the butyl layer would distribute itself and be readily detected. These samples were immersed in water and then tested at intervals of time. Tests of power factor and capacitance were made to determine the rate and degree of moisture penetration through the layer of molded butyl.

The results of these tests are shown in Figures 7, 8, and 9. For a 1/8-inch thick layer of butyl, a period of 29 days' immersion at 75 degrees centigrade was required for an appreciable change (5 per cent) in power factor. In water at room temperature (approximately 25 degrees centigrade) there was no change after im-

Figure 6. Water penetration molded sample. Samples were immersed in water for aging, then tested in air for capacitance and power factor

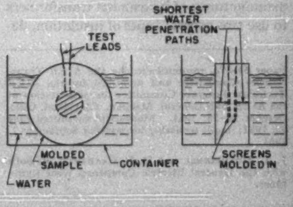

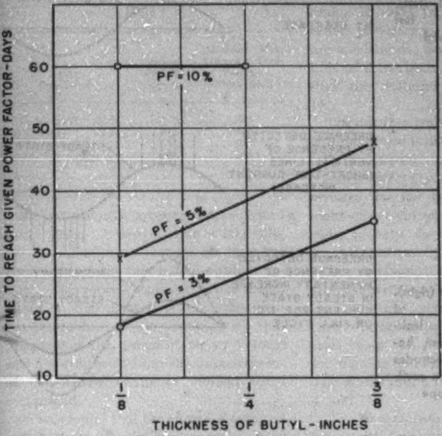

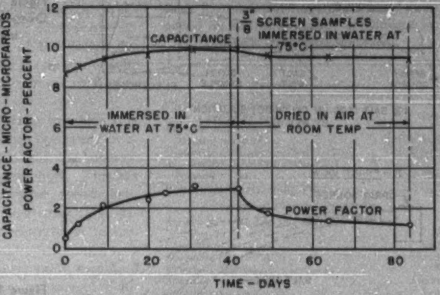

Figure 7 (left). Water penetration of molded butyl at 75-degrees centigrade. Time for wire mesh samples to reach 3, 5, and 10 per cent power factor

Figure 9 (above). Water penetration at 75 degrees centigrade and drying at room temperature of molded butyl

mersion for 55 days. After being immersed in water for a sufficient time to change the power factor, recovery rate by drying was very rapid. This is shown in Figure 9.

In order to provide a waterproof casing for the transformer, the butyl required for insulation on the outside surfaces was increased. An added thickness of approximately 1/8 inch is considered adequate to prevent moisture penetration.

Resistance to Weathering: Resistance to weathering was found to be excellent as determined by accelerated weathering tests made on both material samples and transformer samples. After extended actual weathering in an industrial atmosphere, transformer samples were operating satisfactorily and showed no adverse effects when tested. On an actual outdoor service installation in exceptionally corrosive atmospheres, trial transformers are still operating satisfactorily after more than a year's service.

Mechanical tests made on samples of butyl compound strips showed that the hardness and elasticity improved as shown in Figure 10 after aging for twelve months under various conditions. Examination of sample transformers after three years of outdoor aging showed that the butyl insulation was in excellent mechanical condition.

Watertight Adhesion to Metals: In order to prevent the possibility of moisture entering the transformer, a method was developed for sealing the molded butyl to the protruding metal parts of the transformer. Samples of the seal tested under a pressure of ten feet of water for a continuous period of fourteen days displayed no signs of leakage.

Resistance to Surface Voltage Creepage: One of butyl's most important properties which had to be evaluated was its resistance to voltage creepage. Creepage is the phenomena of leakage current flowing along a surface from one electrical potential to another. On a current transformer, there is a considerable potential difference from the primary to the secondary winding and from the primary to ground. Because of the exposed terminals, the voltage creepage characteristics are of considerable importance.

In this investigation, the critical data have been obtained in order to utilize the creepage characteristics for the utmost benefit in the finished transformer design.

The test method consisted of applying voltage between two parallel bar-type electrodes placed on the surface of the sample. The butyl surface was inclined approximately 15 degrees to the horizontal and subjected to a salt mist. This is shown in Figure 11. The 15-degree slope was used in the tests because it rep-

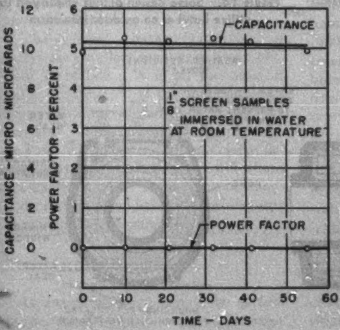

Figure 8 (left). Water penetration of molded butyl at room temperature

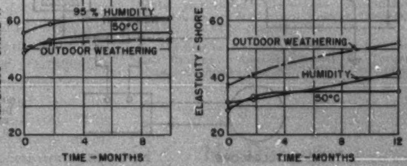

Figure 10 (right). Mechanical properties of molded butyl. Hardness and elasticity versus aging time under various aging conditions

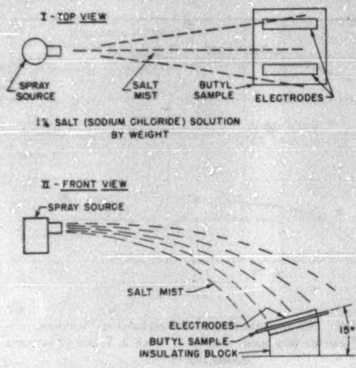
I - TOP VIEW
SPRAY SOURCE
SALT MIST
BUTYL SAMPLE
ELECTRODES
1% SALT (SODIUM CHLORIDE) SOLUTION BY WEIGHT
II - FRONT VIEW
SPRAY SOURCE
SALT MIST
ELECTRODES
BUTYL SAMPLE
INSULATING BLOCK
15°

Figure 11 (left). Creepage test method

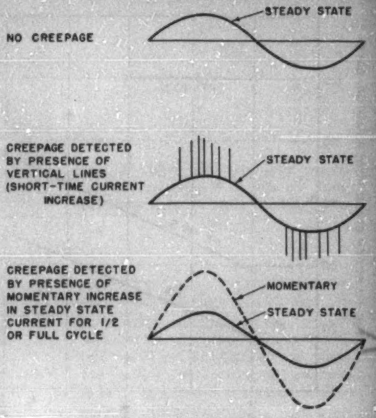
NO CREEPAGE
STEADY STATE
CREEPAGE DETECTED BY PRESENCE OF VERTICAL LINES (SHORT-TIME CURRENT INCREASE)
STEADY STATE
CREEPAGE DETECTED BY PRESENCE OF MOMENTARY INCREASE IN STEADY STATE CURRENT FOR 1/2 OR FULL CYCLE
MOMENTARY
STEADY STATE

Figure 13 (right). Detection of creepage leakage current between electrodes as seen on oscilloscope

resented the worst practical operating condition, since transformer surfaces are designed to have a slope of greater than 15 degrees. A salt solution of 1 per cent sodium chloride by weight was used.

The presence of creepage was determined by viewing the creepage current on an oscilloscope. Figure 12 shows the electrical test circuit used. The creepage was shown on the oscilloscope as very short-time increases in current or as a change in current during a single cycle of applied voltage. The detection of creepage is shown in Figure 13. This test method provides a sensitivity of detection that is not possible by direct visual perception of creepage.

Using this method of testing, the worst creepage condition to be expected during the normal service of outdoor transformers was determined. It consists of a very dirty surface with a water mist directed upon it. Dirt collected in an industrial atmosphere was used for this test. This condition was very unstable, since the dirt washed off rapidly, causing the creepage to stop. It was found that a salt mist was an equally bad condition and, in addition, was stable and reasonably repeatable. The salt spray was, therefore, adopted as a practical test method, since it was equivalent to the typically poor condition of dirt from an industrial atmosphere plus a water mist.

Tests were made to determine at what minimum voltage creepage occurred. It occasionally started at a minimum voltage gradient of 450 volts per inch under the test conditions used. Creepage usually started at a voltage gradient above 800 volts per inch. Visual creepage occasionally occurred at a minimum voltage gradient of 800 volts per inch. Visible creepage usually started at a voltage gradient above 900 volts per inch.

The effects of high-surge voltages added to the impressed 60-cycle voltage were investigated. Tests show that there is no change in the creepage start voltage due to the addition of voltage surges. Flashover or creepage that occurs during voltage surges does not continue after the surge and, therefore, does not cause damage to the surface.

Since creepage starts at a relatively low voltage, tests were made to determine its damaging effects. At a potential gradient of 2,000 volts per inch across the surface, visible creepage occurred and caused visible damage after 80 hours of continuous operation. A potential gradient of 1,000 volts per inch produced creepage that was detectable with the test equipment. After 80 hours of continuous operation, some damage had occurred and sparking was visible occasionally. At 300 volts per inch, creepage was neither visible nor detectable on butyl and produced no effect after 100 hours of continuous operation under the salt mist.

It was concluded, therefore, that a satisfactory butyl outdoor design must operate at a sufficiently low-surface voltage gradient to prevent creepage from occurring. This has been accomplished in the transformer design by allowing

Figure 12. Electrical circuit for creepage test

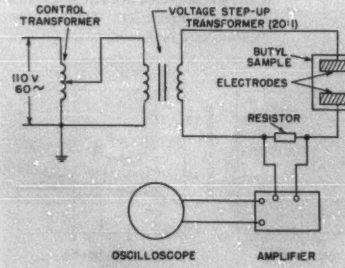
CONTROL TRANSFORMER
VOLTAGE STEP-UP TRANSFORMER (20:1)
110 V 60~
BUTYL SAMPLE
ELECTRODES
RESISTOR
OSCILLOSCOPE
AMPLIFIER

Figure 14. Some design details employed to utilize butyl as an outdoor insulation

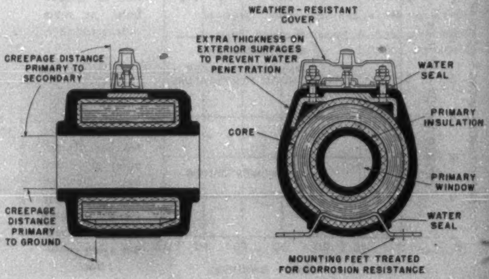
CREEPAGE DISTANCE PRIMARY TO SECONDARY
CREEPAGE DISTANCE PRIMARY TO GROUND
WEATHER - RESISTANT COVER
EXTRA THICKNESS ON EXTERIOR SURFACES TO PREVENT WATER PENETRATION
WATER SEAL
CORE
PRIMARY INSULATION
PRIMARY WINDOW
WATER SEAL
MOUNTING FEET TREATED FOR CORROSION RESISTANCE

Table I

Aging Condition	Aging Period, Years	Absolute Min. Creepage Start Voltage, Volts/Inch
90% humidity, 30°C	3	360
75°C oven	3	350
Outdoor exposure	1/2	400
Room temperature	1/2	450

sufficient distance between terminals and other parts. A design value of 200 volts per inch maximum creepage gradient has been used on the first indoor-outdoor design. This represents conservative design based on the characteristics of the present material. It is anticipated that progress in the design of higher voltage ratings will result from the improvement of this characteristic of molded butyl compound.

It was found that the effects of aging on creepage characteristics were satisfactory for the outdoor use of this material at low voltages. Samples that had been aged for three years under various conditions were tested for creepage start voltage. The results of these tests are shown in Table I.

Tests made on sheet samples that had been subjected to accelerated aging in a weatherometer and a 100-degree centigrade oven showed that butyl has good resistance to creepage. Samples subjected to accelerated aging compared reasonably well with samples aged at room temperature.

The minimum start voltage increased approximately 25 per cent during the 62-day accelerated aging period for both the accelerated and the normally aged samples.

Other Properties: The electrical and chemical properties of this special transformer butyl compound have proved to be satisfactory for use as both indoor and outdoor insulation. These properties are shown in Table II.

The general physical properties of butyl are excellent for its use as an outdoor insulation. It is on the basis of these properties that this material offers many advantages over old materials. By the elimination of metal-porcelain casings, and asphalt-paper insulation, many design and manufacturing simplifications are made possible. These result in standardization and additional improvements in the finished transformer.

Transformer Design

It was necessary to utilize the various properties of butyl in a final transformer design to meet the requirements of excellent performance under adverse operating conditions. Some of the design details used to obtain the maximum benefit from this material are shown in Figure 14.

The outdoor transformer in which this new insulation is used has been very carefully designed to utilize fully the superior characteristics of molded butyl. This has resulted in the successful accomplishment of an entirely new concept in design; namely, an indoor-outdoor instrument transformer.

The mechanical construction combines strength with small size and ease of molding. The high-permeability silicon steel core is fastened to the base by a welded steel strap, providing excellent support for molding and for ruggedness in service. The construction is shown in Figures 2, 4, and 14.

This new transformer combines several important features of both indoor and outdoor current transformers. In addition to being suitable for outdoor use without external housings, it has features that make it excellent for indoor use.

The secondary terminals are located on top for maximum accessibility. The over-all size is small for convenient use in limited space. This transformer essentially meets all requirements of the Edison Electric Institute Specification, MS-2,[6] for low-voltage metering transformers. It fits in the same space and, with an adapter, may be used on the same mounting holes. This design offers the advantages of flexibility, since it may be used with either a cable or a primary bar passing through the primary window, and for certain current ratings may be used for 3-wire single-phase metering applications.

Conclusion

The new insulation developed for use in indoor instrument transformers has been found to be applicable to low-voltage (600 volts and below) outdoor instrument transformers. This insulation, molded butyl compound, is being used in an indoor-outdoor current transformer. This represents an additional advance in the use of this new insulation in instrument transformers.

A careful utilization of the superior properties of molded butyl has made possible many improvements in the finished high accuracy transformer. Outstanding among these are high-thermal rating, small convenient size, and long-time stability of insulation properties. This contribution to the development of insulating materials now offers the many economies of a standardized indoor-outdoor current transformer.

Table II. Important Properties of Butyl Compound for Use as an Indoor or Outdoor Instrument Transformer Insulation

Electrical Properties	
Dielectric strength (Min.), volts per 0.001 inch	400
60-cycle power factor (ASTM D150),[7] per cent	0.3–0.8
Dielectric constant (ASTM D150)	2.5–3.5
Arc tracking (ASTM-D495-42),[8] seconds	130
Volume resistivity, ohms/cm.^3	10^{16}
General Physical Properties	
Tensile strength (ASTM D412),[9] lb./sq. in.	700
Elongation, per cent	680
Hardness (shore "A")	45–60
Elasticity (shore)	38
Abrasion resistance	Good
Specific gravity	1.3
Specific heat	0.36
Thermal conductivity	6.4×10^{-4} Cal./Sec./Cm.^3/Deg. C.
Flexing resistance	Excellent
Resistance to mechanical damage	Excellent
Chemical Properties	
Corona resistance	Good
Flame resistance	Good
Ozone resistance	Good
Sunlight resistance	Good
Resistance to attack by:	
Transil oil	Fair
Sulphuric acid	Good
Sodium hydroxide	Good
Salt spray	Good
Miscellaneous Properties	
Suitability for molding	Good

References

1. A New Dry Type Insulation for Instrument Transformers, R. A. Pfuntner, R. E. Franck, F. R. D'Entremont. *AIEE Transactions*, volume 69, part I, 1950, pages 453–58.

2. Revolutionary Advance in Instrument Transformer Design, I. F. Kinnard. *General Electric Review* (Schenectady, N. Y.), volume 52, June 1949, pages 15–19.

3. Butyl Rubber Engineering Data, E. N. Cunningham, L. B. Turner. *Product Engineering* (New York, N. Y.), November 1945.

4. Structure of Copolymers of Isobutylene and Isoprene (Butyl Rubber), John Rehner, Jr. *Industrial and Engineering Chemistry* (Easton, Pa.), volume 36, 1944.

5. Butyl Rubber, R. M. Thomas, I. E. Lighbown, W. J. Sparks, P. K. Frohlich, E. V. Murphree. *Industrial and Engineering Chemistry* (Easton, Pa.), volume 32, October 1940, page 1, 283.

6. Suggestions for Specifications for Coordinated and Standardized Low-Voltage Metering Current. *Publication MS-2*, Edison Electric Institute (New York, N. Y.), 1940.

7. Methods of Test for Power Factor and Dielectric Constant of Electrical Insulating Materials. American Society for Testing Materials (Philadelphia, Pa.), *ASTM D150*, 1944.

8. Method of Test for Arc Resistance of Solid Electrical Insulating Materials. American Society for Testing Materials (Philadelphia, Pa.), *ASTM D495-42*, 1942.

9. Method of Tension Testing of Vulcanized Rubber. American Society for Testing Materials (Philadelphia, Pa.), *ASTM D412*, 1941.

No Discussion

The Closed Core Reactor

S. BENNON
MEMBER AIEE

Synopsis: This paper indicates the value of a closed iron core reactor as a source of fundamental reactive kilovolt-amperes. The saturation of the core provides a sharp transition point and a steep rise in reactive kilovolt-amperes when operating in the neighborhood of saturation. A practical method of analysis is outlined which permits the design of these reactors with engineering accuracy. Also included is experimental data on a commercial reactor of this type.

FOR APPLICATIONS which require a rapid increase of reactive kilovolt-amperes with moderate increase in voltage, a reactor with a closed iron core represents a practical solution. By operating the core slightly below saturation moderate increments in applied voltage will produce large increments of current by forcing the core to operate above saturation for portions of a cycle. When an oriented steel such as Hipersil[1] is used as the core material, the sharpness of the transition at saturation can be considerably increased.

The current drawn by a reactor of this type will be highly peaked as indicated by the oscillogram in Figure 1, but will, nevertheless, contain a large fundamental component. In 3-phase applications the peaks of line current can be greatly reduced by connecting the reactors in delta, thus providing a path for triple harmonics.

Theoretical Characteristics

In the application of reactors of this type, the fundamental component and the total rms value of exciting current are of primary importance. As both of these quantities are determined almost entirely by the current peaks, it is possible to analyze the performance with engineering accuracy by assuming the impedance infinite below core saturation. The theoretical relations used are based on a hypothetical reactor whose core has the broken straightline characteristic shown in Figure 14(B), and are derived in detail in the Appendix.

If a gradually increasing sine voltage is applied across this hypothetical reactor, the current will remain zero until an rms value $(E_s)_{rms}$ sufficient to bring the core to the effective saturation flux density B_s is reached. This represents the transition point between the two straight-line portions of the core characteristic. Beyond this point the exciting current appears as a series of discrete positive and negative pulses. In this current region beyond saturation, the reactor has an impedance Z, determined by the effective resistance R and the air core reactance X of the winding.

As developed in the Appendix the rms value of the total exciting current and its fundamental component can be expressed in the form,

$$(I_T)_{rms}=K_T\times\frac{E_{rms}}{Z}$$

$$(I_F)_{rms}=K_F\times\frac{E_{rms}}{Z}$$

where

$$Z=\sqrt{R^2+X^2}$$

E_{rms} = rms value of applied voltage

The coefficients K_T and K_F are completely determined by two simple nondimensional ratios. These may be defined as,

$$n=R/X$$

$$s=\frac{E_{rms}}{(E_s)_{rms}}$$

Plotting the characteristic curves in terms of n and s places them in generalized form applicable to any closed core reactor.

As defined above the quantity s is a convenient measure of the excursion beyond core saturation produced by the applied voltage E_{rms}. It also is the reciprocal of the quantity m used in the Appendix. If B_m is the maximum flux density corresponding to the applied voltage E_{rms} the relation is,

$$s=\frac{1}{m}=\frac{B_m}{Bs}$$

As the fundamental component is in general the useful component of the reactor current, the ratio p of the fundamental to the total rms current is indicative of the effectiveness of the reactor.

$$p=\frac{K_F}{K_T}$$

The ratio p is plotted in Figure 2 for values of n of zero, five, and infinity. As can be seen, the fundamental component of the total exciting current is relatively large.

When the applied voltage is increased the duration of the current pulses increases as well as the peak value. Figure 3 is a plot of the pulse duration in degrees for n equal to zero, five, and infinity.

One of the problems encountered in the use of a closed iron core reactor operated in the neighborhood of saturation is the high inrush current which may flow when voltage is first applied. The simplest

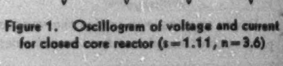

Figure 1. Oscillogram of voltage and current for closed core reactor ($s=1.11$, $n=3.6$)

Paper 51-375, recommended by the AIEE Transformers Committee and approved by the AIEE Technical Program Committee for presentation at the AIEE Fall General Meeting, Cleveland, Ohio, October 22–26, 1951. Manuscript submitted June 19, 1951; made available for printing September 4, 1951.

S. BENNON is with Westinghouse Electric Corporation, Sharon, Pa.

The author wishes to acknowledge the excellent work of M. R. Muhovich on the design of the reactors referred to in the section on Test Data of this paper. Mr. Muhovich is with the Engineering Department, Westinghouse Electric Corporation, Sharon, Pa.

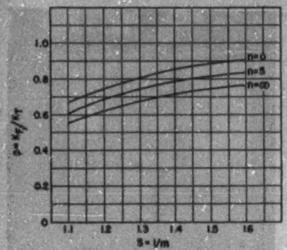

Figure 2. Ratio of fundamental to total current as a function of the excursion beyond core saturation

method of controlling the inrush is to use a series resistor. This not only limits the magnitude of the inrush, but decreases the duration of the transient. Fortunately, the resistor may have a value considerably greater than the air core reactance and still only produce a moderate reduction in the fundamental component of reactor current. Figure 4 indicates the per cent reduction in fundamental current produced by changing from a negligible resistance to values several times the air core reactance. It takes a resistance four times the reactance for $s=1.25$ and six times the reactance for $s=1.11$ to reduce the fundamental component to half its original value. This rather surprising result is due to a compensating variation in the coefficient K_F. As R, and therefore Z, is increased, K_F increases simultaneously. This is illustrated clearly by Figure 5 where values of K_F are plotted for several values of n. For a value of $s=1.25$, the fundamental component would be more than doubled by changing the ratio of resistance to reactance from zero to five, even though the total impedance Z were kept the same. Figure 6 illustrates the modification in pulse shape and amplitude produced by the variation in ratio n, for constant total impedance and $s=1.25$. Proceeding from $n=0$ to $n=\infty$ the pulse shape varies from a sinusoidal segment cut from a sine wave lagging 90 degrees by a line parallel to the time axis, to a sinusoidal segment cut from a sine wave in phase with the voltage by a line perpendicular to the time axis.

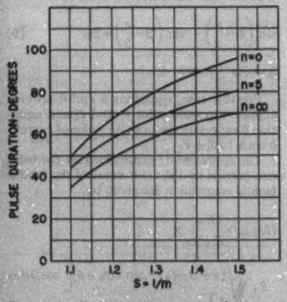

Figure 3. Duration of current pulses as a function of the excursion beyond core saturation

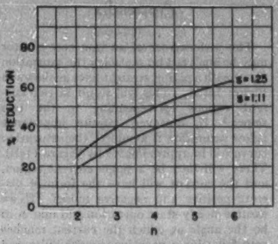

Figure 4. Per cent reduction in fundamental current due to addition of series resistance

The pulse shape for $n=3.33$ illustrates an intermediate step between the two extremes. The large increase in pulse amplitude with increasing n as shown in Figure 6 is the physical process behind the corresponding increase in K_F. This effect is large for values of s in the neighborhood of unity and decreases with increasing s.

The angle of lag α of the fundamental current is a function of s as well as the ratio of resistance to reactance n. When the resistance is negligible, the current will lag the applied voltage by essentially 90 degrees for all values of s. As the resistance increases, the angle of lag decreases, although the decrease is small for small excursions beyond saturation. Figure 7 is a plot of the percentage value of the quadrature component of fundamental current for several values of n.

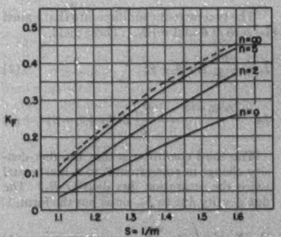

Figure 5. Variation of K_F with magnitude of excursion beyond core saturation

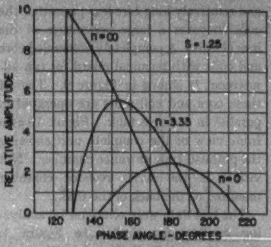

Figure 6. Variation of form and amplitude of a current pulse with ratio of resistance to reactance for $s=1.25$

Test Data

The test results presented in this section were made on closed core reactors built for use as part of an induction motor starting installation. Due to a very weak supply line, a large block of shunt capacitors was required to compensate for the motor lagging kilovolt-amperes drawn during starting. This led to the problem of limiting the voltage rise in the short interval required to switch the capacitor bank after the motor came up to speed. The delta-connected reactors were permanently connected in parallel with the delta-capacitor bank and were designed to draw negligible kilovolt-amperes at the starting voltage, but to draw sufficient kilovolt-amperes after motor start to limit the line voltage to acceptable values until the reactor-capacitor combination could be switched off the line.

An unyoked core and coil assembly is shown in Figure 8. The rectangular section Hipersil core is built with 45-degree angle alternate butt and lap corner joints. Rectangular single layer coils are mounted on each leg. The narrow window opening

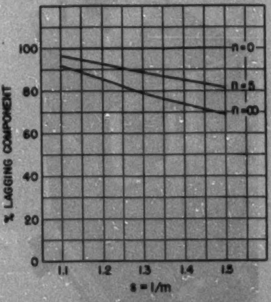

Figure 7. Per cent quadrature component of fundamental current as a function of the excursion beyond core saturation

and relatively long core legs permitted the coils to cover a large percentage of the iron circuit. A completely assembled core and coils with terminal board for tap adjustment is shown in Figure 9. Two of these core and coil units are operated in parallel in a single tank. Figure 10 is a front view of the complete unit showing the pothead type entrance chamber. Not visible is the series resistor chamber mounted at the back of the tank.

The test data were obtained by analyzing oscillograms similar to Figure 1. Test values of K_p indicated in Figure 11 are in fair agreement with the calculated curve. In this test the voltage was maintained constant and the series resistance varied.

In this simplified method of analysis the impedance has been assumed infinite below saturation. The test values would, therefore, be expected to deviate more for values of s in the neighborhood of unity. Although this is true, Figure 12 indicates the deviation is only moderate for small excursions beyond saturation.

The operating curve for the complete reactor is shown in Figure 13. The voltage designated as 100 per cent is the nominal motor voltage at starting and corresponds to core operation slightly below saturation. The sharp transition at saturation is the basic characteristic of this type of reactor. At 110 per cent voltage the fundamental kilovolt-amperes is over 400 per cent. The steep slope of the curve above saturation is important in that it tends to stabilize the operating voltage limits for fluctuations in system conditions. The incremental ratio of fundamental kilovolt-amperes at 115 per cent voltage is over 5 kva per volt.

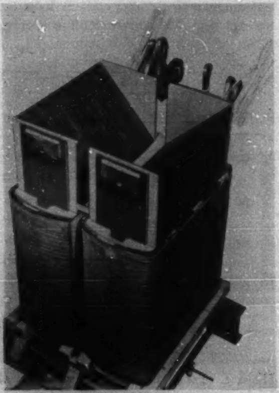

Figure 8. Unyoked core and coil assembly

Appendix

The performance of an iron core reactor may be analyzed by replacing the saturation curve with a pair of straight lines as shown in Figure 14(A). This will result in two current regions corresponding to the two slopes.[2] If, however, infinite impedance below saturation is assumed, the saturation curve will be approximated by Figure 14(B). There will then be a single current region, and the current will have the form of discrete positive and negative pulses. If we assume steady-state operation and take θ_1 to be the angle at which the current reaches zero following a negative current pulse and θ_2 the angle at which the next positive current pulse is initiated, then the positive pulse will last till $\pi+\theta_1$. The current due to a voltage $E_m \sin \omega t$ applied to a series resistance R and reactance X at phase angle θ_2 has the form,

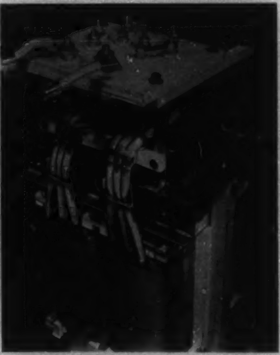

Figure 9. Complete core and coil assembly with terminal board mounted in position

$$i=\frac{E_m}{Z}\sin(\omega t-\beta)+I_t\epsilon^{-\frac{R}{X}(\omega t-\theta_2)} \tag{1}$$

where

$$Z=\sqrt{R^2+X^2}$$

$$\beta=\tan^{-1}\left(\frac{X}{R}\right)$$

The two current conditions are that i must be zero at θ_2 and $\pi+\theta_1$. These yield,

$$I_t=-\frac{E_m}{Z}\sin(\theta_2-\beta) \tag{2}$$

$$I_t\epsilon^{-\frac{R}{X}(\pi+\theta_1-\theta_2)}=-\frac{E_m}{Z}\sin(\pi+\theta_1-\beta) \tag{3}$$

The third condition is that the flux density change in going from θ_1 to θ_2 must equal twice the saturation flux density B_s. The flux density due to $E_m \sin \omega t$ has the form,

$$B=B_m\sin\left(\omega t-\frac{\pi}{2}\right) \tag{4}$$

The flux density relation is, therefore,

Figure 10. Complete reactor unit with pothead-type entrance chamber

$$\sin\left(\theta_2-\frac{\pi}{2}\right)-\sin\left(\theta_1-\frac{\pi}{2}\right)=2m \tag{5}$$

where $m=B_s/B_m$.

The quantity m also is the ratio of the voltage necessary to bring the core to saturation to the actual applied voltage. Substituting equation 2 into equations 1 and 3,

$$i=\frac{E_m}{Z}\left[\sin(\omega_t-\beta)-\sin(\theta_2-\beta)\epsilon^{-\frac{R}{X}(\omega t-\theta_2)}\right] \tag{6}$$

$$\sin(\theta_2-\beta)\epsilon^{-\frac{R}{X}(\pi+\theta_1-\theta_2)}=\sin(\pi+\theta_1-\beta) \tag{7}$$

The two unknown θ_1 and θ_2 in equation 6 can be evaluated using equations 5 and 7. For values of ωt between θ_2 and $\pi+\theta_1$ equation 6 plots a positive current pulse.

Special Case $R \gg X$

If we assume R large enough to make the value of the exponential in equation 7 approximately zero, we have,

$$\sin(\pi+\theta_1-\beta)=0 \qquad \theta_1=\beta \tag{8}$$

From equation 8 and equation 5,

$$\sin\left(\theta_2-\frac{\pi}{2}\right)-\sin\left(\beta-\frac{\pi}{2}\right)=2m \tag{9}$$

$$\theta_2=\cos^{-1}[\cos\beta-2m]$$

For this case, equations 8 and 9 provide explicit expressions for θ_1 and θ_2 and equation 6 expresses the positive pulse of current from θ_2 to $\theta_1+\pi$.

The approximate expressions for the total rms current and the rms value of the fundamental component are given by,

$$(I_T)_{\text{rms}}\simeq\frac{E_m}{Z\sqrt{2\pi}}\times\sqrt{(\pi+\beta-\theta_2)+\sin 2(\theta_2-\beta)\left[\cos 2\beta-\frac{1}{2}\right]+\sin^2(\theta_2-\beta)[\tan\beta-2\sin 2\beta]} \tag{10}$$

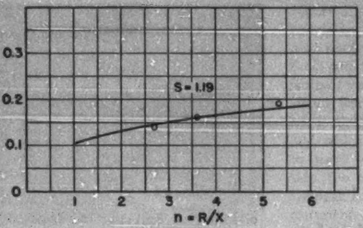

Figure 11 (left). Comparison of test values of K_F with theoretical curve. Variation of K_F with n for s=1.19. (Test values indicated by circles)

$$(I_F)_{rms} \simeq \frac{E_m}{Z\pi\sqrt{2}} \times \sqrt{(\pi+\beta-\theta_2)^2+(\pi+\beta-\theta_2)(\sin 2\theta_2 - \sin 2\beta)+\sin^2(\theta_2+\beta)-\sin 2\beta \sin 2\theta_2} \tag{11}$$

These equations can be written,

$$(I_T)_{rms} = K_T \times \frac{E_{rms}}{Z} \tag{12}$$

$$(I_F)_{rms} = K_F \times \frac{E_{rms}}{Z} \tag{13}$$

$$K_T = \frac{1}{\sqrt{\pi}} \times \sqrt{(\pi+\beta-\theta_2)+\sin 2(\theta_2-\beta)\left[\cos 2\beta-\frac{1}{2}\right]+\sin^2(\theta_2-\beta)\,[\tan \beta - 2\sin 2\beta]} \tag{14}$$

$$K_F = \frac{1}{\pi} \times \sqrt{(\pi+\beta-\theta_2)^2+(\pi+\beta-\theta_2)(\sin 2\theta_2 - \sin 2\beta)+\sin^2(\theta_2+\beta)-\sin 2\beta \sin 2\theta_2} \tag{15}$$

The approximate angle of lag of the fundamental component behind the applied voltage is given by,

$$\alpha = \tan^{-1} \times \left[\frac{(\pi+\beta-\theta_2)\sin\beta+\sin\theta_2 \sin(\theta_2+\beta)-\sin\beta\sin 2\beta}{(\pi+\beta-\theta_2)\cos\beta+\sin\theta_2\cos(\theta_2+\beta)-\sin\beta\cos 2\beta}\right] \tag{16}$$

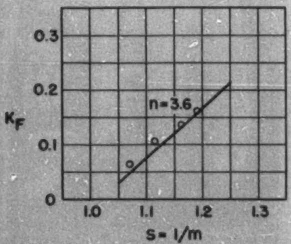

Figure 12. Comparison of test values of K_F with theoretical curve. Variation of K_F with s for n=3.6 (Test values indicated by circles)

Special Case $R=0$ ($n=0$)

For $R=0$, $\beta=\pi/2$ and equation 7 yields

$$\sin\left(\theta_2-\frac{\pi}{2}\right) = -\sin\left(\theta_1-\frac{\pi}{2}\right) \tag{17}$$

$$\theta_2 = \pi-\theta_1$$

while equation 6 becomes,

$$i = \frac{E_m}{X}\left[\sin\left(\omega t-\frac{\pi}{2}\right)-\sin\left(\theta_2-\frac{\pi}{2}\right)\right] \tag{18}$$

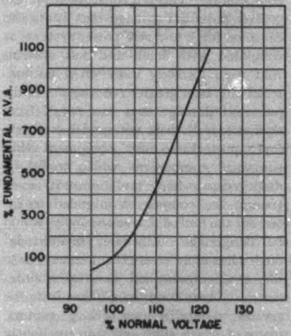

Figure 13. Operating curve of closed core reactor

Substituting equation 17 into equations 5 and 18,

$$\sin\left(\theta_2-\frac{\pi}{2}\right) = m \tag{19}$$

$$i = \frac{E_m}{X}\left[\sin\left(\omega t-\frac{\pi}{2}\right)-m\right] \tag{20}$$

Equation 20, therefore, represents the positive pulse of current between θ_2 and $\pi+\theta_1$. The angles θ_1 and θ_2 are determined from equations 17 and 19.

As in the previous case, the total and fundamental currents can be written,

$$(I_T)_{rms} = K_T \times \frac{E_{rms}}{X} \tag{21}$$

$$(I_F)_{rms} = K_F \times \frac{E_{rms}}{X} \tag{22}$$

$$K_T = \frac{1}{\sqrt{\pi}}\sqrt{2(\pi-\theta_2)(\cos 2\theta_2+2)+3\sin 2\theta_2} \tag{23}$$

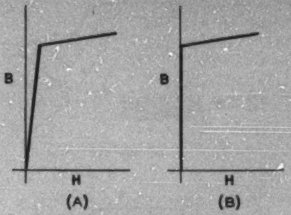

Figure 14. Straight line approximations to saturation curve

$$K_F = \frac{1}{\pi}[2(\pi-\theta_2)+\sin 2\theta_2] \tag{24}$$

$$\alpha = \frac{\pi}{2}$$

Special Case $X=0$ ($n=\infty$)

For $X=0$, $\beta=0$ and equation 7 yields,

$$\sin(\pi+\theta_1) = 0 \tag{25}$$

$$\theta_1 = 0$$

while equation 6 becomes,

$$i = \frac{E_m}{R}\sin\omega t \tag{26}$$

Using equation 25 with equation 5 we obtain,

$$\theta_2 = \cos^{-1}(1-2m) \tag{27}$$

Equation 26, therefore, expresses the positive pulse of current from θ_2 to $\theta_1+\pi$.

Again in this case, we can write,

$$(I_T)_{rms} = K_T \times \frac{E_{rms}}{R} \tag{28}$$

$$(I_F)_{rms} = K_F \times \frac{E_{rms}}{R} \tag{29}$$

$$K_T = \frac{1}{\sqrt{2\pi}}\sqrt{2(\pi-\theta_2)+\sin 2\theta_2} \tag{30}$$

$$K_F = \frac{1}{\pi}\sqrt{(\pi-\theta_2)(\pi-\theta_2+\sin 2\theta_2)+\sin^2\theta_2} \tag{31}$$

The angle of lag of the fundamental component is,

$$\alpha = \tan^{-1}\left[\frac{1-\cos 2\theta_2}{2(\pi-\theta_2)+\sin 2\theta_2}\right] \tag{32}$$

References

1. HIPERSIL A NEW MAGNETIC STEEL AND ITS USE IN TRANSFORMERS, J. K. Hodnette, C. C. Horstman. *Westinghouse Engineer* (East Pittsburgh, Pa.), pages 52–56, August 1941.

2. MATHEMATICAL ANALYSIS OF NON-LINEAR CIRCUITS, A. Boyajian. *General Electric Review* (Schenectady, N. Y.), pages 531–37, September 1931.

No Discussion

A New 5,000-Volt Air-Break Contactor for Industrial Service

LEON J. GOLDBERG
MEMBER AIEE

Synopsis: This paper describes a line of air-break contactors made for controlling 100-horsepower to 3,000-horsepower motors on 2,400-, 4,160- and 4,800-volt systems. The design features compactness, accessibility, and long life. The arc-rupturing structure has a magnetic blowout and an arc chute which confines and interrupts the arc entirely within its boundaries for all currents which it is rated to interrupt.

Application

INDUSTRY has steadily been expanding its use of high-voltage motors and has broadened its requirements for controlling them safely, conveniently, and economically. Many of these motors are started directly across the line and run at a single speed but there is a substantial use of various combinations of full or reduced-voltage start, single or multiple speed, reversing or nonreversing and with or without dynamic braking. Typical applications are drives for rubber mills, plastic mills, large air compressors, hydraulic system pumps, and mine hoists. Sizes of motors that are typical and which can be controlled by this new line of contactors run from 100 horsepower to 3,000 horsepower.

Special Requirements

Controllers for these motors, besides providing the basic functions of starting, stopping and running control, must give a much more nearly complete protection against overloads and faults than had been expected from older and smaller equipments. This is a consequence of the greater potential damage that faults can cause on large and stiff power systems as compared with small and soft systems that were formerly more often encountered and to a greater recognition of the potential damage that can result from equipments that do not render complete fault protection. An equipment that contained components which would be damaged on high fault current, even though the component intended to interrupt the fault did so successfully, would be dangerous. Likewise, modern industry has more severe requirements as to life, compactness, and ease of maintenance. These conditions follow from the greater variety of uses of large motors, many of which start and stop frequently and often have to do so within prescribed starting and stopping times. With the greater variety of applications, many controllers are located close to factory production areas where space is expensive and where outage time, and the labor of maintenance must be kept to a minimum.

Limitations in Former Equipments

Formerly, many controllers for high-voltage motors were built with either circuit breakers or oil-immersed contactors. The new contactor overcomes the deficiencies of both these devices in meeting specific requirements. The circuit breaker, being designed for entirely different purposes, has some qualities that are not required for motor control and lacks very important ones that should be required. Specifically, the circuit breaker has short life in terms of number of operations and is difficult to maintain. The oil-immersed contactor has about 5 per cent the contact life of an equivalent air-break contactor, is very messy to maintain, and has certain hazards associated with the oil. The simple forms of oil-immersed contactors usually do not have adequate ability to interrupt or withstand fault currents to the degree required to make a controller completely integrated and safe. The larger and more complex oil-immersed contactors are not compact. All of these limitations have been overcome with the new contactor. It is as compact as the smallest oil-immersed contactors that are available; it has long life, both in its magnet and mechanical parts as well as in contacts and other electrical parts; it is easy to inspect and to maintain and it has abilities to interrupt and to carry current such that it may be part of a controller fully integrated to give itself and its associated equipment complete protection from the smallest overload to the maximum for which it is rated.

Description of Structure

Figure 1 is a 3-pole contactor for 5,000 volts and 200 amperes. The three poles are side by side and adjacent to a magnet. Similar construction is used for 2-, 4-, or 5-pole forms. The moving parts constitute a single structural assembly

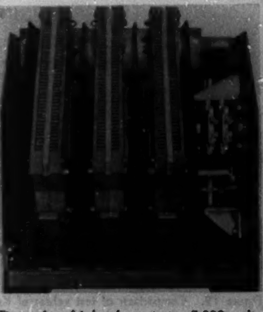

Figure 1. Air-break contactor 5,000 volts, 200 amperes, 3-pole form, with d-c magnet

---

Paper 51-376, recommended by the AIEE Industrial Control Committee and approved by the AIEE Technical Program Committee for presentation at the AIEE Fall General Meeting, Cleveland, Ohio, October 22–26, 1951. Manuscript submitted June 25, 1951; made available for printing September 11, 1951.

Leon J. Goldberg is with General Electric Company, Schenectady, N. Y.

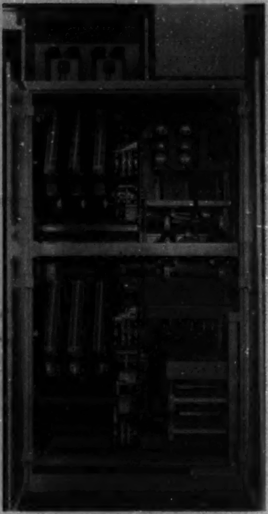

Figure 2. Representative controller with current-limiting power fuses for rubber-mill service. Contactors provide full-voltage reversing control with dynamic braking. The reverse direction contactor and dynamic braking contactor are in a single combined structure

mounted on sealed, precision type self-aligning ball bearings. The stationary structure is basically made from sturdy steel side plates tied together by four substantial channel shaped steel beams. The electrical stationary parts are insulated from this steel frame by pedestal-type heavy-duty-type insulators. The arc rupturing structure on each pole consists of a pair of arcing horns or runners connected to the renewable contacts and associated with an arc chute and magnetic blowout. The magnetic blowout on each pole contains a double-section coil, one section of which carries line current whenever the contactor is closed, and one section of which carries line current only when the arc has started to progress along the arcing horns and is about to be extinguished within the chute. The method of accomplishing this is illustrated in Figure 3. The advantage of the double-coil design is that there is always a strong field ready to move the arc off the contacts onto the arc horns as soon as the arc is first formed, and then there is an extra strong field which appears only when an arc is already formed between the horns and which is available to force the arc to move very rapidly and extinguish inside the chute. Since the extra field strength is set up only when needed, because the current flows in the section of the coil providing this increased strength of field only during the interrupting period, a very strong field can be provided without making a structure big enough to carry the current continuously.

The arc chute is one which causes the arc to be confined and extinguished within its boundaries under all circumstances. The structure of the chute is relatively small. The chute is symmetrical and may be mounted in either of two positions, and the internal parts of the chute are separately renewable. The chute is withdrawn approximately straight forward for inspection. It mounts without the use of bolts or fasteners.

The contacts of this contactor are of the single-break type. Usually in a contactor interrupting more than low voltages, even though the contacts may be of the double-break type, the arc takes the form of a single arc between arcing horns prior to its extinction. Consequently, there is no advantage so far as interruption is concerned in having more than a single-break. There are, however, two very important advantages to having single-break contacts. For a given size of magnet, with its associated impact and wear, greater contact force or greater wipe and depth of wear allowance can be provided for each contact when there is only single-break. Furthermore, the single-break type of construction lends itself readily to contacts having rolling wipe movement. In this form of contact movement the contacts come together at a zone of initial contact when they first touch in closing and roll to another zone of final contact as the magnet seals, see Figure 4. They traverse these zones in reverse order when the contactor opens. This means that the arcing area and the carrying area on each contact are in separate positions.

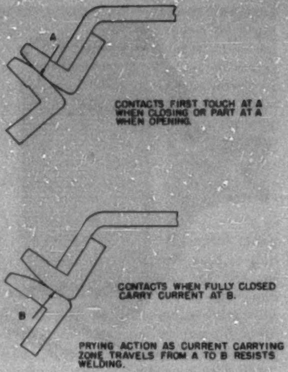
A
CONTACTS FIRST TOUCH AT A WHEN CLOSING OR PART AT A WHEN OPENING.
B
CONTACTS WHEN FULLY CLOSED CARRY CURRENT AT B.
PRYING ACTION AS CURRENT CARRYING ZONE TRAVELS FROM A TO B RESISTS WELDING.

Figure 4. Action of contacts having rolling wipe, showing transfer of current-carrying zone and mechanical action that resists welding

Thus, the current carrying area maintains a cleaner and smoother surface which gives it greater current carrying ability. Contact area is distributed over large sections of metal, and greater volume of expendable contact material can be provided by a magnet of a given size than with double or multiple breaks because the magnet has to wipe-in a smaller number of contacts. Moreover, this type of contact can be made from copper which has both reasonably good ability to resist welding and to carry current. Where special alloys have to be used in contact faces, it is very difficult to find one that is both able to resist welding and to carry current without excessive temperature rise.

The flexible shunt associated with each

Figure 5. Configuration of current path through flexible shunt, showing effect in minimizing magnetic forces to open contacts

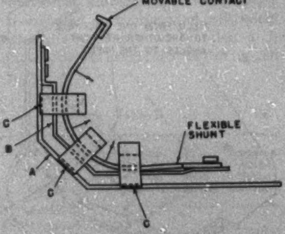
MOVABLE CONTACT
FLEXIBLE SHUNT
C
B
A
C
C

A AND B ARE RIDGID CONDUCTORS.
C ARE INSULATION SUPPORTS.
FORCE ON FLEXIBLE SHUNT IS
IN DIRECTION OF ARROWS.

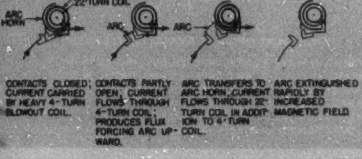
4-TURN COIL
22-TURN COIL
ARC HORN
ARC
ARC
CONTACTS CLOSED; CURRENT CARRIED BY HEAVY 4-TURN BLOWOUT COIL.
CONTACTS PARTLY OPEN; CURRENT FLOWS THROUGH 4-TURN COIL; PRODUCES FLUX FORCING ARC UPWARD.
ARC TRANSFERS TO ARC HORN; CURRENT FLOWS THROUGH 22-TURN COIL IN ADDITION TO 4-TURN COIL.
ARC EXTINGUISHED RAPIDLY BY INCREASED MAGNETIC FIELD.

Figure 3. Action of 2-section blowout coil in automatically providing increased field strength when arc is on the arcing horns. Heavy lines indicate current path

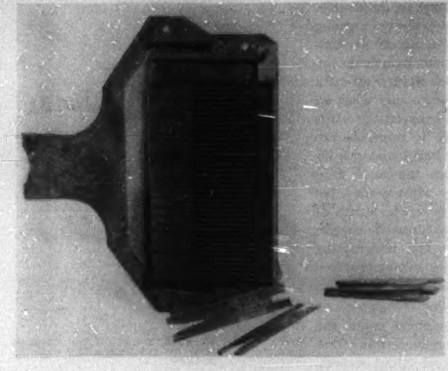

Figure 6 (above). View showing arc chute sides and V-shaped barriers

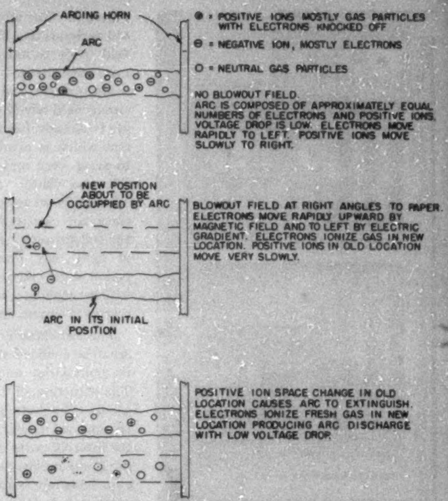
ARCING HORN
ARC
⊕ = POSITIVE IONS MOSTLY GAS PARTICLES WITH ELECTRONS KNOCKED OFF
⊖ = NEGATIVE ION, MOSTLY ELECTRONS
○ = NEUTRAL GAS PARTICLES
NO BLOWOUT FIELD. ARC IS COMPOSED OF APPROXIMATELY EQUAL NUMBERS OF ELECTRONS AND POSITIVE IONS. VOLTAGE DROP IS LOW. ELECTRONS MOVE RAPIDLY TO LEFT. POSITIVE IONS MOVE SLOWLY TO RIGHT.
NEW POSITION ABOUT TO BE OCCUPPIED BY ARC
BLOWOUT FIELD AT RIGHT ANGLES TO PAPER. ELECTRONS MOVE RAPIDLY UPWARD BY MAGNETIC FIELD AND TO LEFT BY ELECTRIC GRADIENT. ELECTRONS IONIZE GAS IN NEW LOCATION. POSITIVE IONS IN OLD LOCATION MOVE VERY SLOWLY.
ARC IN ITS INITIAL POSITION
POSITIVE ION SPACE CHANGE IN OLD LOCATION CAUSES ARC TO EXTINGUISH. ELECTRONS IONIZE FRESH GAS IN NEW LOCATION PRODUCING ARC DISCHARGE WITH LOW VOLTAGE DROP.

Figure 8 (right). Action of the components of an arc as it moves under the influence of a magnetic blowout field

pole on this contactor is confined by sturdy insulation so that it cannot reduce effective electrical clearance. The shunt is part of a circuit so arranged as to prevent the magnetic forces due to current within it and the other conductors from building up strong opening forces on the contacts. Figure 5 illustrates this action.

Theory of Interruption

The arc chute for this contactor consists essentially of an array of refractory insulators so arranged as to present to the arc alternately along its length solid surfaces and open spaces. The particular construction used to accomplish this is an assembly consisting of two side pieces which form the general support and arc enclosure, and a set of V-shaped barriers placed in the chamber formed by the two side pieces. Figure 6 illustrates this. The barriers, made of phosphoasbestos, are intended to be inert refractory insulators. Functionally, so far as arc interruption is concerned, it would be equally satisfactory to make the barriers or portions of them integral with the side pieces. In fact, small arc chutes have been made exactly this way and in these, the barriers take the form of ribs on the arc chute sides. In the large chute, however, separate barriers make possible better control of shape and thickness of the surfaces exposed to the arc and more economical renewal of parts.

In understanding how the chute acts to extinguish the arc, it is essential to consider the progression of an arc within an arc chute associated with arcing horns and

Figure 7. Configuration of current path through blowout coil, contacts, arcing horns, and arc; showing successive positions of arc under influence of the magnetic blowout field

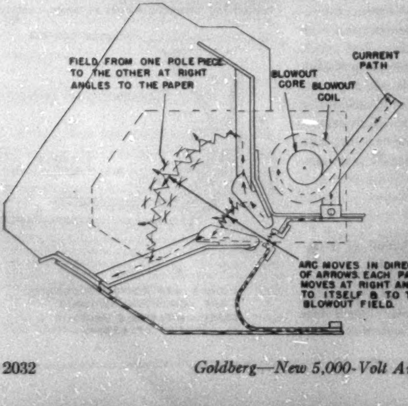
FIELD FROM ONE POLE PIECE TO THE OTHER AT RIGHT ANGLES TO THE PAPER
BLOWOUT CORE
BLOWOUT COIL
CURRENT PATH
ARC MOVES IN DIRECTION OF ARROWS. EACH PART MOVES AT RIGHT ANGLES TO ITSELF & TO THE BLOWOUT FIELD.

Figure 9. Oscillogram of interruption at 5,300 volts and 6,730 amperes (average of three phases), initial current in the arc, amperes rms

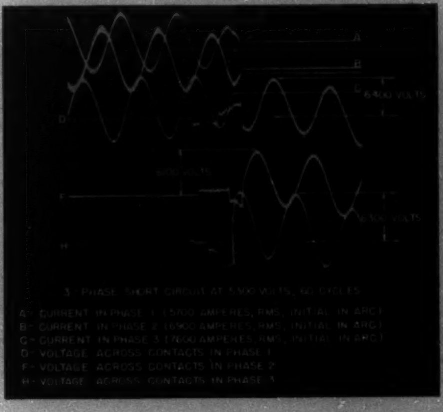

Table I

8-Hour Current-Carrying Amperes	8-Cycle Current-Carrying Amperes, Rms, Asymmetrical	Momentary Withstand Current With Current-Limiting Fuses, Amperes Peak
200	32,000	60,000
400	32,000	60,000

a magnetic blowout. Figure 7 indicates by outline the arrangement of blowout, arcing horns and other parts, and successive positions of the arc in an arc chute with magnetic blowout. In determining the direction in which the arc will move from one position to successive positions, the 3-finger rule* that is used in connection with a solid conductor carrying current in a magnetic field is often applied. Because of this, it is sometimes concluded that the arc moves in the same manner that a solid conductor does. This is not so. The arc consists of a body of hot gas, ionized particles, and electrons. Under the influence of a transverse magnetic field, the electrons, because of their mobility, move very much more rapidly than any of the positive ions. When the electrons are removed from the original location, the body of heated air and ionized particles that remain there can no longer conduct at a low voltage drop. The electrons in the new position now adjacent to the old one, establish a new body of ionized heated particles in which the positive ions and electrons set up a voltage distribution that is characteristic of an arc. This is how an arc progresses. The significant point is that what moves directly under the influence of the magnetic field is a locus of conduction and that in each position of this locus, a new body of air is raised to a high temperature, while in each old position a hot body of air is allowed to cool to a lower temperature.

Within the heated body of air, electrons, and ionized particles that constitute the arc, there is a central cross-section called the core that is at a temperature from 6,000 to 10,000 degrees centigrade. It is known from many studies of arcs and gas ionization that for air at normal pressure the core of an arc must be at this temperature range or the air can not be sufficiently ionized to carry current at the low voltage drop that is the distinguishing characteristic of an arc. Surrounding the core of the arc is a luminous body of air at a temperature below 6,000 degrees centigrade. Surrounding it is air at still lower temperatures. In a moving arc, the air outside the luminous part, say at a distance equal to the diameter of the core, might be in the vicinity of 500 degrees centigrade or less. Although it appears that the main portion of the arc moves continuously without discrete steps, consider what happens over a small finite interval of time during which the arc has moved a finite distance from one locus to a second one nearby as illustrated in Figure 8. At the moment that the arc is in the first locus, the air occupied by the core of the arc is in the vicinity of 7,500 degrees centigrade and the air in the second locus which the arc is about to occupy is in the vicinity of 500 degrees centigrade. At the end of the time interval under consideration, the air in the second locus suddenly has been raised from about 500 degrees centigrade to about 7,500 degrees centigrade. Thus, in accordance with the law of thermodynamics of gases, $PV=RT$, the initial tendency after the transfer of the arc from the first locus to the second is for the air in the second locus to rise from a pressure of one atmosphere to about ten or more atmospheres and, consequently, to start to expand. If the arc chute consists of solid walls adjacent to the arc, the air expanding from the core of the arc in the second locus reflects back from these walls and momentarily forms a dynamic sheath which spaces and insulates the core of the arc from the solid walls. If, however, the walls are not solid but intermittently open, the gases expanding from the core of the arc opposite these openings escape. This makes breaks in the sheath around the arc. Portions of the arc near these breaks come closer to the solid walls of the chute and are rendered non-conducting by processes associated with the cool walls. It is this greater effectiveness in cooling the arc or portions of it to below the critical range of temperature in the vicinity of 6,000 degrees centigrade that makes this chute effective. The V-shaped cross-section of the chute into which the arc is forced makes this process take place gradually as the arc approaches the vertex of the V.

The process of breaking the sheath around the arc by the type of structure described may be called "lateral venting," and the chute may be described as "laterally vented." There are two interesting things worth noting. First, so long as the chute is effective in extinguishing the arc, no part of the core of the arc passes beyond the apex of the "V" in the arc barriers. Secondly, there is no attempt to lengthen the arc to anything more than the straight-line distance between the arcing horns at the level of the apex of the "V". While this arc extinguishes the arc compactly compared with any other arc chute, it is interesting to speculate on the idea that if the chute could cool the arc to well below ionization temperatures with very great efficiency, the length of the arc would not have to be greater than the space required to withstand breakdown of cold air with the same voltage.

Ratings

Voltage

The contactors have a nominal rating of 5,000 volts. They are used, within stated limits, on systems of nominal utilization voltages of 2,400, 4,160, and 4,800. The maximum actual voltage for which these contactors are rated is 5,280. This permits their usage on systems of nominal rating of 4,800 volts with 10 per cent plus tolerance. Although this tolerance is greater than that listed in the Edison Electric Institute—National Electrical Manufacturers Association report on preferred ratings[1] it is realistic at the present time, because there are substantial systems operating at this voltage.

Insulation

The insulation of these contactors are made to withstand the standard NEMA test values for control[2] of 13,250 volts at 60 cycles and 60,000 volts at impulse.

Current Carrying

Forms are available having 8-hour current carrying ratings as shown in the first column of Table I. These forms have abilities to carry current as listed in the second column, without major damage, at any voltage up to 5,280, for any time however short but not more than 0.133 second. The contactors carry currents listed in the third column for the required length of time when used with suitable current-limiting fuses.

All forms may be used in controllers having suitable fuses for interrupting short-circuit current, and other properly co-ordinated accessories, and will safely carry the maximum current that a 3-phase system of listed capacity can furnish

Table II

Voltage	8-Hour Current Rating, Amperes	Kva Symmetrical	Amperes, Rms, Symmetrical
2,400 nominal 2,500 maximum 2,200 minimum	200	25,000	6,000
	400	25,000	6,000
4,800 nominal 5,280 maximum 4,160 minimum	200	25,000	3,500
	400	35,000	4,850

---

*Fleming's left-hand rule for motor action.

to the controller for the length of time permitted by the fuses.

System Voltage	System 3-Phase Available Short-Circuit Capacity, Kva
2,400 nominal 2,500 maximum 2,200 minimum	150,000
4,800 nominal 5,280 maximum 4,160 minimum	250,000

INTERRUPTING

Interrupting ratings are based on actual tests at about eight per cent power factor with static air core reactor loads. This type of test is representative, with suitable margins, of fault conditions that the contactors might be exposed to. Under normal operation conditions these contactors would interrupt motor loads. These are very much less severe, and are interrupted in much shorter arc time. Table II is for 3-phase circuits. The maximum rating is the listed kilovolt-amperes or amperes, whichever is smaller. In order to utilize a uniform method of applying these contactors to a large variety of power systems, the interruption ratings are expressed in terms of the symmetrical component of interrupted kilovolt-amperes or rms amperes with the understanding that the rating includes an ability to interrupt a fault of that symmetrical component plus the worst offset that would be encountered. In establishing this rating an offset multiplier of 1.6 was used.

HORSEPOWER

Table III lists the maximum horsepower 3-phase motors for which each form contactor is rated.

References

1. EEI-NEMA PREFERRED VOLTAGE RATINGS FOR A-C SYSTEMS AND EQUIPMENT. Edison Electric Institute and National Electrical Manufacturers Association (New York, N. Y.), 1949.

2. STANDARDS FOR INDUSTRIAL CONTROL. National Electrical Manufacturers Association (New York, N. Y.), 1949.

3. GASEOUS CONDUCTION (book), J. D. Cobine. McGraw-Hill Book Company, New York, N. Y., 1941.

Table III

Contactor 8-Hour Current Rating, Amperes	Motor Rated Voltage 2,200–2,400			Motor Rated Voltage 4,000–4,600		
	Synchronous		Induction	Synchronous		Induction
	1.0 p	0.8 p		1.0 p	0.8 p	
200	900	700	700	1,500	1,250	1,250
400	1,750	1,500	1,500	3,000	2,500	2,500

No Discussion

The Selection of Field Circuit Resistance for Synchronous Motors

W. A. THOMAS
MEMBER AIEE

O. D. WHITWELL
ASSOCIATE MEMBER AIEE

Synopsis: The first three sections of this paper present a brief description of the methods presently employed by synchronous motor designers to control the starting performance and select the field discharge resistance. Subsequent sections propose a system whereby the designer or the user of a synchronous motor may change the starting performance through selection of the proper field circuit resistance.

THE starting performance of salient pole synchronous motors has been given much study by designers and users of these machines. However, only a few comprehensive articles appear in the literature on the subject. Fechheimer[1] published the first study of the starting characteristics of synchronous motors in 1912. Since that time others have extended these studies in keeping with the developments in synchronous machines. As the theory developed, it became more and more involved with the numerous factors which are now known to enter into the prediction of synchronous motor performance. The result has been a maze through which only those well versed in design have found their way.

After fabrication of the motor is complete, the application engineer has available only a limited number of external factors with which to control the performance of the machine. Among these are the terminal voltage to be applied on starting (including both the method of reducing the starting voltage and the value necessary to compensate for such factors as line voltage drop and system capacity), the exciter voltage, the field rheostat, and the external field circuit resistance. Of these items little information is available concerning the selection of the external field circuit resistance. As will be shown, the external resistance in the field circuit may be of considerable importance in the starting performance of synchronous motors. Since this resistance is one of the variables which the user, or the control manufacturer, may determine, a system for easily selecting this resistance should be devised. This paper develops one possible method.

Synchronous Motor Starting Theory

The starting period of a synchronous motor is defined as the time from the application of voltage of the primary winding, at zero speed, until the rotor speed is 95 per cent of synchronous speed. Practically all present day synchronous motors operate as squirrel cage induction motors during the starting period. As with the induction motor, the torque developed by the rotor is proportional to the inphase component of the rotor current and the rotor resistance. The starting performance may be varied by the designer by changing the squirrel cage resistance and reactance. Low inrush kilovolt-amperes and high starting torque are obtained with a high resistance squirrel cage winding having a low reactance. This is shown in Figure 1.

The d-c field winding on the rotor of the synchronous motor has characteristics opposed to this type of winding. Consequently, the use of the field circuit as a starting winding is undesirable. However, to protect the field winding from the high induced voltages realized at standstill when line voltage is applied, it is customary to close the field circuit through a field discharge resistance. If this resistance is of low value the power factor of the rotor will be low, the field being highly inductive, and the inphase component of the current will be reduced. The use of a high value of resistance in the field circuit will increase the power factor and the starting torque will be increased proportionately.

In either the induction motor or the synchronous motor a higher torque is realized at speeds near synchronism with a low resistance squirrel cage winding, see Figure 1. This phenomena may be explained as being the result of the reduction in rotor reactance at the lower frequency voltages induced in the rotor near synchronism. As a result of this reduced reactance, the power factor of the rotor is improved, the inphase component of current is increased, and the torque, rotor I^2R, is increased. Since this condition is obtained with conditions adverse to the conditions for high starting torque, a double squirrel cage winding may be employed. Windings of this type exhibit the speed-torque characteristics shown in

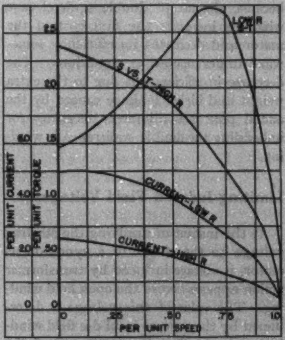

Figure 1. Typical induction motor curves. Single squirrel cage rotor winding

---

Paper 51-377, recommended by the AIEE Industrial Control Committee and approved by the AIEE Technical Program Committee for presentation at the AIEE Fall General Meeting, Cleveland, Ohio, October 22–26, 1951. Manuscript submitted July 30, 1951; made available for printing August 31, 1951.

W. A. THOMAS is with Case Institute of Technology, Cleveland, Ohio, and O. D. WHITWELL is with the Clark Controller Company, Cleveland, Ohio.

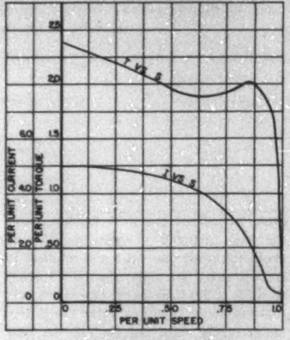

Figure 2. Typical induction motor curves. Double squirrel cage rotor winding

Figure 2. These characteristics result because the rotor has a high effective resistance when starting and a low effective resistance near synchronous speed.

Practice has shown that a synchronous motor having a single squirrel cage winding and the proper resistance across the d-c field may have the same characteristics as the double squirrel cage winding. In Figure 3 it is seen that increasing R_{fe} (field circuit resistance) flattens the cusp of the speed-torque curve and increases both the starting and pull-in torques.

The double squirrel cage starting winding, giving low starting kilovolt-ampere inrush and good starting, accelerating and pull-in torques is an ideal starting winding for synchronous motors. The use of the proper values of R_{fe} with a standard single cage synchronous motor will provide these characteristics at less cost in many applications. This results because the use of double squirrel cage windings increases the first cost of the motor and decreases its efficiency somewhat under operating conditions. The decrease in efficiency is due to the extra weight and higher leakage caused by the added pole face thickness necessary for imbedding the double squirrel cage winding.

Limiting Induced Field Voltages

At the instant of applying the starting voltage to the stator of a synchronous motor, a voltage induced by transformer action appears across the open field winding. The value of this voltage is determined by the ratio of total d-c field winding turns to the effective turns of the stator. A large number of turns are often necessary in the field winding to obtain sufficient excitation, resulting in a high turns ratio and a high induced voltage in the field winding.

This high voltage is detrimental to the field insulation, and precautions are essential in preventing voltages in excess of the rating of the insulation. Although a sectionalized field winding is sometimes employed, the most used provision is a field discharge resistor in series with the field circuit. An approximate value of this resistor may be determined from the ratio of the maximum permissible induced voltage to the current that is induced in the short circuited field on starting with rated voltage applied. The resistance found is a conservative value which will limit the voltage to a value less than that taken as permissible. This is partially corrected by the general practice of subtracting the ohmic value of the internal field resistance from this conservative value

A somewhat more accurate value may be obtained through knowledge of the maximum allowable field current (I_f) and the field impedance ($Z_f = R_f + jX_f$) at rated line frequency. The total required field circuit impedance in ohms will then be

$$Z_T = \frac{\text{maximum allowable induced voltage}}{\text{maximum allowable } I_f}$$

Z_T is composed of the field impedance plus the external field resistance (R_{fe}). Therefore

$$Z_T = R_T + jX_f$$

and

$$R_{fe} = R_T - R_f$$

If complete design is available on a particular class of motors, an equivalent circuit[3-6] such as is shown in Figure 4 may be calculated on a per-unit basis and the necessary discharge resistance predetermined.

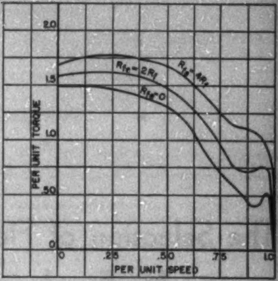

Figure 3. Typical synchronous motor starting performance curves

A discharge resistor is generally connected across the field to limit the induced voltage when the d-c excitation is removed. The same resistor used to limit the induced voltages on starting may be employed in this application provided it is of the proper value. This is readily checked with the familiar equations for d-c transient conditions in circuits containing resistance and inductance in series.

$$e_t = \frac{R_{fe}}{R_f} V \epsilon^{-(R_{fe}+R_f)tL}$$

where

e_t = instantaneous induced voltage
V = rated d-c excitation voltage
R_f and L_f = field resistance and inductance respectively
R_{fe} = external resistance in series with field circuit
t = time after opening field circuit
ϵ = 2.718

The maximum induced voltage occurs at the instant of interrupting the field circuit (at $t=0$), so the maximum induced voltage becomes simply

$$E_m = \frac{R_{fe}}{R_f} V$$

Table I. NEMA Classification of Synchronous Motors and Normal Torque Requirements

		Per Cent of Rated Torque		
Power Factor and Horsepower	Speed, Rpm	Locked Rotor	Pull-in	Pull-out
General Purpose Motors				
1.0 PF to 8 incl. 200 HP	1,800	110	110	150
	1,200–514	110	110	175
0.8 PF to and incl. 150 HP	1,800	110	110	200
	1,200–514	110	110	250
Large High-Speed Motors—514 Rpm and Up				
1.0 PF 250–500 HP	1,800–514	110	110	150
0.8 PF 200–500 HP	1,800–514	125	125	200
1.0 PF 600 HP and up	1,800–514	85	85	150
0.8 PF 600 HP and up	1,800–514	100	100	200
Low-Speed Synchronous Motors—450 Rpm and Lower				
1.0 PF		40	30	150
0.8 PF		40	30	150

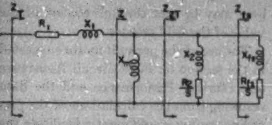

Figure 4. Equivalent circuit of a salient pole synchronous motor having a single squirrel cage starting winding

Field Circuit Resistance and Starting Performance

The equivalent circuits referred to in the section on Limiting Induced Field Voltage present convenient means for calculating the performance of synchronous motors from design or test data. There has been no equivalent circuit or scheme of calculating motor performance proposed which offers an over-all accuracy greater than about five per cent. However, accuracy within five or ten per cent is adequate in modern engineering procedure wherein any precision attained in the calculations is modified by the demands of manufacturing, economics, and standardization. This philosophy prevailing, a proposal for the control of synchronous motor starting performance through selection of the field discharge resistance is presented.

The standard torque specifications for synchronous motors of the National Electrical Manufacturers Association are shown in Table I. As indicated in these tables, all synchronous motors having standard horsepower, speed, and power factor ratings are in three general categories; namely, (1) general purpose synchronous motors, (2) large high-speed synchronous motors, and (3) low-speed synchronous motors. These classifications are subdivided according to speed, horsepower, and power factor ratings.

If ample quantities of design or test data were available to supply the per-unit values of each impedance for a synchronous motor equivalent circuit, an average per-unit motor could be determined based on an average of the individual per unit values from each of a multitude of motors. Comprehensive data encompassing motors with ratings throughout the entire range of National Electrical Manufacturers Association classifications and subdivisions should be compiled and analyzed. If the per-unit values exhibit excessive deviation, further subdivision of the general classifications will be required. The data may also indicate an increase of input reactance (and the resulting decrease in starting inrush current and torque) with increasing horsepower ratings and decreasing speed ratings. This fact alone may necessitate the further subdivisions.

A comprehensive study of the data will result in approximately eight or ten per-unit motors. Supplying the per-unit impedances of each of these average motors in the equivalent circuit provides a means of calculating the motor performance. The torque-speed characteristic is determined by assuming values of slip for each point on the curve and calculating the resulting torque in terms of the rotor power input.

To determine the effect of the external field circuit resistance on the starting performance, it becomes necessary to assume values of external field resistance and then to calculate the resulting torque-speed relation. The starting torque and the pull-in torque are the most important points in the starting period. Therefore, a tabulation of the results calculated at zero speed (slip = 1.0) and at 95 per cent synchronous speed (standard pull-in slip = 0.05) may suffice. The values of external field resistance to assume in performing these calculations should range from a short circuit to a maximum value determined by the dielectric strength of the insulation.

The calculation of complete torque-speed curves for each value of field circuit resistance may be advantageous. The family of curves so revived may illustrate the possibility of using some form of field acceleration in the application of synchronous motors; for example, an application requiring low inrush kilovolt ampere and very high starting torque and also a very high pull-in torque. These conditions are satisfied by utilizing a very high resistance and removing it in steps as the motor comes up to speed.

Table II. Effect of External Field Resistance (R_{fe}) on Synchronous Motor Starting Performance

R_{fe}	Starting Torque	Pull-in Torque	Starting Kva Inrush	Starting Power Factor	Torque Kva Inrush
0	0.87	0.88	6.0	0.254	0.145
1R_f	0.877	1.166	6.0	0.255	0.1462
2R_f	0.888	1.36	6.0	0.256	0.147
3R_f	0.89	1.46	6.0	0.257	0.1473
4R_f	0.896	1.515	6.0	0.259	0.1493
5R_f	0.916	1.71	6.01	0.262	0.153
6R_f	0.911	1.52	6.015	0.262	0.151
7R_f	0.915	1.478	6.01	0.262	0.1528
8R_f	0.914	1.465	6.0	0.262	0.1524
9R_f	0.916	1.455	6.0	0.262	0.153
10R_f	0.928	1.42	6.0	0.264	0.1548
12R_f	0.93	1.368	6.0	0.261	0.155
25R_f	0.009	1.19	6.0	0.279	0.168
100R_f	1.099	1.14	5.85	0.318	0.187
Open Field	1.11	0.818	5.47	0.31	0.19

Table III. Effect of External Field Resistance (R_{fe}) on the Rotor Current (I_2) and the Total Effective Rotor Resistance (R_{2T})

	Starting; Slip = 1.0		Pull-in; Slip = 0.05	
R_{fe}	R_{2T}	I_2	R_{2T}	D_2
0	0.0286	5.52	0.1465	2.45
1R_f	0.02875	5.525	0.193	2.46
2R_f	0.029	5.53	0.236	2.4
3R_f	0.0291	5.53	0.274	2.31
4R_f	0.02922	5.54	0.3095	2.22
5R_f	0.03015	5.53	0.3595	2.18
6R_f	0.0296	5.55	0.37	2.026
7R_f	0.0298	5.54	0.394	1.94
8R_f	0.03	5.52	0.406	1.9
9R_f	0.0302	5.51	0.435	1.83
10R_f	0.0304	5.53	0.461	1.743
12R_f	0.0305	5.52	0.496	1.66
25R_f	0.033	5.53	0.63	1.345
100R_f	0.043	5.45	0.82	1.05
Open Field	0.0455	4.94	0.91	0.948

Example of Effect of Field Resistance on the Starting Performance

In this section the calculation of the effect of changing the field discharge resistance is applied to a per-unit motor in the National Electrical Manufacturers Association classification of general purpose synchronous motor, unity power factor.

The equivalent circuit of Figure 4 was utilized because of its relative simplicity, and its proved ability and accuracy commensurate with practical synchronous motor design. In lieu of comprehensive machine design data from which to determine average per-unit data, design data from a single motor was employed for purposes of illustrating the method.

The results of the computations are found in Table II. Analysis of this tabulated data discloses a number of effects produced by changes in the field circuit resistance.

1. The starting torque increases with increasing d-c field circuit resistance (R_{fe}) because an increasing resistive element in the secondary circuit (Z_{2T}) causes the total equivalent secondary resistance (R_{2T}) to increase, see Table III. The equivalent secondary reactance (X_{2T}) at the starting frequency remains at essentially a constant value of a larger order of magnitude than the effective resistance.

Consequently, the secondary current is practically independent of the magnitude of the resistance. Since the torque developed is proportional to the rotor power $(I_2^2R_{2r})$, the torque will increase with increasing R_{fe}.

2. The starting power factor increases with increasing R_{fe}, a consequence of the increasing resistance reflected into the primary as the secondary resistance is increased.

3. The starting inrush remains essentially constant until large enough values of field resistance exist to increase the input impedance appreciably. Since the effective turns ratio of the sample machine is approximately 25 to 1, this effect is not appreciable in the normal range of R_{fe}.

4. The starting torque per kilovolt-ampere-inrush factor is indicative of the starting efficiency, and is observed to increase steadily in proportion to the increasing starting torque. This is because of the practically constant inrush.

5. Table II indicates that the pull-in torque is not strictly a function of the secondary resistance. At slip frequency, the reactance is nearly constant and equivalent circuit becomes a fixed reactance in series with a variable resistance. The locus of the current in such a circuit is a circle having a diameter proportional to the value of current when the current is lagging 90 degrees behind the applied voltage. As the resistance is increased the current decreases in magnitude from a maximum at 90 degrees lagging to zero at infinite resistance. The power consumed, and consequently the torque of the motor, in such a circuit is then a maximum at the point where the magnitude of the resistance is equal to that of the reactance. The tabular data, see Table II, indicates this point to be at an external field resistance of approximately five times the field resistance.

6. Also of interest is the magnitude of the excursions made by the starting and pull-in torque from the rated values. The starting torque may be reduced 3 per cent and increased 21 per cent (from the 0.90 design value) by variations from short circuit to open field. Over the same range of external resistances, the pull-in torque varies from 60 per cent below to 20 per cent above the design value of 1.5.

Conclusion

The change in starting torque with change in field circuit resistance of normally-used values is small, the starting torque depending primarily upon the resistance and reactance of the squirrel cage winding. However, the field resistance does have an appreciable effect on the pull-in torque. This indicates that the selection of a synchronous motor should be determined primarily from the starting torque requirements of the load. Then the pull-in torque requirements of the load may be met through control of the value of the field resistor.

The use of the per-unit motor suggested in the section on Field Circuit Resistance and Starting Performance and the data resulting from the calculations of the preceding section would greatly facilitate the selection of the correct field circuit resistance for the synchronous motor. It is believed that this proposal is the first comprehensive scheme of application information ever presented for any electric machine. Consequently, the intentions are to indicate the need for such application information and to instigate the prerequisite thought for development of a system of application data which may eventually be applied to all types of electric apparatus.

References

1. **SELF-STARTING SYNCHRONOUS MOTORS, C. J. Fechheimer.** ***AIEE Transactions,*** **volume 31, 1912, pages 529–604.**

2. **BEHAVIOR OF SYNCHRONOUS MOTORS DURING STARTING, F. D. Newbury.** ***AIEE Transactions,*** **volume 32, 1913, pages 1509–25.**

3. **STARTING PERFORMANCE OF SYNCHRONOUS MOTORS, H. V. Putnam.** ***AIEE Transactions,*** **volume 46, 1927, pages 39–59.**

4. **STARTING PERFORMANCE OF SALIENT POLE SYNCHRONOUS MOTORS, T. H. Linville.** ***AIEE Transactions,*** **volume 49, 1930, pages 531–47.**

5. **STARTING PERFORMANCE OF SALIENT POLE SYNCHRONOUS MOTORS, M. K. Liwschitz.** ***AIEE Transactions,*** **volume 59, 1940, pages 913–19.**

6. **DESIGN OF ELECTRICAL APPARATUS, J. H. Kuhlmann. John Wiley and Sons, Inc., New York, N. Y., 1950.**

No Discussion

Evaluation of Manual Methods of Resuscitation

ARCHER S. GORDON
NONMEMBER AIEE

MAX SADOVE
NONMEMBER AIEE

FRANK RAYMON
NONMEMBER AIEE

A. C. IVY
NONMEMBER AIEE

THE ADEQUATE evaluation of manual methods of artificial respiration has been hampered by the inability to produce prolonged periods of apnea during which a group of methods could be appraised comparatively on the same subjects. Previous studies in this laboratory have used fresh corpses and normal subjects with passively suspended respiration to obtain such data. However, vital circulatory processes cannot be studied on the former and, it is generally agreed, the latter give inaccurate results because the conscious subject can assist or resist the manual maneuvers.

Accordingly, a method has been perfected of producing drug-induced apnea for prolonged artificial respiration studies on normal human volunteers. This is accomplished by the use of intermittent injections of intravenous pentothal sodium and curare drugs. The former produces sleep and an amnesia for the procedure, whereas, large enough doses of the curare drugs temporarily paralyze all of the skeletal muscles of the body, including the diaphragm and respiratory muscles. In this state, a subject is provided who is unconscious and unable to breathe and, thereby, closely resembles one who actually requires artificial respiration.

Using this technique on 50 normal healthy adult males, a study was made of a number of manual methods and the Eve Rocking Method.* Studies have included an evaluation of: (1) lung ventilation; (2) circulatory effects; (3) fatigue of the operator; (4) rate of performance; and (5) pedagogical and performance aspects.

Methods of Artificial Respiration Studied

The methods of resuscitation studied included the commonly employed and the newer manual methods. (See Figure 1.) The Eve Rocking Method is, strictly speaking, a mechanical method but was evaluated here because it lends itself readily to these studies and further comparative data on this method are useful. On one group of the volunteers the pole-top method of resuscitation also was studied. All methods were applied to all subjects in each group in order to provide comparative data. In this study, all methods were performed at a rate of 10 to 12 complete cycles per minute.

SCHAFER METHOD (MODIFIED)

The standard Schafer Prone Pressure Method utilizes pressure on the flanks over the floating ribs on the prone subject to induce active expiration; with release of pressure inspiration occurs passively. The use of "back-pressure," in which the pressure is applied over the midback (just below the shoulder blades) with the fingers spread and the thumbs about one inch from the spine, has been found to give almost twice as much ventilation as standard prone pressure. Accordingly, in the Schafer Method and all other prone manual methods this "back-pressure" technique was applied.

ARM-LIFT CHEST-PRESSURE (SILVESTER)

This century-old method is performed with the subject in the supine position. The arms are grasped above the wrists and drawn first upward and then above the victim's head until they touch the floor. They are then brought back to the chest and pressure is exerted in a downward direction.

EVE ROCKING METHOD

In this mechanical method the victim is placed prone on a stretcher and alternately rocked 45 degrees in a head-down position and then 45 degrees in a feet-down position.

ARM-LIFT BACK-PRESSURE (NIELSEN METHOD)

The Danish Nielsen method is applied to the subject who is lying prone with both hands resting under his face. The arms are grasped above the elbows and lifted until firm resistance is met. This induces active inspiration. They are then replaced and back-pressure is exerted to cause active expiration.

HIP-LIFT BACK-PRESSURE METHOD

In this method, the operator places his hands beneath the hips of the prone subject. The hips are lifted four to six inches, which results in active inspiration, and are then replaced on the ground. Back-pressure is then exerted to cause active expiration. A variation of this technique is the Hip-Roll Back-Pressure Method in which the subject is "rolled" up onto the operator's knee or thigh, followed by back-pressure.

POLE-TOP METHOD

This method is used for immediate resuscitation of linemen who are shocked while working on the pole-tops. The rescuer ascends the pole and places the victim astride his own safety belt. He then rhythmically compresses the victim's abdomen with both hands while he is being lowered to the ground for definitive care.

---

* Detailed accounts of these studies are to appear in: Journal of the American Medical Association, Journal of Applied Physiology, and American Journal of Physiology.

Paper 51-378, recommended by the AIEE Safety Committee and approved by the AIEE Technical Program Committee for presentation at the AIEE Fall General Meeting, Cleveland, Ohio, October 22-26, 1951. Manuscript submitted August 15, 1951; made available for printing September 28, 1951.

ARCHER S. GORDON, MAX SADOVE, FRANK RAYMON, and A. C. IVY are all with the University of Illinois College of Medicine, Chicago, Ill.

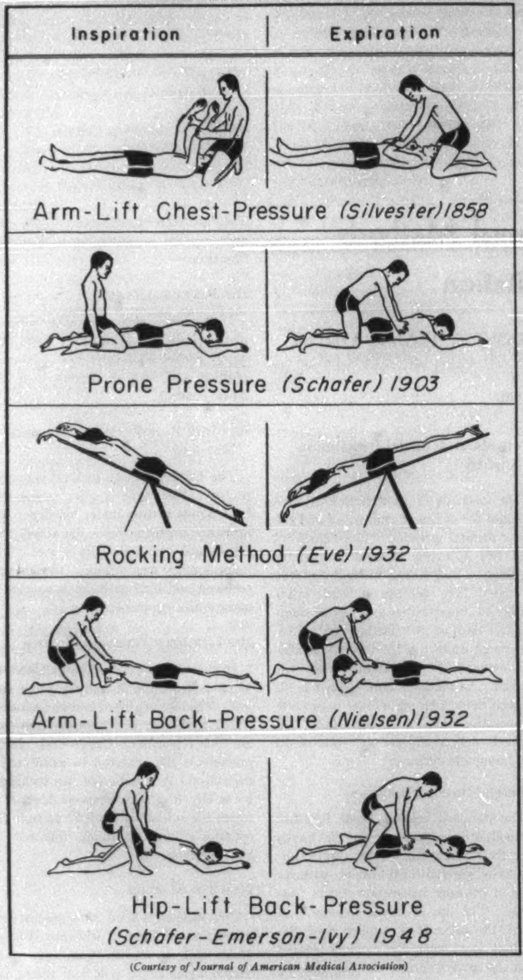
Inspiration
Expiration
Arm-Lift Chest-Pressure *(Silvester)1858*
Prone Pressure *(Schafer) 1903*
Rocking Method *(Eve) 1932*
Arm-Lift Back-Pressure *(Nielsen)1932*
Hip-Lift Back-Pressure
(Schafer-Emerson-Ivy) 1948

(Courtesy of Journal of American Medical Association)

Figure 1. Artificial respiration

Results

LUNG VENTILATION

Table I shows the results of the various methods of artificial respiration on 26 normal adult healthy male volunteers rendered unconscious and totally apneic with pentothal and curare mixtures. All of the "push-pull" methods (Arm-Lift Back-Pressure, Hip-Lift Back-Pressure, Hip-Roll Back-Pressure, and Arm-Lift Chest-Pressure) which use a double maneuver resulting in active inspiration and active expiration are two to three times as efficient in getting air in and out of the lungs as the Schafer Method. This occurred despite the fact that, in this series, the Schafer Method was performed with "back-pressure" and a spring-off or quick-release at the end of the pressure in order to give greater ventilation than with the standard Schafer Prone Pressure. The Eve Rocking Method (mechanical) gave values intermediate between the Schafer and the "push-pull" manual techniques. The Silvester (Arm-Lift Chest-Pressure) Method gave values as great as the better prone methods; however, previous tests have shown that in over one half of the cases the tongue falls back into the throat and prevents air from reaching the lungs.

The Pole-top Method was shown to give adequate ventilation and should be applied immediately in case the victim is on a pole. However, he should be lowered to the ground and one of the "push-pull" methods started as soon as possible, since his position on the pole will impede circulation due to the pooling of blood in the dependent parts of the body.

CIRCULATORY EFFECTS

Although getting air in and out of the lungs remains the prime goal of artificial respiration, it is important to know how much oxygen passes into the blood in the lungs and is carried to the body cells. In 15 subjects whose respirations had been stopped with drugs, each method was performed for 15 minutes. Blood specimens were drawn during and at the end of the procedures. In three out of nine cases in which the Schafer Method (with back-pressure and spring-off release) was used, the artificial respiration was found to be so inadequate that it was necessary to stop the procedure after several minutes because the condition of the subject was deteriorating. In all cases where the Schafer Method was stopped, the "push-pull" method which immediately preceded it and the one which immediately followed it were found to be completely adequate and the patients remained in good condition throughout the 15-minute testing period.

Analysis of the blood specimens revealed that in all of the methods except the Schafer Method, the average values for oxygen saturation of the arterial blood were at near-normal levels. The mean value for the Schafer Method was at an alarmingly low level.

FATIGUE OF THE OPERATOR

From a purely practical standpoint, it is important to know how fatiguing the various methods are. A selected group of average sized operators performed each of the methods on normal victims who were kept asleep with anaesthetic agents. They performed each method for 10 minutes and rested 30 minutes between methods. During the tests the amount of work that the operators performed was measured on a metabolism spirometer by calculating the amount of oxygen they used during the application of each method. They also were asked how much fatigue they felt with the methods.

The results indicated that the Schafer Method was always easiest and produced less fatigue. The Hip-Lift Back-Pressure Method resulted in the greatest expenditure of energy and caused the greatest fatigue; the Hip-Roll Back-Pressure Method was the second most difficult. The Arm-Lift Back-Pressure Method (Nielsen) and the Arm-Lift Chest-Pressure Method (Silvester) occupied an intermediary position. Under the duress of the tests all of the operators, including two female medical students, were able to complete the 10 minute period with all of the methods.

RATE OF PERFORMANCE

Use of the pneumotachograph (sensitive air-flow meter) makes it possible to accurately measure the time required for each phase of the artificial-respiration cycle. The "push-pull" methods each have four phases: (1) Lift, or Roll—Active Inspiration; (2) Release—Passive Expiration; (3) Press—Active Expiration; and (4) Release—Passive Inspiration. Each of these phases was found to require an optimum duration of $1^{1}/_{2}$ seconds, or 6 seconds for the entire cycle. The passive, or release, phases are not important here and may be slightly accelerated, since the next phase is always an active one in the same direction of flow. Thus, a rate of 10 to 12 times per minute with each complete cycle occupying 5 to 6 seconds is found to be best.

PEDAGOGICAL AND PERFORMANCE ASPECTS

In order to appraise the teaching and performance factors concerned with the various methods, 1000 Naval Recruits and Waves were given lecture-demonstrations of the prone "push-pull" methods and were then required to perform each of the methods for ten minutes. Despite the random pairing of operators and subjects, there were only a few cases where the operator could not complete the 10-minute performance period under the pressure of the experiment. The Arm-Lift Back-Pressure Method was found to be the easiest of the prone "push-pull" methods to perform, and it was performed relatively more accurately than the hip methods after short periods of indoctrination. The Hip-Lift Back-Pressure was the most difficult to perform but was applied with fewer errors than the Hip-Roll Back-Pressure Method. This latter method was found to be more difficult to understand and apply correctly, and became awkward with prolonged use.

Table I. Lung Ventilation with Various Methods of Artificial Respiration

Method* (All performed at rate of 10 to 12 complete cycles per minute)	Tidal Volumes, Cubic Centimeters per Complete Respiratory Cycle
Schafer (Back-pressure with spring-off)	485
Eve Rocking†	751
Hip-Roll Back-Pressure	967
Arm-Lift Back-Pressure	1,056
Arm-Lift Chest-Pressure**	1,069
Hip-Lift Back-Pressure	1,140
Pole-top Method‡	725

* Twenty-six cases, except where noted.

† Ten cases only.

** Fifteen cases only.

‡ Five cases only.

Both the Hip-Lift Back-Pressure and Hip-Roll Back-Pressure Methods were significantly easier to perform when an adjunct was used, such as a towel, belt, or rope, under the hips for lifting or rolling.

Summary

A comparative evaluation of manual methods of resuscitation has been made possible by the development of a method for producing prolonged drug-induced apnea in normal human volunteers, using varying amounts of sodium pentothal and curare drugs. This renders the subject unconscious and unable to breathe, in which state he closely resembles the victim who requires artificial respiration.

Tests on lung ventilation have revealed that all of the "push-pull" manual methods are two to three times as effective, as regards getting air in and out of the lungs, as the commonly used Schafer Method. Use of "back-pressure" instead of prone pressure almost doubles the ventilation with the Schafer Method. The Eve Rocking Method, a mechanical method, gives ventilatory volumes intermediary between the Schafer and the "push-pull" methods. The Pole-Top Method gives adequate ventilation and should be started immediately when a lineman requires artificial respiration. However, he should be lowered to the ground as soon as possible and one of the more efficient prone methods should be started.

Tests on the circulatory effects of the methods have indicated that the Schafer Method was so inadequate that it had to be stopped in three out of nine cases because of the deteriorating condition of the subject. In each case one of the "push-pull" techniques was able to adequately sustain the subjects for full 15-minute test periods immediately before and after the Schafer test period which failed. The oxygen saturation of arterial blood was near normal with all other methods, but was alarmingly depressed with the Schafer Method.

The Schafer Method was found to be the least fatiguing and require the least work. The Hip-Lift Back-Pressure and Hip-Roll Back-Pressure Methods were most fatiguing and the most demanding as regards the actual measurement of energy required. The Arm-Lift Back-Pressure and the Arm-Lift Chest-Pressure Methods occupied intermediary positions. Large groups of Naval Recruits and Waves were able to perform the various prone "push-pull" methods for ten minutes each. They found the Arm-Lift Back-Pressure easiest to do, and performed it more accurately than any of the hip methods. Of the latter, the Hip-Lift Back-Pressure was most difficult, but was performed relatively more accurately than the Hip-Roll Back-Pressure, which was more difficult to understand and was awkward with prolonged performance.

Although the Arm-Lift Chest-Pressure (Silvester) Method gives adequate ventilation and has survived for the past century, the use of the supine position predisposes to obstruction of the airway due to the tongue falling into the throat. This makes it impractical for general use.

Of the prone "push-pull" methods, the Arm-Lift Back-Pressure is the easiest method, and has been used successfully for 20 years in the Scandinavian countries. The Hip-Lift Back-Pressure Method gives slightly greater ventilation, but is more difficult to perform; the Hip-Roll Back-Pressure Method is easier but is more difficult to learn and perform correctly.

Trained personnel should probably know several of the manual resuscitation methods. The two preferred methods would be the Arm-Lift Back-Pressure and the Hip-Lift Back-Pressure. These would provide ready alternatives in cases of injury to or inability to manipulate either the arms or the legs. Since time is of prime importance, one of these methods must be started immediately when resuscitation is required. In the case of a lineman on a pole, the pole-top method should be started at once, and as soon as he can be lowered to the ground one of these "push-pull" methods should be substituted.

No Discussion

A Universal Power Circle Diagram

RALPH D. GOODRICH, JR.
MEMBER AIEE

POWER SYSTEM engineers recognize the utility of the circle diagram. At the same time it is generally agreed that the necessity of plotting new circles for every change in transmission line constants or terminal voltages, limits their use considerably. In the diagram to be described the circles are printed or multilithed beforehand. Solution of a circle diagram problem then consists of a selection of the appropriate circle or circles on the diagram and the location of the point from which to measure phasor power. Furthermore, since circles are immediately available for any combination of terminal voltages, the diagram is useful for the plotting of such auxiliary curves as receiving end power versus receiving end voltage or receiving end voltage versus receiving end power factor with all other quantities held constant.

The formulas for the diagram are based on general circuit constants, and consequently the diagram is not restricted to systems containing transmission lines only. Indeed any constant impedance elements such as terminal transformers with or without taps, shunt reactors, or series capacitors may be included.

Fundamental Considerations

The new diagram is based on the translation of the origin from the point of zero phasor power to the centers of the power circles. Hence, all the power circles are concentric since their centers are at the origin, and sending-and-receiving end operating points lie on the same circle because the original receiving- and sending-end circles have the same radii. Furthermore, a very simple relationship exists between the location of the sending- and receiving-end operating points, so that when one has been found the other can be obtained easily.

Any problem in plane analytic geometry can be expressed in either Cartesian or polar co-ordinates. The combination of first one and then the other used in this paper is admittedly arbitrary, but it lends itself both to theoretical considerations and to practical problems.

In Cartesian co-ordinates, the equations of the power circles are expressed as

$$(P_R+P_R')^2+(Q_R+Q_R')^2=r^2 \qquad (1)$$

$$(P_S-P_S')^2+(Q_S-Q_S')^2=r^2 \qquad (2)$$

where

P_R = receiving end power
$P_R'=(e_R/b)^2(AB)_{RP}$
P_S = sending end power
$P_S'=(e_S/b)^2(DB)_{RP}$
$r=e_Se_R/b$
Q_R = receiving end reactive, and is positive for a lagging power factor load
$Q_R'=(e_R/b)^2(AB)_{IP}$
Q_S = sending end reactive
$Q_S'=(e_S/b)^2(DB)_{IP}$
e_R = absolute value of receiving end voltage
e_S = absolute value of sending end voltage

The general circuit constants are defined by

$$A=A_r+jA_i=a\underline{/\alpha}$$
$$B=B_r+jB_i=b\underline{/\beta}$$
$$D=D_r+jD_i=d\underline{/\Delta}$$
$$AB=(AB)_{RP}+j(AB)_{IP}=(A_r-jA_i)(B_r+jB_i)$$
$$DB=(DB)_{RP}+j(DB)_{IP}=(D_r-jD_i)(B_r+jB_i)$$

When the origin is located at the center of the circles, the equations become

$$M_R^2+N_R^2=r^2 \qquad (3)$$

$$M_S^2+N_S^2=r^2 \qquad (4)$$

whence

$M_R=P_R+P_R'$
$M_R=P_S-P_S'$
$N_R=Q_R+Q_R'$
$N_S=Q_S-Q_S'$

Equations 1 and 2 are derived in the appendix in which it also is proved that

$$N_R/M_R=\tan(\beta-\delta) \qquad (5)$$

$$N_S/M_S=\tan(\beta+\delta) \qquad (6)$$

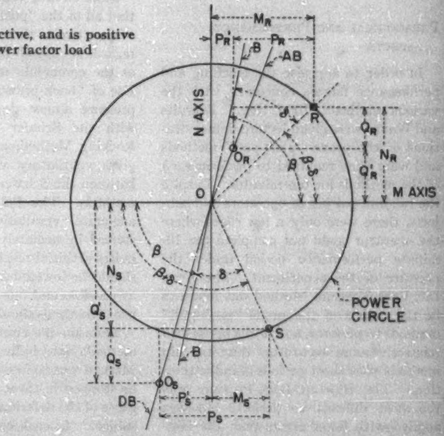

Figure 1. General relations of the universal circle diagram

Paper 51-379, recommended by the AIEE System Engineering Committee and approved by the AIEE Technical Program Committee for presentation at the AIEE Fall General Meeting, Cleveland, Ohio, October 22–26, 1951. Manuscript submitted October 16, 1950; made available for printing August 30, 1951.

Ralph D. Goodrich, Jr. is with United States Bureau of Reclamation, Denver, Colo.

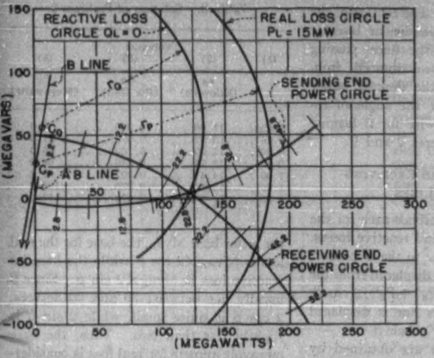

Figure 2. Solution of Problem 1. Sending and receiving end power circles were traced from universal diagram. Note that loss circles are associated with receiving end circle only

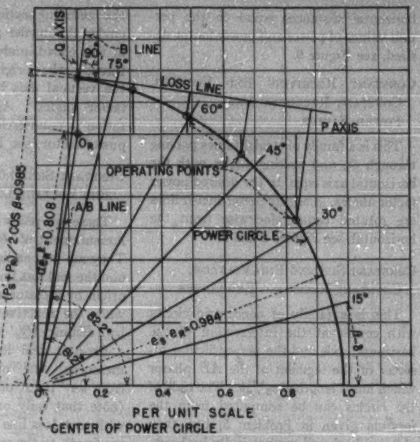

Figure 3. Solution of Problem 2. Illustrates location of O_R, use of loss line, and use of $\beta-\delta$

where δ is the phase angle between e_S and e_R. These general relationships are illustrated in Figure 1.

Besides verifying the preceding formulas and the previously mentioned fact that the receiving-and-sending end operating points "*R*" and "*S*" lie on the same circle the figure lends itself to a number of other important observations.

1. Receiving end conditions occur in the first quadrant.
2. Sending end conditions occur in the third and fourth quadrants.
3. The auxiliary origin for measuring receiving end power and reactive, O_R, lies on the phasor *AB*. (Its distance from the origin is ae_R^2/b.)
4. The auxiliary origin for measuring sending end power and reactive, O_S, lies on the phasor *DB*. (Its distance from the origin is de_S^2/b.)
5. The angular relation between the phasor *B* and corresponding receiving-and-sending end operating points, *R* and *S*, is shown. (The phasor *B* plays an important part in the loss loci described later.) Evidently once the receiving point, *R*, has been found, δ can be determined, and then *S* can be located.

General Use of the Diagram

The diagram consists of a blank sheet containing a set of polar co-ordinates superimposed on Cartesian co-ordinates. In general, the polar co-ordinates are drawn to a greater degree of refinement than the Cartesian, and by including only the first quadrant, a drawing suitable for 3-place accuracy can be obtained without allowing the size to become unwieldy. The diagram is calibrated in per unit, and the megavolt-ampere base is usually selected to make "*b*" equal to 1.00. This choice of base has the obvious advantage of eliminating "*b*" from the denominator of several formulas so that the following hold true:

1. $r = e_S e_R$.
2. Distance from *O* to O_R is ae_R^2.
3. Distance from *O* to O_S is de_S^2.

With O_R and O_S located, (on the phasors *AB* and *DB*), it is a simple matter to scale off horizontal and vertical projections to *R* and *S*, and so obtain per-unit values of phasor power. See subsequent Illustrative Problems 1, 2, 3, 4, and 5.

Table I. Solution of Problem 2

(1)	(2)	(4)	(5)	(6)	(7)	(9)	(10)
P_R (Megawatts)	P_R (Per Unit)	Q_R (Per Unit)	Power Factor Per Cent	$\beta-\delta$ (Degrees)	δ (Degrees)	P_L (Per Unit)	P_L (Megawatts)
0	0.000	+0.176	0.0*	82.2	0.0	0.002	0.15
50	0.176	+0.135	79.3*	71.8	10.4	0.020	1.55
100	0.352	+0.057	98.7*	60.3	21.9	0.071	5.49
150	0.528	−0.066	99.2**	48.3	33.9	0.170	13.14
200	0.704	−0.278	93.7**	31.9	50.3	0.355	27.44

* Lagging power factor

** Leading power factor

Use of the first quadrant only involves special consideration of sending end conditions. A rotation of 180 degrees will superimpose the third quadrant on the first, where *DB* and O_S can be conveniently located. From O_S phasor power is measured positively to the left and positively downward. This is satisfactory until $\beta+\delta$ becomes greater than 90 degrees. Then the operating point passes into the second quadrant where there is no co-ordinate system. One way to solve the difficulty is to locate an image origin with respect to the *N* axis, O_S', in the second quadrant, and allow δ to increase clockwise into the first quadrant. The radii are calibrated with the supplements of their first quadrant values to facilitate this mode of operation.

Special Receiving End Loci

Since circles for any combination of operating voltages are immediately available, it is possible to plot auxiliary curves to describe system operations subject to certain restrictions. Points for these curves lie on one or more of the loci described below. The loci are discussed for receiving end conditions, but similar equations can be obtained for sending end loci.

CONSTANT RECEIVING END POWER

This is a family of straight lines parallel to the *AB* phasor offset to the right by horizontal distances equal to the per-unit values of power and power factor desired, see Figure 9.

CONSTANT RECEIVING END VOLTAGE, CONSTANT RECEIVING END POWER FACTOR

This is a family of straight lines passing through O_R and making angles with the horizontal axis equal to the desired power factor angles. Lagging power factor lines are rotated counterclockwise from the horizontal, see Figures 5 and 7.

CONSTANT SENDING END VOLTAGE, CONSTANT RECEIVING END POWER

This is a family of concentric circles with center at the intersection of the horizontal axis and the perpendicular bisector of the segment of the ***AB*** phasor which has a length of e_S^2/ab. The radii of the circles can be computed from the formula given in Problem 5, but they also can be found geometrically by locating any receiving end points which represent the required amounts of power. These points may be determined, for instance, by the intersection of a Constant Power Line with the Constant Unity Power Factor Circle. When the center and one point on the circumference have been determined, the circle can be drawn, see Figure 9.

CONSTANT SENDING END VOLTAGE, CONSTANT RECEIVING END POWER FACTOR

This is a family of circles containing as a common chord the phasor segment of the ***AB*** line of length e_S^2/ab described in the preceding section. The centers of the circles lie on the perpendicular bisector of this chord, and on the lines passing through the origin and rotated from the vertical axis by the desired power factor angles. Again the angle of rotation is counterclockwise for a lagging power factor, see Figures 7 and 9.

CONSTANT SENDING AND RECEIVING END VOLTAGE LOSS LINES

These are really reference axes for the measurement of real and reactive losses. They are perpendicular to the B phasor; and the real loss line is displaced from the origin by a distance $(P_S'+P_R')/2\cos\beta$, while the reactive loss line is displaced by a distance $(Q_S'+Q_R')/2\sin\beta$.

Per-unit real losses are obtained by measuring the perpendicular distance from any point on the operating circle, (note that only one circle is associated with each loss line because both voltages are fixed), to the real loss line. Similarly, the perpendicular distance to the reactive loss line is the reactive loss in per unit. Since the two loss lines are parallel it follows that P_L-Q_L is a constant equal to $(P_S'+P_R')/2\cos\beta$ minus $(Q_S'+Q_R')/2\sin\beta$, where P_L is the real loss in per unit, and Q_L is the reactive loss in per unit. Hence, only one loss need be measured at each operating point, and the other can be obtained by subtraction. It will be noted that for all practical purposes Q_L is negative below surge impedance loading and positive above it.

A peculiarity of the loss lines is that the megavolt-ampere base is different from the base of the operating circles. Calling the latter base Mva_B, the base for the real loss is $\text{Mva}_B\times 2\cos\beta$ while the base for reactive loss is $\text{Mva}_B\times 2\sin\beta$. Since β usually lies between 70 and 90 degrees, $2\cos\beta$ is quite small, while $2\sin\beta$ is slightly less than two. Thus, the base megavolt-ampere for real loss is considerably smaller than Mva_B, which is equivalent to plotting the losses to a greatly expanded scale. Conversely the reactive losses are plotted to a somewhat compressed scale, but it has been found that their accuracy is quite adequate. See Figure 3.

Table II. Solution of Problem 3

Columns (1)	(2)	(5)	(6)
r	e_S (Kilovolts)	P_R (Per Unit)	P_R (Megawatts)
0.808	11.66	0.000	0.0
0.85	12.27	0.075	21.3
0.90	12.99	0.163	46.3
0.95	13.71	0.240	68.2
1.00	14.44	0.307	87.2
1.05	15.16	0.372	105.7
1.10	15.88	0.436	123.9

CONSTANT RECEIVING END VOLTAGE, LOSS CIRCLES

If the sending end voltage is allowed to vary, then the locus of points on the receiving end diagram with equal losses are concentric circles. It will be convenient to define P_L' as $e_R^2/(\boldsymbol{DB})_{RP}$ and Q_L' as $e_R^2/(\boldsymbol{DB})_{IP}$. Then it can be shown that the center of the real loss circles lies on the B phasor at the distance $P_L'\cos\beta$ from the origin, while the center of the reactive loss circles also lies on the B phasor, but at the distance $Q_L'\sin\beta$ from the origin. The formulas for the radii of

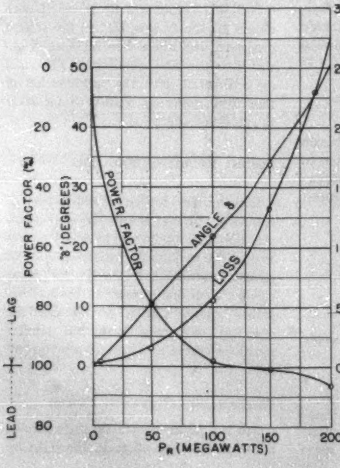

Figure 4 (left). Auxiliary curves for Problem 2 from Figure 3 and Table I. Performance of 230-kv line and transformer with constant sending end voltage of 14.2 kv, constant receiving end voltage of 220 kv

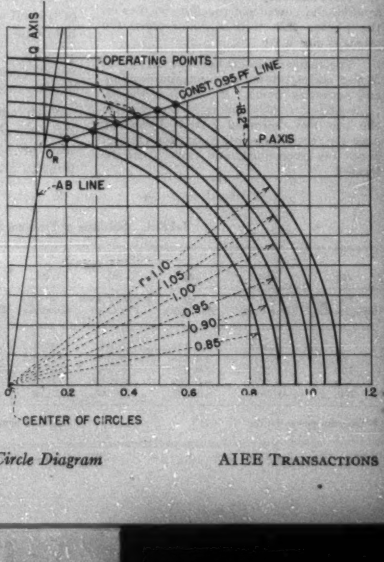

Figure 5 (right). Solution of Problem 3. Illustrates use of constant power factor line and different power circles

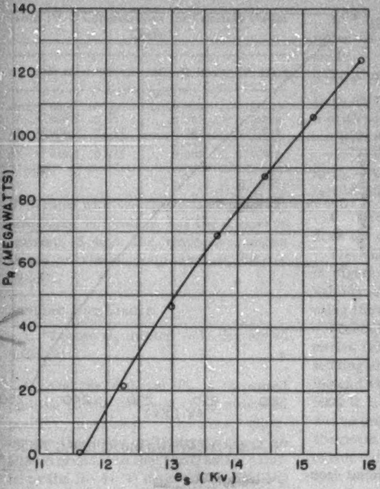

Figure 6 (left). Auxiliary curve for Problem 3 from Figure 5 and Table II. Performance of system with constant receiving end voltage of 200 kv and constant receiving end power factor of 95 per cent lagging

Figure 8 (right). Auxiliary curve for Problem 4 from Figure 7 and Table III. Performance of system with constant sending end voltage of 14.2 kv and constant receiving end power factor of 95 per cent lagging

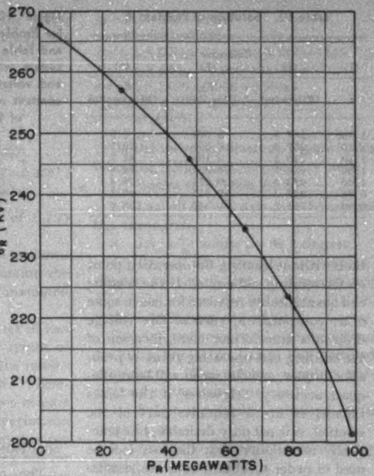

the circles are parabolic functions of the losses, and consequently evaluation is somewhat tedious. However, they can be converted to a standard form which facilitates the computation.

The equations of the real and reactive loss parabolas are

$$(P_L/P_L')=(r_P/P_L')^2+[(AB)_{RP}(DB)_{RP}/b^2-\cos^2\beta] \quad (7)$$

$$(Q_L/Q_L')=(r_Q/Q_L')^2+[(AB)_{IP}(DB)_{IP}/b^2-\sin^2\beta] \quad (8)$$

where

P_L = real loss in per unit
Q_L = reactive loss in per unit
r_P = radius of the real loss circle
r_Q = radius of the reactive loss circle

It can be seen that both of these equations are written in the form:

$$l=m^2+n \quad (9)$$

where

l = ratio of loss to a constant
m = ratio of the radius to the same constant
n = vertical offset of the vertex of the parabola, positive for real losses, negative for reactive losses, and constant for any particular set of line constants. Note that when $b=1$, all quantities in the expression for S are available from previous computations

See Figure 2.

The loss lines and the loss circles make it possible to obtain sending end condi-

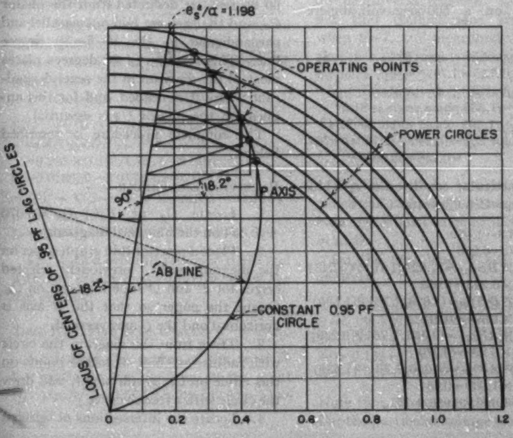
e_S^2/a = 1.198
OPERATING POINTS
POWER CIRCLES
18.2°
P AXIS
90°
LOCUS OF CENTERS OF .95 PF LAG CIRCLES
AB LINE
18.2°
CONSTANT 0.95 PF CIRCLE
0
0.2
0.4
0.6
0.8
1.0
1.2

Figure 7. Solution of Problem 4. Illustrates use of constant power factor circle

Figure 9. Solution of Problem 5. Illustrates use of constant power circle and constant power line

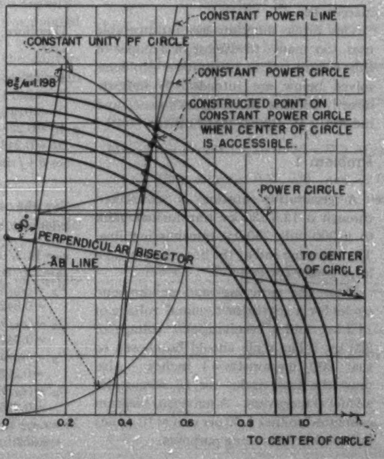
CONSTANT POWER LINE
CONSTANT UNITY PF CIRCLE
e_S^2/a=1.198
CONSTANT POWER CIRCLE
CONSTRUCTED POINT ON CONSTANT POWER CIRCLE WHEN CENTER OF CIRCLE IS ACCESSIBLE.
POWER CIRCLE
90°
PERPENDICULAR BISECTOR
AB LINE
TO CENTER OF CIRCLE
0
0.2
0.4
0.6
0.8
1.0
TO CENTER OF CIRCLE

Table III. Solution of Problem 4

Columns (1) r	(2) e_R (Kilovolts)	(5) P_R (Per Unit)	(6) P_R (Megawatts)
1.198	267.8	0.000	0.0
1.15	257.0	0.092	26.1
1.10	245.8	0.168	47.7
1.05	234.7	0.228	64.8
1.00	223.5	0.276	78.4
0.95	212.3	0.317	90.1
0.90	201.2	0.347	98.6

tions without locating the operating point on the sending end circle. If the sending end quantities are required for use in some other computation, such as the voltage drop in a transformer bank, location of the sending end operating point is probably simpler, and the result will have adequate accuracy. However, if the losses themselves are a requisite part of the solution, it is not only desirable, but practically mandatory that the loss loci be used in order to obtain accurate results. In one study the desired quantities were curves of power loss and receiving-and-sending end reactive versus receiving end power for a large number of different combinations of line constants and terminal voltages. It was found necessary to draw the operating circles on tracing cloth as accurately as possible to a large scale—1.00 per unit = 20 inches. Then transparent overlays were used for the solutions of the separate problems. Loss loci were used to obtain sending end conditions, and spot checks by mathematical computations showed an error of not over ±0.002 in per unit. Other methods were either intolerably laborious, or intolerably inaccurate.

This circle diagram has innumerable uses, too many, to discuss in a paper of this nature. The illustrative problems solved below are intended to indicate directly some of the diagram's uses; and indirectly to suggest many others.

Problem 1

A generating station is connected through a 13.8-230-kv transformer bank to a 200-mile 230-kv transmission line. The receiving end of the line connects to a large power system.

Draw the receiving- and sending-end circles for a generator terminal voltage of 14.2 kv, and a receiving-end voltage of 220 kv. The scale should be chosen so that 200 megawatts = 4 inches. Also draw the loss circles for 15 megawatts and for 0 megavars. A universal diagram calibrated so that 1.00 per unit = 10 inches is available for tracing purposes.

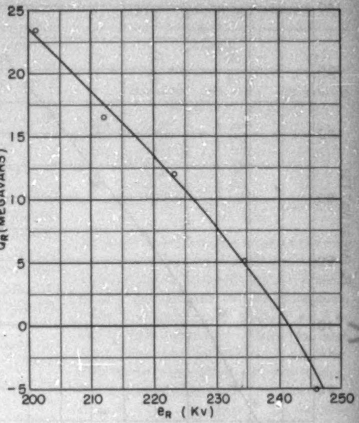

Figure 10. Auxiliary curve for Problem 5 from Figure 9 and Table V. Performance of system with constant sending end voltage of 14.2 kv, and constant receiving end power of 100 megawatts

SOLUTION

The composite general circuit constants for the line and transformer on a 100-megavolt-ampere base are:

$A = 0.884 + j0.015 \quad C = -0.002 + j0.540$
$B = 0.048 + j0.349 \quad D = 0.916 + j0.013$

In order to use the universal diagram for which 1.00 = 10 inches and have 200 megawatts equal 4 inches, it is evident that 500 megawatts must equal 10 inches and hence must equal 1.00 per unit. Therefore, the first operation is to convert the constants to a 500-megavolt-ampere base. For this operation.

A and D remain invariant
$B_{500} = 5B_{100}$
C is not required.

Therefore, on a 500-megavolt-ampere base

$A = 0.884 + j0.015 \qquad a = 0.884$
$B = 0.240 + j1.745 = 1.761\underline{/82.2^\circ}$
$D = 0.916 + j0.013 \qquad d = 0.916$
$\boldsymbol{AB} = 0.238 + j1.539$ phase angle is 81.2°
$\boldsymbol{DB} = 0.243 + j1.595$ phase angle is 81.4°
$\cos\beta + j\sin\beta = B/b = (0.240 + j1.745)/1.761$
$= 0.136 + j0.991$

For the particular condition of $e_S = 14.2$ kilovolts, $e_R = 220$ kilovolts

$e_S = 14.2/13.8 = 1.029$
$e_R = 220/230 = 0.956$
$P_S' = (e_S/b)^2(\boldsymbol{BB})_{RP} = (1.029/1.761)^2(0.243)$
$= 0.342 \times 0.243 = 0.083$
$Q_S' = (e_S/b)^2(\boldsymbol{DB})_{IP} = (1.029/1.761)^2(1.595)$
$= 0.342 \times 1.595 = 0.545$
$P_R' = (e_R/b)^2(\boldsymbol{AB})_{RP} = (0.956/1.761)^2(0.238)$
$= 0.295 \times 0.238 = 0.070$
$Q_R' = (e_R/b)^2(\boldsymbol{AB})_{IP} = (0.956/1.761)^2(1.539)$
$= 0.295 \times 1.539 = 0.454$
$r = e_S e_R/b = 1.029 \times 0.956/1.761$
$= 0.559$

$O_S = de_S^2/b\underline{/(\boldsymbol{DB})} = 0.916 \times 1.029^2/1.761 \times \underline{/81.4^\circ}$
$= 0.551\underline{/81.4^\circ}$
$O_R = ae_R^2/b\underline{/(\boldsymbol{AB})} = 0.884 \times 0.956^2/1.761 \times \underline{/81.2^\circ}$
$= 0.459\underline{/81.2^\circ}$
$P_L' = e_R^2/(\boldsymbol{DB})_{RP} = 0.956^2/0.243 = 3.761$
$Q_L' = e_R^2/(\boldsymbol{DB})_{IP} = 0.956^2/1.595 = 0.573$

On the circle diagram O_S and O_R can be located either by means of the Cartesian co-ordinates $P_S' + jQ_S'$ and $P_R' + jQ_R'$ or by means of the phasors O_S and O_R. The results will be the same and the choice is usually a matter of personal preference. However, it will be found when tracing the sending end circle from the diagram that most of the desired circle lies in the second quadrant. To make the graph fall on a usable part of the diagram, 60 degrees are deducted from the phasor O_S, and the axes are laid out parallel and perpendicular to the $\beta - \delta = 30$ degree line. This rotation of 60 degrees places most of the diagram in the second quadrant where it is needed, and for this application the phasor O_S is essential.

The complete procedure is described below.

RECEIVING END CIRCLE

1. Locate O_R at $P_R' + jQ_R' = 0.070 + j0.454$ on the universal diagram.
2. Place a piece of thin graph paper on the diagram with a previously selected origin for P and Q superimposed on O_R. Orient the paper so that the P axis is horizontal and the Q axis vertical.
3. Trace from the diagram the circle with radius $r = 0.559$, or locate points on this circle on the graph paper, and draw the circle with a french curve.
4. Locate the intersections of selected

Table IV. Computations for Constant Power Circle

	Cos θ	Sin θ	M_1-R_1 Cos θ	R_1 Sin θ
0	1.000	0.000	0.369	0.000
5	0.996	0.087	0.383	0.300
10	0.985	0.174	0.422	0.618
15	0.966	0.259	0.490	0.920
20	0.940	0.342	0.582	1.215

$\beta-\delta$ radii with the circle. Label the intersections in terms of δ as the difference between β and the respective angles shown on the diagram, that is, $\delta=\beta-(\beta-\delta)$.

Sending End Circle

1. Locate O_S rotated −60 degrees at $0.551\underline{/21.4^\circ}$.

2. On the diagram P_S is measured positive to the left, and Q_S is measured positive downward. Therefore, superimpose the origin on the graph paper on O_S and orient it so that the Q axis is parallel to the $\beta-\delta=30$ degree line, with $+Q$ pointed toward the center of the circles.

3. Trace from the graph the circle with radius $r=0.559$.

4. Locate the intersections of selected $\beta+\delta$ radii with the circle. Label the intersections in terms of δ as the difference between the respective angles shown on the diagram and β, that is, $\delta=(\beta+\delta)-\beta$. However, because of the initial rotation of 60 degrees of the whole diagram, an added 60 degrees must be subtracted from each angle.

Fifteen-Megawatt Loss Circle

1. Locate the center of the power loss circle on the diagram at the point $P_L'\cos\beta\underline{/\beta}=3.761\times0.136\underline{/82.2^\circ}=0.511\underline{/82.2^\circ}$.

2. Superimpose the graph paper on the diagram as for the receiving circle and locate the center of the loss circle on the graph paper.

3. Compute

$$l=P_L/P_L'=(15/400)/3.761=0.009970$$
$$n=(AB)_{RP}(DB)_{RP}/b^2-\cos^2\beta$$
$$=0.238\times0.243/1.761^2-0.136^2$$
$$=0.018650-0.018496=0.000154$$
$$r_P/P_L'=\sqrt{l-n}=\sqrt{0.009970-0.000154}$$
$$=0.099$$
$$r_P=0.099P_L'=0.099\times3.761=0.372$$

4. With a per-unit radius of 0.372 and with the center located above, draw the loss circle.

Zero Reactive Loss Circle

1. Locate the center of the reactive loss circle on the diagram at the point $Q_L'\sin\beta\underline{/\beta}=0.573\times0.991\underline{/82.2^\circ}=0.568\underline{/82.2^\circ}$.

2. Locate the center on the graph paper as was done for the power loss circle.

3. Compute

$$l=Q_L/Q_L'=0$$
$$n=(AB)_{IP}(DB)_{IP}/b^2-\sin^2\beta$$
$$=1.539\times1.595/1.761^2-0.991^2$$
$$=0.791584-0.982081=-0.190497$$
$$r_Q/Q_L'=\sqrt{l-n}=\sqrt{0+0.190497}=0.436$$
$$r_Q=0.436Q_L'=0.436\times0.573=0.250$$

4. With a per-unit radius of 0.250 draw the circle.

The completed circle diagram is shown in Figure 2. Check points to assure the validity of the results can be computed using the original constants.

It should be noted that one set of loss circles can be used with any values of sending end voltage so long as the receiving end voltage is held constant. Therefore, it is possible to locate two centers and an origin on the diagram, superimpose the graph paper, and trace off any number of concentric receiving end circles, one for each sending end voltage. Loss circles can then be drawn with appropriate radii to use in predicting sending end conditions.

Problem 2

For the set of constants used in Problem 1 and for the same voltages, draw curves of P_R versus power factor, power losses, and phase angle, δ, between sending and receiving terminals.

Solution

This problem could be solved on the receiving circle plotted for Problem 1, but it is preferable to solve it independently on the universal diagram. It was pointed out that computations are simplified when $b=1$, and accordingly the conversion to a new megavolt-ampere base will be made first.

On 100 megavolt-ampere base:

$$A=0.884+j0.015$$
$$B=0.048+j0.349=0.352\underline{/82.2^\circ}$$
$$D=0.916+j0.013$$

The base is to be changed to the value which will make $b=1$. Therefore, the old base and B must be multiplied by $1/0.352=2.841$.

On the new base of 284.1 megavolt-amperes

$$A=0.884+j0.015 \qquad a=0.884$$
$$B=0.136+j0.992=1.001\underline{/82.2^\circ}$$
$$D=0.916+j0.013 \qquad d=0.916$$
$$AB=0.135+j0.875\underline{/81.2^\circ}$$
$$DB=0.137+j0.907\underline{/81.4^\circ}$$

Note that B now equals $\cos\beta+j\sin\beta$. For the particular voltage conditions:

$$e_S=14.2/13.8=1.029$$
$$e_R=220/230=0.956$$
$$P_S'=e_S^2(DB)_{RP}=1.029^2\times0.137=0.145$$
$$P_R'=e_R^2(AB)_{RP}=0.956^2\times0.135=0.123$$
$$r=e_Se_R=1.029\times0.956=0.984$$
$$O_R=ae_R^2\underline{/AB}=0.884\times0.956^2\underline{/81.2^\circ}=0.808\underline{/81.2^\circ}$$

On the universal diagram, Figure 3, the following initial constructions are made

1. Locate $O_R=0.808\underline{/81.2^\circ}$
2. Lay off the P_R axis as a horizontal line through O_R.
3. Lay off the line $\beta=82.2$ degrees.
4. Lay off the power loss line perpendicular to the β line at the distance $(P_S'+P_R')/2\cos\beta=(0.145+0.123)/2\times0.136=0.985$ from the origin.

Ensuing work can best be accomplished by filling out Table I from this itemized procedure. (The column numbers correspond to the item numbers.)

1. Select appropriate values of P_R in megawatts.
2. Convert to per unit by dividing by 284.1.
3. Lay off these per-unit distances on the P_R axis to the right from O_R, and erect perpendiculars to intersect the power circle $r=0.984$.
4. Measure Q_R, the vertical ordinates from the P_R axis to the circle.
5. Compute power factor = cos (arctan Q_R/P_R).

4(A) and 5(A). As an alternative to items 4 and 5, the constant power factor lines from the operating points to O_R can be drawn, and the power factor angle can be measured with a protractor.

6. Record the angle $\beta-\delta$ from the M axis to each operating point.
7. Compute $\delta=\beta-(\beta-\delta)=82.2-(\beta-\delta)$.
8. Drop perpendiculars from the operating points to the loss line.
9. Measure the per-unit length of the perpendiculars.
10. Obtain loss in megawatts by multiplying the per-unit losses by

$$\text{Mva}_B2\cos\beta=284.1\times2\times0.136=77.3\text{ Mva}$$

11. Plot columns (5), (7), and (10) of Table I versus power received, see Figure 3.

Table V. Solution of Problem 5

Columns (2)	(3)	(5)	(6)
r	e_R (Kilovolts)	Q_R (Per Unit)	Q_R (Megavars)
1.10	245.8	−0.018	−5.1
1.05	234.7	+0.018	+5.1
1.00	223.5	0.042	+11.9
0.95	212.3	0.058	16.5
0.90	201.2	0.082	23.3

Problem 3

With the receiving end voltage held constant at 220 kilovolts, plot sending end voltage versus receiving end power with constant receiving end power factor of 95 per cent lagging.

Solution

The initial data will be the same as for Problem 2.

As in Problem 2, the phasor O_R is laid off, and the horizontal P_R axis is drawn. In addition, the constant 95 per cent power factor line is drawn through O_R at the counterclockwise power factor angle 18.2° from the horizontal, see Figure 5.

In order to use established circles on the diagram, it will be convenient to use the power circle radius, r, as an independent parameter. The procedure is given below with item numbers corresponding to columns in Table II:

1. Select appropriate values of r
2. Compute sending end kilovolts from the formula

$$e_{S(kv)} = e_{S(PU)} \times 13.8 = (r/e_R)13.8 = 13.8r/0.956$$
$$= 14.435r$$

3. Locate the intersections of the constant power factor line with the selected circles.
4. Drop perpendiculars from these intersections to the P_R axis.
5. Measure the distances in per-unit from O_R to the perpendiculars.
6. Multiply the per-unit distances by 284.1 to obtain P_R in megawatts.
7. Plot P_R versus e_S, see Figure 6.

Problem 4

With the sending end voltage held constant at 14.2 kilovolts, plot receiving end power versus receiving end voltage for a constant load power factor of 95 per cent lagging.

Solution

The procedure consists of finding a series of operating points on the constant power factor circle, locating the corresponding O_R's, and measuring the horizontal projection between the two. Since e_R is a variable, O_R is also a variable, but all O_R's will lie on the $\mathbf{AB}$ phasor.

The constant power factor circle is located on Figure 7 as follows:

1. Lay off the phasor

$$e_S^2/a\underline{/\mathbf{AB}} = 1.029^2/0.884\underline{/81.2^\circ} = 1.198\underline{/81.2^\circ}$$

2. Project the perpendicular bisector of this phasor into the second quadrant.
3. Locate the intersection of the perpendicular bisector with the line in the second quadrant rotated across 0.95 = 18.2° from the vertical axis. This point is the center of the desired circle.
4. Draw the circle through the two ends of the $e_S^2/a\underline{/\mathbf{AB}}$ phasor.

Again it is convenient to select values of r for the parameter to allow the use of established circles, see Table III.

1. Select appropriate values of r.
2. Compute $e_R = (r/e_S) \times 230 = 223.5r$.
3. Locate receiving end operating points at the intersections of the operating circles with the constant power factor circle.
4. Draw receiving end operating phasors between the operating points and the $\mathbf{AB}$ phasor.
5. Measure the horizontal projections of these phasors in per unit.
6. Convert to megawatts by multiplying by 284.1.
7. Plot e_R versus P_R.

Problem 5

Plot a curve of receiving end voltage versus receiving end reactive for a constant sending end voltage of 14.2 kilovolts, and a constant received power of 100 megawatts.

Solution

The operating points now lie on the constant power circle, and since the received power is constant, the horizontal projections of the receiving end phasors must lie between the $\mathbf{AB}$ phasor and the constant power line, parallel to the $\mathbf{AB}$ phasor, and to the right of it at the distance 100/284.1 = 0.352.

The center of the constant power circle can be located by finding the intersection of the perpendicular bisector of the $e_S^2/a\underline{/\mathbf{AB}}$ phasor with the horizontal axis, and one point on the circle can be found by locating the interesection of the constant power line and the unity power factor circle. The center of this circle lies at intersection of the above perpendicular bisector with the vertical axis.

However, for this particular problem, the R/X ratio of the line is so low that the perpendicular bisector is very nearly parallel to the horizontal axis. Consequently, the center of the circle is so far away as to be inaccessible, and recourse must be had to the formulas of the center and radius of the circle in order to plot the necessary portion of it.

The center is at the distance $M_1 = e_S^2/2(\mathbf{AB})_{RP}$ from the center of the power circles, and the radius of the circle is

$$R_1 = M_1\sqrt{1 - 2P_R/M_1}$$
$$= M_1 - P_R \text{ when } P_R \text{ is small compared with } M_1$$

By using a parameter, θ, points (X, Y) on the constant power circle can be found from the parametric equations

$$X = M_1 - R_1 \cos\theta$$
$$Y = R_1 \sin\theta$$

For this set of constants

$$M_1 = e_S^2/2(AB)_{RP} = 1.029^2/2 \times 0.135 = 3.921$$
$$R_1 = M_1\sqrt{1 - 2P_R/M_1} = 3.921\sqrt{1 - 2 \times 0.352/3.921}$$
$$= 3.921\sqrt{0.820454} = 3.921 \times 0.906 = 3.552$$

Note that $M_1 - P_R = 3.921 - 0.352 = 3.569$

After drawing the constant power circle:

1. Locate operating points at the intersections of the constant power circle and selected operating circles.
2. Record the radii of these circles.
3. Compute $e_R = 223.5r$.
4. Drop perpendiculars from the operating points to the constant power line.
5. Record the lengths of the perpendiculars.
6. Convert the values to megavars by multiplying by 284.1.
7. Plot e_R versus Q_R, see Figure 10.

It will be seen that the receiving end phasor is not required. However, it has been drawn in for $r = 0.90$ to aid in visualizing the construction.

Beside providing a ready means for plotting power circles and loss loci for general studies the diagram is useful in such specific power system design problems as the selection of transformer taps, the determination of required reactive capacity, and the determination of adequate conductor size.

Appendix

Conversion of General Circuit Constant Formulas to Scalar Form

Let

$$E_S = AE_R + BI_R \qquad (10)$$

Multiply both sides by $\mathbf{E}_R$

$$E_S\mathbf{E}_R = AE_R\mathbf{E}_R + BI_R\mathbf{E}_R$$

Since

$$EI = S = P + jQ$$

Then

$$EI = P - jQ$$

Therefore

$$E_S\mathbf{E}_R = Ae_R^2 + B(P_R - jQ_R)$$

Let E_R be the phasor of phase reference so that

$$E_R = E_R = E_{Rr} + j0 = e_R$$

Therefore

$$e_R(E_{Sr} + jE_{Si}) = e_R^2(A_r + jA_i) + (P_R - jQ_R)(B_r + jB_i) \tag{11}$$

Resolve equation 11 into two equations, one involving real quantities only, the other involving imaginary quantities only

$$e_R E_{Sr} = e_R^2 A_r + P_R B_r + Q_R B_i \tag{12}$$

$$e_R E_{Si} = e_R^2 A_i + P_R B_i - Q_R B_r \tag{13}$$

Square equations 12 and 13:

$$e_R^2 E_{Sr}^2 = e_R^4 A_r^2 + 2e_R^2 P_R A_r B_r + 2e_R^2 Q_R A_r B_i + P_R^2 B_r^2 + 2P_R Q_R B_r B_i + Q_R^2 B_i^2 \tag{14}$$

$$e_R^2 E_{Si}^2 = e_R^4 A^2_i + 2e_R^2 P_R A_i B_i - 2e_R^2 Q_R A_i B_r + P_R^2 B_i^2 - 2P_R Q_R B_r B_i + Q_R^2 B_r^2 \tag{15}$$

Add equations 14 and 15

$$e_R^2 e_S^2 = e_R^4 a^2 + 2e_R^2 P_R(A_r B_r + A_i B_i) + 2e_R^2 Q_R(A_r B_i - A_i B_r) + P_R^2 b^2 + Q_R^2 b^2$$

Since

$$AB = (AB)_{RP} + j(AB)_{IP} = (A_r B_r + A_i B_i) + j(A_r B_i - A_i B_r)$$

$$a^2 e_R^4 + 2e_R^2\,[P_R(AB)_{RP} + Q_R(AB)_{IP}] + b^2 P_R^2 + b^2 Q_R^2 = e_S^2 e_R^2 \tag{16}$$

Collect terms involving P_R and Q_R

$$[b^2 P_R^2 + 2e_R^2(AB)_{RP} P_R] + [b^2 Q_R^2 + 2e_R^2(AB)_{IP} Q_R] + a^2 e_R^4 = e_S^2 e_R^2$$

completing squares

$$[b^2 P_R^2 + 2e_R^2(AB)_{RP} P_R + e_R^4(AB)_{RP}^2/b^2] + [b^2 Q_R^2 + 2e_R^2(AB)_{IP} Q_R + e_R^4(AB)_{IP}^2/b^2] - e_R^4[(AB)_{RP}^2 + (AB)_{IP}^2]/b^2 + a^2 e_R^4 = e_S^2 e_R^2$$

whence

$$[bP_R + (e_R^2/b)(AB)_{RP}]^2 + [bQ_R + (e_R^2/b)(AB)_{IP}]^2 = e_S^2 e_R^2$$

Divide both sides by b^2

$$[P_R + (e_R/b)^2(AB)_{RP}]^2 + [Q_R + (e_R/b)^2(AB)_{IP}]^2 = e_S^2 e_R^2/b^2$$

or

$$(P_R + P_R')^2 + (Q_R + Q_R')^2 = r^2 \tag{1}$$

Similarly

$$(P_S - P_S')^2 + (Q_S - Q_S')^2 = r^2 \tag{2}$$

Derivation of Formulas Involving δ the Angle between E_S and E_R Equations

Let δ be positive when E_R is the phase reference so that

$$E_S = e_S\underline{/\delta} = e_S \cos\delta + je_S \sin\delta = E_{Sr} + jE_{Si}$$

Then when E_S is the phase reference

$$E_R = e_R\underline{/-\delta} = e_R \cos\delta - je_R \sin\delta = E_{Rr} + jE_{Ri}$$

Derivation of equation 5:
Divide equation 13 by equation 12

$$\frac{e_R E_{Si}}{e_R E_{Sr}} = \frac{e_R^2 A_i + P_R B_i - Q_R B_r}{e_R^2 A_r + P_R B_r + Q_R B_i} = \frac{e_R e_S \sin\delta}{e_R e_S \cos\delta}$$

Cross multiply

$$e_R^2 A_i \cos\delta + P_R B_i \cos\delta - Q_R B_r \cos\delta = e_R^2 A_r \sin\delta + P_R B_r \sin\delta + Q_R B_i \sin\delta$$

Collect terms in e_R^2, P_R and Q_R

$$e_R^2(A_i \cos\delta - A_r \sin\delta) + P_R(B_i \cos\delta - B_r \sin\delta) = Q_R(B_r \cos\delta + B_i \sin\delta)$$

$$e_R^2(A_i \cos\delta - A_r \sin\delta) + P_R(b \sin\beta \cos\delta - b \cos\beta \sin\delta) = Q_R(b \cos\beta \cos\delta + b \sin\beta \sin\delta)$$

$$e_R^2(A_i \cos\delta - A_r \sin\delta) + bP_r \sin(\beta-\delta) = bQ_R \cos(\beta-\delta)$$

$$(e_R^2/b)(A_i \cos\delta - A_r \sin\delta) + P_R \sin(\beta-\delta) = Q_R \cos(\beta-\delta)$$

$$(e_R^2/b)(A_i \cos\delta - A_r \sin\delta) - (e_R/b)^2(AB)_{RP} \sin(\beta-\delta) + (e_R/b)^2 \times (AB)_{IP} \cos(\beta-\delta) + P_R \sin(\beta-\delta) + (e_R/b)^2(AB)_{RP} \sin(\beta-\delta) = Q_R \times \cos(\beta-\delta) + (e_R/b)^2(AB)_{IP} \cos(\beta-\delta)$$

$$(e_R^2/b)(A_i \cos\delta - A_r \sin\delta) - (e_R/b)^2 \times [(A_r B_r + A_i B_i) \sin(\beta-\delta) - (A_r B_i - A_i B_r) \cos(\beta-\delta)] + [P_R + (e_R/b)^2(AB)_{RP}] \sin(\beta-\delta) = [Q_R + (e_R/b)^2(AB)_{IP}] \cos(\beta-\delta)$$

$$(e_R^2/b)(A_i \cos\delta - A_r \sin\delta) - (e_R/b)^2 \times [A_r b \cos\beta \sin(\beta-\delta) + A_i b \sin\beta \times \sin(\beta-\delta) - A_r b \sin\beta \cos(\beta-\delta) + A_i b \cos\beta \cos(\beta-\delta)] + M_R \sin(\beta-\delta) = N_R \cos(\beta-\delta)$$

See equations 3 and 4

$$(e_R^2/b)(A_i \cos\delta - A_r \sin\delta) - (e_R^2/b) \times \{A_r[\cos\beta \sin(\beta-\delta) - \sin\beta \cos(\beta-\delta)] + A_i[\sin\beta \sin(\beta-\delta) + \cos\beta \times \cos(\beta-\delta)]\} + M_R \sin(\beta-\delta) = N_R \cos(\beta-\delta)$$

$$(e_R^2/b)(A_i \cos\delta - A_r \sin\delta) - (e_R^2/b)\{A_r \sin[(\beta-\delta)-\beta] + A_i \cos[(\beta-\delta)-\beta]\} + M_R \times \sin(\beta-\delta) = N_R \cos(\beta-\delta)$$

$$(e_R^2/b)(A_i \cos\delta - A_r \sin\delta) - (e_R^2/b)(A_i \cos\delta - A_r \sin\delta) + M_R \sin(\beta-\delta) = N_R \cos(\beta-\delta)$$

$$M_R \sin(\beta-\delta) = N_R \cos(\beta-\delta)$$

$$N_R/M_R = \tan(\beta-\delta) \tag{5}$$

Similarly

$$N_S/M_S = \tan(\beta+\delta) \tag{6}$$

References

1. CIRCLE DIAGRAMS FOR TRANSMISSION SYSTEMS, R. D. Evans, H. K. Sels. *Electric Journal* (Pittsburgh, Pa.), 1922, page 550.

2. THE CIRCLE DIAGRAM OF A TRANSMISSION NETWORK, F. E. Terman. *AIEE Transactions*, volume 45, 1926, pages 1081–92.

3. ELECTRIC CIRCUITS (book), O. G. C. Dahl. McGraw-Hill Book Company, Inc., New York, N. Y., 1938, page 296.

4. ELECTRIC CIRCUITS (book), Electrical Engineering Staff. Massachusetts Institute of Technology, Cambridge, Mass., chapter IX.

5. THE COMPLEX VARIABLE, Sidney Frankel. *Communications* (New York, N. Y.), September 1943, page 62.

6. SOME GRAPHICAL SOLUTIONS OF A-C CIRCUITS, F. W. Loe. *AIEE Transactions*, volume 45, 1936, pages 948–56.

7. PERFORMANCE REQUIREMENTS FOR RELAYS ON UNUSUALLY LONG TRANSMISSION LINES, F. C. Poage, C. A. Streifus, D. M. MacGregor, E. E. George. *Electrical Engineering* (*AIEE Transactions*), volume 62, June 1943, pages 275–83.

8. IMPEDANCES SEEN BY RELAYS DURING POWER SWINGS WITH AND WITHOUT FAULTS, Edith Clarke. *AIEE Transactions*, volume 64, 1945, pages 372–84.

9. NEW TRANSMISSION LINE DIAGRAMS, A. C. Schwager, P. Y. Wang. *Electrical Engineering* (*AIEE Transactions*), volume 64, September 1945, pages 610–15.

Discussion

Eric T. B. Gross (Illinois Institute of Technology, Chicago, Ill): It seems to me that this is a very valuable contribution to an important phase of transmission engineering; it is of help to both the practicing engineer and the more academically inclined engineer since it contains new methods and new results. The author replaces two families of circles in one system of co-ordinates[1] by one family of circles in two systems of co-ordinates; this is of interest to the practicing engineer when he uses these diagrams since it is much easier to draw accurately straight lines than large circles. We have used this method, as suggested by Goodrich, for some time and were able to improve the accuracy of the previously known graphical solutions by changing to Goodrich's circles.

However, this paper contains other facts which are new also. For example, it is pointed out that the locus of the centers of the loss circles lies on the *B*-line, and this knowledge simplifies greatly the drawing of the loss circles. It appears that this locus has not been referred to in previous publications. The author deserves an expression of thanks for making available these improved methods to the industry.

REFERENCE

1. CALCULATIONS, DIAGRAMS, AND REGULATION OF LONG TRANSMISSION LINES, P. Thielemanns. *Revue Generale d'Electricité* (Paris, France), volumes 7–9, 1920, 1921.

R. D. Goodrich: I wish to thank Dr. Gross for the active interest he has taken in this paper; his continued encouragement and comments have been most helpful. It was due to his suggestion that the loss loci were included in the presentation; otherwise the relation of the *B*-line to these loci would not have been discovered.

It is indeed gratifying to have an engineer of his standing recommend this paper both on practical and academic grounds.

Automatic Protection of Refrigerating Machines

T. C. JOHNSON
MEMBER AIEE

G. C. WEDEL
NONMEMBER AIEE

THE growth in scope and complexity of the air conditioning and commercial refrigeration business during the last few years has emphasized a number of important problems of motor application and control which call for increased understanding of this business and its problems by the related electrical businesses. It is the purpose of this paper to discuss some of these problems which confront design and application engineers and for help on which they must turn to the public utilities, the motor manufacturers, and the control manufacturers. Further, since these problems often require the help of municipal authorities, national code authorities, and the standardization efforts of the major engineering technical societies, it is hoped that a free discussion will be of benefit to all.

Automatic operation of air conditioning and refrigeration equipment is desirable for most of the conditions under which it is used, whether it is used for reasons of comfort or necessity. The maximum amount of refrigeration must be obtained from any given apparatus, with trouble-free operation. Such equipment must start and operate automatically (sometimes several times an hour) even though connected to a power supply of limited capacity.

The protection of a motor when driving a refrigeration compressor is essentially no different than when driving any other machine. The overload protective device must protect the motor from stalled conditions imposed by a faultily driven machine, frozen bearing, or something of that nature. On polyphase motors, it must protect against stalled conditions produced by a single-phase line. The overload device must also protect the motor from an overload which causes the motor to heat for such a long time that the insulation is deteriorated. Also, it must allow the motor to stay on the line long enough to accelerate the load and must not be set so close to operating conditions that short, intermittent, and undamaging overloads cause nuisance tripouts.

The foregoing requirements are no different in their statement than those of many other kinds of equipment, but because of the varying load conditions it is possible to operate close to the maximum capacity. Consequently, each application must be designed as accurately as possible to make the most efficient use of the equipment. This statement applies particularly to the electrical portions of the equipment, for usually the cooling capacity required of the driven equipment cannot be determined with anything like the precision with which the possible motor output can be measured.

The importance of this field to the electrical manufacturers and the public utilities can be seen from the fact that air conditioning and commercial refrigeration is rapidly approaching the scale of universal use; the number of industries where refrigeration is a process requirement is growing (the rubber and petroleum industries, for example). Also, department stores and many smaller businesses need air conditioning as a matter of customer demand. Advances in scientific work are beginning to require cooling in large quantities at progressively lower and lower temperatures, and, for the future, there is the heat pump foreseen for possible residential use. The market for motors and controls blossoms with each new application, and the public utilities are finding increasing demands on their services from this type of load.

Scope

To illustrate the problems met when designing and applying this equipment, several situations will be described and the requirements for each examined. Three typical applications are:

1. Beverage cooler with *FHP* (fractional horsepower) open-type compressor.
2. Same with hermetic compressor.
3. Central plant air conditioning system with integral horsepower motors.

The type of equipment that will be discussed within the limits of this paper can be classified from the electrical standpoint as shown in Table I.

There are more varieties of application systems possible than the "standard" kinds chosen for discussion. The differences of these systems are not enough to warrant separate treatment for the purposes of this paper. The discussion here is also confined to systems involving reciprocating compressors only. Centrifugal compressors, which are generally used in the region of, say, 150 horsepower and up, have somewhat different loading characteristics and are not considered here.

The problems of production variations between lots of refrigerating machines, motors, controls, and the effects of changes in power supplies, operating conditions, etc., are important and often take

Table I

	Typical HP Range	Control Features
FHP Open	1/6-3/4	Built-in (Overload and start)
FHP Hermetic	1/6-3/4	"Dome" or Remote (Overload) Remote (Start)
Integral Open	1 up	Remote (Overload and Start)

Paper 51-380, recommended by the AIEE Domestic and Commercial Application Committee and approved by the AIEE Technical Program Committee for presentation at the AIEE Fall General Meeting, Cleveland, Ohio, October 22-26, 1951. Manuscript submitted February 24, 1949; made available for printing September 21, 1951.

T. C. Johnson and G. C. Wedel are with General Electric Company, Bloomfield, N. J.

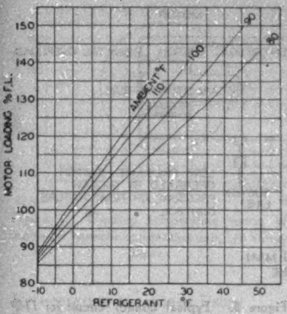

Figure 1. Refrigeration cycle

considerable ingenuity to solve, but will not be discussed in this paper.

Fundamentals of Refrigerating Systems

A brief illustration will suffice to show the load requirements for the motor and the conditions under which the control must allow operation and protection of the motor.

Figure 1 shows an elementary refrigerant circuit in which high pressure, high temperature refrigerant condenses in the lower coil (condenser), thereby giving up heat to some cooling fluid (air, water, or other), and the liquid refrigerant, after going through a suitably controlled valve, evaporates at a low pressure and correspondingly low temperature in the upper coil (evaporator), taking heat from the fluid to be cooled. The low pressure gas then goes back to the compressor to be pumped to high pressure again. Generally, the temperature of the cooling fluid around the condenser is determined by external conditions, such as the weather or temperature of the room in which the equipment is located. Also the temperature of the fluid around the evaporator is maintained at some given value fixed by the application.

For a given evaporator temperature, and the corresponding saturated vapor suction pressure for that refrigerant, the load on the motor increases with increasing condensing temperature. Also, for a given condensing temperature the motor load increases quite rapidly as the suction pressure increases. These two effects are shown on Figure 2, which is typical for a small air-cooled condensing unit driven by an open-type motor, as might be used on a beverage cooler application. Generally, such a unit is designed for "normal" conditions of, say, 90 degrees Fahrenheit ambient air temperature, and 20 degrees Fahrenheit evaporator temperature. Obviously, changing conditions of ambient temperature will greatly change the load on the motor. However, design conditions merely specify the steady-state conditions. When the unit is first started, all parts of the equipment are essentially at ambient temperature, say, 90 degrees Fahrenheit, which is decidedly warmer than the normal operating temperature of 20 degrees Fahrenheit for the evaporator. The motor is saved from the apparent great overload by the refrigerant valve shown in Figure 1 which restricts the flow of refrigerant to the evaporator and compressor somewhat. High loading of the motor does result during start-up, however, and the net effect of a "pull-down," plus cycling which occurs because the capacity of the unit, must be greater than the requirements under steady state, as shown in Figure 3.

The problem at hand is, then, that the refrigerating machine designer must apply motors and controls so as to get the most out of the equipment and yet not cause serious or even nuisance failures under the varying conditions outlined above and the additional problems raised by low or high voltage or other abnormal situations. It is almost as bad to have failures as to have an overload which may cause the control to take the motor off the line but stay just hot enough so that the reset time is excessive. Customers are naturally somewhat annoyed when anything removes their equipment from service when it is needed.

Refrigerating Machines Using FHP Open-Type Motors

Typical installations of units using small open-type motors are beverage coolers, candy merchandisers, reach-in refrigerators, home freezer cabinets, milk coolers (for farm use), room coolers, and many others. These same installations are also the most likely for units using hermetic motors which are discussed in the next section. Figure 4 is a close-up of a typical condensing unit by itself, showing that the motor carries a fan on its shaft extension which pulls cooling air through the condenser and also helps to cool the motor.

The applications for this size unit are characterized by periodic peaks of load with relatively short cycle times (two to three cycles per hour is normal for beverage coolers). Pulldown time on each cycle is quite short so that the motors can be loaded nearly to their full capacity, considering that they have a good blast of air over them. On the other hand, each cycle normally starts with full condensing pressure on the compressor, requiring high torque to start. The motor loading must, therefore, be chosen so that adequate reserve torque is available for starting even under reduced voltage conditions. Commonly, high-starting torque, capacitor-start, induction-run motors or repulsion-start, induction-run motors are applied.

The highest normal load on the motor comes during pulldown from conditions of initial start or when a new load of warm bottles has been charged into the machine, as shown in Figure 3. This situation may occur twice a day. It is not desirable to have to derate the motor for cycling (steady state) conditions in order to handle initial pulldown, therefore, for this brief period the control must allow motor loading and temperatures to rise as high as good practice can dictate. Since the total running time of refrigerating machines in such service is rarely over 40 per cent of the total elapsed time, and since the equipment selling price is often partly dictated by the nominal horsepower rating of the driving motor, there is considerable emphasis on a design that produces the most refrigeration for a given size and price. This makes the setting of the control for adequate protection both critical and difficult.

Maximum allowable motor loadings are not the problem of this paper, but it should be noted that the recommended service factors established by National Electrical Manufacturers Association apply to motors tested in still air, while invariably for air cooled condensing units there is an air blast over the motor.

Figure 2. Performance curves for open-type condensing unit

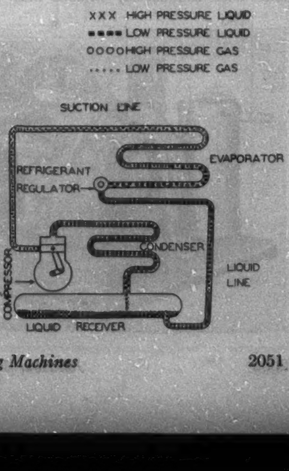

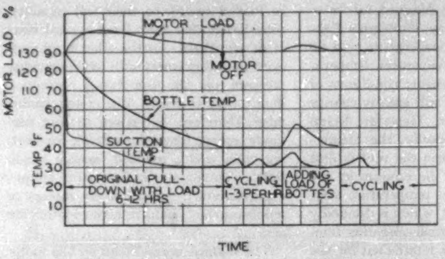

Figure 3. Pull-down and cycling curves for typical beverage cooler

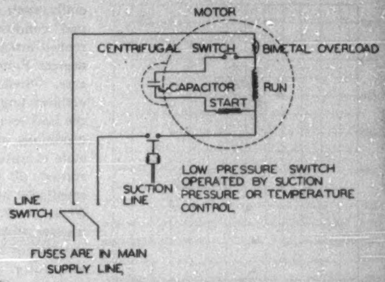
MOTOR
CENTRIFUGAL SWITCH
BIMETAL OVERLOAD
CAPACITOR
RUN
START
LOW PRESSURE SWITCH OPERATED BY SUCTION PRESSURE OR TEMPERATURE CONTROL
SUCTION LINE
LINE SWITCH
FUSES ARE IN MAIN SUPPLY LINE

Figure 5. Typical control circuit for *FHP* capacitor start induction run motor on a refrigeration machine

The control must, therefore, protect the motor from dangerous overload, but allow loading up to a reasonable temperature limit when favorable conditions are imposed. It has been found that some controls adequately protect the motor from high current overloads, but do not reset as fast as the motor itself cools, and may thus keep the motor off the line and the equipment inoperative much longer than is necessary.

Typically, motors for this service are loaded to give maximum rated steady-load conditions. For cases where the pulldown time is of the order of an hour or so, the motor may be loaded temporarily over its normal rating but because of the relative infrequence of this occurrence, no detectable decrease in the life of the motor is found.

Typical performance standards as set by the industry for maximum design operating conditions read as follows: "Tests shall be made at 90, 100, and 110 per cent of rated voltage at the unit service connection, and at rated frequency. Operation shall be continuous for four hours after equilibrium is established. The power supply shall then be interrupted for ten seconds and resumed for one hour. The motors shall operate for four hours continuously without interruption by motor overload, without damage by overheating, and without injury. After the ten-second shutdown and reapplication of power, the unit is to start within five minutes and run for one hour without trip or damage."

The motor and control circuit for an application of this class is shown in Figure 5. Note that the motor is subject to automatic starting whenever the suction line pressure rises high enough to indicate that the fluid surrounding the evaporator demands refrigeration.

Certain applications, such as milk coolers, have such a long pulldown time that special means must be used to avoid either overloading the motor or requiring an oversized motor. Milk coolers commonly have a large water bath which is cooled during the period when milk is not being chilled until an ice bank forms in a thick layer on the evaporator tubes. The addition of several cans of milk at or near "cow" temperature adds a sudden load to the system which is partly carried by melting the ice and warming the water slightly. After the milk is chilled in the required time (approximately three hours) the system must build up a reserve for use at the end of the next 12 hours. Original pulldown time for such a system is commonly 10 to 12 hours so the motor would be badly overloaded if left to operate under conditions shown in Figure 2. Usually a specially adjusted valve which restricts the flow of low pressure gas to the compressor is used to keep the unit working at full capacity for the maximum time.

A typical loading-time curve is shown in Figure 6. While such a control is not strictly part of the motor protection equipment, it does show that every attempt is made to keep the motor loaded to its maximum capacity.

Protection of equipment and personnel sometimes requires other controls such as fusible plugs (or other pressure-relief devices) in the refrigerant high pressure line, or a high-pressure cutout (either hand or automatic reset) in the motor line. Fusible plugs are generally used on small air-cooled condensers to avoid an explosion in case of fan motor failure or stopped-up condensers, while high-pressure cutouts are generally used with water-cooled condensers to protect in case of water failure, although they may also be used on the larger air-cooled units to avoid loss of refrigerant.

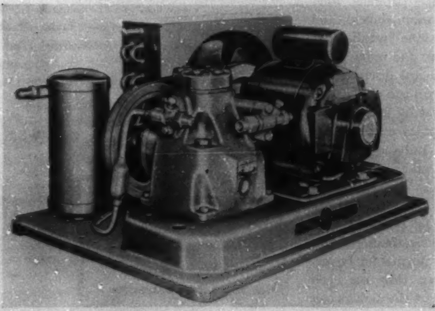

Figure 4 (left). Open-type condensing unit, 1/2 horsepower, air cooled

Figure 6 (below). Typical operation curves for a milk cooler application

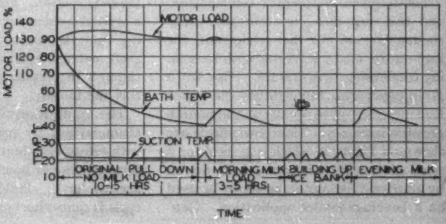

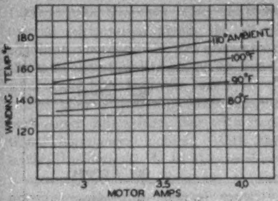

Figure 7. Winding temperature curves of motor for hermetic condensing unit, 1/6 horsepower

Refrigerating Machines Using FHP Hermetic Motors

The typical applications in which *FHP* hermetic motors are used in refrigerating machines are essentially the same as those listed in the previous section. Generally, either type of unit can be used. As mentioned later with certain systems hermetic motor-compressors have some advantages but open-type units will continue to be used widely, especially for the odd power supplies and those applications where easy replacement of motor or compressor, independently of each other, is necessary.

The principal reason for the trend toward hermetics is that in systems which can be made otherwise leak-tight and which use very small refrigerant charges, the use of a hermetic compressor removes one more hazard to long, trouble-free operation.

The essential differences in the systems (as regards the motor) which affect the control problem are: (1) the inclusion of the motor windings in the refrigerant gas (necessitating special care with windings and insulation); (2) better control of motor winding temperatures, partially independent of motor loading; (3) requirement for external starting and overload protection (Centrifugal switches and sliding brushes will not operate in an atmosphere of refrigerant); and (4) the necessity for a fan for condenser air independent of the compressor motor.

With the motor windings surrounded by relatively cool refrigerant, the motor heat goes into the gas with the interesting result that the motor load current is sometimes no longer a good measure of motor temperature as it is in open motors. It is possible under some conditions to keep the motor under safe operating temperatures for all loads up to the stalling point on torque! Such loadings are obviously not reasonable as a sufficient torque margin must be allowed for low voltage and abnormal operating conditions, as well as starting, but the two basic motor limitations of temperature and torque are under nearly separate control. Figure 7 shows the variation of winding temperature in motor current for a particular equipment.

Two methods of overload protection for hermetic motors are currently possible; one (located apart from the motor) depending essentially on motor load current, but with the overload relay adjusted to the requirements of the particular application; and the other ("dome mounted" on the motor compressor case) depending largely on the actual temperature of the windings, but biased partly by current. Both methods have their advantages and their adherents. "Dome" mounted relays are sometimes subject to the varying effect of air flow in different locations, while the "remote" relays subject to current only might tend to reset sooner than motor temperatures would justify at high ambients. Either can give adequate protection if properly designed and applied.

The starting control for hermetic motors is somewhat more difficult for the refrigeration design engineer than for open motors because an external relay operating on motor current or voltage across the starting winding is necessary for the former whereas such control is normally furnished built-in with open motors. The real difficulty comes in the necessary production variation in motors and controls, and the possible voltage changes that must be allowed for. This problem is larger than can be dealt with in this paper. The control circuits for hermetic motors are shown in Figure 8 for the two methods of obtaining switching of the starting winding.

One hazard which may exist on small air-cooled units which do not as yet justify much control expense is failure of the condenser fan motor. If it fails the condenser is not capable of removing enough heat from the refrigerant to prevent very high pressures and temperatures building up, so that the pressure protective device (usually a fusible plug) operates, thereby taking the system completely out of use until it is serviced. The reliability of fan motors is generally high enough so that this hazard is acceptably small, while on larger equipment a high pressure cutout is standard for other

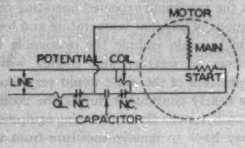

VOLTAGE TYPE RELAY

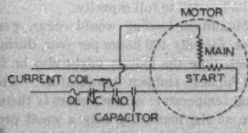

CURRENT TYPE RELAY

Figure 8 (left). Control circuits for hermetic units

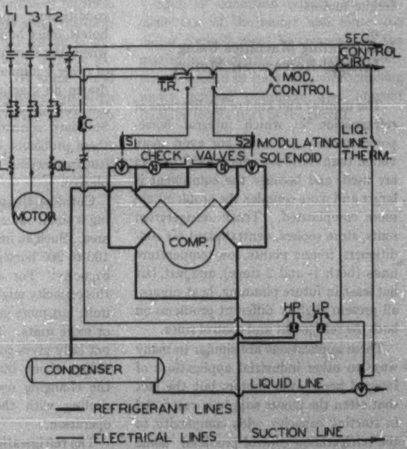

Figure 9 (right). Control circuit for single condensing unit, unloaded start, capacity modulation

reasons and thus provides adequate protection.

The temperature limitations of hermetic motors are not as well standardized yet as they are on open motors. Not long ago one of the refrigeration industry standardizing groups in a draft of a proposed standard stated essentially as follows: "For the purpose of limiting motor loading, the maximum published evaporator temperature for air-cooled units and inlet and outlet water temperature for water-cooled units, should be such that motors provided with class-*A* insulation may be operated continuously for not less than two hours without exceeding a motor-winding temperature of 115 degrees centigrade (239 degrees Fahrenheit) as measured by resistance when tested for performance at rated voltage and frequency under maximum operating conditions." No agreement was reached on this proposal, but it illustrates the difference in conditions and points up the fact that the control and application problems are different for open and hermetic motors.

One of the principal applications of hermetic compressors is in systems using a capillary tube (a long tube with a very fine bore) as a refrigerant control instead of a valve that can be closed. The capillary tube will allow equalizing of pressures on the high and low sides during off periods and thus leaves the compressor motor with a reduced gas compression plus friction and inertia as a starting load. This merely results in the use of a low starting torque motor, however, and although the relay settings are different, their type is the same as for high starting torque motors.

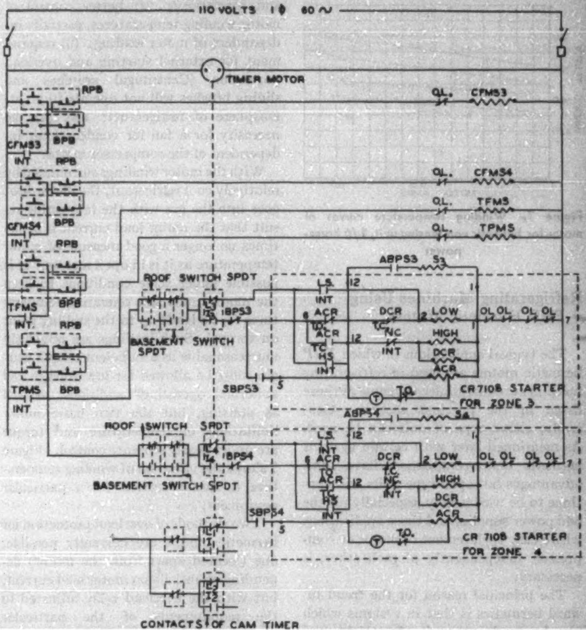

Figure 10. Partial elementary diagram of control circuit for multiple unit system using sequence starting and interlocking controls

Refrigerating Machines Using Integral Horsepower Motors

The number and kind of applications of refrigeration in which integral horsepower motors are used are even more varied than those for which *FHP* motors are used, and because the equipment is larger and more complex the problems are more complicated. Truck refrigeration units, store coolers, central plant air conditioners, freezer plants, low temperature units (both 1- and 2-stage), and last, but not least in future planning, heat pumps, all present slightly different problems on both the refrigerant and control sides.

These applications are similar in many ways to other industrial applications of integral horsepower motors but the fact that often the power supply is restricted in starting capacity adds complexity to the refrigeration control problem. Some very large units have been installed in industry for use in rubber plants, petroleum refineries, etc., but the majority of air conditioning applications are made in hotels, office buildings, stores, and homes where the density of load and proximity of other equipment may limit the power drawn on starting and may even cause low voltage difficulties at certain times. Standard control equipment can handle these problems, but obviously additional features increase the initial cost and complexity.

Consider the problem of air conditioning a small office building in a downtown area. Such an installation might use from 100 to 200 horsepower of installed motor capacity. For air conditioning reasons this capacity might be concentrated in one unit, but more generally would be in two or more units. The multiplicity of units not only gives some protection in case of outage of one, but also more nearly meets the changing needs of the building for cooling with the greatest economy of operation.

The refrigeration units would use water as the means of disposing of the heat and the motors would be located in some machinery room with suitable ventilation, but without other special cooling. For this reason the motor loading would be designed to utilize the service factor at the maximum expected operating conditions of ambient temperature and load, which would include the reasonable extremes of weather and cooling water. Operation of the units would very likely be nearly continuous during the cooling season, for the air conditioning equipment may have to remove moisture from the air even on days when the temperature is not excessive. The loading on the motors would vary sharply with the weather and only for relatively short periods would the units be used to full capacity.

Maximum loading would occur, perhaps, for only 400 hours per year, during which time the motors might also be in the highest ambient temperature. The total temperature of the motors is therefore at the maximum only a small percentage of the time, although the hours of operation under any load might be from

1,000 to 2,000 hours per year. (In commercial refrigeration plants the above conditions are essentially true except that the total operating time might be somewhat above 2,000 hours per year.)

The control problem with integral horsepower differs from that with fractional horsepower motors. With the latter, it is desirable to be able to allow temporary overloads right up to the maximum allowable thermal capacity, but with integral horsepower motors the control function is largely to start the motors, possibly under reduced voltage, and switch them as required to meet the load with the fewest units operating. The overload protection must, of course, be capable of preventing damage due to unusual loads, emergency conditions such as caused by damaged bearings, and special situations such as single-phase operation.

Sometimes instead of switching operating units on and off the refrigeration circuit has its capacity reduced by modulating the capacity of the compressor to pump gas, thereby reducing the load on the motor. The same effect also can be realized by reducing the speed of the driving motor, as with a 2-speed motor. Additional controls are needed for these functions.

As a guide in the application of motors to the refrigeration industry, one of the standards reads as follows: "For the purpose of limiting motor loading, evaporator temperature limits should be established for each published compressor speed and inlet air temperature for air cooled units. This limit should be such that the motor, if provided with class-*A* or class-*B* insulation, may be operated continuously for not less than two hours without exceeding a motor-winding temperature rise of 50 degrees centigrade, and in no event should the ultimate temperature of the motor-winding exceed 90 degrees centigrade (as measured by thermometer) when tested for performance at rated voltage and at conditions specified."

The starting problem for a single unit which is not allowed to be thrown across the line would be relatively straight except that not all public utilities have the same requirements. In most cases the increment starter (resistance, or transformer) is used and the compressor may be left untouched—but it will not turn over until the starter is on the final step because of the high starting torque required. Different limits in the increments allowed in different localities cause considerable problems in stocking and shipping controls. For instance, Philadelphia, Kansas City, Chicago, and New York City all have different requirements. However, in some instances the total starting current is limited and then the compressor must be "unloaded" so it can be started against only friction, inertia, and a very low compression torque. This must be done automatically with the controls interlocked with the starting switch.

During the past year, the increasing load on the public utilities has manifested itself in some localities by voltages which are lower than normal. All equipment must, of course, be designed to operate at ten per cent under normal voltage but sometimes 220-volt motors used on 208-volt networks on which the voltage is below nominal have proved very difficult to protect with overload relays and heaters set by the usual rules. Low voltage is a difficulty to contend with on air conditioning equipment control even under less difficult times, however, for many installations particularly of the smaller horsepowers may be in outlying business areas, or in residences and small business houses where the internal wiring is not capable of taking the load without excessive voltage drop. In some rural areas, even with the intensive campaign in recent years, voltages as low as 75 volts have been reported occasionally. The most frequent complaint in such cases is that the motor will not start or has burned out.

Thus, the problem of applying control which will utilize the potential capacity of the motor and still protect it from damage is made very difficult.

Any one system may be made automatic with nearly perfect success, but it is the production variations between motors, power supplies, and heaters for overloads, for example, that have caused many cases that should have been satisfactory to turn into complaints. In some cases, the manufacturing tolerance build-up in standard controls has prevented a motor from carrying its rated service factor load. The refrigeration design engineer working closely with the motor and control engineers will solve this problem in time, and it will, no doubt, be the valued source of additional published studies.

As an example of the control circuit needed on a single unit Figure 9 is shown. In the other extreme is Figure 10, which is the elementary diagram of a multiple unit system using sequence starting and various interlocking controls on fans, compressors, et cetera.

Refrigeration systems used in low temperature work have an added complication since the pull-down time is long and the load heavy until operating conditions are reached. Often there is no feasible way to accomplish pull-down without overloading the motor so that frequently a 60-horsepower motor must be applied to a job that only draws about 30 horsepower when running under normal rated conditions.

Such a condition results in inefficient use of the motor and since the motor controls must be arranged for the maximum conditions, some extra protection is needed to indicate malfunctioning under normal operation and prevent damage to any part of the circuit.

No Discussion

The 3-Phase Oscilloscope as an Harmonic Analyzer in Power Systems

E. B. KURTZ
FELLOW AIEE

R. H. BURKHARDT
STUDENT MEMBER AIEE

THE purpose of this paper is to show the significance of harmonic patterns produced on a polyphase oscilloscope, to explain how they arise, and to relate the results to symmetrical systems. A series of patterns for various combinations of harmonics is presented.

The 3-phase oscilloscope and its derivatives can be used as a polyphase voltmeter, polyphase ammeter, polyphase power factor meter,[1] polyphase synchroscope,[2] phase sequence indicator, symmetrical component analyzer, and polyphase waveform analyzer. This paper deals with its use as a waveform or harmonic analyzer in polyphase systems. It will be shown how its use makes possible determining (1) the order of the harmonic, if present, (2) the magnitude of the harmonic, and (3) the phase sequence of the harmonic, that is, whether positive or negative with respect to the fundamental.

Three-Phase Oscilloscope

The distinguishing feature of the 3-phase oscilloscope is its deflection system which provides deflections along three axes separated 120 degrees in space. Figure 1 illustrates a 3-phase electromagnetic deflection system.

When sinusoidal 3-phase currents flow in the deflection coil windings, a rotating flux field of constant magnitude and constant angular velocity is produced as in a 3-phase induction motor. The phase sequence of the currents and the connections to the coils determine the direction of field rotation. The electron beam of the cathode ray tube is deflected by this field to produce a circle on the screen. The diameter is directly proportional to the current magnitude.

Harmonic Patterns

Harmonics cause deviations in the circular pattern. When currents of two different frequencies flow in the deflection system, two circular motions of different frequencies are superimposed. This produces a pattern having loops or nodes. Similar patterns are produced in one method of frequency comparison where sources of different frequencies produce superimposed circular motions in a conventional oscilloscope through the use of phase-shift networks.[3–7] Forrest observed 3-phase harmonic patterns with an oscilloscope placed in a 3-phase field.[8] The mathematics of these patterns has been worked out by Rangachari.[9]

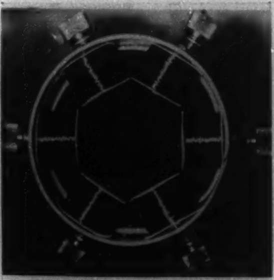

Figure 1. Three-phase electromagnetic deflection system designed for use on 3-inch RCA oscilloscope. Coils are wound to respond to voltage

A process of graphical construction is illustrated in Figure 2 for opposite rotation and in Figure 3 for same rotation for a second harmonic. The vector representing the harmonic rotates around the outer end of the vector representing the fundamental. The fundamental thus may be considered to produce a sweep for the harmonic.

The experimentally produced patterns of Figure 4 were obtained in the laboratory with two 3-phase generators connected in series. The relative speeds and field excitations of the generators determined the frequency ratio and relative magnitudes of the voltages. By observing the motion of the spot on the screen while the generator was moving very slowly the direction of rotation of the spot was established. Opposite rotations were obtained by interchanging any two of the 3-phase leads from the harmonic generator.

Analysis

The ratio of harmonic to fundamental can be calculated from

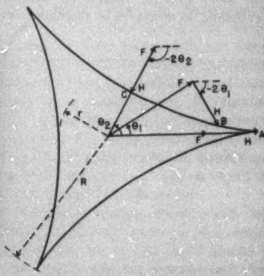

Figure 2. Graphical construction of pattern produced by a fundamental and second harmonic having opposite phase rotation

---

Paper 51-381, recommended by the AIEE Instruments and Measurements Committee and approved by the AIEE Technical Program Committee for presentation at the AIEE Fall General Meeting, Cleveland, Ohio, October 22–26, 1951. Manuscript submitted March 13, 1950; made available for printing September 5, 1951.

E. B. Kurtz and R. H. Burkhardt are with the State University of Iowa, Iowa City, Ia.

Vol. 195

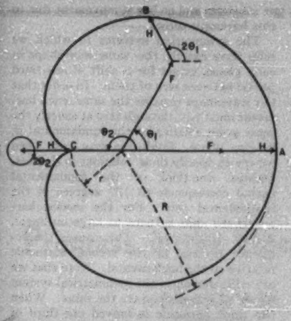

Figure 3. Graphical construction of pattern produced by a fundamental and a second harmonic having same phase rotation

$$\frac{H}{F}=\frac{R-r}{R+r}$$

where R is the maximum radius and r is the minimum radius of the pattern.

A loop or node begins to form as the percentage of the harmonic is increased to $100/n$ per cent of the fundamental where n is the order of the harmonic.[3] This is due to a cancellation of velocities of the superimposed circular motions.

The rule from which phase sequence and harmonic order may be determined is as follows: When the loops are on the outside, phase rotation is opposite and there are $n+1$ loops. When the loops are on the inside, phase rotation is the same and there are $n-1$ loops.[3]

Three-Phase Harmonics

In symmetrical 3-phase circuits each phase is identical with each of the others. Consequently, the currents drawn or voltages generated are identical. The waveform of the phase voltages or currents has the same mathematical expression except for the 120 degree phase shift. It is important to notice that this is actually a time shift and represents 120 electrical degrees for the fundamental only. In a given amount of time a harmonic, because of its higher frequency, travels through more electrical degrees than the fundamental. For the *kth* harmonic the shift is $k\times 120$ degrees.

If the sequence of the fundamental is called positive, then in this symmetrical case, the fourth, seventh, and tenth harmonics also have positive sequences and cause a rotation of their respective magnetic fields in the same direction as the rotation of the fundamental. The second, fifth, and eighth harmonics have negative sequences. The third, sixth, and ninth harmonics are exactly the same in all phases. They may be said to have zero sequences. Zero sequence currents can cause no deflection in the 3-phase oscilloscope since the fields along each axis will be equal at any instant and the vector sum of these fields is zero.

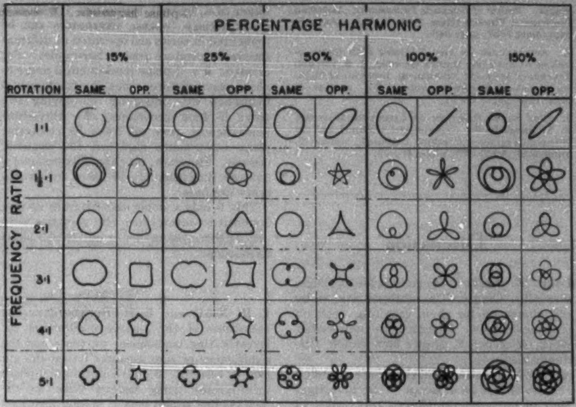

Figure 4. Screen patterns produced by combining 3-phase fundamental and harmonic voltages of different order, varying percentages, and with same and opposite phase rotation

The sequence of any harmonic in a symmetrical system can be determined by the application of the following rule: If $n=1+3m$, the sequence is positive; if $n=2+3m$, the sequence is negative; and if $n=3m$, the sequence is zero, where n is the order of the harmonic and $m=0,1,2,3,\ldots$

Advantages

The main advantages of the polyphase oscilloscope in harmonic analysis may be summarized as follows: (1) The use of the fundamental as a sweep eliminates the need for synchronizing an external sweep generating circuit. (2) The use of the fundamental as a sweep virtually eliminates the fundamental from consideration in the waveform. With a conventional oscilloscope using a linear time sweep, the shape of a complex wave consisting of a fundamental and a single harmonic depends on the relative phase positions of the two components. However, on the 3-phase oscilloscope, phase changes cause merely a rotation of the pattern. This advantage disappears when more than one harmonic is present. (3) The use of all 3 phases of the system permits this oscilloscope to indicate the relative phase sequences of the fundamental and harmonics. (4) The percentage of a single harmonic can be obtained readily from the pattern.

Conclusion

The 3-phase oscilloscope makes possible presenting in a novel manner useful information about the order, sequence, and magnitude of harmonics, if present, in 3-phase systems through its use of revolving flux fields produced in its polyphase deflection system.

References

1. A Polyphase Electronic Power Factor Meter, E. B. Kurtz, P. O. Erickson. *Proceedings*, Fourth National Electronics Conference (Chicago, Ill.), November 1948, pages 437–44.

2. Polyphase Power Synchroscope, E. B. Kurtz and R. H. Burkhardt. *Electronics* (New York, N. Y.), volume 21, August 1948, page 124.

3. Improved Cathode-Ray Tube Methods for the Harmonic Comparison of Frequencies, D. W. Dye. *Proceedings*, Physical Society of London (London, England), volume 37, 1925, pages 158–68.

4. The Harmonic Comparison of Radio Frequencies by the Cathode-Ray Oscillograph, T. S. Rangachari. *Experimental Wireless and the Wireless Engineer* (London, England), volume 5, number 56, May 1928, pages 264–6.

5. A Simple Circuit for Oscillographic Frequency Comparisons, B. Kurrelmeyer. *Review of Scientific Instruments*, American Institute of Physics (New York, N. Y.), volume 7, May 1936, pages 200–01.

6. Circuits for Oscillographic Frequency Comparison, H. J. Reich. *Review of Scientific Instruments*, American Institute of Physics (New York, N. Y.), volume 8, September 1937, pages 348–9.

7. Note on the Proceeding Paper, B. Kurrel-

meyer. *Review of Scientific Instruments*, American Institute of Physics (New York, N. Y.), volume 8, September 1937, page 349.

8. APPLICATION OF THE CATHODE-RAY OSCILLOGRAPH TO ELECTRIC POWER SYSTEMS, J. S. Forrest. *Journal of Scientific Instruments*, Institute of Physics (London, England), volume 20, number 5, Map 1943, pages 69–71.

9. THE SUPER-POSITION OF CIRCULAR MOTIONS, T. S. Rangachari. *Experimental Wireless and the Wireless Engineer* (London, England), volume 6, number 67, April 1929, pages 184–93.

Discussion

Louis N. Stone (Oregon State College, Corvallis, Oreg.): The authors are to be complimented for their very fine work on this oscilloscope. Reference to their earlier work, reference 2, shows how simple this device really is.

I would like to know if they have extended the use of this oscilloscope to the investigation of currents on the various types of 3-phase transformer connections. By using current coils instead of potential coils this type of investigation could be readily carried out.

I believe the authors could clarify an apparent discrepancy that exists between a statement in the text of the paper and figure 4. A statement in the section on 3-phase harmonics indicates that the third, sixth and ninth harmonics are the same in all phases; that they may be said to have zero sequence; and that zero sequence currents can cause no deflection on the 3-phase oscilloscope. The patterns shown in figure 4 for a frequency ratio of 3 to 1 show some very definite deviations in the fundamental frequency deflection pattern as shown in the percentage harmonic columns.

Possibly this discrepancy lies in the definition of a 3-phase harmonic. I wonder if two ordinary 3-phase alternators can be connected in series and operated at different speeds to produce triplen harmonics. For example if a 3-phase fundamental and a 3-phase wave of three times the fundamental frequency are added by employing two series 3-phase generators, the three-time fundamental wave will have its respective phase components displaced 120 electrical degrees. However, the third harmonic of a 3-phase fundamental will have its components in phase.

This is only a minor detail and in no way is meant to detract from the very fine work the authors have done on the 3-phase oscilloscope.

E. B. Kurtz and **R. H. Burkhardt**: The usefulness of the 3-phase oscilloscope for investigating transformer currents and the significance of zero sequence harmonics are closely related. We have obtained 3-phase oscillograms using current coils on the oscilloscope which show a strong fifth harmonic in the exciting currents flowing in a set of transformers connected in a 3-phase system. Any other harmonics having 3-phase relationships will appear in the resulting patterns along with the usual indications of current magnitude and unbalance. However, the prominent third harmonic to be expected in the transformer exciting current does not appear because it is a zero sequence harmonic.

We consider zero sequence harmonics to be those in which the currents or voltages at the harmonic frequency have precisely the same magnitude and angle in all three phases relative to a fixed reference. If a zero sequence harmonic is applied to the 3-phase oscilloscope, the magnetic fields produced along the three axes of the deflection system exactly balance each other at all times and no beam movement due to this harmonic occurs.

The symmetrical systems to which we refer have exactly the same waveshape in each phase, except for a shift of one-third period between each of them. In order that the waveshape remains the same, each harmonic must pass through zero at exactly the same point relative to the fundamental in its own phase. Confusion may arise when we try to specify these relations in degrees, because one-third of the fundamental period corresponds to 120 degrees of the fundamental only. For the second harmonic the shift is twice as large an angle, 240 or -120 degrees. This causes the sequence reversal of the second harmonic relative to the fundamental. Note that we are still referring to the symmetrical system where all waveshapes are the same. When the third harmonic is moved one-third of the fundamental period to maintain the constancy of waveshape, it is really shifted by three times 120 = 360 degrees or one complete cycle of the third harmonic frequency in each phase. Thus all of the third harmonic components in a given set of symmetrical waveforms have the same phase angle when multiples of 360 are removed. This is why the third harmonic is called a zero sequence harmonic in a symmetrical system.

The patterns of Figure 4 show a third harmonic because the method of producing the harmonics, using two 3-phase alternators connected in series, forced the third harmonic currents into 120 degree 3-phase relationships. Physically this means that the three complex waveforms obtained from the alternators were not identical even when the one-third period shift is taken into account. These unsymmetrical or non-identical waveforms were able to produce third harmonic patterns because the third harmonic fields did produce revolving magnetic fields and did not cancel.

Progress in the Electric Power Industry

I. E. MOULTROP
FELLOW AIEE

G. A. ORROK
NONMEMBER AIEE

Synopsis: The subject of this paper concerns the progress that has been made in the generation of electricity by steam and its distribution. It is significant that the two authors selected by your committee to discuss this subject are both power plant designers, and that their two working lifetimes cover the whole history of electric power generation since its beginning. That there has been progress in the electric power industry during this brief span of years is well illustrated by Figure 1, which shows that electrical residential rates on a national basis have a history of continuously lowering during the past 50 years while, at the same time, the cost index has been continuously rising. Where else than in the electric power industry can such a record of progress be shown?

A Story of Progress

Boilers

BEFORE going into a more technical analysis, let us review the physical equipment back of this concrete record of achievement to see if the road behind points out the road ahead. Figure 2 is a model of the first Edison station, the Pearl Street Station in New York. Boilers are tiny, hand-fired, and operated at about 100 pounds steam pressure. Figure 3 shows a Roney stoker under a power boiler. These boilers operated at about 200 pounds pressure and are much larger in size. Figure 4 shows an underfeed stoker-fired boiler, similar to types which were installed through the 1920's. The capacity is up to several hundred thousand pounds per hour, and pressures up to 1,200 pounds; temperatures up to 725 degrees could be obtained. Figure 5 shows a boiler fired by two underfeed stokers. Such boilers were installed in the late 1920's and early 1930's, and some were of very large capacity. Figure 6 shows a boiler, installed in the late 1920's burning pulverized coal. Notice the use of refractory walls. Such furnaces, although practical, required high maintenance and were of small size. Figure 7 shows a modern pulverized coal-fired boiler. Note that the use of refractories has almost disappeared. Such boilers can be made in extremely large sizes, and pressures up to 2,500 pounds, and temperatures up to 1,050 degrees are available today.

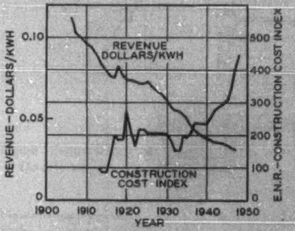

Figure 1. National average residential revenue per kilowatt-hour compared to construction cost index

In thinking over these pictures of the progress of boiler design, we should consider the principal indications or trends in their design. From the very start, continual progress is to larger and larger units. We also note a continued tendency to operate at higher pressures and temperatures. Has there been a continuous improvement in efficiency? Actually, not of any great moment. James Watt's early boilers for pumping-engine service in England had test efficiencies of 86 per cent, while the newest and best boilers today rarely exceed 90 per cent. Although not shown on these pictures, but connected with the boilers and the progress of their design, we should not forget the improvements which have been made by the use of regenerative feed water heating, as well as by the use of the reheat cycle.

Turbogenerators

Let us see what the history of prime movers and generators can show us. Figure 8 shows the first Boston station with Edison Jumbo generators. This is a d-c machine of about 120-kw capacity. Figure 9 shows the Atlantic Avenue engine room some 10 years later. Note that the generator brushes ride on the face of the commutator. Capacities up to 2,000 horsepower were not too uncommon in such large compound steam engines. Figure 10 shows a room full of vertical turbines, first installed about 1905, in operation today for peak loads. The maximum capacity of a single unit is 15,000 kw. Steam conditions are 200 pounds, 525 degrees. Figure 11 shows a turbine room of the late 1920's. The main units operate with 400 pounds, 725 degrees steam. Such 1,800-rpm machines were available up to 150,000-kw capacity. This station also contains three of the early 1,200-pounds 725-degree turbines. These machines were of a type which did not become popular for another 20 years. In other words, they were topping turbines, a small high-pressure unit taking the steam from 1,200 pounds down to approximately 400 pounds, then the steam returning to a header, and in this case, being reheated before going to the low-pressure turbine. Figure 12 shows a modern 3,600-rpm turbine.

The dominant fact brought out by this brief review has been the great extension in the available heat range which is responsible for the great progress in fuel economy. The use of condensers brought the lower level of useful heat downward to low temperatures and very low pressures while the extension to higher temperatures, pressures, and the use of reheat

---

Paper 51-382, recommended by the AIEE Power Generation Committee and approved by the AIEE Technical Program Committee for presentation at the AIEE Fall General Meeting, Cleveland, Ohio, October 22-26, 1951. Manuscript submitted January 2, 1951; made available for printing August 31, 1951.

I. E. Moultrop and G. A. Orrok are with the Boston Edison Company, Boston, Mass.

BOILERS

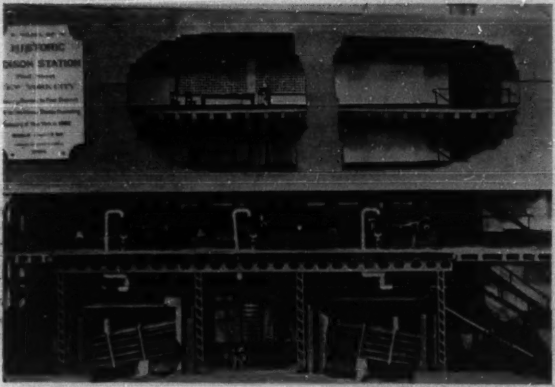
HISTORIC
EDISON STATION
NEW YORK CITY

Figure 2. The first Edison station—Pearl Street model

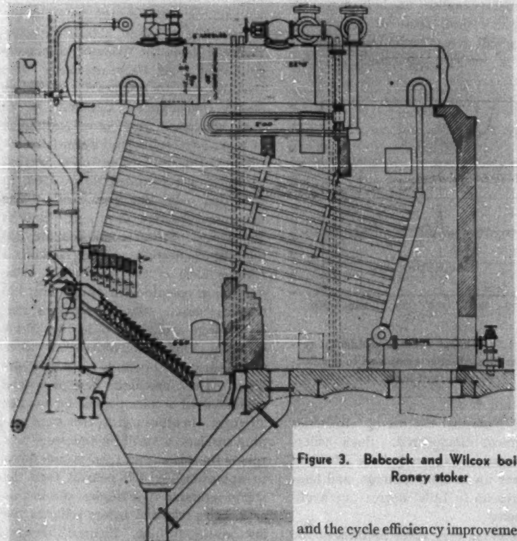

Figure 3. Babcock and Wilcox boiler with Roney stoker

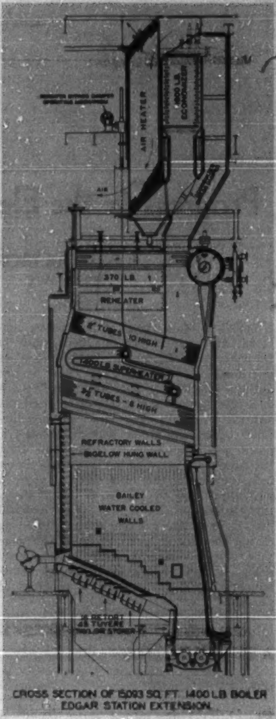
AIR HEATER
1400 LB. ECONOMIZER
AIR
370 LB.
REHEATER
2" TUBES 10 HIGH
1400 LB SUPERHEATER
2½" TUBES – 8 HIGH
REFRACTORY WALLS
BIGELOW HUNG WALL
BAILEY
WATER COOLED
WALLS
16 RETORT
48 TUYERE
TAYLOR STOKER
CROSS SECTION OF 15,093 SQ FT 1400 LB BOILER
EDGAR STATION EXTENSION

Figure 4. Underfeed stoker

raised the upper level of available heat. The efficiency of utilization of the available energy changed moderately from a figure of 70 per cent for a compound engine to perhaps 86 per cent for a modern turbine.

The tendency to large sizes is important and the cycle efficiency improvements due to regenerative feedwater heating should also be noted.

SWITCHING

The electrical side of the power business also has quite a history of progress. Figure 13 shows a Pearl Street switch in 1882. This is quite a far cry from Figure 14 which shows a d-c switch in service today but which was built in the early part of the century. Figure 15 shows 6,900-volt hand-operated oil switches. These were put into service early after the transfer from direct to alternating current and are still in service. Figure 16 shows a 14,000-volt oil circuit breaker. Installed in segregated compartments and fully automatic, these were a great advance over the switches available at the time and many of those installed as early as 1904 are still in daily use. Figure 17 shows a 14,000-volt modern airblast switch at the Mystic Station. These represent the latest available development and have by no means reached the top of their possibilities for rapid operation and capacity of interruption. Figure 18 shows a 69,000-volt outdoor oil switch. These were developed in the late 1920's and are available in this country up to 300,000 volts.

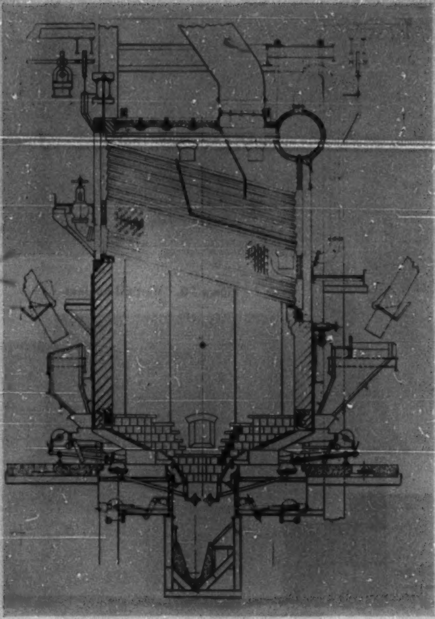

Figure 5 (upper left). Double stoker

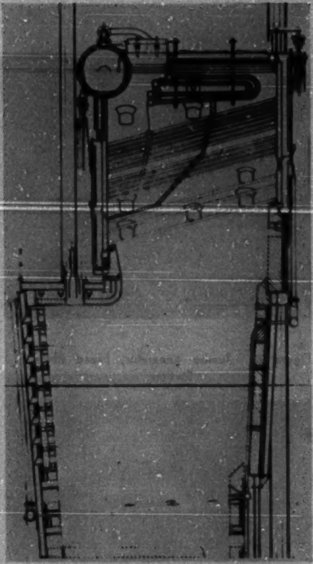

Figure 6 (upper right). Early pulverized-coal boiler

The picture that can be seen from this series of illustrations on the development of switching shows a very similar tendency to the prime mover and generator equipment; in other words, a definite tendency towards larger units and a very definite tendency for an increase in voltage. But it should be noted that the development to a maximum voltage of 250,000 came quite early and there is some indication that voltages much above this figure are far in the future. There has been a steady growth in interrupting capacity and a steady increase in speed of opening and reclosing. There is some indication that the change in types travels in cycles, from air-break switches to oil-break switches and back to air-break again.

TRANSMISSION

An important part of the electrical power business is transmission. Of course in the early stages when direct current was used, there was no transmission as we understand it today and when the transfer from direct to alternating current was

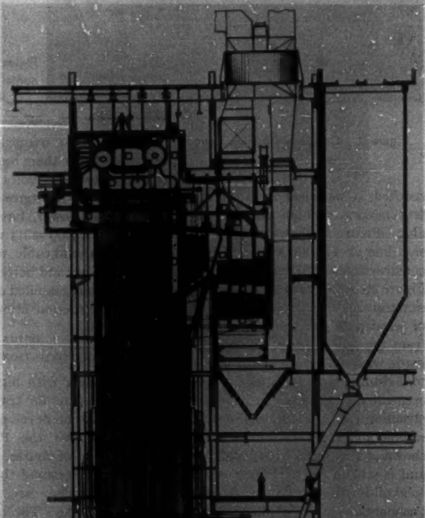

Figure 7 (right). Modern pulverized-coal boiler

TURBOGENERATORS

Figure 8. Jumbo generator, Head Place Station

Figure 11. Horizontal turbines—1,800 rpm

Figure 10. Vertical turbines

Figure 9. Compound engine generators

Figure 12. Modern turbines—3,600 rpm

reached, it was clear from the start that transmission at high voltage was desirable. Figure 19 shows an early transmission line at 110,000 volts. This type of construction is in marked contrast to Figure 20, which shows a modern high-tension transmission line for 110,000 volts but of wood pole construction. The change from the steel towers to wood has been made with an improvement in resistance to lightning and with a substantial decrease in cost. The progress in cable construction is likewise significant. The sample of early transmission cable, as shown in Figure 21, was installed in 1911 and is still in use at 14,000 volts with a solid oil-impregnated insulation. Modern transmission cable, as shown in the cross section in Figure 22, is filled with oil under pressure and has little more insulation thickness for operation at 110,000 volts. Other insulating mediums such as inert gas are used in modern cable. The pictures suggest that the rise in voltage to approximately a maximum of 350,000 volts, a-c overhead occurred quite early and that there has been little tendency to exceed this voltage in present-day practice. Underground cables were somewhat slower, but the maximum voltage of 110,000 volts was reached fairly early with solid cable, modern practice going to cheaper and better construction involving oil and gas-filled cables and the pipe-type construction involving high-pressure gas or oil.

TRANSFORMATION

Along with high-voltage transmission, apparatus for transformation of voltages had to be developed at the start. Figure 23 shows the Pearl Street regulators. These, of course, are not transformers as we understand them in modern a-c practice. They are, in fact, carbon-packed rheostats. The purpose, however, is for the control of the voltage in the individual d-c feeders. The construction is shown for the Pearl Street Station in 1882. With the conversion to alternating current, modern transformers appear. Figure 24 shows an early air-blast transformer of approximately 5,000-kva capacity. Some transformers of this type are still in service. Figure 25 shows a much later, standard oil-filled transformer and Figure 26 shows a modern oil-filled transformer.

A review of the progress of transformer development shows a rapid increase in size and voltage to match transmission requirements. There was a definite change from single-phase to the 3-phase units. From the very start, as indicated by the Pearl Street regulators, there were many special types. From the standpoint of efficiency no piece of apparatus was ever as satisfactory as the transformer. The fundamental principles were early developed and applied to produce practically perfect machines.

The final phase of the electric power business concerns distribution.

DISTRIBUTION

Figure 27 shows Pearl Street connections in 1882. These were the principal d-c feeders leaving Pearl Street Station. D-c distribution, which was in the form of

Figure 13. Pearl Street switching

Figure 14 (left). D-c switch

Figure 15 (right). Hand-operated oil switch

Figure 16 (left). 14,000-volt automatic oil circuit breaker

Figure 17 (right). 14,000-volt automatic air-blast circuit breaker

SWITCHING
(Continued)

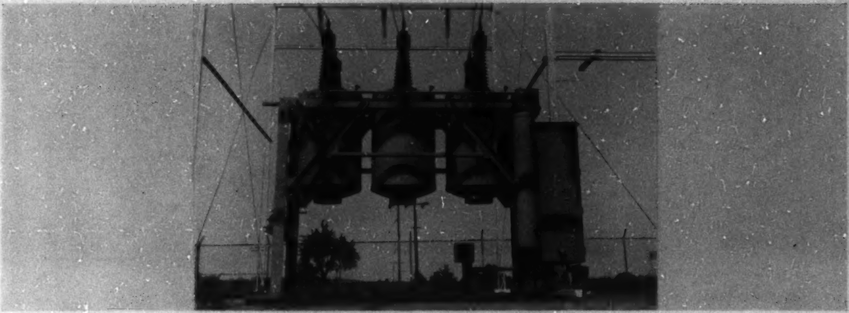

Figure 18. 66,000-volt outdoor oil circuit breaker

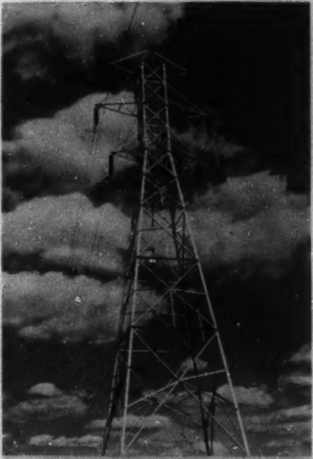

Figure 19 (left). Early 110,000-volt transmission line

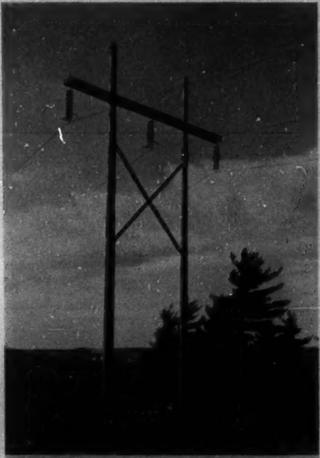

Figure 20 (right). Modern wood pole, 110,000-volt transmission line

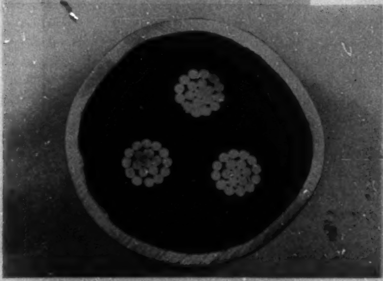

Figure 21. Early solid cable, 14,000-volt service

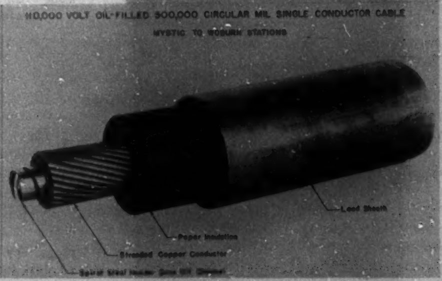
110,000 VOLT OIL-FILLED 500,000 CIRCULAR MIL SINGLE CONDUCTOR CABLE
MYSTIC TO WOBURN STATIONS
Lead Sheath
Paper Insulation
Stranded Copper Conductor

Figure 22. Modern oil-filled cable 110,000-volt service

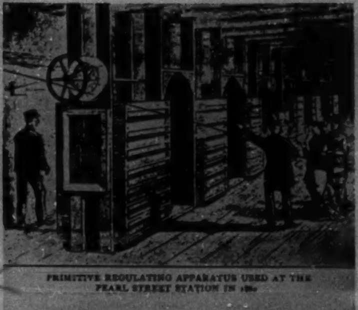
PRIMITIVE REGULATING APPARATUS USED AT THE PEARL STREET STATION IN

Figure 23 (left). Pearl Street regulators

Figure 24 (right). Early air-blast transformers

Figure 25. Oil-filled self-cooled transformer

Figure 26. Large modern oil-filled transformer

a network, was early supported by large storage-battery installations as shown in Figure 28. This is still in operation. As the distances increased and the advantages of a-c distribution became apparent, the departure was to a-c, radial overhead distribution, as shown in Figure 29. The problems of overhead distribution in congested city districts led to the radial underground distribution with transformers set in manholes and with underground ducts. The problem of radial, a-c distribution was met in the early 1920's, as shown in Figure 30, by typical nonattended automatic substations.

The problem is solved today very differently, as shown in Figure 31, by change from radial distribution to the secondary a-c network. Instead of the large substations, the substations consist of entirely automatic underground vaults tied into a network system. Here again, the philosophy of design has turned the full circle back to the substantial networks which were common in the d-c days. Another method of solving the problem is illustrated in Figure 32 which shows an entirely automatic factory-built primary-network substation. Here the network is on the 4,000-volt side. The economies in attendance and care and first cost are apparent from the illustrations. Finally, Figure 33 shows the typical unit-type substation again, factory-built and unattended and fully automatic, which serves radial primaries in the same way that the typical automatic substation of Figure 30 used to do. What can be seen from these few brief illustrations of the progress of distribution?

We see the progress from the early d-c network going to the a-c radial system and back again today to the a-c networks, both on the primary and secondary ends. We see today factory-built unit substations taking the place of the large buildings of the early days. If we wished to take the time, we could have shown you many of the modern tricks of distribution, such as, the banking of transformer secondaries, the improvement in capacity of distribution systems by the addition of capacitors and the widespread use of pole-type voltage regulators.

The Technical Side

We have reviewed the past progress of the electric power industry and commented on certain trends which can be read into the data presented. Let us now see what some of these generalizations mean in their technical aspect.

Large Size

A review of the past has stressed the tendency toward large size. Generally speaking, it is easier to build good and efficient equipment in the larger sizes than it is in small sizes. Many of the friction and loss quantities are fixed by the existence of the machine itself and large size reduces them in proportion to the total output. In addition, large size permits introducing refinements in design

DISTRIBUTION

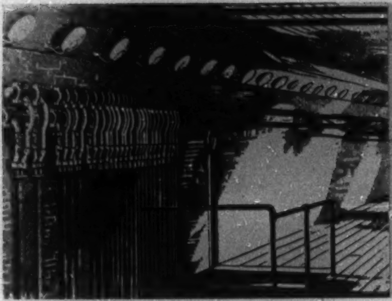
Figure 27. Pearl Street connections

Figure 28. Battery room

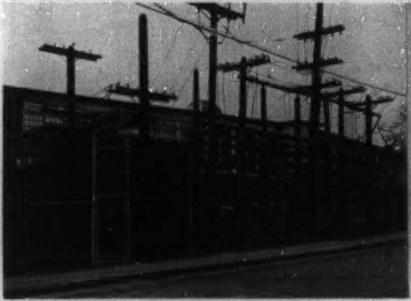
Figure 29. Early a-c radial overhead construction

Figure 30. Radial, manual, and automatic substation

Vol. 7
1951

which would be of so small total effect in smaller equipment that they could not be afforded. This is plain on the mechanical side of the problem with the old 120-kw jumbo generator; it would have been difficult to justify five stages of feedwater heating, even if this concept had been fully appreciated at the time. However, in a modern large-sized turbogenerator of 100,000 or 150,000 kw, it is very simple to go to seven or even nine stages of feed water heating. Similarly, in the use of reheat, certain fixed losses are introduced into the cycle which could not be tolerated in a small unit. In large units these fixed losses are not too much greater, and the possibilities of obtaining the true theoretical gain from reheat can be realized. In such a simple matter as the use of modern feedwater treatment, which is essential to the use of large-capacity, high-tension, high-pressure units, large-scale operation makes possible the employment of suitable personnel and suitable equipment for the complicated feedwater treatment, which could not possibly have been afforded by the small-scale operations 50 years ago.

The Cycle

A review of the progress of the past has shown an increasing use of higher temperatures and pressures. Figure 34 shows the effect of modern pressures and temperatures on the cycle efficiency. The use of this figure, with the engine efficiency ratio shown in Table I, permits the calculating of the performance of any particular cycle which you may desire. The ideal cycle efficiencies are drawn without regenerative feedwater heating and the effect of this is taken care of in the efficiency ratio. The choices between getting better cycle efficiency from increased pressure or increased temperature are clearly indicated. Both are effective if operations are conducted on a large enough scale. One of the early troubles with high pressure was concerned with the leakage losses in the small-capacity machines considered at that time. These are not such important factors in the large-scale machines that are being built today. Suffice it to say that substantial gains in cycle efficiency can be obtained with more certainty by the increase of temperature rather than by pressure.

Prime Mover and Generator

Throughout our review of the past, there has been a continuous increase in prime mover speed and size. With our choice of the 60-cycle frequency for a-c use, we have run into a natural limit on speed of 3,600 revolutions a minute with the 2-pole generator. On the other hand, it is not apparent that we have exploited anywhere near to the limit the size of machines that can be built for this speed.

DISTRIBUTION

(Continued)

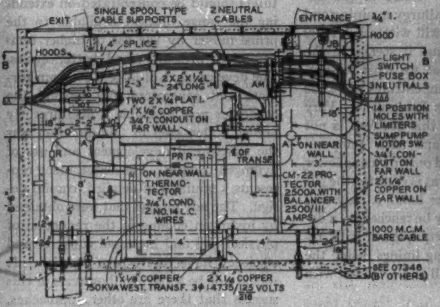
SINGLE SPOOL TYPE CABLE SUPPORTS
2 NEUTRAL CABLES
EXIT
ENTRANCE
3/4" I.
HOOD
4" SPLICE
HOODS
JB
B
LIGHT SWITCH
FUSE BOX
3NEUTRALS
2-3'
2"X2"X1/4"L 24"LONG
AM
TWO 2"X1/4" FLAT I.
1"X1/8" COPPER
3/4" I. CONDUIT ON FAR WALL
14 POSITION MOLES WITH LIMITERS
18"
2'-2"
10"
3'-0"
SUMP PUMP MOTOR SW.
A
A
ON NEAR WALL
3'
R
PR R
℄ OF TRANSF.
3/4" I. CONDUIT ON FAR WALL
ON NEAR WALL THERMO-TECTOR
CM-22 PROTECTOR 2500A. WITH BALANCER. 2500/111 AMPS.
2"X1/4" COPPER ON FAR WALL
8'
8'-6"
5'
3/4" I. COND. 2 NO. 14 L.C. WIRES
12"
1000 M.C.M. BARE CABLE
24"
4'
4'
4'
24"
16"
SEE 07348 (BY OTHERS)
1"X1/8" COPPER
2"X1/4" COPPER
750KVA WEST. TRANSF. 3φ 14735/125/216 VOLTS

Figure 31. Secondary network vault

Figure 32. Primary network unit

Figure 33. Unit substation

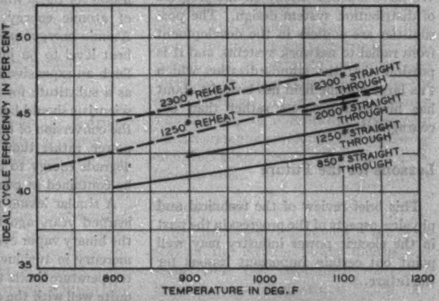

Figure 34. Ideal cycle efficiencies versus temperature for reheat cycles and straight through cycles at various pressures

Under this heading should be discussed the important advantages which have occurred to 3,600-rpm prime movers and generators by the use of hydrogen cooling. This has permitted a marked reduction in physical size or, on the other hand, a marked increase in capacity, and suggests many possibilities for future developments.

ELECTRICAL

In electric equipment, the tendency to larger sizes and capacities has come to match the growth of prime movers. They have had their own advantages in simplicity, in lowered costs of switching and transformation. The efficiency of transmission and distribution after the abandonment of the d-c system was good. There has been no great improvement in this today. As we have indicated in our survey of the past, the rise in voltage occurred quite early in the development of the power industry and presents many technical aspects. The use of higher voltage makes the problems of insulation and of corona discharge much more critical. Higher voltage, of course, permits the use of the same copper to distribute more power with satisfactory losses. There is considerable question as to the future field for use of voltages beyond the 350,000-volt level. It may well be, however, that for local transmission and distribution considerably higher voltages than those now used may prove desirable.

Table I. Annual Plant Net Heat Rates

	Pounds	Degrees	Efficiencies % Cycle	Efficiencies % Ratio	Efficiencies % Plant	Annual Heat Rate Net Btu/-Kwhr
Mystic*	1,250	900	42.3	0.714	30.2	11,300
Port Washington**	1,250	815	42.9	0.757	32.5	10,500
Twin Branch**	2,300	940	45.8	0.738	33.8	10,100
*	2,300	1,100	46.0	0.715	32.9	10,350
	2,000	1,050	45.0	0.715	32.2	10,600
	1,600	1,000	43.5	0.715	31.1	10,950
Proposed						
**	2,300	1,050	47.2	0.725	34.2	9,950
	2,300	1,000	46.5	0.725	33.7	10,100
	2,300	900	45.4	0.725	32.9	10,350
	1,450	1,000	45.3	0.725	32.9	10,380
	1,250	900	43.7	0.725	31.7	10,750

* Straight through. ** Reheat.

From our review, the trend to factory-built substations, prefabricated and prewired, is overwhelming. This trend offers no fundamental electrical problem and its extension is expected. At the same time, the trend to special types and special designs makes factory standardization difficult, especially where the volume is low.

One of the most significant features in transformer design, is the wide variety, such as tap changing under load, transformers for phase-angle shift, and for voltage control. The various means of cooling also are interesting. Many early transformers used forced air. Later transformers were filled with oil, cooled first by natural circulation, then by using forced air, then by forced water. Nowadays we are using forced oil and forced air, and instead of oil, we are using the fireproof Askarels and are even reverting to the straight air-cooled transformers. We have touched briefly on the progress of distribution system design. The possibilities are endless in the development from radial to network systems, and it is possible that the standardization which this large-volume field has brought about has hindered progress rather than encouraged it.

Lessons for the Future

This brief review of the technical and physical aspects of the progress in the past in the electric power industry may well point out certain important lessons for the future.

LARGE SIZE

The lessons of the past undoubtedly suggest that the units of the future will show a continued growth to larger sizes. This, of course, is the present handicap of gas turbines today. Their use for large power systems is largely circumscribed by their small size. Large electric power generating systems today have a peak load of as much as 2,000,000 kw and it would be ridiculous to add units to such a system having much less than 200,000-kw capacity. It will be many a day before gas turbines of 200,000-kw capacity are available, but every effort should be made to develop ordinary steam units for this size and larger.

BETTER CYCLE EFFICIENCY

A very fundamental part of the progress of the electric power industry in the past has been due to continuous improvements in cycle efficiency. It is believed, in the future as in the past, that the major forward steps will come by extending the available heat range upward by increased pressure and particularly increased temperatures. Today, the top temperature that is used for power generation is 1,050 degrees Fahrenheit. There is an immediate need for metallurgy in piping and in equipment which will withstand 1,200 degrees Fahrenheit and it seems, in the very near future, that we must be prepared to consider temperatures up to as high as 2,000 degrees Fahrenheit. Very likely the answer to this problem is not metallurgical. Perhaps such temperatures can be contained only by using lower pressures in the cycle as is done for the gas turbine. On the other hand, it may well be that a solution may be reached by a design of piping and equipment with refractory and insulating linings inside the pressure-resistant shell and provided with local cooling.

In any case, the tendency in the past for higher and higher temperatures is a lesson for those who are planning the use of atomic energy for power purposes. Atomic energy must be used at a high heat level to be justified by the results. Such an expensive fuel cannot be wasted as a substitute for oil and coal. Atomic scientists should bend their efforts toward the conversion of high potential energy to power, rather than considering means to degrade energy to the point where it can be contained in conventional equipment.

A similar lesson might well have been learned years ago by the proponents of the binary vapor cycles, such as the use of mercury in turbines. Between ordinary temperature limits the steam cycle can do quite well with the energy available. The excellent thermodynamic characteristics of mercury should have been utilized at much higher temperature levels.

The hopes for improvements in the steam cycle itself must be placed in the future not only in utilizing higher temperatures and pressures but also in reducing the percentage of heat rejected in the condenser by by-product use and by recirculating heat. By recirculating heat is meant all the varieties of heat traps, such as air heaters, economizers, and boiler feed heaters. It might be well to insert a word of caution that in considering heat traps it is not desirable to push recirculation to the point that the cycle reaches the dilemma which held the gas turbine for so many years. In other words, no net output. The principle of the gas turbine has been well recognized and understood for more than 100 years. During that time, many models were built. The only difficulty was that more power was used in recirculating energy, in the air compressor, than was delivered by the turbine.

PRIME MOVER AND GENERATOR

As the preceding sections have discussed, the first efforts of our manufacturers should be concentrated on extending the range of heat available to the prime mover by the use of higher temperatures, pressures, and better cycles. The development of large 3,600-rpm turbines and generators way beyond the capacities now available is also urgently needed. One step in this direction was the widespread development and use of hydrogen cooling. The design today represents a triumph of detailed, careful design. The advantages that were obtained by hydrogen cooling in the reduction of physical size and increased capacity and efficiency have rarely been excelled. It should not be forgotten, however, in this success that there are other approaches, and other means of generator cooling may well yield equally startling progress.

The progress in generator voltage design has been nowhere near as satisfactory. At a very early stage in their development, 14,000 volts were used in American generators and, while admitting that there may be many technical reasons why extremely high-voltage generators are not practical, it would seem to us that doubling or tripling of present voltages would reduce the amount of copper in our machines, as well as reduce mechanical and cooling stresses.

In the actual detailed construction of generators today, there is a tremendous amount of skilled handwork and techniques which were well developed in 1882. This is typified by the widespread use of hand-split mica. It would seem that modern manufacturing methods and design aimed at improved insulation, improved cooling, and the suppressing of corona could achieve important progress in electric machine design today. There is recent evidence of progress in this direction.

A similar field for modern manufacturing methods lies in the manufacture of laminated cores. The insulation of laminations, their punching and burring and assembly, are awaiting improvements which would lower costs and eliminate vibration and the resulting noise.

The comments so far under this heading have been largely electrical in nature and this proceeds from the idea that turbines can be built much larger in capacity than the generators which are now available. At the same time, we have full realization that the mechanical detailed design of turbines today with the large amount of skilled hand work and fitting could be very largely improved. Careful functional design in such simple matters as blade roots, nozzle block caulking, and sealing strip caulking could easily be transferred from the realm of skilled artistry to mass production.

Switching

The tendency towards larger capacity and faster switching has been clearly brought out by our review. There may be some question as to the ultimate desirable size and interrupting capacity of switching, but there can be no doubt of the desirability of minimizing by faster action and better relaying the burning of cables, windings, and cores that occur in short circuits.

Considering the present rate of load growth, the ultimate size of the electric load cannot be predicted. It may be that, rather than the design of apparatus with larger interrupting capacity, what is needed is a design of transmission and distribution systems which will limit the interrupting capacity thrown on the switching. This is obtained at present by sectionalizing, by limiters, by splitting networks into smaller parts. The opportunity exists for system design of a fundamental nature to anticipate and provide for the growths that the future will bring us.

Mention should be made of porcelain, so widely used as an insulator on our electric systems. It is indeed a difficult engineering material, subject to cracks, absorption, and brittleness and there are few ways to measure its satisfactoriness for service. With the higher voltages, higher speeds, and higher mechanical stresses that are coming in the growth of our electrical industry, some better material is badly needed.

Another bugaboo of the electric system are the moving contacts such as are found in regulators and tap changers and in the switches themselves. The problem of the moving contact has never been solved properly.

Silver plating, wiping contacts, are all improvements, but perhaps the solution is not a matter of detail but of a complete new approach. It may be that the power switching of the future will be done electronically in tubes.

Transmission

The needs for the future in the field of transmission are clearer. Lower-cost cables which can be installed more economically than present practice are necessary. If lower-cost methods of installation could be combined with some method of assuring that the cable is installed without damage from pulling, it would be extremely desirable.

It seems there is a field for standardization in transmission design similar to the unit designs of the distribution substations. On the overhead transmission lines, the control of lightning and of sleet are still none-too-well worked out and could benefit from further effort. The very real limitations on the long distance transmission of large amounts of power suggest an opportunity for fundamental research. It may well be that a continuation of the work on high voltage d-c transmission would prove fruitful.

Distribution

Returning once more to the distribution system of the electrical power industry, this is a mass production item, and because it deals in the lower voltages and with repetitive installations, it is not so glamourous as some of the other fields of endeavor. It should be borne in mind, however, that the extremely large investments which power companies make in their distribution system warrant the most intensive engineering studies. The extremely long life of distribution systems, as in all the equipment of the power industry, is also important. The first installation should provide for future growth without frequent rebuilding.

Perhaps two phases of the distribution system design call for the most immediate attention. One is the great need for lower-cost underground construction. Modern cities' civic pride and indeed the high-density power requirements of a modern city force conversion to underground distribution. If new techniques, new approach, or new modern machinery could develop a lower-cost underground distribution system, it could be put in originally and the high cost of later conversion could be avoided. The second urgent need is for improved reliability in the overhead distribution system. Aerial cable may be one of the answers to this problem. The situation is just the reverse of the underground problem. Modern overhead construction is relatively economical. Furthermore, repairs to the overhead system are quickly and economically made. It is perhaps for this reason that no great improvement in the reliability of the overhead distribution system has been made.

Transformation

The future of transformer design would appear a simple problem and will undoubtedly be a continuation in the development of larger and larger 3-phase units. The problem of the tap changer and of the moving contacts has been discussed. It is certainly desirable that there be an immediate solution to the noise problem. There seems no reason why a piece of nonrotating equipment should present a problem to the acoustical engineers every time it is installed in a residential area.

Conclusions

In summing up this review of the progress of the electric power industry, it seems clear that continued progress to low-cost power as shown on Figure 1 requires a reversal in the upward trend of the cost index. The industry will continue its present rapid growth. Cycle efficiencies are going to increase as will the temperatures utilized. New economies from large-scale operations will be realized as the sizes of equipment increase.

Many of the annoying details that seem important to us today will vanish due to the progress of the arts. Nevertheless there will be, for many and many a year, plenty of work for the designers of the electrical power industry.

Discussion

John M. Drabelle (Iowa Electric Light & Power Company, Cedar Rapids, Ia.): The authors, I. E. Moultrop and G. A. Orrok, have contributed a valuable review to the literature of the electric power industry.

To look backward is to really look forward and see the progress which has been made in the generation, transmission and distribution of electrical energy to the public and to better see what lies ahead. This progress is that of the public utility industry of the country, together with the manufacturers.

The heat cycle in the power station is the real challenge, and as long as we use water and steam, the lower end of the steam cycle does not present any such opportunity of improvement, so we naturally turn to higher temperatures and higher pressures with the regenerative and reheat cycles, together with the various heat traps on the boiler, such as the economizer and the air preheater.

With the standardization program as carried out jointly by the AIEE and The American Society of Mechanical Engineers, the time and effort of the manufacturer's engineers can be devoted to mechanical and internal refinements of the steam turbine and its accompanying generator, rather than devoting all their time to recalculating standard machines for nonstandard conditions and various nonstandard arrangements of extractions for feed water heating that contribute little or nothing in the over-all heat cycle.

As has been pointed out by the authors, the distribution system, both overhead and underground, challenges as yet the ingenuity of the engineering fraternity.

Herbert B. Reynolds (J. G. White Engineering Corporation, New York, N. Y.): The authors have presented a splendid review of the power industry and have pointed the way for further development. However, I would like to mention a few additional milestones in the progress of the art.

First there is the last stand of reciprocating steam engines for central station use in the form of the 7,500-kw units in the 74th Street and 59th Street Power Plants of the Interborough Rapid Transit Company, now part of the New York City Transit System. These engines are the largest ever built for central station use, the diameters of the high and low pressure cylinders being 44 inches and 88 inches respectively, with a common stroke of 60 inches. The diameter of the revolving field is 32 feet. Some of these units are still in use for peak load and standby service.

Another milestone was the addition of 7,500-kw low-pressure turbines to some of these engines so that the exhaust steam from the engines could be used in the turbines, thus doubling the capacity of the units and greatly improving the efficiency, making them the most efficient prime movers at the time. This improvement was conceived by the late Henry G. Stott, a past president of the Institute and one of the pioneers in large power plant work. The installation of Roney stokers under the rear of the existing Roney fired boilers in the 59th Street Power Plant by Mr. Stott was probably the first major step taken in order to increase the capacity of boiler heating surface.

Another great improvement in the power field has been the use of the fully automatic ignitrons in place of the manually operated rotary converters for the conversion of alternating current to direct current.

F. M. Gunby (Chas. T. Main, Inc., Boston, Mass.): We are indebted to the authors for recording so much so well, and also for their disclosure of trends. The picturing of some of the early works and practices is valuable and gives us good back sights.

The growth of loads has made the great increase in the size of generating units feasible.

Standardization within the electric industry is one of the fundamentals upon which the rapid development of this huge industry rests. The authors skillfully give us the shadows from some of the early days before standards emerged.

The team work which met and solved these problems is a memorial to the early figures in the electrical industry. This team work developed largely around the National Engineering Societies and AIEE can be proud of its major share in that team work.

The authors have prepared a comprehensive history or critique of the progress in steam electric power plant development. Since improvements in cycle efficiencies by means of higher temperatures must await the development of new materials, it becomes increasingly important to expand the installation of by-product plants. In large cities there appears to be an important opportunity for utilizing the heat in the steam ordinarily rejected to the condenser as a means of supplying the office-district load which is concentrated in a relatively small area for distribution. Industry has long made use of this cycle and there are examples of its use by utilities.

The authors state that they have confined their work primarily to the generation of electricity by steam. The title, however, is broad enough to warrant a reference to generation of hydroelectric power and some of the transmission problems which have resulted. The following discussion touches on that source of energy which in 1950 accounted for nearly 30 per cent of the total kilowatt-hours.

Progress in hydroelectric development parallels the great advance in thermal station design. The use of horizontal multi-runner turbines of low capacity operating in cylindrical plate steel casings and other early designs are still within the memory of many present-day engineers. Large modern installations use vertical shaft units. Probably no other factor contributed so materially to the advance leading to the modern large size vertical turbine as the advent of the Kingsbury thrust bearing.

The present top of individual unit size is in the 120,000-kva range. Prediction of output limits would be essentially based on improvement in turbine practice resulting in higher speeds. This would increase generator outputs without exceeding present rotor weights, which are fast approaching economic limits of structures and handling methods.

The larger units usually have direct connected stabilized exciters and a closed ventilating system consisting of an air housing and surface air coolers. There have been a few outdoor installations but no distinct trend in that direction.

Most large hydroelectric stations are now of the so-called unit design in which each unit is actually a complete independent installation having its own turbine, governor, generator, exciter, auxiliaries, and step-up transformers. Some are having the metal-clad switchgear connected to the generator air housing.

Progress in hydraulic prime movers has been notable in the trend to large size units. The limitation on the size of Francis type turbines has been fixed principally by the maximum diameter of the runner that can be shipped in a single piece. Larger diameters have been built with split runners but these have been limited to moderate heads.

The development of the propeller-type turbine has increased the speed at which units can operate under moderate heads with resulting economy. The development of the adjustable blade Kaplan unit has made possible the adaptation of the propeller unit to wide variations in flow and head conditions. Recent trends in installation of Kaplan units at heads above 100 feet have increased the adaptability of this type of unit.

Efficiencies of hydraulic turbines have not improved greatly in recent years. The maximum reported efficiency of $94^{1}/_{2}$ per cent was obtained by the installation of the 100,000-horsepower units in Canada.

Improvements in the setting of turbines, increased knowledge from cavitation research, and the development of stainless steel protection against cavitation has resulted in increased speeds for both Francis and propeller-type turbines with consequent economy in both turbine and generator.

Increased capacity of impulse units has resulted from development of multinozzle vertical shaft installations.

Since sites of important hydroelectric developments are usually far from large cities with their large loads, and generally concentrated steam generating facilities, this condition early brought long distance transmission prominently into the picture.

The trend is toward the use of large systems consisting of several stations or group of stations interconnected by heavy transmission lines. Often several such systems, including both steam-electric and hydroelectric generation, are linked up and operated as a single system. The control can be by a system dispatcher using modern aids such as carrier current telephoning and telemetering, supervisory control, automatic load frequency control, proportionate load control, or tie line control.

The protective relaying of these large systems is well understood. Great advances are being made in the field of power dispatching. The simple system of yesterday, where the regulation of the system output was concentrated in an individual, appears doomed for the larger systems. Accelerated by our post-war needs, this country is fast becoming an integrated network of power transmissions of such complexity that automatic equipment is even now assuming the task of coordinating the generation of many far-flung plants.

Where hydroelectric generation with ample pondage is available, it is often economical to increase the installed capacity and operate the hydroelectric plants for peak loads and as reserves. The increased installed capacity at such points can frequently be obtained at additional costs, which are relatively small.

E. G. Bailey (New York, N. Y.): The authors have presented a very pertinent review of progress in an outstanding industry, where engineering, invention, and development, together with progressive management, have resulted in continually lowering the cost of equipment while increasing its output in spite of advances in wage rates and the influence of inflation. The future will require the best of engineering and management to maintain the standards already recorded.

The statement in the paper that boiler efficiencies were 86 per cent in the days of Watt and only 90 per cent now may be misleading to some, because there is more to the story than just these two figures. The average boiler efficiency was probably below 70 per cent throughout all steam generating history until 1900. It is usually in the high 80's today. The over-all thermal efficiency of Watt's pumping unit was about 4 per cent as against 8 per cent for the average in 1920; 20 per cent in 1949, and 37 per cent for the best operating plants last year.

The great reduction in cost of generating steam has been due to the very high output per pound of boiler steel and the reduction in manpower per unit output. The credit for all of this is shared by the manufacturers of all kinds of equipment, as well as by the consulting engineers, management, and operators.

The future improvements likewise will be shared by all in their continuation of interest and contribution of engineering abilities.

The plant operators have striven for a high reliability of equipment, and it has been improved, thereby necessitating only a narrow margin of spare capacity.

As a user who has experienced 40-odd hours outage in supply twice in the past three years, there is still a problem of winning the battle of reliable distribution to the ultimate user against the elements.

N. E. Funk (Philadelphia, Pa.): The authors have presented a very excellent picture of the progress in the electric power industry over the years, for which they should be complimented.

There are several items, however, to which I wish to refer:

(1). In the abstract, the impression is definitely given that the improvement in the efficiency of generating electrical energy has been primarily responsible for the great reduction in the cost to the customer. This is not true. The vast improvement in efficiency has been practically wiped out by the increased price of coal, labor and power plant equipment. Thus, today the bus bar cost, including both operating and annual capital costs, is little different than it was 30 years ago, even with a great improvement in load factor.

As a matter of fact, the reduction in cost has been attained through greater customer density, greater individual customer use, greater individual customer load factor, better diversity factor, and a tremendous increase in total load.

(2). I do not feel that we will move too rapidly into units of 200,000-kw capacity.

The capital cost per kilowatt does not decrease very greatly for unit sizes over 150,000 kw, neither does the operating cost. Thus, the larger size units may require the installation of more capacity to safeguard the system, which at $150 per kilowatt overcomes the small saving from the larger size.

(3). I would not cast the gas turbine aside too lightly because of its size. There may be locations in any large system remote from circulating water where small gas turbines can be placed at a great saving in local transmission and with improvement in service reliability.

(4). Admitted there is an optimum voltage which permits a winding of the best electrical and mechanical characteristics, but it is somewhere between 14,000 and 20,000 volts, and not two or three times the present voltage.

I would assume without having made any calculations that the weight of copper depended upon the speed of the machine and its capacity, and that voltages of 28,000 or 42,000 would increase the copper weight rather than reduce it, because of increased insulation thickness. This would tend to increase the differential expansion of iron and copper; thus accentuating some of our present troubles.

William F. Ryan (Stone & Webster Engineering Corporation, Boston, Mass.): At this moment in history when every engineer in the power industry is overloaded with immediate and pressing problems it is fortunate that somebody has taken the time to review our progress to date and give some thought to long range future developments. We are indebted to Messrs. Moultrop and Orrock, not only for their own thoughtful and factual presentation, but for the stimulus their paper has given all of us who have read it to crystallize our own thoughts regarding future progress. I am sure we all agree that progress will continue at an unslackened pace, but each of us may place more emphasis on particular objectives.

It is possible, for example, that we should place more emphasis on reducing capital costs than on larger capacities or higher efficiency of generating units. The Engineering-News Record Cost Index, shown in Figure 1, has relatively little significance in the power industry. On the one hand it does not reflect the progressive inefficiency of construction labor, which makes actual costs even higher than the index would indicate, and on the other hand it does not allow for the technological advances which have enabled the designers of power plants and power systems to offset, in large part, the rising costs of material and labor. According to our own index of power equipment costs, the boilers which Mr. Moultrop installed at L Street, 50 years ago, would now cost 18.8 times as much as they did in 1901, if anyone should care to install boilers of that size and design. However, the same heating surface would now generate about seven times as much steam, and the latter amount of steam would generate nearly 30 times as much power per square foot of boiler heating surface. Actually, steam generating equipment costs less now, per unit of electrical output, than it did at any time prior to about 1939. The outstanding challenge to designers today is to hold capital costs in line.

Another item which deserves more present thinking for future progress is the cost of maintenance. Our boasts regarding decreased costs of labor and fuel are not matched by decreases in maintenance expense. It is open to question whether the cost of maintenance, per kilowatt year, is any less in our largest and most modern plants than it was in the first plants that Mr. Moultrop, or Mr. Orrock's distinguished father ever designed.

It would appear also that radical advances must be made in the art of local distribution. The traffic on our local distribution systems is increasing faster than it is on the highways, but the systems themselves have more in common with the streets of downtown Boston than they have with the freeways of Los Angeles. Radical developments are required, not only to reduce costs, but because we shall soon be unable to get enough conductors of the present type into our city streets.

As mentioned in the beginning, it is good to find someone who will take the time to look forward. Mr. Moultrop has been doing that for 60 years, and Mr. Orrock will still be doing it 60 years from now if progress in longevity parallels progress in the power industry.

I. E. Moultrop and **G. A. Orrok**: The authors feel very complimented at the caliber and quantity of the discussions presented and wish to thank the discussers.

John M. Drabelle

Mr. Drabelle emphasizes the importance of standardization. We agree with this and his other suggestions.

Herbert B. Reynolds

This discussion makes a very good addition to the paper, amplifying the section on the early reciprocating steam engines and boilers. The engineering work of Mr. H. G. Stott is outstanding in our field.

F. M. Gunby

Mr. Gunby makes a very valuable addition to the paper in discussing the developments in the hydroelectric generation of power.

E. G. Bailey

We can only agree with Mr. Bailey's careful analysis of boiler efficiencies. His discussion adds value to the paper.

N. E. Funk

This valuable discussion brings up several of the debatable points in the paper and we must agree that the efficiency of electrical generation is not the whole story on low cost. Nevertheless, had the generating efficiency not improved, costs would be much higher than they are today. The increase in total load and in load density have been tremendous factors in holding the cost of electricity down. The point we wish to make is that similar growth and increase of load density have been common to other types of industry and other types of product where the same reduction in price of the commodity to the consumer has not ensued. As to the economic size of units this, of course, is a question which can be solved only for each specific unit as it comes up. We must agree that it is very easy to purchase too large a unit for a given installation. On the other hand, for many installations reliable units of a large-enough size have not been available. This discussion sheds more light on the question of gas turbines and on the optimum generator voltage.

William F. Ryan

Mr. Ryan throws additional light on two important problems of electric power station design: the first on capital cost, and the second on the cost of maintenance. The authors have not stressed in the paper the importance of the progress in the design of power plants toward reduced maintenance expense. Actually, a comparison of the operating figures will indicate that the cost of maintenance has varied more in proportion to the capital cost of the equipment installed than with the cost of kilowatthours. This fact is only what might be expected, but the desirability of directing design toward reduced maintenance costs can not be emphasized too strongly.

Many of the discussions emphasize the point with which we would like to close. The development of the power industry has been the result of the collaboration of many individual engineers, of the power companies, of the manufacturers of equipment, the National Engineering Societies, and many others. We can all take pride in our share in this great development.

Transmission Systems of The Hydro-Electric Power Commission of Ontario

J. E. SPROULE
ASSOCIATE MEMBER AIEE

F. L. CODE
ASSOCIATE MEMBER AIEE

THE original transmission system of The Hydro-Electric Power Commission of Ontario was placed in service in 1910. In December 1950 the total peak load of all the Commission's systems was about 2,715,000 kw, exceeding that of the previous year by over 22 per cent. The purpose of this paper is to review the transmission developments of the Commission in both 115-kv and 230-kv classes.

In the field of high-voltage transmission the Commission was one of the pioneers, first in 1910 with its original 115-kv network and later in 1928 with its adoption of 230-kv transmission. The Commission also was one of the pioneers in the development and use of the suspension insulator, which was fundamental in increasing voltages beyond 90 kv.

Today in 1951, the Commission has ten trunk transmission circuits bringing power at 230-kv from eastern generating sources to the load centers in central and western Ontario, as shown in Figure 11. An extensive 230-kv 60-cycle network is being built up, to cover the whole of southern Ontario. When the frequency standardization program, now under way is completed, the five trunk circuits at present operating at 25 cycles will be included in the 60-cycle network.

At present the Commission's transmission systems, include nearly 3,000 circuit miles of 230-kv construction and about 4,600 circuit miles of 115-kv line. Some 492 route miles of 230-kv double circuit construction will have been erected at the end of the present program, as compared to the 45 route miles of double-circuit line previously in service.

Changes in design of the towers and lines are discussed, and the frequency of lightning and other outages has been compared for the various types of construction. The securing of a low tower footing resistance on the Commission's existing 230- and 115-kv lines is the object of a construction program now in progress.

Studies now under way involve a possible 500 miles of additional 230-kv transmission line, which will likely use larger conductor sizes than the 795,000 circular mil steel reinforced aluminum cable which is the present standard.

Stability problems will become less important as the size of the 230-kv network becomes greater. Hence the load carrying capacity per circuit will tend to increase until it reaches a limit set by the system losses. With a high load factor, the system tends to become more sensitive to the cost of transmission losses, and the proposed use of larger conductors seems justified on this basis.

Early 115-Kv Transmission Lines

In 1908, the original 115-kv transmission system of the Commission was designed, to consist of 244 route miles of double circuit and 36 route miles of single-circuit steel tower lines and involved 13 stations and terminals. Suspension insulators were used which were a new and untried field for this voltage at that time. Five static wires were provided during the trial period of this double-circuit construction, but this was changed to only one overhead static wire. The first lines built used a triangular configuration as shown in Figure 1(A), with a span length of 550 feet. Lightning outages on the double-circuit section of these early lines taken over the period from 1941 to 1949 were equivalent to 4.85 lightning outages per 100 circuit-mile-years. Glaze outages were equivalent to 0.89 outage per 100 circuit-mile-years. The lightning outages may involve only momentary loss of facilities, but the glaze outages can result in the loss of the affected circuits for many hours.

Ice loading of conductors produced two kinds of problems. Under certain temperature conditions and in relatively still air when the ice suddenly fell off a heavily ice-loaded circuit, the conductor would jump vertically upwards and contact the conductor above. A second phenomenon now referred to as "galloping or dancing conductors" involved a critical condition of light glaze coating and moderate quartering wind, under which conductors were

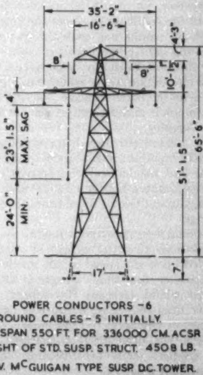
35'-2"
16'-6"
8'
8'
4'-3"
10'-1½"
4'
23'-1.5"
MAX. SAG
24'-0"
MIN.
51'-1.5"
65'-6"
17'
7'
POWER CONDUCTORS -6
GROUND CABLES - 5 INITIALLY.
STD. SPAN 550 FT. FOR 336000 CM. ACSR
WEIGHT OF STD. SUSP. STRUCT. 4508 LB.
115 KV. McGUIGAN TYPE SUSP. DC. TOWER.

Figure 1(A). McGuigan type double-circuit steel tower used on original 115-kv construction in 1910

Paper 51-383, recommended by the AIEE Transmission and Distribution Committee and approved by the AIEE Technical Program Committee for presentation at the AIEE Fall General Meeting, Cleveland, Ohio, October 22-26, 1951. Manuscript submitted April 3, 1951; made available for printing August 30, 1951.

J. E. Sproule and F. L. Code are with The Hydro-Electric Power Commission of Ontario, Toronto, Ont., Canada.

The authors wish to acknowledge the assistance in the preparation of this paper of their colleagues, particularly that of Mr. A. E. Davison, Transmission Consultant of the Commission's electrical engineering department.

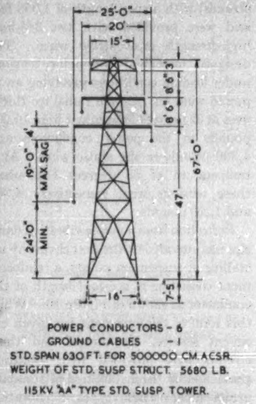
25'-0"
20'
15'
3'
8'6"
8'6"
4'
19'-0"
MAX. SAG
67'-0"
47'
24'-0"
MIN.
16'
7'-5"
POWER CONDUCTORS - 6
GROUND CABLES - 1
STD. SPAN 630 FT. FOR 500000 CM. ACSR.
WEIGHT OF STD. SUSP STRUCT. 5680 LB.
115 KV. "AA" TYPE STD. SUSP. TOWER.

Figure 1(B). "AA" type double-circuit steel tower used on 115-kv lines built in 1914

observed to rise and fall in a rhythmic motion.[1] These critical conditions could persist for hours, and flashovers between conductors in the same vertical plane caused frequent line outages.

In 1914, the designs of the Commission were altered to that shown in Figure 1(B) using a span length of 630 feet. This change was made to increase the clearance between phases and to reduce the angle of protection, as well as to use larger conductors with a longer span length. The performance record for these lines over the same period gave 2.38 lightning outages per 100 circuit-mile-years. These lines were located in good agricultural land, and hence had low tower footing resistance. The outages due to glaze conditions were equivalent to 0.63 outage per 100 circuit-mile-years. Trouble was experienced on this design due to galloping conductors and the vertical spacing was increased by the use of extension bars in the insulator strings.

In 1917, under wartime conditions, the Commission built its first 115-kv wood pole line, 68 miles long, which was a single-pole arrangement sometimes referred to as the "wish-bone" type with a span length of 350 feet and using 3/0 steel reinforced aluminum cable, as shown in Figure 2.

During the period from 1920 to 1928 progress in the design of the Commission's 115-kv circuits involved a trend towards longer spans and towards larger conductors with higher conductor tensions. Tower height was restricted by the prevailing knowledge of lightning phenomena at that time.

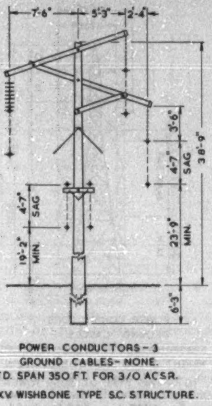
7'-6"
5'-3"
2'-4"
3'-6"
4'-7"
SAG
38'-9"
4'-7"
SAG
19'-2"
MIN.
23'-9"
MIN.
6'-3"
POWER CONDUCTORS - 3
GROUND CABLES - NONE.
STD. SPAN 350 FT. FOR 3/0 ACSR.
115 KV. WISHBONE TYPE S.C. STRUCTURE.

Figure 2. "Wishbone" type single-circuit wood pole structure used on 115-kv line built in 1917. Ground wire generally provided

In order to provide greater separation and also a horizontal displacement sufficient to avoid interference under "galloping" conditions, the 115-kv double-circuit steel tower design was altered in 1920 from that shown in Figure 1(B) to the type shown in Figure 3(A).

The circuits constructed in 1920 were designed for 880-foot spans. The conductors were 605,000 circular mil steel reinforced aluminum cable, and the ruling tensions 8,000 pound maximum under loading conditions involving an 8 pound wind on 1/2-inch radial ice thickness at 32 degrees Fahrenheit, and 3,110 pounds at 60° Fahrenheit. In 1928, the standard span was increased from 880 feet to 1,056 feet with the tower height only increased sufficiently to maintain the same conductor tensions and ground clearances, see Figure 3(B).

Figure 3(A). 1920 type 115-kv double-circuit steel tower

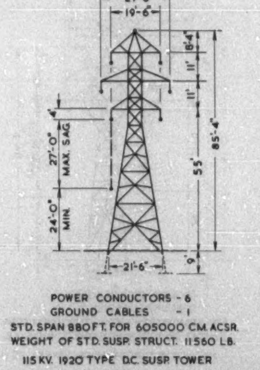
27'-6"
19'-6"
8'-4"
11'
11'
4'
27'-0"
MAX. SAG
55'
85'-4"
24'-0"
MIN.
9'
21'-6"
POWER CONDUCTORS - 6
GROUND CABLES - 1
STD. SPAN 880 FT. FOR 605000 CM. ACSR.
WEIGHT OF STD. SUSP. STRUCT. 11560 LB.
115 KV. 1920 TYPE D.C. SUSP. TOWER

The problem of aeolian vibration of conductors was first experienced seriously with this design. Breakages of individual strands in the conductors of this 1928 design were found even before the line was placed in operation, and the 1920 design with 880 foot spans was then found to be also suffering from individual strand failures. Strand failures due to crystallization have since been minimized by the application of armor rods later supplemented by vibration absorbers.[2]

Data covering the performance of the 115-kv double-circuit construction built between 1920 and 1928 for the 10-year period ending December 31, 1949, show an average of 3.12 outages per 100 circuit-mile-years due to lightning and 1.17 outages per 100 circuit-mile-years due to ice conditions.

Recent 115-Kv Line Construction

Recent 115-kv line construction by the Commission has been designed to incorporate improved lightning protection, with greater clearances so as to minimize outages due to ice conditions and galloping conductors, and with vibration absorbers to decrease the breakage of individual strands in the conductors.

The 115-kv single-circuit steel tower

Figure 3(B). 1928 type 115-kv double-circuit steel tower

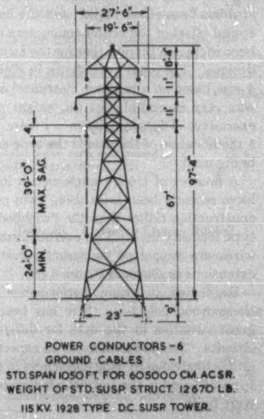
27'-6"
19'-6"
8'-4"
11'
11'
4'
39'-0"
MAX. SAG
67'
97'-4"
24'-0"
MIN.
9'
23'
POWER CONDUCTORS - 6
GROUND CABLES - 1
STD. SPAN 1050 FT. FOR 605000 CM. ACSR.
WEIGHT OF STD. SUSP. STRUCT. 12670 LB.
115 KV. 1928 TYPE D.C. SUSP. TOWER.

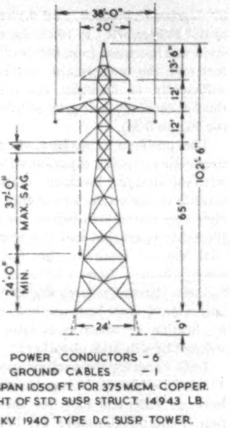
38'-0"
20'
13'-6"
12'
12'
4'
37'-0" MAX. SAG
24'-0" MIN.
65'
102'-6"
24'
9'
POWER CONDUCTORS - 6
GROUND CABLES - 1
STD. SPAN 1050 FT. FOR 375 MCM. COPPER.
WEIGHT OF STD. SUSP. STRUCT. 14943 LB.
115 KV. 1940 TYPE D.C. SUSP. TOWER.

Figure 4. 1940 type 115-kv double-circuit steel tower

construction now uses 1,056-foot spans with 477,000-circular mil steel reinforced aluminum cable as shown in Figure 6(A). This design made use of one high single static wire.

The outage record on these 115-kv single-circuit steel tower lines shows 2.71 lightning outages per 100 circuit-mile-years. There were no outages due to ice conditions during the period from 1941 to 1950 inclusive.

Recent 115-kv double-circuit steel tower construction uses 1,056-foot spans with 605,000 circular mil steel reinforced aluminum cable conductors as shown in Figures 4 and 5. The single static wire also has been raised higher, and the horizontal offset of the center conductors has been increased beyond that for the former designs. The tower type shown in Figure 4 was based on a full loop clearance[1] and was very successful, but the weight was excessive. The tower shown in Figure 5 is a modification of this and is the type now being used.

A number of 115-kv single-circuit lines have recently been built using twin pole construction rather than the "wishbone" type formerly used. Two overhead static wires are supported on structural steel extensions as shown in Figure 6 (B).

Regarding lightning performance of these wood pole lines there has been a great variation in the data for different circuits. This is probably to be expected and is likely due to wide differences in the type of country through which the lines were built.

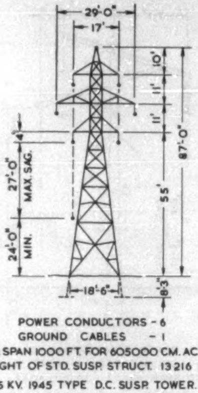
29'-0"
17'
10'
11'
11'
4'
27'-0" MAX. SAG
24'-0" MIN.
55'
87'-0"
18'-6"
8'-3"
POWER CONDUCTORS - 6
GROUND CABLES - 1
STD. SPAN 1000 FT. FOR 605000 CM. ACSR.
WEIGHT OF STD. SUSP. STRUCT. 13216 LB.
115 KV. 1945 TYPE D.C. SUSP. TOWER.

Figure 5. 1945 type 115-kv double-circuit steel tower

Early 230-Kv Single-Circuit Construction

In October 1928, the Commission placed in service its first 230-kv single-circuit steel tower line 230 miles in length to bring 25-cycle power to south-western Ontario from the Paugan Generating Station of the Gatineau Power Company. The initial terminal station was located at Leaside near Toronto. A second single-circuit line paralleling the first was brought into service in July 1930. With the completion of the Chats Falls Generating Station in 1931, a third 230-kv circuit was constructed.

The design of the steel towers for these three original circuits is as shown in Figure 7(A). These lines all used 795,000 circular mil steel reinforced aluminum cable conductors (54 aluminum by seven steel strands) with a span length of 1,056 feet and were provided with two 3/8-inch high-strength steel static wires. The designed maximum conductor tensions under loading conditions involving an 8-pound wind on 1/2-inch radial ice thickness at 32 degrees Fahrenheit were 10,000 pounds in the power conductors and 4,300 pounds in the static wires. At a temperature of 60 degrees Fahrenheit these tensions were respectively 4,360 and 1,250 pounds.

Protection from possible vibration damage was provided on the first circuit by installing at suspension points, a reinforcement consisting of a 6-foot length of the conductor as shown in Figure 10. While this form of reinforcement has given excellent service, the second and third circuits were provided with vibration protection by the installation of standard armor rods. These types of vibration protection have been satisfactory and inspection to date has shown no breaks due to vibration.

These three original 230-kv single-circuit lines covering the total operating period from 1928 to December 31, 1950 show an average of 1.44 lightning outages per 100 circuit-mile-years. Table I gives the classification of the lightning outages into single-line to ground, double-line to ground, and 3-phase. Also this table gives the relative number of lightning outages involving one, two or three circuits. Those outages known to have occurred on the connecting lines in the Province of Quebec, which are not the property of the Commission, have been omitted.

In 1941, a fourth 230-kv trunk circuit was built to bring 25-cycle power directly from the Beauharnois Generating Station to the Leaside terminal. At

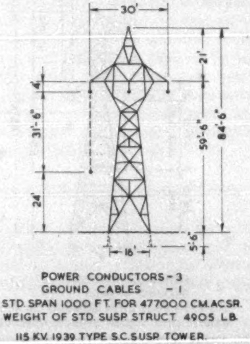
30'
21'
4'
31'-6"
59'-6"
84'-6"
24'
5'-6"
16'
POWER CONDUCTORS - 3
GROUND CABLES - 1
STD. SPAN 1000 FT. FOR 477000 CM.ACSR.
WEIGHT OF STD. SUSP. STRUCT. 4905 LB.
115 KV. 1939 TYPE S.C. SUSP. TOWER.

Figure 6(A) (left). 1939 type 115-kv single-circuit steel tower

Figure 6(B) (below). Twin pole 115-kv single-circuit wood structure

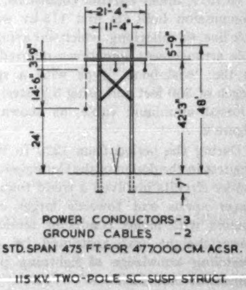
21'-4"
11'-4"
5'-9"
3'-0"
14'-6"
24'
42'-3"
48'
7'
POWER CONDUCTORS - 3
GROUND CABLES - 2
STD. SPAN 475 FT. FOR 477000 CM. ACSR.
115 KV. TWO-POLE S.C. SUSP. STRUCT.

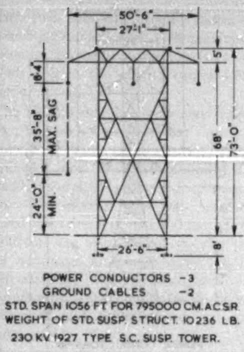
50'-6"
27'-1"
5'
18'-4"
35'-8" MAX. SAG
68'
73'-0"
24'-0" MIN.
8'
26'-6"
POWER CONDUCTORS -3
GROUND CABLES -2
STD. SPAN 1056 FT. FOR 795000 CM. ACSR.
WEIGHT OF STD. SUSP. STRUCT. 10236 LB.
230 KV. 1927 TYPE S.C. SUSP. TOWER.

Figure 7(A). 1927 type 230-kv single-circuit steel tower (Gatineau circuits)

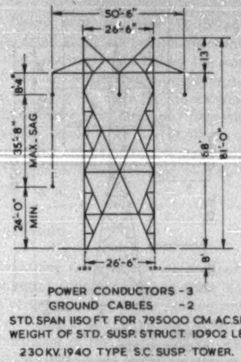
50'-6"
26'-6"
13'
18'-4"
35'-8" MAX. SAG
68'
81'-0"
24'-0" MIN.
8'
26'-6"
POWER CONDUCTORS -3
GROUND CABLES -2
STD. SPAN 1150 FT. FOR 795000 CM. ACSR.
WEIGHT OF STD. SUSP. STRUCT. 10902 LB.
230 KV. 1940 TYPE S.C. SUSP. TOWER.

Figure 7(B). 1940 type 230-kv single-circuit steel tower (Beauharnois circuit)

the same time a second 230-kv terminal station was established at Burlington.

The 1941 single-circuit steel tower design, see Figure 7(B), involved an increase in span length from 1,056 feet to 1,150 feet. In order to maintain the same ground clearance at the longer span, the higher strength (26 aluminum by seven steel strands) 795,000 circular mil steel reinforced aluminum cable was used, strung to a maximum designed tension of 12,000 pounds. The two ground cables of 3/8-inch galvanized steel were elevated eight feet higher than in the previous design in order to remove the loci of the motion[1] of the static wires from those of the power conductors, so as to provide greater clearance under the assumed conditions. Vibration protection was provided by means of vibration absorbers–approximately one-half of the line being equipped with Stockbridge dampers and one-half with T and B torsional dumbbell-type dampers, Figure 10, as developed in the Commission's laboratory.[2] Both dampers were used singly; that is, two per span. The two ground wires were protected against vibration by the use of festoons, see Figure 10.

Tower footing resistances in the earth section at the western end of the line did not generally exceed 15 ohms, but for the rock section covering some 95 miles towards the eastern end continuous counterpoise was laid consisting of two 5/16-inch steel conductors, mostly buried in the ground under the outer phase wires.

Lightning outages on this single circuit 230-kv line built in 1941 up to the end of December 1950, as shown in Table II, are equivalent to an average of 0.30 lightning outage for 100 circuit-mile-years. These outages also are classified as to the number of phases involved.

A fifth 230-kv single circuit steel tower transmission circuit was completed and put into service in December 1948. This circuit transmits power directly from Masson Generating Station to Leaside Receiving Station. For this circuit the towers were of a new design as shown in Figure 8 with a normal span length of 1,100 feet.

First 230-Kv Double-Circuit Construction (1941)

The first 230-kv double-circuit steel tower line built by the Commission was completed in 1941 from Leaside Junction to Burlington, a distance of 45 miles. The use of double-circuit construction was dictated partly by restricted right-of-way and partly by the system interconnection. This double-circuit section was put into service in 1941 shortly after the fourth trunk circuit was completed.

The tower type used is shown in Figure 9 and a relatively conservative design was adopted. As aluminum was not available at this time, the power conductors utilized were type-*HH* segmental hollow core copper of 500,000 circular mil, 1.02 inches outside diameter with seven segments, having an ultimate strength of 21,200 pounds. The span length used was 880 feet and the maximum designed tension, under loading conditions involving an 8 pound wind on 1/2-inch radial ice thickness at 32 degrees Fahrenheit, was 9,500 pounds with a 60 degrees Fahrenheit tension of 4,700 pounds. No particular treatment of the tower footing was considered necessary as the line was all located in good agricultural land.

A single static wire of 3/8-inch steel was located at the tower peak, 30 feet

Figure 8. 1946 type 230-kv single-circuit steel tower

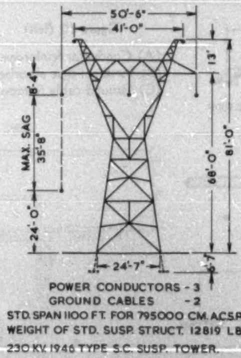
50'-6"
41'-0"
13'
18'-4"
MAX. SAG 35'-8"
68'-0"
81'-0"
24'-0"
24'-7"
6'-7"
POWER CONDUCTORS -3
GROUND CABLES -2
STD. SPAN 1100 FT. FOR 795000 CM. ACSR.
WEIGHT OF STD. SUSP. STRUCT. 12819 LB.
230 KV. 1946 TYPE S.C. SUSP. TOWER.

Table I. Lightning Outage Record

Original Three 230-Kv Single-Circuit Lines, 1928–1931
(1928 to 1950 Inclusive)

	Per Cent
Type of Fault	
Involving one wire and ground	62.4
Involving two wires and ground	28.2
Involving three wires	9.4
Number of Circuits	
Involving one circuit only	91.4
Involving two circuits simultaneously	5.4
Involving three circuits simultaneously	3.2

Table II. Lightning Outage Record

Revised 230-Kv Single-Circuit Line, 1941
(1941 to 1950 Inclusive)

	Per Cent
Type of Fault	
Involving one wire and ground	75
Involving two wires and ground	12.5
Involving three wires	12.5

Table III. Lightning Outage Record

230-Kv Double-Circuit Section, 1941
(45 Miles)

	Per Cent
Type of Fault	
Involving one wire and ground	88.9
Involving two wires and ground	11.1
Involving three wires	
Multiple outages involving both circuits	1

above the point of support of the upper phase conductors. The clearances were based on half-loop movement of the heavy copper power conductors and full loop movement of the relatively light ground cable. No special precautions were taken to protect against conductor vibration.

Lightning outages on this 45-mile double-circuit section up to December 31, 1950, as shown in Table III, were equivalent to an average of 1.09 lightning outages for 100 circuit-mile-years. One multiple outage occurred involving both circuits, but the cause of this multiple outage could not be accurately determined. There were no outages due to glaze or ice conditions.

Recent 230-Kv Single- and Double-Circuit Construction

Five additional 230-kv trunk transmission circuits have been completed and put into operation during 1950, as shown on the system diagram in Figure 11. These bring 60-cycle power from the new hydro-electric generating stations at Des Joachims, La Cave, and Chenaux on the Ottawa River down to the load centers in the central and western parts of southern Ontario. Two single-circuit steel tower lines and one double-circuit steel tower line extend from Des Joachims generating station to a midpoint switching station at Minden. A single-circuit 230-kv line connects La Cave generating station to the Des Joachims 230-kv bus—this line is now in temporary operation at 115-kv, to connect with the Northeastern Region until the La Cave units begin to generate power in 1951. When units number 7 and number 8 at La Cave are ready for service, the addition of a second 230-kv, single-circuit line between La Cave and Des Joachims is contemplated.

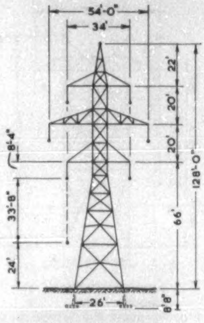
54'-0"
34'
22'
20'
20'
128'-0"
8'-4"
33'-8"
66'
24'
26'
8'8"
POWER CONDUCTORS - 6
GROUND CABLES - 1
STD. SPAN 880 FT. FOR 500 MCM.H.H. CU.
WEIGHT OF STD. SUSP. STRUCT. 22 709 LB.
230 KV. 1940 TYPE D.C. SUSP. TOWER.

Figure 9. 1940 type 230-kv double-circuit steel tower (Burlington to Leaside)

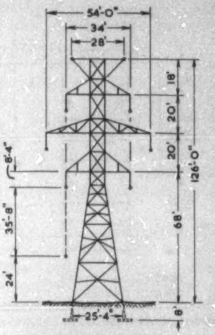
54'-0"
34'
28'
18'
20'
20'
126'-0"
8'-4"
35'-8"
68'
24'
8'
25'-4"
POWER CONDUCTORS - 6
GROUND CABLES - 2
STD. SPAN 1100 FT. FOR 795000 CM. ACSR.
WEIGHT OF STD. SUSP. STRUCT. 24436 LB.
230 KV. 1949 TYPE D.C. SUSP. TOWER.

Figure 9(A). 1949 type 230-kv double-circuit steel tower

From Minden Switching Station two 230-kv circuits extend down to a new 60 cycle receiving station at Kipling and to the existing Burlington station, consisting of two single-circuit lines for part of the distance and double-circuit construction for the remainder. Also from Minden Switching Station, a 230-kv double-circuit steel tower line extends to Essa transformer station and then to the E. V. Buchanan Frequency Changer and Transformer Station at Westminster. A short length of 230-kv double-circuit line extends southwest from Burlington Transformer Station, one circuit branching off to E. V. Buchanan Transformer Station, and the other circuit extending to Allanburg Transformer Station in the Niagara Peninsula, this latter circuit being in temporary use at 115-kv. From E. V. Buchanan Transformer Station a 230-kv double-circuit steel tower line is under construction to the J. Clark Keith steam generating station but only one circuit will be strung at present.

From Chenaux generating station a 230-kv single-circuit steel tower line was built and placed in service to Ross L. Dobbin Transformer Station during 1950. A 230-kv single-circuit steel tower line was also built from Peterboro to Scarboro Frequency Changer and Transformer Station, this circuit being put into temporary operation at 115-kv in January 1951. This 230-kv single-circuit steel tower design has been altered to that shown in Figure 8, with a normal span of 1,100 feet to carry three 795,000 circular mil steel reinforced aluminum cable (26 aluminum by seven steel strands). This tower line

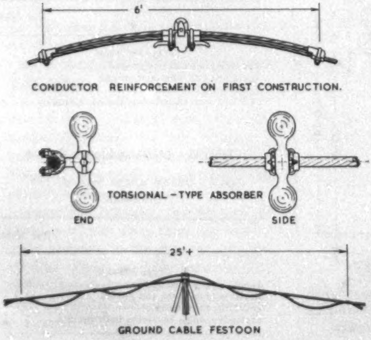
6'
CONDUCTOR REINFORCEMENT ON FIRST CONSTRUCTION.
TORSIONAL - TYPE ABSORBER
END
SIDE
25'+
GROUND CABLE FESTOON

Figure 10 (left)

(A) Conductor reinforcement
(B) Torsional-type absorber
(C) Ground cable festoon

Figure 11 (below). System diagram of 230-kv lines in 1951

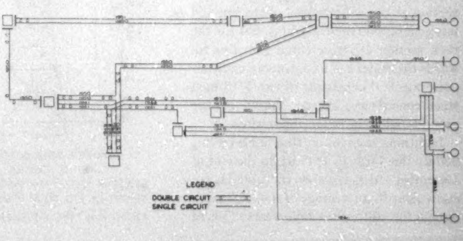
LEGEND
DOUBLE CIRCUIT
SINGLE CIRCUIT

carries two overhead ground cables of 3/8-inch galvanized steel. The maximum tension in the power conductors is 11,000 pounds and in the ground cables 4,880 pounds.

The 230-kv double-circuit steel tower design has been altered to that shown in Figure 9(A) and includes two 3/8-inch galvanized steel overhead ground wires instead of the single ground wire formerly used. The normal span has been increased from 880 feet to 1,100 feet. The conductors are also 795,000 circular mil steel reinforced aluminum cable (26 by seven strands), and the maximum tensions are now 11,000 pounds for the power conductors and 5,000 pounds for the ground cables. In the areas where high footing resistance has been encountered, the tower footing resistance has been reduced to below 20 ohms by the use of counterpoise or crowfoot.

As these new 230-kv 60-cycle circuits have only been put into operation during the latter half of the year 1950, sufficient time has not yet elapsed to obtain any reliable figures covering lightning outages and operating experience.

Standard 5-inch suspension insulators with 11,000 pound mechanical strength are used on the Commission's system and for heavy duty purposes the $5^{3}/_{4}$-inch units rated at 25,000 pounds mechanical strength are used. At 230-kv the standard number of suspension insulator units in a string is 18, while for 115-kv service eight insulator units are used. For strain positions 18 units are used at 230-kv and ten units at 115-kv. Grading rings to protect insulator strings are not used by the Commission.

Conclusion

Lightning outages can be reduced in number by counterpoising or other methods of lowering the tower footing resistance. This is shown by comparing the performance of the fourth 230-kv circuit built in 1941, with that of the original three circuits built in 1928–1931. As various improvements have been incorporated into the design of the 115-kv steel tower circuits the frequency of outages due to lightning has been reduced. A program of construction to improve the performance of the Commission's existing 230- and 115-kv lines by additional counterpoising is now under way. The new 230-kv circuits should provide interesting performance data, particularly on the double-circuit sections, when sufficient time has elapsed to provide reliable service records.

Outages attributed to "galloping or dancing conductors" caused by the rhythmic movement of glaze-coated lines under certain wind conditions have been studied,[1] and changes in circuit configurations and separation distances have been made to minimize this hazard. Breakages of individual conductor strands due to aeolian vibration have been reduced by the application of armour rods or vibration dampers.[2]

Recent changes in the design of the 230-kv transmission system include a much greater use of double-circuit construction due to the restrictions on right-of-way.

Larger conductors than 795,000 circular mil steel reinforced aluminum cable are under consideration for future 230-kv construction. Stability limits increase as the 230-kv network develops, and the increased capacity of the circuits causes transmission losses to become of paramount consideration.

References

1. ICE-COATED ELECTRICAL CONDUCTORS, A. E. Davison. International Conference on Large High Voltage Electric Systems (Paris, France), 1939.

2. MEASUREMENT AND CONTROL OF CONDUCTOR VIBRATION, G. B. Tebo. *AIEE Transactions*, volume 60, 1941, pages 1188–93.

No Discussion

Selection of A-C Motors for Driving Oil Well Pumping Units

M. H. HALDERSON
NONMEMBER AIEE

MANY TYPES of a-c motors have been used for oil well pumping. Open wound-rotor motors were used almost exclusively prior to 1930. Since 1930 the electrical characteristics of motors installed for oil well pumping range from normal torque, normal slip, normal starting current to high torque, 8 to 13 per cent slip. Frame types range from open to explosion-proof. The diversity of types of motors used for oil well pumping suggests that the various types are equally desirable, but this is not the case. Experience and a more fundamental approach to the evaluation of motors now make it possible for oil producers to select the type of motor that costs the least per horsepower capacity and that has the most desirable characteristics for the conditions encountered in driving pumping units.

Factors that must be considered in selecting motors for oil well pumping are the type of load, starting requirement, initial cost of motors, and the fact that the motors must operate in the open. Evaluation of available motors with respect to these factors leads to the conclusion that high torque, 5 to 8 per cent slip motors in a drip-proof or protected frame should be purchased for installations where polyphase electric power is available. 2-value capacitor type motors in a drip-proof or protected frame are preferred where single-phase power must be used.

Motors with 5 to 8 per cent slip are preferred for driving pumping units because they have the best starting characteristics and because, compared to normal slip motors, they will carry 35 per cent more load per name plate rating, will operate with 20 points higher power factor, and will operate with 25 per cent less peak power input. Drip-proof or protected frames are preferred because motors built in these frames have the greatest thermal capacity per dollar invested and because experience has shown that these frames provide ample protection for outdoor operation.

Load characteristics are such that motors installed on pumping units cannot average an output equal to name plate rating without being thermally overloaded. Based on tests in the field, the recommended procedure for sizing the two types of motors most frequently used for oil well pumping is to assume that 5 to 8 per cent slip motors can average an output equal to 76 per cent of name plate rating and that normal slip motors can average an output equal to 56 per cent of name plate rating.

Motors rated 440 volts have been standard for oil well pumping. Consideration of wye connecting 440 volt motors to permit operation at 760 volts is recommended where wells are spaced greater than 660 feet apart and where motors larger than 25 horsepower will be used.

Electrical Characteristics

Electrical characteristics available for polyphase motors include (1) normal torque, normal slip, normal starting current; (2) normal torque, normal slip, low starting current; (3) high torque, normal slip, low starting current; (4) high torque, 5 to 8 per cent slip; and (5) high torque, 8 to 13 per cent slip. Although catalogue literature does not always so state, 5 to 8 per cent slip and 8 to 13 per cent slip motors have low starting current.

Selection of the electrical characteristic best suited for driving pumping units is based on the starting requirement, the performance of motors with the various characteristics when applied to the load encountered on pumping units, and the initial cost of motors. Data on the performance of the high torque, 8 to 13 per cent motors are not available and conclusions regarding 8 to 13 per cent slip motors are based on their initial cost and estimates of their performance compared to other types of motors.

Starting Requirements

Figure 1 is a typical electric motor driven pumping unit. The majority of such installations are started automatically and an essential requirement is that motor starting torque be great enough to start the pumping unit without the assistance of an operator. Measurements of the torque required to start pumping units are not available, but experience has shown that motor starting torque must be greater than that required for ordinary continuous service applications. Numerous installations have been made where pumping units could not be started without rocking the beam of the pumping unit. There have also been instances where motors could not start pumping units even though the motors would have been of sufficient size to operate the units had starting been possible.

Motors for oil well pumping should have both high starting torque and low starting current to insure positive starting and minimum cost for distribution lines. Starting torque developed by a motor installed on a pumping unit is determined by the locked rotor torque of the motor at rated voltage and also by the terminal voltage during the starting period. Line voltage drop during starting is more critical than is sometimes realized because starting torque varies as the square of the voltage and because

---

Paper 51-384, recommended by the AIEE Rotating Machinery Committee and approved by the AIEE Technical Program Committee for presentation at the AIEE Fall General Meeting, Cleveland, Ohio, October 22–26, 1951. Manuscript submitted September 18, 1950; made available for printing September 11, 1951.

M. H. Halderson is with Phillips Petroleum Company, Bartlesville, Okla.

Figure 1. Electric motor - driven pumping unit

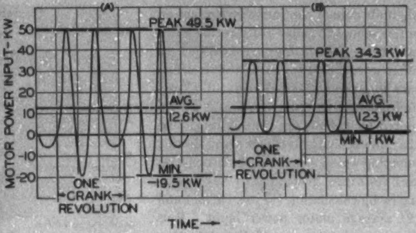

Figure 3. Change in motor load resulting from a change in per cent slip of motor

(A) Power input to a 25-horsepower normal slip motor driving a pumping unit 22.2 strokes per minute

(B) Power input to a 25-horsepower 5 to 8 per cent slip motor driving same unit 21.6 strokes per minute

motors may be as far as a mile from the source of low voltage power. As often as not, the minimum size of wire required for distribution lines is determined by voltage drop on starting rather than voltage drop on running.

Normal torque, normal slip, low starting current motors, which have a locked rotor torque of 135 per cent to 160 per cent of full-load torque, will usually start pumping units providing the motors are sized 50 per cent larger than required to carry the running load without being thermally overloaded and provided the terminal voltage on starting is not less than 84 per cent of rated. The practice of using normal torque motors is not economical because it results in higher initial investment for motors and often requires increased investment in distribution lines.

High torque, normal slip, low starting current motors, which have 200 to 250 per cent starting torque and 525 to 700 per cent starting current, will start pumping units in almost all cases provided voltage on starting is not less than 84 per cent of rated voltage.

High torque, 5 to 8 per cent slip motors have 275 to 350 per cent starting torque and 500 to 625 per cent starting current. These motors have the best starting characteristics and frequently will permit the use of smaller wire for line than that required for high torque normal slip motors.

High torque, 8 to 13 per cent slip motors have starting characteristics similar to 5 to 8 per cent slip motors, but their initial cost is 20 per cent higher than that of 5 to 8 per cent slip motors. The purchase of 8 to 13 per cent slip motors is therefore not justified from the standpoint of starting characteristics.

Pumping Load

Determining the relative merits of the various types of motors for oil well pumping service is difficult because of the type of load encountered. The pumping load is generally characterized by high peaks and wide and rapid load variation. However, the exact load versus time relationship is influenced by many factors and is different for each installation. This makes it impossible to reach general conclusions from a test of one installation.

Figure 2 illustrates the variation of speed reducer torque with time for a counterbalanced pumping unit. Actual curves of reducer torque versus time are irregular in various ways, but the load variation and the relative position of load limits with respect to the average load are typical. Pumping speed ranges in practice from 4 to 30 cycles, or strokes, per minute. During each stroke, there are two peaks and two valleys. The valleys are usually negative, that is, occur at a time when energy is being transferred from the crank to the speed reducer. The ratio of peak load to average load depends on pumping conditions and ranges from 1.8 to 4.0.

Motor Load

The load on a motor that drives a given pumping unit depends upon the electrical characteristic of the motor as well as the load cycle on the speed reducer of the pumping unit. High slip motors vary more in speed with change in load than do normal slip motors. The greater speed change causes the inertia of the rotating parts of the system to store more energy during the minimum load periods and release more energy during the peak load periods. The result is that input power peaks and over-all load variation are always less with 5 to 8 per cent slip motors and 8 to 13 per cent slip motors than with normal slip motors. Averages of field measurements show that peak power input will be 25 per cent less with 5 to 8 per cent slip motors than with normal slip motors. Figure 3 is an example of the reduction in peak load and over-all load variation that resulted from changing the characteristic of the motor driving a given pumping unit from normal slip to 5 to 8 per cent slip. Power input limits and the time relationship of the limits are actual. Curves connecting the power limits are approximate.

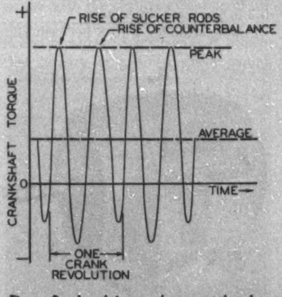

Figure 2. Load imposed on speed reducer of properly counterbalanced pumping unit

Figure 3 and similar exhibits show that the use of high slip motors instead of normal slip motors will result in less fluctuation in line voltage and will result in lower peaks and less load variation on generating plants that are installed in the field to serve a group of oil well pumping units. Other measurements are required to reach conclusions regarding the relative efficiency, power factor, and load carrying capacity of normal slip and high slip motors when used as prime movers for pumping units.

Load Carrying Capacity and Power Factor

Because of the high load peaks and wide load variation, motors that drive pumping units cannot continuously average an output equal to name plate rating without being thermally overloaded. In other words, derating of motors is necessary to prevent thermal overload. Tests under actual pumping conditions are required to find the per cent of rated load that motors can average when driving pumping units. Measurements made on such tests must give either by direct reading or by calculation (1) rms current and (2) average motor power input. Rms current may be measured directly with a thermal ammeter. Average power input may be obtained from a watthour meter with a demand attachment or by calculation after first timing the disk on a watthour meter to get disk revolutions per minute. Having obtained rms current and average motor input, a measurement of terminal voltage will permit the calculation of power factor.

Measurements taken during 17 tests of motors driving pumping units gave results shown in Table I. Normal slip motor sizes ranged from 20 to 60 horsepower, and 5 to 8 per cent slip motor sizes ranged from 10 to 60 horsepower.

Derating factor is defined as the ratio of average motor output on a pumping load to the output that the motor would develop on a steady load at the rms current measured on a pumping load. If rms current is near the rated motor current, the derating factor becomes the factor by which motor name plate rating should be multiplied to give the average output that a motor can develop on a pumping load without being thermally overloaded.

For average oil well pumping applications, the test data show that normal slip motors can develop 58 per cent of name plate rating and that the 5 to 8 per cent slip motors can develop 80 per cent of name plate rating. For the most severe conditions, normal slip motors can carry 51 per cent of rating whereas 5 to 8 per cent slip motors can carry 68 per cent of rating. Derating factors of 0.56 for normal slip motors and 0.76 for 5 to 8 per cent slip motors are considered adequate for 85 to 90 per cent of all pumping unit installations and are recommended for general use.

Table I

	High Torque Normal Slip	High Torque 5–8% Slip
Number of tests	6	11
Average of rms currents in per cent of rated	99	95
Range of rms currents in per cent of rated	80 to 121	83 to 118
Average of power factors	0.499	0.698
Range of power factors	0.43 to 0.57	0.59 to 0.81
Average of derating factors	0.583	0.796
Range of derating factors	0.51 to 0.65	0.68 to 0.91

Derating factors as determined from tests on pumping motors show that 5 to 8 per cent slip motors can average 35 per cent higher output per name plate rating than normal slip motors. Five to eight per cent slip motors cost 2 to 5 per cent more than high torque normal slip motors for sizes up to and including 20 horsepower and, with few exceptions, cost 15 to 17 per cent more than high torque normal slip motors in sizes above 20 horsepower. The net result is that 5 to 8 per cent slip motors give the oil producer 15 to 30 per cent more horsepower capacity per dollar invested than do high torque, normal slip motors. This fact alone justified the purchase of 5 to 8 per cent slip motors for oil well pumping.

Tests on 8 to 13 per cent slip motors are not available, but justification for their purchase in preference to 5 to 8 per cent slip motors is doubtful. Eight to thirteen per cent slip motors cost 20 per cent more than 5 to 8 per cent slip motors and it is not likely that they will have as great a horsepower capacity per dollar initial cost as 5 to 8 per cent slip motors.

Power factor for 5 to 8 per cent slip motors was found on tests on oil pumping operations to be 20 points higher on the average than the power factor for normal slip motors. Therefore, the use of 5 to 8 per cent slip motors instead of high torque normal slip motors will either (1) reduce investment for capacitors if power factor correction is required, (2) permit smaller size of wire for line, or (3) result in less distribution system loss for the same wire size if power factor is not corrected.

Motor Efficiency

The efficiency of high torque normal slip motors on steady loads is 3 to 5 points higher than the efficiency of 5 to 8 per cent slip motors. Which of the two types of motors is the more efficient on the fluctuating load encountered in oil well pumping is still not known with certainty and is difficult to establish. To answer the question, tests must be made on many wells to determine the kilowatt hours used per barrel of liquid lifted by the two types of motors when pumping a given well at the same stroke and strokes per minute. Obtaining such tests is difficult because of the expense and down time required for changing motors, the difficulty of obtaining the motor sizes required to make the test with the two types of motors operating at near the same thermal load, frequent lack of facilities to obtain accurate production tests, and frequent inability to obtain motor sheaves to operate at the same strokes per minute with the two types of motors.

Results of tests on three different wells where kilowatt hours used per barrel of liquid lifted were determined with both normal slip and 5 to 8 per cent slip motors are shown in Table II. These tests were made in an oil field where the productivity of individual wells was practically constant. The time between tests with the two types of motors on a given well ranged from three to five days.

Lift efficiencies of normal and 5 to 8 per cent slip motors were practically the

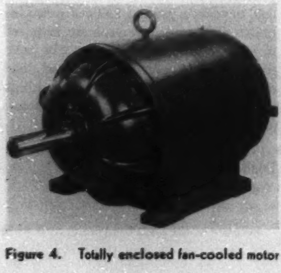
Figure 4. Totally enclosed fan-cooled motor

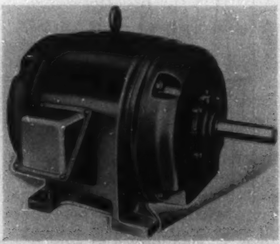
Figure 5. Splash-proof motor

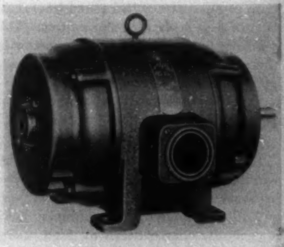
Figure 6. Protected frame motor

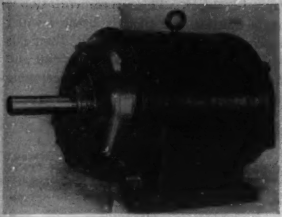

Figure 7. Protected frame motor

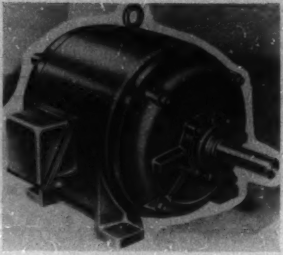

Figure 8. Drip-proof motor

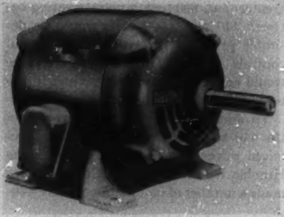

Figure 9. Drip-proof motor

same on the tabulated tests. Thermal load for the two types of motors was nearly the same during only one of the tests and there was some difference in strokes per minute in all cases. Until sufficient tests are made to show a trend one way or another, the efficiencies of normal slip and 5 to 8 per cent slip motors will be considered equal for oil well pumping applications.

Motor Protection

Ordinary thermal overload relays will not protect 5 to 8 per cent slip motors from stalled single phase. This is not necessarily a disadvantage because stalled single phase is prevented by either one or the other of two devices that are usually incorporated in oil well motor controls. One of these devices is the under voltage relay.

The other is the time delay relay, a device that is used to automatically start motors one at a time after restoration of power following an interruption. Where a time delay relay is used, the coil of the magnetic switch is connected across one phase and the time delay relay is connected across another phase. Then, one or both of the elements will not pick up after an outage until 3-phase power is restored.

Single Phase Motors

There are instances where only single-phase power is available. Types of single-phase motors that can be used for oil well pumping service include capacitor start, induction run; repulsion-induction; repulsion start, induction run; and 2-value capacitor, sometimes called capacitor start, capacitor run.

The 2-value capacitor motors are preferred for oil well pumping service. These motors have electrical characteristics similar to three phase high torque, normal slip motors; are as simple in construction as three phase induction motors; operate with 8 to 20 points high power factor than other types of single-phase motors; and sell for the same price as other types of single-phase motors.

Frames

Pumping motors are installed in the open to simplify the entire installation and reduce installation cost. Types of frames that are available for outdoor service include totally enclosed fan-cooled; splash-proof; protected frame; and drip-proof.

Figures 4 to 9 illustrate, respectively, a totally enclosed fan-cooled motor, a splash-proof motor, two makes of protected frame motors, and two makes of drip-proof motors. The various frames obviously give different degrees of protection against entrance of water, but experience has shown that all of the frames illustrated are satisfactory for outdoor service with the possible exception of the rare instances where motors may be buried in snow. Some operators believe that housing is justified where motors may be covered with snow.

Water will enter drip-proof motors during driving rain storms.

This has not been found to cause winding deterioration provided provision is made for drainage of water out of the motor.

In some areas, for example the Borger Field in the Texas Panhandle, rodents will build nests in the air passageways of motors installed on pumping units. Air inlet and outlet openings of any type motor must be covered with quarter inch mesh screen where this condition exists.

Users will get the most horsepower capacity per dollar invested by purchasing protected frame or drip-proof motors. Specifically, drip-proof and protected frame motors have 20 per cent more horsepower capacity per dollar initial cost than splash-proof motors and 61 per cent more capacity per dollar initial cost than totally enclosed fan-cooled motors. Derivation of the percentage figures is shown in Table III.

Horsepower capacity per-unit cost for drip-proof and protected frame motors compared to splash-proof = 1.00/0.83 = 1.20. Horsepower capacity per unit cost for drip-proof and protected frame motors compared to totally enclosed fan-cooled = 1.00/0.62 = 1.61.

Voltage Rating

A rating of 440 volts has been the most widely used for oil well pumping motors. This voltage rating has been adequate for loads up to 25 horsepower and for installations where the distance between wells did not exceed 660 feet, the distance between wells on 10-acre spacing. For loads greater than 25 horsepower and where the distance between wells is

Table II

	Stroke, Inch	Strokes per Minute		Rms Current in Per Cent of Rated		Kwhr/Barrel	
		Normal	5–8%	Normal	5–8%	Normal	5–8%
Well A	110.8	18.6	17.7	110	84.6	0.528	0.525
Well B	44.5	20.7	20.3	68.5	61.8	0.499	0.503
Well C	21.9	17.3	17.0	98.2	81.3	0.633	0.636

Table III

	Protected Frame and Drip-proof	Splash-proof	Totally Enclosed Fan-cooled
Rated temperature rise, centigrade	40	50	55
Relative horse-power capacity	1.00	0.805	0.853
Relative initial cost	1.00	1.08	1.38
Relative horse-power capacity per unit cost	1.00	0.83	0.62

greater than 660 feet, a voltage rating between 440 and 2,400 volts would be desirable provided the cost of motors and controls for the intermediate voltage would not more than offset savings in the cost of distribution lines.

To obtain an operating voltage between the 440 and 2,400 without paying premium prices for motors and controls, the Humble Oil and Refining Company has made a number of installations where 440-volt motors were wye connected to operate at 760 volts. Performance of the 760-volt system has been reported to be satisfactory when the motor neutrals have been grounded, thereby limiting the maximum voltage to ground on any portion of the motor to 440 volts

Consideration of the 760-volt system is recommended for installations where motors will be larger than 25 horsepower, and where the distance between wells will exceed 660 feet. This recommendation is made because the trend is toward wider spacing of wells and, as a result, the fields where a voltage rating between 440 and 2,400 would be desirable are becoming more common.

Reference

1. 762 VERSUS 440-VOLT DISTRIBUTION SYSTEMS, B. L. Moore. *The Oil and Gas Journal* (Tulsa, Okla.), volume 48, November 10, 1949, pages 248–58.

No Discussion

Electrical Features of Modern Automatic Hydro Stations

C. L. GAMBLE
NONMEMBER AIEE

A. G. MELLOR
ASSOCIATE MEMBER AIEE

IN A period of rising labor costs and a shortage of qualified operating personnel willing to accept full time employment at remote station locations, there is continued interest in the subject of automatic operation of hydroelectric power plants.

It is the purpose of this paper to review the various types of automatic hydro stations and some of the factors to be considered, from an electrical standpoint, when developing an automatic hydroelectric station.

Automatic hydro plants may best be classified as to the degree of automatic operation provided, namely, semiautomatic, fully automatic and fully automatic with provision for control of the station from a remote location. Each new development presents special problems that warrant individual attention to arrive at the best solution for the particular station. However, based on many years experience with various types and sizes of automatic hydroelectric stations, certain general conclusions can be made.

Conclusions

1. Over 25 years of operating experience with automatic hydro stations has proved that the automatic features of these stations are very reliable and perform many operations better than can be done under manual operation.

2. The application of automatic features to many different sizes and types of hydro developments has shown an appreciable saving in generating cost per kilowatt hour.

3. The component equipment of a hydroelectric plant is readily adaptable to automatic operation with a resulting improvement in accuracy and speed of operation as compared to manual stations.

4. The degree of automatic operation provided at a hydroelectric station will depend on many factors, such as: the size and importance of the station with respect to the power system; the expected load factor of the station; the relative location of the station with respect to other generating stations and to population centers; special hydraulic problems including any required supervision of dams and other hydraulic works and ice and debris control problems.

5. In installing automatic control equipment at hydro stations, installation time and expense can be reduced by the use of factory assembled, packaged equipments wherever possible.

General

Of the various types of plants used to generate electric power, the hydroelectric station lends itself most readily to automatic operation. Basically, stored energy in the form of water in the forebay can be released and converted to electric power by merely opening the turbine gates under the control of the governor, thus developing horsepower on the prime mover shaft. The generator will produce real power under control of the governor and reactive power under supervision of the voltage regulator. The inherent design of the components involved makes the problem of obtaining automatic, unattended operation a relatively simple and inexpensive application.

The foremost factor in any automatic application is to keep the scheme employed both simple and economical. However, it must be realized that to obtain an automatic plant that is functionally equivalent to a manual station, all operations previously performed by personnel must now be accomplished by mechanical and electrical devices substituted to obtain equivalent operating performance. The automatic scheme thus developed will result in a plant that is as dependable and reliable as the manual station it replaces and in addition will give faster and more precise operation.

The cost of making the electric equipment in the plant automatic to any given degree will not vary appreciably with the actual capacity of the plant; however, as the capacity of the station under consideration increases, other factors such as complications in the mechanical equipment and the desirability of having personnel present at the station for other duties tend to decrease the savings that can be realized by going to automatic control. One eastern utility is now in the process of installing a single-unit fully automatic plant, with remote control, having a capacity of 37,500 kva. At the other end of the range, plants of only a few hundred kilowatts have been made semiautomatic in order to justify economically their operation.

The amount of attendance required at any station will depend to a very large extent on the degree to which the station is made automatic. In general, operators from nearby plants will visit the automatic stations periodically to perform any required manual operating procedures as well as general maintenance duties. Specialized preventative maintenance functions such as relay testing et cetera can be carried out by traveling crews from a central headquarters organization performing similar tasks at automatic substations.

Semiautomatic Plants

The simplest and least expensive type of automatic control used in hydro stations is that found in semiautomatic stations. Stations of this type must be started and put on the line manually by an operator but then may be left unattended.

Paper 51-385, recommended by the AIEE Power Generation Committee and approved by the AIEE Technical Program Committee for presentation at the AIEE Fall General Meeting, Cleveland, Ohio, October 22–26, 1951. Manuscript submitted May 21, 1951; made available for printing September 11, 1951.

C. L. Gamble and A. G. Mellor are with General Electric Company, Schenectady, N. Y.

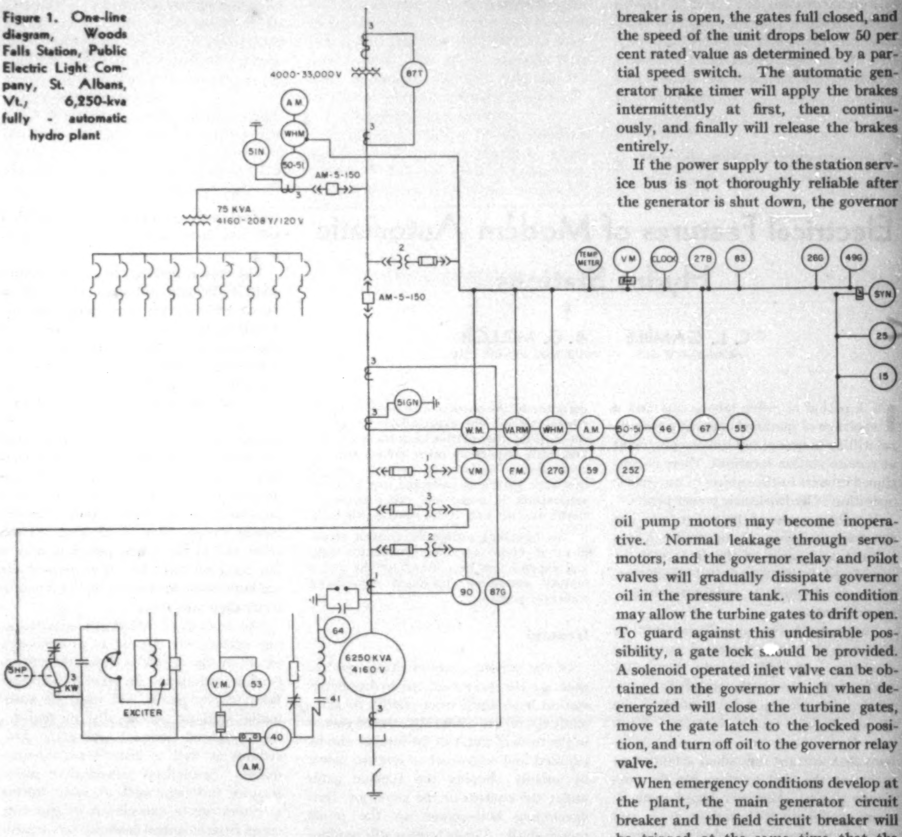

Figure 1. One-line diagram, Woods Falls Station, Public Electric Light Company, St. Albans, Vt., 6,250-kva fully-automatic hydro plant

This type of control is generally applied to stations which are small with respect to the system to which they are connected and thus do not require that their output be coordinated with the system daily load curve. Such stations are often operated for only an 8-hour period each day and thus once they are shut down may not be available to meet emergency conditions on the system unless an operator is available to go to the site to restart the machine.

Machines in stations of this type may be operated on free governor, load limit, or on load limit as controlled by a float-operated device installed to maintain constant forebay water level elevation.

The control must provide means for shutting down the unit automatically on a signal from a time switch or float switch. Sufficient protective devices must also be provided to automatically shut down the station and prevent damage to the equipment under certain abnormal operating conditions. Other abnormal conditions may only result in sounding an alarm.

In the normal automatic shutdown sequence the governor gate limit motor will be energized to close the gates and drop load on the generator. As the gates pass through the no load gate position the main generator circuit breaker and the field circuit breaker will be tripped by the closing of the contacts of a position switch on the governor. The gate limit motor will be de-energized by limit switches when the gates reach the full closed position. When automatic braking is used, the generator brake air valve solenoid should not be energized until the generator circuit breaker is open, the gates full closed, and the speed of the unit drops below 50 per cent rated value as determined by a partial speed switch. The automatic generator brake timer will apply the brakes intermittently at first, then continuously, and finally will release the brakes entirely.

If the power supply to the station service bus is not thoroughly reliable after the generator is shut down, the governor oil pump motors may become inoperative. Normal leakage through servomotors, and the governor relay and pilot valves will gradually dissipate governor oil in the pressure tank. This condition may allow the turbine gates to drift open. To guard against this undesirable possibility, a gate lock should be provided. A solenoid operated inlet valve can be obtained on the governor which when de-energized will close the turbine gates, move the gate latch to the locked position, and turn off oil to the governor relay valve.

When emergency conditions develop at the plant, the main generator circuit breaker and the field circuit breaker will be tripped at the same time that the governor shutdown solenoid is de-energized. As a result, load will be dumped and the unit will tend to overspeed. If a pilot exciter is supplied with the generator, a block of resistance is inserted in the pilot exciter field circuit to limit overvoltage on this device. The governor shutdown solenoid will act directly on the governor pilot valve to close the turbine gates thus by-passing control by the flyballs.

If trouble of a serious nature develops at the station, operation of the protective devices will cause the machine to be shut down and locked out. While it is recognized that each installation will present special problems, the following abnormal conditions should be considered as possibly being serious enough to shut down and lock out the unit.

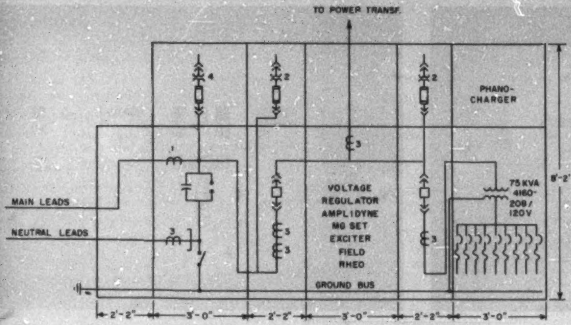

Figure 2. Schematic diagram of Woods Falls Station switchgear

1. Failure of power supply to the governor ballhead.

2. Overheating of generator thrust or guide bearings.

3. Overheating of turbine guide bearing.

4. Speed in excess of calculated full load rejection overspeed.

5. Operation of the generator differential relays.

6. Operation of the transformer differential relays.

7. Generator bus overvoltage.

8. Generator ground current.

9. Loss of generator excitation.

The following conditions may operate protective devices to shut down the unit and prevent restarting until conditions return to normal:

1. Low governor oil pressure.

2. Loss of d-c control bus voltage.

3. Generator reverse power.

4. Generator overcurrent.

5. Generator phase current unbalance.

6. Generator out-of-step.

7. Overheating of generator stator windings.

8. Excessive temperature of generator cooling air.

9. Failure of both d-c and a-c turbine bearing lubricating oil pumps.

10. Excessive temperature of generator thrust bearing oil bath.

Additional devices are generally applied to sound an alarm only when other abnormal conditions exist. A typical list of these conditions includes:

1. Ground on generator field.

2. Battery undervoltage.

3. Low cooling water flow to generator thrust bearing oil bath.

4. Excessive temperature of transformer top oil.

5. Low transformer oil level.

Consideration must also be given to hydraulic conditions at the forebay. The headgates should be designed to close after suitable time delay in the event the unit overspeeds above 105 per cent of the full load rejection overspeed. High forebay water level should sound an alarm and if the condition persists, open the spillway gates automatically by means of a float switch control. Excessive differential of water level on upstream and downstream sides of the trash racks should be noted by means of an alarm.

Fully-Automatic Stations

The control for this type of station offers the advantage of being able to start the plant by means of a signal from a time, float, or frequency device without the presence of an operator at the site.

Automatic starting and synchronizing features must be added to the control scheme previously outlined for semiautomatic stations. A typical control sequence is outlined in the following paragraphs.

After the starting indication has been given, the master control relay will not be energized unless the following operating conditions exist:

1. Adequate governor oil pressure.

2. Adequate d-c control bus voltage.

3. Lock-out relays are in their normal reset position.

4. Automatic auxiliary shutdown relays are in their normal reset position.

When the master control relay is energized it picks up an auxiliary relay which in turn starts the turbine bearing oil pumps and operates a motor-operated

Figure 3. Front and rear views of Woods Falls Station switchgear

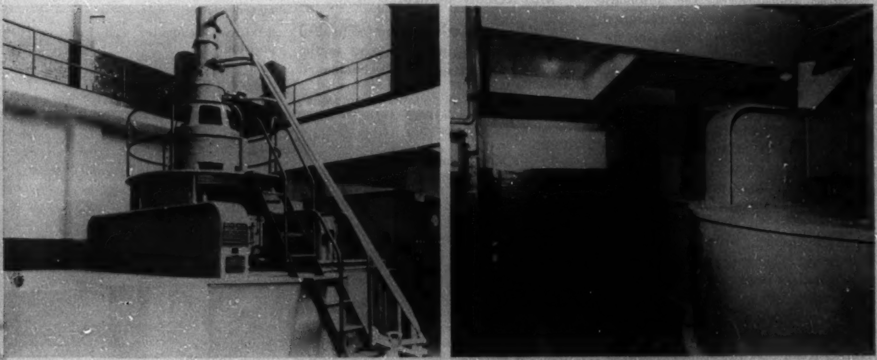

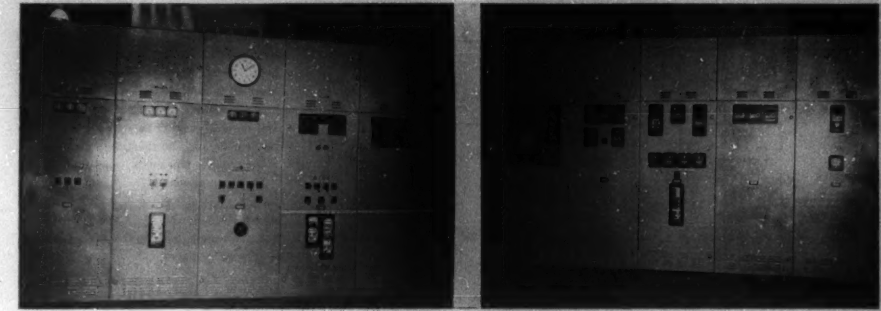

Figure 4. Front and rear views of switchgear, Smith Station, Public Service Company of New Hampshire, Berlin, N. H., 18,750-kva fully-automatic hydro plant

valve, which starts the flow of cooling water to the generator thrust bearing. This auxiliary relay remains picked up whenever the unit is operating and is sealed in through a time delay opening contact of a timer to insure that the turbine bearing oil pumps will maintain operation until the unit comes to a complete stop during the shutdown sequence.

The automatic governor start-stop solenoid is then energized and an automatic governor sequence releases the gate lock and applies oil pressure to the main relay valve. The turbine gates open, at a rate controlled by an accelerating timer provided on the governor mechanism, to the breakaway position and the turbine starts to rotate. When the exciter voltage builds up, a voltage relay closes the generator field circuit breaker. As the machine approaches synchronous speed, it will be under the control of the governor flyballs and the voltage regulator.

When voltage appears on the generator potential transformers, the automatic synchronizing equipment is energized. Speed matching relays adjust the frequency on the machine to that of the bus by giving raise and lower impulses to the governor speed adjusting motor. Impulses are given once each slip cycle and the lengths vary with the slip frequency. The automatic synchronizing relay will give the closing impulse to the generator circuit breaker at the proper phase angle to insure that the circuit breaker main contacts close at approximately zero phase displacement between the machine and the bus. The lead angle at which the closing impulse is given will vary with slip frequency.

If the generator fails to reach synchronous speed and the generator circuit breaker is not closed in a definite time interval after the starting indication is given, the unit will be shut down and locked out by an incomplete sequence timing device. After the generator circuit breaker closes in the normal starting sequence, the synchronizing and speed matching equipments are de-energized. In the event the generator circuit breaker is tripped, the machine cannot be reconnected to the line without going through the synchronizing sequence.

After the machine is on the line, the governor speed adjusting motor will be run to the full raise position and de-energized by limit switches. The machine will pick up load in accordance with a previously set gate limit position or an adjustable gate limit as actuated by a forebay water level float device.

The shutdown sequence will be identical functionally to that described under semiautomatic stations.

Fully-Automatic Stations with Remote Control

A fully-automatic station controlled from a remote point offers most of the operating advantages of an attended manual station. The available water can be used in the most efficient manner by adjusting the output of the station to system load requirements. Added economic advantages can be obtained if severalhydro stations and substations can be controlled from a single control station.

The following general list of functions to be performed from the control station may be considered for any particular installation of a large automatic station:

1. Telephone communication.
2. Start and stop generator and receive indication of position of master control relay (energized or de-energized).
3. Raise and lower load and meter kilowatts.
4. Raise and lower excitation and indicate kilovars.
5. Indicate position of generator circuit breaker.
6. Indicate position of lock-out relay.
7. Meter forebay water level.
8. Raise and lower spillway gates and meter position.
9. Close headgates and indicate closed position.
10. Indicate excessive differential water

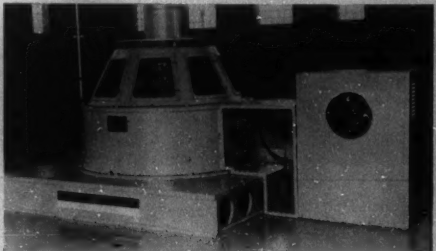

Figure 5. Front view of Smith Station field cubicle

level on upstream and downstream sides of the trash racks.

11. Meter tailrace water level.

12. Raise and lower governor gate limit setting and meter position.

13. Receive general alarm.

To carry out these functions, a communication channel must be set up between the control station and the outlying power plant. This channel may be direct wire, carrier, or microwave.

The number of channels required can be reduced by means of supervisory control equipment which provides a means of selective control and automatic indication of the particular function to be performed. All functions which do not require a continuous meter reading or control operation can be handled over one or two common channels by this method. Coded impulse supervisory equipments prevent false operation that might be caused by control cable faults or inductive interference in direct wire systems.

For distances under 10 miles direct wire connections between the control station and the power station are most commonly used. These circuits may be shielded cable or leased telephone lines when available. Direct current type of telemetering is the least expensive type of remote metering but can be applied only on direct wire circuits. Whenever necessary, shielded control cables are protected by lightning arresters. If there is a possibility of an appreciable difference in ground potential between the control and outlying stations under fault conditions, a neutralizing transformer should be connected in series with the control circuits.

For distances in excess of 10 miles or in cases where the terrain makes the use of direct wire control difficult, either carrier or microwave should be considered. Since transmission lines are constructed to withstand severe weather conditions, the carrier channel should be extremely reliable.

Any required carrier-current relaying functions can also be accomplished over the same common carrier channel.

Physical Arrangement of Electrical Equipment

After the one line diagram and the control circuits for an automatic station have been worked out, consideration must be given to the arrangement and electrical interconnections of the equipment.

For stations about 40,000 kva and smaller, a very compact metal clad switchgear design is available. In this design the control, generator switching equipment, voltage regulator components, exciter rheostats, and protective relaying devices are all mounted and wired in one metalclad switchgear line-up. The field contactor or circuit breaker, generator field ammeter shunt, and discharge resistor and the loss of excitation relay may be located in a separate cubicle mounted on the machine stator cover plates adjacent to the exciter. The length of generator field leads is reduced to a bare minimum by this arrangement.

The front or control side of this switchgear consists of swinging panels on which are mounted the control switches, indicating lights, and meters for the various equipment. Mounted on the rear swinging panels are the protective relays and other control components.

Inside the metal enclosed switchgear are the generator circuit breaker, instrument transformers, generator surge protective equipment, voltage regulator, and battery charger. For plants having a station service requirement of 100 kva maximum, the auxiliary transformer and distribution panelboard can be mounted inside the switchgear. This is a definite advantage for stations obtaining auxiliary power from the generator leads.

Metal enclosed, insulated, nonsegregated phase bus may be used for main power connections between the generator and power transformer for this class of station. The bus duct is easily installed and fully coordinated in design with the switchgear power circuits.

Figure 1 shows the one line diagram of a fully-automatic, remote-controlled hydro station which went into operation in New England during 1948. Present practices would tend to modify this one line to include overlapping transformer and generator differential protection and voltage restrained overcurrent relays for generator back-up protection. Dimensions given on Figure 2 apply specifically to this plant and in general will vary with voltage and breaker ratings as well as size and type of voltage regulator and excitation system components required.

Figures 3 and 4 show existing modern automatic hydro stations employing the switchgear arrangement discussed in the preceding paragraphs.

References

1. AUTOMATIC HYDRO STATIONS PROVE PROFITABLE, G. C. George and S. O. Schamberger. *Electric Light and Power* (Chicago, Ill.), December 1946, pages 76–78.

2. SUPERVISORY CONTROL OF 30,000 KVA HYDROELECTRIC PLANT, C. W. Bohner, A. P. Maness. *Electrical Engineering* (*AIEE Transactions*), volume 65, June 1946, pages 337–42.

3. SPACE CODE SELECTOR SUPERVISORY SYSTEM, E. F. Forrest, P. W. Schirmer. *AIEE Transactions*, volume 68, part II, 1949, pages 1312–16.

4. AUTOMATIC CONTROL OF HYDROELECTRIC GENERATING STATIONS, M. J. Brown, W. A. Derr. *AIEE Transactions*, volume 66, 1947, pages 343–55.

Discussion

Basil Payne (Nepsco Services, Incorporated, Augusta, Maine): The matter of reducing production expense is today of vital importance to each operating company. The application of automatic control to hydro stations is one means to this end, and the authors are to be complimented on their excellent paper on modern practice in this field. The following comments are based on the experience of one operating group.

Of the factors listed as determining the degree to which automatic operation may be justified, the three items of size of unit, its importance to the system, and its location with respect to the system are of first order importance. The larger the unit and the greater its importance to the system the greater will be the justification for direct supervision, whether by manual attendant or by remote control. In milder climates, remote or automatic (that is, unattended) control of head and spillway gates may be practicable and satisfactory. In more severe climates, however, this is not so due to the imperative requirement that the gates be thawed out before being operated. This is particularly true at stations where no open spillway exists, where river control is obtained entirely by means of gates. Stations in this class customarily are attended.

From the operating point of view the terms semiautomatic and fully-automatic control might be reworded, respectively: automatic-stop and automatic start-stop. The remote control feature may as readily be applied to stations of the semiautomatic type as to those full-automatic, and perhaps with greater benefit. In any case the automatic-stop features are identical for all three types of control under consideration, and have the single objective of providing full protection for the unit and its auxiliaries against dangerous or harmful operating conditions. In the manual station these features permit the operator, once having started the unit, to attend to other duties about the station without giving constant attention to the unit itself.

In setting up a remote control system there is a definite advantage in arranging, whenever possible, for at least two separate channels, one for control and one for indication. This enables the operator to observe and follow the extent or effect of the control while it is being operated. With but one channel the controls and indications operate alternately with consequent loss of speed and accuracy.

Probably to a greater extent than in any other type of generating plant the location and arrangement of the component items of equipment in hydrostations are determined by conditions existing at the site. For example, in a deep narrow valley it may be necessary to use a vertical assembly with transformer, switchgear, and generator, one above the other. On the other hand, an arrangement with all items at one level may better lend itself to a power house designed for a wide and open valley. Since the basic conditions determining the most favorable equipment layout are often in a large measure beyond the control of the designer of the station, the need for flexibility between the major equipment items is obvious. Each item may in itself be perfectly standard, but the means of interconnection between the several items must be sufficiently flexible to permit the power house designer to arrange these items to suit the particular conditions existing at the site.

The scheme of placing the field circuit breaker and its accessories in a cabinet located adjacent to the exciter is a very excellent one and there is much to commend it, notably the resulting short length of cable in the field circuit.

In the smaller stations where space is often limited the combined control panel and switchgear assembly works out very nicely. For higher capacity units requiring larger circuit breakers and heavy bus runs there may be advantages in having the switchgear independent of the control and relay switchboard. When separated, each may be located to best advantage. The walk-in duplex switchboard with fixed panels avoids certain objections to the hinged panels of the metal clad type and is especially advantageous where, as sometimes is the case, the control switchboard is made to line up with the governor cabinet.

In smaller stations where local conditions prevent placing the generator, switchgear, and transformer immediately adjacent to each other the main generator leads may consist of single or multiple cables. As the size of unit increases the use of factory built bus duct becomes increasingly attractive and the choice between the two types of construction will depend upon the conditions obtaining at a particular site.

H. L. Hoeppner (Pioneer Service and Engineering Company, Chicago, Ill.): The paper presented by Messrs. Gamble and Mellor presents a compact cross section of present day practice with respect to automatic, unattended hydrostations in the capacities usually encountered in the averages utility system.

Most of the automatic features can also be used advantageously in the larger hydro stations, which are attended because of their importance as a power source and the magnitude of their capital investment.

With respect to the smaller hydro stations, the induction generator presents an opportunity for simplification of the control system and elimination of the excitation system.

The power factor characteristics of the induction generator are probably responsible for its relative infrequent use. However, its power factor characteristics can be offset by the use of shunt capacitors which, in some cases, will be less costly than the more elaborate control and excitation system of the synchronous machine. While not an electrical feature, the use of outdoor equipment will result in a lower capital investment.

C. L. Gamble and **A. G. Mellor:** Mr. Payne's discussion outlines some of the practical problems to be faced by the operating company when designing an automatic plant.

It is recognized that the location of the site will definitely influence the design of the powerhouse and the subsequent location of component electrical equipments. However, the compact arrangement of control, relaying, and switching equipment mentioned and illustrated in the subject paper can often be employed with a resulting saving in powerhouse floor space, as well as installation time and expense. In the unattended plant the actual location of the control and metering panels need not be dictated primarily by operating considerations present in an attended station.

Mr. Hoeppner's discussion brings out the possibility of using induction rather than synchronous generators in the smaller hydro stations. Since the induction machine is excited by the system to which it is connected, no excitation system is required. In some cases the hydraulic turbine used with an induction generator is not controlled by a speed governor. The above tends to simplify the control of the induction generator with respect to that applied to the synchronous machine. Since the induction machine draws reactive power from the system for excitation, a source of reactive power must be available at all times. Generally one kilovar of reactive power must be supplied by the system for each kilowatt of real power supplied by the machine, although the power factor of the induction machine will vary with load and will be affected by design consideration including overspeed requirements. The induction generator will not support voltage on the station bus during system disturbances since it is entirely dependent on the system for excitation.

The Effects of Coupling-Capacitor Potential-Device Transients on Protective-Relay Operation

AIEE COMMITTEE REPORT

THIS subject has been brought up periodically over the years in various AIEE committee meetings. However, no formal approach to the problem was made until the Carrier-Current Committee, at a meeting in Cleveland in 1948, referred the matter to the Joint Subcommittee on Instrument Transformers. The Joint Subcommittee appointed a Working Group on Transient Characteristics of Capacitance Potential Devices, which first met October 27, 1948 to explore its assignment and to organize procedure. This is the report of that Working Group.

Objectives

The Working Group noted: (1) that there was need for data not then available, (2) that there was suspicion that improper relay operation had resulted from potential-device transients, and (3) that there were no performance standards on transient characteristics. Attention was focused principally on class-*A* coupling-capacitor potential devices, since these are used most frequently with high-speed relaying. Unless otherwise stated, this class and type should be assumed whenever the term "potential device" appears hereafter.

The Working Group established the following primary and ultimate objectives:

Primary Objectives

1. To obtain data, in the form of oscillograms, showing the transient characteristics of potential devices available to the trade, under uniform methods of test and with uniform typical burdens and adjustment settings.
2. To formulate a method for defining and expressing the characteristics in significant terms with respect to their effect on relay performance.

Ultimate Objectives

1. To establish standards of potential-device transient performance, consistent with the inherent nature of the equipment and the advancement of the art.
2. To make available data which could be used for guidance in the application of different types of relays and the predetermination of their performance.

To achieve these objectives, two projects were undertaken, as follows:

1. To obtain operating experience and information regarding practice from users of potential devices.
2. To make tests with various burdens and device adjustments. (The actual test procedure is described later in detail.)

Replies to Questionnaire on Operating Experience and Practice

Questionnaires were sent to eight operating companies, and seven replies were received. Of those replying, only four companies had sufficient experience with potential devices for their replies to be useful. Of these four companies, two reported no incorrect relay operations chargeable to potential-device transients, one reported suspicion of some trouble, and another reported some trouble definitely ascribable to potential-device transients. (Much of the trouble, however, having been experienced soon after installation and before corrective measures were undertaken.)

The troubles reported as having been caused (or suspected to have been caused) by potential-device transients are as follows:

1. Improper tripping when a fault was in the nontripping direction (undesired directional-relay operation).
2. Delayed tripping when a fault was in the tripping direction (delayed directional-relay operation).
3. Improper tripping owing to protective-gap spark-over during disconnect-switch operation with no fault on the system.

Involved in these reported troubles were both phase and ground relays. These relays were mostly of the high-speed type, although misoperation of time-delay relays also was reported.

Discussion of Replies to the Questionnaire

Of the three types of reported trouble, the first one, having to do with improper tripping owing to undesired directional-relay operation, has caused the most concern. Delayed tripping seems to be more of a conjecture rather than an actual hard hip. Improper tripping owing to protective-gap spark-over during disconnect-switch operation is subject to correction by proper adjustment of the device and of the length of the protective gap (so long as the length is short enough to protect the equipment); in early models of one manufacture, the auxiliary capacitor unit had some inductance which necessitated replacing the unit to prevent spark-over. In view of the foregoing, this report will concern itself only with the

---

Paper 51-386, recommended by the AIEE Transformers Committee and approved by the AIEE Technical Program Committee for presentation at the AIEE Fall General Meeting, Cleveland, Ohio, October 22–26, 1951. Manuscript submitted May 18, 1951; made available for printing September 28, 1951.

Personnel of the AIEE Working Group on Transient Characteristics of Capacitance Potential Devices: J. E. Clem, *chairman*, J. E. Barkle, C. W. Boadway, J. W. Farr, H. F. Lindemuth, C. J. Miller, Jr., W. M. Terry, T. R. Halman, L. W. Marts, W. A. Morgan, F. C. Poage, F. Von Roeschlaub, F. D. Johnson, C. R. Mason.

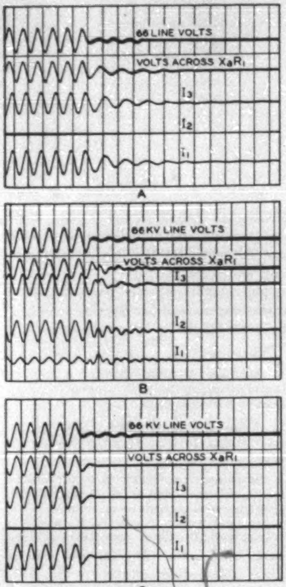

Figure 1. Oscillograms of tests on Make A potential device at 150 volt-amperes burden

(A). Burden power factor 0.25 uncorrected; (B). Burden power factor 0.25 corrected to unity power factor; (C) Burden power factor 1.00 (no correction required)

question of improper tripping for faults in the nontripping direction, or in other words with undesired directional-relay operation.

In so far as operating experience is concerned, the replies to the questionnaire do not throw any new light on the subject. Although the questionnaire was not extensively distributed, it is believed that the replies are representative of general experience. One should not expect to learn much from a questionnaire on this subject. As will be seen later, under rare circumstances, the operation of directional relays can be adversely affected by potential-device transients. In those rare circumstances, it is "touch and go" whether the directional relay operates undesirably or not. Therefore, it is practically impossible for one to say whether a particular relay misoperation was caused by a potential-device transient, or as a consequence of misadjustment of the potential devices, or because of a system transient. In this respect, it is regrettable that the questionnaire did not ask for data as to the types of faults, whether during staged tests or not, and the location of the faults with respect to the location of the relays that misoperated. In the case of those who report no trouble, it is likely that the conditions have never been exactly right to cause trouble.

There is no doubt that relays have operated undesirably because of potential-device transients, and it is not the intent of this report to discount the replies of those who co-operated in answering the questionnaire. However, it is believed that many if not most of the misoperations occurred in early installations where the potential devices had certain undesirable characteristics that have since been corrected. Also, the adjustment and loading of the devices may not have been such as to minimize the likelihood of misoperation. At least the answers to the questionnaire are not very specific on these points. However, there still remains the possibility that directional relays might have misoperated, though rarely, even with modern potential devices having the optimum loading and adjustment.

It is significant that both operating companies who reported trouble have adopted the practice of resistance loading to minimize transients and their consequent effect on directional-relay operation. It is presumed that this practice has proved to be desirable, and if so, it confirms the conclusion reached after the Working Group studied the results of potential-device tests and their significance with regard to directional-relay operation. This will be described later in the report.

It is also significant that users who have reported actual or suspected trouble have not discontinued the use of potential devices for high-speed relaying. However, the user reporting the most trouble reports a "tendency to go back to the use of bus potential transformers on busses at line terminals where the stability considerations are paramount"; the reason for preferring bus potential transformers was not only their freedom from the production of transients, but also that the use of a voltage source connected to a bus permits the "memory action," provided in certain high-speed relaying equipments, to be effective when closing a line in on a fault. That such memory action cannot be effective when voltage is obtained from the line side of the line breaker is well known, and the limitation applies whether potential devices or potential transformers are connected at this location. When one decides to use bus voltage for this reason, it is generally necessary to resort to potential transformers in order to obtain sufficient capacity to supply the relays of all lines connected to the bus. If more than one set of coupling-capacitor potential devices were required to get sufficient output, the economic advantage would be lost. Also, the fact that potential devices cannot be adjusted to correct for the variable burden with ground relays (to be discussed later), is another reason for preferring potential transformers.

The other large user of potential devices who reported suspicion of transient trouble would apparently rather risk occasional relay misoperation because of potential-device transients than to supply the relays of all lines from a single set of bus potential transformers; he fears the possibility of trouble in the potential transformers or the secondary wiring affecting the relaying of all lines. In fact, this user appears to be more concerned

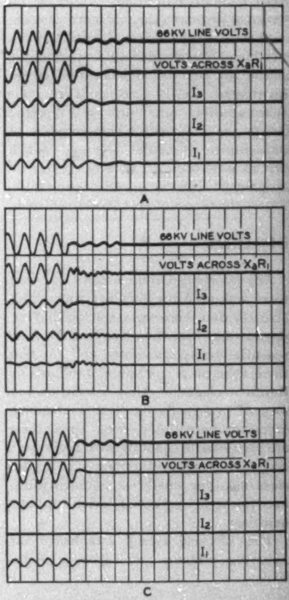

Figure 2. Oscillograms of tests on Make A potential device at 50 volt-amperes burden

(A). Burden power factor 0.25 uncorrected; (B). Burden power factor 0.25 corrected; (C). Burden power factor 1.00 (no correction required)

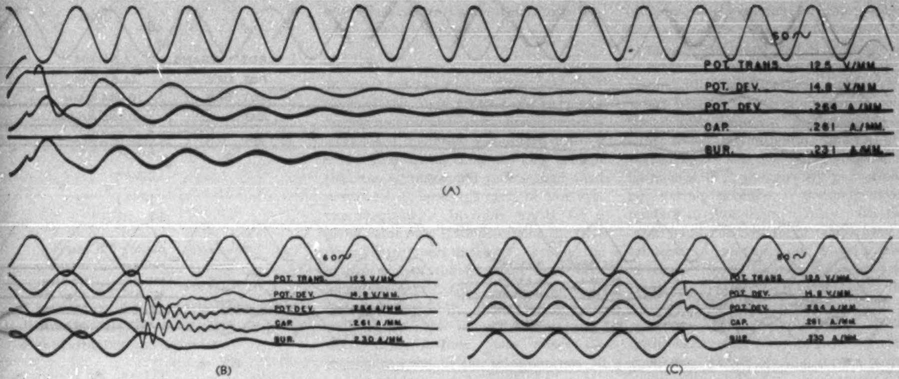

Figure 3. Oscillograms of tests on Make B potential device at 150 volt-amperes burden

(A). Burden power factor 0.25 uncorrected; (B). Burden power factor 0.25 corrected to unity power factor; (C). Burden power factor 1.00 (no correction required)

with delayed tripping than with improper tripping, although the answer to the questionnaire does not report actual trouble of a delay-tripping nature.

In short, neither the answers to the questionnaire nor present-day practice as reflected in the frequent applications of potential devices indicate that misoperation because of transients has been sufficiently objectionable to off-set the economic advantage of such devices.

Results of Tests on Potential Devices

Tests were made by the two major manufacturers of potential devices, under identical conditions of procedure, adjustment of the devices, and loading. In both cases, the devices tested were class-*A* coupling-capacitor potential devices and their associated coupling capacitors, such as would be used for a 115-kv, (66,400 volts-to-ground), 60-cycle circuit. For each test, the device was adjusted to produce rated secondary voltage in phase with the applied high-tension voltage before the short circuit was applied. For each burden used, one test was made by shorting the applied high-tension voltage at or near the zero point of the voltage wave; and for the other test, the short was attempted at the crest of the voltage wave. One series of tests was performed with the burden corrected to unity power factor by capacitance loading, and the other tests were for no power factor correction. The various burdens and their power factors are given in Table I.

Figures 1 to 4 show typical oscillograms for various burdens and adjustments. The potential device of one manufacturer is called "Make A", and the other is called "Make B". Reading from top to bottom, the oscillogram traces have the following significance:

Make A—(1) Line volts (66.4 kv); (2) Potential-device secondary volts; (3) Current through useful part of burden; (4) Current through power factor correction capacitor; (5) Total of (3) and (4).

Make B—(1) 60-cycle timing wave; (2) Line volts (66.4 kv); (3) Potential-device secondary volts; (4) Total of (5) and (6); (5) Current through power factor correction capacitor; (6) Current through useful part of burden.

Trace (1) of Make A appears to show an appreciable remnant of line voltage across the coupling capacitor after the short was applied; actually, the voltage was reduced immediately to zero, but since the oscillograph element of trace (1) was connected to measure the voltage across a tertiary winding of the supply power transformer, some voltage persisted across this winding until the supply breaker was opened. The corresponding trace (2) of Make B was obtained from the secondary of a standard potential transformer connected directly across the coupling capacitor.

As will be noted in Figures 3(A) and 3(C) the short for those tests was actually applied at the crest of the voltage wave instead of at the zero point as intended; that this happened was not discovered until after the tests were finished, and the tests were not repeated. Actually, the size of the transient is not much affected by when the short circuit is applied.

The oscillograms are purposely grouped in Figures 1 to 4 to show the high-frequency-transient components introduced by the power-factor-correction capacitor, and also the reduction of the transient resulting from resistance loading. In order to show the effect of loading on the magnitude and attenuation of the transient, the oscillograms are shown for the tests involving the two extreme burden magnitudes used. The oscillograms for the intermediate-burden power-factor and magnitude are not included, but, as might be expected, they show transients intermediate to those for the extreme conditions.

Analysis of the Tests in Terms of Phase-Relay Operation

The problem immediately resolves itself into a consideration of the effects on high-speed directional relays. Distance-measuring elements are not involved because the tests are for a fault at the relay location, and aside from slowing the operation of such relay elements slightly (and probably not noticeably), the voltage transients have no other effect. But a high-speed directional relay might operate incorrectly either to prevent (or to delay) desired tripping, or to cause undesired tripping. Therefore, this part of the study concerns itself only with the probable operation of high-speed directional relays.

No more than an educated guess of the

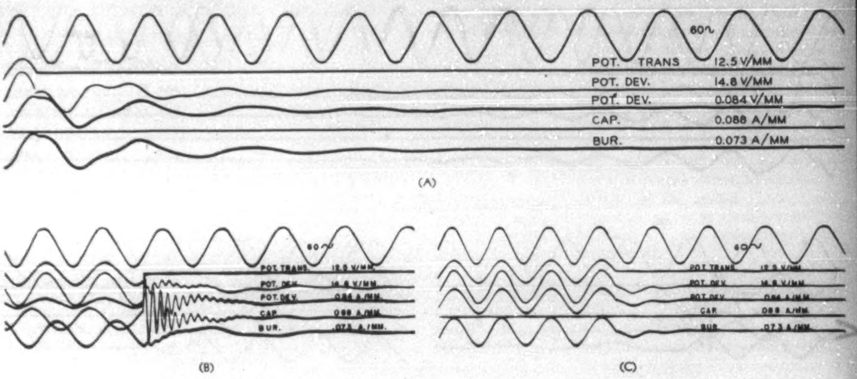

Figure 4. Oscillograms of tests on Make B potential device at 50 volt-amperes burden

(A). Burden power factor 0.25 uncorrected; (B). Burden power factor 0.25 corrected to unity; (C). Burden power factor 1.00 (no correction required)

probable operating tendency of a directional relay will be given here. There are too many variables involved and the art is not sufficiently advanced for one to say definitely what will happen. The Working Group's conclusions follow

1. A high-speed directional relay would operate to cause desired tripping.

2. Undesired tripping is also likely in some cases.

3. The power factor of the burden has more effect than the size of the burden on the possibility of undesired tripping.

4. With a 0.25 power factor burden, undesired tripping is likely, regardless of the size of the burden and whether or not the power factor is corrected to unity by capacitance loading.

5. With a 0.7 power factor burden, undesired tripping may or may not occur. It is not clear whether there is any choice between correcting the power factor to unity or not by capacitance loading.

6. With a 1.0 power factor burden, undesired tripping is unlikely, regardless of the size of the burden.

7. From the foregoing, it is concluded that to reduce the possibility of undesired tripping it would be better where possible to correct the power factor by resistance loading up to the limit of the device. It is not definitely indicated by the tests whether or not capacitive loading also is desirable; however, one member of the Working Group stated that he knew of tests that indicated a slight over-compensation to about 10 degrees lead was beneficial.

Technique of Analysis

The following were estimated from the oscillograms and recorded in Table I.

1. The frequencies of the transients.

2. The crest value of the first half cycle of each transient in per-unit of initial voltage.

3. The number of timing-wave cycles for the transients to decay substantially to zero.

To use these data for estimating directional-relay response, one must know how a directional relay responds when its polarizing voltage has a frequency different from that of the current supplied by the current transformers. There are two different types of high-speed directional relays in use—the single-induction-loop type shown schematically in Figure 5 and the induction-cup or the double loop type of Figure 6. The cup and the double-loop types are represented in Figure 6 by two loops at right angles to one another. The X signifies that current is flowing down in the portion of the loop at right angles to the air-gap flux path, and the circle and dot signify that the current is flowing up. Equations are given on the figures for the instantaneous torques developed in both types of relays. The subscripts of the currents identify the fluxes which induce the currents.

Let us assume that ϕ_1 is produced by coil current from a current transformer having the basic system frequency, and that ϕ_2 is produced by a coil energized from the potential-device voltage; ϕ_2 will be assumed to have a frequency different from that of ϕ_1.

Figure 7 shows approximately the various quantities and the torques produced over a period of time when the flux due to a subnormal-frequency-transient voltage is assumed not to attenuate. Actually, this flux decays to zero after a few cycles, but the analysis is simplified if this decay is neglected. The decay is a very important factor, and is one of the things that makes a definite conclusion impossible, but it can be treated apart from our immediate considerations. The two fluxes are assumed to be such that at the initial instant ($\theta=0$), the net torque is a maximum. The various quantities of Figure 7 can therefore be expressed as

$$\phi_1=\Phi_1 \cos \theta$$
$$\phi_2=\Phi_2 \sin n\theta$$
$$i\phi_1=-K\Phi_1 \sin \theta$$
$$i\phi_2=K\Phi_2 \cos n\theta$$

where n is the per-unit frequency of ϕ_2 based on the frequency of ϕ_1.

It is significant to note that the average torque reverses in the case of any directional relay after a short time. It will be evident that so long as the two fluxes continue unattenuated, the resulting average torque will be a sinusoidal wave periodically reversing its direction.

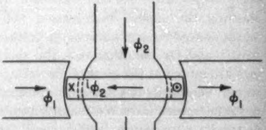

Figure 5. Torque $\propto \phi_1 i\phi_2$

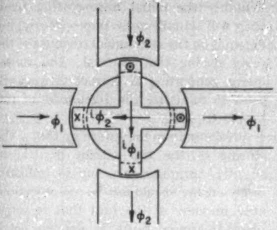

Figure 6. Torque $\propto \phi_1 i\phi_2 - \phi_2 i\phi_1$

In the case of the induction-cup or the double induction-loop relay, the equation of the instantaneous torque is

$$\text{Torque} \propto \cos |(n-1)|\theta$$

where n is the per-unit frequency of the transient based on the normal system frequency. The average torque of the single induction-loop relay will be similarly expressed.

In order to find the length of time represented on Figure 7 for the interval from $\theta=0$ to $\theta=\theta$, which is the length of time taken for the torque to reverse after starting with maximum torque, we can let

$$\cos |(n-1)|\theta = 0$$

or

$$\theta = \frac{90}{|(n-1)|} \text{ degrees}$$

In terms of the base frequency, the time is

$$t = \frac{90}{360|(n-1)|} = \frac{1}{4|(n-1)|} \text{ cycles}$$

This relation is shown in Figure 8. Since the duration of the period from $\theta=0$ to $\theta=\theta$ is one quarter of the total torque cycle, the duration of the torque cycle in terms of the base frequency is $|1/n-1|$, or the actual frequency of the torque is $|n-1|$ times base frequency.

The decisions recorded in Table I as to the possibility of undesired operation were reached in the following manner. It is known that a conventional high-speed directional relay will not operate if the frequency of its torque reversals is equal to the base frequency; if operation were possible, a single induction-loop relay would operate when its actuating quantities were at the zero-torque phase relations. The relay is close to operation, however, because it vibrates quite a bit. At any rate, operation was judged to be impossible if the frequency of the torque was equal to or higher than base frequency, which is to say

$$|n-1| \geq 1$$

or, when $n=2$ or more. This eliminated some of the cases where high-frequency transients were observed. For values of n less than 2, operation was judged possible if the attenuation time was long enough that the torque could reverse and then persist for at least 1/2 cycle of base system frequency. In other words, for a given value of n, if we determine the time from Figure 8 and then add 1/2 cycle, the attenuation of the transient must take longer than that time if the relay is to operate undesirably. Borderline cases are indicated in Table I by a question mark; these cases include those where the maximum crest of the transient was 10 per cent or less.

It is felt that the conclusions probably indicate a greater-than-actual likelihood of undesirable operation, but there are so many variables whose effect cannot be accurately evaluated that it is preferred to let the conclusions stand. For example, all induction-type relays respond best to a certain frequency, and their torque decreases for frequencies on either side of the optimum; this was not taken into account here. The presence of harmonics, even though they produce no net torque, produces a damping effect tending to slow down a relay. On the other hand, all high-speed relays have a tendency to overtravel, and, given a pulse of contact-closing torque, may overtravel enough to close contacts even though the torque decays to zero before the contacts can close. The assumption that at the initial instant the relay is operating with maximum contact-opening torque is not necessarily valid. For a departure from the maximum-torque position, the attenuation time of the transient necessary

Table I

Burden at 120 Volts		Short at Peak Voltage					Short at Zero Voltage					
					Will Relay Mis-operate					Will Relay Mis-operate		Make of
Power Factor	Volt Amperes	n	First Crest	Cycles Duration	Yes	No	n	First Crest	Cycles Duration	Yes	No	Pot. Device
PF Corrected to Unity												
0.25	50	0.43	0.38	5	X		0.47	0.44	5	X		B
		1.17	0.11	5	X		1.46	0.1−	5		?	B
		0.58	0.25	5	X		0.59	0.29	5	X		A
		2.50	0.1−	5		X	2.30	0.1−	5		X	A
	100	0.50	0.30	5	X							B
		1.42	0.20	5	X							B
		1.12	0.30	3	?							B
		0.64	0.28	8	X	X						A
		2.00	0.21	8								B
	150	0.52	0.25	5	X		0.59	0.38	5	X		B
		1.70	0.1−	5		?	1.57	0.1−	5		?	B
		0.58	0.10	5		?	0.64	0.40	7	X		A
		1.75	0.30	8	X		2.00	0.10	7		X	A
0.70	50	1.08	0.29	3.5		X	0.43	0.38	5	X		B
							1.45	0.10	5		?	B
		2.90	0.1−	3		X	Practically none				X	A
	100	0.48	0.40	3	X		0.45	0.27		?		B
		1.44	0.10	3		?	1.30	0.1−	3		?	B
		2.30	0.10	3		X	2.30	0.10	3		X	A
	150	1.41	0.47	2.5	X		0.56	0.47	3	X		B
							1.44	0.10	3		?	B
		2.30	0.35	3		X	1.75	0.56	3	?		A
1.00	50	1.50	0.30	2	?		1.50	0.30	2	?		B
		Practically none				X	1.00	0.29	1		X	A
	100	1.54	0.40	2	?		1.31	0.55	1		X	B
		1.00	0.29	1		X	1.00	0.33	1		X	A
	150	1.31	0.55	2	?							B
		1.23	0.61	2		?						B
		1.00	0.30	2		X	1.0	0.55	1.5		X	A
PF Uncorrected												
0.25	50						0.56	0.67	5	X		B
							0.94	0.10−	∞		?	B
							0.47	0.59	6	X		B
		0.58	0.50	5	X		0.50	0.75	6	X		A
	100	0.86	1.00	10	X		0.78	1.00	10	X		B
		0.55	0.57	10	X		0.55	0.72	10	X		A
	150	0.73	0.82	10	X							B
		1.12	0.75	7	X							B
		0.55	0.75	10	X		0.55	0.75	10	X		A
0.70	50	0.61	0.22	2	?		0.50	0.33	4	X		B
		1.58	0.22	3	?		1.54	0.10	3		?	B
		0.88	0.29	1		X	0.88	0.43	2		X	A
	100	1.14	0.1−	3		?	0.47	0.64	3	X		B
							1.57	0.60	3	X		B
		0.73	0.39	3	?		0.73	0.50	3	?		A
	150	0.67	0.55	3	X		0.71	0.75	3	?		B
		0.87	0.40	3	?		0.86	0.56	3	?		A

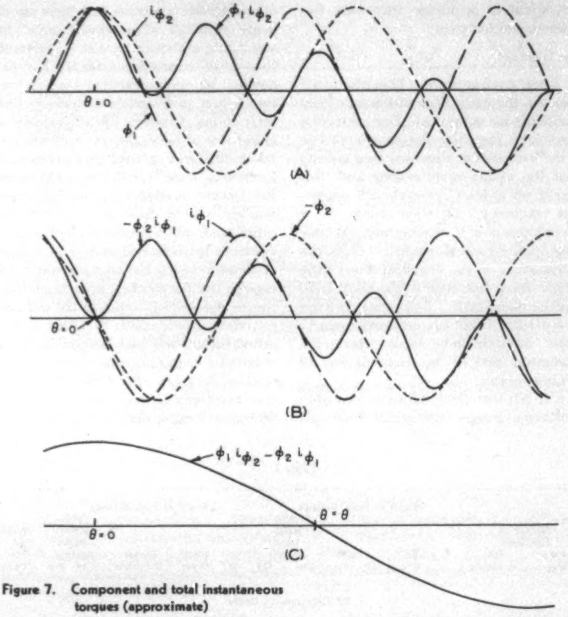

Figure 7. Component and total instantaneous torques (approximate)

to cause undesired operation may be greater or less than that used as a basis for the conclusions of Table I. And finally, the maximum crest, the frequency, and the time to attenuate to zero recorded in Table I were only estimates.

Analysis of the Tests in Terms of Ground-Relay Operation

It has been shown that the cause of phase-relay misoperation is the change in phase of the transient voltage. At the start of the short circuit, the phase relation of the transient voltage is such as to give proper relay operation, but after a certain time the transient voltage changes phase sufficiently to cause misoperation. In this case, the transient voltage is the sole voltage on which the relay relies for its operation.

The operating tendency of a directional-ground relay is just the opposite to that of a phase relay. The presence of a potential-device transient produces a misoperating tendency at the initial instant of the short circuit, but after a very short time the operating tendency becomes correct. In this case, the relay relies for its operation on the vector sum of the voltages from the three potential devices, and the transient voltage of one device introduces the greatest error at the initial instant. The subsequent change in phase of the transient voltage has little if any effect because the voltage attenuates, and therefore, the voltage across the polarizing coil approaches closer to the correct value, which gives proper operation.

Figure 9 shows the three potential-device voltages and the burden voltage before and after a phase-to-ground short circuit on one phase. Also, the voltage across the burden is shown as it would be if the potential device of the shorted phase had no transient. Comparing this voltage with the actual voltage, one will see that at the initial instant and for a fraction of a cycle thereafter, the apparent phase of the actual voltage is very different from what it would be without the transient. It is during this interval that a directional-ground relay may generate a pulse of torque in the wrong direction.

However, immediately after this interval, the voltage closely approaches the true voltage, the difference in phase quickly attenuating to a negligible value, and correct torque will be generated. Whether the initial misoperating tendency will actually cause improper tripping depends on the mechanical response of the relay during that interval; the subsequent generation of correct torque will tend to minimize the likelihood of improper tripping.

It follows from the foregoing that if the closing of the trip circuit is delayed slightly, improper tripping is unlikely. Such a delay should not be too objectionable in view of the fact that a single phase-to-ground fault is not as detrimental to stability as interphase faults; for a two phase-to-ground fault, the phase relaying can operate undelayed. In fact, modern high-speed relaying equipments contain the necessary delay because of the use of auxiliary relays in the tripping functions.

The burden on the auxiliary windings of potential devices supplying polarizing voltage to directional-ground relays cannot be compensated either by resistance or capacitance auxiliary loading so as to minimize the transient. With the broken-delta connection, the same current flows through the auxiliary winding of all three devices when a ground fault occurs, and no matter what the power factor of the burden is, it will be different when referred to each winding since the voltage of each winding has a different phase. If the burdens on the phase-relay windings are properly chosen as to magnitude and power factor, and if the ground-relay burden is a small part of the total, its effect will be negligible.

Otherwise, the steady-state error introduced into the voltage across the ground-relay coils owing to different errors of each of the three devices may be more of a problem than the possibility of transient-voltage error. Such steady-state error is subject to a relatively simple check, however.

The Probability of Relay Misoperation

The foregoing analyses have shown that relay misoperation is possible for the conditions tested. In this respect, the tests merely confirm the prevalent suspicions. But the test results also show that it is almost "touch and go" whether misoperation will occur, even under the most adverse conditions of potential-device loading and adjustment; for the most favorable conditions, misoperation is unlikely. It is appreciated that it will not be possible to use much if any supplementary resistance loading when the useful burden loads the device nearly to full capacity; where such conditions prevail, improper

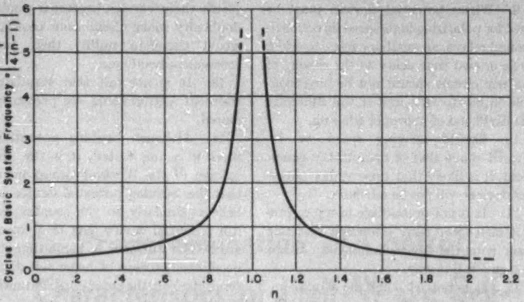

Figure 8. Duration of the period corresponding to that from $\theta=0$ to $\theta=\theta$ of Figure 7(C)

relay operation is likely under the conditions tested.

But lest improper emphasis be placed on the likelihood of misoperation under actual service conditions, one should realize that the conditions tested are rarely if ever duplicated in actual service. Seldom if ever will the high-tension voltage be reduced immediately to zero as in the tests. This will happen only if a maintenance crew forgets to remove grounding protective means connected at the terminals of the coupling capacitors, and the line circuit breaker is closed in on this solid 3-phase short circuit. Or, such a condition might be duplicated in a staged test where a solid short circuit was applied through a circuit breaker at a line terminal. The usual short circuit comprises an arc, and the voltage across the arc will be at least 4 per cent of rated voltage. Moreover, the voltage does not immediately decrease to that low value, and this will still further lessen the severity of the transient-voltage output of the potential device. The probability of even an arcing short circuit occurring at the terminals of the coupling capacitor is very small, and the greater the length of line between the coupling capacitors and the fault, the higher the minimum voltage. Tests have indicated that if the line-to-ground voltage is not reduced below 8 per cent of normal, relay misoperation because of potential-device transients is impossible, even though one does not use the loading methods recommended herein for minimizing the transient.

Coupling-Capacitor Potential Devices versus Potential Transformers

The only justification for using potential devices is to save expense. While the findings of the Working Group would seem to "lay the ghost" of potential-device transients, nevertheless, there will always be a small amount of uncertainty. Furthermore, it should be realized that present-day relay speeds have been assumed; should relay speed be much increased, it is possible that present-day potential devices will not be suitable. Errors arising from the inability to equalize the burdens on the auxiliary windings for ground-relay polarization is another disadvantage of potential devices not shared by potential transformers.

Attainment of Objectives

The primary objectives of the Working Group to obtain data on potential-device transients and their effect on relay operation have been attained. However, the ultimate objectives are only partially attained. This report gives only suggestions for guidance in the loading of potential devices so as to avoid as far as possible the likelihood of relay misoperation. To try to predetermine relay performance except in a general qualitative way is felt to be impracticable.

It is probably possible to establish standards of transient performance, but the Working Group has made no effort in this respect. If such standards were to be devised, they should, in effect, assure as good transient performance as that now provided by the devices tested for this report. It was the opinion of the Working Group that the present investigation has not indicated the necessity of redesigning the potential devices now available, in order to improve their transient performance. Improvement would be possible, but it would result in more costly devices, and this would nullify the economic advantages now enjoyed by potential devices for the higher voltages. It is felt that these devices are generally satisfactory for most high-speed relay applications, and that there is no need at this time for performance standards.

Conclusions

Based on the answers to the questionnaire, the tests and analytical studies, and the knowledge of members of the Working Group as to present-day experience and practices, the following conclusions are presented.

1. Potential transformers should be used in preference to coupling-capacitor potential devices when such use is economically justifiable.
2. Present-day coupling-capacitor-potential devices, properly loaded and adjusted, are suitable for most high-speed relaying applications.
3. Coupling-capacitor devices will, in rare cases, produce transient voltages that will cause undesired tripping by directional-relay operation. Desired tripping will always occur, though with a short-time delay in rare cases.
4. Low power-factor useful burden imposed on potential devices should be kept to a minimum in order that auxiliary resistance loading to the full capacity of the devices can be employed.
5. Power-factor-correction-capacitor loading should be used, but only in addi-

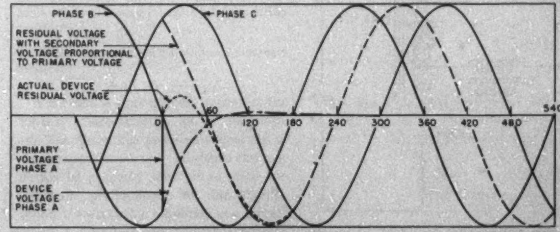

Figure 9

tion to the maximum possible resistance loading, to overcorrect the power factor to approximately 10-degrees lead.

6. The practices of (4) and (5) will minimize the likelihood of improper directional-relay operation.

7. The difficulty of obtaining satisfactory adjustment when directional-ground-relay polarization is involved is more of a detriment to the use of potential devices than their transient performance.

8. Where a suitable power-transformer neutral-current polarizing source is available for directional-ground relays, it should be used in preference to voltage polarization from the auxiliary windings of potential devices.

9. Where potential devices must be used for polarizing high-speed directional-ground relays, an auxiliary relay to add a cycle or two time delay to the closing of the trip circuit should not be objectionable in most cases, and it will minimize the likelihood of improper tripping.

10. Should relaying speed be increased above that of present-day equipment, it is likely that present-day potential devices will not be adequate.

11. It is not practicable to try to predict high-speed-relay operation resulting from potential-device transients, except in a qualitative way.

12. It is not felt that the short comings of potential devices are enough to justify their redesign because it would undoubtedly make them more costly, and would therefore nullify their present economic advantage.

13. It is not felt that standards of transient performance are presently required.

14. Although bushing potential devices were not tested, it is the general opinion of the Working-Group members that the bushing potential device would behave similarly to the coupling-capacitor potential device, but to a lesser degree. The duration of oscillation should be shorter because of faster self-damping resulting from the smaller capacitance and higher loss ratios.

Discussion

A. W. Adams (Bonneville Power Administration, Portland, Oreg.): The members of the Working Group and the manufacturers who co-operated in this report are to be complimented on their work on this extremely difficult problem.

The Bonneville Power Administration has been interested in this problem for a number of years but the large number of variables encountered prevented us from conducting tests that would lead to conclusive results. The Working Group, in this report, has arrived at a fairly definite procedure for improving the performance of potential devices.

It will still be necessary for each utility to decide for themselves whether potential devices or potential transformers should be used where the first cost of potential transformers is higher than the cost of potential device.

On the Bonneville system, we believe that considerable weight should be given to the lack of transients with potential transformers. If high-speed relaying can be speeded up even a fraction of a cycle by replacing potential devices with potential transformers, considerable extra cost can be justified. In many cases, one set of potential transformers can be used for the relays on three or more circuits.

On our system, we have a number of cases of potential devices that have required recalibration even when the burden had not been changed. In most cases, the reason for this change was never fully investigated, but it has influenced our ideas regarding the use of potential devices.

The Committee has recognized the weaknesses of potential devices, such as inaccuracy for polarizing ground directional relays. It also must be recognized that the additional delay in the trip circuit recommended to eliminate improper tripping for ground faults will also delay high-speed reclosing.

The lack of standards for transient performance of potential devices is a serious disadvantage to an agency which must purchase equipment on the basis of the low bid received which meets specifications. If no standards or specifications for transient performance are available, it is possible for a manufacturer to offer us equipment which would be suitable for steady-state performance but entirely unsuitable in its transient performance.

We are sure that the manufacturers will continue their experimental work and the development of potential devices. With the present cost of high-voltage potential transformers, potential devices must be used in their place for many purposes and, if improved devices are available, they will be used for additional purposes.

Predetermination of Control Characteristics of Half-Wave Self-Saturated Magnetic Amplifiers

HENRY LEHMANN
ASSOCIATE MEMBER AIEE

Synopsis: The control characteristic of a self-saturated magnetic amplifier is dependent upon the magnetic properties of the core material. A method is outlined for the experimental determination of the control magnetization curve, a plot of the locus of the minor dynamic hysteresis loops, which may be used with a firing angle analysis to predict the performance of simple magnetic amplifiers with high-control circuit impedance.

DURING the past few years, numerous papers have been written in an attempt to explain the operation of magnetic amplifiers as system elements. Reviewing the literature of this field, one may find waveform analyses of various series and parallel circuits, or relations defining the power gain or speed of response in terms of physical constants of the system. One immediately notices a common property of these papers. In most cases the author accepts a mathematical defeat at the hand of the nonlinear characteristics of the core and rectifier. The author is forced to make rash assumptions regarding the forward and reverse resistances of the rectifier and the *B-H* relationship of the magnetic material. The performance equations derived on the basis of these assumptions establish a clear and simple physical picture, but cannot be used to predict the exact performance of the magnetic amplifier circuit. Methods are available for the approximate calculations of power gains and time constants of a magnetic amplifier, so that its effect on a control system can be ascertained, but the nonlinearities of the magnetic amplifier itself are just beginning to be studied. Systems containing these magnetic elements are being designed and function properly after certain adjustments are made in the laboratory, but one cannot as yet predict exactly what output will be obtained for a given control current.

This situation is not a healthy one. In order to minimize the design efforts and to maximize the utilization of materials, the factors influencing the actual control characteristics must be understood. Two questions thus present themselves:

1. How do the actual control characteristics differ from the theoretical characteristics derived using the usual linearizing assumptions?

2. What causes these differences in characteristics?

A method is thus needed to predict the control characteristics of a magnetic amplifier from the physical properties of the component parts. Only then can materials be properly selected to yield the optimum performance of the circuit. When the magnetic amplifier as a circuit element is understood, the system problems will solve themselves, because a magnetic amplifier of the required characteristics can then be synthesized.

It is the purpose of this paper to develop a semiexperimental method by which the nonlinearities of the magnetic core can be included in the prediction of magnetic amplifier performance. No effort is made to include the nonlinearities of the rectifier.

The Circuit Element Considered

Since this is a study of circuit elements, the simplest type of magnetic amplifier is chosen for the analysis. The scope of this paper is limited to half wave self-saturated magnetic amplifiers with high impedance control circuits. This is the basic component of many complex systems, so that the theory developed for this elementary circuit element should be valid for a broad range of circuits, see Figure 1.

"Self-saturation in a magnetic amplifier refers to the connection of half-wave rectifying circuit elements in series with the output windings of the saturable reactors."[6] The feedback current thus flows through the load winding, resulting in 100 per cent feedback.

From ordinary transformer theory it is known that the average ampere-turns must be balanced out around a core. The direct current flowing in the load winding

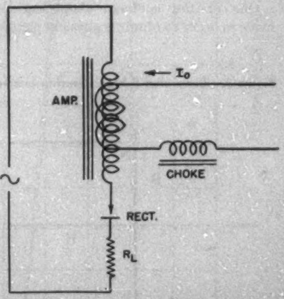

Figure 1. Half-wave self-saturating magnetic amplifier with high control circuit impedance

---

Paper 51-387, recommended by the AIEE Magnetic Amplifiers Committee and approved by the AIEE Technical Program Committee for presentation at the AIEE Fall General Meeting, Cleveland, Ohio, October 22-26, 1951. Manuscript submitted March 27, 1951; made available for printing September 7, 1951.

HENRY LEHMANN is with the General Electric Company, Schenectady, N. Y.

The work forming the basis for this paper was done under the direction of H. W. Lord at the General Electric Research Laboratory while the author was assigned there from the Advanced Engineering Program of the General Electric Company. The author is indebted to F. H. Wright of the Advanced Engineering Program for some of the data included in this paper.

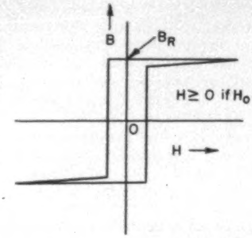

Figure 2. Extremely rectangular hysteresis loop

exactly balances out the load ampere-turns; consequently, the only ampere-turns which need be supplied by the control winding are the magnetizing ampere-turns. Since these are very small for the high grade core materials used, large amounts of power can be controlled with very small control currents, resulting in large power gains.

The choke is included in the circuit of Figure 1 to prevent alternating currents from flowing in the control circuit. Thus, the control current consists only of a direct component. Since the rectifier does not permit negative load currents, the flux density in the core can never fall below the residual point when the control current is zero or positive.

For the rectangular hysteresis loop materials commonly used in high-performance magnetic amplifiers, maximum output is expected when the control magnetizing force, H_o, is equal to zero. Figure 2 indicates that useful control is obtained only for negative values of control ampere-turns.

Assumptions Made in Previous Papers

One of the common simplifications made in order to obtain a physical picture of the amplifier operation is to treat the B-H relationship of the core material as the simple 3-line diagram of Figure 3.[5,9] Other simplified *B-H* curves are Figure 4[8,9], and the actual d-c magnetization curve.[1,2,4] When applied to rectangular hysteresis loop materials, none of these assumptions show that maximum output is obtained with zero control current.

Figure 3. Simplified B-H relationship in core

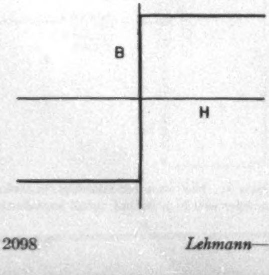

Nomenclature

A_o = dimensionless ratio defining output voltage
B = flux density in core at any instant
B_o = bias flux density equivalent to control magnetizing force
B_f = firing flux density
B_m = maximum flux density associated with supply voltage $E_m/(\omega NA)$
B_r = residual flux density
e_o = instantaneous output voltage
E_o = average output voltage
E_m = maximum value of supply voltage
H_o = control magnetizing force
N = number of turns on load winding
R_L = load resistance
φ_f = firing angle
ω = angular frequency of supply voltage
$E_f = \omega NAB_f$

Only two papers have been found which use the d-c hysteresis loop of the material.[7] The control current is assumed to force the residual flux density down along the upper portion of the hysteresis loop. It will be shown that this is not the actual B-H relationship in the core.

Firing Angle Analysis

In analysing the operation of the magnetic amplifier using the d-c hysteresis loop of the core material, W. J. Dornhoefer[7] treats the amplifier as a thyratron. The following assumptions are made in the analysis:

1. The core material has a rectangular hysteresis loop, that is, the differential permeability is very high and constant until a level is reached where the differential permeability suddenly drops to a very low value.
2. The rectifier has infinite reverse resistance.
3. The applied voltage is sinusoidal.
4. The total load circuit resistance is low compared to the unsaturated coil reactance and high compared to the saturated reactance.
5. The rectifier forward resistance is constant.

Figure 4. Simplified B-H relationship in core

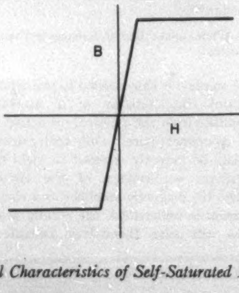

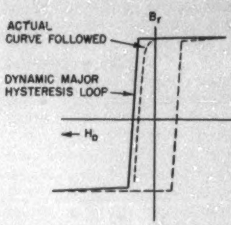

Figure 5. Location of control magnetization curve with respect to major hysteresis loop

As long as the total flux density in the core is below the firing flux density, B_f, at the knee of the hysteresis loop, no current can flow. As soon as the flux density rises above this value, the core permeability drops to a very low value, and the current is limited only by the load circuit resistance.

The angle of the sinusoidal voltage at which firing occurs is given by

$$\theta_f = \cos^{-1}\left(1 - \frac{B_f - B_o}{B_m}\right) \tag{1}$$

The output voltage is thus

$$e_o = E_m \sin \omega t \tag{2}$$

and, in dimensionless form

$$A_o = \frac{2\pi E_o}{E_f} = \frac{2B_m}{B_f} + \frac{B_o}{B_f} - 1 \tag{3}$$

The application of this analysis depends upon the proper determination of B_o and B_f, both properties of the core material.

Determination of B_o—Control Magnetization Curve

Since an alternating voltage is applied to the magnetic amplifier, the flux in the core does not follow the d-c hysteresis loop, so that this curve cannot be used to predict the $B_o - H_o$ relationship in the core. Eddy currents flow in the laminations and must be supplied from the a-c power source. The total a-c magnetizing

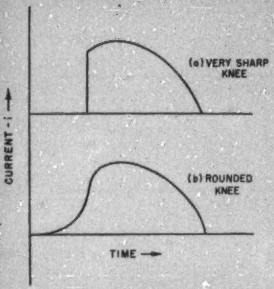

Figure 6. Output current waveforms obtained for hysteresis loop with very sharp and rounded knee

current flowing at any instant is the sum of the current determined from the d-c hysteresis loop and that required to supply the eddy current losses. The latter component is in phase with the voltage and is a maximum when the flux in the core is zero. The maximum widening of the hysteresis loop in going from direct current to power frequency excitation thus occurs at the coercive point.

The reader may be surprised that eddy currents must be considered in studying the performance of magnetic elements constructed of laminations of thicknesses as low as 0.002 inch and operating at 60 cycles per second. However, it is precisely this effect which has resulted in poor agreement between the experimental control characteristics and the theoretical ones based on the d-c hysteresis loop.

The rectangular hysteresis loop materials used in magnetic amplifiers have resistivities approximately the same as the more common transformer steels. The eddy current losses, and their equivalent magnetizing forces, H_e, will thus be the same for two coils, one using transformer steel, and the other a high grade rectangular hysteresis loop material. However, the d-c coercive force of the rectangular loop material is considerably smaller than that of the transformer steel. The eddy current component of coercive force thus represents a larger percentage of the total for the rectangular loop material, so that eddy current effects are of greater importance in high grade magnetic amplifier cores.

Table I. Comparison between D-C and Dynamic Hysteresis Loops*

Material, Inches	Resistivity	D-c H_c	H_e	60 Cycles per Second H_c
		Oersteds		
0.010 Deltamax	50	0.125	0.185	0.310
0.005 Deltamax	50	0.040	0.060	0.100
0.005 Permalloy	25	0.020	0.150	0.170

* It should be noted that the ratio of H_c values for 0.010-inch and 0.005-inch Deltamax at 60 cycles per second is not four as would be expected from the elementary eddy current equations. Further experimental data have substantiated the above implication that for those square loop materials the elementary eddy current equation in which the loss is proportioned to the frequency and thickness squared is inaccurate. A preliminary theoretical investigation has revealed H_e to be a more complicated function of the frequency, lamination thickness, maximum induction, and permeability.

Table I is a compilation of experimentally determined coercive forces of various samples of magnetic amplifier cores. This table indicates that the d-c and dynamic hysteresis loops are entirely different. The coercive force at 60 cycles per second of Deltamax (square loop

Figure 7. Control magnetization curve in relation to d-c and dynamic hysteresis loops for 0.010-inch thick Deltamax

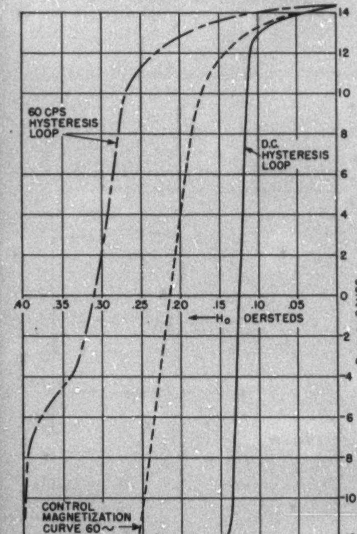

Figure 8. Calculated and measured control characteristics of 1/2-wave magnetic amplifier using 0.010-inch thick ring Deltamax core

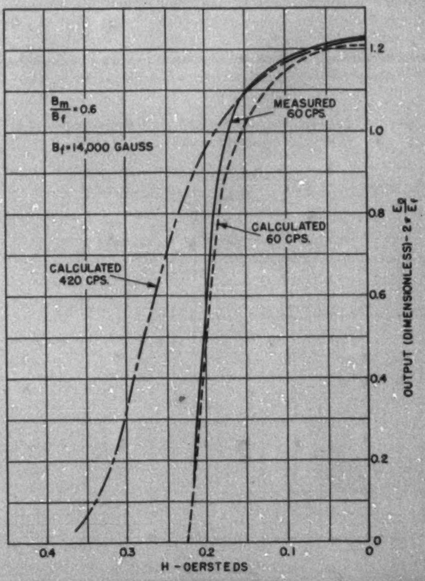

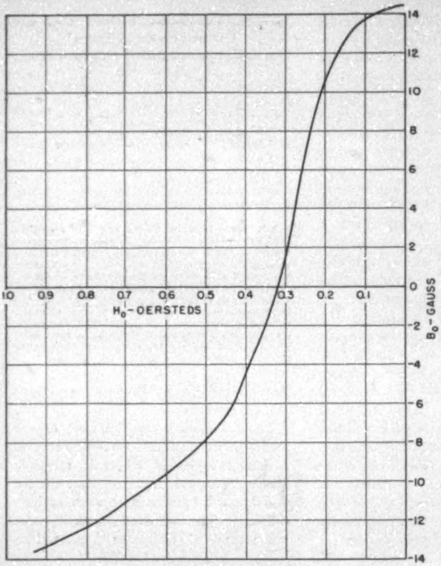

Figure 9. Control magnetization curve of 0.010-inch Deltamax ring core at 420 cycles per second

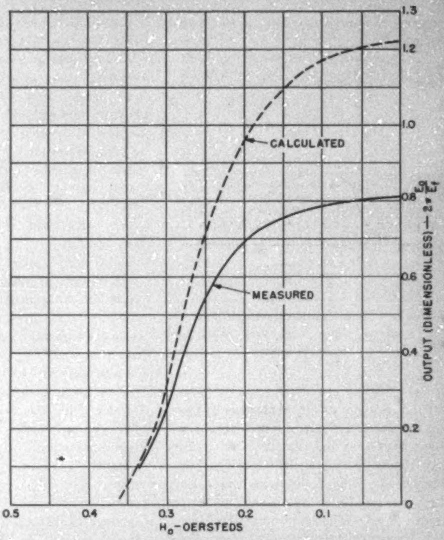

Figure 10. Control characteristics of 1/2-wave magnetic amplifier using 0.010-inch thick Deltamax core at 420 cycles per second

Nicaloi) is about $2^1/_2$ times that under d-c excitation. Permalloy which has a d-c coercive force one half that of Deltamax has, because of its lower resistivity, a 60-cycle-per-second coercive force 1.7 that of Deltamax for the same thickness of lamination. Since the core follows a minor dynamic hysteresis loop in its operating cycle, and since these dynamic loops are widened by the eddy current effects, accurate prediction of the magnetic amplifier control characteristics can thus not be expected using the d-c hysteresis loop.

In order to use the firing angle analysis to predict the control characteristics of a magnetic amplifier, the bias flux density must be known for every value of control magnetizing force, that is, the B_o-H_o re-

Figure 11. D-c hysteresis loop of 0.010-inch Deltamax core used in magnetic amplifier

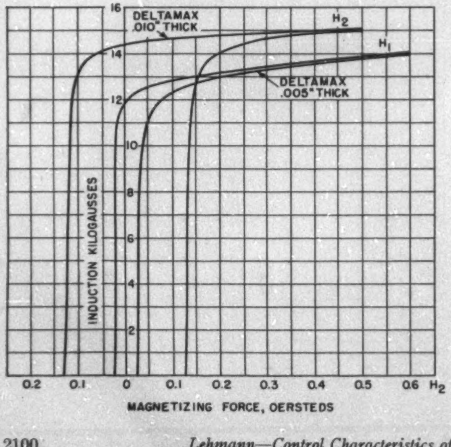

Figure 12. Control characteristics at 60-cycles per second of 0.005-inch Deltamax and Permalloy cores

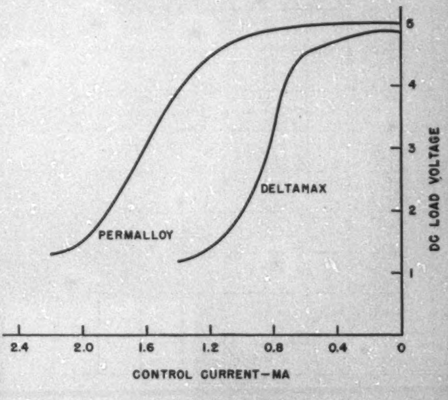

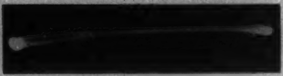

(A). $H_o=0$

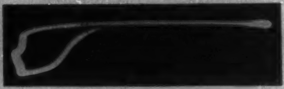

(B). $H_o=0.151$

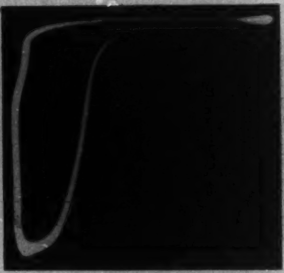

(C). $H_o=0.202$

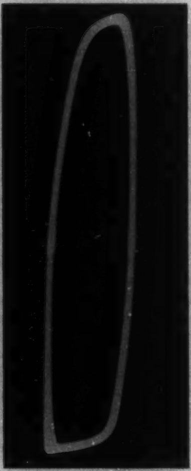

(D). $H_o=0.222$

Figure 13. Dynamic minor hysteresis loops at 60 cycles per second. 0.010-inch Deltamax, $B_m/B_f=0.75$

lationship must be known. It was believed that increasing H_o negatively would cause B_o to follow along the upper half of the major dynamic hysteresis loop obtained at the operating frequency, starting from B_r at $H_o=0$ (see Figure 5). Values of B_o thus obtained were inserted into equation 3, and a control characteristic was constructed. Poor agreement was obtained with the experimental results. The error was in a direction opposite to that obtained using the d-c hysteresis loop.

This led to the conclusion that the B_o-H_o relationship in the core is neither the d-c nor the a-c major hysteresis loop, but lies somewhere between these two curves. This relationship can be obtained only by actually plotting the locus of the bottom tips of the minor hysteresis loops over which the core operates, as shown in Figure 5. This curve has been called the control magnetization curve. This curve must be obtained at the actual frequency of operation of the amplifier. At any other frequency, the eddy current effects will be different and the minor hysteresis loops obtained will not be those over which the core will actually operate.

The value of B_o obtained by this method is used with the actual flux density at the knee of the rectangular dynamic hysteresis loop as B_f, and yields excellent correlation with the measured results.

Determination of B_f

The knee of the hysteresis loop does not occur at a singular point in most commercial magnetic materials. It is thus of interest to know what value of B_f to use when the assumption of perfect rectangularity is not met. The voltage equation around the load circuit is

$$V \sin \omega t = \frac{N d\varphi}{dt} + iR \tag{4}$$

Or

$$V \sin \omega t = N\frac{d\varphi}{di}\frac{di}{dt} + iR \tag{5}$$

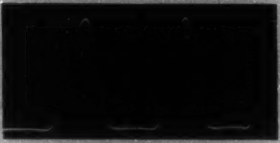

(A). $H_o=0$

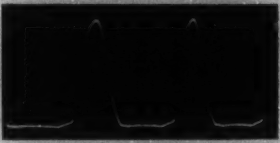

(B). $H_o=0.151$

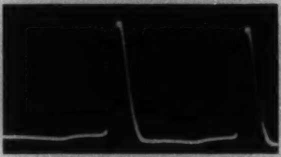

(C). $H_o=0.202$

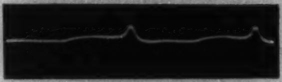

(D). $H_o=0.222$

Figure 14. Load current wave forms at 60 cycles per second of 0.010-inch Deltamax $B_m/B_f=0.75$

Thus, as soon as $d\varphi/di$ starts to decrease, di/dt goes up, producing an increase in current. If the knee is very sharp, $d\varphi/di$ suddenly drops to a very low value, causing a rapid increase in current referred to as firing. However, if the knee is gradual, such sharp firing does not occur, and the current increases more gradually. Two extreme current waveforms are shown in Figure 6. It is difficult to say where firing occurs for the material of Figure 6(B). It is suggested that B_f be taken as the point at which the differential permeability is one half of the maximum core permeability, the latter being determined by drawing a line from the origin tangent to the rising portion of the dynamic major hysteresis loop.

Limitations of Analysis

Only half-wave circuits with high-control circuit impedance have been considered. This method has been applied successfully to parallel full wave circuits with high-control circuit impedance. Little success has been obtained in applying this method to low-control circuit impedance cases, but further effort is being directed along this line.

Infinite reverse rectifier resistance has been assumed. Rectifier reverse leakage will permit negative load current flow

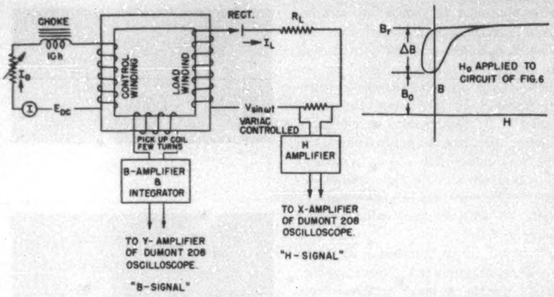

Figure 15. Suggested circuit for determination of control magnetization curve

and will thus permit a net negative magnetizing force in the core when $H_o=0$. This causes a lateral shift in the control characteristic with some modification in the circuit gain. This problem must be considered entirely separately.

Explanation of Results

Figure 7 shows the control magnetization curve in relation to the control regions of major hysteresis loops. This shows clearly that the B_o-H_o relationship can not be approximated by either the d-c or dynamic major loop.

Figure 8 shows the calculated and measured control characteristics at 60 cycles per second. These curves are shown only in the control region and can be extended in both directions of H_o. The curves indicate that the output cannot be reduced to zero. This minimum output is due to the prefiring current, present only because the presaturation inductance is not infinite. This can also be seen from the current waveforms under almost complete cut off of Figure 15. Further increases in H_o cause the output to rise, but at a very low slope. This occurs because B_o is driven into the negative saturation region, and the rectified load current increases instead of decreasing the ampere-turns which must be overcome by the control current. This is a region of low amplifier gain.

The agreement between the measured and calculated curves at 60 cycles per second is good. The error which exists is probably due to rectifier nonlinearity or noninstantaneous firing. The calculated control curve for 420 cycles per second is drawn to the same scale on Figure 8 to show the decreased gain of the amplifier because of eddy current in the core.

Figure 10 shows the control characteristic of the circuit at 420 cycles per second, obtained from the control magnetization curve of Figure 9. The agreement seems to be only fair in the full output region. This occurs because one of the assumptions was not met. Operating at the same flux density, seven times the voltage is used at 420 cycles per second as compared to 60. The reactive voltage drop across the winding after saturation also goes up by a factor of seven. However, in this case the load circuit resistance was only increased by a factor of five, so that the post-saturation inductance has a greater effect in limiting the current at 420 cycles per second. The full supply voltage then does not appear across the circuit resistance.

Figure 11 shows the d-c hysteresis loop of the material used. Ring cores wound of 0.010-inch thick Deltamax were used. B_f is about the same there as on the dynamic loop, and was selected as 14,000 gausses.

Figure 12 shows the control characteristics obtained at 60 cycles per second using 0.005-inch thick Deltamax and Permalloy. Because of the larger eddy current loss in the Permalloy, a greater control current is required for the same output, and the circuit gain is lower.

Figure 13 shows oscillograms of the minor loops for various values of H_o. Figure 14 shows the load current waveforms under the same operating conditions. These photographs were taken at 60 cycles per second with $B_m/B_f=0.75$.

Suggested Procedure for Obtaining Control Magnetization Curve

A circuit used for obtaining the minor dynamic hysteresis loops is shown in Figure 15. For any given H_o, or the directly measurable quantity I_o, the B down from the residual point is measured on the oscilloscope. By knowing the residual flux density of the material, the actual value of B at the bottom of the minor loops are then plotted against H_o, resulting in the control magnetization curves of Figures 7 and 9.

Special Notes on Apparatus Used

Rectifier: This analysis is only for the purpose of determining the effects of the core properties on the magnetic amplifier; all effects of the rectifier should thus be minimized. A high vacuum rectifier should be used to minimize the reverse current. The forward resistance should be essentially constant over the range of load current encountered. If this resistance variation is appreciable, the rectifier forward resistance should be made small compared to R_L so that the total circuit resistance remains essentially constant.

Over-all Circuit Resistance: The total load circuit resistance should be much smaller than the unsaturated amplifier reactance, so that the total applied voltage appears across the amplifier load winding before firing. The load circuit resistance should be sufficiently greater than the saturated coil reactance, so that essentially all of the applied voltage appears across the load resistance after firing. Then, the actual conditions of operation as stated in the analysis are met.

Amplifiers: It is essential that no phase shift be introduced in the amplifiers, so that the true phase relation between B and H is not disturbed. In order to obtain low phase shift the amplifiers must have good low frequency characteristics. Because of the integrating circuit the B amplifier must have high gain, which means that the circuit will be very sensitive to low frequency voltage variations. In order to prevent flicker of the pattern on the oscilloscope, excellent stability of the plate supply is required.

Core: In order for this curve to be of most value, it should be taken on the actual core to be used. This refers to material composition and thickness, anneal, shape, and frequency. A variation in any of these factors will change the B_o-H_o relationship and introduce errors in the calculations. This may appear as a large task, but it is done for hysteresis loops used in transformer, and this curve may be considered as equivalent in importance to the magnetic amplifier designer.

References

1. An Analysis of Transients and Feedback in Magnetic Amplifiers, W. C. Johnson, F. W.

Latson. *AIEE Transactions*, volume 69, part I, 1950, pages 604–12.

2. AN ANALYSIS OF TRANSIENTS IN MAGNETIC AMPLIFIERS, D. W. Ver Planck, L. A. Finzi, D. C. Beaumariage. *AIEE Transactions*, volume 69, part I, 1950, pages 498–503.

3. ANALYTICAL DETERMINATION OF CHARACTERISTICS OF MAGNETIC AMPLIFIERS AND FEEDBACK, D. W. Ver Planck, L. A. Finzi, D. C. Beaumariage. *AIEE Transactions*, volume 68, part I, 1949, pages 565–70.

4. SOME FUNDAMENTALS OF L-C CONTROLLED REACTORS WITH RESISTIVE LOAD, H. F. Storm. *AIEE Transactions*, volume 68, part I, 1949, pages 188–94.

5. SOME FUNDAMENTALS OF A THEORY OF THE TRANSDUCTOR OR MAGNETIC AMPLIFIER. A. Uno Lamm. *AIEE Transactions*, volume 66, part I, 1947, pages 1078–85.

6. PROGRESS REPORT OF THE MAGNETIC AMPLIFIER SUBCOMMITTEE, AIEE Committee Report. *AIEE Transactions*, volume 70, part I, 1951, pages 445–50.

7. SELF SATURATION OF MAGNETIC AMPLIFIERS, W. J. Dornhoefer. *AIEE Transactions*, volume 68, part II, 1949, pages 835–50.

8. THE TRANSDUCTOR, H. R. Rex. *Instruments* (Pittsburgh, Pa.), volume 20, December 1947, pages 1102–09.

9. TRANSDUCTOR FUNDAMENTALS, S. E. Hedstroem, L. F. Borg. *Electronics* (New York, N. Y.), volume 21, September 1948, pages 88–93.

Discussion

R. H. Bueshcer (General Electric Co., Schenectady, N. Y.): Mr. Lehmann has done a good job in devising a method of predicting characteristics of magnetic amplifiers. However, several points in the paper have been made which are worthy of additional consideration.

Concerning the control magnetization curve, Mr. Lehmann reports that it is found by plotting the minor hysteresis loops, by electronic means, then finding the lower most point of those loops, and replotting them for various output levels until the entire desired curve is obtained. Mr. Lehmann then reasons that with this curve, firing angle analysis may be used to predict amplifier characteristics. The firing angle analysis is based on the assumption that when the supply voltage goes through zero, the voltage across the load winding is likewise zero, and hence equation 1 is found. Since eddy currents in the laminations are not necessarily in phase with the supply voltage it would seem more reasonable to find the control magnetization curve from points on the minor loops at times when the supply voltage passes through zero. This could be accomplished by superimposing small blips on the supply voltage, small enough to be negligible in the consideration of the energy storage. Also it is possible to show that for certain shapes of cores and windings that there is considerable after saturation inductance which tends to carry over the current beyond the point at which the supply voltage returns to zero, and the direct firing angle analysis must still be corrected by a factor.

Although the paper's author mentioned some of the limitations of the control magnetization curve approach, the most basic objection should be kept in mind. A good design method should be able to specify the optimum size and shape core which must be used. According to Mr. Lehmann's methods, we must first construct the actual core on which to perform the tests and find the control magnetization curve. This is necessary since variations within even one batch of annealed magnetic material are appreciable. After this has been done only the simplest portion of the design remains. Establishment of the number of turns on the core can usually be found from the desirable magnitude of the supply voltage and from the over-all current gain. Therefore, use of Mr. Lehmann's approach require guessing the most difficult and expensive portion of the design procedure.

It is indeed refreshing to see in this paper that the author, basically an analyst, successfully realizes that the magnetic amplifier is difficult to analyze directly through mathematical relationships, and has taken a large step in the direction of real design simplification.

H. Lehmann: Mr. Bueshcer states that the variations within one batch of annealed magnetic material appreciably affect the control magnetization curve. This may be true, but this would prevent any accurate design of a magnetic device. This is a situation which can be remedied only by better quality control. Until this is achieved, a statistical mean of the magnetic properties of a batch must be used, and it must be realized that actual performance can check with the design predictions only to the degree of uniformity of the batch.

The firing angle analysis based on the control magnetization curve can be used to study the maximum gains and maximum operating range obtainable for a given core. These must be known before other factors can be considered in the selection of a core.

Mr. Bueshcer's comments on the post-saturation inductance are quite accurate. If the hysteresis loops are available from which the post-saturation inductance can be computed, the correction factor in the analysis can easily be determined from the load resistance and this inductance. It is expected that the winding resistance of the reactor and the forward resistance of the rectifier may actually be more important in limiting the output than the post-saturation inductance.

This analysis, as such, will not give good correlation with the experimental results on a practical magnetic amplifier. The most important reason for this is that infinite reverse resistance of the rectifier has been assumed. It may be possible that the effect of the rectifier is of such a magnitude to mask the error introduced by neglecting eddy currents in the consideration of the core

However, to be able to outline a practical design method, each variable must be analyzed separately. Only then can one show quantitatively that one effect is negligible compared to another and can thus be neglected. This paper is an attempt to understand the basic behavior of the core. After this basic understanding is gained, the effect of the assumptions can be studied and the theory reduced to practice.

Bibliography of Magnetic Amplifier Devices and the Saturable Reactor Art

JAMES G. MILES
ASSOCIATE MEMBER AIEE

THIS Bibliography lists all references on Magnetic Amplifier Devices and the Saturable Reactor Art known by or suggested to the author to mid-1951. It was prepared particularly as an aid to the accumulation of information on saturable reactors and saturable transformers as related to the magnetic amplifier art. Included are references on magnetic theory, measurements, core material characteristics, and rectifier characteristics pertinent to the development of magnetic amplifiers.

Entries are arranged chronologically by year of publication, and alphabetically within each year by authors' names. Where there are two or more authors for an item, the item is listed only once, under the first authors' surname.

If a book or article is written in a foreign language, the title has been translated into accepted English terminology and the language of the original has been noted in parenthesis following the English title. Following the title are given the usual bibliographic data on the author or authors, name of publication, date, and pages.

All patents included have been classified according to Table I. The key numbers and letters associated with each patent thus represent information relating to the magnetic amplifier class and circuit type, and to special means for affecting the amplifier characteristics. All patents considered by this author to be outstandingly significant to the magnetic amplifier art are indicated by an asterisk (*) immediately following the reference number.

Table II, shown on pages 2118–20, entitled Significant Patents to Magnetic Amplifier Art lists the outstanding features of each of these patents. The associated magnetic amplifier type designations are so presented, in chart form, to facilitate search for any combination of magnetic amplifier features.

In the Author Section beginning on page 2121 the name of each of the authors is listed, with the reference number or numbers.

Table I. Classification Chart for Saturable Core Devices

I. Magnetic Amplifiers:
  A. Saturable reactors controlled by signal magnetomotive force.
  B. Saturable transformers controlled by signal magnetomotive force.
    B′. Control by varying incremental permeability or by distorting waveform.
    B″. Control of mutual inductance by varying the reluctance of a saturable shunt.
  C. Magnetic modulators with negative resistance characteristics.

General classes A and B contain specific circuit types such as polarized and nonpolarized magnetic amplifiers comprising:

1. Single-sided circuits.
2. Push-pull circuits.
3. Wheatstone-bridge-type circuits.
4. Special magnetic amplifier circuits (such as cross-connected pairs of magnetic amplifiers, magnetic amplifiers in combination with transformers, et cetera).

Amplifier sensitivity, stability, linearity, and speed of response may be affected by incorporating any one or more of the following means:

a. External feedback (amplitude-related and/or phase-related external feedback means terminating in a signal-control winding or special feedback winding).
b. Internal feedback (by rectifiers in series with load windings).
c. Unidirectional bias magnetomotive force of fixed magnitude.
d. A-c bias magnetomotive force at fundamental or harmonic of power supply (carrier) frequency.
e. Off-resonant and ferroresonant means.
f. Frequency-discriminating means.
g. Additional co-operative waveform distorting means.
h. Ultra-carrier frequency means for reduction of hysteresis effects, and to increase the range of incremental permeability variations.

II. Frequency Changers (including peaked-wave forming devices):
  A. Saturating reactors with and without d-c bias.
  B. Saturating transformers with and without d-c bias.

III. Other Devices (including special voltage regulators, phase shifters, "rectifiers," et cetera):
  A. Saturating reactors with and without d-c bias.
  B. Saturating transformers with and without d-c bias.
  C. Saturating and nonsaturating differential transformers.

1887

1. Notes on Electricity and Magnetism—III. On the Behavior of Iron and Steel Under the Operation of Feeble Magnetic Forces, **Lord Rayleigh.** *Philosophical Magazine*, series 5, volume 23, March 1887, page 225.

1900

2. Theory and Calculation of Alternating Current Phenomena (book), (in German), **C. P. Steinmetz.** Berlin, 1900. See also German patent 286,531.

1901

3. System of Electrical Distribution, **A. R. Everest.** United States patent 687,140, November 19, 1901 (M/A Class III,A).

1903

4*. Regulation of Electric Circuits, **C. F. Burgess, B. Frankenfield.** United States patent 720,884, February 17, 1903 (M/A Class I,A,1).

5. Introduction to the Variations of the Self Inductance of Coils (in German), **W. Laymeyer and Company.** German patent 148,791, April 21, 1903 (M/A Class I,A,1).

1905

6. Magnetization by Rapidly Changing Currents, and the Action of Rutherford-Marconi Magnetometers (in German), **E. Madelung.** *Annalen der Physik*, volume 17, 1905, pages 861–90.

1908

7*. Method of Automatic Regulation of Rectifiers and Rotary Converters, **F. B. Crocker.** United States patent 891,797, June 23, 1908 (M/A Class I,B′,1).

Paper 51-388, recommended by the AIEE Magnetic Amplifiers Committee and approved by the AIEE Technical Program Committee for presentation at the AIEE Fall General Meeting, Cleveland, Ohio, October 22–26, 1951. Manuscript submitted July 19, 1951; made available for printing September 14, 1951.

James G. Miles is with Engineering Research Associates, Inc., St. Paul, Minn.

1910

8. The Reduction of Hysteresis Loss by Means of High Frequency Current and the Behavior of Iron Under Longitudinal and Transverse Magnetization, **R. Goldschmidt.** *Elektrotechnische Zeitschrift,* March 3, 1910, page 218.

9. New Resonance Phenomena in Alternating Current Circuits (in German), **O. Martienssen.** *Physikalische Zeitschrift,* volume 11, May 1910, pages 448–60.

1912

10. Hysteresis Loss in Iron Taken Through Unsymmetrical Cycles of Constant Amplitude, **M. Rosenbaum.** *Journal,* Institution of Electrical Engineers, volume 48, January 1912, pages 534–45.

1913

11. Impedance Device for Use With Current-Rectifiers, **F. Conrad, Y. Sakai.** United States patent 1,075,404, October 14, 1913 (M/A Class III,C).

1914

12. Reactors, **J. B. Taylor.** *AIEE Transactions,* volume 33, part 2, 1914, pages 1545–46, discussion, page 1563.

1915

13. The Unsymmetrical Hysteresis Loop, **J. D. Ball.** *AIEE Transactions,* volume 34, part 2, 1915, pages 2693–720.

14. The Effect of Displaced Magnetic Pulsations on the Hysteresis Loss of Sheet Steel, **L. W. Chubb, T. Spooner.** *AIEE Transactions,* volume 34, part 2, 1915, pages 2671–92, discussion, pages 2716–20.

15. Measuring the Current in D-C Circuits, **O. A. Knopp.** *Electrical World,* October 2, 1915, page 751.

1916

16. A Magnetic Amplifier for Radio Telephony, **E. F. W. Alexanderson.** *Proceedings,* Institute of Radio Engineers, volume 4, February 1916, page 101.

17*. Controlling Alternating Currents, **E. F. W. Alexanderson.** United States patent 1,206,643, November 28, 1916 (M/A Class I,A,1,c).

18. A Magnetic Amplifier for Radio Telephony, **E. F. W. Alexanderson, S. P. Nixdorff.** *Proceedings,* Institute of Radio Engineers, volume 4, April 1916, pages 101–29.

19. Frequency Converter, **P. F. Pichon, A. Meissner.** United States patent 1,169,676, January 25, 1916 (M/A Class II,A).

20. Means for Changing the Frequency of Alternating Currents, **A. M. Taylor.** United States patent 1,180,800, April 25, 1916 (M/A Class II,A).

21. Means for Producing High Frequency Currents, **G. von Arco, A. Meissner.** United States patent 1,181,556, May 2, 1916 (M/A Class II,B).

1917

22. Design of Magnetic Control Appliances, **C. B. Bradish.** *General Electric Review,* 1917, pages 282–91.

23. Improvising a Current Limiting Reactor by D-C Excitation of a Pair of Transformers, **F. P. Coffin.** *General Electric Review,* volume 20, October, 1917, pages 821–24.

24. Frequency Conversion System for Electrical Oscillations, **T. Kujirai.** United States patent 1,215,820, February 13, 1917 (M/A Class II,B).

25*. Means for Controlling Alternating Currents, **M. Osnos.** United States patent 1,227,302, May 22, 1917 (M/A Class A).

1918

26*. High Frequency Detector, **G. W. Elmen.** United States patent 1,289,418, December 31, 1918 (M/A Class I,A,3,h).

27*. Modulating System, **R. V. L. Hartley.** United States patent 1,287,982, December 17, 1918 (M/A Class I,B′,1,c,h).

28. Circuitry and Construction of Saturable Reactors Controlled by Direct Current (in German), **M. Osnos.** *Elektrotechnische Zeitschrift,* volume 39, 1918, pages 205–07, 216–18.

29. Method for Multiplying the Frequency of Electric Currents, **I. Schoenberg.** United States patent 1,269,011, June 11, 1918 (M/A Class II,A,1).

30. Transmitting Apparatus for Wireless Telegraphy and Telephony, **G. von Arco, A. Meissner.** United States patent 1,267,018, May 21, 1918 (M/A Class II,B).

1919

31. Measuring Large Direct Currents at Great Distances (in German), **E. Besag.** *Elektrotechnische Zeitschrift,* volume 40, 1919, pages 436–37.

32. Transforming Device, **T. Bodde.** United States patent 1,298,443, March 25, 1919 (M/A Class I,B″,1).

1920

33*. Means for Controlling Alternating Currents, **E. F. W. Alexanderson.** United States patent 1,328,473, January 20, 1920 (M/A Class I,A,1,c,e,f).

34*. Method of and Means for Controlling High-Frequency Alternating Currents, **E. F. W. Alexanderson.** United States patent 1,328,610, January 20, 1920 (M/A Class I,A,1,c,e,f).

35*. Means for Controlling Alternating Currents, **E. F. W. Alexanderson.** United States patent 1,328,797, January 20, 1920 (M/A Class I,A,1,a,c,e).

36. Transoceanic Radio Communication, **E. F. W. Alexanderson.** *General Electric Review,* volume 23, October 1920, pages 794–803.

37. Electric Transformer, **H. B. Brooks.** United States patent 1,357,197, October 26, 1920 (M/A Class III,C).

38. The Alexanderson System for Radio Communication, **E. E. Bucher.** *General Electric Review,* volume 23, October 1920, pages 813–39.

39. Regulating System for Alternating Current Circuits, **E. J. Murphy, L. W. Thompson.** United States patent 1,337,942, April 20, 1920 (M/A Class I,B′,1).

40. Regulating System for Alternating Current Circuits, **L. W. Thompson.** United States patent 1,337,855, April 20, 1920 (M/A Class I,B′,1).

1921

41. Hysteresis Effects With Varying Superposed Magnetizing Forces, **W. Fondiller, W. H. Martin.** *AIEE Journal,* volume 40, February 1921, pages 149–58.

42. Process of and Apparatus for Producing Radiofrequency Current, **L. F. Fuller.** United States patent 1,381,626, June 14, 1921 (M/A Class II,B).

43. Current Regulator, **F. L. ReQua.** United States patent 1,390,543, September 13, 1921 (M/A Class I,A,1).

44. Regulator for Alternating Currents **E. R. Stoekle.** United States patent 1,376,978, May 3, 1921 (M/A Class I,B″,1).

1922

45*. Apparatus for Regulating the Voltage of Metal Vapor Rectifier Installations, **J. Jonas.** United States patent 1,434,346, October 31, 1922 (M/A Class I,A,1,a,b).

46. Regulating System for Alternating Current Circuits, **W. B. Kirke.** United States patent 1,414,652, May 2, 1922 (M/A Class I,B′,2).

47. Oscillating Circuits With Iron-Cored Coils (in German), **H. Schunk, J. Zenneck.** *Jahrbuch der drachtlosen Telegraphie und Telephonie,* volume 19, March 1922, pages 149–58.

48. Speed Regulation of Alternating Current Motors, **L. W. Thompson.** United States patent 1,408,844, March 7, 1922 (M/A Class I,A,1).

1923

49. Transmission System, **G. W. Elmen.** United States patent 1,470,965, October 16, 1923 (M/A Class I,B′,1,c,f).

50. Protective Device for Electric Distribution Systems, **A. S. FitzGerald.** United States patent 1,468,441, 1923 (M/A Class III,C).

51*. Modulating System, **R. V. L. Hartley.** United States patent 1,462,038, July 17, 1923 (M/A Class I,B′,2,c,f).

52. Control of High Frequency Currents by Means of Saturable Iron With Superposed Magnetization (in German), **L. Pungs.** *Elektrotechnische Zeitschrift,* volume 44, 1923, pages 78–81.

53. The Change of Flux in an Iron-Cored Coil With Superposed Direct-Current Magnetization (in German), **H. Schunk.** *Archiv fur Elektrotechnik,* volume 12, 1923, pages 428–33.

1924

54. Applications of Saturable Core Reactors and Regulators, **D. C. Blake.** *AIEE Transactions,* volume 43, 1924, pages 937–46.

55. Theory of D-C Excited Iron Core Reactors and Regulators, **A. Boyajian.** *AIEE Journal,* October 1924, pages 958–66, also *AIEE Transactions,* volume 43, 1924, pages 919–36.

56. Experimental Investigations of Oscillating Circuits With Iron-Cored Coils (in German), **L. Casper, F. Hubmann, J. Zenneck.** *Jahrbuch der drachtlosen Telegraphie und Telephonie,* volume 23, April–May 1924, pages 63–77.

57. Current Limiting Reactors, **M. Dann.** *AIEE Transactions,* volume 43, June 1924, pages 914–18.

58. Control of Electric Switches, **A. S. FitzGerald.** United States patent 1,508,174, September 9, 1924 (M/A Class I,B′,1).

59. Means for Transmitting Signals for Wireless Telegraphy, **H. Gerdien.** United States patent 1,486,134, March 11, 1924 (M/A Class I,B′,1,f).

60. Current-Limiting Reactors, **F. H. Kierstead, H. O. Stephens.** *AIEE Transactions,* volume 43, June 1924, pages 902–13.

61. Current-Limiting Reactor Characteristics, **S. I. Oesterreicher.** *AIEE Transactions,* volume 43, June 1924, pages 892–901.

62. Frequency Multiplier System, **M. Osnos.** United States patent 1,501,569, July 15, 1924 (M/A Class II,A,B).

63. Regulating Means for Direct-Current Circuits, **E. R. Stoekle.** United States patent 1,479,561, January 1, 1924 (M/A Class I,A,1).

1925

64. Effective Permeability and Iron Losses in Sheets and Wires Under Weak Magnetic Fields, **W. Cauer.** *Archiv fur Elektrotechnik,* volume 15, 1925, page 308.

65. Losses in Iron Under the Action of Superposed Alternating and Direct Current Excitations, **O. E. Charlton, J. E. Jackson.** *AIEE Transactions,* volume 44, June 1925, pages 824–29.

66. Multiplying Transformer, **W. Dornig.** United States patent 1,545,040, July 7, 1925 (M/A Class II, A).

67. Method and System for Amplifying Variable Currents, **G. W. Elmen, C. F. Ort.** United States patent 1,544,381, June 30, 1925 (M/A Classes I,A,1,e,f,h; I,A,3,e,f,h).

68. Protective Apparatus, **A. S. FitzGerald.** United States patent 1,539,658, May 26, 1925 (M/A Class III,C).

69. Apparatus for the Protection of Alternating Electric Current Systems, **A. S. FitzGerald.** United States patent 1,549,478, August 11, 1925 (M/A Class III,C).

70. Protective System, **A. S. FitzGerald.** United States patent 1,551,380, August 25, 1925 (M/A Class III,C).

71. Alternating-Electric-Current Protective Apparatus, **A. S. FitzGerald.** United States patent 1,560,934, November 10, 1925 (M/A Class III,C).

72. Effect of a Superposed Alternating Field on Apparent Magnetic Permeability and Hysteresis Loss, **T. Spooner.** *Physical Review,* volume 25, April 1925, pages 527–40.

1926

73. High Frequency Transformer, **W. Dornig.** United States patent 1,587,512, June 8, 1926 (M/A Class II,B).

74. Electromagnetic Device, **G. W. Elmen.** United States patent 1,586,885, June 1, 1926 (M/A Class II,B).

75. High Frequency Three-Phase System, **K. W. Wagner.** United States patent 1,597,937, August 31, 1926 (M/A Class II,A).

1927

76. Voltage Regulator, **E. F. W. Alexanderson.** United States patent 1,652,923, December 13, 1927 (M/A Class I,A,1).

77. Electrical Frequency-Multiplying System, **W. Dornig.** United States patent 1,618,411, February 22, 1927 (M/A Class II,A).

78. Frequency Reducing Arrangement, **J. G. Fallou.** United States patent 1,633,481, June 21, 1927 (M/A Class II,A).

79. Design of Reactances and Transformers Which Carry Direct Current, **C. R. Hanna.** *AIEE Transactions*, volume 46, February 1927, pages 155–60.

80. Arrangement for the Regulation of the Frequency in Frequency Changers, **K. Heegner.** United States patent 1,639,695, August 23, 1927 (M/A Class II,B).

81. Flame-Arc Furnace, **J. Jonas, W. Niggeler.** United States patent 1,650,072, November 22, 1927 (M/A Class I,A,1,a,b).

82. Apparatus for Influencing Alternating Currents, **L. Kuhn.** United States patent 1,653,859, December 27, 1927 (M/A Class I,A,2).

83. Electrical Apparatus, **M. Latour.** United States patent 1,637,828, August 2, 1927 (M/A Classes I; II,A).

84. Regulation of Electric Circuits, **F. L. ReQua.** United States patent 1,625,282, April 19, 1927 (M/A Class I,A,1).

85*. Magnetic Amplifier and Self-Modulator, **J. Slepian.** United States patent 1,645,302, October 11, 1927 (M/A Class I,A,1,a,c,e,f).

86. Magnetic Frequency Changer, **J. Slepian.** United States patent 1,645,303, October 11, 1927 (M/A Class II,B).

87. Properties and Testing of Magnetic Materials (book), **T. Spooner.** McGraw-Hill Book Company, Inc., New York, N. Y., 1927.

1928

88. Voltage Regulator, **G. B. Crouse.** United States patent 1,691,022, November 6, 1928 (M/A Class I,A,1).

89. Regulation of Electric Circuits, **C. T. Evans.** United States patent 1,668,711, May 8, 1928 (M/A Class I,A,1).

90. Earthing Reactor With D-C Excited Iron Core, **M. Ferada.** *Journal*, Institute of Electrical Engineers of Japan, volume 16, 1928, and *Elektrotechnische Zeitschrift*, volume 51, 1930, pages 1726–27.

91*. Arrangement for the Generation of Oscillations, **K. Heegner.** United States patent 1,656,195, January 17, 1928 (M/A Classes I,C; II,B).

92*. Magnetic Amplifying System, **R. A. Heising.** United States patent 1,654,932, January 3, 1928 (M/A Class I,A,1,a,c,e,f).

93. Circuit Arrangement for High-Frequency Systems With Frequency Amplification, **M. Osnos.** United States patent 1,682,768, September 4, 1928 (M/A Class II,B).

94. Electric System, **D. C. Prince.** United States patent 1,655,475, January 10, 1928 (M/A Class I,B′,1,a,c).

95. System of Distribution, **D. C. Prince.** United States patent 1,655,893, April 10, 1928 (M/A Class I,B′,1,c).

96. Electric Regulator, **H. M. Stoller.** United States patent 1,695,035, December 11, 1928 (M/A Class I,A,1).

1929

97*. Electrical Translating Apparatus, **P. H. Dowling.** United States patent 1,739,579, December 17, 1929 (M/A Class I,A,1,a,c,e,f,g).

98. Magnetic Alloys of Iron, Nickel, and Cobalt, **G. W. Elmen.** *Journal*, Franklin Institute, volume 207, May 1929, pages 583–617, also *Bell System Technical Journal*, volume 8, July 1929, pages 435–65.

99. Atomic Physics and Circuit Theory, **R. V. L. Hartley.** *Bell Laboratories Record*, volume 7, February 1929, page 231.

100. A Braun Hysteresigraph, **J. B. Johnson.** *Bell System Technical Journal*, volume 8, 1929, pages 286–308.

101. Coils With Saturated Iron Cores, **F. Ollendorf.** *Archiv fur Elektrotechnik*, volume 23, November 19, 1929, pages 162–80.

102. Arc Welding System, **J. F. Peters.** United States patent 1,709,629, April 16, 1929 (M/A Class III,A).

103. Regulator for Rectifier, **J. C. Schelleng.** United States patent 1,724,968, August 20, 1929 (M/A Class I,A,1,a).

104. Control System, **P. Thomas.** United States patent 1,730,254, October 1, 1929 (M/A Class I,A,1,a).

105*. Synchronizing Relay System, **P. Thomas.** United States patent 1,734,239, November 5, 1929 (M/A Class I,B′,1,d).

106. Generator Voltage Regulator, **C. P. West.** United States patent 1,710,755, April 30, 1929 (M/A Class I,A,1,a).

107. Self-Excited Oscillations in Circuits With Iron-Cored Coils (in German), von **H. Winter-Gunther.** *Jahrbuch der Drachtlosen Telegraphie und Telephonie*, volume 34, August 1929, pages 41–49.

1930

108. Signalling System, **E. T. Burton.** United States patent 1,763,880, June 17, 1930 (M/A Class II,B).

109. ———, **R. Goldschmidt.** *Zeitschrift fur Technische Physik*, volume 11, 1930, pages 8–12.

110. Effect of Direct Current in Transformer Windings, **E. L. Harder.** *Electric Journal*, October 1930.

111. Electric System, **T. C. Lennox.** United States patent 1,783,804, December 2, 1930 (M/A Class I,A,1).

112. Frequency Changer for Short Waves, **M. Osnos, R. Kummich.** United States patent 1,744,668, January 21, 1930 (M/A Class II,A).

113. Electrical System, **D. C. Prince.** United States patent 1,752,109, March 25, 1930 (M/A Classes I,A,1; II,A,B).

114. Variation of the Inductance of Coils Due to the Magnetic Shielding Effect of Eddy Currents in the Cores, **K. L. Scott.** *Proceedings*, Institute of Radio Engineers, volume 18, 1930, pages 1750–64.

115. Regulator System, **H. M. Stoller.** United States patent 1,763,017, June 10, 1930 (M/A Class I,A,3).

1931

116. A New System for D-C Arc Welding, **S. R. Bergman.** *AIEE Transactions*, volume 50, June 1931, pages 678–80.

117. Static Frequency Changer, **R. K. Bonell.** United States patent 1,819,069, August 18, 1931 (M/A Class II,A).

118. Mathematical Analyses of Non-Linear Circuits, **A. Boyajian.** *General Electric Review*, volume 34, 1931, pages 531–37, 745–51.

119. Protective Regulating Means for Alternating Current Rectifier, **W. W. Brown.** United States patent 1,808,522, June 2, 1931 (M/A Class I,A,1).

120. Electrical Translating Apparatus, **P. H. Dowling.** United States patent 1,788,152, January 6, 1931 (M/A Class I,A,1,c,e,f).

121*. Electrical Translating Apparatus, **P. H. Dowling.** United States patent 1,793,213, February 17, 1931 (M/A Class I,B″,3).

122. Electrical Translating Apparatus, **P. H. Dowling.** United States patent 1,812,202, June 30, 1931 (M/A Class I,A,1,c,e,f).

123*. Electrical Translating Apparatus, **P. H. Dowling.** United States patent 1,835,209, December 1931 (M/A Class I,A,1,4).

124. Electrical Regulator, **A. S. FitzGerald.** United States patent 1,824,714, September 22, 1931 (M/A Class I,A,1).

125. Apparatus for Measuring Direct Currents, **A. S. FitzGerald.** United States patent 1,825,514, September 29, 1931 (M/A Class I,A,3).

126. High Power Rectifier System, **L. A. Gebhard.** United States patent 1,822,618, September 8, 1931 (M/A Class I,A,1).

127. Arrangement for Switching in the High Frequency Machine to Frequency Transformers, **R. Herzog.** United States patent 1,830,758, November 10, 1931 (M/A Class II,A).

128. Electric Controlling Apparatus, **H. K. Kouyoumjian.** United States patent 1,812,299, June 30, 1931 (M/A Class I,B′,1,a; III,B).

129. Electric Controlling Apparatus, **H. K. Kouyoumjian.** United States patent 1,828,054, October 20, 1931 (M/A Class I,A,1,3).

130. Electric Controlling Apparatus, **H. K. Kouyoumjian.** United States patent 1,835,115, December 8, 1931 (M/A Class I,B′,1).

131. Electrical Translating Apparatus, **F. W. Lee.** United States patent 1,797,268, March 24, 1931 (M/A Class I,B″,1).

132. Iron-Core Static Frequency Changer, **N. E. Lindenblad.** United States patent 1,787,948, January 6, 1931 (M/A Class II,A).

133. Electric Controlling Apparatus, **V. L. Osgood.** United States patent 1,834,416, December 1, 1931 (M/A Class I,A,1).

134. Wave Modulation and Application Thereof, **E. Peterson.** United States patent 1,810,326, June 16, 1931 (M/A Class I,A,1,c,e,h).

135*. Electrical Translating Apparatus, **A. J. Sorensen.** United States patent 1,824,577, September 22, 1931 (M/A Class I,A,3,c,f).

136. Studies in Non-Linear Circuits, **C. G. Suits.** *AIEE Transactions*, volume 50, June 1931, pages 724–36.

137. Electrical Regulator and Regulating System, **L. W. Thompson.** United States patent 1,836,886, December 15, 1931 (M/A Class I,A,1).

138. Balance Coil or Reactor for Paralleling Transformers, **E. C. Wentz.** *Electric Journal*, volume 28, September 1931.

139. Direct Current Controlled Reactor, **E. C. Wentz.** *Electric Journal*, volume 28, October 1931, pages 561–63.

1932

140. Voltage-Regulating Auto-Transformer, **F. Bedell, J. Kuhn.** *Review of Scientific Instruments*, January 1932, pages 20–23.

141. Combination Electrical Regulator, **T. A. E. Belt.** United States patent 1,849,820, March 15, 1932 (M/A Class I,B″,1).

142. Electrical Regulator, **A. Boyajian, E. V. DeBlieux.** United States patent 1,870,093, August 2, 1932 (M/A Class I,A,1,e).

143. Zero Correcting Circuit, **E. T. Burton.** United States patent 1,858,037, May 10, 1932 (M/A Class III,B).

144. Electrical Circuit Regulator, **B. A. Case.** United States patent 1,874,240, August 30. 1932 (M/A Class I,A,1).

145. Voltage Regulator for Radio Transmitters, **R. L. Davis.** United States patent 1,839,869, January 5, 1932 (M/A Class I,A,1).

146*. Electrical Translating Apparatus, **P. H. Dowling.** United States patent 1,842,392, January 26, 1932 (M/A Class I,A,1,4,d).

147*. Electrical Translating Apparatus, **P. H. Dowling.** United States patent 1,862,211, June 7, 1932 (M/A Class I,A,1,a,e).

148*. Electrical Translating Apparatus, **P. H. Dowling.** United States patent 1,862,212, June 7, 1932 (M/A Class I,B′,1,4,d,e).

149*. Electrical Translating Apparatus, **P. H. Dowling.** United States patent 1,878,764, September 20, 1932 (M/A Class I,A,1,4,a,c,e).

150*. Electrical Translating Apparatus, **P. H. Dowling.** United States patent 1,891,044, December 13, 1932 (M/A Class I,B′,1,4,a,d).

151. Electrical Regulating Apparatus, **R. M. Gilson.** United States patent 1,865,562, July 5, 1932 (M/A Class I,A,1).

152. Electrical Translating Apparatus, **F. W. Lee.** United States patent 1,855,639, April 26. 1932. Reissued as United States patent Re, 19,129, April 3, 1934.

153. Electrical Frequency Changer, **O. P. McCarty, A. Boyajian.** United States patent 1,875,250, August 30, 1932 (M/A Class II,A,B).

154. Rectification of Alternating Currents, **K. B. McEachron.** United States patent 1,857,160, May 10, 1932 (M/A Class III,A).

155*. Magnetic Wave-Amplifying Repeater, **E. Peterson.** United States patent 1,884,844, October 25, 1932 (M/A Class I,C,1,f).

156*. Magnetic Amplifier, **E. Peterson.** United States patent 1,884,845, October 25, 1932 (M/A Class I,C,1,f).

157. Controller for Electric Motors, **E. V. Seegar.** United States patent 1,848,847, March 8, 1932 (M/A Class I,A,1).

158. Measuring Core Loss at High Densities, **B. M. Smith, C. Concordia.** *Electrical Engineering*, January 1932, pages 36–38.

159. Electrical Translating Apparatus, **A. J. Sorensen, P. H. Dowling.** United States patent 1,862,203, June 7, 1932 (M/A Class I,A,2,3,c,f).

160*. Electrical Translating Apparatus, **A. J. Sorensen.** United States patent 1,862,204, June 7, 1932 (M/A Class I,A,4,a,d).

161. Motor Control System, **H. M. Stoller.** United States patent 1,849,646, March 15, 1932 (M/A Class I,A,1).

162. Flashing Lights Without Moving Parts, **C. G. Suits.** *Electrical World*, volume 99, June 1932, pages 1098–99, and volume 101, March 1933, page 321.

163. Oscillation Generator, **C. G. Suits.** United States patent 1,877,703, September 13, 1932 (M/A Class II,A).

164. Control of Constant Current Circuits, **C. G. Suits.** United States patent 1,885,155, November 1, 1932 (M/A Classes I,A,1; II,A).

165. Electrical Regulating Means, **L. W. Thompson.** United States patent 1,843,745, February 2, 1932 (M/A Class I,A,B′,1,4).

166. Electrical Control System, **L. W. Thompson** United States patent 1,844,704, February 9, 1932 (M/A Class I,A,3).

167. Electrical Regulating Means, **L. W. Thompson.** United States patent 1,878,350, September 20, 1932 (M/A Class I,A,1,e).

168. Battery Charging Apparatus, **K. T. Williamson, O. I. Seaverson.** United States patent 1,861,516, June 7, 1932 (M/A Class I,A,1).

169*. Electric Regulator, **M. Zucker.** United States Patent 1,851,692, March 29, 1932 (M/A Class I,A,3).

1933

170. Automatic Railway Block Signalling System, **H. D. Abernethy.** United States patent 1,936,705, November 28, 1933 (M/A Class I,A,1).

171. Electrical Control System, **W. H. Arkenburgh.** United States patent 1,902,485, March 21, 1933 (M/A Class I,A,1).

172. Means for Voltage Regulation in Alternating Current Supplies, **R. I. Bagnall.** United States patent 1,896,995, February 7, 1933 (M/A Class III,A).

173. Phase Shifting Circuits, **B. D. Bedford.** United States patent 1,918,173, July 11, 1933 (M/A Class II,B).

74. Frequency Changer System, **E. T. Burton.** United States patent 1,917,921, July 11, 1933 (M/A Class II,B).

175. Electric Wave Transmission System, **E. T. Burton.** United States patent 1,936,153, November 21, 1933 (M/A Class II,A,B).

176*. Electrical Translating Apparatus, **P. H. Dowling.** United States patent 1,910,381, May 23, 1933 (M/A Class I,A,4).

177. Rectifier and Reactance Combinations Produce Interesting Non-Linear Circuits. *Power Plant Engineering*, volume 37, May 1933, pages 219–20.

178. Electric Translation Circuits, **A. S. FitzGerald.** United States patent 1,893,766, January 10, 1933 (M/A Class I,A,1,4).

179. Electric Regulator, **A. S. FitzGerald, F. L. Gaines.** United States patent 1,893,767, January 10, 1933 (M/A Class I,A,1,3,c).

180. Electric Regulator, **A. S. FitzGerald.** United States patent 1,893,768, January 10, 1933 (M/A Class I,A,3).

181*. Electric Control System, **A. S. FitzGerald.** United States patent 1,914,201, June 13, 1933 (M/A Class I,A,1,4).

182. Exercising Apparatus, **A. S. FitzGerald.** United States patent 1,919,627, July 25, 1933 (M/A Class I,A,3).

183. Electric Fault Responsive Apparatus, **A. S. FitzGerald.** United States patent 1,929,059, October 3, 1933 (M/A Classes I,A,1; II,B).

184. Battery Charging Regulation, **R. M. Gilson.** United States patent 1,916,307, July 4, 1933 (M/A Class I,A,1).

185. Electric Regulating System, **R. C. Griffith.** United States patent 1,926,280, September 12, 1933 (M/A Class I,A,3,e).

186. New Developments in Synchronous Motor Control, **M. N. Halberg.** *General Electric Review*, volume 36, May 1933, pages 244–49.

187. Method of and Apparatus for Controlling Electric Circuits, **R. B. Hunter.** United States patent 1,931,799, October 24, 1933 (M/A Class I,A,1).

188. Motor Starter, **B. W. Jones.** United States patent 1,905,720, April 25, 1933 (M/A Class I,A,1).

189. Electric Controlling Apparatus, **H. K. Kouyoumjian.** United States patent 1,896,316, February 7, 1933 (M/A Class III,B).

190. Principles of Radio Communications (book), **J. H. Morecroft.** John Wiley and Sons, Inc., New York, N. Y., 1933, page 752.

191*. Control System for Alternating Current Motors, **B. V. Nagashev.** United States patent 1,920,803, August 1, 1933 (M/A Class I,A,3).

192*. Variable Reactance Device, **A. Schmidt, Jr.** United States patent 1,921,703, August 8, 1933 (M/A Class I,A,1).

193. Electric Valve Circuits, **A. Schmidt, Jr.** United States patent 1,935,460, November 14, 1933 (M/A Class III,A).

194. An Identification Tag for the Airport, **W. P. Simpson.** *General Electric Review*, volume 36, July 1933, pages 326–27.

195. Voltage Compensator, **J. G. Sola.** United States patent 1,893,251, January 3, 1933 (M/A Class III,B).

196*. Electrical Translating Apparatus, **A. J. Sorensen, P. H. Dowling.** United States patent 1,914,220, June 13, 1933 (M/A Class I,A,B′, 2,3,4,c,e).

197. Nonlinear Circuits Applied to Relays, **C. G. Suits.** *Electrical Engineering*, volume 52, April 1933, pages 244–46.

198. Nonlinear Circuit, **C. G. Suits.** United States patent 1,921,786, August 8, 1933. Reissued as United States patent Re. 20,317, March 30, 1937, which see.

199. Pulsation Apparatus, **C. G. Suits.** United States patent 1,921,787, August 8, 1933 (M/A Class II,A).

200. Electric Control System, **C. G. Suits.** United States patent 1,921,788, August 8, 1933 (M/A Class III,A).

201. Electrical Time Delay Apparatus, **C. G. Suits.** United States patent 1,940,335, December 19, 1933 (M/A Class I,A,1,a).

202. Mathematical Expression of a Saturation Curve, **C. M. Summers.** *General Electric Review*, volume 36, April 1933, pages 182–85.

203. Current-Controlling Apparatus, **R. J. Wensley.** United States patent 1,930,545, October 17, 1933 (M/A Class I,A,1).

1934

204. Two Applications of Non-Linear Circuits, **T. M. Austin, F. W. Cooper.** *Electrical Engineering* (*AIEE Transactions*), volume 53, February 1934, pages 293–300.

205. Dry Rectifier, **F. Bauer, D. W. Kafka.** United States patent 1,947,075, February 13, 1934 (M/A Classes I,A,1; I,B′,1).

206. Motor-Control Scheme, **M. J. Brown.** United States patent 1,955,322, April 17, 1934 (M/A Class I,A,2,d).

207. Voltage Regulation System, **C. F. Cairns.** United States patent 1,942,535, January 9, 1934 (M/A Class III,B).

208. Voltage Regulator, **G. B. Crouse, J. L. Jatlow.** United States patent 1,952,974, March 27, 1934 (M/A Class I,A,1).

209. Automatic Reclosing Circuit Breaker System, **A. S. FitzGerald.** United States patent 1,944,072, January 16, 1934 (M/A Class I,A,3).

210. Regulating System, **A. S. FitzGerald.** United States patent 1,948,372, February 20, 1934 (M/A Class I,A,3).

211. Electroresponsive System, **A. S. FitzGerald.** United States patent 1,980,395, November 13, 1934 (M/A Classes I,A,4; I,A,1,c).

212. Multiple Circuit Proportional Control System, **A. S. FitzGerald.** United States patent 1,985,562, December 25, 1934 (M/A Class I,A,1,c).

213. Electron Tube Motor Control, **F. H. Gulliksen.** *Electronics*, volume 7, June 1934, page 179.

214. Permeability Changes in Ferromagnetic Materials—Heat Treated in Magnetic Fields, **G. A. Kelsall.** *Physics*, volume 5, July 1934, pages 169–72.

215. Shunt Resistors for Reactors—II, **F. H. Kierstead, L. V. Bewley.** *Electrical Engineering* (*AIEE Transactions*), volume 53, March 1934, pages 411–18.

216*. Electrical Translating Apparatus, **F. W. Lee.** United States patent reissue Re. 19,129, April 3, 1934 (from original United States patent 1,855,639, April 26, 1932) (M/A Class I,A,1,4).

217. Electric Controlling Apparatus, **F. G. Logan.** United States patent 1,963,093, June 19, 1934 (M/A Class I,A,1,a).

218. Electric Controlling Apparatus, **F. G. Logan.** United States patent 1,977,193, October 16, 1934 (M/A Class I,A,1).

219*. Electric Controlling Apparatus, **F. G. Logan.** United States patent 1,981,921, November 27, 1934 (M/A Class I,A,1,d).

220. A New Kipp Regulating Coil (in German), **K. Maier.** *Elektrotechnische Zeitschrift*, volume 55, 1934, pages 1026–29.

221. Electric Motor, **B. V. Nagashev.** United States patent 1,969,520, August 7, 1934 (M/A Class I,A,1).

222. Method of Producing an Unsymmetrical Alternating Voltage, **O. Neiss.** United States patent 1,968,346, July 31, 1934 (M/A Class III,B).

223*. Rectifier System, **J. R. Power.** United States patent 1,943,088, January 9, 1934 (M/A Class I,A,3,e).

224. An Experimental Study of Ferro-Resonance (in French). **E. Roulle.** *Revue Generale de l'Electricite*, volume 36, November 24, 1934, pages 715–38; December 1, 1934, pages 763–80; December 8, 1934, pages 795–819; December 15, 1934, pages 841–58.

225. Voltage Regulation by Means of Transformers Excited by Direct Current (in German), **W. Scheuring.** *Elektrotechnik und Maschinenbau*, volume 52, 1934, pages 326–28.

226. Regulated Rectifier Circuit, **H. M. Stoller.** United States patent 1,965,439, July 3, 1934 (M/A Class I,A,3,a).

227*. Control Apparatus for Alternating Current Circuits, **C. G. Suits.** United States patent 1,968,576, July 21, 1934 (M/A Class I,A,1,4,a,e).

228. Voltage Regulating Apparatus, **W. S. Werner.** United States patent 1,967,108, July 17, 1934 (M/A Class III,C).

1935

229. Voltage Regulator, **R. O. Askey.** United States patent 1,995,530, March 26, 1935 (M/A Class I,B′,1,4).

230. Alternating Fields and Eddy Currents in Solid Iron at High Magnetic Saturation, **J. B. Barth.** *Elektroteknish Tidsskrift*, volume 48, March 5, 1935, pages 85–87; and volume 48, March 15, 1935, pages 98–99.

231. Electric Valve Converting System, **B. D. Bedford.** United States patent 1,985,912, January 1, 1935. Reissued as United States patent Re. 20,493, September 7, 1937.

232. Electric Valve Translating Circuit, **B. D. Bedford.** United States patent 1,986,617, January 1, 1935 (M/A Class II,B).

233. Present Status of Electromagnetic Theory, **R. M. Bozorth.** *Electrical Engineering (AIEE Transactions)*, volume 54, November 1935, pages 1251–61.

234. Design of Saturable Core Reactors, **M. J. Brown.** *Radio News*, volume 16, March 1935, pages 540–41.

235. Application of Electron Tubes in Industry, **D. E. Chambers.** *Electrical Engineering (AIEE Transactions)*, volume 54, January 1935, pages 82–92.

236. Electrical Transmitter, **A. M. Cravath.** United States patent 1,987,730, January 15, 1935 (M/A Class I,A,B′,1,c).

237. Means for Controlling the Terminal Pressure of an Electric Device, **P. R. Dijksterhuis.** United States patent 2,018,348, October 22, 1935 (M/A Class I,A,1).

238. Magnetic Alloys of Iron, Nickel and Cobalt, **G. W. Elmen.** *Electrical Engineering (AIEE Transactions)*, volume 54, December 1935, pages 1292–99.

239. Electrical Regulator, **A. A. Emmerling.** United States patent 1,996,041, March 26, 1935 (M/A Class I,A,1).

240. Electric Valve Circuit, **A. S. FitzGerald.** United States patent 1,988,271, January 15, 1935 (M/A Class I,A,1).

241*. Electric Control System, **A. S. FitzGerald.** United States patent 2,021,099, November 12, 1935 (M/A Class I,A,4).

242*. Automatic Regulating System, **A. S. FitzGerald.** United States patent 2,026,124, December 31, 1935 (M/A Class I,A,3,4).

243. Regulator System, **L. L. Fountain.** United States patent 2,015,556, September 24, 1935 (M/A Class I,A,1).

244. Induction of D-C Saturable Reactors, **V. D. Gussakov.** *Elektrichestvoo*, October 1935, pages 47–50.

245. Ferromagnetic Distortion of a Two-Frequency Wave, **R. M. Kalb, W. R. Bennett.** *Bell System Technical Journal*, volume 14, April 1935, pages 322–59.

246. Hysteretic Modulation, I and II, **R. M. Kalb, W. R. Bennett.** *Bell Laboratories Record*, volume 14, October 1935, pages 39–44.

247*. Electric Controlling Apparatus, **F. G. Logan.** United States patent 1,986,112, January 1. 1935 (M/A Class, I,A,1,4,g).

248*. Electric Controlling Apparatus, **F. G. Logan.** United States patent 1,997,179, April 9, 1935 (M/A Class I,A,1,b,d).

249. Electric Controlling Apparatus, **F. G. Logan.** United States patent 2,003,945, June 4, 1935 (M/A Class I,A,1,b,d).

250. Subharmonics in Forced Oscillations in Dissipative Systems, **P. O. Pederson.** *Journal*, Acoustical Society of America, volume 6, April 6, 1935, pages 227–28, and volume 7, July 7, 1935, pages 64–70.

251. Regulated Rectifier, **J. R. Power.** United States patent 2,000,189, May 7, 1935 (M/A Class I,A,3,c).

252. Power Supply System, **W. H. Reichard.** United States patent 1,995,652, March 26, 1935 (M/A Class I,B′,1,d).

253. Regulating System, **O. Schmutz.** United States patent 1,997,657, April 16, 1935 (M/A Class I,A,2,c,d).

254. Coding Apparatus, **W. P. Simpson.** United States patent 2,010,610, August 6, 1935 (M/A Class II,A).

255. Motor Controller, **C. Stansbury.** United States patent 2,013,221, September 3, 1935. Reissued as United States patent Re. 19,853, February 11, 1936.

256. Current Regulation With Thermal Elements and Magnetic Amplifiers (in German), **M. Steenbeck, O. Schmutz.** *Siemens Zeitschrift*, volume 15, 1935, pages 201–04.

257. Voltage Regulator, **H. M. Stoller.** United States patent 1,996,495, April 2, 1935 (M/A Class I,B′,1,4).

258. Electric Translating Circuit, **C. G. Suits.** United States patent 1,989,500, January 29, 1935 (M/A Class I,A,1,d).

259. Control of Constant Current Circuits, **C. G. Suits.** United States patent 2,006,970, July 2, 1935 (M/A Classes I,A,1; II,A).

260. Electric Pulsating Apparatus, **C. G. Suits.** United States patent 2,010,614, August 6, 1935 (M/A Class II,A).

261. Electrical System Providing Sequence Operation, **C. G. Suits.** United States patent 2,011,380, August 13, 1935 (M/A Class I,A,1,a,e).

262. Electric Circuit Control Means, **C. G. Suits.** United States patent 2,021,753, November 19, 1935 (M/A Class II,A).

263*. Direction Responsive System, **H. P. Thomas.** United States patent 2,016,977, October 8, 1935 (M/A Class I,A,3,b,g).

1936

264. On the Control of an Electrical Machine (in Dutch). Allgemeine Elektricitats Gesellschaft, Netherlands patent 38,015, April 15, 1936 (M/A Class II,A).

265*. Magnetic Field Direction and Intensity Finder, **H. Antranikian.** United States patent 2,047,609, July 14, 1936 (M/A Class I,B′,2,b,c).

266*. Electric Circuit Control Means, **A. Boyajian.** United States patent 2,040,684, May 12, 1936 (M/A Classes I,A,1,a,c,e; III,A).

267. Heat Treatment of Magnetic Materials in a Magnetic Field, I and II, **R. M. Bozorth, J. F. Dillinger.** *Metal Progress*, 1936.

268. Potential Control System, **B. S. Burke, C. V. Heck.** United States patent 2,057,512, October 13, 1936 (M/A Class I,A,1).

269. Frequency Tripling Transformers, **J. L. Cantwell.** *Electrical Engineering (AIEE Transactions)*, volume 55, July 1936, pages 784–90.

270. Saturable Reactor Starters for Synchronous Motors, **C. W. Drake.** *Electric Journal*, volume 33, April 1936, pages 178–80.

271. Angle Switching of Synchronous Motors, **C. W. Drake.** *Electric Journal*, volume 33, May 1936, page 213.

272. Electrical Standard, **D. V. Edwards.** United States patent 2,040,768, May 12, 1936 (M/A Class III,B).

273*. Magnetic Amplifier, **A. S. FitzGerald.** United States patent 2,027,311, January 7, 1936 (M/A Class I,A,1,2,3,c).

274*. Magnetic Amplifying and Control System, **A. S. FitzGerald.** United States patent 2,027,312, January 7, 1936 (M/A Class I,A,1,a,c).

275. Descriptive Bulletin Number DB-61, *SATUREX* (book), **A. S. FitzGerald.** Haverford College, Haverford, Pa., June 1936.

276. Automatic Circuit Breaker System, **A. S. FitzGerald.** United States patent 2,050,882, August 1, 1936 (M/A Class I,A,3).

277. Apparatus for Automatic Regulation of Rectifiers, **R. M. Gilson.** United States patent 2,028,541, January 21, 1936 (M/A Class I,B′,1).

278. Oscillations in Systems With Non-Linear Reactance, **R. V. L. Hartley.** *Bell System Technical Journal*, volume 15, July 1936, pages 424–40.

279. Oscillations in Electromechanical Systems, **L. W. Hussey, L. R. Wrathall.** *Bell System Technical Journal*, volume 15, July 1936, pages 441–45.

280*. Direct Current Indicator, **C. W. LaPierre.** United States patent 2,053,154, September 1, 1936 (M/A Class I,B′,2,c,f).

281. Reactors in D-C Service, **R. Lee.** *Electronics*, September 1936, pages 18–20, 76.

282*. Control System, **A. R. Locke.** United States patent 2,044,006, June 16, 1936 (M/A Class I,A,1).

283*. Electric Controlling Apparatus, **F. G. Logan.** United States patent 2,036,708, April 7, 1936 (M/A Class I,A,1,4,d).

284. Rectifier Regulator, **F. G. Logan.** United States patent 2,040,492, May 12, 1936 (M/A Class I,A,1,b,d).

285. Electric Controlling Apparatus, **F. G. Logan.** United States patent 2,047,915, July 14, 1936 (M/A Class I,A,1,4).

286. Electrical Control for Varying Lighting Intensities, **S. R. McCandless, F. M. Wolff.** *Transactions*, Illumination Engineering Society, volume 31, January 1936, pages 41–68.

287. Control System for Arc Welding, **W. E. Pakala.** United States patent 2,036,233, April 7, 1936 (M/A Class I,A,1).

288. Electrical Engineers' Handbook—Electrical Communications and Electronics (book), **H. Pender, K. McIlwain.** John Wiley and Sons, Inc., New York, N. Y., 1936, pages 4–23.

289. Eddy Currents in Composite Laminations, **E. Peterson, L. R. Wrathall.** *Proceedings*, Institute of Radio Engineers, volume 24, 1936, pages 275–86.

290. Electric Control Means, **H. T. Seely.** United States patent 2,031,509, February 18, 1936 (M/A Class I,A,1).

291. Motor Controller, **C. Stansbury.** United States patent Re. 19,853, February 11, 1936 (Reissue of United States patent 2,013,221, September 3, 1935) (M/A Class I,A,1).

292. Secret Signalling, **A. H. Turner.** United States patent 2,026,758, January 7, 1936 (M/A Class I,A,1,c,e).

293. A Generator-Voltage Regulator Without Moving Parts, **C. P. West, I. D. Applegate.** *Electric Journal*, volume 33, 1936, pages 181–83.

294. Arrangement for Maintaining Constant Line Power Transmission, **W. Wiskott, E. Friedlander.** United States patent 2,046,496, July 7, 1936 (M/A Class I,A,1,c).

295. Regulating System, **E. R. Wolfert, E. C. Wentz.** United States patent 2,039,044, April 28, 1936 (M/A Classes I,A,2; I,B′,2).

1937

296. D-C Controlled Reactors, **C. V. Aggers, W. E. Pakala.** *Electric Journal*, February 1937, pages 55–57.

297. Voltage Regulator for Rectifier Circuits, **C. V. Aggers.** United States patent 2,085,-061, June 29, 1937 (M/A Class I,A,1,a,b,d,e).

298. Electrical Control System, **R. D. Amsden.** United States patent 2,082,607, June 1, 1937 (M/A Classes I,A,1,b; I,B′,1,a,c).

299. Electric Valve Converting System, **B. D. Bedford.** United States patent 1,985,912, January 1, 1935. Reissued as United States patent Re. 20,493, September 7, 1937, which see (M/A Class II,B).

300. Constant Current Magnetic Bridge, **B. D. Bedford.** United States patent 2,103,996, December 26, 1937 (M/A Class II,B).

301. Electric Control Circuit, **B. D. Bedford.** United States patent 2,103,997, December 28, 1937 (M/A Class II,B).

302. Control System, **W. T. Croden.** United States patent 2,086,120, July 6, 1937. Reissued as United States patent Re. 21,407, March 26, 1940.

303. Reactance Amplifiers, Editor. *Electronics*, volume 10, October 1937, pages 28–30.

304*. System of Electrical Distribution, **M. A. Edwards, G. A. Kane.** United States patent 2,084,900, June 22, 1937 (M/A Class I,A,1,e).

305. Electric Circuit Control Means, **A. A. Emmerling.** United States patent 2,074,145, March 16, 1937 (M/A Class III,A).

306. Reactance Amplifiers, **A. S. FitzGerald.** *Electronics*, volume 10, 1937, pages 28–30.

307. Electric Elevator Indicating System, **A. S. FitzGerald.** United States patent 2,074,835, March 23, 1937 (M/A Class I,A,3).

308. Control Scheme Uses Tubeless Amplifier, **A. S. FitzGerald.** *Electrical World*, volume 107, May 8, 1937, page 1592.

309. Traffic Control System, **A. S. FitzGerald.** United States patent 2,100,313, November 30, 1937 (M/A Classes I,A,1; III,C).

310. Electrical Control Circuit, **C. B. Foos.** United States patent 2,079,500, May 4, 1937 (M/A Class I,A,1).

311. Voltage Regulating Equipment, **J. W. Graff, S. J. Spurgeon.** United States patent 2,079,206, May 4, 1937 (M/A Classes I,A,1; III,C).

312. Saturable Reactors Magnetized by Direct Current (in German), **G. Hauffe.** *Elektrotechnische Zeitschrift*, volume 58, 1937, pages 937–40, 989–90.

313. Heavy Current Engineering Application of Saturable Coils Magnetized by Direct Current (in German), **G. Hauffe.** *Elektrotechnische Zeitschrift*, volume 58, 1937, pages 990–93.

314. Energizing System, **H. C. Jenks.** United States patent 2,100,715, November 30, 1937 (M/A Class I,A,1).

315. A Simple Direct-Current Converter With Pure Current Conversion Characteristics (in German), **W. Kramer.** *Elektrotechnische Zeitschrift*, volume 58, 1937, pages 1309–13.

316. Electric Controlling Apparatus, **F. G. Logan.** United States patent 2,067,143, January 5, 1937 (M/A Class I,A,1).

317*. Electric Controlling Apparatus, **F. G. Logan.** United States patent 2,068,188, January 19, 1937 (M/A Class I,A,1,a,b,d).

318. Voltage Regulator, **F. G. Logan.** United States patent 2,074,552, March 23, 1937 (M/A Class I,A,1,b,d).

319. Electric Controlling Apparatus, **F. G. Logan.** United States patent 2,078,880, April 27, 1937 (M/A Class I,A,1,b,c,d).

320. Electric Controlling Apparatus, **F. G. Logan.** United States patent 2,092,319, September 7, 1937 (M/A Class I,A,1,b).

321. Phase Shifting Circuit, **E. E. Moyer.** United States patent 2,078,152, April 20, 1937 (M/A Class I,A,3).

322. The Inductance of Iron-Cored Coils Carrying Direct Current, **G. F. Partridge.** *Philosophical Magazine*, volume 23, 1937, pages 99–106.

323. Motor Control System, **W. R. Perry.** United States patent 2,102,911, December 21, 1937 (M/A Class I,A,1).

324. Magnetic Generation of a Group of Harmonics, **E. Peterson, J. M. Manley, L. R. Wrathall.** *Electrical Engineering* (*AIEE Transactions*), volume 56, August 1937, pages 995–1001, also *Bell System Technical Journal*, volume 16, October 1937, pages 437–55.

325. Electrical Control System, **H. E. Phillips.** United States patent 2,079,466, May 4, 1937 (M/A Class I,A,1).

326. Regulating System, **L. V. R. Philpott.** United States patent 2,066,943, January 5, 1937 (M/A Class I,A,1).

327. System of Electrical Distribution, **A. Schmidt, Jr.** United States patent 2,084,870, June 22, 1937 (M/A Class I,A,1,c).

328. Frequency Reducing System, **C. P. Stocker.** United States patent 2,088,618, August 3, 1937 (M/A Class II,A,B).

329. Frequency Reducing System, **C. P. Stocker.** United States patent 2,088,619, August 3, 1937 (M/A Class II,A).

330. Frequency Changing System, **C. P. Stocker.** United States patent 2,088,620, August 3, 1937 (M/A Class II,B).

331*. Non-Linear Circuit, **C. G. Suits.** United States patent 1,921,786, August 8, 1933. Reissued as United States patent Re. 20,317, March 30, 1937 (M/A Class I,A,1,e).

332. Subharmonics in Circuits Containing Iron-Cored Inductors, **Irven Travis, C. N. Weygandt.** *Electrical Engineering* (*AIEE Transactions*), volume 57, August 1938, pages 423–31.

333. The Magnetic Amplifier, **K. Vulfson.** *Journal of Technical Physics*, volume 7, 1937, page 1170.

334. A Qualitative Theory of Saturable Reactors Magnetized by Direct Current (in German), **T. Wasserrab.** *Archiv fur Elektrotechnik*, volume 31, December 1937, pages 814–21.

335. Voltage Regulator Using Magnetic Saturation, **K. J. Way.** *Electronics*, volume 10, July 1937, pages 14–16.

336. Regulating System, **C. P. West.** United States patent 2,066,919, January 5, 1937 (M/A Class I,A,1).

337. Carrier Generation, **L. R. Wrathall.** *Bell Laboratories Record*, July 1937, page 357.

338. Constant Current System, **H. E. Young.** United States patent 2,085,060, June 29, 1937 (M/A Class I,A,1).

1938

339. Battery Charging Regulator, **C. V. Aggers.** United States patent 2,114,827, April 19, 1938 (M/A Class I,A,1,a).

340. Electric Valve Circuits, **B. D. Bedford.** United States patent 2,126,603, August 9, 1938 (M/A Class III,B).

341. Electric Control and Indicating Circuits, **B. D. Bedford.** United States patent 2,130,412, September 20, 1938 (M/A Class III,B).

342. Alternating Current Control Apparatus, **T. A. Behrens.** United States patent 2,107,360, February 8, 1938 (M/A Class I,A,1,e).

343*. Magnetic Device, **E. M. Boardman.** United States patent 2,108,642, February 15, 1938 (M/A Class I,B′,2,b,f,g).

344. On a Method of Amplifying a D-C Voltage, **H. Chonan, Y. Watanabe.** *Nippon Electrical Communication Engineering*, April 1938, page 184.

345*. Electric Regulator, **P. H. Craig.** United States patent 2,138,732, November 29, 1938 (M/A Class I,A,B′,1,d,e).

346*. Change Amplifying Means, **J. W. Dawson.** United States patent 2,140,349, December 13, 1938 (M/A Class I,A,1,a,c).

347. Electric Control System, **A. S. FitzGerald.** United States patent 2,129,920, September 13, 1938 (M/A Class I,A,1,4,a,c).

348. Regulating Means for Current Rectifying or Converting Apparatus, **H. Forssell, H. Ofverholm.** United States patent 2,128,771, August 30, 1938 (M/A Class I,A,3).

349. Electrical Regulating Apparatus for Rectifiers, **L. K. Hedding.** United States patent 2,136,243, November 8, 1938 (M/A Class I,B″,1,a).

350. The Saturation Choke Coil as a Power Amplifier, **G. R. Herzenberg.** *Avtomatika and Telemechanika*, 1938, page 35.

351. Frequency Changer System, **R. M. Kalb.** United States patent 2,112,533, March 29, 1938 (M/A Class II,B).

352. Resonance Theory of Series Non-Linear Circuits, **E. G. Keller.** *Journal*, Franklin Institute, volume 225, May 1938, page 561.

353. Direct Current Measuring Means, **W. Kramer.** United States patent 2,137,878, November 22, 1938 (M/A Class I,A,1,d,e).

354. A New Direct Voltage Converter for Measuring High Direct Voltages (in German), **W. Kramer.** *Elektrotechnische Zeitschrift*, volume 59, 1938, pages 1295–98.

355*. Electric Controlling Apparatus, **F. G. Logan.** United States patent 2,118,440, May 24, 1938 (M/A Class I,A,1,4,d).

356*. Electric Controlling Apparatus, **F. G. Logan.** United States patent 2,126,790, August 16, 1938 (M/A Class I,A,1,b,d).

357. Investigation of High Frequency Coils With Iron Tape Cores Under Variable Direct-Current Magnetization (in German), **G. Maus.** *Elektrische Nachrichten Technik*, volume 15, 1938, pages 369–79.

358. Critical Conditions in Ferroresonance, **P. H. Odessey, E. Weber.** *Electrical Engineering* (*AIEE Transactions*), volume 57, August 1938, pages 444–52.

359. A Controlled Amplifier (in German), **K. Reuss.** *Archiv fur Elektrotechnik*, volume 33, 1938, pages 777–800.

360. Electric Control System, **A. Schmidt, Jr.** United States patent 2,112,051, March 22, 1938 (M/A Class II,B).

361. Electric Valve Circuits, **C. G. Suits** United States patent 2,137,148, November 15 1938 (M/A Class II,A).

362. The Generalized Solution for the Critical Conditions of the Ferroresonant Parallel Circuit, **W. T. Thomson.** *AIEE Transactions*, volume 58, 1939, pages 743–46.

363. Resonant Nonlinear Control Circuits, **W. T. Thomson.** *Electrical Engineering* (*AIEE Transactions*), volume 57, August 1938, pages 469–76.

364. Subharmonics in Circuits Containing Iron-Cored Reactors, **Irven Travis, C. N. Weygandt.** *Electrical Engineering* (*AIEE Transactions*), volume 57, August 1938, pages 423–31. Part II by **Irven Travis.** *AIEE Transactions*, volume 58, 1939, pages 735–42.

365. Contactless Regulator, **C. E. Valentine, V. E. Thornburg.** United States patent 2,137,068, November 15, 1938 (M/A Class I,A,1).

366. Static Transformer for Direct Current (in French), **J. Vassiliere-Arlhac.** *Bulletin*, Societe Francaise des l'Electriciens, volume 8, 1938, pages 834–38, also *Revue Generale de Electricite*, volume 46, 1939, pages 54–56.

367. Harmonic Producer, **L. R. Wrathall.** United States patent 2,117,752, May 17, 1938 (M/A Class II,A).

1939

368. Indicating Device, **L. E. Barton.** United States patent 2,166,674, July 18, 1939 (M/A Class I,A,1).

369. Electric Valve Circuit, **B. D. Bedford.** United States patent 2,157,812, May 9, 1939 (M/A Class II,B).

370. Electric Control and Indicating Means, **B. D. Bedford.** United States patent 2,169,866, August 15, 1939 (M/A Class III,B).

371*. Magnetic Impulse Storing Device, **E. T. Burton.** United States patent 2,147,688, February 21, 1939 (M/A Class I,B′,1,2,a,b).

372*. Magnetic Device, **E. T. Burton.** United States patent 2,164,383, June 4, 1939 (M/A Class I,B′,1,2,a,b,c,e,f).

373. The Transductor, an Electrical Control Apparatus With Multiple Applications (in Swedish), **F. Dahlgren.** *ERA*, volume 12, 1939, pages 51–52.

374*. Regulating System, **F. S. Dellenbaugh, Jr.** United States patent 2,175,379, October 10, 1939 (M/A Class I,A,1,e).

375. Discharge Lamp System, **M. A. Edwards.** United States patent 2,142,837, January 3, 1939 (M/A Class II,A).

376*. Electrical Control System, **M. A. Edwards.** United States patent 2,169,093, August 8, 1939 (M/A Class I,A,1,b,c,e).

377. Electric Indicating and Control System, **A. S. FitzGerald.** United States patent 2,145,591, January 31, 1939 (M/A Class I,A,3).

378*. Pulsating Electrical Control System, **A. S. FitzGerald.** United States patent 2,168,402, August 8, 1939 (M/A Class I,A,4,a,c).

379*. Automatic Regulating Apparatus for Current Supply Systems, **S. M. Hanley.** United States patent 2,144,289, January, 17, 1939 (M/A Class I,A,1,d,g).

380. Automatic Regulating Apparatus for Current Supply Systems, **S. M. Hanley.** United States patent 2,144,290, January 17, 1939 (M/A Class I,A,1,b,d,g).

381. Electrical Regulating System, **S. M. Hanley.** United States patent 2,182,666, December 5, 1939 (M/A Class I,A,1,a,b,d,g).

382. Approximate Calculation of Saturable Reactors With Direct-Current Magnetization (in German), **W. Hartel.** *Archiv fur Elektrotechnik*, volume 33, September 1939, pages 585–92.

383. A Contribution to the Qualitative Theory of Saturable Iron-Cored Coils With Direct-Current Magnetization (in German), **G. Hauffe.** *Archiv fur Elektrotechnik*, volume 33, 1939, pages 41–47.

384*. Voltage-Compensating Transformer, **W. Kalbskopf.** United States patent 2,173,905, September 26, 1939 (M/A Class I,B″,1,a).

385. Electric Valve Control System, **E. Kern.** United States patent 2,148,049, February 21, 1939 (M/A Class II,B).

386. Saturable Core Detector, **C. J. Kettler.** United States patent 2,149,092, February 28, 1939 (M/A Class I,A,3).

387. Externally Excited Current Controller as a Universal Controller for the Oscillography of Pulsating Currents (in German), **W. Kramer.** *Elektrotechnische Zeitschrift*, volume 60, 1939, pages 393–95.

388. Direct Current Measurement Means, **W. Kramer.** United States patent 2,153,377, April 14, 1939 (M/A Class I,A,1,4).

389. Current Responsive Arrangement, **W. Kramer.** United States patent 2,153,378, April 14, 1939 (M/A Class I,A,1).

390. Transductors (in Swedish), **A. U. Lamm.** *ASEA Tidning*, volume 31, 1939, pages 18–31.

391. Transductor and Its Applications, **A. U. Lamm.** *ASEA Journal*, volume 31, May and June 1939.

392. Some Polarization Phenomena in Magnetic Materials With Special Reference to Nickel-Iron Alloys, **T. A. Ledward.** *Journal*, Institute of Electrical Engineers, volume 84, January 1939, page 113. Discussion, page 139.

393. Survey of Magnetic Materials and Applications in the Telephone System, **V. E. Legg.** *Bell System Technical Journal*, volume 18, pages 438–64.

394. Electric Controlling Apparatus, **F. G. Logan.** United States patent 2,161,179, June 6, 1939 (M/A Classes I,A,1,b; III,B).

395. Harmonic Producer, **J. M. Manley.** United States patent 2,150,386, March 14, 1939 (M/A Class II,B).

396. Self-Regulating Battery Charger, **S. J. Murcek.** United States patent 2,179,299, November 7, 1939 (M/A Classes I,A,1; II,A).

397. Harmonic Producing Apparatus, **E. Peterson.** United States patent 2,146,091, February 7, 1939 (M/A Class II,A).

398. Control System, **E. J. Rasmusson.** United States patent 2,165,111, July 4, 1939 (M/A Class I,A,1).

399. Transforming Means, **C. A. Sabbah, L. W. Morton.** United States patent 2,168,173, August 1, 1939 (M/A Class I,B′,1,e).

400. Frequency Changing System, **C. P. Stocker.** United States patent 2,179,386, November 7, 1939 (M/A Class II,A).

401. Electric Valve Circuit, **W. H. Teare, O. W. Livingstone.** United States patent 2,160,688, May 30, 1939 (M/A Class II,B).

402. The Magnetic Voltage Amplifier, **A. A. Teldbaum.** *Avtomatika and Telemechanika*, number 5, 1939, page 29.

403. Similitude of Critical Conditions in Ferroresonant Circuits, **W. T. Thomson.** *Electrical Engineering* (*AIEE Transactions*), volume 58, March 1939, pages 127–30.

404. The Generalized Solution for the Critical Conditions of the Ferroresonant Parallel Circuit, **W. T. Thomson.** *AIEE Transactions*, volume 58, 1939, pages 743–46.

405. Apparatus for Automatically Controlling the Current in an Alternating Current Circuit, **A. H. B. Walker.** United States patent 2,177,556, October 24, 1939 (M/A Class I,A,1,e).

406*. Constant Voltage System, **H. E. Young.** United States patent 2,154,020, April 11, 1939 (M/A Classes I,A,1,4; I,B′,1,4).

1940

407. Electric Valve Circuits, **B. D. Bedford.** United States patent 2,222, 700, November 26, 1940 (M/A Class II,B).

408. Power Converting Unit and System, **T. F. Carmichael.** United States patent 2,222,214, November 19, 1940 (M/A Class III,B).

409. Control System, **W. T. Croden.** United States patent reissue Re. 21,407, March 26, 1940. From original United States patent 2,086,120, July 6, 1937 (M/A Class I,A,1).

410. Control Device for Rectifiers With Ionized Vapor, **M. Demontvignier.** United States patent 2,190,353, February 13, 1940 (M/A Class II,A).

411. Electric Valve Circuit, **M. A. Edwards.** United States patent 2,190,774, February 20, 1940 (M/A Class I,A,1,e).

412. Electric Valve Circuit, **M. A. Edwards.** United States patent 2,190,775, February 20, 1940 (M/A Class II,A).

413. Frequency Compensator, **M. A. Edward, R. W. Porter.** United States patent 2,194,299, March 19, 1940 (M/A Class II,A).

414. Control System, **M. A. Edwards.** United States patent 2,210,805, August 6, 1940 (M/A Class I,A,1).

415. Fundamentals of the Magnetic Amplifier for Measurement and Control, **W. Geyger.** *Wissenschaftliche Veroffentlichungen aus dem Siemens-Konzern*, volume 19, November 1940, pages 226–69.

416. Registration Control System, **F. H. Gulliksen.** United States patent 2,208,420, July 16, 1940 (M/A Classes I,A,3; II,B).

417. Direct Current Regulated Petersen Coils (in German), **W. W. Gusew.** *Elektrotechnische Zeitschrift*, volume 61, 1940, pages 916–17. Also *Elektricheskie Stantsii*, 1940.

418*. Railway Signalling Apparatus, **C. M. Hines.** United States patent 2,215,820, September 24, 1940 (M/A Class I,B″,1,a,c).

419*. Electrical Switching Device, **F. A. Hubbard.** United States patent 2,218,711, October 22, 1940 (M/A Class I,B″,1,c).

420. Rectifier Circuits, **H. Klemperer.** United States patent 2,206,701, July 2, 1940 (M/A Class II,B).

421. The Transductor or Direct-Current Magnetized Reactor—A Static Relay and Regulating Device (in Swedish), **A. U. Lamm.** *Elektroteknisk Tidsskrift*, volume 59, 1940, pages 97–107.

422. The Transductor, A Revived Member of the Electrical Apparatus Family (in Swedish), **A. U. Lamm.** *Teknisk Tidsskrift*, volume 70, 1940, pages 189–93.

423. The Transductor and its Applications (in French), **A. U. Lamm, L. Vellard.** *Revue Generale de l'Electricite*, volume 47, 1940, pages 373–89.

424. Compressed Powdered Molybdenum Permalloy for High Quality Inductance Coils, **V. E. Legg, F. J. Given.** *Bell System Technical Journal*, volume 19, 1940, page 385.

425. Electrical Control System, **L. C. Ludbrok.** United States patent 2,213,882, September 3, 1940 (M/A Class I,A,1,b).

426. Arc Welding System, **H. L. Mills.** United States patent 2,200,632, May 14, 1940 (M/A Class I,A,1).

427. Electric Valve Converting System, **M. M. Morack.** United States patent 2,202,711, May 28, 1940 (M/A Classes I,A,1; III,A).

428. Starting Circuit for Electric Valve Apparatus, **E. E. Moyer.** United States patent 2,190,799, February 20, 1940 (M/A Class III,A).

429*. Railway Signalling Apparatus, **B. E. O'Hagan.** United States patent 2,215,821, September 24, 1940 (M/A Class I,B″,1,2,c).

430*. Railway Signalling Apparatus, **B. E. O'Hagan.** United States patent 2,215,822, September 24, 1940 (M/A Class I,B″,1,c).

431*. Railway Traffic Controlling Apparatus, **B. E. O'Hagan.** United States patent 2,215,-823, September 24, 1940 (M/A Class I,B″,1).

432. Railway Track Circuit Apparatus, **B. E. O'Hagan.** United States patent 2,215,910, September 24, 1940 (M/A Class II,A,B).

433. Railway Signalling Apparatus, **B. E. O'Hagan.** United States patent 2,216,623, October 1, 1940 (M/A Class I,A,1).

434. Electric Circuit, **R. M. Partington.** United States patent 2,202,715, May 28, 1940 (M/A Class III,B).

435. System of Electrical Distribution, **A. Schmidt, Jr.** United States patent 2,193,649, March 12, 1940 (M/A Class II,B).

436. Generator Voltage Regulator, **O. Schmutz.** United States patent 2,217,457, October 8, 1940 (M/A Class I,A,1,e).

437*. Apparatus for the Production of Electric Oscillations, **S. A. Stevens, A. H. B. Walker.** United States patent 2,222,048, November 19, 1940 (M/A Classes I,A,1; II,A).

438. Determination of Magnetic Permeability at 100 Megacycles per Second, **M. J. O. Strutt.** *Physica*, volume 7, 1940, pages 635–54.

439. Converter System, **P. J. Walsh.** United States patent 2,199,121, April 30, 1940 (M/A Class III,A).

440. Electric Control, **M. E. Whitenack.** United States patent 2,208,235, July 16, 1940 (M/A Class I,A,1).

441. Electric Fence, **C. H. Willis.** United States patent 2,196,046, April 2, 1940 (M/A Class II,A).

1941

442. Electric Valve Circuits, **E. F. W. Alexanderson, A. H. Mittag.** United States patent 2,248,600, July 8, 1941 (M/A Class II,A).

443. Method and a Device for Determining the Magnitudes of Magnetic Fields, **G. Barth.** United States patent 2,252,059, August 12, 1941 (M/A Class I,A,B′,1,3,a,c,e).

444. Electron Discharge Apparatus, **A. E. Bowen.** United States patent 2,230,558, February 4, 1941 (M/A Class I,A,B′,1,d).

445. Code Responsive Control Apparatus, **C. C. Buchanan.** United States patent 2,230,860, February 4, 1941 (M/A Class I,A,1,c).

446. Control System, **D. E. Chambers.** United States patent 2,267,395, December 23, 1941 (M/A Class I,A,1,a,e).

447. Electric Control Circuit, **M. A. Edwards.** United States patent 2,262,491, November 11, 1941 (M/A Class II,B).

448. Voltage Regulator, **O. Eisenschmid.** United States patent 2,261,676, November 4, 1941 (M/A Class I,A,1).

449. Rectifier Filter, **J. L. Finch, G. L. Usselman.** United States patent 2,242,881, May 20, 1941 (M/A Class I,A,1).

450. Experimental Investigations of Magnetic Amplifiers for Measurement and Control Purposes (in German), **W. Geyger.** *Wissenschaftliche Veroffentlichungen aus dem Siemens-Konzern*, volume 20, 1941, pages 253–67.

451. Magnetic Amplifiers for Measuring and Control Technique, **W. Geyger.** *Elektrotechnische Zeitschrift*, volume 62, October 23, 1941, page 849, and November 6, 1941, page 891, also *Wireless Engineer*, Abstract 1135, and *Electrical Engineering Abstracts, Section B of Science Abstracts*, number 1851, 1946.

452. Application of Magnetic Amplifiers to the Control and Automatic Regulation of Furnace Temperatures, **H. E. Giroz.** *Bulletin;* Societe Francaise des Electriciens, volume 1, August to October 1941, page 459, also *Electrical Engineering Abstracts, Section B of Science Abstracts*, number 2369, 1946.

453. Reversing Control for Alternating Current Motors, **F. H. Gulliksen.** United States patent 2,228,078, January 7, 1941 (M/A Class I,A,1).

454. Electrical Regulating Apparatus, **L. K. Hedding, P. S. Johnson.** United States patent 2,253,705, August 26, 1941 (M/A Class I,A,B″,1,e).

455. Grid Control System, **B. Heller, J. Ibl.** United States patent 2,231,670, February 11, 1941 (M/A Class III,A,C).

456. Electric Valve Converting System, **C. C. Herskind.** United States patent 2,246,173, June 17, 1941 (M/A Class II,B).

457. Electric Valve Circuit, **O. W. Livingstone.** United States patent 2,250,961, July 29, 1941 (M/A Class II,A).

458*. Electric Controlling Apparatus, **F. G. Logan.** United States patent 2,259,647, October 21, 1941 (M/A Classes I,A,1,d; I,A,3,d).

459. Energy Translating Apparatus, **S. P. Sashoff.** United States patent 2,253,351, August 19, 1941 (M/A Class I,A,B′,1,3).

460. Polarized Iron-Core Chokes for Regulating Circuits (in German), **W. Schilling**

Elektrotechnik und Maschinenbau, volume 59, August 29, 1941, also *Wireless Engineer*, Abstract 428, 1944.

461. Temperature Control System, **E. D. Schneider, A. R. Ryan.** United States patent 2,266,569, December 16, 1941 (M/A Class I,A,1).

462. Welding System, **D. B. Scott.** United States patent 2,265,930, December 9, 1941 (M/A Classes I,A,1; III,A).

463. Variable Voltage Transformer, **C. P. Sweeney.** United States patent 2,227,468, January 7, 1941 (M/A Class I,B′,1).

464. Reactor, **P. A. Vance.** United States patent 2,253,962, August 26, 1941 (M/A Class I,A,1).

465. Arrangement for Controlling the Voltage of Alternating Current Circuits, **O. Werner.** United States patent 2,229,950, January 28, 1941 (M/A Class I,A,1,b,d).

466*. Magnetic Amplifier, **A. L. Whitely, L. C. Ludbrook.** United States patent 2,229,952, January 28, 1941 (M/A Classes I,A,1,b; I,A,2).

467. Wound Motor Rotor Control, **W. R. Wickerham.** United States patent 2,238,613, April 15, 1941 (M/A Class I,A,1,c).

1942

468. AIEE Standard Definitions of Electrical Terms (book). AIEE, 1942.

469. Power Amplifier, **G. Barth.** United States patent 2,287,755, June 23, 1942 (M/A Class I,A,1,a).

470. Speed Responsive Device, **C. E. Baston.** United States patent 2,289,171, July 7, 1942 (M/A Class III,C).

471. Vapor Electric Device, **W. B. Batten.** United States patent 2,285,556, June 9, 1942 (M/A Class III,B).

472. Electric Circuits, **B. D. Bedford.** United States patent 2,284,794, June 2, 1942 (M/A Classes I,A,1; II,A).

473. Electric Circuit, **B. D. Bedford.** United States patent 2,289,090, July 7, 1942 (M/A Class III,B).

474. Direct Current Polarized A-C Choke Coils and Their Feedback (in German), **T. Buchhold.** *Archiv fur Elektrotechnik*, volume 36, April 30, 1942, pages 221–38, 514, also translation, **H. B. Rex.** *Instruments*, volume 20, December 1947, pages 1102–09, and *Wireless Engineer*, Abstract 3547, 1946.

475. Automatic Voltage and Current Regulating Device, **P. H. E. Claesson.** United States patent 2,306,998, December 29, 1942 (M/A Class I,A,B,B″,1,2,a).

476. Electrical Control System, **A. S. FitzGerald.** United States patent 2,277,849, March 31, 1942 (M/A Class I,A,1,2,a,c).

477. Control Apparatus for Electrical Circuits, **W. J. Garlick.** United States patent 2,292,514, August 11, 1942 (M/A Class II,B).

478. Experimental Investigations on Magnetic Amplifiers for Measuring and Control Technique, **W. Geyger.** *Wissenschaftliche Veroffentlichungen aus dem Siemens-Konzern*, volume 20, 1942, page 33, also *Wireless Engineer*, Abstract 123, 1943.

479. A Null Current Magnetic Amplifier of High Sensitivity for Measurement and Regulation Purposes, **W. Geyger.** *Wissenschaftliche Veroffentlichungen aus dem Siemens-Konzern*, volume 21, 1942, page 187, also *Electrical Engineering Abstracts, Section B of Science Abstracts*, number 2343, 1946.

480. Evaluation of Harmonics in Choke Coils Magnetized by Direct Current (in German), **W. Hartel.** *Archiv fur Elektrotechnik*, volume 36, 1942, pages 556–72.

481. Electrical Measuring Apparatus, **C. M. Hathaway.** United States patent 2,272,772, February 10, 1942 (M/A Class I,A,1,b,c).

482. Electrical Regulating Apparatus, **L. K. Hedding.** United States patent 2,282,471, May 12, 1942 (M/A Class I,A,1).

483. Means for Charging Electric Batteries, **R. S. Hinds, A. Mandl.** United States patent 2,272,745, February 10, 1942 (M/A Class I,A,1).

484. Railway Signalling Apparatus, **C. M. Hines.** United States patent 2,297,148, September 29, 1942 (M/A Class I,B″,1,c).

485. Static Frequency Changer, **H. M. Huge.** United States patent 2,274,925, March 3, 1942 (M/A Class II,B).

486. Motor Starting Apparatus, **F. G. Logan.** United States patent 2,299,911, October 27, 1942 (M/A Class I,A,1).

487. Electrical Frequency Changer, **J. M. Manley.** United States patent 2,272,246, February 10, 1942 (M/A Class II,A).

488. Electric Valve Circuits, **E. E. Moyer.** United States patent 2,273,586, February 17, 1942 (M/A Class I,A,3,a,c).

489. Regulating Apparatus, **L. R. Runaldue.** United States patent 2,278,151, March 31, 1942 (M/A Class I,A,1,a,c,d,e).

490. Control System, **E. D. Schneider.** United States patent 2,285,172, June 2, 1942 (M/A Class I,A,1).

491. Electrical Regulating Apparatus, **C. M. Summers.** United States patent 2,272,755, February 10, 1942 (M/A Class II,A).

492. Regulating Apparatus, **C. M. Summers.** United States patent 2,272,756, February 10, 1942 (M/A Class I,A,1,a,e).

1943

493. B-H Curve Tracer for Lamination Samples, **R. Adler.** *Electronics*, volume 16, November 1943, page 128.

494. Regulation of the Amplification of Bi-Directional Alternating Currents by Means of Saturable Reactors Polarized by Direct Current Magnetization, **Allmanna Svenska Elektriska Aktiebolaget.** Switzerland patent 228,082, October 16, 1943 (M/A Class I,A,1,a).

495. Electrical Control System, **R. D. Amsden.** United States patent 2,334,528, November 16, 1943 (M/A Class I,A,1).

496. Electric Controlling Apparatus, **R. A. Andrews.** United States patent 2,309,156, January 26, 1943 (M/A Class I,A,1,a,b).

497. On the Theory of Magnetic Amplifiers, **T. Buchhold.** *Archiv fur Elektrotechnik*, volume 37, 1943, pages 197–211, also *Wireless Engineer*, Abstract 55, 1944, and *Electrical Engineering Abstracts, Section B of Science Abstracts*, number 1599, 1945.

498. Electric Circuit, **M. A. Edwards.** United States patent 2,313,526, March 9, 1943 (M/A Classes I,B′,1; II,A).

499. A High Sensitivity Magnetic Null-Circuit Amplifier for Measuring and Control Technique, **W. Geyger.** *Wissenschaftliche Veroffentlichungen aus dem Siemens-Konzern*, volume 21, 1943, page 47.

500. Static Frequency Changing System, **A. B. Haines.** United States patent 2,309,586, January 26, 1943 (M/A Class II,A).

501. Characteristics and Applications of Selenium-Rectifier Cells, **E. A. Harty.** *AIEE Transactions*, volume 62, October 1943, pages 624–29.

502. Voltage Regulating Apparatus, **L. K. Hedding.** United States patent 2,316,331, April 13, 1943 (M/A Class I,A,B″,1,g).

503. Electrical Regulating Apparatus, **L. K. Hedding.** United States patent 2,322,130, June 15, 1943 (M/A Class I,A,1).

504. Electric Valve Translating Apparatus, **C. C. Herskind.** United States patent 2,335,673, November 30, 1943 (M/A Class II,B).

505*. System of Measurement and/or Control, **A. J. Hornfeck.** United States patent 2,310,955, February 16, 1943 (M/A Class I,A, 1,2,3,a,c,e).

506. Non-Linear Inductance, **H. M. Huge.** United States patent 2,329,537, September 14, 1943 (M/A Class II,A).

507. Constant Current Transformer, **R. A. S. Johnson.** United States patent 2,312,416, March 2, 1943 (M/A Class I,B′,1).

508. The Transductor, D-C Pre-Saturated Reactor With Special Reference to Transductor Control of Rectifiers, **A. U. Lamm.** *Esselte Arktiebolag*, Stockholm, Sweden, 1943, also *Acta Polytechnica*, Second Edition (book), Academy of Engineering Science (Stockholm, Sweden), May 1948.

509. Direct Current Saturated Inductance With Relay Action, **A. U. Lamm.** United States patent 2,337,253, December 21, 1943. Reissued as United States patent Re. 22,768, June 25, 1946.

510. DC/AC Converter, **T. A. Ledward.** *Wireless World*, volume 48, August 1943, page 230.

511. Electromagnetic Inductance Apparatus, **H. J. McCreary.** United States patent 2,324,634, July 20, 1943 (M/A Classes I,A,1,c; II,B).

512. Regulated Rectifier, **L. E. Milarta.** United States patent 2,331,411, October 12, 1943 (M/A Class I,A,1).

513. Electric Regulating Circuit, **E. E. Moyer.** United States patent 2,331,131, 1943 (M/A Class I,A,1).

514. Vapor-Electric Device, **H. C. Myers.** United States patent 2,318,091, May 4, 1943 (M/A Classes I,A,1; II,A).

515. Wave Generating System, **E. Peterson.** United States patent 2,317,482, April 27, 1943 (M/A Class II,A).

516. Electric Valve Circuit, **A. R. Ryan.** United States patent 2,331,731, October 12, 1943 (M/A Class I,A,1,g).

517. Magnesyn Remote Reading Compass, **D. W. Smith.** *Aeronautical Engineering Review*, volume 2, May 1943, pages 31–36.

518. Battery-Charging System, **I. R. Smith.** United States patent 2,333,617, November 2, 1943 (M/A Class I,A,1).

519. Electromagnetic System, **P. J. Walsh.** United States patent 2,329,021, September 7, 1943 (M/A Class III,A).

520. Saturable Core Reactor Now Smaller, More Capable, **E. C. Wentz.** *Westinghouse Engineer*, volume 3, November 1943, page 115.

521. A New Saturable Core Reactor, **E. C. Wentz.** *Westinghouse Engineer*, November 1943.

522. Electric Valve Protective System, **H. Winograd.** United States patent 2,329,735, September 21, 1943 (M/A Class III,B).

1944

523*. Apparatus for Measuring Direct Currents or Voltages, **W. Geyger.** United States patent 2,338,423, January 4, 1944 (M/A Class I,A,3,4,a).

524. Current Supply System, **O. D. Grandstaff, T. W. Gilman, R. H. Herrick.** United States patent 2,343,411, March 7, 1944 (M/A Class I,A,1).

525. Constant Current Control, **E. H. Haug.** United States patent 2,351,681, June 20, 1944 (M/A Class I,A,1,4,e).

526. Regulating Apparatus, **L. K. Hedding.** United States patent 2,346,487, April 11, 1944 (M/A Class I,A,1).

527. Coupling Methods Applied to Regulating Transductors (in Swedish), **S. E. Hedström, U. H. Krabbe.** *ASEA Tidning*, numbers 11–12, 1944.

528. Frequency Reducing System, **R. H. Herrick.** United States patent 2,340,382, February 1, 1944 (M/A Class II,A).

529. Electrical Transmission System, **W. H. T. Holden.** United States patent 2,339,406, January 18, 1944 (M/A Class I,B′,1,a,c).

530. Frequency Reducer, **H. M. Huge.** United States patent 2,364,531, December 5, 1944 (M/A Class II,B).

531. Common Core Frequency Changer, **H. M. Huge.** United States patent 2,364,532, December 5, 1944 (M/A Class II,B).

532. Voltage Stabilizer, **R. Lee.** United States patent 2,351,980, June 20, 1944 (M/A Class I,B′,2).

533. A Continuous-Control Servo System, **J. T. McNaney.** *Electronics*, volume 17, December 1944, pages 118–25.

534. Vapor Electric Device, **H. C. Myers.** United States patent 2,349,633, May 23, 1944 (M/A Classes I,A,2,c,d; II,A).

535. Incremental Permeability Tuning, **W. J. Polydoroff.** *Proceedings*, National Electronics Conference, volume 1, 1944, page 146.

536. Voltage Regulator, **J. E. Priest.** United States patent 2,346,997, April 18, 1944 (M/A Class I,B*,1,a).

537. A Mechanical Integrating System Incorporating a Magnetic Amplifier (Report number 436, OSRD NDRC Division 14), **H. S. Sack, J. W. Trischka.** Cornell University (Ithaca, N. Y.), December 15, 1944.

538. Control Apparatus, **H. T. Sparrow.** United States patent 2,355,567, August 8, 1944 (M/A Class I,A,2,e).

539. Rectifying System, **D. E. Trucksess.** United States patent 2,349,685, May 23, 1944 (M/A Class I,A,3).

1945

540. Orthomagnetic Bushing Current Transformer for Metering, **A. Boyajian, G. Camilli.** *Electrical Engineering* (*AIEE Transactions*), volume 64, March 1945, pages 137–40.

541. Self-Regulating Rectifier, **H. M. Christopher.** United States patent 2,373,383, April 10, 1945 (M/A Class I,A,1,e).

542. Electronics (book), Coyne Electrical School Technical Staff, Chicago, Ill., 1945, page 79.

543. Welding System, **L. O. Dorfman.** United States patent 2,387,889, October 30, 1945 (M/A Class III,A).

544. Electric Valve Control System, **I. K. Dortort.** United States patent 2,373,297, April 10, 1945 (M/A Class I,A,1,e).

545. Protective Circuits for Rectifiers, **J. Dyson.** United States patent 2,371,035, March 6, 1945 (M/A Class I,A,1).

546. Voltage Regulator, **D. E. Garr.** United States patent 2,378,765, June 19, 1945 (M/A Class I,A,1).

547. The Transductor as an Aid in Measurement(in Swedish), **S. E. Hedstrom.** *Teknisk Tidskrift*, volume 18, 1945.

548. DC Saturable Reactors for Control Purposes, **H. Holubow.** *Electronic Industries*, volume 4, March 1945, pages 76–79.

549. The Control of Alternator Frequency on the German Long Range Rocket (Report number EL 1361), **C. S. Hudson, I. A. Mossop.** Royal Aircraft Establishment (Farnborough, England), February 1945.

550. Reactance, **R. W. Keiser.** United States patent 2,387,797, October 30, 1945 (M/A Class III,C).

551. Electromagnetic Engineering (book), **I. W. P. King.** McGraw-Hill Book Company, New York, N. Y., 1945.

552. Equivalent Circuit of a Pulse Transformer Core (Report number 666), Staff, Massachusetts Institute of Technology, Cambridge, Mass., March 22, 1945, also Library of Congress Publication Board Report PB-2719 (Washington, D. C.).

553*. Electromagnetic Apparatus, **H. D. Middel.** United States patent 2,388,070, October 30, 1945 (M/A Class I,A,1,g).

554. Polyphase Direct Current Saturated Inductance, **B. Nordfeldt.** United States patent 2,372,112, March 20, 1945 (M/A Class I,A,1).

555. Ferroinductance as a Variable Electric-Circuit Element, **J. D. Ryder.** *Electrical Engineering* (*AIEE Transactions*), volume 64, October 1945, pages 671–77.

556. Use of a Specially Designed Magnetic Amplifier in Computing Circuits (Report number 437, OSRD NDRC Division 14), **H. S. Sack, R. T. Beyer, G. H. Miller, J. W. Trischka.** Cornell University, Ithaca, N. Y., May 10, 1945.

557. Voltage Regulator Circuit, **T. T. Short.** United States patent 2,367,625, January 16, 1945 (M/A Class III,A).

558. Sustained Subharmonic Response in Non-Linear Series Circuits, **C. F. Spitzer.** *Journal of Applied Physics*, volume 16, February 1945, pages 105–11.

559. Servos With Magnetic Amplifiers (Transductors). *Report Number 206–45*, United States Naval Technical Mission in Europe, September 1945.

560. Hoist Control System, **W. R. Wickerham.** United States patent 2,386,581, October 9, 1945 (M/A Class I,A,1).

561. Variable-Unbalanced-Voltage Control, **W. R. Wickerham.** *Electrical Engineering* (*AIEE Transactions*), volume 64, March 1945, pages 98–102.

1946

562. German Two Stage Magnetic Amplifiers Used in Blind Landing Equipment, **J. Baranawski.** Report Number EL 1392, Royal Aircraft Establishment (Farnborough, England), May 1946.

563. Electric Circuits, **B. D. Bedford.** United States patent 2,405,397, August 6, 1946 (M/A Class III,A).

564. Voltage Regulation, **W. H. Bixby.** United States patent 2,409,610, October 22, 1946 (M/A Class I,A,1,a,c,g).

565. Magnetic Development in Japan During World War II (Report X-34(N)), **R. M. Bozorth, F. T. Chestnut, G. W. Elmen, R. L. Sanford, W. D. Williams.** Naval Technical Mission, Japan, 1946, also Department of Commerce *Report PB 76031*, 1946.

566. On the Theory of Magnetic Amplifiers, **T. Buchhold.** May 6, 1946.

567. Magnetic Amplifier (German patent), **T. Buchhold.** *Bibliography of Scientific and Industrial Reports*, Office of Technical Services, United States Department of Commerce (Washington, D. C.), volume 2, August 2, 1946, page 325 (*PB 12464*).

568. Magnetic Amplifier With Transverse Magnetization (German patent), **T. Buchhold.** *Bibliography of Scientific and Industrial Reports*, Office of Technical Services, United States Department of Commerce (Washington, D. C.), volume 2, August 23, 1946, page 562 (*PB 12487*).

569. Magnetic Amplifier (German patent), **T. Buchhold.** *Bibliography of Scientific and Industrial Reports*, Office of Technical Services, United States Department of Commerce (Washington, D. C.), volume 3, November 15, 1946, page 524 (*PB 12488*).

570. Saturable Reactors for Automatic Control, **W. D. Cockrell.** *Electronic Industries*, volume 5, December 1946, pages 48–53.

571. Vapor-Electric System, **J. H. Cox, H. C. Myers.** United States patent 2,397,089, March 26, 1946 (M/A Classes I,A,1; II,A).

572. Transductor Type Voltage Regulators. Other Types of Transductor Regulators and Power Regulation, Editor. *ASEA Journal*, numbers 1–3, 1946.

573. Applications of Thin Permalloy Tape in Wide-Band Telephone and Pulse Transformers, **A. G. Ganz.** *Electrical Engineering* (*AIEE Transactions*), volume 65, April 1946, pages 177–83.

574. Regulating Apparatus, **L. K. Hedding.** United States patent 2,399,185, April 30, 1946 (M/A Class I,A,B*,1,a,e,g).

575. Electric Control System, **A. Herz.** United States patent 2,401,156, May 28, 1946 (M/A Class I,A,1).

576. Components of UHF Field Meters, **E. Karplus.** *Electronics*, volume 19, November 1946, pages 124–29.

577. The Transductor—Its Operation and Applicability (in Swedish), **U. H. Krabbe.** *ASEA Tidning*, volume 5, 1946, pages 47–60.

578. Electrically Operating Regulating Device, **A. Kurssmann.** United States patent 2,399,872, May 7, 1946 (M/A Class I,A,3).

579. Direct Current Saturated Inductance With Relay Action, **A. U. Lamm.** United States patent Reissue Re. 22,768, June 25, 1946. From original United States patent 2,337,253, December 21, 1943 (M/A Class I,A,1,a,c).

580. Load Current Control, **A. U. Lamm.** United States patent 2,403,891, July 9, 1946 (M/A Class I,A,1,3,a,b).

581. Negative Resistance Effects in Saturable Reactor Circuits, **J. M. Manley, E. Peterson.** *AIEE Transactions*, volume 65, 1946, pages 870–81.

582. Electric Motor Control System, **G. H. Pettibone.** United States patent 2,394,100, February 1946 (M/A Class I,A,3,c).

583. The Magnetic Amplifiers (in French), **L. Schoerer.** *La Radio Francaise*, volume 4, 1946, page 24.

584. Several After-Effect Phenomena and Related Losses in Alternating Fields, **J. L. Snoek, F. K. DuPre.** *Philips Technical Review*, volume 8, February 1946, pages 57–64.

585. Non-Metallic Material for High Frequencies, **J. L. Snoek.** *Philips Technical Review*, volume 8, December 1946, pages 353–60.

586. Electrometer Input Circuits, **H. A. Thomas.** *Electronics*, volume 19, December 1946, pages 130–31.

587. Control System, **W. R. Wickerham.** United States patent 2,408,461, October 1, 1946 (M/A Class I,A,1,3,c).

588. FM by Non-Linear Coils, **L. R. Wrathall.** *Bell Laboratories Record*, volume 24, March 1946, pages 102–05.

1947

589. Electric Control Circuits, **E. F. W. Alexanderson, A. H. Mittag.** United States patent 2,431,903, December 2, 1947 (M/A Classes I,A,3, II,A).

590. Voltage Control Apparatus, **W. C. Anderson.** United States patent 2,428,693, October 7, 1947 (M/A Class I,A,1).

591. Electric Control Circuit, **J. A. Augier.** United States patent 2,427,542, September 16, 1947 (M/A Class II,A).

592. Means Producing a Steep Wave-Front Potential for Control of Electric Discharge Devices, **J. A. Augier.** United States patent 2,428,604, October 7, 1947 (M/A Class II,B).

593. Use of Magnetic Amplifiers in Computing Circuits, **R. T. Beyer.** *Physical Review*, volume 72, September 15, 1947, page 522.

594. Magnetic Developments in Japan During World War II, BIOS Report, number 1283, 1947, page 60.

595. A New Magnetic Material of High Permeability, **O. L. Boothby, R. M. Bozorth.** *Journal of Applied Physics*, volume 18, February 1947.

596. Magnetism, **R. M. Bozorth.** *Review of Modern Physics*, volume 19, January 1947.

597. Direct Current Premagnetized Reactors With and Without Feedback, **T. Buchhold.** (Translated by J. B. Priauf), February 6, 1947, pages 173–76.

598. On the Theory of Eddy Currents in Ferromagnetic Materials, **H. B. G. Casimir.** *Philips Research Report*, volume 2, 1947, pages 42–54.

599. High-Frequency Excitation of Iron Cores, **J. D. Cobine, J. R. Curry, C. J. Gallagher, S. Ruthberg.** *Proceedings*, Institute of Radio Engineers, volume 35, October 1947, pages 1060–67.

600. Battery Charging System, **L. P. Cronvall.** United States patent 2,431,311, November 25, 1947 (M/A Class I,A,1).

601. The Transductor, Principle and Application, Editor. *Publication 7051 E/Reg. 479*, Allmanna Svenska Elektriska Aktiebolaget, March 1947.

602. The Transductor Applied to Electrical Measurement, Editor. *Publication 7126 E/Reg. 479*, Allmanna Sevenska Elektriska Aktiebolaget, 1947.

603. Reactance Amplifiers, Editor. *Electronics*, volume 20, part 2, October 1947.

604. Follow-Up Control System, **M. A. Edwards, H. M. Ogle.** United States patent 2,414,936, January 28, 1947 (M/A Class I,A,2,a,b,c,d).

605. Electrical Control Device, **M. A. Edwards.** United States patent 2,432,399, December 9, 1947 (M/A Class I,A,3).

606. Saturable Reactor System, **A. L. Embry.** United States patent 2,422,958, June 24, 1947 (M/A Class I,A,1).

607. Rectifiers: Selenium and Copper Oxide, **W. H. Falls.** *General Electric Review*, volume 50, February 1947, pages 34–38.

608. Air-Borne Magnetometers, **E. P. Felch, W. J. Means, T. Slonczewski, L. G. Parratt, L. H.**

Rumbaugh, A. J. Tickner. *Electrical Engineering*, volume 66, July 1947, pages 680–85.

609. Magnetic Amplifier Circuits, Neutral Type, **A. S. FitzGerald.** *Journal*, Franklin Institute, volume 244, October 1947, pages 249–65.

610. Some Notes on the Design of Magnetic Amplifiers, **A. S. FitzGerald.** *Journal*, Franklin Institute, volume 244, November 1947, pages 323–62.

611. Magnetic Amplifier Characteristics, Neutral Type, **A. S. FitzGerald.** *Journal*, Franklin Institute, volume 244, December 1947, pages 415–40.

612. Data Storage in Three Dimensions (Report number M-70), **J. W. Forrester.** ONR Contract N5ori-60, Project Whirlwind, Massachusetts Servomechanisms Laboratory, Cambridge, Mass., April 29, 1947.

613. Applications of Magnetic Amplifiers, **W. E. Greene.** *Electronics*, volume 20, September 1947, pages 124–28.

614. Circuit Control Apparatus, **E. H. Haug.** United States patent 2,421,786, June 10, 1947 (M/A Class I,A,1,e).

615. The Transductor Applied to Electrical Measurement, **S. E. Hedström.** *Pamphlet Number 7126E*, Allmanna Svenska Elektriska Aktiebolaget, 1947.

616. Designing Saturable-Core Reactors for Specific Uses, **C. Helber.** *Electronic Industries and Instrumentation*, December 1947, pages 4, 5, 13.

617. Controlled Sources for Heavy Direct Currents, **G. Houck.** *Electronic Industries and Instrumentation*, December 1947, pages 12–13.

618. Frequency Changer, **H. M. Huge.** United States patent 2,418,640, April 8, 1947 (M/A Class II,A,B).

619. Frequency Changer, **H. M. Huge.** United States patent 2,418,641, April 8, 1947 (M/A Class II,A,B).

620. Frequency Reducer, **H. M. Huge.** United States patent 2,418,642, April 8, 1947 (II,B).

621. Magnetic Frequency Changer, **H. M. Huge.** United States patent 2,418,643, April 8, 1947 (M/A Class II,A).

622. Regulating System, **H. C. Jenks.** United States patent 2,420,881, May 20, 1947 (M/A Class I,A,1).

623. Balanced Amplifiers Using Biased Saturable Core Reactors, **H. S. Kirschbaum, E. L. Harder.** *AIEE Transactions*, volume 66, 1947, pages 273–78.

624. The Transductor, Principle and Application, **U. H. Krabbe.** *ASEA Journal*, volume 20, 1947, page 119.

625. The Design of Transductor Circuits, **U. H. Krabbe, S. E. Hedstrom.** *ASEA Journal*, volume 21, 1947, page 3.

626. The Transductor Amplifier (book), **U. H. Krabbe.** Lindhska Boktryckeriet, Orebro, Sweden, 1947, also Einar Munksgaard, Copenhagen, Denmark.

627. Some Fundamentals of and Theory of the Transductor or Magnetic Amplifier, **A. U. Lamm.** *AIEE Transactions*, volume 66, 1947, pages 1078–85.

628. Current Control Apparatus, **K. A. Lang.** United States patent 2,426,937, September 2, 1947 (M/A Class I,A,1,3,e).

629. Electronic Transformers and Circuits (book), **R. Lee.** John Wiley and Sons, Inc., New York, N. Y., 1947.

630. Notes on the Types, General Characteristics, Control, and Some Basic Applications of Saturable Core Reactors, **F. G. Logan.** *Report*, Ward-Leonard Company (Mt. Vernon, N. J.), January 3, 1947.

631. Non-Linear Dynamics (Report number 130, PIB 81.9, ONR Contract N6ori-98, Task Order 4), Staff of the Polytechnic Institute of Brooklyn, Microwave Research Institute, New York, N. Y., September 1947.

632. Non-Linear Electrodynamics (Report number 130, PIB-81.11, ONR Contract N6ori-98, Task Order 4), Staff of the Polytechnic Institute of Brooklyn, Microwave Research Institute, New York, N. Y., 1947. Continued: Report number 130, PIB 81.14, May 25, 1948.

633. Voltage Regulated Rectifier Circuit, **J. A. Potter.** United States patent 2,423,114, July 1, 1947 (M/A Class I,A,B′,1).

634. The Transductor, **H. B. Rex.** *Instruments*, volume 20, December 1947, pages 1102–09.

635. Special Magnetic Amplifiers and Their Use in Computing Circuits, **H. S. Sack, R. T. Beyer, G. H. Miller, J. W. Trischka.** *Proceedings*, Institute of Radio Engineers, volume 35, November 1947, pages 1375–82.

636. New Developments in Ferromagnetic Materials (book), **J. L. Snoek.** Elsevier Publishing Company, New York, N. Y., 1947.

637. Analytical and Experimental Study of Magnetic Amplifiers (Report number R-149, PIB-98, ONR Contract N6ori-98, Task Order 4), **M. Stateman.** Polytechnic Institute of Brooklyn, Microwave Research Institute (New York, N. Y.), June 10, 1947.

638. Saturable Reactors for Load Control, I and II, **P. A. Vance.** *General Electric Review*, volume 50, August 1947, pages 17–21, and September 1947, pages 42–44.

639. Magnetic Amplifiers Part I—The Steady State Performance of Magnetic Amplifiers Without Feedback (ONR Contact N6ori-47, Task Order 5), **D. W. VerPlanck, M. Fishman.** Carnegie Institute of Technology (Pittsburgh, Pa.), February 1947.

640. Magnetic Amplifiers Part II—The Steady State Performance of Magnetic Amplifiers With Feedback (ONR Contract N6ori-47, Task Order 5), **D. W. VerPlanck, M. Fishman.** Carnegie Institute of Technology (Pittsburgh, Pa.), August 1947.

641. On the Crystalline Structure of Ferrites and Analogous Metal Oxides, **E. J. W. Verwey, P. W. Haayman, E. L. Heilman.** *Philips Technical Review*, volume 9, 1947, pages 185–90.

642. Converter System, **P. J. Walsh.** United States patent 2,417,622, March 18, 1947 (M/A Class III,A).

643. A 60-Cycle Hysteresis Loop Tracer for Small Samples of Low Permeability Materials, **D. E. Wiegand, W. W. Hansen.** *AIEE Transactions*, volume 66, 1947, page 119.

644. Accumulator Charging System, **G. Winkler.** United States patent 2,423,134, July 1, 1947 (M/A Class I,A,1).

645. A Cathode Ray B-H Tracer, **J. Zamsky.** *Electrical Engineering*, volume 66, July 1947, pages 678–80.

1948

646. Some Aspects of the Theory of Iron-Testing by Wattmeter and Bridge Methods, **N. F. Astbury.** *Journal*, Institution of Electrical Engineers, volume 95, part 2, October 1948, pages 607–16.

647. Magnetic Amplifiers Part III—The Step-by-Step Calculation of a Magnetic Amplifier (ONR Contract N6ori-47, Task Order 5), **D. C. Beaumariage.** Carnegie Institute of Technology (Pittsburgh, Pa.), April 1948.

648. Simplified Magnetic Amplifier, **D. A. Bell.** *Wireless Engineer*, volume 25, September 1948, pages 303–04.

649. Magnetic Amplifier Development (United States Naval Ordnance Laboratory Report NOLR 1091), **A. O. Black, Jr.** *Conference Paper*, Naval Ordnance Laboratory Magnetic Materials Symposium (Washington, D. C.), June 15, 1948.

650. Effect of Core Materials on Magnetic Amplifier Design, **A. O. Black, Jr.** *Proceedings*, National Electronics Conference, volume 4, 1948, pages 427–35.

651. Some Factors Governing the Achievement of a Rectangular Hysteresis Loop (USNOL Report NOLR 1091), **E. Both.** Naval Ordnance Laboratory Magnetic Materials Symposium (Washington, D. C.), June 15, 1948.

652. Magnetic Materials With a Rectangular Hysteresis Loop (Technical Memo number M-1155 GS), **E. Both.** SCEL Fort Monmouth number 6, Signal Corps Project 152A, D. A. Project number 3-99-15-021, September 1948.

653. Investigation of the Eddy-Current Anomaly in Electrical Sheet Steels, **F. Brailsford.** *Journal*, Institution of Electrical Engineers, volume 95, part 2, February 1948, pages 38–48.

654. The Effects of Overlapping Joints in Laminated Magnetic Cores on the M.M.F. and Power Required for Their A.C. Magnetization, **O. I. Butler, C. Y. Mang.** *Journal*, Institution of Electrical Engineers, volume 95 part 2, February 1948, pages 15–24.

655. Predetermination of the Magnetic Properties of Ferro-Magnetic Laminae at Power and Audio Frequencies, **O. I. Butler, C. Y. Mang.** *Journal*, Institution of Electrical Engineers, volume 95, part 2, February 1948, pages 25–37.

656. Polarization Phenomena in Nickel-Iron Alloys, and Their Effective Elimination, **O. I. Butler.** *Journal*, Institution of Electrical Engineers, volume 95, part 2, October 1948, pages 627–35.

657. The Design of Transductor Circuits, Editor. *Publication 713E/Reg 4795*, Allmanna Svenska Elektriska Aktiebolaget, 1948.

658. Supermalloy, Editor. *Bell Laboratories Record*, volume 26, March 1948, pages 111–13.

659. Magnetic Amplifier, Editor. *Electrical Review*, volume 143, December 3, 1948, pages 880–81.

660. Magnetic Amplifiers for Industrial Controls, Permenorm 5000 Z, Editor. *Electrical World*, volume 130, September 1948, page 103, also *Machinery*, volume 55, September 1948, page 178.

661. Electromagnetic Amplifiers, Editor. *Electronics*, volume 21, January 1948, pages 190–95.

662. Improved Materials for Magnetic Amplifiers, Editor. *Electronics*, volume 21, August 1948, page 128.

663. Magnetic Program at the Naval Ordnance Laboratory (USNOL Report NOLR 1091), **G. W. Elmen.** Naval Ordnance Laboratory Magnetic Materials Symposium (Washington, D. C.), June 15, 1948.

664. Special Magnetic Alloys and Applications, **G. W. Elmen, E. A. Gaugler.** *Electrical Engineering*, volume 67, September 1948, pages 843–45, also *Power Generation*, volume 52, September 1948, pages 64–67.

665. Magnetic Amplifiers Part V—Analytical Predetermination of the Steady State Characteristics of Magnetic Amplifiers (ONR Contract N6ori-47, Task Order 5), **L. A. Finzi, D. C. Beaumariage.** Carnegie Institute of Technology (Pittsburgh, Pa.), December 1948.

666. Magnetic Amplifiers Part IV—The Steady State Performance of Magnetic Amplifiers With Self Feedback (ONR Contract N6ori-47, Task Order 5), **M. Fishman, D. C. Beaumariage.** Carnegie Institute of Technology (Pittsburgh, Pa.), August 1948.

667. The Theory of Magnetic Amplifiers and Some Recent Developments, **E. H. Frost-Smith.** *Journal of Scientific Instruments*, volume 25, August 1948, pages 268–72.

668. Processing of Magnetic Materials at the Naval Ordnance Laboratory (USNOL Report NOLR 1091), **E. A. Gaugler.** Naval Ordnance Laboratory Magnetic Materials Symposium (Washington, D. C.), June 15, 1948.

669. Iron-Loss Measurements by A. C. Bridge and Calorimeter, **J. Grieg, H. Kayser.** *Journal*, Institution of Electrical Engineers, volume 95, part 2, April 1948, pages 205–16.

670. Investigation and Development of Magnetic Amplifiers (Summary Report, Contract NObs 45340, Task Order 1), **J. Grillo.** BuShips, Navy Department, Ward-Leonard Electric Company (Mt. Vernon, N. Y.), August 27, 1948.

671. Transductor Fundamentals, **S. E. Hedström, L. F. Borg.** *Electronics*, volume 21, September 1948, pages 88–93.

672. Standards on Abbreviations, Graphical Symbols, Letter Symbols, and Mathematical Signs (book). Institute of Radio Engineers, New York, N. Y., 1948.

673. Magnetic Properties of Ordered Nickel-Manganese Alloys, **R. J. Jaffee.** *Journal of Applied Physics*, volume 19, October 1948, pages 867–70.

674. The Mechanical Rectifier (USNOL Report NOLR 1091), **O. Jensen.** Naval Ordnance

Laboratory Magnetic Materials Symposium (Washington, D. C.), June 15, 1948.

675. Pulse Transformers (Final report, Contract W28-099 ac-118), **H. S. Kirschbaum, C. E. Warren.** Ohio State University Research Foundation (Columbus, Ohio), November 1948, also *Report R-2230*, Library of Congress, Science and Technology Project, Technical Information Section (Washington, D. C.).

676. The Transductor (book), **A. U. Lamm.** Esselte Aktiebolag, Stockholm, Sweden, second edition 1948.

677. A-C Measurements of Magnetic Properties, **H. W. Lamson.** *Proceedings*, Institute of Radio Engineers, volume 36, February 1948, pages 266–77.

678. The Type 1670—A Magnetic Test Set, **H. W. Lamson.** *General Radio Experimenter*, volume 23, August 1948.

679. Protective System for Current Converters Utilizing Differentially Connected Saturable Reactors, **K. Lerstrup.** United States patent 2,434,214, January 6, 1948 (M/A Class I,A,2,4).

680. The Measurement of Permeability and Magnetic Losses of Non-Conducting Ferromagnetic Material at High Frequencies, **H. J. Lindenhovius, J. C. van der Breggen.** *Philips Research Reports*, volume 3, 1948, pages 37–45.

681. Saturable Reactor and Magnetic Amplifier Circuits (USNOL Report NOLR 1091), **F. G. Logan.** Naval Ordnance Laboratory Magnetic Materials Symposium (Washington, D. C.), June 15, 1948.

682. Saturable Reactors and Magnetic Amplifiers, **F. G. Logan.** *Electronics*, volume 21, October 1948, pages 104–09.

683. Anisotropic Strains Produced by Surface Abrasion, and Their Effect on the Magnetic Properties of Silicon Sheet Steel, **R. C. Martindale.** *Journal*, Institution of Electrical Engineers, volume 95, part 2, October 1948, pages 620–26.

684. Frequency Changer, **H. J. McCreary.** United States patent 2,455,078, November 30, 1948 (M/A Class II,B).

685. The Magnetic Amplifier or Transductor (Memograph L8-11-15, 4711), **W. E. Meserve.** Cornell Aeronautical Laboratory, Inc. (Buffalo, N. Y.), November 15, 1948.

686. Bibliography on Transductors, Magnetic Amplifiers, etc., **H. B. Rex.** *Instruments*, volume 21, April 1948, pages 332, 352–62.

687. Parallel-Tuned Transformer Design, **V. C. Rideout.** *Bell System Technical Journal*, volume 27, January 1948, pages 96–108.

688. Development of Locators of Small Metallic Bodies Buried in the Ground, **B. Roston.** *Journal*, Institution of Electrical Engineers, volume 95, part 2, December 1948, pages 653–67.

689. Voltage Regulator, **S. Saretzky.** United States patent 2,437,837, March 16, 1948 (M/A Class I,A,1,e).

690. Summary Report No. 1, First Phase of Contract NObs 45156 With Addendum Volume 1 and With Addendum Volume 2 (bibliography), (Navy Department, BuShips, Contract NObs 45156), **F. L. Spencer, Jr.** Eclipse-Pioneer Division, Bendix Aviation Corporation (Teterboro, N. J.), March 9, 1948 and October 8, 1948.

691. Eclipse-Pioneer Magnetic Amplifier Applications (Summary Report No. 2, Navy Department, BuShips, First Phase of Contract NObs 45156), **F. L. Spencer, Jr.** Eclipse-Pioneer Division, Bendix Aviation Corporation (Teterboro, N. J.), 1948.

692. Magnetic Amplifier With Feedback Study of Steady-State Conditions (Summary Report 3, Second Phase of Contract NObs 45156), **F. L. Spencer, Jr.** BuShips, Navy Department, Eclipse-Pioneer Division, Bendix Aviation Corporation (Teterboro, N. J.), March 15, 1948.

693. Investigation and Development of Core Construction and Evaluation of Core Materials for Magnetic Amplifiers (Progress Report number 2, Contract NObs 46768), **S. Steinitz, W. J. Dornhoefer.** BuShips, Navy Department, Vickers, Inc. (St. Louis, Mo.), October 11, 1948.

694. Some Fundamentals of D-C Controlled Reactors With Resistive Loads, **H. F. Storm.** *AIEE Transactions*, volume 68, 1949, pages 188–94.

695. Magnetic Amplifiers, **S. E. Tweedy.** *Electronic Engineering*, volume 20, February 1948, pages 38–43, and volume 20, March 1948, pages 84–88, and discussion, volume 20, May 1948.

696. Magnetic Amplifiers—Circuits, Characteristics, Applications (Bulletin number VT-2000), Vickers Electric Division, Vickers, Inc. (St. Louis, Mo.), 1948.

697. Rectifier System, **P. J. Walsh.** United States patent 2,435,062, January 27, 1948 (M/A Class III,A).

698. Investigation and Development of Magnetic Amplifiers and Their Component Elements (Progress Report number 2, Contract NObs 45340, Task Order 1), Ward-Leonard Electric Company (Mt. Vernon, N. Y.), BuShips, Navy Department, March 30, 1948.

699. Investigation and Development of Magnetic Amplifiers (Contract NObs 45340, Task Order 1), Ward-Leonard Electric Company (Mt. Vernon, N.Y.), Navy Department, BuShips, August 27, 1948.

700. Analytical Study of an Unbiased Bridge Type Magnetic Amplifier (Report number R 177-46, PIB-122, Contract N6ori-98, Task Order 4), **E. Weber, M. Stateman.** Polytechnic Institute of Brooklyn, Microwave Research Institute (New York, N. Y.), November 19, 1948.

701. Single-Turn A-C Ring Tester for Magnetic Laminations, **J. H. Wright.** *General Electric Review*, volume 51, November 1948, pages 36–38.

1949

702. Magnetic Amplifier Core Properties, Phase (C) (Report R-207-49, PIB-151, ONR Contract N6ori-98, Task Order 4), **F. Benjamin.** Polytechnic Institute of Brooklyn, Microwave Research Institute (New York, N. Y.), May 13, 1949.

703. The Eddy-Current Anomaly in Ferromagnetic Laminae at High Rates of Change of Flux, **L. R. Blake.** *Proceedings*, Institution of Electrical Engineers, volume 96, part 2, October 1949, pages 705–18.

704. Some Aspects of Magnetic Materials Used in Transductors, **L. F. Borg.** *Proceedings*, Institution of Electrical Engineers, volume 96, part 2, April 1949, pages 316–18.

705. Magnetic Ferrites for High-Frequency Uses, **F. G. Brockman.** *Electrical Engineering*, volume 68, December 1949, pages 1077–80.

706. Magnetic Amplifiers for Naval Shipboard Applications, **L. W. Buechler.** *Electrical Engineering*, volume 68, January 1949, pages 33–37, also *Electrical World*, volume 130, November 6, 1948, page 117.

707. The Use of Rectified Pulses for Control Current in Magnetic Amplifiers (Summary Report, Contract NObsr 46768), **L. W. Buechler, W. J. Dornhoefer.** BuShips, Navy Department, Vickers, Inc. (St. Louis, Mo.), August 20, 1949.

708. Use of Square Deltamax Laminations in Magnetic Amplifier (Summary Report VED S. O. 48–1002, Contract NObs 46768), **L. W. Buechler.** BuShips, Navy Department, Vickers, Inc. (St. Louis, Mo.), November 1, 1949. Continued: Supplementary Report, January 1, 1950.

709. Use of 'U' Laminations in Cores of Magnetic Amplifiers (Summary Report, Contract NObs 46768), **L. W. Buechler, W. J. Dornhoefer.** BuShips, Navy Department, Vickers, Inc. (St. Louis, Mo.), November 1, 1949.

710. Operating Magnetic Amplifiers Over Variable Frequencies at Constant Voltage (Summary Report, Contract NObs 46768), **L. W. Buechler, W. J. Dornhoefer.** BuShips, Navy Department, Vickers, Inc. (St. Louis, Mo.), December 8, 1949.

711. Use of Supermalloy as a Core Material for Magnetic Amplifiers (Interim Report, Contract NObs 46768), **L. W. Buechler, W. J. Dornhoefer.** BuShips, Navy Department, Vickers, Inc. (St. Louis, Mo.), December 30, 1949.

712. Step by Step Method for Investigation of Magnetic Amplifiers (Report R122–49, PIB-166, Contract N6ori-98, Task Order 4), **L. G. Cacho,** Polytechnic Institute of Brooklyn, Microwave Research Institute (New York, N. Y.), July 15, 1949.

713. Saturation Effect of Leakage Reactance, **S. S. L. Chang, T. C. Lloyd.** *AIEE Transactions*, volume 68, 1949, pages 1144–47.

714. A Sensitive Magnetometer for Very Small Areas, **D. M. Chapin.** *Review of Scientific Instruments*, volume 20, December 1949, pages 945–46.

715. An Approach to the Operation of Inductors and Transformers in Terms of the Field Impedance, **W. H. B. Cooper.** *Proceedings*, Institution of Electrical Engineers, volume 96, part 2, June 1949, pages 509–17.

716. Saturating Core Devices (book), **L. R. Crow.** The Scientific Book Publishing Company, Vincennes, Ind., 1949.

717. Magnetic Anisotropy in Cold-Reduced Electrical Sheet Steel, **A. E. DeBarr.** *Proceedings*, Institution of Electrical Engineers, volume 96, part 2, October 1949, pages 719–28.

718. On the Propagation of Large Barkhausen Discontinuities in Ni-Fe Alloys, **L. J. Dijkstra, J. L. Snoek.** *Philips Research Report*, volume 4, October 1949, pages 334–56.

719. Self-Saturation in Magnetic Amplifiers, **W. J. Dornhoefer.** *Electrical Engineering*, volume 68, November 1949, page 988, also *AIEE Transactions*, volume 68, part 2, 1949, pages 835–50.

720. Nonmetallic Materials Developed With Improved Magnetic Properties, Editor. *Materials and Methods*, volume 29, June 1949, pages 54–55.

721. Magnetic Amplifiers for Thermocouples, Editor. *Metallurgia*, volume 41, November 1949, page 34.

722. Steady-State Analysis of a Magnetic Amplifier (Report R-196–49, PIB-140, Contract N6ori-98, Task Order 4), **W. H. Esselman, E. J. Smith.** Polytechnic Institute of Brooklyn, Microwave Research Institute (New York, N. Y.), April 13, 1949.

723. Straight Line Analysis of Full-Wave Magnetic Amplifier (Report R-223–49, PIB-168, Contract N6ori-98, Task Order 4), **W. H. Esselman,** Polytechnic Institute of Brooklyn, Microwave Research Institute (New York, N. Y.), September 8, 1949.

724. Permeability and Eddy Currents in Sheet Metal Cores at Very High Frequencies, **F. Feldtkeller.** *Frequenz*, volume 3, April 1949, pages 111–16, also abstract, number 2808, *Wireless Engineer*, October 1949.

725*. Magnetic Amplifier System, **A. S. FitzGerald.** United States patent 2,461,046, February 8, 1949 (M/A Class I,A,3,4,a).

726*. Magnetic Amplifier, **A. S. FitzGerald.** United States patent 2,464,639, March 15, 1949 (M/A Class I,A,2,a,c,g).

727. Feedback in Magnetic Amplifiers, Parts I–II, **A. S. FitzGerald.** *Journal*, Franklin Institute, volume 247, March 1949, pages 223–43, and volume 247, May 1949, pages 457–71, also *Electrical Communication*, volume 27, December 1950, pages 298–319.

728. An Experimental Study of the Magnetic Amplifier and the Effects of Supply Frequency on Performance, **E. H. Frost-Smith.** *Journal*, British Institution of Radio Engineers, volume 9, December 1949, page 358.

729. Theoretical and Experimental Study of the Series-Connected Magnetic Amplifier, **H. M. Gale, P. D. Atkinson.** *Proceedings*, Institution of Electrical Engineers, volume 96, part 1, May 1949, pages 99–114, continued volume 96, part 2, June 1949, pages 339–54. Discussions: volume 96, part 1, May 1949, pages 115–24; volume 96, part 2, June 1949, pages 355–64; volume 96, part 2, October 1949, pages 767–68; volume 97, part 2, February 1950, pages 14–16; volume 97, part 1, March 1950, pages 85–88; volume 97, part 1, November 1950, pages 302–03; volume 98, part 1, January 1951, pages 41–43; volume 98, part 2, February 1951, pages 100–05.

730. Soft Magnetic Materials, **E. A. Gaugler.** *Product Engineering*, volume 20, July 1949, pages 84–89.

731. Magnetic Amplifiers, **J. Grieg.** *Nature*, volume 163, March 26, 1949, page 501.

732. On the Measurement of Magnetic Permeability at Ultra-High Frequency, **J. S. Guicherd, P. Grivet.** *Comptes Rendus des Seances de l'Academie des Sciences*, volume 228, June 8, 1949, page 1796.

733. Magnetic Amplifier Studies on the Analog Computer, **E. L. Harder, W. H. Hamilton, D. F. Aldrich, J. T. Carleton, F. N. McClure.** *Proceedings*, the National Electronics Conference, volume 5, 1949, pages 222–34.

734. Universal Curves for D-C Controllable Reactors, **W. C. Johnson, B. C. Merrell, R. E. Alley, Jr.** *AIEE Transactions*, volume 68, part 1, 1949, pages 31–40 and *Electrical Engineering*, volume 68, May 1949, page 417.

735. Standardization of Reactor Ratings, **F. H. Kierstead, J. L. Thomason.** *AIEE Transactions*, volume 68, 1949, pages 955–58.

736. Resonant Circuits With Time-Varying Parameters, **R. H. Kingston.** *Proceedings*, Institute of Radio Engineers, volume 37, December 1949, pages 1478–81.

737. The Magnetic Amplifier, **P. M. Kintner, G. H. Fett.** *Radio and Television News*, volume 13, August 1949, pages 14–18, 26–28.

738. A Method for Designing Pulse Transformers, **H. S. Kirschbaum, C. E. Warren.** *AIEE Transactions*, volume 68, 1949, pages 971–78.

739. Physical Theory of Electromagnetic Domains, **C. Kittel.** *Review of Modern Physics*, volume 21, October 1949, pages 541–83.

740. Development of Audio Amplifier Stage (Final Report, Contract NObs 46256, Task Order 1), **W. C. Kluz.** BuShips, Navy Department, Ward-Leonard Electric Company (Mt. Vernon, N. Y.), November 28, 1949.

741. Collected Data on the Magnetic Properties of Non-Metallic Compounds (Memo NOLM 10496), **C. J. Kriessman, Jr.** Naval Ordnance Laboratories, September 26, 1949.

742. Barkhausen Noise and Magnetic Amplifiers: I. Theory of Magnetic Amplifiers, II. Analysis of the Noise, **J. A. Krumhansl, R. T. Beyer.** *Journal of Applied Physics*, volume 20, May 1949, pages 432–36, and volume 20, June 1949, pages 582–86.

743. The Use of Ferrite Cored Coils as Converters, Amplifiers, and Oscillators, **V. D. Landon.** *RCA Review*, volume 10, September 1949, pages 387–96.

744. The Problem of the Magnetic Amplifier and Some Approaches to Its Solution, **M. Liwschitz-Garik, E. J. Smith, E. Weber.** *Proceedings*, National Electronics Conference, volume 5, 1949, pages 235–54.

745. Amplification by Magnetization, **F. N. McClure.** *Westinghouse Engineer*, volume 9, May 1949, pages 92–96.

746. The Magnetic Cross Valve and Its Application to Subfrequency Power Generation, **H. J. McCreary.** *Proceedings*, National Electronics Conference, volume 5, 1949, pages 450–66.

747. Saturable Core Reactors as Digital Computer Elements (Contract Nobsr-42001), **J. G. Miles.** BuShips, Navy Department, Engineering Research Associates, Inc. (St. Paul, Minn.), June 17, 1949.

748. Magnetic Amplifiers, **A. G. Milnes.** *Proceedings*, Institution of Electrical Engineers, volume 96, part 1, May 1949, pages 89–98, and volume 96, part 2, June 1949, pages 329–38, also Discussion: volume 96, part 1, May 1949, pages 115–24; volume 96, part 2, June 1949, pages 355–64; volume 97, part 1, November 1950, pages 302–03; volume 98, part 1, January 1951, pages 40–41; volume 98, part 2, February 1951, pages 100–01; *Electrical Review*, volume 143, December 10, 1948, pages 899–900, also Abstracts: *Electrical Review*, volume 143, December 10, 1948, page 899; *Electrician*, volume 141, December 10, 1948, pages 1739–40; volume 142, April 15, 1949, page 1120.

749. The Amplistat: A Magnetic Amplifier, **R. E. Morgan.** *Electrical Engineering*, volume 68, August 1949, pages 663–67.

750. Instrument Amplifier (Contract NObs-47610), **R. E. Morgan, H. Gottliebsen.** BuShips, Navy Department, General Electric Company (Schenectady, N. Y.), September 14, 1949.

751. Electronic Classifying Cataloging and Counting Systems, **J. H. Parsons.** *Proceedings*, Institute of Radio Engineers, volume 37, May 1949, pages 564–68.

752. Magnetic Amplifier Increases Speed Range of Motor, **J. E. Priest.** *Electrical World*, volume 132, July 16, 1949, page 94, also *Machine Design*, volume 21, August 1949, page 208.

753. Electrical Instrument With Electromagnetic Feedback, **H. B. Rex.** United States patent 2,486,657, October 25, 1949 (M/A Class I,A,1,4,a).

754. Non-Homonic Oscillations as Caused by Magnetic Saturation, **R. Rudenberg.** *AIEE Transactions*, volume 68, 1949, pages 676–85.

755. A Recent Development in Soft Magnetic Materials, **H. H. Scholefield.** *Journal of Scientific Instruments*, volume 26, June 1949, pages 207–09, also Abstract 2810, *Wireless Engineer*, October 1949.

756. A Study of Self-Saturating Magnetic Amplifiers: Part I—Steady-State Response of Half-Wave Circuit (ONR Contract N6ori-98, Task Order 4), **E. J. Smith.** Polytechnic Institute of Brooklyn (Brooklyn, N. Y.), *Report R-229-49, PIB-174*, December 30, 1949.

757. A Study of Self-Saturating Magnetic Amplifiers: Part II—Investigation of Rectifier Reverse Current Flow and Steady State Analysis of Full-Wave and Doubler Circuits (ONR Contract N6ori-98, Task Order 4), **E. J. Smith.** Polytechnic Institute of Brooklyn (Brooklyn, N. Y.), *Report R-230-50, PIB-175*, February 20, 1950.

758. A Study of Self-Saturating Magnetic Amplifiers: Part III—Influence of Control Circuit Resistance on Steady-State Performance (ONR Contract N6ori-98, Task Order 4), **E. J. Smith.** Polytechnic Institute of Brooklyn (Brooklyn, N. Y.), *Report R-231-50, PIB-176*, March 27, 1950.

759. Magnetic Amplifiers (Report UA-514-P-1), **H. J. Smith, J. W. Ford.** Cornell Aeronautical Laboratories, Inc. (Buffalo, N. Y.), August 23, 1949.

760. Magnetic Ferrites-Core Materials for High Frequencies, **C. L. Snyder, E. Albers-Schoenberg, H. A. Goldsmith.** *Electrical Manufacturing*, December 1949.

761. Final Report, First Phase of Contract NObs 45156, **F. L. Spencer, Jr.** BuShips, Navy Department, Eclipse-Pioneer Division, Bendix Aviation Corporation (Teterboro, N. J.), January 20, 1949.

762. Characteristics of Magnetic Amplifiers Employing E-I and D-U Laminated Cores and Grain-Oriented Toroidal Cores (Summary Reports 5–7 and Final Report on Phase 2, Contract NObs 45156), **F. L. Spencer, Jr.** BuShips, Navy Department, Eclipse-Pioneer Division, Bendix Aviation Corporation (Teterboro, N. J.), June 17, 1949.

763. Magnetic Amplifier Characteristics and Application Data (Contract NObs 45156), **F. L. Spencer, Jr.** BuShips, Navy Department, Eclipse-Pioneer Division, Bendix Aviation Corporation (Teterboro, N. J.), December 16, 1949.

764. Magnets From Pure Iron Powder, **R. Steinitz.** *Metal Progress*, volume 55, June 1949, page 858, also Abstract 2816, *Wireless Engineer*, October 1949.

765. A Universal Ceramic Core Sweep Transformer—Parts I and II, **C. E. Torsch.** *Tele-Tech*, volume 8, December 1949, pages 23–25, 49, and volume 9, January 1950, pages 34–35.

766. Magnetic Amplifying Circuits, **S. E. Tweedy.** United States patent 2,475,575, July 5, 1949 (M/A Class I,A,3,a).

767. Analytical Determination of Characteristics of Magnetic Amplifiers With Feedback, **D. W. VerPlanck, L. A. Finzi, D. C. Beaumariage.** *AIEE Transactions*, volume 68, part 1, 1949, pages 565–70.

768. Analysis of Magnetic Amplifiers With Feedback, **D. W. VerPlanck, M. Fishman, D. C. Beaumariage.** *Proceedings*, Institute of Radio Engineers, volume 37, August 1949, pages 862–66, also Report, ONR Contract N6ori-47, Task Order 5, and Abstract, *Proceedings*, National Electronics Conference, November 6, 1948, page 426.

769. Analysis of Interlinked Electric and Magnetic Networks With Application to Magnetic Amplifiers, **D. W. VerPlanck, M. Fishman.** *Proceedings*, Institute of Radio Engineers, volume 37, September 1949, pages 1021–27, also Report, ONR Contract N6ori-47, Task Order 5, and Abstract, *Proceedings*, National Electronics Conference, November 6, 1948, page 426.

770. Magnetic Amplifier Design Handbook (book), Vickers Electric Division, Vickers, Inc. (St. Louis, Mo.), July 1949.

1950

771. Saturable Magnetic Core, **J. Q. Adams.** United States patent 2,498,475, February 21, 1950 (M/A Class I,A,1,c,d).

772. Ferromagnetic Oxide Bodies—A Counterpart to the Ceramic Dielectrics, **E. Albers-Schoenberg.** *Ceramic Age*, volume 56, October 1950, pages 14–16.

773. Improved Core Material for 400-Cycle Airborne Power Transformers (Development of Magnetic Materials) (Progress Report 17), American Rolling Mills Company, Middletown, Ohio, Armco-Navy Contract NOa(s) 8944, March 14, 1950.

774. An Instrument for Measuring Magnetic Hysteresis, **J. W. Apperson, E. F. Hansen.** *General Electric Review*, volume 53, October 1950, pages 53–60:

775. Routine Testing Equipment for Transformer Steels, **N. F. Astbury, T. Emmerson, J. McFarlane.** *Proceedings*, Institution of Electrical Engineers, volume 97, part 2, April 1950, page 221.

776. Theory of the No Load Characteristics of Saturable Reactors With Hysteresis, **I. A. Banos, Jr., W. B. McLean.** *Physical Review*, volume 78, April 15, 1950, page 92.

777. Gyromagnetic Phenomena Occurring With Ferrites, **H. G. Beljers, J. L. Snoek.** *Philips Technical Review*, volume 11, May 1950, pages 313–22.

778. Reactive Circuits as Computers and Analogues, **D. A. Bell.** *Electronic Engineering*, volume 22, June 1950, pages 232–35.

779. Analysis of Saturable Reactor, **L. A. Bessonov.** *Electrishestvoo*, number 5, May 1950, pages 61–65.

780. An Extension of a Theory of Magnetic Amplifiers, **R. T. Beyer, M. Y. Wei.** *Journal*, Franklin Institute, volume 250, July 1950, pages 25–37.

781. Graphical Method to Analyze and Design Saturable Reactors, **A. S. Bogoslovskic.** *Electrichestvoo*, number 10, October 1950, pages 54–61.

782. Factors Affecting Magnetic Quality, **R. M. Bozorth.** *Bell System Technical Journal*, volume 29, April 1950, pages 251–86.

783. Sensing Small Motions: (1) With Variable Reactors, (2) With Differential Transformers, **T. R. Breunich.** *Product Engineering*, volume 21, July 1950, pages 113–17.

784. The Use of a Miniature Lloyd-Fisher Square for Power-Loss Measurements at Audio Frequencies, **O. I. Butler.** *Proceedings*, Institution of Electrical Engineers, volume 97, part 2, April 1950, page 215.

785. The Incremental Magnetic Properties of Silicon-Iron Alloys, **R. O. Cartier.** *Proceedings*, Institution of Electrical Engineers, volume 97, part 2, April 1950, page 199.

786. The Magnetic Amplifier, **N. R. Castellini.** *Proceedings*, Institute of Radio Engineers, volume 38, February 1950, pages 151–58.

787. Noise Figure of the Magnetic Amplifier, **N. R. Castellini.** *Proceedings*, National Electronics Conference, volume 6, 1950, pages 52–58.

788. Recording Fluxmeter of High Accuracy and Sensitivity, **P. P. Cioffi.** *Review of Scientific Instruments*, volume 21, July19 50, pages 624–28.

789. Analysis and Design of Self-Saturable Magnetic Amplifiers, **S. Cohen.** *Conference Paper*, Institute of Radio Engineers National Convention, March 8, 1950.

790. Effect of Rectifier Leakage on Magnetic Amplifier Performance (Summary Report, Contract NObs 46768), **J. Conrath.** BuShips, Navy Department, Vickers, Inc. (St. Louis, Mo.), January 20, 1950.

791. Symposium of Papers on Ferromagnetic Materials, Editor. *Proceedings*, Institution of

Electrical Engineers, volume 97, part 2, April 1950, pages 118–274.

792. Rectifier With Direct-Current Saturable Reactor for Voltage Regulation, **H. Elmlund, A. U. Lamm.** United States patent 2,524,220, October 3, 1950 (M/A Class I,A,1,a,c).

793. The Tracing and Interpretation of Asymmetrical Hysteresis Loops, **G. M. Ettinger.** *Journal of Applied Physics*, volume 21, September 1950, pages 936–37.

794. The Magnetic Amplifier, Transductor Theory, **R. Feinberg.** *Wireless Engineer*, volume 27, April 1950, pages 118–24.

795. A Review of Transductor Principles and Applications, **R. Feinberg.** *Proceedings*, Institution of Electrical Engineers, volume 97, part 2, October 1950, pages 628–44.

796. Inductors, Their Calculation and Losses, **R. F. Field.** *Conference Paper*, Institute of Radio Engineers National Convention, March 8, 1950.

797. General Characteristics of Magnetic Amplifiers, **L. A. Finzi, D. C. Beaumariage.** *AIEE Transactions*, volume 69, 1950, pages 919–27, and Report, ONR Contract N7onr 30306, part 7.

798*. Magnetic Amplifier for Reversible Currents, **H. Forssell.** United States patent 2,504,675, April 18, 1950 (M/A Class I,A,1,2,4,a,c).

799. Magnetic Amplifiers of the Balance Detector Type—Their Basic Principles, Characteristics and Applications, **W. A. Geyger.** *Electrical Engineering*, volume 69, May 1950, page 459.

800. Magnetic Amplifiers With Orthonol Tape Cores, **W. A. Geyger.** *Proceedings*, National Electronics Conference, volume 6, 1950, pages 59–67.

801. Selective Output Saturable Reactor Amplifier Circuit, **P. Glass.** United States patent 2,493,130, January 3, 1950 (M/A Class I,A,2,4).

802. Magnetic Cores of Thin Tape Insulated by Cataphoresis, **H. L. B. Gould.** *Electrical Engineering*, volume 69, June 1950, page 544, also Abstract, *Bell Laboratories Record*, volume 28, July 1950, pages 292–94.

803. D-C Control With Amplistats, **W. L. O. Graves, H. M. Ogle.** *Product Engineering*, volume 21, February 1950, pages 81–84.

804*. Magnetic Amplifier for Inductive Loads, **W. L. O. Graves.** United States patent 2,516,563, July 25, 1950 (M/A Class I,A,1,b,g).

805. Practical Calculation of Magnetizing Force, **A. A. Halacsy.** *Proceedings*, Institution of Electrical Engineers, volume 97, part 1, March 1950, pages 37–42.

806. Laminated Ferromagnetic Cores at Very Low Inductions for Use in Line Communication, **R. J. Halsey.** *Proceedings*, Institution of Electrical Engineers, volume 97, part 2, April 1950, page 141.

807. Response Time of Magnetic Amplifiers, **E. L. Harder, W. F. Horton.** *AIEE Transactions*, volume 69, 1950, pages 1130–41.

808. Saturable Reactor System, **S. V. Hart.** United States patent 2,497,218, February 14, 1950 (M/A Class III,C).

809. Ferromagnetic Spinels for Radio Frequencies, **R. L. Harvey, I. J. Hegyi, H. W. Leverenz.** *RCA Review*, volume 11, September 1950.

810*. Electromagnetic Amplifier, **S. E. Hedström.** United States patent 2,509,864, May 30, 1950 (M/A Class I,A,2,a,b,g).

811. Frequency Compensated Saturable Reactor System, **S. E. Hedström, R. Svensson.** United States patent 2,509,865, May 30, 1950 (M/A Class I,A,1,e,g).

812. A Theory of the Series Transductor, **C. S. Hudson.** *Proceedings*, Institution of Electrical Engineers, volume 97, part 2, December 1950, pages 751–55.

813. A Direct Current Amplifier as Power Amplifier for Temperature Control, **W. Jellinghaus.** *Zeitschrift fur Angewandte Physik*, June 1950, pages 254–61.

814. A Magnetic Amplifier Frequency Control, **L. J. Johnson, H. G. Schafer.** *AIEE Transactions*, volume 69, 1950, pages 613–15, and abstract, *Electrical Engineering*, volume 69, May 1950, page 445.

815. Analysis of Transients and Feedback in Magnetic Amplifiers, **W. C. Johnson, F. W. Latson.** *AIEE Transactions*, volume 69, 1950, pages 604–12, also *Electrical Engineering*, volume 69, April 1950, pages 353–59.

816. Experimental Magnetic-Type DC-AC Signal Inverter, **J. Kauke.** *Radio and Television News*, volume 43, May 1950, pages 64–65.

817. Static Magnetic Amplifier for Regulating Circuits, **H. E. Larson, T. Dunnegan, Jr.** *Iron and Steel Engineer*, volume 27, July 1950, pages 88–102.

818. A Survey of the Possible Applications of Ferrites, **K. E. Latimer, H. B. MacDonald.** *Proceedings*, Institution of Electrical Engineers, volume 97, part 2, April 1950, page 257.

819. Flashtube Triggering Circuits, **H. W. Lord.** United States patent 2,509,005, May 23, 1950 (M/A Class II,A).

820*. Balanced Magnetic Amplifier, **H. W. Lord.** United States patent 2,509,738, May 30, 1950 (M/A Class I,A,3,b,d,e).

821. Three-Dimensional Information Storage Using Magnetic Cores (Summary Report 24, Project Whirlwind, ONR Contract N5ori60, Project NR-048-097), Massachusetts Institute of Technology, Servomechanisms Laboratory (Cambridge, Mass.), Third Quarter, 1950, pages 11–14.

822. Application of Magnetic Amplifiers, **F. N. McClure.** *Electrical Engineering*, volume 69, June 1950, pages 538–43.

823. Magnetic Amplifiers in Industry, **F. N. McClure.** *Westinghouse Engineer*, volume 10, September 1950, pages 201–05.

824. The Measurement and Calculation of Pulse Magnetization Characteristics of Nickel Irons From 0.1 to 5 Microseconds, **W. S. Melville.** *Proceedings*, Institution of Electrical Engineers, volume 97, part 2, April 1950, page 165.

825. A New Theory of the Magnetic Amplifier, **A. G. Milnes.** *Proceedings*, Institution of Electrical Engineers, volume 97, part 2, August 1950, pages 460–83, also Abstract (by author), volume 97, part 3, November 1950, pages 462–64.

826. The Extension of Amplistat Performance by Alternating Current Components, **R. E. Morgan, H. M. Ogle, V. J. Wattenberger.** *AIEE Transactions*, volume 69, 1950, pages 986–91.

827. Oriented Crystals: Their Growth and Their Effects on Magnetic Properties, **W. Morrill.** *General Electric Review*, volume 53, August 1950, pages 16–21.

828. New Developments in the Field of Self-Saturating Magnetic Amplifiers, **R. H. Munch.** *Industrial and Engineering Chemistry*, volume 42 (supplement-107A–108A), September 1950.

829. The Amplistat and Its Application, Parts I, II, III, **H. M. Ogle.** *General Electric Review*, volume 53, February 1950, pages 32–35, and volume 53, August 1950, pages 41–44, and volume 53, October 1950, pages 41–46.

830. A Coincident-Current Magnetic Memory Unit (Project Whirlwind Report R-192, ONR Contract N5ori60), **W. N. Papian.** Massachusetts Institute of Technology, Servomechanisms Laboratory (Cambridge, Mass.), September 8, 1950, also Massachusetts Institute of Technology, Electrical Engineering Department, Master of Science Thesis, August 31, 1950.

831. Influence of Design Parameters on the Performance of Direct Current Transformers, **Y. B. Perets.** *Electrichestvoo*, number 2, February 1950, pages 66–69.

832. The Eddy-Current and Screen Losses of a Screened Single-Layer Solenoid, **F. M. Phillips.** *Proceedings*, Institution of Electrical Engineers, volume 97, part 3, March 1950, pages 77–87.

833. Ferrite Materials, **D. Polder.** *Proceedings*, Institution of Electrical Engineers, volume 97, part 2, April 1950, page 246.

834. Some Metallurgical and Structural Factors Affecting Properties of Soft Magnetic Materials, **W. F. Randall, H. H. Scholefield.** *Proceedings*, Institution of Electrical Engineers, volume 97, part 2, April 1950, page 133.

835. Regulation With Magnetic Amplifiers, **I. I. Ratgaus, S. A. Dohman.** *Electrichestvoo*, number 5, May 1950, pages 44–46.

836. Amplitude Method to Design Saturable Reactors, **A. M. Ribkin.** *Electrichestvoo*, number 8, August 1950, pages 57–63.

837. Some Properties and Tests of Magnetic Powders and Powder Cores, **C. E. Richards, S. E. Buckley, P. R. Bardell, M. A. Lynch.** *Proceedings*, Institution of Electrical Engineers, volume 97, part 2, April 1950, page 236.

838. Determination of Steady-State Performance of Self-Saturating Magnetic Amplifiers, **E. J. Smith.** *AIEE Transactions*, volume 69, 1950, pages 1309–17.

839. The Theory of the Current Transductor and Its Application in the Aluminum Industry, **T. R. Specht, R. N. Wagner.** *AIEE Transactions*, volume 69, 1950, pages 441–52, also *Electrical Engineering*, volume 69, September 1950, pages 828–32.

840. Losses in Electrical Sheet Steel, **K. H. Stewart.** *Proceedings*, Institution of Electrical Engineers, volume 97, part 2, April 1950, page 121.

841. Series Connected Saturable Reactor With Control Source of Comparatively Low Impedance, **H. F. Storm.** *AIEE Transactions*, volume 69, part 2, 1950, pages 756–65.

842. Series Connected Saturable Reactor With Control Source of Comparatively High Impedance, **H. F. Storm.** *AIEE Transactions*, volume 69, 1950, part 2, pages 1299–1309.

843. Ferromagnetic Materials and Ferrites, Properties and Applications, **M. J. O. Strutt.** *Wireless Engineer*, volume 27, December 1950, pages 277–84.

844. Investigations on Reversible Susceptibility of Ferromagnetics, **R. S. Tebble, W. D. Corner.** *Proceedings*, Physical Society, volume 63, December 1, 1950, pages 1005–16.

845*. Binary Counting Circuit, **R. L. Thompson.** United States patent 2,519,513, August 22, 1950 (M/A Class I,A,4,a).

846. An Analysis of Transients in Magnetic Amplifiers (Without Feedback), **D. W. Ver-Planck, L. A. Finzi, D. C. Beaumariage.** *AIEE Transactions*, volume 69, part 1, 1950, pages 498–503, also Report on ONR Contract N6ori-47, part 6.

847. Output Characteristics and Frequency Response of Magnetic Amplifiers, Vickers Electric Division, Vickers, Inc. (St. Louis, Mo.), Supplement to Bulletin 2000 (Under cover of Issue 50D), October 1950, pages 11–14.

848. Static Magnetic Storage and Delay Line, **A. Wang, W. D. Woo.** *Journal of Applied Physics*, volume 21, January 1950, pages 49–54.

849. Static Magnetic Pulse Control and Information Storage, **A. Wang.** *Conference Paper number 75*, Institute of Radio Engineers National Convention, New York, N. Y., March 8, 1950.

850. Magnetic Triggers, **A. Wang.** *Proceedings*, Institute of Radio Engineers, volume 38, June 1950, pages 626–29.

851. Magnetic Amplifiers (ONR Report), **E. Weber.** Polytechnic Institute of Brooklyn, Microwave Research Institute (New York, N. Y.), September 1950.

852. On the Determination of the Complex Permeability of Ferromagnetic Conductors at High Frequencies, **A. Wieberdink.** *Applied Scientific Research*, volume B1, number 6, 1950, pages 439–52.

853. The Fundamental Limitations of the Second-Harmonic Type of Magnetic Modulator as Applied to the Amplification of Small D-C Signals, **F. C. Williams, S. W. Noble.** *Proceedings*, Institution of Electrical Engineers, volume 97, part 2, August 1950, pages 445–59, and discussion, volume 97, part 2, August 1950, pages 474–83, also abstract, volume 97, part 3, November 1950, pages 461–62, and abstract, *Electrical Record*, volume 146, March 1950, page 466.

854. Ferromagnetic Domains, **H. J. Williams.** *Electrical Engineering*, volume 69, September 1950, pages 817–22.

855. Magnetic Amplifier Voltage Regulator, **J. L. Wolff.** *Proceedings*, National Electronics Conference, volume 6, 1950, pages 45–51.

856*. Electrical Trigger, **M. L. Wood.** United States patent 2,524,154, October 3, 1950 (M/A Class 1,A,4,a).

857. Frequency Analysis of Variable Networks, **L. A. Zadeh.** *Proceedings*, Institute of Radio Engineers, volume 38, March 1950, pages 291–99.

1951

858. Progress Report of the AIEE Magnetic Amplifier Subcommittee, **AIEE Magnetic Amplifier Subcommittee.** *AIEE Transactions*, volume 70, part 1, 1951, pages 445–50.

859. Ferromagnetism (book), **R. M. Bozorth.** D. Van Nostrand Company, Inc., New York, N. Y., 1951.

860. Structure and Properties of Ferrites, **F. G. Brockman.** *Electrical Engineering*, volume 70, June 1951, pages 489–94.

861. Saturable Reactors and Control Oscillators, **E. Bukstein.** *Radio and Television News*, volume 45, April 1951, pages 42, 120–21.

862. The C. G. S. Increductor (pamphlet). C. G. S. Laboratories, Inc. (Stamford, Conn.), 1951.

863. H. F. Magnetization of Ferromagnetic Laminae, **H. R. Chablani.** *Wireless Engineer*, volume 28, March 1951, pages 92–97.

864. Experimental Preparation of Ferrites, **Editor.** *Bell Laboratories Record*, volume 29, May 1951, pages 206–08.

865. Prospects for Magnetic Amplifiers, **Editor.** *Product Engineering*, volume 22, May 1951, page 143.

866. Steady-State Analysis of Self-Saturating Magnetic Amplifiers Based on Linear Approximations of the Magnetization Curve, **W. H. Esselman.** *AIEE Transactions*, volume 70, part 1, 1951, pages 451–59.

867. Direct-Current Amplifiers Employing Magnetors, **E. P. Felch, V. E. Legg, F. G. Merrill.** *Conference Paper*, Institute of Radio Engineers National Convention, New York, N. Y., March 1951.

868. Transient Response of Magnetic Amplifiers, **L. A. Finzi, D. P. Chandler, D. C. Beaumariage.** *AIEE Transactions*, volume 70, 1951, pages 934–42.

869. Digital Information Storage in Three Dimensions Using Magnetic Cores, **J. W. Forrester.** *Journal of Applied Physics*, volume 22, January 1951, pages 44–48.

870. Ferromagnetic Ceramics, **H. A. Goldsmith.** *Product Engineering*, volume 22, April 1951, pages 97–102.

871. Investigations for Design of Digital Calculating Machinery (USAF Contracts W-19-122-ac-24 and AF-33(038)9461), Harvard University Computation Laboratory Staff, Progress Reports number 2, August 10, 1948 to November 10, 1948; number 3, November 10, 1948 to February 10, 1949; number 4, February 10, 1949 to May 10, 1949; number 5, May 10, 1949 to August 10, 1949; number 6, August 10, 1949 to November 10, 1949; number 7, November 10, 1949 to February 10, 1950; number 8, February 10, 1950 to May 10, 1950; number 10, May 10, 1950 to August 10, 1950; number 13, August 10, 1950 to November 10, 1950; number 16, November 10, 1950 to February 10, 1951.

872. A Magnetic Scaling Circuit, **H. Hertz.** *Journal of Applied Physics*, volume 22, January 1951, pages 107–08.

873. Static Magnetic Memory, **M. Kincaid, J. M. Alden, R. B. Hanna.** *Electronics*, volume 24, January 1951, pages 108–11.

874. Thin Ferromagnetic Films, **M. J. Klein, R. S. Smith.** *Physical Review*, volume 81, February 1951, pages 378–80.

875. Ferrites: New Magnetic Materials for Communication Engineering, **V. E. Legg.** *Bell Laboratories Record*, volume 29, May 1951, pages 203–06.

876. High Saturation Magnetic Alloy With Rectangular Hysteresis Loop, **J. F. Libsch, E. Both.** *Electrical Engineering*, volume 70, May 1951, pages 420–21.

877. Magnetic Amplifiers Voltage Regulator. Magnetic Amplifiers, Inc. (Long Island City, N. Y.), (Memo-EM234-1951), 1951.

878. Some General Properties of Magnetic Amplifiers, **J. M. Manley.** *Proceedings*, Institute of Radio Engineers, volume 39, March 1951, pages 242–51.

879. The Use of Saturable Reactors as Discharge Devices for Pulse Generators, **W. S. Melville.** *Proceedings*, Institution of Electrical Engineers, volume 98, part 3, May 1951, pages 185–89.

880. Saturable Reactors as Substitutes for Electron Tubes in High Speed Digital Computers, **J. G. Miles.** *Conference Paper*, Institute of Radio Engineers National Convention, New York, N. Y., March 1951.

881. Amplistat Circuits for Voltage Control of Power Rectifiers, **M. J. Mulhern.** *General Electric Review*, volume 54, May 1951, pages 27–33.

882. Ferromagnetic Cores for Three-Dimensional Digital Storage Arrays, **W. N. Papian.** *Conference Paper, number 88*, Institute of Radio Engineers National Convention, New York, N. Y., March 1951.

883. A 300- to 4,000-Kilocycle Electrically Tuned Oscillator, **A. I. Pressman, J. P. Blewett.** *Proceedings*, Institute of Radio Engineers, volume 39, January 1951, pages 74–77.

884. On the Mechanics of Magnetic Amplifier Operation, **R. A. Ramey.** Naval Research Laboratory Report, number 3799, January 22, 1951.

885. The Magnetic Amplifier (book), **J. H. Reyner.** Stewart and Richards, London, England, February 1951.

886. Transient Response of Self-Saturating Magnetic Amplifiers, **E. J. Smith.** *Conference Paper*, Institute of Radio Engineers National Convention, New York, N. Y., March 1951.

887. How Magnetic Amplifiers Operate, **G. H. Stearley.** *Product Engineering*, volume 22, January 1951, pages 132–36.

888. Transient Response of Saturable Reactors With Resistive Load, **H. F. Storm.** *AIEE Transactions*, volume 70, part 1, 1951, pages 95–102, also *Electrical Engineering*, volume 70, May 1951, page 442.

✓889. Magnetic Amplifiers—A Rising Star in Naval Control Equipment (pamphlet), **A. M. Vincent** (United States Navy). Navy BuShips, Electronics Design and Development Division, Code 815, Washington, D. C.

890. Magnetic Delay-Line Storage, **A. Wang.** *Proceedings*, Institute of Radio Engineers, volume 39, April 1951, pages 401–07.

891. A Simple Magnetic Modulator for Conversion of Millivolt D-C Signals, **G. Wennerberg.** *Electrical Engineering*, volume 70, February 1951, pages 144–47.

892. Some Aspects of Magnetic Amplifier Technique, **R. Willheim, F. E. Butcher.** *Conference Paper*, Institute of Radio Engineers National Convention, New York, N. Y., March 1951.

ADDENDA

893. Description of a Graphical Method of Calculating a Transductor (Special Technical Report, number 8), **Lt. H. Allam.** Royal Navy 472.5, British Naval Gunnery Mission.

894. Reactor Drive for Operation of Fuel Pumps, Askania Regulator Company, Supplementary Report on Contract NObs-20970.

895. Final Report Number 864, BIOS, Item numbers 1 and 7, M-473-47.

896. Transductors: D-C Controlled Saturable Reactors for Magnetic Amplifiers (Report EL 1433), **A. G. Milnes.** Royal Aircraft Establishment.

897. Magnetic Amplifier Instrument Amplifier (USN Contract—49), **R. E. Morgan, L. H. Gottlebsen.**

898. Magnetic Amplifiers (Technical Report OANAR 39-47), Office of Naval Research (London, England).

899. A High Grain Magnetic Amplifier to Operate a Relay in an Electronic Torquemeter Circuit (Report EL 1411), Royal Aircraft Establishment (Farnborough, England).

900. Magnetic Amplifier Voltage Regulator (Navy Contract Memo EM 234), **A. A. Stork.**

901. Fuel Pump Reactor Drive (Final Report), Applied Science Research Laboratory, University of Cincinnati, Cincinnati, Ohio.

Table II. Significant Patents to Magnetic Amplifier Art

(Chronological by Filing Date)

Patentee	United States Pat. No.	Filed	Issued	Magnetic Amplifier Type																Reason Selected
				A	B′	B″	C	1	2	3	4	a	b	c	d	e	f	g	h	
Burgess, C. F. & Frankenfield, B.	720,884	6-12-01	2-17-03	A				1												Early d-c saturable reactor. Control circuit decoupling means as follows: series impedance 3-legged and 4-legged cores, hollow annular cores, and magnetic "cross valve" core arrangements
Crocker, F. B.	891,797	7-25-04	6-23-08		B′			1												Early d-c saturable transformer. Control circuit decoupling means utilizing a 3-legged core.
Alexanderson, E. F. W.	1,206,643	12-07-12	11-28-16	A				1						c						First to mention gain properties. Early d-c saturable reactor with d-c bias means. Control circuit decoupling means employing two cores, also 4-legged cores.
Osnos, M.	1,227,302	7-08-15	5-22-17	A																Saturable reactors with 2-core and 3-legged core control circuit decoupling means.
Elmen, G. W.	1,289,418	11-23-15	1-31-18	A						3									h	Early Wheatstone bridge circuit employing signal-controlled reactor in one arm. Novel control means is by controlling the amount of agitating magnetomotive force to obtain variable hysteresis-effect reduction. Hollow annular core for circuit decoupling.
Alexanderson, E. F. W.	1,328,797	11-26-15	1-20-20	A				1				a		c		e				Early illustration of external feedback means. Control circuit decoupling means employing two cores, also 4-legged and 8-legged cores.
Alexanderson, E. F. W.	1,328,610	1-21-16	1-20-20	A				1						c		e	f			Early to claim off-resonant principle for increased gain. Also frequency discriminating means in a-c power supply and control circuits. Early illustration of cascaded magnetic amplifier stages.
Hartley, R. V. L.	1,462,038	12-30-16	7-17-23		B′				2					c			f			A fundamental push-pull magnetic modulator.
Hartley, R. V. L.	1,287,982	2-16-17	12-17-18		B′			1						c					h	D-c saturable transformer with ultra-carrier frequency magnetomotive force means for hysteresis-effect reduction.
Stoekle, E. R.	1,376,978	11-24-17	5-03-21			B″		1												Fundamental d-c saturable transformers with controlled-reluctance shunts; useful embodiments.
Alexanderson, E. F. W.	1,328,473	4-20-18	1-20-20	A				1						c		e	f			Means for utilizing a simple winding for the combined functions of saturation control, d-c bias and as the reactance winding of a d-c saturable reactor.
Jonas, J.	1,434,346	10-04-20	10-31-22	A				1				a	b							Early full-wave d-c saturable reactor circuit with internal feedback. Control by d-c saturating winding.
Slepian, J.	1,645,302	4-21-21	10-11-27	A				1				a		c		e	f			A magnetic "self-modulator" (amplitude modulator) employing phase-controlled external feedback.
Heising, R. A.	1,654,932	6-29-22	1-03-28	A				1				a		c		e	f			A magnetic "self-modulator" (amplitude modulator) with external feedback.
Heegner, K.	1,656,195	10-23-25	1-17-28				C													Fundamental negative-resistance type magnetic self-modulator (amplitude modulator). Basic to the general class of magnetic amplifiers with negative resistance characteristics.
Lee, F. W.	Re.19,129	10-30-26	4-03-34	A				1			4									Early means for obtaining zero output current from a magnetic amplifier in response to zero signal input. One embodiment utilizes "dummy" reactors. Early magnetic amplifier employing, though not claiming, Graetz-connected (full-wave bridge) copper oxide rectifiers for demodulation.
Thomas, P.	1,734,239	9-23-27	11-05-29		B′			1							d					A preferred winding configuration for 3-legged core d-c saturable transformers of class B′.
Dowling, P. H.	1,739,579	6-20-28	12-17-29	A				1				a		c		e	f	g		Novel external feedback means comprising center-leg winding shorted by rectifier (for 3-legged cores only). Also novel d-c balancing means in d-c output circuit. Early permanent magnet d-c bias means. Combination circuits.
Dowling, P. H.	1,862,211	6-20-28	6-07-32	A				1				a				e				External feedback type and ferroresonant type magnetic "self-modulators" (amplitude modulators) in which the moduluting frequency is determined by the R-L or L-C time constant of the control circuit.
Dowling, P. H.	1,878,764	6-20-28	9-20-32	A				1			4	a		c		e				Balanced magnetic amplifier comprising an output transformer with two opposing primary windings one of which is seriesed with the reactance winding of a controlling d-c saturable reactor. Zero stage output for zero control signal.
Peterson, E.	1,884,844	3-30-29	10-25-32				C	1									f			Fundamental negative-resistance type magnetic amplifier.
Dowling, P. H.	1,793,213	11-20-29	2-17-31			B″				3										Magnetic amplifier comprising a Wheatstone-bridge shaped core. Bridge balance is affected by controlling the magnetic reluctance of the bridge arms.
Dowling, P. H.	1,910,381	12-26-29	5-23-33	A							4									Novel magnetic amplifier type coincidence detector. D-c saturable reactors and transformers in novel combinations.
Sorensen, A. J.	1,824,577	2-07-30	9-22-31	A						3				c			f			Early Wheatstone bridge type magnetic amplifier. The four reactance arms of the bridge are the four reactance windings on two 3-legged reactors.
Dowling, P. H.	1,891,044	3-25-30	12-13-32		B′			1			4	a			d					Early counter-acting a-c bias magnetomotive force at power supply frequency; means comprises shorting winding linking d-c control leg. Also novel balanced magnetic amplifier comprising d-c saturable reactor in combination with transformer. Novel core and winding configurations. Early external feedback type flip-flop.
Dowling, P. H.	1,835,209	6-23-30	12-08-31	A				1			4									D-c saturable reactors and transformers n novel combinations. Novel core and winding configurations are used.
Dowling, P. H.	1,862,212	6-23-30	6-07-32		B′			1			4				d	e				Series ferroresonant circuit with flip-flop action. Also a novel d-c saturation controlled-balance transformer with opposing secondary windings.
Sorensen, A. J. & Dowling, P. H.	1,914,220	6-23-30	6-13-33	A	B′				2	3	4			c		e				A group of significant and novel push-pull (balanced) magnetic amplifier circuits.
Peterson, E.	1,884,845	9-23-30	10-25-32				C	1									f			Variations on negative-resistance type magnetic amplifier.
FitzGerald, A. S.	1,914,201	10-02-30	6-13-33	A				1			4									Early phase-shift circuit employing a d-c saturable reactor as variable-L.
Nagashev, B. V.	1,920,803	10-11-30	8-01-33	A						3										Wheatstone bridge type magnetic amplifier comprising a single 3-legged core with two bridge arm windings on each of the outside arms of the magnetic core. Bridge balance is affected by d-c magnetomotive force introduced in the center leg.
Sorensen, A. J.	1,862,204	12-06-30	6-07-32	A							4	a			d					Magnetic amplifier type combination coincidence detector and flip-flop.
Dowling, P. H.	1,842,392	12-12-30	1-26-32	A				1			4				d					D-c saturable reactors and transformers in novel combinations. Novel core and winding configurations are used.

Table II. Significant Patents to Magnetic Amplifier Art (Continued)

Patentee	United States Pat. No.	Filed	Issued	Magnetic Amplifier Type A	B′	B″	C	1	2	3	4	a	b	c	d	e	f	g	h	Reason Selected
Suits, C. G.	Re.20,317	1-21-31	3-30-37	A				1								e				Nonlinear ferroresonant circuits to increase magnetic amplifier control sensitivity.
Zucker, M.	1,851,692	4-17-31	3-29-32	A						3										Wheatstone bridge type R-L phase-shift circuit employing a d-c saturable reactor as variable-L The R-L circuit is energized from a center-tapped impedance or transformer.
Logan, F. G.	1,997,179	5-07-31	4-09-35	A				1					b		d					Early internal feedback magnetic amplifier wherein the amount of positive internal feedback (net unidirectional flux) is controlled by means of a "flux normalizing" or a-c-magnetomotive force-controlling impedance paralleled with the rectifier a-c input.
Schmidt, A.	1,921,703	11-13-31	8-08-33	A				1												Early multiple-saturation means for affecting the linearity and constancy of the reactance versus d-c control magnetomotive force characteristic of d-c saturable reactors.
Thomas, H. P.	2,016,977	12-01-31	10-08-35	A						3			b					g		Wheatstone bridge type magnetic amplifier employing peaked-waveform a-c power supply excitation to excite core to saturation. Nonlinear symmetrical resistive devices provide rectification for internal feedback and d-c output signal.
Logan, F. G.	2,068,188	8-03-32	1-19-37	A				1				a	b		d					Standard 3-legged core embodiment of internal feedback magnetic amplifier with control by saturating winding to supply d-c load.
Logan, F. G.	2,036,708	8-08-32	4-07-36	A				1			4				d					Novel d-c load current control scheme wherein a d-c saturable reactor is employed to variably load the secondary of a specially connected transformer, the primaries of which are seriesed with the a-c input of a full-wave rectifier.
Logan, F. G.	1,981,921	8-10-32	11-27-34	A				1							d					Early use of a-c bias at power supply frequency.
Power, J. R.	1,943,088	9-01-32	1-09-34	A						3						e				Wheatstone bridge type phase-shifter with variable L and parallel C off-resonant phase adjusting means.
Boyajian, A.	2,040,684	12-23-32	5-12-36	A				1				a		c		e				Magnetic amplifier control circuit sensitivity-increasing means comprising series and parallel nonlinear ferroresonant circuits employing saturating reactors with controlled d-c bias. Where the circuit has leading current, it appears as a nonlinear capacitance, or saturating capacitance.
Logan, F. G.	1,986,112	5-11-33	1-01-35	A				1			4							g		Magnetic amplifier control-characteristic-exaggerating means comprising positive temperature coefficient resistor in shunt with d-c saturating (control) winding.
FitzGerald, A. S.	2,027,311	6-21-33	1-07-36	A				1	2	3		a								Schemes for improving the operation of cascaded magnetic amplifier stages. A reverse d-c bias is used in one embodiment to cancel the quiescent signal from the stage ahead. Also Wheatstone bridge and push-pull magnetic amplifiers.
FitzGerald, A. S.	2,021,099	7-27-33	11-12-35	A							4									A magnetic amplifier matrix method for randomly or successively energizing or de-energizing a plurality of loads one at a time from a single pair of d-c controlled inputs.
Antranikian, H.	2,047,609	8-25-33	7-14-36		B′				2				b	c						Novel push-pull magnetic amplifier system employing class B′ d-c saturable transformers with pulsating unidirectional magnetomotive force applied via primary windings. Internal feedback by rectifiers in secondary circuits; novel means for compensating for rectifier leakage.
Suits, C. G.	1,968,576	9-23-33	7-31-34	A				1			4	a				e				Novel external feedback scheme comprising means for variably shunting the feedback circuit input impedance (here the secondary of a current transformer) to make negligible the temperature and aging characteristics of the dry disk rectifier in the feedback circuit. Also novel embodiments: magnetic self-modulator and cascaded load sequencing circuit.
FitzGerald, A. S.	2,026,124	12-01-33	12-31-35	A						3	4									A modified Wheatstone bridge type magnetic amplifier capable of reciprocally and mediately indicating two balance conditions to two respective load circuits.
Burton, E. T.	2,164,383	1-29-34	7-04-39		B′			1	2			a	b	c		e	f			Several "second harmonic" type magnetic amplifiers and binary flip-flops.
FitzGerald, A. S.	2,027,312	7-23-34	1-07-36	A				1				a		c						Single-sided d-c saturable reactor type magnetic flip-flop with two stable states.
Dellenbaugh, F. S., Jr.	2,175,379	12-31-34	10-10-39	A				1								e				Off-resonant type magnetic amplifier with novel means for inductively coupling the "parallel" C in order to make possible the use of a smaller C; the saturation control windings are utilized in the coupling scheme.
LaPierre, C. W.	2,053,154	3-27-35	9-01-36		B′				2					c			f			Early "second harmonic type" magnetic amplifier. Employs a class B′ d-c saturable transformer with opposing secondaries. One embodiment is a magnetometer.
Edwards, M. A.	2,432,399	4-24-35	12-09-47	A						3										Wheatstone bridge type magnetic amplifier wherein the d-c saturating windings form a control bridge and the reactance windings are the reactance arms in the controlled reactance bridge.
Hanley, S. M.	2,144,289	8-26-35	1-17-39	A				1							d			g		Novel 3-legged reactor with unbalanced a-c flux path to purposefully create a-c flux in center leg. Control is by d-c saturating winding and by variably shunted winding on center leg. Two core equivalent is shown.
Edwards, M. A. & Kane, G. A.	2,084,900	10-10-35	6-22-37	A				1		3										Wheatstone bridge type phase shift circuit employing series L and C in one arm of the bridge.
Dawson, J. W.	2,140,349	10-23-35	12-13-38	A				1				a		c						Special magnetic amplifier to amplify changes in a-c power supply voltage. This is a simple external feedback magnetic amplifier without a separate control winding per se.
Logan, F. G.	2,118,440	3-30-36	5-24-38	A				1			4				d					Unique a-c bias means for control of special reactor which in turn controls d-c load. A-c control (bias) here is at magnetic amplifier power supply frequency. One-cycle control response is achieved.
Young, H. E.	2,154,020	4-09-36	4-11-39	A	B′			1			4									Differentially-balanced magnetic amplifier employing buck-boost d-c saturable transformer or d-c saturable reactor-controlled-transformer in a novel circuit arrangement.
Logan, F. G.	2,126,790	6-23-36	8-16-38	A				1					b		d					Basic d-c controlled internal feedback magnetic amplifier to control a-c load.
Boardman, E. M.	2,108,642	8-20-36	2-15-38		B′				2				b				f	g		Two significant push-pull magnetic amplifiers with internal feedback. One of these magnetic amplifiers is of the "second harmonic" type.
Craig, P. H.	2,138,732	9-21-36	11-29-38	A	B′			1							d	e				Magnetic amplifier control circuit sensitivity-increasing means employing series and parallel L-C ferroresonant circuit combinations.
Burton, E. T.	2,147,688	12-02-36	2-21-39		B′			1	2			a	b							Magnetic amplifiers and binary and ternary magnetic flip-flops and delay flop-flops. Some of the devices are of the "second harmonic" type.

Table II. Significant Patents to Magnetic Amplifier Art (Continued)

Patentee	United States Pat. No.	Filed	Issued	Magnetic Amplifier Type																Reason Selected
				A	B′	B″	C	1	2	3	4	a	b	c	d	e	f	g	h	
Edwards, M. A.	2,169,093	1-02-37	8-08-39	A				1					b	c		e				Internal feedback magnetic amplifier to control a-c load. Novel features are d-c bias to compensate for no load magnetizing flux and capacitor to neutralize load winding reactance. The possibility of a resonant-type magnetic amplifier flip-flop is noted.
Kalbskopf, W.	2,173,905	5-28-37	9-26-39			B″		1				a								D-c saturable transformer with opposing secondary windings which are differentially balance-controlled such that the net output voltage is the difference voltage between the two seriesed secondaries. Balanced circuit possibilities exist.
FitzGerald, A. S.	2,168,402	1-11-38	8-08-39	A							4	a		c						Two single-sided flip-flops combined to form a self-oscillating flip-flop or multivibrator. The flip-flops are cross-connected by their saturation control windings.
O'Hagan, B. E.	2,215,823	6-10-38	9-24-40			B″		1												D-c saturable transformer having two load energizing secondaries which are mediately and selectively excited in a reciprocal manner according to the amount of coupling of each with the primary as determined by the amount of d-c control magnetomotive force.
Whitely, A. L. & Ludbrook, L. C.	2,229,952	10-19-38	1-28-41	A				1	2				b							Two novel magnetic amplifiers—One is a non-polarized magnetic amplifier with internal feedback to control a single d-c load. The other is a polarized magnetic amplifier without feedback to control one d-c load or to reciprocally control two d-c loads.
Hubbard, F. A.	2,218,711	12-30-38	10-22-40			B″		1						c						Novel means for the controlled coupling of any one or more of a multiplicity of secondaries to the primary of a d-c saturable transformer. Novel permanent magnet d-c bias means.
Logan, F. G.	2,259,647	2-09-39	10-21-41	A				1		3					d					Unique a-c bias means for control of special reactor which in turn controls a-c load. A-c control (bias) here is at magnetic amplifier power supply frequency. One cycle control response is obtained.
Hines, C. M.	2,215,820	6-23-39	9-24-40			B″		1				a		c						Novel embodiment of d-c saturable transformer having two load energizing secondaries the coupling of which to the primary is mediately, selectively and reciprocally controlled by the amount of d-c control magnetomotive force.
O'Hagan, B. E.	2,215,821	6-24-39	9-24-40			B″		1	2					c						Novel embodiment of differentially balanced d-c saturable transformer having opposing secondary windings; the net output voltage is the difference voltage between the two seriesed secondaries. This is a balanced magnetic amplifier.
O'Hagan, B. E.	2,215,822	6-27-39	9-24-40			B″		1						c						Novel d-c biasing means for class B″ d-c saturable transformers.
Geyger, W.	2,338,423	12-14-39	1-04-44	A						3	4	a								Cascaded Wheatstone bridge magnetic amplifier stages employing novel differentially connected d-c control windings to subsequent stages. Novel external feedback means for Wheatstone bridge magnetic amplifier. Novel Wheatstone bridge output means employing differential transformer.
Hornfeck, A. J.	2,310,955	12-30-39	2-16-43	A				1	2	3		a		c		e				Push-pull magnetic amplifier employing differentially cross-connected external feedback circuits to reciprocally affect one magnetic amplifier regeneratively and the other degeneratively depending on the polarity of the control signal.
McCreary, H. J.	2,324,634	1-31-40	6-20-43	A				1						c						D-c bias means for use in magnetic amplifiers. Permanent magnet bias means. A-c and d-c magnetic circuit separation and isolation means.
Stevens, S. A. & Walker, A. H. B.	2,222,048	2-21-40	11-19-40	A				1												Novel magnetic self-modulators and demodulators.
Krussmann, A.	2,399,872	10-24-40	5-07-46	A						3										Wheatstone bridge magnetic amplifier employing only one set of windings which are used for combined functions as d-c saturable control and as the reactance arms of the bridge.
Middel, H. D.	2,388,070	8-22-41	10-30-45	A				1										g		Novel d-c load controlling magnetic amplifier which does not employ rectifiers, but which employs, instead, symmetrical characteristic current distorting impedances which have no rectifying properties per se. High magnetic amplifier sensitivity is claimed.
Lamm, U.	2,403,891	9-23-42	7-09-46	A				1		3		a	b							Wheatstone bridge magnetic amplifier having external and internal feedback. Also Wheatstone bridge type magnetic flip-flop.
FitzGerald, A. S.	2,464,639	4-13-45	3-15-49	A					2			a		c				g		Novel d-c polarized push-pull magnetic amplifier. Novel features include impedance-coupled external feedback means to the control winding instead of to a special external feedback winding. Novel signal-limiters are used to avoid the deleterious effects of excessive control signals.
FitzGerald, A. S.	2,461,046	5-03-46	2-08-49	A						3	4	a								Novel Wheatstone bridge type magnetic amplifier.
Hedstrom, S. E.	2,509,864	6-19-46	5-30-50	A					2			a	b					g		Novel d-c polarized external feedback magnetic amplifier employing push-pull internal feedback magnetic amplifiers.
Forssell, H.	2,504,675	8-21-47	4-18-50	A				1	2		4	a		c						Novel d-c polarized balanced, single ended and push-pull magnetic amplifiers.
Tweedy, S. E.	2,475,575	10-29-47	7-05-49	A						3		a								Novel d-c polarized Wheatstone bridge type magnetic amplifier.
Graves, W. L. O.	2,516,563	4-19-48	7-25-50	A				1					b					g		Magnetic amplifier for the control of an inductive load. A rectifier limits the negative voltage across the inductive load to establish a mode of operation similar to that for a resistive load.
Lord, H. W.	2,509,738	4-29-48	5-30-50	A						3			b		d	e				Novel Wheatstone bridge magnetic amplifier with internal feedback.
Thompson, R. L.	2,519,513	9-09-48	8-22-50	A							4	a								Two-sided magnetic binary counter (flip-flop) with crossed external feedback.
Wood, M. L.	2,524,154	1-05-49	10-03-50	A							4	a								Two-sided magnetic flip-flop with crossed external feedback.

Author Section

Abernethy, H. D. … 170
Adams, J. Q. … 771
Adler, R. … 493
Aggers, C. V. … 296, 297, 339
Albers-Schoenberg, E. … 760, 772
Alden, J. M. … 873
Alder, R. … 493
Aldrich, D. F. … 733
Alexanderson, E. F. W. … 16, 17, 18, 33, 34, 35, 36, 76, 442, 589
Allam, Lt. H. … 893
Alley, R. E., Jr. … 734
Amsden, R. D. … 298, 495
Anderson, W. C. … 590
Andrews, R. A. … 496
Antranikian, H. … 265
Applegate, I. D. … 293
Apperson, J. W. … 774
Arkenburgh, W. H. … 171
Askey, R. O. … 229
Astbury, N. F. … 646, 775
Atkinson, P. D. … 729
Augier, J. A. … 591, 592
Austin, T. M. … 204

Bagnall, R. I. … 172
Ball, J. D. … 13
Banos, I. A., Jr. … 776
Baranawski, J. … 562
Bardell, P. R. … 837
Barth, G. … 443, 469
Barth, J. B. … 230
Barton, L. E. … 368
Baston, C. E. … 470
Batten, W. B. … 471
Bauer, F. … 205
Beaumariage, D. C. … 647, 665, 666, 767, 768, 797, 846, 868
Bedell, F. … 140
Bedford, B. D. … 173, 231, 232, 299, 300, 301, 340, 341, 369, 370, 407, 472, 473, 563
Behrens, T. A. … 342
Beljers, H. G. … 777
Bell, D. A. … 648, 778
Belt, T. A. E. … 141
Benjamin, F. … 702
Bennett, W. R. … 245, 246
Bergman, S. R. … 116
Besag, E. … 31
Bessonov, L. A. … 779
Bewley, L. V. … 215
Beyer, R. T. … 556, 593, 635, 742, 780
Bixby, W. H. … 564
Black, A. O., Jr. … 649, 650
Blake, D. C. … 54
Blake, L. R. … 703
Blewett, J. P. … 883
Boardman, E. M. … 343
Bodde, T. … 32
Bonell, R. K. … 117
Bogoslovskic, A. S. … 781
Boothby, O. L. … 595
Borg, L. F. … 671, 704
Both, E. … 651, 652, 876
Bowen, A. E. … 444
Boyajian, A. … 55, 118, 142, 153, 266, 540
Bozorth, R. M. … 233, 267, 565, 595, 596, 782, 859
Bradish, C. B. … 22
Brailsford, F. … 653
Breunich, T. R. … 783
Brockman, F. G. … 705, 860
Brooks, H. B. … 37
Brown, M. J. … 206, 234
Brown, W. W. … 119
Buchanan, C. C. … 445
Bucher, E. E. … 38
Buchhold, T. … 474, 497, 566, 567, 568, 569, 597
Buckley, S. E. … 837
Buechler, L. W. … 706, 707, 708, 709, 710, 711
Bukstein, E. … 861
Burgess, C. F. … 4
Burke, B. S. … 268
Burton, E. T. … 108, 143, 174, 175, 371, 372
Butcher, F. E. … 892
Butler, O. I. … 654, 655, 656, 784

Cacho, L. G. … 712
Cairns, C. F. … 207
Camilli, G. … 540
Cantwell, J. L. … 260
Carleton, J. T. … 733
Carmichael, T. F. … 408
Cartier, R. O. … 785
Case, B. A. … 144
Casimir, H. B. G. … 598
Casper, L. … 56
Castellini, N. R. … 786, 787
Cauer, W. … 64
Chablani, H. R. … 863
Chambers, D. E. … 235, 446
Chandler, D. P. … 868
Chang, S. S. L. … 713
Chapin, D. M. … 714
Charlton, O. E. … 65
Chestnut, F. T. … 565
Chonan H, … 344
Christopher, H. M. … 541
Chubb, L. W. … 14
Cioffi, P. P. … 788
Claesson, P. H. E. … 475
Cobine, J. D. … 599
Cockrell, W. D. … 570
Coffin, F. P. … 23
Cohen, S. … 789
Concordia, C. … 158
Conrad, F. … 11
Conrath, J. … 790
Cooper, F. W. … 204
Cooper, W. H. B. … 715
Corner, W. D. … 844
Cox, J. H. … 571
Craig, P. H. … 345
Cravath, A. M. … 236
Crocker, F. B. … 7
Croden, W. T. … 302, 409
Cronvall, L. P. … 600
Crouse, G. B. … 88, 208
Crow, L. R. … 716
Curry, J. R. … 599

Dahlgren, F. … 373
Dann, M. … 57
Davis, R. L. … 145
Dawson, J. W. … 346
DeBarr, A. E. … 717
DeBlieux, E. V. … 142
Dellenbaugh, F. S., Jr. … 374
Demontvignier, M. … 410
Dijksterhuis, P. R. … 237
Dijkstra, L. J. … 718
Dillinger, J. F. … 267
Dohman, S. A. … 835
Dorfman, L. O. … 543
Dornhoefer, W. J. … 693, 707, 709, 710, 711, 719
Dornig, W. … 66, 73, 77
Dortort, I. K. … 544
Dowling, P. H. … 97, 120, 121, 122, 123, 146, 147, 148, 149, 150, 159, 176, 196
Drake, C. W. … 270, 271
Dunnegan, T., Jr. … 817
DuPre, F. K. … 584
Dyson, J. … 545

Edwards, D. V. … 272
Edwards, M. A. … 304, 375, 376, 411, 412, 413, 414, 447, 498, 604, 605
Eisenschmid, O. … 448
Elmen, G. W., 26, 49, 67, 74, 98, 238, 565, 663, 664
Elmlund, H. … 792
Embry, A. L. … 606
Emmerling, A. A. … 239, 305
Emmerson, T. … 775
Esselman, W. H. … 722, 723, 866
Ettinger, G. M. … 793
Evans, C. T. … 89
Everest, A. R. … 3

Fallou, J. G. … 78
Falls, W. H. … 607
Feinberg, R. … 794, 795
Felch, E. P. … 608, 867
Feldtkeller, F. … 724
Ferada, M. … 90
Fett, G. H. … 737
Field, R. F. … 796
Finch, J. L. … 449
Finzi, L. A. … 665, 767, 797, 846, 868
Fishman, M. … 639, 640, 666, 768, 769
FitzGerald, A. S., 50, 58, 68, 69, 70, 71, 124, 125, 178, 179, 180, 181, 182, 183, 209, 210, 211, 212, 240, 241, 242, 273, 274, 275, 276, 306, 307, 308, 309, 347, 377, 378, 476, 609, 610, 611, 725, 726, 727
Fondiller, W. … 41
Foos, C. B. … 310
Ford, J. W. … 759
Forrester, J. W. … 612, 869
Forssell, H. … 348, 798
Fountain, L. L. … 243
Frankenfield, B. … 4
Friedlander, E. … 294
Frost-Smith, E. H. … 667, 728
Fuller, L. F. … 42

Gaines, F. L. … 179
Gale, H. M. … 729
Gallagher, C. J. … 599
Ganz, A. G. … 573
Garlick, W. J. … 477
Garr, D. E. … 546
Gaugler, E. A. … 664, 668, 730
Gebhard, L. A. … 126
Gerdien, H. … 59
Geyger, W. … 415, 450, 451, 478, 479, 499, 523
Geyger, W. A. … 799, 800
Gilman, T. W. … 524
Gilson, R. M. … 151, 184, 277
Giroz, H. E. … 452
Given, F. J. … 424
Glass, P. … 801
Goldschmidt, R. … 8, 100
Goldsmith, H. A. … 760, 870
Gottlebsen, L. H. … 897
Gottliebsen, H. … 750
Gould, H. L. B. … 802
Graff, J. W. … 311
Grandstaff, O. D. … 524
Graves, W. L. O. … 803, 804
Greene, W. E. … 613
Grieg, J. … 669, 731
Griffith, R. C. … 185
Grillo, J. … 670
Grivet, P. … 732
Guicherd, J. S. … 732
Gullikson, F. H. … 213, 416, 453
Gusew, W. W. … 417
Gussakov, V. D. … 244

Haayman, P. W. … 641
Haines, A. B. … 500
Halacsy, A. A. … 805
Halberg, M. N. … 186
Halsey, R. J. … 806
Hamilton, W. H. … 733
Hanley, S. M. … 379, 380, 381
Hanna, R. B. … 873
Hanna, C. R. … 79
Hansen, E. F. … 774
Hansen, W. W. … 643
Harder, E. L. … 110, 623, 733, 807
Hart, S. V. … 808
Hartel, W. … 382, 480
Hartley, R. V. L. … 27, 51, 99, 278
Harty, E. A. … 501
Harvey, R. L. … 809
Hathaway, C. M. … 481
Hauffe, G. … 312, 313, 383
Haug, E. H. … 525, 614
Heck, C. V. … 268
Hedding, L. K. … 349, 454, 482, 502, 503, 526, 574
Hedstrom, S. E. … 527, 547, 615, 625, 671, 810, 811
Heegner, K. … 80, 91
Hegyi, I. J. … 809
Heilman, E. L. … 641
Heising, R. A. … 92
Helber, C. … 616
Heller, B. … 455
Herrick, R. H. … 524, 528
Herskind, C. C. … 456, 504
Hertz, H. … 872
Herz, A. … 575
Herzenberg, G. R. … 350
Herzog, R. … 127
Hinds, R. S. … 483
Hines, C. M. … 418, 484
Holden, W. H. T. … 529
Holubow, H. … 548
Hornfeck, A. J. … 505
Horton, W. F. … 807
Houck, G. … 617
Hubbard, F. A. … 419
Hubmann, F. … 56
Hudson, C. S. … 549, 812
Huge, H. M., 485, 506, 530, 531, 618, 619, 620, 621
Hunter, R. B. … 187
Hussey, L. W. … 279

Ibl, J. … 455

Jackson, J. E. … 65
Jaffee, R. J. … 673
Jatlow, J. L. … 208
Jellinghaus, W. … 813
Jenks, H. C. … 314, 622
Jensen, O. … 674
Johnson, J. B. … 100
Johnson, L. J. … 814
Johnson, P. S. … 454
Johnson, R. A. S. … 507
Johnson, W. C. … 734, 815
Jonas, J. … 45, 81
Jones, B. W. … 188

Kafka, D. W. … 201
Kalb, R. M. … 245, 246, 355

Kalbskopf, W. 384
Kane, G. A. 304
Karplus, E. 576
Kauke, J. 816
Kayser, H. 669
Keiser, R. W. 550
Keller, E. G. 352
Kelsall, G. A. 214
Kern, E. 385
Kettler, C. J. 386
Kierstead, F. H. 60, 215, 735
Kincaid, M. 873
King, I. W. P. 551
Kingston, R. H. 736
Kintner, P. M. 737
Kirke, W. B. 46
Kirschbaum, H. S. 623, 675, 738
Kittel, C. 739
Klemperer, H. 420
Klein, M. J. 874
Kluz, W. C. 740
Knopp, O. A. 15
Kouyoumjian, H. K. 128, 129, 130, 189
Krabbe, U. H. 527, 577, 624, 625, 626
Kramer, W. 315, 353, 354, 387, 388, 389
Kriessman, C. J., Jr. 741
Krumhansl, J. A. 742
Kuhn, J. 140
Kuhn, L. 82
Kujirai, T. 24
Kummich, R. 112
Kurssmann, A. 578

Lamm, A. U. 390, 391,
421, 422, 423, 508, 509, 579, 580, 627, 676, 792
Lamson, H. W. 677, 678
Landon, V. D. 743
Lang, K. A. 628
LaPierre, C. W. 280
Larson, H. E. 817
Latimer, K. E. 818
Latour, M. 83
Latson, F. W. 815
Laymeyer, W., & Co 5
Ledward, T. A. 392, 510
Lee, F. W. 131, 152, 216
Lee, R. 281, 532, 629
Legg, V. E. 393, 424, 867, 875
Lennox, T. C. 111
Lerstrup, K. 679
Leverenz, H. W. 800
Libsch, J. F. 876
Lindenblad, N. E. 132
Lindenhovius, H. J. 680
Livingstone, O. W. 401, 457
Liwschitz-Garik, M. 744
Lloyd, T. C. 713
Locke, A. R. 282
Logan, F. G. 217, 218,
219, 247, 248, 249, 283, 284, 285, 316, 317, 318,
319, 320, 355, 356, 394, 458, 486, 630, 681, 682
Lord, H. W. 819, 820
Ludbrook, L. C. 425, 466
Lynch, M. A. 837

MacDonald, H. B. 818
Madelung, E. 6
Maier, K. 220
Mandl, A. 483
Mang, C. Y. 654, 655
Manley, J. M. 324, 395, 487, 581, 878
Martienssen, O. 9
Martin, W. H. 41
Martindale, R. C. 683
Maus, G. 357
McCandless, S. R. 286
McCarty, O. P. 153
McClure, F. N. 733, 745, 822, 823
McCreary, H. J. 511, 684, 746
McEachron, K. B. 154
McFarlane, J. 775
McIlwain, K. 288
McLean, W. B. 776
McNaney, J. T. 533
Means, W. J. 608
Meissner, A. 19, 21, 30
Melville, W. S. 824, 879
Merrell, B. C. 734
Merrill, F. G. 867
Meserve, W. E. 685
Middel, H. D. 553
Milarta, L. E. 512
Miles, J. G. 747, 880
Miller, G. H. 556, 635
Mills, H. L. 426
Milnes, A. G. 748, 825, 896
Mittag, A. H. 442, 589
Morack, M. M. 427
Morecroft, J. H. 190
Morgan, R. E. 749, 750, 826, 897
Morrill, W. 827
Morton, L. W. 399
Mossop, I. A. 549
Moyer, E. E. 321, 428, 488, 513
Mulhern, M. J. 881
Munch, R. H. 828
Murcek, S. J. 396
Murphy, E. J. 39
Myers, H. C. 514, 534, 571

Nagashev, B. V. 191, 221
Neiss, O. 222
Niggeler, W. 81
Nixdorff, S. P. 18
Noble, S. W. 853
Nordfeldt, B. 554

Odessey, P. H. 358
Oesterreicher, S. I. 61
Ofverholm, H. 348
Ogle, H. M. 604, 803, 826, 829
O'Hagan, B. E. 429, 430, 431, 432, 433
Ollendorf, F. 101
Ort, C. F. 67
Osgood, V. L. 133
Osnos, M. 25, 28, 62, 93, 112

Pakala, W. E. 287, 296
Papian, W. N. 830, 882
Parratt, L. G. 608
Parsons, J. H. 751
Partington, R. M. 434
Partridge, G. F. 322
Pederson, P. O. 250
Pender, H. 288
Perets, Y. B. 831
Perry, W. R. 323
Peters, J. F. 102
Peterson, E. ...134, 155, 156, 289, 324, 397, 515, 581
Pettibone, G. H. 582
Phillips, F. M. 832
Phillips, H. E. 325
Philpott, L. V. R. 326
Pichon, P. F. 19
Polder, D. 833
Polydorof, W. J. 535
Porter, R. W. 413
Potter, J. A. 633
Power, J. R. 223, 251
Pressman, A. I. 883
Priest, J. E. 536, 752
Prince, D. C. 94, 95, 113
Pungs, L. 52

Randall, W. F. 834
Ramey, R. A. 884
Rasmusson, E. J. 398
Ratgaus, I. I. 835
Rayleigh, Lord 1
Reichard, W. H. 252
ReQua, F. L. 43, 84
Reuss, K. 359
Rex, H. B. 474, 634, 686, 753
Reyner, J. H. 885
Ribkin, A. M. 836
Richards, C. E. 837
Rideout, V. C. 687
Rosenbaum, M. 10
Roston, B. 688
Roulle, E. 224
Rudenberg, R. 754
Rumbaugh, L. H. 608
Runaldue, L. R. 489
Ruthberg, S. 599
Ryan, A. R. 461, 516
Ryder, J. D. 555

Sabbah, C. A. 399
Sack, H. S. 537, 556, 635
Sakai, Y. 11
Sanford, R. L. 565
Saretzky, S. 689
Sashoff, S. P. 459
Schafer, H. G. 814
Schelleng, J. C. 103
Scheuring, W. 225
Schilling, W. 460
Schmidt, A., Jr. 192, 193, 327, 360, 435
Schmutz, O. 253, 256, 436
Schneider, E. D. 461, 490
Schoenberg, I. 29
Schoerer, L. 583
Schoelfield, H. H. 755, 834
Schunk, H. 47, 53
Scott, D. B. 462
Scott, K. L. 114
Seaverson, O. I. 168
Seegar, E. V. 157
Seeley, H. T. 290
Short, T. T. 557
Simpson, W. P. 194, 254
Slepian, J. 85, 86
Slonczewski, T. 608
Smith, B. M. 158
Smith, D. W. 517
Smith, E. J. 722, 744, 756, 757, 758, 838, 886
Smith, H. J. 759
Smith, I. R. 518
Smith, R. S. 874
Snoek, J. L. 584, 585, 636, 718, 777
Snyder, C. L. 760
Sola, J. G. 195
Sorensen, A. J. 135, 159, 160, 196
Sparrow, H. T. 538
Specht, T. R. 839
Spencer, F. L., Jr. 690, 691, 692, 761, 762, 763
Spitzer, C. F. 558
Spooner, T. 14, 72, 87
Spurgeon, S. J. 311
Stansbury, C. 255, 291
Stateman, M. 637, 700
Stearley, G. H. 887
Steenbeck, M. 256
Steinmetz, C. P. 2
Steinitz, R. 764
Steinitz, S. 693
Stephens, H. O. 60
Sterk, A. A. 900
Stevens, S. A. 437
Stewart, K. H. 840
Stocker, C. P. 328, 329, 330, 400
Stoekle, E. R. 44, 63
Stoller, H. M. 96, 115, 161, 226, 257
Storm, H. F. 694, 841, 842, 888
Strutt, M. J. O. 438, 843
Suits, C. G. 136, 162, 163, 164, 197, 198, 199,
200, 201, 227, 258, 259, 260, 261, 262, 331, 361
Summers, C. M. 202, 491, 492
Svensson, R. 811
Sweeney, C. P. 463

Taylor, A. M. 20
Taylor, J. B. 12
Teare, W. H. 401
Tebble, R. S. 844
Teldbaum, A. A. 402
Thomas, H. A. 586
Thomas, H. P. 263
Thomas, P. 104, 105
Thomason, J. L. 735
Thompson, L. W. 39, 40, 48, 137, 165, 166, 167
Thompson, R. L. 845
Thomson, W. T. 362, 363, 403, 404
Thornburg, V. E. 365
Tickner, A. J. 608
Torsch, C. E. 765
Travis, I. 332, 364
Trischka, J. W. 537, 556, 635
Trucksess, D. E. 539
Turner, A. H. 292
Tweedy, S. E. 695, 766

Usselman, G. L. 449

Valentine, C. E. 365
Vance, P. A. 464, 638
van der Breggen, J. C. 680
Vassiliere-Arlhac, J. 366
Vellard, L. 423
VerPlanck, D. W. 639, 640, 767, 768, 769, 846
Verwey, E. J. W. 641
Vincent, A. M. 889
Von Arco, G. 21, 30
Vulfson, K. 333

Wagner, K. W. 75
Wagner, R. N. 839
Walker, A. H. B. 405, 437
Walsh, P. J. 439, 519, 642, 697
Wang, A. 848, 849, 850, 890
Warren, C. E. 675, 738
Wasserrab, T. 334
Watanabe, Y. 344
Wattenberger, V. J. 826
Way, K. J. 335
Weber, E. 358, 700, 744, 851
Wei, M. Y. 780
Wennerberg, G. 891
Wensley, R. J. 203
Wentz, E. C. 138, 139, 295, 520, 521
Werner, O. 465
Werner, W. S. 228
West, C. P. 106, 293, 336
Weygandt, C. N. 332, 364
Whitenack, M. E. 440
Whitely, A. L. 466
Wickerham, W. R. 467, 560, 561, 587
Wieberdink, A. 852
Wiegand, D. E. 643
Willheim, R. 892
Williams, F. C. 853
Williams, H. J. 854
Williams, W. D. 565
Williamson, K. T. 168

Willis, C. H. 441
Winkler, G. 644
Winograd, H. 522
Winter-Gunther, von H. 107
Wiskott, W. 294
Wolfert, E. R. 295
Wolff, F. M. 286
Wolff, J. L. 855
Woo, W. D. 848
Wood, M. L. 856
Wrathall, L. R. 279, 289, 324, 337, 367, 588
Wright, J. H. 701

Young, H. E. 338, 406

Zadeh, L. A. 857
Zamsky, J. 645
Zenneck, J. 47, 56
Zucker, M. 169

List of Periodicals

Acta Polytechnica, Stockholm, Sweden
Aeronautical Engineering Review, New York, N. Y.
Allgemeine Elektricitats Gesellschaft, Berlin, Germany
Annalen der Physik, Leipzig, Germany
Applied Scientific Research, The Hague, Holland
Archiv fur Elektrotechnik, Berlin, Germany
ASEA Journal, Vasteras, Sweden and London, England
ASEA Tidning, Vasteras, Sweden
Avtomatika i Telemekhanika, Moscow, USSR
Bell Telephone Laboratories, New York, N. Y.
Bell System Technical Journal, New York, N. Y.
BIOS Reports, London, England
Bulletin de la Societe Francaise des Electriciens, Paris, France
Ceramic Age, Newark, N. J.
Comptes Rendus Hebdomadaire des Seances de l'Academie des Sciences, Paris, France
Electric Journal, Pittsburgh, Pa.
Electrical Communication, New York, N. Y.
Electrical Engineering, New York, N. Y.
Electrical Engineering Abstracts (Section B of Science Abstracts), Institution of Electrical Engineers, London, England
Electrical Manufacturing, New York, N. Y.
Electrical Record, New York. N. Y.
Electrical Review, London, England
Electrical World, New York, N. Y.
Electrician, London, England
Electronic Engineering, London, England
Electronic Industries, New York, N. Y.
Electronics, New York, N. Y.
Elektricheskie Stantsii, Moscow, USSR
Elektrichestvo, Moscow, USSR
Elektrische Nachrichten Technik, Berlin, Germany
Elektrotechnik und Maschinenbau, Vienna, Austria
Elektrotechnische Zeitschrift, Berlin, Germany
Elektroteknisk Tidsskrift, Oslo, Norway
ERA, Stockholm, Sweden.
Esselte Arktiebolag, Stockholm, Sweden
Frequenz, Berlin, Germany
General Electric Review, Schenectady, N. Y.
General Radio Experimenter, Cambridge, Mass.
Industrial and Engineering Chemistry, New York, N. Y.
Instruments, Pittsburgh, Pa.
Iron and Steel Engineer, Pittsburgh, Pa.
Jahrbuch der Drahtlosen Telegraphie und Telephonie, Berlin, Germany
Journal, Acoustical Society of America, New York, N. Y.
Journal, American Institute of Electrical Engineers, New York, N. Y.
Journal, British Institution of Radio Engineers, London, England
Journal, Franklin Institute, Philadelphia, Pa.
Journal, Institute of Electrical Engineers of Japan, Tokyo, Japan
Journal of Applied Physics, New York, N. Y.
Journal of Scientific Instruments, London, England
Journal of Technical Physics, Leningrad, USSR
La Radio Francaise, Paris, France
Machine Design, Cleveland, Ohio
Machinery, New York, N. Y.
Materials and Methods, New York, N. Y.
Metal Progress, Cleveland, Ohio
Metallurgia, Manchester, England
Nature, London, England
Nippon Electrical Communication Engineering, Tokyo, Japan
Philips Technical Review, Eindhoven, Holland
Philosophical Magazine, London, England
Physica, The Hague, Holland
Physical Review, New York, N. Y.
Physikalische Zeitschrift, Leipzig, Germany
Power Generation, New York, N. Y.
Power Plant Engineering, Chicago, Ill.
Proceedings, American Institute of Electrical Engineers, New York, N. Y.
Proceedings, Institute of Radio Engineers, New York, N. Y.
Proceedings, National Electronics Conference, Chicago, Ill.
Proceedings, Physical Society, London, England
Radio and Television News, Chicago, Ill.
Radio News, Chicago, Ill.
RCA Review, Princeton, N. J.
Revue Generale de l'Electricite, Paris, France
Review of Modern Physics, New York, N. Y.
Review of Scientific Instruments, New York, N. Y.
Siemens Zeitschrift, Berlin, Germany
Teknisk Tidsskrift, Stockholm, Sweden
Tele-Tech, New York, N. Y.
Transactions, American Institute of Electrical Engineers, New York, N. Y.
Transactions, Illuminating Engineering Society, New York, N. Y.
Westinghouse Engineer, East Pittsburgh, Pa.
Wireless Engineer, London, England
Wireless World, London, England
Wissenschaftliche Veroffentlichungen aus dem Siemens-Werken, Berlin, Germany
Zeitschrift fur Angewandte Physik, Berlin, Germany
Zeitschrift fur Technische Physik, Leipzig, Germany

On the Control of Magnetic Amplifiers

R. A. RAMEY
MEMBER AIEE

IN A recent paper[1] the author proposed a new theory of magnetic amplifier operation and showed how this theory could be used to predict many new types of magnetic amplifier configuration. This theory is based upon a realistic approach to the treatment of the two major nonlinearities inherent to the ferromagnetic materials used in magnetic amplifiers—saturation and loop magnetization characteristics. It is known that the level of magnetization of a magnetic material in its unsaturated state is not uniquely determined by the magnetomotive force applied to its windings. On the contrary the loop character of the magnetic characteristics of the important ferromagnetic materials destroys any single-valued dependence and makes this dependence almost indeterminate. It is suggested that the history of the reactive voltage across a winding of a magnetic amplifier core be used to determine uniquely the magnetization level. The control or independent variable exhibits its influence in the form of a voltage. The control circuit current is a variable dependent upon the circuit configuration, parameter characteristics, auxiliary circuitry, and control variable.

From consideration of the relatively elementary nonlinear physics involved one can practically tailor an amplifier circuit to his particular problem. There can be many variations falling quite logically within the outlines of the theory. This paper has as its subject some of the many possible control elements and will be illustrated experimentally by a single-core magnetic amplifier electronically controlled. The subject of investigations yet to be reported is the application of the theory to consideration of other elements of magnetic amplifier circuits and some new constraints which may be usefully imposed in conjunction with the magnetic constraints.

The single-core magnetic amplifier used for a basis of illustration is not necessarily the most useful configuration. It does, however, represent a convenient vehicle for highlighting many of the theoretical concepts involved and does represent a startling deviation from ordinary magnetic amplifier practice. Most of the conclusions attained are applicable to multiple-core amplifiers. This amplifier circuit is shown in Figure 1 with its controlled element and magnetizing element in one of the appropriate configurations for resistive load and 1-cycle response and with its control element in an unspecified configuration which will prove useful in demonstrating the operating principles.

The author's use of the word *element* with reference to amplifier segments supplies a means by which various circuit functions may be conveniently separated. Generally a controlled element, Figure 1, consists of a source of electric power, a load and whatever other parameters are needed for desired operation. The magnetizing element ordinarily derives some electrical function from the controlled element and applies it, after appropriate transformation and scale change, to the control circuit. In multiple-core magnetic amplifiers the saturable transformers may be made to take over some or all of the functions of the magnetizing element. A control element is ordinarily a passive circuit parameter or an active parameter in combination with linear and/or nonlinear parameters and in each case contains an independent electrical variable. A gating element is ordinarily one or more saturable transformers or autotransformers. An auxiliary element, not illustrated in Figure 1, is an added circuit or circuit segment providing an additional function, for example, compensation for rectifier leakage or magnetization loop width, rectifier blocking, et cetera.

A type of single-core magnetic amplifier is used for illustration since its various circuit elements can be clearly separated and studied and since its transient operation reaches steady state within a cycle. Most conventional magnetic amplifiers have their circuit elements so closely integrated as to make separation of function difficult and analysis of transients requires consideration of several cycles. To further simplify the analysis it will be assumed that the core material is of the rectangular loop type similar to Deltamax, Orthonol, et cetera Figure 2(B), with complete saturation at a very low, but definite, value of magnetomotive force and the rectifiers are ideal (no forward voltage drop and no reverse current). The magnetizing element will be a transformer with turns ratio the same as that of the gating transformer. The magnitude of the a-c voltage is assumed to be the maximum the gating transformer can absorb without saturation.

Circuit Operation

The operation of the single-core magnetic amplifier is essentially the same as the operation of a single transformer in any other magnetic amplifier. During one period of time its core is caused to saturate and allow output current to flow. In the examples to be discussed this

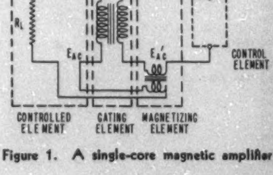

Figure 1. A single-core magnetic amplifier

Paper 51-389, recommended by the AIEE Magnetic Amplifiers Committee and approved by the AIEE Technical Program Committee for presentation at the AIEE Fall General Meeting, Cleveland, Ohio, October 22–26, 1951. Manuscript submitted June 26, 1951; made available for printing September 7, 1951.

ROBERT A. RAMEY, Naval Research Laboratory, Washington, D. C.

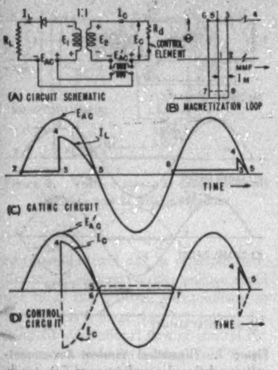

Figure 2. Theoretical transient flux-current-voltage relations for shorting of control element position

saturation will be considered controlled by the a-c line voltage. During a succeeding period of time its core is caused to reset by an amount dependent primarily upon the control circuit functions. With resistive loading these periods of time can be easily visualized. During one half-cycle, saturation occurs; during the succeeding half-cycle, controlled reset occurs.

A mathematical discussion of an example of this circuit type has been presented[1] and will not be iterated here. However, the physics of this circuit operation bears discussion since the design or choice of control elements will be dependent upon the physical factors involved. This discussion is nonmathematical but rather is implemented by simultaneous reference to a set of diagrams. For any given figure: (a) denotes circuit configuration, (b) describes instantaneous core saturation and (c), (d), and (e) show instantaneous voltages and currents.

To facilitate a general discussion of control elements it will be useful to describe circuit operation with the control element position short circuited, Figure 2. From consideration of the dictated modes of operation one can describe useful control elements.

To establish initial conditions, let it be specified that the magnetic core is in unsaturated condition 1, Figure 2(B), at the instant the a-c voltage is applied at the beginning of a positive half-cycle. The instantaneous polarities are shown in Figure 2(A). The following is a verbal description of subsequent nonlinear operation which sets a pattern by which successive figures can be analyzed.

First Half-Cycle

The a-c voltage is immediately applied to the gating transformer. The current I_L flowing in the gating circuit, Figure 2 (C), will be limited to that designated by the magnetization characteristic of the cores I_m, Figure 2(B). The current in the control circuit will be considered zero with E_2 equal and opposite to E_{ac}'. Actually the magnetizing current during this period can flow in either or both circuits depending upon parameter values.

When sufficient voltage integral is applied (one-half of the a-c voltage integral) the gating transformer saturates at 3, Figure 2(B); its terminal voltages become zero (regard the assumptions). The a-c voltage is now applied to the gating circuit resistance R_L causing appropriate output current to flow. The current flowing in the control circuit will be of the same sinusoidal function but its magnitude will be dependent upon the resistance inherent to the control circuit, R_d. It is pointed out that this relatively large counterclockwise control circuit current during a conduction period contributes nothing to the output quantity, does not affect the magnetization level and yet loads the control element. These currents become zero at the end of the first half-cycle and the flux level in the core is at saturation position 5.

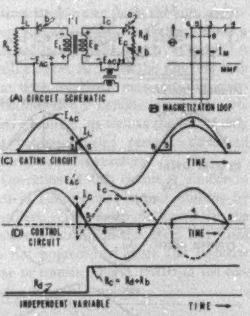

Figure 3. Theoretical transient flux-current-voltage relations for step change of control element resistance

Second Half-Cycle

The polarities of voltages E_{ac} and E_{ac}' now reverse. E_{ac} cannot be applied to the gating transformer in this phase since the rectifier prevents the flow or current in this direction. E_{ac}' can however appear as E_2 and induce voltage E_1 in the gating circuit. E_1 can be no more than equal to E_{ac} under the conditions imposed upon the examples to be considered so no current flows in the gating circuit. The current in this control circuit would be I_c while the magnetization level changes from 6 to 7. This mode of operation will be called reset. I_c equals I_m if all circuit components are ideal. Complete reset is approached at the end of second half-cycle. The integral of voltage I_cR_d during this period prevents complete reset.

Third Half-Cycle

The polarities of the voltages become positive and the a-c voltage is applied again to the gating transformer. Now practically the whole half-wave of a-c voltage is needed to change the core's magnetization level from 8 to 3. The current in the gating circuit is again I_m and the current in the control circuit zero before saturation. The angle of firing will be such as to make the average voltage in the control circuit zero in this steady-state operation.

Succeeding Half-Cycles

Operation in succeeding half-cycles repeats that of the second and third half-cycles since steady-state conditions have been attained.

The two phases of operation being dictated to this circuit are: (1) during positive half-cycles the gating transformer core is caused to saturate by application of part of the integral of the a-c line voltage; subsequent to this saturation, output current flows along with a nonessential control circuit current and (2) during negative half-cycles the gating transformer core is caused to reset an

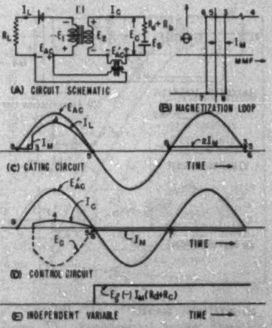

Figure 4. Theoretical transient flux-current-voltage relations for application of E_s

amount dependent upon the integral of the magnetizing voltage and whatever other voltages are present in the control circuit. The degree of reset is inversely proportional to the output quantity. Control of this circuit can be exercised by almost any type of control element which will influence this degree of reset of the saturable transformer.

It is important to note that, for the functioning of the circuit being considered the clockwise flow of current I_c in the control circuit need not exceed the magnetizing current I_m and the counterclockwise flow need never exist at all. In the interest of keeping circuit gain at as high a level as possible one could use nonlinear parameters in the control element which would seek to limit the current in the counterclockwise direction without materially affecting its flow in the clockwise direction. However, choice of parameter will ordinarily be predicated upon an engineering evaluation of each problem. There are many possibilities of such parameters and two which seem to show practical promise in the present state of the art will be used for illustration. A rectifier, shown in dashed outline in Figure 3, or a rectifier combination, Figure 5, could be used to limit current to unidirectional flow or limited bidirectional flow and a reactor combination, Figure 8 could be used to limit current in bidirectional flow. Resistance, Figure 4, would ordinarily be used in more conventional versions of this circuitry.

Variable Resistance as a Control Element

The effect of the normally-small control circuit resistance has been noted. In effect, the control circuit current I_c produced a voltage drop across R_d which subtracted from E_{ac}' and prevented full reset of the saturable transformer core. This resulted in output current proportional to $\int I_cR_d$ for the reset period. If a variable resistance, R_b, is placed in the control element position, Figure 3, the output quantity would be varied throughout its range by variation of R_b. The functional relationship I_c would bear to R_b would be dependent upon all the parameters affecting I_c. If, however, one considers rectifiers to be perfect and the magnetization loop represents the material for all rates of magnetization the magnetization current I_m would indeed be I_c.

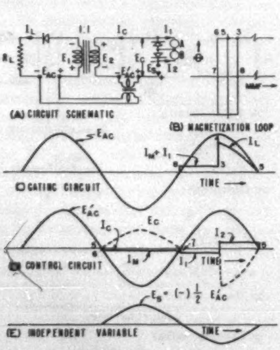

I_L
1:1
I_C
I_1
R_L
E_1
E_2
E_C
E_AC
E'_AC
E_s
I_2
6 5
3
7
8
MMF
(A) CIRCUIT SCHEMATIC
(B) MAGNETIZATION LOOP
E_AC
I_L
I_M+I_1
TIME
(C) GATING CIRCUIT
E'_AC
I_C
E_C
I_2
I_M
I_1
TIME
(D) CONTROL CIRCUIT
E_s = (−) ½ E'_AC
(E) INDEPENDENT VARIABLE
TIME

Figure 5. Theoretical transient flux-current-voltage relations for application of E$_s$

Since I_m and I_c would be constant during reset the integral of I_cR_b would be a readily calculable function of R_b. The effective control voltage E_c would be a sinusoid truncated at $I_m(R_b+R_c)$. The average output current I_L would be proportional to the average control element voltage E_c during the reset half-cycle. During the gating half-cycle a rectifier would prevent control circuit current if inserted as shown in Figure 3.

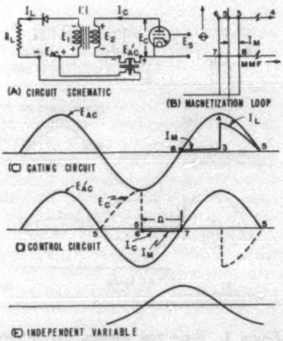

I_L
1:1
I_C
R_L
E_1
E_2
E_C
E_AC
E'_AC
E_s
6 5
3
4
I_M
7
8
MMF
(A) CIRCUIT SCHEMATIC
(B) MAGNETIZATION LOOP
E_AC
I_L
I_M
(C) GATING CIRCUIT
E'_AC
E_C
Ω
(D) CONTROL CIRCUIT
I_C
I_M
(E) INDEPENDENT VARIABLE

Figure 6. Theoretical transient flux-current-voltage relations for application of E$_s$(Ω = 90°) to thyratron grid

Figure 3 shows the voltage-flux-current relations in a transient resulting from a step change of control variable R_c. The resulting transfer characteristic is shown in Figure 9. Initial conditions are the final conditions of the example of Figure 2. The response time is again less than a cycle as dictated by the choice of the magnetizing element and controlled element combination.

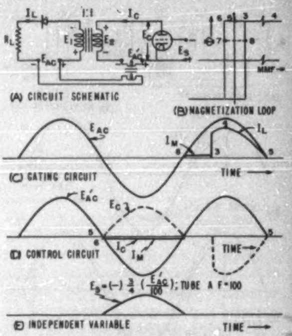

I_L
1:1
I_C
R_L
E_1
E_2
E_C
E_AC
E'_AC
E_s
6 5
3
4
7
8
MMF
(A) CIRCUIT SCHEMATIC
(B) MAGNETIZATION LOOP
E_AC
I_L
I_M
TIME
(C) GATING CIRCUIT
E'_AC
E_C
I_C
I_M
TIME
(D) CONTROL CIRCUIT
E_s = (−) ¾ (E'_AC/100); TUBE A F=100
(E) INDEPENDENT VARIABLE
TIME

Figure 7. Theoretical transient flux-current-voltage relations for application of E$_s$ to triode grid

Voltage Source as a Control Element

Resistance as Series Parameter

For continuity of thought the resistance $R_c = R_b + R_d$ of the previous example will be used as the control circuit resistance and the initial conditions of this example will be the final conditions of the previous example. The same graphical analysis procedure is used.

It can be readily visualized that the existence of any voltage in the control element in addition to that due to I_mR_c will directly affect the reset level. For example, if E_s, Figure 4, were equal to I_mR_c the effect due to the resistance during the reset period would be negated. A transient picture for application of the conditions described above is shown in Figure 4. The resulting transfer characteristic is shown in Figure 9. The application of an a-c voltage would result in different shapes of transfer characteristic depending upon the nature of the a-c voltage. The response time would remain the same.

The steady-state condition of I_c equal to a theoretically constant I_m is characteristic only of the zero-output condition described.

The literature is replete with examples of this type of control. Ordinarily a different magnetizing function is utilized allowing a longer response time. One of the most unfortunate features inherent to this control element is its dependence upon parameter stability.

Rectifiers as Series Parameters

An analysis of this control element has been published[1] for control with single

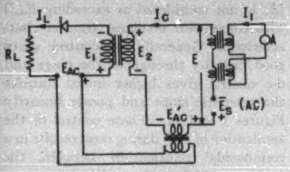

Figure 8. Voltage source as control element with reactors as series parameters

rectifiers and will not be repeated here. Controlled element rectifier leakage would not alter the transfer characteristic so long as this leakage does not exceed I_m. Limited bidirectional flow of control circuit currents can be accomplished by use of a rectifier combination such as shown in Figure 5. This circuit limits current flow to a maximum value I_1 in one direction and I_2 in the other direction as designated by the current sources "A" and "B". This allows controlled circuit rectifier leakage to exceed the magnetization loop width to the value of the counterclockwise control circuit current limit before the transfer characteristic would be appreciably altered.

Figure 5 shows theoretical flux-voltage-current relations for application of E_s in a circuit composed of ideal parameters. For initial conditions the beginning of a magnetizing (negative) half-cycle and core condition 5 are assumed. The effect of control circuit resistance is assumed to be negligible or negated. E_c is chosen a sinusoid of the same frequency as E_{ac}' but of opposite phase. This choice is dictated by a desire to maintain essentially the same conditions of operation as required before, that is, core magnetization during gating by controlled element and core magnetization during reset by control circuit. With current limiting and appropriate control circuit voltages all magnetization currents could be carried by the control circuit. The results of this type of operation are now being analyzed together with auxiliary circuitry useful in altering the resulting transfer characteristic.

REACTORS AS SERIES PARAMETERS

A considerable degree of practical success has been achieved in the laboratory by using reactor combinations for current limiting in control elements with a-c control voltage. An example of this type of circuit is shown in Figure 8. The series reactor combination is designed in such a way as to require larger magnetizing current than that of the gating transformer.

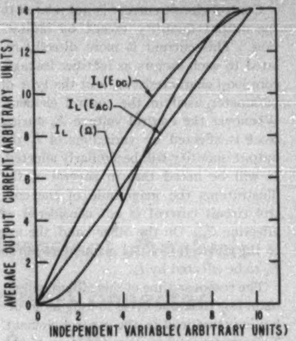

Figure 9. Theoretical transfer characteristics

Normal magnetization current for the gating transformer flows through an appropriately designed reactor combination without appreciable reactive drop. A small current I_b biases the reactors such that their combined magnetization characteristic has a definite break at zero. This condition, as well as the use of only a-c voltages, helps prevent undesired saturation of the reactors.

Operation of this circuit is similar to that of bidirectional current limiting by rectifiers. Transients do occur in the reactor combination flux level but these do not appreciably affect the response time or transfer characteristic of the correctly designed amplifier.

Thyratron as Control Element

As indicated earlier, any variable which will alter the degree of reset of the saturable transformer core may be inserted as a control element. The thyratron offers an interesting example. Before breakdown a thyratron would prevent reset; after breakdown, reset would be a function of E_{ac}'. The plate voltage of the thyratron is a known function (E_{ac}') before breakdown so control of firing time can be readily accomplished, particularly by a grid signal whose phase is the independent variable. Output reproducibility depends upon thyratron stability.

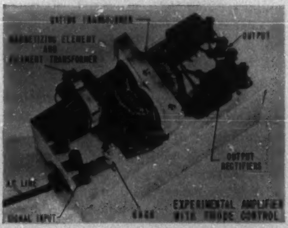
GATING TRANSFORMER
MAGNETIZING ELEMENT AND FILAMENT TRANSFORMER
OUTPUT
OUTPUT RECTIFIERS
AC LINE
SIGNAL INPUT
6AQ6
EXPERIMENTAL AMPLIFIER WITH TRIODE CONTROL

Figure 10. Experimental amplifier with triode control

Figure 6 shows the flux-voltage-current relations resulting from the sudden application of a grid voltage phase which allows thyratron firing at 90 degrees in the a-c wave. Initial conditions are as before with core saturation at 5 at the beginning of a reset period and the circuit parameters are considered ideal.

The transfer characteristic would be a cosinusoidal function of the thyratron firing angle, Figure 9, and the response time would again be less than a cycle of the a-c line frequency.

Triode as Control Element

Another useful device for altering the degree of reset is the triode. It is perhaps one of the most useful of elements when considerable power needs to be controlled by the output of a small electronic device. For a given grid bias the idealized plate characteristics of a triode very closely approximate those of a voltage and single rectifier. There is, however, an important difference. The independent variable, E_s, which controls E_c when plate current exists is applied as a negative signal to the high impedance grid. The power gain of such combination could be made astronomical.

Figure 7 shows the theoretical flux-current-voltage relations existing in transient after a single rectified half-cycle of a-c line frequency and phase is applied to the grid of the triode during reset. The initial conditions are those of the previous example. If this signal is repeated in

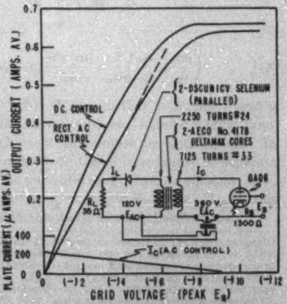

Figure 11. Experimental transfer characteristics with triode control element

each cycle, steady-state current I_L will flow; if the signal is not repeated, the single pulse shown will represent the total output. Programmed pulses on the input will be reproduced in the load with only a half-cycle phase shift.

A 60-cycle amplifier of this type was constructed for demonstration, Figure 10. The time required for 100 per cent response is less than a cycle as predicted. Experimental transfer characteristics for rectified a-c and d-c control are shown in Figure 11. The output power is more than 35 watts and the control element a *6AQ6* miniature voltage amplifier triode whose grid power is practically immeasurable. This is by no means an optimum design and the capabilities of the tube are not even approached. The transfer characteristics show the same general forms predicted theoretically, Figure 9.

REMARKS

The foregoing illustrations have iterated and reiterated one principle of operation: amplifier output is determined by the effective control element voltage during a single reset half-cycle. From consideration of the idealized and somewhat stylized examples one can draw some interesting conclusions.

Control circuit current is not related to the output quantity except by indirection. This current is more directly related to such factors as rectifier leakage, core loop characteristics, and the type of parameter used in the control element. Whenever the control voltage E_c during reset is affected by variations of I_c the output quantity will be similarly affected. It will be noted that in several of the illustrations the magnitude of the control circuit current is not considered as affecting E_c. On the other hand, the use of the resistive control element required E_c to be effected by I_c.

The response time of this circuit will remain less than one cycle so long as no delay is introduced in the control element. This response time is a function of the magnetizing element utilized and is not considered within the scope of this paper.

The average value of a-c voltage applicable to the load is directly determined by the average value of E_c during reset. This gives rise to several types of transfer characteristic depending upon the type of control voltage E_s used. Theoretically, linear relations exist between an a-c voltage E_s, E_c, and the output quantity. Application of a d-c voltage E_s results in an E_c of the form of a truncated sinusoid (E_c is not considered as exceeding E_{ac}') with consequent nonlinear transfer characteristic. Generally a-c control gives good linearity throughout the range and d-c control gives higher initial transfer characteristic slope and poorer linearity Figures 9 and 11. Phase control of the application of E_{ac}' during reset results in a cosinusoidal relationship between the angle at which such application occurs and the output quantity, Figure 9. The output quantity is actually a voltage integral but precedence requires it be indicated as an average current.

It is rather directly discernible that ideal parameters offer clean-out solutions. However most problems involve the use of rectifiers and magnetic materials which do not more than approach these ideals. It is an engineering problem to recognize the inherent deviations and to prevent them from affecting the desired results in more than a second order manner. When E_c is not allowed to be affected by I_c this can usually be accomplished with a high degree of success.

Reference

1. ON THE MECHANICS OF MAGNETIC AMPLIFIER OPERATION, R. A. Ramey. *AIEE Transactions*, volume 70, part II, 1951, pages 1214–23.

No Discussion

Steady-State and Transient Analysis of an Idealized Series-Connected Magnetic Amplifier

LOUIS A. PIPES
MEMBER AIEE

Synopsis: This paper presents a mathematical analysis of an idealized series-connected magnetic amplifier based on certain simplifying assumptions. The methods of nonlinear mechanics are used to obtain expressions for the input and output currents in the transient and steady state. Considerable attention is given to the problems of the existence and nature of time constants associated with the series-connected amplifier.

IN RECENT years magnetic amplifiers have been used more and more extensively as reliable substitutes for vacuum tube amplifiers. The general principles upon which the operation of magnetic amplifiers depends have been known for over 50 years.

In the early literature the magnetic amplifier was more commonly known as the d-c excited reactor. It is only in more recent publications that the name magnetic amplifier has been used. A magnetic amplifier is an arrangement of saturable reactors and metal rectifiers that behaves as an amplifier of steady or varying d-c input power. Many investigators have, in recent years, developed the steady-state theory of magnetic amplifiers. In these treatments the development of the theory is based on simplified idealized circuits and magnetization curves.

In this paper, a mathematical analysis of an idealized series-connected magnetic amplifier in the transient state is attempted. In the course of the investigation, it was found that in considering the transient state it is not possible to neglect the resistance of the windings of the amplifier as is commonly done in investigations of the steady state. The methods of nonlinear mechanics have been applied to the solution of the differential equations that describe the dynamic behavior of the amplifier and certain methods of estimating the time constant of the amplifier under consideration have been developed.

The Basic Equations of the Circuit

The basic equations of the circuit of Figure 1 are obtained by an application of Kirchhoff's voltage laws and Ampere's circuital law for the electric and magnetic loops. The equations are

$$E_o=2R_1i_1+N_1\left(\frac{d\phi_a}{dt}+\frac{d\phi_b}{dt}\right) \tag{1}$$

$$E_m\sin(\omega t)=2R_2i_2+N_2\left(\frac{d\phi_a}{dt}+\frac{d\phi_b}{dt}\right) \tag{2}$$

$$N_1i_1+N_2i_2=lH_a \tag{3}$$

$$N_1i_1-N_2i_2=lH_b \tag{4}$$

where H_a and H_b are the magnetic intensities of cores a and b, ϕ_a and ϕ_b are the magnetic fluxes in the corresponding cores, R_1 and R_2 are the resistances of the windings N_1 and N_2 (turns), and l is the mean length of the magnetic path of the two cores. The remaining quantities are indicated in Figure 1.

In order to carry out a mathematical analysis, it is necessary to postulate an analytical relation between H and ϕ of the cores. An analytical expression that may be adjusted to fit the experimental curves of a large class of materials is

$$H=k_1\phi+k_2\phi^n=F(\phi) \tag{5}$$

where k_1 and k_2 are constants and the number n may usually be given the values $n=3, 5, 9, 11, 15$. In the present analysis the value $n=3$ will be taken; however, the procedure may be modified to take account of other choices of values for the number n. With the choice $n=3$.

$$H_a=k_1\phi_a+k_2\phi_a^3 \tag{6}$$

and

$$H_b=k_1\phi_b+k_2\phi_b^3 \tag{7}$$

We now have a complete set of equations in order to determine the transient and steady-state currents i_1 and i_2.

Separation of the Variables

To simplify the analysis let it be assumed that

$$N_1=N_2=N \tag{8}$$

$$R_1=R_2=R \tag{9}$$

With this assumption

$$E_o=2Ri_1+N\left(\frac{d\phi_a}{dt}+\frac{d\phi_b}{dt}\right) \tag{10}$$

and

$$E_m\sin(\omega t)=2Ri_2+N\left(\frac{d\phi_a}{dt}+\frac{d\phi_b}{dt}\right) \tag{11}$$

If these equations are solved for i_1 and i_2

$$i_1=\frac{E_o}{2R}-\frac{N}{2R}\left(\frac{d\phi_a}{dt}+\frac{d\phi_b}{dt}\right) \tag{12}$$

and

$$i_2=E_m\frac{\sin(\omega t)}{2R}-\frac{N}{2R}\left(\frac{d\phi_a}{dt}+\frac{d\phi_b}{dt}\right) \tag{13}$$

It is thus seen that to obtain i_1 and i_2 the variation of $d\phi_a/dt$ and $d\phi_b/dt$ as functions of time must be determined. In order to do this it is necessary to separate the variables and obtain an equation in ϕ_a and another one in ϕ_b alone. To do this add equations 10 and 11 and obtain

---

Paper 51-390, recommended by the AIEE Magnetic Amplifiers Committee and approved by the AIEE Technical Program Committee for presentation at the AIEE Fall General Meeting, Cleveland, Ohio, October 22–26, 1951. Manuscript submitted June 25, 1951; made available for printing September 13, 1951.

Louis A. Pipes is with the University of California, Los Angeles, Calif.

$$E_o+E_m \sin(\omega t)=2R(i_1+i_2)+2N\dot{\phi}_a \tag{14}$$

However, from equation 3

$$N(i_1+i_2)=lH_a \tag{15}$$

or

$$(i_1+i_2)=\frac{lH_a}{N} \tag{16}$$

If this is substituted into equation 14, one obtains

$$\frac{d\phi_a}{dt}+\frac{RlH_a}{N^2}=\frac{E_o+E_m \sin(\omega t)}{2N} \tag{17}$$

H_a may now be eliminated by the use of equation 6 and equation 17 may be written in the following form

$$\frac{d\phi_a}{dt}+\frac{Rl}{N^2}(k_1\phi_a+k_2\phi_a{}^3)=\frac{E_o+E_m \sin(\omega t)}{2N} \tag{18}$$

In the same way, if equation 11 is subtracted from equation 10 and equations 4 and 7 are used, one obtains

$$\frac{d\phi_b}{dt}+\frac{Rl}{N^2}(k_1\phi_b+k_2\phi_b{}^3)=\frac{E_o-E_m \sin(\omega t)}{2N} \tag{19}$$

Equations 18 and 19 are the desired equations with the variables separated. These equations are nonlinear differential equations of the first order. The importance of the resistance term is apparent from the equations. It does not appear justifiable to neglect the resistance terms as has been done by many writers on the theory of magnetic amplifiers.

Qualitative Discussion of the Time Constant

Before considering the solution of the general problem, it is instructive to consider the notion of the time constant of a magnetic amplifier in a qualitative manner.

In the absence of nonlinearity of the H,ϕ curve, equations 18 and 19 are of the form

$$\frac{d\phi}{dt}+a\phi=\frac{1}{2N}[E_o \pm E_m \sin(\omega t)] \tag{20}$$

where

$$a=\frac{Rlk_1}{N^2} \tag{21}$$

The free growth or decay of the magnetic fluxes of the cores are governed by the homogeneous equation

$$\frac{d\phi}{dt}+a\phi=0 \tag{22}$$

If at $t=0$ we have $\phi=\phi_0$, then the solution of this equation is of the form

$$\phi=\phi_0 e^{-at} \tag{23}$$

In the usual linear discussions involving time constants, a time constant, T, is defined by the equation

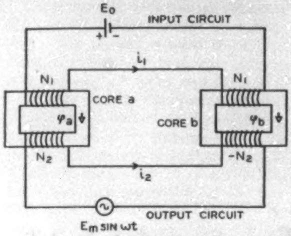

Figure 1. Series-connected magnetic amplifier

$$aT=1 \tag{24}$$

or

$$T=\frac{1}{a}=\frac{N^2}{Rlk_1} \tag{25}$$

This is a measure of the rapidity with which transient disturbances build up or decay. In this linear case

$$H=k_1\phi \tag{26}$$

where k_1 is a measure of the initial slope of the H,ϕ curve. The initial inductance of the circuit is

$$L_0=\frac{N^2}{lk_1}=\frac{N^2S\mu_0}{l} \tag{27}$$

where S is the cross-sectional area of the magnetic cores and u_0 is the initial permeability of the magnetic core material. It is thus seen that the time constant in the linear case varies directly with the initial permeability of the magnetic material.

The nonlinear H,ϕ curve may be represented by the equation

$$H=k_1\phi+k_3\phi^n \tag{28}$$

where n is an odd number. In this case equations 18 and 19 reduce to an equation of the type

$$\frac{d\phi}{dt}+\frac{Rl}{N^2}(k_1\phi+k_3\phi^n)=0 \tag{29}$$

for the free growth or attenuation of the fluxes in the cores. This equation is of the form

$$dx/dt+ax+bx^n=0 \tag{30}$$

where

$$a=\frac{Rlk_1}{N^2} \tag{31}$$

$$b=\frac{Rlk_3}{N^2} \tag{32}$$

Equation 30 may be written

$$\frac{dx}{ax+bx^n}=-dt \tag{33}$$

This may be integrated by placing

$$m=(n-1) \tag{34}$$

and using the following formula

$$\int\frac{dx}{x(a+bx^m)}=\frac{l}{am}\ln\left(\frac{x^m}{a+bx^m}\right) \tag{35}$$

Equation 33 upon integration becomes

$$\frac{x^m}{(a+bx^m)}=Ke^{-amt} \tag{36}$$

where K is an arbitrary constant. This may be written in the more convenient form

$$\frac{a+bx^m}{x^m}=\frac{1}{Ke^{-amt}}=Ce^{amt} \tag{37}$$

or

$$x^m=\frac{a}{(Ce^{amt}-b)} \tag{38}$$

where C is an arbitrary constant. If $x=x_0$ at $t=t_0$, and $t=0$, then

$$C=\frac{a}{x_0{}^m}+b=\frac{a+bx_0{}^m}{x_0{}^m} \tag{39}$$

If this is substituted into equation 38

$$x^m=\frac{a}{(a/x_0{}^m+b)e^{amt}-b} \tag{40}$$

Clearly, the rate of decay depends upon the initial condition x_0. An interesting case is the one in which the H,ϕ curve may be represented by a high power term alone so that

$$H=k_3\phi^n\ (n\ \text{odd}) \tag{41}$$

In this case, the equation to be integrated is

$$dx/dt+bx^n=0 \tag{42}$$

or

$$\frac{dx}{x^n}=-bdt \tag{43}$$

Now if $x=z_0$ at $t=0$,

$$t=\frac{1}{b(n-1)}\left(\frac{1}{x^{n-1}}-\frac{1}{x_0{}^{n-1}}\right) \tag{44}$$

For example let $n=5$ and suppose it is required to determine the time required so that x should drop to one-third its initial value, then

$$x=\frac{x_0}{3} \tag{45}$$

and

$$T=\frac{1}{4b}(3^4/x_0{}^4-1/x_0{}^4)=20/bx_0{}^4 \tag{46}$$

Note that the time required for the decay is a function of the initial conditions and of the values of n and b. The fact that the rates of decay in the nonlinear case are functions of the original excitation makes it rather difficult to define a time constant in a precise manner. In the linear case the time of decay to a fractional part of the initial value is independent of the initial value.

The First Approximation Theory of the Nonlinear Case

Return, now, to equations 18 and 19 and consider an approximate method for the solution of these equations. These equations are of the form

$$\frac{d\phi_a}{dt}+a\phi_a+b\phi_a^3=A+B\sin(\omega t) \tag{47}$$

and

$$\frac{d\phi_b}{dt}+a\phi_b+b\phi_b^3=A-B\sin(\omega t) \tag{48}$$

where

$$a=\frac{Rlk_1}{N^2}=\frac{Rl}{N^2S\mu_0} \tag{49}$$

in this expression μ_0 is the initial permeability of the core material and S is the cross-sectional area of the cores.

$$b=\frac{Rlk_3}{N^3} \tag{50}$$

$$A=\frac{E_0}{2N} \tag{51}$$

$$B=\frac{E_m}{2N} \tag{52}$$

Equations 47 and 48 may be written in the form

$$d\phi_a/dt=A+B\sin(\omega t)-a\phi_a-b\phi_a^3 \tag{53}$$

and

$$d\phi_b/dt=A-B\sin(\omega t)-a\phi_b-b\phi_b^3 \tag{54}$$

Now as a first approximation take

$$d\phi_{a1}/dt+a\phi_{a1}=A+B\sin(\omega t) \tag{55}$$

$$d\phi_{b1}/dt+a\phi_{b1}=A-B\sin(\omega t) \tag{56}$$

The solution of these equations, subject to the initial condition that at $t=0$, $\phi_{a1}=\phi_{b1}=0$, are

$$\phi_{a1}=\frac{A(1-\epsilon^{-at})}{a}+B\omega\left[\frac{\epsilon^{-at}}{Z^2}+\frac{\sin(\omega t-\theta)}{\omega Z}\right] \tag{57}$$

and

$$\phi_{b1}=\frac{A(1-\epsilon^{-at})}{a}-B\omega\left[\frac{\epsilon^{-at}}{Z^2}+\frac{\sin(\omega t-\theta)}{\omega Z}\right] \tag{58}$$

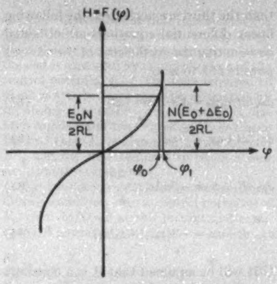

Figure 2. Curves for the graphical determination of the time constant

where

$$\theta=\tan^{-1}(\omega/a) \text{ and } Z=\sqrt{a^2+\omega^2} \tag{59}$$

To obtain the first approximation for $d\phi_a/dt$ and $d\phi_b/dt$ substitute equations 57 and 58 into equations 53 and 54 and obtain

$$d\phi_a/dt=A+B\sin(\omega t)-a\phi_{a1}-b\phi_{a1}^3 \tag{60}$$

and

$$d\phi_b/dt=A-B\sin(\omega t)-a\phi_{b1}-b\phi_{b1}^3 \tag{61}$$

Let $U(t)=(1-\epsilon^{-at})$, then

$$\begin{aligned}d\phi_a/dt=A+B\sin(\omega t)-A\,U(t)-\\ aB\omega\left[\frac{\epsilon^{-at}}{Z^2}+\frac{\sin(\omega t-\theta)}{\omega Z}\right]-b\times\\ \left\{\frac{A\,U}{a}(t)+B\omega\left[\frac{\epsilon^{-at}}{Z^2}+\frac{\sin(\omega t-\theta)}{\omega Z}\right]\right\}^3\end{aligned} \tag{62}$$

In the same manner, or by replacing B by $-B$ in equation 62

$$\begin{aligned}d\phi_b/dt=A-B\sin(\omega t)-A\,U(t)+\\ aB\omega\left[\frac{\epsilon^{-at}}{Z^2}+\frac{\sin(\omega t-\theta)}{\omega Z}\right]-b\times\\ \left\{\frac{A\,U}{a}(t)-B\omega\left[\frac{\epsilon^{-at}}{Z^2}+\frac{\sin(\omega t-\theta)}{\omega Z}\right]\right\}^3\end{aligned} \tag{63}$$

The control current, i_1, and the output current, i_2, are given by

$$i_1=\frac{E_0}{2R}-\frac{N}{2R}\left(\frac{d\phi_a}{dt}+\frac{d\phi_b}{dt}\right) \tag{64}$$

and

$$i_2=\frac{E_m}{2R}\sin(\omega t)-\frac{N}{2R}\left(\frac{d\phi_a}{dt}+\frac{d\phi_b}{dt}\right) \tag{65}$$

If equations 62 and 63 are added, one obtains

$$\begin{aligned}\left(\frac{d\phi_a}{dt}+\frac{d\phi_b}{dt}\right)=2A-2A\,U(t)-b\left\{2\frac{A^3}{a^3}U^3(t)+\right.\\ \left.6\frac{A\,U}{a}(t)B^2\omega^2\left[\frac{\epsilon^{-at}}{Z^2}+\frac{\sin(\omega t-\theta)}{\omega Z}\right]\right\}\end{aligned} \tag{66}$$

The control current is obtained by substituting equation 66 into equation 64 and is

$$\begin{aligned}i_1=E_0\frac{U(t)}{2R}+\frac{bNA\,U(t)}{aR}\left\{A^2\frac{U^2}{a^2}(t)+3B^2\omega^2\times\right.\\ \left.\left[\frac{\epsilon^{-at}}{Z^2}+\frac{\sin(\omega t-\theta)}{\omega Z}\right]^2\right\}\end{aligned} \tag{67}$$

The steady-state control current is obtained by placing $t\rightarrow\infty$ in equation 67. Note that

$$\underset{t\rightarrow\infty}{\text{Limit}}\ U(t)=1 \tag{68}$$

Hence

$$i_1=\frac{E_0}{2R}+\frac{bNA}{aR}\left[\frac{A^2}{a^2}+\frac{3B^2\omega^2\sin^2(\omega t-\theta)}{\omega^2Z^2}\right] \tag{69}$$

or

$$i_1=\frac{E_0}{2R}+\frac{E_0k_3}{Rk_1}\left[\frac{E_0^2N^2}{4R^2l^2k_1^2}+\frac{3B^2}{Z^2}\sin^2(\omega t-\theta)\right] \tag{70}$$

Now since

$$\sin^2(\omega t-\theta)=\frac{1}{2}[1-\cos(2\omega t-2\theta)] \tag{71}$$

and

$$B^2=E_m^2/4N^2 \tag{72}$$

Equation 70 may be written in the following form

$$\begin{aligned}i_1=\frac{E_0}{2R}+\frac{E_0k_3}{Rk_1}\left\{\frac{E_0^2N^2}{4R^2l^2k_1^2}+\right.\\ \left.\frac{3E_m^2}{8N^2Z^2}[1-\cos(2\omega t-\theta)]\right\}\end{aligned} \tag{73}$$

to the first degree of approximation. In the absence of nonlinearity, $k_3=0$ and the current reduces to $E_0/2R$ as it should. It is seen that to the order of the first approximation, the current i_1 contains a second harmonic ripple of the output potential.

The output current, i_2, now may be obtained by substituting equations 62 and 63 into 65. If this is done and some algebraic reductions are performed, one obtains

$$\begin{aligned}i_2=\frac{E_mlk_1\omega}{2N^2}\frac{[\epsilon^{-at}+\sin(\omega t-\theta)]}{\omega Z}+\\ \frac{E_mlk_3\omega}{2N^2}\left\{\frac{E_m\omega^2}{4N^2}\left[\frac{\epsilon^{-at}}{Z^2}+\frac{\sin(\omega t-\theta)}{\omega Z}\right]^3+\right.\\ \left.\frac{3E_0^2U^2(t)}{4R^2l^2k_1^2}\left[\frac{\epsilon^{-at}}{Z^2}+\frac{\sin(\omega t-\theta)}{\omega Z}\right]\right\}\end{aligned} \tag{74}$$

If use is made of equation 68, the steady-state current may be obtained from equation 74 in the form

$$\begin{aligned}i_2=\frac{E_mlk_1}{2N^2}\frac{\sin(\omega t-\theta)}{Z}+\frac{E_m^3lk_3}{8N^4}\frac{\sin^3(\omega t-\theta)}{Z^3}+\\ \frac{3E_mE_0^2lk_3\sin(\omega t-\theta)}{8R^2l^2k_1^2N^2\times Z}\end{aligned} \tag{75}$$

To this degree of approximation it is seen that the effect of nonlinearity is to produce a term in the output current proportional to the square of the control potential. Since

$$\sin^3 A = \frac{(3 \sin A - \sin 3A)}{4} \tag{76}$$

it is seen that the second term of equation 75 leads to a third harmonic term in the output current.

Equations 67 and 74 for the input and output currents are based on the linear plus cubic term representation of the H, ϕ curve and the first order term solutions of the nonlinear differential equations for ϕ_a and ϕ_b. An examination of equation 74 discloses the fact that if a change in E_a is made, then a steady-state is reached when the quantity $U(t)$ approaches unity. Since $U(t) = (1 - \epsilon^{-at})$, it would appear that the quantity

$$T = \frac{1}{a} = \frac{N^2 S \mu_0}{Rl} \tag{77}$$

is a measure of the rapidity of the response of the magnetic amplifier, and the larger the initial permeability, μ_0, of the core material, the slower the response of the amplifier will be.

Solution of the Nonlinear Differential Equations by the Perturbation Method

In this section a more precise solution of the nonlinear differential equations 47 and 48 will be formulated. The standard perturbation method so frequently used in nonlinear mechanics will be used.[1,2,3]

Both equations 47 and 48 are of the form

$$dx/dt + ax + bx^3 = A + B \sin (\omega t) \tag{78}$$

where a, b, A, and B are defined by equations 49–52. Equation 78 may be solved by the perturbation method. The perturbation method consists of assuming a solution of the following form

$$x = x_0(t) + bx_1(t) + b^2x_2(t) + b^3x_3(t) + \ldots \tag{79}$$

This is a power series in the parameter b. If equation 79 is substituted into equation 78 obtains the following result

$$\begin{aligned}\left(\frac{dx_0}{dt} + \frac{bdx_1}{dt} + \frac{b^2dx_2}{dt} + \frac{b^3dx_3}{dt} + \ldots\ldots\right) + \\ a(x_0 + bx_1 + b^2x_2 + b^3x_3 + \ldots) + \\ bx_0^3 + b^2(3x_0^2x_1) + b^3(3x_0x_1^2 + \\ 3x_0^2x_2) + \ldots = +A + B \sin (\omega t)\end{aligned} \tag{80}$$

This equation must hold for any value of the quantity b, and hence every factor for each of the powers of b must be zero. If all terms containing b to powers higher than the third are neglected, the following linear differential equations are obtained on equating the coefficients of the various powers of b to zero:

$$dx_0/dt + ax_0 = A + B \sin (\omega t) \tag{81}$$

$$dx_1/dt + ax_1 = -x_0^3 \tag{82}$$

$$dx_2/dt + ax_2 = -3x_0^2x_1 \tag{83}$$

$$dx_3/dt + ax_3 = -3(x_0x_1^2 + x_0^2x_2) \tag{84}$$

It will be assumed that A is a constant and that at $t = 0$, the circuit is at rest and that there is no residual magnetism. In such a case we have the initial conditions that

$$x(0) = 0 \text{ and } x_i(0) = 0 \quad i = 0,1,2,3,\ldots \tag{85}$$

The solution of the first equation of the above set, equation 81, subject to the above initial condition is

$$x_0 = \frac{A}{a}(1 - \epsilon^{-at}) + B\omega \frac{\epsilon^{-at}}{Z^2} + \frac{B}{Z} \sin (\omega t - \theta) \tag{86}$$

where

$$\tan \theta = \frac{\omega}{a} \text{ and } Z = \sqrt{a^2 + w^2} \tag{87}$$

Equation 86 may be written in the following form

$$x_0 = K_1 + K_2\epsilon^{-at} + K_3 \sin (\omega t - \theta) \tag{88}$$

where

$$K_1 = \frac{A}{a}, \; K_2 = \left(B \frac{\omega}{Z^2} - \frac{A}{a}\right), \quad K_3 = \frac{B}{Z} \tag{89}$$

Now

$$\begin{aligned}x_0^3 = K_1^3 + K_2^3\epsilon^{-3at} + K_3^3 \sin^3 (\omega t - \theta) + \\ 6K_1K_2\epsilon^{-at}K_3 \sin (\omega t - \theta) + \\ 3[K_1^2K_2\epsilon^{-at} + K_1K_2^2\epsilon^{-2at} + \\ K_2^2\epsilon^{-2at}K_3 \sin (\omega t - \theta) + \\ K_2\epsilon^{-at}K_3^2 \sin^2 (\omega t - \theta) + K_1K_3^2 \times \\ \sin^2 (\omega t - \theta) + K_1^2K_3 \sin (\omega t - \theta)] = F(t)\end{aligned} \tag{90}$$

With this notation, the solution of equation 82

$$x_1 = -\int_0^t \epsilon^{-a(t-u)} F(u)du = - \epsilon^{-at} \int_0^t \epsilon^{au} F(u)du \tag{91}$$

On obtaining $x_1(t)$, then equation 83 may be solved and x_2 obtained and so on In the absence of definite numerical values the algebraic manipulations soon become formidable. It is apparent from the form of the solution that the series equation 79 converges rapidly. It is evident that the transient terms all contain the factor ϵ^{-at} or multiples of this factor; it is thus apparent that the fundamental time constant is

$$T = \frac{1}{a} = \frac{N^2 S \mu_0}{Rl} \tag{92}$$

The perturbation method is a laborious one, but if numerical values are available it may be applied to differential equations of the form

$$\frac{dx}{dt} + ax + bx^n = A + B \sin (\omega t) \tag{93}$$

by a modification of the above procedure. Once x is determined, then ϕ_a and ϕ_b are known and the control and output currents can be computed from equations 12 and 13.

Conclusions

This analysis is an attempt to study mathematically the basic differential equations of a series-connected magnetic amplifier based on the assumption that the $H-\phi$ curve of the material of the cores can be represented by an equation of the type

$$H = k_1\phi + k_2\phi^3 \tag{94}$$

The method presented can be easily extended to the case where

$$H = k_1\phi + k_2\phi^n \tag{95}$$

n being an odd positive integer. The effects of hysteresis and leakage are neglected and no feedback is taken into account.

The analysis indicates that in studying the problem from a rigorous point of view in the transient state, the effect of the resistance of the windings cannot be neglected. The results show that if the control potential, E_a, is altered, a new steady-state is not reached until terms of the form ϵ^{-at} where $a = Rl/N^2S\mu_0$ tend to zero.

The concept of a time constant applies to nonlinear systems in a qualitative manner. In an R, L, linear series circuit, the time constant is conventionally taken to be

$$T_0 = \frac{L}{R} \tag{96}$$

where L is the inductance of the system. For such a system the inductance parameter is defined as

$$L = \frac{Nd\phi}{di} = \frac{N^2}{l}\frac{d\phi}{dH} = \frac{N^2 S \mu}{l} \tag{97}$$

where N is the number of turns of the inductor, S the mean cross-sectional area of the magnetic path, l the mean length of the magnetic path and μ the permeability of the linear magnetic material of the core.

Extrapolation from the linear to the nonlinear case cannot be rigorously justified but qualitative results may sometimes be obtained by doing so. Following such a procedure one might define an equivalent inductance in a qualitative manner by computing $d\phi/dH$ from equation 95 and substituting the result into equation 97 and thus obtain

$$L_{\text{equiv}} = \frac{N^2}{1(k_1 + nk_2\phi^{n-1})} \tag{98}$$

Such an inductance would not be a constant but would be a function of the mean operating flux, ϕ. By analogy with equation 96 an equivalent time constant could be defined by

$$T_{\text{equiv}} = \frac{N^2}{Rl(k_1 + nk_2\phi^{n-1})} \tag{99}$$

Since

$$k_1 = \frac{1}{S\mu_0} \tag{100}$$

where μ_0 is the initial permeability of the core material, it can be seen that if the B versus H curve of the material rises very rapidly, then $k_1 \rightarrow 0$ and equation 99 reduces to

$$T_{\text{equiv}} = \frac{N^2}{Rlnk_2\phi^{n-1}} \tag{101}$$

Equation 101 is a possible qualitative definition for a time constant. Since it depends on the existing value of ϕ, the mean operating flux might be taken for ϕ in the equation to obtain an order of magnitude of the time constant defined in this manner. Another approximate method for computing the time constant is given in the appendix.

Appendix

A Suggested Method for Determining the Time Constant of a Series-Connected Magnetic Amplifier

The equation governing the flux distribution of the cores is of the form

$$\frac{d\phi}{dt} + \frac{Rl}{N^2}F(\phi) = A \pm B\sin(\omega t) \tag{102}$$

where $F(\phi)$ expresses the H versus ϕ relation of the material of the cores. To simplify the analysis $F(\phi)$ has been taken to be of the form

$$F(\phi) = k_1\phi + k_2\phi^n \quad (n = 3, 5, 7, 9, \ldots) \tag{103}$$

In the absence of a-c excitation in the output windings $B = 0$, and therefore equation 102 becomes

$$\frac{d\phi}{dt} + \frac{Rl}{N^2}F(\phi) = A = \frac{E_o}{2N} \tag{104}$$

Now suppose that E_o is varied and it is required to determine the time required for the system to acquire a new steady-state. Since the a-c excitation is assumed removed, the flux is produced by the application of the control potential E_o. The time required to reach a steady state may be estimated by supposing that at $t = 0$ an excitation E_o has been applied and that equilibrium has been reached then E_o is increased by an amount ΔE_o and the time required to reach a new steady state is computed.

If at $t = 0$ the system has reached an equilibrium condition with a control potential of E_o, then $d\phi/dt = 0$ at this instant and equation 104 becomes

$$\frac{Rl}{N^2}F(\phi) = \frac{E_o}{2N} \tag{105}$$

The value of the flux at this instant is given by

$$F(\phi_0) = \frac{E_oN}{2Rl} \tag{106}$$

If the curve $F(\phi)$ is given graphically, this may be determined as shown in Figure 2.

Now at $t = 0$, let E_o be increased by an amount ΔE_o. Then

$$\frac{d\phi}{dt} + \frac{Rl}{N^2}F(\phi) = \frac{1}{2N}(E_o + \Delta E_o) \tag{107}$$

or

$$\frac{d\phi}{\dfrac{(E_o + \Delta E_o)}{2N} - \dfrac{Rl}{N^2}F(\phi)} = dt \tag{108}$$

The new equilibrium state is reached when $\frac{d\phi}{dt} = 0$ in equation 107 and the equilibrium flux is now given by

$$F(\phi_1) = \frac{N}{2Rl}(E_o + \Delta E_o) \tag{109}$$

The required time, T, to arrive at a new steady state is obtained by integrating both sides of equation 109 and is given by

$$T = \int_{\phi_0}^{\phi_1} \frac{d\phi}{\dfrac{(E_o + \Delta E_o)}{2N} - \dfrac{Rl}{N^2}F(\phi)} \tag{110}$$

Since at $\phi = \phi_1$ the denominator vanishes, the integral of equation 110 is an improper one. To eliminate the difficulty that this entails in a graphical integration, the time constant, T, could be defined as the time required to reach a fraction (say $0.9\phi_1$) of the final value of the flux as a measure of the rapidity of the response of a magnetic amplifier.

This is analogous to the procedure used in defining the time constants of linear R,L, series circuits where the transients decay by the factors $\epsilon^{-Rt/L}$ and the time constant is arbitrarily defined by setting $T = L/R$ so that the transients die down to ϵ^{-1} of their initial values at the end of $t = T$.

References

1. The Engineer Grapples with Nonlinear Problems, T. von Kármán. *Bulletin*, American Mathematical Society (New York, N. Y.), volume 1, 1946, pages 615–83.

2. Applied Mathematics for Engineers and Physicists (book), L. A. Pipes. McGraw-Hill Book Company, New York, N. Y. Chapter XXII, 1946.

3. Introduction to Nonlinear Mechanics (book), N. Minorsky. Edward Brothers, Ann Arbor, Mich., 1947.

Discussion

L. A. Finzi (Carnegie Institute of Technology, Pittsburgh, Pa.): This is a treatment of a series-connected magnetic amplifier with cores of gradually varying differential permeability. The approach has a character of novelty in so far as the author considers it necessary to take the resistance of the windings into full account in all steps of the analysis. By doing so, a direct integration of the voltage differential equations is rendered impossible and methods of approximation are suggested for the solution.

Truly, engineers concerned with magnetic amplifiers give preference to types of analysis in which the relative influences of factors of design and operation are seen explicitly throughout. Synthesis design is generally their ultimate aim. Methods of approximation are valuable to them if they can be carried out in a symbolic form of comparatively easy physical interpretation. If numerical manipulations are needed, these should not be too lengthy so as to make it feasible to collect copious and sufficiently approximate answers that may be summarized in the form of curves or tabulations expressing trends over a suitably large range of the variables of the problems. Therefore, before accepting the author's suggestion, one should scrutinize whether this somewhat inconvenient method of approach is necessary and whether it is satisfactory in terms of labor and accuracy.

For the first point, the author writes the voltage differential equations of input and output circuits and recognizes that resistive drops do appear formally in the equations written. Hence, he concludes, "The importance of the resistance term is apparent from the equations. It does not appear justifiable to neglect the resistance terms as has been done by many writers on the theory of magnetic amplifiers." Engineers, and physicists and applied mathematicians, may not share the author's impatience. To them a procedure of problem solving appears nonjustifiable only if it leads to errors beyond the range of accuracy expected in the solution. After all, this is what makes engineering different from formal algebra or accounting.

The many writers criticized may have recognized that resistive voltage drops in the windings for any reasonable design of amplifiers with cores of gradually varying differential permeability are small in comparison with the electromotive forces induced by the core fluxes in the steady state and not likely to affect the wave form of these fluxes significantly. They may have checked this point carefully, both by calculations and by experiments, and may have concluded that for the determination of flux

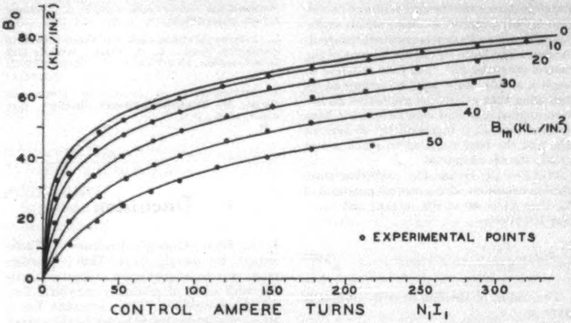

Figure 1. Density of B_0 of flux linked with the control (input) circuit as a function of average control ampere turns for various values of the crest B_m of superposed alternating flux density. The upper curve is the normal magnetization curve of the cores

expressions in the steady state the assumption of negligible winding resistances is not only extremely useful but also very well justified, perhaps more justified than other assumptions concerning hysteresis et cetera which the author does not find objectionable in his idealization. Beyond this step they may have made no further use of the assumption.

Now for the steady stage, there is abundant evidence that variations of the resistance of the input circuit over broad ranges have no noticeable effects on the output of this type of amplifier for any given value of average control current. Moreover, the amplifier in question is essentially a constant current device and therefore in many instances, we can account later for output winding resistance, and for the much more significant influence of loads, by means of corrective load lines procedures applied to no-load characteristics. We agree that these procedures are inadequate in other instances; here methods of successive approximations are used whenever need for this is felt and time is available. And the methods suggested by the author may constitute a valuable tool.

Unfortunately, the author's analysis is initiated only for amplifiers having equal resistances and equal turns in control and output circuit. This limitation is incompatible with the concept of power amplification expected from these devices and should be removed so as to deal with load situations of broader interest. Moreover, the author accepts a much too simple cubic approximation for the normal magnetization curve, while other writers[1,2] have found it necessary to express field intensities H as power series of B that contain a 5th or a 9th or even a 15th power term, even when dealing with comparatively nonsharp core materials. The need for numerical substitutions is recognized by the author already for his overly simplified problem and solution, and the calculations are bound to become much more formidable in more realistic cases. Ultimately the engineer, after having learned from the author that other existing analyses are unjustifiable, may feel driven even more from analytical approaches of any kind into the domain of experimentation alone.

Concerning the transient problem, the paper may convey a wrong impression about the state of the art as it says that, "in the course of the investigation, it has been found impossible to neglect the resistance of the windings," and adds later that the author's "analysis indicates that from a rigorous point of view in the transient state, the effect of the resistance of the windings cannot be neglected."

As far as the input circuit is concerned this is an understatement, as it would be strange if any one would try to carry out an investigation of the transient response of any physical system by neglecting those sinks of energy which constitute the very reason for a gradual transition to the steady state.

Now, a large number of papers have been published in this country and abroad on the subject of the transient response of magnetic amplifiers. All of these papers may be open to some criticism, because of approximations used to obtain comprehensive and conclusive results of sorts. In particular, some moderate and rational use may have been made of relations between fluxes and currents previously derived for the steady state and extended further into the analysis of the practically most interesting slow transients. But I am not aware of any writer who may have tried to neglect input circuit resistances in this aspect of the problem.

Finally, in the Appendix, the author seems to be guided by the concept that the total flux linking the input circuit of the amplifier depends on the control current alone. Hence, a procedure of separation of variables leading to graphical integration is presented which is in common use[3] when dealing with the transient response of a single winding linking a nonlinear core, for example, the field winding of a generator.

In the case of the magnetic amplifier of the kind considered, however, the physical situation is different. The additional alternating magnetization impressed by the output winding modifies and reduces the flux that links the input winding often to a surprisingly great extent. This is not a hair-splitting refinement; it is rather a most striking phenomenon which, one can say, is the very reason for the character of constant current device I have mentioned before. It has been pointed out and explained quantitatively by many writers in their analyses.[4,6] (The very fact that it did not appear clearly to the author seems to support my concern about the advisability of his methods). The phenomenon can be evidenced also with simple experimentation. The circled points of Figure 1, for instance, result from measurements of the flux linked with the input circuit as function of the input current for various values of the crest B_m of alternating component of core flux density for an amplifier with rather nonsharp core material (Hypersil) well within the range of rated operation. The upper curve is the normal magnetization curve of the cores; the other curves result from analytical considerations.

Therefore, any so-called time constant or time of response obtained simply in terms of initial or differential permeabilities of the normal magnetization curve or from an analysis of growth or decay of the flux linked with the input circuit in the absence of a-c excitation, may convey very misleading information as to the rapidity of the response of magnetic amplifiers in which an a-c voltage source normally exists in the output circuit. In fact, such procedures would represent the product of a subconscious temptation to use linear concepts and superposition, which should be avoided in these problems.

Graphical integration procedures can be used in the transient problem, if one so chooses, as shown by others[6,7] who, however, have been aware that the basic relation between input circuit flux linkages and input circuit currents is different for every different value of the a-c excitation voltage.

REFERENCES

1. MAGNETIC AMPLIFIERS, A. G. Milnes. *Proceedings*, Institution of Electrical Engineers (London, England) volume 96, part I, number 99, May 1949.

2. UNIVERSAL CURVES FOR D-C CONTROLLABLE REACTORS, W. C. Johnson, R. C. Merrell, R. E. Alley, Jr. *AIEE Transactions*, volume 68, part I, 1949, pages 31–39.

3. TRANSIENT ELECTRIC CURRENTS (book), H. H. Skilling. McGraw-Hill Book Company, New York, N. Y., 1937, page 241.

4. MAGNETIC AMPLIFIERS, T. Buchold. *Archiv fur Elektrotechnik* (Berlin, Germany), volume 36, 1942, page 221.

5. SOME FUNDAMENTALS OF D-C CONTROLLED REACTORS WITH RESISTIVE LOADS, H. F. Storm. *AIEE Transactions*, volume 68, 1949, pages 188–94. See also discussion of this paper by W. C. Johnson.

6. THE THEORY OF MAGNETIC AMPLIFIERS AND SOME RECENT DEVELOPMENTS, R. M. Frost-Smith. *Journal of Scientific Instruments* (London, England), volume 25, August 1948, page 271.

7. AN ANALYSIS OF TRANSIENTS AND FEEDBACK IN MAGNETIC AMPLIFIERS, W. C. Johnson, Frank M. Latson. *AIEE Transactions*, volume 69, part I, 1950, pages 604–11.

Louis A. Pipes: Mr. Finzi, in his discussion of this paper, seems to take exception to the author's insistence that the resistance terms in the voltage differential equations of the input and output circuits should be considered in this analysis. It is stated by Mr. Finzi that authors who have neglected the resistance terms have done so after convincing themselves, both by calculations and by experiments, that the effects of these terms are negligible. It is unfortunate that these calculations are not included in their analyses. It is customary in the physical sciences for papers that present theoretical discussions of phenomena in a mathematical form to be completely explicit and self contained. If, in the process of solution, a nonlinear differential equation is encountered, it appears reasonable to first attempt to apply known methods to study its behavior before linearizing the problem by eliminating the inconvenient terms. An immediate linearization of the equation by discarding terms may lead to a solution that is greatly in error. It is common knowledge that frequently the slight modification of a term of an equation changes vastly the nature of the solution. It is regrettable that because of the inherent difficulty of the solution of nonlinear differential equations, the use of iterative methods is often imperative in many cases and not only, "whenever need for this is felt and time is available."

The operation of magnetic amplifiers cannot be explained on the basis of classical linear doctrine and the theoretical investigator must resort to nonlinear differential equations to deduce the required information. There is danger in linearizing the differential equations that characterize the behavior of nonlinear physical systems at too early a stage of the analysis because if this is done, jump phenomena, subharmonic response and other effects of a purely nonlinear nature may be missed. To avoid these pitfalls it is safer to apply some of the standard methods of solution to the nonlinear equation before discarding any terms.

The second point raised by Mr. Finzi is that many authors have in some way taken into account the resistance terms in their mathematical analysis of the transient behavior of magnetic amplifiers. This is, of course, true and nothing is said in the paper to the contrary. In many papers, first the steady-state response is obtained by neglecting the resistances of the circuits and account is taken later of their effect. The manner in which this is done is not always very clear but usually the solution obtained is tailored to fit some facts obtained experimentally. As can be easily seen from considering a nonlinear system such as a simple pendulum oscillating through large amplitudes, the response of a nonlinear system is often a function of its initial conditions. A mathematical analysis of a nonlinear dynamical system in which the parameters of the differential equations involved are altered during the process of solution is naturally open to suspicion.

The criticism raised in Mr. Finzi's third point concerning the method suggested in the Appendix for determining the time constant of a magnetic amplifier is well taken. It is not justifiable to neglect the effect of the a-c excitation of the output winding in computing the time constant because only a very rough estimate of the time constant can be obtained by this procedure.

In conclusion, it may be pointed out that some 30 years ago our knowledge of nonlinear differential equations might have been compared with that of linear differential equations at the time of Newton and Leibnitz. However, in recent years problems involving nonlinear dynamical systems have received much attention. In Russia a great deal of work has been done in this field during the last two or three decades by a staff of highly trained scientists and this has resulted in a virtual Russian monopoly. Very recently, the results of these efforts have been made available in English. Research has now started in Britain and in the United States with very promising results. A survey of the accomplishments in this field in the world literature indicates that powerful methods now exist for the solution of certain classes of nonlinear problems. It is the essential purpose of this paper to call attention to some of these methods in the hope that it may give an impetus to their use in the analysis of the response of nonlinear electrical devices.

DISCUSSIONS FROM ABROAD

This section has been established to permit members residing outside of the United States (exclusive of Canada) to submit discussions which could not be received before the closing dates, which are two weeks after the meetings.

Where it is possible to do so, such discussions have been included with the paper, otherwise a footnote has been included at the end of each paper discussed referring to additional discussions in the back of the annual volume (except when the paper is published in a preceding volume).

Dielectric Loading for Waveguide Linear Accelerators

Discussion and author's closure of paper 51-164 by Gail T. Flesher and George I. Cohn at the AIEE Great Lakes District Meeting, Madison, Wis., May 17–19, 1951, and published in AIEE Transactions, 1951, part I, pages 887–93.

R. B. R. Shersby-Harvie, W. Walkinshaw, L. B. Mullett (Ministry of Supply, Great Malvern, Worchestershire, England): The linear accelerator group of the Atomic Energy Research Establishment, Harwell, have been investigating for several years various methods of improving the efficiency of linear electron accelerators in particular the traveling-wave type. Early in 1948 promising theoretical results were obtained for dielectric loaded waveguides and after a long program of theoretical and experimental work, an accelerator of the traveling-wave type was designed and built to give 1,500,000 electron volts in a length of 80 centimeters, operating at the normal wavelengths of 10 centimeters. This was not of course intended to show the improved efficiency which is theoretically possible, but only to demonstrate that dielectric can be used in an accelerator. A current of the order of 150 milliamperes during the pulse was obtained at an energy of approximately 1,500,000 electron volts.

This type of dielectric loading has been reported in Nature[1] and is the substance of several patents.[2–4]

In considering the relative performance of resonant and traveling-wave type accelerators it is important to obtain a criterion which is applicable to both systems, and includes the important economic factors of power and length. We have defined the efficiency of an accelerator as the square of the waverage voltage gained per-unit power dissipated per-unit length, that is, $V^2/P.L.$ This can be related to the shunt impedance of the corrugated waveguide $E_0^2/2\alpha$ for a given length of accelerator section where α is the voltage attenuation coefficient, and E_0 is the axial field per-unit power flow. With all the radio frequency power fed in at one end and the power remaining at the other end being dissipated in a resistive load the efficiency has a maximum value of $0.82E_0^2/2\alpha$ when the length of section L_0 is such that it has an attenuation of 1.25 nepers.

It is obvious that for a traveling-wave accelerator whose section length is determined by frequency tolerance of the radio frequency source, build-up time, space or any other factor in such a way as to be less than L_0 then the efficiency is reduced. In the case of the resonant accelerator, this factor does not occur although there is of course the quite serious time averaging factor involved in obtaining the average voltage. To overcome this loss of efficiency with short section length it is necessary to use a system of radio frequency feedback. This has been successfully employed on two accelerators and consists essentially of a balanced bridge circuit which will combine the power from the end of the accelerator section with the power from the radio frequency source. This has been reported in the Proceedings of the Physical Society[5] and together with practical waveguide bridges which will combine any ratio of powers forms the substance of several patents.[6–8]

The power magnification is limited by losses in the feed-back loop and also by build-up of reflections, but ratios up to four are considered very practical. In some cases the efficiency can be brought more nearly to $E_0^2/2\alpha$ than in the optimum length of accelerator section without feedback, and moreover a large proportion of the difficult problem of stabilizing the frequency of the radio frequency source can be replaced by the relatively simple and automatic operation of stabilizing the phase in the feed-back loop.

In terms of $V^2/P.L.$ the early Stanford traveling-wave machines and those of this establishment had quite low efficiencies of the order of 10 to 20 megohms per meter since they were naturally designed on a conservative basis. The shunt impedance was low (between 40 and 70 megohms/meter) due to deliberately choosing a large hole size and having metal losses considerably greater than theoretically possible; the over-all efficiency was further lowered by choosing a large phase angle between peak accelerating field and stable electron position, and by using lengths less than the optimum L_0 without feedback. For machines in the low-energy high-current range such as those designed for medical purposes the efficiency is by no means an over-riding factor and final efficiencies of 25 megohms per meter have again been chosen in such cases. For really high energy machines where the greatest degree of economy in radio frequency power and length is required theoretical shunt impedances (at 3,000 megacycles) of the order of 100 megohms per meter can be obtained for metal guides with ratio of hole radius to wavelength ≤ 0.1. Every effort has then to be made to keep the efficiency $V^2/P.L.$ as close to this figure as possible by ensuring minimum metal losses and by using a small stable phase angle and optimum length of section (preferably with feedback since some relief is then obtained in the way of frequency stability). It also is possible to maintain the efficiency associated with small hole size and yet increase the group velocity by adding a small gap between the loading disks and the outer metal tube, thus introducing a coaxial line type of power flow outside the disks.

A dielectric loaded accelerator would normally only be considered as a good alternative to metal guides in this high energy range, where shunt impedance and efficiency are the all-important factors. We have therefore to aim at shunt impedances considerably greater than 100 megohms per meter. With solid dielectric and no hole the optimum dielectric constant for minimum metal losses is four. The shunt impedance (obtained by adding the dielectric and metal power loss) is considerably worse than ordinary metal corrugated guides. If, however, the dielectric is effectively made anisotropic by breaking up the dielectric into disks (used in a similar way to metal disks) the metal loss can be greatly reduced and shunt impedances higher than 100 megohms per meter can be obtained. Dielectric constants in the range 10 to 100 seem to offer the greatest possibilities especially since magnesium titanate ($\epsilon/\epsilon_0=15$) and titanium dioxide ($\epsilon/\epsilon_0=95$) are known low-loss materials which will carry large quantities of power and work under vacuum conditions. In the experimental accelerator titanium dioxide was used in disks which were spaced so as to give the required law of phase velocity. The effective dielectric constants were of the order of 50 in the radial direction and little greater than one in the axial direction.

With these dielectric waveguides it is found that accelerating field per-unit power is in general less than that obtained with metal waveguides, and the higher shunt impedance arises from a greatly reduced attenuation constant. The length L_0 therefore increases but the group velocity does not increase in the same proportion. Hence the frequency stability required for a length of section L_0 is increased and it becomes most desirable if not essential to use "feedback."

The theoretical work involved has been considerably more complex than for metal loaded waveguides. We can distinguish three separate regions in a disk loaded dielectric waveguide:

1. The axial region which is free from dielectric.
2. The region between the dielectric disk.
3. The region filled with dielectric.

The method of solution is to obtain a series representation for the field in region 1 and match this to a series representation for the fields in regions 2 and 3 (in terms of symmetrical E (or $T.M.$) modes only). The numerical solution of the infinite determinantal equation thus obtained is much too tedious for practical application.

The approximate theories which have been developed are in order of complexity:

1. The anisotropic solution. If the electrical length of the disks and the spacing between disk centers are small then an accurate solution of Maxwell's equations for an $E_{01}(T.M_{01})$ mode can readily be obtained using dielectric constants in the radial and axial direction averaged by static considerations. The guide with a central hole can then be treated quite simply analytically and numerically, and we can readily calculate the accelerating field, attenuation (due to dielectric and metal losses), shunt impedance, and group velocity. As the disk thickness increases this theory becomes inadequate and will not of course predict the expected π mode cut-off.

In practice these ceramic materials (especially in the case of TiO_2) cannot be ground to such a small thickness that the anisotropic theory can be used entirely, but it is normally adequate to obtain the accelerating field (perhaps with small corrections), the attenuation and the group velocity so that a wide range of the various parameters can be investigated. In designing an accelerator, however, the major requirement is a more accurate wavelength equation.

2. For the case with no hole a solution can be obtained by matching forward and reflected fundamental waves in the dielectric and air-filled sections of the waveguide at the dielectric-air interface. It is then possible to obtain a fairly accurate solution by applying knowledge of what happens in the anisotropic case when a hole is introduced.

3. We also have used a solution in which the first term of an infinite determinant is taken (this reduces to (2) when various approximations are made).

4. A solution obtained by a variational method which should give an upper and lower limit to the correct solution.

For this relatively simple disk loading calculations show that when optimum efficiency is obtained the metal loss may be as high as five to ten times the dielectric loss. It should therefore be possible to devise a means of introducing more dielectric in such a way as to reduce the metal loss for a given axial electric field, until a new optimum is reached where metal loss and dielectric loss are comparable or dielectric loss is dominant. The simplest method is to use the same size of dielectric disks and to support them in a larger metal tube. In the region outside the disks we then have a coaxial line mode (at phase velocity equal to C) and since H_ϕ is continuous across the boundary and falls as $1/\zeta$ in the coaxial line region, the metal loss per-unit length for a given axial electric field falls as $1/\zeta$. The shunt impedance can be considerably increased in this way but unfortunately $D\zeta$ is continuous at this same boundary so that for the high dielectric constant materials there is a very large power flux down the coaxial line compared with that in the dielectric and central hole. The length L_o now becomes quite enormous so that for a practical length of accelerator the feed-back ratio would be very high and consequently inefficient.

A more promising alternative is an application of the alternate high-impedance low-impedance series of quarter wavelength transformers. If we initially ignore the central hole the dielectric waveguide then consists of a central region having disks exactly as before extending to the first zero of E_z (that is, J_o), a second region of more dense dielectric (with a ratio of disk thickness to pitch (K) of the order of 0.9 to 1.0 compared with a value of about 0.3 in the inner region) extending to the first zero of H_ϕ, and a third region extending to the second zero of E_z with a value of K again of about 0.3. It is easy to see that for a given E_z on the axis the magnetic field H_ϕ can be considerably reduced at the second zero of E_z compared with that at the first zero of E_z. A large number of calculations have shown that this reduction of H_ϕ can be so large that it more than overcomes the increase in surface area of the metal tube (the diameter is roughly doubled since the region of dense dielectric is radially quite thin) and in fact the metal loss can be reduced to a negligible factor. The dielectric loss is of course increased especially in the dense region, and it now becomes of primary importance to know the power factor of the dielectric with considerable certainty before the extent of the improvement in shunt impedance can be determined. The accelerating field for a given power flux is not greatly affected by adding the two extra regions of dielectric, but the most disturbing feature is that the attenuation can become so low that the optimum length L_o becomes impracticably long. It is then necessary to use higher feed-back ratios than one would normally consider, and it becomes important to make a reasonable estimate of the losses in the feed-back loop and to base the usefulness of the system on the final efficiency $V^2/P.L.$ and not merely on shunt impedance.

In metal-corrugated waveguides it is normally possible to exclude by design the possibility of obtaining propagated modes having different radial and azimuthal variations, and in general the $E_{01}(T.M_{01})$ mode is the lowest propagated mode to the exclusion of $H_{11}(TE_{11})$ (which would be the lowest mode in a smooth waveguide) and all higher E or H modes. The mode troubles experienced with resonant systems are then confined to longitudinal resonances of E_{01}. In the simple disk loaded waveguide it also is possible to propagate the H_{11} mode so that care must be taken to exclude this mode by symmetrical feeding. With the more complex dielectric structures the possibility of propagating modes with other radial and azimuthal variations will increase.

The problem has so many variables that a very extensive theoretical and numerical investigation has had to be undertaken and at present owing to various uncertainties especially in dielectric power factors, it is impossible to state the exact improvement in efficiency which can be attained or what will be the optimum wavelength, although present indications are that a considerable improvement over the best metal guides can be obtained especially if the wavelength is reduced to the region of 5 centimeters.

References

1. A Proposed New Form of Dielectric-Load Wave Guide for Linear Electron Accelerators, **R. B. R. Shersby-Harvie.** *Nature* (London, England), volume 162, December 4, 1948, page 890.

2. Improvements in or Relating to Dielectric Loading of Wave Propagation Devices, **R. B. R. Shersby-Harvie.** British Patent 9532, 1948.

3. Improvements in or Relating to Dielectric Loaded Waveguides, **R. B. R. Shersby-Harvie.** British Patent 18524, 1950.

4. Improvements in or Relating to Loaded Waveguides for Linear Accelerators, **W. Walkinshaw, L. B. Mullett.** British Patent 18525, 1950.

5. A Traveling Wave Linear Accelerator with Radio Frequency Power Feedback, **R. B. R. Shersby-Harvie, L. B. Mullett.** *Proceedings*, Physical Society (London, England), volume LXII, 1949, page 270.

6. Improvements in or Relating to Feedback in Linear Accelerators, **R. B. R. Shersby-Harvie.** British Patent 27071, 1948.

7. Improvements in or Relating to Microwave Circuits, **L. B. Mullett.** British Patent 6035, 1949.

8. Improvements in or Relating to Automatic Phase Control for Waveguide Rat-Race Arrangements, **L. B. Mullett.** British Patent 7815, 1949.

Gail T. Flesher and **George I. Cohn:** We wish to thank the British group for their most interesting discussion. They have carried out a large amount of research in linear accelerator development. It is to be regretted that more detailed accounts of their developments have not been more widely published.

Report of the Board of Directors

THE BOARD OF DIRECTORS of the American Institute of Electrical Engineers presents to the membership its 67th annual report, covering the fiscal year ending April 30, 1951. It contains a brief summary of the principal activities of the Institute during the year, a general balance sheet showing the financial condition of the Institute at the close of the fiscal year, a statement of cash receipts and disbursements, and a schedule of securities owned. Much additional information regarding the activities appeared in various issues of *Electrical Engineering*.

BOARD OF DIRECTORS' MEETINGS

Five meetings of the Board of Directors were held during the year, two in New York, N. Y., one each in Pasadena, Calif., Oklahoma City, Okla., and Miami Beach, Fla.

Information regarding many of the more important matters which were considered by the Board of Directors appeared in various issues of *Electrical Engineering*.

INSTITUTE POLICY

A report on the 1949 Membership Opinion Poll and a progress report on the membership voting on the following three proposals of policy were published in the 1950 Board of Directors report:

1. To work continually for the unification of the profession.

2. To recognize the fact that the Institute finds its chief reason for existence in the technical field.

3. To handle questions on nontechnical affairs as necessary and as they arise, on an emergency basis, until through unification they can be handled on a general professional basis.

The votes to June 1, 1950, are reported here:

Proposal	Number 1	Number 2	Number 3
Approved	4,062	4,077	4,012
Disapproved	321	349	383

The Board of Directors, at its meeting on June 15, 1950, directed that the tabulation on the 1950 poll be published in *Electrical Engineering*, with the conclusion that the membership, as represented by the poll, endorses the three proposals, and a statement to the effect that the Board of Directors of the AIEE will, therefore, be guided by these three proposals in making all of its decisions concerning Institute activities (*EE, Aug '50, p 669*).

INSTITUTE VISITS

For several years, the Board of Directors has been endeavoring to relieve the President of responsibility for Section visits, and to place this responsibility upon the Vice-Presidents. A resolution to this effect was adopted on June 27, 1946, and appears on page 510 of the 1950 Year Book.

After further discussion at various times, and particularly on April 27, 1950, the Board of Directors took the following action on that date:

> VOTED that it is the sense of the Board of Directors that the President should not be expected to visit Sections or Branches; that those official visits should be made the responsibility of the Vice-Presidents, with the cooperation of Directors, or District Secretaries, or other Institute personnel who may be designated by the Vice-Presidents; and that the President concentrate his attention on general and District meetings, technical conferences, and such other meetings as should, in his discretion, be attended; also that this action be transmitted to all Sections, and that the Finance Committee be requested to make provisions in the 1950–51 budget for such visits.

President LeClair visited certain Sections and attended the general and District meetings. He also attended meetings of the Engineers Joint Council, and represented the Institute at several meetings of various types. The Vice-Presidents visited substantial percentages of the Sections within their Districts, and also many Student Branches.

ANNUAL MEETING

The 66th annual business meeting of the Institute was held in Pasadena, Calif., June 12, 1950. The annual report of the Board of Directors for the fiscal year which ended April 30, 1950, was presented in abstract by Secretary H. H. Henline, who also presented a report of the Committee of Tellers on the vote of the membership on the election of officers whose terms were to begin on August 1, 1950. In the absence of the Treasurer, W. I. Slichter, Secretary Henline also presented a brief report of the Treasurer. President-elect Titus G. LeClair was introduced, and responded with a brief address covering broadly the problems ahead, both in the Institute and in its relations with other organizations.

In commemoration of the 100th anniversary of the birth of Oliver Heaviside, an address was given by Dr. Paul S. Epstein, Professor of Theoretical Physics at the California Institute of Technology since 1921.

The Lamme Medal for 1949 was presented to C. M. Laffoon, Manager of the A-C Engineering Department, Westinghouse Electric Corporation.

Mr. Fairman delivered a message of great importance to the engineering profession in his President's address, "Is Engineering a Profession?"

GENERAL MEETINGS

Three general meetings were held during the year, and a brief report on each follows:

Summer and Pacific General Meeting. The 66th Summer General Meeting was combined with the Pacific General Meeting and held in Pasadena, Calif., June 12–16, 1950, with a registration of 1,665. The program included 31 technical sessions and conferences, an opening ceremony, the annual business meeting of the Institute, ten committee meetings, two Section Delegates sessions, conference of Vice-Presidents and District Secretaries, meeting of the Board of Directors, two student technical sessions, session for presentation of District Branch Prize Papers, numerous inspection trips, banquet, aquacade, and President's Reception, and an extensive schedule of events for the ladies.

Fall General Meeting. The Fourth Fall General Meeting was held in Oklahoma City, Okla., October 23–27, 1950, with a registration of 1,144. In 25 technical and conference sessions 122 papers were presented. Other events were a Forum of Technical Committee Chairmen, 15 committee meetings, general session, meeting of the Board of Directors, meeting of the South West District Executive Committee, joint luncheon with the Oklahoma City Chamber of Commerce, dinner-dance, stag smoker, inspection trips, and a special program for the ladies.

Winter General Meeting. The Winter General Meeting was held in the Hotel Statler, New York, January 22–26, 1951, with the largest program in the history of the Institute, and a registration of 3,334. There were 67 technical sessions, in which 143 formal papers and 160 conference papers were presented. At three general sessions, the Hoover, John Fritz, and Edison Medals were presented. After receiving the Hoover Medal, Dr. Karl T. Compton gave an address on "Engineers and National Security." The Alfred Noble prize and numerous AIEE prizes for papers were presented. Other parts of the meeting were a meeting of the Board of Directors, Forum of Technical Committee Chairmen, 100 committee meetings, smoker, dinner-dance, numerous inspection trips, and special events for the ladies.

DISTRICT MEETINGS

Great Lakes District Meeting. In a 2-day meeting of the Great Lakes District, in Jackson, Mich., May 11–12, 1950, the principal subject was "Transmission and Distribution of Electric Energy on Systems with Low Load Density." Many of the papers in seven technical sessions were directly related to this subject. Other events were a general session, two student sessions in which the Branch Prize winners presented their papers, graduate student session, informal banquet, student banquet, inspection trips, and several features for the ladies. The registration was 536.

Middle Eastern District Meeting. A Middle Eastern District Meeting was held in Baltimore, Md., October 3–5, 1950, with a registration of 972. In 23 sessions 98 papers were presented. In addition, there were a general session on the topic "Developing Engineers for Industry," smoker, cabaret dance, inspection trips, and ladies' events. The Executive Committee of District 2 held an all-day meeting on the day preceding the District Meeting.

Southern District Meeting. A Southern District Meeting was held in Miami Beach, Fla., April 11–13, 1951. The program included a general session with an address by President LeClair, four technical sessions at which 34 papers were presented, a meeting of the Board of Directors, several inspection

Vol
195

and sight-seeing trips, luncheon, banquet, buffet and water show, and a program of events for the ladies. The registration was 421.

SPECIAL TECHNICAL CONFERENCES

"Special Technical Conferences" were inaugurated in 1948, and have proved so successful that they are now planned and conducted as a regular Institute activity. The conferences are intended to be national in interest, technical in character, and concentrated as to subject matter toward one particular industry or objective. This type of meeting is designed to explore thoroughly a limited field and to afford specialists in that field an opportunity to discuss mutual technical problems. The conference may be defined as a program of panel discussions, technical papers, or exhibits under the auspices of a national technical committee, in co-operation with an AIEE local Section, which might act as host to the conference. Operating under the policy and procedure which has been set up, the following conferences were held during the past fiscal year:

Rubber and Plastics Conference. The third annual conference on electrical engineering problems in the rubber and plastics industries was held in Akron, Ohio, May 5, 1950, sponsored by the Subcommittee on Rubber and Plastics Industries of the Committee on General Industry Applications in co-operation with the Akron Section. A diversified program was planned to attract as large an attendance as possible. This resulted in the presentation of eight papers. Some of the subjects covered were calender auxiliary drives, including constant tension winder drives for film and fabric; recent developments in process sequence control; electrostatic casualties in the rubber and plastic industries; and so forth. The conference was attended by 173 persons. No proceedings were published.

Improved Quality Electronic Components Conference. A 3-day conference was held in Washington, D. C., May 9–11, 1950, sponsored by the AIEE, Institute of Radio Engineers, and Radio Manufacturers Association, with active participation by agencies of the United States Department of Defense and the National Bureau of Standards. The main theme of this conference was that components for military electronic equipment must be designed to serve without replacement during the normal life of the equipment if electronics is to continue in its role of increasing importance in modern warfare. The conference was attended by 749 engineers and scientists from all parts of the United States, as well as representatives from Canada, Great Britain, Australia, New Zealand, and Sweden. The five sessions covered dependability in electronics, unitized design and electronic fabrication techniques, components, and panel discussion. During the conference there were also several interesting inspection trips. A complete report of the conference, including papers and discussions, has been prepared and is available at $3.50.

Telemetering Conference. The Philadelphia Section was host to a 3-day telemetering conference in Philadelphia, Pa., May 24–26, 1950, sponsored by the AIEE and the National Telemetering Forum. In conjunction with the conference, eight exhibitors demonstrated their telemetering products in the display room of the Philadelphia Electric Company. The attendance was 205. Two inspection trips were arranged to the Franklin Institute Laboratories for Research and Development and the Raymond Rosen Engineering Products, Inc. Both point-to-point and mobile telemetering were covered at this conference. The five sessions were devoted to general features of telemetering, telemetering systems, telemetering systems and pickups, data presentation, and other topics, including definitions of telemetering terms. Complete proceedings of the conference have been printed in book form and are available at AIEE headquarters at $3.50 per copy.

Domestic Appliances Conference. A conference on domestic appliances was held in Cleveland, Ohio, June 20, 1950, sponsored by a special subcommittee of the Committee on Domestic and Commercial Applications, in co-operation with the Cleveland Section. There was an attendance of 86. The morning session was devoted to automatic washing machines, and the afternoon session was given to electric ranges. During the discussion period, problems of motor drives, controls, and other accessories were covered. Due to the enthusiasm of those attending, the committee is planning to promote such a conference next year as part of its activity.

Conference on Electronic Instrumentation in Nucleonics and Medicine. The third annual joint conference on electronic instrumentation in nucleonics and medicine, sponsored by the AIEE and the Institute of Radio Engineers, was held in New York, N. Y., October 23–25, 1950, with 653 people attending. The first day of the 3-day conference featured papers on subjects in the non-nucleonic phases of electronics in medicine. The second day was devoted to nucleonics and medicine. The last day covered nucleonic development in industry and government laboratories. There were six sessions with a total of 23 papers presented, plus a round-table discussion on the evening of the second day on the subject "Effects of Atomic Weapons." Exhibits of nucleonic apparatus, instruments, and components were shown by 20 manufacturers. No conference proceedings were published.

Machine Tools Conference. The third annual conference on machine tools was held in Worcester, Mass., November 14–16, 1950, sponsored by the AIEE Subcommittee on Machine Tools of the Committee on General Industry Applications and the Worcester Section. The total attendance was more than 200. During the morning session of the first day four papers were presented. The afternoon was devoted to plant visitations in and around Worcester, Mass. Six papers were presented on the second day, and there was a meeting of the Subcommittee on Machine Tools. The subcommittee unanimously considered the conference very successful and made plans for holding future conferences on this subject. Approximately 150 conferees went to Springfield, Vt., for the final day of the conference, which was spent visiting four machine tool plants in the Windsor-Springfield area. No conference proceedings were published.

Electron Tubes for Computers Conference. A conference on electron tubes for computers was held in Atlantic City, N. J., December 11–12, 1950, sponsored by the AIEE and Institute of Radio Engineers, in collaboration with the Panel on Electron Tubes of the Research and Development Board. It was attended by 316 engineers from all parts of the country and from Canada and England. This conference was the result of a survey which indicated that the field of electron tubes for computers was in need of clarification. The sessions included computer experience with electron tubes; electron tube problems; special purpose computer tubes; tube manufacture and crystal diode experience; and Williams type storage. No proceedings were published.

Conference on High-Frequency Measurements. The second conference on high-frequency measurements was held in Washington, D. C., January 10–12, 1951, jointly sponsored by the AIEE, Institute of Radio Engineers (IRE), and National Bureau of Standards. It was evidenced at this second conference that the radio-frequency portion of the spectrum is in a state of expansion. After registration, the members of the conference were invited to the Bureau of Standards where open house was held on Wednesday morning. Here the guests were shown the research and experiments being conducted in magnetism and electricity towards the goal of establishing various constants with a greater accuracy. The sessions were devoted to measurements of frequency and time; measurements of impedance; measurements of power and attenuation; and measurements of transmission and reception. An evening demonstration session also was held. Inspection trips were arranged to the National Bureau of Standards, the Naval Observatory, the Naval Ordnance Laboratory, and the Naval Research Laboratory. There was a total attendance of 549 engineers from all parts of this country and Canada. No conference proceedings were published.

As this was the 50th anniversary of the National Bureau of Standards, President T. G. LeClair of AIEE and President I. E. Coggeshall of IRE presented scrolls to Dr. E. U. Condon, Director of the National Bureau of Standards, at this conference.

Textile Industry Conferences. Two conferences on the textile industry were held in April 1951. The first was held in Philadelphia, Pa., on April 23, on the subjects of static electricity in the textile process and electrical installation practice and problems, and was sponsored jointly by the AIEE Textile Industry Subcommittee of the Committee on General Industry Applications, the Philadelphia Textile Institute, and the Philadelphia Section of AIEE. Papers presented covered principles of static electricity, electric installations on full-fashioned hosiery machines, and so forth. The attendance was 84. The second conference was held in Atlanta, Ga., on April 26 and 27, and also covered static electricity, with the addition of textile mill power systems and maintenance. It was co-sponsored by the Textile Industry Subcommittee, Georgia Institute of Technology, and the Georgia Section of AIEE. Some of the interesting subjects discussed were: static in the woolen industry, design of a textile mill power system, and problems in operation and maintenance of a mill power system. The attendance was 140. No proceedings are to be published.

GENERAL COMMITTEES

BOARD OF EXAMINERS

Board meetings were well attended, and consequently no meetings other than those regularly scheduled were required. In addition to its regular work, the Board prepared a rough draft of proposed amendments to the Constitution relative to the revision of membership classification to conform to the suggested uniform membership grades prepared by the Engineers' Council for Professional Development committee on that subject. This draft was submitted to the Committee on Constitution and By-Laws for preparing the amendments in proper form for the Board of Directors.

Statistics relating to the number of cases handled by the Board are given in Table I. The current total, excluding those enrolled as Student members, is more than 17 per cent greater than in 1949–50. This is largely due to a more than 22 per cent increase in the number of Associate applications. Large Student enrollments of previous years probably account for most of this increase in Associates.

Student enrollment for the current year is more than 35 per cent under that of 1949–50. This is accounted for in large part by the closing out of the GI Bill of Rights and the current build-up of the armed forces.

COMMITTEE ON CODE OF PRINCIPLES OF PROFESSIONAL CONDUCT

The "Statement of Principles of Professional Conduct," which last year's annual report stated was almost complete, was approved by the Board of Directors on August 4, 1950, and published in the Year Book, pages 491–3, and in the February issue of *Electrical Engineering*, pages 171–3.

Since that time there has been only one request for any committee action concerning the Principles as published. That request was for a clarification of Section 27 of the Code, which reads: "He will not use the advantages of a salaried position to compete unfairly with other engineers."

The chairman replied to that request by stating that in his opinion the rule means that engineers who have positions that provide office space or other emoluments should not take advantage of such favors and charge fees for consultations less than the regular charges made by consulting engineers practicing in the region involved.

COMMITTEE ON CONSTITUTION AND BY-LAWS

This committee submitted certain recommendations to the Board of Directors in advance of the meetings, and the By-Laws were amended as follows:

April 27, 1950. The Board "VOTED to adopt in principle the recommendation for elimination from the By-Laws of all provisions for ex-officio memberships, and to instruct the Committee on Constitution and By-Laws to implement this action." This idea is being carried out in any changes that are being made in the By-Laws.

June 15, 1950. A change was made in Section 1 of the By-Laws, clarifying and restricting the use of Institute badges and imprints of the badges.

Section 76 of the By-Laws also was revised, changing the composition of the Committee on Award of Institute Prizes.

Table I. Applications for Admission and Transfer, 1950–1951

Applications for Admission		
Recommended for grade of Associate	4,670	
Re-elected to grade of Associate	77	
Not recommended	8	4,755
Recommended for grade of Member	315	
Re-elected to grade of Member	17	
Not recommended	48	380
Recommended for grade of Fellow	6	
Reinstatement to grade of Fellow	2	
Not recommended	3	11
Applications for Transfer		
Recommended for grade of Member	575	
Not recommended	22	597
Recommended for grade of Fellow	159	
Not recommended	3	162
Students		
Recommended for enrollment as Students		4,988
Total		10,893

August 4, 1950. Section 53 of the By-Laws was amended, raising the Student dues to $5.00 per year.

October 26, 1950. Sections 33, 51, 53, 60, and 84 of the By-Laws, covering Student Branches, were amended to facilitate the operation of the Branches and enable them to complete their organization earlier in the year.

January 25, 1951. This committee recommended certain changes in the Constitution which would transfer the dues and entrance and transfer fees from the Constitution to the By-Laws.

It was recommended that all of Article II of the Constitution and parts of Articles III and IV be revised to establish uniform grades of membership as recommended by Engineers' Council for Professional Development. This recommendation limits the elevation to the grade of Fellow to the method known as proposal by invitation, to be extended by the Board of Directors. It changes the Associate grade to Associate Member and adds a new grade to be known as Affiliate.

A number of minor changes in the Constitution were also recommended to take care of the new grades of membership. The Board approved these proposed amendments to the Constitution, subject to corrections by legal counsel, for submission to the membership for vote. Recommendations were also made and approved for making the corresponding changes in the By-Laws, contingent upon adoption of the Constitutional amendments by the membership.

COMMITTEE ON EDUCATION

During the past year the committee sponsored two conference sessions at general meetings. At the Summer General Meeting, the theme of the conference was "Planning of New Laboratory Facilities." The theme was dealt with by three separate papers, written by well-known authorities in electrical engineering education, describing the planning and the actual facilities included in new laboratory buildings. The session was timely, since a great deal of new construction is currently under way at the engineering colleges, and many of the novel features discussed at the session have been helpful to others in their planning.

At the Winter General Meeting, a conference session on "Graduate Study in Electrical Engineering" was presented. Three papers on various phases of graduate study were presented, each of which discussed distinctly different phases of the graduate curriculum. The session was very well attended, and its timeliness was attested to by the fact that discussion continued from both educators and representatives of industry until it was necessary arbitrarily to terminate the meeting. Also at the Winter General Meeting, the committee acted as joint sponsor at a conference session on electronic education. The papers presented discussed the importance of electronic education from the standpoint of industry, of research, and of the academic field itself.

During the year four subcommittees were appointed to study specific subjects believed to be of current importance. They are: Subcommittee on Graduate Programs in Electrical Engineering, Subcommittee on Accrediting of Curricula, Subcommittee on Specific Objectives of Electrical Engineering Curricula, and Subcommittee on Measurement of Educational Effectiveness. The first three of these subcommittees have actively begun their work. The session held at the Winter General Meeting was sponsored by the first of these subcommittees, and future programs are now being planned as a result of the productive efforts of the other subcommittees.

No sessions are planned for the Summer General Meeting because that meeting conflicts directly with the Annual Meeting of the American Society for Engineering Education.

FINANCE COMMITTEE

With a continuing growth in membership, both the income and the expenses of the Institute increase each year. The growth of expenses was accelerated sharply a few years ago due to the rising costs of most things after the end of World War II. The measures mentioned in previous annual reports were put into effect in an attempt to step up the rate of growth of income to compensate for the accelerated growth of expenses. The unavoidable delays before these measures became effective resulted in substantial deficits during the fiscal years ending April 30, 1948, and 1949. The fiscal year ending 1950 showed income and expenses substantially in balance, and, for the year ending April 30, 1951, there was a margin of income over expenses. This recovery was accomplished, however, at the expense of some curtailment in the services to members and a severe limitation upon the volume of technical publications. A continuation of these restrictions is considered undesirable.

If further increases in unit costs take place, another series of deficits can be expected unless it is possible to adjust income more promptly. Since an amendment to the Constitution increasing the dues would require approximately two years to become effective, the Finance Committee recommended to the Board of Directors on October 26, 1950, that the dues provisions be removed from the Constitution and placed in the By-laws. The Board approved this proposal, and, on February 28, 1951, ballots were mailed to the entire membership covering the necessary amendment to the Constitution.

The Finance Committee made an analysis of income and expenses of the Institute, which was published in *Electrical Engineering*, December 1950, to give the members a clearer understanding of the financial problems of the organization preparatory to the submission of the constitutional amendment.

The amendment of the Social Security Act about the middle of 1950 made it possible for the first time for employees of the Institute to be covered by social security, provided the Board of Directors approved and at least two-thirds of the employees elected to be covered. The Board approved and the necessary two-thirds of the employees voted to be covered. Coverage was made effective as of April 1, 1951.

The financial report for the fiscal year is included in this annual report.

HEADQUARTERS COMMITTEE

The program of modernization of the lighting at AIEE headquarters, started two years ago, has been completed. All office space and the Board of Directors' Room are now equipped with modern fluorescent fixtures with a marked improvement in illumination.

Linoleum floor coverings in rooms 1005, 1007, 1008, and 1009 had deteriorated over the years to such an extent that replacement was necessary, and new linoleum was installed in these rooms during the winter.

Other items in the budget included minor repairs to upholstered chairs in the Members' Room and the Board of Directors' Room, cleaning of draperies, and servicing of air-conditioning units.

There is a slight blistering of the veneer wall covering in the Members' Room and Board of Directors' Room. Repairs were considered, but the price seemed to be too high to warrant any action at this time, as the blisters are not obvious. When this condition becomes objectionable, repairs or refinishing of these rooms will be necessary.

COMMITTEE ON MANAGEMENT

Recognizing the increasing importance of the knowledge of management know-how to electrical engineers, the committee has planned a series of conference programs on this general subject at general and District meetings. These programs will cover the broad field of management, including organization, personnel relations, human relations, government and business, productivity and economy of operations, and related subjects.

The first meeting of the series was held in connection with the Winter General Meeting. William B. Maloney, Manager of Employee Relations Department of The Esso Standard Oil Company, spoke on "Management Development." Mr. Maloney pointed out the need for top-flight management in the future to cope with business competition, the maintenance of excellent management relations with stockholders, employees, customers, and the general public. He also stressed the need for maintaining the type of management personnel which would be capable of assuming active and affirmative leadership in participation in national and community issues, even though these issues were only indirectly related to the problems of business.

In order to achieve a continuing top-flight management, Mr. Maloney suggested a program which included planning the future organizational structure, making an inventory of personnel for management positions, and the training of replacements for management jobs required to be filled in the future. He also pointed out the necessity of recognizing that business philosophies, techniques, and experiences are not static, and that current management personnel requires information to keep pace with the times. This is not only for the purpose of effective management teamwork but also for the purposes of morale values and application of company philosophies and policies to employees. This can be accomplished through 2-way communication between "firing-line" management and executive management and through formalized training.

General Leslie B. Simon, Chief of Ordnance Research and Development Division of the Army, spoke on "An Outline of Army Ordnance Research and Development." General Simon described the intricate and highly organized network of research and development agencies which extends on the one hand all the way up through the General Staff, the Research and Development Board of the Secretary of Defense, to the President as Commander in Chief, and on the other hand down to the laboratories and proving ground in the field. He pointed out that today research and development is a highly organized co-operative process, and he stressed the teamwork between the Ordnance Department and industry and science.

COMMITTEE ON MEMBERS-FOR-LIFE FUND

After a long discussion at a meeting on January 23, the committee unanimously agreed that, with the uncertain conditions now existing, it was undesirable to increase the expenditures of this committee, and therefore voted to recommend that the activities be continued as they have been in the past: considering only the odd-numbered districts one year and the even-numbered districts the next year.

At the time of the meeting, there was available $5,373.00 in cash, with the major expenditures for the year having been made, and none of the income from the members for the year 1950–51 having yet been credited to the account. This would indicate that by the end of the fiscal year there would be over $7,000.00 in cash. For this reason, the committee recommends that $5,000 of the cash be invested until it is desirable to expand the operation of the fund.

MEMBERSHIP COMMITTEE

Membership in the Institute increased by 3,860, an increase of 11.3 per cent, and a slight percentage gain above last year, the largest previous individual year on record. Table II of the membership statistics shows the distribution of the membership changes among the various grades. 6,450 applications were received during the year, of which 4,168 were from Students and 2,082 from others. It is significant that the number of applications received from other than Students has shown a marked decrease.

Members in arrears for dues for the fiscal year ending April 30, 1951, amounted to 1,867, a percentage of 4.9 per cent, as compared with 4.42 per cent reported in the previous year.

Student membership has declined from 20,668 reported in 1950 to 15,028 in 1951. This is of great concern to the Membership Committee, and co-operative efforts will be continued with the Committee on Student Branches to encourage Student membership.

The increase in delinquent memberships and the decline of Student memberships can probably be attributed to the uncertainty which has confronted young engineers and Students during the past year. Recognition must be taken of this and efforts continued to reverse this trend.

Charles Clos, Vice-Chairman of the Membership Committee, participated in the study which resulted in the establishment of the Section Growth Award Plan by the Board of Directors this year.

The committee is appreciative of the efforts of the Section Membership Committees throughout the year, especially since the individuals engaged in this voluntary work have found it increasingly difficult to take time from their normal duties to devote to this activity.

COMMITTEE ON PLANNING AND CO-ORDINATION

The committee sponsored no radical departures either in planning or co-ordinating Institute activities during the past year.

Table II. Membership Statistics for Fiscal Year Ending April 30, 1951

	Honorary Members	Fellows	Members	6-Year Associates	Associates	Subtotals	Totals
Membership							
April 30, 1950	8	1,255	9,186	9,433	14,316		34,198
Additions							
New members qualified		7	235		4,785	5,027	
Former members reinstated or re-elected		3	109	64	84	260	
Subtotals		10	344	64	4,869	5,287	
Transfers		131	633	1,567		2,331	
Totals		141	977	1,631	4,869	7,618	
Deductions							
Died	1	24	86	65	29	205	
Resigned		1	61	154	169	385	
Dropped		2	89	272	474	837	
Subtotals	1	27	236	491	672	1,427	
Transfers			129	537	1,665	2,331	
Totals	1	27	365	1,028	2,337	3,758	
Net Changes	1	114	612	603	2,532	3,860	
Membership							
April 30, 1951	7	1,369	9,798	10,036	16,848		38,058

Table III. Number of Applications Received From Student Members and From All Others

Year Ending April 30	Students	All Others	Total
1951	4,168	2,082	6,250
1950	4,033	2,417	6,450
1949	2,286	2,192	4,478
1948	1,481	2,272	3,753
1947	938	2,331	3,269
1946	308	2,453	2,761
1945	249	2,179	2,428
1944	466	1,908	2,374
1943	783	1,431	2,214

Scheduling of Future Meetings. The future general and District meetings of the Institute have been scheduled through 1953, with some 1954 reservations already on schedule. Once again considerable attention was given to respacing the general meetings, this time with a survey of opinion among the technical advisors. The committee concluded that, with all points of view considered, the Winter General Meeting should continue to be held in general during the last week of January in New York; that, however, if the meeting be moved from New York, then consideration be given to establishing a date several weeks later in the year. The Board of Directors gave its approval.

Centennial of Engineering. The request of the American Society of Civil Engineers (ASCE) to participate in the celebration of its 100th anniversary in Chicago in 1952 was met by the appointment of a local group under the chairmanship of Frank V. Smith to arrange for national participation. The Chicago ASCE meeting will precede the AIEE Fall General Meeting in New Orleans by more than a month.

Election Procedures. At the request of President LeClair, the committee handled a brief opinion survey on the possibility of changing Institute election procedures so as to achieve greater democracy in the operation of the Institute. Of those who responded to the *Electrical Engineering* article on the subject, more than 80 per cent thought that the present system is satisfactory. No change is contemplated.

Presidential Election. At the request of the Board, the committee also investigated various methods heretofore proposed for making known the incoming president more than a year in advance with obvious advantages in committee organization, policy formation, and the like. However, no generally acceptable method was uncovered.

Constitutional Amendments. Several chores in connection with study and analysis, as well as co-ordination, were turned in on the Constitutional amendments currently before the membership.

Forum of Technical Committee Chairmen. This forum, a natural outgrowth of last year's ban on ex officio committee memberships, has held two extremely satisfactory meetings, and the third will be held in June. It provides formal location and proficient participants for discussion of the many problems that continually arise in the administration of the technical work of the Institute. The chairmanship is vested in the President of the Institute, present practice rotating the preparation of the program among the chairmen of the Committees on Publication, Standards, Technical Advisory, Technical Program, and perhaps others.

PROFESSIONAL DIVISION ADVISORY COMMITTEE

In its capacity as an advisory group for the nontechnical committees assigned to it, this committee dealt with several matters of special interest. The subject of means to be taken to broaden the effectiveness of engineers generally and to assist in the development of younger engineers in particular was considered. After a brief survey as to what action should be taken, it was concluded that the program already being formalized by the Engineers' Council for Professional Development should be supported.

Consideration also was given to the matter of consulting engineering fees in the electrical field. After reviewing this from the standpoint of policy and also the extent of membership concerned in this matter, it was agreed to leave consideration of it to organizations already constituted and having such problems in their planned field of operation.

PUBLICATION COMMITTEE

The publication policy which became effective January 1, 1947, has been carried out with minor modifications. The number of pages of published material for the calendar year 1950 is shown in Table VII together with the number of pages published in preceding years for ready comparison. The total number of pages published was 13.8 per cent greater than for the same period of the previous year, because of the increase in the number of technical papers from 202 to 238.

Electrical Engineering. One of the important ways in which a high standard of publication has been maintained is by continuing the policy of not republishing material which has been published previously elsewhere. Table VIII shows the various kinds of material in *Electrical Engineering* during the year: the Special Articles include material of broad interest, the President's messages, and the other contributions which have been submitted or solicited for publication in *Electrical Engineering* only.

Beginning with the January 1951 issue, the trim size of *Electrical Engineering* was reduced from $8^{3}/_{4}$ by $11^{5}/_{8}$ inches to the standard size of $8^{1}/_{4}$ by $11^{1}/_{4}$ inches. Ultimately this will effect a saving of $10,000 annually in the cost of paper and reduced postage. The change also makes for greater uniformity on library shelves and provides increased flexibility to advertisers who furnish bleed plates.

Table IV. Number of Student Members as of April 30

Year	New Applications	Renewals	Total
1951	4,635	10,393	15,028
1950	7,876	12,792	20,668
1949	9,967	9,461	19,428
1948	7,876	6,041	13,917
1947	5,092	3,929	9,021
1946	2,574	2,513	5,087
1945	2,326	2,287	4,613
1944	2,242	2,656	4,898
1943	2,512	3,200	5,712

Table V. Record of AIEE Membership

Year	Total May 1	Year	Total May 1	Year	Total May 1
1884	71	1907	4,521	1929	18,133
1885	209	1908	5,674	1930	18,003
1886	250	1909	6,400	1931	18,334
1887	314	1910	6,681	1932	18,003
1889	333	1911	7,117	1933	17,010
1890	427	1912	7,459	1934	15,230
1891	541	1913	7,654	1935	14,269
1892	615	1914	7,876	1936	14,600
1893	673	1915	8,054	1937	15,308
1894	800	1916	8,202	1938	16,078
1895	944	1917	8,710	1939	16,605
1896	1,035	1918	9,282	1940	17,213
1897	1,073	1919	10,352	1941	17,886
1898	1,098	1920	11,345	1942	18,944
1899	1,133	1921	13,215	1943	20,161
1900	1,183	1922	14,263	1944	21,407
1901	1,260	1923	15,298	1945	23,072
1902	1,549	1924	16,455	1946	25,090
1903	2,229	1925	17,319	1947	26,470
1904	3,027	1926	18,158	1948	28,408
1905	3,460	1927	18,344	1949	30,791
1906	3,870	1928	18,265	1950	34,198
				1951	38,058

The classification of articles in *Electrical Engineering* in seven broad fields is presented in Table IX, which may be compared readily with the report of the previous year. By selecting shorter articles, more highly condensing others, and decreasing the Institute Activities section, a greater number of articles in full or nearly in full has been published. Also, the publication of digests of conference papers was discontinued beginning with the January issue. Experience had proved that digests are of little value unless the complete papers are available, and the deletion of these digests will provide 84 more pages annually for the publication of articles in full. One hundred and fifty-three articles in full or essentially in full were carried, as compared with 119 for the previous year. The number of Science and Electronics articles has increased 18 per cent, and there has been an increase in the number of Industry and General Applications papers. Papers on applications of electronic circuits and vacuum tubes cut across the five major divisions, and a separate analysis of the 153 articles indicates that 56 of the articles could be considered to have a major area of interest in the electronics field. Efforts are being made to increase further the numbers of articles in the fields of electronics, industry, and general applications.

Advertising. The number of pages of advertising during the last eight months of 1950 was about the same as for the corresponding period of the previous year. During the first four months of 1951, there was an increase of 22 pages, or 11.4 per cent more pages, than for the same period during the previous year. The general outlook for 1951 seems quite good. From contacts made during recent trips, the Advertising Director feels that this condition will continue.

Transactions. Volume 69 of the 1950 *Transactions* has been made available in two parts. Part I, which contains the papers presented during the Winter General Meeting of 1950, consisting of 670 pages, was made available for distribution in August. Part II, which contains the remainder of the papers for the year, the Board of Directors' Report, and a complete index, comprising a total of 1,082 pages, was made available for distribution on April 5, 1951.

Table VI. Deaths of AIEE Members Reported in Electrical Engineering

Name	Date of Election	Date of Death	Grade at Death	Obituary Notice in Electrical Engineering
Allen, John E.	A '21	Aug. 6, '50	F	Oct. '50, p. 936
Anderson, Burt T.	A '35	Nov. 8, '50	A	Jan. '51, p. 87
Archibald, Carl G.	A '37	Apr. 12, '50	A	June '50, p. 569
Balogh, Stephen I.	A '44	July 31, '50	A	Oct. '50, p. 936
Batcheller, Birney C.	M '17	Nov. 27, '50	M	Feb. '51, p. 170
Bennett, Edward	A '01	Jan. 10, '51	F	Apr. '51, p. 367
Boykin, Richard M.	A '13	Jan. 29, '50	M	June '50, p. 570
Brown, Frederic S.	A '12	Mar. 4, '51	F	May '51, p. 461
Brueck, Haworth L.	A '42	Apr. 11, '50	A	July '50, p. 659
Burbank, Jerome D.	A '26	Feb. 6, '51	M	May '51, p. 462
Bushnell, Robert J.	A '36	Dec. 5, '50	M	Mar. '51, p. 281
Champe, Willard C.	A '25	May 1, '50	M	July '50, p. 659
Christensen, Carlo P.	A '14	June 16, '50	A	Sept. '50, p. 848
Clark, Walter G.	A '03	Dec. 17, '50	F	Feb. '51, p. 170
Doherty, Robert E.	A '16	Oct. 19, '50	F	Dec. '50, p. 1132
Draper, Ray O.	A '45	Dec. 26, '49	A	June '50, p. 569
Eisenmenger, Hugo E.	A '11	Aug. 28, '50	M	Mar. '51, p. 281
Ellerman, Louis H.	A '28	Mar. 14, '50	M	July '50, p. 660
Fitz, Ervin M.	A '03	July 6, '50	A	Jan. '51, p. 87
Gary, Laurence A.	A '12	Aug. 23, '50	M	Nov. '50, p. 1040
Gill, Sir Frank	A '03	Oct. 25, '50	F	Mar. '51, p. 280
Hannon, Frank R.	A '20	Jan. 5, '51	A	Mar. '51, p. 281
Hare, Robert J.	M '44	Sept. 12, '50	M	Mar. '51, p. 281
Henningsen, Earie S.	A '20	Sept. 23, '50	F	Dec. '50, p. 1133
Hickok, Robert D.	M '16		F	July '50, p. 659
Hill, Stanley C. H.	A '38	Sept. 4, '50	A	Nov. '50, p. 1040
Horle, Lawrence C. F.	A '20	Oct. 28, '50	F	Jan. '51, p. 87
Hotchkiss, Frederick W.	A '20	Nov. 11, '50	M	Jan. '51, p. 87
Hubbard, Albert S.	A '95	Apr. 19, '50	A	July '50, p. 660
Jones, Frederick S.	A '14	Feb. 26, '51	M	May '51, p. 462
Kaehni, William	M '44	Jan. 27, '50	M	June '50, p. 569
Kalantar, Hamaz H.	M '42		M	June '50, p. 569
Kappeyne, Jacobus	M '18	Feb. 22, '51	M	May '51, p. 462
Kent, Walter	M '44	Feb. 10, '50	M	June '50, p. 570
Kinnaird, William R.	A '43	Oct. 19, '50	A	Mar. '51, p. 281
Knightley, William J.	A '37	Jan. 25, '51	M	Apr. '51, p. 368
Laudenslager, Richard L.	A '32	June 2, '50	M	Aug. '50, p. 736
Layman, Waldo A.	A '99	Oct. 25, '50	F	Jan. '51, p. 87
Leilich, Frank T.	A '09	Nov. 19, '50	M	Feb. '51, p. 170
Martin, Lewis G.	A '03	Apr. 1, '50	A	July '50, p. 660
Mason, Ruric C.	A '26	May 12, '50	M	July '50, p. 659
McAfee, William K.	A '16	Feb. 2, '50	M	June '50; p. 569
McBerty, Frank R.	A '01	Feb. 19, '50	F	Nov. '50, p. 1040
McCarter, Robert D.	A '99	Mar. 9, '51	M	May '51, p. 462
McClellan, William	A '04	Nov. 14, '50	F	Jan. '51, p. 87
McIver, Jr., George W.	A '08	July 24, '50	F	Nov. '50, p. 1040
Miller, Alvin A.	A '03	Apr. 5, '50	M	July '50, p. 659
Mills, John H.	A '37	Jan. 6, '51	A	Apr. '51, p. 368
Oboukhoff, Nicholas M.	M '24	July 30, '50	F	Oct. '50, p. 936
Parrack, Vasco R.	A '25	May 11, '50	F	July '50, p. 659
Parsons, John S.	A '27	Aug. 22, '50	M	Oct. '50, p. 936
Pierce, George A.	A '03	Mar. 10, '51	A	May '51, p. 461
Pike, Otis W.	A '30	Oct. 7, '50	M	Dec. '50, p. 1133
Pohnan, Frank J.	M '50	Nov. 26, '50	M	Apr. '51, p. 368
Poor, Walter E.	A '15	Apr. 4, '50	A	June '50, p. 569
Rice, Chester W.	A '13	Mar. 8, '51	F	May '51, p. 461
Rippey, Samuel H.	A '04	May 18, '50	F	Aug. '50, p. 737
Rose, Melvin C.	M '46	Apr. 23, '50	M	July '50, p. 659
Sanderford, Roger M.	A '43	Oct. 12, '50	A	Apr. '51, p. 368
Sawford, Frank	A '10	Aug. 24, '50	M	Nov. '50, p. 1040
Schauss, Stanley L.	A '43	Jan. 24, '51	M	Apr. '51, p. 368
Skinner, Charles E.	A '99	May 12, '50	F	Aug. '50, p. 736
Smith, Alzamora B.	A '40	Aug. 15, '50	A	Oct. '50, p. 936
Spinney, Louis B.	A '03	Jan. 25, '51	M	Apr. '51, p. 367
Streamer, A. Camp	A '10	May 4, '50	M	July '50, p. 658
Timmerman, Arthur H.	A '03	July 18, '50	F	Sept. '50, p. 848
Waldo, Edward H.	A '07	Aug. 30, '50	M	Nov. '50, p. 1040
Waller, James C.	A '44	Apr. 2, '50	A	July '50, p. 660
Warner, Harry O.	M '27	Sept. 16, '50	M	Nov. '50, p. 1040
Williams, John B.	A '40	Sept. 2, '50	A	Nov. '50, p. 1040
Winterroth, William C.	A '36	June 17, '50	A	Dec. '50, p. 1133
Wittig, Gustav F.	A '05	May 30, '50	A	Aug. '50, p. 736
Wolfrom, Carl A.	A '10	Aug. 3, '50	A	Feb. '51, p. 170
Woolston, Louis F.	A '20	Sept. 20, '49	F	July '50, p. 659
Wynant, James W.	A '09	May 1, '50	M	July '50, p. 658
Yensen, Trygve D.	A '09	July 2, '50	M	Aug. '50, p. 736

AIEE Proceedings. During the year, there has been a decrease in the number of *Proceedings* orders received. A total of 6,572 orders was received, representing a distribution of 54,560 copies of papers. This is an 18.4 per cent decrease in the number of order forms received and may be attributable to a smaller number of back orders for the papers of the previous year.

Divisional Publications. The committee has made an extensive study of the possibilities of issuing five divisional publications three or four times a year to take the place of the present *AIEE Proceedings*. A preliminary analysis from a sample of orders for the 1949 papers indicates that most members are ordering in a pattern the papers from three or more divisions. From a calendar of when the 1949 *Proceedings* papers were ready for distribution, it is indicated that many of the papers will be delayed two or more months if bound according to divisions. The data also show that there are not enough papers in some divisions—for example, Industry and General Applications—to issue publications quarterly. The independent survey made by a specially appointed committee, in which some 330 members were questioned, indicated that about 65 per cent of the members questioned were not in favor of incorporated sectional material in packages.

The committee felt that it did not know enough about the problem and it recommended that a survey of the membership be made to determine each member's major area of interest according to the five divisions and to determine to which other divisions each member might subscribe at a nominal annual subscription price of $2 to $3 per division.

Special Publications. During the year, the following six Special Publications have been made available and three more are in prospect. These publications are on a self-supporting basis and are made available to members at cost and in general to nonmembers at double cost through order forms published in *Electrical Engineering* from time to time.

1. Lightning Reference Bibliography, 1936–1949 (4/50)
2. Bibliography on Industrial Control (9/50)
3. AIEE Power Conference—Power Generation and Industrial Power Systems* (8/50)
4. Joint AIEE/NTF Conference on Telemetering* (8/50)
5. Electric Arc and Resistance Welding—II* (12/50)
6. Sources of Electric Energy (1/51)

---

* Conference Reports.

Conference Papers. There are many advantages to the presentation of conference papers; however, for some time the Publication Committee has been concerned with the increase in the number of conference papers and the decline of the formal types of papers as related to the increasing membership. Data on the matter over a 20-year period are shown in Table X. Conference papers provide an easy way of getting material which has not been reviewed on programs. The practice which permits some authors who have good facilities for the reproduction of their papers to distribute them at meetings is unfair to other authors who have good material but lack the facilities for reproduction and distribution. Presentation again by title does not provide a satisfactory solution as most of the discussion is lost, and during the interim the conference paper may have been published elsewhere. Providing conference papers in preprint form is only a partial solution, as it would not preserve the discussion and the permanent record of the paper would be lost when stock is depleted.

During the past 20 years publication costs have more than doubled. There does not seem to be any ready solution to the problem without a considerable increase in appropriations for publication purposes to provide for the increased costs and staff additions. The problem was discussed at the technical forum held during the Winter General Meeting, and it will be further explored at the forum of the Summer General Meeting.

COMMITTEE ON REGISTRATION OF ENGINEERS

The committee has continued its efforts to advise the AIEE membership on the problems of registration.

The committee held a meeting at the Winter General Meeting, which was attended by a large majority of the members.

Supplementing previously published papers sponsored by the committee, a paper by N. L. Freeman entitled "Procedures for Obtaining Registration as a Professional Engineer" was published in the February 1951 issue of *Electrical Engineering*. Reprints are available at Headquarters for use by the Sections and Student Branches and by the membership. It is planned to continue this series of papers with others, each covering some phase of registration. These are to be published in *Electrical Engineering* when approved, and reprints of these will also be available at Headquarters.

In the 1950 issue of the Year Book, for the first time Registered Professional Engineers are indicated by a dagger. Not all who are registered are so indicated, due to the failure of some members to properly fill out their information cards. It is hoped that this will be corrected in the near future.

SECTIONS COMMITTEE

Section Activities. Two new Sections, Sacramento and Northern New Mexico, were formed.

New Subsections were formed as follows: Black Hills (Denver Section), Boise (Utah Section), Eureka (San Francisco Section), Hawaii (San Francisco Section), and Vancouver Island (Vancouver Section). Other Subsections are pending.

Section, Subsection, and membership development has been very active and healthy as noted above and as shown in Table XI.

The western portion of Louisiana, including the Shreveport Section and Lake Charles Subsection, was transferred from District 4 to District 7.

Meetings of the Sections Committee. A meeting of the Sections Committee was held during the Winter General Meeting, and a meeting is scheduled for the Section delegates during the Summer General Meeting.

Special Activities. A new revision of the "Model By-Laws for Sections and Subsections" was printed which not only brought these up-to-date, including by-laws for Subsections, but also suggested a change in the method of electing officers so as to give them a sequence of position which would result in better officer material and more experience.

At the suggestion of a special committee under the chairmanship of C. G. Veinott, a plan was approved by the Board of Directors to award four prizes to the Sections which have been the most outstanding in regard to attendance and membership growth. This will be known as the Plan for Recognition of Section Growth.

Publicity activity has been increasing in each Section, and as a further stimulation they are being offered help by Raymond C. Mayer, the Institute public relations counsel.

A thorough review has been requested of each Section regarding the necessity or advisibility of having local members, and it is hoped that some pattern for future guidance may come from this study.

A Subcommittee of the Sections Committee is studying the question of what officers of a Section should be the official representatives at its District Executive Committee meeting. At present the official delegates are the Chairman and Secretary.

General Conclusions. The figures on the rate of membership growth as well as the membership attendance at meetings are the best indications of active and effective Section operation. Present indications are for even better results in the future.

STANDARDS COMMITTEE

The Standards Committee consists of 26 appointed members and the Secretary. Two meetings have been held so far this year and a third is planned for June.

Completed Standards. Since August 1950, the following Institute Standards or Codes were completed or revised:

AIEE *52* (March 1951), Application Guide for Grounding of Instrument Transformer Secondary Circuits and Cases.

AIEE *551* (August 1950), Master Test Code for Temperature Measurement.

AIEE *601* and *602* (November 1950), Large 3,600-Rpm 3-Phase 60-Cycle Condensing Steam Turbine-Generators.

AIEE *605* (September 1950), Recommended Specifications for Speed-Governing of Hydraulic Turbines Intended to Drive Electric Generators.

AIEE *801* (August 1950), Proposed Test Code for Aircraft Circuit Interrupting Devices.

Revisions of AIEE *20*, Air Circuit Breakers, AIEE *20A*, Low-Voltage Air Circuit Breakers, and AIEE *27*, Switchgear Assemblies, were completed, but approval has been withheld pending the settlement of some questions raised in the Standards Committee.

Work in Progress. It is not possible in this brief report to mention all the standardizing subjects being considered in many of the Institute technical committees. Work in progress which has been reported to the Standards Committee recently by standards co-ordinating committees, by Institute technical committees, and by subcommittees is as follows:

Standards Co-ordinating Committee Number 8, which serves as the AIEE delegation to the AIEE-Edison Electric Institute-National Electrical Manufacturers Association (NEMA) Joint Committee on Co-ordination of Insulation, has continued its study of insulation requirements and the development of basic impulse levels.

The Committee on Instruments and Measurements is preparing a Master Test Code for Power Measurements and a Master Test Code for Speed Measurements. This committee is also studying the markings of varmeters which may result in a standard.

The Committee on Electronics has formed various groups to study vacuum-tube standards. In one group progress is being made on ratings and test methods for pool tubes. Other groups are undertaking the preparation of standards on radiation detection tubes and high vacuum receiving tubes. A proposal on Symbols for X-ray Tubes was completed and submitted to the American Standards Association (ASA) sectional committee. Work on definitions in the X-ray field is also being carried on in co-operation with the ASA Sectional Committee on Definitions of Electrical Terms.

The Committee on Switchgear is considering the preparation of standards for network protectors.

The Committee on Transformers has under preparation certain proposed revisions in the American Standard for Transformers.

Active work is in progress in revising certain of the test codes which are under the jurisdiction of the Committee on Rotating Machinery. These are being co-ordinated with the American Standards for Rotating Machines as they are, in effect, made a part of these standards by references in the latter. This technical committee is also preparing recommendations for the consideration of the ASA sectional committee which is at present engaged in making a revision of the American Standards.

The Standards Subcommittee of the Committee on Industrial Control has been studying possible changes which might be proposed in the American Standard drawing symbols.

A subcommittee of the Standards Committee is correlating standard temperature rises at the terminals of apparatus.

Work With Other Organizations. An Institute Subcommittee on Standard Frequency Bands and Designations has developed a proposed standard which designates each frequency band by a number which is the logarithm of the lowest frequency in the band. This subcommittee has co-operated with an Institute of Radio Engineers (IRE) committee to arrive at this proposed standard, which has been submitted to the Department of State as a joint AIEE-IRE recommendation for the purpose of having it included on the agenda of the

Table VII. Numbers of Pages of Published Material

	Electrical Engineering			Transactions Only		
Year	Technical Articles	News	Transactions Sections	Technical Papers	Discussions	Total
1941	337	281	600	542	268	2,028
1944	246	214	738	493	231	1,922
1945	255	225	736	121	143	1,480
1946	285	315	832	254	120	1,806
1947	806	474		1,600*	153*	3,033
1948	832	395		1,643†	172†	3,042
1949	796	320		1,275‡	167‡	2,558
1950	836	323		1,579**	173**	2,911

* Preprinted 227 papers as *AIEE Proceedings*, except for a 17-page technical paper in *Electrical Engineering*.

† Preprinted 247 papers as *AIEE Proceedings*, requiring a total of 2,090 pages.

‡ Preprinted 202 papers as *AIEE Proceedings*, requiring a total of 1,795 pages.

** Preprinted 238 papers as *AIEE Proceedings*, requiring a total of 2,014 pages.

Table VIII. Material in Electrical Engineering, May 1950 to April 1951

	Number of Articles	Number of Pages	Per Cent Pages
Special Articles	60	216	17.9
Technical Papers	58*	291	24.1
Conference Papers	35**	147	12.2
One-Page Digests	120	120	10.0
Conference Paper Digests		23	1.9
Essays		29	2.4
Filler Items	25	10	0.8
Institute Activities Section		211	17.5
Current Interest Section		85	7.0
Industrial Notes, Trade Literature, and so forth		27	2.2
Title and Highlights Pages	24	24	2.0
1950 Index	1	24	2.0
		1,207	100.0

* 34 of these were condensed.

** 9 of these were condensed.

Table IX. Classification of Articles in Electrical Engineering in Seven Broad Fields

(Exclusive of 1-Page Digests)

	May	June	July	Aug.	Sept.	Oct.	Nov.	Dec.	Jan.	Feb.	Mar.	April	Total
General interest	4	1	3	3	1	2	2	4	2	4	5		31
Educational	1	1						1	1			1	5
Science and electronics	3	3	4	2	6.5	4.5	4	3	1	2	2	3	38
Communication	1	1		1	1		2	1	1	1	3	2	14
Power	5	4	3	2	2.5	3.5	5	2	4	5	4	2	42
Industry	1	2	1	2	1	2		2			1	2	14
General applications	1		1			2	1	1	1			2	9
Totals	16	12	12	10	12	14	14	14	10	12	15	12	153

meeting of the International Consultative Committee on Radiotelephony (CCIR) to be held in Geneva in June, with a view to adoption as an international statement.

Institute representatives serve on a number of committees of other organizations and on some joint committees of other organizations. During the year, a Joint AIEE-IRE Committee was formed to deal with new definitions relating to noise which are coming into use, and an AIEE subcommittee is working with an IRE subcommittee on the preparation of definitions for telemetering.

American Standards Association. The Institute has continued support of the ASA by participation in the work of the ASA Standards Council, the ASA Electrical Standards Committee, the ASA Drawings and Symbols Correlating Committee, and the Mining Standardization Correlating Committee through its representatives on these committees. The Institute is sole sponsor for eight ASA projects, most of which are under sectional committee procedure. A number of these have been active during the year as follows:

The AIEE Committee on Land Transportation has completed a proposed revision of the American Standards for Electric Control Apparatus for Land Transportation Vehicles, ASA *C48*, AIEE *16*, which will be published for trial use. AIEE is proprietary sponsor of this project.

Progress is being made in the tremendous task of revising the Definitions for Electrical Terms, ASA *C42*.

A Sectional Committee on Capacitors has been organized which will consider revision of American Standard *C55*, AIEE *18*, Standards for Capacitors. A proposed revision has been prepared by the Capacitor Subcommittee of the Committee on Transmission and Distribution.

A subcommittee of the Committee on Instruments and Measurements, which also serves as ASA Sectional Committee *C68*, reported that it has prepared a proposed revision of the American Standard for Measurement of Test Voltage in Dielectric Tests, ASA *C68.1*, AIEE *4*.

Upon invitation of ASA, the Institute has recently undertaken to serve as sole sponsor of the project on Electrical Equipment in Metal Mines, *M24*. The sectional committee is being reorganized, and interested organizations are being canvassed to obtain the names of their representatives.

The Institute serves as joint sponsor with the National Fire Protection Association on ASA Project *C5*. This project relates to the Code for Protection against Lightning, a revision of which has been completed and is in the process of approval as an American Standard.

Other ASA projects on which the Institute serves as joint sponsor are *C19*, Industrial Control Apparatus, with NEMA; and *Z32*, Graphical Symbols and Abbreviations for Use on Drawings, *Z32*, with American Society of Mechanical Engineers. The organization and personnel of both of these sectional committees is at present being reviewed in prospect of renewed activity in these subjects.

The Institute is represented on 56 other ASA sectional committees, but no attempt is made in this report to cover the very considerable contributions which AIEE representatives have made to these ASA projects for which the AIEE does not have the responsibility of sponsorship.

Standards Committee Organization. It became apparent that there is a need for some guidance to Institute committees which develop standards in the voting procedure in these committees and in reporting the degree of consensus obtained on standards which they pass to the Standards Committee for approval. The Standards Committee has appointed a subcommittee to study and report on this subject.

The Standards Committee regards its close working relations with the Institute technical committees and its representatives on other committees as highly important. During the year one of the subjects of chief concern was to bring about some form of liaison with these committees comparable to the former relations obtained by ex officio memberships on the Standards Committee.

UNITED STATES NATIONAL COMMITTEE OF THE INTERNATIONAL ELECTROTECHNICAL COMMISSION

Dr. H. S. Osborne, Chief Engineer of the American Telephone and Telegraph Company, was re-elected President of the United States National Committee (USNC) of the International Electrotechnical Commission for the calendar year of 1951. At the same time, P. H. Chase, Chief Engineer of the Philadelphia Electric Company, and R. C. Sogge, Manager of the Standards Division of the General Electric Company, were elected as Vice-Presidents of the USNC for the calendar year of 1951.

At the invitation of the French Electrotechnical Committee, the International Electrotechnical Commission (IEC) held its annual meeting in Paris from July 10 to 21, 1950. This meeting was attended by almost 300 delegates representing 16 nations, and was the largest meeting of the IEC since the war. It comprised meetings of 11 international technical committees, several subcommittees, and the International Special Committee on Radio Interference (CISPR). The IEC Committee of Action, which deals with administrative matters in the interval between meetings of the Council, also met. The United States was represented by 14 technical delegates well versed in their respective fields. The delegation was headed by P. H. Chase, Vice-President of the USNC. Meetings of the following technical committees were held in Paris:

Technical Committee 3—Graphical Symbols
Technical Committee 7—Aluminum
Technical Committee 12—Radio Communication
Technical Committee 23—Electrical Accessories
Technical Committee 24—Electric and Magnetic Magnitudes and Units
Technical Committee 25—Letter Symbols
Technical Committee 28—Co-ordination of Insulation
Technical Committee 32—Fuses
Technical Committee 33—Power Capacitors
Technical Committee 34—Lamps, Lamp Caps, and Holders
Technical Committee 35—Dry Cell Batteries

In addition, a meeting of Technical Committee 5 on Steam Turbines was held in London July 6 to 8, 1950.

Considerable progress has been made in the technical committees during the year. Several proposed international recommendations in the field of radio, electric lamps, letter symbols, turbine-type generators, and electric motors are now before the national committees of the member countries of the IEC for approval as International Standards. Among these are:

Color Code for Fixed Resistors

Specification for Series of Preferred Values and Their Associated Tolerances for Resistors and Capacitors for Apparatus for Radio Communication

Specification for Tungsten Filament Lamps for General Service

International Letter Symbols for Use in Connection with Electricity—Magnitude Symbols, Alphabets, and Letter Type

Table X. Growth of Conference Papers and Decline of Published Papers in Proportion to Membership Over a 20-Year Period

	Calendar Years				
	1930	1935	1940	1944	1950
Number of Conference Papers		64*	58*	88*	284
Number of District Papers		8	12	21	105
Number of ACO Papers	32	3	8	8	44
Total of Unpublished Papers	32	75	78	117	433
Number of Transactions Papers	167	127	155	231	238
Membership as of May 1st	18,003	14,269	17,213	21,407	34,198
Unpublished Papers × 100/Membership	0.178	0.526	0.453	0.546	1.27
Published Papers × 100/Membership	0.93	0.89	0.90	1.08	0.696

* 50 per cent estimated (assumption 4 papers per conference).

Preferred Standard 3,000 Rpm 3-Phase 50-Cycle Turbine Type Generators

Two new subcommittees have been organized: one on Dimensional Standards for Electric Motors, and another on Turbine-Type Generators. Meetings of these groups were held in London in November 1950, and a representative of the USNC was present at both meetings.

During the course of the year, two new member countries have been added to the IEC; namely, Israel and Yugoslavia.

The next annual meeting of the IEC will be held in Estoril, Portugal, during the period of July 4 to 12, 1951. In addition to meetings of the Council and Committee of Action, meetings of the following technical committees have been scheduled to be held at that time:

Technical Committee 1—Nomenclature
Technical Committee 2—Rotating Machinery
  Subcommittee 2A of Technical Committee 2—Turbine-Type Generators
  Subcommittee 2B of Technical Committee 2—Dimensions for Electric Motors
Technical Committee 8—Standard Voltages and Currents
Subcommittee 3 of Technical Committee 12 on Radio Components
Technical Committee 14—Transformers
Technical Committee 15—Insulating Materials
Technical Committee 17—Switchgear
Technical Committee 28—Co-ordination of Insulation

Arrangements have been made for the USNC to be well represented at these meetings.

The invitation extended by the USNC to hold meetings in the United States in 1954 to celebrate the 50th Anniversary of the founding of the IEC (which was founded in St. Louis, Mo., in 1904) has been accepted, and preliminary plans are now being made for these meetings.

UNITED STATES NATIONAL COMMITTEE OF THE INTERNATIONAL COMMISSION OF ILLUMINATION

During the year 1949–1950, the United States National Committee has been actively engaged in preparation for the sessions which are to be held in Stockholm in June 1951. An organization meeting for the Stockholm sessions was held in Amsterdam on January 23. At this meeting, the recommendations of the USNC for separate sessions for papers of general interest received favorable consideration. Five of the six papers submitted by Americans have been accepted for presentation. These are:

The Engineering Evolution of the Fluorescent Lamp by Dr. E. F. Lowry, Sylvania Electric Products, Inc.

The Subjective Appraisal of Brightness by S. K. Guth, General Electric Company

Daylight in Classrooms by Prof. R. L. Biesele, Jr., Southern Methodist University

Home Lighting Practice by Miss Myrtle Fahsbender, Westinghouse Lamp Division

Space Concepts of Lighting by R. G. Slauer, Sylvania Electric Products, Inc.

In addition, the USNC has been requested to invite Doctor Evans of the Eastman Kodak Company to present a paper on color and vision at a special meeting. Present indications are that the USNC will be represented at the Stockholm sessions by an exceptionally large and well-qualified delegation, with at least one outstanding United States expert at every committee meeting.

Table XI. Section and Branch Statistics

	For Fiscal Year Ending April 30					
	1946	1947	1948	1949	1950	1951
Sections						
Number of Sections	75	75	81	84	87	89
Number of meetings held	1,210	1,333	1,340	1,561	1,605	1,716
Total attendance	113,531	155,649	109,637	128,025	135,847	125,779
Branches						
Number of Branches	125	126	127	129	130	132
Number of meetings held	716	1,018	1,172	1,350	1,298	1,281
Total attendance	22,844	40,669	77,040	103,828	80,672	62,630

During the year, it developed that the Central Bureau, which is now located in the United States, lacked both manpower and financial resources to carry on the work. Unusual expenses in connection with the production of the Proceedings and the devaluation of the pound had reduced the available income to an amount far below that necessary for the successful operation of the Bureau. If the International Commission of Illumination is to continue to exist and grow, some arrangements must be made to ensure more adequate and reliable sources of income. The present annual dues from national committees ($6,000) will not support this activity.

Therefore, it was proposed that a committee be constituted to raise funds to assist in financing the Central Bureau from June 1, 1950, to June 1, 1952, these funds to be solicited from firms engaged in the lighting business on an international scale. This proposal was placed before the members of the USNC in the form of a letter ballot and was approved. One of the first activities of this committee was the preparation of an informational brochure. It was originally planned to ask United States firms to underwrite the operation of the Central Bureau in the amount of $24,300, for the period June 1, 1950, to June 1, 1952, only, but it now appears that $30,000 will be needed. A report on the outcome of these solicitations has not been made yet. A system of sustaining membership on an international basis similar to the procedure in use in the Illuminating Engineering Society is also under consideration.

COMMITTEE ON STUDENT BRANCHES

Upon the recommendation of the Committee on Student Branches, the Board of Directors authorized the establishment of four additional Student Branches during the year. These Branches were authorized at the University of Massachusetts, the University of Toledo, and the United States Naval Academy. These additional Branches bring the total number to 133.

Sections 33, 51, 53, 60, and 84 of the By-Laws, relating to Student membership and Student Branches, were amended by the Board of Directors at its meeting on October 26, 1950, in accordance with the recommendations of the Committee on Student Branches and the Committee on Constitution and By-Laws. These changes in the By-Laws clarify certain points regarding Student membership, include the Chairmen of the District Committees on Student Activities as appointed members of the Committee on Student Branches, and adjust the times for nominating and appointing District Committees on Student Activities. The latter adjustments enable the President-elect to appoint the members of the Committee on Student Branches at the same time other committee appointments are made.

A previous amendment of Section 53 of the By-Laws changed the Student membership dues from $3.00 to $5.00 per year. The increase will become effective May 1, 1951. This is the first change in the Student membership dues since that grade of membership was established in 1903. When the dues were increased, the Board of Directors requested the Committee on Student Branches to investigate and report to the Board ways and means by which the Institute may further promote the student program. A subcommittee charged with the responsibility of this investigation has been working on the project since the summer of 1950 and submitted a progress report at the January 23, 1951, committee meeting. The progress report was reviewed and referred back to the subcommittee for further investigation and a report at the June meeting of the committee in Toronto, Canada.

Last year, a subcommittee presented a report on making available to each of the Branches a certificate to be awarded, at their discretion, to a Student member for outstanding activity. After further study, this report was recommended to the Board of Directors and it was approved by the Board at its meeting on January 25, 1951. These certificates were made available to the Branches this year.

The Joint AIEE-IRE Co-ordination Committee at its meeting on November 7, 1950, made the following recommendation to the AIEE and IRE:

> "That a continuing joint subcommittee be established under the Education Committee of the IRE and the Student Branch Committee of the AIEE. The purpose of the subcommittee will be to resolve differences of Joint Student Branches, which are of such magnitude or of such specialized nature that they cannot be settled by the Executive Secretary of the IRE and the Secretary of the AIEE."

The Committee on Student Branches recommended such a joint subcommittee to the Board of Directors, and it was approved by the Board at its meeting on January 25, 1951. The Board of Directors of the IRE had previously approved the joint subcommittee on November 8, 1950, and it has been established.

Because of the number of Student members being called into the armed services, the committee recommended to the Board of Directors that the policy of granting suspended membership for Student members, followed during World War II, be applied in the present national emergency. This recommendation was approved by the Board, to become effective at the beginning of the fiscal year, May 1, 1951.

The committee held two meetings, one in Pasadena, Calif., on June 14, 1950, and the other in New York, N. Y., on January 23, 1951.

TECHNICAL ADVISORY COMMITTEE

Technical Committee Organization. Two new technical committees were established in the Science and Electronics Division to meet the expanding activities of this division. The Subcommittee on Magnetic Amplifiers was transferred to technical committee status, and the Committee on Therapeutics was merged with the Joint Subcommittee on Electrical Aids to Medicine to form the new Committee on Electrical Techniques in Medicine and Biology, thereby increasing the number of active technical committees to a total of 39.

Administration of Joint Subcommittees. Progress was made during the year toward reducing the number of joint subcommittees subject to joint administration. The Joint Subcommittee on Electrical Aids to Medicine was merged into the Committee on Electrical Techniques in Medicine and Biology, as noted above, and the Joint Subcommittee on Instrument Transformers was assigned for administrative purposes to the Committee on Transformers. Joint administration of a limited number of joint subcommittees will continue into the next administrative year, partly to afford additional experience, and partly in anticipation that some subcommittees will be transferred to the status of technical committees.

Special Technical Conferences. Special technical conferences have become a permanent Institute technical activity. On an over-all basis, this activity has been financially self-sustaining.

Member Classification. The lack of a classification of Institute membership according to interest has been a drawback in the preparation of mailing lists to publicize special technical conferences and other technical activities. Various means for establishing a classification are under study. Consideration is being given to the utilization of the tabs on the available addressograph equipment to permit classification according to Division interest as the first step toward a more complete classification.

AIEE Participation in Centennial of Engineering. The Technical Advisory Committee is co-operating with the local committee for the participation of the Institute in the centennial anniversary celebration of the American Society of Civil Engineers scheduled for the week of September 7, 1952, in Chicago. Preliminary plans provide for three days of AIEE-sponsored sessions on subjects appropriate to the occasion. Liaison is being effected by representation from each Division on the local committee.

Committee Scopes. Efforts were continued during the year to bring existing technical committee scopes up to date and to have scopes prepared for subcommittees and working committees where these were lacking. A complete roster of personnel and scopes for these subcommittees has been included in the Year Book for 1950.

Technical Activities. The technical activities of the Institute continued at an increased rate during the year as indicated elsewhere in the annual report. The problem of equal distribution of the burden of technical sessions among the four general meetings of the Institute has been considered. Studies toward effecting a satisfactory solution will be continued.

Technical Conference Papers. The status of technical conference papers has been reviewed, with indications of the need of remedial action. It has become quite apparent that conference papers are no longer being used as originally intended. Instead, they have grown in number to such an extent that they constitute the major form of paper presentation. The effect has been a loss in the *Transactions*, which constitute the permanent record of the advancement in the art of electrical engineering, of some valuable material. Much of the difficulty stems from the fact that the budget does not permit publications to parallel the expansion of the technical activities of the Institute.

Manual of Instructions. The manual of instructions made available to technical committee chairmen, as a source of information for their guidance in the performance of their duties, has been revised and enlarged in light of the experience during the past year. A calendar of dates covering general and District meetings, closing dates for paper submission, and so forth, has been included for the convenience of chairmen.

Forum of Technical Committee Chairmen. Forum meetings of technical committee chairmen with a panel of appropriate general committee chairmen were instituted at the Fall General Meeting. Although originally contemplated as an annual event, the Oklahoma City forum meeting was so successful that it was followed by a meeting in New York City, and a third is to be held in Toronto. The objectives of the forum are to afford an opportunity for the exchange of opinions, the submission of expressions for preferred action on matters relating to technical activities, and the statement by chairmen of general committees of specific problems and the extent of co-operation desired from technical committee chairmen.

The New York City forum is responsible for the recent Board action permitting the waiver of registration fees for nonmember authors who have been invited to present papers before the Institute members.

TECHNICAL PROGRAM COMMITTEE

Papers Presented. Technical activity in the Institute continues to rise, and the past year sets a new record in papers presented and published. This increased activity was especially noticeable at the Winter General Meeting, where there were eight concurrent sessions at many periods on the program, and a total of 68 technical sessions and conferences were held. The two sessions on "Operation of Utilities under Military Attack" were of outstanding interest. A tabulation of papers classified by meetings is given in Table XII.

Conference Papers. A record number of papers has been accepted for *Transactions*, but the increase in conference papers continues to be the outstanding trend. This channel for bringing recent developments promptly to the attention of our membership has been especially important in the Communication and Science and Electronics Divisions. The conference papers presented appear to be appropriate for this channel because only about 10 per cent of them are subsequently presented by title and published in *Transactions*. It should be recognized that much of the material presented in conference papers cannot be made available in any more formal manner.

Relation of Forum and Technical Program Committee. The forum of technical committee chairmen, which held the first meeting in Oklahoma City, provides a valuable opportunity to discuss Institute problems. The discussion of registration fees for nonmember authors at the Winter forum brought the problem to the attention of the Directors who took appropriate action. Conference papers were also considered at the Winter meeting, and will be continued on the agenda at the Summer meeting. The needs of the Technical Program Committee would be served more effectively if this committee held a special forum during September. This meeting should discuss details of handling technical papers, particularly for the information of new committee chairmen. Tentative plans for the technical program for the year could also be made. A forum at the Fall General Meeting comes a little late for best results and may not be well attended by technical committee chairmen.

COMMITTEE ON TRANSFERS

In addition to answering quite a number of communications from Section transfer committees, the committee held two general meetings—one in Pasadena, in June, and the second in New York, in January. At the Pasadena meeting, Lloyd Hunt of the Los Angeles Section described an activity which appeared to have considerable merit. They have formed the Fellows of that area into a group called the Royal W. Sorenson Fellows, having one meeting per year. This meeting provides an opportunity for the Fellows in the Los Angeles area to get together informally and at the same time gives a certain amount of recognition to that group.

At the New York meeting of the committee, it was decided to withhold printing

Table XII. Numbers of Papers Presented During the Year Ending April 30, 1951

Meeting	District	Advance Copy Only	Conference Papers	Transactions	Total	Attendance
Great Lakes District Meeting	21	2		3	25	536
Summer and Pacific General Meeting		13	85	53	151	1,665
Middle Eastern District Meeting	68	3		24	95	972
Fall General Meeting		12	59	51	122	1,144
Winter General Meeting		24	161	119	304	3,334
Southern District Meeting	27	2		5	34	328
Total	116	56	305	255	731	7,979

of the guide for local transfers committees until the proposed changes in membership requirements and the procedure in the election of Fellows had been voted upon by the membership. The committee urges that, as soon as the new requirements and procedures are decided and settled, this guide be revised and issued, as there is a definite need for it.

TECHNICAL DIVISIONS AND COMMITTEES

Communication Division

COMMITTEE ON COMMUNICATION SWITCHING SYSTEMS

One committee meeting was held and two technical sessions were sponsored. The session on the subject of community dial offices referred to in last year's report was held at the Fall General Meeting. There appeared to be considerable general interest in this subject, and the committee is attempting to obtain sufficient papers on it to constitute a second session for the Fall General Meeting. The session sponsored for the Winter General Meeting covered subjects on telegraph switching and supervisory arrangements developed for long-haul telephone trunks. This session was well attended and the discussions were lively and stimulating.

The committee expects to be able to sponsor a symposium of papers on the subject of nation-wide operator toll dialing at the 1952 Winter General Meeting. In view of the wide interest in this subject and its extreme importance in the telephone switching field, it should constitute a meeting of considerable interest.

COMMITTEE ON RADIO COMMUNICATIONS SYSTEMS

The committee held one formal meeting—on January 25, 1951. Mr. Dickieson, Chairman of the Subcommittee on Mobile Radio, submitted a comprehensive report of the work done on the protection of fixed radio stations, intended for mobile radio service, against damage by lightning. This report is now being studied and revised in preparation for publication.

The committee sponsored one session at the Winter General Meeting and one session at the Summer General Meeting, and suggested papers for presentation at the Pacific General Meeting.

COMMITTEE ON SPECIAL COMMUNICATIONS APPLICATIONS

This committee has served to handle subjects that do not logically fall within the scope of other committees in the Communication Division. Activities concerned with recording, public address systems, printer circuits, and various components have been handled during the past year. The committee has processed several papers covering these topics, which cover a wide range of interest.

COMMITTEE ON TELEGRAPH SYSTEMS

The past year's work of this committee culminated during the Winter General Meeting in a well-rounded technical session covering several recent developments in electronic applications to telegraphic communication. A meeting of the committee also was held during the Winter General Meeting to review the progress of the year and set a course for the coming year. It was obvious that considerable interest had been aroused by the several papers presented on multiplex operation, particularly on the subject of the relative merits of frequency versus time-division systems. The committee therefore concluded that it would be worth while to pursue the subject further. It is hoped that this will result in an additional paper on a new time-division system and a paper on recent applications of frequency-shift diplexing, possibly for the Fall General Meeting.

It was agreed that active work should proceed on a collection of reference information on the various types of printers, codes, keyboards, and so forth, used in the operations of American and foreign telegraph carriers. The need for such a collection was recognized in the previous year, but, because of the pressure of other matters, the work of preparation had to be postponed.

Several new developments were brought to the attention of the committee. Short-haul carrier facilities have been developed to alleviate the shortage of d-c physical wires for telephone service, and may provide an interesting paper during the coming year. New terminal equipment is being developed for the rapid setting-up and changing of program networks. Modern traffic engineering aspects of the terminal handling of record communications by printer, facsimile, telephone, and messenger warrant further attention by the committee.

The growing importance of facsimile in both military and civilian applications should be of interest. New continuous recorders, high-speed techniques for transmission of printed matter as well as photographs and drawings, and the application of such equipment to practical telegraph systems, indicate that there may well be material for a future technical session on facsimile. All of these items are being followed closely by the committee.

COMMITTEE ON TELEVISION AND AURAL BROADCASTING SYSTEMS

This committee was newly formed this year, combining the scope of the former two Committees on Television Systems and Aural Broadcasting Systems. One meeting of the committee was held on September 15, 1950, at which plans were made for sponsoring technical sessions. During the Winter General Meeting the committee sponsored a technical session on the more recent developments in the television field. Three papers on color television and one on ultra-high-frequency television were presented and were well received by the large group in attendance. Work is in progress toward sponsoring a session on broadcasting at the Fall General Meeting. A review was prepared, which was subsequently published in *Electrical Engineering*, covering the outstanding developments during 1950 in the field of broadcasting. Since it was thought that standardizing work was being adequately covered by other groups, no new work in this direction was undertaken this year.

COMMITTEE ON WIRE COMMUNICATIONS SYSTEMS

This committee held meetings and sponsored technical sessions at the Summer and Pacific, Fall, and the Winter General Meetings, and plans meetings at the Summer and Pacific General Meetings. These meetings have enabled more members to attend committee sessions than was possible when only New York committee meetings were held. Consideration is being given to establishing standards of various types, and information is being gathered toward that end. While the need for such standards is clear, it is not yet certain that they can be successfully prepared in the present state of the art.

General Applications Division

COMMITTEE ON AIR TRANSPORTATION

The committee met last October at the Middle Eastern District Meeting. Tentative plans were made for the 1951 meeting to be held in Portland, Oregon, in conjunction with the Pacific General Meeting. Since then, the greatly increased activity in the aircraft industry has made it imperative to hold the meeting near the largest possible concentration of aircraft activity. The committee plans to have a special technical conference on aircraft equipment in Los Angeles, Calif., October 8–10.

Aircraft Electrical Rotating Machinery Subcommittee. On March 16, 1951, copies of a Proposed Test Code for D-C Machines was mailed to the members of the Committee on Air Transportation and other interested parties. The subcommittee is presently working with the Systems Subcommittee in the review of the "Aircraft Electric System Guide Report, AIEE *750*."

Principles of Altitude Rating of Electrical Apparatus Subcommittee. A report titled "Generator Blast-Air Cooling" has been compiled, and is now in the process of circulation among the members of the subcommittee for comments. When the comments are received, it will be revised and submitted to the main committee.

Information is being compiled on variation of air temperature with altitude so that a series of curves may be drawn giving realistic temperature limits for use in designing electric apparatus for aircraft.

Aircraft Electrical Systems Subcommittee also is reviewing the "Aircraft Electric System Guide Report, AIEE *750*." It is expected that revised drafts of certain sections of this report and certain new sections will be prepared for consideration by the Committee on Air Transportation.

Aircraft Electrical Control, Protective Devices, and Cable Subcommittee is reviewing the AIEE Preliminary Test Code *801* on circuit breakers for the purpose of co-ordination with the new MIL-C-Specification.

The proposed AIEE Test Code on Aircraft Carbon-Pile Voltage Regulators is being reviewed in light of the comments received following circulation to members of the Committee on Air Transportation.

Sections 400 and 500 of the Aircraft Electric Systems Guide, AIEE Report *750*, are being reviewed.

COMMITTEE ON DOMESTIC AND COMMERCIAL APPLICATIONS

The activities of the committee are carried on by four subcommittees, three of which have been functioning in the past, while one is new.

Subcommittee on Electric Space Heating and Heat Pumps for the Pacific Coast is co-operating with the program committee for the Pacific General Meeting. The subject is timely, especially for that section of the United States, and because of the relative newness of the application there is much opportunity for the exchange of technical information tending to foster engineering progress in this field.

Subcommittee on Electric Space Heating and Heat Pumps for the East sponsored a very successful session at the Winter General Meeting. This followed a similar session a year ago, and the large attendance at both sessions gave evidence of the interest which this subject holds in the East, as well as on the Pacific Coast.

Subcommittee on Domestic Appliances is co-operating with the Columbus Section for a technical conference to be held at Battelle Memorial Institute in Columbus, Ohio, on May 15. A technical conference sponsored by this same subcommittee in June 1950 in Cleveland, Ohio, was well attended. The two subjects were automatic washers and electric ranges. That conference probably was the first AIEE meeting ever devoted solely to the subject of domestic appliances. A considerable segment of the appliance industry does not have adequate outlet for the exchange of technical information, and it is the hope of this committee that this industry will use AIEE as a forum for engineering advances in this important field.

A new Subcommittee on Farm Electrification was formed during the year which has not been active as yet, but the groundwork has been laid for continuance in future years of activity in this field. While AIEE has taken an active part in meetings and papers relating to the problems of bringing electric power to the farm, there has been comparatively little attention paid, technically, to the many and rapidly growing applications for the utilization of electricity in farming. The committee has had a delegate to the National Farm Electrification Conference, L. R. Emmert, who is also chairman of this subcommittee. Future subcommittee activity in this field will include co-operation with other organizations, including the American Society of Agricultural Engineers.

COMMITTEE ON LAND TRANSPORTATION

This committee has been very active during the year in keeping the Institute informed, by papers and reports, of the progress and new developments in land transportation. It participated in the programs of the Summer and Pacific and Winter General Meetings. The papers sponsored and presented by this committee at these two general meetings covered an unusually broad scope. At Pasadena, the papers presented were specifically related to the design features of the electric and Diesel-electric locomotives, by means of which the American railroads are becoming "electrified" rapidly.

The papers presented during the first session of the Winter General Meeting were devoted to heavy traction subjects, which covered the recent improvements in multiple-unit car motors, both a-c and d-c, and their control, a description of a new train performance calculator, and the technical details of the modern cab signaling and train control equipment now in use on many railroads. The second session was devoted to light traction subjects, the papers covering recent progress in design of light-weight rapid transit cars, their motors and control, and the power supply problems of urban trolley-coach operation. All meetings were unusually well attended, and, in the discussion of the papers, the members present indicated by their keen interest that progress is still being made in electric transportation which is now over 55 years old.

In September 1950 a large group of European railway engineers and officials were brought to this country under the auspices of the Economic Co-operation Administration. Many of the members of the committee had the opportunity of meeting with the subgroup studying American railway electrification, and are now keeping in close touch with recent electric transportation developments in Europe.

In addition to sponsoring the presentation of papers, two meetings of the committee were held, the first in Philadelphia in May, where members had the opportunity of inspecting the "Ignitron-rectifier" car with d-c motors in use on the Pennsylvania Railway a-c electrification and the electric train performance calculator which had recently been placed in service on that railroad. New a-c multiple-unit car equipment recently acquired by the Reading Railroad was inspected also. The second meeting of the committee was held during the Winter General Meeting, at which time plans for participation in the Summer General Meeting were outlined. A well-organized program of papers for presentation in two sessions has been prepared.

COMMITTEE ON PRODUCTION AND APPLICATION OF LIGHT

A lively conference session under the auspices of this committee was held during the Winter General Meeting, where there was an open discussion of the problem of the measurement and control of audible noise from fluorescent lighting equipment.

At the annual committee meeting, held during the Winter General Meeting, plans were laid for an added session next year, probably in connection with the Fall General Meeting, to deal with problems of lighting as affected by the critical materials situation. It is probable that this session will be co-sponsored by the Subcommittees on Distribution Systems for Industrial Plants and Distribution Systems for Commercial Buildings of the Committee on Industrial Power Systems.

The subject chosen for the usual session at the next Winter General Meeting is "Ultraviolet Radiations." The Subcommittee on Ultraviolet Radiations will make a formal report at that time.

COMMITTEE ON MARINE TRANSPORTATION

The committee held two well-attended meetings at Institute headquarters, in May and December. It has been working on revisions to "Recommended Practices for Electrical Installation on Shipboard," as issued in December 1948. As the stock of this Standard was exhausted, the committee requested the Institute to reprint the 1948 issue with a supplementary sheet covering corrections for use until such time as the 1948 issue could be revised. It also has been working on the international standardization of electric installations on shipboard.

Subcommittee Activities. Subcommittees consist of: Power Generation, Power Applications, Wires and Cables, Switchboards and Controls, Distribution, Fittings and Appliances, Communications and Alarms, and Navigation Equipment. All of these subcommittees have been quite active, each reviewing the sections of Standard *45* under its cognizance and making reports to the main committee for action.

Industry Division

COMMITTEE ON CHEMICAL, ELECTROCHEMICAL, AND ELECTROTHERMAL APPLICATIONS

The committee held a meeting at the Winter General Meeting, at which it was decided to recommend a shorter committee name. The name of the Arc Furnaces and Electrothermal Processes Subcommittee was changed to the Electrothermal Processes Subcommittee. The name of the Petroleum Refining and Production Subcommittee was changed to the Petroleum Industries Subcommittee.

Sessions were held in Pasadena in conjunction with the Committee on Industrial Power Systems, in Oklahoma City, two at the Winter General Meeting, and one at the Southern District Meeting.

For the coming year, this committee is sponsoring a session each for the Summer, the Pacific, and the Fall General Meetings, and three sessions for the Winter General Meeting.

Electrothermal Processes Subcommittee is continuing its study of the problems of arc furnace application, and is planning a full session with emphasis on operating conditions.

Cathodic Protection Subcommittee held a meeting in Oklahoma City and one at the Winter General Meeting, and has scheduled a meeting for the Fall General Meeting. A 5-year schedule of activities has been worked out, and the subcommittee will co-ordinate its work with that of the National Association of Corrosion Engineers. A full session is scheduled for the Fall General Meeting.

Electrolytic Processes Subcommittee has a full session planned for the Pacific General Meeting on "Electrical Applications in the Aluminum Industry."

Petroleum Industry Subcommittee prepared a full session on "The Petroleum Industry in Canada" for the Summer General Meeting, and is planning two sessions for the Winter General Meeting on "Electrical Applications for Pipe Line Transportation."

Storage Batteries Subcommittee is working on the basic problem of defining storage battery capacity, and is collecting information on various types of accumulators which will appear in one or more papers.

Chemical Industry Subcommittee is planning a full session for the Winter General Meeting, and will present a summary of the properties of cable insulations suitable for chemical plants and refineries.

COMMITTEE ON ELECTRIC HEATING

The committee did not sponsor any sessions at general meetings since it was considering a possible special conference. This was finally postponed for the present because of various difficulties which arose. Instead, sessions are being considered for the Fall and Winter General Meetings.

Induction and Dielectric Heating Subcommittee has completed its work on proposed definitions, and is endeavoring to secure approval. Final assembly of proposed equipment standards is going on at present. A continuing function is co-operation with the Federal Communications Commission on reports of radio interference from heating equipment.

Radiation Measurements Above 300 Megacycles Subcommittee has almost completed its work on Recommended Practice for Measurement of Field Intensities above 300 Megacycles from R. F. Industrial, Scientific and Medical Equipments. It is expected that this will shortly be presented to the Standards Committee for approval.

Radiant Heating Subcommittee is continuing its investigation into basic information over a wide field, covering selective absorption of different wavelengths by various materials, characteristics of different heat sources, and new applications.

Technical Data Subcommittee is a new group organized to gather into working form information on the physical and electrical properties of different materials, in order to assist in solving various electric heating problems.

COMMITTEE ON ELECTRIC WELDING

During the year the "newest" activity has been expressed through the Fundamental Electric Arc Research Subcommittee. Choosing the electric arc as the field that required most work, this subcommittee has stimulated interest in the whole corps of men who are doing fundamental arc research. They have pooled the resources of several important work-centers to begin a card-index bibliography that is running into thousands of references. Summaries and translations are planned for all items. When further need arises, fine classification will be undertaken. Further steps of an ambitious program will begin after the bibliography is well consolidated.

The Subcommittee on Power Supply for Resistance Welding Machines has also made substantial progress: two of the three major sections in the Report on Power Supply for Resistance Welders are nearly complete, and the third section is well under way. It is planned to have this report printed late in 1951 so that it can be presented and fully discussed at the 1952 welding conference.

The key organization for the 1952 welding conference has been set up, and preliminary arrangements and program are under way. The meeting will be held in the Rackham Building of Detroit, as before. Subjects will be chosen in relation to the current electrical problems of the industry. Exhibits under the auspices of the American Welding Society are planned to supplement the technical papers. It is expected that the value of the new conference will at least equal that of past conferences, from which some 15 papers have been recommended for publication in *Transactions*. To carry on this work and to arrange for the technical sessions at general and District meetings, there were four committee and eight subcommittee meetings, well distributed around the northeastern industrial sections of the country.

COMMITTEE ON FEEDBACK CONTROL SYSTEMS

The membership of the committee is widely distributed over the United States and Canada, and includes liaison with the Committees on Industrial Control, Mining and Metal Industry, Basic Sciences, Computing Devices, and Instruments and Measurements, and with The American Society of Mechanical Engineers.

The entire committee met once during the year, at the Winter General Meeting. The next committee meeting is planned to be held at the Summer General Meeting. The committee was represented at the forums of technical committee chairmen held at the Fall General and the Winter General Meetings, and at a meeting of specialists to investigate the application of Nyquist's stability criteria to dynamic systems, which was held March 22 and 23, 1951, in Los Angeles, as well as at the meetings of the Industry Division Committee held at the Fall General and the Winter General Meetings.

Subcommittee on Terminology and Nomenclature. During the year four meetings of this subcommittee were held, with representation from the American Standards Association and The American Society of Mechanical Engineers. A progress report was presented as a conference paper at the Great Lakes District Meeting. The subcommittee also plans to have a report published in the July 1951 issue of *Electrical Engineering*.

Subcommittee on Bibliography. In co-operation with a similar subcommittee under the Committee on Industrial Control, this subcommittee is engaged in compiling a bibliography on feedback control systems.

Technical Papers. The committee sponsored one technical session at the Fall General Meeting and two at the Winter General Meeting. In these sessions, nine *Transactions* papers and five conference papers were presented. Interest in this field appears to be lively, as evidenced by the good attendance and discussions at technical sessions and the large number of requests for preprints and reprints of technical papers. The number of papers being submitted for consideration by the committee also appears to be growing, and enough papers are already available for technical sessions at the coming Summer General and Pacific General Meetings.

Technical paper 50-44, "A Frequency-Response Method for Analyzing and Synthesizing Contactor Servomechanisms" by Ralph J. Kochenburger, sponsored by this committee, received first prize in the Industry Group for the year 1950–51. Doctor Kochenburger also received the Alfred Noble prize for 1950.

Conference on Feedback Control Systems. The committee plans to schedule a conference on feedback control systems in the fall of 1951. The conference will afford an opportunity for persons in the industries employing feedback control systems to discuss the state of the art in its many applications.

COMMITTEE ON GENERAL INDUSTRY APPLICATIONS

The committee held a meeting and sponsored a technical session at the Winter General Meeting. The subject was "Electrical Installations in Hazardous Locations." The session was a continuation of a similar session held at the 1950 Winter General Meeting. In addition, the committee sponsored through its subcommittees two technical sessions and three special technical conferences at the Fall General Meeting. These technical conferences followed the pattern set during preceding years in holding technical conferences apart from the general meetings where industrial electrical engineers can meet others in the same or allied fields and discuss electrical applications peculiar to their branch of industry.

Subcommittee on Machine Tools sponsored a 3-day special conference on machine tools in Worcester, Mass., and Springfield, Vt., on November 14, 15, and 16, 1950, and is planning a similar conference to be held in the fall of 1951 in Rockford, Ill.

Subcommittee on Rubber and Plastics Industry has been relatively inactive during the current year due to illnesses among the personnel of the committee. However, the committee is planning a special technical conference to be held in the spring of 1952.

Subcommittee on Textile Industry. A Northern Textile Conference was held in Philadelphia on April 23, 1951, and a Southern Textile Conference in Atlanta on April 26 and 27, 1951.

Subcommittee on Pulp and Paper Industry has been planning a special technical conference to be held in the fall of 1951 in Kalamazoo, Mich. This conference will feature papers on the maintenance and installation problems encountered in this industry.

Subcommittee on Material Handling. Two technical sessions on the application of freight elevators, hoists, and conveyors are planned for the Fall General Meeting. These sessions will prove to be of interest to engineers who have charge of the selection, operation, and maintenance of material handling equipment in industrial plants and coal and ore unloading facilities.

District 7 Subcommittee. Two well-attended and interesting sessions dealing with electrical applications in the oil industry were held at the Fall General Meeting. These sessions were jointly sponsored by this committee and the Induction Machinery Subcommittee of the Committee on Rotating Machinery. A special technical conference consisting of a 1-day program on this same subject is being planned for presentation in the fall of 1951 in Houston, Tex.

West Coast Subcommittee. Two technical sessions dealing with the lumber industry and corrosion and cathodic protection are being planned by this committee for presentation at the Pacific General Meeting.

Other Activities. The subcommittee work discussed does not cover by any means all the industries which come within the scope of the committee. It is planned to add another Subcommittee on Food Processing Industry during the 1951–52 season, and this subcommittee would sponsor technical sessions for 1952 Summer General Meeting.

Conferences. The Committee on General Industry Applications believes the conferences held apart from AIEE general meetings have proved to be of immense value to industrial electrical engineers.

COMMITTEE ON INDUSTRIAL CONTROL

The committee held two meetings and sponsored technical sessions during the Middle Eastern District Meeting and the Winter General Meeting. Plans are under way for participation in the Summer General Meeting and the Fall General Meeting. The following projects have been worked on by the various subcommittees.

Standards Subcommittee is studying graphical symbols for connection diagrams to determine what symbols are needed by industrial users in addition to those now contained in American Standard *Z32.3*. Several symbols have been suggested by the subcommittee to a task group formed by the American Standards Association (ASA) to study symbols for eventual inclusion in an American Standard.

Electronic Control Subcommittee, through its working groups, has completed its work on definitions of electronic control terms. A list of definitions has been submitted to Subcommittee V of ASA Sectional Committee *C42* for inclusion in the pending revised edition of American Standard *C42* "Definitions of Electrical Terms."

Bibliography Subcommittee has completed its work on the "Bibliography on Industrial Control," which has been issued by the Institute as Publication *S39*. The subcommittee is following the contemporary literature on industrial control preparatory to an eventual revision of the bibliography.

Test Codes Subcommittee studied testing methods for behavior of electric contacts. Several papers were sponsored by the subcommittee on that subject for presentation during the Winter General Meeting. Test code sections on endurance and interrupting ability of a-c contactors and on testing temperature rise are under active discussion now.

Regulators and Feedback Control Systems Subcommittee is engaged in developing definitions of technical terms and system classifications which will eventually be discussed with other technical committees active in related fields.

COMMITTEE ON INDUSTRIAL POWER SYSTEMS

At the Summer and Pacific General Meeting, the committee sponsored one session jointly with the Committee on Chemical, Electrochemical, and Electrothermal Applications on problems in the petroleum industry. The committee also sponsored a session at the Fall General Meeting. At the Winter General Meeting, the committee sponsored one session jointly with the Committee on Relays, and two sessions on industrial power distribution, generation, and relaying. The program for a session at the Summer General Meeting is practically complete.

Executive Subcommittee. Only one meeting was held, and all other matters were settled by correspondence. The subject of an industrial power conference for next year is currently under study.

Industrial Plant Grounding. This new subcommittee has held two meetings, with the following subjects assigned to working groups: (a) System Grounding, (b) Equipment and Structures Grounding, (c) Static Grounding, (d) Earthing. It expects to present results in the form of a special publication in 1952.

Distribution Systems for Industrial Plants Subcommittee. This subcommittee, working on revision of the "Red Book," has run into difficulty with one chapter but expects to have it completed shortly.

Distribution Systems for Commercial Buildings Subcommittee. This subcommittee has not been very active since publication of the "Green Book," Special Publication *S30*, last year. About 4,000 of the 5,000 copies printed have been sold to date. Any problems or criticisms will be welcomed.

Load Characteristics Subcommittee. This newly organized subcommittee has little progress to report to date, but plans for study are being formulated.

Power Supply Subcommittee. This new subcommittee was responsible for two papers.

Codes and Standards Subcommittee. This newly organized subcommittee has a double objective, (a) to study and list minimum standards for industrial use, and (b) to keep in contact with AIEE groups working on standards problems to present the industrial point of view, as in the study made several years ago on transformers' voltage rating and taps.

COMMITTEE ON MINING AND METAL INDUSTRY

During the year the committee held two meetings, the first in Cleveland in September, during the fall meeting of the Association of Iron and Steel Engineers, and the second during the Winter General Meeting. The activity of the committee has consisted principally of extending its organization to cover its large field more effectively.

The mining industry is in two groups separated geographically and in center of interest. The first, or eastern group, located generally east of the Mississippi River, has a large majority of its members engaged in soft coal and anthracite mining. The second group consists of the hard rock miners of the West, engaged in mining copper, potash, lead, silver, gold, and other ores. Separate subcommittees were set up during the year for these two groups.

Two technical sessions on mining at the Summer and Pacific General Meeting and a session at the Fall General Meeting were sponsored by this latter group. Due to the great distances in the west, a subcommittee meeting has not been held, and some time will be required to get the organization complete.

A third group associated with both metals and mining operations is that engaged in the beneficiation of taconite. While the work in this field is developing principally around methods and pilot plants, it is expected that large-scale use of electric power will result. No special group has been set up to cover this work.

The two mining subcommittees have been working through their liaison representative with the American Mining Congress, and some work on standards is under way.

The Metals Subcommittee, in sponsoring the technical session at the Summer and Pacific General Meeting on the steel industry in the Los Angeles area and the aluminum industry in the west, reached the interest of the western segments of these two industries for the first time.

The Western (hard rock) Mining Subcommittee and the Metals Subcommittee both will give support to the Summer and Pacific General Meetings.

Liaison is being maintained with the Association of Iron and Steel engineers in the electrical phases of the steel industry.

Due to the geographical distribution of the membership of this committee, its program does not include a technical session at the Winter General Meeting, but a committee meeting is normally held during this session. Technical programs are scheduled for the Summer and Fall General Meetings, where larger attendance from the industries served is expected. With such geographically widespread membership, a directory of committee membership has been prepared for use within the committee giving a biographical sketch of each member.

Based on the experience of the committee since organization, a manual for committee guidance was prepared during the year outlining organization, scope, and procedure. This information is intended to be of assistance to the subcommittees and incoming officers.

Power Division

COMMITTEE ON CARRIER CURRENT

This committee held two meetings during the year, and plans to call similar meetings on a flexible schedule as required by the work in process. The committee sponsored technical conference sessions on carrier current matters and on microwave applications at the Summer General Meeting.

Full advantage was taken of contacts established with individuals on the West Coast to publicize the activities of this group and to solicit co-operation from interested parties. A vice-chairman representing the West Coast was appointed, and has been most effective in administering the activities among members in that part of the country, particularly in planning technical sessions at District meetings and bringing in new members.

Power-line carrier, in general, is being called upon to assume greater burdens as power systems expand through the addition of new plants, lines, and substations. This, with the tendency toward automatization, requires more channels such as power-line carrier for the burden of conveying telemetering, supervisory control, load control, and relaying signals, in addition to voice communication.

As in the past, the major part of the work has been carried on by subcommittees, each of which has followed actively its assignment.

Subcommittee for Preparation of a General Interest Paper. The work of this group has been completed and the subcommittee will be discontinued.

Subcommittee to Report on Application Guidance for Carrier Current. The work of this group is nearing completion.

Subcommittee on Methods of Measurement is studying further simplification of methods, attempting to make them foolproof, plans to provide more detail in measurements of line characteristics, and will draw up a list of the most suitable instruments for this work.

Subcommittee on High Frequency Characteristics of Power Equipment is making measurements in factories whenever the opportunity presents itself.

Subcommittee on Carrier Current Characteristics of Transmission Lines and Systems has assembled considerable data through a questionnaire and is now busy analyzing these data.

Subcommittee on Long-life Tubes is gathering information from all possible sources and will consider, in addition, tube life in microwave service.

Subcommittee on Use of Microwave Equipment for Relaying, Telemetering, and Supervisory Control. Microwave applications are fast approaching the status of an exact science, such that it is possible to predetermine performance and provide any desired order of reliability. The committee is actively in touch with all developments and will consider methods of co-ordinating with existing facilities such as power-line carrier.

Subcommittee on Operating Experience with Carrier Current Relaying Channels has assembled much information from a questionnaire and a preliminary report is in preparation.

Other Activities. A bibliography of technical material on power-line carrier is in preparation. Liaison has been maintained during the year with the Committee on Radio Communications Systems, the Committee on Relays, and the Committee on Transmission and Distribution.

The committee is planning to hold a symposium in the near future, consisting basically of: (1) One or more papers expressing the general position of power-line carrier and its value in the industry, (2) A history of the evolution of power-line carrier, as produced by the subcommittee for preparation of a general interest paper, and (3) Present status and application guide, as produced by the Subcommittee to Report on Application Guidance.

In general, the committee thinks that, judging from the interest shown, there is an adequate demand for work of the type which it has undertaken, and it is hoped that even more rapid progress can be made in the coming year.

COMMITTEE ON INSULATED CONDUCTORS

The committee has continued its active program through a total of some 90 members and special members and two regular meetings, besides special meetings of subcommittees.

Some progress has been made regarding a number of subjects during the past year, including the following: thermal characteristics of cable installed in conduit and of pipe-type cable systems; methods for determining effects of cable movement on life of sheath in manholes and the use of lead-alloy sheaths to obtain increased life; practices on vertical-riser cables; accessories for insulated wires and cables; bibliography on insulated conductors; impulse testing; and characteristics of synthetic insulations.

In addition to continuing the development of a good number of desirable papers during the past year, the committee has in prospect a fairly large number of worth-while papers for the coming year.

COMMITTEE ON POWER GENERATION

The committee held two meetings, one at the Fall General Meeting and the other at the Winter General Meeting. The activities of the committee, as reported by the various subcommittees, are as follows:

Prime Mover. A session was organized by this subcommittee for the Fall General Meeting, at which recent advances in the control of gas turbines for power generation, thrust bearing problems, and hydrogen cooling problems were discussed.

Station Design. Through the efforts of this subcommittee, a session was organized for the Winter General Meeting on the co-ordination of station design and analysis of plant operation troubles. Recent developments in power generation were discussed, together with needed improvements in stations and machines. This subcommittee is sponsoring a symposium on "Needed Improvements in Power Stations" for the 1952 Winter General Meeting.

Speed Governing. This subcommittee is now obtaining experience data on the governing and control of modern reheat steam units. These data will later form the subject of a report. Progress has been made by this subcommittee jointly with the Excitation Subcommittee in the compilation of terms and definitions.

Excitation Systems. This subcommittee organized a session for the Summer General Meeting, at which papers were presented discussing excitation experience and recent developments.

Application of Probability Methods. A session on hydroelectric plant reserve practices was sponsored by this subcommittee during the Winter General Meeting. Papers sponsored by this subcommittee made contributions to the problem of evaluating reserve savings from interconnections. The subcommittee is now exploring the possibility and desirability of further investigating the effect of station layouts on reserve capacity.

Hydroelectric Systems. A session on underground electric plants was sponsored by this subcommittee at the Summer General Meeting, in which the possibilities of underground generation were explored.

Other Activities of the Committee on Power Generation are: The committee has agreed to participate in the American Society of Civil Engineers Celebration of Centennial of Engineering in Chicago, September 1952, by sponsoring two or three papers. The committee is studying factors affecting economics of generation, and is planning a session on Power Generation Economics for the 1952 Winter General Meeting.

COMMITTEE ON PROTECTIVE DEVICES

The Committee on Protective Devices has sponsored two technical sessions, one at the Winter General Meeting, and one for the forthcoming Summer General Meeting. The committee held a meeting during the Winter General Meeting. The activities of the committee are primarily carried on by three subcommittees. The reports from these subcommittees are as follows:

Fault Limiting Devices. Application guides covering the grounding of synchronous generating systems, the method of grounding transmission systems, and the application of ground-fault neutralizers were presented at the Summer and Pacific General Meeting. These guides have been presented as Advance-Copy-Only papers and issued on a trial basis. The committee has now received comments from the membership, and has started to revise the guides to place them in final form.

The Power System Fault Limitation Working Group completed its report, which was presented at the Winter General Meeting. A survey is being conducted jointly with the Committee on Industrial Power Systems to determine present grounding practices on industrial systems. This survey will determine if there is any accepted practice or agreement in the connection of the power system neutral, that is, whether the neutral should be grounded through a resistor, a reactor, potential transformer, ground-fault neutralizer, or a combination distribution transformer and resistor.

The subcommittee has the following projects under consideration: (a) A project to set forth the factors relative to the necessity for shunting resistors or lightning arresters across reactors used for feeders or generator neutrals, (b) A project to outline the factors which determine the size and rating of grounding transformers, and (c) A project on grounding of voltage regulators on power systems.

A survey is being made jointly with the Committee on Substation Grounding to determine the present-day practices on substation grounding.

Lightning Protective Devices. The Lightning Protective Devices Subcommittee has continued its efforts to unify and co-ordinate information relating to performance characteristics, testing, and application of lightning protective devices. A major step in this program was the publication of the report on the Combined Standard for Valve and Expulsion Arresters, AIEE *28A*. This report has been out for one year, and the working group which developed it has been reactivated to study its effectiveness in the field and to consider recommendations for amendment or modification. The specification of recovery voltage conditions under which power tests of lightning arresters shall be made also will be undertaken at this time, since the necessary information has become available recently.

The performance characteristics of all types of lightning arresters are being reviewed to determine the advisability of issuing a revised report to include new makes of lightning arresters which have entered the field since the last report and the new reduced tolerances which have been established for certain types of lightning arresters.

One of the major projects remaining on the agenda of this subcommittee is that of the Application Guide for the Protection of Substations. This difficult work is nearing completion, and a preliminary report has been scheduled for the Summer General Meeting. Lack of agreement on some points and lack of necessary data have delayed this project considerably. However, recent AIEE papers have made available much of the awaited information, particularly that relating to distance effects between the protective device and the object to be protected. A survey is now under way to determine the extent and effectiveness of the practice of direct stroke shielding of substation and associated lines. This information is needed in order to complete the recommendations to be included in the application guide.

The agenda of the subcommittee includes the following suggestions which have been submitted for its consideration: co-ordination of methods for determining radio influence; rod-gap characteristics in the short-time region; protection of aerial cable; and dry-type transformers.

Co-ordination of Insulation. This subcommittee was formed primarily to keep the members of the main committee informed as to the progress that is being made by the Triple Joint Committee (consisting of EEI, AIEE, and NEMA delegations) on the co-ordination of insulation. For this reason it has not required the establishment of working groups.

COMMITTEE ON RELAYS

The committee held three meetings and sponsored three technical sessions. The technical activities of this committee were carried on through a number of project committees which were appointed to fulfill specific assignments. Following are the reports of the various project committees:

Generator Protection. This committee has completed its investigation of the various methods of a-c generator protection used in this country and Canada. On the basis of a survey made last year, a report was prepared recommending practices preferred for application to new installations, which was presented at the Winter General Meeting. The committee report and the discussions of it have been released for publication in the *Transactions.*

Bibliography of Relay Literature. This project committee presented a "Bibliography of Relay Literature, 1947–49" at the Winter General Meeting. The committee will continue to maintain an up-to-date bibliography in future years.

Co-ordination of Construction and Protection of Distribution Circuits. This project committee is a joint working group of the Committee on Relays, the Distribution Subcommittee, and the Edison Electric Institute Transmission and Distribution Committee.

This working group is now in the process of writing a first draft of a report on the Performance of Distribution Circuits from which operating data were obtained for the year 1949. The report will contain information relative to the number of faults occurring on these circuits and a breakdown of the causes of these faults into the number initiated by lightning, glaze, wind, trees, and other causes. It also will contain information covering the performance of different types of protective devices in preventing faults of a temporary nature from becoming permanent. The first draft of the report is not yet complete, but it is expected to be finished and available for the Fall General Meeting.

Standards for Power Relays. In 1949 this committee completed a revision of ASA Standard *C-37*, American Standard for relays associated with electric power apparatus. During the past year considerable information was gathered on performance specifications which will ultimately be added to the present Standard ASA *C37.1*. In analyzing the material, it became apparent that this phase of the work fell outside the scope of the Committee on Relays, and steps were taken to have a committee in the National Electrical Manufacturers Association take on this phase of the Standard. Such arrangements were made, and a committee is now actively engaged in preparing performance standards for relays.

Transmission-Line Protection. The project committee on transmission-line relaying has as its objective the preparation of a report describing current practice and trends of thinking in transmission-line protection. In order to develop material, two conference sessions and one technical session have been sponsored, and a questionnaire on backup practice has been distributed and replies analyzed. There is still lacking an adequate paper on ground relaying, and a further single question on backup relaying is to be circulated to members of the main committee. Arrangements are being made for a paper on ground relaying and one on backup relaying. When these are available, it will be possible to prepare a final report of the project committee.

Electronic Relay Applications. This project committee was relatively inactive during the past year, its principal function being to follow developments in electronic protective relays. Developments in this area consisted mainly of the use of microwaves in transmission-line relaying and in transferred tripping. New developments in transferred tripping via carrier current are being reported by another project committee.

Relaying of Interconnections Between Industrial and Utility Generating Systems. This project committee, in co-operation with the committee on Industrial Power Systems, sponsored a conference session at the 1951 Winter General Meeting. The project committee presented a conference paper at this session which was based on a questionnaire on the practice of utility-industrial relaying that had been answered by 32 companies. There has been some discussion of the presentation of additional papers on practices of the relaying of interconnecting transmission lines between industrial and utility systems.

Pilot Wires. A questionnaire has been prepared by this committee for circulation to the industry to obtain information relative to operating experience with pilot wire circuits, leased and privately owned, used for protective relays. The questionnaire covers the years 1942–1950 inclusive. It is proposed to prepare a report summarizing the information obtained from the answers to this questionnaire.

Remote Tripping Schemes. The objective of this committee is to collect information on remote tripping schemes and the operating experience that has been obtained. A questionnaire has been prepared, and has been sent to various operating companies, requesting data on the design of equipment that has been installed and on operating experience. The results obtained from this questionnaire will be presented to the Institute in the near future.

Test Methods. This committee has been collecting data from available sources on portable field testing equipment suitable for testing the majority of the more complicated types of relays. The data are being reviewed by the project committee, and it is expected that eventually information on this equipment will be presented to the Committee on Relays.

Consideration is being given to the sponsorship by this committee of a conference session at one of the 1951–52 general meetings. This will make possible an exchange of ideas on test methods and test equipment.

Effect of Vibration and Shock on Relays. This committee was formed to study the effects of vibration and shock on relays used in electric power systems in industrial applications. Some progress has been made in the study of existing installations by making actual measurements of available equipment. A questionnaire has been circulated covering the troubles that have been experienced with relays in existing installations. From the information which is being obtained from various sources, the committee proposes to prepare an Institute paper offering a suggested guide which should be useful to the industry in designing and applying protective relays to avoid difficulty from shock and vibration.

Joint and Associated Projects. The committee participates in the activities of the Instrument Transformer Subcommittee of the Committee on Transformers, with special attention to the relaying performance of current transformers and the transient performance of capacitance potential devices. The latter committee has been very active this past year in examining the problems associated with the use of capacitance potential devices for relaying purposes. The Committee on Relays has maintained close co-ordination with the activities of the Committee on Carrier Current on items of joint interest.

COMMITTEE ON ROTATING MACHINERY

The committee held a meeting during the Winter General Meeting. Committee activity is largely carried on by correspondence and through its subcommittees. The outstanding feature of this year's activity was the group of sessions on insulation at the Winter General Meeting. This old subject needed only an outlet to bring out a torrent of 15 papers on insulation. It is expected that, with present rapid developments, insulation will be an active subject for several years.

One new subcommittee is being formed to cover magnetic fluid couplings and clutches, the magnetic particle clutch, electric coupling, eddy current coupling, eddy current brakes, eddy current dynamometer, and electrically operated friction brakes where the magnetic circuit is part of the brake itself, but to exclude electrically operated friction brakes and clutches where the electrical part is simply a magnet of solenoid providing a pull to operate a completely mechanical device.

Synchronous Machinery Subcommittee. Seven papers were processed and presented. Revisions have been recommended in the test code, and under consideration is a new method for testing subtransient reactances. The first draft of the synchronous section of the revised ASA *C-50* has been received for review. Under consideration is the upward extension of standard voltage ratings for synchronous generators above 90,000 kva. Papers may be solicited on this question.

Insulation Subcommittee. An unusually successful group of sessions was held at the Winter General Meeting. Future projects include a-c and d-c overvoltage testing values for machines in service, overvoltage testing of turn to turn insulation, and a review of classifications of insulation in AIEE Standard *1*.

Induction Machinery Subcommittee. Test Code Number *500* is now almost completely rewritten. Copies of the revised draft will soon be available for general committee review. A symposium has been suggested on the application of motors with particular emphasis on papers of value to the users of motors.

D-C Machinery Subcommittee. Active work is being done on transients and short-circuit currents in d-c machines. Similar work on flashover is being considered. Transients and protection of d-c systems on aircraft are also on the agenda.

Single-Phase and Fractional Horsepower Subcommittee. A special technical conference will be held in Dayton, October 11 and 12, 1951. Application of small motors to refrigeration and pumps is the main topic for this session, which is jointly sponsored with the Domestic Appliances Subcommittee. The test code is being actively revised, still requiring correlation with the master test codes.

Test Code Co-ordinating Subcommittee. This committee is working actively with the ASA *C-50* committee toward revision of test codes so as to be directly usable in the test code section of ASA. Requests have been made for master test codes for radio noise measurement and for speed measurement.

COMMITTEE ON SUBSTATIONS

The status of the projects on which work is in progress in the subcommittees and working groups of this committee is described here.

Automatic and Supervisory Control Subcommittee. This subcommittee concluded work on rectifier reclosing control problems, grounding practices on d-c switching structures, and protection of conversion units feeding high capacity d-c busses.

Distribution and Conversion Substations Subcommittee. The project on "Bus Regulation versus Feeder Regulation" finally culminated in a set of papers at the Winter General Meeting. This project is now closed. Work is still continuing on the project covering "Breakers versus Reclosing Fuses" and "Basic Structural Design of Outdoor Stations." Projects on "Lighting of Substations" and "Standardization of Factory Designed and Constructed Substations" are being pursued to some extent.

Transmission Substation Subcommittee. A report on a project covering "Basic Structural Design of Substations" is expected to be ready soon. Little progress has been made on the "Safety Considerations in Substations" project.

Device Function Numbers Working Group. No activity was necessary during the year.

Substation Grounding Practice Working Group. A questionnaire was circulated and replies are now being studied. A report is forthcoming.

Rectifier Switchgear Working Group is studying grounding practices and recommendations for d-c switchgear in outdoor substations.

Committee Meetings. In addition to meetings of the subcommittees and working groups, meetings of the main committee were held in Pasadena in June 1950, and in New York in January 1951. A technical session under the sponsorship of the committee was held at the Winter General Meeting.

COMMITTEE ON SWITCHGEAR

The activities of the committee have largely comprised work on revision of present AIEE Standards *20*, *25*, *27*, and *50*.

Proposed Standard *20A* on Low Voltage Air Circuit Breakers was published in December 1946, and is still on a trial basis. A complete revision of this standard was approved by the committee on October 17, 1950, and submitted to the Standards Committee on November 21, 1950. No action has as yet been taken by the Standards Committee, but it would seem very desirable to get this standard issued as speedily as feasible, since the present Standard *20* was issued in 1930.

Work is in progress on a revision of Standard *25*, "Fuses above 600 Volts." The subcommittee working on this expects to have the work completed shortly.

A complete revision of Standard *27* on Switchgear Assemblies was also approved by the committee at the October 17th meeting, and submitted to the Standards Committee on November 24, 1950. Action on this standard is very much desired since a considerable amount of new material is contained in the revision which did not appear in the present standard issued in August 1942. The addition to Standard *27* of Standards to cover isolated phase busses is now under consideration.

Proposed Standard *50* for Automatic Circuit Reclosures issued in September 1949 for trial use is being worked on for submission as an approved standard. This work is progressing nicely, and it is hoped that it will be ready in the near future.

It is expected that revisions to Proposed Standards *22A* on Air Switches, Insulator Units, and Bus Supports, issued for trial use in October 1949, will be ready for action during the coming year. A working group is being organized for the purpose of preparing a standard for ice testing of disconnecting switches.

The Circuit Breaker Subcommittee has also completed the work of making revisions in ASA Standard *C-37* on Power Circuit Breakers. This has involved co-operation with other interested committees and standardizing bodies. These proposed changes will be presented shortly for approval. A Test Code for Power Circuit Breakers and one for Low Voltage Air Circuit Breakers are being prepared.

Two committee meetings were held. The committee sponsored one session at the Fall General Meeting and one at the Winter General Meeting. One joint session was also held with the Committee on Transmission and Distribution on the subject of capacitor switching at the Winter General Meeting.

During this year a new subcommittee was formed to consider the design and application of network protectors. The need of some standardization for generator voltage regulators is also being given some consideration by the Switchgear Assemblies Subcommittee.

COMMITTEE ON SYSTEM ENGINEERING

This committee is about to finish its fourth year of existence, and is continuing its original subcommittee organization, which is: (1) Administrative; (2) System Planning; (3) System Operation; (4) System Economics; (5) System Controls; and (6) Interconnection Contracts.

The committee's technical program for the year ending April 30, 1951, began with a session on system planning at the Summer and Pacific General Meeting. During the year it conducted a number of technical and conference sessions on the subjects "The Effect of Low Voltage and Low Frequency on Power Plant Auxiliaries" and "Determination of Reserve Capacity by the Probability Theory"; and a symposium on "Determination of What Units in What Plants should be Used for Loan and Frequency Control."

Three committee meetings were held, an all-day meeting in Chicago on May 4, 1950, with separate subcommittee meetings as part of the agenda, and meetings at the Fall and Winter General Meetings.

In conformity with the committee's general plan of having a subcommittee sponsor a technical session for an individual general meeting, the System Economics Subcommittee is preparing for a session at the Fall General Meeting dealing with the general subject of "What the Basic Factors Should be for the Comparison of Alternate Facilities." The System Planning Subcommittee has undertaken to arrange for a program for the Winter General Meeting.

COMMITTEE ON TRANSFORMERS

The committee has progressed in the various topics under investigation, as indicated by the following reports:

Co-ordinated Study of Life of Transformer Insulation Working Group. A progress report dealing with the co-operative tests on aging of high-temperature insulations was presented at the Winter General Meeting. All of the technical difficulties of getting this started have now been completed, and the tests are under way.

Joint Working Group on Instrument Transformers. A report on the changes in the standards for instrument transformers was presented at the Winter General Meeting. The report deals with the clarification and modification of ASA *C57.13* and *C57.33*. A paper on the study of transient characteristics of potential devices is now complete and will be presented at the Summer General Meeting.

Magnetization Characteristics of Transformers Working Group. The work of this group was presented at the Winter General Meeting. It deals with magnetization characteristics, relaying problems associated with excitation current of transformers, and a survey of air switch practice.

Revision of Dielectric Tests Working Group. A report on the activities of this working group was presented at the Winter General Meeting. The group has submitted a report to the Committee on Transformers for approval.

Guides for the Operation and Maintenance of Dry Type Transformers with Class-B Insulation Working Group. A complete report of this group's activity was submitted at the Winter General Meeting. The group is now awaiting letter-ballot approval by the main committee. This report covers an entirely new field of investigation.

Co-ordination of Insulation Working Group. Work in this group has been completed for the 115-kv basic-impulse-insulation-level range and higher.

Methods of Making Temperature Tests Working Group. The work of this group consisted of general revision of ASA *C57.22* and was issued as a preliminary report at the Winter General Meeting for comments. The report has been revised and the final report will be submitted to the main committee for approval.

Audible Noise in Transformers Working Group has been enlarged to include those having field experience now that the method of conducting the study has been completed. Work is progressing satisfactorily.

Hot Spot Temperature Rise of Class-B Reactors Working Group. The trial period for the 110-degree centigrade hot spot, set more than a year ago, has now expired and this subject will be reviewed again, taking into account all the comments received.

Permissible Maximum Oil Temperature Rise in Service Working Group has almost completed a report which will be issued shortly.

Insulating Fluids Working Group is a new group formed this year to study and make recommendations on some of the problems in which insulating fluids are involved.

COMMITTEE ON TRANSMISSION AND DISTRIBUTION

Considerable progress has been made during the past year in the several fields of activity within the committee scope, through the planning of the main committee, the efforts of the subcommittees, and technical papers which have been presented at practically all the major general meetings of the Institute.

In the lightning and insulator field, the Lightning Bibliography covering 1936–1949 was completed and made available in pamphlet form at Institute headquarters. Copies of this are still available for those who now are, or later expect to be, interested in this field. The committee report on predetermining the lightning performance of transmission lines has been completed and published. Experience in insulator washing under contaminated atmospheric conditions and considerations of insulation co-ordination were presented in papers at the Middle Eastern District Meeting. Other papers on lightning performance of transmission lines have been presented, or are in prospect at the present time.

In the power capacitor field, papers were presented at the Winter General Meeting dealing with features of design and operation of large capacitor banks. A bibliography on this subject is now in the course of preparation. The application of series capacitors to high-voltage lines is to be treated in a series of papers at the Pacific General Meeting.

In the distribution field, a report on rural-line sectionalizing was presented at the Winter General Meeting, and a presentation on economics of primary design is planned for the Summer General Meeting.

Conductor vibration on high-voltage lines has received considerable attention in the Towers, Poles, and Conductors Subcommittee, and a comprehensive symposium was held at the Fall General Meeting. Discussion, work, and further consideration on this subject are still going on. Another subject in which there is considerable interest at the present time is the possibility of more heavily loading transmission-line conductors.

Of outstanding interest during the past year has been the presentation of field test results on corona and radio influence as determined on an experimental high-voltage line operating as high as 525 kv. As a result of these field tests, extending over some three years, the announcement has come of a new high-voltage line designated as 300/315 kv, which probably will operate as high as 345 kv, phase-to-phase. Sections of this line are now under construction.

Looking to the future, the work in the committees of particular interest is: (1) The joint study with the Edison Electric Institute on line outage experience of high-voltage lines over a large part of the country, on which a preliminary report will be presented at the Summer General Meeting; (2) An investigation of rates-of-voltage rise on distribution systems which will be of use in applying lightning protective devices; (3) A study of lightning insulation characteristics of wood, air, and porcelain in series; and (4) Application of series capacitors on high-voltage systems.

The committee is continuing to function, as in the past, with the main committee acting as the discussion and advisory group, where all matters of importance and significance are presented and discussed and then delegated to the subcommittees for the constructive action and carrying through to a conclusion. In addition to the specific work carried on by the committee itself, there have been quite a number of technical papers offered to the committee on more general, but related, subjects. These have been reviewed and processed for publication, or other disposition as recommended. To date, there is no backlog of approved technical papers in the committee which have not been scheduled for publication.

Science and Electronics Division

COMMITTEE ON BASIC SCIENCES

The Committee sponsored eight papers describing advances in the theory of transmission circuits at the Winter General Meeting. The committee also held a meeting at which decisions were taken to establish a Subcommittee on Dielectrics and a Subcommittee on Defense.

It has long been thought that the Subcommittee on the Electrical Properties of Solids and Liquids has too broad a field and that the subject of dielectrics could be properly isolated from this general field and considered apart from metals and semiconductors. Accordingly, the new subcommittee on dielectrics is to have the following scope:

> To foster and promote symposia on the basic aspects of the electric insulation field, to disseminate information on progress being made in the fields of dielectric theory and practice for the general purpose of serving the design and development engineer who will eventually apply this information to practice, to bring to the Institute some of the results of the activities of the National Research Council conference on electric insulation.

The members of the Committee on Basic Sciences, after a talk by Colonel W. M. Young on the problems of the armed services, decided that a Subcommittee on Defense to help the armed services with the basic technical problems should be established with the following scope:

> To make available to the armed services such information on the basic sciences that would expedite their efforts in the solution of defense problems, and to co-operate with the armed services in whatever way they desired in order to strengthen the defense of our country.

It was suggested that three members of the armed services—one from the Army, one from the Navy, and one from the Air Force—be invited to become members of this subcommittee and that the subcommittee recruit as members several civilian experts in various fields of basic knowledge.

The work of the Committee on Basic Sciences is unique. It not only promotes advances in the fields already familiar to the profession but also attempts to acquaint engineers with new developments in the fields of physics and mathematics which are of interest to the profession. Hence, besides these newly established subcommittees, the Committee on Basic Sciences sponsors and co-ordinates the activities of six other subcommittees. The reports of the chairmen of these subcommittees follow.

Subcommittee on Magnetics held one meeting in 1950, and arranged for a symposium on "Magnetic Materials at High Frequencies" which was held during the Winter General Meeting, with four invited papers, and was well attended. Two of the papers are to be published in *Electrical Engineering*. Another project of the subcommittee has been to prepare a list of people in this country who are actively interested in magnetism. The list now comprises about 150 names and is a help to the subcommittee in its work; it is available to members of the Institute. A number of Institute papers on magnetism have been reviewed.

Subcommittee on the Electrical Properties of Solids and Liquids sponsored a conference during the Winter General Meeting at which four conference papers dealing with the properties of semiconductors were presented. The purpose of these papers was to acquaint the profession with new developments in the field of semiconductors. Interest in this field was shown not only by the attendance but also by the discussion of the papers.

Subcommittee on Electric Circuit Theory presented a symposium at the Winter General Meeting on "New Techniques of Network Synthesis," at which four outstanding specialists in network theory presented invited papers. The talks were concerned with the generation of functions suitable for network synthesis and the construction of realizable networks therefrom. The session was well attended and the interest in the papers was manifested by the energetic discussions which took place. At a later meeting of the subcommittee, it was decided to consider the publication of a pamphlet which would contain selected papers presented at this symposium and other successful network symposia held in the last two years. Further, it was decided that, in view of the success of the symposium at the Winter General Meeting, a similar session would be organized for the Fall General Meeting.

Subcommittee on the Electrical Properties of Gases held three meetings. The primary purpose of the first two meetings was to complete plans for a technical conference on electrical breakdown in gases, which was held during the Winter General Meeting, with four conference papers presented. The conference was well attended, and interest in this general topic was shown through the discussions which followed it. The subcommittee also held a meeting of its membership for the purpose of planning a program for the 1952 Winter General Meeting. The tentative subject of this conference is fundamental processes in gas discharge tubes. The subcommittee also reviewed several papers.

Subcommittee on Applied Mathematics has tried to implement the program it proposed during the last year whereby a group of mathematicians would be made available for the solution of problems presented by the AIEE membership. In order to popularize the program, the chairman of the subcommittee published an article in *Electrical Engineering* outlining the proposal and inviting Institute members to take advantage of the free services offered by the mathematicians who were made members of the subcommittee. So far, only four problems have been submitted, and these have been referred to the mathematicians for solution. It is sincerely hoped that more Institute members will take advantage of the opportunity to avail themselves of the free services of outstanding mathematicians.

Subcommittee on Energy Sources held a meeting and sponsored one conference, its fifth, on energy sources during the Fall General Meeting. It is planned to have the sixth conference on energy sources during the 1952 Winter General Meeting.

COMMITTEE ON COMPUTING DEVICES

Work in the field of large-scale computing has progressed rapidly during the year, and many of the projects and applications which were plans only a few years ago have now been achieved, or appear close to achievement. The large-scale computer field has two important aspects: research and development in the production of large-scale computers, and the applications of these machines. In research and development, there have been many improvements, and former potentialities, such as high-speed memories having far greater capacities than even thought of several years ago, now appear to be rather definite possibilities.

In the field of application, there are over and above the applications in the physical sciences for computing, control, and so forth, important applications both present and potential in number theory, mathematical table making, analysis of large-scale data in the field of statistics, business applications, and management applications, as well as a large group of miscellaneous potential uses sometimes of a rather unusual character. In number theory, there have been computations carried out in certain cases which have in a short time doubled all the work done in past years. In table making, the tables issued by the Harvard Computational Laboratory and by others have substantially shown that the big machine is taking over this complete field as far as major projects are concerned. In the handling of large amounts of data, probably the most important single test will be the use of the large electronic machine being built for the Bureau of Census and now nearing completion. If this proves a success, it should be the forerunner of a large number of others for similar applications.

In the field of business, planning usually proposes combining many procedures and making automatic many manual operations by means of large-scale computers, with much saving in time and in cost indicated. In the field of management, problems of the logistics type which often can be linearized into a multitude of simultaneous equations may be handled on large-scale computers to obtain optimum results. One machine for this particular purpose is now being constructed. In addition to all these, there are the simulators and other large special purpose machines, both analogue and digital, the use of which has increased greatly in the last few years. One paper presented an application of a small computer to an economic problem, and it is known one of the Armed Services is actively investigating the use of large-scale computers for determining effects on the entire economy of major changes in industrial requirements.

The Committee on Computing Devices has thought that one of its primary duties is to perform an educational function by calling the attention of members to the computing machine field. To this end, it arranged one or more sessions each at the Summer, Fall, and Winter General Meetings, as well as at three District meetings, and has under way plans for sessions at the 1951 Summer and Pacific General Meetings.

The subcommittee on preparation of a bibliography is preparing a bibliography of a basic character which, though it will not be long or comprehensive, will be selective and of the type which is hoped will enable a fast review of progress to date with a minimum of effort. This bibliography should be available as an AIEE publication during the coming year.

The Committee on Computing Devices was joint sponsor of the conference on electron tubes for computers, held in Atlantic City in December 1950. The committee has an active subcommittee which has taken the initiative in preparing plans, jointly with IRE and Association for Computing Machinery for another conference, probably to be held late in 1951.

COMMITTEE ON ELECTRONIC POWER CONVERTERS

The committee activities have consisted mainly of the preparation of reports summarizing available information and outlining recommended practices, and the presentation of papers describing new developments and applications of interest. One technical session was held at the Summer and Pacific General Meeting, and a conference session on "New Types of Rectifiers" was held at the Winter General Meeting.

Plans for the year were outlined at a meeting of the Administrative Subcommittee held on October 16, 1950, in New York. A meeting of the committee was held during the Winter General Meeting. The committee also met with the Electron Tube Subcommittee of the Committee on Electronics at a joint luncheon meeting on the same date.

The following progress has been made on the various committee projects:

Report on Inductive Co-ordination Aspects of D-C Systems Supplied by Rectifiers. This report has been completed, and it is scheduled for presentation at the Summer General Meeting and publication in *Transactions*. It was prepared by a working group of the Subcommittee on Applications.

Bibliography on Electronic Power Converters. The Subcommittee on Papers and Speakers has begun the preparation of a supplement to the Bibliography for the years 1948, 1949, and 1950.

Standards for Hot-Cathode Power Converters. The Subcommittee on Hot-Cathode Power Converters has prepared a list of definitions for hot-cathode power converters. It is presently engaged in preparing material for sections of standards and test code.

Report on Rectifier Cooling and Corrosion Problems. A working group has been appointed to prepare a report summarizing the available information on rectifier cooling and corrosion problems and outlining recommended practice. It is expected to complete the report sometime within the next year.

Conference on Power Tubes in 1952. The Committee on Electronic Power Converters and the Electronic Tube Subcommittee of the Committee on Electronics are planning to sponsor a joint conference on power tubes in April or May, 1952. This will be a 2-day conference, and is expected to draw an attendance of 200 or more. Committees are now engaged in selecting a location and planning the program.

West Coast Subcommittee. This subcommittee is planning to hold a technical session at the Pacific General Meeting. It is soliciting papers of particular interest to rectifier users.

Subcommittee on Mechanical Rectifiers. In view of the continuing development and growing application of mechanical rectifiers, it has been decided to form a new Subcommittee on Mechanical Rectifiers.

COMMITTEE ON ELECTRONICS

The committee has continued to support specialized 2- or 3-day conferences in specific work areas. Such meetings during the period covered by this report have been:

A 3-day symposium on improved quality electronic components in Washington, D. C., in May 1950.

The third annual joint conference on electronic instrumentation in nucleonics and medicine, held in New York in the fall of 1950.

The annual conference on electron devices, held at the University of Michigan, Ann Arbor, in June 1950. This was sponsored jointly by the IRE Committee on Electron Tubes and Solid State Devices and by the Subcommittee on Electron Tubes of the Committee on Electronics. The attendance was excellent. This was in a sense an experiment on the part of the AIEE group, as for many years this conference has been an annual affair operating entirely within the IRE organization. The 1950 conference represented a very satisfactory co-operative effort.

A 2-day conference on electron tubes for use in electronic computing devices, held in Atlantic City in December 1950.

National Electronics Conference (NEC). This 3-day conference, held annually in the fall in Chicago, is a very large middle-western forum for the presentation of papers of electronic interest, incorporating an extensive manufacturer's display of electronic instruments and new products; the *Proceedings* of the NEC, published annually, contains in complete form the papers presented at the NEC. The Committee on Electronics has continued the policy of giving substantial support to the NEC. During the calendar year 1951, the Chairman of the committee is also serving as Chairman of the Board of Directors of the NEC.

Active plans are currently under way for the following conferences:

A conference on electron tubes for power conversion in industrial control equipment, somewhat similar to the one on electron tubes held in Buffalo in the spring of 1949.

The annual electron devices conference, to be held in June 1951 at the University of New Hampshire.

The conference on electronic instrumentation in nucleonics and medicine has become well established as an annual affair, and plans are in process for holding it again in December 1951.

Meetings of the committee were held at the Summer and Pacific General Meeting; at the National Electronics Conference; and at the Winter General Meeting.

At the fall meeting in Chicago, the primary subject of discussion was the question of the appropriate size for the committee, in view of the objectives it is pursuing. As a result of the discussion, the committee concluded that it is not desirable to separate the electron tube subcommittee activity, because of the very great profit that accrues both to the electron tube group and the circuit activities represented in the committee by their mutual association and contact. Also, it became quite apparent that the committee represents not only activities in very special fields requiring specialized talent for their carrying-out but also serves as a valuable forum for the exchange of opinions and judgments as to the proper future program of electronics activities within the AIEE. Thus, many of the members of the committee are valuable because of the responsibility they feel toward giving advice and counsel to the group as a whole and in helping to orient its program, even though their present participation in work activities is modest.

As to organization, the committee has two types of subcommittees: subcommittees active in special technical fields, and subcommittees having specific functional interests relative to all technical aspects of the committee's work.

The following are the subcommittees in special technical fields.

Electron Tubes. This subcommittee has working groups engaged in the preparation of standards and program planning as follows: (1) High Vacuum Tubes, (2) Cathode-Ray Tubes, (3) Hot-Cathode Gas Tubes, and (4) Mercury-Pool Tubes. It was responsible for two technical sessions at the Winter General Meeting. One of these dealt with radiation detection devices and the other with power tubes for electronic heating. Both sessions were concerned primarily with the design phases. The subcommittee has active working groups on mercury-pool tube standards, and is working on standards for radiation detection devices. It was the responsible agent of the main committee for the 2-day electron devices conference in June 1950 and for the 2-day conference on electron tubes for computers in December 1950.

X-Ray Tubes, Apparatus, and Applications. This subcommittee held three meetings during the year, under environments permitting close association with members of the major societies of medical radiologists. A 5-paper symposium on X-ray equipment and applications was held at the Winter General Meeting, jointly sponsored by this subcommittee and the Committee on Therapeutics. As to standards, a report on X-ray tube graphical symbols has been completed, and the work on definition of terms is being carried forward; it is hoped that this will be completed during 1951. The next study will be that of specifications of characteristics and ratings of tubes used for X-ray equipment.

Electrostatic Processes. This subcommittee arranged two programs involving interesting demonstrations for the Winter General Meeting in January, and has completed arrangements for a technical session at the Summer General Meeting. The standards activity, initiated as an outgrowth of a conference paper presented in January 1950, is continuing, and working groups have been established.

High-Frequency Conductors, Cables, and Connectors. This subcommittee has been active in maintaining AIEE contact with developments within its scope. As a result of discussions at recent meetings of the subcommittee and of the Committee on Electronics, it has seemed desirable to expand the scope of this subcommittee somewhat, and the size of the group is being expanded and reinforced to handle its change of interest. It is expected that a technical session will be organized by the group in the near future.

Liaison with Nucleonics. This is a 1-man subcommittee, the objective of the activity being to maintain an adequate correlation with the work of the Committee on Nucleonics, and similar activities in other professional societies.

Electronic Aids to Navigation. This is a 1-man subcommittee whose function is to maintain adequate correlation with related work within the Committee on Communication, and with appropriate groups in the IRE.

Electronic Aids to Geophysics. This subcommittee, having to do with electronic equipment used in geophysical exploration primarily for the oil industry, is centered in the southwestern part of the United States. Its principal activity has had to do with the planning phases of a technical session sponsored by the Committee on Electronics at the 1950 Fall General Meeting.

Infrared Applications. This subcommittee has continued to study the specific problems of infrared instrumentation, nomenclature, and the broadening of the knowledge of infrared techniques among engineers. A set of definitions has been submitted through appropriate channels to the American Standards Association (ASA) and the American Society for Testing Materials (ASTM) committees on definitions of technical terms, and is being revised and supplemented for possible use as a committee report. A study was started to seek better testing and evaluation standards for photoconductive detectors used in infrared equipment. Liaison with the ASTM-ASA Committee on Nomenclature and Applied Spectroscopy has been continued with particular reference to infrared terminology.

Electronic Methods in Food and Biological Processing. This is a 1-man subcommittee whose responsibility has been to maintain active contact, particularly on the West Coast, with possible electronic methods for the objectives suggested by the title.

Magnetic Amplifiers. This subcommittee has been extremely active, particularly in the sponsorship of technical programs at the Summer and Pacific Meeting and the Winter General Meeting. The work-load of this committee and its importance has grown to a point where it has been made a technical committee of the Institute.

Electronic Applications of Semiconductor Devices. This subcommittee arranged a very successful technical conference as a part of the program of the Winter General Meeting. It has participated in joint standards planning with a similar group in the IRE. This subcommittee has also had an active part in the joint sponsorship, with the IRE, of the conferences on electron devices held in June 1950, and planned for June 1951.

Electronic Heating Liaison. This is a 1-man subcommittee charged with the responsibility of maintaining adequate contact with other groups within the AIEE active in the use of electronics for induction and dielectric heating. This subject matter is the primary responsibility of the Induction and Dielectric Heating Subcommittee of the Committee on Electric Heating. During the past year the AIEE contributions to this activity have included preparation of effective standards required to place this industry on a sound footing. The industry in general is using many of these standards, although they are still in subcommittee status. The subcommittee's liaison has been very successful in keeping the main committee informed in regard to the substantial activities in this field by other committees of the AIEE, and associated groups within the IRE and NEMA.

Electronic Systems Engineering. One of the responsibilities of this subcommittee is to maintain an alert attitude toward making available to the AIEE membership material on electronic systems engineering that has its origin in military needs but which, at an appropriate time, can be declassified and presented to the professional societies. This subcommittee was responsible for the arrangement of a technical session held at the Fall General Meeting.

Electronic Circuit Components. This subcommittee was organized during the past year, its scope involving attention to preparation of standards and planning of technical programs relative to good engineering practice for quality electronic components (passive) including miniaturization. One of the reasons for the organization of this subcommittee was the great interest in passive components apparent at the quality electronic components conference in May 1950.

The following are the functional subcommittees.

Electronic Standards and Definitions. It is the responsibility of this subcommittee to maintain adequate orientation and stimulation among the other subcommittees regarding the general planning of standardization in the electronics field. This subcommittee has periodically presented to the committee as a whole reviews of standards problems in various areas of electronics.

Liaison with IRE. This is a 1-man subcommittee, the objective being to maintain a close contact in regard to policy matters of technical committee work with corresponding groups in the IRE.

Liaison with JETEC. The responsibility of this subcommittee is to maintain an active, informative contact with the Joint Electron Tube Engineering Council, particularly in relation to policy and planning objectives of the committee's work.

Education in Electronics. The objective of this subcommittee is to maintain a continuing review and cognizance of change and reorientation in matters of education in electronics, both in the universities and in the adult education field. This subcommittee periodically arranges conference programs at general meetings of the Institute, the last having been held during the Winter General Meeting. These sessions have been marked by very active discussion and a generally high level of audience participation in the program. The subcommittee also provides liaison with the Committee on Education.

Papers Review. The primary responsibility of this subcommittee is to handle matters connected with review of papers of the *Transactions* type. In addition, this group has organized conference-type meetings as part of general meetings of the Institute. Two such meetings, devoted to "New Electronic Devices," were held at the Winter General Meeting, and one on the general subject of "Research Administration in Electronics" is planned for the Summer General Meeting.

West Coast Subcommittee. This is a relatively informal but very active subcommittee, whose leadership during the past two years has been provided by the West Coast Vice-Chairman of the Committee on Electronics. This subcommittee accepted the entire responsibility for the organization and planning of three technical sessions held at the Summer and Pacific General Meeting. Particular attention was devoted in these sessions to problems in equipment for nuclear particle accelerators, in collaboration with the Committees on Nucleonics and on Electronic Power Converters, and to new instrumentation techniques in the electronics field. All of the meetings were very well attended, and there was active audience participation.

General. The activities in supporting technical and conference sessions at general meetings of the Institute during the past year total 15 full sessions, with four shared by other committees.

COMMITTEE ON INSTRUMENTS AND MEASUREMENTS

The activities of the committee have been quite varied and numerous. The western division of the committee was strengthened to provide adequately for an active instruments and measurements program in that area. Membership is equally divided among educational institutions, government and private laboratories, utilities, and manufacturers, and covers all major fields of instruments and measurements.

The committee has two vice-chairmen, one for the activities of the East and one for the activities of the West. In addition to having a general secretary located in the East, a secretary for the West was appointed to assist the western vice-chairman. The increase in the number of instruments and measurements *Transactions* papers and technical sessions of that area is a definite endorsement of this western expansion policy.

The first committee meeting of the year was held October 2, 1950, to formulate the plans for the coming year. A luncheon meeting was held during the Winter General Meeting. A third meeting was held April 4, 1951, at the National Bureau of Standards, to complete plans for forthcoming meetings and to discuss subcommittee reports. A luncheon and a tour of the Bureau followed the meeting.

Changes

Subcommittee on the Preparation of a Master Test Code for Temperature Measurements has been discontinued, since the Test Code AIEE *551* was issued August 15, 1950.

Subcommittee on Electrical Aids to Medicine, which was a Joint Subcommittee of the Committees on Instruments and Measurements, Electronics, and Therapeutics will become a main committee August 1, 1951. It will be called Committee on Electrical Techniques in Medicine and Biology, and will replace also the Committee on Therapeutics.

Subcommittee on a Master Test Code for Speed Measurements has been established at the request of the Test Code Co-ordinating Subcommittee of the Committee on Rotating Machinery.

Subcommittee on Recorders and Controllers has been created.

Subcommittee on Navigation Instruments has been formed.

Activities of Subcommittees

Subcommittee on Organization is investigating the existing structure of the main committee to determine the feasibility of reorganizing it in a manner somewhat similar to a Division.

Subcommittee on Revision of Standard Number 4, Measurement of Test Voltage in Dielectric Tests is preparing a revised draft of a proposed new standard.

Subcommittee on Watt-hour Meters has prepared a preliminary draft of a bibliography on watt-hour meters covering about 225 periodicals and book references.

Subcommittee on Definitions has been active in assisting in the preparation of the third draft of Group 30 definitions—instruments, meters, and meter testing—being prepared by Subcommittee Number 6 in ASA-*C42*.

Subcommittee on Electrical Tests on Dielectric Measurements has completed a report on a survey which it made to determine current practices in field testing of dielectrics; this report was presented at the Winter General Meeting and will be published in the near future. It sponsored a technical session on insulating oil testing at the Winter General Meeting.

Subcommittee on Recorders and Controllers, while still in the organizational stage, is planning a program for the Fall General Meeting.

Subcommittee on High-Frequency Measurements, acting jointly with the IRE Committee on High-Frequency Measurements, sponsored a very successful conference on high-frequency measurements in Washington, D. C., in January 1951.

Subcommittee on the Marking of Varmeters and Related Instruments completed a report on the results of the survey to determine the practices in marking varmeters. This report was published in *Electrical Engineering*, and was presented at the Winter General Meeting.

Subcommittee on Co-operation with the Instrument Society of America (ISA) sponsored two technical sessions at the ISA conference in Buffalo, N. Y., one on September 20 and the other on September 21, 1950. An AIEE-sponsored luncheon was held on September 21. The average attendance at these three affairs was approximately 65. The Niagara Frontier Section of the AIEE was of invaluable assistance in making the necessary local arrangements.

Subcommittee on a Master Test Code for Power Measurements has made a second draft of a proposed Master Test Code for Power Measurements. At present it is being reviewed by the subcommittee members.

Subcommittee on Industrial Spectroscopy has confined its activities to sponsoring a technical session at the Winter General Meeting.

Subcommittee on a Master Test Code for Speed Measurements is preparing a preliminary draft of a proposed test code.

Subcommittee on Navigation Instruments is still in the organizational stage.

Activities of Joint Subcommittees

Joint Subcommittee on Instrument Transformers has been actively engaged in obtaining *Transactions* papers for various meetings.

Joint Subcommittee on Telemetering has continued active collaboration with the National Telemetering Forum (NTF). The subcommittee is still engaged in completing a glossary of telemetering terms which had been started by the Instrument Research Division of the National Advisory Committee for Aeronautics. The proceedings of the technical conference on telemetering, which conference was sponsored by this subcommittee and the NTF last May in Philadelphia, were edited by this subcommittee and issued early this year. A technical session is being planned for the Summer General Meeting.

Joint Subcommittee on Electronic Instruments is completing work on the specification formats for vacuum-tube voltmeters and for cathode-ray instruments. Similar specification formats for signal sources have been started. The Proceedings of the conference on improved quality electronic components, which conference was jointly sponsored by this subcommittee, the IRE, and Radio Manufacturers Association last May in Washington, D. C., were edited by this subcommittee and issued early this year. This subcommittee also sponsored a technical session at the Winter General Meeting.

Joint Subcommittee on Nucleonic Instruments, working in collaboration with the Joint Subcommittee on Electrical Aids to Medicine and the IRE, sponsored the third annual Joint AIEE-IRE conference on electronic instrumentation in nucleonics and medicine held in New York City last October. This subcommittee is assisting the Civil Defense Administration in the field of nuclear instruments, and has published an article in *Electrical Engineering* on the subject of "Suitable Instruments for Radiation Measurements." It is preparing a set of definitions, standards procedures, and test methods for the scintillation detector to parallel a similar set of definitions formulated by the IRE. It sponsored a technical session at the Winter General Meeting, and is arranging a session for the Summer General Meeting.

Other Activities. The Committee on Instruments and Measurements continued its activities in other fields through its contacts with other committees of the AIEE, the American Standards Association, and The American Society of Mechanical Engineers.

In addition to the previously mentioned eight sessions, the committee sponsored one session at the Middle Eastern District Meeting; part of one session at the Southern District Meeting; two sessions at the Winter General Meeting; one at the Great Lakes District Meeting; and has planned two sessions for the 1951 Summer General Meeting. This makes a total of 15 technical sessions on instruments and measurements for the 1950–51 season.

COMMITTEE ON MAGNETIC AMPLIFIERS

Magnetic amplifier work in the AIEE was organized as a subcommittee of the Committee on Electronics in the fall of 1948. In $2^1/_2$ years it has grown to an Institute technical committee, operating with nine subcommittees, and has produced a progress report covering the initial work on definitions, standards, and application information. Through the committee discussions and the progress report on definitions and standards, much of the loose talk regarding magnetic-amplifier performance has been eliminated, and a majority of the papers and articles are now appearing with information presented in a mutually understandable form. This marks the end of one phase of the committee work. The activity is quite firmly established in the AIEE, and is providing the desired interchange of ideas and progress in standardization.

The principal subcommittees now having active assignments are those on Definition Ratings, Applications, Test Code, Materials, and Non-Linear Circuit Theory arising particularly in magnetic amplifiers. The committee is also sponsoring some bibliography work.

Definitions Subcommittee, having established the basic definitions, must now settle down to the task of providing mutually agreeable terms for many of the commonly used circuit arrangements and principles of operation, and has also been requested to start work on standardization of symbols, both graphical and literal.

Materials Subcommittee is expected, through conference sessions jointly sponsored with other groups, to bring out the vital importance of materials in magnetic amplifiers and to give a clear picture of the limitations and possibilities of the materials, and of their true relationship to obtainable magnetic amplifier performance from a fundamental viewpoint.

Ratings Subcommittee has a real job in working out necessary rating quantities and methods of expressing performance of this essentially nonlinear device. A good start has been made, and a rating can now be given to a magnetic amplifier based on the proposals in the progress report. These recommendations are being used by the principal suppliers. The next job for this group is concerned with rating and expression of the performance of the saturable reactor, which surprisingly appears to present more of a problem than the complete magnetic amplifier.

Test Code Subcommittee has started its work of finding agreed-upon methods of implementing the standards and definitions by generally feasible forms of test.

Application Subcommittee has been formalized recently, although a number of conference and technical papers have dealt with various applications. This subcommittee will continue to work largely in this way, although it may provide a beneficial service by a report showing the scope of application and the limit of performance that has been achieved in various lines such as frequency, sensitivity, freedom from temperature variations, linearity, speed, and the like. Also the number and variety of circuits and uses continue to increase at a tremendous rate, and a group keeping track of this activity will be of considerable benefit to the industry.

Subcommittee on Non-Linear Circuit Theory arose spontaneously within the committee because of a keen interest on the part of some of the members in working mutually on the advanced circuit analysis techniques involved in nonlinear circuits, particularly those of interest in this field.

In the military field, magnetic amplifiers are already an accepted necessity. A large number of naval specifications are now coming out requiring magnetic amplifiers without electronic tube substitutions permitted. In atomic power work, where reliability is paramount, there is a general swing to magnetic amplifiers for many kinds of applications including d-c power supplies and the various control system components. Many applications are being sought in aircraft, and one autopilot operation will use over a million dollars worth of magnetic amplifiers per year. Other applications in aircraft are heater controls, wing flap controls, and so forth.

The reason for applications vary considerably, and the magnetic amplifier is not dependent upon any one characteristic for its acceptance or choice in comparison with other methods. It actually can be built with lower losses, less heat dissipation, and to occupy smaller space than comparable electronic devices such as the power stage for handling small servo motors, and so forth. Thus, space and heat economy are the ruling characteristics in some applications. In others, the comparative shock-proofness is a requisite quality. In other applications, the reliability and long life predominate as the characteristics principally determining the choice of the magnetic amplifier over electronic or rotating devices.

The industrial control application of magnetic amplifiers brings in the cost factor more predominantly than any other field, particularly for the less important control. However, for the more important controls handling important processes or expensive machinery, there is no question about the justification for the magnetic amplifier. The principal deterrent is simply the time required to change over designs from current styles to those incorporating the magnetic amplifier. Already it has found its way into an imposing list of industrial applications including steel mill controls, reel drives of various kinds, motor controls, voltage and frequency regulators, speed regulators, volts per cycle regulators, elevator controls, aircraft controls, paper mill applications, and a host of others.

Its use as the equivalent of a d-c current transformer for heavy current d-c busses likewise has been accepted and is spreading.

There are many unsolved problems in the magnetic amplifier. It is a nonlinear circuit with many facets as yet uncovered. A recent bibliography of literature and patents covers 52 pages of references to technical work bearing on the magnetic amplifier and the associated iron and nonlinear circuit characteristics. Yet today new characteristics and possible performance features are being discovered at a still increasing rate. When it is realized that only the simplest of the nonlinear circuits have been explored at all, and these not thoroughly, it is evident that the magnetic amplifier is only a small start on the application of nonlinear circuit devices involving saturation.

COMMITTEE ON METALLIC RECTIFIERS

A committee meeting was held during the Winter General Meeting, and the committee sponsored a session, which included several papers, at the Summer General Meeting.

Definitions and Test Code Subcommittees reported that standard definitions and test code were reviewed and additions were made to agree with requests for new definitions. A new edition was authorized by the committee.

Miniature Rectifiers Subcommittee. A preliminary report on methods of rating metallic rectifiers using capacitor loads was reviewed. The subcommittee is making a further study of the matter.

Patents Subcommittee. After reviewing the patent list, the committee decided that a new edition should be written.

Bibliography Subcommittee. The preparation of a new edition of the bibliography was authorized by the committee.

COMMITTEE ON NUCLEONICS

The committee has almost completed one of the tasks which it set at the time of its organization. It has reached a state where there seems to be little need for additional papers to bring to electrical engineers the basic concepts of nucleonics. The chief subjects of current interest are: nucleonic instruments, particularly those needed for routine measurement of radiation; isotopic tracers, particularly when used in industrial processes; and nuclear machines of various types, including particle accelerators. To deal with these, the subcommittee organization developed last year has been continued.

The committee was again one of the sponsors for the joint AIEE-IRE special technical conference on electronic instrumentation in nucleonics and medicine, which was held in New York, October 23–25, 1950.

The committee assisted in obtaining two papers for the Great Lakes District Meeting, but has devoted its major effort toward two technical sessions at the Summer General Meeting. A particular effort is being made in this direction because of the opportunity it affords for bringing into the program Canadians working in nucleonic fields.

One annoying, although probably necessary, obstacle to be overcome in obtaining conference or technical papers is that resulting from the necessity of securing "clearance" from the appropriate government agencies. The time that this involves, when added to that necessary to comply with Institute procedures, is so great as to be serious. This is particularly true when there has been a change in subcommittee chairmanship, for the new incumbent requires at least two months to develop the broad outlines of the program for the year.

COMMITTEE ON THERAPEUTICS

The Committee on Therapeutics jointly sponsored a technical conference with the Electronics Subcommittee on X-Ray Tubes, Apparatus, and Applications at the Winter General Meeting. This was a conference relating to X-ray and electromedical applications of electrical engineering. Five papers were presented to about 50 attendants.

The Committee on Therapeutics and the Subcommittee on Electrical Aids to Medicine have jointly recommended combination of their activities into a single Committee on Electrical Techniques in Medicine and Biology. A recommended scope was prepared at the joint meeting of the two committees. The merger of the two committees, its name, and scope have been approved by the Board of Directors. It is believed that the union of these two existing committees into one will eliminate certain overlapping within their scopes and create a stronger committee, which will strengthen the Institute's position in the electromedical manufacturing industry, the application of some equipment, and co-operation between the Institute and the medical profession.

AWARDS

EDISON MEDAL

The Edison Medal for 1950 was awarded to Otto B. Blackwell (retired), American Telephone and Telegraph Company, "for his pioneer contributions to the art of telephone transmission," and was presented to him on January 24, 1951, during the Winter General Meeting.

The medal may be awarded annually for meritorious achievement in electrical science, electrical engineering, or the electrical arts. Awards are made by a committee of 24 members of the Institute.

LAMME MEDAL

The Lamme Medal for 1950 was awarded to Donald I. Bohn, Chief Electrical Engineer, Aluminum Company of America, "for his pioneering development and application of electrical equipment for controlling rectifying systems in the production of aluminum." The medal will be presented to him on June 25, 1951, during the Summer General Meeting.

The medal may be awarded annually by a committee of nine members to a member of the AIEE for "meritorious achievement in the development of electrical apparatus or machinery."

JOHN FRITZ MEDAL

The John Fritz Medal may be awarded annually for notable scientific or industrial achievements by a board of award composed of representatives of the American Society of Civil Engineers (ASCE), The American Society of Mechanical Engineers (ASME), American Institute of Mining and Metallurgical Engineers (AIME), and AIEE. The 1951 medal was awarded to Dr. Vannevar Bush, President of the Carnegie Institution of Washington, "for outstanding contributions to his country and to his fellow men."

The medal was presented, in absentia, January 23, 1951, during the Winter General Meeting.

HOOVER MEDAL

The Hoover Medal for 1950 was awarded to Dr. Karl T. Compton, Chairman of the Corporation of the Massachusetts Institute of Technology, with the following citation: "Great leader in engineering education, who had a profound influence on the development of science and engineering, and has devoted himself wholeheartedly to the welfare of the Nation, both in times of peace and in times of war." The medal was presented to him on January 22, 1951, during the Winter General Meeting.

The Hoover Medal is awarded by a board representing the ASCE, AIME, ASME, and AIEE "for outstanding civic or humanitarian activities constituting distinguished public service."

MARSTON MEDAL BOARD OF AWARD

This medal is presented annually at the commencement exercises of Iowa State College to a graduate of that institution who has achieved success in his field of engineering activity.

The award for the year 1950 was made to C. E. Prudden, a graduate in mechanical engineering, who served Allis-Chalmers Manufacturing Company as Chief Engineer of its Tractor Division, and is now President of the Society of Automotive Engineers.

CHARLES LeGEYT FORTESCUE FELLOWSHIP COMMITTEE

The availability of this award was brought to the attention of all departments of electrical engineering in the country that offer accredited programs. Financial statements were reviewed by the committee members, and it was decided to grant one $1,500 fellowship for the year 1951–52. A total of 11 applications for the award was received. All applicants appeared to be well qualified.

The recipient of the award for the coming year is Mr. Clarence J. Baldwin of the University of Texas. In addition to his outstanding scholastic attainments, Mr. Baldwin has demonstrated exceptional leadership in university student affairs. He will continue his studies at the University of Texas.

ALFRED NOBLE PRIZE

The Alfred Noble Prize for the year ending June 1, 1950, was awarded to Ralph J. Kochenburger, Associate AIEE, for his paper, "A Frequency Response Method for Analyzing and Synthesizing Contactor Servomechanisms." The ceremony was held at the Winter General Meeting in New York on January 2, 1951. The prize is a cash award of $350, accompanied by a certificate signed by the President and Secretary of the American Society of Civil Engineers (which Society has been designated as Trustee of the Fund), and bears the names of the respective societies participating in the award.

The prize was established in 1929 and is awarded to a member of any grade of the ASCE, AIME, ASME, AIEE, or the Western Society of Engineers for a technical paper of exceptional merit presented before one of the societies and published in their technical publications, provided the author has not passed his 31st birthday at the time the paper is submitted.

The recipient of the prize is selected by a committee of five consisting of one representative of each society. The report of the committee is made to the Board of Direction of the ASCE on or before November 1. The presentation is made publicly at a general meeting of the society, of which the recipient is a member, by a representative of the ASCE.

JOINT ACTIVITIES

UNITED ENGINEERING TRUSTEES, INC.

For the four Founder Societies, the United Engineering Trustees, Inc., administers the funds and property in the Engineering Societies Building, the Engineering Societies Library, and the Engineering Foundation. It also serves as Treasurer of the Engineers' Council for Professional Development.

Efforts have been in progress for several years to find ways and means to secure an adequate building for an engineering center which would carry out Andrew Carnegie's ideals.

ENGINEERING FOUNDATION

The Engineering Foundation is a department of the United Engineering Trustees, Inc., and its general objective is "the furtherance of research in science and engineering."

With the income from its endowment funds, it supports a broad range of research projects, now numbering about 14. Some of its most effective contributions are those supporting studies and analyses necessary in the early stages of organizing projects on such bases that financial support from other sources becomes available. During the year 1949–50, the share of the Foundation in the cost of researches sponsored by it was a little less than three per cent.

ENGINEERING SOCIETIES LIBRARY

The library is a department of the United Engineering Trustees, Inc., and was formed by combining the separate libraries of the ASCE, AIME, ASME, and AIEE, and is conducted as a free public reference library.

In addition to affording the use of a large collection of engineering books and periodicals, the library renders special services such as bibliographies, translations, photostats, searches, and book loans by mail.

A revised Library Agreement has been approved by the Library Board, the United Engineering Trustees, Inc., and the Boards of the Founder Societies. In it, the ownership and title to books, documents, equipment, and other property in the custody of the Library are vested in the United Engineering Trustees, Inc., unless specifically prohibited by the original deeds of gift or bequests.

In order to conserve space, the Library is studying more critically new material received, and is discarding little-used material in larger amounts than ever before.

COMMITTEE ON ENGINEERING SOCIETIES MONOGRAPHS

One book was published: "Theory of Flow and Fracture of Solids," volume 1, by A. Nadal. Two books have been accepted and are in process of publication: "The Buckling Strength of Metal Structures," by F. Bleich, and "The Theory of Elasticity," by S. Timoshenko. One manuscript on "Hydraulics Transients" is now under review. Three manuscripts were submitted, but not accepted.

The committee is composed of two representatives each of the ASCE, AIME, ASME, and AIEE. The royalties from the books published are paid to the Engineering Societies Library.

ENGINEERS' COUNCIL FOR PROFESSIONAL DEVELOPMENT

The principal activities of ECPD include programs for the guidance of young persons thinking of entering the engineering field, the accrediting of curricula of engineering schools, and encouragement and assistance to individuals in their engineering and cultural studies during several years following graduation. The council represents ASCE, AIME, ASME, AIEE, The American Institute of Chemical Engineers (AIChE), the Engineering Institute of Canada, the American Society for Engineering Education, and the National Council of State Boards of Engineering Examiners.

ECPD approved and referred to the constituent societies the report of the Committee on Professional Recognition recommending the adoption of uniform grades of membership. The AIEE Board of Directors approved the uniform grades, and submitted to the membership proposed Constitutional amendments including them.

Revisions in the Charter of ECPD were submitted to and approved by the constituent societies.

ENGINEERS JOINT COUNCIL

The membership of this council includes the two most recent available past Presidents and the Secretaries, also the Presidents as ex officio members without votes, of the five societies ASCE, AIME, ASME, AIEE, and AIChE. Its principal functions are to study matters of mutual interest to the member societies, recommend joint action when desirable, and administer activities upon approval of a majority of the societies.

During the past year, the Engineering Manpower Commission was organized to aid in the establishment of policies for the most effective utilization of engineers in the national effort; a survey of selected engineering personnel for the Department of Defense was completed and definitions of 253 fields of specialization, in which 63,689 engineers of high standing listed themselves, were prepared; and the Water Policy Panel submitted a comprehensive report.

The Exploratory Group to Consider Further Unity in the Engineering Profession, which was organized at the invitation of EJC, submitted a report which is being studied by the societies.

Many other matters were considered during the year.

JOINT AIEE-IRE CO-ORDINATION COMMITTEE

The Joint AIEE-IRE Co-ordination Committee was established by the Boards of Directors of the AIEE and the IRE. The first meeting of the committee was held September 5, 1950.

By the establishment of this Joint Coordination Committee, opportunity is provided to discuss subjects of mutual interest and to recommend action thereon.

Recommendation was made that a continuing joint subcommittee be established, under the Education Committee of the IRE and the Committee on Student Branches of the AIEE, to resolve differences which occur in the operation of Joint Student Branches. This recommendation was approved by the respective Boards of Directors, and members of the subcommittee have been appointed.

INTER-SOCIETY CORROSION COMMITTEE

The Inter-Society Corrosion Committee, fostered by the National Association of Corrosion Engineers, was established in 1949, and held its third annual meeting in New York in March 1951. The committee membership now comprises delegates from 30 United States and Canadian engineering and scientific associations and government agencies having an interest in corrosion and its prevention.

During the past year by-laws of the committee were adopted by vote of the societies represented upon it through delegate members. At the meeting in March, a subcommittee reported upon the activities in the field of corrosion of societies represented upon the committee, and further reports of a similar character from delegate members were received. Other subcommittees previously appointed and at work during the past year are those on Standard Definitions and Terminology and on Liaison with Foreign Laboratories and Corrosion Agencies.

In furtherance of one of the main objectives of the committee, namely, the promotion of co-operation and the avoidance of undue duplication of effort, the AIEE delegates to the Inter-Society Corrosion Committee have been in contact during the past year with AIEE committees whose fields of interest were thought to include corrosion in a major or minor degree. In about half of these cases, interest and the desire to be kept further informed were manifested.

REPRESENTATIVES

The Institute is represented in many other joint activities not covered by this report, and a complete list may be found in the Year Book, or in the September issue of *Electrical Engineering.*

APPRECIATION

The continuing rapid increase in membership and expansion in technical activities reflect great credit upon the general and technical committees and the District, Section, and Student Branch officers and committees. The Board of Directors extends to all of these groups and to the membership in general its heartiest congratulations and thanks.

Respectfully submitted for the Board of Directors.

H. H. HENLINE
Secretary

HASKINS & SELLS
CERTIFIED PUBLIC ACCOUNTANTS

250 PARK AVENUE
NEW YORK 17

ACCOUNTANTS' CERTIFICATE

American Institute of Electrical Engineers:

We have examined the balance sheet of American Institute of Electrical Engineers, and schedule of securities owned, as of April 30, 1951, and the related statements of income and operating fund reserve and of restricted fund reserves for the year then ended. Our examination was made in accordance with generally accepted auditing standards, and accordingly included such tests of the accounting records and such other auditing procedures as we considered necessary in the circumstances.

In our opinion, the accompanying balance sheet, schedule of securities owned, and statements of income and operating fund reserve and of restricted fund reserves present fairly the financial position of, and securities owned by, the Institute at April 30, 1951, and the results of its operations for the year then ended, in conformity with generally accepted accounting principles applied on a basis consistent with that of the preceding year.

(*Signed*) HASKINS & SELLS

New York,
May 18, 1951

AMERICAN INSTITUTE OF ELECTRICAL ENGINEERS

Exhibit A

Balance Sheet, April 30, 1951

ASSETS		
Property Fund Assets:		
One-fourth interest in physical properties of United Engineering Trustees, Inc.:		
Land, buildings, and equipment (less depreciation and renewal reserve)	$306,752.07	
Funded depreciation and renewal reserve	191,696.41	
Total	$498,448.48	
Equipment:		
Library (nominal value)	1.00	
Office furniture and fixtures (less reserve for depreciation, $35,335.34)	27,605.84	
Works of art, etc.	3,001.35	
Total property fund assets		$ 529,056.67
Restricted Fund Assets:		
Securities—at cost (quoted market value, $694,582.00)—Schedule 1	$584,660.72	
Cash (including $1,760.83 Canadian funds):		
Reserve capital fund	6,760.09	
Life membership fund	2,314.81	
Member-for-Life fund	2,857.76	
International Electrical Congress of St. Louis Library fund	1,565.99	
Lamme Medal fund	160.00	
Mailloux fund	1,023.44	
Volta Memorial fund	734.01	
Retired employees insurance fund	2,000.00	
Accrued interest receivable	278.51	
Total restricted fund assets		602,355.33
Operating Fund Assets:		
Cash (not including $2,225.01 for Federal taxes withheld from employees)	$ 6,048.32	
Accounts receivable:		
Members—for dues (less reserve, $7,700.00)	15,589.22	
Advertisers	2,966.30	
Miscellaneous	4,574.47	
Accrued interest receivable	2,209.27	
Inventories:		
Transactions, etc.	2,306.00	
Text and cover paper	13,904.90	
Badges	9,204.64	
Deferred charges:		
Production charges for May issue of *Electrical Engineering*	17,578.42	
Travel advances	970.00	
Total operating fund assets		75,351.54
Total		$1,206,763.54

LIABILITIES		
Property Fund Reserve		$ 529,056.67
Restricted Fund Reserves (Exhibit C):		
Reserve capital fund	$548,767.87	
Life membership fund	7,357.51	
Member-for-Life fund	12,719.21	
International Electrical Congress of St. Louis Library fund	6,608.69	
Lamme Medal fund	4,440.44	
Mailloux fund	1,023.44	
Volta Memorial fund	19,438.17	
Retired employees insurance fund	2,000.00	
Total restricted fund reserves		602,355.33
Operating Fund Reserve, Liabilities, Etc.:		
Accounts payable	$ 26,512.75	
Deferred income:		
Dues received in advance	4,719.56	
Entrance fees and dues advanced by applicants for membership	2,884.15	
Subscriptions to publications received in advance	22,657.30	
Miscellaneous (including unallocated receipts)	1,346.27	
Operating fund reserve (Exhibit B)	17,231.51	
Total operating fund reserve, liabilities, etc.		75,351.54
Total		$1,206,763.54

Note: On October 26, 1950, the Board of Directors transferred title to the Institute's books, papers, and so forth, except as to restricted gifts, to United Engineering Trustees, Inc.

AMERICAN INSTITUTE OF ELECTRICAL ENGINEERS

Exhibit B

Statement of Income and Operating Fund Reserve for the Year Ended April 30, 1951

Income:			
Dues (including $207,684.00 allocated to *Electrical Engineering* subscriptions)		$457,552.94	
Advertising in *Electrical Engineering*		202,136.40	
Transactions subscriptions		18,608.45	
Electrical Engineering subscriptions		33,914.81	
Miscellaneous publications (preprints, Standards, and other publications)		53,462.44	
Students' fees		35,254.00	
Entrance fees		18,432.27	
Registration fees—Institute meetings and technical conferences		19,812.62	
Membership badges		4,694.90	
Transfer fees		3,780.00	
Interest and dividends on investments of Reserve Capital Fund		27,594.91	
Total income			$875,243.74
Expenses:			
Publications expense:			
Electrical Engineering text	$191,064.15		
Electrical Engineering advertising	102,203.87	$293,268.02	
Transactions		30,546.65	
Proceedings		38,298.92	
"Year Book"		15,884.32	
Miscellaneous publications (preprints, Standards, and other publications)		38,446.92	
Institute meetings		31,346.53	
Institute Sections		98,522.49	
Institute Branches, including paper prizes, etc.		8,939.18	
Finance Committee		850.00	
Headquarters Committee (including $925 wiring costs—air conditioning)		1,382.46	
Membership Committee		24,688.87	
Transfers Committee		87.67	
Standards Committee		16,654.34	
Technical Committees		15,594.06	
Committee on Public Relations		7,219.18	
Constitution and By-Laws Committee		3,183.06	
Edison Medal Committee		266.35	
Lamme Medal Committee		114.30	
Forward		$625,293.32	$875,243.74

Total Income (forward)		$875,243.74
Expenses (forward)	$625,293.32	
Traveling expenses:		
Geographical Districts:		
Executive Committees	7,732.43	
Vice-Presidents	1,867.90	
Conferences on student activities	10,040.99	
Board of Directors	20,274.25	
Nominating Committee	1,909.50	
President's appropriation	970.62	
Institute representatives	116.32	
Administrative expenses	106,335.00	
Geographical Districts—Branch paper prizes	745.65	
Institute prizes	745.41	
Retirement system AIEE—normal contribution	9,342.45	
American Standards Association	1,500.00	
Canadian Radio Technical Planning Board	10.00	
Engineers' Council for Professional Development	2,163.20	
Engineering Foundation Project—Welding Research	250.00	
Engineers Joint Council	4,916.32	
Hoover Medal	292.43	
John Fritz Medal	181.68	
National Council of State Boards of Engineering Examiners	500.00	
United States National Committee—International Commission on Illumination	300.00	
National Fire Protection Association	100.00	
United Engineering Trustees, Inc.:		
Building assessments	19,803.64	
Library assessments	15,498.35	
Library retirement plan	3,499.45	
Membership badges	4,618.65	
Legal services	250.00	
Rent, etc.—Editorial office, 500 Fifth Avenue	7,007.54	
Exchange allowances	9,574.02	
Provision for doubtful accounts	9,079.95	
Transfer to Property Fund Reserve for furniture and fixtures expenditures	5,150.89	
Total expenses	$870,069.96	
Less—Expenditures for air-conditioning equipment for the two years ended April 30, 1951, originally charged to Operating Fund Reserve, now treated as repayment of loan from Capital Fund Reserve (see below)	10,572.68	
Total expenses (net)		859,497.28
Excess of Income over Expenses for the Year		$ 15,746.46
Operating Fund Reserve, May 1, 1950		12,057.73
Total		$ 27,804.19
Less—Repayment of advances from Reserve Capital Fund (see above)		10,572.68
Operating Fund Reserve, April 30, 1951		$ 17,231.51

AMERICAN INSTITUTE OF ELECTRICAL ENGINEERS

Exhibit C

Statement of Restricted Fund Reserves for the Year Ended April 30, 1951

	Total	Reserve Capital Fund	Member-for-Life Fund	Life Membership Fund	International Electrical Congress of St. Louis Library Fund	Lamme Medal Fund	Mailloux Fund	Volta Memorial Fund	Retired Employee Insurance Fund
Balance, May 1, 1950	$595,145.26	$543,295.65	$11,288.94	$7,610.88	$6,382.33	$4,440.44	$1,021.38	$19,105.64	$2,000.00
Additions:									
Income from bonds	$ 983.82		$ 126.90	$ 138.39	$ 138.53	$ 160.00		$ 420.00	
Interest on bank balances	65.70			45.54			$ 20.16		
Operating fund loan repayments: 1949–1950 (leaving a balance of $19,427.32 due from Operating Fund)	10,572.68	$ 10,572.68							
Allocated portion of dues	2,292.00		2,292.00						
Profit on sale of securities, etc.	5,912.12	5,472.22		213.47	226.43				
Total additions	$ 19,826.32	$ 16,044.90	$ 2,418.90	$ 397.40	$ 364.96	$ 160.00	$ 20.16	$ 420.00	
Total	$614,971.58	$559,340.55	$13,707.84	$8,008.28	$6,747.29	$4,600.44	$1,041.54	$19,525.64	$2,000.00
Deductions:									
Expenditures for air-conditioning equipment made by Operating Fund for account of Reserve Capital Fund	$ 10,572.68	$ 10,572.68							
Authorized withdrawal from life membership fund	650.77			$ 650.77					
Purchase of medal, cost of engraving, etc. (exclusive of $114.30 paid from operating fund)	160.00					$ 160.00			
Library purchases	156.70				$ 138.60		$ 18.10		
Traveling expenses—District Branch prize winners	988.63		$ 988.63						
Costs of printing applications, etc.	87.47							$ 87.47	
Total deductions	$ 12,616.25	$ 10,572.68	$ 988.63	$ 650.77	$ 138.60	$ 160.00	$ 18.10	$ 87.47	
Balance, April 30, 1951 (Exhibit A)	$602,355.33	$548,767.87	$12,719.21	$7,357.51	$6,608.69	$4,440.44	$1,023.44	$19,438.17	$2,000.00

Schedule 1

AMERICAN INSTITUTE OF ELECTRICAL ENGINEERS
Securities Owned, April 30, 1951

	Principal Amount of Bonds or Number of Shares of Stock	Reserve Capital Fund	Restricted Funds: Life Membership Fund	Member-for-Life Fund	International Electrical Congress of St. Louis Library Fund	Lamme Medal Fund	Volta Memorial Fund	Total
Railroad Bonds:								
Atlantic Coast Line first consolidated 4%, due 1952	$ 4,000.00					$4,253.78		$ 4,253.78
Baltimore & Ohio, Pittsburgh, Lake Erie & West Virginia System refunding 4%, due 1980	10,000.00	$ 6,450.00						6,450.00
New York Central Railroad Company 4% series A consolidated mortgage, due 1998	15,000.00	9,812.50						9,812.50
Northern Pacific Railway Company $4^1/_2$% collateral trust, due 1975	15,000.00	15,307.50						15,307.50
Total railroad bonds		$ 31,570.00				$4,253.78		$ 35,823.78
Public Utility Bonds:								
American Telephone & Telegraph Company $2^3/_4$% debentures, due 1971	$ 5,000.00			$4,775.00				$ 4,775.00
American Telephone & Telegraph Company $2^3/_4$% debentures, due 1975	20,000.00	$ 10,062.50	$5,031.25		$5,031.25			20,125.00
Philadelphia Electric Company first refunding $2^3/_4$%, due 1967	10,000.00	10,325.00						10,325.00
Total public utility bonds		$ 20,387.50	$5,031.25	$4,775.00	$5,031.25			$ 35,225.00
Industrial Bonds:								
Shell Union Oil Company $2^1/_2$% debentures, due 1971	$20,000.00	$ 19,800.00						$ 19,800.00
Standard Oil Company of New Jersey $2^3/_8$% debentures, due 1971	20,000.00	19,675.00						19,675.00
Total industrial bonds		$ 39,475.00						$ 39,475.00
United States Government Bonds:								
Treasury bonds 3%, due September 15, 1955/51	$ 2,000.00						$ 2,081.66	$ 2,081.66
Defense bonds series G $2^1/_2$%, due December 1, 1954	18,000.00	$ 13,000.00		$5,000.00				18,000.00
Treasury savings bonds series G $2^1/_2$%, due September 1, 1955	40,000.00	40,000.00						40,000.00
Treasury savings bonds series G $2^1/_2$%, due November 1, 1956	17,000.00	17,000.00						17,000.00
Treasury savings bonds series G $2^1/_2$%, due May 1, 1957	20,000.00	20,000.00						20,000.00
Treasury savings bonds series G $2^1/_2$%, due October 1, 1957	30,000.00	30,000.00						30,000.00
Treasury savings bonds series G $2^1/_2$%, due May 1, 1961	30,000.00	30,000.00						30,000.00
Treasury savings bonds series G $2^1/_2$%, due July 1, 1961	15,000.00	15,000.00						15,000.00
Treasury bonds $2^1/_4$%, due December 15, 1962/59	16,000.00						16,480.00	16,480.00
Total United States Government bonds		$165,000.00		$5,000.00			$18,561.66	$188,561.66
Total bonds		$256,432.50	$5,031.25	$9,775.00	$5,031.25	$4,253.78	$18,561.66	$299,085.44
Capital Stocks:								
Preferred Stocks:								
Atchison, Topeka & Santa Fe Railway Company	200 shares	$ 19,174.71						$ 19,174.71
Dow Chemical $4 cumulative, series A	100 shares	11,547.50						11,547.50
General Motors Corporation $5	200 shares	25,820.00						25,820.00
Ohio Edison Company 4.40%	200 shares	21,279.25						21,279.25
Scoville Manufacturing Company 3.65% cumulative	100 shares	10,111.25						10,111.25
United States Steel Corporation 7% cumulative	100 shares	14,885.00						14,885.00
Total preferred stocks		$102,817.71						$102,817.71
Common Stocks:								
American Can Company	60 shares	$ 4,988.40						$ 4,988.40
American Gas & Electric Company	400 shares	15,069.04						15,069.04
Caterpillar Tractor Company	200 shares	9,361.30						9,361.30
Consolidated Natural Gas Company	100 shares	4,428.80						4,428.80
Eastman Kodak Company	330 shares	9,699.90						9,699.90
E. I. du Pont de Nemours & Company	300 shares	12,278.14						12,278.14
General Electric Company	200 shares	7,748.66						7,748.66
General Motors Corporation	200 shares	4,235.53						4,235.53
Gulf Oil Corporation	200 shares	12,264.20						12,264.20
Insurance Company of North America	120 shares	10,847.50						10,847.50
International Harvester Company	300 shares	5,030.50						5,030.50
International Paper Company	200 shares	9,186.12						9,186.12
Louisville & Nashville Railroad Company	100 shares	6,278.13						6,278.13
Pacific Gas and Electric Company	200 shares	8,316.23						8,316.23
Public Service Electric and Gas Company $1.40 dividend preference common stock	300 shares	9,040.55						9,040.55
Sears, Roebuck and Co.	400 shares	6,014.97						6,014.97
Socony Vacuum Oil Company	400 shares	8,216.87						8,216.87
Standard Oil Company of Indiana	200 shares	8,170.32						8,170.32
Standard Oil Company of New Jersey	252 shares	12,219.99						12,219.99
Swedish Match Company class B	18 shares	100.00						100.00
Union Carbide & Carbon Corporation	300 shares	7,277.42						7,277.42
United Fruit Company	300 shares	11,985.00						11,985.00
Total common stocks		$182,757.57						$182,757.57
Total capital stocks		$285,575.28						$285,575.28
Total		$542,007.78	$5,031.25	$9,775.00	$5,031.25	$4,253.78	$18,561.66	$584,660.72

Officers of A.I.E.E. for 1951–1952

PRESIDENT

F. O. McMILLAN
Corvallis, Oreg.
(*Term expires July 31, 1952*)

PAST PRESIDENTS

James F. Fairman, New York, N. Y.
(*Term expires July 31, 1952*)

Titus G. LeClair, Chicago, Ill.
(*Term expires July 31, 1953*)

VICE-PRESIDENTS

District
1 J. G. Tarboux, Ithaca, N. Y.
3 C. S. Purnell, New York, N. Y.
5 J. R. North, Jackson, Mich.
7 H. R. Fritz, St. Louis, Mo.
9 J. A. McDonald, Salt Lake City, Utah
(*Terms expire July 31, 1952*)

District
2 J. C. Strasbourger, Cleveland, Ohio
4 E. S. Lammers, Jr., Atlanta, Ga.
6 F. W. Norris, Lincoln, Nebr.
8 N. M. Lovell, Tucson, Ariz.
10 W. R. Way, Montreal, Que., Canada
(*Terms expire July 31, 1953*)

DIRECTORS

C. W. Fick, Cleveland, Ohio
A. H. Frampton, St. Catharines, Ont., Canada
M. D. Hooven, Newark, N. J.
(*Terms expire July 31, 1952*)

Ernest W. Davis, Cambridge, Mass.
N. B. Hinson, South Pasadena, Calif.
H. J. Scholz, Birmingham, Ala.
(*Terms expire July 31, 1953*)

Walter J. Barrett, Newark, N. J.
Elgin B. Robertson, Dallas, Tex.
Victor Siegfried, Worcester, Mass.
(*Terms expire July 31, 1954*)

F. R. Benedict, Pittsburgh, Pa.
R. F. Danner, Oklahoma City, Okla.
D. D. Ewing, Lafayette, Ind.
(*Terms expire July 31, 1955*)

TREASURER

W. I. Slichter, New York, N. Y.
(*Term expires July 31, 1952*)

SECRETARY

H. H. Henline, New York, N. Y.
(*Term expires July 31, 1952*)

LOCAL HONORARY SECRETARIES

Australia—V. J. F. Brain, Electricity Authority of N.S.W., Box 2600 G.P.O., Sydney, New South Wales

Brazil—W. L. Simpson, Sao Paulo Tramway Light and Power Company, Caixa Postal 26-B, Sao Paulo

England—Sir A. P. M. Fleming, Metropolitan Vickers Electric Company, Trafford Park, Manchester 17

India, Northern, S. S. Kumar, P.W.D. Electricity Secretariat, Ellerslie, Simla-E, East Punjab

India, Southern—M. S. Thacker, India Institute of Science, Bangalore

Japan—Stetfan Tanabe, 96 San-Chome, Denen-Chofu, Ohta-Ku, Tokyo

New Zealand—R. D. Neale, School of Engineering, Canterbury University College, Christchurch C.1

Pakistan—Mohamed Hussain Khalid, Electricity Department, Mardan

Sweden—Edy Velander, Box 5073, Stockholm 5

Transvaal—Francis E. Ingham, Box 6067, Johannesburg, Transvaal, South Africa

PAST PRESIDENTS—*1884–1951*

*Norvin Green	1884–85–86
*Franklin L. Pope	1886–87
*T. Commerford Martin	1887–88
*Edward Weston	1888–89
*Elihu Thomson	1889–90
*William A. Anthony	1890–91
*Alexander Graham Bell	1891–92
*Frank Julian Sprague	1892–93
*Edwin J. Houston	1893–94–95
*Louis Duncan	1895–96–97
*Francis Bacon Crocker	1897–98
*A. E. Kennelly	1898–1900
*Carl Hering	1900–01
*Charles P. Steinmetz	1901–02
*Charles F. Scott	1902–03
*Bion J. Arnold	1903–04
*John W. Lieb	1904–05
*Schulyer Skaats Wheeler	1905–06
*Samuel Sheldon	1906–07
*Henry G. Stott	1907–08
*Louis A. Ferguson	1908–09
*Lewis B. Stillwell	1909–10
*Dugald C. Jackson	1910–11
Gano Dunn	1911–12
Ralph D. Mershon	1912–13
*C. O. Mailloux	1913–14
*Paul M. Lincoln	1914–15
*John J. Carty	1915–16
H. W. Buck	1916–17
*E. W. Rice, Jr.	1917–18
Comfort A. Adams	1918–19
*Calvert Townley	1919–20
*A. W. Berresford	1920–21
*William McClellan	1921–22
*Frank B. Jewett	1922–23
*Harris J. Ryan	1923–24
*Farley Osgood	1924–25
*M. I. Pupin	1925–26
*C. C. Chesney	1926–27
*Bancroft Gherardi	1927–28
*R. F. Schuchardt	1928–29
*Harold B. Smith	1929–30
*William S. Lee	1930–31
*C. E. Skinner	1931–32
H. P. Charlesworth	1932–33
J. B. Whitehead	1933–34
*J. Allen Johnson	1934–35
*E. B. Meyer	1935–36
A. M. MacCutcheon	1936–37
W. H. Harrison	1937–38
John Castlereagh Parker	1938–39
F. Malcolm Farmer	1939–40
R. W. Sorensen	1940–41
David C. Prince	1941–42
Harold S. Osborne	1942–43
Nevin E. Funk	1943–44
C. A. Powel	1944–45
*W. E. Wickenden	1945–46
J. Elmer Housley	1946–47
B. D. Hull	1947–48
Everett S. Lee	1948–49
James F. Fairman	1949–50
Titus G. LeClair	1950–51

* Deceased.

Past and Present Officers of the Institute

Abbott, Arthur V., *V-P.*, 1900–02.
Adams, Comfort A., *M.*, 1912–15; *V-P.*, 1915–17; *P.*, 1918–19.
*Adsit, C. G., *V-P.*, 1921–23.
Alger, P. L., *D.*, 1944–48.
*Anthony, Wm. A., *V-P.*, 1886–89; *P.*, 1890–91; *V-P.*, 1894–96.
*Armstrong, A. H., *M.*, 1903–06; *V-P.*, 1906–08.
*Arnold, Bion J., *M.*, 1895–98; *V-P.*, 1902–03; *P.*, 1903–04.
Auty, K. A., *V-P.*, 1932–34.

*Babcock, A. H., *V-P.*, 1918–19.
Barker, J. W., *V-P.*, 1940–42.
Barnes, H. H., Jr., *M.*, 1910–13; *V-P.*, 1913–15.
Barrett, Walter J., *D.*, 1949–54.
*Barstow, W. S., *M.*, 1900–03; *V-P.*, 1903–05.
Barton, T. F., *V-P.*, 1939–40; *D.*, 1940–44.
Bates, D. H., *V-P.*, 1885–87.
*Baum, Frank G., *V-P.*, 1906–08.
Beardsley, C. R., *D.*, 1937–41.
Beaver, J. L., *V-P.*, 1927–29.
Bedell, Frederick, *M.*, 1914–17; *V-P.*, 1917–18.
*Behrend, B. A., *M.*, 1913–16; *V-P.*, 1916–18.
*Bell, Alexander G., *V-P.*, 1884–85; *P.*, 1891–92.
*Bell, Louis, *M.*, 1891–94.
Benedict, F. R., *D.*, 1951–55.
Bennett, Edward, *V-P.*, 1924–26.
*Berresford, A. W., *M.*, 1909–12; *V-P.*, 1912–14; *P.*, 1920–21.
Berry, J. H., *V-P.*, 1947–49.
Bettis, A. E., *V-P.*, 1926–28; *D.*, 1928–32.
Bickelhaupt, C. O., *V-P.*, 1927–29.
Bingham, L. A., *V-P.*, 1943–45.
Black, R. G., *M.*, 1910–13.
Blackwell, O. B., *V-P.*, 1936–38.
Blaisdell, L. T., *V-P.*, 1936–38.
Bolton, F. C., *V-P.*, 1938–40.
Bonney, R. B., *V-P.*, 1933–35.
Bower, G. W., *V-P.*, 1947–49.
*Brackett, Cyrus F., *M.*, 1886–89.
*Bradley, Chas. S., *M.*, 1894–97; *V-P.*, 1897–99; *M.*, 1899–1902.
*Brooks, David M., *M.*, 1885–88.
*Brooks, Morgan, *M.*, 1907–10; *V-P.*, 1910–12.
*Brush, Chas. F., *M.*, 1884–87.
Bryant, J. M., *M.*, 1924–28.
Buck, Harold W., *M.*, 1907–10; *V-P.*, 1910–12; *P.*, 1916–17.
*Buckingham, Chas. L., *M.*, 1885–88.
Buckley, O. E., *V-P.*, 1946–48.
Bush, Vannevar, *D.*, 1937–41.
Bussey, H. E., *V-P.*, 1923–25.

Callahan, J. L., *V-P.*, 1948–50.
Carle, N. A., *M.*, 1916–19; *V-P.*, 1919–20.
*Carlton, W. G., *M.*, 1908–11; *V-P.*, 1911–13.
Carpenter, C. B., *V-P.*, 1944–46.
*Carpenter, H. V., *V-P.*, 1930–32.
*Carty, John J., *M.*, 1893–96, 1900–03, 1903–04, 1906–08; *V-P.*, 1904–06, 1908–11; *P.*, 1915–16.
*Chamberlain, J. C., *M.*, 1890–93.
Charlesworth, H. P., *M.*, 1923–27; *V-P.*, 1930–32; *P.*, 1932–33.
*Chesney, C. C., *M.*, 1905–08; *V-P.*, 1908–10; *P.*, 1926–27.
Chesterman, F. J., *D.*, 1926–30.
Christie, C. V., *V-P.*, 1935–37.
Chubb, L. W., *D.*, 1931–35.
Chubbuck, L. B., *V-P.*, 1931–33.
Church, W. Lee, *M.*, 1887–88.
*Clarke, Chas. L., *M.*, 1904–05.
Clifford, H. E., *M.*, 1908–11.
Coldwell, O. B., *V-P.*, 1921–22.
*Compton, Alfred G., *M.*, 1891–94.
Cone, D. I., *V-P.*, 1947–49.
Cooper, A. B., *V-P.*, 1927–29; *D.*, 1930–34.
Coover, M. S., *D.*, 1940–44; *V-P.*, 1944–46.
Copley, A. W., *V-P.*, 1931–33.
*Craft, E. B., *M.*, 1920–24.
Craft, F. M., *V-P.*, 1933–35.
*Crocker, Francis B., *M.*, 1888–90; *V-P.*, 1890–92, 1894–96; *P.*, 1897–98.
*Crosby, Oscar T., *V-P.*, 1892–94.
*Cross, Chas. R., *V-P.*, 1884–85.
*Cuttriss, Chas., *M.*, 1888–91.

Danner, R. F., *V-P.*, 1946–48; *D.*, 1951–55.
Davis, Ernest W., *V-P.*, 1946–48; *D.*, 1949–53.
Dawes, Chester L., *V-P.*, 1938–40.
*Delany, Patrick B., *M.*, 1890–93; *V-P.*, 1893–95.
Del Mar, Wm. A., *M.*, 1917–21; *V-P.*, 1921–22.
*Dewars, A. G., *V-P.*, 1942–44; *D.*, 1950–51.
Dobson, W. P., *V-P.*, 1925–27.
*Dolbear, A. E., *V-P.*, 1885–87.
*Don Carlos, H. C., *D.*, 1926–30.
*Downing, P. M., *V-P.*, 1925–27.
*Duncan, Louis, *P.*, 1895–97.
Dunn, Gano, *M.*, 1897–1900; *V-P.*, 1900–02; *M.*, 1902—05; *V-P.*, 1905–07; *P.*, 1911–12.
DuVall, W. C., *V-P.*, 1949–51.

Eales, H. W., *V-P.*, 1921–26.
*Eckert, W. H., *M.*, 1884–85.
*Edgar, Chas. L., *M.*, 1905–08.
*Edison, Thos. A., *V-P.*, 1884–85.
*Eglin, W. C. L., *M.*, 1903–06; *V-P.*, 1907–09.
Eldredge, M., *V-P.*, 1935–37; *D.*, 1939–43.
Ellestad, I. M., *V-P.*, 1947–49.
*Emmet, W. L. R., *V-P.*, 1900–02.
Evans, Herbert S., *V-P.*, 1929–31.
Evenson, F. F., *V-P.*, 1945–47.
Everitt, W. L., *D.*, 1947–51.
Ewart, F. R., *V-P.*, 1921–23.
Ewing, D. D., *D.*, 1951–55.

*Faccioli, G., *M.*, 1918–22; *V-P.*, 1922–24.
Fair, R. H., *V-P.*, 1935–37.
Fairman, J. F., *V-P.*, 1944–46; *D.*, 1946–49; *P.*, 1949–50.
Farmer, F. M., *D.*, 1934–38; *V-P.*, 1938–39; *P.*, 1939–40.
*Ferguson, Louis A., *M.*, 1904–07; *V-P.*, 1907–08; *P.*, 1908–09.
Ferguson, O. J., *V-P.*, 1927–29.
Fick, C. W., *D.*, 1948–52.
*Field, Stephen D., *M.*, 1884–86.
Fields, E. S., *V-P.*, 1945–47.
*Finney, John H., *M.*, 1914–17; *V-P.*, 1917–18.
*Fisken, John B., *M.*, 1916–19; *V-P.*, 1919–20.
Flanigen, J. M., *D.*, 1945–49.
Fleager, C. E., *V-P.*, 1929–31.
*Foster, Horatio A., *M.*, 1890–93.
*Fowle, F. F., *M.*, 1919–23.
*Fowler, A. C., *M.*, 1887.
Fowler, M. M., *D.*, 1925–29.
Frampton, A. H., *V-P.*, 1949–51; *D.*, 1951–52.
*Freeman, W. E., *V-P.*, 1931–33.
Fritz, H. R., *V-P.*, 1950–52.
Funk, N. E., *D.*, 1934–38; *P.*, 1943–44.

Gamble, Lester R., *V-P.*, 1938–40; *D.*, 1941–45.
Gaylord, J. M., *V-P.*, 1943–45.
Gear, H. B., *D.*, 1934–38.
Geiger, D. G., *V-P.*, 1947–49.
*Geyer, Wm. E., *M.*, 1888–92.
*Gherardi, Bancroft, *M.*, 1905–08; 1914–17; *V-P.*, 1908–10; *P.*, 1927–28.
Gilson, Walter J., *V-P.*, 1943–45.
Goldsborough, W. E., *M.*, 1901–04; *V-P.*, 1904–06.
*Gray, Elisha, *M.*, 1884–86.
*Green, Norvin, *P.*, 1884–86; *V-P.*, 1886–88.
*Greene, S. Dana, *M.*, 1899.

Hall, Walter A., *M.*, 1917–21; *V-P.*, 1921–22.
*Hamblet, Jas., *M.*, 1891–94; *V-P.*, 1894–96.
*Hamilton, George A., *V-P.*, 1884–86; *Natl. Treas.*, 1895–1930.
Hamilton, J. L., *V-P.*, 1940–42.
*Hammer, William J., *V-P.*, 1891–93; *M.*, 1893–96.
Hanker, F. C., *D.*, 1927–31.
Hansen, K. L., *V-P.*, 1940–42; *D.*, 1942–46.
*Harding, C. F., *V-P.*, 1936–38.
*Harisberger, John, *V-P.*, 1924–26.
Harper, J. D., *V-P.*, Aug.–Oct. 1951.
Harrison, W. H., *V-P.*, 1935–37; *P.*, 1937–38.
*Haskins, Chas. H., *V-P.*, 1884–86.
*Hasson, W. F. C., *V-P.*, 1895–97; *M.*, 1897–1900.
*Hazard, Rowland R., *Treas.*, 1884–86; *V-P.*, 1887–89.
*Hellings, M. L., *M.*, 1884–85.
*Hellmund, R. E., *D.*, 1939–42.
*Henderson, S. E. M., *V-P.*, 1923–25.
Henline, H. H., *Act. Secy.*, 1932; *Secy.*, 1933–.
Henry, R. T., *V-P.*, 1944–46; *D.*, 1946–50.
*Hering, Carl, *V-P.*, 1891–93; 1895–98; *P.*, 1900–01.
*Herzog, F. Benedict, *M.*, 1887–92.
Hewitt, Chas., *M.*, 1893–96.
Hibbard, Angus S., *M.*, 1892–95; *V-P.*, 1895–97.
Hibshman, N. S., *V-P.*, 1941–43.
*Higson, C. R., *V-P.*, 1932–34.
Hinson, N. B., *V-P.*, 1935–37; *D.*, 1949–53.
Hitchcock, H. W., *V-P.*, 1939–41.
*Hobart, H. M., *M.*, 1922–26; *V-P.*, 1926–28.
Hooven, M. D., *D.*, 1948–52.
Hopkins, Ralph A., *V-P.*, 1949–51.
Housley, J. E., *V-P.*, 1941–43; *P.*, 1946–47.
*Houston, Edwin J., *M.*, 1884–87; *P.*, 1893–95.
*Howell, John W., *M.*, 1888–90.
Hull, A. H., *V-P.*, 1933–35.
Hull, B. D., *V-P.*, 1928–30; *D.*, 1931–35; *P.*, 1947–48.
*Humphrey, H. H., *V-P.*, 1906–08.
Hunting, F. S., *M.*, 1911–14; *V-P.*, 1914–16.
*Hutchinson, Cary T., *M.*, 1895–98; *V-P.*, 1898–1900.
*Hutchinson, F. L.. *Natl. Secy.*, 1912–32.

*Imlay, L. E., *M.*, 1919–23.

*Jackson, Dugald C., *V-P.*, 1897–99; *P.*, 1910–11.
*Jackson, W. B., *M.*, 1912–15; *V-P.*, 1918–19.
James, Wm. F., *V-P.*, 1923–25.
Jamieson, B. G., *V-P.*, 1926–28.
*Jewett, F. B., *M.*, 1915–18; *V-P.*, 1918–19; *P.*, 1922–23.
Johnson, F. Ellis, *D.*, 1936–39.
*Johnson, J. Allen, *D.*, 1928–32; *V-P.*, 1932–34; *P.*, 1934–35.
Jollyman, J. P., *V-P.*, 1937–39.
Jones, A. L., *V-P.*, 1941–43.
Jones, C. R., *D.*, 1935–39; *V-P.*, 1942–44.
*Jones, Francis W., *M.*, 1884–85; *V-P.*, 1885–87.
*Jorgensen, L. R., *V-P.*, 1919–20.
Juhnke, P. B., *D.*, 1933–37.
*Junkersfeld, P., *M.*, 1913–16; *V-P.*, 1916–18.

Kearns, J. E., *D.*, 1929–33.
*Keith, Nathaniel S., *Secy.*, 1884–85.
*Kelsch, Raymond S., *V-P.*, 1918–19.
*Kennelly, Arthur E., *V-P.*, 1892–94; *M.*, 1894–97; *V-P.*, 1897–98; *P.*, 1898–1900.
Kidder, H. A., *M.*, 1925–28; *V-P.*, 1928–30.
*Knight, G. L., *M.*, 1922–26; *V-P.*, 1926–28.
Knowlton, A. E., *D.*, 1930–34.
Kositzky, G. A., *D.*, 1932–36.
Kouwenhoven, W. B., *V-P.*, 1931–33; *D.*, 1935–39.

Lacy, T. N., *V-P.*, 1930–32.
Laffoon, C. M., *D.*, 1942–47.
*Lamme, Benj. G., *M.*, 1907–10.
Lammers, E. S., Jr., V-P, 1951–53.
Lane, F. H., *D.*, 1937–41.
Lardner, H. A., *M.*, 1913–16.
Lawton, F. L., *V-P.*, 1945–47.
LeClair, T. G., *D.*, 1941–45; *V-P.*, 1946–48 *P.*, 1950–51.
Lee, Everett S., *D.*, 1933–37; *V-P.*, 1940–42; *P.*, 1948–49.
*Lee, William S., *M.*, 1911–14; *D.*, 1929–30; *P.*, 1930–31.
*Leonard, H. Ward, *M.*, 1890–93; *V-P.*, 1893–95.
*Lieb, John W., *M.*, 1896–99; *V-P.*, 1899–1901; *M.*, 1901–03; *V-P.*, 1903–04; *P.*, 1904–05.
*Lighthipe, J. A., *V-P.*, 1913–15.
Lincoln, J. F., *M.*, 1920–24.
*Lincoln, Paul M., *M.*, 1906–09; *V-P.*, 1909–11; *P.*, 1914–15.
Liversidge, H. P., *D.*, 1927–31.
*Lloyd, Herbert, *M.*, 1898–1901.
*Lockwood, Thos. D., *V-P.*, 1886–87; *M.*, 1888–90; *V-P.*, 1891–93.
Lovell, A. H., *D.*, 1932–36; *V-P.*, 1938–40.
Lovell, N. M., *V-P.*, 1951–53.
*Lozier, R. T., *M.*, 1902–04.
Lunn, Ernest, *M.*, 1922–26.

MacCutcheon, A. M., *D.*, 1928–32; *P.*, 1936–37.
*Macdonald, J. E., *V-P.*, 1923–25.
*Macfarlane, Alexander, *M.*, 1897–1900.
Maclachlan, Wills, *V-P.*, 1919–20.
*Magnusson, C. E., *V-P.*, 1920–21.
Mahood, E. T., *V-P.*, 1942–44.
*Mailloux, C. O., *M.*, 1886–89; *V-P.*, 1898–99; *M.*, 1899–1902; *V-P.*, 1902–04; *M.*, 1905–07; *P.*, 1913–14.
*Mapes, L. R., *D.*, 1938–42.
*Martin, T. Commerford, *Act. Secy.*, 1884–85; *M.*, 1885–87; *P.*, 1887–88; *V-P.*, 1888–90.
Martindale, E. H., *M.*, 1917–20; *V-P.*, 1920–21.
*Maver, Wm., Jr., *M.*, 1888–91.
Maxwell, Fred R., Jr., *V-P.*, 1939–41; *D.*, 1941–45.
*Maynard, Geo. C., *V-P.*, 1886–88.
*McAllister, A. S., *M.*, 1914–17; *V-P.*, 1917–18.
McClellan, L. N., *V-P.*, 1937–39.
*McClellan, William, *M.*, 1912–15; *V-P.*, 1915–17; *P.*, 1921–22.
McConahey, W. M., *M.*, 1923–27.
McDonald, J. A., *V-P.*, 1950–52.
McDowell, C. S., *V-P.*, 1920–21.
McEachron, K. B., *D.*, 1936–40; *V-P.*, 1942–44.
McHenry, M. J., *V-P.*, 1937–39; *D.*, 1944–48.
McKay, Richard, *V-P.*, 1948–50.
McMillan, F. O., *V-P.*, 1934–36; *D.*, 1948–51; *P.*, 1951–52.
*Merriam, E. B., *M.*, 1924–28; *V-P.*, 1928–30.
Mershon, Ralph D., *M.*, 1900–03; *V-P.*, 1903–05; *P.*, 1912–13.
*Meyer, E. B., *D.*, 1927–31; *V-P.*, 1932–34; *P.*, 1935–36.
Meyer, F. J., *V-P.*, 1934–36; *D.*, 1939–43.
*Michaelis, O. E., *M.*, 1886–89; *V-P.*, 1889–90.
Mier, C. W., *D.*, 1943–47.
Mills, G. A., *V-P.*, Aug.–Oct. 1932.
Mitchell, W. E., *V-P.*, 1925–27.
Montieth, A. C., *D.*, 1947–51.
*Morehouse, L. F., *M.*, 1919–23; *V-P.*, 1924–26.
*Morrow, L. W. W., *D.*, 1933–37.
Mortensen, S. H., *D.*, 1943–47.
Morton, W. B., *D.*, 1941–46.
Moultrop, I. E., *D.*, 1926–30; *V-P.*, 1930–32.
*Mullin, E. H., *M.*, 1902–04.
*Murray, Wm. S., *M.*, 1908–09; 1909–12; *V-P.*, 1912–14.

Newbury, F. D., *M.*, 1918–22.
*Nichols, E. L., *V-P.*, 1889–91.
Norris, F. W., *V-P.*, 1951–53.
*Norris, H. H., *M.*, 1909–12.
North, J. R., *D.*, 1945–49; *V-P.*, 1950–52.
Northmore, E. R., *V-P.*, 1927–29.

Osborne, H. S., *D.*, 1938–42; *P.*, 1942–43.
*Osgood, Farley, *M.*, 1911–14; *V-P.*, 1914–16; *P.*, 1924–25.
Owens, R. B., *V-P.*, 1898–1900.

Parker, John Castlereagh, *V-P.*, 1921–22; *P.*, 1938–39.
Patton, P. H., *V-P.*, 1931–33.
*Peek, F. W., Jr., *D.*, 1930–33.
Pender, Harold, *M.*, 1915–18; *V-P.*, 1918–19.
*Perrine, Frederick A. C., *M.*, 1898–1900.
*Phelps, Geo. M., Jr., *M.*, 1885–87; *Treas.*, 1886–95.
*Pickernell, F. A., *M.*, 1896–99.
Pierce, A. G., *M.*, 1921–25; *V-P.*, 1925–27.
Pingree, G. N., *V-P.*, 1948–50.
Plumb, H. T., *V-P.*, 1922–24.
*Pope, Franklin L., *V-P.*, 1884–86; *P.*, 1886–87; *V-P.*, 1887–89.
*Pope, Ralph W., *Secy.*, 1885–1911; *Hon. Secy.*, 1911–29.
Post, G. G., *V-P.*, 1934–36.
Powel, C. A., *D.*, 1936–40; *V-P.*, 1942–43; *P.*, 1944–45.
Pratt, H. A., *M.*, 1921–25.

*Prescott, Geo. B., *M.*, 1884.
*Prescott, G. B., Jr., *M.*, 1888–91.
*Price, C. A., *V-P.*, 1941–43.
Prince, D. C., *D.*, 1938–41; *P.*, 1941–42.
*Puffer, Wm. L., *M.*, 1896–99.
*Pupin, Michael I., *M.*, 1892–95; *V-P.*, 1895–97; 1901–03; *P.*, 1925–26.
Purnell, C. S., *V-P.*, 1950–52.

Quarles, D. A., *D.*, 1944–48.
Quinan, G. E., *V-P.*, 1928–30.

*Reber, Samuel, *M.*, 1901–04; *V-P.*, 1904–06.
*Rice, Calvin W., *M.*, 1900–03; *V-P.*, 1903–05.
*Rice, E. W., Jr., *P.*, 1917–18.
Ricker, Claire W., *V-P.*, 1943–45.
Robbins, Chas., *M.*, 1916–20; *V-P.*, 1920–21.
Robertson, Elgin B., *D.*, 1947–51; *D.*, Oct. 1951–54.
Robertson, L. M., *V-P.*, 1945–47.
*Robinson, L. T., *M.*, 1913–16; *V-P.*, 1916–18, 1920–21.
*Rodman, W. S., *V-P.*, 1929–31.
Rogers, C. E., *V-P.*, 1936–38.
*Ruffner, Chas. S., *M.*, 1916–20; *V-P.*, 1920–21.
*Rugg, W. S., *M.*, 1910–13.
*Rushmore, D. B., *M.*, 1908–11; *V-P.*, 1911–13.
*Ryan, Harris J., *M.*, 1893–96; *V-P.*, 1896–98; *P.*, 1923–24.
*Ryan, W. T., *V-P.*, 1928–30.

*Sands, Herbert S., *V-P.*, 1923–27.
*Sargent, W. D., *M.*, 1885–86.
Schilling, E. W., *V-P.*, 1942–44.
*Schoen, A. M., *M.*, 1906–09; *V-P.*, 1919–20.
Scholz, H. J., *D.*, 1949–53.
Schoolfield, H. H., *V-P.*, 1926–28.
*Schuchardt, R. F., *V-P.*, 1922–24; *P.*, 1928–29.
*Scott, Chas. F., *M.*, 1895–98; *V-P.*, 1899–1901; *P.*, 1902–03.
*Scribner, Chas. E., *M.*, 1910–13; *V-P.*, 1913–15.
Seeger, E. W., *V-P.*, 1949–50.
Seeley, W. J., *V-P.*, 1949–51.
Sever, Geo. F., *M.*, 1898–1901; *V-P.*, 1901–03; *M.*, 1903–06.
*Shaad, G. C., *V-P.*, 1930–32; *D.*, 1935–36.
*Shelbourne, Sidney F., *M.*, 1886–87.
*Sheldon, Samuel, *M.*, 1898–1901; *V-P.*, 1901–03; *M.*, 1903–06; *P.*, 1906–07.
Sibley, R., *V-P.*, 1921–23.
Siegfried, Victor, *V-P.*, 1948–50; *D.*, 1950–54.
Sinclair, C. T., *V-P.*, 1939–41.
*Sisson, C. E., *V-P.*, 1929–31.
*Skinner, C. E., *M.*, 1915–19; *V-P.*, 1919–20; *P.*, 1931–32.
Slichter, Walter I., *M.*, 1918–22; *V-P.*, 1922–24; *Treas.*, 1930–.
*Smith, H. B., *M.*, 1920–24; *V-P.*, 1924–26; *P.*, 1929–30.
Smith, Walter Charles, *V-P.*, 1941–43; *D.*, 1945–49.
Smith, W. R., *D.*, 1942–46.
*Smith, W. W., *M.*, 1884–85.
Sorensen, R. W., *V-P.*, 1933–35; *D.*, 1936–40; *P.*, 1940–41.
*Spencer, Paul, *M.*, 1906–09; *V-P.*, 1909–11.
*Sprague, Frank J., *V-P.*, 1890–92; *P.*, 1892–93.
*Springer, F. W., *V-P.*, 1921–23.
*Sprong, S. D., *M.*, 1909–12; *V-P.*, 1912–14.
*Stanley, Wm., *V-P.*, 1898–1900.
Stein, I. Melville, *V-P.*, 1937–39.
*Steinmetz, Chas. P., *M.*, 1892–95; *V-P.*, 1896–98; *M.*, 1898–1901; *P.*, 1901–02.
*Stephens, C. E., *D.*, 1928–33.
Stevens, A. C., *D.*, 1932–36; *V-P.*, 1936–38.
*Stevens, J. Franklin, *M.*, 1912–15; *V-P.*, 1915–17.
*Stillwell, Lewis B., *M.*, 1896–99; *V-P.*, 1899–1901; *P.*, 1909–10.
Stine, Wilbur M., *V-P.*, 1896–98.
Stokes, Stanley, *V-P.*, 1932–34.
*Stone, Chas. W., *M.*, 1908–11; *V-P.*, 1911–13.
Stone, E. C., *D.*, 1925–29; *V-P.*, 1929–31.
*Storer, Norman W., *M.*, 1911–14; *V-P.*, 1914–16, 1921–23.
*Stott, Henry G., *M.*, 1904–07; *P.*, 1907–08.
Strasbourger, J. C., *V-P.*, 1951–53.
Sykes, Wilfred, *M.*, 1917–21.

Tapscott, R. H., *D.*, 1930–34; *V-P.*, 1934–36.
Tarboux, J. G., *V-P.*, 1950–52.
Taylor, A. LeRoy, *V-P.*, 1940–42.
Taylor, John B., *M.*, 1915–18; *V-P.*, 1918–19.
Terrell, C. F., *V-P.*, 1946–48.
*Terry, Chas. A., *N.*, 1902–05; *V-P.*, 1905–07.
Terry, I. A., *V-P.*, 1948.
*Tesla, Nikola, *V-P.*, 1892–94.
*Thomas, B. F., *M.*, 1885–87.
Thomas, Percy H., *M.*, 1907–10; *V-P.* 1910–12.
Thompson, Edward P., *M.*, 1887–88.
*Thomson, Elihu, *V-P.*, 1887–89; *P.*, 1889–90.
Thomson, J. M., *V-P.*, 1939–41.
Timbie, W. H., *V-P.*, 1934–36.
*Townley, Calvert, *M.*, 1905–08; *V-P.*, 1908–10; *P.*, 1919–20.
*Townsend, Henry C., *M.*, 1899–1902.
*Trowbridge, Wm. P., *M.*, 1884–86.
Turner, A. L., *V-P.*, 1939–41.

*Upton, Francis R., *V-P.*, 1889–90; *M.*, 1890–92.

*Vail, Theo. N., *M.*, 1884–86.
*Vanderpoel, W. K., *M.*, 1923–27.
*Van Hoevenbergh, H., *M.*, 1888–90.
Veinott, C. G., *V-P.*, 1949–51.
*Vonsize, W. B., *M.*, 1894–97.

*Wallace, Wm., *V-P.*, 1893–95.
Warner, R. G., *D.*, 1940–44.
Warner, R. W., *V-P.*, 1944–46.
Way, W. R., *V-P.*, 1951–53.
*Weaver, W. D., *M.*, 1894–97; 1899–1902.
Webb, Herbert L., *M.*, 1891–94; 1897–1900.
*Weston, Edward, *M.*, 1884–87; *P.*, 1888–89; *V-P.*, 1889–91.
*Wetzler, Jos., *M.*, 1888–90; *V-P.*, 1890–92.
*Wheeler, Schuyler S., *M.*, 1887–90; *V-P.*, 1890–91; 1902–04; *M.*, 1904–05; *P.*, 1905–06.
*White, Jas. G., *M.*, 1904–07; *V-P.*, 1907–09.
Whitehead, John B., *M.*, 1924–28; *P.*, 1933–34.
*Wickenden, W. E., *V-P.*, 1943–45; *P.*, 1945–46.
*Williamson, R. B., *M.*, 1921–25.
*Wilson, A. M., *V-P.*, 1933–35.
*Wirt, Chas., *M.*, 1892–95.
*Wolcott, Townsend, *M.*, 1902–05; *V-P.*, 1905–07.
Wolf, H. B., *V-P.*, 1945–47.
*Wood, Edwin D., *V-P.*, 1937–39.
*Woodrow, H. R., *D.*, 1931–35.

Yerkes, E. P., *D.*, 1946–50.

Abbreviations: *P.*, President; *V-P.*, Vice-President; *M.*, Manager; *D.*, Director; *Natl. Secy.*, National Secretary; *Secy.*, Secretary; *Hon. Secy.*, Honorary Secretary; *Natl. Treas.*, National Treasurer; *Treas.*, Treasurer.

*Deceased.

Honorary Members, 1884-1951

*Sir William Preece	1884
*Norvin Green	1889
*Moses G. Farmer	1890
*Lord Kelvin	1892
*Cyrus Field	1892
*E. W. von Siemens	1892
*Andre E. Blondel	1912
*C. E. L. Brown	1912
*Emil A. Budde	1912
*S. Z. de Ferranti	1912
*Antonio Pacinotti	1912
*S. P. Thompson	1914
*Guglielmo Marconi	1917
*Oliver Heaviside	1918
*Ferdinand Foch	1921
*Thomas A. Edison	1928
*John J. Carty	1928
*M. I. Pupin	1928
*Ambrose Swasey	1928
*Elihu Thomson	1928
Herbert Hoover	1929
*Charles F. Scott	1929
*Charles F. Brush	1929
Motoji Shibusawa	1929
*Frank J. Sprague	1932
*W. L. R. Emmet	1933
*G. A. Hamilton	1933
*Arthur E. Kennelly	1933
R. A. Millikan	1933
*E. W. Rice, Jr.	1933
*Edward Weston	1933
*Bion J. Arnold	1937
*Alex Dow	1937
*Cummings C. Chesney	1938
Andrew G. L. McNaughton	1942
*Dugald C. Jackson	1944
*Charles E. Skinner	1945
Gano Dunn	1945
*Frank B. Jewett	1945
Vannevar Bush	1949

* Deceased.

See page 132 for information concerning living Honorary Members.

Headquarters Staff

33 West 39th Street, New York 18

Secretary	H. H. Henline
Office Manager and Business Manager of Publications	F. A. Norris
Editor	C. S. Rich
Associate Editor	G. C. Baxter Rowe
Secretary, Technical Program Committee	Edward C. Day
Secretary, Board of Examiners and Standards Committee	J. J. Anderson, Jr.
Technical Committee Activities	R. S. Gardner
Advertising Manager	J. S. Lopes

General Counsel

Simon Presant......55 Liberty St., New York 5

Sections

Name	District	Organized	Membership Aug. 1, 1951	Chairman	Secretary	Secretary's Address
Akron	2	Aug. 12, '20	183	R. F. Miller	P. O. Huss	University of Akron, Akron 4, Ohio
Alabama	4	May 22, '29	298	T. S. Birdsong	E. C. Gentle, Jr.	Southern Bell Tel. & Tel. Co., Birmingham, Ala.
Arizona	8	Mar. 22, '41	209	I. G. Jenkins, Jr.	K. V. Fletcher	General Electric Co., 303 Luhrs Tower, Phoenix, Ariz.
Arkansas	7	Apr. 23, '47	133	R. J. Rhinehart	W. A. Bost	Arkansas Power & Light Co., Searcy, Ark.
Arrowhead	5	Apr. 23, '47	58	Roy B. Wiprud	T. W. Holmes	4709 Gladstone St., Duluth 4, Minn.
Beaumont	7	June 27, '45	87	T. G. Smith	R. W. Sherwood	Gulf States Utilities Co., Beaumont, Texas
Boston	1	Feb. 13, '03	1001	J. F. Archibald	L. J. Weed	Boston Edison Co., 39 Boylston St., Boston 11, Mass.
Canton	2	Nov. 5, '47	103	S. A. Langell	C. J. Muckley	5310 Hilltop Path, N. W., Canton 9, Ohio
Central Illinois	5	June 28, '51	164	J. F. Kruszka	C. R. Schultz	2040 North 22nd St., Springfield, Ill.
Central Indiana	5	Jan. 12, '12	348	C. A. Wilson	P. B. Ewing	Indiana Bell Telephone Co., Indianapolis, Ind.
Chicago	5	1893	1991	W. M. Ballenger	R. R. O'Connor	Illinois Bell Telephone Co., 208 W. Washington St., Chicago 6, Ill.
Cincinnati	2	June 30, '20	269	Sheldon B. Storer	W. A. Farris	111 Farragut Road, Greenhills, Cincinnati 18, Ohio
Cleveland	2	Sept. 27, '07	879	C. J. Beller	L. J. Shaffer	Ohio Bell Telephone Co., 820 Superior Ave., N. W., Cleveland 13, Ohio
Columbus	2	Mar. 17, '22	170	C. E. Warren	A. P. Jerencsik	1597 Meadow Road, Columbus, Ohio
Connecticut	1	Apr. 16, '21	601	E. G. Horton	M. B. Sprague	The Southern New England Telephone Co., 227 Church St., New Haven 6, Conn.
Corpus Christi	7	Oct. 25, '51				
Dayton	2	June 9, '43	415	R. L. Dingle	L. H. Henry	118 Oakview Drive, Dayton 9, Ohio
Denver	6	May 18, '15	474	Evan R. Jones	H. F. Gidlund	Public Service Co. of Colorado, P. O. Box 840, Denver 1, Colo.
East Tennessee	4	Sept. 2, '36	337	F. J. Baker	W. M. Stanley	Tennessee Valley Authority, 204 Power Bldg., Chattanooga 1, Tenn.
El Paso	7	Mar. 7, '40	116	Lee R. Hammond	R. E. Gnauck	4310 Dover St., El Paso, Texas
Erie	2	Jan. 11, '18	192	C. B. Lewis	G. H. Ramandanes	103 East 35th St., Erie, Pa.
Florida	4	Jan. 28, '31	186	J. A. Turner, Sr.	B. N. Darlington	902 Peninsular St., Tampa, Fla.
Fort Wayne	5	Aug. 14, '08	183	R. D. Jones	M. L. Miller	526 Dayton Ave., Fort Wayne, Ind.
Georgia	4	Jan. 14, '04	299	H. P. Peters	W. H. Hickey, Jr.	Southern States Equipment Corp., Hampton, Ga.
Houston	7	Aug. 7, '28	296	W. E. Silvus	T. A. Standish	2106 Swift, Houston 5, Texas
Illinois Valley	5	June 30, '45	90	R. M. King	R. H. Bonney	2011 Isabell Ave., Peoria, Ill.
Iowa	5	June 29, '29	237	J. E. Lagerstrom	F. E. Baird	Northwestern Bell Telephone Co., 816 Telephone Bldg., Des Moines, Iowa
Ithaca	1	Oct. 15, '02	237	S. W. Zimmerman	E. F. Wood	1715 Lovell Terrace, Elmira, N. Y.
Kansas City	7	Apr. 14, '16	343	A. J. Nicholson	J. C. Bibbs	Westinghouse Electric Corp., 101 W. 11th St., Kansas City 6, Mo.
Lehigh Valley	2	Apr. 16, '21	423	J. O. Leslie	W. C. Seymour	Pennsylvania Power & Light Co., 117 East Broad St., Hazelton, Pa.
Los Angeles	8	May 19, '08	1657	E. K. Sadler	C. A. Wells	Pacific Tel. & Tel. Co., 740 South Olive St., Los Angeles 55, Calif.
Louisville	4	Oct. 15, '26	155	W. G. Adair	J. G. Lips	Acme Contracting & Engg. Co., 120 Hillcrest Ave., Louisville 6, Ky.
Lynn	1	Aug. 22, '11	324	A. M. Bjontegard	E. K. Rohr	General Electric Co., 920 Western Ave., Lynn, Mass.
Madison	5	Jan. 8, '09	100	T. J. Higgins	N. L. Schmitz	University of Wisconsin, Madison 6, Wis.
Mansfield	2	Mar. 6, '39	102	F. L. Hanson	E. F. Huston	P. O. Box 431, Mansfield, Ohio
Maryland	2	Dec. 16, '04	768	J. W. Magee	Carl Watchorn	1611 Lexington Bldg., Baltimore 3, Md.
Memphis	4	May 22, '30	109	W. J. Fransioli, Jr.	V. E. Mohler	519 Williamsburg, Memphis 11, Tenn.
Mexico	7	June 29, '22	193	Gonzalo Fortoul	C. R. Arguelles	Palma 33, Despacho 210, Mexico D. F., Mexico
Miami	4	Feb. 3, '49	134	O. T. Ayers, Jr.	C. O. Grannis	1230 N. W. 57th St., Miami, Fla.
Michigan	5	Jan. 13, '11	933	I. B. Baccus	A. P. Fugill	Detroit Edison Co., 2000 Second Ave., Detroit 26, Mich.
Milwaukee	5	Feb. 11, '10	846	C. P. Feldhausen	H. C. Brem	Allis-Chalmers Mfg. Co., Milwaukee 1, Wis.
Minnesota	5	Apr. 7, '02	401	G. B. Germain	R. M. Kalb	4906—37th Ave., South, Minneapolis 17, Minn.
Mississippi	4	June 28, '51	72	W. L. Harp	T. R. Brock	General Elec. Co., 203 West Capitol St., Jackson 12, Miss.
Montana	9	June 24, '31	125	D. E. Kampschror	W. H. Blankmeyer	The Montana Power Co., Butte, Montana
Montreal	10	Apr. 16, '43	356	J. M. Sharpe	Leo Roy	Quebec Hydro-Elec. Commission, 107 Craig St. West, Montreal, Que., Canada
Nashville	4	June 28, '51	74	Walter Criley	J. M. Pinkerton	Nashville Electric Service, 605 Church St., Nashville, Tenn.
Nebraska	6	Jan. 21, '25	173	F. C. Clatterbaugh	A. G. Johnson	Omaha Public Power District, 936 Electric Bldg., Omaha, Nebr.
New Orleans	4	Dec. 8, '33	271	J. R. Rombach, Jr.	H. E. Pritchard, Jr.	5836 General Haig St., New Orleans 19, La.
New York	3	Dec. 10, '19	5503	J. P. Neubauer	Leland Stone	General Electric Co., 744 Broad St., Newark 2, N. J.
Niagara Frontier	1	Feb. 10, '25	299	J. P. Wood	T. O. Zittel	304 East & West Road, West Seneca 24, N. Y.
Niagara International	10	Aug. 5, '48	139	J. A. Williamson	J. A. Armstrong	112½ Geneva Ave., St. Catharines, Ont., Canada
North Carolina	4	Mar. 21, '29	323	Ben Martin	W. C. Burnett	Southern Bell Tel. & Tel. Co., 1701 Johnston Bldg., Charlotte, N.C.
Northeastern Michigan	5	Feb. 1, '50	127	A. E. Stevens	J. E. Young	Consumers Power Co., 600 Federal Ave., Saginaw, Mich.
Northern New Mexico	7	Jan. 25, '51	117	A. D. Taylor	M. L. Favia	Sandia Corp., 919 No. Jefferson, Albuquerque, New Mexico
North Texas	7	May 18, '28	539	E. W. Rogers	J. L. Pratt	1800 North Market St., Dallas, Texas
Oak Ridge	4	Feb. 1950	113	E. W. Parrish	R. B. Somers	102 Norton Road, Oak Ridge, Tenn.
Oklahoma City	7	Feb. 16, '22	223	J. S. Wantland	Bryce Brady	Oklahoma Gas & Elec. Co., Oklahoma City, Okla.
Ottawa	10	June 23, '49	68	C. R. Thornton	J. Rylance	133 Russell Road, Overbrook, Ottawa, Canada
Panhandle Plains	7	June 12, '47	177	H. P. Mathieu	P. S. Sterrett	Southwestern Public Service Co., Clovis, New Mexico
Philadelphia	2	Feb. 18, '03	1700	H. H. Sheppard	W. F. Denkhaus	Bell Telephone Co. of Pa., 1401 Arch St., Philadelphia, Pa.
Pittsburgh	2	Oct. 13, '02	1290	A. A. Johnson	W. J. Lyman	435—6th Ave., Pittsburgh 19, Pa.
Pittsfield	1	Mar. 25, '04	327	W. E. Birchard	W. A. McMorris	95 Strong Ave., Pittsfield, Mass.
Portland	9	May 18, '09	584	Waldo Porter, Jr.	William G. Meyer	Westinghouse Electric Corp., 914 U. S. National Bank Bldg., Portland 4, Oreg.
Providence	1	Mar. 12, '20	167	G. E. Andrews, Jr.	C. B. Leathers	General Electric Co., 111 Westminster St., Providence, R. I.
Richland	9	Apr. 23, '48	126	R. B. Crow	E. P. Peabody	1407 Thayer, Richland, Wash.
Rochester	1	Oct. 9, '14	240	J. A. Gienger	R. H. Rankin	Eastman Kodak Co., Rochester, N. Y.
Rock River Valley	5	Apr. 23, '47	87	C. F. Vinci	V. W. Schmidt	Louis Allis Co., 121 7th St., Rockford, Ill.
Sacramento	8	June 15, '50	114	A. B. Johnson	H. P. Braun	Pacific Gas & Electric Co.,723 S Street, Sacramento 14, Calif.
St. Louis	7	Jan. 14, '03	650	R. N. Slinger	R. C. Hase	1205 Telephone Bldg., St. Louis 1, Mo.
San Diego	8	Jan. 18, '39	189	O. L. Doolittle	I. E. McDougal	7560 Olive Place, La Mesa, Calif.
San Francisco	8	Dec. 23, '04	1361	W. F. Poynter	W. R. Johnson	Pacific Gas & Elec. Co., 245 Market St., San Francisco, Calif.
Schenectady	1	Jan. 26, '03	1047	L. T. Rader	C. C. Herskind	General Elec. Co., Schenectady 5, N. Y.
Seattle	9	Jan. 19, '04	601	C. D. Howe	D. E. Edwards	9402—6th Ave., S. W., Seattle 6, Wash.
Sharon	2	Dec. 11, '25	210	M. M. Morisuye	T. A. Casey	1527 Penn Ave., Sharpsville, Pa.
Shreveport	7	June 12, '47	118	E. D. Nuttall	W. C. Morris, Jr.	388 Atlantic St., Shreveport, La.
South Bend	5	Feb. 26, '41	138	H. R. Neighbours	J. W. Leadbetter	314 Peashway St., South Bend 17, Ind.
South Carolina	4	Mar. 2, '40	166	C. Y. House	G. L. Dibble	141 Meeting Street, Charlotte, S. C.
South Texas	7	May 23, '30	228	R. R. Krezdorn	J. C. Smith	6101 Bull Creek Road, Austin, Texas
Spokane	9	Feb. 14, '13	165	R. M. Gilbert	Charles Uhden	West 303 Joseph Ave., Spokane 12, Wash.
Springfield	1	June 29, '22	114	R. H. Walker	D. L. Ross	Westinghouse Elec. Corp., 26 Vernon St., Springfield 3, Mass.
Syracuse	1	Aug. 12, '20	315	D. A. Gaffney	A. H. Clark	202 Carleton Drive, Syracuse 3, N. Y.
Toledo	2	June 3, '07	151	T. J. Kozak	J. B. Cloer, Jr.	2723 Eldora Drive, Toledo 13, Ohio
Toronto	10	Sept. 30, '03	717	H. R. Osborne	J. T. Fisher	Bell Telephone Co. of Canada, Ltd., 76 Adelaide St. West, Toronto 1, Ont., Canada
Tri-State	2	June 28, '51	63	C. W. Feil	Jack Steelman, Jr.	2010 Enslow Blvd., Huntington 1, W. Va.
Tulsa	7	Oct. 1, '37	175	W. H. Plumer	Harold Furtney	Wagner Elec. Corp., 303 Tuloma Bldg., Tulsa 3, Okla.
Utah	9	Mar. 9, '17	154	R. A. Radford	L. D. Harris	1738 Logan Ave., Salt Lake City, Utah
Vancouver	9	Aug. 22, '11	232	D. S. Smith	H. M. Shockley	Canadian General Electric Co., Ltd., 1065 West Pender St., Vancouver, B. C., Canada
Virginia	4	May 19, '22	228	R. B. Liverman	L. D. Johnson, III	R. F. D. 7, Box 201, Richmond, Va.
Virginia Mountain	4	June 23, '49	101	A. B. Tillett	H. A. Clarke	Appalachian Electric Power Co., Roanoke, Va.
Washington	2	Apr. 9, '03	1110	F. W. Willcutt	W. J. Ellenberger	6419 Barnaby St., N. W., Washington 15, D. C.
West Virginia	2	Apr. 9, '40	119	H. L. Lindsey	John Vodar, Jr.	4614 Noyes Ave., S. E., Charleston, W. Va.
Wichita	7	Sept. 16, '37	128	Berwyn Brewer	O. R. Hantla	Kansas Gas & Elec. Co., Box 208, Wichita, Kansas
Worcester	1	Feb. 18, '20	108	G. R. Blake	D. J. Allia	New England Power Service Co., 66 Faraday St., Worcester, Mass.
Total Sections	93					

Subsections

Name	Chairman	Secretary	Secretary's Address
Baton Rouge (New Orleans Section)	F. E. Reeves	W. S. Syrett	1366 Stephens Ave., Baton Rouge 15, La.
Billings (Montana Section)	C. B. Brown	H. B. Campbell	914 Yale Avenue, Billings, Mont.
Binghamton Area (Ithaca Section)	J. P. Peterson	C. J. Fitch	209 West Edward St., Endicott, N. Y.
Black Hills (Denver Section)	C. L. Gust	E. R. Shields	Homestake Mining Co., Lead, S. Dak.
Boise (Utah Section)			
Boulder City (Los Angeles Section)	F. A. Latham	F. G. Scussel	717 New Mexico, Boulder City, Nevada
Casper, Wyo. (Denver Section)	W. D. Lawrence, Jr.	W. H. Keating	Box 340, Casper, Wyo.
Central Texas (North Texas Section)	C. B. Ingram	Lee Montgomery	2621 Lyle, Waco, Texas
Centre County (Pittsburgh Section)	A. F. Lopez	D. S. Pearson	Pennsylvania State College, State College, Pa.
Charleston (South Carolina Section)			
Charlotte (North Carolina Section)	W. C. Burnett	C. E. Harris	Duke Power Co., Box 2178, Charlotte 1, N. C.
Columbia (South Carolina Section)	J. F. Rader, Jr.	H. G. Eidson, Jr.	Radio Station W.I.S., 1111 Bull St., Columbia 1, S. C.
Eastern Shore (Maryland Section)	McCoy A. Tall	E. S. Mortimer	Mt. Hermon Road, Salisbury, Md.
Eureka Division (San Francisco Section)	M. D. McLellan	J. T. Morgan	Pacific Gas & Elec. Co., 318—5th St., Eureka, Calif.
Fort Worth (North Texas Section)	Karl Ratliff	B. B. Hulsey, Jr.	Texas Elec. Service Co., Box 970, Fort Worth 1, Texas
Fox River Valley (Milwaukee Section)	H. H. Brown	G. S. Johnson	128 Lincoln Circle, Kohler, Wis.
Freeport (Houston Section)	R. T. Windecker	B. S. Kirkpatrick, Jr.	431 Center Way, Lake Jackson, Texas
Fresno Division (San Francisco Section)	G. W. Hayden	F. S. Taylor	1050 Poplar Ave., Fresno 4, Calif.
Great Falls (Montana Section)	D. Sandell	William Sanders	Anaconda Copper Mining Co., Great Falls, Mont.
Hamilton (Toronto Section)	H. W. Macpherson	L. G. Stopps	Canadian Westinghouse Co., Ltd., Hamilton, Ont., Canada
Hampton Roads (Virginia Section)	G. T. Strailman	L. E. Rhinesmith	1119 East Warwick Road, R. D. 1, Box 35, Hilton Village, Va.
Hawaii (San Francisco Section)	Herbert Heinrich	John A. Ray	Hawaiian Pineapple Co., Ltd., Honolulu, Hawaii
Hudson Valley Division (New York Section)	E. W. Paquin	J. R. Vogel	Central Hudson Gas & Elec. Corp., Poughkeepsie, N. Y.
Johnstown (Pittsburgh Section)	R. S. Bogar	G. W. Murdock	Pennsylvania Elec. Co., Johnstown, Pa.
Lake Charles (Beaumont Section)	S. L. Adams	J. H. Ware, Jr.	Mathieson Chemical Corp., Lake Charles, La.
Lancaster-York (Maryland Section)	G. E. Conn, Jr.	K. J. Granbois	Road 2, Conestoga, Pa.
Lima (Dayton Section)	F. C. Horn	E. S. Reed	Westinghouse Elec. Corp., Lima, Ohio
Mid-State (North Carolina Section)	L. L. Browning, Jr.	H. M. Jackson, II	Western Electric Co., Dept. 8140, Winston-Salem, N. C.
Mobile-Pensacola (Alabama Section)	W. L. Sockwell	R. E. Pride	Alabama Power Co., 68 St. Francis St., Mobile 11, Ala.
Muscle Shoals (East Tennessee)	E. B. Foster		
New Hampshire (Boston Section)	P. W. Buxton	Fred Austin	Public Service Co. of N. H., 205 Main St., Nashua, N. H.
New Jersey Division (New York Section)	J. L. Blackburn	A. G. Smith	Weston Electrical Instrument Corp., 614 Frelinghuysen Ave., Newark 5, N. J.
Northwest Arkansas (Arkansas Section)	R. E. Anderson	F. M. Hinkle	411 Rebecca St., Fayetteville, Ark.
Quad-Cities (Iowa Section)	A. W. Kremser	G. F. Fisher	Stanley Engineering Co., Hershey Bldg., Muscatine, Iowa
Racine-Kenosha (Milwaukee Section)	C. B. Lee	J. B. Winther	Dynamatic Corp., Kenosha, Wis.
Red River Valley Division (Minnesota Section)	Robert Falman	K. B. MacKichan	2110 Second Ave. West, Grand Forks, N. Dak.
Richmond (Virginia Section)	C. E. McMurdo	D. N. Rice	P. O. Box 1194, Richmond, Va.
Ridgway (Erie Section)	C. F. McGinnis	J. H. Schneider	Smith St., R. D. #1, Ridgway, Pa.
St. Lawrence International (Syracuse Section)	N. O. Ross	C. I. Bacon	Cornwall St. Ry. Lt. & Pr. Co., Ltd., 16 Second St. East, Cornwall, Ont., Canada
St. Maurice Valley (Montreal Section)	M. T. Ferguson	J. B. Simpson	Northern Electric Co., Ltd., 2620 Notre Dame St., Three Rivers, Que., Canada
San Jose (San Francisco Section)	A. F. Lowe	J. A. Wells	Westinghouse Elec. Corp., Sunnyvale, Calif.
Savannah (Georgia Section)	J. G. Brown	J. K. Walsh	Union Bag & Paper Corp., Savannah, Ga.
Shasta Division (San Francisco Section)	A. A. Craig	C. R. Machen	Pacific Gas & Elec. Co., 301 Main St., Chico, Calif.
Tacoma (Seattle Section)	J. J. Dempsey	E. E. Martin	City of Tacoma Light Div., Tacoma, Wash.
Tampa (Florida Section)			
Vancouver Island (Vancouver Section)	J. B. Hedley	O. B. Bass	747 Lampson St., Esquimalt, B. C., Canada
West Central Texas Division (North Texas Section)	M. E. Mullings	C. A. Glover	1926 Sycamore St., Abilene, Texas
West Michigan (Michigan Section)	Norman MacMillan	L. A. Zahorsky	127 Colfax St. N. E., Grand Rapids, Mich.
Wilmington (Philadelphia Section)	J. M. Rowe	R. E. Seddon	E. I. du Pont de Nemours & Co., Wilmington, Del.
Zanesville (Columbus Section)	R. W. Squibb	J. M. Audi	434 Sunkel Ave., Zanesville, Ohio

Geographical District Executive Committees

District	Chairman (Vice-President, AIEE)	Secretary (District Secretary)	Chairman, District Committee on Student Activities
1 North Eastern	J. G. Tarboux, Cornell University, Ithaca, N. Y.	E. B. Alexander, New York State Elec. & Gas Corp., 62 Henry St., Binghamton, N. Y.	W. H. Erickson, Cornell University, Ithaca, N. Y.
2 Middle Eastern	J. C. Strasbourger, Cleveland Elec. Illuminating Co., 75 Public Square, Cleveland 1, Ohio	J. L. Fuller, Reliance Elec. & Engg. Co., 1088 Ivanhoe Road, Cleveland 10, Ohio	K. A. Fegley, University of Pennsylvania, 200 S. 33rd St., Philadelphia, Pa.
3 New York City	C. S. Purnell, Westinghouse Electric Corp., 40 Wall St., New York 5, N. Y.	D. W. Taylor, Public Service Elec. & Gas Co., 80 Park Place, Newark 1, N. J.	R. T. Weil, Jr., Manhattan College, New York 63, N. Y.
4 Southern	E. S. Lammers, Jr., Westinghouse Electric Corp., 1299 Northside Drive, N. W., Atlanta, Ga.	C. P. Almon, Jr., Tennessee Valley Authority, 707 Power Bldg., Chattanooga 2,Tenn.	D. H. Vliet, Tulane University, New Orleans 15, La.
5 Great Lakes	J. R. North, Commonwealth Services, Inc., 7 Hayes St., Jackson, Mich.	G. M. Chute, General Electric Co., 700 Antoinette St., Detroit 2, Mich.	E. A. Reid, University of Illinois, Urbana, Ill.
6 North Central	F. W. Norris, University of Nebraska, Lincoln, Nebr.	Q. L. Bonness, University of Nebraska, Lincoln, 8, Nebr.	S. I. Pearson, University of Colorado, Boulder, Colo.
7 South West	H. R. Fritz, Southwestern Bell Tel. Co., 2502 Telephone Bldg., St. Louis 1, Mo.	R. C. Meyerand, Union Elec. Co. of Missouri, 315 No. 12th Blvd., St. Louis 1, Mo.	P. M. Honnell, Washington University, St. Louis, Mo.
8 Pacific	N. M. Lovell, Tucson Gas, Elec. Light & Power Co., Tucson, Ariz.	Fred Mahler, P. O. Drawer 869, Phoenix, Ariz.	J. C. Clark, University of Arizona, Tucson, Ariz.
9 North West	J. A. McDonald, General Electric Co., 200 So. Main St., Salt Lake City, Utah	F. O. Wald, Utah Power & Light Co., P. O. Box 899, Salt Lake City 10, Utah	L. N. Stone, Oregon State College, Corvallis, Oreg.
10 Canada	W. R. Way, Shawinigan Water & Power Co., 600 Dorchester St., West, Montreal 2, Que., Canada	L. K. Hart, Square D Co. of Canada, Ltd., 5012 Western Ave., Montreal 28, Que., Canada	

NOTE: Each District Executive Committee includes also the chairman and one other officer (selected by the Section's executive committee) of each Section within the District, the District Vice-Chairman of the AIEE Membership Committee, and a member of the Sections Committee who is resident in the District.

Student Branches

Name and Location	District	Counselor (Member of Faculty)
*Akron, University of, Akron, Ohio	2	K. F. Sibila
Alabama Polytechnic Institute, Auburn	4	James Chadwick
Alabama, University of, University	4	W. F. Gray
*Alberta, University of, Edmonton, Canada	10	
*Arizona, University of, Tucson	8	J. C. Clark
Arkansas, University of, Fayetteville	7	Ross Lanier
*British Columbia, University of, Vancouver, Canada	9	S. C. Morgan
Brooklyn, Polytechnic Institute of, Brooklyn, N. Y., (Day)	3	F. A. Wahlers
Brooklyn, Polytechnic Institute of, Brooklyn, N. Y., (Evening)	3	Anthony B. Giordano
Brown University, Providence, R. I.	1	M. F. Gordon
*Bucknell University, Lewisburg, Pa.	2	B. H. Bueffel, Jr.
California Institute of Technology, Pasadena	8	Gilbert D. McCann
*California, University of, Berkeley	8	R. M. Saunders
*Carnegie Institute of Technology, Pittsburgh, Pa.	2	George H. Royer
Case Institute of Technology, Cleveland, Ohio	2	Rollin W. Waite
Catholic University of America, Washington, D. C.	2	Joseph C. Michalowicz
Cincinnati, University of, Cincinnati, Ohio	2	A. C. Herweh
Clarkson College of Technology, Potsdam, N. Y.	1	J. P. McCormick
Clemson A & M College, Clemson, S. C.	4	F. T. Tingley
Colorado A & M College, Fort Collins	6	C. C. Britton
*Colorado, University of, Boulder	6	S. I. Pearson
*Columbia University, New York, N. Y.	3	Walter A. LaPierre
*Connecticut, University of, Storrs	1	Howard L. Heydt
*Cooper Union, New York, N. Y.	3	E. W. Starr
*Cornell University, Ithaca, N. Y.	1	W. H. Erickson
*Delaware, University of, Newark	2	H. S. Bueche
*Denver, University of, Denver, Colo.	6	A. M. Stiles
*Detroit, University of, Detroit, Mich.	5	Guido Ferrara
*Drexel Institute of Technology, Philadelphia, Pa.	2	F. C. Powell
Duke University, Durham, N. C.	4	Otto Meier, Jr.
Fenn College, Cleveland, Ohio	2	R. W. Schindler
*Florida, University of, Gainesville	4	P. H. Nelson
George Washington University, Washington, D. C.	2	Jerome S. Antel, Jr.
Georgia Institute of Technology, Atlanta	4	H. B. Duling
Harvard University, Cambridge, Mass.	1	Kenneth Johansen
Howard University, Washington, D. C.	2	E. R. Welch
Idaho, University of, Moscow	9	J. Hugo Johnson
Illinois Institute of Technology, Chicago	5	E. T. B. Gross
*Illinois, University of, Urbana, and Chicago Division, Chicago	5	E. A. Reid
*Iowa State College, Ames	5	G. A. Richardson
Iowa, University of, Iowa City	5	E. B. Kurtz
*Johns Hopkins University, Baltimore, Md.	2	John M. Kopper
Kansas State College, Manhattan	7	Earl L. Sitz
*Kansas, University of, Lawrence	7	W. P. Smith
Kentucky, University of, Lexington	4	Gustavus E. Smith
*Lafayette College, Easton, Pa.	2	J. G. Reifsnyder
Lehigh University, Bethlehem, Pa.	2	H. T. MacFarland
Louisiana Polytechnic Institute, Ruston	7	S. P. Gullatt, Jr.
*Louisiana State University, Baton Rouge	4	A. K. Ramsey
Louisville, University of, Louisville, Ky.	4	Thomas R. Bailey
*Maine, University of, Orono	1	P. M. Seal
*Manhattan College, New York, N. Y.	3	R. T. Weil, Jr.
*Marquette University, Milwaukee, Wis.	5	E. W. Kane
*Maryland, University of, College Park	2	L. J. Hodgins
*Massachusetts Institute of Technology, Cambridge	1	Alexander Kusko
Massachusetts, University of, Amherst	1	N. E. Wilson
*Michigan College of Mining and Technology, Houghton	5	G. W. Swenson
*Michigan State College, East Lansing	5	Thomas W. Culpepper
*Michigan, University of, Ann Arbor	5	John J. Carey
Milwaukee School of Engineering, Milwaukee, Wis.	5	R. J. Ungrodt
*Minnesota, University of, Minneapolis	5	Paul A. Cartwright
Mississippi State College, State College	4	P. B. Jacobs, Jr.
*Missouri School of Mines and Metallurgy, Rolla	7	J. W. Rittenhouse
*Missouri, University of, Columbia	7	G. V. Lago
Montana State College, Bozeman	9	E. W. Schilling
*Nebraska, University of, Lincoln	6	E. J. Ballard, Jr.
Nevada, University of, Reno	8	Harold J. Hendriks
Newark College of Engineering, Newark, N. J.	3	Robert E. Anderson
*New Hampshire, University of, Durham	1	John B. Hraba
*New Mexico College of A & M Arts, State College	7	C. D. Crosno
*New Mexico, University of, Albuquerque	7	J. L. Ellis
New York, College of the City of, New York	3	Harold Wolf
*New York University, New York	3	B. James Ley
North Carolina State College, Raleigh	4	A. R. Eckels
North Dakota Agricultural College, Fargo	5	E. M. Anderson
*North Dakota, University of, Grand Forks	5	Raymond A. Berg
*Northeastern University, Boston, Mass.	1	Roland G. Porter
*Northwestern University, Evanston, Ill.	5	A. H. Wing
Norwich University, Northfield, Vt.	1	D. B. Staake
*Notre Dame, University of, Notre Dame, Ind.	5	L. F. Stauder
Ohio Northern University, Ada	2	James Klingenberger
*Ohio State University, Columbus	2	F. C. Weimer
*Ohio University, Athens	2	D. B. Green
*Oklahoma A & M College, Stillwater	7	David L. Johnson
*Oklahoma, University of, Norman	7	J. Bruce Wiley
*Oregon State College, Corvallis	9	L. N. Stone
*Pennsylvania State College, State College	2	A. P. Powell
*Pennsylvania, University of, Philadelphia	2	Kenneth A. Fegley
Pittsburgh, University of, Pittsburgh	2	R. C. Gorham
*Pratt Institute, Brooklyn, N. Y.	3	David Vitrogan
*Princeton University, Princeton, N. J.	2	C. H. Willis
Puerto Rico, University of, Mayaguez	3	Jose Luis Garcia de Quevedo
Purdue University, Lafayette, Ind.	5	Stephen Freeman, Jr.
*Rensselaer Polytechnic Institute, Troy, N. Y.	1	E. D. Broadwell
*Rhode Island, University of, Kingston	1	Robert S. Haas
Rice Institute, Houston, Texas	7	J. S. Waters
Rose Polytechnic Institute, Terre Haute, Ind.	5	R. D. Strum
*Rutgers University, New Brunswick, N. J.	3	P. S. Creager
Santa Clara, University of, Santa Clara, Calif.	8	Henry P. Nettesheim
South Carolina, University of, Columbia	4	J. H. Noland, Jr.
South Dakota School of Mines and Technology, Rapid City	6	J. O. Kammerman
South Dakota State College, Brookings	5	John N. Cheadle
*Southern California, University of, Los Angeles	8	Rodney C. Lewis
*Southern Methodist University, Dallas, Texas	7	F. W. Tatum
*Stanford University, Stanford, Calif.	8	W. G. Hoover
Stevens Institute of Technology, Hoboken, N. J.	3	William L. Sullivan
Swarthmore College, Swarthmore, Pa.	2	R. W. Merriam
*Syracuse University, Syracuse, N. Y.	1	Edward E. Shelton
Tennessee, University of, Knoxville	4	W. O. Leffell
*Texas, A & M College of, College Station	7	N. F. Rode
*Texas Technological College, Lubbock	7	V. D. Wade
*Texas, University of, Austin, and Texas Western College Sub-Branch, El Paso	7	William J. McKune
*Toledo, University of, Toledo, Ohio	2	Tsute Yang
Toronto, University of, Toronto, Ont., Canada	10	
*Tufts College, Medford, Mass.	1	J. L. Warner
*Tulane University, New Orleans, La.	4	D. H. Vliet
Union College, Schenectady, N. Y.	1	Owen G. Owens
United States Naval Academy, Annapolis, Md.	2	D. G. Howard
*Utah, University of, Salt Lake City	9	Seymour B. Hammond
Vanderbilt University, Nashville, Tenn.	4	Walter Criley
Vermont, University of, Burlington	1	R. F. Mosher
Villanova College, Villanova, Pa.	2	John B. Clothier
Virginia Military Institute, Lexington, Va.	4	J. S. Jamison
Virginia Polytechnic Institute, Blacksburg	4	Claudius Lee
*Virginia, University of, Charlottesville	4	G. K. Carter
Washington, State College of, Pullman	9	O. E. Osburn
*Washington, University of, Seattle	9	H. M. Rustebakke
Washington University, St. Louis, Mo.	7	Pierre M. Honnell
*Wayne University, Detroit, Mich.	5	Edward L. Fairchild
West Virginia University, Morgantown	2	Everette C. Dubbe
Wisconsin, University of, Madison	5	John Baird
*Worcester Polytechnic Institute, Worcester, Mass.	1	D. C. Alexander
*Wyoming, University of, Laramie	6	R. K. Beach
*Yale University, New Haven, Conn.	1	R. R. Shank

Total Branches........133

---

*Joint AIEE-IRE Branches.

Committees and Representatives for 1951-52

General Committees

Executive

F. O. McMillan, *Chairman;* Oregon State College, Corvallis, Oreg.

W. J. Barrett	Newark, N. J.
J. F. Fairman	New York, N. Y.
T. G. LeClair	Chicago, Ill.
J. R. North	Jackson, Mich.
C. S. Purnell	New York, N. Y.
W. I. Slichter	New York, N. Y.

Board of Examiners

P. H. Adams, *Chairman;* Public Service Electric and Gas Company, 80 Park Place, Newark 1, N. J.

John J. Anderson, Jr., *Secretary* AIEE Headquarters

A. E. Anderson	Philadelphia, Pa.
R. W. Atkinson	Bayonne, N. J.
R. H. Barclay	New York, N. Y.
J. L. Callahan	New York, N. Y.
W. G. Claytor	New York, N. Y.
H. A. Dambly	Philadelphia, Pa.
A. S. Dana	Seymour, Conn.
E. W. Davis	Cambridge, Mass.
E. D. Doyle	Philadelphia, Pa.
F. M. Feiker	Washington, D. C.
C. W. Franklin	New York, N. Y.
W. N. Goodwin, Jr.	Newark, N. J.
S. B. Griscom	East Pittsburgh, Pa.
R. A. Heising	New York, N. Y.
N. S. Hibshman	Brooklyn, N. Y.
L. F. Hickernell	Hastings-on-Hudson, N. Y.
Lee H. Hill	New York, N. Y.
J. W. Horton	New London, Conn.
H. E. Ives	New York, N. Y.
A. E. Knowlton	Short Beach, Conn.
G. H. Landis	Poughkeepsie, N. Y.
Henry Logan	New York, N. Y.
J. B. MacLean	New York, N. Y.
E. E. Mayer	New Rochelle, N. Y.
L. G. Pacent	New York, N. Y.
F. J. Scudder	Manhasset, N. Y.
B. E. Shackelford	New York, N. Y.
H. W. Tenney	Jersey City, N. J.
Gordon Thompson	New York, N. Y.
Robert Treat	Schenectady, N. Y.
H. M. Trueblood	Dobbs Ferry, N. Y.
B. Van Ness, Jr.	Baltimore, Md.
R. G. Warner	New Haven, Conn.
S. S. Watkins	New York, N. Y.
Roland Whitehurst	Philadelphia, Pa.
Sidney Withington	New Haven, Conn.

Constitution and Bylaws

F. R. Benedict, *Chairman;* Westinghouse Electric Corporation, 306 Fourth Ave., P. O. Box 1017, Pittsburgh 30, Pa.

N. B. Hinson	South Pasadena, Calif.
W. W. Lewis	Schenectady, N. Y.
W. S. Peterson	Los Angeles, Calif.

Finance

W. J. Barrett, *Chairman;* New Jersey Bell Telephone Company, Engineering Department, Room 905, 540 Broad Street, Newark 2, N. J.

M. D. Hooven	Newark, N. J.
C. S. Purnell	New York, N. Y.

Headquarters

D. W. Taylor, *Chairman;* Public Service Electric and Gas Company, 80 Park Place, Newark 1, N. J.

W. J. Barrett	Newark, N. J.
H. H. Henline	New York, N. Y.

Members-for-Life Fund

Mark Eldredge, *Chairman;* 2110 Spencer Road, Silver Spring, Md.

C. L. Dawes	Cambridge, Mass.
N. E. Funk	Philadelphia, Pa.
A. H. Hull	Toronto, Ontario, Canada
L. N. McClellan	Denver, Colo.
S. H. Mortensen	Milwaukee, Wis.
W. I. Slichter	New York, N. Y.
R. W. Sorensen	Pasadena, Calif.
F. C. Weiss	Birmingham, Ala.

(Continued in next column)

Membership

J. C. Woods, *Chairman;* Commonwealth Edison Company, 72 West Adams Street, Chicago 90, Ill.

Charles Clos, *Vice-Chairman* New York, N. Y.

M. J. Adams	Chicago, Ill.
W. C. Bloomquist	Schenectady, N. Y.
G. W. Cross	New York, N. Y.
C. W. Fick	Cleveland, Ohio
W. R. Horrigan	Amarillo, Tex.
C. R. Kingsbury	Seattle, Wash.
J. L. McKinley	Denver, Colo.
E. W. Morris	Los Angeles, Calif.
Russell Ranson	Charlotte, N. C.
C. L. Roach	Montreal, Quebec, Canada
W. E. Scholz	Philadelphia, Pa.

District Vice-Chairmen

1	R. K. Fairley	Schenectady, N. Y.
2	W. A. Dynes	Dayton, Ohio
3	M. A. Jones	Newark, N. J.
4	E. R. Coulbourn	Birmingham, Ala.
5	H. R. Heckendorn	Chicago, Ill.
6	R. W. Shaw	Omaha, Nebr.
7	R. G. Kloeffler	Manhattan, Kans.
8	G. B. Kenline	San Diego, Calif.
9	H. B. Hodgins	Salt Lake City, Utah
10	M. C. Thurling	Toronto, Ontario, Canada

Planning and Co-ordination

M. D. Hooven, *Chairman;* Public Service Electric and Gas Company, 80 Park Place, Newark 1, N. J.

W. J. Barrett	Newark, N. J.
M. M. Brandon	New York, N. Y.
J. L. Callahan	New York, N. Y.
J. F. Fairman	New York, N. Y.
F. E. Harrell	Cleveland, Ohio
H. H. Henline	New York, N. Y.
W. Scott Hill	Pittsfield, Mass.
A. E. Knowlton	Short Beach, Conn.
T. G. LeClair	Chicago, Ill.
K. B. McEachron	Pittsfield, Mass.
Elgin B. Robertson	Dallas, Tex.
M. J. Steinberg	New York, N. Y.

Publication

K. B. McEachron, *Chairman;* General Electric Company, 100 Woodlawn Ave., Pittsfield, Mass.

F. R. Benedict	Pittsburgh, Pa.
D. T. Braymer	New York, N. Y.
H. W. Codding	Newark, N. J.
P. B. Garrett	Chicago, Ill.
L. F. Hickernell	Hastings-on-Hudson, N. Y.
Everett S. Lee	Schenectady, N. Y.
G. R. Meager	Clifton, N. J.
J. R. North	Jackson, Mich.
T. A. O'Halloran	Washington, D. C.
G. C. Quinn	Milwaukee, Wis.
C. S. Rich	New York, N. Y.
J. D. Tebo	New York, N. Y.
G. C. Tenney	San Francisco, Calif.
E. R. Whitehead	Chicago, Ill.
C. H. Willis	Princeton, N. J.

Public Relations

G. T. Minasian, *Chairman;* Consolidated Edison Company of New York, Inc., 4 Irving Place, New York 3, N. Y.

Guy Bartlett	Schenectady, N. Y.
G. W. Bower	Newark, N. J.
V. A. Diggs	Cleveland, Ohio
R. T. Ferris	Philadelphia, Pa.
R. R. Herrmann	Minneapolis, Minn.
R. K. Honaman	New York, N. Y.
J. T. Kimball	Phoenix, Ariz.
A. E. Knowlton	Short Beach, Conn.
G. J. Lowell	New York, N. Y.
H. W. Marquardt	New York, N. Y.
C. A. Mayo	Salem, Mass.
K. B. McEachron	Pittsfield, Mass.
J. P. Neubauer	New York, N. Y.
H. J. Scholz	Birmingham, Ala.
W. B. Stephenson	Oklahoma City, Okla.

(Continued in next column)

Research

J. A. Hutcheson, *Chairman;* Research Laboratories, Westinghouse Electric Corporation, East Pittsburgh, Pa.

B. G. Ballard	Ottawa, Ontario, Canada
F. R. Benedict	Pittsburgh, Pa.
E. W. Boehne	Cambridge, Mass.
Cledo Brunetti	Stanford, Calif.
C. R. Burrows	Ithaca, N. Y.
H. E. Edgerton	Cambridge, Mass.
M. A. Edwards	Schenectady, N. Y.
T. J. Killian	Washington, D. C.
J. T. Littleton	Corning, N. Y.
W. H. Pickering	Pasadena, Calif.
C. S. Schifreen	Philadelphia, Pa.

Safety

Hendley Blackmon, *Chairman;* Westinghouse Electric Corporation, Office 7-L-38, East Pittsburgh 21, Pa.

H. R. Stevenson, *Vice-Chairman* Detroit, Mich.

H. B. Whitaker, *Secretary* Chicago, Ill.

Robin Beach	Brooklyn, N. Y.
M. M. Brandon	New York, N. Y.
W. B. Buchanan	Toronto, Ontario, Canada
C. F. Dalziel	Berkeley, Calif.
G. S. Diehl	Lancaster, Pa.
W. P. Dobson	Toronto, Ontario, Canada
G. W. Elg	New York, N. Y.
C. E. Ganther	Cleveland, Ohio
J. A. Gienger	Rochester, N. Y.
Floyd L. Goss	Los Angeles, Calif.
N. B. Hinson	South Pasadena, Calif.
L. S. Inskip	Murray Hill, N. J.
W. B. Kouwenhoven	Baltimore, Md.
J. O. Leslie	Reading, Pa.
R. L. Lloyd	Bethesda, Md.
T. M. C. Martin	Portland, Oreg.
G. R. Radley	Milwaukee, Wis.
W. T. Rogers	New York, N. Y.
H. H. Watson	Bridgeport, Conn.
H. B. Williams	New York, N. Y.

Division Liaison Representatives

Communication:	
T. J. Boerner	Camden, N. J.
General Applications:	
S. D. Summers	Washington, D. C.
Industry:	
G. W. Heumann	Schenectady, N. Y.
Power:	
E. W. Oesterreich	Pittsburgh, Pa.
Science & Electronics:	
J. T. Lusignan	Mansfield, Ohio

Medical Consultants

Dr. Cecil K. Drinker, P. O. Box 502, Falmouth, Mass.

Dr. Archer Gordon, University of Illinois, Medical Center, Chicago, Ill.

Dr. Jerome Kay, The Johns Hopkins University, Baltimore 18, Md.

Dr. B. L. Vosburgh, General Electric Company, 1 River Road, Schenectady 5, N. Y.

Sections

C. S. Purnell, *Chairman;* Westinghouse Electric Corporation, 40 Wall Street, New York 5, N. Y.

H. A. Dambly, *Vice-Chairman (East)* Philadelphia, Pa.

R. E. Kistler, *Vice-Chairman (West)* Seattle, Wash.

V. L. Ingersoll, *Secretary* New York, N. Y.

D. I. Anzini	San Francisco, Calif.
Francis Aubert	Mexico, D. F., Mexico
F. S. Black	New York, N. Y.
T. C. D. Churchill	Toronto, Ontario, Canada
Bradley Cozzens	Los Angeles, Calif.
R. B. Crow	Richland, Wash.
F. A. Eastom	Boulder, Colo.
D. E. Garr	Schenectady, N. Y.
A. J. Hendry	St. Paul, Minn.
R. C. Horn	St. Louis, Mo.
C. P. Knost	New Orleans, La.
E. L. Michelson	Chicago, Ill.
A. L. O'Banion	Boston, Mass.
F. H. Pumphrey	Gainesville, Fla.
C. L. Reed	Erie, Pa.
F. H. Schlough	Pittsburgh, Pa.
E. T. Sherwood	Milwaukee, Wis.
J. C. Strasbourger	Cleveland, Ohio
J. D. Tebo	New York, N. Y.

(Continued in next column)

Standards

E. B. Paxton, *Chairman;* General Electric Company, 1 River Road, Schenectady 5, N. Y.

M. M. Brandon, *Vice-Chairman* New York, N. Y.

John J. Anderson, Jr., *Secretary* AIEE Headquarters

Joseph Wm. Allen	Teterboro, N. J.
R. W. Atkinson	Bayonne, N. J.
E. L. Bailey	Highland Park, Mich.
Sterling Beckwith	Milwaukee, Wis.
P. L. Bellaschi	Portland, Oreg.
R. C. Bergvall	Pittsburgh, Pa.
R. S. Burnap	Harrison, N. J.
J. E. Clem	Schenectady, N. Y.
H. C. Coleman	East Pittsburgh, Pa.
C. L. Dawes	Cambridge, Mass.
Rodman D. deKay	New York, N. Y.
W. P. Dobson	Toronto, Ontario, Canada
I. W. Gross	New York, N. Y.
R. T. Henry	Buffalo, N. Y.
F. C. Holtz	Springfield, Ill.
W. R. Hough	Cleveland, Ohio
H. R. Huntley	New York, N. Y.
H. E. Kent	New York, N. Y.
W. I. Middleton	Cambridge, Mass.
A. C. Muir	Philadelphia, Pa.
J. R. North	Jackson, Mich.
J. E. O'Brien	Washington, D. C.
R. W. Sherwood	Beaumont, Tex.
F. B. Silsbee	Washington, D. C.

Technical Advisory

L. F. Hickernell, *Chairman;* Anaconda Wire and Cable Company, Hastings-on-Hudson 6, N. Y.

R. S. Gardner, *Secretary* AIEE Headquarters

F. B. Bramhall	New York, N. Y.
W. R. Brownlee	Birmingham, Ala.
E. I. Green	Murray Hill, N. J.
J. R. North	Jackson, Mich.
T. R. Rhea	Schenectady, N. Y.
C. F. Scott	Bridgeport, Conn.
M. J. Steinberg	New York, N. Y.
J. D. Tebo	New York, N. Y.

Technical Program

M. M. Brandon, *Chairman;* Underwriters Laboratories, Inc., 161 Sixth Ave., New York 13, N. Y.

N. S. Hibshman, *Vice-Chairman* Brooklyn, N. Y.

Edward C. Day, *Secretary* AIEE Headquarters

Hendley Blackmon	East Pittsburgh, Pa.
F. B. Bramhall	New York, N. Y.
W. R. Brownlee	Birmingham, Ala.
J. L. Callahan	New York, N. Y.
W. G. Dow	Ann Arbor, Mich.
E. I. Green	Murray Hill, N. J.
J. A. Herrmann	Detroit, Mich.
D. J. Marsden	San Francisco, Calif.
T. R. Rhea	Schenectady, N. Y.
H. I. Romnes	New York, N. Y.
C. F. Scott	Bridgeport, Conn.
J. G. Tarboux	Ithaca, N. Y.

Transfers

C. B. Carpenter, *Chairman;* Pacific Telephone & Telegraph Company, 509 S. W. Oak Street, Portland 4, Oreg.

W. C. Bloomquist	Schenectady, N. Y.
Charles Clos	New York, N. Y.
F. A. Cooper	St. Louis, Mo.
C. W. Fick	Cleveland, Ohio
J. D. Harper	Alcoa, Tenn.
F. S. Himebrook	Dayton, Ohio
M. R. Horne	Dearborn, Mich.
L. F. Hunt	Los Angeles, Calif.

(Continued on page 2172)

C. W. Keller	Denver, Colo.
J. W. Robinson	San Francisco, Calif.
E. W. Stone	De Kalb, Ill.
J. J. Tesar	Cleveland, Ohio
W. W. Walters	Chicago, Ill.
F. W. Willcutt	Washington, D. C.
H. B. Wood	Boston, Mass.

Professional Division Committees

Professional Division Advisory

W. Scott Hill, *Chairman;* Transformer and Allied Products Division, General Electric Company, 100 Woodlawn Ave., Pittsfield, Mass.

F. S. Black, *Vice-Chairman*	New York, N. Y.
C. J. Beller	Cleveland, Ohio
J. F. Calvert	Evanston, Ill.
A. G. Conrad	New Haven, Conn.
N. L. Freeman	Albany, N. Y.
A. H. Kehoe	New York, N. Y.
H. N. Muller, Jr.	East Pittsburgh, Pa.
J. J. Orr	New York, N. Y.
R. W. Sorensen	Pasadena, Calif.
F. W. Tatum	Dallas, Tex.

Charles LeGeyt Fortescue Fellowship

F. W. Bush	Milwaukee, Wis.
A. G. Conrad, *Chairman*	New Haven, Conn.
	(*Terms expire July 31, 1952*)
Guy Kleis	East Pittsburgh, Pa.
F. E. Sanford	Jackson, Mich.
	(*Terms expire July 31, 1953*)
F. H. Pumphrey	Gainesville, Fla.
J. D. Ryder	Urbana, Ill.
	(*Terms expire July 31, 1954*)

Code of Principles of Professional Conduct

R. W. Sorensen, *Chairman;* 384 South Holliston Avenue, Pasadena, Calif.

R. E. Argersinger	Boston, Mass.
Harry Barker	New York, N. Y.
Edith Clarke	Austin, Tex.
F. F. Evenson	San Diego, Calif.
E. S. Fields	Cincinnati, Ohio
C. A. Heinze	Los Angeles, Calif.
W. B. Kouwenhoven	Baltimore, Md.
R. D. Maxson	Chicago, Ill.
J. S. Waters	Houston, Tex.

Edison Medal

Appointed by the President for term of five years

Marvin W. Smith	Philadelphia, Pa.
H. S. Osborne	New York, N. Y.
H. A. Winne	Schenectady, N. Y.
	(*Terms expire July 31, 1952*)
D. I. Cone	San Francisco, Calif.
J. B. MacNeill	East Pittsburgh, Pa.
Philip Sporn	New York, N. Y.
	(*Terms expire July 31, 1953*)
J. L. Callahan	New York, N. Y.
J. M. Flanigen	Atlanta, Ga.
R. I. Wilkinson	New York, N. Y.
	(*Terms expire July 31, 1954*)
J. F. Calvert, *Chairman*	Evanston, Ill.
B. A. Case	Swampscott, Mass.
John Grotzinger	Akron, Ohio
	(*Terms expire July 31, 1955*)
A. H. Frampton	Toronto, Ontario, Canada
J. R. North	Jackson, Mich.
B. R. Teare, Jr.	Pittsburgh, Pa.
	(*Terms expire July 31, 1956*)

Members of Board of Directors elected by the Board for term of two years

M. D. Hooven	Newark, N. J.
F. O. McMillan	Corvallis, Oreg.
C. S. Purnell	New York, N. Y.
	(*Terms expire July 31, 1952*)
F. R. Benedict	Pittsburgh, Pa.
D. D. Ewing	Lafayette, Ind.
Victor Siegfried	Worcester, Mass.
	(*Terms expire July 31, 1953*)

Education

H. N. Muller, Jr., *Chairman;* Westinghouse Electric Corporation, East Pittsburgh, Pa.

E. B. Alexander	Binghamton, N. Y.
E. D. Ayres	Columbus, Ohio
R. D. Bennett	Silver Spring, Md.
R. L. Bieseie	Dallas, Tex.
E. W. Boehne	Cambridge, Mass.
D. S. Bridgman	New York, N. Y.
C. V. Bullen	Lubbock, Tex.
M. S. Coover	Ames, Iowa
W. C. DuVall	Boulder, Colo.
A. W. Friend	Elizabeth, N. J.
Henry E. Hartig	Minneapolis, Minn.
A. R. Hellwarth	Detroit, Mich.
F. C. Lindvall	Pasadena, Calif.
T. C. Lloyd	Springfield, Ohio
K. B. McEachron, Jr.	Schenectady, N. Y.
T. C. McFarland	Berkeley, Calif.
D. W. McLenegan	Richland, Wash.
E. W. Morris	Los Angeles, Calif
H. A. Peterson	Madison, Wis.
Walther Richter	Milwaukee, Wis.
J. D. Ryder	Urbana, Ill.
E. M. Strong	Ithaca, N. Y.
B. R. Teare, Jr.	Pittsburgh, Pa.
G. F. Tracy	Toronto, Ontario, Canada
Eric A. Walker	State College, Pa.
M. L. Waring	New York, N. Y.
S. Reid Warren, Jr.	Philadelphia, Pa.

Lamme Medal

C. B. Jolliffe	Princeton, N. J.
A. H. Kehoe, *Chairman*	New York, N. Y.
J. B. MacNeill	East Pittsburgh, Pa.
	(*Terms expire July 31, 1952*)
W. J. Barrett	Newark, N. J.
L. L. Bosch	Cincinnati, Ohio
Walther Richter	Milwaukee, Wis.
	(*Terms expire July 31, 1953*)
A. M. MacCutcheon	Shaker Heights, Ohio
B. L. Robertson	Berkeley, Calif.
Elgin B. Robertson	Dallas, Texas
	(*Terms expire July 31, 1954*)

Management

C. J. Beller, *Chairman;* Cleveland Electric Illuminating Company, 75 Public Square, Cleveland 13, Ohio

K. P. Applegate	Hartford, Conn.
E. D. Ayres	Columbus, Ohio
R. D. Bennett	Silver Spring, Md.
F. W. Bush	Milwaukee, Wis.
W. L. Cisler	Detroit, Mich.
S. M. Hamill, Jr.	Cincinnati, Ohio
E. E. Hill	New York, N. Y.
H. O. Hodson	Amarillo, Tex.
F. K. McCune	Schenectady, N. Y.
A. C. Monteith	Pittsburgh, Pa.
H. A. Peterson	New York, N. Y.
D. A. Quarles	New York, N. Y.
F. M. Roberts	Schenectady, N. Y.
D. D. Smalley	San Francisco, Calif.
J. B. Wiley	Norman, Okla.

Prizes, Award of Institute

J. J. Orr, *Chairman;* United States Rubber Company, 1230 6th Avenue, New York 20, N. Y.

Edward C. Day, *Secretary*	AIEE Headquarters
H. A. Affel	Murray Hill, N. J.
J. C. Aydelott	Erie, Pa.
G. S. Brown	Cambridge, Mass.
H. F. Brown	New Haven, Conn.
W. R. Brownlee	Birmingham, Ala.
W. G. Dow	Ann Arbor, Mich.
A. J. Maslin	Sharon, Pa.
K. B. McEachron	Pittsfield, Mass.
G. W. Scott, Jr.	Lancaster, Pa.
B. G. A. Skrotzki	New York, N. Y.
A. B. Smith	Chicago, Ill.
S. D. Summers	Washington, D. C.
H. M. Turner	New Haven, Conn.
L. A. Umansky	Schenectady, N. Y.
C. H. Willis	Princeton, N. J.
Harold Winograd	Milwaukee, Wis.

Registration of Engineers

N. L. Freeman, *Chairman;* Board of Examiners of Professional Engineers and Land Surveyors, 23 S. Pearl Street, Albany 7, N. Y.

(*Continued in next column*)

H. A. Carlberg	Richland, Wash.
J. H. Foote	Jackson, Mich.
Ward Harrison	Cleveland, Ohio
K. B. McEachron	Pittsfield, Mass.
E. W. Oesterreich	Pittsburgh, Pa.
Elgin B. Robertson	Dallas, Tex.
C. G. Roush	Kansas City, Mo.
R. V. Shepherd	Schenectady, N. Y.
R. W. Sorensen	Pasadena, Calif.

Student Branches

F. W. Tatum, *Chairman;* Southern Methodist University, Dallas, Tex.

J. C. Clark	Tucson, Ariz.
R. F. Danner	Oklahoma City, Okla.
W. H. Erickson	Ithaca, N. Y.
K. A. Fegley	Philadelphia, Pa.
P. M. Honnell	St. Louis, Mo.
R. C. Lewis	Los Angeles, Calif.
C. A. Mann	Cleveland, Ohio
A. J. McCrocklin, Jr.	Austin, Tex.
H. N. Muller, Jr.	East Pittsburgh, Pa.
S. I. Pearson	Boulder, Colo.
R. G. Porter	Boston, Mass.
E. A. Reid	Urbana, Ill.
J. D. Ryder	Urbana, Ill.
L. N. Stone	Corvallis, Oreg.
J. G. Tarboux	Ithaca, N. Y.
C. F. Terwilliger	Schenectady, N. Y.
D. H. Vliet	New Orleans, La.
R. T. Weil	New York, N. Y.

Volta Scholarship Trustees

C. A. Powel	Boston, Mass.
	(*Term expires July 31, 1953*)
H. S. Osborne, *Chairman*	New York, N. Y.
	(*Term expires July 31, 1955*)
D. D. Ewing	Lafayette, Ind.
	(*Term expires July 31, 1957*)

Technical Committees

Communication Division

Communication Division Committee

F. B. Bramhall, *Chairman;* Western Union Telegraph Company, 60 Hudson Street, New York 13, N. Y.

H. A. Affel, *Vice-Chairman*	Murray Hill, N. J.
I. S. Coggeshall, *Secretary*	New York, N. Y.
L. G. Abraham	Murray Hill, N. J.
W. J. Barrett (*representing Board of Directors*)	Newark, N. J.
J. L. Callahan	New York, N. Y.
E. C. Chamberlin, Jr.	New York, N. Y.
J. B. Coleman	Camden, N. J.
A. T. Lattauzeo	New York, N. Y.
John Meszar	New York, N. Y.
H. I. Romnes	New York, N. Y.
G. T. Royden	New York, N. Y.

Committee on Communication Switching System

John Meszar, *Chairman;* Bell Telephone Laboratories, Inc., 463 West Street, New York 14, N. Y.

A. E. Frost, *Vice-Chairman*	New York, N. Y.
William Keister, *Secretary*	New York, N. Y.
Eric Brooke	Galion, Ohio
L. L. Burns	Dallas, Tex.
R. C. Davis	New York, N. Y.
W. E. Glomski	St. Louis, Mo.
G. H. Gray	Little Falls, N. J.
R. S. Neikirk	Washington, D. C.
H. V. Schofield	New York, N. Y.
J. O'D. Shepherd	Atlanta, Ga.
A. B. Smith	Chicago, Ill.
D. L. Solomon	Alexandria, Va.
W. G. Storey	Chicago, Ill.
C. M. Tomlinson	Philadelphia, Pa.

No subcommittees

Committee on Radio Communications Systems

G. T. Royden, *Chairman;* Mackay Radio and Telegraph Company, 67 Broad Street, New York 4, N. Y.

A. C. Dickieson, *Vice-Chairman*	Murray Hill, N. J.
H. P. Corwith, *Secretary*	New York, N. Y.
C. M. Backer	Philadelphia, Pa.
I. F. Byrnes	New York, N. Y.
R. D. Campbell	New York, N. Y.
Edward Daskam, Jr.	New York, N. Y.
G. E. Dodrill	Washington, D. C.
L. W. Gregory	Baltimore, Md.
L. B. Grew	New Haven, Conn.
D. D. Grieg	Nutley, N. J.
J. W. Kearney	Mineola, L. I., N. Y.
S. C. Leyland	Newark, N. J.
L. P. Morris	Chicago, Ill.
J. E. Reid	Toronto, Ontario, Canada
Hubert Sharp	Denver, Colo.
C. E. Smith	Cleveland, Ohio
L. R. Spaulding	Portland, Oreg.
David Talley	Clifton, N. J.
J. M. Walsh	New York, N. Y.

Mobile Radio Subcommittee

A. C. Dickieson, *Chairman;* Bell Telephone Laboratories, Inc., Murray Hill, N. J.

C. M. Backer	Philadelphia, Pa.
I. F. Byrnes	New York, N. Y.
G. E. Dodrill	Washington, D. C.
L. B. Grew	New Haven, Conn.
J. W. Kearney	Mineola, L. I., N. Y.
L. P. Morris	Chicago, Ill.
J. E. Reid	Toronto, Ontario, Canada
C. E. Smith	Cleveland, Ohio
David Talley	New York, N. Y.

Point-to-Point Radio Subcommittee

H. P. Corwith, *Chairman;* Western Union Telegraph Company, 60 Hudson Street, New York 13, N. Y.

C. M. Backer	Philadelphia, Pa.
R. D. Campbell	New York, N. Y.
Edward Daskam, Jr.	New York, N. Y.
G. E. Dodrill	Washington, D. C.
L. W. Gregory	Baltimore, Md.
D. D. Grieg	Nutley, N. J.
S. C. Leyland	Newark, N. J.
Hubert Sharp	Denver, Colo.
L. R. Spaulding	Portland, Oreg.
J. M. Walsh	New York, N. Y.

Committee on Special Communications Applications

A. T. Lattauzeo, *Chairman;* Westinghouse Electric Corporation, 40 Wall Street, New York 5, N. Y.

Melville Eastham, *Vice-Chairman*	Cambridge, Mass.
L. C. Holmes, *Secretary*	Rochester, N. Y.
A. G. Clavier	Nutley, N. J.
G. J. Crowdes	Cambridge, Mass.
A. A. James	New Haven, Conn.
R. H. Kline	Baltimore, Md.
W. A. Ready	Malden, Mass.
T. W. Stringfield	Portland, Oreg.

Electro-Acoustics Subcommittee

W. A. Ready, *Chairman;* National Company, Inc., 61 Sherman Street, Malden, Mass.

Melville Eastham	Cambridge, Mass.
T. W. Stringfield	Portland, Oreg.

Railroad Communications Subcommittee

R. H. Kline, *Chairman;* Westinghouse Electric Corporation, 3601 Washington Boulevard, Baltimore 27, Md.

W. D. Hailes	Rochester, N. Y.

Special Activities Subcommittee

G. J. Crowdes, *Chairman;* Simplex Wire and Cable Company, 66 Sidney Street, Cambridge, Mass.

A. G. Clavier	Nutley, N. J.
A. A. James	New Haven, Conn.

Committee on Telegraph Systems

E. C. Chamberlin, Jr., *Chairman;* Western Union Telegraph Company, 60 Hudson Street, New York 13, N. Y.

J. A. Duncan, Jr., *Vice-Chairman*	New York, N. Y.
R. B. Shanck, *Secretary*	New York, N. Y.
A. S. Benjamin	Chicago, Ill.
A. G. Cooley	New York, N. Y.
L. C. Edie	Clifton, N. J.
L. G. Erickson	San Carlos, Calif.
D. F. Hazen, Jr.	New York, N. Y.
J. V. L. Hogan	New York, N. Y.
Charles Jelinek, Jr.	New York, N. Y.
Alfred Kahn	New York, N. Y.
R. E. Pierce	New York, N. Y.
L. A. Smith	New York, N. Y.
R. B. Steele	Toronto, Ontario, Canada
E. F. Watson	New York, N. Y.
H. P. Westman, Sr.	New York, N. Y.

Facsimile Subcommittee

A. G. Cooley, *Chairman;* Times Facsimile Corporation, 540 W. 58th Street, New York 19, N. Y.

J. V. L. Hogan	New York, N. Y.
Charles Jelinek, Jr.	New York, N. Y.
E. F. Watson	New York, N. Y.

Committee on Television and Aural Broadcasting Systems

J. B. Coleman, *Chairman;* Radio Corporation of America, R.C.A. Victor Division, Camden, N. J.

I. J. Kaar, *Vice-Chairman*	Syracuse, N. Y.
W. L. Lawrence, *Secretary*	Camden, N. J.
G. H. Brown	Princeton, N. J.
W. F. Cotter	Chicago, Ill.
L. G. Cumming	New York, N. Y.
C. E. Dean	Little Neck, L. I., N. Y.
D. G. Fink	New York, N. Y.
P. C. Goldmark	New York, N. Y.
W. H. Heiser	East Paterson, N. J.
Scott Helt	Passaic, N. J.
K. W. Jarvis	Chicago, Ill.
E. M. Johnson	New York, N. Y.
D. G. Little	Baltimore, Md.
F. H. McIntosh	Washington, D. C.
C. B. Plummer	Washington, D. C.
E. G. Ports	Nutley, N. J.
J. W. Rieke	Murray Hill, N. J.
L. M. Rodgers	Philadelphia, Pa.
R. E. Shelby	New York, N. Y.
F. R. Small	St. Louis, Mo.
S. C. Spielman	Philadelphia, Pa.
V. E. Trouant	Camden, N. J.
J. C. Van Arsdell, Jr.	Erie, Pa.

No subcommittees

Committee on Wire Communications Systems

L. G. Abraham, *Chairman;* Bell Telephone Laboratories, Inc., Murray Hill, N. J.

G. B. Ransom, *Vice-Chairman*	New York, N. Y.
P. G. Edwards, *Secretary*	Murray Hill, N. J.
A. L. Albert	Corvallis, Oreg.
W. M. Allen	New York, N. Y.
E. D. Barcus	Los Angeles, Calif.
Hezzie Clark	Houston, Tex.
A. B. Credle	Ithaca, N. Y.
G. E. Dodrill	Washington, D. C.
H. E. Ellithorn	Notre Dame, Ind.
L. G. Erickson	San Carlos, Calif.
D. G. Geiger	Toronto, Ontario, Canada
R. F. Gosnell	St. Louis, Mo.
G. H. Gray	Little Falls, N. J.
W. D. Hailes	Rochester, N. Y.
E. B. Hansen	Seattle, Wash.
L. M. Hartwell	Dallas, Tex.
H. R. Hunkins	Clifton, N. J.
H. R. Huntley	New York, N. Y.
L. H. Hutchins	Cambridge, Mass.
E. R. Jones	Denver, Colo.
R. R. O'Connor	Chicago, Ill.
W. F. Potter	Boston, Mass.
A. L. Rumsey	Albany, N. Y.
L. M. Schindel	Kansas City, Mo.
L. J. Shaffer	Cleveland, Ohio
A. B. Smith	Chicago, Ill.
L. A. Smith	New York, N. Y.
W. T. Smith	Washington, D. C.
H. W. Sundius	New Haven, Conn.

No subcommittees

General Applications Division

General Applications Division Committee

C. F. Scott, *Chairman;* General Electric Company, 1285 Boston Avenue, Bridgeport 8, Conn.

H. F. Brown, *Vice-Chairman*	New Haven, Conn.
W. H. Reed, *Secretary*	New York, N. Y.
L. W. Birch	Mansfield, Ohio
T. H. Cline	Newark, Ohio
J. B. Feder	Washington, D. C.
C. W. Fick (*representing Board of Directors*)	Cleveland, Ohio
D. E. Fritz	Cleveland, Ohio
R. C. Putnam	Cleveland, Ohio
S. D. Summers	Washington, D. C.
C. C. Whipple	Brooklyn, N. Y.

Committee on Air Transportation

D. E. Fritz, *Chairman;* Jack and Heintz, Inc., Cleveland 1, Ohio

W. L. Berry, *Vice-Chairman*	Culver City, Calif.
R. H. Keith, *Secretary*	Lima, Ohio
J. W. Allen	Teterboro, N. J.
G. W. Almassy	Los Angeles, Calif.
B. O. Austin	Lima, Ohio
E. P. Barlow	Baltimore, Md.
J. H. Blankenbuehler	Troy, Ohio
W. V. Boughton	So. Pasadena, Calif.
W. C. Bryant	Burbank, Calif.
J. P. Dallas	Culver City, Calif.
J. C. Dieffenderfer	Dayton, Ohio
Peter Duyan, Jr.	Santa Monica, Calif.
D. W. Exner	Seattle, Wash.
H. E. Felix	Tulsa, Okla.
Fred Foulon	El Segundo, Calif.
E. A. Freitas	Hawthorne, Calif.
Elio Fueyo	Miami, Fla.
C. E. Gagnier	Torrance, Calif.
S. H. Hanville, Jr.	Washington, D. C.
R. D. Jones	Fort Wayne, Ind.
Irving Kalikow	West Lynn, Mass.
W. B. Keller	Cleveland, Ohio
E. F. Kotnik	San Diego, Calif.
L. R. Larson	Washington, D. C.
Karl Martinez	Seattle, Wash.
John Maxian, Jr.	Los Angeles, Calif.
C. F. McCabe	San Diego, Calif.
R. S. Mead	Kansas City, Mo.
R. A. Millermaster	Milwaukee, Wis.
J. D. Miner	Lima, Ohio
C. R. Moore	Inglewood, Calif.
Joseph Nader	Chicago, Ill.
R. L. Olson	St. Paul, Minn.
G. A. Phillips	Schenectady, N. Y.
H. F. Rempt	Burbank, Calif.
K. R. Smythe	Johnsville, Pa.
G. E. Sylvester	Fort Worth, Tex.
F. H. Walker	Buffalo, N. Y.
S. H. Webster	Teterboro, N. J.

Aircraft Electrical Rotating Machinery Subcommittee

L. R. Larson, *Chairman;* Naval Research Laboratory, Washington, D. C.

S. H. Hanville, Jr.	Washington, D. C.
R. D. Jones	Fort Wayne, Ind.
Irving Kalikow	Lynn, Mass.
R. R. Miille	Lima, Ohio
F. M. Potter	Teterboro, N. J.
R. R. Smith	Baltimore, Md.
H. R. Tragesser	Cleveland, Ohio
L. A. Zahorsky	Grand Rapids, Mich.

Aircraft Electrical Systems Subcommittee

G. A. Phillips, *Chairman;* Aviation Divisions, General Electric Company, Schenectady, N. Y.

Phil. Binderman	Washington, D. C.
R. L. Brown	Teterboro, N. J.
L. M. Cobb	Johnsville, Pa.
D. W. Exner	Seattle, Wash.
L. H. Hildebrandt	Dayton, Ohio
T. H. McNary, Jr.	Wichita, Kan.
C. L. Mershon	Lima, Ohio
Charles Milliken	Burbank, Calif.
R. L. Olson	St. Paul, Minn.
D. H. Scott	Washington, D. C.
O. C. Walley	Cleveland, Ohio

Principles of Altitude Rating of Electrical Apparatus Subcommittee

Karl Martinez, *Chairman;* Boeing Airplane Company, Plant 1, Seattle, Wash.

S. H. Hanville, Jr.	Washington, D. C.
V. C. Holloway	Johnsville, Pa.
G. C. Martin	Cleveland, Ohio
L. Pico	Dayton, Ohio
L. A. Zahorsky	Grand Rapids, Mich.

Aircraft Electrical Control, Protective Devices and Cable Subcommittee

B. O. Austin, *Chairman;* Aviation Engineering Department, Westinghouse Electric Corporation, Lima, Ohio

Earl Barlow	Baltimore, Md.
E. L. Bottemiller	Schenectady, N. Y.
W. V. Bryant	Burbank, Calif.
A. J. Mustard	Miami, Fla.
R. A. Millermaster	Milwaukee, Wis.
W. G. Neild	Teterboro, N. J.
E. R. Olson	Richmond, Ind.
J. Ottmar	Attleboro, Mass.
J. W. Pobst	Johnsville, Pa.
J. C. Thomas	Dayton, Ohio
Omar Wally	Cleveland, Ohio

Committee on Domestic and Commercial Applications

T. H. Cline, *Chairman;* Newark Stove Company, 550 Wehrle Avenue, Newark, Ohio

T. C. Johnson, *Vice-Chairman*	Bloomfield, N. J.
J. P. Harris, *Secretary*	Cleveland, Ohio
J. C. Beckett	San Francisco, Calif.
C. D. Bratiotis	Boston, Mass.
W. B. Buchanan	Toronto, Ontario, Canada
O. K. Buck	Los Angeles, Calif.
V. P. Campbell	Newport, Wash.
W. R. Crawford	Cincinnati, Ohio
L. R. Emmert	East Pittsburgh, Pa.
R. W. Fauquet	Chicago, Ill.
J. F. Frazier	Corning, N. Y.
R. R. Herrmann	Minneapolis, Minn.
H. F. Hoebel	New York, N. Y.
B. H. Martin	Chattanooga, Tenn.
T. L. Matney	Richland, Wash.
W. G. Meese	Detroit, Mich.
C. W. Meytrott	New York, N. Y.
J. H. Oliver	Schenectady, N. Y.
B. F. Parr	Mansfield, Ohio
L. N. Roberson	Seattle, Wash.
G. E. Schall, Jr.	New York, N. Y.
C. F. Scott	Bridgeport, Conn.
W. B. Shepperd	State College, Pa.
G. S. Smith	Seattle, Wash.
T. T. Woodson	Jeffersontown, Ky.
R. F. Zimmerman	Dayton, Ohio

Electric Space Heating and Heat Pumps Subcommittee (West Coast)

V. P. Campbell, *Chairman;* Public Utility District Number 1, Pend Oreille County, Box G, Newport, Wash.

J. C. Beckett	San Francisco, Calif.
O. K. Buck	Los Angeles, Calif.
L. N. Roberson	Seattle, Wash.
G. S. Smith	Seattle, Wash.

Electric Space Heating and Heat Pumps Subcommittee (East Coast)

H. F. Hoebel, *Chairman;* American Gas and Electric Service Corp., 30 Church Street, New York 8, N. Y.

(Personnel to be selected)

Domestic Appliances Subcommittee

T. T. Woodson, *Chairman;* General Electric Company, 1285 Boston Avenue, Bridgeport 2, Conn.

W. B. Buchanan	Toronto, Ontario, Canada
B. F. Parr	Mansfield, Ohio
C. F. Scott	Bridgeport, Conn.
R. F. Zimmerman	Dayton, Ohio

(*Continued in next column*)

Farm Electrification Subcommittee

W. R. Crawford, *Chairman;* Crosley Division, AVCO Manufacturing Company, 1329 Arlington Street, Cincinnati 25, Ohio

L. R. Emmert	East Pittsburgh, Pa.
R. W. Fauquet	Chicago, Ill.
H. H. Kelly	Washington, D. C.
W. G. Meese	Detroit, Mich.
W. B. Shepperd	State College, Pa.

Committee on Land Transportation

L. W. Birch, *Chairman;* Ohio Brass Company, Transportation Department, Mansfield, Ohio

S. R. Negley, *Vice-Chairman*	Philadelphia, Pa.
G. M. Woods, *Secretary*	East Pittsburgh, Pa.
J. C. Aydelott	Erie, Pa.
L. S. Billau	Baltimore, Md.
H. R. Blomquist	Providence, R. I.
W. A. Brecht	East Pittsburgh, Pa.
H. F. Brown	New Haven, Conn.
D. M. Burckett	Boston, Mass.
C. N. Chase	Brooklyn, N. Y.
R. J. Corfield	Garfield, Utah
Andrew Costic	Hoboken, N. J.
Llewellyn Evans	Chattanooga, Tenn.
A. P. Frey	Baltimore, Md.
J. E. Gardner	Chicago, Ill.
K. H. Gordon	Philadelphia, Pa.
P. H. Hatch	Erie, Pa.
G. L. Hoard	Seattle, Wash.
J. G. Inglis	Toronto, Ontario, Canada
A. P. Jerencsik	Columbus, Ohio
Charles Kerr, Jr.	East Pittsburgh, Pa.
R. L. Kimball	New York, N. Y.
S. B. Lent	Boston, Mass.
T. M. C. Martin	Portland, Oreg.
P. A. McGee	New York, N. Y.
E. B. Meissner	St. Louis, Mo.
I. S. Nippes	Ridgway, Pa.
A. G. Oehler	New York, N. Y.
W. R. Simmons	Montreal, Quebec, Canada
Dwight L. Smith	Highwood, Ill.
Jacob Stair, Jr.	Philadelphia, Pa.
M. C. Swanson	Schenectady, N. Y.
J. D. Sylvester	Montreal, Quebec, Canada
R. S. Warren	Elkhart, Ind.
R. A. Williamson	Erie, Pa.
H. P. Wright	Baltimore, Md.
Lawrence Wylie	Seattle, Wash.

Heavy Traction Electrification Data Subcommittee

L. W. Birch, *Chairman;* Ohio Brass Company, Mansfield, Ohio

H. F. Brown	New Haven, Conn.
A. G. Oehler	New York, N. Y.
R. A. Williamson	Erie, Pa.
G. M. Woods	East Pittsburgh, Pa.

Projects:

(*1*). Catenary overhead systems
(*2*). Third rail systems
(*3*). Electric locomotives
(*4*). Substations
(*5*). Power supply

The personnel of the projects is as follows:

(*1*) and (*2*). L. W. Birch, *Chairman*, Ohio Brass Company, Mansfield, Ohio; H. F. Brown, New Haven, Conn.

(*3*), (*4*), and (*5*). A. G. Oehler, New York, N. Y.; R. A. Williamson, Erie, Pa.; G. M. Woods, East Pittsburgh, Pa.

Heavy Traction Papers and Plans Subcommittee

H. F. Brown, *Chairman;* New York, New Haven, and Hartford Railroad, Railroad Station, New Haven, Conn.

W. A. Brecht	East Pittsburgh, Pa.
R. L. Kimball	New York, N. Y.
T. M. C. Martin	Portland, Oreg.
S. R. Negley	Philadelphia, Pa.
M. C. Swanson	Schenectady, N. Y.
Lawrence Wylie	Seattle, Wash.

Light Traction Papers and Plans Subcommittee

G. M. Woods, *Chairman;* Industry Engineering Department 11-L, Westinghouse Electric Corporation, East Pittsburgh, Pa.
J. C. Aydelott Erie, Pa.
H. R. Blomquist Providence, R. I.
J. G. Inglis Toronto, Ontario, Canada
S. B. Lent Boston, Mass.
W. R. Simmons Montreal, Quebec, Canada
Dwight L. Smith Highwood, Ill.

Subcommittee on Revision of AIEE Standard Number 16 (Electric Railway Control Apparatus) ASA C48

R. A. Williamson, *Chairman;* Railroad Rolling Stock Division of Locomotive and Car Equipments Divisions, General Electric Company, Erie, Pa.
P. H. Hatch Erie, Pa.
J. G. Inglis Toronto, Ontario, Canada
G. M. Woods East Pittsburgh, Pa.

Committee on Marine Transportation

J. B. Feder, *Chairman;* United States Coast Guard, Merchant Marine Technical Division, 1300 E Street North West, Washington 25, D. C.
W. E. Jacobsen, *Vice-Chairman* Schenectady, N. Y.
W. N. Zippler, *Secretary* New York, N. Y.
W. B. Armstrong Washington, D. C.
H. C. Coleman East Pittsburgh, Pa.
P. J. DuMont New York, N. Y.
R. W. Frost Amesbury, Mass.
A. R. Gatewood New York, N. Y.
E. A. Geary Camden, N. J.
L. M. Goldsmith Philadelphia, Pa.
P. A. Guise New York, N. Y.
H. F. Harvey, Jr. Newport News, Va.
J. E. Jones Milwaukee, Wis.
Cornelius Krommenhock Brooklyn, N. Y.
V. W. Mayer Washington, D. C.
S. N. Mead Amesbury, Mass.
W. H. Reed New York, N. Y.
E. M. Rothen New York, N. Y.
J. D. Shuster Quincy, Mass.
C. W. Souder Glen Cove, N. Y.
E. H. Stivender Milwaukee, Wis.
G. O. Watson London, England
O. A. Wilde Chester, Pa.

Power Generation Subcommittee

O. A. Wilde, *Chairman;* Sun Shipbuilding and Dry Dock Company, Chester, Pa.
W. B. Armstrong Washington, D. C.
H. C. Coleman East Pittsburgh, Pa.
L. M. Goldsmith Philadelphia, Pa.
W. E. Jacobsen Schenectady, N. Y.
E. H. Stivender Milwaukee, Wis.

Power Application Subcommittee

L. M. Goldsmith, *Chairman;* Atlantic Refining Company, 260 South Broad Street, Philadelphia, Pa.
W. B. Armstrong Washington, D. C.
H. C. Coleman East Pittsburgh, Pa.
W. E. Jacobsen Schenectady, N. Y.
J. E. Jones Milwaukee, Wis.
E. H. Stivender Milwaukee, Wis.

Wires and Cables Subcommittee

W. N. Zippler, *Chairman;* Gibbs and Cox, Inc., 1 Broadway, New York 4, N. Y.
P. J. DuMont New York, N. Y.
J. B. Feder Washington, D. C.
A. R. Gatewood New York, N. Y.
W. E. Jacobsen Schenectady, N. Y.
V. W. Mayer Washington, D. C.
W. H. Reed New York, N. Y.

Switchboards and Control Subcommittee

H. C. Coleman, *Chairman;* Westinghouse Electric Corporation, East Pittsburgh, Pa.
P. J. DuMont New York, N. Y.
H. F. Harvey, Jr. Newport News, Va.
J. E. Jones Milwaukee, Wis.
Cornelius Krommenhock Brooklyn, N. Y.
J. D. Shuster Quincy, Mass.
E. H. Stivender Milwaukee, Wis.

Distribution Subcommittee

H. F. Harvey, Jr., *Chairman;* Newport News Shipbuilding and Dry Dock Company, Newport News, Va.
W. B. Armstrong Washington, D. C.
A. R. Gatewood New York, N. Y.
E. A. Geary Camden, N. J.
L. M. Goldsmith Philadelphia, Pa.
P. A. Guise New York, N. Y.
V. W. Mayer Washington, D. C.
W. N. Zippler New York, N. Y.

Fittings and Appliances Subcommittee

V. W. Mayer, *Chairman;* United States Maritime Commission, Technical Division, United States Department of Commerce Building, Washington, D. C.
P. J. DuMont New York, N. Y.
R. W. Frost Amesbury, Mass.
E. A. Geary Camden, N. J.
P. A. Guise New York, N. Y.
H. F. Harvey, Jr. Newport News, Va.
E. M. Rothen New York, N. Y.
J. D. Shuster Quincy, Mass.
O. A. Wilde Chester, Pa.

Communications and Alarm Subcommittee

W. H. Reed, *Chairman;* Bruce Electric Company, 196 West Houston Street, New York 14, N. Y.
R. W. Frost Amesbury, Mass.
A. R. Gatewood New York, N. Y.
E. A. Geary Camden, N. J.
Cornelius Krommenhock Brooklyn, N. Y.
S. N. Mead Amesbury, Mass.
E. M. Rothen New York, N. Y.
J. D. Shuster Quincy, Mass.
C. W. Souder Great Neck, N. Y.

Navigation Equipment Subcommittee

S. N. Mead, *Chairman;* Sig-Trans, Inc., Haverhill Road, Amesbury, Mass.
R. W. Frost Amesbury, Mass.
P. A. Guise New York, N. Y.
Cornelius Krommenhock Brooklyn, N. Y.
E. M. Rothen New York, N. Y.
C. W. Souder Great Neck, N. Y.

Publicity, Personnel, and History Subcommittee

W. H. Reed, *Chairman;* Bruce Electric Company, 196 West Houston Street, New York 14, N. Y.
H. F. Harvey, Jr. Newport News, Va.
W. N. Zippler New York, N. Y.

Editing Subcommittee

W. N. Zippler, *Chairman;* Gibbs and Cox, Inc., 1 Broadway, New York 4, N. Y.
J. B. Feder Washington, D. C.
H. F. Harvey, Jr. Newport News, Va.
W. H. Reed New York, N. Y.

International Standardization Subcommittee

A. R. Gatewood, *Chairman;* American Bureau of Shipping, 45 Broad Street, New York 4, N. Y.
H. C. Coleman East Pittsburgh, Pa.
H. F. Harvey, Jr. Newport News, Va.
W. N. Zippler New York, N. Y.

Committee on Production and Application of Light

R. C. Putnam, *Chairman;* Case Institute of Technology, Electrical Engineering Department, 10900 Euclid Avenue, Cleveland 6, Ohio
R. L. Oetting, *Secretary* Cleveland, Ohio
J. F. Angier Washington, D. C.
L. H. Brown Stanford, Calif.
S. W. Bruun New York, N. Y.
H. S. Bull Ann Arbor, Mich.
M. D. Clayton Storrs, Conn.
J. F. Dickerhoff Mineola, L. I., N. Y.
G. C. Harvey Fort Wayne, Ind.
O. W. Holden Los Angeles, Calif.
H. E. Mahan West Lynn, Mass.
F. H. Murphy Portland, Oreg.
Harris Reinhardt New York, N. Y.
D. W. Rowten Cleveland, Ohio
E. H. Salter New York, N. Y.
T. C. Sargent Salem, Mass.
E. M. Strong Ithaca, N. Y.
J. D. Thomas Jacksonville, Fla.
H. F. Wall Detroit, Mich.
M. N. Waterman Bloomfield, N. J.
C. C. Whipple Brooklyn, N. Y.

Nomenclature of Electronic Lamps Subcommittee

(Personnel to be selected)

Infrared Radiations Subcommittee

(Personnel to be selected)

Ultraviolet Radiations Subcommittee

(Personnel to be selected)

Industry Division

Industry Division Committee

T. R. Rhea, *Chairman;* Industrial Engineering Department, General Electric Company, Schenectady 5, N. Y.
R. S. Gardner, *Secretary* New York, N. Y.
H. G. Barnett East Pittsburgh, Pa.
C. N. Clark Pittsburgh, Pa.
J. A. Cortelli Cleveland, Ohio
P. H. Goodell Detroit, Mich.
S. W. Herwald Pittsburgh, Pa.
G. W. Heumann Schenectady, N. Y.
V. O. Johnson New York, N. Y.
A. C. Muir Philadelphia, Pa.
L. W. Roush South Charleston, W. Va.
Victor Siegfried (*representing Board of Directors*) Worcester, Mass.

Committee on Chemical, Electrochemical and Electrothermal Applications

L. W. Roush, *Chairman;* P. O. Box 8395, South Charleston 3, W. Va.
J. Z. Linsenmeyer, *Secretary* East Pittsburgh, Pa.
F. V. Andreae Chattanooga, Tenn.
F. M. Baxandall Midland, Mich.
F. R. Benedict Pittsburgh, Pa.
E. C. Benjamin New York, N. Y.
F. T. Bowditch Cleveland, Ohio
E. H. Browning East Pittsburgh, Pa.
A. B. Campbell Houston, Tex.
W. H. Dickinson Linden, N. J.
W. C. Dreyer Houston, Tex.
F. S. Glaza Freeport, Tex.
W. E. Gutzwiller Milwaukee, Wis.
E. A. Hanff Pittsburgh, Pa.
J. D. Harper Alcoa, Tenn.
T. G. Hieronymus Kansas City, Mo.
J. E. Hobson Stanford, Calif.
H. E. Houck Wilmington, Del.
J. D. Huntsberger Trenton, N. J.
M. A. Hyde, Jr. East Pittsburgh, Pa.
F. L. Kaestle Schenectady, N. Y.
R. J. Kuhn New Orleans, La.
F. L. Lawton Montreal, Quebec, Canada
D. H. Levy Dallas, Tex.
J. J. Loustaunau Boston, Mass.
J. A. McLellan Linden, N. J.
F. J. Mollerus Richland, Wash.
Waldo Porter Vancouver, Wash.
H. E. Ramsey Port Arthur, Tex.
R. L. Rayner Detroit, Mich.
H. C. Riggs Philadelphia, Pa.
S. J. Rosch Hastings-on-Hudson, N. Y.
G. B. Scheer Oakland, Calif.
E. O. Scott Welland, Ontario, Canada
Herbert Speight Santa Barbara, Calif.
J. J. Unger Cleveland, Ohio
H. W. Wahlquist New York, N. Y.
R. M. Wainwright Urbana, Ill.
H. H. Zielinski Schenectady, N. Y.

Cathodic Protection Subcommittee

R. M. Wainwright, *Chairman;* College of Engineering, University of Illinois, Urbana, Ill.
F. J. Mollerus, *Secretary* Richland, Wash.
A. E. Archambault New York, N. Y.
J. D. Brance Houston, Tex.
A. S. Brooks Newark, N. J.
A. B. Campbell Houston, Tex.
Guy Corfield Los Angeles, Calif.
G. C. Cox Charleston, W. Va.
I. A. Denison Washington, D. C.
I. C. Dietze Los Angeles, Calif.
L. J. Gorman New York, N. Y.
T. G. Hieronymus Kansas City, Mo.
H. D. Holler Chevy Chase, Md.
R. J. Kuhn New Orleans, La.
R. W. Linney Oklahoma City, Okla.
J. P. Oliver Cleveland, Ohio
R. L. Rayner Detroit, Mich.
H. W. Wahlquist New York, N. Y.

Chemical Industry Subcommittee

L. W. Roush, *Chairman;* P. O. Box 8395, South Charleston 3, W. Va.
J. J. Loustaunau, *Secretary* Boston, Mass.
F. R. Benedict Pittsburgh, Pa.
L. L. Carter Hastings-on-Hudson, N. Y.
I. H. Coen East Pittsburgh, Pa.
F. S. Glaza Freeport, Tex.
R. C. Graham Rome, N. Y.
J. E. Hobson Stanford, Calif.
H. E. Houck Wilmington, Del.
N. D. Kenney Cambridge, Mass.
A. E. Maibauer New York, N. Y.
S. J. Rosch Hastings-on-Hudson, N. Y.
Herbert Speight Santa Barbara, Calif.

Electrochemical Processes Subcommittee

W. E. Gutzwiller, *Chairman;* Allis-Chalmers Manufacturing Company, Box 512, Milwaukee 1, Wis.
G. F. Jones, *Secretary* East Pittsburgh, Pa.
J. R. Auld Montreal, Quebec, Canada
F. M. Baxandall Midland, Mich.
P. M. Fischer Barberton, Ohio
J. N. Fogg Baton Rouge, La.
E. M. Hansford Alloy, W. Va.
A. D. Hargroder Lake Charles, La.
J. D. Harper Alcoa, Tenn.
John Kiefer Jones Mills, Ark.
C. A. Langlois Troutdale, Oreg.
F. L. Lawton Montreal, Quebec, Canada
A. E. Marshall St. Louis, Mo.
Waldo Porter Vancouver, Wash.
G. B. Scheer Oakland, Calif.
J. T. Thwaites Hamilton, Ontario, Canada
J. W. Tracht Wyandotte, Mich.
R. N. Wagner Pittsburgh, Pa.

Electrothermal Processes Subcommittee

E. H. Browning, Jr., *Chairman;* Westinghouse Electric Corporation, 700 Braddock Avenue, East Pittsburgh, Pa.
F. T. Bowditch, *Secretary* Cleveland, Ohio
F. V. Andreae Chattanooga, Tenn.
W. L. Bundy Wilson Dam, Ala.
R. A. Geiselman East Pittsburgh, Pa.
E. A. Hanff Pittsburgh, Pa.
A. R. Oltrogge Schenectady, N. Y.
E. O. Scott Welland, Ontario, Canada
J. J. Unger Cleveland, Ohio

Petroleum Industry Subcommittee

J. Z. Linsenmeyer, *Chairman;* Industrial Engineering Department, Westinghouse Electric Corporation, East Pittsburgh, Pa.
C. R. Olson, *Secretary* East Pittsburgh, Pa.
H. J. Appel New York, N. Y.

(*Continued on page 2175*)

E. C. Benjamin	New York, N. Y.
W. H. Dickinson	Linden, N. J.
W. C. Dreyer	Houston, Tex.
E. R. Hoyle	East Chicago, Ind.
M. A. Hyde, Jr.	East Pittsburgh, Pa.
D. H. Levy	Dallas, Tex.
J. A. McLellan	Linden, N. J.
E. L. Nopper	Philadelphia, Pa.
H. E. Ramsey	Port Arthur, Tex.

Storage Batteries Subcommittee

H. C. Riggs, *Chairman;* Electric Storage Battery Company, 19th and Allegheny Avenues, Philadelphia 32, Pa.

H. H. Zielinski, *Secretary*	Schenectady, N. Y.
J. D. Huntsberger	Trenton, N. J.
L. A. Murray	Providence, R. I.
E. T. Rummel	Cleveland, Ohio
J. J. Unger	Cleveland, Ohio
K. A. Vaughn	Depew, N. Y.

Committee on Electric Heating

Paul H. Goodell, *Chairman;* Jensen Specialties, Inc., 9331 Freeland Avenue, Detroit 28, Mich.

L. P. Hynes, *Vice-Chairman*	Haddonfield, N. J.
Harold Bunte, *Secretary*	Chicago, Ill.
E. L. Bailey	Detroit, Mich.
R. M. Baker	Baltimore, Md.
I. J. Barber	Fostoria, Ohio
E. J. Bates	Dayton, Ohio
Mrs. B. O. Buckland	Schenectady, N. Y.
F. T. Chesnut	Trenton, N. J.
P. E. Dittman	Corning, N. Y.
L. M. Duryee	Waterbury, Conn.
J. E. Eiselein	Camden, N. J.
J. G. Fleming	Waterbury, Conn.
M. M. Greer	Middletown, Conn.
E. M. Guyer	Corning, N. Y.
J. C. Handy	Baltimore, Md.
T. P. Kinn	Baltimore, Md.
G. F. Leland	Schenectady, N. Y.
R. C. Machler	Philadelphia, Pa.
A. D. Moore	Ann Arbor, Mich.
A. E. Opdenweyer	Portland, Oreg.
C. E. Peck	Meadville, Pa.
W. C. Rudd	New Rochelle, N. Y.
R. J. Ruff	Detroit, Mich.
E. H. Scheick	New York, N. Y.
G. W. Scott, Jr.	Lancaster, Pa.
J. T. Vaughan	Cleveland, Ohio
G. E. Walters	Peoria, Ill.

Radiant Heating Subcommittee

I. J. Barber, *Chairman;* Fostoria Pressed Steel Corporation, 1945 Bradner Street, Fostoria, Ohio

E. J. Bates	Dayton, Ohio
P. H. Bowman	Chicago, Ill.
Harold Bunte	Chicago, Ill.
C. S. Cogger	Nutley, N. J.
A. D. Coggeshall	Schenectady, N. Y.
P. E. Dittman	Corning, N. Y.
P. H. Goodell	Detroit, Mich.
J. D. Hall	Bloomfield, N. J.
W. F. Hickes	Foxboro, Mass.
Raymond Joblonski	Detroit, Mich.
W. B. Kennedy	Salem, Mass.
J. E. Kolb	Pittsburgh, Pa.
E. A. Linsday	Cleveland, Ohio
R. C. Machler	Philadelphia, Pa.
H. W. McLarney	St. Louis, Mo.
C. L. Raynor	Detroit, Mich.
C. E. Russell	Philadelphia, Pa.
W. H. Wannamaker	Philadelphia, Pa.

Induction and Dielectric Heating Subcommittee

J. E. Eiselein, *Chairman;* Radio Corporation of America, Victor Division, Building 53-C-1, Camden, N. J.

R. M. Baker	Baltimore, Md.
G. P. Bosomworth	Akron, Ohio
E. W. Chapin	Laurel, Md.
F. T. Chesnut	Trenton, N. J.
L. G. Cumming	New York, N. Y.
M. E. Dunlap	Washington, D. C.
L. M. Duryee	Waterbury, Conn.
C. W. Frick	Schenectady, N. Y.
W. H. Hickok	Louisville, Ky.
C. A. Jorgensen	Kenosha, Wis.
T. P. Kinn	Baltimore, Md.
G. W. Klingaman	Camden, N. J.
Eugene Mittelman	Chicago, Ill.
William Paulin	Toronto, Ontario, Canada
W. C. Rudd	New Rochelle, N. Y.
G. W. Scott, Jr.	Lancaster, Pa.

(*Continued in next column*)

Technical Data Subcommittee

L. P. Hynes, *Chairman;* Consulting Engineer, 36 West End Avenue, Haddonfield, N. J.

F. T. Chesnut	Trenton, N. J.
J. E. Eiselein	Camden, N. J.
C. D. Fawcett	Philadelphia, Pa.
F. J. Jolly	Detroit, Mich.
H. V. Paynter	Philadelphia, Pa.
L. B. Rosseau	Philadelphia, Pa.
G. W. Scott, Jr.	Lancaster, Pa.
Arnold Spillman	Philadelphia, Pa.

Committee on Electric Welding

C. N. Clark, *Chairman;* Duquesne Light Company, 435 Sixth Avenue, Pittsburgh 19, Pa.

E. J. Limpel, *Vice-Chairman*	Milwaukee, Wis.
J. F. Deffenbaugh, *Secretary*	Warren, Ohio
Fritz Albrecht	Baltimore, Md.
J. H. Blankenbuehler	Troy, Ohio
W. G. Bostwick	Cincinnati, Ohio
F. L. Brandt	Lynn, Mass.
C. R. Dixon	New Kensington, Pa.
Earl Ewald	Minneapolis, Minn.
R. C. Freeman	Fitchburg, Mass.
G. W. Garman	Detroit, Mich.
W. B. Kouwenhoven	Baltimore, Md.
R. J. Krieger	Columbus, Ohio
S. W. Luther	Detroit, Mich.
F. W. Maxstadt	Pasadena, Calif.
R. C. McMaster	Columbus, Ohio
C. E. Pflug	Kenosha, Wis.
L. C. Poole	Detroit, Mich.
J. F. Randall	Dearborn, Mich.
C. M. Rhoades, Jr.	Schenectady, N. Y.
M. S. Shane	Cleveland, Ohio
C. B. Stadum	Buffalo, N. Y.
E. F. Steinert	Buffalo, N. Y.
L. K. Stringham	Cleveland, Ohio
G. I. F. Theriault	Dayton, Ohio
H. W. Tietze	Newark, N. J.
J. T. Vaughan	Cleveland, Ohio
L. P. Winsor	Troy, N. Y.
B. L. Wise	Bay City, Mich.
R. E. Young	Kankakee, Ill.
Myron Zucker	Royal Oak, Mich.

Power Supply for Resistance Welding Machines Subcommittee

Myron Zucker, *Chairman;* Myron Zucker Engineering Company, 1708 Crooks Road, Royal Oak, Mich.

E. L. Bailey	Highland Park, Mich.
W. K. Boice	New Haven, Conn.
W. G. Bostwick	Cincinnati, Ohio
C. N. Clark	Pittsburgh, Pa.
J. F. Deffenbaugh	Warren, Ohio
L. E. Fisher	Detroit, Mich.
Julius Heuschkel	East Pittsburgh, Pa.
S. W. Luther	Detroit, Mich.
C. E. Pflug	Kenosha, Wis.
J. L. Solomon	Chicago, Ill.
C. B. Stadum	Buffalo, N. Y.
H. W. Tietze	Newark, N. J.
H. R. Wall	Jackson, Mich.

Fundamental Electric Arc Research Subcommittee

R. C. McMaster, *Chairman;* Battelle Memorial Institute, 505 King Avenue, Columbus 1, Ohio

J. H. Chyle	Milwaukee, Wis.
J. D. Cobine	Schenectady, N. Y.
Wolfgang Finkelnburg	Fort Belvoir, Va.
W. J. Greene	Murray Hill, N. J.
Julius Heuschkel	East Pittsburgh, Pa.
W. B. Kouwenhoven	Baltimore, Md.
Robert Krieger	Columbus, Ohio
J. M. Parks	Chicago, Ill.
S. F. Radtke	Newport, Del.
R. E. Somers	Bethlehem, Pa.
E. H. Wilhelm	Annapolis, Md.
L. P. Winsor	Troy, N. Y.

Committee on Feedback Control Systems

S. W. Herwald, *Chairman;* Westinghouse Electric Corporation, 1844 Ardmore Boulevard, Pittsburgh 21, Pa.

F. E. Crever, *Vice-Chairman*	Schenectady, N. Y.
A. G. Kegel, *Secretary*	Pittsburgh, Pa.
W. R. Ahrendt	College Park, Md.
E. R. Behn	New York, N. Y.
W. W. Bender	Baltimore, Md.
G. S. Brown	Cambridge, Mass.
H. W. Cory	Milwaukee, Wis.
A. P. DiVincenzo	Cleveland, Ohio
W. R. Evans	Downey, Calif.
F. H. Ferguson	Washington, D. C.
J. G. Ferguson	Murray Hill, N. J.
R. M. Hutchinson	Philadelphia, Pa.
R. W. Jones	Evanston, Ill.
R. J. Kochenburger	Storrs, Conn.
O. W. Livingston	Schenectady, N. Y.
J. R. MacIntyre	West Lynn, Mass.
H. T. Marcy	Endicott, N. Y.
G. D. McCann	Pasadena, Calif.
R. C. McMaster	Columbus, Ohio
W. E. Meserve	Ithaca, N. Y.
C. W. Miller	Norwalk, Conn.
R. W. Moore	Buffalo, N. Y.
F. O. Nottingham, Jr.	Atlanta, Ga.
Arthur Porter	Toronto, Ontario, Canada
J. R. Ragazzini	New York, N. Y.
O. H. Schuck	Minneapolis, Minn.
G. L. Stancliff, Jr.	Washington, D. C.
W. H. Surber	Princeton, N. J.
H. I. Tarpley	State College, Pa.
C. E. Warren	Columbus, Ohio
C. N. Weygandt	Philadelphia, Pa.
G. E. White	Los Angeles, Calif.
A. J. Williams, Jr.	Philadelphia, Pa.

Terminology and Nomenclature Subcommittee

F. E. Crever, *Chairman;* General Engineering Laboratory, General Electric Company, Schenectady, N. Y.

W. R. Ahrendt	College Park, Md.
H. W. Cory	Milwaukee, Wis.
A. G. Kegel	Pittsburgh, Pa.
Paul Travers	Cambridge, Mass.
A. J. Williams, Jr.	Philadelphia, Pa.

Bibliography Subcommittee

R. W. Jones, *Chairman;* Northwestern University, Department of Electrical Engineering, Evanston, Ill.

E. R. Behn	New York, N. Y.
F. H. Ferguson	Washington, D. C.
Arthur Porter	Toronto, Ontario, Canada
O. H. Schuck	Minneapolis, Minn.
C. N. Weygandt	Philadelphia, Pa.

Feedback Control Systems Conference Subcommittee

H. T. Marcy, *Chairman;* International Business Machines Corporation, Engineering Department, Endicott, N. Y.

E. R. Behn	New York, N. Y.
A. G. Kegel	Pittsburgh, Pa.
C. W. Miller	Norwalk, Conn.
O. H. Schuck	Minneapolis, Minn.

Committee on General Industry Applications

V. O. Johnson, *Chairman;* United States Rubber Company, 1230 Avenue of the Americas, New York 20, N. Y.

F. D. Snyder, *Vice-Chairman*	Boston, Mass.
E. M. Hays, *Secretary*	Pittsburgh, Pa.
B. T. Anderson	Rockford, Ill.
V. B. Baker	East Pittsburgh, Pa.
L. B. Blalock	Dallas, Tex.
S. P. Blakeman	Philadelphia, Pa.
E. L. Blankenbeker	Pittsburgh, Pa.
S. A. Bobe	Atlanta, Ga.
O. M. Bundy	Cleveland, Ohio
M. A. DeFerranti	Schenectady, N. Y.
J. M. Delfs	Schenectady, N. Y.
R. J. Demartini	Rensselaer, N. Y.
W. J. Dowis	Richland, Wash.
J. C. Fink	Pittsburgh, Pa.
M. H. Fisher	East Pittsburgh, Pa.
A. W. Frankenfield	Wilmington, Del.
R. I. Greenwood	Los Angeles, Calif.
E. L. Happ	Pisgah Forest, N. C.
L. W. Herchenroeder	East Pittsburgh, Pa.
L. T. Jester, Jr.	Boston, Mass.
K. W. John	Detroit, Mich.
T. A. Kauppi	Midland, Mich.
G. W. Knapp	Schenectady, N. Y.
R. E. Koontz	Niles, Mich.
A. F. Lukens	Lynn, Mass.
R. E. Marriott	Port Neches, Tex.
H. B. Mathieu	Lubbock, Tex.
E. F. Mekelburg	Milwaukee, Wis.
J. F. Moore	Toronto, Ontario, Canada
E. K. Murphy	New York, N. Y.
F. S. Parker	Portland, Oreg.
D. R. Percival	Worcester, Mass.
Kennard Pinder	Wilmington, Del.
G. E. Plaisted	San Francisco, Calif.
N. L. Platt	Binghamton, N. Y.
C. G. Plomasen	Rochester, N. Y.
H. A. Rose	Seattle, Wash.
R. G. Rudrow	Wilmington, Del.
A. L. Scott	Idaho Falls, Idaho
A. G. Seifried	Akron, Ohio
H. L. Smith	New York, N. Y.
R. F. Snyder	Akron, Ohio
Ray Stroppel	Cincinnati, Ohio
J. A. Tudor	Portland, Oreg.
H. C. Uhl	Sylacauga, Ala.
L. A. Umansky	Schenectady, N. Y.
B. H. Zacherle	Philadelphia, Pa.

(*Continued in next column*)

Machine Tools Subcommittee

B. T. Anderson, *Chairman;* Sundstrand Machine Tool Company, 2531—11th Street, Rockford, Ill.

R. W. Brown	Windsor, Vt.
J. M. Delfs	Schenectady, N. Y.
R. T. Fenn	Springfield, Vt.
L. W. Herchenroeder	East Pittsburgh, Pa.
J. J. Jaeger	West Hartford, Conn.
E. F. Mekelburg	Milwaukee, Wis.
D. R. Percival	Worcester, Mass.
W. J. Piper	Springfield, Vt.
S. Rice	Worcester, Mass.
E. J. Rivoira	Cincinnati, Ohio
R. E. Stroppel	Cincinnati, Ohio
W. B. Wigton	Cincinnati, Ohio
T. A. Wetzel	Milwaukee, Wis.

Materials Handling Subcommittee

S. P. Blakeman, *Chairman;* Haughton Elevator Company, 1725 Fairmount Avenue, Philadelphia, Pa.

A. R. Dunne	Port Hope, Ontario, Canada
D. C. Gray	St. Paul, Minn.
C. P. Hamilton	Schenectady, N. Y.
E. M. Hays	Pittsburgh, Pa.
J. B. McGinn	Philadelphia, Pa.
G. N. Meyers	Philadelphia, Pa.
Fred A. Miller	Wilmington, Del.
C. B. Risler	East Pittsburgh, Pa.

Pulp and Paper Industry Subcommittee

V. B. Baker, *Chairman;* Westinghouse Electric Corporation, Industrial Engineering Division, East Pittsburgh, Pa.

S. Anderson	New York, N. Y.
H. B. Barrow	Atlanta, Ga.
D. C. Christison	Neenah, Wis.
G. C. Ehemann	Rittman, Ohio
G. W. Knapp	Schenectady, N. Y.
E. K. Murphy	New York, N. Y.
H. A. Rose	Seattle, Wash.
A. P. Schnyder	New York, N. Y.
Eric R. Smith	New York, N. Y.
J. L. Van Nort	Cleveland, Ohio

Rubber and Plastics Industries Subcommittee

R. F. Snyder, *Chairman;* Goodyear Tire and Rubber Company, 1144 East Market Street, Akron, Ohio

L. T. Blalock	Dallas, Texas
B. J. Dalton	Schenectady, N. Y.
K. W. John	Detroit, Mich.
G. V. Kullgren	Akron, Ohio
J. F. Moore	Toronto, Ontario, Canada
H. R. Neighbours	Mishawaka, Ind.
R. G. Rudrow	Wilmington, Del.
W. J. Secrest	Akron, Ohio
R. E. Seddon	Wilmington, Del.
A. G. Seifried	Akron, Ohio
H. L. Smith	New York, N. Y.
W. S. Watkins	Willoughby, Ohio
B. H. Zacherle	Philadelphia, Pa.

Textile Industry Subcommittee

R. J. Demartini, *Chairman;* F. C. Huyck & Sons, Kenwood Mills, Rensselaer, N. Y.

J. D. McConnell, *Secretary,* Greensboro, N. C.

A. T. Bacheler	Buffalo, N. Y.
S. A. Bobe	Atlanta, Ga.
J. M. Bracken	Philadelphia, Pa.
I. S. Bull	Greenville, S. C.
Swaffield Cowan	Charlotte, N. C.
R. B. Flowers	Atlanta, Ga.
A. W. Frankenfield	Wilmington, Del.
L. T. Jester	Boston, Mass.
J. T. Meador	Charlotte, N. C.
R. R. Prechter	Schenectady, N. Y.
V. P. Sepavich	Worcester, Mass.
F. D. Snyder	Boston, Mass.
H. C. Uhl	Sylacanga, Ala.
R. S. White	Providence, R. I.

Committee on Industrial Control

John A. Cortelli, *Chairman;* Clark Controller Company, 1146 East 152nd Street, Cleveland 10, Ohio

H. L. Palmer, *Vice-Chairman* Schehectady, N. Y.

L. H. Matthias, *Secretary* Milwaukee, Wis.

E. H. Alexander	Schenectady, N. Y.
H. H. Angel	Bethlehem, Pa.
E. L. Bailey	Detroit, Mich.
T. H. Bloodworth	Milwaukee, Wis.
G. S. Brown	Cambridge, Mass.
J. R. Dickey	Corpus Christi, Tex.
W. H. Elliot	Milwaukee, Wis.
C. T. Evans	Milwaukee, Wis.
H. G. Frostick	Pittsburgh, Pa.
J. E. Gahagan	Binghamton, N. Y.
J. A. Gienger	Rochester, N. Y.
F. Y. Grepe	Toronto, Ontario, Canada
Walter Hansen	Boston, Mass.
G. W. Heumann	Schenectady, N. Y.
E. W. Hutton	Schenectady, N. Y.
J. J. Jaeger	West Hartford, Conn.
R. W. Jones	Evanston, Ill.
R. W. Kowitz	Dearborn, Mich.
W. E. Lawton	Wenatchee, Wash.
O. W. Livingston	Schenectady, N. Y.
E. F. Mekelburg	Milwaukee, Wis.
R. W. Moore	Buffalo, N. Y.
E. E. Moyer	Troy, N. Y.
A. H. Myles	Cleveland, Ohio
J. J. O'Connor	New York, N. Y.
S. C. Phillips	Peterboro, Ontario, Canada
J. W. Picking	Cleveland, Ohio
Walter Schaelchlin	Buffalo, N. Y.
F. E. Strauss	Oakland, Calif.
E. H. Vedder	Buffalo, N. Y.

Bibliography Subcommittee

R. W. Jones, *Chairman;* Department of Electrical Engineering, Northwestern University, Evanston, Ill.

W. H. Elliott	Milwaukee, Wis.
E. E. Moyer	Troy, N. Y.
J. W. Picking	Cleveland, Ohio
Walter Schaelchlin	East Pittsburgh, Pa.

Electronic Control Subcommittee

E. W. Hutton, *Chairman;* General Electric Company, 1 River Road, Schenectady 5, N. Y.

F. T. Bailey	Buffalo, N. Y.
H. B. Black	Ampere, N. J.
L. H. Dee	Schenectady, N. Y.
J. R. Devoy	Schenectady, N. Y.
W. H. Elliot	Milwaukee, Wis.
William Few	Cleveland, Ohio
L. U. C. Kelling	Schenectady, N. Y.
M. H. A. Lindsay	New York, N. Y.
F. O. Nottingham	Atlanta, Ga.
J. W. Picking	Cleveland, Ohio
L. C. Poole	Detroit, Mich.
E. H. Pritchard	Canton, Mass.
C. A. Schurr	Cleveland, Ohio
P. E. Shields	State College, Pa.
H. I. Stanback	Milwaukee, Wis.
B. B. Stuart	Waltham, Mass.
C. M. Summers	Fort Wayne, Ind.
B. F. Tellkamp	Milwaukee, Wis.
E. H. Vedder	Buffalo, N. Y.
W. M. Walthall	Danville, Ill.
L. L. Worner	Rankin, Ill.

(Continued in next column)

Working Groups:

(1). Electronic Control of D-C Motors

J. W. Picking, *Chairman;* Reliance Electric and Engineering Company, 1068–1088 Ivanhoe Road, Cleveland 10, Ohio

H. B. Black	East Orange, N. J.
L. H. Dee	Schenectady, N. Y.
W. H. Elliot	Milwaukee, Wis.
William Few	Cleveland, Ohio
L. C. Poole	Detroit, Mich.
H. I. Stanback	Milwaukee, Wis.
B. B. Stuart	Waltham, Mass.
B. F. Tellkamp	Milwaukee, Wis.
E. H. Vedder	Buffalo, N. Y.

(2). Photoelectric Pickup Systems

L. U. C. Kelling, *Chairman;* General Electric Company, 1 River Road, Schenectady 5, N. Y.

F. T. Bailey	Buffalo, N. Y.
M. H. A. Lindsay	New York, N. Y.
E. M. Pritchard	Canton, Mass.
W. M. Walthall	Danville, Ill.
L. L. Worner	Rankin, Ill.

(3). Electronic Relaying Devices

J. R. Devoy, *Chairman;* General Electric Company, 1 River Road, Schenectady 5, N. Y.

C. A. Schurr	Cleveland, Ohio
B. F. Tellkamp	Milwaukee, Wis.

Standards Subcommittee

J. J. O'Connor, *Chairman;* Associate Editor, *Power*, McGraw-Hill Publishing Company, 330 West 42nd Street, New York 18, N. Y.

E. L. Bailey	Detroit, Mich.
J. E. Gahagan	Binghamton, N. Y.
J. A. Gienger	Rochester, N. Y.
F. Y. Grepe	Toronto, Ontario, Canada
W. E. Happel	Waynesboro, Pa.
J. J. Jaeger	West Hartford, Conn.
R. W. Kowitz	Dearborn, Mich.
L. H. Matthias	Milwaukee, Wis.

Test Codes Subcommittee

C. T. Evans, *Chairman;* Cutler-Hammer, Inc., 315 North 12th Street, Milwaukee, Wis.

G. C. Armstrong	Buffalo, N. Y.
C. P. Clare	Chicago, Ill.
D. K. Frost	Rockford, Ill.
W. E. Pakala	East Pittsburgh, Pa.
H. E. Rhoads	Schenectady, N. Y.
C. A. Schaefer	Milwaukee, Wis.

Subcommittee on Prize Paper Awards

E. E. Moyer, *Chairman;* Rensselaer Polytechnic Institute, Troy, N. Y.

T. H. Bloodworth	Milwaukee, Wis.
R. W. Jones	Evanston, Ill.

Regulators and Feedback Systems Subcommittee

O. W. Livingston, *Chairman;* General Electric Company, Control Engineering Division, Schenectady 5, N. Y.

S. L. Burgwin	Buffalo, N. Y.
E. T. Davis	Philadelphia, Pa.
W. H. Elliot	Milwaukee, Wis.
William Few	Cleveland, Ohio
J. W. Picking	Cleveland, Ohio

Committee on Industrial Power Systems

H. G. Barnett, *Chairman;* Westinghouse Electric Corporation, Industry Engineering Department, East Pittsburgh, Pa.

S. A. Warner, *Vice-Chairman* New York, N. Y.

R. H. Whaley, *Secretary* Indianapolis, Ind.

D. M. Allison	St. Louis, Mo.
H. H. Angel	Bethlehem, Pa.
D. L. Beeman	Schenectady, N. Y.
Y. T. Chaney	Plainville, Conn.
E. S. Dibble	Los Angeles, Calif.
V. E. Dodson	Seattle, Wash.
Leo Dolkart	Chicago, Ill.
C. W. Elble	Woodland, Maine
W. J. Ellenberger	Washington, D. C.
R. W. Foster	Canton, N. C.
J. E. Gahagan	Binghamton, N. Y.
F. S. Glass	Freeport, Tex.
W. S. Gordon, Jr.	Tacoma, Wash.
J. D. Harper	Alcoa, Tenn.
E. H. Hulse	San Francisco, Calif.
C. R. Johnson	New York, N. Y.
C. M. Lathrop	Linden, N. J.
M. H. Lovelady	Corpus Christi, Tex.
S. W. Luther	Detroit, Mich.
A. E. Marshall	St. Louis, Mo.
J. L. McKeever	Peterboro, Ontario, Canada
T. Y. Merrell	Phoenix, Ariz.
J. S. Morgan	Milwaukee, Wis.
W. A. Mosteller	Detroit, Mich.
A. L. Nelson	Blanco, Tex.
R. R. Nissley	New York, N. Y.
E. P. Peabody	Richland, Wash.
Waldo Porter	Vancouver, Wash.
R. H. Rankin	Rochester, N. Y.
W. H. Rollman	Dallas, Tex.
C. C. Saunders	Wilmington, Del.
T. O. Sweatt	New York, N. Y.
R. B. Temple	Portland, Oreg.
H. B. Thacker	East Pittsburgh, Pa.
H. T. Theis	New York, N. Y.
B. F. Thomas, Jr.	New York, N. Y.
R. C. Waldron	Passaic, N. J.
E. F. Wehr	Cleveland, Ohio
R. T. Woodruff	St. Louis, Mo.
William Zelley	Roebling, N. J.
T. O. Zittel	Lackawanna, N. Y.

(Continued in next column)

Executive Subcommittee

Main Committee Officers:

H. G. Barnett, *Chairman;* Westinghouse Electric Corporation, Industry Engineering Department, East Pittsburgh, Pa.

S. A. Warner, *Vice-Chairman* New York, N. Y.

R. H. Whaley, *Secretary* Indianapolis, Ind.

Subcommittee Chairmen:

D. L. Beeman	Schenectady, N. Y.
W. J. Ellenberger	Washington, D. C.
A. E. Marshall	St. Louis, Mo.
W. A. Mosteller	Detroit, Mich.
B. F. Thomas, Jr.	New York, N. Y.

Power Supply Subcommittee

A. E. Marshall, *Chairman;* Monsanto Chemical Company, 1700 South 2nd Street, St. Louis 4, Mo.

A. J. Claes	East St. Louis, Ill.
R. T. Woodruff	St. Louis, Mo.

Distribution Systems for Industrial Plants Subcommittee

W. A. Mosteller, *Chairman;* General Electric Company, 700 Antoinette Street, Detroit 2, Mich.

Distribution Systems for Commercial Buildings Subcommittee

B. F. Thomas, Jr., *Chairman;* N. A. Lougee and Company, 120 Broadway, New York 5, N. Y.

Allan Coggeshall	New York, N. Y.
L. W. McCullough	New York, N. Y.
A. C. Youngson	New York, N. Y.

Characteristics of Loads Subcommittee

W. J. Ellenberger, *Chairman;* 6419 Barnaby Street, N. W., Washington, D. C.

Industrial Grounding Subcommittee

D. L. Beeman, *Chairman;* General Electric Company, Schenectady 5, N. Y.

H. H. Angel	Bethlehem, Pa.
J. E. Arberry	Pittsburgh, Pa.
K. M. Bausch	San Francisco, Calif.
Fred Heller	New York, N. Y.
E. M. Hunter	Schenectady, N. Y.
L. W. Roush	South Charleston, W. Va.
C. C. Saunders	Wilmington, Del.
J. M. Schmidt	Schenectady, N. Y.
H. M. Stewart	Baytown, Tex.
T. O. Sweatt	New York, N. Y.
H. B. Thacker	East Pittsburgh, Pa.
B. F. Thomas, Jr.	New York, N. Y.
S. A. Warner	New York, N. Y.
Roy Whaley	Indianapolis, Ind.

Codes and Standards Subcommittee

W. J. Ellenberger, *Chairman;* 6419 Barnaby Street, N. W., Washington 15, D. C.

Committee on Mining and Metal Industry

A. C. Muir, *Chairman;* The Berwind-White Coal Mining Company, 1400 Pennsylvania Building, Philadelphia 2, Pa.

W. R. Harris, *Vice-Chairman* East Pittsburgh, Pa.

J. E. Arberry	Pittsburgh, Pa.
H. W. Biskeborn	Newark, Ohio
J. E. Breth	Birmingham, Ala.
A. B. Chafetz	Carlsbad, N. Mex.
R. J. Corfield	Garfield, Utah
F. W. Cramer	Pittsburgh, Pa.
J. M. Downie	Erie, Pa.
J. A. Dunn	Holden, W. Va.
J. H. Edwards	New York, N. Y.
Sam Ein	Chicago, Ill.
Cecil Farrow	Cleveland, Ohio
J. J. FitzGibbon	Washington, D. C.
E. J. Gleim	Pittsburgh, Pa.
Lanier Greer	Cleveland, Ohio
L. N. Grier	Pittsburgh, Pa.
C. L. Gust	Lead, S. Dak.
L. H. Harrison	Birmingham, Ala.
J. G. Ivy	Chicago, Ill.
L. H. James	Scranton, Pa.
G. F. Johnson	Michigan City, Ind.
J. Z. Linsenmeyer	East Pittsburgh, Pa.
W. E. Miller	Schenectady, N. Y.
T. B. Montgomery	Milwaukee, Wis.
R. B. Moore	Schenectady, N. Y.
H. P. Musser	Charleston, W. Va.
M. G. Myers, Jr.	Boston, Mass.
F. C. Nicholson	Wilkes-Barre, Pa.
C. A. Poppino	Phoenix, Ariz.
B. E. Price	Columbus, Ohio
L. W. Roush	So. Charleston, W. Va.
F. O. Schnure	Sparrows Point, Md.
Victor Siegfried	Worcester, Mass.
O. J. Swanson	Gary, W. Va.
C. L. Tyler	Irwin, Pa.
T. R. Weichel	Wilkes-Barre, Pa.
J. R. Wickey	Cleveland, Ohio
W. G. Willson	Phoenix, Ariz.
C. O. Wood	Chicago, Ill.

Metal Industries Subcommittee

W. R. Harris, *Chairman;* Westinghouse Electric Corporation, Department 10-L, East Pittsburgh, Pa.

F. O. Schnure, *Secretary* Sparrows Point, Md.

J. E. Arberry	Pittsburgh, Pa.
H. W. Biskeborn	Newark, Ohio
J. A. Cortelli	Cleveland, Ohio
F. W. Cramer	Pittsburgh, Pa.
E. F. Donatic	Fontana, Calif.
Sam Ein	Chicago, Ill.
R. H. Ellis	Pittsburgh, Pa.
Cecil Farrow	Cleveland, Ohio
R. I. Greenwood	Los Angeles, Calif.
Lanier Greer	Cleveland, Ohio
L. N. Grier	Pittsburgh, Pa.
G. A. Hornbecker	Waterbury, Conn.
D. C. McCrady	Hamilton, Ontario, Canada
W. E. Miller	Schenectady, N. Y.
T. B. Montgomery	Milwaukee, Wis.
M. G. Myers, Jr.	Boston, Mass.
B. E. Price	Columbus, Ohio
E. G. Schlup	Middletown, Ohio
Victor Siegfried	Worcester, Mass.
H. I. Stanback	Milwaukee, Wis.
J. R. Wickey	Cleveland, Ohio

Eastern Mining Subcommittee (Coal)

R. B. Moore, *Chairman;* Industrial Engineering Division, General Electric Company, Schenectady 5, N. Y.

J. E. Breth	Bessemer, Ala.
J. A. Buss	Cleveland, Ohio
E. W. Davis	Cambridge, Mass.
J. M. Downie	Erie, Pa.
J. A. Dunn	Holden, W. Va.
J. H. Edwards	New York, N. Y.
J. J. FitzGibbon	Washington, D. C.
E. J. Gleim	Pittsburgh, Pa.
L. H. Harrison	Birmingham, Ala.
L. H. James	Scranton, Pa.
G. F. Johnson	Michigan City, Ind.
J. Z. Linsenmeyer	East Pittsburgh, Pa.

(Continued on page 2177)

R. C. McMaster Columbus, Ohio
A. C. Muir Philadelphia, Pa.
H. P. Musser Charleston, W. Va.
F. C. Nicholson Wilkes-Barre, Pa.
L. W. Roush South Charleston, W. Va.
O. J. Swanson Gary, W. Va.
C. L. Tyler Irwin, Pa.
T. R. Weichel Wilkes-Barre, Pa.
C. O. Wood Chicago, Ill.

Western Mining Subcommittee (Hard Rock)

A. B. Chafetz, *Chairman;* International Minerals and Chemical Corporation, Potash Division, Carlsbad, N. Mex.
C. A. Poppino, *Secretary* Phoenix, Ariz.
C. H. Bailey Duluth, Minn.
R. D. Call St. Louis, Mo.
R. J. Corfield Garfield, Utah
C. L. Gust Lead, S. Dakota
J. G. Ivy Chicago, Ill.
B. E. Rector East Pittsburgh, Pa.
W. G. Willson Phoenix, Ariz.

Power Division

Power Division Committee

W. R. Brownlee, *Chairman;* Southern Services, Inc., Birmingham, Ala.
B. G. A. Skrotzki, *Vice-Chairman* New York, N. Y.
R. S. Gardner, *Secretary* New York, N. Y.
C. W. Boadway Toronto, Ontario, Canada
Robert Brandt Boston, Mass.
J. A. Brooks New York, N. Y.
S. B. Crary Schenectady, N. Y.
R. C. Ericson Hammond, Ind.
C. T. Hatcher New York, N. Y.
L. F. Hickernell Hastings-on-Hudson, N. Y.
L. F. Kennedy Schenectady, N. Y.
A. J. McConnell Schenectady, N. Y.
E. L. Michelson Chicago, Ill.
H. V. Nye West Allis, Wis.
E. W. Oesterreich Pittsburgh, Pa.
H. J. Scholz (*representing Board of Directors*) Birmingham, Ala.
H. R. Stewart Boston, Mass.
C. G. Veinott Lima, Ohio
F. J. Vogel Milwaukee, Wis.
C. F. Wagner East Pittsburgh, Pa.

Committee on Carrier Current

C. W. Boadway, *Chairman;* Hydro-Electric Power Commission of Ontario, 620 University Avenue, Toronto 2, Ontario, Canada
S. C. Leyland, *Vice-Chairman (East)* Newark, N. J.
R. H. Miller, *Vice-Chairman (West)* San Francisco, Calif.
B. W. Storer, *Secretary* Chicago, Ill.
J. F. Atkinson Washington, D. C.
S. C. Bartlett New York, N. Y.
T. M. Blakeslee Los Angeles, Calif.
W. H. Blankmeyer Butte, Mont.
J. R. Boston Portland, Oreg.
H. A. Brown Rochester, N. Y.
R. C. Cheek Baltimore, Md.
J. A. Doremus Chicago, Ill.
J. M. Dunham New York, N. Y.
G. W. Dupree Amarillo, Tex.
L. G. Eaton Boston, Mass.
J. R. Ellison Oklahoma City, Okla.
G. E. Farmer Chattanooga, Tenn.
O. L. Gierach Charlotte, N. C.
E. T. Gray St. Louis, Mo.
F. B. Gunter Baltimore, Md.
E. W. Kenefake Syracuse, N. Y.
L. F. Kennedy Schenectady, N. Y.
J. V. Kresser San Francisco, Calif.
Samuel Lubin North Adams, Mass.
L. E. Ludekens Los Angeles, Calif.
T. D. MacCoun Brooklyn, N. Y.
D. M. MacGregor New York, N. Y.
T. W. MacLean Spokane, Wash.
O. K. Mangum Phoenix, Ariz.
T. A. Phillips Phoenix, Ariz.
D. C. Pinkerton Syracuse, N. Y.
T. T. Smith Portland, Oreg.
O. A. Starcke Kansas City, Mo.
H. J. Sutton Beaumont, Tex.
T. D. Talmage Chicago, Ill.
Mead Warren, Jr. Alcoa, Tenn.
T. D. Wood, Jr. Birmingham, Ala.
Jean Youngblood Detroit, Mich.

Executive Subcommittee

C. W. Boadway, *Chairman;* Hydro-Electric Power Commission of Ontario, 620 University Avenue, Toronto 2, Ontario, Canada
S. C. Leyland, *Vice-Chairman (East)* Newark, N. J.
R. H. Miller, *Vice-Chairman (West)* San Francisco, Calif.
B. W. Storer, *Secretary* Chicago, Ill.
S. C. Bartlett New York, N. Y.
E. W. Kenefake Syracuse, N. Y.
L. F. Kennedy Schenectady, N. Y.

Subcommittee for Preparation of a General Interest Paper on Carrier Current

M. H. Wood, *Chairman;* Westinghouse Electric Corporation, 2519 Wilkens Avenue, Baltimore 3, Md.
S. C. Bartlett New York, N. Y.
J. D. Booth Baltimore, Md.
L. F. Kennedy Schenectady, N. Y.

Subcommittee to Report on Application Guidance for Carrier Current

D. M. MacGregor, *Chairman;* Ebasco Services, Inc., 2 Rector Street, New York 6, N. Y.
C. W. Boadway Toronto, Ontario, Canada
T. D. Talmage Chicago, Ill.

Methods of Measurement Subcommittee

E. W. Kenefake, *Chairman;* General Electric Company, Electronics Department, Syracuse, N. Y.
S. C. Bartlett New York, N. Y.
C. W. Boadway Toronto, Ontario, Canada
M. H. Wood Baltimore, Md.

High-Frequency Characteristics of Power Equipment Subcommittee

S. C. Leyland, *Chairman;* Westinghouse Electric Corporation, 95 Orange Street, Newark 2, N. J.
T. A. Cramer Schenectady, N. Y.

Carrier Current Characteristics of Transmission Lines and System Subcommittee

T. D. Talmage, *Chairman;* Kellogg Switchboard and Supply Company, 6650 Cicero Avenue, Chicago 38, Ill.
W. H. Blankmeyer Butte, Mont.
R. C. Ericson Hammond, Ind.
W. J. Googe Shreveport, La.
L. E. Ludekens Los Angeles, Calif.

Long Life Tubes Subcommittee

L. G. Eaton, *Chairman;* New England Power Service Company, 441 Stuart Street, Boston 16, Mass.
R. W. Beckwith Syracuse, N. Y.
L. F. Ferri Elyria, Ohio
Samuel Lubin North Adams, Mass.
M. H. Wood Baltimore, Md.

Use of Microwave Equipment for Relaying, Telemetering, and Supervisory Control Subcommittee

S. C. Leyland, *Chairman;* Westinghouse Electric Corporation, 95 Orange Street, Newark 2, N. J.

Operating Experience with Carrier Current Relaying Channels Subcommittee

O. A. Starcke, *Chairman;* Kansas City Power and Light Company, Box 679, Kansas City, Mo.
T. A. Cramer Schenectady, N. Y.
J. R. Curtin Portland, Oreg.
W. J. Googe Shreveport, La.

(Continued in next column)

V. J. Hayes Waterbury, Conn.
H. W. Lensner Newark, N. J.
L. E. Ludekens Los Angeles, Calif.
B. W. Storer Chicago, Ill.
Mead Warren, Jr. Alcoa, Tenn.

Committee on Insulated Conductors

C. T. Hatcher, *Chairman;* Consolidated Edison Company of New York, Inc., 4 Irving Place, New York 3, N. Y.
R. J. Wiseman, *Vice-Chairman* Passaic, N. J.
M. H. McGrath, *Secretary* Perth Amboy, N. J.
M. J. Andrews Los Angeles, Calif.
C. F. Avila Boston, Mass.
H. G. Barnett East Pittsburgh, Pa.
C. E. Baugh San Francisco, Calif.
E. D. Bent Montreal, Quebec, Canada
C. E. Betzer Chicago, Ill.
Andrew Bodicky St. Louis, Mo.
A. S. Brookes Newark, N. J.
W. R. Bullard New York, N. Y.
H. W. Clark Washington, D. C.
E. W. Davis Cambridge, Mass.
W. A. Del Mar Yonkers, N. Y.
C. D. Eash Jackson, Mich.
D. M. Farnham Montreal, Quebec, Canada
G. H. Fiedler Rochester, N. Y.
L. E. Fogg Phillipsdale, R. I.
J. D. Frantz Portland, Oreg.
M. W. Ghen Pittsburgh, Pa.
Herman Halperin Chicago, Ill.
L. F. Hickernell Hastings-on-Hudson, N. Y.
R. A. Hopkins Knoxville, Tenn.
B. R. Hubbard Trenton, N. J.
A. H. Kidder Philadelphia, Pa.
R. H. Kolks Cincinnati, Ohio
L. I. Komives Detroit, Mich.
M. J. Lowenberg Boston, Mass.
R. E. Morse New York, N. Y.
C. T. Nicholson Buffalo, N. Y.
W. T. Peirce Worcester, Mass.
F. L. Phillips Kansas City, Mo.
J. J. Pokorny Cleveland, Ohio
S. J. Rosch Hastings-on-Hudson, N. Y.
J. J. Rueckert Baltimore, Md.
R. A. Schatzel Rome, N. Y.
G. B. Shanklin Schenectady, N. Y.
V. A. Sheals Schenectady, N. Y.
H. D. Short Toronto, Ontario, Canada
F. V. Smith Chicago, Ill.
F. W. Smith Richmond, Va.
G. M. L. Sommerman Evanston, Ill.
E. G. Sturdevant Bristol, R. I.
Gordon Thompson New York, N. Y.
A. J. Warner Nutley, N. J.
H. H. Watson Bridgeport, Conn.
K. S. Wyatt Yonkers, N. Y.
C. W. Zimmerer New York, N. Y.

Administration Subcommittee

C. T. Hatcher, *Chairman;* Consolidated Edison Company of New York, Inc., 4 Irving Place, New York 3, N. Y.
R. J. Wiseman, *Vice-Chairman* Passaic, N. J.
M. H. McGrath, *Secretary* Perth Amboy, N. J.

Subcommittee Chairmen:
C. E. Betzer Chicago, Ill.
W. A. Del Mar Yonkers, N. Y.
L. E. Fogg Phillipsdale, R. I.
M. W. Ghen Pittsburgh, Pa.
Herman Halperin Chicago, Ill.
B. R. Hubbard Trenton, N. J.
L. I. Komives Detroit, Mich.
W. T. Peirce Worcester, Mass.
J. J. Pokorny Cleveland, Ohio
S. J. Rosch Hastings-on-Hudson, N. Y.
R. A. Schatzel Rome, N. Y.
Gordon Thompson New York, N. Y.

Standards and Publications Subcommittee

L. E. Fogg, *Chairman;* Kennecott Wire and Cable Company, Phillipsdale, R. I.
E. D. Bent Montreal, Quebec, Canada
A. S. Brookes Newark, N. J.
M. H. McGrath New York, N. Y.
L. F. Roehmann Hastings-on-Hudson, N. Y.
V. A. Sheals Schenectady, N. Y.
C. W. Zimmerer New York, N. Y.

Cable Characteristics Subcommittee

W. A. Del Mar, *Chairman;* Phelps Dodge Copper Products Company, Habirshaw Cable and Wire Division, Yonkers, N. Y.
M. J. Andrews Los Angeles, Calif.
E. D. Bent Montreal, Quebec, Canada
R. W. Burrell New York, N. Y.
Herman Halperin Chicago, Ill.
A. H. Kidder Philadelphia, Pa.
M. H. McGrath New York, N. Y.
J. H. Neher Philadelphia, Pa.
F. L. Phillips Kansas City, Mo.
G. B. Shanklin Schenectady, N. Y.
F. V. Smith Chicago, Ill.
R. J. Wiseman Passaic, N. J.
F. O. Wollaston Vancouver, B. C., Canada

Conductors Subcommittee

B. R. Hubbard, *Chairman;* J. A. Roebling's Sons Company, Trenton 2, N. J.
G. W. Acock Trenton, N. J.
A. A. Jones Hastings-on-Hudson, N. Y.
G. M. L. Sommerman Evanston, Ill.

Insulations Subcommittee

R. A. Schatzel, *Chairman;* Rome Cable Corporation, Rome, N. Y.
J. C. Balsbaugh Cambridge, Mass.
C. E. Betzer Chicago, Ill.
J. T. Blake Cambridge, Mass.
F. M. Clark Schenectady, N. Y.
A. S. Dana Seymour, Conn.
E. W. Greenfield Hastings-on-Hudson, N. Y.
B. R. Hubbard Trenton, N. J.
Thorstein Larsen Baltimore, Md.
E. L. Lotz Irvington, N. J.
E. E. McIlveen Passaic, N. J.
R. B. McKinley Bridgeport, Conn.
J. D. Piper Detroit, Mich.
S. J. Rosch Hastings-on-Hudson, N. Y.
E. G. Sturdevant Bristol, R. I.
A. J. Warner Nutley, N. J.
K. S. Wyatt Yonkers, N. Y.

Sheaths and Coverings Subcommittee

C. E. Betzer, *Chairman;* Commonwealth Edison Company, 72 West Adams Street, Chicago 90, Ill.
C. F. Avila Boston, Mass.
Andrew Bodicky St. Louis, Mo.
A. S. Brookes Newark, N. J.
G. H. Fiedler Rochester, N. Y.
C. T. Hatcher New York, N. Y.
L. F. Hickernell Hastings-on-Hudson, N. Y.
A. H. Kidder Philadelphia, Pa.
V. A. Sheals Schenectady, N. Y.
H. D. Short Toronto, Ontario, Canada
R. C. Waldron Passaic, N. J.
F. O. Wollaston Vancouver, B. C., Canada
G. W. Zink Yonkers, N. Y.

Cable Supply Systems Subcommittee

L. I. Komives, *Chairman;* Detroit Edison Company, 2000—2d Avenue, Detroit 26, Mich.
C. F. Avila Boston, Mass.
F. A. Bolien Portland, Oreg.
W. R. Bullard New York, N. Y.
H. W. Clark Washington, D. C.
D. M. Farnham Montreal, Quebec, Canada
J. D. Frantz Portland, Oreg.
Herman Halperin Chicago, Ill.
C. T. Hatcher New York, N. Y.
L. F. Hickernell Hastings-on-Hudson, N. Y.
M. J. Lowenberg Boston, Mass.
M. H. McGrath Perth Amboy, N. J.
C. T. Nicholson Buffalo, N. Y.
C. S. Schifreen Philadelphia, Pa.
G. B. Shanklin Schenectady, N. Y.
H. D. Short Toronto, Ontario, Canada
F. W. Smith Richmond, Va.
R. J. Wiseman Passaic, N. J.
K. S. Wyatt Yonkers, N. Y.

Utilization Wiring Systems Subcommittee

S. J. Roach, *Chairman;* Anaconda Wire and Cable Company, Hastings-on-Hudson, N. Y.

H. G. Barnett	East Pittsburgh, Pa.
A. L. Barrett	Franklin, Pa.
T. P. Branch	Washington, D. C.
R. W. Foster	Canton, N. C.
M. J. Lowenberg	Boston, Mass.
E. E. McIlveen	Passaic, N. J.
R. A. Schatzel	Rome, N. Y.
J. J. Tesoriero	New York, N. Y.
J. S. Waddington	Brockville, Ontario, Canada
H. H. Watson	Bridgeport, Conn.
C. W. Zimmerer	New York, N. Y.

Special-Purpose Cable Subcommittee

W. T. Peirce, *Chairman;* American Steel and Wire Company, Worcester, Mass.

J. F. Atkinson	Washington, D. C.
A. L. Barrett	Franklin, Pa.
E. D. Bent	Montreal, Quebec, Canada
E. W. Davis	Cambridge, Mass.
H. S. Eubank	New York, N. Y.
R. A. Hopkins	Knoxville, Tenn.
R. H. Kolks	Cincinnati, Ohio
R. B. McKinley	Bridgeport, Conn.
F. L. Phillips	Kansas City, Mo.
F. V. Smith	Chicago, Ill.
E. G. Sturdevant	Bristol, R. I.
J. J. Tesoriero	New York, N. Y.
R. C. Waldron	Passaic, N. J.
A. J. Warner	Nutley, N. J.
G. W. Zink	Yonkers, N. Y.

Accessories Subcommittee

M. W. Ghen, *Chairman;* Duquesne Light Company, 1241 Reedsdale Street, N. S., Pittsburgh 33, Pa.

P. N. Bosworth	Pittsfield, Mass.
C. Christensen	Melrose Park, Ill.
C. D. Eash	Jackson, Mich.
J. D. Frantz	Portland, Oreg.
R. W. Gillette	New York, N. Y.
Fred Heller	New York, N. Y.
J. E. Johnson	Philadelphia, Pa.
S. C. Killian	Chicago, Ill.
R. H. Kolks	Cincinnati, Ohio
L. E. Leinbach	Detroit, Mich.
E. L. Lotz	Irvington, N. J.
H. E. Martin	Brooklyn, N. Y.
R. E. Morse	New York, N. Y.
J. H. Nicholas	Chicago, Ill.
J. J. Pokorny	Cleveland, Ohio
D. S. Young	Toronto, Ontario, Canada
S. Zysk	Schenectady, N. Y.

Structures Subcommittee

J. J. Pokorny, *Chairman;* Cleveland Electric Illuminating Company, Cleveland, Ohio

M. J. Andrews	Los Angeles, Calif.
C. E. Baugh	San Francisco, Calif.
Andrew Bodicky	St. Louis, Mo.
H. W. Clark	Washington, D. C.
C. D. Eash	Jackson, Mich.
H. S. Eubank	New York, N. Y.
G. H. Fiedler	Rochester, N. Y.
R. W. Gillette	New York, N. Y.
C. T. Nicholson	Buffalo, N. Y.
F. L. Phillips	Kansas City, Mo.
F. W. Smith	Richmond, Va.
L. G. Smith	Baltimore, Md.

Tests and Measurements Subcommittee

Gordon Thompson, *Chairman;* Electrical Testing Laboratories, Inc., 2 West End Avenue, New York 21, N. Y.

J. C. Balsbaugh	Cambridge, Mass.
A. S. Dana	Seymour, Conn.
E. W. Davis	Cambridge, Mass.
W. A. Del Mar	Yonkers, N. Y.
W. N. Eddy	Cambridge, Mass.
E. W. Greenfield	Hastings-on-Hudson, N. Y.
Thorstein Larsen	Baltimore, Md.
C. G. Mansfield	Los Angeles, Calif.
J. C. Parker	Memphis, Tenn.
L. F. Roehmann	Hastings-on-Hudson, N. Y.
G. M. L. Sommerman	Evanston, Ill.
R. F. Tener	Washington, D. C.
C. W. Zimmerer	New York, N. Y.

Committee on Power Generation

J. A. Brooks, *Chairman;* Consolidated Edison Company of New York, Inc., 4 Irving Place, New York 3, N. Y.

J. B. McClure, *Vice-Chairman*	Schenectady, N. Y.
H. R. Harris, *Secretary*	Detroit, Mich.
R. E. Appleyard	Milwaukee, Wis.
J. E. Barkle, Jr.	East Pittsburgh, Pa.
E. P. Bryant	Los Angeles, Calif.
Giuseppe Calabrese	New York, N. Y.
A. D. Caskey	Chicago, Ill.
H. E. Deardorff	Dayton, Ohio
S. M. Denton	Denver, Colo.
E. F. Dissmeyer	Jackson, Mich.
Alex Dovjikov	Portland, Oreg.
C. B. Fontaine	Lynn, Mass.
G. P. Gamble	St. Louis, Mo.
W. P. Hammond	Atlanta, Ga.
C. A. Harrington	Cleveland, Ohio
A. P. Hayward	Pittsburgh, Pa.
J. A. Hooper	Portland, Oreg.
G. W. Kerr	Walla Walla, Wash.
C. E. Kilbourne	Schenectady, N. Y.
A. J. Krupy	Chicago, Ill.
F. L. Lawton	Montreal, Quebec, Canada
J. T. Madill	Montreal, Quebec, Canada
E. F. Maryatt	San Francisco, Calif.
A. H. Mergenthaler	Birmingham, Ala.
I. E. Moultrop	Belmont, Mass.
D. R. Pattison	Johnstown, Pa.
A. L. Pollard	Seattle, Wash.
C. S. Randall	Washington, D. C.
M. D. Ross	East Pittsburgh, Pa.
G. E. Schmitt	Austin, Tex.
R. C. Schuknecht	Portland, Oreg.
B. G. A. Skrotzki	New York, N. Y.
W. E. Taylor	Toronto, Ontario, Canada
C. W. Watchorn	Baltimore, Md.
W. F. Wetmore	Detroit, Mich.
R. R. Wisner	Boston, Mass.
G. R. Woodman	Los Angeles, Calif.

Prime Movers Subcommittee

B. G. A. Skrotzki, *Chairman;* Associate Editor, *Power*, 330 West 42d Street, New York 18, N. Y.

E. P. Bryant	Los Angeles, Calif.
A. D. Caskey	Chicago, Ill.
G. P. Gamble	St. Louis, Mo.
J. A. Hooper	Portland, Oreg.
I. E. Moultrop	Belmont, Mass.
C. S. Randall	Washington, D. C.
R. R. Wisner	Boston, Mass.

Speed Governing Subcommittee

J. B. McClure, *Chairman;* General Electric Company, Central Station Engineering Division, Schenectady 5, N. Y.

R. E. Appleyard	Milwaukee, Wis.
C. P. Almon, Jr.	Chattanooga, Tenn.
R. M. Beville	Chicago, Ill.
A. P. Hayward	Pittsburgh, Pa.
T. H. Mawson	Birmingham, Ala.
G. H. McDaniel	New York, N. Y.
F. L. Reinmann	Michigan City, Ind.

Excitation Systems Subcommittee

A. J. Krupy, *Chairman;* Commonwealth Edison Company, 72 West Adams Street, Chicago 90, Ill.

J. E. Barkle, Jr., *Vice-Chairman*	East Pittsburgh, Pa.
H. W. Cory	Milwaukee, Wis.
S. M. Denton	Denver, Colo.
E. F. Dissmeyer	Jackson, Mich.
Alex Dovjikov	Portland, Oreg.
C. B. Fontaine, Jr.	Lynn, Mass.
J. H. Kinghorn	New York, N. Y.
C. J. Manner	Los Angeles, Calif.
J. B. McClure	Schenectady, N. Y.
C. E. Valentine	East Pittsburgh, Pa.

Station Design Subcommittee

D. R. Pattison, *Chairman;* Pennsylvania Electric Company, 222 Livergood Street, Johnstown, Pa.

H. E. Deardorff	Dayton, Ohio
C. A. Harrington	Cleveland, Ohio
H. R. Harris	Detroit, Mich.
W. W. Perry	Binghamton, N. Y.
R. R. Wisner	Boston, Mass.

Hydroelectric Systems Subcommittee

F. L. Lawton, *Chairman;* Aluminum Laboratories, Ltd., 1800 Sun Life Building, Montreal, Quebec, Canada

S. M. Denton	Denver, Colo.
J. D. Harper	Alcoa, Tenn.
J. T. Madill	Shipshaw, Quebec, Canada
E. F. Maryatt	San Francisco, Calif.
A. L. Pollard	Seattle, Wash.
G. F. Simson	Toronto, Ontario, Canada
G. R. Woodman	Los Angeles, Calif.

Pacific Coast Subcommittee

E. P. Bryant, *Chairman;* Department of Water and Power, City of Los Angeles, 207 South Broadway, Los Angeles 12, Calif.

S. M. Denton	Denver, Colo.
Alex Dovjikov	Portland, Oreg.
V. H. Estcourt	San Francisco, Calif.
N. G. Holmdahl	Coulee Dam, Wash.
E. F. Maryatt	San Francisco, Calif.
A. L. Pollard	Seattle, Wash.
G. R. Woodman	Los Angeles, Calif.

Power Generation Liaison Representative to Gas Turbine Power Division of ASME

B. G. A. Skrotzki, c/o "Power," 330 West 42nd Street, New York 18, N. Y.

Committee on Protective Devices

H. R. Stewart, *Chairman;* New England Power Service Company, 441 Stuart Street, Boston 16, Mass.

A. A. Johnson, *Vice-Chairman*	East Pittsburgh, Pa.
E. H. Yonkers, *Secretary*	Chicago, Ill.
S. E. Caldwell	Portland, Oreg.
D. D. Clarke	Kansas City, Mo.
J. E. Clem	Schenectady, N. Y.
J. O'R. Coleman	Boston, Mass.
L. M. Connors	Toronto, Ontario, Canada
H. A. Cornelius	Chicago, Ill.
F. M. Defandorf	Washington, D. C.
G. K. Ditlow	Washington, D. C.
G. B. Dodds	Pittsburgh, Pa.
J. R. Eaton	Lafayette, Ind.
T. I. Eldridge	Philadelphia, Pa.
Byron Evans	Denver, Colo.
O. L. Giersch	Charlotte, N. C.
E. M. Hunter	Schenectady, N. Y.
P. A. Jeanne	New York, N. Y.
K. H. Kidd	Toronto, Ontario, Canada
W. A. Lewis, Jr.	Chicago, Ill.
F. R. Longley	Springfield, Mass.
W. A. McMorris	Pittsfield, Mass.
R. H. Mertz	Detroit, Mich.
R. E. Neidig	Reading, Pa.
Einar Nilsson	San Francisco, Calif.
E. G. Norell	Chicago, Ill.
A. M. Opsahl	East Pittsburgh, Pa.
H. L. Rorden	Portland, Oreg.
H. O. Stoelting	South Milwaukee, Wis.
J. M. Towner	Baltimore, Md.
S. S. Watkins	New York, N. Y.

Fault Limiting Devices Subcommittee

E. M. Hunter, *Chairman;* General Electric Company, Schenectady, N. Y.

L. J. Blaize	Dallas, Tex.
V. J. Cissna	Chattanooga, Tenn.
J. E. Clem	Schenectady, N. Y.
C. L. Derrick	Hartford, Conn.
Byron Evans	Denver, Colo.
L. F. Ferri	Jackson, Mich.
O. L. Giersch	Charlotte, N. C.
E. T. B. Gross	Chicago, Ill.
W. D. Hardaway	Denver, Colo.
P. A. Jeanne	New York, N. Y.
A. A. Johnson	East Pittsburgh, Pa.
C. C. Jones	Birmingham, Ala.
W. A. Lewis, Jr.	Chicago, Ill.
F. R. Longley	Springfield, Mass.
Cort Lowerison	Los Angeles, Calif.
Corbett McLean	Portland, Oreg.
R. E. Neidig	Reading, Pa.
Einar Nilsson	San Francisco, Calif.
E. G. Norell	Chicago, Ill.
H. D. Ruger	Sparrows Point, Md.
J. C. Russ	Pittsfield, Mass.
L. E. Saver	Sharon, Pa.
O. L. Sidenfaden	Los Angeles, Calif.
S. S. Watkins	New York, N. Y.

Working Groups:

(1). *Application Guide on Methods of Neutral Grounding Transmission Systems*

E. M. Hunter, *Chairman;* General Electric Company, Schenectady, N. Y.

H. W. Hartzell	Jackson, Mich.
A. A. Johnson	East Pittsburgh, Pa.
R. E. Neidig	Reading, Pa.

(2). *Application Guide for the Grounding of Synchronous Generator Systems*

A. A. Johnson, *Chairman;* Westinghouse Electric Corporation, East Pittsburgh, Pa.

E. M. Hunter	Schenectady, N. Y.
D. M. MacGregor	New York, N. Y.
E. G. Norell	Chicago, Ill.
W. T. Smith	Washington, D. C.

(3). *Guide for Application of Ground-Fault Neutralizers*

J. E. Clem, *Chairman;* General Electric Company, Schenectady, N. Y.

H. H. Brown	Cedar Rapids, Iowa
S. S. Cook	Sharon, Pa.
N. E. Dillow	Schenectady, N. Y.
W. D. Hardaway	Denver, Colo.
R. E. Neidig	Reading, Pa.
P. B. Speer	Minneapolis, Minn.

Lightning Protective Devices Subcommittee

J. M. Towner, *Chairman;* Consolidated Gas, Electric Light and Power Company, Madison Street Building, Baltimore 3, Md.

E. H. Grosser, *Secretary*	Chicago, Ill.
S. E. Caldwell	Portland, Oreg.
L. M. Connors	Toronto, Ontario, Canada
H. A. Cornelius	Chicago, Ill.
F. M. Defandorf	Washington, D. C.
G. K. Ditlow	Washington, D. C.
J. R. Eaton	Lafayette, Ind.
T. I. Eldridge	Philadelphia, Pa.
W. F. Griffard	Jackson, Mich.
I. W. Gross	New York, N. Y.
S. B. Howard	Pittsfield, Mass.
R. F. Huber	Chicago, Ill.
L. S. Inskip	New York, N. Y.
C. M. Jackson	Pittsburgh, Pa.
I. B. Johnson	Schenectady, N. Y.
J. W. Kalb	Barberton, Ohio
F. N. McClure	East Pittsburgh, Pa.
R. H. Mertz	Detroit, Mich.
A. M. Opsahl	East Pittsburgh, Pa.
H. L. Rorden	Portland, Oreg.
H. O. Stoelting	South Milwaukee, Wis.

Working Groups:

(1). *Lightning Arrester Performance Characteristics*

E. H. Grosser, *Chairman;* Commonwealth Edison Company, Chicago, Ill.

T. I. Eldridge	Philadelphia, Pa.
S. B. Howard	Pittsfield, Mass.
J. W. Kalb	Barberton, Ohio
A. M. Opsahl	East Pittsburgh, Pa.
H. O. Stoelting	South Milwaukee, Wis.

(2). *Survey of Direct Stroke Shielding of Substations*

J. R. Eaton, *Chairman;* Purdue University, Lafayette, Ind.

J. W. Kalb	Barberton, Ohio
F. E. Leib	Glassport, Pa.
T. H. Mawson	Birmingham, Ala.
A. M. Opsahl	East Pittsburgh, Pa.
H. L. Rorden	Portland, Oreg.

(3). *Combined Lightning Arrester Standard*

E. M. Defandorf, *Chairman;* National Bureau of Standards, Washington, D. C.

L. B. Crann	Alexandria, Va.
T. I. Eldridge	Philadelphia, Pa.
I. W. Gross	New York, N. Y.
E. H. Grosser	Chicago, Ill.
S. B. Howard	Pittsfield, Mass.
A. M. Opsahl	East Pittsburgh, Pa.
H. O. Stoelting	South Milwaukee, Wis.
E. H. Yonkers	Chicago, Ill.

(4). *Application Guide for Protection of Substations*

H. A. Cornelius, *Chairman;* Public Service Company of Northern Illinois, Chicago, Ill.

W. F. Griffard	Jackson, Mich.
S. B. Howard	Pittsfield, Mass.
R. H. Mertz	Detroit, Mich.
A. M. Opsahl	East Pittsburgh, Pa.
P. M. Ross	Mansfield, Ohio
E. R. Whitehead	Chicago, Ill.

Co-ordination of Insulation Subcommittee

J. E. Clem, *Chairman;* Central Station Engineering Division, General Electric Company, Schenectady 5, N. Y.

(Members to be selected at need)

Committee on Relays

A. J. McConnell, *Chairman;* General Electric Company, 1 River Road, Schenectady 5, N. Y.

W. E. Marter, *Vice-Chairman*	Pittsburgh, Pa.
Frank von Roeschlaub, *Secretary*	New York, N. Y.
A. W. Adams	Portland, Oreg.
J. E. Barkle, Jr.	East Pittsburgh, Pa.
M. A. Bostwick	Portland, Oreg.
J. W. Bowman	Fort Wayne, Ind.
R. J. Cooper	Atlanta, Ga.
R. E. Cordray	Philadelphia, Pa.
G. E. Dana	Binghamton, N. Y.
L. L. Draper	Los Angeles, Calif.
M. A. Faucett	Urbana, Ill.
F. S. Fehr	Reading, Pa.
L. F. Ferri	Jackson, Mich.
L. L. Fountain	East Pittsburgh, Pa.
Sidney Goldsmith	Cincinnati, Ohio
E. T. B. Gross	Chicago, Ill.
T. R. Halman	Detroit, Mich.
G. W. Hampe	Chicago, Ill.
V. J. Hayes	Waterbury, Conn.
B. C. Hicks	Montreal, Quebec, Canada
R. O. Hopkins	Beaumont, Tex.
J. H. Kinghorn	New York, N. Y.
R. A. Larner	Fort Worth, Tex.
S. C. Leyland	Newark, N. J.
H. F. Lindemuth	New York, N. Y.
J. R. Linders	Cleveland, Ohio
Cort Lowerison	Los Angeles, Calif.
H. A. McLaughlin	Poughkeepsie, N. Y.
G. W. McKenna	Philadelphia, Pa.
M. S. Merritt	Chattanooga, Tenn.
M. P. Osburn	Toronto, Ontario, Canada
C. E. Parks	Plainfield, Ind.
H. P. Sleeper	Newark, N. J.
W. K. Sonnemann	Newark, N. J.
G. S. Steeb	Buffalo, N. Y.
R. W. World	Denver, Colo.

Project Committee on Bibliography of Relay Literature

E. T. B. Gross, *Chairman* and *Sponsor;* Illinois Institute of Technology, 3300 Federal Street, Chicago 16, Ill.

Sidney Goldsmith	Cincinnati, Ohio
C. E. Parks	Indianapolis, Ind.
C. L. Smith	Rochester, N. Y.

Project Committee on Co-ordination of Construction and Protection of Distribution Circuits (Joint with Distribution Subcommittee and Edison Electric Institute)

G. B. Dodds, AIEE *Chairman* and *Sponsor;* Duquesne Light Company, 435 Sixth Avenue, Pittsburgh 19, Pa.

R. O. Askey	Chicago, Ill.
G. G. Auer	Schenectady, N. Y.
T. J. Brosnan	Buffalo, N. Y.
Harold Cole	Detroit, Mich.
C. L. Headley	Baltimore, Md.
Cort Lowerison	Los Angeles, Calif.
H. F. Ostman	St. Louis, Mo.
C. L. Smith	Rochester, N. Y.

C. J. Beller, EEI *Chairman* and *Sponsor;* Cleveland Electric Illuminating Company, 75 Public Square, Cleveland 1, Ohio

G. E. Dean	Newark, N. J.
G. H. Fiedler	Rochester, N. Y.
W. P. Holben	Pittsburgh, Pa.
A. L. Malmstrom	Detroit, Mich.

Project Committee on Revision of Standards for Power Relays

J. R. Linders, *Chairman* and *Sponsor;* Cleveland Electric Illuminating Company, 75 Public Square, Cleveland 1, Ohio

R. E. Cordray	Philadelphia, Pa.
V. L. Cox	Philadelphia, Pa.
L. L. Fountain	East Pittsburgh, Pa.
W. A. Lewis	Chicago, Ill.
S. C. Leyland	Newark, N. J.
E. L. Michelson	Chicago, Ill.
W. A. Morgan	Denver, Colo.
H. P. Sleeper	Newark, N. J.
G. S. Steeb	Buffalo, N. Y.

Project Committee on Transmission-Line Protection

J. H. Kinghorn, *Chairman* and *Sponsor;* American Gas and Electric Service Corporation, 30 Church Street, New York 7, N. Y.

L. J. Audlin	Syracuse, N. Y.
J. E. Barkle, Jr.	East Pittsburgh, Pa.
W. R. Brownlee	Birmingham, Ala.
B. C. Hicks	Montreal, Quebec, Canada
W. A. Lewis	Chicago, Ill.
W. E. Marter	Pittsburgh, Pa.
A. J. McConnell	Schenectady, N. Y.
M. S. Merritt	Chattanooga, Tenn.
E. L. Michelson	Chicago, Ill.
C. E. Parks	Indianapolis, Ind.
K. N. Reardon	Pittsburgh, Pa.

Project Committee on Electronic Relay Applications

F. S. Fehr, *Chairman* and *Sponsor;* Metropolitan Edison Company, 412 Washington Street, Reading, Pa.

J. E. Barkle, Jr.	East Pittsburgh, Pa.
R. J. Cooper	Atlanta, Ga.
L. F. Ferri	Jackson, Mich.
E. L. Harder	East Pittsburgh, Pa.
J. H. Kinghorn	New York, N. Y.
D. M. MacGregor	New York, N. Y.
E. L. Michelson	Chicago, Ill.

Project Committee on Relaying of Interconnections Between Industrial and Utility Generating Systems

T. R. Halman, *Chairman* and *Sponsor;* Detroit Edison Company, 2000 Second Avenue, Detroit 26, Mich.

J. E. Barkle, Jr.	East Pittsburgh, Pa.
G. E. Dana	Binghamton, N. Y.
F. S. Fehr	Reading, Pa.
J. R. Linders	Lakewood, Ohio

Project Committee on Relaying Performance of Current Transformers (Emphasis on High Impedance Secondary Types)

W. E. Marter, *Chairman* and *Sponsor;* Duquesne Light Company, 435—6th Avenue, Pittsburgh 19, Pa.

J. E. Barkle, Jr.	East Pittsburgh, Pa.
J. E. Clem	Schenectady, N. Y.
R. E. Cordray	Philadelphia, Pa.
W. K. Dickinson	Lynn, Mass.
T. R. Halman	Detroit, Mich.
W. A. Lewis	Chicago, Ill.
W. K. Sonnemann	Newark, N. J.
E. C. Wentz	Sharon, Pa.

Project Committee on Remote Tripping Schemes

H. P. Sleeper, *Chairman* and *Sponsor;* Public Service Gas and Electric Company, 80 Park Place, Newark 2, N. J.

J. L. Blackburn	Newark, N. J.
M. A. Bostwick	Portland, Oreg.
T. A. Cramer	Schenectady, N. Y.
Sidney Goldsmith	Cincinnati, Ohio
G. W. Hampe	Chicago, Ill.
V. J. Hayes	Waterbury, Conn.
S. C. Leyland	Newark, N. J.

Project Committee on Pilot Wires

H. F. Lindemuth, *Chairman* and *Sponsor;* Consolidated Edison Company of New York, Inc., 4 Irving Place, New York 3, N. Y.

M. A. Bostwick	Portland, Oreg.
J. L. Davidson, Jr.	Mineola, N. Y.
W. E. Marter	Pittsburgh, Pa.
A. J. McConnell	Schenectady, N. Y.
J. L. McKee	New York, N. Y.
G. W. McKenna	Philadelphia, Pa.
E. L. Michelson	Chicago, Ill.
W. K. Sonnemann	Newark, N. J.

Project Committee on Effect of Shock and Vibration on Relays

C. E. Asbury, *Chairman* and *Sponsor;* Commonwealth Services, Inc., 7 Hayes Street, Jackson, Mich.

R. E. Cordray	Philadelphia, Pa.
M. A. Faucett	Urbana, Ill.
T. R. Halman	Detroit, Mich.
H. F. Lindemuth	New York, N. Y.
W. K. Sonnemann	Newark, N. J.
G. S. Steeb	Buffalo, N. Y.
R. I. Ward	Chicago, Ill.

Project Committee on Test Methods

G. E. Dana, *Chairman* and *Sponsor;* New York State Electric and Gas Corporation, 62 Henry Street, Binghamton, N. Y.

R. E. Cordray	Philadelphia, Pa.
L. F. Ferri	Jackson, Mich.
T. R. Halman	Detroit, Mich.
J. E. Lange	Pittsburgh, Pa.
R. A. Larner	Fort Worth, Texas
W. A. Morgan	Denver, Colo.
W. K. Sonnemann	Newark, N. J.

Committee on Rotating Machinery

C. G. Veinott, *Chairman;* Induction Motor Section, Westinghouse Electric Corporation, Lima, Ohio

E. I. Pollard, *Vice-Chairman*	Ridgway, Pa.
L. W. Buchanan, *Secretary*	Lima, Ohio
P. L. Alger	Schenectady, N. Y.
W. R. Appleman	Dayton, Ohio
R. E. Arnold	Lynn, Mass.
C. E. Asbury	Jackson, Mich.
M. A. Baker	Fort Wayne, Ind.
Sterling Beckwith	Milwaukee, Wis.
L. J. Berberich	East Pittsburgh, Pa.
B. H. Caldwell	Schenectady, N. Y.
C. F. Cameron	Stillwater, Okla.
E. A. Crellin	San Francisco, Calif.
James DeKiep	Minneapolis, Minn.
L. O. Dorfman	New York, N. Y.
W. H. Fifer	Washington, D. C.
L. T. Fisher	Portland, Oreg.
D. E. Fritz	Cleveland, Ohio
J. L. Fuller	Cleveland, Ohio
R. W. Gaskins	St. Louis, Mo.
Lanier Greer	Cleveland, Ohio
A. M. Harrison	East Pittsburgh, Pa.
C. B. Hathaway	Buffalo, N. Y.
S. F. Henderson	Buffalo, N. Y.
W. R. Hough	Cleveland, Ohio
J. W. Jones	Philadelphia, Pa.
G. H. Jump	Boston, Mass.
Richard Lamborn	Erie, Pa.
I. M. Levy	Dayton, Ohio
T. M. Linville	Schenectady, N. Y.
M. R. Lory	East Pittsburgh, Pa.
W. E. Meserve	Ithaca, N. Y.
C. F. Miller	Baltimore, Md.
R. C. Moore	Milwaukee, Wis.
R. F. Munier	St. Louis, Mo.
J. G. Noest	New York, N. Y.
C. P. Potter	St. Louis, Mo.
F. C. Rushing	Buffalo, N. Y.
M. L. Schmidt	Fort Wayne, Ind.
H. R. Sills	Peterboro, Ontario, Canada
P. H. Trickey	St. Louis, Mo.
J. J. Unger	Cleveland, Ohio
J. H. Vivian	Los Angeles, Calif.
R. W. Wieseman	Schenectady, N. Y.
W. W. Wishard	Chicago, Ill.

Administrative Subcommittee

C. G. Veinott, *Chairman;* Induction Motor Section, Westinghouse Electric Corporation, Lima, Ohio

E. I. Pollard, *Vice-Chairman*	Ridgway, Pa.
L. W. Buchanan, *Secretary*	Lima, Ohio
R. E. Arnold	Lynn, Mass.
L. J. Berberich	East Pittsburgh, Pa.
Lanier Greer	Cleveland, Ohio
S. F. Henderson	Buffalo, N. Y.
M. R. Lory	East Pittsburgh, Pa.
R. F. Munier	St. Louis, Mo.
E. I. Pollard	Ridgway, Pa.
P. H. Trickey	St. Louis, Mo.

Synchronous Machinery Subcommittee

M. R. Lory, *Chairman;* Westinghouse Electric Corporation, East Pittsburgh, Pa.

C. E. Asbury	Jackson, Mich.
Sterling Beckwith	Milwaukee, Wis.
J. F. Calvert	Evanston, Ill.
S. B. Crary	Schenectady, N. Y.
E. A. Crellin	San Francisco, Calif.
James DeKiep	Minneapolis, Minn.
L. O. Dorfman	New York, N. Y.
L. T. Fisher	Portland, Oreg.
R. W. Gaskins	St. Louis, Mo.
E. L. Harder	East Pittsburgh, Pa.
D. B. Harrington	Schenectady, N. Y.
J. W. Jones	Philadelphia, Pa.
C. E. Kilbourne	Schenectady, N. Y.
L. B. LeVesconte	Chicago, Ill.
J. G. Noest	New York, N. Y.
E. I. Pollard	Ridgway, Pa.
R. V. Shepherd	Schenectady, N. Y.
C. L. Sidway	Los Angeles, Calif.
H. R. Sills	Peterboro, Ontario, Canada
J. H. Vivian	Los Angeles, Calif.
E. C. Whitney	East Pittsburgh, Pa.
S. S. Wolff	Reading, Pa.

Induction Machinery Subcommittee

S. F. Henderson, *Chairman;* Westinghouse Electric Corporation, Buffalo, N. Y.

P. L. Alger	Schenectady, N. Y.
E. C. Barnes	Cleveland, Ohio
L. A. Burckmyer, Jr.	Ithaca, N. Y.
C. F. Cameron	Stillwater, Okla.
R. W. Gaskins	St. Louis, Mo.
W. R. Hough	Cleveland, Ohio
J. J. Kirkish	Milwaukee, Wis.
C. J. Koch	Schenectady, N. Y.
I. M. Levy	Dayton, Ohio
T. C. Lloyd	Springfield, Ohio
R. C. Moore	Milwaukee, Wis.
J. G. Noest	New York, N. Y.
E. I. Pollard	Ridgway, Pa.
C. P. Potter	St. Louis, Mo.
F. C. Rushing	Buffalo, N. Y.
P. H. Trickey	St. Louis, Mo.
S. S. Wolff	Reading, Pa.

D-C Machinery Subcommittee

Lanier Greer, *Chairman;* Reliance Electric and Engineering Company, 1088 Ivanhoe Road, Cleveland 10, Ohio

M. A. Baker	Fort Wayne, Ind.
B. H. Caldwell, Jr.	Schenectady, N. Y.
C. F. Cobb	Cincinnati, Ohio
W. H. Fifer	Washington, D. C.
D. E. Fritz	Cleveland, Ohio
A. M. Harrison	East Pittsburgh, Pa.
C. B. Hathaway	Buffalo, N. Y.
L. H. Hirsch	St. Louis, Mo.
H. E. Koenig	Urbana, Ill.
Richard Lamborn	Erie, Pa.
Paul Lebenbaum, Jr.	Lynn, Mass.
T. J. Martin	Seattle, Wash.
A. T. McClinton	Washington, D. C.
W. E. Meserve	Ithaca, N. Y.
L. G. Opel	Buffalo, N. Y.
W. J. Prise	New York, N. Y.
R. M. Saunders	Berkeley, Calif.
J. H. Schneider	Ridgway, Pa.
G. O. Schwandt	Wausau, Wis.
J. J. Unger	Cleveland, Ohio

Single-Phase and Fractional-Horsepower Subcommittee

R. F. Munier, *Chairman;* Emerson Manufacturing Company, 8100 Florissant Avenue, St. Louis 21, Mo.

W. R. Appleman	Dayton, Ohio
Nick Bratu	Chicago, Ill.
C. F. Cameron	Stillwater, Okla.
E. P. Codling	Cleveland Heights, Ohio
L. H. Hirsch	St. Louis, Mo.
E. E. Kimberly	Columbus, Ohio
I. M. Levy	Dayton, Ohio
T. C. Lloyd	Springfield, Ohio
C. F. Miller	Baltimore, Md.
L. C. Packer	Springfield, Mass.
C. P. Potter	St. Louis, Mo.
L. C. Schaefer	Lima, Ohio
M. L. Schmidt	Fort Wayne, Ind.
P. H. Trickey	St. Louis, Mo.

Test Code Subcommittee

R. E. Arnold, *Chairman;* General Electric Company, 920 Western Avenue, West Lynn, Mass.

T. E. M. Carville	Lima, Ohio
J. L. Fuller	Cleveland, Ohio
H. C. Marcroft	Lancaster, Pa.
R. F. Munier	St. Louis, Mo.
E. H. Myers	East Pittsburgh, Pa.
E. B. Paxton	Schenectady, N. Y.
E. I. Pollard	Ridgway, Pa.

Insulation Subcommittee

L. J. Berberich, *Chairman;* Westinghouse Electric Corporation, Research Laboratories, East Pittsburgh, Pa.

P. L. Alger	Schenectady, N. Y.
O. D. Butler	Chicago, Ill.
E. A. Crellin	San Francisco, Calif.
E. B. Curdts	Philadelphia, Pa.
P. A. Emmons	Badin, N. C.
W. T. Gordon	Lima, Ohio
D. D. Higgins	Chicago, Ill.
W. R. Hough	Cleveland, Ohio
J. W. Jones	Philadelphia, Pa.
T. A. Kauppi	Midland, Mich.
M. S. Kirwen	Jackson, Mich.
J. L. Kuehlthau	Milwaukee, Wis.
H. C. Marcroft	Lancaster, Pa.
G. L. Moses	East Pittsburgh, Pa.
E. I. Pollard	Ridgway, Pa.
E. H. Povey	Belmont, Mass.
C. L. Sidway	Los Angeles, Calif.
J. B. Swering	Hartford, Conn.
H. R. Tomlinson	Boston, Mass.
A. L. VanEmden	Washington, D. C.
R. W. Wieseman	Schenectady, N. Y.

Electric Coupling Subcommittee

P. H. Trickey, *Chairman;* Vickers Electric Division, St. Louis, Mo.

James DeKiep	Minneapolis, Minn.
R. F. Edwards	Ridgway, Pa.
E. H. Fredericks	Kenosha, Wis.
L. M. Goldsmith	Philadelphia, Pa.
R. L. Jaeschke	Kenosha, Wis.
M. R. Lory	East Pittsburgh, Pa.
J. A. Mason	Beloit, Wis.
Jacob Rabinow	Washington, D. C.
M. L. Schmidt	Fort Wayne, Ind.

Bibliography and Publicity Subcommittee

E. I. Pollard, *Chairman;* Elliot Company, Ridgway, Pa.

R. E. Arnold	Lynn, Mass.
M. A. Baker	Fort Wayne, Ind.
R. A. Farrell	Cleveland, Ohio
J. W. Jones	Philadelphia, Pa.
I. M. Levy	Dayton, Ohio
M. R. Lory	East Pittsburgh, Pa.
E. C. Starr	Corvallis, Oreg.

Committee on Substations

R. C. Ericson, *Chairman;* Northern Indiana Public Service Company, 5265 Hohman Avenue, Hammond, Ind.

K. L. Wheeler, *Vice-Chairman*	Cleveland, Ohio
N. G. Larson, *Secretary*	Chicago, Ill.
T. J. Allen	Atlanta, Ga.
Herman Bany	Philadelphia, Pa.
Harris Barber	Boston, Mass.
R. O. Bell	Milwaukee, Wis.
F. J. Berger	Philadelphia, Pa.
J. L. Buckley	San Francisco, Calif.
H. P. Cadario	Toronto, Ontario, Canada
F. J. Chapin	Albany, N. Y.
C. C. Crane	Madison, Wis.
M. V. Eardley	Los Angeles, Calif.
G. P. Fallon	Baltimore, Md.
H. F. Gidlund	Denver, Colo.
E. M. Hunter	Schenectady, N. Y.
S. C. Killian	Chicago, Ill.
W. M. Larson	Minneapolis, Minn.
R. F. Lawrence	East Pittsburgh, Pa.
F. W. Linder	LaCrosse, Wis.
F. J. Maas	Portland, Oreg.
W. M. McCauley	Greensburg, Pa.
J. L. McKee	New York, N. Y.
I. S. Mendenhall	Detroit, Mich.
K. E. Personius	Elmira, N. Y.
P. R. Pierson	East Pittsburgh, Pa.
M. E. Reagan	East Pittsburgh, Pa.
J. H. Rixse, Jr.	Washington, D. C.
O. J. Rotty	St. Louis, Mo.
W. S. Scheering	Springfield, Mass.
C. H. Smoke	Portsmouth, Va.
R. F. Stevens	Portland, Oreg.

(*Continued in next column*)

Executive Subcommittee

R. C. Ericson, *Chairman;* Northern Indiana Public Service Company, 5265 Hohman Avenue, Hammond, Ind.

M. V. Eardley	Los Angeles, Calif.
N. G. Larson	Chicago, Ill.
I. S. Mendenhall	Detroit, Mich.
M. E. Reagan	East Pittsburgh, Pa.
K. L. Wheeler	Cleveland, Ohio

Automatic and Supervisory Control Subcommittee

M. E. Reagan, *Chairman;* Switchboard Engineering Department, Westinghouse Electric Corporation, East Pittsburgh, Pa.

T. J. Allen	Atlanta, Ga.
Herman Bany	Philadelphia, Pa.
R. O. Bell	Milwaukee, Wis.
J. F. Bracken	Chicago, Ill.
B. D. Dexter	San Francisco, Calif.
W. M. Larson	Minneapolis, Minn.
J. L. McKee	New York, N. Y.
J. W. Savage	Los Angeles, Calif.

Distribution and Conversion Substation Subcommittee

W. S. Scheering, *Chairman;* Western Massachusetts Electric Company, Springfield, Mass.

T. J. Allen	Atlanta, Ga.
Herman Bany	Philadelphia, Pa.
R. O. Bell	Milwaukee, Wis.
F. J. Chapin	Albany, N. Y.
E. R. Coop	Providence, R. I.
C. C. Crane	Madison, Wis.
M. V. Eardley	Los Angeles, Calif.
G. P. Fallon	Baltimore, Md.
E. M. Hunter	Schenectady, N. Y.
F. W. Linder	LaCrosse, Wis.
I. S. Mendenhall	Detroit, Mich.
P. R. Pierson	East Pittsburgh, Pa.
O. J. Rotty	St. Louis, Mo.

Transmission Substation Subcommittee

I. S. Mendenhall, *Chairman;* The Detroit Edison Company, 2000 Second Avenue, Detroit 26, Mich.

T. J. Allen	Atlanta, Ga.
Harris Barber	Boston, Mass.
F. J. Berger	Philadelphia, Pa.
J. L. Buckley	San Francisco, Calif.
H. P. Cadario	Toronto, Ontario, Canada
H. F. Gidlund	Denver, Colo.
E. M. Hunter	Schenectady, N. Y.
S. C. Killian	Chicago, Ill.
N. G. Larson	Chicago, Ill.
F. W. Linder	LaCrosse, Wis.
W. M. McCauley	Greensburg, Pa.
J. H. Rixse, Jr.	Washington, D. C.
W. S. Scheering	Springfield, Mass.
R. F. Stevens	Portland, Oreg.

A. Working Group on Device Function Numbers

Herman Bany, *Chairman;* General Electric Company, 6901 Elmwood Avenue, Philadelphia 42, Pa.

L. B. LeVesconte	Chicago, Ill.
M. E. Reagan	East Pittsburgh, Pa.
M. S. Schneider	Cincinnati, Ohio

B. Working Group on Substation Grounding Practice

H. F. Gidlund, *Chairman;* Public Service Company of Colorado, 810—15th Street, Denver 2, Colo.

F. J. Berger	Philadelphia, Pa.
M. K. Brown	Buffalo, N. Y.
F. R. Longley	Springfield, Mass.
J. M. Towner	Baltimore, Md.

C. Working Group on Rectifier Switchgear

M. E. Reagan, *Chairman;* Switchgear Engineering Department, Westinghouse Electric Corporation, East Pittsburgh, Pa.

D. C. Hoffman	Philadelphia, Pa.

D. Working Group on Project 10—Basic Structural Design of Outdoor Stations

R. F. Stevens, *Chairman;* Bonneville Power Administration, Portland, Oreg.

F. J. Chapin	Albany, N. Y.

E. Working Group on Project 11—Breakers versus Reclosing Fuses

Herman Bany, *Chairman;* General Electric Company, Philadelphia, Pa.

T. J. Allen	Atlanta, Ga.
F. J. Chapin	Albany, N. Y.
C. C. Crane	Madison, Wis.
I. S. Mendenhall	Detroit, Mich.
M. E. Reagan	East Pittsburgh, Pa.

F. Working Group on Project 20—Standardization of Factory-Designed Substations

R. O. Bell, *Chairman;* Allis-Chalmers Manufacturing Company, Milwaukee, Wis.

D. W. Anderson	Hammond, Ind.
E. M. Hunter	Schenectady, N. Y.
P. R. Pierson	East Pittsburgh, Pa.
W. S. Scheering	Springfield, Mass.

G. Working Group on Project 21—Safety Considerations in Substations

H. P. Cadario, *Chairman*; Hydro-Electric Power Commission of Ontario, 620 University Avenue, Toronto, Ontario, Canada

N. G. Larson	Chicago, Ill.
J. H. Rixse, Jr.	Washington, D. C.
R. F. Stevens	Portland, Oreg.

H. Working Group on Project 51.1—Recommended Minimum Clearances

S. C. Killian, *Chairman;* Delta-Star Electric Company, Chicago, Ill.

T. J. Allen	Atlanta, Ga.
F. J. Berger	Philadelphia, Pa.
E. M. Hunter	Schenectady, N. Y.
K. E. Personius	Elmira, N. Y.
C. H. Smoke	Portsmouth, Va.

Committee on Switchgear

H. V. Nye, *Chairman;* Allis-Chalmers Manufacturing Company, West Allis, Wis.

R. L. Webb, *Vice-Chairman*	New York, N. Y.
J. M. Geiger, *Secretary*	Buffalo, N. Y.
R. M. Bennett	Philadelphia, Pa.
F. S. Benson	San Francisco, Calif.
H. F. Brown	New Haven, Conn.
J. S. Brown	Pittsburgh, Pa.
E. A. Childerhose	Boston, Mass.
H. W. Codding	Newark, N. J.
V. L. Cox	Philadelphia, Pa.
G. K. Ditlow	Washington, D. C.
J. A. Elzi	Jackson, Mich.
W. E. Enns	Portland, Oreg.
K. J. C. Falck	Philadelphia, Pa.
W. J. Gilson	Toronto, Ontario, Canada
J. W. Graff	Birmingham, Ala.
C. W. Gragg	Amarillo, Tex.
V. J. Hayes	Waterbury, Conn.
M. H. Hobbs	East Pittsburgh, Pa.
W. G. Hoover	Stanford, Calif.
C. L. Killgore	Denver, Colo.
I. T. Knight	Kansas City, Mo.
F. A. Lane	New York, N. Y.
W. G. Lewis	Hyde Park, Mass.
H. L. Lowe	New York, N. Y.
F. W. McCloska	Chicago, Ill.
W. J. McLachlan	Schenectady, N. Y.
D. J. Marsden	San Francisco, Calif.
R. G. Meyerand	St. Louis, Mo.
E. F. Miller	Davenport, Iowa
V. J. Muzznay	Schenectady, N. Y.
E. K. Sadler	Los Angeles, Calif.
A. W. Shelhorse	Atlanta, Ga.
J. F. Sinnott	San Diego, Calif.
Garland Stamper	Dayton, Ohio
E. A. Stroberg	Boston, Mass.
Anthony Van Ryan	So. Milwaukee, Wis.
J. H. Vivian	Los Angeles, Calif.
C. P. West	East Pittsburgh, Pa.
W. F. Wetmore	Detroit, Mich.
C. E. Winegartner	Cleveland, Ohio
J. D. Wood	Philadelphia, Pa.
J. C. Woods	Chicago, Ill.
S. W. Zimmerman	Ithaca, N. Y.

Administrative Subcommittee

R. L. Webb, *Chairman;* Consolidated Edison Company of New York, Inc., 4 Irving Place, New York 3, N. Y.

R. M. Bennett	Philadelphia, Pa.
K. J. C. Falk	Philadelphia, Pa.
Anthony Van Ryan	South Milwaukee, Wis.
C. P. West	East Pittsburgh, Pa.
J. D. Wood	Philadelphia, Pa.
J. C. Woods	Chicago, Ill.

Power Circuit Breakers Subcommittee

R. M. Bennett, *Chairman;* General Electric Company, 6901 Elmwood Avenue, Philadelphia 42, Pa.

E. A. Childerhose	Boston, Mass.
J. A. Elzi	Jackson, Mich.
R. M. Ferrill	Chattanooga, Tenn.
S. B. Griscom	East Pittsburgh, Pa.
E. J. Harrington	Portland, Oreg.
A. W. Hill	East Pittsburgh, Pa.
C. L. Killgore	Denver, Colo.
F. A. Lane	New York, N. Y.
W. G. Lewis	Boston, Mass.
H. H. Mitchell	Los Angeles, Calif.
D. M. Umphrey	San Francisco, Calif.
O. B. Vikoren	Philadelphia, Pa.
J. D. Wood	Philadelphia, Pa.
C. A. Woodrow	Schenectady, N. Y.

Low Voltage Air Circuit Breakers Subcommittee

J. D. Wood, *Chairman;* I-T-E Circuit Breaker Company, 19th and Hamilton Streets, Philadelphia, Pa.

Sam Ein	East Chicago, Ind.
C. L. Killgore	Denver, Colo.
H. F. Lingal	East Pittsburgh, Pa.
F. W. McCloska	Chicago, Ill.
R. G. Meyerand	St. Louis, Mo.
J. W. Timmerman, Jr.	Waukesha, Wis.
B. W. Wyman	Philadelphia, Pa.
S. W. Zimmerman	Ithaca, N. Y.

Automatic Reclosures Subcommittee

Anthony Van Ryan, *Chairman;* Line Material Company, Division of McGraw Electric Company, c/o Kyle Products Plant, South Milwaukee, Wis.

C. E. Asbury	Jackson, Mich.
L. L. Baird	Philadelphia, Pa.
L. B. Crann	Washington, D. C.
E. J. Field	Greensburg, Pa.
J. T. Finley	St. Louis, Mo.
Chase Hutchinson	New York, N. Y.
J. M. Wallace	East Pittsburgh, Pa.
C. E. Winegartner	Cleveland, Ohio

Switchgear Assemblies Subcommittee

C. P. West, *Chairman;* Switchboard Engineering Division, Westinghouse Electric Corporation, East Pittsburgh, Pa.

H. G. Frus	Pittsburgh, Pa.
J. M. Geiger	Buffalo, N. Y.
M. G. Lewis	San Francisco, Calif.
H. L. Lowe	New York, N. Y.
F. W. McCloska	Chicago, Ill.
G. M. Reed	Philadelphia, Pa.
Garland Stamper	Dayton, Ohio
B. K. Sturgis	Philadelphia, Pa.
J. W. Timmerman, Jr.	Waukesha, Wis.
W. F. Wetmore	Detroit, Mich.

Switches, Fuses and Insulators Subcommittee

K. J. C. Falck, *Chairman;* Philadelphia Electric Company, 900 Sansom Street, Philadelphia 7, Pa.

R. H. Amundson	So. Milwaukee, Wis.
T. E. Curtis	Hampton, Ga.
H. W. Graybill	Greensburg, Pa.
G. L. Hill	Emeryville, Calif.
J. B. Owens	East Pittsburgh, Pa.
A. H. Powell	Philadelphia, Pa.
J. C. Woods	Chicago, Ill.
C. P. Zimmerman	New York, N. Y.

Network Protectors Subcommittee

J. C. Woods, *Chairman;* Commonwealth Edison Company, 72 West Adams Street, Chicago 90, Ill.

B. S. Beall, III	Philadelphia, Pa.
G. G. Grissinger	East Pittsburgh, Pa.
D. L. Levine	Chicago, Ill.
R. E. Morse	New York, N. Y.
B. L. Peter	San Francisco, Calif.

Committee on System Engineering

Robert Brandt, *Chairman;* New England Power Company, 441 Stuart Street, Boston 16, Mass.

H. L. Harrington, *Vice-Chairman*	Buffalo, N. Y.
O. W. Manz, Jr., *Secretary*	New York, N. Y.
D. W. Alden	Pawtucket, R. I.
C. P. Almon, Jr.	Chattanooga, Tenn.
G. E. Bishop	Santa Cruz, Calif.
E. F. Bossuyt	Portland, Oreg.
E. C. Brown	Hartford, Conn.
D. H. Cameron	Kansas City, Mo.
O. E. Charlton	Birmingham, Ala.
S. B. Farnham	Schenectady, N. Y.
W. B. Fisk	New York, N. Y.
G. D. Floyd	Toronto, Ontario, Canada
A. P. Fugill	Detroit, Mich.
E. E. George	New York, N. Y.
S. M. Hamill, Jr.	Cincinnati, Ohio
A. C. Hartranft	Philadelphia, Pa.
A. P. Hayward	Pittsburgh, Pa.
R. G. Hooke	Newark, N. J.
L. R. Janes	Chicago, Ill.
W. R. Johnson	San Francisco, Calif.
J. C. Jones	Portland, Oreg.
C. B. Kelley	Des Moines, Iowa
H. J. Klumb	Rochester, N. Y.
R. F. Lawrence	East Pittsburgh, Pa.
H. A. Lott	Los Angeles, Calif.
M. H. Lovelady	Corpus Christi, Tex.
C. W. Mayott	Hartford, Conn.
G. H. McDaniel	New York, N. Y.
E. L. Michelson	Chicago, Ill.
W. E. Montgomery	Los Angeles, Calif.
S. B. Morehouse	Philadelphia, Pa.
W. A. Morgan	Denver, Colo.
W. H. Osterle	Pittsburgh, Pa.
L. R. Patterson	Denver, Colo.
H. P. Peters	Atlanta, Ga.
Noel Pike	Phoenix, Arizona
R. T. Purdy	Chicago, Ill.
G. F. Switzer	Indianapolis, Ind.
G. M. Tatum	Richmond, Va.
J. J. Tesar	Cleveland, Ohio
D. C. Vaughan	Washington, D. C.
R. M. Walker	El Paso, Tex.
H. R. Wall	Jackson, Mich.
J. B. Ward	Lafayette, Ind.
C. W. Watchorn	Baltimore, Md.
W. R. Way	Montreal, Quebec, Canada
G. S. Whitlow	St. Louis, Mo.
A. L. Williams	Los Angeles, Calif.

Administrative Subcommittee

Robert Brandt, *Chairman;* New England Power Company, 441 Stuart Street, Boston 16, Mass.

W. B. Fisk	New York, N. Y.
H. L. Harrington	Buffalo, N. Y.
C. B. Kelley	Des Moines, Iowa
H. A. Lott	Los Angeles, Calif.
O. W. Manz, Jr.	New York, N. Y.
C. W. Mayott	Hartford, Conn.
G. H. McDaniel	New York, N. Y.
C. N. Metcalf	New York, N. Y.
C. W. Watchorn	Baltimore, Md.

System Planning Subcommittee

W. B. Fisk, *Chairman;* Consolidated Edison Company of New York, Inc., 4 Irving Place, New York 3, N. Y.

O. E. Charlton	Birmingham, Ala.
S. B. Farnham	Schenectady, N. Y.
A. P. Fugill	Detroit, Mich.
R. G. Hooke	Newark, N. J.
L. R. Janes	Chicago, Ill.
H. J. Klumb	Rochester, N. Y.
R. F. Lawrence	East Pittsburgh, Pa.
W. J. Lyman	Pittsburgh, Pa.
W. A. Morgan	Denver, Colo.
W. H. Osterle	Pittsburgh, Pa.
L. R. Patterson	Denver, Colo.
H. P. St. Clair	New York, N. Y.
G. F. Switzer	Indianapolis, Ind.
J. J. Tesar	Cleveland, Ohio
D. C. Vaughan	Washington, D. C.
R. M. Walker	El Paso, Texas

(Continued in next column)

System Operations Subcommittee

C. B. Kelley, *Chairman;* Interchange Power Service, P. O. Box 616, Des Moines, Iowa

D. W. Alden	Pawtucket, R. I.
F. A. Andrews	Baltimore, Md.
E. C. Brown	Hartford, Conn.
G. D. Floyd	Toronto, Ontario, Canada
S. M. Hamill, Jr.	Cincinnati, Ohio
A. C. Hartranft	Philadelphia, Pa.
W. R. Johnson	San Francisco, Calif.
J. C. Jones	Portland, Oreg.
O. W. Manz, Jr.	New York, N. Y.
E. L. Michelson	Chicago, Ill.
W. E. Montgomery	Los Angeles, Calif.
Noel Pike	Phoenix, Ariz.
G. M. Tatum	Richmond, Va.

System Economics Subcommittee

C. W. Watchorn, *Chairman;* Pennsylvania Water and Power Company, 1611 Lexington Building, Baltimore, Md.

G. E. Bishop	Santa Cruz, Calif.
E. C. Brown	Hartford, Conn.
E. E. George	New York, N. Y.
A. P. Hayward	Pittsburgh, Pa.
H. P. Peters	Atlanta, Ga.
R. T. Purdy	Chicago, Ill.
J. A. Rose	Newark, N. J.
H. R. Wall	Jackson, Mich.
J. B. Ward	Lafayette, Ind.
W. R. Way	Montreal, Quebec, Canada
A. L. Williams	Los Angeles, Calif.

System Controls Subcommittee

G. H. McDaniel, *Chairman;* American Gas and Electric Service Corporation, 30 Church Street, New York 8, N. Y.

C. P. Almon, Jr.	Chattanooga, Tenn.
E. S. Bossuyt	Portland, Oreg.
D. H. Cameron	Kansas City, Mo.
R. F. Lawrence	East Pittsburgh, Pa.
C. N. Metcalf	New York, N. Y.
S. B. Morehouse	Philadelphia, Pa.
G. S. Whitlow	St. Louis, Mo.

Interconnection Contracts Subcommittee

C. W. Mayott, *Chairman;* Hartford Electric Light Company, 266 Pearl Street, Hartford, Conn.

Bradley Cozzens	Los Angeles, Calif.
E. D. Early	Birmingham, Ala.
E. E. George	New York, N. Y.
C. B. Kelley	Des Moines, Iowa
M. H. Lovelady	Corpus Christi, Tex.

Committee on Transformers

F. J. Vogel, *Chairman;* Transformer Engineering Department, Allis-Chalmers Manufacturing Company, Milwaukee 1, Wis.

M. K. Brown, *Vice-Chairman*	Buffalo, N. Y.
J. R. Meador, *Secretary*	Pittsfield, Mass.
J. A. Adams	Philadelphia, Pa.
H. E. Bonheimer	Cleveland, Ohio
R. J. Brown	Toronto, Ontario, Canada
J. L. Cantwell	Pittsfield, Mass.
R. B. Carson	Toronto, Ontario, Canada
J. H. Chiles, Jr.	Sharon, Pa.
J. E. Clem	Schenectady, N. Y
G. W. Clothier	Milwaukee, Wis.
J. A. Elzi	Jackson, Mich.
Byron Evans	Denver, Colo.
I. W. Gross	New York, N. Y.
E. M. Gue	Pittsburgh, Pa.
J. B. Hodtum	Pittsburgh, Pa.
A. A. Johnson	East Pittsburgh, Pa.
H. B. Keath	St. Louis, Mo.
D. L. Levine	Chicago, Ill.
C. M. Lovell	St. Louis, Mo.
C. W. Maller	Sharon, Pa.
V. M. Montsinger	Pittsfield, Mass.
H. R. Osborne	Toronto, Ontario, Canada
M. H. Pratt	Syracuse, N. Y.
T. D. Reimers	New York, N. Y.
S. E. Schultz	Portland, Oreg.
W. C. Sealey	Milwaukee, Wis.
P. D. Smith	Mimico, Ontario, Canada
F. L. Snyder	Sharon, Pa.
K. M. Stevens	Alhambra, Calif.
J. M. Towner	Baltimore, Md.
V. A. Treat	San Francisco, Calif.
P. A. Vance	Fort Wayne, Ind.
H. H. Wagner	Canonsburg, Pa.
P. L. Weir	Washington, D. C.
Harry Wells	Phoenix, Ariz.
W. C. Whitman	Boston, Mass.

(Continued in next column)

Insulation Tests Subcommittee

F. J. Vogel, *Chairman;* Transformer Engineering Department, Allis-Chalmers Manufacturing Company, Milwaukee 1, Wis.

J. A. Adams	Philadelphia, Pa.
V. J. Christen	St. Louis, Mo.
J. E. Clem	Schenectady, N. Y.
I. W. Gross	New York, N. Y.
J. H. Hagenguth	Pittsfield, Mass.
D. C. MacGregor	New York, N. Y.
W. R. McCarty	St. Louis, Mo.
J. R. Meador	Pittsfield, Mass.
C. W. Miller	Sharon, Pa.
V. M. Montsinger	Sarasota, Fla.
W. C. Sealey	Milwaukee, Wis.
W. L. Teague	Sharon, Pa.

Insulation Life Subcommittee

J. A. Adams, *Chairman;* Philadelphia Electric Company, 900 Sansom Street, Philadelphia 5, Pa.

Working Group on Life of Materials:

J. F. Cantwell, *Chairman;* General Electric Company, 100 Woodlawn Avenue, Pittsfield, Mass.

C. E. Arntzen	East Pittsburgh, Pa.
F. M. Clark	Pittsfield, Mass.
J. F. Dexter	Midland, Mich.
C. F. Hill	East Pittsburgh, Pa.
Myron Kin	Midland, Mich.
M. L. Manning	Canonsburg, Pa.
V. M. Montsinger	Sarasota, Fla.
J. S. Parkinson	Manville, N. J.
J. R. Perkins	Wilmington, Del.
T. D. Reimers	New York, N. Y.
W. W. Satterlee	Sharon, Pa.
W. M. Terry, Jr.	Pittsburgh, Pa.
F. J. Vogel	Milwaukee, Wis.
T. R. Walters	Pittsfield, Mass.
H. G. Zambell	Pittsburgh, Pa.

Working Group on Methods of Making Temperature Rise Tests:

J. E. Clem, *Chairman;* Central Station Engineering Division, General Electric Company, Schenectady 5, N. Y.

J. A. Adams	Philadelphia, Pa.
M. F. Beavers	Pittsfield, Mass.
H. B. Keath	St. Louis, Mo.
A. J. Maslin	Sharon, Pa.
W. H. Mutschler	Pittsburgh, Pa.
Paul Narbut, *Alternate*	Sharon, Pa.
S. O. Schamberger	Albany, N. Y.
R. C. Smith, *Alternate*	Philadelphia, Pa.
W. C. Whitman	Boston, Mass.

Working Group on Temperature Rise of Class-B Reactors:

D. L. Levine, *Chairman;* Commonwealth Edison Company, 72 West Adams Street, Chicago 90, Ill.

F. H. Kierstead	Pittsfield, Mass.
J. C. Russ	Pittsfield, Mass.
L. E. Sauer	Sharon, Pa.

Insulation Fluids Subcommittee

J. R. Meador, *Chairman;* General Electric Company, 100 Woodlawn Avenue, Pittsfield, Mass.

Working Group on Permissible Maximum Oil Temperature in Service:

M. H. Pratt, *Chairman;* Niagara Mohawk Power Company, 300 Erie Boulevard, Syracuse 2, N. Y.

A. J. Maslin	Sharon, Pa.
J. R. Meador	Pittsfield, Mass.

Working Group on Insulation Fluids:

J. R. Meador, *Chairman;* General Electric Company, 100 Woodlawn Avenue, Pittsfield, Mass.

J. G. Ford	Sharon, Pa.
I. W. Gross	New York, N. Y.
M. H. Pratt	Syracuse, N. Y.
E. L. Raab	Pittsfield, Mass.
W. W. Satterlee	Sharon, Pa.

(Continued from next column)

Liaison Members from Other Committees:

F. C. Doble	Belmont, Mass.
(Instruments and Measurements representative)	
D. R. Pattison	Johnstown, Pa.
(Power Generation representative)	
V. L. Cox	Philadelphia, Pa.
(Switchgear representative)	

Magnetic Circuit Behavior Subcommittee

J. H. Chiles, Jr., *Chairman;* Westinghouse Electric Corporation, Transformer Engineering Department, Sharon, Pa.

Working Group on Magnetization Characteristics:

J. E. Clem, *Chairman;* General Electric Company, Central Station Engineering Divisions, Schenectady 5, N. Y.

J. A. Elzi	Jackson, Mich.
T. D. Gordy	Pittsfield, Mass.
S. C. Killian	Chicago, Ill.
J. H. Kinghorn	New York, N. Y.
W. E. Marter	Pittsburgh, Pa.
A. J. Maslin	Sharon, Pa.
W. W. Perry	Binghamton, N. Y.
A. H. Powell	Philadelphia, Pa.
R. J. Salsbury	Pittsburgh, Pa.
W. C. Sealey	Milwaukee, Wis.
H. T. Seeley	Philadelphia, Pa.
W. K. Sonneman	Newark, N. J.
D. W. Taylor	Newark, N. J.
J. M. Wallace	East Pittsburgh, Pa.

Working Group on Audible Noise:

J. H. Chiles, *Chairman;* Transformer Engineering Department, Westinghouse Electric Corporation, Sharon, Pa.

J. E. Clem	Schenectady, N. Y.
T. D. Gordy	Pittsfield, Mass.
D. L. Levine	Chicago, Ill.
A. J. Maslin	Sharon, Pa.
T. D. Reimers	New York, N. Y.
J. M. Towner	Baltimore, Md.
H. E. Noren	Maywood, Ill.
Frank Von Voigtlander	Jackson, Mich.

Performance Characteristics Subcommittee

M. H. Pratt, *Chairman;* Niagara Mohawk Power Corporation, 300 Erie Boulevard, Syracuse 2, N. Y.

Working Group on Instrument Transformers:

J. E. Clem, *Chairman;* General Electric Company, Central Station Engineering Division, Schenectady 5, N. Y.

Herman Bany	Philadelphia, Pa.
J. H. Chiles	Sharon, Pa.
R. E. Cordray	Philadelphia, Pa.
A. B. Craig	Boston, Mass.
F. E. Davis, Jr.	Jackson, Mich.
K. J. C. Falck	Philadelphia, Pa.
R. E. Franck	Lynn, Mass.
J. M. Geiger	Buffalo, N. Y.
T. R. Halman	Detroit, Mich.
E. K. Huntington	Rochester, N. Y.
L. F. Kennedy	Schenectady, N. Y.
J. H. Kinghorn	New York, N. Y.
D. B. Masters	Jackson, Mich.
J. P. Scott	St. Louis, Mo.
F. B. Silsbee	Washington, D. C.
W. K. Sonnemann	Newark, N. J.
W. M. Terry	Pittsburgh, Pa.
E. C. Wentz	Sharon, Pa.
C. A. Woods	East Pittsburgh, Pa.

Working Group on Dry Type Transformers:

J. A. Adams, *Chairman;* Philadelphia Electric Company, 900 Sansom Street, Philadelphia 5, Pa.

G. J. Johnson	Pittsburgh, Pa.
T. D. Reimers	New York, N. Y.
T. E. Rodhouse	Pittsfield, Mass.
W. W. Satterlee	Sharon, Pa.
H. H. Wagner	Canonsburg, Pa.
C. E. Winegartner	Cleveland, Ohio

Liaison Representative on Converters:

W. C. Sealey	Milwaukee, Wis.
(Electronic Power Converters Committee)	

Committee on Transmission and Distribution

S. B. Crary, *Chairman;* General Electric Company, 1 River Road, Schenectady 5, N. Y.

(Continued on page 2182)

F. V. Smith, *Vice-Chairman*	Chicago, Ill.
E. K. Huntington, *Secretary*	Rochester, N. Y.
H. G. Barnett	East Pittsburgh, Pa.
C. E. Baugh	San Francisco, Calif.
P. L. Bellaschi	Portland, Oreg.
H. C. Bingham	Cleveland, Ohio
D. K. Blake	Schenectady, N. Y.
C. A. Booker	Boston, Mass.
Bryce Brady	Oklahoma City, Okla.
T. J. Brosnan	Buffalo, N. Y.
L. L. Carter	Hastings-on-Hudson, N. Y.
Harold Cole	Detroit, Mich.
E. R. Coulbourn	Birmingham, Ala.
P. J. Croft	Toronto, Ontario, Canada
A. E. Curtis	Shawinigan Falls, Quebec, Canada
H. L. Davis, Jr.	Philadelphia, Pa.
A. E. Davison	Toronto, Ontario, Canada
G. E. Dean	Newark, N. J.
T. C. Duncan	New York, N. Y.
H. A. Frey	Baltimore, Md.
E. T. B. Gross	Chicago, Ill.
I. W. Gross	New York, N. Y.
J. H. Hagenguth	Pittsfield, Mass.
K. E. Hapgood	Chattanooga, Tenn.
E. R. Hendrickson	Maywood, Ill.
P. A. Jeanne	New York, N. Y.
E. L. Kanouse	Los Angeles, Calif.
C. H. Kraft	St. Louis, Mo.
A. V. Lambert	Portland, Oreg.
J. T. Lusignan, Jr.	Mansfield, Ohio
W. A. Morgan	Denver, Colo.
D. W. Nethercut	Jackson, Mich.
J. E. O'Brien	Washington, D. C.
E. W. Oesterreich	Pittsburgh, Pa.
A. A. Osipovich	Portland, Oreg.
C. E. Parks	Plainfield, Ind.
R. E. Pierce	New York, N. Y.
C. K. Poarch	New York, N. Y.
J. A. Rawls	Richmond, Va.
L. M. Robertson	Denver, Colo.
E. V. Sayles	Jackson, Mich.
A. N. Shealy	Baltimore, Md.
D. M. Simmons	New York, N. Y.
E. C. Starr	Corvallis, Oreg.
H. B. Thacker	East Pittsburgh, Pa.
C. F. Wagner	East Pittsburgh, Pa.
P. G. Wallace	Dallas, Tex.
L. J. Weed	Boston, Mass.
R. L. Witzke	East Pittsburgh, Pa.

Transmission and Distribution

Capacitor Subcommittee

C. E. Parks, *Chairman;* Public Service Company of Indiana, Inc., 110 East Main Street, Plainfield, Ind.

Glen Appleman	Allentown, Pa.
P. L. Bellaschi	Portland, Oreg.
L. F. Billman	South Plainfield, N. J.
E. R. Coop	Providence, R. I.
H. V. Dryer	So. Milwaukee, Wis.
K. E. Hapgood	Chattanooga, Tenn.
D. A. Leeds	Hammond, Ind.
M. F. Leftwich	Charlotte, N. C.
R. E. Marbury	East Pittsburgh, Pa.
D. B. Masters	Jackson, Mich.
Leon Podolsky	North Adams, Mass.
M. E. Scoville	Pittsfield, Mass.
F. V. Smith	Chicago, Ill.
H. E. Smith	Chicago, Ill.
P. H. Underwood	Houston, Tex.

Distribution Subcommittee

T. J Brosnan, *Chairman;* Niagara Mohawk Power Corporacion, 300 Electric Building, Buffalo, N. Y.

H. G. Barnett	East Pittsburgh, Pa.
C. E. Baugh	San Francisco, Calif.
H. C. Bingham	Cleveland, Ohio
D. K. Blake	Schenectady, N. Y.
Bryce Brady	Oklahoma City, Okla.
W. R. Bullard	New York, N. Y.
L. L. Carter	Hastings-on-Hudson, N. Y.
Harold Cole	Detroit, Mich.
H. L. Davis, Jr.	Philadelphia, Pa.
E. R. Hendrickson	Maywood, Ill.
J. B. Hodtum	Pittsburgh, Pa.
E. K. Huntington	Rochester, N. Y.
C. H. Kraft	St. Louis, Mo.
J. E. O'Brien	Washington, D. C.
E. W. Oesterreich	Pittsburgh, Pa.
E. V. Sayles	Jackson, Mich.
M. F. Schonefeld	Fort Wayne, Ind.
A. F. Sedgwick	New Haven, Conn.
H. E. Smith	Chicago, Ill.
A. H. Thayer	Los Angeles, Calif.

General Systems Subcommittee

R. L. Witzke, *Chairman;* Industry Engineering Department, Westinghouse Electric Corporation, East Pittsburgh, Pa.

P. W. Blye	New York, N. Y.
R. W. Caswell	Chicago, Ill.
F. L. Code	Toronto, Ontario, Canada
O. A. Demuth	Portland, Oreg.
R. G. Hooke	Newerk, N. J.
E. K. Huntington	Rochester, N. Y.
I. B. Johnson	Schenectady, N. Y.
A. A. Kroneberg	Los Angeles, Calif.
L. B. LeVesconte	Chicago, Ill.
F. H. Linsley	Waterbury, Conn.
L. M. Robertson	Denver, Colo.

Lightning and Insulator Subcommittee

J. T. Lusignan, Jr., *Chairman;* Ohio Brass Company, Engineering Department, Mansfield, Ohio

L. V. Bewley	Bethlehem, Pa.
H. N. Ekvall	Philadelphia, Pa.
H. A. Frey	Baltimore, Md.
I. W. Gross	New York, N. Y.
J. H. Hagenguth	Pittsfield, Mass.
E. L. Harder	East Pittsburgh, Pa.
W. W. Lewis	Schenectady, N. Y.
H. L. Rorden	Portland, Oreg.
S. K. Waldorf	Baltimore, Md.
E. R. Whitehead	Chicago, Ill.

Towers, Poles, and Conductors Subcommittee

E. L. Kanouse, *Chairman;* Water and Power Department, City of Los Angeles, 207 South Broadway, Los Angeles 13, Calif.

H. W. Adams	Louisville, Ky.
H. W. Biskeborn	Newark, Ohio
C. A. Booker	Boston, Mass.
L. L. Carter	Hastings-on-Hudson, N. Y.
P. J. Croft	Toronto, Ontario, Canada
A. E. Davison	Toronto, Ontario, Canada
K. T. Deutch	Denver, Colo.
S. E. Goodell	Chicago, Ill.
K. E. Hapgood	Chattanooga, Tenn.
C. A. Jordan	Perth Amboy, N. J.
J. E. O'Brien	Washington, D. C.
A. A. Osipovich	Portland, Oreg.
T. F. Peterson	Cleveland, Ohio
J. A. Rawls	Richmond, Va.
L. M. Robertson	Denver, Colo.
A. S. Runciman	Montreal, Quebec, Canada
A. N. Shealy	Baltimore, Md.
Joel Tompkins	Massena, N. Y.
E. M. Wright	San Francisco, Calif.
R. G. Yerke	Seward, Neb.

Science and Electronics Division

Science and Electronics Division Committee

E. I. Green, *Chairman;* Bell Telephone Laboratories, Inc., Murray Hill, N. J.

W. R. Clark, *Vice-Chairman*	Philadelphia, Pa.
W. F. Bonner, *Secretary*	Clifton, N. J.
W. F. Davidson	New York, N. Y.
I. K. Dortort	Philadelphia, Pa.
W. G. Dow	Ann Arbor, Mich.
E. L. Harder	East Pittsburgh, Pa.
J. T. Lusignan, Jr.	Mansfield, Ohio
W. H. MacWilliams, Jr.	Whippany, N. J.
M. G. Malti	Ithaca, N. Y.
J. H. Miller	Newark, N. J.
J. G. Tarboux (*representing Board of Directors*)	Ithaca, N. Y.
J. D. Tebo	New York, N. Y.
J. T. Thwaites	Hamilton, Ontario, Canada
S. Reid Warren, Jr.	Philadelphia, Pa.

Committee on Basic Sciences

M. G. Malti, *Chairman;* School of Electrical Engineering, Cornell University, Ithaca, N. Y.

(*Continued in next column*)

R. M. Bozorth, *Vice-Chairman*	Murray Hill, N. J.
W. C. Johnson, *Secretary*	Princeton, N. J.
J. A. Becker	Murray Hill, N. J.
L. J. Berberich	East Pittsburgh, Pa.
L. V. Bewley	Bethlehem, Pa.
Aram Boyajian	Pittsfield, Mass.
J. G. Brainerd	Philadelphia, Pa.
C. B. Brown	White Oak, Md.
C. R. Burrows	Ithaca, N. Y.
H. J. Carlin	Brooklyn, N. Y.
F. M. Clark	Schenectady, N. Y.
Charles Concordia	Schenectady, N. Y.
P. C. Cromwell	Knoxville, Tenn.
W. C. Dunlap	Schenectady, N. Y.
L. A. Finzi	Pittsburgh, Pa.
M. F. Gardner	Cambridge, Mass.
E. A. Guillemin	Cambridge, Mass.
C. R. Hanna	East Pittsburgh, Pa.
C. W. Hansell	Rocky Point, L. I., N. Y.
E. L. Harder	East Pittsburgh, Pa.
F. K. Harris	Washington, D. C.
V. P. Hessler	Urbana, Ill.
N. S. Hibshman	Brooklyn, N. Y.
T. J. Higgins	Madison, Wis.
G. B. Hoadley	Raleigh, N. C.
T. B. Jones	Baltimore, Md.
R. M. Kalb	St. Paul, Minn.
E. W. Kimbark	Sao Paulo, Brazil, South America
W. R. LePage	East Syracuse, N. Y.
W. H. MacWilliams, Jr.	Whippany, N. J.
P. C. Magnusson	Corvallis, Oreg.
L. W. Matsch	Chicago, Ill.
H. F. Mathis	Chicago, Ill.
G. D. McCann	Pasadena, Calif.
W. E. Phillips	Philadelphia, Pa.
L. A. Pipes	Los Angeles, Calif.
H. J. Plumley	Silver Spring, Md.
Dimiter Ramadanoff	Cleveland, Ohio
Walther Richter	Milwaukee, Wis.
H. H. Skilling	Stanford, Calif.
J. J. Smith	Schenectady, N. Y.
V. G. Smith	Toronto, Ontario, Canada
G. M. L. Sommerman	Evanston, Ill.
E. C. Starr	Corvallis, Oreg.
W. L. Sullivan	Hoboken, N. J.
W. A. Thomas	Cleveland, Ohio
G. S. Timoshenko	Storrs, Conn.
J. S. Waters	Houston, Tex.
A. H. Waynick	State College, Pa.
J. H. Wright	Lynn, Mass.
W. M. Young	Falls Church, Va.

Applied Mathematics Subcommittee

M. G. Malti, *Chairman;* School of Electrical Engineering, Cornell University, Ithaca, N. Y.

Mathematicians

Garrett Birkhoff	Cambridge, Mass.
D. G. Bourgin	Urbana, Ill.
R. J. Duffin	Pittsburgh, Pa.
A. E. Heins	Pittsburgh, Pa.
Mark Kac	Ithaca, N. Y.
Harry Pollard	Ithaca, N. Y.
J. J. Stoker	New York, N. Y.
J. W. Tukey	Princeton, N. J.
John Von Neumann	Princeton, N. J.
D. V. Widder	Cambridge, Mass.
Norbert Wiener	Cambridge, Mass.
Max Woodbury	Princeton, N. J.

Electrical Engineers

P. L. Alger	Schenectady, N. Y.
Murray Gardner	Cambridge, Mass.
H. B. Hansteen	New York, N. Y.
E. W. Kimbark	São Paulo, Brazil, S. A.
H. F. Mathis	Chicago, Ill.
Louis Pipes	Los Angeles, Calif.
J. J. Smith	Schenectady, N. Y.
Harry Sohon	Philadelphia, Pa.

Electric Circuit Theory Subcommittee

H. J. Carlin, *Chairman;* Microwave Research Institute, Polytechnic Institute of Brooklyn, 55 Johnson Street, Brooklyn 1, N. Y.

J. G. Brainerd	Philadelphia, Pa.
R. L. Dietzold	Murray Hill, N. J.
A. B. Giordano	Brooklyn, N. Y.
E. A. Guillemin	Cambridge, Mass.
T. J. Higgins	Madison, Wis.
G. B. Hoadley	Raleigh, N. C.
Robert Kahal	St. Louis, Mo.
Milton Mohr	Culver City, Calif.
P. F. Ordung	New Haven, Conn.

Electrical Properties of Gases Subcommittee

T. B. Jones, *Chairman;* School of Electrical Engineering, Johns Hopkins University, Baltimore 18, Md.

L. J. Berberich	East Pittsburgh, Pa.
J. D. Cobine	Schenectady, N. Y.
L. H. Fisher	New York, N. Y.
L. H. Germer	Murray Hill, N. J.
L. Malter	Harrison, N. J.
Joseph Slepian	East Pittsburgh, Pa.

Energy Sources Subcommittee

L. W. Matsch, *Chairman;* Illinois Institute of Technology, Department of Electrical Engineering, Chicago 16, Ill.

W. C. Brown	Point Mugu, Calif.
M. A. Garstens	Washington, D. C.
W. A. Lewis, Jr.	Chicago, Ill.
Walther Richter	Milwaukee, Wis.
J. J. Smith	Schenectady, N. Y.
B. R. Teare	Pittsburgh, Pa.
J. D. Tebo	New York, N. Y.
Milton Tenzer	Fort Monmouth, N. J.

Magnetics Subcommittee

R. M. Bozorth, *Chairman;* Bell Telephone Laboratories, Inc., Murray Hill, N. J.

A. C. Beiler	East Pittsburgh, Pa.
F. G. Brockman	Irvington-on-Hudson, N. Y.
R. A. Chegwidden	Murray Hill, N. J.
G. H. Cole	Middletown, Ohio
E. A. Gaugler	Butler, Pa.
J. E. Goldman	Pittsburgh, Pa.
W. Morrill	Pittsfield, Mass.
J. A. Osborn	Washington, D. C.
W. E. Ruder	Schenectady, N. Y.
C. W. Stoker	Pittsburgh, Pa.

Dielectrics Subcommittee

L. J. Berberich, *Chairman;* Liaison Engineering Department 7-L, Westinghouse Electric Corporation, East Pittsburgh, Pa.

J. C. Balsbaugh	Cambridge, Mass.
T. D. Callinan	Washington, D. C.
T. W. Dakin	East Pittsburgh, Pa.
J. W. Deaderick	Chattanooga, Tenn.
J. F. Dexter	Midland, Mich.
M. Getting, Jr.	Pittsburgh, Pa.
H. F. Jones	Waterford, N. Y.
G. T. Kohman	Murray Hill, N. J.
J. R. Perkins	Wilmington, Del.
J. D. Robinson	New York, N. Y.
A. W. Rogers	Fort Monmouth, N. J.
A. H. Scott	Washington, D. C.
A. H. Sharbaugh	Schenectady, N. Y.
G. M. L. Sommerman	Evanston, Ill.
Joseph Sticher	Detroit, Mich.
A. J. Warner	Nutley, N. J.

Semiconductors and Transistors Subcommittee

W. C. Dunlap, *Chairman;* Research Laboratory, General Electric Company, Schenectady 5, N. Y.

John Bardeen	Urbana, Ill.
J. A. Becker	Murray Hill, N. J.
C. B. Brown	White Oak, Md.
R. W. Engstrom	Lancaster, Pa.
K. Lark-Horovitz	Lafayette, Ind.
P. H. Miller, Jr.	Philadelphia, Pa.
Lloyd Smith	Ithaca, N. Y.
D. W. Wooldridge	Culver City, Calif.

Committee on Computing Devices

W. H. MacWilliams, Jr., *Chairman;* Bell Telephone Laboratories, Inc., Whippany, N. J.

J. C. McPherson, *Vice-Chairman*	New York, N. Y.
F. J. Maginniss, *Secretary*	Schenectady, N. Y.
S. N. Alexander	Washington, D. C.
J. G. Brainerd	Philadelphia, Pa.
S. H. Caldwell	Cambridge, Mass.
J. M. Coombs	St. Paul, Minn.
W. G. Dow	Ann Arbor, Mich.
G. V. Eltgroth	Philadelphia, Pa.
E. L. Harder	East Pittsburgh, Pa.
J. W. Mauchly	Ambler, Pa.
G. D. McCann	Pasadena, Calif.

(*Continued on page 2183*)

M. S. McIlroy	Ithaca, N. Y.
P. L. Morton	Berkeley, Calif.
J. D. Ryder	Urbana, Ill.
V. G. Smith	Toronto, Ontario, Canada
Irven Travis	Philadelphia, Pa.

Analog Computers Subcommittee

G. D. McCann, *Chairman;* California Institute of Technology, Pasadena 4, Calif.

S. H. Caldwell	Cambridge, Mass.
E. L. Harder	East Pittsburgh, Pa.
F. J. Maginniss	Schenectady, N. Y.
M. S. McIlroy	Ithaca, N. Y.

Computer Bibliography Subcommittee

W. H. MacWilliams, Jr., *Chairman;* Bell Telephone Laboratories, Inc., Whippany, N. J.

Digital Computers Subcommittee

M. Coombs, *Chairman;* Engineering Research Associates, 1902 West Minnehaha Avenue, St. Paul 4, Minn.

S. N. Alexander	Washington, D. C.
J. G. Brainerd	Philadelphia, Pa.
G. V. Eltgroth	Philadelphia, Pa.
J. W. Mauchly	Philadelphia, Pa.
G. D. McCann	Pasadena, Calif.
P. L. Morton	Berkeley, Calif.
J. D. Ryder	Urbana, Ill.
V. G. Smith	Toronto, Ontario, Canada
Irven Travis	Philadelphia, Pa.

Committee on Electrical Techniques in Medicine and Biology

S. Reid Warren, Jr., *Chairman;* Moore School of Electrical Engineering, University of Pennsylvania, 200 South 33rd Street, Philadelphia 4, Pa.

A. M. Zarem, *Vice-Chairman*	Los Angeles, Calif.
Scott W. Smith, *Secretary*	Washington, D. C.
G. W. Dunlap	Schenectady, N. Y.
L. F. Ehrke	Bloomfield, N. J.
W. A. Geohegan	New York, N. Y.
J. P. Hervey	Baltimore, Md.
L. H. Montgomery	Nashville, Tenn.
H. D. Moreland	Baltimore, Md.
G. A. Morton	Princeton, N. J.
J. G. Reid, Jr.	Washington, D. C.
J. A. Reynolds	White Plains, N. Y.
T. H. Rogers	Springdale, Conn.
E. D. Trout	Milwaukee, Wis.
R. E. Watson	Philadelphia, Pa.

(No subcommittees)

Committee on Electronic Power Converters

I. K. Dortort, *Chairman;* I-T-E Circuit Breaker Company, 19th and Hamilton Streets, Philadelphia 30, Pa.

C. R. Marcum, *Vice-Chairman*	East Pittsburgh, Pa.
J. B. Pitman, *Secretary*	Massena, N. Y.
B. D. Bedford	Schenectady, N. Y.
W. E. Bloecker	New York, N. Y.
H. R. Blomquist	Providence, R. I.
W. F. Bonner	Clifton, N. J.
J. L. Boyer	East Pittsburgh, Pa.
F. W. Cramer	Pittsburgh, Pa.
A. G. Dickinson	Trail, British Columbia, Canada
J. B. Donnelly	Philadelphia, Pa.
W. J. Gilson	Toronto, Ontario, Canada
F. S. Glaza	Freeport, Tex.
W. E. Gutzwiller	Milwaukee, Wis.
J. D. Harper	Alcoa, Tenn.
C. C. Herskind	Schenectady, N. Y.
G. N. Hughes	Alcoa, Tenn.
Otto Jensen	Philadelphia, Pa.
F. D. Kaiser	Sharon, Pa.
Armin Leuthold	Montreal, Quebec, Canada
D. E. Marshall	Bloomfield, N. J.
L. W. Morton	Schenectady, N. Y.
J. B. Nayler	Arvida, Quebec, Canada

(Continued in next column)

R. A. Nelson	Pittsfield, Mass.
F. O. Nottingham, Jr.	Atlanta, Ga.
Waldo Porter	Vancouver, Wash.
M. E. Reagan	East Pittsburgh, Pa.
W. J. L. Rupprecht	Midland, Mich.
August Schmidt, Jr.	Schenectady, N. Y.
W. C. Sealey	Milwaukee, Wis.
F. W. Smith	Easton, Pa.
S. L. Smith	Philadelphia, Pa.
H. C. Steiner	Schenectady, N. Y.
O. J. Swanson	Gary, W. Va.
J. T. Thwaites	Hamilton, Ontario, Canada
D. E. Trucksess	New York, N. Y.
J. C. Walter	Camden, N. J.
C. H. Willis	Princeton, N. J.
Harold Winograd	Milwaukee, Wis.

Administrative Subcommittee

Main Committee Officers:

I. K. Dortort, *Chairman;* I-T-E Circuit Breaker Company, 19th and Hamilton Streets, Philadelphia 30, Pa.

C. R. Marcum, *Vice-Chairman*	East Pittsburgh, Pa.
J. B. Pitman, *Secretary*	Massena, N. Y.
C. C. Herskind, *Preceding Chairman*	Schenectady, N. Y.

Subcommittee Chairmen:

B. D. Bedford	Schenectady, N. Y.
Otto Jensen	Philadelphia, Pa.
Waldo Porter	Vancouver, Wash.
August Schmidt, Jr.	Schenectady, N. Y.
J. C. Walter	Camden, N. J.

Others:

Harold Winograd	Milwaukee, Wis.

Papers and Speakers Subcommittee

August Schmidt, Jr., *Chairman;* General Electric Company, 1 River Road, Schenectady 5, N. Y.

J. B. Rice	West Allis, Wis.
J. T. Thwaites	Hamilton, Ontario, Canada
H. E. Zuvers	Schenectady, N. Y.

Electronic Converter Circuits Subcommittee

B. D. Bedford, *Chairman;* General Electric Company, 1 River Road, Schenectady 5, N. Y.

W. E. Bloecker	New York, N. Y.
W. F. Bonner	Clifton, N. J.
J. L. Boyer	East Pittsburgh, Pa.
E. J. Diebold	Philadelphia, Pa.
G. N. Hughes	Alcoa, Tenn.
F. D. Kaiser	Sharon, Pa.
A. H. Mittag	Schenectady, N. Y.
R. A. Nelson	Pittsfield, Mass.
M. E. Reagan	East Pittsburgh, Pa.
August Schmidt, Jr.	Schenectady, N. Y.
W. C. Sealey	Milwaukee, Wis.
C. H. Willis	Princeton, N. J.

Mercury Arc Converters Subcommittee

C. R. Marcum, *Chairman;* Westinghouse Electric Corporation, East Pittsburgh, Pa.

J. L. Boyer	East Pittsburgh, Pa.
E. H. Coxe, Jr.	Baton Rouge, La.
F. W. Cramer	Pittsburgh, Pa.
J. B. Donnelly	Philadelphia, Pa.
W. E. Gutzwiller	Milwaukee, Wis.
C. C. Herskind	Schenectady, N. Y.
A. D. Howry	Conshohocken, Pa.
R. N. Hunter	New York, N. Y.
Armin Leuthold	Montreal, Quebec, Canada
E. J. Remscheid	Schenectady, N. Y.
W. J. L. Rupprecht	Midland, Mich.
O. J. Swanson	Gary, W. Va.
J. T. Thwaites	Hamilton, Ontario, Canada
Harold Winograd	Milwaukee, Wis.

Hot-Cathode Power Converter Subcommittee

J. C. Walter, *Chairman;* Radio Corporation of America, Camden, N. J.

R. W. Barker	Pittsfield, Mass.
W. H. Bixby	Detroit, Mich.
H. R. Butler	Newark, N. J.

(Continued in next column)

F. W. Cramer	Pittsburgh, Pa.
D. V. Edwards	Newark, N. J.
C. E. Hamann	Lynn, Mass.
J. F. Harris	Newark, N. J.
E. W. Hutton	Schenectady, N. Y.
W. E. Large	East Pittsburgh, Pa.
F. G. Logan	St. Louis, Mo.
E. J. Rathsack	Milwaukee, Wis.
F. M. Rives	Schenectady, N. Y.
W. C. Rudd	New Rochelle, N. Y.
J. W. Sanborn	Camden, N. J.
D. H. Smith	Schenectady, N. Y.
H. C. Steiner	Schenectady, N. Y.
H. L. Thorson	Schenectady, N. Y.
D. E. Trucksess	New York, N. Y.

Mechanical Rectifier Subcommittee

Otto Jensen, *Chairman;* I-T-E Circuit Breaker Company, 501 North 19th Street, Philadelphia 30, Pa.

E. J. Diebold	Philadelphia, Pa.
W. J. Gilson	Toronto, Ontario, Canada
D. H. Smith	New York, N. Y.

West Coast Subcommittee

Waldo Porter, *Chairman;* Aluminum Company of America, P. O. Box 120, Vancouver, Wash.

W. M. Allen	New York, N. Y.
E. D. Barcus	Los Angeles, Calif.
E. S. Benson	San Francisco, Calif.
H. L. Burris	Pittsburg, Calif.
R. J. Corfield	Garfield, Utah
J. H. Cox	Sunnyvale, Calif.
R. H. Denyer	Portland, Oreg.
A. G. Dickinson	Trail, British Columbia, Canada
E. F. Donatic	Ontario, Calif.
Alex. Dovjikov	Portland, Oreg.
R. H. Duguid	Los Angeles, Calif.
S. R. Durand	Milwaukee, Wis.
L. E. Dye	Los Angeles, Calif.
T. F. Hadwin	Vancouver, British Columbia, Canada
D. R. Hoopes	Salt Lake City, Utah
J. V. Kresser	San Francisco, Calif.
C. A. Langlois	Troutdale, Oreg.
H. F. Lickey	Pullman, Wash.
M. McCoy	Portland, Oreg.
A. L. Munn	San Leandro, Calif.
S. J. Pope	Spokane, Wash.
H. H. Skilling	Stanford, Calif.
E. C. Starr	Corvallis, Oreg.
H. V. Strandberg	Seattle, Wash.
J. R. Tenney	Geneva, Utah

Working Group on Cooling and Corrosion

E. J. Remscheid, *Chairman;* General Electric Company, Schenectady, N. Y.

A. P. Colaiaco	East Pittsburgh, Pa.
A. G. Dickinson	Trail, British Columbia, Canada
J. Y. Doran	Toronto, Ontario, Canada
G. N. Hughes	Alcoa, Tenn.
J. Klotz	Philadelphia, Pa.
R. J. Nix	Indiana, Pa.
M. W. Rew	Cleveland, Ohio
Mark Sareault	Providence, R. I.
Harold Winograd	Milwaukee, Wis.

Committee on Electronics

J. T. Thwaites, *Chairman;* Canadian Westinghouse Company, Ltd., Research and Development Laboratory, Electronics Division, Aberdeen Avenue, Hamilton, Ontario, Canada

H. C. Steiner *Vice-Chairman (East)*	Schenectady, N. Y.
J. D. Ryder, *Vice-Chairman (West)*	Urbana, Ill.
D. G. Wilson, *Secretary*	Lawrence, Kans.
W. R. G. Baker	Syracuse, N. Y.
R. W. Barker	Pittsfield, Mass.
E. M. Boone	Columbus, Ohio
John Boykin	Baltimore, Md.
C. J. Breitwieser	Indianapolis, Ind.
C. B. Brown	White Oak, Md.
Cledo Brunetti	Stanford, Calif.
R. S. Burnap	Harrison, N. J.
J. M. Cage	Lafayette, Ind.
A. H. Canada	Schenectady, N. Y.
W. R. Clark	Philadelphia, Pa.
L. G. Cowles	Houston, Tex.

(Continued in next column)

G. J. Crowdes	Cambridge, Mass.
W. G. Dow	Ann Arbor, Mich.
A. V. Eastman	Seattle, Wash.
G. V. Eltgroth	Philadelphia, Pa.
W. T. Evans	Beaumont, Tex.
Rudolf Feldt	Clifton, N. J.
G. H. Fett	Urbana, Ill.
W. J. Field	St. Paul, Minn.
D. G. Fink	New York, N. Y.
H. L. Flowers	Akron, Ohio
W. A. Geohegan	New York, N. Y.
E. L. Harder	East Pittsburgh, Pa.
Victor Harris	Bethesda, Md.
G. W. Hewitt	East Pittsburgh, Pa.
J. E. Hobson	Stanford, Calif.
A. J. Humphrey	Cleveland, Ohio
J. R. Hyneman	New York, N. Y.
T. P. Kinn	Baltimore, Md.
K. S. Koon	Endicott, N. Y.
O. W. Livingston	Schenectady, N. Y.
D. E. Marshall	Bloomfield, N. J.
R. E. McCoy	Los Angeles, Calif.
H. R. Meahl	Schenectady, N. Y.
H. R. Mimno	Cambridge, Mass.
G. A. Morton	Princeton, N. J.
R. E. Mumma	Dayton, Ohio
J. B. Nayler	Isle Maligne, Quebec, Canada
R. A. Nielsen	Pasadena, Calif.
E. K. Northrop	Ithaca, N. Y.
David Packard	Palo Alto, Calif.
G. W. Penney	Pittsburgh, Pa.
W. H. Pickering	Pasadena, Calif.
A. J. Quigley	Notre Dame, Ind.
Simon Ramo	Culver City, Calif.
J. G. Reid, Jr.	Washington, D. C.
L. E. Reukema	Berkeley, Calif.
R. W. Reynolds	Wilmington, Del.
E. T. Sherwood	Milwaukee, Wis.
Scott W. Smith	Washington, D. C.
E. P. Spandau	Los Angeles, Calif.
C. F. Spitzer	Syracuse, N. Y.
J. R. Steen	New York, N. Y.
C. M. Summers	Fort Wayne, Ind.
E. R. Thomas	New York, N. Y.
Irven Travis	Philadelphia, Pa.
D. E. Trucksess	New York, N. Y.
D. C. Ulrey	Harrison, N. J.
W. C. White	Schenectady, N. Y.
C. H. Willis	Princeton, N. J.
Harold Winograd	Milwaukee, Wis.
A. M. Zarem	Los Angeles, Calif.

Electron Tube Subcommittee

Scott Helt, *Chairman;* Allen B. DuMont Laboratories, Inc., Research Division, 2 Main Avenue, Passaic, N. J.

R. E. Higgs, *Secretary*	Harrison, N. J.
A. Y. Bentley	Clifton, N. J.
W. R. Clark	Philadelphia, Pa.
W. G. Dow	Ann Arbor, Mich.
D. V. Edwards	Newark, N. J.
A. M. Glover	Lancaster, Pa
R. E. Graham	Kew Gardens, N. Y.
William Happe, Jr.	Clifton, N. J.
L. B. Headrick	Lancaster, Pa.
J. H. Hutchings	Geneva, Ill.
E. O. Johnson	Princeton, N. J.
K. S. Koon	Endicott, N. Y.
O. W. Livingston	Schenectady, N. Y.
C. R. Marcum	East Pittsburgh, Pa.
D. E. Marshall	Bloomfield, N. J.
D. S. Peck	Allentown, Pa.
August Schmidt, Jr.	Schenectady, N. Y.
J. R. Steen	New York, N. Y.
H. C. Steiner	Schenectady, N. Y.
J. T. Thwaites	Hamilton, Ontario, Canada
Simeon Weston	Brooklyn, N. Y.
C. H. Willis	Princeton, N. J.
Harold Winograd	Milwaukee, Wis.

Industrial X-Ray Subcommittee

Scott W. Smith, *Chairman;* X-Ray Section, National Bureau of Standards, Washington 25, D. C.

Z. J. Atlee	Chicago, Ill.
Arthur Klinckermann	Chicago, Ill.
Joseph Lempert	Bloomfield, N. J.
G. E. Maxim	Cleveland, Ohio
T. H. Rogers	Springdale, Conn.
David Sussin	Covington, Ky.
R. F. Wilson	Milwaukee, Wis.

Electrostatic Processes Subcommittee

G. W. Hewitt, *Chairman;* Research Laboratories, Westinghouse Electric Corporation, East Pittsburgh, Pa.

(Continued on page 2184)

J. O. Amstutz	Troy, N. Y.
J. K. Coolidge, Jr.	State College, Pa.
E. P. Miller	Indianapolis, Ind.
H. V. Nelson	Schenectady, N. Y.
S. R. Orem, Jr.	Greenwich, Conn.
G. W. Penney	Pittsburgh, Pa.
E. R. Thomas	New York, N. Y.
J. B. Thomas	Baltimore, Md.
H. J. White	Bound Brook, N. J.

Liaison with Nucleonics Subcommittee

G. A. Morton, *Chairman;* R. C. A. Laboratories, Princeton, N. J.

Liaison with Electronic Heating Subcommittee

T. P. Kinn, *Chairman;* Electronics and X-Ray Division, Westinghouse Electric Corporation, 2519 Wilkens Avenue, Baltimore 3, Md.

R. M. Baker	Baltimore, Md.
W. C. Rudd	New Rochelle, N. Y.

Liaison with Standards Subcommittee

C. H. Willis, *Chairman;* Princeton University, Princeton, N. J.

Liaison with IRE Subcommittee

R. S. Burnap, *Chairman;* Radio Corporation of America, R. C. A. Victor Division, Harrison, N. J.

Liaison with JETEC Subcommittee

D. E. Marshall, *Chairman;* Westinghouse Electric Corporation, Bloomfield, N. J.

Papers Review Subcommittee

W. C. White, *Chairman;* General Electric Research Laboratory, The Knolls, Schenectady, N. Y.

W. R. Clark	Philadelphia, Pa.
H. F. Dart	Bloomfield, N. J.
Rudolf Feldt	Clifton, N. J.
R. E. Graham	Kew Gardens, N. Y.
S. B. Ingram	Murray Hill, N. J.
L. A. Kilgore	East Pittsburgh, Pa.
H. L. Palmer	Schenectady, N. Y.
H. C. Steiner	Schenectady, N. Y.
Dayton Ulrey	Lancaster, Pa.
Harold Winograd	Milwaukee, Wis.

Education in Electronics Subcommittee

J. D. Ryder, *Chairman;* Electrical Engineering Dept., University of Illinois, Urbana, Ill.

E. M. Boone	Columbus, Ohio
M. A. Honnell	Atlanta, Ga.
B. K. Northrop	Ithaca, N. Y.
A. J. Quigley	Notre Dame, Ind.
J. T. Thwaites	Hamilton, Ontario, Canada
D. G. Wilson	Lawrence, Kans.

Electronic Systems Engineering Subcommittee

H. L. Flowers, *Chairman;* Aerophysics Department, Goodyear Aircraft Corporation, Akron 15, Ohio

Victor Harris	Silver Spring, Md.

Electronic Semi-Conductor Devices Subcommittee

J. P. Jordan, *Chairman;* Electronics Laboratory, General Electric Company, Electronics Park, Syracuse, N. Y.

C. B. Brown	White Oak, Md.
Harold Goldberg	Washington, D. C.
J. R. Hyneman	New York, N. Y.
G. D. O'Neill	Kew Gardens, N. Y.

West Coast Subcommittee

T. H. Morrin, *Chairman;* Department of Electrical Engineering, Stanford Research Institute, Stanford, Calif.

Infrared Applications Subcommittee

A. H. Canada, *Chairman;* General Engineering Laboratory, General Electric Company, Schenectady 5, N. Y.

A. R. Dennett	Newport, R. I.
W. A. Dynes	Dayton, Ohio
W. G. Fastie	Philadelphia, Pa.
B. J. Goldfarb	Dayton, Ohio
E. D. Wilson	East Pittsburgh, Pa.
C. S. Woodside	Washington, D. C.

Electronic Aids to Navigation Subcommittee

H. R. Mimno, *Chairman;* Cruft Laboratory, Harvard University, Cambridge 38, Mass.

High Frequency Conductors, Cables, and Connectors Subcommittee

G. J. Crowdes, *Chairman;* Simplex Wire and Cable Company, 79 Sidney Street, Cambridge 39, Mass.

W. R. Dohan	Camden, N. J.
E. W. Greenfield	Newark, Ohio
J. D. Heibel	Erie, Pa.
B. A. Jackson	New York, N. Y.
W. J. King	Murray Hill, N. J.
H. B. Slade	Passaic, N. J.
M. Tenzer	Fort Monmouth, N. J.
W. R. Thurston	New York, N. Y.

Committee on Instruments and Measurements

J. H. Miller, *Chairman:* Weston Electrical Instrument Corporation, 614 Frelinghuysen Avenue, Newark 5, N. J.

J. G. Reid, Jr., *Vice-Chairman (East)*	Washington, D. C.
J. E. Hobson, *Vice-Chairman (West)*	Stanford, Calif.
Ernst Weber, *Secretary (East)*	Brooklyn, N. Y.
W. S. Pritchett, *Secretary (West)*	Berkeley, Calif.
S. P. Bartles	Rochester, N. Y.
P. L. Bellaschi	Portland, Oreg.
H. W. Berry	Minneapolis, Minn.
P. A. Borden	Waterbury, Conn.
D. L. Brown	Portland, Oreg.
L. A. Burckmyer, Jr.	Ithaca, N. Y.
D. T. Canfield	West Lafayette, Ind.
J. H. Chiles, Jr.	Sharon, Pa.
W. R. Clark	Philadelphia, Pa.
J. E. Clem	Schenectady, N. Y.
Nello Coda	Erie, Pa.
A. B. Craig	Boston, Mass.
E. B. Curdts	Philadelphia, Pa.
C. L. Dawes	Cambridge, Mass.
L. M. Dearing	Hollywood, Calif.
F. C. Doble	Belmont, Mass.
C. K. Duff	Toronto, Ontario, Canada
I. G. Easton	Cambridge, Mass.
W. N. Eddy	Cambridge, Mass.
G. V. Eltgroth	Philadelphia, Pa.
J. H. Enns	Ann Arbor, Mich.
R. K. Fairley	Schenectady, N. Y.
E. P. Felch, Jr.	Murray Hill, N. J.
Rudolf Feldt	Clifton, N. J.
J. G. Ferguson	Murray Hill, N. J.
F. J. Gaffney	Brooklyn, N. Y.
W. A. Geohegan	New York, N. Y.
T. S. Gray	Cambridge, Mass.
Ferdinand Hamburger, Jr.	Baltimore, Md.
F. K. Harris	Washington, D. C.
C. E. Hastings	Hampton, Va.
C. M. Hathaway	Denver, Colo.
A. J. Hornfeck	Cleveland, Ohio
W. G. Knickerbocker	Detroit, Mich.
H. C. Koenig	New York, N. Y.
F. X. Lamb	Newark, N. J.
G. L. Lane	Spokane, Wash.
Everett S. Lee	Schenectady, N. Y.
B. E. Lenehan	Newark, N. J.
W. N. Lindblad	Emeryville, Calif.
J. T. Lusignan, Jr.	Mansfield, Ohio
Harold Lyons	Washington, D. C.
N. W. Matthews	Washington, D. C.
W. J. Mayo-Wells	Silver Spring, Md.
G. A. Morton	Princeton, N. J.
L. J. Neuman	Houston, Tex.
David Packard	Palo Alto, Calif.
H. J. Plumley	White Oak, Md.
F. A. Redding	Alhambra, Calif.
C. F. Savage, Jr.	West Lynn, Mass.
F. B. Silsbee	Washington, D. C.
G. S. Smith	Seattle, Wash.
Harry Sohon	Philadelphia, Pa.
Carroll Stansbury	Washington, D. C.
K. M. Stevens	Alhambra, Calif.
L. N. Stone	Corvallis, Oreg.
J. M. Vanderleck	Toronto, Ontario, Canada
W. H. Wickham	Chicago, Ill.
A. H. Wing, Jr.	Evanston, Ill.
C. J. Zeller	New York, N. Y.

(Continued in next column)

Organization Subcommittee

T. S. Gray, *Chairman;* Massachusetts Institute of Technology, Cambridge 39, Mass.

C. F. Savage, *Secretary*	Lynn, Mass.
W. R. Clark	Philadelphia, Pa.
E. I. Green	Murray Hill, N. J.
H. C. Koenig	New York, N. Y.
E. S. Lee	Schenectady, N. Y.
J. H. Miller (ex officio)	Newark, N. J.
J. G. Reid, Jr. (ex officio)	Washington, D. C.

Co-operation with Instrument Society of America Subcommittee

(Personnel to be selected)

Definitions Subcommittee

C. L. Dawes, *Chairman;* Harvard University, Cambridge 39, Mass.

J. E. Clem	Schenectady, N. Y.
A. B. Craig	Boston, Mass.
H. C. Dickinson	Lynn, Mass.
R. K. Fairley	Schenectady, N. Y.
W. N. Goodwin, Jr.	Newark, N. J.
B. E. Lenehan	Newark, N. J.
F. B. Silsbee	Washington, D. C.

Dielectric Measurements in the Field Subcommittee

E. B. Curdts, *Chairman;* James G. Biddle Company, 1316 Arch Street, Philadelphia 7, Pa.

W. G. Amey	Philadelphia, Pa.
J. E. Clem	Schenectady, N. Y.
F. C. Doble	Belmont, Mass.
C. A. Duke	Chattanooga, Tenn.
W. F. Dunkle	Hazleton, Pa.
I. G. Easton	Cambridge, Mass.
W. N. Eddy	Cambridge, Mass.
I. W. Gross	New York, N. Y.
H. J. Klumb	Rochester, N. Y.
W. N. Lindblad	Emeryville, Calif.
H. C. Marcroft	Lancaster, Pa.
J. H. McWhirter	Sharon, Pa.
R. L. Murray	Birmingham, Ala.
W. H. Wickham	Chicago, Ill.

High Frequency Measurements Subcommittee

Ferdinand Hamburger, Jr., *Chairman;* The Johns Hopkins University, School of Engineering, Baltimore 18, Md.

R. G. Fellers	Washington, D. C.
R. K. Hellmann	Little Neck, N. Y.
J. W. Kearney	Mineola, N. Y.
H. Lyons	Washington, D. C.
H. R. Meahl	Schenectady, N. Y.
D. C. Ports	Washington, D. C.
Ernst Weber	Brooklyn, N. Y.
A. J. Wing, Jr.	Evanston, Ill.

Industrial Spectroscopy Subcommittee

J. H. Enns, *Chairman;* Randall Laboratory, University of Michigan, Ann Arbor, Mich.

H. M. Bedell	Cleveland, Ohio
G. D. Butler	New York, N. Y.
D. K. Coles	East Pittsburgh, Pa.
C. H. Corliss	Washington, D. C.
H. M. Crosswhite	Baltimore, Md.
W. G. Fastie	Philadelphia, Pa.
W. D. Hershberger	Berkeley, Calif.
E. K. Jaycox	Murray Hill, N. J.
L. W. McNair	Wood River, Ill.
J. Sherman	Philadelphia, Pa.
John Sterner	Cambridge, Mass.
Van Zandt Williams	Glenbrook, Conn.

Marking of Varmeters and Related Instruments Subcommittee

A. B. Craig, *Chairman;* Boston Edison Company, 39 Boylston Street, Boston, Mass.

A. L. Brownlee	Chicago, Ill.
A. L. Carvill	Lynn, Mass.
W. G. Knickerbocker	Detroit, Mich.
A. E. Knowlton	New York, N. Y.
F. A. Redding	Los Angeles, Calif.
F. B. Silsbee	Washington, D. C.
H. B. Smith	Buffalo, N. Y.

Master Test Code for Power Measurements Subcommittee

C. J. Zeller, *Chairman;* Consolidated Edison Company of N. Y., Inc., 708 First Avenue, New York 17, N. Y.

A. G. Christie	Baltimore, Md.
J. L. Fuller	Cleveland, Ohio
W. G. Knickerbocker	Detroit, Mich.
H. C. Koenig	New York, N. Y.
B. E. Lenehan	Newark, N. J.
L. W. Match	Chicago, Ill.
J. H. Miller	Newark, N. J.
C. F. Savage, Jr.	West Lynn, Mass.
H. Sohon	Philadelphia, Pa.
L. N. Stone	Corvallis, Oreg.

Revision of Standard No. 4 Subcommittee (Measurement of Test Voltage in Dielectric Tests (ASA C-68A))

J. T. Lusignan, Jr., *Chairman;* Ohio Brass Company, Mansfield, Ohio

P. L. Bellaschi	Portland, Oreg.
J. S. Carroll	Stanford, Calif.
J. J. Clark	East Pittsburgh, Pa.
J. E. Clem	Schenectady, N. Y.
E. W. Davis	Cambridge, Mass.
C. M. Foust	Schenectady, N. Y.
H. A. Frey	Baltimore, Md.
M. Getting, Jr.	Pittsburgh, Pa.
I. W. Gross	New York, N. Y.
J. H. Hagenguth	Pittsfield, Mass.
W. B. Kouwenhoven	Baltimore, Md.
W. W. Lewis	Schenectady, N. Y.
G. D. McCann, Jr.	Pasadena, Calif.
M. M. Newman	Minneapolis, Minn.
J. H. Park	Washington, D. C.
W. C. Sealey	Milwaukee, Wis.
C. S. Sprague	Lafayette, Ind.
W. L. Teague	Sharon, Pa.
W. H. Wickham	Chicago, Ill.
S. W. Zimmerman	Ithaca, N. Y.

Master Test Code for Speed Measurements Subcommittee

(Personnel to be selected)

Watthour Meters Subcommittee

B. E. Lenehan, *Chairman;* Westinghouse Electric Corporation, 95 Orange Street, Newark, N. J.

H. A. Brown	Rochester, N. Y.
G. N. Burkhart, Jr.	Lafayette, Ind.
D. T. Canfield	Lafayette, Ind.
A. B. Craig	Boston, Mass.
F. C. Holtz	Springfield, Ill.
W. G. Knickerbocker	Detroit, Mich.
H. C. Koenig	New York, N. Y.
W. N. Lindblad	Emeryville, Calif.
F. H. Rogers	Baltimore, Md.
C. F. Savage, Jr.	West Lynn, Mass.
K. M. Stevens	Alhambra, Calif.
M. B. Stout	Ann Arbor, Mich.
J. M. Vanderleck	Toronto, Ontario, Canada

Navigation Instruments Subcommittee

C. E. Hastings, *Chairman;* Hastings Instrument Company, Super Highway and Pine Avenue, Hampton, Va.

J. L. Anast	Dayton, Ohio
W. H. Bigger	Cedar Rapids, Iowa
W. C. Blaisdell	New York, N. Y.
R. T. Brown	Washington, D. C.
J. B. Coleman	Camden, N. J.
J. H. Dellinger	Chevy Chase, Md.
J. B. Feder	Washington, D. C.
W. P. Frantz	Great Neck, L. I., N. Y.
W. N. Hubbard	Essex, Conn.

(Continued on page 2185)

C. M. Jansky, Jr.	Washington, D. C.
J. W. Leas	Camden, N. J.
K. A. Norton	Boulder, Colo.
J. D. Peterson	Teterboro, N. J.
P. C. Sandretto	Nutley, N. J.
W. H. Skidmore	Newark, N. J.
A. F. VanDyck	New York, N. Y.
A. H. Warner	Cocoa, Fla.
P. V. H. Weems	Annapolis, Md.
H. S. Whitehead	Lynn, Mass.

Recorders and Controllers Subcommittee

A. J. Hornfeck, *Chairman;* Bailey Meter Company, 1050 Ivanhoe Road, Cleveland 10, Ohio

R. F. Wild, *Secretary*	Wilmington, Del.
E. F. Adams	Newark, N. J.
P. A. Borden	Waterbury, Conn.
G. L. Broomell	Philadelphia, Pa.
R. K. Fairley	Schenectady, N. Y.
J. G. Ferguson	Murray Hill, N. J.
Albert Hansen, Jr.	West Lynn, Mass.
W. H. Howe	Foxboro, Mass.
H. C. Koenig	New York, N. Y.
T. L. Mell	Philadelphia, Pa.
F. A. Ransom	Washington, D. C.
W. A. Stelzer	Midland, Mich.
J. M. Vanderleck	Toronto, Ontario, Canada
W. G. Walker	Philadelphia, Pa.

Instruments and Measurements Representatives on other Committees

Standard Frequency Bands and Designations Joint Subcommittee: I. G. Easton, General Radio Company, Cambridge, Mass.

ASA Instrument Transformer: J. H. Chiles, Jr., Westinghouse Electric Corporation, Sharon, Pa.

ASA Revision of C-39.1: H. C. Koenig, Electrical Laboratories, New York, N. Y.

ASA Revision C-39.2: H. C. Koenig, Electrical Laboratories, New York, N. Y.

AIEE Computing Devices Committee: G. V. Eltgroth, Remington Rand, Inc., Philadelphia, Pa.

ASME Industrial Instruments and Regulators: E. S. Lee, General Electric Review, Schenectady, N. Y.

Joint AIEE-IRE Noise Definitions Committee: I. G. Easton, General Radio Company, Cambridge, Mass.

Test and Measurements Subcommittee of Insulated Conductors Committee: W. N. Eddy, Simplex Wire and Cable Company, Cambridge, Mass.

Feedback Control Systems Committee, AIEE: J. G. Ferguson, Bell Telephone Laboratories, Inc., Murray Hill, N. J.

ASME Power Test Code Committee: C. J. Zeller, Consolidated Edison Company of New York, Inc., New York, N. Y.

AIEE Transformers Insulating Fluids Subcommittee: F. C. Doble, Doble Engineering Company, Belmont, Mass.

ASA Subcommittee C-63.1 on Noise Measurements: I. G. Easton, General Radio Company, Cambridge, Mass.

AIEE Committee on Electrical Techniques in Medicine and Biology: G. A. Morton, RCA Laboratories, Princeton, N. J.

Committee on Magnetic Amplifiers

E. L. Harder, *Chairman;* Westinghouse Electric Corporation, Industry Engineering Department 11-L, East Pittsburgh, Pa.

W. J. Dornhoefer, *Vice-Chairman*	Mt. Vernon, N. Y.

(Continued in next column)

E. V. Weir, *Secretary*	Butler, Pa.
A. O. Black, Jr.	Butler, Pa.
L. W. Buechler	St. Louis, Mo.
W. J. Field	St. Paul, Minn.
L. A. Finzi	Pittsburgh, Pa.
A. S. Fitzgerald	San Francisco, Calif.
W. A. Geyger	Silver Spring, Md.
A. B. Haines	Murray Hill, N. J.
J. E. Hart	Washington, D. C.
W. C. Johnson	Princeton, N. J.
H. W. Lord	Schenectady, N. Y.
F. S. Malick	Pittsburgh, Pa.
R. W. Moore	Buffalo, N. Y.
H. M. Ogle	Schenectady, N. Y.
P. L. Schmidt	East Pittsburgh, Pa.
C. F. Spitzer	Syracuse, N. Y.

Applications Subcommittee

R. W. Moore, *Chairman;* Westinghouse Electric Corporation, 4457 Genesee Street, Buffalo 5, N. Y.

W. J. Dornhoefer	Mount Vernon, N. Y.
L. A. Finzi	Pittsburgh, Pa.
A. S. Fitzgerald	San Francisco, Calif.
A. B. Haines	Murray Hill, N. J.
A. D. Hitt, Jr.	Washington, D. C.
W. F. Horton	Wilkinsburg, Pa.
H. M. Ogle	Schenectady, N. Y.
E. V. Weir	Butler, Pa.

Definitions Subcommittee

W. J. Dornhoefer, *Chairman;* Regulator Equipment Corporation, 55 MacQuesten Parkway South, Mount Vernon, N. Y.

W. J. Field	St. Paul, Minn.
L. A. Finzi	Pittsburgh, Pa.
A. B. Haines	Murray Hill, N. J.
E. L. Harder	East Pittsburgh, Pa.
H. W. Lord	Schenectady, N. Y.
E. V. Weir	Butler, Pa.

Listing of Principal Groups Subcommittee

A. O. Black, Jr., *Chairman;* Magnetics Inc., Butler, Pa.

L. W. Buechler	St. Louis, Mo.
H. W. Lord	Schenectady, N. Y.
P. L. Schmidt	East Pittsburgh, Pa.

Materials Subcommittee

P. L. Schmidt, *Chairman;* Westinghouse Electric Corporation, Materials Engineering Department, East Pittsburgh, Pa.

E. Albers-Schoenberg	Keasby, N. J.
A. O. Black, Jr.	Butler, Pa.
F. Brockman	Irving-on-Hudson, N. Y.
J. Conrath	St. Louis, Mo.
E. A. Gaugler	Butler, Pa.
H. A. Goldsmith	Long Island City, N. Y.
H. W. Lord	Schenectady, N. Y.

Non-Linear Circuit Theory Subcommittee

W. C. Johnson, *Chairman;* Princeton University, School of Engineering, Princeton, N. J.

W. J. Dornhoefer	Mount Vernon, N. Y.
L. A. Finzi	Pittsburgh, Pa.
A. B. Haines	Murray Hill, N. J.
E. L. Harder	East Pittsburgh, Pa.
R. A. Ramey	Washington, D. C.
H. F. Storm	Schenectady, N. Y.

Ratings Subcommittee

R. W. Wolke, *Chairman;* General Electric Company, 1 River Road, Schenectady 5, N. Y.

W. J. Dornhoefer	Mount Vernon, N. Y.
W. J. Field	St. Paul, Minn.
L. A. Finzi	Pittsburgh, Pa.
J. E. Hart	Washington, D. C.
R. W. Moore	Buffalo, N. Y.
B. E. Stevens	Murray Hill, N. J.

Test Code Subcommittee

H. M. Ogle, *Chairman;* General Electric Company, General Engineering Laboratory, Schenectady 5, N. Y.

L. W. Buechler	St. Louis, Mo.
L. A. Finzi	Pittsburgh, Pa.
F. S. Malick	Pittsburgh, Pa.
E. V. Weir	Butler, Pa.

Speed of Response, Figure of Merit Subcommittee

L. A. Finzi, *Chairman;* Carnegie Institute of Technology, Electrical Engineering Department, Schenley Park, Pittsburgh 13, Pa.

W. J. Dornhoefer	Mount Vernon, N. Y.
E. L. Harder	East Pittsburgh, Pa.
W. C. Johnson	Princeton, N. J.
H. B. Rex	Washington, D. C.
E. V. Weir	Butler, Pa.

Committee on Metallic Rectifiers

W. F. Bonner, *Chairman;* Selenium-Intelin Division, Federal Telephone and Radio Corporation, 100 Kingsland Avenue, Clifton, N. J.

Glen Ramsey, *Vice-Chairman*	North Chicago, Ill.
E. A. Harty, *Secretary*	West Lynn, Mass.
P. R. Brown	Hamilton, Ontario, Canada
L. W. Burton	Lynn, Mass.
J. T. Cataldo	Fort Monmouth, N. J.
P. G. Cobb	Newark, N. J.
M. E. Gamble	Indianapolis, Ind.
K. S. Geiges	New York, N. Y.
E. A. Groeteke	St. Louis, Mo.
C. E. Hamann	Lynn, Mass.
C. W. Hansell	Rocky Point, L. I., N. Y.
L. K. Hedding	Pittsburgh, Pa.
C. C. Herskind	Schenectady, N. Y.
C. K. Hooper	Baltimore, Md.
I. R. Smith	Buffalo, N. Y.
D. E. Trucksess	New York, N. Y.
J. L. Wagner	Endicott, N. Y.

Technical Information Subcommittee

C. E. Hamann, *Chairman;* Rectifier Division, General Electric Company, 920 Western Avenue, Lynn 3, Mass.

M. E. Gamble	Indianapolis, Ind.
L. K. Hedding	Pittsburgh, Pa.
J. L. Wagner	Endicott, N. Y.

Miniature Rectifiers Subcommittee

P. G. Cobb, *Chairman;* Weston Electrical Instrument Corporation, 614 Frelinghuysen Avenue, Newark 5, N. J.

Definitions Subcommittee

D. E. Trucksess, *Chairman;* Bell Telephone Laboratories, Inc., 463 West Street, New York 14, N. Y.

W. F. Bonner	Clifton, N. J.
C. W. Hansell	Rocky Point, L. I., N. Y.

Bibliography Subcommittee

E. A. Harty, *Chairman;* Rectifier Engineering Division, General Electric Company, River Works, West Lynn 3, Mass.

Test Code Subcommittee

I. R. Smith, *Chairman;* Motor Engineering Department, Westinghouse Electric Corporation, Buffalo, N. Y.

J. T. Cataldo	Fort Monmouth, N. J.
K. S. Geiges	New York, N. Y.

Patents Subcommittee

Glen Ramsey, *Chairman;* Fansteel Metallurgical Corporation, Rectifier Division, North Chicago, Ill.

Papers and Meetings Subcommittee

L. W. Burton, *Chairman;* General Electric Company, River Works, 920 Western Avenue, Lynn, Mass.

E. A. Groeteke	St. Louis, Mo.
Glen Ramsey	North Chicago, Ill.

Committee on Nucleonics

W. F. Davidson, *Chairman;* Consolidated Edison Company of New York, Inc., 4 Irving Place, New York 3, N. Y.

(Continued in next column)

G. W. Dunlap, *Vice-Chairman*	Schenectady, N. Y.
W. E. Barbour, Jr., *Secretary*	Boston, Mass.
H. W. Bibber	Schenectady, N. Y.
H. W. Brackney	Chevy Chase, Md.
D. W. Cardwell	Oak Ridge, Tenn.
J. O'R. Coleman	Boston, Mass.
T. S. Gray	Cambridge, Mass.
J. G. Hutton	Schenectady, N. Y.
T. R. Kohler	Irvington-on-Hudson, N. Y.
C. V. Larrick	Richland, Wash.
R. G. Lorraine	Schenectady, N. Y.
L. C. Marshall	Berkeley, Calif.
M. S. Oldacre	Chicago, Ill.
J. K. Pickard	Washington, D. C.
Walther Richter	Milwaukee, Wis.
P. N. Ross	Pittsburgh, Pa.
W. E. Shoupp	Pittsburgh, Pa.
Abe Tilles	San Francisco, Calif.
J. G. Trump	Cambridge, Mass.
R. E. Watson	Philadelphia, Pa.

Isotopic Tracers Subcommittee

R. E. Watson, *Chairman;* Research Department, Leeds and Northrup Company, 4901 Stenton Avenue, Philadelphia 44, Pa.

(Personnel to be selected)

Nuclear Theory Subcommittee

P. N. Ross, *Chairman;* Atomic Power Division, Westinghouse Electric Corporation, Bettis Field, P. O. Box 1468, Pittsburgh 30, Pa.

Nuclear Machines Subcommittee

J. G. Hutton, *Chairman;* General Engineering Laboratory, General Electric Company, Schenectady 5, N. Y.

(Personnel to be selected)

Joint Subcommittees

Joint Subcommittee on Applications of Probability Methods to Power-System Problems (Joint with Power Generation and System Engineering Committees)

G. Calabrese, *Chairman;* Electrical Engineering Department, New York University, University Heights, New York 53, N. Y.

W. R. Blakely	Toronto, Ontario, Canada
V. M. Cook	New York, N. Y.
Howard Duryea	Birmingham, Ala.
R. G. Hooke	Newark, N. J.
F. J. Leerburger	New York, N. Y.
H. A. Lott	Los Angeles, Calif.
W. J. Lyman	Pittsburgh, Pa.
Bela Mohr	Oklahoma City, Okla.
H. W. Phillips	Philadelphia, Pa.
H. B. Smith	Buffalo, N. Y.
V. A. Thiemann	New York, N. Y.
C. W. Watchorn	Baltimore, Md.

Joint Subcommittee on Electronic Instruments (Joint with Electronics and Instruments and Measurements Committees)

Rudolf Feldt, *Chairman;* Allen B. DuMont Laboratories, Inc., 1000 Main Avenue, Clifton, N. J.

W. H. Tidd, *Vice-Chairman*	Murray Hill, N. J.
P. K. McElroy, *Secretary*	Cambridge, Mass.
M. J. Ackerman	Camden, N. J.
G. E. Beggs, Jr.	Philadelphia, Pa.
C. C. Chambers	Philadelphia, Pa.
Edward Durbin	Great Neck, L. I., N. Y.
G. V. Eltgroth	Philadelphia, Pa.
M. L. Greenough	Washington, D. C.
R. R. Haberland	Silver Spring, Md.
C. E. Hastings	Hampton, Va.
C. M. Hathaway	Denver, Colo.
D. M. Hill	Boonton, N. J.
G. B. Hoadley	Raleigh, N. C.

(Continued on page 2186)

N. W. Matthews	Washington, D. C.
Edmund Osterland	Boonton, N. J.
E. R. Thomas	New York, N. Y.
J. T. Thwaites	Hamilton, Ontario, Canada
Howard Vollum	Portland, Oreg.
A. H. Waynick	State College, Pa.
W. P. Wills	Philadelphia, Pa.

Joint Subcommittee on Carbon Brushes (Joint AIEE Technical Committees on Air Transportation and Rotating Machinery, and in Co-operation with NEMA on Codes)

T. M. Linville, *Chairman;* General Electric Company, 1 River Road, Schenectady 5, N. Y.

W. T. Appleman	Dayton, Ohio
W. H. Austry	St. Marys, Pa.
R. J. Blais	New York, N. Y.
H. R. Brown	Seattle, Wash.
W. E. Clancy	St. Marys, Pa.
J. V. Dobson	St. Marys, Pa.
H. M. Elsey	East Pittsburgh, Pa.
C. B. Hathaway	Buffalo, N. Y.
L. A. Heath	Long Island City, N. Y.
B. C. Henry	Ironton, Ohio
C. J. Herman	Fort Wayne, Ind.
V. P. Hessler	Urbana, Ill.
L. H. Hilderbrandt	Dayton, Ohio
H. T. Hulbert	St. Marys, Pa.
R. E. Klokow	Lima, Ohio
E. A. Lapham	Long Island City, N. Y.
L. R. Larson	Washington, D. C.
I. M. Levy	Dayton, Ohio
K. Lugosch	Johnsville, Pa.
Clarence Lynn	East Pittsburgh, Pa.
I. H. Manfredo	Brooklyn, N. Y.
M. S. May	St. Marys, Pa.
H. F. Mitchel	Saginaw, Mich.
E. H. Myers	East Pittsburgh, Pa.
L. C. Novak	West Lynn, Mass.
H. R. Partridge	Boonton, N. J.
Dimiter Ramadanoff	Cleveland, Ohio
O. C. Rutledge	Schenectady, N. Y.
S. D. Summers	Washington, D. C.
F. R. Terrant	Cleveland, Ohio
H. R. Tragesser	Cleveland, Ohio
A. L. VanEmden	Washington, D. C.
W. W. Walker	Yonkers, N. Y.

Joint Subcommittee on Nucleonic Instruments (Joint with Nucleonics and Instruments & Measurements Committees)

G. A. Morton, *Chairman;* Radio Corporation of America, RCA Laboratories Division, Princeton, N. J.

R. L. Butenhoff	Washington, D. C.
D. L. Collins	Cleveland, Ohio
L. F. Curtiss	Washington, D. C.
P. W. Davison	Princeton, N. J.
F. D. Lewis	Cambridge, Mass.
A. Lovoff	Washington, D. C.
M. A. Schultz	Pittsburgh, Pa.
W. W. Schultz	Schenectady, N. Y.

Joint Subcommittee on Telemetering (Joint with Instruments & Measurements, Carrier Current, and Substations Committees)

W. J. Mayo-Wells, *Chairman;* Applied Physics Laboratory, The Johns Hopkins University, 10,010 Georgia Avenue, Silver Spring 18, Md.

E. E. Lynch, *Secretary*	West Lynn, Mass.
J. L. Blackburn	Newark, N. J.
P. A. Borden	Waterbury, Conn.
M. A. Bostwick	Portland, Oreg.
Robert Brandt	Boston, Mass.
W. A. Derr	East Pittsburgh, Pa.
C. K. Duff	Toronto, Ontario, Canada
A. J. Hornfeck	Cleveland, Ohio
R. K. Klumb	Los Angeles, Calif.
G. S. Lunge	Schenectady, N. Y.
C. A. Mabey	Newark, N. J.
J. L. McKee	New York, N. Y.
J. W. Peckham	Los Angeles, Calif.
W. E. Phillips	Philadelphia, Pa.
G. M. Thynell	Silver Spring, Md.
G. E. Winegartner	Cleveland, Ohio

AIEE-IRE Subcommittee on Telemetering Terms

W. J. Mayo-Wells (*AIEE-IRE*), *Chairman;* Applied Physics Laboratory, The Johns Hopkins University, 10,010 Georgia Avenue, Silver Spring 18, Md.

J. L. Blackburn (*AIEE*)	Newark, N. J.
J. F. Brinster (*IRE*)	Princeton, N. J.
R. E. Colander (*AIEE-IRE*)	Burbank, Calif.
C. K. Duff (*IRE*)	Toronto, Ontario, Canada
A. P. Gruer (*AIEE-IRE*)	Albuquerque, New Mex.
R. L. Harding (*AIEE-IRE*)	Mishawaka, Ind.
C. H. Hoeppner (*IRE*)	Newton, Mass.
M. V. Kiebert (*AIEE-IRE*)	Detroit, Mich.
F. Lehan (*AIEE-IRE*)	Pasadena, Calif.
E. E. Lynch (*AIEE*)	West Lynn, Mass.
M. G. Pawley (*AIEE-IRE*)	Corona, Calif.
W. E. Phillips (*AIEE*)	Philadelphia, Pa.
G. M. Thynell (*AIEE-IRE*)	Silver Spring, Md.
F. L. Verwiebe (*AIEE-IRE*)	Silver Spring, Md.
G. F. C. Weedon (*AIEE-IRE*)	Toronto, Ontario, Canada
G. E. White (*IRE*)	Los Angeles, Calif.
W. A. Wildhack (*AIEE-IRE*)	Washington, D. C.

AIEE-IRE Joint Committee on High Frequency Measurements

E. P. Felch, *General Chairman;* Bell Telephone Laboratories, Inc., Murray Hill, N. J.

AIEE

Ferdinand Hamburger, Jr., *Chairman;* School of Electrical Engineering, The Johns Hopkins University, Homewood, Baltimore, Md.

R. G. Fellers	Washington, D. C.
R. K. Hellmann	Little Neck, L. I., N. Y.
J. W. Kearney	Mineola, N. Y.
Harold Lyons	Washington, D. C.
H. R. Meahl	Schenectady, N. Y.
D. C. Ports	Washington, D. C.
Ernst Weber	Brooklyn, N. Y.
A. H. Wing, Jr.	Evanston, Ill.

IRE

E. I. Green, *Chairman;* Bell Telephone Laboratories, Inc., Murray Hill, N. J.

R. W. Lowman, *Secretary*	Mineola, N. Y.
R. A. Braden	Princeton, N. J.
I. G. Easton	Cambridge, Mass.
F. J. Gaffney	Brooklyn, N. Y.
G. B. Hoadley	Raleigh, N. C.
E. W. Houghton	Murray Hill, N. J.
B. Parzen	Nutley, N. J.
H. E. Webber	Great Neck, L. I., N. Y.

AIEE-ASME Joint Subcommittee on Recommended Specifications for the Speed Governing of Prime Movers

M. J. Steinberg (*AIEE*), *Chairman;* Consolidated Edison Company of New York, Inc., 4 Irving Place, New York 3, N. Y.

W. C. Astley (*ASME*)	Philadelphia, Pa.
C. L. Avery (*ASME*)	Rockford, Ill.
S. B. Griscom (*AIEE*)	East Pittsburgh, Pa.
A. P. Hayward (*AIEE*)	Pittsburgh, Pa.
C. E. Kenney (*ASME*)	Milwaukee, Wis.
J. B. McClure (*AIEE*)	Schenectady, N. Y.
G. H. McDaniel (*AIEE*)	New York, N. Y.
A. F. Schwendner (*ASME*)	Philadelphia, Pa.
Raymond Sheppard (*ASME*)	Schenectady, N. Y.

AIEE Representatives

APPOINTED BY THE BOARD OF DIRECTORS

Alfred Noble Prize Committee, ASCE

T. M. Linville	Schenectady, N. Y.

American Association for the Advancement of Science, Council

J. W. Barker	New York, N. Y.
I. Melville Stein	Philadelphia, Pa.

American Research Committee on Grounding

C. T. Sinclair	Pittsburgh, Pa.

American Standards Association, Standards Council

F. E. Harrell	Cleveland, Ohio
Charles Rufus Harte	New Haven, Conn.
R. T. Henry	Buffalo, N. Y.

Alternates

R. C. Bergvall	Pittsburgh, Pa.
J. R. North	Jackson, Mich.
E. B. Paxton	Schenectady, N. Y.

American Year Book, Advisory Board

H. H. Henline	New York, N. Y.

Conference of Representatives From Engineering Societies of Western Europe and USA

F. O. McMillan	Corvallis, Oreg.
H. H. Henline	New York, N. Y.

Construction Industry Advisory Council

H. H. Henline	New York, N. Y.

Engineering Foundation Board

J. W. Barker	New York, N. Y.
C. G. Suits	Schenectady, N. Y.

Engineering Societies Monographs Committee

W. F. Davidson	New York, N. Y.
W. I. Slichter	New York, N. Y.

Engineers' Council for Professional Development

R. H. Barclay	New York, N. Y.
M. S. Coover	Ames, Iowa (*Until Annual Meeting, Oct. '51*)
D. D. Ewing	Lafayette, Ind. (*After Annual Meeting, Oct. '51*)
M. D. Hooven	Newark, N. J.

Engineers Joint Council

J. F. Fairman	New York, N. Y.
H. H. Henline	New York, N. Y.
T. G. LeClair	Chicago, Ill.
F. O. McMillan	Corvallis, Oreg.

Alternates

W. J. Barrett	Newark, N. J.
J. L. Callahan	New York, N. Y.

General Electric Educational Fund Fellowship Committee

John L. Callahan	New York, N. Y.

Hertz Award Committee

M. S. Coover	Ames, Iowa

Hoover Medal Board of Award

T. G. LeClair	Chicago, Ill.
D. C. Prince	Schenectady, N. Y.
J. G. Tarboux	Ithaca, N. Y.

John Fritz Medal Board of Award

J. F. Fairman	New York, N. Y.
B. D. Hull	Dallas, Tex.
T. G. LeClair	Chicago, Ill.
Everett S. Lee	Schenectady, N. Y.

Joint AIEE-IRE Co-ordination Committee

W. J. Barrett	Newark, N. J.
Everett S. Lee	Schenectady, N. Y.

Library Board, United Engineering Trustees, Inc.

N. S. Hibshman	Brooklyn, N. Y.
W. G. Vieth	New York, N. Y.

Marston Medal Board of Award

Harry B. Gear	Chicago, Ill.

National Association of Corrosion Engineers, Inter-Society Committee on Corrosion

L. J. Gorman	New York, N. Y.
H. M. Trueblood	Dobbs Ferry, N. Y.

National Bureau of Engineering Registration, Advisory Board

N. L. Freeman	Albany, N. Y.

National Electronics Conference, Board of Directors

W. G. Dow	Ann Arbor, Mich.

National Engineering Advisory Committee

A. H. Kehoe	New York, N. Y.

National Fire Waste Council

Hendley Blackmon	East Pittsburgh, Pa.
W. B. Kouwenhoven	Baltimore, Md.

National Research Council, Division of Engineering and Industrial Research

W. B. Kouwenhoven	Baltimore, Md.

Quarterly of Applied Mathematics

M. G. Malti	Ithaca, N. Y.

United Engineering Trustees, Inc.

W. J. Barrett	Newark, N. J.
A. G. Oehler	New York, N. Y.
D. A. Quarles	New York, N. Y.

U. S. National Committee of the International Commission on Illumination

Ward Harrison	Cleveland, Ohio
R. C. Putnam	Cleveland, Ohio
E. H. Salter	New York, N. Y.

Washington Award Commission

W. L. Everitt	Urbana, Ill.
Frank V. Smith	Chicago, Ill.

World Power Conference, Executive Committee of United States National Committee

F. O. McMillan	Corvallis, Oreg.

APPOINTED BY STANDARDS COMMITTEE

Aeronautical Electrical Equipment Standardization

D. E. Fritz, liaison with NASC and SAE Cleveland, Ohio

Electrical Standards Committee, ASA and U. S. National Committee of the International Electrotechnical Commission

F. E. Harrell	Cleveland, Ohio
E. B. Paxton	Schenectady, N. Y.
J. J. Pilliod	New York, N. Y.

Alternates

R. D. deKay	New York, N. Y.
I. W. Gross	New York, N. Y.

Division Assignment

Communication and Electronics Division

R. D. deKay	New York, N. Y.
F. E. Harrell	Cleveland, Ohio
J. J. Pilliod	New York, N. Y.

Power Division

I. W. Gross	New York, N. Y.
E. B. Paxton	Schenectady, N. Y.

Industry Committee on Interior Wiring Design

M. M. Brandon	New York, N. Y.
L. C. Peterman	New York, N. Y.

Joint Committee for Development of Statistical Applications in Engineering and Manufacturing

W. P. Dobson	Toronto, Ontario, Canada

National Fire Protection Association, Electrical Section

Robin Beach	Brooklyn, N. Y.
W. B. Kouwenhoven	Baltimore, Md.